DAMIAN E. DUPUY
YUMAN FONG
WILLIAM N. MCMULLEN
EDITORS

Image-Guided Cancer Therapy

A Multidisciplinary Approach

Springer Reference

Image-Guided Cancer Therapy

Damian E. Dupuy • Yuman Fong
William N. McMullen
Editors

Image-Guided Cancer Therapy

A Multidisciplinary Approach

With 394 Figures and 71 Tables

Springer Reference

Editors
Damian E. Dupuy
Department of Diagnostic Imaging
Rhode Island Hospital
The Warren Alpert Medical School of
Brown University
Providence, RI, USA

Yuman Fong
Department of Surgery and Radiology
Memorial Sloan Kettering Cancer Center
New York, NY, USA

William N. McMullen
McMullen Consulting, LLC
Surprise, AZ, USA

ISBN 978-1-4419-0750-9 ISBN 978-1-4419-0751-6 (eBook)
ISBN 978-1-4419-0752-3 (print and electronic bundle)
DOI 10.1007/978-1-4419-0751-6
Springer New York Heidelberg Dordrecht London

Library of Congress Control Number: 2013937941

Printed on acid-free paper

Springer is part of Springer Science+Business Media (www.springer.com)

We all have known several people who over the years motivate and drive us to continue our work in alleviating the pain and suffering of those with cancer. One of my former co-workers and good friend, Paul R. Morrison, was one of those.

Paul was a medical physicist in the Department of Radiology at Brigham & Women's Hospital. He received his M.Sc. in Physics from Illinois Institute of Technology in 1987. On graduating, he worked as a laser specialist in the Department of Dermatology at Boston University Medical Center. Thereafter, he moved across town and began work in the Department of Surgery at BWH, focusing on laser applications in otolaryngology. This quickly evolved into a series of clinical projects involving image-guided surgery as well as experiments in MRI of thermal events in tissue at the genesis of a growing collaboration between Surgery and Radiology. This collaboration evolved into what is now the Image Guided Therapy Program headed by Dr. Ferenc Jolesz. In 2000, he moved over to the Department of Radiology, with primary duties in the Cross-sectional Interventional Radiology Service and the Tumor Ablation Program. He is focused on image-guided thermal ablation (e.g., cryotherapy, radiofrequency, and laser) from both a clinical and experimental perspective. Over the years, he has been involved in hundreds of clinical procedures.

Paul is a member of the American Association of Physicists in Medicine. He has co-authored over 35 original articles on a range of related topics that include cryotherapy, radiofrequency ablation, laser, image-guided surgery, computer-assisted visualization, and computer-assisted

navigation in a range of organs and systems. In addition to a number of reviews and posters, he has been involved with over 50 scientific abstracts and has given presentations in a variety of academic and professional venues.

Paul was one of those rare individuals who emulates the highest qualities of a medical professional in the attitude in which he carried himself with his colleagues and patients. I always enjoyed his dry sense of humor and intellectual comments based on his unique viewpoint. He was one of the most intelligent people I have ever worked with. Paul lost his courageous battle with cancer on September 24, 2012. In addition to his vital role at BWH, he was a warm, thoughtful, and sensitive colleague and friend who will be deeply missed.

—William N. McMullen

Foreword

This book which has the "who's who" in interventional oncology as its editors, and, importantly, as its authors, incorporate a unique style and a completely integrated approach to this relatively new and fascinating field. Interventional oncology has literally rocketed to the forefront of interventional radiology, surgical oncology, radiation therapy, and oncology. There is not one meeting, nationally or internationally, in any of these specialties that does not address this subject.

What makes a book like this good? It's a combination of the editors and the authors. This is not just a book put together without thought with authors who are only slightly familiar with a topic. Indeed, the editors represent leaders in the field of interventional oncology and individuals who put this subspecialty on the map. They have carefully chosen outstanding leaders in the field to thoroughly address this new specialty. The reader will be exposed to all aspects of the specialty from interventional radiology to radiation therapy.

Led by Damian E. Dupuy, this group of editors have corralled this sometimes difficult and complicated subject into digestible bits that will allow interested physicians to understand and use them when needed. The book is organized topically, allowing the reader to become educated in all aspects of interventional oncology. Current areas of interest such as liver tumors, bone tumors, metastatic tumors, etc. allows the reader to easily access commonly seen disease processes that are nicely updated and categorized in this opus.

However, this is not a standard textbook with standard coverage. It goes much beyond that. The first section describes the theories and science behind several techniques including the newest, "electroporation," which is so new that few monographs have described it. The second part of the book explores an area which is extremely important, but is not discussed in enough detail in most books. These include the development of clinical practice, the interaction with anesthesia, and patient management issues in cancer patients who are undergoing these techniques. This is one of the more neglected areas of discussion in most books and one of the most difficult parts of any interventional oncology procedure. The total management of the patient is not an area which is well discussed or taught in the review courses set up in most societal meetings.

The format is both readable and practical in that the book is divided into both organ-based topics such as liver, kidney, and lung and specific topics that the reader can turn to such as treatment of metastasis; the chapter on "alternatives and novel therapies of the liver" is a great example of the total scope

of the book; where else can you get a review of cryotherapy of liver or the use of laser therapy? The senior authors are all world-renowned experts in interventional oncology which is another example of the high-quality authorship and experience that is brought to this book.

The later chapters discuss therapies that are simply not covered in any other source: Everyone who is doing or wants to do ablation therapies and interventional oncology will face a time when they will be asked to use their expertise in less used and less investigated areas. There is nowhere else where the reader can get information on the prostate, breast, gynecologic areas, and especially pediatrics. These chapters offer an outstanding compliment to the basic material described earlier in the book.

This book is an outstanding contribution to the literature and will become a "must read" for all physicians who are interested in interventional oncology.

Boston, Massachusetts
USA

Peter R. Mueller, MD

Preface

Multidisciplinary care for cancer is no longer just surgery, chemotherapy, and radiotherapy. Interventional oncology is a rapidly growing field that is already indispensible in the care of the patient with a malignancy. Needle- and catheter-based therapies provide palliation of symptoms, cyto-reduction in cases of incurable cancers, and potential cure in cancers discovered at an early enough stage. This book is an attempt at summarizing the state of the art in terms of physical and biologic basis of practice and current clinical delivery. This book does not only present the data for use of interventional procedure, but also tries to placed these procedures within the context of other modalities for treatment of cancer.

The authorship of this book includes surgeons, oncologists, radiation therapists, in addition to the leaders in interventional radiology. It is an authorship that reflects the multidisciplinary nature of the book and of the field of cancer care. We, the editors, thank the contributors for writing their thorough chapters in a timely fashion while juggling their day-to-day activities of being busy clinicians and scientists. We understand how busy professionals have ever-changing lives and ever-increasing tasks related to their jobs and personal life may make it hard to "write another chapter." Our book, *Image-Guided Cancer Therapy*: *A Multidisciplinary Approach*, is a testament to the patience, understanding, and hard work of the editors, associate editors, section editors, and authors, for without whom this book would never have come to completion. We all share a vision that having the current practice of interventional oncology summarized in a comprehensive textbook is timely and important.

We would be remiss not to thank our families, loved ones, coworkers and support staff whose love and support allowed us to take the extra time needed to bring together this important body of work which we feel is a very comprehensive source of information for cancer practitioners today. Thus, to our wives Cathy, Nicole, and Kris, we particularly say thanks. We would also be negligent if we didn't thank the thousands of courageous cancer patients who have undergone some of these advanced therapies as part of clinical trials or as part of their cancer care. As with many fields that rely on state-of-the-art technology, this field is rapidly growing and changing.

Hopefully, this book is the first of many future editions that addresses this ever-changing , evolving, and exciting field of medicine.

Damian E. Dupuy, MD, FACR
Yuman Fong, MD, FACS
William N. McMullen

Editors

Damian E. Dupuy, MD, FACR, Director of Tumor Ablation, Department of Diagnostic Imaging, Rhode Island Hospital, The Warren Alpert Medical School of Brown University, Providence, Rhode Island, USA

Damian E. Dupuy is the director of tumor ablation at Rhode Island Hospital and a professor of diagnostic imaging at The Warren Alpert Medical School of Brown University.

Dr. Dupuy received his medical degree from the University of Massachusetts Medical School in 1988 and completed his residency in radiology at The New England Deaconess Hospital and Harvard Medical School in 1993. After residency Dr. Dupuy joined the staff at Massachusetts General Hospital where he worked in the Abdominal Imaging and Bone and Joint Divisions.

In 1997 Dr. Dupuy joined the Department of Diagnostic Imaging at Rhode Island Hospital and Brown University.

Dr. Dupuy, a pioneer in the use of image-guided ablation, helped broaden clinical applications to successfully combat cancer involving the kidney, liver, lung, head and neck, adrenal, and skeleton. Other newer technologies such as percutaneous microwave ablation, cryoablation, and combination therapies using RFA with external radiation or brachytherapy have been pioneered by Dr. Dupuy, who has been the principal investigator of two multicenter trials funded by the National Cancer Institute.

Dr. Dupuy has received national awards for research and teaching from the American College of Radiology Imaging Network and the Radiological Society of North America (RSNA) where he is currently the chair of the Interventional Oncology Symposium featured at the Annual Meeting of the RSNA and fellow of the American College of Radiology.

Dr. Dupuy is a member of the RSNA, The New England Roentgen Ray Society, the American College of Radiology, Rhode Island Radiological Society, and the Society of Interventional Radiology.

Dr. Dupuy has published over 150 publications and given over 120 invited lectures in the field of radiology and image-guided ablation both nationally and internationally.

Yuman Fong, MD, Murray F. Brennan Chair in Surgery, Department of Surgery and Radiology, Memorial Sloan Kettering Cancer Center, New York, New York, USA

Dr. Yuman Fong is an attending surgeon at the Memorial Sloan-Kettering Cancer Center (MSKCC), where he holds the Murray F. Brennan Chair in Surgery. He is a professor of surgery at Weill Cornell Medical College. Dr. Fong received a B.A. in medieval literature from Brown University in 1981, and an M.D. from Cornell University Medical College in 1984. This was followed by surgical training at the New York Hospital/Cornell Medical Center and a surgical oncology fellowship at MSKCC.

Dr. Fong is best known clinically for his extensive work in the field of hepatobiliary surgery—especially for hepatocellular carcinoma, hepatic metastases from colorectal cancer, gallbladder cancer, cholangiocarcinoma, and pancreatic cancer. He has pioneered many surgical, laparoscopic, and ablative therapies for these cancers.

Dr. Fong leads an active laboratory studying the use of genetically modified viruses for the killing of cancer. He was one of the first investigators to administer engineered viruses into the blood stream of humans for treatment of cancer. He is active at coordinating trials of such novel viruses in international clinical trials.

Dr. Fong has co-authored over 600 peer-reviewed articles and 11 textbooks. He has been on the editorial boards of 14 journals. He is a member of numerous scientific and medical societies including the American Surgical Association, Southern Surgical Association, and American Society for Clinical Investigation. He has received many honors and awards including the James IV Surgical Traveler, and the Shipley Award from the Southern Surgical Association. He has served on the board of the Society for Surgery of the Alimentary Tract and the board of the James IV Society of Surgeons. He is currently Chair of the recombinant DNA advisory committee of the National Institutes of Health.

William N. McMullen, Owner/Consultant, McMullen Consulting, LLC, Surprise, Arizona, USA

Bill McMullen is currently the owner and consultant for McMullen Consulting, LLC. In this role, he provides technical advice, clinical guidance, and market analysis for companies and investors, competitive product assessment, risk analysis, FDA, and global regulatory guidance.

McMullen started out his career in the mid-1970s working to promote and launch ultrasound as a diagnostic tool for physicians. Later, he was a part of the pioneering team to develop the first U.S. Food and Drug Administration (FDA)-cleared ultrasound contrast agent. Remaining true to his ultrasound background, he assisted in the development of the first laparoscopic ultrasound system in the United States for surgeons.

McMullen continued his work acquiring global experience developing thermal ablative techniques in the fields of radiology, surgery, and interventional oncology; specializing in device operations, prototyping, technology assessment, clinical education, and commercialization at a senior level for leading companies.

McMullen's past experience included serving as vice president, Ablation Market Development, DFINE, Inc., senior vice president of interventional oncology for Microsulis Medical (Acquired by AngioDynamics), director of operations – tumor ablation at Radionics (now Covidien), and director of clinical marketing for RITA Medical Systems (also acquired by AngioDynamics, Inc.). In these roles, he helped develop and launch the first FDA-cleared RF ablation system and coordinated worldwide sales, marketing, clinical trials, customer education, manufacturing, regulatory, and engineering operations for RF ablation products.

McMullen is the founder and co-program director for Fire, Ice & Beyond: The Future of Interventional Oncology. This program involves some of the world's foremost clinicians and institutions interested in adding ablation therapies and interventional programs to a radiology or surgical practice. He sits on several editorial and review boards and has coedited highly regarded publications, including *Tumor Ablation: Principles and Practice*

and *Image-Guided Cancer Therapy: A Multidisciplinary Approach*. In addition, he is the founder and administrator of Radiological Society of North America Working Group on Image-Guided Tumor Ablation, an international consortium composed of like-minded physicians, scientists, and dedicated to investigating the potential uses of image-guided tumor ablation therapies.

Associate Editors

David Lu Professor of Radiology; Director, CT and Cross Sectional IR; Director HIFU and Tumor Ablation Program, Ronald Reagan Medical Center, UCLA Healthcare, Los Angeles, California, USA

Riccardo Lencioni Professor of Radiology, Division of Diagnostic Imaging and Intervention, Pisa University Hospital and School of Medicine, Pisa, Italy

Jordan Berlin Associate Professor, Division of Hematology and Oncology, Department of Medicine, Vanderbilt University, Nashville, Tennessee, USA

Section Editors

Shraga Nahum Goldberg Section Chief, Image-Guided Therapy and Interventional Oncology, Department of Radiology, Hebrew University-Hadassah Medical Center, Jerusalem, Israel

Matthew Callstrom Associate Professor of Radiology, Department of Radiology, Mayo Clinic, Rochester, Minnesota, USA

E. David Crawford Head, Section of Urologic Oncology; and Professor of Urologic and Radiation Oncology, University of Colorado at Denver, University of Colorado Hospital, Aurora, Colorado, USA

Debra A. Gervais Division Chief, Abdominal Imaging and Intervention, Division Chief, Pediatric Imaging; and Assistant Program Director, MGH Radiology Residency, Boston, Massachusett, USA

Chul S. Ha Professor and Chairman, Department of Radiation Oncology, Cancer Therapy and Research Center at the University of Texas Health Science Center, San Antonio, TX, USA

Robert L. Worthington-Kirsch Medical Director, Vein Clinics of America, Wayne, Pennsylvania, USA

Peter J. Littrup Director, Imaging Core and Radiological Research; and Director, Image Guided Therapy Program, Karmanos Cancer Institute, Imaging Division, Detroit, Michigan, USA

Contents

† Deceased

Contributors

Fereidoun Abtin Department of Radiological Sciences, Ronald Reagan UCLA Medical Center, Los Angeles, CA, USA

Muneeb Ahmed Department of Radiology, WCC 308-B, Beth Israel Deaconess Medical Center, Section of Interventional Radiology, Boston, MA, USA

Munther Ajlouni Department of Radiation Oncology, Henry Ford Health Systems, Detroit, MI, USA

Rosalinda Alvarado Department of General Surgery, Rush University Medical Center, Chicago, IL, USA

Yasuaki Arai Department of Diagnostic Radiology, National Cancer Center Hospital, Tokyo, Japan

Thomas D. Atwell Department of Diagnostic Radiology, Mayo Clinic, Rochester, MN, USA

Tushar C. Barot Mount Sinai Medical Center, Miami Beach, FL, USA

Daniel Baseman Department of Radiation Oncology, Cancer Therapy and Research Center & The University of Texas Health Science Center at San Antonio, San Antonio, TX, USA

Jordan Berlin Department of Medicine, Division of Hematology and Oncology, Vanderbilt University Medical Center, Nashville, TN, USA

Jeffrey Berman Jeffrey Berman Architect, New York, NY, USA

Chris L. Brace Department of Radiology, University of Wisconsin – Madison, Madison, WI, USA

David J. Breen Department of Radiology, Southampton University Hospitals, Southampton, UK

Daniel B. Brown Department of Radiology, Thomas Jefferson University, Philadelphia, PA, USA

Matthew Callstrom Department of Diagnostic Radiology, Mayo Clinic, Rochester, MN, USA

Raphael Catane Oncology Institute, Sheba Medical Center, Tel Hashomer, Ramat Gan, Israel

Indrin J. Chetty Department of Radiation Oncology, Henry Ford Health Systems, Detroit, MI, USA

Jonathan A. Coleman Department of Surgery, Urology Division, Weill Cornell/Memorial Sloan Kettering Cancer Center, New York, NY, USA

Erik N. K. Cressman Department of Radiology, University of Minnesota Medical Center, Minneapolis, MN, USA

Laura Crocetti Division of Diagnostic Imaging and Intervention, School of Medicine, University of Pisa, Cisanello Hospital, Pisa, IT, Italy

Farshid Dayyani Division of Hematology-Oncology, The University of Texas MD Anderson Cancer Center, Houston, TX, USA

Seyed Saeid Dianat Department of Urology, New York University VA University Hospital, New York, NY, USA

Elizabeth A. Dick Department of MRI, St. Mary's Hospital Imperial College Healthcare NHS Trust, London, UK

Thomas A. DiPetrillo Department of Radiation Oncology, Rhode Island Hospital, Providence, RI, USA

Bob Djavan Department of Urology, New York University VA University Hospital, New York, NY, USA

Gerald Dodd, III Department of Radiology, University of Colorado, Denver, Aurora, CO, USA

Kambiz Dowlatshahi Department of General Surgery, Rush University Medical Center, Chicago, IL, USA

Melinda Dunlap Department of Medicine, Division of Hematology and Oncology, Vanderbilt University Medical Center, Nashville, TN, USA

Damian E. Dupuy Department of Diagnostic Imaging, Rhode Island Hospital, The Warren Alpert Medical School of Brown University, Providence, RI, USA

Tony Y. Eng Department of Radiation Oncology, Cancer Therapy and Research Center & The University of Texas Health Science Center at San Antonio, San Antonio, TX, USA

Fiona M. Fennessy Department of Radiation, Brigham and Women's Hospital, Boston, MA, USA

Richard S. Finn Department of Medicine, Geffen School of Medicine at UCLA Ronald Regan Medical Center at UCLA, Los Angeles, CA, USA

Mary Fischer Department of Anesthesia and Critical Care, Memorial Sloan-Kettering Cancer Center, New York, NY, USA

Yuman Fong Department of Surgery and Radiology, Memorial Sloan Kettering Cancer Center, New York, NY, USA

Martin Fuss Department of Radiation Medicine, Oregon Health and Science University, Portland, OR, USA

Wadyslaw M. W. Gedroyc Department of Radiology, St. Mary's Hospital Imperial College Healthcare NHS Trust, London, UK

S. Nahum Goldberg Department of Radiology, Hebrew University-Hadassah Medical Center, Jerusalem, Israel

David J. Grand Department of Diagnostic Radiology, Warren Alpert School of Medicine, Brown University, Providence, RI, USA

Seza A. Gulec Department of Surgical Oncology, The Herbert Wertheim College of Medicine Florida International University, Miami, FL, USA

Rajan K. Gupta Department of Radiology, University of Colorado, Denver, Aurora, CO, USA

Antonio Gutierrez Department of Radiological Sciences, Ronald Reagan UCLA Medical Center, Los Angeles, CA, USA

Chul S. Ha Department of Radiation Oncology, Cancer Therapy and Research Center at the University of Texas Health Science Center, San Antonio, TX, USA

Subarna Hamid Eisaman Department of Radiation Oncology, University of Pittsburgh Medical Center- Regional Cancer Center, Johnstown, PA, USA

Arik Hananel Insightec Ltd., Tirat Carmel, Haifa, Israel

J. Louis Hinshaw Department of Radiology, University of Wisconsin School of Medicine and Public Health, Madison, WI, USA

Mohammad Hjouj School of Computer Science and Engineering, Hebrew University of Jerusalem, Jerusalem, Israel

Department of Medical Imaging, Al–Quds University, Abu–Dis, Palestine

Mark J. Hogan Department of Radiology, School of Medicine, The University of Toledo Medical Center, Columbus, OH, USA

Mark D. Hurwitz Department of Radiation Oncology, Dana-Farber/ Brigham and Women's Cancer Center, Boston, MA, USA

Michael J. Hutchinson Division of Abdominal Imaging and Intervention, Department of Radiology, Brigham and Women's Hospital, Harvard Medical School, Boston, MA, USA

Anne Smith Hutchison South Carolina Oncology Associates, Columbia, SC, USA

Yael Inbar Imaging Institute, Sheba Medical Center, Tel Hashomer, Ramat Gan, Israel

Yu Jie Department of Interventional Ultrasound, Chinese PLA General Hospital, Beijing, China

Eric Jonasch Division of Hematology-Oncology, The University of Texas MD Anderson Cancer Center, Houston, TX, USA

Alexandra Jost Department of Diagnostic and Interventional Radiology, University Hospital of Frankfurt, Frankfurt am Main, Germany

Brian D. Kavanagh Department of Radiation Oncology, University of Colorado School of Medicine, Aurora, CO, USA

Stephen T. Kee Department of Radiology, UCLA Medical Center, Los Angeles, CA, USA

Fady Khoury-Collado Gynecology Service, Department of Surgery, Memorial Sloan-Kettering Cancer Center, New York, NY, USA

Katherine Kopckash Department of Surgery, Rush University Medical Center, Chicago, IL, USA

Alan Kotin Department of Anesthesia and Critical Care, Memorial Sloan-Kettering Cancer Center, New York, NY, USA

Ming Kuang Department of Hepatobiliary Surgery and Division of Interventional Ultrasound, The First Affiliated Hospital of Sun Yat-sen University, Guangzhou, China

Corey J. Langer Department of Medicine, Division of Hematology-Oncology, Hospital of the University of Pennsylvania, Philadelphia, PA, USA

Christopher Lee Department of Radiology, Body Division, Keck School of Medicine USC University Hospital, Los Angeles, CA, USA

Edward Wolfgang Lee Department of Radiology, UCLA Medical Center, Los Angeles, CA, USA

Fred T. Lee, Jr. Department of Radiology, University of Wisconsin, Madison, WI, USA

Riccardo Lencioni Division of Diagnostic Imaging and Intervention, School of Medicine, University of Pisa, Cisanello Hospital, Pisa, IT, Italy

Herbert Lepor Department of Urology, New York University Langone Medical Center, New York, NY, USA

Robert J. Lewandowski Department of Radiology, Northwestern Memorial Hospital, Chicago, IL, USA

Ying Li Department of Radiation Oncology, University of Texas Health Science Center at San Antonio, San Antonio, TX, USA

Peter J. Littrup Imaging Division, Karmanos Cancer Institute, Detroit, MI, USA

Ming-De Lu Institute of Diagnostic and Interventional Ultrasound, The First Affiliated Hospital of Sun Yat-sen University, Guangzhou, China

Meghan G. Lubner Department of Radiology, University of Wisconsin School of Medicine and Public Health, Madison, WI, USA

Homer A. Macapinlac Department of Nuclear Medicine, University of Texas MD Anderson Cancer Center, Houston, TX, USA

Ronit Machtinger Department of Obstetrics and Gynecology, Brigham and Women's Hospital, Boston, MA, USA

Martin G. Mack Department of Diagnostic and Interventional Radiology, University Hospital of Frankfurt, Frankfurt am Main, Germany

Samuel McGrath Department of Radiation Oncology, William Beaumont Hospital, Royal Oak, MI, USA

Laleh G. Melstrom Department of Surgery, Robert Wood Johnson and the Cancer Institute of New Jersey, New Brunswick, NJ, USA

Khairuddin Memon Department of Radiology, Northwestern Memorial Hospital, Chicago, IL, USA

Paul R. Morrison[†]

Benjamin Movsas Department of Radiation Oncology, Henry Ford Health Systems, Detroit, MI, USA

Mohamed Nabil Department of Diagnostic and Interventional Radiology, University Hospital of Frankfurt, Frankfurt am Main, Germany

Zeina Nahleh Department of Internal Medicine, Division of Hematology-Oncology, TTUHSC-Paul L. Foster School of Medicine, El Paso, TX, USA

Dominic Nguyen Department of Radiation Oncology, Cancer Therapy and Research Center & The University of Texas Health Science Center at San Antonio, San Antonio, TX, USA

Peter Osborn Department of Diagnostic Imaging, Queen Alexandra Hospital, Portsmouth, Hampshire, UK

Gyan Pareek Department of Surgery, Division of Urology, Warren Alpert Medical School of Brown University, Providence, RI, USA

Bernard J. Park Department of Surgery, Hackensack University Medical Center, Hackensack, NJ, USA

Henrik Petrowsky Swiss Hepato-Pancreato-Biliray and Transplant Center, Department of Surgery, University Hospital Zürich, Zürich, Switzerland

[†]Deceased

M. Raphael Pfeffer Oncology Institute, Sheba Medical Center, Tel Hashomer, Ramat Gan, Israel

Liang Ping Department of Interventional Ultrasound, Chinese PLA General Hospital, Beijing, China

Tatiana Rabin Oncology Institute, Sheba Medical Center, Tel Hashomer, Ramat Gan, Israel

Steven S. Raman Department of Radiological Sciences, Ronald Regan UCLA Medical Center, Los Angeles, CA, USA

Paul S. Rava Department of Radiation Oncology, Tufts Medical Center and Rhode Island Hospital, Boston, MA, USA

Lei Ren Department of Radiation Oncology, Duke University, Durham, NC, USA

Ahsun Riaz Department of Radiology, Northwestern Memorial Hospital, Chicago, IL, USA

Boris Rubinsky Department of Mechanical Engineering, University of California at Berkeley, Berkeley, CA, USA

Paul Russo Cornell Weill School of Medicine, Memorial Sloan Kettering Cancer Center, New York, NY, USA

Thomas P. Ryan FreeFall Consulting, Austin, TX, USA

Samuel Ryu Department of Radiation Oncology and Neurosurgery, Henry Ford Hospital, Detroit, MI, USA

Riad Salem Department of Radiology, Northwestern Memorial Hospital, Chicago, IL, USA

Tracey E. Schefter Department of Radiation Oncology, University of Colorado School of Medicine, Aurora, CO, USA

Gabriel Schnickel Department of Transplant Surgery, Henry Ford Transplant Institute, Detroit, MI, USA

Helmut Schoellnast Department of Radiology, Memorial Sloan-Kettering Cancer Center, New York, NY, USA

Chirag Shah Department of Radiation Oncology, William Beaumont Hospital, Royal Oak, MI, USA

William E. Shiels, II Department of Radiology, School of Medicine, The University of Toledo Medical Center, Columbus, OH, USA

Paul B. Shyn Division of Abdominal Imaging and Intervention, Department of Radiology, Brigham and Women's Hospital, Harvard Medical School, Boston, MA, USA

Farzan Siddiqui Department of Radiation Oncology, Henry Ford Health Systems, Detroit, MI, USA

Stuart G. Silverman Division of Abdominal Imaging and Intervention, Department of Radiology, Brigham and Women's Hospital, Harvard Medical School, Boston, MA, USA

Anna Simeonova Department of Radiation Oncology, University Medical Center Mannheim, Mannheim, Germany

Luigi Solbiati Department of Diagnostic Imaging and Interventional Oncologic Radiology, General Hospital of Busto Arsizio, Busto Arsizio, VA, Italy

Stephen B. Solomon Department of Radiology, Memorial Sloan-Kettering Cancer Center, New York, NY, USA

Yukio Sonoda Gynecology Service, Department of Surgery, Memorial Sloan-Kettering Cancer Center, New York, NY, USA

Robert Suh Department of Radiological Sciences, Ronald Reagan UCLA Medical Center, Los Angeles, CA, USA

Gregory P. Swanson Department of Radiation Oncology, Cancer Therapy and Research Center at the University of Texas Health Science Center, San Antonio, TX, USA

Nelly Tan Department of Radiological Sciences, Ronald Regan UCLA Medical Center, Los Angeles, CA, USA

Beenish Tasawwar Department of Radiology, Beth Israel Deaconess Medical Center, Harvard Medical School Section of Interventional Radiology, Boston, MA, USA

Servet Tatli Department of Abdominal Imaging and Intervention, Brigham and Women's Hospital, Boston, MA, USA

Derek Tessier Department of Radiology, Rhode Island Hospital, Providence, RI, USA

Simone Thavaseelan Department of Surgery, Division of Urology, Warren Alpert Medical School of Brown University, Providence, RI, USA

Tania Tondolo Department of Biomedical Sciences and Technologies, Section of Radiological Science, School of Medicine, University of Milan, Milan, MI, Italy

Frank Vicini Department of Radiation Oncology, William Beaumont Hospital, Royal Oak, MI, USA

Thomas J. Vogl Department of Diagnostic and Interventional Radiology, University Hospital of Frankfurt, Frankfurt am Main, Germany

Kien Vuu Department of Radiological Sciences, Ronald Reagan UCLA Medical Center, Los Angeles, CA, USA

Jared Weiss Department of Medicine, Division of Hematology-Oncology, University of North Carolina at Chapel Hill, Chapel Hill, NC, USA

Ronald S. Winokur Department of Diagnostic Radiology, Thomas Jefferson University, Philadelphia, PA, USA

Daphne Wong Department of Radiology, UCLA Medical Center, Los Angeles, CA, USA

Robert L. Worthington-Kirsch Vein Clinics of America, Wayne, PA, USA

Reza Zare Department of Urology, New York University VA University Hospital, New York, NY, USA

Tumor Ablation: An Evolving Technology

1

Muneeb Ahmed, Beenish Tasawwar, and S. Nahum Goldberg

Abstract

Image-guided tumor ablation is a minimally invasive strategy to treat focal tumors by inducing irreversible cellular injury through the application of thermal, and more recently, nonthermal energy or chemical injection. This approach has become a widely accepted technique and is incorporated into the treatment of a range of clinical circumstances, including in the treatment of focal tumors in the liver, lung, kidney, bone, and adrenal glands. Given the multiplicity of treatment types and potential complexity of paradigms in oncology, and the wider application of thermal ablation techniques, a thorough understanding of the basic principles and recent advances in thermal ablation is a necessary prerequisite for their effective clinical use. This chapter will review several of these key concepts related to tumor ablation, including those that relate to performing a clinical ablation, such as understanding the goals of therapy and mechanisms of tissue heating or tumor destruction, and understanding the proper role of tumor ablation and the strategies that are being pursued to improve overall ablation outcome.

M. Ahmed (✉)
Department of Radiology, WCC 308-B, Beth Israel Deaconess Medical Center, Section of Interventional Radiology, Boston, MA, USA
e-mail: mahmed@bidmc.harvard.edu

B. Tasawwar
Department of Radiology, Beth Israel Deaconess Medical Center, Harvard Medical School Section of Interventional Radiology, Boston, MA, USA
e-mail: btasawwa@bidmc.harvard.edu

S.N. Goldberg
Department of Radiology, Hebrew University-Hadassah Medical Center, Jerusalem, Israel
e-mail: snahum@hadassah.org.il

Understanding Tumor Ablation: An Overview

Image-guided tumor ablation is a minimally invasive strategy to treat focal tumors by inducing irreversible cellular injury through the application of thermal, and more recently, nonthermal energy or chemical injection. This approach has become a widely accepted technique and is incorporated into the treatment of a range of clinical circumstances, including in the treatment of focal tumors in the liver, lung, kidney, bone, and adrenal glands [1–6]. Benefits of minimally invasive therapies compared to surgical resection

D.E. Dupuy et al. (eds.), *Image-Guided Cancer Therapy*, DOI 10.1007/978-1-4419-0751-6_3,

include lesser mortality and morbidity, lower cost, and the ability to perform procedures on outpatients who are not good candidates for surgery [7]. However, additional work is required to improve outcomes and overcome limitations in ablative efficacy, including persistent growth of residual tumor at the ablation margin, the inability to effectively treat larger tumors, and variability in complete treatment based upon tumor location [7].

Given the multiplicity of treatment types and potential complexity of paradigms in oncology, and the wider application of thermal ablation techniques, a thorough understanding of the basic principles and recent advances in thermal ablation is a necessary prerequisite for their effective clinical use. These key concepts related to tumor ablation can be broadly divided into (1) those that relate to performing a clinical ablation, such as understanding the goals of therapy and mechanisms of tissue heating or tumor destruction, and (2) understanding the proper role of tumor ablation and the strategies that are being pursued to improve overall ablation outcome. These latter concepts include a systematic approach to technological development, understanding and using the biophysiologic environment to maximize ablation outcome, combining tumor ablation with adjuvant therapies to synergistically increase tumor destruction, and improving tumor visualization and targeting through image navigation and fusion technology. Given that the greatest experimental and clinical experience exists for radiofrequency (RF)-based ablation, this will be the representative model used to discuss many of these concepts. However, many of these principles also apply when using alternative ablative modalities, as will be discussed in subsequent chapters.

Goals of Minimally Invasive Therapy

The overall goal of minimally invasive focal tumor ablation encompasses several specific aims. First and foremost, a successful ablation completely treats all malignant cells within the target. This includes both achieving homogenous ablation within the tumor (so that no focal areas of viable tumor remain) and adequately treating a rim of apparently "normal" tissue around the tumor which often contains microscopic invasion of malignant cells at the tumor periphery. Thus, based upon examinations of tumor progression in patients undergoing surgical resection and the demonstration of viable malignant cells beyond visible tumor boundaries, in most cases (or except when otherwise indicated) tumor ablation therapies attempt to include at least a 0.5–1.0 cm "ablative" margin of seemingly normal tissue for liver and lung, though less may be needed for some tumors in the kidney [8, 9].

A secondary goal is to ensure accuracy of therapy to minimize the damage to "non-target" normal tissue surrounding the ablative zone. As such, one significant advantage of percutaneous ablative therapies over conventional standard surgical resection is the potential to remove or destroy only a minimal amount of normal tissue. This is critical in clinical situations where the functional state of the background organ parenchyma is as important in determining patient outcome as the primary tumor. Examples of clinical situations where this is relevant include focal hepatic tumors in patients with underlying cirrhosis and limited hepatic reserve, patients with Von Hippel Lindau Syndrome who have limited renal function and required treatment of multiple renal tumors, and patients with primary lung tumors with extensive underlying emphysema and limited lung function [10–12]. Many of these patients are not surgical candidates due to limited native organ functional reserve placing them at a higher risk for postoperative complications or organ failure. Other clinical circumstances in which high specificity and accuracy of targeting have proven useful include providing symptomatic relief for patients with symptomatic osseous metastases or hormonally active neuroendocrine tumors and using percutaneous therapies to improve focal interstitial drug delivery [13–15].

Finally, maximizing ablation efficiency is an additional consideration. For example, appropriate and complete tumor destruction only occurs when the entire target tumor is exposed to appropriate temperatures, and therefore determined by

the pattern of tissue heating in the target tumor. For larger tumors (usually defined to be larger than 3–5 cm in diameter), a single ablation treatment may not be sufficient to entirely encompass the target volume [3]. In these cases, multiple overlapping ablations or simultaneous use of multiple applicators may be required to successfully treat the entire tumor and achieve an ablative margin, though accurate targeting and probe placement can often be technically challenging [16]. Tumor biology can also affect ablation efficiency. Growth patterns of the tumor itself can influence overall treatment outcomes, with slow growing tumors more amenable to multiple treatment sessions over longer periods of time. Optimizing ablation efficiency is applicable to a wide range of ablative technologies, including both thermal and nonthermal strategies.

Principles of Tissue Heating in Thermal Ablation

Ablative tissue heating occurs through two specific mechanisms. First, an applicator placed within the center of the target tumor delivers energy that interacts with tissue to generate focal heat immediately around it. This approach is similar for all thermal ablation strategies, regardless of the type of energy source used, though specific mechanisms of heat induction are energy specific [17]. For example, as RF current travels from the electrode applicator to the remote grounding pad, local tissue resistance to current flow results in frictional heat generation. In microwave-based systems, the needle antenna applies electromagnetic energy to the tissue, and as molecules with an intrinsic dipole moment (such as water) are forced to continuously align to the externally applied magnetic field, the kinetic energy that is generated results in local tissue heating, which extends deeper into tissues around the antennae (compared to, e.g., RF energy). Laser ablation uses emission of laser energy from optic fibers to generate tissue heat immediately around the fiber tip. Ultrasound-based systems induce tissue heating by applying a focused beam of ultrasound energy with a high peak intensity, either directly around a percutaneously placed applicator (like for other ablative systems), or transcutaneously by directing several ultrasound beams of lower intensity from different directions so that they converge at the target tumor, where the ultrasound energy is absorbed by the tissue and converted to heat. The second mechanism of tissue heating in thermal ablation uses thermal tissue conduction [18]. Heat generated around the electrode diffuses through the tumor and results in additional high-temperature heating separate from the direct energy-tissue interactions that occur around the electrode. The contribution of thermal conduction to overall tissue ablation is determined by several factors. Tissue heating patterns vary based upon the specific energy source used – for example, microwave-based systems induce tissue heating at a much faster rate than RF-based systems, and so thermal conduction contributes less to overall tissue heating [18]. Additionally, tumor and tissue characteristics also affect thermal conduction. As an example, primary hepatic tumors (hepatocellular carcinoma) transmit heat better than the surrounding cirrhotic hepatic parenchyma [3, 19].

Regardless of the energy source used, the endpoint of thermal ablation is adequate tissue heating so as to induce coagulative necrosis throughout the defined target area. Relatively mild increases in tissue temperature above baseline (40–42 °C) can be tolerated by normal cellular homeostatic mechanisms [20]. Low-temperature hyperthermia (42–45 °C) results in reversible cellular injury, though this can increase cellular susceptibility to additional adjuvant therapies such as chemotherapy and radiation [21, 22]. Irreversible cellular injury occurs when cells are heated to 46–48 °C for 55–60 min, and occurs more rapidly as the temperature rises, so that most cell types die in a few minutes when heated at 50 °C (Fig. 1.1) [23]. Immediate cellular damage centers on protein coagulation of cytosolic and mitochondrial enzymes, and nucleic acid-histone protein complexes, which triggers cellular death over the course of several days [24]. “Heat fixation” or “coagulation necrosis” is used to describe this thermal damage,

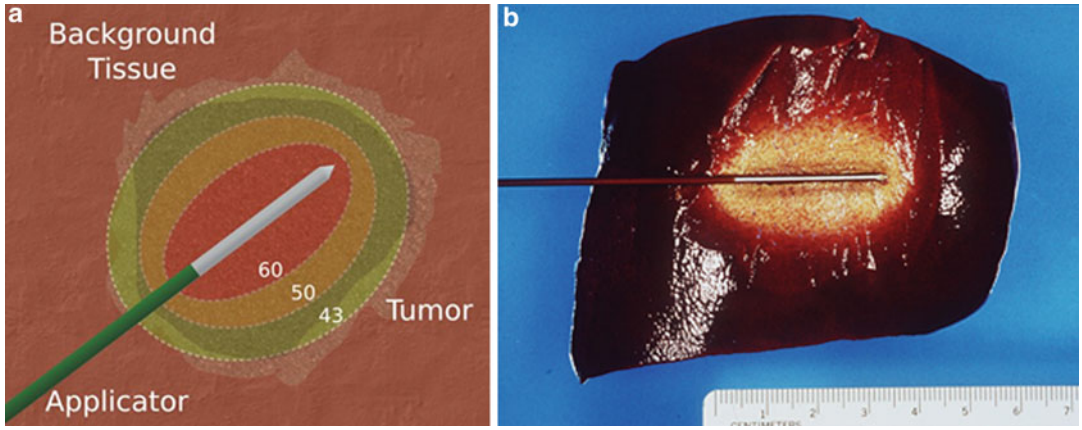

Fig. 1.1 *Schematic* (**a**) *and pictorial* (**b**) *representation of focal thermal ablation therapy*. Electrode applicators are positioned either with image-guidance or direct visualization within the target tumor, and thermal energy is applied via the electrode. This creates a central zone of high temperatures in the tissue immediately around the electrode (they can exceed 100 °C), and surrounded by more peripheral zones of sublethal tissue heating (<50 °C) and background liver parenchyma (Images reprinted with permission from Ref. [7])

even though ultimate manifestations of cell death may not fulfill strict histopathologic criteria of coagulative necrosis [25]. This has implications with regard to clinical practice, as percutaneous biopsy and standard histopathologic interpretation may not be a reliable measure of adequate ablation [25]. Therefore, optimal temperatures for ablation range likely exceed 50 °C. On the other end of the temperature spectrum, tissue vaporization occurs at temperatures >110 °C, which in turn, limits further current deposition in RF-based systems (as compared to, e.g., microwave systems that do not have this limitation).

The exact temperature at which cell death occurs is multifactorial and tissue specific. Based upon prior studies demonstrating that tissue coagulation can be induced by focal tissue heating to 50 °C for 4–6 min [26], this has become the standard surrogate endpoint for thermal ablation therapies in both experimental studies and in current clinical paradigms. However, studies have shown that depending on heating time, the rate of heat increase, and the tissue being heated, maximum temperatures at the edge of ablation are variable. For example, maximum temperatures at the edge of ablation zone, known as the "critical temperature," have been shown to range from 30 °C to 77 °C for normal tissues and from 41 °C to 64 °C for tumor models (a 23 °C difference) [27, 28]. Likewise, the total amount of heat administered for a given time, known as the thermal dose, varies significantly between different tissues [27, 28]. Thus, the threshold target temperature of 50 °C should be used only as a general guideline. This conceptual framework is also clearly applicable in determining optimal energy delivery paradigms for nonthermal energy sources as well [29].

Applying the Principles of the Bioheat Equation to Achieve Meaningful Volumes of Tumor Ablation

Complete and adequate destruction by thermal ablation requires that the entire tumor (and usually an ablative margin) be subjected to cytotoxic temperatures. Success of thermal ablation is contingent upon adequate heat delivery. The ability to heat large volumes of tissue in different environments is dependent on several factors encompassing both energy delivery and local physiological tissue characteristics. The relationship between this set of parameters, as described by the Bio-heat equation [30], can be simplified to describe the basic relationship guiding thermal

ablation–induced coagulation necrosis as: "coagulation necrosis = (energy deposited × local tissue interactions) – heat loss" [31]. Based on this relationship, a three-pronged approach to increase the ability to ablate larger tumors has been pursued. These encompass (1) technological developments, including modification of energy input algorithms and electrode design to deposit more energy into the tissue; (2) improved understanding and subsequent modification of the biophysiologic environment to increase tissue heating; and (3) incorporation of adjuvant therapies to increase uniformity of tumor cellular injury in the ablation zone, along with increasing cellular destruction in the nonlethal hyperthermic zone around the ablation. While the RF ablation platform will be the example used below, this three-pronged approach serves as a successful model for the development of other ablation systems as well.

Advances in RF Ablation: A Model for Technological Evolution

Most investigation to improve thermal ablation outcomes has focused on device development, much of which has been, as noted above, for RF-based ablation systems. Technologic efforts to increase ablation size have focused on modifying energy deposition algorithms and electrode designs to increase both the amount of tissue exposed to the active electrode and the overall amount of energy that can be safely deposited into the target tissue.

Refinement of energy application algorithms: The algorithm by which energy is applied during thermal ablation is dependent on the energy source, device, and type of electrode that is being used. While initial power algorithms for RF-based systems were based upon a continuous and constant high energy input, tissue overheating and vaporization ultimately interferes with continued energy input due to high impedance to current flow from gas formation. Therefore, several strategies to maximize energy deposition have been developed and, in some cases, incorporated into commercially available devices.

Applying high levels of energy in a pulsed manner, separated by periods of lower energy, is one such strategy that has been used with RF-based systems to increase the mean intensity of energy deposition [32]. If a proper balance between high and low energy deposition is achieved, preferential tissue cooling occurs adjacent to the electrode during periods of minimal energy deposition without significantly decreasing heating deeper in the tissue. Thus, even greater energy can be applied during periods of high energy deposition thereby enabling deeper heat penetration and greater tissue coagulation [33]. Synergy between a combination of both internal cooling of the electrode and pulsing has resulted in even greater coagulation necrosis and tumor destruction than either method alone [33]. Pulsed-energy techniques have also been successfully used for microwave and laser-based systems.

Another strategy is to slowly increase (or "ramp-up") the RF energy application in a continuous manner, until the impedance to RF current flow increases prohibitively [34, 35]. This approach is often paired with multi-tined expandable electrodes, which have a greater contact surface area with tissue, and in which the goal is to achieve smaller ablation zones around multiple small electrode tines. This algorithm is also often combined with a staged expansion of the electrode system such that each small ablation occurs in a slightly different location within the tumor (with the overall goal being ablating the entire target region).

"Electrode switching" is an additional technique that is incorporated into pulsing algorithms to further increase RF tissue heating [36]. In this, multiple independently placed RF electrodes are connected to a single RF generator, and RF current is applied to a single electrode until an impedance spike is detected at which point current application is applied to the next electrode and so forth. Several studies have demonstrated significant increases in ablation zone size and a reduction in application time using this technique [36, 37]. For example, Brace et al. also show larger and more circular ablation zones with the switching application with more rapid

heating being 74 % faster than the sequential heating (12 vs. 46 min) [36].

Finally, continued device development has also led to increases in the overall maximum amount of power that can be delivered [38, 39]. For RF-based devices, the maximum amount of RF current that can be delivered is dependent on both the generator output and the electrode surface area, as higher surface areas reduce the current density, and therefore adequate tissue heating around the electrode cannot be achieved. While initial systems had maximum power outputs of less than 200 W, subsequent investigation suggests that higher current output and larger ablation zones can be achieved if higher-powered generators are coupled with larger-surface-area electrodes. For example, Solazzo et al. used a 500-kHz (1,000 W) high-powered generator in an in vivo porcine model and achieved larger coagulation zones with a 4 cm tip cluster electrode (5.2 ± 0.8 cm) compared to a 2.5 cm cluster electrode (3.9 ± 0.3 cm) [39]. Similar gains in ablation size have been seen in higher-powered versions of microwave-based systems [40].

Electrode modification: Development of ablation applicators (electrodes for RF, antennae for microwave, and diffuser tips for laser-based systems) has contributed significantly to the ability to reliably achieve larger ablation zones. Several strategies to increase the amount of energy deposition and the overall ablation size have been balanced with the need for smaller caliber electrodes to permit the continued use of these devices in a percutaneous and minimally invasive manner. These include the use of multiple electrodes simultaneously, either adjacent to each other or as part of an expandable device through a single introducer needle; the use of cooling systems to minimize tissue and electrode overheating; or the use of bipolar systems for RF ablation to increase tissue heating in the target zone (Fig. 1.2).

Originally, simply lengthening the electrode tip increased coagulation in an asymmetric and preferentially longitudinal geometry. Use of a single electrode inserted multiple times to perform overlapping ablations requires significantly greater time and effort, making it impractical for routine use in a clinical setting. Therefore, the use of multiple electrodes simultaneously in a preset configuration represents a significant step forward in increasing overall ablation size. Initial work with multiple electrodes demonstrated that placement of several monopolar electrodes in a clustered arrangement (no more than 1.5 cm apart) with simultaneous RF application could increase coagulation volume by over 800 % compared to a single electrode [41]. Subsequently, working to overcome the technical challenges of multiprobe application, multi-tined expandable RF electrodes have been developed [42]. These systems involve the deployment of a varying number of multiple thin, curved tines in the shape of an umbrella or more complex geometries from a central cannula [43, 44]. This surmounts earlier difficulties by allowing easy placement of multiple probes to create large, reproducible volumes of necrosis. Leveen et al., using a 12-hook array, were able to produce lesions measuring up to 3.5 cm in diameter in in vivo porcine liver by administering increasing amounts of RF energy from a 50 W RF generator for 10 min [45]. More recently, Applebaum et al. were able to achieve >5 cm of coagulation in in vivo porcine liver using currently commercially available expandable electrodes with optimized stepped-extension and power input algorithms [46].

While the majority of conventional RF systems use monopolar electrodes (where the current runs to remotely placed grounding pads placed on the patient's thighs to complete the circuit), several studies have reported results using bipolar arrays to increase the volume of coagulation created by RF application. In these systems, applied RF current runs from an active electrode to a second grounding electrode in place of a grounding pad. Heat is generated around both electrodes, creating elliptical lesions. McGahan et al. used this method in ex vivo liver to induce necrosis of up to 4.0 cm in the long axis diameter, but could only achieve 1.4 cm of necrosis in the short diameter [47]. Though this increases the overall size of coagulation volume, the shape of necrosis is unsuitable for actual tumors making the gains in coagulation less clinically significant.

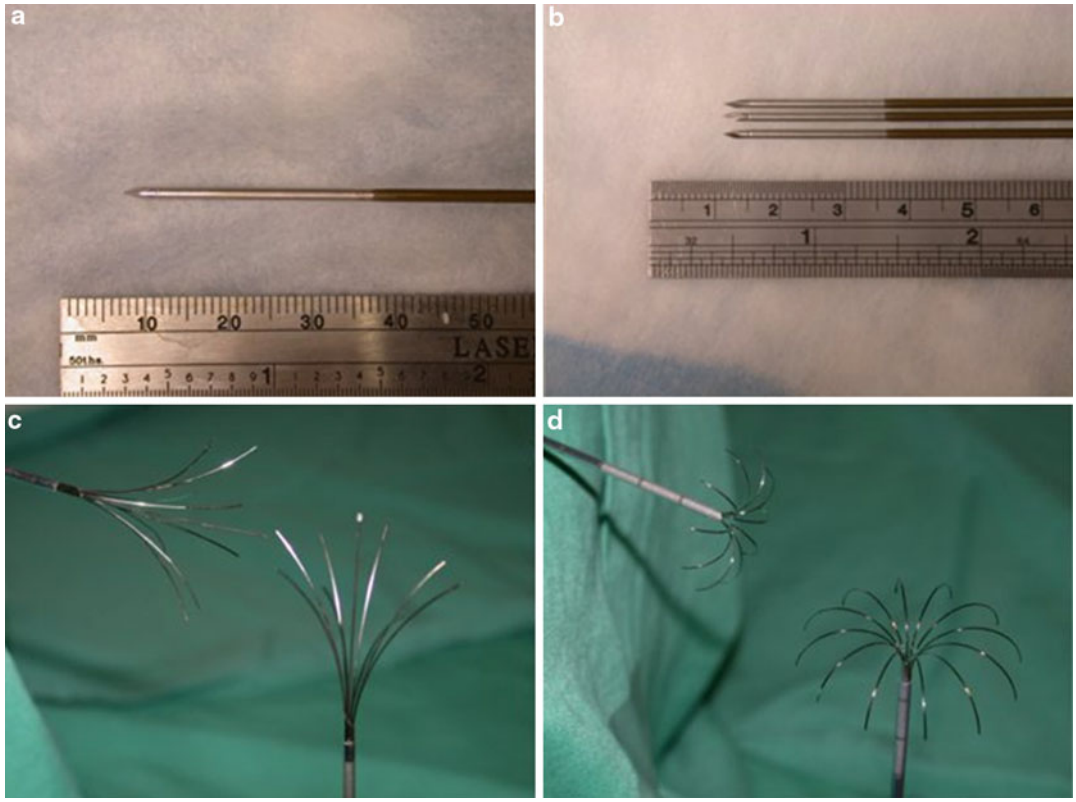

Fig. 1.2 *Various RF electrode designs*. Commonly used and commercially available electrode designs, including (**a**) a single internally cooled electrode with a 3 cm active tip (Cool-tip™ system, Valleylab, Boulder, CO), (**b**) a cluster internally cooled electrode system with three 2.5 cm active tips (Cluster™ electrode system, Valleylab, Boulder, CO), and two variations of an expandable electrode system (**c**: Starburst™, RITA Medical Systems, Mountain View, CA; **d**: LeVeen™, Boston Scientific Corp, Natick, MA) (Images reprinted with permission from Ref. [7])

Desinger et al. have described another bipolar array that contains both the active and return electrodes on the same 2 mm diameter probe [48]. Lee et al. used two multi-tined active and return electrodes to increase coagulation during bipolar RF ablation [49]. Finally, several studies have used a multipolar (more than two) array of electrodes (multi-tined and single internally cooled) during RF ablation to achieve even greater volumes of coagulation [50, 51].

One of the limitations for RF-based systems has been overheating surrounding the active electrode leading to tissue charring, rising impedance, and RF circuit interruption and ultimately limiting overall RF energy deposition. One successful strategy to address this has been the use of internal electrode cooling, where electrodes contain two hollow lumens that permit continuous internal cooling of the tip with a chilled perfusate, and the removal of warmed effluent to a collection unit outside of the body [52]. This reduces heating directly around the electrode, tissue charring, and rising impedance; allows greater RF energy deposition; and shifts the peak tissue temperature farther into the tumor, contributing to a broader depth of tissue heating from thermal conduction. In initial studies using cooling of 18 gauge single or clustered electrode needles using chilled saline perfusate, significant increases in RF energy deposition and ablation zone size were observed compared to conventional monopolar uncooled electrodes in ex vivo liver, with findings subsequently confirmed in in vivo large animal models and clinical studies [33, 52].

Similar results were observed when chilled saline was infused in combination with expandable electrode systems (referred to as an "internally cooled wet electrode"), though infusion of fluid around the electrode is more difficult to control and makes the reproducibility of results more variable [53]. Most recently, several investigators have used alternative cooling agents (e.g., argon or nitrogen gas) to achieve even greater cooling, and therefore larger zones of ablation, around the RF electrode tip [54]. As for RF-based systems, cooling of antennae shaft for microwave applicators have also been developed with reduced shaft heating (and associated complications such as skin burns) while allowing increased power deposition through smaller caliber antennae.

While many of these technological advances have been developed independently of each other, they may often be used concurrently to achieve even larger ablation zones. Furthermore, while much of this work has been based upon RF technology, specific techniques can be used for other thermal ablative therapies. For example, multiple electrodes and applicator cooling have been effectively applied in microwave-based systems, as well [55, 56].

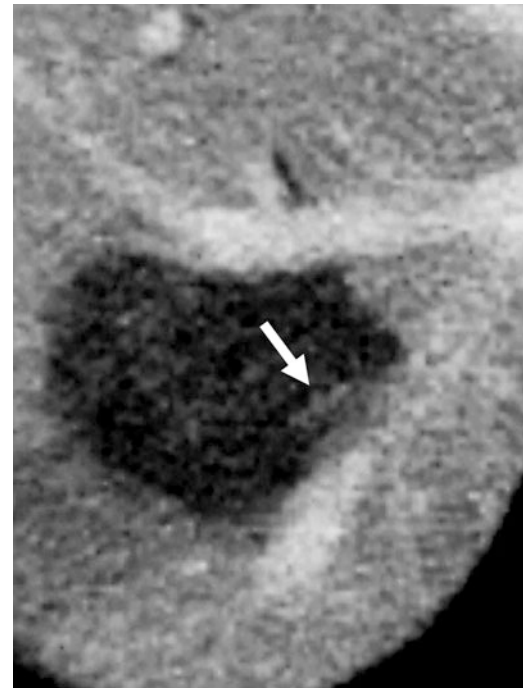

Fig. 1.3 *Example of local tumor progression at the edge of the RF ablation zone due to the heat sink effect*. This is a clinical example in a patient who underwent focal RF tumor ablation of a single colorectal metastasis. Follow-up contrast-enhanced CT imaging 6 months after RF ablation demonstrates a focal area of local tumor progression (*Arrow*) from incomplete treatment and persistently viable tumor cells due to vessel-mediated cooling from the abutting of the adjacent right hepatic vein

Modification of the Biophysiologic Environment

While larger coagulation zones have been created through modifying electrode design in ablative procedures, there are limitations due to the tumor physiology itself. Recent investigations have centered on altering underlying tumor physiology as a means to improve thermal ablation. Current studies have focused on the effects of tissue characteristics in the setting of temperature-based therapies such as tissue perfusion, thermal conductivity, and system-specific characteristics such as electrical conductivity for RF-based ablation.

Tissue perfusion: The leading factor constraining thermal ablation coagulation size in tumors continues to be tissue blood flow which has two effects: a large vessel heat sink effect and a microvascular perfusion–mediated tissue cooling effect. Firstly, larger-diameter blood vessels with higher flow act as heat sinks, drawing away heat from the ablative area (Fig. 1.3). Lu et al. show this in an in vivo porcine model by examining the effect of hepatic vessel diameter on RF ablation outcome. Using CT and histopathologic analysis, more complete thermal heating and a reduced heat-sink effect was seen when the heating zone was <3 mm in diameter [57]. In contrast, vessels >3 mm in diameter had higher patency rates, less endothelial injury, and greater viability of surrounding hepatocytes after RF ablation. Studies confirm the effect of hepatic blood flow on RF-induced coagulation in which increased coagulation volumes were obtained with decreased hepatic blood flow, either by embolotherapy, angiographic balloon occlusion,

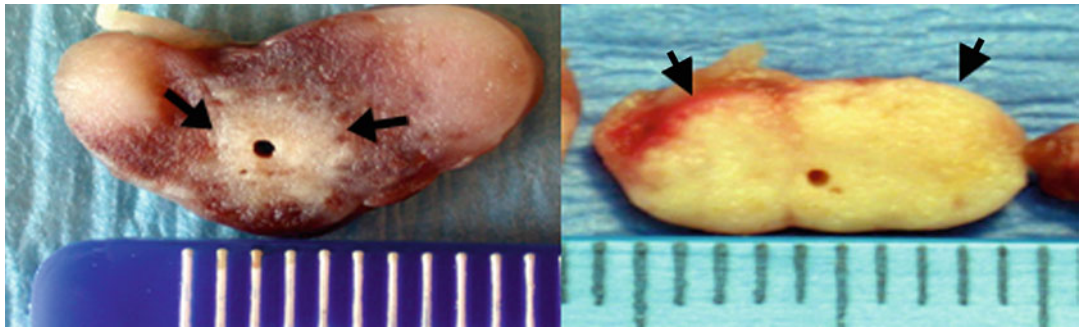

Fig. 1.4 *Reducing the negative effects of tumor microvascular perfusion on tissue heating by combining antiangiogenic therapy with RF ablation*. RF ablation combined with anti-angiogenic therapies such as Sorafenib, a VEGF receptor inhibitor, results in significantly increased tumor coagulation (*right image*: 9 mm, *black arrows*) compared to RF ablation alone (4 mm, *left image*, *black arrows*) in this small animal tumor model (Reprinted with permission from Hakimé A, Hines-Peralta A, Peddi H, et al. Combination of radiofrequency ablation with antiangiogenic therapy for tumor ablation efficacy: study in mice. *Radiology* 2007;244:464–470)

coil embolization, or the Pringle maneuver (total portal inflow occlusion) [58, 59]. The second effect of tissue vasculature is a result of perfusion-mediated tissue cooling (capillary vascular flow) that also functions as a heat sink. By drawing heat from the treatment zone, this effect reduces the volume of tissue that receives the required minimal thermal dose for coagulation. Targeted microvascular perfusion by using pharmacological alteration of blood flow can also improve overall RF ablation efficacy. Goldberg et al. modulated hepatic blood flow using intraarterial vasopressin and high dose halothane in conjunction with RF ablation in in vivo porcine liver [60]. Horkan et al. has modulated the use of arsenic trioxide showing reduced blood flow and increased tumor destruction [61]. More recently, another antiangiogenic drug, Sorafenib, has been combined with RF ablation to increase overall tumor coagulation in small animal models (Fig. 1.4) [62]. In this regard, newer nonthermal energy sources, such as irreversible electroporation, have been shown to be less affected by these effects, and will likely provide an alternative in clinical situations where perfusion-mediated cooling impacts ablation outcome [63].

Thermal conductivity: Initial clinical studies using RF ablation for hepatocellular carcinoma in the setting of underlying cirrhosis noted an "oven" effect (i.e., increased heating efficacy for tumors surrounded by cirrhotic liver or fat, such as exophytic renal cell carcinomas), or altered thermal transmission at the junction of tumor tissue and surrounding tissue [3]. Subsequent experimental studies in ex vivo agar phantoms and bovine liver have confirmed the effects of varying tumor and surrounding tissue thermal conductivity on effective heat transmission during RF ablation, and further demonstrated the role of "optimal" thermal conductivity characteristics on ablation outcome [19, 64]. For example, very poor tumor thermal conductivity limits heat transmission centrifugally away from the electrode with marked heating in the central portion of the tumor and limited, potentially incomplete heating in peripheral portions of the tumor. In contrast, increased thermal conductivity (such as in cystic lesions) results in fast heat transmission (i.e., heat dissipation), with potentially incomplete and heterogeneous tumor heating. Furthermore, in agar phantom and computer modeling studies, Liu et al. demonstrated that differences in thermal conductivity between the tumor and surrounding background tissue (specifically, decreased thermal conductivity from increased fat content of surrounding tissue) results in increased temperatures at the tumor margin. However, heating was limited in the surrounding medium, making a 1 cm "ablative" margin more difficult to achieve [64]. An understanding of the role of thermal conductivity, and tissue- and tumor-specific characteristics,

on tissue heating may be useful when trying to predict ablation outcome in varying clinical settings (e.g., in exophytic renal cell carcinomas surrounded by perirenal fat, lung tumors surrounded by aerated normal parenchyma, or osseous metastases surrounded by cortical bone) [19].

Electrical conductivity: The power deposition in RF-induced tissue heating is strongly dependent on the local electrical conductivity. The effect of local electrical conductivity can be divided into two main categories. First, altering the electrical activity environment immediately around the RF electrode with ionic agents can increase electrical conductivity prior to or during RF ablation. High local saline concentration increases the area of the active surface electrode, allowing greater energy deposition, thereby increasing the extent of coagulation necrosis [65]. Saline may be beneficial when ablating cavitary lesions which might not have a sufficient current path. However, it should be noted that saline infusion is not always a predictable process, as fluid can migrate to unintended locations and cause complications if not used properly [66]. Second, different electrical conductivities between the tumor and surrounding background organ can affect tissue heating at the tumor margin. Several studies show increases in tissue heating at the tumor-organ interface when the surrounding medium is characterized by reduced lower electrical conductivity [67]. In certain clinical settings, such as treating focal tumors in either lung or bone, marked differences in electrical conductivity may result in variable heating at the tumor/organ interface, and, indeed, limit heating in the surrounding organ, and may make obtaining a 1.0 cm ablative margin difficult. Lastly, electrical conductivity must be taken into account when using techniques such as hydrodissection to protect adjacent organs. Non-ionic fluids can be used to protect tissues adjacent to the ablation zone (such as diaphragm or bowel) from thermal injury. For this application, fluids with low ion content, such as 5 % dextrose in water (D5W) should be used, since they have been proven to electrically force RF current away from the protected organ, decrease the size and incidence of burns on the diaphragm and bowel, and reduce pain scores in patients treated with D5W when compared to ionic solutions, such as saline [36, 37]. Ionic solutions like 0.9 % saline should not be used for hydrodissection since, as noted above, they actually increase RF current flow [68].

Tissue fluid content: Microwave-based systems use electromagnetic energy to forcibly align molecules with an intrinsic dipole moment (such as water) to the externally applied magnetic field, which generates kinetic energy and results in local tissue heating. Therefore, higher tissue water content influences the rates and maximum amounts of achievable tissue heating in these systems [69]. Incorporating tissue internal water content into computer modeling of tumor ablation to more accurately predict tissue heating has also been proposed [70]. In addition, Brace et al. have demonstrated that greater dehydration (and resultant contraction of the ablation zone) occurs with microwave ablation compared to RF-based systems [71]. Optimization of microwave heating by modulating the tissue fluid content is also being investigated [72].

Combining Tumor Ablation with Adjuvant Therapies

Strategies to modify ablative systems and the biologic environment have been successful in improving the clinical utility of percutaneous ablation but limitations in clinical efficacy persist. For example, with further long-term follow-up of patients undergoing ablation therapy, there has been an increased incidence of detection of persistent local tumor growth of ablated tumors suggesting that there are residual foci of viable, untreated tumor tissue within and around the treatment zone [3]. As such, additional strategies are required to improve RF ablation efficacy by targeting these residual foci of viable malignant cells.

Investigators have studied the effects of combining thermal ablation with adjuvant therapies such as chemotherapy and radiation [73, 74]. Currently, thermal ablation only takes advantage

of temperatures that are sufficient by themselves to induce coagulation necrosis (>50 °C). Yet, based upon the exponential decrease in RF tissue heating, there is a steep thermal gradient in tissues surrounding an RF electrode. Hence, there is substantial flattening of the curve below 50 °C, with a much larger tissue volume encompassed by the 45 °C isotherm. Modeling studies demonstrate that were the threshold for cell death to be decreased by as few as 5 °C, tumor coagulation could be increased up to 1.5 cm (up to a 59 % increase in spherical volume of the ablation zone) [67]. Therefore, target tumors can be conceptually divided into three zones: (1) a central area, predominantly treated by thermal ablation, which undergoes heat-induced coagulation necrosis; (2) a peripheral rim, which undergoes reversible changes from sublethal hyperthermia; and (3) surrounding tumor or normal tissue that is unaffected by focal ablation, though still exposed to adjuvant systemic therapies.

Several studies show that tumor destruction may be achieved by combining RF thermal ablation with adjuvant chemotherapy or radiation [13, 74–76]. The goal of this combined approach is to increase tumor destruction occurring in the peripheral rim of sublethal temperatures (i.e., largely reversible cell damage induced by mildly elevating tissue temperatures to 41–45 °C) surrounding the coagulation zone [75]. Heterogeneity of thermal diffusion with high-temperature heating (in the presence of vascularity) prevents adequate ablation. Since local control requires complete tumor destruction, ablation may be inadequate even if large zones of ablation that encompass the entire tumor are created. By killing tumor cells at lower temperatures, this combined paradigm will not only increase necrosis volume, but may also create a more complete area of tumor destruction by filling in untreated gaps within the ablation zone. Combined treatment also has the potential to achieve equivalent tumor destruction with a concomitant reduction of the duration or course of therapy.

Combining thermal ablation with adjuvant chemotherapy: Several investigators have combined RF thermal ablation with adjuvant chemotherapy, most commonly using doxorubicin [75, 77]. In an initial study, Goldberg et al. performed RF ablation in conjunction with percutaneous intratumoral injection of free doxorubicin demonstrating a significant increase when treated with both RF and intratumoral doxorubicin (11.4 mm) as compared to RF alone (6.7 mm) [77]. However, many difficulties have been encountered in the clinical setting with image-guided direct intratumoral injection including nonuniform drug diffusion and limited control of drug distribution. Systemic intravenous injection of free chemotherapy is also associated with dose-limiting side effects. Therefore, the use of doxorubicin encapsulated within a liposome as an adjuvant to RF ablation has also been advanced. Advantages of using liposome nanoparticles as a delivery vehicle is that they are completely biocompatible, cause very little toxic or antigenic reaction, and are biologically inert. Water-soluble drugs can be trapped in the inner aqueous compartment, whereas lipophilic compounds may be incorporated into the liposomal lipid membrane. Additionally, incorporation of polyethylene-glycol surface modifications minimizes plasma protein absorption on liposome surfaces and subsequent recognition and uptake of liposomes by the reticuloendothelial system, which further reduces systemic phagocytosis and results in prolonged circulation time, selective agent delivery through the leaky tumor endothelium (an enhanced permeability and retention effect), as well as reduced toxicity profiles. Therefore, liposomal doxorubicin has proved beneficial in the clinical setting.

Several studies have focused on combining RF ablation with a commercially available preparation of liposomal doxorubicin (Doxil) or thermosensitive (preparations designed to release their contents when exposed to specific temperatures, such as 37–41 °C) liposomal doxorubicin [78–80] (Fig. 1.5). Experiments in rat mammary adenocarcinoma have showed a significant increase in mean tumor diameter from combination RF/Doxil therapy (13.1 mm) than from RF alone (6.7 mm) [81]. Interestingly, RF ablation combined with adjuvant empty liposomes also increased coagulation over RF alone but less than RF/Doxil. In a large animal canine

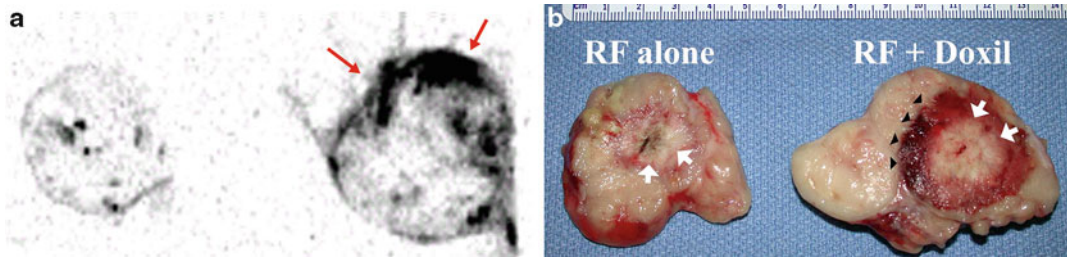

Fig. 1.5 *Combination RF ablation and IV liposomal doxorubicin*. (**a**) Autoradiography of two paired tumors from the same animal 24 h following the IV administration of tritiated liposomes, without (*left*) and with (*right*) RF ablation immediately preceding liposome injection. For the RF ablated tumor, the central zone with little uptake corresponds to the zone of RF coagulation, with a peripheral rim of increased liposome uptake seen (*small red arrows*) (Reprinted with permission from Ref. [83]). (**b**) Observed effects of combined RF/IV liposomal doxorubicin therapy (*right*) compared to RF alone (*left*, 12 min RF application, 1 cm internally cooled electrode) in subcutaneous canine venereal sarcoma tumors. The central white zone (*arrows*) that corresponds to RF-induced coagulation is slightly larger (3 mm) in the combined therapy tumor, while the peripheral red zone is dramatically increased in size (0.21–0.93 cm). In the combined therapy tumor, this red zone of increased tumor destruction is comprised of frank coagulative necrosis (Reprinted with permission from Ref. [73])

subcutaneous sarcoma model, combination therapy increased mean tumor coagulation diameter from 23 mm with RF alone to 37 mm with RF/Doxil, representing an increase of 212 % in necrosis volume, with most of the gain occurring in the larger peripheral periablative zone [73]. Additionally, D'Ippolito et al. reported increases in animal endpoint survival for rat R3230 adenocarcinoma tumors treated with combined RF/IV liposomal chemotherapy (28 days) compared to either RF or IV liposomal chemotherapy alone (18 days each) [82].

A pilot study was conducted combining RF ablation (using internally cooled electrodes) with adjuvant Doxil therapy in 10 patients who were randomized into two treatment groups of RF alone and RF with pretreatment Doxil (24 h pre RF) [13] (Fig. 1.6). Patients receiving Doxil therapy with RF ablation showed a 25 % increase in coagulation volume 4 weeks post ablation compared to a decrease of 76–88 % in patients treated with RF alone. Additional clinically beneficial findings were also observed only in the combination therapy group, including increased diameter of the treatment effect for multiple tumor types, improved completeness of tumor destruction particularly adjacent to intratumoral vessels, and increased treatment effect including the peritumoral liver parenchyma (suggesting a contribution to achieving an adequate ablative margin).

Additional studies on this combination therapy demonstrated greatest coagulation effect when given post-RF, pointing to a potential two-hit effect, with initial reversible cell injury inflicted by sublethal doses of heat in the more peripheral ablation zone, followed by irreversible injury by doxorubicin on already susceptible cells. Studies in both small and large animal models have demonstrated up to a 5.6-fold increase in intratumoral doxorubicin accumulation following RF ablation, with (1) the greatest amount of intratumoral doxorubicin occurring in the zone immediately peripheral to the central RF area and (2) smaller amounts of doxorubicin occurring in the central RF-coagulated area, suggesting drug deposition in areas with residual, patent vasculature [73, 75, 83]. These findings help explain why liposomal doxorubicin is likely to be complementary to RF ablation. Finally, several liposomal formulations are available that have chemical structures designed to release their contents at specific hyperthermic temperatures (42–45 °C), further increasing the specificity of targeting periablational tumor [84].

A second synergistic effect of adjuvant Doxil with RF ablation lies in the ability to cause increased tumor destruction, most notably by

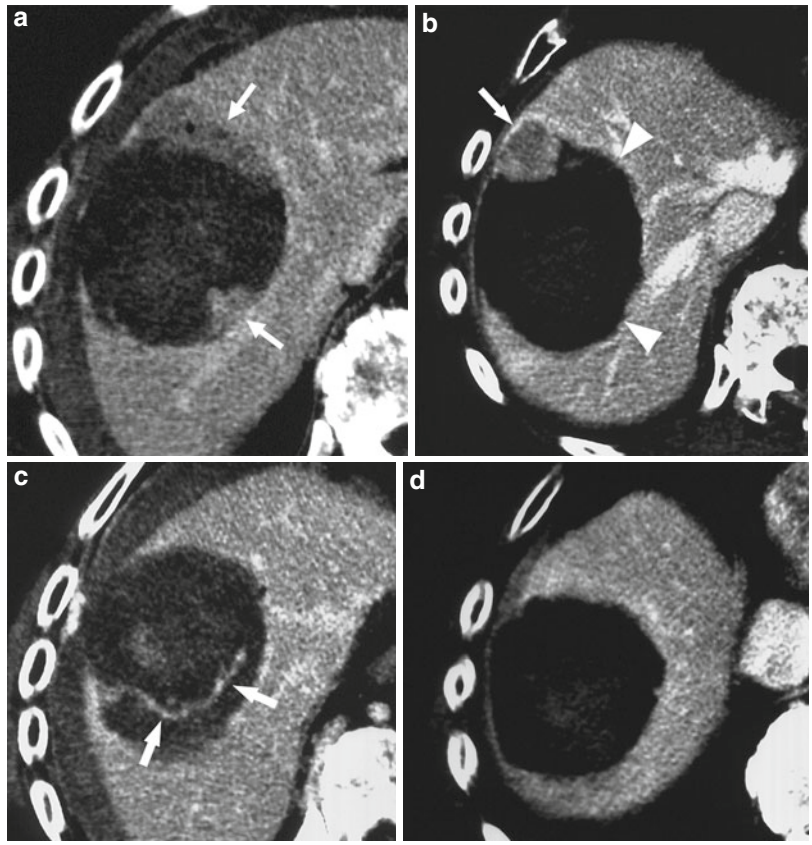

Fig. 1.6 *Increased tumor destruction with combined RF and liposomal doxorubicin*. An 82-year-old male with an 8.2 cm vascular hepatoma. (**a**) CT image obtained immediately following RF ablation shows persistent regions of residual untreated tumor (*white arrows*; *black zone* = ablated region). (**b**) Two weeks following therapy, there is interval increase in coagulation as the 1.5 cm inferior region of residual tumor and the 1.2 cm anteromedial portion of the tumor no longer enhance (*white arrowheads*). A persistent nodule of viable tumor is identified (*white arrow*). This was successfully treated with a course of RF ablation. (**c**) CT image obtained immediately following RF ablation demonstrates the persistence of a large vessel (*white arrows*) coursing through the non-enhancing ablated lesion. (**d**) Two weeks post therapy, there is no enhancement throughout this region, and no vessel was seen on any of the three phases of contrast enhancement. No evidence of local tumor recurrence was identified at 48 months of follow-up (Reprinted with permission from American Journal of Roentgenology [13])

increased cell stress (caused by upregulation of nitrative and oxidative pathways) leading to apoptosis. Recently, Solazzo et al. performed immunohistochemical staining of rat breast tumors treated with RF ablation with and without adjuvant Doxil for markers of cellular stress [85]. In the periablational rim surrounding the ablation zone, combination RF/Doxil increased markers of DNA breakage and oxidative and nitrative stress early (~4 h) after RF ablation, with subsequent co-localization staining for cleaved caspase 3 (a marker for apoptosis), suggesting that these areas later underwent apoptosis. N-acetyl cystiene (NAC) was also administered in some animals, and reductions in both cellular stress pathways and apoptosis confirmed the causatory relationship between the two processes. Additionally, increased heat-shock protein production in a concentric ring of still-viable tumor surrounding the ablation zone, and immediately peripheral to the rim of apoptosis, was also observed.

This increased understanding in the underlying mechanisms has led to successful

investigations of adding other adjuvant chemotherapies that specifically target cellular stress pathways. In a recent study, Yang et al. combined RF ablation with IV liposomal paclitaxel (showing proapoptotic and anti-heat shock protein effects) in rat mammary adenocarcinoma tumors which demonstrated increased tumor coagulation and animal endpoint survival over RF or paclitaxel alone [86]. Even greater gains were observed when triple therapy with paclitaxel-RF-Doxil was conducted. Interestingly, immunohistochemistry demonstrated reduced heat shock protein expression and increased apoptosis for treatment combinations that included paclitaxel. Most recently, combining RF ablation with IV liposomal quercetin (a flavanoid agent with known anti-heat shock protein effects) also reduced heat shock protein expression and increased tumor coagulation and survival [85].

Finally, RF ablation has also been combined with direct intra-arterial chemotherapy in the form of chemoembolization (either using lipiodol-based regimens or, more recently, drug-eluting particles) in a number of clinical studies. Mostafa et al. combined RF ablation with transarterial chemoembolization or bland embolization for VX2 tumors implanted in the liver of a rabbit animal model and found that the greatest tumor necrosis was achieved with transarterial chemoembolization performed before RF ablation [59]. These results likely relate to both a reduction in perfusion-mediated vascular cooling from prior embolization and the combined cytotoxic effects of hyperthermia and chemotherapy. Ahrar et al. have further demonstrated that chemotherapy agents commonly used for chemoembolization (such as cisplatin, doxorubicin, or mitomycin) are either not affected by high-temperature heating or are degraded only after prolonged exposure (>60 min at 100 °C), reflecting heating times that do not occur clinically [87]. Recent clinical studies performing transarterial chemoembolization followed by RF ablation for larger tumors have demonstrated promising results [88, 89].

Combining thermal ablation with adjuvant radiation: Several studies have reported early investigation into combination RF ablation and radiation therapy with promising results [74, 76, 90, 91]. There are known synergistic effects of combined external-beam radiation therapy and low-temperature hyperthermia [92]. Experimental animal studies have demonstrated increased tumor necrosis, reduced tumor growth, and improved animal survival with combined external beam radiation and RF ablation when compared to either therapy alone [74, 93]. For example, in a rat breast adenocarcinoma model, Horkan et al. demonstrated significantly longer mean endpoint-survival for animals treated with combination RF ablation and 20-Gy external beam radiation (94 days) compared to either radiation (40 days) or RF ablation (20 days) alone (Fig. 1.7). Preliminary clinical studies in primary lung malignancies confirm the synergistic effects of these therapies [76]. Potential causes for the synergy include the sensitization of the tumor to subsequent radiation due to the increased oxygenation resulting from hyperthermia-induced increased blood flow to the tumor [94]. Another possible mechanism, which has been seen in animal tumor models, is an inhibition of radiation-induced repair and recovery and increased free radical formation [85]. Future work is needed to identify the optimal temperature for ablation and optimal radiation dose, as well as the most effective method of administering radiation therapy (external-beam radiation therapy, brachytherapy, or yttrium microspheres) on an organ-by-organ basis. For a more complete clinical overview of the combination of radiation and ablation for lung cancer, see Chap. 39, "Lung Resection."

Improving Image Guidance and Tumor Targeting

Thermal ablation is commonly performed with a percutaneous approach using imaging guidance with a single or combination of modalities (CT, ultrasound, or MRI). A successful ablation is contingent upon the operator's ability to visualize the tumor, position the electrode within the target, and accurately evaluate the treatment zone upon ablation completion. Several significant challenges to performing a successful ablation

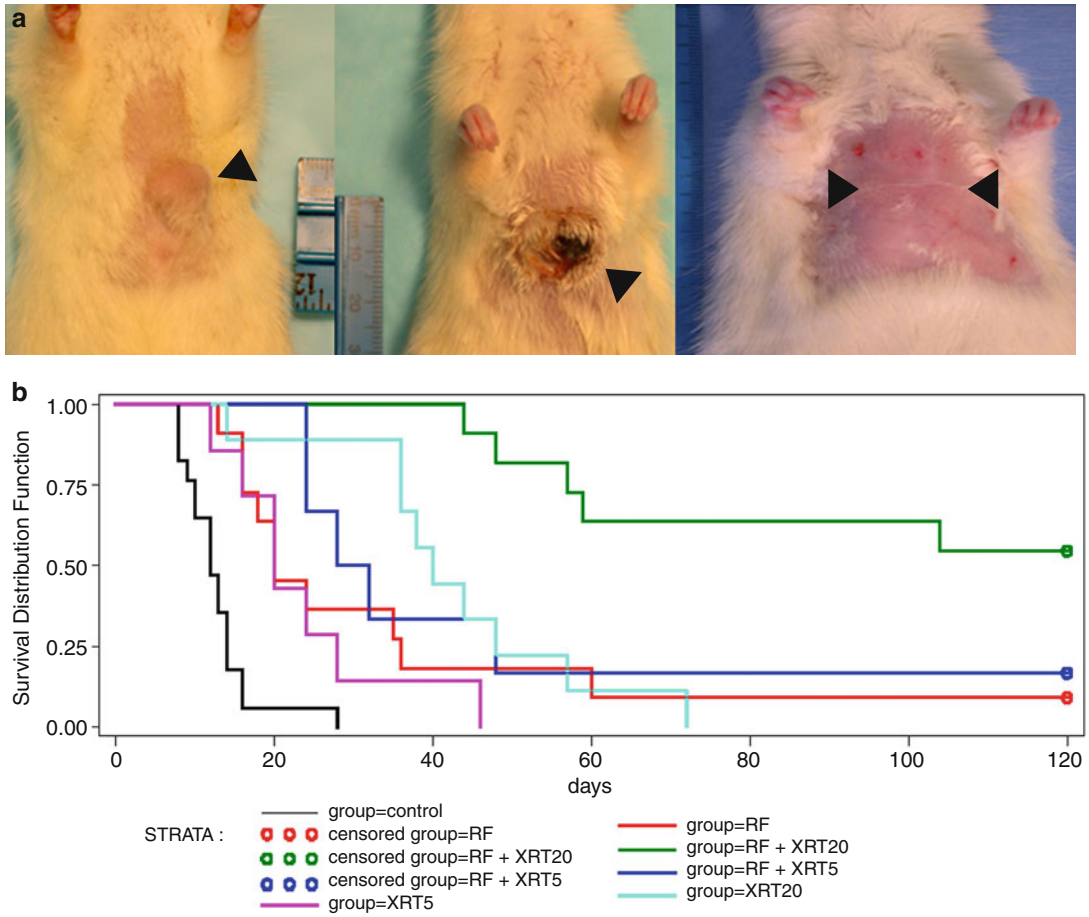

Fig. 1.7 *Combining RF ablation with external beam radiation*. (**a**) Sequential images demonstrate a subcutaneously implanted R3230 rat mammary adenocarcinoma tumor before treatment (*left*, *arrowhead*), following RF ablation combined with external beam radiation immediately after treatment (*middle*, *arrowhead*), and 120 days after therapy (*right*, *arrowheads*). Post-treatment images demonstrate complete dissolution of the tumor. (**b**) Kaplan-Meier analysis demonstrates significantly increased animal survival for R3230 tumors treated with RF ablation combined with external beam radiation compared with either therapy alone or no treatment (Reprinted with permission from Ref. [74])

exist at each of these steps. For example, diagnostic imaging studies are often obtained with modalities that are separate from the modality being used for treatment (e.g., diagnostic MRI and ablation being performed with CT or US), positional variations between diagnostic and treatment imaging precludes an exact overlay of different imaging studies, and target tumors often have variable visibility with or without contrast on ultrasound, CT, and/or MRI. Electrode positioning often requires traversing a narrow course or window in a three-dimensional trajectory when only two-dimensional, real-time imaging is available, often when the target is moving from respiratory motion. Finally, correlating the immediate post-procedure imaging to prior diagnostic imaging to determine adequacy of treatment, especially at the tumor margin, can often be difficult. All of these factors make treating some lesions extremely technically challenging [95].

Several technologies are being developed to address some of these difficulties [95]. Image-fusion software is now becoming commercially available to allow image overlay of two different

imaging modalities for diagnostic interpretation. Multimodality image-fusion for procedural guidance takes this further by pairing an existing data set from a prior diagnostic study to the "real-time" modality being used for the procedure. CT-ultrasound fusion systems often use a sensor in the ultrasound transducer and initial landmark localization to fuse a prior CT scan (which allows multiplanar reconstruction from the CT data set) with real-time ultrasound images (Fig. 1.3). Finally, needle tracking systems are also being developed using either electromagnetic (EM) or optical (infrared-based) tracking technology [96]. In these systems, the needle-tip is identified and localized in three-dimensional space and the needle trajectory overlays existing imaging. EM-based devices use a small field generator to create a rapidly changing magnetic field, in which a sensor coil in the needle tip creates an electrical current, allowing localization within three-dimensional space. Several of these devices have been tested for simple procedures such as joint injection or biopsy, and can likely be applied to ablative procedures as well, especially when coupled with predictive modeling software [97, 98].

Conclusion

Thermal ablation is being more widely accepted in clinical practices for the treatment of a range of tumors in various organ sites. However, a good conceptual framework that includes an understanding of the goals of tumor ablation and the mechanisms of tissue destruction that occur with ablation are a necessary prerequisite to its successful clinical application. The development of RF ablation serves as an excellent model for the evolution and development of additional ablation modalities (such as microwave, IRE, and cryotherapy-based systems). Several successful strategies have been used to improve thermal ablation efficacy including technological advancements in ablation devices, including electrode and navigation-system developments and modifications of tissue and tumor environment. Finally, thermal ablation has been successfully combined with adjuvant chemotherapy and radiation, and future investigation will explore tailoring specific adjuvant therapies based upon a mechanistic rationale.

References

1. Gervais DA, et al. Renal cell carcinoma: clinical experience and technical success with radio-frequency ablation of 42 tumors. Radiology. 2003;226(2):417–24.
2. Kurup AN, Callstrom MR. Ablation of skeletal metastases: current status. J Vasc Interv Radiol. 2010;21(8 suppl):S242–50.
3. Livraghi T, et al. Hepatocellular carcinoma: radiofrequency ablation of medium and large lesions. Radiology. 2000;214:761–8.
4. Solbiati L, et al. Percutaneous radiofrequency ablation of hepatic metastases from colorectal cancer: long term results in 117 patients. Radiology. 2001;221:159–66.
5. Venkatesan AM, et al. Percutaneous ablation of adrenal tumors. Tech Vasc Interv Radiol. 2010;13(2):89–99.
6. Zemlyak A, Moore WH, Bilfinger TV. Comparison of survival after sublobar resections and ablative therapies for stage I non-small cell lung cancer. J Am Coll Surg. 2010;211(1):68–72.
7. Ahmed M, et al. Principles of and advances in percutaneous ablation. Radiology. 2010;258(2):351–69.
8. Dodd 3rd GD, et al. Minimally invasive treatment of malignant hepatic tumors: at the threshold of a major breakthrough. Radiographics. 2000;20(1):9–27.
9. Shimada K, et al. Role of the width of the surgical margin in a hepatectomy for small hepatocellular carcinomas eligible for percutaneous local ablative therapy. Am J Surg. 2008;195(6):775–81.
10. Gervais DA, et al. Radiofrequency ablation of renal cell carcinoma: part 1, Indications, results, and role in patient management over a 6-year period and ablation of 100 tumors. AJR Am J Roentgenol. 2005;185(1):64–71.
11. Lencioni R, et al. Early-stage hepatocellular carcinoma in patients with cirrhosis: long-term results of percutaneous image-guided radiofrequency ablation. Radiology. 2005;234(3):961–7.
12. Lencioni R, et al. Response to radiofrequency ablation of pulmonary tumours: a prospective, intention-to-treat, multicentre clinical trial (the RAPTURE study). Lancet Oncol. 2008;9(7):621–8.
13. Goldberg SN, et al. Radiofrequency ablation of hepatic tumors: increased tumor destruction with adjuvant liposomal doxorubicin therapy. AJR Am J Roentgenol. 2002;179(1):93–101.
14. Callstrom MR, Charboneau JW. Image-guided palliation of painful metastases using percutaneous ablation. Tech Vasc Interv Radiol. 2007;10(2):120–31.

15. Gillams A, et al. Radiofrequency ablation of neuroendocrine liver metastases: the Middlesex experience. Abdom Imaging. 2005;30(4):435–41.
16. Dodd 3rd GD, et al. Radiofrequency thermal ablation: computer analysis of the size of the thermal injury created by overlapping ablations. AJR Am J Roentgenol. 2001;177(4):777–82.
17. Goldberg SN, et al. Image-guided tumor ablation: standardization of terminology and reporting criteria. J Vasc Interv Radiol. 2009;20(7 suppl):S377–90.
18. Schramm W, Yang D, Haemmerich D. Contribution of direct heating, thermal conduction and perfusion during radiofrequency and microwave ablation. Conf Proc IEEE Eng Med Biol Soc. 2006;1:5013–6.
19. Ahmed M, et al. Computer modeling of the combined effects of perfusion, electrical conductivity, and thermal conductivity on tissue heating patterns in radiofrequency tumor ablation. Int J Hyperthermia. 2008;24(7):577–88.
20. Thrall DE, et al. A comparison of temperatures in canine solid tumours during local and whole-body hyperthermia administered alone and simultaneously. Int J Hyperthermia. 1990;6(2):305–17.
21. Seegenschmiedt M, Brady L, Sauer R. Interstitial thermoradiotherapy: review on technical and clinical aspects. Am J Clin Oncol. 1990;13:352–63.
22. Trembley B, Ryan T, Strohbehn J. Interstitial hyperthermia: physics, biology, and clinical aspects. Hyperth Oncol. 1992;3:11–98. Utrecht: VSP.
23. Larson T, Bostwick D, Corcia A. Temperature-correlated histopathologic changes following microwave thermoablation of obstructive tissues in patients with benign prostatic hyperplasia. Urology. 1996; 47:463–9.
24. Zevas N, Kuwayama A. Pathologic analysis of experimental thermal lesions: comparison of induction heating and radiofrequency electrocoagulation. J Neurosurg. 1972;37:418–22.
25. Goldberg SN, et al. Treatment of intrahepatic malignancy with radiofrequency ablation: radiologic-pathologic correlation. Cancer. 2000;88:2452–63.
26. Goldberg SN, et al. Radiofrequency tissue ablation: importance of local temperature along the electrode tip exposure in determining lesion shape and size. Acad Radiol. 1996;3:212–8.
27. Mertyna P, et al. Radiofrequency ablation: the effect of distance and baseline temperature on thermal dose required for coagulation. Int J Hyperthermia. 2008; 24(7):550–9.
28. Mertyna P, et al. Radiofrequency ablation: variability in heat sensitivity in tumors and tissues. J Vasc Interv Radiol. 2007;18(5):647–54.
29. Daniels C, Rubinsky B. Electrical field and temperature model of nonthermal irreversible electroporation in heterogeneous tissues. J Biomech Eng. 2009; 131(7):071006.
30. Pennes H. Analysis of tissue and arterial blood temperatures in the resting human forearm. J Appl Physiol. 1948;1:93–122.
31. Goldberg SN, Gazelle GS, Mueller PR. Thermal ablation therapy for focal malignancy: a unified approach to underlying principles, technqiues, and diagnostic imaging guidance. Am J Radiol. 2000;174:323–31.
32. Goldberg SN, et al. Percutaneous radiofrequency tissue ablation: optimization of pulsed-RF technique to increase coagulation necrosis. JVIR. 1999;10:907–16.
33. Goldberg SN, et al. Large-volume tissue ablation with radiofrequency by using a clustered, internally-cooled electrode technique: laboratory and clinical experience in liver metastases. Radiology. 1998;209:371–9.
34. Gulesserian T, et al. Comparison of expandable electrodes in percutaneous radiofrequency ablation of renal cell carcinoma. Eur J Radiol. 2006;59(2):133–9.
35. McGahan JP, et al. Maximizing parameters for tissue ablation by using an internally cooled electrode. Radiology. 2010;256(2):397–405.
36. Brace CL, et al. Radiofrequency ablation: simultaneous application of multiple electrodes via switching creates larger, more confluent ablations than sequential application in a large animal model. J Vasc Interv Radiol. 2009;20(1):118–24.
37. Laeseke PF, et al. Multiple-electrode radiofrequency ablation creates confluent areas of necrosis: in vivo porcine liver results. Radiology. 2006;241(1):116–24.
38. Brace CL, et al. Radiofrequency ablation with a high-power generator: device efficacy in an in vivo porcine liver model. Int J Hyperthermia. 2007;23(4):387–94.
39. Solazzo SA, et al. High-power generator for radiofrequency ablation: larger electrodes and pulsing algorithms in bovine ex vivo and porcine in vivo settings. Radiology. 2007;242(3):743–50.
40. Laeseke PF, et al. Microwave ablation versus radiofrequency ablation in the kidney: high-power triaxial antennas create larger ablation zones than similarly sized internally cooled electrodes. J Vasc Interv Radiol. 2009;20(9):1224–9.
41. Goldberg SN, et al. Radiofrequency tissue ablation using multiprobe arrays: greater tissue destruction than multiple probes operating alone. Acad Radiol. 1995;2:670–4.
42. Bangard C, et al. Large-volume multi-tined expandable RF ablation in pig livers: comparison of 2D and volumetric measurements of the ablation zone. Eur Radiol. 2010;20(5):1073–8.
43. Rossi S, Buscarini E, Garbagnati F. Percutaneous treatment of small hepatic tumors by an expandable RF needle electrode. AJR Am J Roentgenol. 1998;170:1015–22.
44. Siperstein AE, et al. Laparoscopic thermal ablation of hepatic neuroendocrine tumor metastases. Surgery. 1997;122:1147–55.
45. Leveen RF. Laser hyperthermia and radiofrequency ablation of hepatic lesions. Semin Interv Radiol. 1997;12:313–24.
46. Appelbaum L, et al. Algorithm optimization for multitined radiofrequency ablation: comparative study in ex vivo and in vivo bovine liver. Radiology. 2010;254(2):430–40.

47. McGahan JP, et al. Hepatic ablation using bipolar radiofrequency electrocautery. Acad Radiol. 1996; 3(5):418–22.
48. Desinger K, et al. Interstitial bipolar RF-thermotherapy (REITT) therapy by planning by computer simulation and MRI-monitoring – a new concept for minimally invasive procedures. Proc SPIE. 1999;3249:147–60.
49. Lee JM, et al. Bipolar radiofrequency ablation using wet-cooled electrodes: an in vitro experimental study in bovine liver. AJR Am J Roentgenol. 2005; 184(2):391–7.
50. Seror O, et al. Large (>or = 5.0-cm) HCCs: multipolar RF ablation with three internally cooled bipolar electrodes – initial experience in 26 patients. Radiology. 2008;248(1):288–96.
51. Lee JM, et al. Multiple-electrode radiofrequency ablation of in vivo porcine liver: comparative studies of consecutive monopolar, switching monopolar versus multipolar modes. Invest Radiol. 2007;42(10): 676–83.
52. Goldberg SN, et al. Radiofrequency tissue ablation: increased lesion diameter with a perfusion electrode. Acad Radiol. 1996;3:636–44.
53. Hsieh CL, et al. Effectiveness of ultrasound-guided aspiration and sclerotherapy with 95 % ethanol for treatment of recurrent ovarian endometriomas. Fertil Steril. 2009;91(6):2709–13.
54. Hines-Peralta A, et al. Hybrid radiofrequency and cryoablation device: preliminary results in an animal model. J Vasc Interv Radiol. 2004;15(10): 1111–20.
55. Tsai WL, et al. Clinical trial: percutaneous acetic acid injection versus percutaneous ethanol injection for small hepatocellular carcinoma - a long-term follow-up study. Aliment Pharmacol Ther 2008; 28(3): 304–11.
56. He N, et al. Microwave ablation: an experimental comparative study on internally cooled antenna versus non-internally cooled antenna in liver models. Acad Radiol. 2010;17(7):894–9.
57. Lu DS, et al. Influence of large peritumoral vessels on outcome of radiofrequency ablation of liver tumors. J Vasc Interv Radiol. 2003;14(10):1267–74.
58. Patterson EJ, et al. Radiofrequency ablation of porcine liver in vivo: effects of blood flow and treatment time on lesion size. Ann Surg. 1998;227(4):559–65.
59. Mostafa EM, et al. Optimal strategies for combining transcatheter arterial chemoembolization and radiofrequency ablation in rabbit VX2 hepatic tumors. J Vasc Interv Radiol. 2008;19(12):1740–8.
60. Goldberg SN, et al. Radio-frequency tissue ablation: effect of pharmacologic modulation of blood flow on coagulation diameter. Radiology. 1998;209(3): 761–7.
61. Horkan C, et al. Radiofrequency ablation: effect of pharmacologic modulation of hepatic and renal blood flow on coagulation diameter in a VX2 tumor model. J Vasc Interv Radiol. 2004;15(3):269–74.
62. Hakime A, et al. Combination of radiofrequency ablation with antiangiogenic therapy for tumor ablation efficacy: study in mice. Radiology. 2007;244(2): 464–70.
63. Lee EW, et al. Advanced hepatic ablation technique for creating complete cell death: irreversible electroporation. Radiology. 2010;255(2):426–33.
64. Liu YJ, et al. Thermal characteristics of microwave ablation in the vicinity of an arterial bifurcation. Int J Hyperthermia. 2006;22(6):491–506.
65. Aube C, et al. Influence of NaCl concentrations on coagulation, temperature, and electrical conductivity using a perfusion radiofrequency ablation system: an ex vivo experimental study. Cardiovasc Intervent Radiol. 2007;30(1):92–7.
66. Gillams AR, Lees WR. CT mapping of the distribution of saline during radiofrequency ablation with perfusion electrodes. Cardiovasc Intervent Radiol. 2005;28(4):476–80.
67. Liu Z, et al. Radiofrequency tumor ablation: insight into improved efficacy using computer modeling. AJR Am J Roentgenol. 2005;184(4):1347–52.
68. Laeseke PF, et al. Use of dextrose 5 % in water instead of saline to protect against inadvertent radiofrequency injuries. AJR Am J Roentgenol. 2005;184(3):1026–7.
69. Yang D, et al. Measurement and analysis of tissue temperature during microwave liver ablation. IEEE Trans Biomed Eng. 2007;54(1):150–5.
70. Yang D, et al. Expanding the bioheat equation to include tissue internal water evaporation during heating. IEEE Trans Biomed Eng. 2007;54(8): 1382–8.
71. Brace CL, et al. Tissue contraction caused by radiofrequency and microwave ablation: a laboratory study in liver and lung. J Vasc Interv Radiol. 2010;21(8):1280–6.
72. Isfort P, et al. [In vitro experiments on fluid-modulated microwave ablation]. Rofo. 2010;182(6):518–24.
73. Ahmed M, et al. Combination radiofrequency ablation with intratumoral liposomal doxorubicin: effect on drug accumulation and coagulation in multiple tissues and tumor types in animals. Radiology. 2005;235(2): 469–77.
74. Horkan C, et al. Reduced tumor growth with combined radiofrequency ablation and radiation therapy in a rat breast tumor model. Radiology. 2005;235(1):81–8.
75. Ahmed M, Goldberg SN. Combination radiofrequency thermal ablation and adjuvant IV liposomal doxorubicin increases tissue coagulation and intratumoural drug accumulation. Int J Hyperthermia. 2004;20(7):781–802.
76. Dupuy DE, et al. Radiofrequency ablation followed by conventional radiotherapy for medically inoperable stage I non-small cell lung cancer. Chest. 2006; 129(3):738–45.
77. Goldberg SN, et al. Radiofrequency thermal ablation with adjuvant saline injection: effect of electrical conductivity on tissue heating and coagulation. Radiology. 2001;219:157–65.

78. Gaber MH, et al. Thermosensitive liposomes: extravasation and release of contents in tumor microvascular networks. Int J Radiat Oncol Biol Phys. 1996;36(5): 1177–87.
79. Negussie AH, et al. Formulation and characterisation of magnetic resonance imageable thermally sensitive liposomes for use with magnetic resonance-guided high intensity focused ultrasound. Int J Hyperthermia. 2011;27(2):140–55.
80. Gasselhuber A, et al. Mathematical spatio-temporal model of drug delivery from low temperature sensitive liposomes during radiofrequency tumour ablation. Int J Hyperthermia. 2010;26(5):499–513.
81. Ahmed M, et al. Radiofrequency thermal ablation sharply increases intratumoral liposomal doxorubicin accumulation and tumor coagulation. Cancer Res. 2003;63(19):6327–33.
82. D'Ippolito G, et al. Percutaneous tumor ablation: reduced tumor growth with combined radio-frequency ablation and liposomal doxorubicin in a rat breast tumor model. Radiology. 2003;228(1):112–8.
83. Monsky WL, et al. Radio-frequency ablation increases intratumoral liposomal doxorubicin accumulation in a rat breast tumor model. Radiology. 2002;224(3):823–9.
84. Poon RT, Borys N. Lyso-thermosensitive liposomal doxorubicin: a novel approach to enhance efficacy of thermal ablation of liver cancer. Expert Opin Pharmacother. 2009;10(2):333–43.
85. Solazzo S, et al. Liposomal doxorubicin increases radiofrequency ablation-induced tumor destruction by increasing cellular oxidative and nitrative stress and accelerating apoptotic pathways. Radiology. 2010;255:62–74.
86. Yang W, et al. Do liposomal apoptotic enhancers increase tumor coagulation and end-point survival in percutaneous radiofrequency ablation of tumors in a rat tumor model? Radiology. 2010;257(3):685–96.
87. Ahrar K, et al. Dr. Gary J. Becker Young Investigator Award: relative thermosensitivity of cytotoxic drugs used in transcatheter arterial chemoembolization. J Vasc Interv Radiol. 2004;15(9):901–5.
88. Kim JH, et al. Medium-sized (3.1–5.0 cm) hepatocellular carcinoma: transarterial chemoembolization plus radiofrequency ablation versus radiofrequency ablation alone. Ann Surg Oncol. 2011;18:1624–9.
89. Morimoto M, et al. Midterm outcomes in patients with intermediate-sized hepatocellular carcinoma: a randomized controlled trial for determining the efficacy of radiofrequency ablation combined with transcatheter arterial chemoembolization. Cancer. 2010;116(23):5452–60.
90. Chan MD, et al. Combined radiofrequency ablation and high-dose rate brachytherapy for early-stage non-small-cell lung cancer. Brachytherapy. 2011;10: 253–9.
91. Grieco CA, et al. Percutaneous image-guided thermal ablation and radiation therapy: outcomes of combined treatment for 41 patients with inoperable stage I/II non-small-cell lung cancer. J Vasc Interv Radiol. 2006;17(7):1117–24.
92. Algan O, et al. External beam radiotherapy and hyperthermia in the treatment of patients with locally advanced prostate carcinoma. Cancer. 2000;89(2): 399–403.
93. Solazzo S, et al. RF ablation with adjuvant therapy: comparison of external beam radiation and liposomal doxorubicin on ablation efficacy in an animal tumor model. Int J Hyperthermia. 2008;24(7):560–7.
94. Mayer R, et al. Hyperbaric oxygen and radiotherapy. Strahlenther Onkol. 2005;181(2):113–23.
95. Wood BJ, et al. Navigation systems for ablation. J Vasc Interv Radiol. 2010;21(8 suppl):S257–63.
96. Krucker J, et al. Electromagnetic tracking for thermal ablation and biopsy guidance: clinical evaluation of spatial accuracy. J Vasc Interv Radiol. 2007;18(9): 1141–50.
97. Klauser AS, et al. Fusion of real-time US with CT images to guide sacroiliac joint injection in vitro and in vivo. Radiology. 2010;256(2):547–53.
98. Khan MF, et al. Navigation-based needle puncture of a cadaver using a hybrid tracking navigational system. Invest Radiol. 2006;41(10):713–20.

Electroporation

2

Mohammad Hjouj and Boris Rubinsky

Abstract

Nonthermal irreversible electroporation (NTIRE) is a minimally invasive tissue ablation modality in which high field strength, nanosecond to millisecond long pulsed electric fields are delivered across the cell to produce nanoscale defects in the cell membrane and thereby induce cell death. An important attribute of this technique is its ability to ablate cells in volumes of tissues while leaving intact the extracellular scaffold, including the mechanical scaffold of blood vessels and ducts. This is a review of the technology with a special emphasis on medical imaging. The review contains a background on the technology, mathematical modeling for treatment planning, fundamental findings from animal studies, first clinical results, and aspects of medical imaging.

Introduction

Electroporation is an electric field-induced biophysical phenomenon in which the cell membrane permeability to transmembrane molecular transport is increased by exposing the cell to short nanosecond to millisecond scale and high field, kV/cm scale, electric pulses [1, 2]. Such increase in permeability [3] is, presumably [4], related to the formation of nanoscale defects or pores in the cell membrane, from which the term electro-"poration" [5] stems. For certain electric pulses, membrane permeabilization is permanent, and the process leads to cell lysis. It is in this sense of permanent permeabilization that most authors define irreversible electroporation (IRE). However, it must be noted that temporary permeabilization can also cause a severe disruption of the cell homeostasis which can finally result in cell death, either necrotic or apoptotic. Therefore, in a broader sense, IRE could be defined as the permanent or temporal membrane electroporation process that causes cells to die.

The phenomenon of irreversible electroporation – cell death due to the applications of short electric pulses – has been recognized, in various forms, for centuries and until

M. Hjouj (✉)
School of Computer Science and Engineering, Hebrew University of Jerusalem, Jerusalem, Israel

Department of Medical Imaging, Al–Quds University, Abu–Dis, Palestine
e-mail: mhjouj@hotmail.com

B. Rubinsky
Department of Mechanical Engineering, University of California at Berkeley, Berkeley, CA, USA
e-mail: rubinsky@me.berkeley.edu; brubinsky@gmail.com

D.E. Dupuy et al. (eds.), *Image-Guided Cancer Therapy*, DOI 10.1007/978-1-4419-0751-6_4,

recently used primarily in the food industry [6]. The biophysical phenomenon referred in medical applications as "irreversible electroporation" is known in food technology as *pulsed electric field* processing or *electroplasmolysis*, in reference to the lysis of cell membranes in tissue, for extracting their contents, or the bactericidal effect in treatment of fluids [7]. The "pulsed electrical field" concept is broader than just irreversible electroporation. It has been recently shown to include also the effects of nanoscale pulses on intracellular components [8]. The interest of the food industry in the so-called bactericidal action of electrical fields motivated a series of three seminal papers by Sale and Hamilton [9–11]. These papers are extraordinary in that they set the basis for the field of irreversible electroporation and contain the ingredients of many of the future studies in what subsequently was called the field of electroporation in general.

Recently, nonthermal irreversible electroporation (NTIRE) has begun to be employed as a new tool in the surgical armamentarium for minimally invasive ablation of undesirable tissue [12]. In NTIRE, the primary use of irreversible electroporation is to induce undesirable cell death by affecting selectively only the cell membrane without causing a possible thermal mode of damage due to excessive electric current-induced Joule heating. Specifically, care is given to choosing electric pulse parameters that induce irreversible electroporation without causing thermal damage [13, 14]. The research in the field of nonthermal irreversible electroporation in medicine has recognized that while the final outcome of irreversible electroporation and thermal damage on cell viability is the same, cell death, there are many very important aspects at the microscale which are different. Unlike electroporation that affects only one type of molecule in the treated volume – the cell membrane lipid bilayer – thermal, radiation, as well as chemical (alcohol) ablation indiscriminately affect every molecule in the treated volume. Therefore, when a volume of tissue is ablated by irreversible electroporation only, the procedure has molecular selectivity (i.e., it targets one type of molecule only, the cell membrane lipid bilayer). Having a minimally invasive technique that can ablate only one certain type of molecule, the cell membrane, is advantageous – because it spares important other tissue components such as the extracellular matrix and electrically nonconductive molecular structures. An intact extracellular matrix after NTIRE treatment allows such structures as ducts, large blood vessels, or nerve conduits to continue to serve their physical function, even in the absence of cells. This facilitates the treatment of tumors that abut large blood vessels in previously inaccessible parts and organs of the body such as the pancreas [15, 16], near large blood vessels in the liver [17–19], and kidney [20]. Retaining the patency of the large blood vessels also facilitates a much faster response of the immune system and sometimes healing without the formation of scar tissue [21]. It was also shown that the selectivity of NTIRE can lead to survival and regeneration of nerves [22–24]. The intact extracellular matrix can also serve as a template for cell regeneration after NTIRE. For instance, Maor and colleagues have shown that the carotid artery continues to serve as an effective blood conduit after NTIRE [25, 26]. Furthermore, endothelial cells regenerate and grow along the NTIRE-treated blood vessel on the intact extracellular matrix [25, 26].

Typical NTIRE procedures employ two or more electrodes inserted in tissue in such a way as to confine the undesirable tissues between them [21]. The electrodes can be mounted on one probe (e.g., [25–27]) or on several probes (Fig. 2.1) [21]. The process of tissue ablation occurs between electrodes and is usually confined by the electrodes (Fig. 2.2). In this respect, NTIRE is different from most of the other ablation techniques in which the ablation propagates as a function of time from the probe outward. NTIRE is also different from other minimally invasive tissue ablation techniques by the time scale in which the procedure occurs. The electric pulses that induce NTIRE are on the length scale of nanosecond to milliseconds. NTIRE is delivered as a set of pulses rather than continuously. Current clinical practice employs between 8 and 90 pulses of 70–100 μs length, delivered at a frequency of 1 Hz [17, 19, 28]. In contrast,

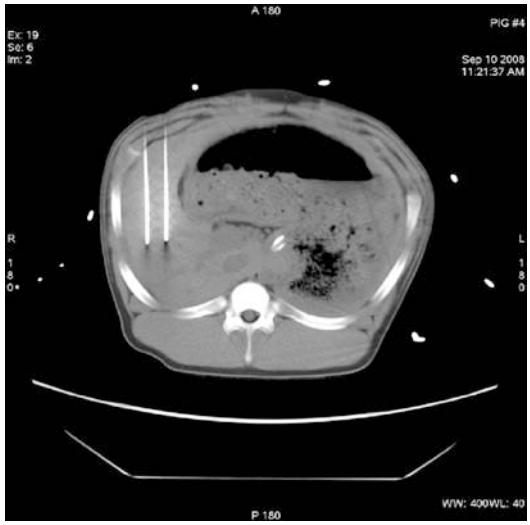

Fig. 2.1 Two NTIRE copper, 1 mm diameter, electrodes (*bright lines*) inserted into a pig liver (Courtesy Dr. Stephen Solomon, *Memorial Sloan-Kettering Cancer Center*)

thermal ablation procedures employ time scales from minutes to tens of minutes. Because NTIRE is conceptually different from other more established tissue ablation procedures, such as cryosurgery, radiofrequency ablation, or radiation, it is important for those with experience in the other techniques to understand the particular attributes of NTIRE and how it is different from the other tissue ablation techniques.

We will introduce next the mathematical modeling required for treatment planning of NTIRE. Treatment planning, which is important in every minimally invasive tissue ablation procedure, is essential for correct use of NTIRE. This is followed by a description of fundamental experimental results of NTIRE and a brief survey of clinical results produced so far. Lastly, we will discuss medical imaging of NTIRE with respect to two key aspects: placement of electrodes and procedural follow-up.

Mathematical Models for Nonthermal Irreversible Electroporation

As with other minimally invasive tissue ablation techniques, treatment planning is of great importance and can benefit from mathematical modeling. NTIRE treatment planning mathematical modeling requires the solution of the electric field equation to determine the electric field produced during the procedure. In addition to the field equation in order to avoid thermal damage, the bio-heat equation coupled with a kinetic equation is solved to evaluate if thermal damage occurs [13, 14, 29–32]. In this section, we will first present the set of equations used in NTIRE treatment planning. This is followed by some illustrative examples.

The electric field equation is,

$$\nabla \cdot (\sigma \nabla \phi) = 0 \tag{2.1}$$

subject to voltage boundary conditions on the electrodes:

$$\phi(electrodes) = prescribed \tag{2.2}$$

where σ is the electrical conductivity of the tissue and ϕ is the local electrical potential. It should be emphasized that the electrical conductivity of the tissue can change during the process of electroporation, and therefore the problem may become nonlinear as the local conductivity may become related to the local electrical field. In addition, the boundary conditions prescribed here are of the first kind. It is possible that contact impedance between the electrodes and the tissue may be a more appropriate boundary, e.g., Somersalo et al. [33]. The boundaries of the domain that are not in contact with the electrodes are treated as either infinite or insulated.

The local electrical field, E, can be calculated from the electrical potential:

$$E = \nabla \phi \tag{2.3}$$

This electrical field affects the local conductivity through electroporation effects and makes the problem nonlinear. In addition, it yields a local heat source, P, through Joule heating. The local electrical power dissipation is given by:

$$P = \sigma(|\nabla \phi|)^2 \tag{2.4}$$

The equation most commonly used to calculate the temperature during electroporation in

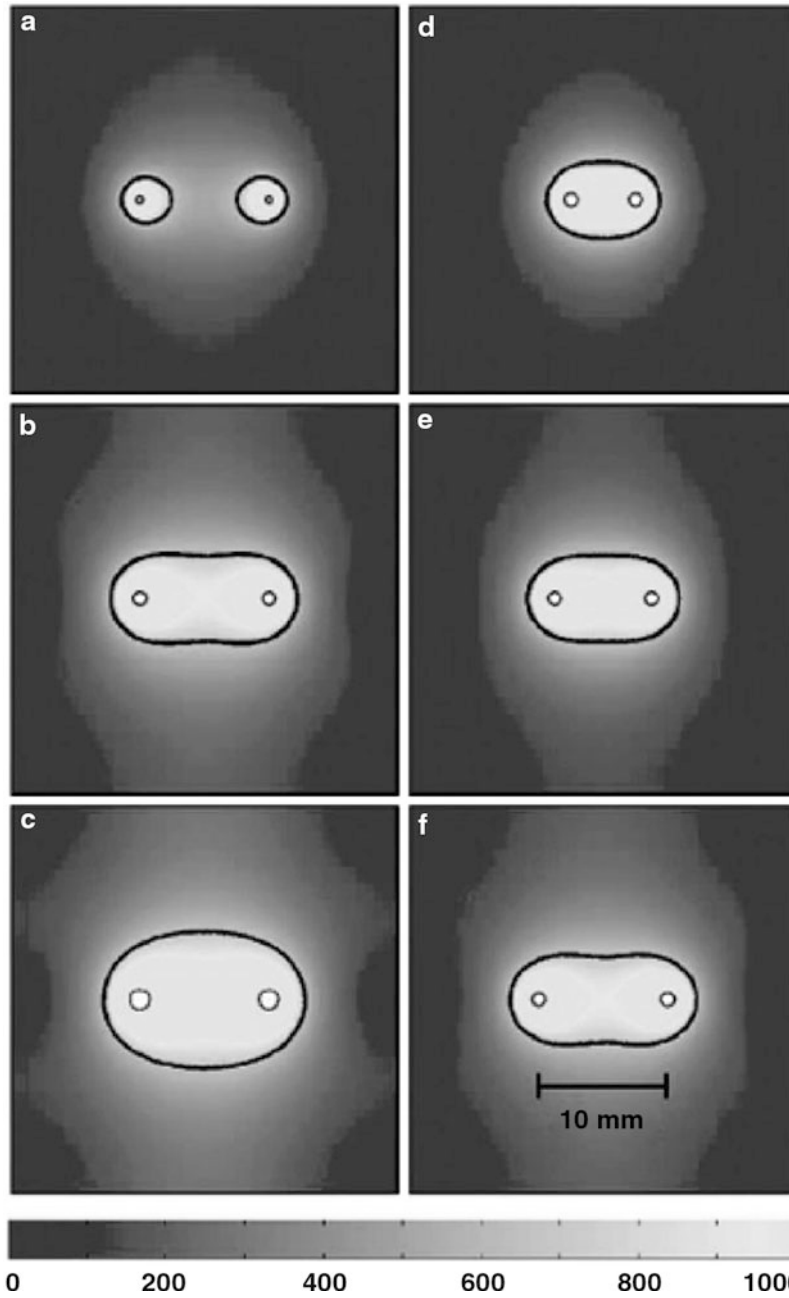

Fig. 2.2 Typical NTIRE ablation zone shapes that can be obtained with two electrodes. The *dark line* shows the interface between the areas that was irreversible electroporated and that was reversible electroporated. The elliptic shape is typical to the treated region, when the electroporation is induced by two electrodes. The lighter area beyond the *dark line* illustrates the reversible electroporated domain. This area may become important in the future uses of reversible electroporation as it allows the incorporation of drugs or genes around the area treated with NTIRE, in the mode of electrochemotherapy (Modified with permission from Ref. [13])

biological tissues is the bio-heat equation [34] to which the local power dissipation is added as a heat source:

$$\nabla \cdot (k\nabla T) + w_b c_b (T_a - T) + q'' + P = \rho c_p \frac{\partial T}{\partial t} \tag{2.5}$$

where k is the thermal conductivity of the tissue, T is temperature, $w_b c_b$ are the product of the volumetric mass flow of blood and blood heat capacity, q'' is the volumetric metabolic heat, t is time, and ρc_p is the product of tissue density and heat capacity of tissue.

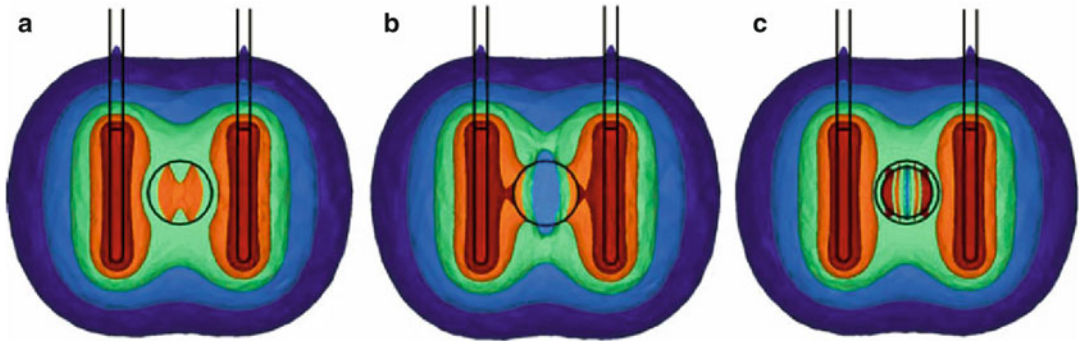

Fig. 2.3 Effect of a heterogeneous tissue conductivity on the electric field distribution. Each graph depicts the surfaces of constant electric field strength (for 100, 200, 400, 800, and 1,600 V/cm) that would result from the presence of a 5-mm-diameter spherical inclusion, located halfway between the electrodes. The inclusion is composed of tissue with one fifth or five times the background electrical conductivity in graphs (**a**) and (**b**), respectively, while (**c**) the third graph is similar to (**a**) but with a nested 4-mm-diameter sphere of five times normal conductivity (With permission from Ref. [32])

This equation is solved subject to initial temperature conditions, which in case of the living body is often taken as 37 °C. The boundary conditions are taken as either 37 °C or adiabatic (no heat transfer occurs). A review of various models of the bio-heat equation can be found in [35].

Once the time-dependent temperature is calculated, it can be introduced into an Arrhenius type of chemical reaction kinetics equation that correlates tissue damage, Ω, to temperature, T, and time, t [36]

$$\Omega = \int \zeta e^{-E/RT} dt \tag{2.6}$$

where ζ is a frequency factor, E is the activation energy, and R is the universal gas constant. It should be emphasized that the thermal damage is a function of both time and temperature and long-term exposure to temperatures as low as 42 °C can cause thermal damage. Nevertheless, when the exposure time is on the order of magnitude of seconds, 50 °C is sometimes taken as a target temperature [37].

Figure 2.2 illustrates typical NTIRE ablation zone shapes that can be obtained with two electrodes [13]. Studies on the treated region shapes that can be obtained with various electrode configurations are found in several publications [13, 14, 29, 32]. It is particularly interesting to note that under certain parameters, the treatment can be incomplete and a zone of untreated tissue can occur between the electrodes (Fig. 2.2a). The lighter area beyond the dark line illustrates the reversible electroporated domain. This area may become important in the future uses of reversible electroporation as it allows the incorporation of drugs or genes around the area treated with NTIRE, in the mode of electrochemotherapy.

Heterogeneities, for instance, a metal clip in the treated area, can affect the treated zone as illustrated in Fig. 2.3 [30, 32]. It is important to understand that in NTIRE, as in other ablation methods, the shape of the electrodes, the placement of the electrodes, and the voltages set on the electrodes will all affect the outcome of the procedure.

Experimental and First Clinical Results of Nonthermal Irreversible Electroporation

This section will highlight first the unique aspects of nonthermal irreversible electroporation, which can be directly attributed to the unique "molecular selective" mode of this procedure. Figure 2.4 is from the first animal study of NTIRE [31] and the results are typical of all the later studies as well. In the study, a rat liver was exposed to a 20-ms NTIRE pulse, and the rat was killed a couple of hours later. The liver

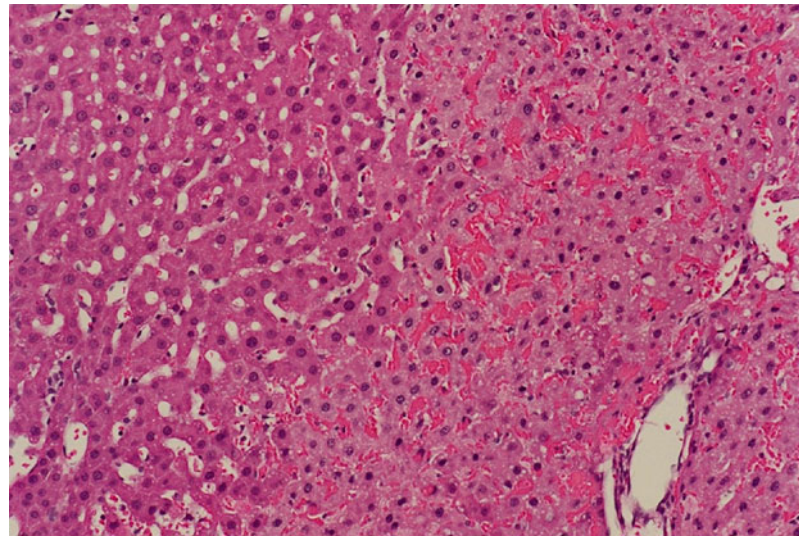

Fig. 2.4 H&E stained liver that has undergone NTIRE. The left-hand side is the normal liver, and the right-hand side is the electroporated liver. Note the sharp line of distinction between the treated and untreated areas. Red blood cells are destroyed and occlude the sinusoids on the right hand while they are open on the left. However, the large blood vessel in the treated area has remained morphologically intact. The *right panels* show an intact vein

was flushed through its vasculature prior to embedding and H&E staining.

Figure 2.4 shows the margin of the NTIRE-treated liver. The light spaces between cells on the left side are the intact sinusoids that were flushed of red blood cells. The hepatocytes around the intact sinusoids are also intact. On the other hand, on the right-hand side, the sinusoids are filled with destroyed red blood cells and other cellular debris. Flushing did not remove the debris from the sinusoids. However, as predicted for the NTIRE mode, the procedure did not affect the extracellular matrix and other tissue molecules, except the cell membrane. Therefore, the mechanical integrity of large blood vessels remains intact. The patency of the large blood vessels and ducts is evident from the bottom right-hand side images of clear large blood vessels in the midst of the NTIRE-treated region. Because of the unique aspects of NTIRE, the mechanical structure of these blood vessels remained intact and accessible to flushing.

The results from the first chronic study of NTIRE in a large animal model are shown in Fig. 2.5, and they are also typical of all the subsequent findings [21].

Figure 2.5 shows a pig liver treated with NTIRE and also flushed prior to embedding in formalin. The top and bottom rows show the macroscopic and H&E stained cross section of the liver at various times after the procedure. The treated areas are outlined. A most unusual aspect of NTIRE, relative to other minimally ablation surgical modalities, which is also being confirmed in clinical studies [19], is how fast the treated liver regenerates. It is particularly interesting to see in the second and third columns that NTIRE can ablate tissue all the way to the margin of the larger blood vessels – an aspect of tissue ablation of great importance in treating of unresectable tumors near large blood vessels [19] and in the pancreas [15, 16]. As in the case of the flushed rat liver, the flushed pig liver had also patent and open large blood vessels within the treated area. Such open and mechanically intact large blood vessels do not occur during thermal treatment with radio frequency, focused ultrasound, or microwave. The availability of such open conduits allows the immune system excellent access to all the parts of the treated tumor tissue, through the blood flow. In other modes of ablation – the immune system needs to remove the dead cells by diffusion through the volume of treated tissue from the outer margin of the treated tissue. In NTIRE, the entire volume of the treated tissue is accessible through the large blood vessels, and the immune system can remove the dead cells through the entire treated system. This effect is evident from the bottom row of Fig. 2.5, which shows the lymph nodes.

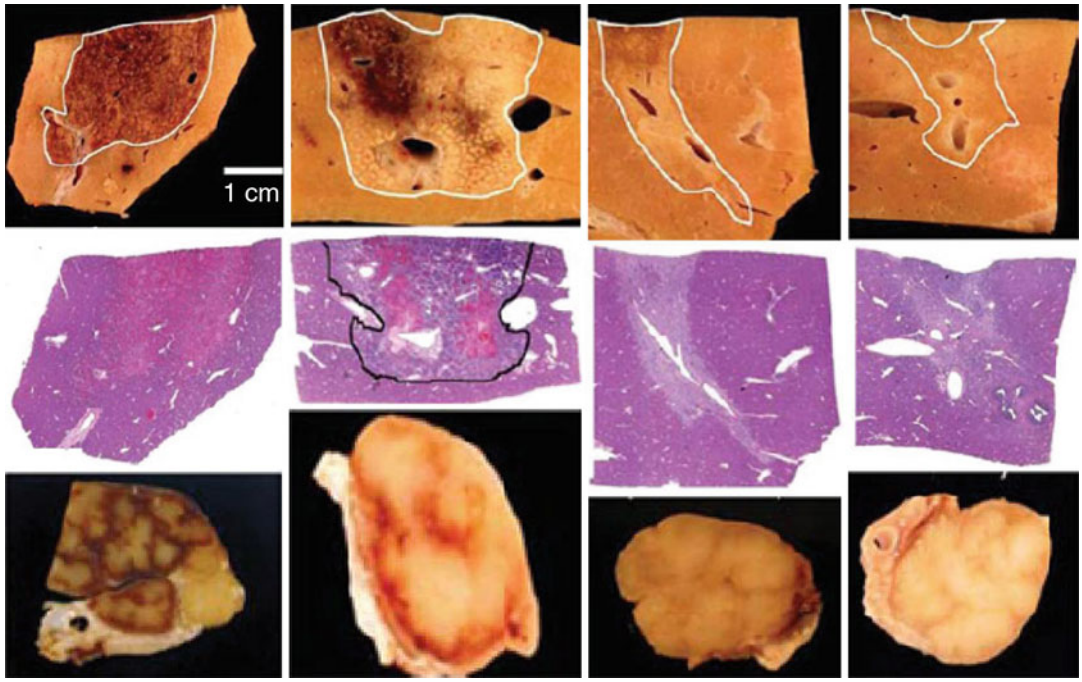

Fig. 2.5 Cross section through NTIRE-treated pig liver after 24 h (first column from *left*), 3 days (second column), 7 days (third column), 14 days (fourth column). *Top row* – macroscopic cross section: *middle row* – H&E stained section: *bottom row* – lymph nodes (Reprinted from Ref. [21])

It is evident that after 24 h, the lymph nodes are inflamed and active. However, within a week, the inflammation has disappeared.

Figure 2.6 shows that bile ducts as well as arteries remain intact in the NTIRE-treated volume of tissue.

At the time this review is written, NTIRE has been already used to treat a variety of malignant tumors including, liver, kidney, lymph nodes, lung, and prostate in well over 800 patients. However, very few scientific reports have been published so far. Nevertheless, published clinical studies [17, 19, 28, 38, 39] produce observations that are consistent with the results from animal experiments.

Brausi et al. confirmed the safety of NTIRE in treatment of prostate cancer [28]. The clinical work of Onik [38] in the prostate confirmed many of the advantages seen in the animal studies treated using NTIRE. In terms of tissue destruction, animal studies showed that IRE lesions are characterized by uniform necrosis throughout, with a very narrow zone of transition to

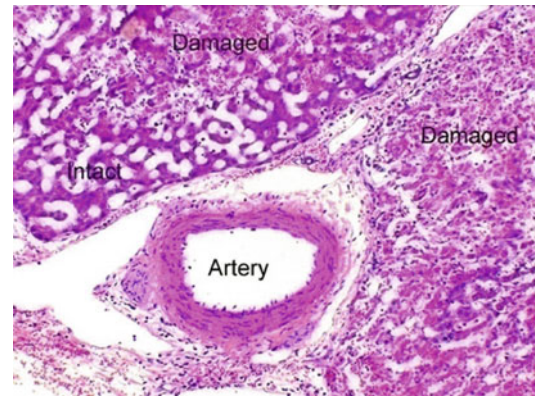

Fig. 2.6 Intact bile ducts and arteries within NTIRE-treated tissue

unaffected tissue. Two postoperative biopsies in patients showed complete epithelial cell ablation in all the cores taken from all patients. No viable glandular elements were identified, although ghosts of glandular structures were still identifiable. Of interest is that these results were independent of Gleason score with successful

treatment of patients with Gleason score of seven and eight. Despite the uniform destruction of glandular cellular elements evidenced in biopsies, sparing of normal structures was also demonstrated. Post-op pathology and color Doppler US demonstrated intact and functioning micro- and macrovasculature, particularly in the prostate neurovascular bundle. This characteristic appears to be unique to NTIRE lesions. While IRE does cause endothelial cell death, it does not cause vessel occlusion. Also noted on the biopsies was the preservation of nerves and ganglion cells within the NTIRE lesions despite them being included in the NTIRE lesion. All the patients who were potent prior to treatment were immediately potent after treatment, while it did take approximately 6 months for two patients who were treated bilaterally to regain their potency. A number of patients were successfully treated despite tumors being adjacent to the urethra. Of note is that two of the patients were also radiation failures. In one of the patients, the tumor involved the midline ejaculatory duct region. Despite very aggressive treatment in this area, the patient's ejaculatory ducts remained intact, allowing for normal ejaculation postoperatively. This is unique to IRE ablation. Nevertheless, animal studies suggest a need for cautions. IRE will ablate both smooth and striated muscle. Although all patients in this initial experience were continent immediately, care still needs to be taken not to destroy both the internal and external sphincter which would result in incontinence because NTIRE can ablate muscle cells. From a technical point of view, NTIRE is similar to other transperineal ultrasound-guided procedures such as cryosurgery and brachytherapy. However, it is important to emphasize that general anesthesia with patient paralysis is needed due to the muscle contraction associated with the electrical pulsing. The speed of the IRE procedure is however impressive compared to cryoablation and HIFU. The multiple pulses for the treatment are delivered in a few minutes rather than the much longer process of freezing and thawing associated with cryoablation or the numerous small ablation zones necessary in HIFU. The Albert Hospital group of Dr. Kenneth Thomson has produced by far, the majority of peer reviewed reports on clinical use of NTIRE [17, 19, 39]. They have used general anesthesia with muscular paralysis to ensure that the energy applied to the electrodes did not cause severe muscle contraction. Even with the patient fully paralyzed, the energy delivered by the IRE is sufficient to cause contraction of a muscle in the immediate vicinity of the electrodes. Additional patient monitoring using BIS monitors and a direct arterial pressure monitor was used as during the application of the electroporation, the electrocardiogram tracing was significantly distorted by the electrical energy. In a few patients, the electrical energy generated extra systoles and in one patient, a series of contractions which did not provide adequate cardiac output for several seconds. As a result of these cardiac arrhythmias, an ECG synchronizing device was used to deliver the IRE energy 50 μs following the peak of the R wave. While this device prevented the arrhythmias, the delivery of the energy was markedly delayed as in most patients, only one or two pulses could be delivered per heartbeat. In practice however, the time of delivery of the energy is not a rate-limiting factor.

Thomson reports that "The promise of preservation of the structural integrity of the tissue was achieved and as a result of this we have been able to place the electrodes in an extremely aggressive manner with respect to vital organs. Where a tumor lies adjacent to a large bile duct, blood vessel or other vital structure, with imaging guidance it is a simple matter to position the electrodes in such a way as not to puncture the vessel or structure yet provide a zone of electroporation which involves the region of the vessel structure. Likewise lesions adjacent to the gall bladder, stomach, diaphragm and right atrium have been accessed effectively without evidence of damage to these adjacent vital structures…The most remarkable feature of recovery following irreversible electroporation… is the almost complete absence of post-ablation pain. In this group of patients who have been subjected to most other alternatives including chemotherapy, surgery and thermal ablation, this feature of (IRE) is most remarkable. From a histological point of view,

tissue biopsies taken one month after the procedure demonstrated 'coagulate necrosis' with preservation of tissue structure. On CT follow-up at periods between 1 and 8 months, there has been no evidence of residual damage to blood vessels or bile ducts. Since the biliary endothelium would have suffered the same fate as the tumor cells with electroporation, it is surprising that we have not seen evidence of bile duct stricture. Vascular endothelium and smooth muscle should also be ablated with irreversible electroporation but we have not been able to detect any deleterious effect to blood vessels in our patients." In a follow-up study, Ball et al. [19] conclude that "Relaxant general anesthesia is required for IRE of the liver, lung, and kidney. An electrocardiogram synchronizer should be used to minimize the risk of arrhythmias. Attention to the position of the arms is required to maximize CT scan quality but minimize brachial plexus strain. Simple postoperative analgesia is all that is required in most patients."

The group of Davalos produced a recent series of reports on clinical use of NTIRE in dogs with tumors in their brain. The results are very promising showing that, e.g., the procedure can successfully treat a large sarcoma [40].

Medical Imaging in Nonthermal Irreversible Electroporation

Similar to other minimally invasive tissue ablation techniques, IRE is also dependent on two important aspects of medical imaging. The first is placement of the IRE probes (electrodes), and the second is imaging the outcome of the procedure. Unlike thermal tissue ablation modalities such as cryosurgery or radiofrequency, IRE requires the use of two electrodes and not only one enabling probe. In IRE, the two electrodes bound the tissue that is ablated, and the ablation is virtually instantaneous. In the thermal modalities, the tissue ablation process propagates as a function of time from the thermal probe outward. This affects the mode of placing the probes. In IRE, the probe needs to be placed in such a way that the tissue to be ablated is between the

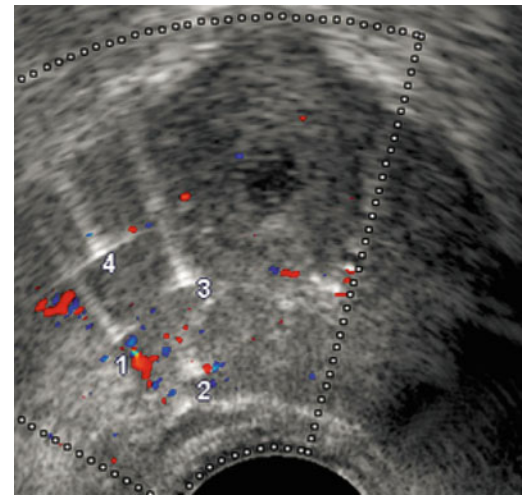

Fig. 2.7 Ultrasound showing the IRE probes (*bright numbered points*) in a parallelogram pattern bracing the area of the know tumor (With permission from Ref. [38])

electrodes, i.e., they are at the periphery of the tissue to be ablated. In contrast, in thermal ablation, the probes are placed in the core of the tissue that needs to be ablated so that the ablation propagates in time from the core to the periphery. Placement of the probes is done with imaging (as shown in Fig. 2.1).

Oni [38] reports that in the prostate procedure, patients were placed in the dorsal lithotomy position, and 18-gauge IRE electrodes were placed under transrectal ultrasound guidance percutaneously through the perineum. IRE probes were placed to cover the known area of cancer location based on the patients mapping biopsy. Four probes were placed in a roughly square array, 1–1.5 cm apart, with the known area of cancer in the center of the array (Fig. 2.7).

Thomson [17, 19, 39] reports that in his experience, in humans, especially in the case of metastases from colorectal carcinoma, ultrasound visualization solutions were difficult, and therefore, computed tomography was used for image guidance. This was even more necessary in the lungs and in most of the renal tumors that were treated (Fig. 2.8).

The other complicating factor in the group of patients chosen for treatment was the inability to reliably place a grid pattern of electrodes

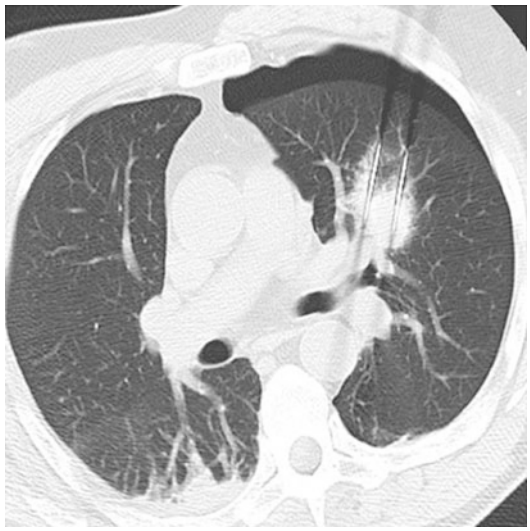

Fig. 2.8 Solitary hilar metastasis with electrodes in position astride the *upper pole* pulmonary artery. No hemoptysis after the IRE procedure. Pneumothorax resolved on drainage in 24 h (From Ref. [39] with permission, Reprinted with permission from Thomson [22])

over the tumor. This was because of the overlying ribs, scapula, and other vital organs. "Unlike the prostate, where a rectangular grid could be used to accurately space the electrodes throughout the gland, in the liver, the spacing of the electrodes was usually performed in an oblique manner from a limited access point in the intercostal space. This aspect of the treatment remains the most difficult in terms of planning and execution. As our experience has grown, we have moved from planning a "slab-to-slab" delivery to planning a "point-to-point" delivery of electroporation. We have also reduced the electrode exposure from 40 to 20–30 mm" [19]. Thomson, as well as Onik, found that positioning the electrodes through the tumor mass remains the most time-consuming facet of the procedure. Anecdotal reports from other physicians performing NTIRE confirm this observation. Placement of the electrodes under imaging is the part of the procedure which is most prone to mistakes and requires radiology skills from the interventional physicians. Since the distance between the electrodes is of importance, when the probes are not within the allowed distance, untreated regions can occur between the electrodes as in (Fig. 2.2a). Thomson [39] reports that early in their experience, this scenario resulted in what he terms "skip lesions" as the entire tumor had not been completely electroporated. This further illustrates the challenges facing the physicians using imaging to place the multiple electrodes for ablation. Developing imaging-assisted skills for optimal probe placement is an important area of clinical research, whose successful completion will substantially improve the outcome of NTIRE.

Perhaps one of the most important advances in minimally invasive surgery was made when imaging was first used to detect the extent of freezing during cryosurgery [41, 42]. Although in cryosurgery the extent of freezing is not equivalent to the extent of tissue ablation, it nevertheless provides a measure of control over the procedure. Therefore, we tried to determine, early in developing IRE, if the outcome of the procedure can be visualized with imaging modalities. Most interesting was the finding that immediately following pulse application ultrasound showed a markedly hypoechoic lesion in the expected location of the IRE lesion [Fig. 2.9b (axial) and Fig. 2.9c (sagittal)] [21]. At 24 h, the ultrasound image showed the hypoechoic lesion had changed character and was now uniformly hyperechoic [21].

Histology as well as mathematical modeling of treatment planning has shown that the hypoechoic lesion seen immediately after NTIRE on ultrasound corresponds well with the region of predicted and measured tissue ablation (Fig. 2.10) [21]. Similar observations on ultrasound imaging of IRE were reported by Lee et al. [43]. Thomson [17, 19, 39] also reports that in those patients in whom ultrasound could be used, similar findings were observed in terms of immediate loss of ultrasound echogenicity with electroporation. While the mechanism which gives rise to the image is not certain, it is most possible related to the destruction of the red blood cells in the small blood vessels. This would be more pronounced in vascular organs as the liver, although it was also observed in the kidney and to a lesser degree in the prostate. Thomson [39] has found that computer tomography (CT)

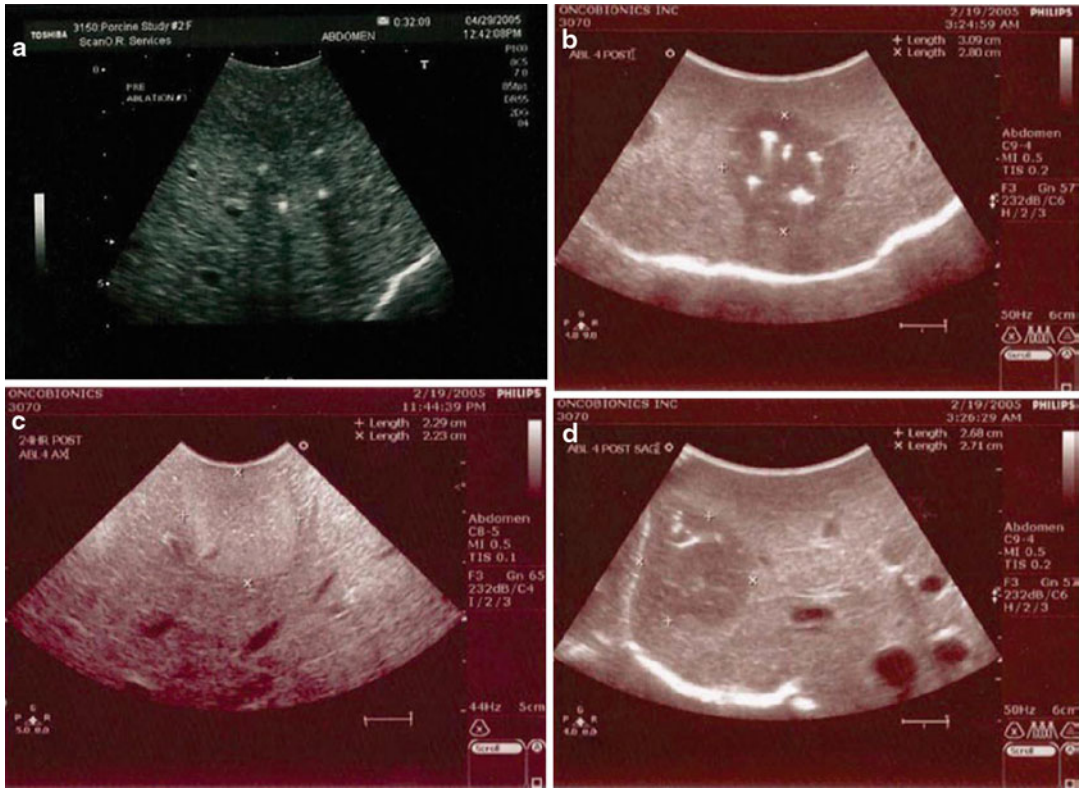

Fig. 2.9 Ultrasound imaging of IRE ablation in the pig liver. (**a**) The placement of the electroporation probes under ultrasound, *hyperechoic dots* represents the electroporation needles. (**b**) Shows axial ultrasound with four hyperechoic dots representing the four needles tracks. The hypoechoic appearance of the expected area of the IRE lesion is noted. (**c**) Sagittal view of the same lesion. The hypoechoic appearance of the expected area of the IRE lesion is noted. (**d**) Sagittal view of the treated area taken 24 h post-IRE. Lesion has now become hyperechoic. Seems to have shrunk by about 4–5 mm. Scale bar 1 cm (From Ref. [21] with permission)

also produces similar images of NTIRE (Fig. 2.11). The group of Kee et al. [18] has also shown that essentially every imaging modality (e.g., MRI, CT, and ultrasound) produces images of the NTIRE-treated areas.

In two recent papers [44, 45], the group of Larson has investigated the use of MRI, with and without contrast material, in a rodent animal model to detect the extent of the treated tissue regions after irreversible electroporation (IRE). Using MR imaging compatible electrodes, the IRE procedure was imaged with T1- and T2-weighted images acquired before and immediately after application of the IRE pulses. MR imaging measurements were compared with both finite element modeling (FEM)-anticipated ablation zones and histologically confirmed ablation zones at necropsy. MR imaging measurements permitted immediate depiction of IRE ablation zones that were hypointense on T1-weighted images and hyperintense on T2-weighted images. MR imaging-based measurements demonstrated excellent consistency with FEM-anticipated ablation zones (for both T1- and T2-weighted images). MR imaging measurements were also highly correlated with histologically confirmed ablation zone measurements. In the contrast material-enhanced magnetic resonance (MR) imaging study, IRE was monitored with conventional T1-weighted gradient-recalled echo (GRE) and inversion recovery (IR)-prepared GRE methods to quantitatively measure the size of irreversible electroporation. IRE ablation zones were produced by using

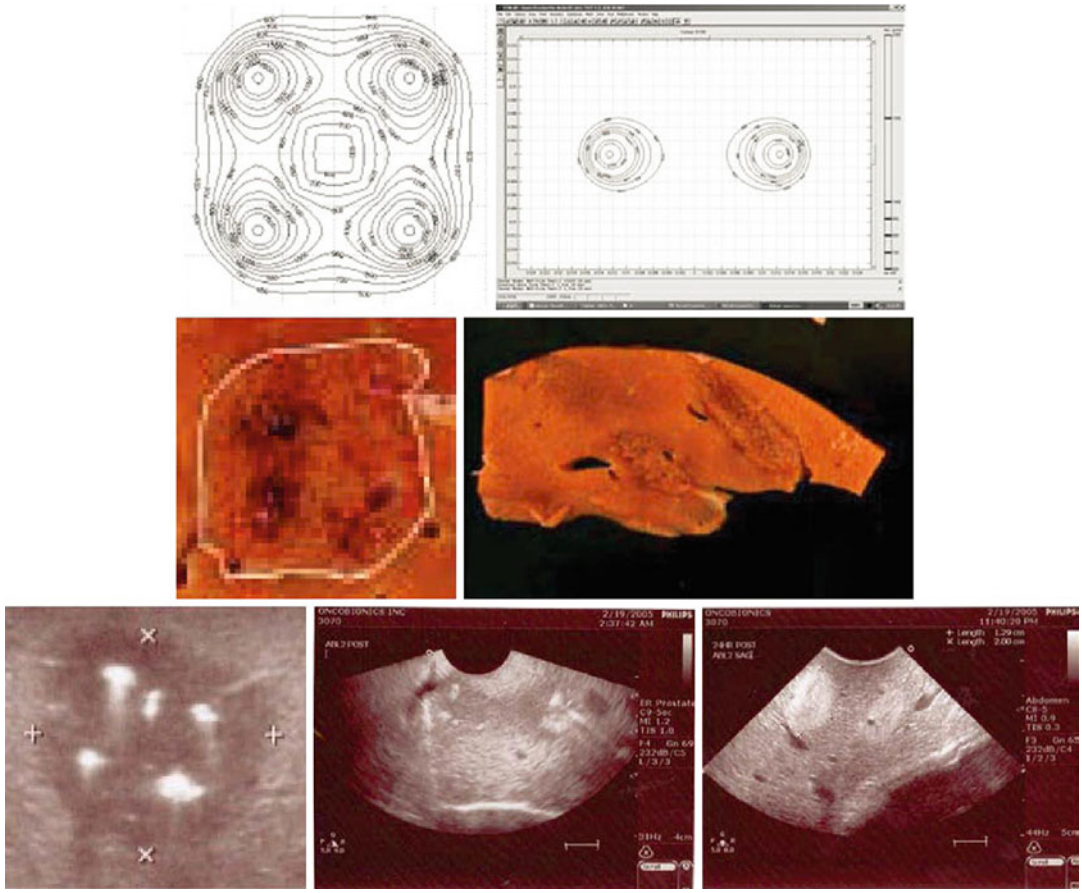

Fig. 2.10 Comparison between: *top* mathematical prediction of the extent of IRE ablation. *Outer* isoline is for 600 V/Cm, and each increment is 100 V/Cm. *Middle* is gross histology of the ablated area 24 h past ablation. *Bottom* is ultrasound images. The first column deals with the four electroporation probes case. For scale comparison, use the distance between the electroporation probes, which is 1.5 cm. The *right part* of the figure deals with a two-needle electroporation case in which the needles are separated by 2.5 cm. The pulse parameters are the same as in the left-hand case. Here, the ultrasound images show *left* ultrasound immediately after electroporation and *right* ultrasound immediately prior to necropsies. For scale compare the distance between electrodes which is 2.5 cm (From Ref. [21] with permission)

different IRE parameters after gadopentetate dimeglumine administration. Controls underwent IRE ablation without prior gadopentetate dimeglumine. MR imaging measurements (with conventional T1-weighted GRE and IR-prepared GRE methods) were performed 2 h after IRE to assess the IRE ablation zones, which were correlated with pathology-confirmed necrosis areas 24 h after IRE. The analysis shows that necrotic areas measured on the pathology images were well correlated with the hyperintense regions measured on T1-weighted GRE images and normal tissue-nulled IR images. Pathology measurements were also well correlated with the smaller hyperintense regions measured on those IR images with inversion times specifically selected to null signal from the peripheral penumbra surrounding the ablation zone. Bland-Altman plots indicated that these penumbra-nulled IR images provided more accurate predictions of IRE ablation zones, with T1-weighted GRE measurements tending to overestimate ablation zone sizes.

Electroporation is a complex biophysical process that occurs first at the nanoscale and within

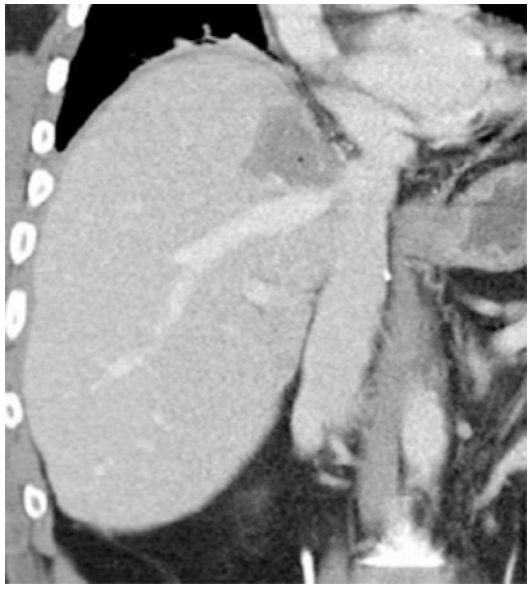

Fig. 2.11 CT image of post-IRE treatment (*dark area*) of a colorectal carcinoma near right atrium, diaphragm, and hepatic vein IVC confluence. Successful procedure without damage to these structures and no post-procedure pain (From Ref. [39] with permission)

microseconds. Therefore, while conventional medical imaging seems to produce a signature of the process of electroporation, it would be beneficial to develop a fundamental understanding of what the various imaging modalities show.

The potato, which has been long used as a model system for studying electroporation, is a good first model to study on the fundamentals of MRI of electroporation of cells, without systemic effects. When IRE is performed on a potato, the intracellular milieu containing melanin compounds is released and upon oxidation produces a visible dark area of the treated region (Fig. 2.12).

Our original choice of the MRI sequences was based on the assumption that the primary effect is related to the IRE damage to the cellular membrane and to the consequent release of intracellular content. It was anticipated that the main changes on MRI would be related to disruption of the cell membrane and a possible change in the signal from the phospholipids that form the cell membrane or from chemical changes due to the release of the intracellular contents – such as that related to the release of intracellular iron compounds and the eventual formation of melanin. To this end, we chose sequences that assume that NTIRE caused cell membrane chemical composition-related relaxation effects, i.e., shortening of relaxation times T1 and T2 [46]. Therefore, we used conventional spin echo, T1- and T2-weighted, FLAIR MRI sequences. To determine if the signal comes from phospholipids (lipid bilayer) or molecules with lipid like T1, we used a STIR sequence. STIR is used to eliminate signal from lipid or molecules with a T1 similar to that of lipid. The MRI acquisition parameters used in this study are listed as follows:

TE 19 ms, BW 10.4 kHz, TR 350 ms, NSA 3, matrix 192 × 256 for SE T1W images;

TE 125 ms, BW 20.8 kHz, TR 3,500 ms, NSA 3, matrix 256 × 256, for FSE T2W images;

TI 1800, TE 96 ms, BW 20.8, TR 8,000 ms, NSA 1, matrix 256 × 256 for FLAIR images; and

TI 225150 ms, TE 10.5 ms, BW 25, TR 2,800 ms, NSA 2, matrix 192 × 256 for STIR images (for all sequences, a 20-cm FOV, 3-mm slice thickness, and no gap were used). The results have shown that the MRI signals are lost from the electroporated region in imaging with the STIR sequence which is a special case of the inversion recovery-spin echo (IR-SE) pulse sequence. In this sequence, TI is chosen to have such a value that the signal from lipid or any tissue with T1 similar to lipid is suppressed. In contrast, strong signals were seen in the treated area on T1 and FLAIR sequences. Because any bright image in the ROI (region of interest) is lost in STIR-MRI, and strong signals are seen on T1 and FLAIR in the ROI, they could be caused by either lipids released from the cell membrane or by a molecule with T1 similar to that of lipid, released from the interior of the cell following disruption of the cell membrane. Regardless of the mechanism involved in the imaging process, it is obvious that MRI has the potential to produce images related to cell membrane disruption induced by NTIRE.

Electrical impedance tomography (EIT) is another imaging modality that has the potential to produce an image of the process of electroporation that is related to the cell membrane disruption due

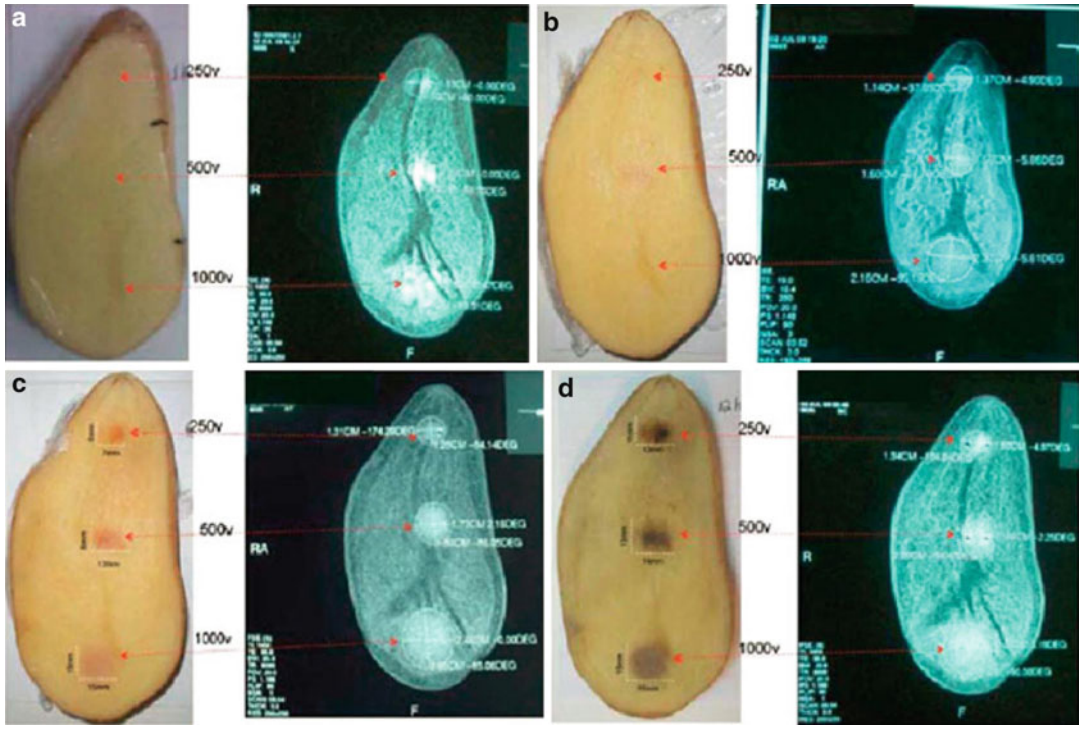

Fig. 2.12 Comparison between photographic images of the IRE-treated potato (*left*) and FLAIR-MRIs (*right*). The voltage used for electroporation is listed. The affected region is *dark* on the photographs due to oxidation and *bright* on the MRI due to either the signals from the lipids or some intracellular components. The dimensions of the affected areas are listed on the images. Times after IRE: (**a**) 1 h, (**b**) 3 h, (**c**) 6 h, (**d**) 12 h

to IRE. EIT produces a map of the tissue impedance. In an EIT implementation, electrodes are placed around the tissue, and very small currents are injected into the tissue while the voltage on the tissue boundary is measured [47]. Using the finite elements method, the impedance of the entire tissue is modeled, and a solution for the most likely configuration that fits the problem is obtained [48]. EIT is known as a suitable technique for imaging fast dynamic phenomena in three dimensions [49]. While IRE can produce various biophysical phenomena, the first event of importance is the permeabilization of the cell membrane. We have shown that the permeabilization of the cell membrane by electroporation produces a change in the electrical impedance of the cell because it provides a new path for ionic currents [50]. Therefore, we have suggested and demonstrated that EIT can produce an instantaneous image of the cell membrane permeabilization [51].

Summary

The goal of this brief review was to introduce the new minimally invasive tissue ablation modality of nonthermal irreversible electroporation and various important aspects related to the clinical use of this modality. NTIRE has several unique attributes that do not exist in other tissue ablation modalities; it can ablate large volumes of tissue rapidly, and it affects only the cell membrane. While this is very promising, substantial further research is needed to take full advantage of the special attributes of the technique. Among them are developing a fundamental understanding of the biophysics of the process, developing advanced treatment planning mathematical algorithms, and developing medical-imaging technologies optimized for NTIRE.

Cross-References

- Anesthesia Challenges in Interventional Oncology
- Cryoablation
- Devices and Equipment in Interventional Oncology and Their Operation
- Emerging Technologies in the Treatment of Cancer
- Image-Guided High-Intensity Focused Ultrasound in the Treatment of Cancer
- Imaging of Interventional Therapies in Oncology: Computed Tomography
- Imaging of Interventional Therapies in Oncology: Magnetic Resonance Imaging
- Imaging of Interventional Therapies in Oncology: Positron Emission Tomography/Computed Tomography
- Imaging of Interventional Therapies in Oncology: Ultrasound
- Microwave Ablation for Cancer: Physics, Performance, Innovation, and the Future
- Tumor Ablation: An Evolving Technology

References

1. Weaver J, Chizmadzhev YA. Theory of electroporation: a review. Bioelectrochem Bioenerg. 1996;41:135–60.
2. Chen C, Smye SW, Robinson MP, Evans JA. Membrane electroporation theories: a review. Med Biol Eng Comput. 2006;44:5–14.
3. Stopper H, Zimmermann U, Wecker E. High yields of DNA-transfer into mouse L cells by electropermeabilization. Z Naturforsch C. 1985;40:929–32.
4. Teissie J, Golzio M, Rols MP. Mechanisms of cell membrane electropermeabilization: a minireview of our present (lack of?) knowledge. Biochim Biophys Acta. 2005;1724:270–80.
5. Neumann E, Schaeffer-Ridder M, Wany Y, Hofschneider PH. Gene transfer into mouse lymphoma cells by electroporation in high electric fields. EMBO J. 1982;1:841–5.
6. Rubinsky B. Irreversible electroporation in medicine. Technol Cancer Res Treat. 2007;6(4):255–60.
7. Lelieveld HLM, Netermans S, de Haan SWH, editors. Food preservation by pulsed electric fields. From research to applications. Cambridge: Woodhead; 2007.
8. Beebe SJ, Fox PM, Rec LJ, Somers K, Stark RH, Schoenbach KH. Nanosecond pulsed electric field (nsPEF) effects on cells and tissues: apoptosis induction and tumor growth inhibition. IEEE Trans Plasma Sci. 2002;30:286–92.
9. Hamilton WA, Sale AJH. Effects of high electric fields on microorganisms. 2. Mechanism of action of the lethal effect. Biochim Biophys Acta. 1967;148:789–800.
10. Sale AJ, Hamilton WA. Effects of high electric fields on microorganisms. 1. Killing of bacteria and yeasts. Biochim Biophys Acta. 1967;148:781–8.
11. Sale AJ, Hamilton WA. Effects of high electric fields on microorganisms. 3. Lysis of erythrocytes and protoplasts. Biochim Biophys Acta. 1968;163:37–43.
12. Rubinsky B, editor. Irreversible electroporation, Series in biomedical engineering. New York: Springer; 2010. p. 314.
13. Davalos RV, Mir L, Rubinsky B. Tissue ablation with irreversible electroporation. Ann Biomed Eng. 2005;33(2):223–31.
14. Davalos RV, Rubinsky B. Temperature considerations during irreversible electroporation. Int J Heat Mass Transfer. 2008;51(23–24):5617–22.
15. Bower M, Sherwood L, Li Y, Martin R. Irreversible electroporation of the pancreas: definitive local therapy without systemic effects. J Surg Oncol. 2011;104(1):22–8.
16. Charpentier KP, Wolf F, Noble L, Winn B, Resnick M, Dupuy DE. Irreversible electroporation of the pancreas in swine: a pilot study. HPB. 2010;12(5):348–51.
17. Ball C, Thomson K, Kavnoudias H. Irreversible electroporation: a new challenge in "out of operating theater" anesthesia. Anesth Analg. 2010;110:1305–9.
18. Lee EW, Chen C, Prieto VE, Dry SM, Loh CT, Kee ST. Advanced hepatic ablation technique for creating complete cell death: irreversible electroporation. Radiology. 2010;255(2):426–33.
19. Thomson KR, Cheung W, Ellis SJ, Federman D, Kavnoudias H, Loader-Oliver D, Roberts S, Evans P, Ball C, Haydon A. Investigation of the safety of irreversible electroporation in humans. J Vasc Interv Radiol. 2011;22(5):611–21.
20. Tracy CR, Kabbani W, Cadeddu JA. Irreversible electroporation (IRE): a novel method for renal tissue ablation. BJU Int. 2011;107(12):1982–7.
21. Rubinsky B, Onik G, Mikus P. Irreversible electroporation: a new ablation modality–clinical implications. Technol Cancer Res Treat. 2007;6(1):37–48.
22. Onik G, Mikus P, Rubinsky B. Irreversible electroporation: implications for prostate ablation. Technol Cancer Res Treat. 2007;6(4):295–300.
23. Schoellnast H, Monette S, Ezell PC, Deodhar A, Maybody M, Erinjeri JP, Stubblefield MD, Single GW, Hamilton WC, Solomon SB. Acute and subacute effects of irreversible electroporation on nerves: experimental study in a pig. Radiology. 2011;260(2):421–7.
24. Li W, Fan QY, Ji ZW, Qiu X, Li Z. The effects of irreversible electroporation (IRE) on nerves. PLoS One. 2011;6(4):e18831. doi:10.1371/journal.pone.0018831.
25. Maor E, Ivorra A, Leor J, Rubinsky B. Irreversible electroporation attenuates neointimal formation after

angioplasty. IEEE Trans Biomed Eng. 2008;55(9): 2268–74.
26. Maor E, Ivorra A, Rubinsky B. Non thermal irreversible electroporation: novel technology for vascular smooth muscle cells ablation. PLoS One. 2009;4(3): e4757.
27. Neal RE, Singh R, Hatcher HC, Kock ND, Torti SV, Davalos RV. Treatment of breast cancer through the application of irreversible electroporation using a novel minimally invasive single needle electrode. Breast Cancer Res Treat. 2010;123(1):295–301.
28. Brausi M, Gilberto GL, Simonini GL, Botticelli L, Gregorio C. Irreversible electroporation, a novel technology for focal ablation of prostate cancer: results of an interim pilot safety study in low-risk patients. Anticancer Res. 2011;31(5):1834–5.
29. Becker SM, Kuznetsov AV. Thermal damage reduction associated with in vivo skin electroporation: a numerical investigation justifying aggressive precooling. Int J Heat Mass Transfer. 2007;50:105–16.
30. Daniels CR, Rubinsky B. Electrical field and temperature model of nonthermal irreversible electroporation in heterogeneous tissues. J Biomech Eng. 2009; 131(7):071006.
31. Edd JF, Horowitz L, Davalos RV, Mir LM, Rubinsky B. In vivo results of a new focal tissue ablation technique: irreversible electroporation. IEEE Trans Biomed Eng. 2006;53(7):1409–15.
32. Edd JF, Davalos RV. Mathematical modeling of irreversible electroporation for treatment planning. Technol Cancer Res Treat. 2007;6:275–86.
33. Somersalo E, Cheney M, Isaacson D. Existence and uniqueness for electrode models for electric current computed tomography. SIAM J Appl Math. 1992; 52:1023–40.
34. Pennes HH. Analysis of tissue and arterial blood temperatures in the resting forearm. J Appl Physiol. 1948;1:93–122.
35. Rubinsky B. Numerical bio-heat transfer. In: Minkowycz WJ, Sparrow EM, Murthy JY, editors. John Wiley ed. Handbook of numerical heat transfer. 2nd ed. Hoboken, NJ: Wiley; 2006, p. 851–93.
36. Henriques FC, Moritz AR. Studies in thermal injuries: the predictability and the significance of thermally induced rate processes leading to irreversible epidermal damage. Arch Pathol. 1947;43:489–502.
37. Diller KR. Modeling of bioheat transfer processes at high and low temperatures. In: Choi YI, editor. Bioengineering heat transfer. Boston: Academic; 1992. p. 157–357.
38. Onik G, Rubinsky B. Irreversible electroporation: first patient experience focal therapy of prostate cancer. In: Rubinsky B, editor. Irreversible electroporation, Series in biomedical engineering. Berlin: Springer; 2010.
39. Thomson K. Human experience with irreversible electroporation. In: Rubinsky B, editor. Irreversible electroporation, Series in biomedical engineering. Berlin: Springer; 2010.
40. Rossmeisl JH, Garcia PA, Lanz OI, Hena-Guerrero N, Davalos VR. Successful treatment of a large soft tissue sarcoma with irreversible electroporation. J Clin Oncol. 2011;29(13):E372–7.
41. Onik CC, Goldenberg HI, Moss AA, Rubinsky B, Christianson M. Ultrasonic characteristics of frozen liver. Cryobiology. 1984;21:321–8.
42. Gilbert JC, Onik GH, Haddick WK, Rubinsky B. The use of ultrasonic imaging for monitoring cryosurgery. IEEE Trans Biomed Eng. 1984;8:563.
43. Lee EW, Loh CT, Kee ST. Imaging guided percutaneous irreversible electroporation: ultrasound and immunohistological correlation. Technol Cancer Res Treat. 2007;6(4):287–94.
44. Zhang Y, Guo Y, Ragin AB, Lewandowski RJ, Yang GY, Nijm GM, Sahakian AV, Yang GY, Omary RA, Larson AC. MR imaging to assess immediate response to irreversible electroporation for targeted ablation of liver tissue: preclinical feasibility studies in a rodent model. Radiology. 2010;256(2): 424–32.
45. Guo Y, Zhang Y, Nijm GM, Shakian AV, Yang GY, Omary RA, Larson AC. Irreversible electroporation in the liver: contrast inversion imaging approaches to differentiate reversible electroporation penumbra from irreversible electroporation zones. Radiology. 2011;258(2):461–8.
46. Hjouj M, Rubinsky B. Magnetic resonance imaging characteristics of non-thermal irreversible electroporation in vegetable tissue. J Membr Biol. 2010; 236(1):137–46.
47. Jossinet J, Marry E, Matias A. Electrical impedance endotomography. Phys Med Biol. 2002;47:2189–202.
48. Lionheart WR. EIT reconstruction algorithms: pitfalls, challenges and recent developments. Physiol Meas. 2004;25:125–42.
49. Metherall P, Barber DC, Smallwood RH, Brown BH. Three-dimensional electrical impedance tomography. Nature. 1996;380:509–12.
50. Huang Y, Rubinsky B. Micro-electroporation: improving the efficiency and understanding of electrical permeabilization of cells. Biomed Microdevices. 1999;2(2):145–50.
51. Granot Y, Ivorra A, Maor E, Rubinsky B. In vivo imaging of irreversible electroporation by means of electrical impedance tomography. Phys Med Biol. 2009;54(16):4927–43.

Microwave Ablation for Cancer: Physics, Performance, Innovation, and the Future

3

Thomas P. Ryan

Abstract

Microwave treatment (MW) for cancer dates back to the 1970s, with continuous development, innovation, and clinical improvements ongoing to the present day. MW physics is reviewed to demonstrate the inherent performance advantages with significant penetration and time-savings compared to competing energy sources which have pioneered contemporary ablation therapy. A review of current antenna designs and their performance is covered, as well as historical designs that provide much of the basis of current clinical use. To address ever larger tumors, the transition from single to multiple antennas is discussed, including antenna arrays powered synchronously versus asynchronous operation and the advantages. The progression from low power (5–15 W) to high power (60–200 W) in the present day systems is discussed, as well as the differentiation among frequencies of 433, 915 and 2,450 MHz, including antenna dimensions and practicality in relation to various treatment target sites. The utilization of numerical modeling is shown both for power deposition patterns, temperature distribution predictions, and predictions of ablation coverage. To optimize MW thermal therapy, several aspects of localization and treatment are discussed, which are slowly evolving to aid in more precise treatment, guided by real-time assessment. Evolutionary aspects of treatment include treatment planning, image guidance, coregistration, navigation, and real-time treatment assessment. Many of these aspects are under development and will provide the new and needed capabilities necessary for future systems incorporating imaging and ablation tools for the physician.

Introduction

Thermal therapy as a treatment for cancer is a viable treatment paradigm with a variety of energy-based technologies available and undergoing continuous development. The goal of the

T.P. Ryan
FreeFall Consulting, Austin, TX, USA
e-mail: tryan@ieee.org

D.E. Dupuy et al. (eds.), *Image-Guided Cancer Therapy*, DOI 10.1007/978-1-4419-0751-6_5,

thermal treatment is ablation, defined as the heating of the target tissue to toxic levels such that coagulation necrosis occurs. The tissue is left in place to resorb and/or fibrose. The target is often an unresectable tumor with 5- or 10-mm ablative margin added to the imaged boundaries for ablation.

Recent advances in systems and applicator technology for thermal therapy give clinicians more opportunity to affect larger volumes of tissue in less time with either radio frequency (RF) or microwave (MW) systems. Modern ablation paradigms take place much more rapidly. For MW clinical use, several features are available: cooling, multiple applicators, greater power levels, power modulation, and new applicator designs.

Ablation has shown to be a valuable treatment option in liver, kidney, breast, bone, and lung. Interstitial ablation is the direct targeting of tumors and is practiced by both interventional radiologists and surgeons. Surgeons may resect some tumors in the liver, for example, and then ablate the remaining without further section, all of this under intraoperative or laparoscopic ultrasound guidance. Interventional radiologists, on the other hand, perform ablations percutaneously, often with CT, MR, or ultrasound guidance. Through this direct targeting of the tumor, localization is assured, and significant levels of energy can be applied to address a 4–5-cm ablation diameter in 5 min. In fact, the greatest heating per unit time is achieved via MW interstitial heating. For smaller targets, the ablation is easily scalable by cutting back time or power. As ablation has evolved, benefits are seen over surgical resection, including the reduction in morbidity and mortality, as well as lower cost and suitability for real-time image guidance. Combining this with the ability to easily perform ablative procedures on patients creates a potential application in a wide spectrum of sites, especially with nonsurgical patients with few viable options [1].

An extensive body of literature exists on the use of microwave energy in anatomical structures, including esophagus, prostate, bile duct, blood vessels, breast, and heart. These applications require flexible antennas and a plastic coating that is both nonstick and sterilizable. Antenna designs are required to meet user needs regarding durability and antenna geometry (size, shape, and diameter). In addition to these sites, other high-water-content tissues like liver and uterus are common treatment targets, as well as lung [2–13]. Lastly, ablative techniques have also been utilized in the treatment of bone cancers and are becoming a viable treatment for patients with both benign and malignant forms of bone cancer [14, 15]. These early efforts in cancer treatment demonstrated the successful use of small antennas for ablation [16, 17].

The latest technology options include MW systems, whose sheer treatment volume capacity and speed bring the thermal treatment of cancer into new frontiers. Reviewing recent clinical experience in ablation, liver tumors have been the most common target, with either hepatocellular carcinoma (HCC, primary liver cancer) or metastases from colorectal cancer being the most common cancers in the liver. In many cases, if no treatment is given, the prognosis is poor with a nearly 100 % death rate at 5 years. Conventional therapies such as radiation or chemotherapy have been less than effective. Recent improvements in imaging technology have enabled the development of minimally invasive tumor therapies in a number of sites, relying on image guidance for accurate placement of thermal ablation applicators [18]. The advantages are several: viable alternative for nonsurgical candidates requiring either ablation or palliation, reduction in morbidity and costs, improvement in the quality of life, and performed as outpatient procedures.

Microwave ablation represents the most recent addition to ablative technologies in the lung. Microwave treatment offers several key advantages: consistently higher intratumoral temperatures, larger ablation volumes, reduced treatment times, and improved convection profiles [19]. Additionally, in a clinical study with 50 patients, it was shown that microwave ablation is effective and may be safely applied to lung tumors [20].

MW Historical Overview

The use of microwaves has its origins during World War II with test data from MIT that indicated that the absorption of microwaves at 2,450 MHz in water was 7,000 times that of short wave diathermy operating at 27 MHz, which was popular for thermal therapy in that era. The FCC subsequently reserved this frequency for physical medicine due to its therapeutic value. Microwave ovens also adopted this frequency [21].

The extensive medical literature on microwave treatment technology dates back as early as 1979. In the early years, the use of hyperthermia to heat tissue and target cancerous tumors was undertaken. In 1979, an animal study showed coagulation necrosis in tissue by the application of energy from implanted microwave antennas [22, 23].

Some of the early work with microwave heating of tissue began with Strohbehn et al. [22], who developed a sharp tip antenna powered at 3–10 W which was inserted directly into tissue in 1979. They also suggested the possibility of treating with much higher temperatures, as long as the heat source was localized in the tumor with small antennas. These antennas permitted even deep-seated tumors to be treated with minimal risk and discomfort. Their work with MW antennas utilized direct insertion into tumors in animal models, creating high temperatures and showing therapeutic effectiveness [22]. Further work by Douple et al. investigated thermal distributions produced by the antennas in a tumor model implanted in mice. The therapeutic efficacy of heating was demonstrated by comparing tumor diameters in mice following control, sham, or heat treatment, the results verifying that the system could be employed clinically to provide very localized heating of deep-seated tumors [23]. Other work in the 1970s used a microwave antenna made out of a hollow hypodermic needle that could not only heat tissue but could simultaneously inject agents such as chemotherapeutic agents [24].

By the mid-1980s, commercial systems using microwave antennas in tissue were available, some which had automatic control of target site temperatures by automated power adjustment. Some of the early clinical systems included numerical models, so the power deposition and heating patterns of particular antennas could be visualized for pretreatment planning [25–27]. Early microwave ablation work began in 1985 as a treatment for benign prostate disease [28]. There were a great number of published studies showing physicians adopted MW thermal therapy as the standard treatment for benign prostatic hyperplasia [29].

In fact, there were many clinical studies in Japan (161 papers dating from 1986 to 2009) based on the use of a single, rigid microwave antenna which they termed percutaneous microwave coagulation therapy (PMCT). These studies demonstrated the successful use of a sharp tip MW antenna for ablation in clinical applications and established a basis for current microwave ablation therapies. The studies also incorporated methods using 60 W of power during withdrawal in order to coagulate the insertion track to prevent bleeding and tumor cell seeding [30, 31].

Early work with MW antennas was more concerned with hyperthermia (mild heating to ~43 °C), than with ablation. There are several factors to consider when considering the history of hyperthermia and the transition to solo ablation. Hyperthermia treatments were typically 60 min once temperatures were attained. This allowed frequent temperature sweeps to be mapped with points at 1–2 mm resolution. Ablation takes place much more rapidly (i.e., minutes), and the temperatures are more transient; thus, these types of spatial temperature measurements could not be evaluated properly. Ablation is more concerned with the coagulation boundary, and often temperatures are not measured in any location. Ablation also may use multiple applicators, either sequentially or together to treat the entire volume. Hyperthermia used antenna arrays of 2–5, even 12 antennas, to cover the entire volume with a single treatment. Hyperthermia antennas in catheters were placed in well-spaced, insertion grids with parallel placement assured. This is challenging in ablation, with freehand placement of antennas and

with sequential treatment, combined with limited a priori knowledge of where the previous insertion and heating took place. Hyperthermia utilized treatment planning, with carefully laid out placement of the antennas, and then calculations of the power deposition and heating patterns were made. Ablation treatment systems do not have this planning feature, and thus more technology needs to be developed.

It is important to note that hyperthermia and ablation use the same frequencies, the same antennas, the same type of treatment systems, and the same numerical models for prediction of power deposition and heating patterns. This is an evolution that incorporates well-understood technology with better guidance and much higher power and temperatures.

Solo ablation has many advantages over hyperthermia. One of the big advantages is that the current ablation technology incorporates image guidance into its procedures. Thus, technology is moving toward more spatially accurate, controlled heating systems, combined with image guidance and treatment verification [32]. There is great potential for the combination of ablation and/or radiation and/or chemotherapy or other drugs. Hyperthermia and ablation may be combined in some cases.

MW Compared to RF

RF ablation has emerged as the most effective method for local tumor destruction and is currently used as the primary ablative modality at most institutions [33]. Historically, RF has been the most widely used ablation technology worldwide, although microwaves have been used extensively in Asia for more than 20 years. The number and variety of MW applicators commercially available to clinicians are now dramatically proliferating.

With the either technology, multiple applicators allow coagulation necrosis of larger zones in shorter time periods. Recently, there have been some higher power, single MW applicators that provide increased performance. Thus, MW ablation of liver tumors may also become an adjunct or alternative to resection in patients with primary or secondary metastatic cancers. With high-power applicators, it has been shown that a large, localized coagulation with a single insertion of a MW applicator has significantly shorter time than comparable treatments [34–36].

Microwaves have several advantages over RF electrode heating: (1) deep penetration; (2) no direct electrical contact required (thus, all metallic surfaces may be coated with nonstick coatings, thus easy to remove following the ablation); (3) rapid heating (much faster than RF systems which are only slightly better than conductive heating systems); (4) any tissue charring does not reduce power delivery, (unlike RF systems which are often limited by the surface temperature of the electrode [$\sim$100 °C]); (5) the near field tissue region may have severe desiccation (which is hypothesized to create an opportunity for deeper penetration due to an increase in transparency to microwaves); (6) antennas may be used in arrays and provide advantages due to the phase relationships between antennas (allowing constructive or destructive interference and the focus or defocus of power, respectively); (7) a number of unique antenna designs that each afford a customized heating pattern; and (8) choice of frequency to control penetration depth [37]. Further advantages include high thermal efficiency, higher capability of coagulating blood vessels [38], shorter ablation times, and improved convection profile which induces large ablation volumes and yields local tumor control [37, 38].

Unlike RF, MW applicators have cable losses resulting in cable heating which often requires cooling of the shaft to mitigate. In addition, unlike RF applicators which can be made almost any length, MW applicator active length is more closely prescribed by frequency and design.

From a more technical standpoint, the customization of microwave interstitial antennas and arrays allows the power distribution in both axial and radial directions to be altered by changing antenna designs. This was shown by Ryan [39] with several different antenna types compared, showing differences in tip, center, and insertion point values of power deposited,

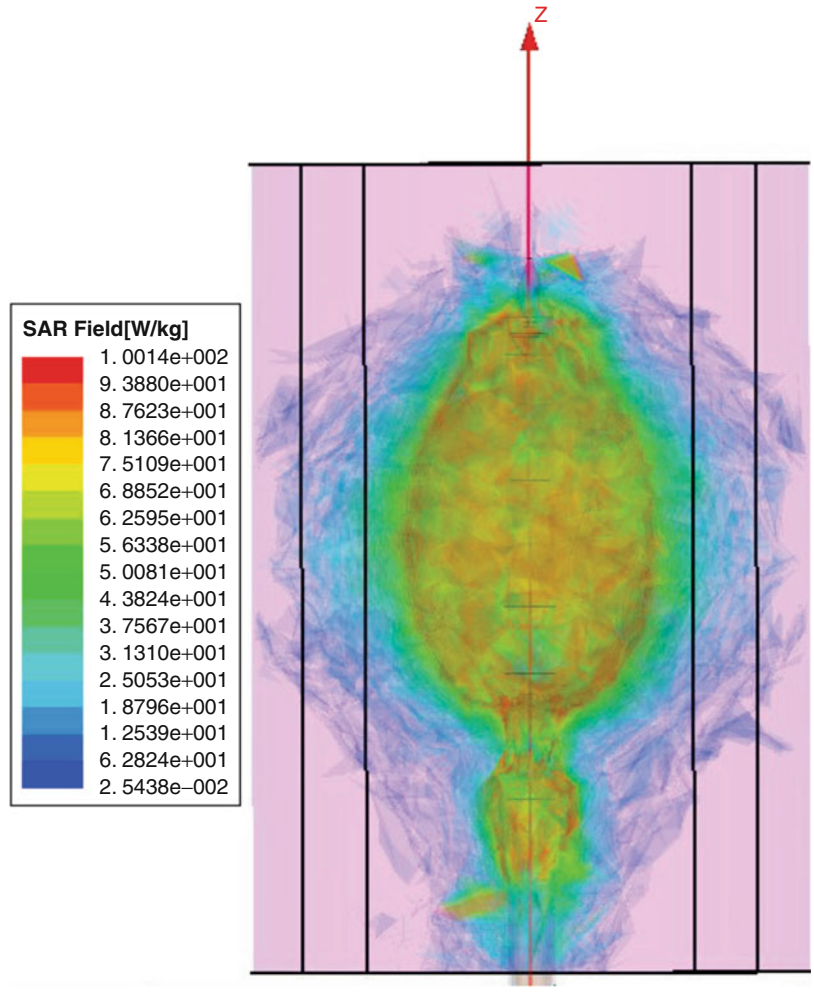

Fig. 3.1 Shows Specific Absorption Rate (SAR), the power deposition pattern of a MW applicator. The SAR coloration is shown in the legends in units of W/kg. The microwave applicator shows the penetration to a radius of 10–20 mm of active heating. Power falls off as 1/r (r = radius from the antenna)

as well as array behavior due to the phase relationships among antennas in an array. Depending on the antenna design, the heating at the insertion point may be affected, an important consideration in percutaneous procedures [39].

In summary, MW applicators are becoming more prevalent in cancer ablation therapy today and used both by surgeons and interventional radiologists. This is due to factors of penetration and shortened treatment time. These applicators create the largest zones of necrosis of any available energy sources [37, 40] (Figs. 3.1 and 3.2).

With RF, power falls off as $1/r^2$ [41]. The SAR infers the heating pattern for short activation times [39, 42, 43] (Fig. 3.2). RF has shallow tissue penetration combined with convective heat losses from the heat sink of local blood flow presents a challenge with RF heating, necessitating longer heating times since thermal conduction is relied upon to extend the heating to deeper aspects of the target volume. Thermal conduction is an inefficient process though, which is why microwaves, with their much larger active zone of heating, do not rely solely on thermal conduction for ablation. Thus, microwave ablation is less prone to convective heat loss from blood flow [44, 45] (Reproduced from Ref. [46]).

Although RF and MW techniques are safe and effective and easy to use, RF treatment is poorly visualized with diagnostic ultrasound due to the artifact caused by the activation of the RF power, making the procedure difficult to monitor.

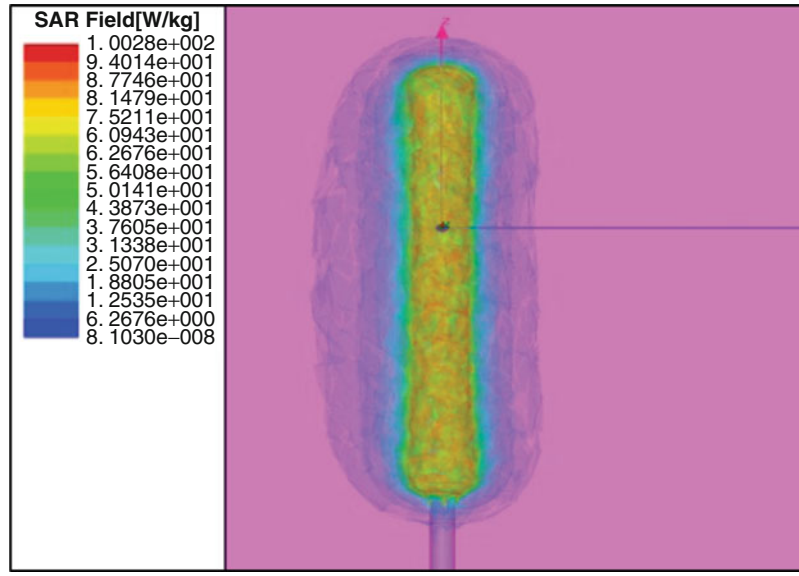

Fig. 3.2 Shows Specific Absorption Rate (SAR), the power deposition pattern of an RF applicator. The SAR coloration is shown in the legends in units of W/kg. Power falls off as $1/r^2$ (r = radius from the antenna). The RF applicator shows the penetration to a radius of 1–2 mm of active heating

In some cases, microwaves do not interfere with the ultrasound signal, so visualization can occur in real-time during microwave usage [47]. High-frequency ultrasound was found in one study to provide excellent visualization of the interface between normal and ablated liver with resolution to the submillimeter level [37].

As a performance indicator, one study had a goal of ablation diameters of 3–4 cm, which were readily achieved with MW between 1.5 and 4 min., but with usage of RF would require a much longer time [36].

MW Physics

In the USA, the main frequencies for MW systems for thermal therapy are 915 and 2,450 MHz, although there is some work at 433 MHz. In Europe and Asia, the frequency of choice is 2,450 MHz, since in Europe, 915 MHz is at the edge of the GSM band used for cellular phones. Lower frequencies provide the advantage of greater penetration, although the antennas are typically longer and have to be placed further in tissue to operate. Antennas used for MW thermal therapy have deeper penetration than RF or laser sources, thus providing the potential for a single applicator to heat large volumes (Fig. 3.1).

MW antennas are independent sources that launch a wave into tissue. Unlike RF sources which require a grounding pad or return electrode, the antennas are self-contained and need no other conductor.

MW Heating of Tissue

The three figures below (Fig. 3.4a–c) demonstrate microwave heating in tissue (Fig. 3.3). Figure 3.4a shows the orientation of charges and the induced, rapidly alternating microwave field as the gray curve in the background. Figure 3.4b shows simultaneous rotation of all the dipoles in tissue, aligning with the electric field. Figure 3.4c shows the dipoles as molecular heating sources, with the area below the dotted line being in the high amplitude MW field and heating tissue directly. Above the dotted line, the field is weaker, and the area relies more on thermal conduction. Thermal conduction will bring the heat further out resulting in deeper penetration over time [46].

Electromagnetic properties of tissue are governed by structural components including cellular membranes, proteins, and water content. Each of these polarizable components responds to an imposed electromagnetic field. As explained above, when MW power is turned on,

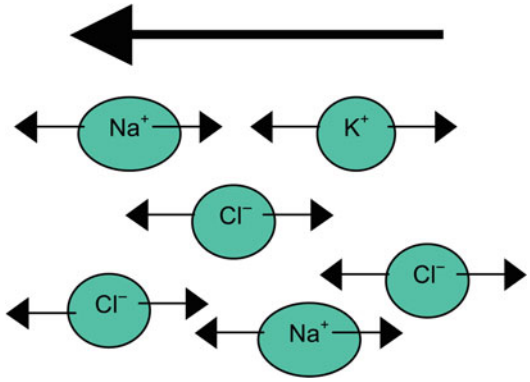

Fig. 3.3 RF-induced heating in tissue is shown. The picture shows ions found in tissue, in locations that are intracellular as well as extracellular. When an alternating electric field is applied during RF power-on, the current direction moves the ions back and forth [46]. The result is ionic agitation which causes heating by friction of the particles (Reproduced from Ref. [46])

the polar molecules in tissue begin to heat immediately at both near and far locations. The electromagnetic field propagates out from the antenna at the speed of light to a radius of about 10–20 mm. This rapid heating results in coagulation necrosis of tissue as temperatures exceed ~55 °C. The power deposition pattern of a MW antenna together with the heat conduction determines the temperature and resulting damage to the treated tissue [48, 50, 51] (Fig. 3.5a, b).

MW System Requirements

The user needs for practical and predictable ablation has the following requirements:

1. Easy setup of microwave system, including cabling, antenna cooling, and user interface programming.
2. Simple insertion of antennas.
3. Compatible with imaging systems, including imaging while power is on.
4. Antennas reliably remain in target zone.
5. Antennas need not be placed beyond target zone.
6. Antenna insertion point in skin does not heat (active cooling is likely).
7. Multiple use without degradation, no cleaning or tissue adherence (nonstick).
8. The following are predictable:
   (a) Heating pattern (antenna to antenna)
   (b) Power output (as measured by calorimetry)
9. Heating pattern is independent of insertion depth in tissue.
10. Antenna diameter suitable for organ site.
11. Custom antennas available, providing heating-pattern, geometry selection.
12. Antenna interaction understood.
    (a) Synchronous (in-phase) or asynchronous
    (b) Tip convergence effects

MW Antenna Performance

Methods to Evaluate Antennas

MW antennas are characterized by their power deposition pattern, also known as specific absorption rate (SAR). One experimental method is performed with a MW antenna placed into a tissue equivalent phantom, with the same electromagnetic (dielectric constant and electrical conductivity) and thermal (thermal conductivity and specific heat) properties as tissue. The method uses a short burst of power (less than 60 s) and then measures the heating at localized points in the phantoms. The temperature rise over the short time interval is proportional to power deposited at the measurement point. A second method uses the same power and technique but utilizes a split phantom that is quickly opened and assessed by a thermographic camera, which captures an entire plane of heating. A third method utilizes a miniature electric field probe which is capable of resolving the x, y, and z components of the measured electric field. These systems use automated movement systems or a robotic arm to move the probe around the phantom container with a low level power applied. More recently, ablation devices, whether RF or MW, have instead had their performance assessed by the extent of coagulation and the pattern of coagulation during ablation of ex vivo or in vivo tissue such as liver.

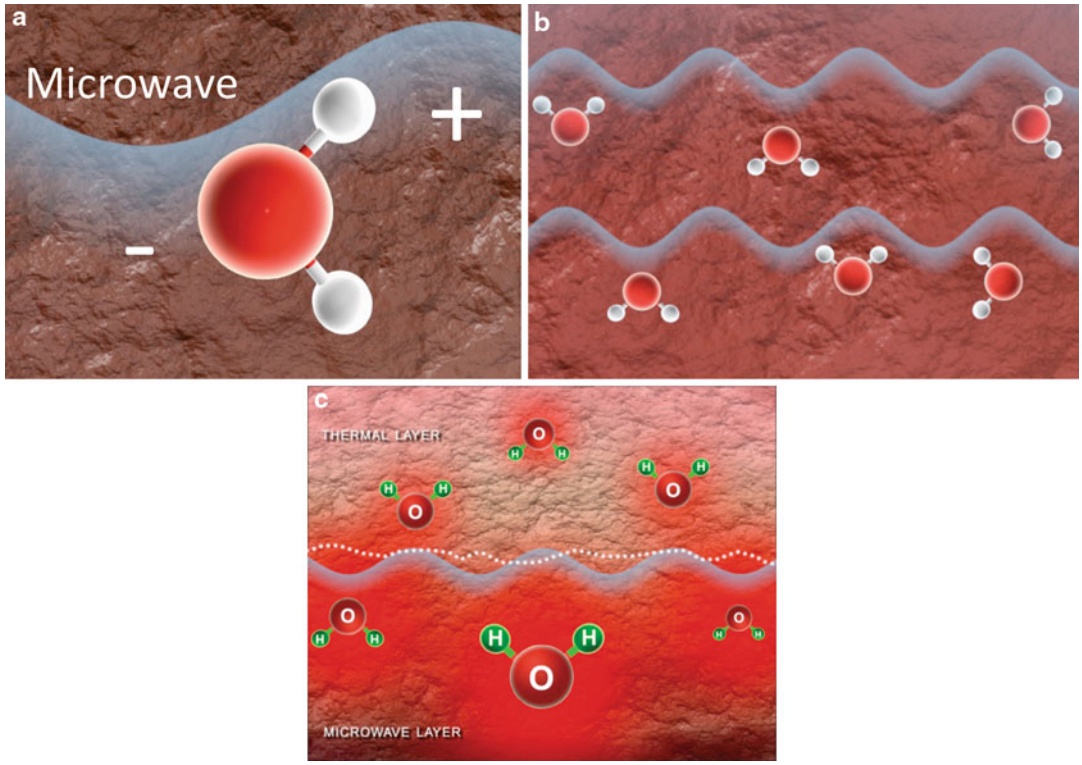

Fig. 3.4 (**a**) Shows a water molecule with an angle between the hydrogen bonds of 105°. If microwaves are applied to tissue as a rapidly alternating field at 2.45 GHz, the dipole polar molecules attempt to align with the rotating electromagnetic field. (**b**) Inertia and binding forces found inside the cells dominate, along with intermolecular bonds, all of which resist movement resulting in friction and heating. Heating is proportional to MW power level and is quite efficient since each dipole becomes a heating source. (**c**) Thus, MW can heat near and far simultaneously since all the dipoles are heating at the molecular level [48, 49]. This heating at a distance contributes to the penetration advantages of MW over other technologies (i.e., RF and light) (Reproduced from Ref. [46])

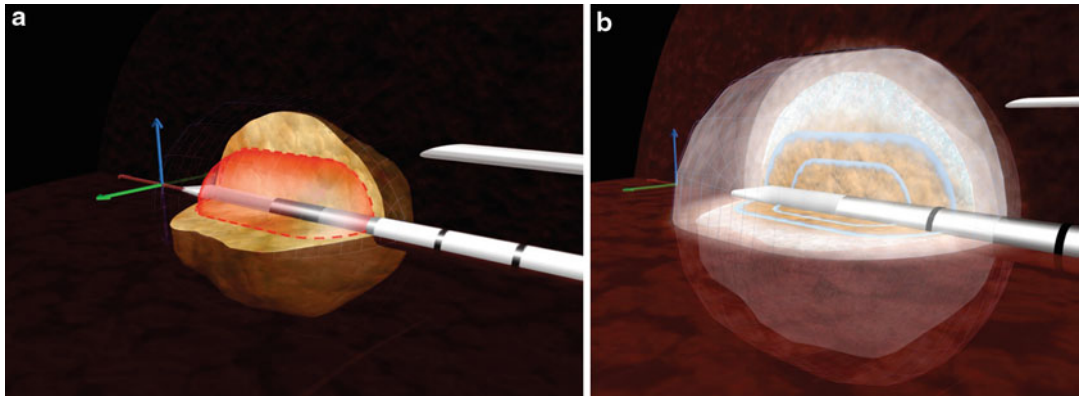

Fig. 3.5 (**a**) Shows a microwave applicator inserted into a tumor. The *red* zone shows the actual penetration of microwaves and immediate heating of the dipoles in the tissue [46]. (**b**) Shows thermal conduction. The entire tumor is ablated, given sufficient time for thermal conduction and heat to penetrate (Reproduced from Ref. [46])

Single MW Antenna Designs and Performance

There are a number of MW antenna designs and new work every year with new antennas that offer a wide range of heating patterns to meet the needs of the clinician and anatomical site or tumor size. Many of the current designs have been in use clinically for a number of years including dipole, monopole, helical, and modified dipoles with the helical tip that successfully combine the phase relationship of a dipole and the tip heating of a helical antenna [39, 52]. Other antennas have been designed and tested to improve performance and give a broader range of choices for clinicians (Fig. 3.7). These include choke [39], hybrid [39], sliding choke [53, 54], folded dipole [6, 8], high-dielectric ceramic materials (Fig. 3.6) [37, 55], floating sleeve [56], and triaxial [57, 58]. Some of these designs allow choices of the length of axial heating and ultimately the ablation volume shape (i.e., the choice between more spherical or more cylindrical shape).

There have been advances in improving the capability of the single antenna. These methods include cooling which allows one to raise the power to significant levels in order to greatly increase the ablation volume with a single antenna, as well as increasing antenna size or putting ceramic materials to enable very high power levels. For some antenna types though, there is a limit to power and thus the heating volume and will require multiple antennas in an array [37].

Numerical Models and Simulations

The other benchmark for antenna performance is the numerical model which has been used for a number of years to predict the SAR distribution as a guide for both antenna design and performance, as well as for clinical guidance via treatment planning for therapy. The numerical model is a computer simulation that utilizes the energy distribution from a single or from multiple antennas to predict the SAR or power deposition pattern as well as the resulting heating pattern with time.

The inputs to the model have several categories:

(a) Antenna selection (each antenna has a particular power deposition pattern).
(b) Frequency (this will determine penetration and antenna performance).
(c) Number of antennas and spacing (will determine how the antennas will interact).
(d) Antenna power level (or power control based on temperature at a specified location).
(e) Tissue type (various tissues have different electrical and thermal properties and blood flow).
(f) Tumor type (various tumors have different electrical and thermal properties and blood flow).
(g) Time (the heating pattern grows over time, so the transient spatial patterns are important).

It is easy to see that the numerical model can be run to verify experimental work. In addition, these methods are particularly useful in treatment planning for the placement of microwave interstitial antennas to better understand the effect of changing each parameter mentioned above. This in turn provides improved understanding of microwave ablation procedures in clinical practice, especially with limited positioning and trajectory and such variables as applicator spacing, nonparallel alignment, variation in phase for synchronous phase, the use of asynchronous arrays, frequency, active antenna elements, specific antenna designs, and may model the variable blood flow in normal and tumor tissue.

Antenna designs may be thus chosen to obtain a particular heating pattern depending on the clinical need. The helical antennas may also have longer or shorter lengths of the helix to customize the heating pattern [60, 61]. In addition, changing from 915 to 2,450 MHz with the same helical antenna will change its heating pattern, giving the user added flexibility [48]. For illustrative purposes, antennas are pictured next to the SAR results, when in fact the antenna is located at a radial distance of 0 on the *y*-axis (Fig. 3.8).

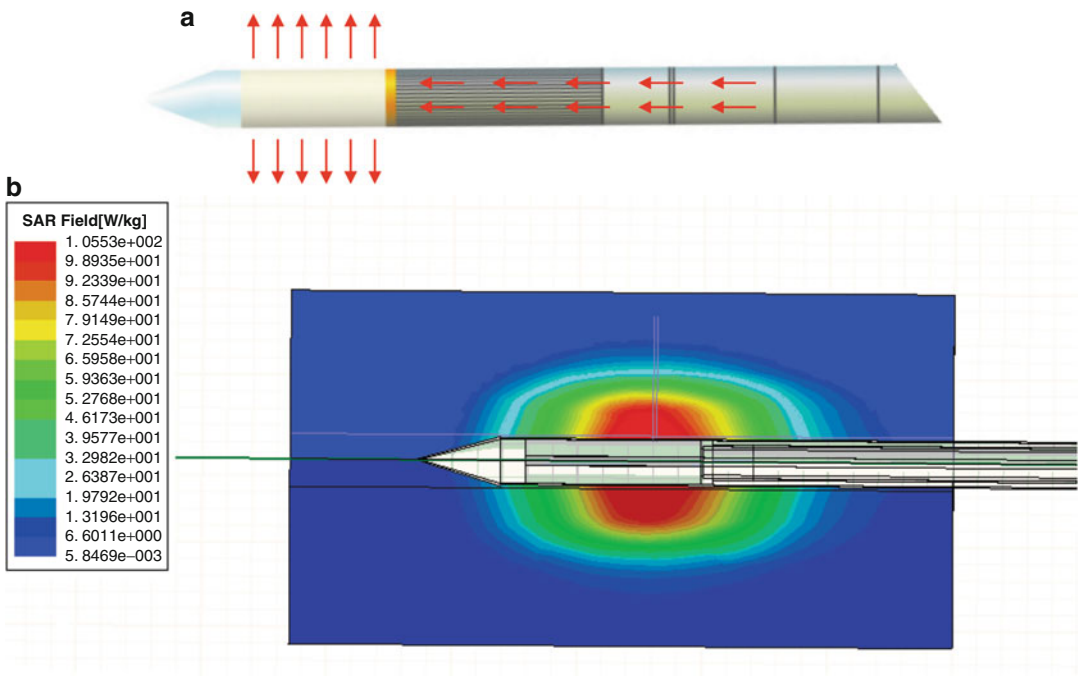

Fig. 3.6 (**a**) The MW dipole antenna operates at 2,450 MHz at powers up to 100–200 W. The diagram shows microwave energy coming down the feedline and emitting through the high-dielectric ceramic into the tissue (*red arrows*). (**b**) shows the SAR (power deposition pattern) results in liver using a numerical model. The central zone emanates from the white ceramic portion of the MW antenna. The ceramic has a high-dielectric constant of 25 [59]. This SAR pattern helps to predict what the heating pattern will look like when the MW applicator is activated in tissue for a short time [41] (Reproduced from Ref. [46])

Helical antennas were shown to give improved localization of heating over a range of insertion depths (Figs. 3.7, 3.8) [60, 61]. Another design not shown above provides an alternate design to the dipole antennas. It is a hybrid, being a dipole antenna with a helix at the tip [48].

MW antennas are typically used in catheters or have their own dielectric (plastic) coating which will change the match with tissue. For dipole antennas, being resonant will provide optimal efficiency and will minimize the heating along the feedline of the antenna. Dipole antennas are composed of two resonant quarter wavelength sections as calculated by Trembly [48, 62]. The results were 6.8, 3.5, and 1.7 cm for 433, 915, and 2,450 MHz, respectively. Thus, the frequency selection will affect the antenna lengths for dipole antennas. From a practical standpoint, the 433 MHz dipoles are typically too long for practical use.

MW Array Designs and Performance

There may be a limit to how much a single antenna can heat tissue unless it can handle 100–200 W. Thus, arrays of antennas have been designed and tested for thermal therapy, with extensive clinical use over the years. An array of antennas may number from 2 to 6, although typically would be three or four antennas. Arrays not only allow for larger treatment volumes to be treated all at once, but arrays also allow conformability to irregularly shaped tumor volumes and tumors deep within the body by flexibility in placement along with the number of antennas implanted [39].

Overview of Phased Arrays (Synchronous Versus Asynchronous)

In an array of dipole antennas, whether with two or three or four antennas, constructive or

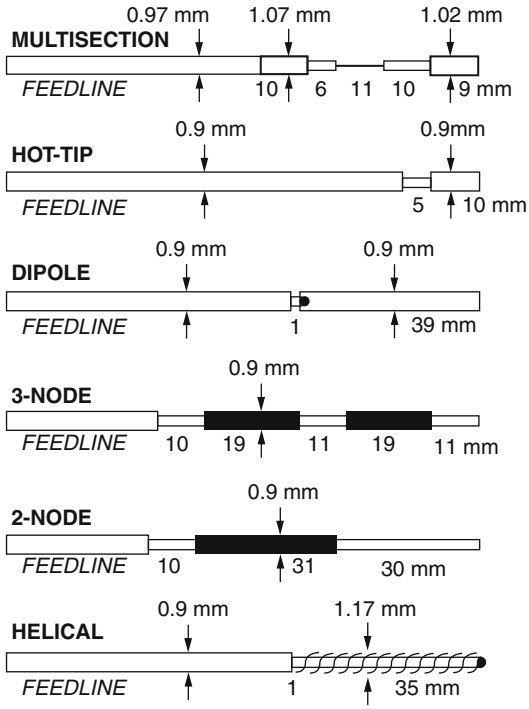

Fig. 3.7 Shows 6 antenna designs which have a variety of SAR patterns, especially axial falloff and locations of zones with greater or less intensity (Reproduced from Ref. [39])

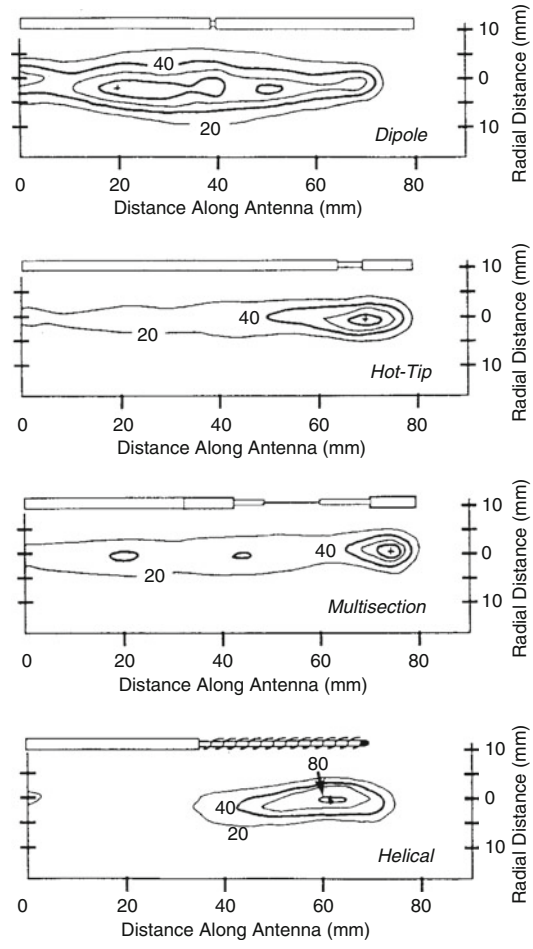

Fig. 3.8 Shows four antenna designs with their associated power deposition patterns. The dipole has the longest pattern, inferring that its heating pattern may be the longest of the four antennas. The hot tip and helical designs show a concentration of power near the tip, as does the multi-section antenna

destructive interference is achieved when each antenna is simultaneously active and synchronized in phase (phase synchronous). Constructive interference is the adding of power fields of neighboring antennas if they are in phase. Imagine the wake of two boats in which neither boat is ahead and they are traveling at the same speed. The wakes will meet and create a higher wave in the center. Destructive interference is the subtracting (cancellation) between waves. Imagine one boat is now ahead of the other and the two wakes meet such that the high point of one and the low point of the other intersect and actually subtract.

Phase synchronous antennas are synchronized in time. Asynchronous phase is the condition when the antennas are not simultaneously active and do not have constructive interference. For example, if one antenna at a time is powered on, then there is no phase relationship between antennas. Asynchronous arrays can also be achieved by using applicators that are powered by independent sources, typically separate generators which are at slightly different frequency and timing. Typically when three generators are used for three antennas, these generators are asynchronous (not synchronized in time).

In arrays, 915 MHz antennas are most effective at heating medium length tumors, especially tumors with high blood flow. The dielectric properties of tissue change with temperature and are determined by the combined effects of tissue water and small proteins. Coagulation may change the dielectric properties with elevated

temperatures which will lead to structural changes in tissue. Electrical conductivity may increase by a factor of 1.5 as temperatures approach 60–70 °C. The changes are often irreversible as temperatures exceed ~50 °C. This coincides with irreversible changes with elevated temperatures also found at lower frequencies [38, 63] with RF. So to conclude, as the tissue desiccates with RF heating, higher impedance will be seen at the interface of the tissue and the RF electrodes such that the higher impedance becomes a barrier to continued heating with RF. With MW systems however, the desiccated tissue is more transparent to microwaves (due to higher electrical conductivity) and will therefore radiate more efficiently due to increased penetration.

Arrays of 2–6 Antennas

An example of two dipole antennas in phase, and operated synchronously, would be a pair of antennas where the maximum power is in between the two antennas (Fig. 3.9a). If the same two antennas were operated asynchronously, the maximum power would be at each of the antennas, not in between. In this synchronous case, a phase relationship between the two antennas is established. One could change the phase slightly between antennas and actually move the power back and forth between antennas, a means of phase focusing of power (Fig. 3.9b, c). This could also be done for three antennas or four antennas, assuming that they were synchronous and had an established phase relationship to begin with (Figs. 3.9a–c and 3.10a–c).

The dipole antennas below show a good phase relationship, such that the maximum power is at the center of the array and not at the antennas themselves (Fig. 3.10a, b). The antennas were operated in phase (synchronous). The center has maximum power due to constructive interference, as a result of resonant dipole antenna selection, the 2.0 cm spacing between antennas, and the frequency of 915 MHz. The helical antennas do not have the same phase relationship as the dipoles and show little difference when driven synchronously (in-phase) or asynchronously (Fig. 3.10c).

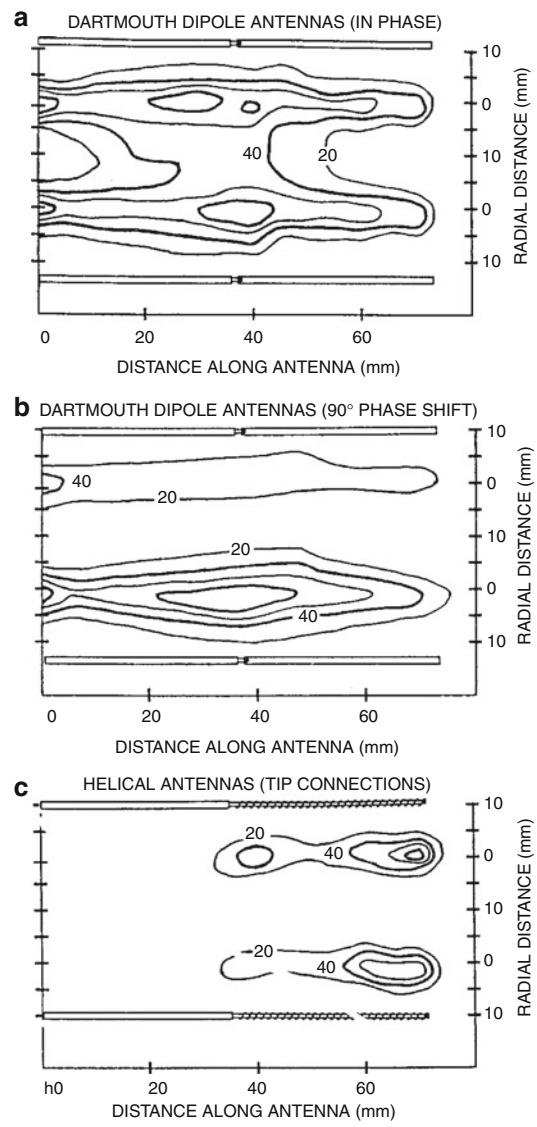

Fig. 3.9 (**a**–**c**) These three figures demonstrate phase relationships and phase shifting. Experimental SARs are shown for a pair of antennas spaced in a plane, 2 cm apart (antennas are pictured next to the SAR results, when in fact the antennas are located at a radial distance of 0 along the *y*-axis.). (**a**, *upper*): Maximum SAR in the center is 20–80 SAR, depending on axial position (**b**, *middle*): This is the same setup as the upper figure except that there is now a 90° phase shift between antennas. Due to the phase shift, power is now steered away from the center and preferentially near to one of the antennas. This demonstrates phase focusing and power steering with synchronous antennas by changing phase. (**c**, *lower*): Shows two helical antennas driven in phase. There is no central power deposition or SAR due to the lack of a phase relationship between antennas (Reproduced from Ref. [48])

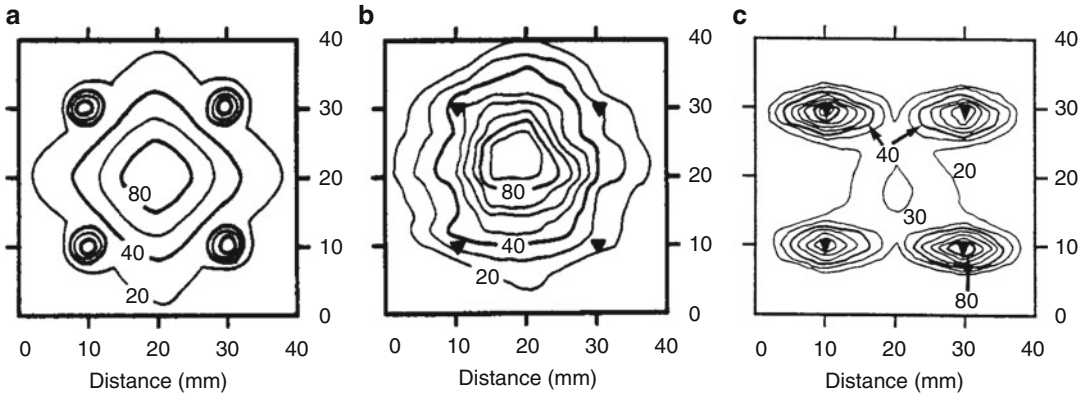

Fig. 3.10 Shows SAR results for an array of four antennas going into the page at locations marked by small circles or triangles. The contours represent 20–80 % SAR (percent of maximum power deposition). (**a**, *left*) shows the theoretical plot from computer simulations, and (**b**, *middle*) shows the experimental results for the same dipole antennas at 915 MHz. In the theoretical plot, the central SAR reaches 80 % SAR. The experimental results reach 90 % SAR, although the amount of power around the individual antennas is minimal. The plane of measurement is the midplane of the dipole, perpendicular to the angle of insertion. Lastly, (**c**, *right*) shows an array of helical antennas with SAR measurements in a plane near the tips. Note the central power is only 30 % SAR, and high values of SAR are found around the antennas themselves (Reproduced from Ref. [39])

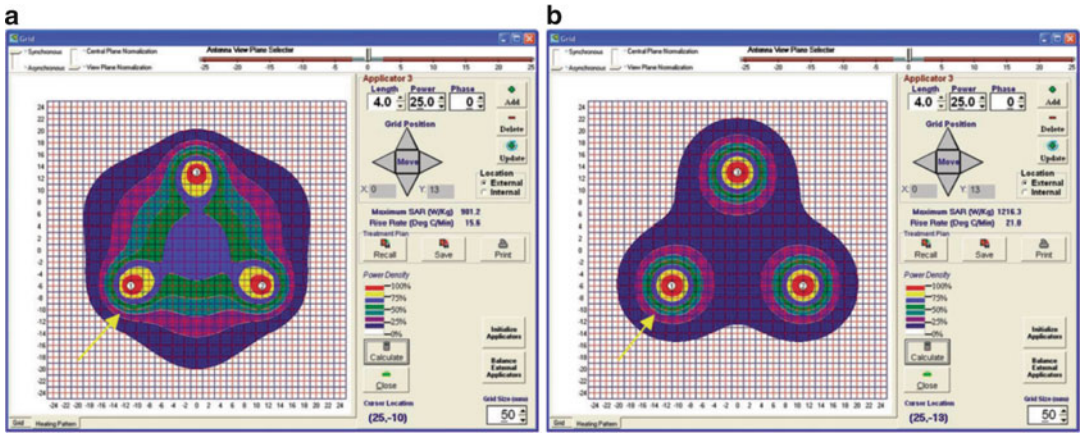

Fig. 3.11 Three antenna simulations showing synchronous versus asynchronous results. (**a**) The predicted SAR pattern with three synchronous antennas (see *arrow* for antenna location) spaced 2.2 cm on a side with triangular cross section. (**b**) The predicted SAR pattern with three asynchronous antennas (see *arrow*) spaced 2.2 cm on a side with triangular cross section [64] (Reproduced from Ref. ([64])

In the simulation results for three antennas (Fig. 3.11, right side), the asynchronous case had no phase relationship between antennas and no central constructive interference almost as if the antennas were turned on at separate times. In the synchronous case (in the left figure), the central SAR is nearly 75 %. In the asynchronous case, the central area has only 25 % SAR and may have trouble heating. Most of the power is concentrated around the antennas, and there is no constructive interference among the antenna sources. This program is also used for treatment planning and provides the user with tools to change the antenna geometry and layout, interactively on a workstation, to plan a patient treatment.

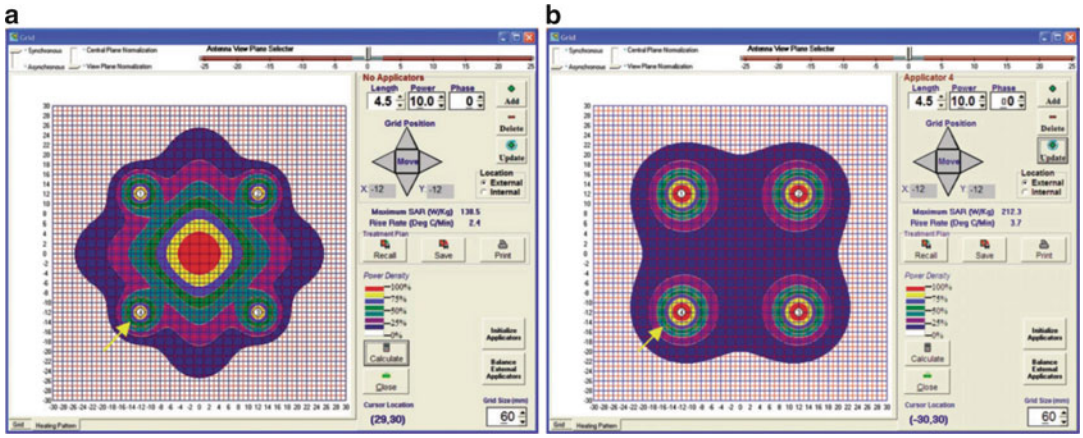

Fig. 3.12 Four antenna simulations showing synchronous versus asynchronous. (**a**) The predicted SAR pattern with four synchronous antennas (see *arrow*) spaced 2.4 cm on a side with square cross section. (**b**) The predicted SAR pattern with four asynchronous antennas (see *arrow*) spaced 2.4 cm on a side with square cross section [64] (Reproduced from Ref. [64])

In the simulation results for four antennas (Fig. 3.12, right side), the asynchronous antennas once again have no phase relationship and no central power deposition advantage, covered only by 25 % SAR. Power remains concentrated around the antennas as in the three antenna case. In the synchronous case (on the left), central power is at 100 % SAR. Thus, maximum heating will take place in the center of the array and not at the antennas themselves.

The use of MW antennas allows shaping of the heating pattern. In the cases where antennas were in asynchronous mode, no useful phase relationship exists between antennas. If it operates synchronously, this allows better control of the power deposition. Already there is a high level of power applied in the array center, and this can be refocused and steered within the array (see Fig. 3.9). Control of the power deposition pattern or SAR during ablation will give the clinician more flexibility in planning and applying ablation techniques, although a viable feedback mechanism still needs to be implemented to track performance and heating [48].

Constructive interference among microwave antennas when using arrays for synchronous use is advantageous. Heating the entire tumor has often been a challenge, especially as volumes are of greater size. One study showed that tumors treated with a diameter of 3 cm had only 48 % complete necrosis following MW ablation. If the tumors were larger, 5 cm or greater, the complete necrosis rate dropped to 25 %. This infers that large ablations are not being successfully targeted [65] and remain a challenge.

Antenna Cooling

Cooling was a feature added to microwave antennas for one of two reasons: (1) to preserve tissue in the vicinity of the antenna, for example, to preserve the urethra during transurethral prostate heating or (2) to cool the shaft at the proximal end of the MW antenna to spare the skin entry. Cooling could be accomplished with either flowing air or fluid. As an example, one group used a MW antenna which was cooled by 4 °C saline. They compared heating volumes both with and without cooling at 60 W for 5 min. With no cooling, heat tracked up the shaft and the ablation volume had a tail, proximally. With cooling, the ablation was more spherical with no tracking up the shaft [66].

It was also found that cooling significantly improves the radial uniformity of the temperature

distribution of a single antenna or could increase the area raised to a given temperature by a factor of four with air cooling [67, 68]. Cooled sources allow larger volumes by better distributing heat and keeping devices cool that are in contact with the patient's skin.

Other recent work with MW arrays showed the comparison among ablation results with cooling versus noncooling as well as synchronous versus asynchronous. With cooling, the power could be raised from 33 up to 60 W per antenna for percutaneous applications and still avoid skin damage. With cooled antennas, comparing three antennas operated synchronously versus three antennas operated asynchronously, in the synchronous case, the ablation was 4.2 × 5.5 cm; in the asynchronous case, the ablation size was 2.7 × 6 cm [64].

A large 433-MHz applicator with water cooling was used more than 25 years ago, developed for the treatment of prostate cancer. The control system directly modulated the power output to avoid damage to the tissue around the prostate, especially the periurethral tissue and the tissue between the prostate and the rectum. About 60 experiments with male dogs were completed, demonstrating that local heating of the prostate was possible without any damage to the urethra if cooling was used [69].

Clinical Performance with MW Applicators

Real-Time Ultrasound Imaging

With high-frequency ultrasound using a 12-MHz transducer, resolution was at the submillimeter level (Fig. 3.13). This high-frequency applicator demonstrated three distinct, concentric zones of injury: edema, hemorrhagic rim, and desiccated zone. The zones of injury were identifiable both on ultrasound, as well as on gross histology. The ultrasound monitoring also observed tracking along small hepatic veins; from the core ablation zone, heat tracking led to the formation of venous thrombus in small vessels [38].

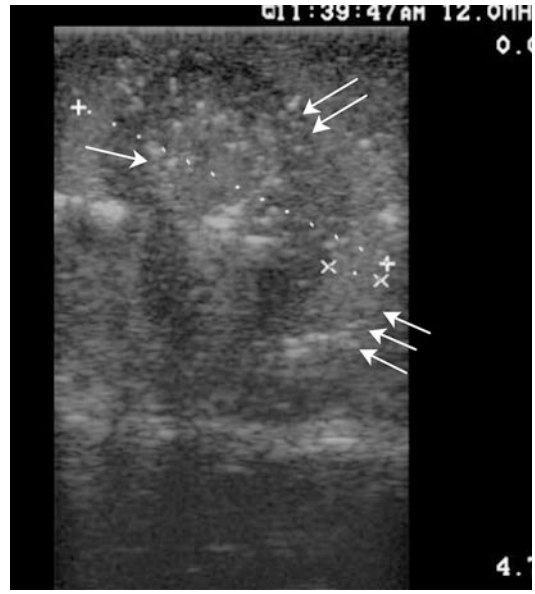

Fig. 3.13 The picture above shows an ultrasound scan immediately following a MW thermal treatment with 100 W at 4 min (in vivo porcine liver). Three distinct zones of injury are seen with the 12-MHz transducer (B-K ultrasound). The *single arrow* shows the zone of desiccation, *dual arrows* show the hemorrhagic rim, and *triple arrows* show the zone of edema [38] (Reproduced from Ref. [38])

Ex Vivo and In Vivo Results with MW Antennas

A study was done in fresh tissue (ex vivo) and in vivo in a porcine model with a single MW antenna at 2,450 MHz. Treatment duration ranged from 2 to 20 min, and power was one of three levels: 50, 100, or 150 W. Results are shown in Fig. 3.14a–c.

Another study showed the results of microwave heating of a single high-power applicator at 2.45 GHz [35] Figure 3.15.

Clinical Results

Using MW applicators in a patient series, ablation of large 5 cm tumors was accomplished in a short period of time. The MW applicator ablated tumors reproducibly and safely, highlighting the

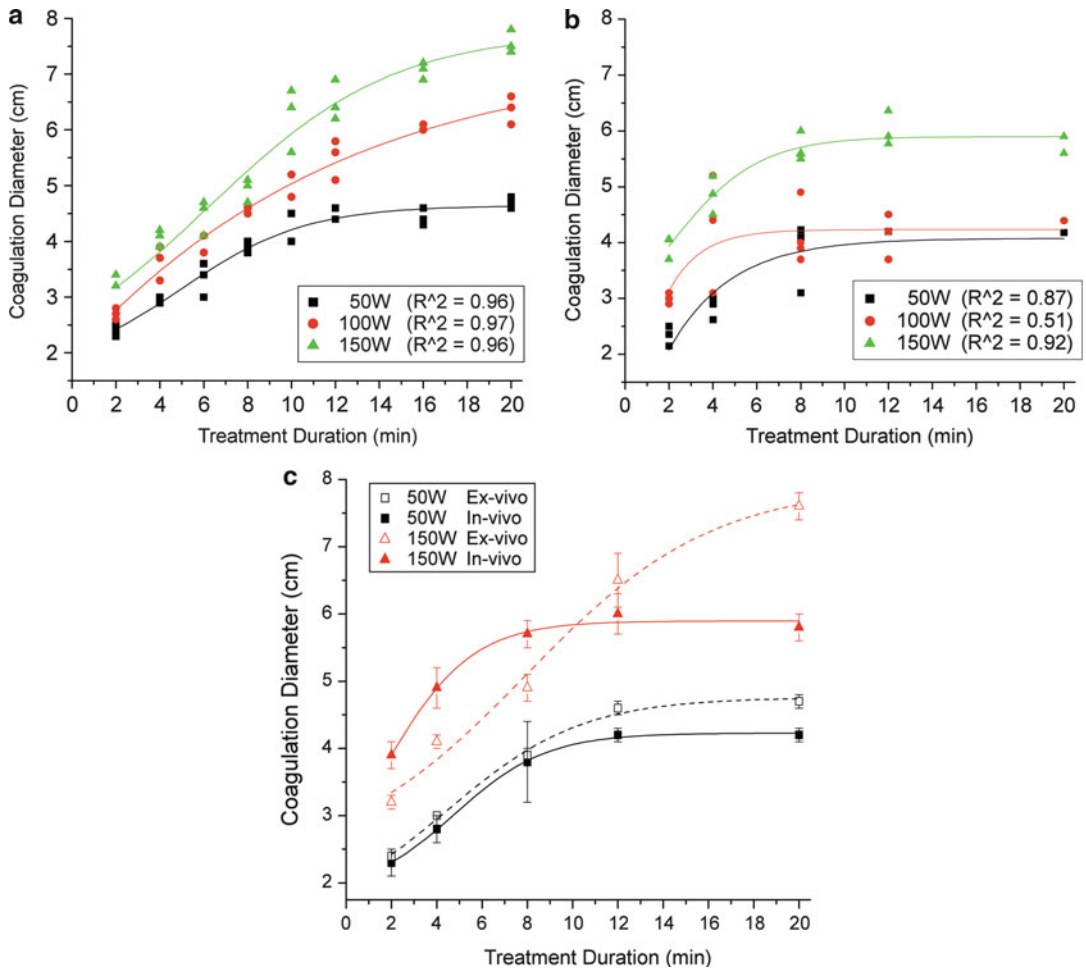

Fig. 3.14 (**a**) Shows ex vivo results with power and time increase. (**b**) Shows in vivo results, also for increasing power and time. The *x*-axis shows the treatment duration in minutes, while the *y*-axis shows the coagulation diameter in centimeters. On the left side in the ex vivo model, there is a near-linear increase in coagulation cross-section diameter with time increase. Each increase in power will also increase coagulation diameter. The figure on the right shows an increasing coagulation diameter up to about 4–8 min of treatment. After this point, the coagulation diameter does not increase with additional time. Thus, we see a steady-state condition where power activation only needs to be on for 4–8 min to achieve maximum results [55] (Reproduced from Ref. [55]). (**c**) Summarizes treatment duration versus coagulation diameter at 50 or 150 W. Ex vivo results are shown with dotted lines and in vivo results are shown with *solid lines*. At 150 W and at times less than 10 min, the in vivo results of ablation diameter exceeded the ex vivo results. This is also seen at 100 W, although not shown. It is also clear that after about 8 min of ablation time, in the in vivo cases, the ablation size plateaus and does not increase, indicating that the only means to increase lesion size would be to increase power [55] (Reproduced from Ref. [55])

potential of microwave systems as a viable treatment for unresectable liver tumors. Liver tumors as large as 6 cm were successfully treated with a single MW antenna at 150 W and 4 min at 2,450 MHz. Patient follow-up showed no tumor recurrence at 24 months [70, 71].

In clinical treatments for spherical tumors, a single central antenna is preferred. If tumors are irregularly shaped or very close to large vessels or near vulnerable structures, the clinician may choose multiple sources for more accurate control of the shape and size of the ablation.

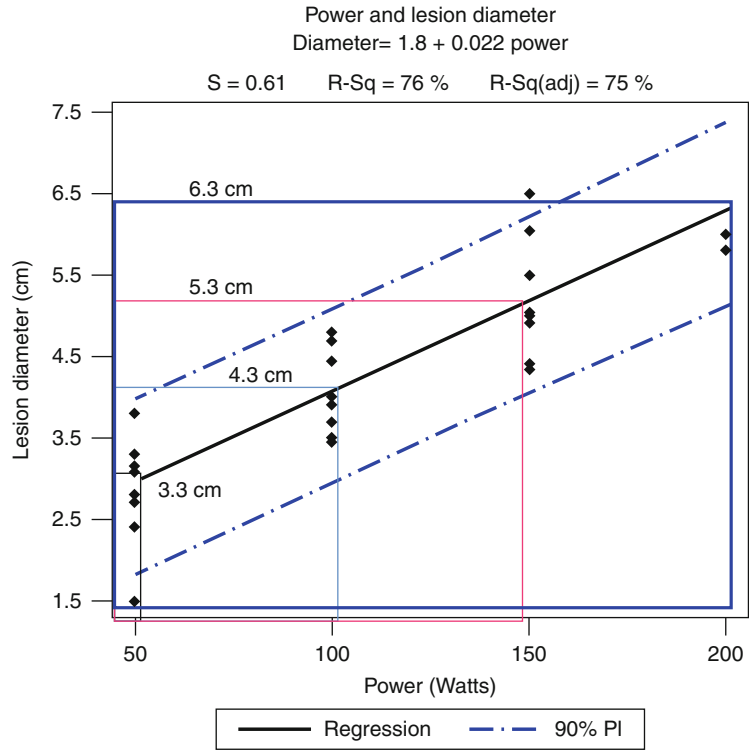

Fig. 3.15 Shows the results of in vivo porcine experiments with a single MW applicator where 50–200 W of power was applied for 4 min and the lesion diameter assessed. Note that for 50, 100, 150, and 200 W, the ablation diameters are 3.3, 4.3, 5.3, and 6.3 cm, respectively, and shown by the *colored boxes* [35]. Thus, as shown in animal studies, the system was able to scale the ablation diameter by varying power and keeping time the same, with a single high-power MW applicator, in a controlled and dose-dependent manner [35] (Reproduced from Ref. [35])

MW applicators can utilize very high power, resulting in very hot temperatures at the tissue interface, potentially exceeding 150–200 °C. MW ablation performance is unaffected by tissue desiccation and can achieve higher intratumoral temperatures, faster ablation times, and larger ablation volumes than other energy sources. In fact, desiccated tissue in the near field of the applicator is absent of water content and will actually be more transparent to microwaves, thus providing deeper penetration during ablation [72].

Ablation Near Vessels and Ducts and Thermal Tracking

In many tumor locations in the liver, blood vessels or ducts present a particular challenge to practitioners. The vessels may be of sufficient diameter to cool themselves (and self-protect), and clinicians may depend on this heat sink to spare large vessels carrying critical blood supply. When using RF applicators, tumors that are too close to major blood vessels will show incomplete ablation due to the blood flow cooling of the vessels.

But new evidence is coming out that MW applicators have sufficient penetration to change these suppositions. In the study below [38], they deliberately inserted the microwave applicator within 2 cm of large blood vessels in order to evaluate the heat sink effect on ablation performance (Fig. 3.16).

The study found that the shape of the ablation appeared unaffected by the blood flow in these large vessels. Microscopic examination revealed uniform coagulation necrosis circumferentially around both arteries and veins, indicating the ablation was not impaired by this heat sink from local blood flow. Thus, despite being in close proximity to large blood vessels, the ablation zone remained uniform in size and of 3–4 cm in diameter, related to power delivery only.

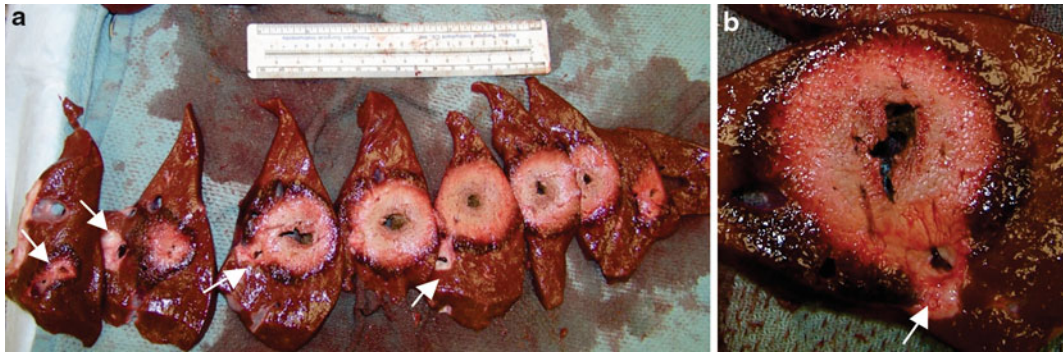

Fig. 3.16 Shows the result of a single MW applicator in an in vivo porcine model. The tissue is breadloafed following the ablation, with 1-cm slices. (**a**) Shows an ablation of 100 W and 4 min with the Pringle maneuver applied using a single MW applicator. The hemorrhagic rim was 5.6 cm and the tan zone was 4.5 cm. Tracking evidence is shown by *white arrows*. (**b**) Shows a close-up of a slice showing the vessel tracking (*white arrow*), with an additional ablation zone evident [38]. The tracking creates its own lesions. This is seen in the LEFT figure above, looking at the two slices on the left which show a separate lesion due to tracking up and away from the main body of the ablation (Reproduced from Ref. [38])

The reduction of blood flow by the Pringle maneuver resulted in a 70 % increase in gross diameter in the ablation zones [38].

With microwave ablation, vessels next to the ablation zone were also found to be included in the ablation, thus increasing the ablation size locally. Thus, microwaves may be superior to RF in terms of treating tumor blood vessel margins and limiting recurrence of these locations.

The evidence of tracking along vessels as seen in the above figures may be due to the creation of high-temperature water vapor that follows blood vessels along the path of least resistance in the direction away from the ablation site. The phenomenon is of some concern as it poses the risk of venous coagulation and hepatic infarction [38]. Thermal tracking was also reported by Wright who noted tracking along small hepatic vessels extending beyond the main body of the lesion [73]. This phenomenon could alter the expected spherical shape of the ablation [65, 72].

3D Treatment Planning

In the field of ablation, treatment planning is in its infancy. In thermal therapy for cancer, MW antennas are usually inserted parallel to one another, with tips in the same plane [39]. If one deviates from either of the conditions of parallel insertion or tip alignment, treatment planning is recommended to help predict the consequences, especially the presence of cold spots that may cause recurrence. The typical elliptical shape of ablation that MW applicators have may be advantageous for some tumor shapes [48]. As described in the MW historical review paper [64], the direct insertion of MW antennas into tumors along with high-temperature heating, antenna cooling, synchronous and asynchronous array operation, as well as treatment planning, has been in practice for 20 or 30 years. Current ablation procedures now incorporate real-time image guidance but lack extensive treatment planning and temperature monitoring as historically found in hyperthermia treatments. Future systems are expected to incorporate advanced features in three dimensions that may include treatment planning, image-guided placement, system knowledge of actual applicator location and trajectory along with target localization, real-time thermography, necrosis boundary imaging, as well as flexibility and applicator locations with power deposition control for conformability with the target [64] (additionally, see Refs. [74–76], including robotic placement [77]).

Thermal Mapping

For ablations performed in an MR scanner, software is available to use the real-time MR imaging to infer 3D temperature distributions. MR thermography is a rather recent tool based on the linear relationship between measured temperatures and phase angle change of the proton-resonance frequency shift, the modality used to ascertain temperature from MR scanning. MR scanning creates millimeter resolution slices for thermography, with power off for 20 s after every 4 min of scanning. During patient treatments, imaging showed a large non-enhancing region, implying necrosis, but sparing normal tissue [78]. Thus, MR images are observed even during MW ablation, as well as thermography assessment in real time [79].

Image Guidance and Navigation

There are different elements that need to dovetail for the combination of image guidance and navigation. Virtually all of the present ablation procedures utilize image guidance, whether ultrasound, CT, or MR, or a combination thereof. Ideally, the system is coregistered with patient space and antenna positions can then be tracked based on an initial treatment plan, and the treatment plan could be updated based on the *actual* implant as it progresses. One modern system described by Sato et al. [80] used real-time MR imaging in two orthogonal planes which showed the MW applicator insertion in real time. The system utilized an optical tracking positioning system for applicator trajectory and depth information of the applicators. Ablation was performed with temperature monitoring in 3D by MR thermography. All these features still need to be integrated into a user-friendly, commercially available system [80]. Others used an open MR scanner combining treatment planning, detecting the orientation and location of the treatment area, and monitoring with temperature and thermal dose visualization in near real time [81, 82], plus optical tracking for navigation [83]. Robotics are also being applied to MW antenna placement. One group used MR-guided, robotic needle insertion and therapy, using 3D visualization of the current needle visualization, followed by treatment monitoring in real time [84–88]. When comparing robotic needle insertion versus computer-aided navigation, the accuracy for the robot and computer navigation was 1.2 and 5.8 mm, respectively, while time to reach the target was 37 s versus 108 s, respectively. The robot was faster, more accurate, and less user dependent than the navigation system [89].

Next-Generation Systems Operating in 3D

New systems are needed that do the following in a time-efficient, user-friendly manner: (a) coregister devices with patient space; (b) allow treatment planning including MW applicator number, orientation, depth, antenna type, and frequency; (c) provide temperature calculations using the bioheat equation in real time; (d) provide real-time tracking and navigation of antennas from skin insertion to insertion trajectory and depth to reach target; (e) include 3D thermography showing the extent of heating and an ablation monitor showing the border of coagulation necrosis relative to the treatment plan; and (f) incorporate multiple antennas for power focusing and defocusing, with changes in the power to individual antennas to shape the temperature distribution within the volume. This can be done in a closed-loop fashion from the temperature imaging information.

Conclusions

In the future, systems will be available for clinical use that combine imaging, image guidance and navigation for the placement of applicators and monitoring of the ablation. The first step is treatment planning, and all of this will be incorporated into the treatment system, a user-friendly, time-saving system that will increase local control by

increasing the complete necrosis of the target, while sparing sensitive structures and reducing morbidity. This may benefit the patient by having shorter procedure times and less anesthesia.

References

1. D'Ippolito G, Goldberg SN. Radiofrequency ablation of hepatic tumors. Tech Vasc Interv Radiol. 2002;5:141–55.
2. Nardone DT, Smith DL, Martinez-Hernandez A, Consigny PM, Kosman Z, Rosen A, Walinsky P. Microwave thermal balloon angioplasty in the atherosclerotic rabbit. Am Heart J. 1994;127:198–203.
3. Smith DL, Walinsky P, Martinez-Hernandez A, Rosen A, Sterzer F, Kosman Z. Microwave thermal balloon angioplasty in the normal rabbit. Am Heart J. 1992;123:1516–21.
4. Landau C, Currier JW, Haudenschild CC, Minihab AC, Heymann D, Faxon DP. Microwave balloon angioplasty effectively seals arterial dissections in an atherosclerotic rabbit model. J Am Coll Cardiol. 1994;23:1700–7.
5. Young LA, Boehm RF. A finite difference heat transfer analysis of a percutaneous transluminal microwave angioplasty system. J Biomech Eng. 1993;115:441–6.
6. Lin JC. Catheter microwave ablation therapy for cardiac arrhythmias. Bioelectromagnetics. 1999; 20(Suppl 4):120–32.
7. Thomas SP, Clout R, Deery C, Mohan AS, Ross DL. Microwave ablation of myocardial tissue: the effect of element design, tissue coupling, blood flow, power, and duration of exposure on lesion size. J Cardiovasc Electrophysiol. 1999;10:72–8.
8. Lin JC, Beckman KJ, Hariman RJ, Bharati S, Lev M, Wang YJ. Microwave ablation of the atrioventricular junction in open-chest dogs. Bioelectromagnetics. 1995;16:97–105.
9. Herron DM, Grabowy R, Connolly R, Schwaitzberg SD. The limits of bloodwarming: maximally heating blood with an inline microwave bloodwarmer. J Trauma. 1997;43:219–26.
10. Holzman S, Connolly RJ, Schwaitzberg SD. The effect of in-line microwave energy on blood: a potential modality for blood warming. J Trauma. 1992;33:89–93.
11. Langberg JJ, Wonnell T, Chin MC, Finkbeiner W, Scheinman M, Stauffer P. Catheter ablation of the atrioventricular junction using a helical microwave antenna: a novel means of coupling energy to the endocardium. Pacing Clin Electrophysiol. 1991; 14:2105–13.
12. Larson TR, Blute ML, Tri JL, Whotlock SV. Contrasting heating patterns and efficiency of the Prostatron and Targis microwave antennae for thermal treatment of benign prostatic hyperplasia. Urology. 1998;6:908–15.
13. Djavan B, Larson TR, Blute ML, Marberger M. Transurethral microwave thermotherapy: what role should it play versus medical management in the treatment of benign prostatic hyperplasia? Urology. 1998;52: 935–47.
14. Simon CJ, Dupuy DE. Percutaneous minimally invasive therapies in the treatment of bone tumors: thermal ablation. Semin Musculoskelet Radiol. 2006;10: 137–44.
15. Simon CJ, Dupuy DE, Mayo-Smith WW. Microwave ablation: principles and applications. Radiographics. 2005;25:S69–83.
16. Dong BW, Liang P, Yu XL, Zeng XQ, Wang PJ, Su L, Wang XD, Xin H, Li S. Sonographically guided microwave coagulation treatment of liver cancer: an experimental and clinical study. AJR Am J Roentgenol. 1998;171:449–54.
17. Matsukawa T, Yamashita Y, Arakawa A, Nishiharu T, Urata J, Murakami R, Takahashi M, Yoshimatsu S. Percutaneous microwave coagulation therapy in liver tumors. A 3-year experience. Acta Radiol. 1997; 38:410–5.
18. Boss A, Clasen S, Kuczyk M, Schick F, Pereira PL. Image-guided radiofrequency ablation of renal cell carcinoma. Eur Radiol. 2007;17:725–33.
19. Wasser EJ, Dupuy DE. Microwave ablation in the treatment of primary lung tumors. Semin Respir Crit Care Med. 2008;29:384–94.
20. Wolf FJ, Grand DJ, Machan JT, Dipetrillo TA, Mayo-Smith WW, Dupuy DE. Microwave ablation of lung malignancies: effectiveness, CT findings, and safety in 50 patients. Radiology. 2008;247: 871–9.
21. Guy AW, Lehmann JF, Stonebridge JB. Therapeutic applications of electromagnetic power. Proc IEEE. 1974;62:55–75.
22. Strohbehn JW, Bowers ED, Walsh JE, Douple EB. An invasive microwave antenna for locally-induced hyperthermia for cancer therapy. J Microw Power. 1979;14:339–50.
23. Douple EB, Strohbehn JW, Bowers ED, Walsh JE. Cancer therapy with localized hyperthermia using an invasive microwave system. J Microw Power. 1979;14:181–6.
24. Bigu-del-Blanco J, Romero-Sierra C. The design of a monopole radiator to investigate the effect of microwave radiation in biological systems. J Bioeng. 1977;1:1181–4.
25. Turner P. Interstitial equal-phase arrays for EM hyperthermia. IEEE Trans Microw Theory Tech. 1986;MTT-34:572–8.
26. Emami B, Stauffer P, Dewhirst MW, Prionas S, Ryan T, Corry P, Herman T, Kapp DS, Myerson RJ, Samulski T, et al. RTOG quality assurance guidelines for interstitial hyperthermia. Int J Radiat Oncol Biol Phys. 1991;20:1117–24.
27. Scott RM, Cheung AY, Samaras GM. Clinical local heating by microwaves. Natl Cancer Inst Monogr. 1982;61:351–5.

28. Harada T, Etori K, Kumazaki T, Nishizawa O, Noto H, Tsuchidas S. Microwave surgical treatment of diseases of prostate. Urology. 1985;26:572–6.
29. Sapozink MD, Boyd SD, Astrahan MA, Jozsef G, Petrovich Z. Transurethral hyperthermia for benign prostatic hyperplasia: preliminary clinical results. J Urol. 1990;143:944–9.
30. Tabuse Y, Tabuse K, Mori K, Nagai Y, Kobayashi Y, Egawa H, Noguchi H, Yamaue H, Katsumi M, Nagasaki Y. Percutaneous microwave tissue coagulation in liver biopsy: experimental and clinical studies. Nippon Geka Hokan. 1986;55:381–92.
31. Murakami R, Yoshimatsu S, Yamashita Y, Matsukawa T, Takahashi M, Sagara K. Treatment of hepatocellular carcinoma: value of percutaneous microwave coagulation. AJR Am J Roentgenol. 1995;164:1159–64.
32. Diederich CJ. Thermal ablation and high-temperature thermal therapy: overview of technology and clinical implementation. Int J Hyperthermia. 2005; 21:745–53.
33. Lencioni R, Crocetti L. Image-guided thermal ablation of hepatocellular carcinoma. Crit Rev Oncol Hematol. 2008;66:200–7.
34. Swift B, Strickland A, West K, Clegg P, Cronin N, Lloyd D. The histological features of microwave coagulation therapy: an assessment of a new applicator design. Int J Exp Pathol. 2003;84:17–30.
35. Strickland AD, Clegg PJ, Cronin NJ, Swift B, Festing M, West KP, Robertson GS, Lloyd DM. Experimental study of large-volume microwave ablation in the liver. Br J Surg. 2002;89:1003–7.
36. Ahmad F, Strickland AD, Wright GM, Elabassy M, Kiruparan P, Bell PRF, Lloyd DM. Laparoscopic microwave tissue ablation of hepatic metastasis from a parathyroid carcinoma. Eur J Surg Oncol (EJSO). 2005;31:321–2.
37. Ryan TP, Clegg P. Novel microwave applicators for thermal therapy, ablation, and hemostasis. In: Ryan TP, editor. Thermal treatment of tissue: energy delivery and assessment V, vol. 6440. Bellingham: SPIE Press; 2009.
38. Garrean S, Hering J, Saeid A, Hoopes PJ, Helton WS, Ryan TP, Espat NJ. Ultrasound monitoring of a novel microwave ablation (MWA) device in porcine liver: lessons learned and phenomena observed on ablative effects near major hepatic vessels. J Gastorintest Surg. 2009;13:334–40.
39. Ryan TP. Comparison of six microwave antennas for hyperthermia treatment of cancer: SAR results for single antennas and arrays. Int J Radiat Oncol Biol Phys. 1991;21:403–13.
40. Chen JC, Moriarty JA, Derbyshire JA, Peters RD, Trachenberg J, Bell SD, Doyle J, Arrelano R, Wright GA, Henkleman RM, Hinks RS, Lok SY, Toi A, Kucharczyk W. Prostate cancer: MR imaging and thermometry during microwave thermal ablation-initial experience. Radiology. 2000;214: 290–7.
41. Clegg PJ. Microwave ablation therapy for liver cancers [doctoral dissertation]. University of Bath, UK; 2002.
42. Tamaki K, Shimizu I, Oshio A, Fukuno H, Inoue H, Tsutsui A, Shibata H, Sano N, Ito S. Influence of large intrahepatic blood vessels on the gross and histological characteristics of lesions produced by radiofrequency ablation in a pig liver model. Liver Int. 2004;24:696–701.
43. Chinn SB, Lee Jr FT, Kennedy GD, Chinn C, Johnson CD, Winter 3rd TC, Warner TF, Mahvi DM. Effect of vascular occlusion on radiofrequency ablation of the liver: results in a porcine model. AJR Am J Roentgenol. 2001;176:789–95.
44. Tungjitkusolmun S, Staelin ST, Haemmerich D, Tsai JZ, Webster JG, Lee Jr FT, Mahvi DM, Vorperian VR. Three-dimensional finite-element analyses for radiofrequency hepatic tumor ablation. IEEE Trans Biomed Eng. 2002;49:3–9.
45. Skinner MG, Lizuka MN, Kolios MC, Sherar MD. A theoretical comparison of energy sources – microwave, ultrasound and laser – for interstitial thermal therapy. Phys Med Biol. 1998;43:3535–47.
46. Ryan T. A tutorial on recent advances in thermal therapy systems. In: Ryan TP, editor. Thermal treatment of tissue: energy delivery and assessment IV, vol. 6440. Bellingham: SPIE Press; 2007. p. 1–19.
47. Cha CH, Lee Jr FT, Gurney JM, Markhardt BK, Warner TF, Kelcz F, Mahvi DM. CT versus sonography for monitoring radiofrequency ablation in a porcine liver. AJR Am J Roentgenol. 2000;175:705–11.
48. Trembly BS, Ryan TP, Strohbehn JW. Physics of microwave hyperthermia. In: Urano M, Douple E, editors. Hyperthermia and oncology. Volume 3. Interstitial hyperthermia: physics, biology and clinical aspects. New York: VSP Press; 1991. p. 11–98.
49. Thuéry J, Grant EH. Microwaves: industrial, scientific and medical applications. Boston: Artech House; 1992.
50. Chin L, Sherar M. Changes in dielectric properties of ex vivo bovine liver at 915 MHz during heating. Phys Med Biol. 2001;46:197–211.
51. Moore JE, Zouridakis G. Biomedical technology devices handbook. Boca Raton: CRC Press; 2003. p. 31–2.
52. Ryan TP, Hoopes PJ, Taylor JH, Strohbehn JW, Roberts DW, Douple EB, Coughlin CT. Experimental brain hyperthermia: techniques for heat delivery and thermometry. Int J Radiat Oncol Biol Phys. 1991;20:739–50.
53. Prakash P, Converse MC, Webster JG, Mahvi DM. An optimal sliding choke antenna for hepatic microwave ablation. IEEE Trans Biomed Eng. 2009;56:2470–6.
54. Prakash P, Deng G, Converse MC, Webster JG, Mahvi DM, Ferris MC. Design optimization of a robust sleeve antenna for hepatic microwave ablation. Phys Med Biol. 2008;53:1057–69.
55. Hines-Peralta AU, Pirani N, Clegg P, Cronin N, Ryan TP, Liu Z, Goldberg SN. Microwave ablation: results with a 2.45-GHz applicator in ex vivo bovine and in vivo porcine liver. Radiology. 2006;239:94–102.

56. Yang JM, Bertram JM, Converse MC, O'Rourke AP, Webster JG, Hagness S, Will JA, Mahvi DV. A floating sleeve antenna yields localized hepatic microwave ablation. IEEE Trans Biomed Eng. 2006;53:533–7.
57. Durick NA, Laeseke PF, Broderick LS, Lee Jr FT, Sampson LA, Frey TM, Warner TF, Fine JP, van der Weide DW, Brace CL. Microwave ablation with triaxial antennas tuned for lung: results in an in-vivo porcine model. Radiology. 2008;247:80–7.
58. Laeseke PF, Lee Jr FT, Sampson LA, van der Weide DW, Brace CL. Microwave ablation versus radiofrequency ablation in the kidney: high-power triaxial antennas create larger ablation zones than similarly sized internally cooled electrodes. J Vasc Interv Radiol. 2009;20:1224–9.
59. Hardie D, Sangster AJ, Cronin NJ. Coupled field analysis of heat flow in the near field of a microwave applicator for tumor ablation. Electromagn Biol Med. 2006;25:1–15.
60. Satoh T, Stauffer PR, Fike JR. Thermal distribution studies of helical coil microwave for interstitial hyperthermia. Int J Radiat Oncol Biol Phys. 1988;15: 1209–18.
61. Satoh T, Seilman TM, Stauffer PR, Sneed PK, Fike JR. Interstitial helical coil microwave antenna for experimental brain hyperthermia. Neurosurgery. 1988;23: 564–9.
62. Trembly BS. The effects of driving frequency and antenna length on power deposition within a microwave antenna array used for hyperthermia. IEEE Trans Biomed Eng. 1985;MTT-32:152–7.
63. Dadd JS, Ryan TP, Platt R. Tissue impedance as a function of temperature and time. Biomed Sci Instrum. 1996;32:205–14.
64. Ryan TP, Turner PF, Hamilton B. Interstitial microwave transition from hyperthermia to ablation: historical perspectives and current trends in thermal therapy. Int J Hyperthermia. 2010;26:415–33.
65. McGahan JP, Dodd GD. Radiofrequency of the liver: current status. AJR Am J Roentgenol. 2001;176:3–16.
66. Kuang M, Lu MD, Xie XY, Xu XY, Mo HX, Liu GJ, Xu ZF, Zheng YL, Liang JY. Liver cancer: increased microwave delivery to ablation zone with cooled-shaft antenna: experimental and clinical studies. Radiology. 2007;242:914–24.
67. Eppert V, Trembly BS, Richter HJ. Air cooling for an interstitial microwave hyperthermia antenna: theory and experiment. IEEE Trans Biomed Eng. 1991;38:450–60.
68. Trembly BS, Douple EB, Hoopes PJ. The effect of air cooling on the radial temperature distribution of a single microwave hyperthermia antenna in vivo. Int J Hyperthermia. 1991;7:343–54.
69. Scheiblich J, Petrowicz O. Radiofrequency-induced hyperthermia in the prostate. J Microw Power. 1982; 17:203–9.
70. Strickland AD, Clegg PJ, Cronin NJ, Elabassy M, Lloyd DM. Rapid microwave ablation of large hepatocellular carcinoma in a high-risk patient. Asian J Surg. 2005;28:151–3.
71. Grieco CA, Simon CJ, Mayo-Smith WW, DiPetrillo TA, Ready NE, Dupuy DE. Percutaneous image-guided thermal ablation and radiation therapy: outcomes of combined treatment for 41 patients with inoperable stage I/II non-small-cell lung cancer. J Vasc Interv Radiol. 2006;17:1117–24.
72. Haemmerich D, Lee FT. Multiple applicator approaches for radiofrequency and microwave ablation. Int J Hyperthermia. 2005;21:93–106.
73. Wright AS, Lee Jr FT, Mahvi DM. Hepatic microwave ablation with multiple antennae results in synergistically larger zones of coagulation necrosis. Ann Surg Oncol. 2003;10:275–83.
74. Dodd 3rd GD, Frank MS, Aribandi M, Chopra S, Chintapalli KN. Radiofrequency thermal ablation: computer analysis of the size of the thermal injury created by overlapping ablations. AJR Am J Roentgenol. 2001;177:777–82.
75. Cen MH, Yang W, Yan K, Zou MW, Solbiati L, Liu JB, Dai Y. Large liver tumors: protocol for radiofrequency ablation and its clinical application in 110 patients – mathematic model, overlapping mode, and electrode placement process. Radiology. 2004;232:260–71.
76. Zhai W, Xu J, Zhao Y, Song Y, Sheng L, Jia P. Preoperative surgery planning for percutaneous hepatic microwave ablation. Med Image Comput Comput Assist Interv. 2008;11(Pt 2):569–77.
77. Xu J, Jia ZZ, Song ZJ, Yang XD, Chen K, Liang P. Three-dimensional ultrasound image-guided robotic system for accurate microwave coagulation of malignant liver tumours. Int J Med Robot. 2010;6: 256–68.
78. Laing P, Wang Y. Microwave ablation of hepatocellular carcinoma. Oncology. 2007;72:124–31.
79. Morikawa S, Inubushi T, Kurumi Y, Naka S, Sato K, Tani T, Yamamoto I, Fujimura M. MR-guided microwave thermocoagulation therapy of liver tumors: initial clinical experiences using a 0.5 T open MR system. J Magn Reson Imaging. 2002; 16:576–83.
80. Sato K, Morikawa S, Inubushi T, Karumi Y, Naka S, Haque HA, Demura K, Tani T. Alternate bipolar MR navigation for microwave ablation of liver tumors. Magn Reson Med Sci. 2005;4:89–94.
81. Keserci BM, Kokuryo D, Suzuki K, Kumamoto E, Okada A, Khankan AA, Kuroda K. Near-real-time feedback control system for liver thermal ablations based on self-referenced temperature imaging. Eur J Radiol. 2006;59:175–82.
82. Abe H, Kurumi Y, Naka S, Shiomi H, Umeda T, Naitoh H, Endo Y, Hanasawa K, Morikawa S, Tani T. Open-configuration MR-guided microwave thermocoagulation therapy for metastatic liver tumors from breast cancer. Breast Cancer. 2005;12(1):26–31.
83. Morikawa S, Inubushi T, Kurumi Y, Naka S, Sato K, Tani T, Haque HA, Tokuda J, Hata N. New assistive

devices for MR-guided microwave thermocoagulation of liver tumors. Acad Radiol. 2003;10:180–8.
84. Naka S, Kurumi Y, Shimizu T, Kondo H, Mekata E, Naito H, Kawaguchi A, Abe H, Endo Y, Hanasawa K, Tani T, Morikawa S, Ishizuka Y, Yamazaki M, Furukawa K. Tumor ablation with MRI navigation–a novel method of microwave coagulation therapy for hepatic tumor. Gan To Kagaku Ryoho. 2001;28:1591–4.
85. Morikawa S, Naka S, Murakami K, Kurumi Y, Shiomi H, Tani T, Haque HA, Tokuda J, Hata N, Inubushi T. Preliminary clinical experiences of a motorized manipulator for magnetic resonance image-guided microwave coagulation therapy of liver tumors. Am J Surg. 2009;198:340–7.
86. Tokuda J, Fischer GS, DiMaio SP, Gobbi DG, Csoma C, Mewes PW, Fichtinger G, Tempany CM, Hata N. Integrated navigation and control software system for MRI-guided robotic prostate interventions. Comput Med Imaging Graph. 2010;34:3–8.
87. Masamune K, Fichtinger G, Patriciu A, Susil RC, Taylor RH, Kavoussi LR, Anderson JH, Sakuma I, Dohi T, Stoianovici D. System for robotically assisted percutaneous procedures with computed tomography guidance. Comput Aided Surg. 2001;6:370–83.
88. Boctor EM, Choti MA, Burdette EC, Webster Iii RJ. Three-dimensional ultrasound-guided robotic needle placement: an experimental evaluation. Int J Med Robot. 2008;4:180–91.
89. Pollock R, Mozer P, Guzzo TJ, Marx J, Matlaga B, Petrisor D, Vigaru B, Badaan S, Stoianovici D, Allaf ME. Prospects in percutaneous ablative targeting: comparison of a computer-assisted navigation system and the AcuBot Robotic System. J Endourol. 2010;24:1269–72.

Cryoablation

4

Meghan G. Lubner, J. Louis Hinshaw, Chris L. Brace, and Fred T. Lee, Jr.

Abstract

Cryotherapy is a controlled destruction of tissue by freezing. Due to the excellent visualization of the ice ball on imaging and the close correlation between the ice ball and the zone of necrosis, this is a very precise ablation modality. In addition, multiple probes can be used to generate larger ablation zones, and probes can be controlled individually allowing some sculpting of the ice ball. Cryotherapy may be less sensitive to "cold sink" effects. However, cryoablation lacks the natural cautery effect of heat-based modalities, may be more time consuming and expensive than radiofrequency ablation, and has risk for cryoshock with large volume ablations. In this chapter, we will review the indications, technique, and management of patients undergoing cryoablation.

Introduction

Controlled destruction of tissue by freezing is widely practiced for a variety of purposes ranging from treatment of dermatologic lesions to ablation of tumors. Cryoablation is one of the oldest available tumor ablation modalities, with its origins in the 1800s when advanced carcinomas of the breast and cervix were treated with iced saline solutions [1, 2]. The last 50 years have seen great advances in the knowledge of the biological effects of freezing and the introduction of new technology. The purpose of this chapter is to review the principles, technique, applications, advantages, and complications of cryoablation.

M.G. Lubner (✉) • J.L. Hinshaw
Department of Radiology, University of Wisconsin School of Medicine and Public Health, Madison, WI, USA
e-mail: mlubner@uwhealth.org; jhinshaw@uwhealth.org

C.L. Brace
Department of Radiology, University of Wisconsin – Madison, Madison, WI, USA
e-mail: clbrace@wisc.edu

F.T. Lee, Jr.
Department of Radiology, University of Wisconsin, Madison, WI, USA
e-mail: flee@uwhealth.org

Principles of Cryotherapy

Tissue freezing during cryoablation causes both intracellular and extracellular formation of ice. The mechanism of cell death varies with the rate

D.E. Dupuy et al. (eds.), *Image-Guided Cancer Therapy*, DOI 10.1007/978-1-4419-0751-6_6,

and final temperature of freezing. Freezing at faster rates and to lower temperatures leads to formation of intracellular ice crystals. Intracellular ice crystals cause direct damage to the cell membrane and organelles producing cell death. Slower rates of freezing produce extracellular ice crystals, which leaves the rest of the extracellular milieu hyperosmolar to the intracellular compartment. This leads to cell dehydration and death [1, 3]. The critical cell kill temperature at which cells are irreversibly destroyed varies with cell and tissue type, ranging from approximately −20 °C for water-rich tissues [4, 5] to −40 °C for more fibrous tissues [5, 6].

Cryoprobes freeze tissue via circulation of a cryogen in a closed system. Early cryoprobes used liquid nitrogen as a cryogen. Early nitrogen systems demonstrated the promise of focal cryotherapy. Disadvantages of nitrogen systems included a relatively large probe diameter (5 mm and greater) which limited percutaneous applications, slow freezing and thawing due to the high viscosity of liquid nitrogen, and large heavy dewars associated with early devices. More recently, cryoablation systems have become available which utilize the Joule-Thomson phenomenon of expanding gases. In these probes, high-pressure gas (argon) is forced down the narrow shaft into an expansion chamber at the tip of the cryoprobe. As argon expands, very cold temperatures (approximately −150 °C) are generated. Due to the low viscosity of argon gas, smaller feed lines became possible, resulting in cryoprobes of reduced diameter (13–17 gauge). Smaller probes have led to an increased interest in percutaneous applications (Fig. 4.1). Modern cryoablation systems support the simultaneous use of multiple probes, and the resulting thermal synergy between closely spaced cryoprobes makes possible the creation of very large ablation zones. Thawing can be active, where warming is created by the Joule-Thomson expansion of helium inside the cryoprobe, or passive, relying only on thermal diffusion from the surrounding tissue.

There is continuing research and development in cryoablation focusing on novel cryogens and applicators. One of the more promising technologies utilizes "near-critical nitrogen." The very low viscosity of near-critical nitrogen will potentially allow smaller diameter applicators, but with improved freeze capacity as compared with current argon systems, but this has not yet been successfully incorporated into a clinical system.

Technique

Probe Placement

The number of probes utilized to treat a tumor varies with the type and location of the tumor, and the approach and size of the probe being used. In addition, performance may vary with the type of system being used. The "1–2" rule described by *Wang* et al. is a useful guide for planning probe placement [7]. This rule states that cryoprobes should be placed no more than 1 cm from the tumor edge, and no farther than 2 cm from the nearest adjacent cryoprobe. Placement in this configuration allows synergistic effects between the probes, providing a greater rate of freezing and a larger lethal isotherm. Because of the "cold sink" effect of large vessels, it is recommended that the spacing between probes and between the probe and the edge of the tumor be decreased along any border with a large vessel.

Probe placement can be performed using US, CT, or MRI guidance. US has the advantage of real-time feedback regarding both the cryoprobe position during placement and the growing ice ball and, in comparison to non-contrast CT, can potentially allow for superior visualization of the soft tissue tumor. Although intraoperative approaches are sometimes required, percutaneous probe placement has been shown to be equally efficacious to laparoscopic or open approaches, with lower complication rates, lower cost, and shorter hospital stay [8–12]. If intraoperative ultrasound (IOUS) probe placement is necessary or if cryoablation is being performed in conjunction with surgical resection, some advantages can be afforded by laparotomy. A combination of direct visualization and tactile evaluation can be used to assist with probe placement, and IOUS is highly sensitive in the detection of unexpected tumors [13, 14]. In addition, larger probes with more

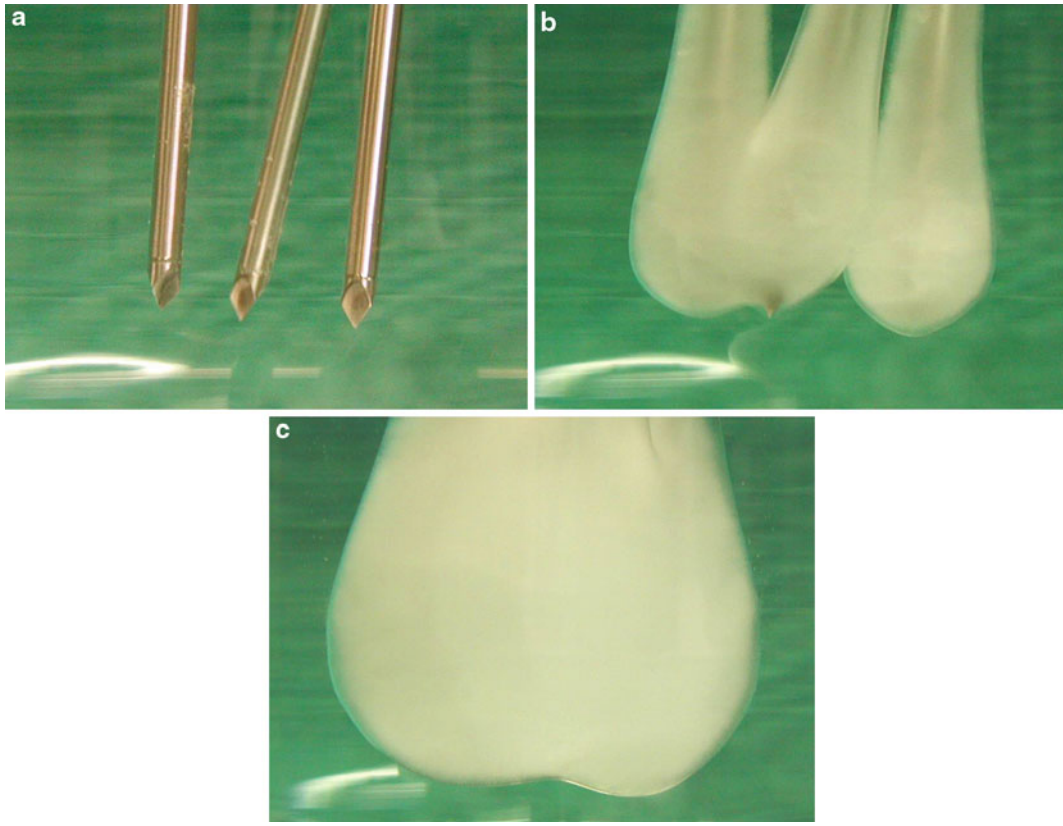

Fig. 4.1 Three 12-gauge cryoprobes are seen in a water bath prior to freezing (**a**). Ice formation is seen on each probe early in the freeze cycle (**b**) which eventually becomes a confluent ice ball as time progresses (**c**)

freezing capacity (10–13 gauge) can be used with this approach. Cryoprobe placement with the conventional or laparoscopic intraoperative ultrasound can be technically challenging and may require multiple repositionings with associated prolongation of procedure time and theoretical increased risk of bleeding and tumor seeding.

Monitoring

Once the probes are in place, freezing can be monitored with US, CT, and/or MRI. The visible ice ball corresponds well with the zone of necrosis at gross pathology [5, 15, 16]. Specifically, the −20° isotherm lies approximately 3 mm inside the ice ball edge, and the −40° isotherm lies approximately 8 mm inside the ice ball edge, although the exact distance will vary somewhat based upon the cooling power of the cryoprobe, number of cryoprobes used, and the tissue type [5, 17, 18]. When monitoring with US, the ice ball produces a hyperechoic line along its anterior margin with dense posterior acoustic shadowing that makes evaluation of the deep margin difficult (Fig. 4.2). On CT, the ice ball is low in attenuation, near water density, and is well seen in solid parenchymal organs even without intravenous contrast (Fig. 4.3) [16]. The interface of the ice ball and any adjacent fatty tissue may be more difficult to visualize with CT due to similar density values. At MRI, the ice ball demonstrates a prominent signal void on all sequences, and given the inherent tissue contrast, the margins of the tumor with respect to the ice ball are often very well seen [15, 19, 20].

One advantage of cryoablation is that when real-time monitoring is utilized, adjustments can be

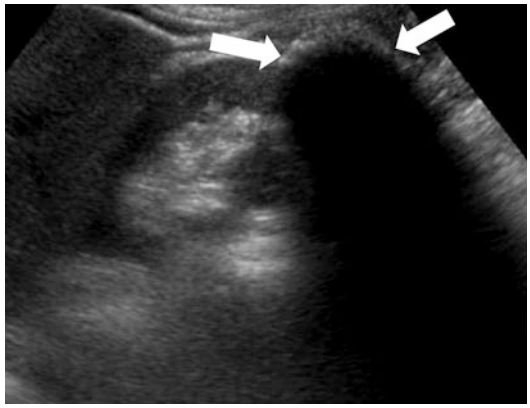

Fig. 4.2 US image demonstrates a cryoablation zone in the right kidney. Note the hyperechoic line at the anterior margin (*arrows*) with dense posterior acoustic shadowing

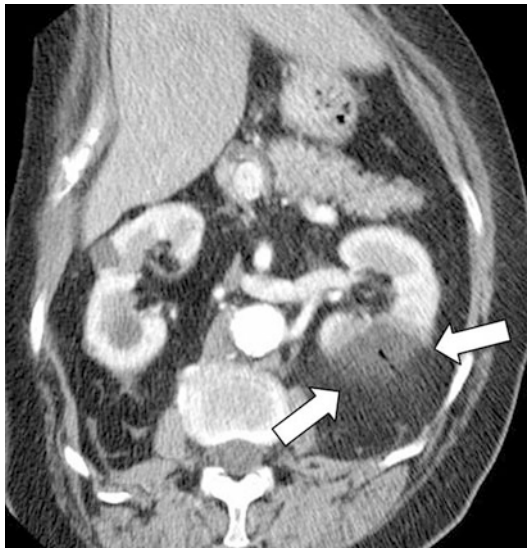

Fig. 4.3 Contrast-enhanced CT image obtained immediately post-ablation demonstrates a low-attenuation ice ball (*arrows*) along the posterior margin of the left kidney

made to both the duration and intensity of freezing of individual probes, which allows some level of control of the ultimate size and shape of the ice ball. This ability to control the size and shape of the ice ball as well as the correlation between the ice ball and the zone of necrosis allows a degree of precision that can be difficult to obtain with heat-based modalities. A 100 % duty cycle should be used whenever possible, since rapid freezing is associated with more effective cytotoxicity [21].

Multiple freeze cycles are preferred because the later freezes are associated with a faster rate of freezing and a larger zone of necrosis than a single freeze of similar total duration [22]. This practice is based on limited data but has been effective clinically [18, 23, 24]. Note that additional freezes can be performed but will result in exponentially smaller gains with each freeze [25]. Therefore, if residual tumor remains after two freeze cycles, additional probes should be placed into any untreated areas. Since frozen tissue will deflect the additional probes, the ice ball may need to be at least partially thawed before additional probes can be placed.

Periprocedural and Post-procedure Management

Unlike radiofrequency ablation (RFA), cryoablation is associated with relatively little pain once the adjacent sensory nerves have been frozen and can be performed under conscious sedation [26]. Some centers use general anesthesia due to patient comfort during prolonged procedures and more controlled breath holding which decreases movement of the target during probe placement and ablation. Post-ablation monitoring and care differs between procedure types and providers. Some centers perform cryoablation as an outpatient procedure, while others keep patients utilize a short stay admission.

Imaging follow-up is even more variable but should include an imaging examination within a month of the ablation (this can be performed on the table at the time of ablation), followed by imaging at 3–6 month intervals for the next 2 years depending on the target tumor type and technical outcome. Of note, immediately following cryoablation and thawing, the ablation zone often becomes transiently hyperemic (Fig. 4.4). Over the next several days, these vessels thrombose and the treated area becomes hypovascular. A thin, relatively uniform peripheral rim of enhancement related to acute inflammation and subsequent granulation often persists for a month or more. This should be distinguished from nodular enhancement concerning for residual disease

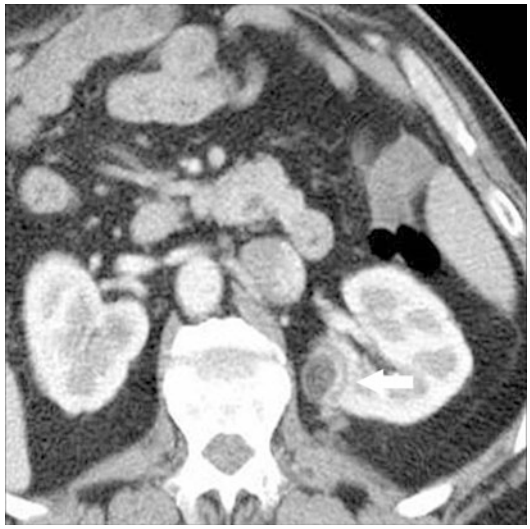

Fig. 4.4 CT image obtained immediately post-ablation demonstrates peripheral enhancement (*arrow*) due to transient hyperemia

and geographic zones of enhancement which can be related to adjacent small vessel changes and shunt formation [27, 28].

The ablation zone should slowly decrease in size in the months and years following the ablation (Fig. 4.5) [29]. Nodular or crescentic enhancement in the setting of a prior hypervascular tumor is concerning for residual or recurrent disease. For low-attenuation or hypovascular tumor types, residual or recurrent tumor may cause enlargement of or asymmetric changes in a hypoattenuating ablation zone (Fig. 4.6) [30, 31].

Organ-Specific Applications

Kidney

The incidence of renal cell carcinoma is increasing due to both increased detection of incidental small renal masses and an underlying increase in the incidence of renal cancers. While surgical resection remains the standard of care for most patients, cryoablation and radiofrequency ablation have emerged as minimally invasive treatments with excellent short- and intermediate-term results [11, 32–40]. Several studies have shown 97–100 % technical success and short- and intermediate-term local control in 92–100 % of patients [32, 36, 41, 42].

Patient selection for ablation is based on both tumor (size, location, and tumor type) and patient-related factors (comorbidities, renal function/reserve, and presence of multiple tumors or conditions predisposing to multiple tumors). The advantages of cryoablation in these patients are that it is well tolerated, has an excellent safety profile, has minimal effect on renal function, and can be repeated as needed.

Numerous studies have shown that large tumors can be successfully treated but that the risk for residual or recurrent tumor increases significantly in tumors over 4 cm [34, 43]. In addition to the problem of obtaining adequate local control, larger tumors typically have unfavorable histology [44].

Tumor location is also a critical consideration. Peripheral, exophytic, and posterior tumors are technically the simplest tumors to target and ablate. Central tumors are more likely to be associated with local tumor progression, probably related to central heat sink effects, but a central location should not be considered a contraindication if the tumor is otherwise amenable to cryoablation [34, 40]. Anterior tumor location was historically considered a relative contraindication to percutaneous ablation due to the close proximity of vulnerable structures and the difficulty of percutaneous access. However, adjunctive techniques such as changes in patient positioning, use of probes for tumor displacement with retraction or leverage, and hydrodissection have allowed for safe treatment of many anterior tumors (Fig. 4.7) [45–52]. Placement of a ureteric stent with pyeloperfusion using warm saline or sterile water has also been utilized to protect the ureter when treating central, anterior, or inferior tumors [50, 53, 54].

Although both RF and cryoablation can be effective in the treatment of renal tumors, cryoablation has the advantage of precision due to the high visibility of the ice ball, and renal cell carcinoma appears to be particularly vulnerable to cold damage. A recent meta-analysis of 1,375 kidney tumors demonstrated that cryoablation may require fewer treatment sessions and have a slightly lower rate of local tumor progression

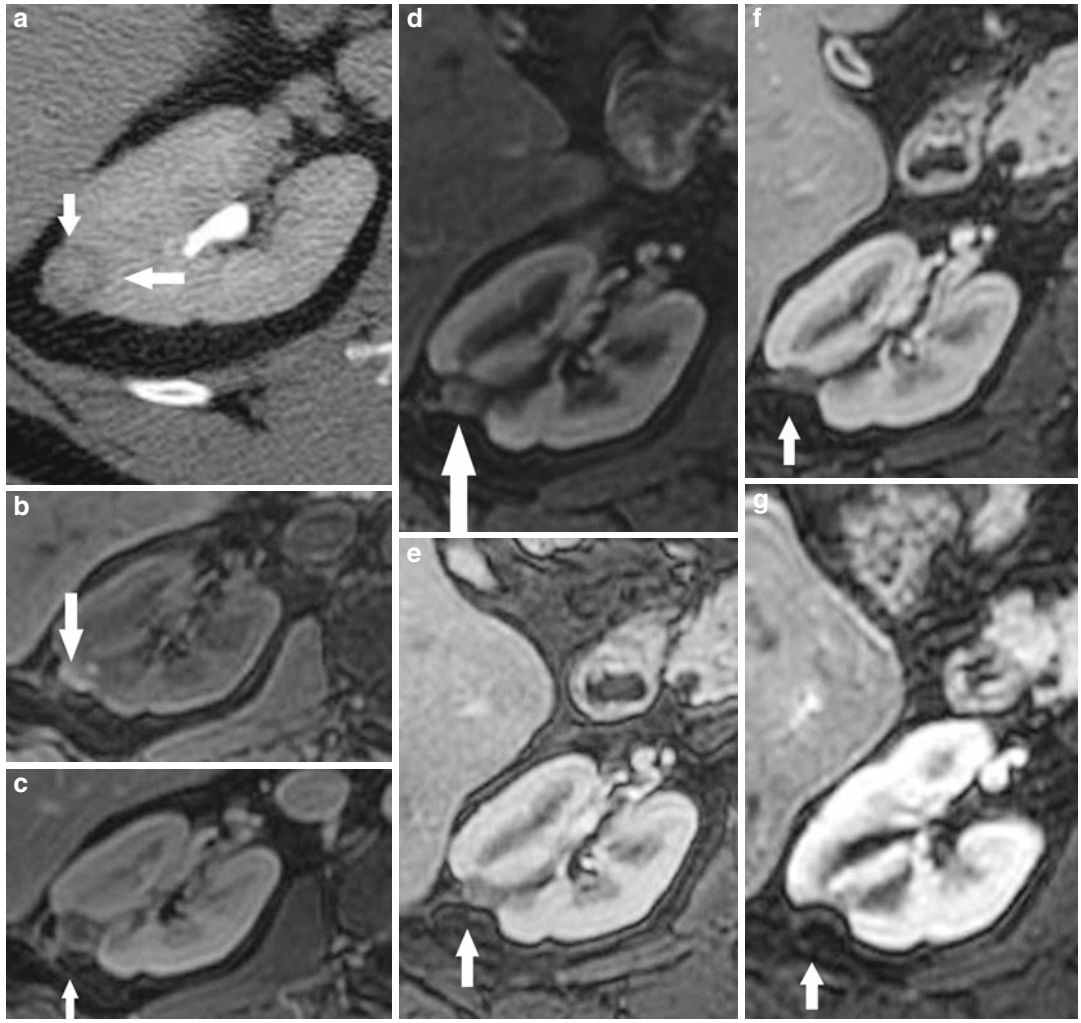

Fig. 4.5 Normal evolution of the ablation zone over time. Pretreatment imaging demonstrates a peripheral enhancing tumor (*arrow* on all images) (**a**). Pre- (**b**) and post- (**c**) contrast imaging at 3 months post-ablation demonstrates high T1 signal in the ablation zone without residual enhancement. The ablation zone gradually evolves and decreases in size at 6, 9, and 12 (**d–f**) months posttreatment with almost no residual ablation zone seen at 24 months posttreatment (**g**)

[55]. The majority of cryoablations (65 %) in this study were performed laparoscopically, but multiple studies have shown that percutaneous and laparoscopic techniques are comparable in efficacy, but with fewer complications, lower costs, and shorter hospital stays seen with percutaneous techniques [9, 11, 12, 37]. Similarly, cryoablation is a less painful treatment option than RFA, with one group showing lower pain and sedative medication requirements during procedures performed with cryoablation [26]. In addition, cryoablation is theoretically less damaging to the collecting system, which can be advantageous in the treatment of central tumors [56] although ureteral strictures have been reported [57].

Disadvantages of cryoablation include a longer procedure time, a higher theoretical risk of bleeding due to a lack of microvascular coagulation, and higher procedural costs due to the need for compressed gas [58].

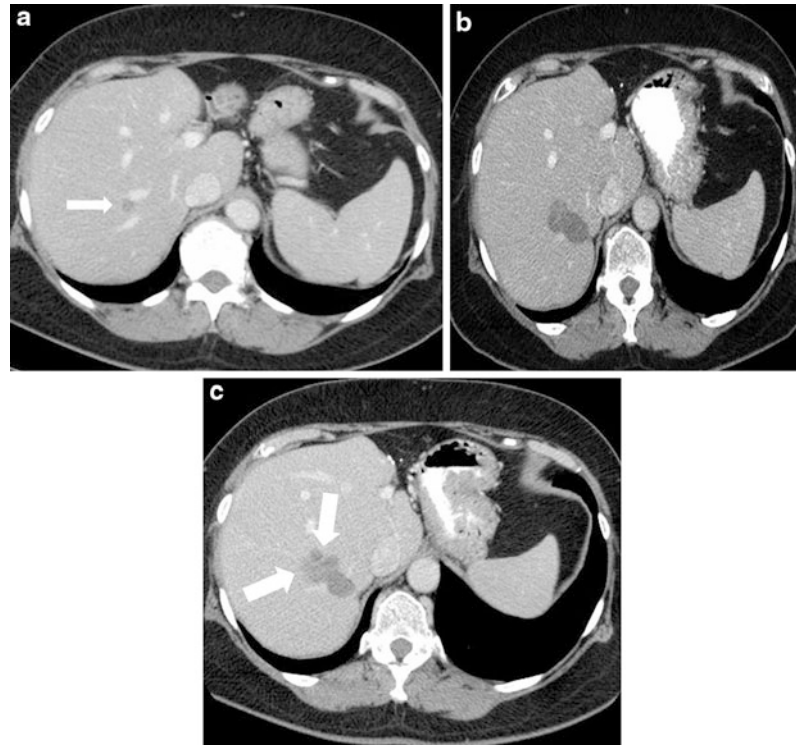

Fig. 4.6 Post-ablation recurrence. CT image demonstrates a small low-attenuation tumor in the right lobe between branches of the right hepatic vein (*arrow*) (**a**). Image obtained post-ablation shows a bilobed low-attenuation ablation zone (**b**). Follow-up imaging demonstrates gradual enlargement of the ablation zone with irregular tentacular margins (*arrows*) (**c**) consistent with recurrent disease

Liver

Hepatic tumors can be divided into primary hepatic neoplasms and metastatic disease. Hepatocellular carcinoma (HCC) accounts for the majority of primary hepatic malignancies, with steadily increasing incidence due to increases in hepatitis B and C infection [59, 60]. These patients often develop synchronous or metachronous sites of disease due to the field effect of chronic liver disease [61].

Colon cancer is the most common metastatic liver tumor, and because of the pattern of portal blood flow, the liver may be the only site of metastatic disease. Other metastatic liver tumors such as melanoma, carcinoid, sarcoma, renal cell carcinoma, and pancreatic adenocarcinoma are highly associated with systemic spread which may make locoregional therapies less effective [62]. Therefore, the focus of this discussion is metastatic colorectal cancer, although occasionally there will be times when the ablation of other metastatic malignancies is appropriate.

Hepatocellular Carcinoma

The preferred and only truly curative treatment for hepatocellular carcinoma in patients with limited disease is hepatic transplant when possible [63, 64]. However, many patients are not eligible for transplant or may have a prolonged wait time prior to a transplant, and for these patients, resection or locoregional therapy should be considered. Many of these patients are not eligible for hepatic resection due to limited hepatic reserve, proximity of the tumor to major intrahepatic vessels, or high surgical risk. In these cases, locoregional or liver-directed therapies including ablation or intra-arterial therapy such as transarterial chemoembolization, bland embolization, or radio embolization are preferred. Given the range of treatment options available, involvement of a multispecialty group is critical to selecting the best possible treatment for each patient.

Ablation is generally the locoregional treatment of choice for small tumors less than 3 cm, as complete cellular necrosis can be consistently

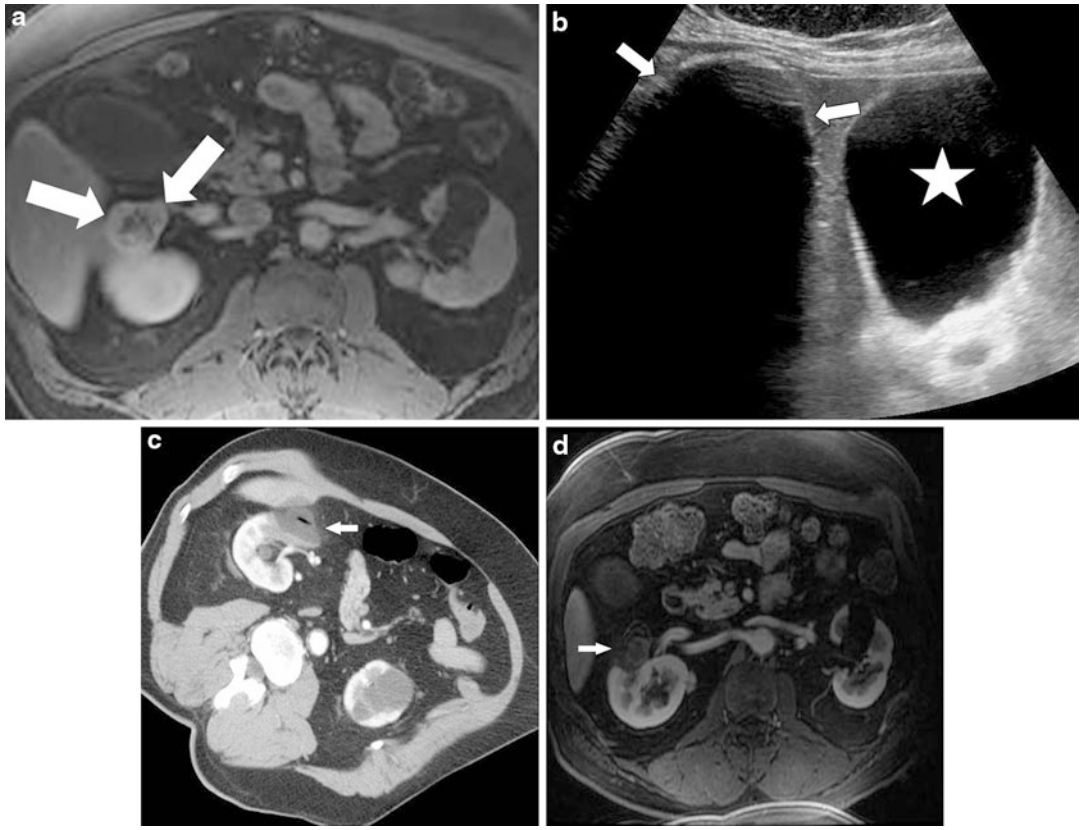

Fig. 4.7 Anterior renal tumor. T1 post-contrast MRI image demonstrates a peripherally enhancing anterior renal mass (*arrows*) (**a**). Ultrasound image obtained during ablation demonstrates the echogenic ice ball (*arrows*) adjacent to the gallbladder (*star*) (**b**). Probe retraction aided in maintaining a safe distance from the gallbladder. Nonenhancing ablation zone seen on the immediate post-ablation CT scan (**c**) and on 3-month post-contrast MRI follow-up imaging (*arrow*) (**d**)

achieved with minimal complications [65]. However, in the setting of liver disease, heat-based thermal ablation modalities such as RF are preferred over cryoablation. This is related to the cautery effect of heat which decreases the risk of bleeding in these patients who are often coagulopathic, the susceptibility of these patients to post-ablation systemic effects, and the ability to take advantage of the "oven effect" associated with ablating an HCC in a cirrhotic liver [66]. If a tumor is closely adjacent to the biliary tree, then chemical ablation with an agent such as ethanol may be preferred.

Metastatic Disease

Cryoablation is most likely to be of benefit in patients with colorectal metastases and a small subset of patients with relatively indolent non-colorectal metastases such as breast cancer, neuroendocrine tumors, or indolent renal cell carcinoma. Ablative therapy has been shown to increase survival in these patients [67–69].

Surgical resection is considered first-line therapy in eligible patients with hepatic metastatic colorectal cancer, and several series have demonstrated mean 5-year survivals of 32–58 % [70–73], much better than the dismal outcomes in the 80 % of patients who are not eligible for surgical resection [74, 75]. Systemic chemotherapy with current regimens has a mean survival of 16–20 months, which can be improved beyond 24 months with the addition of angiogenesis inhibitors [76–78]. Given the success of surgery, it makes sense that ablation should be able to

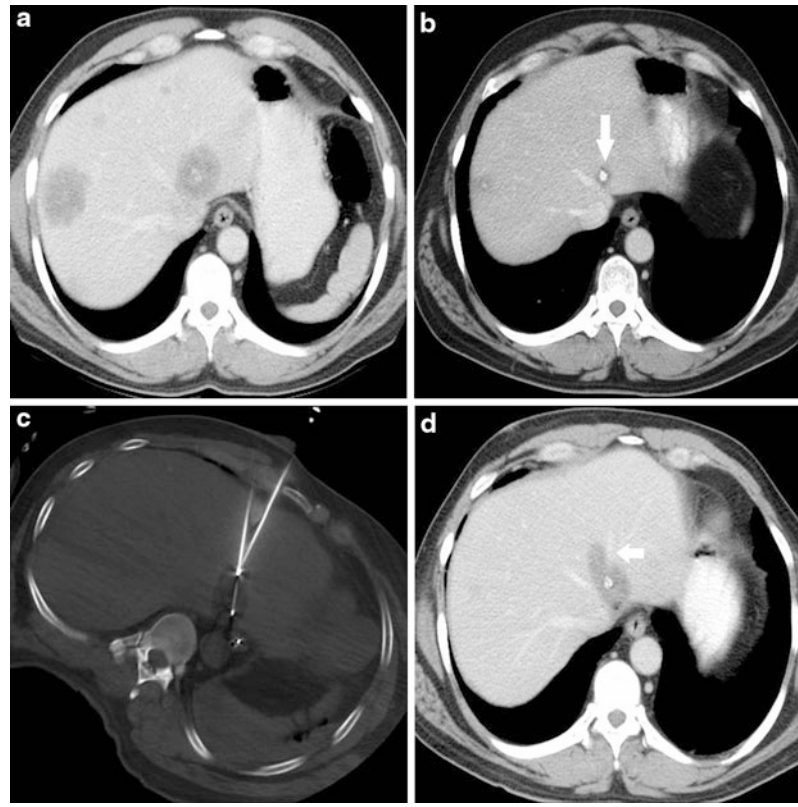

Fig. 4.8 Hepatic colorectal metastatic disease. CT image from a young patient with newly diagnosed colorectal cancer demonstrates multiple large low-attenuation tumors (**a**). These tumors show interval decrease in size and central calcification with chemotherapy (**b**). Given the response and the location of the majority of the tumors in the right lobe, the patient was felt to be a candidate for right hepatectomy. However, a single tumor was present in the left hepatic lobe near the left hepatic vein (*arrow*, **b**). This tumor was treated with cryoablation (**c**), with stable ablation zone posttreatment (**d**), prior to proceeding with surgery. Note the cold sink effect, causing indentation on the ablation zone (*arrow*), due to the left hepatic vein

achieve comparable results if all sites of disease can be controlled. Another role for ablation is in combination with surgery (i.e., ablation of a tumor in the left lobe of a patient undergoing right hepatectomy) (Fig. 4.8). Ablation is generally contraindicated in patients with uncontrolled extrahepatic disease.

As with renal tumors, tumors less than 4 cm in size are the best targets for ablation, with increased risk of local recurrence in larger tumors [79]. Ablation of metastatic disease requires a 1-cm "surgical" treatment margin to be confident of a complete treatment. Although an increase in the number of tumors treated has not been shown to increase risk of recurrence [80], there is a limit to the number of tumors that can be safely treated in one session. Treatment of a larger tumor or more numerous tumors may be indicated in a patient who is symptomatic from metastatic neuroendocrine malignancy. Tumor debulking in these cases may improve symptom control.

Lung

Cryoablation has been utilized for the treatment of primary non-resectable lung cancer as well as pulmonary metastatic tumors (Fig. 4.9). However, relatively limited data is available due to small sample sizes and short follow-up periods. Studies have shown that it is easier to achieve a technically successful treatment with smaller (3 cm or less) and more peripheral tumors, but even large, central tumors can be successfully treated with appropriate technique [81]. There is some evidence to suggest that a triple freeze-thaw technique may be helpful in the lung [82]. The primary theoretical advantage of a triple freeze is that the initial freezes are associated with alveolar pulmonary hemorrhage, which results in improved thermal conductivity (fluid vs. air) as well as decreased aeration of the target portion of the lung and thus less ventilation-mediated cooling. However, note that this has not been validated in human lung tumors.

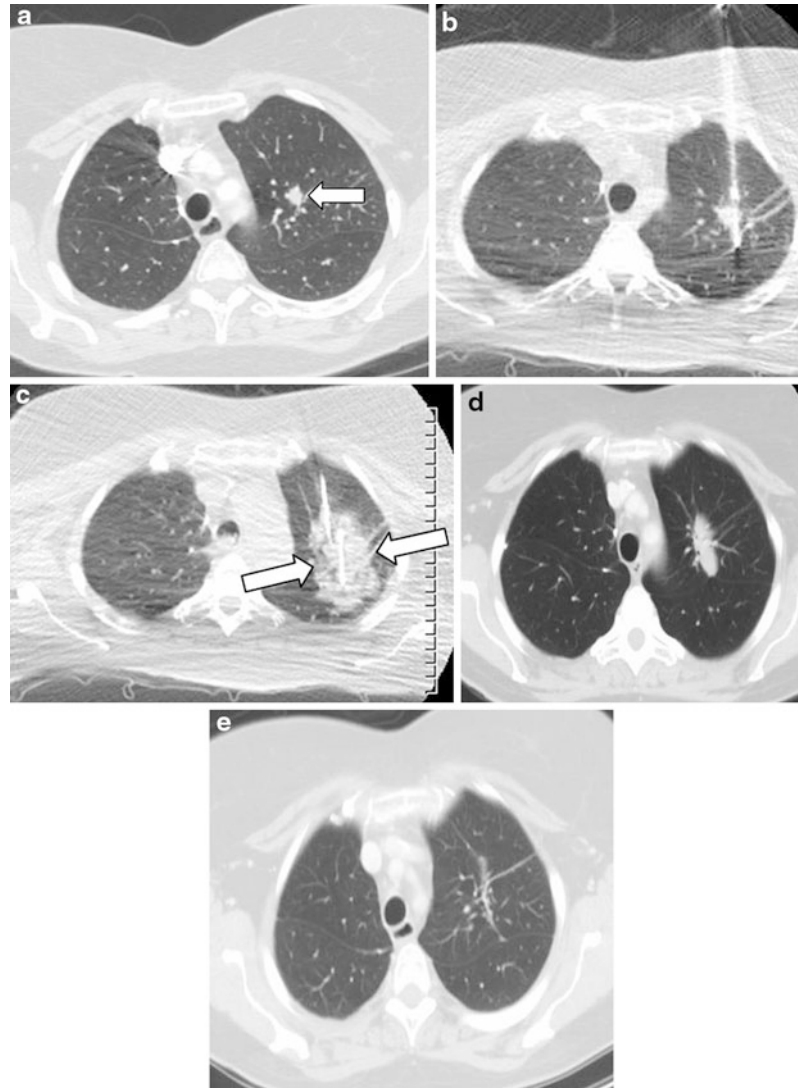

Fig. 4.9 Metastatic colorectal cancer to the lung. CT image demonstrates a small pulmonary nodule in a patient with known colorectal cancer metastatic disease (*arrow*) (**a**). This was treated with two cryoprobes (**b**) and multiple freeze cycles producing surrounding hemorrhage (*arrows*) (**c**). Follow-up imaging over time demonstrates gradual regression of the ablation zone (**d**, **e**)

Bone

Painful skeletal metastases are a common problem for cancer patients. External beam radiation is considered the standard of care for cancer patients with localized bone pain. However, it is associated with very high expense, a significant side effect profile, and may not control symptoms [83, 84]. As a result, there has been an interest in developing other treatments for this problem, and percutaneous ablation has shown significant promise even in patient's refractory to other therapies [85, 86]. Skeletal metastatic disease at risk for impending fracture may be treated surgically with internal fixation [86].

Ablation works best in patients with moderate to severe pain, localized to one or two sites. Patients with diffuse metastatic disease are better served with systemic therapies rather than a focal approach. Osteolytic, mixed osteolytic-osteoblastic, or primarily soft tissue tumors respond best (Fig. 4.10), while osteoblastic tumors are more difficult to treat. The tumor should be accessible percutaneously and be safely distant from

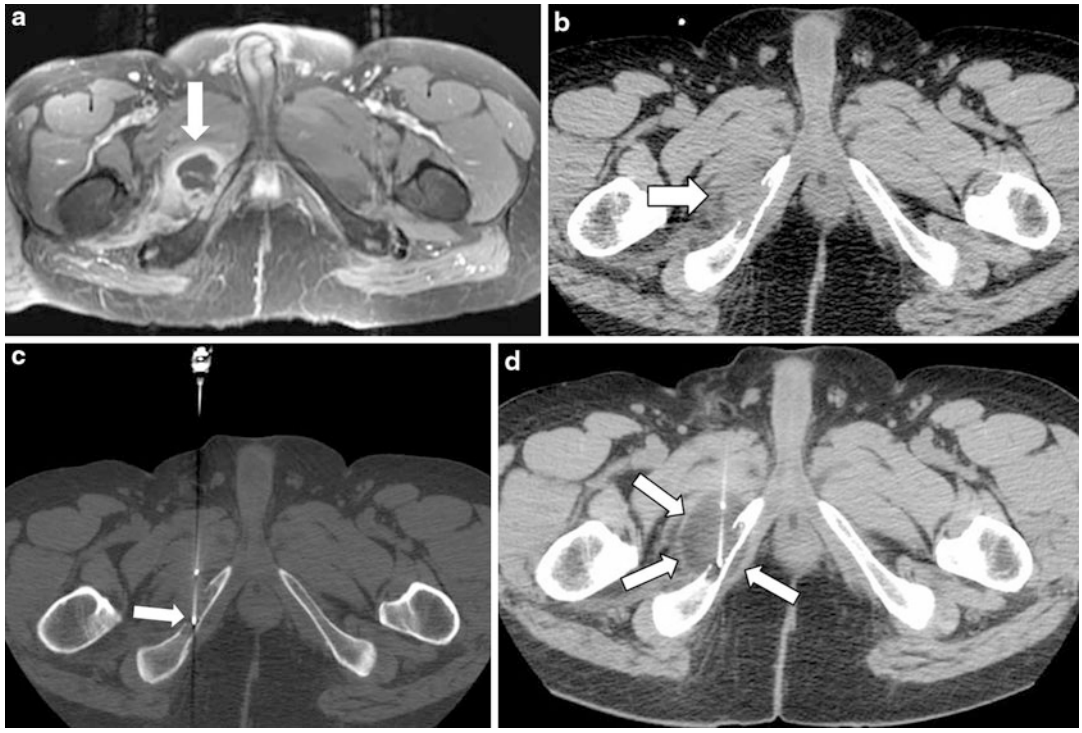

Fig. 4.10 Cryoablation of osseous metastatic disease in a patient with metastatic chordoma. T1 post-contrast MR image of the pelvis demonstrates an osseous tumor with a rim-enhancing soft tissue component (*arrow*) (**a**). CT image (**b**) redemonstrates the tumor, with a lytic osseous component (*arrow*) (**b**). Given that this tumor was quite painful, it was treated with cryoablation, with placement of two probes, one of which is seen on this non-contrast CT image (*arrow*) (**c**). Generation of the low-attenuation ice ball is seen to encompass the tumor (*arrows*) (**d**)

the spinal cord, major nerves, artery of Adamkiewicz, and other vulnerable structures previously discussed [83].

During probe placement, particular attention should be pain to the bone-tumor interface. Probes are often placed in parallel along the long axis of the tumor. Probe spacing is similar to that used in the liver and kidney. Shorter or longer freeze times may be used, depending on the tumor coverage. As with the other organs discussed, the precision of ablation zone sculpting and the ease of ablation zone monitoring using ice give it an advantage over heat-based modalities in the treatment of these tumors, particularly when the tumor is adjacent to vulnerable structures or larger than 5 cm. In addition, patients treated with cryoablation may experience more rapid pain relief than those treated with heat-based modalities [83].

Although some primary bone tumors have been treated with cryoablation, often in combination with a surgical approach, ablation is not generally indicated in this setting [87–90]. Benign bone tumors such as osteoid osteomas can also be treated with cryoablation [91], although RFA is the preferred modality for treatment [92].

Other Applications

A developing indication for cryoablation is pain relief in patients with post-thoracotomy pain syndrome and chronic inguinal pain from the genitofemoral nerve. In this setting, selective cryoablation of the offending nerves has been used to effectively and safely relieve pain symptoms [93–95].

In addition, cryoablation has been applied to a variety of other applications including treatment of prostate cancers where there is actually a fairly robust clinical experience [96–105], focal breast tumors, especially fibroadenomas [106, 107], fibroids, endometrial pathologies [108–110], and primary and metastatic extrahepatic tumors in the abdomen and pelvis [111–113].

Complications

Risks of cryoablation can be divided into those that are inherent to any percutaneous ablation modality and those that are specific to cryoablation. The rate of procedure-related mortality is low, with one pooled review documenting 1.6 % mortality rate in 869 patients from different series [114]. The most common cause of periprocedural mortality in this review was acute myocardial infarction. Certain complications may be organ specific, and risks may vary given the proximity of the tumor being treated to adjacent vulnerable structures.

Hemorrhage

Post-procedure hemorrhage is a possibility with almost any percutaneous ablation procedure. The risk may be higher when working in vascular organs, such as the lung, liver, or kidney, or when working in coagulopathic patients. In patients with cirrhosis and poor associated hepatic function, the relative decrease in clotting factors can lead to significantly increased risk of hemorrhage. Cryoablation has traditionally been considered to have a higher risk of hemorrhage than the heat-based ablation modalities, and there probably is a subtle increased risk of bleeding; however, experimental evaluation in a non-cirrhotic porcine model failed to demonstrate a significant difference between cryoablation and RF ablation [58]. Several large clinical series have demonstrated the risk for major hemorrhage to be less than 5 % [114, 115]. Capsular cracking has been described in the liver and kidney, which may be related to the mechanical stress imposed by the rapid freeze-thaw cycle. This is a rare event, but when it occurs, it can lead to massive, rapid blood loss [116]. Fortunately, post-ablation hemorrhage is usually self-limited and can be treated with blood transfusions and factor replacement in most cases.

Abscess

Cryoablation creates a pocket of necrotic tissue, which can be susceptible to infection. However, the rate of abscess formation is low, and those who develop an abscess often have identifiable risk factors. In the liver, patients with history of a biliary procedure that compromises the sphincter of Oddi (sphincterotomy, biliary stent, or biliary enteric anastomosis) are at increased risk of infection [117]. This is presumably due to colonization of the biliary system by gastrointestinal flora with retrograde infection of the ablation zone. There is a high likelihood (up to 50 % even with prophylactic antibiotics) that an abscess will develop in these patients, and it may require treatment with percutaneous drainage [118]. Prophylactic dose of a first-generation cephalosporin (or alternative such as clindamycin in patients with allergy) immediately prior to ablation can be performed to treat skin flora.

Tumor Lysis Syndrome (Cryoshock)

Cryoshock is a potentially fatal tumor lysis syndrome that is unique to cryoablation. Because cryoablation does not cauterize vessels in the ablation zone, the necrotic contents of the ablation zone are exposed to the systemic circulation. This can lead to a systemic inflammatory response which can result in severe coagulopathy, thrombocytopenia, disseminated intravascular coagulation, shock, lung injury, and multisystem organ failure [119]. This is an uncommon complication, seen in less than 1 % of patients, and appears to be related to the volume of tissue cryoablated [120].

Tumor Seeding

Tumor seeding is a potential concern with any percutaneous intervention on malignant tumors, including biopsy, RF, and cryoablation. However, the risk is exceedingly low, approximately 0.5 % for RFA in several large case series [121, 122] and lower than the risk of tumor seeding during open resection [123–125]. Subcapsular or peripheral tumors with little overlying normal parenchyma are at greater risk of tumor seeding. The risk increases with larger probes and multiple punctures.

Post-ablation Syndrome

Post-ablation syndrome is a well-described collection of symptoms that occur in the post-ablation period. Symptoms generally start 48–72 h post-ablation, last up to 5 days, and include low-grade fever, malaise, chills, nausea, and delayed pain [126]. The exact underlying mechanism is unknown, but it is thought to be a milder version of the systemic inflammatory response that produces cryoshock [119]. These symptoms should not be confused with infection or developing abscess unless the fever is high grade and persists beyond 10 days or the patient has other associated risk factors or symptoms.

Nontarget Ablation

A risk of all ablation procedures is extension of the ablation zone into adjacent vulnerable structures. In the liver, the primary structures at risk include the central biliary tree, gallbladder, stomach, and large bowel. If small peripheral biliary ducts are involved in the ablation zone, there is an approximately 3 % risk of biloma development [120], and if the central ducts are involved, this may lead to stricture or obstruction, although less frequently than with heat-based ablation modalities [127, 128]. In the kidney, the collecting system and ureter are at risk, although once again, cryoablation has been suggested to be less damaging to the renal collecting system than heat [56]. It appears safe to perform ablations that involve the calyceal system, but if the central renal collecting system or ureter is in close proximity to the ice ball, stent placement and pyeloperfusion can be considered [53, 54, 129].

Ablation of the adrenal gland, either purposeful or nontarget as can be seen with treatment of upper pole renal tumors, can produce malignant hypertension during thawing [130]. Therefore, when adrenal freezing is possible, an arterial line can be placed for close monitoring of the blood pressure and pretreatment with alpha-adrenergic blocking medications (i.e., phenoxybenzamine) can be considered. If the patient has not been pretreated and becomes hypertensive during the thaw, a repeat freeze will often halt the hypertensive crisis so that the patient can be medicated with alpha-blockers prior to reinitiating the thaw. One group describes development of Takotsubo syndrome as a result of this adrenergic outpouring [131].

Caution must be used around the bowel, as transmural freezing can lead to perforation, infection, and even death [132]. Ablation zones involving the pancreas could induce pancreatitis. These structures may be protected using hydrodissection, probe leverage or retraction, and patient positioning [45–48, 51, 133, 134].

Conclusion

Tumor ablation is a minimally invasive technique that is becoming increasingly utilized in the treatment of malignant and benign conditions. Multiple modalities are available to perform ablation, including chemical or thermal, which can be further divided into heat and cold. Each ablation modality has particular strengths and weaknesses, which the practitioner should be aware of prior to performing these procedures. Cryoablation allows precise sculpting and monitoring of the ice ball. In addition, multiple probes can be used to generate large treatment zones when needed. Cryoablation lacks the natural cautery effect seen with heat-based modalities, may be more time consuming and expensive than heat-based ablation, can lead to cryoshock in the setting

of large volume ablations, and has reimbursement challenges related to a lack of percutaneous CPT (Current Procedural Terminology) codes for use in the bone, lung, and liver. Given the spectrum of treatment options available to these patients, cases should ideally be reviewed at a multidisciplinary conference where tumor size, location, histology, and associated comorbidities are considered. Cryoablation can be utilized for most patients being treated with ablation therapy but is particularly advantageous for the treatment of tumors >5 cm, tumors in a location requiring a high degree of precision, tumors adjacent to large vessels, and tumors ablated in the operating room. In this chapter, we have reviewed the indications, technique, and management of patients undergoing cryoablation.

Cross-References

- ▶ Breast Ablation for Breast Imagers and Interventional Radiologists
- ▶ Cryoablation of Bone Tumors
- ▶ Cryoablation of Liver Tumors
- ▶ Percutaneous Interventional Radiology: The Lung
- ▶ Percutaneous Renal Cryoablation

References

1. Hoffmann NE, Bischof JC. The cryobiology of cryosurgical injury. Urology. 2002;60(2 Suppl 1):40–9.
2. Cooper SM, Dawber RP. The history of cryosurgery. J R Soc Med. 2001;94(4):196–201.
3. Rupp CC, Hoffmann NE, Schmidlin FR, Swanlund DJ, Bischof JC, Coad JE. Cryosurgical changes in the porcine kidney: histologic analysis with thermal history correlation. Cryobiology. 2002;45(2):167–82.
4. Rubinsky B, Lee CY, Bastacky J, Onik G. The process of freezing and the mechanism of damage during hepatic cryosurgery. Cryobiology. 1990;27(1):85–97.
5. Weber SM, Lee Jr FT, Warner TF, Chosy SG, Mahvi DM. Hepatic cryoablation: US monitoring of extent of necrosis in normal pig liver. Radiology. 1998; 207(1):73–7.
6. Zacarian SA. The observation of freeze-thaw cycles upon cancer-cell suspensions. J Dermatol Surg Oncol. 1977;3(2):173–4.
7. Wang H, Littrup PJ, Duan Y, Zhang Y, Feng H, Nie Z. Thoracic masses treated with percutaneous cryotherapy: initial experience with more than 200 procedures. Radiology. 2005;235(1):289–98.
8. Badwan K, Maxwell K, Venkatesh R, et al. Comparison of laparoscopic and percutaneous cryoablation of renal tumors: a cost analysis. J Endourol. 2008;22(6):1275–7.
9. Bandi G, Hedican S, Moon T, Lee FT, Nakada SY. Comparison of postoperative pain, convalescence, and patient satisfaction after laparoscopic and percutaneous ablation of small renal masses. J Endourol. 2008;22(5):963–7.
10. Finley DS, Beck S, Box G, et al. Percutaneous and laparoscopic cryoablation of small renal masses. J Urol. 2008;180(2):492–8. discussion 8.
11. Hinshaw JL, Shadid AM, Nakada SY, Hedican SP, Winter 3rd TC, Lee Jr FT. Comparison of percutaneous and laparoscopic cryoablation for the treatment of solid renal masses. AJR Am J Roentgenol. 2008;191(4):1159–68.
12. Hui GC, Tuncali K, Tatli S, Morrison PR, Silverman SG. Comparison of percutaneous and surgical approaches to renal tumor ablation: metaanalysis of effectiveness and complication rates. J Vasc Interv Radiol. 2008;19(9):1311–20.
13. Cervone A, Sardi A, Conaway GL. Intraoperative ultrasound (IOUS) is essential in the management of metastatic colorectal liver lesions. Am Surg. 2000;66(7):611–5.
14. Leen E, Ceccotti P, Moug SJ, et al. Potential value of contrast-enhanced intraoperative ultrasonography during partial hepatectomy for metastases: an essential investigation before resection? Ann Surg. 2006;243(2):236–40.
15. Silverman SG, Tuncali K, Adams DF, et al. MR imaging-guided percutaneous cryotherapy of liver tumors: initial experience. Radiology. 2000;217(3): 657–64.
16. Lee Jr FT, Chosy SG, Littrup PJ, Warner TF, Kuhlman JE, Mahvi DM. CT-monitored percutaneous cryoablation in a pig liver model: pilot study. Radiology. 1999;211(3):687–92.
17. Littrup PJ, Jallad B, Vorugu V, et al. Lethal isotherms of cryoablation in a phantom study: effects of heat load, probe size, and number. J Vasc Interv Radiol. 2009;20(10):1343–51.
18. Auge BK, Santa-Cruz RW, Polascik TJ. Effect of freeze time during renal cryoablation: a swine model. J Endourol. 2006;20(12):1101–5.
19. Silverman SG, Tuncali K, van Sonnenberg E, et al. Renal tumors: MR imaging-guided percutaneous cryotherapy–initial experience in 23 patients. Radiology. 2005;236(2):716–24.
20. Silverman SG, Sun MR, Tuncali K, et al. Three-dimensional assessment of MRI-guided percutaneous cryotherapy of liver metastases. AJR Am J Roentgenol. 2004;183(3):707–12.
21. Neel 3rd HB, Ketcham AS, Hammond WG. Requisites for successful cryogenic surgery of cancer. Arch Surg. 1971;102(1):45–8.

22. Mala T, Edwin B, Tillung T, Kristian Hol P, Soreide O, Gladhaug I. Percutaneous cryoablation of colorectal liver metastases: potentiated by two consecutive freeze-thaw cycles. Cryobiology. 2003;46(1):99–102.
23. Robinson D, Halperin N, Nevo Z. Two freezing cycles ensure interface sterilization by cryosurgery during bone tumor resection. Cryobiology. 2001;43(1):4–10.
24. Woolley ML, Schulsinger DA, Durand DB, Zeltser IS, Waltzer WC. Effect of freezing parameters (freeze cycle and thaw process) on tissue destruction following renal cryoablation. J Endourol. 2002; 16(7):519–22.
25. Cooper IS, Hirose T. Application of cryogenic surgery to resection of parenchymal organs. N Engl J Med. 1966;274(1):15–8.
26. Allaf ME, Varkarakis IM, Bhayani SB, Inagaki T, Kavoussi LR, Solomon SB. Pain control requirements for percutaneous ablation of renal tumors: cryoablation versus radiofrequency ablation–initial observations. Radiology. 2005;237(1):366–70.
27. Kuszyk BS, Choti MA, Urban BA, et al. Hepatic tumors treated by cryosurgery: normal CT appearance. AJR Am J Roentgenol. 1996;166(2):363–8.
28. McLoughlin RF, Saliken JF, McKinnon G, Wiseman D, Temple W. CT of the liver after cryotherapy of hepatic metastases: imaging findings. AJR Am J Roentgenol. 1995;165(2):329–32.
29. Dromain C, de Baere T, Elias D, et al. Hepatic tumors treated with percutaneous radio-frequency ablation: CT and MR imaging follow-up. Radiology. 2002; 223(1):255–62.
30. Goldberg SN, Charboneau JW, Dodd 3rd GD, et al. Image-guided tumor ablation: proposal for standardization of terms and reporting criteria. Radiology. 2003;228(2):335–45.
31. Goldberg SN, Grassi CJ, Cardella JF, et al. Image-guided tumor ablation: standardization of terminology and reporting criteria. Radiology. 2005;235(3): 728–39.
32. Atwell TD, Farrell MA, Leibovich BC, et al. Percutaneous renal cryoablation: experience treating 115 tumors. J Urol. 2008;179(6):2136–40. discussion 40–1.
33. Breen DJ, Rutherford EE, Stedman B, et al. Management of renal tumors by image-guided radiofrequency ablation: experience in 105 tumors. Cardiovasc Intervent Radiol. 2007;30(5):936–42.
34. Gervais DA, McGovern FJ, Arellano RS, McDougal WS, Mueller PR. Radiofrequency ablation of renal cell carcinoma: part 1, Indications, results, and role in patient management over a 6-year period and ablation of 100 tumors. AJR Am J Roentgenol. 2005; 185(1):64–71.
35. Gill IS, Remer EM, Hasan WA, et al. Renal cryoablation: outcome at 3 years. J Urol. 2005; 173(6):1903–7.
36. Littrup PJ, Ahmed A, Aoun HD, et al. CT-guided percutaneous cryotherapy of renal masses. J Vasc Interv Radiol. 2007;18(3):383–92.
37. Malcolm JB, Berry TT, Williams MB, et al. Single center experience with percutaneous and laparoscopic cryoablation of small renal masses. J Endourol. 2009;23(6):907–11.
38. Mayo-Smith WW, Dupuy DE, Parikh PM, Pezzullo JA, Cronan JJ. Imaging-guided percutaneous radiofrequency ablation of solid renal masses: techniques and outcomes of 38 treatment sessions in 32 consecutive patients. AJR Am J Roentgenol. 2003; 180(6):1503–8.
39. Park S, Anderson JK, Matsumoto ED, Lotan Y, Josephs S, Cadeddu JA. Radiofrequency ablation of renal tumors: intermediate-term results. J Endourol. 2006;20(8):569–73.
40. Zagoria RJ, Traver MA, Werle DM, Perini M, Hayasaka S, Clark PE. Oncologic efficacy of CT-guided percutaneous radiofrequency ablation of renal cell carcinomas. AJR Am J Roentgenol. 2007;189(2):429–36.
41. Atwell TD, Farrell MA, Callstrom MR, et al. Percutaneous cryoablation of 40 solid renal tumors with US guidance and CT monitoring: initial experience. Radiology. 2007;243(1):276–83.
42. Gupta A, Allaf ME, Kavoussi LR, et al. Computerized tomography guided percutaneous renal cryoablation with the patient under conscious sedation: initial clinical experience. J Urol. 2006; 175(2):447–52. discussion 52–3.
43. Atwell TD, Farrell MA, Callstrom MR, et al. Percutaneous cryoablation of large renal masses: technical feasibility and short-term outcome. AJR Am J Roentgenol. 2007;188(5):1195–200.
44. Frank I, Blute ML, Cheville JC, Lohse CM, Weaver AL, Zincke H. Solid renal tumors: an analysis of pathological features related to tumor size. J Urol. 2003;170(6 Pt 1):2217–20.
45. Allaf ME, Lang E. Bowel separation before percutaneous renal cryoablation. J Urol. 2008; 180(2):721.
46. Arellano RS, Garcia RG, Gervais DA, Mueller PR. Percutaneous CT-guided radiofrequency ablation of renal cell carcinoma: efficacy of organ displacement by injection of 5% dextrose in water into the retroperitoneum. AJR Am J Roentgenol. 2009; 193(6):1686–90.
47. Farrell MA, Charboneau JW, Callstrom MR, Reading CC, Engen DE, Blute ML. Paranephric water instillation: a technique to prevent bowel injury during percutaneous renal radiofrequency ablation. AJR Am J Roentgenol. 2003;181(5):1315–7.
48. Ginat DT, Saad W, Davies M, Walman D, Erturk E. Bowel displacement for CT-guided tumor radiofrequency ablation: techniques and anatomic considerations. J Endourol. 2009;23(8):1259–64.
49. Lee SJ, Choyke LT, Locklin JK, Wood BJ. Use of hydrodissection to prevent nerve and muscular damage during radiofrequency ablation of kidney tumors. J Vasc Interv Radiol. 2006; 17(12):1967–9.

50. Park BK, Kim CK. Complications of image-guided radiofrequency ablation of renal cell carcinoma: causes, imaging features and prevention methods. Eur Radiol. 2009;19(9):2180–90.
51. Park BK, Kim SH, Byun JY, Kim YS, Kwon GY, Jang IS. CT-guided instillation of 5% dextrose in water into the anterior pararenal space before renal radiofrequency ablation in a porcine model: positive and negative effects. J Vasc Interv Radiol. 2007;18(12):1561–9.
52. DeBenedectis CM, Beland MD, Dupuy DE, Mayo-Smith WW. Utility of iodinated contrast medium in hydrodissection fluid when performing renal tumor ablation. J Vasc Interv Radiol. 2010;21(5):745–7.
53. Cantwell CP, Wah TM, Gervais DA, et al. Protecting the ureter during radiofrequency ablation of renal cell cancer: a pilot study of retrograde pyeloperfusion with cooled dextrose 5% in water. J Vasc Interv Radiol. 2008;19(7):1034–40.
54. Wah TM, Koenig P, Irving HC, Gervais DA, Mueller PR. Radiofrequency ablation of a central renal tumor: protection of the collecting system with a retrograde cold dextrose pyeloperfusion technique. J Vasc Interv Radiol. 2005;16(11):1551–5.
55. Kunkle DA, Uzzo RG. Cryoablation or radiofrequency ablation of the small renal mass: a meta-analysis. Cancer. 2008;113(10):2671–80.
56. Sung GT, Gill IS, Hsu TH, et al. Effect of intentional cryo-injury to the renal collecting system. J Urol. 2003;170(2 Pt 1):619–22.
57. Georgiades CS, Hong K, Bizzell C, Geschwind JF, Rodriguez R. Safety and efficacy of CT-guided percutaneous cryoablation for renal cell carcinoma. J Vasc Interv Radiol. 2008;19(9):1302–10.
58. Shock SA, Laeseke PF, Sampson LA, et al. Hepatic hemorrhage caused by percutaneous tumor ablation: radiofrequency ablation versus cryoablation in a porcine model. Radiology. 2005;236(1):125–31.
59. Davila JA, Morgan RO, Shaib Y, McGlynn KA, El-Serag HB. Hepatitis C infection and the increasing incidence of hepatocellular carcinoma: a population-based study. Gastroenterology. 2004;127(5): 1372–80.
60. El-Serag HB, Mason AC. Rising incidence of hepatocellular carcinoma in the United States. N Engl J Med. 1999;340(10):745–50.
61. Winter TC, Laeseke PF, Lee Jr FT. Focal tumor ablation: a new era in cancer therapy. Ultrasound Q. 2006;22(3):195–217.
62. Cagol PP, Pasqual E, Bacchetti S. Natural history of the neoplastic locoregional disease: clinical and pathological patterns. J Exp Clin Cancer Res. 2003;22(4 Suppl):1–4.
63. Duffy JP, Vardanian A, Benjamin E, et al. Liver transplantation criteria for hepatocellular carcinoma should be expanded: a 22-year experience with 467 patients at UCLA. Ann Surg. 2007;246(3):502–9. discussion 9–11.
64. Baccarani U, Benzoni E, Adani GL, et al. Superiority of transplantation versus resection for the treatment of small hepatocellular carcinoma. Transplant Proc. 2007;39(6):1898–900.
65. Komorizono Y, Oketani M, Sako K, et al. Risk factors for local recurrence of small hepatocellular carcinoma tumors after a single session, single application of percutaneous radiofrequency ablation. Cancer. 2003;97(5):1253–62.
66. Livraghi T, Goldberg SN, Lazzaroni S, Meloni F, Solbiati L, Gazelle GS. Small hepatocellular carcinoma: treatment with radio-frequency ablation versus ethanol injection. Radiology. 1999;210(3): 655–61.
67. Lawes D, Chopada A, Gillams A, Lees W, Taylor I. Radiofrequency ablation (RFA) as a cytoreductive strategy for hepatic metastasis from breast cancer. Ann R Coll Surg Engl. 2006;88(7):639–42.
68. Livraghi T, Goldberg SN, Solbiati L, Meloni F, Ierace T, Gazelle GS. Percutaneous radio-frequency ablation of liver metastases from breast cancer: initial experience in 24 patients. Radiology. 2001;220(1): 145–9.
69. Alseidi A, Helton WS, Espat NJ. Does the literature support an indication for hepatic metastasectomy other than for colorectal primary? J Gastrointest Surg. 2006;10(1):99–104.
70. Ahmad A, Chen SL, Bilchik AJ. Role of repeated hepatectomy in the multimodal treatment of hepatic colorectal metastases. Arch Surg. 2007;142(6): 526–31. discussion 31–2.
71. Ravikumar TS, Kane R, Cady B, Jenkins R, Clouse M, Steele Jr G. A 5-year study of cryosurgery in the treatment of liver tumors. Arch Surg. 1991;126(12): 1520–3. discussion 3–4.
72. Tuttle TM, Curley SA, Roh MS. Repeat hepatic resection as effective treatment of recurrent colorectal liver metastases. Ann Surg Oncol. 1997;4(2): 125–30.
73. Pawlik TM, Choti MA. Surgical therapy for colorectal metastases to the liver. J Gastrointest Surg. 2007;11(8):1057–77.
74. Stangl R, Altendorf-Hofmann A, Charnley RM, Scheele J. Factors influencing the natural history of colorectal liver metastases. Lancet. 1994;343(8910): 1405–10.
75. Ballantyne GH, Quin J. Surgical treatment of liver metastases in patients with colorectal cancer. Cancer. 1993;71(12 Suppl):4252–66.
76. Aggarwal S, Chu E. Current therapies for advanced colorectal cancer. Oncology (Williston Park). 2005;19(5):589–95.
77. Goldberg RM. Advances in the treatment of metastatic colorectal cancer. Oncologist. 2005;10(Suppl 3):40–8.
78. Emmanouilides C, Sfakiotaki G, Androulakis N, et al. Front-line bevacizumab in combination with oxaliplatin, leucovorin and 5-fluorouracil (FOLFOX) in patients with metastatic colorectal cancer: a multicenter phase II study. BMC Cancer. 2007;7:91.

79. Adam R, Akpinar E, Johann M, Kunstlinger F, Majno P, Bismuth H. Place of cryosurgery in the treatment of malignant liver tumors. Ann Surg. 1997;225(1): 39–8. discussion 48–50.
80. Seifert JK, Morris DL. Indicators of recurrence following cryotherapy for hepatic metastases from colorectal cancer. Br J Surg. 1999;86(2):234–40.
81. Choe YH, Kim SR, Lee KS, et al. The use of PTC and RFA as treatment alternatives with low procedural morbidity in non-small cell lung cancer. Eur J Cancer. 2009;45(10):1773–9.
82. Permpongkosol S, Nicol TL, Link RE, et al. Differences in ablation size in porcine kidney, liver, and lung after cryoablation using the same ablation protocol. AJR Am J Roentgenol. 2007;188(4):1028–32.
83. Callstrom MR, Kurup AN. Percutaneous ablation for bone and soft tissue metastases–why cryoablation? Skeletal Radiol. 2009;38(9):835–9.
84. Tong D, Gillick L, Hendrickson FR. The palliation of symptomatic osseous metastases: final results of the Study by the Radiation Therapy Oncology Group. Cancer. 1982;50(5):893–9.
85. Callstrom MR, Charboneau JW. Image-guided palliation of painful metastases using percutaneous ablation. Tech Vasc Interv Radiol. 2007;10(2):120–31.
86. Callstrom MR, Charboneau JW, Goetz MP, et al. Image-guided ablation of painful metastatic bone tumors: a new and effective approach to a difficult problem. Skeletal Radiol. 2006;35(1):1–15.
87. Lessard AM, Gilchrist J, Schaefer L, Dupuy DE. Palliation of recurrent Ewing sarcoma of the pelvis with cryoablation and somatosensory-evoked potentials. J Pediatr Hematol Oncol. 2009;31(1):18–21.
88. Meller I, Weinbroum A, Bickels J, et al. Fifteen years of bone tumor cryosurgery: a single-center experience of 440 procedures and long-term follow-up. Eur J Surg Oncol. 2008;34(8):921–7.
89. Souna BS, Belot N, Duval H, Langlais F, Thomazeau H. No recurrences in selected patients after curettage with cryotherapy for grade I chondrosarcomas. Clin Orthop Relat Res. 2010;458:1956–62.
90. van der Geest IC, de Valk MH, de Rooy JW, Pruszczynski M, Veth RP, Schreuder HW. Oncological and functional results of cryosurgical therapy of enchondromas and chondrosarcomas grade 1. J Surg Oncol. 2008;98(6):421–6.
91. Liu DM, Kee ST, Loh CT, et al. Cryoablation of osteoid osteoma: two case reports. J Vasc Interv Radiol. 2010;21(4):586–9.
92. Rybak LD. Fire and ice: thermal ablation of musculoskeletal tumors. Radiol Clin North Am. 2009;47(3):455–69.
93. Byas-Smith MG, Gulati A. Ultrasound-guided intercostal nerve cryoablation. Anesth Analg. 2006; 103(4):1033–5.
94. Moore W, Kolnick D, Tan J, Yu HS. CT guided percutaneous cryoneurolysis for post thoracotomy pain syndrome early experience and effectiveness. Acad Radiol. 2010;17:603–6.
95. Hunt I, Eaton D, Maiwand O, Anikin V. Video-assisted intercostal nerve cryoablation in managing intractable chest wall pain. J Thorac Cardiovasc Surg. 2010;139(3):774–5.
96. Robinson JW, Donnelly BJ, Siever JE, et al. A randomized trial of external beam radiotherapy versus cryoablation in patients with localized prostate cancer: quality of life outcomes. Cancer. 2009;115(20):4695–704.
97. Bahn DK, Lee F, Silverman P, et al. Salvage cryosurgery for recurrent prostate cancer after radiation therapy: a seven-year follow-up. Clin Prostate Cancer. 2003;2(2):111–4.
98. Bahn DK, Lee F, Badalament R, Kumar A, Greski J, Chernick M. Targeted cryoablation of the prostate: 7-year outcomes in the primary treatment of prostate cancer. Urology. 2002;60(2 Suppl 1):3–11.
99. Cohen JK. Cryosurgery of the prostate: techniques and indications. Rev Urol. 2004;6(Suppl 4):S20–6.
100. Donnelly BJ, Saliken JC, Brasher PM, et al. A randomized trial of external beam radiotherapy versus cryoablation in patients with localized prostate cancer. Cancer. 2010;116(2):323–30.
101. Finley DS, Pouliot F, Miller DC, Belldegrun AS. Primary and salvage cryotherapy for prostate cancer. Urol Clin North Am. 2010;37(1):67–82. Table of Contents.
102. Kimura M, Mouraviev V, Tsivian M, Mayes JM, Satoh T, Polascik TJ. Current salvage methods for recurrent prostate cancer after failure of primary radiotherapy. BJU Int. 2010;105(2):191–201.
103. Onik G, Vaughan D, Lotenfoe R, Dineen M, Brady J. The "male lumpectomy": focal therapy for prostate cancer using cryoablation results in 48 patients with at least 2-year follow-up. Urol Oncol. 2008;26(5):500–5.
104. Ritch CR, Katz AE. Update on cryotherapy for localized prostate cancer. Curr Urol Rep. 2009;10(3):206–11.
105. Rukstalis DB. The case for cryoablation of prostate cancer. J Endourol. 2008;22(9):2057–8. discussion 9.
106. Littrup PJ, Freeman-Gibb L, Andea A, et al. Cryotherapy for breast fibroadenomas. Radiology. 2005;234(1):63–72.
107. Littrup PJ, Jallad B, Chandiwala-Mody P, D'Agostini M, Adam BA, Bouwman D. Cryotherapy for breast cancer: a feasibility study without excision. J Vasc Interv Radiol. 2009;20(10):1329–41.
108. Zupi E, Piredda A, Marconi D, et al. Directed laparoscopic cryomyolysis: a possible alternative to myomectomy and/or hysterectomy for symptomatic leiomyomas. Am J Obstet Gynecol. 2004;190(3): 639–43.
109. Pansky M, Cowan BD, Frank M, Hampton HL, Zimberg S. Laparoscopically assisted uterine fibroid cryoablation. Am J Obstet Gynecol. 2009;201(6):571 e1–7.
110. Kumar S, Suneetha PV, Dadhwal V, Mittal S. Endometrial cryoablation in the treatment of dysfunctional

uterine bleeding. Int J Gynaecol Obstet. 2002; 76(2):189–90.
111. Beland MD, Dupuy DE, Mayo-Smith WW. Percutaneous cryoablation of symptomatic extraabdominal metastatic disease: preliminary results. AJR Am J Roentgenol. 2005;184(3):926–30.
112. Kujak JL, Liu PT, Johnson GB, Callstrom MR. Early experience with percutaneous cryoablation of extra-abdominal desmoid tumors. Skeletal Radiol. 2010;39(2):175–82.
113. Beland MD, Mayo-Smith WW. Ablation of adrenal neoplasms. Abdom Imaging. 2009;34(5):588–92.
114. Seifert JK, Junginger T, Morris DL. A collective review of the world literature on hepatic cryotherapy. J R Coll Surg Edinb. 1998;43(3):141–54.
115. Zhou XD, Tang ZY, Yang BH, et al. Experience of 1000 patients who underwent hepatectomy for small hepatocellular carcinoma. Cancer. 2001;91(8): 1479–86.
116. Xu KC, Niu LZ, He WB, Guo ZQ, Hu YZ, Zuo JS. Percutaneous cryoablation in combination with ethanol injection for unresectable hepatocellular carcinoma. World J Gastroenterol. 2003;9(12): 2686–9.
117. Riley DK, Babinchak TJ, Zemel R, Weaver ML, Rotheram EB. Infectious complications of hepatic cryosurgery. Clin Infect Dis. 1997;24(5):1001–3.
118. Elias D, Di Pietroantonio D, Gachot B, Menegon P, Hakime A, De Baere T. Liver abscess after radiofrequency ablation of tumors in patients with a biliary tract procedure. Gastroenterol Clin Biol. 2006;30(6–7):823–7.
119. Glasgow SC, Ramachandran S, Csontos KA, Jia J, Mohanakumar T, Chapman WC. Interleukin-1beta is prominent in the early pulmonary inflammatory response after hepatic injury. Surgery. 2005;138(1): 64–70.
120. Seifert JK, Morris DL. World survey on the complications of hepatic and prostate cryotherapy. World J Surg. 1999;23(2):109–13. discussion 13–4.
121. Livraghi T, Solbiati L, Meloni MF, Gazelle GS, Halpern EF, Goldberg SN. Treatment of focal liver tumors with percutaneous radio-frequency ablation: complications encountered in a multicenter study. Radiology. 2003;226(2):441–51.
122. de Baere T, Risse O, Kuoch V, et al. Adverse events during radiofrequency treatment of 582 hepatic tumors. AJR Am J Roentgenol. 2003;181(3):695–700.
123. Yeh CN, Chen MF. Resection of peritoneal implantation of hepatocellular carcinoma after hepatic resection: risk factors and prognostic analysis. World J Surg. 2004;28(4):382–6.
124. Yeh CN, Chen MF, Jeng LB. Resection of peritoneal implantation from hepatocellular carcinoma. Ann Surg Oncol. 2002;9(9):863–8.
125. Cha C, Fong Y, Jarnagin WR, Blumgart LH, DeMatteo RP. Predictors and patterns of recurrence after resection of hepatocellular carcinoma. J Am Coll Surg. 2003;197(5):753–8.
126. Dodd 3rd GD, Napier D, Schoolfield JD, Hubbard L. Percutaneous radiofrequency ablation of hepatic tumors: postablation syndrome. AJR Am J Roentgenol. 2005;185(1):51–7.
127. Kahlenberg MS, Volpe C, Klippenstein DL, Penetrante RB, Petrelli NJ, Rodriguez-Bigas MA. Clinicopathologic effects of cryotherapy on hepatic vessels and bile ducts in a porcine model. Ann Surg Oncol. 1998;5(8):713–8.
128. Akahane M, Koga H, Kato N, et al. Complications of percutaneous radiofrequency ablation for hepatocellular carcinoma: imaging spectrum and management. Radiographics. 2005;25(Suppl 1):S57–68.
129. Rouviere O, Badet L, Murat FJ, et al. Radiofrequency ablation of renal tumors with an expandable multitined electrode: results, complications, and pilot evaluation of cooled pyeloperfusion for collecting system protection. Cardiovasc Intervent Radiol. 2008;31(3):595–603.
130. Atwell TD, Wass CT, Charboneau JW, Callstrom MR, Farrell MA, Sengupta S. Malignant hypertension during cryoablation of an adrenal gland tumor. J Vasc Interv Radiol. 2006;17(3):573–5.
131. Tsoumakidou G, Buy X, Zickler P, Zupan M, Douchet MP, Gangi A. Life-threatening complication during percutaneous ablation of adrenal gland metastasis: Takotsubo syndrome. Cardiovasc Intervent Radiol. 2009;33:646–9.
132. Moszkowicz D, Balian C, Dugue L, Maftouh A, Masmoudi H, Charlier A. [Colonic perforation after radiofrequency ablation of a renal cancer]. J Chir (Paris). 2008;145(4):407–8.
133. Bodily KD, Atwell TD, Mandrekar JN, et al. Hydrodisplacement in the percutaneous cryoablation of 50 renal tumors. AJR Am J Roentgenol. 2010;194(3):779–83.
134. Froemming A, Atwell T, Farrell M, Callstrom M, Leibovich B, Charboneau W. Probe retraction during renal tumor cryoablation: a technique to minimize direct ureteral injury. J Vasc Interv Radiol. 2010;21(1):148–51.

Image-Guided High-Intensity Focused Ultrasound in the Treatment of Cancer

5

M. Raphael Pfeffer, Tatiana Rabin, Yael Inbar, Arik Hananel, and Raphael Catane

Abstract

High-intensity focused ultrasound (HIFU) is a noninvasive technique delivering acoustic energy for localized thermal ablation of tumors. The targeted volume reaches temperatures above 70 °C within a fraction of a second resulting in coagulative necrosis and ablation of the target and minimal side effects to nontargeted tissues. Available systems use either ultrasound or magnetic resonance imaging (MRI) to define the target and guide the treatment. MR-guided HIFU has the additional advantage of real-time thermometry which allows measurement and adjustment of the deposited energy during therapy. Several HIFU devices are commercially available, and the clinical use of HIFU is approved in many countries for the treatment of benign uterine fibroids and for the treatment of adenomyosis and painful bone metastases. Clinical studies are investigating the use of MR-guided HIFU for the treatment of painful bone metastases, primary breast cancer, and primary prostate cancer. Ultrasound-guided transrectal HIFU devices are in use in several countries to treat benign prostatic hypertrophy as well as primary and locally recurrent prostate cancer. The use of HIFU in cancer treatment is expanding due to advances in technology and accumulating clinical experience. In this chapter, we will review the technology and clinical experience of HIFU in cancer treatment.

M.R. Pfeffer (✉) • T. Rabin • R. Catane
Oncology Institute, Sheba Medical Center, Tel Hashomer, Ramat Gan, Israel
e-mail: raphipf@sheba.health.gov.il; tatiana.rabin@sheba.health.gov.il; raphael.catane@sheba.health.gov.il

Y. Inbar
Imaging Institute, Sheba Medical Center, Tel Hashomer, Ramat Gan, Israel
e-mail: yael.inbar@sheba.health.gov.il

A. Hananel
Insightec Ltd., Tirat Carmel, Haifa, Israel
e-mail: arikh@insightec.com

Introduction

High-intensity focused ultrasound (HIFU) is a noninvasive technique that focuses acoustic energy precisely at a targeted tumor volume, thereby heating the target and destroying it by localized thermal ablation (similar to using a magnifying glass to focus energy from the sun) (Fig. 5.1). HIFU causes tissue damage through conversion of mechanical energy to heat and through acoustic cavitation of the

D.E. Dupuy et al. (eds.), *Image-Guided Cancer Therapy*, DOI 10.1007/978-1-4419-0751-6_7,

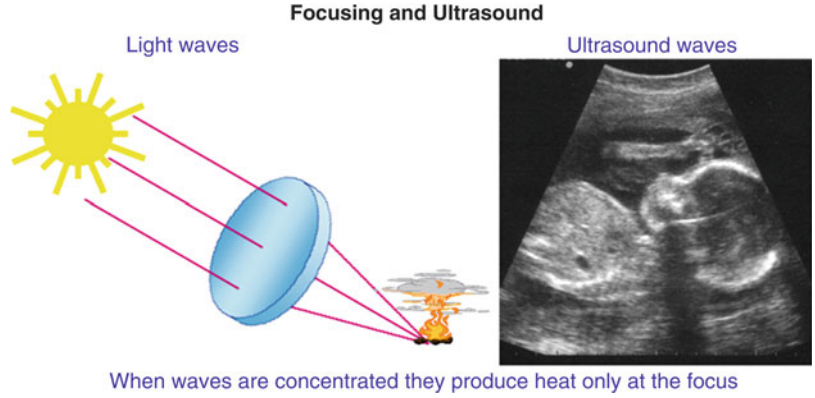

Fig. 5.1 Focusing thermal ultrasonic energy waves can be compared to using a magnifying glass to focus solar energy on a small target (With permission from Insightec Ltd)

targeted tissue. The temperature elevation in the targeted volume (>70 °C) results in irreversible coagulative necrosis and ablation of the targeted structure within a fraction of a second. The thermal energy decreases sharply outside the focal zone; thus, the overlying and surrounding tissues are minimally affected. This creates a sharp demarcation between the targeted and nontargeted tissues. The size of the thermal lesion can be controlled by adjusting the power and duration of the ultrasound pulse. Studies using HIFU to destroy cancerous tissues have shown no increase in the risk of metastatic spread. An essential component of HIFU is image guidance. Available systems use either ultrasound or magnetic resonance imaging (MRI) to define the target and guide the treatment. Several HIFU devices are commercially available, and the clinical use of HIFU is approved in many countries. The InSightec ExAblate MR-guided focused ultrasound (MRgFUS) system is approved in the USA and Asia for the treatment of benign uterine fibroids and in Europe for the same indication as well as for the treatment of adenomyosis and painful bone metastases. Currently, there are additional clinical studies under way to investigate the use of MRgFUS for the treatment of painful bone metastases, primary breast cancer, and primary prostate cancer. Philips and Siemens are also developing MR-guided HIFU systems as well. Ultrasound-guided transrectal HIFU devices have been in use for more than 10 years, particularly in European countries, to treat benign prostatic hypertrophy as well as for the treatment of primary and locally recurrent prostate cancer. Clinical trials of HIFU for malignant diseases that are registered at the NIH (clinicaltrials.gov) include studies of transrectal ultrasound-guided HIFU for early-stage and locally recurrent prostate cancer and MR-guided HIFU for the treatment of bone pain and breast cancer. Most of these studies include small numbers of patients.

This chapter will describe the development of HIFU and review the clinical experience in the tumor sites where it has been studied. This chapter will not discuss HIFU devices that require laparoscopic or surgical intervention.

History

Conventional hyperthermia treatment aims to deliver temperatures around 43–44 °C, and treatment duration must be 60 min or longer in order to achieve a meaningful antitumor effect. At such temperatures, hyperthermia alone has limited efficacy although it can potentiate the effect of both chemotherapeutic agents and radiation [1]. The clinical use of hyperthermia was hampered by the lack of an effective heat delivery system allowing selective heating of the tumor target and by the lack of an accurate noninvasive method of monitoring the endpoint of the energy delivered (i.e., the actual temperature achieved in the target and in the surrounding tissues). During the time period required for conventional hyperthermia (minutes to hours), the heat delivered to the target dissipates into the surrounding tissues, thereby

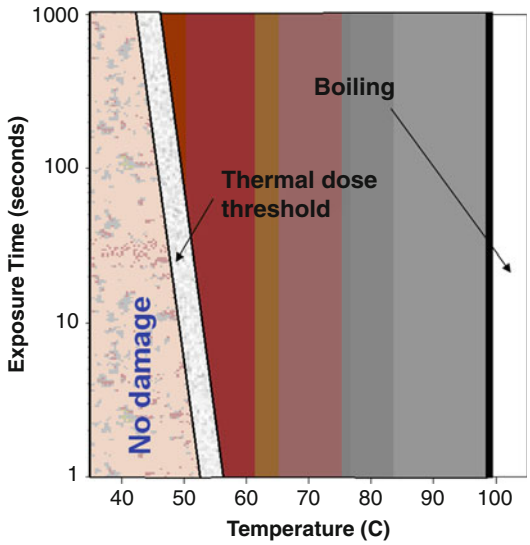

Fig. 5.2 Thermal ablation occurs when tissue temperature is higher from a certain threshold for a distinct period of time (At 43 °C–240 min, at 54 °C–3 s, at 57 °C–1 s) (Adapted from Ref. [6])

reducing the specificity of the treatment against the tumor target. Hyperthermia has therefore been limited to use as a regional therapy potentiating the effect of chemotherapy [2].

The concept of focusing ultrasound waves to deliver acoustic energy in order to heat a target to ablative temperatures was described over 50 years ago [3]. In 1954, Fry and colleagues reported on the clinical use of HIFU to produce focally destructive, deep CNS lesions to treat Parkinson's disease [4]. In 1956, Burov suggested that HIFU be used to treat malignant tumors, but it required many more years until the technology was adequately developed to make it clinically practical [5]. Focused ultrasound allows the delivery of a large amount of thermal energy to small selected volumes, achieving temperatures of over 70 °C in the target. At these temperatures, focused ultrasound results in target ablation via coagulative necrosis in a fraction of a second before the thermal energy can dissipate to surrounding tissues, and the effect is substantially different from that of conventional hyperthermia (Fig. 5.2). The basic requirements for HIFU include real-time target imaging during treatment and a method for assessing the immediate effects of the HIFU on the treated tissue. This is achieved either with ultrasound guidance or more recently with MRI guidance. MR has the added benefit of MR thermometry which can monitor the temperature achieved in the target and adjacent areas and ensure the effective and safe delivery of the thermal energy.

Noninvasive image-guided delivery of thermal energy has gradually entered intensive clinical evaluation as a modality for cancer treatment over the last 15 years. The development of image-guided HIFU paralleled the development of focused image-guided radiotherapy (SBRT), which allows the delivery of ablative doses of radiation (radiosurgery) to small targets and is changing the practice of radiotherapy today. The mechanism of tumor destruction with radiosurgery, which is believed to be through tumor ablation or vascular impairment, differs from the radiobiological effects of classic radiotherapy and may be closer to other ablative technologies such as HIFU. Nevertheless, there are several important differences between stereotactic high-dose radiotherapy (radiosurgery) and HIFU, which deem these treatments complimentary. To date, SBRT has been mostly applied for treating brain, spine, and lung lesions. HIFU with the current technology is contraindicated in CNS lesions, although some researchers are evaluating the feasibility of performing trans-skull thermal ablation in the brain for malignant and functional indications using a helmetlike transducer. Neither can HIFU be used for targets where the ultrasound wave must cross air cavities such as in lung tumors.

Experimental systems have shown that heating tumors to cytotoxic temperatures can result in an antitumor immune response, which may add a systemic antitumor effect to HIFU treatment. However, this has not yet been systematically studied in human subjects [7].

Principles of Focused Ultrasound

Ultrasound is a high-frequency pressure wave above the range of audible hearing. Ultrasound waves are produced by applying a radiofrequency

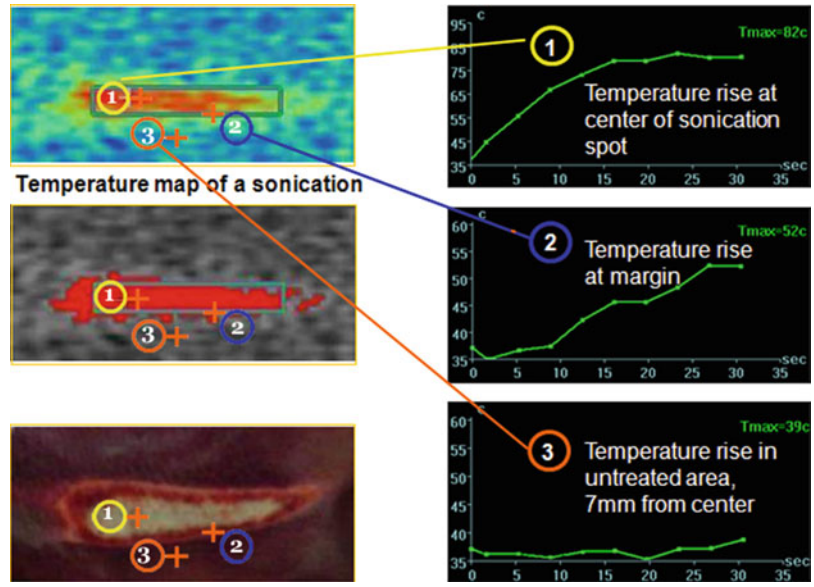

Fig. 5.3 MR thermometry demonstrating a clear correlation of high temperature within the target (resulting in tissue ablation) and steep temperature gradient with low temperature in surrounding tissue resulting in sharp edges of sonication (With permission from Insightec Ltd)

across piezoelectric material that expands and contracts with applied voltage. The wave transmits mechanical motion via compression and decompression of adjacent molecules. The attenuation and direction of the ultrasound wave is affected by the tissue absorption capacity (i.e., ultrasound waves in most HIFU systems cannot cross air cavities) and the difference in speed of sound between different tissues (i.e., fat vs. muscle). Therapeutic focused ultrasound systems use a transducer several centimeters in diameter to direct the acoustic energy to a predetermined depth without depositing a substantial amount of energy along the beam path. The acoustic energy is deposited as thermal energy in a small target volume, resulting in heating of the target at the focal point with a sharp energy gradient around the target resulting in a precise lesion (Fig. 5.3). The properties of the ultrasound wave can be modulated by changing its frequency and wavelength and by the size of the transducer. By selecting the transducer properties, it is possible to optimize energy delivery depending on the specific clinical application. The behavior of the ultrasound beam is less predictable when it crosses soft tissue interfaces with bone or air. Targeting and monitoring of the tissue effects is therefore needed to provide feedback of the actual in vivo effects [8].

Technologies for HIFU

The commercially available technologies for noninvasive image-guided HIFU use either MRI or ultrasound for tissue targeting and evaluation of treatment effect. Imaging allows identification of the tumor target and is necessary to avoid the ultrasound beams crossing air cavities, such as bowel, which would interfere with their transmission. For percutaneous delivery, the ultrasound waves originate from multiple transducer elements (phased arrays) located on and in contact with the surface of the body. For prostate therapy, the transducer is introduced transrectally and is situated in contact with the rectal surface facing the prostate. By controlling the different elements' phases and amplitudes, the ultrasound energy is focused at a predesignated point deep inside the body. At the point where the ultrasound beams converge, there is a substantial temperature rise that results in tissue necrosis. Beyond the

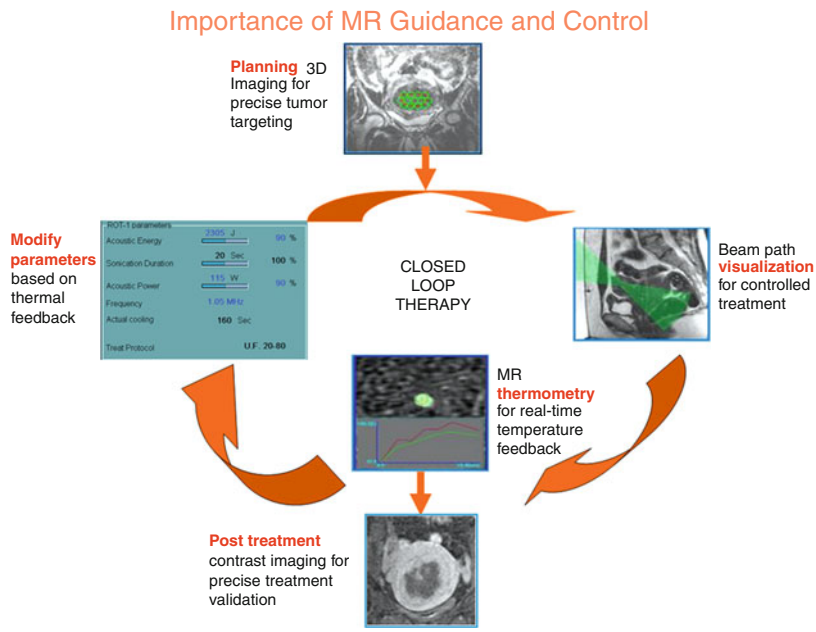

Fig. 5.4 Closed loop feedback system for controlled delivery of focused ultrasound with imaging and real-time thermometry (With permission from Insightec Ltd)

focal point of the beams, the deposited energy is too low to lead to a significant increase in temperature compared to the body's natural state.

MR-Guided Focused Ultrasound (MRGFUS)

Jolesz and Hynynen developed the concept of MR-guided focused ultrasound (MRgFUS) almost 20 years ago [9, 10]. The advantages of MRgFUS compared to ultrasound-guided HIFU include not only more accurate target imaging with MRI but also the capacity to monitor temperature changes in the target and surrounding areas during treatment with real-time MR thermometry. This allows the operator to monitor the intensity of the temperature rise at the treatment site to the desired level (65–80 °C) and ensures that the target receives a sufficient ablative dose of energy to cause coagulative necrosis, while the normal tissues surrounding the target are spared [11]. The major disadvantage of MRgFUS compared to ultrasound-guided systems is the increased cost of the MR-based system.

MRgFUS constitutes a closed loop system (Fig. 5.4). The patient is positioned on the MRI table with the lesion to be targeted lying on top of the transducer. A set of MR images is acquired to define the three-dimensional target volume to be treated, and the operating physician draws the desired treatment contours. The planning system calculates the number, position, and size of the sonications required to deliver adequate thermal energy to the three-dimensional target volume. The required number of adjacent focal spots depends on the target volume. Treatment volumes vary with clinical application, but can be as high as 1,000 cm^3 for a single session of uterine fibroid ablation. During the actual treatment, several small, oval volumes of sonication are treated in a sequential manner to cover the entire target. Each sonication lasts several seconds. Discrete areas in the tumor are consecutively treated at operator-controlled time intervals to prevent significant heat accumulation in surrounding tissue. Because the beam is focused on the treatment area, there is no significant heating effect on pain-sensitive areas such as adjacent normal tissue or skin.

After approval of the treatment plan, a series of sonications delivers a low dose of energy to the target to result in a small, non-ablative, temperature rise. The temperature-sensitive MRI phase

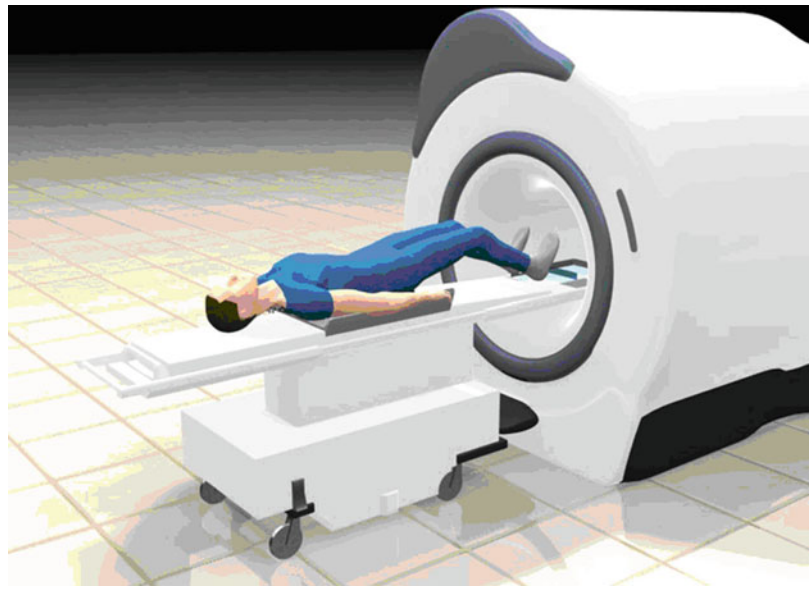

Fig. 5.5 Integrated MR imaging and focused ultrasound therapy unit (With permission from Insightec Ltd)

sequence locates the focal point of the beam and its position relative to the planned target point. The location of the focal spot can be corrected at this point to remove errors arising from mechanical alignment of the patient or tissue acoustic aberration. A full-dose sonication is then delivered to this volume, and the temperature is monitored until the required ablative temperature is reached. During the sonications, there is continuous feedback of the energy delivery and the progress of the treatment, confirming the planned target ablation. Once a volume is ablated, the transducer can be targeted to an adjacent location and the process repeated until the entire tumor volume is heated to between 65 °C and 80 °C to induce thermal coagulation. The treating physician can take advantage of the data acquired during therapy to individually adjust treatment parameters and to achieve the desired ablative effect in the target.

After the final sonication, the physician can evaluate the accumulated dose map and may decide to add additional points to complete the layer or to end the treatment. On completion of the treatment, the ablated volume is verified using contrast-enhanced MRI scans. Since treatment has ablated the tissue and coagulated the small blood vessels in the target volume, the treated volume does not undergo contrast enhancement.

MRgFUS has been shown to be clinically effective in treating uterine fibroids [12] and is currently being evaluated for the treatment of painful bone metastases [13], primary breast cancer [14], and prostate cancer. In vivo animal studies and preliminary clinical studies have been carried out in systems designed to treat liver [15] and brain tumors [16].

The first commercially available MRI-monitored and MRI-controlled FUS system (ExAblate 2000) was developed by InSightec Ltd. (Tirat Carmel, Israel), in collaboration with the Brigham and Women's MRI division, and is compatible with a General Electric MR scanner (Fig. 5.5). Siemens [17] and Philips Medical Systems also have MRI-guided FUS research and development programs and have begun clinical studies. The Phillips MRgFUS system is undergoing initial clinical evaluation for uterine fibroids and bone metastases and is in preclinical studies of a novel application in combination with drugs encapsulated in heat-sensitive liposomes [18].

The present second-generation ExAblate system incorporates phased-array technology for electronic focusing, tissue aberration correction, and electronic steering. The ExAblate 2000 has a concave, 120-mm diameter, phased-array transducer with over 200 elements. The integration of

the treatment system with the MR scanner allows both energy delivery and treatment monitoring to be coordinated in a single system (Fig. 5.5). The ExAblate 2000 uses a transducer that can be directed from under the treatment couch toward the targeted tissue. A new generation conformal transducer is undergoing phase II clinical study for the treatment of bone metastases. This can be positioned over the targeted bone metastasis to treat targets for which the patient could not be comfortably treated using the couch-based system that necessitates lying with the lesion positioned over the transducer.

Ultrasound-Guided HIFU Systems

There are two ultrasound-guided HIFU systems in clinical use for the treatment of prostate cancer. These single-focus systems are manufactured by Focus Surgery (Sonablate, Indianapolis, Indiana) [19] and EDAP (Ablatherm, Lyon, France) [20]. Both devices use a spherically curved transducer that combines both ultrasound imaging and therapeutic capability. The transducer is positioned in the rectum to deliver sonications of the prostate tissue through the rectal wall. The ultrasound imaging allows delineation and mapping of the prostate and guides the therapy beam, but it does not aid in temperature-sensitive imaging or in making thermal dose calculations.

The Sonablate 500 transrectal HIFU device (US HIFU) is undergoing phase III study in the USA and is commercially available in several other countries for the treatment of de novo and recurrent prostate cancer. The Sonablate version 4 (SB500 V4) module includes an ultrasound power generator, transrectal probes, the probe positioning system, and a continuous cooling system. The transrectal HIFU probes use single transducer with low-energy ultrasound (4 MHz) for imaging of the prostate and for the delivery of high-energy ablative pulses (site intensity, 1,300–2,200 W/cm^2). The single piezoelectric crystal alternates between high-energy power for ablative and low energy for ultrasound imaging. The size of each focus lesion, requiring around 5 s to treat, is 3 × 3 × 12 mm (0.108 cc). The transducer can be angled to 90° to treat the whole prostate without probe repositioning. Bidirectional color Doppler is used to detect blood vessels surrounding the neurovascular bundle. The physician can review and refine the prostate treatment plan during ongoing treatment and add or remove individual treatment sites to the treatment plan as required.

The EDAP Ablatherm device contains two ultrasound transducers; a 7.5-MHz ultrasound provides real-time integrated imaging of the prostate, while a 3-MHz high-intensity ultrasound is used to deliver focused thermal energy through the rectal wall to the targeted prostate area. The targeted zone for each focused lesion is 1.7 mm in width and 1.7 mm in thickness and can be varied in height from 19 to 24 mm depending on the target size. A total of 400–600 pulses are generally required to cover the entire prostate tumor. The system incorporates a rectal temperature probe to prevent overheating of the rectal wall which may result in tissue damage. The duration of treatment is 1–3 h depending on the total target volume.

The Model JC ultrasound-based transdermal HIFU system developed in China (Chongqing Haifu Technology, Chongqing, China) is now entering clinical use in Europe, primarily for the treatment of benign lesions such as uterine fibromas and breast adenofibromas. Studies in bone tumors with this system have recently been reported (see below). This system is guided by real-time ultrasonographic imaging. The ultrasonic imaging device is situated in the center of the HIFU transducer. Focused ultrasound is produced by a piezoelectric ceramic transducer (12 cm in diameter with a focal length of 135 mm) at a frequency of 0.8 MHz (continuous wave) producing an ellipsoid focal region with dimensions of 3.3 × 1.1 mm. The skin is prepared by defatting and degassing to reduce the refraction of ultrasound and enhance the accuracy of focusing. Real-time ultrasonography is used to target the tumor, which is divided into sections with 5 mm of separation. The targeted regions are then ablated by the HIFU scanning beam. This process is repeated section by section to achieve complete ablation of the tumor volume.

This system does not measure the actual thermal energy delivered or the temperature reached in the target; however, real-time ultrasonographic scans are obtained during HIFU ablation, immediately before and after the individual exposures. These are compared to ensure treatment of the desired area and to determine whether the echogenic changes to the HIFU-treated region indicate coagulative necrosis.

Primary and Metastatic Bone Tumors

Bone metastases are a common manifestation of advanced cancer. The most common symptom is pain which may be severe enough to require treatment with opioid analgesics and may also result in mechanical bone impairment [21]. Thirty percent of all cancer patients will develop bone metastases and 50–57 % of these suffer from significant pain [22, 23]. Improvements in systemic cancer therapies have greatly increased the life expectancy of patients with metastatic disease of most common cancer types. This has contributed to a growth in the number of patients with symptomatic bone metastases requiring palliation. An increased emphasis on the quality of life of cancer patients has led to a search for effective pain palliation for clinically active bone metastases, with fewer short- and long-term side effects [24]. Palliation of bone metastases can be achieved with systemic therapies such as analgesics, chemotherapy, hormonal therapy, and bisphosphonates, but local pain control is usually achieved with radiation therapy although surgical stabilization is sometimes required [25, 26]. Radiofrequency ablation is being investigated for the treatment of bone pain, but since this is an invasive procedure, it may not be appropriate for many patients with bone metastases [27].

The current standard of care for clinically active bone metastases is external beam radiation; however, more than one-third of the patients do not experience significant pain relief, and in a further 27 % pain may recur [28]. A recent meta-analysis reporting 16 randomized trials totaling 5,000 patients randomized between single-fraction and multiple-fraction radiotherapy for bone metastases showed that 58–59 % had some pain relief but only 23–24 % had a complete response [29]. Re-irradiation may sometimes achieve a further palliative effect, but the use of re-irradiation is limited due to concerns about the cumulative dose of radiation to the bone and surrounding tissues.

Treating bone lesions with HIFU, in contrast to treating soft tissue lesions, has certain advantages, such as higher absorption of the acoustic energy (up to 50 times higher absorption in bone than in soft tissue) and low thermal conductivity of bone tissue [19]. These differences lead to limited penetration into normal cortical bone when using the soft tissue tumor MRgFUS system. Delivering acoustic energy on the bone surface results in a temperature rise in the part of the bone cortex enclosed in the beam path zone, thus indirectly ablating the adjacent periosteum and tumor tissue. Since the bone periosteum is considered to be a major source of pain in patients with metastatic bone lesions, ablating the source of pain should produce lasting pain relief [20].

Several centers, including Sheba Medical Center in Israel, are participating in studies with MRgFUS for bone metastases using the ExAblate 2000 system (InSightec Ltd., Haifa, Israel), which has a focused ultrasound phased-array system integrated with an MRI scanner (GE 1.5-T MRI, Milwaukee, WI, USA). In a phase 1–2 study, 31 patients with painful bone metastasis were treated with MRgFUS in three medical centers: the Sheba Medical Center (Tel Hashomer, Tel Aviv, Israel), Toronto General Hospital (Toronto, Ontario, Canada), and Charite Hospital (Berlin, Germany). The main inclusion criteria were clinically identifiable painful bone metastatic lesions in patients who had exhausted or refused all other pain palliation methods including external beam radiation. Exclusion criteria included weight-bearing bone and targets within 1 cm of the skin, spinal cord, or major nerves.

The procedure is performed with the patient lying inside the MRI scanner, under conscious sedation and analgesia including IV midazolam and morphine sulfate. The targeted region is identified based on pretreatment MRI and computed

tomography (CT) screening images. The patient is placed on the MRI table with the targeted lesion positioned over a water bath containing the ultrasound transducer. Acoustic coupling is accomplished by placing a coupling gel pad between the patient and patient table. The position of the patient and the sonication pathway are checked using MR imaging (standard T2-weighted fast spin-echo images), and the images are loaded into the MRgFUS workstation, where the target area and bone contour are delineated for treatment. Following this, the workstation generates an individualized, patient-specific treatment plan avoiding damage to nontarget tissue while optimizing the required energy level and the number of sonications. At the beginning of each procedure, a number of low-power sonications are performed to ensure the targeting accuracy in three dimensions. Treatment at therapeutic power levels begins after a mild increase in the temperature as the expected position is detected. Throughout the treatment, each sonication's location and the temperature elevation in the tissue adjacent to the targeted bone are monitored in real time using the proton resonance frequency (PRF) shift temperature measurement method. In response to the resulting temperature map, the treating physician can then modify the treatment parameters such as power, frequency, sonication duration, or spot size.

At the end of each procedure, contrast-enhanced MRI scans (fat-suppressed T1-weighted contrast-enhanced spoiled gradient-recalled-echo images) are performed to ensure that the extent of ablation is confined to target tissue and that there is no substantial damage to the tissue surrounding the target.

In the above phase I–II study, the average length of the treatment was 66 min (range = 22–162 min). The average number of sonications was 17.3 (range = 8–32), with an average sonication energy of 1,135 J (range = 440–1,890 J). The mean follow-up time was 108 days after treatment. No device-related severe adverse events were recorded in any of the patients. The clinical indications for treatment were the presence of clinically identifiable painful bone metastatic lesions in patients who had exhausted or refused all other pain palliation methods including external beam radiation. Treatment response was categorized using the endpoint criteria defined by the International Bone Metastases Working Party guidelines on palliative radiotherapy endpoints for future clinical trials [13]. A partial response is defined as a drop of two points in the VAS (visual analog scale) score without an increase in pain medication or a drop of 25 % in pain medication without an increase in the reported pain score. A complete response is defined as a pain score of 0 on the VAS score without an increase in pain medication. Treatment safety was monitored by recording the incidence of any device-related morbidity, either local or systemic, at each follow-up point.

Thirty-six treatments in 31 patients were conducted, targeting 32 metastatic lesions [30, 31]. The primary tumors included breast, prostate, lung, and renal cell carcinoma. All patients except two tolerated the MRgFUS treatment using only conscious sedation. Two patients died before reaching the 3-month follow-up examination due to progressive systemic disease. Twenty-five patients who had full treatment and reached the 3-month follow-up visit were evaluated with the 11-point VAS scale. The mean VAS score before treatment was 5.9 (range = 3.5–8.5). The mean VAS score 3 days after treatment was 3.8 (range = 0–8.5), and by the 3-month posttreatment follow-up, the VAS score had dropped to 1.8 (range = 0–8) (Figs. 5.6 and 5.7).

Eighteen (72 %) of these patients had a significant (>2 points) reduction in pain at the 3-month follow-up, and nine patients (36 %) reported a posttreatment VAS score of 0. Similarly, when combining both the medication and VAS score, 36 % of patients had a partial response, and 36 % had a complete response, according to the working group criteria (Fig. 5.5). No difference in response was seen between the tumor types (breast, prostate, renal, and lung cancer) treated in this study. There was no difference in response rate between osteoblastic and osteolytic metastases. It is noteworthy to point out that 52 % of patients reported substantial pain relief as early as 3 days posttreatment. Immediate posttreatment

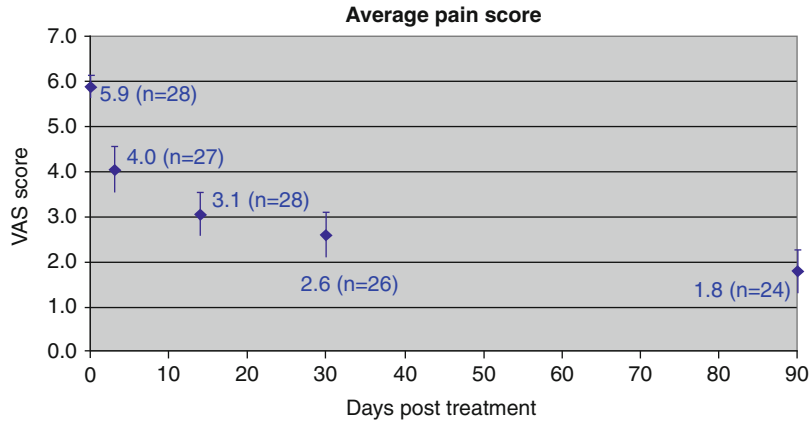

Fig. 5.6 VAS pain score following MRgFUS for bone metastases (With permission from Insightec Ltd)

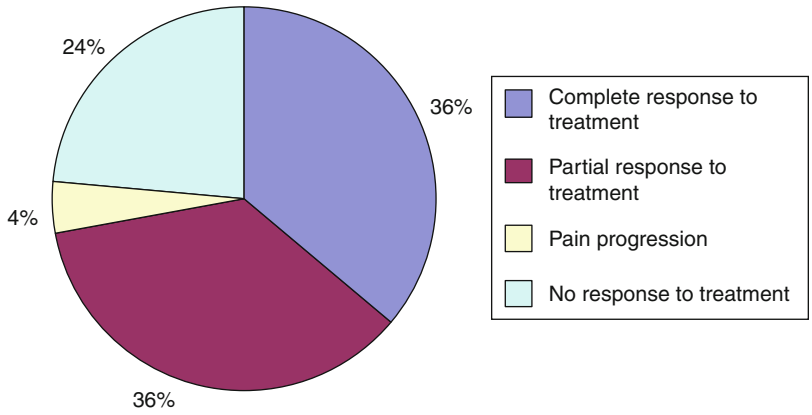

Fig. 5.7 VAS pain score response of bone metastases patients (With permission from Insightec Ltd)

contrast-enhanced MR images showed edema at the target area and in some cases minor localized ablation. MR images at 3 months did not show evidence of lasting damage, and follow-up CT images showed some cases of calcification of targeted tissue.

The Chongqing Haifu Model JC ultrasound-guided HIFU system has been investigated to treat both primary and metastatic bone tumors. Chen and colleagues reported on a series of 80 patients with primary bone tumors, mostly osteogenic sarcoma, treated with ultrasound-guided HIFU [32]. Most of the patients also received chemotherapy and were patients for whom surgical resection was contraindicated or refused. The treatment volume included the bone lesion with 3–5 cm of normal bone adjacent to the lesion and 1–2 cm of normal tissue. HIFU treatment was performed with patients under general anesthesia to prevent the patient from experiencing pain and to ensure immobilization. Prior to HIFU treatment, the skin surrounding the area to be treated was prepared by degassing and defatting to reduce the refraction of ultrasound and enhance the accuracy of focusing. Degassed water was applied to the target area to wet the skin, and a disk suction device with holes was connected to the vacuum extractor which was used to degas the skin. A transparent film was then applied to the degassed area to block the air. The treated area of skin was greater than the target area by 3–5 cm. The tumor was divided into sections separated by 5 mm and targeted with real-time ultrasonography by moving the integrated probe. The targeted regions in each section were completely ablated by the HIFU scanning beam. This process was repeated section by section to achieve complete ablation of the tumor volume.

During HIFU ablation, real-time ultrasound images obtained immediately before and after the individual exposures were compared to determine whether the echogenic changes to the HIFU-treated region were indicative of coagulative necrosis and to ensure that treatment covered the desired area.

Two weeks after the initial HIFU treatment, patients were assessed using MR and SPECT imaging, and they were retreated if residual tumor activity was seen. Twenty-six patients (32 %) with residual disease required retreatment for up to a total of four treatments. Splint support was used for 3–6 months to allow bone healing after treatment. Complete necrosis was achieved in 69 (86 %) of patients, five of whom later progressed. The most common complication was mild local pain for several days after treatment. Seventeen patients had skin toxicity including one with third-degree burns. Ten patients had peripheral nerve damage, nine of which regained some nerve function. All the damaged nerves were within 10 mm of the tumor margin. Other complications included bone fracture in six patients and ligamentous laxity, epiphysiolysis, or secondary infection in seven patients. Eleven patients (14 %) required surgical intervention to treat side effects of the HIFU. Li and colleagues reported a series of 25 patients with painful bone tumors, which included 13 patients with primary bone tumors and 12 patients with bone metastases [33]. These treatments were also monitored with real-time ultrasound, which determined whether there was coagulative necrosis of the lesion. Similarly to the previous study, the HIFU target included normal bone tissue 2–3 cm from the tumor and normal soft tissue 2 cm from the edge of tumor. Seven patients (28 %) required more than one HIFU session due to inadequate effectiveness of the initial treatments based on clinical factors and tumor imaging. Antitumor effect was evaluated clinically and by MRI or PET-CT. Twenty-one out of 24 patients were reported to have complete pain relief. Eleven out of 13 patients (85 %) with primary bone tumors had objective imaging responses, with six patients exhibiting complete remission and five exhibiting partial remission. Nine out of twelve patients (75 %) with bone metastases had objective imaging responses, five of which had complete remission and four of which had partial remission.

When comparing the experience with ultrasound-guided HIFU and MR-guided HIFU for bone lesions, there is a major difference in the target definition. A significant volume of normal tissue around the tumor was included in the target for ultrasound-guided treatment, whereas in the MRgFUS study, only the actual tumor was targeted. No margin of tissue is needed for MRgFUS since the target is accurately defined using MRI, and the delivery of an ablative dose of thermal energy to the tumor with MR thermometry can be verified in real time. Additionally, the studies using ultrasound-guided HIFU required the skin to be thoroughly prepared by defatting and degassing to improve the ultrasonic visualization of the target. The average treatment time with ultrasound-guided treatment was 230 min compared to 66 min with MRgFUS. The larger treatment volume required for ultrasound-guided HIFU may contribute to the much higher toxicity rate seen in these studies compared to the experience with MRgFUS. To date, over 200 patients have been treated as part of various studies on MRgFUS for bone metastases, with only two patients (where the skin was within 1 cm of the target) suffering a second-degree skin reaction and one patient experiencing post-procedural fracture of the upper part of the pelvic spine. At this stage, it is still unclear whether the fracture was related to the MRgFUS treatment. Aside from reports of pain, there were no other toxic or adverse reactions experienced during the procedure (unpublished data on file at Insightec).

The response rate in both the primary tumors treated in the two Chinese HIFU studies and in the multicenter MRgFUS studies are impressive. HIFU can be considered an option for patients with primary bone tumors who are unable to undergo surgical resection. The rate of pain control achieved with MRgFUS is particularly notable considering that most of these patients had persistent or recurrent pain following previous radiotherapy. As with any new cancer treatment,

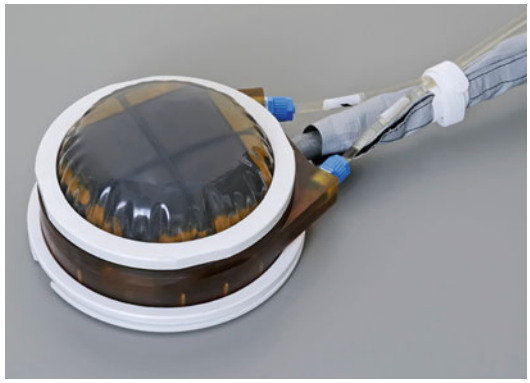

Fig. 5.8 Conformal bone applicator (With permission from Insightec Ltd)

the results should be validated in prospective randomized studies. A phase III FDA-approved randomized study, comparing MRgFUS to sham treatment in patients with painful bone metastases who have exhausted or refused all other pain palliation methods including external beam radiation, is expected to complete accrual soon. The patient is blinded as to whether he/she will receive treatment or undergo a sham procedure in which he undergoes the same procedure in the MRI machine as patients receiving the HIFU treatment with the only difference being that no sonications are performed. In this study, patients who have inadequate pain relief following treatment are allowed to be unblinded as to the actual treatment and may cross over to the actual treatment if they have received a sham treatment.

Two additional studies for patients with painful bone metastases are also under way. The first of these studies is designed to test the next generation bone system, using a conformal transducer (Fig. 5.8), and the second study is a multicenter prospective phase III randomized study of patients with painful bone metastases and no prior radiotherapy who receive either conventional radiotherapy or MRgFUS. The endpoint of this study includes tumor response by MRI at 3 and 6 months post-therapy as well as pain control according to the International Bone Metastases Working Party guidelines. Patients with inadequate pain relief from the assigned arm are allowed to cross over to the other treatment arm.

Pain palliation is one of the most important factors influencing the quality of life in patients with metastatic bone lesions. MRgFUS treatment has the advantage of circumventing the side effects caused by other therapies, by using noninvasive, nonionizing, accurate, controlled ablation. It is possible that the rapid improvement of pain is due to local bone denervation, caused by the heat denaturation of the periosteum layer in the treated area. Since the energy is nonionizing, there is no upper limit to the accumulated acoustic energy allowed to pass through adjacent soft tissue, as long as tissue temperature is kept at the safe level. Thus, the treatment can be repeated as needed, without reaching a maximal cumulative dose, as is the case with external beam radiation therapy. Due to the low thermal conductivity and high absorption rate of the bone cortex, it is possible to use lower energy levels for this treatment, compared to soft tissue treatments, thereby improving the safety profile by reducing the thermal damage around the treated bone site.

Temperature monitoring during bone treatment is limited to the soft tissue adjacent to the targeted bone since it is practically impossible to calculate the temperature in bone cortex, due to its low water content, and temperature measurements in bone marrow are unreliable. Nonetheless, the thermal feedback from soft tissue was sufficient to allow control over the location of the actual sonication and minimize damage to nontarget tissues. In this multicenter study, the mean VAS score dropped from 5.9 at baseline to 1.8 after 3 months. Even considering the relatively few patients in this study, VAS score reduction was statistically significant for a two-point change ($P < 0.003$). Despite the fact that most of the patients had persistent pain following prior radiotherapy, we observed a favorable response in 72 % of patients treated. It is important to note that most patients reported substantial pain relief as early as 3 days after treatment, such that only one treatment session was required in most cases, with pain relief continued for at least 3 months. No device-related serious adverse events occurred in any of the patients that were treated.

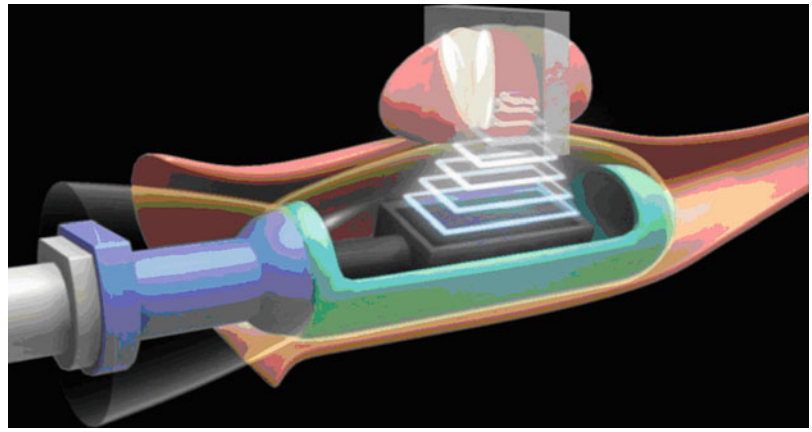

Fig. 5.9 Focused ultrasound delivered via transrectal probe inserted into prostate results in a series of ellipses of ablation in order to cover the target (With permission from Insightec Ltd)

Issues that will need to be answered in future studies include durability of pain relief and evaluation of tumor ablation over a longer follow-up period, with a larger patient population, and correlation between the site of metastases or primary tumor type and treatment outcome. Another interesting area to explore is the potential synergy between MRgFUS and other cancer therapies, such as chemotherapy or radiation. We have seen cases of long-term antitumor response, but larger studies are needed to further clarify and potentially predict the extent of such an effect.

In summary, the above results show that MRgFUS technology has the potential to be an important tool in treating painful bone metastases.

Prostate Cancer

Prostate cancer is well suited for treatment with HIFU. A transrectal transducer can be brought close to the prostate, with no structures or air cavities lying between the rectum and the prostate (Fig. 5.9), and the prostate can be visualized on ultrasonography. On the other hand, a major limitation of transrectally delivered HIFU for prostate cancer is the difficulty in delivering effective therapy to the anterior portion of the prostate, especially in patients with moderately large prostates. HIFU has usually been limited to patients with low- and intermediate-risk prostate cancer who are poor surgical candidates or refuse other treatment modalities.

Yerushalmi and colleagues reported the first use of thermal energy to treat localized prostate cancer in combination with external beam radiation [34]. These early efforts with conventional hyperthermia were disappointing. Long-term results showed no benefit of hyperthermia to 42.5 °C when added to external beam radiation for treating prostate cancer, and the initial enthusiasm for hyperthermia waned [35].

At significantly higher temperatures, Gelet and colleagues demonstrated coagulative necrosis in the benign prostate, with the degree of necrosis dependent on the dose of thermal energy delivery [36]. Madersbacher and colleagues reported focal tissue ablation in prostatectomy specimens of 29 patients receiving HIFU prior to surgical prostatectomy. Transrectal HIFU lesions consistently demonstrated sharply delineated intraprostatic coagulative necrosis of the entire target zone, with no changes in the periprostatic structures in the resected specimens. Tumor ablation with HIFU was then attempted in 10 additional patients with unilateral localized (T2a or T2b) prostate cancer. Of these 10 patients, histologic evaluation after prostatectomy showed that despite adequate targeting of the tumor, complete ablation was evident in only three patients [37]. In a recent study of 25 prostate cancer patients, coagulative necrosis often accompanied by acute, chronic, or granulomatous inflammation and mild or moderate fibrosis was seen in 72 % of prostate biopsies taken 180 days after HIFU treatment. Nevertheless, residual prostatic carcinoma was found in 11 patients (44 %),

nine of which had no apparent treatment effects [38].

The use of transrectal HIFU to treat prostate cancer has recently been reviewed [39], and two reports on large patient cohorts have been updated since then. Additionally, several groups have published short-term results after HIFU treatment for prostate cancer. The Sonablate and Ablatherm ultrasound-guided HIFU systems are in clinical use for the treatment of prostate cancer. The current models of both devices are single-focus systems that use a spherically curved transducer that combines both ultrasound imaging and therapeutic capability, with both systems using similar techniques. Treatment is performed under general or epidural anesthesia or deep sedation. Prior to treatment, a urethral catheter is put in place, and the rectum is evacuated with enemas to reduce interference with the transrectal probe. The rectal transducer is positioned in the rectum and covered by a condom or balloon, following which degassed, cooled water is circulated within it to eliminate air pockets which could interfere with the ultrasound waves between the transducer and the rectal mucosa. In addition, the circulating water cools the rectal wall, thereby preventing rectal toxicity.

Gelet's group in France pioneered the treatment of prostate cancer using the Ablatherm HIFU device. They overcame the difficulty of reaching the anterior parts of the prostate by flattening the prostate with an intrarectal condom and restricting the use of HIFU to patients with small to moderately sized prostates ($<40\ cm^3$). In addition, patients underwent transurethral resection (TURP), usually at the same sitting as the HIFU therapy. TURP allows more complete treatment of the anterior prostate and reduces the risk of urinary retention necessitating prolonged catheter drainage.

The long-term oncological outcome of a multicenter database including 803 patients treated with various Ablatherm devices since 1993 has recently been published [40]. Eighty patients were treated before 1999 with prototype devices. Patients treated since 2000 underwent TURP of the transitional zone followed by HIFU using a commercially available device. The first 446 patients on this protocol were treated with the first-generation Ablatherm device, and since 2005, a further 255 patients were treated with a second-generation device that includes integrated imaging technology, which allows real-time control of therapy. The whole prostate gland was treated within a 4–6-mm safety margin for the treatment of the apex. Five hundred and twenty-one patients (64.9 %) were treated in one session; 255 patients (31.7 %) required two sessions, and 27 (3.4 %) required three or more sessions. On average, 496 sonications were delivered during the first HIFU session, corresponding to an average treated volume of 26.8 ml (equivalent to 109 % of the prostate volume at the time of treatment).

Patients in this series had early-stage (T1–T2, N0, M0) prostate cancer and were not candidates for radical surgery according to age and general status, and did not receive neoadjuvant hormone therapy. The median age was 71 years. There were 481 patients (59.9 %) with T1 disease and 322 (40.1 %) with T2 disease. Sixty-four percent of patients had a Gleason score of 6, 30 % had a Gleason score of 7, and 6 % had a Gleason score of 8. The median serum prostate-specific antigen (PSA) level was 7.7 ng/ml (mean 9.1 $\pm$ 5.9). Thus, most of the patients in this series have a low risk for recurrence and may have been eligible for a protocol of active surveillance. Patients were followed for at least 2 years to track PSA levels and underwent prostate sextant biopsies 6 months after HIFU treatment, regardless of PSA level and/or in the case of three successive rises in PSA level. Patients with a positive prostate biopsy during follow-up without evidence of metastasis received retreatment with HIFU. The mean follow-up was 42 months. After HIFU treatment, the prostate volume (assessed by transrectal ultrasound) decreased on average from 24.5 $\pm$ 10 ml to 13.6 $\pm$ 13.1 ml. Interestingly, the need for retreatment in the initial group of patients treated with the prototype machine was 77 %. The retreatment rate was 42 % with the first-generation commercial machine and 15 % with the second-generation machine, which incorporates ultrasound-guided imaging during therapy.

The mean PSA nadir was reached within 6 months after HIFU in all patients and was 1.0 ± 2.8 ng/ml, with a median of 0.25 ng/ml. For the overall population, 436 patients (54.3 %) had a nadir PSA < 0.3 ng/ml. PSA nadir was a major predictive factor for HIFU success. Post-HIFU prostatic biopsies were performed on 589 patients (73.3 %). The biopsies were negative in 459 patients (77.9 %) and positive in 130 patients (22.1 %).

The long-term clinical outcome reported in this multicenter study does not include toxicity data, but toxicity data are included in an earlier report on 402 patients from this group. Posttreatment urinary retention was seen in all patients for a median of 5 days in patients treated with a Foley catheter and 34 days in those treated with a suprapubic catheter. Urinary retention was prolonged in 8.6 % of patients. Rectourethral fistulas developed in five patients, and urethral strictures developed in 4 % [41]. Blana and colleagues previously reported outcome and toxicity data on 140 patients treated with the Ablatherm system at their institution [42]. Thirty-four percent of patients had at least one episode of incontinence in the 3 months following HIFU. With longer follow-up, 94 % of patients recovered normal urinary continence, 5 % had grade 1 incontinence (loss of urine under heavy exercise), and one patient had grade 2 incontinence (loss of urine under light exercise using more than 1 pad/day). Urinary obstruction associated with stricture developed in 13.6 % of patients, 5.7 % had pelvic pain for more than 6 months, and 26 % of previously potent patients developed severe erectile dysfunction. Rectourethral fistulas occurred in 1 % of patients.

Patients from the Ablatherm multicenter study group who relapsed after treatment with HIFU received salvage therapy with either external beam radiotherapy (EBRT) to a median dose of 72 Gy if they demonstrated local recurrence and long life expectancy (84 patients) or androgen deprivation if there was no biopsy-proven local relapse or poor general status (98 patients). Progression-free survival at 5 years (defined as three consecutive rises in PSA with a velocity of >0.4 ng/ml or PSA > 1.5 ng/ml) of the group receiving EBRT after failure of HIFU was 72.5 % (93, 67, and 55 % for low-, intermediate-, and high-risk patients, respectively). Late GI toxicity was grade 1–10 % and grade 2–2 %. Late GU toxicity was grade 1–24 %, grade 2–23 %, and grade 3–6 % [43]. The incidence of severe erectile dysfunction was 14 % before HIFU therapy, 51.9 % after HIFU and before EBRT, and 82.3 % after EBRT.

The largest series of prostate cancer patients treated with the Sonablate device has recently been updated by Uchida and colleagues from Japan. This series of 517 patients with T1c–T3 tumors included 38 % with intermediate-risk and 34 % with high-risk tumors (based on pretreatment PSA, Gleason score, and T stage). Two-thirds of patients in this series received neoadjuvant hormonal therapy. Patients were treated using three generations of Sonablate HIFU devices, and the median follow-up time was 24.0 months (range = 2–88). The biochemical disease-free rate (BDFR) in all patients at 5 years was 72 %. The BDFR in patients with stage T1c, T2a, T2b, T2c, and T3 groups at 5 years were 74 %, 79 %, 72 %, 24 %, and 33 %, respectively ($P < 0.0001$). The BDFR in patients in the low-, intermediate-, and high-risk groups at 5 years were 84 %, 64 %, and 45 %, respectively ($P < 0.0001$). Similar to the Ablatherm series, patients treated more recently with the third-generation SB500 version 4 had better outcome than patients treated with earlier versions. The authors attribute this to a feature allowing changes in the treatment plan during therapy. In addition, there is a learning curve related to both technique and patient selection, which may contribute to improved outcomes over time. Postoperative erectile dysfunction was noted in 33 out of 114 patients (28.9 %) who were preoperatively potent [44]. In this study, only 0.6 % of patients had prolonged urinary retention although 22 % had strictures necessitating periodic urethral dilation, and 6 % complained of epididymitis.

Ahmed and colleagues reported on 172 prostate cancer patients treated in the UK with the Sonablate system. As with the Japanese series, this study includes about one-third patients with an intermediate risk of disease and one-third with

a high risk. The median follow-up time was less than 1 year, which is too early to evaluate a clinical response, especially since an unspecified number of patients received neoadjuvant hormonal therapy. The main side effect was urinary obstruction, which required catheterization for a mean of 2 weeks after treatment. Thirty percent required interventions for either a stricture or necrotic tissue within the prostate cavity. Grade 1 stress urinary incontinence occurred in 13 out of 172 patients (7.6 %), with one patient suffering grade 3 stress urinary incontinence that required an artificial urinary sphincter. The International Prostate Symptom Score (IPSS) significantly deteriorated at 3 and 6 months but returned to baseline at 9 and 12 months [45].

Nineteen patients with early-stage prostate cancer were treated on a phase I/II study at Indiana University School of Medicine using the Sonablate 500 system. One to three treatments were required for each patient. Two patients had transient urinary retention over 30 days, and rectal injury occurred in one patient. Forty-two percent of the patients achieved a PSA level of less than 0.5 ng/ml and a negative prostate biopsy [46].

Both the Ablatherm and the Sonablate reports used the Phoenix criteria (nadir PSA + 2.0 ng/ml) to define biochemical failure-free survival (BFFS). According to these criteria, the 5-year and 7-year BFFS for low-, intermediate-, and high-risk patients were 83–75 %,72–63 %, and 68–62 %, respectively ($P = 0.03$). The Phoenix criteria were validated for patients receiving external beam radiotherapy. The Phoenix criteria consensus panel specifically stated that the definitions are "not recommended for patients treated with other modalities such as cryotherapy or radical prostatectomy [47]". The behavior of serum PSA levels after radiotherapy is different from that seen after ablative therapies such as prostatectomy, cryotherapy, or HIFU. In addition, the consensus conference recommended "to avoid the artifacts resulting from short follow-up, the reported date of control should be listed as 2 years short of the median follow-up." The Ablatherm series does not report the median follow-up, but the mean follow-up was only 43 months. One of the reasons for the use of the Phoenix criteria is to avoid artifacts due to PSA bounce. Crouzet and colleagues note that since "PSA bounce is never observed after HIFU treatment" it is therefore inappropriate to use Phoenix criteria in these patients. The 5-year and 7-year additional treatment-free survival rates, which therefore more accurately reflect the true local control, were 84–79 %, 68–61 %, and 52–54 %, respectively, for low-, intermediate-, and high-risk patients. These results are less than those seen with modern dose escalated external beam radiation in patients with low PSA T1, T2 N0 prostate cancer [48].

HIFU has been used as a salvage therapy for patients with local recurrence of prostate cancer following external beam radiotherapy. Gelet's group published toxicity data on 167 patients with recurrent prostate cancer treated with the Ablatherm ultrasound-guided HIFU system at their institution [49]. Fifty-five percent of them received adjuvant hormone therapy. Local control was achieved in 73 % for a median follow-up of 18 months. Half the patients had urinary incontinence which was grade 2 or 3 in 31.5 %. Five patients treated in the earlier years of the study developed a urethrorectal fistula, and 8 % had urinary retention requiring prolonged catheterization. Zacharakis and colleagues investigated the oncological and functional outcome of HIFU in 31 men with biopsy-proven locally recurrent prostate cancer following external beam radiation therapy. The mean pre-therapy PSA level was 7.73 (range = 0.20–20) ng/mL [50]. The patients were followed for a mean of 7.4 months. Eleven of the 31 patients (35 %) developed stricture or required intervention to remove obstructing necrotic tissue, 8 (26 %) had urinary tract infection or dysuria syndrome, and 2 (6 %) suffered from urinary incontinence. Rectourethral fistulae occurred in two men (7 %). Overall, 71 % had no evidence of disease following salvage HIFU.

Urinary retention appears to be one of the most common side effects of HIFU, developing in almost all patients [51]. Grade I and II urinary stress incontinence occurs in about 12 % of

patients. If TURP is not performed prophylactically, many patients require subsequent TURP or bladder neck incision. Postoperative impotence occurs in 55–70 % of patients.

The place of HIFU in the treatment of prostate cancer remains undefined. A review of new treatments for prostate cancer published at the end of 2008 describes the importance of patient selection for HIFU treatment [52].

Many of the early-stage patients included in these series that refused surgery and radiation therapy would have been appropriate for active surveillance protocols. It is clear from the work of both large groups that there has been an improvement in results with improved patient selection and technical advances, in particular imaging of the prostate during therapy. Illing and colleagues proposed a standard for carrying out ultrasound-guided transrectal HIFU for prostate cancer. They describe the importance of ultrasonically monitoring the changes induced in the prostate by HIFU and adapting the treatment parameters based on these changes [53]. Further technological developments such as MR guidance, which increases the precision of targeting and uses magnetic resonance thermography to monitor the temperature in the rectum, urinary tract, and neurovascular bundles during treatment, may improve clinical outcome and reduce adverse events related to transrectal HIFU for prostate cancer. In addition to the ability to detect changes due to intraprostatic tumor, MRI is considered by many experts to be the gold standard for determining prostate volume [54].

Prospective randomized studies comparing image-guided HIFU to other modalities (radiotherapy or active surveillance) appropriate to the specific group of elderly patients with limited volume of prostate cancer are needed to evaluate the comparative efficiency and toxicity of alternative therapies. None of the published studies included prospective evaluation using validated quality-of-life (QOL) questionnaires; therefore, the consequences of HIFU on quality of life – especially sexual, urinary, and bowel function – and on the overall health of these patients remain poorly documented. Currently, there are several nonrandomized clinical trials being conducted in the United States to determine the safety and efficacy of a minimally invasive prostate cancer treatment using high-intensity focused ultrasound. These include patients with primary prostate cancer and patients with recurrent prostate cancer. However, most are planned to accrue small numbers of patients. Unfortunately, it has been difficult to accrue prostate cancer patients to studies randomizing between competing therapies such as surgical resection, radiotherapy, cryotherapy, active surveillance, or HIFU. Nevertheless, future studies will need to include validated QOL measurements in order to define the place of HIFU among the treatment options for early prostate cancer.

The current European Urological Association Guidelines for 2010 consider HIFU for prostate cancer to still be experimental or investigational in the initial treatment of localized disease, and a longer follow-up is mandatory to assess its role in the management of prostate cancer. In the setting of local relapse following radiotherapy, HIFU might be an alternative option; however, patients must be informed about the experimental nature of this treatment modality due to the short follow-up periods reported. HIFU seems appropriate in patients with localized recurrence following radiotherapy, particularly when an actual recurrence can be identified with biopsy and imaging.

Breast Cancer

Focal therapy has an increasing place in the overall course of treatment of early-stage breast cancer. Traditionally, a 6–7-week regimen of radiotherapy is delivered to the whole breast after surgical resection of the breast tumor. In recent years, the use of partial breast irradiation (PBI), in which the tumor bed alone is treated, has established a role for focal therapy in breast cancer. MRI is the most sensitive imaging modality for identifying and delineating breast cancer, and Hynynen and colleagues initially described the feasibility of MRgFUS for treating breast lesion [55]. Several centers have reported on patient cohorts treated with MRgFUS prior to surgical

resection [56]. In 2001, Huber and colleagues described a sheep animal model and reported the first clinical treatment of breast cancer [57]. Zippel and colleagues described a series of 10 patients receiving MRgFUS 1 week prior to tumor resection, with only two of them having complete tumor necrosis [58]. Gianfelice and colleagues described a series of women receiving MRgFUS prior to lumpectomy. Their initial report of the first 12 patients concluded that "residual viable cancer was found outside the targeted area when targeting was poor or not perfect and at the periphery of the tumor when targeting was completely accurate [59]". Subsequent analyses of a total of 25 women suggested that posttreatment MRI can accurately assess residual tumor tissue after MRgFUS if performed more than 7 days after treatment [60]. This information may help to select patients requiring retreatment with HIFU. Furusawa and colleagues treated a group of women with MRgFUS prior to surgery to a target that included a 5-mm margin around the tumor. Among 25 breast carcinomas that received adequate treatment according to protocol, the mean necrosis of ablated tumor was 98 % with 15 of them (60 %) having 100 % necrosis. Review of the treatment plan for the single patient whose tumor had less than 95 % necrosis showed that the sonication did not cover the entire tumor and margin [61]. Wu and colleagues described a randomized study including 48 patients with breast tumors, 23 of whom received ultrasound-guided HIFU prior to mastectomy. The target included the tumor with a 1.5–2.0-cm margin of normal tissue. In all 23 patients, complete coagulative necrosis of the tumor was seen [62]. All these studies performed surgical resection within a couple of weeks after HIFU. An ongoing study is testing the delivery of MRgFUS HIFU to early breast cancer patients with no additional tumor resection or radiotherapy. Patients were followed up every 3 months with ultrasound and MRI. A report with a median follow-up of 14 months for the first 21 patients treated on this study showed one case of recurrence of pure mucinous carcinoma [63].

The need to address breast cancer cells outside the main tumor mass was noted by Holland and colleagues, who found that in 20 % of breast cancer specimens, tumor foci were present up to 2 cm away from the clinical tumor mass and in 43 % of specimens, tumor was found more than 2 cm away [64]. This is part of the rationale for the need to add radiation to the tumor bed following lumpectomy for early breast cancer. From the above HIFU studies, it can be concluded that as long as the entire tumor with margins is included in the targeted volume, HIFU can successfully ablate cancerous breast lesions, provided that the targeted lesion includes a margin of at least 5 mm of healthy tissue around the tumor. It is possible that with longer follow-up, a greater degree of necrosis will be seen even in patients receiving treatment to the tumor alone, without a margin of healthy tissue. Indeed, animal studies have shown that HIFU induces an immunological response outside of the targeted tumor. This may involve tumor antigens released from damaged tumor cells that activate dendritic cells and may lead to destruction of residual tumor cells surviving HIFU [65].

Brain Tumors

The initial clinical experience with HIFU almost 60 years ago was to produce CNS lesions in patients with functional disorders. The main limitation to the use of HIFU for brain tumors is the attenuation of the ultrasound beam by the intervening bony tissue of the skull, requiring removal of a small portion of the skull to access the brain. Using the InSightec MRgFUS system, a preclinical study in pigs [66] and a small clinical study have been carried out at Sheba Medical Center in Israel. In the clinical study, three patients with recurrent glioma were treated. Focal lesions were seen on images of the targeted tissue, and coagulative necrosis was seen on histological examination, but one patient developed a secondary focus of heating in the beam path outside the targeted area [67].

In 1981, Fry and colleagues described a method of producing focal brain lesions with the ultrasound beam crossing the skull, thus avoiding the need for craniectomy [68]. Hynynen

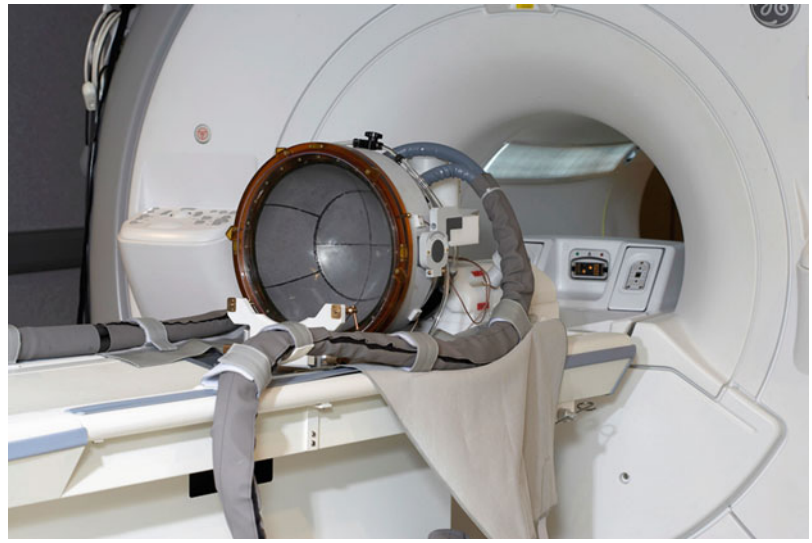

Fig. 5.10 A clinical prototype brain treatment system (ExAblate 3000, InSightec, Inc., Haifa, Israel)

and colleagues further developed this concept [69], and a study on primates with the InSightec MRgFUS system showed the feasibility of the transcranial approach for delivering focused ultrasound to CNS lesions (Fig. 5.10). Primary brain tumors which tend to infiltrate the surrounding healthy brain are not ideal lesions for treatment with focused therapy such as HIFU. The clinical use of HIFU in brain disease may be more appropriate for reversible blood–brain barrier opening, to enable a more efficient chemotherapeutic effect in the brain, benign noncancerous lesions, or as a tool for functional neurosurgery.

Conclusions

The technology exists today to deliver high doses of thermal energy to effectively destroy cancerous lesions in tissues. This requires image guidance using either ultrasound or MRI to image the target tumor and to evaluate the clinical response to therapy. An increasing number of manufacturers are developing systems for image-guided HIFU. MRI has the added advantage of allowing real-time temperature measurement during therapy, thereby enabling more accurate energy deposition and better control of the lesions produced. Clinical studies have confirmed the feasibility of image-guided HIFU for the treatment of both primary and metastatic tumors. The greatest experience has been obtained in treating primary and metastatic bone tumors and in treating prostatic carcinoma. Ongoing clinical studies will help to define the place of image-guided HIFU in the spectrum of cancer therapies.

References

1. Pfeffer MR, Teicher BA, Holden SA, Al-Achi A, Herman TS. The interaction of cisplatin plus etoposide with radiation +/− hyperthermia. Int J Radiat Oncol Biol Phys. 1990;19:1439–47.
2. Wust P, Hildebrandt B, Sreenivasa G, Rau B, Gellermann J, Riess H, Felix R, Schlag PM. Hyperthermia in combined treatment of cancer. Lancet Oncol. 2002;3:487–97.
3. Lynn JG, Zwemer RL, Chick AJ, et al. A new method for the generation and use of focused ultrasound in experimental biology. J Gen Physiol. 1942;26:179.
4. Fry WJ, Mosberg Jr WH, Barnard JW, Fry FJ. Production of focal destructive lesions in the central nervous system with ultrasound. J Neurosurg. 1954;11:471–8.
5. Burov AK. High intensity ultrasonic oscillations for the treatment of malignant tumors in animal and man. Dokl Akad Nauk SSSR. 1956;106:239.
6. Sapareto SA, Dewey WC. Thermal dose determination in cancer therapy. Int J Rad Oncol Biol Phys. 1984;10:787–800.
7. Zhang HG, Mehta K, Cohen P, Guha C. Hyperthermia on immune regulation: a temperature's story. Cancer Lett. 2008;271:191–204.

8. Hynynen K, Watmough DJ, Mallard JR. Design of ultrasonic transducers for local hyperthermia. Ultrasound Med Biol. 1981;7:397–402.
9. Hynynen K, Darkazanli A, Unger E, et al. MRI-guided noninvasive ultrasound surgery. Med Phys. 1993; 20:107–15.
10. Cline HE, Schenck JF, Hynynen K, et al. MR-guided focused ultrasound surgery. J Comput Assist Tomogr. 1992;16:956–65.
11. Jolesz F, Hynynen K. Focused ultrasound. In: DeVita VT, Lawrence TS, Rosenberg SA, editors. Cancer principles and practice of oncology. 8th ed. Philadelphia: Lippincott Williams & Wilkins; 2008. p. 2991–3000.
12. Stewart EA, Gostout B, Rabinovici J, et al., for the MRgFUS for Uterine Fibroids Group. Sustained relief of leiomyoma symptoms by using focused ultrasound surgery. Obstet Gynecol. 2007;110:279–87.
13. Chow E, Wu JS, Hoskin P, et al. International consensus on palliative radiotherapy endpoints for future clinical trials in bone metastases. Radiother Oncol. 2002;64:275–80.
14. Gianfelice D, Khiat A, Boulanger Y, et al. MR imaging-guided focused ultrasound surgery of breast cancer: correlation between dynamic contrast-enhanced MRI and histopathologic findings. Breast Cancer Res Treat. 2003;82:93–101.
15. Kopelman D, Inbar Y, Hanannel A, et al. Magnetic resonance guided focused ultrasound surgery (MRgFUS). Four ablation treatments of a single canine hepatocellular adenoma. HPB. 2006;8:292–8.
16. Cohen ZR, Zaubermann J, Harnof S, et al. Magnetic resonance imaging-guided focused ultrasound for thermal ablation in the brain: a feasibility study in a swine model. Neurosurgery. 2007;60:593–600.
17. Huber PE, Jenne JW, Rastert R, et al. A new noninvasive approach in breast cancer therapy using magnetic resonance imaging-guided focused ultrasound surgery. Cancer Res. 2001;61:8441–7.
18. Böhmer MR, Klibanov AL, Tiemann K, Hall CS, Gruell H, Steinbach OC. Ultrasound triggered image-guided drug delivery. Eur J Radiol. 2009;70:242–53.
19. Smith NB, Temkin JM, Shapiro F, et al. Thermal effects of focused ultrasound energy on bone tissue. Ultrasound Med Biol. 2001;27:1427–33.
20. Lipton A. Management of bone metastasis in breast cancer, current treatment options. Oncology. 2005; 6:161–71.
21. Roodman GD. Mechanisms of bone metastasis. N Engl J Med. 2004;350:1655–64.
22. Falkmer U, Jarhult J, Wersall P, et al. A systematic overview of radiation therapy effects in skeletal metastases. Acta Oncol. 2003;42:620–33.
23. Chow E, Hoskin P, van der Linden Y, et al. Quality of life and symptom end points in palliative bone metastases trials. Clin Oncol (R Coll Radiol). 2006;18:67–9.
24. Mundy GR. Metastasis to bone, causes, consequences, and therapeutic opportunities. Nat Rev Cancer. 2002; 2:584–93.
25. Konski A. Radiotherapy is a cost-effective palliative treatment for patients with bone metastasis from prostate cancer. Int J Radiat Oncol Biol Phys. 2004;60:1373–8.
26. Sze WM, Shelley MD, Held I, et al. Palliation of metastatic bone pain: single fraction versus multifraction radiotherapy – a systematic review of randomised trials. Clin Oncol. 2003;15:345–52.
27. Ahrar K. The role and limitations of radiofrequency ablation in treatment of bone and soft tissue tumors. Curr Oncol Rep. 2004;6:315–20.
28. Saarti T, Janes R, Tenhunen M, et al. Palliative radiotherapy in treatment of skeletal metastasis. Eur J Pain. 2002;6:323–30.
29. Chow E, Harris K, Fan G, Tsao M, Sze WM. Palliative radiotherapy trials for bone metastases: a systemic review. J Clin Oncol. 2007;25(11):1423.
30. Liberman B, Gianfelice D, Inbar Y, et al. Pain palliation in patients with bone metastases using MR-guided focused ultrasound surgery: a multicenter study. Ann Surg Oncol. 2009;16:140–6.
31. Catane R, Beck A, Inbar Y, et al. MR-guided focused ultrasound surgery (MRgFUS) for the palliation of pain in patients with bone metastases-preliminary clinical experience. Ann Oncol. 2007;18:163–7.
32. Chen W, Zhu H, Zhang L, et al. Primary bone malignancy: effective treatment with high-intensity focused ultrasound ablation. Radiology. 2010;255(3):967–78.
33. Li C, Zhang W, Fan W, et al. Noninvasive treatment of malignant bone tumors using high-intensity focused ultrasound. Cancer. 2010;116:3934–42.
34. Yerushalmi A, Servadio C, Leib Z, Fishelovitz Y, Rokowsky E, Stein JA. Local hyperthermia for treatment of carcinoma of prostate: a preliminary report. Prostate. 1982;3:623–6.
35. Algan O, Fosmie H, Hynynen K, et al. External beam radiotherapy and hyperthermia in the treatment of patients with locally advanced prostate carcinoma. Cancer. 2000;89:399–403.
36. Gelet A, Chapelon JY, Margonari J, et al. High intensity focused ultrasound experimentation on human benign prostatic hypertrophy. Eur Urol. 1993;23:44–7.
37. Madersbacher S, Pedevilla M, Vingers L, Susani M, Marberger M. Effect of high-intensity focused ultrasound on human prostate cancer in vivo. Cancer Res. 1995;55(15):3346–51.
38. Biermann K, Montinori R, Lopez-Beltran A, Zhang S, Cheng L. Histopathological findings after treatment of prostate cancer using high-intensity focused ultrasound (HIFU). Prostate. 2010;70:1196–200.
39. Rebillard X, Soulié M, Chartier-Kastler E, et al. High-intensity focused ultrasound in prostate cancer; a systematic literature review of the French Association of Urology. BJU Int. 2008;101:1205–13.
40. Crouzet S, Rebillard X, Chevallier D, et al. Multicentric oncologic outcomes of high-intensity focused ultrasound for localized prostate cancer in 803 patients. Eur Urol. 2010;58:559–66.
41. Thuroff S, Chaussy C, Vallancien G, et al. High-intensity focused ultrasound and localized prostate

cancer: efficacy results from the European multicentric study. J Endourol. 2003;17:673–7.
42. Blana A, Murat F-J, Waler B, et al. First analysis of the long-term results with transrectal HIFU in patients with localized prostate cancer. Eur Urol. 2008;53:1194–203.
43. Riviere J, Bernhard JC, Robert G, et al. Salvage radiotherapy after high-intensity focused ultrasound for recurrent localized prostate cancer. Eur Urol. 2010; 58:567–73.
44. Uchida T, Shoji S, Nakano M, et al. Transrectal high-intensity focused ultrasound for the treatment of localized prostate cancer: eight-year experience. Int J Urol. 2009;16(11):881–6.
45. Ahmed HU, Zacharakis E, Dudderidge T, et al. High-intensity-focused ultrasound in the treatment of primary prostate cancer: the first UK series. Br J Cancer. 2009;101:19–26.
46. Koch MO, Gardner T, Cheng L, et al. A phase I/II trial of high intensity focused ultrasound for the treatment of previously untreated localized prostate cancer. J Urol. 2007;178(6):2366–70.
47. Roach M, Hanks G, Walter B, et al. Defining biochemical failure following radiotherapy with or without hormonal therapy in men with clinically localized prostate cancer: recommendations of the RTOG-ASTRO Phoenix Consensus Conference. Int J Radiat Oncol Biol Phys. 2006;65:965–74.
48. Eade TN, Hanlon AL, Horwutz EM, et al. What dose of external beam radiation is high enough for prostate cancer? Int J Radiat Oncol Biol Phys. 2007;68:682–9.
49. Murat F-J, Poisonnier L, Rabilloud M, et al. Mid-term results demonstrate salvage high-intensity focused ultrasound as an effective and acceptably morbid salvage treatment for locally recurrent prostate cancer. Eur Urol. 2009;55:640–9.
50. Zacharakis E, Ahmed HU, Ishaq A, Scott R, Illing R, Freeman A, Allen C, Emberton M. The feasibility and safety of high-intensity focused ultrasound as salvage therapy for recurrent prostate cancer following external beam radiotherapy. BJU Int. 2008;102(7):786–92.
51. Poissonnier L, Chapelon JY, Rouviere O, Curiel L, et al. Control of prostate cancer by transrectal HIFU: high-intensity focused ultrasound in 227 patients. Eur Urol. 2007;51(2):381–7.
52. Marberger M, Carroll PR, Zelefsky MJ, et al. New treatments for localized prostate cancer. Urology. 2008;72(Suppl 6A):36–43.
53. Illing OW, Leslie TA, Kennedy JE, et al. Visually directed high-intensity focused ultrasound for organ-confined prostate cancer: a proposed standard for the conduct of therapy. BJU Int. 2006;98:1187–92.
54. Van As N, Parker C, De Souza N. Magnetic resonance imaging is the modality of choice for accurate assessment of prostate volume. Clin Oncol. 2007;19:S4.
55. Hynynen K, Freund W, Cline HE, et al. A clinical noninvasive MRI monitored ultrasound surgery method. Radiographics. 1996;16:185.
56. Schmitz AC, Gianfelice D, Daniel BL, Mali WP, van den Bosch MA. Image-guided focused ultrasound ablation of breast cancer: current status, challenges, and future directions. Eur Radiol. 2008; 18:1431–41.
57. Zippel DB, Papa MZ. The use of MR imaging guided focused ultrasound on breast cancer patients; a preliminary phase one study and review. Breast Cancer. 2005;12:32–8.
58. Gianfelice D, Khiat A, Amara M, Belblidia A, Boulanger Y. MR imaging-guided focused US ablation of breast cancer: histopathologic assessment of effectiveness–initial experience. Radiology. 2003; 227:849–55.
59. Khiat A, Gianfelice D, Amara M, Boulanger Y. Influence of posttreatment delay on the evaluation of the response to focused ultrasound surgery of breast cancer by dynamic contrast enhanced MRI. Br J Radiol. 2006;79:308–14.
60. Furusawa H, Namba K, Thomsen S, et al. Magnetic resonance- guided focused ultrasound surgery of breast cancer: reliability and effectiveness. J Am Coll Surg. 2006;203:54–63.
61. Wu F, Wang Z, Cao Y, Chen W, Bai J, Zou J, Zhu H. A randomised clinical trial of high-intensity focused ultrasound ablation for the treatment of patients with localised breast cancer. Br J Cancer. 2003;89: 2227–33.
62. Furusawa H, Namba K, Nakahara H, et al. The evolving nonsurgical ablation of breast cancer: MR guided focused ultrasound (MRgFUS). Breast Cancer. 2007; 14:55–8.
63. Holland R, Veling SH, Mravunac M, Hendriks JH. Histologic multifocality of Tis, T1-2 breast carcinomas. Implications for clinical trials of breast-conserving surgery. Cancer. 1985;56:979–90.
64. Hu Z, Yang XY, Liu Y, et al. Investigation of HIFU-induced anti-tumour immunity in a murine tumour model. J Trans Med. 2007;5:34–9.
65. Cohen ZR, Zaubermann J, Harnof S, et al. Magnetic resonance imaging-guided focused ultrasound for thermal ablation in the brain: a feasibility study in a swine model. Neurosurgery. 2006;60: 593–600.
66. Ram Z, Cohen ZR, Harnof S, et al. Magnetic resonance imaging-guided, high intensity focused ultrasound for brain tumor therapy. Neurosurgery. 2006; 59:949–55.
67. Fry JF, Goss SP, Patrick JT. Transkull focal lesions in cat brain produced by ultrasound. J Neurosurg. 1981; 54:659–63.
68. Hynynen K, Clement G. Clinical applications of focused ultrasound – the brain. Int J Hyperthermia. 2007;23:193–202.
69. Hynynen K, McDannold N, Clement G, et al. Preclinical testing of a phased-array ultrasound system for MRI-guided noninvasive surgery of the brain-a primate study. Eur J Radiol. 2006;59:149–56.

Embolic Therapies

6

Ahsun Riaz, Khairuddin Memon, Robert J. Lewandowski, and Riad Salem

Abstract

Primary and secondary liver cancers pose a challenge in terms of treatment options for the following reasons: (1) most patients are unresectable at presentation not only due to tumor stage but also because of comorbidities (cirrhosis) and (2) there exist limitations in systemic chemotherapy (adverse events) and external radiation (dose delivered to normal tissue). Given this, embolic therapies involve the transarterial delivery of high-dose toxic material directly to the tumor and thereby sparing the normal hepatic tissue as well as rest of the body from possible adverse reactions. Embolic therapies require knowledge of vascular anatomy, technical aspects of targeting the tumor for delivery of toxic material, physical properties of available devices, and clinical aspects of patient selection, response assessment, patient monitoring, and complications. Embolic therapy includes bland embolization, chemoembolization (conventional and drug-eluting beads), and radioembolization. This chapter covers the basic concepts associated with each of these treatment modalities. This chapter also gives a brief overview of utilization of embolic therapies in extrahepatic neoplasms.

Embolic Therapies for Hepatic Malignancies

The incidence of primary and secondary liver tumors continues to increase [1]. Surgery and systemic chemotherapy have limited role in the management of liver tumors [2, 3]. Hence, image-guided locoregional therapies are establishing their roles in their management. Locoregional therapies have been shown to have a palliative role and may also have a potentially curative role [4–8]. This chapter is focused on hepatic embolic therapies used in the field of interventional oncology. Table 6.1 summarizes some of the available embolic locoregional therapies. These targeted therapies decrease the rates of systemic toxicity without compromising tumoricidal effect.

A. Riaz (✉) • K. Memon • R.J. Lewandowski • R. Salem
Department of Radiology, Northwestern Memorial Hospital, Chicago, IL, USA
e-mail: ahsun.riaz@gmail.com; khairuddin.kd@gmail.com; r-lewandowski@northwestern.edu; r-salem@northwestern.edu

D.E. Dupuy et al. (eds.), *Image-Guided Cancer Therapy*, DOI 10.1007/978-1-4419-0751-6_8,

Table 6.1 Summary of image-guided therapies

Type of treatment	Treatment	Primary liver tumors	Secondary liver tumors
Catheter-based therapies	Transarterial bland embolization	HCC	Neuroendocrine, metastatic sarcoma
	Transarterial chemoembolization	HCC	Neuroendocrine, CRC, mixed
	Transarterial chemoembolization with drug-eluting beads	HCC	CRC
	Radioembolization	HCC, ICC	CRC, neuroendocrine, mixed

Anatomy of the Liver

Hepatic malignancies have been the predominant target of interventional oncologists partly due to the favorable anatomy of the liver making image-guided approaches to tumors possible. The vascular supply of the tumors is predominantly by the hepatic artery. The normal parenchyma is predominantly supplied in contrast by the portal vein. This unique blood supply to the liver allows the hepatocytes to carry out their metabolic functions on the substrates absorbed from the gastrointestinal tract. It also predisposes the liver to become a predominant site for metastases [9–11].

An overview of the arterial supply of the liver is important to understand the use of transcatheter therapies for the treatment of liver malignancies. The celiac trunk is the first anterior branch of the abdominal aorta. It gives off the common hepatic artery which becomes the proper hepatic artery which subsequently branches into the right and left hepatic arteries. These supply the corresponding lobes of the liver by giving off segmental branches. The cystic artery supplying the gallbladder usually arises from the right hepatic artery. Hepatic tumors are hypervascular structures which can also parasitize arterial flow from the surrounding tissue.

The role of injecting embolic material in the main hepatic artery is extremely limited due to the increased toxic effects on normal parenchyma. Injecting embolic material into the right or left lobar arteries is also limited. However, radiation lobectomy is a relatively new concept in which radioembolic material is injected into the right or left lobar artery to cause tumor necrosis with shrinkage of the tumor-containing lobe and hypertrophy of the normal contralateral hepatic lobe. Selective arterial embolization is preferred whenever possible. Advances in imaging such as C-arm angiographic CT have allowed for superselective embolization and hence further facilitating tumor targeting and decreasing toxicity to normal hepatic parenchyma [12].

Diagnosis and Staging of Liver Tumors

The following gives a brief overview of the various liver tumors currently treated using targeted therapies. The management of liver tumors is now a multidisciplinary task with the involvement of hepatologists, medical and surgical oncologists, transplant surgeons, and interventional radiologists. The patients should be selected for a specific targeted therapy after multidisciplinary consensus. The evidence-based criteria for patient selection are discussed separately with each treatment below.

Primary Liver Tumors

Hepatocellular Carcinoma (HCC)

The details of diagnosis and staging of the liver tumors are beyond the scope of this chapter. Previously published and well-established

guidelines are followed for diagnosing and staging [13]. The use of laboratory tests to assess the liver function status and radiologic studies (contrast-enhanced CT or MRI) to diagnose and stage the HCC is of optimal importance. The tumor markers for HCC, i.e., alpha-fetoprotein (AFP) and protein induced by vitamin K absence (PIVKA-II), have a role in diagnosing HCC.

Patients within Milan criteria, i.e., single lesion less than 5 cm or up to three lesions all less than 3 cm, are eligible for orthotopic liver transplantation (OLT) [14]. Resection is possible only if liver function is well compensated. The use of surgical options is considered gold standard for these patients. The limited availability of donor organs for OLT and the dropout of patients due to tumor progression limit the role of OLT.

Patients who are outside transplant criteria but do not have malignant PVT or metastatic HCC are also candidates for some targeted therapies. Locoregional therapies in these patients have been shown to downstage the disease within transplant criteria [15, 16]. This use allows the patients who were initially outside Milan criteria to be eligible for transplant. Recurrence-free and overall survivals after OLT in the downstaged patients are yet to be compared to those of patients who were already within transplant criteria to determine the efficacy of downstaging. This group of patients may also have a survival benefit following treatment even without downstaging.

Systemic therapy with sorafenib has been shown to have a significant improvement in survival in patients with advanced disease [3]. Patients with advanced disease benefit from targeted therapies. The presence of PVT excludes these patients from receiving curative surgical therapies. The presence of distant metastases, i.e., lung and adrenals, is a contraindication to most local treatments, as there has not been a survival benefit seen in this group of patients.

Intrahepatic Cholangiocarcinoma (ICC)

Interventional oncology has been shown to be effective in the treatment of HCC, but its role in the management of ICC has not been extensively studied.

Secondary Liver Tumors

Metastatic Colorectal Carcinoma (CRC)

Less than 10 % of hepatic metastatic CRC are resectable [17]. Systemic chemotherapy for this disease includes fluorouracil (5-FU), oxaliplatin, irinotecan (CPT-11), bevacizumab, cetuximab, and capecitabine. Some treatment modalities used in interventional oncology have established their role in the treatment of metastatic CRC to the liver.

Metastatic Neuroendocrine Tumors

Neuroendocrine tumors commonly metastasize to the liver. The production of hormones makes these tumors cause a variety of symptoms. Carcinoid, VIPomas, gastrinomas, and somatostatinomas are some examples. Systemic chemotherapy and ablative procedures have been shown to have a modest benefit in these patients. Patients with unresectable disease are candidates for chemoembolization, bland embolization, and radioembolization.

Other Primary Tumors

Many secondary tumors to the liver have been treated using interventional oncology techniques, but only metastatic breast cancer has been studied in detail. Metastatic melanoma, sarcoma, and renal cell carcinoma are some other examples.

Monitoring Response to Treatment

Tumor Markers

The baseline tumor markers are often compared to the posttreatment values to analyze treatment efficacy. Recent studies have shown that alpha-fetoprotein is a valuable marker for response assessment in HCC [18]. There may be a role of tumor markers such as CA-19-9 and carcinoembryonic antigen (CEA) in response assessment following treatment of secondary liver tumors as well.

Radiological Monitoring

Image-guided therapies utilize live imaging techniques to guide and target the lesion during

treatment. The response to treatment is monitored clinically and radiologically. The first radiologic study is usually performed 1 month after treatment to assess response. Patients are then followed with scans every 3 months to assess response to treatment or progression of disease. The use of the WHO size criteria and the EASL necrosis criteria is used to assess response in the target lesions [19]. Recently, the concept of response in the "primary index lesion" as a tumor marker in HCC has been suggested [20]. Conventional anatomic imaging studies may not able to assess tumor response until 6 weeks have elapsed after treatment. The use of functional MRI may have a role in earlier detection of tumor response [21].

In a recent study at our center, various combinations of WHO, EASL, and RECIST guidelines were studied in order to understand correlation between radiological response and actual pathological necrosis. Various scoring systems were devised based on the combinations of these radiological guidelines. It was concluded that EASL × WHO scoring system provides a simple and clinically acceptable method of response assessment and radiological-pathological correlation [22].

Embolic Therapies

Transarterial (Bland) Embolization

Introduction

This is a therapy which occludes the blood vessels and induces tumor ischemia by the transcatheter injection of bland embolic material into the tumor-feeding vessel. This was first used in the 1950s and is the basis for all transcatheter therapies [23].

Procedure

There is a trend towards an increased survival using transarterial chemoembolization when compared to bland embolization, but no study has been able to demonstrate a difference in survival in the two treatments [24, 25]. After staging of the tumor, the vascular anatomy of the region and the tumor is meticulously studied using angiography. After localizing and identifying the vascular supply of the tumor, the bland embolic material is injected into the tumor using the feeding vessel. Some of the embolic agents used are polyvinyl alcohol particles, Embospheres (BioSphere Medical, Inc., Rockland, MA), and Gelfoam (Pharmacia and Upjohn Company, Kalamazoo, MI). Bland embolization has been shown to induce tumor ischemia and cell death but may also lead to neoangiogenesis due to an increase in angiogenic factors [26].

Indications for Bland Embolization

A randomized controlled trial comparing bland embolization with symptomatic treatment failed to show a survival benefit of using bland embolization in patients with HCC belonging to Child-Turcotte-Pugh class A [27]. As mentioned above, the use of chemoembolization has not shown to have a difference in survival when compared to bland embolization. Maluccio et al. concluded that bland embolization was effective in treating patients with unresectable HCC and that bland particles may be the critical component of intra-arterial embolotherapy [28]. It has also been used for pain relief and control of symptoms in hepatic metastases from neuroendocrine tumors and sarcomas [29].

Complications

Patients may experience a mild post-embolic syndrome which consists of the following clinical signs and symptoms: fatigue, nausea, vomiting, anorexia, fever, abdominal discomfort, and cachexia. There might be right upper quadrant pain. This is usually mild and resolves without clinical intervention. In select cases, it may require inpatient care. Other complications may include injury to the groin when gaining or closing the access to the vessel [30] and abscess formation.

Transarterial Chemoembolization

Introduction

Chemoembolization allows the delivery of a high dose of chemotherapeutic agents to the tumor with minimal systemic bioavailability. It is

being used since the 1980s [31, 32]. This is an inpatient procedure.

Procedure

After meticulous evaluation of the baseline characteristics and stage of the malignancy using clinical and radiologic data, angiography is performed to study the vascular anatomy of the region and the tumor. The chemotherapeutic drug is mixed with Lipiodol and injected into the tumor-feeding vessel during angiography. Lipiodol is a poppy-seed oil containing 38 % iodine by weight. It is a radiopaque substance and is visualized on posttreatment CT scans in the target lesion. This is followed by the injection of bland embolic particles to prevent washout of the drug and to induce ischemic necrosis [33].

Indications for Chemoembolization

In general, absolute contraindications to chemoembolization include the absence of hepatopetal flow or compensatory collaterals, encephalopathy, and biliary obstruction. The relative contraindications include elevated serum bilirubin (>2 mg/dL), elevated lactate dehydrogenase (>425 U/L), elevated aspartate aminotransferase (>100 U/L), tumor burden exceeding >50 % of the liver, ascites, bleeding varices, thrombocytopenia, or cardiac or renal insufficiency [34]. Doxorubicin alone as the chemotherapeutic is commonly used worldwide, whereas the combination of mitomycin C, doxorubicin, and cisplatin is preferred in the United States [35]. The best patients for chemoembolization are those with good performance status, preserved liver function, and no evidence of vascular invasion or extrahepatic metastasis. Llovet et al. compared survival outcomes in patients treated with fixed interval (intention-to-treat) chemoembolization, embolization, and conservative measures [8]. The authors concluded that chemoembolization and embolization significantly improved survival in select patients with unresectable HCC. Takayasu et al. published data from a large cohort study of 8,510 HCC patients treated with chemoembolization and showed that prognosticators of survival included degree of liver damage, alpha-fetoprotein value, maximum tumor size, number of lesions, and portal vein invasion [36].

The role of chemoembolization in cholangiocarcinoma is relatively ill explored. In a recent two-center study, Kiefer et al. treated 62 patients of unresectable cholangiocarcinoma with lobar or segmental chemoembolization. They concluded that chemoembolization provided local disease control (PR + SD) of intrahepatic cholangiocarcinoma. Overall survival after chemoembolization showed the best outcomes for those receiving multidisciplinary integrated liver-directed and systemic therapies [37].

There are data on patients treated with chemoembolization for metastatic disease. Geschwind et al. demonstrated that chemoembolization can prolong survival of patients with colorectal metastases even in patients who had not responded to systemic chemotherapy [38]. Liapi et al. analyzed imaging responses and determined outcomes of 26 patients with neuroendocrine metastases treated with chemoembolization and showed a mean patient survival of 78 months [39]. The imaging response to treatment using WHO (bidimensional) and RECIST (unidimensional) criteria was seen in only one-third of the cohort. Patients with breast metastasis to the liver unresponsive to standard of care chemotherapy have been treated with chemoembolization, and the survival benefit seen is not impressive as most patients develop extrahepatic metastases [40, 41]. Burger et al. have reported on their experience of treating 17 patients with unresectable cholangiocarcinoma treated with chemoembolization and concluded that chemoembolization was effective in prolonging survival in these patients [42].

Combination Therapies

Chemoembolization/RFA

Chemoembolization has been used prior to RFA to decrease the tumor size and vascularity making it more susceptible to the effects of RF ablation [43]. Kagawa et al. reported their comparison o of 62 patients who received TACE and RFA and 55 patients who underwent surgical resection [44]. They found out that 1, 3, and 5 years in the TACE + RFA group were similar

($P = .788$) to those in the resection group (92.5 %, 82.7 %, and 76.9 %, respectively). They concluded that RFA combined with TACE is an efficient and safe treatment.

Chemoembolization/Surgery

Chemoembolization has the potential of bridging patients to OLT allowing longer waiting times. It also has shown ability to downstage patients to the Milan criteria, thus allowing them to undergo OLT [45].

Chemoembolization/Ethanol Ablation

A randomized control trial comparing chemoembolization alone with the combination of chemoembolization and percutaneous ethanol ablation showed significantly higher response rates and less recurrence following the combination [46].

Complications

Post-embolization syndrome is seen after TACE and is usually managed during the hospitalization. Other complications may include (a) bile duct injury [30], up to 5.3 % patients may develop biliary complications following TACE; [47] (b) liver abscesses are rare but are possible after TACE especially in patients who have undergone biliary interventions; [30] (c) the inadvertent deposition of the chemotherapeutic drug to the gastrointestinal tract may cause duodenal or gastric ulcers and may even lead to perforation in severe cases; [30] (d) intra-arterial approach increases the risk of vascular injury in all transcatheter techniques, and [30] chemotherapeutic agents may also have a role in causing this complication; [48] (e) tumor rupture (0.15 %) following TACE; [30] and pulmonary artery embolism may occur and the patient may present with cough and dyspnea [30].

Chemoembolization with Drug-Eluting Beads

Introduction

Drug-eluting beads are chemotherapeutic agent-loaded microspheres which are delivered intra-arterially. This allows the delivery of the agent in a controlled and sustained manner. Some available drug-eluting beads include (a) a copolymer microsphere (QuadraSphere, Biosphere Medical, Rockland, Massachusetts) and (b) doxorubicin-capable (DC) bead. The latter has also been loaded with irinotecan, and an acceptable safety profile has been reported following their use in management of colorectal metastases to the liver [12].

Procedure

The procedure is similar to conventional chemoembolization described above and is delivered after angiographic evaluation of the vascular anatomy. Studies have shown significant reductions in the peak plasma concentrations with drug-eluting beads when compared to conventional chemoembolization [49].

Indications for Drug-Eluting Beads

The doxorubicin-loaded beads have a promising role in the treatment of inoperable HCC [50, 51]. Patient selection is similar to that for conventional chemoembolization. Poon et al. reported a 63 % response using the modified RECIST criteria which takes tumor necrosis into account [4]. A recent randomized controlled trial on 200 patients comparing conventional chemoembolization with drug-eluting beads failed to show a significant survival benefit (PRECISION V). There were fewer adverse events seen after chemoembolization with drug-eluting beads when compared to conventional chemoembolization.

Varela et al. investigated the use of chemoembolization with DEBs in a series of 27 patients with HCC and Child-Pugh A cirrhosis. They demonstrated that response rate was 75 % by CT at 6 months; doxorubicin Cmax and AUC were significantly lower than conventional TACE, and 1- and 2-year survival rates were 92.5 % and 88.9 %, respectively, with a median follow-up of 27.6 months. They concluded that chemoembolization using DEBs is an effective procedure with a favorable pharmacokinetic profile [52].

In a single-center phase II trial of chemoembolization with DEBs, Reyes et al. evaluated its safety and efficacy in a series of 20 patients

with unresectable HCC. They demonstrated that at 1 month, partial response and stable disease was seen in 10 % and 90 %, respectively, using RECIST guidelines, whereas by EASL guidelines, 60 % had objective tumor response and 40 % had stable disease. Overall survival rates at 1 and 2 years were 65 % and 55 %, respectively; median overall survival was 26 months. They concluded that DEB-TACE is safe and effective in achieving local tumor control [53].

Malagari et al. performed a prospective randomized trial comparing DEB with bland embolization in two groups of patients each with 41 and 43 patients, respectively. EASL complete and partial response was seen in 26.8 % and 46.3 % of patients treated with DEB versus 14 % and 41.9 % of those treated with bland embolization. Recurrence rate and time to progression were found to be higher for bland embolization and DEB groups, respectively. They concluded that DEB presents a better local response, fewer recurrences, and a longer TTP than bland embolization [54].

DEB has also been investigated for colorectal metastases to liver. In a recent multicenter series of 55 patients with liver metastases of colorectal cancer with prior chemotherapy, Martin et al. investigated 99 treatment sessions with DEBIRI (drug-eluting bead, irinotecan). Adverse events occurred in 28 %, response rates were 66 % and 75 % at 6 and 12 months, and overall and progression-free survival was 19 and 11 months, respectively. Authors concluded that hepatic arterial drug-eluting bead, irinotecan (DEBIRI) was safe and effective in treatment of metastatic colorectal cancer refractory to multiple lines of systemic chemotherapy [55].

Complications

The toxicity profile is similar to that seen after chemoembolization, and preliminary data according to the PRECISION V trial may indicate that this is a safer therapy when compared to conventional chemoembolization. Some of the complications may be GI ulcers, hepatobiliary toxicity, abscess formation, vascular injury, and tumor rupture.

Radioembolization

Introduction

Radioembolization uses various vehicles carrying radionuclides for delivery of a concentrated radiation dose to the target lesion. There is a very high incidence of radiation-induced liver disease after external radiation, and radioembolization minimizes the incidence of this complication. Radioembolization is an outpatient procedure.

Procedure

The inadvertent spread of the radioactive microspheres is prevented by meticulous study of the vascular anatomy of the liver and collateral nontarget flow [56]. Coil embolization of nontarget vessels may be necessitated to decrease the unintended deposition of microspheres. Technetium-99m-labeled macroaggregated albumin (^{99m}Tc-MAA) is used to assess splanchnic shunting and pulmonary shunting. This pretreatment nuclear scan is important to prevent potential complications associated with the treatment and to calculate the lung shunt fraction (LSF). All the hepatic vessels are assessed during the angiogram, and the arteries feeding the tumor are studied in detail [9–11].

Available Devices

^{90}Y is a pure beta emitter with a half-life of 64.2 h. The range of tissue penetration of the emissions is 2.5–11 mm. It is the most commonly used radionuclide. There are two forms available. TheraSphere® (MDS Nordion, Ottawa, Canada) consists of nonbiodegradable glass microspheres that have a diameter between 20 and 30 μm. It was approved by the FDA in 1999 as a bridge to transplantation and recently has been approved for use in HCC patients with PVT. Each microsphere has an activity of 2,500 Bq at the time of calibration. SIR-Spheres® consist of resin microspheres that are biodegradable. The spheres have slightly increased diameter and lower specific gravity per microsphere than TheraSphere®. The use of SIR-Spheres® was approved by the FDA for metastatic colorectal cancer to the liver in 2002. Yttrium microspheres have minimal embolic effect and thus have deeper tissue penetration. The technical

details of the procedure and dosimetry are beyond the scope of this chapter [33]. The procedure is performed on an outpatient basis [57].

Although yttrium-90 is the most clinically studied of the radioactive treatments for liver tumors, other radiopharmaceuticals still under investigation include iodine-131-labeled iodized oil (I-131 Lipiodol), rhenium-188 HDD-labeled iodized oil, phosphorus-32 glass microspheres, and Millican/holmium-166 microspheres (HoMS).

Indications for Radioembolization

Hepatocellular Carcinoma

The use of radioembolization has been shown to limit progression of the disease. This allows the patient more time to wait for donor organs [58] and thus increases their chance of undergoing OLT. Thus, it has a role of bridging the patient to OLT. Patients beyond transplant criteria have been shown to be downstaged to be eligible for transplant after radioembolization. There is an increase in overall survival in these patients as well [58]. Patients with PVT have been shown to have a good response to treatment after radioembolization. A survival benefit has been shown with the use of radioembolization in patients with malignant vascular involvement [59].

In a recent comparative effectiveness analysis, Salem et al. compared 123 patients who received radioembolization versus 122 patients who received chemoembolization for HCC and concluded that survival outcomes between two therapies are similar, but radioembolization leads to longer time to progression and lesser toxicities [5]. This study presented a comprehensive comparison of two therapies and tried to answer one of the most commonly asked questions, i.e., if either of the two therapies is superior in terms of efficacy and safety.

Intrahepatic Cholangiocarcinoma

A pilot study analyzing the use of ^{90}Y in 24 patients with biopsy-proven ICC has shown a favorable response to treatment and favorable survival outcomes [60]. The patients with a better performance status according to the Eastern Cooperation Oncology Group (ECOG) had a significantly better survival in this study. A second study of 25 patients with ICC demonstrated the safety and efficacy of ^{90}Y radioembolization. They concluded that ^{90}Y may be a safe and efficacious treatment for unresectable ICC with a median survival of 9.3 months and low incidence of grade III toxicities [61].

Colorectal Carcinoma

The patients who have unresectable disease and are on systemic chemotherapy or have failed to respond to first-line or second-line chemotherapeutic agents are considered as candidates for radioembolization. The combination of radioembolization with systemic chemotherapy has been shown to have a significantly better tumor response, a longer time to progression, survival benefit, and an acceptable safety profile [62]. The use of radioembolization alone has also been published in many series and has shown promising results [63]. Dose escalation studies have shown a better response with increasing doses [64].

Sharma et al. performed a phase I study analyzing the combination of radioembolization with modified FOLFOX4 systemic chemotherapy in patients with unresectable CRC metastases in liver in a series of 20 patients with the primary endpoint of toxicity [65]. Five patients experienced National Cancer Institute (NCI; Bethesda, MD) grade 3 abdominal pain, two of whom had microsphere-induced gastric ulcers; grade 3 or 4 neutropenia was recorded in 12 patients; one episode of transient grade 3 hepatotoxicity was recorded. Partial responses were demonstrated in 18 patients and stable disease in two patients. Median progression-free survival was 9.3 months, and median time to progression in the liver was 12.3 months. They concluded that this chemoradiation regime merits phase II–III trials.

In a recent multicenter phase III randomized trial comprising of 46 patients with unresectable liver-limited metastatic colorectal cancer, Hendlisz et al. compared intravenous fluorouracil alone with combination of radioembolization and

intravenous fluorouracil. They concluded that combination therapy is well tolerated and significantly improves time to progression compared with fluorouracil alone and this procedure is valid therapeutic option for chemotherapy-refractory liver metastases of CRC [66].

Metastatic Neuroendocrine Tumors

Radioembolization of metastatic disease to the liver from a neuroendocrine neoplasia has been shown to be effective and safe. A prolonged response to treatment, i.e., greater than 2 years, has also been seen [67, 68].

Mixed Neoplasia

Breast cancer is the most common cancer in women. It has a tendency to metastasize to the liver. Radioembolization is an efficacious treatment for unresectable breast cancer metastasis to the liver [69]. There is a significant radiologic response after radioembolization, but the survival benefit of this treatment in these patients has not been established. Radioembolization has been used to treat secondary liver tumors from various primary sources. This mode of treatment gives an effective alternative to patients who have failed chemotherapy or have become chemorefractory [70]. The data suggests a similar benefit in survival and tumor response in metastatic liver tumors from the mixed neoplasia.

Complications

The post-embolization syndrome occurs less commonly after radioembolization due to the small size of the particles, and these patients seldom require hospitalization [71–73]. Other serious adverse events related to radioembolization may include (a) radiation-induced liver disease [74, 75], with ascites development; [74] (b) fibrosis that may lead to portal hypertension with variable time to development; [76] (c) bilomas, abscess, and cholecystitis; [21] (d) radiation pneumonitis with high LSF; [77] (e) gastrointestinal ulceration with nontarget flow; [78, 79] and (f) vascular injury occurs less commonly but may be seen in patients who were already on systemic chemotherapy [80].

Embolic Therapies for Extrahepatic Tumors

Retinoblastoma

Recently selective ophthalmic artery chemotherapy with melphalan has been proposed as an alternative to intravenous chemoreduction, enucleation, or external beam radiotherapy for intraocular retinoblastoma. The authors suggest that it should only be used in advanced cases and administered in one eye due to the potential of loss of sight [81].

Laryngeal Carcinoma

Rapid infusion chemoradiotherapy to advanced laryngeal carcinomas via the superior thyroid artery may aid in preservation of the larynx [82].

Renal Malignancies

The role of embolic therapies in renal cell carcinoma is limited due to the availability of percutaneous techniques such as cryoablation and radiofrequency ablation. There have been analyses that have shown benefit of transcatheter embolization for radioactive interstitial implantation of iodine 125 in inoperable renal cell carcinoma [83]. There is a role of preoperative embolization of hypervascular renal tumors to facilitate resection. A recent retrospective analysis has suggested that preoperative chemoembolization with Lipiodol-pirarubicin-vindesine emulsion with short-term chemotherapy increases the rates of complete tumor resection and recurrence-free survivals in patients with advanced Wilm's tumors [84].

Osseous Tumors

Embolization has been suggested as a primary or palliative treatment and as an adjunct to surgical resection for primary and metastatic osseous neoplasms. The authors recommended using N-2-butyl cyanoacrylate (NBCA) in 33 % Lipiodol [85].

Benign Tumors

Transarterial embolization has also been used for benign tumors. Embolization of nasopharyngeal angiofibromas has been shown to decrease intraoperative bleeding during surgical resection [86]. Embolization of large renal angiomyolipomas is a relatively new concept which can be used to cause tumor shrinkage [87]. The therapeutic role of uterine fibroid embolization is well known [88]. However, embolic treatment of uterine or adnexal malignancies is limited by ovarian arterial supply.

Conclusion

Careful patient selection and preparation for targeted therapies will result in an optimal risk-benefit ratio for the patient. For patients presenting with hepatocellular carcinoma, the treatment of advancing disease must be balanced against the often-compromised functional liver reserve due to underlying cirrhosis. Selection of patients with adequate hepatic reserve and good functional status will maximize the beneficial therapeutic effect of this therapy with minimal risk to normal liver parenchyma. These treatments have also shown to be beneficial for patients presenting with metastatic disease who have intrahepatic progression despite standard of care chemotherapy. The clinical benefit and potential for enhancing quality of life represents an exciting opportunity for all disciplines involved in the management of liver tumors including hepatobiliary, medical, surgical, radiation, and interventional oncology. As indicated in the end of this chapter, there is a potential role for transarterial embolic therapies in many extrahepatic tumors. Further research is needed to establish these roles.

References

1. El-Serag HB. Hepatocellular carcinoma and hepatitis C in the United States. Hepatology. 2002;36(5 Suppl 1):S74–83.
2. Cheng AL, Kang YK, Chen Z, et al. Efficacy and safety of sorafenib in patients in the Asia-Pacific region with advanced hepatocellular carcinoma: a phase III randomised, double-blind, placebo-controlled trial. Lancet Oncol. 2009;10(1):25–34.
3. Llovet JM, Ricci S, Mazzaferro V, et al. Sorafenib in advanced hepatocellular carcinoma. N Engl J Med. 2008;359(4):378–90.
4. Lo CM, Ngan H, Tso WK, et al. Randomized controlled trial of transarterial lipiodol chemoembolization for unresectable hepatocellular carcinoma. Hepatology. 2002;35(5):1164–71.
5. Salem R, Lewandowski RJ, Kulik L, et al. Radioembolization results in longer time-to-progression and reduced toxicity compared with chemoembolization in patients with hepatocellular carcinoma. Gastroenterology. 2011;140(2):497–507 e492.
6. Salem R, Lewandowski RJ, Mulcahy MF, et al. Radioembolization for hepatocellular carcinoma using Yttrium-90 microspheres: a comprehensive report of long-term outcomes. Gastroenterology. 2010;138(1):52–64.
7. Lewandowski RJ, Mulcahy MF, Kulik LM, et al. Chemoembolization for hepatocellular carcinoma: comprehensive imaging and survival analysis in a 172-patient cohort. Radiology. 2010;255(3):955–65.
8. Llovet JM, Real MI, Montana X, et al. Arterial embolisation or chemoembolisation versus symptomatic treatment in patients with unresectable hepatocellular carcinoma: a randomised controlled trial. Lancet. 2002;359(9319):1734–9.
9. Salem R, Lewandowski RJ, Sato KT, et al. Technical aspects of radioembolization with ^{90}Y microspheres. Tech Vasc Interv Radiol. 2007;10(1):12–29.
10. Lewandowski RJ, Sato KT, Atassi B, et al. Radioembolization with (90)y microspheres: angiographic and technical considerations. Cardiovasc Intervent Radiol. 2007;30(4):571–92.
11. Liu DM, Salem R, Bui JT, et al. Angiographic considerations in patients undergoing liver-directed therapy. J Vasc Interv Radiol. 2005;16(7):911–35.
12. Lewandowski RJ, Geschwind JF, Liapi E, Salem R. Transcatheter intraarterial therapies: rationale and overview. Radiology. 2011;259(3):641–57.
13. Llovet JM, Di Bisceglie AM, Bruix J, et al. Design and endpoints of clinical trials in hepatocellular carcinoma. J Natl Cancer Inst. 2008;100(10):698–711.
14. Mazzaferro V, Regalia E, Doci R, et al. Liver transplantation for the treatment of small hepatocellular carcinomas in patients with cirrhosis. N Engl J Med. 1996;334(11):693–9.

15. Chapman WC, Majella Doyle MB, Stuart JE, et al. Outcomes of neoadjuvant transarterial chemoembolization to downstage hepatocellular carcinoma before liver transplantation. Ann Surg. 2008;248(4):617–25.
16. Lewandowski RJ, Kulik LM, Riaz A, et al. A comparative analysis of transarterial downstaging for hepatocellular carcinoma: chemoembolization versus radioembolization. Am J Transplant. 2009;9(8):1920–8.
17. Welsh JS, Kennedy AS, Thomadsen B. Selective Internal Radiation Therapy (SIRT) for liver metastases secondary to colorectal adenocarcinoma. Int J Radiat Oncol Biol Phys. 2006;66(2 Suppl):S62–73.
18. Riaz A, Ryu RK, Kulik LM, et al. Alpha-fetoprotein response after locoregional therapy for hepatocellular carcinoma: oncologic marker of radiologic response, progression, and survival. J Clin Oncol. 2009; 27(34):5734–42.
19. Ibrahim SM, Nikolaidis P, Miller FH, et al. Radiologic findings following Y90 radioembolization for primary liver malignancies. Abdom Imaging. 2009; 34(5):566–81.
20. Riaz A, Miller FH, Kulik LM, et al. Imaging response in the primary index lesion and clinical outcomes following transarterial locoregional therapy for hepatocellular carcinoma. JAMA. 2010;303(11):1062–9.
21. Rhee TK, Naik NK, Deng J, et al. Tumor response after yttrium-90 radioembolization for hepatocellular carcinoma: comparison of diffusion-weighted functional MR imaging with anatomic MR imaging. J Vasc Interv Radiol. 2008;19(8):1180–6.
22. Riaz A, Memon K, Miller FH, et al. Role of the EASL, RECIST, and WHO response guidelines alone or in combination for hepatocellular carcinoma: radiologic–pathologic correlation. J Hepatol. 2011; 54(4):695–704.
23. Markowitz J. The hepatic artery. Surg Gynecol Obstet. 1952;95(5):644–6.
24. Brown KT, Nevins AB, Getrajdman GI, et al. Particle embolization for hepatocellular carcinoma. J Vasc Interv Radiol. 1998;9(5):822–8.
25. Camma C, Schepis F, Orlando A, et al. Transarterial chemoembolization for unresectable hepatocellular carcinoma: meta-analysis of randomized controlled trials. Radiology. 2002;224(1):47–54.
26. Erler JT, Bennewith KL, Nicolau M, et al. Lysyl oxidase is essential for hypoxia-induced metastasis. Nature. 2006;440(7088):1222–6.
27. Bruix J, Llovet JM, Castells A, et al. Transarterial embolization versus symptomatic treatment in patients with advanced hepatocellular carcinoma: results of a randomized, controlled trial in a single institution. Hepatology. 1998;27(6):1578–83.
28. Maluccio MA, Covey AM, Porat LB, et al. Transcatheter arterial embolization with only particles for the treatment of unresectable hepatocellular carcinoma. J Vasc Interv Radiol. 2008;19(6):862–9.
29. Maluccio MA, Covey AM, Schubert J, et al. Treatment of metastatic sarcoma to the liver with bland embolization. Cancer. 2006;107(7):1617–23.
30. Xia J, Ren Z, Ye S, et al. Study of severe and rare complications of transarterial chemoembolization (TACE) for liver cancer. Eur J Radiol. 2006;59(3): 407–12.
31. Eksborg S, Cedermark BJ, Strandler HS. Intrahepatic and intravenous administration of adriamycin–a comparative pharmacokinetic study in patients with malignant liver tumours. Med Oncol Tumor Pharmacother. 1985;2(1):47–54.
32. Ensminger W. Hepatic arterial chemotherapy for primary and metastatic liver cancers. Cancer Chemother Pharmacol. 1989;23(Suppl):S68–73.
33. Coldwell DM, Stokes KR, Yakes WF. Embolotherapy: agents, clinical applications, and techniques. Radiographics. 1994;14(3):623–43. quiz 645–626.
34. Soulen MC. Chemoembolization of hepatic malignancies. Oncology (Williston Park). 1994;8(4):77–84. discussion 84, 89–90 passim.
35. Solomon B, Soulen MC, Baum RA, Haskal ZJ, Shlansky-Goldberg RD, Cope C. Chemoembolization of hepatocellular carcinoma with cisplatin, doxorubicin, mitomycin-C, ethiodol, and polyvinyl alcohol: prospective evaluation of response and survival in a U.S. population. J Vasc Interv Radiol. 1999;10(6):793–8.
36. Takayasu K, Arii S, Ikai I, et al. Prospective cohort study of transarterial chemoembolization for unresectable hepatocellular carcinoma in 8510 patients. Gastroenterology. 2006;131(2):461–9.
37. Kiefer MV, Albert M, McNally M, et al. Chemoembolization of intrahepatic cholangiocarcinoma with cisplatinum, doxorubicin, mitomycin C, ethiodol, and polyvinyl alcohol. Cancer. 2011;117(7):1498–505.
38. Geschwind J, Hong K, Georgiades C. Utility of transcatheter arterial chemoembolization for liver dominant colorectal metastatic adenocarcinoma in the salvage setting. American Society of Clinical Oncology Gastrointestinal Cancers Symposium. San Francisco; 26–28 Jan 2006.
39. Liapi E, Geschwind J-F, Vossen JA, et al. Functional MRI evaluation of tumor response in patients with neuroendocrine hepatic metastasis treated with transcatheter arterial chemoembolization. AJR Am J Roentgenol. 2008;190(1):67–73.
40. Giroux MF, Baum RA, Soulen MC. Chemoembolization of liver metastasis from breast carcinoma. J Vasc Interv Radiol. 2004;15(3):289–91.
41. Buijs M, Kamel IR, Vossen JA, Georgiades CS, Hong K, Geschwind JF. Assessment of metastatic breast cancer response to chemoembolization with contrast agent enhanced and diffusion-weighted MR imaging. J Vasc Interv Radiol. 2007;18(8):957–63.
42. Burger I, Hong K, Schulick R, et al. Transcatheter arterial chemoembolization in unresectable cholangiocarcinoma: initial experience in a single institution. J Vasc Interv Radiol. 2005;16(3):353–61.
43. Murakami T, Ishimaru H, Sakamoto I, et al. Percutaneous radiofrequency ablation and transcatheter

arterial chemoembolization for hypervascular hepatocellular carcinoma: rate and risk factors for local recurrence. Cardiovasc Intervent Radiol. 2007; 30(4):696–704.
44. Kagawa T, Koizumi J, Kojima S, et al. Transcatheter arterial chemoembolization plus radiofrequency ablation therapy for early stage hepatocellular carcinoma: comparison with surgical resection. Cancer. 2010;116(15):3638–44.
45. Heckman JT, Devera MB, Marsh JW, et al. Bridging locoregional therapy for hepatocellular carcinoma prior to liver transplantation. Ann Surg Oncol. 2008;15(11):3169–77.
46. Bartolozzi C, Lencioni R, Caramella D, et al. Treatment of large HCC: transcatheter arterial chemoembolization combined with percutaneous ethanol injection versus repeated transcatheter arterial chemoembolization. Radiology. 1995;197(3):812–8.
47. Kim HK, Chung YH, Song BC, et al. Ischemic bile duct injury as a serious complication after transarterial chemoembolization in patients with hepatocellular carcinoma. J Clin Gastroenterol. 2001;32(5):423–7.
48. Belli L, Magistretti G, Puricelli GP, Damiani G, Colombo E, Cornalba GP. Arteritis following intra-arterial chemotherapy for liver tumors. Eur Radiol. 1997;7(3):323–6.
49. Hong K, Georgiades CS, Geschwind JF. Technology insight: Image-guided therapies for hepatocellular carcinoma–intra-arterial and ablative techniques. Nat Clin Pract Oncol. 2006;3(6):315–24.
50. Constantin M, Fundueanu G, Bortolotti F, Cortesi R, Ascenzi P, Menegatti E. Preparation and characterisation of poly(vinyl alcohol)/cyclodextrin microspheres as matrix for inclusion and separation of drugs. Int J Pharm. 2004;285(1–2):87–96.
51. Gonzalez MV, Tang Y, Phillips GJ, et al. Doxorubicin eluting beads-2: methods for evaluating drug elution and in-vitro:in-vivo correlation. J Mater Sci Mater Med. 2008;19(2):767–75.
52. Varela M, Real MI, Burrel M, et al. Chemoembolization of hepatocellular carcinoma with drug eluting beads: efficacy and doxorubicin pharmacokinetics. J Hepatol. 2007;46(3):474–81.
53. Reyes DK, Vossen JA, Kamel IR, et al. Single-center phase II trial of transarterial chemoembolization with drug-eluting beads for patients with unresectable hepatocellular carcinoma: initial experience in the United States. Cancer J. 2009;15(6):526–32.
54. Malagari K, Pomoni M, Kelekis A, et al. Prospective randomized comparison of chemoembolization with doxorubicin-eluting beads and bland embolization with BeadBlock for hepatocellular carcinoma. Cardiovasc Intervent Radiol. 2010;33(3):541–51.
55. Martin RC, Joshi J, Robbins K, et al. Hepatic intra-arterial injection of drug-eluting bead, irinotecan (DEBIRI) in unresectable colorectal liver metastases refractory to systemic chemotherapy: results of multi-institutional study. Ann Surg Oncol. 2011;18(1): 192–8.
56. Covey AM, Brody LA, Maluccio MA, Getrajdman GI, Brown KT. Variant hepatic arterial anatomy revisited: digital subtraction angiography performed in 600 patients. Radiology. 2002;224(2):542–7.
57. Salem R, Thurston KG, Carr BI, Goin JE, Geschwind JF. Yttrium-90 microspheres: radiation therapy for unresectable liver cancer. J Vasc Interv Radiol. 2002;13(9 Pt 2):S223–9.
58. Kulik LM, Atassi B, van Holsbeeck L, et al. Yttrium-90 microspheres (TheraSphere(R)) treatment of unresectable hepatocellular carcinoma: downstaging to resection, RFA and bridge to transplantation. J Surg Oncol. 2006;94(7):572–86.
59. Kulik LM, Carr BI, Mulcahy MF, et al. Safety and efficacy of (90)Y radiotherapy for hepatocellular carcinoma with and without portal vein thrombosis. Hepatology. 2007;47(1):71–81.
60. Ibrahim SM, Mulcahy MF, Lewandowski RJ, et al. Treatment of unresectable cholangiocarcinoma using yttrium-90 microspheres: results from a pilot study. Cancer. 2008;113(8):2119–28.
61. Saxena A, Bester L, Chua TC, Chu FC, Morris DL. Yttrium-90 radiotherapy for unresectable intrahepatic cholangiocarcinoma: a preliminary assessment of this novel treatment option. Ann Surg Oncol. 2010;17(2):484–91.
62. Gray B, Van Hazel G, Hope M, et al. Randomised trial of SIR-Spheres plus chemotherapy vs. chemotherapy alone for treating patients with liver metastases from primary large bowel cancer. Ann Oncol. 2001;12(12):1711–20.
63. Kennedy A, Coldwell D, Nutting C, Overton C, Sailer S. Liver brachytherapy for unresectable colorectal metastases: US results 2000–2004. Paper presented at: ASCO GI Symposium. Miami; 27–29 Jan 2005.
64. Goin JE, Dancey JE, Hermann GA, Sickles CJ, Roberts CA, MacDonald JS. Treatment of unresectable metastatic colorectal carcinoma to the liver with intrahepatic Y-90 microspheres: a dose-ranging study. World J Nuc Med. 2003;2:216–25.
65. Sharma RA, Van Hazel GA, Morgan B, et al. Radioembolization of liver metastases from colorectal cancer using yttrium-90 microspheres with concomitant systemic oxaliplatin, fluorouracil, and leucovorin chemotherapy. J Clin Oncol. 2007;25(9):1099–106.
66. Hendlisz A, Van den Eynde M, Peeters M, et al. Phase III trial comparing protracted intravenous fluorouracil infusion alone or with yttrium-90 resin microspheres radioembolization for liver-limited metastatic colorectal cancer refractory to standard chemotherapy. J Clin Oncol. 2010;28(23):3687–94.
67. Rhee TK, Lewandowski RJ, Liu DM, et al. ^{90}Y Radioembolization for metastatic neuroendocrine liver tumors: preliminary results from a multi-institutional experience. Ann Surg. 2008;247(6): 1029–35.
68. Kennedy AS, Dezarn WA, McNeillie P, et al. Radioembolization for unresectable neuroendocrine hepatic metastases using resin ^{90}Y-microspheres: early

results in 148 patients. Am J Clin Oncol. 2008;31(3):271–9.
69. Coldwell D, Nutting C, Kennedy AK. Treatment of hepatic metastases from breast cancer with yttrium-90 SIR-Spheres radioembolization. Paper presented at: Society of Interventional Radiology Annual Meeting. New Orleans; 31 Mar–5 Apr 2005.
70. Sato KT, Lewandowski RJ, Mulcahy MF, et al. Unresectable chemorefractory liver metastases: radioembolization with ^{90}Y microspheres–safety, efficacy, and survival. Radiology. 2008;247(2):507–15.
71. Salem R, Lewandowski RJ, Atassi B, et al. Treatment of unresectable hepatocellular carcinoma with use of ^{90}Y microspheres (TheraSphere): safety, tumor response, and survival. J Vasc Interv Radiol. 2005;16(12):1627–39.
72. Kennedy AS, Coldwell D, Nutting C, et al. Resin ^{90}Y-microsphere brachytherapy for unresectable colorectal liver metastases: modern USA experience. Int J Radiat Oncol Biol Phys. 2006;65(2):412–25.
73. Murthy R, Xiong H, Nunez R, et al. Yttrium 90 resin microspheres for the treatment of unresectable colorectal hepatic metastases after failure of multiple chemotherapy regimens: preliminary results. J Vasc Interv Radiol. 2005;16(7):937–45.
74. Sangro B, Gil-Alzugaray B, Rodriguez J, et al. Liver disease induced by radioembolization of liver tumors: description and possible risk factors. Cancer. 2008;112(7):1538–46.
75. Young JY, Rhee TK, Atassi B, et al. Radiation dose limits and liver toxicities resulting from multiple yttrium-90 radioembolization treatments for hepatocellular carcinoma. J Vasc Interv Radiol. 2007;18(11):1375–82.
76. Jakobs TF, Saleem S, Atassi B, et al. Fibrosis, portal hypertension, and hepatic volume changes induced by intra-arterial radiotherapy with (90)yttrium microspheres. Dig Dis Sci. 2008;53(9):2556–63.
77. TheraSphere Yttrium-90 microspheres package insert, MDS Nordion, Kanata, Canada; 2004.
78. Murthy R, Brown DB, Salem R, et al. Gastrointestinal complications associated with hepatic arterial Yttrium-90 microsphere therapy. J Vasc Interv Radiol. 2007;18(4):553–61. quiz 562.
79. Carretero C, Munoz-Navas M, Betes M, et al. Gastroduodenal injury after radioembolization of hepatic tumors. Am J Gastroenterol. 2007;102(6):1216–20.
80. Murthy R, Eng C, Krishnan S, et al. Hepatic yttrium-90 radioembolotherapy in metastatic colorectal cancer treated with cetuximab or bevacizumab. J Vasc Interv Radiol. 2007;18(12):1588–91.
81. Munier FL, Beck-Popovic M, Balmer A, Gaillard MC, Bovey E, Binaghi S. Occurrence of sectoral choroidal occlusive vasculopathy and retinal arteriolar embolization after superselective ophthalmic artery chemotherapy for advanced intraocular retinoblastoma. Retina. 2011;31(3):566–73.
82. Nakashima T, Mihoki T, Ono T, Umeno H, Tanaka N. Selective (intra-arterial), rapid infusion chemoradiotherapy to preserve the larynx in advanced laryngeal carcinoma: preliminary results. J Laryngol Otol Suppl. 2009;31:30–4.
83. Lang EK, Sullivan J. Management of primary and metastatic renal cell carcinoma by transcatheter embolization with iodine 125. Cancer. 1988;62(2):274–82.
84. Li MJ, Zhou YB, Huang Y, et al. A retrospective study of the preoperative treatment of advanced Wilms tumor in children with chemotherapy versus transcatheter arterial chemoembolization alone or combined with short-term systemic chemotherapy. J Vasc Interv Radiol. 2011;22(3):279–86.
85. Rossi G, Mavrogenis AF, Rimondi E, et al. Selective arterial embolisation for bone tumours: experience of 454 cases. Radiol Med. 2011;116(5):793–808.
86. Roche PH, Paris J, Regis J, et al. Management of invasive juvenile nasopharyngeal angiofibromas: the role of a multimodality approach. Neurosurgery. 2007;61(4):768–77. discussion 777.
87. Lee SY, Hsu HH, Chen YC, et al. Embolization of renal angiomyolipomas: short-term and long-term outcomes, complications, and tumor shrinkage. Cardiovasc Intervent Radiol. 2009;32(6):1171–8.
88. Watkinson A, Nicholson A. Uterine artery embolisation to treat symptomatic uterine fibroids. BMJ. 2007;335(7622):720–2.

Emerging Technologies in the Treatment of Cancer

7

Erik N. K. Cressman

Abstract

Emerging technologies in interventional oncology span a broad range of topics. In the broadest sense, most have a common underlying theme converging around energy and tissues. This chapter covers new areas related to energy deposition, guidance, monitoring, new sources of energy, and ways to alter cellular and tissue responses to these interventions to improve outcomes for patients. In addition, upcoming developments in new embolic agents are highlighted from both an imaging perspective and a pharmacokinetic point of view.

Technology development in interventional oncology is an extremely active area with many aspects to consider. For purposes of this chapter, the theme of energy in tissues serves as a useful guiding concept for developing a discussion on emerging technologies. These emerging technologies generally can be grouped into the following:

- New ways to guide/target energy deposition
- New energy sources
- New ways to deposit energy
- New ways to deplete energy in cells
- New ways to sensitize cells to energy inputs or alter how energy interacts with tissues
- New ways to determine where energy has been deposited, how much, and if treatment is adequate

Each of these will be examined in turn. The chapter will then conclude with a discussion of areas that fit outside of this paradigm, particularly the evolution of embolic materials.

New Ways to Guide/Target Energy Deposition

This is a very active area that has seen tremendous growth within the last decade. Solomon et al. described the early uses of electromagnetic instrument tracking for interventional procedures [1–3], and this topic is covered in much greater detail in part III of this volume. Most major imaging equipment vendors are developing or have recently introduced products in this area. The majority of these rely on electromagnetic tracking as the mechanism for spatial

E.N.K. Cressman
Department of Radiology, University of Minnesota Medical Center, Minneapolis, MN, USA
e-mail: cress013@umn.edu

D.E. Dupuy et al. (eds.), *Image-Guided Cancer Therapy*, DOI 10.1007/978-1-4419-0751-6_9,

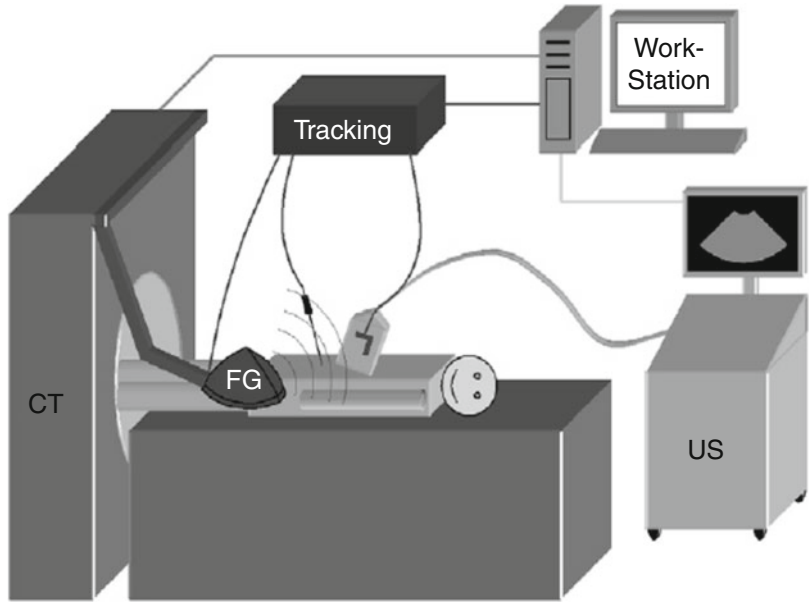

Fig. 7.1 Scheme illustrating a combination for electromagnetic tracking. Positioning is determined in space by a field generator detecting the probe, and the information is fused with ultrasound and CT guidance for real-time feedback (Reprinted with permission from Krücker J, et al. J Vasc Interv Radiol. 2007;18(9):1142–50, © 2007 Elsevier)

localization. Nearly all employ some version of fusion of prior images (CT, MR, and/or US, typically but not always obtained with contrast) and real-time acquisition of procedural images to allow more accurate positioning, much like a GPS.

The common theme is user interfaces that allow in-plane and out-of-plane targeting and real-time instrument tracking as a needle or device is advanced to the desired target. Most rely on some variation of position-sensing coils, and several are now able to or soon will be able to account for physiologic motion such as cardiac or respiratory motion, for example. The reporter coil position is detected by a detector panel positioned near the patient, and fused images allow for real-time adjustments of position. Figure 7.1 is an example of such a system. Examples include the Philips PercuNav (previously Traxtal), Siemens iGuide CAPPA, Veran Medical ig4 navigation system, St. Jude Medical/Mediguide, and the GE LOGIQ E9 systems, to name a few. On the optical imaging side, the ActiSight system by ActiViews takes advantage of a small, reusable camera to guide device placement based on a disposable targeting template that is applied to the patient's skin. Changes in trajectory are calculated based on the relationships of the target markers in four quadrants. When the device deviates off target, the distances to the markers become asymmetrical, and this difference is indicated by the display to allow for real-time correction. Figure 7.2 is an example of the typical setup.

Banovac and colleagues have focused on interventional assist systems (robotics) that could aid in delivery of biopsy needles and RF ablation electrodes, as examples, into a target with high precision and accuracy [4, 5]. Wood and colleagues showed the feasibility of this technology in image-guided biopsy and ablation and demonstrated a targeting error of 3.5 $\pm$ 1.9 mm suggesting that the spatial tracking accuracy is sufficient to display clinically relevant pre-procedural imaging information during needle-based procedures [6]. Using computer-assisted methods for volumetric planning, they developed a physician-assist system that allows for pre-procedural planning and real-time assistance of electrode insertion into predetermined locations in the tumor. This theoretically makes possible volumetric "sculpting" of multiple ablation zones to cover a tumor and the desired margin.

The added cost of such technologies will have to be offset by improvement in clinical outcomes given the expected future climate of health-care economics. Factors to consider include an

Fig. 7.2 The ActiSight (ActiViews, Haifa Israel) navigation positioning is determined by mapping the 2D coordinates of the colored reference markers in the camera image to the coordinates of the radio-opaque prints of the same markers in the 3D computed tomography images

increasing awareness of the risks of exposure to ionizing radiation and that it is well known that many CT-guided procedures can result in substantial radiation doses. These combine to strengthen the case for faster, more accurate interventions that would decrease exposure to ionizing radiation. Presumably, the lower doses and more accurate treatments will extrapolate to decreased future complications resulting from such procedures. By extension, overall cost for care would likely go down. It is difficult, however, to ascribe costs and calculate benefits accurately when the overall outcomes may never be truly known. The time savings per procedure, while yet not rigorously quantified, could be tracked with relative ease by comparison.

While the previous discussion focused on guiding device placement, alternative methods for targeting energy from an external source are beginning to achieve practical application. For example, MR-guided high-intensity focused ultrasound (variably referred to as MRgUS or since MR is very commonly integral, HIFU) is already in clinical use for treatment of a benign condition, symptomatic uterine fibroids. An example of an emerging area is HIFU that is guided not by MR but rather by ultrasound. Early clinical experience seems encouraging [7–11].

Several designs have been proposed generally with a gap in the center for placement of a diagnostic probe. Two of the newest developments in this area are integrated arrays as shown in Fig. 7.3a [12] and a dual-mode ultrasound array (DMUA), shown in Fig. 7.3b that has intrinsic self-registration of images in real time [13–15]. A 64-element array transducer can be used to serve both diagnostic and therapeutic functions. In other words, a single handheld device can image and ablate at the same time. The treating physician would be able to watch the effects in tissue as they are happening. Work remains to be done in terms of the diagnostic image since the early results are based on imaging at 1 MHz, which is at the same frequency as the therapeutic usage but is not the optimal frequency for the anticipated eventual use in vivo.

Despite the above limitations, the feasibility of DMUAs for image-guided noninvasive therapy has been demonstrated using the 1 MHz prototype. In particular, in vitro experimental verification of DMUA capabilities has been achieved:

- Imaging of changes in tissue echogenicity upon volumetric coagulum formation using full synthetic aperture (SA) imaging [16]. Figure 7.4 shows one example of imaging target tissue before and after coagulum formation using SA imaging. Freshly excised, degassed porcine liver samples were secured in gel phantom holder and backed with a sponge absorber. A volumetric (approximately 1 cm^3) coagulum was formed using nine shots of 3-s HIFU beams in a 33-element

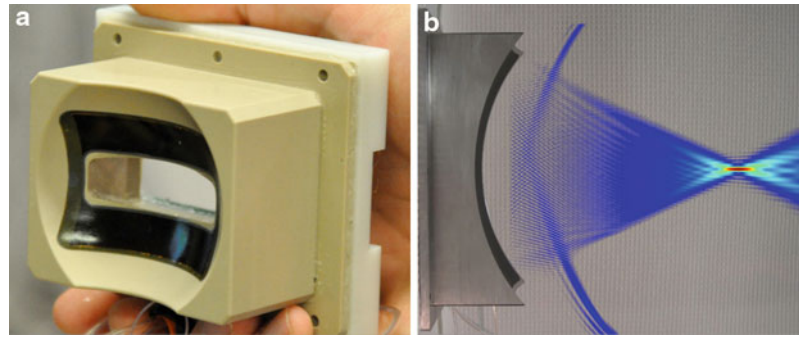

Fig. 7.3 (**a**) Fenestrated array for HIFU clearly showing the opening through which a separate but integrated diagnostic transducer can be affixed (**b**) dual-mode array capable of both imaging and therapeutic ultrasound (**b**. Courtesy of Prof. Emad Ebbini, University of Minnesota)

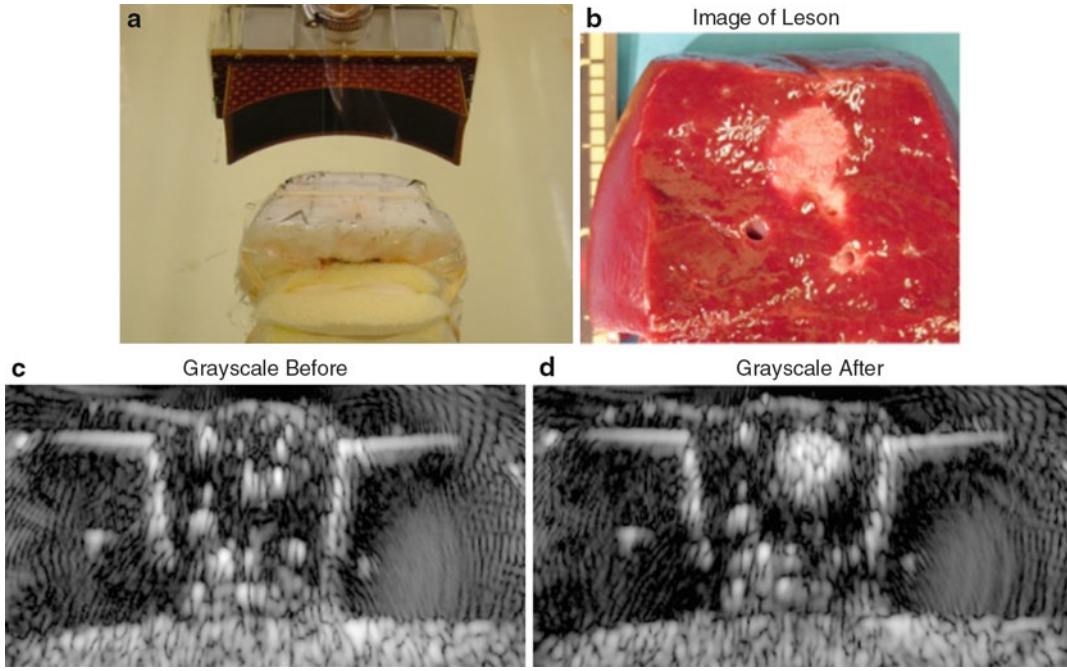

Fig. 7.4 Results from a volumetric HIFU sonication experiment using the 64-element, 1-MHz DMUA in freshly excised and degassed porcine liver sample. (**a**) The DMUA and the tissue positioned in the sample holder. (**b**) A cut through the central plane of the target volume with the lesion visible as change in color. (**c**) and (**d**) grayscale synthetic aperture images (50 dB) of the tissue sample at the center plane of the target zone before and after sonication, respectively (Courtesy of Prof. Emad Ebbini, University of Minnesota)

matrix (1-min wait time between shots). Figure 7.4b shows a cross section of the tissue sample with the HIFU-induced coagulum completely within the sample, i.e., the intervening tissue was spared. SA images using the DMUA were acquired before and after lesion formation and are shown in Fig. 7.4c, d, respectively. The change in echogenicity is quite visible, and it corresponds to the location and shape of the induced zone of coagulation.

- Imaging of changes in tissue echogenicity upon discrete (single-shot) ablation treatment using single-transmit focus (STF) imaging [16]. STF imaging is a new mode in which the HIFU beam is used as a transmit focus (at a diagnostic level) and dynamic focusing

is used on receive only. This has several advantages in noninvasive HIFU treatment:
  - High sensitivity to changes in echoes from the assumed lesion location (at the HIFU focus), including nonlinear response due to the formation of cavitation bubbles. This was well demonstrated in a series of experiments of freshly excised, degassed porcine liver tissues treated by DMUA-generated therapeutic HIFU beams [16].
  - Identification of strongly scattering objects in the path of the HIFU beam, e.g., the ribs when targeting liver or kidney tumors. The echogenicity from these objects serves as a form of feedback to assess their exposure to HIFU at subtherapeutic levels before the therapeutic beam is applied.
  - With the recent completion of a real-time 64-channel transmit/receive interface for the DMUA prototype, STF offers practically continuous monitoring of tissue response to HIFU sonication (STF frame data can be collected in less than 1 ms minimizing interruption to the therapeutic HIFU beam).
- An image-based optimal refocusing method was developed to maximize the power deposition at the target location while minimizing the exposure to the ribs in transthoracic focusing [15]. This form of feedback is unique to DMUAs due to the inherent registration between the imaging and therapeutic coordinate systems used in beamforming the refocused HIFU beams.

It should also be noted that as these techniques improve, the entire field of noninvasive local drug delivery using thermally sensitive delivery systems will expand. This will likely therefore incorporate many non-oncologic applications of both low- and high-temperature hyperthermia in the future.

New Energy Sources

Most of the commercially available technologies make use of energy somewhere on the electromagnetic spectrum and apply it in a focused manner to achieve the desired therapeutic effect. Exploiting the energy released from certain chemical reactions is an area that is just beginning to be explored. The general concept, termed thermochemical ablation, encompasses many classes of reactions. The ones most studied to date are acid–base neutralization reactions. These can be done either sequentially [17] or simultaneously [18] and can produce substantial exotherms. Sequential technique is simpler but has the distinct disadvantage that incomplete reaction of an acidic or basic reagent can result in systemic exposure and poor control over the completion of the reaction.

The amount of energy released depends on three variables. These are the strength of the reagents used, the concentration, and the amount. The molar heat of formation of water is in the range of 55 kJ/mol, and this is the approximate amount released using strong acids and bases together. In clinical and practical terms, this translates to enough energy to quickly boil water using small amounts at relatively modest concentrations. The reaction of weak acids and bases is rather less exothermic but by no means insignificant. The difference is attributed to energy lost for ionization of weak reagents that must occur before reaction can take place, and this is in the range of 30 kJ/mol. At about half the amount of energy evolved as with strong reagents, it takes higher concentrations of weak reagents to achieve the same results, but it is clearly possible. As might be expected, using one strong component and one weak component results in an intermediate amount of energy released, on the order of 40–45 kJ/mol. Acetic acid and sodium hydroxide provide just such an example of an intermediate combination, in which early, as yet unpublished in vivo work in the author's laboratory has shown that temperatures as high as 105 °C are attainable. This result was obtained using just 1 cc each of 15 M concentration reagents. Higher temperatures should therefore be possible with either higher concentrations or different reagents, but such extremes may not be necessary.

Duration of the thermal excursion lasts as long as the reagents are reacting together and releasing

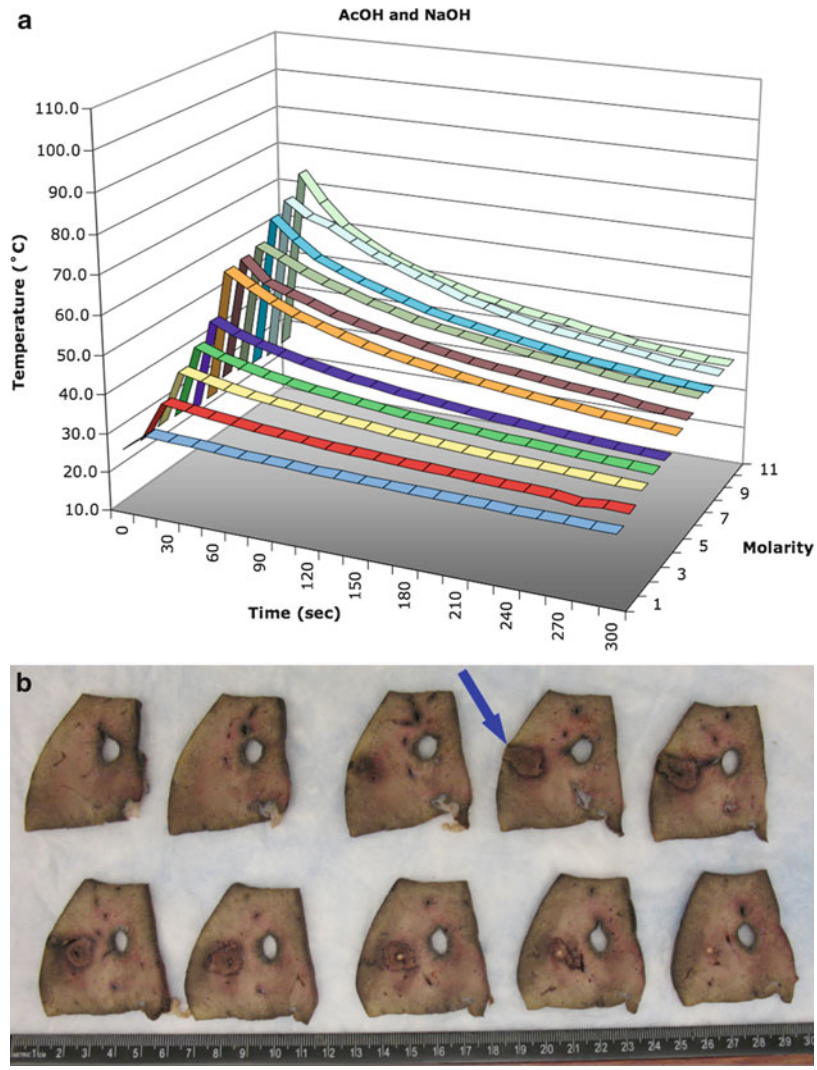

Fig. 7.5 (**a**) Gel phantom temperature profiles of increasing concentrations of acetic acid (a weak acid) and sodium hydroxide (a strong base). At 5 M concentration, on the low end of the tested range, the temperature increase is in the range of 15 °C above baseline (peak temp 45 °C measured) but quickly decays (**b**) acute in vivo results from 5-M simultaneous injections of 0.5 cc each of the same reagents. *Blue arrow* denotes the zone of coagulation readily seen on adjacent slices of the specimen. Sample was fixed in formalin prior to sectioning

energy into the system. This will be related to a number of variables and may only last a few minutes since reaction is essentially instantaneous and is complete when the injection is finished. Thermal dose defined strictly in terms of time at temperature may serve as a starting point for understanding this technique, but the actual effects cannot be accurately summarized based on time and temperature alone.

Thermochemical ablation using an acid and base is a multifactorial process that produces a salt and water in addition to releasing the energy. If equal concentrations and volumes are used, it follows that the salt product will be formed at half the concentration of the starting materials. The particular salt remaining in the tissues is expected to have local hyperosmolar effects due to the concentration and also have intrinsic protein denaturing capability. In many cases, it is possible to produce salts at or above their solubility limits in aqueous solution. These hyperosmolar and denaturing effects are expected to persist for a considerable but yet unknown time in the local milieu after the relatively brief temperature excursion resulting from the reaction. This is illustrated in Fig. 7.5a, which depicts the temperature/concentration relationship of a weak acid and strong base in a gel

phantom, and Fig. 7.5b showing the acute, in vivo effects of simultaneous injection of only 0.5 cc each of 5 M acetic acid and sodium hydroxide in a porcine liver model. Note that the temperature change at this low concentration based on the graph is relatively mild but the tissue effects are nevertheless substantial.

Systemic effects from these reactions are likewise under investigation. At issue are both any exposure to unreacted materials and understanding the products with respect to any salt load that must be handled. Thoughtful selection of reagents may provide adequate local coagulation effects with inert substances that have little, if any, systemic effect. In the same manner as with RF ablation, one could also contemplate combined therapy with embolization via the transarterial route. The reduction in perfusion-mediated cooling in a large vascular territory may lead to adequate coverage of a larger tumor volume.

Another category recently examined is oxidation-reduction chemistry, more commonly called redox chemistry. Changes in oxidation states of various metals can be orders of magnitude more exothermic than neutralization chemistry, and this could translate to requiring smaller amounts of the reagents. Unlike the acid–base example described above, reactions are not so clear-cut with well-defined products. Although precise energetics are therefore challenging to calculate, low concentrations of reagents easily reach boiling temperatures in a number of cases. The products vary according to the reaction employed and can themselves have significant tumoricidal properties [19–22].

In all of the thermochemical methods other than those using implantable solids, issues arise concerning tracking of instilled reagents along paths of least resistance as is known from the chemical ablation literature with percutaneous ethanol therapy. The lack of precise control of fluid distribution is one of the reasons that purely thermal therapies have become favored over ethanol in current practice. However, if the volumes can be kept relatively small with energy release high, conditions may be discovered that rely primarily on a conductive effect which would be much more predictable in nature. The ability to perform an ablation without the requirement for either a costly power source or one that did not need any cabling or tubing extending off of a sterile procedural field has much practical appeal if this area can be successfully developed. Weighed against these benefits is the lack of a refined device and the issues with approval by governmental agencies such as the FDA for reagents at the doses that might be contemplated.

New Ways to Deposit Energy

Established methods such as radiofrequency ablation, microwave ablation, lasers, cryotherapy, and ionizing radiation are outside the scope of this chapter. A relatively new method, electroporation, is likewise covered in a separate chapter. Two new experimental areas that could reach clinical use in the near future are conductive interstitial tumor therapy (CITT) and RF capacitance heating of nanoparticles.

CITT relies purely on conductive effects in tissues using a device designed for deployment in a surgical bed to treat tissue margins such as for breast tumor lumpectomy or similar enucleation procedures [23, 24].

Temperatures are significantly higher than those seen in radiofrequency ablation (they can be in excess of 150 °C), and charring does occur to some extent. However, while charring interferes with radiofrequency energy deposition, this is much less of an issue with pure conduction. In one device, deployable pins are utilized to increase contact area and thereby increase the size of an ablation as shown in Fig. 7.6. A possible advantage of this approach is the predictability and uniformity of conduction through tissues rather than energy absorption per se as the means of heating. This is most likely to see utility in diseases such as breast cancer to treat a surgical resection bed, but other possibilities such as head and neck cancer are being studied. Much remains to be done if this approach is to be adapted to a percutaneous method able to treat larger size tumors.

Noninvasive, noncontact techniques combining nanoparticles and electromagnetic energy in the kHz and MHz range to ablate tumors have been evolving at a rapid rate since the early reports [25–27]. In one technique, gold nanoparticles have been identified as highly efficient radiofrequency energy absorbers in the MHz range. In this method, the energy is delivered in a way similar to RF capacitive heating at radiofrequencies that penetrate tissue with much lower absorption than at GHz frequencies. Figure 7.7 shows time-lapse-infrared images of the rapid heating possible in vitro. In another technique, alternating magnetic fields (AMFs) at high kHz frequencies are used in conjunction with magnetic nanoparticles to deliver energy [28–31]. This area appears very promising, but several issues must be surmounted. A key one is targeting. Image guidance may prove necessary until such time as the particles achieve the required pharmacokinetic and pharmacodynamic profiles. This assumes that adequate loading of particles into cells can be accomplished in a meaningful time frame for treatment. This in turn is directly related to the strength of the applied field. Eddy currents seen at higher AMF fields can cause unintended heating of nontarget areas, and in numerous experiments, unintentional heating occurs in cells and tissues that do not contain the nanoparticles exposed to these RF fields.

Fig. 7.6 Conductive interstitial thermal therapy device with tines to distribute heat in a larger volume (Courtesy of Dr. Gal Shafirstein, Arkansas Children's Hospital, Little Rock, AK)

There are many unanswered questions concerning the toxicology of such particles although it is true that certain types appear to be relatively safe based on available data [32]. Understanding both the mechanisms of action for these materials, the optimal conditions for the most beneficial result, and to some extent the toxicity profile will therefore be necessary before they are widely adopted. Some studies

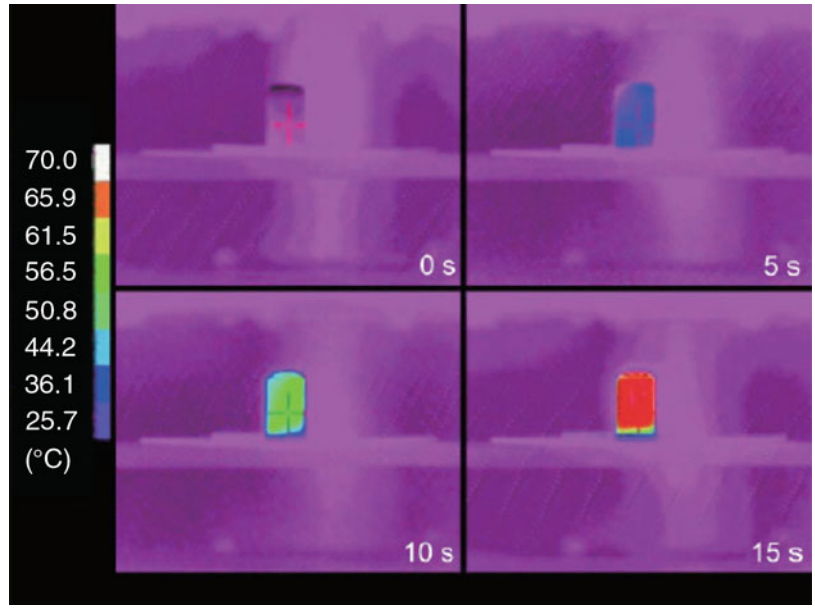

Fig. 7.7 Time-lapse-infrared images (5 s intervals) demonstrating heating potential of RF capacitance heating using 10-nm gold nanoparticles. Particles were exposed to a 15 kV/m RF field at a concentration of 36 ppm in a cuvette (Reprinted with permission from Moran CH, et al. Nano Res. 2009;2(5):400–5)

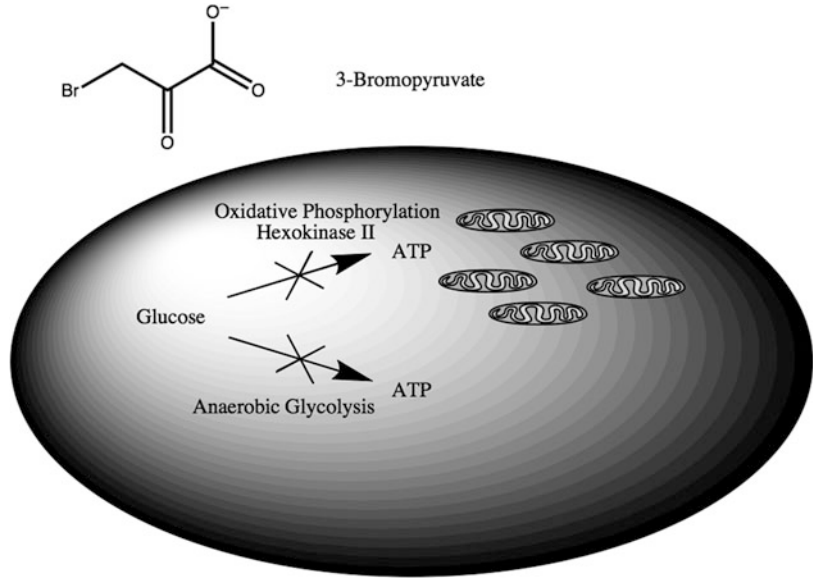

Fig. 7.8 Scheme depicting two of the presumed mechanisms of action for 3-Bromopyruvate. Glycolysis and mitochondrial targets are involved, depleting cells of ATP produced from both anaerobic and aerobic pathways

suggest that intracellular heating is occurring, but this is extremely challenging to document. Ohmic effects for RF heating of gold nanoparticles have been postulated, but evidence remains inconclusive [33]. Overall, the basic science appears very promising. It is likely, however, that there will be a role for image-guided application of such materials for the foreseeable future even after targeting methods are improved given the heterogeneity of tumor tissues, issues with irregular tumor vascularity and penetration, and therapeutic index.

A final subcategory is the use of RF energy within a magnet. Using the RF coils of the magnet itself as the energy source for hyperthermia, 9L gliosarcoma tumors were treated in a rat model [34]. This completely noninvasive method also allows for flexibility in monitoring the metabolic response by several markers.

New Ways to Deplete Energy in Cells

In the early part of the twentieth century, Otto Warburg observed a peculiar aspect regarding metabolism in neoplastic cells. For reasons still poorly understood, the inefficient glycolytic pathway is preferentially used over oxidative phosphorylation to generate ATP. This results in accumulation of lactate in the extracellular environment and a resulting drop in extracellular pH within many tumors. Early work by Pederson identified an opportunity to exploit this vulnerability and potential selectivity for malignancies. After a concerted effort, 3-bromopyruvate was identified as an effective compound that is undergoing extensive investigation [35]. This compound is approaching clinical trials after successful demonstration in several animal models. While it appears that there is more than one location and possibly more than one target for this compound, one mode of action is inhibition of mitochondrial hexokinase type 2 as shown in Fig. 7.8 and presumably thereby depletion of energy [36, 37].

New Ways to Sensitize Cells to Energy Inputs or Alter How Energy Interacts with Tissues

In considering the general class of sensitizers, it becomes important to make a mechanistic distinction between lowering the threshold for thermally based damage and altering in a biological sense the susceptibility or response of the treated cells to an intervention. It is also useful to

consider the actual target, whether it is the tumor, the vasculature supplying the tumor, or both.

Several of the techniques discussed below take advantage of the fact that while there is essentially no therapeutic index for heat in ablation, it succeeds as well as it does in ablation because there is a critical spatial and temporal component of thermal ablations that limits the thermal exposure to the entire body.

Mechanism-based enhancements to intervention have only recently attracted a modest amount of attention despite the potential in this area. These can be divided into tissue level and the cellular/molecular level areas. At the tissue level, previous work in RF ablation attempted to improve on existing results by instilling adjuvants such as hypertonic saline or acetic acid. The underlying hypothesis in many of these investigations was that such materials could enhance energy deposition and improve conduction through the tissues [38, 39]. While some conditions do show an improvement in ablation volume, the concept has not achieved widespread acceptance due to a reported lack of predictability in regard to ablation shape.

Much more predictable is the application of temperature-sensitive liposomes loaded with a drug. Since the seminal report of the concept by Yatvin and colleagues more than 30 years ago [40], the idea has been developed and a commercial product loaded with doxorubicin as the active agent, ThermoDox® (Celsion), has been granted orphan drug status by the FDA. A global, 600 patient, stage III clinical trial of the loaded liposome plus RFA compared to RFA alone is underway and is estimated to be completed in mid-2011. The primary endpoint is progression-free survival. Solazzo et al. recently reported on the effects of doxorubicin-loaded liposomes used in conjunction with RF ablation [41] building on the earlier work of Monsky et al. [42]. Data point toward increasing oxidative stress and activation of apoptotic pathways as mechanisms for the effects, but care must be taken interpreting the results. ThermoDox® with RF delivers doxorubicin very quickly, whereas other protocols may involve slow release of contents over time. With a longer temporal window, there is an opportunity to take advantage of mechanisms related to oxidative stress and apoptosis.

Efforts at quantifying the amount of drug delivered in tissues from various interventions continue to progress as well [43–45], and we can expect to see future studies using combinations of drugs with thermal therapies proliferating. Figure 7.9 illustrates one method exploiting microcapillary electrophoresis using a laser to detect doxorubicin in tissues at a remarkably small scale.

Photodynamic therapy has a long history particularly in superficial tumors such as head and neck cancers. This usually has taken the form of porphyrin derivatives that harvest light and generate singlet oxygen as the presumed mechanism of action. In the past few years, attention has turned toward percutaneous application of light energy via LED technology. Talaporfin sodium [46–48] is an example of a molecule with improved water solubility and targeting capability that may allow treatment of deeper solid tumors using this technique. The hope is that with such local activation, fewer problems with systemic toxicity and photosensitivity will be found. Practical concerns remain, as the treatment times are proposed on the scale of hours, data from clinical trials underway are not yet conclusive, and the rate and degree of side effect occurrence are not clearly defined. Figure 7.10 illustrates the underlying concepts of this type of treatment.

Recently, new approaches to increasing ablation volumes have been reported. These are somewhat more mechanism based as to their mode of action and effects on cell membranes. Here it is worth noting that a general distinction at the cellular level holds between antiangiogenic agents such as bevacizumab and arsenic trioxide and more acute vascular disrupting agents [49–51]. Both are likely to see increased use in conjunction with treatments such as hyperthermia. Still at the experimental level, block copolymers such as Pluronic P85® have been shown to increase ablation volumes over controls. Either direct intratumoral injection or intravenous administration was performed using

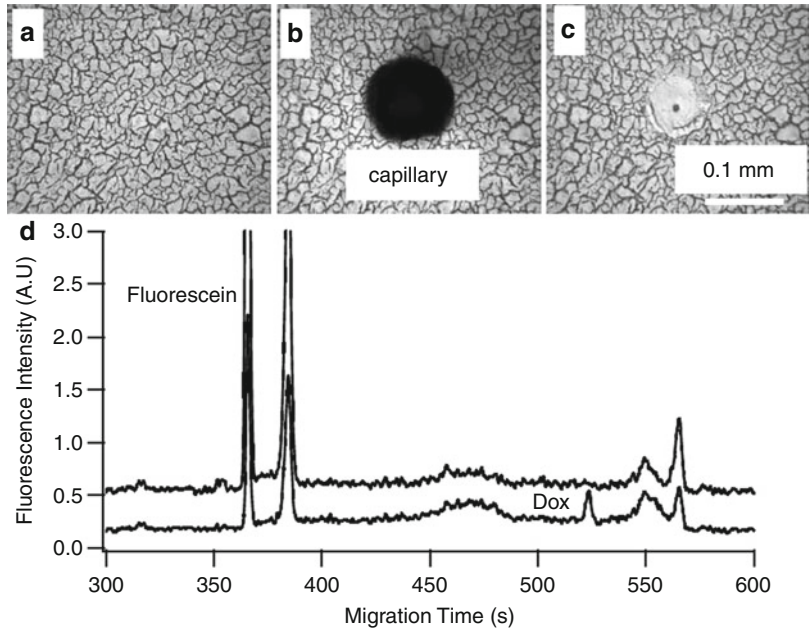

Fig. 7.9 (**a**–**d**) Direct tissue sampling using micellar electrokinetic chromatography with laser-induced fluorescence (MEKC-LIF). Histologic specimen in (**a**) was treated with doxorubicin. In (**b**), the microcapillary is positioned over the sample to aspirate a small volume leaving a void seen in (**c**). The peak for doxorubicin can be seen compared to a control in the electropherogram (**d**) (Reprinted with permission from Wang Y, et al. Anal Chem. 2009;81:3321–8, Fig. 5, p. 3325)

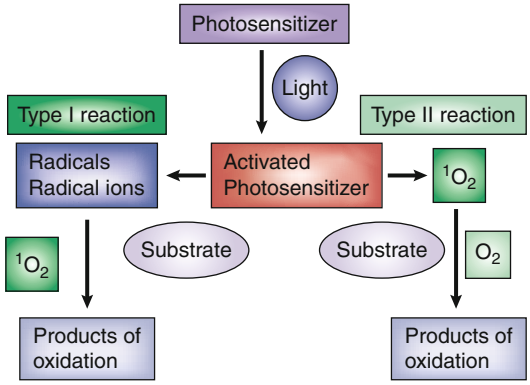

Fig. 7.10 Depiction of two possible modes of action for photodynamic therapy after light is absorbed, generally via structures based on a porphyrin ring (talaporfin sodium is but one example). Direct generation of free radicals (type I) and generation of singlet oxygen (type II) both lead to oxidative damage in the tissue (Reprinted with permission from Dolmans DEJGJ, et al. Photodynamic therapy for cancer. Nat Rev Cancer 2003;3(5):380–87)

low-temperature hyperthermia in combination with temperature-sensitive liposomal doxorubicin, but the detailed mechanism of the combination has not yet been determined [52]. A simple, 15-membered ring macrolactone used in the perfume industry, cyclopentadecanolide, has been shown to function both as a thermal sensitizer by lowering the threshold for damage (shown in Fig. 7.11) and in a role that is likely closely related as a permeability enhancing agent [53].

Heat shock proteins play an important role in response to thermal ablation. Some of these are expressed constitutively, and others are quickly upregulated after a thermal excursion or other stress. At the center of an ablation, thermal fixation occurs, but at the edge where temperature gradients drop into the nonlethal range, multiple pathways are activated. It is therefore logical to investigate modulation of this response and potentially improve outcomes. Early work in this area by Ahmed and Goldberg to suppress HSP 70 using the drug quercetin has resulted in an increase in ablation volumes in an animal model [54]. Quercetin is one compound that may suppress HSP70, but it may also modulate NF-kappa B and AP-1/JNK pathways as the primary modes of action based on data from HepG2 cells [55].

Much of this chapter is focused on hyperthermic methods, but progress continues in cryoablation as well. The particular challenges in cryoablation are centered on size of ice ball and new ways to expand the lethal zone well within the visualized area out to the edge of the

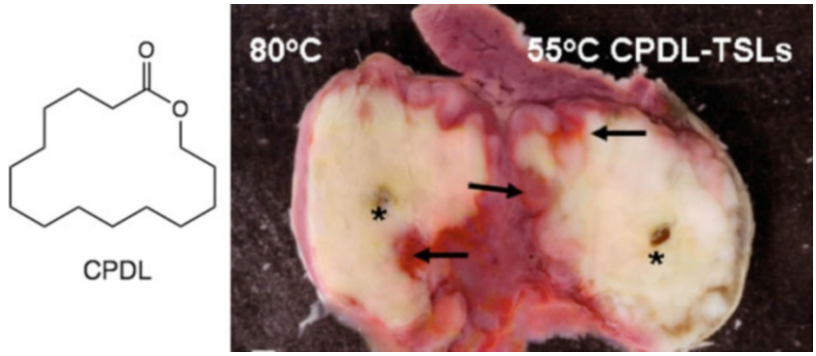

Fig. 7.11 Cyclopentadecanolide (CPDL, CAS # 106-02-5) as a thermal sensitizer: two RF ablations were performed in a single Walker 256 tumor grown in the liver of a male Wistar rat. The first ablation (*left*) was produced by delivering a 500-kHz sinusoidal signal to the 20-g RFA needle and adjusting the delivered power rapidly so that a thermocouple in the needle tip recorded 80 °C. Ablation was then *continued for 15 min* with the power adjusted to maintain the temperature at 80 °C. After the temperature returned to 37 °C, a 300 μl dose of 1 μm diameter temperature-sensitive liposomes containing a 3 % CPDL emulsion was given IV. The second ablation (*right*) was then performed identical to the first except that power to the RFA needle was adjusted such that the thermocouple recorded a temperature of 55 °C. *Arrows* indicate blood vessels, and **s* indicate needle tracts (Courtesy of Michael Borrelli)

visible ice ball. This would provide cryoablation with a distinct advantage over hyperthermic methods where it is typically difficult to assess the size of the treated area. Considerable progress has been made with CYT-6091, a gold nanoparticle conjugated to TNF alpha [56].

New Ways to Determine Where the Energy Has Been Deposited, How Much, and if Treatment Is Adequate

Knowing when tissue has been adequately treated but without damaging adjacent nontarget areas is critical to the ultimate success of an ablation procedure. It must be kept in mind that temperature is in fact a surrogate marker for tissue damage and loss of viability. Both ultrasound and CT are limited in their ability to delineate where adequate treatment has been delivered with respect to hyperthermic methods. Ice ball formation is readily visualized and one of the advantages to cryoablation (shown in Fig. 7.12), yet the lethal zone within an ice ball is considerably smaller than the visualized area.

MRI methods can provide this type of information in detail not currently possible by other means. The principles underlying MR thermography are already well established even if the facilities are not widely available. Disadvantages to MR thermography also necessarily include having MR-compatible materials for treatment that can add considerably to the cost. There is, therefore, an opportunity for other noninvasive methods of temperature monitoring. One such technique is ultrasound thermometry, and the field is advancing at a rapid pace [57, 58]. A key issue is addressing motion artifacts given the small differences in time constants that are exploited. Furthermore, much as the DMUA arrays described earlier represent a compromise, adding a thermography component to the same transducer will be challenging. Briefly, these methods relay on the temperature dependence of the speed of sound, attenuation, or shear modulus. These changes may be estimated using several methods that are beyond the scope of this discussion. Nevertheless, once these obstacles are overcome, the potential for noninvasive treatment will be substantial. The concept of "dose painting" developed primarily at the NIH and Duke University with MR imaging and shown in Fig. 7.13 [59–61] will become translatable to the world of ultrasound as well.

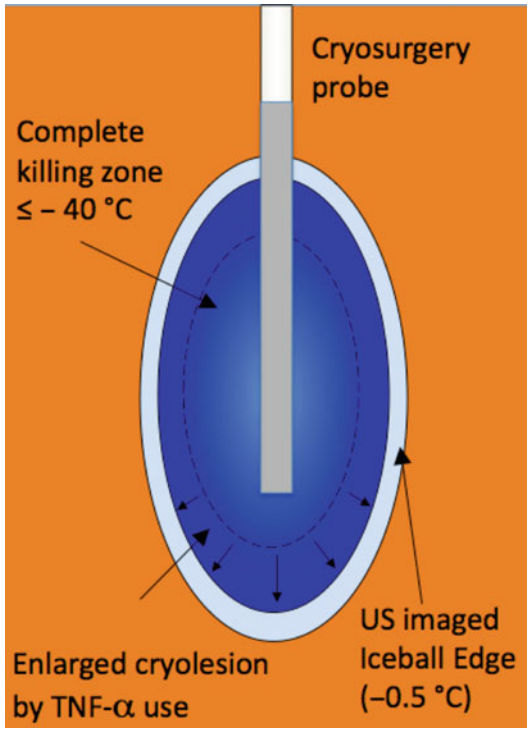

Fig. 7.12 In cryoablation, the lethal zone is significantly smaller than the visualized ice ball. Use of sensitizers such as a gold nanoparticles coated with TNF alpha extends the lethal zone closer to the margin of the visualized treatment area (Reprinted with permission from Hoffmann NE, Bischof JC. Mechanisms of injury caused by in vivo freezing, Chapter 16. In: Fuller BB, Lane N, editors. Life in the frozen state. London: Taylor & Francis; 2004. p. 455–82)

An example of real-time temperature imaging produced by the system described by Liu and Ebbini [57] is given in Fig. 7.14. With the diagnostic probe positioned so that the imaging plane intersects the axis of the therapeutic transducer (a), real-time (2D + Time) temperature data were generated in response to subtherapeutic HIFU beams designed to produce low-temperature rise in an ex vivo porcine heart tissue sample before and after therapeutic HIFU application that resulted in a zone of coagulation at the focus. The temperature images shown in Fig. 7.13b, c show the 2D temperature maps resulting from the application of subtherapeutic HIFU before and after sonication, respectively. The exposure parameters (intensity and duration) for the subtherapeutic HIFU were identical, but the temperature rise at the focus is higher after lesion formation. This can be easily seen from the temperature history profiles at the focus (>30 % change) indicating a significant change in absorption after lesion formation.

This result demonstrates several aspects of the use of US thermography in monitoring, control, and guidance of thermal therapy. Before lesion formation, temperature imaging of (short-exposure) subtherapeutic HIFU heating can be use to localize and characterize the quality of the HIFU focus before the application of the therapeutic HIFU. This can be used in

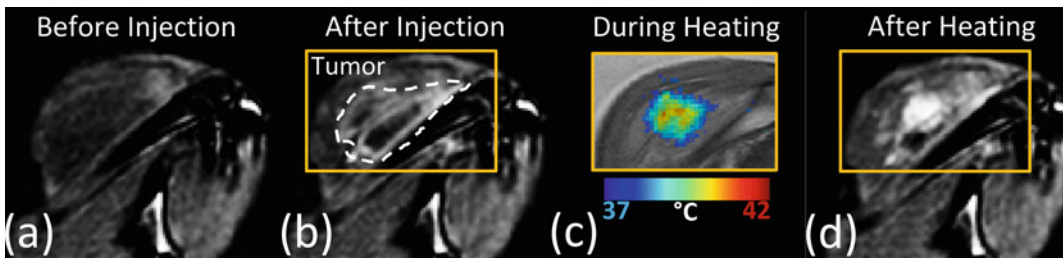

Fig. 7.13 Dose painting with temperature-sensitive liposomes loaded with contrast agent. MR signal intensity before and after liposome injection and heating with MR-HIFU. Signal intensity (**a**) before injection and (**b**) after injection. (**c**) Example of temperature map during heating overlaid on signal intensity obtained with a treatment planning proton density-weighted scan. (**d**) Signal intensity after a single 10-min heating session. Note that (**a**), (**b**), and (**d**) depict T1-weighted images whereas (**c**) shows a proton density-weighted image (Courtesy of Prof. Mark Dewhirst and his student, Pavel Yarmolenko)

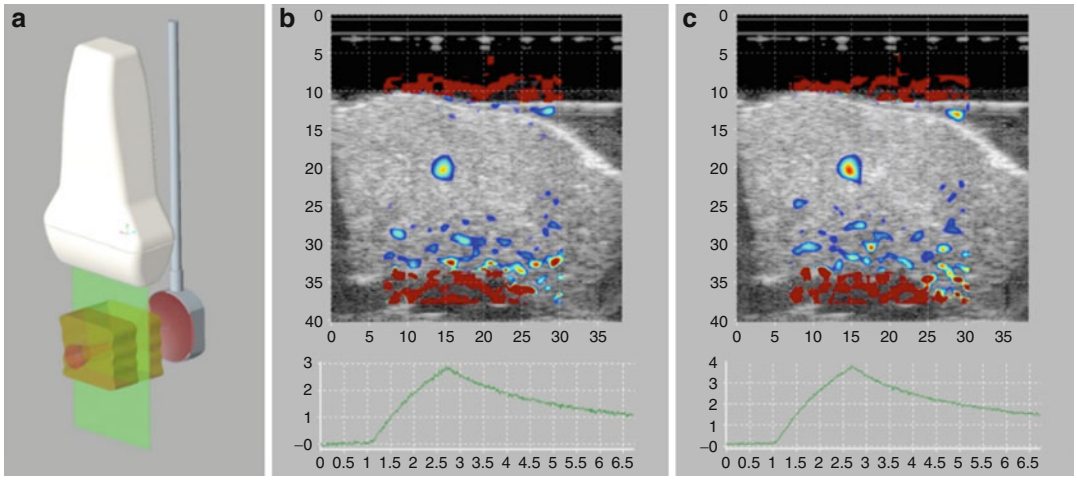

Fig. 7.14 (**a**) Diagnostic probe positioned so that the imaging plane intersects the axis of the therapeutic transducer, (**b**) and (**c**) show the 2D temperature maps resulting from the application of subtherapeutic HIFU before and after sonication, respectively (Courtesy of Prof. Emad Ebbini, University of Minnesota)

repositioning or refocusing the HIFU beam to maximize its efficacy in therapeutic mode. After sonication, the change in the heating rate and/or maximum temperature can be used to estimate the change in absorption, which may serve as a marker for tissue damage, especially for coagulative necrosis. This offers the possibility of immediate damage assessment upon the formation of each HIFU target volume in the course of the treatment. Note that these advantages are almost independent of the limitations mentioned above and, given that it is available in real time, it is ready for deployment in vivo.

Changes on unenhanced CT have been known for quite some time. Differences in the range of 0.25–0.5 HU/°C are subtle but well documented. Overall, changes less than 5 HU are difficult to reliably perceive, but changes due to ablation are greater than this, in the range of 10–20 HU. In an effort to improve the sensitivity, low-dose contrast/multiple low-dose scans have been developed in a protocol known as HYPR [62]. Reconstruction algorithms allow for significant improvements in the signal-to-noise ratio, but a drawback to the method is the inherent reliance on the use of additional ionizing radiation. The requirement for repeated scans also leaves the method vulnerable to misregistration artifacts from motion.

New Developments in Embolic Materials and Oncolytic Therapies

Transarterial chemoembolization or TACE is an accepted method with a survival benefit in malignancies such as hepatocellular carcinoma (HCC). Protocols vary widely around the world with no standardization of drugs, embolic particles, or how they are delivered. Further complicating the picture of what constitutes the best care is the arrival of drug-eluting beads on the market as discussed elsewhere in this volume. It is not known if so-called permanent embolic particles lead to the best outcomes. Beyond clinical trials of drug-eluting beads and combination therapies with agents such as sorafenib or bevacizumab, new areas for investigation are those of resorbable beads and imageable beads.

Resorbable beads may be beneficial for a controlled, temporary occlusion, but the area is new enough that the exact role for such technology remains to be defined. Some possible applications would include uterine fibroid embolization, chemoembolization, and trauma. Carboxymethyl cellulose (CMC) and chitosan (CN) are well-known biodegradable and biocompatible biomaterials and for these reasons have been used as starting materials. Microspheres from CMC and

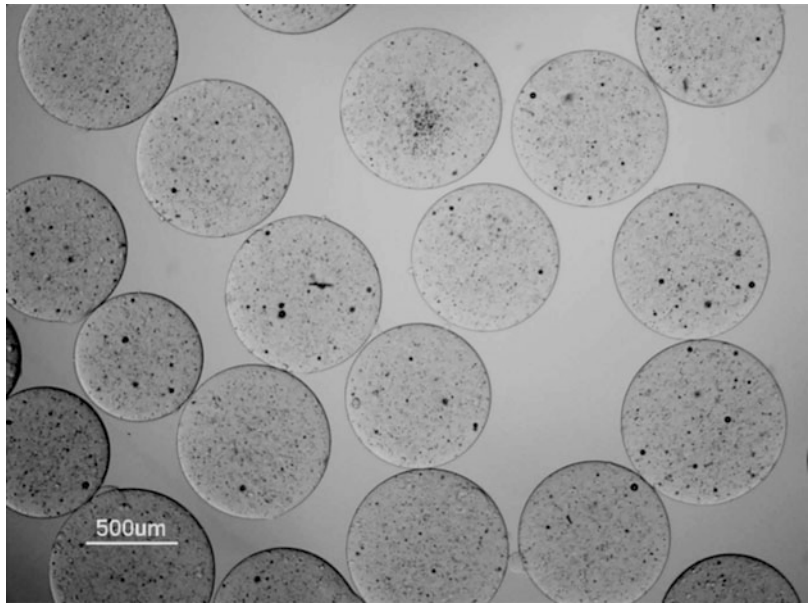

Fig. 7.15 Photomicrograph of resorbable CMC/CN microspheres showing relatively uniform size after sieving (Courtesy of Prof. Jafar Golzarian, University of Minnesota)

CN have recently been prepared and will presumably be bioresorbable. These may be differentiated from conventional spherical embolic materials due to their temporary characteristics and possibility of restoration of the vessel integrity after embolization. In regard to the transient nature, they are somewhat similar to liposomes but may have a longer half-life, larger size, and rather than having a discrete bilayered membrane, they have a continuous, cross-linked hydrogel structure.

Preliminary results show that these microspheres are fairly uniform in size distribution after sieving, in isolated or unloaded form are nontoxic in cell culture, and are degradable, compressible, colorable, and injectable. As shown in Fig. 7.15, 99 % of the microspheres exhibit a very round shape. The diameter of the microspheres ranges from 100 to 1,550 μm, and the fracture force, or the amount of force required to destroy the integrity of the bead, can reach 0.58–0.88 N (corresponding to a mass range of 60–90 g). Fracture deformation varies from approximately 70 % to 95 % of the original size. These microspheres can be colored by Evan's blue and form a stable suspension in a 4:6 contrast/saline mixture, which can be easily injected through microcatheters (2 F, 3 F) without aggregating or clogging. As show in Fig. 7.16, they are biodegradable with a significant change in their morphology. Depending on their composition, the degradation time varies from 2 weeks to 2 months.

Due to the existence of functional groups on the microsphere matrix, it is also possible to load them with a drug such as doxorubicin as with many other drug-eluting beads. As depicted in Fig. 7.17, microspheres loaded with doxorubicin exhibit a red color under fluorescence microscopy, indicating successful loading with doxorubicin. The microspheres can reach 90 % of maximum loading (0.3–0.7 mg doxorubicin per mg dry spheres depending on the size of the microspheres) in about 2 h. In vitro, the maximum doxorubicin release can be reached within 2 weeks, and the overall doxorubicin release can last up to 1 month. A potential advantage to such an approach beyond resorption is that a loaded drug would theoretically be 100 % available. This would presumably translate to better control of the kinetics of the treatment and improved outcomes. Based on these results,

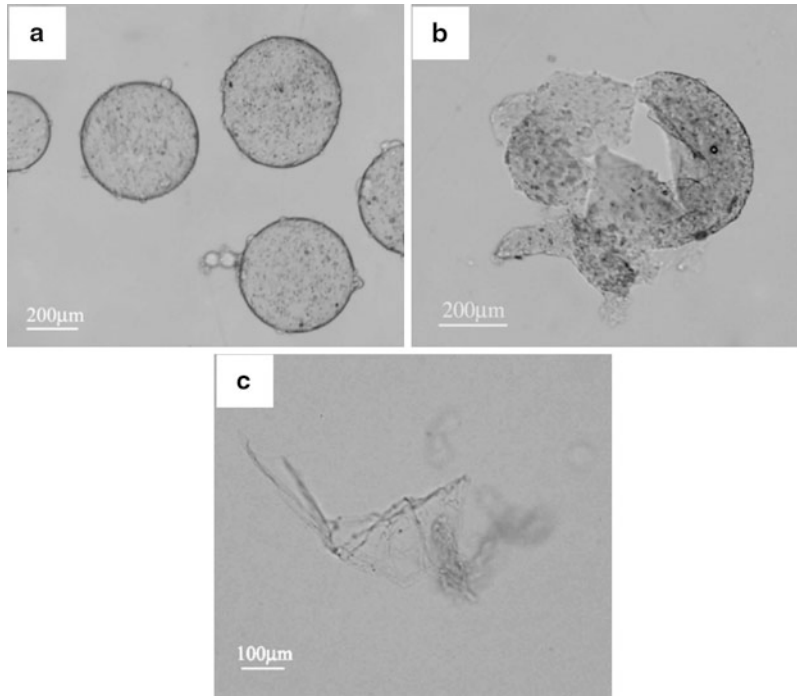

Fig. 7.16 Photomicrograph demonstrating degradation of resorbable microspheres over time (day 0, day 9, and day 14) (Courtesy of Prof. Jafar Golzarian, University of Minnesota)

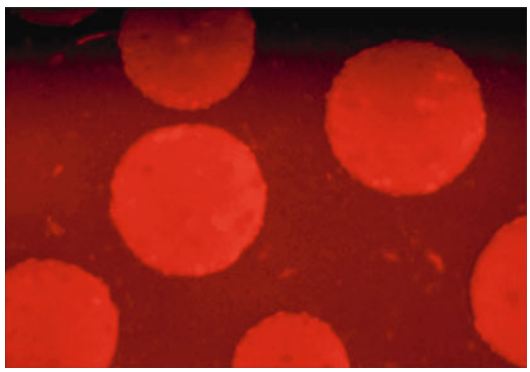

Fig. 7.17 Fluorescence microscopy image showing *red* color attributable to resorbable beads loaded with doxorubicin (Courtesy of Prof. Jafar Golzarian, University of Minnesota)

CMC/CN hydrogel microspheres appear to be a promising material for temporary therapeutic embolization. However, many questions remain about optimization of components, fate of the breakdown products, the ideal time profile with respect to breakdown of the products, and drug release kinetics in vivo. In the future, it may be possible to fuse both the resorbability and imaging as described below.

Another area that has received attention is improving the visibility of the beads themselves. Recent work at the NIH Center for Interventional Oncology in cooperation with Biocompatibles has produced a category of imageable beads known as iBeads™ that incorporate iodine to increase the density. The beads themselves are somewhat difficult to perceive in real time at fluoroscopy during an embolization procedure, but they can be seen by fluoroscopy at the presumed final location and are visualized quite readily with CT as shown in Fig. 7.18. Efforts are underway to improve contrast and at the same time load the beads with a drug as is becoming more commonplace for embolization procedures. Such beads will allow for more accurate assessments of vascularity, distribution of particles, actual territory embolized, and standardization of procedural endpoints [63].

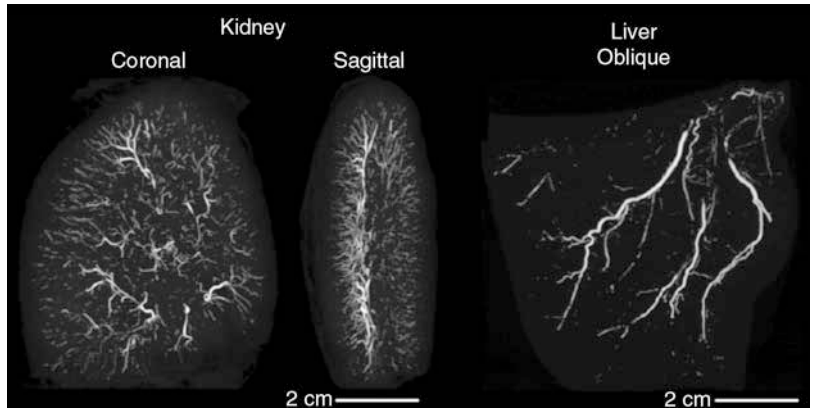

Fig. 7.18 Imageable beads on micro-CT in healthy kidney and liver tissues. Bead size is within the 50-μm resolution limit of the equipment, allowing resolution of individual beads (Reprinted with permission from Sharma KV, Dreher MR, Yiqing Tang Y, et al. J Vasc Interv Radiol. 2010;21:865–76. Copyright © 2010 Elsevier)

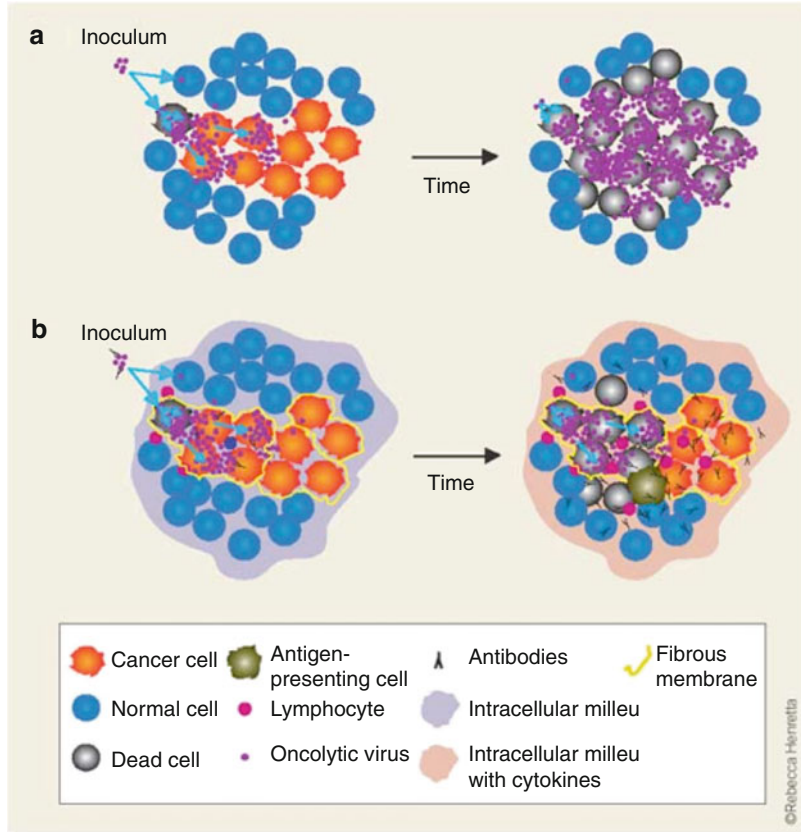

Fig. 7.19 Generalized scheme for oncolytic treatment strategies. In the upper images (**a**), an idealized situation is shown in which a virus replicates in and thereby destroys all the viable tumor tissue. In (**b**), confounding factors such as host immune responses and the microenvironment are shown which hinder the effects of the treatment (Reprinted with permission from Aguilar-Cordova E. Nat Biotechnol. 2003;21(7):756–7)

The appeal of targeted oncolytic viral therapy is significant, and therefore, it has attracted considerable attention and investment by biotechnology companies over the past few years. Several generations of vectors have now resulted in improved activity, and human clinical trials are ongoing for a subset of these. Of over a dozen different types of vectors, variants of herpes and vaccinia viruses appear promising, but the measles virus, vesicular stomatitis virus [64], Newcastle disease virus [65, 66], and several adenoviruses also have potential based on data from animal models. In general, the strategies encompass mutations that allow for selective replication of a virus in tumoral tissue as shown in Fig. 7.19. The infected cells then either

undergo apoptosis directly or become susceptible to an otherwise ineffective drug therapy as a consequence of infection. Inflammatory responses often ensue. It is not yet clear if this is beneficial or counterproductive, when, for how long, and under what circumstances.

One especially appealing aspect of oncolytic viral therapy is the theoretical advantage of spread throughout tumor at both the local and systemic levels. Thus, the virus can be delivered in a small volume by any of several methods: directly into the tumor, via the transarterial route, portal venous route, retrograde by way of a hepatic vein, intravenous route, or even the biliary ductal system. It must be pointed out that this approach stands in marked contrast to the use of viruses in conventional gene therapy, where replicative potential is considered a health risk and therefore avoided if at all possible. The underlying assumption is that the genetically crippled, modified virus will only reproduce in the tumor cells.

One of the challenges for treatment of hepatocellular carcinoma (HCC) in particular is hepatotoxicity in the setting of an already diseased liver, a common problem with many interventions for this disease. The diverse molecular biology of malignancies such as HCC and the heterogeneity within a given tumor also present significant obstacles. Eventually one could imagine an intranasal administration or equally elegant route (depending on the type of virus and its mechanism of spread) obviating the need for an image-guided intervention. Factors such as required dosages, clearance by various routes, and antibody neutralization of a virus will need to be addressed. Such a goal, however, appears to be many years in the future.

In conclusion, the future of interventional oncology holds much promise and is rapidly advancing on many fronts. Therapies on the horizon will become even less invasive, provide better outcomes, and at the same time reduce the burden of cancer on society. We can expect to see more overlap in sensitizing methods used in related fields such as radiation biology/oncology and more collaboration with medical oncology using systemic adjuvants and immune modifiers. Until the day when molecular therapies reach perfection and prevention and early detection are optimized, image-guided intervention will play a key role in the treatment of malignancies.

Acknowledgments A number of physicians, scientists, and engineers contributed insight and discussion in the preparation of this chapter. In particular, the author would like to thank the following: Dr. Fil Banovac, Dr. Karun Sharma, Dr. Matt Dreher, Dr. Dan Sze, Dr. Jafar Golzarian, Dr. Muneeb Ahmed, Dr. Lihui Weng, Dr. Emad Ebbini, Dr. Rob Griffin, Dr. Chris Brace, Dr. Dustin Kruse, and Dr. John Bischof.

Cross-References

- ▶ Combination Therapies in the Treatment of Primary Liver Cancers
- ▶ Cryoablation
- ▶ Embolic Therapies
- ▶ Embolic Therapy for the Treatment of Liver Metastases
- ▶ Embolotherapy in the Management of Gynecologic Neoplasms
- ▶ Focused Ultrasound of Liver
- ▶ High-Intensity Focused Ultrasound Treatment for Bone Metastases
- ▶ Image-Guided High-Intensity Focused Ultrasound in the Treatment of Cancer
- ▶ Imaging of Interventional Therapies in Oncology: Image Guidance, Robotics, and Fusion Systems
- ▶ Magnetic Resonance-Guided High-Intensity Focused Ultrasound: Gynecological Applications
- ▶ Percutaneous Ethanol Injection Injectables in the Treatment of Primary Liver Cancers

References

1. Solomon SB, White Jr P, Acker DE, Strandberg J, Venbrux AC. Real-time bronchoscope tip localization enables three-dimensional CT image guidance for transbronchial needle aspiration in swine. Chest. 1998;114(5):1405–10.
2. Solomon SB, Magee C, Acker DE, Venbrux AC. TIPS placement in swine, guided by electromagnetic real-time needle tip localization displayed on previously acquired 3-D CT. Cardiovasc Intervent Radiol. 1999;22(5):411–4.

3. Solomon SB, Magee CA, Acker DE, Venbrux AC. Experimental nonfluoroscopic placement of inferior vena cava filters: use of an electromagnetic navigation system with previous CT data. J Vasc Interv Radiol. 1999;10(1):92–5.
4. Banovac F, Tang J, Xu S, et al. Precision targeting of liver lesions using a novel electromagnetic navigation device in physiologic phantom and swine. Med Phys. 2005;32(8):2698–705.
5. Banovac F, Cheng P, Campos-Nanez E, et al. Radiofrequency ablation of lung tumors in swine assisted by a navigation device with preprocedural volumetric planning. J Vasc Interv Radiol. 2010;21(1):122–9.
6. Krucker J, Xu S, Glossop N, et al. Electromagnetic tracking for thermal ablation and biopsy guidance: clinical evaluation of spatial accuracy. J Vasc Interv Radiol. 2007;18(9):1141–50.
7. Fischer K, Gedroyc W, Jolesz FA. Focused ultrasound as a local therapy for liver cancer. Cancer J. 2010;16(2):118–24.
8. Illing RO, Kennedy JE, Wu F, et al. The safety and feasibility of extracorporeal high-intensity focused ultrasound (HIFU) for the treatment of liver and kidney tumours in a Western population. Br J Cancer. 2005;93(8):890–5.
9. Wu F, Wang ZB, Chen WZ, et al. Advanced hepatocellular carcinoma: treatment with high-intensity focused ultrasound ablation combined with transcatheter arterial embolization. Radiology. 2005;235(2):659–67.
10. Orgera G, Curigliano G, Krokidis M, et al. High-intensity focused ultrasound effect in breast cancer nodal metastasis. Cardiovasc Intervent Radiol. 2010;33(2):447–9.
11. Orgera G, Krokidis M, Monfardini L, et al. High intensity focused ultrasound ablation of pancreatic neuroendocrine tumours: report of two cases. Cardiovasc Intervent Radiol. 2010;34:419–23.
12. Jeong JS, Chang JH, Shung KK. Ultrasound transducer and system for real-time simultaneous therapy and diagnosis for noninvasive surgery of prostate tissue. IEEE Trans Ultrason Ferroelectr Freq Control. 2009;56(9):1913–22.
13. Jeong JS, Cannata JM, Shung KK. Adaptive HIFU noise cancellation for simultaneous therapy and imaging using an integrated HIFU/imaging transducer. Phys Med Biol. 2010;55(7):1889–902.
14. Owen NR, Chapelon JY, Bouchoux G, Berriet R, Fleury G, Lafon C. Dual-mode transducers for ultrasound imaging and thermal therapy. Ultrasonics. 2010;50(2):216–20.
15. Ballard JR, Casper AJ, Ebbini ES. Monitoring and guidance of HIFU beams with dual-mode ultrasound arrays. Conf Proc IEEE Eng Med Biol Soc. 2009;2009:137–40.
16. Ebbini ES, Yao H, Shrestha A. Dual-mode ultrasound phased arrays for image-guided surgery. Ultrason Imaging. 2006;28(2):65–82.
17. Deng ZS, Liu J. Minimally invasive thermotherapy method for tumor treatment based on an exothermic chemical reaction. Minim Invasive Ther Allied Technol. 2007;16(1):1–6.
18. Farnam JL, Smith BC, Johnson BR, et al. Thermochemical ablation in an ex-vivo porcine liver model using acetic acid and sodium hydroxide: proof of concept. J Vasc Interv Radiol. 2010;21:1573–8.
19. Rao W, Liu J. Tumor thermal ablation therapy using alkali metals as powerful self-heating seeds. Minim Invasive Ther Allied Technol. 2008;17(1):43–9.
20. Rao W, Liu J, Zhou YX, Yang Y, Zhang H. Anti-tumor effect of sodium-induced thermochemical ablation therapy. Int J Hyperthermia. 2008;24(8):675–81.
21. Rao W, Liu J. Injectable liquid alkali alloy based-tumor thermal ablation therapy. Minim Invasive Ther Allied Technol. 2009;18(1):30–5.
22. Cressman EN, Tseng HJ, Talaie R, Henderson BM. A new heat source for thermochemical ablation based on redox chemistry: initial studies using permanganate. Int J Hyperthermia. 2010;26(4):327–37.
23. Shafirstein G, Kaufmann Y, Hennings L, et al. Conductive interstitial thermal therapy (CITT) inhibits recurrence and metastasis in rabbit VX2 carcinoma model. Int J Hyperthermia. 2009;25(6):446–54.
24. Shafirstein G, Novak P, Moros EG, et al. Conductive interstitial thermal therapy device for surgical margin ablation: in vivo verification of a theoretical model. Int J Hyperthermia. 2007;23(6):477–92.
25. Cherukuri P, Curley SA. Use of nanoparticles for targeted, noninvasive thermal destruction of malignant cells. Methods Mol Biol. 2010;624:359–73.
26. Curley SA, Cherukuri P, Briggs K, et al. Noninvasive radiofrequency field-induced hyperthermic cytotoxicity in human cancer cells using cetuximab-targeted gold nanoparticles. J Exp Ther Oncol. 2008;7(4):313–26.
27. Gannon CJ, Cherukuri P, Yakobson BI, et al. Carbon nanotube-enhanced thermal destruction of cancer cells in a noninvasive radiofrequency field. Cancer. 2007;110(12):2654–65.
28. Kawashita M, Domi S, Saito Y, et al. In vitro heat generation by ferrimagnetic maghemite microspheres for hyperthermic treatment of cancer under an alternating magnetic field. J Mater Sci Mater Med. 2008;19(5):1897–903.
29. Fortin JP, Gazeau F, Wilhelm C. Intracellular heating of living cells through Neel relaxation of magnetic nanoparticles. Eur Biophys J. 2008;37(2):223–8.
30. Wilhelm C, Fortin JP, Gazeau F. Tumour cell toxicity of intracellular hyperthermia mediated by magnetic nanoparticles. J Nanosci Nanotechnol. 2007;7(8):2933–7.
31. Jing Y, He S, Kline T, Xu Y, Wang JP. High-magnetic-moment nanoparticles for biomedicine. Conf Proc IEEE Eng Med Biol Soc. 2009;2009:4483–6.
32. Dennis CL, Jackson AJ, Borchers JA, et al. Nearly complete regression of tumors via collective behavior of magnetic nanoparticles in hyperthermia. Nanotechnology. 2009;20(39):395103.

33. Moran CH, Wainerdi SM, Cherukuri TK, et al. Size-dependent joule heating of gold nanoparticles using capacitively coupled radiofrequency fields. Nano Res. 2009;2(5):400–5.
34. James JR, Gao Y, Soon VC, Topper SM, Babsky A, Bansal N. Controlled radio-frequency hyperthermia using an MR scanner and simultaneous monitoring of temperature and therapy response by (1)H, (23)Na and (31)P magnetic resonance spectroscopy in subcutaneously implanted 9L-gliosarcoma. Int J Hyperthermia. 2010;26(1):79–90.
35. Ko YH, Smith BL, Wang Y, et al. Advanced cancers: eradication in all cases using 3-bromopyruvate therapy to deplete ATP. Biochem Biophys Res Commun. 2004;324(1):269–75.
36. Mathupala SP, Ko YH, Pedersen PL. The pivotal roles of mitochondria in cancer: Warburg and beyond and encouraging prospects for effective therapies. Biochim Biophys Acta. 2010;1797:1225–30.
37. Mathupala SP, Ko YH, Pedersen PL. Hexokinase-2 bound to mitochondria: cancer's stygian link to the "Warburg effect" and a pivotal target for effective therapy. Semin Cancer Biol. 2009;19(1):17–24.
38. Nour SG, Goldberg SN, Wacker FK, et al. MR monitoring of NaCl-enhanced radiofrequency ablations: observations on low- and high-field-strength MR images with pathologic correlation. Radiology. 2010;254(2):449–59.
39. Wood MA, Goldberg SM, Parvez B, et al. Effect of electrode orientation on lesion sizes produced by irrigated radiofrequency ablation catheters. J Cardiovasc Electrophysiol. 2009;20:1262–8.
40. Yatvin MB, Weinstein JN, Dennis WH, Blumenthal R. Design of liposomes for enhanced local release of drugs by hyperthermia. Science. 1978;202(4374):1290–3.
41. Solazzo SA, Ahmed M, Schor-Bardach R, et al. Liposomal doxorubicin increases radiofrequency ablation-induced tumor destruction by increasing cellular oxidative and nitrative stress and accelerating apoptotic pathways. Radiology. 2010;255(1):62–74.
42. Monsky WL, Kruskal JB, Lukyanov AN, et al. Radiofrequency ablation increases intratumoral liposomal doxorubicin accumulation in a rat breast tumor model 1. Radiology. 2002;224(3):823–9.
43. Head HW, Dodd 3rd GD, Bao A, et al. Combination radiofrequency ablation and intravenous radiolabeled liposomal Doxorubicin: imaging and quantification of increased drug delivery to tumors. Radiology. 2010;255(2):405–14.
44. Wang Y, Hong J, Cressman EN, Arriaga EA. Direct sampling from human liver tissue cross sections for electrophoretic analysis of doxorubicin. Anal Chem. 2009;81(9):3321–8.
45. Namur J, Wassef M, Millot JM, Lewis AL, Manfait M, Laurent A. Drug-eluting beads for liver embolization: concentration of doxorubicin in tissue and in beads in a pig model. J Vasc Interv Radiol. 2010;21(2):259–67.
46. Wang S, Bromley E, Xu L, Chen JC, Keltner L. Talaporfin sodium. Expert Opin Pharmacother. 2010;11(1):133–40.
47. Kujundzic M, Vogl TJ, Stimac D, et al. A Phase II safety and effect on time to tumor progression study of intratumoral light infusion technology using talaporfin sodium in patients with metastatic colorectal cancer. J Surg Oncol. 2007;96(6):518–24.
48. Chen J, Keltner L, Christophersen J, et al. New technology for deep light distribution in tissue for phototherapy. Cancer J. 2002;8(2):154–63.
49. Siemann DW, Horsman MR. Vascular targeted therapies in oncology. Cell Tissue Res. 2009;335(1):241–8.
50. Siemann DW, Shi W. Efficacy of combined antiangiogenic and vascular disrupting agents in treatment of solid tumors. Int J Radiat Oncol Biol Phys. 2004;60(4):1233–40.
51. Siemann DW, Bibby MC, Dark GG, et al. Differentiation and definition of vascular-targeted therapies. Clin Cancer Res. 2005;11(2 Pt 1):416–20.
52. Weinberg BD, Krupka TM, Haaga JR, Exner AA. Combination of sensitizing pretreatment and radiofrequency tumor ablation: evaluation in rat model. Radiology. 2008;246(3):796.
53. Heberlein WE, Borrelli MJ, Wu J, Bernock LJ. Localized injection of a tissue permeabilizer reduces the threshold temperature required to ablate solid tissue. J Vasc Interv Radiol. 2010;21(2):S36.
54. Yang W, Ahmed M, Tasawwar B, Levchenko T, Sawant RR, Collins M, Signoretti S, Torchilin V, Goldberg SN. Radiofrequency ablation combined with liposomal quercetin to increase tumour destruction by modulation of heat shock protein production in a small animal model. Int J Hyperth. 2011; 27 (6):527–538.
55. Granado-Serrano AB, Martin MA, Bravo L, Goya L, Ramos S. Quercetin modulates NF-kappa B and AP-1/JNK pathways to induce cell death in human hepatoma cells. Nutr Cancer. 2010;62(3):390–401.
56. Goel R, Swanlund D, Coad J, Paciotti GF, Bischof JC. TNF-alpha-based accentuation in cryoinjury–dose, delivery, and response. Mol Cancer Ther. 2007;6(7):2039–47.
57. Liu D, Ebbini ES. Real-time 2-D temperature imaging using ultrasound. IEEE Trans Biomed Eng. 2010;57(1):12–6.
58. Anand A, Kaczkowski PJ. Noninvasive determination of in situ heating rate using kHz acoustic emissions and focused ultrasound. Ultrasound Med Biol. 2009;35(10):1662–71.
59. Ponce AM, Viglianti BL, Yu D, et al. Magnetic resonance imaging of temperature-sensitive liposome release: drug dose painting and antitumor effects. J Natl Cancer Inst. 2007;99(1):53–63.
60. Viglianti BL, Abraham SA, Michelich CR, et al. In vivo monitoring of tissue pharmacokinetics of liposome/drug using MRI: illustration of targeted delivery. Magn Reson Med. 2004;51(6):1153–62.

61. de Smet M, Langereis S, van den Bosch S, Grull H. Temperature-sensitive liposomes for doxorubicin delivery under MRI guidance. J Control Release. 2010;143(1):120–7.
62. Brace CL, Mistretta CA, Hinshaw JL, Lee Jr FT. Periodic contrast-enhanced computed tomography for thermal ablation monitoring: a feasibility study. Conf Proc IEEE Eng Med Biol Soc. 2009;2009:4299–302.
63. Sharma KV, Dreher MR, Tang Y, et al. Development of "imageable" beads for transcatheter embolotherapy. J Vasc Interv Radiol. 2010;21(6):865–76.
64. Jenks N, Myers R, Greiner SM, et al. Safety studies on intrahepatic or intratumoral injection of oncolytic vesicular stomatitis virus expressing interferon-beta in rodents and nonhuman primates. Hum Gene Ther. 2010;21(4):451–62.
65. Chang JF, Chen PJ, Sze DY, et al. Oncolytic virotherapy for advanced liver tumours. J Cell Mol Med. 2009;13(7):1238–47.
66. Altomonte J, Marozin S, Schmid RM, Ebert O. Engineered newcastle disease virus as an improved oncolytic agent against hepatocellular carcinoma. Mol Ther. 2010;18(2):275–84.

Radiation Therapy: Intensity-Modulated Radiotherapy, Cyberknife, Gamma Knife, and Proton Beam

8

Lei Ren and Samuel Ryu

Abstract

Radiosurgery is a medical procedure of accurate targeting of a well-defined volume with radiation. It requires a decision-making based on the patient's clinical presentation, medical status, and imaging studies. Practically, radiosurgery requires reliable patient positioning and immobilization, stereotactic target tumor localization, computerized radiation planning and calculation, and delivery of the designed radiation with rapid dose falloff outside the target. Recent advances of computer science, radiation delivery technology, and image guidance made it possible to apply the radiosurgery to the extracranial body sites as well as brain. The technology has been evolving rapidly. In this entry, the currently available radiosurgery equipments are described. It is helpful for the practitioners to understand the different design of the technology for radiosurgery for a better clinical application.

Introduction

The physical hallmark of radiosurgery is rapid radiation dose falloff outside the target. It is usually represented by the distance between the point of high radiation dose and the other point of low radiation dose, 90–50 % isodose lines, for example. It is usually within a few millimeters between those two points of isodose lines. With this physical property of radiation dose falloff, radiosurgery can deliver high radiation dose which is not used in conventional radiotherapy. On the other hand, radiosurgery requires accurate targeting and the ability of achieving a high conformality of radiation distribution to the target volume. This conformality provides three-dimensional shaping of the target volume with the radiation dose shaping to the target. While conformality of radiosurgery provides necessary therapeutic radiation to the tumor, rapid dose falloff provides high selectivity of radiosurgery for optimum management of the small volume targets. Thus, high radiation dose can be delivered to the gross tumor volume or a clinically well-defined target. With these physical properties, radiosurgery has

L. Ren (✉)
Department of Radiation Oncology, Duke University, Durham, NC, USA
e-mail: lei.ren@duke.edu

S. Ryu
Department of Radiation Oncology and Neurosurgery, Henry Ford Hospital, Detroit, MI, USA
e-mail: sryu1@hfhs.org

D.E. Dupuy et al. (eds.), *Image-Guided Cancer Therapy*, DOI 10.1007/978-1-4419-0751-6_10,

been used exclusively for treatment of intracranial targets by using rigid stereotactic frame.

For brain radiosurgery, patient is usually immobilized using a carbon fiber or metallic head ring rigidly attached to the skull (frame-based method) or a mask (frameless-based method). Attached to the frames is the localizer box, which defines a 3D coordinate system used for treatment planning and image registration between different imaging modalities (e.g., CT, MRI, angiography). With the accuracy of submillimeter range, the brain radiosurgery has been used for treatment of benign and malignant tumors, vascular lesions, and functional disorders.

In the recent years, radiosurgery has been applied to the extracranial targets, most notably to the spine, lung, and liver, among others [1–4]. To be used for the body sites, several obstacles had to be overcome. Immobilization and positioning becomes the first task to overcome in order to stereotactically target the lesions without rigid frames. They include the establishment of a fiducial system for target localization, stereotactic imaging, dosimetric planning, and radiation treatment. There also exists difficulty of beam delivery to the moving lesions with the internal organ movement mostly associated with breathing. The use of a micro multi-leaf collimator (μMLC) or pencil beam techniques also made it possible to three-dimensionally shape the target lesions and modulate the radiation beam intensity. Progress of imaging studies became available for a better visualization of the target tumor tissue in relation to the surrounding normal tissue which may be the dose-limiting organ in radiation therapy. Technological development of computerized treatment planning of radiation beam intensity modulation and the development of radiation delivery system made the application of radiosurgery to the targets in the body possible by dosimetric precision to the tumor and the adjacent normal tissue. Radiosurgery of body sites is now called stereotactic body radiation therapy (SBRT) by American Society of Therapeutic Radiology and Oncology (ASTRO). It is not possible to describe all the details of radiosurgery equipments. In this entry, the basic structure and clinical applicability of the available radiosurgery units are introduced.

Advance of Image-Guided Radiotherapy

Radiation therapy is a local treatment, compared to the systemic treatment with chemotherapy. The ultimate goal of radiotherapy is to treat the defined tumor and spare the surrounding normal tissue. In the practice of radiotherapy, however, there can be many factors that may cause discrepancy between the planned dose distribution and the actual delivered dose distribution. One such factor is uncertainty in patient position on the treatment unit. Guiding the placement of the treatment field is not a new concept. Conventional radiotherapy used surface and skin markers such as tattooing the isocenter point on the skin and portal films, and more recently, electronic portal imaging has been used. To target the tumor more accurately, image-guided localization, known as image-guided radiation therapy (IGRT), has become a component of the radiation therapy process that incorporates imaging coordinates from the treatment plan to be delivered in order to ensure the patient is properly aligned in the treatment room. The goal of the IGRT process is to improve the accuracy of the radiation field placement, thus improving tumor control and decreasing radiation to the surrounding normal tissues.

Currently, many radiation therapy techniques employ the process of IMRT (described above). This form of radiation therapy can shape the radiation beam according to the tumor shape and sculpt a three-dimensional radiation dose map, specific to the target's location, including the organ motion characteristics. The utmost form of treatment can be radiosurgery or SBRT, which requires precision targeting, a direct by-product of noninvasive image guidance. IGRT also generates an increased amount of data collected throughout the course of therapy. This allows the continued assessment and refinement of the radiation delivery, so-called adaptive radiotherapy. The clinical benefit for the patient is the ability to monitor and adapt to changes that may occur during the course of radiation treatment. IGRT technique has a great potential of further development, coupled with sophisticated radiation delivery technique,

to incorporate the change of tumor shrinkage during the course, and visualizing and tracking the movement of tumors and organs during the actual radiation delivery. Image guidance can also be used for brachytherapy (placement of radiation sources within the tumor). Gold or radioopaque fiducial placement can also be used. Placement of fiducial is performed mostly by fluoroscopic guidance. It can also be done with CT, ultrasound, or other imaging modalities. It was mostly used during the initial developing phase of the body radiosurgery equipment, such as CyberKnife or Novalis, and is largely replaced by noninvasive image-guided localization methods, i.e., IGRT. However, it can be useful when there is no anatomical landmark in the vicinity of the target tissue. The radioopaque fiducial can serve for image guidance.

IGRT is a distinct use of images from the delineation of targets and organs for planning of radiation therapy to the delivery of radiation to the desired target. Various images including CT, MRI, or PET are acquired and fused between each other. An example technique includes cone-beam CT (CBCT) images, which images the attainable volume of tissue containing the target tumors and reconstruct the 2D images into 3D ones, using either the megavoltage from the linear accelerator or the mounted kilovoltage imager. High-quality CBCT images are produced with only a modest dose to the patient. Such images can be used to more accurately setup patients based on internal anatomy rather than the external markers.

Most of the currently available radiosurgery systems use image-guidance system with one or combined methods. These are more equipped with radiosurgery systems with linear accelerator such as Novalis, CyberKnife, or tomotherapy, as described below.

Concepts of 3D-CRT, IMRT, and Dynamic Arc

Advances of precision image guidance for patient localization and targeting tumors were coupled with the development of more accurate radiation dose delivery with techniques such as three-dimensional conformal radiotherapy (3D-CRT), intensity-modulated radiotherapy (IMRT), or dynamic arc therapy. There are several types of treatments that can be delivered by a radiotherapy machine. Either a cone or multi-leaf collimator (MLC) can be used to shape the beam during the delivery. A multi-leaf collimator is a device made up of individual "leaves" of a high atomic number material, usually tungsten. These leaves move independently in and out of the path of a radiation beam in order to shape the beam opening, as shown in Fig. 8.1 [5, 6]. Different delivery techniques can be designed in MLC-based treatments such as 3D-CRT, IMRT, or dynamic arc therapy [7, 8].

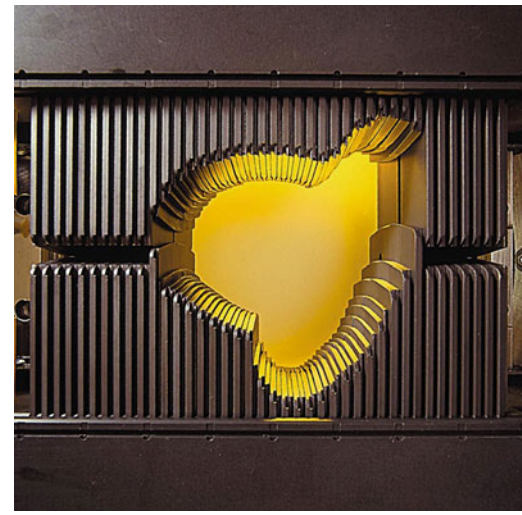

Fig. 8.1 A high-definition multi-leaf collimator (From Varian Medical System)

In 3D-CRT, the gantry delivers several beams from different angles with the beam opening defined by MLC conformed, in beam's eye view, to the tumor. The radiation beam intensity within each beam opening is uniform. The dose weighting for each beam is then adjusted in a trial-and-error fashion to refine the plan. 3D-CRT is performed by the traditional forward planning process and calculates the dose to the target and normal tissue based on predefined treatment plan parameters including various beam weight, and energy configurations [9–12].

The next step of advancement was intensity modulation of radiation beam. It is called intensity-modulated radiotherapy (IMRT), in which the radiation fluence intensity in each beam is modulated by moving the MLC during the delivery [9, 13, 14]. IMRT is achieved by the inverse treatment planning which the computerized treatment algorithm searches for the optimal treatment plan based on clinical target dose prescription and normal tissue avoidance parameters in contrast to the forward planning system used for 3D-CRT. In the IMRT treatment planning process, the user sets dose constraints that permit a maximum dose to the target and restrict the dose to the adjacent normal tissue structures. The planning computer, through numerous optimization iterations, comes up with the best possible dynamic MLC motion pattern that modulates the radiation fluence to meet the dose constraints. As a result, radiation fluence intensity modulation occurs in the plane of each beam aperture. IMRT has a wide range of potential clinical applications, particularly in central nervous system, head and neck, breast, and prostate cancer patients, where intrafraction target motion is minimal and normal tissue toxicity is of major concern. Thus, 3D conformal approach with IMRT allows radiation dose escalation which can improve local tumor control, with greater sparing of critical structures surrounding the tumor [15].

Dynamic arc therapy is a radiation therapy delivery technique that combines gantry rotation with MLC motion. Each treatment is composed of several arcs, and within each arc, the gantry continuously rotates with the MLC moving to shape the beam opening to match with the tumor at various gantry angles during the delivery. Note that the beam fluence intensity at each angle is uniform in this delivery.

Before the radiation treatment, patient is immobilized by different immobilization devices, including stereotactic frame, mask, alpha cradle, and BlueBAG™ *BodyFIX*® vacuum [16, 17]. Several in-room imaging devices can be used to correct the patient positioning errors before the treatment, such as BrainLab ExacTrac and onboard cone-beam CT (CBCT).

Available Technologies

Gamma Knife

Since the first introduction in the 1950s, there have been modifications in the design of the system [18]. Although the physical appearances of the current models differ (models U, B, C, 4C, and Perfexion®), there is only minimal difference in the dose profiles. There is an array of 60Co sources (201 sources in the U, B, and C models, 192 in the Perfexion) aligned with a tungsten collimation (plug) system within the external collimator helmets of 4, 8, 14, and 18-mm nominal aperture size. Modification of the isodose distribution is achieved by using combinations of isocenters using different collimators, different stereotactic locations, and different dwell times. In the new Perfexion, the external helmet collimators have been replaced by a single internal collimation system. Rather than being fixed, the cobalt sources are grouped into eight sectors. Each sector can move in a linear direction back and forth over the internal collimation system, with several stopping positions. This eliminated manual change of collimators. Perfexion is also able to create composite shots with different collimator sizes to improve the conformality of the dose distribution [19].

For positioning and immobilization, a stereotactic head frame is affixed to the patient's head. This frame defines a reference coordinate system [20]. During imaging procedure, fiducial markers are used with the frame to locate the areas of interest within the attainable images to the stereotactic space. A computerized planning system is used to calculate precise dose distributions to the target of interest. During the treatment, patient lies on a couch with the head frame attached to the couch. Movement of the patient couch in and out of the radiation unit, and opening of the shielding door, is performed with high precision. The unit directs gamma radiation to the target point based on the treatment plan. The accuracy of dose delivery using the gamma knife has been reported approximately 0.25 mm. Mechanical accuracy as dictated by the manufacturer is less than 0.3 mm.

Advantage of the gamma knife is the ability to create conformal and irregular dose plans using multiple target points. The unit aims sharply focused sources of cobalt-60 photon radiation at tumors of variable shapes and sizes ranging from several millimeters to more than 3 cm in diameter. The dose each patient receives is custom designed and can vary by the technique of plugging and dosimetric planning – usually performed by neurosurgeon, medical physicist, and radiation oncologist. Disadvantage of gamma knife is that the treatment time becomes protracted with the radioactive decay of the cobalt-60 radioisotopes which has half-life of 5.27 years.

Robotic Arm Mounted Linear Accelerator System

The lightweight miniature 6MV linac (Schonberg Radiation Inc., Santa Clara, CA) operates in the X-band (9,300 MHz), and it is much smaller and lighter than a conventional S-band (2,856 MHz) medical linear accelerators [21, 22]. The prototype is CyberKnife unit (Accuray Inc., Sunnyvale, California) which has the uses of the 6-MV linear accelerator mounted on a robotic arm. The parameters of the radiation beam for the CyberKnife and conventional linacs are comparable except that the CyberKnife system has a lower beam output. The industrial robotic arm manufactured by GMF (GMFanuc Robotics Corporation, Auburn Hills, MI) is capable of movement with 6° of freedom, allowing a radiation beam to approach up to 100 locations in the patient from up to 12 trajectories for each location without the need of a mechanical isocenter [23, 24].

For image-guided localization, CyberKnife uses two orthogonal kilovoltage X-ray tubes installed in the ceiling and flat panel detectors. Orthogonal X-ray projections can be acquired before and during the treatment to monitor and track the treatment target. Fiducial markers are sometimes implanted in the patient to facilitate the tracking. The patient positioning errors are determined and can be corrected in real time.

Positioning and immobilization techniques are not different from other radiosurgery methods. Noninvasive devices are used for patient immobilization. The manufacturer reported an overall spatial treatment accuracy of 0.95 mm. The CyberKnife treatment has been reported to be lengthy.

Gantry-Based Linear Accelerator (Linac) Radiosurgery Systems

Gantry-based linear accelerator (LINAC) treatments are prevalent throughout the world [25]. It can be designed to be a general purpose radiation delivery machine or a dedicated machine for radiosurgery [26]. The gantry where the megavoltage radiation is produced rotates around the patient, delivering radiation beams from different angles. Initially, a radiosurgery cone was attached to the gantry in order to make the sharper radiation beam. More recently, MLC technology was made easier to manipulate the radiation beam shaping. Micro-MLC (mMLC) is usually used for radiosurgery which has a width of 2–3 mm. mMLC enables three-dimensional target shaping function and radiation beam intensity modulation within the already small beam opening. This system is able to use a larger field sizes and thus makes it easier to treat larger tumors more uniformly with rapid dose falloff outside of the target.

The image-guided positioning system can be an integration of different imaging modalities including infrared optical tracking devices, 2D X-ray imaging, and 3D cone-beam CT imaging system [27–32]. The integrated image-guided and positioning system achieves the targeting accuracy within submillimeter level. For patient immobilization, either frame-based or frameless methods can be used [33]. For frame-based immobilization, rigid stereotactic head frame is affixed to the patient's head for both immobilization and target localization. For frameless targeting, individually custom-made mask and head-and-neck localizer box can be used for brain radiosurgery, and body positioning method can be used for extracranial radiosurgery. A dedicated radiation planning systems usually accompany the radiosurgery equipment. Most planning systems use technology

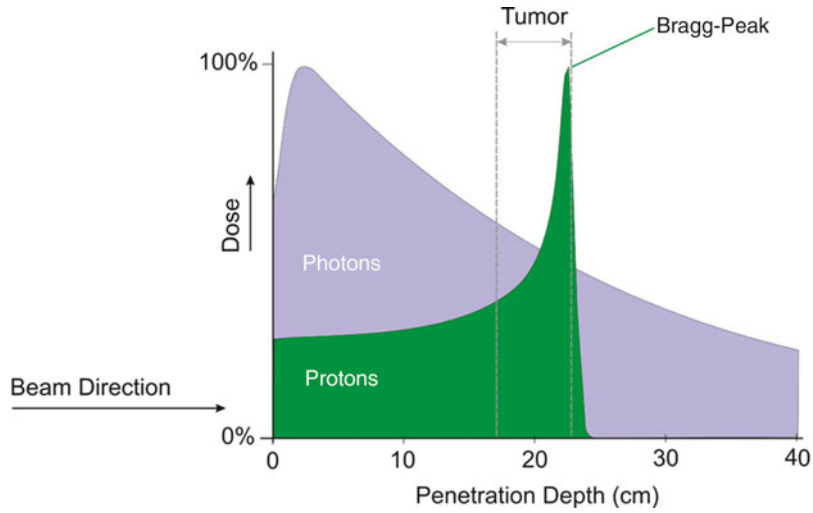

Fig. 8.2 Dose deposition at different depths for proton and photon beams (From Varian Medical System)

of image fusion with the diagnostic image and digitally reconstructed simulation image taken with stereotactic positioning device.

Tomotherapy

The concept of computed tomography (CT) imaging which used low energy photon was extended to mount the high energy photons in a binary opening of pencil beams. Tomotherapy uses a 6-MV fan beam delivery pattern by mounting a linear accelerator on CT style ring gantry that rotates around patients as they advance slowly through the ring [34, 35]. Photon radiation is produced by the linear accelerator, which travels in multiple circles all the way around the gantry ring. The beam intensity is modulated with a 64-leaf binary MLC. This collimator system has two sets of interlaced leaves that move in and out to constantly modulate the radiation beam. Thus, tomotherapy combines IMRT with a helical (or spiral) delivery pattern to deliver the radiation treatment. The helical delivery of the intensity-modulated fan beam allows the treatment of extended volumes in the cephalo–caudad direction without the need for junctioning between the radiation fields. The couch translates at a constant speed (usually much less than 1 mm/s) in the longitudinal direction, guiding the patient slowly through the center of the ring. The gantry also rotates at a constant speed during the treatment delivery with a period ranging 15–60 s. So each time the linac comes around, the beam is on at a slightly different axial plane.

Patient positioning is similar to other radiosurgery technologies. It starts with mechanical/optical system involving fitting the rigid mask on the patient and using the laser system for alignment. Then, helical megavoltage CT is performed to verify the position of the target.

Proton Beam Radiosurgery

The main physical characteristic of proton therapy is Bragg peak which can be located geometrically within the target. The pattern of energy distribution of a proton beam consists of an entrance region of a slowly rising dose, a rapid rise to a maximum (known as the Bragg peak), and a fall to near zero, whereas patterns of energy deposition by photons follow the law of exponential decay, as shown in Fig. 8.2; Bragg peak is also produced by heavy-charged particles, and some of them are also in medical use such as alpha particle and carbon ions. Bragg and Kleeman originally reported the correlation between the particle path length and its initial energy and the sharp increase of energy

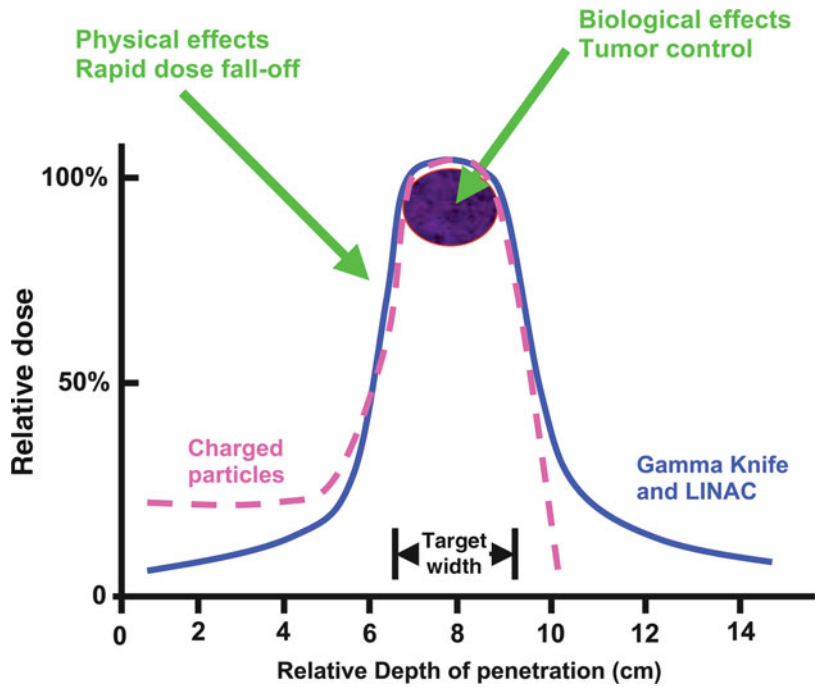

Fig. 8.3 Diagram of radiation profile by various radiation modalities, relating to the target volume

deposition near the end of the particle track. The sharpness of the Bragg peak from monoenergetic proton beam can irradiate a very small area around the tumor. However, in order to treat a larger tumor, the size of Bragg peak should be increased by the use of higher energy proton, which increases the entrance dose. To reduce the high entrance dose and spread out the Bragg peak, multiple proton beams of different energies are used. To make irradiation of the proton beam from all angles available, a mobile beam source mounted on a gantry was developed for proton therapy treatment. While the major advantage of proton therapy comes from the physical characteristics of radiation dose accumulation, the gain of biological effectiveness is not clearly defined over the photon treatment.

In general, the steps involved in proton-based SRS are similar to those of photon-based SRS. Due to the time required for customization of proton beams, imaging and treatment are usually done on separate days for proton treatments. Main disadvantage of this technique is the cost of the equipment. Proton therapy has been primarily used for pediatric tumors in an attempt to protect the normal tissues [36, 37]. More recently, there is a trend of using proton beams for adult tumors. Although there is physical advantage of Bragg peak effect, proton has never been tested with the modern intensity-modulated radiation therapy. Therefore, it is not possible to conclude if the benefit of proton therapy is from the physical characteristics or the biological effectiveness.

Clinical Application

When radiosurgery is considered, one tends to think only the physical characteristics, i.e., rapid dose falloff and accuracy. The result of this technology is indeed an accumulation of high radiation dose to the defined target volume. Therefore, the physical property of radiosurgery is closely connected with the biological aspects – the radiation dose and the target volume. The diagram shown in Fig. 8.3 shows the relationship of the physical and biological effects of radiosurgery. Stereotactic radiosurgery has two fundamental concepts; one is the technology of stereotactic

targeting of focused radiation to a defined volume with accuracy, and the other is the biological consequences resulting from high radiation doses. Therefore, biology of radiosurgery cannot be separated from the inherent physical advantage of reduced target volume of radiosurgery. Main clinical advantage of radiosurgery is from the fact that normal tissues are virtually not included in the target volume. The understanding of cell-killing mechanism of radiosurgery by high radiation dose has been changing recently with modern biological experimentations. This is beyond the scope of this entry. Briefly, the main radiation-induced cell-killing mechanism is double-strand DNA break, which is basically from the fractionated radiation therapy. This results in reproductive cell death or sometimes called mitotic cell death and becomes the predominant mode of cellular loss in the majority of human tumors (other than lymphoid and germinal tumors) following X irradiation. Apoptosis is another important mode of cell death in normal tissues and some tumors, particularly during the acute phase of radiation response. Stem cells of self-renewal normal tissues such as hematopoietic and intestinal crypt cells undergo apoptosis following a moderate dose of radiation exposure. Studies of in vivo murine or human tumors and clinical experience have shown an increased tumor control rates following single-fraction dose of radiation. Recent evidences have shown that there can be additional cell-killing mechanism from the high radiosurgical doses. A radiation-induced endothelial apoptosis in the irradiated microvasculature is considered to be an obligatory process in achieving tumor cure in some tumors through sphingomyelinase ceramide pathway [38]. Ionizing radiation can cause DNA strand breakage or distortion of the DNA nucleoprotein conformation, events which would trigger the expression of cellular stress response signals. Further studies have also shown that radiation can cause molecular damage to any molecule in a cell. The initial molecular events include rapid upregulation of gene transcription for inflammatory cytokines, angiogenic factors, secondary transcriptional activators, and gene products involved in the repair of damaged DNA [39–41]. Thus, understanding of radiobiology by radiosurgical high dose radiation will help design the radiosurgery with multimodality approach of modern cancer treatment.

In making the decision of radiosurgery, one has to consider if the tumor or target lesion is a clinically and biologically suitable target or not. Radiosurgery may not be suitable for tumors with high tendency of infiltrating to the surrounding tissue. The other important factor is the goal of radiosurgery – tumor control (tumor disappearance versus stabilization), pain control, or functional improvement or preservation, etc. The use of technology and biological consideration can also vary depending on what needs to be achieved by radiosurgery. Technically, the most fundamental requirements are immobilization and positioning of the patients in relation to the defined center of the equipment as well as careful radiosurgical treatment planning. With the progress of positioning and image-guided localization method coupled with the control of internal organ motion, the radiosurgery has been applied to the various body sites such as lung, liver, spine, and other organs. There is room for further improvement with research and progress for a better understanding of biological effects of high radiation doses, better image guidance, and technical developments.

Cross-References

- ▶ Image-Guided Radiation Therapy for Lung Cancer
- ▶ Image-Guided Radiation Therapy for Renal Cell Carcinoma
- ▶ Image-Guided Radiation Therapy in Gynecology Applications
- ▶ Image-Guided Radiotherapy and Prostate Cancer
- ▶ Radiation Oncology in Breast Cancer
- ▶ Radiation Therapy in the Treatment of Primary Liver Cancers
- ▶ Role of Combination Therapies in the Treatment of Non-small Cell Lung Cancer and Thoracic Metastasis
- ▶ Stereotactic Body Radiation Therapy for Liver Metastases

References

1. Hof H, et al. Stereotactic single-dose radiotherapy of stage I non-small-cell lung cancer (NSCLC). Int J Radiat Oncol Biol Phys. 2003;56:335–41.
2. Lee SW, et al. Stereotactic body frame based fractionated radiosurgery on consecutive days for primary or metastatic tumors in the lung. Lung Cancer. 2003;40:309–15.
3. Schweikard A, et al. Robotic motion compensation for respiratory movement during radiosurgery. Comput Aided Surg. 2000;5:263–77.
4. Shell M, et al. AAPM Report No. 54, Stereotactic Radiosurgery: Report of AAPM Task Group 42. 1995.
5. Jordan TJ, Williams PC. The design and performance characteristics of a multileaf collimator. Phys Med Biol. 1994;39:231–51.
6. Boyer AL, et al. Clinical dosimetry for implementation of a multileaf collimator. Med Phys. 1992;19:1255–61.
7. Bel A, et al. Target margins for random geometrical treatment uncertainties in conformal radiotherapy. Med Phys. 1996;23:1537–45.
8. Ling CC, et al. Conformal radiation treatment of prostate cancer using inversely-planned intensity-modulated photon beams produced with dynamic multileaf collimation. Int J Radiat Oncol Biol Phys. 1996;35:721–30.
9. Purdy JA. 3D treatment planning and intensity-modulated radiation therapy. Oncology (Williston Park). 1999;13:155–68.
10. Bortfeld T. Optimizing planning using physical objectives and constraints. Sem Radiat Oncol. 1999;9:15.
11. Llacer J. Inverse radiation treatment planning using the dynamically penalized likelihood method. Med Phys. 1997;24:1751–64.
12. Hilbig M, et al. IMRT-Inverse planning based on linear programming. Z Medizinische Physik. 2002;12:8.
13. The BS, et al. Intensity modulated radiation therapy (IMRT): a new promising technology in radiation oncology. Oncologist. 1999;4:433–42.
14. Grant W. Commissioning and quality assurance of an IMRT system. Madison: Advanced Medical Publishing; 1997.
15. Low DA, et al. Phantoms for IMRT dose distribution measurement and treatment verification. Int J Radiat Oncol Biol Phys. 1998;40:1231–5.
16. Nevinny-Stickel M, et al. Reproducibility of patient positioning for fractionated extracranial stereotactic radiotherapy using a double-vacuum technique. Strahlenther Onkol. 2004;180:117–22.
17. Fuss M, et al. Repositioning accuracy of a commercially available double-vacuum whole body immobilization system for stereotactic body radiation therapy. Technol Cancer Res Treat. 2004;3:59–67.
18. Lindquist C. Gamma knife radiosurgery. Semin Radiat Oncol. 1995;5:197–202.
19. Van Dyk J. The modern technology of radiation oncology: a compendium for medical physicists and radiation oncologists. Medical Physics Publishing; 2005.
20. Leksell L, et al. A new fixation device for the Leksell stereotaxic system. Technical note. J Neurosurg. 1987;66:626–9.
21. Adler Jr JR, et al. The Cyberknife: a frameless robotic system for radiosurgery. Stereotact Funct Neurosurg. 1997;69:124–8.
22. Webb S. Conformal intensity-modulated radiotherapy (IMRT) delivered by robotic linac–conformality versus efficiency of dose delivery. Phys Med Biol. 2000;45:1715–30.
23. Degen JW, et al. CyberKnife stereotactic radiosurgical treatment of spinal tumors for pain control and quality of life. J Neurosurg Spine. 2005;2:540–9.
24. Gerszten PC, et al. CyberKnife frameless single-fraction stereotactic radiosurgery for benign tumors of the spine. Neurosurg Focus. 2003;14:e16.
25. Winston KR, Lutz W. Linear accelerator as a neurosurgical tool for stereotactic radiosurgery. Neurosurgery. 1988;22:454–64.
26. Yin FF, et al. A technique of intensity-modulated radiosurgery (IMRS) for spinal tumors. Med Phys. 2002;29:2815–22.
27. Schweikard A, et al. Planning for camera-guided robotic radiosurgery. IEEE Trans Robot Autom. 1998;14:12.
28. Wang LT, et al. Infrared patient positioning for stereotactic radiosurgery of extracranial tumors. Comput Biol Med. 2001;31:101–11.
29. Ryu S, et al. Image-guided and intensity-modulated radiosurgery for patients with spinal metastasis. Cancer. 2003;97:2013–8.
30. Jaffray DA, et al. Flat-panel cone-beam computed tomography for image-guided radiation therapy. Int J Radiat Oncol Biol Phys. 2002;53:1337–49.
31. Penny GP, et al. A comparison of similarity measures for use in 2D-3D medical image registration. IEEE Trans Med Img. 1998;17:10.
32. Lam KL, et al. Automated determination of patient setup errors in radiation therapy using spherical radio-opaque markers. Med Phys. 1993;20:1145–52.
33. Takeuchi H, et al. Frameless stereotactic radiosurgery with mobile CT, mask immobilization and micro-multileaf collimators. Minim Invasive Neurosurg. 2003;46:82–5.
34. Mackie TR, et al. Tomotherapy. Semin Radiat Oncol. 1999;9:108–17.
35. Salter BJ, et al. An oblique arc capable patient positioning system for sequential tomotherapy. Med Phys. 2001;28:2475–88.
36. Harsh G, et al. Stereotactic proton radiosurgery. Neurosurg Clin N Am. 1999;10:243–56.

37. Chen CC, et al. Proton radiosurgery in neurosurgery. Neurosurg Focus. 2007;23:E5.
38. Garcia-Barros M, Kolesnick R, Fuks Z, et al. Tumor response to radiotherapy regulated by endothelial cell apoptosis. Science. 2003;300:1155–9.
39. Hallahan DE, Haimovitz A, Kufe DW, et al. The role of cytokines in radiation oncology. Important Adv Oncol. 1993:71–81.
40. Gorski DH, Beckett NT, Jaskowiak DP, et al. Blockade of vascular endothelial growth factor stress response increases the antitumor effects of ionizing radiation. Cancer Res. 1999; 59:3374–8.
41. Dalton TP, Shertzer HG, Puge A. Regulation of gene expression by reactive oxygen. Annu Rev Pharmacol Toxicol. 1999;39:67–101.

Anesthesia Challenges in Interventional Oncology

9

Mary Fischer and Alan Kotin

Abstract

Better technology and imaging has allowed image-guided cancer therapy once only performed in the traditional operating room to be performed as minimally invasive procedures in other locales. The complexity of the procedures, the level of sedation required, and the comorbidities of the patients have created a need for the anesthesia care provider's presence. This chapter discusses the role and challenges of the anesthesiologist in interventional oncology for procedures outside the traditional operating room.

Technological advancement and movement toward closed body, minimally invasive surgery has moved interventional oncology procedures, once only performed in the operating room (OR), to nontraditional locales. Historically, patient sedation in the interventional operating room has been performed under the supervision of the interventional physician. Complex procedures and the Joint Commission on Accreditation of Healthcare Organization (JCAHO) regulations led to the anesthesiology and interventional physicians working more closely together [1]. Despite the apparent simplicity of this new relationship, working outside the main operating room can be very complex. In order for the anesthesiologist to guarantee the same level of safety for the patient, the anesthesiologist must be familiar with the procedure, the location, and the potential complications. The interventionalist must be familiar with the practice guidelines and standard of anesthesia care. This chapter provides the extensive list of issues that must be addressed before the anesthesia image-guided oncology team begins patient care as well as the unique anesthetic considerations of patients undergoing image-guided cancer therapy.

M. Fischer (✉) • A. Kotin
Department of Anesthesia and Critical Care, Memorial Sloan-Kettering Cancer Center, New York, NY, USA
e-mail: fischerm@mskcc.org; kotina@mskcc.org

D.E. Dupuy et al. (eds.), *Image-Guided Cancer Therapy*, DOI 10.1007/978-1-4419-0751-6_11,

Practice Guidelines

The American Society of Anesthesiology (ASA) has long been an advocate for patient safety. Although anesthesiologists may not be directly involved in the care of all patients receiving sedation/analgesia for a procedure, there is a high likelihood that they are involved in creating, revising, and organizing sedation services in all hospitals. JCAHO, the American Pediatric Guidelines, and the American College of Radiology (ACR) contain recommendations made by the ASA for the safe administration and monitoring of sedation/analgesia outside the operating room [2]. The key components of these guidelines and regulations are defining the continuum for sedation/anesthesia and the qualifications for those administering sedation/analgesia. Because sedation is a continuum, it is not always possible to predict how an individual patient will respond; therefore, the practitioner administering sedation must be qualified to "rescue" the patient from the next level of sedation. The JCAHO guidelines state: "Practitioners intending to induce moderate sedation are competent to manage a compromised airway and inadequate oxygenation and ventilation." This requirement states that qualified individuals must have competency-based education, training, and experience in evaluation of patients, in performing sedation, and to rescue the patient from the next level of sedation. "Practitioners intending to induce deep sedation are competent to rescue a patient from general anesthesia, being able to manage an unstable cardiovascular system as well as a compromised airway and inadequate oxygenation and ventilation".

Screening

The updated JCAHO regulations require similar assessment and care of patient standards for moderate and deep sedation as are used for patients having general anesthesia [1]. Specifically, new regulations for moderate and deep sedation include pre-sedation assessment, candidate appropriate for sedation, immediate reevaluation, recovery area admission and discharge assessment, sedation planned and communicated among providers, patient understands options and risks(education), patient's physiologic status is monitored, post-procedure and post-discharge status assessed, and outcomes collected to improve patient care [2].

At the present time, there are several commonly used approaches to screening patients scheduled for surgery. These include facility visit prior to the day of surgery [3], office visit prior to the day of the procedure [4], telephone interviews, no visit [5], review of health survey/no visit [6], preoperative screening and visit on the morning of surgery [7], and computer-assisted information gathering [8]. Each option has its own advantages and disadvantages. In order to satisfy JCAHO requirements, interventionalists will select one of these approaches. Just like surgeons, some interventionalists may choose to have a clinic for consultation prior to the actual day of the procedure. The preprocedural assessment reviews medical history, medications, allergies, and NPO guidelines and determines the need for an anesthesiologist. In the traditional OR, the anesthesia care provider is always present and will select the type of anesthesia considering patient and surgeon requests. Interventional oncology procedures differ in that the interventionalist or the patient must recognize the need for an anesthesia care provider in order to request this service. For a procedure that mandates deep sedation or a general anesthetic, the consultation is clear; however, what patient factors should determine the need for the anesthesia care provider for minimal or moderate sedation is not well defined. JCAHO guidelines state: "If risk factors for an adverse event are present, supervision by an anesthesiologist should be considered" [1].

The ASA Task Force on Sedation and Analgesia by Non-Anesthesiologists has developed guidelines to assist the interventionalist to identify higher-risk patients: major comorbidity, abnormal airway, and tolerance to pain medications that may require the presence of an anesthesia care provider [1]. Other factors that may contribute to the need for anesthesia services are

patients with special needs, pediatric patients, morbid obesity/sleep apnea, the prone position, claustrophobia, family history of difficulty with anesthesia, or those who have had prior difficulties with nurse administered sedation. These guidelines should be transformed into an algorithm that is followed during the pre-procedural assessment in order to schedule the need for an anesthesiologist during the procedure.

Scheduling procedures between anesthesia and interventional departments can be challenging. Anesthesia departments typically have clinical coordinators who are responsible for scheduling and staffing needs. In anesthesia departments, this position is a daily assignment of one individual or a small group who share this responsibility. The same is true for Interventional Radiology Department and is often referred to as the "traffic coordinator." Anesthesia clinical coordinators responsible for staffing and scheduling prefer a full day of cases for efficient use of personnel. It is also ideal that interventional radiology procedures requiring anesthesia services be performed as "first cases." The interventional radiology schedule typically prefers to schedule outpatient procedures prior to inpatient procedures and must take into consideration the availability of certain modalities and the individual expertise of the interventionalist. While the number of interventional cases requiring anesthesia services is increasing, there may not be a day's worth of procedures to require a dedicated anesthesia team. Anesthesia departments handle these scheduling challenges differently with some dedicating a "utility" anesthesiologist that will service all remote sites. Creating a schedule requires daily communication between the IR "traffic" coordinator and the anesthesia coordinator and utility anesthesiologist. The IR traffic coordinator and the anesthesia coordinator share the responsibility to keep both services on schedule. In our institution, each interventionalist will have a suite assigned to them. The need for anesthesia personnel in a suite is determined by whether at least one of the procedures requires anesthesia services. The anesthesia team will then care for all the patients scheduled for that particular suite. This allows for efficient usage of anesthesia staff. It also allows for the Interventional Radiology Department to staff the other rooms requiring minimal or moderate sedation effectively.

Anesthesia Provider Evaluation

Although sometimes difficult to arrange, the pre-procedural interview and evaluation by an anesthesiologist can be extraordinarily beneficial. In addition to lessening anxiety about the treatment and anesthesia, the anesthesiologist will be able to identify potential medical problems in advance, determine their etiology, and if indicated initiate appropriate corrective measures, thereby minimizing the numbers of delays, cancellations, as well as complications on the day of the procedure. For nontraditional locales, it is often the anesthesiologist who is most involved in the direct medical care of the patient, the physician who must ensure that the patient is appropriately screened, evaluated, and informed prior to the procedure. Indeed, the anesthesiologist/patient relationship often takes on a primary care quality.

An important component of the preanesthesia evaluation is assigning the ASA physical status (Table 9.1). The anesthetic risk attributed to a procedure depends on the preoperative status of the patient. The presence of comorbidities that may influence the incidence of postoperative morbidity and mortality needs to be recognized at the preoperative visit and then clinically optimized before the procedure. Although it is not possible to alter all, there are modifiable risk factors. Detailed evaluation of these major organ systems with a focus on corrective measures is combined with selected pharmacologic agents, anesthetic technique, and monitoring to provide optimal care. As anesthesiologists have become more experienced with anesthetic management of the problem patient, the list of unacceptable patients has dwindled and it is difficult to identify the unacceptable patient for interventional oncology. Extrapolating from the traditional and ambulatory surgery literature, even geriatric and higher-risk (physical status 3 and 4) patients may be considered acceptable candidates for

Table 9.1 (ASA) Physical status classification system

I	Normal healthy patient
II	Patient with mild systemic disease
III	Patient with severe systemic disease
	Examples: History of angina pectoris, myocardial infarction or cerebrovascular accident, congestive heart failure over 6 months ago, slight chronic obstructive pulmonary disease, and controlled insulin-dependent diabetes or hypertension will need medical consultation
IV	Patient with severe systemic disease that is a constant threat to life
	This classification represents a "*red flag*" – a warning flag indicating that the risk involved in treating the patient is too great to allow elective care to proceed. *Examples*: History of unstable angina pectoris, myocardial infarction or cerebrovascular accident within the last 6 months, severe congestive heart failure, moderate to severe chronic obstructive pulmonary disease, and uncontrolled diabetes, hypertension, epilepsy, or thyroid condition. If emergency treatment is needed, medical consultation is indicated
V	Moribund patient who is not expected to survive without surgery
VI	Patient declared brain-dead whose organs are removed for donor purposes

Source: American Society of Anesthesiologists. New classification of physical status. Anesthesiology. 1963; 24:111, material is in the public domain

interventional oncology if their systemic diseases are well controlled and the patient's medical condition is optimized preoperatively [4, 5]. Often, it is the presence of comorbidities that makes the risk/benefit of a closed, image-guided cancer therapy more acceptable than traditional surgery. The anesthesiologist is in a position to have an informed discussion with the patient about the increased risk of morbidity and mortality and work with other members of the patient's care team to determine whether any consultations or pre-procedural therapies should be initiated before the day of the scheduled procedure in an effort to minimize the risk of anesthesia. The anesthesiologist may be asked to care for a patient whose illness is overwhelming and the intervention's intention may be palliative. For those procedures aimed at getting rid of pain or loss of function caused by a tumor and therefore improving the patient's quality of life, the anesthesia care provider needs common sense, flexibility, and complex case management skills. At our institution, we individualize our decision with regard to each patient; with few exceptions, the appropriateness of a case for interventional oncology is determined by a combination of factors including patient considerations, interventional procedure, anesthetic technique, anesthetic risk, and the anesthesiologist's comfort level.

Cardiac Evaluation

The risk of periprocedural cardiac complications is the summation of an individual patient's risk and cardiac stress related to the procedure. The basic clinical evaluation obtained by history, physical examination, and review of the electrocardiogram usually provides enough data to estimate cardiac risk. There are active cardiac conditions that may cancel surgery unless the surgery is emergent, but most stable patient's cardiac risk can be derived from the Revised Cardiac Risk Index [9]. This simple index identifies six independent risk factors: history of ischemic heart disease, history of congestive heart failure, history of cerebrovascular disease, diabetes mellitus, renal insufficiency, and high-risk surgery. Each factor receives one point. If the score is 3 or greater, the patient has an 11 % risk of a major cardiac event. For those patients with clinical risk factors, the 2007 ACC/AHA guidelines on perioperative cardiovascular evaluation and care for noncardiac surgery are an excellent framework for evaluating cardiac risk in the preoperative period [10].

Over the years, perioperative management has shifted from assessing and treating coronary obstruction toward medical therapy aiming at prevention of myocardial oxygen supply and demand mismatch and coronary plaque stabilization. Today, preoperative cardiac testing, cardiac stenting, and coronary revascularization are performed for the same indications as the nonoperative setting [11]. Instead, beta-blockers, statins, and aspirin are widely used in the perioperative setting. Beta-blocker therapy has been

shown to reduce the incidence of perioperative ischemic events and myocardial infarction [12]. Recently, the risk benefit of this therapy in patients without coronary artery disease has been challenged. The perioperative ischemic evaluation (POISE) study showed an increased incidence of ischemic stroke in combination with intraoperative bradycardia and hypotension [13]. In a retrospective review of patients who underwent noncardiac surgery, perioperative beta-blockers showed no benefit and possible harm in low-risk patients but a benefit in high-risk patients [14]. Management of the patient with coronary artery stents is a balancing act of the risk/benefit ratio of dual antiplatelet therapy interruption versus continuation. Aspirin should never be interrupted unless the risk of bleeding far outweighs the risk of stent thrombosis [15]. The presence of a cardiac pacemaker and internal defibrillator excludes patients from MRI-guided intervention. These patients require magnet conversion during ablations with other imaging.

Pulmonary Evaluation

Patients with respiratory disease are at an increased risk for postoperative pulmonary complications (PPCs). Indeed, postoperative pulmonary complications may rival cardiovascular complications in frequency and severity. There are many limitations of studies that examine risk factors for PPCs. However, there are some consistent patterns. The three most important risk factors for PPCs are the presence of pulmonary disease, cigarette smoking, and the site of surgery, with abdominal surgery being one of the highest [16]. Avoiding open surgery by doing a less invasive procedure, one would expect to reduce, but not eliminate risk. Pulmonary function testing per se is not useful in predicting risk [17]. Thus, routine pulmonary function testing is not justified unless it is part of an effort to optimize preoperative status. The definition of optimization depends on the type of respiratory disease and the individual patient. Consultation with the interventionalist and pulmonologist will help guide whether a course of systemic corticosteroids or antibiotics is warranted perioperatively. Despite an increased risk of pulmonary complications in patients with respiratory disease, there is no level of pulmonary function for which the risk of the procedure is prohibitive [18]. A prospective study did not find an elevated $PaCO_2$ to be a risk factor among surgical candidates; hence, clinicians should not use arterial blood gas analyses to identify patients for whom the risk of a less invasive procedure is contraindicated [19]. Obese patients are at risk of suffering from a number of respiratory derangements, including obstructive sleep apnea (OSA) and obesity-hypoventilation syndrome. Many patients with OSA are undiagnosed, but there is a strong relationship between obesity and OSA [20]. Given the association of obesity and OSA with multiple medical conditions, increased risk of venous stasis, pulmonary embolism, hypertension, cerebral vascular accidents, cardiomyopathy, arrhythmias, and ischemic heart disease [20–22], the ASA has practice guidelines for including assessment of patients for possible OSA before anesthesia and careful postoperative monitoring for those suspected at risk [23]. Polysomnography is the gold standard for diagnosis of OSA, but it is expensive and a limited resource. The most reasonable approach would be to check room-air pulse oximetry. If the patient has an oxygen saturation level less than 96 %, further evaluation may be warranted. A 2-week period of CPAP therapy has been shown to be effective in correcting abnormal ventilatory drive and improving cardiac function [24, 25]. Deep venous thrombosis prophylaxis should be considered.

Hepatic Evaluation

Percutaneous ablation therapy is often indicated for nonsurgical patients who have primary or metastatic liver cancer. Risk factors and symptoms of liver disease are not as well defined as in other organ systems. Liver function tests can measure different aspects of hepatic function, but these biochemical markers cannot quantify the hepatic disease. A high degree of suspicion of preexisting liver disease in patients with

hepatocellular carcinoma (HCC) is warranted given the propensity of HCC to develop in the cirrhotic liver [26]. Coagulation abnormalities must be identified and corrected whenever possible. The liver synthesizes vitamin K-dependent factors II, VII, IX, and X; protein S; and protein C. Improvements in coagulation may be achieved with vitamin K (10 mg/day). If this fails to correct a prolonged international normalized ratio after 2–3 days, vitamin K administration should be stopped, and additional causes should be sought. In addition to the vitamin K-dependent factors, the liver also synthesizes antithrombin III and factor I (fibrinogen). In this setting, fresh frozen plasma may be administered at a dose 12–20 mL/kg (2–6U) with the goal of decreasing the prothrombin time to within 3 seconds of control. If coagulopathy persists, dysfibrinogenemia should be entertained and vasopressin peri-procedure may be needed. In contrast, anesthesiologists are often confronted with abnormal hepatic function tests in asymptomatic patients. In general, for asymptomatic patients with mildly elevated alanine and aspartate aminotransferase levels and a normal bilirubin concentration, further work-up or cancellation of the intervention is rarely indicated.

Renal Evaluation

Most interventional procedures cannot be performed without an intravascular contrast agent. Except for MRI procedures, these agents are iodinated and considered potentially nephrotoxic. The contrast dye has an osmotic effect precipitating dehydration. Patients already dehydrated or with an elevated bun and creatinine are at an increased risk, and contrast should be avoided if possible. Patients with moderate to end-stage kidney diseases who receive a gadolinium-based contrast agent during a magnetic resonance imaging scan (MRI) or magnetic resonance angiography (MRA) are at risk for developing a serious systemic fibrosing disease called nephrogenic systemic fibrosis/nephrogenic fibrosing dermopathy (NSF/NFD). The need for gadolinium will be determined on an individual basis by the interventionalist.

Image-Guided Operating Room

The anesthesiologist must adopt a new mind-set in order to work in the interventional oncology operating room. The traditional OR is scheduled with elective surgeries, and patient's preoperative preparation is optimized in advance of the scheduled date. Emergent and urgent add-on cases do exist, but these typically represent a small proportion of the OR schedule. The interventional radiology schedule performs elective procedures but also typically has an "add-on" schedule of urgent and emergent procedures that may represent at least half of the schedule. These in patients are often quite ill with multiple medical issues resulting from previous surgery or medical management. The interventional procedures often offer a cure to many of these acutely debilitated patients so that optimizing their medical issues pre-procedure is unlikely. The anesthesiologist offering care for this patient population often must be flexible in interpreting clinical practice guidelines. In addition to the comorbidities of the patients, the challenges include working with a new team, the actual location and design of the interventional suites, and providing the standards for basic anesthetic monitoring.

The Team

The interventionalist and anesthesiologist are unfamiliar with one another in both practice and personality. The IR suite is staffed by technicians, registered nurses (RN), and interventional radiologists. Patients will receive moderate sedation with medications ordered by interventional radiologists but administered by RN's according to the institutional sedation policy. The interventional radiology nurse is responsible for monitoring and patient safety during the procedure. The technician assists with the positioning and technical aspects to optimize success of the treatment. The standard IR table is fixed, and the equipment used such as fluoroscopy and CT scanners may make positioning technically difficult.

Patients may be positioned prone, supine, and lateral with their arms or legs placed in unusual positions. The use of moderate sedation allows the patients to vocalize any discomfort from positioning or pain from the procedure.

The presence of anesthesia care providers alters this paradigm. An anesthesiologist may work alone or supervise a nurse anesthetist or resident. Anesthesia care providers are often fearful outside the confines of their well-equipped traditional OR environment. In order for these procedures to be done safely, the role of the anesthesia technical support staff becomes increasingly important in the planning and day-to-day operations of these procedures since the anesthesia machine, equipment, supply carts, and pharmacy services are typically not part of the IR suite. The IR procedure will dictate patient position. The choice of anesthesia may be a monitored anesthesia care (MAC) or a general anesthetic. Depending on the required position, the location, (MRI), and the actual design of the interventional suite, the anesthetic may occur on a stretcher with all required monitors and equipment in place and then the anesthetized patient is positioned. The anesthesiologist and the technician must work together to provide the best position for the interventionist's success with the least patient harm from malposition. Depending on the procedure, the positioning may be done more than once, moving the patient from prone to lateral or from head to toe to toe to head.

Location

Traditional operating rooms are designed in a similar manner and based upon where the anesthesiologist will be situated. The anesthesia machine is positioned on the right side of the patient. Physiologic monitors are typically attached to the anesthesia machine so that all cables and wires begin on the patients' right side. The older IR suites have not typically been designed with the intent of having anesthesia services. The IR table is fixed and is unable to function like the typical OR bed. In newer interventional oncology ORs, the IR table is fixed, but provisions for the anesthesia machine to be located in any of the four quadrants surrounding the imaging have been made; therefore, knowing the laterality of the intervention allows for machine setup. Almost all interventional radiological procedures are carried out in special fluoroscopy suites with built-in oxygen, suction, and ventilator outlets. Wall oxygen and vacuum are typically present, but other gases, including air and nitrous oxide, are typically not part of the design. In order to provide a safe environment, communication of needs for each procedure between the IR, IR tech, anesthesiologist, and anesthesia support staff is vital. The goal is to situate the anesthesia equipment to emulate the traditional OR room design as much as possible. In addition to standard monitoring and equipment carts, it is imperative that there be emergency equipment and code carts easily accessible and available. Dedicated emergency airway equipment including fiber-optic bronchoscope with light source, intubating laryngeal mask airways, glide scopes, and other lifesaving airway equipment should be in close proximity and be maintained and checked on a regular basis.

The MRI suite is particularly challenging for the anesthesiologist. The excellent resolution of MR can be severely degraded by any patient movement. In addition, the required intense magnetic fields create unique problems with the use of physiologic monitors, standard anesthesia machines, and ventilators. Because of the strong magnetic field, no objects that can be attracted by a magnet can be brought into the MRI room. All anesthesia equipment must be MRI compatible. The anesthesiologist prepares the patient using either a ferromagnetic pump outside of the MRI room, and once stable and deeply sedated, the patient is transported to the MRI room or employs a MRI compatible infusion pump inside the MRI. Remote monitoring must meet basic anesthesia standards.

Communication needs for the anesthesiologist in remote environments is an increasingly important consideration. Emergency situations, equipment malfunctions, or other needs require a well-thought-out communication strategy. Anesthesia personnel must have a mechanism of

communicating with one another and with anesthesia technical support staff. Anesthesia staff should be familiar with the location of remote sites. Pagers, phones, or other communication devices should be dependable and tested on a regular basis.

Anesthesia care providers in the traditional operating room setting rely on an OR pharmacy or drug delivery systems such as Pyxis for dispensing necessary medications. In remote sites, the anesthesiologist and pharmacist must work together to assemble a portable medication kit that anticipates potential medications that may be needed.

Basic Anesthesia Monitoring

The ASA has issued standards for basic anesthetic monitoring intended for any and all types of anesthetic [27]:

Standard I: Qualified anesthesia personnel shall be present in the room throughout the conduct of all general anesthetics, regional anesthetics, and monitored anesthesia care.

Standard II: During all anesthetics, the patient's oxygenation, ventilation, circulation, and temperature shall be continually evaluated.

Effective July 1, 2011, the current standard for basic anesthetic monitoring reads as follows: during regional anesthesia (with no sedation) or local anesthesia (with no sedation), the adequacy of ventilation shall be evaluated by continual observation of qualitative clinical signs. During moderate or deep sedation, the adequacy of ventilation shall be evaluated by continual observation of qualitative clinical signs and monitoring for the presence of exhaled carbon dioxide unless precluded or invalidated by the nature of the patient, procedure or equipment.

Objective

Because of the rapid changes in patient status during anesthesia, qualified anesthesia personnel shall be continuously present to monitor the patient and provide anesthesia care. In the event there is a direct known hazard, e.g., radiation, to the anesthesia personnel which might require intermittent remote observation of the patient, some provision for monitoring the patient must be made. In the event that an emergency requires the temporary absence of the person primarily responsible for the anesthetic, the best judgment of the anesthesiologist will be exercised in comparing the emergency with the anesthetized patient's condition and in the selection of the person left responsible for the anesthetic during the temporary absence [27].

Certain monitors are required for all anesthetic techniques. Cases requiring general anesthesia (GA) with an anesthesia machine have certain additional requirements, and if an endotracheal tube (ET) or laryngeal mask airway (LMA) are used, there are further requirements. Patients receiving GA with or without an LMA or ET tube need to be continuously monitored for adequacy of ventilation. "End-tidal CO_2 monitoring should be used always unless the procedure, patient, or equipment prohibits its use." EKG should always be continuously monitored and displayed from the anesthesia start until the anesthesia end. Blood pressure and heart rate are to be assessed and documented at least every 5 min. Circulatory function must also be continuously assessed. Pulse oximetry with its pulse tracing and its distinctive tones is an invaluable monitor and satisfies this requirement. Temperature should also be monitored when significant temperature changes are anticipated.

The frequent use of imaging modalities such as CT scans and fluoroscopy and the risk of radiation exposure are unsettling for anesthesia personnel. Proper shielding and protection with lead aprons, thyroid shields, and protective eyewear are essential. Exiting the procedure room during imaging and keeping an adequate distance from the radiation source are advisable. Since there is so much movement in and out of the room, positioning monitors so they are easily viewable is recommended. In addition, setting high audible alarm volumes is also good practice. A physiological slave monitor placed in the control room of the procedure room allows for easy monitoring. These measures can provide a level of comfort for involved staff concerning radiation safety and also meet the standards for basic anesthetic monitoring.

Table 9.2 Definitions of levels of sedation adapted from guidelines for sedation and analgesia by non-anesthesiologists ASA and JCAHO continuum of sedation

	Minimal sedation ("anxiolysis")	Moderate sedation ("conscious sedation")	Deep sedation	General anesthesia
Responsiveness	Normal response to verbal stimulation	Purposeful response to verbal or tactile stimulation	Purposeful response following repeated or painful stimulation	Unarousable, even with painful stimulus
Airway patency	Unaffected	No intervention required	Intervention may be required	Intervention often required
Spontaneous ventilation	Unaffected	Adequate	May be inadequate	Frequently inadequate
Cardiovascular function	Unaffected	Usually maintained	Usually maintained	May be impaired

Source: Guidelines for sedation and analgesia for non-anesthesiologists; 2002 is reprinted with permission of the American Society of Anesthesiologists

Intraoperative Management: Choice of Anesthetic Method

The definitions of the four levels of sedation and anesthesia (Table 9.2) are:

Minimal sedation (anxiolysis): A drug-induced state during which patients respond normally to verbal commands. Although cognitive function and coordination may be impaired, ventilatory and cardiovascular functions are unaffected.

Moderate sedation/analgesia: A drug-induced depression of consciousness during which patients respond purposefully to verbal commands, either alone or accompanied by light tactile stimulation. No interventions are required to maintain a patent airway, spontaneous ventilation is adequate, and cardiovascular function is usually maintained. This level of sedation was referred to as conscious sedation in the past. The old terminology is confusing and inaccurate and is no longer used.

Deep sedation/analgesia: A drug-induced depression of consciousness during which patients cannot be easily aroused but respond purposefully following repeated or painful stimulations. Reflex withdrawal is not considered a purposeful response. The ability to independently maintain ventilatory function may be impaired. Patients may require assistance in maintaining a patent airway, and spontaneous ventilation may be inadequate. Cardiovascular function is usually maintained.

General anesthesia: A drug-induced loss of consciousness during which patients are not arousal, even by painful stimulation. The ability to independently maintain ventilatory function is often impaired. Patients often require assistance in maintaining a patent airway, and positive pressure ventilation may be required because of depressed spontaneous ventilation or drug-induced depression of neuromuscular function. Cardiovascular function may be impaired.

In order to understand the continuum of sedation, a distinction must be made between sedation and analgesia. Regional and local anesthesia or analgesics can be used for painful procedures with or without sedation. However, sedation alone or a failed regional technique for painful procedures may lead to a confused, restless, uncooperative patient. There are several choices among anesthetic methods for image-guided tumor treatment: local, general, or regional anesthesia. All three types are equally safe; therefore, the choice made by the team is to provide immobility, safety, and comfort for the patient while achieving the best image-guided treatment. In order to make this choice, the anesthesiologist needs to know from the interventionalist the position of the patient, the pain of the procedure, the length of the procedure, the need for a pneumothorax, the need for immobility of the patient, and if the patient will be discharged home or admitted to the hospital following the procedure.

MAC

While MAC (monitored anesthesia care) may include the administration of sedatives and/or analgesics often used for moderate sedation, it is distinguished from moderate sedation in several ways. The provider of MAC must be prepared and qualified to convert to general anesthesia when necessary. Like all anesthesia services, MAC includes an array of post-procedure responsibilities beyond the expectations of practitioners providing moderate sedation, including assuring a return to full consciousness, relief of pain, management of adverse physiological responses or side effects from medications administered during the procedure, as well as diagnosis and treatment of coexisting medical problems.

In anesthesiology, unlike most medical disciplines, pharmacodynamic drug interactions are frequently produced by design. Anesthesiologists take advantage of the pharmacodynamic synergy that results when two drugs with different mechanisms of action but similar therapeutic effects are combined. These synergistic combinations can be advantageous because the therapeutic goals of the anesthetic can often be achieved with less toxicity and faster recovery than when the individual drugs are used alone in higher doses. In fact, except for specific limited clinical circumstances wherein a volatile vapor or propofol alone is an acceptable approach, modern-day anesthesia is at least a two-drug process consisting of an analgesic (typically an opioid) and a hypnotic agent. Newer anesthetics have made total intravenous anesthesia (TIVA), a workable alternative to the traditional practice of general anesthesia with a volatile vapor. This is especially relevant if nerve monitoring will be used during the tumor treatment. Volatile vapors interfere with nerve monitoring.

The popularity of propofol in part relates to its half-life: The elimination half-life of propofol is 1–3 h, shorter than that of methohexital (6–8 h) or thiopental (10–12 h). The sedative/hypnotic effect and the fast onset and extremely short duration of propofol administered at 50–200 mcg/kg/min I.V. are extremely useful for deep sedation. Propofol has no analgesic effects and is often combined with opioids, such as fentanyl. There is presently a desire for clinicians other than anesthesiologists to use propofol for sedation. Because propofol can rapidly cause apnea even in low sedative doses, the most recent ASA statement on sedation with propofol says that "propofol is an anesthetic drug, and the ASA believes that the involvement of an anesthesiologist in the care of every patient undergoing anesthesia is optimal" [28].

General Anesthesia

General anesthesia may be considered in the context of four stages of anesthesia: preoperative patient management, induction, maintenance, and recovery. These stages are not independent: Actions taken during one stage may influence the next stage.

Preoperative Patient Management

The anesthesia care provider must obtain the patient's trust in a short period of time. Psychological techniques to allay anxiety can be extraordinarily useful adjuncts to the sedation plan. Commonly, a normal (terrified) adult will receive midazolam premedication. But midazolam administration extracts a price. Its administration may delay awakening and discharge from the postanesthesia care unit (PACU), particularly after brief procedures [29].

Induction of Anesthesia

Induction of anesthesia should rapidly, safely, and pleasantly achieve the anesthetic state, concurrently anticipating issues of maintenance and recovery from anesthesia. Induction of anesthesia is accomplished with an intravenous induction agent such as propofol or inhalation of a volatile vapor. Adult patients prefer intravenous. A rapidly acting opioid, often fentanyl, adds two desirable qualities to induction. Fifty to 100 mcg of fentanyl synergistically decreases the concentration of an inhaled anesthetic required to produce immobility in the face of noxious stimulation, and such doses also decrease perception of factors that otherwise might illicit airway responses such as coughing or laryngospasm [30].

The intravenous induction is followed by inhalation of a volatile vapor with oxygen or air/oxygen or nitrous oxide/oxygen. During induction with sevoflurane or isoflurane, there is a dose-related decrease in blood pressure and heart rate which returns to normal with a noxious stimulus. However, induction of anesthesia with desflurane produces a transient dose-related elevation of blood pressure and heart rate [31].

Maintenance

Maintenance of anesthesia has both immediate and long-range goals. MAC is the minimum alveolar concentration (partial pressure) of an inhaled anesthetic at 1 atm. that prevents skeletal muscle movement in response to a noxious stimulus (surgical skin incision) in 50 % of patients [32]. MAC values for combinations of inhaled anesthetics are additive. For example, 0.5 MAC nitrous oxide plus 0.5 MAC isoflurane has the same effect at the brain as either used alone. Because 50 % of patients would move with a noxious stimulus at 1 MAC concentration, a MAC greater than 1 is used clinically. Administration of approximately 1.3 MAC prevents movement in nearly all patients. The cardiorespiratory effects of potent inhaled anesthetics tend to be similar. Blood pressure tends to fall during maintenance in direct relation to depth of anesthesia due to peripheral vasodilation, but cardiac rhythm remains stable. With controlled respiration and normal $PaCO_2$, cardiac output tends to be maintained despite increasing depth of anesthesia, primarily through a rise in heart rate. However, after 8 h of 1.25 MAC, desflurane and sevoflurane anesthesia in volunteers produces indistinguishable effects on heart rate and blood pressure [33]. Potent inhaled anesthetics share many respiratory effects. All can increase $PaCO_2$. With spontaneous respiration, the resulting hypercapnia may increase heart rate and cardiac output above awake levels. All can dilate constricted bronchi and thus are useful in the management of patients with asthma or chronic obstructive pulmonary disease [34]. Some anesthetics at higher MAC can irritate the airways. Since maintenance of anesthesia usually requires less than1 MAC, irritation of the airway is not a problem. During maintenance, the incidence of coughing while breathing spontaneously through a laryngeal mask airway (LMA) is 5 % or less and not affected by anesthetic choice [35–38].

Recovery from Anesthesia

A rapid recovery from anesthesia carries several advantages. It may allow the earlier assessment and management of pain. It may permit a more rapid transit through the interventional suite and PACU. It may add to safety by restoration of airway support and reflexes and thereby decrease a propensity to oxyhemoglobin desaturation. Even a small concentration of anesthetic, a quarter of MAC awake, may produce pharyngeal dysfunction, and protective airway reflexes return sooner after anesthesia with a less soluble anesthetic [39, 40]. Two features, sedative potency and solubility, characterize recovery from inhaled anesthetics. MAC awake, the minimum alveolar concentration of inhaled anesthetic that permits appropriate response to commands (“open your eyes”), defines the sedative character of inhaled anesthetics. Nitrous oxide has a MAC awake approximately two-thirds of MAC, whereas desflurane, isoflurane, and sevoflurane have MAC awake values of approximately one-third of MAC [41, 42]. The equivalent value for propofol is less than 20 % of the value required to suppress movement [43]. A high MAC awake/MAC value accelerates awakening because awakening requires removal of a lesser fraction of the anesthetic. Thus, all things being equal, awakening occurs most rapidly with nitrous oxide and slowest with propofol. However, an anesthetic with a high MAC awake/MAC value is more likely to permit awareness during anesthesia than an anesthetic with a low MAC awake/MAC. Awareness may occur with 70 % nitrous oxide, but not with an equivalent concentration of propofol [43].

Nitrous oxide and desflurane have lower lean tissue solubilities than all other currently used inhaled anesthetics, but desflurane is ten times more soluble in fat than nitrous oxide. Sevoflurane has approximately twice the solubility of desflurane in all tissues, and isoflurane has twice the solubility of sevoflurane. Thus, recovery from sevoflurane is quicker than recovery from

isoflurane, and recovery from desflurane is quicker than recovery from sevoflurane or isoflurane [42]. A more rapid recovery from sevoflurane than from isoflurane occurs with both brief and prolonged anesthetics [44, 45]. Obesity does not change these relationships [46].

A safe recovery requires that residual neuromuscular blockade does not compromise ventilation or the ability to maintain a patent airway. Thus, the anesthesiologist usually maintains at least 1 twitch for a train –of –four twitches to ensure a capacity to reverse residual effect with neostigmine. The ability of inhaled anesthetics to cause relaxation and their ability to enhance the effects of neuromuscular blocking agents add to the safety of anesthesia with inhaled agents. Thus, elimination of a potent inhaled anesthetic decreases the paralysis produced by a given blood concentration of a neuromuscular agent.

Recovery also must consider untoward effects such as coughing on removal of the tracheal tube, postoperative nausea and vomiting (PONV), and postoperative pain. Removal of the endotracheal tube at peak lung inflation is helpful since it ensures that the next respiratory maneuver must be an exhalation that would push any foreign material (phlegm) into the pharynx rather than draw it into the larynx/trachea. Nausea with or without vomiting is the number one reason that patients scheduled to go home after a procedure need to be admitted to the hospital. Several factors predispose to PONV. The young female having laparoscopic surgery who receives substantial doses of drugs that predispose to PONV (opioids, nitrous oxide, and neostigmine) is the perfect storm. Obviously, the anesthesia care provider controls only some of these factors. Management of PONV includes decreased administration of drugs that predispose to PONV. It may also include administration of multiple receptor blockers [35] because diverse receptors probably mediate PONV. Males may report more postoperative pain than females, Caucasians more than African Americans or Orientals [47]. Complaints of pain are more likely after major versus minor procedures, after longer versus shorter procedures, and after procedures in which no opioid has been used or where no opioid has been administered recently [47]. Management of pain assumes a prediction for the degree of pain. Mild pain may be managed by nonspecific NSAIDS such as ketorolac. More severe pain may require administration of opioids titrated to a level of respiratory rate. The interventionalist may assist in the management of pain by injecting with local anesthetic which greatly reduces the requirement for systemic analgesics. Maximum doses should be calculated and not exceeded in order to avoid toxicity. The toxic effects of local anesthetics are additive.

Regional Techniques

Regional techniques include spinal, epidural, local infiltration, and peripheral nerve blocks. Performing a block takes longer than monitored anesthesia care or inducing general anesthesia, and the incidence of failure is higher. Unnecessary delays can be obviated by performing the block beforehand in a pre-procedural holding area. Resurgence in the popularity of regional anesthesia techniques has occurred in conjunction with an increased emphasis on perioperative pain relief, the desire to discharge ambulatory patients with minimal discomfort, and to maintain a "stress-free" physiologic environment for both ambulatory and inpatients. Regional anesthesia can be employed to obtain pre-, intra-, and postoperative pain relief with the use of single, intermittent, or continuous techniques. With the increased emphasis on regional anesthesia, both new and old issues arise and need to be addressed. Current issues in regional anesthesia include whether to perform blocks in anesthetized patients; choice of regional blocks for postoperative pain; choice of technique peripheral nerve stimulator, paresthesia, or ultrasound; and the performance of regional techniques in a patient taking anticoagulant or antiplatelet medication.

Special Considerations

Interventional tumor therapy is viewed as procedures with low anesthetic risk. While these procedures are noninvasive and lack many of

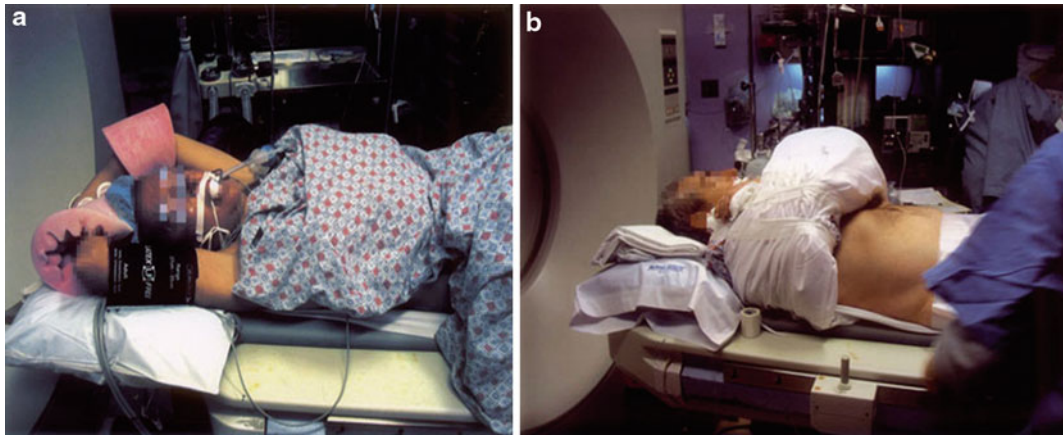

Fig. 9.1 (**a**) Incorrect positioning with the patient's arm raised above his head. This position resulted in brachial plexus injury. (**b**) Modified positioning with the patient's arms folded across his chest. This position is an acceptable compromise to avoid brachial plexus injury while avoiding artifacts on the CT images (From Shankar et al., Brachial plexus injury from CT guided radiofrequency ablation under general anesthesia. CVIR. 2005;28:646–48, reprinted with permission from Springer Science+Business Media)

the known anesthetic risks of open surgery, there are special anesthetic considerations related to the procedure, location, and mechanism of action of the intervention (percutaneous direct injection of toxic substances, transarterial embolization, percutaneous delivery of thermal energy, internal radiotherapy).

Positioning

Tremendous care must be taken during the positioning. If positioning is performed after induction of general anesthesia, the move requires that the ET tube be well secured, and the head, eyes, nose, and other facial structures are well padded and protected. The neck must also be in neutral position to prevent any cervical spine complications. Chest rolls and abdominal rolls should be placed so that ventilatory support is uncompromised. Extreme vigilance is required to make sure that all body parts are properly positioned and there should be frequent checks to ensure proper positioning. The arms are typically placed in a neutral position to avoid brachial plexus injury and allow easy use of a CT scanner or fluoroscopy machine (Fig. 9.1a, b). The arm, elbows, and hands must be well padded and secure. A pillow should be placed below the ankle so that there is flexion of the knee to prevent any peroneal injury. Gel pads should be placed before the knees to prevent pressure injuries.

Respiratory Events

Analysis of the data from the ASA Closed Claims Project Database exploring the patterns of injury and liability associated with anesthesia provided in remote locations compared to the standard OR documented that respiratory events were twice as likely to occur in remote locations as in operating rooms [48]. The most common event was inadequate oxygenation/ventilation. In 30 % of the remote location claims, an absolute or relative overdose of sedative, hypnotic, and/or analgesic drugs led to respiratory depression. Seventy percent of the cases that occurred in radiology involved over sedation. The remaining events were esophageal intubation, difficult intubation, and aspiration of gastric contents. Nonoperating room anesthesia claims were more often judged as having substandard care and being preventable by better monitoring [48].

Non-anesthesia-related potential respiratory complications range from a simple pneumothorax

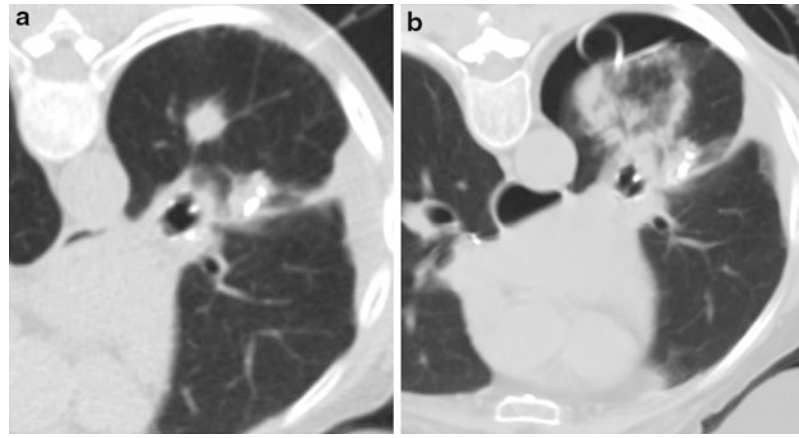

Fig. 9.2 (**a**) Lung expansion prior to RFA. (**b**) Pneumothorax after removal of RFA probe (Courtesy of Stephen Solomon, MD)

or self-limiting hemoptysis to life-threatening pulmonary hemorrhage or air embolism. Pneumothorax is both a complication and, at times, a planned intervention. It is typically discussed with patients during the consent. Procedures performed that are in close proximity to the dome of the diaphragm such as liver RFA will require the interventionalist to deliberately create a pneumothorax in order to gain adequate exposure to the site of treatment. Again, communication among the anesthesia team and the interventional team is essential. The anesthesia team must be aware so that any untoward hemodynamic or respiratory instability can quickly be reversed. The imaging equipment allows the interventionalist to control the degree of pneumothorax so that optimal exposure to the treatment site is maximized while maintaining hemodynamic and respiratory stability. Pneumothorax may also be unintentional, and the anesthesia team must be vigilant and recognize the clinical signs (Fig. 9.2a, b). During controlled ventilation, high peak ventilatory pressure is a warning sign of pneumothorax. In spontaneous or controlled ventilation, a drop in oxygen saturation, hypotension, and/or bradycardia are all signs that a pneumothorax may be present. When recognized, this complication is easily treated by aspirating the air in the pleural space. Depending on both the severity of the intra-procedural pneumothorax and if a residual pneumothorax exists after treatment, a chest tube may be placed. This is a benefit of treatment under image guidance because this imaging can also detect untoward effects of the therapy and assist the anesthesiologist in diagnosing and treating. Upon transfer of care to the PACU team, communication of a residual pneumothorax is essential. An initial chest x-ray is obtained upon arrival to the PACU, and a subsequent film is done 2 h later. The interventionalist may inject air into the abdominal cavity to move uninvolved organs away from the tumor. A sudden drop in end-tidal CO_2 may indicate an air embolism.

The success of the interventional treatment depends on locating the tumor with imaging. Low tidal volume, atelectasis, and endobronchial intubation can camouflage tumors of the lung, liver, or kidney. The anesthesiologist can contribute to the success and completion of the procedure with maneuvers such as repositioning the ETT, Valsalva for lung expansion, increasing tidal volume, or changing the patient's position (Figs. 9.3a, b and 9.4a, b).

Physiologic Instability

Sedation and/or analgesia that is inadequate or certain tumor manipulation may provoke the autonomic stress response (hypertension, tachycardia). RFA of solid organs may create transient hypertension during the treatment phase which responds to deepening the anesthesia. During RFA of the adrenal or any neuroendocrine tumor, the anesthesiologist should anticipate and be prepared to treat hypertensive crisis with vasoactive medications. RFA of nonsecreting

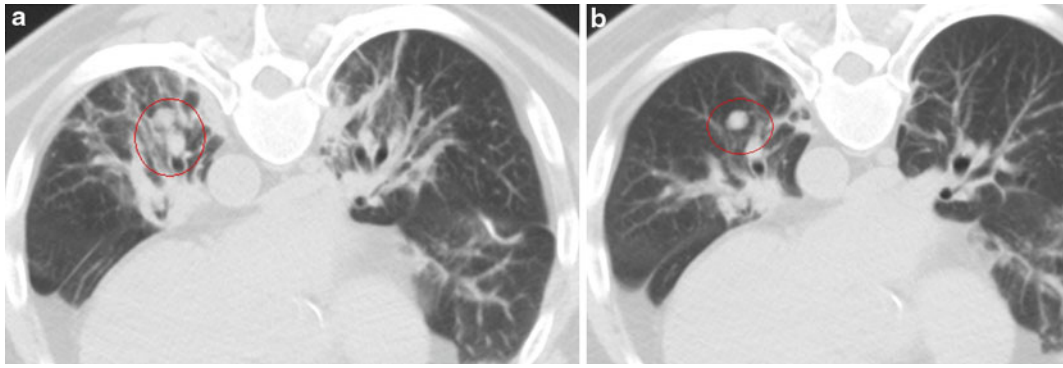

Fig. 9.3 (**a**) Low tidal volume creates atelectasis and camouflages nodule. (**b**) Increasing the tidal volume expands lung, and nodule is visualized (Courtesy of Stephen Solomon, MD)

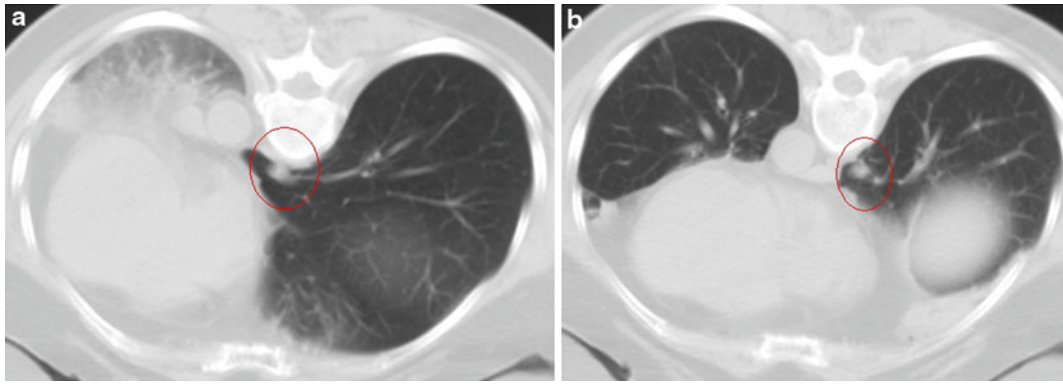

Fig. 9.4 (**a**) Low lung volume shows nodule to the *left* of vertebral body. (**b**) Expanding the *left* lung shifts nodule form *left* of vertebral body to *right* side (Courtesy of Stephen Solomon, MD)

adrenal, hepatic, or renal tumors [49, 50] may create catecholamine release from adjacent normal adrenal tissue. Embolizations for metastatic carcinoid to the liver may be complicated by carcinoid syndrome. In our institution, we pretreat these patients with octreotide. Signs of flushing, sweating, and hypertension may be observed during the procedure or post-procedure and will require treatment with additional doses of octreotide.

Metastatic pheochromocytosis is an exception. These patients should be pretreated for this minimally invasive procedure similar to being prepped for an open or laparoscopic adrenalectomy. The metastases of pheochromocytoma most commonly affect targets that can be treated with radiofrequency ablation. Preparation for hypertensive crisis with arterial monitoring and vasoactive medications is essential. In addition, in our institution, we use a technique of ceasing the current if signs of catecholamine release exist [51]. If the heart rate or blood pressure begins to rise, vasoactive substances are immediately administered. We will frequently bolus both esmolol and nicardipine (100 umg/cc). Treatment will continue only after the patient has returned to their baseline hemodynamic. In addition, RFA of nonsecreting adrenal tumors may create catecholamine release from adjacent normal adrenal tissue, and we recommend invasive monitoring and available direct acting vasodilators and short-acting beta-blockers.

On the other hand, sedatives and analgesics may blunt an appropriate response to hypovolemia or

procedure-related stresses. Anytime a needle is inserted into an organ, bleeding may occur.

Bleeding can include massive hemoperitoneum, hemothorax, or hemoptysis. All patients need good intravenous access, known coagulation profile with correction if needed, and type and screen. More commonly, there is mild intrapulmonary hemorrhage with transient hemoptysis during pulmonary RFA and mild intraperitoneal hemorrhage during liver RFA; both are treated conservatively.

Percutaneous ethanol injection (PEI) is used in patients with hepatocellular carcinoma. The choice of anesthesia and the complications will depend on the volume of ethanol injected. A single session with a large-volume injection demands a general anesthetic. This is extremely painful and may generate nausea and vomiting during the procedure as well as alcohol toxicity. Similar to RFA of the liver, intraperitoneal hemorrhage or hemothorax may occur. Unique to this procedure is the risk of variceal bleeding.

Adverse drug reactions are common; however, only 6–10 % are immunologically mediated. Unlike most adverse drug reactions, allergic drug reactions are unpredictable. Predictable adverse drug reactions are dose-dependent, related to the known pharmacologic actions of the drug, occur in otherwise normal patients, and account for approximately 80 % of the adverse drug effects. Most serious predictable adverse drug reactions are toxic in nature and either directly related to either the amount of drug in the body (overdosage), inadvertent route of administration, or known side effects (i.e., opioid-related nausea). However, some drugs have effects that are indirect consequences of the drug's primary pharmacologic action (i.e., drug-mediated histamine release from mast cells or drug interactions). Patients often refer to any adverse drug effects as being allergic in nature. Anesthetic drugs also have the potential to produce direct effects on the cardiovascular system (propofol-induced vasodilation) complicating the diagnosis of perioperative adverse drug reactions.

Any substance that patients are exposed to during the periprocedural period including drugs, blood products, or latex can produce anaphylaxis. Most anesthetic drugs and agents have been reported in the literature to produce anaphylactic and anaphylactoid reactions [52]. Therefore, a plan for treatment of anaphylactic or anaphylactoid reactions must be established before the event [53]. Because any parentally administered agent can cause death form anaphylaxis, anesthesiologists must diagnose and treat the acute cardiopulmonary changes that can occur.

Airway maintenance, 100 % oxygen administration, intravascular volume expansion, and epinephrine are essential to treat the hypotension and hypoxia that results from the increased capillary permeability and bronchospasm [53].

Regular monitoring of vital signs, adequate intravenous access, blood availability, resuscitative drugs, and team communication should allow appropriate treatment and decrease the likelihood of adverse outcomes from any complication [1].

Magnetic Resonance Imaging

MRI is utilized for a multitude of interventions. The MRI suite is particularly challenging for the anesthesiologist. In order to practice safely in the MRI environment, all equipment must be MRI compatible. In addition, patients and personnel entering these rooms must be screened constantly. An MRI compatible anesthesia machine has become a more integral component of the MRI suite. Remote monitoring must meet basic anesthesia standards. The monitoring systems and IV pumps must also be MRI compatible. In our institution, we use the in vivo monitoring system which consists of a wireless 4 lead EKG and wireless pulse oximetry. $ETCO_2$, noninvasive and invasive BP, and temperature are all hardwired components of this system. There is a slave monitor that communicates wirelessly with the base unit which can be placed in the MRI control room and is easily seen by the anesthesia team. We use Pyxis for our drug delivery system, and these non-MRI compatible units are kept in the MRI control room which is outside of the MRI scanner. The equipment cart used and all items stocked must be MRI compatible. MRI laryngoscopes and blades are essential. If all monitors and equipment are MRI compatible

and personnel have been properly screened, then the induction of any type of anesthesia can be safely performed directly inside the MRI suite which is preferable to inducing general anesthesia outside the suite and moving the unconscious patient into the scanner.

Adults will often present for MRI with anxiety due to claustrophobia, or they may have pain syndromes that prevent them from lying flat and still for prolonged periods which often requires a GA. In addition, new advances in IR procedures such as MRI laser ablation may necessitate long periods of apnea that can only be done if a patient is having a GA. MR imaging data is acquired in 8–10-min sequences. If patient movement occurs during that time, the entire sequence must be repeated. Prolonged studies with inaccessibility to the patient can be problematic. CPR must be performed outside the MRI scanner.

Radiation Exposure

Radiation protection measures are necessary for all individuals who work in the interventional fluoroscopy suite. This includes anesthesiologists who may only be in the radiation environment occasionally. Radiation protection tools such as a protective apron and thyroid shield should be worn, and the anesthesiologist should stay as far away from the X-ray beam as possible in a low scatter area. In order to know one is working safely, personal dosimetry should be recorded to determine level of exposure.

Conclusion

As technology advances and more noninvasive image-guided therapies become available, it is important for anesthesiologists and interventional physicians to work together to offer a safe environment for this increasing patient population. Optimizing the patient's comorbidities, being familiar with the interventional procedure and location, and creating a safe anesthesia work area outside the traditional operating room are preemptive measures to lessen any anesthetic risk. Intervention oncology has been referred to as the surgery of the future. This next generation of interventional physicians will be well served by anesthesiologists who are able to adapt to this rapidly changing field. It is essential that these anesthesiologists possess communication and complex case management skills to develop an anesthetic plan that achieves the desired treatment goal and causes no harm for the individual patient.

References

1. Procedure for Intravenous Conscious Sedation. Comprehensive Accreditation Manual for Hospitals: The Official Handbook. The Joint Commission on Accreditation of Healthcare Organizations.
2. American Society of Anesthesiologists Task Force on Sedation and Analgesia by Non-Anesthesiologists. Practice guidelines for sedation and analgesia by non-anesthesiologists. Anesthesiology. 2002;96:1004–17.
3. Meridy HW. Criteria for selecting of ambulatory surgical patients and guidelines. Anesth Analg. 1982;61:921–6.
4. Natof HE. Ambulatory surgery: patients with pre-existing medical problems. Ill Med J. 1984;166:101.
5. Federated Ambulatory Surgery Association. FASA special study 1. Alexandria: FASA; 1987.
6. Chung F, Mezei G, Tong D. Pre-existing medical conditions as predictors of adverse events in day-case surgery. Br J Anaesth. 1999;83:262–70.
7. Chung F, Mezei G. Factors contributing to a prolonged stay after ambulatory surgery. Anesth Analg. 1999;6: 1352–9.
8. Lichtor JL. Anesthesia for ambulatory surgery. In: Barash PG, Cullen BF, Stoelting RK, editors. Clinical anesthesia. 6th ed. Philadelphia: Lippincott Williams & Wilkins; 2009.
9. Lee TH. Reducing cardiac risk in noncardiac surgery. N Engl J Med. 1999;341:1838–40.
10. Fleischer LA, Beckman JA, Brown KA, et al. ACC/AHA 2007 guidelines on preoperative cardiovascular evaluation for noncardiac surgery. Circulation. 2007;116:418–500.
11. Schouten O, Jeroen JB, Poldermans D, et al. Assessment of cardiac risk before noncardiac surgery. Heart. 2006;92:1866–72.
12. Auerbach A, Goldman L. Assessing and reducing the cardiac risk of noncardiac surgery. Circulation. 2006;113:1361–76.
13. Devereaux PJ, Yang H, Guyatt GH, et al. Rationale, design, and organization of the perioperative ischemic evaluation (POISE) trail; a randomized controlled trial of metoprolol versus placebo in patients undergoing noncardiac surgery. Am Heart J. 2006;152:223–30.
14. Lindenauer PK, Pekow P, Wang K, et al. Perioperative beta-blockade therapy and mortality after noncardiac surgery. N Engl J Med. 2005;353:349–61.

15. Newsome LT, Weller RS, Gerancher JC, et al. Coronary artery stents: II. Perioperative considerations and management. Anesth Analg. 2008;107:570–90.
16. Warner DO. Preventing postoperative pulmonary complications: the role of the anesthesiologist. Anesthesiology. 2000;92:1467–72.
17. McAlister FA, Khan NA, Straus SE, et al. Accuracy of preoperative assessment in predicting pulmonary risk after nonthoracic surgery. Am J Resp Crit Care Med. 2003;167:741–4.
18. Kroenke K, Lawrence VA, Theroux JF, et al. Postoperative complications after thoracic and major abdominal surgery in patients with and without obstructive lung disease. Chest. 1993;104:1445–51.
19. Kearney DJ, Lee TH, Reilly JJ, et al. Assessment of operative risk in patients undergoing lung resection: importance of predicted pulmonary function. Chest. 1994;105:753–9.
20. Stroh KP, Redline S. Recognition of obstructive sleep apnea. Am J Resp Crit Care Med. 1996;154:279–89.
21. Ortego LD, Carnevali-Ruiz D, Gallego ED. Sleep apnea and the risk for perioperative myocardial infarction. Ann Intern Med. 1993;119:953.
22. Gupta RM, Parvizi J, Hanssen AD, et al. Postoperative complications in patients with obstructive sleep apnea syndrome undergoing hip or knee replacement. Mayo Clin Proc. 2001;76:897–905.
23. Gross JB, Bachenberg KL, Benumof JL, et al. Practice guidelines for the perioperative management of patients with sleep apnea. Anesthesiology. 2006;104:1081–93.
24. Lin CC. Effect of CPAP on ventilatory drive in normocapnic and hypercapnic patients with obstructive sleep apnea syndrome. Eur Respir J. 1994;7:2005–10.
25. Loadsman JA, Hillman DR. Anesthesia and sleep apnea. Br J Anaesth. 2001;86:254–66.
26. Fattowich G. Natural history and prognosis of hepatitis B. Semin Liver Dis. 2003;23:47–58.
27. Standards for Basic Anesthetic Monitoring (amended by ASA House of Delegates Oct 2010). www.asahq.org/publicationsAndServices/standards/02.PDF. Accessed October 2004.
28. Philip BK. Sedation with propofol: a new ASA statement. ASA Newsl. 2005;69:29–30.
29. Fredman B, Lahav M, Zohar E, et al. The effect of midazolam premedication on mental and psychomotor recovery in geriatric patients undergoing brief surgical procedures. Anesth Analg. 1999;89:1161–6.
30. Katoh T, Kobayashi S, Suzuki A, et al. The effect of fentanyl on sevoflurane requirements for somatic and sympathetic responses to surgical incision. Anesthesiology. 1999;90:398–405.
31. Ebert TJ, Muzi M, Lopatka CW. Neurocirculatory responses to sevoflurane in humans. A comparison to desflurane. Anesthesiology. 1995;83:88–95.
32. Merkel G, Eger EI. A comparative effect of halothane and halopropane anesthesia. Introducing method for determining equipotency. Anesthesiology. 1963;24:346–57.
33. Eger EI, Bowland T, Ionescu P, et al. Recovery and kinetic characteristics of desflurane and sevoflurane in volunteers after 8 hour exposure, including kinetics of degradation products. Anesthesiology. 1997;87:517–26.
34. Habre W, Petak F, Sly PD, et al. Protective effects of volatile agents against methacholine-induced bronchoconstriction in rats. Anesthesiology. 2001;94:348–53.
35. Tang J, White PF, Wender RH, et al. Fast-track office based anesthesia: a comparison of propofol versus desflurane with antiemetic prophylaxis in spontaneously breathing patients. Anesth Analg. 2001;92:95–9.
36. Ashworth J, Smith I. Comparison of desflurane with isoflurane or propofol in spontaneously breathing ambulatory patients. Anesth Analg. 1998;87:312–8.
37. Tang J, Chen L, White PF, et al. Recovery profile, costs, and patient satisfaction with propofol and sevoflurane for fast-track office-based anesthesia. Anesthesiology. 1999;91:253–61.
38. Eshima RW, Maurer A, King T, et al. Comparison of airway responses during desflurane and sevoflurane administration via a laryngeal mask airway (LMA) for maintenance of anesthesia. Anesth Analg. 2003;96:701–5.
39. Sundman E, Witt H, Sandin R, et al. Pharyngeal function and airway protection during sub hypnotic concentrations of propofol, isoflurane, and sevoflurane. Volunteers examined by pharyngeal videoradiography and simultaneous manometry. Anesthesiology. 2001;95:1125–32.
40. Mckay RE, Large MJ, Balea MC, et al. Airway reflexes return more rapidly after desflurane anesthesia than after sevoflurane anesthesia. Anesth Analg. 2005;100:697–700.
41. Dwyer R, Bennett HL, Eger EI, et al. Effects of isoflurane and nitrous oxide in sub anesthetic concentrations on memory and responsiveness in volunteers. Anesthesiology. 1992;77:888–98.
42. Eger EI, et al. The pharmacology of inhaled anesthetics. Chicago: Healthcare Press; 2002.
43. Chortkoff BS, Eger EI, Crankshaw DP, et al. Concentrations of desflurane and propofol that suppress response to command in humans. Anesth Analg. 1995;81:737–43.
44. Philip BK, Kallar SK, Bogetz MS, et al. A multicenter comparison of maintenance and recovery with sevoflurane or isoflurane for adult ambulatory anesthesia. Anesth Analg. 1997;83:314–9.
45. Ebert TJ, Robinson BJ, Uhrich TD, et al. Recovery from sevoflurane anesthesia. A comparison to isoflurane and propofol anesthesia. Anesthesiology. 1998;89:1524–31.
46. Strum EM, Szenohradszki J, Kaufman WA, et al. Emergence and recovery characteristics of desflurane versus sevoflurane in morbidly obese adult surgical patients: a prospective, randomized study. Anesth Analg. 2004;99:1848–53.

47. Dahmani S, Dupont H, Mantz J, et al. Predictive factors of early morphine requirements in the post – anesthesia care unit. Br J Anesth. 2001;87: 385–9.
48. Metzner J, Posner KL, Domino KB, et al. The risk and safety of anesthesia at remote locations: the US closed claims analysis. Curr Opin Anaesthesiol. 2009;22:502–8.
49. Onik G, Onik C, Medary I, et al. Life-threatening hypertensive crises in two patients undergoing hepatic radiofrequency ablation. AJR Am J Roentgenol. 2003;181:495–7.
50. Chini EN, Brown MJ, Farrell MA, et al. Hypertensive crisis in a patient undergoing percutaneous radiofrequency ablation of an adrenal mass under general anesthesia. Anesth Analg. 2004;99:1867–9.
51. Venkatesan AM, Locklin J, Lai EW, et al. Radiofrequency ablation of metastatic pheochromocytoma. J Vasc Interv Radiol. 2009;20:1483–90.
52. Levy JH. Anaphylactic reactions in anesthesia and intensive care. 2nd ed. Stoneham: Butterworth-Heinemann; 1992.
53. Stark BJ, Sullivan TJ. Biphasic and protracted anaphylaxis. J Allergy Clin Immunol. 1986;78:76–83.

Management of the Oncologic Patient 10

Derek Tessier

Abstract

The purpose of this chapter is to provide the interventional radiologist and his or her ancillary staff with the basic requirements and knowledge to successfully establish an image-guided tumor service within their radiology practice. The focus is on a hospital-based practice although a private ablation center is conceivable. The objective of this chapter outlines the process of how a referral-based ablation practice functions. It offers ideas on how to improve communication, consultation, ablation process itself, and post-ablation follow-up care and imaging.

Like the technology of ablation, the management of an image-guided tumor ablation service is ever evolving. There is the art of performing the technical aspects of ablation as well as the art of managing patients undergoing the ablation process. Establishing and managing a reliable ablation service are important aspects that provide the referring physician and patient the information and knowledge required to successfully navigate through the ablation process. Maintaining structure within the ablation service provides the interventionalist, patient, and referring providers a consistency, which in turn provides a stability where expectations are established and met. In addition to acquiring a patient base and being adequately reimbursed for your efforts, it remains very important to provide a dedicated clinical point person managing your clinical ablation program [1].

Although ablation procedures are minimally invasive, they remain surgical procedures nonetheless and should be treated as such. Patients and referring providers are not always aware of the comprehensive planning and follow-up care that ablation procedures require. We have formulated ablation guidelines that we currently utilize in our ablation service at Rhode Island Hospital that will help assist the provider and the patient through one of potentially many treatments in our battle against cancer. Updates to ablation guidelines are as necessary a part of this process as personalizing a patient's care plan. This chapter is meant to take you through the comprehensive steps we take from the time of referral to the continued management of post-ablation care and imaging.

Whether you have a well-established or fledgling image-guided tumor ablation (IGTA) service, the referral process at your institution should strive to be well organized and efficient. The necessary

D. Tessier
Department of Radiology, Rhode Island Hospital, Providence, RI, USA
e-mail: dtessier@lifespan.org

D.E. Dupuy et al. (eds.), *Image-Guided Cancer Therapy*, DOI 10.1007/978-1-4419-0751-6_12,

ingredients for a successful service start with dedicated well-trained staff, who can make the whole referral process as seamless and expedited as possible for the patient and referring and consulting physician. We, like many other institutions, receive our referrals from an array of multidisciplinary sources. Tumor board is one avenue in which patients are referred to our service. In addition to medical, surgical, and radiation oncology, other referral sources include urology, pulmonology, gastroenterology, and lastly, self-referrals.

In our institution, our surgery department also utilizes intraoperative ablation. In some instances, the interventional radiologist has even made themselves available to assist during these surgical procedures. This is certainly not mandatory; however, it provides for an open two-way communication and potential avenues of referrals between radiology and surgery departments.

In many, if not a majority of cases, of our referrals are by way of tumor board. This most certainly allows for a multidisciplinary and comprehensive approach to each patient's individual cancer scenario. This also allows for combination treatments or therapies to be achieved. Ablation can be used with concurrent or subsequently to surgery [2], radiation [3], and systemic or local chemotherapy [4].

Gathering information for self- and physician-referred patients has subtle differences that will be discussed separately. Having a self-referred patient basis indicates that you are reaching out to community networks and the Internet. These alternative, less formal avenues of referrals tend to inform the consumer of available treatments that they or their medical providers may not have been previously aware. This creates a whole separate referral source and with it, potential problems. It is important to keep in mind that self-referrals can be time consuming and daunting as many of them have come to a roadblock in their cancer care and have resorted to the Internet to find alternative treatments to the care that is currently being offered to them. We also know that the Internet can be a double-edged sword where on one hand it provides a vast amount of information and on the other hand not always providing the patient with accurate or unbiased information. Even a relatively well-informed consumer can have difficulty wading through copious amounts of information available on the Internet. This makes for a potentially overwhelming and difficult time. All the while, patients and families are still trying to deal with the psychological and physical effects of cancer.

We have helped design a web site and appropriate links for self-referrals, and others who are trying to obtain additional information. Your web site should be developed with patients in mind. It should include some basic information about you, your institution, and a brief description of what ablation is all about. It also helps to have a direct e-mail link to a clinical resource such as a nurse practitioner to facilitate communication and respond to inquiries. In addition to being a source of new patient referrals, your web site and midlevel will educate the health-care consumer and potentially save the interventionalist a great deal of time. Once the self-referrals contact our institution, they are sent a form letter (Table 10.1) requesting additional pertinent, necessary clinical and demographic information. In addition to the imaging, it is oftentimes necessary to collect the patient's past medical information and treatments they may have received as part of their cancer care. Reviewing both the medical history and imaging is a relatively small investment of time up front but will save time for you, patient, and the referring physician in the long run. If patients are not ideal candidates for ablation, they can then be referred to the appropriate specialist.

Once we are aware of the patient's initial and current cancer staging, we are able to determine if ablation would be curative or palliative. We can also suggest additional interventions such as radiation or chemotherapy, which may be necessary as adjunct therapy. If it has not already occurred, we oftentimes take this opportunity to discuss our patient's individual needs at tumor board. This allows for additional multidisciplinary clinical input and individualizes the patient's treatment choices and options to fit their medical needs [5]. We will also inform patients that other treatments or surgery may be more appropriate for their

Table 10.1 Self-referral form letter example

I am sorry to hear about your present circumstances. We may be able treat your current medical condition with either radiofrequency ablation (heating), microwave ablation (heating), cryoablation (freezing), or irreversible electroporation (IRE) depending on tumor location, number, and extent of disease (staging). You may want to let your treating physician know you are looking into ablation as a potential treatment option
It is very important that you provide us with all the following requested information/reports. Failure to do so will result in a delayed review of your medical information. Because this is all being done as a courtesy for you and due to time constraints, we will be unable to contact your providers for any information. It is your responsibility to get requested information to us. Please do not provide more information than what is requested
We will need the following additional information from you:
1. The most recent two notes only from the physician(s) that is currently treating your cancer – medical, surgical, and radiation oncologist (please do not send the whole chart)
2. The latest CT or MRI scans *and* reports (do not send images without the reports)
3. PET or PET/CT scan *and* reports
I will then review your information with the doctor and get back in touch with you. We will then let you know whether we can or cannot treat the tumor(s) safely and effectively and whether you are an appropriate candidate for our procedure. Please be patient for a response as this is being done as a courtesy for you. Typically, you should expect to hear from us within 1 week of receiving the above information. Please refer to fax and phone number and address below to send the above requested information
Please check with your insurer to ensure the procedure you are requesting would be covered out of state
Best regards,
Please refer to following web sites for additional information:
http://www.lifespan.org/Services/Oncology/Default.htm
http://www.lifespan.org
http://www.diagnosticimaging.com/ablation/
http://www.mayoclinic.org/radiofrequency-ablation/
http://www.cc.nih.gov/drd/rfa/
http://www.lungcanceronline.org/treatment-experimental/rfa.html
http://www.angiodynamics.com/pages/patients/IRE.asp
e-mail:
Phone #:
Fax #:

particular tumor. Once a more definitive determination is made whether IGTA is the appropriate choice, we can then set up a consult and ablation date. Since most self-referrals tend to come from out of state, it is important to determine candidacy for not only clinical but travel reasons. We take every step ahead of time to ensure patients traveling from out of state are candidates for ablation before they arrive. It is also helpful to get their treating physician's contact information (e.g., spelling of name, phone numbers, fax numbers, and mailing addresses). This will ensure proper communication and makes them aware of their patient's intentions.

In addition to gathering self- and physician-referred patient's medical information, the midlevel acts as a clinical and administrative point person. This allows for effective communication between the referring source and the ablative service. To address a patient's problem and deal with this in a timely manner, medical notes, imaging, and biopsy reports are gathered within a short time of the referral. We have developed a guideline for each major tumor type. The guideline outlines the imaging and testing we require before, during, and after treatment. For example, if a patient with a lung nodule is being referred, it is ideal to have a CT of the chest, staging PET/CT, brain MR, pulmonary function tests, and biopsy-proven diagnosis (Table 10.2).

It is necessary to have medical information ahead of time in order to make a clinical determination of patient candidacy for IGTA. It is also recommended that patient has been evaluated by pulmonology, medical oncology, or thoracic surgery. This will help determine if patient is inoperable or is a high-risk surgical candidate due to comorbidities. Once we have all this information, there are few if any hurdles to obtain prior authorization or deal with insurance companies. As an aside, if one aspect of imaging or testing has yet to be performed and it will cause a significant delay in patient being seen, it may be better to have imaging performed on day of consult. We remain aware that patient and providers alike are anxious to be seen and treated in the most expedited fashion.

Table 10.2 Lung cancer (NSCLC)

A. *Patient referred*
1. Gather pertinent medical info from referring and other involved MDs and gather imaging and perform preliminary review with MD
Obtain oncology, radiation oncology, pulmonary, thoracic surgery, and PCP notes
2. Review chest, abdomen, and pelvic CT
3. Review PET/CT (if PET > 60 days, order PET/CT)
4. Review biopsy report
5. Confirm staging and determine previous or future treatments with chemoradiation
6. Order chest CT at time of consult if > 60 days
7. Order PET/CT 1 week prior to consult if > 60 days
8. Stage 1a or 1b NSCLC and schedule PFTs prior to day of consult (if spirometry/PFTs > 90 days) and 4 month f/u spirometry to coincide with 4 month f/u chest CT
B. *Consult*
1. CT chest day of consult if previous CT > 60 days
2. Perform H & P
3. Consult with MD and NP candidate for RFA or microwave ablation in CT
4. Thoracic surgery referral
5. Pulmonology or medical referral as indicated
6. Pulmonary function tests
7. Radiation oncology referral as indicated
8. Pulmonology and/or medical referral to admitting RI Hospital physician for patients referred from outside referral source/outside institution at time of consult prior to biopsy and/or ablation
9. Cardiology referral as indicated (? EKG, echocardiogram, stress test)
10. Schedule procedure in CT
11. Lab work: CBC, BUN/creat, PT/PTT/INR
12. Determine method (microwave or RFA and applicator size) and dictate in clinical visit and on procedure booking sheet
13. Determine if concomitant brachytherapy or pre/post external beam radiation is indicated
14. Determine positioning of patient during procedure and dictate in clinical visit and on procedure booking sheet
15. Anticipate admission and get pulmonology involved/ referral as indicated
16. Dictate post consult note and fax to referring and other docs involved
17. Write letter of necessity to insurer if indicated
C. *Image-guided thermal ablation procedure of lung*
1. Consent patient
2. Perform scheduled ablation procedure (with on-site pathology if indicated)
3. Two-hour post-ablation CXR
4. Assess in recovery and discharge to home/floor with d/c instructions and scripts
5. Schedule follow-up imaging
6. Schedule post-ablation f/u visit
7. Admit patient as indicated in conjunction with pulmonology for pneumothorax, respiratory distress, pain control, and other chronic medical issues
D. *Follow-up imaging ALWAYS WITH and WITHOUT contrast (unless contraindicated)*
1. CT of chest: with and without contrast in 2–3 weeks, then alternate chest CT I – I + with PET/CT every 3 months thereafter

Once the medical information and imaging is received, it is organized by the midlevel. It is comprehensively reviewed with the interventionalist. The interventionalist will decide if any further studies are needed and review as indicated once they are performed. The midlevel can track the patient and ensure that not only is the appropriate study being ordered but ordered the appropriate way. The interventionalist will then make the ultimate decision to treat or refer as deemed appropriate. To ensure the information received prior to consult is still up to date and disease has remained stable, patient information should be re-reviewed as you get closer to the day of consultation and treatment.

Self-referred patients are kindly asked to gather all the necessary information and imaging. Unfortunately, not very many offices have the resources or time to call or collect all the treating physicians notes or imaging from multiple sites. As it stands, this review of information is being done at no charge and as a courtesy to the patient. Once they have gathered all necessary medical information, we then have them mail to our hospital for our review. Otherwise, for physician-referred patients, we ask the referring office to mail us the imaging. As a second option, we will contact the institution where the imaging was performed and ask them to send us the imaging directly. As a last resort, if the imaging center requires patients to release this information, we have the patients to either mail or bring us the

images. We always prescreen imaging and very rarely have we had the patient bring their imaging on the day of consult.

In addition to educating patients, it is also important to ensure that the referring physicians are also kept up to date. Due to the relative novelty of IGTA, we cannot assume that all physicians are aware of ablation or know which patients are best suited for IGTA based on above criteria. A good way to combat this problem is to have the interventionalist or midlevel perform grand rounds, speak in the community, and be present at tumor board. Basic inservices for radiology staff are also helpful and provide the technical knowledge for CT scan or ultrasound technologists to participate in ablations. It is also important to educate or inform the radiology recovery nurses how ablation works and what expected and unexpected outcomes are. Ablation is a minimally invasive surgical procedure and should be treated as such.

When dealing with the imaging aspect of cancer and ablation, it is ideal to have all necessary imaging performed prior to consultation. Sometimes this is not possible, and you may need to order additional imaging at time of consult. When consults require imaging or restaging, most of the pre- and post-ablation imaging requires contrast. It is helpful to have a recent creatinine and estimated glomerular filtration rate (eGFR). In the event patients have decreased kidney function, eGFR less than 60 mL/min, we utilize hydration guidelines (Table 10.3). If you do require additional imaging prior to consultation, you may ultimately save time by having the referring physician's office order the imaging. This is particularly true when patient medication requires adjusting or prior approval from the patient's insurance company is necessary. When you do not have sufficient medical or demographic information on a new patient, obtaining prior authorization may prove to be more difficult and time consuming than you would think.

Prior to their consultation, all of our patients are provided with a reminder letter, which includes the date and time of consult and imaging. The letter also includes explicit instructions, directions to and within the hospital, parking, and as indicated local accommodations and places of interest. We always strongly encourage patients to bring along a family member or friend. A health history form is mailed ahead of consultation with the reminder letter. We request patient's medical history, surgeries, medications, demographics, and insurance. This information is reconciled at time of consultation. A phone call reminding the patient of their consult date and time is made ahead of time as well.

The patient will meet with the nurse practitioner and receive a comprehensive history and physical examination as well as an overview of all pertinent available treatment options, in particular IGTA.

Table 10.3 Guidelines for administering IV contrast

For patients with eGFR > 60: No special preparation
For patients with eGFR < 60:
1. Consider low-osmolality CT contrast (Visipaque)
(a) Hospitalized patients for elective imaging in CT department:
Consider holding loop diuretics and NSAIDS 48 h prior to scanning
500 mL of 0.45 % normal saline pre *and* post contrast (total 1 l)
Recheck creatinine in 24–48 h. Encourage oral intake as indicated. Nephrology referral as indicated
(b) Outpatient CT scanning:
For patients *with* cardiac history (CAD, CHF):
Consider holding loop diuretics and NSAIDS 48 h prior to contrast
Day before CT contrast, instruct oral hydration 1–2 l of water
Day of CT, administer 500 mL 0.45 % normal saline bolus prior to *and* post contrast
Patient oral hydration 500–1,000 mL of water on the day of CT and day after
No history of CAD or CHF:
500 mL bolus NS 0.9 % before *and* after CT contrast
Patient oral hydration 1,000 mL day of and after CT contrast
2. Recheck creatinine in 24–48 h

Source: Department of Diagnostic Imaging, Rhode Island Hospital, Brown Medical School Residency Manual. Most recent review and revision June 2010. Hydration recommendations, pp. 42–43 from Katzberg, R. Lecture at ARRS Boston, 2009

Table 10.4 Consult note for radiologist from referring physician

Full result: Interventional radiology tumor ablation services new patient consultation for biopsy confirmed 1.8-cm left lower lobe adenocarcinoma with bronchoalveolar features
HPI: Mrs. L is a pleasant 74-year-old female who is accompanied by her daughter today. Patient was originally referred to tumor ablation services by pulmonologist Dr. WD. Apparently, patient developed some abdominal pain this past spring and underwent a CT of the abdomen which demonstrated an incidental nodule in the left lower lobe. CT performed at XRA on 04/09/2010 demonstrated a 1.8-cm left lower lobe nodule. Biopsy of left lower lobe nodule was performed at Rhode Island Hospital on 04/30/2010. Final pathology was consistent with well-differentiated adenocarcinoma with bronchoalveolar features. PET/CT performed on 05/21/2010 redemonstrated left lower lobe nodule with mild FDG activity. No evidence of distal disease
Currently, other than chronic shortness of breath associated with her emphysema, patient remains without any dry or productive cough, pain, or hemoptysis
Past medical history: Non-small cell lung cancer, chronic obstructive pulmonary disease/emphysema, hypertension, anxiety, IBS, osteoarthritis, hypertension
Past surgical history: Cholecystectomy
Social history: Widowed, 8 children, retired, lives in her own condo independently
Family history: Negative
Habits: 2–1/2 packs per day × 35 years, quit 1988, 1–2 drinks per day, stopped walking and swimming about 2 weeks ago
Medications: Spiriva once daily, Symbicort 2 puffs 1–2 times daily, Ativan 0.5 mg 2 tablets qhs and prn, albuterol prn, metoprolol 50 mg twice daily, Diovan/HCT 0320/25 mg once daily, Prilosec 20 mg once daily, Tylenol prn, Bentyl prn, OTC sleep fast prn
Allergies: Adverse reaction to Benadryl causing jitters, no known drug allergies, no known IV contrast allergy
Diagnostic and clinical tests: CT, PET/CT, and pathology as above. On 05/12/2010, pulmonary function tests FEV1 43 % of predicted and DLCO 30 %
Labs: 04/27/2010: PT 10.6, INR 0.97, PTT 28.8, platelet 324,000, creat 1.2
Physical exam: Temperature 98, pulse 68, respirations 16, blood pressure 130/68
General: Patient alert, oriented × 3 in NAD. Skin: warm, dry, and intact. Neurological: grossly intact and nonfocal. HEENT: PERRLA, sclera anicteric. Oropharynx clear. Neck: supple, negative carotid bruit, no lymphadenopathy or thyromegaly. Chest: CTA, no rhonchi, rales, or wheezes. Heart: RRR, S1 S2, no S3 S4, no GRM. Abdomen: no HSM, no palpable masses. MSK: full ROM. Extremities: no clubbing, cyanosis, or edema
(*continued*)

Table 10.4 (continued)

Total face time spent with patient was over 60 min. After meeting with myself and Dr. DD and reviewing patient's past medical history, current health status, and current imaging, patient is deemed an appropriate candidate for percutaneous CT-guided radiofrequency ablation of 1.8-cm left lower lobe lung tumor. The ablation procedure was explained in great depth and detail; any and all questions were answered. Alternatives to ablation procedure were discussed. Patient was consulted by thoracic surgery; patient is not an optimal surgical candidate and is not interested in pursuing surgery. Benefits, limitations, and risks of the ablation procedure were discussed. They include, but are not limited to, infection, hemorrhage, incomplete treatment, nerve damage, diaphragmatic injury, intestinal perforation, surrounding soft tissue and organ damage, pneumothorax, chest tube insertion, cavitation, bronchopleural fistula, hospitalization, temporary or permanent oxygen dependence, respiratory failure, and remote chance for death. A tentative date for ablation has been scheduled for Monday, June 7 at 10:00 a.m. Pre-procedure instructions were given and reviewed. Medication instructions were reviewed. Patient/family were instructed to contact office with any questions
Impression: 1.8-cm left lower lobe non-small cell lung cancer. Lesion is technically amenable to percutaneous CT-guided radiofrequency ablation scheduled as above. Cluster electrode will be utilized

One hour, at minimum, should be allotted for the midlevel to take an accurate history, explain the procedure, and perform a physical exam. They will then meet with the interventional radiologist to answer any remaining questions. He/she will discuss whether treatment with ablation is aimed at cure or palliation or, in other words, whether we expect partial or total response from IGTA. We will also inform the referring physician if additional or adjunct therapies such as surgery, radiation, or chemotherapy may be necessary to augment our treatment. Please see example of a consult note (Table 10.4). This consult method saves the treating radiologist a significant amount of time and allows them to literally step out of the reading room for a few moments or see a patient in between procedures for a relative short amount of time. At the end of the consultation, specific written pre-procedure ablation instructions are given and reviewed with the patient and family (Appendix 10.1).

Department of Diagnostic Imaging/Interventional Radiology

Rhode Island Hospital
A Lifespan Partner

CT Guided Thermal Ablation Preparation Instruction Sheet

We have scheduled you to have an image guided tumor ablation to be performed in the CT Department of Rhode Island Hospital.

Procedure: _____

Procedure Date: _____ Arrival Time: _____

The Week Before:

1. You will need to ***STOP***
   Your last dose of
2. You will also need to ***STOP***
   Last dose of
3. It is OK to take acetaminophen (Tylenol) or other prescription pain medications as directed.
4. Blood work due by.
   You do not need to fast for this blood work. Please take the enclosed lab slip with you to the lab of your choice.

The Night Before:

1. Nothing to eat or drink after midnight.

The Day of the Procedure:

1. In addition to the above medication instructions, see below:
   _____
   _____
   _____
2. Morning of procedure, you may have sips of water with your medications EXCEPT those listed above.
3. If you have any inhalers, then please take ALL of your inhalers as prescribed.
4. **Bring a list of your current or newly added medications with you and a list of any medication allergies.**
5. If you do not speak English, please bring a family/friend who does speak English.
6. Morning of the procedure, report to the second floor CT/Ultrasound Department on the second floor of the Meehan Building and check in. You will then be escorted to the Radiology Recovery Room.
7. The procedure and recovery time varies, but can take up to 5–6 hours. For any complications, a hospital admission may be required.
8. **You will need someone to drive you home and stay with you the night of the procedure.**

If you have any questions, please call Tumor Ablation Services at (401)444-5707.

Appendix 10.1

Although my personal role is managing the Rhode Island Hospital IGTA service, I continue to act as an interdepartmental liaison to ensure comprehensive evaluation and care. When we are coordinating consults for in-state and out-of-state patients alike, we try to consolidate the patient's visit to the hospital to include any other necessary medical consults or testing on the same day. Coordinating this care and schedules can be more daunting than it first presents, but it does provide the patient with the ease and convenience of a true comprehensive cancer care experience [6].

For out-of-state patients, a 3-day visit is planned. On the first day, any necessary imaging is performed along with the consultation. On the second day, the ablation procedure is performed. On the third day, any necessary follow-up imaging is ordered prior to follow-up visit, and a physical exam is performed to assess patient's response to treatment. Patients are also made aware that they may require more than one ablation procedure to entirely rid them of their tumor; hospitalization or a delay in returning home may also occur.

Unless patient condition warrants, we book procedures 1–2 weeks out from initial consultation. This allows time for referring physicians to be notified, insurance companies to be contacted, prior approval to be obtained, and any other necessary hospital resources to be set in place (e.g., electrophysiology for interrogation of pacemakers). If a patient requires general anesthesia for their ablation procedure, this is arranged by the midlevel. From our experience, it takes about 2–3 weeks to coordinate an elective CT procedure with general anesthesia at our hospital. If you do need to schedule a procedure with anesthesia, we have found that it is more efficient to perform lab work, EKG, and any other pre-procedure testing ourselves. We then touch base with anesthesia via e-mail and send our history and physical and lab results. If patient condition (i.e., age, cardiovascular disease) warrants, anesthesiologist will request a consultation with them. Otherwise, younger or relatively healthier patients are seen the morning of the procedure. For all procedures, we order any necessary lab work (e.g., creatinine, complete blood count, and coagulation studies). We also make any necessary medication adjustments (i.e., insulin, warfarin, platelet aggregation inhibitors, nonsteroidals, etc.) Our secretary faxes the imaging reports and consults notes to all doctors involved. This way all the providers are kept abreast of their patient's care. Our midlevel fills out all the appropriate booking sheets to ensure accurate description of procedure and to cut down or eliminate the incorrect procedure from being ordered.

Another variable to factor in to scheduling ablations and consults are the interventionalists' schedules. Ideally, one should make every effort to have doctors here on consistent days for ablations and consults. For a routine ablation, we block a 2-h time slot in CT scan or ultrasound. If you are relatively new to ablation procedures, you are not equipped with CT fluoroscopy, the tumor is above average size, or you are planning cryoablation, you may want to allow for more time. Initially, it also helps to have an industry representative at hand to troubleshoot any technical or equipment issues during the ablation until you are comfortable with the technology.

We prefer to perform ablations in the mornings as this allows patients time to recover and be discharged by the afternoon. It also allows time to admit the patient under the appropriate service if patient condition warrants. We prefer not to admit to the radiology service when patients have significant medical comorbidities but, instead, comanage the patients with appropriate medical service (i.e., medical oncology, pulmonology, or medicine). For routine overnight observation due to prolonged post-procedural pain, nausea, or somnolence, we admit to our own service.

On the day of their ablation procedure, patients report to the hospital 2 h prior to their procedure to allow for parking, registration, and any other unforeseen delays. Patients are consented either at the time of consultation or on the morning of their procedure in the presence of a family member by the midlevel practitioner. We have a designated radiology preparatory and recovery area staffed by recovery and sedation nurses where our patients are seen pre-procedurally. Greater than 95 % of our procedures are performed with conscious sedation on an outpatient basis. The midlevel manages and discharges patients in the recovery area. We have specific post-ablation discharge instructions that are always reviewed with patient and family member or friend (Appendix 10.2). In the event the patient is admitted, the midlevel can assist the resident or attending physician in writing admitting orders in conjunction with the admitting medical specialty. They also round on the patient with radiology residents. If the patient is admitted, the midlevel will provide specific ablation discharge instructions in the inpatient units with a family member present.

Rhode Island Hospital
A Lifespan Partner

ABLATION DISCHARGE INSTRUCTIONS

You have had an ablation of your_____

You may experience some of the following post procedure symptoms:
Localized redness, tenderness, or pain at or around puncture site.
Numbness and/or tingling may occur at site of treatment.
In some instances, you may experience flu like symptoms including fatigue and fever up to 102, typically lasting for less than 72 hours. Treatment is rest, fluids, and Tylenol as directed.

More specific to your particular procedure, you may experience the following:
___ Lung: productive and/or blood tinged sputum for one to two weeks.
___ Kidney: you may have blood tinged urine for the next several days.
___ Bone: increased swelling or pain.

Post procedure puncture care should include changing the band-aid after 24 hours, gently cleansing with soap and water, rinse, dry, and apply antibiotic cream and band-aid once daily until healed.
You may shower after 24 hours.
You may take_____ for pain. _____ pills every ____ hours
You may also take Tylenol (acetaminophen) as directed.
You may take _____ as directed, for bowels/constipation.
You should resume all your usual medications. See below for any specific medication instructions.
You may restart _____ on_____
Blood work due on _____
Additional Medication instructions:_____
_____

Your activity level should progress as tolerated. Light normal activity is encouraged. No driving for 48 hours or as long as you are taking pain medication. No lifting anything heavier than 10 lbs for 7 days.

If experience any of the following or feel that your problem is severe or cannot wait until the next day, you should go directly to the emergency room/dial 911. Bring this discharge sheet with you.
___ Severe shortness of breath, severe pain, fever persisting greater than 4 days. Excessive redness, warmth or discharge from puncture site
___ *Lung*: severe pain or severe shortness of breath.
___ *Kidney*: increased difficulty or inability to urinate, blood in your urine after 4 days.
___ *Liver*: fluid build up in your abdomen, yellow tinged skin (jaundice).
___ *Bone*: inability to move affected limb, excessive swelling, severe pain.

You will be called and scheduled for follow up appointments and radiographic exams.
For questions/clarifications, Monday-Friday, 8 am-4:30 pm. please call 401-444-5707
After hours/weekends to reach the interventional radiologist call 401-444-4000 or 401-444-3434.

Our department will call you the day after your procedure to check on your status.

_____ _____ _____
Physician Signature Patient Signature Date

Appendix 10.2

At our institution, all interventional procedures, including ablations, are discussed at morning report prior to all procedures scheduled for that day. Patient position and modality of treatment (i.e., radiofrequency ablation, microwave ablation, cryoablation) are reviewed and finalized. In addition to ablations being performed as outpatient procedures, it has been our overwhelming experience that a majority of patients tolerate the ablation with conscious sedation. We utilize lorazepam pre-procedurally and midazolam and fentanyl intraprocedurally. This cuts down on the time it takes to schedule an ablation since we do not have to rely on the anesthesia department's schedule. Conscious sedation also cuts down on patient recovery time. Specially trained and certified sedation nurses are present during the procedures to monitor patient's condition, blood pressure, heart rhythm, and pulse oximetry. In addition to the sedation nurse, a radiology resident/fellow and a CT technologist are present during the ablation to assist the interventionalist.

Once the procedure has been completed, the treating interventionalist meets with the family to inform and update them on how the procedure went. Patients recover in the designated radiology recovery area where they are closely monitored. Barring any complications, patients are discharged about 3–4 h after their procedure. The interventionalist sees the patient prior to discharge. The midlevel then reviews specific post-ablation discharge instructions with the patient and family. Patients and families are also provided with contact numbers where they can reach an interventionalist after hours or on weekends. Our department insists that patients make arrangements with family or friends to be with them the night of the procedure. The midlevel calls the patient the following day to assess how they are recovering. A follow-up appointment is scheduled in 2–3 weeks or as necessary. Typically, the first post-ablation follow-up imaging is performed at this visit if it was not performed immediately after the procedure. It is up to the treating interventionalist's discretion as to whether immediate or 2–4-week post-ablation imaging is performed.

There are no universal post-ablation imaging guidelines. We do have our recommended guidelines that we will review. Essentially, post-ablation imaging is done in conjunction with the referring and treating physicians to avoid unnecessary duplication of imaging. We prefer our IGTA department to order post-ablation imaging, as we prefer it to be performed in specific ways to aid in our determining the effectiveness of ablation treatment and to assess for any residual or recurrent tumor. In most if not all circumstances and in order to establish a post-ablation baseline study, a 2–3-week post-ablation CT or MR is performed at the time of follow-up visit. In optimal conditions, results of the imaging are discussed and reviewed with the treating interventionalist. We then discuss results with patients and their family.

From that point on, patients who have undergone an ablation specifically for lung cancer will have follow-up imaging approximately every 3 months. Depending on the pathology and PET/CT avidity, we alternate between CT of chest without and with contrast and PET/CT. Patients who have undergone ablation of lung metastasis (e.g., colorectal, melanoma, carcinoid) have CT of chest without and with imaging alternating with PET/CT typically every 3–4 months. Patients who have undergone ablation of primary liver tumors or metastatic liver tumors that are not PET/CT avid are scheduled for 3-phase liver CT every 3–4 months. In addition to their 2–4 week follow-up CT, patients who are post-ablation for primary renal cell carcinoma undergo 3-phase kidney CT at 6 months and then every 12 months. Depending on physician preference, patient age, and sensitivity, MR may also be utilized to decrease radiation exposure.

The management of an image-guided tumor ablation service remains as evolutionary as the technology. The above is a general outline of what service you may expect. There will ultimately be exceptions and variations to every patient's care which providers must take into consideration. I hope this information is helpful in setting up or guiding your current IGTA service. Please visit our web site at www.lifespan.org for additional information about our ablation service at Rhode Island Hospital.

References

1. van Sonnenberg E, McMullen W, Solbiati L (eds). Image guided tumor ablation: how to build a practice. Tumor ablation principles and practice. New York: Springer; 2005:59–63.
2. Simon C, Dupuy D, Dipetrillo T, et al. Pulmonary RFA: long-term safety and efficacy in 153 patients. Radiology. 2007;243:268–75.
3. Elias D, Baton O, Sideris L, et al. Hepatectomy plus intraoperative radiofrequency ablation and chemotherapy to treat technically unresectable multiple colorectal liver metastases. J Surg Oncol. 2005;90(1):36–42.
4. Ahmend M, Lukyanov A, Torchilin V, Tournier H, Schneider A, Goldberg SN. Combined radiofrequency ablation and adjuvant liposomal chemotherapy: effect of chemotherapeutic agent, nanoparticle size, and circulation time. J Vasc Inter Radiol. 2005;16(10):1365–71.
5. Massachusetts Medical Society Tumor Board Guidelines. 28 Apr 2006. http://www.massmed.org/Content/NavigationMenu/ContinuingEducation/Accreditation/CommitteeonAccreditationReview/Tumor_Board_Guidelin.htm
6. National Coalition for Cancer Survivorship. What is comprehensive cancer care? 2009 policy priorities. http://www.canceradvocacy.org/take-action/nccs-policy/comprehensive.html

Devices and Equipment in Interventional Oncology and Their Operation

11

Paul R. Morrison†

Abstract

This chapter focuses on ablation devices, equipment, and their operation. It exhibits less the principles of ablation than it does with the principal features of the technologies that are employed by the physician-user. These features include the device's "applicator" (or probe) and the user interface. Applicator is a general term given to that element of the overall system that delivers the therapeutic agent to the tumor. The user interface is that with which the physician interacts to control the system to govern the treatment and to monitor the ablation based on feedback from the display.

Ablation can be divided into two main categories: (a) thermal and (b) nonthermal. Thermal ablation is a general term referring to a focal treatment involving an energy exchange with tissue that results in raising or lowering the temperature of the target. Various physical agents can be used as pyrogens and cryogens. Nonthermal ablation involves neither heating nor freezing. Nonthermal approaches include chemical ablation via intratumoral injection, intravenously injected drug-based ablation, and high-voltage electroporation.

Introduction

This chapter focuses on ablation devices, equipment, and their operation. It exhibits less the principles of ablation than it does with the principal features of the technologies that are employed by the physician-user. Throughout the chapter, these features include (a) the applicator and (b) the user interface. (a) Here, applicator (also "probe") is a general term given to that element of the overall system that delivers the therapeutic agent to the tumor. Typically, the applicator is a tool manipulated by the physician and thus navigated through tissues by hand – placing the applicator's active element within the tumor. Of course, tumor identification and instrument navigation are usually performed under some noninvasive imaging modality (US, CT, PET/CT, MRI). (b) The user interface is typically the front panel/display of an electrically powered medical system; overall, the system governs the output of the therapeutic agent to the applicator. The physician interacts with the

†Deceased

D.E. Dupuy et al. (eds.), *Image-Guided Cancer Therapy*, DOI 10.1007/978-1-4419-0751-6_13,

user interface to control the system further (setting/adjusting parameters or activating treatment) and to monitor the ablation based on feedback from the display. The limited feedback from the user interface is often complemented by intraprocedural radiologic images.

Ablation can be divided into two main categories: (a) thermal and (b) nonthermal. (a) Thermal ablation is a general term referring to a focal treatment involving an energy exchange with tissue that results in raising or lowering the temperature of the target. Various physical agents are used as pyrogens for heating tissues; these include electrical current (radiofrequency alternating current (AC)), electromagnetic (EM) radiation (laser light or microwaves), and mechanical waves (high-intensity ultrasound). Contemporary cryoablation devices use high-pressure gas as a cryogen to freeze tissues. The tip of the ablation applicator acts as a heat source to heat or heat sink to freeze; this creates extreme focal temperatures so that cytodestructive temperatures are achieved at a distance from the tip, thus treating a volume of tissue. Generally, a therapeutic effect (tissue destruction) is achieved at or above +60 °C (pyroablation) and at or below −40 °C (cryoablation). (b) Nonthermal ablation involves neither heating nor freezing. Nonthermal approaches include chemical ablation via intratumoral injection, intravenously injected drug-based ablation, and high-voltage electroporation.

Thermal Ablation

Radiofrequency Ablation (RFA)

Radiofrequency ac near 450 kHz has long been utilized as a means to heat tissue for ablation. The various clinical RFA systems involve an electrical circuit that includes a patient's tissues; an RF generator is wired to the RF applicator ("active" electrode) placed within the tumor. A high current density is established within millimeters of this electrode causing ionic agitation and resistive heating. This heat conducts to adjacent tissue creating a volume of ablation. The electrical circuit is closed by having the patient wired back to the RF generator. This is typically accomplished by placing large conductive "dispersive" electrodes ("grounding pads") on the patient, usually adhered to the patient's thighs; this allows the current to exit through the skin with a low current density as it is distributed over the large area of the pads.

In general, the active electrodes are sharp and rigid enough so as to pass through tissue. They are manufactured in a variety of configurations; the primary geometries are "needle" and "array" type. They are electrically insulated along their shaft up to the distal exposed segment whereby the current passes into the tissue; the length of the exposed segments allows for various sizes of ablation volume. Various overall shaft lengths allow for reaching various depths within the body from an insertion site on the skin.

Covidien Cool-tip RF Ablation System

Longstanding in the field is the Cool-tip RF ablation system (Covidien, Boulder, CO). See Fig. 11.1. The standard electrical generator provides up to 200 W of power and 2 A of current at 480 kHz [1]. The system features needlelike active electrodes that are internally water cooled. Cooling these electrodes (at ∼100 mL/min) allows a higher current density at the exposed tip (thus more heat and larger ablation volumes) and yet prevents the carbonization (charring) of tissues immediately adjacent to the tip which would impede current flow and limit the volume of ablation.

The basic "single" electrode (overall length, 10–25 cm) is a 17-G needle with exposed tips 0.7–3.0 cm long; a given length is selected based on the volume to be ablated. The "cluster" electrode combines three parallel single electrodes (each 2.5-cm tip) in one handle; these share the power, are activated simultaneously, and act synergistically. This concept of multiple electrodes for larger ablation volumes is extended with the Cool-tip Switching Controller, an add-on device that allows the use of up to three separate single electrodes (each with a 3.0-cm tip).

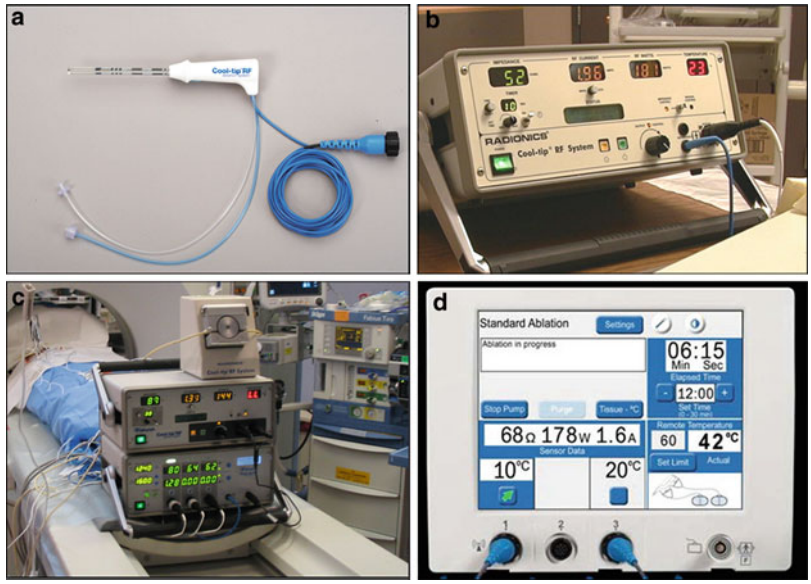

Fig. 11.1 Covidien Cool-tip RF ablation. (**a**) A "cluster" electrode comprised of three individual 17-G electrodes in one handle. *Light blue* and clear tubing provide for flow of coolant to and from electrode tips, respectively. (**b**) Standard Cool-tip generator powers one electrode. Control panel displays time, impedance, current, power, and temperature. (**c**) Standard generator atop switching controller provides power distribution for up to three single RF electrodes for multi-probe RFA. (The peristaltic pump, on top of the standard generator, is for pumping coolant.) (**d**) *Front panel* of the E-Series generator with inherent three-probe capability – connectors (1, 2, 3) seen along *bottom left of panel*. System also displays reading from optional Remote Temperature Probe (here, 42 °C) (Figure parts (**a**) and (**d**) courtesy Covidien, Boulder, CO)

The latter are manually set into tissue at ~1.5-cm distance from each other. Synergy is achieved by cycling full power to each at approximately 30-s intervals.

The Cool-tip RF system can be used in either of two operating modes. Ablation is most often performed in the "impedance control" mode in which the system automatically sets and adjusts the power output. The user selects the duration of the activation (usually 12 min; 16 min for multiple electrodes with the switching controller). The user interface of this system is the front panel of the generator. This offers a set of LED displays that continuously report the tissue impedance (ohms, Ω), current (amps), power (watts, W), elapsed time (minutes), and temperature (C) at the electrode's tip. Notable is that during a typical cooled-tip ablation, the temperature displayed is that of the chilled water. The tissue temperature is evident as the ablation is completed and the coolant flow is stopped. In "manual mode," the user sets the power and duration. This is typically selected when the electrode is purposefully not water cooled, and the user is interested in monitoring and controlling the tip temperature.

A new platform for the Cool-tip is the Covidien E-Series generator (CE cleared; FDA pending) [2]. This system can itself manage up to three individual electrodes. Added feedback features include a button-activated query of tissue temperature during a cooled-tip ablation; current and coolant flow are stopped to allow a read of the tissue temperature from the electrode's thermal sensor. Also, this system supports a separate 20.5-G needlelike Remote Temperature Probe (RTP) to monitor the temperature at the edge of the ablation zone or near a critical structure during ablation – warning the user at some user-defined temperature limit or shutting off the RF power directly. For non-cooled applications and

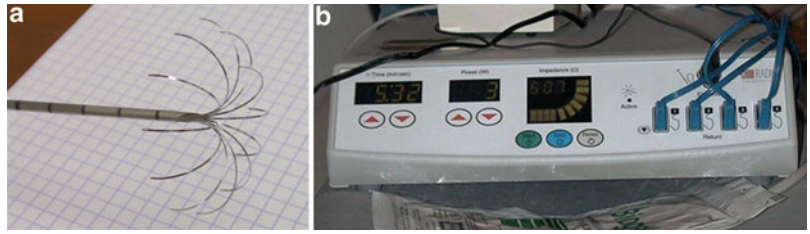

Fig. 11.2 Boston Scientific RF ablation. (**a**) The LeVeen RF electrode is shown with tines deployed forming a 4.0-cm-diameter array. (**b**) RF 3000 generator. From *left to right*, readouts on the front panel show elapsed time, power, and impedance. Rightmost on the panel are the electrical connections for the electrode (*black wire*) and the four grounding pads (*blue*). Time and power are set by the user; however, the display of the tissue impedance provides feedback to the user that serves as the clinical endpoint for the treatment

electrode-track coagulation, the E-Series offers automated self-regulation of electrode temperatures to a user-defined preset value.

Boston Scientific RF 3000 Radiofrequency Ablation System

The RF 3000 (Boston Scientific Corporation, Natick, MA) RFA system provides up to 200 W at 460 kHz. It is historically identified by its array-type LeVeen electrode and its use of tissue impedance as a clinical endpoint [3]. See Fig. 11.2. The electrode is not water cooled. Tissue charring is prevented by the distribution of the current over the multiple tines of the array and by a gradual ramping up of the power from a relatively low initial value.

The applicator is comprised of a sharp bevel-tipped, electrically insulated outer cannula (~13-G dia, 12–25-cm length). After inserting it into the tumor, the physician manipulates a mechanical plunger in the electrode's handle to deploy multiple non-insulated metallic tines out from the cannula's tip. The tines exit radially – though arcing back to form an umbrellalike array from which the current flows. A range of array diameters (2–5 cm) allow for various volumes to be ablated. The electrodes also come in a CoAccess™ version in which the insulated cannula is separate and provides a sharp handleless introducer to accommodate limited CT gantry clearance and can also provide a track through which pre-ablation needle biopsy or injection can be performed. The system also supports a single needle-type electrode (0.9-cm active tip, Soloist™) for small volume ablations.

The most prominent element of the user interface on the BSC RF 3000 generator is the display for the readout of the tissue impedance. At the outset of the ablation, the physician sets the power output to an initial value and then gradually increases it stepwise, manually. The initial power, increments, and maximum settings depend on the size of the array selected. During the ablation, the tissue impedance is monitored. The impedance is observed to rise suddenly by an order of magnitude, indicating tissue coagulation around the electrode; the power is shut off. After a brief pause, a second similar phase of power deposition is applied to assure a thorough ablation – again with the marked increase in tissue impedance as the endpoint for the ablation.

Angiodynamics StarBurst

The StarBurst® Radiofrequency Ablation System (AngioDynamics, Inc., Latham, NY) operates at 460 kHz and provides up to 250 W of power [4]. The system is known for its array-type electrodes and multipoint temperature feedback [5]. See Fig. 11.3. Exemplary is the StarBurst XL 5-cm-diameter array electrode. Housed in an insulated 14-G cannula (10-, 15-, 25-cm overall lengths), the non-insulated array is deployed via a mechanism in instrument's handle. It can be extended partially or fully to achieve a 3-, 4- or 5-cm-diameter ablation. Of its nine tines, five have thermal sensors in their tips. Separately notable is that the distal 5 mm of the cannula itself is non-insulated and can be activated during probe removal for track coagulation.

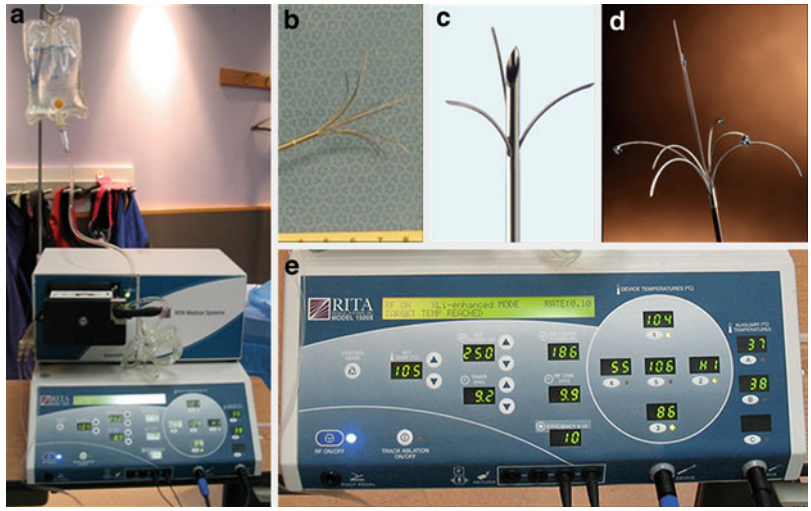

Fig. 11.3 AngioDynamics RF ablation. (**a**) The StarBurst RF ablation system is shown underneath its companion IntelliFlow pump which is connected to a small bag of saline suspended above. (**b**) The StarBurst array-type electrode shown with tines projecting forward from the insulated cannula. Thermocouples in the tips of alternating tines provide temperature readings during RFA. (**c**) The SDE or side-deployed array electrode offers, as its name suggests, an alternative to the standard forward projection of the tines. (**d**) The XLi version utilizes the pump seen in figure part (**a**). A slow perfusion of saline adds to the conductivity to the tissue. (**e**) The user interface of the AngioDynamics generator allows the user to set a desired average ablation temperature (far *left* display; here, 105 °C). Contained within the *circle on the right* are measured temperature values reported from the thermal sensors in the array (Figure parts (**c**) and (**d**) courtesy AngioDynamics, Inc., Latham, NY)

Variations on the StarBurst include the Semi-Flex – the cannula of which has two sections: a distal rigid 12 cm for tissue penetration and a proximal 13 cm that is flexible. A bend of the flex portion can assist in situations with limited CT gantry clearance. Both the XL and the Semi-Flex electrodes are available in MRI-safe versions for magnetic field strengths of up to 1.5 T. The StarBurst "XLi enhanced," intended for treating large tumors, is a 7-cm-diameter saline-perfused array. An external pump provides a slow drip of saline into tissue from the tips of certain tines during the ablation to add conductivity to the tissue. (Note that the saline is not used for the purpose of cooling the XLi electrode).

The most prominent feature of the generator's front panel is the display of the five temperature readings from the thermal sensors in the tines of the array. Automatic temperature control (ATC) mode allows the user to define a target temperature (say, 95 °C) in the range 50–120 °C (instructions for use provide lookup tables for recommended temperature, duration, and power limit). On activation, the system ramps up the power until the temperatures average 95 whereupon the output is modulated to sustain that temperature. It is sustained for a preset duration (say, 7 min) to complete the ablation. If needed, individual thermal sensors in individual tines can be turned off so as not to contribute to the calculation of the average. Separately, (a) the device has automated-track coagulation mode for use during probe removal (tines withdrawn), and (b) the device can support the AngioDynamics 17-G UniBlate electrode intended for small tumor ablations. This is a needlelike electrode with a single thermal sensor. The tip has an adjustable active length (1–2.5 cm).

Celon Power System

The Celon *Power* System (Celon AG Medical Instruments/Olympus Surgical, Teltow, Germany) is a 470-kHz RF generator providing up to 250 W [6]. The system powers the needle-type Celon Pro *Surge* RFA electrode [7].

Fig. 11.4 Celon Power System RF ablation. (**a**) Three Pro Surge bipolar electrodes shown traversing a *thin plastic template* for proper inter-probe spacing. (**b**) Mobile cart transports generator (and optional laptop) and coolant pump system. (**c**) The system's front panel LED displays provide readouts of ablation power, energy, and time. Underneath the readouts are a socket for a footswitch and the plug-ins for up to three electrodes for multi-probe RFA (Images courtesy Celon AG Medical Instruments/ Olympus Surgical, Teltow, Germany)

See Fig. 11.4. In contrast to the monopolar RF applicators described above, the Pro *Surge* electrode is a bipolar device. That is, rather than having the current flow from the active electrode to the separate dispersive electrode(s) located remotely on the patient's body, the current flows between positive and negative elements located together on the needle tip. Grounding pads are not used with the Pro Surge electrodes.

The Pro *Surge* and the MRI-safe *Surge MRI* are 15 G in diameter and 10–25 cm long and are electrically insulated proximally along the shaft to the final few centimeters. The non-insulated active tip (2, 3, or 4 cm) is made up of two adjacent electrodes (one positive, one negative) separated from each other by a small spacer. For smaller and larger volumes of ablation, there is the *Micro Surge* applicator with a sub-cm active tip and the thicker *Surge Plus* at ten French for open procedures, respectively. All these devices are internally cooled with pumped (30 ml/min) room temperature water to prevent tissue charring adjacent to the probes.

The Celon system is a multi-probe system – with connections for up to three bipolar applicators for simultaneous use in treating large tumors. When two or three are used, current flows not only between the elements of an individual bipolar applicator but also between elements of separate probes in an alternating fashion. The system is typically run in its automatic RCAP (resistance controlled automatic power)

mode – whereby the system regulates the power output in response to its internal monitoring of the electrical resistance in the tissue. RCAP mode reduces power when tissue impedance exceeds program limits. RCAP can be turned off for manual power control for end-of-procedure track ablation. A lookup table for setting target RF power and duration is provided by the manufacturer. During treatment, the user interface displays the power, energy (Joules; W-s), and elapsed time; an audible tone provides added feedback about impedance status.

Cryoablation

In contrast with pyrogenic devices are cryogenic systems designed to focally ablate tissues by freezing. In general, contemporary clinical cryoablation systems use a high-pressure gas as a cryogen. The room temperature, high-pressure gas is circulated to multiple needlelike applicators (cryoprobes, cryoneedles). The gas flows from a regulated tank in the room through a micro-tube to the probe's tip where it exits the micro-tube into the small relatively low-pressure space within the probe's tip, and flows back out into the room. Freezing occurs at the site within the probe where the gas exits the micro-tube. This "throttling" of the gas and the resulting drop in temperature are in accord with the Joule-Thomson (J-T) effect. Certain gases such as nitrous oxide, carbon dioxide, and argon have a positive J-T coefficient at room temperature and are suitable cryogens for these clinical systems. (Gas is not released into the patient's body).

While gas-based systems predominate in the field, other cryogens offer alternative solutions. Technologies arriving in the market include the new IceSense3 (*IceCure Medical*, Caesarea, Israel) which uses low-pressure liquid nitrogen for freezing of a single cryoprobe. Separately, a work in progress of note is *CryoMedix, LLC* (Albuquerque, NM) development of refrigerated "single-phase" liquid cooling agents that are circulated in a closed loop offering the potential for adjustable cooling through both rigid and flexible catheters.

Galil Medical SeedNet

The SeedNet cryoablation system (Galil Medical, Arden Hills, MN) is an argon gas-based system [8]. See Fig. 11.5. It and its kin, the Presice and the MRI SeedNet, support the simultaneous independent activation of multiple (as many as 25) cryoprobes. While high-pressure (∼3,500 psi) argon gas is used as the cryogen, high-pressure helium gas (∼2,200 psi) can be used to warm the probes. (Helium has a negative J-T coefficient.) Thus, this two-gas configuration system can first freeze the tissue for treatment and then deliver an active thaw for a quick release of the probes from the frozen tissue. The Presice model is a single gas system that offers a helium-free thaw (i-Thaw) – using warmed low-pressure argon gas to actively thaw the probes after treatment.

The needlelike Galil cryoprobes are 17 G in diameter with an overall shaft length of 17.5 cm and are available with straight or right-angled handles. A thin lightweight gas line leads from the handle to one of the connection ports on the side of the main body of the system. Various probe models (i.e., IceSeed, IceSphere, and IceRod) provide various iceball sizes that can be used in multiple-probe applications to create larger or sculpted ice formations. MRI-safe versions of the IceSeed and IceRod cryoneedles are available for use with the MRI SeedNet system.

The SeedNet's user interface is a computer screen with a touchpad mouse. The system manages the flow of gases to five groups of probes with as many as five probes per group. During treatment, the user can control the five groups independently, selecting from among options of freezing with a full flow of argon gas or actively thawing with helium. Also, the flow of argon to any of the probe groups can be reduced from 100 % to 80 % (or 60 %, 40 %, 20 %, 0 %) for control of ice growth. Additional feedback for the control of the ablation can be obtained using the thermal sensors (TS) and multi-point thermal sensors (MTS). The disposable 17-G sensors can be placed interstitially to provide single-point temperature readings (four separate readings for the MTS). These readings appear on the console to monitor user-defined critical temperatures and can also be used by the system in

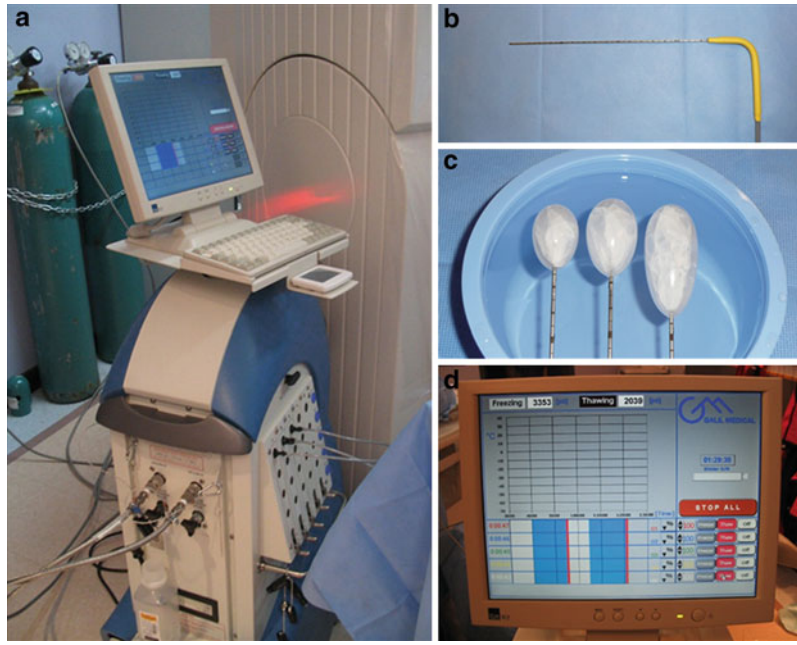

Fig. 11.5 Galil Medical cryoablation. (**a**) SeedNet system with swivel monitor and keyboard. The back of the system is in the foreground showing hoses for argon gas (for freezing) and helium (for active thawing) exiting the system and leading to gas source tanks (*green*) in the background. On the *right-hand side* of the system, the connections for multiple probes can be seen. (**b**) 17-G *right angle* "cryoneedle." (**c**) Sample iceballs formed in water at distal tips of IceSeed, IceSphere, and IceRod. (**d**) Lower half of screen displays treatment history of a freeze, thaw – freeze, thaw cycle (*blue*, *red*, *grey pattern*); probe status (percent flow, freeze, thaw, off) is shown toward the *right*

a controlled mode to automatically adjust gas flow to maintain/limit temperature in a TS' location. The Presice system offers additional on-screen features to the user for treatment planning in kidney and prostate procedures including visualization of intra-procedural US images.

Microwave Ablation (MWA)

Microwave energy delivery for ablation is distinct from RFA. Unlike an RF electrode from which electric current flows into tissue, the MWA applicator is an antenna, electrically driven, that emits electromagnetic (EM) radiation – essentially broadcasting from its tip into the surrounding tissue. No grounding pads are necessary for MWA since the antenna itself is a complete circuit. While the microwave portion of the EM spectrum is broad, ranging from 300 MHz to 300 GHz, clinical MW ablation systems typically operate at one of two frequencies: 915 MHz and 2.45 GHz. Contemporary antennae are all needlelike and range from 17-G thin to 13-G thick. The microwaves are generated by a magnetron within the MWA system and fed to the antenna. Currently marketed systems provide power connections for 1–3 antennae. When activated, dielectric tissue heating occurs – the electric dipole moment of molecules in the tissue (primarily H_2O) oscillates rapidly with the EM waves, transferring energy to adjacent nonpolar molecules.

Most MWA systems, though not all, employ a circulating liquid- or gas-cooling mechanism to prevent the shaft of the probe from overheating; this cooling is to protect the patient and healthcare personnel from burns. The shaft can heat up due to power that is reflected back from tissue during activation of the antenna in turn due to an "impedance mismatch" between the metal antenna and the tissue.

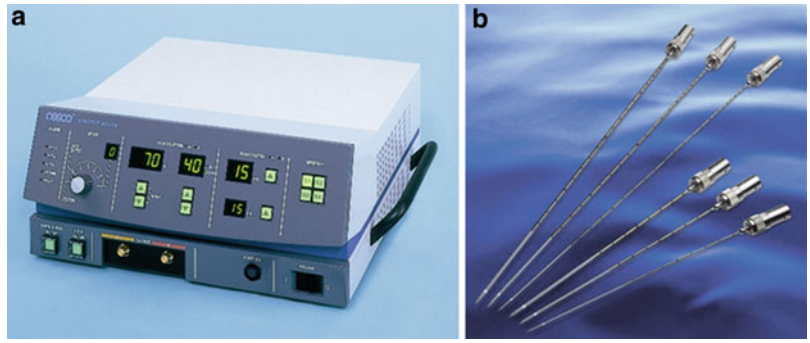

Fig. 11.6 Alfresa Pharma microwave ablation. (**a**) The Microtaze microwave generator provides up to 110 W at 2.45 GHz. Model shown (AZM-520) allows for two antennae to be used simultaneously. The system can have several user-defined preset patterns of ablation power and duration. (**b**) Various needle-type -coated antennae for percutaneous MWA (Images courtesy Alfresa Pharma Corporation, Osaka, Japan)

Alfresa Pharma Corporation AZM-550

The Microtaze AZM-550 MWA system (Alfresa Pharma Corporation, Osaka, Japan) generates 10–110 W of power at a frequency of 2.45 (±50) GHz [9]. See Fig. 11.6. Antennae with various tip geometries are available for hemostasis, tissue resection, and tissue coagulation in open and laparoscopic surgical settings as well as for percutaneous tumor ablation. The system includes a unique "dissociation" feature that is intended to prevent a probe tip from adhering to the ablated tissue – a small direct current is used so as to pull water molecules toward the probe by electroosmosis and thus to soften the coagulum.

The percutaneous MW ablation applicators are needlelike dipole MW antennae. They are available in a disposable version, NESCO Percu-Pro DP, with diameters of 1, 1.6, and 2 mm and overall shaft lengths of 15 and 25. Sterilizable, reusable antennae for interstitial ablation are also available. The probe shafts are not cooled; the manufacturer recommends applying saline to the skin insertion site during ablation to cool the site. The distal tips of the Percu-Pro series are coated in Teflon to provide a nonstick surface which obviates the need for the system's electrical dissociation feature as might be used with other probes. Coaxial cables carry power to the antennae from the system/generator. The AZM-550 can power a single antenna (the 550's predecessor, the AZM-520, powers two antennae simultaneously).

The prominent display components on the front panel of the Alfresa's Microtaze system are the MW "coagulation" power and duration; these can be set at between 10–110 W and 0–15 min, respectively. A separate display shows values of the dissociation current and its duration of between 0–20 mA and 0–60 s, respectively. Typical settings could be 70 W for 60-s coagulation and 15 s at 15-mA dissociation. The coagulation and dissociation can be set to alternate or to run simultaneously; patterns and the repetition of patterns can be selected from preset modes or user-defined cycles that can be stored in memory for frequent use. There is also a slow coagulation function that automatically ramps up the power slowly from zero to a preset value.

Covidien Evident

The Evident Microwave Ablation System (Covidien, Valleylab, Inc., Boulder, CO) operates at 915 MHz and can power a single dipole MW antenna at up to 60 W [10, 11]. See Fig. 11.7. The single-use antennae are available in both a 13-G surgical (VTS series) and a 14-G percutaneous (VT) version. The radiating section of the VTS is 3.7 cm long (shaft length 17 cm), while that of the percutaneous VT (shaft lengths 12, 17, 22 cm) is available as 3.7 as well as 2.0 cm. The shaft of the percutaneous antennae is water cooled during energy deposition from a small reservoir by an external peristaltic pump. A thin power cable exits the handle of

Fig. 11.7 Covidien Evident microwave ablation. (**a**) Sample 14-G antenna for percutaneous ablation at 915 MHz. (**b**) Pair of generators for multi-probe ablation. Display on each shows planned and elapsed durations as well as power setting(s). A single peristaltic pump for antennae shaft cooling sits atop both generators; the small tubular reservoir for the coolant hangs suspended to the *left* of the pump

the probe and leads back to the generator. This electric cable (and the inflow-outflow water tubing in the case of the percutaneous VT) is guarded by an accordion-like thin plastic guide intended to serve as a spacer and protective shield should the cable heat up.

The user interface of the evident generator primarily allows the user to set the power to the antenna and the duration. The timer can be set for up to 30 min. The system indicates when the unit is active and displays the elapsed time. Note that the percutaneous antennae are limited to 45 W and 10 min. Utilization of multiple probes for a procedure requires multiple generators, one for each probe. The peristaltic pump can provide sufficient flow to accommodate three antennae. For multi-probe procedures, small templates are available that can be placed at the skin insertion sites to establish a set spacing between probes, that is, a 1.5-cm distance for the VT probes. Single- and multiple-probe configurations warrant various power-time combinations depending on the desired size of the ablation – the manufacturer's lookup tables provide recommended combinations for planned ablation sizes.

HS Medical AMICA

The HS AMICA, an acronym for Apparatus for Microwave Ablation, is a 2.45-GHz microwave ablation system (HS Hospital Service SpA., Aprilia, Italy) that delivers up to 140 W to a single needle-like MW antenna, the AMICA-PROBE [12].

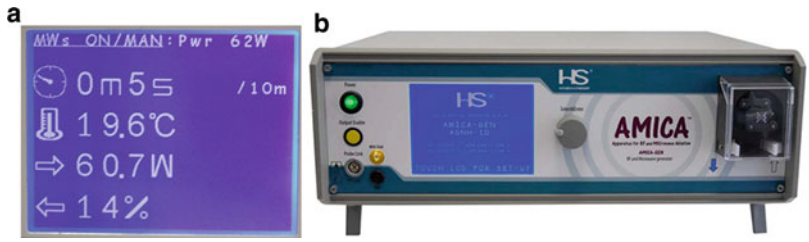

Fig. 11.8 HS Medical microwave ablation. (**a**) Liquid crystal display and touch screen for the HS Medical AMICA-GEN AGN-3.0 2.45-GHz MWA system. Here, the interface reports on elapsed time, probe coolant temperature, output power, and reflected power. (**b**) The new hybrid AMICA AGN-H-1.0 offers 200 W at 450 kHz to a needlelike cooled-tip RF electrode in addition to the MWA capabilities of the AGN-3.0 2.45-GHz MWA device (Images courtesy HS Hospital Service SpA., Aprilia, Italy)

See Fig. 11.8. The AMICA-PROBE is a coaxial dipole microwave antenna, available as 11, 14, and 16 G for surgical and percutaneous applications. A flexible 2.5-mm-diameter probe is available for endoscopic ablation. Probe heating due to reflected power is addressed structurally in the probe's manufacture by a "quarter-wave coaxial 'choke'" at the probe tip which electrically suppresses reflected power, although, in addition, the probe shaft is water cooled by a closed circuit of pump-driven water.

The AMICA-GEN, the system's MW power source and control unit, comes in 100-W (AGN-2.1) and 140-W (AGN-3.0) versions, the latter having an integrated coolant pump rather than an external peristaltic pump (AMICA-PUMP). An LCD touch screen and control/select knob serves as the user interface. The operator can select from manual and automatic modes. A lookup table for power settings and ablation durations is available when selecting the manual mode in which these parameters are user defined. In the automatic mode, a target tissue temperature can be selected, and the device will modify its output based on an internal thermal sensor in the tip. Also, a separate external thermal sensor can be connected to the device to assist in monitoring tissue adjacent to the ablation zone. The user can define a maximum allowable temperature for the thermal sensors or set limits on treatment duration or power output. The LCD screen reports on elapsed time, power, and probe temperature.

In a unique recent development, HS Medical has released, in Europe, a dual modality system that is a hybrid relative to the AMICA-GEN – a single unit that offers a selection of either RFA at 450 kHz or MWA at 2.45 GHz.

NeuWave Medical Certus 140

The Certus 140 2.45-GHz Ablation System (NeuWave Medical, Madison, WI) is equipped with a microwave generator that provides for up to three antennae that can be used simultaneously [13]. See Fig. 11.9. The "triaxial" needlelike antennae (consisting of three concentric longitudinal elements) are manufactured so as to be "tuned" to specific tissues for ablation efficiency (i.e., less reflected power) [14, 15]. These include the 17-G Certus^{LK} for the liver and kidney and the Certus^{LN} antenna for the lung. The radiating segment at the distal tip of either probe type is available as 2.0 or 3.7 cm in length (15 or 20 cm in overall shaft length; with a 13-G 25-cm antenna also available).

The probes connect into the compact Power Distribution Module which can be attached to the patient table (but remains tethered to the generator); this offers plug-in near the interventional field while keeping the main body of the system relatively remote. Each MW antenna shaft is cooled by a CO_2 gas system using the J-T effect instead of flowing water. In addition to a deep cooling that allows for more power to be applied, the CO_2 gas can get as cold as −10 °C so as to freeze part of the distal end of the probe to enable the user to lock it in place, the Tissu-Loc function. Each probe is equipped with three thermal sensors: one to monitor the temperature of this

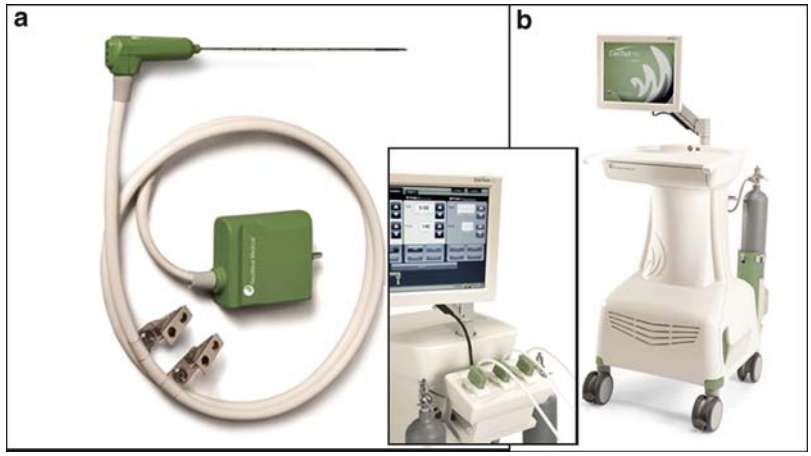

Fig. 11.9 NeuWave Medical microwave ablation. (**a**) NeuWave 17-G Certus antenna. (**b**) Certus 140 system at 2.45 GHz with adjustable computer screen for user interface. Cart supports the small CO_2 tanks (*grey*) for probe cooling during ablation, *inset*. Power Distribution Module on back of cart (shown between CO_2 tanks with three antennae plugged in) can be detached from the back of the cart and attached to CT table near the interventional field (Images courtesy NeuWave Medical, Madison, WI)

Tissu-Loc feature, one in the tip at the site of ablation, and one in the handle for user safety.

As noted above, the system has multi-probe capability. It provides up to a maximum of 140 W of power for a single-antenna ablation. If three probes are used, the generator can deliver a total output of up to 195 W with each channel receiving up to 65 W. The system is controlled and monitored via a computer touch-screen user interface; power and duration are set based on the number of probes and as per lookup tables provided by the manufacturer (i.e., 140 W for 5 min with one probe, 65 W for 10 min with three probes). Visual cues on the control screen as well as on the probe handle itself alert to user to the active delivery of MW energy. The device also features a cauterize mode for needle-track coagulation.

MedWaves AveCure

The AveCure (MedWaves, Inc., San Diego, CA) microwave ablation system features proprietary software that monitors tissue temperature and reflected power during ablation to optimize power delivery to result in more transmitted energy into tissue. See Fig. 11.10. This involves adjustments to the operating frequency over a range of 902–928 MHz (centered at 915 MHz) [16]. The system is designed to power a single monopole antenna at up to 32 W. No cooling of the shaft is required.

The needlelike antennae are 12, 14, and 16 G in diameter with shaft lengths of 15–30 cm. They include integrated temperature sensors. The system can thus be run in a temperature control or power control mode in which the device uses data to modulate MW output to maintain a constant user-defined temperature or power for a prescribed time. A typical ablation protocol is 32 W set for 10 min.

Microsulis Acculis

The Acculis Sulis V^{pMTA} ablation system Control Unit (Microsulis Medical Ltd., Hampshire, UK) provides up to 180 W at a frequency of 2.45 GHz to a single MW applicator [17]. See Fig. 11.11. The system can also support certain surgical applicators such as the 5.6-mm-diameter Accu5i antenna intended for open procedures. The Accu2i is Microsulis' percutaneous dipole antenna: 1.4-cm active tip, 1.8-mm diameter, water cooled, and with overall shaft lengths of 14 and 29 cm. The system monitors the reflected energy back to the antenna as well as the

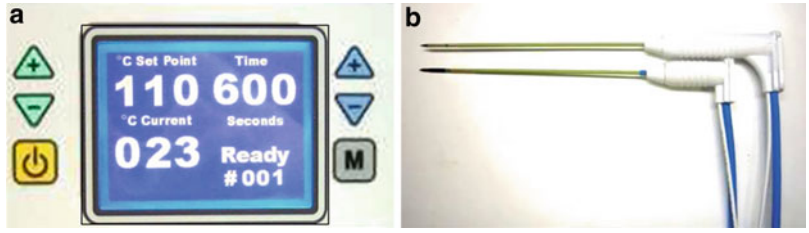

Fig. 11.10 MedWaves microwave ablation. (**a**) Liquid crystal display for the single-antenna MedWaves AveCure 915-MHz system. In temperature control mode, a target temperature (here 110 °C) for the antenna tip can be preset. (**b**) Sample antennae (range 12–16 G) (Images courtesy MedWaves, Inc., San Diego, CA)

Fig. 11.11 Microsulis microwave ablation. (**a**) The 2.45-GHz Sulis V system powers a single MWA antenna. The control panel allows the user to set and monitor ablation duration and power. The bottom row of the panel shows temperature readouts from up to two separate 18-G thermal sensors that can be placed adjacent to ablation volume for added feedback on tissue status (Images courtesy Microsulis Medical Ltd., Hampshire, UK)

temperature of the probe shaft and that of the water coolant. These readings provide feedback to the device for automatic shutdown should values fall outside of a prescribed range.

The control unit houses a touch-screen user interface. Here, the duration and power can be set for a given ablation. Manufacturer's instructions include lookup tables that list desired ablation diameters as functions of power, time, and tissue type (liver, muscle, kidney), that is, a typical liver setting is 120 W for 6 min. During ablation, the touch screen reports time, power, and temperatures. Notably, the unit can support up to two independent 18-G thermal sensors (MTA temperature probes) which can be placed near the ablation field to help in tissue monitoring.

BSD MicroThermX

The MicroThermX Microwave Ablation System (BSD Medical Corporation, Salt Lake City, UT) operates at 915 MHz [18]. See Fig. 11.12. It offers the simultaneous use of up to three probes at a time. When two or three antennae are activated, they operate in a "synchronous" mode such that the electromagnetic waves from each probe have not only the same 915-MHz frequency but also the same phase. Superimposing

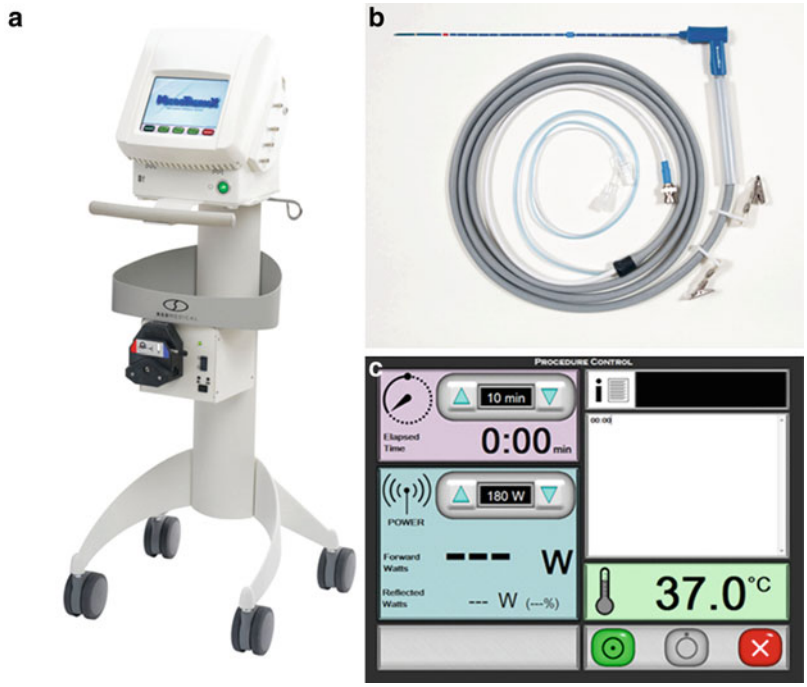

Fig. 11.12 BSD MicroThermX microwave ablation. (**a**) The mobile MicroThermX 915-MHz MWA system. The head of the system includes the touch-screen control panel. On the *right-hand side* of the head are seen connectors for up to three MWA antennae. Just below the waist of the cart in the front is the pump for water cooling of probe shafts during ablation. (**b**) Sample SynchroWave antenna with electrical connection for power and tubing for coolant flow in and out. (**c**) Control panel close-up. Duration and power can be set and monitored on the *left side* of the screen; this includes a report of reflected power. The *right-hand side* of the screen has an information field and readout of the optional 18-G thermal sensor (Images courtesy BSD Medical Corporation, Salt Lake City, UT)

waves with the same phase contribute to constructive interference – whereby the waves add together to enhance power deposition in tissue.

The 14-G SynchroWave antennae are needle-like with a 5-cm active length. Overall shaft lengths range 10–25 cm. These probes are internally cooled with sterile saline via a peristaltic pump to control heating due to power reflected back along the shaft. The generator provides 180 W, up to 60 W to each of three probes. An ablation zone chart provided by the manufacturer guides the user as to probe spacing and parameters. The latter can be set by the user via the procedure control screen which also displays power, time, and temperature during the ablation. Also, there is an optional 18-G TempSure Temperature Sensor that can be used to perform a point measurement of temperature during ablation to monitor adjacent structures. The antenna can perform tract coagulation for coagulating the probe tract on removal post-ablation.

Laser Ablation (ILT, LITT, ILP)

LASER is an acronym for Light Amplification by Stimulated Emission of Radiation. Laser is the noun used to refer to the device whereby the LASER process occurs, and the light energy emitted from a laser is EM radiation. Laser light is typically characterized by its wavelength in microns or nanometers (as opposed to it frequency in Hz as referred to above in discussing microwaves). Depending on the laser system, a range of wavelengths are possible: from the invisible ultraviolet to the invisible far infrared with the visible colors in between. The wavelength of the light that is selected for a medical

application is due to the absorption characteristics of the tissue involved (water content, presence of blood, other chromophores) and the desired endpoint. For interstitial tissue ablation, lasers that emit are the near infrared which are most common – such as the neodymium-doped yttrium aluminum garnet (Nd:YAG) laser at 1,064 nm or diode laser at 980 nm. These wavelengths typically allow for a deeper penetration in tissue. The photons are absorbed and the energy is converted into heat. The light is delivered to tissue by means of a fiber optic cable from the output of the laser system to the distal end. For effective delivery over a volume of tissue and to help prevent charring, the working end usually involves a light-diffusing element whereby the light is emitted radially over the distal few centimeters of the optic. It is possible to use multiple fibers by splitting a primary beam or by using multiple laser systems. For higher energy throughput, the fiber can be cooled (such as by pumped water) so that a higher photon density can be achieved and charring avoided. A historic mainstay for the interstitial delivery of laser light is the water-cooled MR Power Laser Application catheter (Somatex Medical Technologies GMBH, Teltow, Germany), also available in a non-cooled and non-MR versions). More recent to market with an MRI focus on LITT is the Visualase Thermal Therapy System (Visualase, Inc., Houston, TX) [19] and, separately, the AutoLITT (Monteris Medical Inc., Winnipeg, MB Canada). See Fig. 11.13.

Ultrasound Ablation

High-frequency sound waves can serve as mechanical agents of thermal ablation. In procedures commonly dubbed high-intensity focused ultrasound ablation (HIFU) or focused ultrasound surgery (FUS), mechanical waves are transmitted through and absorbed by tissues. In a most common configuration, for transcutaneous treatment, the HIFU energy source is an ultrasonic transducer with a large surface area (*low-intensity* US) that is extracorporeal and is acoustically coupled to the patient's skin "above" the target. The physical shape of the transducer and its associated electronics can focus the transmitted ultrasound beam like a lens to a focal spot (*high-intensity* US) within the body. Further, the transducer can be tilted and translated, and the beam delivery parameters can be modified such that the energy can be delivered as a single (small or large) ellipsoidal focus (a "sonication") or as a timed combination of multiple sonications whereby a volume can be treated.

Important to the delivery of therapeutic levels of ultrasound energy for heating or disrupting tissues is radiological imaging for control of the spatial distribution of the effects. As seen in the sections that follow, MRI can serve to target and monitor the ablation. Alternatively, ultrasound itself can play the roles of both diagnostic and therapeutic components of an ablation system. The latter is exemplified in the Haifu JC Focused Ultrasound Therapeutic System (Chongqing Haifu (HIFU) Technology Co., Ltd., Chongqing, China).

Under a separate paradigm, ultrasound technology can be rendered into an interstitial or intraluminal ablation modality. One promising example is a work in progress (Profound Medical, Inc., Toronto, Canada) utilizing a linear array of small planar ultrasound transducers in an applicator thin enough for transurethral ablation in the prostate. The device adds spatial selectivity to ablation by varying the wavelength of the ultrasound waves applied and can be monitored and controlled by MR imaging feedback.

InSightec ExAblate

The ExAblate magnetic resonance image-guided focused ultrasound surgery (MRgFUS) system (Model 2000 and 2100, InSightec Ltd., Tirat Carmel, Israel) integrates the FUS system with a General Electric MRI scanner (1.5 or 3.0 T) whereby imaging can assist in both targeting the tumor and monitoring the tissue heating [20]. See Fig. 11.14. The FUS system's workstation can communicate with the MRI scanner for control of image acquisition and image data transfer.

The treatment source for the ExAblate is a 10-cm-diameter 211 multielement phased-array transducer (1.61 MHz) located in a dedicated

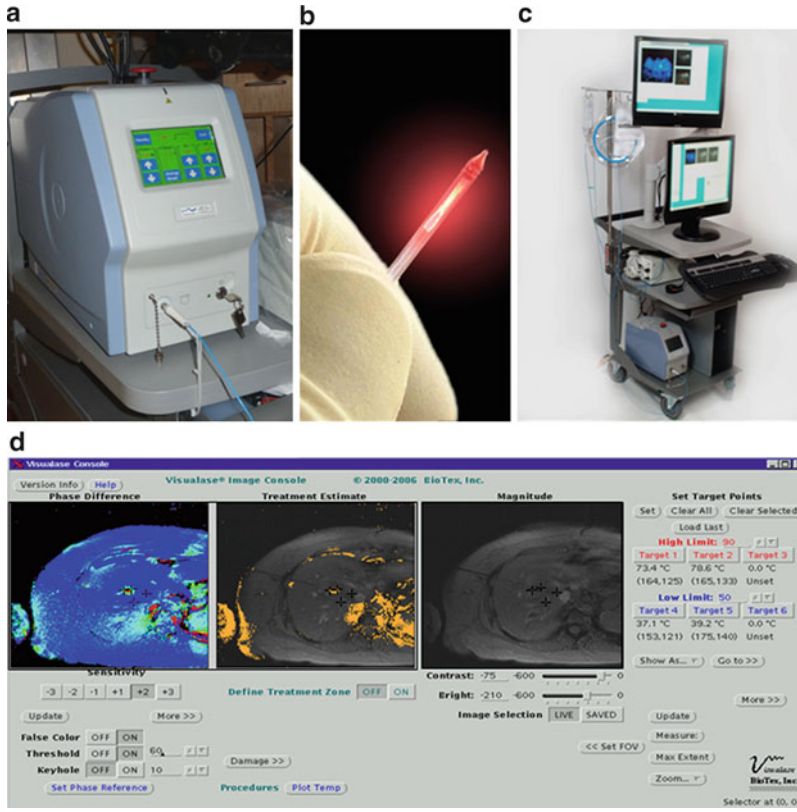

Fig. 11.13 Visualase laser ablation. (**a**) The PhoTex 30 diode laser provides up to 30 W of near-infrared light (980 nm) to a single fiber. A touch control screen provides access to set-up features and for setting output power and duration. (**b**) Visible (*red*) aiming beam illustrates the light-diffusing fiber tip; the sharp catheter in which the fiber is contained is water cooled to prevent charring. (**c**) The complete Visualase system includes a computer workstation for communicating with MRI scanner for thermal mapping during ablation. The laser is seen on the cart's *bottom* shelf. (**d**) The system displays MRI-based temperature map (*left image*) and total thermal dose (*center image*). The user can mark individual voxels in the image for numeric display of temperatures at points in or near the ablation field (Figure parts (**b**), (**c**), and (**d**) courtesy Visualase, Inc., Houston, TX)

MRI patient table and controlled by the FUS system computer workstation near the MRI control console. Images can be acquired prior to and during sonications. The location of the sonications can be adjusted by manipulating the angle (and pitch and roll) of the transducer. Computerized control of the multiple elements of the array provides electronic control over the size of the focal spot (ranging $\sim 2 \times 2 \times 4$–$10 \times 10 \times 35$ mm) and also the depth of the focal spot into tissue (5–20 cm). A sample set of parameters for a sonication is 70 W for 20 s over a $5.6 \times 5.6 \times 28$ mm focus. Multiple adjacent foci can be delivered to ablate a volume of tissue.

The FUS workstation provides a user interface for managing parameters and monitoring the treatment. It receives images from the scanner for treatment planning that help the user assess suitable beam paths and to select input parameters such as acoustic power, duration, interval between sonications, and focal spot size. The user can also fine-tune the energy deposition with modifications to the selected frequency to adjust for defocusing of the beam due to various tissues in the path. The FUS workstation provides image feedback during treatment that includes thermal maps calculated from the thermally sensitive MRI scans acquired during sonication and thermal dose maps based on time-temperature profiles.

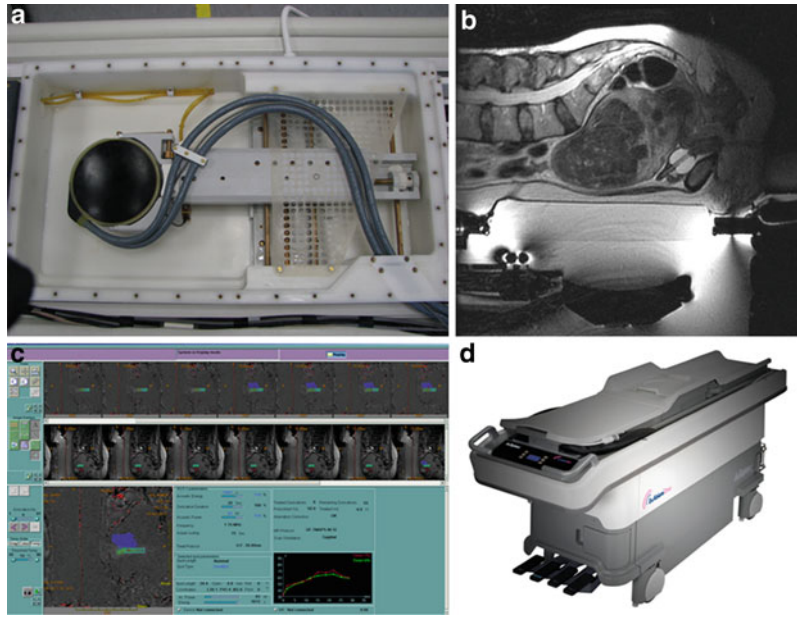

Fig. 11.14 InSightec ExAblate focused ultrasound surgery. (**a**) Multielement 10-cm-diameter phased array transducer built into MRI scanner's patient table. Computer control provides translation and angulation of the treatment beam. (**b**) MRI image illustrates relative position of anatomy above and FUS transducer (seen in cross section as *curved black silhouette*) below. (**c**) Computer software displays MRI-derived heat and dose maps. Lower *left image* displays temperature of current sonication (*green*) with background of previous treated regions (*blue*). (**d**) ExAblate one table replaces standard MRI scanner table (Figure parts (**a**), (**c**), and (**d**) courtesy InSightec Ltd., Tirat Carmel, Israel)

Philips Sonalleve

The Sonalleve MR-guided high-intensity focused ultrasound (MR-HIFU) system (Philips Medical Systems, Andover, MA) is an option that is available for the Philips 1.5- and 3.0-T Achieva MRI scanners [21]. See Fig. 11.15. The HIFU source is a 13-cm-diameter spherically shaped ultrasound transducer that operates at a primary frequency of 1.2 MHz and is composed of 256 individual elements. It is incorporated into a special add-on MRI scanner tabletop and can be mechanically moved within the confines of the tabletop by horizontal and vertical translation and tilting. Computerized control of the transducer's elements and its position within the table allow for individual sonicated volumes of ablation, "treatment cells," of various diameters (4, 8, 12, 16 mm). Larger cells can be treated in a "volumetric" sonication in which the US beam follows a spiral "trajectory" outward from the cell center.

The user interface for the Sonalleve is a computer workstation that provides the user with a selection of sonication modes and parameters of power, duration, and limits. MRI images identify the orientation of the transducer in the table, and thus, the ultrasound beam path can be reviewed by the user. The path and planned treatment cells can be adjusted to avoid critical structures and optimize the treatment. During sonication, temperature data (calculated from the MRI image data) can be updated rapidly (∼every 3.5 s or less). In addition to this temperature feedback, thermal dose maps based on time and temperature can be displayed to view cumulative effects. An individual sonication's duration can also be controlled automatically by this MRI-temperature feedback – whereby the beam can be made to advance to another part of the target based on some preset limit on temperature or dose. The system also reports on various parameters such as reflected power to assist in assessing efficacy and safety.

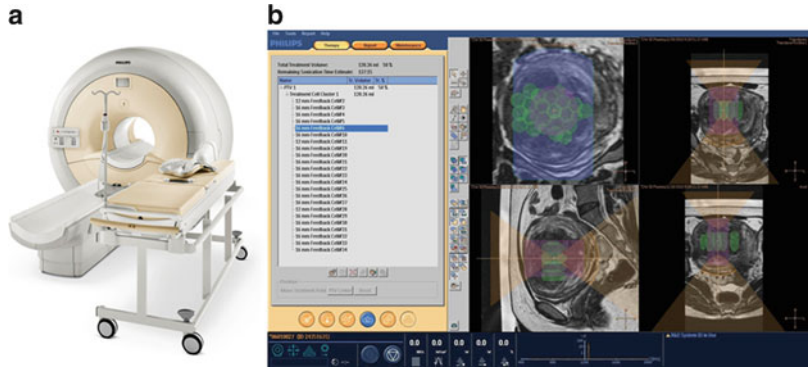

Fig. 11.15 Philips Sonalleve's high-intensity focused ultrasound ablation. (**a**) Philips HIFU tabletop adjacent to standard scanner table for MRI-guided ablation. (**b**) The user interface is computer based, providing sophisticated image-based planning, dosimetry, and monitoring. In the planning mode shown, multiple sonications are planned for throughout a volume. The ovoid sonications are seen as *green circles* in cross section in the coronal planning image (*upper left*) and as *green ovals* in the sagittal image (*lower left*) (Images courtesy Philips Medical Systems, Andover, MA)

Nonthermal Ablation

Irreversible Electroporation

AngioDynamics NanoKnife

Irreversible electroporation (IRE), as an ablative modality, is a nonthermal treatment in which the permeability of cell membranes is affected. The ablative agent is a series of high-voltage pulses delivered by a pair (or pairs) of interstitially placed electrodes. Thus, within a volume of tissue, cell membranes are exposed to a pulsed electric field above the threshold at which the cells' permeability to ions and macromolecules is increased irreversibly with a negative impact on the health of the cell. Various operating parameters impact the outcome of the effects. These include electric field strength (in volts per centimeters, V/cm), pulse duration (microseconds), frequency of pulses (Hz), and total number of pulses or duration of exposure. Of interest is that the IRE tissue ablation effect is not susceptible to heat sink or heat source effects as can be the case for thermal ablation methods, and the architecture of connective tissues is spared since the tissue is not coagulated by heat.

The NanoKnife system (AngioDynamics, Inc., Queensbury, NY) includes a generator and applicators designed for the controlled delivery of pulses of energy for the clinical implementation of IRE [22]. See Fig. 11.16. The applicators are needlelike, and the basic configuration is a pair of electrodes 15-mm apart between which the voltage is established [23]. (Notably, no grounding pads are needed as a return path to the generator). Up to six probes can be connected; system software coordinates the voltage between possible pairings. Aside from the number of electrodes, the user selects the electrode type based on the length of the non-insulated tip (ranging up to 4 cm). The NanoKnife pulse generator can deliver 10–100 high-voltage 20–100 μs long electrical pulses at a frequency of greater than 90 pulses per minute and at field strengths of 500–3,000 V/cm. Manufacturer's lookup tables provide information about optimal probe spacing and the various ablation parameters.

The system interface is a keyboard and LCD computer screen. The interface provides for an interactive probe placement process with a planning grid to determine the number of probes for a given target with click-and-drag probe adjustments. The plan can be further modified as the actual probe configuration is observed during the procedure. The Pulse Generation Screen enables settings and provides a test pulse of energy to check impedance. The system

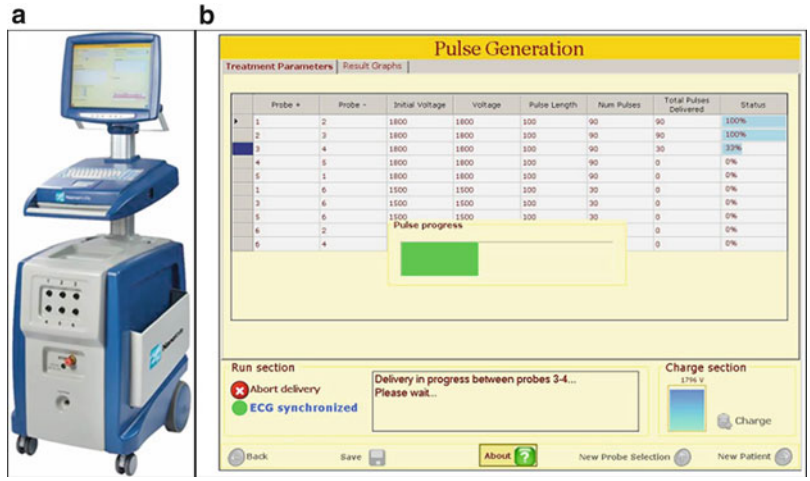

Fig. 11.16 AngioDynamics IRE. (**a**) NanoKnife system for nonthermal ablation by irreversible electroporation. Ports for as many as six electrodes are seen on the front of the main body of the system. (**b**) Progress of the ablation is monitored as the percent completion of planned high-voltage pulses between possible pairings between all electrodes placed (Images courtesy AngioDynamics, Inc., Queensbury, NY)

then tracks the overall progress of the ablation, the number of pulses for various pairs, and the percentage of the planned pulse count for the various pairs.

Photo-Activated Drugs

Light Sciences Oncology Aptocine

Aptocine (Light Sciences Oncology, Bellevue, WA) is a drug (talaporfin sodium) that is currently under investigation for ablation of solid tumors in various organ systems [24]. When activated by its disposable light source, the energized drug generates singlet oxygen within a volume of tissue – this presents direct cytotoxic effects as well as secondary vascular damage and a possible antitumor immunologic response. The photoactivation of the drug is nonthermal – the drug provides no treatment unless activated, and the light itself is not therapeutic in the absence of the drug.

The applicator for the treatment, the drug activator, is a 1.2-mm-diameter linear array of tiny 664-nm red light-emitting diodes (LED) tethered by a microwire to a very small on/off control unit. See Fig. 11.17. The LED array can fit within a catheter and can thus be placed interstitially. Multiple activators can be used simultaneously to treat larger volumes. Once the activators are in place, Aptocine at ~1 mg/kg is injected into the patient intravenously and the LEDs are powered on (at ~20 mW/cm) for a preset time (targeting a total energy of ~200 J/cm). A small liquid crystal display on the power supply keeps time as the endpoint for the exposure.

Injectables

Rex Medical Quadra-Fuse

Quadra-Fuse (Rex Medical, Conshohocken, PA) is a mechanical device. It is an injection needle in an array-type configuration engineered to provide a more even distribution of injected liquid agents such as ETOH over that of a simple straight needle [25]. See Fig. 11.18. After placement of the 18-G cannula in tissue, the three tines of the array are deployed by manipulating the handle. The tines are not in fact solid but are fine 27-G stainless steel tubes with four machined micro-holes at each tip through which fluid can be injected. While the symmetry of the three tines about the axis of the cannula helps the distribution of the liquid, a more homogeneous distribution can

Fig. 11.17 Life Science Oncology. A small power/supply with clock is shown wired to the 1.2-mm-diameter array of LEDs (*red light*). The latter is placed interstitially, and treatment is effected by activation of intravenously injected Aptocine (vial) by the light (Image courtesy Light Sciences Oncology, Bellevue, WA)

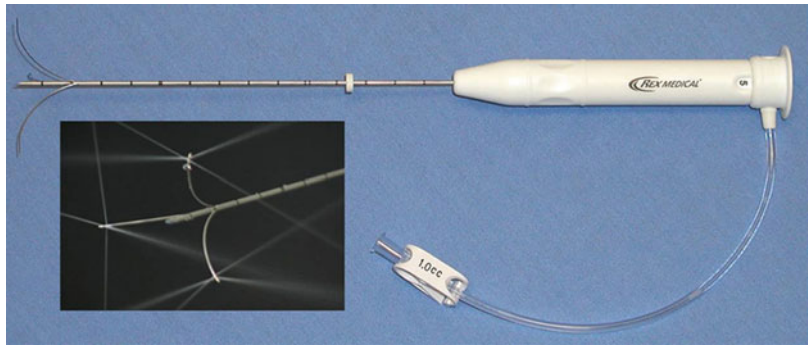

Fig. 11.18 Rex Medical Quadra-Fuse. The array-type configuration of the hollow tines of the device allows for a more even delivery of liquids (such as ETOH) in tissue, *inset*. Micro-holes in each of the tines assist in the distribution. Further, tine deployment can be done incrementally for staged deposition over a volume (Images courtesy Light Sciences Oncology, Bellevue, WA)

be achieved by a staged deployment of the array. As an example, the standard Quadra-Fuse needle deploys fully to 5 cm, but it is designed to open stepwise as 1, 2, 3, 4, and 5 cm – thus providing for partial injections throughout the volume. To withdraw the tines and to redeploy after a rotation of the cannula can also assist in the distribution. Overall shaft lengths available for the cannulae are 10, 15, and 20 cm. The alternative short tip model deploys to a maximum of 2 cm.

Closing

This chapter attempts to sweep the full spectrum of today's technical approaches to ablation. While the reader may thus appreciate the breadth and diversity of this topic, it is difficult to have a definitive and exhaustive list of companies, products, and device features in any snapshot of a field. Also, there are always advances coming to market and new ideas being implemented.

Examples include ablation devices specialized for certain disease states such as the versatile M1004 (RF Medical Co., Ltd., Seoul, Korea) for myolysis and, separately, the Halt Fibroid RFA System (Brentwood, CA); novel new designs such as the spiral elements of the bipolar RFA Encage System (Trod Medical, Bradenton, FL); and also devices based in eastern markets such as the 2.45-GHz Forsea MTC-3 (Forsea Microwave & Electronic Research Institute, Nanjing, CH). Readers are encouraged to investigate the device marketplace beyond this chapter to pursue details, to recognize their own preferences, and to assess the suitability of an approach for one's given clinical environment (e.g., OR vs. IR). Lastly, beyond the devices and their operation, readers are also encouraged to study the physical principles behind a chosen modality to be certain of the full scope of a given device's utility (or limitations).

References

1. Valleylab cool-tip RF ablation system user's guide. Valleylab, Inc.; 2009.
2. Covidien cool-tip RF ablation system series E user's guide and maintenance instructions. Valleylab, Inc.; 2009.
3. Instructions for use – the LeVeen family of electrodes. Boston Scientific Corporation; 2004.
4. RITA 1500X user's guide and service manual 160–103990 Rev03. AngioDynamics, Inc.
5. RITA® StarBurst® Model 75, StarBurst® SDE electrosurgical device, StarBurst® XL electrosurgical device, MRI compatible StarBurst® XL device, MRI compatible StarBurst® SEMI-FLEX electrosurgical device instructions for use 160–104121 Rev 02. AngioDynamics, Inc.
6. Olympus Celon LabPower instructions for use WB135400-W11 (2010–03). Celon AG Medical Instruments/Olympus Surgical; 2003.
7. Olympus Celon LabSurge BiPolar coagulation electrode instructions for use WB135418-W11 (2010–02). Celon AG Medical Instruments/Olympus Surgical; 2009.
8. PresIce user manual DOC000134B-ASMCH0477 Rev B. Galil Medical Ltd.; 2009.
9. Operation manual Microtaze AZM-520. NESCO Co.
10. User's guide MW ablation generator 1012655. Valleylab, Inc.; 2008.
11. Evident MWA percutaneous antenna instructions for use 1011085. Valleylab, Inc.; 2009.
12. HS AMICA user's manual release 2.1. HS Hospital Service SpA; 2010.
13. Certus 140 microwave ablation system user reference manual [Software Version 1.0.0.337]. NeuWave Medical, Inc.; Draft 3/10/10.
14. Certus 140 percutaneous ablation probes instructions for use. NeuWave Medical, Inc.; Draft 10/04/10.
15. Certus 140 surgical ablation probes instructions for use. NeuWave Medical, Inc.; Draft 10/04/10.
16. MedWaves microwave ablation system (MWA) system description. MedWaves Inc.
17. Acculis Accu2i pMTA percutaneous microwave tissue ablation applicator instructions for use 62836-09-001 Issue 2.0. MicroSulis Medical Ltd.
18. BSD medical MicroThermX microwave ablation system instructions for use (IFU) #10-17258 Rev G. BSD Medical Corporation; 2010.
19. Visualase thermal therapy system instructions for use. Visualase, Inc.; 2010.
20. ExAblate 2000/2100 1.5 and 3.0 T information for prescribers [System Version 4.2 2009]. InSightec; 2009.
21. Sonalleve Release 2.1 MR-HIFU Fibroid therapy system instructions for use 4510 000 79024 998112D/781. Royal Philips Electronics N.V.; 2010.
22. User manual United States Edition [Software Version 160–103720 Rev 01 2.1.0]. AngioDynamics, Inc.; 2009.
23. Single electrode probe NanoKnife irreversible electroporation instructions for use IC 038 Rev D. AngioDynamics, Inc.; 2010.
24. Light sciences oncology company background and information. Light Sciences Oncology; 2010.
25. QuadraFuse/QuadraFuse ST instructions for use P-4018-0166-00-Rev B. Rex Medical.

Designing Interventional Environments in the Treatment of Cancer

12

Jeffrey Berman and Yuman Fong

Abstract

The last two decades have seen remarkable advances in imaging and procedural-guidance technology. Enhancements in computing, sensors, and data processing now allow many imaging modalities to produce information that can be displayed, transmitted, and utilized in real time. This has allowed the immediate use of imaging modalities to guide surgery and interventional therapies, with improvements in patient care and outcome. Until recently, diagnostic imaging, surgery, endoscopy, and interventional radiology had developed and evolved fairly independently. In the past, procedural rooms were generally designed with a single discipline in mind. We are now asked to construct enhanced work environments which support multidisciplinary workflow and novel-navigated therapeutic procedures. In these new image-enhanced working environments, the collection, processing, and display of information are rapidly evolving. Accompanying these changes in the workflow is increased demands on staff, on infrastructure, and on additional equipment needed to support integration of new technologies. This chapter discusses the design of these rooms. The goal in interventional OR design is to produce functional spaces that are safe and efficient and that have the capacity to support the development and evolution of new technologies and equipment with minimal construction changes.

Introduction

Operating rooms, diagnostic radiology facilities, and interventional radiology suites each have their common and unique elements. As imaging equipment and image processing improves in speed to allow real-time use of images for navigation and monitoring, and with increasing intersection of the needs of interventionists from many disciplines for similar expensive

J. Berman (✉)
Jeffrey Berman Architect, New York, NY, USA
e-mail: jberman@jbarch.com

Y. Fong
Department of Surgery and Radiology, Memorial Sloan Kettering Cancer Center, New York, NY, USA
e-mail: fongy@mskcc.org

D.E. Dupuy et al. (eds.), *Image-Guided Cancer Therapy*, DOI 10.1007/978-1-4419-0751-6_14,

Fig. 12.1 *Preoperative preparation and postoperative recovery room.* For procedures of short duration, a combined pre- and postoperative (universal) room allows for efficient flow of patients and management of morning and afternoon peak patient loads. Private rooms create a comfortable setting for patient and family (Photograph courtesy of John Bartelstone Photography)

equipment, there has arisen a demand for complex, image-guided, interventional rooms [1–5]. The facilities designer is now confronted with technical design and operational challenges not encountered in single discipline rooms. An understanding of the components of room design is particularly important now for clinicians, to allow them to effectively collaborate with the architect in the building of such complex interventional environments. In order to produce useful and efficient hybrid interventional oncology facilities, all members of the design team, including the physicians, must have an understanding of regulatory as well as the facility issues. When doctors, engineers of new technology, and facilities designers collaborate and pool their resources, the result is an optimally functioning facility [6]. The academic therapeutic oncologist designing new technology or novel use of current technology must have even a better grasp of facilities issues to collaborate in the design of these experimental facilities. In this chapter, we will discuss the main considerations in designing the interventional room.

Overview of the Interventional Center

The basic functional and space program for an interventional suite has three major components:

1. *Patient preparation, holding, and recovery areas*: A well-designed preparation and recovery area is essential for efficient flow of patients, which is important for the high turnover reality of modern interventional practices. Such areas require space for reception, waiting, interview and consult rooms, exam rooms, dressing rooms, holding areas, and PACU beds (Fig. 12.1). When well designed, this area provides support for private discussions to alleviate anxieties of families and patients.
2. *Procedure rooms*: Designs of procedure rooms must also account for scrub areas (Fig. 12.2), clean supply, storage, control rooms, and observation space for staff. Additional space must be provided for diagnostic equipment, infrastructure, and storage space for portable or mobile equipment not always in use or fixed in the procedure room.
3. *Support areas*: These areas include staff offices, clean and soiled work rooms, instrument cleaning and processing, clean and sterile supply storage and delivery, waste handling and cleanup, locker and changing rooms for staff, and janitor's closets.

In this chapter, we will restrict our remarks mainly to the procedure rooms. For discussion of the other two areas, the reader is referred to standard texts on these subjects.

Fig. 12.2 *Operating room clean core and work area.* This area provides for scrub sinks, storage area for essential and emergency equipment, as well as quiet work areas for the clinician in proximity to the procedure rooms (Photograph courtesy of John Bartelstone Photography)

Regulatory Issues and Guidelines

Procedure rooms have clearly existed separately in surgical suites, endoscopy areas, and radiology departments. There are common elements for preparation and recovery of the patients and support of staff. These are governed by the Facilities Guidelines Institute and published as "Guidelines for Design and Construction of Health Care Facilities" [7]. This set of guidelines, which sets minimum standards for hospitals, has been adopted by most states. In the past, there were differences between facilities based on the type of procedure performed. Their construction used to be guided by different standards depending on the invasiveness of the procedure, the equipment needs, and the level of anesthesia and life support required for the procedure. More recently, there has been a shift to a common standard for guiding sterile or operating room environments for all invasive procedures with the major design differences related to room sizes. The layouts will vary according to equipment and staffing differences related to the procedure and type of anesthesia used. The time required to complete the procedure and recover the patient will affect infrastructure of the facility, such as emergency power requirements. Generally, in the design of these facilities, we work to produce a unified work environment with consistent work processes, material flows, and computer/device interfaces in each room. Modularity is also used to allow for flexibility of staffing assignments and efficiency in training and orientation.

Definition of the Level of Care: The size and optimal location of the procedure rooms is generally determined by the level of care to be provided. The levels of care as defined by the American College of Surgeons in the FGI "Guidelines" 2010 edition [7] are as follows:

Class A: Provides for minor surgical procedures performed under topical, local, or regional anesthesia without preoperative sedation. Excluded are intravenous, spinal, and epidural routes; these methods are appropriate for Class B and Class C facilities.

Class B: Provides for minor or major surgical procedures performed in conjunction with oral, parenteral, or intravenous sedation or under analgesic or dissociative drugs.

Class C: Provides for major surgical procedures that require general or regional block anesthesia and support of vital bodily functions.

The level of care also affects infrastructure and utility requirements that we will discuss in a separate section.

Size of Rooms: Operating rooms generally start with a minimum floor area of 400 ft^2 (Fig. 12.3a) by modern minimum standards and are regularly built at 600 ft^2 to accommodate

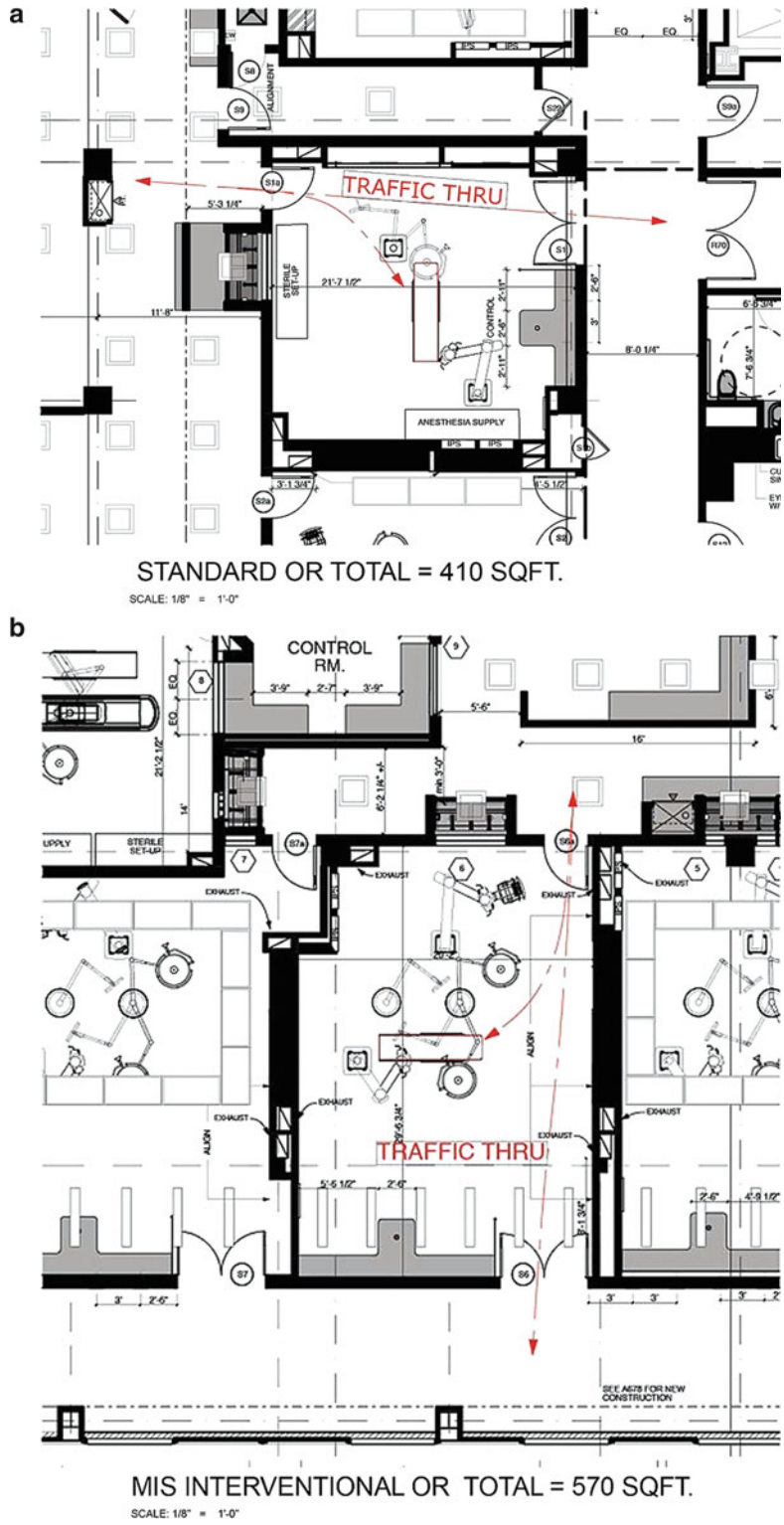

Fig. 12.3 (continued)

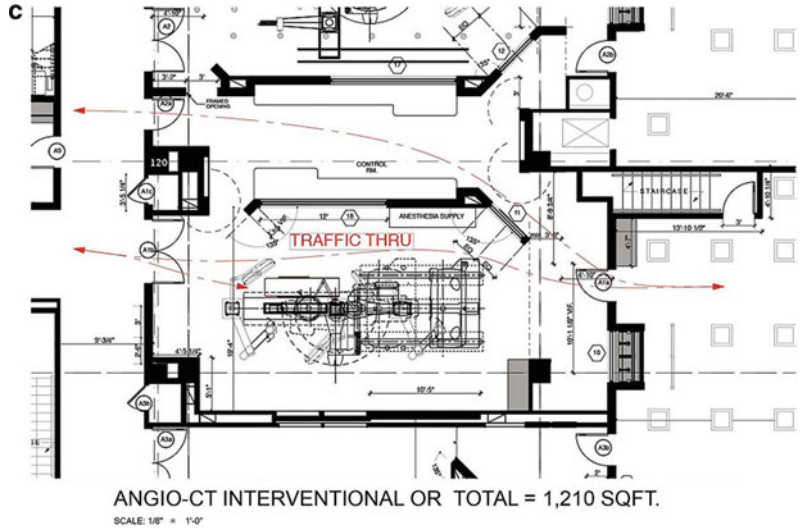

Fig. 12.3 *Typical size and designs of procedure rooms*. (**a**) Illustrates a typical operating room for conventional surgery of approximately 400 ft^2. (**b**) Illustrates a typical room for laparoscopy of approximately 600 ft^2. (**c**) Illustrates a complex imaging procedure room of approximately 1,200 ft^2

Fig. 12.4 *Typical laparoscopic/MIS/general operating room*. This photograph illustrates lighting requirements including ceiling lights, spot LED lights, and green light for dimmed environments. Ceiling mounts in the center of the room for laminar ceiling to floor air flow are also seen (Photograph courtesy of John Bartelstone Photography)

additional personnel and equipment for procedures (Figs. 12.3b and 12.4). Diagnostic rooms start at 200 ft^2 and get as large as 600 ft^2 for modalities such as MRI (Fig. 12.5).

The size of hybrid image-guided interventional rooms is substantially larger and generally will not fit into the footprint of existing ORs or diagnostic rooms they are replacing. Trying to retrofit them into existing suites originally planned for single function spaces is a difficult proposition because these hybrid rooms must accommodate both the functionality of sterile procedure rooms (ORs) and full-size diagnostic equipment (Fig. 12.3c).

Fig. 12.5 *PET/CT procedure room*. This photograph illustrates the challenges of monitoring the patient when large view-obstructing equipment is involved. Note the anesthesia boom in the *middle* of picture, which is mobile and can be moved to provide electrical, vital signs monitors, and gases from any of 360° around the gantry (Photograph courtesy of John Bartelstone Photography)

The difficulty is to provide adequate space to support the equipment, the procedure, the staff, and the supplies without compromising adjacent rooms or functions.

Basic Considerations in Design

The precedents for the design of image-guided interventional facilities are interventional radiology rooms, the integrated image management-based laparoscopic ORs, and the first generation hybrid and intraoperative ORs built for special purposes and specific procedures. The integrated OR provides a good starting model for thinking about image guidance in that the OR provides a well-understood workflow and system approach to providing therapy and controlling the environment as it affects the treatment. There is a well-developed information management system for the creation of visual images and their display at the bedside for the use of the surgeon. The protocols and controls are understood by the staff and have generally been developed to support the process and needs of each individual institution. Moving forward, this is a good starting point for live image guidance. It is important for the facilities designer to understand the new imaging equipment to be added to the therapy environment, how it works and how its information is produced and used in the treatment of the patients.

The image-guided therapies discussed in other chapters of this book can be sorted into several major categories for the purposes of room planning and process design. Most therapies under consideration are mobile and involve movable equipment and instruments that move from room to room and are brought to the imaging and guidance systems. Rooms for these therapies need to be flexible, designed with sufficient work space, storage, and power sources for the nomadic equipment. Design for fixed therapeutic technology is more straightforward. These involve installed therapies, such as linear accelerators or focused ultrasound, and are usually integrated into imaging modalities such as CT, PET, or MR systems; however, these systems must also be designed to support the nomads when they visit.

The greatest challenge in design is that due in large part to the new and developmental nature of image-guided procedure rooms and the small market for equipment, there is a lack of equipment and systems designed and manufactured to support these uses. Thus, design of novel guidance procedures usually involves large bulky diagnostic equipment that has big space requirements and poor ergonomics for the proceduralist [8]. The imaging equipment in the best case is designed for

interventional radiology procedures that may require the use of an angio system or cath lab. Other modalities will require a room based system to provide visual guidance information to the physician.

Lighting

Lighting consists of two major elements: the fixtures and the controls. Both are necessary to get the system to function correctly and support the procedures to be performed. As a rule, controls and specialty fixtures like OR lights should be consistent from room to room within a facility in order to prevent staff fatigue and errors and to allow for ease of maintenance (Fig. 12.4).

The two most important characteristics of lighting are color and intensity. For overhead lights, the light sources generally used now are fluorescent because they have long life, are easily controlled and dimmed, and have very consistent color from lamp to lamp. They are also the most efficient light source on lumens produced per watt of electricity. In the next 5 years, however, LED will become competitive in this application.

In general, overhead fluorescent lamps serve well for illuminating setup, cleaning, and equipment service: functions that require uniform bright light throughout the room. A common design is for the fluorescent lights in a room to have the ability to be dimmed and controlled in small, localized zones for lighting of specific tasks in the room during a procedure. When all the lights are switched on at high intensity, uniform, general lighting of the room is achieved. The dimming control system is selected so that groups of lights can be dimmed to 10 % of maximum brightness without flicker or color shift. This will enable support of the image-guided and interventional procedures where the information displayed on video screens is at lower light levels. Lowering the room lights reduces glare and helps with highlighting the detail and color rendition from the video displays.

In all procedures and surgeries, there are staff circulating about the room. Thus, a consistent low level of lighting across the entire room is necessary to allow for this travel without accidents. Beyond this, there is the need for task lighting of certain areas to permit the operation of equipment to complete chart notes, to operate equipment, or to prepare instruments and supplies. Ideally, the general lighting can be set at a sufficient level to support these functions using spot lighting that is brighter than the room lighting. Separate ceiling-mounted task lights should have controls that allow them to be turned on and off as needed by the person working in areas such as the anesthesiologists, technicians preparing case carts, nurses managing notes, or imaging personnel operating control consoles [9, 10].

For lighting of the procedure area itself, the controls should be not only adjustable but also programmable so that the usual setups or operating modes of the room can be preset. This allows a quick transition between lighting programs and provides a consistent work environment from room to room and from day to day. This programming should include general and task specific lights throughout the room and control room. The essential lighting and equipment should also be configured on emergency power to allow the procedure to continue without interruption even in the event of a power outage. The lighting and controls should also be designed to function through the transition between power sources and function identically on normal or emergency power [11, 12].

For novel interventional environments such as those with MRIs, the electrical and lighting considerations are even more complex. Filtered, dimmable LED lighting systems for illumination of the work environment within the high magnetic field are now available. Fiber-optic switching networks and RF-shielded direct fiber-optic-fed monitors for MRI images are necessary.

Sterile Work Environment

The design standard for clean work environments requires a laminar flow air supply and a HEPA filtration system to clean the air and remove almost all particulates [13]. The laminar flow system is based on a special air supply diffuser mounted in

the ceiling that supplies air in a non-aspirating curtain that falls vertically toward the floor until it is past the table (Fig. 12.4). The curtain is then drawn horizontally away from the field to low return grills in the corners of the room. To be effective, the diffusers must form a closed ring and extend 2 ft beyond the work area. These procedure rooms have a code requirement of 20 air changes per hour, which is a large quantity of air. Care must be taken in the design of this system to control air velocity and thereby to reduce noise. The white noise produced by an air supply system not properly sized or balanced can mask speech. The large diffuser in the ceiling, general and task lighting, boom-mounted displays, and other equipment must be coordinated with imaging equipment and the planned working positions to provide convenient access to the utility connections and sight lines to the displays.

Other design challenges have to do with the control of equipment and process heat loads. To the extent possible, these should be isolated from the procedure space in separately air-conditioned rooms. These mechanical rooms also allow access for service without disturbing the procedure rooms. In both the equipment and the procedure spaces, the designer needs to be aware that the equipment heat loads vary dramatically over time. The imaging systems idle at low power when not in use but produce large heat outputs during imaging. The load profiles are inconsistent from room to room, so the zoning for the controls must be by individual room, not groups of adjacent rooms.

Imaging and Image Processing

The diagnostic image is the principal output from the radiology equipment such as an MRI scanner, CT, PET/CT, or C-arm. Depending on how it is to be used in the room, care must be given to display and routing of this signal to maintain its quality and consistency. The simplest way to do this is with a dedicated display chain provided by the equipment manufacturer that is not routed or switched in the room. The dedicated chain provides the radiology staff with a single visual reference point or "live image" for calibration and comparison of all of the displays and image routing equipment within each room.

The image storage and picture archiving and communication system (PACS) serves a dual role in interventional suites. It is the system that brings the diagnostic information already collected and interpreted to the procedure room for use in guidance systems or as reference information in an image-guided procedure. PACS also functions as an integral part of the medical record of the procedure. Thus, in this environment, the PACS interface is a two-way interactive system providing images previously archived from other modalities as well as storing records from the procedure in progress and storing images at the conclusion. The PACS images generated in the room have the same quality control requirements as standard diagnostic images.

Once the acquired images are displayed and stored in PACS in their native format, they are also often exported to separate diagnostic displays at different scales for use on guidance systems [14]. Therefore, there should be a way to set up an image or an image set in PACS and then route it anywhere while maintaining its proportions and fidelity. Many of the imaging system data sets are post-processed into other views or 3D images as part of the treatment planning or pre-procedure diagnostic work. These computers are generally separate workstations and have different display systems from the diagnostic tools they support. In interventional work often the ability to reprocess a new view will be helpful in resolving an anatomy question or some visually ambiguous image. The ability to do this independent of the ongoing procedure and imaging is an important asset. This is best done from the control room (Fig. 12.6), out of the traffic of the case, and displayed at the bedside or elsewhere in the procedure room.

Visual Information Management

The information necessary to guide a case needs to be displayable at the bedside and at multiple other locations in the room so that all of the staff is aware of what was going on and where in the procedure they were at the moment [15–17].

Fig. 12.6 *Angiography/CT procedure room*. The different displays needed in an advanced image-guided procedure room are highlighted. There needs to be PACS displays (*left*), boom-mounted displays with processed images (*right*), and patient information wall displays. Spot lights also will need to be mobile because of the mobile area of therapeutic interest (Photograph courtesy of John Bartelstone Photography)

Fig. 12.7 *Common control room*. The entire procedure must be visible from the control room. Work space must be provided not only for the imaging technicians and the interventional physicians but also for anesthesiologists and medical physicists. Sharing of a common control room between two or more procedure rooms can reduce personnel and equipment requirements. In designing common control rooms, it is important to be sure that patients within the procedure room cannot look through to adjacent procedure rooms (Photograph courtesy of John Bartelstone Photography)

Ideally, there should be a large display visible to all in the room with essential data relevant to all personnel. Such a "wall of knowledge" should display important background data on a patient such as allergies and brief history, as well as live data such as ongoing vital signs. This system uses data already in systems at the hospital and displays it in a standard format for the staff to use in monitoring the patient and organizing their schedule and workflow (Fig. 12.7).

The live and near live images to be displayed in the modern interventional environment include

not only radiologic images but also images from ceiling, operative light-mounted, and laparoscopic cameras. Thus, monitors must support display of almost every video format. There is also the need to provide remote viewing access for visiting physicians and students, which can be optimized by displaying the working images at strategic points in the room and on multiple displays around the patient. The optimal visual working distance for the fine details on video displays is much shorter than the distance from which one watches television images. Keeping the working distances consistent from eye to hand and eye to display and maintaining a uniform light level from display to working field and from display to display is important in reducing fatigue and eyestrain caused by refocusing or adjusting to different illumination as you work.

Image Displays

Resolutions of image displays have been improving rapidly. 1080P HD video displays have become standard – a substantial upgrade in image quality over the previous PC display standards used in integrated ORs. Video and other working images are migrating to this standard. It is more than likely that in the near future, consumer 3D television display systems will migrate into these image-guided rooms for display of the post-processed 3D radiology images. Even with glasses, these systems will be useful for virtual reality overlay imaging (and even better once co-registration software is perfected). 3D displays not requiring glasses are also available, and their implementation is only awaiting further improvements in resolution and decrease in cost.

Design in placement of displays depends mainly on sizes needed to provide working information at the distance from which the display would be viewed. Boom-mounted displays are usually smaller than wall-mounted displays but should be the same resolution and aspect ratios (Fig. 12.6). The signals coming from each piece of equipment should optimally be preprocessed to a standard HD format compatible with the displays and switchable through the video system. This allows for equipment to travel from room to room. The use of a standard signal in the switching systems also makes it easy to route images produced by different systems and display them consistently throughout the facility.

Composite procedures are those that include multiple therapies or modalities simultaneously to accomplish something that one specialist could not do alone. Examples include the use of catheters or laparoscopes to manipulate and protect an adjacent structure to enhance tumor ablation. Other examples include combined endoscopic ultrasound and CT guidance to provide multiple image planes and real-time updating of transbronchial procedures. The composite element adds people to the procedure room and requires additional displays in the field to display images and information for each of the simultaneous processes.

Because most imaging equipment was developed as diagnostic equipment, the specifications of room sizes and configurations necessary to house much of the imaging hardware are not well defined and not optimal for interventional rooms. Even the length of cable becomes an issue when equipment is isolated and the work area is enlarged to support sterile instruments and a sterile field. This creates a planning and functional hardship that the equipment vendors should be pressured to address. The cable currently connecting many cross-sectional imaging machines and tables to the support computer equipment is sufficiently short that it restricts room size or dictates that equipment closets be placed in the spaces immediately adjacent to the procedure rooms, which is better used for staff and ancillary supplies and equipment.

A number of pending changes are likely to greatly impact this field. Future use of fiber-optic cabling to allow direct fiber-fed equipment and fiber switching will reduce latency and improve bandwidth and connectivity between rooms within the suite. Remote surgery by human-operated "robotics" will be employed to address and resolve the challenges posed by working in the small bores of scanners, to reduce the radiation exposures to the staff, and to increase accuracy of procedures. The "no-touch" controllers, similar to the controller-less interfaces new this season in consumer

video games, will likely be applied in the future to allow control of equipment information and images while maintaining sterility.

Equipment Noise and Acoustics

Acoustics in sterile environments are compromised by need for washable and wet-cleanable hard surfaces that generally reflect and amplify sound. Noise from systems and equipment in the room must be minimized at the sources and in the equipment design in order to maintain a comfortable work space, since the ability to dampen and control sound with finishes and materials is limited. Walls between rooms and doors to corridors need to be substantial to attenuate sound transmission between rooms and through walls and corridors. Special construction details are required in the walls of rooms containing noise-producing equipment such as MRI, where gradient coils can produce noise at 60 dB (subway train volume) so that staff in adjacent rooms is not disturbed.

Magnetic and radiofrequency shielding and radiation protection all require continuity and closure which conflicts with the requirements for the distribution of and access to the utilities and infrastructure in the walls. A design solution that addresses this is a multilayered wall where the shielding was isolated in the center where it could be installed early in construction and inspected. Then the individual rooms and their cabling and piping could be installed in the room. These free-standing layered walls will enhance sound attenuation between rooms. In the future, we expect this will enhance our ability to work in the rooms and update systems and equipment one room at a time without disturbing procedures in adjacent rooms.

Challenge of Large Equipment and Nomadic Equipment

Several workflow challenges in the design and operation of image-guided environments that do not exist in traditional ORs are related to the mechanics and need to move the patient through large immobile imaging equipment. Unlike traditional surgery where the operative field is generally placed in the middle of the room and personnel as well as therapeutic equipment are brought to the field, in interventional environments, the operative field is not usually fixed in space and is rarely in the center of the room. The patient and therapeutic field are usually brought to the imaging machine. The work site can be in the center of the imaging machine for percutaneous therapies or at some distance for catheter-based treatments. Depending on the procedure, patients may be head in or head out of the imaging equipment. Reorienting the patient causes all of the staff to move as well. The most difficult of these displacements is in anesthesia where the staff is tethered at both ends since their equipment has connections both to the patient and the room utilities. In some rooms, there are multiple locations where anesthesia utilities support must be provided to support the variety of procedures performed.

The increased sizes of the working fields resulting from equipment having several optional working locations require us to provide duplications of utilities and infrastructure that are not needed in standard ORs. Once the optimal location for the anesthesia setup for a case has been determined, issues relating to cable and tubing management around and to the patient as well as the movement of the patient for imaging during the case must be resolved. These include maintaining the connections for routing cables so they do not pass through the sterile fields or work areas during the procedure. These are routed so they do not create image artifacts. Routing should also be planned to minimize need for handling and to protect them from impact.

There are also many pieces of equipment that are shared among many rooms, such as ablation generators, ultrasounds, or C-arms. Such nomadic therapy and imaging equipment need a place to live when in the room and a method to connect to the infrastructure without blocking circulation paths around the room. Surgical booms and ceiling-mounted displays address some of these needs. Manufacturers of fixed equipment need to provide

space for utilities infrastructure and connectivity to support the ancillary equipment, so it does not need connections to walls.

The Patient Experience

The quality of the patient experience or "hospitality" component of the hospital is a significant component of the design of new facilities. Along with an expectation of excellent medical care, there is an expectation of quality personal care. A well-planned modern work environment that is more efficient allows both expectations to be fulfilled and produces better, more consistent outcomes.

Where a patient is to recover after a procedure is a very important consideration in patient flow. It has been shown that fewer transfers between stretchers tables and beds make the patient more comfortable and reduce complications caused by movement. During the entire treatment day, the patients should be provided the utmost privacy and the ability to be accompanied by a family member or friend. They should be able to talk with staff and physicians in private settings to preserve their confidentiality. These expectations are reflected in evolving standards that now call for private rooms and closed consultation and interview rooms [8]. Patients' expectations for the care of their clothing and belongings, adequate space for dressing in private and preparing oneself to leave the hospital include personal care items, such as a mirror to check one's appearance and a chair to sit on while getting dressed, as well as adequate space for someone to assist them in these activities, must be reflected in the design.

PACU/recovery is the place where patients spend the majority of their conscious time in the interventional suite. Ideally, these spaces should be designed as private rooms with solid walls and doors (Fig. 12.1). Patients are often accompanied by family members in these areas and need to talk with them and the staff responsible for their care. These conversations require privacy, and patients recovering from anesthesia require quiet and isolation from the traffic and noise produced by others in the area and need an appropriate area to be cared for in private.

Other Adjacencies Necessary to Support This Work

A plan for immediate interaction with pathology is essential for any modern interventional suite. There is the need for expedited delivery of excised or biopsied tissue to pathology for immediate analysis. A live information connection for consultation and reporting of results in real time to the OR/procedure room is required [15, 18].

Central sterile supply and instrument processing facilities need to be located so that materials can move between them and procedure rooms simply by cart or elevator. A process such as case carts or "just in time" ordering and delivery must be planned to meet the needs for supplies and instruments for procedures. Regularly needed equipment or equipment needed in an emergency (such as specialty angiographic catheters) should be placed in close proximity to the procedure [6].

Planning room placement and sharing of control rooms for rooms where similar procedures are performed will enhance efficiency and minimize personnel and stocking costs. This will also allow for sharing of high-cost mobile equipment and other specialized items. Intra-procedural consultations can then also be facilitated in difficult cases (Fig. 12.7).

Equally important are quiet workspaces away from the procedure room for charting post-processing images and data and for discussions and phone calls. These areas make it possible to complete those administrative and social tasks that accompany our daily work without the acoustical challenges in the procedure room (Fig. 12.6).

Conclusion

The development of image-guided operating rooms began with laparoscopic/MIS and interventional radiology suites. As increasingly larger,

more expensive and sophisticated imaging equipment became standard in the interventional environment, simple procedure rooms evolved to interventional suites, and now multimodality interventional platforms. Obstacles to development include the fact that many traditional imaging companies often see a sufficient market for these special purpose imaging systems to spend money on development but will continue to focus on improving their core diagnostic imaging market. The field of therapy applications will have to figure out how to function and adapt in this predominately diagnostic environment.

Because of the high cost of the construction, operation, and maintenance of these rooms, they must necessarily be shared facilities that cross disciplines. These comprehensive surgical, endoscopic, and image-guided interventional ORs are also designed to serve both inpatients and outpatients. Uniform standards and equipment should be selected, and workflow, room controls, and charting information systems are standardized to support collaboration between the specialties and to provide support for the application of new and developing therapies. For efficiency and further cost reduction, some groups have started to design rooms and workflow that would allow a number of patients being treated in adjacent rooms to be transported to a central area with a large immobile imaging machine only when scanning is necessary. The next evolution in this area is likely to involve development of mobile, high-resolution, imaging equipment that will travel between and service a number of procedures simultaneously. Both models would move away from the current one room, one machine model of intra-procedural imaging, to a less costly many rooms, one machine model.

References

1. Kpodonu J. Hybrid cardiovascular suite: the operating room of the future. J Card Surg. 2010;25(6):704–9.
2. Sikkink CJ, Reijnen MM, Zeebregts CJ. The creation of the optimal dedicated endovascular suite. Eur J Vasc Endovasc Surg. 2008;35(2):198–204.
3. Bonatti J, Vassiliades T, Nifong W, Jakob H, Erbel R, Fosse E, et al. How to build a cath-lab operating room. Heart Surg Forum. 2007;10(4):E344–8.
4. Nollert G, Wich S. Planning a cardiovascular hybrid operating room: the technical point of view. Heart Surg Forum. 2009;12(3):E125–30.
5. Hudorovic N, Rogan SA, Lovricevic I, Zovak M, Schmidt S. The vascular hybrid room – operating room of the future. Acta Clin Croat. 2010;49(3):289–98.
6. Matern U, Koneczny S. Safety, hazards and ergonomics in the operating room. Surg Endosc. 2007;21(11):1965–9.
7. Facilities Guideline Institute. Guidelines for design and construction of health care facilities. Dallas: FGI; 2010.
8. Fillinger MF, Weaver JB. Imaging equipment and techniques for optimal intraoperative imaging during endovascular interventions. Semin Vasc Surg. 1999;12(4):315–26.
9. Surgical lights. An illuminating look at the LED marketplace. Health Devices. 2010;39(11):390–402.
10. Hadjipanayis CG, Jiang H, Roberts DW, Yang L. Current and future clinical applications for optical imaging of cancer: from intraoperative surgical guidance to cancer screening. Semin Oncol. 2011;38(1):109–18.
11. Riley RH. Power failure to a tertiary hospital's operating suite. Anaesth Intensive Care. 2010;38(4):785.
12. Eichhorn JH, Hessel EA. Electrical power failure in the operating room: a neglected topic in anesthesia safety. Anesth Analg. 2010;110(6):1519–21.
13. Dalstrom DJ, Venkatarayappa I, Manternach AL, Palcic MS, Heyse BA, Prayson MJ. Time-dependent contamination of opened sterile operating-room trays. J Bone Joint Surg Am. 2008;90(5):1022–5.
14. Lemke HU, Berliner L. PACS for surgery and interventional radiology: features of a therapy imaging and model management system (TIMMS). Eur J Radiol. 2011;78(2):239–42.
15. Kranzfelder M, Schneider A, Gillen S, Feussner H. New technologies for information retrieval to achieve situational awareness and higher patient safety in the surgical operating room: the MRI institutional approach and review of the literature. Surg Endosc. 2011;25(3):696–705.
16. Balust J, Macario A. Can anesthesia information management systems improve quality in the surgical suite? Curr Opin Anaesthesiol. 2009;22(2):215–22.
17. Seim AR, Sandberg WS. Shaping the operating room and perioperative systems of the future: innovating for improved competitiveness. Curr Opin Anaesthesiol. 2010;23(6):765–71.
18. Tamariz F, Merrell R, Popescu I, Onisor D, Flerov Y, Boanca C, et al. Design and implementation of a web-based system for intraoperative consultation. World J Surg. 2009;33(3):448–54.

Imaging of Interventional Therapies in Oncology: Ultrasound

13

Luigi Solbiati and Tania Tondolo

Abstract

Ultrasonography (US) and contrast-enhanced ultrasonography (CEUS) play a key role at each step of imaging-guided therapies. Ultrasound (US) is actually the most widely diffused imaging technique for the guidance of percutaneous ablation as it allows for real-time visualization of the ablation device insertion and monitoring of the procedure and does not require ionizing radiation.

CEUS allows to diagnose focal lesions on the basis of enhancement patterns that are analogous to those typically seen on contrast-enhanced CT and MRI. Compared to CT and MRI, CEUS has the limitation to enable the study of one lesion at a time, but it has the advantage to be a real-time technique. CEUS is usefully employed before ablation for detection and characterization of lesions, pre-procedure planning, intra-procedure targeting (particularly for difficult and/or small lesions) and monitoring and, immediately after ablation, correct assessment of the volume of necrosis achieved, and detection of possible residual foci of untreated tumor.

CEUS can also implement B-mode US when real-time US-CT/MRI fusion imaging (or "virtual navigation") is employed: Real-time US is co-registered with previously acquired contrast-enhanced CT or MRI scans multiplanarly reconstructed and transferred to the US machine.

In conclusion, for interventional therapies of lesions and organs that can be imaged with US, CEUS is a very valuable tool in all the phases of treatments. When follow-up contrast-enhanced CT or MRI are contraindicated or not conclusive, CEUS can also be used in follow-up protocols.

L. Solbiati (✉)
Department of Diagnostic Imaging and Interventional Oncologic Radiology, General Hospital of Busto Arsizio, Busto Arsizio, VA, Italy
e-mail: lusolbia@tin.it

T. Tondolo
Department of Biomedical Sciences and Technologies, Section of Radiological Science, School of Medicine, University of Milan, Milan, MI, Italy
e-mail: tania.tondolo@gmail.com

Priorities of medical imaging in interventional oncology are different from those required for diagnostic studies. Patients sent to interventional procedures have always preliminarily undergone high-quality diagnostic imaging. For interventional procedures, lower-resolution imaging restricted to the region of interest is an acceptable compromise, but easy access to the patient,

D.E. Dupuy et al. (eds.), *Image-Guided Cancer Therapy*, DOI 10.1007/978-1-4419-0751-6_15,

real-time imaging, precision of guidance, image feedback of the therapy (preferably in real time), and low radiation dose are the priority properties needed. In this scenario, ultrasonography (US) and contrast-enhanced ultrasonography (CEUS) play a key role at each step of image-guided therapies: (1) pre-procedure planning, (2) intraprocedural targeting, (3) intraprocedural monitoring (to assess tissue changes caused by the treatment) and control (to make adjustments during the procedure), and (4) post-procedure assessment [1].

Pre-procedure Planning

Pre-procedure planning has as main purposes those of establishing if the procedure is indicated and technically feasible, what is the best approach to the target, and if there are potential risks to the structures surrounding the neoplastic target(s). In order to achieve this information, high-quality diagnostic imaging is recommended, mostly anatomic (US, CT, MRI) but occasionally also physiologic (PET, SPECT). Multiphasic contrast-enhanced helical CT and dynamic gadolinium-enhanced MRI represent the mainstay for staging of hepatic and extrahepatic neoplastic involvement, whereas the use of hepatobiliary and reticuloendothelial-specific MR contrast agents may be helpful in selected patients to maximize lesion detection [2]. FDG-PET/CT is also of great importance particularly for the pre-procedure staging of metastatic lesions, even if its sensitivity declines rapidly for lesions smaller than 1 cm [2]. Unenhanced B-mode ultrasound is widely employed for screening of abdominal diseases but cannot generally be employed for the pre-procedure planning of interventional procedures because of some intrinsic limitations: level of diagnostic quality related to patient's body habitus and bowel gas distention, insufficient sensitivity for the detection of small lesions mostly in some conditions (like obesity, underlying diffuse parenchymal disease, history of previous treatments affecting organ structure), limited accuracy for the characterization of focal lesions, field of view too restricted for the staging of neoplastic diseases within large organs, and operator dependence [3]. Color and spectral Doppler US are also often poorly helpful, principally because of their inability to demonstrate blood flow at parenchymal level.

CEUS provides more information for lesion detection and characterization than either B-mode or color Doppler US do and can be usefully employed for pre-procedure planning of interventional therapies for some peculiar purposes. Second-generation microbubble contrast agents have high harmonic emission capabilities and prolonged longevity (4–5 min) thanks to the elasticity of the bubbles' shell and the very low acoustic power that limits microbubble destruction provided by the contrast-specific ultrasound software systems developed by the major ultrasound companies. These systems, based on the principle of wideband harmonic US, allow to visualize microbubble enhancement with optimal contrast and spatial resolution in real-time continuous mode, displaying both macro- (vascular imaging) and microcirculation (tissue perfusion imaging) in all the vascular phases, cancelling the signals coming from stationary tissues and without the motion and blooming artifacts characteristic of color and power Doppler US [4, 5]. In addition, US contrast agents are nontoxic, easy to use, and well tolerated by patients, and repeat injections can be safely performed either before or during interventional procedures.

CEUS allows to diagnose focal lesions on the basis of enhancement patterns that are analogous to those typically seen on contrast-enhanced CT and MRI (Figs. 13.1 and 13.2). Compared to CT and MRI, CEUS has the limitation to be able to study one lesion at a time but also the advantage to be a real-time study, capable of catching, for each lesion, the instant of the enhancement phase crucial for lesion characterization. In addition, CEUS has a sensitivity for the detection of small sub-centimetric focal lesions (particularly of hypovascular metastases in the liver) much greater to that of B-mode US and at least as good as CT [5, 6]. Consequently, in addition to

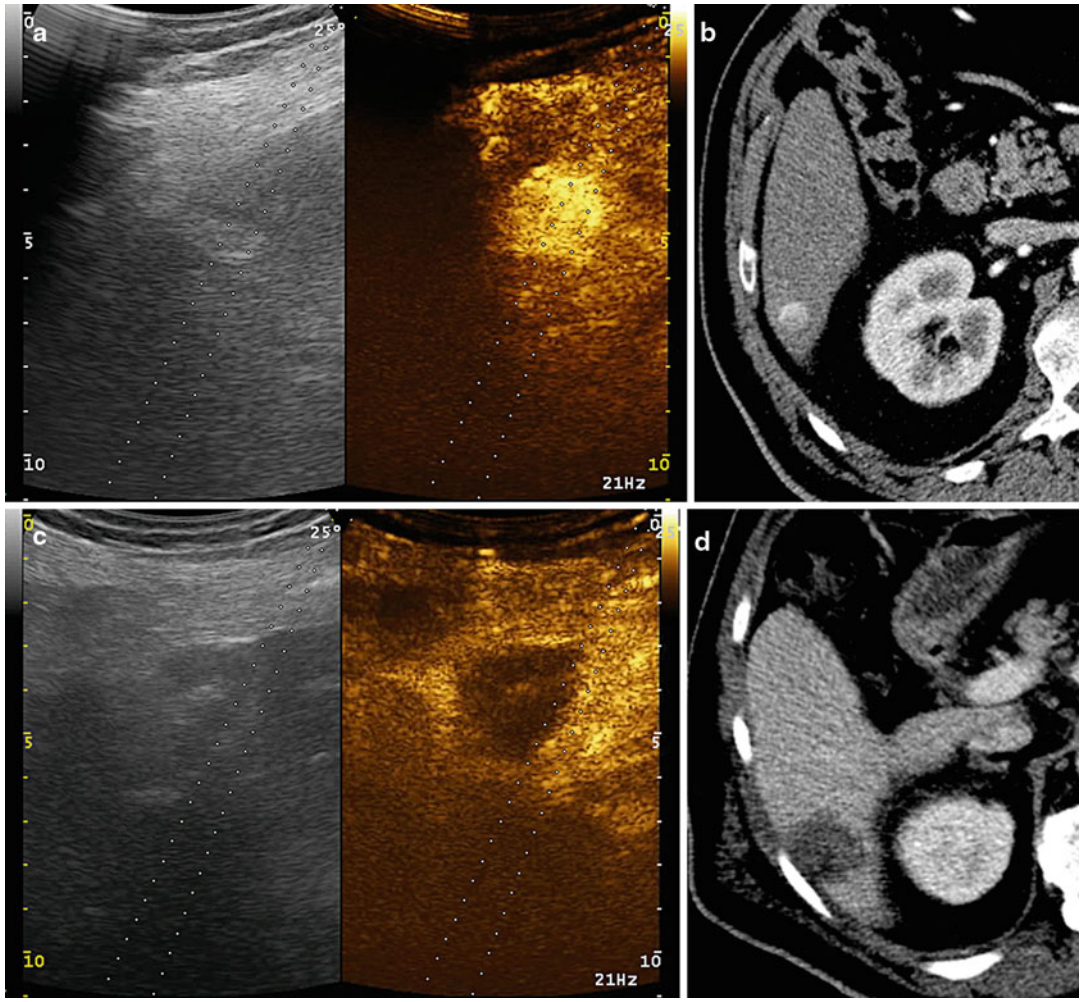

Fig. 13.1 Small, subcapsular hepatocellular carcinoma (HCC) at segment 6. On B-mode US (**a**, *left*), the nodule is poorly visible, while on CEUS in arterial phase (**a**, *right*), it shows the typical early, intense, and homogeneous enhancement pattern of HCCs. (**b**) On multidetector CT scan in arterial phase, the nodule is clearly seen. (**c**) Six minutes after withdrawing the microwave antenna for ablation, few gas bubbles still remain in the treatment area. The actual volume of necrosis achieved cannot be defined on B-mode US (*left*), while it is clearly depicted on CEUS (*right*) in portal phase, slightly underestimated in size in comparison with that showed on the 24-h follow-up CT scan (**d**)

contrast-enhanced CT or MRI, in the pre-procedure diagnostic work-up, particularly when US is the diagnostic modality chosen for guiding the interventional procedure, the addition of CEUS can be very helpful to define [4, 6–9]:

- Actual number and size of the lesions to be treated, including the perilesional hypervascular halo with washout which represents the most actively growing part of tumors (see Fig. 13.2)
- Degree of enhancement and presence of areas of necrosis, in order to facilitate the comparison of pre- and post-therapy patterns at the end of treatment (Fig. 13.3b)
- Tumor margins, mostly for subcapsular and exophytic tumors, in order to thoroughly assess the relationships of tumors with surrounding structures and to adopt appropriate treatment strategies, reducing the risk of complications

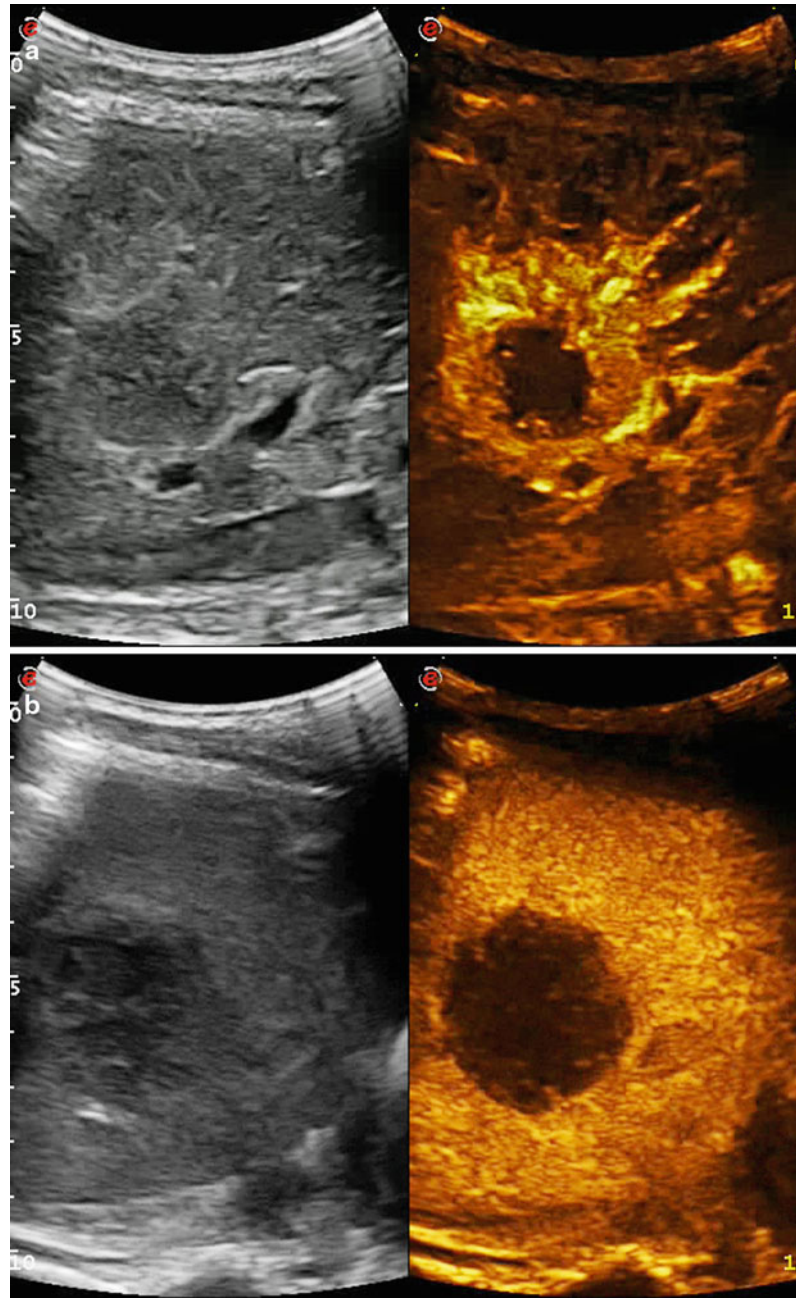

Fig. 13.2 Metastasis from colon carcinoma in the right hepatic lobe examined with B-mode US (*left*) and CEUS (*right*) in both arterial (**a**) and portal (**b**) phase. On CEUS, the peripheral hypervascular halo (with echogenicity decreasing from the arterial to the portal phase) and the central area of necrosis, unenhancing in both phases, are depicted

– Zones of local tumor progression or residual tumors following previous locoregional treatments

Pretreatment planning (number of devices needed to treat each tumor, path to target for each treatment device, and planning of overlapping contiguous treatment volumes) can be performed with US through real-time volumetric (4D) studies [10, 11] or, more recently, using the systems of real-time US-CT/MRI fusion imaging [12–16]. These systems (so-called virtual navigation systems) combine real-time US with previously acquired contrast-enhanced CT or MRI volumetric scans

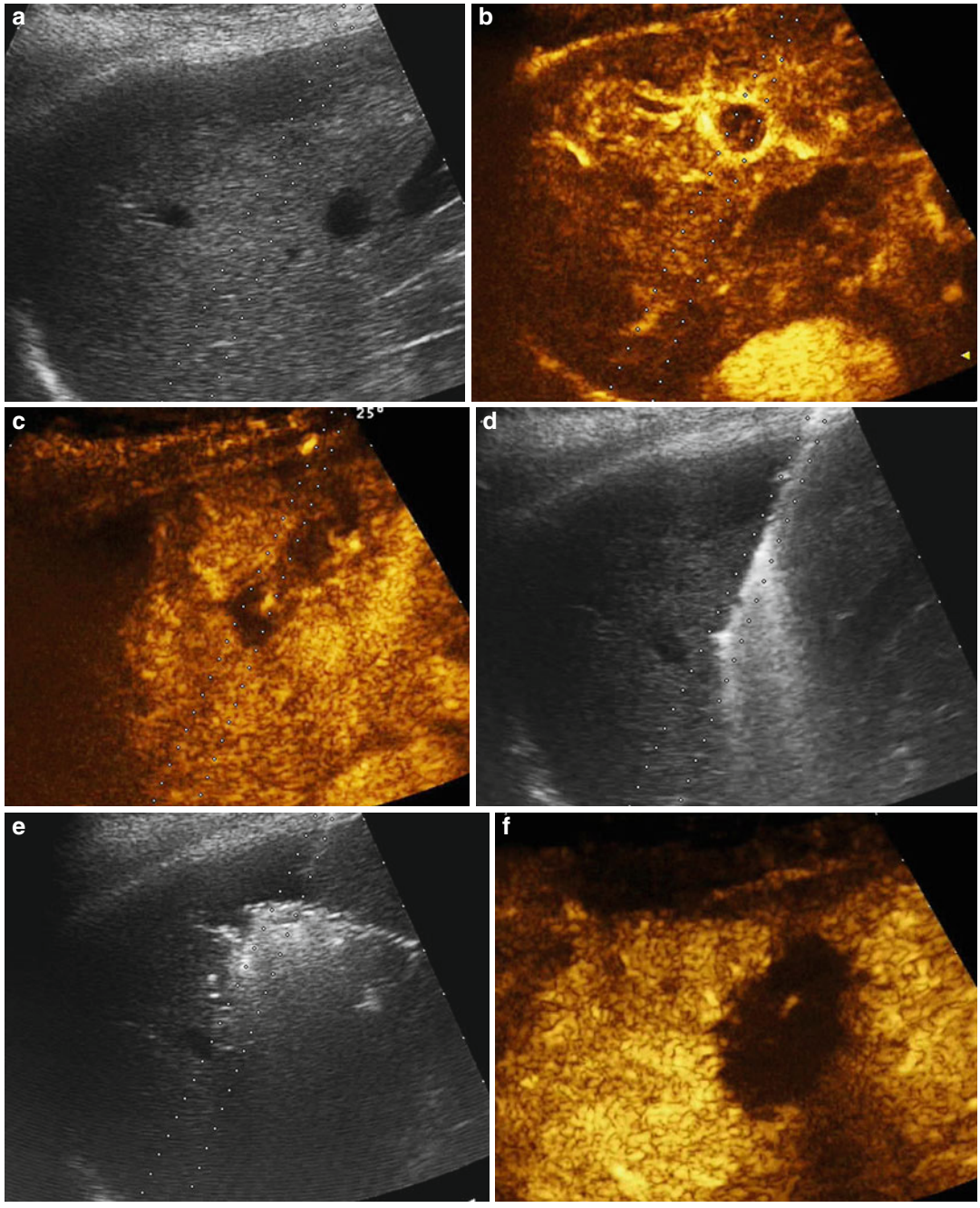

Fig. 13.3 1.5-cm metastasis from breast carcinoma in the right hepatic lobe, undetectable on B-mode US (**a**) and clearly seen on CEUS in arterial phase (**b**), with peripheral enhancing rim and wide central unenhancing area, due to necrosis. Real-time positioning of microwave antenna is performed on portal phase CEUS (**c**), but switching back to B-mode US facilitates the visualization of the inserted antenna. (**d**) Six minutes after starting energy deposition, a large hyperechoic "cloud" due to gas bubble formation covers the treatment area (**e**) and prevents from assessing the real volume of coagulative necrosis achieved that is instead distinctly appraised on CEUS in portal phase, performed 7 min after withdrawing the antenna (**f**)

multiplanarly reconstructed and transferred to the US machine. Co-registration, achieved through anatomical landmarks detected on both US and CT or MRI, is provided by electromagnetic tracking systems consisting of a magnetic field transmitter, fixed to the operation bed, and electromagnetic sensors applied to the ultrasound probes and to the ablation applicators. The position and orientation of the ultrasound probes in space is determined in relation to the transmitter, and real-time matched US-CT/MRI images are generated. Prior to performing the interventional procedure, the anticipated path of the interventional device and a virtual treatment volume based upon the different dimensions and shape of the anticipated zone of ablation produced by the various ablation applicators can be drawn and overlapped on the real-time CT/MRI scans, simulating the needle placement and the ablation volume potentially achievable. This is of particular importance when multiple overlapped treatment volumes produced by a single applicator or the placement of multiple simultaneous applicators are needed to treat the whole tumor (Fig. 13.4).

In pre-procedure planning, when the target lesion is not visualized by B-mode US because of small size or difficult anatomic location, real-time US-CT/MRI fusion imaging can help detect the lesion and perform a subsequent "targeted" CEUS aimed at defining the features above described of the tumor before treatment.

Intraprocedural Targeting

Due to its nearly universal availability, portability, ease of use, and low cost, US represents the most commonly used imaging modality for the guidance of interventional procedures performed in organs visible with US. Fast and easy real-time visualization of electrode positioning is a characteristic feature of US, whereas the same procedure may be cumbersome in CT and MRI environments (Figs. 13.3d and 13.5).

Pretreatment CEUS is usually repeated as the initial step of the interventional session during the induction of anesthesia or sedation, in order to confirm the mapping of lesions as shown on CT/MRI scans. Images or movie clips are digitally stored to be compared with immediate post-ablation study [17].

When the tumor is hardly seen with B-mode US because of small size, isoechogenicity to the surrounding normal parenchyma, or critical location, CEUS facilitates real-time positioning of the interventional device during the vascular phase in which the lesion is better detected (e.g., arterial phase for hepatocellular carcinomas and delayed phase for hypovascular metastases) [17] (Fig. 13.3c). At peak enhancement, device tip detection may become difficult due to the strong enhancement of the normal parenchyma where the lesion is located and it is useful to switch back to high-power conventional B-mode US (Fig. 13.3c, d).

CEUS as guidance modality is also particularly useful when the target is a locally recurrent or progressing tumor after previous local treatments (either interventional or surgical) because the presence of contrast enhancement is the only feature which allows to distinguish viable tumor from adjacent necrotic tissue.

When lesion targeting is particularly challenging, visualization of the "virtual" device (electrode, antenna, cryoprobe, etc.) provided by real-time US-CT/MRI fusion imaging can significantly facilitate the procedure (Figs. 13.6 and 13.7). Also in these occurrences, CEUS can be performed in combination with real-time fusion imaging with additional increase of the operator's confidence [14].

Using CEUS as guidance for interventional procedures instead of B-mode US, the complete necrosis rate after one session reportedly increases from 65 % to 94.7 % [7].

Intraprocedural Monitoring and Control and Post-procedure Assessment

One of the most critical challenges for image-guided interventional therapies is knowing during the procedure when the treatment has been sufficient, with the clear endpoint of the complete

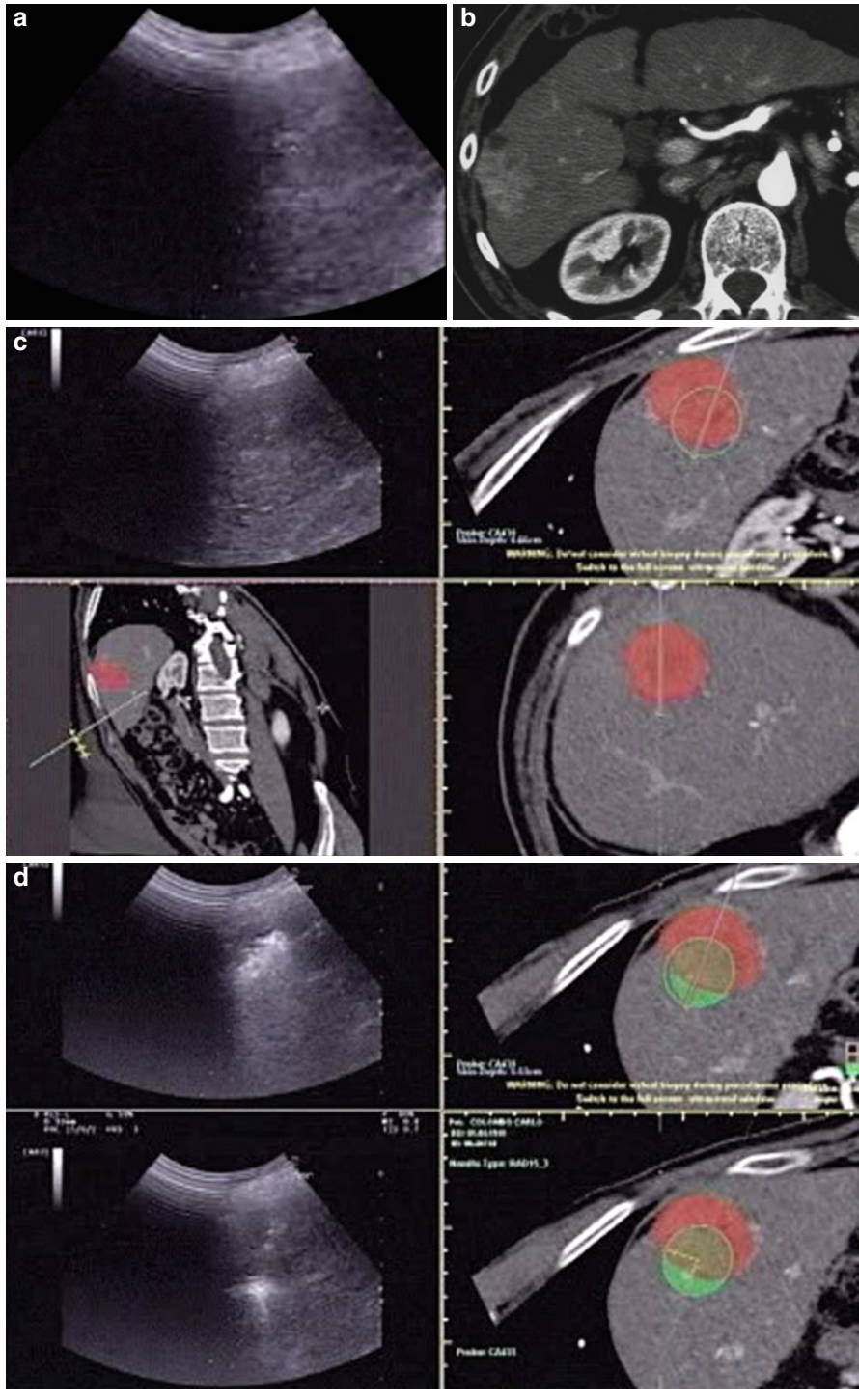

Fig. 13.4 (continued)

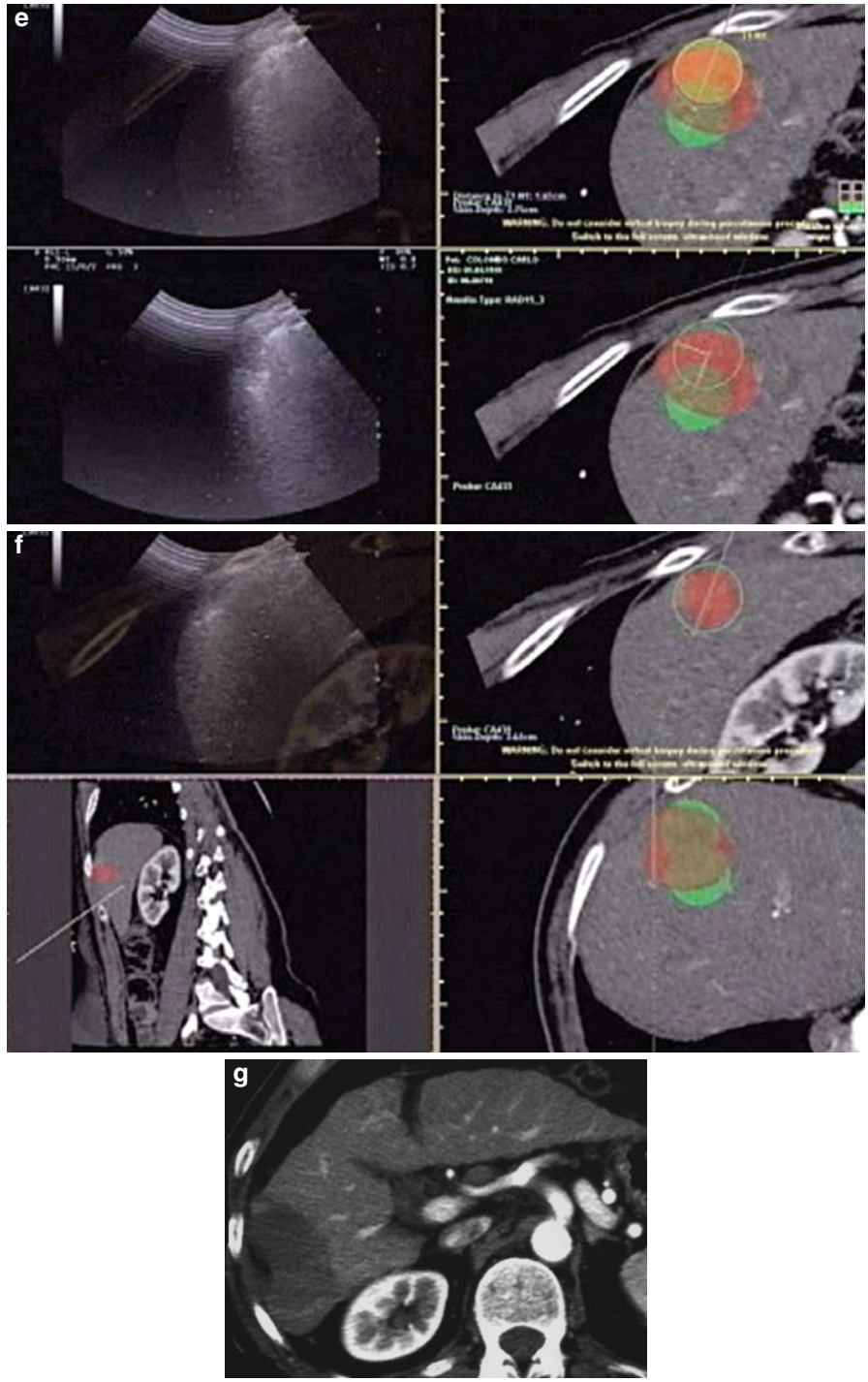

Fig. 13.4 Large, subcapsular HCC in the right hepatic lobe, poorly seen on B-mode US (**a**) and well depicted on multidetector CT scan in arterial phase (**b**). Given the large size, the mass is ablated with multiple insertions of single cool-tip radiofrequency electrode, using the real-time US-CT image fusion (**c**–**f**). Thanks to the "virtual needle" showed on CT scans, several insertions are performed, based upon the size of the anticipated zone of ablation produced by the electrode used for the procedure. The ablation volume achieved by each insertion is

disruption of the tumor mass. The term "monitoring" means to visualize by imaging during the procedure the changes resulting from the treatment in order to know "that the tumor is being treated appropriately and that the surrounding normal structures are not being affected more than is necessary to complete the treatment effectively and safely" [1]. On the other hand, "control" means to make the needed adjustments during the procedure.

The problem of local treatments is the induction of sufficiently large necrotic zones with safe destruction of the tumor tissue with an adequate 0.5- to 1-cm "safety margin" of ablated peritumoral normal tissue in order to destroy microscopically infiltrating tumor and therefore limit the incidence of local progression [18, 19].

The assessment of vascularization and tissue perfusion is crucial to differentiate necrosis from residual viable tumor. Consequently, unenhanced B-mode US, even combined with color/power Doppler, cannot provide any reliable information about the outcome of interventional procedures, being unable to differentiate coagulation necrosis from viable tumor. During thermal ablative treatments, a progressively increasing hyperechoic "cloud" corresponding to gas bubble formation and tissue vaporization is visible with B-mode US around the distal probe and may persist for some minutes. However, the size of this area of gas bubbles cannot be used to assess the amount of necrosis achieved, since it tends to extend beyond the margins of the actual ablation and thus can lead to overestimation of the real volume of necrosis (Figs. 13.3e and 13.5d). Using real-time US-CT/MRI fusion imaging during the procedure, it is possible to perform an adequate "control" of the treatment, repositioning the applicator immediately or modifying its effects (if needed) without having to wait for the reabsorption of gas bubbles before reinserting the applicator (see Fig. 13.4).

For all the interventional procedures performed under US guidance, the most important imaging finding that indicates complete ablation is the disappearance of any previously visualized intralesional enhancement on CEUS (performed 5–10 min after the end of the interventional procedure) throughout the whole volume of the treated tumor in all the vascular phases [4, 18, 20–25] (see Figs. 13.1c, 13.3f, and 13.5e). Residual unablated tumor is seen as one or more irregular nodular areas displaying the native, characteristic enhancement pattern of the pretreatment tumor, while coagulation necrosis is avascular (Fig. 13.8).

The size of the posttreatment avascular volume of the necrosis achieved has to be compared with the size of pretreatment volume of tumor(s) (Fig. 13.9). The simultaneous display of tissue and contrast signals is of particular value for short- and long-term follow-up of treated lesions, to ascertain whether persistent enhancing portions of tissue are inside or outside the ablated lesion. Using real-time fusion imaging, it is also possible to precisely compare the volume of necrosis achieved with the pretreatment volume of the same lesion on contrast-enhanced CT or MRI [26] (Fig. 13.10). Compared to posttreatment contrast-enhanced CT or MRI, CEUS has limited sensitivity (60–75 %) for the detection of residual, incompletely treated tumor tissue, but very high specificity (94–100 %) [20–25].

If even questionable residual tumor foci with enhancement or vascular supply are depicted, it is highly recommended to perform immediate, CEUS-guided targeted re-treatment in the same session up to the demonstration of complete tumor avascularity on CEUS. In fact, delayed

Fig. 13.4 (continued) represented as a green-colored sphere overlapped over the large *red-colored* tumoral mass. When the overlapped green spheres cover the whole red mass, the procedure is stopped. During the treatment, US (on the *left side* of **c–f**) cannot be used to target the multiple insertions because the "cloud" of gas bubbles generated by the ablation makes the whole tumor completely invisible. (**g**) 24-h follow-up CT scan demonstrates the completeness of ablation. The volume of coagulative necrosis achieved is larger than the original HCC

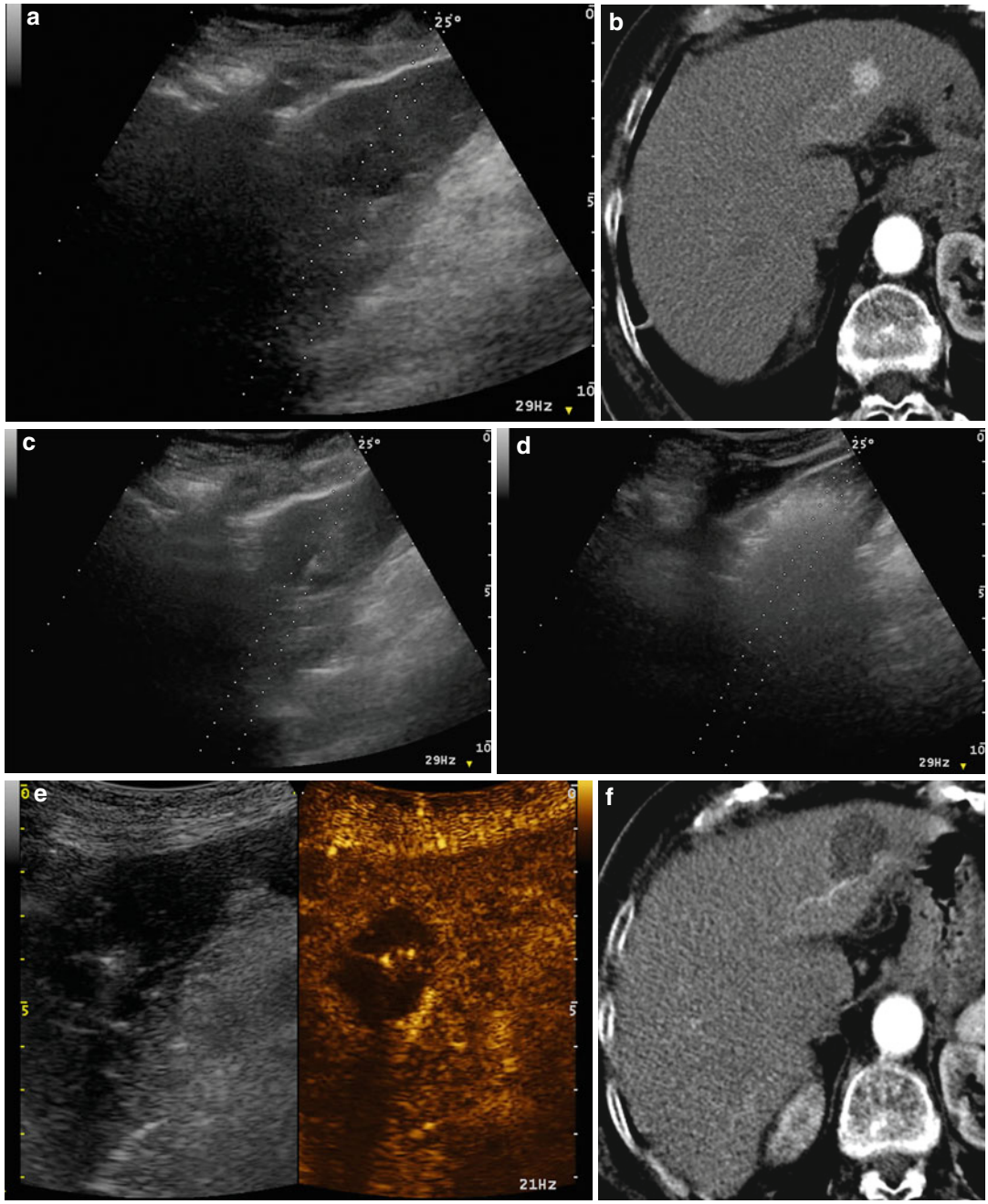

Fig. 13.5 1.9-cm HCC in the left hepatic lobe, seen on B-mode US (**a**) and contrast-enhanced CT in arterial phase (**b**) and precisely targeted with US guidance (**c**). A wide cloud of gas bubbles is seen on US during ablation (**d**). Few minutes after the end of energy deposition, CEUS demonstrates complete ablation (**e**) with a volume of necrosis larger than the pretreatment HCC, as confirmed by the 24-h contrast-enhanced CT scan (**f**)

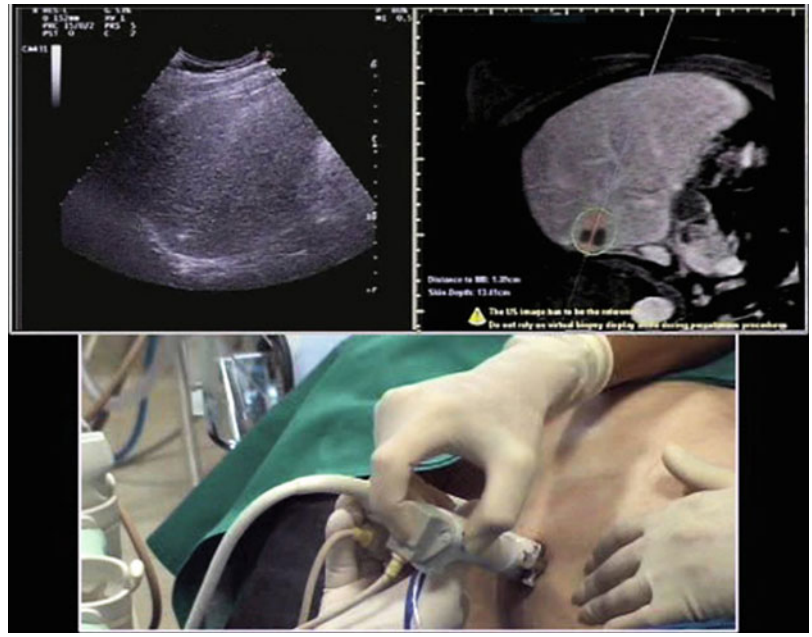

Fig. 13.6 Using the "virtual needle" (*top right*) of the real-time US-CT image fusion system (*bottom*), a small metastasis from rectal carcinoma in subphrenic location, undetectable with B-mode US, is precisely targeted and ablated with cool-tip radiofrequency

re-treatment is often technically difficult owing to the difficulty to differentiate active tumor from coagulation necrosis and has a higher rate of failure. Thanks to its high contrast and temporal resolution, CEUS is very helpful to reduce the duration of the re-treatment and provide high success rate.

In the early (e.g., within the first 30 days) post-ablative evaluation using CEUS, a thin and uniform enhancing rim due to reactive hyperemia can be visible along the periphery of the necrotic area, similar to findings on contrast-enhanced CT or MRI. Misinterpretation of this perilesional hyperemic halo as residual viable tumor can be avoided by comparing post-ablation images with pre-ablation scans.

Contrast-enhanced CT and MRI are the mainstay for imaging *follow-up* of treated patients for the detection of local tumor progressions or the occurrence of new tumors in the same organ or in other organs. Unfortunately, the absence of enhancement immediately after the procedure and in the following 24–48 h does not always indicate real, complete ablation and cannot exclude the presence of residual tumor tissue that will lead to a recurrence. Today, there is no clear consensus nor any evidence-based criteria for how and when posttreatment surveillance imaging should be performed. Generally, imaging studies (mostly CT or MRI) are performed at 3-, 6-, and 12 months to confirm the success of the interventional procedure.

B-mode US cannot be employed for this purpose because of its inability to differentiate areas of coagulative necrosis from local tumor progressions.

CEUS is very helpful for this differentiation, but, compared to CT and MRI, does not have the sufficiently large field of view which enables to thoroughly explore large organs and detect new lesions in organs different from the one treated. However, it may be helpful to obtain a CEUS study for each treated lesion shortly after treatment to which later CEUS examinations can be compared. CEUS can be usefully employed on long-term follow-up in patients allergic to iodine or with renal failure or when contrast-enhanced CT or MRI shows questionable patterns.

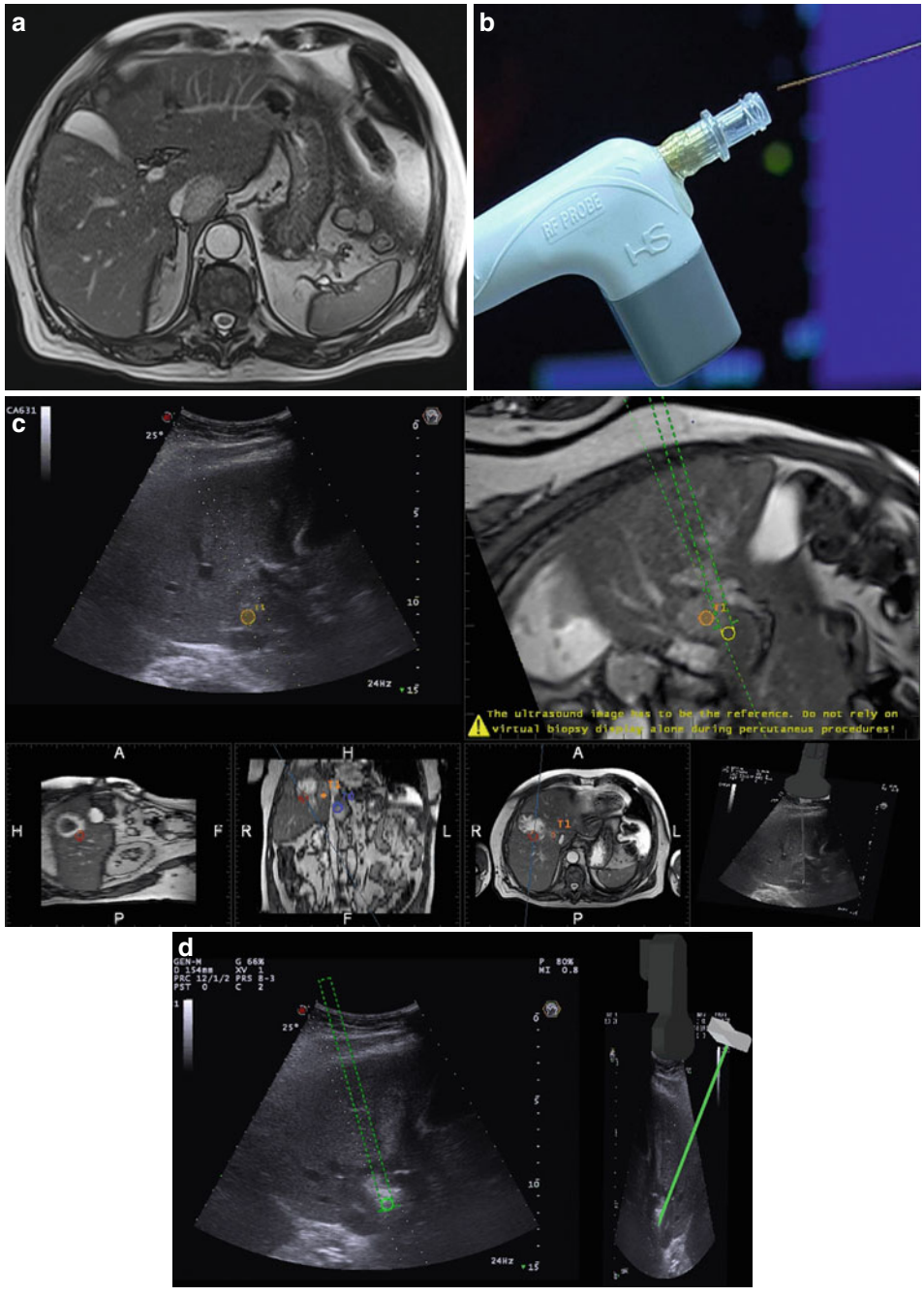

Fig. 13.7 (**a**) Contrast-enhanced MRI shows a 2.5-cm metastasis from lung carcinoma unresponsive to chemotherapy that entirely occupies the caudate lobe. Given the complexity and the high risk of the ablative procedure, a prototype RF electrode with internal canal allowing to insert a micro-electromagnetic sensor mounted on tip of a stylet (Hospital Service HS, Aprilia, Italy) (**b**) is used in combination with a real-time US-MRI image fusion system (Esaote, Genoa, Italy). The correct path of the electrode to the target (*green dotted line*) and the precise real-time positioning of the electrode tip (*yellow circle* in **c** on the *right side* and *green circle* in **d** on the *left image*) are seen both on the real-time US-MRI-fused scans (**c**) and on the two orthogonal real-time US scans (**d**)

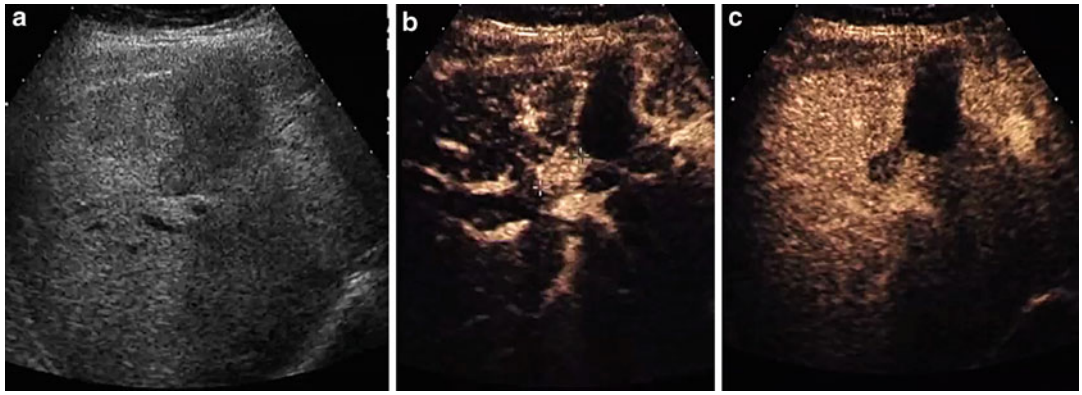

Fig. 13.8 Metastasis from colon cancer in the right hepatic lobe studied with B-mode US (**a**) and CEUS (**b**, **c**), 15 min after the end of radiofrequency ablation. US shows the complete disappearance of gas bubbles produced by ablation, but does not allow to assess the completeness of treatment (**a**). CEUS shows a wide, oval, unenhancing volume of necrosis but also (posteriorly) a rounded, 1.2-cm nodule with early and intense enhancement in arterial phase (**b**) and early washout in portal phase (**b**), representing residual, unablated portion of the metastasis

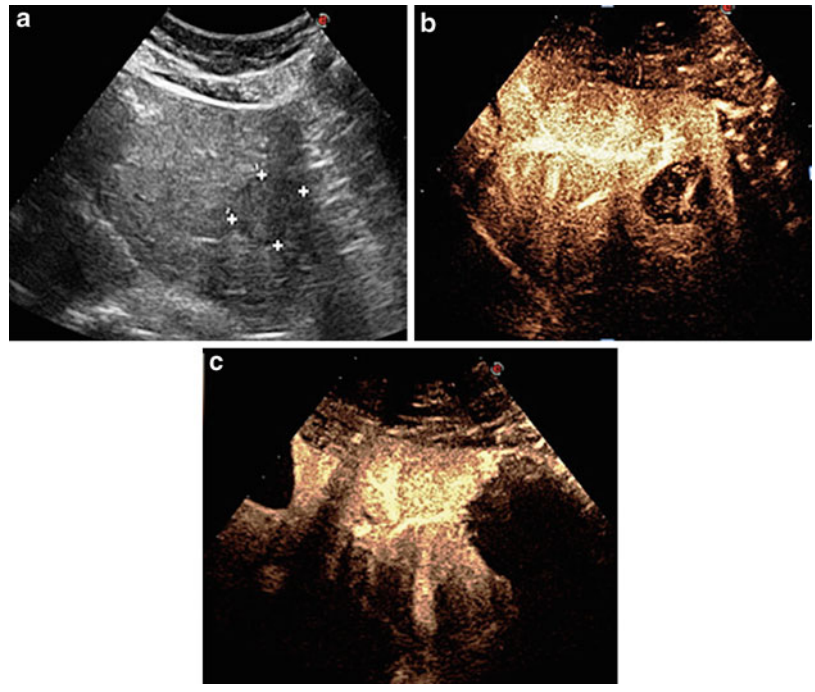

Fig. 13.9 (**a**) Pre-ablation US scan of 2.9-cm metastasis from colon carcinoma in the right hepatic lobe. (**b**) Few minutes after ablative treatment with cool-tip radiofrequency, CEUS shows an avascular volume of coagulative necrosis approximately of the same size of the pretreatment metastasis, thus insufficient to achieve local control of the tumor. (**c**) Immediate, CEUS-guided re-treatment is performed, and at the end, CEUS shows a much larger volume of necrosis, certainly adequate for local control

The RECIST guidelines [27] for the assessment of tumor response are no longer adequate for interventional procedures because of the poor relationship between necrosis and tumor size: completely necrotic tumors may remain unchanged in size, while tumors that shrunk may still be viable. Three patterns can suggest the presence of residual/recurrent viable tumor: (a) nodular enhancement at the periphery of the lesion, (b) thick, irregular rim of enhancement

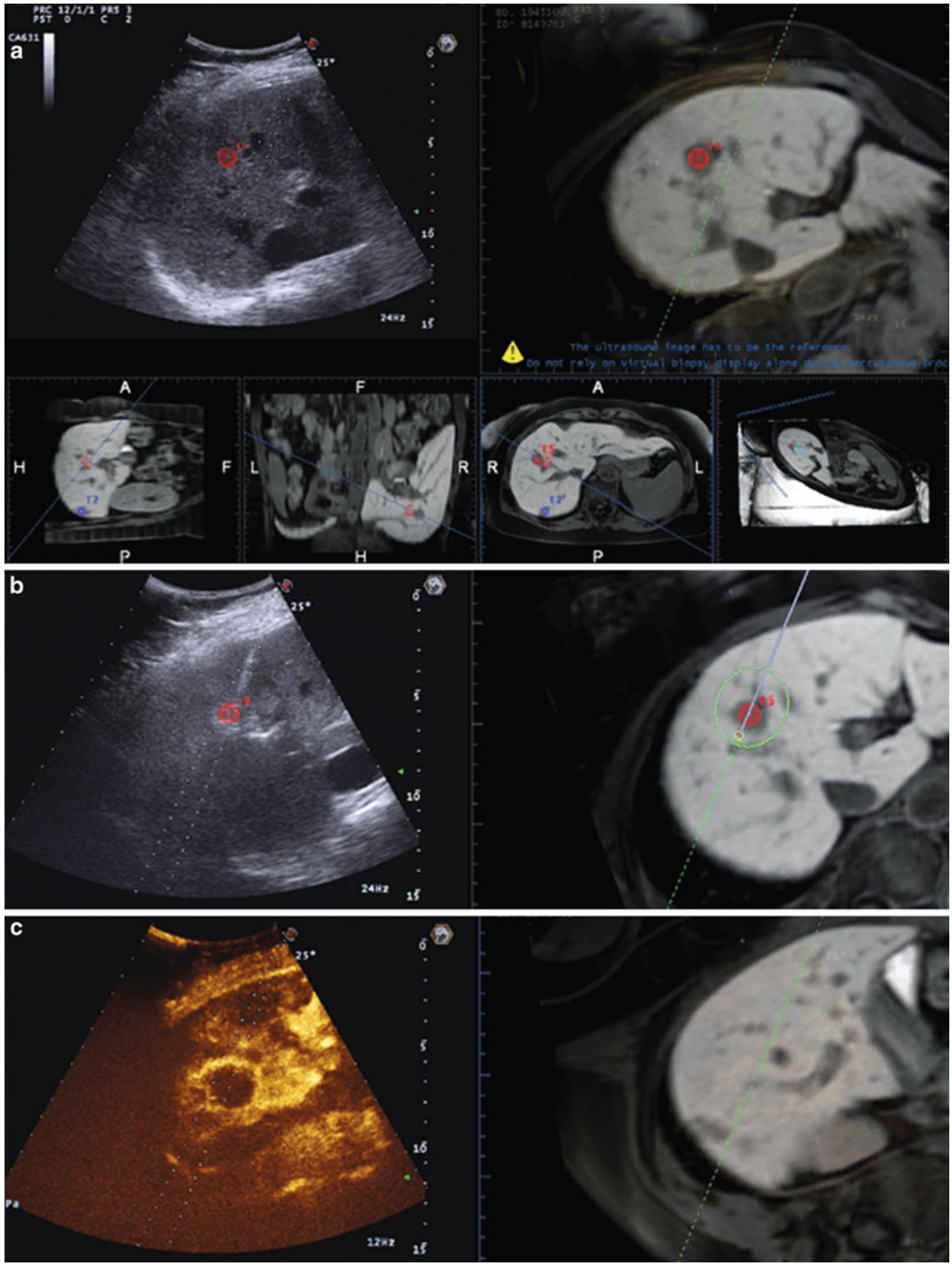

Fig. 13.10 Small metastasis from breast carcinoma detected before ablation (**a**) and precisely targeted (**b**) thanks to the real-time US-MRI image fusion system (Esaote, Genoa, Italy). Few minutes after ablation, CEUS is performed (**c**, on the *left*), and the size of the volume of necrosis showed by CEUS can be easily compared to the size of the pretreatment metastasis on MRI (**c**, on the *right*), clearly demonstrating complete ablation with wide peripheral "safety halo" of necrosis

around the ablated area, and (c) increase in gross enlargement of the ablated area in comparison to prior imaging examination.

CEUS is fast, easily available; allows real-time imaging, any type of angulation for biopsy/ablation; and is characterized by high natural contrast among parenchyma, tumors, cyst, calcification, and vessels. On the other hand, CT plays an important role, especially in interventions, which cannot be adequately guided by fluoroscopy or US.

In conclusion, in interventional therapies, B-mode US is the most widely employed imaging modality for guiding treatments, but cannot be used either for pre-procedure planning or intraprocedural monitoring and post-procedure follow-up. In interventional therapies of lesions and organs that can be imaged with US, CEUS is helpful as a complement to contrast-enhanced CT or MRI for pre-procedure staging and assessment of target lesion vascularity and can facilitate needle positioning in difficult occurrences. In addition, CEUS is particularly indicated as routine imaging modality for the assessment of immediate post-procedure treatment effect and the guidance of immediate re-treatment of residual unablated tumor. When follow-up contrast-enhanced CT or MRI is contraindicated or not conclusive, CEUS can be used in follow-up protocols.

Recent real-time US-CT/MRI fusion imaging systems have already gained a role (and will be increasingly used) for accurate pretreatment planning, precise targeting of difficult lesions, intraprocedural monitoring and control of treatment completeness, and immediate post-procedure assessment of necrosis achieved.

References

1. Solomon SB, Silverman SG. Imaging in interventional oncology. Radiology. 2010;257:624–40.
2. Wiering B, Ruers TJ, Krabbe PF, Dekker HM, Oyen WJ. Comparison of multiphase CT, FDG-PET and intra-operative ultrasound in patients with colorectal liver metastases selected for surgery. Ann Surg Oncol. 2007;14(2):818–26.
3. Harvey CJ, Albrecht T. Ultrasound of focal liver lesions. Eur Radiol. 2001;11:1578–93.
4. Solbiati L, Tonolini M, Cova L, Goldberg SN. The role of contrast-enhanced ultrasound in the detection of focal liver lesions. Eur Radiol. 2001;11 Suppl 3:E15–26.
5. Lencioni R, Cioni D, Bartolozzi C. Tissue harmonic and contrast-specific imaging: back to gray scale in ultrasound. Eur Radiol. 2002;12:151–65.
6. Maruyama H, Takahashi M, Ishibashi H, et al. Ultrasound-guided treatments under low acoustic power contrast harmonic imaging for hepatocellular carcinomas undetected by B-mode ultrasonography. Liver Int. 2009;29:708–14.
7. Minami Y, Kudo M, Chung H, et al. Contrast harmonic sonography-guided radiofrequency ablation therapy versus B-mode sonography in hepatocellular carcinoma: prospective randomized controlled trial. AJR Am J Roentgenol. 2007;188:489–94.
8. Numata K, Morimoto M, Ogura T, et al. Ablation therapy guided by contrast-enhanced sonography with Sonazoid for hepatocellular carcinoma lesions not detected by conventional sonography. J Ultrasound Med. 2008;27:395–406.
9. Chen MH, Wu W, Yang W, et al. The use of contrast-enhanced ultrasonography in the selection of patients with hepatocellular carcinoma for radiofrequency ablation therapy. J Ultrasound Med. 2007;26:1055–63.
10. Chen MH, Yang W, Yan K, et al. The role of contrast-enhanced ultrasound in planning treatment protocols for hepatocellular carcinoma before radiofrequency ablation. Clin Radiol. 2007;62:752–60.
11. Luo W, Numata K, Morimoto M, et al. Clinical utility of contrast-enhanced three-dimensional ultrasound imaging with Sonazoid: findings on hepatocellular carcinoma lesions. Eur J Radiol. 2009;72:425–31.
12. Hakime A, Deschamps F, De Carvalho EG, Teriitehau C, Auperin A, De Baere T. Clinical evaluation of spatial accuracy of a fusion imaging technique combining previously acquired computed tomography and real-time ultrasound for imaging of liver metastases. Cardiovasc Intervent Radiol. 2011;34(2):338–44.
13. Kawasoe H, Eguchi Y, Mizuta T, et al. Radiofrequency ablation with real-time virtual sonography system for treating hepatocellular carcinoma difficult to detect by ultrasonography. J Clin Biochem Nutr. 2007;40(1):66–72.
14. Liu FY, Yu XL, Liang P, et al. Microwave ablation assisted by a real-time virtual navigation system for hepatocellular carcinoma undetectable by conventional ultrasonography. Eur J Radiol. 2012;81(7):1455–9.
15. Minami Y, Chung H, Kudo M. Radiofrequency ablation of hepatocellular carcinoma: value of virtual CT sonography with magnetic navigation. AJR Am J Roentgenol. 2008;190(6):335–41.
16. Wood BJ, Kruecker J, Abi-Jaoudeh N, et al. Navigation systems for ablation. J Vasc Interv Radiol. 2010;21(8 Suppl):S257–63.
17. Claudon M, Cosgrove D, Albrecht T, et al. Guidelines and good clinical practice recommendations for contrast enhanced ultrasound (CEUS) – update 2008. Ultraschall Med. 2008;29:28–44.

18. Solbiati L, Tonolini M, Cova L. Monitoring RF ablation. Eur Radiol. 2004;14 Suppl 8:P34–42.
19. Rhim H, Goldberg SN, Dodd GD, Solbiati L, Lim HK, Tonolini M, Cho OK. Essential techniques for successful radiofrequency thermal ablation of malignant hepatic tumors. Radiographics. 2001;21:S17–31.
20. Andreana L, Kudo M, Hanataka K, et al. Contrast-enhanced ultrasound techniques for guiding and assessing response to locoregional treatments for hepatocellular carcinoma. Oncology. 2010;78 Suppl 1: 68–77.
21. Kim HJ, Kim TK, Kim PN, et al. Assessment of the therapeutic response of hepatocellular carcinoma treated with transcatheter arterial chemoembolization. Comparison of contrast-enhanced sonography and 3-phase computed tomography. J Ultrasound Med. 2006;25:477–86.
22. Miyamoto N, Hiramatsu K, Tsuchiya K, et al. Contrast-enhanced sonography-guided radiofrequency ablation for the local recurrence of previously treated hepatocellular carcinoma undetected by B-mode sonography. J Clin Ultrasound. 2010;38:339–45.
23. Ricci P, Cantisani V, Drudi F, et al. Is contrast-enhanced US alternative to spiral CT in the assessment of treatment outcome of radiofrequency ablation in hepatocellular carcinoma? Ultraschall Med. 2009;30: 252–8.
24. Shiozawa K, Watanabe M, Takayama R, et al. Evaluation of local recurrence after treatment for hepatocellular carcinoma by contrast-enhanced ultrasonography using Sonazoid: comparison with dynamic computed tomography. J Clin Ultrasound. 2010;38:182–9.
25. Vilana R, Bianchi L, Varela M, BCLC Group, et al. Is microbubble-enhanced ultrasonography sufficient for assessment of response to percutaneous treatment in patients with early hepatocellular carcinoma? Eur Radiol. 2006;16:2454–62.
26. Kisaka Y, Hirooka M, Koizumi Y, et al. Contrast-enhanced sonography with abdominal virtual sonography in monitoring radiofrequency ablation of hepatocellular carcinoma. J Clin Ultrasound. 2010; 38:138–44.
27. Therasse P, Arbuck SG, Eisenhauer EA, et al. New guidelines to evaluate the response to treatment in solid tumors. European Organization for Research and Treatment of Cancer, National Cancer Institute of the United States, National Cancer Institute of Canada. J Natl Cancer Inst. 2000;92:205–16.

Imaging of Interventional Therapies in Oncology: Computed Tomography

14

David J. Grand

Abstract

Computed tomography (CT), particularly multi-detector CT (MDCT), rapidly provides exquisite diagnostic information. Continued growth of percutaneous oncologic therapies requires detailed understanding of the CT appearance of tumors both before and after treatment. The purpose of this chapter is to familiarize the radiologist with current techniques for tumor diagnoses as well as well as posttreatment evaluation of percutaneously treated lesions.

Introduction

In the past two decades, the use of computed tomography (CT) has grown exponentially, becoming the fundamental workhorse of all major radiology departments. Multi-detector CT (MDCT) provides fast, accurate, noninvasive assessment of nearly every organ system with sub-mm resolution and typically does so in less than 1 min. For these reasons, in addition to widespread availability and excellent patient tolerance, MDCT plays a critical role in the diagnosis, staging, and percutaneous treatment of malignancies of multiple organ systems including the lung, liver, kidney, and musculoskeletal systems. Finally, MDCT is the modality most commonly used to judge both the initial success of percutaneous intervention and the durability of treatment response and potential need for subsequent intervention.

D.J. Grand
Department of Diagnostic Radiology, Warren Alpert School of Medicine, Brown University, Providence, RI, USA
e-mail: dgrand@lifespan.org

Diagnosis

Lung

MDCT has revolutionized the detection of both primary bronchogenic carcinoma and metastatic disease to the lungs. The ability of MDCT to detect small cancers is beyond question. Its efficacy is underscored by numerous national and international trials using MDCT to screen asymptomatic, high-risk patients in hopes of earlier detection and higher cure rates [1–3]. Importantly, IV contrast is not necessary to detect parenchymal lung disease, although it is helpful in delineating nodal disease within the mediastinum.

For practical purposes, MDCT is the only clinically relevant imaging modality for the lung. Ultrasound may be used to guide biopsy of

D.E. Dupuy et al. (eds.), *Image-Guided Cancer Therapy*, DOI 10.1007/978-1-4419-0751-6_16,

pleural-based masses, but otherwise ultrasound is "blinded" by the diffuse scatter of sound waves at interfaces with air. Likewise, MRI is adversely affected by air which causes inhomogeneity in the magnetic field. While it may also be useful for chest wall or pleural-based masses, it is not useful for intraparenchymal lesions.

Though exquisitely sensitive, MDCT is plagued by low specificity [4, 5]. Incidental, inconsequential pulmonary nodules are a common and frustrating finding resulting in (anxiety-provoking) follow-up examinations and lung biopsies.

When pulmonary nodules/masses are detected by MDCT, the most commonly used criteria to assess malignant potential are size and growth. Patients with nodules greater than 1 cm without definite benign features (classic calcification patterns and/or macroscopic fat) typically undergo PET/CT (to evaluate for metabolic activity) or percutaneous biopsy. Patients with nodules smaller than 1 cm undergo serial MDCT follow-up examinations, attempting to establish 2-year stability. If the nodule is noted to enlarge in this interval, biopsy is performed. Specific guidelines for the management of pulmonary nodules have been issued by the Fleischner Society and have been widely accepted [6].

There have been promising studies using dynamic contrast enhancement to quantify the risk of malignancy in pulmonary nodules [7]. As we will discuss, this technique is used following percutaneous therapy; however, dynamic assessment of pulmonary nodules has not gained widespread acceptance and is not routinely performed.

Liver

Contrast-enhanced MDCT is an excellent test for the detection of primary and metastatic disease to the liver. While MRI may demonstrate higher sensitivity and specificity, the rapid anatomic coverage of CT is unparalleled, allowing for comprehensive radiologic staging in a single exam. The routine use of IV contrast is mandatory for adequate sensitivity. If IV contrast cannot be administered, MRI should be recommended for its superior inherent soft-tissue contrast. It is also worth noting that hepatic steatosis can decrease the sensitivity of MDCT [8, 9].

Primary malignancies of the liver require dynamic imaging for adequate evaluation. At a minimum, pre-contrast, arterial phase and portal venous phase imaging should be performed, and delayed imaging should be considered. Hepatocellular carcinoma is most commonly hypervascular and therefore most conspicuous on arterial phase imaging. Small lesions and satellite lesions can be invisible on portal phase images [10]. Delayed images should be critically reviewed as accelerated "washout" of contrast is as worrisome a feature as rapid "wash in." In contrast, cholangiocarcinoma may have a significant fibrous component and enhance on delayed images [11].

Dynamic imaging is not necessary for detection of metastatic disease from most primary malignancies [12]. Lesions are most conspicuous on the portal venous phase, approximately 60–90 s following IV injection, and therefore, a single time point is adequate [13]. Only hypervascular lesions (most commonly neuroendocrine malignancies) require multiphase exams as metastases from these tumors may be undetectable on portal phase studies.

Kidney

In large part because of the widespread use of MDCT, most renal masses are now discovered incidentally [14]. MDCT is the gold-standard imaging test for the detection and characterization of renal masses. Some centers report increased sensitivity with multiple phases of contrast enhancement, but, at a minimum, pre- and post-contrast imaging must be performed [15]. Imaging characterization of renal masses is straightforward and best approached by first categorizing masses as either cystic or solid.

Solid masses which contain macroscopic fat are benign angiomyolipomas. Solid, enhancing renal masses without macroscopic fat are malignant until proven otherwise. The differential diagnosis for a solid, enhancing renal mass without macroscopic fat includes renal cell carcinoma,

oncocytoma, and lipid-poor angiomyolipoma. Practically, renal cell carcinoma and oncocytoma receive identical, definitive treatment. Lipid-poor angiomyolipoma constitutes a relatively small number of enhancing renal masses but, if pathologically proven via biopsy, can be safely ignored. If the patient has a known primary malignancy, metastases must be considered in the differential diagnosis, and biopsy should be performed.

Cystic renal lesions are categorized by the Bosniak criteria. Simple cysts are well-defined, measure <20 HU, and contain no internal septations or calcifications. Complex cysts contain proteinaceous debris or hemorrhage but lack significant enhancement (<20 HU increased density following contrast administration). Thin, enhancing septations and smooth, mural calcification are common within cystic lesions and are not indicative of malignancy. Thick or nodular septations may indicate cystic renal cell carcinoma and should be followed or biopsied. Cystic lesions which enhance between 10 and 20 HU are indeterminate and should be followed radiographically. Cystic lesions which enhance >20 HU are considered to be malignant [16, 17].

After establishing a confident imaging or pathologic diagnosis, MDCT is critical for preprocedural planning. Whenever possible, images should be obtained with isotropic voxels (identical resolution in *x*-, *y*-, and *z*-axis) conducive to multi-planar reconstructions. This allows confident assessment of the proximity of important structures such as the renal pelvis, ureter, and bowel.

MRI is excellent for the detection and characterization of renal lesions but plays a secondary role to MDCT at most institutions. Renal MRI is best used in two clinical scenarios: first, to evaluate cystic lesions which demonstrate indeterminate enhancement at CT and, second, to definitively assess enhancement in hemorrhagic/proteinaceous cysts.

Post-procedural Imaging

Post-procedural imaging is critical to assure immediate procedural success as well as monitor for disease reoccurrence. The interpreting radiologist should be aware of common appearances of successfully treated lesions, which can vary between organ systems, to avoid false-positive interpretations. The ideal imaging modality for detecting tumor reoccurrence remains undetermined and likely varies based on the origin of the tumor. For example, PET/CT may be the most useful modality for monitoring treatment response in colorectal metastases to the liver, but is not helpful for hepatocellular carcinoma. Despite, or perhaps because of, the current unknowns as well as the ease and widespread availability of CT, CT remains the most common modality used to monitor treatment response. Specific discussion of tumor types and individual organs follows; however, in general, nodular enhancement at the treatment margin indicates recurrent disease.

Lung

Posttreatment evaluation of percutaneously treated lung lesions, primary or metastatic, is fraught with difficulty due to often profound architectural changes in the surrounding lung parenchyma. In the immediate posttreatment setting, lung lesions may appear to have increased in size as the thermal treatment zone is surrounded by inflammatory, ground-glass changes which can occupy large segments of adjacent lung [18]. It is critical to review the pretreatment images as well as the images obtained during treatment to avoid mistaking these changes for residual or recurrent disease. Cavitation is also a fairly common sequelae of percutaneous therapy estimated to occur in 14–52 % of treatment sessions, typically within the first month following treatment (Fig. 14.1). Patients at highest risk for cavitation include those with primary lung cancer, emphysema, and subpleural lesions [19].

Over time, the change in lung parenchyma dissipates as inflammation decreases and is replaced by scar tissue [20]. Features considered indicative of residual or recurrent disease include true increase in lesion size or enhancing nodularity along the lesion margin [21]. Obtaining multiple phases of contrast enhancement may be helpful to

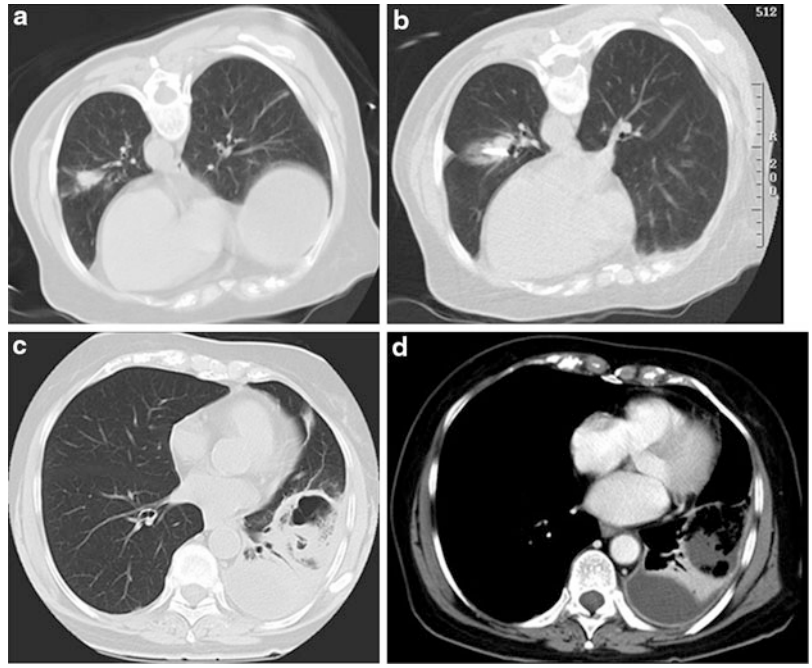

Fig. 14.1 Axial pre-procedural (**a**) and intraprocedural (**b**) images with patient in prone position. A mass is noted within the right lower lobe. Please note tip of ablation device within lesion on image (**b**). Axial follow-up images at 3 months (**c**, **d**) demonstrate typical changes of cavitation and small pleural effusion with no evidence of enhancing solid tissue to suggest recurrent disease

increase reader confidence (Fig. 14.2). Of note, a thin rim of symmetric peritumoral enhancement is a common and benign finding seen in the first 6 months following treatment [22]. Of course, in addition to evaluation of the ablation site, it is critical to search carefully for the appearance of distant nodules/masses and adenopathy.

Liver

Recurrence following percutaneous therapy may be categorized as one of three types: local intrahepatic, remote intrahepatic, and extrahepatic. Local intrahepatic recurrence will be discussed here as it is the most challenging to detect and differentiate from normal posttreatment changes. If the treated lesion was initially arterially hyperenhancing (e.g., HCC), three-phase CT should be performed for follow-up. Otherwise, a portal venous phase CT will suffice [23]. Meta-analysis suggests that the incidence of local tumor progression at the site of treatment is between 2 % and 60 % and most commonly occurs within 6–12 months of treatment [24].

In contrast to the lung and kidney, there are two different percutaneous techniques available for treatment of hepatic tumors: transarterial chemoembolization (TACE) and ablation. Fundamentally, the posttreatment appearance of recurrent disease is the same, nodular foci of residual enhancement, though each technique warrants a brief, separate discussion.

TACE exploits the preference of liver tumors for a hepatic arterial, rather than portal venous, blood supply. Most commonly, chemotherapeutic agents are mixed with lipiodol and injected into a specific, feeding hepatic artery, thereby delivering higher local doses of chemotherapy than could be achieved systemically. Embolic agents may or may not then be administered to decrease the hepatic arterial flow to the tumor. Careful examination of pre-contrast images is crucial in the posttreatment setting as lipiodol is hyperattenuating on CT and can impair detection of residual enhancement [25]. Transarterial therapy may also now be performed using embolic

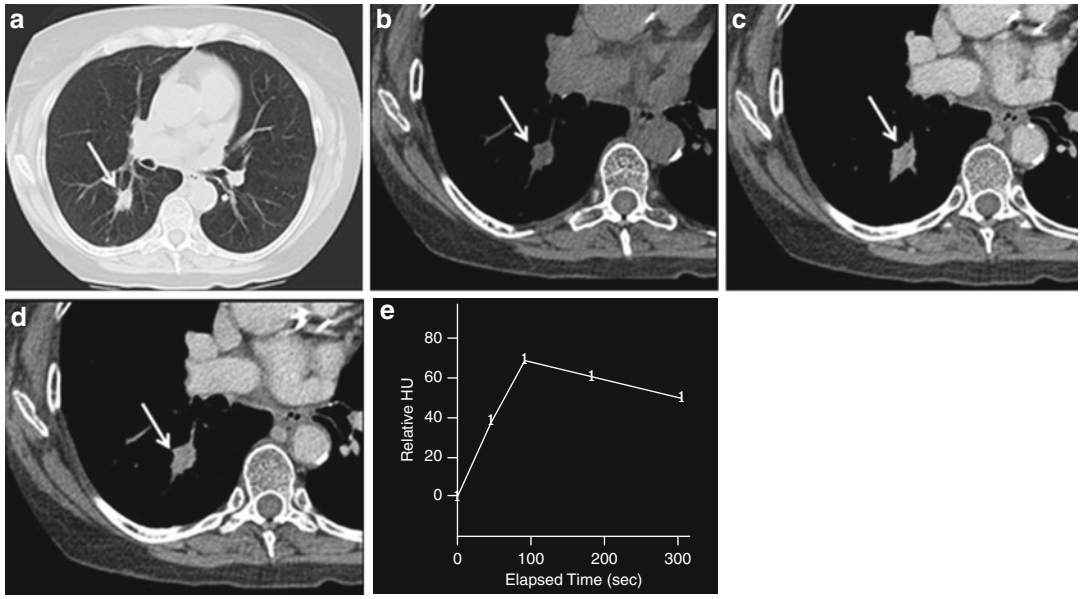

Fig. 14.2 Axial pre-contrast (**a**, **b**) and dynamically acquired post-contrast images (**c**, **d**) with graph of enhancement (**e**). Significant enhancement (greater than 20 HU) is indicative of residual tumor

beads impregnated with chemotherapy or yttrium which delivers high doses of local radiation. These options do not use lipiodol. Viability is again judged by residual enhancement.

Established recommendations are for percutaneous ablation to treat a margin of healthy tissue between 0.5 and 1.0 cm beyond the suspected tumor margin [26]. As in the lung, this then creates an ablation defect which will initially appear larger than the treated lesion itself. Treated (dead) liver tissue does not enhance; however, "debris" from thermal coagulation may be dense. This debris typically occurs in the center of the ablation zone and is amorphous rather than nodular; however, in case of confusion, a multiphase exam can be performed to confirm lack of enhancement (Fig. 14.3).

Identification of local recurrence is based on patterns described as nodular, halo, or gross enlargement. The nodular pattern consists of a new, focal mass, protruding from the ablation margin. The halo type describes a discernible rim of tissue at the margin of the ablation zone which enhances differently from the liver parenchyma or ablation zone itself. Gross enlargement refers to an overall increase in tumor size, taking into account that at the time of the first follow-up scan, the ablation zone is expected to be larger than the initial lesion [27].

Of course, it is critical to fully assess the liver for remote intrahepatic recurrence as well as the remainder of the chest, abdomen, and pelvis for extrahepatic disease. Finally, it should be noted that the performance of CT for detection of local recurrence following percutaneous therapy is imperfect and other modalities (MRI, PET/CT) may be more advantageous depending upon the initial tumor type. For example, MRI is an excellent modality for detecting recurrence of HCC in addition to detecting satellite lesions.

Kidney

Post-procedural follow-up of ablated renal lesions requires at least pre- and post-contrast imaging. Ablated renal lesions are typically higher in attenuation than normal renal parenchyma on pre-contrast imaging; however, they do not

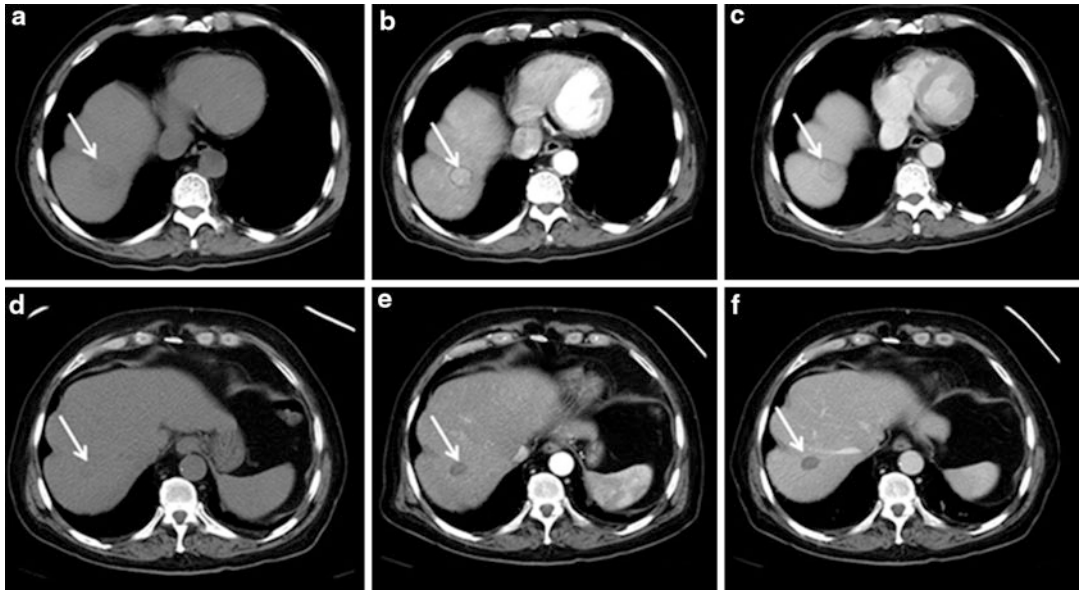

Fig. 14.3 Pre-procedural axial CT obtained non-contrast (**a**), as well as in the arterial (**b**) and venous phases (**c**). Please note extensive enhancement on the arterial phase with washout on the delayed phase indicative of hepatocellular carcinoma. Corresponding posttreatment images (**d–f**) demonstrate mild hyperattenuating material within the ablation site without evidence of enhancement compatible with complete tumor kill

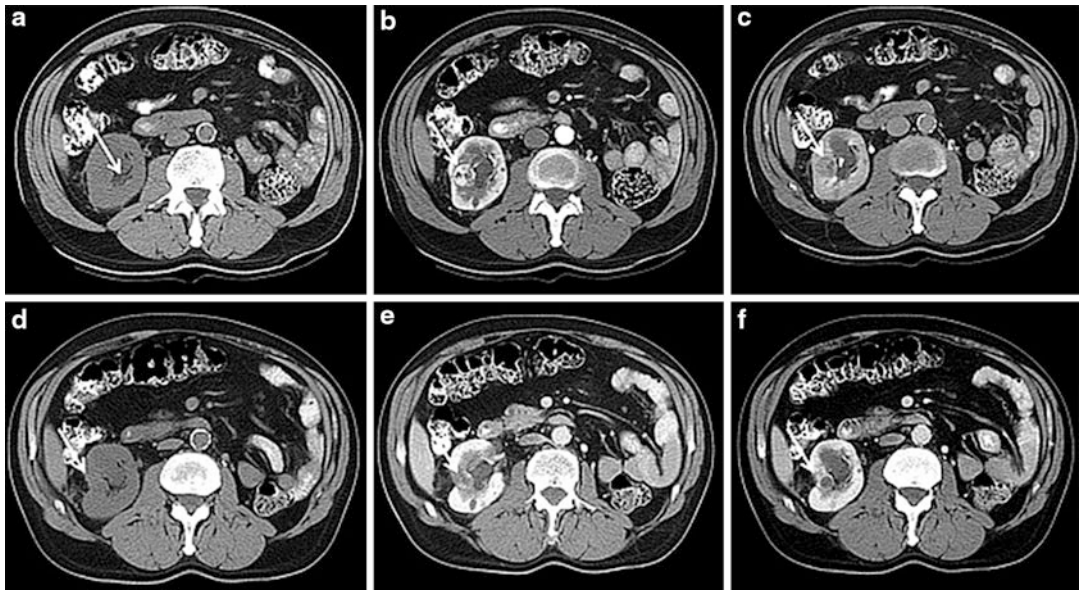

Fig. 14.4 Pre-procedural imaging-performed pre-contrast (**a**) as well as in the arterial (**b**) and delayed phases demonstrates an enhancing mass in the interpolar region of the right kidney. Corresponding post-procedural imaging demonstrates no evidence of residual enhancement indicative of excellent response

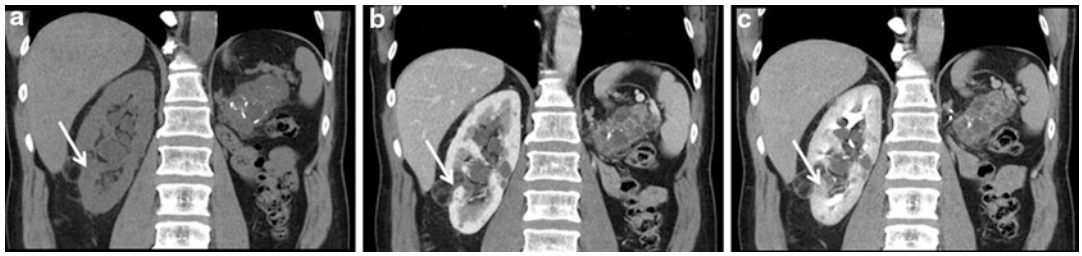

Fig. 14.5 Coronal follow-up images of same patient at 2 years obtained pre-contrast (**a**) as well as in the arterial (**b**) and delayed (**c**) phases demonstrate nodular enhancement at the medial margin of the ablation site compatible with recurrent disease

enhance. As previously discussed, the ablation zone will often appear larger than the initial lesion and tends to decrease in size over time. Perinephric stranding is a common and benign post-procedural finding [28].

As in the liver, findings suspicious for local recurrence include foci of enhancing nodularity or crescentic enhancement typically at the margin of the ablation zone (Figs. 14.4 and 14.5) [29]. One unique feature of posttreatment renal imaging is the appearance of the "halo" sign which occurs in up to 75 % of patients and consists of macroscopic fat surrounded by a thin, smooth rim of soft tissue at the ablation site [30]. This should not be mistaken for tumor reoccurrence or (more commonly) an angiomyolipoma. Careful attention should be paid to identification of metachronous lesions in the treated or contralateral kidney.

MDCT is so effective that MRI likely does not confer any additional benefit in terms of detection of recurrence or new lesions. However, RCC is unique in that it is most commonly an incidentally detected mass which, once successfully treated, will likely not affect the patient's life span. (Consider this in contrast to HCC, which even if successfully treated usually arises in a background of comorbid conditions such as cirrhosis.) In this context, given that patients currently undergo surveillance imaging with multiphase MDCT for the remainder of their lives, MRI may be used to reduce radiation exposure. This is particularly important for younger patients, although the definition of "young" is quite variable and personal.

Conclusion

Due to its relative simplicity and availability, CT is and will likely remain the most common imaging modality for identification of malignancy as well as monitoring treatment response. Although there are minor variations in treatment appearance depending on the organ of interest, fundamentally treatment zones should be well-defined and lack enhancement. Growth at or of the treatment site or development of nodular foci of enhancement should be considered suspicious for recurrent disease.

References

1. Menezes RJ, Roberts HC, Paul NS, et al. Lung cancer screening using low-dose computed tomography in at-risk individuals: the Toronto experience. Lung Cancer. 2010;67:177–83.
2. Fujikawa A, Takiguchi Y, Mizuno S, et al. Lung cancer screening – comparison of computed tomography and X-ray. Lung Cancer. 2006;61:195–201.
3. Diederich S, Thomas M, Semik M, et al. Screening for early lung cancer with low-dose spiral computed tomography: results of annual follow-up; examinations in asymptomatic smokers. Eur Radiol. 2004;14:691–702.
4. Crosswell JM, Baker SG, Marcus PM, et al. Cumulative incidence of false-positive test results in lung cancer screening. Ann Intern Med. 2010;152(8):505–12.
5. Wahidi MM, Govert JA, Goudar RK, et al. Evidence for the treatment of patients with pulmonary nodules: when is it lung cancer? Chest. 2007;132:94S–107.
6. MacMahon H, Austin JH, Gamsu G, et al. Guidelines for management of small pulmonary nodules detected on CT scans: a statement from the Fleischner Society. Radiology. 2005;237(2):395–400.

7. Swenson SJ, Viggiano RW, Midthun DE, et al. Lung nodule enhancement at CT: multicenter study. Radiology. 2000;214:73–80.
8. Angliviel B, Benoist S, Penna C, El Hajjam M, Chagnon S, Julie C, Beauchet A, Rougier P, Nordlinger B. Impact of chemotherapy on the accuracy of computed tomography scan for the evaluation of colorectal liver metastases. Ann Surg Oncol. 2009;16:1247–53.
9. Yates CK, Streight RA. Focal fatty infiltration of the liver simulating metastatic disease. Radiology. 1986;159:83–4.
10. Kim MJ, Choi JY, Lim JS, et al. Optimal scan window for detection of hypervascular hepatocellular carcinomas during MDCT examination. AJR. 2006;187(1):198–206.
11. Motosugi U, Ichikawa T, Nakajima H, et al. Cholangiolocellular carcinoma of the liver: imaging findings. J Comput Assist Tomogr. 2009;33(5):682–8.
12. Ch'en IY, Katz DS, Jeffrey Jr RB, Daniel BL, Li KC, Beaulieu CF, Mindelzun RE, Yao D, Olcott EW. Do arterial phase helical CT images improve detection or characterization of colorectal liver metastases? J Comput Assist Tomogr. 1997;21(3):391–7.
13. Soyer P, Poccard M, Boudiaf M, Abitbol M, Hamzi L, Panis Y, Valleur P, Rymer R. Detection of hypovascular hepatic metastases at triple-phase helical CT: sensitivity of phases and comparison with surgical and histopathologic findings. Radiology. 2004;341:413–20.
14. Smith SJ, Bosniak MA, Megibow AJ, et al. Renal cell carcinoma. Earlier discovery and increased detection. Radiology. 1989;170:699–703.
15. Kopka L, Fischer U, Zoeller G, et al. Dual-phase helical CT of the kidney: value of the corticomedullary and nephrographic phase for evaluation of renal lesions and preoperative staging of renal cell carcinoma. AJR. 1997;169:1573–8.
16. Silverman SG, Israel GM, Herts BR, et al. Management of the incidental renal mass. Radiology. 2008;249(1):16–31.
17. Israel GM, Bosniak MA. An update of the bosniak renal cyst classification system. Urology. 2005;66: 484–8.
18. Wolf FJ, Grand DJ, Machan JT. Microwave ablation of lung malignancies: effectiveness, CT findings and safety in 50 patients. Radiology. 2008;247:871–9.
19. Okuma T, Matsuoka T, Yamamoto A. Factors contributing to cavitation after CT-guided percutaneous radiofrequency ablation for lung tumors. J Vasc Interv Radiol. 2007;18:399–404.
20. Bojarski JD, Dupuy DE, Mayo-Smith WM. CT imaging findings of pulmonary neoplasm after treatment with radiofrequency ablation: results in 32 tumors. AJR. 2005;185:466–71.
21. Yamakado K, Hase S, Matsuoka T, et al. Radiofrequency ablation for the treatment of unresectable lung metastases in patients with colorectal cancer: a multicenter study in Japan. J Vasc Interv Radiol. 2007;18:393–8.
22. Goldberg SN, Grassi C, Cardella J, et al. Image-guided tumor ablation: standardization of terminology and reporting criteria. J Vasc Interv Radiol. 2005;16:765–78.
23. Schraml C, Clasen S, Schwenzer NF. Diagnostic performance of contrast-enhanced computed tomography in the immediate assessment of radiofrequency ablation success in colorectal liver metastases. Abdom Imaging. 2008;33:643–51.
24. Muller S, Ni Y, Jamart J, et al. Local recurrence after hepatic radiofrequency coagulation: multivariate meta-analysis and review of contributing factors. Ann Surg. 2005;242:158–71.
25. Chen CY, Li CW, Kuo YT, et al. Early response of hepatocellular carcinoma to transcatheter arterial chemoembolization: choline levels and MR diffusion constants – initial experience. Radiology. 2006; 239(2):448–56.
26. Cady B, Jenkins RL, Steele Jr GD, et al. Surgical margin in hepatic resection for colorectal metastasis: a critical and improvable determinant of outcome. Ann Surg. 1998;277:566–71.
27. Chopra S, Dodd GD, Chintapalli KN. Tumor recurrence after radiofrequency thermal ablation of hepatic tumors: spectrum of findings on dual-phase contrast-enhanced CT. AJR. 2001;177:381–7.
28. Davenport MS, Caoili EM, Cohan RH, et al. MRI and CT characteristics of successfully ablated renal masses: imaging surveillance after radiofrequency ablation. AJR. 2009;192:1571–8.
29. Wile GE, Leyendecker JR, Krehbiel KA, et al. CT and MR imaging after imaging-guided thermal ablation of renal neoplasms. Radiographics. 2007;27:325–41.
30. Schirmang TC, Mayo-Smith WW, Dupuy DE, et al. Kidney neoplasms: renal halo sign after percutaneous radiofrequency ablation – incidence and clinical importance in 101 consecutive patients. Radiology. 2009;253:263–9.

Imaging of Interventional Therapies in Oncology: Magnetic Resonance Imaging

15

Servet Tatli and Stuart G. Silverman

Abstract

MRI is one of the main pillars of oncologic imaging and plays a vital role in the care of patients with cancer. Due to intrinsic proprieties such as superior soft tissue contrast resolution, multiplanar capability, functional imaging ability, and lack of ionizing radiation, MRI has become indispensible in the management of oncologic diseases. As the technology advances, its role will continue to expand at virtually every stage of patient care. In this chapter, we review the essential features of MRI in oncologic imaging and discuss the clinical use of MRI in the diagnosis, staging, treatment, and surveillance of common oncologic diseases. We also discuss recent and forthcoming advances in oncologic MRI.

Introduction

Imaging plays a crucial role in the care of patients with cancer and is being used in virtually every stage of the management of oncologic diseases including screening, diagnosis, staging, treatment, and surveillance. Imaging frequently is used to guide biopsies to obtain tissue samples for histopathologic diagnosis, to plan invasive therapies including surgery and radiotherapy, and to plan and execute percutaneous therapies such as tumor ablations.

X-ray radiography is widely available, but the information is limited and generally helpful only in certain organs, such as breast, bones, and lungs. Ultrasound utilizes no ionizing radiation, but its clinical use is also limited to certain organs such as thyroid, liver, kidney, and pelvic organs. CT is the most commonly used imaging modality in the care of patients with oncologic diseases; it is fast, widely available, and well tolerated, but its soft tissue contrast resolution is not adequate to detect and characterize some tumors. Tissue proprieties displayed by CT are limited to attenuation and enhancement. MRI, like US, uses no ionizing radiation and provides images with excellent soft tissue contrast in multiple planes. However, MRI yields more information about

S. Tatli (✉)
Department of Abdominal Imaging and Intervention, Brigham and Women's Hospital, Boston, MA, USA
e-mail: statli@partners.org

S.G. Silverman
Division of Abdominal Imaging and Intervention, Department of Radiology, Brigham and Women's Hospital, Harvard Medical School, Boston, MA, USA
e-mail: sgsilverman@partners.org

D.E. Dupuy et al. (eds.), *Image-Guided Cancer Therapy*, DOI 10.1007/978-1-4419-0751-6_17,

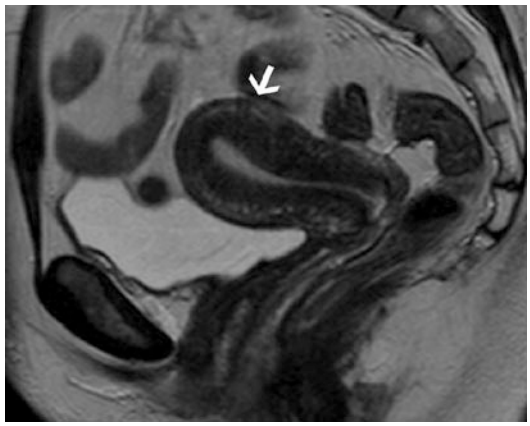

Fig. 15.1 Normal female pelvis. Sagittal T2-weighted MR image demonstrates excellent soft tissue contrast resolution allowing visualization of the substructural anatomy of the uterus (*arrow*), which has a central hyperintense endometrial stripe surrounded by hypointense junctional zone

tissue proprieties including T1 and T2 signal intensity, enhancement, and information about the presence of fat, water, and other substances.

Using pulse sequences used in clinical practice, MRI is based on different resonance capabilities of hydrogen protons in a strong magnetic field. The protons are excited with various radiofrequency pulses and allowed to relax to their equilibrium state. Depending on their molecular environment, excited protons return to their equilibrium state at different rate. This difference can be detected by receiver coils, and an MR image can be constructed. Therefore, an MR image reflects molecular differences in tissues and demonstrates high soft tissue contrast between tissues containing different molecules. Many cancers can be detected by MRI due to their molecular differences relative to their surrounding tissues.

Soft tissue contrast resolution of MRI surpasses all other available imaging modalities. Anatomic details of the major substructure of the organs such as the brain, head and neck, and female and male pelvic organs can be visualized better with MRI (Fig. 15.1). MRI allows visualization of certain tumors of the liver, breast, and prostate gland that are simply not visible with other imaging modalities (Fig. 15.2). Due to its excellent soft tissue resolution, MRI helps characterize masses detected with other imaging modalities and prevents unnecessary invasive procedures (Figs. 15.3 and 15.4).

MRI is helpful also in staging cancers, identifying local extension, lymph node involvement, and distant metastases. The multiplanar capability of MRI helps to define the local extent of the tumor (Fig. 15.5). In addition, imaging plane in any desired plane has been found useful in planning surgery and radiation therapy and guiding interventional procedures [1].

MRI is particularly helpful in patients for whom contrast-enhanced CT scan cannot be performed because of iodinated contrast material allergy or renal insufficiency and pregnant patients to prevent harmful effect of radiation to the fetus. Perhaps MRI's important advantage is that it does not use ionizing radiation. Cumulative radiation doses resulting from multiple CT scans used to diagnose and follow patients with cancer can be substantial and are thought to increase the risk of the development of secondary cancer, particularly in children and young adults [2]. In the future, it is likely that MRI will be used more frequently in lieu of CT.

Initial MRI investigators thought that with development of variety of pulse sequences would increase soft tissue contrast ability of MRI and the use of any contrast agent would be unnecessary. However, subsequently it was realized that contrast agent provides physiologic information, and significantly increases the ability of MRI in the detection and characterization of abnormal masses by increasing contrast between tumors and background soft tissues. Gadolinium-based compounds such as gadopentetate dimeglumine (Gd-DTPA) are the main contrast agent used in MRI. The sequences following intravenous administration of contrast agent are currently the backbone of most MRI protocols and commonly utilized during routine MRI evaluation of almost every organs of the patients with cancer.

Gadolinium-based contrast agents are well tolerated by patients and have very high safety profile compare to iodine-based contrast agents [3]. The total prevalence of adverse

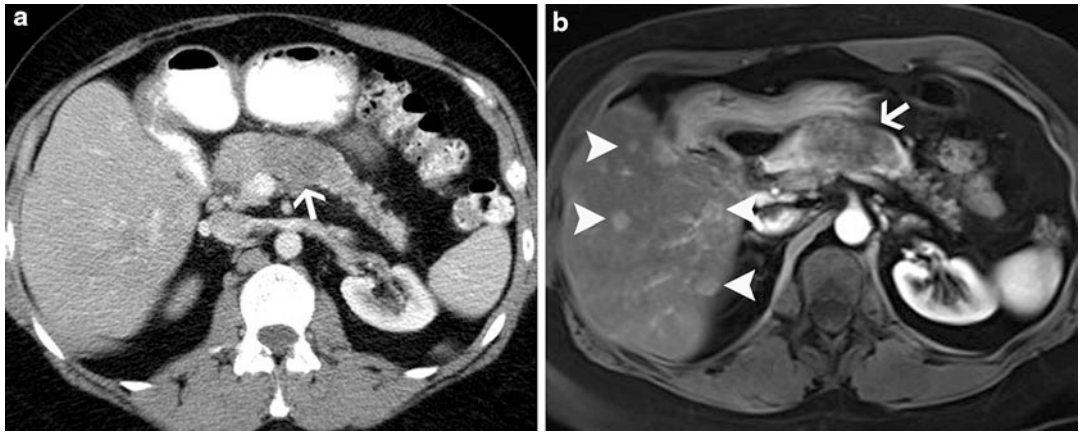

Fig. 15.2 Pancreatic neuroendocrine tumor. Axial enhanced CT (**a**) shows hypodense mass (*arrow*) in the body of the pancreas proven to be a neuroendocrine tumor. Axial, fat-suppressed, enhanced MRI (**b**) at the same level of the CT image shows in addition to the pancreatic mass (*arrow*) multiple liver metastases (*arrowheads*) that were not seen at CT

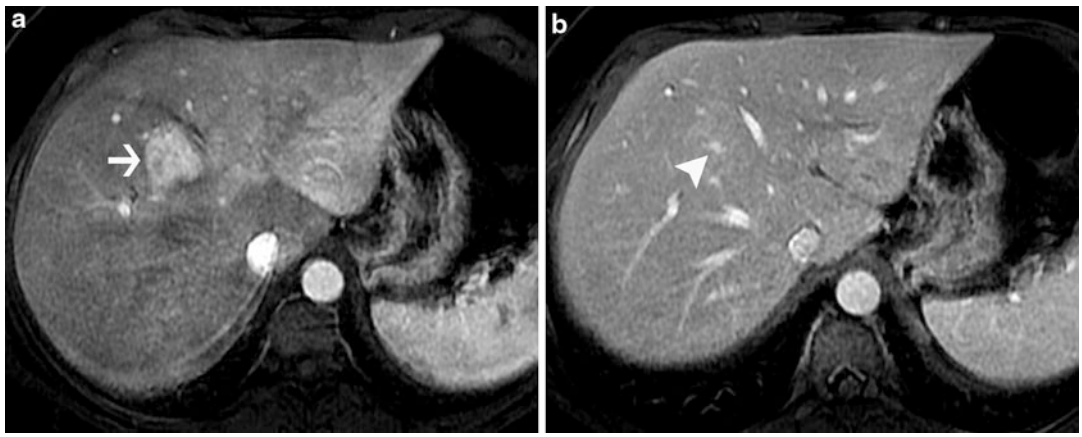

Fig. 15.3 Focal nodular hyperplasia (FNH). A liver mass was seen incidentally on abdominal US in a 26-year-old woman who presented with abdominal pain. The patient was referred to liver MRI for further characterization. Axial, fat-suppressed, enhanced MRI (**a**) at early arterial phase shows markedly and diffusely enhancing mass (*arrow*) in the liver. Axial, fat-suppressed, enhanced MRI (**b**) during portal-venous phase shows that the mass become isointense with the rest of the liver but has central enhancing focus (*arrowhead*). The appearance is typical for FNH, and the central enhancing focus represents vascular central scar

reactions of all types is approximately 2.4 %, and most includes minor symptoms such as headache, nausea, vomiting, local burning or cool sensation, and hives [3]. Adverse events after intravenous injection of gadolinium seem to be more common in patients who had previous reaction to MR contrast agents [4]. All patients with asthma, allergic respiratory histories, and prior iodinated- and/or gadolinium-based contrast reactions should be followed more closely as they carry higher risk of adverse reaction [4].

Recently, an important late but serious adverse reaction to gadolinium-based contrast agents has been described, nephrogenic systemic fibrosis (NSF) [5, 6]. NSF is caused by excessive accumulation of gadolinium in soft tissues because of impaired renal elimination in

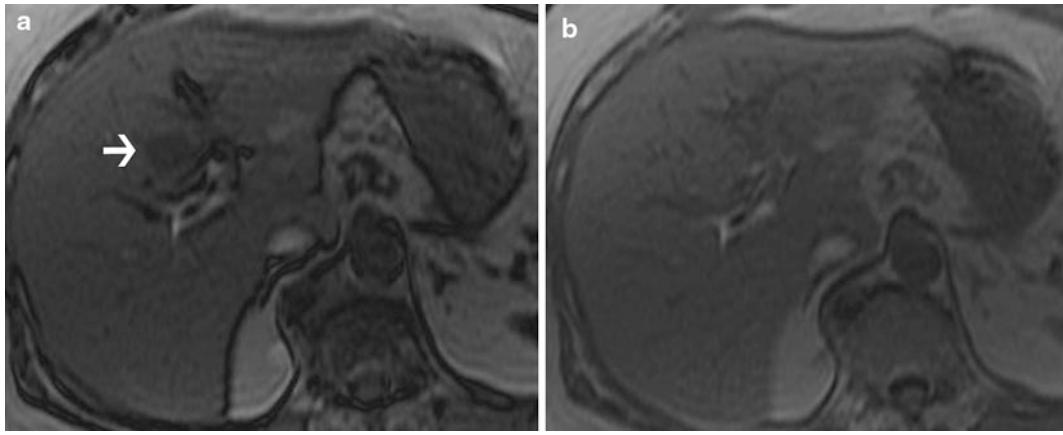

Fig. 15.4 A focal fat. A 65-year-old woman with history of lymphoma. MRI was performed to characterize a liver mass adjacent to porta hepatis seen on surveillance CT scan (not shown). Axial, out-of-phase T1-weighted gradient echo MR image (**a**) shows that the mass drops signal and appears hypointense in comparison to in-phase MR image (**b**) consistent with focal fat deposition rather than a lymphomatous deposit

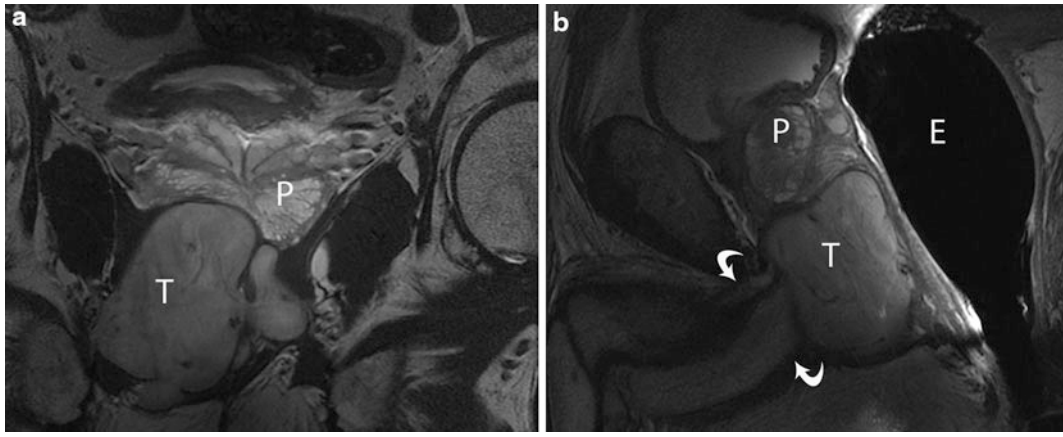

Fig. 15.5 Endorectal coil MRI in a 75-year-old man with pelvic spindle cell carcinoma. Coronal (**a**) and sagittal (**b**) T2-weighted MR image clearly demonstrates the extent of hyperintense, well-marginated tumor (*T*), which is located inferior to the prostate (*P*), posterior to the penile root (*curved arrow*), and anterior to the rectum with endorectal coil (*E*)

patients with severe, acute, or chronic kidney diseases. It is a progressive condition causing extraneous growth of fibrous tissue on the skin and internal organs, which can be painful, and debilitating, and often is exhibited by pronounced thickening and hardening of skin [7]. Because of NSF concern, gadolinium-based contrast agents should be used cautiously in patients carrying risk of impaired renal function (e.g., age >60 years, hypertension, diabetes). Gadolinium-based contrast agents are not recommended for patients on dialyses or with glomerular filtration rate (GFR) below than 30. Most radiology departments have updated their policy and implemented questionnaire and laboratory evaluation such as eGFR to their pre-MRI screening algorithm to identify such high-risk patients. Table 15.1 summarizes the potential risks of magnetic field and MRI contrast agents.

Table 15.1 Adverse effects of MRI and gadolinium-containing MRI contrast agents. Items with (*) demonstrate absolute contraindications to MRI

MRI feature	Type of force	Harmful interaction	Effected object	Possible result
Magnetic field strength	Translational force	Projectile effect	Ferromagnetic objects (e.g., gas cylinders, cleaning trolleys, chairs, and scissors)	Damage the magnet, injure patient and personnel
	Deflection or torsion	Twisting	Intracranial vascular clips*	Damage the adjacent soft tissues
			Cochlear implants*	
			Metallic (e.g., intracranial-orbital*) foreign bodies, stents, or prostheses	
	Electronic or magnetic	Device malfunction	Pacemakers*, implantable defibrillators (ICD)*	Dysrhythmias
			Implanted stimulators*	Suspension of drug infusion
			Implanted infusion devices*	Voltage inductions
RF waves	Energy transmission	Excessive heating	Soft tissues, particularly adjacent to a device or wire	Burns
Gradients	Induced electric currents	Neuromuscular stimulation	Peripheral nerves	Tingling/tapping sensation
	Impact of the gradients coils to their mountings	Acoustic noise	Inner ears	Anxiety, temporary or potentially permanent hearing loss
Contrast agent	Immune system	Allergic reaction	Skin, mucosa, and air ways	A spectrum of adverse effects from hives to anaphylactic shock
	Elevated level of free gadolinium	Extraneous growth of fibrous tissue	Soft tissue and internal organs of individuals with kidney failure	Nephrogenic systemic fibrosis

MRI In Diagnosis of Cancer

Although used to detect and characterize masses throughout the body, MRI has been found to be superior to other modalities in imaging of malignancies of certain organs.

Central Nervous System Cancers

Although due to its widespread availability, CT is often the first imaging technique used; however, MRI is essential in the diagnosis of brain and spinal tumors because of its superior soft tissue resolution [8, 9] (Fig. 15.6). Multiplanar capability of MRI offers superior localization of the tumor and allows the accurate detection of its extent. Advanced functional MRI techniques such as magnetic resonance spectroscopy (MRS) and diffusion-weighted imaging (DWI) aid in characterizing tumors [8]. Diffusion tensor tractography can demonstrate crucial cortical tracts and may be helpful in surgical planning such that these crucial structures are not injured [8, 10].

Head and Neck Cancers

Contrast-enhanced CT with multidetector technology is usually considered the initial study in the evaluation of head and neck cancers. CT shows bony structures better than MRI. However, MRI is often utilized when evaluating local tumor spread, particularly in tumors of the base of the tongue, floor of the mouth, nasopharynx, parapharyngeal spaces, and skull base [11].

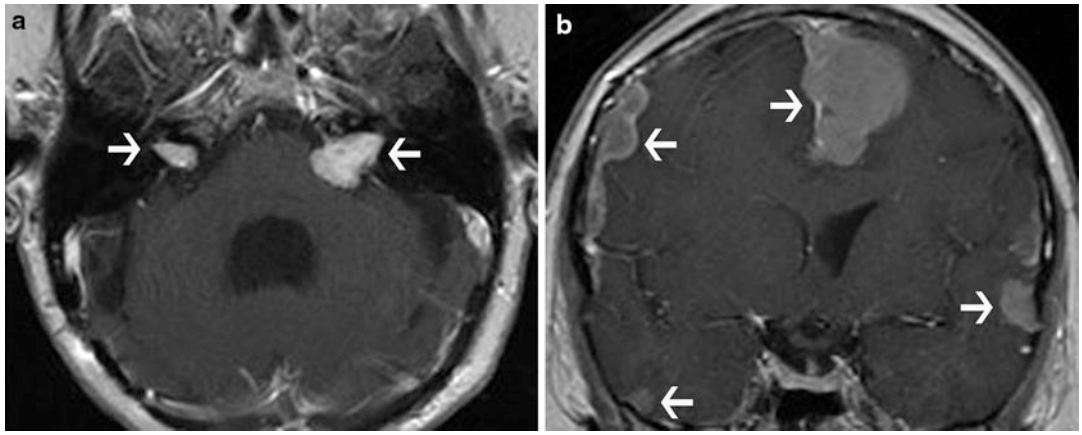

Fig. 15.6 A 57-year-old woman with a history of neurofibromatosis (NF) 2. Axial, enhanced MRI (**a**) shows enhancing masses (*arrows*) in both internal acoustic canals consistent with vestibular schwannomas. Coronal, enhanced T1-weighted MRI (**b**) shows multiple meningeal-based enhancing masses (*arrow*) consistent with meningiomas

MRI is preferred in imaging tumors in or near the skull base and is considered the modality of choice for evaluating perineural tumor invasion [12].

Breast Cancers

Mammography and ultrasound are the mainstay imaging modalities of the breast; however, recently, particularly after development of special breast phased-array coils and dynamic, contrast-enhanced subtraction sequences, breast MRI has been found widespread clinical use [13]. MRI can identify additional breast cancer foci in up to 10 % of cases [14].

Current American College of Radiology (ACR) guidelines recommend that breast MRI be used to screen high-risk patients (individuals with genetic predisposition to breast cancer by either gene testing, BRCA 1 or 2, or family pedigree, or individuals with a history of mantle radiation to the chest for Hodgkin's disease between the ages of 10 and 30 years) [15]. Breast MRI is recommended to screen the contralateral breast in patients diagnosed with a breast malignancy, and patients with breast augmentation [15]. The guidelines also recommend diagnostic breast MRI to assess extent of the disease in patients with invasive carcinoma or ductal carcinoma in situ (DCIS), invasion of deep fascia, post lumpectomy with positive margins, and following patients with neoadjuvant chemotherapy [15]. In addition, MRI may be used as a problem-solving tool in certain clinical scenarios such as differentiating scar versus recurrence at the lumpectomy site in patients in whom mammography is indeterminate, and detecting mammography- and ultrasound-occult primary breast cancers in patients presenting with metastatic adenopathy of unknown primary [13].

Lung and Cardiac Cancers

Lung cancer accounts for more deaths than any other cancer in both men and women [16]. CT is the main imaging modality in the evaluation of lung cancers. FDG-PET improves the detection of nodal and distant metastases [17]. MRI has a secondary role and can be helpful in defining the extent of local invasion into the chest wall, mediastinum, and heart [18]. MRI is particularly helpful in defining the local extent of superior sulcus tumors and can be used to assess the degree of involvement of the brachial plexus, subclavian vessels, and vertebral bodies [18].

US often is the initial imaging modality to evaluate the heart. However, US's ability to

characterize soft tissues is limited [19]. A limited acoustic window (due to bony and air-filled surroundings structures) restricts the field of view and hinders visualization of adjacent mediastinal structures [19]. US is also limited in large patients. MR imaging's ability to assess primary and secondary cardiac and pericardiac neoplasms is well established [19, 20].

Gastrointestinal System Cancers

MRI plays an important role in the evaluation of both primary and secondary liver malignancies. MRI is often complementary to CT and may be superior in the detection and characterization of focal liver lesions [21]. The liver is a common site of metastases. Hepatocellular carcinoma (HCC) is the most common primary liver malignancy, and it is usually found in the setting of cirrhosis [22]. Although overall survival of HCC is poor, survival significantly increases when the disease is diagnosed and treated early [22]. MRI has been widely used in the surveillance of patients with cirrhosis [22]. Management options for HCC include percutaneous tumor ablation, surgical resection, liver transplantation, embolization, and chemotherapy [22].

Primary cancers of the biliary system are most commonly adenocarcinomas and can arise from the gall bladder and extrahepatic or intrahepatic bile ducts. An MRI examination of the pancreaticobiliary tree includes T1-weighted images, T2-weighted images (also called MR cholangiopancreatography (MRCP)), and images before and after IV contrast material [23]. MRCP is a fluid-sensitive MR technique that relies on the inherent contrast-related properties of fluid-filled compartments; no administration of exogenous contrast agents is required. Endoscopic retrograde cholangiopancreatography (ERCP) has been used traditionally in the assessment of the pancreaticobiliary tree owing to its high spatial resolution and potential for image-guided therapy; however, ERCP is an invasive technique with a risk of complications. MRCP has a high sensitivity and specificity for the evaluation of various pancreaticobiliary pathologies and is now being used in lieu of ERCP in many patients, unless an intervention or tissue sampling is known to be required. Together with MRCP, MRI provides a thorough evaluation of pancreaticobiliary system and upper abdomen and is often the modality of choice for assessment of surgical resectability and postsurgical evaluation of the cancers of the pancreatic and biliary systems [24] (Fig. 15.7).

Gadolinium-based contrast agents (Gd-DTPA) used for routine enhanced MRI distributes rapidly in the extracellular space but their hepatocellular uptake and biliary excretion negligible. In order to improve the diagnostic ability of MRI, liver-specific MR contrast agents targeting hepatocytes or reticuloendothelial system have been developed and shown helpful in the detection and characterization of focal liver lesions [25–29]. Several liver-specific MR contrast agents with different magnetic properties are currently available. These includes the agents that are specifically taken up by hepatocytes and excreted into the bile (hepatobiliary agents) such as mangafodipir trisodium (Mn-DPDP, Teslascan), gadobenate dimeglumine (Gd-BOPTA, MultihHance), and gadoxetate (Gd-EOB-DTPA, Eovist), and superparamagnetic nanoparticles that are predominantly accumulate into Kupffer cells of the liver (reticuloendothelial agents) [30].

In recent years, preoperative radiochemotherapy has become standard of care for locally advanced rectal cancer [31]. Therefore, preoperative staging is crucial for prognosis and treatment planning. T and N stage are two independent predictors of outcome. Preoperative chemoradiotherapy is typically recommended for tumors extending beyond the rectal wall and/or regional lymph node involvement. To avoid the morbidity of unnecessary chemoradiation, MRI with endorectal and/or phased-array coil can be used to locally stage rectal cancer and accurately differentiate tumors confined to the rectal wall (T1-2) from tumors with mesorectal invasion (T3-4), and identifies lymph node involvement [32] (Fig. 15.8).

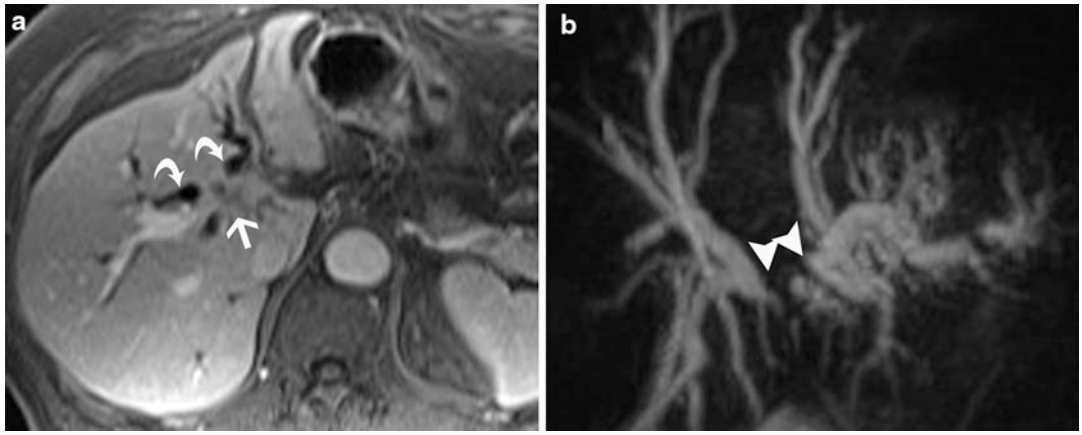

Fig. 15.7 A 73-year-old man presenting with obstructive jaundice. Axial, fat-suppressed, enhanced T1-weighted MR image (**a**) shows slightly enhancing mass (*arrow*) involving the biliary bifurcation and dilated intrahepatic bile ducts (*curved arrows*) consistent with cholangiocarcinoma, Klatskin type. Coronal, thick-slap MRCP image (**b**) shows markedly dilated intrahepatic bile ducts that taper and obstruct at the hilum (*arrowheads*)

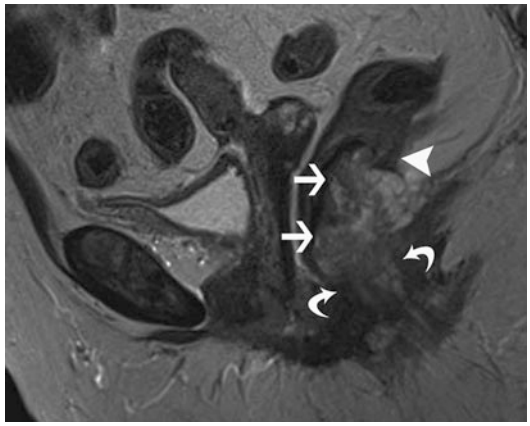

Fig. 15.8 A 70-year-old woman with rectal cancer. Sagittal T2-weighted MR image shows a large heterogeneous tumor (*arrows*) in the posterior wall of the lower rectum. The tumor arises just above the anorectal junction (*curved arrow*), invades the muscularis propria, seen as hypointense layer (*arrowhead*), and extends into mesorectal fat suggestive of T3 disease

Genitourinary System Cancers

CT is currently the imaging modality of choice in the initial work-up of renal cell carcinoma (RCC). However, MRI is useful in several aspects of renal cancer evaluation and may have some advantages, especially in differentiating benign from malignant lesions; in staging, particularly inferior vena cava (IVC) invasion; and in surveillance following percutaneous ablations [33, 34].

Most bladder tumors are malignant; urothelial carcinoma is the most common. Cystoscopy is the gold standard for the detection of bladder cancer [35]. Biopsy during cystoscopy establishes the pathologic diagnosis and local extent of the tumor. However, imaging plays an important role in the overall staging of bladder carcinoma [35]. Upper urinary tract evaluation is also needed to exclude synchronous and multifocal cancers; this can be achieved by retrograde pyelography at the time of cystoscopy or with excretory urography (EU). CT urography is rapidly replacing EU in the evaluation of these patients [36]. For local bladder tumor, MRI is considered superior to CT in detecting extravesical tumor extension, surrounding organ invasion, and distinguishing superficial tumors from those with muscle invasion [37, 38] (Fig. 15.9). The latter is an important distinction; patients with muscle invasion disease typically require cystectomy. MR urography (MRU) using fluid-sensitive and contrast-enhanced sequences of the kidneys, ureters, and bladders used to both locally stage the bladder tumor and evaluate the upper tracts. Intravenous administration of saline, furosemide, or both before the acquisition of MRI sequences distends the collecting systems,

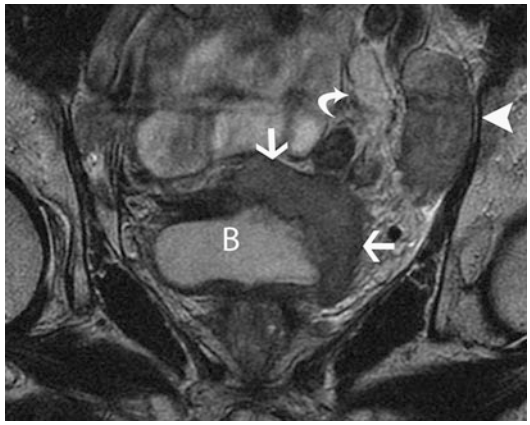

Fig. 15.9 An 85-year-old man with urothelial carcinoma of the urinary bladder cancer. Coronal T2-weighted MR shows large, intermediate signal intensity mass (*arrows*) in *left* urinary bladder (*B*) wall that extends into perivesical fat suggestive of T3 disease. There is also *left* obturator lymphadenopathy (*arrowhead*) and markedly dilated left ureter (*curved arrow*)

ureters, and bladder and allows better evaluation of small urothelial lesions [35].

The adrenal gland is one of the most common sites of metastatic disease in the body after the lung, liver, and bone [39]. Tumors that spread commonly to the adrenal gland include lung, breast and colon cancers and melanoma [40]. Because of the high prevalence of clinically silent adrenal adenomas, most adrenal masses are benign, even in patients with known malignancy [39]. Accurate characterization of an adrenal mass may not be critical if the gland is one of many sites of metastases, but if the adrenal gland is the only possible site, precise characterization is crucial for management. Chemical-shift MRI is a technique used to identify cells with intracytoplasmic lipid and is the most sensitive and specific MR imaging technique for differentiating adrenal adenomas [41] from metastases because most adenomas are rich in intracytoplasmic lipid and most metastases are not [42]. Chemical-shift MRI can be used to differentiate adrenal adenomas from metastases with the sensitivity and specificity at 81–100 % and 94–100 %, respectively [42].

The current principal role of MRI in prostate cancer is to stage biopsy-proven cancer. An endorectal coil offers higher signal-to-noise ratio and improves the accuracy of the examination [43]. Prostate cancers are typically T2 hypointense and can be detected in background of normal T2-hyperintense peripheral zone of prostate gland. Most recently, diffusion-weighted imaging and dynamic contrast-enhanced sequences can also be used [44–47]. Prostate cancers typically demonstrate restricted diffusion and enhance and wash out rapidly [44–47]. Once the tumor is identified, MRI is used to detect extracapsular extension, lymph node and seminal vesicle involvement, and regional bone metastases.

MR imaging is used also to stage uterine malignancies. It has been shown to be effective for preoperative characterization and staging of endometrial and cervical carcinoma [48–50]. The most common gynecologic malignancy, endometrial carcinoma, typically occurs in postmenopausal women and presents with abnormal bleeding. Prognosis depends on histological grade, extension into the cervical stroma, and depth of myometrial invasion, which independently predicts lymph node involvement, recurrence, and 5-year survival [48]. The presence of deep myometrial invasion is well evaluated with MR imaging [49].

Cervical cancer is the third most common gynecologic malignancy. Preoperative assessment of tumor stage influences the prognosis and choice of treatment. Compared to CT, MRI has been shown to perform significantly better for tumor visualization, detection of depth of stromal and parametrial invasion [51]. However, in a recent multicenter study, both imaging modalities performed similarly in overall staging [51]. In this study, accuracy of International Federation of Gynecology and Obstetrics (FIGO) clinical staging was also found higher than previously reported. The authors concluded that FIGO staging was influenced by CT and MRI findings since the majority of patients had their final FIGO clinical staging results submitted after CT or MRI was done [51].

Ultrasonography, particularly using a transvaginal approach, is the first-line imaging technique for detecting and characterizing ovarian tumors. However, when an US-detected lesion is complex or large, MRI is often needed to characterize the mass further [52, 53]. Furthermore, US may be limited in large patients and transvaginal

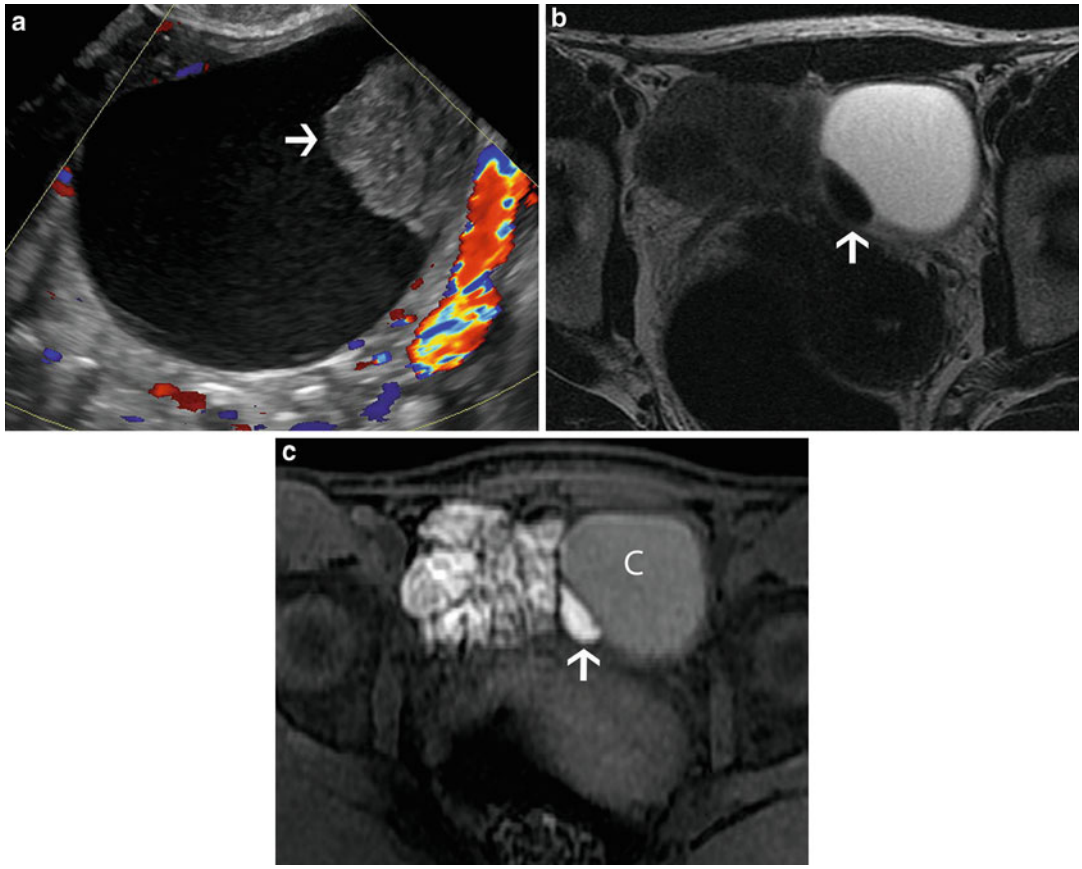

Fig. 15.10 A 44-year-old woman with pelvic pain. Transvaginal color Doppler US (**a**) shows an ovarian cyst with an intracystic solid component (*arrow*) that could represent clot or soft tissue. The solid component (*arrow*) is hypointense on axial T2-weighted MR image (**b**) and hyperintense on fat-suppressed, T1-weighted MR image consistent with blood clot. Note: the cyst (**c**) is also slightly hyperintense on the T1-weighted images due to its hemorrhagic content

approach may not be possible in virgins. MR imaging is superior to CT for assessing complex ovarian masses because of its better soft tissue resolution [52] (Fig. 15.10). The overall accuracy of MRI for distinguishing benign from malignant ovarian lesions approaches 90 % [53].

Musculoskeletal System Cancers

Radiographs remain the initial imaging modality in detecting and characterizing primary and secondary bone tumors. MRI plays a valuable role in evaluating bone tumors, particularly in assessing in extent of bony, intramedullary, joint, and soft tissue involvement [54, 55]. MRI examination should include the entire bone from joint to joint to evaluate for skip lesions and to assess the longitudinal extent of the tumor for surgical planning (Fig. 15.11). Contrast material is helpful in defining areas of viable tumor and tumor necrosis to determine the optimal biopsy site [56]. MRI is best performed prior to surgical biopsy to prevent distortion of tumor by the intervention.

MRI in Percutaneous Oncologic Interventions

Due to the imaging advantages described above, MRI has been considered a useful imaging tool to guide percutaneous oncologic intervention [57–60].

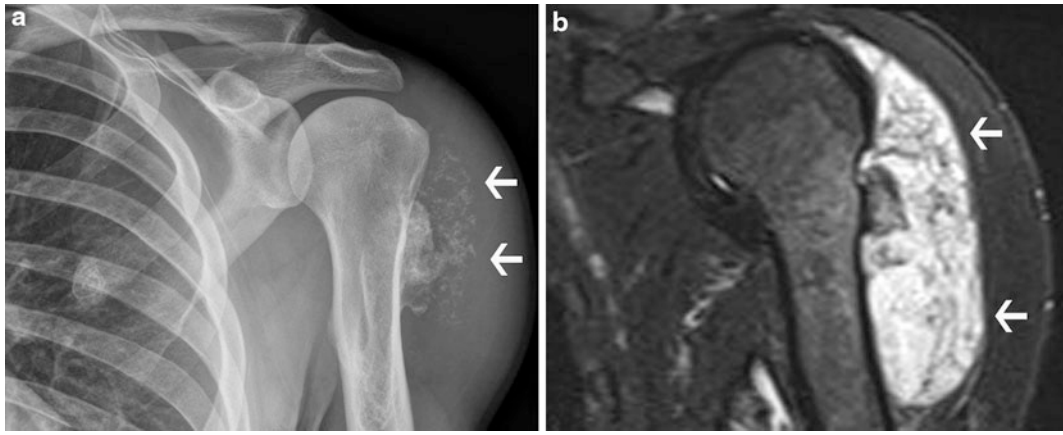

Fig. 15.11 A 43-year old man with a history of multiple osteochondromas complaining of a painful, enlarging mass in the left shoulder. A plain radiography (**a**) shows a soft tissue mass (*arrows*) with chondroid mineralization in the proximal humerus. Coronal, T2-weighted MR image (**b**) shows that the tumor (*arrows*) has mostly high signal with bands of low-signal intensity consistent with chondroid matrix. Note excellent delineation of the extent of the tumor. Biopsy revealed chondrosarcoma likely developing in preexisting osteochondroma

Currently, CT and US are often used to guide percutaneous interventions. However, some lesions detected with MRI (e.g., some breast, liver, and prostate cancers) may not be visible with US or unenhanced CT. Contrast-enhanced CT may demonstrate such masses, but this method suffers from the fact that contrast material enhancement of masses is generally transient and therefore insufficient to guide the entire length of the procedure. Poor visualization of the lesions during biopsy may result in inadequate sampling and false-negative results. Poor visualization during percutaneous ablations may lead to inadequate treatment or inadvertent injury to adjacent critical structures. MRI's superb soft tissue contrast capability allows visualization of many tumors and anatomic details of many organs and their relationships with adjacent critical structures that is not possible with other imaging modalities.

Regarding targeting, multiplanar capability of MRI allows angling superiorly to lesions in the liver dome, adrenal gland, and upper pole of the kidney and, as a result, avoids traversing pleural space or lung [60]. MRI allows images to be obtained in virtually any plan. This helps visualize the entire length of the biopsy needle or ablation applicator.

MRI is particularly suited to guide percutaneous ablations. During tumor ablations, MRI may facilitate procedures during all phases including planning, targeting, monitoring, and controlling [61]. Cryoablation, the process of freezing tissues to lethal temperatures, is particularly well suited for MRI [61]. The effect of freezing during cryoablation, called an iceball, is visualized well with MRI as an area of signal void on all conventional pulse sequences. Visualization of the iceball allows intraprocedural monitoring to assure adequate coverage of the tumor and minimize adjacent organ injury [62]. Similarly, heat-sensitive MRI sequences have been developed and used during certain ablation procedures such as high-intensity focused ultrasound ablation [63].

Since MRI does not involve ionizing radiation, the interventional radiologist can be present in the procedure room alongside the patient during image acquisition. This feature enables the interventionalist to perform certain maneuvers such as manual external compression during interventions to displace adjacent bowel loops to prevent injury [64].

Although closed-bore magnets can be used to guide percutaneous intervention, open interventional MRI systems have been developed [65, 66] (Fig. 15.12). Two principal types of open MRI

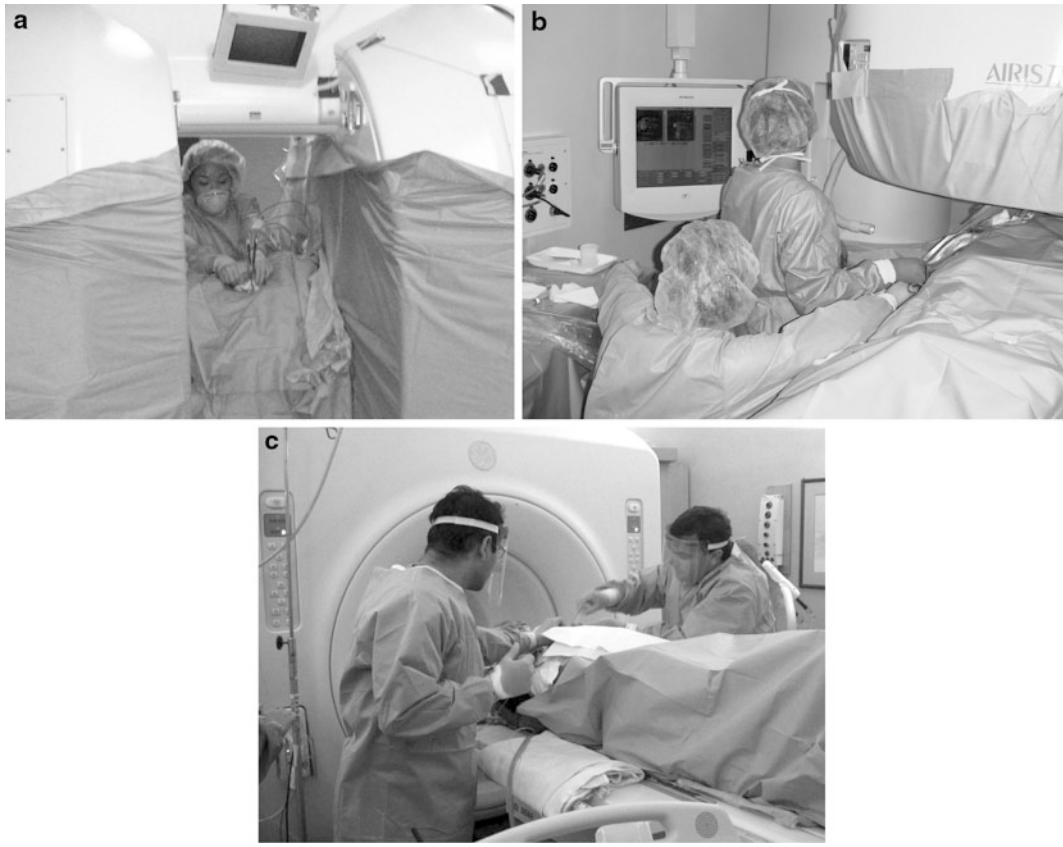

Fig. 15.12 MRI systems for intervention. "Vertically open" 0.5 T interventional MRI system (Signa SP, GE Healthcare, Milwaukee, WI) (**a**) provides bedside access to the patient while the patient is being imaged and treated with percutaneous intervention. The 56-cm distance between the sidewalls of the scanner provides space for needle/probe placement and display monitors to view images. "Horizontally open" 0.3 T MRI system (AIRIS II, Hitachi, Tokyo, JP) (**b**) also provides bedside access for interventional procedures including cryoablation. The 43-cm space between the poles of the magnet favors lateral approach (Photo courtesy of Dr. Yusuke Sakuhara, Radiology, Hokkaido University Hospital, Sapporo, JP). "Closed bore" 1.5 T MRI system (Signa, GE Healthcare, Milwaukee, WI) (**c**) allows little-to-no access to the patient while scanning. Procedures are performed by pausing the scanning and advancing the patient out of the bore, similar to CT-guided interventions (Figures were published in Tatli S, Morrison PR, Tuncali K, Silverman SG. Interventional MRI for oncologic applications. Tech Vasc Interv Radiol. 2007;10(2):159–70. Copyright Elsevier (2007))

systems have been produced: horizontally open and vertically open systems. Open MRI systems allow interventional radiologists access to patients during instrument manipulation as well as image acquisition. Also, relative to closed systems, open MRI helps accommodate large patients and provides sufficient space for instrument such as biopsy needles, ablation applicators and anesthesia, and patient monitoring equipments when necessary [66]. However, open systems contain either low- or midfield magnetic strengths that result in a lower signal-to-noise ratio. Therefore, some tumors detected with high-field, closed-bore magnets may not be visualized with these magnets. In addition, homogeneous fat suppression may not be achieved with open MRI systems. Some advanced MRI sequences such as temperature-sensitive, diffusion-weighted sequences and MR spectroscopy may not be performed.

Despite the physical advantages of open MRI systems, most MRI-guided procedures currently

are being performed using high-field, closed-bore MRI systems to take advantage of their better and faster image quality, and advanced imaging techniques [67–69]. Typically these systems are used similar to CT; patients are moved into the gantry for imaging acquisition and out for needle or applicator manipulation. A relatively new interventional MRI system (IMRIS, Winnipeg, AB, Canada) employs a unique approach: a wide-bore magnet is mounted on ceiling rails and moves to the patient during imaging acquisition and out for needle or other instrument manipulation [70].

Since MRI involves powerful magnetic fields, MRI-guided intervention can pose a safety risk to patients and personnel. Major risks include projectiles, patient burns, dislodged ferromagnetic implants, and medical device malfunction and failure [71]. Therefore, all equipment in the interventional MR room must be MR safe [72, 73]. In addition, instrumentation used during intervention should not adversely affect image quality. If the instrument is both MR safe and does not affect image quality, it is considered "MR compatible" [71].

MRI-Guided Biopsy

Although it can be used to guide biopsy of masses in any organ, MRI has been used mostly in the breast [74–77] and prostate gland [78–81]. Widespread use is limited by availability of MR scanner time, issues related to equipment and instrumentation compatibility, patient body habitus, and cost. In addition, CT and ultrasound are readily available and satisfactory in most cases. However, MRI guidance may be necessary for lesions in other organs (e.g., liver, kidney, bone) that are not seen or seen poorly with CT and ultrasound (Fig. 15.13).

The use of MRI to guide breast biopsies has increased in the last few years. When lesions are identified on diagnostic breast MRI that are occult or poorly seen on mammography and ultrasound, MR is used to perform vacuum-assisted large needle biopsy and preoperative wire localization prior to surgical excision [82–86] (Fig. 15.14).

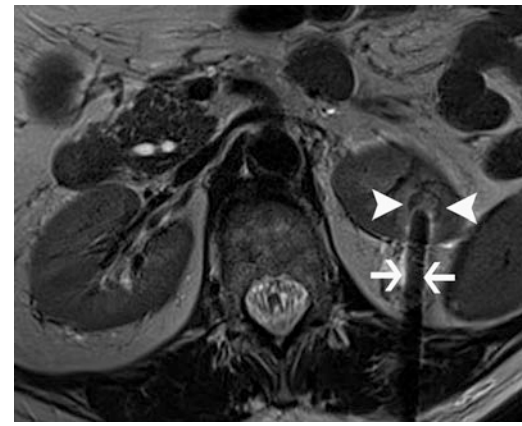

Fig. 15.13 A 65-year-old woman with incidentally detected left renal mass. Since the mass was better seen with MRI, biopsy was performed using 3 T MRI guidance. Axial T2-weighted MRI shows the tip of biopsy needle (*arrows*) within the mass (*arrowheads*)

Transrectal (TR) US-guided prostate biopsy has become a universally accepted tool in the diagnosis of prostate cancer in patients with an abnormal digital examination or elevated serum-prostate specific antigen (PSA). However, US-guided biopsy may be falsely negative, and MRI-guided biopsy may be helpful [87–92]. MRI allows visualization of the substructural anatomy of the prostate and may demonstrate suspicious nodules that are not seen with ultrasound [87]. As a result, MRI can be utilized to biopsy patients with increasing PSA levels and negative TRUS-guided prostate biopsies [88–92]. A transperineal or transgluteal approach can also be used in patients without a rectum due to prior surgery and those who are reluctant to undergo transrectal biopsy because of its recognized complications such as infections, hematuria, and rectal bleeding [92].

MRI-Guided Tumor Ablation

Although RF ablation is probably the most commonly used percutaneous tumor ablation technique worldwide, the utilization of RF ablation under MRI guidance has been limited due to the fact that RF signals generated by the ablation device distort the MR image [1, 93]. As a result,

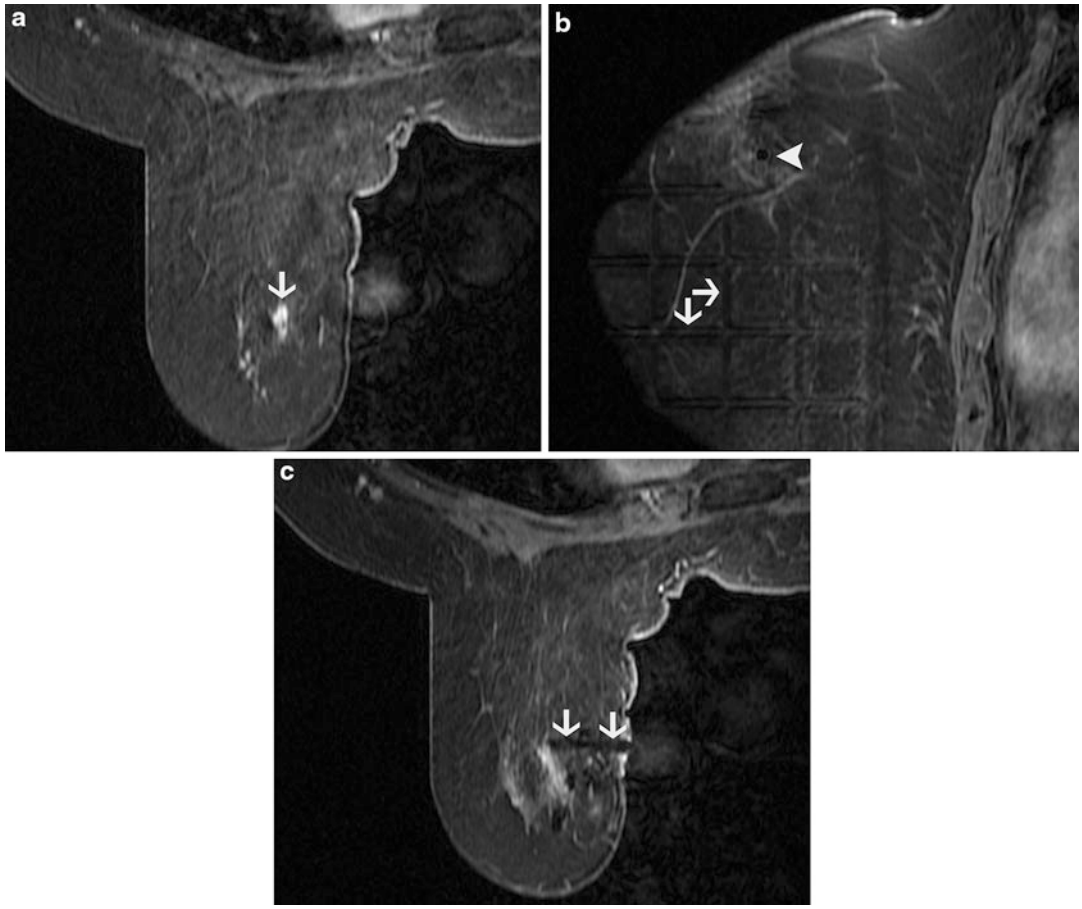

Fig. 15.14 MRI guided breast biopsy in a 69-year-old female with a 1.8-cm clumped segmental area of enhancement on MRI. The patient had a family history of breast cancer and a group of suspicious microcalcifications on mammography. Contrast-enhanced, fat-suppressed T1-weighted axial image (**a**) shows area of abnormal enhancement. Contrast-enhanced, fat-suppressed T1-weighted sagittal image (**b**) shows compression grid as low-signal intensity lines at skin surface (*arrows*) and signal void introducer (ATEC, Suros Surgical System, Indianapolis, IN) (*arrowhead*). Contrast-enhanced, fat-suppressed T1-weighted axial image (**c**) shows introducer (*arrows*). The vacuum-assisted biopsy device (ATEC, Suros Surgical System, Indianapolis, IN) was inserted through the introducer, and sampling was performed (Figures 14b–c were published in Tatli S, Morrison PR, Tuncali K, Silverman SG. Interventional MRI for oncologic applications. Tech Vasc Interv Radiol. 2007;10(2):159–70. Copyright Elsevier (2007))

during MRI-guided RF ablation, the RF energy deposition has to be discontinued during imaging acquisition. Intermittent discontinuation of ablation could adversely affect its effectiveness. Alternatively, postponing imaging until the RF ablation is completed prevents the ablation from being monitored. This also could hinder its effectiveness and might also increase the risk of complications. Despite several efforts to pulse the RF intermittently in a rapid fashion or use either filters for the RF generators, MRI-guided RFA has not gained wide acceptance [93].

Unlike RF ablation, cryoablation does not adversely affect MRI imaging. MRI-guided cryoablation has been shown to be safe and effective in selected patients with a variety of cancers including those of the liver, kidney, and musculoskeletal system [94–99]. In addition to the fact that the iceball is well seen with MRI, cryoablation has several other advantages

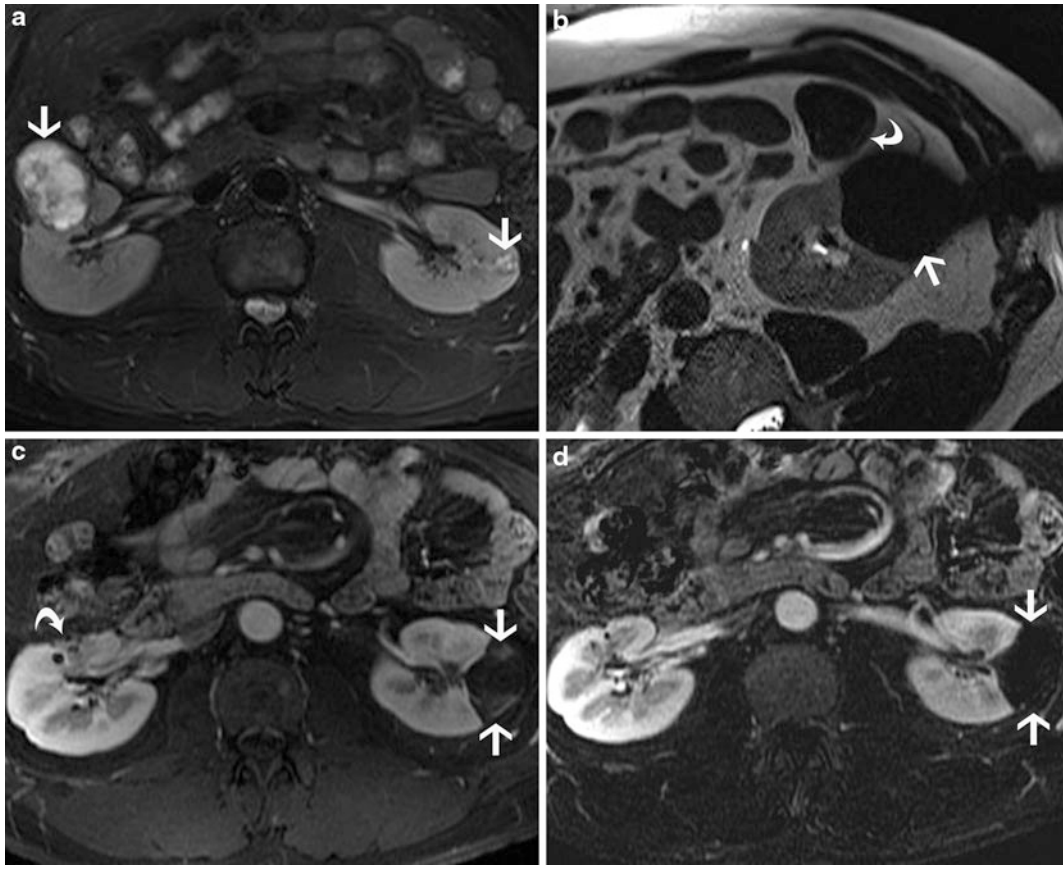

Fig. 15.15 A 51-year-old man with a history of lymphoma. Axial, fat-suppressed, T2-weighted MRI (**a**) shows bilateral renal masses (*arrows*). The patient underwent right partial nephrectomy and pathology revealed renal cell carcinoma. 3 T MRI-guided cryoablation performed since the lesion was better seen with MRI. Axial, T2-weighted MR image (**b**) obtained during procedure shows signal void area of the iceball (*arrow*) covering the tumor and abutting the adjacent colon (*curved arrow*). Axial, fat-suppressed, enhanced 3 T MRI (**c**) obtained 24 h after the ablation shows ablation zone (*arrow*) with some hyperintense areas. Note postsurgical changes in the right kidney (*curved arrow*). Axial subtraction MR image (**d**) reveals that there is no enhancement within the ablation

including the ability to place and control multiple applicators individually, and the ability to adjust the cryogen gas rate (for each probe) to control the size and shape of the iceball (Fig. 15.15). If intraprocedural imaging demonstrates that the iceball does not completely treat the tumor, cryoprobes can be repositioned or additional cryoprobes can be placed. Alternatively, when the iceball extends too close to critical adjacent structures, the cryogen gas rate of those individual probes can be decreased or ceased. The ability to monitor and control the ablation is the principal reason why cryoablation is preferred in the treatment of tumors close to critical structures [62].

Recently, MRI-guided focused ultrasound ablation has been developed and applied successfully in several clinical scenarios including uterine fibroids, breast neoplasms, and bone metastases [100–110] (Fig. 15.16). In focused ultrasound ablation, high-frequency ultrasound beams are focused through skin to a predefined small target to generate localized high temperatures. Each energy delivery is called a sonication and can only ablate a small area of tumor, typically less than a centimeter in diameter. By applying

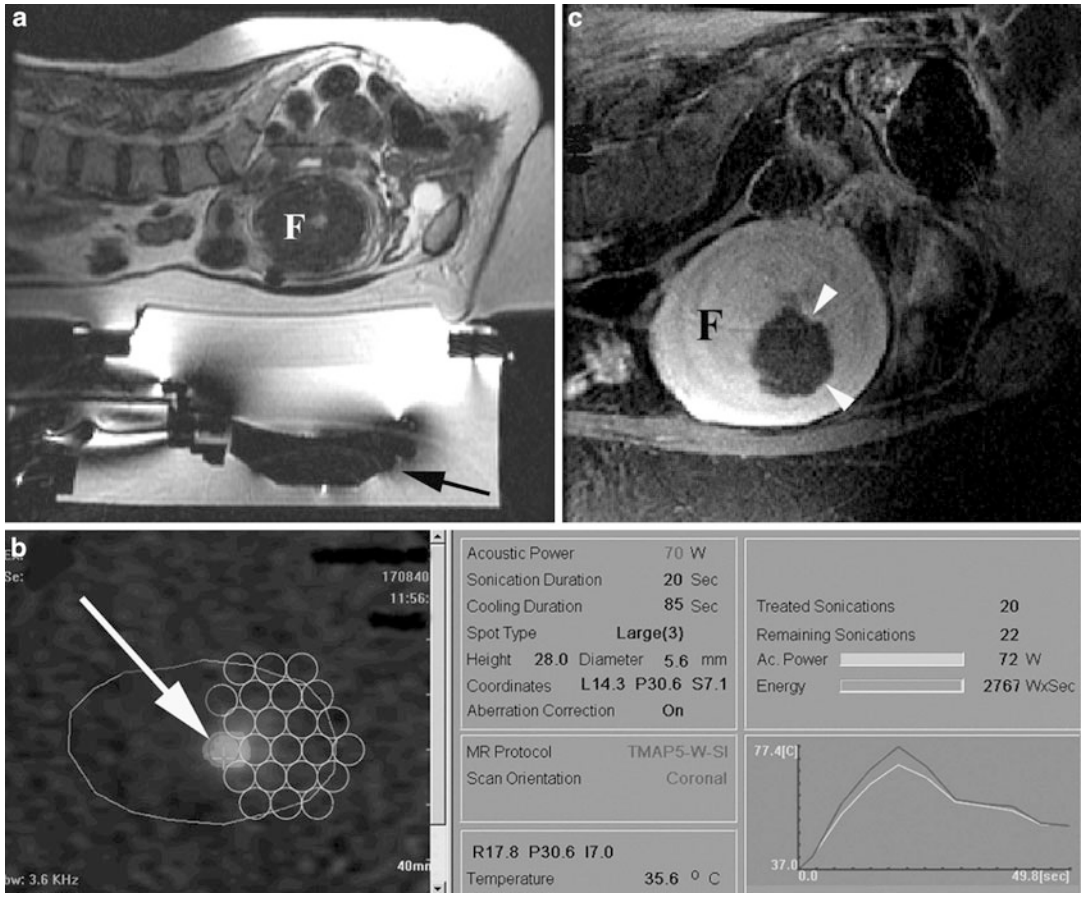

Fig. 15.16 Focused ultrasound ablation of uterine fibroid in a 39-year-old female. Sagittal T2-weighted MR image (**a**) shows that the patient lying prone on MRI scanner bed with targeted fibroid (*F*) placed above the ultrasound transducer (*arrow*). The transducer (Insightec, Israel) focuses high-intensity ultrasound through the skin into the fibroid. The onscreen display of the focused ultrasound system (**b**) shows the treated region (*arrow*). The display also provides a visual record of the previously sonicated areas and those yet to be treated (*hollow circles*). The graph at the *right* shows the temperature within the transducer's focus as a function of time. Contrast-enhanced, fat-suppressed T1-weighted MR image (**c**) acquired post-procedurally showing that part of the fibroid (*F*) that was treated (*arrowheads*) no longer enhancing (Photos courtesy of the Focused Ultrasound Laboratory, Brigham & Women's Hospital [**a** and **c**] and Insightec, Inc. [**b**]) (Figures were published in Tatli S, Morrison PR, Tuncali K, Silverman SG. Interventional MRI for oncologic applications. Tech Vasc Interv Radiol. 2007;10(2):159–70. Copyright Elsevier (2007))

multiple sonications, monitored by temperature-sensitive MRI sequences, larger ablation zones can be created. Although the potential of focused ultrasound ablation had been touted since the 1940s, clinical acceptance was delayed until MRI guidance was suggested [100]. Using conventional pulse and temperature-sensitive sequences, MRI can be used to monitor each focal sonication while targeting precisely and providing feedback about thermal damage [102, 103]. MRI-based temperature monitoring before, during, and after each sonication provides assurance that adequate temperatures have been reached in the target and effects in normal tissue have been minimized. MRI-guided focused ultrasound also has the potential to be used throughout the body, including the central nervous, genitourinary, and musculoskeletal systems because it is transcutaneous [111–113]. Focused ultrasound has the potential to be the least invasive of all ablation techniques.

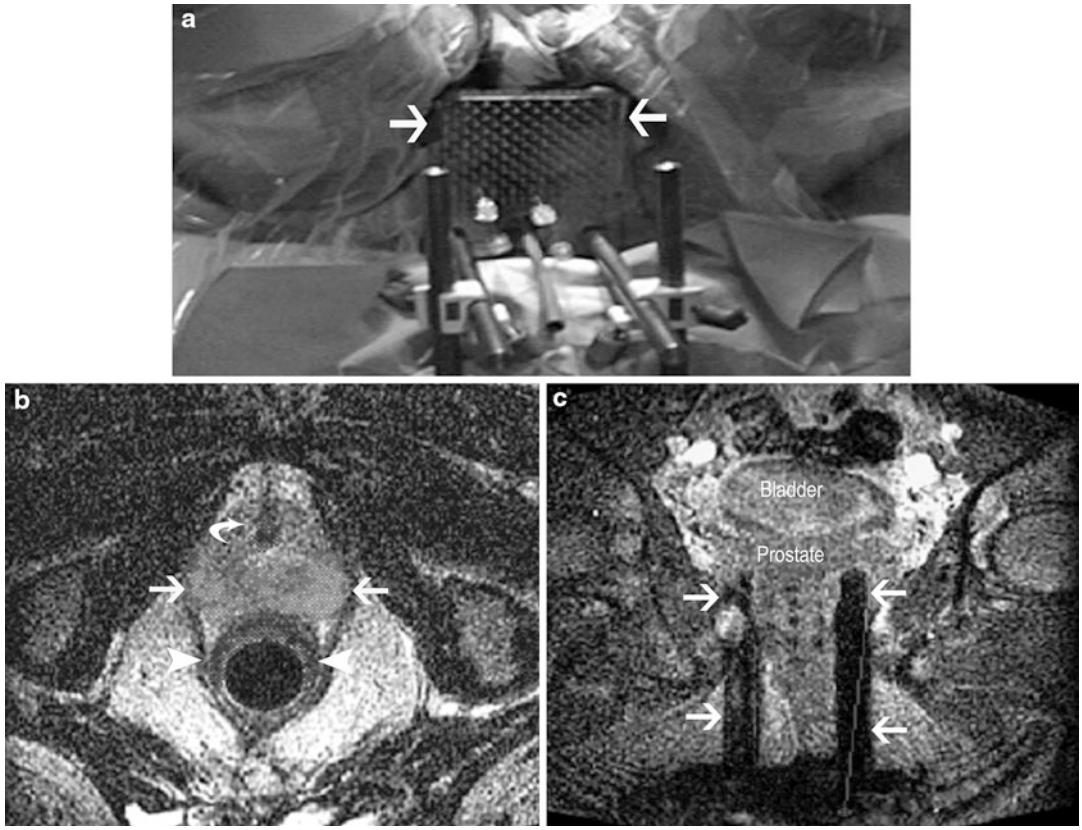

Fig. 15.17 MRI-guided brachytherapy of a 75-year-old man with prostate cancer. The template (*arrows* in **a**) is placed against the patient's perineum and secured to the MRI scanner table. Axial T2-weighted MR image (**b**) obtained and using special software a radiologist marked the peripheral zone of the prostate gland (*arrows*), urethra (*curved arrow*), and rectal wall (*arrowheads*). With designated planning software, a medical physicist generated a treatment plan. Coronal MRI show (**c**) the needles (*arrows*) containing brachytherapy seeds inserted into the desired location of the patient's prostate gland through the holes of the template according to the treatment plan (Figures were published in Tatli S, Morrison PR, Tuncali K, Silverman SG. Interventional MRI for oncologic applications. Tech Vasc Interv Radiol. 2007;10(2):159–70. Copyright Elsevier (2007))

MRI-Guided Brachytherapy

Brachytherapy is an established interstitial radiation treatment for certain indications including prostate and cervical cancer [114–116]. In most centers, brachytherapy seeds are placed under transrectal ultrasound guidance [117]. However, MRI guidance provides superior visualization of the target organ, its substructure, and surrounding tissues (Fig. 15.17). In the treatment of prostate cancer with brachytherapy, MRI has been shown to improve targeting, maximize the tissue destruction effect of radioactive seeds, and reduce the damage of adjacent normal structures such as rectal mucosa, urethra, and neurovascular bundles [118–123].

MRI-Guided Surgery

Imaging guidance during surgical procedures provides many advantages including more accurate lesion localization, assessment of the completeness of the procedure, and lessening the risk of complication [70, 124]. Most intraoperative MR systems have been designed and used for neurosurgery [125–127]. Two intraoperative

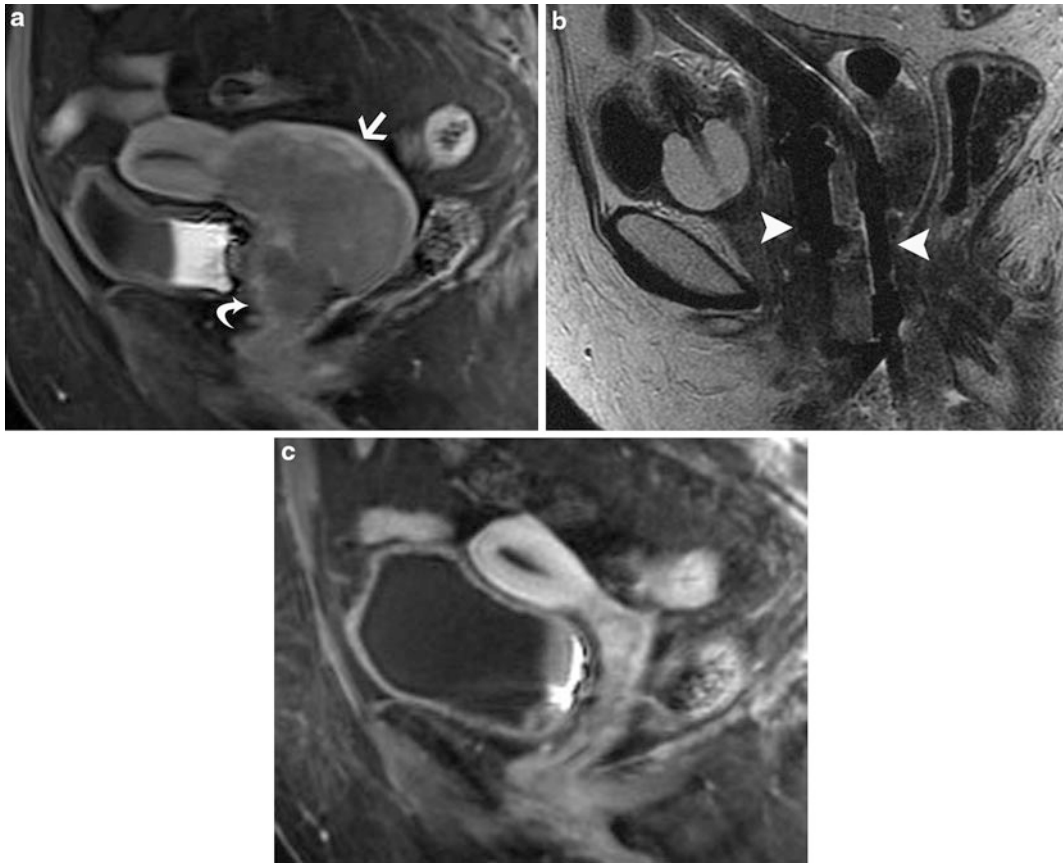

Fig. 15.18 A 63-year-old woman with cervical cancer. Sagittal, enhanced MRI (**a**) shows a large enhancing mass (*arrow*) in the cervix extends inferiorly into the lower vagina (*curved arrow*). Sagittal T2-weighted MRI (**b**) after the placement of intracavitary brachytherapy applicator (*arrowheads*). Sagittal, enhanced MRI (**c**) performed 3 months after completion of brachytherapy shows no residual mass

MR imaging approaches have been described: (1) separate operating room and MRI suite with the safe transfer between the rooms of a special table that can be used for both surgery and MRI, and (2) MR scanners that are designed for surgery within an operating room [70]. While moving the patients (or scanner) permits only intermittent MR imaging without continues real-time imaging monitoring, the latter approach allows direct access to patients and near real-time imaging guidance throughout the surgical procedures.

Intraoperative MR imaging is currently applied for a variety of neurosurgical procedures, such as brain tumor biopsies and resections, cyst drainage, transsphenoidal pituitary resections, functional brain surgery, and intraparenchymal drug and cell delivery [70]. Apart from its application in neurosurgery, intraoperative MR imaging has been used successfully to guide endoscopic procedures in paranasal sinus surgery and to monitor skull base surgery in otolaryngology [128–131]. In addition, intraoperative MRI has been demonstrated to be suitable for lumpectomy guidance in malignant breast tumors [132].

MRI Surveillance Following Cancer Treatment

Imaging surveillance is crucial in the management of oncologic diseases. Although clinical history, physical examination, and laboratory

tests such as tumor markers (e.g., CEA in colon cancer, AFP in hepatocellular carcinoma, and PSA in prostate cancer) provide useful information about treatment response, patient care relies heavily on imaging surveillance. The role of imaging surveillance after cancer treatment is to determine any change in tumor size (or presence of residual tumor), detect distant metastases, and identify side effects or complications of the therapy (Fig. 15.18).

Currently, CT is the most commonly used imaging modality in the surveillance of patients with cancer. Unfortunately, CT largely relies on size criteria such as the Response Evaluation Criteria in Solid Tumors (RECIST) to assess treatment response, and contrast enhancement changes are not yet widely used [133]. However, tumor size measurements do not provide functional information; indeed, tumors may be well treated, but not change in size. In addition, CT findings may not provide adequate information to be able to differentiate posttreatment changes such as granulation tissue or fibrosis from residual or recurrent tumor. FDG PET/CT is being used more frequently in the surveillance of patients with various cancers because of additional metabolic information provides. However, PET may be falsely negative in small (<1 cm) lesions and falsely positive due to treatment effects [131–136]. MRI is preferred in certain cancers such as those of the brain, head and neck, breast, and prostate and used as a problem-solving tool in many scenarios. In addition, due to the potential cancer-causing effects of radiation exposure in patients requiring long-term CT or PET/CT follow-up, MRI will likely be used more in cancer surveillance following treatment, particularly in young patients.

MRI is particularly preferred following percutaneous tumor ablation and embolization. Ablation-induced necrosis is manifested by a lack of enhancement in tissues that enhanced before the ablation [1]. The use of subtraction MRI techniques is helpful to confirm lack of enhancement and detect subtle areas of residual enhancement [1]. Following ablation, coagulation necrosis may appear as regions of increase T1 signal and mimic enhancement if only enhanced images were reviewed. Subtraction techniques electronically remove these hyperintense regions (Fig. 15.15).

MRI: Recent and Forthcoming Advances

Although MRI is playing an increasingly important function in oncologic imaging, with ongoing developments in magnet, surface coil, software, and contrast material technology, the role of MRI in the diagnosis, treatment, and posttreatments surveillance of cancer will likely to expend even further.

High-Field Systems

There has been movement toward higher-field (3 T) MRI systems. The essential advantage of 3 T MRI, relative to 1.5 T, is an increased signal-to-noise ratio that can be used to obtain either finer anatomical detail or decreased acquisition time [137]. MRI at 3 T simply outperforms 1.5 T MRI in many ways, particularly in neurological and musculoskeletal imaging [138–140]. 3 T MRI systems may allow IV contrast material doses to be reduced [137]. MR sequences such as MR spectroscopy, diffusion-weighted, and perfusion imaging are also more robust at 3 T [137, 141].

Parallel Imaging

Parallel imaging is considered one of the most important innovations in MRI technology in the last decade [142, 143]. Using special radiofrequency surface coils and image reconstruction algorithms, signals coming from different part of body volume are combined, and the acquisition time can be significantly shortened or spatial resolution increased.

Dynamic Contrast-Enhanced MRI

Dynamic contrast-enhanced (DCE) MRI can be used to investigate tumor vascular characteristics

quantitatively by performing sequential MRI scans before, during, and following intravenous administering contrast material [144]. DCE MRI can be performed using T1- or T2*-weighted sequences and most commonly utilizes a low-molecular-weight gadolinium-containing compound such as gadopentetate dimeglumine [145]. Tracer kinetics principles can be used to provide estimates of relative blood volume (rBV), relative blood flow (rBF), and mean transit time (MTT) derived from the first pass of the contrast material through the microcirculation of tumors. Experience in quantitative T2* DCE MRI is accumulating more in neurological practice [144]. High tumor rCBV correlates with mitotic activity and vascularity and is seen much higher in high-grade than low-grade gliomas. Other potential uses of T2*-weighted DCE MRI in patients with brain tumors include distinguishing radiation necrosis from recurrent disease, determining prognosis, and monitoring response to therapy [144]. Although analysis of enhancement seen on T1-weighted DCE MRI has been investigated in a number of clinical situations, its role has been more established in distinguishing benign from malignant breast lesions [144, 146]. Signal intensity time curves have shown that malignant breast tissue generally enhance early, with rapid and large increases in signal intensity compared with benign tissues, which in general show a slower increase in signal intensity [144]. DCE MRI also has been found to be valuable in the staging of gynecological malignancies, bladder, and prostate cancers [38, 147, 148].

Diffusion-Weighted Imaging

Diffusion-weighted (DW) MRI relies on the microscopic movement of water molecules. Certain pathological processes can decrease the motion of water molecules and can be detected on DW MRI as restricted diffusion. DW MRI was first introduced in the mid-1990s as a highly sensitive way to detect acute ischemic stroke [149]. More recently, its value has been shown for evaluating tumors [150, 151]. Malignant tissue generally exhibits hypercellularity and increase in the amount of macromolecular proteins, resulting in decreased diffusion in the extra- and intracellular compartments [149, 152]. However, restricted diffusion is not specific to malignancy and can be seen in other benign entities such as infection and inflammation as well as ischemia [152]. Although routine use of DW MR imaging for abdominopelvic oncologic imaging is being evaluated, studies have documented the value of DW MR imaging in the detection of various malignancies including liver, renal, prostate, colorectal, pancreatic, uterine, ovarian and lung cancer, and lymph node metastases [153] (Fig. 15.19). DW MR imaging has been suggested in helping depict recurrent tumor, assessment of treatment response, and tumor characterization [154]. Whole-body imaging using diffusion has been suggested as a way to evaluate for metastases [155]. Although its oncological applications are currently under investigation, initial studies, with comparison with PET/CT, are reporting promising results [156].

MR Lymphography

In most patients with cancer, lymph node metastases affect the prognosis and planned therapy significantly. Therefore, detection of nodal involvement is crucial before planning any treatment. Current cross-sectional imaging modalities including US, CT, and MRI rely on size criteria and thus are not a reliable way of identifying nodal involvement. Small nodes can be involved with cancer and nodes may be enlarged due to reactive hyperplasia. Although PET/CT can help to differentiate nodal metastases in some cancers, small metastatic nodes may be missed due to limited spatial resolution of current PET/CT scanners.

MRI lymphography using ultrasmall supermagnetic iron oxide (USPIO) has been described as a promising method to identify nodal metastases, even for small nodes [157]. Since USPIO particles are taken up by macrophages, normal nodes appear hypointense on T2*-weighted images; metastatic nodes are

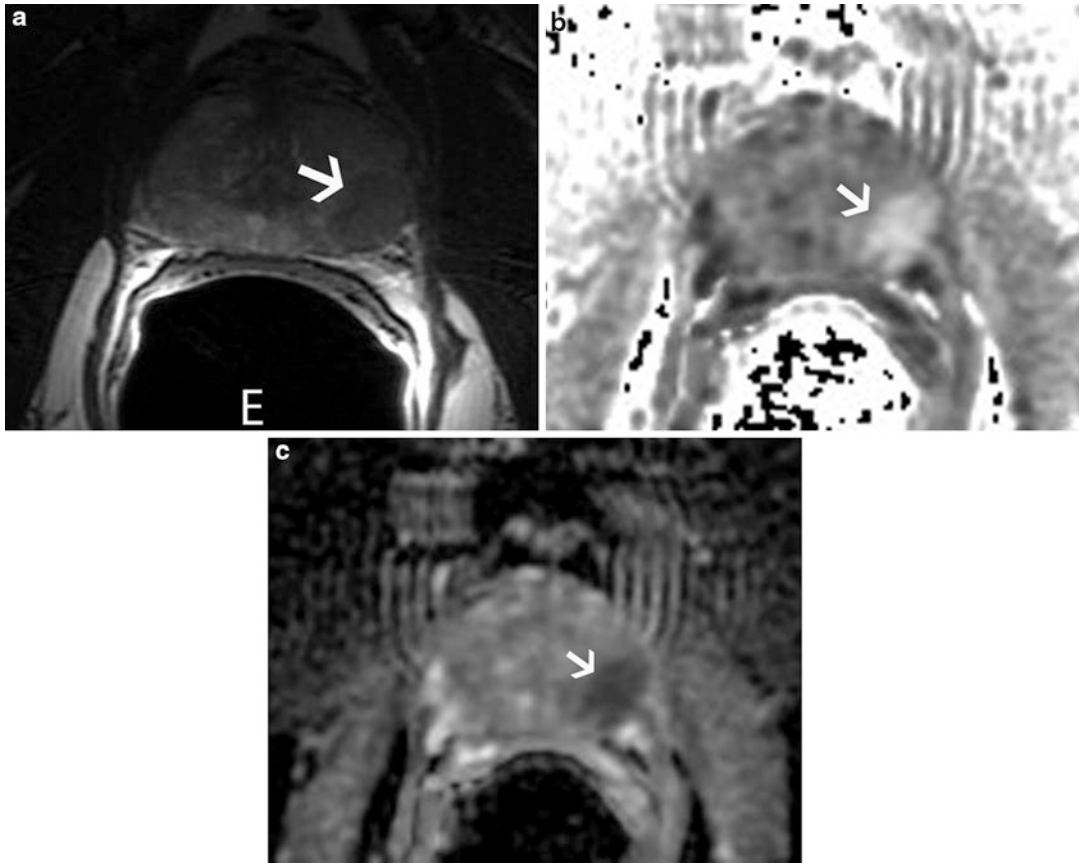

Fig. 15.19 A 57-year-old man with prostate cancer. Axial, T2-weighted MRI (**a**) obtained with endorectal coil shows a low-signal intensity area (*arrow*), which may represent patient's known cancer. The abnormal area shows restricted diffusion and manifest as hyperintense on diffusion-weighted image (**b**) and hypointense on apparent diffusion coefficient (ADC) map image (**c**). Note signal void endorectal coil (*E*)

hyperintense because of lack of uptake. Despite its great potential in oncologic imaging, USPIO has not been approved for human use by the FDA.

Other Recent or Forthcoming Advances in MRI

Recent advances in surface coil and scanner table design and improvements in computer technology and acquisition software have allowed development of high-quality, whole-body MRI algorithms in 30 min [158, 159]. Whole-body MRI examinations can be used in oncologic imaging for initial staging or follow-up. Alternatively, using specific software, MR image can be co-registered and fused with whole-body PET images [160]. There has been also a strong interest in developing combine PET/MR imaging. A prototype scanner, which obtains PET and MRI of brain images simultaneously, has already been developed, and potential clinical applications are under investigation [161]. A whole-body PET/MR is currently under development.

Conclusion

MRI is one of the main pillars of oncologic imaging and plays a vital role in the care of patients with cancer. Due to intrinsic proprieties such as superior soft tissue contrast resolution, multiplanar

capability, functional imaging ability, and lack of ionizing radiation, MRI has become indispensible in the management of oncologic diseases. As the technology advances, its role will continue to expand at virtually every stage of patient care including initial diagnosis, planning of therapy, guiding of treatment, and posttreatment surveillance.

Cross-References

- Cryoablation
- Cryoablation of Liver Tumors
- Emerging Technologies in the Treatment of Cancer
- Image-Guided High-Intensity Focused Ultrasound in the Treatment of Cancer
- Imaging of Interventional Therapies in Oncology: Computed Tomography
- Magnetic Resonance-Guided High-Intensity Focused Ultrasound: Gynecological Applications
- Tumor Ablation: An Evolving Technology

References

1. Tatli S, Morrison PR, Tuncali K, Silverman SG. Interventional MRI for oncologic applications. Tech Vasc Interv Radiol. 2007;10(2):159–70.
2. Brenner DJ, Hall EJ. Computed tomography – an increasing source of radiation exposure. N Engl J Med. 2007;357:2277–84.
3. Kanal E, Shellock FG, Talagala L. Safety considerations in MR imaging. Radiology. 1990;176(3):593–606.
4. Kanal E, Borgstede JP, Barkovich AJ, American College of Radiology, et al. American College of Radiology white paper on MR safety. AJR Am J Roentgenol. 2002;178(6):1335–47.
5. Cowper SE, Robin HS, Steinberg SM, Su LD, Gupta S, LeBoit PE. Scleromyxoedema-like cutaneous diseases in renal-dialysis patients. Lancet. 2000;356(9234):1000–1.
6. Marckmann P, Skov L, Rossen K, Dupont A, Damholt MB, Heaf JG, Thomsen HS. Nephrogenic systemic fibrosis: suspected causative role of gadodiamide used for contrast-enhanced magnetic resonance imaging. J Am Soc Nephrol. 2006;17(9):2359–62.
7. Shellock FG, Spinazzi A. MRI safety update 2008: part 1, MRI contrast agents and nephrogenic systemic fibrosis. AJR Am J Roentgenol. 2008;191(4):1129–39.
8. Cha S. Update on brain tumor imaging: from anatomy to physiology. AJNR Am J Neuroradiol. 2006;27:475–87.
9. Koeller KK, Rosenblum RS, Morrison AL. Neoplasms of the spinal cord and filum terminale: radiologic-pathologic correlation. Radiographics. 2000;20(6):1721–49.
10. Thurnher MM, Law M. Diffusion-weighted imaging, diffusion-tensor imaging, and fiber tractography of the spinal cord. Magn Reson Imaging Clin N Am. 2009;17(2):225–44.
11. Caldemeyer KS, Mathews VP, Righi PD, Smith RR. Imaging features and clinical significance of perineural spread or extension of head and neck tumors. Radiographics. 1998;18(1):97–110.
12. Ginsberg LE. MR imaging of perineural tumor spread. Magn Reson Imaging Clin N Am. 2002;10(3):511–25.
13. Yeh ED. Breast magnetic resonance imaging: current clinical indications. Magn Reson Imaging Clin N Am. 2010;18(2):155–69.
14. Fischer U, Kopka L, Grabbe E. Breast carcinoma: effect of preoperative contrast-enhanced MR imaging on the therapeutic approach. Radiology. 1999;213:881–8.
15. American College of Radiology. http://www.acr.org/. Accessed 1 Dec 2010.
16. American Cancer Society, Cancer Facts & Figures 2010. http://www.cancer.org/acs. Accessed 1 Dec 2010.
17. Antoch G, Stattaus J, Nemat AT, et al. Non-small cell lung cancer: dual-modality PET/CT in preoperative staging. Radiology. 2003;229:526–33.
18. Godelman A, Haramati LB. MR imaging in diagnosis and staging of pulmonary carcinoma. Magn Reson Imaging Clin N Am. 2008;16(2):309–17.
19. Syed IS, Feng D, Harris SR, et al. MR imaging of cardiac masses. Magn Reson Imaging Clin N Am. 2008;16(2):137–64.
20. Hoffmann U, Globits S, Schima W, et al. Usefulness of magnetic resonance imaging of cardiac and paracardiac masses. Am J Cardiol. 2003;92(7):890–5.
21. El-Serag HB, Marrero JA, Rudolph L, Reddy KR. Diagnosis and treatment of hepatocellular carcinoma. Gastroenterology. 2008;134(6):1752–63.
22. Semelka RC, Martin DR, Balci C, Lance T. Focal liver lesions: comparison of dual-phase CT and multisequence multiplanar MR imaging including dynamic gadolinium enhancement. J Magn Reson Imaging. 2001;13(3):397–401.
23. Barish MA, Yucel EK, Ferrucci JT. Magnetic resonance cholangiopancreatography. N Engl J Med. 1999;341(4):258–64.
24. Sahni VA, Mortele KJ. Magnetic resonance cholangiopancreatography: current use and future applications. Clin Gastroenterol Hepatol. 2008;6(9):967–77.
25. Federle M, Chezmar J, Rubin D, et al. Efficacy and safety of mangafodipir trisodium (MnDPDP)

injection for hepatic MRI in adults: results of the U.S. multicenter phase III clinical trials. Efficacy of early imaging. J Magn Reson Imaging. 2000;12(5): 689–701.
26. Hagspiel KD, Neidl KF, Eichenberger AC, Weder W, Marincek B. Detection of liver metastases: comparison of superparamagnetic iron oxide-enhanced and unenhanced MR imaging at 1.5 T with dynamic CT, intraoperative US, and percutaneous US. Radiology. 1995;196(2):471–8.
27. Nakayama M, Yamashita Y, Mitsuzaki K, Yi T, Arakawa A, Katahira K, Nakayama Y, Takahashi M. Improved tissue characterization of focal liver lesions with ferumoxide-enhanced T1 and T2-weighted MR imaging. J Magn Reson Imaging. 2000;11(6):647–54.
28. Reimer P, Rummeny EJ, Daldrup HE, Hesse T, Balzer T, Tombach B, Peters PE. Enhancement characteristics of liver metastases, hepatocellular carcinomas, and hemangiomas with Gd-EOB-DTPA: preliminary results with dynamic MR imaging. Eur Radiol. 1997;7(2):275–80.
29. Runge VM. A comparison of two MR hepatobiliary gadolinium chelates: Gd-BOPTA and Gd-EOB-DTPA. J Comput Assist Tomogr. 1998;22(4): 643–50.
30. Ji H, Ros PR. Magnetic resonance imaging. Liver-specific contrast agents. Clin Liver Dis. 2002;6(1): 73–90.
31. Sauer R, Fietkau R, Wittekind C, German Rectal Cancer Group, et al. Adjuvant vs. neoadjuvant radiochemotherapy for locally advanced rectal cancer: the German trial CAO/ARO/AIO-94. Colorectal Dis. 2003;5:406–15.
32. Tatli S, Mortele KJ, Breen EL, Bleday R, Silverman SG. Local staging of rectal cancer using combined pelvic phased-array and endorectal coil MRI. J Magn Reson Imaging. 2006;23(4): 534–40.
33. Eisner BH, Kurtz MP, Harisinghani MG. Evolving role of magnetic resonance imaging in renal cancer imaging. J Endourol. 2010;24(5):707–11.
34. Silverman SG, Israel GM, Herts BR, Richie JP. Management of the incidental renal mass. Radiology. 2008;249(1):16–31.
35. Jacobs BL, Lee CT, Montie JE. Bladder cancer in 2010: how far have we come? CA Cancer J Clin. 2010;60(4):244–72.
36. Silverman SG, Leyendecker JR, Amis Jr ES. What is the current role of CT urography and MR urography in the evaluation of the urinary tract? Radiology. 2009;250(2):309–23.
37. Setty BN, Holalkere NS, Sahani DV, Uppot RN, Harisinghani M, Blake MA. State-of-the-art cross-sectional imaging in bladder cancer. Curr Probl Diagn Radiol. 2007;36(2):83–96.
38. Tekes A, Kamel I, Imam K, et al. Dynamic MRI of bladder cancer: evaluation of staging accuracy. AJR Am J Roentgenol. 2005;184(1):121–7.
39. Hussain HK, Korobkin M. MR imaging of the adrenal glands. Magn Reson Imaging Clin N Am. 2004;12(3):515–44.
40. Korobkin M. Overview of imaging/CT. Urol Radiol. 1989;4:221–6.
41. Mayo-Smith WW, Lee MJ, McNicholas MMJ, Hahn PF, Boland GW, Saini S. Characterization of masses (<5 cm) by use of chemical shift MR imaging Observer performance versus quantitative measure. Am J Roentgenol. 1995;165(1):91–5.
42. Outwater EK, Siegelman ES, Radecki PD, Piccoli CW, Mitchell DG. Distinction between benign and malignant adrenal masses: value of T1-weighted chemical-shift MR imaging. AJR Am J Roentgenol. 1995;165(3):579–83.
43. Hricak H, White S, Vigneron D, et al. Carcinoma of the prostate gland: MR imaging with pelvic phased-array coils versus integrated endorectal–pelvic phased-array coils. Radiology. 1994;193(3):703–9.
44. Shimofusa R, Fujimoto H, Akamata H, Motoori K, Yamamoto S, Ueda T, Ito H. Diffusion-weighted imaging of prostate cancer. J Comput Assist Tomogr. 2005;29(2):149–53.
45. Lim HK, Kim JK, Kim KA, Cho KS. Prostate cancer: apparent diffusion coefficient map with T2-weighted images for detection – a multireader study. Radiology. 2009;250(1):145–51.
46. Jager GJ, Ruijter ET, van de Kaa CA, et al. Dynamic TurboFLASH subtraction technique for contrast-enhanced MR imaging of the prostate: correlation with histopathologic results. Radiology. 1997; 203(3):645–52.
47. Engelbrecht MR, Huisman HJ, Laheij RJ, et al. Discrimination of prostate cancer from normal peripheral zone and central gland tissue by using dynamic contrast-enhanced MR imaging. Radiology. 2003;229(1):248–54.
48. Amant F, Moerman P, Neven P, et al. Endometrial cancer. Lancet. 2005;366(9484):491–505.
49. Frei KA, Kinkel K, Bonél HM, Lu Y, Zaloudek C, Hricak H. Prediction of deep myometrial invasion in patients with endometrial cancer: clinical utility of contrast-enhanced MR imaging-a meta-analysis and Bayesian analysis. Radiology. 2000;216(2):444–9.
50. Hricak H, Gatsonis C, Chi DS, American College of Radiology Imaging Network 6651, Gynecologic Oncology Group 183, et al. Role of imaging in pretreatment evaluation of early invasive cervical cancer: results of the intergroup study American College of Radiology Imaging Network 6651-Gynecologic Oncology Group 183. J Clin Oncol. 2005;23(36):9329–37.
51. Hricak H, Gatsonis C, Coakley FV, et al. Early invasive cervical cancer: CT and MR imaging in preoperative evaluation – ACRIN/GOG comparative study of diagnostic performance and interobserver variability. Radiology. 2007;245(2):491–8.
52. Rieber A, Nüssle K, Stöhr I, et al. Preoperative diagnosis of ovarian tumors with MR imaging: comparison

with transvaginal sonography, positron emission tomography, and histologic findings. AJR Am J Roentgenol. 2001;177(1):123–9.
53. Hricak H, Chen M, Coakley FV, et al. Complex adnexal masses: detection and characterization with MR imaging–multivariate analysis. Radiology. 2000;214(1):39–46.
54. Ma LD. Magnetic resonance imaging of musculoskeletal tumors: skeletal and soft tissue masses. Curr Probl Diagn Radiol. 1999;28(2):29–62.
55. Alyas F, James SL, Davies AM, Saifuddin A. The role of MR imaging in the diagnostic characterisation of appendicular bone tumours and tumour-like conditions. Eur Radiol. 2007;17(10):2675–86.
56. Wootton-Gorges SL. MR imaging of primary bone tumors and tumor-like conditions in children. Magn Reson Imaging Clin N Am. 2009;17(3):469–87.
57. Hagspiel KD, Kandarpa K, Jolesz FA. Interventional MR imaging. J Vasc Interv Radiol. 1997;8:745–58.
58. McDannold NJ, Jolesz FA. Magnetic resonance image-guided thermal ablations. Top Magn Reson Imaging. 2000;11:191–202.
59. Hynynen K, Kettenbach J, Kacher DF, et al. Interventional and intraoperative magnetic resonance imaging. Annu Rev Biomed Eng. 2000;2:661–90.
60. Lu DS, Lee H, Farahani K, et al. Biopsy of hepatic dome lesions: semi-real-time coronal MR guidance technique. AJR Am J Roentgenol. 1997;168:737–9.
61. Silverman SG, Tuncali K, Morrison PR. MR Imaging-guided percutaneous tumor ablation. Acad Radiol. 2005;12:1100–19.
62. Morrison PR, Silverman SG, Tuncali K, Tatli S. MRI-guided cryotherapy. J Magn Reson Imaging. 2008;27(2):410–20.
63. Tempany CM, Stewart EA, McDannold N, Quade BJ, Jolesz FA, Hynynen K. MR imaging-guided focused ultrasound surgery of uterine leiomyomas: a feasibility study. Radiology. 2003;226(3):897–905.
64. Tuncali K, Morrison PR, Tatli S, Silverman SG. MRI-guided percutaneous cryoablation of renal tumors: use of external manual displacement of adjacent bowel loops. Eur J Radiol. 2006;59(2):198–202.
65. Silverman SG, Jolesz FA, Newman RW, et al. Design and implementation of an interventional MR imaging suite. AJR Am J Roentgenol. 1997;168:1465–71.
66. Silverman SG, Collick BD, Figueira MR, et al. Interactive MR-guided biopsy in an open-configuration MR imaging system. Radiology. 1995;197:175–81.
67. Wallis F, Gilbert FJ. Magnetic resonance imaging in oncology: an overview. J R Coll Surg Edinb. 1999;44(2):117–25.
68. Salomonowitz E. MR imaging-guided biopsy and therapeutic intervention in a closed-configuration magnet: single-center series of 361 punctures. AJR Am J Roentgenol. 2001;177:159–63.
69. Solomon SB, Silverman SG. Imaging in interventional oncology. Radiology. 2010;257(3):624–40.
70. Fenchel S, Boll DT, Lewin JS. Intraoperative MR imaging. Magn Reson Imaging Clin N Am. 2003;11(3):431–47.
71. Johnston T, Moser R, Moeller K, Moriarty TM. Intraoperative MRI: safety. Neurosurg Clin N Am. 2009;20(2):147–53.
72. Jolesz FA, Morrison PR, Koran SJ, et al. Compatible instrumentation for intraoperative MRI: expanding resources. J Magn Reson Imaging. 1998;8:8–11.
73. Keeler EK, Casey FX, Engels H, et al. Accessory equipment considerations with respect to MRI compatibility. J Magn Reson Imaging. 1998;8:12–8.
74. Bedrosian I, Schlencker J, Spitz FR, et al. Magnetic resonance imaging-guided biopsy of mammographically and clinically occult breast lesions. Ann Surg Oncol. 2002;9(5):457–61.
75. Liberman L, Bracero N, Morris E, Thornton C, Dershaw DD. MRI-guided 9-gauge vacuum-assisted breast biopsy: initial clinical experience. AJR Am J Roentgenol. 2005;185(1):183–93.
76. Kuhl CK, Morakkabati N, Leutner CC, et al. MR imaging–guided large-core (14-gauge) needle biopsy of small lesions visible at breast MR imaging alone. Radiology. 2001;220:31–9.
77. Perlet C, Heywang-Kobrunner SH, Heinig A, et al. Magnetic resonance-guided, vacuum-assisted breast biopsy: results from a European multicenter study of 538 lesions. Cancer. 2006;106:982–90.
78. Hata N, Jinzaki M, Kacher D, et al. MR imaging-guided prostate biopsy with surgical navigation software: device validation and feasibility. Radiology. 2001;220(1):263–8.
79. Cormack RA, D'Amico AV, Hata N, Silverman S, Weinstein M, Tempany CM. Feasibility of transperineal prostate biopsy under interventional magnetic resonance guidance. Urology. 2000;56(4):663–4.
80. D'Amico AV, Tempany CM, Cormack R, et al. Transperineal magnetic resonance image guided prostate biopsy. J Urol. 2000;164:385–7.
81. Lichy MP, Anastasiadis AG, Aschoff P, et al. Morphologic, functional, and metabolic magnetic resonance imaging-guided prostate biopsy in a patient with prior negative transrectal ultrasound-guided biopsies and persistently elevated prostate-specific antigen levels. Urology. 2007;69(6):1208.e5–8.
82. Buchanan CL, Morris EA, Dorn PL, et al. Utility of breast magnetic resonance imaging in patients with occult primary breast cancer. Ann Surg Oncol. 2005;12:1045–53.
83. Eby PR, Lehman C. MRI-guided breast interventions. Semin Ultrasound CT MR. 2006;27:339–50.
84. Meeuwis C, Peters NH, Mali WP, et al. Targeting difficult accessible breast lesions: MRI-guided needle localization using a freehand technique in a 3.0 T closed bore magnet. Eur J Radiol. 2007;62:283–8.
85. Bloom S, Morrow M. A clinical oncologic perspective on breast magnetic resonance imaging. Magn Reson Imaging Clin N Am. 2010;18(2):277–94.

86. Philpotts LE. MR intervention: indications, technique, correlation and histologic. Magn Reson Imaging Clin N Am. 2010;18(2):323–32.
87. Ellis JH, Tempany C, Sarin MS, Gatsonis C, Rifkin MD, McNeil BJ. MR imaging and sonography of early prostatic cancer: pathologic and imaging features that influence identification and diagnosis. AJR Am J Roentgenol. 1994;162(4):865–72.
88. Haker SJ, Mulkern RV, Roebuck JR, Barnes AS, Dimaio S, Hata N, Tempany CM. Magnetic resonance-guided prostate interventions. Top Magn Reson Imaging. 2005;16(5):355–68.
89. Zangos S, Herzog C, Eichler K, et al. MR-compatible assistance system for punction in a high-field system: device and feasibility of transgluteal biopsies of the prostate gland. Eur Radiol. 2007;17:1118–24.
90. Barnes AS, Haker SJ, Mulkern RV, et al. Magnetic resonance spectroscopy-guided transperineal prostate biopsy and brachytherapy for recurrent prostate cancer. Urology. 2005;66:1319.
91. Susil RC, Menard C, Krieger A, et al. Transrectal prostate biopsy and fiducial marker placement in a standard 1.5 T magnetic resonance imaging scanner. J Urol. 2006;175:113–20.
92. Fennessy FM, Tuncali K, Morrison PR, Tempany CM. MR imaging-guided interventions in the genitourinary tract: an evolving concept. Magn Reson Imaging Clin N Am. 2010;18(1):11–28.
93. Zhang Q, Chung YC, Lewin JS, Duerk JL. A method for simultaneous RF ablation and MRI. J Magn Reson Imaging. 1998;8(1):110–14.
94. Silverman SG, Tuncali K, Adams DF, et al. MR imaging-guided percutaneous cryotherapy of liver tumors: initial experience. Radiology. 2000;217:657–64.
95. Silverman SG, Tuncali K, vanSonnenberg E, et al. Renal tumors: MR imaging-guided percutaneous cryotherapy – initial experience in 23 patients. Radiology. 2005;236:716–24.
96. Han KR, Cohen JK, Miller RJ, et al. Treatment of organ confined prostate cancer with third generation cryosurgery: preliminary multicenter experience. J Urol. 2003;170:1126–30.
97. Nurko J, Mabry CD, Whitworth P, et al. Interim results from the FibroAdenoma Cryoablation Treatment Registry. Am J Surg. 2005;190:647–51.
98. Tuncali K, Morrison PR, Winalski CS, et al. MRI-guided percutaneous cryotherapy for soft-tissue and bone metastases: initial experience. AJR Am J Roentgenol. 2007;189:232–9.
99. Sakuhara Y, Shimizu T, Kodama Y, et al. Magnetic resonance-guided percutaneous cryoablation of uterine fibroids: early clinical experiences. Cardiovasc Intervent Radiol. 2006;29:552–8.
100. Cline HE, Schenck JF, Hynynen K, et al. MR-guided focused ultrasound surgery. J Comput Assist Tomogr. 1992;16:956–65.
101. Cline HE, Hynynen K, Hardy CJ, et al. MR temperature mapping of focused ultrasound surgery. Magn Reson Med. 1994;31:628–36.
102. Tempany CM, Stewart EA, McDannold N, et al. MR imaging-guided focused ultrasound surgery of uterine leiomyomas: a feasibility study. Radiology. 2003;226:897–905.
103. Mulkern RV, Panych LP, McDannold NJ, et al. Tissue temperature monitoring with multiple gradient-echo imaging sequences. J Magn Reson Imaging. 1998;8:493–502.
104. Kuroda K, Oshio K, Chung AH, et al. Temperature mapping using the water proton chemical shift: a chemical shift selective phase mapping method. Magn Reson Med. 1997;38:845–51.
105. Jolesz FA, Hynynen K, McDannold N, et al. MR imaging-controlled focused ultrasound ablation: a noninvasive image-guided surgery. Magn Reson Imaging Clin N Am. 2005;13:545–60.
106. Hynynen K, Pomeroy O, Smith DN, et al. MR imaging-guided focused ultrasound surgery of fibroadenomas in the breast: a feasibility study. Radiology. 2001;219:176–85.
107. Zippel DB, Papa MZ. The use of MR imaging guided focused ultrasound in breast cancer patients; a preliminary phase one study and review. Breast Cancer. 2005;12:32–8.
108. Fennessy FM, Tempany CM, McDannold NJ, et al. Uterine leiomyomas: MR imaging-guided focused ultrasound surgery – results of different treatment protocols. Radiology. 2007;243:885–93.
109. Catane R, Beck A, Inbar Y, Rabin T, Shabshin N, Hengst S, Pfeffer RM, Hanannel A, Dogadkin O, Liberman B, Kopelman D. MR-guided focused ultrasound surgery (MRgFUS) for the palliation of pain in patients with bone metastases – preliminary clinical experience. Ann Oncol. 2007;18(1):163–7.
110. Gianfelice D, Gupta C, Kucharczyk W, Bret P, Havill D, Clemons M. Palliative treatment of painful bone metastases with MR imaging – guided focused ultrasound. Radiology. 2008;249(1):355–63.
111. Watkin NA, Morris SB, Rivens IH, et al. High-intensity focused ultrasound ablation of the kidney in a large animal model. J Endourol. 1997;11:191–6.
112. Kopelman D, Inbar Y, Hanannel A, et al. Magnetic resonance-guided focused ultrasound surgery (MRgFUS): ablation of liver tissue in a porcine model. Eur J Radiol. 2006;59:157–62.
113. McDannold N, Moss M, Killiany R, et al. MRI-guided focused ultrasound surgery in the brain: tests in a primate model. Magn Reson Med. 2003;49:1188–91.
114. Nag S, Cardenes H, Chang S, Image-Guided Brachytherapy Working Group, et al. Proposed guidelines for image-based intracavitary brachytherapy for cervical carcinoma: report from Image-Guided Brachytherapy Working Group. Int J Radiat Oncol Biol Phys. 2004;60(4):1160–72.
115. Cormack RA. Quality assurance issues for computed tomography-, ultrasound-, and magnetic resonance imaging-guided brachytherapy. Int J Radiat Oncol Biol Phys. 2008;71(1 Suppl):S136–41.

116. Stokes SH. Comparison of biochemical disease-free survival of patients with localized carcinoma of the prostate undergoing radical prostatectomy, transperineal ultrasound-guided radioactive seed implantation, or definitive external beam irradiation. Int J Radiat Oncol Biol Phys. 2000;47:129–36.
117. Pfeiffer D, Sutlief S, Feng W, Pierce HM, Kofler J. AAPM Task Group 128: quality assurance tests for prostate brachytherapy ultrasound systems. Med Phys. 2008;35(12):5471–89.
118. D'amico AV, Tempany CM, Schultz D, et al. Comparing PSA outcome after radical prostatectomy or magnetic resonance imaging-guided partial prostatic irradiation in select patients with clinically localized adenocarcinoma of the prostate. Urology. 2003;62:1063–7.
119. Talcott JA, Clark JA, Stark PC, et al. Long-term treatment related complications of brachytherapy for early prostate cancer: a survey of patients previously treated. J Urol. 2001;166:494–9.
120. Hurwitz MD, Cormack R, Tempany CM, et al. Three-dimensional real-time magnetic resonance-guided interstitial prostate brachytherapy optimizes radiation dose distribution resulting in a favorable acute side-effect profile in patients with clinically localized prostate cancer. Tech Urol. 2000;6:89–94.
121. D'Amico AV, Cormack RA, Tempany CM. MRI-guided diagnosis and treatment of prostate cancer. N Engl J Med. 2001;344:776–7.
122. Cormack RA, Kooy H, Tempany CM, et al. A clinical method for real-time dosimetric guidance of transperineal 125I prostate implants using interventional magnetic resonance imaging. Int J Radiat Oncol Biol Phys. 2000;46:207–14.
123. D'Amico AV, Cormack R, Tempany CM, et al. Real-time magnetic resonance image-guided interstitial brachytherapy in the treatment of select patients with clinically localized prostate cancer. Int J Radiat Oncol Biol Phys. 1998;42:507–15.
124. Mislow JM, Golby AJ, Black PM. Origins of intraoperative MRI. Neurosurg Clin N Am. 2009;20(2):137–46.
125. Black PM, Moriarty T, Alexander 3rd E, et al. Development and implementation of intraoperative magnetic resonance imaging and its neurosurgical applications. Neurosurgery. 1997;41(4):831–42.
126. Schwartz RB, Hsu L, Wong TZ, et al. Intraoperative MR imaging guidance for intracranial neurosurgery: experience with the first 200 cases. Radiology. 1999;211(2):477–88.
127. Pergolizzi Jr RS, Nabavi A, Schwartz RB, et al. Intraoperative MR guidance during trans-sphenoidal pituitary resection: preliminary results. J Magn Reson Imaging. 2001;13(1):136–41.
128. Bootz F, Schulz T, Weber A, Scheffler B, Keiner S. The use of open MRI in otorhinolaryngology: initial experience. Comput Aided Surg. 2001;6(5): 297–304.
129. Schulz T, Schneider JP, Bootz F, et al. Transnasal and transsphenoidal MRI-guided biopsies of petroclival tumors. J Magn Reson Imaging. 2001; 13(1):3–11.
130. Dort JC, Sutherland GR. Intraoperative magnetic resonance imaging for skull base surgery. Laryngoscope. 2001;111(9):1570–5.
131. Fried MP, Topulos G, Hsu L, et al. Endoscopic sinus surgery with magnetic resonance imaging guidance: initial patient experience. Otolaryngol Head Neck Surg. 1998;119(4):374–80.
132. Gould SW, Lamb G, Lomax D, Gedroyc W, Darzi A. Interventional MR-guided excisional biopsy of breast lesions. J Magn Reson Imaging. 1998;8(1): 26–30.
133. Therasse P, Arbuck SG, Eisenhauer EA, et al. New guidelines to evaluate the response to treatment in solid tumors. European Organization for Research and Treatment of Cancer, National Cancer Institute of the United States, National Cancer Institute of Canada. J Natl Cancer Inst. 2000;92(3):205–16.
134. Klaeser B, Mueller MD, Schmid RA, Guevara C, Krause T, Wiskirchen J. PET-CT-guided interventions in the management of FDG-positive lesions in patients suffering from solid malignancies: initial experience. Eur Radiol. 2009;19:1780–5.
135. Selzner M, Hany TF, Wildbrett P, McCormack L, Kadry Z, Clavien PA. Does the novel PET/CT imaging modality impact on the treatment of patients with metastatic colorectal cancer of the liver? Ann Surg. 2004;240(6):1027–34.
136. Tatli S, Gerbaudo VH, Mamede M, Tuncali K, Shyn PB, Silverman SG. Abdominal masses sampled at PET/CT-guided percutaneous biopsy: initial experience with registration of prior PET/CT images. Radiology. 2010;256(1):305–11.
137. Soher BJ, Dale BM, Merkle EM. A review of MR physics: 3 T versus 1.5 T. Magn Reson Imaging Clin N Am. 2007;15(3):277–90.
138. DeLano MC, Fisher C. 3 T MR imaging of the brain. Magn Reson Imaging Clin N Am. 2006;14(1):77–88.
139. Nagae-Poetscher LM, Jiang H, Wakana S, Golay X, van Zijl PC, Mori S. High-resolution diffusion tensor imaging of the brain stem at 3 T. AJNR Am J Neuroradiol. 2004;25(8):1325–30.
140. Ramnath RR. 3 T MR imaging of the musculoskeletal system (Part II): clinical applications. Magn Reson Imaging Clin N Am. 2006;14(1):41–62.
141. Sosna J, Pedrosa I, Dewolf WC, Mahallati H, Lenkinski RE, Rofsky NM. MR imaging of the prostate at 3 Tesla: comparison of an external phased-array coil to imaging with an endorectal coil at 1.5 Tesla. Acad Radiol. 2004;11(8):857–62.
142. Bammer R, Schoenberg SO. Current concepts and advances in clinical parallel magnetic resonance imaging. Top Magn Reson Imaging. 2004;15(3):129–58.
143. Glockner JF, Hu HH, Stanley DW, Angelos L, King K. Parallel MR imaging: a user's guide. Radiographics. 2005;25(5):1279–97.

144. Padhani AR. Dynamic contrast-enhanced MRI in clinical oncology: current status and future directions. J Magn Reson Imaging. 2002;16(4):407–22.
145. Kwee TC, Takahara T, Klomp DW, Luijten PR. Cancer imaging: novel concepts in clinical magnetic resonance imaging. J Intern Med. 2010;268(2): 120–32.
146. Kuhl CK, Mielcareck P, Klaschik S, et al. Dynamic breast MR imaging; a signal intensity time course data useful for differential diagnosis of enhancing lesions? Radiology. 1999;211:101–10.
147. Bloch BN, Furman-Haran E, Helbich TH, et al. Prostate cancer: accurate determination of extracapsular extension with high-spatial-resolution dynamic contrast-enhanced and T2-weighted MR imaging–initial results. Radiology. 2007;245(1):176–85.
148. Thomassin-Naggara I, Daraï E, Cuenod CA, Rouzier R, Callard P, Bazot M. Dynamic contrast-enhanced magnetic resonance imaging: a useful tool for characterizing ovarian epithelial tumors. J Magn Reson Imaging. 2008;28(1):111–20.
149. Schaefer PW, Grant PE, Gonzalez RG. Diffusion-weighted MR imaging of the brain. Radiology. 2000;217(2):331–45.
150. Kono K, Inoue Y, Nakayama K, et al. The role of diffusion-weighted imaging in patients with brain tumors. AJNR Am J Neuroradiol. 2001;22: 1081–8.
151. Stadnik TW, Chaskis C, Michotte A, et al. Diffusion-weighted MR imaging of intracerebral masses: comparison with conventional MR imaging and histologic findings. AJNR Am J Neuroradiol. 2001;22: 969–76.
152. Provenzale JM, Mukundan S, Barboriak DP. Diffusion-weighted and perfusion MR imaging for brain tumor characterization and assessment of treatment response. Radiology. 2006;239(3):632–49.
153. Low RN, Gurney J. Diffusion-weighted MRI (DWI) in the oncology patient: value of breathhold DWI compared to unenhanced and gadolinium-enhanced MRI. J Magn Reson Imaging. 2007; 25(4):848–58.
154. Low RN. Diffusion-weighted MR, imaging for whole body metastatic disease and lymphadenopathy. Magn Reson Imaging Clin N Am. 2009;17(2): 245–61.
155. Takahara T, Imai Y, Yamashita T, Yasuda S, Nasu S, Van Cauteren M. Diffusion weighted whole body imaging with background body signal suppression (DWIBS): technical improvement using free breathing, STIR and high resolution 3D display. Radiat Med. 2004;22(4):275–82.
156. Komori T, Narabayashi I, Matsumura K, et al. 2-[Fluorine-18]-fluoro-2-deoxy-D-glucose positron emission tomography/computed tomography versus whole-body diffusion-weighted MRI for detection of malignant lesions: initial experience. Ann Nucl Med. 2007;21(4):209–15.
157. Harisinghani MG, Saini S, Weissleder R, et al. MR lymphangiography using ultrasmall superparamagnetic iron oxide in patients with primary abdominal and pelvic malignancies: radiographic-pathologic correlation. AJR Am J Roentgenol. 1999;172(5):1347–51.
158. Schick F. Whole-body MRI, at high field: technical limits and clinical potential. Eur Radiol. 2005;15(5):946–59.
159. Lauenstein TC, Goehde SC, Herborn CU, et al. Whole-body MR imaging: evaluation of patients for metastases. Radiology. 2004;233(1):139–48.
160. Antoch G, Vogt FM, Freudenberg LS, et al. Whole-body dual-modality PET/CT and whole-body MRI for tumor staging in oncology. J Am Med Assoc. 2003;290(24):3199–206.
161. Raylman RR, Majewski S, Velan SS, et al. Simultaneous acquisition of magnetic resonance spectroscopy (MRS) data and positron emission tomography (PET) images with a prototype MR-compatible, small animal PET imager. J Magn Reson. 2007;186(2):305–10.

Imaging of Interventional Therapies in Oncology: Positron Emission Tomography/Computed Tomography

16

Homer A. Macapinlac

Abstract

This chapter is intended to illustrate the utility of positron emission tomography (PET) in image-guided therapies. PET imaging provides functional images of the body allowing us to identify alterations in metabolism which better characterizes the presence of cancer, its prognosis, and early response to multimodality therapy. PET imaging is the most widely used clinical technique for molecular imaging and, in conjunction with traditional anatomic modalities such as computed tomography (CT), provides a better assessment of the status of oncology patients. PET/CT imaging has become widely available, particularly with the use of fluorodeoxyglucose (FDG) as an analogue to glucose metabolism, which in turn allows us to identify the presence of cancer and measure response to therapy. This chapter provides an overview of the biologic mechanisms which occur in cancer, and by using PET imaging, we take advantage of this altered biochemistry to improve our ability to stage the extent of cancer and direct appropriate biopsies of the primary tumor. PET/CT imaging can also provide a road map to allow nodal sampling which can be useful to stage and determine type of therapy. PET/CT has also been used to direct biopsy or verify suspected distant metastases which can allow earlier management decisions between potentially curative and palliative therapies. Finally, the minimally invasive therapies using image guidance can benefit by PET/CT to determine target delineation and any residual or recurrent disease. The future direction, particularly with the clinical use of novel radiotracers, is discussed as it pertains to imaging hypoxia to identify radiation resistant parts of tumor, DNA or proliferation imaging to assess early response, and angiogenesis PET imaging for targeted therapies.

H.A. Macapinlac
Department of Nuclear Medicine, University of Texas
MD Anderson Cancer Center, Houston, TX, USA
e-mail: hmacapinlac@mdanderson.org

D.E. Dupuy et al. (eds.), *Image-Guided Cancer Therapy*, DOI 10.1007/978-1-4419-0751-6_18,

Introduction

Positron emission tomography (PET) is a nuclear medicine technique which produces functional images of the body by detecting gamma rays produced by positron-emitting tracers like fluorine-18. The most widely utilized tracer is the glucose analogue 2-fluoro-2-deoxy-D-glucose (FDG). When FDG is injected into fasting patients (Fig. 16.1), glucose utilization is seen in the brain, muscle, and some in the liver and is mainly excreted in the urine via the kidneys and bladder. We note that most normal cells have low levels of FDG uptake. A patient with lung cancer (Fig. 16.2) shows the high FDG retention in tumor as compared to the surrounding normal cells. This phenomenon of glucose hypermetabolism was first described by Warburg [1] et al. in the 1920s but has only been used to image cancer in humans in the 1980s [2, 3]. FDG is rapidly taken up by cancer cells via glucose transporters and then phosphorylated (like glucose) via hexokinase, "trapping" the

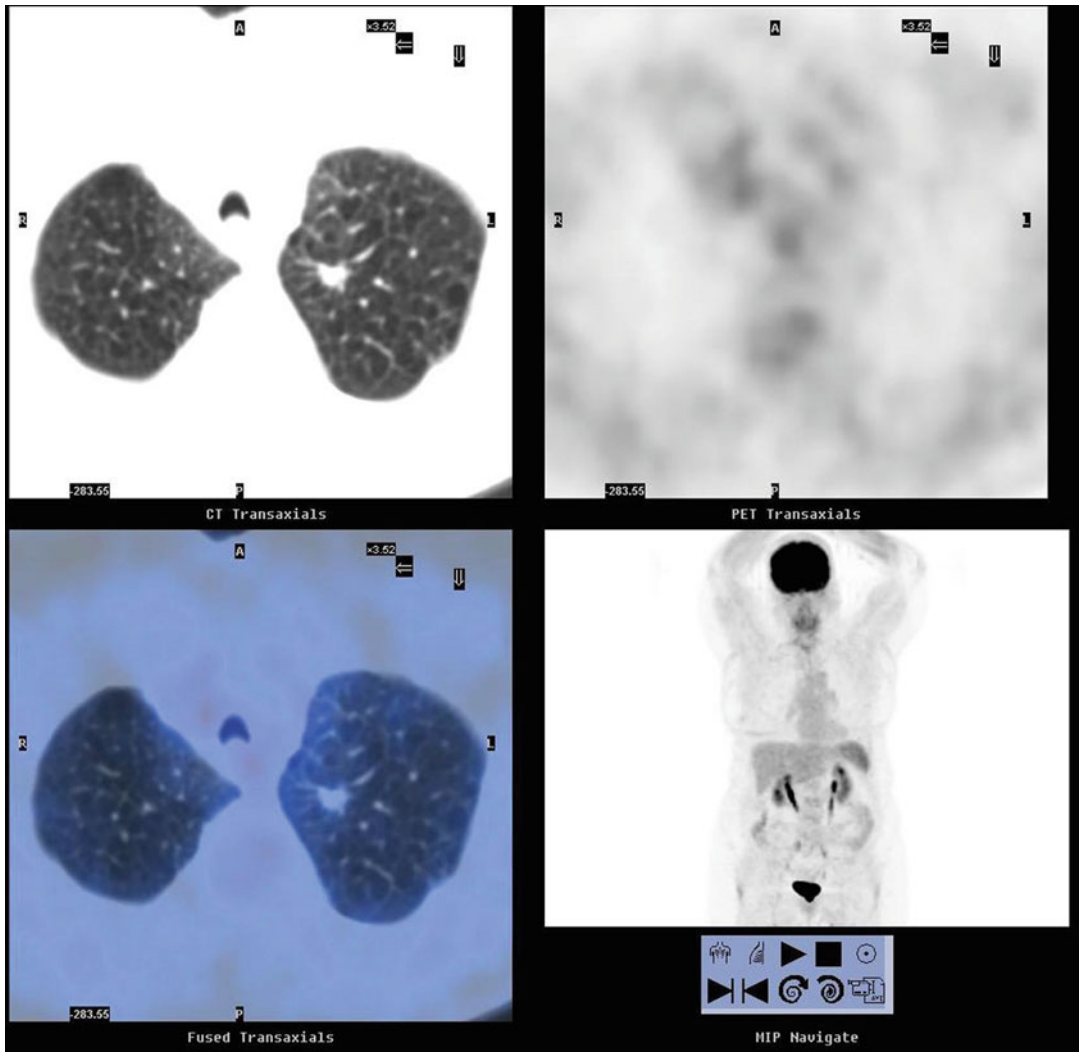

Fig. 16.1 PET/CT scan of a patient with NSCLC treated with chemotherapy and radiation. The FDG PET scan (*lower right*) shows normal activity in the brain, liver, spleen, kidneys, and bladder. The residual lung mass in the left upper lobe (*upper left*) shows no FDG uptake on the PET scan (*upper right*) and fused PET/CT image (*lower left*)

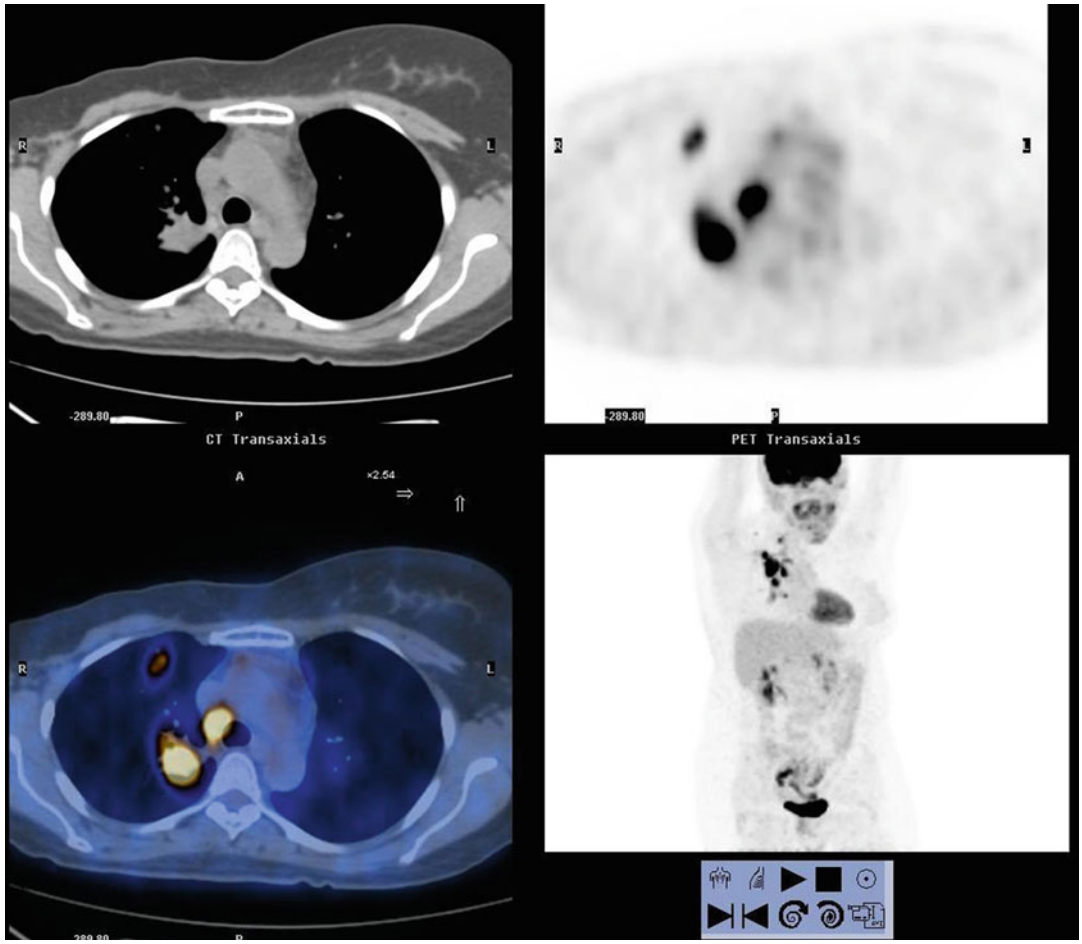

Fig. 16.2 This is a patient with a right upper lobe lung cancer with FDG avid mediastinal nodes (*lower right*). The PET/CT image (*lower right*) shows the FDG uptake in the primary and right paratracheal nodes

FDG-6P within these cells. This process is also enhanced by the relative hypoxia in tumors which activates this anaerobic glycolytic pathway. In relative low concentration of glucose-6-phosphatase in cancer cells, a reverse dephosphorylation reaction does not occur, allowing this "trapping" to occur. Therefore, FDG is a marker for enhanced glycolytic activity of tumors. The intensity of FDG uptake in tumors appears to correlate with more aggressive tumors and poor prognosis [4]. However, well-differentiated and mucinous tumors may demonstrate low FDG uptake as in bronchoalveolar cell cancers of the lung. Hence, FDG PET imaging in these tumors will be limited [5].

Use of PET increased dramatically after the Centers for Medicare & Medicaid Services (CMS) approved its use in diagnosis, staging, and restaging of non-small-cell lung cancer, esophageal cancer, lymphoma, melanoma, and head and neck cancers.

Most recently, in April 2009, CMS expanded coverage to include the use of FDG PET to evaluate the initial treatment strategy (formerly diagnosis and initial staging) of patients with nearly all solid tumors and also the use of PET in subsequent evaluations of treatment strategy (formerly restaging, detection of suspected recurrence, and treatment monitoring) for additional cancer types. CMS also specifically identified noncoverage

for screening for cancer detection, surveillance of patients with cancer history, staging of prostate cancer, diagnosis of breast cancer, and evaluation of regional nodes for breast cancer and melanoma [6].

It is important to remember that good patient preparation which includes fasting for at least 6 h and standardized imaging technique is crucial for the success in managing both individual patients and patients in imaging trials [7].

More recently, integrated PET and CT machines allow co-registration of the anatomic (CT) and functional (PET) images to improve our ability to identify tumor, evaluate its extent, differentiate posttreatment changes from recurrence, and monitor response to therapy. The primary reason for the CT acquisition is to provide attenuation correction and image reconstruction [8].

FDG PET-Directed Biopsy for Cancer Diagnosis

The fusion of CT and FDG PET images allows very good correlation and localization of abnormal glucose activity which can be very useful in directing a biopsy which would likely yield the malignant cells. More importantly, if one is dealing with a large heterogenous tumor or multiple nodes, the biopsy can be directed toward the most aggressive component of the tumor which is usually more FDG avid than the rest of the tumor (see Figs. 16.3 and 16.4). FDG PET-directed biopsies have been demonstrated to be useful for various tumor types including gliomas [9] and lung cancer [10]. When a brain tumor biopsy is equivocal or yields a mixed type of tumor such as an oligodendroglioma, an FDG PET-directed biopsy may be necessary to identify an anaplastic component thereby changing management. Early studies have shown the feasibility of using FDG PET to identify malignant degeneration of low-grade gliomas which can allow the appropriately directed biopsy prior to treatment decision making [11]. FDG PET/CT could differentiate between CNS lymphomas and infections such as toxoplasmosis in patients with HIV/AIDS. In this setting, both disease entities may demonstrate similar characteristics on CT or MR, and thus, it would be crucial to make the differential diagnosis as the treatments are very different [4].

Non-small-cell lung cancers usually have a necrotic component. Therefore, an FDG PET-directed biopsy may yield better results as FDG retaining cells are usually viable. In certain instances, benign FDG uptake in brown fat may mimic tumor uptake. The PET/CT technique has been useful in identifying these variants in patients with chest tumors allowing more appropriately directed biopsies and avoiding benign tissue-mimicking tumor [12].

Patients presenting with cervical nodes and an unknown primary would benefit from FDG PET/CT scans to identify the primary. A meta-analysis has demonstrated that in up to a third of these previously unknown tumors which could be identified, the appropriate biopsy followed by correctly indicated therapy was done for these patients [13]. Furthermore, patients would benefit from knowing the origin of the cancer cells as well as in lieu of empiric therapy, having the correct therapy administered.

Patients presenting with multi-compartmental adenopathy may also benefit from FDG PET/CT-directed biopsy. A good example would be patients with chronic lymphocytic leukemia who may present with increasing adenopathy. Performing FDG PET/CT allows for the identification of FDG avid nodes which at biopsy would likely harbor lymphoma cells in a setting of Richter's transformation. The correct treatment could then be given, plus the repeat FDG PET/CT at the end of chemotherapy may be useful for monitoring response and prognostication [14]. FDG PET imaging has become an integral imaging component of assessing response in patients with lymphoma as outlined by the recently revised international harmonization criteria [15].

An active area of implementation is the use of FDG PET/CT as a guide to the biopsy of mediastinal nodes using endobronchial ultrasound with transbronchial nodal assessment (EUS/TBNA). This minimally invasive technique has become the preferred method for staging the mediastinum

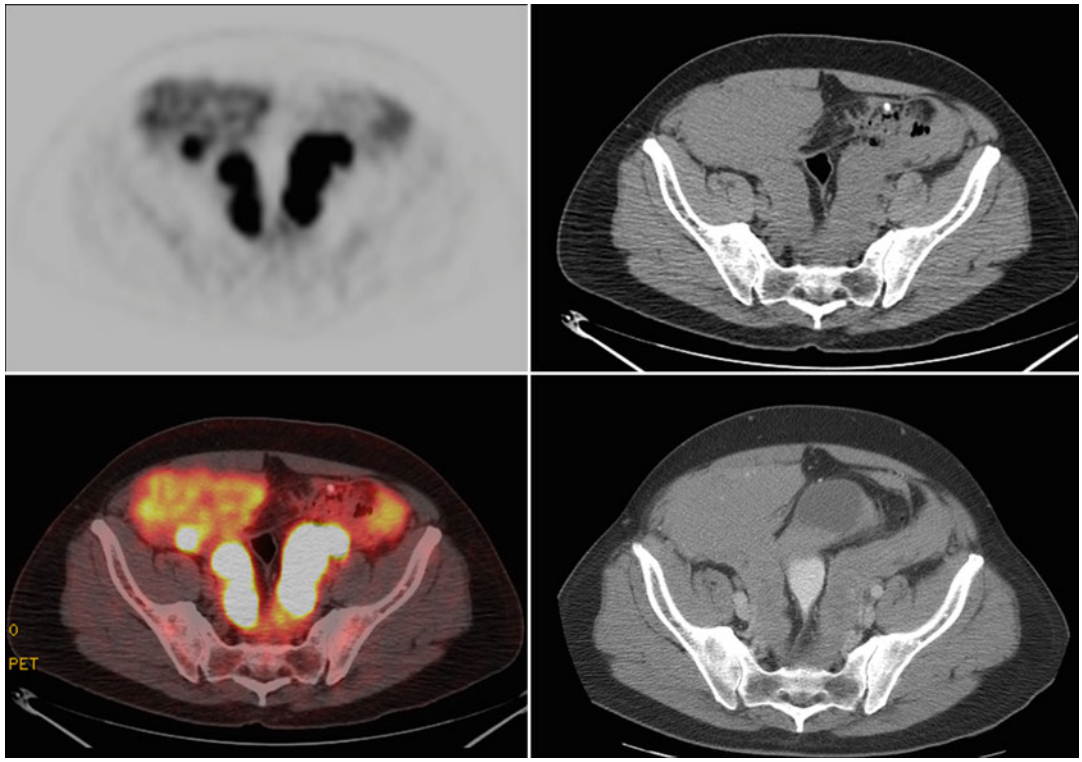

Fig. 16.3 This is a patient presenting with multi-compartmental adenopathy and a diagnosis of low-grade lymphoma. The rapid development of symptoms was discordant with that of a low-grade lymphoma; hence, an FDG PET/CT was done showing both a low-grade FDG component and high-grade FDG component best seen on the combined PET/CT image (*right lower*). The non-contrast- and contrast-enhanced CT (*upper right* and *lower right*, respectively) cannot demonstrate any morphologic difference in these confluent nodes

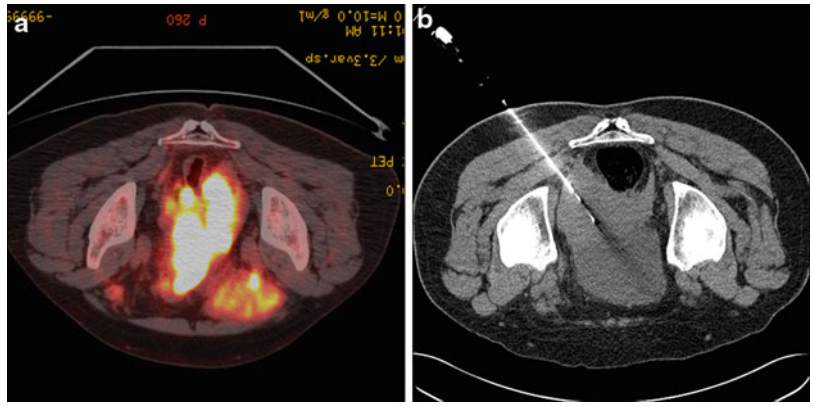

Fig. 16.4 This patient underwent a PET/CT-directed biopsy under CT guidance (**b**), note the flipped PET/CT image used as a guide (**a**). The core biopsy result showed diffuse large B cell lymphoma

in lieu of more invasive techniques such as bronchoscopy or open thoracotomy. The FDG PET/CT scan is useful in identifying FDG avid borderline-/normal-sized nodes or enlarged non-FDG avid nodes which may harbor malignancy for more accurate assessment of mediastinal nodal status which will determine the type of therapy in patients with NSCLC [16]. It is important to emphasize that FDG PET/CT imaging of nodal involvement has its limitations

as it cannot identify microscopic disease and may miss tumors with low FDG uptake as in mucinous tumors.

FDG PET/CT has been valuable in identifying unsuspected distant metastases which allows better patient management. In thoracic tumors such as esophageal cancer [17] and NSCLC [10], FDG PET/CT can identify distant metastases between 10 % and 15 % of patients. By directing the appropriate biopsy, one can avoid futile surgeries and potentially change treatment plans from curative to palliative. When PET/CT has been applied to RT planning in non-small-cell lung cancers, the treatment volume can change by as much as 15–60 % as it may limit or expand the treated areas depending on the identification of malignancy both intra- and extrathoracic [18]. FDG PET/CT is better than CT alone in identifying adrenal metastases from various malignancies [19, 20]. In summary, FDG PET/CT can direct the appropriate biopsy to identify the most aggressive part of a tumor. This technique can guide appropriate nodal sampling to assess stage and identify more aggressive malignancy. Finally, FDG PET/CT can directly affect patient management by identifying unsuspected distant metastases which can be missed by conventional imaging techniques.

FDG PET/CT in Image-Guided Therapies

Various minimally invasive ablative techniques provide inherent advantages of effective therapy in localized tumors, and may provide an alternative for patients who are poor surgical candidates.

The use of FDG PET/CT in patients undergoing radio frequency ablation has demonstrated some utility in assessing the extent of disease up front as FDG uptake is well documented in NSCLC. It may serve as a guide for needle placement prior to RFA [21]. However, it is equally well documented that this technique is unsuitable for patients with bronchoalveolar cancer which can manifest as ground glass opacities with or without a solid component. It is somewhat useful in the immediate post RFA setting to identify any residual tumors [10]. FDG activity is expected in the rim around the treated lung which is posttreatment inflammation. This may be minimal and/or diffuse, but sometimes mildly heterogeneous. This low-grade activity may persist, but we try to identify any increasing or focal activity associated with CT changes corresponding to the site of original tumor which may allow us to identify early tumor recurrence [22]. Respiratory motion can degrade the image quality of the PET scan, particularly for small nodules (<1 cm) and those found in the lung bases as this is the part of the lung which has the greatest movement. Gating techniques such as average CT [23] have demonstrated the ability to compensate for the FDG counts in the PET study, allowing greater confidence in interpretation and better correlation of the CT with the PET study by eliminating misalignment artifacts. This may be useful in the delivery of focused radiotherapy such as 3D conformal RT, stereotactic RT techniques, and if available, proton therapy.

Ablative techniques have been applied to primary and more commonly metastatic liver tumors usually from colorectal cancer. The liver presents a unique organ as it has low-grade FDG activity which may limit our ability to identify small (<1 cm) tumors, tumors with low FDG uptake such as hepatocellular cancer, and like the lungs, respiratory motion can degrade the PET images [24]. Nevertheless, it has been shown to be a useful technique for identifying hepatic metastases and any extrahepatic metastases as well. As little as one day after radiofrequency ablation, FDG PET/CT can identify residual tumor thus aiding in assessment of completeness of local therapy and close follow-up of patients which may harbor residual disease. A complete ablation usually results in a photopenic area in the liver FDG PET study, and a rim of minimal FDG activity is also expected due to inflammation (Fig. 16.5). A nodular focal area of FDG activity will likely indicate residual or recurrent tumor [25]. Performing the CT component of the study with intravenous contrast and multiphasic technique did not appear to be significantly more accurate than FDG PET/CT in the evaluation of these hepatic metastases [26].

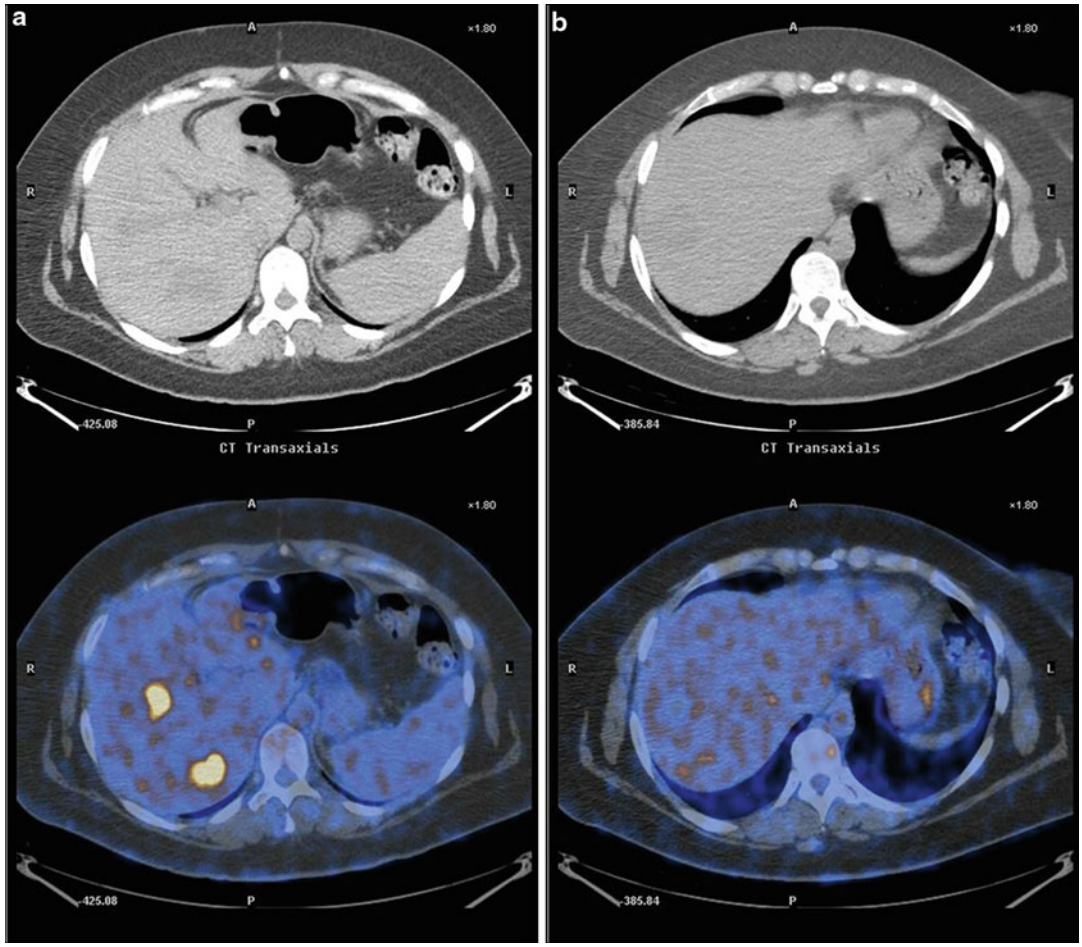

Fig. 16.5 This is a patient with multiple hepatic metastases with colon cancer. She was previously treated with RFA in the right lobe seen as a low-density lesion (**b**, *upper*) and the PET/CT (**b**, *lower*) showing a circular rim of activity. In the same patient, new FDG avid lesions are seen in two sites (**a**, *upper* and *lower*), indicating metastatic lesions

Future Directions

One of the advantages of PET imaging is the large number of radiopharmaceuticals developed to interrogate various processes which allow better diagnosis and early treatment response. There are tumors which are known to have low FDG activity such as prostate cancer. F-18 choline PET has shown to have improved accuracy in preoperative staging [27] and better identification of bony metastases [28]. This could potentially improve guidance of biopsy of the primary, nodes, or distant bony metastases, all of which could affect subsequent patient management.

Another low FDG uptake tumor category would be the neuroendocrine-type tumors or those expressing somatostatin-type receptors such as the gastroenteropancreatic neuroendocrine tumors (GEPNET) which currently are imaged in the USA with In-111 pentetreotide SPECT. These tumors are now better imaged with greater accuracy than conventional imaging with Ga-68-labeled somatostatin analogues [^{68}Ga-DOTA^{0},Tyr^{3}] octreotate or [^{68}Ga-DOTA^{0},Tyr^{3}]octreotide PET.

These analogues when labeled with Y-90, In-111, or Lu-177 are promising therapy agents for these tumors [29].

3′-deoxy-3′-[^{18}F] fluorothymidine positron emission tomography (FLT PET) has been developed for imaging cell proliferation, and findings correlate strongly with the Ki-67 labeling index in breast cancer. The advantage of FLT PET is that it could be used to as a method of early response assessment prior to the changes seen with standard or conventional modalities such as CT or MRI. Clinical FLT PET studies have demonstrated its potential to demonstrate response as early as a week after starting therapy in various tumors including breast cancer [30]. Multiple tracers for various parameters have been done in a clinical setting including hypoxia PET for RT planning [31], and alpha v beta 3 integrin (angiogenesis) PET for targeted therapy evaluation [32].

In summary, the challenges to imaging are continuously evolving as novel personalized therapies and multimodality regimens are developed. However, the scientific limitations and economic realities burden us with the need to provide proof of principle, of which imaging is an integral part of the daily care and the design of various clinical trials to treat cancer patients. The ability of imaging to provide a proper diagnosis and indices to response such as tumor size, perfusion, and more recently functional imaging with PET makes it a standard component of clinical practice and assessment of novel therapies. This central role is best exemplified by the multidisciplinary approach to the management of cancer patients. The integration of surgery, pathology, imaging, medical oncology, radiation oncology, and medical physics to cancer patient care attests to the complex nature of the disease and the need to bring together the expertise of a group in lieu of the traditional models which singular patient physician relationships are developed, followed by subspecialist referrals. The traditional subspecialty designations in diagnostic imaging have and continue to be anatomic regions, i.e., neuroradiology (head and/or neck), thoracic (chest), body (abdomen/pelvis), etc. However, cancer imaging demands expertise beyond specific anatomic areas but also expertise in other modalities such as US, MRI, CT, X-ray plain films, and nuclear medicine, including PET/CT. This multimodality ability is now supported by the ready availability of images via PACS and electronic medical records and when necessary, ready access to other imaging specialists as it may be difficult to manage expertise in so many modalities. Interventional techniques in the future will constitute a more integral part of cancer care as it will allow the confirmation of the molecular signature of cancer, which in turn will allow the assignment of potentially more effective targeted therapy. The early monitoring of response will still require image-guided biopsy to confirm the effectiveness of the targeted treatments in a trial setting which hopefully will lead to more significant outcomes for oncology patients.

References

1. Warburg O, Wind F, Negelein E. The metabolism of tumors in the body. J Gen Physiol. 1927;8(6):519–30.
2. Yonekura Y, Benua RS, Brill AB, Som P, Yeh SD, Kemeny NE, Fowler JS, MacGregor RR, Stamm R, Christman DR, Wolf AP. Increased accumulation of 2-deoxy-2-[^{18}F]Fluoro-D-glucose in liver metastases from colon carcinoma. J Nucl Med. 1982;23(12):1133–7.
3. DiChiro GD, DeLaPaz RL, Brooks RA. Glucose utilization of cerebral gliomas measured by [18] fluorodeoxyglucose and positron emission tomography. Neurology. 1982;32:1323–9.
4. Macapinlac HA. Positron emission tomography of the brain. Neuroimaging Clin N Am. 2006;16(4):591–603.
5. Goudarzi B, Jacene HA, Wahl RL. Diagnosis and differentiation of bronchioloalveolar carcinoma from adenocarcinoma with bronchioloalveolar components with metabolic and anatomic characteristics using PET/CT. J Nucl Med. 2008;49(10):1585–92.
6. Tunis S, Whicher D. The National oncologic PET registry: lessons learned for coverage with evidence development. J Am Coll Radiol. 2009;6(5):360–5.
7. Shankar LK, Hoffman JM, Bacharach S, et al. Consensus recommendations for the use of ^{18}F-FDG PET as an indicator of therapeutic response in patients in National Cancer Institute trials. J Nucl Med. 2006;47:1059–66.

8. Mawlawi O, Podoloff DA, Kohlmyer S, Williams JJ, Stearns CW, Culp RF, Macapinlac H. Performance characteristics of a newly developed PET/CT scanner using NEMA standards in 2D and 3D modes. J Nucl Med. 2004;45(10):1734–42.
9. Pirotte B, Goldman S, Massager N, David P, Wikler D, Lipszyc M, Salmon I, Brotchi J, Levivier M. Combined use of ^{18}F-fluorodeoxyglucose and ^{11}C-methionine in 45 positron emission tomography-guided stereotactic brain biopsies. J Neurosurg. 2004;101(3):476–83.
10. Erasmus JJ, Macapinlac HA, Swisher SG. Positron emission tomography imaging in nonsmall-cell lung cancer. Cancer. 2007;110(10):2155–68. PMID: 17896784.
11. Francavilla TL, Miletich RS, Di Chiro G, Patronas NJ, Rizzoli HV, Wright DC. Positron emission tomography in the detection of malignant degeneration of low-grade gliomas. Neurosurgery. 1989;24(1):1–5.
12. Truong MT, Erasmus JJ, Munden RF, Marom EM, Sabloff BS, Gladish GW, Podoloff DA, Macapinlac HA. Focal FDG uptake in mediastinal brown fat mimicking malignancy: a potential pitfall resolved on PET/CT. AJR Am J Roentgenol. 2004;183(4):1127–32.
13. Kwee TC, Kwee RM. Combined FDG-PET/CT for the detection of unknown primary tumors: systematic review and meta-analysis. Eur Radiol. 2009;19(3):731–44.
14. Bruzzi JF, Macapinlac H, Tsimberidou AM, Truong MT, Keating MJ, Marom EM, Munden RF. Detection of Richter's transformation of chronic lymphocytic leukemia by PET/CT. J Nucl Med. 2006;47(8):1267–73.
15. Juweid ME, Stroobants S, Hoekstra OS, Mottaghy FM, Dietlein M, Guermazi A, Wiseman GA, Kostakoglu L, Scheidhauer K, Buck A, Naumann R, Spaepen K, Hicks RJ, Weber WA, Reske SN, Schwaiger M, Schwartz LH, Zijlstra JM, Siegel BA, Cheson BD. Imaging subcommittee of international harmonization project in lymphoma. Use of positron emission tomography for response assessment of lymphoma: consensus of the imaging subcommittee of international harmonization project in lymphoma. J Clin Oncol. 2007;25(5):571–8.
16. De Leyn P, Lardinois D, Van Schil PE, Rami-Porta R, Passlick B, Zielinski M, Waller DA, Lerut T, Weder W. ESTS guidelines for preoperative lymph node staging for non-small cell lung cancer. Eur J Cardiothorac Surg. 2007;32(1):1–8.
17. Munden RF, Macapinlac HA, Erasmus JJ. Esophageal cancer: the role of integrated CT-PET in initial staging and response assessment after preoperative therapy. J Thorac Imaging. 2006;21(2):137–45.
18. Macapinlac HA. Clinical applications of positron emission tomography/computed tomography treatment planning. Semin Nucl Med. 2008; 38(2):137–40.
19. Vikram R, Yeung HD, Macapinlac HA, Iyer RB. Utility of PET/CT in differentiating benign from malignant adrenal nodules in patients with cancer. AJR Am J Roentgenol. 2008;191(5):1545–51.
20. Ansquer C, Scigliano S, Mirallié E, Taïeb D, Brunaud L, Sebag F, Leux C, Drui D, Dupas B, Renaudin K, Kraeber-Bodéré F. ^{18}F-FDG PET/CT in the characterization and surgical decision concerning adrenal masses: a prospective multicentre evaluation. Eur J Nucl Med Mol Imaging. 2010;37(9):1669–78.
21. Schoellnast H, Larson SM, Nehmeh SA, Carrasquillo JA, Thornton RH, Solomon SB. Radiofrequency ablation of non-small-cell carcinoma of the lung under real-time FDG PET CT guidance. Cardiovasc Intervent Radiol. 2011;34 Suppl 2:S182–5.
22. Singnurkar A, Solomon SB, Gönen M, Larson SM, Schöder H. ^{18}F-FDG PET/CT for the prediction and detection of local recurrence after radiofrequency ablation of malignant lung lesions. J Nucl Med. 2010;51(12):1833–40.
23. Chi PC, Mawlawi O, Luo D, Liao Z, Macapinlac HA, Pan T. Effects of respiration-averaged computed tomography on positron emission tomography/-computed tomography quantification and its potential impact on gross tumor volume delineation. Int J Radiat Oncol Biol Phys. 2008;71(3):890–9.
24. Tonkopi E, Chi PC, Mawlawi O, Riegel AC, Rohren EM, Macapinlac HA, Pan T. Average CT in PET studies of colorectal cancer patients with metastasis in the liver and esophageal cancer patients. J Appl Clin Med Phys. 2010;11(1):3073.
25. Purandare NC, Rangarajan V, Shah SA, Sharma AR, Kulkarni SS, Kulkarni AV, Dua SG. Therapeutic response to radiofrequency ablation of neoplastic lesions: FDG PET/CT findings. Radiographics. 2011;31(1):201–13.
26. Kuehl H, Rosenbaum-Krumme S, Veit-Haibach P, Stergar H, Forsting M, Bockisch A, Antoch G. Impact of whole-body imaging on treatment decision to radio-frequency ablation in patients with malignant liver tumors: comparison of [^{18}F] fluorodeoxyglucose – PET/computed tomography, PET and computed tomography. Nucl Med Commun. 2008;29(7):599–606.
27. Beheshti M, Imamovic L, Broinger G, Vali R, Waldenberger P, Stoiber F, Nader M, Gruy B, Janetschek G, Langsteger W. ^{18}F choline PET/CT in the preoperative staging of prostate cancer in patients with intermediate or high risk of extracapsular disease: a prospective study of 130 patients. Radiology. 2010;254(3):925–33.
28. Beheshti M, Vali R, Waldenberger P, Fitz F, Nader M, Hammer J, Loidl W, Pirich C, Fogelman I, Langsteger W. The use of F-18 choline PET in the assessment of bone metastases in prostate cancer: correlation with morphological changes on CT. Mol Imaging Biol. 2010;12(1):98–107.

29. Kwekkeboom DJ, Kam BL, van Essen M, Teunissen JJ, van Eijck CH, Valkema R, de Jong M, de Herder WW, Krenning EP. Somatostatin-receptor-based imaging and therapy of gastroenteropancreatic neuroendocrine tumors. Endocr Relat Cancer. 2010;17(1):R53–73.
30. Kenny L, Coombes RC, Vigushin DM, Al-Nahhas A, Shousha S, Aboagye EO. Imaging early changes in proliferation at 1 week post chemotherapy: a pilot study in breast cancer patients with 3′-deoxy-3′-[^{18}F] fluorothymidine positron emission tomography. Eur J Nucl Med Mol Imaging. 2007;34(9):1339–47.
31. Grégoire V, Chiti A. Molecular imaging in radiotherapy planning for head and neck tumors. J Nucl Med. 2011;52(3):331–4.
32. Beer AJ, Schwaiger M. PET imaging of αvβ3 expression in cancer patients. Methods Mol Biol. 2011;680:183–200.

Imaging of Interventional Therapies in Oncology: Image Guidance, Robotics, and Fusion Systems

17

Helmut Schoellnast and Stephen B. Solomon

Abstract

Image-guided therapies play an increasingly important role in oncology. Several imaging tools for interventional oncology procedures are available or in development which influence the success of the procedures and, therefore, influence the implementation of the procedures into oncologic treatment strategies. In this chapter, a detailed review of medical imaging strategies during an interventional oncology procedure is provided including use of contrast agents for improved tumor visualization, real-time imaging, three-dimensional imaging, fusion of images of different imaging modalities, navigation of devices during interventions, movement of devices by robots, and intraprocedural imaging monitoring. Furthermore, problems of image guidance such as physician access to the patient and radiation exposure are discussed.

In general, the ideal properties of medical imaging during an interventional oncology procedure include (1) sufficient image quality to visualize the tumor targeted as well as the interventional tools and important structures around the tumor; (2) image feedback of the therapy, preferentially in real time, displayed to the interventionalist in the procedure room; and (3) access to the patient by both the interventionalist performing the procedure and other health-care personnel, for example, anesthetist and nurses, during the procedure. In contrast to diagnostic imaging, lower image quality is an acceptable compromise for real-time imaging for interventional procedures. Patients have already undergone high-quality diagnostic imaging when they are referred to interventional therapies. High-quality diagnostic imaging may require more time and more radiation dose than fast imaging of a restricted region of interest as performed for image guidance of interventions.

Ideally imaging for interventions would provide real-time, three-dimensional displays of information that include the depiction of the target, the interventional tools, and the surrounding anatomy and perhaps for some applications physiologic information indicating areas of contrast enhancement or areas of metabolic activity. The latter is particularly helpful in differentiating viable from necrotic tissue for guiding biopsy or ablation therapy. Although current imaging

H. Schoellnast (✉) • S.B. Solomon
Department of Radiology, Memorial Sloan-Kettering Cancer Center, New York, NY, USA
e-mail: helmut.schoellnast@gmail.com; solomons@mskcc.org

D.E. Dupuy et al. (eds.), *Image-Guided Cancer Therapy*, DOI 10.1007/978-1-4419-0751-6_19,

systems provide some of these features, none provides all of them. Ultrasound (US) is a real-time, multi-planar technique that provides full access, but the depiction of some tumors is limited especially near bone- and gas-containing structures. In addition, real-time, three-dimensional imaging is limited for interventional applications. CT provides partial access and can be used to guide procedures intermittently, while CT fluoroscopy is near real time, but both have the potential disadvantage of the need for ionizing radiation, which requires one to limit radiation exposure to patients and personnel [1, 2]. CT also is primarily a two-dimensional planar tool; real-time, three-dimensional imaging is not yet fully integrated into interventional CT applications. Open MRI systems have been developed and allow full access to the patient [3], but many MRI-guided interventions today are performed in systems created for diagnostic imaging, and access is limited [4]. Currently, US, CT, and MRI are rarely used with three-dimensional images.

Technical advances of the following areas aim to improve imaging equipment to better meet interventional imaging requirements.

Physician Access to Patient

Physicians must have access to the patient in most interventional oncology procedures to allow real-time guidance as the interventional oncologist places and advances a device. The degree to which the patient is accessible varies from modality to modality. For instance, US and X-ray fluoroscopy provide the most access. During CT-guided procedures, access to patients is more limited due to the gantry surrounding the patient. For example, CT imaging may not be possible during the placement of devices such as long biopsy needles, drainage catheters, and ablation applicators that do not fit in the space between the patient's body surface and the gantry (Fig. 17.1). This is also the major limiting factor to the use of closed-bore MRI systems. MRI allows interventions to be performed for tumors that are visible only with MRI and provides thermal monitoring of ablations [5-10]. MRI offers advantages related to superior soft tissue contrast. However, physician access to the patient in closed-bore, high-, or

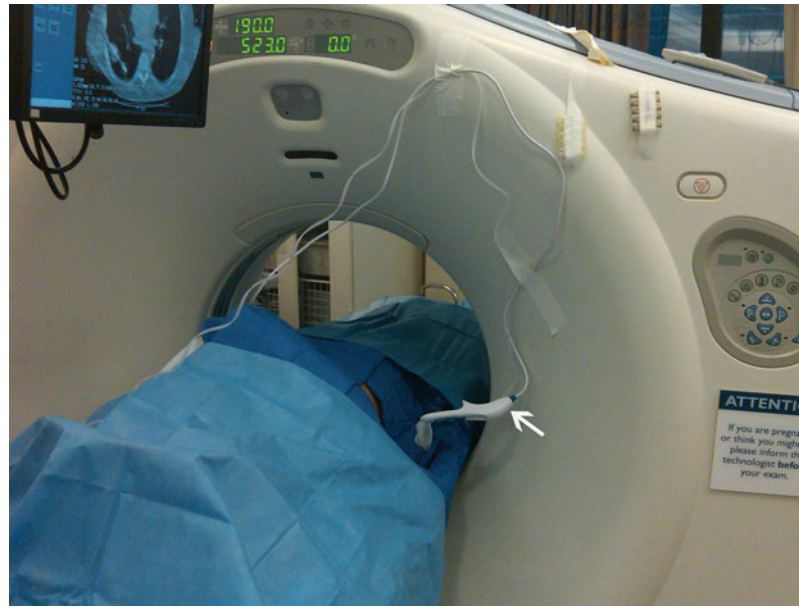

Fig. 17.1 Demonstrates how cumbersome current diagnostic imaging equipment may be for performing interventional procedures. The *arrow* shows how the radiofrequency ablation probe cannot fit within the gantry with the patient due to the limited access. The probe needs to be taped to the bore to keep the top-heavy handle from torquing the probe out of the patient

intermediate-field strength MRI systems is a limitation; this has been partially overcome with newer systems [11, 12]. Older "double-doughnut" and open magnets provide access but have lower field strengths (0.5–1.0 T) than recent wider bore magnets (70 cm) with higher field magnets (1.5 T). These systems have been utilized to provide improved access with higher image quality and are facilitating interventional procedures [13, 14]. Many other impediments to MRI-guided intervention, such as the development of MR-compatible instrumentation, have also been solved; some hurdles still remain. Instrument visualization issues still persist whether due to too much artifact or too little conspicuity [15-17]. Noise generated during scanning is potentially harmful to the interventional radiologist, especially with newer high-field (3T) systems [18, 19]. Other challenges still exist such as electrical noise from ablation devices interfering with MR imaging [20]. Similarly to MRI scanners, some newer CT scanners offer 82–cm bores, which provide extended room for interventional procedures. Other solutions make use of semiflexible devices that can bend to accommodate a closed gantry environment [21].

Contrast Agents

Contrast agents are increasingly being applied as interactive tools during intervention. With diagnostic applications, a contrast agent is administered typically once at the beginning of imaging; however, with interventions repeated, smaller contrast doses given intermittently during a procedure may sometimes be helpful. Contrast agents can be used to highlight a target that is not visualized well on non-contrast scans. However, the benefit of most contrast agents in interventional procedures is limited, as they are rapidly cleared and their effects are often transient. Since the use of these agents is dose limited due to renal toxicity, the volume administered during a procedure must be carefully monitored. New fusion systems that allow overlay of needles on previously acquired enhanced CT imaging may be able to account for the transient nature of contrast enhancement during an intervention.

Contrast agents already play an important role in diagnostic imaging, and new contrast agents are becoming available for all imaging modalities. US contrast agents are comparable to iodine contrast agents concerning tissue enhancement characteristics without subjecting patients to the risk of nephrotoxicity posed by iodinated contrast agents. Contrast agents have been used in US to plan, target, and monitor RF ablations [22-25]. It has been reported that with the routine adoption of contrast-enhanced US, a rate of partial necrosis of 5.9 % was achieved, in comparison with a 16.1 % rate achieved without the real-time management of ablations of hepatocellular and metastatic liver lesions [25]. New, blood-pool, iodinated agents that stay in the vascular space for an extended time and that are hepatocyte selective (such as iodinated triglyceride (ITG)-dual [26]) may be used during CT-guided interventions to delineate blood vessels throughout the procedure or to improve tumor conspicuity in the future [26, 27]. Similar agents are being developed for use in MRI [28]. MRI contrast agents that are aimed at Kupffer cell uptake (superparamagnetic iron oxide particles, SPIO) and agents for the hepatobiliary tree (hepatobiliary-specific MR contrast agents) provide new tools that can be applied to specific cases [29]. Additionally, new thermosensitive MR contrast agents can offer a monitoring tool during thermal ablation by, for example, releasing a contrast agent from a liposome under certain thermal [30-32]. Lastly, advances in molecular imaging are likely to provide improved targeting opportunities that are specific and personalized. For example, new radiotracer-labeled antibodies (such as huA33 and cG250) can specifically target colon cancers or clear cell renal cancers and guide interventions [33, 34].

Real-Time Imaging

CT fluoroscopy, in which real-time CT images are displayed, allows the interventional radiologist to continuously monitor needle placement and has replaced repeated scanning after needle incremental advance as required with standard CT interventions. CT fluoroscopy for interventional procedures was introduced in the early 1990s [35], and it is now widely evaluated for various interventional procedures including the lung, abdominal organs, and the spine [2, 36, 37]. It has been reported that in CT fluoroscopy-guided biopsy of pulmonary lesions with 20-gauge coaxial cutting needles, the biopsy results were nondiagnostic in only 0.6 % of the lesions. The sensitivity and specificity for the diagnosis of malignancy were 94.2 % and 99.1 %, respectively [36].

The downside to CT fluoroscopy is the increased radiation dose and the lack of three-dimensional reconstructions [38]. Attempts to reduce radiation exposure during CT fluoroscopy by lowering the dose applied per section, by implementing angular beam modulation which enables adaption of the tube current to the course of beam and the patient's habitus, and by providing arm extenders have been demonstrated [39-42]. MRI fluoroscopy also provides real-time imaging. Its advantages over CT include the ability to freely select the imaging planes along the needle pathway and the absence of ionizing radiation for the patient [43].

Three-Dimensional Imaging

While US, CT, and MRI are still primarily used in two-dimensional, planar mode, efforts are under way to make more use of three-dimensional imaging. For example, in order for a tumor ablation procedure to be successful, the entire tumor volume needs to be treated, without affecting nearby critical structures. Therefore, intraprocedural displays of the tumor in its entire three-dimensional extension and its surroundings would likely improve ablation outcomes. Preliminary work suggests that three-dimensional imaging is beneficial and assists with applicator placement. One of the limitations to the use of three-dimensional imaging is the time required to create the images and present them to the interventionalist in the procedure suite. The ability to rapidly reconstruct three-dimensional images from these two-dimensional views will further aid image-guided therapy. Rotational flat-panel CT (or cone-beam CT) combine the real-time imaging advantages of fluoroscopy with computed tomography imaging [44-46]. Three-dimensional rotational angiography has been widely applied in neuroradiological interventions. Recent advances in the technology of angiographic equipment have made it feasible to conduct rotational angiography with a large diameter image intensifier allowing coverage of the hepatic vessels [45, 47-51]. It has been reported that 3D rotational flat-panel CT can improve chemoembolization procedure in patients with hepatocellular carcinoma [47, 48, 52]. Software is in evaluation which can be used to segment out the vessels feeding the tumor in 3D angiography images and thereby provide a guide for transcatheter therapy [53]. Providing planar and 3D "CT-like" images with patient access typical of fluoroscopy will allow these machines to take on an even more powerful role in the interventional oncology imaging armamentarium. Although visualization of dense structures such as bone and contrast-filled vessels on these systems is adequate, challenges still remain in soft tissue resolution. As this relatively new technology improves, the need for helical CT to guide many interventional procedures may be reduced.

Image Registration and Fusion

Image registration is defined as aligning two imaging data sets spatially to each other. Fusion is defined as overlaying them and visualizing them as one image. Image fusion may be performed to combine metabolic imaging with anatomical imaging (e.g., fluorodeoxyglucose (FDG) PET with CT) or to combine real-time

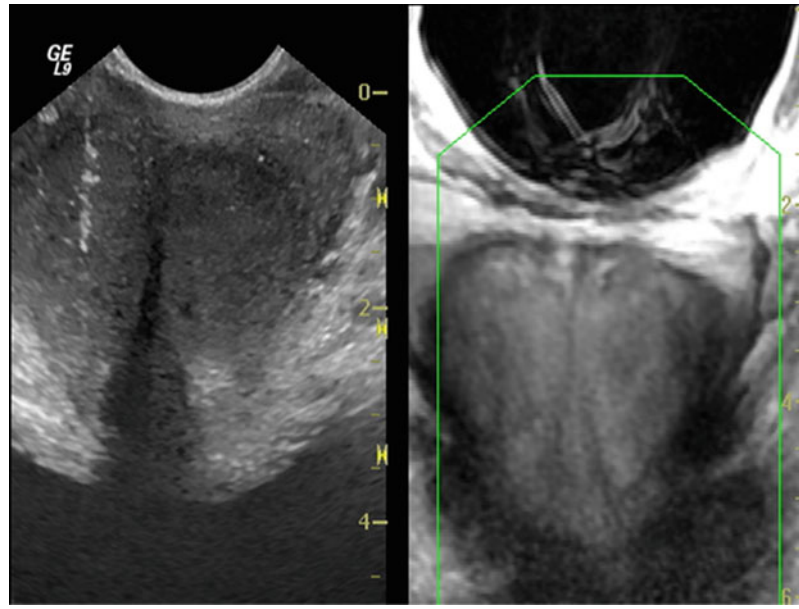

Fig. 17.2 Demonstrates image registration to guide prostate biopsy. The *left* image shows time transrectal ultrasound of the prostate; the *right* image shows prior acquired endorectal MRI which is aligned to the real-time ultrasound image on the *left*

anatomic imaging with non-real-time imaging of a second anatomic imaging modality (e.g., US with CT). While metabolic imaging such as fluorodeoxyglucose (FDG) PET has had a major impact on detecting and staging cancers, its role in interventional radiology has been limited because of the lack of sufficient anatomic detail required for image guidance. While combined PET/CT, SPECT/CT, or even PET/MR systems exist, interventions usually occur in CT or MR systems independent of PET or SPECT equipment. To best utilize these PET images for imaging guidance, they must be fused with the CT images. Fusion, or overlay, of PET images with CT or MR images allows the utilization of both the anatomic detail of CT or MRI and the physiologic information of PET [54-56]. US images also may be fused with CT images obtained preprocedurally to gain the real-time, nonionizing radiation information of US with the anatomic detail of a contrast-enhanced CT [57, 58]. This potential benefit in combining these modalities may be used for image-guided interventions. US systems in which a previously recorded CT or MRI examination is shown simultaneously with real-time US are commercially available from different vendors. An existing CT or MRI data set is loaded into the system, and the CT or MRI images are reformatted in a projection to fit the live sonography images. The advantage of this method is that structures that are difficult to outline on US are shown on the CT or MRI images, and yet real-time ultrasound imaging can still be utilized. In a phantom study using a fusion navigating system [59], a rate of success in obtaining biopsies from US invisible spheres of 72 % has been reported for the first needle pass and of 88 % within two needle passes. In a clinical study [60] in patients with prostate cancer, transrectal US images were registered with pre-procedural-acquired endorectal MRI for biopsy guidance. The authors concluded that the fusion of real-time transrectal US and prior MR images of the prostate (dynamic contrast-enhanced maps, or T2-weighted or MR spectroscopy images) is feasible and enables MRI-guided interventions outside of the MRI suite [60] (Fig. 17.2).

Also, MR images may be fused with intraprocedural, unenhanced CT to provide better depiction of tumor margins for targeting as MRI features higher soft tissue resolution than CT [61]. Fusion has also been used to overlay fluoroscopy with cone-beam CT, CT, or MRI to provide additional guidance during embolization procedures (Fig. 17.3) [62]. Multimodality image fusion may aid interventional radiologists substantially, but

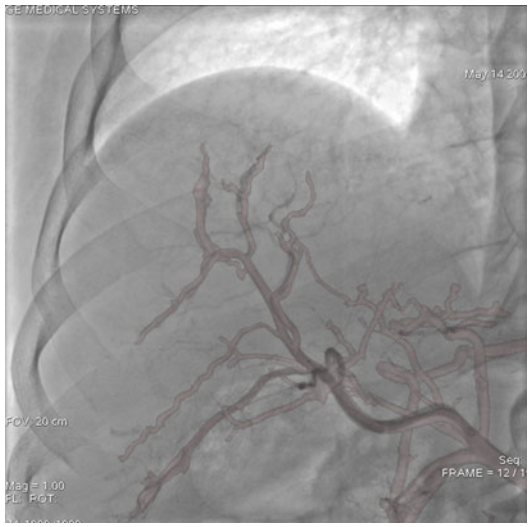

Fig. 17.3 Shows a fused image of a contrast-enhanced cone-beam CT and a live 2D-fluoroscopy image. The cone-beam CT has been segmented to demonstrate the enhanced hepatic arterial tree. It is registered with the fluoroscopy image automatically by maintaining the same table for both imaging studies

patient breathing, patient positioning, organ shift, and even procedure-/instrument-related motion challenge image registration and fusion [63, 64]. The challenge of multimodality fusion is simplified when both imaging data sets are obtained on the same patient bed through the use of multimodality imaging suites. These hybrids, combination suites with CT and fluoroscopy or MR and fluoroscopy, are being used and offer easier image registration since patients remain on the same table and in the same position for both imaging studies. However, these hybrid units are costly limiting their practicality.

Navigation

The integration of position sensors with interventional devices such as needles and ablation applicators allows them to be tracked real time with imaging obtained during a procedure. Tracking displays the needle or applicator location in relation to the pre-procedural-acquired images. Tracking can be accomplished with mechanical arms, with optical systems, or with electromagnetic systems. Electromagnetic tracking allows tracking of internal medical devices, whereas optical tracking requires direct line of sight, which is less useful for image-guided therapy which may utilize flexible needles [65]. Miniaturization of electromagnetic sensors and needles with sensors integrated inside the tip has enabled spatial tracking of needles. Internalized needle-tip sensors actually track and follow the motion of the needle itself and do not rely on the estimation of needle position on the basis of external needle hub position. This can correct for needle bending, organ motion, and respiration [66] (Fig. 17.4).

When used with multimodality image fusion, the coordinates of the device's tip can be superimposed on previously acquired images or on real-time imaging. When a pre-procedural CT scan is fused with real-time US, the position of the device can be tracked in real time such that its position is known in relationship to anatomy displayed both on CT and US. It may also allow the physiologic images such as PET to be incorporated into an intervention. Additionally, device tracking may allow out-of-plane trajectory imaging such as directing a needle to the dome of the liver without transgressing pleura. Navigation has even been reported on cone-beam CT images to further enable procedures in fluoroscopy rooms [67]. However, all these navigation tools face the same image registration engineering challenges that image fusion does [65, 68-72].

Robotics

According to the Robotic Institute of America (1979), a robot is "a reprogrammable, multifunctional manipulator designed to move materials, parts, tools, or other specialized devices through various programmed motions for the performance of a variety of tasks." Robotics have been applied to several areas of medicine [73]. Since modern medical imaging is digital and robots function in a digital world, it makes sense that robotics can be applied to interventional oncology. Robots in interventional oncology, currently, have two potential roles. First, they may

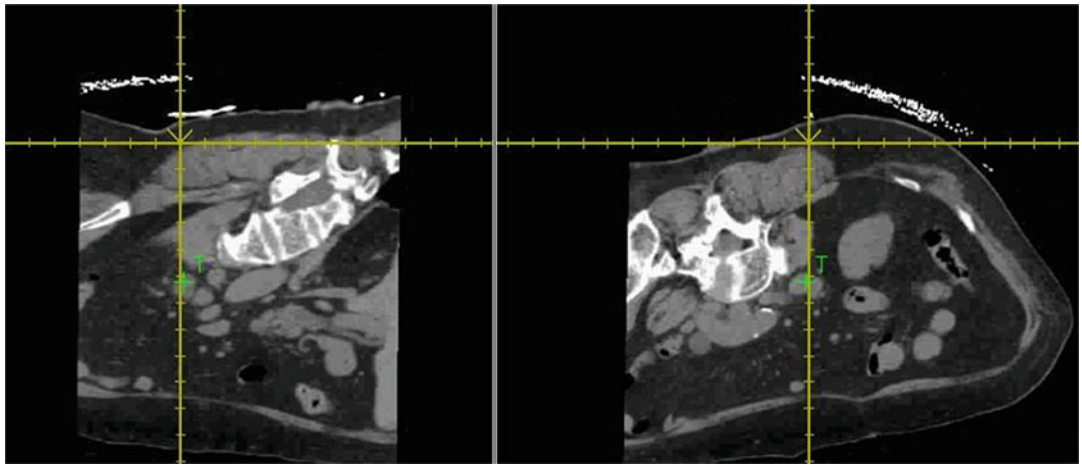

Fig. 17.4 Shows two images from a navigation study where an electromagnetic system was used to guide a needle to a retroperitoneal lymph node (*arrow*). The needle tip is at the skin prior to entry with the *arrow* showing the direction to the lymph node (*T* target). *Left* image shows sagittal-oblique view; *right* image shows transverse–oblique view

act as "arm extenders" during fluoroscopy and CT-guided interventions and thereby limit physician radiation exposure. Second, robots may improve the accuracy of device placement [64, 74, 75]. Using integrated software systems, the coordinates of targets can be chosen, and then the robot can deliver a device to the prescribed location. Robotic precision may be helpful to ensure overlapping ablations and ensure safe probe separation. Robots have been applied to CT, MRI, fluoroscopy, and even US-guided procedures [76-78]. Accurate targeting, however, requires that the image used for planning is registered with the patient and accounts for patient motion. These, therefore, are the same engineering challenges that are faced with navigation and fusion enhancements.

While medical robots have been applied in many fields such as neurosurgery, orthopedics, and urology, they are not the standard of care in any field. Studies on phantoms and animals as well as clinical trials have been performed using fluoroscopy, US, CT, and MRI as imaging modality. The AcuBot robot has been developed in the URobotics Laboratory at Johns Hopkins Medical Institutions (Baltimore, USA) (Fig. 17.5) [64]. Four clinical cases of CT-guided kidney and spine biopsy and radiofrequency ablation and a nephrostomy tube placement were successfully performed with no complications [79]. Another study showed that the use of the robot in CT-guided core biopsies and radiofrequency ablations reduced radiation exposure for the patient and medical personnel [75]. The B-Rob system which has been developed by ARC Seibersdorf Research (Seibersdorf, Austria) enables CT-guided and US-guided biopsies. The first in vitro trials of the system show a high accuracy (0.66 ± 0.27 mm) in image-guided positioning of a biopsy, and a risk analysis of the complete system did not find any major risks [64, 80]. A series of quantitative evaluation studies is currently in process at different research centers. The robotic instrument-guiding system INNOMOTION (Innomedic, Herxheim and FZK Karlsruhe, Germany) has been developed to provide MRI compatibility. The system has shown a precision of the insertion site in the axial plane was +/2 1 mm (0.5–3 mm). The angular deviation in the transverse plane of the cannulae was $\pm$ 1° (0.5°–3°) [64]. The MrBot robot has been developed at URobotics Laboratory at Johns Hopkins Medical Institutions (Baltimore, USA) for fully automated image-guided transperineal access of the prostate gland, and a recent robot developed by this research group is under way for transrectal access. In the future, this robot may enable better targeted prostate image-guided therapies.

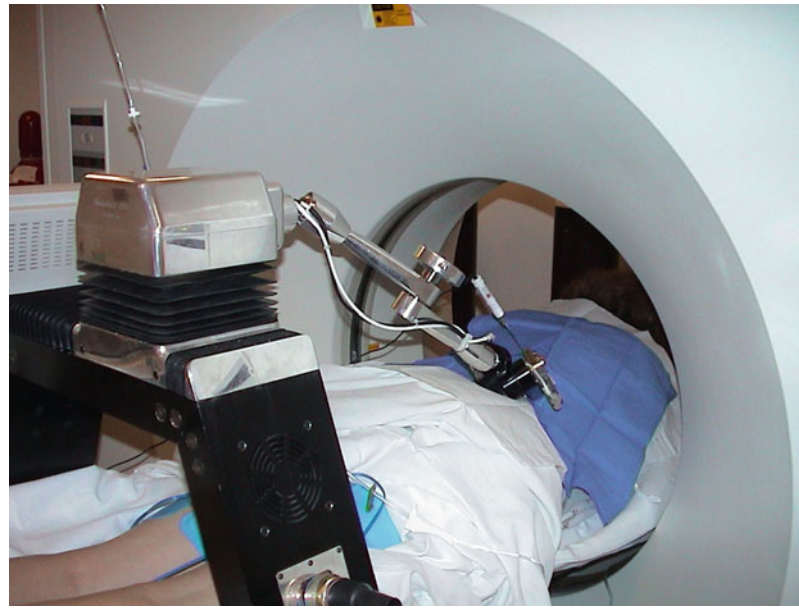

Fig. 17.5 Depicts the AcuBot which is a CT robot for needle placement. The robot is mounted to the CT table and can be registered with the CT image

Intraprocedural Monitoring

Evaluation of treatment success during and immediately after the procedure is an important challenge in most interventional oncologic therapies. Ideally there would be some clear endpoint for therapy completion. Imaging is a preferable potential solution in this matter due to its noninvasive measure of completeness. The term monitoring can be defined as imaging that is used during the procedure and immediately after the procedure that visualizes changes that result from the procedure. The goal of monitoring is to not only determine if the treatment is complete but also display the surrounding critical structures that should not be affected more than is necessary to complete the treatment effectively and safely.

Several imaging modalities have been used to assess completeness of therapy. These primarily revolve around measures of blood flow. Angiography after (chemo-)embolization of hypervascular tumors can show hemostasis and a completely embolized tumor bed. Lipiodol or contrast laden-embolic material uptake may be used to visualize progress during chemoembolization and bland embolization procedures, respectively (Fig. 17.6). This may be especially well visualized on 3D rotational flat-panel CT. Recently combined MR–X-ray systems have allowed intraprocedural transcatheter intra-arterial perfusion MRI to be performed during hepatic artery embolization to permit intraprocedural perfusion changes and monitoring [81].

With US, Doppler flow and contrast agents have been used to assess blood flow and determine when a tumor no longer has a viable blood supply after an ablation [25, 82]. US may also be used without contrast to monitor the effects of an ablation based on changes in echogenicity. During RF ablation, increased echogenicity can be seen in the ablation zone which diameter correlates with the diameter of necrosis [83]. However, the solitary diameter of the echogenic response may be greater than the smallest diameter and less than the largest diameter of the area of tissue necrosis. Therefore, the echogenic response associated with radiofrequency ablation should be viewed only as a rough approximation of the area of induced tissue necrosis; the final assessment of the adequacy of ablation should be deferred to an alternative imaging technique [83]. Furthermore, this increased echogenicity may

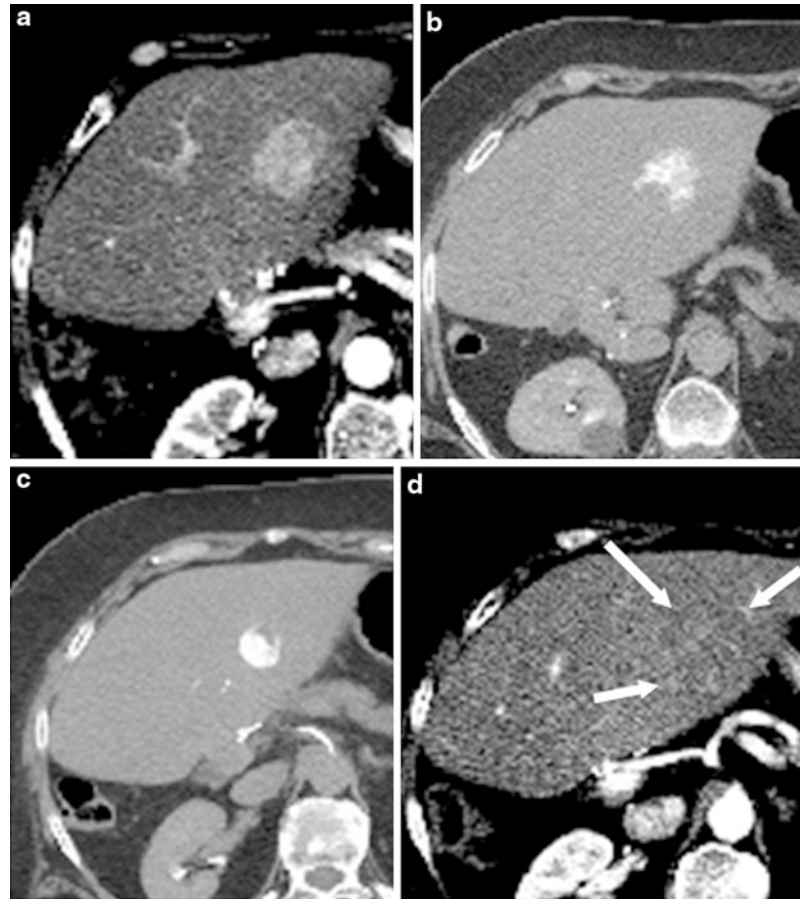

Fig. 17.6 (**a–d**) Shows the importance of intraprocedural monitoring to determine completeness of an image-guided bland embolization procedure. (**a**) Pre-procedure contrast-enhanced CT indicating an enhancing hepatocellular carcinoma, (**b**) mid-procedure non-contrast CT image with contrast laden particles showing a partially embolized tumor, (**c**) mid-procedure CT image with contrast laden particles filling the rest of the tumor, and (**d**) contrast-enhanced CT after the embolization procedure without enhancement of the tumor. Fusing these mid-procedure images (**b–c**) can help guide the interventionalist to a complete treatment

obscure imaging during the procedure and hinder probe replacement. During cryotherapy, an echogenic mass-like structure with distal acoustic shadowing representing the ice ball formation may be noted.

Like US, CT and MRI can also provide intraprocedural imaging feedback during a therapy. Contrast agents may be used in CT and MRI to assess vascularity of the treatment zone. Unlike US, the cryotherapy ice ball can be viewed in its entirety using both CT and MRI [10, 84]. Intraprocedural T2-weighted fast spin-echo images can be obtained every 2–3 min, which allow real-time ice ball monitoring and accurate prediction of the region of cryo-necrosis [85]. During ethanol-ablation procedures, CT low attenuation associated with percutaneous ethanol injection can guide procedure termination [86-88]. Conceivably nuclear medicine agents in the future, such as [15]O-H2O, might be useful to measure tumor viability during a procedure and guide therapy completion. The short, 2-min half-life of [15]O makes it possible to perform repeated PET imaging at 20-min intervals at multiple time points before and after image-guided therapy. [15]O-water PET demonstrates the ablated tumor region, whereas the unablated tumor continued to show high [15]O-water accumulation [89].

More recently imaging has also been used to measure tissue temperatures; these techniques can help monitor thermal ablations and assure that the tumor is completely treated and critical structures not harmed [90]. Since maintaining temperatures of ~54 °C or higher for longer than one second is believed to cause cell death, measuring temperature with MRI can provide a quantitative noninvasive method of evaluating

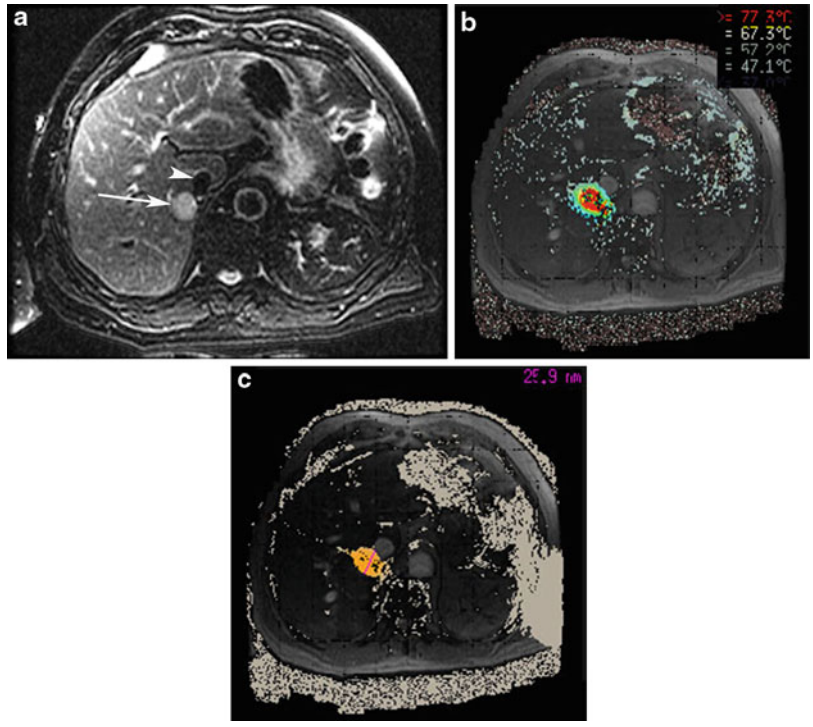

Fig. 17.7 (**a–c**) Demonstrates MRI-guided laser ablation of solitary liver metastases. (**a**) Pretreatment T2-weighted fat-suppressed imaging reveals the hyperintense lesion (*arrow*) adjacent to the inferior vena cava (*arrowhead*). (**b**) MR thermometry during ablation was used to ensure adequate heating and avoidance of critical structures. *Colors* represent different levels of temperature. (**c**) Image after ablation shows tissue where the temperature was above 60 °C in orange to estimate the ablation area

the completeness of a thermal ablation. Understanding the thermal dose delivered may even facilitate some selectivity of tissue destruction since different tissues have different thresholds for death [91]. While a number of temperature-sensitive MR techniques, based on the relaxation time T(1), the diffusion coefficient (D), or proton resonance frequency (PRF) of tissue water, have also been used, proton resonance frequency changes are probably most commonly used clinically [92]. The excellent linearity of the temperature dependency of the proton resonance frequency (PRF) and its near independence with respect to tissue type make the PRF-based methods the preferred choice for many applications. A standard deviation of less than 1 °C, for a temporal resolution below 1 s and a spatial resolution of approximately 2 mm, is feasible for immobile tissues [93]. MR thermometry has been primarily developed for use with high-intensity focused US [31, 94] but has also been applied to other ablative agents, such as radiofrequency, laser, microwave, and hot saline [95-101] (Fig. 17.7). Limitations of MR thermometry still exist due to motion, magnetic field inhomogeneities created by ablation tools or fatty environments, and those due to the limited temporal resolution of the technique.

Although less developed to date and not yet in clinical practice, both CT and US have been suggested as noninvasive modalities to measure tissue temperatures. CT attenuation and sound velocity have both been shown to correlate with temperature [102, 103].

Radiation Exposure

Many procedures are best done using CT or X-ray fluoroscopy as the guidance modality. Their inherent limitation is the radiation exposure to physician and patient. For example, excessive radiation exposure to physician and patient can occur during CT fluoroscopy because of continuous exposure at a single anatomic location. On the other hand, excessively low radiation doses lead to inferior image quality and result in interference with IR procedures. In addition to wearing lead aprons and other protective garb, physician exposure can be diminished further during CT

fluoroscopy-guided procedures by placing a lead shield on the patient just below the imaging plane to reduce scatter radiation and by using "arm extenders" such as robots described above [2]. Modifications to the imaging protocol can also be employed to limit radiation exposure. Lowering tube current and tube potential and reducing the time the beam is on during a rotation reduce radiation exposure directly. On the basis of the As Low As Reasonably Achievable (ALARA) principle, one should use the CT fluoroscopic scan parameters which provide acceptable image quality at the lowest possible radiation exposure. For example, acceptable image quality can be achieved with a tube voltage of 135 kV and a tube current of 10 mA (1.48 mGy/s) for CT fluoroscopy in lung interventional procedures [40]. Adapting the tube load to the patient's size and shape with the aim to keep image noise constant throughout the entire study has also proved to lower the radiation dose to the minimum required. Both in-plane (XY-axis) and longitudinal (Z-axis) dose modulation are embedded in 64-slice CTs [39]. In addition, the use of navigation software and fusion imaging may potentially reduce the time required to do the procedure, thereby indirectly reducing radiation exposure [104, 105].

The dose for rotational flat-panel CT is similar to those used for corresponding MDCT scans with comparable slice thickness [106]. The effect of rotational flat-panel CT on overall patient dose remains to be seen. On the one hand, judicious use of in-suite rotational flat-panel CT may actually result in a decrease in patient dose by providing critical diagnostic information that obviates the need for excessive fluoroscopy. Alternatively, the simple availability of this technique may lead to overuse and increased patient radiation [107].

Conclusion

Imaging plays a critical role in interventional oncology procedures. It is needed for guidance and monitoring. As these tools are adapted from diagnostic roles to interventional ones, they require modification. Some of these modifications have begun to occur, while others are still in their infancy. Image fusion and robotics, for example, represent two areas of potential applicability to interventional oncology procedures. As imaging evolves to meet the needs of interventional oncology, the interventionalist will be enabled to accomplish even more with image-guided, less invasive techniques.

References

1. Nawfel RD, Judy PF, Silverman SG, Hooton S, Tuncali K, Adams DF. Patient and personnel exposure during CT fluoroscopy-guided interventional procedures. Radiology. 2000;216:180–4.
2. Silverman SG, Tuncali K, Adams DF, Nawfel RD, Zou KH, Judy PF. CT fluoroscopy-guided abdominal interventions: techniques, results, and radiation exposure. Radiology. 1999;212:673–81.
3. Lewin JS, Nour SG, Connell CF, et al. Phase II clinical trial of interactive MR imaging-guided interstitial radiofrequency thermal ablation of primary kidney tumors: initial experience. Radiology. 2004;232:835–45.
4. Tatli S, Morrison PR, Tuncali K, Silverman SG. Interventional MRI for oncologic applications. Tech Vasc Interv Radiol. 2007;10:159–70.
5. Gedroyc WM. Magnetic resonance guidance of thermal ablation. Top Magn Reson Imaging. 2005; 16:339–53.
6. Mougenot C, Quesson B, de Senneville BD, et al. Three-dimensional spatial and temporal temperature control with MR thermometry-guided focused ultrasound (MRgHIFU). Magn Reson Med. 2009;61:603–14.
7. Pech M, Wieners G, Freund T, et al. MR-guided interstitial laser thermotherapy of colorectal liver metastases: efficiency, safety and patient survival. Eur J Med Res. 2007;12:161–8.
8. Puls R, Langner S, Rosenberg C, et al. Laser ablation of liver metastases from colorectal cancer with MR thermometry: 5-year survival. J Vasc Interv Radiol. 2009;20:225–34.
9. Silverman SG, Tuncali K, Adams DF, et al. MR imaging-guided percutaneous cryotherapy of liver tumors: initial experience. Radiology. 2000; 217:657–64.
10. Silverman SG, Tuncali K, Morrison PR. MR Imaging-guided percutaneous tumor ablation. Acad Radiol. 2005;12:1100–9.
11. Boss A, Clasen S, Kuczyk M, et al. Magnetic resonance-guided percutaneous radiofrequency ablation of renal cell carcinomas: a pilot clinical study. Invest Radiol. 2005;40:583–90.
12. Morrison PR, Silverman SG, Tuncali K, Tatli S. MRI-guided cryotherapy. J Magn Reson Imaging. 2008;27:410–20.

13. Fritz J, Clasen S, Boss A, et al. Real-time MR fluoroscopy-navigated lumbar facet joint injections: feasibility and technical properties. Eur Radiol. 2008;18:1513–18.
14. Stattaus J, Maderwald S, Forsting M, Barkhausen J, Ladd ME. MR-guided core biopsy with MR fluoroscopy using a short, wide-bore 1.5-Tesla scanner: feasibility and initial results. J Magn Reson Imaging. 2008;27:1181–7.
15. Smits HF, Bos C, van der Weide R, Bakker CJ. Interventional MR: vascular applications. Eur Radiol. 1999;9:1488–95.
16. Thomas C, Springer F, Röthke M, et al. In vitro assessment of needle artifacts with an interactive three-dimensional MR fluoroscopy system. J Vasc Interv Radiol. 2010;21:375–80.
17. Weiss CR, Nour SG, Lewin JS. MR-guided biopsy: a review of current techniques and applications. J Magn Reson Imaging. 2008;27:311–25.
18. Moelker A, Maas RAJJ, Lethimonnier F, Pattynama PMT. Interventional MR imaging at 15 T: quantification of sound exposure. Radiology. 2002;224:889–95.
19. Moelker A, Wielopolski PA, Pattynama PMT. Relationship between magnetic field strength and magnetic-resonance-related acoustic noise levels. Magn Reson Mater Phys Biol Med. 2003;16:52–5.
20. Nour SG, Lewin JS. Radiofrequency thermal ablation: the role of MR imaging in guiding and monitoring tumor therapy. Magn Reson Imaging Clin N Am. 2005;13:561–81.
21. Gaffke G, Gebauer B, Knollmann FD, et al. Use of semiflexible applicators for radiofrequency ablation of liver tumors. Cardiovasc Intervent Radiol. 2006;29:270–5.
22. Chen MH, Yang W, Yan K, et al. The role of contrast-enhanced ultrasound in planning treatment protocols for hepatocellular carcinoma before radiofrequency ablation. Clin Radiol. 2007;62:752–60.
23. Liu JB, Wansaicheong G, Merton DA, et al. Canine prostate: contrast-enhanced US-guided radiofrequency ablation with urethral and neurovascular cooling–initial experience. Radiology. 2008;247:717–25.
24. Numata K, Isozaki T, Ozawa Y, et al. Percutaneous ablation therapy guided by contrast-enhanced sonography for patients with hepatocellular carcinoma. AJR Am J Roentgenol. 2003;180:143–9.
25. Solbiati L, Ierace T, Tonolini M, Cova L. Guidance and monitoring of radiofrequency liver tumor ablation with contrast-enhanced ultrasound. Eur J Radiol. 2004;51(Suppl):S19–23.
26. Weichert JP, Lee FT, Chosy SG, et al. Combined hepatocyte-selective and blood-pool contrast agents for the CT detection of experimental liver tumors in rabbits1. Radiology. 2000;216:865–71.
27. Fu Y, Nitecki DE, Maltby D, et al. Dendritic iodinated contrast agents with PEG-cores for CT imaging: synthesis and preliminary characterization. Bioconjug Chem. 2006;17:1043–56.
28. Burtea C, Laurent S, Vander Elst L, Muller RN. Contrast agents: magnetic resonance. In: Semmler W, Schwaiger M, editors. Molecular imaging I: handbook of experimental pharmacology. Berlin/Heidelberg: Springer; 2008. p. 135–65.
29. Bartolozzi C, Crocetti L, Lencioni R, Cioni D, Della Pina C, Campani D. Biliary and reticuloendothelial impairment in hepatocarcinogenesis: the diagnostic role of tissue-specific MR contrast media. Eur Radiol. 2007;17:2519–30.
30. Lindner LH, Reinl HM, Schlemmer M, Stahl R, Peller M. Paramagnetic thermosensitive liposomes for MR-thermometry. Int J Hyperthermia. 2005;21:575–88.
31. McDannold N, Tempany CM, Fennessy FM, et al. Uterine leiomyomas: MR imaging-based thermometry and thermal dosimetry during focused ultrasound thermal ablation. Radiology. 2006;240:263–72.
32. Needham D, Dewhirst MW. The development and testing of a new temperature-sensitive drug delivery system for the treatment of solid tumors. Adv Drug Deliv Rev. 2001;53:285–305.
33. Strong VE, Humm J, Russo P, et al. A novel method to localize antibody-targeted cancer deposits intraoperatively using handheld PET beta and gamma probes. Surg Endosc Inter Tech. 2008;22:386–91.
34. Wendler T, Traub J, Ziegler SI, Navab N. Navigated three dimensional beta probe for optimal cancer resection. Med Image Comput Comput Assist Interv. 2006;9:561–9.
35. Katada K, Kato R, Anno H, et al. Guidance with real-time CT fluoroscopy: early clinical experience. Radiology. 1996;200:851–6.
36. Hiraki T, Mimura H, Gobara H, et al. CT Fluoroscopy-guided biopsy of 1,000 pulmonary lesions performed with 20-gauge coaxial cutting needles. Chest. 2009;136:1612–17.
37. Trumm CG, Jakobs TF, Zech CJ, Helmberger TK, Reiser MF, Hoffmann R-T. CT Fluoroscopy-guided percutaneous vertebroplasty for the treatment of osteolytic breast cancer metastases: results in 62 sessions with 86 vertebrae treated. J Vasc Interv Radiol. 2008;19:1596–606.
38. de Mey J, Op de Beeck B, Meysman M, et al. Real time CT-fluoroscopy: diagnostic and therapeutic applications. Eur J Radiol. 2000;34:32–40.
39. Hohl C, Suess C, Wildberger JE, et al. Dose reduction during CT fluoroscopy: phantom study of angular beam modulation. Radiology. 2008;246:519–25.
40. Yamato Y, Yamakado K, Takaki H, et al. Optimal scan parameters for CT fluoroscopy in lung interventional radiologic procedures: relationship between radiation dose and image quality. Radiology. 2010;255:233–41.
41. Neeman Z, Dromi SA, Sarin S, Wood BJ. CT fluoroscopy shielding: decreases in scattered radiation for the patient and operator. J Vasc Interv Radiol. 2006;17:1999–2004.

42. Irie T, Kajitani M, Itai Y. CT fluoroscopy-guided intervention: marked reduction of scattered radiation dose to the physician's hand by use of a lead plate and an improved I-I device. J Vasc Interv Radiol. 2001;12:1417–21.
43. Yutzy SR, Duerk JL. Pulse sequences and system interfaces for interventional and real-time MRI. J Magn Reson Imaging. 2008;27:267–75.
44. Beldi G, Styner M, Schindera S, Inderbitzin D, Candinas D. Intraoperative three-dimensional fluoroscopic cholangiography. Hepatogastroenterology. 2006;53:157–9.
45. Liapi E, Hong K, Georgiades CS, Geschwind JF. Three-dimensional rotational angiography: introduction of an adjunctive tool for successful transarterial chemoembolization. J Vasc Interv Radiol. 2005;16:1241–5.
46. Wallace MJ. C-arm computed tomography for guiding hepatic vascular interventions. Tech Vasc Interv Radiol. 2007;10:79–86.
47. Iwazawa J, Ohue S, Mitani T, et al. Identifying feeding arteries during TACE of hepatic tumors: comparison of C-arm CT and digital subtraction angiography. AJR Am J Roentgenol. 2009;192:1057–63.
48. Kakeda S, Korogi Y, Hatakeyama Y, et al. The usefulness of three-dimensional angiography with a flat panel detector of direct conversion type in a transcatheter arterial chemoembolization procedure for hepatocellular carcinoma: initial experience. Cardiovasc Intervent Radiol. 2008;31:281–8.
49. Kakeda S, Korogi Y, Ohnari N, et al. Usefulness of cone-beam volume CT with flat panel detectors in conjunction with catheter angiography for transcatheter arterial embolization. J Vasc Interv Radiol. 2007;18:1508–16.
50. Kim HC, Chung JW, Park JH, et al. Transcatheter arterial chemoembolization for hepatocellular carcinoma: prospective assessment of the right inferior phrenic artery with C-arm CT. J Vasc Interv Radiol. 2009;20:888–95.
51. Matsui O, Kadoya M, Yoshikawa J, et al. Small hepatocellular carcinoma: treatment with subsegmental transcatheter arterial embolization. Radiology. 1993;188:79–83.
52. Tanigawa N, Komemushi A, Kojima H, Kariya S, Sawada S. Three-dimensional angiography using rotational digital subtraction angiography: usefulness in transarterial embolization of hepatic tumors. Acta Radiol. 2004;45:602–7.
53. Solomon S, Thornton R, Deschamps F, et al. A treatment planning system for transcatheter hepatic therapies: pilot study. J Interv Oncol. 2008;1:12–8.
54. Heron DE, Smith RP, Andrade RS. Advances in image-guided radiation therapy – the role of PET-CT. Medical Dosimetry. 2006;31:3–11.
55. Veit P, Kuehle C, Beyer T, Kuehl H, Bockisch A, Antoch G. Accuracy of combined PET/CT in image-guided interventions of liver lesions: an ex-vivo study. World J Gastroenterol. 2006;12:2388–93.
56. Yap JT, Carney JPJ, Hall NC, Townsend DW. Image-guided cancer therapy using PET/CT. Cancer J. 2004;10:221–33.
57. Crocetti L, Lencioni R, DeBeni S, See TC, Della Pina C, Bartolozzi C. Targeting liver lesions for radiofrequency ablation – an experimental feasibility study using a CT-US fusion imaging system. Invest Radiol. 2008;43:33–9.
58. Wein W, Roper B, Navab N. Automatic registration and fusion of ultrasound with CT for radiotherapy. Med Image Comput Comput Assist Interv. 2005;8(Pt 2):303–11.
59. Ewertsen C, Grossjohann HS, Nielsen KR, Torp-Pedersen S, Nielsen MB. Biopsy guided by real-time sonography fused with MRI: a phantom study. Am J Roentgenol. 2008;190:1671–4.
60. Singh AK, Kruecker J, Xu S, et al. Initial clinical experience with real-time transrectal ultrasonography-magnetic resonance imaging fusion-guided prostate biopsy. BJU Int. 2008;101:841–5.
61. Archip N, Tatli S, Morrison P, Jolesz F, Warfield SK, Silverman S. Non-rigid registration of pre-procedural MR images with intra-procedural unenhanced CT images for improved targeting of tumors during liver radiofrequency ablations. Med Image Comput Comput Assist Interv. 2007;10:969–77.
62. Gutierrez LF, Silva R, Ozturk C, et al. Technology preview: X-ray fused with magnetic resonance during invasive cardiovascular procedures. Catheter Cardiovasc Interv. 2007;70:773–82.
63. Solomon SB, Incorporating CT. MR imaging, and positron emission tomography into minimally invasive therapies. J Vasc Interv Radiol. 2005;16:445–7.
64. Cleary K, Melzer A, Watson V, Kronreif G, Stoianovici D. Interventional robotic systems: applications and technology state-of-the art. Minim Invasive Ther Allied Technol. 2006;15:101–13.
65. Wood B, Locklin J, Viswanathan A, et al. Technologies for guidance of radiofrequency ablation in the multimodality interventional suite of the future. J Vasc Interv Radiol. 2007;18:9–24.
66. Kruecker J, Xu S, Glossop N, et al. Electromagnetic tracking for thermal ablation and biopsy guidance: clinical evaluation of spatial accuracy. J Vasc Interv Radiol. 2007;18:1141–50.
67. Meyer BC, Peter O, Nagel M, et al. Electromagnetic field-based navigation for percutaneous punctures on C-arm CT: experimental evaluation and clinical application. Eur Radiol. 2008;18:2855–64.
68. Borgert J, Kruger S, Timinger H, et al. Respiratory motion compensation with tracked internal and external sensors during CT-guided procedures. Comput Aided Surg. 2006;11:119–25.
69. Mogami T, Dohi M, Harada J. A new image navigation system for MR-guided cryosurgery. Magn Reson Med Sci. 2002;1:191–7.

70. Peters TM. Image-guidance for surgical procedures. Phys Med Biol. 2006;51:R505–40.
71. Solomon SB. Interactive images in the operating room. J Endourol. 1999;13:471–5.
72. Zhang H, Banovac F, Lin R, et al. Electromagnetic tracking for abdominal interventions in computer aided surgery. Comput Aided Surg. 2006;11:127–36.
73. Marohn MR, Hanly EJ. Twenty-first century surgery using twenty-first century technology: surgical robotics. Curr Surg. 2004;61:466–73.
74. Hempel E, Fischer H, Gumb L, et al. An MRI-compatible surgical robot for precise radiological interventions. Comput Aided Surg. 2003;8:180–91.
75. Solomon SB, Patriciu A, Bohlman ME, Kavoussi LR, Stoianovici D. Robotically driven interventions: a method of using CT fluoroscopy without radiation exposure to the physician. Radiology. 2002;225: 277–82.
76. Boctor EM, Choti MA, Burdette EC, Webster Iii RJ. Three-dimensional ultrasound-guided robotic needle placement: an experimental evaluation. Int J Med Robot. 2008;4:180–91.
77. DiMaio SP, Pieper S, Chinzei K, et al. Robot-assisted needle placement in open MRI: system architecture, integration and validation. Comput Aided Surg. 2007;12:15–24.
78. Stoianovici D. Multi-imager compatible actuation principles in surgical robotics. Int J Med Robot. 2005;1:86–100.
79. Patriciu A, Solomon S, Kavoussi LR, Stoianovici D. Robotic kidney and spine percutaneous procedures using a new laser-based CT registration method. In: Niessen W, Viergever MA, editors. Medical image computing and computer-assisted intervention, Lecture notes in computer science, vol. 2208. Utrecht: Springer; 2001. p. 249–58.
80. Korb W, Kornfeld M, Birkfellner W, et al. Risk analysis and safety assessment in surgical robotics: a case study on a biopsy robot. Minim Invasive Ther Allied Technol. 2005;14:23–31.
81. Larson AC, Wang D, Atassi B, et al. Transcatheter intraarterial perfusion: MR monitoring of chemoembolization for hepatocellular carcinoma–-feasibility of initial clinical translation. Radiology. 2008;246:964–71.
82. Kim CK, Choi D, Lim HK, et al. Therapeutic response assessment of percutaneous radiofrequency ablation for hepatocellular carcinoma: utility of contrast-enhanced agent detection imaging. Eur J Radiol. 2005;56:66–73.
83. Leyendecker JR, Dodd 3rd GD, Halff GA, et al. Sonographically observed echogenic response during intraoperative radiofrequency ablation of cirrhotic livers: pathologic correlation. AJR Am J Roentgenol. 2002;178:1147–51.
84. Permpongkosol S, Nielsen ME, Solomon SB. Percutaneous renal cryoablation. Urology. 2006;68: 19–25.
85. Saksena M, Gervais D. Percutaneous renal tumor ablation. Abdom Imaging. 2009;34:582–7.
86. Hahn PF, Gazelle GS, Jiang DY, Compton CC, Goldberg SN, Mueller PR. Liver tumor ablation: real-time monitoring with dynamic CT. Acad Radiol. 1997;4:634–8.
87. Hamuro M, Kaminou T, Nakamura K, et al. Percutaneous ethanol injection under CT fluoroscopy for hypervascular hepatocellular carcinoma following transcatheter arterial embolization. Hepatogastroenterology. 2002;49:752–7.
88. Tsai H-M, Lin X-Z, Chen C-Y. Computed tomography demonstration of immediate and delayed complications of computed tomography-guided transthoracic percutaneous ethanol injection of hepatocellular carcinoma at the liver dome. [Miscellaneous Article].
89. Bao A, Goins B, Dodd 3rd GD, et al. Real-time iterative monitoring of radiofrequency ablation tumor therapy with 15O-water PET imaging. J Nucl Med. 2008;49:1723–9.
90. de Senneville BD, Mougenot C, Quesson B, Dragonu I, Grenier N, Moonen CT. MR thermometry for monitoring tumor ablation. Eur Radiol. 2007;17:2401–10.
91. Dewey WC. Arrhenius relationships from the molecule and cell to the clinic. Int J Hyperthermia. 1994;10:457–83.
92. Quesson B, de Zwart JA, Moonen CT. Magnetic resonance temperature imaging for guidance of thermotherapy. J Magn Reson Imaging. 2000;12: 525–33.
93. Denis de Senneville B, Quesson B, Moonen CTW. Magnetic resonance temperature imaging. Int J Hyperthermia. 2005;21:515–31.
94. Rieke V, Butts Pauly K. MR thermometry. J Magn Reson Imaging. 2008;27:376–90.
95. Boss A, Rempp H, Martirosian P, et al. Wide-bore 1.5 Tesla MR imagers for guidance and monitoring of radiofrequency ablation of renal cell carcinoma: initial experience on feasibility. Eur Radiol. 2008;18:1449–55.
96. Liu HY, Hall WA, Martin AJ, Maxwell RE, Truwit CL. MR-guided and MR-monitored neurosurgical procedures at 1.5 T. J Comput Assist Tomogr. 2000;24:909–18.
97. Mack MG, Straub R, Eichler K, Sollner O, Lehnert T, Vogl TJ. Breast cancer metastases in liver: laser-induced interstitial thermotherapy–local tumor control rate and survival data. Radiology. 2004;233:400–9.
98. Morikawa S, Inubushi T, Kurumi Y, et al. MR-guided microwave thermocoagulation therapy of liver tumors: Initial clinical experiences using a 0.5 T open MR system. J Magn Reson Imaging. 2002;16:576–83.
99. Okuda S, Kuroda K, Oshio K, et al. MR-based temperature monitoring for hot saline injection therapy. J Magn Reson Imaging. 2000;12:330–8.

100. Seror O, Lepetit-Coiffe M, Le Bail B, et al. Real time monitoring of radiofrequency ablation based on MR thermometry and thermal dose in the pig liver in vivo. Eur Radiol. 2008;18:408–16.
101. Vogl TJ, Straub R, Eichler K, Sollner O, Mack MG. Colorectal carcinoma metastases in liver: laser-induced interstitial thermotherapy – local tumor control rate and survival data. Radiology. 2004;230: 450–8.
102. Arthur RM, Straube WL, Trobaugh JW, Moros EG. Non-invasive estimation of hyperthermia temperatures with ultrasound. Int J Hyperthermia. 2005;21: 589–600.
103. Fallone BG, Moran PR, Podgorsak EB. Noninvasive thermometry with a clinical x-ray CT scanner. Med Phys. 1982;9:715–21.
104. Efstathopoulos EP, Brountzos EN, Alexopoulou E, et al. Patient radiation exposure measurements during interventional procedures: a prospective study. Health Phys. 2006;91:36–40.
105. Stoeckelhuber BM, Leibecke T, Schulz E, et al. Radiation dose to the radiologist's hand during continuous CT fluoroscopy-guided interventions. Cardiovasc Intervent Radiol. 2005;28:589–94.
106. Gupta R, Grasruck M, Suess C, et al. Ultra-high resolution flat-panel volume CT: fundamental principles, design architecture, and system characterization. Eur Radiol. 2006;16:1191–205.
107. Orth RC, Wallace MJ, Kuo MD. C-arm cone-beam CT: general principles and technical considerations for use in interventional radiology. J Vasc Interv Radiol. 2008;19:814–20.

Percutaneous Radiofrequency Ablation in the Treatment of Primary Liver Cancers

18

Laura Crocetti and Riccardo Lencioni

Abstract

The development of image-guided percutaneous techniques for local tumor ablation has been one of the major advances in the treatment of liver malignancies. Among these methods, radiofrequency (RF) ablation is currently established as the primary ablative modality at most institutions. In the setting of patients of very early and early-stage hepatocellular carcinoma (HCC) – according to the Barcelona Clinic Liver Cancer (BCLC) staging system image-guided tumor ablation is recommended when patients are excluded from surgical options. The goal of RF ablation is to induce thermal injury to the tissue through electromagnetic energy deposition. One or multiple electrodes have to be inserted directly into the tumor to deliver RF energy current. Electrodes are coupled with RF generators and can be monopolar or bipolar, and they can have different designs (multitined expandable, internally cooled, perfused). Targeting of the lesion can be performed with US, CT, or MR imaging. The guidance system is chosen largely on the basis of operator preference and local availability of dedicated equipment such as fluoro-CT or open MR systems. RF ablation has shown superior anticancer effect and greater survival benefit with respect to the seminal percutaneous technique, ethanol injection, in meta-analyses of randomized controlled trials (RCTs), and is currently established as the standard method for local tumor treatment.

Introduction

The development of image-guided percutaneous techniques for local tumor ablation has been one of the major advances in the treatment of liver malignancies. Among these methods, radiofrequency (RF) ablation is currently established as the primary ablative modality at

L. Crocetti (✉) • R. Lencioni
Division of Diagnostic Imaging and Intervention, School of Medicine, University of Pisa, Cisanello Hospital, Pisa, IT, Italy
e-mail: laura.crocetti@med.unipi.it; riccardo.lencioni@med.unipi.it

D.E. Dupuy et al. (eds.), *Image-Guided Cancer Therapy*, DOI 10.1007/978-1-4419-0751-6_20,

most institutions. In the setting of patients of very early and early-stage hepatocellular carcinoma (HCC) – according to the Barcelona Clinic Liver Cancer (BCLC) staging system [1] (Table 18.1) – image-guided tumor ablation is recommended when patients are excluded from surgical options. RF ablation has shown superior anticancer effect and greater survival benefit with respect to the seminal percutaneous technique, ethanol injection, in meta-analyses of randomized controlled trials (RCTs), and is currently established as the standard method for local tumor treatment [2–6]. In the following chapter, indications, contraindications, procedure, and complications of RF ablation will be covered together with the clinical results of the technique in the treatment of HCC.

Table 18.1 BCLC classification in patients diagnosed with HCC

Very early stage	PS 0, Child–Pugh A, single HCC <2 cm
Early stage	PS 0, Child–Pugh A–B, single HCC or 3 nodules <3 cm
Intermediate stage	PS 0, Child–Pugh A–B, multinodular HCC
Advanced stage	PS 1–2, Child–Pugh A–B, portal neoplastic invasion, nodal metastases, distant metastases
Terminal stage	PS > 2, Child–Pugh C

PS performance status

Table 18.2 Absolute and relative contraindications for RF ablation

	Absolute contraindications	Relative contraindications
Lesion-related	Tumor located <1 cm main biliary duct	Superficial lesions
	Intrahepatic bile duct dilation	Superficial lesions that are adjacent to any part of the gastrointestinal tract
	Anterior exophytic location of the tumor	Tumors located in the vicinity of the gallbladder
Patient-related	Untreatable/ unmanageable coagulopathy	Bilioenteric anastomosis

Indications and Contraindications

RF ablation is the therapy of choice in very early and early HCC according to the Barcelona Clinic Liver Cancer (BCLC) classification (Table 18.1) when patients are not candidates for either liver resection or transplantation. In very early-stage HCC, the presence of a solitary small nodule, less than <2 cm in diameter, in Child–Pugh A patients, the absence of microvascular invasion and dissemination offers the highest likelihood of cure. Early-stage disease includes patients with preserved liver function (Child–Pugh A and B) with solitary HCC or up to 3 nodules <3 cm in size [7].

Contraindications for RF ablation can be lesion-related or patient-related. Lesion location should be carefully assessed during pretreatment evaluation due to the risk of determining thermal damage with respect to surrounding structures [8]. Lesions located on the surface of the liver can be considered for thermal ablation, although their treatment requires adequate expertise and may be associated with a higher risk of complications [3]. It has been suggested that thermal ablation of superficial lesions that are adjacent to any part of the gastrointestinal tract should be avoided because of the risk of thermal injury of the gastric or bowel wall. The use of special techniques – such as intraperitoneal injection of dextrose to displace the bowel – can be considered in such instances [2, 8]. Treatment of lesions adjacent to the hepatic hilum increases the risk of thermal injury of the biliary tract, with the delayed occurrence of main biliary duct stenosis. In experienced hands, thermal ablation of tumors located in the vicinity of the gallbladder has been shown to be feasible, although associated in most cases with self-limited iatrogenic cholecystitis. Thermal ablation of lesions adjacent to hepatic vessels is possible, since flowing blood usually protects the vascular wall from thermal injury: in these cases, however, the risk of incomplete treatment of the neoplastic tissue close to the vessel may increase because of the heat loss by convection [2, 8, 9].

Patient-related contraindications are mainly related to the presence of an untreatable coagulopathy, not uncommon in patient with liver cirrhosis. When platelet count is below 50,000/μL and a PT ratio (normal time/patient's time) <50 %, the risk of hemorrhage is considered high and the procedure is contraindicated. Patients bearing a bilioenteric anastomosis have a high likelihood of infection with the occurrence of hepatic abscesses after an RF ablation procedure: this condition represents therefore a relative contraindication for the ablative procedure [2]. Absolute and relative, lesion- and patient-related contraindications are summed up in Table 18.2.

Table 18.3 American Society of Anesthesiologists (ASA) physical status classification system

I	A normal healthy patient
II	A patient with mild systemic disease
III	A patient with severe systemic disease
IV	A patient with severe systemic disease that is a constant threat to life
V	A moribund patient who is not expected to survive without the operation
VI	A declared brain-dead patient whose organs are being removed for donor purposes

Procedure

Anesthesiology Care

RF ablation is usually performed under intravenous sedation or general anesthesia with standard cardiac, pressure, and oxygen monitoring. In some centers, general anesthesia with tracheal intubation is used. American Society of Anesthesiologists (ASA) score (Table 18.3) can be used to assess patient physical status prior to thermal ablation. Patients up to ASA III score can be treated [2].

Technique

The goal of RF ablation is to induce thermal injury to the tissue through electromagnetic energy deposition. In RF ablation, the patient is part of a closed-loop circuit that includes an RF generator, an electrode needle, and a large dispersive electrode (ground pads). An alternating electric field is created within the tissue of the patient. Because of the relatively high electrical resistance of tissue in comparison with the metal electrodes, there is marked agitation of the ions present in the target tissue that surrounds the electrode, since the tissue ions attempt to follow the changes in direction of alternating electric current. The agitation results in frictional heat around the electrode. The discrepancy between the small surface area of the needle electrode and the large area of the ground pads causes the generated heat to be focused and concentrated around the needle electrode [8]. The thermal damage caused by RF heating is dependent on both the tissue temperature achieved and the duration of heating. Heating of tissue at 50–55 °C for 4–6 min produces irreversible cellular damage. At temperatures between 60 °C and 100 °C, near immediate coagulation of tissue is induced, with irreversible damage to mitochondrial and cytosolic enzymes of the cells. At more than 100–110 °C, tissue vaporizes and carbonizes. For adequate destruction of tumor tissue, the entire target volume must be subjected to cytotoxic temperatures. Thus, an essential objective of ablative therapy is achievement and maintenance of a 50–100 °C temperature throughout the entire target volume for at least 4–6 min. However, the relatively slow thermal conduction from the electrode surface through the tissues increases the duration of application to 10–20 min. To accomplish the increase of energy deposition into tissues, the RF output of all commercially available generators has been increased to 150–250 W. On the other hand, the tissue temperature should not be superior to 100–110 °C to avoid carbonization, with significant gas production that both serves as an insulator and retards the ability to effectively establish an RF field [8]. Another important factor that affects the success of RF thermal ablation is the heat loss through convection by means of blood circulation, the so-called heat sink effect. This may consistently limit the volume of ablation and therefore the ability

of RF ablation to ablate all viable tumor tissue and an adequate tumor-free margin. To achieve rates of local tumor recurrence with RF ablation that are comparable to those obtained with hepatic resection, physicians should produce a 360°, 0.5–1-cm-thick tumor-free margin around each tumor. This cuff will assure that all microscopic invasions around the periphery of a tumor have been eradicated. Thus, the target diameter of an ablation must be ideally 1–2 cm larger than the diameter of the tumor that undergoes treatment [8]. After activation, the generators are run by automate programs, designed to modulate the released power relying on direct temperature measurement or on electrical measurement of tissue impedance, to avoid overheating and carbonization. At the end of the procedure, the coagulation of the needle track is performed, to prevent tumor seeding [8]. To minimize heat loss by heat sink effect, several strategies for reducing blood flow during ablation therapy have been proposed. Total portal inflow occlusion (Pringle maneuver) has been used at open laparotomy and at laparoscopy. Angiographic balloon catheter occlusion of the hepatic artery or embolization of the tumor feeding artery has also been shown to be useful in hypervascularized tumors [10]. In the setting of HCC, combining thermal ablation with other therapies such as chemoembolization or transarterial administration of drug-eluting beads has shown very promising results in early clinical investigation [11]. Further research to determine optimal methods of combining chemotherapeutic regimens (both agent and route of administration) with RF ablation is ongoing.

Types of RF Electrode

One or multiple electrodes have to be inserted directly into the tumor to deliver RF energy current. Electrodes are coupled with RF generators and can be monopolar or bipolar, and they can have different designs (multitined expandable, internally cooled, perfused) [2]:

(a) Monopolar electrode: there is a single active electrode, with current dissipated at one or several return grounding pads.
(b) Bipolar electrode: there are two active electrode applicators, which have to be placed in proximity.
(c) Multitined expandable electrode: multiple electrode tines that expand from a larger needle cannula. They permit the deposition of this energy over a larger volume and ensure more uniform heating that relies less on heat conduction over a large distance.
(d) Internally cooled electrode: the electrode has an internal lumen which is perfused by saline without coming into direct contact with patient tissues. They have been designed to minimize carbonization and gas formation around the needle tip by eliminating excess heat near the electrode.
(e) Perfused electrode: the tip of the electrode has small apertures that allow the fluid (usually saline) to come in contact with the tissue. Administration of saline solution during the application of RF current increases tissue conductivity and thereby allows greater deposition of RF current and increased tissue heating and coagulation.

Imaging Guidance/Monitoring

Targeting of the lesion can be performed with US, CT, or MR imaging [12]. The guidance system is chosen largely on the basis of operator preference and local availability of dedicated equipment such as fluoro-CT or open MR systems. During the procedure, important aspects to be monitored include how well the tumor is being covered and whether any adjacent normal structures are being affected at the same time. While the transient hyperechoic zone that is seen at US within and surrounding a tumor during and immediately after RF ablation can be used as a rough guide to the extent of tumor destruction, MR is currently the only imaging modality with validated techniques for real-time temperature monitoring. Contrast-enhanced US performed after the end of the procedure may allow an initial

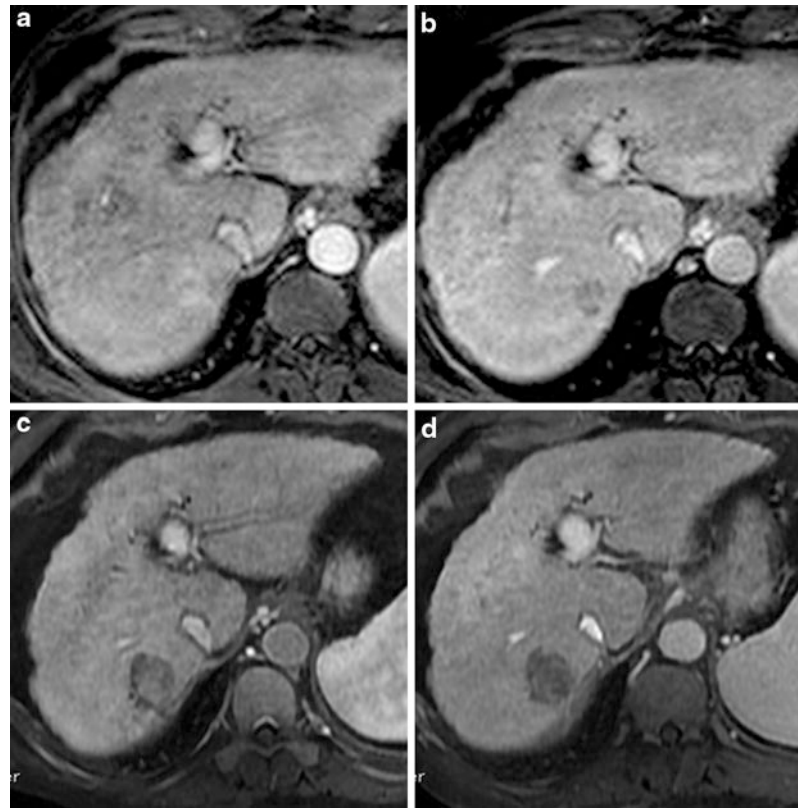

Fig. 18.1 *RF ablation of HCC*. Pretreatment dynamic MR shows the lesion as a small hypervascular nodule (**a**) in the arterial phase with hypointense appearance in portal-venous phase (**b**) in segment 7. On dynamic MR images obtained in the arterial (**c**) and the portal venous phase (**d**) 1 month after percutaneous RF treatment, the tumor is replaced by a nonenhancing ablation zone that exceeds in size the diameter of the naïve tumor. The findings are consistent with complete response

evaluation of treatment effects. However, contrast-enhanced CT or MR imaging is recognized as the standard modalities to assess treatment outcome [12] (Fig. 18.1).

Tumor Response Evaluation

CT and MR images obtained 4–8 weeks after treatment show successful ablation as a nonenhancing area with or without peripheral enhancing rim [13, 14] (Fig. 18.1). The enhancing rim that may be observed along the periphery of the ablation zone appears a relatively concentric, symmetric, and uniform process in an area with smooth inner margins. This is a transient finding that represents a benign physiologic response to thermal injury (initially, reactive hyperemia; subsequently, fibrosis and giant cell reaction). Benign periablational enhancement needs to be differentiated from irregular peripheral enhancement due to residual tumor that occurs at the treatment margin. In contrast to benign periablational enhancement, residual unablated tumor often grows in scattered, nodular, or eccentric patterns [12]. Later follow-up imaging studies should be aimed at detecting the recurrence of the treated lesion (i.e., local tumor progression), the development of new hepatic lesions, or the emergence of extrahepatic disease. Evaluation of tumor response should be performed following criteria originally developed by a panel of experts of the EASL [15]. According to the panel, the optimal method to assess treatment response was to estimate the reduction in viable tumor area using contrast-enhanced radiologic imaging. Viable tumor was defined as uptake of contrast agent in the arterial phase of dynamic CT or MR [15]. Subsequently, this concept has been endorsed by the AASLD and the AASLD practice guidelines on the management of HCC stated

that the evaluation of the treatment response should take into account the induction of intratumoral necrotic areas in estimating the decrease in tumor load and not just a reduction in overall tumor size [7]. The first formal modification of the assessment of response based in the RECIST criteria was published in 2008, and an expanded and detailed description of the proposed amendments, the so-called mRECIST, has been recently published [13, 14].

Complications

Early major complications associated with RF ablation occur in 2.2–3.1 % of patients and include intraperitoneal bleeding, liver abscess, intestinal perforation, pneumo-/hemothorax, and bile duct stenosis [16–18]. An uncommon late complication of RF ablation can be tumor seeding along the needle track. In patients with HCC, tumor seeding occurred in 8 (0.5 %) of 1,610 cases in a multicenter survey [16] and in 1 (0.5 %) of 187 cases in a single-institution series [19]. Lesions with subcapsular location and an invasive tumoral pattern, as shown by a poor differentiation degree, seem to be at higher risk for such a complication [20]. The minor complication rate ranges from 5 % to 8.9 %. They include pain, fever, asymptomatic pleural effusion, and asymptomatic self-limiting intraperitoneal bleeding [16–18]. The procedure mortality rate is 0.1–0.5 %. The most common causes of death are sepsis, hepatic failure, colon perforation, and portal vein thrombosis (particularly in patients submitted to RF ablation with surgical approach and Pringle maneuver) [16–18].

Results

The therapeutic effect of RF ablation in HCC has been assessed by studies that evaluated the outcome of treatment at the histological level and by randomized or cohort studies that investigated the long-term survival outcomes of treated patients. Histological data from explanted liver specimens in patients who underwent RF ablation showed that tumor size and presence of large (3 mm or more) abutting vessels significantly affect local treatment effect. Complete tumor necrosis was pathologically shown in 83 % of tumors <3 cm and 88 % of tumors in nonperivascular location [9]. Comparison with percutaneous ethanol injection (PEI) in five randomized trials [21–25] has shown that RF ablation had higher local anticancer effect than PEI, leading to a better local control of the disease. These data were recently pooled in three independent meta-analysis, and the survival benefit for patients with small HCC submitted to RF ablation was confirmed [3–5]. Therefore, RF ablation appears as the preferred percutaneous treatment for patients with early-stage HCC on the basis of a more consistent local tumor control and better survival outcomes. Recently, the long-term survival outcomes of RF ablation-treated patients were reported (Table 18.4) and were useful to elucidate factors influencing patient prognosis [19, 26–31]. The severity of the underlying cirrhosis and occurrence of new lesions represent the most important prognostic factors. Recent reports on long-term outcomes of RF-treated patients have shown that in patients with Child–Pugh class A and early-stage HCC, 5-year survival rates are as high as 51–64 % and may reach 76 % in patients who meet the BCLC criteria for surgical resection [18, 19, 26, 31] (Table 18.4). Therefore, an open question is whether RF ablation can compete with surgical resection as first line for patients with early-stage, solitary HCC. An RCT comparing resection versus ablation in Child A patients with single HCC 5 cm or less in diameter has failed to show statistically significant differences in overall survival and disease-free survival between the two treatment arms [32]. Conversely, a recent RCT comparing RF ablation and resection in patients conforming to Milan criteria suggested that surgical resection may provide better survival and lower recurrence rates than RFA [33].

An important factor that affects the success of RF ablation is the ability to ablate all viable tumor tissue and possibly an adequate tumor-free margin. The target tumor should not exceed

Table 18.4 Studies reporting long-term survival outcomes of patients with early-stage HCC who underwent percutaneous RF ablation

Author	No. of patients	Survival (%)		
		1 year	3 years	5 years
Tateishi et al. [26]				
Naive patients[a]	319	95	78	54
Nonnaive patients[b]	345	92	62	38
Lencioni et al. [19]				
Child A, 1 HCC < 5 cm or 3 < 3 cm	144	100	76	51
1 HCC < 5 cm	116	100	89	61
Child B, 1 HCC < 5 cm or 3 < 3 cm	43	89	46	31
Cabassa et al. [27]	59	94	65	43
Choi et al. [28]				
Child A, 1 HCC < 5 cm or 3 < 3 cm	359	NA	78	64
Child B, 1 HCC < 5 cm or 3 < 3 cm	160	NA	49	38
Takahashi et al. [29]				
Child A, 1 HCC < 5 cm or 3 < 3 cm	171	99	91	77
Hiraoka et al. [30]				
Child–Pugh A–B	105	NA	88	59
N'Kontchou G [31]	235	NA	60	40
Pt fitting BCLC criteria for resection	67	NA	82	76
Unresectable pts	168	NA	49	27

NA not available
[a]Patients who received radiofrequency ablation as primary treatment
[b]Patients who received radiofrequency ablation for recurrent tumor after previous treatment including resection, ethanol injection, microwave ablation, and transarterial embolization

3 cm at its longest axis to achieve best rates of complete ablation using most of the currently available devices [2]. Moreover, even in small tumors, the ability of RF ablation to achieve a complete tumor eradication appears to be dependent on tumor location. Histological studies performed in liver specimens of patients who underwent RF ablation as bridge treatment to transplantation showed that the presence of large (3 mm or more) abutting vessels results in a drop of the rate of complete tumor necrosis to less than 50 %, because of the heat loss due to perfusion-mediated tissue cooling within the area to be ablated [9]. Therefore, in patients with solitary HCC >3 cm and <5 cm in size, the success rate of RF alone is decreased; combination with intra-arterial treatment could be considered in these patients when surgery and transplantation are not feasible options [10, 11, 34–36]. A combination of TACE followed by RF ablation has been used to minimize heat loss due to perfusion-mediated tissue cooling and increase the therapeutic effect of RF ablation [10, 34–36]. On the other hand, TACE with drug-eluting beads has been performed after an RF ablation procedure to increase tumor necrosis by exposing to high drug concentration the peripheral part of the tumor, where only sublethal temperatures may be achieved in a standard RF ablation treatment [11]. Further research to determine optimal methods of combining chemotherapeutic regimens (both agent and route of administration) with RF ablation is needed. In particular, a phase III, randomized, double-blinded, dummy-controlled study investigating the efficacy and safety of thermally sensitive liposomal doxorubicin in combination with RF ablation compared to RF ablation alone in the treatment of nonresectable HCC is ongoing [37].

In very early HCCs, single nodule with diameter <2 cm, there are the optimal conditions for radical local therapies, as the probability of

microvascular invasion and microsatellites is very low. In patient with very early HCC, the complete response rate approaches 97 %, with 5 years survival rates of 68 % [38]. In such small tumors therefore, RF ablation seems to challenge the role of surgical resection, and in many centers RF ablation, it is offered even in operable patients. Recently, confirmatory information about the respective role of resection and RF ablation in the clinical management of very early HCC has been provided by a decision analysis study. Cho et al. concluded that RF ablation and hepatic resection are to be considered equally effective for the treatment of very early HCC. It has also been pointed out as individual components belonging to each patient (e.g., whether the tumor is central or peripheral, close or distant form bile ducts, in patient who is lean or overweight, presenting with or without portal hypertension) influence the results of each treatment making it better or worse than average [38, 39]. If clinical experiences have suggested that treatment by RF ablation of HCC tumors in subcapsular location or adjacent to the gallbladder is associated with an increased risk of major complications and incomplete ablation [20, 40–43], such tumor locations are considered favorable for hepatic resection. Therefore, in patients with very early HCC, RF ablation seems to represent a complementary rather than an alternate treatment, and treatment should be chosen considering individual variables, including lesion location [44].

References

1. Llovet JM, Brú C, Bruix J. Prognosis of hepatocellular carcinoma: the BCLC staging classification. Semin Liver Dis. 1999;19:329–38.
2. Crocetti L, de Baere T, Lencioni R. Quality improvement guidelines for radiofrequency ablation of liver tumours. Cardiovasc Intervent Radiol. 2010;33:11–7.
3. Orlando A, Leandro G, Olivo M, et al. Radiofrequency thermal ablation vs. percutaneous ethanol injection for small hepatocellular carcinoma in cirrhosis: meta-analysis of randomized controlled trials. Am J Gastroenterol. 2009;104:514–24.
4. Cho YK, Kim JK, Kim MY, et al. Systematic review of randomized trials for hepatocellular carcinoma treated with percutaneous ablation therapies. Hepatology. 2009;49:453–9.
5. Germani G, Pleguezuelo M, Gurusamy K, et al. Clinical outcomes of radiofrequency ablation, percutaneous alcohol and acetic acid injection for hepatocelullar carcinoma: a meta-analysis. J Hepatol. 2010;52:380–8.
6. Lencioni R. Loco-regional treatment of hepatocellular carcinoma. Hepatology. 2010;52:762–73.
7. Bruix J, Sherman M. Management of hepatocellular carcinoma. Hepatology. 2005;42:1208–36.
8. Lencioni R, Crocetti L, Pina MC, et al. Percutaneous image-guided radiofrequency ablation of liver tumors. Abdom Imaging. 2009;34:547–56.
9. Lu DS, Yu NC, Raman SS, et al. Radiofrequency ablation of hepatocellular carcinoma: treatment success as defined by histologic examination of the explanted liver. Radiology. 2005;234:954–60.
10. Rossi S, Garbagnati F, Lencioni R, et al. Percutaneous radio-frequency thermal ablation of nonresectable hepatocellular carcinoma after occlusion of tumor blood supply. Radiology. 2000;217:119–26.
11. Lencioni R, Crocetti L, Petruzzi P, et al. Doxorubicin-eluting bead-enhanced radiofrequency ablation of hepatocellular carcinoma: a pilot clinical study. J Hepatol. 2008;49:217–22.
12. Crocetti L, Della Pina C, Cioni D, et al. Peri-intraprocedural imaging: US, CT, and MRI. Abdom Imaging. 2011;36:648–60.
13. Llovet JM, Di Bisceglie AM, Bruix J, et al. Panel of experts in HCC-design clinical trials. Design and endpoints of clinical trials in hepatocellular carcinoma. J Natl Cancer Inst. 2008;100:698–711.
14. Lencioni R, Llovet JM. Modified RECIST (mRECIST) assessment for hepatocellular carcinoma. Semin Liver Dis. 2010;30:52–60.
15. Bruix J, Sherman M, Llovet JM, et al. EASL panel of experts on HCC. Clinical management of hepatocellular carcinoma. Conclusions of the Barcelona-2000 EASL conference. J Hepatol. 2001;35:421–30.
16. Livraghi T, Solbiati L, Meloni MF, et al. Treatment of focal liver tumors with percutaneous radio-frequency ablation: complications encountered in a multicentre study. Radiology. 2003;26:441–51.
17. De Baere T, Risse O, Kuoch V, et al. Adverse events during radiofrequency treatment of 582 hepatic tumors. AJR Am J Roentgenol. 2003;181:695–700.
18. Bleicher RJ, Allegra DP, Nora DT, et al. Radiofrequency ablation in 447 complex unresectable liver tumors: lessons learned. Ann Surg Oncol. 2003;10:52–8.
19. Lencioni R, Cioni D, Crocetti L, et al. Early-stage hepatocellular carcinoma in cirrhosis: long-term results of percutaneous image-guided radiofrequency ablation. Radiology. 2005;234:961–7.
20. Llovet JM, Vilana R, Bru C, et al. Barcelona clinic liver cancer (BCLC) group. Increased risk of tumor seeding after percutaneous radiofrequency ablation for

single hepatocellular carcinoma. Hepatology. 2001; 33:1124–29.
21. Lencioni R, Allgaier HP, Cioni D, et al. Small hepatocellular carcinoma in cirrhosis: randomized comparison of radiofrequency thermal ablation versus percutaneous ethanol injection. Radiology. 2003;228:235–40.
22. Lin SM, Lin CJ, Lin CC, et al. Radiofrequency ablation improves prognosis compared with ethanol injection for hepatocellular carcinoma < or =4 cm. Gastroenterology. 2004;127:1714–23.
23. Shiina S, Teratani T, Obi S, et al. A randomized controlled trial of radiofrequency ablation versus ethanol injection for small hepatocellular carcinoma. Gastroenterology. 2005;129:122–30.
24. Lin SM, Lin CJ, Lin CC, et al. Randomised controlled trial comparing percutaneous radiofrequency thermal ablation, percutaneous ethanol injection, and percutaneous acetic acid injection to treat hepatocellular carcinoma of 3 cm or less. Gut. 2005;54:1151–6.
25. Brunello F, Veltri A, Carucci P, et al. Radiofrequency ablation versus ethanol injection for early hepatocellular carcinoma: a randomized controlled trial. Scand J Gastroenterol. 2008;43:727–35.
26. Tateishi R, Shiina S, Teratani T, et al. Percutaneous radiofrequency ablation for hepatocellular carcinoma. Cancer. 2005;103:1201–9.
27. Cabassa P, Donato F, Simeone F, et al. Radiofrequency ablation of hepatocellular carcinoma: long-term experience with expandable needle electrodes. AJR Am J Roentgenol. 2006;185:S316–21.
28. Choi D, Lim HK, Rhim H, et al. Percutaneous radiofrequency ablation for early-stage hepatocellular carcinoma as a first- line treatment: long-term results and prognostic factors in a large single-institution series. Eur Radiol. 2007;17:684–92.
29. Takahashi S, Kudo M, Chung H, et al. Initial treatment response is essential to improve survival in patients with hepatocellular carcinoma who underwent curative radiofrequency ablation therapy. Oncology. 2007;72:S98–103.
30. Hiraoka A, Horiike N, Yamashita Y, et al. Efficacy of radiofrequency ablation therapy compared to surgical resection in 164 patients in Japan with single hepatocellular carcinoma smaller than 3 cm, along with report of complications. Hepatogastroenterology. 2008;55:2171–4.
31. N'Kontchou G, Mahamoudi A, Aout M, et al. Radiofrequency ablation of hepatocellular carcinoma: long-term results and prognostic factors in 235 Western patients with cirrhosis. Hepatology. 2009;50:1475–83.
32. Chen MS, Li JQ, Zheng Y, et al. A prospective randomized trial comparing percutaneous local ablative therapy and partial hepatectomy for small hepatocellular carcinoma. Ann Surg. 2006;243:321–8.
33. Huang J, Yan L, Cheng Z, et al. A randomized trial comparing radiofrequency ablation and surgical resection for HCC conforming to the Milan criteria. Ann Surg. 2010;252:903–12.
34. Yamasaki T, Kurokawa F, Shirahashi H, et al. Percutaneous radiofrequency ablation therapy for patients with hepatocellular carcinoma during occlusion of hepatic blood flow. Comparison with standard percutaneous radiofrequency ablation therapy. Cancer. 2002;95:2353–60.
35. Veltri A, Moretto P, Doriguzzi A, et al. Radiofrequency thermal ablation (RFA) after transarterial chemoembolization (TACE) as a combined therapy for unresectable non-early hepatocellular carcinoma (HCC). Eur Radiol. 2006;16:661–9.
36. Helmberger T, Dogan S, Straub G, et al. Liver resection or combined chemoembolization and radiofrequency ablation improve survival in patients with hepatocellular carcinoma. Digestion. 2007;75:104–12.
37. http://www.clinicaltrial.gov/ct2/show/NCT00617981. Accessed July 2011.
38. Livraghi T, Meloni F, Di Stasi M, et al. Sustained complete response and complications rates after radiofrequency ablation of very early hepatocellular carcinoma in cirrhosis: is resection still the treatment of choice? Hepatology. 2008;47:82–9.
39. Cho YK, Kim JK, Kim WT, et al. Hepatic resection versus radiofrequency ablation for very early stage hepatocellular carcinoma: a Markov model analysis. Hepatology. 2010;51:1284–90.
40. Majno PE, Mentha G, Mazzaferro V. Partial hepatectomy versus radiofrequency ablation for hepatocellular carcinoma: confirming the trial that will never be, and some comments on the indications for liver resection. Hepatology. 2010;51:1116–8.
41. Komorizono Y, Oketani M, Sako K, et al. Risk factors for local recurrence of small hepatocellular carcinoma tumors after a single session, single application of percutaneous radiofrequency ablation. Cancer. 2003;97:1253–62.
42. Kim SW, Rhim H, Park M, et al. Percutaneous radiofrequency ablation of hepatocellular carcinomas adjacent to the gallbladder with internally cooled electrodes: assessment of safety and therapeutic efficacy. Korean J Radiol. 2009;10:366–76.
43. Teratani T, Yoshida H, Shiina S, et al. Radiofrequency ablation for hepatocellular carcinoma in so-called high-risk locations. Hepatology. 2006;43:1101–8.
44. Lencioni R, Crocetti L. Local-regional treatment of hepatocellular carcinoma. Radiology. 2012;262:43–58.

Microwave in the Treatment of Primary Liver Cancers

19

Liang Ping and Yu Jie

Abstract

The majority of patients suffering from liver tumors are not candidates for surgery. Currently, minimal invasive techniques have become available for local destruction of hepatic tumors. Microwave ablation (MWA) is a relatively low-risk procedure that utilizes high temperatures to ablate tumors. The aim of this chapter is to review the basic principles; the state of the art of different device technologies, approaches, and treatment strategies; current therapeutic status; and future trends of microwave ablation for primary liver cancer. MWA has achieved similar effect compared with surgery, radiofrequency ablation (RFA), and ethanol injection treatment for hepatocellular carcinoma (HCC). For tumors adjacent to vital structures, MWA has achieved favorable results with low complications as well. Because of several advantages including high thermal efficiency, higher capability of coagulating blood vessels, faster ablation time, and simultaneous application of multiple antennae, MWA could be a promising minimally invasive technique for the treatment of HCC. Long-term survival data and large-scale prospectively RCTs comparing it with other modalities, especially with RFA for ultimately determining its effectiveness, are earnestly anticipated.

Background

Microwave ablation (MWA) is the term used for all electromagnetic methods of inducing tumor destruction by using devices with frequencies greater than or equal to 900 kHz. The microwave coagulation was initially developed in the early 1970s to achieve hemostasis along the plane of transection during hepatic resection [1]. However, microwave coagulation of tissue surfaces was slower than electrocautery units and produced deeper areas of tissue necrosis which has led to further investigation of the application of MWA to treat hepatic malignancies since the 1990s. In recent years with the advance in technique and equipment, MWA has become popularized in many institutions in the Far East countries and part of western countries with

L. Ping (✉) • Y. Jie
Department of Interventional Ultrasound, Chinese PLA General Hospital, Beijing, China
e-mail: liangping301@hotmail.com; yu-jie301@hotmail.com

D.E. Dupuy et al. (eds.), *Image-Guided Cancer Therapy*, DOI 10.1007/978-1-4419-0751-6_21,

a high incidence of hepatocellular carcinoma because of its favorable therapeutic efficacy [2–5].

Mechanism and Principles

Microwave radiation as a high-frequency electromagnetic wave exerts its function by inducing frictional heating from its interaction with polar molecules [6, 7]. Water molecules are polar molecules with the hydrogen side of the molecule carrying a positive charge and the oxygen side of the molecule carrying a negative charge. When microwave radiation hits the water molecules, they oscillate between two and five billion times to align themselves with the fluctuating microwave field. This rapid molecular rotation generates and uniformly distributes heat leading to cell death through coagulation necrosis, which is instantaneous and continuous until the radiation is stopped. Another mechanism responsible for heat generation is ionic polarization which occurs when ions move in response to the applied electric field of microwave. Displacement of ions causes collision with other ions, converting kinetic energy into heat. However, it is a far less important mechanism than the dipole rotation in living tissue. Heating of tissue at 50–55 °C for 4–6 min produces irreversible cellular damage. At temperatures between 60 °C and 100 °C nearly immediate coagulation of tissue is induced, with irreversible damage to mitochondrial and cytosolic enzymes of the cells. At more than 100–110 °C, tissue vaporizes and carbonizes [8]. The high temperature produced by microwave irradiation creates an ablation area around the needle in a column or round shape, depending on the type of needle used and the generating power [9].

Although MWA offers the same benefits as radiofrequency ablation (RFA), it has several theoretical advantages compared with RFA for the treatment of hepatic tumors. In RF ablation, the high-frequency alternating electrical current is used to create heat via ionic agitation within tissue resulting in intense active heating (with carbonization and vaporization) immediately adjacent to the electrode. However, this heating markedly diminishes – by a factor of approximately four – with increased distance from the electrode tip, and the majority of tissue heating occurs via thermal conduction from the active zone of heating to achieve subsequent tissue necrosis [10, 11]. Thereafter, MWA heating is primarily active, whereas RFA heating is primarily passive. The theoretical advantages shared by MWA include the following: (1) MWA has a much broader zone of active heating by not relying on the conduction of electricity into the tissue; thus, the transmission of this energy is less subject to impedance effects produced by tissue desiccation and charring [9, 12]. Therefore, consistently greater intratumoral temperatures can lead to a larger zone of ablation over a shorter treatment time [9, 13]. (2) Thermal conduction is an inefficient process; not only does it decrease exponentially away from its source but it is also very susceptible to heat sink from local blood flow. MWA, by contrast, has a deeper energy deposition and does not rely solely on thermal conduction for ablation. Another significant advantage of MWA over RFA is it is less prone to convective heat loss from blood flow with the ablation zone remaining uniform [14, 15]. Impaired ablation zone by heat sink which can result in residual tumor cells at the tumor periphery and blood vessel margins [16]. (3) The simultaneous treatment of multiple tumors is feasible with multiple microwave antennae, which is not possible with the majority of monopolar RFA. This shortens the treatment time and leads to synergistically larger more spherical ablation zones for larger tumor treatment [17]. (4) Unlike most of RF equipment, MWA does not require the placement of grounding pads, which can result in skin burns; meanwhile, MWA is not contraindicated by the metallic materials like surgical clips or implantable cardiac devices.

Equipment Development

The goal of MWA is to destroy the entire tumor as well as a 5–10-mm sufficient margin of surrounding healthy tissue along the entire boundary

Table 19.1 Ablation characteristics of variety of microwave antennae in in vivo porcine liver

Study	Antenna type	Active-tip length(cm)	Antenna diameter in mm or (gauge)	Frequency (MHz)	Power (W)	Ablation time(min)	Ablation zone(cm)
Dong et al. [21]	Non-cooled-shaft	?	1.4 mm	2,450	60	5	3.74 × 2.58
He et al. [22]	Non-cooled-shaft	1.5	14 G	2,450	50	8	5.8 × 2.8
	Cooled-shaft	1.5	14 G	2,450	50	8	5.0 × 3.4
Kuang et al. [23]	Cooled-shaft	1.5	14 G	2,450	60	5	3.3 × 2.2
	Cooled-shaft	1.5	14 G	2,450	70	20	5.8 × 3.3
Wang et al. [24]	Cooled-shaft	1.1	15 G	2,450	60	10	4.02 × 2.35
Wright et al. [17]	Non-cooled-shaft	3.6	13 G	915	40	10	2.1 × 1.5
Sun et al. [26]	Cooled-shaft	2.5	15 G	915	60	10	5.17 × 3.83
	Cooled-shaft	1.1	15 G	2,450	60	10	4.15 × 2.35
Jie et al. [9]	Cooled-shaft	1.1	15 G	2,450	60	10	3.86 × 2.35
	Cooled-shaft	2.2	15 G	915	60	10	5.79 × 2.95
Shock et al. [27]	Loop		24 G		60	7	3.4 × 1.1
Jiao et al. [25]	Cooled-shaft	1.5	14 G	2,450	60	10	2.67 × 3.73
Brace et al. [28]	Triaxial antenna	1.23	17 G	2,450	68	10	2.27 × 1.25

of the tumor [18]. All MWA systems are composed of three basic elements – microwave generator, low-loss flexible coaxial cable, and microwave antenna. Microwave energy is generated by a magnetron. The antenna is connected via a low-loss coaxial cable to the microwave machine and transmits the microwave energy from the magnetron into the tissue. Antenna design is crucial to the therapeutic efficacy. The coaxial choke is a conductor surrounding the outer conductor of the coaxial antenna feed line separated by a dielectric insulator at the proximal end. Its length is commonly a quarter wavelength, which constrains wave propagation along the outside of the outer conductor and leads to a more spherical ablation zone [19, 20].

Over the years, there have been continued efforts focusing on increasing the coagulation diameters by refinement of the antenna and generator. The characteristics of several microwave system were summarized in Table 19.1. The first generation system including Microtaze (Heiwa Denshi Kogyo, Osaka, Japan), UMC-I, and FORSEA system (both produced in China) with the needle antenna 1.4–2 mm in diameter could create a coagulation zone of (3.7–5.8) × (2.6–2.8) cm in diameter, which both operated at 2,450 MHz in in vivo porcine liver [21, 22]. However, it was plagued by higher power feedback leading to conductive heating of the antenna shaft which would cause elongation of the coagulation zone and possible skin burn. Consequently, protective cooling of the skin is routinely used during MWA. Charring along the needle shaft may decrease energy deposited in the direction perpendicular to the shaft and reduce the short-axis diameter of coagulation. To avoid overheating of the antenna shaft and enlarging the ablation zone, cooled-shaft coaxial-based interstitial antennae have become the design focus in recent years (Fig. 19.1). Inside the shaft lumen, there are dual channels through

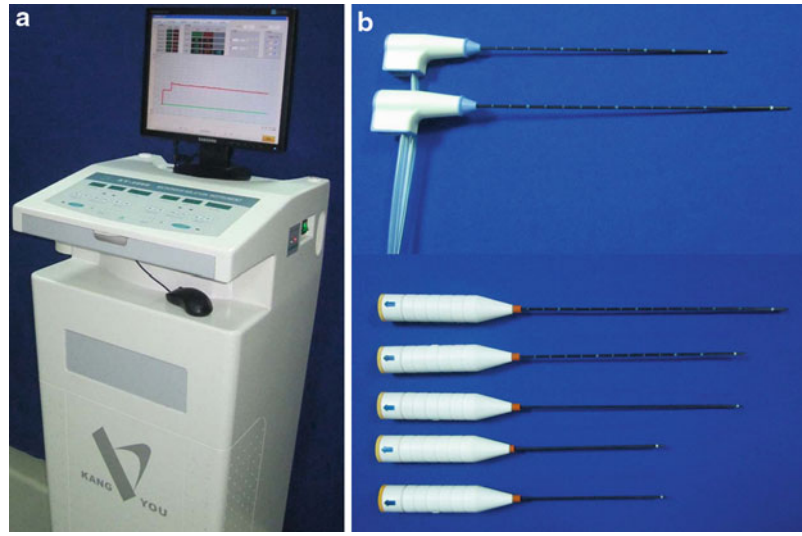

Fig. 19.1 Photographs of microwave applicator. (**a**) Intelligent microwave generator. (**b**) Prototype 15-gauge internally cooled MW antenna with different shaft length and active tip

which chilled saline is circulated by a peristaltic pump continuously cooling the shaft. As shaft temperature can be effectively kept low, higher power output and longer treatment duration are allowed which can deliver more energy into the tissue without causing skin burn. The cooled-shaft antenna could yield more spherical ablation zones than non-cooled-shaft antenna with the coagulation zone of (3.7–5.8) × (2.4–3.4) cm in diameter, which also operated at 2,450 MHz in in vivo porcine liver [9, 22–26]. With further improvement, 915-MHz microwave equipment has shown significant advantages in that it can penetrate more deeply than the commonly adopted 2,450-MHz microwave and may yield larger ablation zones with the size of (5.2–5.8) × (3.0–3.8) cm [9, 26]. Though MWA was mainly clinically used in eastern Asian countries, western countries have recently attached more importance to it and have begun to develop their own MWA systems [5, 17], several of which have been approved for surgical soft tissue coagulation by the U.S. Food and Drug Administration (FDA) but with a relative small literature reports. MedWaves 915-MHz system made from the USA is a non-cooled microwave equipment, which uses intelligent power and frequency control and integrated real-time process control (temperature, power, time) to optimize energy delivery and can produce large ablation zone with a single probe. MTX-180 cooled 915-MHz microwave system from BSD Medical of the USA uses synchronous energy set by the operator utilizing an interactive touch-screen monitor, which allows the operator to quickly and easily control the treatment. The BSD-2000 systems, though being actively prepared for FDA approval, have a broad clinical application perspective. They create a central focusing of energy that can be adjusted to target the three-dimensional shape, size, and location of the tumor and thus can provide dynamic control of the heating delivered to the tumor region. Two of 2,450-MHz microwave system, Acculis MTA System (Microsulis Medical Limited, Hampshire, United Kingdom) and Certus 140 System (NeuWave Medical, Madison WI, USA) with cooled applicators, can produce up to 4.0 × 4.5 cm coagulation zone in 6 min at 60 W based on ex vivo tests. And some other types of antennae such as loop-shaped antennae and triaxial antenna were also proposed but had not acquired wide use clinically [27, 28].

Clinical Procedure

Indications and Contraindications

Several criteria of the operative indications for MWA have been proposed, but they all eventually seem to rely on the policy and expertise of

each ablation team. The indications for MWA depend mainly on three factors: the hepatic functional reserve, the anatomic location, and size of the tumor. From the aspect of the hepatic functional reserve, criteria is defined as follows: (1) absence of ascites or the depth of ascites on ultrasound detection less than 4 cm, (2) a normal serum total bilirubin level or less than 3.5 mg/dl, and (3) a normal albumin level or not less than 30 g/L. From the aspect of the degree of extension of the tumor, the following criteria need to be met: (1) for radical treatment of primary liver cancer, a single lesion of 7 cm or smaller [29], three or fewer multiple hepatocellular carcinoma (HCC) lesions with a maximum diameter of 4 cm or less and absence of portal vein thrombosis or extrahepatic metastases; (2) for palliative treatment of primary liver cancer, the aim is to reduce the tumor burden and prolong the survival for later stage patients. Those with large or multiple lesions, suffering multiple metastasis and unsuitable for other modalities, can be considered to have MWA on the condition of significant hepatic reserve to tolerate the procedure.

Contraindications related to general conditions are advanced cirrhosis or proneness to severe bleeding including marked portal hypertension, esophageal varices at risk of bleeding, severe coagulation disorders, enhanced fibrinolysis, cardiac ischemia, and severe cardiac arrhythmias.

Technique

Similar to RFA, MWA can be performed percutaneously, laparoscopically, thoracoscopically, or at laparotomy [3–5, 30] as well. Whenever possible, MWA should be performed percutaneously to be less invasive at a lower cost and with the opportunity for repeatability. General anesthesia with mechanical ventilation is required for the laparoscopic or laparotomy approach. However, intravenous anesthesia combined with local anesthesia is usually sufficient for the percutaneous approach. Local anesthesia is induced first with 1 % lidocaine from the insertion point at the skin to the peritoneum along the puncture line before inserting the antennae. Then after nicking the skin with a small lancet, the antenna is introduced into the chosen area of the tumor. With a multiple needle procedure, local anesthesia along two or three prefixed puncture trajectories is done as previously described. Two or three active needle antennae directly connected to the MW generator are inserted into the tumor in parallel 1.0–2.5 cm apart. Needle access can be intercostal or subcostal. After placing all the antennae, venous anesthesia is induced with propofol and ketamine or midazolam and fentanyl depending whether an anesthesiologist is present or not. The insertion of the needle antennae in the tumor is performed under US, CT (computed tomography), or MRI (magnetic resonance imaging) guidance. Ultrasound is most commonly employed as it is convenient and allows real-time depiction of the entire treatment process. CT and MR guidance can be useful for the treatment of HCC invisible on ultrasound [31, 32]. New cooled-probe antennae without guide needle can be inserted directly.

At each insertion, the tip of the needle is placed in the deepest part of the tumor. Multiple thermal lesions are created along the needle antenna's major axis by simply withdrawing the needle from the preceding thermal lesion and reactivating the MW generator. When necessary, due to tumor size, to envelope the entire tumor with a safety margin, multiple overlapping ablations are usually needed. Size of the ablation zone can be roughly judged by the expanding hyperechoic area during ablation. For accurate assessment of the treatment efficacy, a thermal monitoring system attached to the MW generator can be used during MWA. One to three thermocouples are placed at different sites 5–10 mm outside the tumor. If the measured temperature does not Creach 60 °C by the end of treatment or does not remain at 54 °C for at least 3 min, treatment time is prolonged until the desired temperature is reached [33]. Overheating can also be avoided through thermal monitoring, thus decreasing the incidence of complications. In recent years, contrast-enhanced ultrasound (CEUS) has been employed for immediate assessment of treatment efficacy which is performed 10–15 min after MWA [34]. If residual tumor is found, additional ablations are performed.

Therapeutic Efficacy Assessment

Contrast-enhanced imaging is performed at 1 month after the last course of a defined ablation protocol. If irregular peripheral enhancement occurs, this represents residual unablated tumor often growing in a scattered, nodular, or eccentric pattern. This sign indicates incomplete local treatment and further ablation should be considered as soon as possible if the patient still meets the criteria for MWA. On the contrary, if complete ablation is achieved, then routine contrasted US, CT, or MRI and serum α-fetoprotein (AFP) are repeated at 1 month and 3 months after MWA and then at 6-month intervals. The increasing serum AFP level may warn of tumor recurrence. US is the preferred baseline examination method for the ablation zone in our institution. During follow-up, the treated HCCs slowly diminish in size, becoming undetectable by US or appearing only as small hyperechoic areas or isoechoic areas with a hypoechoic rim or simply as nonhomogeneous areas. On contrast-enhanced imaging the ablation zone presents even non-enhancement area.

Results

Compared with RFA, MWA is less frequently used and is one of the most recent and exciting advances in the field of thermoablative technology. Currently the overwhelming majority of reports concerning MWA of HCC are from Japan and China. As the microwave systems differ significantly between the institutions, the clinical results were different accordingly (Table 19.2).

Total Therapeutic Efficacy

Physicians in Asia using Microtaze system, FORSEA system, or KY-2000 system and in United Kingdom have reported their MWA experience mainly with 2.45-GHz systems, whereas in the USA, the bulk of the published experience involves 915-MHz models. Percutaneous MWA of HCC was first reported in 1994 by Seki et al. [2], which consisted of 18 patients with solitary small HCC (≤2 cm). Follow-up CT scans showed complete ablations in all the patients. According to the report of the 12th–15th nationwide follow-up survey of the Liver Cancer Study Group of Japan (including 791 institutions), the 1-, 2-, 3-, 4-, and 5-year survival rates of 1,751 patients treated by MWA were 94.2 %, 84.0 %, 72.9 %, 57.6 %, and 44.1 %, respectively. The complete ablation (CA) rate was 75.1 % [35]. Compared with the Japanese Microtaze microwave system, the Chinese microwave systems seem to yield larger ablation diameters [17, 23, 24]; thus, more patients can meet the inclusion criteria; studies conducted in China usually included a large patient number which may allow more reliable assessment of the therapeutic efficacy of MWA [3, 4, 21, 23]. The largest reported series of MWA for HCC in a single institution [4] comprised 288 patients with 477 tumors. The 1-, 2-, 3-, 4-, and 5-year cumulative survival rates were 93 %, 82 %, 72 %, 63 %, and 51 %, respectively. Local tumor progression (LTP) was observed in 8 % of the patients. Patients with single tumors measuring 4.0 cm or less and a Child A cirrhosis had higher probability of long-term survival. Using cooled-shaft microwave antenna, Kuang et al. [23] treated 90 patients with unresectable liver cancers, most of them (82 %, 74 patients) had HCC. The CA rates were 94 %, 91 %, and 92 % for small (≤3 cm), intermediate (3.1–5.0 cm), and large (5.1–8.0 cm) liver cancers. LTP occurred in seven (5 %) treated cancers. As this study is pretty new, no long-term survival rates are available. Zhang et al. [36] demonstrated that 8 (9.3 %) patients had local tumor recurrence among 86 liver cancer patients treated by cool-tip microwave antenna ablation. Jiao D et al. [25] evaluated effects of MWA with a 2,450-MHz internally cooled-shaft antenna in treating 60 HCC lesions with the size 1–8 cm. During a mean follow-up period of 17.17 ± 6.52 months, CA rates in small (≤3.0 cm), intermediate (3.1–5.0 cm), and large (5.1–8.0 cm) liver cancers were 97.06 %, 93.34 %, and 81.82 %, respectively. LTP occurred in four (6.67 %) treated cancers. A 2,450-MHz microwave ablation can achieve effective local tumor control based on previous reports.

Table 19.2 MWA of liver cancer studies reported since 1998 including at least 40 patients

Study	Patient number	Mean tumor size (cm)	Antenna type	Frequency (MHz)	Power (W)	CA (%)	LTP (%)	Survival (%)				
								1-year	2-year	3-year	4-year	5-year
Ikai et al. [35]	1,751					75.1		94.2	84	72.9	57.6	44.1
Kuang et al. [23]	90	2.7 ± 1.5	Cooled-shaft	2,450	70–80	93.2	5					
Dong et al. [21]	41	4.3 ± 1.2	Non-cooled-shaft	2,450	60	84.2		97.6	92.7			
Lu et al. [3]	50	2.7 ± 1.5	Non-cooled-shaft	2,450	60	94.9	11.8	81.6	61.2	50.5	36.8	
Liang et al. [4]	288	3.75 ± 1.58	Non-cooled-shaft	2,450	60		8	93	82	72	63	51
Zhang et al. [36]	160	5.3	Cooled-shaft	2,450	50–0	100	6.3	91.8				
Jiao et al. [25]	60	3.2 ± 0.17	Cooled-shaft	2,450	70–5	92.71	5.21	100	95			
Iannitti et al. [37]	87	3.6	Non-cooled and cooled-shaft	915	45	91.9	2.7	70.1(19 months)				
Martin et al. [5]	100	3.0	Non-cooled-shaft cooled-shaft	915		98	5	Median overall survival 41 months				

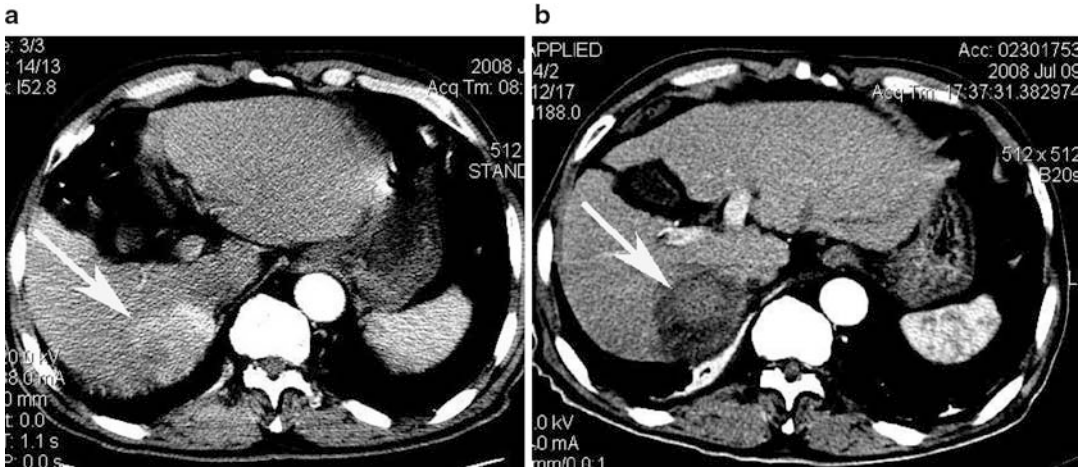

Fig. 19.2 915-MHz microwave ablation in a 66-year-old man with a large HCC in the right hepatic lobe. (**a**) Contrast-enhanced CT before MWA shows a 5.8 × 5.2 cm arterially enhancing tumor (*arrow*) (**b**) contrast-enhanced CT showed no enhancement of the ablation zone at 24 months after treatment (*arrow*)

According to the published experience involving 915-MHz MWA, Iannitti et al. [37] reported the outcomes from the first clinical trial in the United States using MWA and a 915-MHz generator (VivaWave™ System). Eighty-seven patients with 224 hepatic tumors (mean 3.6 cm) were performed MWA by open (45 %), laparoscopic (7 %), and percutaneous (48 %) approaches. Local recurrence occurred in 6 (2.7 %) tumors, and the overall mortality rate was 2.3 %. 41 (47 %) patients were alive with no evidence of disease with a mean follow-up of 19 months. Martin et al. [5] performed a long-term investigation for MWA of hepatic malignancies by using an improved 915-MHz platform based on the VivaWave technology (Evident™ system). One hundred patients underwent combination resection and MWA or ablation alone with median tumor size 3.0 (range, 0.6–6.0) cm. After a median follow-up of 36 months, 5 patients (5 %) had incomplete ablation, 2 (2 %) had local recurrence, and median overall survival was 41 months for HCC patients (Fig. 19.2).

MWA for Tumors in Dangerous Sites

Hepatic tumors in dangerous site refer to the tumors adjacent to important organs and tissues including diaphragm, gastrointestinal tract, hilum, and major bile duct or vessels. Because the thermal energy may spread into surrounding structures, the major concern for MWA of such tumors lies in the increasing opportunity of thermal injury for these important structures. However, combined with artificial ascites, artificial pleural effusion, intermittent emission of microwave antenna, and temperature monitoring assisted with combination low-dose ethanol infusion techniques, it becomes feasible for MWA of dangerous site tumors without sacrificing the therapeutic efficacy (Figs. 19.3 and 19.4). Zhou et al. [38] reported MWA of 53 tumors adjacent to the gastrointestinal tract, with a reported high complete ablation rate (88.7 %) without immediate or delayed complications. Complete ablation of tumors surrounding major hepatic vessels (without vascular occlusion) using microwave radiation through a triple antenna has been reported [39]. In addition, to facilitate the use of MWA for liver tumors in the hepatic dome, MWA in combination with the artificial hydrothorax, intraperitoneal saline infusion, and a thoracoscopic method has achieved successful treatment with the complete ablation rate more than 92 % with a quite low recurrence rate [40–42]. However, there are no literature reports

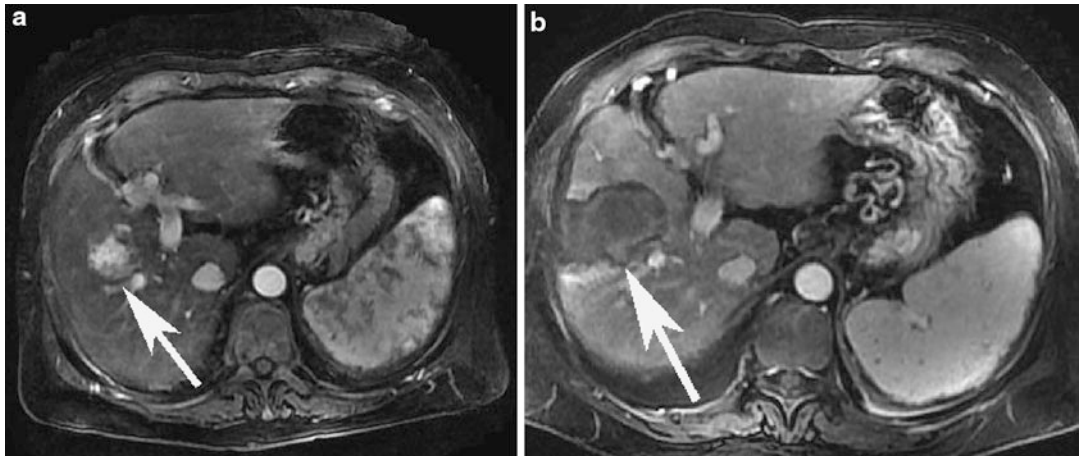

Fig. 19.3 MWA in a 60-year-old woman with HCC adjacent to the hepatic hilum. (**a**) Contrast-enhanced MRI before MWA shows a 3.6 × 3.5 cm arterially enhancing tumor (*arrow*). (**b**) Contrast-enhanced MRI shows no enhancement of the ablation zone at 18 months after treatment (*arrow*)

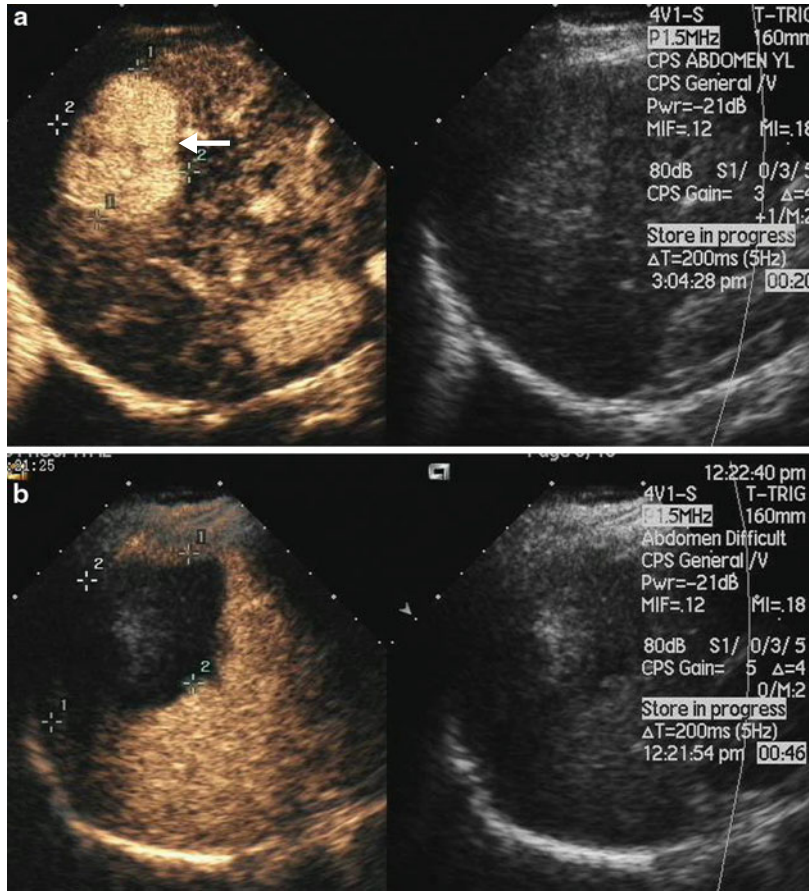

Fig. 19.4 Microwave ablation in a 75-year-old man with HCC adjacent to diaphragm. (**a**) Contrast-enhanced US before MWA shows 4.7 × 4.3 cm arterially enhancing tumor (*arrow*). (**b**) Contrast-enhanced US shows no enhancement of the ablation zone at 12 months after treatment (*arrow*)

for MWA of tumors adjacent to the hepatic hilum. Therefore, a further multicenter study of MWA for dangerous site hepatic tumors with a larger number of patients and a prolonged observation time is required.

Comparative Study with Other Modalities

Only one randomized controlled trial (RCT) compared the effectiveness of MWA with that of RFA [43]. Seventy-two patients with 94 HCC nodules were randomly assigned to RFA and MWA groups. No statistically significant differences were observed with respect to the efficacy of the two procedures. Lu et al. [44] had retrospectively analyzed the comparisons of MWA and RFA for 102 patients, and the local tumor control, complications related to treatment, and long-term results showed equivalent results for the two modalities. Ohmoto et al. [45] performed another retrospective study between MWA and RFA for less than 2 cm HCC. Results showed that significantly fewer treatment sessions, a lower local recurrence rate, and a higher cumulative survival rate were achieved in RFA group. The different results from the studies may be related to the different generator used, and in the report of Ohmoto et al., cool-tip radiofrequency electrode was compared with the first microwave needle antenna (Microtaze system), which produced relatively smaller ablation areas compared with the new cooled-probe antenna.

One retrospective study [46] showed that 1-, 3-, and 5-year disease-free survival rates of patients with single HCC of diameter <5 cm showed no significant difference between MWA group and resection group. The result of multivariate analysis showed that differentiation degree of HCC and the expressions of VEGF (vascular endothelial growth factor) and c-Met in HCC tissues could be used as the independent prognostic factors affecting metastasis and recurrence in patients with small HCC, whereas the methods of therapy had no impact on prognosis.

Another study compared microwave ablation and percutaneous ethanol injection (PEI) in a retrospective evaluation of 90 patients with small HCC [47]. The overall 5-year survival rates for patients with well-differentiated HCC treated with microwave ablation and PEI were not significantly different. However, among the patients with moderately or poorly differentiated HCC, overall survival with microwave ablation was significantly better than with PEI.

Although MWA therapies have gained fairly wide acceptance as an effective treatment for small HCC, there have been only a few clinical studies comparing the response to microwave ablation therapy with other modalities including RFA, PEI, and surgery. The lack of adequate comparative ablation studies for HCC between MW and other recently developed thermal ablation techniques, such as laser-induced interstitial thermotherapy (LITT) and cryoablation, means more research is required to perform a rigorous assessment of MWA's future as a treatment modality for hepatic malignancies.

Complications and Side Effects

Besides local tumor progression (Fig. 19.5a), MWA and RFA share similar low complication rates. Major complications include bile duct stenosis, uncontrollable bleeding, liver abscess, colon perforation, skin burn, and tumor seeding [23, 48–50]. Postoperative death due to liver failure is reported to be 0–0.18 % for percutaneous and endoscopic MWA [49, 51]. Data summarized in Table 19.3 showed the detailed major complication rate as follows: intraperitoneal uncontrollable bleeding (0–0.92 %), bile duct injury requiring drainage (0–2.78 %), colon perforation (0–1.11 %), liver abscess (0–2.78 %), skin burn (0–3.45 %), and antenna track tumor seeding (0–0.44 %). Prophylactic strategies are useful for decreasing the complication rate. As mentioned above, thermal monitoring can prevent collateral damage to adjacent organs such as bile duct and bowel. To minimize tumor and needle tract seeding (Fig. 19.5b), the needle track should be routinely and adequately coagulated when withdrawing the antennae. Skin burns can be prevented by using newly cooled-shaft

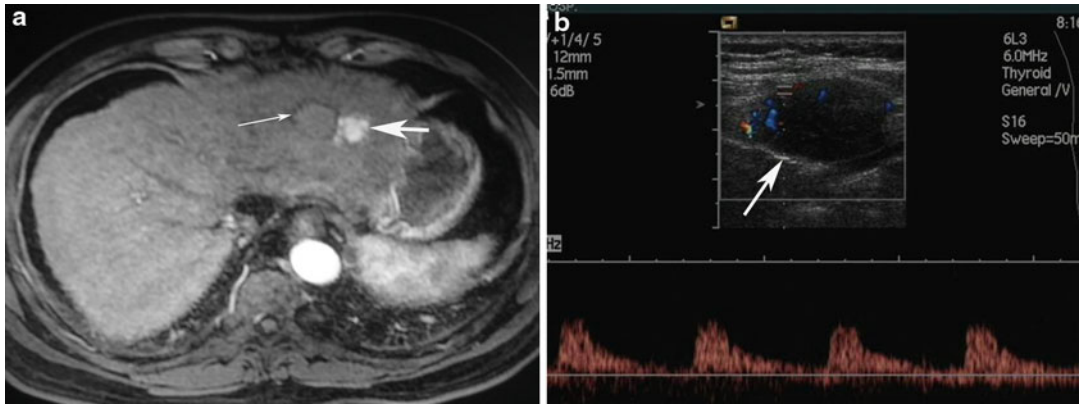

Fig. 19.5 Suboptimal clinical outcomes and complications of MWA for HCC. (**a**) Nodular hyperattenuation consistent with recurrence (*thick arrow*) was detected by contrast-enhanced MRI in the peripheral ablation zone (*thin arrow*) 6 months after MWA for left lobe HCC which was treated by another MWA. (**b**) Tumor seeding in a 44-year-old man with HCC in the abdominal wall. Conventional US scan obtained 18 months after MWA for right hepatic lobe tumor adjacent to the diaphragm shows a hypoechoic 2.4 × 1.9 cm lesion with arterial vascularization (*arrow*), which was treated by resection. Pathology confirmed hepatocellular carcinoma felt to be seeding along the antenna tract

Table 19.3 Procedure-related complications for MWA of hepatic malignancies

Study	Intraperitoneal bleeding (%)	Bile duct injury (%)	Colon perforation (%)	Liver abscess (%)	Skin burn (%)	Tumor seeding (%)	Symptomatic pleural effusion (%)	Perioperative mortality (%)
Kuang et al. [23]	0	0	1.11	1.11	0	0	2.22	0
Dong et al. [50]	0	0	0	0	0.85	0	0	0
Liang et al. [49]	0.09	0.18	0.18	0.44	0.26	0.44	1.06	0.18
Zhang et al. [36]	0	1.25	0	0	0	0	0.63	0
Iannitti et al. [37]	0	0	0	0	3.45	0	0	0
Martin et al. [5]	0	0	0	2	0	0	0	0
Yin et al. [29]	0.92	0.92	0	0	0.92	0	3.67	0
Sakaguchi et al. [51]	0.51	0.26	0	0.26	0.77	0	1.28	0
Shibata et al. [43]	0	2.78	0	2.78	2.78	0	0	0

antennae [23] and making sure the antennae shaft are deep enough and appropriately spaced as skin burns can still occur in these instances. Careful patient selection, choice of the most appropriate imaging modality, and the best approach may also help prevent complications.

Side effects of MWA include pain, postablation syndrome, and asymptomatic pleural effusions

which are usually self-limiting and require no treatment. Low-grade fever and general malaise are common manifestations of postablation syndrome. The duration of postablation syndrome depends on the volume of necrosis induced by MWA and the overall condition of the patient. Patients with large tumors or poor hepatic reserve are likely to be symptomatic for longer periods of time.

Conclusions

MWA of HCC has shown great potential in its relatively short clinical existence by producing an ideal ablation in shorter treatment times with a low complication rate. The survival benefit of HCC patients undergoing resection or ablation treatment is directly dependent on tumor size, which reflects the need of radical tumor ablation including a safety margin. So it is clear that commercially available generators and antenna design will continue to evolve to increase the speed and volume of coagulation necrosis. This combined with the development of improved image guidance methods, such as computer-aided navigation systems and intraprocedure CEUS for precise tumor targeting and deployment of the antennae, helps make microwave techniques safer and their clinical applications better understood. Long-term survival data and large-scale prospective RCTs comparing MWA with other modalities, especially with RFA for ultimately determining its effectiveness, are earnestly anticipated.

Cross-References

- ▶ Designing Interventional Environments in the Treatment of Cancer
- ▶ Devices and Equipment in Interventional Oncology and Their Operation
- ▶ Imaging of Interventional Therapies in Oncology: Ultrasound
- ▶ Microwave Ablation for Cancer: Physics, Performance, Innovation, and the Future

References

1. Tabuse K, Katsumi M, Kobayashi Y, et al. Microwave surgery: hepatectomy using a microwave tissue coagulator. World J Surg. 1985;9:136–43.
2. Seki T, Wakabayashi M, Nakagawa T, et al. Ultrasonically guided percutaneous microwave coagulation therapy for small hepatocellular carcinoma. Cancer. 1994;74:817–25.
3. Lu MD, Chen JW, Xie XY, et al. Hepatocellular carcinoma: US-guided percutaneous microwave coagulation therapy. Radiology. 2001;221:167–72.
4. Liang P, Dong B, Yu X, et al. Prognostic factors for survival in patients with hepatocellular carcinoma after percutaneous microwave ablation. Radiology. 2005;235:299–307.
5. Martin RC, Scoggins CR, McMasters KM. Safety and efficacy of microwave ablation of hepatic tumors: a prospective review of a 5-year experience. Ann Surg Oncol. 2010;17(1):171–8.
6. English NJ, MacElroy JM. Molecular dynamics simulations of microwave heating of water. J Chem Phys. 2003;118:1589–92.
7. Diederich CJ. Thermal ablation and high-temperature thermal therapy: overview of technology and clinical implementation. Int J Hyperthermia. 2005;21:745–53.
8. Goldberg SN, Gazelle GS, Mueller PR. Thermal ablation therapy for focal malignancies: a unified approach to underlying principles, techniques, and diagnostic imaging guidance. AJR Am J Roentgenol. 2000; 174:323–31.
9. Yu J, Liang P, Yu X, Liu F, Chen L, Wang Y, et al. A comparison of microwave ablation and bipolar radiofrequency ablation both with an internally cooled probe: results in ex vivo and in vivo porcine livers. Eur J Radiol. 2011;79:124–30.
10. Haines DE, Watson DD. Tissue heating during radiofrequency catheter ablation: a thermodynamic model and observations in isolated perfused and superfused canine right ventricular free wall. Pacing Clin Electrophysiol. 1989;12:962–76.
11. Organ LW. Electrophysiologic principles of radiofrequency lesion marking. Appl Neurophysiol. 1976;39:69–76.
12. Skinner MG, Iizuka MN, Kolios MC, Sherar MD. A theoretical comparison of energy sources–-microwave, ultrasound and laser–for interstitial thermal therapy. Phys Med Biol. 1998;43:3535–47.
13. Wright AS, Sampson LA, Warner TF, Mahvi DM, Lee Jr FT. Radiofrequency versus microwave ablation in a hepatic porcine model. Radiology. 2005;236:132–9.
14. Garrean S, Hering J, Saied A, Hoopes PJ, Helton WS, Ryan TP, Espat NJ. Ultrasound monitoring of a novel microwave ablation (MWA) device in porcine liver: lessons learned and phenomena observed on ablative effects near major intrahepatic vessels. J Gastrointest Surg. 2009;13(2):334–40.

15. Yu NC, Raman SS, Kim YJ, Lassman C, Chang X, Lu DS. Microwave liver ablation: influence of hepatic vein size on heat-sink effect in a porcine model. J Vasc Interv Radiol. 2008;19(7):1087–92.
16. Solbiati L, Ierace T, Goldberg SN, Sironi S, Livraghi T, Fiocca R, Servadio G, Rizzatto G, Mueller PR, Del Maschio A, Gazelle GS. Percutaneous US-guided radio-frequency tissue ablation of liver metastases: treatment and follow-up in 16 patients. Radiology. 1997;202(1):195–203.
17. Wright AS, Lee Jr FT, Mahvi DM. Hepatic microwave ablation with multiple antennae results in synergistically larger zones of coagulation necrosis. Ann Surg Oncol. 2003;10:275–83.
18. Ikeda K, Seki T, Umehara H, Inokuchi R, Tamai T, Sakaida N, Uemura Y, Kamiyama Y, Okazaki K. Clinicopathologic study of small hepatocellular carcinoma with microscopic satellite nodules to determine the extent of tumor ablation by local therapy. Int J Oncol. 2007;31(3):485–91.
19. Bertram JM, Yang D, Converse MC, Webster JG, Mahvi D. A review of coaxial-based interstitial antennas for hepatic microwave ablation. Crit Rev Biomed Eng. 2006;34:187–213.
20. Longo I, Gentili GB, Cerretelli M, Tosoratti N. A coaxial antenna with miniaturized choke for minimally invasive interstitial heating. IEEE Trans Biomed Eng. 2003;50:82–8.
21. Dong BW, Liang P, Yu XL, Zeng XQ, Wang PJ, Su L, Wang XD, Xin H, Li S. Sonographically guided microwave coagualtion treatment of liver cancer: an experimental and clinical study. AJR Am J Roentgenol. 1998;171:449–54.
22. He N, Wang W, Ji Z, Li C, Huang B. Microwave ablation: an experimental comparative study on internally cooled antenna versus non-internally cooled antenna in liver models. Acad Radiol. 2010; 17(7):894–9.
23. Kuang M, Lu MD, Xie XY, et al. Liver cancer: increased microwave delivery to ablation zone with cooled-shaft antenna – experimental and clinical studies. Radiology. 2007;242:914–24.
24. Wang Y, Sun Y, Feng L, Gao Y, Ni X, Liang P. Internally cooled antenna for microwave ablation: results in ex vivo and in vivo porcine livers. Eur J Radiol. 2008;67(2):357–61.
25. Jiao D, Qian L, Zhang Y, et al. Microwave ablation treatment of liver cancer with 2,450-MHz cooled-shaft antenna: an experimental and clinical study. J Cancer Res Clin Oncol. 2010;136:1507–16.
26. Sun Y, Wang Y, Ni X, et al. Comparison of ablation zone between 915- and 2,450-MHz cooled-shaft microwave antenna: results in in vivo porcine livers. AJR Am J Roentgenol. 2009;192(2):511–14.
27. Shock SA, Meredith K, Warner TF, Sampson LA, et al. Microwave ablation with loop antenna: in vivo porcine liver model. Radiology. 2004;231:143–9.
28. Brace CL, Laeseke PF, Sampson LA, Frey TM, van der Weide DW, Lee Jr FT. Microwave ablation with a single small-gauge triaxial antenna: in vivo porcine liver model. Radiology. 2007;242:435–40.
29. Yin XY, Xie XY, Lu MD, et al. Percutaneous thermal ablation of medium and large hepatocellular carcinoma: long-term outcome and prognostic factors. Cancer. 2009;115(9):1914–23.
30. Aramaki M, Kawano K, Ohno T, et al. Microwave coagulation therapy for unresectable hepatocellular carcinoma. Hepatogastroenterology. 2004;51: 1784–7.
31. Sato M, Watanabe Y, Tokui K, Kawachi K, Sugata S, Ikezoe J. CT-guided treatment of ultrasonically invisible hepatocellular carcinoma. AJR Am J Roentgenol. 2000;95:2102–6.
32. Kurumi Y, Tani T, Naka S, et al. MR-guided microwave ablation for malignancies. Int J Clin Oncol. 2007;12:85–93.
33. Godlewski G, Rouy S, Pignodel C, Ould-Said H, Eledjam JJ, Bourgeois JM, Sambuc P. Deep localized neodymium (Nd)-YAG laser photocoagulation in liver using a new water cooled and echoguided handpiece. Lasers Surg Med. 1998;8(5):501–9.
34. Lu MD, Yu XL, Li AH, et al. Comparison of contrast enhanced ultrasound and contrast enhanced CT or MRI in monitoring percutaneous thermal ablation procedure in patients with hepatocellular carcinoma: a multi-center study in China. Ultrasound Med Biol. 2007;33(11):1736–49.
35. Ikai I, Itai Y, Okita K, et al. Report of the 15th follow-up survey of primary liver cancer. Hepatol Res. 2004;28:21–9.
36. Zhang X, Chen B, Hu S, et al. Microwave ablation with cooled-tip electrode for liver cancer: an analysis of 160 cases. Hepatogastroenterology. 2008;55(88): 2184–7.
37. Iannitti DA, Martin RC, Simon CJ, et al. Hepatic tumor ablation with clustered microwave antennae: the US Phase II Trial. HPB (Oxford). 2007; 9(2):120–4.
38. Zhou P, Liang P, Yu X, Wang Y, Dong B. Percutaneous microwave ablation of liver cancer adjacent to the gastrointestinal tract. J Gastrointest Surg. 2009;13(2): 318–24.
39. Simon CJ, Dupuy DE, Iannitti DA, et al. Intraoperative triple antenna hepatic microwave ablation. AJR Am J Roentgenol. 2006;187:W333–40.
40. Shiomi H, Naka S, Sato K, et al. Thoracoscopy-assisted magnetic resonance guided microwave coagulation therapy for hepatic tumors. Am J Surg. 2008;195(6):854–60.
41. Shimada S, Hirota M, Beppu T, et al. A new procedure of percutaneous microwave coagulation therapy under artificial hydrothorax for patients with liver tumors in the hepatic dome. Surg Today. 2001;31(1):40–4.
42. Ohmoto K, Tsuzuki M, Yamamoto S. Percutaneous microwave coagulation therapy with intraperitoneal saline infusion for hepatocellular carcinoma in the hepatic dome. AJR Am J Roentgenol. 1999; 172(1):65–6.

43. Shibata T, Iimuro Y, Yamamoto Y, Maetani Y, Ametani F, Itoh K, Konishi J. Small hepatocellular carcinoma: comparison of radio-frequency ablation and percutaneous microwave coagulation therapy. Radiology. 2002;223:331–7.
44. Lu MD, Xu HX, Xie XY, et al. Percutaneous microwave and radiofrequency ablation for hepatocellular carcinoma: a retrospective comparative study. J Gastroenterol. 2005;40:1054–60.
45. Ohmoto K, Yoshioka N, Tomiyama Y, et al. Comparison of therapeutic effects between radiofrequency ablation and percutaneous microwave coagulation therapy for small hepatocellular carcinomas. J Gastroenterol Hepatol. 2009;24(2):223–7.
46. Wang ZL, Liang P, Dong BW, Yu XL, Yu DJ. Prognostic factors and recurrence of small hepatocellular carcinoma after hepatic resection or microwave ablation: a retrospective study. J Gastrointest Surg. 2008;12(2):327–37.
47. Seki T, Wakabayashi M, Nakagawa T, et al. Percutaneous microwave coagulation therapy for patients with small hepatocellular carcinoma: comparison with percutaneous ethanol injection therapy. Cancer. 1999;85:1694–702.
48. Shimada S, Hirota M, Beppu T, Matsuda T, Hayashi N. Complications and management of microwave coagulation therapy for primary and metastatic liver tumors. Surg Today. 1998;28:1130–7.
49. Liang P, Wang Y, Yu X, Dong B. Malignant Liver Tumors: treatment with percutaneous microwave ablation–complications among cohort of 1136 patients. Radiology. 2009;251(3):933–40.
50. Dong B, Liang P, Yu X, et al. Percutaneous sonographically guided microwave coagulation therapy for hepatocellular carcinoma: results in 234 patients. AJR Am J Roentgenol. 2003;180(6):1547–55.
51. Sakaguchi H, Seki S, Tsuji K, et al. Endoscopic thermal ablation therapies for hepatocellular carcinoma: a multi-center study. Hepatol Res. 2009;39(1):47–52.

Percutaneous Ethanol Injection in the Treatment of Primary Liver Cancers

20

Ming Kuang and Ming-De Lu

Abstract

Percutaneous local ablation therapy is the best treatment option for patients with early-stage hepatocellular carcinoma (HCC) who are not suitable for resection or transplantation. Percutaneous ethanol injection (PEI) is the first mainstream modality of ablation and used to be a standard alternative therapy for unresectable small HCCs since the 1980s. To achieve complete devitalization of the tumor, conventional PEI using a fine needle usually needs multiple treatment sessions dependent on the tumor size, typically 4–12 sessions at twice-weekly interval. Conventional PEI offers satisfactory local efficacy and long-term survival in treating tumors smaller than 3 cm, but unsatisfactory complete response of tumors larger than 3 cm, mainly because of the influence of intratumoral septa. There have been major efforts to develop new methods for solving this problem. Single-session high-dose PEI using a single needle, simultaneous multiple needles, and a multi-pronged needle was subsequently applied. The latest multi-pronged PEI injection devices achieve better local efficacy than conventional PEI and are able to treat early-stage or recurrent HCC up to 5 cm effectively and safely, even for lesions at high-risk locations. Combined use of PEI with radio-frequency ablation may potentially improve the local efficacy of both techniques. Compared with radio-frequency ablation, PEI has the advantages of minor side effects, simplicity, and low cost. Local efficacy of PEI has been improved by innovative technique. Therefore, PEI will continue to play a role in the treatment of HCC.

M. Kuang (✉)
Department of Hepatobiliary Surgery and Division of Interventional Ultrasound, The First Affiliated Hospital of Sun Yat-sen University, Guangzhou, China
e-mail: kuangminda@hotmail.com

M.-D. Lu
Institute of Diagnostic and Interventional Ultrasound, The First Affiliated Hospital of Sun Yat-sen University, Guangzhou, China
e-mail: lumd@live.com

Introduction

Hepatocellular carcinoma (HCC) is one of the most common cancers worldwide and its incidence in developed countries is rising [1–3]. Early diagnosis of HCC is possible in countries where ultrasound (US) screening is performed for populations at risk, while advanced stage of HCC

D.E. Dupuy et al. (eds.), *Image-Guided Cancer Therapy*, DOI 10.1007/978-1-4419-0751-6_22,

with clinical manifestations is usually found at the first diagnosis in other countries. Only patients at early stage of HCC (one nodule $\leq$5.0 cm in diameter or three nodules $\leq$3.0 cm in diameter each) benefit from curative therapies such as hepatic resection, liver transplantation, or local ablation [4–6]. Resection remains the first choice in treatment of HCC [7, 8], but only a minority of patients are suitable for resection at their first diagnosis because of inoperable factors such as tumor progression, inadequate liver function reserve, concomitance of other diseases, patient refusal, and high surgical risk. Liver transplantation is best indicated in small HCC associated with severe cirrhosis and offers a satisfactory long-term survival outcome [9, 10], but the high cost and donor shortage limit its wide use.

Percutaneous local ablation therapy is the best treatment option for patients with early-stage HCC who are not suitable for resection or transplantation. Besides, about half of patients develop tumor recurrence within 2 years after resection, and the incidence rises to 70–85 % within 5 years [11–13]. Although repeated hepatectomy is the most effective treatment for recurrent HCC, impaired liver function and/or the presence of multicentric tumors limits its use in more than 80 % of recurrent cases [14]. Percutaneous ablation is particularly suitable for treating recurrent HCC because postsurgical recurrence can be detected at an early stage while the nodules are still small and, therefore, amenable to percutaneous ablation [15]. Local ablation achieves destruction of tumor tissue by intratumoral injection of chemical agent such as ethanol, acetic acid, and boiling saline or modification of local temperature with radio frequency (RF), microwave, laser, cryotherapy, etc.

Conventional PEI

In the mid-1980s, two groups of Japanese and Italian doctors independently developed percutaneous ethanol injection (PEI) for treatment of HCC [16, 17]. These initial results showed that injection of absolute ethanol directly into the tumor through a fine-gauge needle under US guidance was able to induce chemical necrosis of small, nodular HCC lesions. PEI is the first mainstream modality of ablation and used to be a standard alternative therapy for unresectable small tumors.

The basic principles of PEI have been described in detail. Alcohol acts by diffusion within the cells, which causes immediate dehydration of cytoplasmic proteins. There is also consequent coagulation necrosis followed by fibrosis, resulting from infiltration of the local vessels, which induces necrosis of endothelial cells and platelet aggregation with consequent thrombosis of small vessels followed by ischemia of the neoplastic tissue.

Two characteristics of HCC favor the toxic action of ethanol: hypervascularization and the different consistency of neoplastic and cirrhotic tissue. Since the neoplastic tissue of HCC is softer than the surrounding cirrhotic tissue, ethanol diffuses within it easily and selectively, whereas at the same time hypervascularization facilitates its uniform distribution within the rich network of neoplastic vessels [18].

Conventional PEI is usually performed under US guidance and local anesthesia. Sterile 95–99.5 % ethanol is slowly injected into the tumor with a 20–22-gauge thin-walled needle (Fig. 20.1) or a 21-gauge needle with a closed conical tip and three terminal side holes [18, 19]. The dose of ethanol injected depends on the size and number of the lesions, usually using 2 ml of ethanol for treating 1 cm of tumor per session. The ethanol usually diffuses for a radius of 2–3 cm around the needle tip toward the periphery of the tumor, which is visible as a cloud of hyperechogenicity. The injection is stopped if there is a significant leakage of ethanol outside the lesion or when diffusion is not clearly visible and the injection can be continued after a few minutes. Since alcohol reflux can cause pain, the needle is left within the tumor for 10–60 s after the injection, particularly in the case of superficial tumors, and then slowly removed. Each session generally requires 10–20 min, and the patient remains in the waiting room for 1–2 h. Ethanol injection was usually repeated twice a week for up to six sessions for treatment of

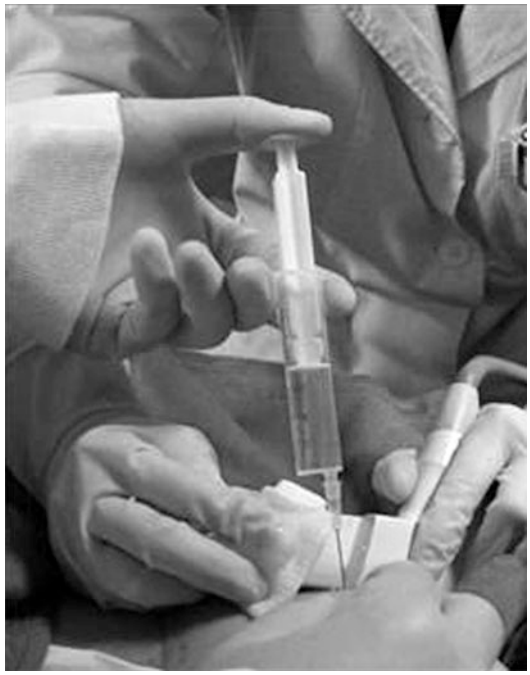

Fig. 20.1 Conventional PEI using a 21-gauge fine injection needle and 99.5 % of ethanol

HCC lesions ≤3 cm in diameter and 6–12 sessions for larger tumors [17–19].

The efficacy of PEI is well documented by numerous reports. PEI achieves necrosis rate of 90–100 % of HCC smaller than 2 cm, 70–80 % in tumors between 2 and 3 cm, but only 50 % in those between 3 and 5 cm [20–23]. Although multiple sessions with repeated injections are performed to achieve the complete eradication of the target tumor, local tumor progression (LTP) rate ranges from 10 % to 33 % in tumors smaller than 3 cm and reaches up to 44–50 % in those larger than 3 cm [19, 24, 25]. The poorer local efficacy of PEI in treating larger tumors is probably attributed to incomplete ethanol infiltration inside the whole tumor tissue that results from the incapability of disrupting the intratumoral septa and/or inadequate placement of the needle [5, 22].

An overall 5-year survival rate of PEI in large series could reach 41–48 %, for tumors meeting Milan criteria [21, 26]. The 5-year survival rate is significantly greater in patients with tumors smaller than 3 cm as compared with those between 3 and 5 cm, being 40–54 % vs. 32–37 % (Table 20.1) [21, 26]. In a series involving 4,037 patients treated by PEI, Japanese authors reported a 5-year survival rate of 54 % for 767 patients with solitary HCC ≤ 2 cm, as compared with 39 % for 587 with those between 2 and 5 cm [27]. Recently, one study analyzed 270 patients with tumor less than 3 cm treated by PEI based on 20-year observation and showed an overall 5-year survival rate of 60 %. The 5-year survival even reaches as high as 78 % among the patients with Child-Pugh grade A and solitary HCC ≤ 2 cm [19]. This evidence indicates that conventional PEI is highly effective and offers a good long-term survival in treating tumors smaller than 3 cm, especially less than 2 cm. This compares well with the outcome of resection in those candidates who do not fit the optimal surgical profile [27]. Therefore, PEI has been used as the first-line treatment option for small HCC in some Asian centers [19].

Technique Improvement

The local effectiveness of conventional PEI for treatment of HCC > 3 cm is less satisfactory owing to limited spread of ethanol. There have been major efforts to develop new methods for solving this problem. To disrupt septa and facilitate ethanol infiltration, some authors have proposed that PEI should be combined with arterial embolization in large HCC [28]. Complete response rate is enhanced, but development of viable intratumoral nests or distant recurrence is common during follow-up and the long-term outcome is not different from PEI alone.

Large-Volume Ethanol Injection

In an Italian study, a large volume of ethanol was injected within a single session under general anesthesia for treatment of HCC > 5 cm [29]. A total of 108 patients were treated, and the amount of alcohol administered per patient ranged from 20 to 165 mL (mean, 62 mL). The total volume of ethanol was smaller than that of

Table 20.1 Long-term outcomes of PEI for small hepatocellular carcinoma

Study (year)	Patients (n)	Tumor number/size	Overall survival rates (%)		References
			3 years	5 years	
Livraghi (1995)	628 (total)	Milan criteria[a]	NA	48	[21]
	246 (total)	Single/≤3 cm	68	40[b]	
	224 (total)	Single/3–5 cm	57	37	
Lencioni (1997)	184 (total)	Milan criteria[a]	67	41	[26]
	94 (total)	Single/≤3 cm	78	54[b]	
	50 (total)	Single/3–5 cm	61	32	
Arii (2000)	767 (clinical stage I)	Single/≤2 cm	81	54	[27]
	587 (clinical stage I)	Single/2–5 cm	NA	39	
Pompili (2001)	111	≤2/<5 cm	62	41	[25]
Ebara (2005)	270 (total)	≤3/≤3 cm	82	60	[19]
	96 (Child-Pugh grade A)	Single/≤2 cm	87	78	

[a]Single tumor, diameter <5 cm or ≤3 nodules, each ≤3 cm
[b]$p < 0.05$ when compared with patients with single tumor of 3–5 cm
Source: Reprinted from Kuang M, Lu, M-D, Xie X- Y, et al. *Radiology* 2009; 253:552–561, with permission from the Radiological Society of North America (RSNA®)

the tumor. The number of injections ranged from 8 to 22 (mean, 13 injections). Time required for the procedure was 20–50 min (mean, 30 min). Complete necrosis of tumor was achieved in 58 % of patients. The 4-year survival rate was 44 % in patients with encapsulated HCC and 18 % in those with infiltrating tumors.

Multiple-needle insertion method was used in some studies [30–32]. Higher-dose ethanol was injected into various parts of the tumor by inserting 2–3 fine needles in HCC > 3 cm to enable the ethanol to distribute throughout the lesion rapidly. Higher-dose PEI achieved complete necrosis of 72 % in tumors <4 cm and the LTP rate was 24 % [31]. It seems that PEI with high-dose ethanol via simultaneous multiple needle injection may improve the effectiveness and require fewer sessions.

Recently, a retractable multi-pronged injection needle (Fig. 20.2) known as Quadra-Fuse has been developed [33]. The device is an 18-gauge puncture needle with three retractable prongs to be deployed up to 5 cm of area, and each prong has four terminal side holes for agent perfusion which enables even distribution of ethanol inside the target tumor. By using this Quadra-Fuse multi-pronged needle, some authors treated 12 HCCs sized from 3.5 to 9 cm with PEI and achieved a complete response of 67 % at an average of 2.3 treatment sessions [34].

In a study, 141 patients with 164 primary or recurrent HCC ranged 1.3–5.0 cm (mean, 2.9 cm ± 0.9) were treated by multi-pronged PEI with a high-dose strategy [35]. Fifty-nine percent of tumors were located at unfavorable sites (Figs. 20.3 and 20.4). After position of the needle in tumor, the three tines were deployed initially at the preplanned maximum extent and then gradually withdrawn with a 1-cm deployment interval. With the use of "injection-rotation-injection" maneuver, ethanol was injected until the whole tumor appeared completely hyperechoic, and the intended ethanol amount depended on the tumor size and patient compliance. For tumors ≤3 cm in diameter, the amount of injected ethanol was calculated as volume of a sphere: $V_1 = 4/3\pi [(D/2 + 0.5)^3]$, V is volume and D is the largest tumor dimension. For tumors 3.1–5.0 cm in diameter, the least amount of ethanol was equal to the volume of the index tumor ($V_2 = 4/3\pi [(D/2)^3]$). Mean treatment sessions were 1.1. The average volume of injected ethanol per tumor was 31 mL (range, 8–68 mL). Primary treatment effectiveness was achieved in 95 % of patients and significantly associated with presence of tumor capsule. After a mean follow-up period of 25 months, LTP rate was 9 % in tumors ≤3 cm in size and 17 % in tumors sized 3.1–5.0 cm (Table 20.2). Major complication rate was 2 %. This high-dose single-session

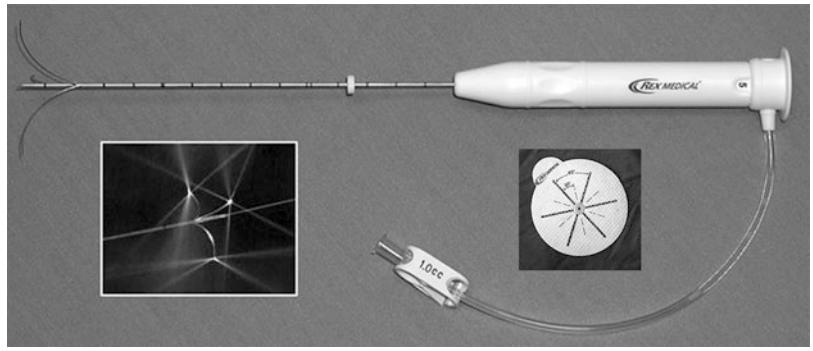

Fig. 20.2 Multi-pronged injection needle used for PEI. The 18-gauge puncture needle consists of three retractable tines each with four fluid exits and a connector with extension tubing clamp (Reprinted with permission from Yin X, Lu M-D. *Expert Rev Gastroenterol Hepatol* 2009; 3:1–9)

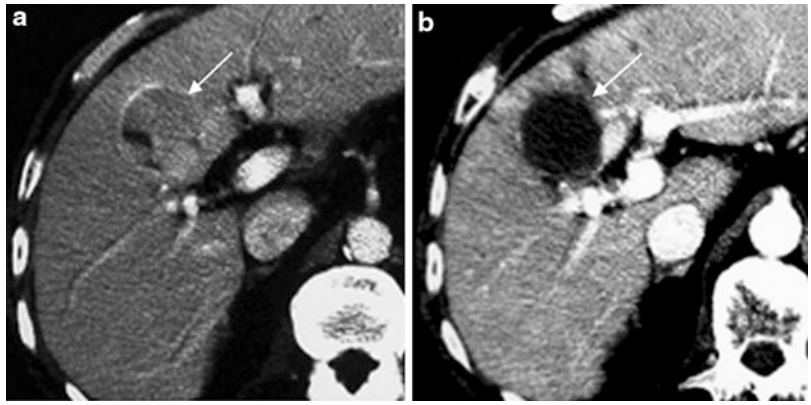

Fig. 20.3 Transverse contrast-enhanced CT scans in a patient who underwent multi-pronged PEI of unfavorable HCC. (**a**) Preablation scan shows a 4.0 × 4.2-cm tumor (*arrow*) located close to porta hepatis. (**b**) Scan obtained 1 month after ablation (1 session, 35 mL of ethanol injected) shows a hypoattenuating ablation zone completely enveloping target tumor site (*arrow*) (Reprinted with permission from Yin X, Lu M-D. *Expert Rev Gastroenterol Hepatol* 2009; 3:1–9)

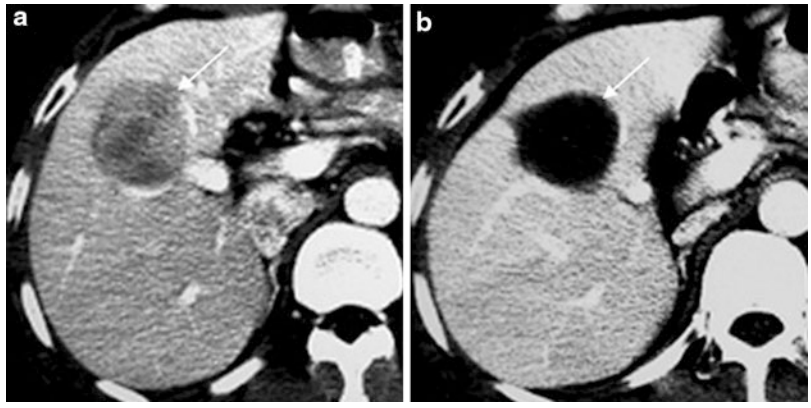

Fig. 20.4 Transverse contrast-enhanced CT scans in a patient who underwent multi-pronged PEI of unfavorable HCC. (**a**) Portal venous phase preablation image shows a 4.1 × 4.5-cm tumor (*arrow*) located above bifurcation of left and right portal veins. (**b**) Image obtained 1 month after a single-session 40-mL ethanol ablation shows hypoattenuating change of the whole target tumor area (*arrow*) (Reprinted with permission from Yin X, Lu M-D. *Expert Rev Gastroenterol Hepatol* 2009; 3:1–9)

Table 20.2 Local effectiveness of multi-pronged PEI of HCC

	Total (n = 141)	Tumor size ≤ 3.0 cm (n = 81)	Tumor size 3.1–5.0 cm (n = 60)
Tumor size (cm)	2.9 ± 0.9	2.3 ± 0.5	3.8 ± 0.6
Ethanol volume per tumor (mL)	31 ± 12	24 ± 7	40 ± 10
Compete ablation rate[a] (%)	88 (124/141)	91 (74/81)	83 (50/60)
Primary effectiveness rate[b] (%)	95 (134/141)	99 (80/81)	90 (54/60)
Local tumor progression rate (%)	12 (16/134)	9 (7/80)	17 (9/54)

[a]Complete ablation rate after the first session of multi-pronged PEI
[b]Complete ablation rate after two sessions of multi-pronged PEI
Source: Reprinted with permission from Yin X, Lu M-D. *Expert Rev Gastroenterol Hepatol* 2009; 3:1–9

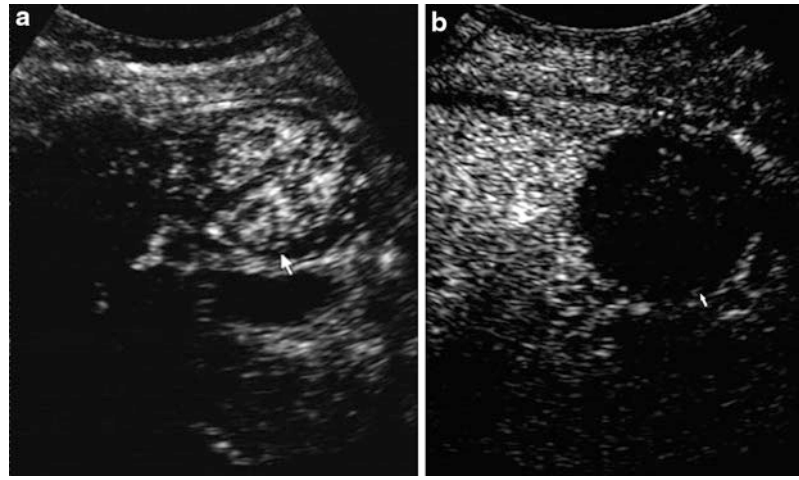

Fig. 20.5 Contrast-enhanced ultrasound images in a patient who underwent combined PEI-RF ablation of HCC. (**a**) Arterial phase image shows a subcapsular 3.8 × 4.5-cm tumor (*arrow*). (**b**) Image obtained 1 month after the treatment shows a coagulation zone of 4.8 × 5.7 cm (*arrow*)

multi-pronged PEI achieves better local efficacy than conventional PEI and is able to treat early-stage or recurrent HCC up to 5 cm effectively and safely, even for lesions at high-risk locations.

Combined PEI and RF Ablation

Combined use of PEI with radio-frequency (RF) ablation may potentially improve the local efficacy of both techniques. It is reported that prior injection of ethanol before RF ablation could significantly increase the coagulation area than RF ablation alone in treating small HCC [36]. The volume of coagulated necrosis was significantly larger in group with high-dose ethanol than that with low-dose ethanol, when radio-frequency energy deliveries were comparable. This combined technique works mainly by shortening the time and energy requirement for RF ablation using the expandable electrode. In a randomized clinical trial for HCC patients, some authors reported that the 5-year overall survival rate in RF ablation plus conventional PEI group was significantly better than that in RF ablation alone [37]. However, the complete response rate after the first session of RF ablation combining conventional PEI was only 75 %. Local efficacy of such combined treatments requires further improvement.

In a preliminary clinical study (not published), 22 HCCs with a mean size of 4.4 cm ± 1.1 (range, 3.1–7.0 cm) were treated by combined use of multi-pronged PEI and RF ablation. A multi-pronged needle and an RF electrode were inserted through a guiding needle into the target tumor one after another, and multi-pronged PEI and RF ablation were subsequently performed in succession. Ethanol was injected until the whole tumor appears completely

Table 20.3 Randomized control studies comparing RFA and PEI for small hepatocellular carcinoma

Study (year)	Treatment type	Patients (n)	Tumor size (cm)	Complete ablation rate (%)	Treatment sessions (n = means)	Local recurrence at 2 years		Overall survival at 3 years		References
						%	*p*-value	%	*p*-value	
Lencioni (2003)	RFA	52	≤5	91	1.1	4	<0.05	64[a]	<0.05	[38]
	PEI	50	≤5	82	5.4	38		43[a]		
Lin (2004)	RFA	52	≤4	96	1.6	18	<0.05	74(59[b])	<0.05	[31]
	Conventional PEI	52	≤4	88	6.5	45		50(42[b])		
	Higher-dose PEI	53	≤4	92	2.7	33		55(45[b])		
Shiina (2005)	RFA	118	≤3	100	2.1	RR = 0.122[c]	<0.05	74[d]	<0.05	[32]
	PEI	114	≤3	100	6.4			57[d]		
Lin (2005)	RFA	62	≤3	96	1.3	14	<0.05	74(43[b])	<0.05	[39]
	PEI	62	≤3	88	4.9	34		51(21[b])		
	PAI	63	≤3	92	2.5	31		53(23[b])		
Brulleno (2008)	RFA	70	≤3	96	13[e]	26	<0.05	59	<0.05	[40]
	PEI	69	≤3	66	14[e]	51		57		

PAI percutaneous acetic acid injection, *PEI* percutaneous ethanol injection, *RFA* radio-frequency ablation
[a]2-year cancer-free survival
[b]Cancer-free survival
[c]Relative risk = 0.12 as compared with PEI
[d]4-year overall survival rate.
[e]Percentage of patients needs 2 treatment cycles
Source: Reprinted from Kuang M, Lu, M-D, Xie X- Y, et al. *Radiology* 2009; 253:552–561, with permission from the Radiological Society of North America (RSNA®)

perfused on the ultrasound image. The average number of needle puncture was 1.5 ± 0.5. The average volume of injected ethanol and the average time of RF ablation were 15 mL ± 6 and 26 min ± 13, respectively. The mean size of coagulation zone was 5.5 cm ± 1.3 (Fig. 20.5), and a complete response rate of 95 % was achieved with one treatment session. It is presumed that the combined use of multi-pronged PEI technique with RF ablation may have potential advantage in treating intermediate and large HCC.

Comparison with RF Ablation

RF ablation has been the major competitor for PEI since their introduction in clinical application from the mid-1990s. Conventional PEI and RF ablation are equal in treating HCC < 2 cm in diameter, but the latter has advantages in treating larger tumor because of better local control. Recently, several randomized clinical trials have revealed that a higher rate of complete response with fewer treatment sessions and better survivals, compared with conventional PEI, can be achieved with RF ablation (Table 20.3) [31, 32, 38–40].

The following points constitute present characteristics of PEI in ablation of HCC:

(a) PEI is a low-risk procedure. RF ablation of tumors at a subcapsular location or adjacent to a critical structure, such as the hepatic hilum or gallbladder, increases the complication rate above the reported baseline of 7–10 % [41–43]. It is reported in an intention-to-treat analysis that 9 % of tumors could not be treated by using RF ablation because of the high-risk location of the tumor [44]. On the contrary, conventional PEI is associated with a major complication rate of 1.3–3.2 % and a mortality rate of 0.09 % [21, 45]. Even for those high-dose PEI techniques, the mortality rates were 0–0.7 % and major complication rates were 2–4.6 % [29, 35]. Conventional PEI can also be used for the treatment of neoplastic portal thrombosis without severe side effects [18].

(b) Local efficacy of innovative PEI is equivalent to RF ablation for treatment of HCC up to 5 cm in size. RF ablation is now the most popular ablation modality, which could achieve a complete response rate of 90 % and a LTP rate of 10–14 % with 1.1 sessions in early-stage HCC [31, 38]. High-dose multi-pronged PEI achieves similar local efficacy, session number, and complication rate to RF ablation. Moreover, this PEI technique has advantages in treating tumors at high-risk locations. Thus, multi-pronged PEI could be used as a useful alternative option to RF ablation.

(c) PEI is inexpensive. The cost of one conventional PEI cycle in Italy, Japan, and China is about USD 1,000 [18], USD 759 [18], and USD 380, while one session of multi-pronged PEI in China costs about USD 1400, all are much cheaper than either resection or RF ablation.

Conclusion

The low cost, easy availability of the necessary material, and simplicity of the PEI technique make it possible to perform it anywhere, even in peripheral centers. Large-volume ethanol injection technique is equivalent to RF ablation in treatment of HCC no more than 5 cm. Combined use of PEI and RF ablation improves local efficacy of both techniques. Therefore, PEI will continue to play a role in the treatment of HCC.

References

1. El-Serag HB, Mason AC. Rising incidence of hepatocellular carcinoma in the United States. N Engl J Med. 1999;340:745–50.
2. Peto J. Cancer epidemiology in the last century and the next decades. Nature. 2001;411:390–5.
3. Bosch FX, Ribes J, Diaz M, Cleries R. Primary liver cancer: worldwide incidence and trends. Gastroenterology. 2004;127(5 Suppl 1):S5–16.
4. Bruix J, Sherman M. Management of hepatocellular carcinoma. Hepatology. 2005;42:1208–36.
5. Llovet JM, Fuster J, Bruix J of the Barcelona-Clı′nic Liver Cancer Group. The Barcelona approach:

diagnosis, staging, and treatment of hepatocellular carcinoma. Liver Transpl. 2004;10:S115–20.
6. Llovet JM, Burroughs A, Bruix J. Hepatocellular carcinoma. Lancet. 2003;362:1907–17.
7. Zhou XD, Tang ZY, Yang BH, Lin ZY, Ma ZC, Ye SL, et al. Experience of 1000 patients who underwent hepatectomy for small hepatocellular carcinoma. Cancer. 2001;91:1479–86.
8. Lang BH, Poon RT, Fan ST, Wong J. Perioperative and long-term outcome of major hepatic resection for small solitary hepatocellular carcinoma in patients with cirrhosis. Arch Surg. 2003;138: 1207–13.
9. Mazzaferro V, Regalia E, Doci R, et al. Liver transplantation for the treatment of small hepatocellular carcinoma in patients with cirrhosis. N Engl J Med. 1996;334:693–9.
10. Llovet JM, Fuster J, Bruix J. Intention-to-treat analysis of surgical treatment for early hepatocellular carcinoma: resection versus transplantation. Hepatology. 1999;30:1434–40.
11. Bruix J, Llovet JM. Prognostic prediction and treatment strategy in hepatocellular carcinoma. Hepatology. 2002;35:519–24.
12. Fong Y, Sun RL, Jarnagin W, Blumgart LH. An analysis of 412 cases of hepatocellular carcinoma at a Western center. Ann Surg. 1999;229:790–800.
13. Lee WC, Jeng LB, Chen MF. Estimation of prognosis after hepatectomy for hepatocellular carcinoma. Br J Surg. 2002;89:311–6.
14. Jarnagin WR, Fong Y. Repeat resection for liver tumors. In: Clavien PA, editor. Malignant liver tumors: current and emerging therapies. Boston: Blackwell Science; 1999. p. 150–8.
15. Lu MD, Yin XY, Xie XY, et al. Percutaneous thermal ablation for recurrent hepatocellular carcinoma after hepatectomy. Br J Surg. 2005;92:1393–138.
16. Sugiura N, Takara K, Ohto M, Okuda K, Hirooka N. Ultrasound guided ethanol injection for the treatment of small hepatocellular carcinoma. Acta Hepatol Jpn. 1983;21:920.
17. Livraghi T, Festi D, Monti F, Salmi A, Vettori C. US-guided percutaneous alcohol injection of small hepatic and abdominal tumors. Radiology. 1986;161: 309–12.
18. Livraghi T. Role of percutaneous ethanol injection in the treatment of hepatocellular carcinoma. Dig Dis. 2001;19:292–300.
19. Ebara M, Okabe S, Kita K, et al. Percutaneous ethanol injection for small hepatocellular carcinoma: therapeutic efficacy based on 20-year observation. J Hepatol. 2005;43:458–64.
20. Lencioni R, Llovet JM. Percutaneous ethanol injection for hepatocellular carcinoma: alive or dead? J Hepatol. 2005;43:377–80.
21. Livraghi T, Giorgio A, Marin G, et al. Hepatocellular carcinoma and cirrhosis in 746 patients: long-term results of percutaneous ethanol injection. Radiology. 1995;197:101–8.
22. Sala M, Llovet JM, Vilana R, Bianchi L, Sole M, Ayuso C, Barcelona Clinic Liver Cancer Group, et al. Initial response to percutaneous ablation predicts survival in patients with hepatocellular carcinoma. Hepatology. 2004;40:1352–60.
23. El–Serag HB, Marrero JA, Rudolph L, Reddy KR. Diagnosis and treatment of hepatocellular carcinoma. Gastroenterology. 2008;134:1752–63.
24. Khan KN, Yatsuhashi H, Yamasaki K, et al. Prospective analysis of risk factors for early intrahepatic recurrence of hepatocellular carcinoma following ethanol injection. J Hepatol. 2000;32:269–78.
25. Pompili M, Rapaccini GL, Covino M, et al. Prognostic factors for survival in patients with compensated cirrhosis and small hepatocellular carcinoma after percutaneous ethanol injection therapy. Cancer. 2001;92:126–35.
26. Lencioni R, Pinto F, Armillotta N, et al. Long-term results of percutaneous ethanol injection therapy for hepatocellular carcinoma in cirrhosis: a European experience. Eur Radiol. 1997;7:514–9.
27. Arii S, Yamaoka Y, Futagawa S, et al. Results of surgical and nonsurgical treatment for small-sized hepatocellular carcinomas: a retrospective and nationwide survey in Japan. The Liver Cancer Study Group of Japan. Hepatology. 2000;32:1224–9.
28. Lencioni R, Vignali C, Caramella D, Cioni R, Mazzeo S, Bartolozzi C. Transcatheter arterial embolization followed by percutaneous ethanol injection in the treatment of hepatocellular carcinoma. Cardiovasc Intervent Radiol. 1994;17:70–5.
29. Livraghi T, Benedini V, Lazzaroni S, Meloni F, Torzilli G, Vettori C. Long term results of single session percutaneous ethanol injection in patients with large hepatocellular carcinoma. Cancer. 1998;83:48–57.
30. Shiina S, Hata Y, Niwa Y, et al. Multiple-needle insertion method in percutaneous ethanol injection therapy for liver neoplasms. Gastroenterol Jpn. 1991;26:47–50.
31. Lin SM, Lin CJ, Lin CC, Hsu CW, Chen YC. Radiofrequency ablation improves prognosis compared with ethanol injection for hepatocellular carcinoma < or = 4 cm. Gastroenterology. 2004;127:1714–23.
32. Shiina S, Teratani T, Obi S, Sato S, Tateishi R, Fujishima T. A randomized controlled trial of radiofrequency ablation with ethanol injection for small hepatocellular carcinoma. Gastroenterology. 2005;129:122–30.
33. Hines-Peralta A, Liu ZJ, Horkan C, Solazzo S, Goldberg SN. Chemical tumor ablation with use of a novel multiple-tine infusion system in a canine sarcoma model. J Vasc Interv Radiol. 2006;17:351–8.
34. Ho CS, Kachura JR, Gallinger S, et al. Percutaneous ethanol injection of unresectable medium-to-large-sized hepatomas using a multipronged needle: efficacy and safety. Cardiovasc Intervent Radiol. 2007;30: 241–7.

35. Kuang M, Lu MD, Xie XY, et al. Ethanol ablation of hepatocellular carcinoma sized up to 5 cm by using a multi-pronged injection needle with high-dose strategy. Radiology. 2009;253:552–61.
36. Kurokohchi K, Watanabe S, Masaki T, et al. Comparison between combination therapy of percutaneous ethanol injection and radiofrequency ablation and radiofrequency ablation alone for patients with hepatocellular carcinoma. World J Gastroenterol. 2005;11:1426–32.
37. Zhang YJ, Liang HH, Chen MS, et al. Hepatocellular carcinoma treated with radiofrequency ablation with or without ethanol injection: a prospective randomized trial. Radiology. 2007;244:599–607.
38. Lencioni RA, Allgaier HP, Cioni D, et al. Small hepatocellular carcinoma in cirrhosis: randomized comparison of radio-frequency thermal ablation versus percutaneous ethanol injection. Radiology. 2003;228:235–40.
39. Lin SM, Lin CJ, Lin CC, Hsu CW, Chen YC. Randomised controlled trial comparing percutaneous radiofrequency thermal ablation, percutaneous ethanol injection, and percutaneous acetic acid injection to treat hepatocellular carcinoma of 3 cm or less. Gut. 2005;54:1151–6.
40. Brunello F, Veltri A, Carucci P, et al. Radiofrequency ablation versus ethanol injection for early hepatocellular carcinoma: a randomized controlled trial. Scand J Gastroenterol. 2008;43:727–35.
41. Livraghi T, Solbiati L, Meloni MF, Gazelle GS, Halpern EF, Goldberg SN. Treatment of focal liver tumors with percutaneous radio-frequency ablation: complications encountered in a multicenter study. Radiology. 2003;226:441–51.
42. Tateishi R, Shiina S, Teratani T, et al. Percutaneous radiofrequency ablation for hepatocellular carcinoma. An analysis of 1000 cases. Cancer. 2005;103:1201–9.
43. Llovet JM, Vilana R, et al. Increased risk of tumor seeding after radiofrequency thermal ablation for single hepatocellular carcinoma. Hepatology. 2001;33:1124–9.
44. Lencioni R, Cioni D, Crocetti L, et al. Early-stage hepatocellular carcinoma in cirrhosis: long term results of percutaneous image-guided radiofrequency ablation. Radiology. 2005;234:961–7.
45. Di Stasi M, Buscarini L, Livraghi T, et al. Percutaneous ethanol injection in the treatment of hepatocellular carcinoma: a multicenter survey of evaluation practices and complications rates. Scand J Gastroenterol. 1997;32:1168–73.

Chemoembolization and Radioembolization in the Treatment of Primary Liver Cancers

21

Khairuddin Memon, Ahsun Riaz, Robert J. Lewandowski, and Riad Salem

Abstract

The incidence of hepatocellular carcinoma is increasing worldwide. Chemoembolization and radioembolization represent two novel transarterial therapies which are primarily based on a similar basic concept of the direct delivery of toxic material to the tumor via the hepatic artery and its branches. This concept exploits the fact that normal hepatic parenchyma derives its blood supply primarily from portal vein, whereas hepatic tumors are hypervascular relying primarily on hepatic arterial blood. Chemoembolization involves the delivery of a combination of chemotherapeutic drugs directly to the vessel feeding the tumor. Another variety of this technique involves drug-eluting beads which are microspheres loaded with the chemotherapeutic drug. Radioembolization involves the delivery of micron-sized radioactive particles to the tumor. While both therapies seem similar upfront, there are distinct differences in the indications, patient selection, technique, patient monitoring, and complications. These therapies have led to an encouraging response in terms of tumor necrosis, progression-free and overall survival, quality of life, and incidence of complications; they are therefore gaining wide acceptance for treating appropriately selected patients with hepatocellular carcinoma.

Introduction

Hepatocellular carcinoma (HCC) is the most common primary liver cancer. It is the sixth most common malignancy worldwide and the third most common cause of cancer-related mortality [1, 2]. Liver transplantation provides a standard method of cure, but many patients are precluded from this treatment either because of unresectability or comorbidities. Also, limited number of available donors increases the chances of patient dropout due to tumor progression beyond acceptable criteria [3, 4]. Systemic chemotherapy has a limited role in HCC [5, 6]. Locoregional therapies are establishing their role in the treatment of liver malignancies; two

K. Memon (✉) • A. Riaz • R.J. Lewandowski • R. Salem
Department of Radiology, Northwestern Memorial Hospital, Chicago, IL, USA
e-mail: k-memon@northwestern.edu

D.E. Dupuy et al. (eds.), *Image-Guided Cancer Therapy*, DOI 10.1007/978-1-4419-0751-6_23,

of the most widely used intra-arterial techniques (chemoembolization and radioembolization) are discussed in this chapter. These techniques permit the delivery of higher toxic dose to the malignant tissue while sparing the normal hepatic parenchyma and also decrease the chances of systemic toxicity. These therapies have been shown to have a palliative role and may also prove to have a potentially curative role as numerous investigators have shown survival benefit with their use [7–12].

A brief overview of liver anatomy, diagnosis, and staging of liver tumors is provided first followed by a detailed discussion on chemoembolization and radioembolization and monitoring their treatment response.

Vascular Anatomy of the Liver

The anatomy of liver has several favorable aspects that make locoregional therapies possible. The relative superficial nature of the liver makes percutaneous techniques feasible. Secondly, cancer cells are predominantly supplied by an arterial source, whereas the normal hepatic parenchyma derives its perfusion from portal venous blood. This fact allows us to direct the locoregional therapies via the hepatic artery and its branches to the cancer cells. The hypervascularity prioritizes flow to the tumor cells with limited exposure to healthy tissue.

The liver is primarily supplied by the hepatic artery proper, a continuation of common hepatic artery which in turn is a branch of the celiac trunk. The proper hepatic artery branches into the right and left hepatic arteries. These supply the corresponding lobes of the liver by giving off segmental branches. Cystic artery which is a branch of right hepatic artery normally supplies the gallbladder. However, the anatomical variations of hepatic vascular supply are very common; a detailed angiography is required before any transarterial therapy [13–15]. Also hepatic tumors are hypervascular and often parasitize arterial supply not only from the surrounding liver parenchyma but also from the surrounding tissues and organs.

Diagnosis and Staging of Liver Tumors

HCC is diagnosed on imaging if there is a lesion greater than 2 cm with arterial-phase enhancement and venous washout. Biopsy is performed in lesions that do not have the typical radiologic findings as defined by the European Association for the Study of the Liver and American Association for the Study of Liver Diseases guidelines [16, 17]. The role of alpha-fetoprotein in diagnosis of HCC is not yet established but is being investigated [18]. This is followed by a thorough evaluation of the patient including history and physical examination, assessment of laboratory values, imaging techniques, and determination of baseline performance status in order to stage the tumor. A multidisciplinary team including hepatologists, medical and surgical oncologists, transplant surgeons, and interventional radiologists is involved in the management of liver tumors. Selection of a specific therapy is based on the patient and tumor characteristics, staging, and performance status of the patient.

Primary Liver Tumors

Hepatocellular Carcinoma (HCC)

Standard guidelines are followed for the diagnosis and appropriate staging of HCC; these may include imaging techniques, tissue diagnosis, and tumor markers (AFP, PIVKA-II) [19]. The performance status of patient is also taken into account. The technical details of diagnosis and staging are beyond the scope of this chapter.

The use of **surgical options** is the gold standard of treatment for these patients which includes liver transplantation or resection. Milan criteria are used to decide whether patients are eligible for transplantation (single lesion <5 cm, three lesions all <3 cm) [20]. Resection is possible only if liver function is well compensated. The limited availability of donor organs for orthotopic liver transplantation (OLT) and the dropout of patients due to tumor progression limit the number

of patients who initially were within transplant criteria and are able to undergo OLT.

Systemic therapy with sorafenib has been shown to have a significant improvement in survival in patients with advanced disease [21]. Patients who have advanced disease, PVT, and metastatic disease may benefit from sorafenib.

Due to the limited role of surgical and systemic therapies, **locoregional therapies** (LRTs) have assumed an important role in the management of liver tumors. They can be used to slow the progression of the disease in patients who are unable to undergo OLT or resection. They can also be used to downstage the disease within transplant criteria [22, 23]. This allows the patients who were initially outside Milan criteria to be eligible for transplant. Recurrence-free and overall survivals after OLT in the downstaged patients are yet to be compared to those of patients who were already within transplant criteria to determine the efficacy of downstaging. This group of patients may also have a survival benefit following treatment even without downstaging.

Intrahepatic Cholangiocarcinoma (ICC)

The role of chemoembolization and radioembolization is significant in HCC, but their role in treating ICC has not been extensively studied. Preliminary data are discussed.

Catheter-Based Therapies

Transarterial Chemoembolization (TACE)

Introduction

TACE is used to deliver potent anticancer drugs directly to the cancer cells while systemic exposure is minimized. It has been used since the 1980s [24, 25]. Although controversial, the most commonly used drugs used for TACE include doxorubicin alone or in combination with mitomycin C and cisplatin. The drug combination is preferred in the USA [26].

Patient Selection

TACE is best suited for patients with good performance status, preserved liver function, and no evidence of vascular invasion and extrahepatic metastasis. It is generally contraindicated in patients with PVT, absence of hepatopedal flow or compensatory collaterals, encephalopathy, or biliary obstruction. Relative contraindications include serum bilirubin >2 mg/dL, lactate dehydrogenase >425 U/L, aspartate aminotransferase >100 U/L, tumor burden exceeding >50 % of liver, ascites, bleeding varices, thrombocytopenia, or cardiac or renal insufficiency [27].

Procedure

The procedure is initiated with a thorough evaluation; this includes assessment of the baseline characteristics and stage of the patient using clinical and radiologic data and performance status. Angiography is performed to study the normal vascular anatomy and possible variations. The vehicle used for the delivery of chemotherapeutic drug is Lipiodol which is a poppy-seed oil containing 38 % iodine by weight. The drug is emulsified with Lipiodol and injected in the tumor-feeding vessel during angiography. Lipiodol permits the concentration of the drug in the tumor and is retained for weeks while the normal hepatocytes are able to excrete it within 7 days. In addition, there is stasis associated with Lipiodol and hence an embolic effect. It is a radiopaque substance and is visualized on posttreatment CT scans in the target lesion. This is followed by the injection of bland embolic particles to prevent washout of the drug and to induce ischemic necrosis [28].

Indications for TACE

Lewandowski et al. performed a comprehensive imaging and long-term survival analysis in a cohort of 172 patients following chemoembolization for HCC. Median survival was significantly different between patients with BCLC stages A, B, and C disease (stage A, 40.0 months;

B, 17.4 months; C, 6.3 months, $P < .0001$). The study concluded that chemoembolization was safe and effective in patients with HCC; however, the determination of time to progression (TTP) and survival in patients with HCC is confounded by tumor biology and background cirrhosis [7]. Llovet et al. studied the survival outcomes in patients treated with fixed interval (intention to treat) chemoembolization, particle embolization, and conservative measures [11]. The authors of this study concluded that TACE and embolization significantly improved survival in select patients with unresectable HCC. Takayasu et al. published data from a large cohort study of 8,510 HCC patients treated with TACE and showed that prognosticators of survival included degree of liver damage, alpha-fetoprotein value, maximum tumor size, number of lesions, and portal vein invasion [29]. A meta-analysis of seven published randomized controlled trials concluded that TACE was an effective palliative treatment modality for unresectable HCC [21].

The role of chemoembolization in cholangiocarcinoma is relatively ill explored. In a recent two-center study, Kiefer et al. treated 62 patients of unresectable cholangiocarcinoma with lobar or segmental chemoembolization. They concluded that chemoembolization provided local disease control (PR+SD) of intrahepatic cholangiocarcinoma. Overall survival after chemoembolization showed the best outcomes for those receiving multidisciplinary integrated liver-directed and systemic therapies [30].

Combination Therapies

TACE/RFA

TACE has been used prior to RFA to decrease the tumor size and vascularity making it more susceptible to the effects of RF ablation [31]. TACE may be given before RF ablation in tumors 3–5 cm to decrease the size and perfusion of the tumor leading to increased sensitivity to RF ablation. Kagawa et al. presented a recent series of 62 patients who received TACE+RFA with 55 patients who underwent surgical resection [32]. They found out that 1, 3, and 5 years in the TACE+RFA group (100 %, 94.8 %, and 64.6 %, respectively) were similar ($P = .788$) to those in the resection group (92.5 %, 82.7 %, and 76.9 %, respectively). They concluded that RFA combined with TACE is an efficient and safe treatment.

TACE/Surgery

TACE can be used as a neoadjuvant to surgery. It has shown the ability to downstage patients to the Milan criteria, thus allowing them to undergo OLT [33].

TACE/Ethanol Ablation

A randomized controlled trial comparing TACE alone with the combination of TACE and PEI showed significantly higher response rates and less recurrence following the combination [34].

Complications

Post-embolization syndrome is seen after TACE and is usually managed during the hospitalization. Other complications may include the following: (a) in bile duct injury [35], up to 5.3 % patients may develop biliary complications following TACE [36]; (b) liver abscesses are rare but are possible after TACE, especially in patients who have undergone biliary interventions [35]; (c) the inadvertent deposition of the chemotherapeutic drug to the gastrointestinal tract may cause duodenal or gastric ulcers and may even lead to perforation in severe cases [35]; (d) the intra-arterial approach increases the risk of vascular injury in all transcatheter techniques [35]. Chemotherapeutic agents may also have a role in causing this complication [37]; and (e) tumor rupture (0.15 %) following TACE [35] and pulmonary artery embolism may occur, and the patient may present with cough and dyspnea [35].

TACE with Drug-Eluting Beads (DEBs)

Introduction

The concept of DEBs is to load microspheres with chemotherapeutic agents and deliver them

intra-arterially in a controlled manner. The unique properties of beads allow for fixed dosing and release of the drug in a sustained manner; this leads to a significant reduction in peak plasma concentration when compared with conventional TACE [26].

Procedure

Both patient selection and procedural aspects are similar to conventional TACE; the microspheres are delivered to the tumor after angiographic evaluation of the vascular anatomy. The microspheres are composed of PVA polymers modified with sulfonate groups. By an ion exchange process, the sulfonate groups actively sequester doxorubicin from solution [38].

Indications for DEB

The published data shows that doxorubicin-loaded DEBs have a promising role in the treatment of inoperable HCC [39, 40]. Although this technique is new, it represents a paradigm shift from the conventional TACE to DEB because of both increased intra-tumoral retention and decreased bioavailability which consequently leads to lower toxicity levels. Poon et al. reported a 63 % response using the modified RECIST criteria which take tumor necrosis into account [12]. A recent randomized controlled trial on 212 patients comparing conventional TACE with DEBs failed to show a significant survival benefit (PRECISION V). However, the ability to tolerate treatment was higher in more advanced patients [10]. Dhanasekran et al. in a recent study concluded that transcatheter therapy with DEB offers a survival benefit over conventional chemoembolization in patients with unresectable HCC [41]. There were fewer adverse events seen after DEBs when compared to conventional TACE. DEBs loaded with irinotecan are being investigated for the treatment of patients with colorectal hepatic metastases [42].

Varela et al. investigated the use of chemoembolization with DEBs in a series of 27 patients with HCC and Child-Pugh A cirrhosis. They demonstrated that response rate was 75 % by CT at 6 months; doxorubicin Cmax and AUC were significantly lower than conventional TACE and 1- and 2-year survival rates were 92.5 % and 88.9 %, respectively, with a median follow-up of 27.6 months. They concluded that chemoembolization using DEBs is an effective procedure with a favorable pharmacokinetic profile [43].

In a single-center phase II trial of chemoembolization with DEBs, Reyes et al. evaluated its safety and efficacy in a series of 20 patients with unresectable HCC. They demonstrated that at 1 month, partial response and stable disease were seen in 10 % and 90 %, respectively, using RECIST guidelines, whereas by EASL guidelines, 60 % had objective tumor response and 40 % had stable disease. Overall survival rates at 1 and 2 years were 65 % and 55 %, respectively; median overall survival was 26 months. They concluded that DEB-TACE is safe and effective in achieving local tumor control [44].

Recently, Malagari et al. performed a prospective randomized trial comparing DEB with bland embolization in two groups of patients each with 41 and 43 patients, respectively. EASL complete and partial response was seen in 26.8 % and 46.3 % of patients treated with DEB versus 14 % and 41.9 % of those treated with bland embolization. Recurrence rate and time to progression were found to be higher for bland embolization and DEB groups, respectively. They concluded that DEB presents a better local response, fewer recurrences, and a longer TTP than bland embolization [45].

Outcomes of conventional and DEB chemoembolization are summarized in Table 21.1.

Complications

The toxicity profile is similar to that seen after TACE, and preliminary data according to the PRECISION V trial may indicate that this is a safer therapy when compared to conventional TACE, particularly in more advanced patients (Child score, performance status). Some of the toxicities associated with DEB may include GI ulcers, vascular injury, hepatic failure, abscess formation, and tumor rupture.

Table 21.1 Outcomes of chemoembolization

	Takayasu et al. [29]	Lewandowski et al. [7]	Lammer et al. [10]	Malagari et al. [45]
Purpose	To analyze survival after TACE	To determine imaging and survival outcome after TACE for (HCC)	To compare response rate and toxicities of cTACE with DC Bead TACE	To compare DEB-TACE with bland embolization
Disease	HCC	HCC	HCC	HCC
Patients	8,510	172	cTACE:108	DEB-TACE: 41
			DC Bead TACE: 93	Bland embolization: 43
Response rate	–	WHO: 31 %	cTACE: 22 %	DEB-TACE: 73.1 %
		EASL: 64 %	DC Bead TACE: 27 %	Bland embolization: 60 %
TTP (*months*)	–	7.9	–	DEB-TACE: 42.4
				Bland embolization: 36.2
Survival	1 year: 82 %	BCLC A: 40.0 mo	–	No difference between two groups within 1 year
	3 years: 47 %	BCLC B: 17.4 mo		
	5 years: 47 %	BCLC C: 6.3 mo		

BCLC Barcelona Clinic Liver Cancer, *cTACE* conventional transarterial chemoembolization, *DC* Bead, doxorubicin-loaded bead, *EASL* European Association for the Study of the Liver diseases, *HCC* hepatocellular carcinoma, *TACE* transarterial chemoembolization, *WHO* World Health Organization

Radioembolization

Introduction

Radioembolization is the delivery of high-dose radiation internally as compared to external radiation therapy. High-dose radioactive particles are delivered to the tumor via the arterial route. External radiation has played an inconsequential role in liver malignancies due to the radiosensitivity demonstrated by hepatic tissue and consequent development of radiation-induced liver disease (RILD), a clinical syndrome of ascites, anicteric hepatomegaly, and elevation of liver enzymes [46, 47]. Besides, the dose given via external radiation is not sufficient to kill cancer cells. Radioembolization helps overcome both of these issues to a great extent. Radioembolization is an outpatient procedure.

Pretreatment Evaluation

Clinical evaluation is required, and patients with Eastern Cooperative Oncology Group (ECOG) status >2 are not considered ideal for this treatment. The performance of radioembolization is a complex process; the inadvertent spread of radioactive microspheres is prevented by meticulous study of the vascular anatomy of the liver and collateral nontarget flow [48]. The aortogram is done to assess the tortuosity and the presence of atherosclerosis in the aorta. The superior mesenteric and celiac trunk angiograms allow interventional radiologists an opportunity to study the vascular anatomy of the liver. The patency of the portal vein and the presence of arterio-portal shunting are also assessed. Coil embolization of nontarget vessels may be necessitated to decrease the unintended deposition of microspheres. Commonly embolized vessels are gastroduodenal artery, right gastric artery, falciform artery, and others as required. Technetium-99-labeled macroaggregated albumin (^{99}Tc-MAA) is used to assess splanchnic shunting and pulmonary shunting. This pretreatment nuclear scan is important to prevent the complications associated with the treatment and to calculate the lung shunt fraction (LSF). All the hepatic vessels are assessed during the angiogram, and the arteries feeding the tumor are studied in detail [13–15].

Patient Selection

Radioembolization is contraindicated in patients with exaggerated hepatopulmonary shunting and/or non-correctable GI flow, i.e., if >30 Gy or >50 Gy of radiation is predicted to be delivered to lungs in a single or as a cumulative dose over multiple sessions [49], respectively, or if nontarget gastric radiation seems inevitable. Relative contraindications include compromised pulmonary function, inadequate liver reserve, serum creatinine >2.0 mg/dL, and thrombocytopenia.

Available Devices

^{90}Y is a pure beta emitter with a half-life of 64.2 h and with a tissue penetration of 2.5–11 mm. There are two forms available: (1) **TheraSphere® (MDS Nordion, Ottawa, Canada)** consisting of glass microspheres that have a diameter of 20–30 μm, approved for unresectable HCC, and (2) **SIR-Sphere® (Sirtex, Lane Cove, Australia)** consisting of resin microspheres with a diameter slightly larger and less dense than glass. This device is approved for metastatic colorectal cancer to the liver. The technical details of the procedure and dosimetry are beyond the scope of this chapter and are described elsewhere [33]. The procedure is performed on an outpatient basis, and the patient is discharged on the same day [50].

Indications for Radioembolization

HCC

The use of radioembolization has been shown to limit progression of the disease. This helps in bridging the patient to OLT as it allows the patient more time to wait for donor organs [51]. Lewandowski et al. compared chemoembolization to radioembolization in their retrospective analysis of patients with HCC beyond Milan criteria [22]. Radioembolization was shown to be a better tool than chemoembolization for downstaging the disease to within transplant criteria.

In a study analyzing the long-term outcomes of 291 patients treated with ^{90}Y for HCC, Salem et al. concluded that patients with Child-Pugh A disease, with or without PVT, benefited most from the treatment, patients with Child-Pugh B disease who had PVT had poor outcomes, whereas TTP and overall survival varied by patient age at baseline [9]. Malignant vascular invasion in patients with advanced HCC is an exclusion criterion for transplant. Embolic therapies are also relatively contraindicated as they may lead to further deterioration of blood supply to already compromised liver parenchyma. However, patient with vascular invasion may benefit from ^{90}Y as it is not a macroembolic procedure [52]. In another study, Hilgard et al. analyzed the safety and efficacy of radioembolization in 108 European patients. They observed a response rate of 40 % (EASL), TTP of 10 months, and overall survival of 16.4 months. They concluded that radioembolization is safe and effective treatment for patients with advanced HCC [53]. In a recent multicenter European study of 325 HCC patients treated with radioembolization, Sangro et al. found a median survival of 12.8 months overall which highly varied by patients' baseline BCLC stage (BCLC A, 24.4 months; BCLC B, 16.9 months; BCLC C, 10.0 months). They found ECOG status, tumor burden, INR, and extrahepatic disease as the most significant independent predictors of survival [54].

Salem et al. recently performed a comparative effectiveness analysis of radioembolization and chemoembolization for HCC and concluded that although the survival outcomes of two therapies are similar, radioembolization resulted in longer time to progression and less toxicity than chemoembolization. Post hoc analyses of sample size indicated that a randomized study with >1,000 patients would be required to establish equivalence of survival times between patients given the different therapies [8].

Intrahepatic Cholangiocarcinoma (ICC)

A pilot study analyzing the use of ^{90}Y in 24 patients with biopsy-proven ICC has shown a favorable response to treatment and favorable survival outcomes [55]. The patients with a better

Table 21.2 Outcomes of radioembolization

	Salem et al. [9]	Hilgard et al. [53]	Sangro et al. [54]	Salem et al. [8]	Saxena et al. [56]
Purpose	To assess clinical outcomes of HCC patients treated with 90Y	To assess clinical outcomes of HCC patients treated with 90Y in Europe	To evaluate prognostic factors of survival after 90Y for HCC patients in Europe	To compare the effectiveness of 90Y versus TACE in HCC patients	To assess safety and efficacy of 90Y for unresectable cholangio-carcinoma
Disease	HCC	HCC	HCC	HCC	Cholangio-carcinoma
Patients	291	108	325	90Y: 123	25
				TACE: 122	
Response rate	WHO: 42 %	EASL: 40 %	–	90Y: 49 %	RECIST: 24 %
	EASL: 57 %			TACE: 36 %	
TTP (*months*)	7.9	10	–	90Y: 13.3	–
				TACE: 8.4	
Survival (*months*)		16.4	12.8 (overall)		9.3
	Child-Pugh A:17.2		BCLC A: 24.4	90Y:20.5	
	Child-Pugh B:7.7		BCLC B: 16.9	TACE: 17.4	
			BCLC C: 10.0		

BCLC Barcelona Clinic Liver Cancer, *EASL* European Association for the Study of the Liver Diseases, *HCC* hepatocellular carcinoma, *RECIST* Response Evaluation Criteria in Solid Tumors, *TACE* transarterial chemoembolization, *TTP* time to progression, *WHO* World Health Organization

performance status according to the Eastern Cooperation Oncology Group (ECOG) had a significantly better survival in this study. A second 25 patient study assessed the safety and efficacy of ^{90}Y radioembolization. They concluded that ^{90}Y may be a safe and efficacious treatment for unresectable ICC with a median survival of 9.3 months and low incidence of grade III toxicities. Further investigation would be required for this treatment modality for ICC [56].

Outcomes of radioembolization are summarized in Table 21.2.

Complications

The post-embolization syndrome occurs less commonly after radioembolization due to the small size of the particles, seldom requiring hospitalization [57–59]. Other serious adverse events related to radioembolization may include (a) radiation-induced liver disease in 15–20 % [60, 61] with the clinical appearance of ascites and jaundice, sometimes the hepatic toxicity may be severe and lead to significant morbidity and mortality [60]; (b) fibrosis that may lead to portal hypertension with variable time to development [62]; (c) bilomas, abscess, and cholecystitis [63]; (d) radiation pneumonitis in a few cases with a predisposing high LSF if treated with resin microspheres [49]; (e) the inadvertent spread of microspheres to the gastrointestinal tract may lead to ulceration [64, 65]; and (f) vascular injury occurs less commonly but may be seen in patients who were already on systemic chemotherapy [66].

Monitoring Response Following Chemoembolization and Radioembolization

The response to treatment is monitored clinically and radiologically. The first radiologic study is done 1 month after treatment to assess response or lack thereof. The patients are then followed with scans and laboratory panel every 3 months to assess response to treatment or progression of disease. Given the lack of standardization of functional imaging in HCC, anatomical methods

are still considered the gold standard for response assessment. In 1979, the World Health Organization (WHO) (bidimensional perpendicular measurements) published guidance on the anatomical assessment of tumor response to therapy [67]. In 2000, the Response Evaluation Criteria in Solid Tumors (RECIST) guidelines (unidimensional measurements) were published, updating the WHO document [68]. European Association for Study of the Liver (EASL) guidelines were published in 2001 and were based on percent change in amount of enhancing tumoral tissue posttreatment [17, 68, 69]. The EASL guidelines address the limitations of WHO and RECIST guidelines as they were intended for systemic therapies, and there were limitations in applying them for locoregional therapies. Recently, American Association for the Study of Liver Diseases (AASLD) developed a set of guidelines referred to as modified RECIST assessment (mRECIST). These guidelines adapt the concept of viable tumor tissue showing uptake in arterial phase of contrast-enhanced radiologic imaging techniques and are aimed at providing a common framework for the design of clinical trials in HCC [70].

In a series of 245 patients treated with locoregional therapies, Riaz et al. investigated the concept of index lesion and inter-method agreement between RECIST, WHO, and EASL guidelines. They concluded that there is high agreement between RECIST and WHO guidelines but low between each of these and EASL. Moreover, primary index lesion, which is the dominant lesion, can be used to measure response to therapy by applying the above-mentioned guidelines [71].

In a recent study, Riaz et al. concluded that post-radioembolization imaging findings of response by EASL and WHO criteria are predictive of the degree of pathologic necrosis after chemoembolization and radioembolization with ^{90}Y [72, 73]. In another recent study at our center, various combinations of WHO, EASL, and RECIST guidelines were studied, and scoring systems were devised based on the combinations of these guidelines. It was concluded that EASL × WHO scoring system provides a simple and clinically acceptable method of response assessment and radiological-pathological correlation [74]. In another study, Riaz et al. also concluded that AFP response seen after locoregional therapy can also be used as an ancillary method of assessing tumor response and survival, as well as an early objective screening tool for progression by imaging [18].

Conclusion

Treatment of HCC and other hepatic tumors poses a challenging task since they often present at an advanced stage where curative surgical options such as resection or OLT are deemed unsuitable. Chemoembolization and radioembolization are novel transarterial locoregional therapies that have gained widespread recognition for the treatment of hepatic tumors in the palliative setting despite several comorbidities and advanced stage. Drawing a comparison between these two intra-arterial therapies is difficult since there are no randomized controlled trials comparing them directly in a controlled manner; there is however a comparative effectiveness analysis recently published [8]. Studies involving the combination of locoregional therapies with several systemic therapies targeted at molecular level are under way. Results from these studies may lead to a better anticipation of enhanced clinical outcomes and survival benefits for patients. The clinical benefit and potential for improving quality of life represent an exciting opportunity for all disciplines involved in the management of liver tumors including hepatobiliary, medical, surgical, radiation, and interventional oncology.

References

1. Parkin DM, Bray F, Ferlay J, Pisani P. Global cancer statistics, 2002. CA Cancer J Clin. 2005;55(2):74–108.
2. Bosch FX, Ribes J, Diaz M, Cleries R. Primary liver cancer: worldwide incidence and trends. Gastroenterology. 2004;127(5 Suppl 1):S5–16.
3. Yao FY, Bass NM, Nikolai B, et al. A follow-up analysis of the pattern and predictors of dropout from the waiting list for liver transplantation in patients with hepatocellular carcinoma: implications for the current organ allocation policy. Liver Transpl. 2003;9(7):684–92.

4. Maddala YK, Stadheim L, Andrews JC, et al. Drop-out rates of patients with hepatocellular cancer listed for liver transplantation: outcome with chemoembolization. Liver Transpl. 2004;10(3):449–55.
5. Llovet JM, Ricci S, Mazzaferro V, et al. Sorafenib in advanced hepatocellular carcinoma. N Engl J Med. 2008;359(4):378–90.
6. Cheng AL, Kang YK, Chen Z, et al. Efficacy and safety of sorafenib in patients in the Asia-Pacific region with advanced hepatocellular carcinoma: a phase III randomised, double-blind, placebo-controlled trial. Lancet Oncol. 2009;10(1):25–34.
7. Lewandowski RJ, Mulcahy MF, Kulik LM, et al. Chemoembolization for hepatocellular carcinoma: comprehensive imaging and survival analysis in a 172-patient cohort. Radiology. 2010; 255(3):955–65.
8. Salem R, Lewandowski RJ, Kulik L, et al. Radioembolization results in longer time-to-progression and reduced toxicity compared with chemoembolization in patients with hepatocellular carcinoma. Gastroenterology. 2011;140(2):497–507. e492.
9. Salem R, Lewandowski RJ, Mulcahy MF, et al. Radioembolization for hepatocellular carcinoma using yttrium-90 microspheres: a comprehensive report of long-term outcomes. Gastroenterology. 2010;138(1):52–64.
10. Lammer J, Malagari K, Vogl T, et al. Prospective randomized study of Doxorubicin-Eluting-Bead embolization in the treatment of hepatocellular carcinoma: results of the PRECISION V study. Cardiovasc Intervent Radiol. 2010;33(1):41–52.
11. Llovet JM, Real MI, Montana X, et al. Arterial embolisation or chemoembolisation versus symptomatic treatment in patients with unresectable hepatocellular carcinoma: a randomised controlled trial. Lancet. 2002;359(9319):1734–9.
12. Lo CM, Ngan H, Tso WK, et al. Randomized controlled trial of transarterial lipiodol chemoembolization for unresectable hepatocellular carcinoma. Hepatology. 2002;35(5):1164–71.
13. Liu DM, Salem R, Bui JT, et al. Angiographic considerations in patients undergoing liver-directed therapy. J Vasc Interv Radiol. 2005;16(7):911–35.
14. Lewandowski RJ, Sato KT, Atassi B, et al. Radioembolization with (90)y microspheres: angiographic and technical considerations. Cardiovasc Inter Rad. 2007;30(4):571–92.
15. Salem R, Lewandowski RJ, Sato KT, et al. Technical aspects of radioembolization with 90Y microspheres. Tech Vasc Interv Radiol. 2007;10(1): 12–29.
16. Bruix J, Sherman M. Management of hepatocellular carcinoma. Hepatology. 2005;42(5):1208–36.
17. Bruix J, Sherman M, Llovet JM, et al. Clinical management of hepatocellular carcinoma. Conclusions of the Barcelona-2000 EASL conference. European Association for the Study of the Liver. J Hepatol. 2001;35(3):421–430.
18. Riaz A, Ryu RK, Kulik LM, et al. Alpha-fetoprotein response after locoregional therapy for hepatocellular carcinoma: oncologic marker of radiologic response, progression, and survival. J Clin Oncol. 2009;27(34): 5734–42.
19. Llovet JM, Di Bisceglie AM, Bruix J, et al. Design and endpoints of clinical trials in hepatocellular carcinoma. J Natl Cancer Inst. 2008;100(10):698–711.
20. Mazzaferro V, Regalia E, Doci R, et al. Liver transplantation for the treatment of small hepatocellular carcinomas in patients with cirrhosis. N Engl J Med. 1996;334(11):693–9.
21. Llovet JM, Bruix J. Systematic review of randomized trials for unresectable hepatocellular carcinoma: chemoembolization improves survival. Hepatology. 2003;37(2):429–42.
22. Lewandowski RJ, Kulik LM, Riaz A, et al. A comparative analysis of transarterial downstaging for hepatocellular carcinoma: chemoembolization versus radioembolization. Am J Transplant. 2009; 9(8):1920–8.
23. Chapman WC, Majella Doyle MB, Stuart JE, et al. Outcomes of neoadjuvant transarterial chemoembolization to downstage hepatocellular carcinoma before liver transplantation. Ann Surg. 2008;248(4): 617–25.
24. Ensminger W. Hepatic arterial chemotherapy for primary and metastatic liver cancers. Cancer Chemother Pharmacol. 1989;23(Suppl):S68–73.
25. Eksborg S, Cedermark BJ, Strandler HS. Intrahepatic and intravenous administration of adriamycin–a comparative pharmacokinetic study in patients with malignant liver tumours. Med Oncol Tumor Pharmacother. 1985;2(1):47–54.
26. Solomon B, Soulen MC, Baum RA, Haskal ZJ, Shlansky-Goldberg RD, Cope C, et al. Chemoembolization of hepatocellular carcinoma with cisplatin, doxorubicin, mitomycin-C, ethiodol, and polyvinyl alcohol: prospective evaluation of response and survival in a U.S. population. J Vasc Interv Radiol. 1999;10(6):793–8.
27. Soulen MC. Chemoembolization of hepatic malignancies. Oncology (Williston Park). 1994;8(4):77–84; discussion 84, 89–90 passim.
28. Coldwell DM, Stokes KR, Yakes WF. Embolotherapy: agents, clinical applications, and techniques. Radiographics. 1994;14(3):623–43. quiz 645–26.
29. Takayasu K, Arii S, Ikai I, et al. Prospective cohort study of transarterial chemoembolization for unresectable hepatocellular carcinoma in 8510 patients. Gastroenterology. 2006;131(2):461–9.
30. Kiefer MV, Albert M, McNally M, et al. Chemoembolization of intrahepatic cholangiocarcinoma with cisplatinum, doxorubicin, mitomycin C, ethiodol, and polyvinyl alcohol. Cancer. 2011;117(7):1498–505.
31. Murakami T, Ishimaru H, Sakamoto I, et al. Percutaneous radiofrequency ablation and transcatheter arterial chemoembolization for hypervascular

hepatocellular carcinoma: rate and risk factors for local recurrence. Cardiovasc Intervent Radiol. 2007;30(4):696–704.
32. Kagawa T, Koizumi J, Kojima S, et al. Transcatheter arterial chemoembolization plus radiofrequency ablation therapy for early stage hepatocellular carcinoma: comparison with surgical resection. Cancer. 2010;116(15):3638–44.
33. Heckman JT, Devera MB, Marsh JW, et al. Bridging locoregional therapy for hepatocellular carcinoma prior to liver transplantation. Ann Surg Oncol. 2008;15(11):3169–77.
34. Bartolozzi C, Lencioni R, Caramella D, et al. Treatment of large HCC: transcatheter arterial chemoembolization combined with percutaneous ethanol injection versus repeated transcatheter arterial chemoembolization. Radiology. 1995;197(3):812–8.
35. Xia J, Ren Z, Ye S, et al. Study of severe and rare complications of transarterial chemoembolization (TACE) for liver cancer. Eur J Radiol. 2006;59(3): 407–12.
36. Kim HK, Chung YH, Song BC, et al. Ischemic bile duct injury as a serious complication after transarterial chemoembolization in patients with hepatocellular carcinoma. J Clin Gastroenterol. 2001;32(5):423–7.
37. Belli L, Magistretti G, Puricelli GP, Damiani G, Colombo E, Cornalba GP. Arteritis following intra-arterial chemotherapy for liver tumors. Eur Radiol. 1997;7(3):323–6.
38. Lencioni R, Crocetti L, Petruzzi P, et al. Doxorubicin-eluting bead-enhanced radiofrequency ablation of hepatocellular carcinoma: a pilot clinical study. J Hepatol. 2008;49(2):217–22.
39. Constantin M, Fundueanu G, Bortolotti F, Cortesi R, Ascenzi P, Menegatti E. Preparation and characterisation of poly(vinyl alcohol)/cyclodextrin microspheres as matrix for inclusion and separation of drugs. Int J Pharm. 2004;285(1–2):87–96.
40. Gonzalez MV, Tang Y, Phillips GJ, et al. Doxorubicin eluting beads-2: methods for evaluating drug elution and in-vitro:in-vivo correlation. J Mater Sci Mater Med. 2008;19(2):767–75.
41. Dhanasekaran RM. Comparison of conventional transarterial chemoembolization (TACE) and chemoembolization with doxorubicin drug eluting beads (DEB) for unresectable hepatocellular carcinoma (HCC). J Surg Oncol. 2010;101(6):476–80.
42. Taylor RR, Tang Y, Gonzalez MV, Stratford PW, Lewis AL. Irinotecan drug eluting beads for use in chemoembolization: in vitro and in vivo evaluation of drug release properties. Eur J Pharm Sci. 2007;30(1):7–14.
43. Varela M, Real MI, Burrel M, et al. Chemoembolization of hepatocellular carcinoma with drug eluting beads: efficacy and doxorubicin pharmacokinetics. J Hepatol. 2007;46(3):474–81.
44. Reyes DK, Vossen JA, Kamel IR, et al. Single-center phase II trial of transarterial chemoembolization with drug-eluting beads for patients with unresectable hepatocellular carcinoma: initial experience in the United States. Cancer J. 2009;15(6):526–32.
45. Malagari K, Pomoni M, Kelekis A, et al. Prospective randomized comparison of chemoembolization with doxorubicin-eluting beads and bland embolization with BeadBlock for hepatocellular carcinoma. Cardiovasc Intervent Radiol. 2010;33(3):541–51.
46. Ingold JA, Reed GB, Kaplan HS, Bagshaw MA. Radiation hepatitis. Am J Roentgenol Radium Ther Nucl Med. 1965;93:200–8.
47. Geschwind JF, Salem R, Carr BI, et al. Yttrium-90 microspheres for the treatment of hepatocellular carcinoma. Gastroenterology. 2004;127(5 Suppl 1): S194–205.
48. Covey AM, Brody LA, Maluccio MA, Getrajdman GI, Brown KT. Variant hepatic arterial anatomy revisited: digital subtraction angiography performed in 600 patients. Radiology. 2002;224(2):542–7.
49. TheraSphere Yttrium-90 microspheres package insert. Kanata, Canada: MDS Nordion; 2004.
50. Salem R, Thurston KG, Carr BI, Goin JE, Geschwind JF. Yttrium-90 microspheres: radiation therapy for unresectable liver cancer. J Vasc Interv Radiol. 2002;13(9 Pt 2):S223–9.
51. Kulik LM, Atassi B, van Holsbeeck L, et al. Yttrium-90 microspheres (TheraSphere(R)) treatment of unresectable hepatocellular carcinoma: downstaging to resection, RFA and bridge to transplantation. J Surg Oncol. 2006;94(7):572–86.
52. Kulik LM, Carr BI, Mulcahy MF, et al. Safety and efficacy of (90)Y radiotherapy for hepatocellular carcinoma with and without portal vein thrombosis. Hepatology. 2007;47(1):71–81.
53. Hilgard P, Hamami M, Fouly AE, et al. Radioembolization with yttrium-90 glass microspheres in hepatocellular carcinoma: European experience on safety and long-term survival. Hepatology. 2010;52(5): 1741–9.
54. Sangro B, Carpanese L, Cianni R, et al. Survival after yttrium-90 resin microsphere radioembolization of hepatocellular carcinoma across Barcelona clinic liver cancer stages: a European evaluation. Hepatology. 2011;54(3):868–78.
55. Ibrahim SM, Nikolaidis P, Miller FH, et al. Radiologic findings following Y90 radioembolization for primary liver malignancies. Abdom Imaging. 2009;34(5): 566–81.
56. Saxena A, Bester L, Chua TC, Chu FC, Morris DL. Yttrium-90 radiotherapy for unresectable intrahepatic cholangiocarcinoma: a preliminary assessment of this novel treatment option. Ann Surg Oncol. 2010;17(2): 484–91.
57. Salem R, Lewandowski RJ, Atassi B, et al. Treatment of unresectable hepatocellular carcinoma with use of 90Y microspheres (TheraSphere): safety, tumor response, and survival. J Vasc Interv Radiol. 2005; 16(12):1627–39.
58. Kennedy AS, Coldwell D, Nutting C, et al. Resin 90Y-microsphere brachytherapy for unresectable

colorectal liver metastases: modern USA experience. Int J Radiat Oncol Biol Phys. 2006; 65(2):412–25.
59. Murthy R, Xiong H, Nunez R, et al. Yttrium 90 resin microspheres for the treatment of unresectable colorectal hepatic metastases after failure of multiple chemotherapy regimens: preliminary results. J Vasc Interv Radiol. 2005;16(7):937–45.
60. Sangro B, Gil-Alzugaray B, Rodriguez J, et al. Liver disease induced by radioembolization of liver tumors: description and possible risk factors. Cancer. 2008; 112(7):1538–46.
61. Young JY, Rhee TK, Atassi B, et al. Radiation dose limits and liver toxicities resulting from multiple yttrium-90 radioembolization treatments for hepatocellular carcinoma. J Vasc Interv Radiol. 2007;18(11): 1375–82.
62. Jakobs TF, Saleem S, Atassi B, et al. Fibrosis, portal hypertension, and hepatic volume changes induced by intra-arterial radiotherapy with (90)yttrium microspheres. Dig Dis Sci. 2008;53(9):2556–63.
63. Rhee TK, Naik NK, Deng J, et al. Tumor response after yttrium-90 radioembolization for hepatocellular carcinoma: comparison of diffusion-weighted functional MR imaging with anatomic MR imaging. J Vasc Interv Radiol. 2008;19(8):1180–6.
64. Murthy R, Brown DB, Salem R, et al. Gastrointestinal complications associated with hepatic arterial yttrium-90 microsphere therapy. J Vasc Interv Radiol. 2007; 18(4):553–61. quiz 562.
65. Carretero C, Munoz-Navas M, Betes M, et al. Gastroduodenal injury after radioembolization of hepatic tumors. Am J Gastroenterol. 2007;102(6): 1216–20.
66. Murthy R, Eng C, Krishnan S, et al. Hepatic yttrium-90 radioembolotherapy in metastatic colorectal cancer treated with cetuximab or bevacizumab. J Vasc Interv Radiol. 2007;18(12):1588–91.
67. WHO. WHO handbook for reporting results of cancer treatment. Geneva: WHO Offset Publication; 1979. No.48.
68. Therasse P, Arbuck SG, Eisenhauer EA, et al. New guidelines to evaluate the response to treatment in solid tumors. European organization for research and treatment of cancer, National Cancer Institute of the United States, National Cancer Institute of Canada. J Natl Cancer Inst. 2000;92(3):205–16.
69. Forner A, Ayuso C, Varela M, et al. Evaluation of tumor response after locoregional therapies in hepatocellular carcinoma: are response evaluation criteria in solid tumors reliable? Cancer. 2009;115(3):616–23.
70. Lencioni R, Llovet JM. Modified RECIST (mRECIST) assessment for hepatocellular carcinoma. Semin Liver Dis. 2010;30(1):52–60.
71. Riaz A, Miller FH, Kulik LM, et al. Imaging response in the primary index lesion and clinical outcomes following transarterial locoregional therapy for hepatocellular carcinoma. JAMA. 2010;303(11): 1062–9.
72. Riaz A, Lewandowski RJ, Kulik L, et al. Radiologic-pathologic correlation of hepatocellular carcinoma treated with chemoembolization. Cardiovasc Intervent Radiol. 2010;33(6):1143–52.
73. Riaz A, Kulik L, Lewandowski RJ, et al. Radiologic-pathologic correlation of hepatocellular carcinoma treated with internal radiation using yttrium-90 microspheres. Hepatology. 2009;49(4):1185–93.
74. Riaz A, Memon K, Miller FH, et al. Role of the EASL, RECIST, and WHO response guidelines alone or in combination for hepatocellular carcinoma: radiologic–pathologic correlation. J Hepatol. 2011; 54(4):695–704.

Combination Therapies in the Treatment of Primary Liver Cancers

22

Riccardo Lencioni and Laura Crocetti

Abstract

Several combined treatment strategies have been used in the treatment of hepatocellular carcinoma (HCC). These include various combinations of locoregional interventions as well as the association of locoregional and systemic therapies. Radio-frequency ablation (RFA) is currently accepted as the best therapeutic choice for nonsurgical patients with early-stage HCC. Nevertheless, the rate of complete tumor eradication is highly dependent on tumor size and presence of large abutting vessels. Several attempts have been made to increase the effect of RFA in HCC treatment. Given that HCC is mostly nourished by the hepatic artery, a combination of RFA and balloon catheter occlusion of the tumor arterial supply or prior transcatheter arterial embolization or chemoembolization has been used to increase heat efficiency. A different strategy is to adominister intrarterially an embolic, drug-eluting bead (DEB) within 24 h of RFA to take advantage of the reactive hyperemia induced by RFA to facilitate delivery of the microspheres to the tumor-bearing area. Investigators have also suggested the combined use of percutaneous approaches, such as ethanol injection and RFA. Despite the advances in locoregional treatments, long-term outcomes of patients with early or intermediate-stage HCC remain unsatisfactory because of the high rate of tumor recurrence. To date, studies of sorafenib, a tyrosine kinase inhibitor with anti-angiogenetic properties, have demonstrated its efficacy in advanced HCC; however, there may also be a role for this agent – or other molecular targeted drugs – in earlier-stage disease, either as adjuvant treatment after curative therapy or in combination with trans-arterial chemoembolization.

R. Lencioni (✉) • L. Crocetti
Division of Diagnostic Imaging and Intervention, School of Medicine, University of Pisa, Cisanello Hospital, Pisa, IT, Italy
e-mail: riccardo.lencioni@med.unipi.it; laura.crocetti@med.unipi.it

Several combined treatment strategies have been used in the treatment of hepatocellular carcinoma (HCC). These include various combinations of locoregional interventions as well as the association of locoregional and systemic therapies. Despite combined treatments are widely used in

D.E. Dupuy et al. (eds.), *Image-Guided Cancer Therapy*, DOI 10.1007/978-1-4419-0751-6_24,

clinical practice, unequivocal evidence of clinical benefit associated with such strategies is lacking, as no robust phase III randomized clinical trials have been completed so far [1].

Combination of Transcatheter Treatments and Image-Guided Ablation

Radio-frequency ablation (RFA) is currently accepted as the best therapeutic choice for nonsurgical patients with early-stage HCC [2]. Randomized trials comparing RFA versus ethanol injection showed that RFA has higher local anticancer effect, leading to a better local control of the disease [3–7]. Reports on long-term outcomes of RFA-treated patients confirmed that survival of naive patients with well-compensated cirrhosis bearing early-stage HCC is similar to that reported in surgical series [8–10].

Nevertheless, histological studies performed in liver specimens of patients who underwent RFA as bridge treatment for transplantation showed that the rate of complete tumor eradication is highly dependent on tumor size and presence of large (3 mm or more) abutting vessels [11]. In fact, vessels adjacent to the target tumor cause heat loss due to perfusion-mediated tissue cooling within the area to be ablated.

Several attempts have been made to increase the effect of RFA in HCC treatment. Since heat efficiency is the difference between the amount of heat produced and the amount of heat lost, most investigators devoted their attention to strategies that aim primarily at minimizing heat loss due to perfusion-mediated tissue cooling [12]. When a laparotomy or a laparoscopy approach is used to perform RF ablation, heat loss can be minimized by performing a Pringle maneuver [12]. In percutaneous procedures, given that HCC is mostly nourished by the hepatic artery, a combination of RF ablation and balloon catheter occlusion of the tumor arterial supply or prior transcatheter arterial embolization or chemoembolization has been used to increase heat efficiency [13–16].

In a standard RFA, one can take advantage of only those temperatures that are sufficient by themselves to induce coagulative necrosis (>50 °C). However, there are large zones of sublethal heating created during RF application in tissues surrounding the electrode that are not being used to achieve sustained treatment effect. Experimental studies in animal tumor models have shown that lowering the temperature threshold at which cell death occurs by combining sublethal temperature with cell exposure to chemotherapeutic agents increases tumor necrosis, apparently occurring in tissues heated to 45–50 °C [17, 18]. In a recent pilot clinical trial, an embolic, drug-eluting bead (DEB) for hepatic arterial administration has been used to explore such a synergy in human HCC. DEB was injected within 24 h of RFA to take advantage of the reactive hyperemia induced by RFA to facilitate delivery of the microspheres to the tumor-bearing area. DEB administration resulted in substantial increase in tissue destruction, leading to confirmed complete responses in patients bearing large tumors refractory to standard RFA [19].

Other investigators have also suggested the combined use of percutaneous approaches, such as ethanol injection and RFA. In one randomized trial, such a combination resulted in higher rates of overall survival and lower rates of tumor recurrence compared to RFA alone [20] (Fig. 22.1).

Combination of Locoregional and Systemic Treatments

Despite the advances in locoregional treatments, long-term outcomes of patients with early or intermediate-stage HCC remain unsatisfactory because of the high rate of tumor recurrence. After local ablation of early-stage HCC, tumor recurrence rate exceeds 80 % at 5 years, similar to post-resection figures [8]. Molecular studies have shown that early recurrences – occurring within the first 2 years after curative treatment – are mainly due to the spread of the original tumor, while late recurrences are more frequently due to the development of metachronous tumors independent of the previous cancer. On the other hand, in patients with large or multinodular tumor at the intermediate-stage HCC who

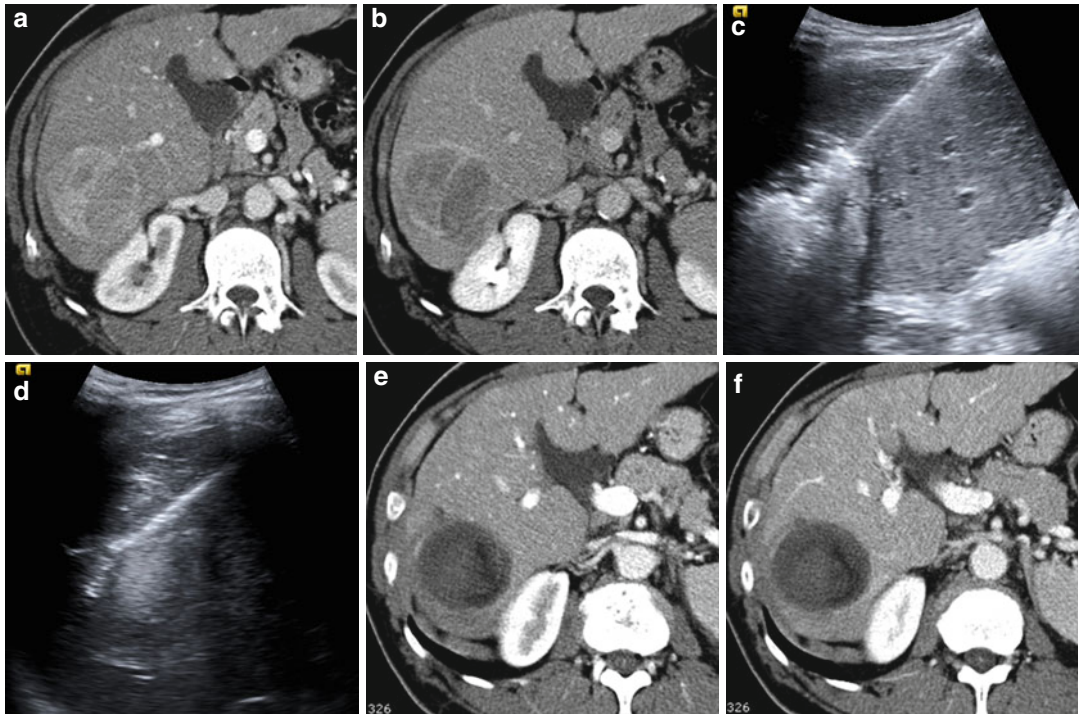

Fig. 22.1 *Combined ethanol injection and RF ablation of HCC*. Pretreatment contrast-enhanced CT shows the lesion as a hypervascular nodule (**a**) in the arterial phase with hypodense appearance in portal-venous phase (**b**). Under ultrasound guidance, ethanol injection (**c**) followed by RF ablation with expandable needle (**d**) is performed. On contrast-enhanced CT images obtained in the arterial (**e**) and the portal-venous phase (**f**) 1 month after percutaneous RF treatment, the tumor is replaced by a non-enhancing ablation zone. The findings are consistent with complete response

received transcatheter arterial chemoembolization (TACE), tumor recurrence or progression is almost inevitable, leading to an overall survival rate of less than 30 % at 3 years [21].

Angiogenesis plays a pivotal role in the development, progression, and prognosis of HCC due to the vascularity of these tumors. Upregulation of angiogenesis is first detected in dysplastic nodules, whereas malignant transformation leads to arterialization of its blood supply and sinusoidal capillarization. Vascular endothelial growth factor (VEGF) plays a critical role in this process. Growth factor signal receptors and their downstream transduction pathways play a central role in the development and progression of HCC. Among the most prominent contributors are the Ras/Raf/MEK/ERK, PI3/AKT/mTOR, and JAK/STAT receptor tyrosine kinase-activated pathways [22]. Signal transduction via the Ras/Raf/MEK/ERK pathway, which includes several ubiquitous enzymes, is involved in the development, progression, and maintenance of HCC. These pathways can be activated by binding of growth factors such as epidermal growth factor (EGF), hepatocyte growth factor (HGF), platelet-derived growth factor (PDGF), and VEGF, which are secreted in an autocrine or paracrine fashion by the tumor or surrounding tissues. These findings suggested that inhibitors of these pathways, particularly of the tyrosine kinases bound by growth factors, may inhibit the progression of HCC.

The first tyrosine kinase inhibitor developed for the treatment of HCC was sorafenib. This small-molecule multikinase inhibitor was shown to significantly inhibit the activity of Raf-1, wild-type and oncogenic BRAF, VEGFR-1 and VEGFR-2, PDGFR, Flt-3, and c-Kit, as well as the phosphorylation of MEK and ERK, both

in vivo and in vitro [23–25]. Moreover, its antitumor activity in human HCC xenografts in nude mice correlated with its inhibition of MAP signaling [25]. Two large, phase III, randomized, placebo-controlled clinical trials have evaluated the efficacy and safety of sorafenib in patients with advanced HCC. In the Sorafenib HCC Assessment Randomized Protocol (SHARP) trial, 602 previously untreated patients with advanced HCC were randomized 1:1 to receive either sorafenib 400 mg or matching placebo twice daily on a continuous basis [26]. Both median overall survival (OS) and median time to disease progression (TTP) were significantly longer in the sorafenib group than in the placebo group. In the Sorafenib Asia-Pacific trial, 271 patients from the Asia-Pacific region with advanced HCC were randomized 2:1 to receive either sorafenib 400 mg or matching placebo twice daily on a continuous basis [27]. As in the SHARP trial, median OS and TTP were significantly longer in the sorafenib group than in the placebo group. Thus, both trials showed that sorafenib is an appropriate option for the systemic treatment of patients with advanced HCC.

To date, studies of sorafenib have demonstrated its efficacy in advanced HCC; however, there may also be a role for this agent – or other molecular targeted drugs – in earlier-stage disease, either as adjuvant treatment after curative therapy or in combination with TACE. Because the amount of oxygen supplied to a tumor is a function of the distance of the tumor cells from the local blood vessel, hypoxia in tumor cells that remain and are distant from the feeding blood vessel increases following TACE [28]. Surrogate markers of tissue hypoxia that increase after TACE include hypoxia-inducible factor 1 alpha (HIF-1α) [29] and both plasma and hepatic VEGF [30, 31]. Hypoxia in HCC can lead to neoangiogenesis, suggesting that inhibition of angiogenesis may be synergistic with TACE in patients with HCC [32].

Treatment with an anti-angiogenic agent such as sorafenib may therefore complement TACE. An anti-angiogenic agent may inhibit TACE-induced angiogenesis and the development of tumor-feeding vessels associated with tumor cell proliferation. In addition, anti-angiogenic agents may target lesions distant from the site of TACE. However, initiating anti-angiogenic therapy before TACE may have potential drawbacks, including the reduction in size and number of blood vessels feeding the tumor, thus reducing the efficacy of TACE. Among the anti-angiogenic agents that have been tested, are being tested, or are scheduled to be tested in combination with TACE in patients with HCC are the tyrosine kinase inhibitors sorafenib, sunitinib, axitinib, brivanib, and TSU-68, as well as thalidomide, TAC-101, and the anti-VEGF antibody bevacizumab [33]. Sorafenib is also currently investigated as adjuvant treatment in early-stage HCC in patients who have undergone successful surgical resection or local ablation. These ongoing trials are the first significant studies in which an interventional locoregional treatment is evaluated in combination with a systemically active molecular targeted drug in HCC. The outcomes of these combination studies are eagerly awaited, as they have the potential to revolutionize treatment of HCC.

References

1. Lencioni R. Loco-regional treatment of hepatocellular carcinoma. Hepatology. 2010;52:762–73.
2. Crocetti L, De Baere T, Lencioni R. Quality improvement guidelines for radiofrequency ablation of liver tumours. Cardiovasc Intervent Radiol. 2010;33:11–7.
3. Lencioni R, Allgaier HP, Cioni D, et al. Small hepatocellular carcinoma in cirrhosis: randomized comparison of radiofrequency thermal ablation versus percutaneous ethanol injection. Radiology. 2003;228:235–40.
4. Lin SM, Lin CJ, Lin CC, et al. Radiofrequency ablation improves prognosis compared with ethanol injection for hepatocellular carcinoma < or = 4 cm. Gastroenterology. 2004;127:1714–23.
5. Shiina S, Teratani T, Obi S, et al. A randomized controlled trial of radiofrequency ablation versus ethanol injection for small hepatocellular carcinoma. Gastroenterology. 2005;129:122–30.
6. Lin SM, Lin CJ, Lin CC, et al. Randomised controlled trial comparing percutaneous radiofrequency thermal ablation, percutaneous ethanol injection, and percutaneous acetic acid injection to treat hepatocellular carcinoma of 3 cm or less. Gut. 2005;54:1151–6.

7. Brunello F, Veltri A, Carucci P, et al. Radiofrequency ablation versus ethanol injection for early hepatocellular carcinoma: a randomized controlled trial. Scand J Gastroenterol. 2008;43:727–35.
8. Lencioni R, Cioni D, Crocetti L, et al. Early-stage hepatocellular carcinoma in cirrhosis: long-term results of percutaneous image-guided radiofrequency ablation. Radiology. 2005;234:961–7.
9. Choi D, Lim HK, Rhim H, et al. Percutaneous radiofrequency ablation for early-stage hepatocellular carcinoma as a first-line treatment: long-term results and prognostic factors in a large single-institution series. Eur Radiol. 2007;17:684–92.
10. N'Kontchou G, Mahamoudi A, Aout M, et al. Radiofrequency ablation of hepatocellular carcinoma: long-term results and prognostic factors in 235 Western patients with cirrhosis. Hepatology. 2009;50:1475–83.
11. Lu DS, Yu NC, Raman SS, et al. Radiofrequency ablation of hepatocellular carcinoma: treatment success as defined by histologic examination of the explanted liver. Radiology. 2005;234:954–60.
12. Goldberg SN, Hahn PF, Tanabe KK, et al. Percutaneous radiofrequency tissue ablation: does perfusion-mediated tissue cooling limit coagulation necrosis? J Vasc Interv Radiol. 1998;9:101–11.
13. Rossi S, Garbagnati F, Lencioni R, et al. Percutaneous radio-frequency thermal ablation of nonresectable hepatocellular carcinoma after occlusion of tumor blood supply. Radiology. 2000;217:119–26.
14. Veltri A, Moretto P, Doriguzzi A, et al. Radiofrequency thermal ablation (RFA) after transarterial chemoembolization (TACE) as a combined therapy for unresectable non-early hepatocellular carcinoma (HCC). Eur Radiol. 2006;16:661–9.
15. Helmberger T, Dogan S, Straub G, et al. Liver resection or combined chemoembolization and radiofrequency ablation improve survival in patients with hepatocellular carcinoma. Digestion. 2007;75:104–12.
16. Yamasaki T, Kurokawa F, Shirahashi H, et al. Percutaneous radiofrequency ablation therapy for patients with hepatocellular carcinoma during occlusion of hepatic blood flow. Comparison with standard percutaneous radiofrequency ablation therapy. Cancer. 2002;95:2353–60.
17. Goldberg SN, Girnan GD, Lukyanov AN, et al. Percutaneous tumor ablation: increased necrosis with combined radio-frequency ablation and intravenous liposomal doxorubicin in a rat breast tumor model. Radiology. 2002;222:797–804.
18. Ahmed M, Liu Z, Lukyanov AN, et al. Combination radiofrequency ablation with intratumoral liposomal doxorubicin: effect on drug accumulation and coagulation in multiple tissues and tumor types in animals. Radiology. 2005;235:469–77.
19. Lencioni R, Crocetti L, Petruzzi P, et al. Doxorubicin-eluting bead-enhanced radiofrequency ablation of hepatocellular carcinoma: a pilot clinical study. J Hepatol. 2008;49:217–22.
20. Zhang YJ, Liang HH, Chen MS, et al. Hepatocellular carcinoma treated with radiofrequency ablation with or without ethanol injection: a prospective randomized trial. Radiology. 2007;244:599–607.
21. Llovet JM, Real MI, Montana X, et al. Arterial embolisation or chemoembolisation versus symptomatic treatment in patients with unresectable hepatocellular carcinoma: a randomised controlled trial. Lancet. 2002;359:1734–9.
22. Wilhelm SM, Adnane L, Newell P, et al. Preclinical overview of sorafenib, a multikinase inhibitor that targets both Raf and VEGF and PDGF receptor tyrosine kinase signaling. Mol Cancer Ther. 2008;7:3129–40.
23. Wilhelm SM, Carter C, Tang L, et al. BAY 43–9006 exhibits broad spectrum oral antitumor activity and targets the RAF/MEK/ERK pathway and receptor tyrosine kinases involved in tumor progression and angiogenesis. Cancer Res. 2004;64:7099–109.
24. Liu L, Cao Y, Chen C, et al. Sorafenib blocks the RAF/MEK/ERK pathway, inhibits tumor angiogenesis, and induces tumor cell apoptosis in hepatocellular carcinoma model PLC/PRF/5. Cancer Res. 2006;66:11851–8.
25. Wilhelm S, Carter C, Lynch M, et al. Discovery and development of sorafenib: a multikinase inhibitor for treating cancer. Nat Rev Drug Discov. 2006;5:835–44.
26. Llovet JM, Ricci S, Mazzaferro V, et al. Sorafenib in advanced hepatocellular carcinoma. N Engl J Med. 2008;359:378–90.
27. Cheng AL, Kang YK, Chen Z, et al. Efficacy and safety of sorafenib in patients in the Asia-Pacific region with advanced hepatocellular carcinoma: a phase III randomised, double-blind, placebo-controlled trial. Lancet Oncol. 2009;10:25–34.
28. Carmeliet P, Jain RK. Angiogenesis in cancer and other diseases. Nature. 2000;407:249–57.
29. Rhee TK, Young JY, Larson AC, et al. Effect of transcatheter arterial embolization on levels of hypoxia-inducible factor-1alpha in rabbit VX2 liver tumors. J Vasc Interv Radiol. 2007;18:639–45.
30. Li X, Feng GS, Zheng CS, Zhuo CK, Liu X. Expression of plasma vascular endothelial growth factor in patients with hepatocellular carcinoma and effect of transcatheter arterial chemoembolization therapy on plasma vascular endothelial growth factor level. World J Gastroenterol. 2004;10:2878–82.
31. Wang B, Xu H, Gao ZQ, et al. Increased expression of vascular endothelial growth factor in hepatocellular carcinoma after transcatheter arterial chemoembolization. Acta Radiol. 2008;49:523–9.
32. Jiang H, Meng Q, Tan H, et al. Antiangiogenic therapy enhances the efficacy of transcatheter arterial embolization for hepatocellular carcinomas. Int J Cancer. 2007;121:416–24.
33. Lencioni R, Zou J, Leberre M, et al. Sorafenib (SOR) or placebo (PL) in combination with transarterial chemoembolization (TACE) for intermediate-stage hepatocellular carcinoma (SPACE). J Clin Oncol. 2010;28: TPS178 [Abstract].

Resection Transplant in the Treatment of Primary Liver Cancers

23

Gabriel Schnickel and Henrik Petrowsky

Abstract

Hepatocellular carcinoma (HCC) is the third leading cause of cancer-related deaths worldwide. Liver resection and orthotopic liver transplantation (OLT) for HCC are the most effective therapies which can achieve cure or long-term survival. Ideal candidates for liver resection are patients with compensated liver function (Child-Turcotte-Pugh [CTP] class A) and absence of portal hypertension. Portal vein embolization (PVE) and sequential use of transarterial chemoembolization (TACE) followed by PVE are adjunctive modalities to surgical resection which can be used for patient selection, making resection safer in cirrhotic patients. Although liver resection for HCC achieves a 5-year survival rate of 30–50 %, tumor recurrence is common affecting 70–80 % of patients. OLT has the advantage of simultaneous removal of tumor and diseased liver; however, this treatment can be offered only to a small proportion of patients due to tumor stage beyond accepted criteria and donor organ shortage. The Milan (single lesion $\leq$5 cm, or no more than three lesions $\leq$3 cm) and UCSF criteria (single lesion $\leq$6.5 cm, or no more than three lesions $\leq$4.5 cm and a total diameter of 8 cm) are the most widely accepted criteria defining the candidacy of patients with HCC for OLT. Whether liver resection or OLT should be used as primary therapy of patients with HCC within the Milan or UCSF criteria is hotly debated. While OLT is favored as primary therapy for small HCC in the United States, many European and Asian centers use primary liver resection with salvage transplantation for recurrence as favored treatment approach in patients with reasonable liver

G. Schnickel
Department of Transplant Surgery, Henry Ford Transplant Institute, Detroit, MI, USA
e-mail: gschnic1@hfhs.org

H. Petrowsky (✉)
Swiss Hepato-Pancreato-Biliray and Transplant Center, Department of Surgery, University Hospital Zürich, Zürich, Switzerland
e-mail: Henrik.Petrowsky@usz.ch

D.E. Dupuy et al. (eds.), *Image-Guided Cancer Therapy*, DOI 10.1007/978-1-4419-0751-6_25,

function (CTP class A) and absence of portal hypertension. Cirrhotic patients with small HCC who have decompensated liver function (CTP class B and C) and portal hypertension should be primarily considered for OLT.

Introduction

Hepatocellular carcinoma (HCC) is the third leading cause of cancer-related deaths worldwide and is on the rise secondary to chronic Hepatitis B virus (HBV) and Hepatitis C virus (HCV) infections [1]. Untreated HCC has a dismal prognosis with a 5-year survival rate below 10 % (Fig. 23.1) [2]. The majority of patients develop HCC in the setting of cirrhosis adding significant complexity to the optimal treatment algorithms. There has been significant progress in recent years in, not only, the understanding of the disease, but in the treatment options for patients with HCC. The current armamentarium for treatment of patients with HCC includes surgical resection, liver transplantation, radiologic directed local regional therapies, and chemotherapy. If HCC is localized and not multifocal, surgical resection and orthotopic liver transplantation (OLT) are the gold standard therapies for patients with HCC.

Surgical Resection for HCC

Patient Selection for Hepatic Resection

Recent advances in diagnosis, imaging, anesthesia, and surgical techniques have improved perioperative outcomes for liver resection. The critical considerations that must be addressed when evaluating surgical resection for HCC are patient-, liver-, and tumor-related factors.

Liver resection is the preferred surgical treatment for non-cirrhotic patients with HCC. The selection of non-cirrhotic patients with HCC for surgical resection follows the same principles as for other non-HCC malignant lesions. Those patients generally have normal liver function without portal hypertension and tolerate extended liver resections with a comparable morbidity. If extended liver resections for large HCC, with a potential remnant liver volume of less than 30 %, have to be considered, patients should undergo portal vein embolization (PVE) to increase the potential remnant liver volume (Fig. 23.2) [3]. A recently published meta-analysis of 1,088 pooled patients demonstrated that PVE is a safe and effective procedure [4]. There is also growing evidence that PVE improves respectability and reduces the risk for postoperative hepatic failure after major resection for HCC [5, 6].

The indication for hepatic resection for HCC in cirrhotic patients is primarily dictated by the function of the diseased liver and the presence of portal hypertension. While cirrhotic patients with well-compensated liver function (Child-Turcotte-Pugh (CTP) score A) are potential candidates for hepatic resection, resection in patients with significant hepatic functional compromise (CTP score B) or decompensated disease (CTP score C) is associated with poor outcome [3]. In addition, the presence of portal hypertension demonstrates a barrier for resection in many institutions since previous studies reported a poor outcome in those patients [7, 8]. Therefore, the published guidelines of the AASLD (American Association for the Study of Liver Diseases) and the EASL (European Association for the Study of the Liver) consider well-compensated liver function (CTP score A) and absence of portal hypertension as mandatory elements for resection [9, 10]. Portal hypertension can be indirectly assessed by presence of splenomegaly, esophagogastric varices, and low platelet count ($<100.000/mm^3$) or directly determined by hepatic venous gradient measurement ($\geq$10 mmHg). Despite these facts, there is growing evidence that liver resection for HCC in well-selected patients with mild portal hypertension is safe and can achieve a comparable outcome as in patients without portal hypertension [11, 12].

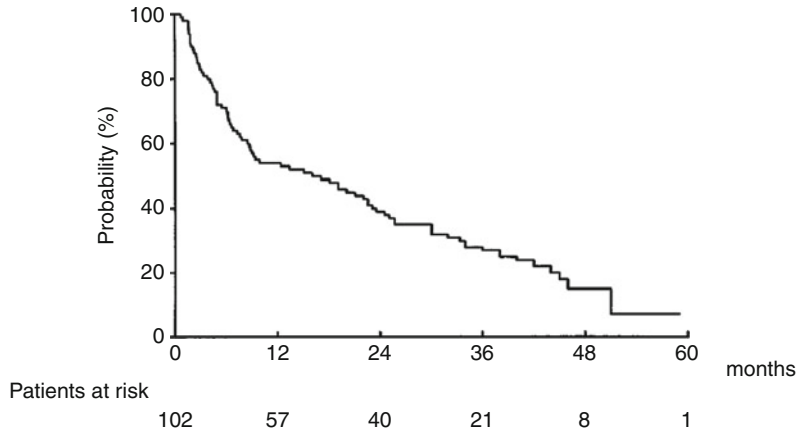

Fig. 23.1 Overall survival probability of 102 patients with untreated HCC (Reprinted from Llovet et al [2] Natural history of untreated nonsurgical hepatocellular carcinoma: rational for the design and evaluation of therapeutic trials. Hepatology 1999;29:62–67, Fig. 1, with permission from John Wiley and Sons)

In addition to liver function and portal hypertension, the future remnant liver mass is another important factor which has to be considered in cirrhotic patients before resection. A volumetric study in patients with HCC revealed that a too small remnant liver volume was associated with a significantly increased risk for post-resectional liver failure (Fig. 23.3) [13]. There is worldwide consensus that the critical remnant liver volume in cirrhotic patients should be above 50 % [14]. If the future remnant liver volume would be below 50 %, PVE might be considered to increase the remnant volume (Fig. 23.2). Several reports have documented the benefit of preoperative (PVE) for improved perioperative outcome and survival in cirrhotic patients with HCC [5, 6, 15, 16]. Another strategy in HCC patients is the sequential application of transarterial chemoembolization (TACE) and PVE followed by surgical resection [15, 16]. This combined approach offers tumor treatment and hypertrophy induction of the future remnant liver. Belghiti et al. have shown that sequential use of TACE and PVE results in more efficient hypertrophy of the future remnant liver compared to PVE alone. Furthermore, cirrhotic patients who failed to respond had a 50 % mortality rate after resection for HCC, while the perioperative mortality in patients with good or mild volume response was zero or significantly lower (13 %). These findings illustrate that PVE with or without TACE might be used as preoperative dynamic liver test for selection of cirrhotic patients who should or should not undergo major liver resection. This presumes that patients, who fail to respond with hypertrophy, will also fail to regenerate after hepatic resection [3].

Dynamic liver function tests such as indocyanine green (ICG) test, breath tests, and GSA scintigraphy are also used as complementary assessment of liver function in cirrhotic patients [3, 14]. The ICG test is a frequently utilized test in many Asian (73 %) and European liver centers (43 %) as a mandatory element of liver function assessment before surgical resection [14, 17]. An ICG retention rate of less than 14 % proved to be a safe indicator for major hepatectomy in cirrhotic patients, whereas retention rates above 20 % should be considered as contraindication for major hepatectomy (Fig. 23.2) [18–20].

Patient-related factors involve many of the same considerations that must be given to any patient undergoing a major surgery. Several studies have looked specifically at patient-related risk factors predictive of outcome following liver resection for HCC. Age and gender have been found to be independent risk factors on multivariate analyses in several large studies [21]. With that finding in mind, Hanazaki et al. looked at their experience with 103 patients over the age of 70 and found that, with careful patient selection, elderly patients benefit as much from resection as do younger patients [22]. A comprehensive review of published studies underscores that liver resection for HCC can be safely performed in well-selected elderly patients (age >70 years)

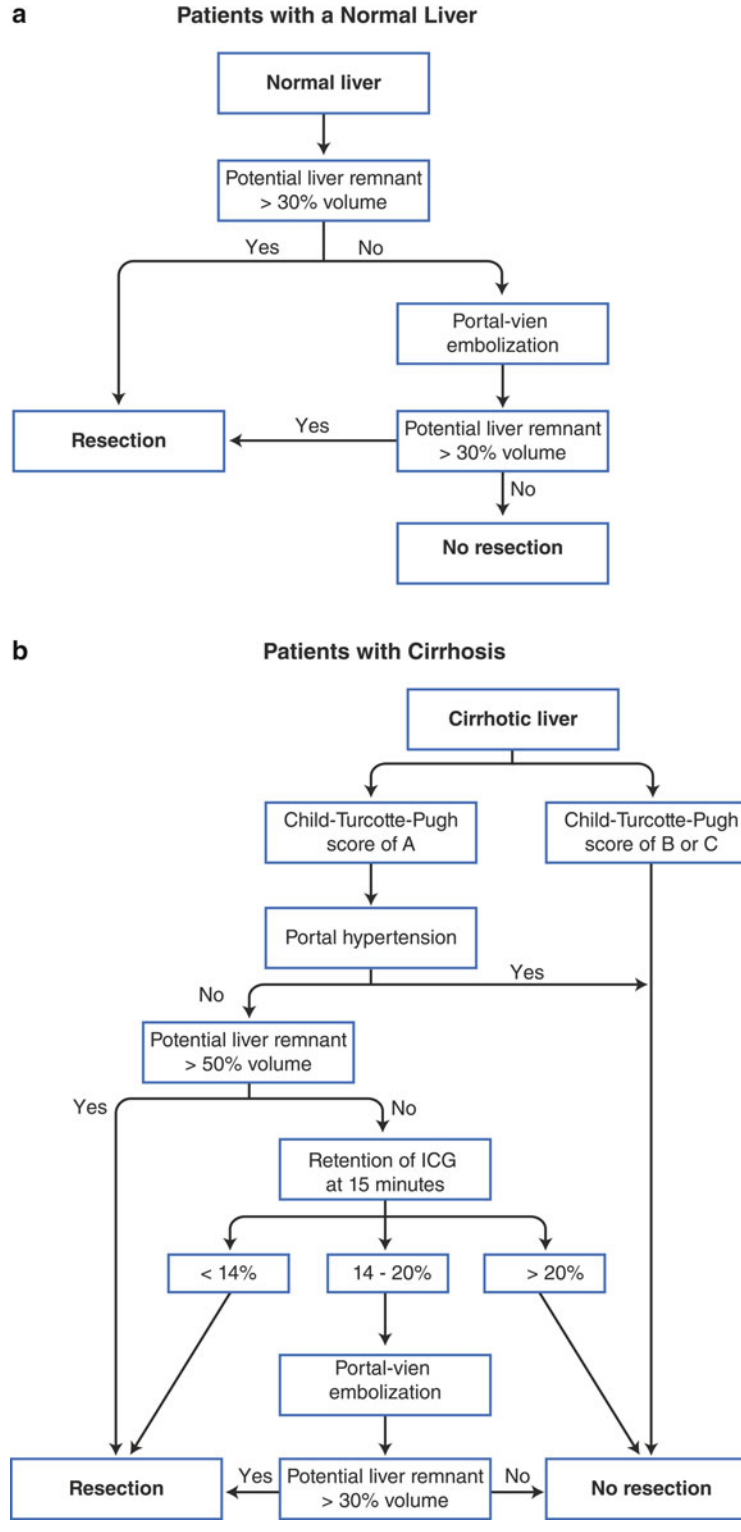

Fig. 23.2 Treatment algorithm for major hepatectomy in patients with normal and cirrhotic livers (Reprinted from Clavien et al [3] Strategies for safer liver surgery and partial liver transplantation. N Engl J Med 2007;356:1545–59, Fig. 3, with permission from Massachusetts Medical Society)

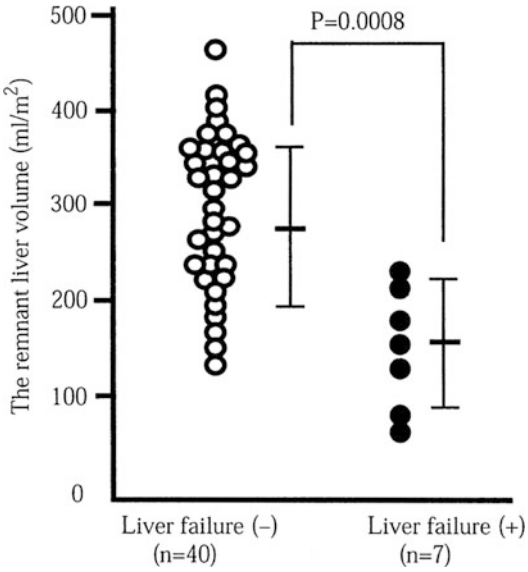

Fig. 23.3 Comparison of remnant liver volumes of patients who died of liver failure (163 ± 63 mL/m^2) and those without liver failure (285 ± 82 mL/m^2) after a right hepatectomy for HCC (Reprinted from Shirabe et al [13] Postoperative liver failure after major hepatic resection for hepatocellular carcinoma in the modern era with special reference to remnant liver volume. J Am Coll Surg 1999;188:304–7, Fig. 1, with permission from Elsevier, UK)

with comparable outcome to younger patients [23]. Comorbidities as represented by American society of anesthesiologists (ASA) grade have also been shown to impact disease-free survival [24]. When considering all of these factors, major liver resection is high-risk operation that can be performed safely with careful patient assessment.

With better patient selection, the perioperative mortality and outcome of hepatic resection for HCC has been continuously improved during the past two decades. Large series of the past 10 years show that resection can roughly achieve a 30–50 % overall survival rate (Table 23.1) which is similar to hepatic resection of colorectal liver metastases. Most of these studies report an acceptable perioperative mortality rate of less than 7 %.

Resection Margin

Tumor biology impacts patient survival and is represented by TNM staging at presentation, macro- and microvascular invasion, number of tumors, and depth of surgical margins. HCC is known to spread via the portal venous system

Table 23.1 Selected series of hepatic resection for HCC with more than 200 patients over the past decade

First author	Year	Study period	No. of pts	Cirrhosis	Minor resections[a]	Mortality	5-year OS rate
Zhou [74]	2001	1967–1998	2,366	-	72 %	2.7 %	50 %
Kanematsu [75]	2002	1985–2000	303	55 %	76 %	1.6 %	51 %
Belghiti [76]	2002	1990–2004	328	50 %	-	6.4 %	37 %
Wayne [77]	2002	1980–1998	249	73 %	73 %	6.1 %	41 %
Ercolani [24]	2003	1983–1999	224	100 %	-	-	42 %
Chen [78][b]	2004	1972–2000	525	91 %	22 %	2.7 %	17 %
Wu [79]	2005	1991–2002	426	100 %	55 %	1.6 %	46–61 %[c]
Capussotti [80]	2005	1985–2001	216	100 %	24 %	8.3 %	34 %
Hasegawa [26]	2005	1994–2001	210	39 %	-	0.0 %	35–66 %[c]
Nathan [81]	2009	1988–2005	788	-	-	-	39 %
Yang [82]	2009	1992–2002	481	77 %	-	1.7 %	20–48 %[c]
Wang [83]	2010	1991–2004	438	-	-	7.5 %	43 %

- Not defined, *pts* patients, *OS* overall survival
[a]Minor resections are defined as ≤ segmentectomy
[b]This study included only HCC >10 cm
[c]Range of 5-year OS among different subgroups

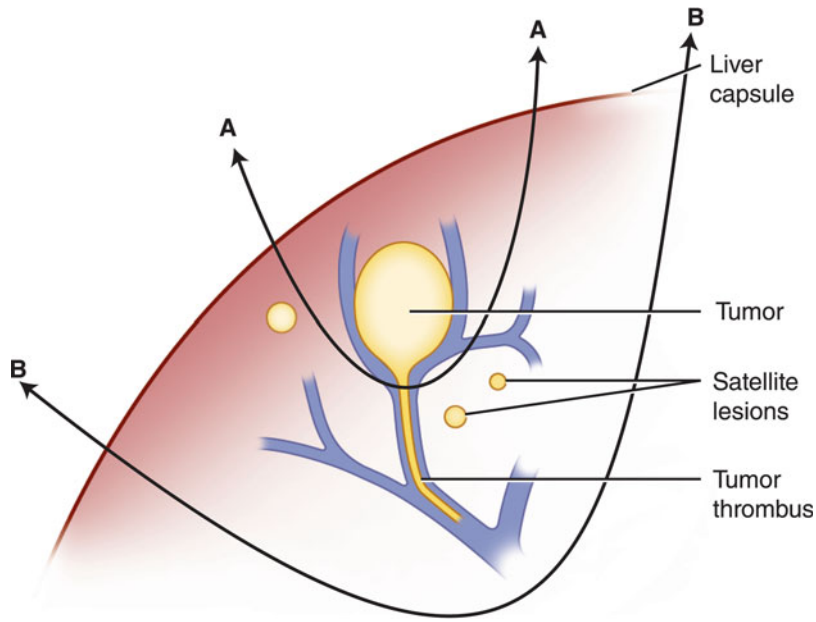

Fig. 23.4 Limited (*A*) versus anatomic (*B*) liver resection for HCC in the settings of satellite lesions and tumor invasion (tumor thrombus) into portal venous branches. Limited resection (*A*) might fail to address tumor thrombus and satellite lesions

and is frequently associated with small satellite tumors that may not be appreciated on preoperative imaging. Patients treated with surgical resection have a high incidence of postoperative recurrence, associated with poor long-term survival. There is no clear margin size that has been universally agreed upon, but there is a great deal of evidence that shows the benefit of an R0 resection [25]. One large Japanese study of 225 patients with HCC found a 77 % versus 21 % 3-year survival of patients with a 1-cm or greater resection margin versus those with less than a 1-cm margin, respectively [26]. Shi et al. report on a randomized controlled trial comparing a 2-cm versus 1-cm resection margin; they found a significant decrease in recurrence as well as improved survival with a greater margin [27].

Anatomic Versus Nonanatomic Liver Resection for HCC

HCC spreads through the portal venous system, has a high frequency of unrecognized satellite tumors and venous tumor thrombus, and requires an adequate resection margin. Patients with no evidence of cirrhosis can tolerate removal of up to two thirds of the liver without functional consequence. In this population anatomic resection is the gold standard. However, because of the frequency of HCC in the setting of cirrhosis, resection may be limited by functional reserve and the risk of resultant postoperative liver failure. Several quality studies have demonstrated improved outcome with anatomic versus nonanatomic resection for HCC; when possible, this is still considered the optimal treatment [28]. Hasegawa et al. looked at hepatic resection for 210 patients with HCC and found a significant difference in the 5-year overall and disease-free survival rates (66 % vs. 35 % in the anatomic resection and nonanatomic resection groups, respectively) [26]. Similar observations in favor of anatomic resection were reported by a French study [29]. Conversely, Kang and colleagues found this is not necessarily the case for smaller solitary tumors, reporting equivalent outcomes in 167 patients with a single small tumor treated with anatomic versus nonanatomic resection [30]. Anatomic resection remains the preferred treatment since this approach addresses potential tumor thrombus and satellite lesions better than limited resections (Fig. 23.4). However, in cirrhotic patients this may not be safe, and if the

tumor is smaller and solitary, a nonanatomic resection should be considered a viable, safe, and effective option.

Liver Transplantation for HCC

Patient Selection Based on Tumor Burden and Outcome

Liver transplantation would seem to be the ideal therapy for HCC because it involves removing the entire liver, yielding an ideal oncologic resection. However, the early experience with transplant yielded dismal results. While the early survival was reasonable, the recurrence rates, and therefore long-term outcomes, were quite poor. Because of the limits of donor availability and the impact on all potential liver recipients, liver transplant should be considered only for those patients who have a predicted survival comparable to non-HCC transplant recipients. Bismuth was one of the first to consider that tumor biology may be at the root of the problem when they demonstrated that patients with small uninodular or binodular tumors <3 cm had much better outcomes with transplant than resection (83 % vs. 18 %). This group also found that patients with diffuse form HCC, more than two nodules >3 cm, or those patients with portal venous thrombus had a much higher rate of recurrence leading to poor long-term outcomes [31].

Mazzaferro et al. reported on their experience with 48 patients with cirrhosis and unresectable HCC who underwent transplantation [32]. This study found a 4-year actuarial survival rate of 85 % and recurrence-free survival rate of 92 % in those patients who met a predetermined criterion (Fig. 23.5). In those patients that were found, on explant, to go beyond that criterion, survival was significantly worse at 50 % and 59 %. These standards became the basis for the Milan criteria, defined by a single tumor less than 5 cm, or 3 or fewer tumors all individually less than 3 cm (Fig. 23.6). The, so-called, Milan criteria have subsequently been adopted by the United Network for Organ Sharing (UNOS) as selection criteria for HCC patients evaluated for transplant.

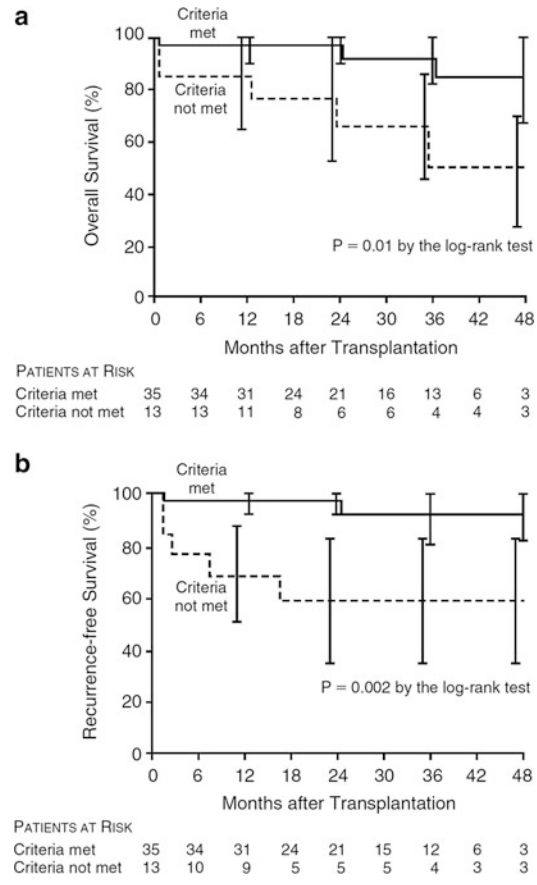

Fig. 23.5 Overall survival (**a**) and recurrence-free survival (**b**) of patients after liver transplantation for HCC within and outside the Milan criteria (Reprinted from Mazzaferro et al. [32] Liver transplantation for the treatment of small hepatocellular carcinoma in patients with cirrhosis. N Engl J Med 1996;334:693–9, Fig. 3, with permission from Massachusetts Medical Society)

The survival benefits of these criteria have been demonstrated in numerous studies [33, 34]. The excellent outcomes of HCC patients within the criteria led many to believe that perhaps the Milan criteria were too restrictive, and reasonable outcomes could be established with even more inclusive standards [35].

The University of California San Francisco (UCSF) group went further and demonstrated excellent results with an even more expanded criteria of tumor burden. Their study proposed the following criteria: solitary tumor $\leq$ to 6.5 cm, three or fewer nodules with the largest $\leq$ to 4.5 cm, and total tumor diameter $\leq$ to 8 cm (Fig. 23.6).

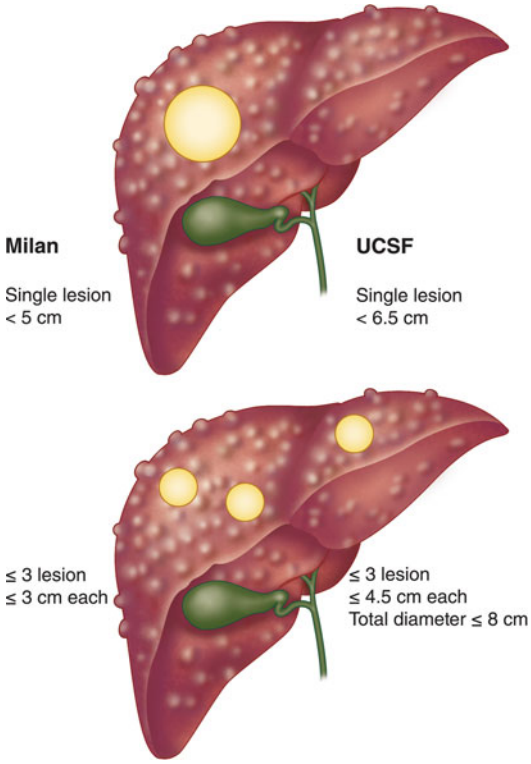

Fig. 23.6 Milan (single lesion ≤5 cm, or no more than three lesions ≤3 cm) and UCSF criteria (single lesion ≤6.5 cm, or no more than three lesions ≤4.5 cm and a total diameter of 8 cm) for patients with HCC and undergoing liver transplantation

This established the UCSF criteria and demonstrated a survival rate of 90 % and 75 % at 1 and 5 years, respectively, compared to 50 % 1-year survival for those with tumors exceeding those limits [35]. This study, however, was based on explant evaluation, something that could not reasonably be established prior to transplant. Further evaluation by the same group subsequently validated these good outcomes, in 2007, using the same size criteria but based measurements taken on preoperative imaging [36].

The largest experience to assess the efficacy of transplantation for HCC and evaluate previously established criteria was reported from the University of California, Los Angeles (UCLA) transplant center [37]. This study looked at 467 transplants for HCC with an overall 1-, 3-, and 5-year survival of 82 %, 65 %, and 52 %, respectively. Their analysis found that patients meeting the Milan criteria had similar survival to those patients meeting UCSF criteria by both preoperative imaging and explant evaluation. They further confirmed tumors beyond UCSF criteria portended survival below 50 %. A multivariate analysis demonstrated that tumor number, lymphovascular invasion, and poor differentiation independently predicted poor survival.

Organ Allocation in the United States: MELD and HCC

The Model for End-Stage Liver Disease (MELD) is a scoring system designed originally to predict the survival of patients with liver failure undergoing TIPS procedure [38]. It was subsequently adopted by UNOS for prioritizing organ allocation for liver transplantation. Because so many of the patients with HCC have reasonably well-compensated cirrhosis, this scoring system does not reasonably assess their true risk of death on the waiting list. With this in mind, the first MELD exception criteria for HCC were established [39]. This initial scoring system assumed a 15 % risk of disease progression within 3 months for stage I disease; therefore, these patients were given a MELD score of 24. For those with stage II disease, a 30 % risk of progression was assumed; this cohort received a MELD of 29. In addition, for each 3 months patients remained on the wait list, they were assessed another 10 % risk, and therefore, the score was increased. This allocation system led to a dramatic swing in the number of transplants performed for HCC from 7 % to 22 % [40]. The system was felt by many to give too great an advantage to HCC patients relative to those with decompensated cirrhosis whose MELD score was physiologic [41]. The allocation for MELD was revised in 2003, resulting in stage I disease receiving a score of 20 and stage II a MELD of 24. This alteration led to a drop from 22 % to 14 % of all transplants performed for HCC. A pathologic review of explanted livers found that those with presumed stage I HCC had no demonstrable tumor 31 % of the time [40]. Therefore, the exception points were further modified to exclude those with stage I HCC.

The current guidelines for MELD score for patients with HCC are as follows: points are awarded for a tumor burden within Milan criteria, tumors within UCSF, but greater than Milan must be downstaged to Milan; 22 points are awarded for tumors >2 cm with an automatic increase for every 3 months spent on the wait list.

The number of patients on the liver transplant wait list continues to increase annually, while the number of viable donors remains static. At this writing there are currently over 16,000 patients on the waiting list for liver transplantation, while only 6,291 patients received a liver transplant in 2010 (UNOS database). Because of the shortage of deceased donors, living donor liver transplant (LDLT) has become an increasingly utilized modality for treatment of patients with decompensated cirrhosis, as well as those with unresectable HCC. Overall, outcomes for all patients undergoing LDLT are comparable to the results with deceased donors [42]. There have been a number of studies that have demonstrated a survival benefit for LDLT in the setting of HCC [43]. The concern is, of course, the risk to the living donor, with morbidity rates as high as 40 %. Many have also expressed a concern for LDLT for patients who are outside of the established Milan or UCSF criteria both in terms of recipient outcomes and donor risk. One must consider if there is a selection bias for those patients with established wait time on the transplant list; this may result in selection of favorable tumor biology as those with more aggressive tumors drop out prior to transplant [44]. This important selection factor may be lost if LDLT is rushed, and those with unfavorable tumor biology are transplanted before they can declare themselves with aggressive tumor progression.

Wait List Management for HCC

To guarantee an accurate preoperative evaluation, there are specific guidelines that must be met for listing patients with HCC for OLT. Patients must be assessed radiologically to evaluate the number and size of tumors and to rule out extrahepatic disease and vascular involvement. Definitive tissue diagnosis is not required, but if no biopsy is available, one of the following must be fulfilled: AFP >200 mg/mL, arteriogram confirming the tumor or arterial enhancement followed by portal venous washout on CT or MRI, or a history of locoregional treatment. Those patients with no demonstrable tumor on imaging may be given MELD exception points if their AFP is > 500 mg/mL. Patients with tumors less than 2 cm or patients beyond Milan criteria can be listed for transplant, but they will receive no additional MELD points for the tumor. All patients must be deemed unresectable, and there must be documentation of the tumor every 3 months by CT or MRI to assure there has been no progression of disease beyond the established criteria.

Patients with unresectable HCC who are on the wait list for transplantation must be carefully followed for disease progression. Because of the time spent on the wait list with, perhaps, a relatively low MELD score, patients with HCC are at risk for tumor progression. This progression leads to poor outcome following transplantation or dropout secondary to disease progression beyond acceptable transplantation criteria. Therefore, local treatment of the tumor to control progression is commonly pursued in transplant centers that anticipate a significant wait time. Local treatment options include TACE, percutaneous radio-frequency ablation (RFA), or percutaneous ethanol injection (PEI).

TACE, which will be discussed in more depths in separate chapters, is a selective embolization of the arterial inflow feeding the hepatoma with chemotherapeutic agents, usually cisplatin of doxorubicin. This embolization results in ischemic insult to the tumor in combination with localized chemotherapy that has little systemic effect. TACE has been shown to lead to complete necrosis, in some cases, and size reduction in 50 % of patients with HCC [45]. TACE can be used with three treatment effects in mind, limiting wait list dropout, improving posttransplant results by decreasing recurrence, and downstaging HCC that is beyond established criteria; so patients in this population can be transplanted (Fig. 23.7).

There is reasonable evidence that TACE can be effectively used as a bridge to transplant. A series of 54 patients at the Mayo clinic treated with

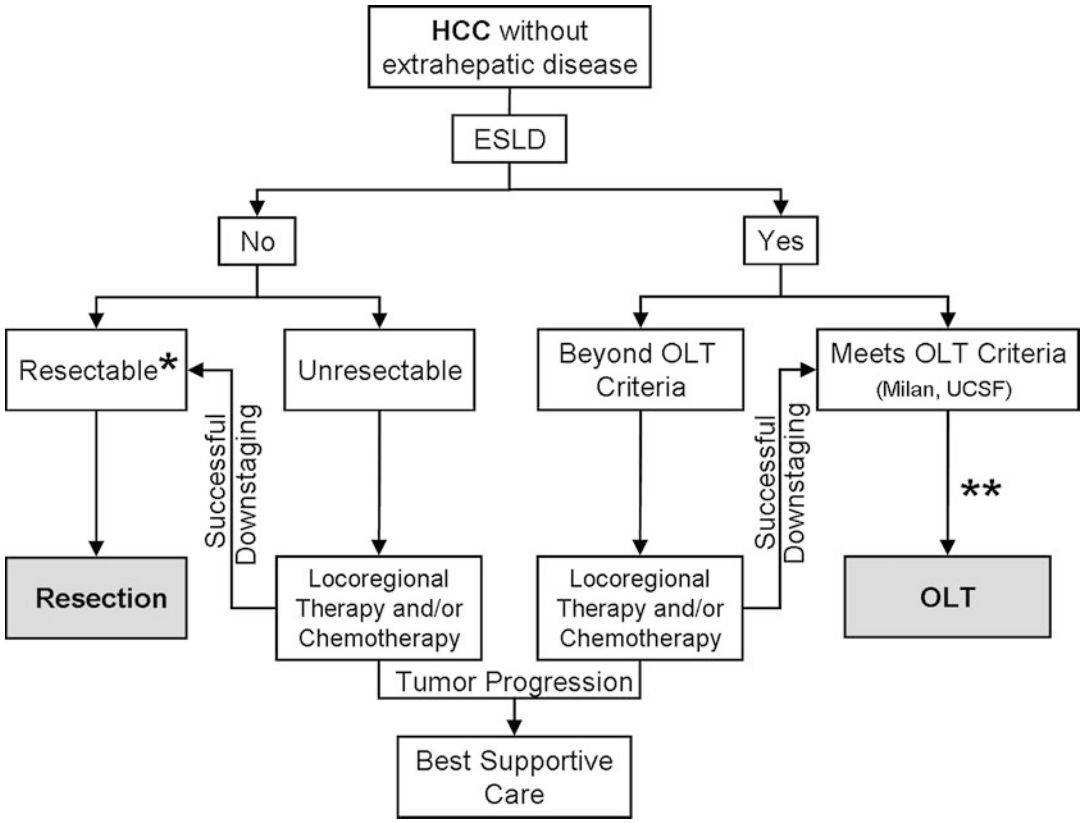

Fig. 23.7 Treatment algorithm of HCC without extrahepatic tumor involvement at the University of California, Los Angeles (UCLA). *, follow treatment algorithm for patients with normal liver (Fig. 23.2a). **, patients with HCC on the waiting list will be reimaged every 3 months. Locoregional therapies (TACE, RFA, PEI) are used as bridging procedures to control the tumor burden within Milan or UCSF criteria (Abbreviations: *ESLD* end-stage liver disease, *OLT* orthotopic liver transplantation)

TACE had a dropout rate of 14 % which compares favorably to the Barcelona Liver Cancer Study group who reported a 38 % 12-month dropout probability with observation alone [8, 46]. Another study of 116 patients with HCC listed for OLT and treated with TACE found a dropout rate of 2.9 % in patients within Milan criteria and 12 % in patients outside of Milan, but within UCSF criteria. This study, however, also found that patients that were downstaged to Milan criteria fared worse posttransplant, with a 5-year survival of only 25 % [47]. The evidence is not overwhelming since there has not been a randomized controlled trial to assess dropout rates with and without TACE, but the evidence does favor intervention particularly since TACE is well tolerated with a low rate of complication and side effects.

PEI is the therapy with the least amount of experiential data in the bridge to transplant setting. It is a modality with an attractive side effect and complication profile, in theory, but it is seldom mentioned in published data. It is an effective treatment option for liver tumors with up to 80 % necrosis in small tumors [48]. It is less invasive than most, utilizing a fine needle which may limit the theoretical concern of track seeding. However, it requires multiple treatment sessions and has been largely replaced, in most centers with RFA, and therefore is unlikely to accumulate any notable data to bolster its use as a bridging therapy.

RFA is another effective treatment option for liver tumors that is being used as a bridge to transplant for patients with HCC. UCLA reported its experience with 52 consecutive patients with 87 tumors. They had a dropout rate of 5.8 % at 12 months due to tumor progression with a 3-year survival of 76 % for 41 patients from this group that made it to transplant with no recurrences within the established follow-up time period [49]. Mazzaferro et al. reviewed their experience with RFA pre-transplant and found no dropout due to tumor progression with a 3-year survival of 83 % [50]. RFA will be discussed in greater detail in other chapters, but it can be used safely and effectively for bridging patients with small tumors awaiting transplant.

The greatest benefit to any treatment modality used as a bridge to transplant is seen with longer wait times. In those centers that are able to rush patients with HCC to transplant, there is little convincing evidence that pretreatment with any of the aforementioned options provides a survival or recurrence benefit. With this in mind fast tracking patients with aggressive tumor biology and at the edge or beyond Milan criteria may be associated with increased recurrence. Most centers are treating HCC patients with a bridging therapy prior to transplant, but at this time there is no evidence to suggest which is superior.

Surgical Resection Versus Liver Transplantation for HCC

Although OLT is currently the best treatment modality for patients with HCC and underlying end-stage liver disease (ESLD), this treatment can be offered only to a small proportion of patients due to tumor stage beyond accepted criteria and donor organ shortage. Therefore, liver resection remains the most important surgical therapy in patients with well-preserved liver function (CTP score A) and absence of portal hypertension (Fig. 23.7) [3].

It was proposed that liver resection can be used in conjunction with transplantation in three clinical scenarios of small HCC [51]: (1) as first-line treatment with salvage transplantation for recurrence, (2) as a diagnostic tool to gain histopathological information of the tumor for appropriate selection for OLT, and (3) as bridge therapy before OLT to control the tumor burden in patients who fulfill the Milan [32] or UCSF [35] criteria.

Liver resection versus liver transplantation as primary therapy for patients with small HCC and adequate hepatic reserve is hotly debated. The "first-line resection with salvage transplantation for recurrence" approach has to be considered especially for geographic regions with a high incidence of HCC and a low donation rate [52]. The rationale behind this approach is that longer waiting times after listing translate into higher risk for tumor progression beyond the accepted criteria for transplantation. Although resection does not remove the underlying liver disease, several studies report comparable overall survival rates for primary resection and primary OLT for transplantable HCC (Table 23.2) [53–55]. The experience of a large Asian transplant center showed that the majority of patients (79 %) who develop tumor recurrence after resection of small HCC were still eligible for salvage transplantation [56]. Conversely, the strategy of initial resection and salvage OLT has no clinical significance in geographic regions, such as the United States, with a low proportion of patients with HCC on the waiting list (10 %) and a relatively short median time of listing to transplantation (3 months) [52]. Therefore, the choice of primary resection with salvage OLT or primary OLT for small HCC is dictated by geographic factors rather than the preferred attitude of the transplant center toward either approach.

Another advantage of primary resection is the opportunity to gain pathological information of the tumor and adjacent liver tissue [51]. Micro- and macrovascular invasion as well as satellite nodules are important prognostic features which are associated with unfavorable outcome. This information can be used to accept or deny patients for salvage liver transplantation in the case of recurrent tumor disease.

Belghiti also proposed liver resection as bridge therapy before OLT [51]. However, this strategy only makes sense if the patient on the waiting list would keep their priority even after complete tumor resection. In the United States

Table 23.2 Recent studies comparing long-term outcome of patients with HCC treated primarily with resection (and salvage transplantation) or primary liver transplantation (Adapted from Rahbari et al [84]. Hepatocellular carcinoma. Current management and perspectives for the future. Ann Surg 2011;253:453–69, Table 3, with permission from Lippincott Williams & Wilkins, US)

First author	Year	Study period	Primary therapy	Sample size	5-year OS rate	5-year DFS rate
Lee [85]	2010	1997–2007	Transplantation	78	68 %	75 %[a]
			Resection	130	52 %	50 %
Facciuto [86][b]	2009	1997–2007	Transplantation	119	62 %	–
			Resection	60	61 %	–
Del Gaudio [87]	2008	1996–2005	Transplantation	147	58 %	54 %
			Resection	80	66 %	41 %
Shah [88]	2007	1995–2005	Transplantation	140	64 %	78 %[a]
			Resection	121	56 %	60 %
Poon [89]	2007	1995–2004	Transplantation	85	44 %	–
			Resection	228	60 %	–
Margarit [55]	2005	1988–2002	Transplantation	36	50 %	64 %[a]
			Resection	37	78 %	39 %
Bigourdan [90]	2003	1991–1999	Transplantation	17	71 %	80 %[a]
			Resection	20	36 %	40 %[a]
Adam [91]	2003	1984–2000	Transplantation	195	61 %[b]	58 %[a]
			Resection	98	50 %	18 %
Belghiti [92]	2003		Transplantation	70	–	59 %
		1991–2001	Resection	18	–	61 %
Figueras [93]	2000		Transplantation	85	60 %	60 %[a]
		1990–1999	Resection	35	51 %	31 %

DFS indicates disease-free survival, *OS* indicates overall survival
[a]Significant difference as reported in the original study
[b]4-year survival rates are reported for patients meeting the Milan criteria

where additional points are added to the physiological MELD score for HCC, a complete tumor resection would result in losing the exception points for HCC and the priority on the waiting list. Therefore, listed patients with HCC are mainly managed with locoregional therapies such as TACE and RFA to control the tumor burden during the waiting time.

Patients with large HCC beyond the Milan or UCSF criteria have a more unfavorable outcome than those with small HCC [32, 35]. In the United States, patients outside the accepted criteria can be principally transplanted based on the physiological MELD score but do not receive any exception points for HCC. A comparative analysis of patients with HCC exceeding the Milan criteria was performed for a cohort undergoing resection versus OLT [57]. In this study, 94 patients who underwent hepatic resection were compared to 92 patients who underwent OLT during the same study period. The mean maximal tumor size was 10 cm for the resection group and 6.4 cm for the OLT group. The overall survival rate was 66 % for both groups. Although this study has many drawbacks in terms of comparability, the results suggest that resection and OLT in patients with HCC beyond the Milan criteria have similar outcomes.

Primary Liver Resection Versus Ablative Therapy for HCC

Locoregional ablative treatment modalities such as RFA have been increasingly performed for the treatment of primary liver cancer during the last decade and have been shown to be effective for local tumor control. In contrast to hepatic resection, percutaneous ablative techniques are less invasive and do not require general anesthesia

or hospitalization. These advantages made percutaneous ablation popular especially for the treatment of primary liver cancer. Despite the encouraging results of ablation, there is growing evidence that hepatic resection is superior to ablation in the treatment for small HCC in terms of recurrence and survival [58, 59]. There are several retrospective studies comparing hepatic resection and percutaneous ablation [60–64]. Although all studies report a better outcome for the resection group in terms of recurrence or survival, a subgroup analysis of small HCC ($\leq$2–3 cm) in three of these studies suggests an equivalent outcome for resection and RFA [60, 63, 64]. However, the results have to be carefully interpreted due to the retrospective nature of the studies. A recently published large survey study by the Liver Cancer Study Group of Japan compared the outcome hepatic resection (n = 2,857), percutaneous RFA (n = 3,022), and PEI (n = 1,306) for patients with HCC meeting the Milan criteria [65]. The study revealed a significantly lower 2-year-time-to-recurrence rate for the resection group. The multivariate analysis of this study showed that percutaneous ablation was an independent predictor of increased recurrence.

The concept of RFA and hepatic resection for small HCC has been recently investigated in a randomized controlled trial [66]. In this trial, HCC patients with liver function CTP A or B and within the Milan criteria (Fig. 23.6) were randomized either to surgical resection (n = 115) or percutaneous RFA (n = 115). The RFA group had a significantly shorter hospital stay (7 vs. 15 days) and a lower complication rate (5/115 vs. 32/115), while the resection group had a significantly better 5-year recurrence (42 % vs. 63 %) and overall survival (76 % vs. 55 %) rate than the RFA group. In addition, resection was found to be an independent predictor for favorable outcome in the multivariate analysis.

These data demonstrate that hepatic resection offers better outcome in terms of recurrence and survival than ablation. However, the advantages of percutaneous ablation are its less invasive nature, shorter length of hospitalization, and lower complication rate.

Re-resection for Recurrent HCC

In geographic regions with a high incidence of HCC and difficult access to liver transplantation or LDLT as only transplant option such as in Japan, liver resection is the preferred surgical treatment over OLT for many patients with HCC. Despite the documented benefit of liver resection for HCC, tumor recurrence is common, affecting 70–80 % of patients after liver surgery. Unlike metastatic colorectal cancer to the liver, where extrahepatic recurrence after initial hepatic resection is common, the vast majority of patients with HCC have recurrence in the remnant liver [24, 67, 68]. For many Asian patients with recurrent HCC, salvage liver transplantation is not an option, and re-resection of recurrent HCC should be carefully considered. Therefore, it is not surprising that the most experience with re-resection for recurrent HCC has been reported from Asia (Table 23.3). However, re-resection is possible only in a minority of patients (10–20 %) who experience recurrence after initial resection [69].

Repeat liver resection for recurrent HCC is increasing in frequency, although it has only recently considered as a safe and effective therapy. However, underlying hepatic disease is a problem for patients with recurrent HCC since those patients often face progression of their hepatic dysfunction and portal hypertension after primary resection. Many series of the past decade revealed that repeat liver resection can be safely performed in well-selected patients with a low perioperative mortality rate below 1 % (Table 23.3). The critical assessment of liver- and tumor-related factors is of paramount importance for selecting patients for repeat resection. As for initial hepatectomy, the liver function of the diseased liver, the portal hypertension, and the potential remnant liver volume have to be considered to minimize the risk for post-resection liver failure (Fig. 23.2b). Although anatomic resections for HCC result in superior oncologic outcome [26, 29], the maximal preservation of remnant liver tissue should be the primary principle for repeat resection. Therefore, the

Table 23.3 Selected series of repeat hepatic resection for HCC with more than 20 patients

First author	Year	Study period	No. of pts (initial resection)	No. of pts (repeat resection)	Cirrhosis	Minor resections[a]	Mortality	5-year OS rate
Shimada [71]	1998	1978–1995	312	41 (13 %)	59 %	95 %	-	42 %
Sugimachi [94]	2001	1984–2000	474	78 (16 %)	-	-	0 %	47 %
Minagawa [73]	2003	1994–2000	334	67 (20 %)	69 %	91 %	0 %	56 %
Itamoto [72]	2007	1990–2004	483	84 (17 %)	67 %	87 %	0 %	50 %
Liang [95]	2008	1999–2007	853	44 (5 %)	-	82 %	0 %	28 %
Wu [96]	2009	1990–2007	1,177	149 (13 %)	78 %	83 %	1 %	59 %
Nagano [70]	2009	1992–2005	231	24 (10 %)	-	96 %	0 %	51 %
Faber [97]	2011	1990–2009	483	27 (6 %)	59 %	52 %	0 %	42 %

- Not defined, *pts* patients, *OS* overall survival
[a] Minor resections are defined as $\leq$ segmentectomy

proportion of patients with minor liver resections ($\leq$ segmentectomy) is significantly higher for repeat resections compared to that of initial resections (Tables 23.1 and 23.3). There is growing evidence that portal vein invasion at time of initial [70, 71] or repeat resection [71–73] is an independent predictor for poor outcome. But also a short disease-free interval of $\leq$1 year after primary resection appears to be associated with an unfavorable outcome after repeat resection for recurrent HCC [73]. With appropriate selection, repeat resection for recurrent HCC can result in long-term survival which is comparable to that after primary resection for HCC (Tables 23.1 and 23.3). If resection cannot be performed or is associated with a high risk for perioperative mortality, locoregional therapies and chemotherapy have to be considered.

References

1. Parkin DM, Bray F, Ferlay J, Pisani P. Global cancer statistics, 2002. CA Cancer J Clin. 2005;55:74–108.
2. Llovet JM, Bustamante J, Castells A, et al. Natural history of untreated nonsurgical hepatocellular carcinoma: rationale for the design and evaluation of therapeutic trials. Hepatology. 1999;29:62–7.
3. Clavien PA, Petrowsky H, DeOliveira ML, Graf R. Strategies for safer liver surgery and partial liver transplantation. N Engl J Med. 2007;356:1545–59.
4. Abulkhir A, Limongelli P, Healey AJ, et al. Preoperative portal vein embolization for major liver resection: a meta-analysis. Ann Surg. 2008;247:49–57.
5. Palavecino M, Chun YS, Madoff DC, et al. Major hepatic resection for hepatocellular carcinoma with or without portal vein embolization: Perioperative outcome and survival. Surgery. 2009;145:399–405.
6. Seo DD, Lee HC, Jang MK, et al. Preoperative portal vein embolization and surgical resection in patients with hepatocellular carcinoma and small future liver remnant volume: comparison with transarterial chemoembolization. Ann Surg Oncol. 2007;14:3501–9.
7. Bruix J, Castells A, Bosch J, et al. Surgical resection of hepatocellular carcinoma in cirrhotic patients: prognostic value of preoperative portal pressure. Gastroenterology. 1996;111:1018–22.
8. Llovet JM, Fuster J, Bruix J. Intention-to-treat analysis of surgical treatment for early hepatocellular carcinoma: resection versus transplantation. Hepatology. 1999;30:1434–40.
9. Bruix J, Sherman M. Management of hepatocellular carcinoma. Hepatology. 2005;42:1208–36.
10. Bruix J, Sherman M, Llovet JM, et al. Clinical management of hepatocellular carcinoma. Conclusions of the Barcelona-2000 EASL conference. European Association for the Study of the Liver. J Hepatol. 2001;35:421–30.
11. Capussotti L, Ferrero A, Vigano L, Polastri R, Tabone M. Liver resection for HCC with cirrhosis: surgical perspectives out of EASL/AASLD guidelines. Eur J Surg Oncol. 2009;35:11–5.

12. Cucchetti A, Ercolani G, Vivarelli M, et al. Is portal hypertension a contraindication to hepatic resection? Ann Surg. 2009;250:922–8.
13. Shirabe K, Shimada M, Gion T, et al. Postoperative liver failure after major hepatic resection for hepatocellular carcinoma in the modern era with special reference to remnant liver volume. J Am Coll Surg. 1999;188:304–9.
14. Breitenstein S, Apestegui C, Petrowsky H, Clavien PA. "State of the art" in liver resection and living donor liver transplantation: a worldwide survey of 100 liver centers. World J Surg. 2009;33: 797–803.
15. Aoki T, Imamura H, Hasegawa K, et al. Sequential preoperative arterial and portal venous embolizations in patients with hepatocellular carcinoma. Arch Surg. 2004;139:766–74.
16. Ogata S, Belghiti J, Farges O, Varma D, Sibert A, Vilgrain V. Sequential arterial and portal vein embolizations before right hepatectomy in patients with cirrhosis and hepatocellular carcinoma. Br J Surg. 2006;93:1091–8.
17. Imamura H, Sano K, Sugawara Y, Kokudo N, Makuuchi M. Assessment of hepatic reserve for indication of hepatic resection: decision tree incorporating indocyanine green test. J Hepatobiliary Pancreat Surg. 2005;12:16–22.
18. Fan ST, Lo CM, Liu CL, et al. Hepatectomy for hepatocellular carcinoma: toward zero hospital deaths. Ann Surg. 1999;229:322–30.
19. Poon RT, Fan ST. Assessment of hepatic reserve for indication of hepatic resection: how I do it. J Hepatobiliary Pancreat Surg. 2005;12:31–7.
20. Yamanaka N, Okamoto E, Toyosaka A, et al. Prognostic factors after hepatectomy for hepatocellular carcinomas. A univariate and multivariate analysis. Cancer. 1990;65:1104–10.
21. Liu JH, Chen PW, Asch SM, Busuttil RW, Ko CY. Surgery for hepatocellular carcinoma: does it improve survival? Ann Surg Oncol. 2004;11:298–303.
22. Hanazaki K, Kajikawa S, Shimozawa N, et al. Hepatic resection for hepatocellular carcinoma in the elderly. J Am Coll Surg. 2001;192:38–46.
23. Petrowsky H, Clavien PA. Should we deny surgery for malignant hepato-pancreaticobiliary tumors to elderly patients? World J Surg. 2005; 29:1093–100.
24. Ercolani G, Grazi GL, Ravaioli M, et al. Liver resection for hepatocellular carcinoma on cirrhosis: univariate and multivariate analysis of risk factors for intrahepatic recurrence. Ann Surg. 2003;237:536–43.
25. Lise M, Bacchetti S, Da Pian P, Nitti D, Pilati PL, Pigato P. Prognostic factors affecting long term outcome after liver resection for hepatocellular carcinoma: results in a series of 100 Italian patients. Cancer. 1998;82:1028–36.
26. Hasegawa K, Kokudo N, Imamura H, et al. Prognostic impact of anatomic resection for hepatocellular carcinoma. Ann Surg. 2005;242:252–9.
27. Shi M, Guo RP, Lin XJ, et al. Partial hepatectomy with wide versus narrow resection margin for solitary hepatocellular carcinoma: a prospective randomized trial. Ann Surg. 2007;245:36–43.
28. Ikai I, Arii S, Kojiro M, et al. Reevaluation of prognostic factors for survival after liver resection in patients with hepatocellular carcinoma in a Japanese nationwide survey. Cancer. 2004;101:796–802.
29. Regimbeau JM, Kianmanesh R, Farges O, Dondero F, Sauvanet A, Belghiti J. Extent of liver resection influences the outcome in patients with cirrhosis and small hepatocellular carcinoma. Surgery. 2002;131: 311–7.
30. Kang CM, Choi GH, Kim DH, et al. Revisiting the role of nonanatomic resection of small ($<$ or $=$ 4 cm) and single hepatocellular carcinoma in patients with well-preserved liver function. J Surg Res. 2010;160:81–9.
31. Bismuth H, Chiche L, Adam R, Castaing D, Diamond T, Dennison A. Liver resection versus transplantation for hepatocellular carcinoma in cirrhotic patients. Ann Surg. 1993;218:145–51.
32. Mazzaferro V, Regalia E, Doci R, et al. Liver transplantation for the treatment of small hepatocellular carcinomas in patients with cirrhosis. N Engl J Med. 1996;334:693–9.
33. Cillo U, Vitale A, Bassanello M, et al. Liver transplantation for the treatment of moderately or well-differentiated hepatocellular carcinoma. Ann Surg. 2004;239:150–9.
34. Hemming AW, Cattral MS, Reed AI, Van Der Werf WJ, Greig PD, Howard RJ. Liver transplantation for hepatocellular carcinoma. Ann Surg. 2001;233:652–9.
35. Yao FY, Ferrell L, Bass NM, et al. Liver transplantation for hepatocellular carcinoma: expansion of the tumor size limits does not adversely impact survival. Hepatology. 2001;33:1394–403.
36. Yao FY, Xiao L, Bass NM, Kerlan R, Ascher NL, Roberts JP. Liver transplantation for hepatocellular carcinoma: validation of the UCSF-expanded criteria based on preoperative imaging. Am J Transplant. 2007;7:2587–96.
37. Duffy JP, Vardanian A, Benjamin E, et al. Liver transplantation criteria for hepatocellular carcinoma should be expanded: a 22-year experience with 467 patients at UCLA. Ann Surg. 2007;246:502–9. discussion 9–11.
38. Malinchoc M, Kamath PS, Gordon FD, Peine CJ, Rank J, ter Borg PC. A model to predict poor survival in patients undergoing transjugular intrahepatic portosystemic shunts. Hepatology. 2000;31:864–71.
39. Wiesner R, Edwards E, Freeman R, et al. Model for end-stage liver disease (MELD) and allocation of donor livers. Gastroenterology. 2003;124:91–6.
40. Wiesner RH, Freeman RB, Mulligan DC. Liver transplantation for hepatocellular cancer: the impact of the MELD allocation policy. Gastroenterology. 2004;127:S261–7.
41. Sharma P, Balan V, Hernandez JL, et al. Liver transplantation for hepatocellular carcinoma: the MELD impact. Liver Transpl. 2004;10:36–41.

42. Olthoff KM, Merion RM, Ghobrial RM, et al. Outcomes of 385 adult-to-adult living donor liver transplant recipients: a report from the A2ALL consortium. Ann Surg. 2005;242:314–23. discussion 23–5.
43. Sarasin FP, Majno PE, Llovet JM, Bruix J, Mentha G, Hadengue A. Living donor liver transplantation for early hepatocellular carcinoma: a life-expectancy and cost-effectiveness perspective. Hepatology. 2001;33:1073–9.
44. Kulik L, Abecassis M. Living donor liver transplantation for hepatocellular carcinoma. Gastroenterology. 2004;127:S277–82.
45. Lo CM, Ngan H, Tso WK, et al. Randomized controlled trial of transarterial lipiodol chemoembolization for unresectable hepatocellular carcinoma. Hepatology. 2002;35:1164–71.
46. Maddala YK, Stadheim L, Andrews JC, et al. Drop-out rates of patients with hepatocellular cancer listed for liver transplantation: outcome with chemoembolization. Liver Transpl. 2004;10:449–55.
47. Millonig G, Graziadei IW, Freund MC, et al. Response to preoperative chemoembolization correlates with outcome after liver transplantation in patients with hepatocellular carcinoma. Liver Transpl. 2007;13:272–9.
48. Vilana R, Bruix J, Bru C, Ayuso C, Sole M, Rodes J. Tumor size determines the efficacy of percutaneous ethanol injection for the treatment of small hepatocellular carcinoma. Hepatology. 1992;16:353–7.
49. Lu DS, Yu NC, Raman SS, et al. Radiofrequency ablation of hepatocellular carcinoma: treatment success as defined by histologic examination of the explanted liver. Radiology. 2005;234:954–60.
50. Mazzaferro V, Battiston C, Perrone S, et al. Radiofrequency ablation of small hepatocellular carcinoma in cirrhotic patients awaiting liver transplantation: a prospective study. Ann Surg. 2004;240:900–9.
51. Belghiti J. Resection and liver transplantation for HCC. J Gastroenterol. 2009;44 Suppl 19:132–5.
52. Cucchetti A, Vitale A, Gaudio MD, et al. Harm and benefits of primary liver resection and salvage transplantation for hepatocellular carcinoma. Am J Transplant. 2010;10:619–27.
53. Cherqui D, Laurent A, Mocellin N, et al. Liver resection for transplantable hepatocellular carcinoma: long-term survival and role of secondary liver transplantation. Ann Surg. 2009;250:738–46.
54. Chua TC, Saxena A, Chu F, Morris DL. Hepatic resection for transplantable hepatocellular carcinoma for patients within Milan and UCSF criteria. Am J Clin Oncol. 2012;35(2):141–5.
55. Margarit C, Escartin A, Castells L, Vargas V, Allende E, Bilbao I. Resection for hepatocellular carcinoma is a good option in Child-Turcotte-Pugh class A patients with cirrhosis who are eligible for liver transplantation. Liver Transpl. 2005;11:1242–51.
56. Poon RT, Fan ST, Lo CM, Liu CL, Wong J. Long-term survival and pattern of recurrence after resection of small hepatocellular carcinoma in patients with preserved liver function: implications for a strategy of salvage transplantation. Ann Surg. 2002;235:373–82.
57. Canter RJ, Patel SA, Kennedy T, et al. Comparative analysis of outcome in patients with hepatocellular carcinoma exceeding the Milan criteria treated with liver transplantation versus partial hepatectomy. Am J Clin Oncol. 2010;34(5):466–71.
58. Gravante G, Overton J, Sorge R, et al. Radiofrequency ablation versus resection for liver tumours: an evidence-based approach to retrospective comparative studies. J Gastrointest Surg. 2011;15:378–87.
59. Petrowsky H, Busuttil RW. Resection or ablation of small hepatocellular carcinoma: what is the better treatment? J Hepatol. 2008;49:502–4.
60. Guglielmi A, Ruzzenente A, Valdegamberi A, et al. Radiofrequency ablation versus surgical resection for the treatment of hepatocellular carcinoma in cirrhosis. J Gastrointest Surg. 2008;12:192–8.
61. Hong SN, Lee SY, Choi MS, et al. Comparing the outcomes of radiofrequency ablation and surgery in patients with a single small hepatocellular carcinoma and well-preserved hepatic function. J Clin Gastroenterol. 2005;39:247–52.
62. Lupo L, Panzera P, Giannelli G, Memeo M, Gentile A, Memeo V. Single hepatocellular carcinoma ranging from 3 to 5 cm: radiofrequency ablation or resection? HPB (Oxford). 2007;9:429–34.
63. Vivarelli M, Guglielmi A, Ruzzenente A, et al. Surgical resection versus percutaneous radiofrequency ablation in the treatment of hepatocellular carcinoma on cirrhotic liver. Ann Surg. 2004;240:102–7.
64. Wakai T, Shirai Y, Suda T, et al. Long-term outcomes of hepatectomy vs percutaneous ablation for treatment of hepatocellular carcinoma $<$ or $=$4 cm. World J Gastroenterol. 2006;12:546–52.
65. Hasegawa K, Makuuchi M, Takayama T. Surgical resection vs. percutaneous ablation for hepatocellular carcinoma: a preliminary report of the Japanese nationwide survey. J Hepatol. 2008;49:589–94.
66. Huang J, Yan L, Cheng Z, et al. A randomized trial comparing radiofrequency ablation and surgical resection for HCC conforming to the Milan criteria. Ann Surg. 2010;252:903–12.
67. Fong Y, Sun RL, Jarnagin W, Blumgart LH. An analysis of 412 cases of hepatocellular carcinoma at a Western center. Ann Surg. 1999;229:790–9. discussion 9–800.
68. Poon RT, Fan ST, Lo CM, et al. Improving survival results after resection of hepatocellular carcinoma: a prospective study of 377 patients over 10 years. Ann Surg. 2001;234:63–70.
69. Lesurtel M, Petrowsky H, et al. Repeat resection for malignant liver tumors. In: Clavien PA, Breitenstein S, Belghiti J, editors. Malignant liver tumors: current and emerging therapies. 3rd ed. Oxford: Wiley-Blackwell; 2010. p. 216–26.
70. Nagano Y, Shimada H, Ueda M, et al. Efficacy of repeat hepatic resection for recurrent hepatocellular carcinomas. ANZ J Surg. 2009;79:729–33.

71. Shimada M, Takenaka K, Taguchi K, et al. Prognostic factors after repeat hepatectomy for recurrent hepatocellular carcinoma. Ann Surg. 1998;227:80–5.
72. Itamoto T, Nakahara H, Amano H, et al. Repeat hepatectomy for recurrent hepatocellular carcinoma. Surgery. 2007;141:589–97.
73. Minagawa M, Makuuchi M, Takayama T, Kokudo N. Selection criteria for repeat hepatectomy in patients with recurrent hepatocellular carcinoma. Ann Surg. 2003;238:703–10.
74. Zhou XD, Tang ZY, Yang BH, et al. Experience of 1000 patients who underwent hepatectomy for small hepatocellular carcinoma. Cancer. 2001;91: 1479–86.
75. Kanematsu T, Furui J, Yanaga K, Okudaira S, Shimada M, Shirabe K. A 16-year experience in performing hepatic resection in 303 patients with hepatocellular carcinoma: 1985–2000. Surgery. 2002;131:S153–8.
76. Belghiti J, Regimbeau JM, Durand F, et al. Resection of hepatocellular carcinoma: a European experience on 328 cases. Hepatogastroenterology. 2002;49:41–6.
77. Wayne JD, Lauwers GY, Ikai I, et al. Preoperative predictors of survival after resection of small hepatocellular carcinomas. Ann Surg. 2002;235: 722–30. discussion 30–1.
78. Chen XP, Qiu FZ, Wu ZD, Zhang BX. Chinese experience with hepatectomy for huge hepatocellular carcinoma. Br J Surg. 2004;91:322–6.
79. Wu CC, Cheng SB, Ho WM, Chen JT, Liu TJ, P'Eng FK. Liver resection for hepatocellular carcinoma in patients with cirrhosis. Br J Surg. 2005;92:348–55.
80. Capussotti L, Muratore A, Amisano M, Polastri R, Bouzari H, Massucco P. Liver resection for hepatocellular carcinoma on cirrhosis: analysis of mortality, morbidity and survival–a European single center experience. Eur J Surg Oncol. 2005;31:986–93.
81. Nathan H, Schulick RD, Choti MA, Pawlik TM. Predictors of survival after resection of early hepatocellular carcinoma. Ann Surg. 2009;249:799–805.
82. Yang LY, Fang F, Ou DP, Wu W, Zeng ZJ, Wu F. Solitary large hepatocellular carcinoma: a specific subtype of hepatocellular carcinoma with good outcome after hepatic resection. Ann Surg. 2009;249: 118–23.
83. Wang J, Xu LB, Liu C, Pang HW, Chen YJ, Ou QJ. Prognostic factors and outcome of 438 Chinese patients with hepatocellular carcinoma underwent partial hepatectomy in a single center. World J Surg. 2010;34:2434–41.
84. Rahbari NN, Mehrabi A, Mollberg NM, et al. Hepatocellular carcinoma: current management and perspectives for the future. Ann Surg. 2011;253:453–69.
85. Lee KK, Kim DG, Moon IS, Lee MD, Park JH. Liver transplantation versus liver resection for the treatment of hepatocellular carcinoma. J Surg Oncol. 2010;101: 47–53.
86. Facciuto ME, Rochon C, Pandey M, et al. Surgical dilemma: liver resection or liver transplantation for hepatocellular carcinoma and cirrhosis. Intention-to-treat analysis in patients within and outwith Milan criteria. HPB (Oxford). 2009;11:398–404.
87. Del Gaudio M, Ercolani G, Ravaioli M, et al. Liver transplantation for recurrent hepatocellular carcinoma on cirrhosis after liver resection: University of Bologna experience. Am J Transplant. 2008;8: 1177–85.
88. Shah SA, Cleary SP, Tan JC, et al. An analysis of resection vs transplantation for early hepatocellular carcinoma: defining the optimal therapy at a single institution. Ann Surg Oncol. 2007;14:2608–14.
89. Poon RT, Fan ST, Lo CM, Liu CL, Wong J. Difference in tumor invasiveness in cirrhotic patients with hepatocellular carcinoma fulfilling the Milan criteria treated by resection and transplantation: impact on long-term survival. Ann Surg. 2007;245: 51–8.
90. Bigourdan JM, Jaeck D, Meyer N, et al. Small hepatocellular carcinoma in child A cirrhotic patients: hepatic resection versus transplantation. Liver Transpl. 2003;9:513–20.
91. Adam R, Azoulay D, Castaing D, et al. Liver resection as a bridge to transplantation for hepatocellular carcinoma on cirrhosis: a reasonable strategy? Ann Surg. 2003;238:508–18. discussion 18–9.
92. Belghiti J, Cortes A, Abdalla EK, et al. Resection prior to liver transplantation for hepatocellular carcinoma. Ann Surg. 2003;238:885–92. discussion 92–3.
93. Figueras J, Jaurrieta E, Valls C, et al. Resection or transplantation for hepatocellular carcinoma in cirrhotic patients: outcomes based on indicated treatment strategy. J Am Coll Surg. 2000;190:580–7.
94. Sugimachi K, Maehara S, Tanaka S, Shimada M. Repeat hepatectomy is the most useful treatment for recurrent hepatocellular carcinoma. J Hepatobiliary Pancreat Surg. 2001;8:410–6.
95. Liang HH, Chen MS, Peng ZW, et al. Percutaneous radiofrequency ablation versus repeat hepatectomy for recurrent hepatocellular carcinoma: a retrospective study. Ann Surg Oncol. 2008;15:3484–93.
96. Wu CC, Cheng SB, Yeh DC, Wang J, P'Eng FK. Second and third hepatectomies for recurrent hepatocellular carcinoma are justified. Br J Surg. 2009;96:1049–57.
97. Faber W, Seehofer D, Neuhaus P, et al. Repeated liver resection for recurrent hepatocellular carcinoma. J Gastroenterol Hepatol. 2011;26(7):1189–94.

Biologic and Systemic Therapies for the Treatment of Hepatocellular Carcinoma

24

Richard S. Finn

Abstract

Hepatocellular carcinoma (HCC) is one of the most common malignancies worldwide, yet systemic treatment options for the disease are limited. Only recently, sorafenib, an oral, small-molecule tyrosine kinase inhibitor of several intracellular proteins suspected to be important in HCC progression, including the platelet-derived growth factor receptor-β (PDGFR), "Raf" kinase, and the vascular endothelial growth factor receptors (VEGFR) including VEGFR 1, 2, and 3, was shown to prolong survival in HCC. While the benefit of sorafenib over placebo is modest (the median survival increased from 7.9 to 10.7 months), it was a significant advance, becoming the first systemic agent to prolong survival in this setting, and has spurred an increase in research at all stages of the disease. Currently, there are an unprecedented number of clinical studies of new agents in HCC. In addition to evaluating these agents in combination with sorafenib, they are being compared directly to sorafenib, after progression on sorafenib, and in combination with locally ablative therapies such as transarterial chemoembolization (TACE) and radio-frequency ablation (RFA) and surgical resection. With this robust activity, we are increasing our understanding of HCC and will likely see significant improvements on the initial observations made with sorafenib. As highlighted here, this will take careful study design, patient selection, and a rational selection of new therapeutic targets.

Introduction

More than any other malignancy, the proper management of patients with hepatocellular carcinoma (HCC) requires a multidisciplinary approach. The disease remains a clinical challenge because it presents as two intimately related medical problems: (1) variable degrees of liver dysfunction and (2) cancer. Liver transplantation remains the

R.S. Finn
Department of Medicine, Geffen School of Medicine at UCLA Ronald Regan Medical Center at UCLA, Los Angeles, CA, USA
e-mail: rfinn@mednet.ucla.edu

D.E. Dupuy et al. (eds.), *Image-Guided Cancer Therapy*, DOI 10.1007/978-1-4419-0751-6_26,

treatment of choice for most patients as it provides a means of correcting both problems. However, most patients are beyond tumor criteria for transplant at presentation, and many that are listed face the reality that they will come off the list while waiting because of tumor progression. Locally ablative therapies such as transarterial chemoembolization (TACE), radio-frequency ablation (RFA), and percutaneous ethanol ablation (PEI) all play a role in managing patients with liver-confined disease but in general are not felt to be curative for most patients. With the above in mind, most patients with HCC will require systemic treatment of their disease at sometime in their disease course. This includes patients that present with advanced disease and also those that have received curative or local therapies and eventually progress. Since the approval of sorafenib, the first systemic agent to improve survival in advanced HCC, interest in HCC as a target for drug development has opened opportunities for the development of new agents in the frontline setting, in second-line setting, and in combination with TACE, RFA, and surgery.

Historical Perspective: Systemic Agents

For many years, HCC has been considered an "orphan disease" in the West. Its incidence has generally been low compared to other tumor types with estimated 16,000 cases of HCC in 2009 versus 219,000, 194,000, 146,000, in lung, breast, and colorectal cancer, respectively, in the United States alone [1]. Nevertheless, many clinical studies have been performed with traditional cytotoxic agents [2]. These studies were often not randomized, but single-arm phase II studies for patients with "unresectable HCC." Even the few studies that were randomized did not show any benefit of newer agents over older ones nor did they demonstrate significant benefit for combinations over single agents.

The reason for the clinical failure of cytotoxics in this disease can be linked to several factors. For one, cytotoxics are associated with significant side effects including bone marrow suppression resulting in infections (from neutropenia) and bleeding (from thrombocytopenia) events, renal insufficiency, and, in some cases, direct hepatotoxicity. In a group of patients with often marginal physiologic reserve, these toxicities are often intolerable. In addition, until recently, studies have assumed that "unresectable" HCC represents one disease entity. Besides the issue of variable outcomes based on liver dysfunction (as measured by either Child-Pugh score or Model for End-Stage Liver Disease (MELD) score), "unresectable" HCC includes patients that have disease that is often associated with variable outcomes based on their tumor burden alone. For example, a patient unresectable because of tumor location will have a different natural history than a patient with portal vein thrombosis and still different from a patient with clear extrahepatic/metastatic spread [3]. Many studies in the past did not stratify for these characteristics and therefore included heterogeneous groups of patients. For this reason, single-arm studies are very difficult to interpret in terms of survival endpoints.

In addition, related to the above two issues is the use of composite endpoints in oncology clinical studies. Endpoints such as progression-free survival (PFS) are commonly used in HCC studies. PFS is typically defined as the time from randomization to either radiographic progression or death from any cause. Given the impact of underlying liver disease on survival, this endpoint may not reflect the true benefit of an anticancer therapy and is clearly affected by patient selection [4].

Other clinical trial factors have to be considered in interpreting clinical trials with systemic agents. One, radiographic evaluation of HCC may require and benefit from newer methods of assessment. While most clinical trials with systemic agents have based clinical activity on response rate, this is not necessarily the most accurate assessment of anticancer activity. Historically bidimensional measurements were used (WHO classification of response) [5] and more recently unidimensional measurements based on the sum of the longest dimensions as defined by RECIST [6]. Several years ago, the European

Association for the Study of the Liver (EASL) put forward newer criteria, taking into account changes in the size of "viable tumor" as measured by enhancement in the arterial phase [7]. This concept again has been put forward as a "modified RECIST" criteria and may have more relevance with the development of novel agents in HCC [8]. Finally, the lack of the use of a consistent staging system has made assessing response across studies challenging. While several staging systems have been proposed, none has been consistently applied to clinical trials. Most recently, the Barcelona Clinic Liver Cancer (BCLC) classification is being adopted in many prospective studies [4].

New Systemic Approaches: Molecular-Targeted Therapeutics

Similar to drug development in other solid-tumor types, new treatment modalities in HCC are focusing on molecularly targeted agents. For years, various cytotoxic agents have been evaluated in HCC based not on any unique biologic characteristics of liver cancer but on the fact that these agents have had activity in other tumor types. However, this empiric approach to drug development has not moved us any further toward improving outcome for patients with liver cancer [2]. Only in the past several years, with the development of sorafenib have we seen for the first time an improvement in overall survival with a systemic agent. This is the result of a well-conducted study with appropriate patient selection, appropriate endpoints, and the use of an agent with biologic rationale for activity in HCC. Table 24.1 compares several agents that are either approved or in advanced-stage clinical evaluation in HCC, and Table 24.2 summarizes selected ongoing clinical trials in HCC.

Table 24.1 Novel systemic agents in development for HCC. *VEGF* vascular endothelial growth factor, *VEGFR* VEGF receptor, *FGFR* fibroblast growth factor receptor, *mTOR* mammalian target of rapamycin, *PDGFR* platelet-derived growth factor receptor, *CSF1R* colony-stimulating factor 1 receptor

Agent	Class	Mechanism of action	Target(s)
Bevacizumab	Monoclonal antibody	Blocks VEGF binding toVEGF receptor	VEGF
Brivanib	Small molecule	Tyrosine kinase inhibitor	VEGFR1-3, FGFR1-3
Everolimus	Small molecule	Serine-threonine kinase inhibitor	mTOR
Linifanib	Small molecule	Tyrosine kinase inhibitor	VEGFR-2, PDGFRα-β, FLT3-4, c-kit, CSF1R
Ramucirimab	Monoclonal antibody	Blocks VEGF receptor 2 activation	VEGFR2
Sorafenib	Small molecule	Tyrosine kinase inhibitor	VEGFR2, VEGFR3, PDGFR, FLT-3, c-kit, raf
TSU-68	Small molecule	Tyrosine kinase inhibitor	VEGFR2, FGFR1, PDGFRβ

Sorafenib

Sorafenib is an oral, small-molecule tyrosine kinase inhibitor of several intracellular proteins suspected to be important in tumor progression, including the platelet-derived growth factor receptor-β (PDGFR), "Raf" kinase, and the vascular endothelial growth factor receptors (VEGFR) including VEGFR 1, 2, and 3 [9]. The proposed mechanism of action of sorafenib is shown in Fig. 24.1. This includes potential inhibition of growth-promoting signals within the tumor cell itself as well as inhibition of the tumor vasculature by its ability to block the VEGFR on endothelial cells. Preclinical models have demonstrated the ability of sorafenib to do both, but the actual effects in human tissue have not been assessed [10].

Two large randomized studies have proven a benefit for sorafenib in BCLC stage C liver cancer.

Table 24.2 Selected ongoing clinical trials in HCC

Agent	Clinical development	Study design	Trial ID
Bevacizumab/erlotinib	Phase II	First-line bevacizumab+ erlotinib versus sorafenib	NCT00881751
Brivanib	Phase III	First-line versus sorafenib	NCT00858871
		Second-line after sorafenib, versus placebo	NCT00825955
		Combo with TACE vs TACE + placebo	NCT00908752
Everolimus	Phase III	Second-line after sorafenib, versus placebo	NCT01035229
Linifanib	Phase III	First-line versus sorafenib	NCT01009593
Ramucirimab	Phase III	Second-line after sorafenib, versus placebo	NCT01140347
Sorafenib[a]	Phase III	First-line sorafenib+ erlotinib versus sorafenib	NCT00126620
	Phase III	First-line sorafenib+ doxorubicin versus sorafenib	NCT01015833
	Phase III	Sorafenib or placebo as adjuvant to resection or RFA	NCT0692770
	Phase II	Sorafenib or placebo in combination with TACE	NCT00855218
Lyso-thermo- sensitive doxorubicin	Phase III	Lyso-thermosensitive doxorubicin or placebo in combination with RFA	NCT00617981

[a]currently approved for advanced HCC

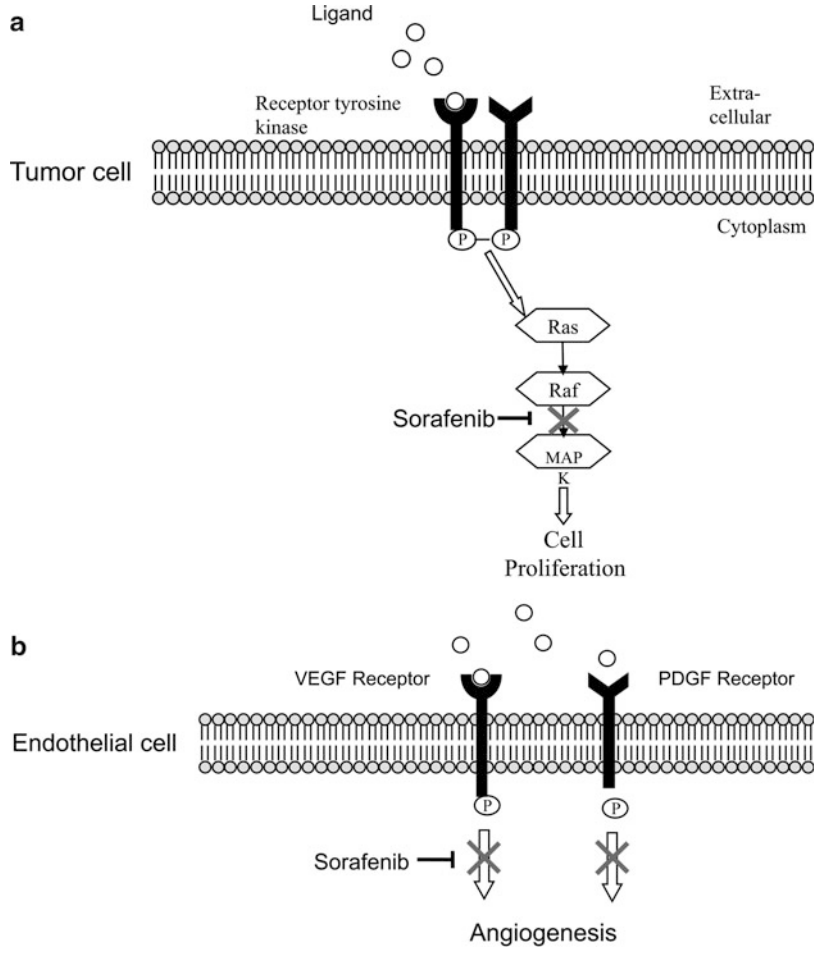

Fig. 24.1 Proposed mechanism of action of the multikinase inhibitor sorafenib. (**a**) Tumor cell, (**b**) endothelial cell (Reproduced with permission from American Association for Cancer Research: Wilhelm SM, et al. Mol cancer ther. October 2008)

Both studies required well-compensated liver disease (Child-Pugh A) at study entry. The Europe-North American study, SHARP, enrolled over 600 patients and randomized them between placebo and sorafenib 400 mg orally twice a day [11]. Patients were stratified for region, performance status, and the presence or absence of macroscopic vascular invasion (portal vein or branches). Patients underwent imaging every 6 weeks to assess radiographic time to tumor progression (TTP). Patients were also assessed for symptomatic endpoints based on a questionnaire. The primary endpoints to the study were overall survival (OS) and the time to symptomatic progression. This study was the first to demonstrate a significant improvement in overall survival with a median OS of 10.7 months in the sorafenib group and 7.9 months in the placebo group (hazard ratio (HR) 0.69; 95 % confidence interval, 0.55–0.87; $p < 0.001$). There was no significant difference in the time to symptomatic progression. The median TTP which was 2.8 months in the placebo group increased to 5.5 months in the sorafenib group ($p < 0.001$). Interestingly, this benefit was not driven by an increase in tumor shrinkage on imaging using standard clinical trial criteria, suggesting the benefit was largely driven by inducing stable disease and slowing progression. Common and predictable toxicities in this population included hand-foot skin reaction, anorexia, and diarrhea. Importantly, there was no significant difference in changes in liver dysfunction or bleeding events between the two groups. Seven hundred and sixty five of patients in the sorafenib group received more than 80 % of the planned daily dose.

A second study that evaluated sorafenib in advanced disease was performed in Asia, in a predominantly hepatitis B population [12]. The dosage of sorafenib was the same, and again only patients with Child-Pugh A cirrhosis were selected. Similar to the SHARP study, sorafenib improved OS (6.5 months for patients treated with sorafenib, compared with 4.2 months in the placebo group) (HR 0.68; 95 % CI 5.56–7.56; $p = 0.014$), and the median TTP was 2.8 months in the sorafenib-treated group compared to 1.4 months in the placebo group ($p = 0.0005$). While the magnitude of benefit was the same in both studies as represented by the hazard ratios of 0.69 and 0.68, respectively, both control and treated groups in the Asian study had a lower survival than the corresponding arms in the SHARP study. One explanation for this is the fact that more of the patients in the Asian study had BCLC stage C than in SHARP, which included a population of BCLC stage B patients. Again, the toxicities seen in the Asian study were similar to the SHARP study though there was an increased incidence of any grade hand-foot skin reaction, 45 % in Asia versus 21 % in SHARP. Of note, the wholesale acquisition cost (WAC) in the United States for a 30-day supply of sorafenib 400 mg twice daily is $6,660.95.

A phase II study comparing sorafenib and doxorubicin versus doxorubicin has been completed [13]. This study included 96 patients and randomized them to doxorubicin 60 mg/m^2 every 21 days versus the same dose of doxorubicin with sorafenib 400 mg twice daily. Results showed a median time to progression of 8.6 months in the combination and 4.8 months in the control arm, and the median overall survival was 13.7 months and 6.5 months, respectively. There was a signal for increased cardiac toxicity in the combination arm. There are plans to evaluate this in comparison to sorafenib in the frontline setting in a randomized phase III study (NCT01015833). In addition, there is an ongoing, randomized phase III study comparing the combination of sorafenib and the EGFR small-molecule tyrosine kinase inhibitor erlotinib versus sorafenib alone in patients with advanced HCC (SEARCH study, NCT00126620).

Brivanib

Brivanib is a small-molecule tyrosine kinase inhibitor which is characterized as the first dual-specific kinase with activity against the vascular endothelial growth factor receptors (VEGFR) 1–3 in addition to the fibroblast growth factor receptors (FGFR) 1–3 [14]. A single-agent study evaluated brivanib in the first-line treatment as well as in patients who progressed following one prior anti-angiogenic agent (sorafenib or thalidomide in

a small number of patients). In the first cohort, a largely Asian population of 55 patients with advanced HCC, first-line treatment with brivanib was associated with a median TTP of 2.8 months, a disease control rate of 60 % (47 evaluable patients), and median OS of 10 months [15]. Though not randomized, these data are promising and compare favorably with the results of sorafenib in an Asian-Pacific population [12]. In 46 patients with HCC that was primary refractory to sorafenib (63 %) or refractory to sorafenib after initial benefit (35 %), second-line treatment with brivanib was associated with a disease control rate of 46 % (37 evaluable patients), a median investigator-assessed TTP of 2.7 months, and a median OS of 9.8 months [16]. Brivanib was well tolerated, the most common adverse events being fatigue and diarrhea of generally common toxicity criteria grade 1 or 2. Currently brivanib is in several randomized phase III studies including head-to-head against sorafenib in the frontline setting (NCT00858871) and in the second-line setting versus placebo for patients that progressed on or are intolerant of sorafenib (NCT00825955). These studies build on laboratory data that suggest that FGF signaling is able to mediate resistance to VEGF-targeted therapies [17] and brivanib's ability to block FGFR signaling is one possible mechanism for its activity [18].

Everolimus

Everolimus is an oral small-molecule serine-threonine kinase inhibitor of mTOR (mammalian target of rapamycin) [19]. mTOR is downstream from several receptor tyrosine kinases and is part of the PI3-kinase/AKT signaling cascade. In addition, several studies have suggested that increased mTOR activity is associated with outcome in HCC [20–22]. mTOR is a potent inducer of angiogenesis via its upregulation of the hypoxia-induced gene *HIF1-α*. The mTOR inhibitors rapamycin [23] and everolimus (RAD001) [24] have shown preclinical activity in HCC. Two early-phase single-agent, nonrandomized studies in patients with both treated and untreated HCC defined the toxicity and maximum tolerated dose of everolimus in a well-compensated population. These studies were small and efficacy is difficult to assess. One study compared daily and weekly dosing in 39 patients [25]. The maximum tolerated dose of each was 7.5 and 70 mg, respectively. Common toxicities included stomatitis, rash, diarrhea, and thrombocytopenia. Reactivation of hepatitis B was also observed requiring prophylaxis in future studies. Disease control rates for the daily and weekly cohorts were reported as 71 % and 44 %, respectively. A second study was a phase I/II study evaluating safety and efficacy in 28 patients [26]. This study expanded a cohort at 10 mg daily and reported a median progression-free survival of 3.8 months and median overall survival of 8.4 months. This included a mixed population of sorafenib-naïve and sorafenib-treated patients. These studies have served as a backbone for a newly initiated phase III study of everolimus 7.5 mg daily or placebo in the second-line setting (NCT01035229). In addition, an ongoing study is evaluating the combination of sorafenib and everolimus in the frontline setting (NCT00828594).

Ramucirumab

Ramucirumab is a recombinant human monoclonal antibody that binds to the extracellular domain of the VEGF receptor 2. It was evaluated as a first-line therapy in patients with advanced HCC [27]. The study treated 42 of 43 enrolled patients. The median PFS was 4.0 months (3.9 months for patients with BCLC C and Child-Pugh A and 2.6 months for patients with BCLC C and Child-Pugh B). The median overall survival was 15 months (51 % 1-year survival): 18 months (63 % 1-year survival) for patients with BCLC C and Child-Pugh A and 4 months (0 % 1-year survival) for patients with BCLC C and Child-Pugh B. Three patients (7 %) with extrahepatic disease and BCLC C had partial response, and 18 patients (43 %) had stable disease (50 % disease control rate). The most frequent adverse events were fatigue (67 %), hypertension (41 %), and headache (38 %), and serious adverse events $\geq$ grade 3 in at least 2 patients included ascites (5 % G3),

gastrointestinal (GI) bleeding (5 % G3; 2 % G5), infusion-related reaction (5 % G3), hypoxia (5 % G3), and hypertension (2 % G2, 2 % G3, and 2 % G4). Like everolimus and brivanib, ramucirumab is being evaluated in a phase III study in the second-line treatment for advanced HCC (NCT01140347).

Bevacizumab

Single-agent studies with the monoclonal antibody to VEGF have shown some disease stabilization. One study evaluated two dosages of bevacizumab, 5 and 10 mg/kg administered intravenously once every 2 weeks [28]. Of the 46 patients enrolled, six had objective responses with a response rate of 13 % (95 % CI, 3 %–23 %), and the median survival was 12.4 months (95 % CI, 9.4–19.9 months). In another preliminary study, an early experience uses bevacizumab as a single agent in HCC in a phase II study [29]. Among the 24 patients evaluable for efficacy, 3 (12.5 %) had PR, and 7 (29 %) had SD of at least of 16 weeks.

The combination of bevacizumab and the small-molecule epidermal growth factor receptor (EGFR) inhibitor erlotinib has been studied as well. This combination is based on the scientific hypothesis that there is cross talk between the EGFR and VEGF families. A phase II study of bevacizumab and erlotinib in patients with advanced HCC was studied [30]. Bevacizumab was given at 10 mg/kg intravenously once every 14 days and erlotinib at 150 mg orally daily. Of the 40 patients evaluable for efficacy, 10 patients had PRs with a 25 % response rate. The median PFS was 9 months and OS 15.65 months. This combination is now being evaluated in a randomized phase II study versus sorafenib (NCT00881751).

Linifanib

Linifanib, ABT-869, is a receptor tyrosine kinase inhibitor of VEGFR and PDGFR receptor families [31]. It has been evaluated in a single-arm phase II study in advanced HCC [32]. Data presented reported an interim analysis on 34 of 44 enrolled patients. The majority were Child-Pugh A and 74 % had not received prior treatment. The median TTP was 112 days and median overall survival was 295 days. Some of the most common adverse events were hypertension, fatigue, diarrhea, rash, and proteinuria. A phase III randomized study versus sorafenib is planned (NCT01009593).

Combining Systemic Agents with Other Treatment Modalities

Recognizing that surgical resection and locally ablative techniques are not curative (but life-prolonging), there is obvious interest in improving on these approaches. As in other malignancies, systemic agents added as adjuvants to definitive therapy have been shown to improve survival and, in some case, the cure rate. To date, the lack of active systemic agents has limited the ability to improve on current techniques. However, now that there are active systemic agents, studies are in progress evaluating this hypothesis. While there are numerous smaller phase I and phase II studies, we will highlight the larger studies aimed at registration below.

STORM

The STORM study is a randomized, double-blind, placebo-controlled study of sorafenib as adjuvant treatment of HCC after curative therapy including surgical resection or RFA (NCT0692770). The study builds on sorafenib's proven efficacy in advanced disease. It aims at enrolling 1,100 patients globally. It aims at treating patients with either sorafenib 400 mg orally twice daily or placebo for a total of 4 years or until recurrence. The primary endpoint will be recurrence-free survival.

SPACE

Like the STORM study, the SPACE study is evaluating a proven systemic therapy, sorafenib, in patients with intermediate-stage HCC (NCT00855218). The study is a phase II study

randomizing patients to either a regimen of TACE with DC beads and doxorubicin versus the same regimen and sorafenib. The study is of scientific interest given the role angiogenesis may play in progression after TACE. The interval, timing, and number of TACE are dictated by the protocol. This study will build on data recently presented that did not demonstrate any benefit of sorafenib added to TACE in an Asian study, though adherence to that protocol seemed poor [33].

BRISK-TA

Brivanib is an oral small-molecule inhibitor of the VEGFR and FGFR that has been studied in a phase II study in advanced untreated and treated HCC. Preliminary activity has initiated a large registration program. Like the SPACE study, the hypothesis is that anti-vascular therapy with TACE can be enhanced with the use of pharmacologic inhibition of angiogenesis with a molecular agent. The BRISK-TA (*B*rivanib Study for Patients at *R*isk-*TA*CE, NCT00908752) study will randomize 870 patients globally with unrespectable HCC to TACE and placebo versus TACE alone. The primary endpoint of the study is overall survival. Unlike the SPACE study that has a regimented TACE schedule, the BRISK study allows for more leeway and is built around TACE "as needed" based on investigator assessment and imaging. Key inclusions are Child-Pugh A or B liver disease and one lesion $\geq$5 cm or multinodular disease with at least one $>$ 3 cm. When completed, it will be the largest TACE study ever completed and will inform us not only about the role of brivanib in this population but also about the natural history of TACE and HCC in this population of patients.

HEAT

Early studies evaluated the sensitizing effects of systemic chemotherapy to thermal ablation to liver tissue [34, 35]. These studies proposed the concept that the area of tissue destruction by radio-frequency ablation (RFA) alone could be achieved by the simultaneous administration of systemic doxorubicin during RFA. This concept is currently being evaluated in a phase III randomized controlled study. The formulation of the study drug in evaluation (*T*hermoDox®) involves the delivery of lyso-thermosensitive doxorubicin in a proprietary liposome that releases drug in the presence of elevated temperatures [36]. The HEAT (*He*patocellular Carcinoma Study of RF*A* and *T*hermoDox, NCT00617981) study is a 600-patient study randomizing patients with larger tumors between RFA and placebo or RFA with simultaneous ThermoDox administration. Key inclusion criteria are Child-Pugh A or B liver disease and no more than four lesions, with at least one $\geq$ 3 cm and none $>$ 7 cm. The primary endpoint of the study is progression-free survival with overall survival as a secondary endpoint. Unfortunately, the sponsoring company Celsion publicly reported on January 31, 2013 that there were no significant differences in progression free survival between the two groups. The overall survival endpoints are unknown at this time.

TSU-68

TSU-68 is an oral small-molecule inhibitor of VEGFR, PDGFR, and FGFR with preliminary single-agent activity in HCC [37]. A phase II study enrolled 101 patients with both Child-Pugh A and B liver disease and randomized them to TACE alone or TACE followed by TSU-68 [38]. The median PFS was 5.2 months with combination versus 4.0 months for TACE alone. The combination seemed well tolerated with the most common serious adverse events being fatigue and liver function abnormalities. A larger study to evaluate its impact on overall survival is required.

Conclusions

The approval of sorafenib has highlighted the unmet medical needs for patient with all stages of HCC. In what was once viewed as a difficult

disease to show benefits in, there are now multiple phase III studies and even more phase I and II studies of newer agents. Currently, the majority of agents in development are antiangiogenic. In principal, the data with sorafenib has validated this class of agent as active in HCC. Now the challenge is improving on sorafenib's impact. To that end, new agents with different chemical properties and targets are being evaluated. These include agents with activity against the FGF and mTOR pathways. While direct comparisons to sorafenib are required in the frontline setting, in the population of patients that progress on sorafenib, there is no proven agent and placebo-controlled trials are required. In addition, new combinations of targeted agents hold promise for exploiting several oncogenic pathways simultaneously. It is possible that the greatest gains in survival will come from the use of these agents in earlier stage of disease. These studies are ongoing as newer agents show promising activity; they will be introduced in these settings as well.

References

1. Jemal A, Siegel R, Ward E, Hao Y, Xu J, Thun MJ. Cancer statistics, 2009. CA Cancer J Clin. 2009;59:225–49.
2. Thomas MB, Zhu AX. Hepatocellular carcinoma: the need for progress. J Clin Oncol. 2005;23:2892–9.
3. Llovet JM, Bru C, Bruix J. Prognosis of hepatocellular carcinoma: the BCLC staging classification. Semin Liver Dis. 1999;19:329–38.
4. Llovet JM, Di Bisceglie AM, Bruix J, Kramer BS, Lencioni R, Zhu AX, Sherman M, et al. Design and endpoints of clinical trials in hepatocellular carcinoma. J Natl Cancer Inst. 2008;100:698–711.
5. Miller AB, Hoogstraten B, Staquet M, Winkler A. Reporting results of cancer treatment. Cancer. 1981;47:207–14.
6. James K, Eisenhauer E, Christian M, Terenziani M, Vena D, Muldal A, Therasse P. Measuring response in solid tumors: unidimensional versus bidimensional measurement. J Natl Cancer Inst. 1999;91:523–8.
7. Bruix J, Sherman M, Llovet JM, Beaugrand M, Lencioni R, Burroughs AK, Christensen E, et al. Clinical management of hepatocellular carcinoma. Conclusions of the Barcelona-2000 EASL conference. European Association for the Study of the Liver. J Hepatol. 2001;35:421–30.
8. Lencioni R, Llovet JM. Modified RECIST (mRECIST) assessment for hepatocellular carcinoma. Semin Liver Dis. 2010;30:52–60.
9. Wilhelm SM, Adnane L, Newell P, Villanueva A, Llovet JM, Lynch M. Preclinical overview of sorafenib, a multikinase inhibitor that targets both Raf and VEGF and PDGF receptor tyrosine kinase signaling. Mol Cancer Ther. 2008;7:3129–40.
10. Wilhelm SM, Carter C, Tang L, Wilkie D, McNabola A, Rong H, Chen C, et al. BAY 43–9006 exhibits broad spectrum oral antitumor activity and targets the RAF/MEK/ERK pathway and receptor tyrosine kinases involved in tumor progression and angiogenesis. Cancer Res. 2004;64:7099–109.
11. Llovet JM, Ricci S, Mazzaferro V, Hilgard P, Gane E, Blanc JF, de Oliveira AC, et al. Sorafenib in advanced hepatocellular carcinoma. N Engl J Med. 2008; 359:378–90.
12. Cheng AL, Kang YK, Chen Z, Tsao CJ, Qin S, Kim JS, Luo R, et al. Efficacy and safety of sorafenib in patients in the Asia-Pacific region with advanced hepatocellular carcinoma: a phase III randomised, double-blind, placebo-controlled trial. Lancet Oncol. 2009;10:25–34.
13. Abou-Alfa GK, Johnson P, Knox JJ, Capanu M, Davidenko I, Lacava J, Leung T, et al. Doxorubicin plus sorafenib vs doxorubicin alone in patients with advanced hepatocellular carcinoma: a randomized trial. JAMA 2010;304(19):2154–60.
14. Cai ZW, Zhang Y, Borzilleri RM, Qian L, Barbosa S, Wei D, Zheng X, et al. Discovery of brivanib alaninate ((S)-((R)-1-(4-(4-fluoro-2-methyl-1H-indol-5-yloxy)-5-methylpyrrolo[2,1-f] [1,2,4]triazin-6-yloxy)propan-2-yl)2-aminopropanoate), a novel prodrug of dual vascular endothelial growth factor receptor-2 and fibroblast growth factor receptor-1 kinase inhibitor (BMS-540215). J Med Chem. 2008;51:1976–80.
15. Raoul JL, Finn RS, Kang YK, et al. An open-label phase II study of first- and second-line treatment with brivanib in patients with hepatocellular carcinoma (HCC). J Clin Oncol. 2009;27:4577.
16. Finn RS, Kang YK,Mulcahy M, Polite BN, Lim HY, Walters I, Baudelet C, et al. Phase II, open-label study of brivanib as second-line therapy in patients with advanced hepatocellular carcinoma. Clin Cancer Res. 2012;18(7):2090–8.
17. Casanovas O, Hicklin DJ, Bergers G, Hanahan D. Drug resistance by evasion of antiangiogenic targeting of VEGF signaling in late-stage pancreatic islet tumors. Cancer Cell. 2005;8:299–309.
18. Huynh H, Ngo VC, Fargnoli J, Ayers M, Soo KC, Koong HN, Thng CH, et al. Brivanib alaninate, a dual inhibitor of vascular endothelial growth factor receptor and fibroblast growth factor receptor tyrosine kinases, induces growth inhibition in mouse models of human hepatocellular carcinoma. Clin Cancer Res. 2008;14:6146–53.
19. Yuan TL, Cantley LC. PI3K pathway alterations in cancer: variations on a theme. Oncogene. 2008;27:5497–510.

20. Sahin F, Kannangai R, Adegbola O, Wang J, Su G, Torbenson M. mTOR and P70 S6 kinase expression in primary liver neoplasms. Clin Cancer Res. 2004;10:8421–5.
21. Sieghart W, Fuereder T, Schmid K, Cejka D, Werzowa J, Wrba F, Wang X, et al. Mammalian target of rapamycin pathway activity in hepatocellular carcinomas of patients undergoing liver transplantation. Transplantation. 2007;83:425–32.
22. Villanueva A, Chiang DY, Newell P, Peix J, Thung S, Alsinet C, Tovar V, et al. Pivotal role of mTOR signaling in hepatocellular carcinoma. Gastroenterology. 2008;135:1972–83, 1983 e1971–11.
23. Wang Z, Zhou J, Fan J, Qiu SJ, Yu Y, Huang XW, Tang ZY. Effect of rapamycin alone and in combination with sorafenib in an orthotopic model of human hepatocellular carcinoma. Clin Cancer Res. 2008; 14:5124–30.
24. Huynh H, Chow KH, Soo KC, Toh HC, Choo SP, Foo KF, Poon D, et al. RAD001 (everolimus) inhibits tumour growth in xenograft models of human hepatocellular carcinoma. J Cell Mol Med. 2009; 13:1371–80.
25. Chen L, Shiah HS, Chen CY, et al. Randomized, phase I, and pharmacokinetic (PK) study of RAD001, and mTOR inhibitor, in patients (pts) with advanced hepatocellular carcinoma (HCC). J Clin Oncol. 2009;27:4587.
26. Blaszkowsky LS, Abrams TA, Miksad RA, et al. Phase I/II study of everolimus in patients with advanced hepatocellular carcinoma (HCC). J Clin Oncol. 2010;28:e14542.
27. Zhu AX, Finn RS, Mulcahy MF, et al. A phase II study of ramucirumab as first-line monotherapy in patients (pts) with advanced hepatocellular carcinoma (HCC). J Clin Oncol. 2010;28:4083.
28. Siegel AB, Cohen EI, Ocean A, Lehrer D, Goldenberg A, Knox JJ, Chen H, et al. Phase II trial evaluating the clinical and biologic effects of bevacizumab in unresectable hepatocellular carcinoma. J Clin Oncol. 2008;26:2992–8.
29. Malka D, Dromain C, Farace F, Horn S, Pignon J, Ducreux M, Boige V. Bevacizumab in patients (pts) with advanced hepatocellular carcinoma (HCC): preliminary results of a phase II study with circulating endothelial cell (CEC) monitoring. J Clin Oncol. 2007;25:4570.
30. Thomas MB, Morris JS, Chadha R, Iwasaki M, Kaur H, Lin E, Kaseb A, et al. Phase II trial of the combination of bevacizumab and erlotinib in patients who have advanced hepatocellular carcinoma. J Clin Oncol. 2009;27(6):843–50.
31. Albert DH, Tapang P, Magoc TJ, Pease LJ, Reuter DR, Wei RQ, Li J, et al. Preclinical activity of ABT-869, a multitargeted receptor tyrosine kinase inhibitor. Mol Cancer Ther. 2006;5:995–1006.
32. Toh H, Chen P, Carr BI, et al. A phase II study of ABT-869 in hepatocellular carcinoma (HCC): interim analysis. J Clin Oncol. 2009;27:4581.
33. Kudo M, Imanaka K, Chida N, Nakachi K, Tak WY, Takayama T, Yoon JH, et al. Phase III study of sorafenib after transarterial chemoembolisation in Japanese and Korean patients with unresctable hepatocellular carcinoma. Eur J Cancer. 2011;47(14): 2117–27.
34. Ahmed M, Monsky WE, Girnun G, Lukyanov A, D'Ippolito G, Kruskal JB, Stuart KE, et al. Radiofrequency thermal ablation sharply increases intratumoral liposomal doxorubicin accumulation and tumor coagulation. Cancer Res. 2003;63:6327–33.
35. Goldberg SN, Kamel IR, Kruskal JB, Reynolds K, Monsky WL, Stuart KE, Ahmed M, et al. Radiofrequency ablation of hepatic tumors: increased tumor destruction with adjuvant liposomal doxorubicin therapy. AJR Am J Roentgenol. 2002;179:93–101.
36. Poon RT, Borys N. Lyso-thermosensitive liposomal doxorubicin: a novel approach to enhance efficacy of thermal ablation of liver cancer. Expert Opin Pharmacother. 2009;10:333–43.
37. Kanai F, Yoshida H, Tateishi R, Sato S, Kawabe T, Obi S, Kondo Y, et al. A phase I/II trial of the oral antiangiogenic agent TSU-68 in patients with advanced hepatocellular carcinoma. Cancer Chemother Pharmacol. 2011;67:315–24.
38. Arai Y, Inaba T, Yamamoto T, et al. A randomized Phase II study of TSU-68 in patients (Pts) with hepatocellular carcinoma (HCC) treated by transarterial chemoembolization (TACE). J Clin Oncol. 2010; 28:4030.

Radiation Therapy in the Treatment of Primary Liver Cancers

25

Brian D. Kavanagh and Tracey E. Schefter

Abstract

Radiation therapy (RT), either in the form of external beam treatment or brachytherapy, is an effective modality for the treatment of primary hepatocellular cancer, and a meta-analysis has shown that the addition of RT in combination with other therapy enhances survival for HCC patients. The application of modern treatment delivery techniques has enabled the safe administration of faster, more potent hypofractionated RT regimens. Newer techniques such as selective internal radiation therapy (SIRT) and stereotactic body radiation therapy (SBRT) are especially promising, and the combination of RT and molecular-targeted therapies is currently under investigation.

Introduction

Hepatocellular cancer (HCC) ranks high among the major causes of cancer deaths worldwide. According to the International Agency for Cancer Research, in 2008, HCC ranked third in total cancer mortality behind lung and stomach cancer [1]. The estimated total number of deaths from HCC was approximately 700,000 in 2008, corresponding to a worldwide age-standardized rate of 10 per 100,000. A particularly high incidence of HCC is seen in East and Southeast Asia and parts of Central and Western Africa. The incidence and mortality of HCC are much lower in the United States. Here, the predominant risk factor is nonalcoholic fatty liver disease, followed by diabetes, hepatitis C, alcoholic cirrhosis, and hepatitis B [2].

For appropriately selected patients with disease localized within the liver and good baseline liver function, partial hepatectomy or liver transplant can offer a good chance of long-term survival with generally low risk of operative mortality [3]. However, a high percentage of patients with liver-only disease are medically unfit for resection or need to wait for an available organ for transplantation. In this group of patients, a variety of nonoperative local therapies may be considered either as definitive treatment or as a means of bridge to liver transplantation. Radiofrequency ablation, trans-arterial chemoembolization (TACE), and ethanol injection are among the available options. Also included among the alternatives to be considered is the use of radiation

B.D. Kavanagh (✉) • T.E. Schefter
Department of Radiation Oncology, University of Colorado School of Medicine, Aurora, CO, USA
e-mail: brian.kavanagh@ucdenver.edu

D.E. Dupuy et al. (eds.), *Image-Guided Cancer Therapy*, DOI 10.1007/978-1-4419-0751-6_27,

therapy (RT), either in the form or external beam treatment or brachytherapy (via infusion of radionuclides or temporary radioactive implant). The focus of the present chapter is the use of RT for nonmetastatic HCC.

Natural History of Untreated HCC

The natural history of untreated HCC has been described for Asian and non-Asian populations. In a multi-institutional series from Japan, Okuda and colleagues described the clinical outcomes for 229 patients who received no specific therapy for HCC [4]. A staging system was applied that identified four key negative prognostic factors: tumor size >50 % of the liver, presence of ascites, serum albumin <3 g/dL, and serum bilirubin >3 mg/dL. Stage I patients had no negative prognostic factors, stage II patients had 1 or 2, and stage III patients had 3 or 4. The median survivals for untreated stage I, II, and III patients were 8.3, 2.0, and 0.7 months, respectively.

Yeung and colleagues from the Center for the Study of Liver Disease in China reported outcomes for 106 patients with HCC not amenable to curative treatment who were managed symptomatically as control-arm patients in several randomized studies [5]. The most common causes of death were tumor progression (63.2 %) and liver failure (31.1 %). The overall median survival was 3 months, and the 1-year survival was 8 %. The Okuda staging system again identified subgroups with different prognoses: the median survivals for untreated Okuda stage I, II, and III patients were 5.2, 2.7, and 1.0 months, respectively.

Ruzzenente and colleagues from the University of Verona Medical School in Italy likewise reported a large series of patients treated for advanced, nonmetastatic HCC [6]. Among 464 patients with HCC, 88 received only supportive care. Multivariate analysis revealed the following to be significant prognostic factors favoring longer overall survival: alpha-fetoprotein <100 ng/mL, smaller tumor size, single lesion, and use of resection or locally ablative therapy versus supportive therapy alone. The median survival among patients who received only supportive therapy was 8 months, with a 5-year survival of 3 %.

Early Radiation Therapy Studies

In the 1980s, the Radiation Therapy Oncology Group (RTOG) conducted a study of the combination of external beam RT to the whole liver (21 Gy in 7 fractions or, later, 24 Gy in 20 fractions given at a dose of 1.2 Gy bid) [7]. The population studied included roughly 30 % who had been previously treated with chemotherapy; half of the patients had extrahepatic metastatic disease. Low-dose chemotherapy was given concurrently in conjunction with the RT on days 1, 3, 5, and 7 and consisted of Adriamycin, 15 mg IV and 5-FU, 500 mg IV. There was no difference in radiographic response between the once-daily and hyperfractionated groups, and there was higher acute toxicity with hyperfractionated treatment.

The Johns Hopkins group studied the use of external beam RT (21 Gy/7 fractions) combined with IV cisplatin (50 mg/m^2) given on day 1 of RT and then continued monthly at the same dose given via intrahepatic arterial infusion [8]. The target volume included the tumor plus a 2-cm margin, which frequently involved whole liver RT. Among 76 patients treated, 21 had extrahepatic metastasis at the time of treatment. The median survivals for Okuda stage I, II, and III patients were 15.8, 5.4, and 4.2 months, respectively, suggesting an improvement over untreated historical controls.

High-Dose Conventionally Fractionated RT

Improvements in the ability to plan and deliver RT with a 3-dimensional knowledge of the location of the tumor and adjacent normal tissue anatomy allowed for studies involving an escalation of the RT dose given to HCC. Typically, patients were selected for treatment if they were ineligible for either surgery or another locally

ablative treatment modality. Doses on the order of 40–60 Gy were given in fractions of 1.5–2.0 Gy, sometimes with concomitant intrahepatic arterial chemotherapy, and median survivals in the range of 12–20 months were reported, with much longer survival for the Okuda stage I patients [9–12].

Tumor thrombosis into the portal vein (PV) or inferior vena cava (IVC) and lymph node metastases are recognized adverse prognostic factors, and in this setting, management is particularly challenging. Zeng and colleagues at Fudan University in Shanghai, China, treated 136 patients with HCC who had either PV or IVC tumor thrombus from HCC [13]. Nearly all had had prior resection and/or TACE as initial therapy for HCC. The tumor thrombus was considered the intended target volume, and the liver primary itself was also treated if feasible without unacceptable risk of toxicity. A median dose of 50 Gy (range, 30–60 Gy) was given in 2 Gy fractions. A complete response at the site of tumor thrombus was observed in 41 patients (30 %), and a partial response was observed in 36 patients (27 %). A median survival of 9.7 months was achieved in this heavily pretreated population with very advanced disease.

Similarly, Han and colleagues at Yonsei University in Seoul, Korea, treated 40 patients with PV thrombosis from HCC [14]. They visualized the target lesion using hepatic angiography and took into account intra-fraction motion in planning the RT. The dose of RT was 45 Gy in 25 fractions, given in combination with continuous infusion hepatic arterial 5-FU (500 mg/day). This combination was followed by monthly hepatic arterial infusion of 5-FU (500 mg/m^2 × 3 days) and cisplatin (60 mg/m^2). A median survival of 13 months and 3-year survival of 24 % were observed.

Regarding the challenge of lymph node metastases from HCC, the group from Fudan University also reported outcomes in this setting [15]. Among 125 patients with HCC metastasis to regional lymph nodes, outcomes for a group of 62 patients who were treated with external beam RT were compared to a group of 63 patients who did not receive RT. The RT dose given ranged from 40 to 60 Gy and was given in daily 2.0-Gy fractions. The median survival was 9.4 months for the EBRT group and 3.3 month for the non-EBRT group ($p < 0.001$).

Recently, McIntosh and colleagues from the University of Virginia reported a pilot experience of combining chronomodulated capecitabine with external beam RT in a cohort of patients with very large HCC primary tumors [16]. Patients were prescribed 1 g of capecitabine in the morning and 2 g at night. The rationale for the use of this schedule was the known circadian variation in the metabolism of 5-FU by dihydropyrimidine dehydrogenase [17]. The RT was given in a modestly accelerated regimen, 50 Gy in 20 fractions of 2.5 Gy, using intensity modulation to provide good coverage of the tumor volume and adequate normal tissue sparing. Among 20 patients treated, 11 were Child-Pugh A and 9 were Child-Pugh B at the time of treatment. More than half of the patients had received 1–3 treatments via TACE previously. The median tumor diameter before RT was 9.5 cm (range, 1.3–17.4 cm). There were no instances of grade 3 or higher treatment-induced toxicity. The median survivals for patients who had Child-Pugh class A and B disease were 22.5 months and 8 months, respectively.

Hypofractionated Radiation Therapy for HCC

Within the last two decades, refinements in the integration of patient imaging and treatment delivery technology have allowed for investigations into more efficient and more intense regimens of external beam RT whereby daily doses of 3 Gy or more are given in fewer total treatments. This approach is known as hypofractionated RT and requires extra attention to conforming and administering the prescription dose tightly around the tumor to be treated while minimizing the dose to adjacent normal structures in order to lessen the risk of injury. In the most extreme sense, with the incorporation of techniques to account for breathing-related motion, daily image guidance prior to each treatment to achieve

accurate target relocalization within a few mm, and compression of the entire course of treatment into five or fewer fractions, the term that applies to this approach is stereotactic body radiation therapy (SBRT) [18].

Hypofractionated RT given in 5–10 treatments has been investigated at several centers. The expected biological effect would be higher than what is expected for the same total dose given in smaller dose per fraction. An example would be the study of Liang and colleagues of Guangxi Medical University, who treated 128 patients with technically or medically unresectable HCC [19]. All patients had AJCC stage T3 ($n = 83$) or T4 ($n = 45$) primary lesions; Child-Pugh class A status was present in 108 cases, and the remaining 20 were Child-Pugh class B. Approximately one third of patients had prior TACE therapy. The tumors were large (mean volume, 459 cc). The typical fractionation scheme was 4–5 Gy per fraction, given 3 days per week, to a total dose of 50 Gy prescribed to the isocenter. The actual dose covering the planning target volume that included the tumor plus a 0.5–1.5-cm margin for motion was approximately 90 % of this prescription dose. For the entire group, a 2-year survival of 43 % was observed. On multivariate analysis, smaller tumor volume and Child-Pugh class A were independent predictors for overall survival. A similar regimen was employed by Choi and colleagues at the Catholic University of Korea [20]. A dose of 50 Gy in 10 fractions was given to 18 patients with HCC, and a dose of 50 Gy in 5 fractions was given to 2 patients. Fiducial markers were placed to facilitate image-guided patient relocalization prior to treatment. No patients experienced grade 3 or 4 toxicity. The median survival was 20 months; the 2-year survival was 43 %.

Charged particles have also been used when administering hypofractionated RT for HCC. Bush and colleagues at Loma Linda University gave a 63 cobalt-Gy equivalent in 15 fractions to 34 patients with HCC via proton beam (4.2 cobalt-Gy equivalent per fraction) [21]. The average tumor diameter was 5.7 cm (range, 1.5–10 cm). Two-year survival was 55 %; among six patients who underwent orthotopic liver transplant following treatment, two of the explanted livers had no detectable residual tumor in the treated volume. Fukumitsu and colleagues from the University of Tsukuba gave a higher proton beam dose of RT, 66 cobalt-Gy equivalent, in 10 fractions to 51 patients with HCC diagnosed by biopsy or combination of radiographic findings and serum markers who met the following criteria: (1) solitary HCC or multiple tumor foci (up to 2), where all lesions could be included in a single irradiation field with no other uncontrolled HCC; (2) a maximal tumor diameter of $\leq$ 10.0 cm; (3) tumor located $\geq$ 2 cm away from the porta hepatis or digestive tract; (4) Child-Pugh class A or B; and (5) the European Organization for Research and Treatment of Cancer performance status of 0–2 [22]. Tumors in this study were somewhat smaller than most other series (median diameter, 2.8 cm; range, 0.8–9.3 cm). Forty patients did not change Child-Pugh class, 3/10 patients improved from Child-Pugh class B to A, and 8/41 patients deteriorated from Child-Pugh class A to B; no patients deteriorated to class C. Rib fracture occurred in three patients. Local control and overall survival at 3 years were 95 % and 49 %, respectively.

Tse and colleagues from Princess Margaret Hospital consolidated treatment into a 6-fraction regimen and conducted a phase I study in patients with HCC ($n = 31$) or intrahepatic cholangiocarcinoma ($n - 10$) [23]. The intent was to escalate dose according to the risk of radiation-induced liver disease (RILD), employing a normal tissue complication probability model that was based on analyses of conventionally fractionated RT to the liver. The median dose to the tumor was 36 Gy (range, 24–54 Gy). Although 5/31 patients deteriorated from Child-Pugh class A to B, there were no instances of RILD observed despite the model-based prediction that up to 20 % of patients in certain cohorts would have had RILD. Thus, it seems unlikely that the same predictive models of toxicity relevant to conventionally fractionated RT apply for hypofractionated RT. In any case, in a group of heavily pretreated patients (over 60 % had had at least one prior therapy for HCC), an encouraging median survival of 12 months was achieved.

SBRT, as defined above, has been investigated for application in the management of HCC at

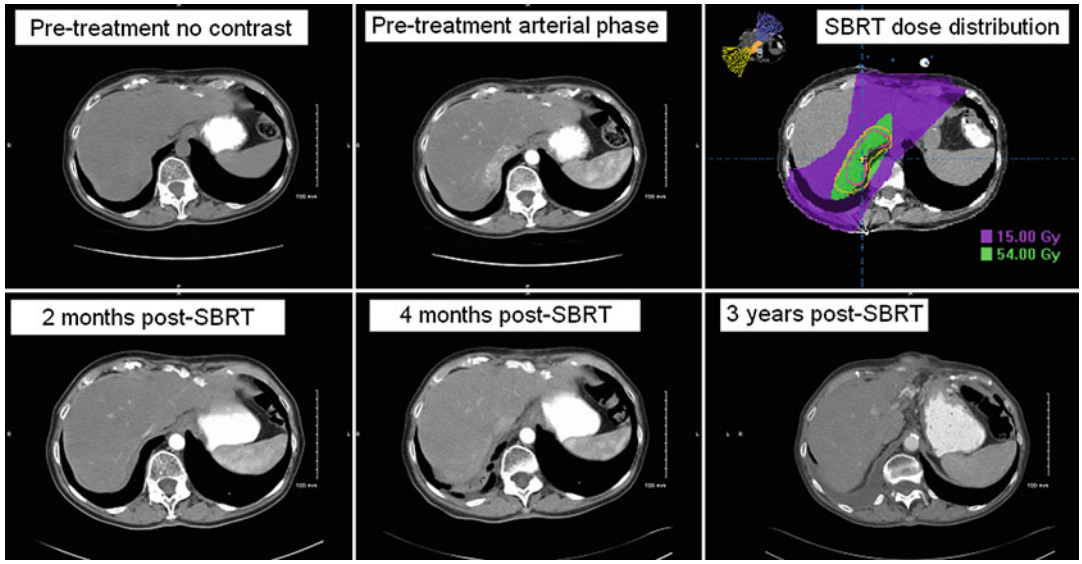

Fig. 25.1 Pretreatment scans, planning images for stereotactic body radiation therapy (SBRT), and posttreatment images for a patient treated with SBRT for recurrent hepatocellular carcinoma. The small pleural effusion seen in the lower right image has been stable for 2 years and is unrelated to disease activity

institutions in Europe, North America, and Asia. Méndez Romero and colleagues at Erasmus University Medical Center in the Netherlands treated 8 patients with 11 separate lesions of HCC in 3–5 fractions to a dose of 25–37.5 Gy; three patients had vascular invasion [24]. This strategy produced a 1-year local control rate of 75 %, which corresponded to a 1-year survival rate of 75 %. In a more recent publication from Choi and colleagues at the Catholic University of Korea, 23 patients with 32 individual lesions of HCC were treated in a 3-fraction regimen to a median dose of 36 Gy (range, 30–39 Gy) [25]. Nine of the patients had portal vein tumor thrombus; follow-up was limited (median, 11 months), but no patient experienced severe toxicity. In a subsequent analysis focused on toxicity, this same group observed that the most important predictor for a decrease in Child-Pugh class was the volume of normal liver receiving 18 Gy or more (V18). The rate of negative impact on Child-Pugh class escalated sharply when the V18 exceeded 800 cc [26].

Cardenes and colleagues reported a multiinstitutional phase I dose-escalation study of SBRT given in 3 fractions for HCC [27]. Eligible patients had Child-Pugh class A or B, were not candidates for resection, and had 1–3 lesions and cumulative tumor diameter $\leq$ 6 cm. Dose escalation started at 12 Gy per fraction. A total of 17 patients with 25 lesions were enrolled. Dose was escalated to 48 Gy (16 Gy/fraction) in Child-Pugh class A patients without any dose-limiting toxicity. Two patients with Child-Pugh class B disease developed grade 3 hepatic toxicity at the 42-Gy (14 Gy/fraction) level. As a result, the investigators decided to reduce the dose to 40 Gy in 5 fractions; still, one patient with Child-Pugh class B experienced progressive liver failure, though 4 additional patients were enrolled at that dose level and tolerated the SBRT without serious incident. Six patients underwent a liver transplant after SBRT. No patients progressed locally within the treated volume. The 2-year overall survival for the entire group was 60 %.

Figure 25.1 is an illustration of a patient with HCC treated with SBRT. The patient was a 77-year-old female who had recurred in a site previously treated with cryotherapy and later unsuccessfully with TACE. The pretreatment AFP had risen to 293. The patient received a dose of 54 Gy in 3 fractions of SBRT, after

which the AFP declined to a level below 2, where it has remained during subsequent surveillance. The figure includes pretreatment images, SBRT planning images showing the prescription dose and 15-Gy dose volume, and posttreatment follow-up imaging. The patient remains alive with no evidence of disease over 5 years after SBRT.

Many of the series above included patients who had had TACE prior to RT. A recent meta-analysis by Meng and colleagues suggested a survival benefit from the combination of TACE + RT relative to TACE alone [28]. A wide variety of RT schedules were used in the randomized studies analyzed, mostly conventionally fractionated regimens. However, there have been recent reports focused only on patients who received a combination of hypofractionated RT and TACE. Oh and colleagues at Sungkyunkwan University School of Medicine in Korea treated patients with unresectable HCC who failed 1 or 2 courses of TACE, giving the RT soon after progression. In 40 patients with 43 lesions, a median dose of 54 Gy in 18 fractions was given; an overall survival rate was 72.0 % at 1 year that was achieved with acceptably low toxicity [29]. Ren and colleagues at Fudan University Shanghai Cancer Center conducted a formal dose-escalation study among HCC patients with Child-Pugh class A status who had received 1–4 courses of TACE previously [30]. The maximum tolerated dose (MTD) for patients with tumor diameter <10 cm was 62 Gy in 10 fractions, and the MTD for tumors ≥ 10 cm was 52 Gy/10 fractions. The in-field progression-free rate was 100 % at 1 year and 93 % at 2 years; overall survival rates for 1 year and 2 years were 72 % and 62 %, respectively.

The established beneficial clinical activity of sorafenib for HCC [31] has prompted investigations into the combination of RT and this or similar agents. Chi and colleagues at National Yang-Ming University in Taipei reported a retrospective analysis of 23 HCC patients, most of whom had 2 or more hepatic lesions, who received 25 mg of sunitinib at least 1 week before, during, and 2 weeks after RT [32]. Thirteen patients continued maintenance sunitinib after RT until disease progression. A median hypofractionated RT dose of 52.5 Gy in 15 fractions was administered. In general, the combination was well tolerated, though 2 patients had grade 3 upper gastrointestinal bleeding and one had grade 3 pancreatitis. Zhao and colleagues from Fudan University have launched a study involving maintenance sorafenib after TACE and RT for HCC [33].

Interstitial and Hepatic Artery Infusional Brachytherapy for HCC

Mohnike and colleagues from Otto von Guericke University in Germany treated HCC patients with interstitial high-dose-rate (HDR) brachytherapy with an iridium-192 source [34]. Most patients had recurred after other prior therapy. The tumor dose was adjusted based on considerations of the normal tissue dose distribution: notably, not more than two third of the normal liver tissue received >5 Gy. Among 75 evaluable patients, only 5 local recurrences were noted.

The median overall survival was 19.4 months for the entire group but higher for the subgroup of patients with the best baseline liver function.

Radioembolization, also called selective internal radiation therapy (SIRT), using yttrium-90 microspheres is another form of brachytherapy which capitalizes on the unique dual blood supply of the liver (portal vein and hepatic artery), coupled with the fact that tumors are almost always fed primarily by the hepatic arterial system [35–37]. Yttrium-90, primarily a beta emitter, is administered via a catheter placed in the hepatic artery. Tumor cell kill is by the combination of beta radiation and embolization, though the relative contribution of the former versus latter is not precisely known.

There are two commercially available yttrium-90 products which obtained FDA approval through two very different mechanisms. TheraSphere (MDS Nordion, Kanata, ON, Canada) obtained approval under a humanitarian device exemption (HDE) in 1999 for the treatment of unresectable HCC. FDA approval for SIR-Spheres (Sirtex Medical, Lane Cove, Australia) was obtained in 2002 but through a mechanism typically used for

approval of drugs, including chemotherapy. SIR-Spheres approval was limited to liver metastases from colorectal primaries. While there are some differences between the two formulations (resin versus glass and size of the particles, TheraSpheres being smaller), there is no scientific rationale why one would work better for metastases versus primary tumors. However, the majority of the clinical experience to date for HCC has been with TheraSpheres.

The early literature is well summarized in a review paper published in 2006 [37]. Pooled analysis of a 121-patient cohort from the HDE database identified several factors that predicted for high 3-month mortality rate: infiltrative tumor, $\geq$ 70 % of the liver with tumor involvement, increase in liver enzyme levels (aspartate or alanine aminotransferase level $>5 \times$ upper limit of normal), a combination of $\geq$ 50 % of the liver with tumor involvement and albumin < 3 g/l, total bilirubin ≥ 2 mg/dL, or predicted lung dose > 30 Gy [38]. The authors concluded that patients with the aforementioned risk factors are not well suited for yttrium-90 treatment as they are likely to experience early liver disease or cancer-related death and are at high risk of treatment toxicity. This data provided a useful guide in patient selection.

Until recently, survival and toxicity parameters have been used as the primary endpoints for most studies since it can be difficult to assess response and local control. Clinical and clinic-pathologic studies have shown that early posttreatment necrosis, indicated by a reduction in arterial enhancement and conversion to hypodensity on CT, is the most important indicator of response. A simple change in size by imaging is not predictive because lesions often appear larger initially posttreatment, not unlike other radioablative therapies [39–41].

The vast majority of patients with HCC have underlying liver disease, but mild to moderate liver dysfunction is not necessarily a contraindication to liver transplant [42]. However, because there can be delays of unpredictable length while a patient waits for a donor liver, therapies like SIRT have been considered as a potential "bridge" to transplant or as a means of downstaging for patients with advanced disease not initially eligible for transplant. Lewandowski and colleagues compared the downstaging achieved with TACE ($n = 43$) versus ytrrium-90 radioembolization ($n = 43$) at a single institution [43]. While not a randomized study and therefore subject to selection bias, there was a statistically demonstrable advantage favoring yttrium-90 radioembolization in partial response (61 % vs. 37 %), time to progression by the United Network for Organ Sharing (UNOS) criteria (18.2 mos vs. 33.3 mos) and overall survival (35.7 mos vs. 18.7 mos).

Summary

Radiation therapy, in the form of external beam treatment or brachytherapy, has been shown to provide effective treatment for selected patients with HCC. Typically, RT has been employed for patients with advanced disease who are unsuitable for other therapies or have recurred after other therapies, and so it is difficult to compare results from RT with outcomes achieved by other modalities. However, recent technologic developments in the area of intensified external bream RT and also in the field of radioembolization using yttrium-90 have yielded very encouraging results either as definitive therapy or as a temporizing (bridge) or downstaging modality prior to transplantation. Investigations in these areas and in the area of strategic combinations of RT and active systemic therapy are currently ongoing and promise to add insights into how the role of RT might expand in the future to help more patients with HCC.

References

1. International Agency for Cancer Research. GLOBOCAN 2008: cancer incidence and mortality worldwide in 2008. http://globocan.iarc.fr. Accessed 31 July 2010.
2. Sanyal A, Poklepovic A, Moyneur E, Barghout V. Population-based risk factors and resource utilization for HCC: US perspective. Curr Med Res Opin. 2010;26(9):2183–91. Epub ahead of print.
3. Hasegawa K, Kokudo N. Surgical treatment of hepatocellular carcinoma. Surg Today. 2009;39(10): 833–43. Epub 2009 Sep 27.

4. Okuda K, Ohtsuki T, Obata H, et al. Natural history of hepatocellular carcinoma and prognosis in relation to treatment. Study of 850 patients. Cancer. 1985;56(4): 918–28.
5. Yeung YP, Lo CM, Liu CL, et al. Natural history of untreated nonsurgical hepatocellular carcinoma. J Gastroenterol. 2005;100(9):1995–2004.
6. Ruzzenente A, Capra F, Pachera S, et al. Is liver resection justified in advanced hepatocellular carcinoma? Results of an observational study in 464 patients. J Gastrointest Surg. 2009;13(7): 1313–20.
7. Stillwagon GB, Order SE, Guse C, et al. 194 hepatocellular cancers treated by radiation and chemotherapy combinations: toxicity and response: A Radiation Therapy Oncology Group study. Int J Radiat Oncol Biol Phys. 1989;17(6):1223–9.
8. Abrams RA, Cardinale RM, Enger C, et al. Influence of prognostic groupings and treatment results in the management of unresectable hepatoma: experience with Cisplatinum-based chemoradiotherapy in 76 patients. Int J Radiat Oncol Biol Phys. 1997;39(5): 1077–85.
9. Liu MT, Li SH, Chu TC, et al. Three-dimensional conformal radiation therapy for unresectable hepatocellular carcinoma patients who had failed with or were unsuited for transcatheter arterial chemoembolization. Jpn J Clin Oncol. 2004;34(9):532–9.
10. Ben-Josef E, Normolle D, Ensminger WD, et al. Phase II trial of high-dose conformal radiation therapy with concurrent hepatic artery floxuridine for unresectable intrahepatic malignancies. J Clin Oncol. 2005;23: 8739–47.
11. Hsu W, Chan S, Ting L, et al. Results of three-dimensional conformal radiotherapy and thalidomide for advanced hepatocellular carcinoma. Jpn J Clin Oncol. 2006;36(2):93–9.
12. Seo YS, Kim JN, Keum B, et al. Radiotherapy for 65 patients with advanced unresectable hepatocellular carcinoma. World J Gastroenterol. 2008;14(15): 2394–400.
13. Zeng Z, Fan J, Tang Z, et al. Prognostic factors for patients with hepatocellular carcinoma with macroscopic portal vein or inferior vena cava tumor thrombi receiving external-beam radiation therapy. Cancer Sci. 2008;99(12):2510–7.
14. Han K, Seong J, Kim JK, et al. Chemoradiation therapy for locally advanced hepatocellular carcinoma with portal vein thrombosis. Cancer. 2008;113: 995–1003.
15. Zeng ZC, Tang ZY, Fan J, Qin LX, Ye SL, Zhou J, Sun HC, Wang BL, Wang JH. Consideration of role of radiotherapy for lymph node metastases in patients with HCC: retrospective analysis for prognostic factors from 125 patients. Int J Radiat Oncol Biol Phys. 2005;63(4):1067–76.
16. McIntosh A, Hagspiel KD, Al-Osaimi AM, et al. Accelerated treatment using intensity-modulated radiation therapy plus concurrent capecitabine for unresectable hepatocellular carcinoma. Cancer. 2009; 115:5117–25.
17. Rich TA, Shepard RC, Mosley ST. Four decades of continuing innovation with fluorouracil: current and future approaches to fluorouracil chemoradiation therapy. J Clin Oncol. 2004;22:2214–32.
18. Kavanagh BD, Timmerman RD. Stereotactic body radiation therapy. Philadelphia: Lippincott Williams & Wilkins; 2005.
19. Liang S-X, Jiang GL, Zhu X-D, et al. Hypofractionated 3-dimensional conformal radiation therapy for primary liver carcinoma. Cancer. 2005;103: 2181–8.
20. Choi BO, Jang HS, Kang KM, et al. Fractionated stereotactic radiotherapy in patients with primary hepatocellular carcinoma. Jpn J Clin Oncol. 2006;36(3):154–8.
21. Bush DA, Hillebrand DJ, Slater JM, et al. High-dose proton beam radiotherapy of hepatocellular carcinoma: preliminary results of a phase II trial. Gastroenterology. 2004;127:S189–93.
22. Fukumitsu N, Sugahara S, Nakayama H, et al. A prospective study of hypofractionated proton beam therapy for patients with hepatocellular carcinoma. Int J Radiat Oncol Biol Phys. 2009;74(3):831–6.
23. Tse RV, Hawkins M, Lockwood G, et al. Phase I study of individualized stereotactic body radiotherapy for hepatocellular carcinoma and intrahepatic cholangiocarcinoma. J Clin Oncol. 2008;26:657–64.
24. Méndez Romero A, Wunderink W, Hussain SM, et al. Stereotactic body radiation therapy for primary and metastatic liver tumors: a single institution phase i-ii study. Acta Oncol. 2006;45(7):831–7.
25. Choi BO, Choi BI, Jang HS, et al. Stereotactic body radiation therapy with or without transarterial chemoembolization for patients with primary hepatocellular carcinoma: preliminary analysis. BMC Cancer. 2008;8:351.
26. Son SH, Choi BO, Ryu MR, et al. Stereotactic body radiotherapy for patients with unresectable primary hepatocellular carcinoma: dose-volumetric parameters predicting the hepatic complication. Int J Radiat Oncol Biol Phys. 2010;78(4):1073–80. Epub ahead of print.
27. Cardenes HR, Price TR, Perkins SM, et al. Phase I feasibility trial of stereotactic body radiation therapy for primary hepatocellular carcinoma. Clin Transl Oncol. 2010;12(3):218–25.
28. Meng M, Cui Y, She B, et al. Transcatheter arterial chemoembolization in combination with radiotherapy for unresectable hepatocellular carcinoma: a systematic review and meta-analysis. Radiother Oncol. 2009;92(2):184–94.
29. Oh D, Lim d H, Park HC. Early three-dimensional conformal radiotherapy for patients with unresectable hepatocellular carcinoma after incomplete transcatheter arterial chemoembolization: a prospective evaluation of efficacy and toxicity. Am J Clin Oncol. 2010;33(4): 370–5.

30. Ren Z, Zhao H, Chen Z, et al. Three-dimensional conformal radiation therapy and intensity-modulated radiation therapy combined with transcatheter arterial chemoembolization for locally advanced hepatocellular carcinoma: an irradiation dose escalation study. Int J Radiat Oncol Biol Phys. 2010. [Epub ahead of print].
31. Llovet JM, Ricci S, Mazzaferro V, et al. Sorafenib in advanced hepatocellular carcinoma. N Engl J Med. 2008;359:378–90.
32. Chi K, Liao C, Chand C, et al. Angiogenic blockade and radiotherapy in hepatocellular carcinoma. Int J Radiat Oncol Biol Phys. 2010;78(1):188–93. Epub ahead of print.
33. Zhao J, Liu J, Ren Z, et al. Maintenance of Sorafenib following combined therapy of three-dimensional conformal radiation therapy/intensity-modulated radiation therapy and transcatheter arterial chemoembolization in patients with locally advanced hepatocellular carcinoma: a phase I/II study. Radiat Oncol. 2010;5:12. doi:10.1186/1748-717X-5-12.
34. Mohnike K, Wieners G, Schwartz F, et al. Computed tomography–guided high-dose-rate brachytherapy in hepatocellular carcinoma: safety, efficacy, and effect on survival. Int J Radiat Oncol Biol Phys. 2010;78(1):172. Epub ahead of print.
35. Salem R, Thurston KG. Radioembolization with ^{90}Yttrium microspheres: a state-of-the-art brachytherapy treatment for primary and secondary liver malignancies part 1: technical and methodologic considerations treatment is administered via the hepatic artery. J Vasc Interv Radiol. 2006;17:1251–78.
36. Salem R, Thurston KG. Radioembolization with ^{90}Yttrium microspheres: a state-of-the-art brachytherapy treatment for primary and secondary liver malignancies part 2: special topics. J Vasc Interv Radiol. 2006;17:1425–39.
37. Salem R, Thurston KG. Radioembolization with ^{90}Yttrium microspheres: a state-of-the-art brachytherapy treatment for primary and secondary liver malignancies part 3: comprehensive literature review and future direction. J Vasc Interv Radiol. 2006;17:1571–94.
38. Goin JE, Salem R, Carr BI, et al. Treatment of unresectable hepatocellular carcinoma with intrahepatic yttrium 90 microspheres: a risk-stratification analysis. J Vasc Interv Radiol. 2005;16:195–203.
39. Keppke AL, Salem R, Reddy D, et al. Imaging of hepatocellular carcinoma after treatment with yttrium-90 microspheres. Am J Roentgenol (AJR). 2007;188:768–75.
40. Welsh JS. Radiographically identified necrosis after ^{90}Y microsphere brachytherapy: a new standard for oncologic response assessment? Am J Roentgenol (AJR). 2007;188:765–7.
41. Riaz A, Kulick L, Lewandowski RJ, et al. Radiologic-pathologic correlation of hepatocellular carcinoma treated with internal radiation using Yttrium-90 microspheres. Hepatology. 2009;49:1–9.
42. Detry O, De Roover A, Delwaide J, et al. Absolute and relative contraindications to liver transplantation. A perpetually moving frontier. Acta Gastroenterol Belg. 2002;65:133–4.
43. Lewandowski RJ, Kulik LM, Riaz SS, et al. A comparative analysis of transarterial downstaging for hepatocellular carcinoma: chemoembolization versus radioembolization. Am J Transplant. 2009;9:1–9.

Radiofrequency Ablation of Hepatic Metastasis

26

Rajan K. Gupta and Gerald Dodd, III

Abstract

Treatment of metastatic liver disease is a commonly encountered problem in oncologic practice. Numerous studies, particularly in the treatment of colorectal hepatic metastasis, have demonstrated that resection of isolated hepatic metastasis can improve survival compared with conventional chemotherapy alone. These observations have led to the basis for obtaining local treatment of isolated hepatic metastasis. Although surgical treatment of isolated hepatic metastatic disease generally remains the gold standard, other minimally invasive treatment options including ablative therapies have evolved and have been used to treat patients who are not surgical candidates. Many retrospective and observational series suggest that local ablation of isolated liver metastasis provides a survival benefit compared to conventional chemotherapy alone and these therapies have rapidly been incorporated into clinical practice. Radiofrequency ablation (RFA) remains the most widely studied and used ablation technology in the liver worldwide. Patient selection is critical and is often carried out in a multidisciplinary forum. The majority of clinical experience and literature regarding ablation of metastatic liver disease is with colorectal liver metastasis, although there is increasing experience with larger populations of patients with breast cancer and neuroendocrine tumors. Clinical efficacy with various tumor types, considerations regarding patient selection, imaging follow-up, patterns of recurrence, and complications are reviewed.

Introduction

Treatment of metastatic liver disease is one of the most commonly encountered problems in oncologic practice. Metastasis to the liver is second only to metastasis to regional lymph nodes and is far more common than primary liver cancer [1]. It is estimated that 40–50 % of all malignancies are complicated by liver metastasis [1].

R.K. Gupta (✉) • G. Dodd, III
Department of Radiology, University of Colorado, Denver, Aurora, CO, USA
e-mail: Rajan.Gupta@ucdenver.edu; Gerald.Dodd@ucdenver.edu

D.E. Dupuy et al. (eds.), *Image-Guided Cancer Therapy*, DOI 10.1007/978-1-4419-0751-6_28,

After treatment of the primary malignancy, patients with a variety of malignancies may present with isolated liver metastasis and may be candidates for additional therapy beyond systemic chemotherapy alone [1].

Numerous studies, particularly in the treatment of colorectal hepatic metastasis, have demonstrated that resection of isolated hepatic metastasis, or metastasectomy, can improve survival compared with conventional chemotherapy alone and may even result in long-term cure in a subset of patients [2–7]. These observations have led to the basis for obtaining local treatment of isolated hepatic metastasis. Local therapy of hepatic metastasis has been applied to other malignancies including neuroendocrine carcinoma, breast cancer, melanoma, sarcomas, and others, albeit with limited evidence [8–21].

Although surgical treatment of isolated hepatic metastatic disease generally remains the gold standard, other minimally invasive treatment options including ablative therapies, transarterial chemoembolization or radioembolization, radiation therapy, or combination therapies have evolved and have been used to treat patients who are not surgical candidates. Of these therapies, ablative and combination therapies are considered to be potentially curative. Many retrospective and observational series suggest that local ablation of isolated liver metastasis provides survival benefit compared to conventional chemotherapy alone and these therapies have rapidly been incorporated into clinical practice [13, 18, 22–25].

Many ablation technologies are currently available including ethanol ablation, cryoablation, microwave ablation, laser ablation, and radiofrequency ablation. Radiofrequency ablation (RFA) remains the most widely studied and used ablation technology in the liver worldwide. RFA utilizes an alternating electrical current to create local ionic frictional heating, which induces thermal damage leading to coagulative necrosis. RFA can be performed from a variety of approaches including open surgical, laparoscopic, or percutaneous routes. Operator experience, local resources, and lesion characteristics often guide approach, although image-guided percutaneous approaches appear to be the dominant technique.

Patient Selection

The two main goals for treatment of patients with metastatic liver disease are improving survival and providing palliation of symptoms. The importance of a team approach to evaluation of oncologic patients at a multidisciplinary tumor board cannot be overemphasized for optimal patient selection and management. Indications and contraindications for radiofrequency ablation of hepatic metastasis are listed in Table 26.1.

The ability to confer a survival benefit by treating metastatic liver disease infers that patients have limited disease and the potential for improved survival. Extrahepatic disease is typically associated with a poor prognosis and is generally considered to be a contraindication to ablation. Major exceptions to this rule include neuroendocrine tumors and breast cancer, which will be discussed in the relevant sections of the text. Additionally, select patients with colorectal liver and lung metastasis may be candidates for ablation if the disease is felt to be curable. In general, patients should have liver dominant disease that is felt to be prognostic of their survival or symptoms that may be improved with ablative therapies [26]. Patients with estimated life expectancy of less than 6 months or those with poor performance status (ECOG >2) are also unlikely to benefit from hepatic ablation, and the risk of treatment outweighs any marginal benefit that may be obtained. An exception to this rule is in neuroendocrine tumors, where poor performance status related to severe hormonal symptoms may actually improve after treatment.

Given a lack of randomized controlled data and generally superior results of surgical resection in terms of improved survival and lower local recurrence, surgical resection of isolated metastatic disease remains the reference standard of treatment. Most practitioners reserve ablative therapies for those who are not surgical candidates or those who refuse resection. There is, however, a shifting pendulum toward ablative therapy to preserve functional liver when the expected rate of new metastatic lesions is high. A relative indication for ablation over surgery is a small tumor that may require a large resection due to location. Unless the

Table 26.1 Indications and contraindications for RFA of liver metastasis

Indications:
Therapy goals:
Survival benefit:
Liver dominant metastatic disease
Liver metastasis felt to be a primary determinant of survival
Palliation:
Tumor bulk symptoms
Hormonal symptoms
Tumor visible with imaging that can be used for guidance:
US, CT, MRI, fusion technologies
Nonsurgical candidate or patient refusal of surgery
Residual/recurrent tumor after prior ablation or hepatic resection
Tumor characteristics:
Size and number:
Best results: tumors <3 cm, 3 or fewer metastases
Intermediate results: tumors <5 cm, 5 or fewer metastases
Potential indications for RFA:
Small tumor requiring a large resection
Combined strategy with resection
Bridging strategy to resection
Contraindications:
Extrahepatic disease:
Exceptions:
Breast cancer with bone/lung metastases stable >6 months
Neuroendocrine metastasis
Select cases of colorectal carcinoma with liver and lung metastasis
Risks for infection:
Incompetent/disrupted biliary sphincter:
Biliary-enteric anastomosis (Whipple, transplant, etc.)
Biliary sphincterotomy/stent
Biliary obstruction
Concurrent bowel resection
Active infection
Uncorrectable coagulopathy
Anatomically unfavorable lesions:
Close proximity (<2 cm) to central bile ducts:
Exception: nasobiliary cooling possible
Close proximity to bowel or stomach with inability to separate:
Exception: ability to separate structures with open or laparoscopic means, changes in positioning, or percutaneous means (D5W infusion, CO_2, balloon separation)
Short life expectancy (<6 months)
Poor performance status (ECOG >2)
Insufficient hepatic reserve
Pregnancy

goal is palliation of tumor bulk or hormonal symptoms, all tumors should be accessible to ablation as the goal is to eliminate all residual disease, similar to an R0 (complete) surgical resection. Relative advantages of ablation compared to surgical resection include lower morbidity and mortality, lower complication rates, shorter hospitalization, lower cost, greater preservation of hepatic parenchyma, and greater repeatability. Relative advantages of surgery include lower local recurrence rates, the ability to treat larger lesions, high sensitivity of intraoperative ultrasound for lesion detection, and the ability to examine the peritoneal cavity for staging.

A number of factors are predictive of local success and are similar for primary liver tumors. Lesion size is likely more important than number largely because local recurrence is strongly correlated with tumor size. Tumors <3 cm in size can typically be treated in one session with low rates of recurrence. Tumors 3–5 cm often need multiple overlapping ablations and have moderate rates of recurrence, and tumors >5 cm are technically challenging to treat and have frequent local recurrence. Tumor number is less important, although incremental survival benefits likely decrease and complications of therapy increase when treating more tumors. When performed for survival benefit, most centers limit treatment to five or fewer tumors. The best results are obtained in those with less than 3 masses, all less than 3 cm in size, although this selection criterion is not uniformly agreed upon and is dependent on goals of ablation. Proximity of masses within 5 mm of larger vessels (>3–5 mm) is correlated to higher recurrence rates due to thermal sink effects.

Anatomic selection factors regarding suitability for ablation are similar for ablation of primary liver tumors and include proximity to structures

that are heat sensitive, most importantly central bile ducts and the gastrointestinal tract. Biliary injury can lead to stenosis, abscess, biloma, sepsis, and liver failure. Peripheral biliary injury is often clinically silent and associated with chronic atrophy of the affected liver segment. Central biliary injury, however, is associated with jaundice and liver failure and can lead to substantial morbidity. Bile ducts travel adjacent to portal veins although their exact relationship is not consistent. The exact relationship can be defined with MRCP if needed. Tumors in the hepatic hilum or those within 2 cm of central portal veins should be avoided due to risks of biliary injury. Prophylactic cooling of the biliary tree to protect it from thermal damage is possible with a nasobiliary or percutaneous tube to infuse chilled saline during ablation [27, 28]. Biliary cooling may decrease the incidence of biliary injury from approximately 40 % to less than 3 % [27, 28]. Although the technique appears promising, long-term follow-up is not yet available and additional risks from ERCP placement of a biliary tube such as pancreatitis and possibly increased risk of abscess formation are present. Thermal damage to the colon, small bowel, or stomach may lead to perforation, sepsis, peritonitis, and death. The colon appears to be the most sensitive to heat, followed by small bowel and then stomach. Ablation of tumors near the gallbladder has been shown to be safe in experienced hands although a self-limited cholecystitis is common [29–31]. Ablation of tumors near the pericardium requires extreme care not to perforate the pericardium with a needle or tine, which may result in pericardial hemorrhage and tamponade. Care should be taken with other surrounding organs such as the kidney, adrenal glands, and diaphragm as well, although significant complications are less common. Open and laparoscopic approaches facilitate mechanical separation of vital structures although percutaneous techniques to protect adjacent structures are possible including the induction of artificial ascites with D5W, separation with CO_2, or balloon interposition [32–34]. Often changes in patient positioning (i.e., decubitus) or decompression of bowel with a nasogastric tube will permit safe ablation. Patients with prior abdominal surgery may have adhesions rendering these techniques ineffective. The needle path should traverse normal hepatic parenchyma, and direct tumor puncture of subcapsular lesions should be avoided due to the theoretical higher risks of tumor tract seeding and hemorrhage. Although more technically challenging, subcapsular lesions can be ablated utilizing an indirect approach that includes a mantle of normal hepatic parenchyma between the capsular puncture and the tumor. Dome lesions can be ablated safely, but caution is required not to perforate the diaphragm with a tine, which can lead to diaphragmatic injury or biliary-pleural fistula. This is particularly true with expandable probes where it is more challenging to predict in three dimensions how an expandable array will deploy in relationship to the curved surface of the diaphragm. The authors prefer to use real-time imaging guidance and single or multiple straight antenna probes in this circumstance. Adjacent vascular structures are not a specific contraindication unless in relation to a central bile duct, although heat sink effects increase rates of local treatment failure. An incompetent biliary sphincter or previous biliary-enteric anastomosis predisposes to a very high rate of abscess development and should be viewed as a contraindication to ablation. Complications are further discussed in the relevant section of the chapter.

High-quality recent imaging is important for both treatment planning and patient selection. Metastatic disease may often be followed with PET imaging, although the sensitivity for detection of lesions less than 1 cm is reduced. PET is important to detect occult extrahepatic disease, which is critical in patient selection. Dynamic contrast-enhanced CT or MRI within 1 month of the procedure is recommended to avoid significant interval progression of disease and ensure that staging of liver disease is appropriate. The tumor should be visible with the imaging intended for the guidance, most commonly either ultrasound or CT. Although MRI can be utilized for guidance, special MRI compatible equipment is needed which is not widely available. MRI is, however, the only imaging guidance that currently allows for real-time temperature monitoring. Recent advances in

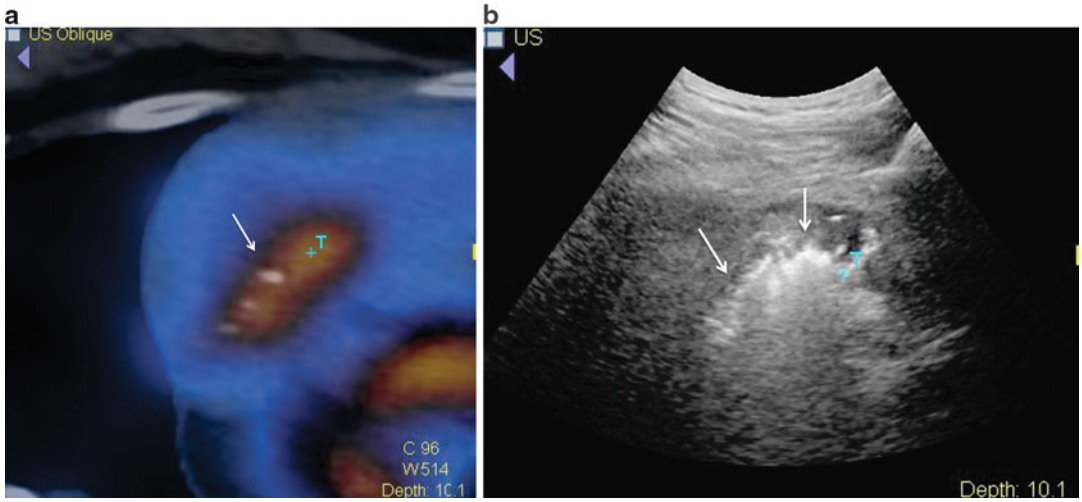

Fig. 26.1 (**a**) Fused imaging (Philips Percunav system) overlay of a positive octreotide SPECT scan with an ultrasound image to visualize a neuroendocrine tumor (*arrow*) liver metastasis that was not visible on ultrasound or CT. Fusion imaging made it possible to perform RFA on this lesion. (**b**) Unfused ultrasound image during RF ablation demonstrates a hyperechoic region (*arrows*) roughly corresponding to the area of ablation

imaging guidance allow fusion of 3-D data sets from CT, MRI, PET, or SPECT imaging with ultrasound imaging that can then be used for guidance of lesions, which are not visible sonographically (Fig. 26.1). If percutaneous ultrasound ablation is planned, preoperative ultrasound by the operator performing the procedure is helpful for planning of approach and ensuring that the mass will be visible at the time of ablation.

Liver insufficiency is rarely a problem in patients with metastatic disease, as patients are typically not cirrhotic. Patients with significant liver compromise often have diffuse hepatic disease and are not candidates for ablative therapies. An adequate coagulation profile with platelet count >50,000 and INR <1.8 is recommended to decrease hemorrhagic complications. Fresh frozen plasma and platelets can be given to correct coagulopathies in appropriate situations.

Clinical Efficacy

Interpretation of published literature for percutaneous ablation for metastatic liver is difficult. Only a single phase II prospective randomized trial has been published comparing RFA combined with chemotherapy to chemotherapy alone for unresectable colorectal liver metastasis, but it was inadequately powered to detect a difference in overall survival [35]. The majority of data supporting the use of RFA for hepatic metastases comes from observational studies, case series, and retrospective data, which are subject to numerous inherent biases and demonstrate significant variability in reporting with a lack of intent-to-treat data. Additionally, the techniques of ablation, ablation systems, and chemotherapy regimens have continued to evolve rapidly. By the time a study has been published with sufficient follow-up, both chemotherapy regimens and ablation systems may have substantially changed. Additionally, the quality of imaging follow-up has varied across studies making direct comparison between studies difficult. Lastly, an evolving understanding of the reasons for local failure and recognizing high risk factors that lead to complications have led to changes in patient selection, which may improve overall results. Reasons for difficulty in data interpretation are summarized in Table 26.2.

Table 26.2 Clinical efficacy of RFA for metastatic disease: factors affecting interpretation of published data

Lack of quality data:
Only a single, underpowered randomized trial for CRC mets has been published
Remaining data is from case series, retrospective, and observational studies
Variable, inconsistent reporting
Variable ablative techniques dependent upon:
Operator experience/skill
Approach (open, laparoscopic, percutaneous)
Device used
Variable chemotherapy and biologic agents
Improved imaging:
Earlier detection of metastasis and local failure
Improved guidance:
Improved ultrasound/CT systems
Fusion navigation systems
Ultrasound contrast agents (not available in USA)
Better patient selection (lessons learned):
Best results in:
Tumors <3 cm
Tumors >5 mm from larger (3 mm) vessels
Larger (>1 cm) ablative margin
Complications:
Incompetent biliary sphincter/biliary-enteric anastomosis → abscess

Colorectal Cancer Hepatic Metastasis

Colon cancer is the third most common malignancy in the US contributing to nearly 10 % of all cancer deaths [25]. Fifteen to twenty-five percent of patients have evidence of liver metastasis at presentation, and 50 % will develop liver metastasis at some point during the course of their disease [25, 36]. Historical median survival in these patients without treatment is 5 months; however, median survival can be prolonged nearly 2 years with modern chemotherapy and biologic agents [24, 25, 37].

Retrospective and prospective data from surgical series have demonstrated that hepatic resection improves overall survival, particularly in patients without extrahepatic disease. Median survival after resection is reported to be from 33 to 46 months, overall 3-year survival ranges from 45 % to 57 %, and overall 5-year survival ranges from 22 % to 58 % [24, 25]. A subset of patients achieves a long-term cure with 10-year survival of approximately 20 % [25]. Despite encouraging results, only 10–25 % of patients are candidates for surgical resection, although technical advancements such as portal vein embolization, multistage approaches at resection, and improvements in chemotherapy leading to downstaging of disease have allowed for greater rates of hepatic resection [38, 39]. Mortality from hepatic resection remains low reported from 0 % to 5 %, although morbidity of resection is moderate ranging from 17 % to 37 %. Additionally, the rate of new metachronous lesions is high. These observations have led to significant interest in alternative therapies including ablative and intra-arterial therapies.

Radiofrequency ablation is the most widely used and studied ablative therapy in the liver. The majority of the existing evidence for RFA of colorectal hepatic metastasis is from single-arm, retrospective, and prospective trials. Ruers et al. recently reported the only prospective randomized trial (EORTC 40004) that has been performed to investigate the benefits of radiofrequency ablation in patients with non-resectable colorectal liver metastasis [35]. This multicenter European study began as a phase III study but was downsized to a phase II design given slow accrual, largely due to strong preferences for a specific treatment arm-limiting referral for trial participation. From 2002 to 2007, 119 patients with non-resectable colorectal liver metastasis were randomly assigned to systemic treatment alone (control group) or combined systemic treatment plus RFA (treatment group). RFA was performed alone or with hepatic resection when required to achieve complete removal of intrahepatic metastatic disease. Patients in the systemic treatment arm were permitted to undergo surgical resection if the disease was converted to resectable by chemotherapy alone. The primary endpoint was to achieve a 30-month overall survival of greater than 38 % in the treatment group. This endpoint was achieved with 30-month overall survival rate of 61.7 % in the treatment group; however, the 30-month overall

survival for control group was higher than expected at 57.6 %. This was partly due to an increase in second-line therapies at the time of disease progression that were not anticipated at the time that the study was designed. Median overall survival was 45.3 months for treatment group and 40.5 months for the control group, which did not achieve statistical significance ($p = 0.22$) given that the phase II design was not adequately powered to detect a difference in overall survival. Progression-free survival at 3 years was, however, significantly longer ($p = 0.025$) in the treatment arm (27.6 %) compared to the control arm (10.6 %). Median progression-free survival was 16.8 months in the treatment arm compared to 9.9 months in the control arm. Of note, reporting of survival statistics was on an intent-to-treat basis, and salvage treatments were unbalanced between the two treatment arms. The results of this trial demonstrate that RFA +/− resection in combination with chemotherapy results in a statistically significant increase in progression-free survival compared to chemotherapy alone in patients with unresectable colorectal hepatic metastases. Although there is a trend in increased overall survival, it was not shown to be statistically significant. Only long-term follow-up may answer this question. The difficulty in recruitment for this and other prospective randomized trials also casts serious doubt on the likelihood for additional randomized data to prove the efficacy of RFA.

Many comprehensive reviews have been published summarizing the numerous retrospective and observational series present in the literature regarding the outcomes for RFA of colorectal hepatic metastases [22, 24, 25]. These reviews include table summaries of the majority of published literature [22, 24, 25]. The most comprehensive review is from the ASCO 2009 review by Wong et al., which reviews available literature for RFA of colorectal liver metastasis (CRLM) from 1996 up through April 2007 [25]. This review included 46 unique data sets from 73 articles with greater than 1,200 patients with CRLM. Reported median overall survival is 18–39 months, 3-year overall survival ranges from 25 % to 68 %, and 5-year overall survival ranges from 17 % to 31 %. More recently, Gillams et al. reported a 5-year survival of 40 % after percutaneous RFA of solitary colorectal hepatic metastasis <4 cm [40]. These results are higher than any published results for chemotherapy alone and provide indirect evidence for survival benefit of RFA. It is important to emphasize that direct comparison of outcomes from RFA compared to resection is not possible due to different patient cohorts, as the majority of patients treated with RFA had unresectable liver metastases.

Table 26.3 2009 ASCO review panel summary: RFA of colorectal hepatic metastasis – survival and local recurrence are related to:

Size of metastases
Number of metastases:
Best outcome in solitary mass
Reasonable outcome in 2–3 mets
Poorest outcome in >3 mets
Location of metastases:
High local failure near blood vessels >1 cm diameter[a]
Approach (risk of local recurrence)
Open < laparoscopic < percutaneous
Physician experience
Inversely related to local tumor recurrence

Wong et al. [25]
[a]Many authors consider peritumoral vessels of 3–5 mm to be of sufficient size to increase local failure [29, 40–42]

Conclusions of the ASCO review panel are summarized in Table 26.3 [25]. The panel found no compelling evidence for use of RFA in patients with viable extrahepatic disease. They found that survival and local recurrence are related to metastasis size, number, location, approach, and physician experience. The best outcome was reported in patients with a small solitary mass. Tumors smaller than 3 cm seemed to respond best with high rates of local control substantiated in a number of reports. Tumors 3–5 cm in size demonstrated moderate local recurrence, and tumors >5 cm in size had very high local failure rates. The number of metastatic lesions also correlated with both survival and local recurrence, with the best outcome in solitary masses, reasonable outcome in 3 or fewer lesions,

and poor outcomes in patients with more than three metastases. The location of tumors adjacent to blood vessels >1 cm in size was associated with high local failure rates, likely due to heat sink effect. Many authors, however, consider smaller peritumoral vessels (3–5 mm) to have significant heat sink effects that increase risks of local failure [30, 41–43]. Overall, surgical and laparoscopic approaches were associated with lower recurrence, although no randomized comparison is available and single-arm studies had overlapping rates of recurrence. Physician experience appeared to be inversely related to recurrence after RFA.

Neuroendocrine Tumor Hepatic Metastasis

Neuroendocrine tumors (NET) are rare, slow-growing tumors arising from primitive neuroectodermal cells, which may secrete proteins with hormonal activity resulting in characteristic clinical syndromes [44]. Over half of all neuroendocrine tumors will eventually metastasize to the liver. Neuroendocrine tumors are generally classified based on the location of the primary tumor, stage of differentiation, and presence or absence of hormonal secretion [45]. The majority of tumors can be broadly divided into carcinoid tumors of the gastrointestinal tract and islet cell carcinomas arising from the pancreas. In contrast to other carcinomas, neuroendocrine tumors demonstrate slow progression and have been called "cancers in slow motion." Despite relatively indolent growth, the presence of unresectable liver metastasis is associated with 5-year survival ranging from 11 % to 40 % [46]. With advances in medical therapy and various locoregional therapies to control hormonal symptoms, liver failure from progressive liver disease is now the leading cause of death in these patients.

The liver will typically metabolize the majority of hormones secreted into the portal system, and hormonal symptoms are often absent until liver metastases are present. Greater overall tumor burden increases the risk of hormonal symptoms as well. Carcinoid syndrome is related to excess serotonin production and may present with episodic flushing; diarrhea; bronchospasm; and in advanced disease, cardiac fibrosis and valvular incompetence. Although pancreatic cell islet carcinomas are histologically similar to carcinoid tumors, they produce a variety of distinct clinical syndromes.

Liver-directed therapy has an important role in treatment of neuroendocrine tumors as it allows targeted treatment of the disease that causes the most morbidity and mortality [44]. Control of neuroendocrine liver metastasis has been shown to improve quality of life by reducing or eliminating hormonal symptoms, and observational evidence suggests survival improvement [47]. The main options for control of liver disease include surgical resection, ablation, arterial embolization, and medical therapy with somatostatin analogs and/or interferon therapy. While medical therapy is often initially effective, most patients become refractory to therapy. Chemotherapy demonstrates poor overall response rates. Five-year survival with medical therapy alone is reported from 0 % to 30 % [48, 49].

Literature regarding surgical resection of NET liver metastases reports 5-year survival rates ranging from 40 % to 85 % [44]. Unfortunately, curative resection is possible in only approximately 10 % of patients due to diffuse disease at presentation [46, 48, 49]. Unlike with other malignancies, cytoreductive strategies with a goal of destruction of greater than 90 % of the tumor may be indicated in hepatic metastases from NET as this will often result in symptomatic response [49].

Interventional therapies for NET liver metastasis include ablation and intra-arterial therapies such as chemoembolization and radioembolization. There is little published evidence regarding outcomes of RFA for neuroendocrine liver metastasis. The largest series by Mazzaglia et al. reported long-term outcomes in 63 patients with 452 neuroendocrine hepatic metastases who underwent 80 laparoscopic RF ablations [17]. In this series, 67 % of patients had hormonal syndromes with 92 % of those patients experiencing partial or total relief after RFA. Duration of

benefit lasted a median of 11 months. Importantly, 67 % of symptomatic patients undergoing repeat ablation for recurrent disease had resolution of symptoms. Five-year overall survival was 48 % after RFA and 57 % after the diagnosis of liver metastasis. Of note, 38 % of patients had extrahepatic disease. Smaller series by Gillams (25 patients, both RFA and LITT) and Henn (7 patients) reported symptomatic response rates of approximately 70 % [10, 12]. Eriksson et al. reported on 73 patients who underwent surgical resection, RFA, or combined surgery and resection [50]. Symptomatic response was present in approximately 70 % in those with carcinoid syndrome. Although limited, this data suggests a high degree of symptomatic response and survival benefit of RFA, even in the presence of extrahepatic disease.

Periprocedural management of patients undergoing RFA of NET hepatic metastasis is unique among metastatic disease. There is a high propensity for hormonal release during both needle placement and thermal ablation. Precipitation of carcinoid crisis can lead to blood pressure instability, cardiac dysrhythmias, and other hormonal symptoms that require advanced planning and special care. These are further discussed in the complications section.

Breast Cancer Hepatic Metastases

Breast cancer affects one in eight women and is the second leading cause of cancer death in women of the Western world [11, 18, 51]. Breast cancer associated with liver metastatic disease is generally associated with a poor prognosis [52]. With modern hormonal and chemotherapeutic treatment, median survival ranges from 5 to 31 months [18].

The most common sites of breast metastases are bones, liver, lungs, brain, and subcutaneous tissues [18]. While liver metastases are present in greater than 50 % of those with disseminated disease, only 5–20 % of patients will present with disease confined to the liver [13]. Liver failure is ultimately responsible for death in 20 % of patients [20].

Retrospective series of surgical resection have suggested moderate benefits in survival in those with liver only metastasis with 5-year survival ranging from 18 % to 80 % [13, 52, 53]. These observations have increased interest in less invasive ablative techniques such as RFA. There is a paucity of published data on outcomes regarding RFA of hepatic metastases. Only six reports specifically related to RFA of hepatic metastases from breast metastases have been published and are summarized in Table 26.4 [11, 13, 15, 16, 18, 20]. Survival data are inconsistently reported and are not available for all studies. Two studies report 5-year survival of 27–30 % after RFA [18, 20]. Reported median survival after RFA in the studies ranges from 30 to 60 months [13, 18, 20]. Unlike in liver metastasis from other sources, concomitant stable bone or lung metastasis is not felt to be predictors of survival and may not be contraindications to resection or RFA of breast cancer liver metastasis. Stable extrahepatic disease was present in 28–83 % of patients across these published studies. This confounds comparison with surgical literature where resection candidates typically do not have extrahepatic disease. Extrahepatic disease should be stable on chemotherapy or hormonal therapy for at least 6 months prior to consideration for ablation. Compared with the available literature for RFA and breast cancer liver metastases, Mack et al. have reported a relatively large experience with MR-guided laser-induced interstitial thermotherapy (LITT) for breast cancer hepatic metastases. Given that the principles of LITT are similar to RFA, this series of 232 patients with 578 metastases from breast cancer is of significant interest. In this series, tumor size ranged up to 5 cm, with 76.4 % of tumors 3 cm or smaller. Reported mean survival time for this cohort was 4.9 years from the time of diagnosis and 4.2 years from the time of first ablation. Local recurrence in this series was impressively low at less than 5 % for all tumor sizes with no correlation with recurrence and size. Although there is no randomized controlled data and available evidence is quite limited, this data suggests that RFA of liver metastasis from breast cancer does show promise for improving survival in selected patients. Surgical resection

Table 26.4 RFA for breast cancer liver metastases

Author	Year	Study type	App	Pts	Mean # Tumors	Mean tumor size	Max tumor size	Median FU after RFA	Ablation success	Median overall survival after RFA	Local rec	Extrahepatic disease
Livraghi	2001	Pro obs	P	24	2.7	1.9 cm	6.6 cm	19 months	92 %	NR	8 %	33 %
Lawes	2006	Retro	P	19	2.4	NR	7.3 cm	15 months	NR	2.5-year survival 41.6 %	NR	57.9 %
Gunabushanam	2007	Pro obs	P	14	1.1	1.9 cm	4.0 cm	19 months	88 %	1-year survival 64 %[a]	14 %	28 %
Sofocleous	2007	Retro	P	12	1.2	NR	6.4 cm	22.5 months	92.8 %	60 months	50 %	83 %
										3, 5-year survival after RFA 70 %, 30 %		
Jokobs	2008	Pro obs	P	43	2.6	2.1 cm	8.5 cm	37 months	96 %	Extrahepatic Dz: 36.4 months	13.5 %	41.9 %
										No extrahepatic Dz (except skeletal mets): 58 months		
Meloni	2009	Retro	P	52	1.7	2.5 cm	5 cm	19.1 months	95 %	29.9 months	25 %	52 %
										1, 3, 5-year survival after RFA 68 %, 43 %, 27 %		

P percutaneous, *Retro* retrospective, *Pro obs* prospective observational, *NR* not reported, *Local rec* local recurrence
[a]Median survival not reached in FU

remains the gold standard when possible, although high rates of metachronous lesions make RFA an attractive treatment strategy.

Other Hepatic Metastasis

There is little data to guide the use of RFA in patients with isolated liver metastases from other sources. Reports have described ablation of isolated hepatic metastases from a variety of tumors, including sarcoma, esophageal carcinoma, melanoma, lung cancer, gynecologic cancers, pancreatic carcinoma, and carcinoma from unknown primary sources. Berber et al. reported on 53 patients undergoing laparoscopic RFA for 192 hepatic masses from non-colorectal, non-neuroendocrine, and non-hepatocellular primaries [9]. The overall median survival was 33 months for all patients, 51 months for breast cancer, and 25 months for sarcoma. Local recurrence was present in 17 % of patients over mean follow-up period of 24 months [9]. Rath et al. reported a retrospective series of 40 patients with hepatic metastases for a variety of tumors undergoing 52 RF ablations with a median tumor size of 1.5 cm (0.75 cm to 4.0 cm) [54]. At 2-year follow-up, there was a local recurrence in 7.5 % of patients and survival data was not reported. Numerous other reports have included RFA of hepatic metastases but have not segmented out data from colorectal metastases or primary liver carcinomas. Data from these small, heterogeneous groups are impossible to synthesize into meaningful recommendations. RF ablation of hepatic metastatic disease from other primary tumors should be made on a case-by-case basis in a multidisciplinary setting.

Imaging Follow-Up and Patterns of Recurrence

Imaging surveillance is performed to identify both local recurrence and new intrahepatic or extrahepatic disease, ideally when it is small and still treatable. Local recurrence most commonly presents at the ablation margin. Dynamic enhanced CT and MRI provide the best spatial resolution for evaluating the margins and are therefore the most commonly employed modalities for ablation follow-up.

With CT, the ablation zone is typically sharply marginated and of low attenuation before and after the administration of intravenous contrast material. Some ablation lesions demonstrate central linear high-attenuation areas immediately adjacent to the track of the RFA probe, which are believed to be caused by local protein coagulation [54]. This finding tends to become less apparent with time. For most non-hypervascular metastasis, portal venous phase imaging offers the best delineation of the RFA lesion as well as detection of residual or recurrent tumor. With noncontrast MRI, the ablation zone is of variable signal intensity on T1-weighted images and typically of dark signal intensity of T2-weighted images [55]. With both contrast-enhanced CT and MRI, a thin, uniform rim of peri-ablation enhancement in the first several months after RFA is common and reflects inflammatory hyperemia [36, 55, 56]. This typically regresses with time. A tumor-free ablation is evidenced by a lack of enhancement and stability or regression of the ablation defect over time.

Local tumor recurrence presents with several patterns: nodular enhancement along the ablation margin, focal/diffuse enlargement of the ablation zone over time, or irregular/thick halolike enhancement (Figs. 26.2, 26.3, and 26.4) [37, 55, 57]. On MRI, viable tumor is most often detected as a focal area of high signal intensity on T2-weighted images and/or as a region of focal enhancement during dynamic post-contrast imaging [55].

Remote recurrence (Fig. 26.5) is more frequent when treating metastatic hepatic disease than primary hepatocellular carcinoma, and common locations of extrahepatic recurrences are tumor specific. Tumor spread is also possible through tract seeding (Fig. 26.6) or from tine extension outside of the liver when treating subcapsular lesions (Fig. 26.7).

PET-CT has gained importance in monitoring whole-body treatment response in a variety of cancers and is now integral in follow-up of

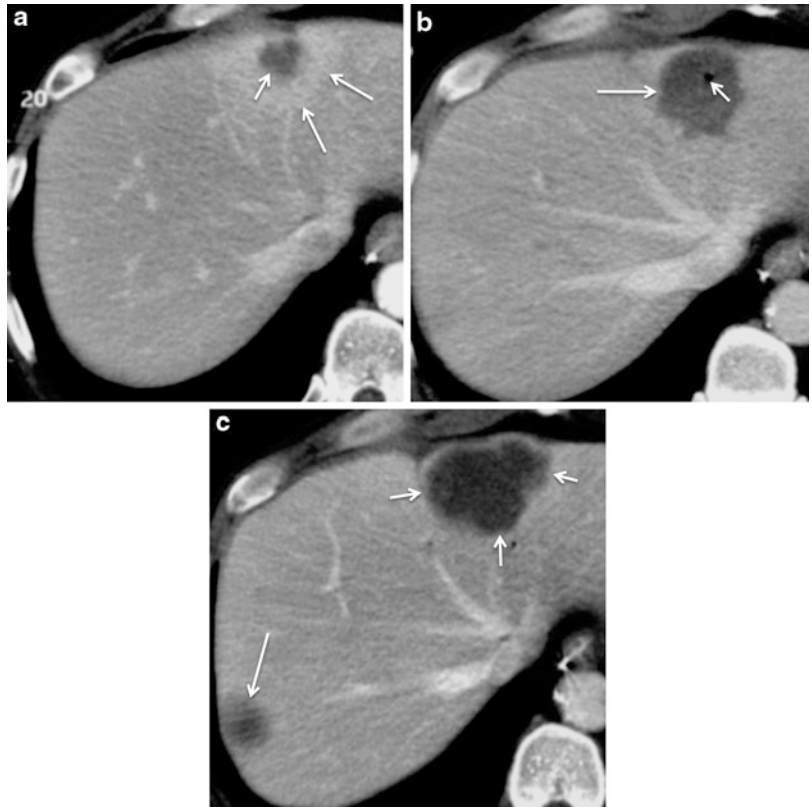

Fig. 26.2 (**a**) Pretreatment CT from a patient with pancreatic carcinoma and a hypovascular left lobe liver metastasis (*short arrow*). This lesion is subcapsular and requires an indirect approach through normal parenchyma for safe ablation. The hazy enhancement surrounding the low-attenuation center (*long arrows*) suggests that the margins of the metastasis are larger than the hypovascular lesion alone. (**b**) Twenty four-hour post ablation CT demonstrating a sharply marginated hypovascular ablation zone (*long arrow*). The small amount of central gas in the ablation zone (*short arrow*) is common on immediate post ablation scans. (**c**) Two-month post ablation CT demonstrating diffuse enlargement of the ablation zone (*short arrows*). This case represented local tumor recurrence although the differential diagnosis includes biloma. A separate hypovascular ablation zone is visible in the right lobe (*long arrow*)

patients with a variety of tumors. Although early retrospective reports of PET to evaluate post ablation recurrence were quite encouraging, more recent studies suggest that multiphase enhanced CT and MRI are comparable to PET-CT in terms of accuracy and sensitivity for detection of recurrence, all of which are superior to PET alone [57–62]. Most physicians currently use PET-CT as a problem-solving tool (Fig. 26.8) or interleave it with conventional multiphase enhanced CT or MRI.

Post ablation imaging within 24 h of the procedure is optional and is obtained by many physicians. This is most often performed with CT since patients who have recently undergone anesthesia are less able to hold their breath and limit their motion, which can substantially degrade MRI imaging. Immediate imaging allows for initial assessment of ablation success; helps to exclude local complications such as hemorrhage, pneumothorax, or injury to adjacent structures; and provides a baseline exam for future comparison. The ablation zone should be larger than the initial lesion, ideally with margins of 1 cm. An ablation zone similar in size to the initial lesion is predictive of future local recurrence. Imaging is often performed at 1 month, then at 3-month intervals for the first year, and at increasing

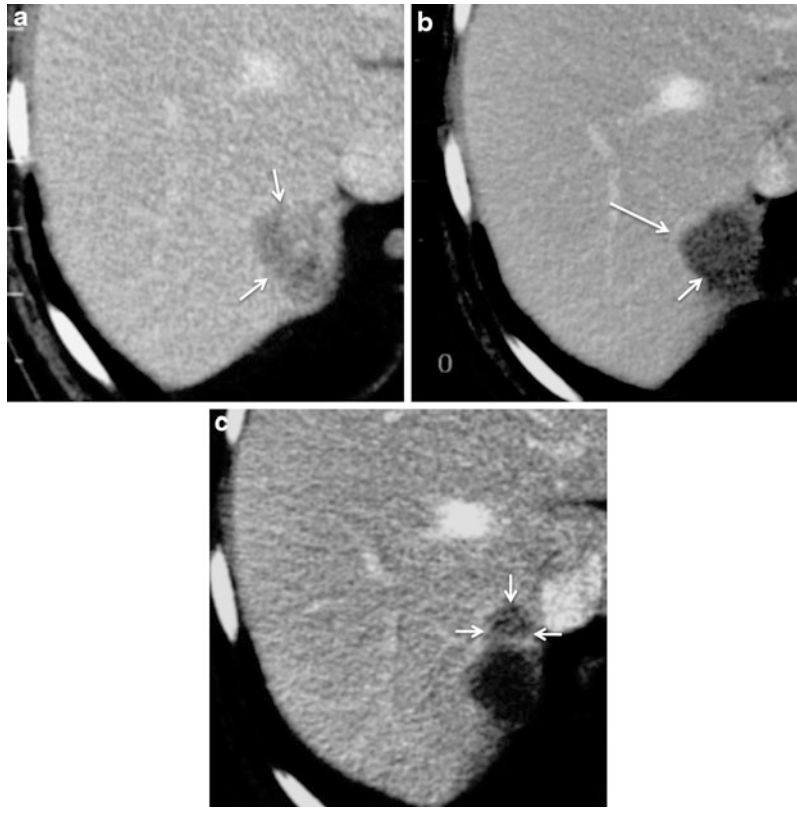

Fig. 26.3 (**a**) Pretreatment CT from a patient with colon carcinoma and a hypovascular subcapsular right lobe metastasis (*arrows*) adjacent to the IVC. The subcapsular nature of the metastasis and the proximity to the IVC (heat sink) are considerations for ablation. (**b**) One-month post ablation CT scan demonstrating an ablation defect (*short arrow*) similar in size to the original tumor. This is suggestive of an inadequate ablation margin. Note the faint thin rim of uniform enhancement (*long arrow*) surrounding the ablation margin. This is common on early imaging and is reflective of hyperemia. (**c**) Two-month post ablation CT scan demonstrating focal expansion and nodular enhancement (*arrows*) of the ablation zone with nodular enhancement. This represents local recurrence. Local heat sink effect of the adjacent IVC likely contributed to this recurrence

intervals thereafter. The optimal regimen for follow-up may be influenced by tumor- and patient-specific factors.

Complications

Numerous reports have been published describing the complications from liver RFA. Although overall reported complication rates are generally low, a thorough understanding of known complications can aid in patient selection, risk stratification, help guide approach, and aid in early recognition and management of adverse events. Additionally, a variety of techniques can be utilized to improve safety in appropriate situations. With an adequate understanding of complications, many complications may be preventable.

Complications may be classified in a variety of ways. They may be categorized based on general type (vascular, biliary, extrahepatic), cause (related to probe placement, related to thermal injury), timing (acute <24 h, subacute <30 days, delayed >30 days), and severity (major, minor). Major complications are defined as adverse events that if left untreated, may threaten the patient's life, lead to substantial morbidity and disability, result in hospital admission, or substantially lengthen hospital stay [63, 64]. Several large multicenter surveys have reported

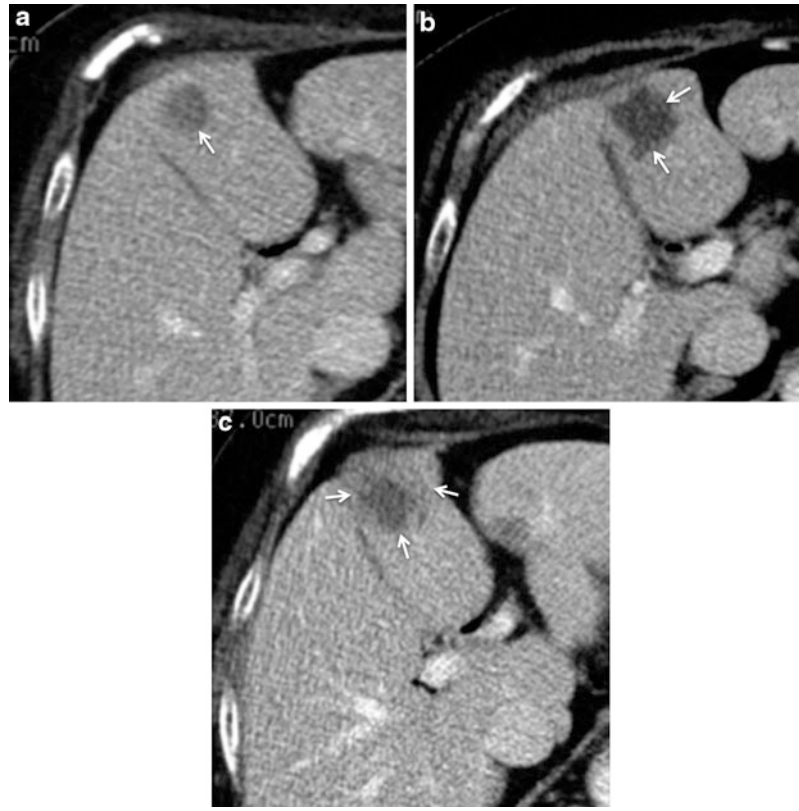

Fig. 26.4 (**a**) Pretreatment CT from a patient with colon carcinoma and a segment 4 hypovascular liver metastasis (*arrow*). (**b**) One-month post ablation CT scan demonstrating an ablation zone (*arrows*) only marginally larger than the initial metastasis. (**c**) Three-month post ablation CT scan demonstrating diffuse, thick, hazy enhancement around the ablation margin (*arrows*). This represents local recurrence. Visualization of the ablation zone and recurrence is optimal in portal venous phase

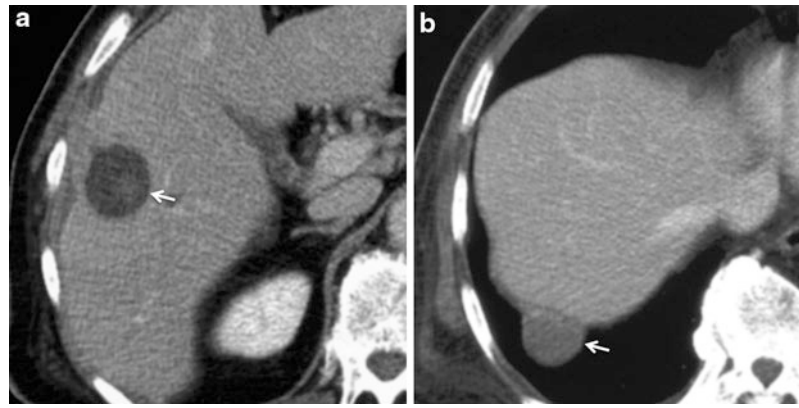

Fig. 26.5 (**a**) Post ablation CT scan in a patient with colon cancer demonstrates a well-marginated ablation zone (*arrow*) in the liver. (**b**) Post ablation CT scan in the same patient demonstrates a pulmonary metastasis (*arrow*) as a site of distant recurrence

mortality rates of 0.1–0.5 %, major complication rate of 2.2–3.1 %, and minor complication rates of 5–8.9 % [64–68].

Vascular complications from RFA include hemorrhagic complications (intraperitoneal, subcapsular, intrahepatic) and less commonly thrombotic vascular complications. Hemorrhagic complications are reported to occur at a rate of 0.46–1.6 % [64, 67, 68]. Intraperitoneal hemorrhage is typically from bleeding through the needle tract and may be managed with immediate needle replacement and cautery of the puncture site, arterial embolization, or surgical intervention when clinically significant. Tract cautery and

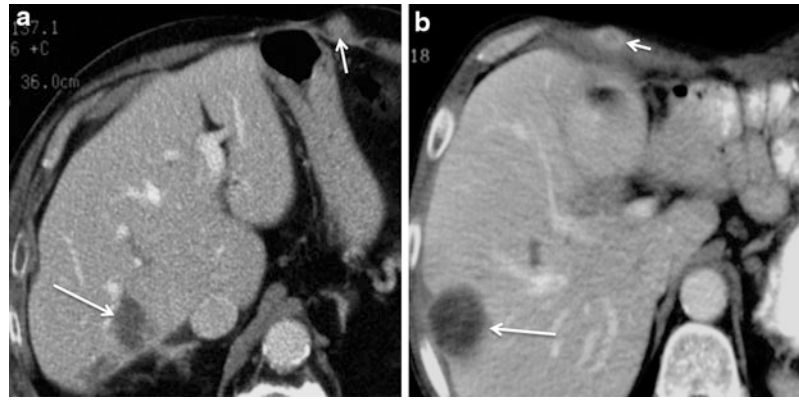

Fig. 26.6 (**a**, **b**) Two separate patients with skin implantation (*arrows*) in a patient who has undergone several ablations for hepatic metastases. Ablation zones are marked with *long arrows*

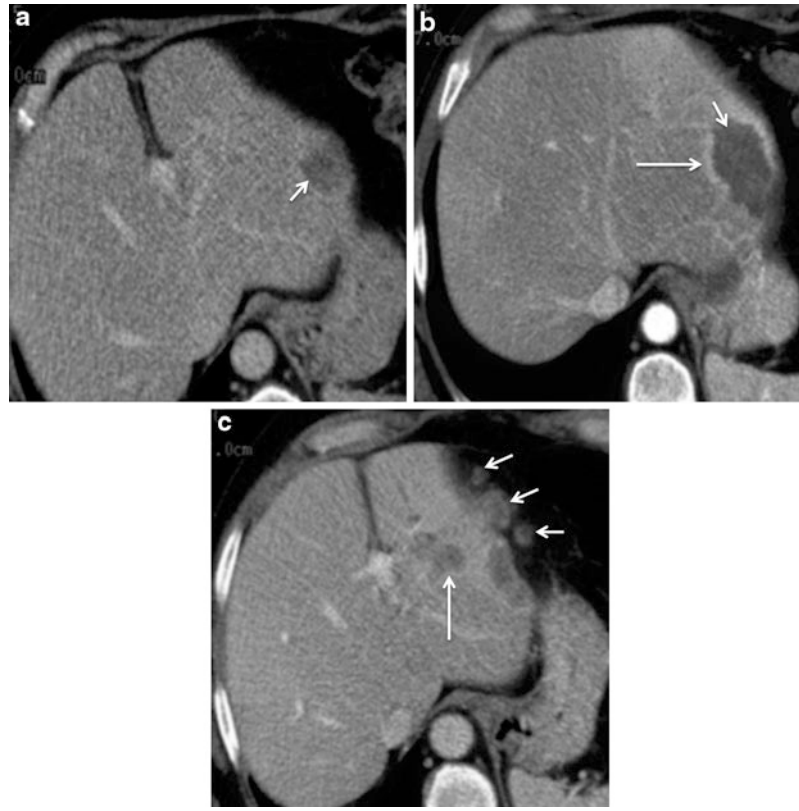

Fig. 26.7 (**a**) Pretreatment CT scan demonstrating marginal recurrence (*arrow*) after hepatic resection in a patient with colon carcinoma. (**b**) Twenty four-hour post ablation CT demonstrates thin regular enhancement (*long arrow*) around the ablation zone (*short arrow*) consistent with hyperemia. (**c**) Five-month post ablation CT demonstrating local recurrence at the ablation zone (*long arrow*) and peritoneal seeding (*short arrows*). This patient was treated with a multi-tined electrode. Peritoneal seeding is likely due to tines penetrating the liver margin during ablation

puncture through a sufficient tract of normal liver parenchyma appears to decrease these risks [64, 69]. Subcapsular hemorrhage is most often reported after treatment of subcapsular lesions, although it may occur after direct trauma to larger intrahepatic vessels (Fig. 26.9) and is often either managed conservatively or with embolization or surgical intervention when indicated [67, 70]. Arterioportal shunting (Fig. 26.10) is often asymptomatic and detected on imaging although it may be associated with hemorrhage [66, 67]. Thrombotic complications, such as portal vein occlusion, are associated with prolonged Pringle maneuver, mechanical damage to central venous structures, and central ablation and are more common in cirrhotic patients [67, 70].

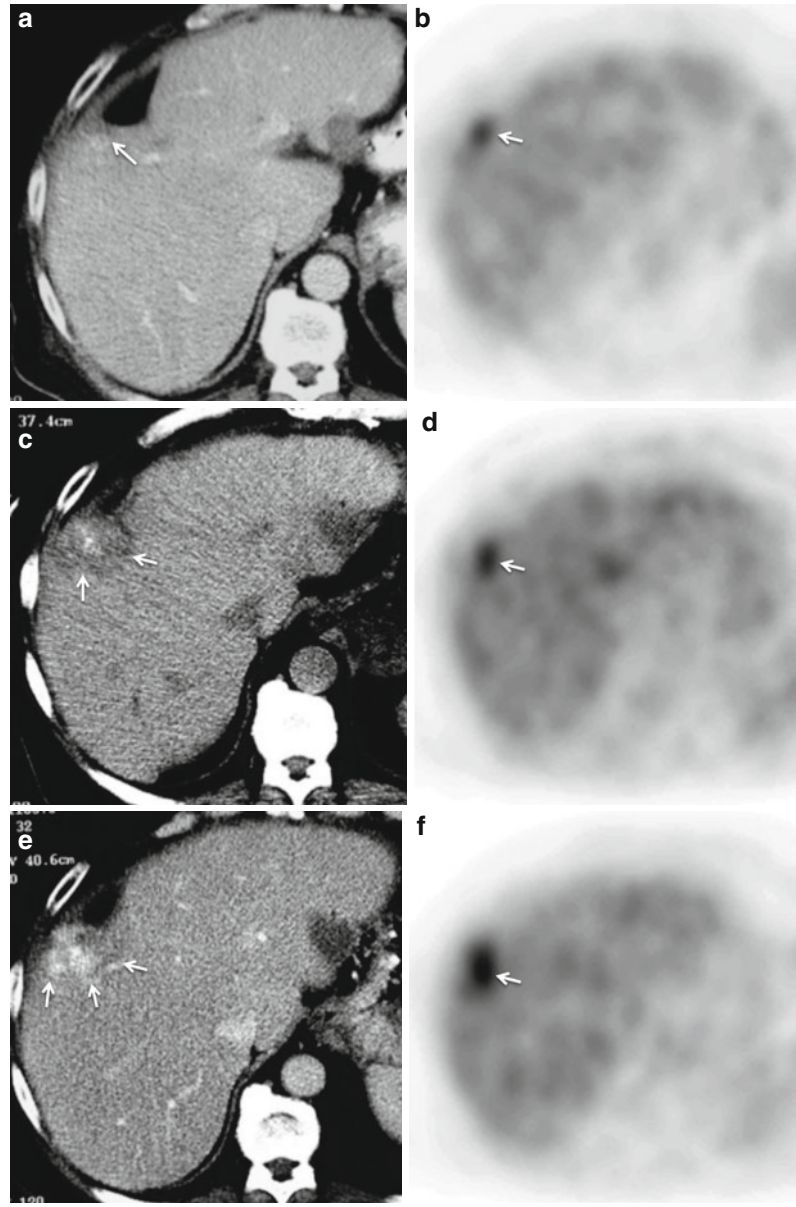

Fig. 26.8 (**a**) Pretreatment CT from a patient with colon cancer and a partially calcified liver metastasis (*arrow*) adjacent to a prior site of resection. (**b**) Pretreatment PET demonstrates hypermetabolic focus (*arrow*) corresponding to the CT abnormality. (**c**) Two-month noncontrast post ablation CT demonstrates a hazy, poorly defined ablation zone (*arrow*) with increasing central calcification suggestive of residual tumor. (**d**) Two-month post ablation PET demonstrates persistent hypermetabolic activity (*arrow*). In this time period, increased PET activity at the ablation margin may represent inflammation or residual tumor. (**e**) Six-month post ablation contrasted CT demonstrating increased density consistent with calcification and diffuse enhancement of the ablation zone, which was enlarging (*arrows*). These findings are consistent with recurrence. (**f**) Six-month post ablation PET demonstrates further increased activity (*arrow*) consistent with residual tumor. Reactive inflammatory hypermetabolic activity would be expected to decrease over time

Hepatic venous thrombosis is rare and frequently does not require therapy.

Biliary complications include intrahepatic abscess, biliary stenosis, and biloma formation and are reported to occur in approximately 0.86–2.1 % of patients [67, 68, 71]. Intrahepatic abscess is one of the most common major complications of RFA (Fig. 26.11). Major risk factors include an incompetent biliary sphincter (biliary stent, biliary-enteric anastomosis, prior sphincterotomy, pneumobilia) and biliary obstruction. Given the high rate of complications in these patients, many authors consider this to be a contraindication to ablation. Concurrent hepatic resection with RFA may increase risk of abscess formation, but this is not widely agreed upon [71]. Diabetes may also be

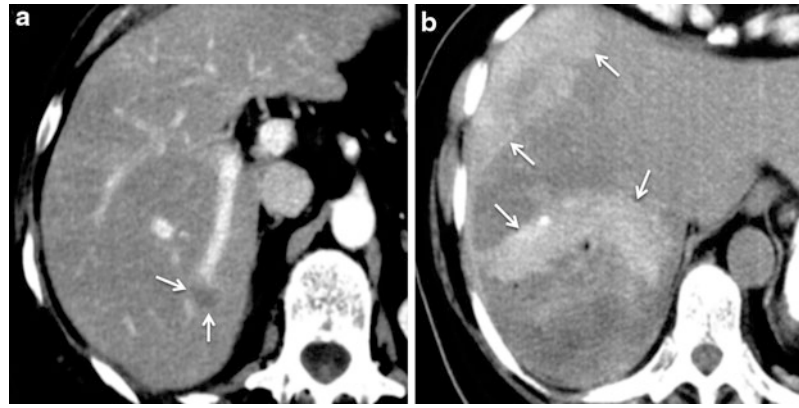

Fig. 26.9 (**a**) Pretreatment CT demonstrating a hypovascular liver metastasis (*arrows*) immediately adjacent to the right hepatic vein. Considerations for this ablation include a large local heat sink. (**b**) Immediate postprocedural CT demonstrating large subcapsular hemorrhage (*arrows*)

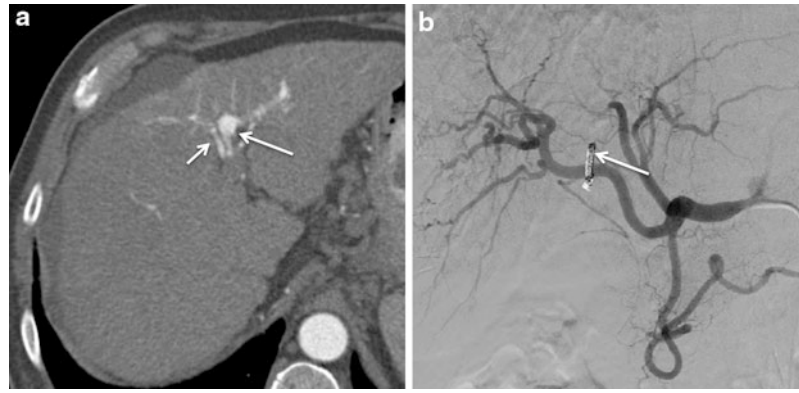

Fig. 26.10 (**a**) Seventy eight-year-old patient post segment 4 ablation. Follow-up imaging demonstrated a large hepatic arterial (*short arrow*) to portal venous (*long arrow*) fistula. (**b**) Angiographic embolization was performed with coils (*arrow*) without complication. This patient was asymptomatic

an independent risk factor for abscess formation [66, 68, 70]. Abscess often presents in the subacute time frame, from 1 to 6 weeks post ablation. Intravenous antibiotics, percutaneous drainage, and relief of any biliary obstruction are principles for management. Bile ducts are very susceptible to thermal injury. While peripheral biliary injury may be asymptomatic and present in a delayed fashion (Fig. 26.12), central biliary injury often leads to cholangitis, intrahepatic biloma formation, and a protracted clinical course (Fig. 26.13). Management is typically with percutaneous drainage of bilomas or abscesses and either percutaneous or endoscopic stenting of biliary strictures. For this reason, tumors in the hepatic hilum or <2 cm from major portal veins (given that biliary ducts are adjacent to portal veins) are poor candidates for ablative therapy. Prophylactic cooling of biliary ducts with nasobiliary or percutaneous tubes and infusion of chilled saline has been reported and may decrease biliary stenosis from 40 % to approximately 3 % [27, 28]. Although these techniques appear promising, long-term data are lacking.

Extrahepatic complications include a variety of injuries. Thermal injury to the GI tract is an uncommon but major complication that may be fatal when associated with perforation. The colon appears the most sensitive to thermal injury, followed by the small bowel and stomach. Previous abdominal surgery may increase risks of thermal injury due to fixation of the bowel due to adhesions [66]. Numerous techniques have been described to prevent injury, including infusion of D5W infusion, balloon interposition, or changes in positioning (decubitus), which may facilitate mechanical separation [32–34]. Adhesions may make these techniques ineffective, and laparoscopic or open surgical ablation may be preferable

in these circumstances. Bowel perforation may occur several days after ablation, and close clinical observation is required in these patients. Ablation of lesions near the gallbladder is possible in experienced hands, and several reports describe safe ablation of lesions adjacent to the gallbladder although self-limited cholecystitis is common [29, 31]. Significant thermal ablation to the kidney is uncommon. Although rare, thermal injury to the adrenal gland may result in massive catecholamine release and subsequent hypertensive crisis [72]. Preparation for this complication includes intra-arterial pressure monitoring, advanced warning for the anesthesia team, and IV beta-blockers or peripheral vasodilators on hand to treat a hypertensive crisis [72]. Ablation should be temporarily stopped if hypertensive crisis is observed.

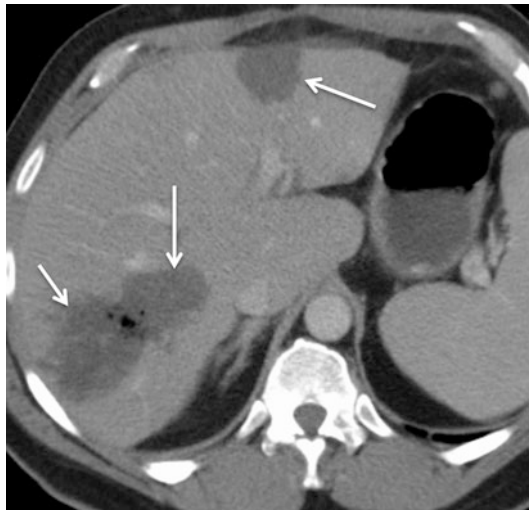

Fig. 26.11 Fifty nine-year-old male with metastatic rectal cancer 1-week post open partial hepatic resection and ablation of several hepatic metastases. Ablation zones (*long arrows*) have sharp margination, while a new low-attenuation lesion with hazy borders and gas represents an abscess (*short arrow*). This was managed with percutaneous drainage and antibiotics. This patient's risk factors for abscess included concurrent hepatic resection and a history or ERCPs

Pulmonary complications occur in approximately 0.8 % of patients and include pneumothorax, pleural effusion, hemothorax, and diaphragmatic injury [67]. Dome lesions are technically challenging to ablate given the difficulty with ultrasound visualization of the dome and challenges with needle placement in CT out of the axial imaging plane. Care should be taken to prevent needle tine perforation of the diaphragm. The authors prefer the use of single or multiple antenna probes with real-time guidance, although some operators prefer to protect the diaphragm through separation with D5W infusion [33]. Hemothorax is often from injury to intercostal arteries, which may be managed by arterial embolization [66]. Biliary-pleural and biliary-bronchial fistulae are rare but are often clinically symptomatic (Fig. 26.14).

A major delayed complication is tumor tract seeding (Figs. 26.6 and 26.7) which is reported to occur 0.2–0.5 % of cases in larger series although higher rates have been reported [66, 67]. Risk factors include subcapsular location, increased number of punctures, poor tumor differentiation, lack of tract cautery, concurrent biopsy, tine perforation of the capsule, and repetitive repositioning of the needle [66, 70]. Every attempt

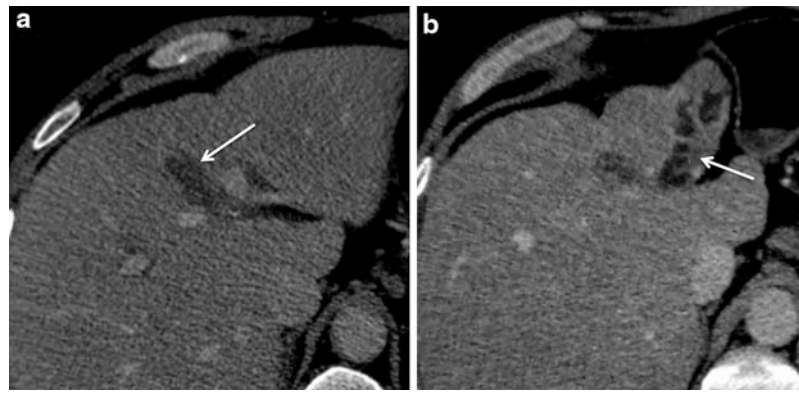

Fig. 26.12 (**a**) Immediate postprocedural CT of ablation of segment 4A mass. The inferior margin of the ablation zone (*arrow*) is adjacent to the main left portal vein. (**b**) One year later, asymptomatic biliary dilation (*arrow*) is noted in the atrophied left lobe

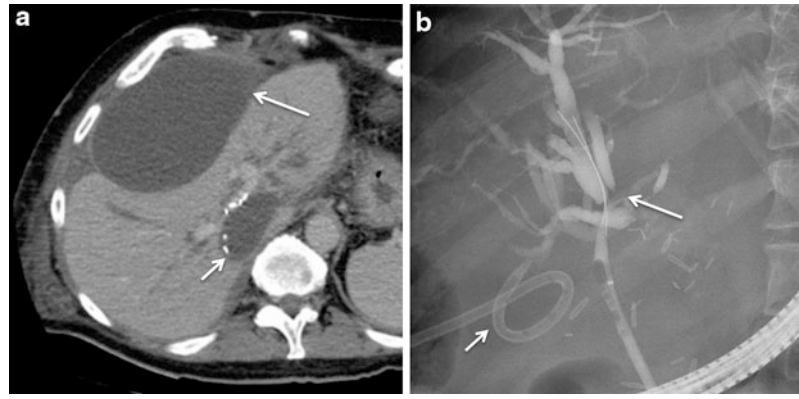

Fig. 26.13 (**a**) Patient with metastatic colorectal carcinoma post open surgical RFA of a central hepatic lesion (*short arrow*) causing central biliary stenosis, diffuse biliary dilation, sepsis, and a large biloma (*long arrow*). (**b**) This patient was managed with a percutaneous biloma drain (*short arrow*) and ERCP drainage of central biliary strictures (*long arrow*)

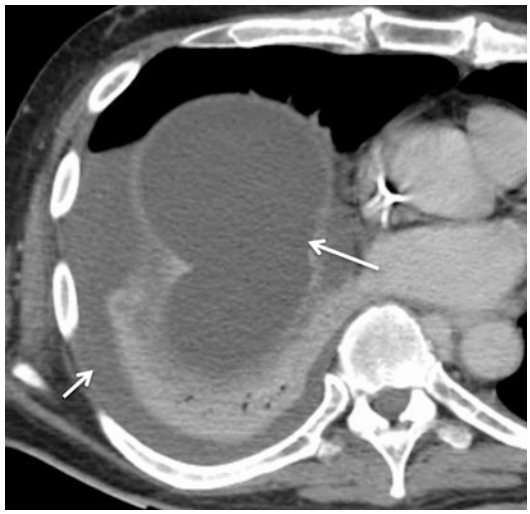

Fig. 26.14 Patient with metastatic colorectal carcinoma post intraoperative ablation of a dome lesion. A large fluid collection representing a biloma is present at the dome (*long arrow*) with pleural fluid (*short arrow*). After drainage, the pleural fluid was noted to be bilious consistent with biliary-pleural fistula

should be made to place needles through tumor with a single pass, and cautery may be used if the needle needs to be repositioned. Traversal of a normal mantle of liver tissue with care not to perforate the capsule with needle tines and tract ablation is recommended to minimize risk.

Liver failure is reported to occur in 0.8 % of patients, most often in patients with hepatocellular carcinoma and underlying liver insufficiency [67]. It is uncommon in patients with metastatic disease unless there are associated vascular, biliary, or infectious complications (portal thrombosis, hepatic infarction, biliary stenosis, sepsis, etc.).

Skin burns are reported to occur in 0.2–0.6 % of cases and are more common in the early RFA experience [67, 68]. Larger and more numerous grounding pads are now typically used with higher output (>50 W) generators which have minimized such complications [67]. Grounding pads should be placed horizontally to increase the leading edge surface to dissipate current, and care should be taken to ensure they are at the same level so current is not preferentially dissipated on a single pad [64, 67]. A prosthetic hip implant may increase current dissipation in the nearby grounding pad(s) and may predispose to grounding pad burn [66]. Skin burns at the needle site are associated with poor technique in tract cautery.

Hormonal complications are unique to treatment of neuroendocrine tumors and require special attention given their serious and potentially fatal nature. In patients with carcinoid syndrome, induction of anesthesia, needle puncture, and thermal ablation of metastatic lesions may precipitate carcinoid crisis [10]. Carcinoid crisis manifests with hemodynamic instability (hypotension or hypertension), cardiac dysrhythmias, flushing, and bronchospasm. Prophylactic octreotide administration (300 mcg subcutaneously) may help to minimize these effects, although additional intraprocedural octreotide IV bolus administration or continuous drips may be required for management. Rapid administration of IV fluids, plasma, or alpha/beta blockade may be required to normalize pressure.

Gillams et al. reported that 62 % of patients treated for NET liver metastases with carcinoid syndrome became hemodynamically unstable during the procedure despite preprocedural administration of octreotide, particularly during needle insertion and thermal ablation [10]. Intra-arterial pressure monitoring and adequate vascular access are strongly recommended. Postprocedural monitoring of these patients for up to 48 h in an intensive care setting is also advocated [67]. Similarly, patients with hormonal syndromes related to islet cell tumors may require unique periprocedural management with IV dextrose administration and frequent blood glucose monitoring with treatment of insulinomas, IV insulin administration with glucagonoma, and H2 blocker and proton pump inhibitor administration with gastrinomas.

Arcing to local metallic surgical clips has been reported and may result in unpredictable and large burns that may predispose to unexpected local thermal injury. Recommendations from experimental studies are to keep the active tip of the RFA probe at least 2 cm from adjacent surgical clips [73].

Post ablation syndrome is a self-limited constellation of findings present in approximately one third of patients after ablation and is related to ablation volume [74]. It presents with low-grade fever, abdominal pain, and a flu-like illness, which is typically self-limited; peaks on day 3; and lasts 5–10 days [74, 75]. Intractable pain is uncommon and may be associated with injury to the abdominal wall or diaphragm.

Conclusion

Despite a lack of randomized data, observational evidence and clinical experience suggest that RFA of isolated hepatic metastatic disease has clinical benefit when used in appropriately selected patients. Given its advantages as a minimally invasive and well-tolerated procedure, it has rapidly been incorporated into clinical practice. The majority of clinical experience and literature regarding ablation of metastatic liver disease is with colorectal liver metastasis, although there is increasing experience with larger populations of patients with breast cancer and neuroendocrine tumors. A multidisciplinary approach to patients is critical to optimizing patient therapy and proper patient selection [24, 30, 44].

References

1. Bhattacharya R, Rao S, Kowdley KV. Liver involvement in patients with solid tumors of nonhepatic origin. Clin Liver Dis. 2002;6(4):1033–43, x.
2. Wei AC, et al. Survival after hepatic resection for colorectal metastases: a 10-year experience. Ann Surg Oncol. 2006;13(5):668–76.
3. Tomlinson JS, et al. Actual 10-year survival after resection of colorectal liver metastases defines cure. J Clin Oncol. 2007;25(29):4575–80.
4. Simmonds PC, et al. Surgical resection of hepatic metastases from colorectal cancer: a systematic review of published studies. Br J Cancer. 2006;94(7):982–99.
5. Rees M, et al. Evaluation of long-term survival after hepatic resection for metastatic colorectal cancer: a multifactorial model of 929 patients. Ann Surg. 2008;247(1):125–35.
6. Morris EJ, et al. Surgical management and outcomes of colorectal cancer liver metastases. Br J Surg. 2010;97(7):1110–8.
7. Cummings LC, Payes JD, Cooper GS. Survival after hepatic resection in metastatic colorectal cancer: a population-based study. Cancer. 2007;109(4):718–26.
8. Bauditz J, Quinkler M, Wermke W. Radiofrequency thermal ablation of hepatic metastases of adrenocortical cancer–a case report and review of the literature. Exp Clin Endocrinol Diabetes. 2009;117(7):316–9.
9. Berber E, et al. Laparoscopic radiofrequency thermal ablation for unusual hepatic tumors: operative indications and outcomes. Surg Endosc. 2005;19(12):1613–7.
10. Gillams A, et al. Radiofrequency ablation of neuroendocrine liver metastases: the Middlesex experience. Abdom Imaging. 2005;30(4):435–41.
11. Gunabushanam G, et al. Radiofrequency ablation of liver metastases from breast cancer: results in 14 patients. J Vasc Interv Radiol. 2007;18(1 Pt 1):67–72.
12. Henn AR, et al. Percutaneous radiofrequency ablation of hepatic metastases for symptomatic relief of neuroendocrine syndromes. AJR Am J Roentgenol. 2003;181(4):1005–10.
13. Jakobs TF, et al. CT-guided radiofrequency ablation in patients with hepatic metastases from breast cancer. Cardiovasc Intervent Radiol. 2009;32(1):38–46.
14. Kim HO, et al. Radiofrequency ablation for metachronous hepatic metastases from gastric cancer. Surg Laparosc Endosc Percutan Tech. 2009;19(3):208–12.
15. Lawes D, et al. Radiofrequency ablation (RFA) as a cytoreductive strategy for hepatic metastasis from breast cancer. Ann R Coll Surg Engl. 2006;88(7):639–42.

16. Livraghi T, et al. Percutaneous radio-frequency ablation of liver metastases from breast cancer: initial experience in 24 patients. Radiology. 2001;220(1): 145–9.
17. Mazzaglia PJ, et al. Laparoscopic radiofrequency ablation of neuroendocrine liver metastases: a 10-year experience evaluating predictors of survival. Surgery. 2007;142(1):10–9.
18. Meloni MF, et al. Breast cancer liver metastases: US-guided percutaneous radiofrequency ablation–intermediate and long-term survival rates. Radiology. 2009;253(3):861–9.
19. Pawlik TM, et al. Results of a single-center experience with resection and ablation for sarcoma metastatic to the liver. Arch Surg. 2006;141(6):537–43. discussion 543–4.
20. Sofocleous CT, et al. Radiofrequency ablation in the management of liver metastases from breast cancer. AJR Am J Roentgenol. 2007;189(4):883–9.
21. Wertenbroek MW, et al. Radiofrequency ablation of hepatic metastases from thyroid carcinoma. Thyroid. 2008;18(10):1105–10.
22. Guenette JP, Dupuy DE. Radiofrequency ablation of colorectal hepatic metastases. J Surg Oncol. 2010; 102(8):978–87.
23. Qian J. Interventional therapies of unresectable liver metastases. J Cancer Res Clin Oncol. 2011;137(12): 1763–72.
24. Stang A, et al. A systematic review on the clinical benefit and role of radiofrequency ablation as treatment of colorectal liver metastases. Eur J Cancer. 2009;45(10):1748–56.
25. Wong SL, et al. American Society of Clinical Oncology 2009 clinical evidence review on radiofrequency ablation of hepatic metastases from colorectal cancer. J Clin Oncol. 2009;28(3):493–508.
26. Berber E, Pelley R, Siperstein AE. Predictors of survival after radiofrequency thermal ablation of colorectal cancer metastases to the liver: a prospective study. J Clin Oncol. 2005;23(7):1358–64.
27. Ogawa T, et al. Prevention of biliary complication in radiofrequency ablation for hepatocellular carcinoma-cooling effect by endoscopic nasobiliary drainage tube. Eur J Radiol. 2010;73(2):385–90.
28. Ohnishi T, et al. Intraductal chilled saline perfusion to prevent bile duct injury during percutaneous radiofrequency ablation for hepatocellular carcinoma. J Gastroenterol Hepatol. 2008;23(8 Pt 2):e410–5.
29. Chopra S, et al. Radiofrequency ablation of hepatic tumors adjacent to the gallbladder: feasibility and safety. AJR Am J Roentgenol. 2003;180(3):697–701.
30. Crocetti L, de Baere T, Lencioni R. Quality improvement guidelines for radiofrequency ablation of liver tumours. Cardiovasc Intervent Radiol. 2010;33(1):11–7.
31. Kim SW, et al. Percutaneous radiofrequency ablation of hepatocellular carcinomas adjacent to the gallbladder with internally cooled electrodes: assessment of safety and therapeutic efficacy. Korean J Radiol. 2009;10(4):366–76.
32. Yamakado K, et al. Percutaneous radiofrequency ablation of liver neoplasms adjacent to the gastrointestinal tract after balloon catheter interposition. J Vasc Interv Radiol. 2003;14(9 Pt 1):1183–6.
33. Song I, et al. Percutaneous radiofrequency ablation of hepatocellular carcinoma abutting the diaphragm and gastrointestinal tracts with the use of artificial ascites: safety and technical efficacy in 143 patients. Eur Radiol. 2009;19(11):2630–40.
34. Chen EA, et al. Thermal protection with 5 % dextrose solution blanket during radiofrequency ablation. Cardiovasc Intervent Radiol. 2006;29(6):1093–6.
35. Ruers T, et al. Radiofrequency ablation combined with systemic treatment versus systemic treatment alone in patients with non-resectable colorectal liver metastases: a randomized EORTC Intergroup phase II study (EORTC 40004). Ann Oncol. 2012;3(10):2619–26.
36. Park MH, et al. Spectrum of CT findings after radiofrequency ablation of hepatic tumors. Radiographics. 2008;28(2):379–90. discussion 390–2.
37. Schima W, et al. Post-treatment imaging of liver tumours. Cancer Imaging. 2007;7(Spec No A): S28–36.
38. Tanaka K, Ichikawa Y, Endo I. Liver resection for advanced or aggressive colorectal cancer metastases in the era of effective chemotherapy: a review. Int J Clin Oncol. 2011;16(5):452–63.
39. Misiakos EP, Karidis NP, Kouraklis G. Current treatment for colorectal liver metastases. World J Gastroenterol. 2011;17(36):4067–75.
40. Gillams AR, Lees WR. Five-year survival following radiofrequency ablation of small, solitary, hepatic colorectal metastases. J Vasc Interv Radiol. 2008; 19(5):712–7.
41. Berber E, Siperstein A. Local recurrence after laparoscopic radiofrequency ablation of liver tumors: an analysis of 1032 tumors. Ann Surg Oncol. 2008;15(10):2757–64.
42. Lu DS, et al. Influence of large peritumoral vessels on outcome of radiofrequency ablation of liver tumors. J Vasc Interv Radiol. 2003;14(10):1267–74.
43. Lu DS, et al. Radiofrequency ablation of hepatocellular carcinoma: treatment success as defined by histologic examination of the explanted liver. Radiology. 2005;234(3):954–60.
44. Garrot C, Stuart K. Liver-directed therapies for metastatic neuroendocrine tumors. Hematol Oncol Clin North Am. 2007;21(3):545–60; ix-x.
45. Knigge U, Hansen CP, Stadil F. Interventional treatment of neuroendocrine liver metastases. Surgeon. 2008;6(4):232–9.
46. Siperstein AE, Berber E. Cryoablation, percutaneous alcohol injection, and radiofrequency ablation for treatment of neuroendocrine liver metastases. World J Surg. 2001;25(6):693–6.
47. Vogl TJ, et al. Liver metastases of neuroendocrine carcinomas: interventional treatment via transarterial embolization, chemoembolization and thermal ablation. Eur J Radiol. 2009;72(3):517–28.

48. Atwell TD, et al. Treatment of neuroendocrine cancer metastatic to the liver: the role of ablative techniques. Cardiovasc Intervent Radiol. 2005;28(4):409–21.
49. Maithel SK, Fong Y. Hepatic ablation for neuroendocrine tumor metastases. J Surg Oncol. 2009;100(8):635–8.
50. Eriksson J, et al. Surgery and radiofrequency ablation for treatment of liver metastases from midgut and foregut carcinoids and endocrine pancreatic tumors. World J Surg. 2008;32(5):930–8.
51. Jemal A, et al. Cancer statistics, 2008. CA Cancer J Clin. 2008;58(2):71–96.
52. Sabel MS, et al. Metastatic breast cancer: Local treatment. In: UpToDate2012.
53. Vlastos G, et al. Long-term survival after an aggressive surgical approach in patients with breast cancer hepatic metastases. Ann Surg Oncol. 2004;11(9):869–74.
54. Rath GK, et al. Radiofrequency ablation of hepatic metastasis: results of treatment in forty patients. J Cancer Res Ther. 2008;4(1):14–7.
55. Gervais DA, Kalva S, Thabet A. Percutaneous image-guided therapy of intra-abdominal malignancy: imaging evaluation of treatment response. Abdom Imaging. 2009;34(5):593–609.
56. Kim YS, Rhim H, Lim HK. Imaging after radiofrequency ablation of hepatic tumors. Semin Ultrasound CT MR. 2009;30(2):49–66.
57. Kei SK, et al. Local tumor progression after radiofrequency ablation of liver tumors: analysis of morphologic pattern and site of recurrence. AJR Am J Roentgenol. 2008;190(6):1544–51.
58. Kuehl H, et al. Impact of whole-body imaging on treatment decision to radio-frequency ablation in patients with malignant liver tumors: comparison of [18F]fluorodeoxyglucose-PET/computed tomography, PET and computed tomography. Nucl Med Commun. 2008;29(7):599–606.
59. Kuehl H, et al. Comparison of FDG-PET, PET/CT and MRI for follow-up of colorectal liver metastases treated with radiofrequency ablation: initial results. Eur J Radiol. 2008;67(2):362–71.
60. Donckier V, et al. [F-18] fluorodeoxyglucose positron emission tomography as a tool for early recognition of incomplete tumor destruction after radiofrequency ablation for liver metastases. J Surg Oncol. 2003;84(4):215–23.
61. Langenhoff BS, et al. Efficacy of fluorine-18-deoxyglucose positron emission tomography in detecting tumor recurrence after local ablative therapy for liver metastases: a prospective study. J Clin Oncol. 2002;20(22):4453–8.
62. Anderson GS, et al. FDG positron emission tomography in the surveillance of hepatic tumors treated with radiofrequency ablation. Clin Nucl Med. 2003;28(3):192–7.
63. Goldberg SN, et al. Image-guided tumor ablation: proposal for standardization of terms and reporting criteria. Radiology. 2003;228(2):335–45.
64. Rhim H. Complications of radiofrequency ablation in hepatocellular carcinoma. Abdom Imaging. 2005;30(4):409–18.
65. de Baere T, et al. Adverse events during radiofrequency treatment of 582 hepatic tumors. AJR Am J Roentgenol. 2003;181(3):695–700.
66. Livraghi T, et al. Treatment of focal liver tumors with percutaneous radio-frequency ablation: complications encountered in a multicenter study. Radiology. 2003;226(2):441–51.
67. Mulier S, et al. Complications of radiofrequency coagulation of liver tumours. Br J Surg. 2002;89(10):1206–22.
68. Rhim H, et al. Major complications after radio-frequency thermal ablation of hepatic tumors: spectrum of imaging findings. Radiographics. 2003;23(1):123–34. discussion 134–6.
69. Rhim H, et al. Radiofrequency thermal ablation of abdominal tumors: lessons learned from complications. Radiographics. 2004;24(1):41–52.
70. Akahane M, et al. Complications of percutaneous radiofrequency ablation for hepato-cellular carcinoma: imaging spectrum and management. Radiographics. 2005;25(Suppl 1):S57–68.
71. Curley SA, et al. Early and late complications after radiofrequency ablation of malignant liver tumors in 608 patients. Ann Surg. 2004;239(4):450–8.
72. Onik G, et al. Life-threatening hypertensive crises in two patients undergoing hepatic radiofrequency ablation. AJR Am J Roentgenol. 2003;181(2):495–7.
73. Boll DT, et al. Do surgical clips interfere with radiofrequency thermal ablation? AJR Am J Roentgenol. 2003;180(6):1557–60.
74. Dodd 3rd GD, et al. Percutaneous radiofrequency ablation of hepatic tumors: postablation syndrome. AJR Am J Roentgenol. 2005;185(1):51–7.
75. Wah TM, et al. Image-guided percutaneous radiofrequency ablation and incidence of post-radiofrequency ablation syndrome: prospective survey. Radiology. 2005;237(3):1097–102.

Embolic Therapy for the Treatment of Liver Metastases

27

Ronald S. Winokur and Daniel B. Brown

Abstract

Transarterial therapies are playing a larger role for patients with unresectable metastatic disease to the liver. An understanding of treatment options, outcomes, and toxicities is important in a comprehensive treatment environment. The current review discusses existing treatment options including chemoembolization, embolization, and radioembolization. Additionally, outcomes with these different therapies are reviewed for a variety of metastatic processes to the liver. Disease states discussed include colorectal cancer, neuroendocrine tumors, breast cancer, and metastatic uveal melanoma. With each pathologic entity, the relative role of transarterial therapies both individually and as a group in comparison to other treatment methods such as resection and systemic chemotherapy is discussed. Expected side effects and toxicities from transarterial therapies in this diverse group of patients are reviewed as well.

Introduction

In the United States, metastases to the liver are 40 times more common than primary hepatic malignancy [1]. The liver is the primary and solitary site of metastatic disease in many malignancies including colorectal cancer, neuroendocrine malignancies, and ocular melanoma. Approximately 145,000 cases of colorectal cancer are diagnosed each year with an estimated incidence of hepatic metastases in as many as 50,000 patients per year [2, 3]. Neuroendocrine malignancies, such as carcinoid tumors, develop liver metastases in as many as 75 % of cases [4]. Ocular melanoma is a rare disease, which has a rapid progression upon development of liver metastases in up to 50 % of individuals [5–10].

Transarterial therapies including embolization, chemoembolization, and radioembolization with yttrium-90 (^{90}Y) microspheres are an important group of procedures in interventional oncology for the treatment of both primary and secondary malignancies of the liver. Since the liver is the dominant site of metastatic disease and surgical treatment is frequently not possible, catheter-based treatment

R.S. Winokur (✉)
Department of Diagnostic Radiology, Thomas Jefferson University, Philadelphia, PA, USA
e-mail: ronald.winokur@jefferson.edu

D.B. Brown
Department of Radiology, Thomas Jefferson University, Philadelphia, PA, USA
e-mail: daniel.brown@jefferson.edu

D.E. Dupuy et al. (eds.), *Image-Guided Cancer Therapy*, DOI 10.1007/978-1-4419-0751-6_29,

options are increasingly utilized. Due to the dual blood supply to the liver by the portal vein and the hepatic arteries (75 % portal vein and 25 % hepatic arteries) and the fact that tumors primarily receive their blood supply from the hepatic arteries, embolic therapy via the hepatic arteries has been proven to be an effective treatment strategy that limits toxicity to normal liver parenchyma [2, 11–16]. In addition, direct infusion of chemotherapeutic agents through the hepatic arteries allows high concentrations of chemotherapy to reach the tumor and avoids first-pass metabolism that would occur with oral or intravenous administration [2].

Table 27.1 ECOG scoring system

Score	ECOG
0	Fully active, able to carry on all pre-disease performance without restriction
1	Restricted in physically strenuous activity but ambulatory and able to carry out work of a light or sedentary nature, e.g., light housework or office work
2	Ambulatory and capable of all self-care but unable to carry out any work activities, up and about > 50 % of waking hours
3	Capable of only limited self-care, confined to bed or chair > 50 % of waking hours
4	Completely disabled, cannot carry on any self-care, totally confined to bed or chair
5	Dead

Indications and Patient Selection

Transarterial therapies are used to treat patients with unresectable primary and secondary malignancies of the liver [13]. In the case of hepatic metastases, the treatment can be palliative for symptom relief or to maximize survival [4, 6, 8, 10, 17–19]. The ideal candidates for treatment are patients with liver-dominant disease, adequate liver function, and no vascular invasion by tumor [13]. Patients should have an Eastern Cooperative Oncology Group (ECOG) performance status of 0–1 to undergo treatment. ECOG performance status of 2 is acceptable if transarterial chemoembolization (TACE) is expected to improve this score. Refer to Table 27.1 for ECOG performance status grades (Table 27.1).

Absolute contraindications to performing hepatic chemoembolization include liver failure, severe infection, and main portal vein thrombosis without collateral flow [13]. Relative contraindications include biliary obstruction, uncorrectable coagulopathy, severe thrombocytopenia, poor performance status, renal insufficiency, and anaphylaxis to contrast media [13, 20]. Biliary obstruction, incompetent sphincter of Oddi, or prior biliary surgery with bilioenteric anastamosis significantly increase the risk of hepatic abscess following treatment [13]. The main portal vein should be patent or have cavernous transformation with flow directed toward the liver (aka hepatopedal) in collateral vessels [12, 13, 20, 21]. Catheter angiography performed prior to treatment can confirm portal vein patency if it is unclear by other imaging modalities.

Exclusion criteria based upon laboratory values are not definitively established. However, the constellation of greater than 50 % tumor burden, bilirubin greater than 2 mg/dL, lactate dehydrogenase greater 425 mg/dL, and aspartate aminotransferase level greater than 100 IU/L may be associated with increased post-procedural mortality following treatment of hepatocellular carcinoma (HCC) [22]. Individual abnormalities in these parameters have not been shown to predict adverse outcomes related to arterial chemoembolization therapy for HCC [23]. Similar research has not been performed for patients with metastatic disease. However, given that unresectable metastases are frequently multifocal, an operator attempting treatment on a patient with elevated bilirubin and metastatic disease should proceed carefully, if at all.

Variations of Tumor Embolization

Arterial embolization is a useful treatment strategy in liver-dominant metastatic disease as described previously due to the unique blood supply to normal liver parenchyma and malignant tissue.

Local intra-arterial therapy can be performed using bland embolization. Bland embolization

refers to infusion of permanent or degradable materials that result in static or slow flow within the vessels. Consequent tumor ischemia is the primary mode of tumor killing. Agents that can be used for bland embolization include gelatin sponge, starch spheres, Ethiodol (Guerbet, Roissy, France), polyvinyl alcohol, and calibrated microspheres [14]. Ethiodol contains iodine organically combined with ethyl esters of the fatty acids of poppy-seed oil. Approximately 1–15 ml of Ethiodol is administered according to tumor size with 1 ml given per cm of tumor diameter for superselective transarterial embolization [13].

Chemoembolization (TACE)

The addition of cytotoxic drugs to bland embolization defines chemoembolization. Direct infusion of chemotherapeutic agents to the hepatic arteries results in a higher concentration of therapy delivered to the malignant tissue. Subsequent bland embolization slows flow within the liver, allowing for reduced washout and increased dwell time of the chemotherapeutic agent. The agents to be used for chemoembolization are not standardized. A partial list of described agents include 5-fluorouracil, cisplatin, doxorubicin, streptozotocin, mitomycin-C, and BCNU for ocular melanoma [8, 17–19, 24]. Chemotherapeutic agents are traditionally delivered in an Ethiodol solution as either a bolus or infusion. More recently, the development of drug-eluting microspheres has been used for chemoembolization. Current configurations allow loading of either doxorubicin or irinotecan with the ability to obtain a sustained release over a long period of time [2].

Radioembolization

Radioembolization utilizes radioisotopes such as ^{90}Y in addition to embolization for intra-arterial treatment. ^{90}Y microspheres are 20–40-μm particles that emit β-radiation for selective internal brachytherapy to the liver. Two products are available in the United States: TheraSpheres (Nordion, Ottawa, ON) and SIR-Spheres (Sirtex Medical, Wilmington, MA). These agents are quite different with relevant review within Table 27.2 (Table 27.2). TheraSpheres are FDA approved to treat HCC, while SIR-Spheres are approved to treat colorectal cancer along with infusion of intra-arterial floxuridine. Off-label use of both types of ^{90}Y-microspheres is being studied in a number of other hepatic metastases for efficacy.

Table 27.2 Differences in radioembolic agents used in the United States

TheraSpheres	SIR-Spheres
Diameter 20–30 μm	Diameter 20–60 μm
Glass bead	Resin bead
1.2–8 million spheres/vial	40–80 million spheres/vial
2,500 Bq/sphere	50 Bq/sphere
Non-embolic	Embolic
FDA approved for HCC	FDA approved for CRC with intra-arterial chemotherapy

Immunoembolization

Early studies have been performed analyzing the utility of immunoembolization therapy with granulocyte-macrophage colony-stimulating factor (GM-CSF) for the treatment of metastatic uveal melanoma. GM-CSF is a glycoprotein that is secreted principally by activated T cells and stimulates immune cells, such as macrophages and dendritic cells [10]. The intra-arterial administration of GM-CSF is thought to attract and stimulate antigen-presenting cells to liver tumors with improved uptake of tumor antigens released from necrotic tumor cells [10]. In addition, local stimulation of the immune system may produce a systemic immune response against tumor cells and suppress the development of extrahepatic disease [10].

Procedural Considerations

Premedication with intravenous fluids, antiemetics, and steroids prior to transarterial embolization and chemoembolization is standard. Hydration is

usually provided with normal saline solution infused at a rate of approximately 150–300 mL/h. Preprocedure antibiotics are not required before the majority of transarterial procedures. However, patients with increased risk for developing hepatic abscess due to prior biliary surgery benefit from preprocedural antibiotics [25–28]. Patients receiving chemoembolization for treatment of neuroendocrine metastases, such as carcinoid, will require pretreatment with octreotide (150 μg subcutaneously) to limit carcinoid crisis that results from the hormonal release after tumor necrosis [17]. Even if the patient is asymptomatic from carcinoid metastases, pretreatment with octreotide is still recommended as a larger quantity of serotonin or bradykinin may be released into the bloodstream after treatment.

Prior to embolization, high-quality diagnostic arteriography of the celiac and superior mesenteric arteries is recommended to evaluate for variant anatomy, vascular supply to the tumors, and origins of extrahepatic vessels to minimize the risk of nontarget embolization. Imaging should continue during the arteriograms through the portal-venous phase to confirm patency or the presence of hepatopedal collaterals prior to treatment. Practice patterns vary, but treatment with the therapeutic agent can be performed in a superselective manner or lobar manner depending on the type and number of lesions being treated. Treatment of the entire liver in one session is associated with an increase in mortality [21]. If treatment of the hepatic arteries leads to irreversible complete occlusion, several collateral pathways can develop including the inferior phrenic, internal mammary, and intercostal arteries [29–31]. Bland embolization should be favored over chemoembolization if any of the collateral pathways communicate with the skin to prevent ischemic cutaneous ulceration [29]. The cystic artery may be included in the treatment field if it cannot be avoided. The major risk associated with cystic artery embolization is pain, which may lengthen the hospital stay. However, the incidence of cholecystitis requiring cholecystectomy or cholecystostomy drain placement is extremely rare [32].

Ethiodol (Guerbet, Bloomington, IN) is typically mixed with chemotherapeutic agents during TACE. It is used because it acts as both an embolic agent and a carrier of the chemotherapeutic agent to the tumor. Ethiodol enters small arteries and peritumoral sinusoids blocking blood flow to tumors [33]. Improved patient survival and treatment response is reported for tumors that retain greater than 50 % Ethiodol following treatment [34]. Temporary or permanent embolic agents are also employed for TACE in order to render the tumors ischemic. Ischemia causes the disruption of the intracellular glycoprotein pumps, which inhibits tumor cells from expelling chemotherapeutic agents and results in prolonged exposure of the tumors to chemotherapy drugs. A study by Sasaki et al. [35]. reported a sixfold increase in cisplatin retention within resected tumors as compared to adjacent liver parenchyma following TACE with gelfoam. Although both temporary and permanent embolic materials can be used for TACE, a study performed in patients with hepatocellular carcinoma showed a trend of improved survival in patients treated with gelfoam versus those treated with polyvinyl alcohol [36]. Other studies have shown no difference in survival when comparing gelfoam powder and polyvinyl alcohol [37].

Following TACE, patients are admitted overnight for observation. Antiemetics and analgesics should be available to control symptoms of the postembolization syndrome. Postprocedural imaging should be performed 4–6 weeks following treatment. Signs of successful chemoembolization include Ethiodol uptake and absence of arterial phase enhancement on CT [36, 38, 39]. If the original lesion did not enhance, obvious tumor enlargement or nodular enhancement during the portal-venous and delayed phases has been described following radiofrequency ablation [40]. Similar findings may be present with recurrent or residual tumor post transarterial therapy.

Prior to treatment with ^{90}Y microspheres for radioembolization, diagnostic mesenteric arteriography is performed to evaluate for variant anatomy and identify the origins of extrahepatic vessels arising from the hepatic arteries. Nontarget infusion of the radioactive microspheres in these vessels can result in radiation ulcers which can be devastating to patients. One institution

reported an incidence of significant lung shunting in both hepatocellular carcinoma and metastatic disease to be less than 10 % [41]. The lungs can tolerate a dose of 30 Gy per treatment session and a cumulative dose of 50 Gy [42]. High uptake of ^{99m}Tc-MAA in non-tumorous liver segments may increase the risk of radiation-induced liver damage [43]. During the same procedure, prophylactic coil embolization of extrahepatic vessels that may lead to nontarget embolization is recommended. For example, embolization of the gastroduodenal artery and right gastric artery should be performed in all cases to prevent gastric or duodenal ulceration [43, 44]. The rich vascular arcade supplying the gastric and intestinal mucosa allows for adequate blood supply following embolization resulting in nonexistent clinical sequelae and an enormous safety benefit [44]. Poor preprocedure performance status, bulky or invasive tumor, and liver dysfunction correlate with increased procedure-related mortality [41, 44]. Prior treatment with capecitabine has been a contraindication to the subsequent treatment with SIR-Spheres, but this may be overly cautious. The required activity of ^{90}Y microspheres relates to the desired tumor dose, extent of hepatosystemic shunting, tumor mass, embolized liver mass, body surface area, and device used. Occasionally, the cystic artery may need to be addressed prior to treatment with radioembolization due to anatomic considerations. Inclusion of the cystic artery in the treatment field with ^{90}Y microspheres can result in radiation cholecystitis in a small number of patients [41]. One group recommends prophylactic embolization of the cystic artery in these cases to prevent the 0.5 % incidence of cholecystitis [41].

Outcomes with Specific Tumor Types

Colorectal Carcinoma Metastases

Liver metastases can be found in up to 80 % of patients with colorectal carcinoma, and the liver is the second most common site of metastatic disease. Patients with liver-isolated disease should be evaluated for potential resection as resection is the only chance for cure. However, only 20 % of patients are candidates for curative treatment with resection due to the number/location of their lesions, hepatic function, or comorbid illness [1, 19]. With careful prescreening, 5-year survivals following resection of 58 % have been reported [45]. For patients who are not surgical candidates, the standard of care is to treat liver metastases with systemic chemotherapy. First-line therapy is typically centered on the drug oxaliplatin and second-line therapy is based on irinotecan. However, patients eventually have progression of disease on these therapies. Also, a number of patients will have toxicity while on therapy requiring a chemotherapy "holiday." These patients are potential candidates for transarterial therapies (Fig. 27.1).

A summary of treatment outcomes for colorectal carcinoma is provided in Table 27.3. Chemoembolization has been specifically studied in the unresectable metastatic colorectal carcinoma population for palliative therapy. Overall response rates are approximately 50 % [1]. Numerous factors are predictive of outcomes regardless of transarterial treatment strategy. For example, patients with an ECOG performance status of 0 or 1 have a significantly longer survival. Sanz-Altamira [46] described a median survival of 24 months for patients with an ECOG score of 0 or 1 as compared to 3 months for those with an ECOG performance status of 2. The presence of extrahepatic metastases also predicts a worse prognosis with a median survival of 3 months, versus 14 months in patients with isolated hepatic disease [46]. A study by Salman et al. [47] showed an estimated survival of 15 months following treatment for patients with solitary hepatic involvement, while survival was only 8 months for patients with extrahepatic metastases. Given that metastatic colorectal cancer is a systemic process, addition of a systemic agent to transarterial therapies to limit extrahepatic progression may be of benefit.

A number of studies are encouraging for the utility of chemoembolization with 1-year survival rates ranging from 68 % to 86 % [46, 48, 49]; 2-year survival rates range from

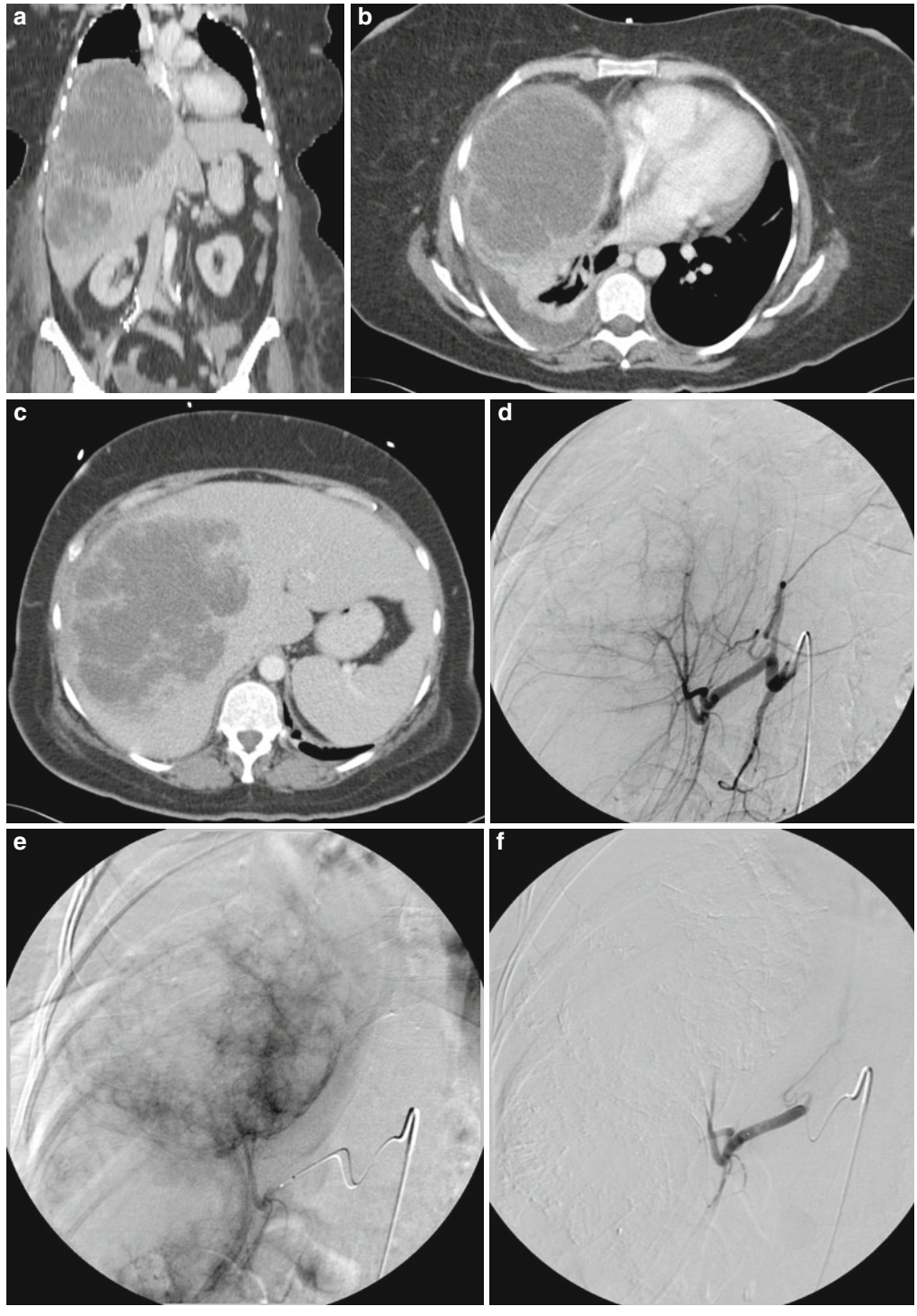

Fig. 27.1 (continued)

37 % to 61 %; a 3 year survival rate of 23 % has also been reported [49]. A study by Tellez et al. [50] reported survival of 29 months after diagnosis, which is comparable to results by Soulen et al. [49] of 24 months. Each study used a different combination of agents in their therapy. Sanz-Altamira et al. [46] used 5-fluorouracil, mitomycin-C, Ethiodol, and gelfoam; Tellez et al. [50] used cisplatin, doxorubicin, mitomycin-C, and bovine collagen; Soulen et al. [49] used cisplatin, doxorubicin, mitomycin-C, Ethiodol, and polyvinyl alcohol; and Lang et al [48]. used doxorubicin and Ethiodol. More recently, the development of drug-eluting beads that allow for the loading of microspheres with a desired chemotherapeutic agent has produced a new method for transarterial local therapy [51]. Response rates of 75 % and 66 % were reported at 3 and 6 months using modified RECIST criteria after treatment with irinotecan-loaded beads [51]. A 50 % drop in CEA levels was also reported to persist up to 6 months following therapy [51]. A phase II clinical trial in 20 patients treated with irinotecan-loaded beads reported an 80 % response rate by changes on posttreatment imaging [52].

A small cohort has also been performed comparing the outcome of bland embolization with either polyvinyl alcohol (PVA) particles or gelfoam to chemoembolization. Salman et al. [47] showed no significant difference in survival between bland embolization with polyvinyl alcohol and chemoembolization with polyvinyl alcohol combined with 5-fluorouracil and interferon. Another study also showed no difference in response between bland embolization with polyvinyl alcohol particles and polyvinyl alcohol plus 5-fluorouracil and interferon [53]. Twenty-five percent of patients in this study had an objective response to therapy, and 46 % had stabilization of disease [53].

Radioembolization with ^{90}Y microspheres is another option in the treatment of patients with colorectal carcinoma metastases to the liver [54, 55]. A comprehensive review article found that more patients have been reported following treatment with SIR-Spheres than with TheraSpheres [56]. The studies utilized different treatment paradigms as well as different outcome measures, which makes comparison of the studies extremely difficult. The only study reporting SIR-Spheres with floxuridine was the trial that led to FDA approval for SIR-Spheres in this combination. Since that point, virtually all publications use the radioembolic agent alone. Gray et al. [57] compared hepatic artery infusion of floxuridine (FUDR) and FUDR plus 1 treatment with resin microspheres and showed improved responses in patients undergoing combined therapy by CT and CEA levels. The median time to disease progression in the liver was significantly longer for patients who received microspheres in addition to intra-arterial chemotherapy with 1-year, 2-year, 3-year, and 5-year survival rates of 72 %, 39 %, 17 %, and 3.5 %, respectively [57].

Overall, a number of studies with encouraging results have been reported, particularly when ^{90}Y microspheres are used in either chemotherapy-naive patients or after failure of 1–2 lines of therapy, a finding that has also been demonstrated with chemoembolization [58, 59]. Analysis of response to therapy varies between the use of imaging modalities, such as CT/MRI, and functional imaging such as PET/CT. One study reported that PET is a more sensitive and accurate indicator of tumor response following radioembolization [60]. At least a partial response was seen in 74 % of patients

Fig. 27.1 Seventy three-year-old female with liver-dominant colorectal cancer metastases. (**a**) Coronal reconstruction and axial images (**b**, **c**) from a CT scan demonstrate the extensive disease. Catheter angiography in the celiac origin (**d**) demonstrates the right hepatic artery. Imaging later in the same run (**e**) reveals the hypervascularity at the margins of the tumors. Following oily chemoembolization, the right hepatic artery is truncated (**f**). A final spot image demonstrates the Ethiodol within the treated tumors

Table 27.3 Outcomes with intra-arterial techniques for patients with colorectal cancer

Trial	Agent(s)	n patients	Overall survival	Time to progression	Toxicities	30-day mortality: n patients and (% patients)
Lang [48]	Doxorubicin	46	58 % 1 year	59 % by 1 year	15/46 patients (33 %)	NR
	Ethiodol		22 % 2 years		Bone marrow suppression in 6	
					Liver failure in 6	
					Renal failure in 2	
Sanz-Altamira [46]	5-fluorouracil, mitomycin-C, Ethiodol, Gelfoam	40	10 months median	7 months median	12/40 patients (30 %)	3 (7.5 %)
					6 worsened ascites	
					1 peritonitis	
					1 gangrenous cholecystitis	
					3 deaths within 30 days	
Tellez [50]	Cisplatin, doxorubicin	30	8.6 months median	NR	ECOG criteria:	0 (0 %)
	Mitomycin-C, bovine collagen				13.8 % grade III anemia	
					13.3 % grade III/IV thrombocytopenia	
Albert [58]	Cisplatin, doxorubicin, mitomycin-C, Ethiodol, polyvinyl alcohol	121	9 months median	3 months	CTCAE:	4 (3.6 %)
					1 % grade III/IV bilirubin	
					2 % grade III/IV alkaline phosphatase	
					3 % grade III/IV AST/ALT	
Mulcahy [59]	^{90}Y glass beads	72	14.5 months	15.4 months (liver only)	CTCAE:	0 (0 %)
					9/72 (13 %) grade III/IV bilirubin	
					6/72 (8 %) grade III/IV alkaline phosphatase	
					4/72 (6 %) grade III/IV ALT/AST	
Cianni [54]	^{90}Y resin beads	41	11.8 months	9.3 months	1/41 (2.4 %) grade IV hepatic failure	0 (0 %)
Jakobs [55]	^{90}Y resin beads	41	10.5 months	NR	1/41 (2.4 %) grade IV cholecystitis	0 (0 %)

by PET imaging, while 26 % showed no response [61]. When using imaging criteria, such as RECIST, response rates varied from 33 % to 48 % [57, 62–64]. In patients that either failed chemoembolization or in patients naïve to intra-arterial therapy, a partial response was seen in 35–65 % of patients [56, 65, 66]. One study that combined SIR-Spheres with first-line FOLFOX4 chemotherapy in chemotherapy-naive patients resulted in a partial response in 90 % of patients [67]. Reported survival times are as long as 24.6 and 29.4 months from diagnosis in two studies [66, 68].

Neuroendocrine Tumor Metastases

Neuroendocrine tumors (NET), such as carcinoid and islet cell carcinomas, have a strong predilection for developing liver metastases with reports of up to a 78 % incidence [4, 18, 69]. The majority of patients with symptomatic disease have diffuse metastases at the time of diagnosis and surgery is not feasible [12, 18]. The presence of liver metastases is associated with a poor prognosis and results in a significant deterioration of patient's quality of life. The 5-year survival rate of patients with neuroendocrine metastases to the liver is less than 20 % [70]. Systemic chemotherapy has a limited role in the treatment of patients with neuroendocrine tumors as carcinoid metastases are resistant to cytotoxic chemotherapy and islet cell tumors have a response rate of 30–70 % [71]. Transarterial procedures such as embolization and chemoembolization are a recognized method of controlling hormonal symptoms associated with NET as well as ameliorating pain related to tumor bulk [4, 21].

Surgical resection of carcinoid and islet cell tumor metastases can result in improved quality of life and relief of symptoms, and appropriate patients should undergo resection. However, a large number of patients are not candidates for surgery and transarterial procedures are employed. Relevant outcomes are reviewed in Table 27.4. Symptomatic relief from hormonal symptoms has been shown in 59–100 % of patients [72]. This effective response is due to a reduction in the expression of hormonal levels such as 5-hydroxyindoleacetic acid (5-HIAA), which is elevated in approximately 51–91 % of patients with carcinoid syndrome [72]. In addition to control of hormonal symptoms, there is also a reported improvement in abdominal pain symptoms related to tumor bulk in 63–66 % of patients [17, 71]. There is a wide range of survival data following chemoembolization for neuroendocrine malignancies, which is likely related to the heterogeneous nature of these tumors. The median survival ranges from 31 months to 50 months [17, 71, 73–76]. One-year, 2-year, and 5-year survival rates are 78–93 %, 62–69 %, and 24–48 %, respectively [4, 17, 71, 74, 77]. In studies that separated carcinoid from islet cell malignancies, outcomes were slightly better for carcinoid metastases [71, 74, 78]. A recent study using drug-eluting doxorubicin beads showed a partial response rate of 80 %, stable disease in 15 %, and progression in 5 % at 3-month follow-up [79]. Progression-free survival was 15 months, which is similar to the rates reported with traditional chemoembolization and bland embolization of 17–20 months [17, 71, 79].

Although numerous studies have shown a benefit of hepatic arterial embolization and hepatic arterial chemoembolization, it is not completely clear if the addition of intra-arterial chemotherapy adds any therapeutic advantage over bland embolization alone (Fig. 27.2). Brown et al. [21] showed an 89 % response rate to bland embolization for hormonal symptoms, and all patients treated for pain alone responded to therapy. Chemoembolization has been thought to be more beneficial because of the initial study by Moertel et al. [80], which showed a greater regression rate and longer duration of regression with systemic chemotherapy after hepatic artery occlusion. Gupta et al. [78] showed that the addition of intra-arterial chemotherapy did not improve overall survival or progression-free survival in patients with carcinoid tumors, but found a tendency toward prolonged survival and improved response rate in patients with pancreatic islet cell tumors treated with chemoembolization. They qualified these findings by stating that the bland embolization group had more extensive liver disease.

Table 27.4 Outcomes for patients receiving intra-arterial techniques for neuroendocrine tumors. In Refs. [71] and [81], chemotherapy agents included cisplatin, doxorubicin, mitomycin-C, Ethiodol, and polyvinyl alcohol particles

Trial	Agent(s)	n patients	Overall survival	Time to progression	Toxicities	30-day mortality: n patients and (% patients)
Gupta [78]	Embolization or chemoembolization at physician discretion	69 carcinoid	33.8 months	22.7 months	Serious adverse following 25 procedures (8.5 %)	1 (0.8 %)
		54 islet cell	23.2 months	16.1 months	No difference between embolization and chemoembolization	
Ho [71]	Embolization or chemoembolization at physician discretion	46	36 months	18.8 months	8 major complications (8.6 %)	4 (4.3 %)
Ruutianinen [81]	Embolization or chemoembolization at physician discretion	67	44 months	12 months	CTCAE: grade III or worse complications in 22 % embolization and 25 % chemoembolization	3 (4.5 %)
Kennedy [82]	^{90}Y resin beads	148	70 months	NR	CTCAE: grade III:	NR
					6.5 % fatigue	
					3.2 % nausea	
					2.7 % pain	
					0.5 % ascites	
Rhee [83]	22 patients: ^{90}Y glass microspheres	42	22 months, glass	NR	CTCAE: Grade III in 6/42 patients (14.3 %)	2 (4.8 %)
	20 patients: ^{90}Y resin microspheres		28 months, resin			
King [84]	^{90}Y resin microspheres	34	27.6 months	NR	3 patients (8.8 %) developed ulcers	1 (2.9 %)
					2 patients (5.9 %) developed jaundice	

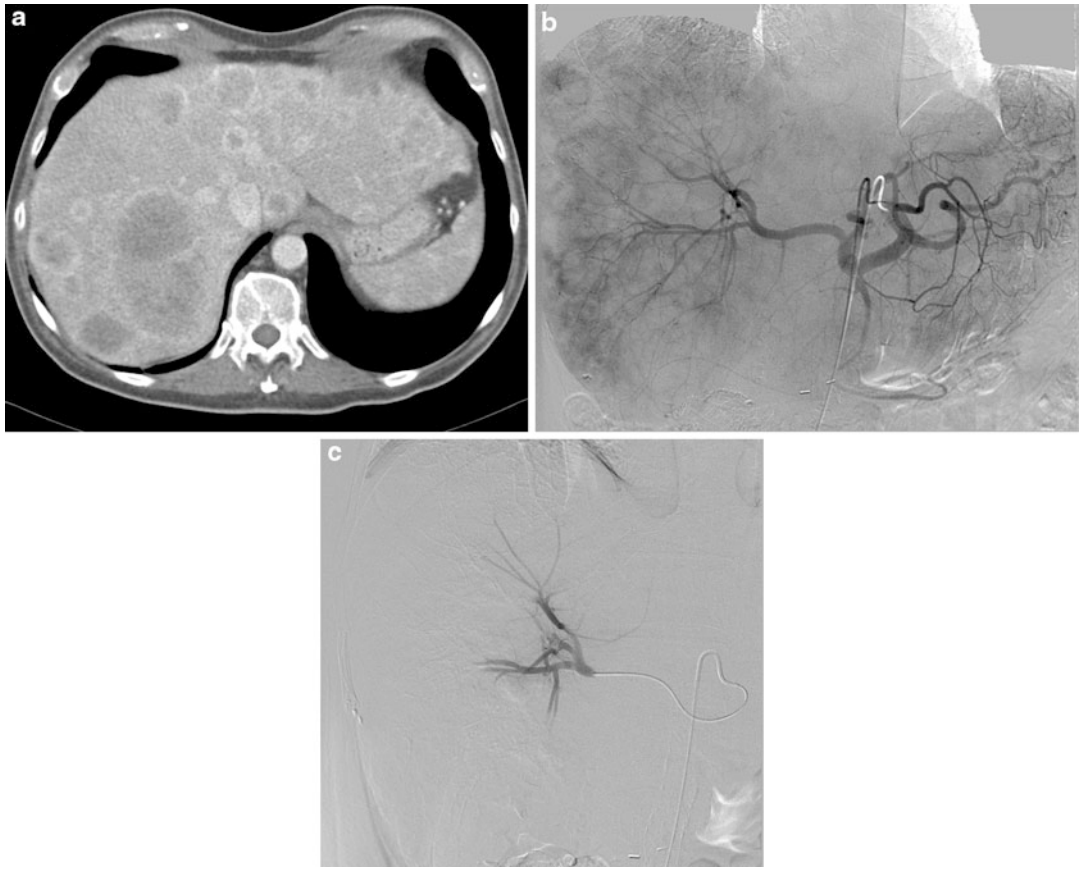

Fig. 27.2 Fifty three-year-old male with metastatic carcinoid tumor. CT (**a**) outlines the involvement of the liver. Celiac angiography (**b**) confirms the vascularity of the tumors. Following bland embolization, the right hepatic artery is truncated (**c**)

Other studies showed no statistically significant difference in median overall survival between the bland embolization and chemoembolization groups in both carcinoid and islet cell tumors [74, 81]. There was also no difference in symptom relief following either procedure [74].

Early studies with ^{90}Y microspheres have demonstrated encouraging response rates and overall survival. One study showed partial response in 60.5 % of patients, stable disease in 22.7 % of patients, complete response in 2.7 % of patients, and disease progression in 4.9 % of patients [82]. That same study showed a median survival of 70 months [82]. Another study using resin and glass microspheres showed response rates of 92 % and 94 % at 6-month follow-up [83]. Median survival from the time of diagnosis of liver metastases was reported as 27.6 months in one study and 36.5 months in another [18, 84]. Symptomatic response to treatment was reported as 50 % at 3 months and 55 % at 6 months [84].

Breast Cancer Metastases

Breast carcinoma is the most common malignancy affecting women in the United States and is the second leading cause of cancer-related mortality among women in industrialized countries [85]. Approximately 50 % of patients will develop metastatic disease with the liver being the most common intra-abdominal site. Liver metastases occur in as many as 20 % of patients [86–88]. Survival following the development of

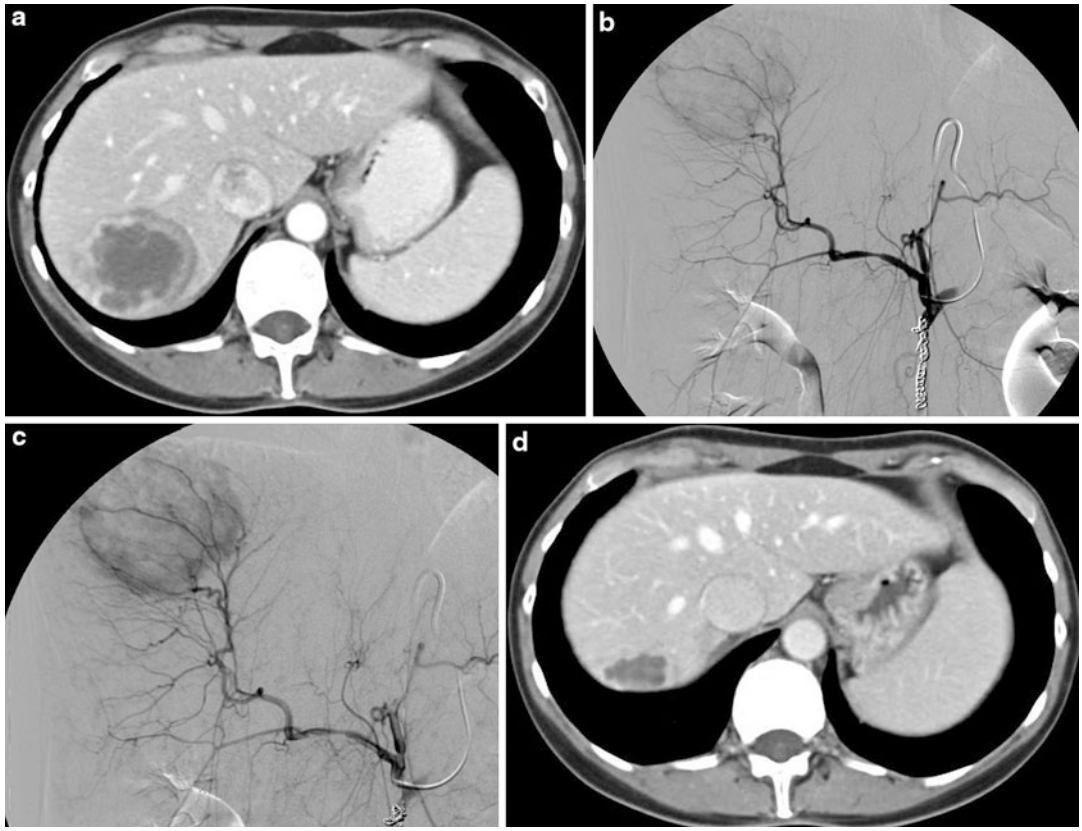

Fig. 27.3 Forty four-year-old female with unresectable metastatic breast cancer who has undergone multiple cycles of chemotherapy. (**a**) CT scan prior to treatment demonstrates a dominant right-sided tumor. The patient was treated with radioembolization. (**b**) Early and (**c**) late images outline the hypervascular mass at the dome of the liver. Follow-up CT 3 months after treatment demonstrates decrease in the size of the treated tumor (**d**)

liver metastases is poor with an estimated median survival time from weeks to 20 months [89, 90]. Metastatic breast cancer remains incurable and treatment is aimed at ameliorating symptoms, delaying tumor proliferation, improving/maintaining quality of life, and improving survival. Transarterial chemoembolization is an option in patients with solely hepatic metastases because many are unresectable. Limited data is available regarding responses to TACE, but they are promising for inducing tumor necrosis and maximizing survival. Partial response rates using RECIST criteria range from 26 % [91] to 35.7 % [92]. A study by Vogl et al. [93] showed partial response in 13 %, stable disease in 50.5 %, and disease progression in 36.5 % of patients. The response induced by TACE can allow patients to become candidates for local ablative therapies such as LITT and RFA [94]. A survival benefit was suggested by outcomes in multiple studies for TACE with a median survival of 25 months after treatment [91, 93]. In one case study of a patient with hepatic-dominant breast metastases, radioembolization with ^{90}Y SIR-Spheres was performed resulting in radiographically and clinical stable disease 13 months following treatment [95]. This report and results of radioembolization of other metastatic lesions may lead to future therapy of breast metastases with radioactive microspheres (Fig. 27.3).

Metastatic Uveal Melanoma

Uveal melanoma is the most common primary intraocular malignancy in adults with an annual

incidence of 1 per 100,000 persons in the United States [8, 96]. Approximately 50 % of patients with uveal melanoma will develop hepatic metastases, and in up to 90 % of patients, it will be the sole site of metastatic disease [97]. Liver metastases can occur years after treatment of the primary tumor. In general, uveal melanoma metastases do not respond to systemic chemotherapy, and patients have a life expectancy of 2–7 months without treatment [5, 98]. In a review of 201 patients, prolonged survival was demonstrated for chemoembolization versus other treatment methods such as systemic chemotherapy or intra-arterial chemotherapy [99]. Another study using cisplatin and polyvinyl alcohol particles showed a 46 % response rate and median survival of 11 months following diagnosis of metastases (Fig. 27.4) [6]. However, follow-up studies with the same treatment regimen failed to reproduce the same results [8]. A study using cisplatin/carboplatin followed by PVA particles in 14 patients showed a partial response in 8 patients (57 %), stable disease in 4 patients (29 %), and 2 patients with immediate disease progression (14 %) [100]. The reported median survival of all patients was 11.5 months from the time of first TACE and 18.5 months from the time of diagnosis of liver metastases [100]. A study of BCNU dissolved in Ethiodol followed by gelfoam sponge embolization showed a response rate of 20.4 % in evaluable patients [8]. The median survival of those patients was 7.4 months [8]. Although the overall survival rate was not much improved over lack of treatment, in patients with less than 20 % liver involvement, a response rate of 33.3 % and median survival of 19 months were observed [8]. Huppert et al. [100] showed similar findings with a median survival of 11 months after TACE for greater than 20 lesions versus 17 months for patients with fewer than 10 lesions. These outcomes suggest that patients with uveal melanoma should be under close surveillance for the development of liver metastases as early treatment when tumor burden is low results in improved outcome. A study by Vogl et al. [101] demonstrated a median survival of 21 months from the time of TACE with mitomycin-C. A study using drug-eluting beads loaded with irinotecan was performed on 10 patients, resulting in 3 patients with greater than 90 % reduction in metastases, 3 patients with 80 % reduction, and 4 patients with 60–70 % reduction [102]. Immunoembolization of the hepatic arteries with granulocyte-macrophage colony-stimulating factor (GM-CSF) and gelfoam has also produced promising results with an overall response rate of 32 %, median survival of 14.4 months, and a 1-year survival rate of 62 % [10]. No direct comparison of immunoembolization and chemoembolization has been reported.

Toxicities and Management

Transarterial therapies of the liver have been performed for decades for a variety of indications and are generally well tolerated. Postembolization syndrome (PES) consists of a constellation of symptoms following therapy including:

1. Fever
2. Nausea and vomiting
3. Right upper quadrant pain

This outcome is expected following embolization in any solid organ and is therefore considered a side effect rather than a complication of therapy [12, 103]. PES is independent of embolic material, drugs used, or tumor type. The etiology of the postembolization syndrome is not fully understood, but theories include a combination of tissue ischemia and an inflammatory response to chemoembolization [13, 32, 104]. Although the symptoms can be managed supportively, a significant percentage of patients require parenteral narcotic and intravenous hydration with symptoms persisting as long as 10 days [32]. The majority of patients have self-limited symptoms that allow discharge on the first posttreatment day [16]. PES requiring extended hospital stay or readmission generally occurs in less than 5 % of patients [21]. In an attempt to predict patients who will have PES that results in prolonged hospitalization, two studies analyzed preprocedural and procedural data and found inclusion of the gallbladder in the embolization field as well as higher chemoembolic dose were associated with severity of PES [32, 104]. No difference in severity of

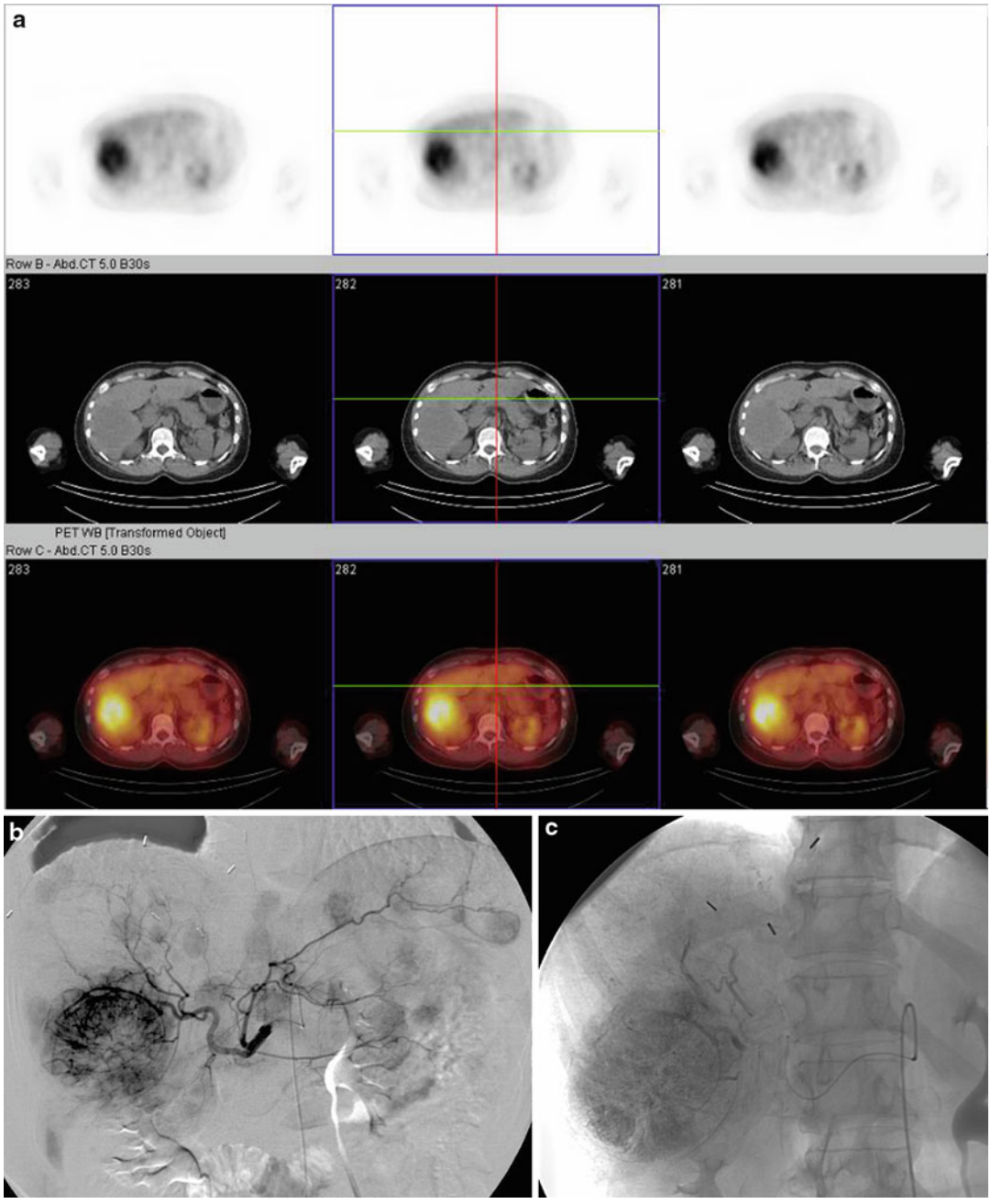

Fig. 27.4 (continued)

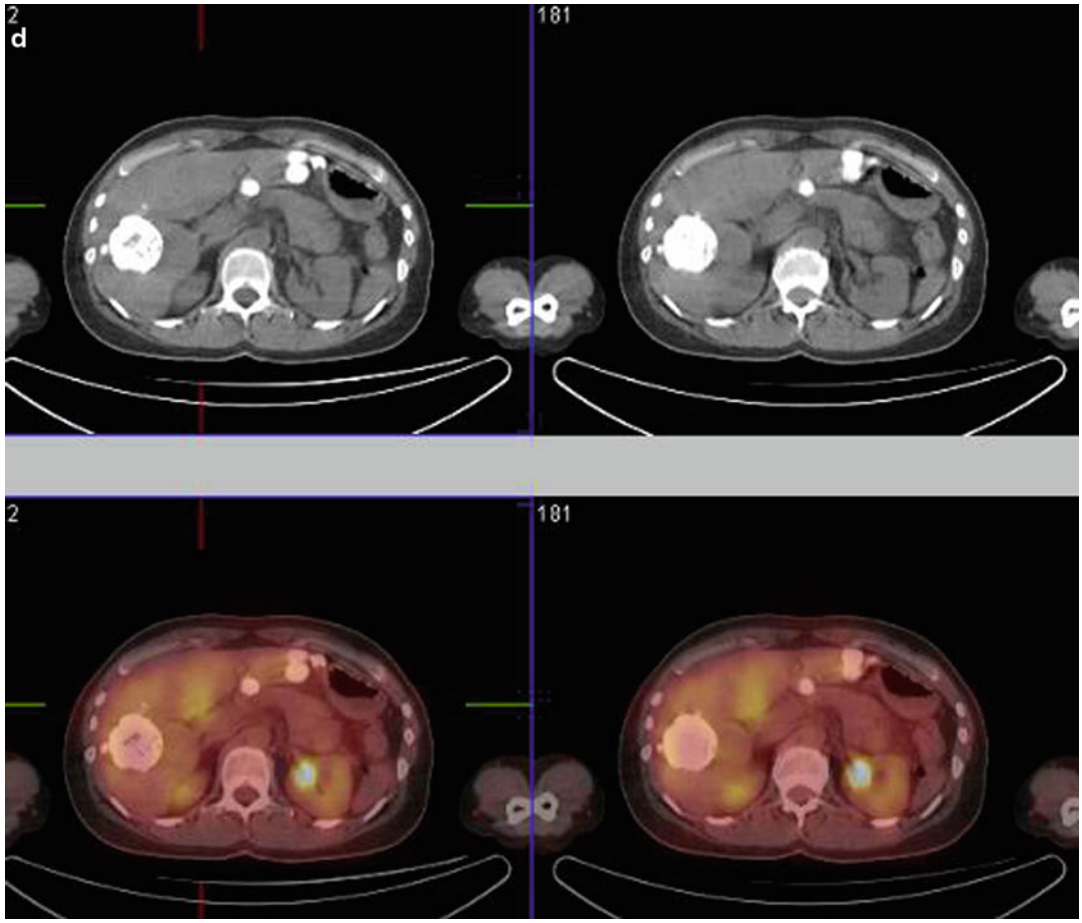

Fig. 27.4 Fifty-year-old female with metastatic uveal melanoma. Pretreatment PET/CT fusion imaging (**a**) demonstrates a dominant right lobe tumor. Multiple satellite nodules are identified at hepatic angiography (**b**). Following right lobe chemoembolization (**c**), there is dense Ethiodol uptake in the dominant tumor. At follow-up PET/CT, (**d**) there is no residual activity in the treated tumor

PES was found for particulate embolization combined with chemotherapy or bland embolization alone [104]. The percentage of liver volume embolized nor the percentage of tumor within the embolized territory were predictive of PES severity [32]. One study showed a reduced risk of PES and extended length of hospitalization in patients with prior embolization therapy, while another study showed no difference [32, 104]. In the author's experience, PES is usually most severe following the initial treatment in a given vascular bed since the arteries are maximal in capacitance at that time.

Liver function tests may be transiently affected by chemoembolization therapy with an increase in liver aminotransferase levels 3–5 days after therapy, returning to baseline by 10–14 days after treatment [16]. The cumulative extrahepatic toxicity of intra-arterial therapy is much less than systemic treatment with little bone marrow suppression. Major complications including hepatic abscess, hepatic failure or infarction, tumor rupture, and nontarget embolization occur in 4–7 % of procedures with a 30-day mortality rate of approximately 1 % [105]. Nontarget embolization is the inadvertent reflux of chemotherapeutic

agents and/or embolic material into unintended territories. For this reason, high-quality diagnostic arteriography as described in the procedural considerations is essential for identifying variant anatomy and origins of extrahepatic vessels. Gastrointestinal ischemia due to nontarget embolization of gastroduodenal arteries has been reported in less than 1 % of patients with chemoembolization or embolization [106]. The right gastric artery arising from the left hepatic arteries should also be searched for to prevent mucosal lesions or ulcerations [105]. Vessels such as the hepatic falciform ligament artery and left inferior phrenic artery are causes of supraumbilical skin irritation and shoulder pain, atelectasis, and left pleural effusion that can be avoided by superselective technique or coil/gelfoam embolization of extrahepatic vessels [107, 108]. Other sites of nontarget embolization resulting in splenic infarct and pulmonary embolism can rarely occur [105, 106].

Acute hepatic failure is a major complication that has been reported to occur in up to 2.6 % of patients and is more likely to occur in patients with greater tumor burden, impaired hepatic function, or compromised portal vein flow [13, 22, 105, 106]. Death within the first 30 days postembolization has been reported in up to 1 % of patients and is mostly related to acute hepatic failure or tumor lysis syndrome [12, 106]. In the case of radioembolization, there is a risk of life-threatening radiation-induced liver disease (RILD), which has been historically described with external beam radiation and presents with anicteric ascites, elevated liver function tests, thrombocytopenia, and venoocclusive disease 2 weeks to 4 months following exposure [41, 109–111]. Patients with hepatic metastases can tolerate 45.8 Gy of external beam radiation without the occurrence of RILD [112], and the incidence of radioembolization toxicity can be up to 20 % [111]. A greater association has been seen with tumor volume occupying greater than 70 % of the liver, higher total bilirubin level, and delivered dose of 150 Gy or greater [109, 113, 114]. Medical treatment should include general supportive care and diuretics, while other therapies are currently unproven [41, 111].

A history of prior bilioenteric anastamosis from Whipple procedure is a major risk factor for the development of liver abscess following chemoembolization with an 800-fold increased risk despite antibiotic prophylaxis [115]. Other interventions that lead to colonized biliary ducts also increase the risk of abscess formation including sphincterotomy, endoscopic stent placement, or percutaneous biliary drainage. The overall rate of development of liver abscess after transarterial embolization therapy is approximately 2 % of cases [16, 115]. However, one study showed that 6 out of 7 patients (85.7 %) who developed liver abscess had a Whipple procedure before chemoembolization [115]. Therefore, this subgroup of patients requires aggressive antibiotic prophylaxis and close posttreatment monitoring.

Conclusion

The role of intra-arterial treatments for liver-dominant metastases is evolving with demonstration of benefit for appropriately selected patients. While embolization and chemoembolization have historically been first-line choices for this patient group, the role of radioembolization with ^{90}Y microspheres is evolving and will be an area of focus over the next decade. Similarly, patient experiences with drug-eluting beads are currently limited and longer-term follow-up with this therapy will eventually determine the ultimate utility of this technology.

In patients with systemic processes such as colorectal cancer, progression of extrahepatic disease is a problem during periods where the focus is on liver-directed therapy. Future research in these disease processes will almost certainly involve combined systemic and locoregional therapy to maximize control of liver and extrahepatic disease. Since patients undergoing liver-directed therapy have better outcomes after 1–2 lines of systemic therapy, future studies should focus on the combination either as a first-line approach to delay disease progression or after second-line therapy to maintain the best chance at durable salvage.

References

1. Stuart K. Chemoembolization in the management of liver tumors. Oncologist. 2003;8:425–37.
2. Kalva SP, Thabet A, Wicky S. Recent advances in transarterial therapy of primary and secondary liver malignancies. Radiographics. 2008;28:101–17.
3. Fong Y, Cohen AM, Fortner JG, et al. Liver resection for colorectal metastases. J Clin Oncol. 1997;15: 938–46.
4. Landry CS, Scoggins CR, McMasters KM, Martin 2nd RC. Management of hepatic metastasis of gastrointestinal carcinoid tumors. J Surg Oncol. 2008;97:253–8.
5. Kath R, Hayungs J, Bornfeld N, Sauerwein W, Hoffken K, Seeber S. Prognosis and treatment of disseminated uveal melanoma. Cancer. 1993;72:2219–23.
6. Mavligit GM, Charnsangavej C, Carrasco CH, Patt YZ, Benjamin RS, Wallace S. Regression of ocular melanoma metastatic to the liver after hepatic arterial chemoembolization with cisplatin and polyvinyl sponge. JAMA. 1988;260:974–6.
7. Patel JK, Didolkar MS, Pickren JW, Moore RH. Metastatic pattern of malignant melanoma. A study of 216 autopsy cases. Am J Surg. 1978;135:807–10.
8. Patel K, Sullivan K, Berd D, et al. Chemoembolization of the hepatic artery with BCNU for metastatic uveal melanoma: results of a phase II study. Melanoma Res. 2005;15:297–304.
9. Rietschel P, Panageas KS, Hanlon C, Patel A, Abramson DH, Chapman PB. Variates of survival in metastatic uveal melanoma. J Clin Oncol. 2005;23: 8076–80.
10. Sato T, Eschelman DJ, Gonsalves CF, et al. Immunoembolization of malignant liver tumors, including uveal melanoma, using granulocyte-macrophage colony-stimulating factor. J Clin Oncol. 2008;26:5436–42.
11. Breedis C, Young G. The blood supply of neoplasms in the liver. Am J Pathol. 1954;30:969–77.
12. Brown DB, Cardella JF, Sacks D, et al. Quality improvement guidelines for transhepatic arterial chemoembolization, embolization, and chemotherapeutic infusion for hepatic malignancy. J Vasc Interv Radiol. 2006;17:225–32.
13. Gonsalves CF, Brown DB. Chemoembolization of hepatic malignancy. Abdom Imaging. 2009;34: 557–65.
14. Gunven P. Liver embolizations in oncology: a review. Part I. Arterial (chemo)embolizations. Med Oncol. 2008;25:1–11.
15. Ramsey DE, Kernagis LY, Soulen MC, Geschwind JF. Chemoembolization of hepatocellular carcinoma. J Vasc Interv Radiol. 2002;13:S211–21.
16. Brown DB, Cardella JF, Sacks D, et al. Quality improvement guidelines for transhepatic arterial chemoembolization, embolization, and chemotherapeutic infusion for hepatic malignancy. J Vasc Interv Radiol. 2009;20:S219–26, S26 e1–10.
17. Gupta S, Yao JC, Ahrar K, et al. Hepatic artery embolization and chemoembolization for treatment of patients with metastatic carcinoid tumors: the M.D. Anderson experience. Cancer J. 2003;9:261–7.
18. Murthy R, Kamat P, Nunez R, et al. Yttrium-90 microsphere radioembolotherapy of hepatic metastatic neuroendocrine carcinomas after hepatic arterial embolization. J Vasc Interv Radiol. 2008;19:145–51.
19. Vogl TJ, Zangos S, Eichler K, Yakoub D, Nabil M. Colorectal liver metastases: regional chemotherapy via transarterial chemoembolization (TACE) and hepatic chemoperfusion: an update. Eur Radiol. 2007;17:1025–34.
20. al-Bassam SH, Munk PL, Sallomi DF, et al. Chemoembolization of hepatic tumours. Australas Radiol. 1999;43:165–74.
21. Brown KT, Koh BY, Brody LA, et al. Particle embolization of hepatic neuroendocrine metastases for control of pain and hormonal symptoms. J Vasc Interv Radiol. 1999;10:397–403.
22. Berger DH, Carrasco CH, Hohn DC, Curley SA. Hepatic artery chemoembolization or embolization for primary and metastatic liver tumors: post-treatment management and complications. J Surg Oncol. 1995;60:116–21.
23. Brown DB, Fundakowski CE, Lisker-Melman M, et al. Comparison of MELD and Child-Pugh scores to predict survival after chemoembolization for hepatocellular carcinoma. J Vasc Interv Radiol. 2004;15:1209–18.
24. Burger I, Hong K, Schulick R, et al. Transcatheter arterial chemoembolization in unresectable cholangiocarcinoma: initial experience in a single institution. J Vasc Interv Radiol. 2005;16:353–61.
25. Geschwind JF, Kaushik S, Ramsey DE, Choti MA, Fishman EK, Kobeiter H. Influence of a new prophylactic antibiotic therapy on the incidence of liver abscesses after chemoembolization treatment of liver tumors. J Vasc Interv Radiol. 2002;13:1163–6.
26. Patel S, Tuite CM, Mondschein JI, Soulen MC. Effectiveness of an aggressive antibiotic regimen for chemoembolization in patients with previous biliary intervention. J Vasc Interv Radiol. 2006;17:1931–4.
27. Reed RA, Teitelbaum GP, Daniels JR, Pentecost MJ, Katz MD. Prevalence of infection following hepatic chemoembolization with cross-linked collagen with administration of prophylactic antibiotics. J Vasc Interv Radiol. 1994;5:367–71.
28. Ryan JM, Ryan BM, Smith TP. Antibiotic prophylaxis in interventional radiology. J Vasc Interv Radiol. 2004;15:547–56.
29. Arora R, Soulen MC, Haskal ZJ. Cutaneous complications of hepatic chemoembolization via extrahepatic collaterals. J Vasc Interv Radiol. 1999;10:1351–6.
30. Chung JW, Park JH, Han JK, Choi BI, Kim TK, Han MC. Transcatheter oily chemoembolization of the inferior phrenic artery in hepatocellular

carcinoma: the safety and potential therapeutic role. J Vasc Interv Radiol. 1998;9:495–500.
31. Tajima T, Honda H, Kuroiwa T, et al. Pulmonary complications after hepatic artery chemoembolization or infusion via the inferior phrenic artery for primary liver cancer. J Vasc Interv Radiol. 2002;13:893–900.
32. Leung DA, Goin JE, Sickles C, Raskay BJ, Soulen MC. Determinants of postembolization syndrome after hepatic chemoembolization. J Vasc Interv Radiol. 2001;12:321–6.
33. Chen MS, Li JQ, Zhang YQ, et al. High-dose iodized oil transcatheter arterial chemoembolization for patients with large hepatocellular carcinoma. World J Gastroenterol. 2002;8:74–8.
34. Higashi S, Tabata N, Kondo KH, et al. Size of lipid microdroplets effects results of hepatic arterial chemotherapy with an anticancer agent in water-in-oil-in-water emulsion to hepatocellular carcinoma. J Pharmacol Exp Ther. 1999;289:816–9.
35. Sasaki Y, Imaoka S, Kasugai H, et al. A new approach to chemoembolization therapy for hepatoma using ethiodized oil, cisplatin, and gelatin sponge. Cancer. 1987;60:1194–203.
36. Higuchi T, Kikuchi M, Okazaki M. Hepatocellular carcinoma after transcatheter hepatic arterial embolization. A histopathologic study of 84 resected cases. Cancer. 1994;73:2259–67.
37. Brown DB, Cai SR, Fundakowski CE, Zamboni WC, Strychor S, McLeod HL. Pharmacokinetics after endovascular lung perfusion with Cisplatin. J Vasc Interv Radiol. 2006;17:883–8.
38. Kubota K, Hisa N, Nishikawa T, et al. Evaluation of hepatocellular carcinoma after treatment with transcatheter arterial chemoembolization: comparison of Lipiodol-CT, power Doppler sonography, and dynamic MRI. Abdom Imaging. 2001;26:184–90.
39. Takayasu K, Arii S, Matsuo N, et al. Comparison of CT findings with resected specimens after chemoembolization with iodized oil for hepatocellular carcinoma. AJR Am J Roentgenol. 2000;175:699–704.
40. Chopra S, Dodd 3rd GD, Chintapalli KN, Leyendecker JR, Karahan OI, Rhim H. Tumor recurrence after radiofrequency thermal ablation of hepatic tumors: spectrum of findings on dual-phase contrast-enhanced CT. AJR Am J Roentgenol. 2001;177:381–7.
41. Salem R, Thurston KG. Radioembolization with ^{90}yttrium microspheres: a state-of-the-art brachytherapy treatment for primary and secondary liver malignancies. Part 2: special topics. J Vasc Interv Radiol. 2006;17:1425–39.
42. Ho S, Lau WY, Leung TW, Chan M, Johnson PJ, Li AK. Clinical evaluation of the partition model for estimating radiation doses from yttrium-90 microspheres in the treatment of hepatic cancer. Eur J Nucl Med. 1997;24:293–8.
43. Gunven P. Liver embolizations in oncology. A review. Part II. Arterial radioembolizations, portal venous embolizations, experimental arterial embolization procedures. Med Oncol. 2007;24:287–96.
44. Salem R, Thurston KG. Radioembolization with ^{90}Yttrium microspheres: a state-of-the-art brachytherapy treatment for primary and secondary liver malignancies. Part 1: technical and methodologic considerations. J Vasc Interv Radiol. 2006;17:1251–78.
45. Fernandez FG, Drebin JA, Linehan DC, Dehdashti F, Siegel BA, Strasberg SM. Five-year survival after resection of hepatic metastases from colorectal cancer in patients screened by positron emission tomography with F-18 fluorodeoxyglucose (FDG-PET). Ann Surg. 2004;240:438–47. discussion 47–50.
46. Sanz-Altamira PM, Spence LD, Huberman MS, et al. Selective chemoembolization in the management of hepatic metastases in refractory colorectal carcinoma: a phase II trial. Dis Colon Rectum. 1997;40:770–5.
47. Salman HS, Cynamon J, Jagust M, et al. Randomized phase II trial of embolization therapy versus chemoembolization therapy in previously treated patients with colorectal carcinoma metastatic to the liver. Clin Colorectal Cancer. 2002;2:173–9.
48. Lang EK, Brown Jr CL. Colorectal metastases to the liver: selective chemoembolization. Radiology. 1993;189:417–22.
49. Soulen MC. Chemoembolization of hepatic malignancies. Semin Interv Radiol. 1997;14:305–11.
50. Tellez C, Benson 3rd AB, Lyster MT, et al. Phase II trial of chemoembolization for the treatment of metastatic colorectal carcinoma to the liver and review of the literature. Cancer. 1998;82:1250–9.
51. Martin RC, Joshi J, Robbins K, Tomalty D, O'Hara R, Tatum C. Transarterial chemoembolization of metastatic colorectal carcinoma with drug-eluting beads, irinotecan (DEBIRI): multi-institutional registry. J Oncol. 2009;2009:539795.
52. Fiorentini G, Aliberti C, Turrisi G, et al. Intraarterial hepatic chemoembolization of liver metastases from colorectal cancer adopting irinotecan-eluting beads: results of a phase II clinical study. In Vivo. 2007;21:1085–91.
53. Martinelli DJ, Wadler S, Bakal CW, et al. Utility of embolization or chemoembolization as second-line treatment in patients with advanced or recurrent colorectal carcinoma. Cancer. 1994;74:1706–12.
54. Cianni R, Urigo C, Notarianni E, et al. Selective internal radiation therapy with SIR-spheres for the treatment of unresectable colorectal hepatic metastases. Cardiovasc Intervent Radiol. 2009;32:1179–86.
55. Jakobs TF, Hoffmann RT, Dehm K, et al. Hepatic yttrium-90 radioembolization of chemotherapy-refractory colorectal cancer liver metastases. J Vasc Interv Radiol. 2008;19:1187–95.
56. Salem R, Thurston KG. Radioembolization with yttrium-90 microspheres: a state-of-the-art brachytherapy treatment for primary and secondary liver malignancies: part 3: comprehensive literature

review and future direction. J Vasc Interv Radiol. 2006;17:1571–93.
57. Gray B, Van Hazel G. Randomised trial of SIR-Spheres plus chemotherapy vs. chemotherapy alone for treating patients with liver metastases from primary large bowel cancer. Ann Oncol. 2001;12:1711–20.
58. Albert M, Kiefer MV, Sun W, et al. Chemoembolization of colorectal liver metastases with cisplatin, doxorubicin, mitomycin C, ethiodol, and polyvinyl alcohol. Cancer. 2010;117:343–52.
59. Mulcahy MF, Lewandowski RJ, Ibrahim SM, et al. Radioembolization of colorectal hepatic metastases using yttrium-90 microspheres. Cancer. 2009;115:1849–58.
60. Wong CY, Salem R, Raman S, Gates VL, Dworkin HJ. Evaluating ^{90}Y-glass microsphere treatment response of unresectable colorectal liver metastases by [18F]FDG PET: a comparison with CT or MRI. Eur J Nucl Med Mol Imaging. 2002;29:815–20.
61. Wong CY, Salem R, Qing F, et al. Metabolic response after intraarterial ^{90}Y-glass microsphere treatment for colorectal liver metastases: comparison of quantitative and visual analyses by 18F-FDG PET. J Nucl Med. 2004;45:1892–7.
62. Gray BN, Anderson JE, Burton MA, et al. Regression of liver metastases following treatment with yttrium-90 microspheres. Aust N Z J Surg. 1992;62:105–10.
63. Kennedy AS, Coldwell D, Nutting C, et al. Resin ^{90}Y-microsphere brachytherapy for unresectable colorectal liver metastases: modern USA experience. Int J Radiat Oncol Biol Phys. 2006;65:412–25.
64. Lim L, Gibbs P, Yip D, et al. Prospective study of treatment with selective internal radiation therapy spheres in patients with unresectable primary or secondary hepatic malignancies. Intern Med J. 2005;35:222–7.
65. Lewandowski RJ, Thurston KG, Goin JE, et al. ^{90}Y microsphere (TheraSphere) treatment for unresectable colorectal cancer metastases of the liver: response to treatment at targeted doses of 135–150 Gy as measured by [18 F]fluorodeoxyglucose positron emission tomography and computed tomographic imaging. J Vasc Interv Radiol. 2005;16:1641–51.
66. Van Hazel G, Blackwell A, Anderson J, et al. Randomised phase 2 trial of SIR-Spheres plus fluorouracil/leucovorin chemotherapy versus fluorouracil/leucovorin chemotherapy alone in advanced colorectal cancer. J Surg Oncol. 2004;88:78–85.
67. Sharma RA, Van Hazel GA, Morgan B, et al. Radioembolization of liver metastases from colorectal cancer using yttrium-90 microspheres with concomitant systemic oxaliplatin, fluorouracil and leucovorin chemotherapy. J Clin Oncol. 2007;25:1099–1106.
68. Murthy R, Xiong H, Nunez R, et al. Yttrium 90 resin microspheres for the treatment of unresectable colorectal hepatic metastases after failure of multiple chemotherapy regimens: preliminary results. J Vasc Interv Radiol. 2005;16:937–45.
69. Chu QD, Hill HC, Douglass Jr HO, et al. Predictive factors associated with long-term survival in patients with neuroendocrine tumors of the pancreas. Ann Surg Oncol. 2002;9:855–62.
70. Oberg K. Neuroendocrine gastrointestinal tumors–a condensed overview of diagnosis and treatment. Ann Oncol. 1999;10(Suppl 2):S3–8.
71. Ho AS, Picus J, Darcy MD, et al. Long-term outcome after chemoembolization and embolization of hepatic metastatic lesions from neuroendocrine tumors. AJR Am J Roentgenol. 2007;188:1201–7.
72. Kvols LK, Turaga KK, Strosberg J, Choi J. Role of interventional radiology in the treatment of patients with neuroendocrine metastases in the liver. J Natl Compr Canc Netw. 2009;7:765–72.
73. Hajarizadeh H, Ivancev K, Mueller CR, Fletcher WS, Woltering EA. Effective palliative treatment of metastatic carcinoid tumors with intra-arterial chemotherapy/chemoembolization combined with octreotide acetate. Am J Surg. 1992;163:479–83.
74. Pitt SC, Knuth J, Keily JM, et al. Hepatic neuroendocrine metastases: chemo- or bland embolization? J Gastrointest Surg. 2008;12:1951–60.
75. Seldinger SI. Catheter replacement of the needle in percutaneous arteriography; a new technique. Acta Radiol. 1953;39:368–76.
76. Touzios JG, Kiely JM, Pitt SC, et al. Neuroendocrine hepatic metastases: does aggressive management improve survival? Ann Surg. 2005;241:776–83. discussion 83–5.
77. Kress O, Wagner HJ, Wied M, Klose KJ, Arnold R, Alfke H. Transarterial chemoembolization of advanced liver metastases of neuroendocrine tumors–a retrospective single-center analysis. Digestion. 2003;68:94–101.
78. Gupta S, Johnson MM, Murthy R, et al. Hepatic arterial embolization and chemoembolization for the treatment of patients with metastatic neuroendocrine tumors: variables affecting response rates and survival. Cancer. 2005;104:1590–602.
79. de Baere T, Deschamps F, Teriitheau C, et al. Transarterial chemoembolization of liver metastases from well differentiated gastroenteropancreatic endocrine tumors with doxorubicin-eluting beads: preliminary results. J Vasc Interv Radiol. 2008;19:855–61.
80. Moertel CG, Johnson CM, McKusick MA, et al. The management of patients with advanced carcinoid tumors and islet cell carcinomas. Ann Intern Med. 1994;120:302–9.
81. Ruutiainen AT, Soulen MC, Tuite CM, et al. Chemoembolization and bland embolization of neuroendocrine tumor metastases to the liver. J Vasc Interv Radiol. 2007;18:847–55.
82. Kennedy AS, Dezarn WA, McNeillie P, et al. Radioembolization for unresectable neuroendocrine hepatic metastases using resin ^{90}Y-microspheres: early

results in 148 patients. Am J Clin Oncol. 2008; 31:271–9.
83. Rhee TK, Lewandowski RJ, Liu DM, et al. ^{90}Y Radioembolization for metastatic neuroendocrine liver tumors: preliminary results from a multi-institutional experience. Ann Surg. 2008;247: 1029–35.
84. King J, Quinn R, Glenn DM, et al. Radioembolization with selective internal radiation microspheres for neuroendocrine liver metastases. Cancer. 2008;113:921–9.
85. Smith AR, Giusti R. The epidemiology of breast cancer. In: Bassett LW, Jackson V, Bralow L, editors. Diagnosis of diseases of the breast. Philadelphia: WB Saunders; 1997. p. 293–16.
86. Carty NJ, Foggitt A, Hamilton CR, Royle GT, Taylor I. Patterns of clinical metastasis in breast cancer: an analysis of 100 patients. Eur J Surg Oncol. 1995;21:607–8.
87. Patanaphan V, Salazar OM, Risco R. Breast cancer: metastatic patterns and their prognosis. South Med J. 1988;81:1109–12.
88. Zinser JW, Hortobagyi GN, Buzdar AU, Smith TL, Fraschini G. Clinical course of breast cancer patients with liver metastases. J Clin Oncol. 1987;5:773–82.
89. Hoe AL, Royle GT, Taylor I. Breast liver metastases–incidence, diagnosis and outcome. J R Soc Med. 1991;84:714–6.
90. Wyld L, Gutteridge E, Pinder SE, et al. Prognostic factors for patients with hepatic metastases from breast cancer. Br J Cancer. 2003;89:284–90.
91. Buijs M, Kamel IR, Vossen JA, Georgiades CS, Hong K, Geschwind JF. Assessment of metastatic breast cancer response to chemoembolization with contrast agent enhanced and diffusion-weighted MR imaging. J Vasc Interv Radiol. 2007;18:957–63.
92. Li XP, Meng ZQ, Guo WJ, Li J. Treatment for liver metastases from breast cancer: results and prognostic factors. World J Gastroenterol. 2005;11: 3782–7.
93. Vogl TJ, Naguib NN, Nour-Eldin NE, Eichler K, Zangos S, Gruber-Rouh T. Transarterial chemoembolization (TACE) with mitomycin C and gemcitabine for liver metastases in breast cancer. Eur Radiol. 2010;20:173–80.
94. Vogl TJ, Mack MG, Balzer JO, et al. Liver metastases: neoadjuvant downsizing with transarterial chemoembolization before laser-induced thermotherapy. Radiology. 2003;229: 457–64.
95. Rubin D, Nutting C, Jones B. Metastatic breast cancer in a 54-year-old woman: integrative treatment with yttrium-90 radioembolization. Integr Cancer Ther. 2004;3:262–7.
96. Shields JA, Shields CL. Introduction to melanocytic tumors of the uvea. In: Shields JA, Shields CL, editors. Intraocular tumors: a text and atlas. Philadelphia: W.B. Saunders; 1992. p. 45–59.
97. Diener-West M, Reynolds SM, Agugliaro DJ, et al. Development of metastatic disease after enrollment in the COMS trials for treatment of choroidal melanoma: Collaborative Ocular Melanoma Study Group Report No. 26. Arch Ophthalmol. 2005;123: 1639–43.
98. Gragoudas ES, Egan KM, Seddon JM, et al. Survival of patients with metastases from uveal melanoma. Ophthalmology. 1991;98:383–9.
99. Bedikian AY, Legha SS, Mavligit G, et al. Treatment of uveal melanoma metastatic to the liver: a review of the M. D. Anderson Cancer Center experience and prognostic factors. Cancer. 1995;76:1665–70.
100. Huppert PE, Fierlbeck G, Pereira P, et al. Transarterial chemoembolization of liver metastases in patients with uveal melanoma. Eur J Radiol. 2010;74:e38–44.
101. Vogl T, Eichler K, Zangos S, et al. Preliminary experience with transarterial chemoembolization (TACE) in liver metastases of uveal malignant melanoma: local tumor control and survival. J Cancer Res Clin Oncol. 2007;133:177–84.
102. Fiorentini G, Aliberti C, Del Conte A, et al. Intra-arterial hepatic chemoembolization (TACE) of liver metastases from ocular melanoma with slow-release irinotecan-eluting beads. Early results of a phase II clinical study. In Vivo. 2009;23:131–7.
103. Brown DB, Gould JE, Gervais DA, et al. Transcatheter therapy for hepatic malignancy: standardization of terminology and reporting criteria. J Vasc Interv Radiol. 2009;20:S425–34.
104. Patel NH, Hahn D, Rapp S, Bergan K, Coldwell DM. Hepatic artery embolization: factors predisposing to postembolization pain and nausea. J Vasc Interv Radiol. 2000;11:453–60.
105. Sakamoto I, Aso N, Nagaoki K, et al. Complications associated with transcatheter arterial embolization for hepatic tumors. Radiographics. 1998;18:605–19.
106. Chung JW, Park JH, Han JK, et al. Hepatic tumors: predisposing factors for complications of transcatheter oily chemoembolization. Radiology. 1996;198:33–40.
107. Ibukuro K, Tsukiyama T, Mori K, Inoue Y. Hepatic falciform ligament artery: angiographic anatomy and clinical importance. Surg Radiol Anat. 1998;20: 367–71.
108. Song SY, Chung JW, Lim HG, Park JH. Nonhepatic arteries originating from the hepatic arteries: angiographic analysis in 250 patients. J Vasc Interv Radiol. 2006;17:461–9.
109. Kennedy AS, McNeillie P, Dezarn WA, et al. Treatment parameters and outcome in 680 treatments of internal radiation with resin ^{90}Y-microspheres for unresectable hepatic tumors. Int J Radiat Oncol Biol Phys. 2009;74:1494–500.
110. Lawrence TS, Robertson JM, Anscher MS, Jirtle RL, Ensminger WD, Fajardo LF. Hepatic toxicity

resulting from cancer treatment. Int J Radiat Oncol Biol Phys. 1995;31:1237–48.
111. Sangro B, Gil-Alzugaray B, Rodriguez J, et al. Liver disease induced by radioembolization of liver tumors: description and possible risk factors. Cancer. 2008;112:1538–46.
112. Dawson LA, Normolle D, Balter JM, McGinn CJ, Lawrence TS, Ten Haken RK. Analysis of radiation-induced liver disease using the Lyman NTCP model. Int J Radiat Oncol Biol Phys. 2002;53:810–21.
113. Goin JE, Salem R, Carr BI, et al. Treatment of unresectable hepatocellular carcinoma with intrahepatic yttrium 90 microspheres: factors associated with liver toxicities. J Vasc Interv Radiol. 2005;16:205–13.
114. Goin JE, Salem R, Carr BI, et al. Treatment of unresectable hepatocellular carcinoma with intrahepatic yttrium 90 microspheres: a risk-stratification analysis. J Vasc Interv Radiol. 2005;16:195–203.
115. Kim W, Clark TW, Baum RA, Soulen MC. Risk factors for liver abscess formation after hepatic chemoembolization. J Vasc Interv Radiol. 2001;12:965–8.

Surgical Therapies for Hepatic Colorectal Metastasis

28

Laleh G. Melstrom and Yuman Fong

Abstract

The liver is the most frequent site of metastases in patients with primary colorectal cancer. Surgical resection for isolated liver disease has become progressively safer, more effective, and potentially curative. Better outcomes have prompted expansion of indications for surgery to include patients in their 70s and 80s, with multi-lobar disease, and with a small future liver remnant that are hypertrophied with portal vein embolization techniques. The clinical risk score takes into account five elements that can better predict and facilitate selection of patients who may benefit the most from surgical resection.

Simultaneous colon and liver resection in synchronous metastases has been demonstrated to be safe and the approach of choice in many high-volume centers. Ablative techniques are also being utilized with good results in patients with smaller tumors and prohibitive operative risk factors or with bilobar disease not amenable to resection. These local therapies are deemed to have better outcomes than chemotherapy alone. However, chemotherapy remains the standard adjuvant therapy in patients with resected stage IV disease. Chemotherapy is also currently being used to downstage patients who initially present with unresectable disease. However, the entity of chemotherapy-associated steatohepatitis (CASH) has been increasingly recognized and therefore *preoperative* chemotherapy for resectable stage IV disease has not been definitively established as the optimal approach. After resection of liver metastases, the primary sites of recurrence are the liver and lung. The best approach to optimize survival is therefore multimodal with a combination of surgery or ablative techniques for focal disease and systemic adjuvant therapy thereafter.

L.G. Melstrom (✉)
Department of Surgery, Robert Wood Johnson and the Cancer Institute of New Jersey, New Brunswick, NJ, USA
e-mail: lgolkar@hotmail.com

Y. Fong
Department of Surgery and Radiology, Memorial Sloan Kettering Cancer Center, New York, NY, USA
e-mail: fongy@mskcc.org

Introduction

Nearly 50 % of patients with primary colorectal cancer will present with hepatic metastasis [1]. Although this may be deemed a systemic disease, up to 25 % have metastases localized only to the

D.E. Dupuy et al. (eds.), *Image-Guided Cancer Therapy*, DOI 10.1007/978-1-4419-0751-6_30,

liver [2]. The liver is the most frequent site of disease as the portal vein provides venous drainage from the colon and rectum directly to the liver. In these patients, local therapy (i.e., liver resection) has been well established as part of the algorithm for long-term survival and potential cure. Furthermore, in the past 30 years, surgical resection has proven to be the treatment of choice for isolated liver metastases [2–5].

This chapter will focus on the indications and safety of liver resection with potentially complimentary ablative approaches in the management of metastatic colorectal cancer to the liver. More efficient and less morbid hepatectomies are allowing combined resections of the primary cancer and synchronous hepatic metastases. The development of complimentary neoadjuvant chemotherapy regimens, parenchymal-sparing techniques, and combined hepatectomy/ablative therapies will be reviewed. These strategies have increased the potential indications and candidates for resection and have expanded the pool of patients provided the opportunity for extension of life and potential cure. The long-term outcomes and recurrence patterns for the patients treated with curative intent will be reviewed to identify the shortcomings of current therapy. Lastly, the areas of current controversy while formulating an algorithm of current care will be discussed and will further be put in context of costs of care.

Surgical Therapy for Hepatic Colorectal Metastases: Safe, Effective, and Potentially Curative

Approximately, 25 % of patients with primary colorectal carcinoma will present with synchronous hepatic metastasis. Furthermore, nearly 50 % of patients will develop metachronous liver metastases after undergoing resection of the colorectal primary [6, 7]. Several series have detailed the outcome of untreated liver metastases from colorectal cancer. The median survival can range from 5 to 10 months and is clearly related tumor burden. Prior to the 1990s, it was not appreciated that the liver functions as an efficient filter for tumor cells – necessitating millions of tumor cells to reach the liver in order for only a few tumor deposits to proliferate [8]. Therefore, many patients will present with a limited number of liver metastases that are amenable to local therapy in the form of surgery alone or in conjunction with some ablative techniques.

In the past three decades, surgery has proven to be the most effective and durable component of the multimodality treatment of hepatic colorectal metastases [3, 5, 9]. Specifically, the actual 10-year survival after resection of colorectal liver metastases has been documented in at least 1 out of 6 patients [10]. Despite the vast improvements in systemic therapies, few patients with hepatic metastases are ever cured with chemotherapy and/or biologic therapies [11, 12].

At present, the median survival for patients treated with chemotherapy is approximately 18 months [11, 12], and few patients survive beyond 3 years. Complete resection has resulted in median survival of over 40 months, a 5-year survival of 30–55 % (Table 28.1) [3–5, 9, 13–20], and cure in approximately 20–25 % of patients [9, 10, 21].

Resection for hepatic colorectal metastases has also proven to be very safe. Most recent series report an operative mortality less than 5 % [3–5, 9, 13–20] (Table 28.1). Patients also recover quickly and return to a good quality of life [22]. For high-volume centers, the median hospital stay is 5–7 days for minor liver resection and 7–10 days for major resection [4, 14–17].

Good Clinical Outcomes for Hepatectomy Has Allowed Expanding Indications of Resection

As safety and long-term cancer-related outcome become better, clinicians are extending the medical and oncologic indications for hepatectomy. Whereas advanced age was once a relative contraindication, hepatectomies are now routinely performed for patients in their 1970s and 1980s [23].

Table 28.1 Results of hepatic resection for metastatic colorectal cancer

Study	n	Operative mortality (%)	1-year survival (%)	3-year survival (%)	5-year survival (%)	10-year survival (%)	Median months
Hughes 1986 [20]	607	–	–	–	33	–	–
Gayowski 1994 [19]	204	0	91	–	32	–	33
Scheele 1995 [9]	434	4	85	45	33	20	40
Nordlinger 1995 [3]	1,568	2	80	–	28	–	40
Jamison 1997 [18]	280	4	84	–	27	20	33
Fong 1999 [5]	1,001	2.8	89	57	36	22	42
Minagawa 2000 [17]	235	0.85	–	51	38	26	
Choti 2002 [16]	226	1	93	57	40	26	46
Kato 2003 [15]	585	0	–	–	33	–	–
Adam 2001 [14]	335	1	91	66	48	30	52
House 2010-Era 1	1,037	2.5	–	57	37	26[a]	43
House 2010-Era 2	563	1	–	69	51	37[a]	64

[a]8-year survival

Aggressive surgery is also increasingly offered to patients with more extensive disease. Previously only patients with few lesions and long disease-free intervals were resected; however, now it is not uncommon for patients with multiple, synchronous disease to be treated with hepatectomy [24]. In spite of the expanding medical and cancer indications for surgery, the overall survival of patients has not changed for the worse in most series. Therefore, an increasing number of patients are being treated without compromising safety or cancer outcome.

In general, patients who are otherwise medically fit and with completely resectable metastases are now offered resections at most major centers.

Increasing Indications for Resection Necessitate More Applicable Clinical Staging Criteria

Despite the progressively more heterogeneous population undergoing hepatic resection, all patients with hepatic colorectal metastases are classified as stage IV by the American Joint Committee on Cancer (AJCC) staging criteria. There are a substantive number of patients that are cured after hepatectomy [10]. Thus, this is one of the few disease conditions where a stage IV patient is frequently cured. This heterogeneity in the stage IV population has generated a problem with regard to choosing patients for therapies and trials, as well as in comparing data from various institutions. In order to address this challenge, many investigators have generated improved staging systems for this disease.

There have been many patient studies that have developed scoring systems for staging patients with hepatic colorectal metastases. Two of these studies are sufficiently robust and have similar findings. Both studies arrived at staging systems that are based on clinical variables associated with the primary cancer, on the presentation of liver metastases, and on characteristics of the liver metastases [3, 5]. The common elements to both systems consisted of five elements used in the clinical risk score (CRS) (Table 28.2) [5]: (1) nodal metastases from primary cancer [25], (2) short disease-free interval [2, 20, 26, 27], (3) size of the largest liver tumor [20, 28], (4) more than one liver metastasis [20, 27], and (5) high CEA [3, 20].

The simplicity and versatility of the CRS has led to its widespread use among clinicians and investigators as a method of more specifically differentiating these stage IV patients. Investigators from Norway and Italy have independently verified this prognostic scoring system. [29, 30]. In addition to providing prognostic information

Table 28.2 Clinical risk score (CRS): prognostic scoring system for hepatic colorectal metastases[a]

Node-positive primary tumor
Disease-free interval less than 12 months between colon resection and appearance of metastases
Size of largest lesion >5 cm
More than one tumor
Carcinoembryonic antigen >200 ng/dl

[a]One point assigned for each positive criterion. Sum of points is CRS

for resection, the CRS has also been proven to be helpful in prognostics for tumor ablation [31]. More recently, the CRS was proven useful for the selection of expensive preoperative staging techniques such as ^{18}F-fluorodeoxyglucose positron emission tomography (FDG-PET) scanning [32] or laparoscopic staging [33]. The CRS may function as a way of identifying patients who would most benefit from having such costly staging tests and can be helpful in optimizing care as well as minimizing cost.

Synchronous Metastases: Simultaneous Colon and Liver Resection Is Safe and Is the Therapy of Choice

The simultaneous surgical approach to the treatment of patients presenting with synchronous liver metastases has become less controversial as hepatectomy has become faster and safer. The operative mortality was reported to be up to 17 % in studies published as late as the 1990s for combining resection of the primary with major hepatectomy [34]. Thus, many clinicians were reluctant to offer major hepatectomies with resection of the primary.

Similar to increasing the safety of hepatectomies overall, there have been many changes in surgical technique in order to improve the outcome of combined liver and colon resection. The majority of liver surgeons are no longer strictly utilizing a subcostal incision as it has become evident that even the most extensive liver resections in even a hostile abdomen can be safely performed via long midline incision extending from xiphoid to symphysis. In addition, to the approach, most experienced liver surgeons have recognized the importance of timing the liver resection prior to the resection of the primary tumor during a combination procedure. Proceeding with the hepatic resection first allows for low central venous pressure anesthesia to decrease blood loss. Subsequently, the colorectal resection may occur during the fluid resuscitation phase. This approach limits the periods of hypovolemia and low splanchnic perfusion. Addressing the liver resection first also has practical advantages by allowing for a single setup of surgical instruments, as the procedure will proceed from the "clean" hepatectomy to the "dirty" colorectal resection.

It is evident from recent data that in well-selected patients, such simultaneous resections provide for fewer complications, less mortality, and a reduced time to recovery and start of appropriate adjuvant chemotherapy. In a series from the Memorial Sloan-Kettering Cancer Center, 134 patients treated with simultaneous resection were compared to 106 patients treated by staged resection. There were no significant differences in mortality or complications; however, there was a decrease in total hospital stay and blood loss in the simultaneous resection group [35]. Additionally, the outcomes of the 45 patients who underwent simultaneous major liver resections were also clearly superior to the 75 patients with sequential resections.

Reddy and his colleagues described the experience of simultaneous resections from three centers across a 20-year period [36]. They reviewed data from 135 patients and found that resection of the colorectal primary in combination with minor liver resection shortened total hospitalization without compromising safety: nine days as compared with 14 days for staged surgery [36]. Data from the University of Louisville demonstrated similar findings and further supported such simultaneous resections [37]. These authors

reviewed 230 patients with synchronous hepatic metastases [37]. Seventy patients who underwent simultaneous resection were compared with 160 patients who underwent staged resections. Similar to other reported series, the patients undergoing simultaneous resections had a shorter total hospital stay (10 vs. 18 days, $p = 0.001$) without any significant increases in morbidity or mortality.

Tumor Ablation: An Effective and Complimentary Less Invasive Procedure

An alternative and sometimes complimentary approach in addressing multiple hepatic metastases is ablation; either alone or in conjunction with surgical resection to render patients tumor free. The technology in the clinical delivery of tumor ablation has significantly advanced over the last decade. There are currently commercially available and widely utilized tumor ablation systems that deliver cancer killing using cryoablation [38], radiofrequency ablation (RFA) [39], and microwave ablation [40]. RFA is the most frequently used method due to the inexpensive equipment, safety, and technical ease for practitioners. This technique has become adequately adopted such that the American Society of Clinical Oncology (ASCO) recently published guidelines for its use [41].

There have been large series documenting the safety of RFA. In a series of 3,554 ablations in 2,320 patients, the mortality rate was 0.3 % and major morbidity 2 % [42]. In the treatment of hepatocellular carcinoma, surgeons are often willing to ablate tumors that are technically resectable for various reasons. In this setting, there is evidence that ablation is equivalent to resection for cancer outcome but with much less morbidity and length of hospital stay [43].

The utility of RFA for colorectal metastases is somewhat more controversial. For cirrhotic patients with HCC, surgeons had been more than happy to ablate rather than to resect for a multitude of reasons. However, unlike HCC, most patients with hepatic colorectal metastases do not have baseline liver dysfunction, and intuitively resection would seem to be better than ablation. This controversy has resulted in the highly variable practices of clinicians treating these liver metastases. Most centers were amenable to ablating lesions that were deemed unresectable. These same patients with the large, poorly placed tumors are the most likely to recur regardless of the therapeutic approach utilized. Alternatively, other centers have been more selective about addressing tumors most likely to be completely treated by ablation. These are generally smaller lesions that are a reasonable distance from major vasculature. The non-standardized approach may account for the highly variable results seen in the literature (review by Decadt) [39]. Extensive data have demonstrated that the likelihood of a good response to ablation is a function of both smaller size and fewer number of lesions [39]. Surgical or laparoscopic approaches have the lowest local recurrence rates [44, 45]; however, this is at a cost of greater morbidity and a longer recovery.

With more experience, data is beginning to emerge for resectable hepatic metastases treated by RFA. Many clinicians are advocating laparoscopic or percutaneous ablation for those patients with medical contraindications to open resection or for those otherwise requiring a major resection for small deep lesions [46]. The benefits of this approach are highlighted in a retrospective comparative study of RFA versus resection for solitary hepatic metastases, where the complication rates were found to be 3 % versus 30 %, respectively, and with no difference in survival ($p = 0.3$) [47].

There is less controversy in the utilization of ablation for patients with recurrent or bilateral hepatic colorectal metastases. The use of ablation has clearly improved outcomes in this population. The most common site for recurrence after resection of colorectal metastases is the liver [6, 7, 48]. In 45–75 % of cases, the liver will be involved as a site of recurrence after liver

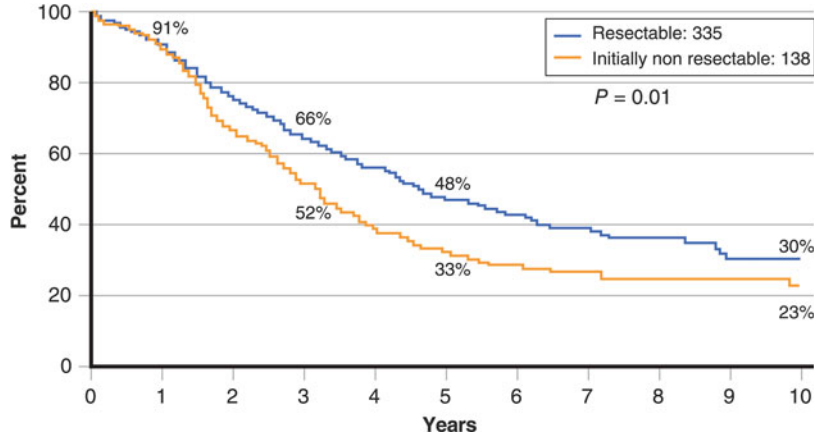

Fig. 28.1 Outcomes of patients treated by downstaging chemotherapy and subsequent resection compared to those initially resectable (Adapted from Adam et al. [14])

resection [6, 7, 48–50]. In 15–40 % of cases, the liver is the only site of recurrence. Only 5–10 % of recurrences can be treated by further, repeat hepatic resection [49–57]. Therefore, recurrences are also being treated by percutaneous ablation. This allows for treatment of more patients and for control of liver disease without undue morbidity.

With expanding criteria for resection, tumor ablation is also increasingly utilized in combination with resection. Rivoire and his colleagues [58] first suggested this in a paper involving 24 patients treated with combined resection and cryoablation. The median survival was reported as 39 months, with very reasonable 1-, 3-, and 4-year survival of 92 %, 50 %, and 36 %, respectively. Pawlik reported on 124 patients with hepatic colorectal metastasis treated by combined resection and RFA [59]. He found the group to have a median survival of 38 %, with an associated operative mortality of 2 %. In a subsequent paper from the same group (Fig. 28.1), the authors compared the outcomes of patients subjected to resection alone versus those treated by combined resection and ablation or by chemotherapy alone [60]. The strategy of this group for treating patients that are not completely resectable is with resection and ablation. It is evident that although those patients treated with ablation had worse long-term outcome than those completely resected, their survival was significantly better than those treated by chemotherapy alone. Thus, RFA improved outcome by increasing the number of patients treatable by hepatic cytoreduction.

In order to preserve liver parenchyma, several groups are now using RFA in conjunction with resection in patients who are completely resectable. Whether this surgical treatment approach is equivalent or superior to complete resection will soon be addressable by data.

In terms of recurrence, Kingham et al. reviewed the experience of recurrence patterns after the use of ablation for colorectal metastases [4]. Factors associated with local recurrence were size of tumor >1 cm, lack of postoperative chemotherapy, and use of cryotherapy. It may then be reasonable to address small central tumors with ablation techniques – in order to both minimize local recurrence and maximize parenchymal preservation.

Adjuvant Systemic Chemotherapy

The utility of adjuvant chemotherapy after liver resection for metastatic colorectal cancer to the liver has been evaluated in five recent studies. The first trial examined the utility of adjuvant 5-fluorouracil (5-FU) and leucovorin (LV) as adjuvant after resection as compared to resection alone [61, 62]. In this study, 173 patients were randomized to receiving either 5-FU/LV or no adjuvant chemotherapy after hepatectomy. There was a significant difference in recurrence-free survival (34 % vs. 27 %, $p < 0.03$). However, due to the small sample size in this trial, the overall survival was not found to be significantly

different (51 % vs. 41 %, $p = 0.1$). In a similar paper evaluating the same question, adjuvant therapy was significantly associated with improved overall and disease-free survival [62]. In this study, patients from an American center, where the majority of patients are given adjuvant therapy, were compared to outcomes from a center in Scotland, where patients were not given chemotherapy [61]. A total of 792 patients were reviewed. For patients treated with chemotherapy, the median survival was 47 months compared to 36 months for no chemotherapy ($p = 0.007$). In patients with a high clinical risk score (CRS) (4 or 5), the median survival was 37 months for patients treated with adjuvant therapy and 20 months for those not receiving adjuvant chemotherapy ($p = 0.007$).

The European Organization for Research and Treatment of Cancer (EORTC) recently published a trial that compared patients with resection alone to those treated with 3 months of preoperative 5-FU/LV plus oxaliplatin (FOLFOX) chemotherapy followed by resection and then 3 more months of chemotherapy postoperatively [63]. The patient population that received chemotherapy demonstrated a longer survival. This study can only be interpreted to indicate that perioperative chemotherapy is superior to resection alone as there was not an arm for adjuvant chemotherapy. Therefore, optimal timing of the chemotherapy remains a question.

Lastly, there have also been two randomized trials evaluating the utility of regional hepatic arterial infusional (HAI) floxuridine (FUDR) chemotherapy as an adjuvant modality after liver resection [64, 65]. One of these trials compared the incorporation of postoperative regional chemotherapy to no adjuvant therapy [64], whereas the other compared the use of systemic 5-FU/LV to the combination of HAI FUDR and systemic 5-FU/LV [65]. In both of these studies, it was quite evident that the use of regional chemotherapy was associated with a very high rate of disease control in the liver and significantly prolonged disease-free survival [64, 65].

Overall, irrespective of the timing or modality, the various data suggest that adjuvant chemotherapy is a reasonable treatment option for patients with resected stage IV colorectal cancer. The majority of data are with the use of systemic 5-FU/LV in patients who are naive to this regimen. However, most oncologists in the United States are using systemic FOLFOX as the adjuvant regimen. This approach is primarily supported by trials of adjuvant therapy for stage III cancer and in part by the EORTC trial [63]. FOLFOX may also be considered for those whose disease has progressed while receiving 5-FU/LV. Additionally, in patients who have not responded to first-line therapy, regional FUDR is a compelling choice at centers with the appropriate expertise in delivering HAI.

Chemotherapy Can Downstage Patients Who Initial Presentation of Unresectable Disease

The use of oxaliplatin and other newer chemotherapies has led to suggestions that a proportion of cases may be convertible from unresectable to resectable. In a report in 2000, Bismuth and colleagues first proposed the possibility of downstaging unresectable patients to resectable by examining 330 consecutive unresectable patients. In this study, 53 patients were converted to resectable with a combination of folinic acid, leucovorin, and oxaliplatin. The most encouraging was that the long-term outcomes of these initially unresectable patients were similar to those patients who were found to be resectable on presentation [66, 67]. Since this initial report, several other series have described FOLFOX as well as other regimens for such downstaging of disease [14, 67–70] (Fig. 28.2 and Table 28.3). Even more impressive is the potential of regional chemotherapy for converting unresectable patients to resectable. Clavien et al. demonstrated a conversion rate of nearly 30 % for regional hepatic arterial infusion (HAI) FUDR [68], while Kemeny reported a rate of over 50 % for a regimen combining HAI FUDR with systemic FOLFOX [69].

Current data indicate that modern chemotherapeutic regimens can downstage 15–50 % of patients to resectable. Issues that remain under

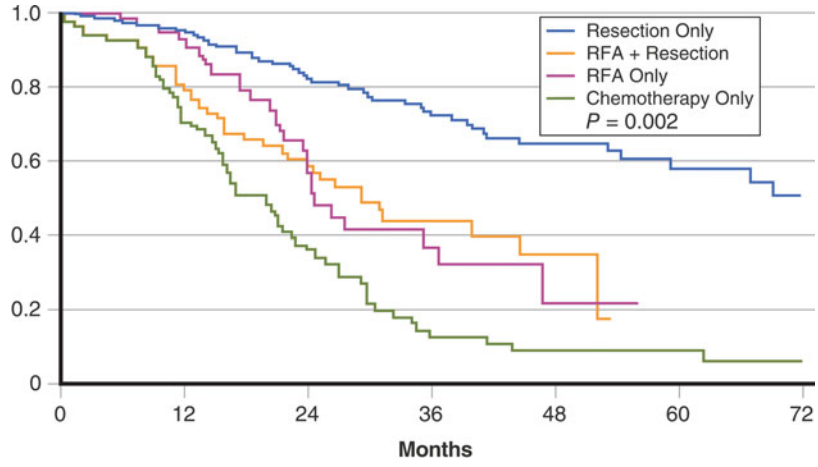

Fig. 28.2 Results of patients treated by combined resection and ablation (Adapted from Abdalla et al. [60]. Patients treated by RFA were deemed not completely resectable. Numbers of patients: resection, 190; RFA + resection, 101; RFA, 57; chemotherapy, 70)

Table 28.3 Results of downstaging chemotherapy

Year and journal	Author	n	Chemotherapeutic agent	N (%) converted to resectable	5-year survival
1996 *Ann Surg*	Bismuth, H. et al. [66]	330	5-FU	53 (16 %)	OS, 40 %
			Leucovorin		
			Oxaliplatin		DFS, 36 %
2001 *Ann Surg Oncol*	Adam, R. et al. [14]	701	5-FU	95 (13.5 %)	OS, 35–60 % large tumors, 49 % ill-located, 34 % multinodular disease 18 % extrahepatic disease + resected liver mets
			Leucovorin		
			Oxaliplatin		DFS, 22 %
2002 *Surgery*	Clavien, P.A. et al. [68]	23	Floxuridine[a]	6 (26 %)	–
2004 *Ann Surg*	Adam, R. et al. [67]	1,104	5-FU + oxaliplatin (70 %)	138 (12.5 %)	OS, 33 %
			5-FU + irinotecan (7 %)		
			5-FU + both (4 %)		DFS, 22 %
2009 *J Clin Oncol*	Kemeny, N. et al. [69]	49	Floxuridine[a]	23 (47 %)	(Median f/u 26 m)
			Oxaliplatin		Median OS, 39.8 m
			Irinotecan		
2005 *J Clin Oncol*	Alberts, S.R. et al. [70]	42	5-FU	17 (40 %)	(Median f/u 22 m)
			Leucovorin		Median OS (all pts), 26 m
			Oxaliplatin		
			(FOLFOX4)		
2007 *J Br Canc*	Barone, C. [74]	40	5-FU Leucovorin	19 (47.5 %)	Last f/u (5 year) OS, 62 %
			Irinotecan		DFS, 46 %

5-FU fluorouracil, *DFS* disease-free survival, *f/u* follow-up, *mets* metastases, *pts* patients, *OS* overall survival
[a]Administered via hepatic arterial infusion (HAI)

debate are the optimal time period that ought to elapse while on downstaging therapy and the ideal chemotherapy regimen. The two competing approaches are resection as soon as lesions become resectable, while others waiver between a waiting for a period of time for maximum response (usually 4 months) and first or subsequent progression (usually 9 months).

Not All Patients Require Preoperative Chemotherapy

Based on the favorable data for use of chemotherapy to downstage patients with unresectable disease (downstaging strategy), many authors have also promoted the use of preoperative chemotherapy in initially resectable disease (neoadjuvant strategy). Advocates of the neoadjuvant approach note that the EORTC demonstrated a survival advantage for perioperative chemotherapy. However, they neglect to acknowledge that this trial did not have an arm with only postoperative chemotherapy [63]. They also note several other theoretical advantages, including the following: (1) A potential that allows in vivo chemosensitivity determination by observing for response of tumors still unresected. (2) The additional time allows distant disease to present itself – demonstrating disease that is not resectable for cure. (3) The preoperative chemotherapy may address microscopic undetectable disease earlier. (4) Chemotherapy after recent colectomy may allow patients a time interval to recover prior to undergoing liver resection.

Of these, only the last argument has proven applicable clinically. To address the question of assessing chemosensitivity, 72 % of patients respond to cetuximab and FOLFOX chemotherapy as first-line therapy, and another 23 % may have stable disease [71]. Therefore, it is unusual for patients to progress (5 %). In another study, this was again demonstrated that with perioperative chemotherapy, there was only 7 % progression of disease [63]. In this study, the interval during chemotherapy only identified 2 % of patients progressing such that they were not resectable [63]. Therefore, the concept of "in vivo" chemosensitivity is only reasonable in the context of failure after first-line therapy.

It has now been recognized that that the use of preoperative chemotherapy may potentially negatively affect the normal liver parenchyma. Chemotherapy-associated steatohepatitis (CASH) presents as hepatic steatosis, splenomegaly, and thrombocytopenia [72]. This syndrome is a function of liver damage and yields some portal hypertension. There is also some growing evidence that the existence of CASH may have effects on complications and postoperative recovery after liver resection [73]. As there are no definitive trials of neoadjuvant chemotherapy demonstrating a clear advantage and with considerable morbidity, this approach should not be considered as the standard of care.

Algorithms of Care

Figure 28.3 presents an algorithm in the approach to managing patients with synchronous liver metastases. If the primary colorectal cancer has already been resected, a delay in hepatectomy for synchronous secondaries may be reasonable in order to recover from the primary resection or if the patients have comorbidities that require medical optimization. If the patient has synchronous primary and liver metastasis that can be safely addressed concurrently, a combined resection is justified [35].

In patients presenting with metachronous metastases, preoperative chemotherapy is only currently justified if disease is borderline resectable or unresectable based on technical or medical issues (Fig. 28.4). The majority of patients should therefore have resection followed by adjuvant chemotherapy except in the context of a trial.

Patterns of Recurrence

The management of patients with hepatic colorectal metastases has produced prolonged survival even in patients who are not necessarily cured. Although the patterns of initial recurrence

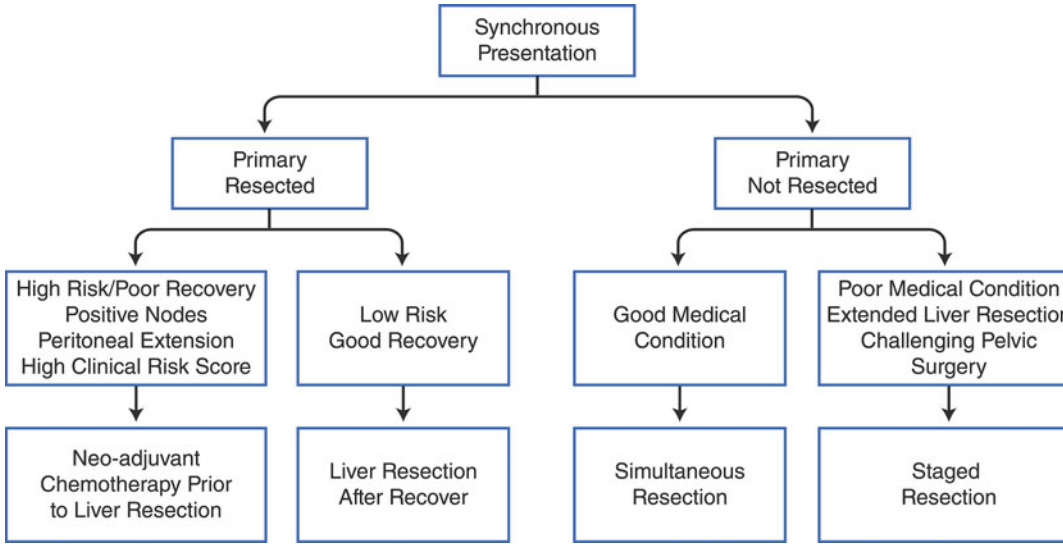

Fig. 28.3 Algorithm of treatment for patients with resectable synchronous hepatic colorectal metastases. Resection and resectable denotes completely cytoreduction by resection, ablation, or combination of both

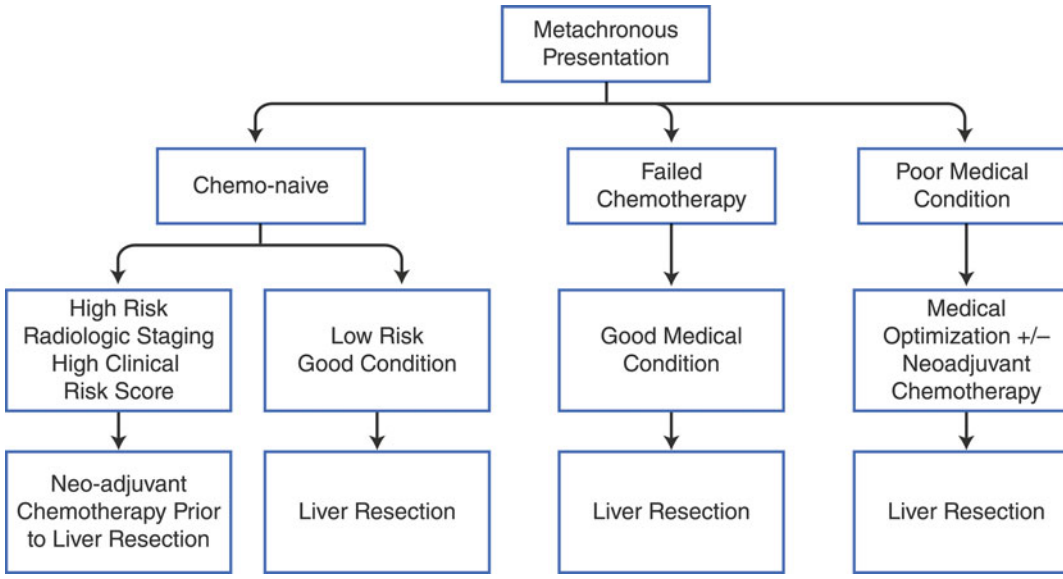

Fig. 28.4 Algorithm of treatment for patients with resectable metachronous hepatic colorectal metastases. Resection and resectable denotes completely cytoreduction by resection, ablation, or combination of both

have been well described, the subsequent history of patients was not well understood until recently. Identifying and describing the patterns of further recurrences highlights locations of additional, residual disease that require treatment targeting and long-term surveillance. In a series of 275 patients followed at a single institution after hepatectomy for colorectal cancer liver metastases

Table 28.4 Sites of recurrences after liver resection. Series of 275 patients subjected to hepatectomy with curative intent for colorectal metastases followed until death with recurrence documented up to five recurrences. The data is the cumulative recurrence by site. Data indicates that 206 patients (75 %) eventually recur within the liver

	Liver	Lung	Anastomosis	Abdominal	Bone	Brain	Others
Total n	206	189	14	170	61	37	54
% of patients	75	68	5	62	22	13	20
% of all recurrences	28	26	2	23	8	5	7

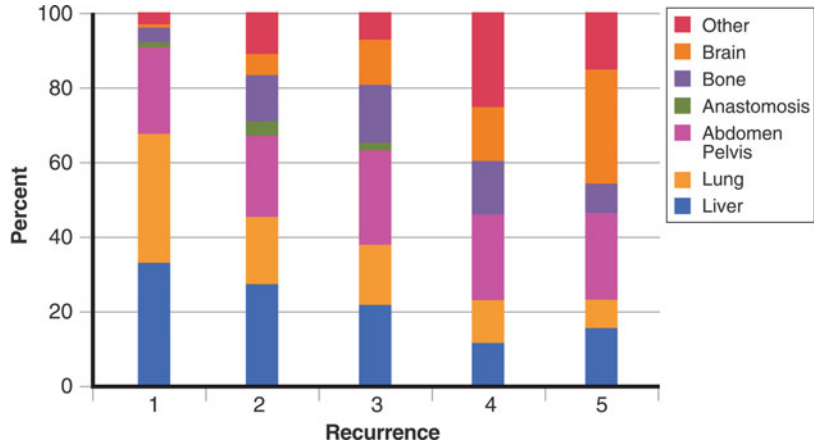

Fig. 28.5 Patterns of recurrence after resection of hepatic colorectal metastases (Data from 275 patients followed until death. Cumulative data in Table 28.4)

until death, we reviewed the patterns of disease progression. A total of 731 sites of recurrences were identified. Median time to 1st recurrence was 16 ± 1 months and to the 2nd, 3rd, 4th, and 5th recurrences were 31 ± 2, 42 ± 3, 48 ± 4, and 54 ± 9 months, respectively.

The majority (75 %) of patients eventually recur in the liver, and two-thirds in the lungs (Table 28.4). Figure 28.5 delineates the patterns of recurrence through the fifth recurrence and illustrates recurrence sites typically late in the disease course including brain and others (e.g., mediastinum). There are some sites that have traditionally been thought to be rare for recurrence. However, this is more likely due to poor documentation of late sites of recurrence. Twenty-two percent of patients eventually present with bone and 13 % brain metastases (Table 28.4). Although the liver is the initial solitary site of clinical presentation with colorectal metastases, systemic dissemination has already occurred in the majority of patients. Thus, two facts are clear. Control of liver disease can provide for long-term survival in patients with metastatic colorectal cancer. Most patients also recur in extrahepatic sites. Thus, treatment strategies directed at local liver disease combined with regional and systemic adjuvant therapy provide the best chance to increase survival and cure.

Cross-References

- ▶ Embolic Therapies
- ▶ Microwave Ablation for Cancer: Physics, Performance, Innovation, and the Future
- ▶ Microwave in the Treatment of Primary Liver Cancers
- ▶ Radiofrequency Ablation of Hepatic Metastasis
- ▶ Tumor Ablation: An Evolving Technology

References

1. Steele GJ, Ravikumar TS. Resection of hepatic metastases from colorectal cancer: biologic perspectives. Ann Surg. 1989;210(2):127–38.
2. Scheele J, Stangl R, Altendorf-Hofmann A, Gall FP. Indicators of prognosis after hepatic resection for colorectal secondaries. Surgery. 1991;110:13–29.
3. Nordlinger B, Guiguet M, Vaillant JC, Balladur P, Boudjema K, Bachellier P, et al. Surgical resection of colorectal carcinoma metastases to the liver. A prognostic scoring system to improve case selection, based on 1568 patients. Association Francaise de Chirurgie. Cancer. 1996;77(7):1254–62.
4. House MG, Ito H, Gonen M, Fong Y, Allen PJ, DeMatteo RP, et al. Survival after hepatic resection for metastatic colorectal cancer: trends in outcomes for 1,600 patients during two decades at a single institution. J Am Coll Surg. 2010;210(5):744–5.
5. Fong Y, Fortner J, Sun RL, Brennan MF, Blumgart LH. Clinical score for predicting recurrence after hepatic resection for metastatic colorectal cancer: analysis of 1001 consecutive cases. Ann Surg. 1999;230(3):309–18.
6. Ekberg H, Tranberg KG, Andersson R, Lundstedt C, Hagerstrand I, Ranstam J, et al. Pattern of recurrence in liver resection for colorectal secondaries. World J Surg. 1987;11:541–7.
7. Bozzetti F, Bignami P, Morabito A, Doci R, Gennari L. Patterns of failure following surgical resection of colorectal cancer liver metastases. Ann Surg. 1987;205:264–70.
8. Picardo A, Karpoff HM, Ng B, Lee J, Brennan MF, Fong Y. Partial hepatectomy accelerates local tumor growth: potential roles of local cytokine activation. Surgery. 1998;124(1):57–64.
9. Scheele J, Stang R, Altendorf-Hofmann A, Paul M. Resection of colorectal liver metastases. World J Surg. 1995;19:59–71.
10. Tomlinson JS, Jarnagin WR, DeMatteo RP, Fong Y, Kornprat P, Gonen M, et al. Actual 10-year survival after resection of colorectal liver metastases defines cure. J Clin Oncol. 2007;25(29):4575–80.
11. Saltz LB, Cox JV, Blanke C, Rosen LS, Fehrenbacher L, Moore MJ, et al. Irinotecan plus fluorouracil and leucovorin for metastatic colorectal cancer. Irinotecan Study Group. N Engl J Med. 2000;343(13):905–14.
12. Saltz LB, Clarke S, az-Rubio E, Scheithauer W, Figer A, Wong R. Bevacizumab in combination with oxaliplatin-based chemotherapy as first-line therapy in metastatic colorectal cancer: a randomized phase III study. J Clin Oncol. 2008; 26(12):2013–9.
13. Fernandez FG, Drebin JA, Linehan DC, Dehdashti F, Siegel BA, Strasberg SM. Five-year survival after resection of hepatic metastases from colorectal cancer in patients screened by positron emission tomography with F-18 fluorodeoxyglucose (FDG-PET). Ann Surg. 2004;240(3):438–47.
14. Adam R, Avisar E, Ariche A, Giachetti S, Azoulay D, Castaing D, et al. Five-year survival following hepatic resection after neoadjuvant therapy for nonresectable colorectal [liver] metastases. Ann Surg Oncol. 2001;8(4):347–53.
15. Kato T, Yasui K, Hirai T, Kanemitsu Y, Mori T, Sugihara K, et al. Therapeutic results for hepatic metastasis of colorectal cancer with special reference to effectiveness of hepatectomy: analysis of prognostic factors for 763 cases recorded at 18 institutions. Dis Colon Rectum. 2003;46(10 Suppl):S22–31.
16. Choti MA, Sitzmann JV, Tiburi MF, Sumetchotimetha W, Rangsin R, Schulick RD, et al. Trends in long-term survival following liver resection for hepatic colorectal metastases. Ann Surg. 2002;235(6):759–66.
17. Minagawa M, Makuuchi M, Torzilli G, Takayama T, Kawasaki S, Kosuge T, et al. Extension of the frontiers of surgical indications in the treatment of liver metastases from colorectal cancer: long-term results. Ann Surg. 2000;231(4):487–99.
18. Jamison RL, Donohue JH, Nagorney DM, Rosen CB, Harmsen WS, Ilstrup DM. Hepatic resection for metastatic colorectal cancer results in cure for some patients. Arch Surg. 1997;132:505–11.
19. Gayowski TJ, Iwatsuki S, Madariaga JR, Selby R, Todo S, Irish W, et al. Experience in hepatic resection for metastatic colorectal cancer: analysis of clinical and pathological risk factors. Surgery. 1994;116:703–11.
20. Hughes KS, Simon R, Songhorabodi S, Adson MA, Ilstrup DM, Fortner JG, et al. Resection of the liver for colorectal carcinoma metastases: a multi-institutional study of patterns of recurrence. Surgery. 1986; 100:278–84.
21. Fortner JG, Fong Y. Twenty-five year follow-up for liver resection: the personal series of Dr. Joseph G. Fortner. Ann Surg. 2009;250:908–13.
22. Fong Y, Gonen M, Rubin D, Radzyner D, Brennan MF. Long-term survival is superior after resection for cancer in high volume centers. Ann Surg. 2005;242(4):540–7.
23. Fong Y, Blumgart LH, Fortner JG, Brennan MF. Pancreatic or liver resection for malignancy is safe and effective in the elderly. Ann Surg. 1995;222(4): 426–37.
24. Weber SM, Jarnagin WR, DeMatteo RP, Blumgart LH, Fong Y. Survival after resection of multiple hepatic colorectal metastases. Ann Surg Oncol. 2000;7(9):643–50.
25. Hughes K, Scheele J, Sugarbaker PH. Surgery for colorectal cancer metastatic to the liver. Surg Clin North Am. 1989;69:339–59.
26. Ballantyne GH, Quin J. Surgical treatment of liver metastases in patients with colorectal cancer. Cancer. 1993;71(S12):4252–66.
27. Rosen CB, Nagorney DM, Taswell HF, Helgeson SL, Ilstrup DM, Van Heerden JA, et al. Perioperative blood transfusion and determinants of survival after

liver resection for metastatic colorectal carcinoma. Ann Surg. 1992;216:492–505.
28. Stephenson KR, Steinberg SM, Hughes KS, Vetto JT, Sugarbaker PH, Chang AE. Perioperative blood transfusions are associated with decreased time to recurrence and decreased survival after resection of colorectal liver metastases. Ann Surg. 1988; 208:679–87.
29. Mala T, Bohler G, Mathisen O, Bergan A, Soreide O. Hepatic resection for colorectal metastases: can preoperative scoring predict patient outcome? World J Surg. 2002;26(11):1348–53.
30. Arru M, Aldrighetti L, Castoldi R, Di PS, Orsenigo E, Stella M, et al. Analysis of prognostic factors influencing long-term survival after hepatic resection for metastatic colorectal cancer. World J Surg. 2008;32(1):93–103.
31. Chen YY, Perera DS, Yan TD, Schmidt LM, Morris DL. Applying Fong's CRS score in patients with colorectal liver metastases treated by cryotherapy. Asian J Surg. 2006;29:238–41.
32. Schussler-Fiorenza CM, Mahvi DM, Niederhuber J, Rikkers LF, Weber SM. Clinical risk score correlates with yield of PET scan in patients with colorectal hepatic metastases. J Gastrointest Surg. 2004;8(2): 150–7.
33. Jarnagin WR, Conlon K, Bodniewicz J, Dougherty E, DeMatteo RP, Blumgart LH, et al. A clinical scoring system predicts the yield of diagnostic laparoscopy in patients with potentially resectable hepatic colorectal metastases. Cancer. 2001;91(6):1121–8.
34. Bolton JS, Fuhrman GM. Survival after resection of multiple bilobar hepatic metastases from colorectal carcinoma. Ann Surg. 2000;231(5):743–51.
35. Martin R, Paty P, Fong Y, Grace A, Cohen A, DeMatteo R, et al. Simultaneous liver and colorectal resections are safe for synchronous colorectal liver metastasis. J Am Coll Surg. 2003;197(2):233–41.
36. Reddy S, Zorzi D, Lum YW, Barbas A, Pawlik T, Ribero D, et al. Timing of multimodality therapy for resectable synchronous colorectal liver metastases: a retrospective multi-institutional analysis. Ann Surg Oncol. 2009;16(7):1809–19.
37. Martin RC, Augenstein V, Reuter NP, Scoggins CR, McMasters KM. Simultaneous versus staged resection for synchronous colorectal cancer liver metastases. J Am Coll Surg. 2009;208(5):842–50.
38. Mala T. Cryoablation of liver tumours – a review of mechanisms, techniques and clinical outcome. Minim Invasive Ther Allied Technol. 2006;15(1):9–17.
39. Decadt B, Siriwardena AK. Radiofrequency ablation of liver tumours: systematic review. Lancet Oncol. 2004;5(9):550–60.
40. Martin RC, Scoggins CR, McMasters KM. Safety and efficacy of microwave ablation of hepatic tumors: a prospective review of a 5-year experience. Ann Surg Oncol. 2009;17(1):171–8.
41. Wong SL, Mangu PB, Choti MA, Crocenzi TS, Dodd III GD, Dorfman GS, et al. American society of clinical oncology 2009 clinical evidence review on radiofrequency ablation of hepatic metastases from colorectal cancer. J Clin Oncol. 2009;28(3): 493–508.
42. Livraghi T, Solbiati L, Meloni MF, Gazelle GS, Halpern EF, Goldberg SN. Treatment of focal liver tumors with percutaneous radio-frequency ablation: complications encountered in a multicenter study. Radiology. 2003;226(2):441–51.
43. Chen MS, Li JQ, Zheng Y, Guo RP, Liang HH, Zhang YQ, et al. A prospective randomized trial comparing percutaneous local ablative therapy and partial hepatectomy for small hepatocellular carcinoma. Ann Surg. 2006;243(3):321–8.
44. Berber E, Siperstein A. Local recurrence after laparoscopic radiofrequency ablation of liver tumors: an analysis of 1032 tumors. Ann Surg Oncol. 2008;15(10):2757–64.
45. Curley SA. Radiofrequency ablation of malignant liver tumors. Ann Surg Oncol. 2003;10(4):338–47.
46. Siperstein AE, Berber E, Ballem N, Parikh RT. Survival after radiofrequency ablation of colorectal liver metastases: 10-year experience. Ann Surg. 2007; 246(4):559–65.
47. Berber E, Tsinberg M, Tellioglu G, Simpfendorfer CH, Siperstein AE. Resection versus laparoscopic radiofrequency thermal ablation of solitary colorectal liver metastasis. J Gastrointest Surg. 2008; 12(11):1967–72.
48. Maeda T, Hasebe Y, Hanawa S, Watanabe M, Nakazaki H, Kuramoto S, et al. Trial of percutaneous hepatic cryotherapy: preliminary report. Nippon Geka Gakkai Zasshi – J Jpn Surg Soc. 1992;93:666.
49. Hohenberger P, Schlag P, Schwarz V, Herfarth C. Tumor recurrence and options for further treatment after resection of liver metastases in patients with colorectal cancer. J Surg Oncol. 1990;44:245–51.
50. Nordlinger B, Parc R, Delva E, Quilichini M, Hannoun L, Huguet C. Hepatic resection for colorectal liver metastases. Ann Surg. 1987;205:256–63.
51. Butler J, Attiyeh FF, Daly JM. Hepatic resection for metastases of the colon and rectum. Surg Gynecol Obstet. 1986;162:109–13.
52. Griffith KD, Sugarbaker PH, Chang AE. Repeat hepatic resections for colorectal metastases. Br J Surg. 1990;77:230–3.
53. Fortner JG. Recurrence of colorectal cancer after hepatic resection. Am J Surg. 1988;155:378–82.
54. Lange JF, Leese T, Castaing D, Bismuth H. Repeat hepatectomy for recurrent malignant tumors of the liver. Surg Gynecol Obstet. 1989;169:119–26.
55. Pastana C, Reitmeier RJ, Moertel CG, et al. The natural history of carcinoma of the colon and rectum. Am J Surg. 1964;108:826–9.
56. Wagner JS, Adson MA, Van Heerden JA, et al. The natural history of hepatic metastases from colorectal cancers. Arch Surg. 1976;111:330–4.
57. Scheele J, Strangl R, Altendor-Hofman A. Hepatic metastases from colorectal carcinoma: impact of

surgical resection on natural history. Br J Surg. 1990;77:1241–6.
58. Rivoire M, De CF, Meeus P, Negrier S, Sebban H, Kaemmerlen P. Combination of neoadjuvant chemotherapy with cryotherapy and surgical resection for the treatment of unresectable liver metastases from colorectal carcinoma. Cancer. 2002;95(11):2283–92.
59. Pawlik TM, Izzo F, Cohen DS, Morris JS, Curley SA. Combined resection and radiofrequency ablation for advanced hepatic malignancies: results in 172 patients. Ann Surg Oncol. 2003;10(9):1059–69.
60. Abdalla EK, Vauthey JN, Ellis LM, Ellis V, Pollock R, Broglio KR, et al. Recurrence and outcomes following hepatic resection, radiofrequency ablation, and combined resection/ablation for colorectal liver metastases. Ann Surg. 2004;239(6):818–25.
61. Portier G, Elias D, Bouche O, Rougier P, Bosset JF, Saric J, et al. Multicenter randomized trial of adjuvant fluorouracil and folinic acid compared with surgery alone after resection of colorectal liver metastases: FFCD ACHBTH AURC 9002 trial. J Clin Oncol. 2006;24(31):4976–82.
62. Park R, Gonen M, Kemeny N, Jarnagin W, D'Angelica M, DeMatteo R, et al. Adjuvant chemotherapy improves survival after resection of hepatic colorectal metastases: analysis of data from two continents. J Am Coll Surg. 2007;204:753–61.
63. Nordlinger B, Sorbye H, Glimelius B, Poston GJ, Schlag PM, Rougier P, et al. Perioperative chemotherapy with FOLFOX4 and surgery versus surgery alone for resectable liver metastases from colorectal cancer (EORTC Intergroup trial 40983): a randomised controlled trial. Lancet. 2008;371(9617):1007–16.
64. Kemeny MM, Adak S, Lipsitz S, MacDonald J, Benson AB. Results of the intergroup [Eastern Cooperative Oncology Group (ECOG) and Southwest Oncology Group (SWOG)] prospective randomized study of surgery alone versus continuous hepatic artery infusion of FUDR and continuous systemic infusion of 5FU after hepatic resection for colorectal metastases. Proc Am Soc Clin Oncol. 1999;18:264a. Abstract.
65. Bozzetti F, Bignami P, Montalto F, Doci R, Gennari L. Repeated hepatic resection for recurrent metastases from colorectal cancer. Br J Surg. 1992;79(2):146–8.
66. Bismuth H, Adam R, Levi F, Farabos C, Waechter F, Castaing D, et al. Resection of nonresectable liver metastases from colorectal cancer after neoadjuvant chemotherapy. Ann Surg. 1996;224(4):509–20.
67. Adam R, Delvart V, Pascal G, Valeanu A, Castaing D, Azoulay D, et al. Rescue surgery for unresectable colorectal liver metastases downstaged by chemotherapy: a model to predict long-term survival. Ann Surg. 2004;240(4):644–57.
68. Clavien PA, Selzner N, Morse M, Selzner M, Paulson E. Downstaging of hepatocellular carcinoma and liver metastases from colorectal cancer by selective intra-arterial chemotherapy. Surgery. 2002; 131(4):433–42.
69. Kemeny NE, Huitzil Melendez FD, Capanu M, Paty PB, Fong Y, Schwartz LH. Conversion to resectability using hepatic artery infusion plus systemic chemotherapy for the treatment of unresectable liver metastases from colorectal carcinoma. J Clin Oncol. 2009;27(21):3465–71.
70. Alberts SR, Horvath WL, Sternfeld WC, Goldberg RM, Mahoney MR, Dakhil SR, et al. Oxaliplatin, fluorouracil, and leucovorin for patients with unresectable liver-only metastases from colorectal cancer: a North Central Cancer Treatment Group phase II study. J Clin Oncol. 2005;23(36):9243–9.
71. Tabernero J, Van CE, az-Rubio E, Cervantes A, Humblet Y, Andre T, et al. Phase II trial of cetuximab in combination with fluorouracil, leucovorin, and oxaliplatin in the first-line treatment of metastatic colorectal cancer. J Clin Oncol. 2007;25(33):5225–32.
72. Fong Y, Bentrem DJ. CASH (chemotherapy-associated steatohepatitis) costs. Ann Surg. 2006;243(1):8–9.
73. Khan AZ, Morris-Stiff G, Makuuchi M. Patterns of chemotherapy-induced hepatic injury and their implications for patients undergoing liver resection for colorectal liver metastases. J Hepatobiliary Pancreat Surg. 2009;16(2):137–44
74. Barone C, Nuzzo G, Cassano A, Basso M, Schinzari G, Giuliante F, et al. Final analysis of colorectal cancer patients treated with irinotecan and 5-fluorouracil plus folinic acid neoadjuvant chemotherapy for unresectable liver metastases. Br J Cancer. 2007; 97(8):1035–9.

Y-90 Radiomicrosphere Therapy of Colorectal Cancer: Liver Metastases

29

Seza A. Gulec and Tushar C. Barot

Abstract

Our objective is to discuss the basic concepts involved in the development of yttrium-90 (Y-90) microsphere selective internal radiation treatment (SIRT) and review the clinical data pertaining to its application in hepatic colorectal cancer metastases. Selective internal radiation treatment is a promising new modality in the treatment of patients with hepatic colorectal cancer metastases as part of a multimodality approach. A chemoselective internal radiation treatment neoadjuvant approach has the potential to improve therapeutic outcomes. Clinical studies in neoadjuvant and salvage settings are needed for more concrete outcome data and design of optimal multimodality treatment strategies. This chapter will discuss the principles of Y-90 therapy, pretreatment evaluation of patients including various imaging techniques, treatment technique studies, and potential complications of radiomicrosphere therapy. It will also review studies previously done in the field of radiomicrosphere therapy.

Principles of Y-90 Radiomicrosphere Therapy

Y-90 radiomicrosphere treatment (RMT) refers to intrahepatic arterial administration of Y-90 radiomicrospheres. Yttrium-90 (Y-90) is a high-energy beta particle radiating radioisotope. It is incorporated in biocompatible microspheres measuring 30–40 μm. The intellectual basis of Y-90 RMT is the preferential distribution of microspheres, when injected intra-arterially into the liver, yielding much higher concentrations in the tumor compartment than the normal liver parenchyma. This selectivity is due to the fact that the tumor blood supply is overwhelmingly derived from the hepatic artery since the neovasculature of angiogenesis is rooted from the hepatic artery branches. Intrahepatic arterially administered Y-90 microspheres are entrapped in the microvasculature and release beta radiation (energy maximum, 2.27 MeV; mean, 0.9367 MeV) with an average penetration range of 2.5 mm and a maximum range of 11 mm

S.A. Gulec (✉)
Department of Surgical Oncology, The Herbert Wertheim College of Medicine Florida International University, Miami, FL, USA
e-mail: sgulec@fiu.edu

T.C. Barot
Mount Sinai Medical Center, Miami Beach, FL, USA
e-mail: tcbarot@gmail.com

D.E. Dupuy et al. (eds.), *Image-Guided Cancer Therapy*, DOI 10.1007/978-1-4419-0751-6_31,

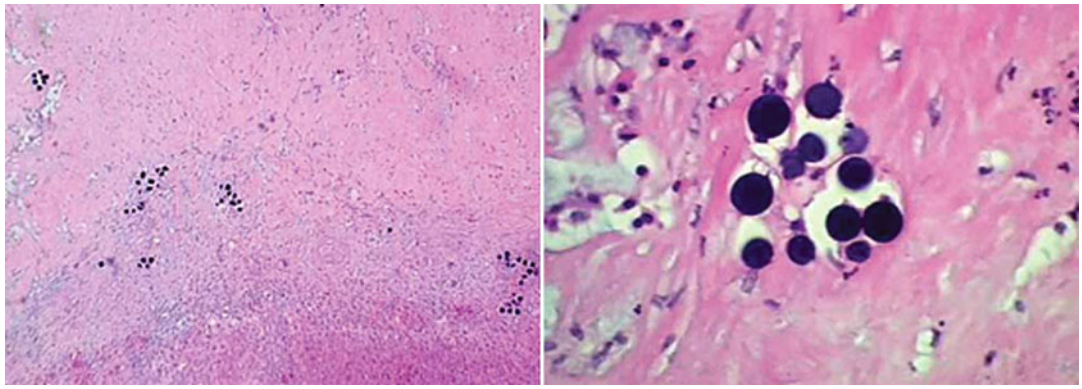

Fig. 29.1 Clustered microspheres lodged in precapillary arterioles. The surrounding tissue exposed to beta radiation is necrotic

in tissue. Y-90 has a physical half-life of 64.2 h (2.67 days). In therapeutic use, 94 % of the radiation is delivered over 11 days. The high tumor-to-liver concentration ratio of Y-90 radiomicrospheres results in an effective tumoricidal radiation absorbed dose while limiting the radiation injury to the normal liver (Fig. 29.1).

There are currently two commercially available Y-90 radiomicrosphere products: glass microspheres (TheraSphere; MDS Nordion, Ottawa, Ontario, Canada) and resin microspheres (SIR-Spheres; Sirtex Medical, Sydney, Australia). Both microspheres have relatively consistent size ranging from 20 to 40 μm, and neither is metabolized or excreted but remains in the liver permanently. The main differences are in the density (g/cc) and specific activity (activity/sphere). The glass microspheres are three times heavier per volume and carry 50 times more activity per weight than resin microspheres.

Pretreatment Evaluation

Evaluation of Liver Function/Reserve

Liver reserve might be and often is affected due to neoplastic replacement and prior hepatotoxic treatments. ALT/AST and alkaline phosphatase/GGT are the markers for acute and subacute hepatocellular and biliocanalicular injury, respectively. More difficult to evaluate is the real "functional volume" in the anatomically intact appearing liver region(s). Bilirubin is a composite marker of liver reserve and has been widely used in many classification systems as a predictive measure. A bilirubin level above 2 mg/dl in the absence of correctable obstructive etiology precludes RMT. Contraindications to the radiomicrosphere therapy are shown in Table 29.1.

Multiphase Liver Scan

Currently, the optimal imaging protocol for Y-90 radiomicrosphere work-up is combined FDG-PET and contrast-enhanced CT. A comprehensive protocol includes FDG-PET/CT where FDG serves as a "metabolic contrast" and a three-phase (arterial, portal, equilibrium phases) contrast-enhanced CT.

Angiography

Angiography is of paramount importance in the planning and administration of RMT. All patients undergo a standard mesenteric angiography, which involves an abdominal aortogram, a superior mesenteric angiogram, and a celiac angiogram followed by a common hepatic angiogram. This initial step allows assessment of first- and second-order anatomy and variations. The second step of angiography involves

Table 29.1 Contraindications to the radiomicrosphere therapy

Contraindication	Comment
Clinical liver failure	Absolute contraindication
Markedly abnormal synthetic and excretory liver function tests; bilirubin >2 mg/dl	Unless abnormalities are due to correctible biliary obstruction
Greater than 20 % lung shunting of the hepatic artery blood flow determined by Tc-99 m MAA scan	For lesser degree shunting, a dose reduction could be considered
Gastrointestinal uptake on Tc-99 m MAA scan	Requires careful review of diagnostic angiogram searching for the criminal vessel(s). May proceed if the vessel is found and coil embolized
Pre-assessment angiogram that demonstrates vascular anatomy that would result in significant reflux of hepatic arterial blood to the GI tract	If coil embolization of these branches are technically not possible or have failed
Portal vein thrombosis	Not an absolute contraindication. More important factor is the associated liver dysfunction
Previous radiation therapy to the liver	Relative contraindication. Previous target, total dose should be evaluated
Extensive extrahepatic malignant disease	Relative contraindication

selective catheterization of left and right hepatic branches. The assessment of segmental blood flow and third-order vascular anatomy is then performed with identification of smaller GI branches such as falciform, phrenic, right, or accessory gastric arteries and supraduodenal, retroduodenal, retroportal, and cystic arteries. An aggressive prophylactic embolization of vessels before therapy is highly recommended, such that any and all hepaticoenteric arterial communications are completely disconnected (Fig. 29.2). The flux of Y-90 radiomicrospheres into unrecognized collateral vessels results in clinical toxicities if proper angiographic protocols are not followed. These might include gastrointestinal ulceration, pancreatitis, cholecystitis, esophagitis, and skin irritation.

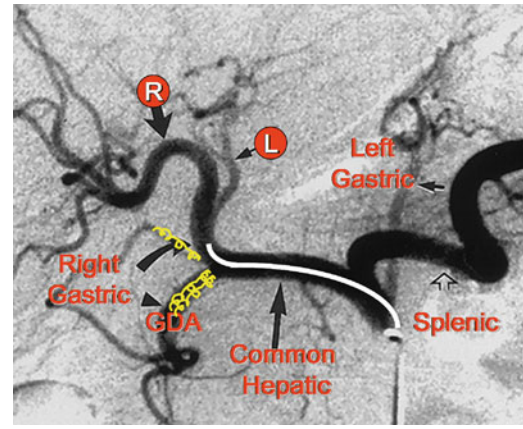

Fig. 29.2 Hepatic angiogram performed prior to Y-90 microsphere treatment. Gastroduodenal artery and right gastric artery are coiled to prevent reflux into the GI tract. Other identifiable GI branches are also coiled if their takeoff is close to the planned administration site of Y-90 microspheres

Tc-99 m MAA Hepatic Scintigraphy

Macroaggregate albumin (MAA) is a particulate form of albumin with an average size of 20–40 μm. Its density is close to that of resin microspheres, and the number of particles per unit volume can be adjusted to a desirable range. Labeled with Tc-99 m, MAA constitutes a reasonable surrogate diagnostic radiopharmaceutical to simulate Y-90 radiomicrosphere distribution when injected in the hepatic artery. Tc-99 m MAA is injected via the hepatic arterial catheter at the completion of the visceral angiography. Shortly after the administration, anterior-posterior planar images of chest and abdomen and SPECT images of liver are obtained. There are three objectives of Tc-99 m MAA study. First and foremost is the detection and quantitation of intrahepatic shunting that would result in escape of radioactive particles to the lungs. Hepatocellular carcinoma and hypervascular metastases may be associated with intrahepatic arteriovenous shunting. Fortunately, the incidence and degree of shunt is less than 5 % with no shunting occurring in the majority of patients. Shunt fraction is determined by ROI analysis on Tc-99 m MAA planar images (Fig. 29.3). The second objective of Tc-99 m MAA imaging is the

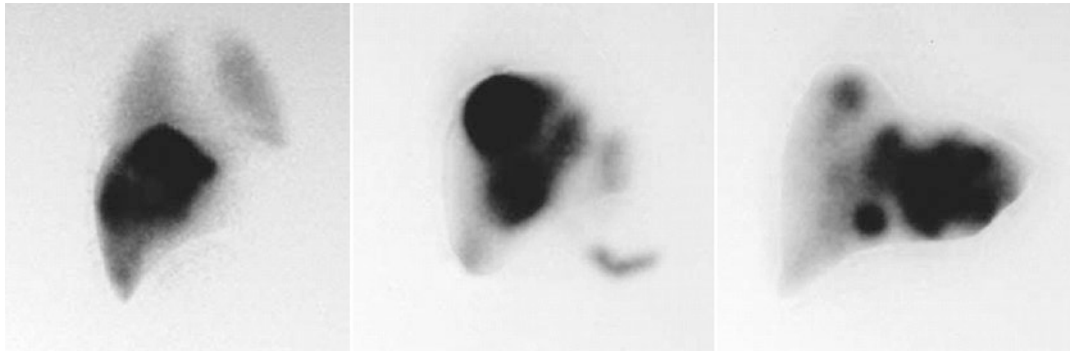

Fig. 29.3 Tc-99 m MAA planar image. The radiopharmaceutical was injected in the right lobe. The image shows distribution in the right lobe of the liver and bilateral pulmonary activity due to intrahepatic shunting. The shunt fraction is calculated using planar images obtaining counts over the lung fields and total counts (shunt fraction = lung counts/total counts). Planar images also demonstrate extrahepatic gastrointestinal activity if GI reflux occurs (not present in this case)

identification of extrahepatic GI uptake which might be caused by an unrecognized hepatofugal vascular runoff. This finding, depending on its size, might preclude further treatment with Y-90 radiomicrospheres unless a safe interventional plan for prevention of extrahepatic flux can be made. The third use of Tc-99 m MAA hepatic scintigraphy is the determination of blood flow ratio between the tumor and normal hepatic parenchyma, which is the major determinant of degree of "selectivity" of RMT.

Treatment Technique

The administration of the Y-90 radiomicrospheres is performed in an angiography suite. The catheter is usually placed in a position determined by the choice of the treatment mode (whole liver, lobar, or segmental). Both Y-90 radiomicrosphere products have their own dedicated apparatus designed to facilitate the administration. Because the resin microspheres have much higher number of microspheres per unit dose, there is an embolic tendency, especially toward the last stages of the administration which is performed in a manually controlled manner with angio-fluoroscopic guidance. Observation of increasing reflux is a sign of increased risk for hepatofugal flux; therefore, this might be an indication to discontinue the administration. Strict adherence to radiation safety guidelines is critically important in patient and personnel safety.

Y-90 radiomicrosphere treatment usually is an outpatient treatment. Patients who experience moderate embolic syndrome could be admitted for under 24 h. Symptomatic treatment might be indicated for pain or nausea. Routine prophylactic use of antibiotics, proton pump inhibitors, or steroids is not indicated. Patients are provided with radiation safety instructions upon discharge.

Complications of RMT

In approximately one-third of patients, administration of RMT causes mild short-term abdominal pain requiring narcotic analgesia. This side effect is more common with increasing number of microspheres administered. Post-RMT treatment lethargy is also common; symptoms can last up to 10 days and may require medication. Most patients develop a mild fever for several days following RMT administration that does not require treatment. Distant organs are not subjected to beta radiation due to the short range of beta particles. Radiation doses to the gonads are unlikely, given the distance from the liver and very short range of beta particles of Y-90. The most serious complications are gastric/duodenal ulcer resulting from reflux of Y-90

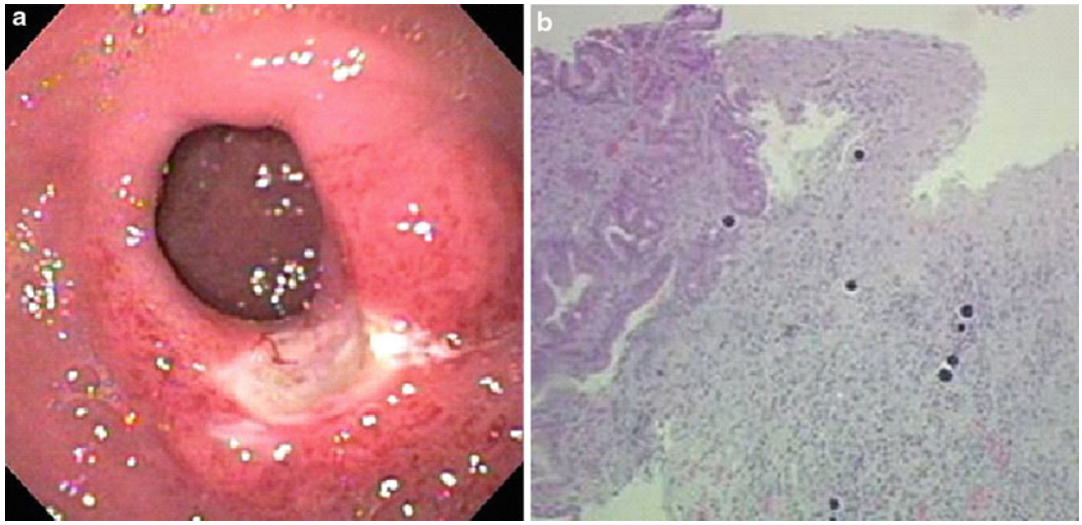

Fig. 29.4 Gastric/duodenal ulcer resulting from reflux of Y-90 radiomicrospheres into the GI vascular bed. (**a**) Endoscopic appearance of a gastric ulceration caused by Y-90 microspheres; (**b**) H&E microscopy of the ulcer showing microspheres in the necrotic (ulcerated) mucosa. The adjacent mucosa preserves its viability

radiomicrospheres into the GI vascular bed (Fig. 29.4) and radiation hepatitis resulting from a radiation overdose to the normal liver parenchyma.

GI Complications

The most common GI complication is gastroduodenitis and gastroduodenal ulcers (5 %). This is related to reflux of radiomicrospheres into hepatofugal branches, primarily gastroduodenal artery and right gastric artery. Cystic artery could also be involved. Subclinical cholecystitis is probably more common than previously thought, but severe, surgical treatment requiring cholecystitis is rare. Pancreatitis has been listed as a potential complication, but it is even more uncommon than cholecystitis.

Radiomicrosphere-Induced Liver Disease

The pathogenesis of radiation damage to the liver from conventional external beam radiation is dominated by vascular injury in the central vein region. Early alterations in the central vein caused by external beam radiation are an intimal damage that leads to an eccentric wall thickening. This process, when diffuse and progressive, results in clinical "veno-occlusive disease" characterized by development of portal hypertension, ascites, and deterioration in liver function [1]. Radiomicrosphere-associated radiation injury has a different pattern. Radiation from microspheres is deposited primarily in the region of the portal triad and away from the central vein, thus minimizing the damage pattern seen in radiation hepatitis from external beam sources [2]. Macroscopically, there is infarction necrosis and fibrosis with nodularity and firmness. Microscopically, radiomicrosphere-induced liver disease (RMILD) is characterized by microinfarcts and a chronic inflammatory infiltrate dominating in the portal areas. The radiation dose to healthy liver parenchyma is determined by the number of microspheres present, the distance of microspheres from one another, and the cumulative activity of the microspheres implanted. Microspheres lodge preferentially in the growing rim of the tumor, as the center may become necrotic and avascular as the tumor size increases. The highest dose exposure is at the zone immediately surrounding the tumor. The damage to this area of parenchyma is unavoidable. The remainder of the

Table 29.2 Adverse events/complications following microsphere therapy

Adverse event/ complication	Incidence
Flu-like symptoms	
Fatigue	
Low-grade fever	50 %
Nausea/vomiting	
Mild abdominal pain	
Post-embolic syndrome	1–2 % with resin microspheres
	None with glass microspheres
Ulceration	0–20 % (median 5 %)
Cholecystitis	<1 %
Radiation-induced liver disease	Classic radiation-induced liver disease (characterized by veno-occlusive disease), <1 %
	Radiomicrosphere-induced liver disease (characterized by portal triaditis), 0–10 % (median 5 %)
Radiation pneumonitis	<1 %

liver receives less radiation than would be predicted from assuming a homogeneous distribution of radiation dose throughout the parenchyma. Clinical veno-occlusive disease is uncommon with RMT. Adverse events and complications are shown in Table 29.2.

Radiation Pneumonitis

The second organ of concern is the lung, as a fraction of microspheres might shunt through the liver and into the lung. It is important to ensure that the radiation dose to the lung is kept to a tolerable limit. This can be calculated from the hepatic MAA scintigraphy. Radiation pneumonitis has been reported to occur at an estimated lung dose level of 30 Gy [3].

Clinical Studies with Y-90 RMT

Selective targeting of metastases with RMT induces substantial objective responses as measured by decrease in functional (by FDG-PET/CT) and anatomic (by CECT or MRI) tumor volume in the liver and significantly prolongs time to tumor progression (TTP), progression-free survival (PFS), and overall survival (OS). RMT in CRCLM can be administered as a stand-alone treatment in a salvage setting or can be administered in conjunction with systemic chemotherapy. The efficacy of the treatment has been demonstrated in both settings.

Chemo-RMT

To date, there have been five structured clinical trials with RMT using Y-90 resin microspheres: a randomized phase III study using hepatic artery chemotherapy with FUDR, a randomized phase II trial comparing systemic chemotherapy with 5-FU/LV with or without SIR-Spheres™, a phase I/II dose escalation study with oxaliplatin, a phase I/II dose escalation study with irinotecan, and a phase II study with FOLFOX-6 or FOLFIRI regimens [4–8].

The first randomized phase III trial in 74 patients with colorectal liver metastases compared RMT (2–3 GBq of Y-90 activity) plus hepatic artery chemotherapy (HAC) with FUDR 0.3 mg/kg/day for 12 days and repeated every 4 weeks for 18 months versus HAC alone (FUDR 0.3 mg/kg/day for 12 days and repeated every 4 weeks for 18 months). The outcome analysis showed significant improvement resulting from the addition of RMT to systemic chemotherapy. Toxicity data showed no difference in any of the grade 3 or 4 toxicity between the two treatment arms. There was a significant increase in the complete and partial response rate (17.6–44 %, $p = 0.01$) and prolongation of time-to-disease progression (9.7 months to 15.9 months, $p = 0.001$) in the liver for patients receiving the combination treatment. Although the trial design was not of sufficient statistical power to detect a survival difference, there was a trend observed toward improved survival for the combination treatment arm [4]. The tumor response, survival, and in-liver disease progression data from this study are given in Fig. 29.5a, b.

The second study combining RMT with systemic chemotherapy was designed as

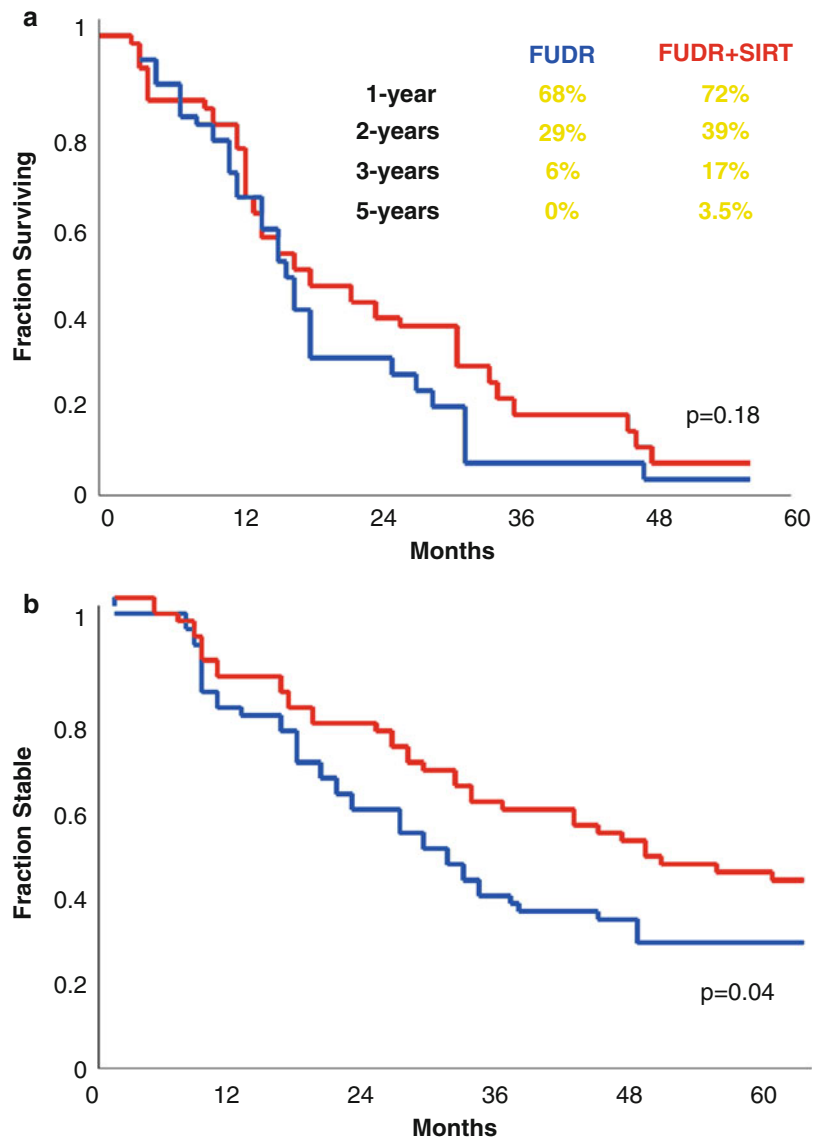

Fig. 29.5 (**a**) Survival curves in FUDR versus FUDR + RMT phase III randomized study. The difference is most significant in years 2 and 3. The 5-year survival difference is not significant largely due to the progression of extrahepatic disease. (**b**) The in-liver progression curves in FUDR versus FUDR + RMT phase III randomized study. The difference is significant in years 2–5

a randomized phase II/III trial in which RMT was used in combination with systemic chemotherapy using 5-FU and LV. This trial accrued 21 patients and closed prematurely due to the paradigm shift in the systemic therapy of metastatic CRC which involved new-generation chemotherapy agents. The toxicity profile was higher in patients receiving the combination treatment, although a dose modification of RMT decreased the toxicity profile to an acceptable level. Furthermore, the objective response rate in this small phase II trial for patients treated with the combination of RMT plus 5-FU/LV was high. Progression-free survival in the combination therapy arm was 18.6 months compared to 3.4 months in the chemotherapy alone arm ($p < 0.0005$). Overall median survival was 29.4 months in the combination therapy arm, compared to 12.8 months in the chemotherapy alone arm ($p = 0.02$) [5]. The survival data from this study are given in Fig. 29.6.

A phase I/II dose escalation trial of systemic chemotherapy using FOLFOX-4 + RMT was recently completed. Twenty patients were

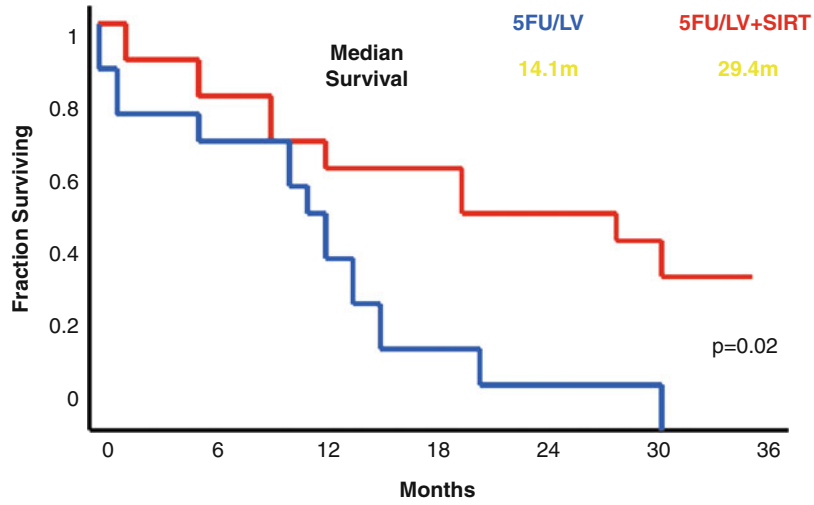

Fig. 29.6 Survival curves in 5FU/LV versus 5FU/LV + RMT phase II randomized study. The difference is significant in year 3

entered from Australia and the United Kingdom. The study population comprised of patients with non-resectable liver-dominant metastatic colorectal adenocarcinoma, who had not previously been treated with chemotherapy. This trial was successfully escalated up to the standard FOLFOX-4 oxaliplatin dose (85 mg/m^2) and demonstrated a safety profile very similar to that observed in other phase III trials of FOLFOX-4 alone. The overall RECIST response rate for the trial was 90 % (partial response + complete response), with the remaining patients (10 %) having stable disease. Of significance is the fact that 2 of the 20 patients in this study had their disease downstaged to the extent that the liver disease was subsequently surgically resected [7].

A second phase I/II dose escalation trial of systemic chemotherapy was done using irinotecan + RMT. Twenty-five patients who had failed previous chemotherapy were entered into the study. Irinotecan was given weekly twice every 3 weeks, starting the day before RMT, for a maximum of nine cycles. Irinotecan dose was escalated from 50 to 100 mg/m^2, and this was well tolerated. Partial responses were seen in 9 out of 17 patients, median time to liver progression was 7.5 months, and median survival was 12 months [6].

A phase II study combining RMT with FOLFOX-6 or FOLFIRI in a frontline setting enrolled 20 patients. The patients received RMT in one of the two liver lobes 24 h after starting chemotherapy. This study was implemented to demonstrate the relative efficacies of chemotherapy and chemotherapy combined with Y-90 radiomicrosphere therapy. By virtue of its design, comparing right and left liver lobes receiving different treatments in individual patients, the study provided clear data in terms of objective responses. The evaluation of objective treatment response in this study included accurate measurements of functional and anatomic tumor volume changes. Eighteen patients were treated in the first-line setting with FOLFOX-6 chemotherapy, and two patients were treated in the second-line setting with FOLFIRI chemotherapy. A decrease in functional tumor volume on FDG-PET/CT imaging was seen in all except one patient. The mean decrease in functional tumor values in the tumors receiving chemo-SIRT and chemo-only treatment is shown in Table 29.3. Comparative anatomic changes in chemo-SIRT and

Table 29.3 The mean decrease (%) in functional tumor values in the tumors receiving chemo-SIRT and chemo-only treatment

Functional volume decrease (%)			
Posttreatment	Chemo-SIRT	Chemo-only	*p* Value
1 month	80.47 ± 25.67	41.32 ± 58.46	0.0128
2–4 months	90.67 ± 17.01	46.67 ± 60.59	0.0076
6–12 months	82.22 ± 38.85	56.00 ± 28.93	0.0873

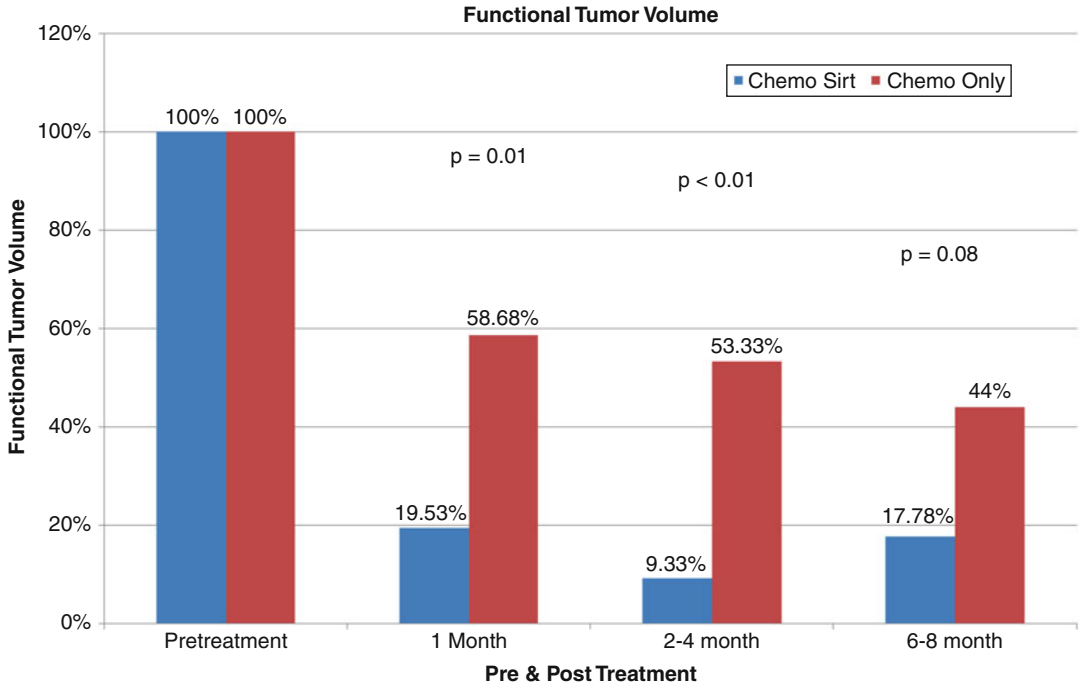

Fig. 29.7 Functional tumor volume (%): pretreatment and posttreatment at 4 weeks, 2–4 months, and 6–8 months

chemo-only lobes are shown in (Figs. 29.7, 29.8, and 29.9). The study demonstrated that, under near identical conditions in terms of patient and tumor characteristics, the chemo-RMT combination produced superior objective responses compared to chemo-only treatment in a frontline treatment setting in patients with CRCLM [8].

RMT Alone

RMT alone is usually administered in the salvage setting in chemorefractory patients. In a large multicenter retrospective review involving 208 patients with unresectable disease, the majority of which had received at least 3 lines of prior chemotherapy and had also failed local-regional therapy, RMT produced objective responses by CT in 35.5 % of patients and disease stabilization in a further 55 % of patients at 3-month follow-up. Response by FDG-PET was observed in 85 % of patients. The treatment response after RMT was highly predictive of prolonged survival, with a median survival of 10.5 months among responders versus 4.5 months for nonresponders or historical controls ($p < 0.0001$) [9].

In a prospective phase II trial, RMT significantly extended both overall survival (OS) and progression-free survival (PFS) of 29 chemorefractory patients with a tumor burden of 20–50 % compared to 29 patients receiving supportive care [10]. Patients in both arms had received a median of 3 regimens prior chemotherapy (range, 2–6), with no significant difference in their experience to chemotherapy and biologic agents. Median PFS was increased from 2.1 months with supportive care to 5.5 months after RMT ($p < 0.001$), and median survival was similarly prolonged from 5.5 to 8.3 months, respectively ($p < 0.001$) [11]. The survival benefit was clearly evident at 3 months (59 % vs. 97 %) and sustained through 12-month follow-up (0 % vs. 24 %). On multivariate analysis, RMT was the most significant predictor of survival ($p < 0.001$). RMT was well tolerated, with a low incidence of adverse events, including thrombocytopenia and sepsis (3 %) and abdominal pain (3 %). Three possible cases of

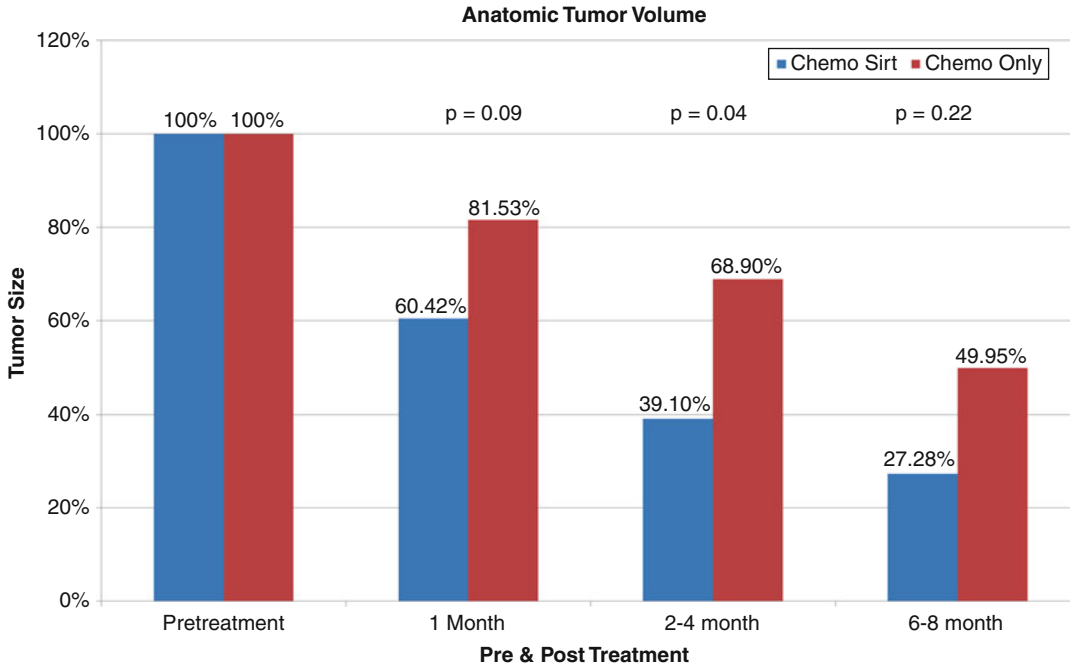

Fig. 29.8 Anatomical tumor volume (%): pretreatment and posttreatment at 4 weeks, 2–4 months, and 6–8 months

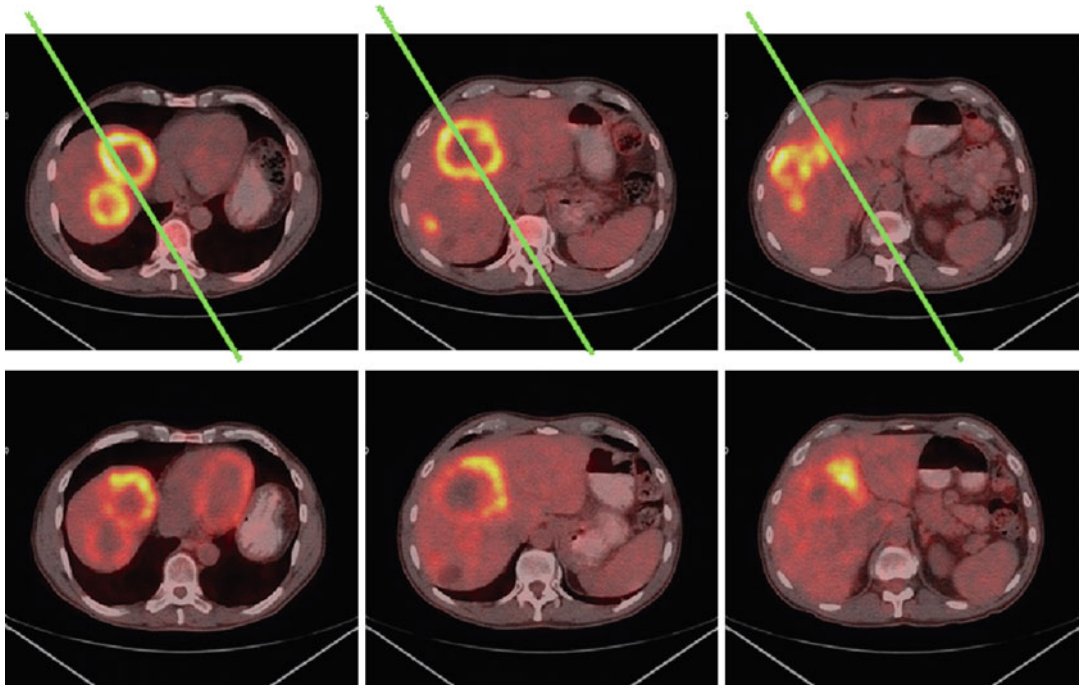

Fig. 29.9 Differential visual response in chemo-SIRT treated lobe versus chemo-only lobe. The line delineates right and lobe border. There is a good response in the right lobe treated with combination protocol

radiation-induced liver disease were managed medically and were not considered life-threatening (median survival, 9.8 months; range, 9.0–16.6) [10].

In a prospective phase II multicenter collaborative-group trial in 50 highly chemorefractory patients who had failed prior oxaliplatin- and irinotecan-based chemotherapy regimens, the overall response rate after a single administration of RMT was 24 % (range, 12.2–35.8 %) with stable disease (SD) reported in a further 24 % of patients. Two patients were sufficiently downsized to a subsequent surgical resection. The Kaplan-Meier median OS was 13 (range, 7–18) months with a 2-year survival of 19.6 %. Similar to the first study, the treatment response with RMT was highly predictive of prolonged survival, with a median survival of 16 (range, 13–19) months among responders compared with 8 (range, 4–12) months among nonresponders ($p < 0.0006$) [12].

A retrospective study of 41 patients with chemotherapy refractory colorectal cancer liver metastases (CRCLM) also reported similar outcomes, with an objective response rate of 17 % measured by response evaluation criteria in solid tumors (RECIST) and a median OS of 10.5 months after RMT [13].

RMT for Preoperative Tumor Downsizing and Future Liver Remnant Recruitment

The extent of resection of liver metastases is restricted by the volume of the future liver remnant (FLR). Among different strategies, portal vein embolization (PVE) has gained wider acceptance to achieve the goal of increasing the volume of the FLR. Induction of hypertrophy of the nondiseased portion of the liver reduces the risk of hepatic insufficiency and associated complications after resection. Clinically adequate compensatory hypertrophy occurs approximately 2–3 weeks postinduction (Fig. 29.10). An FLR of >20 % in patients with an otherwise normal liver, >30 % for those who have received extensive chemotherapy, and >40 % in patients with hepatic fibrosis/cirrhosis is recommended for a safe major hepatic resection. A recent meta-analysis concluded that PVE is a safe and effective procedure for inducing liver hypertrophy to prevent postresection liver failure due to insufficient liver remnant. The controversy over the possibility of tumor progression in nonembolized (and also in embolized) segments during the induction period, however, remains unresolved. RMT was proposed as an alternative novel approach to effectively control the tumor growth and, with appropriate scaling of radiation absorbed dose to the lobar portal microvascular bed, to induce contralateral lobe hypertrophy. The simultaneous accomplishment of tumor control and FLR recruitment might offer a better therapeutic profile compared with that of PVE [14]. Clinical indications, patient selection criteria, and dosimetry for this therapeutic intervention needs to be further investigated.

The Role of RMT in the Contemporary Management of CRCLM

The natural course of untreated metastatic liver disease is poor. Data from sixties and seventies show that the median survival of patients receiving no treatment ranges from 3 to 12 months, with an overall median survival of 7 months [15]. Liver resection provides the most favorable outcomes in appropriately selected patients. With the advancements in surgical, anesthetic, and perioperative care and in medical imaging which allowed better patient selection and surgical planning, liver resections have become accepted as standard therapy [16]. Increasingly, aggressive resections are being performed with an operative mortality less than 5 %. At many centers, more than two-thirds of resections now consist of major hepatectomies. While the liver resection has been accepted to be the only treatment with a chance of long-term survival in patients with CRCLM, the resectability rate of metastases at the time of diagnosis has been low, accounting for the low proportion of patients who may benefit from a surgical approach. Until recently, patients initially considered as

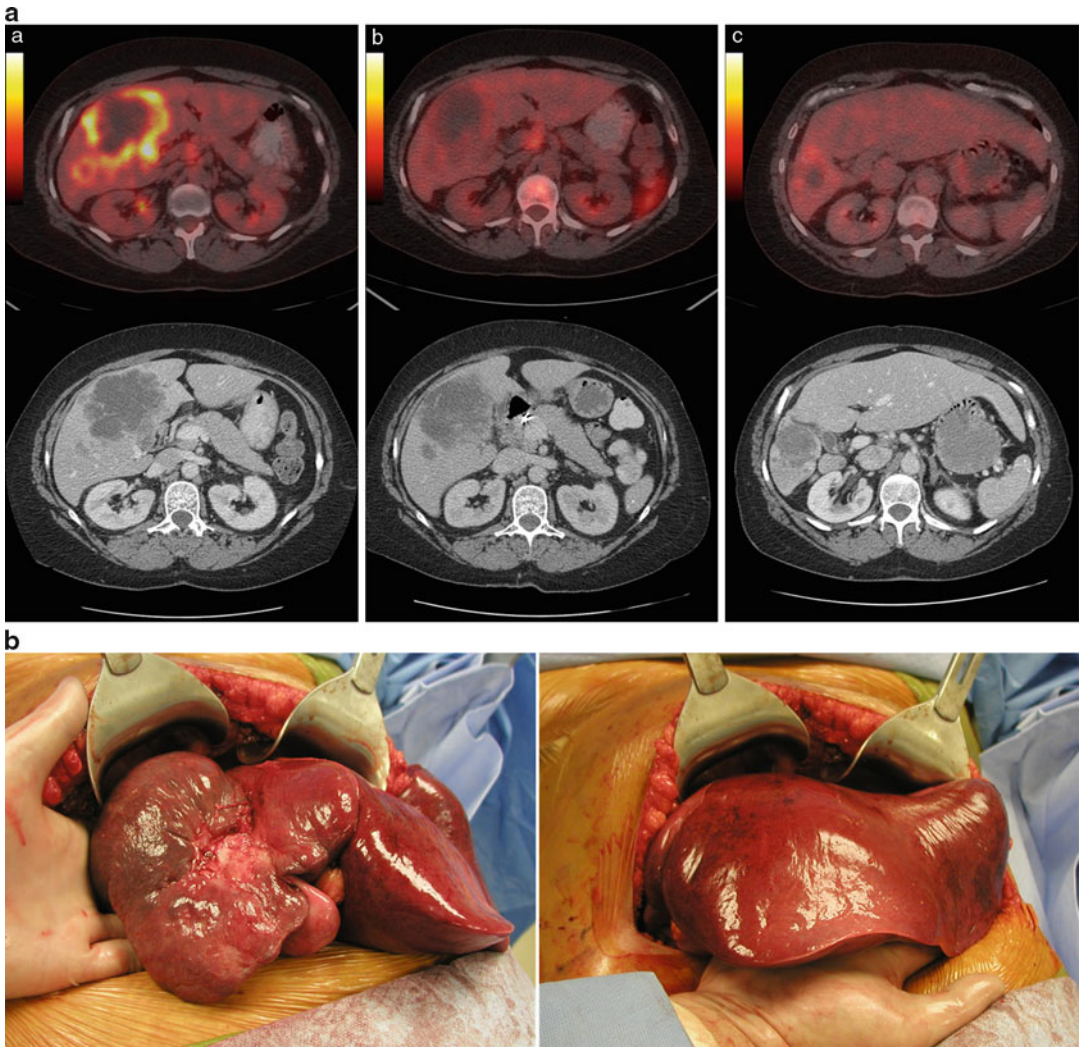

Fig. 29.10 (**a**) FDG-PET/CT image sets demonstrating progressive decrease in the functional and anatomic volume of the tumor with concurrent left lobe hypertrophy. *a*: pretreatment, *b*: 4 weeks after first SIRT treatment, *c*: at the completion of the full course of the treatment. (**b**) Intraoperative pictures demonstrating significantly downsized tumor with scarring and major left lobe hypertrophy

unresectable were treated by palliative chemotherapy, with poor response rates and obviously little chance of 5-year survival. Chemotherapy as a first-line treatment of metastatic colorectal cancer has greatly changed within the last decade. Oxaliplatin- and irinotecan-based combination regimens have improved the effzicacy of systemic treatment not only allowing increased patient survival in a palliative setting but have also offered a possibility of cure to previously unresectable patients with liver surgery after tumor downsizing [17–19]. By reconsidering the initial unresectability of patients who strongly respond to chemotherapy, Adam et al. have shown that survival could be achieved by liver resection in a significant proportion of patients otherwise destined to a poor outcome [20]. This group analyzed a consecutive series of 1,439 patients with CRLM managed in a single institution during an 11-year period (1988–1999). Metastatic disease was determined to be resectable in 335 (23 %) of the patients at initial presentation.

Remaining 1,104 (77 %) were treated by chemotherapy, involving new-generation protocols. Among 1,104 unresectable patients, 138 (12.5 %) underwent secondary hepatic resection after an average of 10 courses of chemotherapy. Seventy-five percent of procedures were major hepatectomies. Portal embolization and ablative treatments were liberally used as adjunct modalities. Currently, an average 5-year overall survival rate of 33 % has been achieved with a wide use of repeat hepatectomies and extrahepatic resections. These results indicate that multimodality approach with aggressive surgical and nonsurgical interventions can be justified toward the goal of improving the survival of patients with CRCLM. Also, significant number of patients can be downsized for a potentially curative resection provided that a successful neoadjuvant strategy can be employed.

At present, the neoadjuvant treatment for unresectable CRCLM involves new-generation chemotherapy regimens combined with targeted therapies such as bevacizumab (Avastin™) and cetuximab (Erbitux™). Radiation therapy has not been considered a viable treatment modality due to its unacceptably high hepatic toxicity and the long-standing dogma that chemoradiation cannot be an oncological strategy for a stage IV disease. Selective internal radiation treatment with Y-90 radiomicrospheres has emerged as an effective liver-directed therapy with a favorable therapeutic ratio. Since its early clinical trials, it has demonstrated improved response rates when used in conjunction with systemic or regional chemotherapy. Chemo-RMT might prove to be a successful neoadjuvant strategy.

References

1. Ingold JA, Reed GB, Kaplan HS, et al. Radiation hepatitis. Am J Roentgenol Radium Ther Nucl Med. 1965;93:200–8.
2. Gray BN, Burton MA, Kelleher D, et al. Tolerance of the liver to the effects of Yttrium-90 radiation. Int J Radiat Oncol Biol Phys. 1990;18:619–23.
3. Dancey JE, Shepherd FA, Paul K, et al. Treatment of nonresectable hepatocellular carcinoma with intrahepatic ^{90}Y-microspheres. J Nucl Med. 2000; 41:1673–81.
4. Gray B, et al. Randomized trial of SIR-Spheres plus chemotherapy vs. chemotherapy alone for treating patients with liver metastases from primary large bowel cancer. Ann Oncol. 2001; 12:1711–20.
5. Van Hazel G, et al. Randomized phase 2 trial of SIR-Spheres plus Fluorouracil/Leucovorin chemotherapy versus Fluorouracil/Leucovorin chemotherapy alone in advanced colorectal cancer. J Surg Oncol. 2004;88:78–85.
6. Van HG, et al. Selective internal radiation therapy (RMT) plus systemic chemotherapy with irinotecan. A phase I dose escalation study. ASCO GI Symposium 2005.
7. Van HG, et al. Selective internal radiation therapy (RMT) plus systemic chemotherapy with oxaliplatin, 5-fluorouracil and leucovorin: a phase I dose escalation study. ASCO GI Symposium 2005.
8. Gulec SA, Pennington K, Bruetman D, et al. Yttrium 90 microsphere selective internal radiation therapy with chemo therapy (chemo-SIRT) for colorectal cancer liver metastases; a phase II trial. (Manuscript Submitted for publication).
9. Kennedy A, Coldwell D, Nutting C, et al. Resin Y-90-microsphere brachytherapy for unresectable colorectal liver metastases: modern USA experience. Int J Radiat Oncol Biol Phys. 2006;65(2):412–25. doi:10.1016/j.ijrobp. 2005.12.051.
10. Ricke J, Rühl R, Seidensticker M, et al. Extensive liver-dominant colorectal (CRC) metastases failing multiple lines of systemic chemotherapy treated by ^{90}Y Radioembolisation: a matched-pair analysis. Poster presentation, 11th World Congress of Gastrointestinal Cancer. Ann Oncol. 2009;20(Suppl 6:vi24): Abs. PD-002.
11. Folprecht G, Grothey A, Alberts S, et al. Neoadjuvant treatment of unresectable colorectal liver metastases: correlation between tumour response and resection rates. Ann Oncol. 2005;16:1311–9.
12. Cosimelli M, Golfieri R, Cagol PP, et al. Multi-centre phase II clinical trial of yttrium-90 resin microspheres alone in unresectable, chemotherapy refractory colorectal liver metastases. Br J Cancer. 2010;103(3): 324–31.
13. Jakobs TF, Hoffmann RT, Dehm K, et al. Hepatic yttrium-90 radioembolization of chemotherapy-refractory colorectal cancer liver metastases. J Vasc Interv Radiol. 2008;19:1187–95.
14. Gulec SA, Pennington K, Hall M, Fong Y. Preoperative Y-90 microsphere selective internal radiation treatment for tumor downsizing and future liver remnant recruitment: a novel approach to improving the safety of major hepatic resections. World J Surg Oncol. 2009;7:6.
15. Gray BN. Colorectal cancer: the natural history of disseminated disease. Aust N Z J Surg. 1980;50: 643–6.
16. Fong Y. Surgical therapy of hepatic colorectal metastasis. CA Cancer J Clin. 1999;49:231–55.

17. Alberts SR, Horvath WL, Sternfeld WC, et al. Oxaliplatin, Fluorouracil, and Leucovorin for patients with unresectable liver-only metastases from colorectal cancer: a North Cdentral Cancer Treatment Group Phase II Study. J Clin Oncol. 2005;23:9243–9.
18. Bismuth H, Adam R. Reduction of non-resectable liver metastases from colorectal cancer after Oxaliplatin chemotherapy. Semin Oncol. 1998;25:40–6.
19. Delanoult T, Alberts SR, Sargent DJ, et al. Chemotherapy permits resection of metastatic colorectal cancer: experience from intergroup N9741. Ann Oncol. 2005;16:425–9.
20. Adam R, Delvart V, Pascal G, et al. Rescue surgery for unresectable colorectal liver metastases downstaged by chemotherapy: a model to predict long-term survival. Ann Surg. 2004;240:644–57.

Stereotactic Body Radiation Therapy for Liver Metastases

30

Martin Fuss, Anna Simeonova, and Samuel Ryu

Abstract

The concept and technique of stereotactic body radiation therapy (SBRT) is presented. This focally tumor-ablative radiation approach is delivered in a few fractions of high radiation doses to a limited volume of metastatic disease to the liver. Indications include one to five metastatic lesions with maximum diameters up to 5 cm. While clinical experience is limited with few larger case series, preliminary outcomes with respect to tumor control and normal liver sparing are encouraging. This new treatment modality offers patients an alternate noninvasive treatment modality promising high local tumor control rates.

Concept of Stereotactic Body Radiation Therapy (SBRT)

Stereotactic body radiation therapy (SBRT) is a relatively novel concept in which high doses of radiation are directed focally onto malignant lesions in organ sites other than the brain, including lung, liver, and spine tumors. The concept of SBRT is derived from the experience in treating metastatic lesions in the brain by stereotactic radiosurgery (SRS). In SRS, very high radiation doses are delivered to small brain lesions in a single session, with the intent to ablate all malignant tumor cells in one setting. The success rates of this treatment approach, with local tumor control rates as high as 93.3 %, have made SRS a standard of care for limited metastatic disease to the brain [1–3]. Similar antitumor efficacy should be achievable for metastatic lesions in organs other than the brain, when high radiation doses are comparably confined to a small tumor. In this chapter, an attempt is made to summarize the clinical experience with SBRT for metastases to the liver. The indications, technical considerations, as well as outcomes of SBRT for liver metastases are discussed, including available data of prospectively designed clinical trials.

SBRT as discussed here will largely adhere to the accepted definition in the United States as the

M. Fuss (✉)
Department of Radiation Medicine, Oregon Health and Science University, Portland, OR, USA
e-mail: fussm@ohsu.edu

A. Simeonova
Department of Radiation Oncology, University Medical Center Mannheim, Mannheim, Germany
e-mail: anna.simeonova@umm.de

S. Ryu
Department of Radiation Oncology and Neurosurgery, Henry Ford Hospital, Detroit, MI, USA
e-mail: sryu1@hfhs.org

D.E. Dupuy et al. (eds.), *Image-Guided Cancer Therapy*, DOI 10.1007/978-1-4419-0751-6_32,

delivery of high-dose focused radiation in 1–5 fractions onto small malignant lesions. The high-dose aspect of delivery, as well as what constitutes a small lesion, is less clearly defined. High-dose delivery is most often understood as single-fraction doses exceeding 5 Gray (Gy). Small lesions are most often defined as being less than 5 cm in maximum diameter. Focal radiation delivery refers to the ability to deliver tumoricidal radiation doses in a highly conformal manner, so that a target volume delineated in CT, MRI, or PET imaging is exposed to high, tumor-ablative doses of radiation, while steep dose gradients toward normal tissues afford sparing the organ harboring the disease from radiation injury. However, highly precise dose planning also requires similarly accurate dose delivery. Unique to the concept of SBRT is the stipulation of image-guidance in the context of dose delivery. As such, SBRT is currently the only radiation therapy concept for which a target has to be directly or indirectly localized before the radiation dose is delivered.

Liver Metastases: Incidence and Established Treatment Options

The liver is second only to regional lymph nodes as a site for metastatic disease for a variety of primary malignancies [4]. For colorectal cancer, the liver is often the first site of metastatic disease manifestation, with 15–25 % of patients harboring liver metastases at the time of diagnosis [5]. At autopsy, liver metastases are found in 25–50 % of patients who have died from cancer [6]. For patients diagnosed with liver metastases, the life expectancy without treatment is poor at about 5 months [7].

Surgical resection is the standard therapy for solitary or few lesions confined to the liver with favorable survival rates at 5 years of 25–35 % [5]. Unfortunately, 80–90 % of patients diagnosed with metastatic disease to the liver are not resection candidates, either due to the extent of metastatic disease, multiorgan metastatic disease, insufficient functional liver reserve, or general medical condition [4, 5].

Alternate liver-directed treatment options for patients with limited but unresectable liver metastases include radiofrequency ablation (RFA) [8], transarterial embolization (TAE) with or without transarterial chemotherapy administration (TACE), and radioembolization [6, 7, 9, 10] (Fig. 30.1). Local tumor control rates for RFA are comparable with surgery for lesions less than 3 cm, but lesions in close proximity to large vessels and the diaphragm, as well as subcapsular location, can be relative contraindications for this technique. Cryotherapy has been largely used in the past for palliation of unresectable liver tumors, but high local recurrence rates and peculiar systemic complications have determined its progressive abandonment. Despite long-term clinical use, the optimum number of freeze-thaw cycles, the role of inflow occlusion, and the potential corrupting effects of intralesional or proximal blood vessels on ablation morphology are still controversial [11].

For patients with multifocal liver metastases that are not candidates for liver-directed therapy, chemotherapy represents the only viable treatment option. Advances in chemotherapy treatment have been impressive for a variety of tumors. For patients with metastatic colorectal cancer, for example, the median survival has been improved from 10 to 20 months after the introduction of new chemotherapeutic agents and targeted therapies [10]. Unfortunately, these results are not seen for most other malignancies.

Radiation Therapy for Liver Metastases: From Conventional Radiation to SBRT

For decades, radiation therapy has had a limited role in the treatment of hepatic metastases because of the limited tolerance of the liver. The entire liver will not tolerate more than 30–35 Gy of conventionally fractionated radiation. At higher doses, radiation-induced liver disease (RILD) occurs frequently. RILD describes a clinical syndrome of anicteric hepatomegaly, ascites, and elevated liver enzymes (particularly serum alkaline phosphatase) occurring from

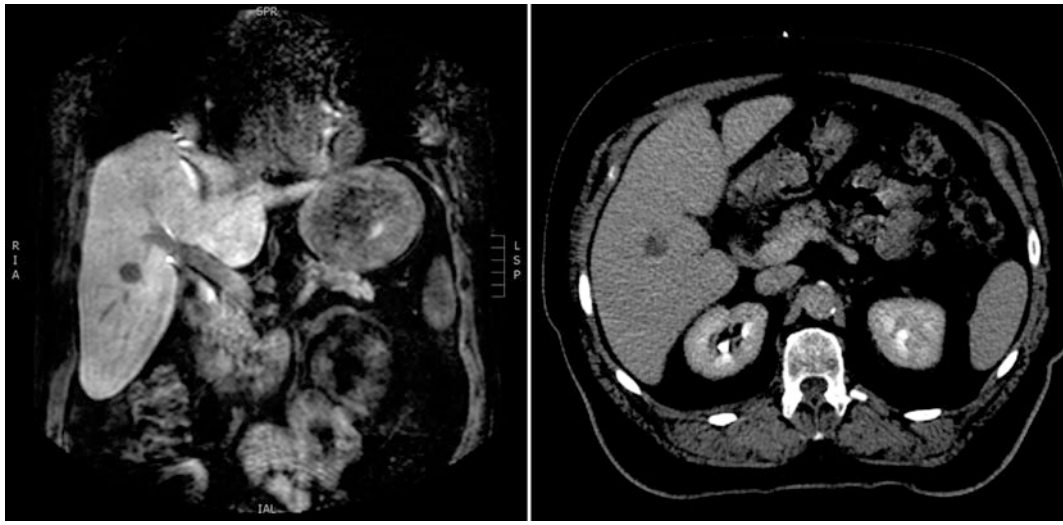

Fig. 30.1 Solitary non-small-cell lung cancer liver metastasis. The lesion is depicted in a coronal reconstruction T1-weighted delayed-phase contrast-enhanced MRI, as well as a delayed-phase post-contrast axial CT. By size (10 mm) and location, this is a candidate lesion for consideration of SBRT. Since at the time of assessment, this lesion represented the only site of systemic disease with locally controlled primary tumor, this could be considered a case of oligometastasis

2 weeks to 3 months following external beam radiation. Diuretics and steroids are often used in therapeutic intent, although evidence is lacking that they change the natural history of RILD. Most cases resolve with conservative, supportive treatment, but some cases lead to irreversible liver failure and occasionally death.

Focal radiation dose delivery to only parts of the liver allows for sufficient normal liver sparing, with an associated lowered risk for chronic liver damage. Recent developments in radiotherapy such as optimized patient immobilization and four-dimensional imaging techniques allow radiation oncologists to assess liver organ motion. Also, three-dimensional treatment planning, image-guidance, and gated or breath-hold radiation delivery have been critical to the high-precision focal irradiation of liver lesions performed with SBRT [12]. In prospective clinical trials, doses prescribed to focal liver lesions could be escalated to 60 Gy in 6 fractions, using modern radiation treatment techniques [13].

Steep dose gradients between liver lesions and surrounding normal liver tissue are a hallmark of SBRT dose distributions and afford excellent liver sparing. This is accomplished by using multiple radiation beams which are shaped according to the tumor outline and are all centered upon a liver lesion (Fig. 30.2). While each of the radiation beams delivers a small fraction of the cumulative radiation dose, the dose at the target, where all radiation beams intersect, is summed up to high tumoricidal dose levels (Fig. 30.3). Similar dose concentrations can be achieved using arc delivery techniques during which a multi-leaf collimator, or radiation beam-shaping device, continually adjusts the radiation port to the shape of the target from a given beam's eye view. SBRT radiation plans use 7–11 individual radiation beams arranged coplanar or noncoplanar around the target lesion, with little incremental plan quality improvement when the number of radiation ports exceeds nine [14–18].

While conventional radiation therapy protocols that are delivered over multiple weeks are computed with homogeneous dose distributions (which expose all aspects of a clinical target volume (CTV) to the same radiation dose), dose distribution used for SBRT often employs heterogeneous dose planning in which the center of a target volume is intentionally exposed to

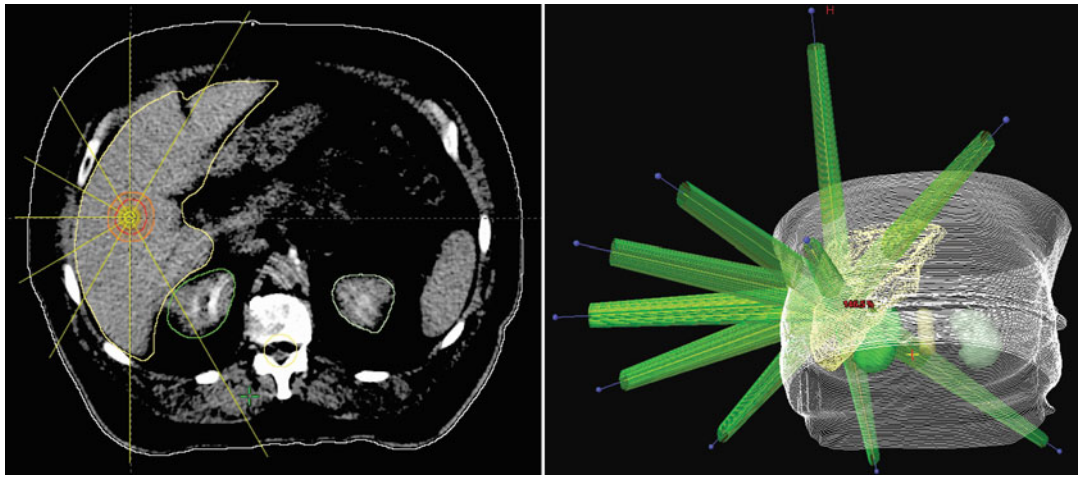

Fig. 30.2 Multi-beam arrangement for SBRT of liver metastases. Here, 10 isocentric beams intersect at the liver metastasis. Each individual beam is shaped to the beam's eye-view outline of the radiation target volume. Eight beams are arranged in a coplanar way, with two additional noncoplanar beams entering from superior anterior and inferior anterior

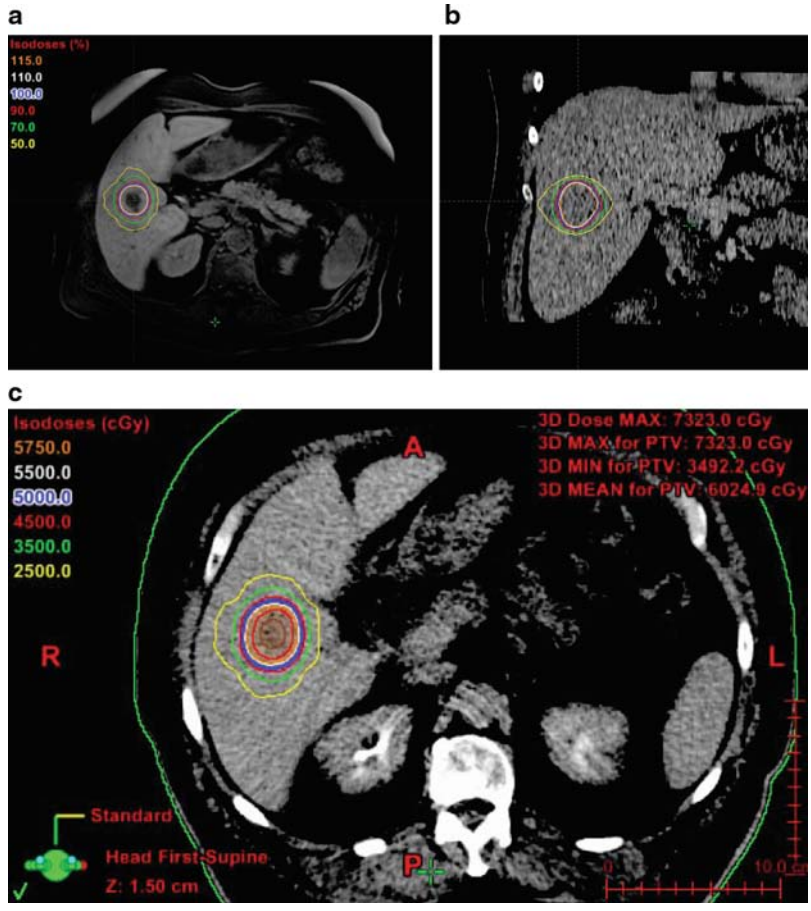

Fig. 30.3 Typical radiation dose distribution for SBRT of liver metastases superimposed onto representative axial and coronal CT slices (**b** and **c**) as well as a co-registered axial MRI (**a**). The *blue, red, green*, and *yellow* lines represent the 50 Gy (100 % of prescribed dose), 45 Gy (90 %), 35 Gy (70 %), and 25 Gy (50 %) radiation dose. Note the steep radiation dose fall off toward the surrounding normal liver, resulting in highly effective healthy liver sparing

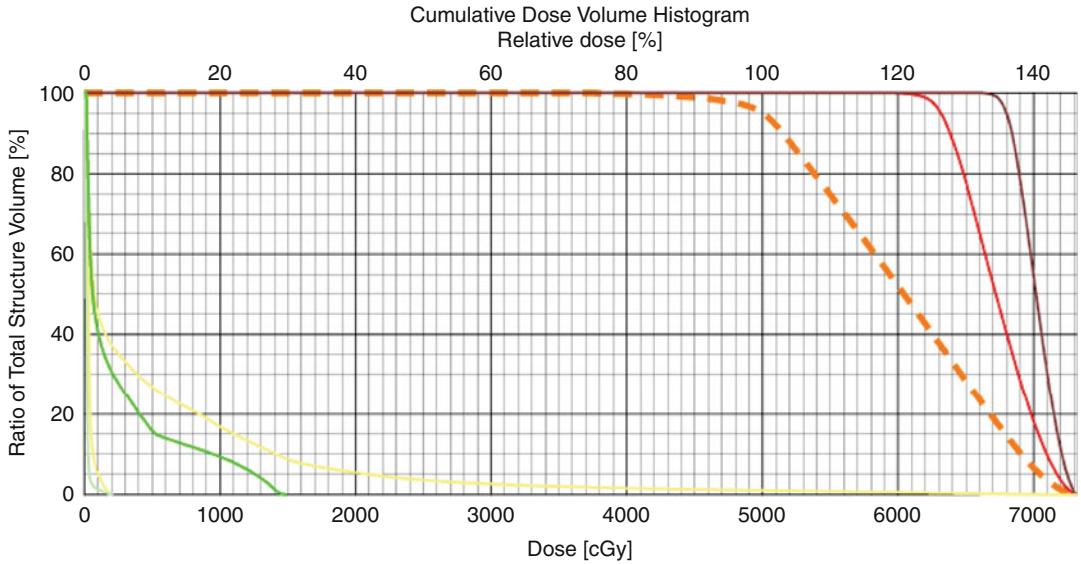

Fig. 30.4 Dose volume histogram (DVH) for SBRT planning of liver metastases. The *orange line* represents the planning target volume (PTV) to which a radiation dose of 50 Gy in 5 fractions is prescribed (95 % of the PTV is exposed to 50 Gy or more). The *red* and *brown* lines represent the target volume and an area delineated for heterogeneous radiation dose prescription. The *yellow* and *green* lines represent liver and right kidney, respectively, with less than 20 % of either organ exposed to more than 20 % of the prescribed dose

25–50 % higher doses than the edge of the target volume [19, 20] (Figs. 30.3 and 30.4). Such heterogeneous dose distributions afford the delivery of higher radiation doses to central tumor aspects that may be hypoxic and protect malignant cells from radiation injury, potentially increasing the clinical efficacy of SBRT [21].

Most SBRT treatments in the US are delivered in 3–5 fraction schedules, with dose delivery every other day or in even lesser numbers of fractions/week [18, 22, 23]. This is in contrast to some European sites pursuing single-dose SBRT for primary and metastatic liver tumors [24–27]. At this point in time, optimal dose scheduling has not been established, and single-dose delivery may result in comparable outcomes to hypofractionated SBRT schedules.

Indications for SBRT of Liver Metastases

Similar to indications for surgery, and other liver-directed therapy options for liver metastases, indications for SBRT include solitary or a low number (<5) of liver lesions. Ideal candidates have metastatic disease limited to the liver or liver lesions considered most life-limiting in the setting of multiorgan systemic disease. Interesting in establishing an indication for SBRT of liver metastases is the concept of oligometastases. The clinical state of oligometastatic disease was proposed in 1995 by Hellman and Weichselbaum as a transitional state between localized and widespread systemic disease [28]. Oligometastatic disease has the potential of progressing to widespread metastatic disease. Thus, local control of oligometastases may yield improved systemic control [29, 30]. While indications for SBRT overlap with many other treatment modalities, there are distinct exceptions which deserve discussion. Primarily, there is no strict size limitation for the use of radiation therapy. While an upper size limit of a liver metastasis of 5 cm is defined in most prospective clinical trials for eligibility of SBRT, larger lesions could be treated using the exact planning techniques and technology used to deliver SBRT [12, 24, 26]. The challenge in treating larger lesions with SBRT techniques is

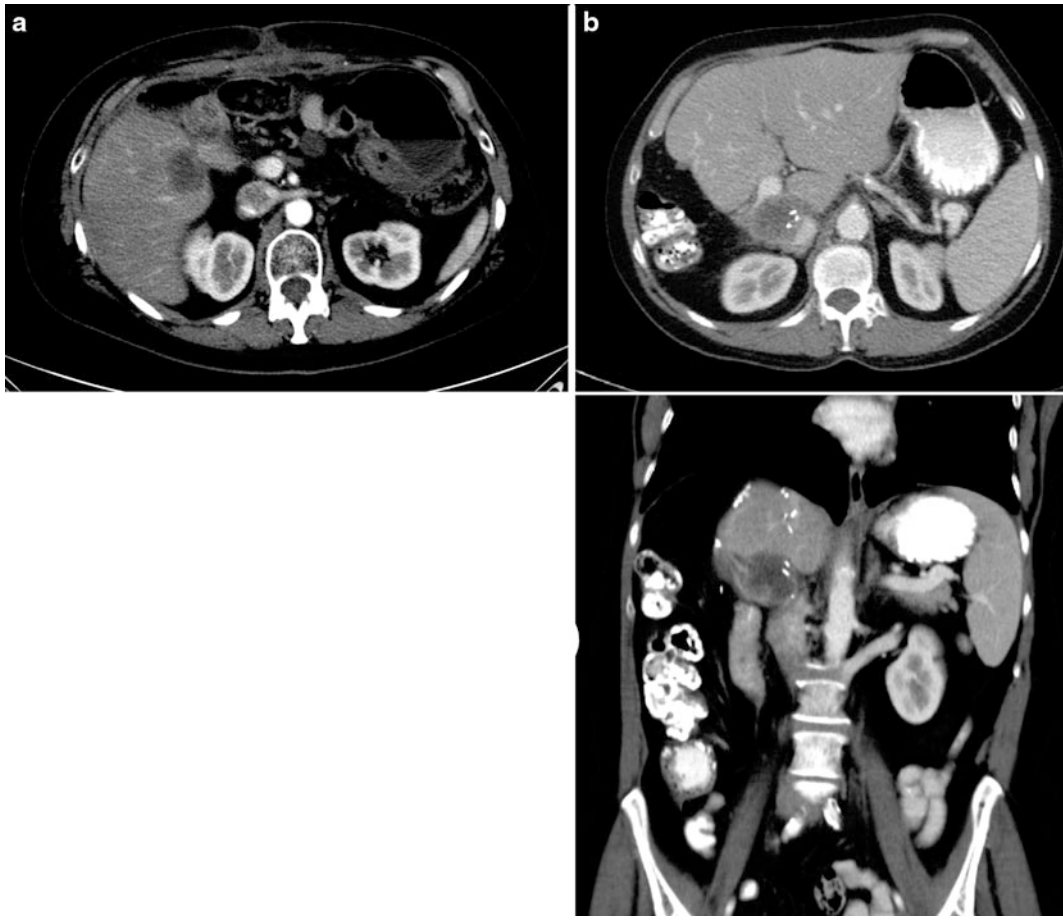

Fig. 30.5 Contraindication for SBRT of liver tumors. While subcapsular location in itself does not represent a contraindication for SBRT, proximity to hollow organs such as stomach or small and large bowel does. Figures (**a**) and (**b**) represent two cases in which a lesion (*arrows*) which is suitable by size for SBRT is located close to bowel loops. Note that the axial slice in figure B does not indicate the close proximity of a resection margin recurrence of metastatic colon cancer to a small bowel loop as well; this becomes more evident in coronal CT reconstruction

the sparing of normal liver volume and avoidance of exposing bowel or other lesion to potentially harmful radiation levels. These limitations often force lowering radiation dose prescription for treatment of large liver metastases, with subsequent lowered tumor control probability. Lesion location within the liver may be less critical for SBRT treatment than for alternate modalities such as RFA or cryoablation. Specifically subcapsular and subdiaphragmatic lesion locations in close proximity to large blood vessels and central lesion location are not definitive contraindications to SBRT. The key consideration when evaluating patients for an indication for SBRT is the proximity of the lesion to hollow organs such as the colon, stomach, or the duodenum (Fig. 30.5). If maximum radiation dose exposure to an aspect of those organs exceeds safe dose limits, SBRT would be contraindicated and radiation therapy may be denied or a more conventionally fractionated treatment course may be recommended. The second most important consideration is residual normal liver volume and underlying liver function. Most prospective clinical trials stipulate a minimum non-tumor liver volume of

700–1,000 cm^3 and reasonable baseline liver function (total bilirubin less than 3 mg/dL, albumin greater than 2.5 g/dL, and normal prothrombin/partial thromboplastin times (unless on anticoagulants) and serum liver enzymes less than three times the upper limit of normal) [22, 23].

SBRT for Liver Metastases: Challenges and Technical Considerations

Owing to the higher tumor-ablative doses delivered with SBRT, knowledge about the target's location and assurance that the patient will not move during radiation dose delivery are critical components of the safe integration of SBRT into the management of liver metastases. It is critical that the SBRT dose is actually delivered onto the target lesion and not accidentally into normal tissues. These challenges can be addressed at least partially by immobilizing the patient's body, preferably by use of whole-body immobilization devices [31–34]. However, while immobilization of the patient's body will locate a target volume close to a predicted treatment position relative to the linear accelerator radiation beam geometry, tumors in the liver can move relative to the bony skeleton rendering an assessment of the patient's position by bony X-ray analysis unreliable [24, 31, 35–38].

Image-guidance, a stipulated component of SBRT delivery in the US, can be used to assess the position of a liver target either by direct visualization or indirectly by assessing the position of the liver or liver lobe harboring the target through radio-opaque fiducials implanted within close proximity to the liver metastases. The obvious challenge here is that liver metastases may or may not be visualized on non-contrast imaging. If an imaging modality other than a diagnostic grade CT scanner is used for image-guidance, such as megavoltage port films, kilovoltage X-ray-based images, or on-board cone-beam CT (CBCT) units, the liver soft tissue contrast will likely be insufficient to depict a liver lesion. The only alternate modality capable of rendering soft tissue structures in the liver is ultrasound. Consequently, two-dimensional ultrasound-based image-guidance has been successfully implemented into the image-guidance workflow for SBRT at select institutions [39].

Liver motion due to breathing during treatment simulation and delivery can be substantial. In order to treat small liver lesions with a focal radiation approach, liver tumor motion must be accounted for to ensure proper delivery of the radiation dose to the tumor and to avoid unnecessary dose exposure of normal tissues. Further complicating this issue is the observation that substantial variations in breathing motion are seen among patients, with motion amplitudes ranging from 5 to 35 mm. Motion occurs predominantly in the cranio-caudal direction, followed by the anterior-posterior direction [40, 41]. In order to account for liver motion during respiration, several approaches can be chosen. The most conventional measure is the addition of so-called planning target volume (PTV) safety margins on a defined liver target volume. The creation of a PTV extends the target volume by adding between 5- and 10-mm margins into the surrounding normal tissues. To develop individual PTV margins, the organ motion during respiration needs to be measured by acquiring imaging studies during inhalation and exhalation or by using fluoroscopy. Other approaches employ means to restrict organ motion such as exerting pressure upon the upper abdomen or using breath-hold imaging and delivery techniques. All of these measures aim at minimizing PTV margins which are exclusively comprised of normal tissues at risk for radiation-induced damage [38].

More recently, it has become possible to define organ motion based on so-called four-dimensional CT (4DCT) studies by sorting an oversampled CT image dataset into phases of a breathing cycle. Delineating a target in all phases of the breathing cycle allows deriving an internal target volume (ITV). An ITV is representative of the motion envelope containing the tumor at all times during the breathing cycle. Use of a 4DCT for SBRT planning also allows identifying the subset of a breathing cycle during which a target volume or the liver moves only to a smaller degree. The concept of gating uses

this information and will enable radiation beam delivery only when the liver and thus the target are in a defined proportion of the breathing cycle [42]. Such a technique minimizes the volume of an ITV and also the additional liver volume included in a PTV [43, 44]. A major drawback to this technique is a prolongation of treatment delivery, as often up to 70 % of the potential beam delivery time is disabled [45]. Thus, overall treatment times may be prolonged by up to three times over non-gated delivery. Additional concern exists regarding the reliability of 4DCT-based SBRT planning. Both ITV-based planning concept and gated treatment delivery assume a reproducible amount of organ motion during respiration to afford PTV margin reduction. However, in a worst-case scenario, margins may need to be increased to accommodate inter-fraction variations in respiration [46].

Breath-hold planning and delivery techniques require patient compliance, but do not prolong overall treatment delivery when the patient can hold their breath for reasonable amounts of time. Typical patients can hold their breath for 20–35 s, which is sufficient to deliver a respective radiation field from a given gantry angle [47–49]. For rotational radiation administration, the beam delivery needs to be interrupted, and the arc broken into shorter arc segments according to the patient's ability to hold their breath. The adaptation of the treatment planning and delivery process for breath-hold must be done with caution. First, the reproducibility of the breath-hold must be established on a patient specific basis. Not all patients are suitable candidates for breath-hold; for some patients, the target positional variation resulting from various breath-hold maneuvers within the same treatment session is as large as the breathing motion [50].

Real-time tumor tracking during radiation treatment delivery is another approach to reduce adverse effects of organ motion. Motion tracking is driven by the correlation between the location of fiducial markers near the tumor, as detected in orthogonal X-rays, and the location of external markers on the patient's chest. The correlation model is built just after patient setup and is updated throughout the treatment session each time verification X-rays are obtained. Several technical solutions to tumor tracking are realized or subject to ongoing research, including moving the entire linear accelerator, continuous adjustment of the couch position, or use of the multileaf collimator (MLC) to track the shape of a lesion as it moves with respiration [51–55].

Clinical Experience with SBRT of Liver Metastases: Early Institutional Experience

In 1995, Blomgren and Lax published the results of a landmark pilot study researching the potential to establish the use of extracranial stereotactic radiotherapy [56]. The pilot study included patients with primary liver tumors, as well as liver metastases and reported outcomes after 20–45 Gy in 1–4 fractions. In 9 patients, 12 tumors ranging from 5 to 622 cm^3 were treated. Complete response was observed early in follow-up for small tumors (Fig. 30.6 depicts a comparable case), but the time to maximal response was prolonged for larger tumors. In 1998, the Karolinska group updated the data after a median follow-up of 9.6 months for 17 patients with liver metastases. Stable disease was seen in 10 tumors, partial response in 4, and the local control rate was 95 % with a mean survival of 17.8 months [26].

The University of Heidelberg group reported outcomes on 60 liver tumors including 56 metastases in 37 patients treated in a phase 1 dose escalation study [24] . Median target volume was 10 cm^3, with a range from 1 to 130 cm^3. Single-dose delivery was escalated from 14 to 26 Gy. At the 26 Gy dose level, further dose escalation was stopped, despite the fact that a maximally tolerated dose (MTD) was not established. There were no major side effects. Eleven patients experienced an intermittent loss of appetite or mild nausea for 1–3 weeks after therapy. Two patients with tumors close to the diaphragm experienced moderate singultus for 2–3 days after therapy. One patient developed fever lasting for 2 days after therapy. None of the treated patients developed clinically

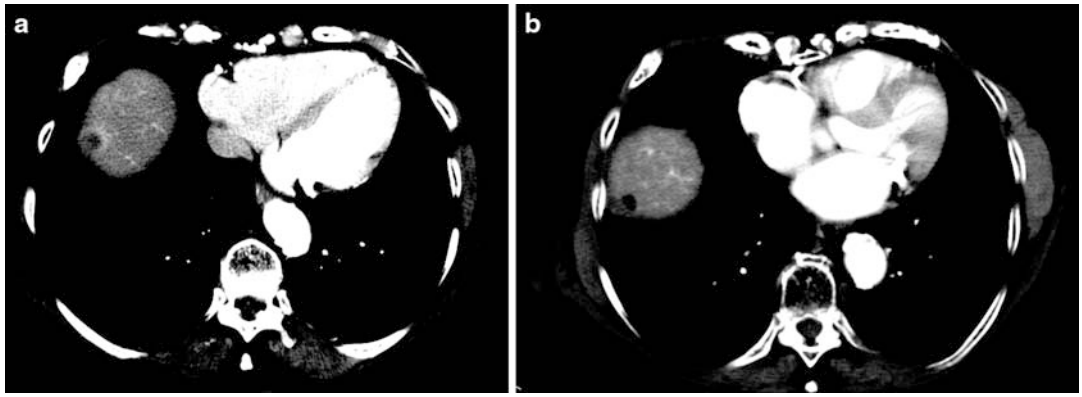

Fig. 30.6 Endometrial cancer liver metastasis before (**a**) and 9 months after SBRT (**b**). Note the loss of rim contrast enhancement in post contrast arterial phase CT scans. A cyst-like remnant can be observed after SBRT

detectable radiation-induced liver disease. Fifty-four (98 %) of 55 tumors were locally controlled after 6 weeks at the initial follow-up based on the CT findings with 22 cases of stable disease, 28 partial responses, and 4 complete responses. The actuarial local tumor control rate was 81 % at 18 months after therapy. A total of 12 local failures were observed during follow-up.

Investigators from the University of Wuerzburg in Germany included 39 patients with 51 hepatic metastases into a prospective study of single- and multi-fraction SBRT [12, 57]. Actual doses prescribed were 30 Gy in 3 fractions (n = 24) and 28 Gy in 4 fractions (n = 1) in a total of 25 lesions, and these patients were analyzed as a low-dose cohort. Patients considered in a high-dose cohort received doses of 37.5 Gy in 3 fractions (n = 13) or 26 Gy in a single setting (n = 8). Mean clinical target volume was 83 cm^3. At a median follow-up of 15 months, nine local failures were observed. Actuarial tumor control was 92 % and 66 % at 1 and 2 years. Eight local recurrences were observed in the low-dose group, with 50 % of colorectal liver metastases in this group experiencing local failure. In 11 colorectal cancer metastases in the high-dose group, no local failure was documented. Consequently, local tumor control was higher in the high-dose group with 100 % and 82 % at 1 and 2 years than in the low-dose group with 86 % and 58 % local control rate at 1 and 2 years. No acute grade 3–5 side effects were observed. Also, no late toxicity clearly related to radiation was documented. Overall survival was 71 % and 41 % at 1 and 2 years.

These landmark series have provided encouraging early outcomes for SBRT treatment of liver metastases. Since the early inception in Sweden, and Germany in the 1990s, additional institutional data and retrospective series analyses have become available.

At Erasmus University, 17 patients with 34 metastatic liver tumors were treated in a phase 1–2 institutional trial to doses of 30–37.5 Gy in 3 fractions [58]. All but 3 patients were diagnosed with metastatic colorectal cancer, and the liver was the only site of metastases at time of treatment. Liver metastases ranged from 0.5 to 6.2 in maximum diameter, and up to 4 lesions were treated. The dose was prescribed to the 65 % isodose surrounding the PTV, resulting in a dose maximum of 150 % at the center of the lesions. For the patients with metastases, the 1- and 2-year actuarial local control rates were 100 % and 86 %, respectively. Local relapse was observed in two metastases after initial complete remission. Overall survival was reported as 85 % and 62 % at 1 and 2 years, respectively. Grade 3 toxicity was observed in two patients with elevation of gamma-glutamyltransferase, potentially related to exposure of 47 % and 40 % of normal liver to doses higher than 15 Gy. This relatively high exposure of the normal liver was a consequence of treating 2 lesions

simultaneously in one patient and presence of a small, post-resection liver volume in the second patient. One case of grade 3 asthenia was observed in a patient who was treated with chemotherapy and resection prior to SBRT. In a 2010 update including at least some of the above-summarized patient population, but with longer follow-up, the 1-year local control rate remained at 100 %, but the 2-year local control (defined as an increase in size based on contrast-enhanced CT or MRI studies) was reduced to 74 % [59]. At a median and maximum follow-up of 26 and 57 months, 9 of 20 patients analyzed had died. Median survival was 34 months, with 2-year survival of 83 %. The same group of investigators studied quality of life following SBRT for liver lesions, including 19 patients with 38 liver metastases [60]. While data were not reported and stratified by primary versus secondary liver lesions, quality of life was maintained for 6 months in patients with continued local tumor control. This finding provided the rationale for further research in a larger multi-institutional study in Europe.

In a recently published phase I study from the Princess Margaret Hospital in Toronto, 68 patients with colorectal cancer liver metastases were treated in a 6-fraction SBRT regimen [13]. Eligible patients had exhausted or were refractory to standard treatment. If extrahepatic systemic disease was present, the largest disease burden had to be hepatic. Individualized radiation dose prescription was based on estimated risk levels for development of RILD and ranged between 27.7 Gy and 60 Gy. The median SBRT dose was 41.8 Gy delivered over 2 weeks. Overall, the investigators found this treatment to be well tolerated, with no acute/subacute RILD, other serious liver toxicity, or any dose-limiting toxicity observed. However, in longer follow-up, one duodenal bleeding event was observed in a patient with progression and invasion of a treated liver metastasis into the organ and another case of delayed small bowel obstruction. Two patients experienced nontraumatic rib fractures, potentially related to chest wall radiation exposure. Tumor response was observed in 49 % of cases with predominantly partial tumor responses or disease stabilization. Complete tumor response was rare and only observed in 4 cases. Median time to maximum response was 6.2 months, and the 1-year local control rate was 71 %. Local control was improved in smaller tumor volumes and in patients that received higher radiation doses. Based on these pilot data, a phase II trial from these investigators is currently underway.

Investigators from the University of Rochester summarized the outcomes of 69 patients with 174 liver metastases treated by a 10-fraction hypofractionated radiation regimen to a total dose of 50 Gy. While this dose delivery schedule would not be considered under the SBRT paradigm, dose planning and delivery techniques match all aspects of typical SBRT. As such, this large retrospective series is included in this review. Dose was prescribed to the 100 % isodose line (IDL), with the 80 % IDL covering the gross tumor volume with a minimum margin of 7 mm. The median overall survival time in this series was 14.5 months, and the actuarial in-field local control rates were 76 % and 57 % at 10 and 20 months, respectively. Complete responses were rare and only observed in five patients. The majority of patients showed partial response ($n = 15$) or stable disease ($n = 33$). In-field recurrence after initial response or disease stabilization was observed in five patients, with median time to relapse of 6.6 months. The limitations of any focal treatment regimen for liver metastases are highlighted by the fact that in 75 % of patients, new hepatic disease manifests during follow-up. The progression-free survival rates were 46 % and 24 % at 6 and 12 months, respectively. While grade 1 or 2 liver function test elevations were noted in 28 % of patients, no grade 3 or higher hepatic toxicity was observed [23].

Prospective Multicenter and Cooperative Group Clinical Trials

The Aarhus University group published results of a multi-institutional phase 2 study on SBRT for colorectal cancer metastases [27]. The study

enrolled 46 patients for treatment of liver metastases between 1999 and 2003. While initial patient enrollment was limited to liver-only metastatic disease, patients were also accepted later when no more than two organ sites (none of them necessarily the liver) were involved in systemic disease. Total dose was 45 Gy in 3 fractions prescribed to the isocenter, with the edge of the PTV receiving no less than 67 % of the prescribed dose (roughly 10 Gy × 3). Outcomes were not reported for lesions by organ site, and enrollment included approximately 30 % of patients with non-hepatic lesion location. Median time to progression was 6.5 months, with most patients developing distant failures or new lesions in the same organ. Median survival was 1.6 years. Hepatic metastases inferred a poorer survival than extrahepatic systemic disease. While one death and three serious adverse events (colonic and duodenal ulcerations) were recorded, the overall morbidity associated with SBRT was considered moderate.

In a multicenter phase I/II clinical trial led by investigators at the University of Colorado and Indiana University, 18 patients with liver metastases were treated on an initial phase I dose escalation protocol; an additional 29 patients were subsequently enrolled in the phase II component of the study [22, 61, 62]. Eligible patients had one to three hepatic metastases, with maximum individual lesion diameter less than 6 cm. In the phase I study, radiation doses were escalated from 36 to 60 Gy in 3 fractions; all patients in phase II were treated to 60 Gy. The dose was prescribed to the 80–90 % isodose (equivalent to 80–90 % of prescribed dose), and at least 700 cm^3 of normal liver had to receive a total dose less than 15 Gy. Results of the phase I component of the study indicated that doses of up to 60 Gy in 3 fraction regimens could be delivered safely for hepatic metastases [23]. While the maximum tolerated dose was not reached, the study successfully enrolled at the highest predefined dose level. The primary phase II study endpoint was in-field tumor control. At a median follow-up of 16 months, local progression was observed in only three of 49 assessable lesions [62]. Median time to progression was 7.5 months after SBRT. Actuarial in-field local control rates at 1 and 2 years after SBRT were 95 % and 92 %, respectively. Among lesions with maximal diameter of 3 cm or less, 2-year local control was 100 %. Median survival was 20.5 months, although 45 % of the patients had active extrahepatic disease at the time of treatment.

In summary, the published results on SBRT of liver metastases are encouraging with respect to offering patients an alternate noninvasive treatment modality promising high local tumor control rates. However, the range of different doses and fractionation schedules used demonstrates the current lack of a consensus regarding the optimal SBRT protocol for liver metastases. Further studies are necessary to define the ideal dose fractionation schedule to achieve optimal tumor control with minimal side effects.

References

1. Li B, Yu J, Suntharalingam M, et al. Comparison of three treatment options for single brain metastasis from lung cancer. Int J Cancer. 2000;90(1):37–45.
2. Rades D, Pluemer A, Veninga T, et al. Whole-brain radiotherapy versus stereotactic radiosurgery for patients in recursive partitioning analysis classes 1 and 2 with 1 to 3 brain metastases. Cancer. 2007;110(10):2285–92.
3. Wang LG, Guo Y, Zhang X, et al. Brain metastasis: experience of the Xi-Jing hospital. Stereotact Funct Neurosurg. 2002;78(2):70–83.
4. Small R, Lubezky N, Ben-Haim M. Current controversies in the surgical management of colorectal cancer metastases to the liver. Isr Med Assoc J. 2007;9(10):742–7.
5. Yoon SS, Tanabe KK. Surgical treatment and other regional treatments for colorectal cancer liver metastases. Oncologist. 1999;4(3):197–208.
6. Vogl TJ, Straub R, Eichler K, et al. Colorectal carcinoma metastases in liver: laser-induced interstitial thermotherapy–local tumor control rate and survival data. Radiology. 2004;230(2):450–8.
7. Solbiati L, Livraghi T, Goldberg SN, et al. Percutaneous radio-frequency ablation of hepatic metastases from colorectal cancer: long-term results in 117 patients. Radiology. 2001;221(1):159–66.
8. Wong SL, Mangu PB, Choti MA, et al. American Society of Clinical Oncology 2009 clinical evidence review on radiofrequency ablation of hepatic metastases from colorectal cancer. J Clin Oncol. 2010;28(3):493–508.

9. Mulier S, Ruers T, Jamart J, et al. Radiofrequency ablation versus resection for resectable colorectal liver metastases: time for a randomized trial? An update. Dig Surg. 2008;25(6):445–60.
10. Kelly H, Goldberg RM. Systemic therapy for metastatic colorectal cancer: current options, current evidence. J Clin Oncol. 2005;23(20):4553–60.
11. Bhardwaj N, Gravante G, Strickland AD, et al. Cryotherapy of the liver: a histological review. Cryobiology. 2010; In print.
12. Wulf J, Hädinger U, Oppitz U, et al. Stereotactic radiotherapy of targets in the lung and liver. Strahlenth Onkol. 2001;177(12):645–55.
13. Lee MT, Kim JJ, Dinniwell R, et al. Phase I study of individualized stereotactic body radiotherapy of liver metastases. J Clin Oncol. 2009;27(10):1585–91.
14. Papiez L, Timmerman R. Hypofractionation in radiation therapy and its impact. Med Phys. 2008;35(1): 112–8.
15. de Pooter JA, Méndez Romero A, Jansen WP, et al. Computer optimization of noncoplanar beam setups improves stereotactic treatment of liver tumors. Int J Radiat Oncol Biol Phys. 2006;66(3):913–22.
16. de Pooter JA, Méndez Romero A, Wunderink W, de Pooter JA, Méndez Romero A, Wunderink W, et al. Automated non-coplanar beam direction optimization improves IMRT in SBRT of liver metastasis. Radiother Oncol. 2008;88(3):376–81.
17. Liu R, Buatti JM, Howes TL, et al. Optimal number of beams for stereotactic body radiotherapy of lung and liver lesions. Int J Radiat Oncol Biol Phys. 2006;66(3):906–12.
18. Chang BK, Timmerman RD. Stereotactic body radiation therapy: a comprehensive review. Am J Clin Oncol. 2007;30(6):637–44.
19. Lax I. Target dose versus extratarget dose in stereotactic radiosurgery. Acta Oncol. 1993;32(4):453–7.
20. de Pooter JA, Wunderink W, Méndez Romero A, et al. PTV dose prescription strategies for SBRT of metastatic liver tumours. Radiother Oncol. 2007;85(2): 260–6.
21. van Laarhoven HW, Kaanders JH, Lok J, et al. Hypoxia in relation to vasculature and proliferation in liver metastases in patients with colorectal cancer. Int J Radiat Oncol Biol Phys. 2006;64(2):473–82.
22. Schefter TE, Kavanagh BD, Timmerman RD, et al. A phase I trial of stereotactic body radiation therapy (SBRT) for liver metastases. Int J Radiat Oncol Biol Phys. 2005;62(5):1371–8.
23. Katz AW, Carey-Sampson M, Muhs AG, et al. Hypofractionated stereotactic body radiation therapy (SBRT) for limited hepatic metastases. Int J Radiat Oncol Biol Phys. 2007;67(3):793–8.
24. Herfarth KK, Debus J, Lohr F, et al. Stereotactic single-dose radiation therapy of liver tumors: results of a phase I/II trial. J Clin Oncol. 2001;19(1):164–70.
25. Fritz P, Kraus HJ, Mühlnickel W, et al. Stereotactic, single-dose irradiation of stage I non-small cell lung cancer and lung metastases. Radiat Oncol. 2006;1:30.
26. Blomgren H, Lax I, Göranson H, et al. Radiosurgery for tumors in the body: clinical experience using a new method. J Radiosurg. 1998;1(1):63–74.
27. Hoyer M, Roed H, Traberg Hansen A, et al. Phase II study on stereotactic body radiotherapy of colorectal metastases. Acta Oncol. 2006;45(7):823–30.
28. Hellman S, Weichselbaum RR. Oligometastases. J Clin Oncol. 1995;13(1):8–10.
29. Mehta N, Mauer AM, Hellman S, et al. Analysis of further disease progression in metastatic non-small cell lung cancer: implications for locoregional treatment. Int J Oncol. 2004;25(6):1677–83.
30. Milano MT, Katz AW, Muhs AG, et al. A prospective pilot study of curative-intent stereotactic body radiation therapy in patients with 5 or fewer oligometastatic lesions. Cancer. 2008;112(3):650–8.
31. Fuss M, Thomas Jr CR. Stereotactic body radiation therapy: an ablative treatment option for primary and secondary liver tumors. Ann Surg Oncol. 2004;11(2): 130–8.
32. Nevinny-Stickel M, Sweeney RA, Bale RJ, et al. Reproducibility of patient positioning for fractionated extracranial stereotactic radiotherapy using a double-vacuum technique. Strahlenther Onkol. 2004;180(2): 117–22.
33. Lax I, Blomgren H, Näslund I, et al. Stereotactic radiotherapy of malignancies in the abdomen. Methodological aspects. Acta Oncol. 1994;33(6):677–83.
34. Fuss M, Salter BJ, Rassiah P, et al. Repositioning accuracy of a commercially available double-vacuum whole body immobilization system for stereotactic body radiation therapy. Technol Cancer Res Treat. 2004;3(1):59–67.
35. Purdie TG, Bissonnette JP, Franks K, et al. Cone-beam computed tomography for on-line image guidance of lung stereotactic radiotherapy: localization, verification, and intrafraction tumor position. Int J Radiat Oncol Biol Phys. 2007;68(1):243–52.
36. Guckenberger M, Sweeney RA, Wilbert J, et al. Image-guided radiotherapy for liver cancer using respiratory-correlated computed tomography and cone-beam computed tomography. Int J Radiat Oncol Biol Phys. 2008;17(1):297–304.
37. Case RB, Sonke JJ, Moseley DJ, et al. Inter- and intrafraction variability in liver position in non-breath-hold stereotactic body radiotherapy. Int J Radiat Oncol Biol Phys. 2009;75(1):302–8.
38. Brock KK, Dawson LA. Adaptive management of liver cancer radiotherapy. Semin Radiat Oncol. 2010; 20(2):107–15.
39. Fuss M, Boda-Heggemann J, Papanikolau N, et al. Image-guidance for stereotactic body radiation therapy. Med Dosim. 2007;32(2):102–10.
40. Booth JT, Zavgorodni SF. Set-up error & organ motion uncertainty: a review. Australas Phys Eng Sci Med. 1999;22(2):29–47.
41. Langen KM, Jones DT. Organ motion and its management. Int J Radiat Oncol Biol Phys. 2001;50(1): 265–78.

42. Briere TM, Beddar S, Balter P, et al. Respiratory gating with EPID-based verification: the MDACC experience. Phys Med Biol. 2009;54(11):3379–91.
43. Guckenberger M, Krieger T, Richter A, et al. Potential of image-guidance, gating and real-time tracking to improve accuracy in pulmonary stereotactic body radiotherapy. Radiother Oncol. 2009;91(3):288–95.
44. Wurm RE, Gum F, Erbel S, et al. Image guided respiratory gated hypofractionated Stereotactic Body Radiation Therapy (H-SBRT) for liver and lung tumors: initial experience. Acta Oncol. 2006;45(7):881–9.
45. Dawood O, Mahadevan A, Goodman KA. Stereotactic body radiation therapy for liver metastases. Eur J Cancer. 2009;45(17):2947–59.
46. Korreman SS, Juhler-Nøttrup T, Boyer AL. Respiratory gated beam delivery cannot facilitate margin reduction, unless combined with respiratory correlated image guidance. Radiother Oncol. 2008;86(1):61–8.
47. Eccles C, Brock KK, Bissonnette JP, et al. Reproducibility of liver position using active breathing coordinator for liver cancer radiotherapy. Int J Radiat Oncol Biol Phys. 2006;64(3):751–9.
48. Dawson LA, Eccles C, Bissonnette JP, et al. Accuracy of daily image guidance for hypofractionated liver radiotherapy with active breathing control. Int J Radiat Oncol Biol Phys. 2005;62(4):1247–52.
49. Boda-Heggemann J, Walter C, Mai S, et al. Frameless stereotactic radiosurgery of a solitary liver metastasis using active breathing control and stereotactic ultrasound. Strahlenther Onkol. 2006;182(4):216–21.
50. Heinzerling JH, Anderson JF, Papiez L, et al. Four-dimensional computed tomography scan analysis of tumor and organ motion at varying levels of abdominal compression during stereotactic treatment of lung and liver. Int J Radiat Oncol Biol Phys. 2008;70(5):1571–8.
51. Lieskovsky YC, Koong A, Fisher G, et al. Phase I Dose escalation study of CyberKnife Stereotactic Radiosurgery for liver malignancies. Int J Radiat Oncol Biol Phys. 2005;63(Suppl 1):S283.
52. Nioutsikou E, Seppenwoolde Y, Symonds-Tayler JR, et al. Dosimetric investigation of lung tumor motion compensation with a robotic respiratory tracking system: an experimental study. Med Phys. 2008; 35(4):1232–40.
53. Seppenwoolde Y, Berbeco RI, Nishioka S, et al. Accuracy of tumor motion compensation algorithm from a robotic respiratory tracking system: a simulation study. Med Phys. 2007;34(7):2774–84.
54. Keall PJ, Sawant A, Cho B, et al. Electromagnetic-guided dynamic multileaf collimator tracking enables motion management for intensity-modulated arc therapy. Int J Radiat Oncol Biol Phys. 2010; In Press.
55. Fenwick JD, Tomé WA, Jaradat HA, et al. Quality assurance of a helical tomotherapy machine. Phys Med Biol. 2004;49(13):2933–53.
56. Blomgren H, Lax I, Näslund I, et al. Stereotactic high dose fraction radiation therapy of extracranial tumors using an accelerator. Clinical experience of the first thirty-one patients. Acta Oncol. 1995; 34(6):861–70.
57. Wulf J, Guckenberger M, Haedinger U, et al. Stereotactic radiotherapy of primary liver cancer and hepatic metastases. Acta Oncol. 2006;45(7):838–47.
58. Méndez Romero A, Wunderink W, Hussain SM, et al. Stereotactic body radiation therapy for primary and metastatic liver tumors: a single institution phase i–ii study. Acta Oncol. 2006;45(7):831–7.
59. van der Pool AE, Méndez Romero A, Wunderink W, et al. Stereotactic body radiation therapy for colorectal liver metastases. Br J Surg. 2010;97(3):377–82.
60. Méndez Romero A, Wunderink W, van Os RM, et al. Quality of life after stereotactic body radiation therapy for primary and metastatic liver tumors. Int J Radiat Oncol Biol Phys. 2008;70(5):1447–52.
61. Kavanagh BD, Schefter TE, Cardenes HR, et al. Interim analysis of a prospective phase I/II trial of SBRT for liver metastases. Acta Oncol. 2006;45(7): 848–55.
62. Rusthoven KE, Kavanagh BD, Cardenes H, et al. Multi-institutional phase I/II trial of stereotactic body radiation therapy for liver metastases. J Clin Oncol. 2009;27(10):1572–8.

Combination Therapy for Liver Metastases: Chemotherapy and Radiologic Interventions

31

Melinda Dunlap and Jordan Berlin

Abstract

The liver is a likely site of metastases for almost every malignancy. However, some cancers are more likely to metastasize to liver than others. Additionally, for some cancers, liver may be the only site of metastases giving a unique opportunity to treat a tumor with more of a regional focus. Particularly in the case of colorectal cancer, this has become increasingly common as full disease control may be achieved. However, whenever cancer has metastasized to the liver, there is always the possibility that it has spread systemically. Therefore, approaches to isolated liver metastases have varied, largely due to the natural history of the disease involved. Approaches include regional therapy only, systemic therapy, and combinations of regional and systemic therapy. Liver metastasis secondary to primary breast, lung, melanoma, and gastrointestinal tumors including colon, esophageal, and gastric are being studied with dual therapy of HAI (hepatic arterial infusion) and systemic chemotherapy. The research describing liver metastasis from solid tumors includes only case studies and phase I trials. Given the paucity of literature for these tumors, this chapter will focus largely on colorectal cancer and the combination approach as there are chapters to focus on regional approaches as well as the principles of systemic approaches in each of the diseases.

Systemic and localized chemotherapy in combination with radiologic interventions for the treatment of cancers that have metastasized to the liver focuses on colorectal cancer.

Introduction

The liver is a likely site of metastases for almost every malignancy. However, some cancers are more likely to metastasize to liver than others. Additionally, for some cancers, liver may be the only site of metastases giving a unique opportunity to treat a tumor with more of a regional focus.

M. Dunlap (✉) • J. Berlin
Department of Medicine, Division of Hematology and Oncology, Vanderbilt University Medical Center, Nashville, TN, USA
e-mail: melinda.dunlap@vanderbilt.edu; jordan.berlin@vanderbilt.edu

D.E. Dupuy et al. (eds.), *Image-Guided Cancer Therapy*, DOI 10.1007/978-1-4419-0751-6_33,

Particularly in the case of colorectal cancer, this has become increasingly common as full disease control may be achieved. However, whenever cancer has metastasized to the liver, there is always the possibility that it has spread systemically. Therefore, approaches to isolated liver metastases have varied, largely due to the natural history of the disease involved. Approaches include regional therapy only, systemic therapy, and combinations of regional and systemic therapy. Liver metastasis secondary to primary breast, lung, melanoma, and gastrointestinal tumors including colon, esophageal, and gastric are being studied with dual therapy of HAI (hepatic arterial infusion) and systemic chemotherapy. The research describing liver metastasis from solid tumors includes only case studies and phase I trials [1–6]. Given the paucity of literature for these tumors, this chapter will focus largely on colorectal cancer and the combination approach as there are chapters to focus on regional approaches as well as the principles of systemic approaches in each of the diseases.

Rationale for Combined Modality Approach

Multimodality treatment with chemotherapy and interventional oncology procedures offers a unique and innovative approach toward metastatic cancers from other sites. In some diseases, such as colorectal cancer, neuroendocrine tumors, and melanoma, surgical resection if possible has become a standard approach for curative intent; however, few patients are candidates. The patient's tumor must be limited to the liver and represent the only site of metastasis to be eligible for resection. Other factors, such as extrahepatic disease, tumor size, number of lesions, vascular invasion, portal hypertension, and underlying hepatic function, are also critical factors in determining resectability [7–9]. However, if the tumors are unresectable, approaches have been developed that take advantage of the liver's dual blood supply, capability of significant first-pass metabolism of drugs, and its regenerative capabilities to aggressively treat the visible disease. However, any tumor spread to another organ represents the capability for the cancer to spread throughout the system. Treating regional disease while ignoring the potential for unseen systemic disease is unlikely to produce long-term disease control. Therefore, combined modality approaches that require integration of disciplines, including surgical, medical, and radiologic specialities, are of growing interest.

Principles of Systemic Therapy

Systemic therapy used to be synonymous with chemotherapy, but new developments in treating cancer have changed that. First, we have long used hormonal therapies in the treatment of prostate and breast cancers. Second, for decades therapies that take advantage of the immune system to kill the cancer have been studied, though few have yielded successes. Most recently, cancer has been treated with a class of agents, called biologics or targeted agents for lack of a better nomenclature. While chemotherapy is designed to affect the DNA and mechanisms that are involved in cellular division, the targeted agents focus on proteins that are abnormal in a variety of ways in cancers. The proteins can be overexpressed, mutated due to genetic alterations within the cancer cells, or constitutively active/dysregulated. In turn, these proteins may affect the abilities for the cancer cells to grow, invade, or affect their environment. Additionally, some of the novel targets are found on the cells of the stroma, the blood vessels, or within the host environment within which the cancer is growing. Finally, some cancers such as breast and prostate cancer may be treated with hormonal therapies. It is beyond the scope of this chapter to discuss all the potential systemic therapies for all the cancers that might spread to the liver. Instead, this chapter will focus on the integration of systemic therapies with locoregional interventions within the liver in the limited number of cancers in which these studies have been conducted.

Colorectal Cancer

Approximately 50 % of patients diagnosed with colorectal cancer eventually develop liver metastasis. Hence, interventional oncology techniques have been studied extensively in this population [10]. Colorectal cancer is the third most common type of cancer in the United States and is the third leading cause of cancer-related death in both men and women. Just under 150,000 new cases of colorectal cancer (106,000 colon cases; 40,800 rectal cases) are diagnosed annually, and approximately 50,000 will die from the disease. Of these patients, 15–25 % develop synchronous liver metastases [11–14], and anywhere from 20 % to 25 % develop metachronous hepatic tumors [11, 15–17]. In 30 % of patients with either synchronous or metachronous liver metastases, the liver represents the only site of metastasis [11, 18]. From 10 % to 20 % of patients with liver metastasis are usually considered resection candidates with intent to cure [19]. When patients undergo liver metastasectomy, within the first 2 years, up to two-thirds of the patients have recurrence, and 5-year survival is roughly 30–40 % [20].

If liver resection is not an option, alternative approaches for treatment have been developed. Options including hepatic arterial infusion, chemoembolization, radioembolization, radiofrequency ablation, and cryotherapy have been studied. While these interventions may reduce tumor burden within the liver, local reoccurrence of cancer as well as extrahepatic tumor spread can still occur. Therefore, the addition of systemic therapy to locoregional intervention techniques either sequentially or concurrently is being studied to improve the patient outcomes.

Systemic therapy for colorectal cancer was historically fluoropyrimidine-based, usually 5-fluorouracil (5-FU) given with modulators of 5-FU, most commonly leucovorin (folinic acid). However, in recent years, two other chemotherapy agents, irinotecan and oxaliplatin, were proven to increase the efficacy of 5-FU. Systemic therapy now most often consists of couplet chemotherapy combining 5-FU with either oxaliplatin or irinotecan, although single-agent therapy with 5-FU or with irinotecan is still used, and on occasion, all 3 chemotherapy agents are used together. In addition, while intravenous infusion of 5-FU is still the most common method of administration, oral formulations of 5-FU prodrugs alone (capecitabine) or in combination with modulators of 5-FU (S-1) are now available in different parts of the world. Finally, new targeted agents have demonstrated benefit in colorectal cancer. Bevacizumab, an antibody to the vascular endothelial growth factor, adds to the effectiveness of either first-line or second-line chemotherapy regimens for metastatic disease. Cetuximab and panitumumab, monoclonal antibodies to the epidermal growth factor receptor, have both demonstrated single-agent activity and benefit when added to chemotherapy in certain settings.

Hepatic Arterial Infusion (HAI) Alone for Metastatic Colorectal Cancer Disease

The underlying principle for HAI focuses on the notion that normal hepatocytes receive their blood supply from both the hepatic artery and portal vein with the majority provided by the portal venous system. In contrast, liver metastases are almost solely perfused by the hepatic artery. Ideally, infusion of chemotherapy through the hepatic artery would maximize cytotoxicity to the sites of malignant cells, while normal liver tissue with its dual blood supply would experience less chemotoxicity. Drugs with a high clearance rate that are metabolized in the liver are recommended for HAI. These agents that are principally metabolized in the liver will have very limited exposure if infused into the liver directly (first-pass effect). FUDR (floxuridine) is one of the most commonly used drugs for hepatic regional therapy because approximately 94–99 % is extracted during the first pass through the liver. In contrast, 5-fluorouracil (5-FU) has only 19–55 % drug extraction with its first pass through the liver, thus allowing for a considerable amount of drug to enter the systemic circulation [21, 22]. When a significant amount of drug is not cleared rapidly and enters

systemic circulation, the advantages of HAI relative to systemic therapy are diminished.

Although HAI has fewer systemic toxicities relative to SCT (systemic chemotherapy), significant side effects can still occur. Approximately 20 % of patients experience gastritis or duodenitis depending on the collateral blood supply directed toward the stomach and duodenum [23]. Elevation of serum aspartate aminotransferase (AST) and bilirubin occurs frequently when HAI is administered, and sclerosing cholangitis has been reported in 5–29 % of patients [24]. A study at Memorial Sloan-Kettering reports that 70 % of patients needed a dose reduction or treatment delay within the first 3 months of therapy. It is hypothesized that the bile ducts are more sensitive to HAI chemotherapy because their blood supply is primarily derived from the hepatic artery. Hepatocytes, in contrast, are perfused by both the hepatic artery and portal vein. Kemeny et al. performed a randomized trial using HAI of FUDR and dexamethasone (DEX) versus FUDR alone. Patients treated with FUDR and DEX were less likely to have elevated bilirubin (bilirubin >200% from baseline; 30 % vs. 9 %, $p = 0.07$) and sclerosing cholangitis (6 % vs. 0 %). Furthermore, partial and complete responses as well as overall survival were better in the group that received DEX and FUDR (CR 4 % vs. 8 %; PR 36 % vs. 63 %; $p = 0.03$; OS 15 months vs. 23 months $p = 0.06$) [24].

Multiple randomized clinical trials (RCT) have compared HAI to systemic chemotherapy. Studies initially utilized percutaneous hepatic arterial lines which were fraught with complications including bleeding and thrombosis. Subsequently, implantable infusion pumps were developed and are now the mainstay for HAI chemotherapy. In 2007, a meta-analysis reviewed ten randomized controlled trials that compared HAI and systemic chemotherapy [25]. In nine of the studies, floxuridine (FUDR) was used for HAI, while fluorouracil (5-FU) and leucovorin were used in one trial. Different types of systemic chemotherapy (SCT) were used in the ten trials and included FUDR, 5-FU, 5-FU/leucovorin, and 5-FU/supportive care. Tumor response was 42.9 % and 18.4 % in the HAI and SCT groups, respectively. Unfortunately, the 2007 meta-analysis indicated that although HAI yielded significant response rates, it did not increase overall survival (OS) relative to SCT. Further, the SCT at the time of these studies was limited to fluoropyrimidines. More recent therapies that incorporate oxaliplatin and irinotecan into the SCT regimen produce tumor responses similar to or higher than those observed with fluoropyrimidine HAI [26, 27].

HAI in Combination with Chemotherapy for Metastatic Colorectal Cancer

Systemic chemotherapy, either given sequentially or concurrently with HAI, offers the advantage of locoregional therapy to hepatic metastasis along with systemic treatment of extrahepatic lesions. O'Connell et al. [28] studied a sequential regimen of HAI FUDR given for 14 consecutive days followed by a 1-week break from therapy and then initiation of daily × 5 days of systemic chemotherapy with 5-FU and leucovorin. FUDR was repeated 3 weeks after completion of the prior FUDR, and the systemic chemotherapy was given at 5-week intervals. Forty patients were treated with this sequential regimen, and 62 % had regression of liver metastases. Median time to progression (TTP) and median overall survival (OS) were 9 and 18 months, respectively. Porta et al. performed a similar phase II study treating 32 patients with sequential HAI FUDR and SCT with 5-FU and leucovorin [29]. They reported a 53 % objective response and 25 % disease stabilization rate. Median TTP and median OS were 7.5 and 9 months, respectively. In a small study, Shimonov et al. also utilized sequential treatment with HAI and systemic chemotherapy. However, they employed HAI irinotecan and added carboplatin to the SCT of 5-FU and leucovorin [30]. Fifteen patients (5 chemo-naive) with colorectal cancer and isolated liver metastases were treated with partial responses noted in 40 % of the patients.

More recent studies of HAI therapy have attempted to integrate the newer systemic agents. Ducreux et al. used concurrent systemic and HAI

chemotherapy when treating colorectal cancer patients with non-operable liver metastases [31]. Patients received oxaliplatin HAI combined with the LV5FU2 (5-fluorouracil both bolus and infusional along with intravenous leucovorin given every 2 weeks). The response rate was 64 %. Median overall survival was 27 months.

HAI in Combination with Systemic Chemotherapy for Resectable Colorectal Liver Metastases

With the high rates of response in hepatic metastases, a logical next step was to evaluate HAI therapy as a neoadjuvant or adjuvant treatment for resectable/resected liver metastases. Downsizing colorectal cancer with liver-only metastases to convert unresectable disease to resectable is a relatively new goal brought on by advances in surgical techniques and more effective chemotherapy regimens with higher response rates that are more durable. At Hopital Paul Brousse, a review of their experience with newer systemic regimens given to 1,104 patients with unresectable liver-only metastases from colorectal cancer, 138 (12.5 %) were downsized to resectability with 5- and 10-year survival rates of 33 % and 23 %, respectively [32].

In the aforementioned Ducreux study of HAI oxaliplatin combined with systemic LV5FU2, five patients (19 %) deemed inoperable before treatment were converted to resectable after therapy [31]. Kemeny et al. performed a phase I trial administering HAI floxuridine (FUDR) and dexamethasone in combination with SCT consisting of either oxaliplatin and irinotecan (group A) or oxaliplatin, 5-FU, and leucovorin (group B). The complete and partial response rates totaled were 90 % and 87 % for groups A and B, respectively. Median TTP was 36 and 22 months, and seven patients in group A were able to undergo liver resection [33]. With such high response rates, Kemeny et al. further explored systemic oxaliplatin and irinotecan with concurrent HAI of FUDR/DEX to determine if unresectable liver metastasis could be converted to resectable. The patient population had extensive liver disease (73 % $>$ 5 liver lesions, 98 % with bilobar disease, 86 % $>$ 6 segments involved). Both chemotherapy-naïve and heavily pretreated patients were included and had a 57 % and 47 % conversion to resectability, respectively [34]. Similarly, in a retrospective analysis of concurrent HAI and systemic irinotecan in non-operable, heavily pretreated patients, partial response rates of 44 % resulted in surgical resection for 18 % of the patients [35]. Accounting for the fact that the definitions of resectable versus unresectable liver metastases vary among surgeons and institutions, there is significant promise for the use of these therapies to downsize tumors to the point of resectability and potential for long-term disease control.

HAI has also been evaluated in the adjuvant setting for colorectal liver metastases. Retrospective and prospective studies recently have been reviewed by N. E. Kemeny [36]. One of the retrospective study from 1991 to 2002 by Memorial Sloan-Kettering Cancer Center (MSKCC) revealed a benefit from HAI following resection of CRC metastasis in the liver. The multivariate analysis showed that postoperative HAI was a significant factor in survival (68 months vs. 50 months in adjuvant HAI vs. no HAI; HR 0.64; 95 % CI, 0.51–0.81; $P < 0.001$) [37]. House et al. also performed a retrospective study from 2001 to 2005 on 250 colorectal cancer patients. Following resection of liver mets, patient received systemic therapy with FOLFOX or FOLFIRI alone or in combination with HAI. Five-year overall survival was 72 % versus 52 %, respectively [38]. Additional smaller retrospective and meta-analysis have shown improvements in OS and DFS when HAI was employed in the adjuvant setting [39–41].

Prospective studies have also examined the use of HAI in the adjuvant setting. ECOG conducted a study including 109 CRC patients that had resection of anywhere from 1 to 3 liver mets. Patients were randomly assigned to receive HAI plus SCT versus observation. In the patients that tolerated HAI pump therapy, the DFS at 4 years was 46 % versus 25 % for the observation group ($p = 0.04$) [42]. An additional study in Germany evaluated 226 patients and showed no improvement in median TTP at the 18-month

interim analysis. Of note, patients received HAI through a PORT instead of an internal catheter which decreased the time of infusion. Moreover, FU, which has poorer hepatic extraction than FUDR, was employed. These factors may have contributed to the limited success of the German study [43]. An additional prospective trial was performed by MSKCC. Patients who had undergone liver resection were randomized to either 6 months of HAI (FUDR/Decadron) and SCT (FU/LV) or SCT (FU/LV) alone. Toxicities were similar in both groups with the expection of increased diarrhea in the HAI group. Overall survival at 10 years was 41 % and 27.2 % for the HAI/SCT and SCT-alone groups, respectively [36, 44]. Lygidakis et al. performed a prospective randomized trial including 122 patients. Four-year survival was 73 % for the HAI plus SCT group and 60 % for the SCT-alone group ($p = 0.05$) [45].

Addition of molecularly targeted therapies to HAI and systemic chemotherapy is being explored in metastatic colorectal cancer. Kemeny et al. completed a randomized phase II trial evaluating adjuvant therapy in patients with resected hepatic metastases from colorectal cancer. Patients were randomly assigned to systemic chemotherapy (FOLFOX) plus HAI (FUDR/Decadron) with or without bevacizumab. Four-year survival was 81 % and 85 % ($p = 0.5$), and DFS at 1 year was 71 % and 83 % for patients with and without bevacizumab, respectively. Patients receiving bevacizumab had a higher rate of biliary toxicity (5/35 patients vs. 0/38 patients; $p = 0.2$) [46]. Although this initial study incorporating bevacizumab into the HAI/systemic chemotherapy regimen did not improve disease-free survival or overall survival, further efforts including other molecularly targeted therapies should not be abandoned.

Chemoembolization and Systemic Therapy

Another modality of treatment that takes advantage of the dual blood supply to the liver and single supply to the tumor is chemoembolization or bland embolization. In bland embolization, the hepatic artery is accessed, and through a variety of methods, the artery feeding the tumor is embolized. In chemoembolization, either chemotherapy is infused into the tumor of the feeding branch of the hepatic artery followed by embolization or, more recently, drug-eluting beads (DEBs) impregnated with the chemotherapy of choice are used to simultaneously deliver chemotherapy locally and embolize the tumor. These techniques are discussed in more detail in Chapter 27.

Radioembolization and Systemic Therapy

A newer advance on bland embolization is the development of radiation-impregnated beads that allows delivery of radioactivity directly to the liver metastases via the hepatic artery while simultaneously at least partially embolizing the tumors. Two forms of radiation-labeled beads have been approved for use in cancer, but only yttrium-labeled selective internal radiolabeled (SIR) beads have been approved for colorectal cancer. Seventy-four patients were analyzed in a first, small randomized trial comparing systemic 5-FU and leucovorin to the same regimen in combination with radioembolization with SIR beads. In this study, response rates were higher for the SIR + SCT arm compared to the SCT-alone arm [47].

Radiofrequency Ablation

Surgical resection of metastatic liver tumors continues to be the most effective therapy; however, only 10–20 % of patients with colorectal liver metastases are candidates for liver resection based on patient performance status and number, size, and location of metastatic lesions [48]. Radiofrequency ablation (RFA) is an alternative option for treating unresectable liver metastases. RFA transmits electrical current from a radiofrequency generator to a probe tip in the tumor, and the high-frequency (400 kHz) current

causes ionic vibrations, thus increasing the temperature within the tumor. This technique is described in greater detail in Chapter 26. Extrahepatic metastasis, local recurrence, and new hepatic lesions can still occur following RFA therapy.

RFA and Systemic Chemotherapy

Radiofrequency ablation has been explored before and after systemic chemotherapy. There is a paucity of literature describing the optimal treatment protocol including sequence of therapy, extent of RFA, and choice of chemotherapy. Machi et al. performed a prospective trial in which RFA and chemotherapy together in first-line and second-line therapy were used to treat patients with unresectable liver metastases from colon cancers [49]. The data from Machi's study was evaluated retrospectively. Systemic therapy consisted of 5-FU, leucovorin, and/or irinotecan and/or eventually oxaliplatin (not available at initiation of study). For patients receiving first-line RFA and SCT, median survival was 48 months which compared favorably with patients receiving first-line chemotherapy alone (median survival of 19–22 months) [50, 51]. In patients receiving SCT followed by second-line RFA, the median survival was 22 months which compares favorably with studies using second-line chemotherapy alone (11–15 months median survival) [52, 53].

RFA provides a useful method of reducing hepatic tumor burden in patients with unresectable metastatic colorectal cancer. When combined with chemotherapy, initial studies are encouraging that it may be able to affect the natural history of colorectal cancer. The best timing of RFA therapy in combination with chemotherapy has yet to be determined. Data from EORTC 40004 (closed in June 2007, phase II randomized trial comparing treatment of CRC liver metastasis with either chemotherapy alone or chemotherapy and radiofrequency) is pending [54]. Further studies evaluating RFA in combination with chemotherapy and the results from EORTC 40004 will be necessary to elucidate the optimal combination of these modalities.

Neuroendocrine Cancers

Neuroendocrine tumors (NET) encompass a diverse group of malignancies that range from well- to poorly differentiated subtypes. Synthesis and secretion of hormonally active polypeptides is characteristic of these tumors [55]. Since neuroendocrine cells exist throughout the body, tumors can arise from practically any site. The most common sites include small bowel, lung, appendix, and pancreas. The WHO classification of NETs describes three subsets – well-differentiated tumor (carcinoid), well-differentiated neuroendocrine carcinoma (malignant carcinoid), and poorly differentiated carcinoid [56]. The two well-differentiated subsets are distinguished from one another based on the grade and behavior of the mass. The well-differentiated tumors include carcinoid, pheochromocytoma, medullary thyroid, paragangliomas, and pancreatic islet cell tumors (gastrinoma, insulinoma, glucagonoma, VIPoma, and somatostatinoma). The majority of well-differentiated tumors arise in the gastrointestinal tract and are thus referred to as gastroenteropancreatic neuroendocrine tumors or carcinoid tumors. These tumors are often considered benign secondary to slow growth, and the absence of metastasis or local invasion. Well-differentiated neuroendocrine carcinomas, in contrast, have locoregional spread or metastasis. As for the poorly differentiated neuroendocrine carcinomas, they are considered high grade and have undifferentiated or anaplastic small cells.

Gastroenteropancreatic neuroendocrine tumors, as mentioned above, are well-differentiated tumors usually classified as benign based on their behavior. Although less common, malignant behavior (large tumor burden, metastases, mitotic rate, perineural and lymphovascular invasion) is observed in some gastroenteropancreatic NETs. Initial diagnosis is often delayed since patients are often asymptomatic or have vague abdominal symptoms, and approximately 50 % of patients have metastatic disease at diagnosis. Clinical course is extremely variable. Patients can remain asymptomatic for

years with indolent tumors. In contrast, large tumor burden, metastatic disease, and secretion of peptide hormones can cause significant morbidity necessitating therapy.

Surgical resection, targeted radiation, and chemical therapies have been employed for the treatment of carcinoids. Localized tumors that are amenable to resection should be surgically removed. Removal of primary tumors and hepatic metastases also has been shown to improve the quality of life and survival; however, patients with hepatic metastases will reoccur [57]. Radiation therapy appears to have limited benefit toward visceral lesions but has been used for lytic bone lesions to improve quality of life. Further, neuroendocrine tumors of the GI tract are fairly resistant to traditional chemotherapies. Single-agent therapies with doxorubicin, etoposide, 5-fluorouracil, streptozocin, or dacarbazine have only mild response (8–30 %) [58]. Combination chemotherapy has been explored, but the benefit over single-agent modality remains uncertain.

Since neuroendocrine tumors of the GI tract are often resistant to standard chemotherapies and can eventually become life-threatening depending on their location and impact on surrounding tissues, molecular-targeted agents represent an innovative approach toward these tumors. Molecular-targeted agents are currently being explored as an alternative to cytotoxic chemotherapy. Therapies directed at PDGFR, EGFR, VEGFR, c-KIT, and mTOR have shown some promise for neuroendocrine tumors [59]. For instance, PDGF expression has been discovered in approximately 70 % of carcinoid tumor [60].

Multi-targeted tyrosine kinase inhibitors, imatinib and sunitinib, are being explored in pancreatic neuroendocrine tumors. Kulke et al. found that patients with advanced neuroendocrine tumors who were treated with sunitinib showed a 10 % response rate and an 81 % disease stabilization based on CT imaging [61]. Furthermore, Kulke et al. performed a two-cohort, phase II study evaluating the effects of sunitinib in advanced carcinoid and pancreatic neuroendocrine tumors [62]. Patients (41 carcinoid and 66 pancreatic endocrine tumor) received 6-week cycles of sunitinib (50 mg daily × 4 weeks, off 2 weeks). In the pancreatic endocrine patients, an objective response of 16.7 % (11 of 66) was seen and stable disease in 68 % (45 of 66). The objective response rate in carcinoid tumors was only 2.4 % (1 of 41 patients), and stable disease was seen in 83 % of patients (34 of 41). While sunitinib showed activity against pancreatic neuroendocrine tumors, its effectiveness against carcinoid tumors was uncertain. A multinational, randomized, double-blind, placebo-controlled phase three trial in patients with advanced pancreatic neuroendocrine tumors has now been published. A total of 171 patients were randomized (1:1) to receive sunitinib (37.5 mg daily) versus placebo. The study was discontinued early when more serious events in the placebo group were observed. Median progression-free survival was 11.4 months versus 5.5 months in the sunitinib and placebo groups, respectively ($p < 0.001$) [63]. VEGF also plays a significant role in the biological activity of carcinoid tumors. Expression of VEGF in tumors was noted to correlate with decreased progression-free survival and metastases [64]. Further, a phase II trial utilizing bevacizumab (monoclonal antibody against VEGF-A) plus octreotide versus peg-interferon and octreotide showed improved progression-free survival at 18 weeks (96 % vs. 68 % respectively) [65]. Patients who progressed on interferon actually demonstrated disease stabilization on bevacizumab. Currently, a randomized phase III trial comparing interferon a-2b plus octreotide to octreotide plus bevacizumab is underway.

Abnormalities in the mTOR pathway have also been reported in neuroendocrine tumors. A phase II study using mTOR inhibitors, everolimus, with or without octreotide LAR in patients with neuroendocrine tumors has shown antitumor activity. A 10 % partial response and 68 % disease stabilization were seen in the everolimus without octreotide patients. The group that utilized octreotide in addition to everolimus had a 4 % partial response and 80 % disease stabilization [66]. Everolimus has further been studied in a phase III prospective randomized trial. Patients with pancreatic neuroendocrine tumors were randomized to everolimus

10 mg daily (207 patients) or placebo (203 patients). The median progression-free survival was 11 and 4.6 months in the everolimus and placebo groups, respectively ($p < 0.001$) [67].

Melanoma

Melanoma is a complex disease originally from almost any cutaneous surface of the body though most commonly from sun-exposed skin. In addition, it can arise from internal organs on rare occasion and from the eye. Melanoma can metastasize to the liver without evidence of distant spread elsewhere. While most of the patients who present this way have cutaneous melanoma, this is due to the relative incidence compared to ocular melanoma that almost exclusively metastasizes to the liver but is a rare form.

Melanoma has traditionally been resistant to cytotoxic chemotherapies. One of the older agents, dacarbazine (DTIC), results in response rates of 10 % or less but has traditionally been considered a standard treatment option. Very little has demonstrated benefit when compared to dacarbazine. However, melanoma has unique characteristics that make it potentially more susceptible to immune modulation therapy. Interferon and interleukin-2 (IL2) have both met with limited success but for a long time have been the mainstay of therapy when needed.

Use of molecularly targeted agents has shown some promising results in patients with metastatic melanoma. A phase III trial using ipilimumab in patients with metastatic melanoma has shown an increase in median overall survival. The trial had three arms which included ipilimumab monotherapy, ipilimumab plus gp100 peptide vaccine, and gp100 peptide vaccine monotherapy. Patients receiving ipilimumab plus vaccine versus vaccine monotherapy had a median overall survival of 10.0 months and 6.4 months, respectively ($p < 0.001$) [68]. The study arm with ipilimumab monotherapy had a 10.1-month survival ($p = 0.003$ when compared to vaccine monotherapy). The two arms containing ipilimumab with or without the vaccine showed no difference in overall survival.

Conclusion

Combinatorial therapy with systemic chemotherapy and interventional oncology procedures offers a new approach to tumors that have metastasized to the liver. The majority of literature describes metastatic colorectal cancer, but data is limited still. With the exception of HAI therapy, the majority of these treatments are approved with minimal data as they are considered devices rather than requiring the burden of proof necessary to get a new drug approved. This ironically negatively impacts our knowledge of the true efficacy of the regimens. Rather than having well-conducted prospective trials, single-institution experiences and retrospective reviews dominate the literature. Patients are highly selected, and it becomes difficult to fully interpret the data and have a truly informed discussion with patients about the risk/benefit ratio from these newer modalities of therapy. This is a dangerous approach that actually hampers the capability of deciding on the best approach to patients and should be replaced with well-designed prospective trials. While done with the best of intentions, this lack of systematic study represents a failure of the medical community to maintain the scientific standards upon which the field was built. Aside from HAI plus systemic therapy, it is difficult to recommend any of the regimens in this chapter outside the auspices of a well-conducted clinical trial. Alternatively, HAI therapy has its own difficulties. Placement of the HAI pumps is conducted at only a select few institutions, and the placement and use of these pumps has a learning curve. In addition, management of the toxicities of HAI therapy must be part of a vigilant multidisciplinary team. This and the fact that studies take a long time to complete allowing systemic therapy to advance prior to positive data has limited the use of HAI therapy from becoming widespread. It is extremely important that these patients be treated by a multidisciplinary team whether on or off a clinical trial to maximize the potential benefits of such regimens while minimizing toxicities.

References

1. Tokito T, Ichiki M, Sakata S, Nakamura M, et al. A case of small cell lung cancer (extensive disease) with liver metastasis acquiring stable disease by hepatic arterial infusion chemotherapy. Gan To Kagaku Ryoho. 2010;37(3):495. Japanese.
2. Minagawa R, Hasegawa H, Anegawa G, Ito S, et al. A case of multiple liver and celiac lymph node metastases after curative esophagectomy for esophageal cancer successfully treated with hepatic arterial infusion and radiation therapy. Gan To Kagaku Ryoho. 2009;36(12):2049. Japanese.
3. Ota T, Shuto K, Ohira G, Natsume T, et al. Evaluation of hepatic arterial infusion chemotherapy for liver metastasis from gastric cancer. Gan To Kagaku Ryoho. 2009;36(12):2019. Japanese.
4. Terakura M, Kaneko M, Ikebe T, Yoshioka H, et al. A case of unresectable advanced gallbladder cancer successfully treated by oral S-1 and hepatic arterial infusion (HAI) of low-dose CDDP therapy. Gan To Kagaku Ryoho. 2008;35(4):645. Japanese.
5. Tsimberidou AM, Fu S, Ng C, Lim JA, et al. A phase 1 study of hepatic arterial infusion of oxaliplatin in combination with systemic 5-fluorouracil, leucovorin, and bevacizumab in patients with advanced solid tumors metastatic to the liver. Cancer. 2010;116:4086–94.
6. Tsimberidou AM, Moulder S, Fu S, Wen S. Phase I clinical trial of hepatic arterial infusion of cisplatin in combination with intravenous liposomal doxorubicin in patients with advanced cancer and dominant liver involvement. Cancer Chemother Pharmacol. 2010;66:1087–93.
7. Vauthey JN, Klimstra D, Franceschi D, Tao Y. Factors affecting long-term outcome after hepatic resection for hepatocellular carcinoma. Am J Surg. 1995;169(1):28.
8. Bruix J, Castells A, Bosch J, Feu F, et al. Surgical resection of hepatocellular carcinoma in cirrhotic patients: prognostic value of preoperative portal pressure. Gastroenterology. 1996;111(4):1018–22.
9. Bruix J. Treatment of hepatocellular carcinoma. Hepatology. 1997;25:259.
10. Edge SB, Byrd DR, Compton CC, AJCC (American Joint Committee on Cancer), et al., editors. AJCC (American Joint Committee on Cancer) cancer staging manual. 7th ed. New York: Springer; 2010. p. 143.
11. Pawlik TM, Choti MA. Surgical therapy for colorectal metastases to the liver. J Gastrointest Surg. 2007;11:1057.
12. Cady B, Monson DO, Swinton NW. Survival of patients after colonic resection for carcinoma with simultaneous liver metastases. Surg Gynecol Obstet. 1970;131:697.
13. Blumgart LH, Allison DJ. Resection and embolization in the management of secondary hepatic tumors. World J Surg. 1982;6:32–45.
14. Jatzko G, Wette V, Muller M, Lisborg P, Klimpfinger M, Denk H. Simultaneous resection of colorectal carcinoma and synchronous liver metastases in a district hospital. Int J Colorectal Dis. 1991;6:111.
15. Finlay IG, McArdle CS. Occult hepatic metastases in colorectal carcinoma. Br J Surg. 1986;73:732–5.
16. Scheele J, Stang R, Altendorf-Hofmann A, Paul M. Resection of colorectal liver metastases. World J Surg. 1995;19:59–71.
17. Altendorf-Hofmann A, Scheele J. A critical review of the major indicators of prognosis after resection of hepatic metastases from colorectal carcinoma. Surg Oncol Clin N Am. 2003;12:165. xi.
18. Scheele J, Stangl R, Altendorf-Hofmann A, Gall FP. Indicators of prognosis after hepatic resection for colorectal secondaries. Surgery. 1991;110:13–29.
19. Lochan R, White SA, Manas DM. Liver resection for colorectal liver metastasis. Surg Oncol. 2007;16:33.
20. Khatri VP, Chee KG, Petrelli NJ. Modern multimodality approach to hepatic colorectal metastases: solutions and controversies. Surg Oncol. 2007;16:71.
21. Collins JM. Pharmacologic rationale for regional drug delivery. J Clin Oncol. 1984;2(5):498.
22. Kemeny N, Fata F. Hepatic arterial chemotherapy. Lancet Oncol. 2001;2:418.
23. Kemeny N, Daly J, Oderman P, Shike M, et al. Hepatic artery pump infusion: toxicity and results in patients with metastatic colorectal carcinoma. J Clin Oncol. 1984;2:595.
24. Kemeny N, Seiter K, Niedzwiecki D, Chapman D, et al. A randomized trial of intrahepatic infusion of fluorodeoxyuridine with dexamethasone versus fluorodeoxyuridine alone in the treatment of metastatic colorectal cancer. Cancer. 1992;69(2):327.
25. Mocellin S, Pilati P, Lise M, Nitti D. Meta-analysis of hepatic arterial infusion for unresectable liver metastases from colorectal cancer: the end of an era? J Clin Oncol. 2007;25(35):5649.
26. Holen KD, Saltz LB. New therapies, new directions: advances in the systemic treatment of metastatic colorectal cancer. Lancet Oncol. 2001;2:290.
27. Kelly H, Goldberg RM. Systemic therapy for metastatic colorectal cancer: current options, current evidence. J Clin Oncol. 2005;23:4553.
28. O'Connell MJ, Nagorney DM, Bernath AM, Schroeder G, et al. Sequential intrahepatic fluorodeoxyuridine and systemic fluorouracil plus leucovorin for the treatment of metastatic colorectal cancer confined to the liver. J Clin Oncol. 1998;16(7):2528.
29. Porta C, Danova M, Accurso S, Tinelli C, et al. Sequential intrahepatic and systemic fluoropyrimidine-based chemotherapy for metastatic colorectal cancer confined to the liver. A phase II study. Cancer Chemother Pharmacol. 2001;47:423.
30. Shimonov M, Hayat H, Chaitchik S, Brener J, et al. Combined systemic chronotherapy and hepatic artery infusion for the treatment of metastatic colorectal cancer confined to the liver. Chemotherapy. 2005;51:111.

31. Ducreux M, Ychou M, Laplanche A, Gamelin E. Hepatic arterial oxaliplatin infusion plus intravenous chemotherapy in colorectal cancer with inoperable hepatic metastases: a trial of the gastrointestinal group of the Federation Nationale des Centres de Lutte Contre le Cancer. J Clin Oncol. 2005;23:4881.
32. Adam R, Delvart V, Pascal G, Aleanu A. Rescue surgery for unresectable colorectal liver metastases downstaged by chemotherapy. Ann Surg. 2004;240:644.
33. Kemeny N, Jarnagin W, Paty P, Gonen M, et al. Phase I trial of systemic oxaliplatin combination chemotherapy with hepatic arterial infusion in patients with unresectable liver metastasis from colorectal cancer. J Clin Oncol. 2005;23(22):4888.
34. Kemeny N, Huitzil-Melendez FD, Capanu M, Paty PB. Conversion to resectability using hepatic artery infusion plus systemic chemotherapy for the treatment of unresectable liver metastases from colorectal carcinoma. J Clin Oncol. 2009;27(21):3465.
35. Gallagher DJ, Capanu M, Raggio G, Kemeny N. Hepatic arterial infusion plus systemic irinotecan in patients with unresectable hepatic metastases from colorectal cancer previously treated with systemic oxaliplatin: a retrospective analysis. Ann Oncol. 2007;18:1995.
36. Kemeny NE, Gonen M. Hepatic arterial infusion after liver resection. N Engl J Med. 2005;352:734.
37. Jarnagin WR, Gonen M, Fong Y, DeMatteo RP, et al. Improvement in perioperative outcome after hepatic resection: analysis of 1803 consecutive cases over the past decade. Ann Surg. 2002;236(4):397.
38. House MG, Kemeny N, Jarnagin WR, et al. Comparison of adjuvant systemic chemotherapy with or without hepatic arterial infusion chemotherapy after hepatic resection for metastatic colorectal cancer [abstract]. Presented at the 2009 Gastrointestinal Cancer Symposium; 2009 Jan 15–17; San Francisco, CA. Abstract 383.
39. Mariani P, Guetz D, Uzzan B, Nicolas P, et al. Systemic or hepatic arterial chemotherapy after curative resection of liver metastases from colorectal cancer. A meta-analysis of randomized controlled trials. J Clin Oncol. 2008; ASCO Annual Meeting Proceedings (Post-Meeting Edition). 2008;26(15S) (May 20 Supplement):4077.
40. Cummings FJ, Varker K, Begossi G, Taneja C, Wanebo HJ. Hepatic artery infusion in surgical therapy of hepatic metastases from colorectal cancer. J Clin Oncol. ASCO Annual Meeting Proceedings (Post-Meeting Edition). 2008;26(15S) (May 20 Supplement):15077.
41. Tomlinson JS, Jarnagin WR, DeMatteo RP, Fong Y. Actual 10-year survival after resection of colorectal liver metastases defines cure. J Clin Oncol. 2007; 25(29):4575.
42. Kemeny N, Adak S, Gray B, MacDonald JS, et al. Combined-Modality treatment of resectable metastatic colorectal carcinoma to the liver: surgical resection of hepatic metastases in combination with continuous infusion of chemotherapy-an intergroup study. J Clin Oncol. 2002;20:1499–505.
43. Lorenz M, Muller HH, Schramm H, Gassel HJ, et al. Randomized trial of surgery versus surgery followed by adjuvant hepatic arterial infusion with 5-fluorouracil and folinic acid for liver metastases of colorectal cancer. German Cooperative on liver metastases. Ann Surg. 1998;228(6):756.
44. Kemeny N, Huang Y, Cohen AM, Shi W, Conti JA, et al. Hepatic arterial infusion of chemotherapy after resection of hepatic metastases from colorectal cancer. N Engl J Med. 1999;341:2039.
45. Lygidakis NJ, Sjourakis G, Vlachos L, Raptis S, et al. Metastatic liver disease of colorectal origin: the value of local immunochemotherapy combined with systemic chemotherapy following liver resection. Results of a prospective randomized study. Hepatogastroenterology. 2001;48:1685.
46. Kemeny NE, Jarnagin WR, Capanu M, Fong Y, et al. Randomized phase II trial of adjuvant hepatic arterial infusion and systemic chemotherapy with or without bevacizumab in patients with resected hepatic metastases from colorectal cancer. J Clin Oncol. 2011;29(7):884.
47. Gray BN, Van Hazel G, Hope M, Burton M, et al. Randomized trial of SIR-Spheres plus chemotherapy vs. chemotherapy alone for treating patients with liver metastases from primary large bowel cancer. Ann Oncol. 2001;12(12):1711.
48. Machi J, Oishi AJ, Sumida K, Sakamoto K, et al. Long term outcome of radiofrequency ablation for unresectable liver metastasis from colorectal cancer: evaluation of prognostic factors and effectiveness in first- and second-line management. Cancer J. 2006;12(4):318.
49. Grothey A, Sargent D, Goldbert RM, et al. Survival of patients with advanced colorectal cancer improves with availability of fluorouracil-leucovorin, irinotecan, and oxaliplatin in the course of treatment. J Clin Oncol. 2004;22:1209.
50. Hurwitz H, Fehrenbacher L, Novotny W, et al. Bevacizumab plus irinotecan, fluorouracil, and leucovorin for metastatic colorectal cancer. N Engl J Med. 2004;350:2335.
51. Rougier P, Lepille D, Bennouna J, et al. Antitumor activity of three second line treatment combinations in patients with metastatic colorectal cancer after optimal 5FU regimen failure: a randomized, multicentre phase II study. Ann Oncol. 2002;13:1558.
52. Pitot HC, Rowland KM, Sargent DJ, et al. N9841: a randomized phase III equivalence trial of irinotecan (CPT-11) versus oxaliplatin/5 fluorouracil (FU)/ leucovorin (FOLFOX4) in patients with advanced colorectal cancer previously treated with 5FU [abstract 3506]. Proceeding ASCO 2005.
53. Giantonio BJ, Catalano PJ. Meropol NJ High dose bevacizumab improves survival when combined with FOLFOX 4 in previously treated advanced colorectal cancer: results from ECOG study E3200 [abstract 2]. Proceeding ASCO 2005.

54. EORTC 40004. Randomized phase II study investigating the role of local treatment of liver metastases by radiofrequency combined with chemotherapy and of chemotherapy alone in patients with unresectable colorectal liver metastases. Brussel 1200 Bruxelles, Belgique. Open trial from 2002 Apr to 2007 June.
55. Talamonti MS, Stuart K, Yao JC. Neuroendocrine tumors of the gastrointestinal tract: how aggressive should we be? In: Perry M, editor. American society of clinical oncology 2004 education book. Alexandria: American Society of Clinical Oncology; 2004. p. 206.
56. Kleppel G, Perren A, Heitz PU. The gastroenteropancreatic neuroendocrine cell system and its tumors: the WHO classification. Ann NY Acad Sci. 2004;1014:13.
57. Que FG, Nagorney DM, Batts KP, et al. Hepatic resection for metastatic neuroendocrine carcinomas. Am J Surg. 1995;169:36.
58. Kulke MH, Mayer RJ. Carcinoid tumors. N Engl J Med. 1999;340(11):858.
59. Yao JC, Hoff PM. Molecular targeted therapy for neuroendocrine tumors. Hematol Oncol Clin North Am. 2007;21:575.
60. Chaudhry A, Funa K, Oberg K. Expression of growth factor peptides and their receptors in neuroendocrine tumors of the digestive system. Acta Oncol. 1993; 32(2):107.
61. Kulke MH, Lenz HJ, Meropol NJ, et al. A phase 2 study to evaluate the efficacy and safety of SU11248 in patients with unresectable neuroendocrine tumors (NETs). J Clin Oncol. 2005;23(16s):210s.
62. Kulke MH, Lenz HJ, Meropol NJ, Posey J, et al. Activity of sunitinib in patients with advanced neuroendocrine tumors. J Clin Oncol. 2008;26(20):3403.
63. Raymond E, Dahan L, Raoul JL, Bang YJ, et al. Sunitinib Malate for the treatment of pancreatic neuroendocrine tumors. N Engl J Med. 2011;364(6):501.
64. Phan AT, Wang L, Xie K, et al. Association of VEGF expression with poor prognosis among patients with low grade neuroendocrine carcinoma. Paper presented at annual meeting of American Society of Clinical Oncology; Atlanta, 2006 June 2.
65. Konno H, Arai T, Tanaka T, et al. Antitumor effect of a neutralizing antibody to vascular endothelial growth factor on liver metastasis of endocrine neoplasm. Jpn J Cancer Res. 1998;89(9):933.
66. Yao JC, Lombard-Bohas C, Baudin E, Kvols LK, et al. Daily oral everolimus activity in patients with metastatic pancreatic neuroendocrine tumors after failure of cytotoxic chemotherapy: a phase II trial. J Clin Oncol. 2010;28(1):69.
67. Yao JC, Shah MH, Ito T, Lombard-Bohas C, et al. Everolimus for advanced pancreatic neuroendocrine tumors. N Engl J Med. 2011;364(6):514.
68. Hodi FS, O'Day SJ, McDermott DF, Weber RW, et al. Improved survival with ipilimumab in patients with metastatic melanoma. N Engl J Med. 2010; 363(8):711–723.

Intra-arterial Pump Infusional Chemotherapy

32

Yasuaki Arai

Abstract

Intra-arterial infusion chemotherapy has a long history since 1950s, and it has been performed with surgical catheter and pump implantation. The percutaneous approach has been developed with techniques of interventional radiology since 1980s. Interventional radiology can provide minimally invasive and accurate intra-arterial infusion chemotherapy consisted of arterial redistribution, percutaneous catheter placement, and drug distribution management. With these techniques, some small studies showed promising data especially in the treatment of liver metastases, but any larger study has not been done yet. Since modern systemic chemotherapy is well advanced, the role of intra-arterial infusion chemotherapy is not much recognized in the field of medical oncology. However, intra-arterial infusion chemotherapy cannot be done without accurate knowledge and techniques. To evaluate this treatment modality correctly at the present and to decide the new role of intra-arterial infusion chemotherapy, interventional radiologists should understand their very important role on intra-arterial infusion chemotherapy.

Introduction

The role of hepatic arterial infusion chemotherapy has not been widely accepted, and it is used in very limited situations at the present, because its efficacy for liver metastases from colorectal cancer has not been established by the most of randomized trials comparing with systemic chemotherapy [1–14]. Only one randomized trial has succeeded to show significant prolongation of survival with hepatic arterial infusion chemotherapy, but no modern strong chemotherapeutic agents was used in the systemic chemotherapy group [9]. Thus, there has no clear answer about the role of hepatic arterial infusion chemotherapy on the treatment of liver metastases. Additionally, in these trials, only surgical procedures have been employed for port–catheter implantation.

Y. Arai
Department of Diagnostic Radiology, National Cancer Center Hospital, Tokyo, Japan
e-mail: arai-y3111@mvh.biglobe.ne.jp

D.E. Dupuy et al. (eds.), *Image-Guided Cancer Therapy*, DOI 10.1007/978-1-4419-0751-6_34,

As the surgical procedure, an indwelling catheter was generally inserted into the hepatic artery via the gastroduodenal artery under laparotomy with general anesthesia, and an implantable continuous infusion pump or port was implanted in the abdominal wall. On the other hand, interventional radiological procedures for port–catheter implantation have been well established [15, 16], and they allow minimally invasive and accurate hepatic arterial infusion chemotherapy. In this chapter, concept, technique, and therapeutic results of port–catheter implantation in hepatic arterial infusion chemotherapy are described.

Concept

Hepatic arterial infusion chemotherapy achieves significantly higher antitumor activity with limited systemic toxicity. The pharmacological rationale of hepatic arterial infusion is explained with two theories of "first-pass effect" and "increased local concentration without first-pass effect" [17]. To realize the advantage in the clinical setting, administrated drug must be distributed only to the whole liver, but not to extrahepatic organs. Port–catheter implantation with interventional radiological techniques is aimed at achieving three distinct processes of (1) arterial redistribution, (2) percutaneous catheter placement, and (3) evaluation and management of drug distribution. After all three processes are well completed, the "optimal drug distribution" can be achieved, and hepatic arterial infusion chemotherapy can show its essential efficacy.

Techniques

Arterial Redistribution

The purposes of arterial redistribution are to convert multiple hepatic arteries if present into a single vascular supply and to occlude arteries arising from the hepatic arterial region and supplying extrahepatic organs (Fig. 32.1).

Conversion of Multiple Hepatic Arteries into a Single Vascular Supply

To convert multiple hepatic arteries into a single vascular supply, all hepatic arteries except the one to be used for drug administration must be embolized with coils. The replaced right hepatic artery (rep. RHA), the accessory right hepatic artery (acc. RHA) that arises from the superior mesenteric artery (SMA) or the common hepatic artery (CHA), and the replaced left hepatic artery (rep. LHA) that arises from the left gastric artery are common target arteries in this procedure. Since intrahepatic arterial communications exist between hepatic arteries, the embolized region can receive arterial blood supply from the remaining non-occluded hepatic artery immediately through these communications. In this mechanism, the liver supplied with multiple hepatic arteries can be changed to receive arterial blood supply from the one remaining artery, and then the liver can be completely perfused by a single indwelling catheter. However, the incidence of hepatic arterial occlusion is high if an indwelling catheter is placed into the replaced hepatic artery; therefore, in a case with the proper hepatic artery and the replaced hepatic artery, the replaced hepatic artery should be embolized to make the proper hepatic artery as the remaining hepatic artery.

Occlusion of Arteries Arising from the Hepatic Artery and Supplying Extrahepatic Organs

To prevent toxic events caused by infusion of chemotherapeutic agents into extrahepatic organs such as stomach, duodenum, or pancreas, arteries should be embolized if they are arised from the artery for an indwelling catheter or supply to extrahepatic organs. The gastroduodenal artery (GDA), the right gastric artery (RGA), the accessory left gastric artery (acc. LGA), the superior duodenal artery (SDA), the posterior superior pancreaticoduodenal artery (PSPDA), and the dorsal pancreatic artery (DPA) should be considered as target arteries of this procedure. To embolize small artery such as the RGA, the use of microcatheter system and microcoils is efficient to make the procedure easier. In cases with

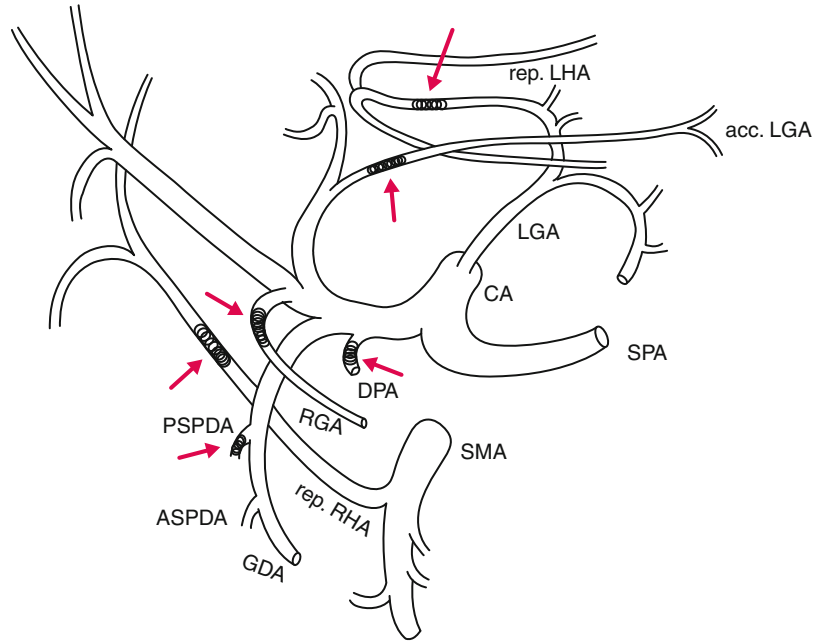

Fig. 32.1 Arterial redistribution with steel coils. When the indwelling catheter tip is fixed with the gastroduodenal artery, steel coils should be positioned in the arteries with *arrows*. *rep. LHA* the replaced left hepatic artery, *acc. LGA* the accessory left gastric artery, *LGA* the left gastric artery, *CA* the Celiac artery, *SPA* the splenic artery, *DPA* the dorsal pancreatic artery, *RGA* the right gastric artery, *SMA* the superior mesenteric artery, *rep. RHA* the replaced right hepatic artery, *PSPDA* the posterior superior pancreaticoduodenal artery, *ASPDA* the anterior superior pancreaticoduodenal artery

difficulties to insert even microcatheter into such small arteries, glue can also be used carefully instead of microcoils. As glue, NBCA (n-butyl-2-cyanoacrylate)–lipiodol mixture (diluted 2–3 times with lipiodol) is usually used.

Percutaneous Catheter Placement

The most important advantage of the percutaneous placement of an indwelling catheter is less invasiveness compared to open surgery under general anesthesia and laparotomy. However, there are unexpected complications associated with an indwelling catheter, such as hepatic arterial occlusion, catheter dislocation, and catheter kinking. There are three technical tips to prevent these complications. First of all, "tip-fixation method" is fundamental. Hepatic arterial occlusion is usually caused by the mechanical stimulation of catheter tip against the vascular endothelium by patients' movement and breathing. In "tip-fixation method", an indwelling catheter with a side-hole is inserted, not into the hepatic artery but commonly into the GDA, adjusting the position of side-hole to CHA, and then fixing the distal tip of the indwelling catheter with the GDA using coils. Thus, this method can reduce the mechanical stimulation of catheter tip against the hepatic artery. Secondly, we should keep enough length of an indwelling catheter in the aorta. Enough length of an indwelling catheter avoids excessive tension to the indwelling catheter by patient's movement can be avoided, leading to the reduction of catheter dislocation risk. The third point is to avoid routes with a wide range of motion (e.g., shoulder or hip joint) in the region where an indwelling catheter is traversing. From this point of view, a route via the subclavian artery or the inferior epigastric artery is more suitable to avoid catheter kinking than that via the femoral artery. However, if the "tip-fixation method" and keeping enough length of an indwelling catheter in the aorta are employed, the risk of catheter dislocation and kinking is limited also in the access via the femoral artery. By applying these techniques, the incidence of complications associated with an indwelling catheter can be remarkably decreased.

Access to the Subclavian Artery

The left subclavian artery is commonly used to avoid complications to the intracranial circulation. The traditional approach is to make a surgical cutdown, which makes a 3-cm skin

incision 2 cm below the left clavicle on the anterior chest wall under the local anesthesia; insert an indwelling catheter via a branch of the subclavian artery, such as the thoracic acromial artery; and fix the catheter by ligation of the branch over the catheter. The direct puncture of the left subclavian artery is also possible under sonographic or fluoroscopic guidance; however, in case of fluoroscopic guidance, insertion of guidewire into the subclavian artery via a separate access is necessary to make a target of puncture. The direct puncture access is simple and easier than surgical cutdown; however, incompleted fixation caused by lack of ligation with a branch sometimes leads to complications such as bleeding, catheter dislocation, and rarely intracranial thrombosis.

Access to the Inferior Epigastric Artery

A "retrograde guidewire guiding method" is useful for interventional radiologists to access to the inferior epigastric artery. In this method, a guidewire is inserted into the inferior epigastric artery by the conventional angiographic manner via the femoral artery, and then the inferior epigastric artery is exposed by a cutdown procedure under fluoroscopic localization of the guidewire. Pulling out the guidewire through the inferior epigastric artery, the angiographic catheter can be easily inserted into the abdominal aorta through the inferior epigastric artery using an over the guidewire technique. After the placement of the indwelling catheter at the appropriate position, the catheter is fixed with the inferior epigastric artery by ligation of over the artery.

Access to the Femoral Artery

Access to the femoral artery for the indwelling catheter placement is essentially the same as that for the conventional angiography. However, to avoid bleeding after the placement of the indwelling catheter, the smaller-sized guiding catheter and introducer systems comparing with the indwelling catheter should be used.

Insertion of the Indwelling Catheter

There are two types of indwelling catheter. One is Anthron PU catheter (B. Braun Medical S.A.S Chasseneuil, France, manufactured by Toray Industries, Inc., Chiba, Japan) and W-spiral catheter (Piolax Medical Device, Inc., Kanagawa, Japan). There are many types of catheters; however, commonly a tapered-type catheter (5 Fr in outer diameter and tapered to 2.7 Fr at distal tip of 20 cm) is used. The indwelling catheter must have a side-hole to flow out anticancer agents. If using a catheter without a side-hole, a side-hole must be opened by scissors-cut manipulation (or using the side-hole opener set in the catheter kit of W-spiral catheter). The tip of the indwelling catheter must be cut to an adequate length for subsequent tip fixation. Based on the angiography images via the celiac and the superior mesenteric arteries, the artery most suitable for indwelling catheter fixation will be chosen. The prepared side-holed catheter is inserted by using the catheter exchange method with a 0.018-in. or smaller guidewire (if a non-tapered indwelling catheter is employed, 0.035-in. guidewire can be used). Commonly, the occlusion of an end-hole of indwelling catheter is not necessary if a tapered indwelling catheter is used. However, if a non-tapered 5-Fr indwelling catheter is used, the end-hole of the indwelling catheter should be occluded with microcoils inserted into the distal portion to the side-hole of the indwelling catheter inserted via a microcatheter placed coaxially. In addition, if using the left subclavian arterial approach, a 5-Fr curved long introducer should be used to prevent kinking in the aortic arch.

Tip Fixation

The GDA is the most commonly used for fixation of the tip of the indwelling catheter. Other arteries such as the SA, the LGA, and the acc. LGA can be used for the tip fixation, if needed. When an indwelling side-holed catheter is inserted into the GDA, the side-hole should be placed within the CHA. Then, the GDA is embolized with coils and NBCA–lipiodol mixture as necessary. If a second catheter can be inserted via the other access, coils and NBC–lipiodol mixture can be administered through the second catheter (Fig. 32.2). If this process is performed without the use of additional catheter, the indwelling catheter with a side-hole at the 5-Fr portion is first inserted into the GDA, and then,

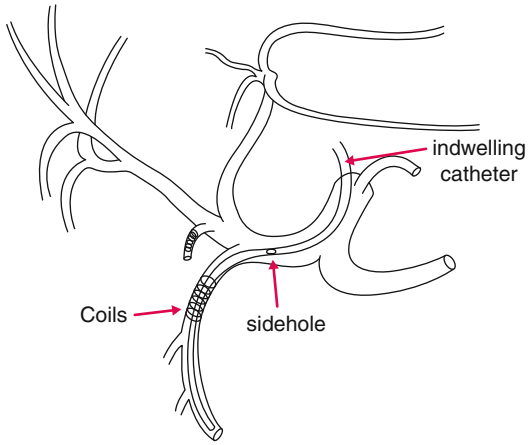

Fig. 32.2 Tip fixation of the indwelling catheter with the gastroduodenal artery using steel coils

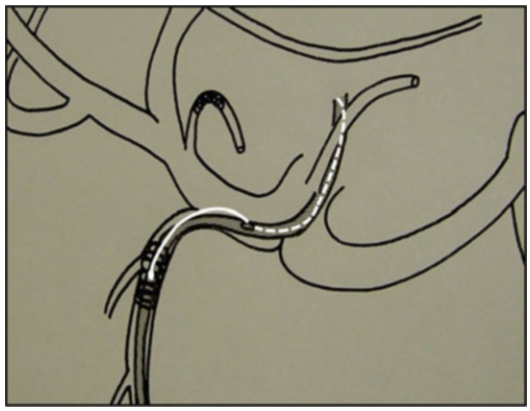

Fig. 32.3 Coaxial access to the gastroduodenal artery with microcatheter system. A microcatheter can be inserted into the gastroduodenal artery through the indwelling catheter coaxially and passed through the side-hole (Reprinted with permission from Arai Y. Interventional radiological procedures for port-catheter implantation. In: Stephen FO, Aigner KR, editors. Induction chemotherapy. New York: Springer; 2011)

a microcatheter is coaxially inserted into the GDA through the indwelling catheter and passed through the side-hole (Fig. 32.3). After the tip fixation, the indwelling catheter should form a loop in the aorta to prevent a direct transmission of patient's movement to the distal portion inserted into the CHA (Fig. 32.4).

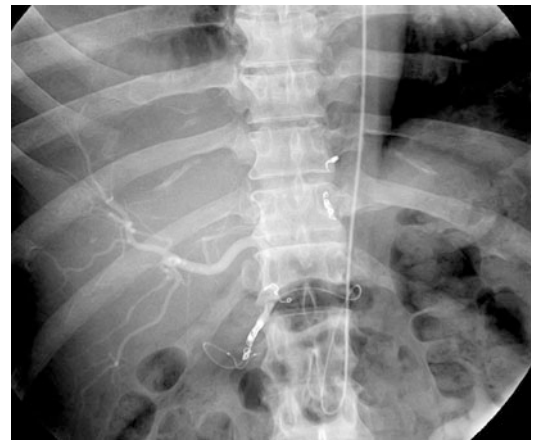

Fig. 32.4 Loop formation of the indwelling catheter in the aorta (Reprinted with permission from Arai Y. Interventional radiological procedures for port-catheter implantation. In: Stephen FO, Aigner KR, editors. Induction chemotherapy. New York: Springer; 2011)

Occlusion of the Indwelling Catheter End-Hole

The end-hole of the placed indwelling catheter maybe naturally occluded with thrombus between a side-hole and an end-hole, if using a tapered type indwelling catheter. However, if a non-tapered 5-Fr catheter is used, the end-hole of the indwelling catheter should be occluded using a microcoil inserted through a coaxial microcatheter.

Connection with a Port System

The proximal end of the indwelling catheter is connected to the implantable port system. Keeping a natural course of the catheter is very important to prevent troubles such as catheter kinking and breakage. It is also important to have a distance from the joints with wide range of motion (e.g., hip joint, shoulder joint). A Huber-point needle must be used to puncture a silicone septum of the port. After administration of chemotherapeutic agents, enough volume of saline must be flushed to wash the inner lumen of the catheter and port system, and 2 ml (2,000 U) of heparin must be injected into the system at least every 2 weeks to prevent thrombosis of the catheter.

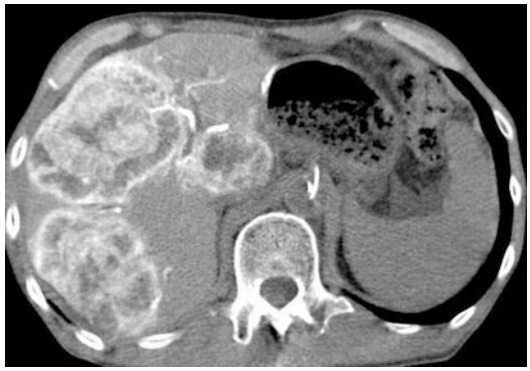

Fig. 32.5 Evaluation of drug distribution with angio-CT via the catheter/port system (Reprinted with permission from Arai Y. Interventional radiological procedures for port-catheter implantation. In: Stephen FO, Aigner KR, editors. Induction chemotherapy. New York: Springer; 2011)

Evaluation and Management of Drug Distribution

During long-term hepatic arterial infusion chemotherapy, drug distribution via the indwelling catheter and port system sometimes changes, due to the development of collateral and/or parasitic blood supply to the liver. To achieve good therapeutic results, the "optimal drug distribution" must be maintained.

Evaluation of Drug Distribution

In the evaluation of drug distribution, a computed tomography during angiography (CTA) via the indwelling catheter–port system is needed as two-dimensional imaging (Fig. 32.5). The digital subtraction angiography (DSA) via the indwelling catheter–port system is insufficient to detect the accurate drug distribution into the liver and surrounding organs. The volume and rate of contrast medium is determined by the scanning time and pitch of the CT scanner. Commonly, 10–20 mL volume of 30–50 % diluted contrast medium is injected via the indwelling catheter–port system at the rate of 0.5–1.5 mL/s. The "optimal drug distribution" in hepatic arterial infusion chemotherapy, defined by CTA, should show contrast enhancement of the entire liver without enhancement of extrahepatic organs. Furthermore, to prevent drug-related complications, it is mandatory to make a thorough evaluation identifying for contrast enhancement within the stomach wall, duodenum, or pancreas. On the other hand, it is not easy with CTA to find the dislocation of the indwelling catheter, the arterial stenosis, and the slowdown of blood flow. Therefore, both DSA and CTA are needed to confirm the causes of troubles of indwelling catheter and port system.

Drug distribution surveillance should be performed at least every 3 months to detect any catheter or vascular troubles. Additionally, when a patient complains unusual clinical symptoms such as abdominal pain, nausea, or fever during and/or after infusion chemotherapy, DSA via the indwelling catheter/port system must be performed immediately. If there is an area without contrast enhancement in the liver, the presence of parasitic or collateral blood supply in this area should be strongly suspected. In such cases, selective angiography must be performed not only to reveal arteries supplying blood into this area but also to revise the drug distribution. Selective angiography become mandatory to look for parasitic or collateral blood supply to the liver including CA, the SMA, the inferior phrenic artery, the right renal artery, the right adrenal artery, and, if necessary, the internal mammary artery.

Contrast medium should be injected at the same infusion rate as that for the given chemotherapeutic agent, because the distribution of contrast medium should accurately simulate the distribution of chemotherapeutic agent. However, performing CTA at less than 1 mL/min infusion rate such as the continuous infusion of 5-fluorouracil (5-FU) or 5-fluorodeoxyuridine (FUDR) is impossible. In such slow infusion rate, MRI with contrast medium injected via the indwelling catheter system may show more accurate distribution of chemotherapeutic agents than CTA [18].

Management of Drug Distribution

If a parasitic or collateral artery supplies blood to a part of the liver, embolization of this artery must be performed to revise the drug distribution (Fig. 32.6). However, such parasitic or collateral

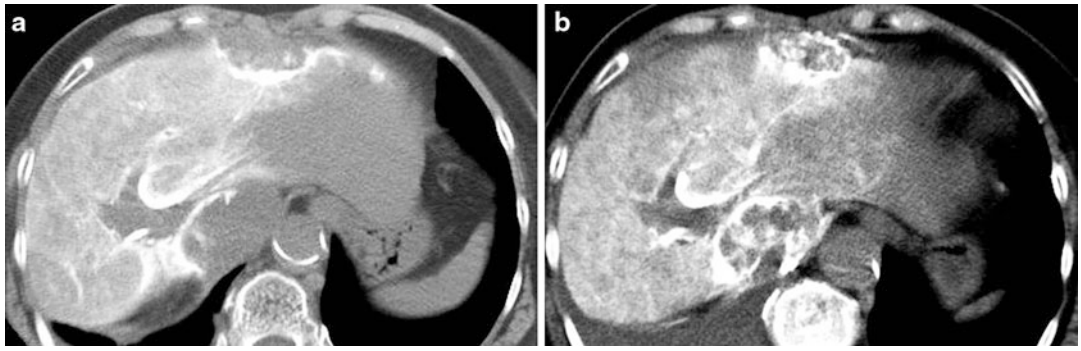

Fig. 32.6 Management of drug distribution by the embolization of parasitic artery with NBCA–lipiodol mixture. (**a**) CTA via the indwelling catheter/port system shows the intrahepatic areas without contrast enhancement. (**b**) CTA via the indwelling catheter/port system after the embolization of the right inferior phrenic artery and the left internal mammary artery shows the significant better drug distribution. Non-enhanced areas before the embolization are enhanced in this study (reprinted with permission from Arai Y. Interventional radiological procedures for port-catheter implantation. In: Stephen FO, Aigner KR, editors. Induction chemotherapy. New York: Springer; 2011)

arteries often have multiple communications with other vessels. Also, proximal embolization with coils may not be enough to stop its blood supply to the liver. Therefore, for the embolization of such parasitic or collateral artery, a complete embolization cast using a NBCA–lipiodol mixture (diluted 6–10 times with lipiodol) should be performed. If successful embolization of the artery is performed and there is no artery supplying blood to the liver (with the exception of the hepatic artery where drug is infused via the system), improved drug distribution will be seen on CTA.

In cases of extrahepatic organ enhancement on CTA via the indwelling catheter system, the branch artery supplying to the extrahepatic organ should be detected by conventional angiography and embolized. For this embolization, it is usually sufficient to occlude the proximal portion of the artery using microcoils. Yet when the artery is too small to insert a microcoil, embolization may be performed using NBCA–lipiodol mixture (diluted 2–3 times with lipiodol).

Removal of the Indwelling Catheter and Port System

When the indwelling catheter and port system become unnecessary, it is possible to remove them even if the catheter tip is fixed to the artery using coils and NBCA–lipiodol mixture. However, it is important to consider that potential risk of thrombus around the indwelling catheter [19]. Especially, if the indwelling catheter is inserted via the left subclavian artery. It is not allowed to pull out the indwelling catheter via the subclavian artery is not allowed. In such case, the indwelling catheter must be removed via the femoral artery using an device such as a vascular loop snare after cutting the proximal side of the indwelling catheter.

Agents for Hepatic Arterial Infusion Chemotherapy

As the initial pharmacokinetic considerations, the overall advantage of intra-arterial administration is composed of the increased local concentration and/or the decreased systemic concentration. These are influenced with the regional and systemic circulating blood volume, flow rate, the extraction rate through liver and whole body, the pharmacokinetic pathway and metabolism of each agent, and administration schedule. (Table 32.1) Many kinds of agents have been used for hepatic arterial infusion chemotherapy depending on a variety of administration schedules. However, the agents and administration

Table 32.1 Regional drug delivery advantage [1]

Total body clearance (ml/min)	Agent	Regional drug delivery advantage	
		Organ blood flow (100 ml/min)	Organ blood flow (1,000 ml/min)
40,000	Thymidine	401	41
25,000	FUDR	251	26
4,000	5-FU	41	5
3,000	Ara-C	31	4
1,000	BCNU	11	2
900	ADM	10	1.9
400	AZQ	5	1.4
400	CDDP	5	1.4
200	Methotrexate	3	1.2

schedule on hepatic arterial infusion chemotherapy should be decided based on the outcomes of clinical trials.

Technical and Therapeutic Results

For hepatic arterial infusion chemotherapy, percutaneous image-guided catheter placement is a technically safe and a viable alternative to traditional methods of hepatic artery access [20, 21]. There have been many reports of percutaneous hepatic arterial catheter placement with techniques of interventional radiology. The technical success rate of catheter placement and 1-year functioning rate that the indwelling catheters–ports can be used were approximately 97–99 % and 78–81 %, respectively [22–24]. However, to ensure the high likelihood of tumor-only delivery of chemotherapy, a complete knowledge of hepatic arterial anatomy, potential blood flow complications, and infusion device management is required. As the therapeutic results of hepatic arterial infusion chemotherapy using interventional catheter/port placement, there are several reports of the treatments for liver metastases from colorectal cancer and gastric cancer. For liver metastases from colorectal cancer, the response rate and the median survival were reported 78–83 % and 25.8–26.0 months, respectively, with 5FU 1,000 mg/m^2 for 5-h continuous infusion qw [25, 26]. For liver metastases from gastric cancer, the response rate and the median survival were reported 56–72 % and 10.5–15 months, respectively, with 5FU 330 mg/m^2 qw, MMC 2.7 mg/m^2 q2w, and epirubicin 30 mg/m^2 q4w with bolus injection [27, 28]. However, these data are all reported over 10 years ago, and the situation of chemotherapy has been changed with powerful new drugs and molecular target agents. Recently, there has been some promising results of hepatic arterial infusion chemotherapy with new drugs reported (Table 32.2). Thus, the field of hepatic arterial infusion chemotherapy with interventional techniques of catheter/port placement using new agents or combining with agents is quite unexplored and challenging.

Table 32.2 Remarkable results of hepatic arterial infusion chemotherapy for colorectal liver metastases

Reference	Protocol	Median survival (months)	Notes
Kemeny et al. [9]	FUDR HAI + LV + Dex	24.4	RCT
Arai et al. [26]	5-FU 1,000 mg/m^2/5 h qw	26	Single arm
Kemeny et al. [29]	FUDR HAI + systemic L-OHP + CPT-11	36	RCT
Ducreux et al. [30]	L-OHP 100 mg/m^2 HAI + systemic LV5FU2	27	Single arm

References

1. Hohn DC, Stagg RJ, Friedman MA, et al. A randomized trial of continuous intravenous versus hepatic intraarterial floxuridine in patients with colorectal cancer metastatic to the liver: the Northern California Oncology Group trial. J Clin Oncol. 1989;7:1646–54.

2. Kemeny N, Daly J, Reichman B, et al. Intrahepatic or systemic infusion of fluorodeoxyuridine in patients with liver metastases from colorectal carcinoma. A randomized trial. Ann Intern Med. 1987;107:459–65.
3. Martin Jr JK, O'Connell MJ, Wieand HS, et al. Intra-arterial floxuridine vs systemic fluorouracil for hepatic metastases from colorectal cancer. A randomized trial. Arch Surg. 1990;125:1022–7.
4. Chang AE, Schneider PD, Sugarbaker PH, et al. A prospective randomized trial of regional versus systemic continuous 5-fluorodeoxyuridine chemotherapy in the treatment of colorectal liver metastases. Ann Surg. 1987;206:685–93.
5. Kemeny MM, Goldberg D, Beatty JD, et al. Results of a prospective randomized trial of continuous regional chemotherapy and hepatic resection as treatment of hepatic metastases from colorectal primaries. Cancer. 1986;57:492–8.
6. Rougier P, Laplanche A, Huguier M, et al. Hepatic arterial infusion of floxuridine in patients with liver metastases from colorectal carcinoma: long-term results of a prospective randomized trial. J Clin Oncol. 1992;10:1112–8.
7. Allen-Mersh TG, Earlam S, Fordy C, et al. Quality of life and survival with continuous hepatic-artery floxuridine infusion for colorectal liver metastases. Lancet. 1994;344:1255–60.
8. Kerr DJ, McArdle CS, Ledermann J, et al. Intrahepatic arterial versus intravenous fluorouracil and folinic acid for colorectal cancer liver metastases: a multicentre randomised trial. Lancet. 2003;361:368–73.
9. Kemeny NE, Niedzwiecki D, Hollis DR, et al. Hepatic arterial infusion versus systemic therapy for hepatic metastases from colorectal cancer: a randomized trial of efficacy, quality of life, and molecular markers (CALGB 9481). J Clin Oncol. 2006;24:1395–403.
10. Lorenz M, Muller HH. Randomized, multicenter trial of fluorouracil plus leucovorin administered either via hepatic arterial or intravenous infusion versus fluorodeoxyuridine administered via hepatic arterial infusion in patients with nonresectable liver metastases from colorectal carcinoma. J Clin Oncol. 2000;18:243–54.
11. Allen-Mersh TG, Glover C, Fordy C, et al. Randomized trial of regional plus systemic fluorinated pyrimidine compared with systemic fluorinated pyrimidine in treatment of colorectal liver metastases. Eur J Surg Oncol. 2000;26:468–73.
12. Reappraisal of hepatic arterial infusion in the treatment of nonresectable liver metastases from colorectal cancer. Meta-analysis group in cancer. J Natl Cancer Inst. 1996;88:252–8.
13. Harmantas A, Rotstein LE, Langer B. Regional versus systemic chemotherapy in the treatment of colorectal carcinoma metastatic to the liver. Is there a survival difference? Meta-analysis of the published literature. Cancer. 1996;78:1639–45.
14. Mocellin S, Pilati P, Lise M, et al. Meta-analysis of hepatic arterial infusion for unresectable liver metastases from colorectal cancer: the end of an era? J Clin Oncol. 2007;25:5649–54.
15. Arai Y, Inaba Y, Takeuchi Y. Interventional techniques for hepatic arterial infusion chemotherapy. In: Castaneda-Zuniga WR, Tadavarthy SM, editors. Interventional radiology. 3rd ed. Baltimore: Williams & Wilkins; 1997. p. 192–205.
16. Arai Y, Takeuchi Y, Inaba Y, et al. Percutaneous catheter placement for hepatic arterial infusion chemotherapy. Tech Vasc Interv Radiol. 2007;10:30–7.
17. Collins JM. Pharmacologic rationale for regional drug delivery. J Clin Oncol. 1984;2:498–504.
18. Seki H, Ozaki T, Takaki S, et al. Using slow-infusion MR arteriography and an implantable port system to assess drug distribution at hepatic arterial infusion chemotherapy. AJR Am J Roentgenol. 2003;180:681–6.
19. Hirota T, Yamagami T, Tanaka O, et al. Brain infarction after percutaneous implantation of port-catheter system via the left subclavian artery. Br J Radiol. 2002;75:799–804.
20. Seki H, Kimura M, Yoshimura N, et al. Hepatic arterial infusion chemotherapy using percutaneous catheter placement with an implantable port: assessment of factors affecting patency of the hepatic artery. Clin Radiol. 1999;54:221–7.
21. Yamagami T, Iida S, Kato T, et al. Using n-butyl cyanoacrylate and the fixed-catheter-tip technique in percutaneous implantation of a port-catheter system in patients undergoing repeated hepatic arterial chemotherapy. AJR Am J Roentgenol. 2002;179:1611–7.
22. Tanaka T, Arai Y, Inaba Y, et al. Radiologic placement of side-hole catheter with tip fixation for hepatic arterial infusion chemotherapy. J Vasc Interv Radiol. 2003;14:63–8.
23. Ganeshan A, Upponi S, Hon LQ, et al. Hepatic arterial infusion of chemotherapy: the role of diagnostic and interventional radiology. Ann Oncol. 2008;19:847–51.
24. Deschamps F, Elias D, Goere D, et al. Intra-arterial hepatic chemotherapy: a comparison of percutaneous versus surgical implantation of port-catheters. Cardiovasc Intervent Radiol. 2010;34(5):973–9.
25. Arai Y, Inaba Y, Takeuchi Y, et al. Intermittent hepatic arterial infusion of high-dose 5FU on a weekly schedule for liver metastases from colorectal cancer. Cancer Chemother Pharmacol. 1997;40:526–30.

26. Arai Y, Inaba Y, Matsueda K, et al. Weekly 5 hour hepatic arterial infusion of high dose 5FU for unresectable liver metastases from colorectal cancer in patients without extra-hepatic lesions. (ASCO 1998 abstract No. 1098). ASCO, 1998, p. 285a.
27. Arai Y, Sone Y, Tohyama N, et al. Hepatic arterial infusion for unresectable liver metastases from gastric cancer. Proc ASCO. 1992;11:176.
28. Kumada T, Arai Y, Itoh K, et al. Phase II study of combined administration of 5-fluorouracil, epirubicin and mitomycin-C by hepatic artery infusion in patients with liver metastases of gastric cancer. Oncology. 1999;57:216–23.
29. Kemeny N, Jarnagin W, Paty P, et al. Phase I trial of systemic oxaliplatin combination chemotherapy with hepatic arterial infusion in patients with unresectable liver metastases from colorectal cancer. J Clin Oncol. 2005;23: 4888–96.
30. Ducreux M, Ychou M, Laplanche A, et al. Hepatic arterial oxaliplatin infusion puls intravenous chemotherapy in colorectal cancer with inoperable hepatic metastases: a trial of the gastrointestinal group of the Federation Nationale des Centres de Lutte Contre le Cancer. J Clin Oncol. 2005;23: 4815–7.

Cryoablation of Liver Tumors

33

Michael J. Hutchinson, Paul B. Shyn, and Stuart G. Silverman

Abstract

Cryoablation refers to the destruction of tissues by rapid freezing and has been used in the treatment of both metastatic and primary hepatic tumors for several decades. Historically, cryoablation was performed in an open surgical setting and was shown to be an efficacious and generally safe treatment. However, severe but relatively infrequent complications did occur. These early complications led to a better understanding of the biochemistry and predisposing factors that led to the complications. This improved understanding allowed for better patient selection as well as improved post treatment care in avoiding or managing complications. While certain complications, including thrombocytopenia, hemorrhage and cryoshock, are unique to or more common in cryoablation than other ablative modalities, most of these complications are now readily treatable or can be avoided with proper patient screening. Recent technological advances have allowed for cryoablation to be performed percutaneously under imaging guidance. Cryoablation zones are exceptionally well visualized using MR or CT. The precision of cryoablation zone monitoring afforded by CT or MRI guidance provides the operator a degree of intraprocedural confidence regarding ablation zone margins and safety that is not generally possible with other ablation technologies. The placement and powering of individual cryoprobes allows for greater flexibility in avoiding critical structures as well as creating a sufficient ablation zone margin. Cryoablation also causes less pain than radiofrequency ablation, allowing for tumors near the diaphragm, or in a perihepatic location, to be treated with lower doses of intraprocedural and post-procedural analgesic medications. As the stigma of historical problems associated with surgical

M.J. Hutchinson • P.B. Shyn (✉) • S.G. Silverman
Division of Abdominal Imaging and Intervention, Department of Radiology, Brigham and Women's Hospital, Harvard Medical School, Boston, MA, USA
e-mail: hutch1588@yahoo.com; pshyn@partners.org; sgsilverman@partners.org

D.E. Dupuy et al. (eds.), *Image-Guided Cancer Therapy*, DOI 10.1007/978-1-4419-0751-6_35,

cryoablation using old technology recedes, a gradually developing body of experience with newer cryoablation technology applied percutaneously and with optimal imaging guidance is stimulating renewed interest in this minimally invasive treatment option for malignant liver tumors.

Introduction

Cryoablation, also known as cryotherapy, refers to the destruction of tissues by rapid freezing and has been used successfully in multiple organs including the kidney and prostate gland since the mid-1960s. Cryoablation of liver tumors has also been performed for several decades and gained more widespread use in the 1970s and 1980s. Although initially performed intraoperatively using large-diameter cryoprobes (historically referred to as cryosurgery because the procedure was performed in an open surgical setting), cryoablation can now be performed percutaneously using thin cryoprobes. Cryoablation systems employ either liquid nitrogen or argon gas-based technology. In argon-based systems, the Joule-Thomson effect is exploited to reduce the temperature in the active tip of the cryoprobe to less than −100°C [1]. Helium is used to increase the temperature of the cryoprobe actively. Since the frozen cryoprobe typically becomes adherent to tissues during freezing, an active thaw is applied to aid cryoprobe removal [1]. Cryoablations are typically performed by inducing an initial rapid freeze, followed by a slow thaw, and then followed by a second rapid freeze. This two-freeze cycle has been shown to increase overall cell death within the ablation zone relative to a single freeze [2, 3].

The mechanisms of cell death in cryoablation appear to include immediate and delayed components. Immediate mechanisms include direct cellular injury from intracellular and extracellular ice crystal formation. It is believed that temperatures of approximately −50°C induce complete irreversible injury and death of all malignant cells; however, this varies depending on tissue type and local factors, with temperatures in the −20° to −40° range being lethal under some circumstances [4]. Initially, ice crystals form only extracellularly, leading to metabolic disturbances and cell death, as the cells lose intracellular water through osmotic effects to the hypertonic extracellular spaces [5]. Intracellular ice formation then results in near-uniform cell death as the cell organelles and the cell membranes become disrupted, causing irreversible damage [4, 6]. Relative to older systems that utilized liquid nitrogen, higher cooling rates in current argon-based systems allow for increased intracellular ice formation. Delayed mechanisms include injury to the microcirculation causing vascular stasis and ischemia. Inflammatory changes, cytokine-regulated effects, immune-mediated mechanisms, and apoptosis may contribute to cell death as well [4]. The degree of tissue damage is increased with a higher rate of cooling, lower minimum temperature, longer duration of freezing, slower thaw rate, and repetition of the freeze-thaw cycle [4].

Cryosurgery Experience

Cryosurgery of the liver was initially used as an alternative to definitive hepatic resection since as few as 10–25 % of all patients with primary or metastatic liver neoplasms were suitable candidates for surgical resection. Cryosurgery was performed in tumors that would otherwise be unresectable due to size, location, or number of lesions. Large, typically 5–10-mm diameter, cryoprobe sizes of early cryoablation systems necessitated an open surgical approach. Intraoperative ultrasound facilitated real-time monitoring of the treatment, later allowing for cryoablation during laparoscopy [7]. Early studies of liver cryosurgery resulted in disease-free survivals of 25–37.7 % at 1–2 years and overall survival rates of 50–70 % at 2 years [8–10]. This was compared to 1 % survival at 5 years without treatment [11].

In a large randomized controlled study of patients with unresectable tumors, cryosurgery, with or without surgical resection, yielded improved survival compared with surgical resection alone [12]. Cryosurgery, therefore, became a viable treatment option in those patients with otherwise unresectable liver tumors.

Local recurrence rates following cryosurgery have been quite variable, ranging from 14 % up to 42 % [13–16]. Recurrence rates are generally higher for metastatic disease than for primary liver tumors, such as hepatocellular carcinoma (HCC) [14]. Many surgical studies are difficult to analyze because of the inclusion of surgical resection or other treatments in addition to cryotherapy as well as mixing of different tumor types within the same study. Due to lack of randomized controlled studies comparing cryotherapy to other modalities such as radiofrequency ablation (RFA) and inconsistent reporting of different tumor types in different series, comparing recurrence rates in cryotherapy relative to RFA is difficult. In a prospective, non-randomized comparison of 146 patients with primary or metastatic liver malignancies undergoing surgical RFA or surgical cryotherapy, local recurrence rates were 13.6 % in patients following cryosurgery and 2.2 % following RFA [13]. The majority of these recurrences were in lesions that were adjacent to major vessels, suggesting that a "cold sink" effect prevented treatment of the lesion. However, heat sinks pose a similar problem with RFA, so this factor may not account for the differing success rates. This study, however, was performed using intraoperative ultrasound, and one reason for increased recurrence rates with cryoablation may have been the inability of the operator to visualize the deep margin of the iceball. Ultrasound is limited in this regard; the front edge of the iceball is visualized, but the remaining volume is hidden by distal acoustic shadowing.

While open or laparoscopic cryosurgery has been shown to be effective in treating unresectable liver tumors, it has been prone to complications. The more severe complications included disseminated intravascular coagulation (DIC), thrombocytopenia, sepsis, renal failure, hypothermia, and hemorrhage, often due to liver capsule cracking. Major complication rates were high, ranging from 15 % to 50 %, with mortality ranging from 1 % to 3 % [13–16]. Many of these complications, including death, occurred in patients in whom a large volume of both tumor and liver was frozen [13, 16]. Patients with complications requiring blood transfusions were shown to have worse outcomes than those not requiring transfusions [17].

These early, cryosurgical complication rates led to further study and an increased understanding of the biochemical effects of cryoablation. Thrombocytopenia is a well-known complication of liver cryosurgery [12–16, 18]. The mechanism of cryoablation-induced thrombocytopenia may, in part, be due to platelet trapping within the cryoablated lesion and platelet sequestration within the reticuloendothelial system [19, 20].

Another known effect of liver cryoablation is myoglobinemia and myoglobinuria. While the liver does not contain myocytes or myoglobin, a rise in serum myoglobin level is frequently observed following cryoablation of liver tumors [8, 13, 14]. Myoglobinuria occurred in nearly all early cases of open cryosurgery, prompting routine prophylactic treatment with alkalinization of urine and diuresis [8]. While myoglobinuria is a transient phenomenon, it can produce renal tubule occlusion and permanent renal impairment. Alkalinization of the urine and diuresis are often performed to help prevent permanent renal damage [8]. The severity of renal impairment correlates with the amount of tissue ablated, with greater renal impairment occurring after ablation of tumors with larger cross-sectional areas [21].

Multiorgan failure, or so-called cryoshock, is the most severe, but fortunately uncommon, complication of large-volume hepatic cryoablation. This complication appears to be unique to cryoablation and is not seen with other ablative therapies. Cryoshock consists of a syndrome of pleural effusions, thrombocytopenia, DIC, acute renal failure, myoglobinemia, liver failure, acute respiratory distress syndrome, and hypotension resembling sepsis but without an infectious etiology. Thrombocytopenia is the most common

component of this syndrome [14]. A large-scale survey conducted among those performing surgical cryoablation during the late 1990s revealed a cryoshock incidence of approximately 1 %, leading to death in approximately 30 % of affected patients [14]. Cryoshock may be related to the degree of inflammatory cytokine release, including tumor necrosis factor-alpha (TNF-α) and interleukins, occurring after treatment. Most of the reported deaths following cryoablation are related to hemorrhage or cryoshock [14, 22].

Percutaneous Cryoablation

As mentioned above, cryoprobes used during liver cryosurgery employed liquid nitrogen, which necessitated large-caliber probes of 3–10 mm in diameter [23]. Newer technology uses argon gas that allows for thinner cryoprobes with current applicators now as thin as 17 gauge. The decrease in cryoprobe diameter allowed for a percutaneous approach instead of an open or laparoscopic approach beginning in the late 1990s [24]. The percutaneous approach also takes greater advantage of imaging guidance using ultrasound (US), computed tomography (CT), or magnetic resonance imaging (MRI) (Table 33.1) [25]. MRI is ideal for guiding cryoablation because, unlike US, the entire iceball can be visualized. Unlike CT, the signal void of the iceball can be discriminated from tumor using conventional MRI pulse sequences. Using CT, both the tumor and the iceball are hypodense. Using MRI and T2-weighted imaging, a T2-hyperintense tumor can be distinguished from the signal void iceball throughout the procedure. This allows the interventionalist to know precisely when the tumor is treated completely.

Using current technology, multiple cryoprobes can be placed percutaneously during one procedure, allowing for large zones of ablation. More than one cryoprobe is almost always needed for tumors larger than 1 cm, and synergy between multiple cryoprobes enables creation of a colder central isotherm than with the use of a single cryoprobe [26, 27]. Two principal manufacturers of cryoablation systems currently available in the USA employ argon gas-based cooling and helium gas-based heating technologies. There are a variety of cryoprobes currently available. In addition to gauge, the length of the active tip also varies; both relate to the corresponding size of the iceball achievable. For example, one manufacturer offers a 17 gauge, 3 cm long active tip cryoprobe that can generate an iceball approximately 2.0 cm in diameter (perpendicular to the axis of the cryoprobe) and 3.0 cm in length. When three of these cryoprobes are placed in parallel with spacing of approximately 1.5 cm, an iceball approximately 4.0 cm in diameter and 4.5 cm in length can be achieved. A single cryoprobe with 4-cm active tip can create an iceball approximately 3.0 cm in diameter and 4.5 cm in length. Three of these cryoprobes placed in parallel can create an iceball 5.0 cm in diameter and 6.0 cm in length. The size of the iceball ultimately achieved, however, depends on several factors including the target organ, target tumor, tissue perfusion, as well as presence of adjacent blood vessels. Cryoablation units are available that can accommodate up to 25 cryoprobes, although we have found that when more than seven to ten probes are used, the freezing power of individual probes may begin to decrease. Cryoprobes are available with handles

Table 33.1 Characteristics of cross-sectional imaging modalities used to guide tumor cryoablation

Visualization	US	CT	MRI
Tissue changes	Yes	Yes	Yes
Entire iceball	No	Yes	Yes
Iceball and tumor	No	No	Yes
Real-time	Yes	No	Yes
Multiplanar	Yes	Yes	Yes

Effective image-guided ablation requires imaging that provides full visualization of the tumor and ablation effects. In particular, only MRI can be used to optimally distinguish cryotherapy effects from tumor. In addition, real-time CT scanning, using CT fluoroscopy, can be used to only a limited extent because of radiation exposure to the patient and interventional radiologist

Modified and reprinted from Academic Radiology, 12 (9), Silverman, Tuncali, Morrison, MR Imaging-guided Percutaneous Tumor Ablation, September 2005, with permission from Elsevier

that are straight or angled at 90°. Right angled probes are particularly helpful in large patients in whom the distance between the patient and the edge of the CT gantry is short. MRI-compatible 17-gauge cryoprobes are available with 90° angled handles also. This is an important feature when performing percutaneous MRI-guided cryoablations in a standard-bore MRI scanner. A thermosensor may be available within the cryoprobe, or alternatively, a separate thermosensor can be inserted into the liver adjacent to the iceball to monitor temperatures at the margin or near critical structures [26, 28].

Advantages of Cryoablation

One of the most important advantages of cryoablation, compared to other ablative technologies, is the ability to clearly visualize the iceball throughout the procedure and thus optimally monitor the treatment (Table 33.1). Monitoring iceball formation allows the interventional radiologist to completely freeze an entire tumor with adequate margins while minimizing damage to surrounding structures. The real-time imaging capabilities of ultrasound can be used to facilitate rapid, accurate cryoprobe placement into target tumors located in the liver. Unfortunately, as mentioned above, ultrasound is less useful for ablation zone monitoring due to acoustic shadowing caused by the near margin of the developing iceball [7].

Using CT, the iceball is low in attenuation compared to normal liver tissue and is therefore well visualized on noncontrast CT. Iceball visualization is less than optimal within fat and bone tissues on CT; however, this is rarely problematic during liver cryoablation procedures. If necessary, iceball visualization in fat can be improved by the injection of saline into the relevant fatty tissues prior to freezing [25].

The round or teardrop-shaped iceball is seen as a signal void on all conventional MRI sequences. MRI has the advantage of excellent iceball visualization in all tissue types and in any imaging plane. The visualized iceball correlates well with the post-procedural zone of hypoenhancement on contrast-enhanced scans [29, 30]. Accordingly, MRI allows for superior visualization and monitoring of the ablation zone throughout the procedure.

Excellent iceball visualization on both CT and MRI helps the interventional radiologist avoid complications. The zero-degree isotherm at the outer edge of the visible iceball can be closely monitored, enabling the avoidance of iceball extension into critical structures. If necessary, the flow rate and pressure of gas to one or more cryoprobes can be reduced or stopped completely during the ablation to adjust the size and shape of the ablation zone as appropriate for the tumor and surrounding structures. By adjusting the flow of gas, the temperature at the active tip of the cryoprobe and therefore the extent of the lethal isotherm are adjusted. The ability to monitor the ablation zone with imaging during cryoablation gives the interventionalist a degree of intraprocedural confidence regarding adequacy and safety of ablation zone margins not generally possible with other ablation technologies (Fig. 33.1). It should be noted that most radiofrequency ablation systems are not MRI compatible at present, leaving cryoablation as the ideal technology for use in the MRI environment.

Another advantage of cryoablation is less intraprocedural and post-procedural pain when compared to RFA. In a study performed in patients undergoing percutaneous ablation of small renal tumors, less analgesic medication was required during cryoablation than RFA. This was true for both intraprocedural and post-procedural analgesics [31]. Although the literature is more limited for percutaneous hepatic cryoablation, we have observed anecdotally that patients undergoing liver cryoablation procedures also experience less pain than with similar RFA procedures. This observation is particularly important when performing ablation of tumors adjacent to the liver capsule or diaphragm. The use of RFA in these locations can result in substantial pain. The use of cryoablation to treat tumors in these locations can be accomplished

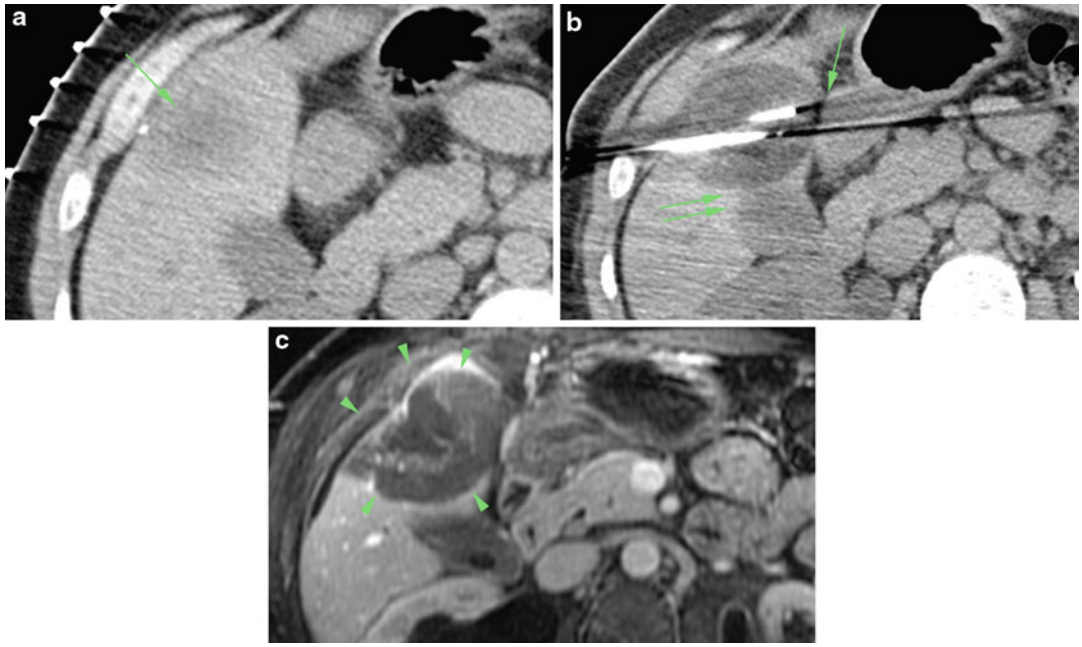

Fig. 33.1 A 46-year-old woman with history of metastatic ovarian papillary adenocarcinoma and multiple prior surgical resections in the abdomen and pelvis presents with an enlarging metastasis in segment IVB of the liver. (**a**) A 3.5-cm mass (*arrow*) is located just anterior and superior to the gallbladder and near the gastric antrum. (**b**) Four cryoprobes were employed to create an iceball that completely encompasses the mass with greater than 5.0-mm margins on all sides. The hypodense iceball extends to the medial liver capsule (*arrow*) ensuring adequate margins but does not extend into the adjacent wall of the gastric antrum. Similarly, the iceball is allowed to abut the gallbladder wall (*double arrow*) along its hepatic surface without extension of the iceball to the peritoneal surface of the gallbladder. (**c**) Contrast-enhanced MRI obtained the following morning demonstrates a hypoenhancing ablation zone (*arrow heads*) which completely covers the tumor. Residual enhancement of the tumor is commonly seen and will gradually resolve over weeks to months. The gallbladder and stomach are not injured. The iceball did extend through the liver capsule and into the adjacent body wall ensuring complete ablation of the subcapsular tumor but without adverse sequelae

without substantial pain even if the iceball extends through the diaphragm and slightly into the adjacent lung parenchyma. Cryoablation involving the diaphragm typically causes a pleural effusion and rise in serum myoglobin, but we have not observed severe pain, pneumothorax, or other adverse clinical sequelae [30, 32].

Percutaneous cryoablation can also be safe and effective in treating metastatic peritoneal tumors, typically from ovarian cancer, which may or may not invade the liver parenchyma [33]. These tumors often require freezing of large peritoneal surfaces, portions of the diaphragm, body wall, liver, and even lung. Nevertheless, the iceball is shaped through carefully planned cryoprobe placements to fully encompass the perihepatic or exophytic liver tumor. The iceball is then monitored and allowed to extend into these adjacent structures as needed to achieve adequate ablation margins around the tumor (Fig. 33.2). Such treatments for gynecologic perihepatic metastases yield low local recurrence rates of <10 % and can even ameliorate pain. There are some data that indicate combining chemotherapy, and local ablation may have a synergistic effect in treating gynecologic metastases [33].

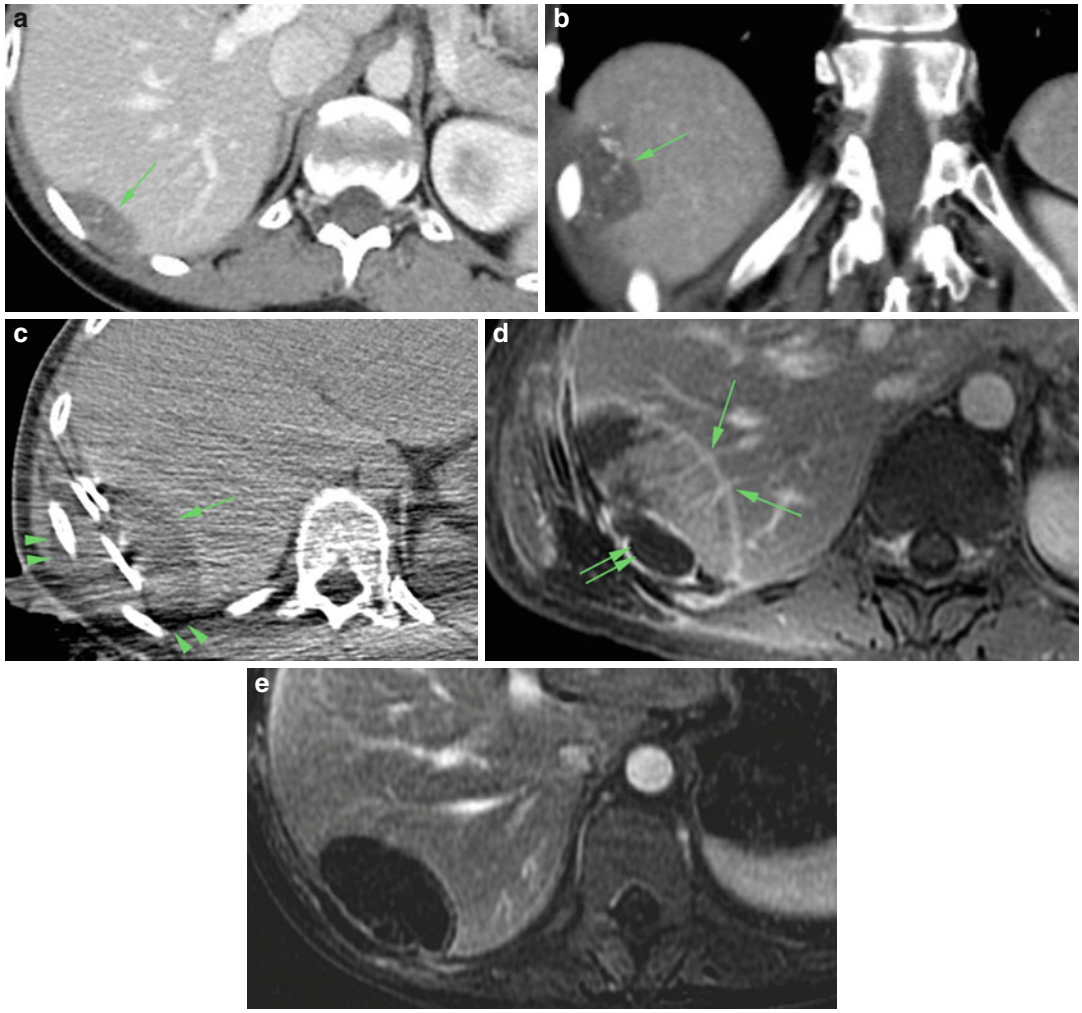

Fig. 33.2 A 50-year-old woman with poorly differentiated mullerian carcinoma of the peritoneum diagnosed 2 years earlier. She presented following surgical resection of recurrent pelvic tumor for cryoablation of a perihepatic metastasis situated between the right hepatic lobe and the lower right hemidiaphragm. (**a**) Contrast-enhanced axial CT image demonstrates the tumor, measuring 1.5 cm by 3.7 cm. (**b**) A coronal CT image reveals calcification within the tumor and a cranio-caudal dimension of 3.7 cm. (**c**) Noncontrast CT during the cryoablation procedure demonstrates extension of the iceball into the liver medially (*arrow*) and the body wall laterally (*arrow heads*), ensuring adequate margins around the peritoneal metastasis. (**d**) Contrast-enhanced MRI obtained the following day demonstrates the centrally non-enhancing tumor (*double arrow*) with peripheral rim enhancement surrounded by a large ablation zone. The hepatic margins of the ablation zone (*arrows*) are traversed by vessels which are not yet thrombosed. These vessels cross the hyperemic rim surrounding the ablation zone. Note that there is patchy residual enhancement within the hepatic ablation zone which will gradually decrease over time. The iceball extended into the body wall but was not allowed to approach the skin. (**e**) Six weeks later, a contrast-enhanced T1-weighted subtraction MRI image reveals absence of enhancement throughout the ablation zone

Unlike most RF applicators, multiple cryoprobes can be active simultaneously allowing for a larger ablation zone with multiple cryoprobes than with a single RF applicator. Since the ablation zone can be monitored, the interventionalist can treat multiple lesions or one large lesion in a single freeze-thaw-freeze cycle, rather than performing multiple overlapping ablations, as RFA would require.

Disadvantages of Cryoablation

While cryotherapy was initially embraced in the surgical arena for the treatment of unresectable liver tumors, it is not commonly employed in the operating room today because of relatively high cryosurgical complication rates and the availability of RFA devices. Although to date there have been no large-scale randomized controlled trials comparing the safety and efficacy of percutaneous RFA relative to percutaneous cryoablation for hepatic neoplasms, RFA is the predominant technology in use today. Data are beginning to accumulate regarding the safety and efficacy of percutaneous image-guided cryoablation in the liver [30, 33–36]; however, there are some disadvantages of cryoablation that must be considered.

As described above, cryoablation can induce thrombocytopenia and therefore should be avoided in patients with baseline thrombocytopenia. The degree of thrombocytopenia closely correlates with immediate posttreatment serum aspartate transaminase (AST) levels. The posttreatment AST rise correlates with the volume of liver tissue that has been ablated and the degree of hepatocellular injury [3, 18, 20]. This complication can be avoided by limiting the volume of liver ablated [18]. On the other hand, thrombocytopenia can almost always be managed successfully with platelet transfusions if the platelet level decreases to less than 50,000/μL. While cryosurgical rates of thrombocytopenia were reported as high as 44 %, other smaller percutaneous cryoablation series do not report thrombocytopenia as common a problem, with incidences of 0–18 % and often not requiring platelet transfusions [16, 18, 30, 34, 35]. While thrombocytopenia is generally successfully managed with platelet transfusions, there are reported cases of patients progressing to DIC following percutaneous cryoablation [18, 36]. Initially described in the surgical literature, cryoshock has been reported with percutaneous cryoablation but occurs less frequently than the 1 % rate reported after surgery. This may be due to smaller ablation volumes, involvement of less normal liver parenchyma, or other factors related to the nonsurgical approach [35, 37].

The risk of hemorrhage is of potentially greater concern with cryoablation than other ablative techniques; however, there are limited data to support this. Historically, an open surgical approach sometimes resulted in hemorrhage, severe enough to warrant hepatic suturing or surgical packing due to cracking of the liver capsule. With a percutaneous approach and smaller cryoprobe diameters, major hemorrhage is uncommon, particularly if care is taken to avoid traversing major portal triads with the cryoprobes. We have not observed severe bleeding when ablating peripheral hepatic tumors close to the liver capsule. This could be explained by the fact that the percutaneous approach does not subject the liver to the deforming forces or air-liver interfaces that can occur in surgery increasing the chance of liver cracking. Unlike RFA, there is no track ablation feature available with current cryoprobe designs, although such track ablation technology is being considered for new cryoprobe designs. No prospective, randomized controlled trials have been performed to compare degree of hemorrhage in percutaneous cryoablation versus RFA, but data from a porcine model study demonstrated a slightly increased risk of bleeding with a 13-gauge cryoprobe compared with single 17-gauge RFA applicator; the greater risk could have been simply due to the larger diameter cryoprobe. Since thinner cryoprobes are currently in use, the risk of hemorrhage may not be as much of a concern with today's cryoablation devices [38].

Hemorrhage and renal failure are of particular concern in cirrhotic patients, where underlying liver and, possibly, renal function are compromised. The amount of blood loss in cirrhotics has been found to be more closely associated with liver dysfunction than the number of cryoprobes used [22]. It is, in part, because of this concern regarding hemorrhage that some may prefer to avoid cryoablation in patients with advanced cirrhosis. While no large trials have been performed to compare cryoablation complication rates in patients with or without cirrhosis, reported cryoablation complication and mortality rates have generally been similar in treated populations with hepatocellular carcinoma and metastatic colon cancer [36, 37, 39]. Patients with Child-Pugh class C cirrhosis are rarely considered

for any available liver ablation technology, including cryoablation, due to lack of hepatic reserve and overall poor prognosis. Patients with cirrhosis are selectively treated with cryoablation in our practice if there is no coagulopathy, thrombocytopenia, renal insufficiency, or class C cirrhosis. Cryoablation is considered on a case-by-case basis if iceball visualization is expected to provide significant advantages in ablation monitoring or safety when compared to RFA. Some previous concerns regarding the use of cryoablation in cirrhotic livers are now outdated, such as inability or difficulty placing a large-diameter cryoprobe through a fibrotic liver; this is no longer a concern since the diameter of cryoprobes is now comparable to other ablation applicators [22].

Cryoablation also has the potential to induce myoglobinemia, leading to myoglobinuria, and ultimately renal failure [36]. However, renal failure was uncommon following surgical cryotherapy with proper postoperative management and is even less common with percutaneous ablation, where ablation zones are generally smaller. In either case, myoglobinuria can be successfully managed with hydration, diuresis, and alkalinization of the urine [18, 36].

Another potential disadvantage of cryoablation is that procedures may be longer in duration than comparable RFA procedures employing a single applicator. Radiofrequency ablation, using an internally cooled cluster applicator, typically requires a minimum 12-min treatment time for small tumors less than or equal to 3 cm in diameter. Only very small tumors of approximately 1 cm in diameter can be treated with a single cryoprobe; even 3-cm-diameter tumors require the use of at least two to three cryoprobes. The placement of multiple cryoprobes can be time-consuming, particularly when using CT or MRI guidance. The double freeze cycle is also time-consuming, typically including a 15-min freeze–10-min thaw–15-min freeze cycle, adding up to a 40-min treatment time. However, cryoablation may actually facilitate shorter procedure times in some cases where the placement of multiple cryoprobes enables complete ablation of a large tumor in one double freeze cycle, a treatment which would otherwise require multiple overlapping RFA applications. The use of ultrasound in the initial placement of cryoprobes can also substantially reduce procedure time.

While data are more limited for percutaneous cryoablation than for cryosurgery, 1-year recurrence rates have been reported from 23 % to 53 % [34–36]. The largest comparison of percutaneous RFA and percutaneous cryoablation compared 64 patients in a retrospective study. This study showed a slightly higher, but not significantly different, procedural complication rate for cryoablation and identical initial success rates between the two modalities. The 53 % rate of local recurrence following cryoablation was significantly higher than the 18 % reported for the RFA group. However, there was no significant difference in 1-year survival between the two groups with the cryoablation group demonstrating a trend toward a slightly better survival rate [37]. When applied in the percutaneous setting, using CT or MRI guidance, the advantages of cryoablation relative to RFA in terms of ablation zone monitoring could be expected to improve local recurrence rates. Studies are needed to confirm this concept.

The initial capital costs for cryoablation systems are greater than for RFA systems, and maintenance is also slightly more expensive and complex than for a comparable microwave or RFA system. Unit costs are also generally higher per procedure for cryoablation when compared to RFA since a larger number of disposable cryoprobes are often used and there is the additional cost of storing and maintaining argon and helium gases.

Percutaneous Liver Cryoablation Procedures

Periprocedural Considerations

In evaluating a patient for possible liver cryoablation, the malignancy should first be appropriately staged. PET/CT using 18F-fluorodeoxyglucose can be helpful in the evaluation of extrahepatic disease. Contrast-enhanced

CT or MRI of the abdomen is then obtained to evaluate the number, size, and location of lesions, as well as potential percutaneous access pathways. CT and MRI also depict the proximity of the tumors to critical structures such as the diaphragm, bowel, adrenal gland, gallbladder, and large portal triads. Biliary-enteric anastomosis is a contraindication, and biliary obstruction is a relative contraindication for most hepatic ablation techniques due to increased risk of bacterial seeding and liver abscess formation.

The size of the tumor is important in evaluating the number and type of cryoprobes required. In selecting an appropriate approach, care is taken to avoid placement of cryoprobes into or through visible portal triads in the liver. If a tumor is subcapsular in location, an access route is planned that will traverse normal liver before entering the tumor. This will minimize the risk of tumor seeding of the peritoneum and, in the case of hypervascular tumors, lessen the risk of bleeding. Ideally, cryoprobes are positioned in parallel and approximately 1.5 cm apart from each other, but not more than 2 cm apart [40]. The cryoprobes should not be placed more than 2 cm apart as spacing greater than 2 cm has been shown to result in inadequate or patchy lethal isotherms between the cryoprobes [27]. It is important to note that the lethal isotherm may lie up to 5 mm or more inside the outer edge of the visible iceball. The outer edge of the visible iceball represents the 0° isotherm and should not be allowed to extend into adjacent critical structures. For spherical tumors, probes are placed in a radial pattern with each probe positioned less than 1 cm inside the peripheral margin of tumor. In general, a guideline for the number of cryoprobes needed is to add one to the lesion diameter measured in centimeters. For example, in treating tumors that are 1 cm or less in diameter, one to two cryoprobes can be used. For 3-cm tumors, four cryoprobes are used. For 5-cm tumors, six to seven cryoprobes can be used. The number of cryoprobes required is affected by the type of cryoprobe used, the shape of the tumor, its location relative to critical structures, and perfusion of the relevant tissues. In addition to the length and number of freeze-thaw cycles, the flow rate and pressure of gas can be adjusted to modify the size and shape of the iceball.

Prior to the procedure, laboratory tests are obtained including a complete blood count and coagulation parameters. A prothrombin time with international normalization ratio (INR) of less than 1.5 is required along with a platelet count of at least 150,000/μl. Hematocrit should preferably be at least 30 % prior to the procedure. While we do not follow strict guidelines with regard to partial thromboplastin time (PTT), PTT should ideally be less than 1.5 times control values. Coumadin, low molecular weight heparin, acetylsalicylic acid, clopidogrel, and other anticoagulants should be discontinued unless required for secondary prophylaxis. If they cannot be discontinued, for example, due to recent coronary artery stent placement, then percutaneous ablation may have to be reconsidered. Alternatively, a heparin bridge strategy might be considered perhaps in consultation with the cardiovascular and hematology services. Liver enzymes and, in particular, serum bilirubin and albumin should be checked in patients with cirrhosis or hepatocellular carcinoma and used to help determine the Child-Pugh score. Child-Pugh class C cirrhotics are rarely eligible for ablative therapy. Renal function must also be adequate, preferably with an estimated glomerular filtration rate in the normal range.

In planning anesthesia, intravenous conscious sedation (IVCS) using fentanyl and midazolam, monitored anesthesia care (MAC), and general anesthesia are all viable options. As cryoablation is less painful than other ablation methods, IVCS can be used for smaller, more peripheral tumors, and MAC or general anesthesia can be employed for larger or more difficult-to-access tumors or where the duration of the procedure may be extended.

Percutaneous, MR-guided cryoablation procedures require careful planning with participation of all members of the healthcare team including interventional radiologists, anesthesiologists, physicists, nurses, and technologists. All equipment used in the MRI suite must be MRI compatible. Cryoablation installations require that the cryoablation unit and gas tanks be

installed outside the interventional MRI suite with MRI-compatible gas lines and peripheral equipment located inside the interventional MRI suite [25].

Post-procedure Care

After the procedure, vital signs are monitored in the recovery area. A complete blood count, serum myoglobin, basic metabolic panel, and liver enzymes are obtained approximately 2 and 18 h post-procedure. We observe patients overnight. If the serum myoglobin level exceeds 1,000 ng/ml, the patient is hydrated intravenously, and the urine is alkalinized. Our regimen for managing this degree of myoglobinemia is to add 150 mEq of sodium bicarbonate to each liter of 5 % dextrose water and hydrate the patient with this solution at 150 ml/h. Mannitol can also be administered to enhance diuresis [8]. If a pneumothorax is suspected, a follow-up chest radiograph is obtained.

As stated above, some decrease in platelet level is expected after cryoablation. The platelet nadir typically occurs 1–3 days following ablation and returns to normal within 1–2 weeks [18]. If the patient's platelets drop below 50,000/μL, platelets are transfused.

While post-procedural pain from cryoablation is generally less than that following RFA, patients may, nevertheless, experience pain in the post-procedure period. At our institution, such pain is usually managed with intravenous morphine or hydromorphone as needed sometimes in the form of patient-controlled analgesia (PCA) delivery systems.

Contrast-enhanced MRI or CT is performed the morning after the procedure to assess the results of the ablation, to evaluate for potential complications, and to provide a baseline for comparison on follow-up imaging. The ablation zone is well visualized with a contrast-enhanced CT or MRI. The key features to evaluate on the immediate post-ablation imaging are the size of ablation zone and the margins around the tumor. The ablation zone should be larger than and completely inclusive of the lesion [41]. At our institution, MRI is generally preferred when possible.

The ablation zone on T1-weighted, contrast-enhanced MRI appears as a relatively hypoenhancing region when compared to normal liver. This hypoenhancing area correlates closely with the area of signal void caused by the iceball during the procedure [30]. These MRI findings correspond to coagulative necrosis histologically [42]. In early follow-up imaging, the lesion may appear T2 hyperintense due to edema, liquefactive necrosis, or granulation tissue [42, 43].

We have observed that enhancement with gadolinium-based contrast agents on post-procedure MRI may be present within the ablation zone 24 h or more after cryoablation and likely reflects variable reperfusion after thawing. The degree of enhancement decreases over the following months. This is similar to published data regarding MRI contrast enhancement findings seen following renal tumor cryoablation [44]. As long as the tumor is fully contained by the hypoenhancing ablation zone with adequate margins, the presence of residual tumor enhancement on MRI has not been associated with local recurrence in our experience. We have also observed that peak liver tumor contrast enhancement on 24-h post-cryoablation MRI tends to occur later in the dynamic MRI scan than prior to ablation, possibly reflecting reperfusion of damaged, leaky vasculature. In the immediate post-ablation setting, benign periablational enhancement is often seen at the peripheral margin of the ablation zone, reflecting hyperemia [42]. This rim of enhancement does not indicate residual tumor or capsule formation and is similar to the periablational enhancement observed following RFA. On later follow-up imaging, the two main features indicative of local recurrence or incomplete treatment are nodular enhancement within or, more commonly, at the margins of the ablation zone and an increase in the ablation zone size [43]. It should be noted, however, that an increase in ablation zone size may be indicative of recurrence but may also result from infection or fluid within the lesion (e.g., bile) without associated recurrence.

The ablation zone as visualized on contrast-enhanced CT is a well-demarcated region of hypoenhancement. This zone may be round or teardrop shaped, depending on the shape of the cryoablation iceball. This area of hypoenhancement correlates well with areas of coagulative necrosis. High-attenuation areas within the ablation zone on noncontrast CT are common and typically represent desiccated tissue or less commonly hemorrhage. Small gas bubbles may be seen within the ablation zone in the first several days after ablation and usually are the result of necrosis. If these do not resolve within a few weeks, a superimposed infection may be present [41]. After the 24-h scan, subsequent imaging is generally performed at 3, 6, 9, 12, 18, and 24 months. These scans, in the absence of recurrence, usually show a gradual decrease in the size of the cryoablation zone. Peripheral, small bile duct dilatation may be seen after cryoablation and may be due to cryoablation-induced injury of ducts or due to obstruction by the primary lesion.

In conclusion, percutaneous image-guided cryoablation is a safe and effective treatment option for both primary and metastatic neoplasms of the liver in many patients. The patient selection criteria and post-procedure management issues are somewhat different for cryoablation when compared to RFA, and the utilization of cryoablation is potentially more expensive and involved than that of RFA. On the other hand, cryoablation offers several important advantages including superior intraprocedural visualization of the developing ablation zone, less procedural and post-procedural pain, and the capability of treating tumors extensively abutting the diaphragm. As the stigma of historical problems associated with surgical cryoablation using old technology recedes, a gradually developing body of experience with newer cryoablation technology applied percutaneously and with optimal imaging guidance is stimulating renewed interest in this minimally invasive treatment option for malignant liver tumors.

References

1. Mala T. Cryoablation of liver tumours – a review of mechanisms, techniques and clinical outcome. Minimal Invasiv Ther. 2006;15:9–17.
2. Neel HB, Ketcham AS, Hammond WG. Requisites for successful cryogenic surgery of cancer. Arch Surg. 1971;102:45–8.
3. Stewart GJ, Preketes A, Horton M, Ross WB, Morris DL. Hepatic cryotherapy: double-freeze cycles achieve greater hepatocellular injury in man. Cryobiology. 1995;32:215–9.
4. Gage AA, Baust J. Mechanisms of tissue injury in cryosurgery. Cryobiology. 1998;37:171–86.
5. Whittaker DK. Mechanisms of tissue destruction following cryosurgery. Ann Roy Coll Surg Eng. 1984;66:313–8.
6. Mazur P. The role of intracellular freezing in the death of cells cooled at supraoptimal rates. Cryobiology. 1977;14:251–72.
7. Gilbert JC, Onik GM, Hoddick WK, et al. Real time ultrasonic monitoring of hepatic cryosurgery. Cryobiology. 1985;22:319–30.
8. Onik GM. Cryosurgery of liver cancer. Semin Surg Oncol. 1993;9:309–17.
9. Ravikumar TS, Steele Jr G, Kane R, King V. Experimental and clinical observations on hepatic cryosurgery for colorectal metastases. Cancer Res. 1991;51:6323–7.
10. Zhou XD, Tang ZY, Yu YQ, Ma ZC. Clinical evaluation of cryosurgery in the treatment of primary liver cancer: report of 60 cases. Cancer. 1988;61:1889–92.
11. Wagner JS, Adson MA, Van Heerden AJ, Adson MH, Ilstrup DM. The natural history of hepatic metastases from colorectal cancer: a comparison with resective treatment. Ann Surg. 1984;199:502–7.
12. Korpan NN. Hepatic cryosurgery for liver metastases: long-term follow-up. Ann Surg. 1997;225:193–201.
13. Pearson AS, Frencesco I, Fleming D, et al. Intraoperative radiofrequency ablation or cryoablation for hepatic malignancies. Am J Surg. 1999;178:592–8.
14. Seifert JK, Morris DL. World survey on the complications of hepatic and prostate cryotherapy. World J Surg. 1999;23:109–14.
15. Ruers TJM, Joosten J, Jager GJ, Wobbes J. Long-term results of treating hepatic colorectal metastases with cryosurgery. Brit J Surg. 2001;88:844–9.
16. Bilchik AJ, Wood TF, Allegra D, et al. Cryosurgical ablation and radiofrequency ablation for unresectable hepatic malignant neoplasms: a proposed algorithm. Arch Surg. 2000;135:657–64.
17. Kerkar S, Carlin AM, Sohn RL, et al. Long-term follow up and prognostic factors for cryotherapy of malignant liver tumors. Surgery. 2004;136:770–9.
18. Nair RT, Silverman SG, Tuncali K, Obuchowski NA, VanSonnenberg E, Shankar S. Biochemical and

hematologic alteration following percutaneous cryoablation of liver tumors: experience in 48 procedures. Radiology. 2008;248:303–11.
19. Pistorious GA, Alexander C, Krisch CM, et al. Local platelet trapping as the cause of thrombocytopenia after hepatic cryotherapy. World J Surg. 2005;29:657–61.
20. Cozzi PJ, Stewart GJ, Morris DL. Thrombocytopenia after hepatic cryotherapy for colorectal metastases: correlates with hepatocellular injury. World J Surg. 1994;18:774–6.
21. Sohn RL, Carlin AM, Steffes C, et al. The extent of cryosurgery increases the complication rate after hepatic cryoablation. Am Surg. 2003;69:317–22.
22. Wong WS, Patel SC, Cruz FS, Gala DV, Turner AF. Cryosurgery as a treatment for advanced stage hepatocellular carcinoma. Cancer. 1998;82:1268–78.
23. Ross WB, Horton M, Bertolino P, Morris DL. Cryotherapy of liver tumours: a practical guide. HPB Surg. 1995;8:167–73.
24. Adam R, Majno P, Castaing D, et al. Treatment of irresectable liver tumours by percutaneous cryosurgery. Br J Surg. 1998;85:1493–4.
25. Silverman SG, Tuncali K, Morrison PR. MR imaging-guided percutaneous tumor ablation. Acad Radiol. 2005;12:1100–9.
26. Hinshaw JL, Lee FT. Cryoablation for liver cancer. Tech Vasc Interv Rad. 2007;10:47–57.
27. Permpongkosol S, Nicol TL, Khurana H, et al. Thermal maps around two adjacent cryoprobes creating overlapping ablations in porcine liver, lung and kidney. J Vasc Interv Radiol (JVIR). 2007;18:283–7.
28. O'Rourke AP, Haemmerich D, Prakash P, Converse MC, Mahvi DM, Webster JG. Current status of liver ablation devices. Expert Rev Med Devices. 2007;4:523–37.
29. Silverman SG, Sun MR, Tuncali K, et al. Three dimensional assessment of MRI-guided percutaneous cryotherapy of liver metastases. AJR Am J Roentgenol. 2004;183:707–12.
30. Silverman SG, Tuncali K, Adams DF, et al. MR imaging-guided percutaneous cryotherapy of liver tumors: initial experience. Radiology. 2000;217:657–64.
31. Allaf ME, Varkarakis IM, Bhayani SB, Inagaki T, Kavoussi LR, Solomon SB. Pain control requirements for percutaneous ablation of renal tumors: cryoablation versus radiofrequency ablation- initial observations. Radiology. 2005;237:366–70.
32. Tatli S, Acar M, Tuncali K, Morrison PR, Silverman SG. Percutaneous cryoablation techniques and clinical applications. Diagn Interv Radiol. 2010;16:90–5.
33. Soloman LA, Munkarah AR, Vorugu VR, et al. Image-guided percutaneous cryotherapy for the management of gynecologic cancer metastases. Gynecol Oncol. 2008;111:202–7.
34. Xu KC, Niu LZ, He WB, et al. Percutaneous cryoablation in combination with ethanol injection for unresectable hepatocellular carcinoma. World J Gastroenterol. 2003;9:2686–9.
35. Xu KC, Niu LZ, He WB, Hu YZ, Zuo JS. Percutaneous cryosurgery for the treatment of hepatic colorectal metastases. World J Gastroenterol. 2008;14:1430–6.
36. Xu KJ, Niu LZ, Zhou Q, et al. Sequential use of transarterial chemoembolization and percutaneous cryosurgery for hepatocellular carcinoma. World J Gastroenterol. 2009;15:3664–9.
37. Adam R, Hagopian EJ, Linhares M, et al. A comparison of percutaneous cryosurgery and percutaneous radiofrequency for unresectable hepatic malignancies. Arch Surg. 2002;137:1332–9.
38. Shock SA, Laeseke PF, Sampson LA, et al. Hepatic hemorrhage caused by percutaneous tumor ablation: radiofrequency ablation versus cryoablation in a porcine model. Radiology. 2005;236:125–31.
39. Adam RA, Akpinar E, Johann M, Kunstlinger F, Majno P, Bismuth H. Place of cryosurgery in the treatment of malignant liver tumors. Ann Surg. 1997;225:39–50.
40. Wang H, Littrup PJ, Duan Y, et al. Thoracic masses treated with percutaneous cryotherapy: initial experience with more than 200 procedures. Radiology. 2005;235:289–98.
41. McLoughlin RF, Saliken JF, McKinnon G, Wiseman D, Temple W. CT of the liver after cryotherapy of hepatic metastases: imaging findings. AJR Am J Roentgenol. 1995;165:329–32.
42. Tacke J, Adam G, Haage P, Sellhaus B, Grobkortenhaus S, Gunther RW. MR-guided percutaneous cryotherapy of the liver: in vivo evaluation with histologic correlation in an animal model. J Magn Reson Imaging (JMRI). 2001;13:50–6.
43. Kuszyk BS, Boitnott JK, Choti MA, et al. Local tumor recurrence following hepatic cryoablation: radiologic-histopathologic correlation in a rabbit model. Radiology. 2000;217:477–86.
44. Porter CA, Woodrum DA, Callstrom MR, et al. MRI after technically successful renal cryoablation: early contrast enhancement as a common finding. AJR Am J Roentgenol. 2010;194:790–3.

Laser-Induced Interstitial Thermotherapy

34

Thomas J. Vogl, Alexandra Jost, Mohamed Nabil, and Martin G. Mack

Abstract

Image-guided thermal ablation of hepatic malignancies has been successfully performed with laser applicators. Local control rates after laser ablation of HCC and hepatic metastases as well as 1-, 3-, and 5-year survival rates are now available, and they support a competitive role to other methods of ablative therapy in the management of hepatic malignancies with an acceptably low rate of major complications.

Introduction

The liver, due to its unique location, function, and circulation, is one of the organs most frequently involved by neoplastic diseases, especially metastatic spread. Among the primary tumors metastasizing to the liver, digestive system malignancies, especially colon cell carcinoma, are the most common [1].

The degree of metastatic involvement of the liver has a major influence on the survival time and quality of life of cancer patients. Hence, while putting forth a treatment strategy of this condition, utmost consideration should be given to sparing more healthy liver parenchyma while simultaneously eliminating more malignant tissue, since hepatic failure is potentially lethal and defeats the palliative intent of the intervention.

Surgery including different grades of resection or even transplantation is still the essential curative treatment method of liver malignancy [2, 3]. If surgery is contraindicated or not feasible, alternative palliative therapeutic measures are to be considered which can be divided into two categories: transarterial chemotherapy [4–7] or percutaneous ablation such as thermal ablation or local alcohol injection [8–14].

Ideally therapeutic alternatives should be less invasive than resection, which entails being applicable under local anesthesia, on an outpatient basis, and with a lower complication rate. They should be capable of achieving similar results, preferably at lower costs. MR-guided laser ablation for hepatic malignant lesions fulfills all those criteria.

The indications of laser ablation in primary or secondary liver malignancies can be classified into (neo)adjuvant, palliative, and/or symptomatic. The curative potential of laser ablation can be defined

T.J. Vogl (✉) • A. Jost • M. Nabil • M.G. Mack
Department of Diagnostic and Interventional Radiology, University Hospital of Frankfurt, Frankfurt am Main, Germany
e-mail: t.vogl@em.uni-frankfurt.de; alexandrajost@gmx.net; mnabil73@hotmail.com; m.mack@em.uni-frankfurt.de

D.E. Dupuy et al. (eds.), *Image-Guided Cancer Therapy*, DOI 10.1007/978-1-4419-0751-6_36,

as the achievement of long-term survival associated with effective local control. In a patient with such a grave condition, this can be a goal worth achieving or at least pursuing. However, the chances of a complete cure in disseminated malignancies are limited because of the constant threat of new metastases developing in the treated organ or in any other organ and the possibility of residual disease after incomplete ablation. Thus, cure does not have to be the primary intention of laser ablation application in all patients even though complete remission can be achieved in some cases.

Laser ablation as neoadjuvant treatment usually combined with surgery mainly aims at converting inoperable cases with extensive liver involvement into operable ones. An example of this is a patient with bilateral involvement of both hepatic lobes. The ablation of a solitary lesion in one of these lobes would spare this lobe from resection and hence preserve more functioning hepatic tissue. In other words, neoadjuvant laser ablation can minimize the extent of surgical resection, downgrading it from a complete resection and transplant into a lobectomy and from lobectomy to segmentectomy or localized resection. Laser ablation can be used as an adjuvant measure to systemic chemotherapy especially in the presence of extrahepatic spread aiming at reducing the hepatic tumorload and thus optimizing treatment success.

On the other hand, it can be used as a palliative measure in cases of inoperability, postsurgical recurrence, or failed systemic chemotherapy to achieve symptomatic relief or just to improve the quality of life.

Recently, a combination of transarterial chemoembolization (TACE) and laser ablation proved its success when TACE was used as a neoadjuvant measure to downsize liver tumors which were beyond the size limit of laser ablation so that they could be subsequently ablated through laser ablation [15].

Physical and Technical Principles

The physical mechanism of thermal ablation is coagulation necrosis through temperature elevation within the tumor core.

Laser ablation is performed using neodymium–yttrium aluminum garnet laser (Nd:YAG) light with a wavelength of 1,064 nm. The light is delivered through 12-m-long fibers terminated by a specially developed diffuser, which emits laser light to an effective distance of up to 12–15 mm [16]. Manufacturers of these laser systems include Dornier (Dornier mediLas 5060, Dornier mediLas 5100; Dornier Medizintechnik, Germering, Germany), DEKA, (DEKA_M.E.L.A.; Florence, Italy [17, 18]), Elesta (Elesta; Florence, Italy) [19], and Visualase Inc. (Houston, USA), all of which produce a similar laser beam to the one previously described.

In contrast to radiofrequency ablation (RFA), the laser functions with the irradiation of coherent monochromatic light, which is appropriately absorbed by the tissue and works independently of the impedance rise at the transition zone between tumor and parenchyma. Hence, further energy deposition is not limited by this phenomenon [16, 20].

Evaluation of MR thermometry data during MR-guided laser-induced thermotherapy demonstrates that metastatic tissue is very sensitive to heat, showing earlier and more widespread temperature distribution than does surrounding liver parenchyma. In most cases, an area of decreased signal intensity appears during laser ablation treatment, which is identical with the area shown to represent coagulative necrosis [1, 20].

The location of the lesion technically influences the procedure. The procedure is most simple if the lesion is surrounded by sufficient normal liver parenchyma with no close vicinity to any of the critical structures such as inferior vena cava, liver capsule, gall bladder, or major portal veins and bile ducts. Unfortunately, this is encountered only in a minority of cases. A lesion is defined as subcardial if it is located in liver segment II with a distance of less than 8 mm to the pericardium.

One laser ablation session is defined as ablation performed on 1 day with 1 or multiple laser applicators of 1 or more lesions simultaneously. A laser application is defined as laser treatment

at one certain position. Pulling the applicator backward and performing another laser treatment to enlarge the necrosis area is considered a second laser application. One ablation round includes all ablation sessions which are necessary to get all visible metastases treated as planned. If new metastases are encountered during follow-up after the initial round, ablation of these lesions is considered a second ablation round.

Equipment and Laser Set

Laser coagulation is accomplished using an Nd:YAG laser light (1,064 nm) delivered through 12-m-long optic fibers terminated by a specially developed diffuser. A flexible diffuser tip of 1.0 mm in diameter makes the laser applications much easier by reducing the risk of damage to the diffuser tip to almost zero. The active length of the diffuser tip ranges between 20 and 40 mm in length. The laser power is adjusted to 12 W per cm active length of the laser applicator. The length of the diffuser dome should cover the diameter of the lesion in the access direction with an additional safety margin of 1 cm. By choosing the applicator length, it must be considered that the segment remaining outside should fit into the gantry [20].

The laser application kit (SOMATEX, Berlin, Germany) consists of a cannulation needle, a sheath system, and a protective catheter which prevents direct contact of the laser applicator with the treated tissues in addition to acting as a tip-cooling system. The closed end of the protective catheter allows complete removal of the applicator at the end of the procedure even if the fiber is damaged (Fig. 34.1).

Systems are available for simultaneous multiple application (Dornier Medizintechnik, Germering, Germany). Using a beam splitter TT SWITCH 3 (Trumpf medical systems), up to six applicators can operate together [20]. The application systems are available in various sizes ranging from 5.5 to 9 F. One-step systems were developed especially for application in the lung so as to provide, in addition to smaller caliber, lesser manipulation during puncture [21, 22].

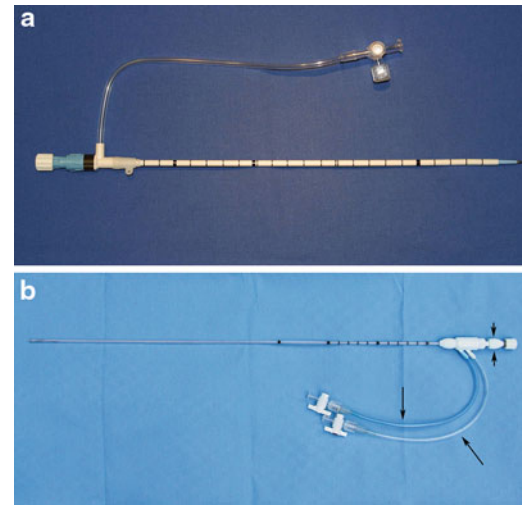

Fig. 34.1 (**a**) A 9F sheath as a part of laser applicator set (*SOMATEX, Berlin, Germany*). A side port with a valve is used for flushing with saline to keep the system airtight. (**b**) Double-lumen protective catheter with the mandarin still in place (*short arrows*). The mandarin is removed to allow the laser fiber to be introduced. Internal cooling is achieved through circulating room-temperature sodium chloride solution within the double-lumen catheter through inlet and outlet tubing (*long arrows*)

Prior to the procedure, all patients are examined using an MR protocol including T1- and T2-weighted images, gradient-echo (GE) T1, and contrast-enhanced T1 for localizing the target lesion and planning the procedure.

The real advantage of MR over CT and ultrasound lies in its heat-sensitive signal changes, which enables accurate monitoring of the degree of induced necrosis. Rapid, near real-time documentation of laser ablation effect confirms complete ablation of the entire lesion and detects residual tissue which can be immediately treated through applicator repositioning under MR guidance.

MR provides unparalleled topographic accuracy due to its excellent soft tissue contrast and high spatial resolution which allows the identification and protection of vital structures during ablation.

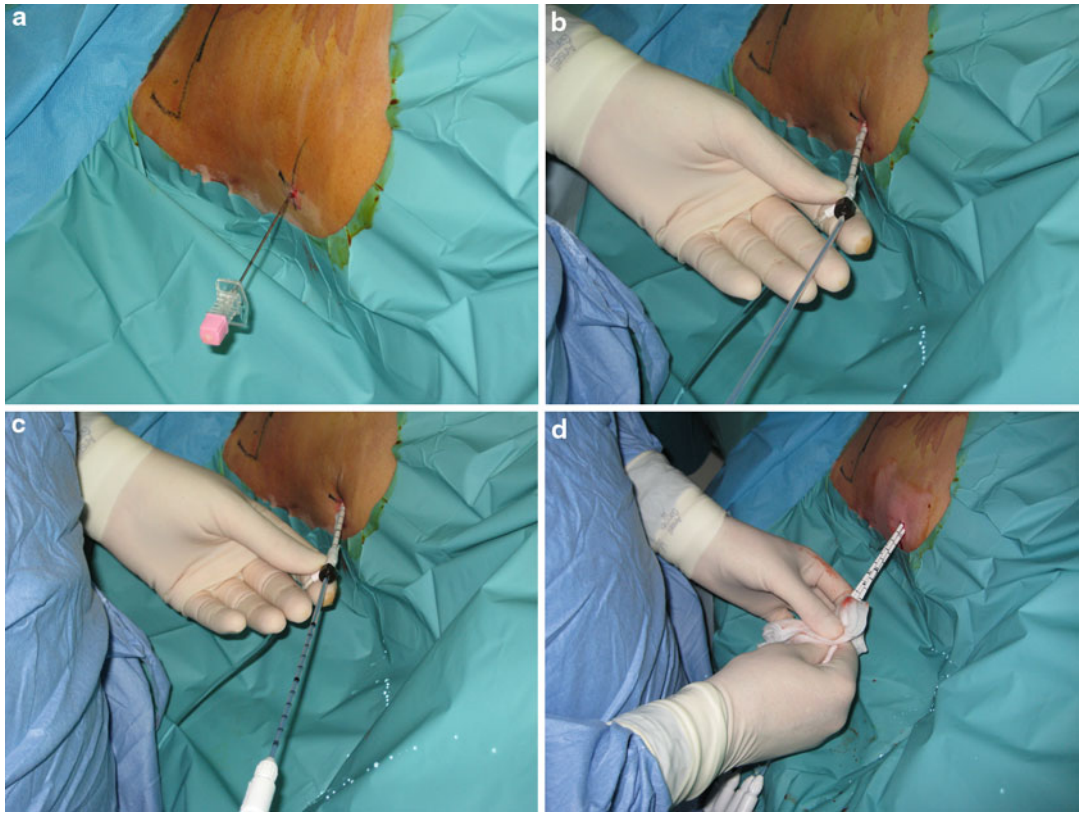

Fig. 34.2 The steps of positioning the laser applicator (Seldinger technique). (**a**) Needle advanced into the lesion. (**b**) Using the Seldinger technique, the guidewire is advanced inside the lumen of the needle to its distal tip. The needle is then removed. (**c**) The sheath is placed over the wire. (**d**) The thermostable protective catheter is introduced within the sheath

Ablation Procedure

Investigations that should be performed prior to the procedure are staging CT or MRI, laboratory evaluation of tumor markers, coagulation values, and electrocardiogram (why? Are all cases done under general anesthesia? No, only sedation under mild analgosedation). Pulmonary function should be intact (what does that mean – do you use values of FEV1 for liver ablations?) before starting the procedure. Patients attend the procedure on an empty stomach.

The puncture site and route is planned on CT images. Local anesthesia is applied. Under CT guidance, the required number of laser application systems is placed in position using the Seldinger technique (Fig. 34.2). Then, the patient is transferred to the MRI unit, where the laser fiber is inserted into the protective catheter. MR sequences are performed in three perpendicular orientations before starting the ablation and then regularly during laser energy application to assess the progress of necrosis manifested by signal loss in the T1-weighted gradient-echo images (Fig. 34.3). Depending on the geometry and intensity of the signal loss, the position of the laser fibers, the laser power, and the cooling rate can be readjusted. Treatment is

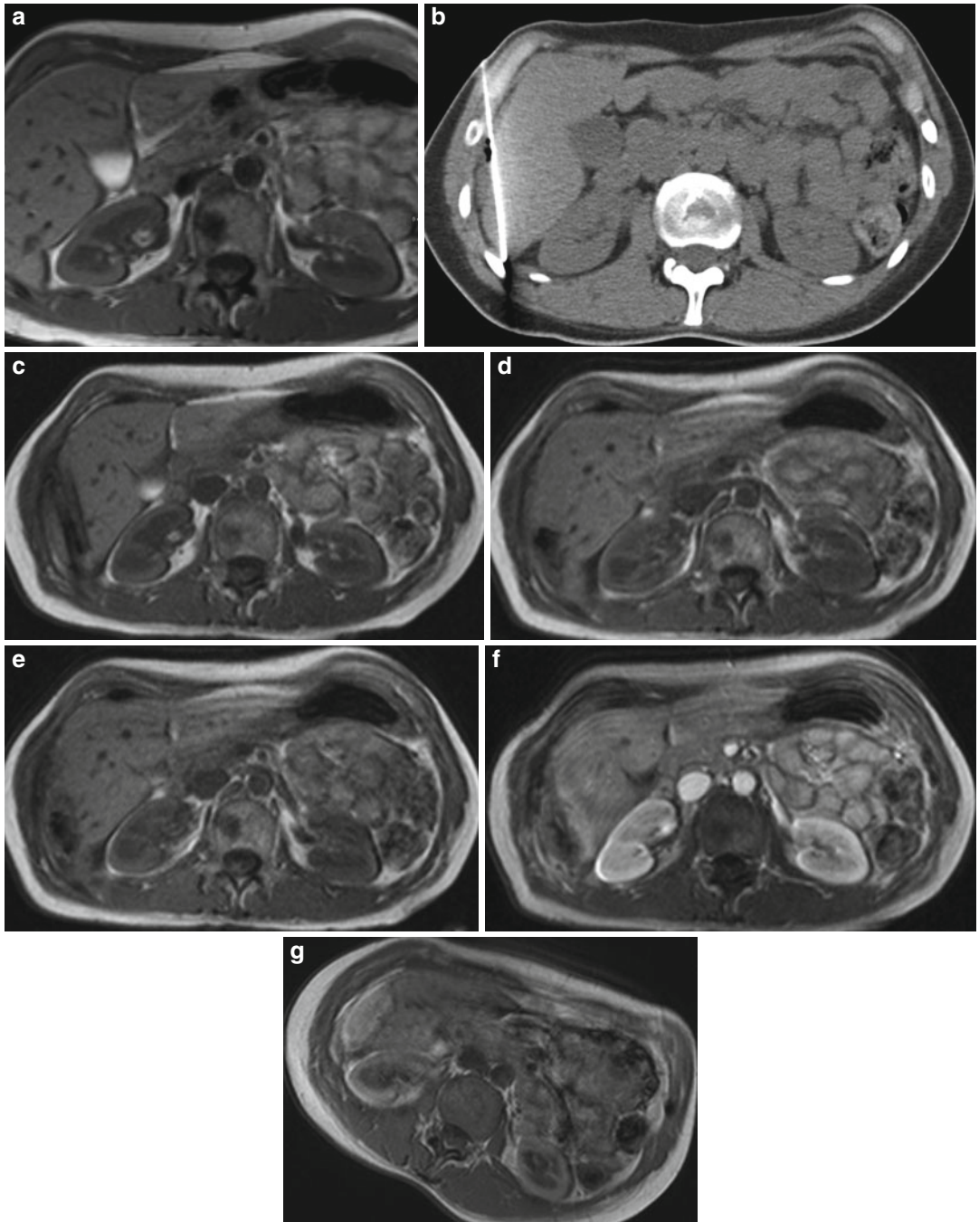

Fig. 34.3 Female patient with liver metastases of breast cancer origin. (**a**) T1W1 before laser ablation showing a small lesion in the right lobe. (**b**) CT-guided puncture of the liver lesion. (**c**) T1W1 at the beginning of the ablation depicting two applicators placed in the center of the lesion. (**d**) After 19-min ablation time, signal reduction is shown. (**e**) T1W1 thermometry image after 21-min ablation time showing signal reduction in a larger area. (**f**) Gd-enhanced T1W1 thermometry image after 24-min ablation time showing signal loss in the area of the former lesion including a safety margin of 1 cm with no Gd enhancement. (**g**) T1W1 24 h after laser ablation showing the area of necrosis. The signal enhancement depicts a possible hematoma

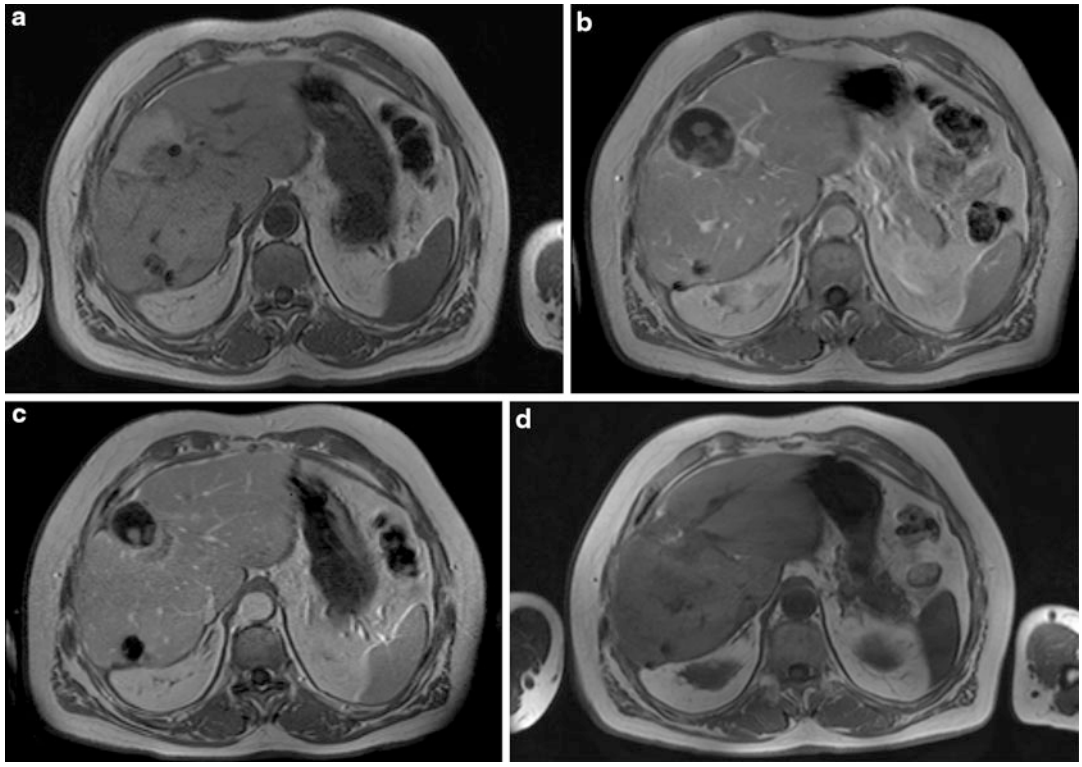

Fig. 34.4 Colorectal liver metastases follow-up after laser ablation. (**a**) T1WI 24 h after laser ablation. (**b**) Gd-enhanced T1WI 3 months and (**c**) 6 months after laser ablation showing signal reduction indicating resorption with no enhancing residual or recurrent tumor mass. (**d**) T1WI 9 months after laser ablation showing scar tissue with no sign of a residual or recurrent tumor mass

stopped after total coagulation of the lesion including a surrounding safety margin of 5–15 mm.

After switching off the laser, T1-weighted contrast-enhanced FLASH-2D images are obtained for verifying the induced necrosis. Follow-up MRI using plain and contrast-enhanced sequences are performed after 24–48 h and every 3 months following the laser ablation procedure. Parameters including size, morphology, signal behavior, and contrast enhancement are evaluated as indicators of treatment success.

The approach to the lesion depends on its location. Transpleural approaches are avoided in all our cases. The most common approach to lesions located in liver segments seven and eight was the cranially angulated lateral approach. The most common approach for lesions located in the left liver lobe segments two and three is a ventral one [1].

Outcome

From October 1998, all laser ablation patients in our institute have been exclusively treated on an outpatient basis. In the process, a number of patients having up to six metastases were treated. In some cases, more than five laser applicators were necessary for the treatment of a single metastatic lesion to achieve a reliable safety margin [1].

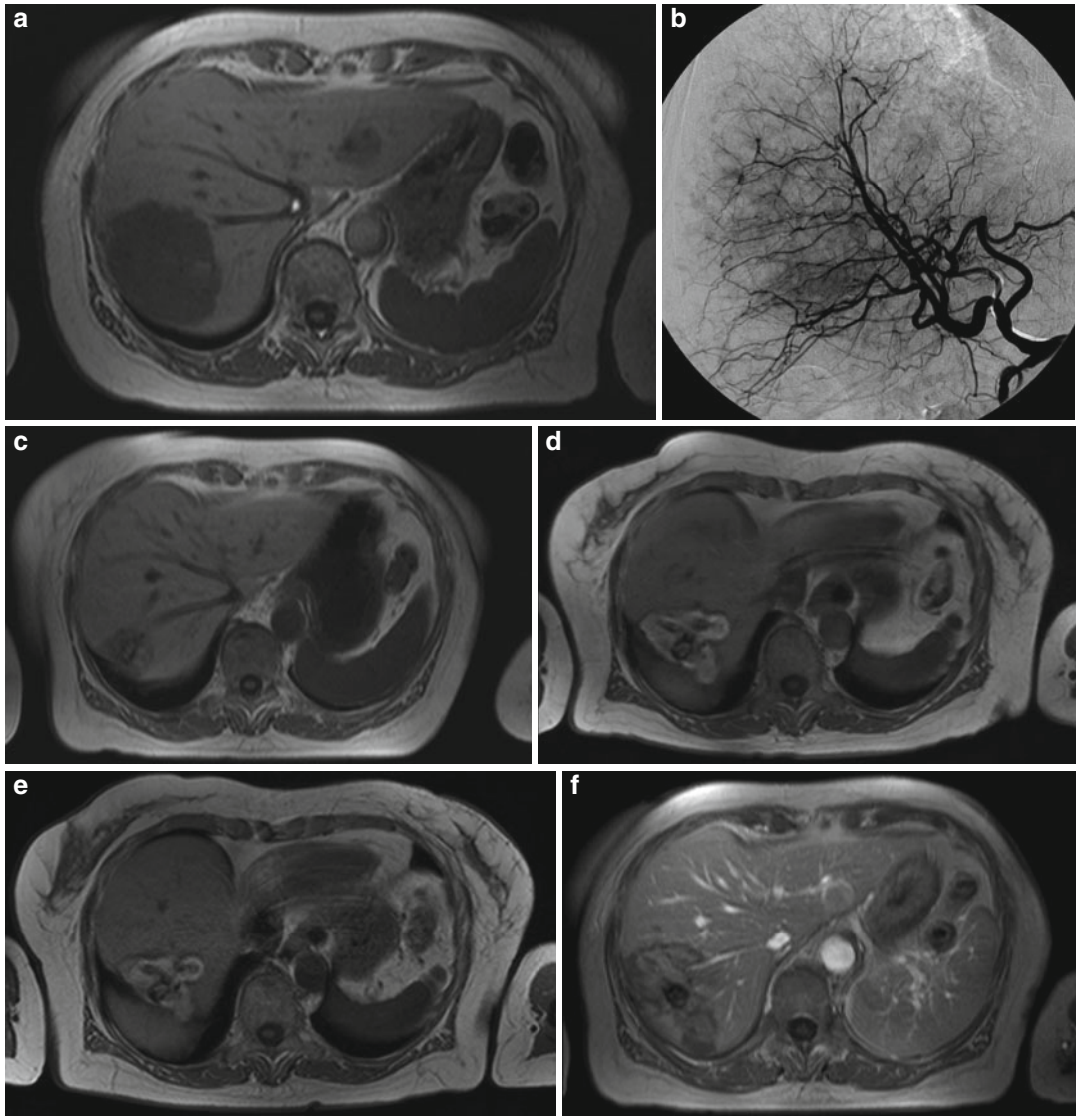

Fig. 34.5 Female patient with liver metastases from left breast carcinoma. (**a**) Before TACE: a huge metastatic lesion in the right lobe more than 5 cm in diameter (**b**) Angiographic demonstration of the hepatic artery and feeders during TACE. (**c**) After TACE: effective downsizing of the lesion. (**d**) T1WI 24 h after laser ablation. (**e**) Three months after laser ablation with constant size of the post-laser ablation lesion. (**f**) Gd-T1WI 6 months after laser ablation showing patchy contrast enhancement and minimal enlargement which was attributed to newly developed metastasis adjacent to the treated lesion

Local Tumor Control and Survival

Contrast-enhanced MRI performed on a 3-month basis after treatment to evaluate local tumor control rate shows an improvement of tumor control rate from 45.1 up to 98 % even in long-term follow-up, reflecting the effective development of the laser application systems and the improving learning curve of the operators (Figs. 34.4 and 34.5). In a large multicenter study including 9 Italian centers, 520 patients with 647 HCC

nodules of different sizes (small, 0–3 cm; intermediate, >3–5 cm; large, >5 cm) received laser ablation. Complete necrosis was achieved in 60 % of nodules regardless of size and in 81.1 % of the small nodules [23]. In a subgroup, 432 of those patients with HCC on top of cirrhosis, initial complete response after laser ablation was achieved in 338 patients (78 %), and median overall survival time was 47 months (95 % confidence interval: 41–53 months). The 3- and 5-year cumulative survival rates were 61 % and 34 %, respectively [24]. Results in our institute were a mean survival rate of 4.4 years (95 % CI: 3.6–5.2) in a series of 39 patients with 61 presumed HCCs and a complete ablation rate of 97.5 % after treatment with laser ablation [25].

Survival curves evaluated using the Kaplan–Meier method showed a mean cumulative survival rate in patients with colorectal liver metastases of up to 4 years. The 1-year survival rate is up to 95 %, the 2-year survival rate is 76 %, the 3-year survival rate is 53 %, and the 5-year survival is 27 % [26]. The overall mean survival rate in liver metastases from breast cancer is 4.6 years after starting treatment [19]. Maximum survival is 83.4 months [26].

Superior survival is to be expected in patients with one or two initial metastases (compared to those with three or more), in patients with metachronous metastases (compared with synchronous metastases), in patients with N0 or N1 primary lymph node stages (compared to N2 and N3 patients), and in patients refusing surgery compared to patients with recurrences after surgical resection [1, 24, 25].

Complications

All patients tolerate the intervention well under local anesthesia. Clinically relevant complications such as bleeding, intra-abdominal or intrahepatic hematoma, liver abscess, injury to bile duct, biliary fistulas, as well as pleural effusion, and pneumothorax are documented in less than 1 % (based on the number of treatment sessions). The overall complication rate is 1.5 %. Complications are mostly treatable either by drainage (in case of pleural effusion, pneumothorax, or abscess), percutaneous biliary stent (in case of biliary injury), transarterial embolization (in case of significant non-self-limiting bleeding), and intravenous antibiotics (in case of infection at the puncture site). Thirty-day mortality is extremely rare. No seeding of metastases was found in our patients [1].

Summary

There are both advantages and disadvantages of laser ablation compared to other local ablation modalities like radiofrequency ablation (RFA), which is the major modality of thermal ablation. In summary, laser ablation competes well with other thermal ablation technologies. As compared to radiofrequency ablation, which is the most established form of ablation technique, laser ablation holds a key advantage in its suitability for MR thermometry and monitoring, although applicator sizes are larger and the procedure itself is more complex. It can play an important role in the management of hepatic malignancy, as a complementary or alternative method to the established treatment modalities, mainly surgical resection and chemoembolization. It is an innovative and promising technique that possesses many advantages with only limited complications.

References

1. Vogl TJ, Straub R, Eichler K, Mack MG. Laser-induced interstitial thermotherapy (LITT) of liver lesions – technique and application data-clinical data. Percutaneous Tumor Ablation in Medical Radiology, vol. VI. Berlin/Heidelberg: Springer; 2007. p. 139–44.
2. Bismuth H, Chiche L, Adam R, Castaing D, Diamond T, Dennison A. Liver resection versus transplantation for hepatocellular carcinoma in cirrhotic patients. Ann Surg. 1993;218:145–51.
3. Ramsey WH, Wu GY. Hepatocellular carcinoma: update on diagnosis and treatment. Dig Dis. 1995;13:81–91.
4. De Cobelli F, Castrucci M, Sironi S, et al. Role of magnetic resonance in the follow-up of hepatocarcinoma treated with percutaneous ethanol

injection (PEI) or transarterial chemoembolization (TACE). Radiol-Med-Torino. 1994;88:806–17.
5. Dodd 3rd GD, Soulen MC, Kane RA, et al. Minimally invasive treatment of malignant hepatic tumors: at the threshold of a major breakthrough. Radiographics. 2000;20:9–27.
6. Kawai S, Tani M, Okumura J, Ogawa M, et al. Prospective and randomized clinical trial of lipiodol-transcatheter arterial chemoembolization for treatment of hepatocellular carcinoma: a comparison of epirubicin and doxorubicin (second cooperative study). Semin Oncol. 1997;24:38–45.
7. Lorenz M, Waldeyer M, Muller HH. Comparison of lipiodol-assisted chemoembolization versus only conservative therapy in patients with nonresectable hepatocellular carcinomas. Z Gastroenterol. 1996;34:205–6.
8. Amin Z, Lees WR, Bown SG. Hepatocellular carcinoma: CT appearance after percutaneous ethanol ablation therapy. Radiology. 1993;188:882–3.
9. Bartolozzi C, Lencioni R. Ethanol injection for the treatment of hepatic tumors. Eur Radiol. 1996;6:682–96.
10. Livraghi T, Lazzaroni S, Vettori C. Percutaneous ethanol injection of small hepatocellular carcinoma. Rays. 1990;15:405–10.
11. Sato M, Watanabe Y, Tokui K, Kawachi K, Sugata S, Ikezoe J. CT-guided treatment of ultrasonically invisible hepatocellular carcinoma. Am J Gastroenterol. 2000;95:2102–6.
12. Shiina S, Tagawa K, Unama T, et al. Percutaneous ethanol injection therapy of hepatocellular carcinoma: analysis of 77 patients. AJR. 1990;155:1221–6.
13. Sironi S, Livraghi T, DelMaschio A. Small hepatocellular carcinoma treated with percutaneous ethanol injection: MR imaging findings. Radiology. 1991;180:333–6.
14. Livraghi T, Goldberg SN, Lazzaroni S, Meloni F, Solbiati L, Gazelle GS. Small hepatocellular carcinoma: treatment with radio-frequency ablation versus ethanol injection. Radiology. 1999;210:655–61.
15. Vogl TJ, Mack MG, Balzer JO, Engelmann K, Straub R, Eichler K, Woitaschek D, Zangos S. Liver metastases: neoadjuvant downsizing with transarterial chemoembolization before laser-induced thermotherapy. Radiology. 2003;229(2):457–64.
16. Knappe V, Mols A. Laser therapy of the lung: biophysical background. Radiologe. 2004;44(7): 677–83.
17. Vogl TJ, Straub R, Lehnert T, Eichler K, Luder-Luhr T, Peters J, Zangos S, Sollner O, Mack M. Percutaneous thermoablation of pulmonary metastases. Experience with the application of laser-induced thermotherapy (LITT) and radiofrequency ablation (RFA), and a literature review. Rofo. 2004;176(11):1658–66.
18. Mack MG, Eichler K, Zangos S, Lehnert T, Vogl TJ. Long-term results of MR-guided laser ablation (LITT) of liver metastases of breast cancer. J Clin Oncol. 2008;26(15S):1037. May 20 Supplement.
19. Mensel B, Weigel C, Heidecke CD, Stier A, Hosten N. Laser-induced thermotherapy (LITT) of tumors of the liver in central location: results and complications. Rofo. 2005;177(9):1267–75.
20. Vogl TJ, Straub R, Lehnert T, Eichler K, Luder-Luhr T, Peters J, Zangos S, Söllner O, Mack MG. Percutaneous thermoablation of pulmonary metastases. Experience with the application of laser-induced thermotherapy (LITT) and radiofrequency ablation (RFA), and a literature review. RoFo. 2004;176(11): 1658–66.
21. Vogl TJ, Fieguth HG, Eichler K, Straub R, Lehnert T, Zangos S, Mack MG. Laser-induced thermometry of lung metastases and primary lung tumors. Radiologe. 2004;44(7):693–9.
22. Hosten N, Stier A, Weigel C, Kirsch M, PULs R, Nerger U, Jahn D, Stroszczynski C, Heidecke CD, Speck U. Laser-induced thermometry (LITT) of lung metastases: description of a miniaturized applicator, optimization, and initial treatment of patients [in German]. RoFo. 2003;175:393–400.
23. Arienti V, Pretolani S, Pacella CM, Magnolfi F, Caspani B, Francica G, Megna AS, Regine R, Sponza M, Antico E, Di Lascio FM. Complications of laser ablation for hepatocellular carcinoma. Radiology. 2008;246(3):947–55.
24. Pacella CM, Francica G, Di Lascio FM, Arienti V, Antico E, Caspani B, Magnolfi F, Megna AS, Pretolani S, Regine R, Sponza M, Stasi R. Long-term outcome of cirrhotic patients with early hepatocellular carcinoma treated with ultrasound-guided percutaneous laser ablation: a retrospective analysis. J Clin Oncol. 2009;27(16):2615–21.
25. Eichler K, Mack MG, Straub R, Engelmann K, Zangos S, Woitaschek D. Vogl TJ [Oligonodular hepatocellular carcinoma (HCC): MR-controlled laser-induced thermotherapy]. Radiologe. 2001;41:915–22.
26. Mack MG, Eichler K, Zangos S, Lehnert T, Vogl TJ. Long-term results of MR-guided laser ablation (LITT) of liver metastases of breast cancer. J Clin Oncol. 2008; 26, Mo 15S (May 20 Supplement):1037.

Irreversible Electroporation in Liver Tumor

35

Edward Wolfgang Lee, Daphne Wong, and Stephen T. Kee

Abstract

As cancer-related deaths continue to increase around the world, providing an effective and cost-efficient treatment remains a top priority. Specifically in relation to ablation techniques, one such modality that is receiving increased attention is irreversible electroporation (IRE). In recent years, IRE has elicited excitement as a potential treatment for malignant tumors due to its advantages of utilizing nonthermal energy, achieving complete cell death and the ability to image the effects in near real time. In this chapter, we will discuss a brief overview of IRE in liver ablation.

Introduction

Cellular homeostasis is achieved by the precise communication between intra and extracellular compartments controlled by physiological transmembrane potentials. When a strong external electric field is applied to targeted cells, a voltage potential difference is created across the plasma membrane of the cell [1, 2]. Once this voltage reaches a threshold, both innate transmembrane pores/channels and electroporation-induced nanopores are opened, and permeabilization of the cell membrane occurs. Depending on the strength of the applied external electric field, the permeabilization becomes transient, reversible electroporation or permanent, irreversible electroporation (IRE) causing cell death [3–5].

In the early history of electroporation, IRE was not widely applied since the majority of studies focused on applications necessitating the restoration of induced pores (reversible electroporation); therefore, irreversible pore formation was considered an undesirable result. However, medical applications of IRE have recently been studied as a minimally invasive method to eliminate cancer cells without the use of adjuvant chemotherapy agents as seen in reversible electroporation [6]. In this chapter, we will explore and summarize the current research on IRE in liver ablation.

Swine Model Studies

Our preliminary IRE ablation study in normal swine liver has revealed several important key findings in using IRE as a potential clinical liver

E.W. Lee (✉) • D. Wong • S.T. Kee
Department of Radiology, UCLA Medical Center, Los Angeles, CA, USA
e-mail: EdwardLee@mednet.ucla.edu; DaphneLWong@gmail.com; Skee@mednet.ucla.edu

D.E. Dupuy et al. (eds.), *Image-Guided Cancer Therapy*, DOI 10.1007/978-1-4419-0751-6_37,

ablation method. Our swine IRE study used either a monopolar (18-gauge probe) or bipolar (16-gauge probe) system to ablate the left or right lobes, while the developing, hypoechogenic ablation zone was continuously monitored with ultrasound imaging. Immunohistological analysis of the ablated tissues showed that real-time ultrasound estimation of the ablation zone correlated closely with gross tissue measurements and preplanning computational measurements. Gross and macroscopic evaluation of the IRE-ablated swine liver demonstrated (1) visible discoloration of the ablation zone suggesting changes in overall cellular structure, (2) a negligible temperature rise of 2–3 °C supporting the nonthermal mechanism for cell death, and (3) acute damage to parenchyma consistent with hepatocyte cell death [7]. In addition, histological findings including TUNEL immunoassay in IRE-ablated cells revealed pyknotic nuclei suggesting apoptosis [7]. IRE-ablated hepatocytes had indistinct membranes and vacuolar degeneration demonstrating that an influx of the extracellular environment contributes to cell death (Fig. 35.1). Intravascular endothelial cells in the ablated zones showed signs of cell death with increased diapedesis and thrombus formation, but overall vascular architecture was maintained (Fig. 35.2) [7]. As early as 1 h after the IRE ablation, histopathological findings showed clearly demarcated IRE-ablated zone from the normal tissue by triphenyltetrazolium chloride (TTC) staining. TTC staining demonstrated normal liver parenchyma with red staining, whereas the ablated zone was unable to retain TTC due to cell death (unpublished data). No peri- or post-procedure complications were encountered for the complete ablation sessions, supporting IRE as a relatively quick, well-controlled, image-guided, and highly effective clinical ablation method that can be used with real-time monitoring.

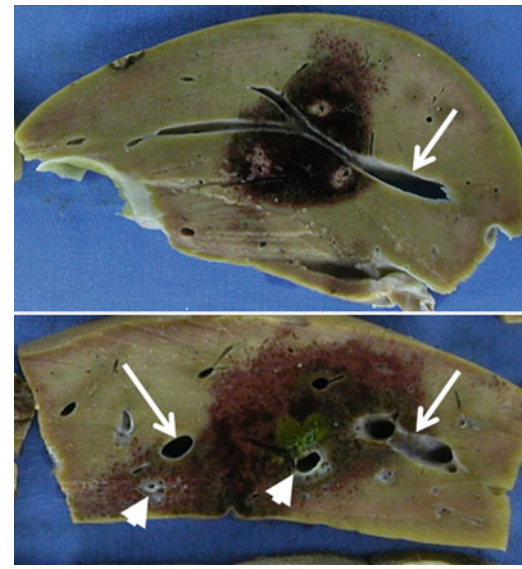

Fig. 35.1 Gross pathologic images of IRE-ablated swine liver in different locations demonstrate a sharp margin of IRE ablation. A clear demarcation between the ablated and non-ablated zone is noted uniformly in all IRE-ablated tissues. As demonstrated in these images, the large vessels (*arrow*) and bile ducts (*arrowhead*) traversing the ablated zone are intact and preserved with its structure. In addition, numerous small vessels and bile ducts as small as 1 mm in size are structurally preserved

Another swine study conducted by our group further observed the radiologic-pathologic correlation of IRE liver ablation [8]. First, the use of real-time ultrasound imaging during and post-IRE ablation was further solidified. Ultrasound in IRE ablation re-demonstrated its advantage as it imaged the IRE ablation zone without any thermally induced microbubble artifacts obscuring the ablation margin. This provides an accurate method of monitoring during IRE ablation. In addition, peri- and post-ablation ultrasound findings and measurements correlated well with pathologic measurements which add significant benefit to IRE ablation for accurate peri- and post-ablation monitoring. Furthermore, use of contrast-enhanced multidetector computer tomography (CT) and magnetic resonance imaging (MRI) were evaluated. CT images demonstrated a hypoattenuating IRE-ablated zone best demarcated post-iodinated contrast administration. MRI findings in several different sequences including post-contrast fat-saturated T1-weighted gradient-echo imaging corresponded with the CT findings with a hypointense IRE-ablated zone with marginal enhancement (Fig. 35.3).

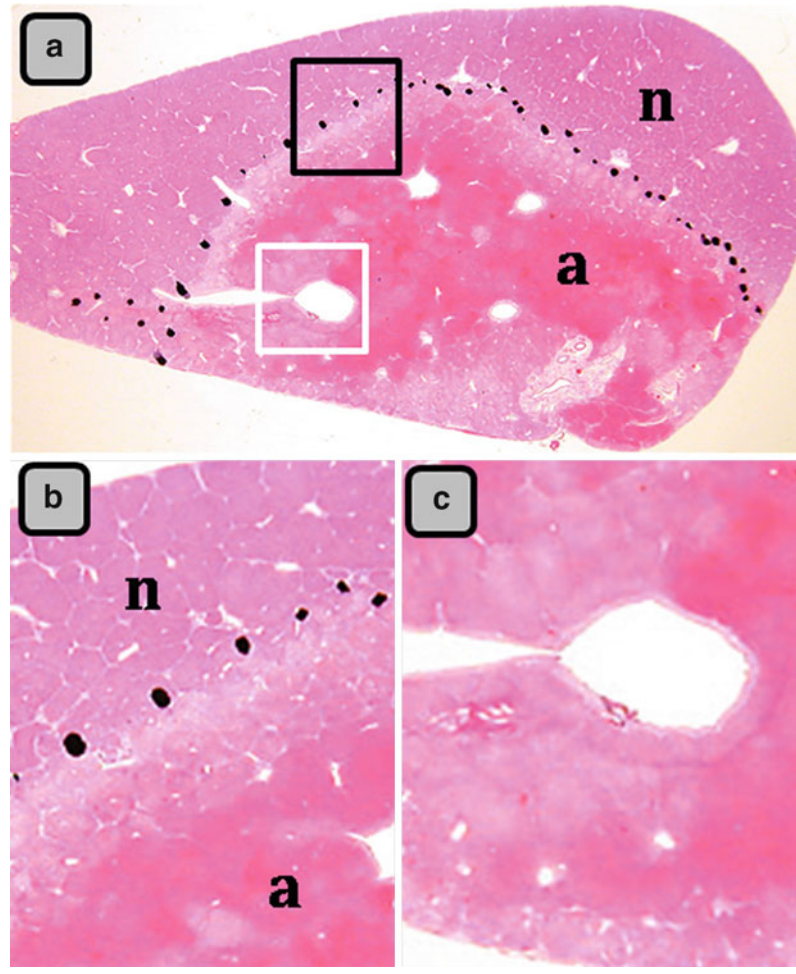

Fig. 35.2 Histological images (hematoxylin and eosin (H&E) staining. **a**–**c**) of IRE-ablated liver show a sharp demarcation between the ablated (a) and non-ablated, normal liver (n). All hepatocytes within the ablated zone (a) are microscopically pyknotic and karyorrhexis, suggestive of complete cell death. (**b**) High magnification of the ablation margin shows normal liver and ablated liver separated by a sharp margin. (**c**) a large vessel within the ablated zone is completely preserved demonstrated in both macro- and microscopic evaluation

Histopathologically, gross specimen examination showed signs of vascular congestion and hemorrhagic changes as early as 3 h post-IRE ablation which may persists up to 72 h after ablation but resolved completely in 14 days following ablation. Other histological examinations demonstrated several important key points in the pathophysiology of IRE ablation. First, complete cell death was indicated by extracellular mineralization of calcium shown in positive Von Kossa staining in the ablated zones. Apoptotic cell death of ablated tissue was demonstrated by positive BCL-2 staining and TUNEL assays (Fig. 35.4). Lastly, preservation of vital vascular structures was verified with positive von Willebrand factor staining.

The above study confirmed our previous findings regarding the mechanism of cell death, real-time monitoring feasibility, and the use of CT/MRI in observing the ablation zone, all of which are essential information in translating IRE into the clinical setting.

Because the potential for preservation of hepatic vessels and bile ducts would enable treatment of tumors centrally in the liver hilum that are contraindicated with other ablative devices, several groups have further studied the safety profile of IRE specifically in this setting. Charpentier reported an initial study where IRE were performed in the porta hepatis with short-term follow-up and demonstrated central ducts and portal vessels to be resistant to significant injury [9]. Lu and his group

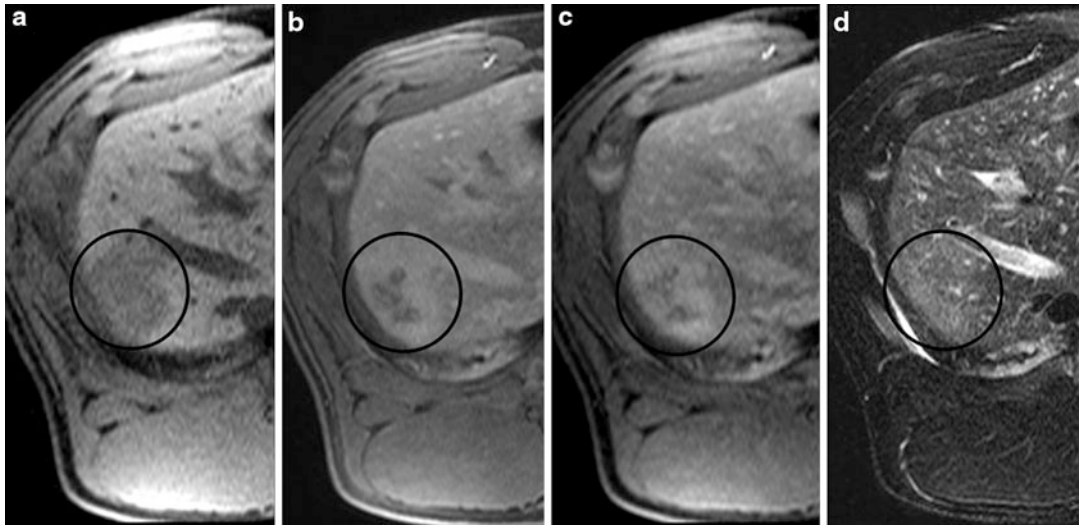

Fig. 35.3 Representative MR images of IRE-ablated zone in the swine liver. (**a**) T1-weighted GRE fat-saturated image (TR 262/TE 2.32) demonstrates a zone of T1 hypointensity, within which there is peripheral contrast enhancement and central hypointensity seen post-gadolinium administration (**b**). (**c**) similar findings are shown with T1-weighted VIBE fat-saturated image post gadolinium (TR 4.59/TE 1.84) after the procedure. (**d**) T2-weighted TSE fat-saturated image (TR5007/TE104) demonstrates diffuse T2 hyperintensity at IRE site

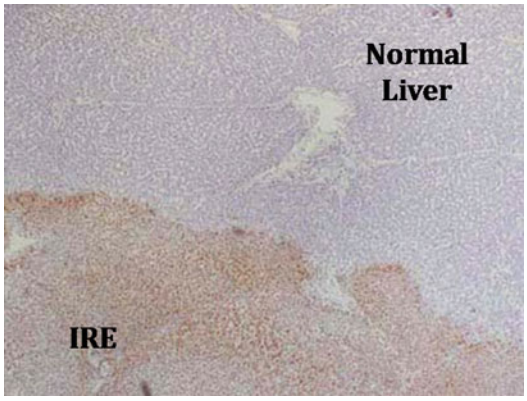

Fig. 35.4 High-magnification image at the margin of IRE-ablated zone demonstrates IRE-ablated zone with markedly increased TUNEL positive (*brown*) stained cells (IRE) compared to the normal liver cells with a minimal TUNEL positive staining. We have hypothesized the involvement of apoptosis in IRE-ablated cell death based on TUNEL assay, caspase, and BCL-2 immunohistochemistry

studied in more detail the long-term effects of IRE on hepatic vessels and bile ducts up to 8 weeks, using a prototype generator (Ethicon Endosurgery, Cincinnati Ohio) [10–12]. They showed that large hepatic veins may show initial narrowing, but they uniformly recovered their caliber without late thrombosis [10]. For central hilar bile ducts, using a CT cholangiography model, there was no immediate narrowing following IRE, although late stricturing is possible, but only if the electrodes were within 3 mm to the bile ducts [11]. This phenomenon may be explained by the finding of a zone which can be seen as an area of different discoloration immediately around the electrode track on gross pathology specimens, the pathophysiologic mechanism of which is currently incompletely understood [12]. Nevertheless, these experiments showed that IRE can be performed safely around central hilar ducts without clinically significant long-term structuring, as long as electrodes could be precisely and appropriately placed.

Rabbit VX2 Tumor Liver Study

With the promising results from our swine studies, we further investigated the effects of IRE on a liver tumor model. The rabbit VX2 liver tumor model was the most appropriate for this study since it was one of the few well-accepted large animal tumor models. With a phylogenetically

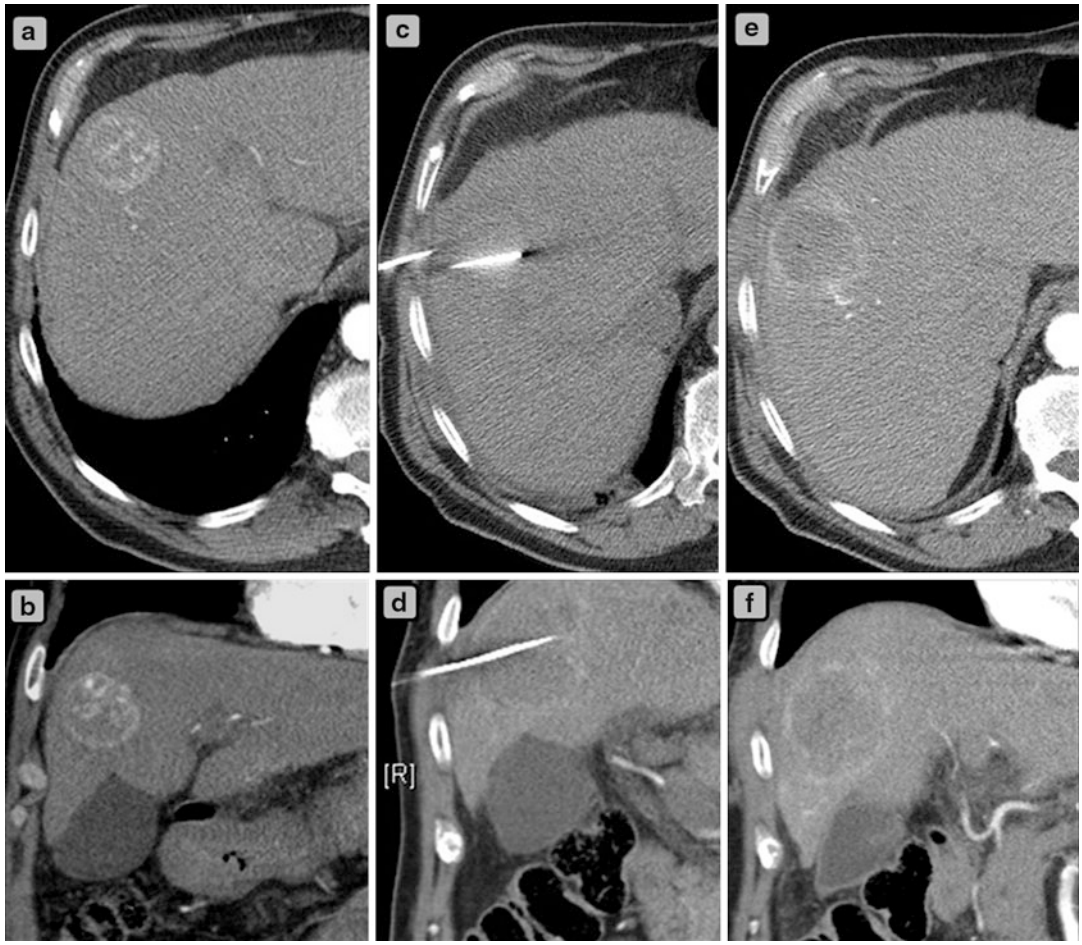

Fig. 35.5 Axial and coronal contrast-enhanced CT images of (**a**, **b**), a hypervascular liver tumor prior to IRE ablation; (**c**, **d**) during the IRE monopolar probe placement; and (**e**, **f**) post-IRE ablation with evidence of mild peri-ablation enhancement with hypodense ablation defect

similar hepatic anatomy to humans and swine, using the rabbit model also allowed us to easily translate our previous swine study findings. In addition, VX2 tumors can grow rapidly up to 1 cm of growth in about a week, and therefore, the model can be well controlled and monitored to obtain a consistent tumor size.

Over 100 New Zealand white rabbits were utilized in this study where all parameters and results from the swine study were tested and verified. Major findings include the following: (1) IRE consistently produced complete cell death in the ablated zone with a distinct margin, (2) IRE ablation is not affected by the heat-sink effect, and (3) IRE ablation holds the possibility of real-time monitoring using US imaging and contrast-enhanced CT (CECT) to monitor and evaluate ablation as early as 24 h post-procedure. Complete cell death was confirmed with both gross and histological analyses, and it was defined as no residual tumor cells within the ablated zone including perivascular tumor cells (Fig. 35.5). Additionally, no evidence of synchronous or metachronous metastatic tumors were seen within the liver or lung demonstrating that the IRE ablation resulted in a complete remission of the VX2 tumor, an extremely aggressive tumor shown to have both intrahepatic and distant metastases in every rabbit in the control and sham groups. A complete tumor ablation is the most important feature of IRE in

translating this technology into the clinical setting as many currently existing thermal ablative techniques lack this due to the heat-sink effect and inability to perform real-time monitoring. The ability to evaluate and monitor the ablation zone in real time was also an advantage of IRE as it allowed us to adjust the probes and ablation parameters and reablate immediately after the first ablation if necessary.

Another clinically important finding of our rabbit VX2 tumor studies was the reaffirmation of our swine studies in the preservation of critical intrahepatic structures such as bile ducts and vessels. Hepatic arteries, hepatic veins, portal veins, and bile ducts were all seen intact within IRE-ablated areas. Small-vessel (less than 2 mm) vasculitis was evident, but any vessels greater than 3 mm in diameter showed either no structural damage or very mild narrowing. These findings were confirmed using CECT as well as both gross and microscopic analysis. Multiple vascular wall markers (vWF, VEGFR, and Masson's trichrome stain) were also used to validate architectural preservation of the vessels and bile ducts. Moreover, normally flowing blood and contrast materials in different phases (arterial, venous versus delayed phase) were seen in larger vessels without compromised hemodynamicity through the use of CECT.

N1-S1 Rodent Liver Model Study

Using an N1-S1 rodent hepatoma model, Guo et al. studied the effect of IRE in the treatment of liver tumor of Sprague–Dawley rats [13]. Thirty rats with hepatoma were used and subsequently divided into different groups including control and IRE-ablated groups with different parameters. Through immunohistochemistry, they were also able to observe clear demarcations between the IRE-treated and untreated areas [13]. Furthermore, five of six rodents that underwent IRE treatment demonstrated no remnant viable tumor 15 days posttreatment with one lesion containing <5 % viable tumor tissue volume [13]. Interestingly, caspase-3 staining, a marker for active apoptosis, showed extensive activity 1-day posttreatment suggesting that there may be more to the mechanism of cell death including apoptosis than just membrane permeabilization as we suggested in our prior studies [13]. This finding helps validate the prospect of natural cell death or apoptosis initiation through IRE. MR imaging also showed a significant reduction of tumor size within 15 days post-IRE treatment [13, 14]. Through this study, Guo et al. concluded that IRE can be a potentially effective ablative treatment for HCC.

Preliminary Clinical Studies of IRE

Thomson et al. have recently published a landmark paper of their findings on the first clinical use of IRE. Twenty-five patients underwent IRE treatment in the preliminary clinical study to evaluate the safety of IRE conducted by Thomson et al. [15]. Fifteen of eighteen tumors treated demonstrated complete tumor ablation with preservation of vital structures including intrahepatic vessels and bile ducts. However, colorectal liver metastases >5 cm did not show a response to tumor control [15]. Interestingly, regeneration of the liver after IRE as seen in patients who did not have severe cirrhosis or previous chemoembolization [15]. The use of ECG synchronization was shown to combat cardiac arrhythmias that were seen as limitations in the early studies of IRE [15]. In addition to the Thomson group, Narayanan et al. [16] have presented their early findings on the safety and effectiveness of IRE in treating patients with HCC. In treating 21 patients with HCC with 35 lesions, 66 % of the treated patients had a complete response based on RECIST criteria, and 14 % had a partial response with at least 4 weeks follow-up [15]. Overall, both early preliminary clinical studies concluded that IRE is a safe and effective ablative method for liver tumors.

Limitations

Despite the described studies of IRE, limitations still exist. When releasing electrical impulses into the body, the electrical signals can have negative

effects on electrically sensitive systems. Muscle contraction can be elicited from the electrical stimuli produced during IRE. However, this can be overcome by administering muscle relaxants before and during the procedure [17, 18]. In human patients, the need for proper muscle neuromuscular blockage is necessary to prevent muscular contractions when performing liver, kidney, or lung ablation [18]. As studied by Thomson et al., electrical impulses can also reach the heart and potentially cause deleterious arrhythmias, particularly ventricular fibrillation. To solve this issue, cardiac synchronization is employed to guarantee that impulses are delivered in tune with the natural heart rhythm. Analysis of the patient's electrocardiogram (ECG) produces an accurate model of the cardiac rhythm [18, 19]. This model can then be used to properly release IRE pulses during the safe period in the QRS complex. Additionally, cardiac synchronization can prevent electrical discharge if an abnormal heartbeat is encountered since electrical stimuli released during such instances are associated with more adverse effects [19]. Even with cardiac synchronization, however, potential for minor arrhythmias or EKG changes may not be entirely eliminated, and additional safety can be provided by placing the electrodes more than 1.7 cm away from the heart [20]. This may have implications for IRE of lesions high up in the liver dome.

Another limitation that has been recently highlighted also relates to the potential for more deleterious tissue effects immediately adjacent to the electrodes, such as the possibility for delayed bile duct structuring [11, 12]. However, this appears to be limited to within only a few millimeters to the electrode and can be avoided by precise electrode placement, or possibly future refinements to IRE technology. With these improvements and continued studies, the knowledge of IRE will only continue to grow, allowing for continued clinical translation.

References

1. Lee RC. Cell injury by electric forces. Ann N Y Acad Sci. 2005;1066:85–91.
2. Gaylor DC, Prakah-Asante K, Lee RC. Significance of cell size and tissue structure in electrical trauma. J Theor Biol. 1988;133(2):223–37.
3. Gabriel B, Teissie J. Direct observation in the millisecond time range of fluorescent molecule asymmetrical interaction with the electropermeabilized cell membrane. Biophys J. 1997;73(5):2630–7.
4. Teissie J, Rols MP. An experimental evaluation of the critical potential difference inducing cell membrane electropermeabilization. Biophys J. 1993;65(1):409–13.
5. Rols MP. Electropermeabilization, a physical method for the delivery of therapeutic molecules into cells. Biochim Biophys Acta. 2006;1758(3):423–8.
6. Davalos RV, Mir IL, Rubinsky B. Tissue ablation with irreversible electroporation. Ann Biomed Eng. 2005;33(2):223–31.
7. Lee EW, Loh CT, Kee ST. Imaging guided percutaneous irreversible electroporation: ultrasound and immunohistological correlation. Technol Cancer Res Treat. 2007;6(4):287–94.
8. Lee EW, et al. Advanced hepatic ablation technique for creating complete cell death: irreversible electroporation. Radiology. 2010;255(2):426–33.
9. Chapentier KP, et al. Irreversible electroporation of the liver and liver hilum in swine. HPB. 2011;13(1):168–73.
10. Lee YJ. et al. Irreversible electroporation in porcine liver: short and long term effects on hepatic veins and adjacent tissue by CT with pathological correlation. Proceedings of the WCIO Annual Meeting, Philadelphia; 2010.
11. Choi JW, et al. Assessment of short and long term effects of irreversible electroporation on Hilar bile ducts in a porcine model. Proceedings of the SIR Annual Meeting, Philaelphia; 2011.
12. Lu DS, et al. Irreversible electroporation in porcine Liver: lesion appearance on CT with pathological correlation. Proceedings of the WCIO Annual Meeting, Philadelphia; 2010.
13. Guo Y, et al. Irreversible electroporation therapy in the liver: longitudinal efficacy studies in a rat model of hepatocellular carcinoma. Cancer Res. 2010;70(4):1555–63.
14. Guo Y, et al. Irreversible electroporation in the liver: contrast-enhanced inversion-recovery MR imaging approaches to differentiate reversibly electroporated penumbra from irreversibly electroporated ablation zones. Radiology. 2011;258(2):461–8.
15. Thomson KR, et al. Investigation of the safety of irreversible electroporation in humans. J Vasc Interv Radiol. 2011;22(5):611–21.
16. Narayanan G, et al. Safety and efficacy of irreversible electroporation in the treatment of primary HCC. In: SIR 36th Annual scientific meeting 2011. Chicago: J Vasc Inter Radiol.

17. Charpentier KP, et al. Irreversible electroporation of the pancreas in swine: a pilot study. HPB (Oxford). 2010;12(5):348–51.
18. Ball C, Thomson KR, Kavnoudias H. Irreversible electroporation: a new challenge in "out of operating theater" anesthesia. Anesth Analg. 2010;110(5): 1305–9.
19. Mali B, et al. The effect of electroporation pulses on functioning of the heart. Med Biol Eng Comput. 2008;46(8):745–57.
20. Deodhar A, et al. Irreversible electroporation near the heart: ventricular arrhythmias can be prevented with ECG synchronization. AJR Am J Roentgenol. 2011;196(3):W330–5.

Focused Ultrasound of Liver

36

Wadyslaw M. W. Gedroyc and Elizabeth A. Dick

Abstract

This chapter examines the use of high-energy focused ultrasound as a method of thermal ablation of liver tumors. This modality holds out the promise of destroying liver tumors without any invasion across the skin at all so that patients could be treated as an outpatient and yet still have substantial destruction of their liver tumor created without any damage to adjacent tissue.

Various manifestations of this technology are discussed, and the potential of using MR guidance to improve safety and accuracy with online thermal mapping helping to visualize tissue response is described. Technological innovations required to take this modality forward to become a clinical reality are described as well as early work in this field.

Introduction

High-intensity focused ultrasound or focused ultrasound surgery (FUS), which is an alternative name for the same technology, is a technique which uses extremely high-power ultrasound waves focused to a very small point in the tissues. The tissues at the focus are heated very rapidly due to molecular vibration at the focal spot, leading to a sharp rapid rise in local temperature, resulting in precipitation of vital cellular proteins and therefore local coagulative cell necrosis. The huge advantage of this procedure is that it is completely noninvasive and can produce areas of destruction in tissues without any requirement for needles or other probes to be passed through tissues as long as a suitable acoustic window free of bowel and bone shielding is available to reach the target area.

Percutaneous ablative techniques that also use local heating to destroy tissues such as radiofrequency, microwave, or laser have shown us that it is possible to use this type of locally destructive energy to treat liver tumors. FUS represents a further technological development in this field of ablative therapy but is completely noninvasive, not requiring significant sized probes placed through the skin in order to deliver heating to the target area.

W.M.W. Gedroyc (✉)
Department of Radiology, St. Mary's Hospital Imperial College Healthcare NHS Trust, London, UK
e-mail: w.gedrogr@imperial.ac.uk

E.A. Dick
Department of MRI, St. Mary's Hospital Imperial College Healthcare NHS Trust, London, UK
e-mail: e.dick@imperial.ac.uk

D.E. Dupuy et al. (eds.), *Image-Guided Cancer Therapy*, DOI 10.1007/978-1-4419-0751-6_38,

The ability to deliver therapy noninvasively profoundly changes the paradigm of how we can deliver locally destructive therapy into the tissues. Surgery is avoided and so are large needle punctures therefore minimizing patient morbidity and mortality. There is also the potential that many of these procedures can be carried out entirely on an outpatient basis, keeping more patients out of the hospital or for much shorter times, therefore not only improving the patient experience but also substantially the cost-effectiveness of such procedures.

This technique therefore potentially allows the creation of a procedure that can treat liver tumors in a safe and repeatable manner with minimal postprocedure morbidity. The hope is that such an innovative approach may ultimately be demonstrated to not only improve survival but also quality of life of many patients with malignant liver tumors compared to current conventional methods.

General Principles of Focused Ultrasound Surgery/High-Intensity Focused Ultrasound (FUS/HIFU)

The biological and chemical effects of acoustic energy were first described in 1927 [1]. By the 1950s, early workers had applied focused ultrasound surgery (FUS) in the brain [2]. FUS is a form of ultrasound (US) with significantly higher intensities in the focal region than with conventional diagnostic ultrasound [3]. While diagnostic transducers deliver ultrasound intensities with time-averaged intensities of 0.1–100 mW/cm^2, FUS transducers deliver US intensities between 100 and 10,000 W/cm^2 to the focal region. The high acoustic energy is absorbed in the tissue resulting in heat generation and rapid temperature elevation to 60 °C or higher. This causes coagulative necrosis within a few seconds. Focusing of the energy produces high intensities at specific locations and over a small volume (up to 1 mm diameter). There is minimal energy deposition outside the focal point and therefore minimal potential for damage. Other phenomena which occur at high intensities are cavitation, microstreaming, and radiation forces. In combination with coagulative necrosis, these effects result in cell apoptosis and lysis [4].

Each time period for continuous delivery of acoustic energy to a defined volume of tissue is termed "sonication." During clinical treatments, the delivery of multiple sonications needs to be optimized, and this can be achieved in various ways. A smaller focal point or shorter time period increases the accuracy of the ablative volume. Short exposure times reduce the cooling heat sink effect due to surrounding blood vessels, which results in a more homogenous temperature range within the target and hence crisp margins of the treated volume. The focal volumes of treatment are applied systematically to the entire targeted organ to ensure confluence of treated tissues [5]. Since each sonication has to be followed by a cooling period to ensure that energy summation in surrounding tissues does not occur, treatment planning has to be strategized to choose nonadjacent treatment volumes and hence reduce cooling/waiting times between sonications [6].

FUS is delivered from a piezoelectric transducer which becomes deformed when electrically polarized. The resulting vibration within the piezoelectric material produces acoustic pressure waves. Current FUS systems use multiphasic, multielement phased array transducers with built-in ability to electronically steer the focus and allow for variation in focal spot size and shapes. Increasing the number of elements increases the speed of treatment and accuracy of targeting [7].

Monitoring

While FUS of the liver has to date been more widely applied under ultrasound guidance, ultrasound guidance has the disadvantage of being unable to accurately detect heat at the focal sonication point, with only the development of an ill-defined hyperechogenicity as a sign of treatment [8], and unable to correlate precisely to the extent of thermal destruction. This increases the likelihood of inaccurate targeting and inadvertent heating of adjacent structures.

The use of MRI to guide FUS brings the advantage of not only treatment planning but also the ability to monitor temperature changes at the focal site and surrounding tissues. The excellent soft tissue contrast capabilities of MRI enable the margins of the targeted tumor to be clearly defined so that treatment can be accurately planned. Temperature can also be monitored by MRI with a temporal resolution up to 500 msec, by which rapid updating of 2D or 3D temperature maps can be achieved. The so-called "phase shift" thermal mapping is independent of the temperature history of the tissue and produces a linear temperature measurement above the threshold for coagulation. MR thermal mapping can therefore enable individualized tailoring of each sonication by adjusting intensity, duration, and size of focus [9, 10].

The Problem

Liver tumors are extremely common in all parts of the world. Hepatocellular carcinoma(HCC) has a global incidence of 0.5 million new cases every year [3] with 21,00 new cases every year in the USA alone. Hepatic secondaries which are more common in the Western world have an annual incidence of approximately 100,000 new cases each year in the USA [3].

HCC is the third leading cause of cancer-related deaths worldwide, and its incidence is rising rapidly in the Western world concomitant with the rise in hepatitis C virus infection and the resultant cirrhosis produced by this virus. Almost no untreated patients with documented liver malignancies survive in 5 years [11]. Conventional oncological management using radiotherapy or chemotherapy also has a similar poor outcome especially in hepatocellular carcinoma, although newer systemic agents have recently shown slight improvement in response to the treatment of HCC. Local therapies using in situ tumor ablation or chemoembolization (TACE) have therefore been enthusiastically investigated because they offer treatment options to patients who may otherwise not receive any specific therapy.

Early Ablative Techniques

Percutaneous ablation procedures come in several different guises and can use radiofrequency energy, microwave energy, or laser energy for heat ablation or can utilize freezing as a destructive energy using appropriate cryotherapy probes. All of these modalities have their advantages and disadvantages which are beyond the scope of this article. They all consist of a procedure which targets the liver mass by the placement of one or more probes percutaneously into the target using ultrasound, CT, or MRI for image guidance. Energy is then delivered into the target to produce coagulative necrosis of tumor tissue. These procedures are carried out under conscious to deep sedation, or even general anesthesia (GA), using very short hospital stays (overnight). Determining how much actual heating is being produced during energy deposition in these types of procedures is problematic since neither CT nor ultrasound imaging is sufficiently sensitive to heat changes to provide real-time thermal mapping during the procedure. MR imaging, on the other hand, can achieve this relatively easily through thermal-sensitive sequences, but if this modality is to be used, it means that the whole procedure must be carried out in the more restricted confines of an MR scanner using MR-compatible tools [12].

Percutaneous therapies can therefore provide in situ local therapy in patients with local disease. They allow minimally invasive procedures to be performed in patients who are unsuitable for more complex procedures such as surgery either due to extent of disease or due to severity of underlying medical conditions. This is particularly relevant in patients with HCC who invariably have severe liver dysfunction and in whom injudicious surgery may commonly causes liver decompensation with all its attendant severe problems and high mortality [13, 14]. A growing body of literature is confirming the effectiveness of these percutaneous procedures in the liver, demonstrating the principle of using local ablative therapies to treat local disease, enabling substantial gains in patient survival without the need for larger and more complex surgical procedures.

Although percutaneous ablation procedures have a much lower morbidity and mortality than liver surgery in the same group of patients, often in patients with poor coagulation abilities due to their underlying liver impairment, these studies still require physical needle puncture through the liver which is a highly vascular organ. The size of the needle used to place radiofrequency, microwave probes, etc., is often surprisingly large (up to 14 gauge), and multiple needle punctures are often required to cover a moderately large target lesion. Complications of these punctures such as hemorrhage, infection (abscess), vascular damage, and tumor seeding, while less frequent and severe than the complications seen following liver surgery, still occur in any large practice [15, 16–19]. Despite these problems, percutaneous ablative procedures have substantially increased the numbers of patients receiving specific treatment for liver tumors especially in the patient groups who are not suitable for surgery. These drawbacks open the door to the concept of a totally noninvasive local ablation technique, that is, focused ultrasound.

Available FUS Technology and Its Problems

There are two main types of FUS machine available commercially which have been used to date to treat liver tumors:

1. Ultrasound-guided machines which do not have thermometric capabilities
2. MR-guided FUS machines which also use MR thermometry to monitor the whole ablative process

These two categories encompass the majority of machine setups, although several other machine configurations are currently in research and development phases. Below discusses the advantages and disadvantages of each of these two dominate categories of devices:

1. A typical ultrasound-guided machine consists of a 3.5-MHz diagnostic transducer coupled with an approximately 12-cm-diameter piezoelectric ceramic treatment transducer with a frequency of between 1.8 and 1.6 MHz [8]. The diagnostic transducer is used both to guide targeting and to monitor tissue changes during the procedure, the latter by visualizing the development of microbubbles. Tissue response to FUS can be very variable depending on the exact nature of the tissue, but the rise in temperature within the target tissue is not effectively visualized with sufficient degree of precision by sonography and does not allow sufficient feedback to the operator to guide adjustments in sonication parameters. Despite this drawback, the large majority of FUS liver cases that have been carried out in the world to date have been performed in China using precisely this type of technology with reasonable promising early results [20, 21].
2. Several MR-guided FUS systems are now in existence. The predominant machine in this field currently is the ExAblate 2000 (Fig. 36.1) manufactured by InSightec [Haifa, Israel] although other machines from other manufacturers such as Philips and Supersonics using this configuration are also now becoming available. The principle utilized in these machines is that MR imaging with its unsurpassed soft tissue discrimination is used for (1) precise lesion targeting and (2) real-time thermal mapping. The information allows the operator to visualize tissue response during the procedure itself and to adjust FUS parameters accordingly in response to the thermal imaging in order to produce optimal and reliable results in the targeted tissue.

Regardless of the imaging modality used for guidance and monitoring, all present FUS machines use an array of electronic transducers or large single-element transducers with a large footprint, such that a coherent focused ultrasound beam cannot be easily delivered through the rib cage that overlies the vast majority of the liver. Bone absorbs focused ultrasound 50 times more avidly than soft tissue, so ribs in the pathway of the focused ultrasound beam completely destroy the beam coherence. If high enough power is used, the ribs may also undergo damage due to avascular necrosis, and the amount of heating

Fig. 36.1 Image of patient in MR scanner about to undergo MR-guided focused ultrasound. This patient is about to receive FUS as a treatment for uterine fibroids. Note the modified MR table which contains the MR-compatible focused ultrasound. The patient in this case is lying facedown so that the anterior abdominal wall is opposed to the water bath which contains the transducer (Courtesy of InSightec, Ltd.)

produced within the ribs may be so great that the heat is conducted through the adjacent subcutaneous fat to the skin resulting in skin burns.

To overcome this problem, the early investigators in China using ultrasound-guided machines would frequently resect the lower ribs prior to a treatment to produce a suitable acoustic window [8]. Few investigators now use this approach, but the barrier of the ribs remains the greatest single problem to overcome in order to allow more widespread implementation of focused ultrasound technology in the treatment of liver tumors.

Respiratory movement of the liver is the other main problem in the application of FUS to the liver. Voluntary respiratory control is not reliable enough to guarantee return of the liver to the same position for accurate sequential sonications to be produced. Therefore, general anesthesia and artificial ventilation are commonly used at the moment so that the degree of respiratory excursion can be carefully controlled. This technique is used in both the ultrasound-guided and the MR-guided procedures to regain 3D spatial control of the process in a reliable manner.

If a good acoustic window is achievable to allow FUS sonication into the liver, it is relatively easy to produce significant areas of thermal destruction. Multiple early papers from China in this field have clearly proved this principle [8, 22, 23], and thermal effects on tissue are now well understood based on extensive worldwide literature on the use of percutaneous thermal ablation techniques in the liver [15, 24].

Results of Liver FUS

Almost the entirety of the current published work in FUS ablation of liver tumors comes from the work in China using ultrasound-guided machines described above. Many of these papers describe promising early results in both small and large hepatocellular carcinomas, with significant improvements in survival in patients with large untreatable liver masses [21]. These procedures, however, are being described in the literature as often lengthy, lasting as long as 8 h [22]. Skin burns commonly occurred in these long procedures, particularly in patients who have had previous radiotherapy to the same area. These results have proved to be difficult to replicate by other practitioners across the world and particularly in the West. This may be because the Western body habitus is significantly different from that of the majority of Chinese patients receiving these early

treatments. Nevertheless, the results produced by these early innovators are extremely promising and offer a clear glimpse of what may be achieved by applying this technology to the liver in the future.

Early pilot work using MR-guided FUS machines has been carried out in the authors unit. We have used a conventional ExAblate 2000 system targeted at liver tumors which are not covered by ribs. This restricts treatment to tumors that predominantly occur in the mid- and anterior part of the left lobe where the liver may be subcostal, thus allowing an unobstructed acoustic window into the liver parenchyma. General anesthesia for the control of respiration as described above is used to control the exact spatial location of the target lesion throughout the procedure. The ventilator always returns the diaphragm to the exact same position for serial sonications allowing thermal destruction to be carried out in a controlled manner. Overlapping sonications can be easily produced with intra-procedure thermal maps guiding the procedure. Sonication times to the liver for a 3-cm lesion are approximately 2 h currently (see Fig. 36.2a). To date, six procedures have been carried out. 5 of 6 patients treated are still alive up to 2 years beyond the treatment date. Although the study is not intended for treatment efficacy and survival analysis, it did achieve its aim to demonstrate that MR-guided FUS in the liver is a feasible and potentially safe approach [no complications to date) which can be accurately controlled by thermal mapping in suitable patients.

Improvements and Future Developments

The two main types of FUS machines that are applied to the treatment of the liver at the moment really reflect the basic differences in the physical properties between diagnostic ultrasound and diagnostic MRI. FUS applied with diagnostic ultrasound targeting and control is a much simpler technological exercise than when MRI is involved. The procedure as a result is easier and cheaper to set up and perform but has several substantial drawbacks. The accuracy of depicting each individual target lesion with ultrasound is often suboptimal compared to that available with MRI. The same applies to the visualization of the different tissues within and adjacent to the proposed acoustic pathway. This is particularly true of gas-containing viscera which are relatively poorly depicted with ultrasound but are very clearly seen in multiple planes with MRI. The recognition of gas in the acoustic pathway for focused ultrasound is particularly important in complex situations since gas causes unpredictable reflection of focused ultrasound power and can cause bowel perforation if a gas-containing loop of bowel is inadvertently allowed into the full primary acoustic pathway.

In the liver, the use of ultrasound contrast agents can improve lesion targeting temporarily while the ultrasound contrast agent is circulating [5]. This however is not a feasible method to maintain accurate targeting for multiple lesions over a more lengthy procedure, particularly for a procedure which is already notorious for requiring many long hours.

Currently, diagnostic ultrasound monitoring techniques do not allow effective measurement of tissue temperature. Assessment of tissue response by temperature monitoring following sonication is therefore impractical with this technique. Unfortunately, there is significant tissue variability in heating response both between patients and within the same patient due to multiple factors, and it would be advantageous to be able to directly visualize such tissue responses in real time during the procedure. This ability enables operator interaction to maximize tissue heating at any site and attempts to overcome the inevitable variations in tissue response to FUS power. It may be possible in the future to produce some form of thermal mapping using diagnostic ultrasound alone by utilizing techniques such as tissue elasticity or other methods. As yet these techniques are relatively undeveloped and have yet to be effectively applied in the clinical arena.

The thermal mapping abilities of MRI (see above) are inherently much more effective and simple to apply compared to ultrasound methods. MR thermal mapping techniques have already

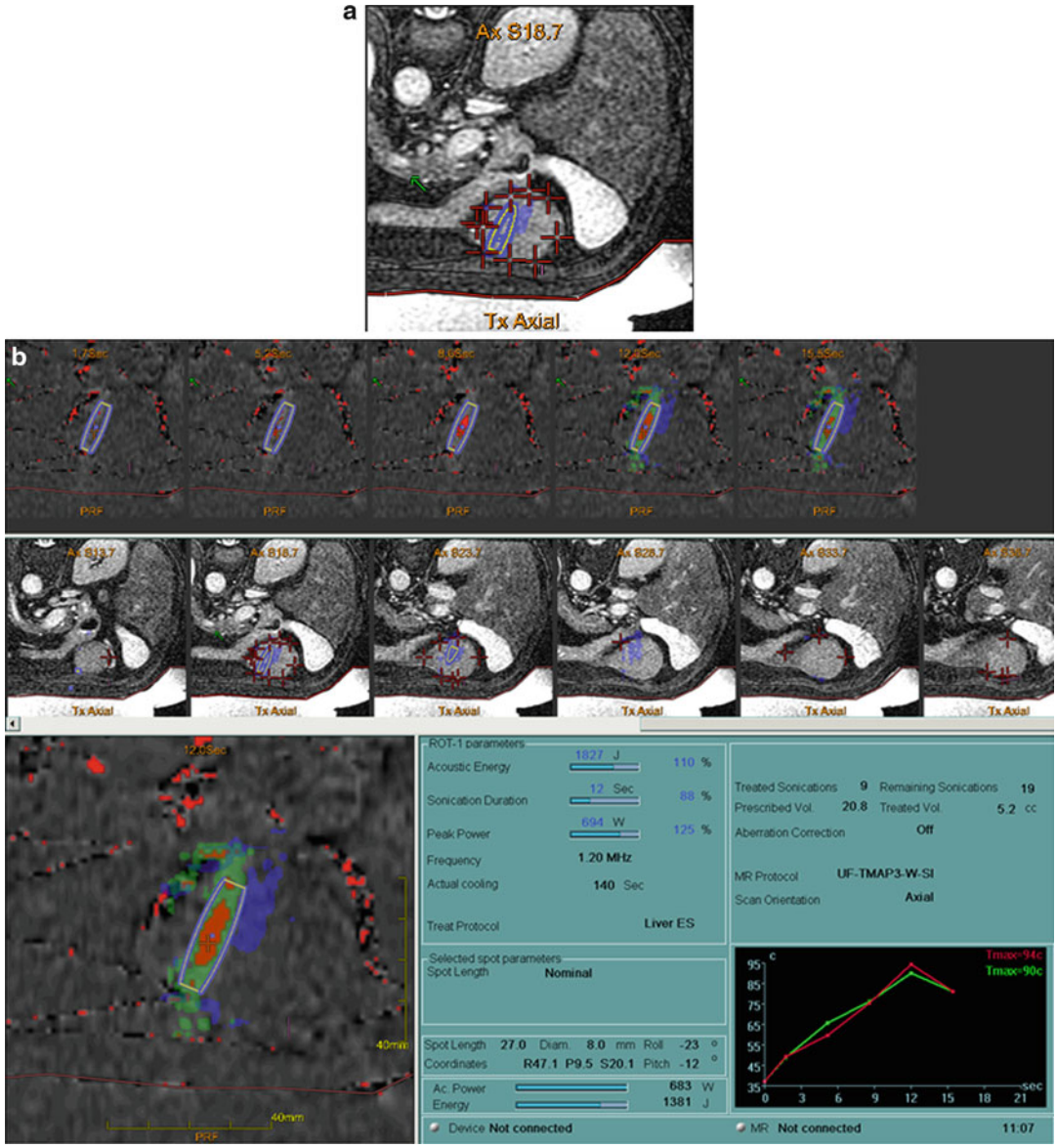

Fig. 36.2 (**a**) Thermal map superimposed on the image of hepatocellular carcinoma of patient in Fig. 36.2. The *blue* areas represent portions of tumor that have been heated to above 55 °C for one second and are therefore coagulated. The *red* crosses surrounding the lesion are fiducial markers which are placed electronically around the lesion margins to make sure that no significant unrecognized movement is occurring between images. (**b**) Screen capture from the image console during MR-guided focused ultrasound procedure to the above patient showing the current lesion *bottom left* in *red* adjacent to previous areas of coagulation in *blue*. In *bottom right* of the image, there is a graphical representation of the temperature achieved during the sonication

been used extensively in more than 5,000 clinical cases worldwide in the treatment of uterine fibroids. It has proved to be robust and reliable and produces repeatable thermal images of the sonicated area so that decisions can be immediately made on how to titrate FUS indices to maximize tissue response.

MR also has the inherent advantage of high soft tissue contrast and the ability to measure multiple tissue parameters such as T1, T2,

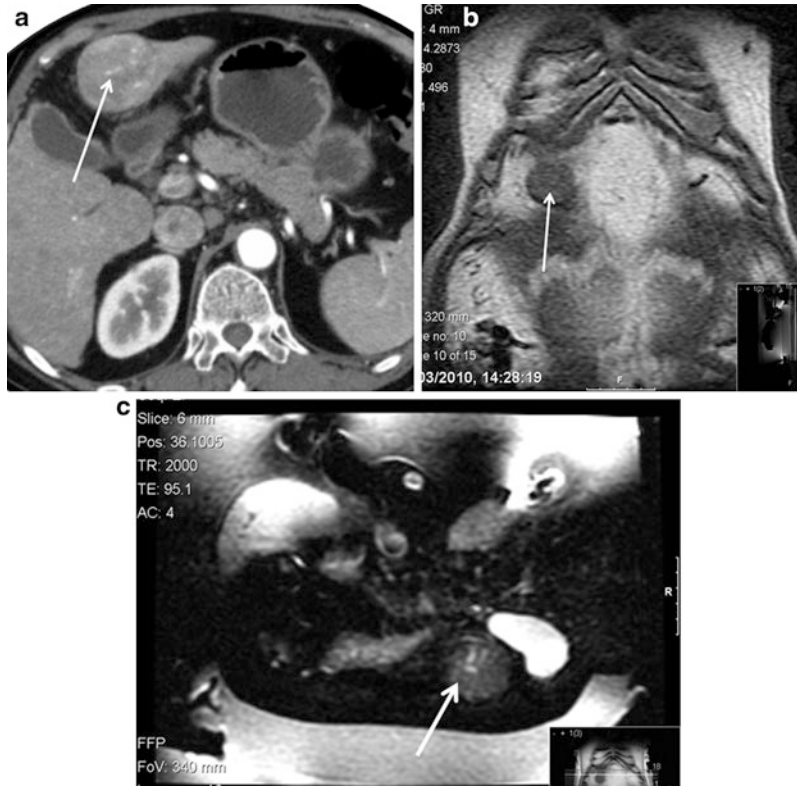

Fig. 36.3 (**a**) CT examination of the liver showing a 4-cm-diameter hepatocellular carcinoma in the anterior aspect of the left lobe (*white arrow*) largely uncovered by ribs allowing MR FUS access to this site with very little interference from overlying ribs. (**b**) Coronal MRI of liver showing position of above mass (*white arrow*) in relation to anterior rib cage which partially covers the left lobe of the liver. The majority of the lesion is not covered by ribs, but its superior more anterior part is behind the lower ribs which are not visualized on this slice but were seen more anteriorly. (**c**) Same patient as above showing restricted diffusion in the left lobe of the liver within the hepatocellular carcinoma (*white arrow*). The signal intensity here altered immediately post thermal ablation indicating that change in diffusion is an almost immediate change post ablation

diffusion, susceptibility, etc., thus enabling visualization of hepatic lesions with great clarity. MR-guided FUS machines, however, inevitably are more complex technologically since they must use MR-compatible materials for their construction. The very high magnetic field of an MR scanner is a hostile environment for any form of additional technology. No ferrous materials can be utilized; motors and other electrical components must be carefully constructed with appropriate shielding, or better still not used at all, because the extraneous radiofrequency energy they produce can completely disrupt the MR images produced. The transducer in MR-guided systems, for example, is usually moved by either piezoelectric motors or some form of hydraulic system so that minimal disruption to the MR imaging field is produced. To carry out general anesthesia in the MR environment is also more complex than when using simple ultrasound-guided systems. Despite these and similar drawbacks, most of the problems of the MR environment are now sufficiently overcome and do not present the problems they once did.

The most difficult problem common to both guiding techniques in the liver is the interference posed by the bony barrier of the ribs (Figs. 36.3, 36.4, and 36.5). Bone absorbs ultrasound 50 times more avidly than soft tissue and completely distorts focused ultrasound beams that try to pass

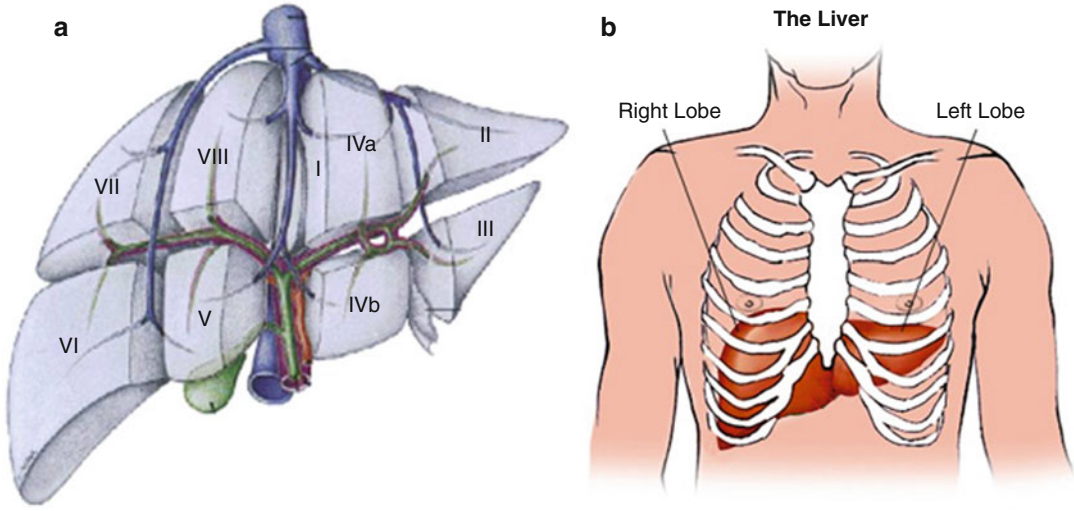

Fig. 36.4 (**a**) Diagrammatic representation of the different segments of the liver. It is only lesions that lie in segments three and four and occasionally segment two that can really be accessed with current technology of MR-guided focused ultrasound (Courtesy of InSightec, Ltd.). (**b**) Liver shown with overlying rib cage

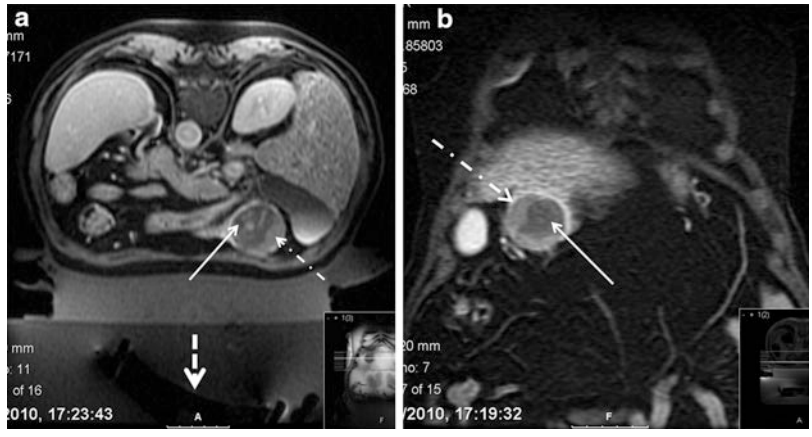

Fig. 36.5 (**a**) Postcontrast axial FS PGR dynamic sequence showing the previously well-perfused hepatocellular carcinoma now with no perfusion post ablation in its medial two thirds (*white arrow*). There is however retained perfusion in the lateral one third (*dashed arrow*) where ribs have covered this portion preventing focused ultrasound from reaching this area. Note the angle of the transducer (*broad dashed arrow*) in the water bath which had to be utilized to reach the target without transgressing the ribs. (**b**) Postcontrast coronal image obtained immediately after **a** showing same findings in a different plane (*arrows* as in Fig. **a**)

through the barrier of the ribs resulting in a defocused nontherapeutic sonication. It seems likely that this problem will be solved in the relatively near future by the development of large arrays of electronic ultrasound transducers which can be placed close to the lower thoracic and abdominal wall. The exact position of each rib will be determined, and rows of transducers will be activated to fire in between ribs (with no bony absorption therefore) while those transducers directly overlying ribs will not be fired at the same time. Such a process should therefore allow coherent sonication spots to be created within the liver and should allow electronic

focusing at multiple target sites, hopefully with the potential of reaching most parts of all segments of the liver. It is nevertheless likely that lesions high under the diaphragm in patients with overexpanded lungs will remain problematic, because of the interruption of the acoustic pathway by lung extending downward around the liver dome. Similarly, bowel extending upward anteriorly in front of the liver may continue to limit acoustic access.

Experimental work to date with MR-guided FUS suggests that lesions adjacent to vessels can be treated right up to the vessel margin and across the border of large vessels without significant damage to the vessel itself, which is protected by the cooling blood flow [25]. This is similar to percutaneous thermal ablation procedures. However, complete eradication of tumor cells close to vessels is known to be relatively problematic for some percutaneous ablation techniques, since the heat sink produced by the flowing blood may also not allow sufficient heating of these perivascular tumor cells. In focused ultrasound, because individual sonications are small and they can be densely overlapped, vascular cooling effects may be better overcome resulting in better coagulation right up to vessel margins.

General anesthesia is commonly used to control respiratory movement in liver FUS at the moment. While this is quite effective in allowing the operator to have spatial control of the procedure, it does introduce potential complications of anesthesia itself into the procedure. In other clinical applications of FUS, such as the treatment of uterine fibroids, procedures are normally performed using only conscious sedation on an outpatient basis [26]. To be able to treat liver tumors without anesthesia as an outpatient, one must develop a technique that overcomes the problems posed by unreliable voluntary respiratory motion. In the MR field, this will require the development of an extremely rapid lesion tracking sequence, probably using rapid Echo planar imaging, in which an operator can effectively lock on to the position of the targeted tumor over multiple respiratory phases in a repeatable manner. This would allow the target lesion to be continuously and clearly identified at a known site so that even if respiration is variable, the target tumor can be effectively visualized. Such a procedure theoretically may then be performed with voluntary respiratory suspension during which time individual sonications can be rapidly carried out. Of course in practice, such a procedure will also require a technique for updating the exact position of the ribs relative to the target at all times.

The technological improvements required to achieve most of the goals described in the above section are quite complex, but each one of them is perfectly feasible in isolation, and it is the combination of all these individual solutions into a unified whole that will be challenging. Early research and development work is already well underway in multiple establishments to solve these issues and amalgamate them into a potentially clinically effective product which will allow this whole field to move forward.

Conclusions

Liver tumors are common, and for the majority of patients, treatment options have been lacking. Although percutaneous ablation techniques are simultaneously advancing, the prospect of FUS for the treatment of liver tumors may radically change the current treatment paradigms in this field. This will be particularly beneficial in patients with substantial liver impairment, especially with associated coagulation abnormalities, and will allow operators to deliver locally destructive tissue therapy without any cutting through the liver.

This application of FUS technology is still very much in its infancy and still requires substantial further technological development to overcome the problems described in this chapter. We anticipate that a mature range of FUS systems will emerge that can effectively treat the majority of liver masses at most sites within the liver within the next few years. The integral use of MRI will add accuracy of targeting and thermal monitoring and therefore allow very accurate control of FUS power deposition.

The widespread implementation of FUS techniques to the liver will represent a giant step forward in the treatment of patients with liver tumors. This technique may potentially provide noninvasive liver tumor destruction as an outpatient irrespective of the presence of bleeding disorder commonly seen in severe liver dysfunction and in a procedure that can be repeated multiple times so that large tumors or multiple tumors can be treated in an effective and safe manner.

References

1. Wood R, Loomis L. The physical and biological effects of high frequency sound waves of great intensity. Philos Mag. 1927;4:417–36.
2. Fry W, Barnard J, Fry F. Ultrasonically produced localised selective lesions in the central nervous system. Am J Phys Med. 1955;34:413–26.
3. Padma S, Martinie J, Iannitti D. Liver tumour ablation: percutaneous and open approaches. J Surg Oncol. 2009;100:619–34.
4. Dubinsky T, Cuevas C, Dighe M. High intensity focused ultrasound: current potential and oncological applications. Am J Roentgenol. 2008;190:191–9.
5. Fischer K, Gedroyc W, Jolesz F. Focused ultrasound as a local therapy for liver cancer. Cancer J. 2010;16(2):118–24.
6. Cline H, Schenck J, Hynynen K. MR-guided focused ultrasound surgery. J Comput Assist Tomogr. 1992;194:731–7.
7. Hynynen K, Clement G, McDannold N. 500-element ultrasound phased array system for noninvasive focal surgery of the brain: a preliminary rabbit study with ex vivo human skulls. Magn Reson Med. 2004;2:100–7.
8. Wu F, Wang Z, Chen W. Extracorporeal focused ultrasound surgery for treatment of human solid carcinomas: early Chinese experience. Ultrasound Med Biol. 2004;30:245–60.
9. McDannold N, Jolesz F. Magnetic resonance image-guided thermal ablations. Top Magn Reson Imaging. 2000;11:191–202.
10. Jolesz F. MRI guided focused ultrasound surgery. Annu Rev Med. 2009;60:417–30.
11. Nagorney D, van Heerden J, Illstrup D. Primary hepatic malignancy: surgical management and determinants of survival. Surgery. 1989;106:740–8.
12. Dupuy D, Goldberg S. Image-guided radiofrequency tumour ablation:challenges and opportunities- part II. J Vasc Interv Radiol. 2001;12:1135–48.
13. Lu D, Yu NR, Raman SS, et al. Percutaneous radiofrequency ablation of hepatocellular carcinoma as a bridge to liver transplantation. Hepatology. 2005;41:1130–7.
14. Pompili M, Mirante V, Rondinara G. Percutaneous ablation procedures in cirrhotic patients with hepatocellular carcinoma submitted to liver transplantation: assessment of efficacy at explant analysis and of safety for tumour recurrence. Liver Transpl. 2005;11: 1117–26.
15. Iannitti D, Dupuy D, Mayo-Smith W. Hepatic radiofrequency ablation. Arch Surg. 2002;137:422–6.
16. Lu M, Kuang M, Liang L. Surgical resection versus percutaneous thermal ablation for early stage hepatocellular carcinoma: a randomized clinical trial. Zhonghua Yi Xue Za Zhi. 2006;86:801–5.
17. Chen M, Li J, Zheng Y. Surgical resection versus percutaneous thermal ablation for early-stage hepatocellular carcinoma: a randomized controlled trial. Ann Surg. 2006;243:321–8.
18. Livraghi T, Meloni F, Di Stasi M, Rolle E, Solbiati L, Tinelli C, et al. Sustained complete response and complication rates after RFA of very early hepatocellular carcinoma in cirrhosis: is resection still the treatment of choice? Hepatology. 2008;47:82–9.
19. Mullier S, Ni Y, Jamart J. RFA versus resection for resectable colorectal metastases: time for a randomized controlled trial? Ann Surg Oncol. 2008; 15:144–57.
20. Wu F, Wang Z, Chen W. Extracorporeal high intensity focused ultrasound ablation in the treatment of patients with large HCCs. Ann Surg Oncol. 2004;11: 1061–9.
21. Wu F, Wang Z, Chen W. Advanced HCC: treatment with high intensity focused ultrasound ablation combined with transcatheter arterial embolization. Radiology. 2005;265:659–67.
22. Li Y, Sha W, Zhou Y. Short and long term efficacy of high intensity focused ultrasound therapy for advanced hepatocellular carcinoma. J Gastroenterol Hepatol. 2007;22:2148–54.
23. Zhang L, Zhu H, Jin C, Zhou K, Li K, Su H, et al. High intensity focused ultrasound (HIFU) effective and safe treatment for hepatocellular carcinoma adjacent to major hepatic veins. Eur Radiol. 2009;19(2):437–41.
24. Livraghi T, Giorgio A, Marin G. HCC and cirrhosis in 746 patients: long term results of percutaneous ethanol injection. Radiology. 1995;197:101–8.
25. Kopelman D, Inbar Y, Hanannel A. MR-guided FUS: ablation of liver tissue in a porcine model. Eur Radiol. 2006;59:157–62.
26. Stewart EA, Gostout B, Rabinovici J, Kim HS, Regan L, Tempany CM. Sustained relief of leiomyoma symptoms by using focused ultrasound surgery. Obstet Gynecol. 2007;110(2 Pt 1):279–87.

Percutaneous Interventional Radiology: The Lung

37

Kien Vuu, Antonio Gutierrez, Fereidoun Abtin, Christopher Lee, and Robert Suh

Abstract

Percutaneous ablation techniques have emerged as a viable treatment option for primary and secondary lung malignancies. Utilizing minimally invasive image-guided approaches, these techniques allow for the precise placement of ablation devices with the goal of total tumor necrosis and local control, offering in some instances curative potential. The different ablative technologies used in the thorax are based on application of thermal energies, chemical lysis, and alteration of cell permeability, the thermal energies most extensively studied thus far. These ablative techniques provide a valuable stand-alone alternative to conventional surgical resection or an adjunct to surgery, chemotherapy, or radiotherapy. The development of these and additional novel therapies has resulted in a multidisciplinary approach for the treatment of primary and secondary pulmonary malignancies with percutaneous ablative techniques proving to be a robust therapeutic option. To date, radiofrequency ablation (RFA) is the best developed and most widely used thermal ablation technique in the lung. Using radiofrequency ablation as a model for thermal ablation, this chapter will outline the principles of thermal ablation, the role of thermal ablation in the treatment of primary and secondary pulmonary malignancies, the procedural-related complications of thermal ablation within the lung, post-ablation follow-up and treatment results, as well as a brief discussion and comparison of the different ablative technologies.

K. Vuu (✉) • A. Gutierrez • F. Abtin • R. Suh
Department of Radiological Sciences, Ronald Reagan UCLA Medical Center, Los Angeles, CA, USA
e-mail: kvuu@mednet.ucla.edu; angutierrez@mednet.ucla.ed; fabtin@mednet.ucla.edu; rsuh@mednet.ucla.edu

C. Lee
Department of Radiology, Body Division, Keck School of Medicine USC University Hospital, Los Angeles, CA, USA
e-mail: chrisleemd@gmail.com

Introduction

Percutaneous ablation techniques have emerged as a viable treatment option for primary and secondary lung malignancies. Utilizing minimally invasive image-guided approaches, these techniques allow for the precise placement of ablation probes with the goal of total tumor necrosis and local control, offering in some

D.E. Dupuy et al. (eds.), *Image-Guided Cancer Therapy*, DOI 10.1007/978-1-4419-0751-6_39,

instances curative potential. The different ablative technologies used in the thorax are based on application of thermal energies, chemical lysis, and alteration of cell permeability, the thermal energies most extensively studied thus far. These ablative techniques provide a valuable stand-alone alternative to conventional surgical resection or an adjunct to surgery, chemotherapy, or radiotherapy. The development of these and additional novel therapies has resulted in a multidisciplinary approach for the treatment of primary and secondary pulmonary malignancies with percutaneous ablative techniques proving to be a robust therapeutic option. To date, radiofrequency ablation (RFA) is the best developed and most widely used thermal ablation technique in the lung. Using radiofrequency ablation as a model for thermal ablation, this chapter will outline the principles of thermal ablation, the role of thermal ablation in the treatment of primary and secondary pulmonary malignancies, the procedural-related complications of thermal ablation within the lung, post-ablation follow-up and treatment results, as well as a brief discussion and comparison of the different ablative technologies.

Lung Cancer Demographics and Treatment Options

Percutaneous RF ablation is used to treat both primary and secondary lung tumors. In 2010, the Surveillance Epidemiology and End Results (SEER) database estimates that approximately 222,520 Americans will be diagnosed with lung cancer and 157,300 people will die of the disease, making primary cancer of the lung or bronchi the leading cause of cancer death in men and women, accounting for approximately one-third of all cancer deaths [1]. Despite advances in cancer care, 5-year survival for newly diagnosed lung cancer has marginally improved, currently at its peak at 15 % [2, 3]. In addition to primary lung cancer, the lungs are the second most common organ for metastases from extrapulmonary solid tumors [4, 5]. Thus, a clear understanding of traditional non-ablative therapies for both primary and secondary lung malignancies is required to better place into context the role of percutaneous ablative techniques.

Non-Small Cell Lung Cancer

The prognosis and treatment of primary lung tumors primarily depends on the histologic type of the tumor, clinical but more so the pathological stage of the tumor, and the cardiorespiratory reserve of the patient [6, 7]. Non-small lung cancers (NSCLC) are staged via the International Staging System for Lung Cancer [8, 9] (Table 37.1). For stages 1 and 2 disease, surgery remains the treatment of choice with 5-year survival of approximately 75 % and 50 %, respectively. For stage 3A disease, a combination of radiotherapy, chemotherapy, and surgery offers a 5-year survival of 10–15 %. Stage 3B disease is not treated with surgery, but with a combination of chemotherapy and radiotherapy, resulting at best a 5-year survival of 5 %. Palliative chemotherapy is occasionally used in stage 4 disease, and the median survival remains relatively poor at approximately 8 months from the time of diagnosis [10]. The optimal surgical resection for stages 1 and 2 disease is lobectomy complemented with hilar and mediastinal lymph node sampling [11–13]; however, eligibility for resection is relatively low with only one-third of lung cancer patients meeting the pulmonary guidelines to withstand surgical resection of their tumors. Others are simply not candidates for lobectomy, suffering from poor reserve related to extensive comorbid lung and/or heart disease, often in particular from smoking. For some of the patients not suitable for lobectomy, smaller anatomic and nonanatomic resections, specifically segmentectomy and wedge resection, may be performed but are viewed as operations of "compromise," given higher rates of local recurrence and diminished long-term survival [14, 15]. Despite comorbidities, better survival outcomes are demonstrated for those patients who receive earlier treatment than no treatment at all [16]. Therefore, a cohort of patients with surgically

Table 37.1 International staging system for lung cancer

	Definitions	N0	N1	N2	N3
T1	Any tumor less than or equal to 3 cm	IA	IIA	IIIA	IIIB
T2	T2a: tumor $>$ 3 but $\leq$ 5 cm	IB	IIA	IIIA	IIIB
	T2b: tumor $>$ 5 but $\leq$ 7 cm	IIA	IIB	IIIA	IIIB
T3	Any tumor greater than 7 cm, invading the chest wall, diaphragm, phrenic nerve, mediastinal pleura, or parietal pericardium. Tumor in the main bronchus $<$ 2 cm distal to the carina or causing obstructive pneumonia of the entire lung. Ipsilobular satellite nodules	IIB	IIIA	IIIA	IIIB
T4	Any size tumor with invasion of heart, great vessels, trachea, recurrent laryngeal nerve, esophagus, vertebral body, or carina	IIIA	IIIA	IIIB	IIIB
M1	Any distant metastasis	IV	IV	IV	IV

N0 No lymph node involvement
N1 Ipsilateral bronchopulmonary or hilar nodes
N2 Ipsilateral mediastinal or subcarinal nodes
N3 Contralateral hilar, contralateral mediastinal, or supraclavicular nodes
Source: Data from Detterbeck [72]

resectable but medically inoperable cancer may benefit from nonsurgical lung-sparing local therapies, such as RFA.

Small Cell Lung Cancer

For small cell lung cancer (SCLC), surgical resection, or for that matter other local therapies, plays a limited role in the treatment of stage 1 disease without benefit for limited disease beyond stage 1 and extensive disease. Limited disease is usually treated with combination chemotherapy, usually combined with radiotherapy, together yielding a median survival of 18–24 months and 2-year survival ranging between 40 % and 50 % [8, 17].

Lung Metastases

Metastatic disease to the lung is common as the pulmonary capillary bed is the first bed to receive lymphatic or blood-borne malignant cells from the systemic circulation [18]. The most common tumor types that metastasize to the lung include melanoma, colorectal carcinoma, osteosarcoma, kidney, breast, and testicular carcinomas [4]. For the most part, metastatic disease, with the exception of those patients with solitary or oligometastatic colorectal cancer to the liver, is excluded from surgical resection. However, approximately 20 % of patients have metastatic disease limited to the lung at the time of initial diagnosis or during the course of therapy and may benefit from pulmonary metastasectomy, provided that their primary tumor has been resected with good control and little or no extrapulmonary tumor [4]. Depending on the location and extent of metastatic disease, surgical approaches include video-assisted thoracoscopic surgery and open metastasectomy with segmentectomy, lobectomy, or pneumonectomy, but unlike primary lung carcinoma, significant benefit does not occur with larger resections [5, 19, 20]. Surgical resections are largely limited by the number and the location of metastases (Fig. 37.1) with central metastases requiring larger resections than peripheral ones and patient comorbidities including extensive or multiple prior resections (Fig. 37.2) diminishing pulmonary reserve. In these situations, lung-sparing ablative techniques may be of significant benefit.

Principles of Thermal Ablation

According to the standardization of terms regarding image-guided tumor ablation [21], the definition of tumor ablation is the direct application of chemical or thermal therapies to a specific tumor (or tumors) in an attempt to achieve eradication or substantial tumor destruction. Tumor destructive mechanisms include thermal energy deposition, chemical injection, photodynamic therapy, and ionization radiation. Of these technologies, thermal sources of heat, including radiofrequency, microwave, and laser

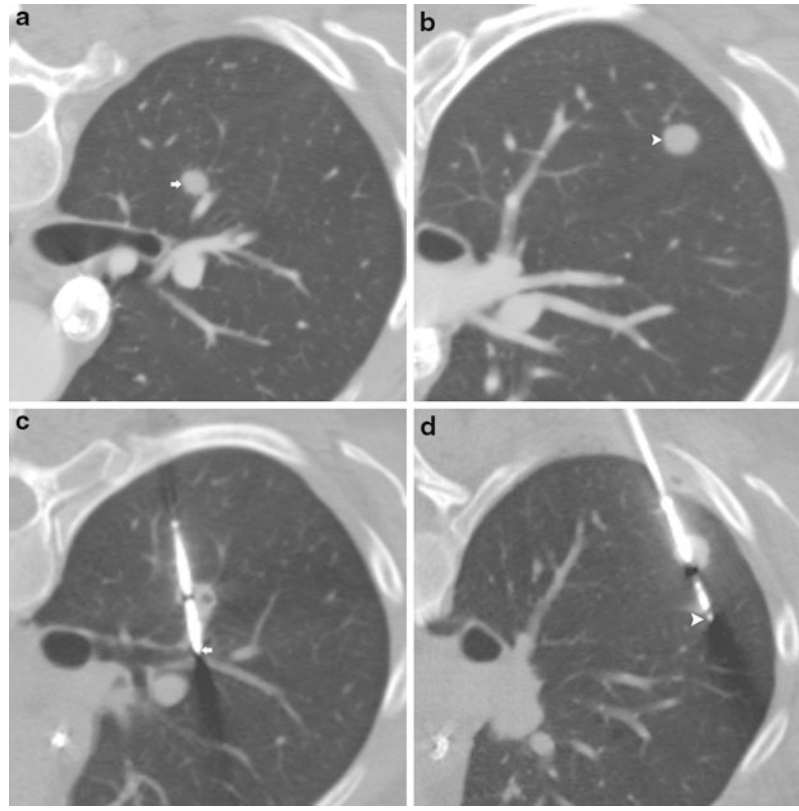

Fig. 37.1 Metastases: 68-year-old woman with colorectal pulmonary metastases involving different lobes. Axial images (**a** and **b**) demonstrate left upper lobe (*arrow*) and left lower lobe (*arrowhead*) nodules, consistent with colorectal metastases. Axial images (**c** and **d**) demonstrate placement of microwave antennas through the left upper lobe nodule (*arrow*) and left lower lobe nodule (*arrowhead*) prior to ablation

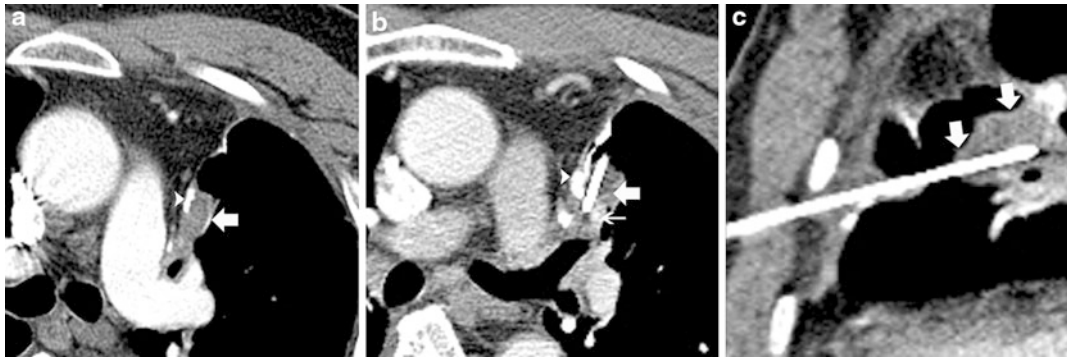

Fig. 37.2 Recurrent metastatic disease: 70-year-old man with colorectal carcinoma status post left upper lobe wedge resection for metastatic disease who presents with recurrence at the resection margin. (**a**) Axial image with contrast demonstrates nodular soft tissue (*arrow*) along the resection margin with note made of surgical suture (*arrowhead*). (**b**) Axial image with contrast demonstrates interval placement of a radiofrequency electrode within the soft tissue nodule adjacent to a segmental pulmonary artery laterally (*long arrow*) and surgical material medially (*arrowhead*). (**c**) Sagittal image confirms placement of the electrode within the soft tissue recurrence (*arrows*)

energies, and sources of cold, specifically cryotherapy or cryoablation, have been the most widely used and studied in the lung and thorax. In general, these energies are delivered through needle-like probes, or "applicators," which are carefully placed into or adjacent to the target tumor typically under image guidance. The term "applicator" broadly refers to all ablation needles, but, more specifically,

is dependent on the energy source; thus, radiofrequency applicators are electrodes, microwave applicators antennas, cryoablation applicators, cryoprobes, and laser applicators fibers.

Radiofrequency Ablation

Physics and Physiology of Radiofrequency Ablation

Radiofrequency ablation is based on a thermal energy delivery system that applies a high-frequency alternating current (460–500 kHz or radio wave spectrum) supplied by a radiofrequency generator and delivered through a needle electrode, causing local tissue destruction by controlled heating. The needle electrode is introduced and confirmed into the target tumor under image guidance, which for the most part is computed tomography (CT), the preferred guidance modality for the lung and the thorax. Depending on the number and type of electrode utilized, time of ablation, generator used, and guidelines specific to each manufacturer, ablation zones of different shapes and sizes are achieved when the alternating current is applied. The concentration of the radiofrequency (RF) current is focused on the non-insulated tip of the electrode, and the circuit is completed to grounding, or dispersive, pads placed on the patient's back or thighs (monopolar system) or a grounding electrode (bipolar system).

The RF current causes agitation of ionic dipolar molecules, resulting in frictional heating of the surrounding tissues and fluids, concentrated most at the non-insulated tip of the electrode [22]. Coagulation necrosis, protein denaturation, and apoptosis are achieved when living tissue is heated to more than 50 °C for at least 5 min. For effective tumor ablation, tissue temperatures typically range from 60 °C to 100 °C [22, 23]. If too much energy is delivered and temperatures reach an excess of 105–115 °C, tissue charring and carbonization occur, leaving pockets of gas and desiccated tissue which can reduce thermal penetration resulting in incomplete ablation and residual non-ablated tumor [24].

Principles of impedance and heat dissipation become central in lung tissue ablation, in particular at the interface between normal lung and tumor, given the disparity in tissue characteristics between the two. For the most part, the normally aerated lung parenchyma acts as an insulator for heat energy deposited largely due to its naturally high impedance, thus requiring less power to achieve adequate ablation [25]. Conversely, when the lesion is in contact with non-aerated tissue, greater heat dissipation occurs and more energy is required to ablate the same volume of tumor. Conversely, non-aerated tumor, although in general carrying lower tissue impedance, has higher heat dissipation, ultimately requiring more power to ablate the same volume of tumor. While ablation within homogeneous tissue, whether normal lung or tumor, occurs with relative ease, difficulty arises at the margins of the tumor, particularly in achieving a 1-cm surgical margin of encompassment; the low resistance tumor will readily ablate, especially given the added benefit of surrounding lung insulation, or "oven" effect, until heat energy reaches the adjacent aerated lung, where the sudden change of resistance from low to high of the surrounding air may prevent further tissue burn, thereby failing to accomplish a true margin of safety. In addition, tissue cooling occurs more rapidly when the ablation is performed adjacent to large blood vessels, a phenomenon referred to as "heat-sink effect," and to a lesser extent, large airways, and can potentially result in incomplete tumor ablation [26].

Given the imperfections and idiosyncrasies of radiofrequency energy and its delivery into heterogeneous tissue zones, other energies including microwave, laser, and cold have been increasingly studied, in hopes to emerge as alternate, viable, and improved energy sources for tumor ablation [27–31].

Other Thermal Ablative Technologies

As reference, the principles of RF energy, specifically its application and delivery for tumor therapy, can facilitate discussion and understanding

of other thermal ablative technologies. Although the applicators used in other thermal ablative technologies are different, image-guided placement of cryoprobes in cryoablation, antennas in microwave ablation, and fibers in laser ablation is similar to the electrode placement in RFA. Furthermore, since these techniques are additional methods for locoregional thermal energy deposition in attempts for local control, the patient selection criteria and complication profile of these methods overlap significantly with those of RFA.

Cryoablation

Cryoablation uses the extremes of cold temperature dissipation to induce thermal injury in tumor tissue. As a technical goal, cryoablation reduces the temperature of the neoplastic target tissue and the surrounding non-neoplastic tissue to lethal levels, and although lethality varies based of vascularity and density of tissue, complete and uniform cell death for the most part can be achieved at temperatures below approximately −20 °C to −25 °C (or −4 °F to −13 °F). Cytotoxicity is mediated via various mechanisms, including ischemia, denaturing of protein structures, and the breakdown of cellular and intracellular proteins due to the formation of ice crystals. For the most part, cryoablation preserves the extracellular architecture of tissue rather than the indiscriminate destruction that occurs with radiofrequency or other heat-based ablations, theoretically allowing for cellular repopulation.

Currently, the most widely used cryoablation systems are helium-argon based. Argon gas is forcefully conducted through the cryoprobe, and through the Joule-Thomson effect, forms an ice ball reaching subzero temperatures. Helium gas is used for thawing the ice ball or in combination with bursts of argon to produce smaller ice balls. Due to dependence on gas, these systems require large metal containers or tanks, which can on occasion be cumbersome. Cell death occurs by post-thaw-freeze rupture, followed by coagulation necrosis [28, 29]. Since the cryoablation system does not impart an electrical current, its system can be safely used in patients with pacemakers and implantable cardiac devices. In addition, since freezing does not disrupt the collagenous architecture of tissue, cryoablation has been shown to be safer when used in proximity of bronchi and nerves and, thus, can be associated with less pain. One potential disadvantage of cryoablation within the lung is poor visualization of the ice ball from dissipation of ice within the air-filled alveolar sacs. To overcome this, an initial 2 min of cryoablation can be performed followed by an immediate thaw phase to allow for the development of fluid and hemorrhage surrounding the tumor; this allows for greater dissipation of cold temperature into the surrounding tissue and results in a larger ice ball formation after completion of a full 10-min cryoablation cycle (Fig. 37.3).

The most common complications associated with cryoablation include cough, hemoptysis, fever, and hypertension [29]. Additional less commonly reported complications include pleural effusion (14 %) and pneumothorax (12 %). Interestingly, self-limited hemoptysis (62 %) and ablation-related hypertension occur at significantly higher frequencies as compared to radiofrequency and microwave ablation, requiring special efforts to monitor and particularly control blood pressure.

Microwave Ablation

Microwave ablation involves induction of microwave energy (900–2,450 MHz) to cause dipole excitation, thereby creating frictional heating and tissue hyperthermia [27]. The microwave antenna emits electromagnetic radiation into tissue without the necessity of an electrical current, and thus carbonization and gas pockets around the antenna do not interfere as much with energy deposition, resulting in higher intratumoral temperatures as compared to RFA. The zone of active heating in RFA extends only a few millimeters from the electrode with the remainder of tissue heating reliant on thermal conduction, and comparatively, the zone of active heating in microwave ablation at 915 Mhz can extend up to 2 cm

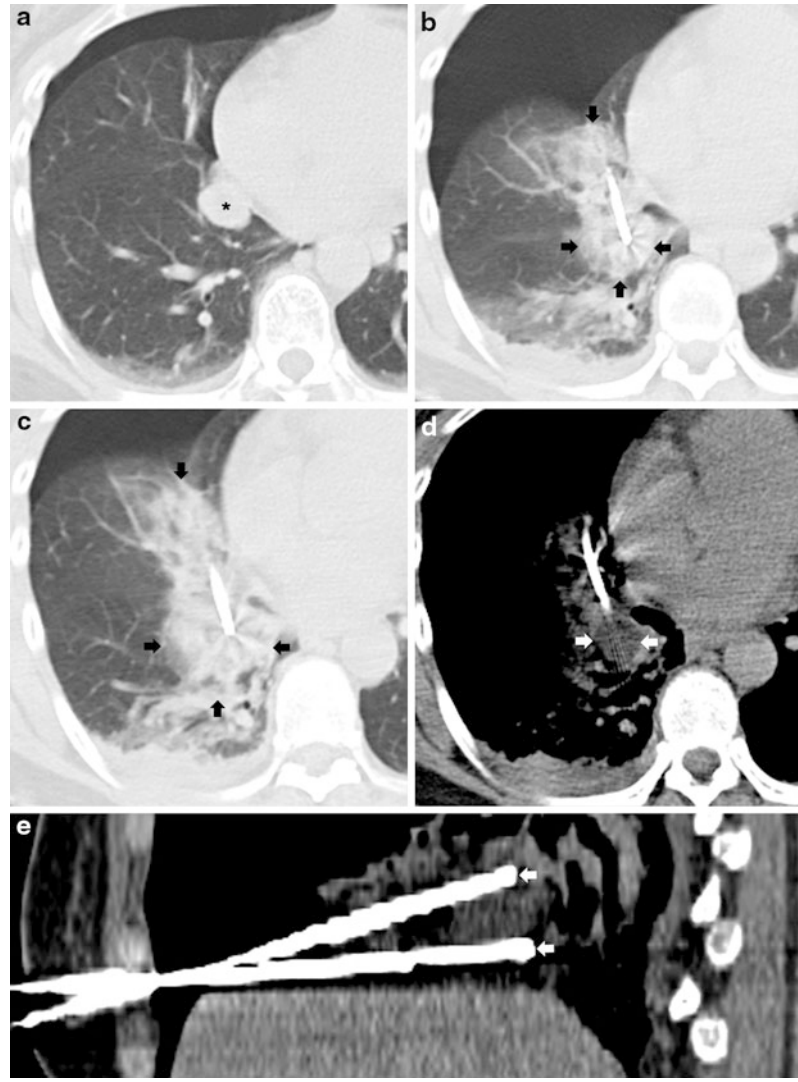

Fig. 37.3 Cryoablation technique: 65-year-old woman with a history of uterine sarcoma with a right lower lobe metastasis adjacent to the right atrium. (**a**) Axial CT image shows a soft tissue metastasis adjacent to the right atrium (*) with a residual pneumothorax from a prior procedure. (**b**) Axial CT image following an initial 2 min of cryoablation and thaw phase demonstrates development of airspace and ground-glass opacity (*arrows*) surrounding the nodule, consistent with hemorrhage. (**c**) Axial CT image following a full cryoablation cycle demonstrates enlargement of the airspace and ground-glass opacity (*arrows*) consistent with an adequate ablation zone. (**d**) Axial CT image demonstrates interval development of low attenuation in the target lesion, consistent with ice ball (*arrows*) formation. (**e**) Sagittal reconstruction confirms the position of the two cryoprobes at the superior (*arrow*) and inferior (*arrow*) surface of the target lesion with the ice ball encompassing the nodule

in solid tissue surrounding the antenna due to a broader field of power density.

Microwave generators allow multiple antennas to be connected and simultaneously activated, thereby allowing for larger ablation volumes with shorter ablation times. Since electrical energy is not utilized, dispersive or grounding pads are not necessary, the danger of secondary burns and skin necrosis significantly reduced as compared to RFA. In addition, microwave ablation confers less pain than RFA during operation, presumably due to the lack of intercostal nerve stimulation by alternating current that passes through the patient with RFA.

Complications from microwave ablation include pneumothorax (33–39 %), mild skin burns (3 %), self-limited hemoptysis, empyema, acute respiratory distress (<5 %), and post-ablation syndrome (2 %) [32].

Laser Ablation

Laser ablation, also known as laser-induced interstitial thermotherapy, employs optical fibers to deliver high-energy laser radiation to the targeted tissues, the fibers positioned through hollow applicators resembling coaxial needles. Once applicators

Table 37.2 Comparison between various factors which influence the choice of ablative modality from less favorable (+) to more favorable (+++). Asterisk (*) designates the number of simultaneous applicators for each respective therapeutic modality

Comparative technologies			
Parameter(s)	Radiofrequency	Microwave	Cryoablation
≤3 cm	+++	+++	+++
>3 cm	+ (up to 3)*	+++ (up to 3)*	++ (up to 25)*
≤1.5 cm pleura	+ (pain)	+ (air leak)	+++
Chest wall & pleura	+	++	+++
Mediastinum	+	+	++
Sinks	+	+++	++
Pacer & AICD	+	++	+++
Coagulopathy	+++	+++	+

are in place, the central trocar is removed and replaced with the laser fiber, which results in tissue heating and causes coagulation necrosis of the tumor. Neodymium-doped yttrium aluminum garnet (Nd: YAG) laser light (wavelength, 1,064 nm) is the most commonly used light source delivered from the fiber. Unlike RFA, laser is not dependent on electrical conductivity for tissue heating and propagation and yields a more predictable and reproducible zone of ablation, the emitted light with an effective distance of up to 12–15 mm [33]. Laser ablation's magnetic resonance (MR) compatibility holds a major advantage over other ablation devices, offering real-time monitoring and thus enabling optimal adjustment of imparted energy throughout the ablation cycle. And as an additional theoretical advantage, tumoricidal liquids could be instilled through the open tip of the applicator when the laser fiber is removed as has been studied in bladder cancer therapy with laser ablation and chemotherapy [34]. Disadvantages of the laser ablation system include the use of larger gauge applicators compared with RF electrodes and the relatively longer time to perform the ablation; both are factors that increase the incidence of pneumothorax and bleeding [35].

Role and Choice of Thermal Ablation

The treatment of primary and secondary malignancies will continue to evolve as longitudinal data and experience with percutaneous ablation techniques emerge. Along with surgical, chemotherapeutic, and radiotherapeutic approaches, it is clear that the treatment of lung malignancies has developed into a multidisciplinary endeavor. This "team approach" to lung cancer treatment has served as a model for multispecialty thoracic tumor boards utilized by many institutions to personalize therapy for each patient's disease. Careful patient and tumor selection with attention paid to specific therapeutic goals and contraindications should be considered in the ablation candidate.

In addition to and on occasion overlapping considerations for patient and tumor selection, a number of factors can influence an operator's preference in the choice of ablative technique and include size of the lesion, distance from pleura, location in chest wall, pleura or mediastinum, potential for heat- and cold-sink effect from proximity to vessels and airways, presence of pacemaker, AICD, and other electronic medical devices and patient conditions, such as coagulopathy (Table 37.2).

Patient Selection

To date, within the medical literature, a number of indications regarding thermal ablation for the treatment of primary and secondary malignancies within the lung and thorax have emerged in addition to resection of traditionally accepted surgical disease in the medically ineligible patient.

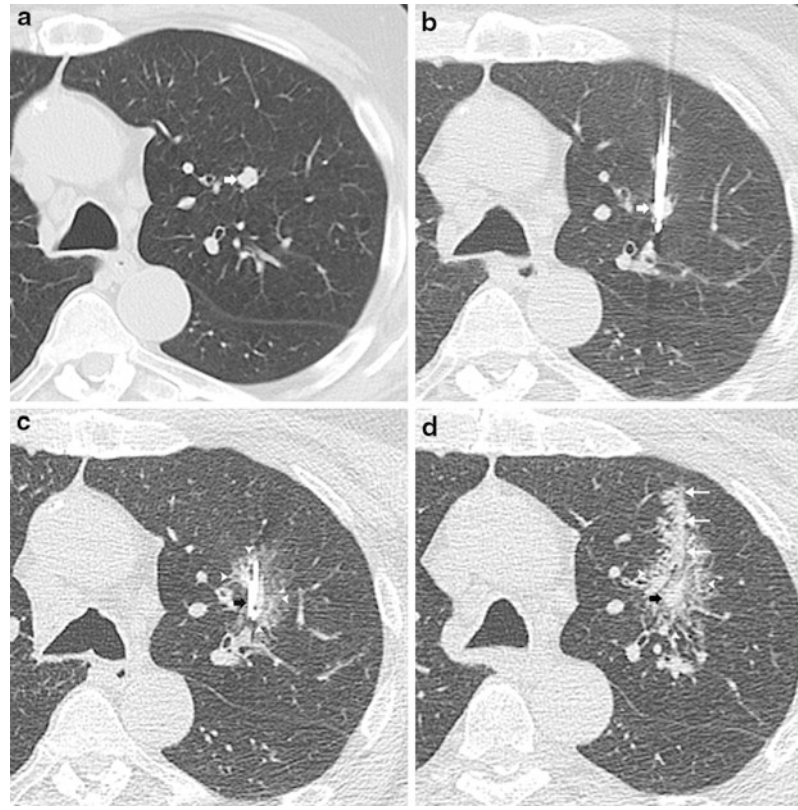

Fig. 37.4 Primary NSCLC: 77-year-old man with Stage 1A left upper lobe adenocarcinoma. (**a**) Supine axial CT image demonstrates a centrally located left upper lobe primary adenocarcinoma (*arrow*). (**b**) Ablation image demonstrates placement of a radiofrequency electrode in the bronchogenic carcinoma.(**c**) Post-ablation image shows peri-nodule airspace and ground-glass opacity (*arrowheads*) encompassing the nodule (*arrow*) and extending beyond the lesion. (**d**) Post-electrode removal CT image demonstrates a spherical ablation zone (*arrowheads*) surrounding the nodule (*arrow*) with changes, consistent with tract cauterization (*long arrows*)

With the understanding that ablation provides only locoregional control of the tumor, therapeutic goals include potential for cure in limited or early stage NSCLC (Fig. 37.4); prolongation of survival in those patients with limited recurrent or metastatic disease to the lung (Fig. 37.1); palliation of symptoms, specifically pain (Fig. 37.5), dyspnea, hemoptysis, and cough [36]; cytoreduction of large tumors in anticipation for adjuvant therapies, potentially improving susceptibility of the remaining viable tumor to chemotherapy or radiotherapy [37, 38]; and prevention of morbid airway or organ compromise, as a preemptive strike prior to invasion (Fig. 37.3).

Tumor Selection

Although limited long-term data is available regarding the tumor characteristics that are most amenable to thermal ablation, several key trends have emerged. Most importantly, the ideal lesion for ablation is completely intraparenchymal and smaller than 3.0–3.5 cm, with studies documenting that these lesions, when treated, have higher rates of complete necrosis and longer length of patient survival [36, 39]. For tumors larger than 3.0 cm, interestingly, improved survival has been shown with a combination of RFA and radiotherapy [40]. For pleural and chest wall lesions given their proximity to intercostal nerves and the somatically innervated parietal pleura, cryoablation has been shown to be associated with less patient discomfort and pain-related complications compared with the heat-based ablative techniques [37]. Tumors treated adjacent to pulmonary or mediastinal and hilar vessels larger than 3.0 mm [38] and/or large bronchi [41] may be susceptible to incomplete or partial ablation due to the heat-sink effect. Within the surgical literature on pulmonary metastasectomy and accordingly for thermal ablation, or "thermal metastasectomy," histology or tumor cell type has been shown to impact patient survival,

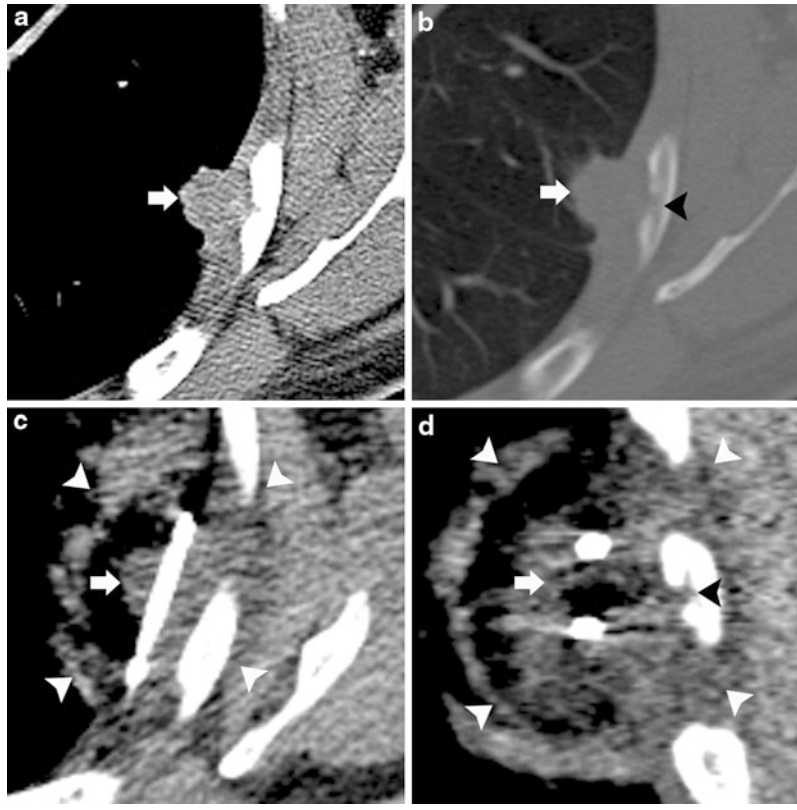

Fig. 37.5 Palliation: 75-year-old man with esophageal carcinoma with pulmonary metastases, who presents with severe left chest wall pain. (**a**) Axial CT image in soft tissue window shows a left lower lobe pulmonary nodule (*arrow*) with associated pleural thickening. (**b**) Axial CT image in bone window shows the left lower lobe nodule (*arrow*) eroding into the adjacent rib (*arrowhead*), accounting for the patient's pain. (**c**) Axial ablation CT image demonstrates interval placement of a cryoprobe within the pulmonary nodule (*arrow*) with development of an ice ball (*arrowheads*) that encompasses the nodule and adjacent rib. (**d**) Coronal ablation CT image confirms the placement of two cryoprobes within the soft tissue nodule (*arrow*) with formation of an ice ball (*arrowheads*) that encompasses the nodule and rib (*black arrowheads*). Post-procedure the patient reported immediate relief of his left chest wall pain

the patients with resected germ cell tumors having the best overall survival followed by breast and colorectal carcinomas. In addition, patients undergoing pulmonary metastasectomy for a single metastasis enjoy better overall survival outcomes than those with multiple metastases with limited benefit for patients with more than six metastases [4]. Ideally, patients being considered for thermal ablation of pulmonary metastases should demonstrate control of their primary tumor site, a lengthy disease-free interval from the treatment of their primary tumor, limited or no extrapulmonary metastases but if present a feasible management plan should exist for control of these sites, and finally, a controllable or manageable tumor burden, for example six or less metastatic deposits, that can be completely eradicated with ablation.

Contraindications

In general, patients who can undergo an image-guided biopsy could be theoretically considered as candidates for image-guided thermal ablation, and for the most part, lung RFA has few relative and absolute contraindications, acute pneumonia and severe pulmonary arterial hypertension (>40 mmHg) being the most notable latter.

Relative contraindications include poor lung function. An FEV1 >1.0 L is preferred for patients to tolerate pulmonary hemorrhage and notable pleural complications, specifically pneumothorax and/or hemothorax. Other relative contraindications include uncorrectable coagulopathy or pneumonectomy or a single-functioning lung. Pacemaker or pacemaker wires may conduct electrical current produced during RFA and may result in thermal injury to tissue not formally a part of the ablation target or damage to the pacemaker itself. In patients with a pacemaker, RFA can be feasible if pacemaker wires are relatively remote to the area targeted for ablation or if the pacemaker is turned off before the application of radiofrequency energy [42]. With cryoablation, bleeding is a relatively more common complication, and coagulopathies pose greater contraindication than with other ablative techniques.

Procedural Details and Follow-Up

Pre-procedural Evaluation

When considering thermal ablation, pre-procedural evaluation of a patient consists of a directed patient history with particular attention to cardiopulmonary status, bleeding diatheses, concurrent pulmonary infections, and medications. Electrocardiogram(s) and pulmonary function tests should be reviewed, particularly in patients with preexistent lung disease or resection, to assess the adequacy of oxygenation, pulmonary reserve, flow volume spirometry, and the fitness of general anesthesia. Anticoagulant and antiplatelet medications should be discontinued prior to the procedure. Warfarin should be converted to subcutaneous or low molecular weight heparin, which is stopped at least 24 h prior to the procedure. Pre-procedural imaging should include a chest CT scan obtained ideally within 4 weeks of the anticipated procedure to assess amenability of ablation, including tumor size and shape, number of tumors, and locally adjacent vital structures and to aid in the assessment for comorbid disease. Abdominal pelvic CT and/or whole-body F-18 fluorodeoxyglucose positron emission tomography (FDG-PET) should be obtained whenever possible for the detection of extrapulmonary disease, and when in question, histopathologic diagnosis should be obtained and/or confirmed. Coagulation profile and platelet count should be obtained within 7 days of the procedure. If intravenous iodinated contrast is required to delineate vascular structures or tumor margins, a serum creatinine must be obtained beforehand. Periprocedural broad spectrum antibiotics are not universally used.

Anesthesia

Radiofrequency ablation within the chest is largely performed under conscious sedation, to a lesser extent general anesthesia, and on occasion, with little or no anesthesia, and the choice of procedural anesthesia is quite dependent on operator experience, availability, and on patient comorbidities, comfort, and the potential for complications requiring assisted management [43, 44]. Whichever anesthesia is chosen, successful RFA procedures are highly dependent on accurate electrode placement, routinely necessitating a fine balance between controlling pain and maximizing reproducibility of target tumor position. Advantages of general anesthesia include improved airway control, better intra-procedural comfort and immobility, and immediately available cardiopulmonary expertise to help manage potential complications. Disadvantages of general anesthesia include higher cost, increased logistical challenges of involving a second service, longer set-up and procedural times, heightened risk of pneumothorax related to positive pressure ventilation, and the added overall risk of general anesthesia compared with conscious sedation.

Choice of Imaging Modality

Computed tomography is the modality of choice for image-guided placement of electrodes within and around the target tumor within the chest.

CT offers excellent tumor conspicuity, especially when juxtaposed against normally aerated lung, and with newer CT platforms, the ability to quickly acquire volumetric data in rendering multiplanar reformations to accurately portray tumor-electrode relationships. Moreover, CT fluoroscopy and navigational systems [45] may enable real-time or near real-time visualization, respectively, for electrode manipulation and proper placement. Although ultrasound (US) offers real-time imaging capability, its lack of acoustic penetration in the aerated lung handicaps its usefulness as a guidance modality unless the target tumor is embedded within the chest wall or adjacent to the pleura [46] with little or no intervening lung. Magnetic resonance imaging (MRI) has the ability to display good tumor conspicuity and, as a theoretical advantage, thermal ablative changes [47–49]; however, there are no commercially available MR-compatible RF applicators.

Intra-procedural Technique

If possible, preferential positioning of the patient on the CT table should allow the RF electrode to be introduced along a line that represents the shortest distance from the skin to the target tumor. With all factors considered equal, a posterior approach with the patient in the prone position is favorable to the supine position, as the posterior ribs are subject to less respiratory variation. Regardless of position, upper extremity placement should be performed with care to avoid damage to the brachial plexus [50]. A well-developed ablation electrode path should pass over the superior aspect of the rib to avoid injury to the subcostal neurovascular bundle, avoid traversal of bullae or fissures to reduce the risk of pneumothorax, and safely eschew critical intrathoracic structures.

Dispersive, large surface area grounding pads need to be carefully applied over the patient's body avoiding underlying bone prominences, and excess hair should be removed prior to pad placement to facilitate skin adhesion and ensure firm contact. Intermittently during the procedure, the operator should verify that the pads do not peel away from the skin due to excessive sweating, causing undue heat buildup and potential serious skin burn injuries since the electric current is concentrated at the leading edge of the pads [51, 52].

Once the patient is comfortably positioned on the CT table, an intake CT is obtained, and a site of skin entry is marked using a radiopaque marker. Following confirmation, the skin entry site is then prepared with antiseptic solution and draped with sterile towels. Local anesthesia is usually achieved with 1 % lidocaine solution, and a 19 gauge or smaller coaxial needle is carefully guided to the parietal pleura, where a generous amount (5–10 cc) of local anesthetic is administered to achieve pleural anesthesia. The electrode is then positioned into or adjacent to the target tumor usually via tandem needle advancement technique along the tissue tract of the initial localization needle or on occasion through a larger insulated coaxial cannula [44]. Electrodes can be deployable with tines emanating from the tip of the cannula or from the shaft of the cannula proximal to the leading tip (LeVeen-Boston Scientific; Starburst and Talon-Angiodynamics) or non-deployable as straight needles placed as single electrode (Covidien Cool-tip), a mated triple cluster, or individually up to 3 electrodes at a given time. Once the electrode(s) are well positioned and all margins confirmed by CT, radiofrequency energy is applied to attempt to achieve homogeneous coagulation necrosis of the entire tumor with a 1-cm margin of surrounding noncancerous lung (Fig. 37.4).

Parameters determining the endpoint for a given ablation vary for each electrode design [26] but, for the most part, rely on impedance, time, and temperature. With all RFA devices, tissues will inevitably all reach complete desiccation, at which time no further electrical current can be imparted due to extremely high impedances; however, determination of the uniformity of resultant coagulation necrosis can be somewhat challenging. Unfortunately, CT is somewhat limited in its assessment of intra-procedural adequacy of tumor ablation, and to

date, the best inference of the margins of the immediate impart of thermal energy is the development of density attenuating the normal appearance of surrounding aerated lung, better known or referred to as "ground-glass halo." Ideally, ground-glass attenuation should envelop the entire tumor and its margins and should extend at least 5 mm [36], but optimally 10–15 mm, since the area of ground-glass attenuation overestimates the area of true coagulation necrosis by an average of 4.1 mm in animal studies [53].

Once RFA is deemed to be complete, "tract cauterization" (Fig. 37.4) can be performed if bleeding arises, by slowly retracting the electrode at low power to cauterize the parenchyma and pleural tract, theoretically reducing the risk of tumor seeding, hemorrhage, and pneumothorax, although there is no scientific evidence to prove this point. Following removal of the electrode, a post-procedural CT scan is performed to assess for procedural-related complications.

Post-procedural Monitoring and Care

After ablation, patients are recovered and observed within the posttreatment care unit with graduated monitoring of vital signs and oxygenation. For pulmonary ablations, chest radiographs are generally obtained at 2 and 4 h post-procedure but may be acquired less frequently in certain situations, such as ablations within the chest wall. On occasion, if symptomatic, a chest radiograph may be useful at 24 and/or 48 h following the ablation to assess for the development of pleural effusion, parenchymal infiltrates, or delayed or progressive pneumothorax. For suspected blood loss, hemoglobin and hematocrit levels may be necessary. Oral analgesics can manage most post-procedural pain associated with ablation, but on occasion with elevated or escalating pain, patient-controlled analgesia (PCA) pumps or oral narcotics may be required.

With expected clinical course, most patients may be discharged home on the same day of the procedure with close interval follow-up. Nonsteroidal anti-inflammatory medications (NSAIDS), such as ibuprofen, are routinely recommended for 3–5 days to suppress post-procedural inflammation of the pleura, thereby reducing pleuritic pain and the potential for pleural effusion. When the lung has been punctured during the ablation, patients are advised to avoid air travel for at least 3 weeks, as the underpressurized air cabin may lead to the development of a pneumothorax or cause expansion of a preexistent one [54]. If air travel cannot be avoided within the 3-week time frame, a chest radiograph should be obtained prior to the flight to exclude an unsuspected pneumothorax or to confirm resolution of a known pneumothorax.

Complications

Pneumothorax remains the most common complication associated with pulmonary RFA, and to some degree, often minor, is present in almost all treated patients when the lung has been directly or indirectly punctured during the ablation (Fig. 37.6). However, the far majority of post-procedural pneumothoraces can be simply observed or conservatively managed with only 10–20 % of pneumothoraces requiring manual aspiration or thoracostomy or pleural tube placement (Fig. 37.6) [45, 55]. Risk factors implicated with increased rates of pneumothorax include longer length of traversed pulmonary parenchyma, traversal of fissures and emphysematous lung and bullae, greater number of tumors ablated within a single ablation session, increased number of electrode manipulations, use of positive pressure ventilation, and possibly the lack of tract ablation during electrode removal [56].

Collectively referred to as "post-ablative syndrome" (PAS), approximately 40 % of patients may experience a commonly occurring constellation of symptoms after ablation, consisting of low-grade fever, malaise, chills, myalgia, anorexia, and nausea. Thought to be related to the release of burn-mediated cytokines into the systemic circulation, symptoms of varying severity generally ensue within the first 24–48 h following the ablation and typically last 7–14 days and on occasion several weeks [26]. In many patients, a chronic but self-limited cough may

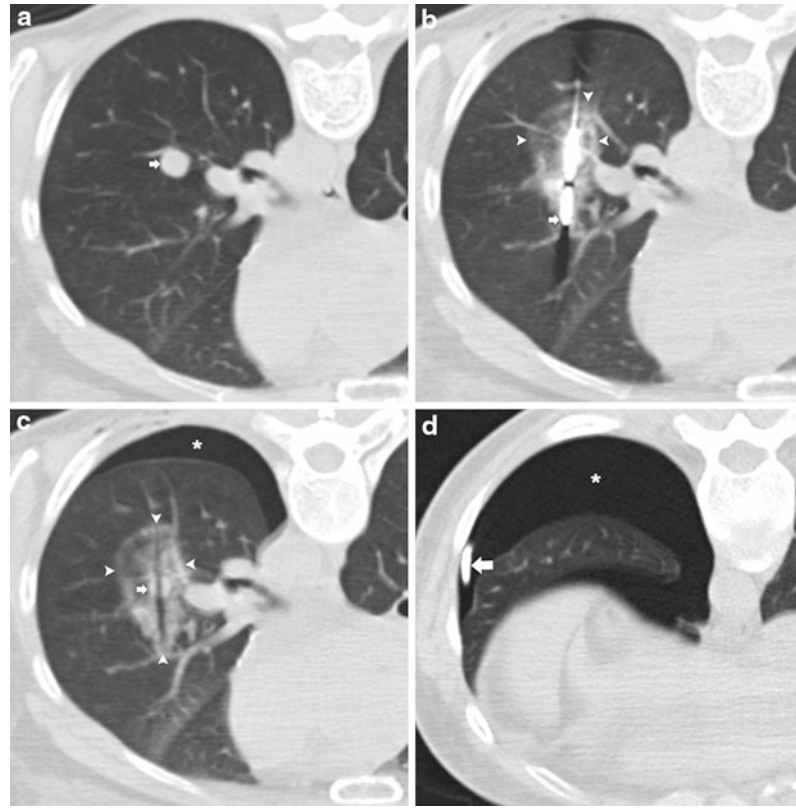

Fig. 37.6 Pneumothorax (**a**) Pre-ablation axial prone CT image shows a right lower lobe adenocarcinoma (*arrow*). (**b**) Ablation axial prone CT image shows interval placement of a single microwave antenna (*arrow*) into the pulmonary nodule with peri-nodule airspace and ground-glass opacity, consistent with the ablation zone (*arrowheads*). (**c**) Post-ablation image following antenna removal demonstrates development of a pneumothorax (*) with increasing airspace and ground-glass opacity (*arrowheads*) surrounding the nodule (*arrow*). (**d**) Repeat post-ablation image demonstrates an enlarging pneumothorax (*), requiring chest tube placement (*arrowhead*)

accompany the symptoms of PAS and is often productive of rust-colored sputum, which represents expectorated necrotic debris from the ablation zone. For PAS and associated cough, management is largely supportive with adequate pain control, antipyretics, antitussives, and antiemetics, as needed.

In approximately 15 % of patients, a gradual pleural effusion may develop after the ablation, primarily due to a sympathetic response to tissue inflammation. In very few instances, however, post-procedural pleural effusions require escalation of care in the form of thoracentesis or thoracostomy tube for symptomatic relief or pleurodesis in that almost all pleural effusions gradually fade by 6 months (Fig. 37.7).

Damage to intercostal or chest wall arteries may result in a hematoma, but more dauntingly, a hemothorax. Hemorrhage into the pleural space can be rapid due to the large potential volume of the recipient hemithorax and further accentuated by the constant negative intrapleural pressure, and not surprisingly, a hemothorax may be fatal if not detected early [44]. Therefore, a rapidly accumulating pleural effusion detected by CT or radiograph during the immediate post-procedural period should warrant expedited clinical evaluation to exclude a potentially lethal hemothorax and to prompt immediate intervention, such as embolization or ligation of the bleeding vessel, if required.

Less common complications include infection, bronchopleural fistula, pulmonary hemorrhage, nerve injury, tumor seeding, and air embolism. Following an ablation, the devitalized tissue of the ablation zone may serve as a nidus for bacterial growth and thus a source for infection, specifically pneumonia or, on occasion, a pulmonary abscess, particularly when the ablated tumor and subsequent ablation zone are quite large [40]. If the ablation zone is adjacent to and/or communicates with the pleural space, an empyema may ensue. However, routine antibiotic prophylaxis remains unsubstantiated.

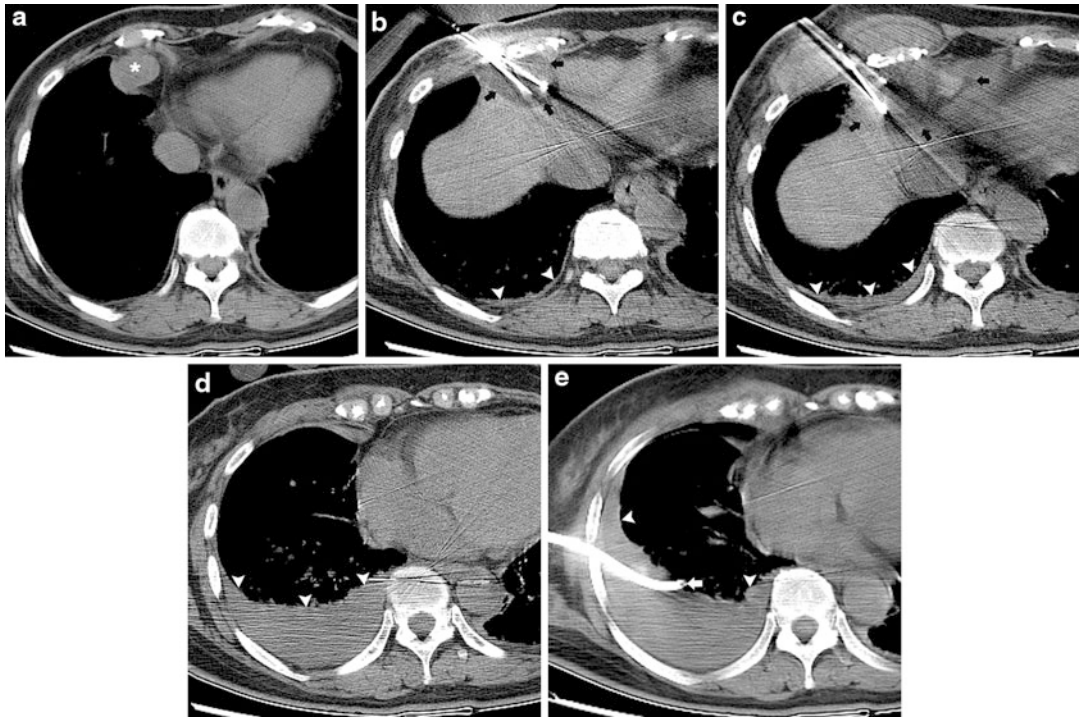

Fig. 37.7 Pleural Effusion (**a**) Supine CT image demonstrates a metastatic right cardiophrenic angle lymph node (*). (**b**) Supine CT image shows interval placement of two cryoablation probes with ice ball formation (*arrows*). There is a trace right pleural effusion (*arrowheads*). (**c**) Soft tissue axial image demonstrates enlargement of the ice ball following repositioning of the medial cryoprobe (*arrows*) with interval enlargement of the right pleural effusion (*arrowheads*). (**d**) Post-cryoablation image demonstrates a large high density effusion, consistent with a hemothorax (*arrowheads*). (**e**) Post-cryoablation image with interval placement of a chest tube (*arrow*) with enlargement of the high density pleural effusion (*arrowheads*)

Bronchopleural fistula has been reported after aggressive ablation and sloughing of the necrotic remnants of a peripheral tumor, resulting in communication between the subtending airway and the pleural space [55] (Fig. 37.8). The reported incidence of intraparenchymal hemorrhage is <1 % [31, 58] and usually results from electrode positioning rather than the ablation itself. Isolated injuries to the brachial plexus, phrenic nerve, recurrent laryngeal nerve, and fibers of sympathetic ganglion have been reported.

Tumor seeding of the ablation tract and pleura has been described in the chest, and although its occurrence is less frequently reported than with hepatic ablation, tract ablation may theoretically further diminish its already low risk, although this has not been scientifically substantiated [56]. Although rare, air embolism related to lung RFA has been reported and is quite different in occurrence, severity, and scope than gas microembolization, which occurs with relatively high frequency as gas micro-emboli created within the ablation bed enter the systemic circulation without sustained neurological deficit or cerebral infarction on both CT and MR [57–60].

Over the course of follow-up after pulmonary ablation, no significant permanent deterioration in pulmonary function, specifically FEV1 and FVC, has been reported in the majority of those patients treated without preexistent lung disease, but more importantly, in those with comorbid lung disease. Although some decline was seen compared to baseline values in the latter group, this has been attributed to progression of underlying chronic lung disease rather than to the after-effects of ablation [61].

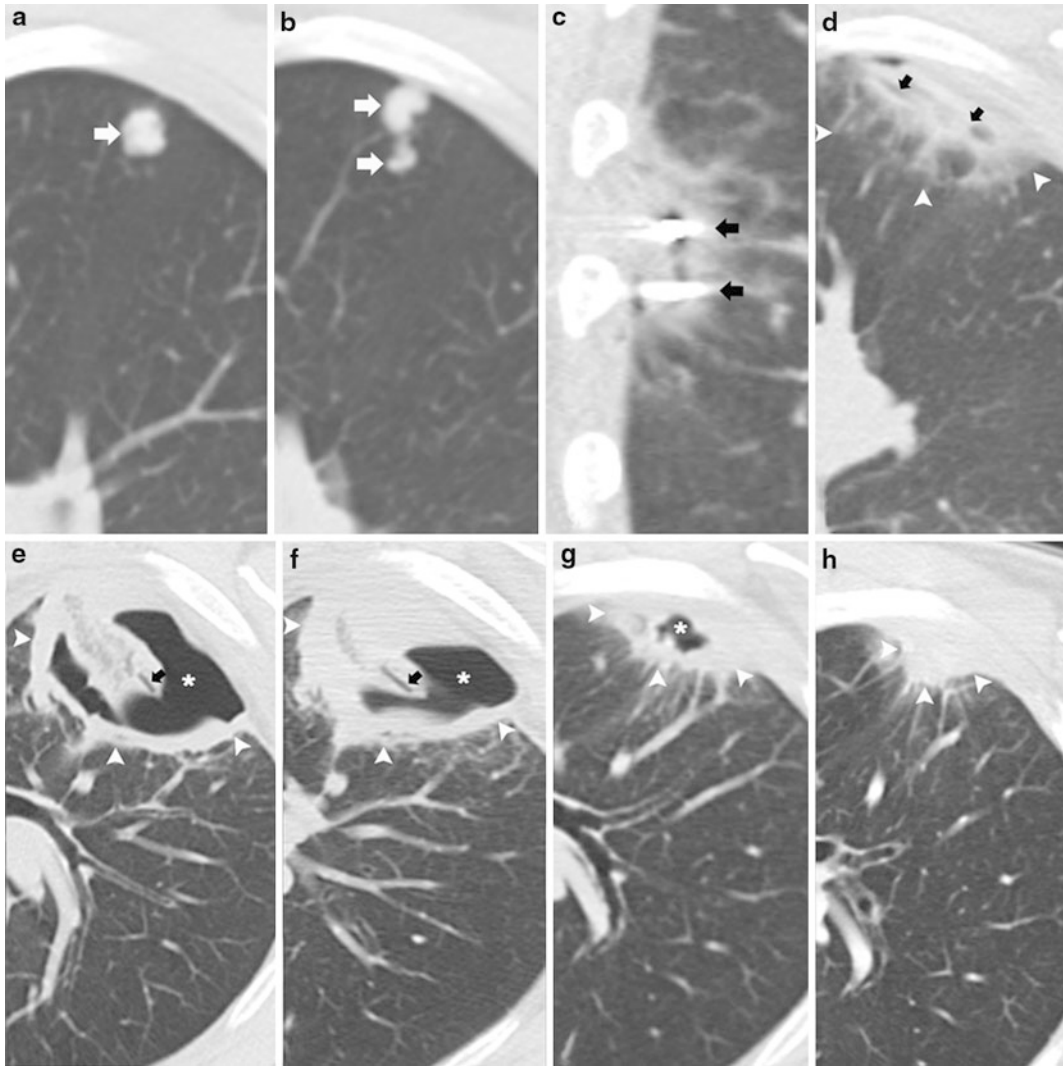

Fig. 37.8 Evolution of the RF ablation zone over 1 year: 55-year-old man with right lower renal cell metastases. (**a** and **b**) Axial CT pre-ablation images demonstrate 3 right lower lobe pulmonary nodules, consistent with biopsy proven renal cell metastases (*arrows*). (**c**) Coronal ablation image confirms placement of two RF electrodes within the pulmonary nodules (*arrows*) with development of surrounding ground-glass opacity, consistent with the ablation zone. (**d**) Immediate post-ablation image demonstrates the electrode tract centrally (*arrows*) with surrounding ground-glass and airspace opacity (*arrowheads*). (**e**) Follow-up image at 1 week demonstrates a heterogeneous ablation zone that is larger than the original nodules with the electrode tract within the central portion of the ablation zone (*arrow*) and development of a localized pneumothorax (*), presumably a contained bronchopleural fistula with surrounding soft tissue rim (*arrowheads*). (**f**) At 3 months, there has been interval decrease in size of the ablation zone with decrease in the localized pleural air (*) but a persistent soft tissue rim (*arrowheads*) and the electrode tract still visualized within the central zone (*arrow*). (**g**) At 6 months, there has been further decrease in size of the ablation zone including the localized pleural air (*) with further retraction of the ablation zone (arrowheads). (**h**) At 12 months, there has been resolution of the localized pleural air with further decrease in size of the ablation zone now seen as a nodular stellate scar (*arrowheads*)

Imaging Follow-Up After Thermal Ablation

Contrast-enhanced CT with nodule or ablation zone densitometry may be utilized pre- and post-ablation in patients with solitary tumors and in whom iodinated contrast is not contraindicated. Originally developed as a method for indeterminate nodule characterization, this technique requires dynamic measurement of tumor enhancement after the administration of a standardized volume of iodinated contrast and can aid in the differentiation between benign and malignant disease based on differences in vascularity and blood flow, those lesions with low likelihood for malignancy when contrast enhancement $\leq$15 Hounsfield Units (HU) and with high likelihood for malignancy when contrast enhancement is vigorous. By using contrast densitometry in the setting of ablation, an additional parameter for subsequent evaluation following treatment is established, especially given that size of the ablation zone is misleading and confounded by profound post-ablative inflammation. In other words, the utility of the test is not to determine benign versus malignant disease, per se, but to establish the maximum degree of contrast enhancement of the original tumor for future reference; in that, the ablation zone should never exceed that of the original tumor after ablative eradication, and if so, suggestive for incomplete ablation and tumor progression (Fig. 37.9). In addition, the radiographic findings, specifically size and contrast enhancement, of the ablation zone demonstrate constant evolution, size generally decreasing following its maximum peak almost immediately after ablation and contrast enhancement markedly diminishing at 1–2 months post-ablation and marginally rising after 3–6 months, although still less than that of the original tumor [43]. Thereafter, contrast enhancement continues to diminish.

In addition to CT, whole-body FDG-PET and, more recently, whole-body CT-PET allows for staging, surveillance for extrapulmonary metastatic and/or recurrent disease, and evaluation of therapeutic response, and in cases where CT imaging results of the ablation zone are ambiguous, FDG-PET and CT-PET may be used as a second-line modality to provide necessary clarity. FDG-PET performed 6 months after ablation may provide valuable assessment of ablation adequacy, and many authors advocate the use of PET in conjunction with CT to optimize correlation between metabolic function and spatial resolution, respectively. Peripheral, or ring-shaped, hypermetabolism at the edge of the ablation zone beyond the margin of the initial tumor can be expected immediately following the ablation with standardized uptake value (SUV) peaking by 2 weeks and continually declining to blood pool levels by 3 months, but this may last even up to 6 months. Significant metabolic activity beyond 3 months, residual activity centrally at the region of ablated tumor, or development of nodular activity is suggestive of incomplete ablation. Additionally, a less than 60 % reduction of FDG uptake at 2 months relative to baseline may be predictive for tumor progression on follow-up CT at 6 months [62]. The role of FDG-PET in primary versus metastatic lung tumors has yet to be completely established.

Although a regimen for follow-up of the ablated tumor has not been standardized or universally accepted, the most prudent algorithm requires a combination of chest CT and whole-body CT-PET with initial post-ablation CT-PET at 2 months, followed by chest CT at 4 months. From then, whole-body CT-PET occur at 6 and 12 months and at 6-month intervals beyond the first year after ablation, alternating with chest CT at 9 months and at 6-month intervals beyond the first year (Fig. 37.10). In metastatic colorectal carcinoma to the lung treated by ablation, therapeutic response has been monitored with carcinoembryonic antigen (CEA), if elevated prior to ablation.

Although the MRI appearance of the ablation zone has been described in both rabbit and porcine lung and in limited human case series, MRI at this time is not in general clinical use as routine imaging assessment of the post-ablation zone, primarily due to poor visualization of lung parenchyma, high cost, and limited availability.

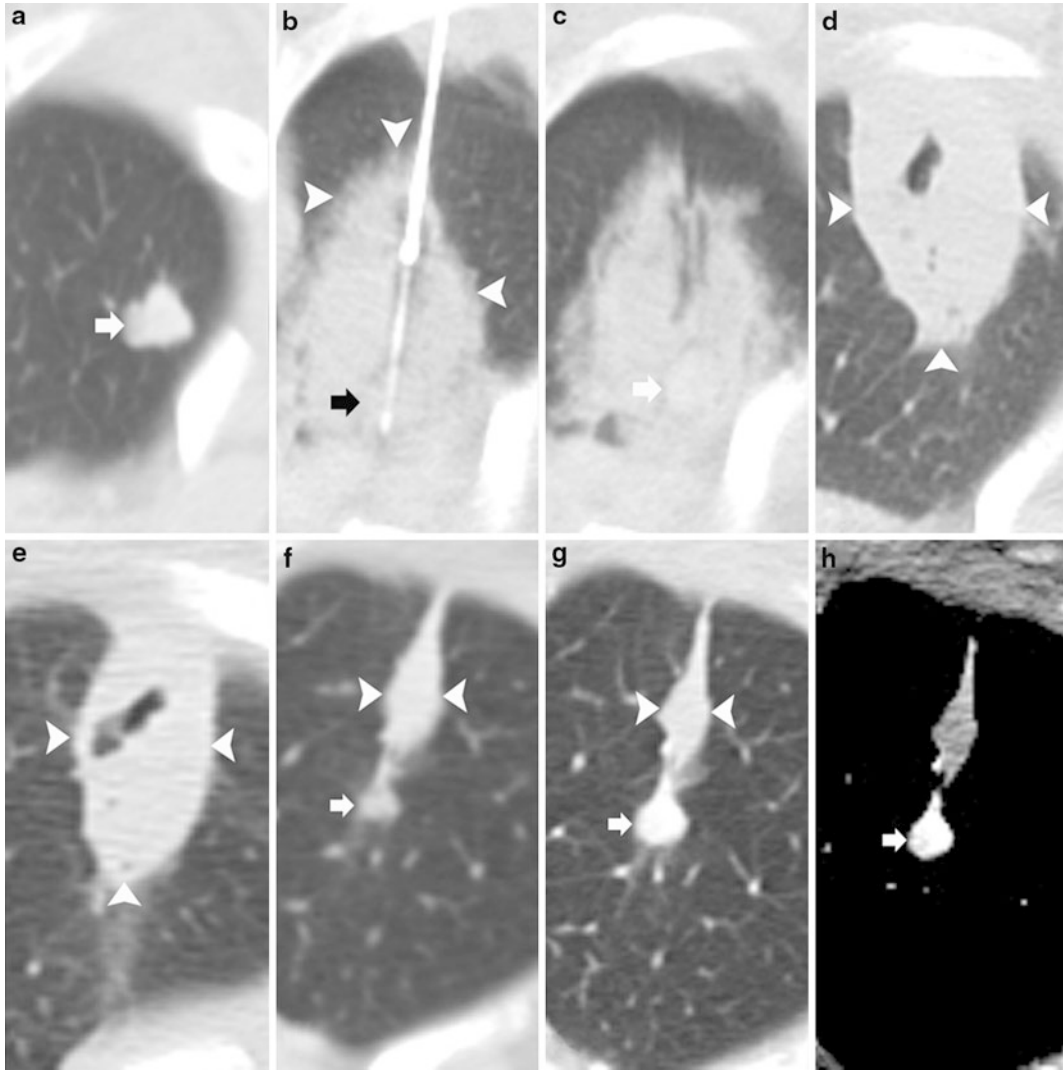

Fig. 37.9 Follow-up tumor recurrence: 65-year-old man with a right upper lobe renal cell metastasis. (**a**) Baseline supine axial CT image demonstrates a right upper lobe pulmonary nodule, consistent with renal cell metastasis. (**b**) Prone ablation CT image demonstrates interval placement of a cryoablation probe within the nodule (*arrow*) with development of surrounding peri-nodule hemorrhage (*arrowheads*). (**c**) Immediate post-ablation image demonstrates the nodule (*arrow*) with surrounding peri-nodule hemorrhage, consistent with the ablation zone. (**d**) Supine post-ablation 1-month follow-up image demonstrates a soft tissue mass (*arrowheads*) larger than the original nodule with central cavitation. (**e**) Supine post-ablation 3-month follow-up image demonstrates interval decrease in size of the ablation zone (*arrowheads*) with persistent central cavitation. (**f**) Supine post-ablation 6-month follow-up demonstrates further decrease in size of the ablation zone now seen as a linear scar (*arrowheads*) with interval development of a nodular component at the anterior aspect (*arrow*), concerning for recurrence. (**g**) Supine post-ablation 9-month follow-up demonstrates further decrease in size of the linear scar (*arrowheads*) with interval enlargement of the nodule at the anterior aspect of the scar (*arrow*). (**h**) Supine post-ablation 9-month follow-up status post intravenous contrast administration shows enhancement within the nodule (*arrow*), consistent with recurrence

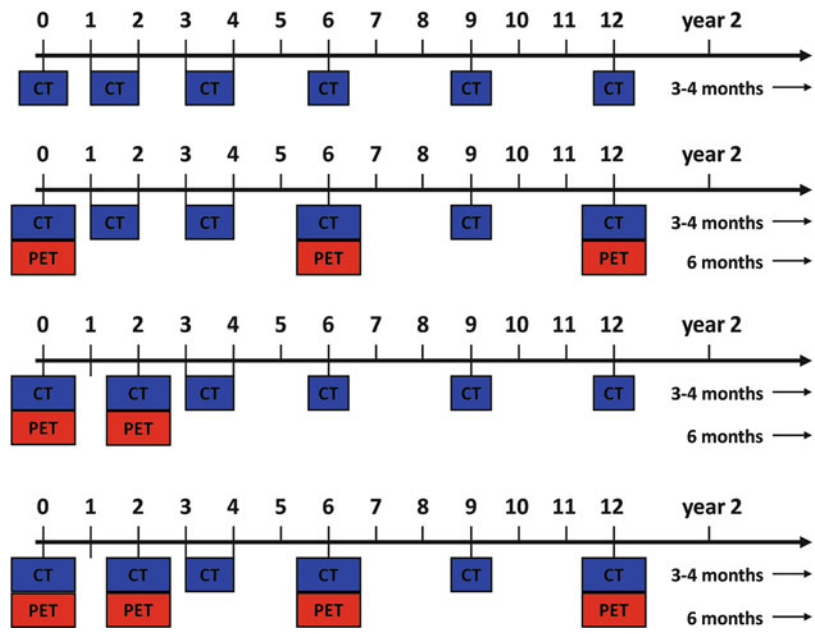

Fig. 37.10 Follow-up imaging algorithm: timetables for follow-up may have a number of different appearances utilizing CT alone or in combination with CT-PET

More recently, MRI diffusion-weighted imaging (DWI) has shown promise with apparent diffusion coefficient (ADC) mapping showing significantly higher values in ablation zones without local progression compared to those with local progression after RFA, and thus, suggesting that the ADC may be predictive of RFA response [63].

Results Following Thermal Ablation

Radiofrequency Ablation

Much of our experience and long-term data with thermal ablation has been with RFA. Patients with stage 1A or 1B NSCLC have a potential for cure with better survival associated with those patients with smaller baseline tumors, which carry the theoretical advantage of better achieving complete necrosis. Simon et al. reported median survival for stage 1 NSCLC at 29 months and 1-, 2-, 3-, 4-, and 5-year survival rates at 75 %, 57 %, 36 %, 27 %, and 27 %, respectively, in medically inoperable patients. Reemphasizing the importance of initial tumor size, 1-, 2-, 3-, 4-, and 5-year survival rates were significantly better for those patients with tumors $\leq$3 cm at 83 %, 64 %, 57 %, 47 %, and 47 %, respectively [64].

Although a number of factors influencing survival and local control in those patients undergoing RFA in the setting of pulmonary metastatic disease have been cited following univariate analyses, multivariate scrutiny identifies very few independent factors of significance. Significant independent factors that are associated with improved short, intermediate, and long-term survival are baseline tumor size $\leq$3 cm [67], the absence of extrapulmonary metastases at the time of ablation [65], single metastasis [66], normal CEA prior to therapy [66], prolonged disease-free interval between primary therapy and the development of first metastases [67], and initial complete response to ablation [67]. In a similar vein, significant independent factors that determine enhanced local control include smaller tumor size ($\leq$1.5–3.5 cm) and lack of contact with an adjacent or subtending bronchus >2 mm [68]. Common to both improved survival and enhanced local control groups, initial tumor size is the main and most important determinant for better prognosis, those patients ablated with smaller tumors demonstrating significantly better results in virtually all measured categories than

those with larger tumors. Simon et al. reported a median time to local tumor progression of 45 months for tumors ≤3 cm in diameter, compared to 12 months for tumors >3 cm [64]. Yamakado et al. reported local tumor progression in metastatic disease following ablation to be 11 % in patients with metastasis ≤3 cm, compared to 50 % in patients with metastases >3–6 cm [65]. Survival data from these two studies reported the following survival rates in ablating colorectal carcinoma metastases: 1-, 2-, and 3-year at 84 %, 64 %, and 46 % [65], and 1-, 2-, 3-, 4-, and 5-year at 87 %, 78 %, 57 %, 57 %, and 57 % [64]. The relationship between RFA and adjunctive chemotherapy is largely unclear. However, Inoue et al. demonstrated a significant difference in survival between those patients with colorectal carcinoma receiving chemotherapy alone and in those receiving chemotherapy and RFA at 33 % and 88 %, respectively, at 3 years [69]. More recently, Chua et al. identified adjuvant chemotherapy as a significant independent factor for improved survival [70].

Cryoablation

Intermediate and long-term data is not available for cryoablation; however, some initial longitudinal data have been published. Initial experience in over 200 patients treated with cryoablation, Wang et al. showed that the general health status as measured by the Karnofsky Performance Scale had significantly improved at 1 week after treatment [29]. Cryoablation has also been shown to be effective means of local metastatic disease control with a 1-year survival rate of 89.4 % at published by Kawamura et al. [73]. In 2010, Zemlyak et al. published that the 3-year survival for the subtotal lung resection, radiofrequency ablation, and cryoablation for high-risk patients with stage I NSCLC and was 87.1 %, 87.5 %, and 77 %, respectively [74].

Microwave Ablation

In 2008, Wolf et al. who reported overall 1-, 2-, and 3-year survival at 65 %, 55 %, and 45 %, respectively, and 1-, 2-, and 3-year cancer-specific survival at 83 %, 73 %, and 61 %, respectively [32]. Residual enhancing tumor was more commonly found at follow-up of treated tumors larger than 3 cm; however, no significant relationship between initial tumor size and patient survival was established. Theoretical advantages of microwave ablation over other heat-based modalities included the faster and larger volume of tissue heating with a given applicator. With higher heat potential with microwave energy, effects of heat-sink effects may be reduced and larger tumor volumes could be ablated. Results from Brace et al. in a preclinical model suggest that microwave energy, compared with RF energy, is a more effective means of ablation in the lung [75]; however, randomized prospective comparative studies would be needed to validate these suggestions.

Laser Ablation

As of this printing, very few long-term studies regarding laser ablation have been published, most recently in 2009, in which Rosenberg et al. reporting 5-year experience in a total 120 percutaneous procedures to manage 108 lung metastases of different primaries. With a median tumor size of 2.0 cm, 1-, 2-, 3-, 4-, and 5-year survival 81 %, 59 %, 44 %, 44 %, and 27 %, respectively. The median progression-free interval was 7.4 months [30]. In addition, Vogl et al. reported both RFA and laser ablation being robust modalities for treating lung metastasis with 6-month local tumor control rates of 85 % with RFA and 91 % with laser ablation [76].

Future Directions

In part, due to the current limitations of treating patients with larger tumors, future exploration in ablation must address improving the currently available thermal technologies for larger and more efficient energy delivery and reliability, new ablative technologies such irreversible electroporation, image guidance and navigation, intra-ablative tissue monitoring, modalities and

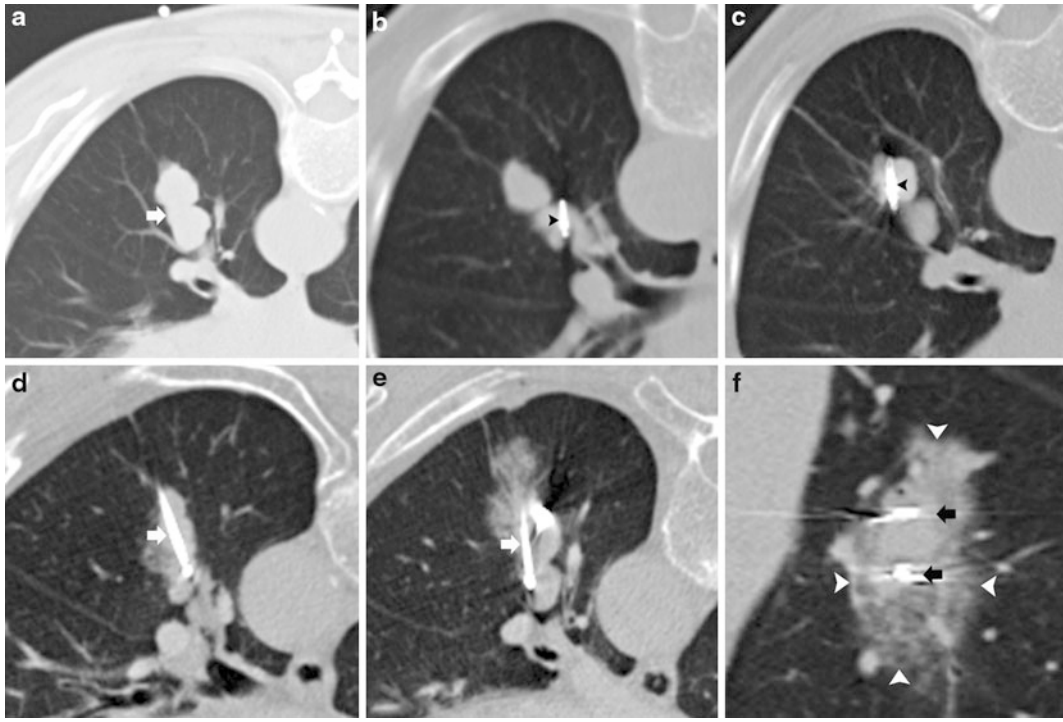

Figure 37.11 Combined radiotherapy and RF ablation for right lower lobe colorectal metastases: (**a**) Prone axial CT image demonstrates two right lower lobe nodules (*white arrow*). (**b**) Interval placement of a fiducial marker in the superior and medial pulmonary nodule (*arrowhead*) for stereotacic radiotherapy. (**c**) Interval placement of a fiducial marker in the inferior and lateral pulmonary nodule (*arrowhead*) for stereotactic radiotherapy. (**d**) Post-radiotherapy CT image shows interval placement of a single radiofrequency electrode in the superior aspect of the right lower lobe metastasis (*arrow*). (**e**) Post-radiotherapy CT image shows interval placement of a single radiofrequency electrode in the inferior aspect of the right lower lobe metastasis (*arrow*). (**f**) Post-ablation coronal image confirms the location of the two electrodes within the right lower metastasis with interval development of surrounding ground glass, consistent with the ablation zone (*arrowheads*)

methods for imaging follow-up, and potential complementary and synergistic combination of therapies, specifically adjuvant chemotherapy, biopharmacologic agents, immunomodulation, and combined thermoablative techniques and radiotherapy (Fig. 37.11), including standard external beam, stereotactic body and brachytherapy as discussed in Chap. 38, "Role of Combination Therapies in the Treatment of Non-small Cell Lung Cancer and Thoracic Metastasis."

Summary

Radiofrequency ablation is clearly safe and technically highly successful in terms of initial ablation, and most complications are readily treatable. Long-term local control or complete necrosis rates drop considerably when tumors are larger than 3 cm, although repeat ablations can be performed. The results regarding RFA are comparable to other therapies currently available, particularly for the conventionally unresectable or high-risk lung cancer population. Multicenter prospective trials are needed, with more homogeneous and standardized patient populations to gauge true local control rates, the role for cytoreduction, and the occurrence of distant nodal or extrathoracic disease when faced with pre-procedural staging with imaging modalities alone, particularly in the high-risk comorbid cardiopulmonary disease group that may be most appropriate for RFA. Trials with adjunctive therapies such as chemotherapy, biopharmacologic

agents, and/or radiotherapy can also be envisioned. With refinements in technology, patient selection, clinical applications, and methods of follow-up, percutaneous thermal ablation will continue to flourish as a potentially viable stand-alone or complementary therapy for both primary and secondary thoracic malignancies in both standard and high-risk populations.

References

1. American Cancer Society, Cancer Facts and Figures. 2010. www.cancer.org.
2. Jemal A, Taylor M, Ward E, et al. Cancer statistics 2005. CA Cancer J Clin. 2005; Jan-Feb;55:10–30. Erratum in: CA Cancer J Clin. 2005 Jul-Aug;55:259.
3. Willis RA. Secondary tumours of the lung. In: Willa RA, editor. The spread of tumours in the human body. London: Butterworths; 1973. p. 167–74.
4. Figlin RA, Holmes EC, Turrisi AT, et al. Neoplasms of the lung, pleura, and mediastinum. In: Haskell CM, editor. Cancer treatment. 4th ed. Philadelphia: WB Saunders; 1995. p. 385–413.
5. Pass HI, Donington JS. Metastatic cancer of the lung. In: DeVita Jr VT, Hellman S, Rosenberg SA, editors. Cancer: principles and practice of oncology. Philadelphia: Lippincott-Raven; 1997. p. 2536–51.
6. Zierhut D, Bettscheider C, Schubert K, et al. Radiation therapy of stage I and II non-small cell lung cancer. Lung Cancer. 2001;34:39–43.
7. Spira A, Ettinger DS. Multidisciplinary management of lung cancer. N Engl J Med. 2004;350:379–92.
8. Mountain CF. Revisions in the international system for staging lung cancer. Chest. 1997;111:1710–7.
9. Mountain CF. A new international staging system for lung cancer. Chest. 1986;89(suppl):225S–33.
10. Schiller JH, Harrington D, Belani CP, et al. Comparison of four chemotherapy regimens for advanced non-small-cell lung cancer. N Engl J Med. 2002; 346(2):92–8.
11. Ginsberg RJ, Port JL. Surgical therapy of stage I, and non-T3 NO stage II non-small lung cancer. In: Pass H, Mitchell JB, Johnson DH, editors. Lung cancer: principles and practice of oncology. 2nd ed. Philadelphia: Lippincott Williams & Wilkins; 2000. p. 682–93.
12. Ihde DC, Pass HI, Glatstein E. Small cell lung cancer. In: DeVita Jr VT, Hellman S, Rosenber SA, editors. Cancer: principles and practice of oncology. 5th ed. Philadelphia: Lippincott-Raven; 1997. p. 911–49.
13. Deslauriers J. Current surgical treatment of nonsmall cell lung cancer 2001. Eur Respir J. 2002;19(suppl): 61S–70.
14. Lung. In: American joint committee on cancer: AJCC cancer staging manual. 7th ed. New York: Springer; 2009. p 253–70.
15. Ginsberg RJ, Rubinstein LV, Lung Cancer Study Group. Randomized trial of lobectomy versus limited resection for T1 N0 nonsmall cell lung cancer. Ann Thorac Surg. 1995;60:615–23.
16. McGarry RC, et al. Observation-only management of early stage, medically inoperable lung cancer: poor outcome. Chest. 2002;121:1155–8.
17. Boring CC, Squires TS, Tong T, Montgomery S. Cancer statistics, 1994. CA Cancer J Clin. 1994;44:7–26.
18. Morgan-Parkes JH. Metastases: mechanisms, pathways, and cascades. AJR Am J Roentgenol. 1995; 164:1075–82.
19. Chen PW, Pass HI. Indications for resection of pulmonary metastases. In: Baue AE, Stanford CT, editors. Glenn's thoracic and cardiovascular surgery. 6th ed. Stanford: Appleton & Lange; 1996. p. 499–510.
20. Landreneau RJ, De Giacomo T, Mack MJ, et al. Therapeutic video-assisted thoracoscopic surgical resection of colorectal pulmonary metastases. Eur J Cardiothorac Surg. 2000;18:671–7.
21. Goldberg SN, et al. Image-guided tumor ablation: proposal for standardization of terms and reporting criteria. Radiology. 2003;228:335–54.
22. Goldberg SN, Dupuy DE. Image-guided radiofrequency tumor ablation: challenges and opportunities–part I. J Vasc Interv Radiol. 2001;12: 1021–32.
23. Mountain CF, McMurtrey MJ, Hermes KE. Surgery for pulmonary metastasis: a 20-year experience. Ann Thorac Surg. 1984;38:323–30.
24. Goldberg SN, Gazelle GS, Mueller PR. Thermal ablation therapy for foal malignancy: a unified approach to underlying principles, techniques and diagnostic imaging guidance. AJR Am J Roentgentol. 2000;174:323–31.
25. Goldberg SN, Gazell GS, Compton CC, et al. Radiofrequency tissue ablation of VX2 tumor nodules in the rabbit lung. Acad Radiol. 1996;3:929–35.
26. Rose SC, Thistlethwaite PA, Sewell PE, et al. Lung cancer and radiofrequency ablation. J Vasc Interv Radiol. 2006;17:927–51.
27. Simon CJ, Dupuy DE, Mayo-Smith WW. Microwave ablation: principles and applications. Radiographics. 2005;25:s69–83.
28. Kawamura M, Izumi Y, Tsukada N, Asakura K, Sugiura H, et al. Percutaneous cryoablation of small pulmonary tumors under computed tomographic guidance with local anesthesia for nonsurgical candidates. J Thorac Cardiol Surg. 2006;131:1007–13.
29. Wang H, Littrup P, Duan Y, et al. Thoracic masses treated with percutaneous cryotherapy: initial experience with more than 200 procedures. Radiology. 2005;235:289–98.
30. Rosenberg C, et al. Laser ablation of metastatic lesions of the lung: long-term outcome. Am J Roentegenol. 2009;192:785–92.
31. Vogl TJ, Mack MG, Nabil M. Laser induced thermotherapy in lung metastases. In: Vogl TJ, Helmberger TK, Mack MG, Reiser MF, editors.

Percutaneous tumor ablation in medical radiology. 1st ed. Berlin/Heidelberg: Springer; 2008. p. 197–205.
32. Wolf FJ, Grand DJ, Machan JT, Dipetrillo TA, Mayo-Smith WW, Dupuy DE. Microwave ablation of lung malignancies: effectiveness, CT findings, and safety in 50 patients. Radiology. 2008;247(3):871–9.
33. Knappe V, Mol A. Laser therapy of the lung: biophysical background. Radiology. 2004;44:677–83.
34. Gofrit ON, Shapiro A, Pode D, et al. Combined local bladder hyperthermia and intravesical chemotherapy for the treatment of high-grade superficial bladder cancer. Urology. 2004;63(3):466–71.
35. Weigel C, Rosenberg C, Langner S, et al. Laser ablation of lung metastases: resultsaccording to diameter and location. Eur Radiol. 2006;16:1769–78.
36. Lee JM, Jin GY, Goldberg SN, et al. Percutaneous radiofrequency ablation for inoperable non-small cell lung cancer and metastases: preliminary report. Radiology. 2004;230:125–34.
37. Abtin F, Wu C, Golshan A, Suh R. CT guided percutaneous cryoablation of thoracic tumors: technical feasibility, early efficacy and imaging of 27 treated tumors. Scientific session 8, #713, 2nd World congress of thoracic imaging and siagnosis in chest disease. Valencia May 30–June 2, 2009.
38. Steinke K, Haghighi KS, Wulf S, Morris DL. Effect of vessel diameter on the creation of ovine lung radiofrequency lesions in vivo: preliminary results. J Surg Res. 2005;124(1):85–91.
39. Akeboshi M, Yamakado K, Nakatsuka A, et al. Percutaneous radiofrequency ablation of lung neoplasms: initial therapeutic response. J Vasc Interv Radiol. 2004;15:463–70.
40. Grieco CA, Simon CJ, Mayo-Smith WW, DiPetrillo TA, Ready NE, Dupuy DE. Percutaneous image-guided thermal ablation and radiation therapy: outcomes of combined treatment for 41 patients with inoperable stage I/II non-small cell lung cancer. J Vasc Interv Radiol. 2006;17:1117–24.
41. Oshima F, Yamakado K, Akeboshi M, et al. Lung radiofrequency ablation with and without bronchial occlusion: experimental study in porcine lungs. J Vasc Interv Radiol. 2004;15(12):1451–6.
42. Skonieczki BD, Wells C, Wasser EJ, Dupuy DE. Radiofrequency and microwave tumor ablation in patient with implanted cardiac devices: is it safe? Eur J Radiol. April 2010 (epub ahead of print).
43. Suh RD, Wallace AB, Sheehan RE, Heinze SB, Goldin JG. Unresectable pulmonary malignancies: CT-guided percutaneous radiofrequency ablation – preliminary results. Radiology. 2003;229: 821–9.
44. Liao WY, Chen MZ, Chang YL, et al. US-guided transthoracic cutting biopsy for peripheral thoracic lesions less than 3 cm in diameter. Radiology. 2000;217:685–91.
45. Wacker FK, Reither K, Ritz JP, et al. MR-guided interstitial laser-induced thermotherapy of hepatic metastasis combined with arterial blood flow reduction: technique and first clinical results in an open MR system. J Magn Reson Imaging. 2001;13:31–6.
46. Vogl TJ, Struab R, Eichler K, et al. Malignant liver tumors treated with MR imaging-guided laser-induced thermotherapy: experience with complication in 899 patients (2,520 lesions). Radiology. 2002;225:367–77.
47. Silverman SG, Sun MR, Tuncali K, et al. Three-dimensional assessment of MRI-guided percutaneous cryotherapy of liver metastases. AJR Am J Roentgenol. 2004;183:707–12.
48. Shankar S, van Sonnenberg E, Silverman SG, et al. Brachial plexus injury from CT-guided RF ablation under general anesthesia. Cardiovasc Intervent Radiol. 2005;28:646–8.
49. Arata MA, Nisenbaum HL, Clark TW, et al. Percutaneous radiofrequency ablation of liver tumors with the LeVeen probe: is roll-off predictive of response? J Vasc Interv Radiol. 2001;12:455–8.
50. Goldberg SN, Solbiati L, Halpern EF, et al. Variables affecting proper system grounding for radiofrequency ablation in an animal model. J Vasc Interv Radiol. 2000;11:169–1075.
51. Yamamoto A, Nakamura K, et al. Radiofrequency ablation in a porcine lung model: correlation between CT and histopathologic findings. Am J Roentgenol. 2005;185:1299–306.
52. Aerospace Medical Association Medical Guidelines Task Force. Medical Guidelines for Airline Travel, 2nd edition. Aviat Space Environ Med. 2003;74(5): A1–19.
53. Simon CJ, Dupuy DE, Dipetrillo TA, et al. Pulmonary radiofrequency ablation: long-term safety and efficacy in 153 Patients. Radiology. 2007;243:268–78.
54. Hiraki T, Tajiri N, et al. Pneumothorax, pleural effusion, and chest tube placement after rf ablation of lung tumors: incidence and risk factors. Radiology. 2006;241:275–83.
55. Sakurai J, Hiraki T, Mukai T. Intractable pneumothorax due to bronchopleural fistula after radiofrequency ablation of lung tumors. J Vasc Interv Radiol. 2007;18(1 Pt 1):141–5.
56. Yamakado A, Nakatsuka A, et al. Tumor seeding following lung radiofrequency ablation: a case report. Cardiovasc Intervent Radiol. 2005;28:530–2.
57. Rose SC, Foothill M, Levin DL, Harrell JH. Cerebral microembolization during radiofrequency ablation of lung malignancies. J Vasc Interv Radiol. 2002;13: 1051–4.
58. Dupuy DE, Mayo-Smith WW, Abott GF, et al. Clinical applications of radio-frequency tumor ablation in the thorax. Radiographics. 2002;22:259–69.
59. Yamamoto A, Matsuoka T, Toyoshima M, et al. Assessment of cerebral microembolism during percutaneous radiofrequency ablation of lung tumors using diffusion-weighted Imaging. AJR Am J Roentgenol. 2004;183:1785–9.
60. Ahrar K, Stafford RJ, Tinkey PT, et al. Evaluation of cerebral microemboli during radiofrequency ablation

of lung tumors in a canine model with use of impedance-controlled devices. J Vasc Interv Radiol. 2007; 18(7):929–35.
61. Lencioni R. CC07c – Debate: lung cancer will always remain a surgery first disease versus radiofrequency ablation will shrink the role of surgery more than you know. Society of Interventional Radiology 32nd Annual Scientific Meeting, Seattle, March 3, 2007.
62. Okuma T, Okamura T, et al. Fluorine-18-fluorodeoxyglucose positron emission tomography for assessment of patients with unresectable recurrent or metastatic lung cancers after CT-guided radiofrequency ablation: preliminary results. Ann Nucl Med. 2006;20(2):115–21.
63. Okuma T, Matsuoka T, et al. Assessment of early treatment response after CT-guided radiofrequency ablation of unresectable lung tumours by diffusion-weighted MRI: a pilot study. Br J Radiol. 2009;82: 989–94.
64. Yamakado K, Hase S, Matsuoka T, et al. Radiofrequency ablation for the treatment of unresectable lung metastasis in patients with colorectal cancer: a multicenter study in Japan. J Vasc Interv Radiol. 2007;18:393–8.
65. Yamakado K, Inoue Y, et al. Long-term results of radiofrequency ablation in colorectal lung metastases: single center experience. Oncol Rep. 2009;22:885–91.
66. Suh R, Reckamp K, Zeidler M, Cameron R. Radiofrequency ablation in lung cancer: promising results in safety and efficacy. Oncology. 2005; 19(11):1–10.
67. Chua TC, Sarkar A, Saxena A, Glenn D, Zhao J, Morris DL. Long-term outcome of image-guided percutaneous radiofrequency ablation of lung metastases: an open-labeled prospective trial of 148 patients. Ann Oncol. 2010;21(10):2017–22. Epub 2010 Mar 24.
68. Sakurai J, Hiraki T, et al. Radiofrequency ablation of small lung metastases by a single application of a 2-cm expandable electrode: determination of favorable responders. J Vasc Interv Radiol. 2010;21:281–6.
69. Inoue Y, Tanaka K, et al. Improved survival using multi-modality therapy in patients with lung metastases from colorectal cancer: a preliminary study. Oncol Rep. 2005;14:1571–6.
70. Chua TC, Thornbury K, et al. Radiofrequency ablation as an adjunct to systemic chemotherapy for colorectal pulmonary metastases. Cancer. 2010;116(9):2106–14.
71. Davalos R, Mir IL, Rubinsky B. Tissue ablation with irreversible electroporation. Ann Biomed Eng. 2005;33:223–31.
72. Detterbeck FC, Botta DJ, Tanoue LT. The new lung cancer staging system. Chest. 2009;136(1):260–71.
73. Kawamura M, Izumi Y, Tsukada N, et al. Percutaneous cryoablation of small pulmonary malignant tumors under computed tomographic guidance with local anesthesia for nonsurgical candidates. J Thorac Cardiovasc Surg. 2006;131:1007–13.
74. Zemlyak A, Moore WH, Bilfinger TV. Comparison of survival after sublobar resections and ablative therapies for stage I non-small cell lung cancer. J Am Coll Surg. 2010;211(1):68–72.
75. Brace C, Hinshaw JL, Laesee PF, Sampson LA, Lee FT. Pulmonary thermal ablation: comparison of radiofrequency and microwave devices by using gross pathologic and CT findings in a swine model. Radiology. 2009;251:705–71.
76. Vogl TJ, Straub R, Lehnert T, et al. Percutaneous thermoablation of pulmonary metastases. Experience with the application of laser-induced thermotherapy (LITT) and radiofrequency ablation (RFA) and a literature review. ROFO. 2004;176:1658–66.

Role of Combination Therapies in the Treatment of Non-small Cell Lung Cancer and Thoracic Metastasis

38

Subarna Hamid Eisaman and Damian E. Dupuy

Abstract

Lung cancer is the most common cancer worldwide, accounting for 1.3 million deaths annually. It is also a disease of the elderly, with 81 % of those living with lung cancer being ≥60 years of age, making them poor surgical candidates. Various alternative combined modalities are being investigated including limited resection with brachytherapy, RFA with conventional RT, and RFA with SBRT. This chapter reviews the basic principles underlying these promising combination therapies.

Introduction

It is estimated that in the United States alone, 219,440 men and women will be diagnosed with cancer of the lung and bronchus in 2009. Furthermore, per the 2002–2006 SEER Cancer Statistics, a staggering 81.5 % of those diagnosed were within the 55–84-year-old age-group [1]. It is not surprising that this age-group has over 75 % prevalence of cardiovascular disease (NHANES 2003–2006) [2], making them poor candidates for potentially curative surgical interventions. The largest body of data for the treatment of lung cancers exists for the traditional options of surgery, conventional radiation therapy (RT), and recently chemotherapy. These modalities have been used in various combinations for local, regional, and metastatic disease. However, even with utilization of the best current therapies, the overall 5-year relative survival rate for 1999–2005 from 17 SEER geographic areas was only 15.6 % [1]. Briefly summarizing the combination treatment trends in early, locally advanced, and metastatic non-small cell lung cancers (NSCLC):

S. Hamid Eisaman (✉)
Department of Radiation Oncology, University of Pittsburgh Medical Center- Regional Cancer Center, Johnstown, PA, USA
e-mail: eisamansh@upmc.edu

D.E. Dupuy
Department of Diagnostic Imaging, Rhode Island Hospital, The Warren Alpert Medical School of Brown University, Providence, RI, USA
e-mail: DDupuy@lifespan.org

Early NSCLC

Although only around 15 % [1] of lung cancers are diagnosed at the "early" stage (usually implying AJCC stages IA, B, and IIA), these are the subsets of patients most likely to be cured. Hence, a large part of the efforts have been concentrated on this group. Multiple randomized

D.E. Dupuy et al. (eds.), *Image-Guided Cancer Therapy*, DOI 10.1007/978-1-4419-0751-6_40,

prospective trials including the North American Lung Cancer Study Group 821 trial [3] showed that the best recurrence-free survival and overall survival is with surgery – specifically lobectomy rather than limited resections. They reported overall survival of 61 % versus 70 % ($p = 0.09$ in one-sided test with $p < 0.1$) and locoregional recurrence of 17 % versus 6 % for limited resection versus lobectomy, respectively. That established the standard of care for early operable non-small cell lung cancers in general. As the overall survivals were still pretty dismal, different combination treatments were investigated for improvement in survival. Preoperative RT [4, 5] showed no difference in survival. The role of postoperative external-beam radiation therapy (EBRT) is more difficult to interpret due to conflicting data about the benefit of EBRT after surgery [6]. Generally, the addition of EBRT with a small field size may be considered for patients with pN2 disease. There does not appear to be a role of EBRT following surgery patients with pN0 or pN1 [7, 8]. Additionally, not all patients with early-stage NSCLC are medically fit to have a lobectomy secondary to medical comorbidities. In such cases, limited resection in combination with some form of adjuvant RT is a reasonable option. To that end, post-resection brachytherapy and external-beam RT have both been investigated. The CALGB 9335 phase II study [9] concluded that EBRT after limited resection incurred significant pulmonary toxicities (11 % rate of severe dyspnea and 4 % pneumonitis) without notable clinical benefit. However, multiple retrospective analyses for stage I NSCLC showed promising reduction in local recurrence with the combination of limited resection and brachytherapy. Fernando et al. [10] reported a statistically significant decrease in local recurrence rate from 17.2 % without brachytherapy to 3.3 % with combination of brachytherapy with a mean follow-up of 34 months. Currently, a large national prospective randomized trial (ACOSOG Z4032) is under way to investigate limited resection along with brachytherapy to treat early-stage lung cancer.

Locally Advanced NSCLC

Multiple randomized prospective multi-institutional studies [11–14] have been reported with the results of combining surgery with adjuvant chemotherapy and chemoradiation therapy for more advanced stage NSCLC. One such study is the Adjuvant Navelbine International Trialist Association (ANITA) [15] which compared surgery +/− cisplatin and vinorelbine which included patients with stages IB–IIIA (36 % IB, 24 % II, 39 % IIIA) disease. Although they report a significant 5-year overall survival difference between surgery only versus surgery with chemotherapy of 51 % and 43 %, respectively, there was no benefit for stage IB on subgroup analysis (5-year OS 62 % vs. 64 %). Therefore, postoperative chemotherapy alone may be beneficial for more advanced disease, but the final data to date are still unclear.

The other combination that is being investigated includes the addition of chemoradiation following resection for NSCLC. The 2007 CALGB 9734 [16] ($n = 44$) compared surgical resection and paclitaxel/carboplatin chemotherapy with or without adjuvant radiation therapy for resected stage III NSCLC. There was no significant difference in disease-free survival or overall survival. The INT 0115 [17] trial came to the same conclusion. Therefore, the use of combination chemoradiation therapy following surgery for locally advanced NSCL cancer also remains investigational.

Metastatic Disease

Seventy-five percent of lung and bronchus cancers are diagnosed with regional or distant disease [18] – both of which can involve painful direct invasion or metastasis into the chest wall. Although radiation therapy is considered the standard for malignant bone pain, maximal response is achieved in only 40–60 % [19] of patients and may be delayed by 4–12 weeks [20]. Novel approaches using RFA alone have been used successfully to palliate osseous

disease [21]. In addition, Gandhi et al. [22] reported a case of combination RT and RFA effectively used for pain palliation of a recurrent Wilms' tumor impinging on the celiac plexus. However, there is still a great need for such combination approaches to palliate and improve quality of life in patients with metastatic disease.

Therefore, the poor response to current treatments and the high prevalence of cardiovascular disease limiting curative surgical options necessitates the need for novel minimally invasive combination therapies. This chapter will briefly review the emerging data for image-guided thermal ablation in combination with RT for medically inoperable NSCLC cancers and chest wall metastases. The details of each thermal ablation technique are discussed in prior chapters of the text.

Biologic Rationale for Combination of Thermal Ablation and RT

Theoretically, multimodality insult to tumor cells can only serve to increase the potential for cell death. Synergy between chemotherapeutic agents and hyperthermic temperatures (42–45 °C) has already been established [23, 24]. Combining radiofrequency ablation (RFA) with additional therapies is one of the many topics of ablation currently under research, intended to mirror the current literature supporting the multidisciplinary approach that includes surgery, chemotherapy, and RT. Preliminary results are already suggesting that combination therapy with RFA and RT has improved local control and survival rates as compared to RT alone, without any additional major side effects [25, 26].

Local tissue factors and vital adjacent structures can limit the volume of tumor necrosis, leaving incomplete tumor margins with potential for residual disease with single therapies like RFA and RT, leading to local control failures. Biologically, upfront cytoreduction with an ablative technique may improve the chances of local control. Hypoxic cells are more resistant to radiation therapy. The central hypoxic regions of the tumor can be destroyed with an ablative technique such as RFA. Residual tumor after RFA, if present, would tend to be at the periphery, which would then be in a more suitable environment (e.g., increased blood flow and increased oxygen) for radiation to work effectively. This provides ample argument for the combining thermal therapy with other treatments, including chemotherapy, chemoembolization, and RT. Microwave ablation produces a field of tissue heating that is not dependent on conduction, but this theoretical advantage has undergone only limited study [27].

Treatment of Medically Inoperable Non-small Cell Lung Cancer

Conventional RT Alone

RT alone has long been the cornerstone of NSCL cancer treatment in patients who are too high-risk for surgical intervention. However, a study of 71 node-negative patients who received at least 60 Gy showed 3-year and 5-year survival rates to be 19 % and 12 %, respectively [28]. In a meta-analysis determining the effectiveness of radical radiotherapy alone for stage I/II medically inoperable NSCLC patients, overall 5-year survival ranged from 0 % to 42 %, with complete response rates of 33–61 % and local failure rates ranging from 6 to as high as 70 % [29]. Yet another study [30] showed a median survival time of 19.9 months and 14.2 months with radiotherapy alone and no treatment, respectively, in early-stage NSCLC. The difference between groups was not statistically significant ($p = 0.447$). Recently, survival rates of 34 % at 3 years for stage I NSCLC and a median survival time of 20.8 months for stage I/IIA NSCLC have been reported after standard RT [31], indicating further the need for additional alternatives. Interstitial brachytherapy has been studied as an adjuvant therapy for NSCLC. Low dose rate remotely afterloaded brachytherapy directed at the surgical margins after limited lung resection for early-stage NSCLC has resulted in decreased recurrence and improved survival compared with RT alone [32]. The results reported have been positive and are consistent with

previous experience [33], but statistical comparison between the RT modalities will remain underpowered until more patients treated with brachytherapy can be followed up. These are just a few examples that illustrate limitations of RT alone and the need for more robust approaches for minimally invasive combined treatment options.

Stereotactic Body Radiotherapy (SBRT) Alone

SBRT was first developed in the 1950s for the treatment of intracranial lesions. Technological developments in planning and treatment delivery of radiation therapy in the last decade have led to the application of this technique to extracranial sites including the thorax and abdomen. SBRT is a form of high-precision radiotherapy delivery. It is an area under active research for inoperable [34–36] NSCLC. Several phase I and II studies have shown excellent local control with this highly focused noninvasive technique, even for the elderly population [37]. However, this regimen should not be used for tumors near central airways (<2 cm) due to excessive toxicity [34]. Careful radiological follow-up of patients is paramount in patients who are treated using SBRT, because salvage surgery, mediastinal RT, or thermal ablation might still be possible in cases of local or regional recurrence. The combination of SBRT and thermal ablation techniques is currently being investigated. There is preliminary evidence that in a subset of patients with limited extracranial metastases or oligometastases, local ablative therapy in combination with systemic therapy may improve treatment outcomes [38].

RT and Conventional Hyperthermia Combination

Conventional hyperthermia has been used in combination with RT for its synergistic antitumor effect in various types of cancers, notably breast [39], cervix [40], rectum [41], and head and neck region [42]. Conventional hyperthermia refers to heating a region of the body affected by cancer up to a tolerable temperature of approximately 43 °C. The rationale is based on a direct cell-killing effect, radiosensitization, and increased blood flow under hyperthermia temperatures above 41–42 °C [43]. A recent prospective Dutch Deep Hyperthermia Trial [44] reported their 12-year follow-up of advanced cervical cancer in patients not eligible for chemotherapy: Local control 37 % versus 56 % ($p = 0.01$) and survival 20 % versus 37 % ($p = 0.03$) with radiation alone and combined radiation/hyperthermia, respectively. Intracavitary and superficial tumors can be heated more easily by means of antennas or applicators emitting mostly microwaves or radio waves placed on their surfaces with a contacting medium. However, for tumors located deeper like the non-peripheral lung or pelvic lesions, reaching temperatures uniformly above the systemic temperature of 37.5 °C has been a continuing technical challenge. Wust et al. [45] have a comprehensive summary of some of these hyperthermia techniques. Unlike conventional hyperthermia, RFA can target deeper tumors with significantly improved precision and tolerability leading to a much higher core temperature within the tumor itself, while sparing adjacent normal structures. This makes RFA a promising thermal technique to combine with other established NSCL cancer modalities.

RT and RFA Combination

The thermal ablation techniques in combination with more traditional noninvasive radiation therapy are being applied with increasing frequency for a number of cancers. Horkan et al. [46] published an elegant in vivo experiment using a rat breast tumor model directly comparing treatment with RT alone, RFA alone, and combination of RT and RFA with the appropriate controls. Eighty-two percent (nine of eleven) of the tumors treated with combined therapy had local control with a medial survival time of 120 days, relative to 0 % local control and <50 day median survival

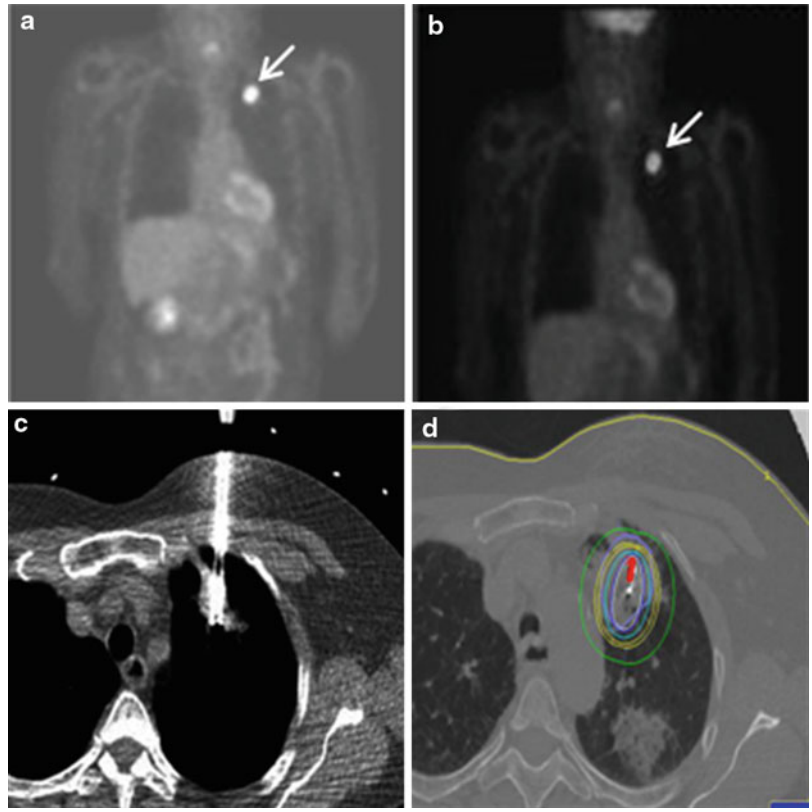

Fig. 38.1 74 year old female with newly diagnosed, inoperable, left upper lobe nonsmall cell lung cancer (Stage IA, T1 N0) presenting in 2004. (**a**, **b**) Pre-treatment PET scans in 2004 demonstrating avid-FDG uptake by tumor (*white arrows*). (**c**) CT image during 2004 RFA procedure. (**d**) Brachytherapy isodose distribution post-RFA (single catheter)

for both modalities alone. Thermal treatment in the form of RFA in combination with RT is the most common technique being used for NSCL cancers. Dupuy et al. first reported using RFA followed by conventional RT in medically inoperable stage I NSCL cancer [25] to prospectively study potential synergy between the two modalities. They reported 2- and 5-year cumulative survival rates as high as 50 % and 39 %, respectively, with twenty-four medically inoperable patients. All patients received RFA followed by three-dimensional conformal radiotherapy. There were no treatment-related deaths or grade 3/4 toxicities. Pneumothorax requiring chest tubes developed in three patients (12.5 %). At a mean follow-up period of 26.7 months (range 6–65 months), 14 patients (58.3 %) died, with cumulative survival rates of 50 % and 39 % at the end of 2 years and 5 years, respectively. Ten of the deaths were cancer related. Two patients had local recurrence (8.3 %), while nine patients had systemic metastatic disease. Additional retrospective data for such combination was reported by Grieco et al. [26]. Forty-one patients with inoperable stage I/II NSCLC tumors were treated with thermal ablation and RT at a single institution between 1998 and 2005. Notably, thirty-seven patients had RFA while four had MWA procedures. All ablations were then followed by standard-fraction external-beam RT within 90 days ($n = 27$) or postprocedural brachytherapy ($n = 14$). With a median follow-up of 19.5 months, the overall survival rates were 97.6 % at 6 months, 86.8 % at 1 year, 70.4 % at 2 years, and 57.1 % at 3 years. Local recurrence occurred in 11.8 % of tumors smaller than 3 cm after an average of 45.6 months and in 33.3 % of the larger tumors after an average of 34.0 months ($p = 0.03$). Outcomes in the brachytherapy and external-beam RT groups did not differ significantly. A representative case of

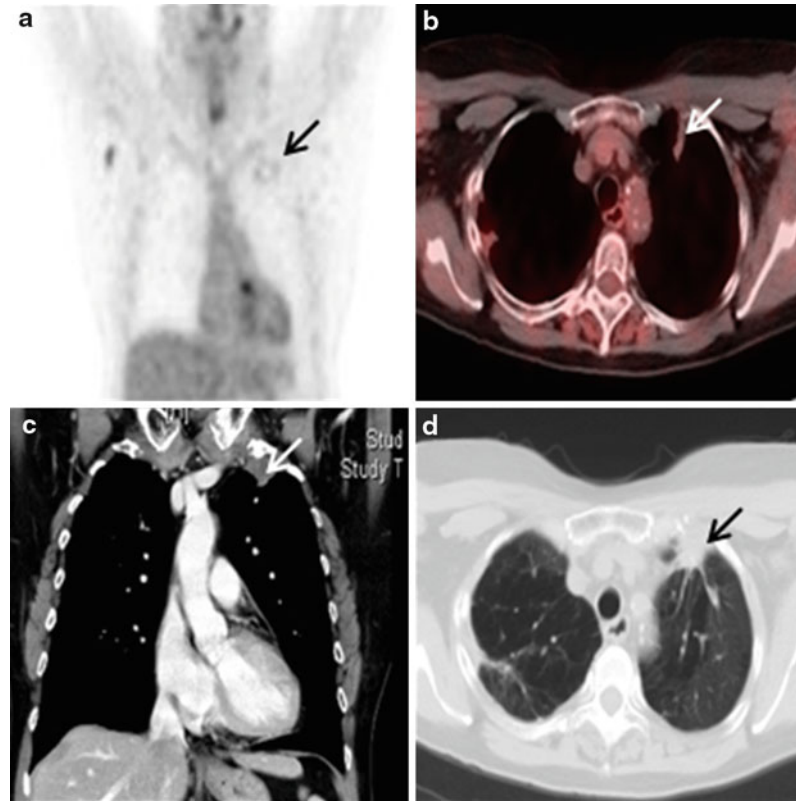

Fig. 38.2 Patient from Fig. 38.1, two years after completion of combined RFA and brachytherapy treatment demonstrating no PET-avid disease (**a**) in the coronal plane (*black arrow*), (**b**) and axial plane (*white arrow*). Corresponding CT scan demonstrating fibrosis along the left anterior chest wall secondary to previous combined treatment (**c**) in the coronal plane (*white arrow*), (**d**) and axial plane (*black arrow*)

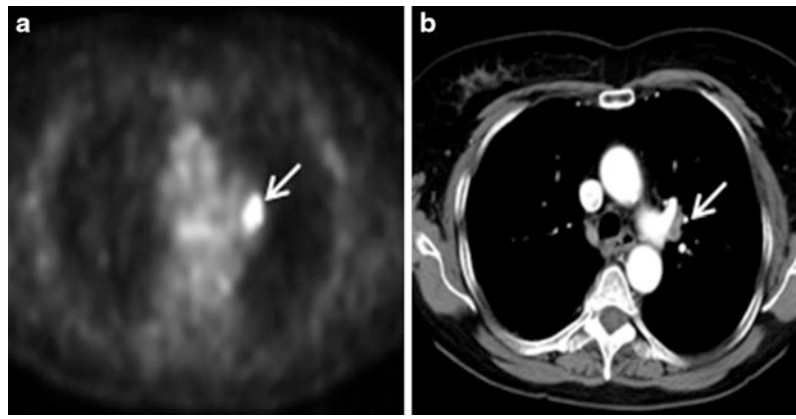

Fig. 38.3 Same patient from Fig. 38.1 presented with new mediastinal recurrence, out of previous treatment field, in 2006 and was treated with SBRT alone. (**a**, **b**) 2006 PET and CT (*white arrows*) images showing FDG-avid tumor recurrence along the left mediastinum, respectively

combination RFA and brachytherapy treatment for primary inoperable NSCL cancer, followed by SBRT alone for a new recurrence treated at Rhode Island Hospital, is illustrated in Figs. 38.1, 38.2, 38.3, and 38.4.

Complications

Radiation therapy alone can lead to pulmonary toxicity. The most common side effect of radiation alone is pneumonitis, which has been

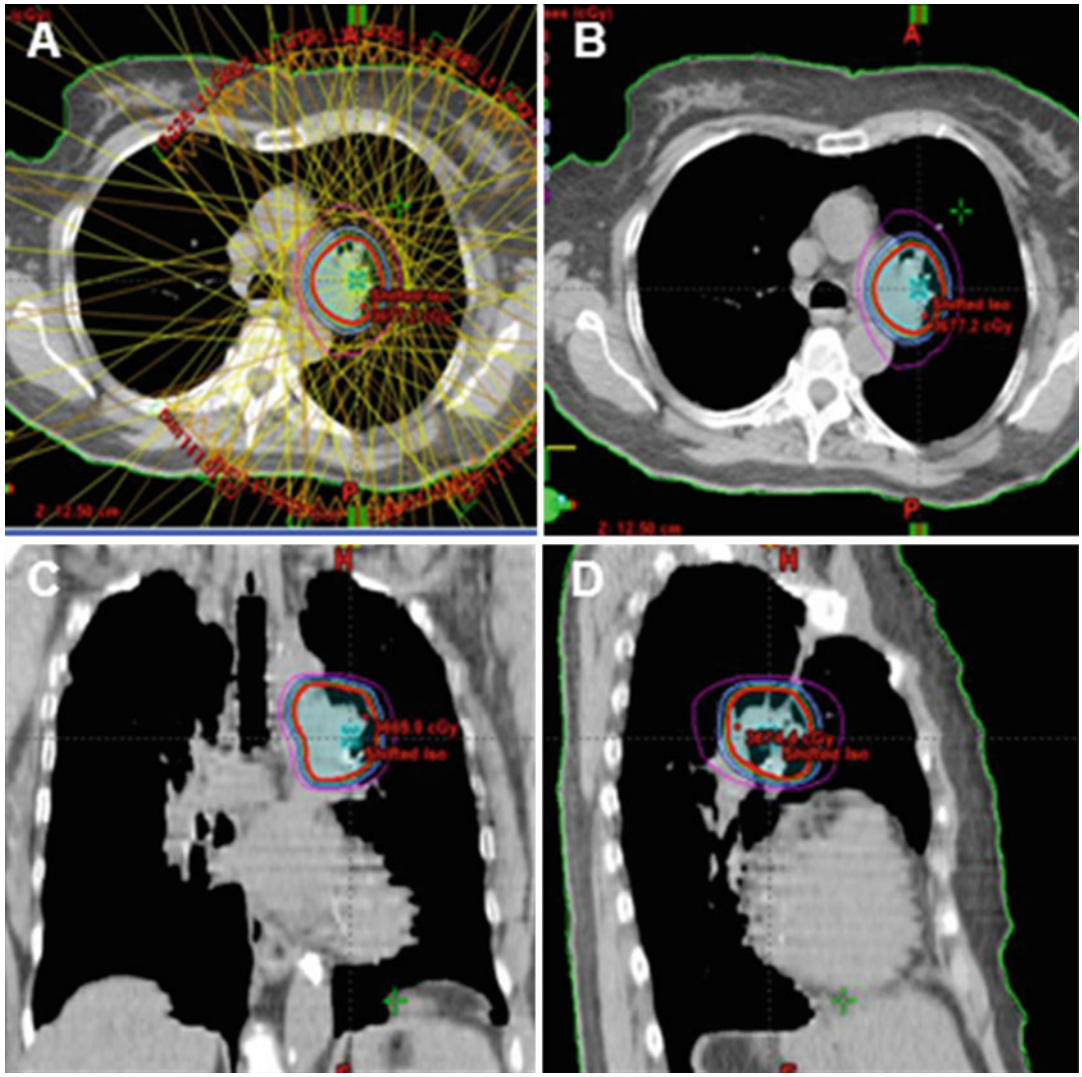

Fig. 38.4 (**a**, **b**) Axial views of 2006 SBRT beam arrangement and treatment isodose distribution used to deliver a total dose of 35 Gy in 5 fractions, respectively. (**c**, **d**) corresponding coronal and sagittal isodose distribution, respectively (*red* 100 %, *light blue* 85 %, *dark blue* 80 % and *pink* 60 % isodose lines). Patient is alive with stable performance status but requires continuous oxygen support, 2L by nasal cannula at rest

reported to occur in 5–15 % of patients [47]. Radiation pneumonitis, when it occurs, is a significant and potentially life-threatening complication of radiation.

With RFA, pneumothorax is the most commonly observed complication. A recent international study surveying nearly 500 pulmonary thermal ablations reported pneumothoraces in 30 % of the cases, a third of which ultimately required chest tube drainage [48]. Other studies report pneumothoraces in approximately 20–35 % of patients after RF ablation [49–52] with approximately 6–16 % requiring placement of a chest catheter [53]. It should be noted that the patient cohorts in these combination studies almost universally carry an underlying diagnosis of emphysema, a known risk factor for pneumothorax after thoracic procedures [54]. One rare, potential risk postulated after RF ablation within the lung is systemic embolization

due to microbubbles generated with the arteries, increasing the potential risk for stroke. Yamamoto et al. [55] prospectively monitored 17 patients who underwent RF ablation of lung tumors with carotid sonography, noting echogenic microbubbles ascending the carotid arteries of 3 patients (who all had larger tumor diameters ranging from 2.5 cm to 6.5 cm). None of their patients demonstrated any evidence of acute infarct on MRI imaging which was performed within 24 h.

Combination of RFA and conventional RT does not appear to have significantly higher rates of complications relative to the modalities alone. Dupuy et al. [25] reported 29 % pneumothoraces after RFA as part of their combined treatment. Three of them required chest tube drainage for clinically significant pneumothorax either during the procedure or immediately following the procedure after a 2-h chest radiograph follow-up. There was no acute respiratory compromise as a result of RFA. All 24 patients completed a full course of RT without any cases of acute pulmonary toxicity secondary to the radiotherapy. Radiographic evidence of radiation fibrosis developed at 6 months in two patients, but they remained asymptomatic.

Summary

Lung cancer mortality exceeds that of breast cancer, prostate cancer, and colon cancer combined. A large majority of patients with this disease have significant medical comorbidities that severely limit treatment options for local control as well as palliation. Complete resection with lobectomy or pneumonectomy is the current standard of care if possible, but only a small percentage of patients qualify. Alternative single modalities of treatment with conventional RT and thermal ablation are being investigated. However, the preliminary results have not been very promising when these modalities are used alone. In addition, the natural ability of clonal expansion tumors with even the least amount of residual disease makes it an ideal candidate for combination therapies with different mechanisms of cell killing. Some of the promising combination therapies for NSCLC under current investigation include limited resection with brachytherapy [56], RFA with conventional RT [26, 27], and RFA with SBRT [57].

Cross-References

- ▶ Image-Guided Radiation Therapy for Lung Cancer
- ▶ Percutaneous Interventional Radiology: The Lung
- ▶ Radiation Therapy: Intensity-Modulated Radiotherapy, Cyberknife, Gamma Knife, and Proton Beam
- ▶ Stereotactic Body Radiation Therapy for Liver Metastases

References

1. Horner MJ, et al. SEER Cancer statistics review, 1975–2006, National Cancer Institute. Bethesda. http://seer.cancer.gov/csr/1975_2006/, based on 2008 Nov SEER data submission, posted to the SEER web site, 2009.
2. Lloyd-Jones D, et al. Circulation. Heart disease and stroke statistics – 2010 update. A report from the American Heart Association. 2009 Dec 17.
3. Ginsberg RJ, et al. Randomized trial of lobectomy versus limited resection for T1 N0 non-small cell lung cancer. Lung cancer study group. Ann Thorac Surg. 1995;60(3):615–22; 622–3.
4. Warram J. Preoperative irradiation of cancer of the lung: final report of a therapeutic trial. A collaborative study. Cancer. 1975;36(3):914–25.
5. Kazem I, et al. Evaluation of short-course preoperative irradiation in the treatment of resectable bronchus carcinoma: long-term analysis of a randomized pilot-study. Int J Radiat Oncol Biol Phys. 1984;10(7):981–5.
6. PORT Meta-analysis Trialists Group. Postoperative radiotherapy for non-small cell lung cancer. Cochrane Database Syst Rev. 2005;2:CD002142.
7. Douillard JY, et al. Impact of postoperative radiation therapy on survival in patients with complete resection and stage I, II, or IIIA non-small-cell lung cancer treated with adjuvant chemotherapy: the adjuvant Navelbine International Trialist Association (ANITA) randomized trial. Int J Radiat Oncol Biol Phys. 2008;72(3):695–701. Epub 2008 Apr 24.
8. Machtay M, et al. Risk of death from intercurrent disease is not excessively increased by modern postoperative radiotherapy for high-risk resected non-smallcell lung carcinoma. J Clin Oncol. 2001;19(19):3912–7.

9. Shennib H, et al. Video-assisted wedge resection and local radiotherapy for peripheral lung cancer in high-risk patients: the Cancer and Leukemia Group B (CALGB) 9335, a phase II, multi-institutional cooperative group study. J Thorac Cardiovasc Surg. 2005;129(4):813–8.
10. Fernando HC, et al. Lobar and sublobar resection with and without brachytherapy for small stage IA non-small cell lung cancer. J Thorac Cardiovasc Surg. 2005;129(2):261–7.
11. Strauss GM, et al. Adjuvant paclitaxel plus carboplatin compared with observation in stage IB non-small-cell lung cancer: CALGB 9633 with the cancer and leukemia group B, Radiation therapy oncology group, and north central cancer treatment group study groups. J Clin Oncol. 2008;26(31):5043–51. Epub 2008 Sep 22.
12. Arriagada R, et al. Cisplatin-based adjuvant chemotherapy in patients with completely resected non-small-cell lung cancer. N Engl J Med. 2004;350(4):351–60.
13. Winton T, et al. Vinorelbine plus cisplatin vs. observation in resected non-small-cell lung cancer. N Engl J Med. 2005;352(25):2589–97.
14. Waller D, et al. Chemotherapy for patients with non-small cell lung cancer: the surgical setting of the big lung trial. Eur J Cardiothorac Surg. 2004;26(1):173–82.
15. Douillard JY, et al. Adjuvant vinorelbine plus cisplatin versus observation in patients with completely resected stage IB-IIIA non-small-cell lung cancer (Adjuvant Navelbine International Trialist Association [ANITA]): a randomised controlled trial. Lancet Oncol. 2006;7(9):719–27.
16. Perry MC, et al. A phase III study of surgical resection and paclitaxel/carboplatin chemotherapy with or without adjuvant radiation therapy for resected stage III non-small-cell lung cancer: cancer and leukemia group B 9734. Clin Lung Cancer. 2007;8(4):268–72.
17. Keller SM, et al. A randomized trial of postoperative adjuvant therapy in patients with completely resected stage II or IIIA non-small-cell lung cancer. Eastern cooperative oncology group. N Engl J Med. 2000;343(17):1217–22.
18. http://seer.cancer.gov
19. Janjan NA. Bone metastases: approaches to management. Semin Oncol. 2001;28:28–34.
20. Janjan NA. Radiation for bone metastases: conventional techniques and the role of systemic radiopharmaceuticals. Cancer. 1997;80(suppl 5):1628–45.
21. Dupuy DE, et al. Percutaneous radiofrequency ablation of painful osseous metastases: a multicenter American College of Radiology Imaging Network trial. Cancer. 2010;116(4):989–97.
22. Gandhi S, et al. Combined computed tomography-guided radiofrequency ablation and brachytherapy in a child with multiple recurrences of Wilms' tumor. J Pediatr Hematol Oncol. 2005;27:377–9.
23. Seegenschmiedt MH, Brady LW, Sauer R. Interstitial thermoradiotherapy: review on technical and clinical aspects. Am J Clin Oncol. 1990;13:352–63.
24. Trembley BS, Ryan TP, Strohbehn JW. Interstitial hyperthermia: physics, biology and clinical aspects. In: Urano M, Douple E, editors. Physics of microwave hyperthermia in hyperthermia and oncology, vol. 3. Utrecht: Springer; 1992. p. 11–98.
25. Dupuy D, DiPetrillo T, Gandhi S, Ready N, Ng T, Donat W, Mayo-Smith W. Radiofrequency ablation followed by conventional radiotherapy for medically inoperable stage I non-small cell lung cancer. Chest. 2006;129:738–45.
26. Grieco CA, Simon CJ, Mayo-Smith WW, DiPetrillo TA, Ready N, Dupuy D. Percutaneous image-guided thermal ablation and radiation therapy: outcomes of combined treatment for 41 patients with inoperable stage I/II non-small-cell lung cancer. J Vasc Interv Radiol. 2006;17:1117–24.
27. Simon CJ, Dupuy DE, Mayo-Smith WW. Microwave ablation: principles and applications. Radiographics. 2005;25(suppl):69–83.
28. Kupelian PA, et al. Prognostic factors in the treatment of node-negative non-small cell lung carcinoma with radiotherapy alone. Int J Radiat Oncol Biol Phys. 1996;36:607–13.
29. Rowell NP, et al. Radical radiotherapy for stage I/II non-small cell lung cancer in patients not sufficiently fit for or declining surgery (medically inoperable): a systematic review. Thorax. 2001;56:628–38.
30. McGarry RC, et al. Observation-only management of early stage, medically inoperable lung cancer: poor outcome. Chest. 2002;121:1155–8.
31. Senan S, Lagerwaard FJ. The role of radiotherapy in non-small-cell lung cancer. Ann Oncol. 2005;16(Suppl 2):223–8.
32. Lee W, Daly BDT, DiPetrillo TA, et al. Limited resection for non-small cell lung cancer; observed local control with implantation of I-125 brachytherapy seeds. Ann Thorac Surg. 2003;75:237–43.
33. Jain SK, Dupuy DE, Cardarelli GA, et al. Percutaneous radiofrequency ablation of pulmonary malignancies: combined treatment with brachytherapy. AJR Am J Roentgenol. 2003;181:711–5.
34. Timmerman R, et al. Excessive toxicity when treating central tumors in a phase II study of stereotactic body radiation therapy for medically inoperable early-stage lung cancer. J Clin Oncol. 2006;24(30):4833–9.
35. Hoopes DJ, et al. FDG-PET and stereotactic body radiotherapy (SBRT) for stage I non-small-cell lung cancer. Lung Cancer. 2007;56(2):229–34. Epub 2007 Mar 13.
36. Onishi H, et al. Hypofractionated stereotactic radiotherapy (HypoFXSRT) for stage I non-small cell lung cancer: updated results of 257 patients in a Japanese multi-institutional study. J Thorac Oncol. 2007;2(7 Suppl 3):S94–100.
37. Haasbeek CJ, et al. Stage I nonsmall cell lung cancer in patients aged >/=75 years: outcomes after stereotactic radiotherapy. Cancer. 2010;116(2):406–14.
38. Lo SS, et al. Stereotactic body radiation therapy for oligometastases. Expert Rev Anticancer Ther. 2009;9(5):621–35.

39. Kapp DS, Cox RS. Thermal treatment parameters are most predictive of outcome in patients with single tumor nodules per treatment field in recurrent adenocarcinoma of the breast. Int J Radiat Oncol Biol Phys. 1995;33:887–99.
40. Kapp DS, Lawrence R. Temperature elevation during brachytherapy for carcinoma of the uterine cervix: adverse effect on survival and enhancement of distant metastasis. Int J Radiat Oncol Biol Phys. 1984;10:2281–92.
41. Berdov BA, Menteshashvili GZ. Thermoradiotherapy of patients with locally advanced carcinoma of the rectum. Int J Hyperthermia. 1990;6:881–90.
42. Datta NR, Bose AK, Kapoor HK, et al. Head and neck cancers: results of thermoradiotherapy versus radiotherapy. Int J Hyperthermia. 1990;6:479–86.
43. Dewey WC. Arrhenius relationships from the molecule and cell to the clinic. Int J Hyperthermia. 1994;10:457–83.
44. Franckena M, et al. Long-term improvement in treatment outcome after radiotherapy and hyperthermia in locoregionally advanced cervix cancer: an update of the dutch deep hyperthermia trial. Int J Radiat Oncol Biol Phys. 2008;70(4):1176–82.
45. Wust P, et al. Hyperthermia in combined treatment of cancer. Lancet Oncol. 2002;3:487–97.
46. Horkan C, et al. Reduced tumor growth with combined radiofrequency ablation and radiation therapy in a rat breast tumor model. Radiology. 2005;235:81–8.
47. Kocak Z, Evans ES, Zhou SM, et al. Challenges in defining radiation pneumonitis in patients with lung cancer. Int J Radiat Oncol Biol Phys. 2005;623:635–8.
48. Steinke K, Sewell PE, Dupuy DE. Pulmonary radiofrequency ablation: an international study survey. Anticancer Res. 2004;24:339–43.
49. Steinke K, King J, Glenn D, et al. Percutaneous radiofrequency ablation of lung tumors with expandable needle electrodes: tips from preliminary experience. AJR Am J Roentgenol. 2004; 183:605–11.
50. Lee JM, Jin GY, Goldberg SN, et al. Percutaneous radiofrequency ablation for inoperable non-small cell lung cancer and metastases: preliminary report. Radiology. 2004;230:125–34.
51. Akeboshi M, Yamakado K, Nakatsuka A, et al. Percutaneous radiofrequency ablation of lung neoplasms: initial therapeutic response. J Vasc Interv Radiol. 2004;15:463–70.
52. Kotaro Y, Susumu K, Yoshifumi S, et al. Thoracic tumors treated with CT-guided radiofrequency ablation: initial experience. Radiology. 2004;231:850–7.
53. Cosmo G, Vittorio M, Giuseppe C, et al. Radiofrequency ablation of 40 lung neoplasms: preliminary results. AJR Am J Roentgenol. 2004;183:361–8.
54. Cox JE, Chiles C, McManus CM, et al. Transthoracic needle aspiration biopsy: variables that affect risk of pneumothorax. Radiology. 1999;212:165–8.
55. Yamamoto A, Matsuoka T, Toyoshima M, et al. Assessment of cerebral microembolism during percutaneous radiofrequency ablation of lung tumors using diffusion weighted imaging. Am J Roentgenol. 2004;183:1785–9.
56. Parashar B, et al. Limited resection followed by intraoperative seed implantation is comparable to stereotactic body radiotherapy for solitary lung cancer. Cancer. 2010;116(21):5047–53.
57. Abbas G, et al. Ablative treatments for lung tumors: radiofrequency ablation, stereotactic radiosurgery, and microwave ablation. Thorac Surg Clin. 2007 May;17(2):261–71.

Lung Resection

39

Bernard J. Park

Abstract

Non-small cell lung cancer (NSCLC) remains one of the leading causes of cancer-related mortality worldwide. Despite recent advances in molecular characterization and systemic therapies, surgical resection remains the mainstay of curative treatment. Anatomic lobectomy is the reference standard surgical approach to localized disease. Sublobar resections (wedge, segmentectomy) may be acceptable in patients who have marginal cardiopulmonary reserve or in those with exceptionally small tumors. Minimally invasive video-assisted thoracic surgery (VATS) techniques, in particular VATS lobectomy, are being increasingly utilized and championed over traditional thoracotomy approaches in the treatment of localized NSCLC for the reported benefits of lower operative morbidity, accelerated postoperative recovery, and oncologic equivalence. This chapter will review the various operative approaches with a focus on the benefits of minimally invasive techniques.

Lung cancer remains one of the leading causes of cancer-related mortality among both men and women worldwide. In the United States, there were an estimated 219,450 new cases and 159,390 deaths in 2009 [1], and non-small cell lung cancer (NSCLC) accounts for roughly 80 % of all lung cancer cases. Given that 50 % of NSCLC patients are older than 65 years old at diagnosis and that the proportion of individuals over 65 years of age in the USA is rising, it is clear that the number of lung cancer patients will only grow [2–4]. Despite recent advances in molecular profiling, targeted therapy and the efficacy of adjuvant chemotherapy surgical resection remains the best option for cure.

Anatomic pulmonary resection is the preferred surgical approach for isolated, early stage lung cancer with lobectomy being the reference standard in patients with adequate cardiopulmonary status. For patients who are high operative risk and have smaller tumors, sublobar resections, such as segmentectomy and wedge resection, are acceptable as long as a complete resection with adequate margins can be achieved. Pneumonectomy can be undertaken in appropriately selected patients with locally advanced

B.J. Park
Department of Surgery, Hackensack University Medical Center, Hackensack, NJ, USA
e-mail: bpark@humed.com

D.E. Dupuy et al. (eds.), *Image-Guided Cancer Therapy*, DOI 10.1007/978-1-4419-0751-6_41,

disease. This chapter will summarize the techniques, indications, and outcomes of surgical resection in the treatment of localized NSCLC with a particular focus on lobectomy and the indications, outcomes, and benefits of minimally invasive techniques.

Video-Assisted Thoracic Surgery (VATS)

Traditionally, the standard incisional approach to NSCLC resection has been via rib-spreading thoracotomy to allow for individual hilar dissection through direct vision. While there are many types of thoracotomies, including anterior, anterolateral, posterolateral, axillary, and vertical, posterolateral is the most commonly employed. All may be performed with sparing of the large muscle groups. Large modern surgical series where thoracotomy was predominantly employed revealed low mortality rates, but substantial postoperative morbidity rates as high as 32 % [5–7]. In an effort to lower the morbidity associated with thoracotomy, several authors in the early 1990s simultaneously developed less invasive VATS techniques for lobectomy for NSCLC [8–11]. The original impetus for the development of these approaches was to minimize or eliminate rib spreading associated with thoracotomy and, thus, reduce the perioperative consequences for the patient. Therefore, the initial techniques reported all employed a thoracoscope for visualization and avoided rib spreading. Following these initial reports, wide variability in VATS lobectomy techniques developed and still exists to this day.

In an effort to standardize the approach to VATS lobectomy, the Cancer and Leukemia Group B (CALGB) undertook a prospective, multi-institutional registry study (CALGB 39802) designed to elucidate the feasibility of VATS lobectomy for early stage NSCLC (peripheral tumors ≤ 3 cm) and to define a unified set of criteria that defines the technique [12]. The standardized definition included a three-incision technique (one 4–8-cm access incision with two 0.5-cm port incisions) that mandated videoscopic guidance and traditional hilar dissection without rib spreading. The results for 127 patients undergoing surgery revealed a perioperative mortality rate of 2.7 %, grade 3 or higher complication rate of 7.4 %, and long-term survival comparable to historical thoracotomy controls, leading the authors to conclude that such a standard technique was both feasible and safe.

Subsequently, there has been a substantial amount of data reported in the literature regarding VATS lobectomy supporting its feasibility in the surgical management of NSCLC, its oncologic equivalence to thoracotomy, and its benefits in postoperative recovery. This has led to increased utilization of VATS, but in spite of this, 70 % of lobectomies are still performed via thoracotomy [7].

The author routinely performs VATS lobectomy for clinical stage I NSCLC or other isolated lesions utilizing an approach consistent with the CALGB 39802 standardized definition: anatomic pulmonary lobectomy is performed using a video thoracoscope and three non-rib-spreading incisions, the largest of which is 3–4 cm (Fig. 39.1). A combination of conventional and specialized thoracoscopic instruments are used to achieve individual dissection and ligation of the hilar structures, including the pulmonary vasculature and airway followed by routine, systematic mediastinal lymph node dissection for NSCLC. The detailed sequence of steps for VATS anatomic pulmonary resection has been previously described elsewhere [13].

Image Guidance and VATS: Preoperative Localization

The main advantage of VATS with respect to patient recovery is lack of rib spreading. This, however, eliminates the possibility of bimanual palpation, making localization of certain pulmonary lesions more difficult. The first are semisolid or ground-glass opacities that are difficult to palpate, even via thoracotomy. The second are smaller, typically subcentimeter

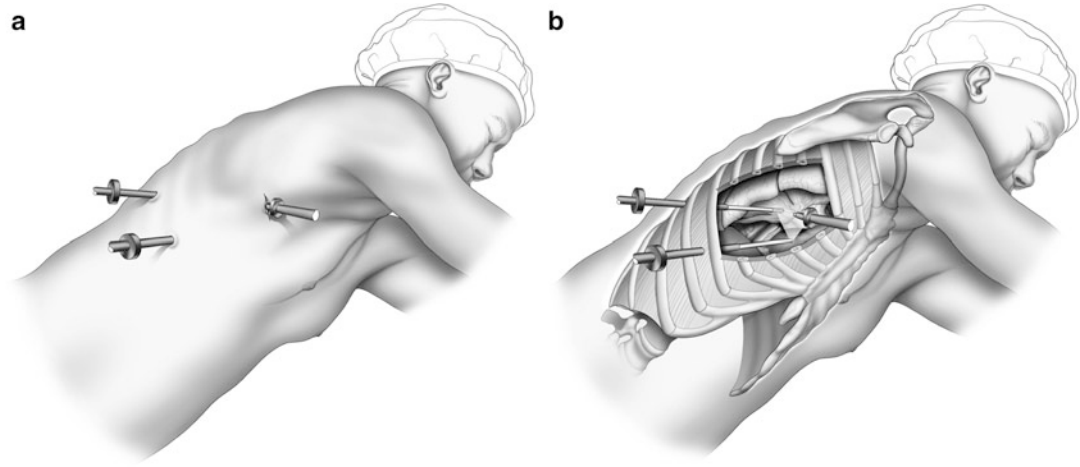

Fig. 39.1 Typical incisions for VATS lobectomy

lesions located deeper than 5 mm from the pleural surface. Given the increase in utilization of CT scans for other indications (e.g., coronary artery scans) and for screening high-risk populations, it is very likely that increasingly smaller lesions will need to be evaluated. There are a number of preoperative localization techniques to guide VATS resection of these abnormalities, but none have been uniformly adopted or utilized.

One category of preoperative image-guided localization is through injection of dye, contrast, or radionuclides. The various materials are injected during a preoperative localization CT on the day of the VATS procedure. Methods of intraoperative identification include visual in the case of methylene blue dye [14], fluoroscopic for iodinated contrast or barium [15], and via probe for radionuclide [16]. Each of these approaches is somewhat limited by the potential for the substances to diffuse away from the nodule over time, requiring a short interval between injection and resection and the potential risks of anaphylactic reactions and systemic embolization. Additionally, methylene blue can be difficult to identify in patients with extensive anthracotic pigmentation, and radionuclide use requires extensive equipment, training, and radiation safety requirements.

The oldest and most reported technique of localization is percutaneous placement of hook wires [17–19]. The wire is placed in the lung close to the nodule of interest and either the wire itself or an attached suture extends through the chest wall. The wire is placed anywhere between 10 and 20 mm deep to, but not through, the lesion itself so as not to interfere with pathological analysis. Complications associated with this method include wire dislodgement, pneumothorax, and intraparenchymal hemorrhage. Success of localization and resection of the target lesions is approximately 96 % [17, 18]. Factors associated with success include increasing size of the lesions, decreasing distance between the visceral pleural surface and the inferior border of the nodule, and increased density of the lesion by CT [19]. A variation of the wire technique involves placement of fiber-coated microcoils completed contained within the lung parenchyma, allowing intraoperative fluoroscopic-guided VATS resection [20]. The advantage over conventional hook wire techniques is lack of dislodgement. Mayo and colleagues demonstrated 100 % localization using microcoils and 97 % successful excision by VATS in a series of 69 patients. Complications included pneumothorax requiring chest tube placement (3 %) and asymptomatic hemothorax in one patient.

Lobectomy: VATS Versus Thoracotomy

Since the initial technique was reported, there have been many large series of VATS lobectomy reporting morbidity rates ranging from 3 % to 13.3 % and operative mortality rates from 0 % to 2 % [21–25] (Table 39.1) that compare favorably to the historical results from a thoracotomy approach [5]. Two of the largest case series of VATS lobectomy for NSCLC demonstrated its feasibility and safety as a procedure [26, 27]. McKenna and colleagues reported the largest series of VATS lobectomies to date with 1,048 cases out of 1,100 VATS anatomic resections, the majority of which (1,015) were for primary lung cancer [26]. Eighty-eight percent of the patients were clinical stage I prior to exploration. The mean age of the patients was 72.1 years with a slight female predominance (54.1 %). The median length of stay was 3 days, and the morbidity rate was 15.3 %. Only 4.1 % of patients required blood transfusion, and readmission rate was 1.1 % (13/1,100). Perioperative mortality was 0.8 % (9/1,100) with no intraoperative deaths.

Similarly, Onaitis and coauthors summarized the Duke University experience with 500 consecutive patients undergoing attempted VATS lobectomy to determine safety, efficacy, and versatility [27]. In this retrospective review, the majority of procedures (416/500) were performed for NSCLC. Successful thoracoscopic lobectomy was achieved in 492 patients (1.6 % conversion rate). The median chest tube and length of hospitalization were both 3 days. Operative mortality was 1.2 % (6/492), and a total of 119 patients (24 %) had complications. The most common complication was atrial fibrillation (52/492, 10 %).

While there are several large series of VATS lobectomy from various authors and centers, there are precious few direct comparisons of the two techniques and virtually no randomized controlled trials. There have been some reports attempting to compare prospectively the two operative approaches in a similar cohort of patients [28–32]. Although the majority of these reports had small sample sizes, nearly all showed that operative time between the approaches was similar and the duration of chest tube drainage and, consequently, length of stay favored the VATS group. VATS patients had shorter chest tube duration and length of stay compared with thoracotomy patients. In the only prospective randomized trial comparing perioperative outcomes of VATS versus thoracotomy for lobectomy, Kirby and associates compared 55 patients with clinical stage I NSCLC randomized to either a VATS (25) or muscle-sparing thoracotomy (30) [29]. Mean operative times were shorter for VATS (161 vs. 175 min), as was mean chest tube duration (4.6 vs. 6.5 days) and mean length of stay (7.1 vs. 8.3 days), although because of the small sample size, none of these differences were statistically significant. The postoperative complication rate was significantly higher in the thoracotomy group ($p < 0.5$), the majority of which were prolonged air leaks. The authors concluded that while there may be some benefits to a closed-chest approach, there was a need for more critical evaluation of the role of VATS for major pulmonary resection.

One of the largest series comparing patients undergoing VATS versus thoracotomy for early stage NSCLC is a retrospective comparison by Flores and colleagues [33]. Over a 5-year period from May 2002 to August 2007, 741 patients underwent either VATS (328) or thoracotomy (413) for clinical stage I NSCLC. Patient characteristics were well matched with identical median age of the patients (67 years), female predominance (63 % VATS, 64 % thoracotomy), and distribution of pathologic stage (84 % I VATS,

Table 39.1 Feasibility of VATS lobectomy

Author	Year	N	Morbidity (%)	Mortality (%)
Lewis [21]	1999	250	11.2	0
McKenna [22]	1998	298	12.4	0.4
Walker [23]	1998	150	13.3	2.0
Kaseda [24]	1998	128	3.0	0.8
Yim [25]	1997	78	6.4	1.3

80 % I thoracotomy). Intent-to-treat and propensity score-matched analyses revealed that the overall complication rate in the VATS patients was significantly lower (22 % VATS vs. 31 % thoracotomy, $p = 0.01$), as was median length of stay (5 days VATS vs. 7 days thoracotomy, $p = 0.001$). This study provided further evidence via direct comparison that not only is VATS a feasible approach to these patients, but that there may be some benefit over thoracotomy.

Oncologic Efficacy of VATS Lobectomy

One of the most important issues with respect to the utilization of VATS for primary surgical treatment of early stage NSCLC is whether the long-term survival outcome is equivalent to thoracotomy. There are no large, randomized controlled trials of VATS versus thoracotomy designed to evaluate oncologic equivalence in NSCLC, and it is unclear if there ever will be. Barriers to development of such trials include failure of equipoise among experts in advanced VATS techniques, inability to randomize secondary to patient preference for the minimally invasive approach, and lack of a standardized approach to the procedure. There have been a number of retrospective, single-institution series looking at overall survival of VATS lobectomy in early stage NSCLC [21, 26, 27, 33–36] and one randomized prospective trial of VATS versus thoracotomy and long-term survival in stage I patients [37]. If one analyzes the studies performed before the advent of routine adjuvant chemotherapy for higher stage disease, in the subset of patients with pathological stage I, the majority of reports show excellent predicted 5-year survival that is comparable to those results historically seen with thoracotomy (Table 39.2). In fact, a few of the series show better than expected survival [21, 34, 37].

One of these studies by Sugi and coauthors is to date the only randomized trial of VATS versus thoracotomy to evaluate long-term cancer outcome [37]. Patients with clinical stage I NSCLC were randomly assigned to lobectomy either by standard rib-spreading thoracotomy ($n = 52$) or by a VATS approach ($n = 48$). Of note, the VATS technique in the study employed an 8-cm access incision. Though underpowered to show statistical equivalence, with a median follow-up period of 60 months, the study suggested that long-term survival outcomes were similar between the VATS (90 %) and thoracotomy (85 %) groups. Unfortunately, no other perioperative information was reported with respect to complication rate or quality of life.

Table 39.2 VATS lobectomy and pathologic stage I survival

Author	Year	N	% 5-year survival	Follow-up (months)
Lewis [21]	1999	92	92[a]	34
Kaseda [34]	2000	50	97	30
Sugi [37][b]	2000	48	90	60
Walker [35]	2003	117	78	38
McKenna [26]	2006	742	78	NR
Onaitis [27]	2007	330	85[c]	24

NR not reported
[a]Actuarial
[b]Randomized
[c]2-year survival

Two relatively large retrospective series analyzed long-term oncologic outcome of VATS versus thoracotomy for early NSCLC [33, 36]. The first by Thomas and coauthors attempted to determine the prognosis of patients treated by VATS versus open lung resections for pathological stage I NSCLC over a 10-year period [36]. There were 110 patients in the VATS group and 405 in the thoracotomy group, and the majority of procedures were lobectomies (390 total, 92 VATS). The overall 5-year survival rates associated with VATS and thoracotomy were 62.9 % (CI, 51.4 %–74.4 %) and 62.8 % (CI, 56.8 %–68.7 %), respectively, ($p = 0.6$). Stage IA patients had survivals of 64.9 % (CI, 47.3 %–82.5 %) following VATS and 79.7 % (CI, 69.6 %–89.9 %) after thoracotomy ($p = 0.15$), whereas stage IB had 5-year survivals of 61.2 % (CI, 45.9 %–76.5 %) and 58.1 % (CI, 51.2 %–65 %), respectively ($p = 0.4$). Despite the favorable results, closer inspection of this study reveals several differences between the patient groups that make its conclusions difficult to

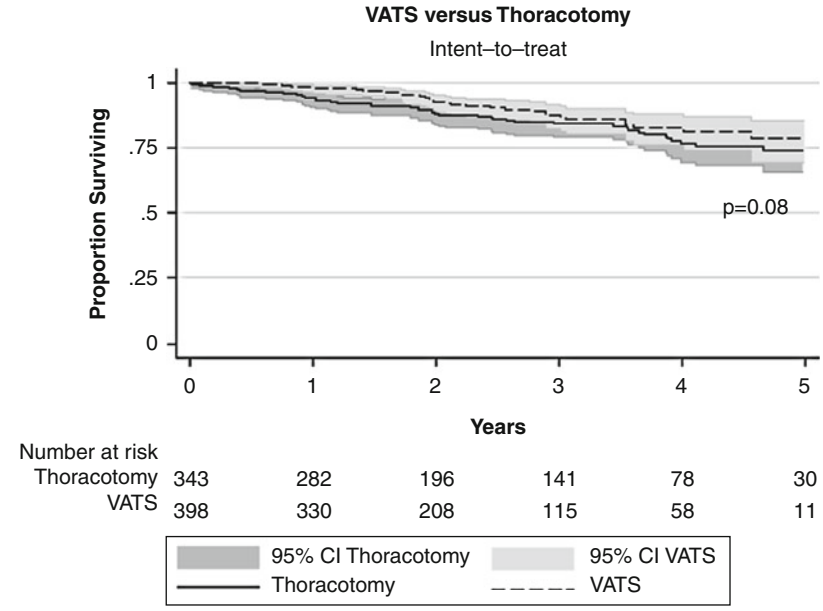

Fig. 39.2 VATS versus thoracotomy. Intent-to-treat. VATS, video-assisted thoracic surgery; CI, confidence intervals (From Flores RM, et al. JTCVS 2009;138:11–18, reprinted with permission from Elsevier)

accept. First, the investigators limited the use of VATS to patients whose tumors were less than 5 cm and in whom the fissures were complete. This is reflected in the fact that the VATS group had statistically significantly smaller proportionally more T1 tumors. Second, their VATS technique included a utility thoracotomy with rib spreading. Lastly, the thoracotomy group had a statistically significantly higher rate of pneumonectomy (21 % vs. 10 %, $p = 0.03$). Clearly, these were two different groups of patients.

By contrast, the series of patients reported by Flores and colleagues consisted of VATS and thoracotomy groups that were well matched with respect to preoperative characteristics, pathological stage, histology, and tumor size [33]. Kaplan-Meier analysis demonstrated a 79 % 5-year survival for the VATS group and a 75 % 5-year survival for the thoracotomy group (log rank; $p = 0.8$) (Fig. 39.2). Furthermore, the authors performed propensity score-matched analysis that demonstrated similar survival between VATS and thoracotomy groups and confirmed the results of the raw data. Outside of a prospective, randomized controlled trial, this provides compelling evidence that a VATS approach is equivalent to thoracotomy in terms of long-term oncologic outcome.

Benefits of VATS

In addition to shorter chest tube duration and length of hospital stay, proponents of VATS feel the benefits also include advantages such as decreased complications, enhanced ability to treat high-risk patients, increased tolerance of adjuvant systemic therapy, and superior quality of life.

Decreased Perioperative Morbidity

There have been multiple published series of VATS anatomic pulmonary resection that suggest that the minimally invasive approach is associated with fewer postoperative complications. Most were large, single-arm retrospective studies [26, 27] and, until recently, those that formally compared VATS to thoracotomy contained small numbers of patients in unmatched analyses [28–32]. Recent efforts have analyzed the two approaches with greater numbers of patients [33, 38] and in matched cohorts to offset the traditional selection bias inherent with individual surgeon choice of VATS versus thoracotomy [39, 40].

Whitson and coauthors evaluated retrospectively their single-institution experience with 147 lobectomies for clinical stage I NSCLC performed by thoracotomy (88) versus by VATS (59) [38]. Although this was an unmatched comparison, the two groups were similar in demographics, preoperative lung function, and pathologic stage. In fact, it was the VATS patients who had a higher incidence of hypertension and chronic renal insufficiency. The VATS group had significantly less postoperative pneumonia (3.4 % vs. 19.3 %, $p = 0.0023$) compared with the thoracotomy group. The rates of prolonged air leak, atrial fibrillation, reoperation, and myocardial infarction were not different between groups. The VATS patients showed a trend toward decreased length of hospital stay, but paradoxically, had a small but significantly increase in the number of intensive care unit days. This study likely suffered from small numbers and the fact that the VATS patients represented the authors' initial experience with the technique.

In an effort to address this, authors from the same institution undertook a systematic review of the literature in order to compare outcomes after VATS or thoracotomy for lobectomy [39]. They identified 39 studies (22 VATS, 27 thoracotomy, 10 both) that contained relevant and adequate data for analysis on a total of 6,370 patients (3,114 VATS, 3,256 thoracotomy). The two groups were similar with respect to mean age, gender distribution, and proportion of adenocarcinoma, but the thoracotomy group did have a higher proportion of squamous cell carcinoma. Consistent with previous reports, univariate analysis demonstrated VATS was associated with shorter duration of chest tube drainage and hospital stay. Moreover, the authors observed that the overall complication rate after VATS lobectomy was significantly lower than thoracotomy lobectomy (16.4 % vs. 31.2 %, $p = 0.018$). The rates of specific complications, such as atrial fibrillation, pneumonia, and persistent air leak, however, were not significantly different between groups.

Park and coauthors were one of the first to attempt to evaluate the two techniques in a matched analysis, reporting on 389 consecutive patients who underwent lobectomy over a 5-year period by either VATS or thoracotomy [40]. Patients were matched by age and gender, leaving 122 patients in each arm. The VATS patients had higher preoperative DLCO and lower rate of receipt of induction therapy. The total complication rate was lower in the VATS group (17.2 % vs. 27.9 %, $p = 0.046$) as was the mean length of stay (4.9 days vs. 7.2 days, $p = 0.01$). As seen in the systematic review, the rates of specific complications were not statistically different between the cohorts. In particular, the rates of postoperative atrial fibrillation between groups were similar (12 % VATS, 16 % thoracotomy), suggesting that the pathogenesis of atrial fibrillation following anatomic pulmonary resection has more to do with autonomic denervation and stress-mediated neurohumoral mechanisms, rather than incision-related effects.

Flores and colleagues from the same institution later reported an update on a larger number of patients ($n = 741$) in order to evaluate any differences between VATS (398) and thoracotomy (346) with respect to perioperative outcomes, as well as survival [33]. Intent-to-treat analysis of the raw data showed that overall complication rate was higher in the thoracotomy group (30 % vs. 24 %, $p = 0.05$) with the most common complications in both groups being atrial arrhythmias, respiratory failure, and prolonged air leaks. Two percent (8/398) of VATS patients had major complications compared to 3.8 % (13/343) of thoracotomy patients. Following propensity scored-matched analysis to compensate for inherent differences between the groups, a logistic regression model for complication demonstrated an odds ratio of 0.67 (CI 0.45–0.98, $p = 0.4$) in favor of VATS.

Perhaps, the most exhaustive examination of the potential differences between VATS and thoracotomy with respect to complications was recently reported by Villamizar and colleagues [41]. Reviewing a 10-year experience from 1999 to 2009 from a single institution, they identified 1,079 patients, 697 of whom underwent lobectomy by VATS. Propensity score matching was done in an in-to-treat method and resulted in 284 patients in each group that had no discernable

Table 39.3 Postoperative complications VATS versus thoracotomy

Complications	THOR ($n = 284$)	VATS ($n = 284$)	*P* value
Atrial fibrillation, n (%)	61 (21)	37 (13)	0.01
Atelectasis, n (%)	34 (12)	15 (5)	0.006
Prolonged air leak, n (%)	55 (19)	37 (13)	0.05
Bleeding, n (%)	3 (1)	3 (1)	
Transfusion, n (%)	36 (13)	11 (4)	0.002
Pneumonia, n (%)	27 (10)	14 (5)	0.05
Empyema, n (%)	2 (0.8)	2 (0.8)	
Bronchopleural fistula, n (%)	3 (1)	1 (0.4)	0.62
Sepsis, n (%)	6 (2)	1 (0.4)	0.12
Renal failure, n (%)	15 (5)	4 (1.4)	0.02
CVA, n (%)	3 (1)	2 (1)	1.0
MI, n (%)	0 (0)	1 (0.4)	0.50
Ventricular arrhythmia, n (%)	2 (0.8)	2 (0.8)	
DVT, n (%)	2 (0.8)	0 (0)	0.50
PE, n (%)	3 (1)	1 (0.4)	0.62
Chest tube duration, median days (25th, 75th quartile)	4 (3, 6)	3 (2, 4)	0.0001[a]
Length of hospital stay, median days (25th, 75th quartile)	5 (4, 7)	4 (3, 6)	0.0001[a]
Death, n (%)	15 (5)	8 (3)	0.20
Patients with no complication, n (%)	144 (51)	196 (69)	0.0001

From Villamizar et al. J Thorac Cardiovasc Surg 2009;138:419–425, reprinted with permission from Elsevier
THOR conventional thoracotomy, *VATS* video-assisted thoracoscopic surgery, *CVA* cerebrovascular accident, *MI* myocardial infarction, *DVT* deep venous thrombosis, *PE* pulmonary embolism
[a]Wilcoxon signed-rank test

inequities with respect to age, gender, use of preoperative therapy, comorbid conditions, lung function, or clinical stage. When these two groups were then compared for occurrence of postoperative complications, the VATS patients not only had a lower overall complication rate (31 % vs. 49 %, $p = 0.0001$) but also had lower incidences of atrial fibrillation, atelectasis, prolonged air leak, pneumonia, transfusion requirement, and renal failure (Table 39.3). Perioperative mortality was similar between groups.

High-Risk Patient Populations

With emerging evidence that a VATS approach seems to be associated with decreased overall complications, there has been speculation that the minimally invasive approach might, therefore, allow borderline, high-risk patients who might otherwise have prohibitive complications following thoracotomy to undergo major lung resection by VATS. One such group is the elderly patient. Given that the incidence of lung cancer continues to remain substantial and the increasing proportion of the elderly population, it is inevitable that the average patient will continue to get older. It is well established that operative morbidity and mortality rates for pulmonary resections rise with advancing patient age. Ginsberg and colleagues for the Lung Cancer Study Group observed a 7.1 % 30-day operative mortality rate in patients (most of whom underwent thoracotomy) greater than or equal to 70 years ($n = 453$) versus 1.3 % for patients younger than 60 years and 3.7 % overall for 2,200 patients undergoing lung resection [5]. Similarly, Damhuis and coauthors noted from a series of 1,577 lung cancer patients undergoing resection that age and extent of resection were the major determinants of

operative risk [6]. Operative mortality in that series was 4.0 % for patients age 70 years and older ($n = 521$) versus 1.4 % for patients younger than 60 years.

A number of studies have reviewed outcomes of VATS lobectomy in older patients, primarily 70 years or older, showing acceptable morbidity and mortality [42–45]. All demonstrated acceptable results employing minimally invasive techniques. McVay and colleagues reported an overall complication rate of only 18 % and operative mortality of 1.8 % in 159 consecutive octogenarians undergoing VATS lobectomy [43], suggesting not only that absolute age is not a contraindication to aggressive surgical treatment of lung cancer, but that there may be some advantages to a less invasive approach. Koizumi and coauthors published the first study attempting to compare elderly patients undergoing VATS versus those having standard thoracotomy [44]. Chest tube duration, length of stay, and change in performance status postoperative were significantly better in patients undergoing VATS. However, there were no differences in overall complication rate and occurrence of specific complications, such as air leak, pneumonia, and arrhythmia. However, the study was quite small (17 VATS, 15 thoracotomy), and this likely limited the statistical power to determine a difference. Of not, the operative mortality rate was 5.9 % in the VATS group and 20 % in the thoracotomy group.

More recently, Cattaneo and coauthors performed a matched analysis of 333 consecutive patients 70 years or older who underwent lobectomy for NSCLC by either VATS or thoracotomy [45]. Matching based on age, gender, comorbidities, and preoperative stage, they identified 164 eligible patients, 82 in each group. Comparison of the two revealed that postoperative complications following pulmonary lobectomy in an elderly patient population occur with a lower frequency with a minimally invasive VATS approach compared with a traditional, rib-spreading thoracotomy. The overall morbidity rate was 28 % in the VATS patients versus 45 % ($p = 0.04$) in those undergoing thoracotomy. In addition, the VATS group not only had a lower complication rate but a lower proportion of patients with one or more complications and lower grades of complications compared with patients undergoing thoracotomy (0 % vs. 7 % grade 3 or higher complications, $p = 0.007$). The exact mechanisms by which complications were reduced were not identified, but also observed was that the rate of pulmonary complications in the thoracotomy group was higher than in the VATS group. This suggested that perhaps limiting chest wall trauma by employing VATS may help reduce pulmonary morbidity, which in turn reduces the overall rate of operative complications.

Postoperative Pain and Quality of Life (QOL)

Even though it is widely accepted that VATS patients experience less acute postoperative pain, there have been few studies using validated measures to analyze differences between VATS and thoracotomy. Landreneau and coauthors attempted to assess the advantage of VATS with respect to postoperative pain-related morbidity by reviewing 138 patients that underwent VATS ($n = 81$) or limited lateral thoracotomy ($n = 57$) [46]. Only 7 patients underwent VATS lobectomy, while 38 had thoracotomy and lobectomy. Pain was quantified by postoperative narcotic requirements, the need for intercostal/epidural analgesia and patient perception of pain index scoring. VATS patients experienced significantly less pain with none requiring intercostal/epidural analgesia compared with 31 (54 %) thoracotomy patients ($p = 0.001$). Overall narcotic requirements were less, and this correlated with lower perception of pain index in the VATS group. In a similar analysis, Stammberger and colleagues retrospectively polled 173 patients that had undergone a VATS procedure a mean of 18 months (range 3–38) previously [47]. Only 16 patients underwent lobectomy, but nonetheless, at 6 months postoperatively, 75 % of patients had no complaints, and postthoracoscopy pain rate

was 25 %. This decreased such that postthoracoscopy pain occurred in only 5 % and 4 % at 1 and 2 years postoperatively, respectively. The major weakness of this study was the fact that questionnaires were not validated measures of pain. Lastly, Nagahiro and coauthors prospectively studied acute postoperative pain in 22 consecutive patients undergoing lobectomy by VATS ($n = 13$) or thoracotomy ($n = 9$) [48]. Pain was assessed on postoperative days 0, 1, 2, 4, 7, and 14 using an 11-point scale, and amount of analgesic use was recorded. VATS patients required significantly less amounts of analgesics postoperatively, and postoperative pain levels were also less at every time point. Unfortunately, no long-term follow-up was performed.

There have been precious few studies on postoperative QOL. Two attempts at evaluating QOL following VATS versus thoracotomy patients came from Asia [49, 50]. Sugiura and others studied 44 consecutive patients with clinical stage I lung cancer who underwent lobectomy by either VATS ($n = 22$) or thoracotomy ($n = 22$) [49]. Long-term QOL was measured retrospectively using a non-validated questionnaire consisting of six primary questions about return to preoperative level of activity; pain, arm, or shoulder dysfunction; and satisfaction with the procedure. Median follow-up was 12.5 months for the VATS patients and 33.6 months for the thoracotomy patients. VATS patients had shorter average time to resumption of preoperative activity (2.5 ± 1.7 vs. 7.8 ± 8.6 days), greater satisfaction with the size of the scar ($p = 0.001$), and a more favorable overall impression of the procedure compared to thoracotomy ($p = 0.03$). The only other prospective evaluation of QOL following VATS versus thoracotomy was from Li and colleagues from the Prince of Wales Hospital [50]. QOL was assessed in 51 patients (27 VATS, 24 thoracotomy) at mean follow-up time of 33.5 months (range 6–84.2 months) in the VATS group and 39.4 months (range 7–75.1 months) in the thoracotomy group. VATS patients displayed a trend toward higher scores on QOL and functioning scales and less chronic pain medication use, but these did not reach statistical significance.

Tolerance of Adjuvant Chemotherapy

Since the advent of adjuvant systemic chemotherapy as standard of care following complete resection of pathologic stage II and higher NSCLC, the issue of whether superior recovery following VATS resection translates into better delivery and tolerance of adjuvant therapy is an important one. Since it is clear that adjuvant therapy for node-positive NSCLC does in fact increase chances of survival [51, 52], and it is equally clear that it is difficult to deliver all intended therapy in the postoperative setting, if a VATS approach enhances a patient's ability to receive such therapy, its routine use can lead to increased survival on that basis alone. There have been only two studies that have evaluated this formally [53, 54]. The first by Petersen and others conducted a retrospective study of 100 consecutive patients with NSCLC who underwent a complete resection via lobectomy and received adjuvant chemotherapy in a 5-year period [53]. Fifty-seven patients had thoracoscopy, while 43 patients had thoracotomy. The patients were similar with respect to age, gender, presence of comorbid conditions, and preoperative pulmonary function. However, the thoracotomy group had a higher proportion of squamous cell carcinoma and a much higher proportion of pathologic stage III patients (47 % vs. 24 %, $p = 0.05$) compared to VATS. Analyzing surrogates of chemotherapy compliance, the authors observed that VATS patients had a lower rate of delayed doses (18 % vs. 58 %, $p < 0.001$), lower rate of reduced doses (26 % vs. 49 %, $p = 0.02$), and a greater percentage that received >75 % of the total planned regimen (61 % vs. 40 %, $p = 0.03$). There were no differences between groups with respect to time to initiation of chemotherapy, percentage of planned regimen ultimately received, or toxicity of treatment.

A later and less comprehensive study by Nicastri and others reported on 26 patients in a single-institution series of 127 patients with NSCLC that underwent VATS lobectomy [54]. Sixteen of the 127 patients had pathologic stage IIA or higher disease, and 26 ultimately received chemotherapy, although it is not clear from the

report what the indications were. Of the 26 patients, 19 (73 %) received the full-planned dose on schedule, while (12 %) were given the full course with a delay in one cycle or more. Twenty-two patients (85 %) received all intended cycles. The results of both of these studies showed superior delivery of adjuvant chemotherapy compared with the roughly 60 % delivery of all therapy in the large adjuvant therapy trials [51, 52], implying that use of VATS allows for enhanced delivery of chemotherapy, but the evidence is preliminary, retrospective, and therefore quite susceptible to selection bias and must be viewed with caution. Further studies are needed on this topic.

Sublobar Resections

The seminal work demonstrating the superiority of lobectomy for early stage lung cancer was reported by Ginsberg and Rubinstein on behalf of the Lung Cancer Study Group [55]. In a prospective, randomized study of clinically node-negative tumors 3 cm or less in diameter, patients were assigned to either lobectomy or sublobar resection (wedge or segmentectomy). The results revealed a 75 % increase in recurrence rate ($p = 0.02$, one-sided) attributable to a threefold increase in local recurrence with limited resection ($p = 0.008$, two-sided). Recent work by authors from Japan has supported, however, potential acceptability of segmental resections for small, peripheral node-negative tumors [56, 57]. There are ongoing randomized trials to address this issue, but limited resection should only be employed for small (less than 2 cm) peripheral tumors at this time.

Data on VATS segmentectomy and pneumonectomy are few, although authors have reported on patients undergoing both in their larger series of VATS resections [26, 58]. McKenna and coauthors reported one of the first series that included segmentectomies and pneumonectomy in a study of 282 consecutive patients that underwent VATS anatomic resections, including 262 standard lobotomies, 15 segmentectomies, 3 sleeve resections, 1 bilobectomy, and 1 pneumonectomy [58]. For the overall group, the median length of stay was 3 days (range 2–23 days), overall morbidity rate was 11 %, and the perioperative mortality rate was 0.6 %. The outcomes of the non-lobectomy patients were not reported separately.

Subsequently, there have been four studies focusing on the results of VATS segmentectomies [59–62]. Watanabe and colleagues performed a feasibility study of 41 consecutive patients undergoing anatomic VATS segmentectomy for NSCLC with a tumor diameter of ≤ 2 cm [57]. Mean operative time was 220 min (range 100–306), and mean chest tube duration was 3 ± 2 days. There were no perioperative deaths, and a 10 % morbidity rate (2 prolonged air leaks, 2 with atrial fibrillation). The 5-year survival for pathologic stage IA patients was 90 %, very similar to previous studies of VATS lobectomy for small tumors, leading the authors to conclude that VATS segmentectomy for small, peripheral NSCLCs was both feasible and oncologically sound. Schubert and others reported their single-institution series of 182 anatomic segmentectomies (114 open, 68 VATS) over a 4-year period for stage I NSCLC and compared them with 246 lobectomies also for stage I disease [60]. The segmentectomy patients tended to have a higher percentage of stage IA disease (60 % vs. 46 %, $p = 0.004$) and smaller mean tumor size (2.3 cm vs. 3.1 cm, $p < 0.0001$) compared with lobectomy. Operative time and blood loss were less with segmentectomy, and morbidity and mortality rates were similar between groups. The overall survival and recurrence rates were not different.

Atkins and coauthors compared segmentectomy done by VATS and thoracotomy in order to assess any advantages to a minimally invasive approach [61]. There were a total of 77 consecutive patients (48 VATS, 29 thoracotomy) that had similar baseline demographics. There were no conversions in the series. Operative times, blood loss, and chest tube duration were similar between groups. Hospital length of stay was significantly less among the VATS patients (4.3 ± 3 days vs. 6.8 ± 6 days, $p = 0.03$). Interestingly, there was no difference in overall or individual complication rates. The 30-day

mortality rate was 6.9 % for the thoracotomy group compared with 0 % for the VATS group, although this was not statistically significantly different. Lastly, Shapiro and others reported their series of VATS segmentectomies ($n = 31$) compared with similar patients undergoing VATS lobectomy ($n = 113$) for small stage I NSCLC [62]. Not surprisingly, lobectomy patients had better preoperative lung function and larger tumors. Moreover, 10 % of the segmentectomy patients had undergone previous pulmonary resections on the contralateral side. The two groups had similar perioperative results in terms of chest tube duration, total complications, and length of stay. Locoregional recurrence rate was similar between VATS segmentectomy and lobectomy (3.5 % vs. 3.6 %, $p = 0.71$), and overall and disease-free survivals at a median follow-up of 21 months were also similar. These results suggested that for small, stage IA tumors, VATS segmentectomy is a reasonable alternative to lobectomy.

There are no reported series of VATS pneumonectomy. As stated previously, a couple of authors reported on VATS pneumonectomy as part of a larger series of VATS pulmonary resections [36, 58]. Thomas and colleagues reported on 511 patients who underwent 515 lung resections [36], 81 of whom had pneumonectomies, 10 by VATS. Unfortunately, no technical or perioperative data on the VATS pneumonectomy patients was given.

Telerobotic Surgery

Limitations of minimally invasive surgical (MIS) approaches for performance of major thoracic procedures include two-dimensional imaging, an unsteady camera platform, and limited maneuverability of instruments used through small non-rib-spreading incisions. In an effort to improve standard MIS techniques, telerobotic surgery evolved. The da Vinci® Surgical System (Intuitive Surgical®, Sunnyvale, CA) is an FDA-approved telerobotic system consisting of four components, including a vision system with a true three-dimensional (3-D) endoscope providing a high-definition, binocular view of the surgical field and the EndoWrist® instrument system capable of seven degrees of freedom and two degrees of axial rotation in order to replicate human wrist-like movements [63]. The advanced articulation of the robotic instruments is clearly its greatest potential improvement over straight instruments employed in conventional VATS procedures. Because of this, the da Vinci® system was initially designed for use in closed-chest cardiac surgery, and the earliest published experience was in the area of coronary artery bypass grafting [64]. Subsequently, however, telerobotic assistance to MIS has had its greatest impact on the fields of urology (robotic prostatectomy) and gynecology.

In the field of general thoracic surgery, however, utilization of robotics was and remains gradual in a way that mirrors advanced VATS techniques. The initial reports of robotic-assisted VATS procedures were limited to case reports [65–67]. For VATS anatomic pulmonary resections, there are some emerging data regarding its feasibility and outcomes. Park and colleagues published the first large series of robotic-assisted VATS lobectomies that described a reproducible technique and reviewed their initial results [13]. Employing a 3-incision, non-rib-spreading VATS technique, robotic assistance was performed on 34 consecutive patients with localized tumors, the majority of which (32/34, 94 %) were NSCLC. Conversion rate to thoracotomy was 12 % (4/34), median number of lymph node stations removed was 4 (range 2–7), and there were no perioperative deaths. Morbidity rate was 26 % and median chest tube duration was 3 days (range 2–12 days) with a median length of stay of 4.5 days (range 2–14 days). Median operative time was 218 min (range 155–350). This report revealed that telerobotic assistance for VATS lobectomy was feasible, safe, and achieved results comparable with the literature for VATS lobectomy. A similar study done by Gharagozloo and coauthors reviewed their experience with robotic assistance in 100 consecutive patients with stage I and II NSCLC that underwent VATS lobectomy [67]. The robotic portion of the procedure was limited to

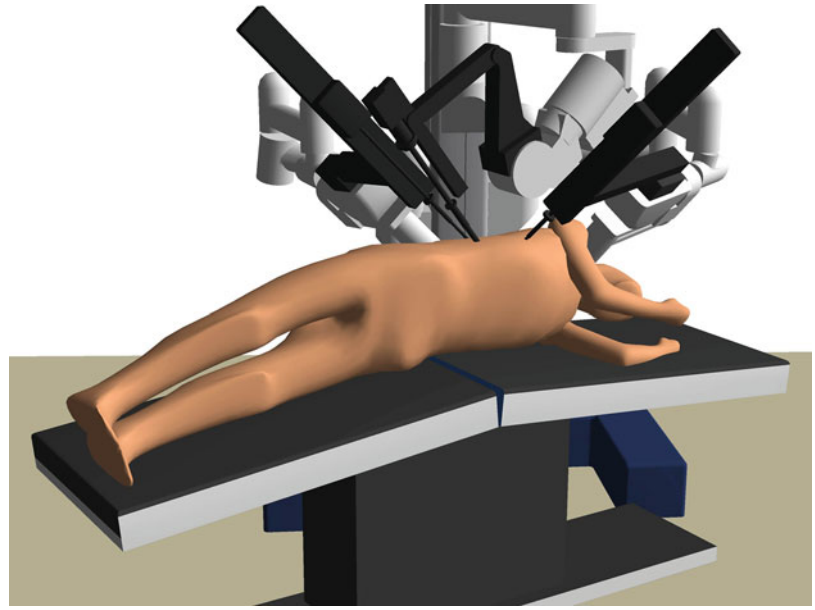

Fig. 39.3 Robotic-assisted VATS lobectomy – incisions and positioning of the da Vinci system (From Park BJ et al. J Thorac Cardiovasc Surg. 2006;131:54–9, reprinted with permission from Elsevier)

mediastinal lymph node dissection and dissection of the oblique fissure. Mean operative time was 216 ± 27 min with a conversion rate of 1 %. Total complication rate was 21 % (21/100), the most common complication being atrial fibrillation in 13 % of patients. Operative mortality was 3 %. This provided further evidence that robotic assistance to complex VATS anatomic resection is indeed feasible and safe. Whether there is a routine role for telerobotic assistance for major VATS, resections is still a matter of controversy and requires further prospective study (Fig. 39.3).

Summary and Conclusions

The incidence of NSCLC remains high, and with improvements in imaging, the possibility of increased screening, and aging of the population, it is likely that the number of patients with early stage disease will continue to increase. Surgical resection in these patients remains the foundation of curative treatment. Utilization of a minimally invasive VATS approach is also likely to increase because it is well established that, compared with thoracotomy, use of VATS for anatomic pulmonary resection of NSCLC results in decreased chest tube duration and length of hospitalization while achieving equivalent oncologic results. There is compelling evidence that VATS is associated with fewer complications, particularly in high-risk and elderly patients and may also lead to better delivery and tolerance of adjuvant therapy. While lobectomy remains the most common indication for advanced VATS, the approach is being increasingly employed for other anatomic resections, such as segmentectomy and even pneumonectomy. Moreover, detection of smaller lesions will also allow for sublobar resections aided by preoperative image guidance. Advances in technologic innovations, such as telerobotics, may lead to further advancements in and expansion of complex minimally invasive procedures [13, 64].

References

1. Jemal A, Siegel R, Ward E, Hao Y, Xu J, Thun M. Cancer statistics, 2009. CA Cancer J Clin. 2009;59:225–49.
2. Gridelli C, Perrone F, Monfardini S. Lung cancer in the elderly. Eur J Cancer. 1997;33:2313–4.
3. Gridelli C. Chemotherapy of non-small cell lung cancer in the elderly. Lung Cancer. 2002;38(suppl 3): S67–70.
4. Yancik R, Ries LA. Aging and cancer in America. Demographic and epidemiologic perspectives. Hematol Oncol Clin North Am. 2000;14:17–23.

5. Ginsberg RJ, Hill LD, Eagan RT, Thomas P, Mountain CF, Deslauriers J, et al. Modern thirty-day operative mortality for surgical resections in lung cancer. J Thorac Cardiovasc Surg. 1983;86:654–8.
6. Damhuis RA, Schutte PR. Resection rates and postoperative mortality in 7899 patients with lung cancer. Eur Respir J. 1996;9:7–10.
7. Boffa DJ, Allen MS, Grab JD, Gaissert HA, Harpole DH, Wright CD. Data from The Society of Thoracic Surgeons general thoracic surgery database: the surgical management of primary lung tumors. J Thorac Cardiovasc Surg. 2008;135:247–54.
8. Kirby TJ, Rice TW. Thoracoscopic lobectomy. Ann Thorac Surg. 1993;56:784–6.
9. Walker WS, Carnochan FM, Pugh GC. Thoracoscopic pulmonary lobectomy. J Thorac Cardiovasc Surg. 1993;106:1111–7.
10. McKenna RJ. Lobectomy by video-assisted thoracic surgery with mediastinal node sampling for lung cancer. J Thorac Cardiovasc Surg. 1994;107:879–82.
11. Lewis RJ. Simultaneously stapled lobectomy: a safe technique for video-assisted thoracic surgery. J Thorac Cardiovasc Surg. 1995;109:619–25.
12. Swanson SJ, Herndon JE, D'Amico TA, Demmy TL, McKenna RJ, Green MR, et al. Video-assisted thoracic surgery lobectomy: report of CALGB 39802-a prospective, multi-institutional feasibility trial. J Clin Oncol. 2007;25:4993–7.
13. Park BJ, Flores RM, Rusch VW. Robotic assistance for video-assisted thoracic surgical lobectomy: technique and initial results. J Thorac Cardiovasc Surg. 2006;131:54–9.
14. Magistrelli P, D'Ambra L, Berti S, et al. Use of India ink during preoperative computed tomography localization of small peripheral undiagnosed pulmonary nodules for thoracoscopic resection. World J Surg. 2009;33:1421–4.
15. Choi BG, Kim HH, Kim BS, et al. Pulmonary nodules: CT-guided contrast material localization for thoracoscopic resection. Radiology. 1998;208: 399–401.
16. Chella A, Lucchi M, Ambrogi MC, et al. A pilot study of the role of TC-99 radionuclide in localization of pulmonary nodular lesions for thoracoscopic resection. Eur J Cardiothorac Surg. 2000;18:17–21.
17. Pittet O, Christodoulou M, Pezzetta E, et al. Video-assisted thoracoscopic resection of a small pulmonary nodule after computed tomography-guided localization with a hook-wire system. Experience in 45 consecutive patients. World J Surg. 2007;31:75708.
18. Chen YR, Yeow KM, Lee JY, et al. CT-guided hook wire localization of subpleural lung lesions for video-assisted thoracoscopic surgery (VATS). J Formos Med Assoc. 2007;106:911–8.
19. Nakashima S, Watanabe A, Obama T, et al. Need for preoperative computed tomography-guided localization in video-assisted thoracoscopic surgery pulmonary resections of metastatic pulmonary nodules. Ann Thorac Surg. 2010;89:212–9.
20. Mayo JR, Clifton JC, Powell TI, et al. Lung nodules: CT-guided placement of microcoils to direct video-assisted thoracoscopic surgical resection. Radiology. 2009;250:576–85.
21. Lewis RJ, Caccavale RJ, Bocage J, Widmann MD. Video assisted thoracic surgical non rib spreading simultaneously stapled lobectomy. Chest. 1999;116:119–1124.
22. Walker WS. Video-assisted thoracic surgery (VATS) lobectomy: the Edinburgh experience. Semin Thorac Cardiovasc Surg. 1998;10:291–9.
23. Kaseda S, Aoki T, Hangai N. Video-assisted thoracic surgery (VATS) lobectomy: the Japanese experience. Semin Thorac Cardiovasc Surg. 1998; 10:300–4.
24. McKenna RJ, Wolf RK, Brenner M, Fischel RJ, Wurnig P. Is lobectomy by video-assisted thoracic surgery an adequate cancer operation? Ann Thorac Surg. 1998;66:1903–8.
25. Yim AP, Liu HP. Thoracoscopic major lung resection-indications, technique and early results: experience from two centers in Asia. Surg Laparosc Endosc. 1997;7:241–4.
26. McKenna Jr RJ, Houck W, Fuller CB. Video-assisted thoracic surgery lobectomy: experience with 1,100 cases. Ann Thorac Surg. 2006;81:421–6.
27. Onaitis MW, Petersen RP, Balderson SS, Toloza E, Burfeind WR, Harpole DH, D'Amico TA. Thoracoscopic lobectomy is a safe and versatile procedure. Ann Surg. 2006;244:420–5.
28. Giudicelli R, Thomas P, Lonjon T, Ragni J, Morati N, Ottomani R, et al. Video-assisted minithoracotomy versus muscle-sparing thoracotomy for performing lobectomy. Ann Thorac Surg. 1994;58:712–7.
29. Kirby TJ, Mack MJ, Landreneau RJ, Rice TW. Lobectomy–video-assisted thoracic surgery versus muscle-sparing thoracotomy. A randomized trial. J Thorac Cardiovasc Surg. 1995;109:997–1001.
30. Ohbuchi T, Morikawa T, Takeuchi E, Kato H. Lobectomy: video-assisted thoracic surgery versus posterolateral thoracotomy. Jpn J Thorac Cardiovasc Surg. 1998;46:519–22.
31. Demmy TL, Curtis JJ. Minimally invasive lobectomy directed toward frail and high-risk patients: a case–control study. Ann Thorac Surg. 1999;68:194–200.
32. Nagahiro I, Andou A, Aoe M, Sano Y, Date H, Shimizu N. Pulmonary function, postoperative pain, and serum cytokine level after lobectomy: a comparison of VATS and conventional procedure. Ann Thorac Surg. 2001;72:362–5.
33. Flores RM, Park BJ, Dycoco J, Aronova A, Hirth Y, Rizk NP, et al. Lobectomy by video-assisted thoracic surgery (VATS) versus thoracotomy for lung cancer. J Thorac Cardiovasc Surg. 2009;138:11–8.
34. Kaseda S, Aoki T, Hangai N, Shimizu K. Better pulmonary function and prognosis with video-assisted thoracic surgery than with thoracotomy. Ann Thorac Surg. 2000;70:1644–6.

35. Walker WS, Codispoti M, Soon SY, Stamenkovic S, Camochan F, Pugh G. Long-term outcomes following VATS lobectomy for non-small cell bronchogenic carcinoma. Eur J Cardiothorac Surg. 2003; 23:397–402.
36. Thomas P, Doddoli C, Yena S, Thirion X, Sebag F, Fuentes P, Giudicelli R. VATS is an adequate oncological operation for stage I non-small cell lung cancer. Eur J Cardiothorac Surg. 2002;21:1094–9.
37. Sugi K, Kaneda Y, Esato K. Video-assisted thoracoscopic lobectomy achieves a satisfactory long-term prognosis in patients with clinical stage IA lung cancer. World J Surg. 2000;24:27–31.
38. Whitson BA, Andrade RS, Boettcher A, Bardales R, Kratzke RA, Dahlberg PS, Maddaus MA. Video-assisted thoracoscopic surgery is more favorable than thoracotomy for resection of clinical stage I non-small cell lung cancer. Ann Thorac Surg. 2007;83:1965–70.
39. Whitson BA, Groth SS, Duval SJ, Swanson SJ, Maddaus MA. Surgery for early-stage non-small cell lung cancer: a systematic review of the video-assisted thoracoscopic surgery versus thoracotomy approaches to lobectomy. Ann Thorac Surg. 2008;86:2008–18.
40. Park BJ, Zhang H, Rusch VW, Amar D. Video-assisted thoracic surgery does not reduce the incidence of postoperative atrial fibrillation after pulmonary lobectomy. J Thorac Cardiovasc Surg. 2007; 133:775–9.
41. Villamizar NR, Darrabie MD, Burfeind WR, Peterson RP, Onaitis MW, Toloza E, et al. Thoracoscopic lobectomy is associated with lower morbidity compared with thoracotomy. J Thorac Cardiovasc Surg. 2009;138:419–25.
42. Koren JP, Bocage JP, Geis WP, Caccavale RJ. Major thoracic surgery in octogenarians. The video-assisted thoracic surgery (VATS) approach. Surg Endosc. 2003;17:632–5.
43. McVay CL, Pickens A, Fuller C, Houck W, McKenna R. VATS anatomic pulmonary resection in octogenarians. Am Surg. 2005;71:791–3.
44. Koizumi K, Haraguchi S, Hirata T, Hirai K, Mikami I, Fukushima M, et al. Lobectomy by video-assisted thoracic surgery for lung cancer patients aged 80 years or more. Ann Thorac Cardiovasc Surg. 2003;9:14–21.
45. Cattaneo SM, Park BJ, Wilton AS, Seshan VE, Bains MS, Downey RJ, et al. Use of video-assisted thoracic surgery for lobectomy in the elderly results in fewer complications. Ann Thorac Surg. 2008;85:231–6.
46. Landreneau RJ, Hazelrigg SR, Mack MJ, Dowling RD, Burke D, Gavlick J, et al. Postoperative pain-related morbidity: video-assisted thoracic surgery versus thoracotomy. Ann Thorac Surg. 1993;56:1285–9.
47. Stammberger U, Steinacher C, Hillinger S, Schmid RA, Kinsbergen T, Weder W. Early and long-term complaints following video-assisted thoracoscopic surgery: evaluation in 173 patients. Eur J Cardiothorac Surg. 2000;18:7–11.
48. Suguira H, Morikawa T, Kaji M, Sasamura Y, Kondo S, Katoh H. Long-term benefits for the quality of life after video-assisted thoracoscopic lobectomy in patients with lung cancer. Surg Laparosc Endosc Percutan Tech. 1999;9:403–8.
49. Li WW, Lee TW, Lam SS, NG CS, Sihoe AD, Wan IY, Yim AP. Quality of life following lung cancer resection. Chest. 2002;122:584–9.
50. The International Adjuvant Lung Cancer Trial Collaborative Group. Cisplatin-based adjuvant chemotherapy in patients with completely resected non-small cell lung cancer. N Engl J Med. 2004; 350:351–60.
51. Winton T, Livingston R, Johnson D, Rigas J, Johnston M, Butts C, et al. Vinorelbine plus cisplatin vs. observation in resected non-small-cell lung cancer. N Engl J Med. 2005;352:2589–97.
52. Petersen RP, Pham D, Burfeind WR, Hanish SI, Toloza EM, Harpole DH, D'Amico TA. Thoracoscopic lobectomy facilitates the delivery of chemotherapy after resection for lung cancer. Ann Thorac Surg. 2007;83:1245–50.
53. Nicastri DG, Wisnivesky JP, Little V, Yun J, Chin C, Dembitzer FR, Swanson SJ. Thoracoscopic lobectomy: report on safety, discharge independence, pain and chemotherapy tolerance. J Thorac Cardiovasc Surg. 2008;135:642–7.
54. Ginsberg RJ, Rubinstein LV. Randomized trial of lobectomy versus limited resection for T1N0 non small cell lung cancer. Lung cancer study group. Ann Thorac Surg. 1995;60:615–22.
55. Koike T, Yamato Y, Yoshiya K, et al. Intentional limited pulmonary resection for peripheral T1N0M0 small sized lung cancer. J Thorac Cardiovasc Surg. 2003;125:924–8.
56. Watanabe T, Okada A, Imakire T, et al. Intentional limited resection for small peripheral lung cancer based on intraoperative pathologic exploration. Jpn J Thorac Cardiovasc Surg. 2005;53:29–35.
57. McKenna RJ, Mahtabifard A, Pickens A, Kusuanco D, Fuller CB. Fast-tracking after video-assisted thoracoscopic surgery lobectomy, segmentectomy and pneumonectomy. Ann Thorac Surg. 2007; 84:1663–7.
58. Watanabe A, Ohori S, Nakashima S, Mawatari T, Inoue N, Kurimoto Y, Higami T. Feasibility of video-assisted thoracoscopic surgery segmentectomy for selected peripheral lung carcinomas. Eur J Cardiothorac Surg. 2009;35:775–80.
59. Schuchert MJ, Pettiford BL, Keeley S, D'Amato TA, Kilic A, Close J, et al. Anatomic segmentectomy in the treatment of stage I non-small cell lung cancer. Ann Thorac Surg. 2007;84:926–33.
60. Atkins BZ, Harpole DH, Mangum JH, Toloza EM, D'Amico TA, Burfeind WR. Pulmonary segmentectomy by thoracotomy or thoracoscopy: reduced hospital length of stay with a minimally-invasive approach. Ann Thorac Surg. 2007; 84:1107–13.

61. Shapiro M, Weiser T, Wisnivesky JP, Chin C, Arustmyan M, Swanson S. Thoracoscopic segmentectomy compares favorably with thoracoscopic lobectomy for patients with small stage I lung cancer. J Thorac Cardiovasc Surg. 2009;137:1388–93.
62. Ballantyne GH. Robotic surgery, telerobotic surgery, telepresence and telementoring. Surg Endosc. 2002;16:1389–402.
63. Mohr FW, Falk V, Diegeler A, Walther T, Gummert JF, Bucerius J, et al. Computer-enhanced "robotic" cardiac surgery: experience in 148 patients. J Thorac Cardiovasc Surg. 2001;121:842–53.
64. Melfi FM, Menconi GF, Mariani AM, Angeletti CA. Early experience with robotic technology for thoracoscopic surgery. Eur J Cardiothorac Surg. 2002;21:864–8.
65. Morgan JA, Ginsburg ME, Sonett JR, Argenziano M. Advanced thoracoscopic procedures are facilitated by computer-aided robotic technology. Eur J Cardiothorac Surg. 2003;23:883–7.
66. Bodner J, Wykypiel H, Wetscher G, Schmid T. First experiences with the da Vinci™ operating robot in thoracic surgery. Eur J Cardiothorac Surg. 2004;25:844–51.
67. Gharagozloo F, Margolis M, Tempesta B, Strother E, Najam F. Robot-assisted lobectomy for early-stage lung cancer: report of 100 consecutive cases. Ann Thorac Surg. 2009;88:380–4.

Image-Guided Radiation Therapy for Lung Cancer

40

Farzan Siddiqui, Indrin J. Chetty, Munther Ajlouni, and Benjamin Movsas

Abstract

Lung cancer is a major global health problem. Image-guided radiation therapy (IGRT), including stereotactic body radiation therapy and adaptive radiation therapy, is emerging as an important technique to try and deliver precise high-dose radiation to the tumor volume while minimizing dose to the normal structures. This chapter intends to highlight some of the features of IGRT including simulation for treatment planning, immobilization devices, target delineation for IGRT, setup and image verification, treatment delivery, radiobiology and physics considerations, clinical outcomes, and ongoing research.

Introduction

Lung cancer has been the most common cancer across the world since 1985 [1]. According to global statistics, there were 1.5 million new cases diagnosed, accounting for 12 % of all cancer diagnoses with about 975,000 male and 376,000 female deaths [2]. In the United States, an estimated 219,440 cases occurred with 159,390 people dying from lung cancer in 2009 [3]. Approximately 80–85 % of lung cancers are non-small cell histology, with the rest being small cell lung cancers.

The role of external beam radiation therapy (EBRT) had previously been mostly confined to later stages of lung cancer, in which surgery was not deemed beneficial or feasible. Recently, it is emerging as a viable treatment option even in selected patients with early-stage non-small cell lung cancers (NSCLC).

Treatment of lung cancer with EBRT has evolved considerably over the past few decades. Previously, using two-dimensional (2D) treatment planning and simple open field arrangements, the conventional doses that could be delivered were limited to about 60 Gy. Yet, a randomized trial comparing conventional EBRT alone versus chemotherapy followed by the same dose of radiation reported histological local control rates of 15 % and 17 %, respectively, at 1 year [4].

The high incidence of radiation pneumonitis and esophagitis using 2D techniques essentially prevented further dose escalation. Over time, the development of 3-dimensional conformal radiation therapy (3D-CRT) permitted dose-escalation

F. Siddiqui (✉) • I.J. Chetty • M. Ajlouni • B. Movsas
Department of Radiation Oncology, Henry Ford Health Systems, Detroit, MI, USA
e-mail: fsiddiq2@hfhs.org; ichetty1@hfhs.org; majiloun1@hfhs.org; bmovas1@hfhs.org

D.E. Dupuy et al. (eds.), *Image-Guided Cancer Therapy*, DOI 10.1007/978-1-4419-0751-6_42,

studies in lung cancer. An RTOG phase I/II study escalated the dose in patients with stage I–III NSCLC based on the estimated risk of pneumonitis [5]. In the group of patients with a volume of lung receiving a dose of 20 Gy (V20) of less than 25 %, the dose-limiting toxicity was reached at 90.3 Gy. In patients with a V20 of 25–36 %, the dose was safely escalated to 77.4 Gy using fraction sizes of 2.15 Gy.

In a study in 104 patients with stage I–IIIB NSCLC, the dose was escalated from 70.2 to 90 Gy using 3D-CRT [6]. As in the RTOG study, unacceptable toxicity was seen at the 90-Gy level, with 84 Gy being the maximum tolerated dose. However, the 2-year local control and overall survival rates increased in a dose-dependent manner, with a cutoff noted at the 80-Gy dose level. Patients who received less than 80 Gy had a 14 % local control compared to 88 % for $\geq$80 Gy. Overall survival at 2 years in stage I–II patients was 60 % for $<$80 Gy and 66 % for $\geq$80 Gy ($p = 0.05$) with median survivals of 25.0 months versus 53.6 months. Hayman et al., in a phase I trial, have been able to safely escalate doses up to 103 Gy using volume bins to limit the risks [7]. A total of 109 patients were treated and followed for a median of 110 months. The grade 2–3 pneumonitis and fibrosis rates were less than 15 %, and no grade 4–5 lung toxicity was seen [8]. The RTOG is also currently conducting a phase III randomized trial comparing 60 Gy versus 74-Gy external beam radiation therapy with concurrent and consolidation carboplatin/paclitaxel with or without cetuximab in patients with stage III non-small cell lung cancer (RTOG 0617).

The existence of a radiation dose–response relationship for local tumor control underscores the importance of trying to deliver a higher dose of radiation, while minimizing dose to the normal lung, esophagus, and heart. Intensity-modulated radiation therapy (IMRT) and stereotactic body radiation therapy (SBRT) are now being increasingly used in the treatment of lung cancer [9]. A recent report from the MD Anderson Cancer Center analyzed their retrospective experience in 381 patients treated using 3D-CRT and 91 patients treated using IMRT [10]. A significant decrease in grade 3 or higher pneumonitis was noted using IMRT. Further studies need to be done to evaluate newer radiation treatment technologies in lung cancer.

Image-guided radiation therapy (IGRT) is a novel strategy that has been developed over the past few years to afford radiation oncologists a higher degree of confidence when delivering radiation by imaging the area of interest being treated. In this way, the margins around the target volume to account for setup errors during treatment can be reduced and normal tissue toxicity minimized while giving the same or higher doses.

The term IGRT is hard to define as it is not confined to any one particular technique, modality, or method. At its basic core is the fact that some form of radiologic imaging is being used at some or all steps of the radiation treatment delivery. This includes, but is not limited to, diagnosing and staging of the cancer, computed tomography (CT)-based simulation for RT planning, target delineation using CT/ MRI/ PET-CT information, and visualization of the tumor and surrounding normal structures during radiation therapy itself. Even during radiation therapy, IGRT could be used to verify the position of the target volume before daily treatment (interfraction), during the delivery of treatment (intrafraction), or over the course of therapy to modify volumes if necessary (adaptive radiation therapy).

The aim of this chapter is to provide an overview of IGRT and its use at various steps in the treatment of lung cancer using radiation therapy.

Imaging (PET-CT Scan)-Based Staging

Staging of lung cancer is essential prior to initiation of therapy. Plain film radiographs served as the main imaging modality for many decades before the development and widespread use of CT scans. More recently, positron emission tomography (PET) and PET-CT scanning technology have become mainstream and are being increasingly used for lung cancer staging.

PET technology utilizes a positron-emitting radioisotope (fluorine-18) conjugated to

a deoxyglucose sugar to identify areas of increased cellular metabolism. Lung cancer cells generally have a higher rate of metabolism, and they incorporate the ^{18}F-FDG (fluorodeoxyglucose). The increased uptake can be imaged with a PET or hybrid PET-CT scanner. The limit of detection for lesions, depending on the avidity of radiotracer uptake, is approximately 5–8 mm depending upon scanner type. PET scans can be used to assess the nature of solitary pulmonary nodules with a sensitivity and specificity of 97 % and 78 %, respectively, for diagnosing a malignancy [11]. PET scans also play an important role in determining the presence or absence of disease in mediastinal lymph nodes. CT scans have a low sensitivity and specificity for diagnosing mediastinal disease. A meta-analysis by Toloza et al. noted that PET scans have a sensitivity and specificity of 84 % and 89 %, respectively, for staging the mediastinum [12]. This compares favorably to the sensitivity (57 %) and specificity (82 %) for CT scans and endoscopic ultrasound (sensitivity – 78 %, specificity – 71 %). This was also confirmed in another meta-analysis [13].

PET-positive mediastinal lymphadenopathy needs to be confirmed pathologically by a mediastinoscopy [14]. The high negative predictive value of PET scans for mediastinal disease permits omission of mediastinoscopy in patients with a PET-negative mediastinum. PET scans also enable detection of extracranial distant metastases. Brain MRIs should be performed to rule out the presence of intracranial metastases (Fig. 40.1).

Simulation/4D CT

A gating system connected to a regular CT scanner can be used for acquisition of 4D-CT scans. This system uses infrared markers placed on the surface of the patient which are tracked using ceiling- or couch-mounted infrared cameras. The infrared markers move with respiration, and their motion is tracked by the cameras which, in turn, are analyzed by the tracking software which generates the motion cycle signal. An amplitude-based gating algorithm is used to generate gating signals to control the CT scanner.

During the simulation procedure, the patient lies on an Alpha Cradle or a Vac-Lok bag in a supine position. Infrared markers are placed on the surface of the thoracic/abdominal area. The infrared markers have two purposes: (1) They are used as the markers for the initial setup of the image-guided radiotherapy procedure. In this case, the markers are placed at locations with minimal movement. (2) They are used as the external motion surrogate for gated CT. In this case, some of the makers are placed at locations with maximal movement. Generally, two markers are placed on the chest surface, and three markers are placed in the upper abdominal area. The average vertical movement of the markers is used as the external motion signal so that the couch movement in longitudinal direction during scanning does not affect the motion signal.

A regular spiral CT including the entire thorax section with the markers placed on the chest surface is then obtained, and the slice at the center of the target is identified. The center of the target is then marked on the patient's skin and used as the isocenter for treatment. A gated CT is then performed to include the target with 3–4 cm extension in each direction. Gated CTs with different trigger points corresponding to the end of expiration phase, the end of inspiration phase, and one or two middle phases are carried out for each patient. During the entire procedure, the patient is breathing normally. Patient coaching is not required except for an explanation of the procedure by the physician or a technologist. The spiral CT image set and the 3–4 gated image sets along with the isocenter information are imported into the treatment planning system (TPS). The gated CT image sets are then registered to the spiral CT image set using an autofusion tool in the TPS system. The fusion result is verified by reviewing the match of the vertebral bodies in the two images. The precision of the registration is estimated to be within 1–1.5 mm. This estimation is based on the observation that manually shifting one image set 1–1.5 mm in any directions would induce a visible mismatch between two image sets.

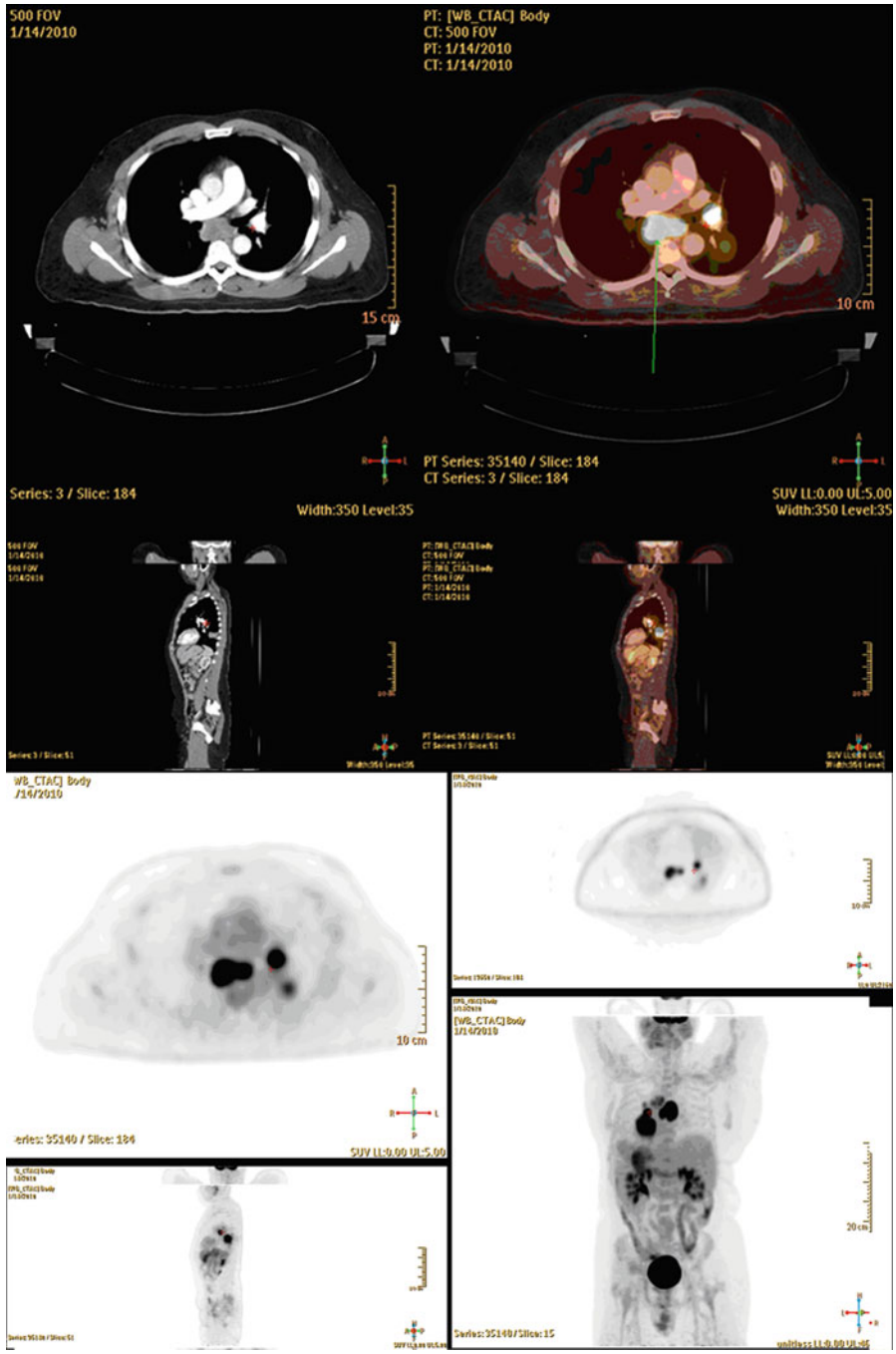

Fig. 40.1 A PET-CT scan demonstrating the primary site of disease in the left lung and the mediastinum

The diagnostic PET-CT images are also loaded into the TPS and fused with the simulation CT images. To fuse the PET images, the diagnostic CT image and the simulation CT images are fused first, followed by fusion of the PET with its diagnostic CT images. The visible tumor in each gated CT and spiral CT image set is contoured, and the internal target volume (ITV) is then drawn

slice by slice in the spiral CT image set to conformally encompass all the contoured targets superimposed on the image. A 3 mm setup uncertainty margin plus a 0–2 mm residual motion margin (overall 3–5 mm margin) is usually applied to the ITV to form a planning target volume (PTV). The residual motion is mainly due to patient breathing irregularity. Some patients could have relatively greater breathing irregularity, which would require a relatively larger residual margin for PTV expansion. IMRT or 3D conformal technique with 6–8 fields is used to treat the patient. The organs at risk (lung, esophagus, and cord) are delineated based on the regular spiral CT image set. The dose calculation is also based on this image set.

The Varian Real-Time Position Management (RPM) Respiratory Gating System (Varian Medical Systems, Palo Alto, CA) is designed for regular free breathing. This system uses a block with two to six circular reflective markers. The block is placed on the patient's abdomen, approximately midway between the xiphoid process and the umbilicus, and its motion with respiration is tracked using an infrared charge-coupled device (CCD) camera.

Immobilization Devices

Proper patient immobilization is essential when treating with EBRT. This is more important when delivering large doses per fraction as in image-guided SBRT. In the thoracic and upper abdominal regions, respiratory motion also needs to be taken into account. Careful attention must be paid to patient comfort, as a patient in a comfortable position is less likely to move about during treatment delivery. SBRT treatment delivery may take 30 min or longer, and the patients need to maintain position for that period of time. Placement of the arms – by the side or above the head – needs to be planned depending on the target location, patients' general health, and other medical conditions, like arthritis or shoulder problems.

Many immobilization devices are available and commonly used for IGRT. The Alpha Cradle system (Smithers Medical Products, Inc., Akron, Ohio) uses foaming agents, which conform to the body shape and harden. Each patient has an individualized Alpha Cradle which cannot be reused for other patients. Bentel et al. compared positional accuracy for lung cancer patients with or without Alpha Cradle immobilization and found a reduced number of isocenter shifts requested by physicians on port films for the immobilized patients. The greatest impact of immobilization was noted for the oblique port films [15].

Another system that is frequently used is the vacuum bean bag systems, like the Vac-Lok (Civco Medical Solutions, Orange, Iowa) or BodyFIX® (Medical Intelligence, Schwabmünchen, Germany). This system uses a bag which is the full length of the patient. After the patient lies on the bag, a vacuum pump is connected to draw air out of the bag. The small bean balls in the bag conform to the patient's shape and can be maintained for the duration a patient is undergoing therapy. Upon completion, the vacuum seal is opened and the bag can be reused for another patient. Additionally, a plastic sheet connected to a continuous vacuum system can be placed on the patient to compress on the body and cause further immobilization.

The BodyFIX® system was evaluated in 53 patients, and a reduction in lung tumor motion was noted in both cranio-caudal and right-left directions [16]. The average tumor motion was 9.2 mm ± 7.1 mm in the cranio-caudal direction and 2.7 mm ± 1.9 mm in the right-left direction. This was reduced to 7.5 mm ± 6.4 mm and 2.1 mm ± 1.2 mm with the BodyFIX® system with a plastic sheet. This 2 mm difference was found to be statistically significant.

Elekta has developed the Stereotactic Body Frame™ (Elekta Medical Systems, Sweden) which has built-in reference indicators for CT and MRI which help with accurate determination of target coordinates. Abdominal compression can also be applied to reduce diaphragm excursion to further reduce tumor motion. Elekta also provides a device called the Active Breathing Coordinator™ for patient-controlled inspiration and expiration.

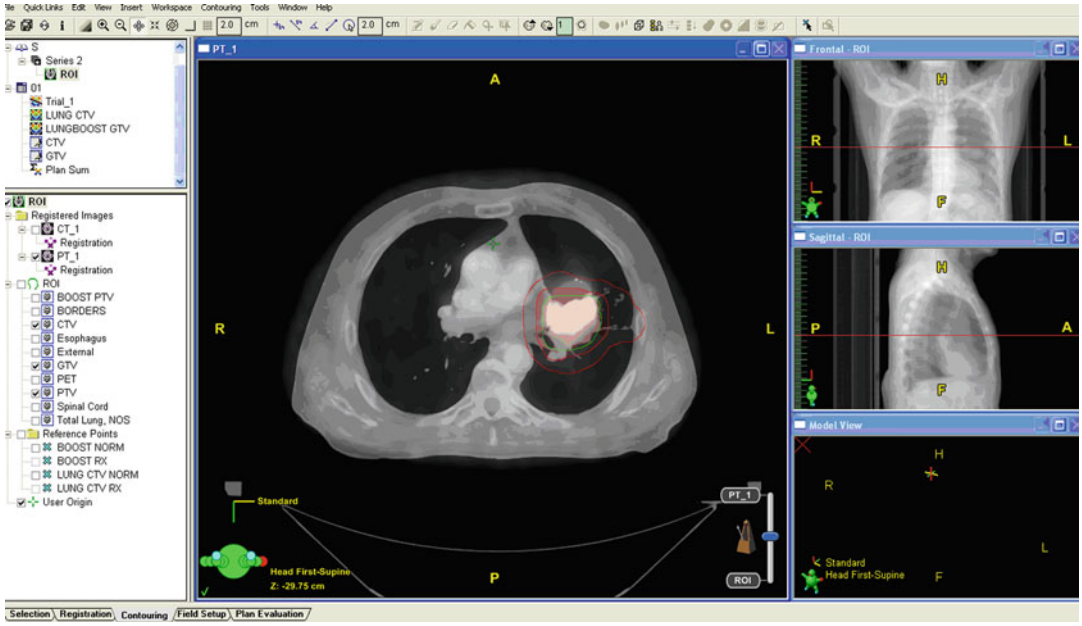

Fig. 40.2 The PET-CT scan is often fused with the CT scan obtained at time of simulation. This allows for more accurate volume definition as part of radiation therapy treatment planning. The FDG-avid tumor volume can be differentiated from areas of atelectasis which do not need to be included as part of the target volume

The physiological state of the patient must always be considered when designing the immobilization device. Lung cancer patients typically have a compromised baseline pulmonary function status. Overzealous chest or abdominal compression to try and reduce tumor motion may cause patient anxiety and discomfort and may paradoxically increase tumor motion due to deeper inspiration and expiration.

Target Delineation for IGRT

Advances in diagnostic imaging technology have readily been incorporated into radiation oncology practices to better define the tumor and target and identify avoidance structures. Previously, tumors were identified on plain x-ray films based on information obtained from diagnostic CT scans and used for 2D planning. Fluoroscopy-based simulation was used to define treatment portals. The development of CT scan-based simulation permitted better visualization of the tumors and normal structures and thus 3D treatment planning.

The most exciting development in recent years has been the introduction of PET scanning and PET-CT fusions which are now being increasingly used for target delineation in lung cancers. PET-CT scans provide information about the biological activity of tumors in addition to showing anatomic abnormalities. While this has proved to be an invaluable tool for radiation oncologists, some technical issues should be kept in mind when utilizing PET scans to outline tumors (Fig. 40.2).

Diagnostic PET-CT scans are usually not obtained in the radiation treatment position with immobilization devices. This introduces the first variable to be taken into account when fusing PET-CT images with simulation CT images for target definition. Various techniques for image registration and fusion have been described, including manual or interactive registration, landmark-based, surface-based, volume-based, and deformable registration [17].

After confirming proper image fusion and registration, the next step is target delineation by the radiation oncologist. Defining the edge of the tumor is challenging, as changing the window/level on a PET scan can change the apparent extent of the tumor. Various methods have been used to define PET-based tumor extent including using a single value of the standardized uptake value (SUV) [18] or a certain percentage of the maximum SUV [5]. Nestle et al. compared four commonly used methods to define PET-based gross tumor volumes (GTV) [19]. PET-CT scans were obtained in the treatment position for 25 patients. GTVs were defined as follows: GTVvis, visual; GTV_{40}, applying a threshold of 40 % of the maximum of SUV; $GTV_{2.5}$, applying an isocontour of SUV = 2.5 all around the tumor; and GTVbg, based on an algorithm taking into account mean tumor PET intensity and background intensity. They noted statistically significant differences in the GTV volumes ranging from 53.6 mL for GTV_{40} to 164.6 mL for $GTV_{2.5}$. The authors concluded that none of these methods are ideal, however, cautioned against the use of GTV_{40} as this led to inadequate tumor coverage.

Caution also needs to be exercised when deciding whether or not to include a small volume which may show up as enlarged on a CT scan but may not be FDG avid or be below the limit of detection of PET scans. This dilemma is frequently encountered in the mediastinal nodal areas. In a recent report, the sensitivity, specificity, and positive and negative predictive values of PET-CT scans for the diagnosis of mediastinal lymph nodes in NSCLC were noted to be 65 %, 96.8 %, 78.5 %, and 90 %, respectively [20].

Another possible source of error is the fact that PET image acquisition takes several minutes. During this time, the patient is freely breathing resulting in "smearing" of the FDG-avid area. This also makes tumor edge delineation difficult. There is a fear that this "smearing" effect may result in an increase in the defined GTV, thus negating the possible benefits of IGRT in reducing normal tissue dose. This was indeed found to be true in one study where the PET data resulted in an increase in target volumes by up to 15 mm in 34 % of the patients [21]. However, in a study of 92 patients, a reduction in GTV was noted in 23 % and an increase in 26 %. Factors responsible for these changes were the presence or absence of atelectasis or the detection of occult mediastinal lymph nodes [22]. Another study also noted similar findings with a reduction in GTV in 12 % and increase in 46 % [23]. Interestingly, PET-CT changed AJCC staging in 31 % patients with 8 % having distant metastases.

The RTOG conducted a study (RTOG 0515) to compare GTV definition with or without PET fusion for patients with NSCLC. Bradley et al. recently presented the data from this study [24]. CT-only-based GTV definition resulted in a mean tumor volume of 98.7 cc versus 86.2 cc for PET-CT-based volume definition ($p < 0.0001$). Consequently, the mean lung dose, V20, and mean esophageal doses were 19 Gy versus 17.8 Gy, 32 % versus 30.8 %, and 28.7 Gy versus 27.1 Gy, respectively, for CT-only- versus PET-CT-based GTV definition.

The internal target volume (ITV) and planning target volume (PTV) are then generated from the GTV. At our institution, we generally add a 3 mm margin in the anterior-posterior direction and a 5 mm margin in the superior-inferior direction to the ITV to form the PTV (PTV_{ITV}) [25]. At some institutions, a 10 mm margin in all directions is used for patients when motion information is not available [26]. Prior to the availability of gated CT scans, we used an individualized PTV (PTV_{indiv}) created from an expansion of the GTV based on motion observed on fluoroscopy.

The maximum intensity projection (MIP) is a treatment planning software-generated image that reflects the highest data value present in the viewing ray for each pixel of volumetric data. This results in an image that is a sum of all GTV excursions in various phases of respiration. Underberg et al. analyzed 10-phase GTV contouring versus MIP contouring and found that MIP scans are reliable and fast clinical tools for generating ITVs from 4D CT data [27] (Figs. 40.3, 40.4, and 40.5).

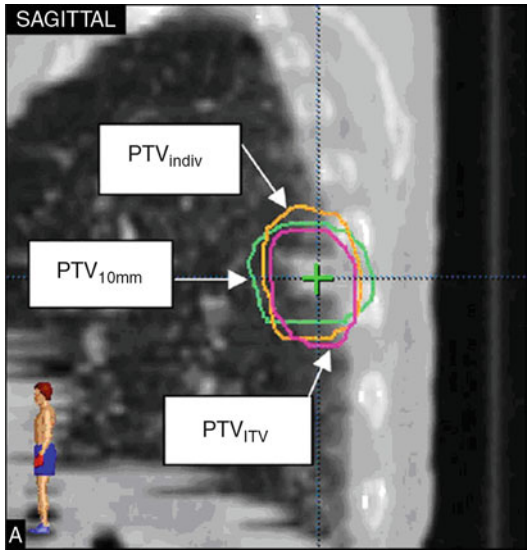

Fig. 40.3 The contours of PTV_{ITV}, $PTV_{10\ mm}$, and PTV_{indiv} of the patient in a regular spiral CT image's coronal view

Image Verification and Treatment Devices

Conventional Portal Films

Imaging of radiation treatment field using portal films was probably the first step in image-guided verification of setup accuracy. Patients are placed in the treatment position, the isocenter and treatment fields are set, and a film placed beyond the patient is exposed to megavoltage radiation. The developed film is then compared to the treatment planning films or digitally reconstructed radiographs (DRRs). Special techniques, skill, and expertise of the radiation therapist are required to obtain satisfactory images using MV film-based portal imaging. Proper film and screen combinations are needed to image different

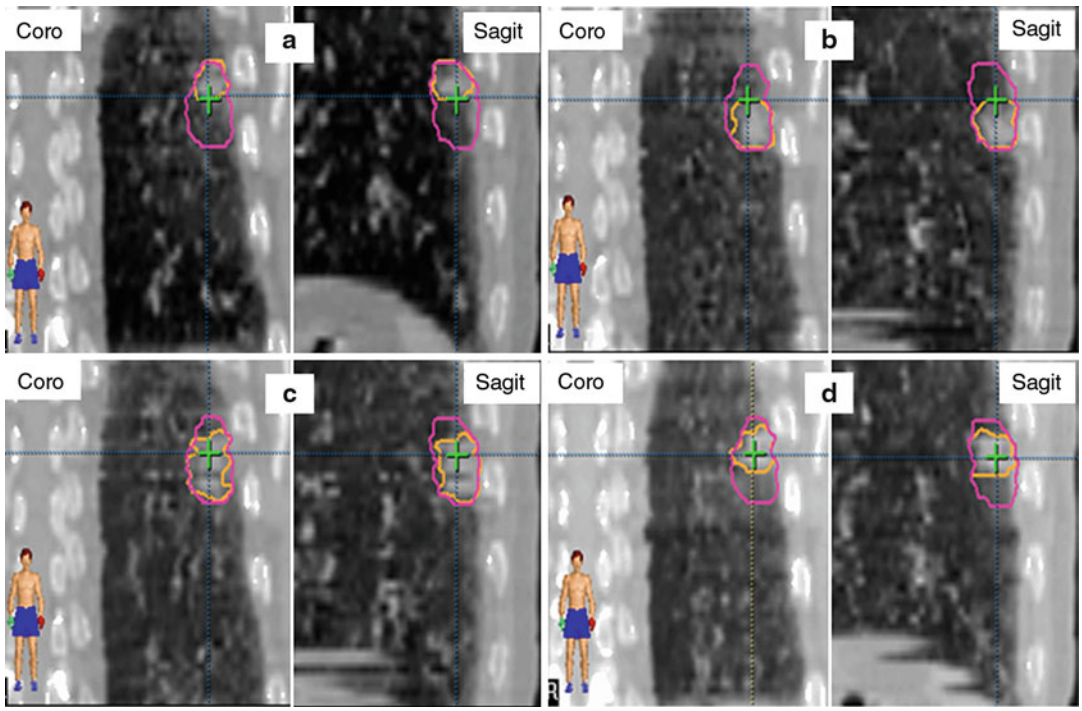

Fig. 40.4 Coronal and sagittal plane views of the CT images of a patient at different gating phases with corresponding GTV and ITV delineated. (**a**) Gated at the expiration phase, (**b**) gated at the inspiration phase, (**c**) gated at a middle phase, and (**d**) a regular spiral scan

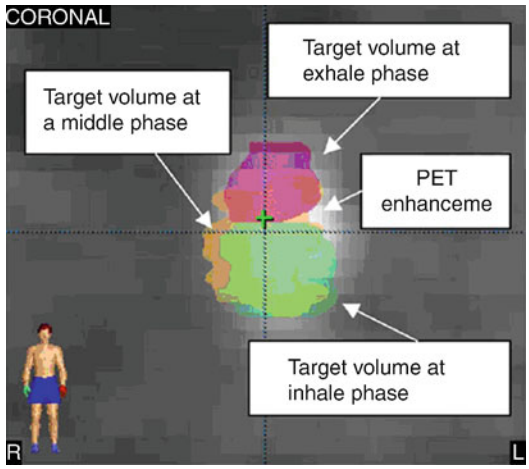

Fig. 40.5 Coronal plane view of the PET images of a patient with the contours of GTV of CT images at different phases superimposed

parts of the body [28, 29]. Examples of such films used for radiation oncology purposes are the Kodak EDR2 and XV-2 films.

This method of image guidance using port films has the advantage of a permanent physical record of the radiation treatment fields. However, it also has certain disadvantages including (1) poor quality of images at megavoltage (MV) energies; (2) only bony structures can be identified with little or no soft-tissue imaging; (3) recurring expense of films; (4) need to maintain a dark room with developers and chemicals and their associated costs; (5) extra time required during treatment to obtain, develop, and verify setup; (6) inability to change contrast/brightness setting on the physical films to obtain satisfactory images; and (7) daily image verification is cumbersome and not practical.

Electronic Portal Imaging Devices (EPID)

Electronic portal imaging overcomes some of the disadvantages of film-based portal imaging. These images can be obtained prior to daily treatment for a patient, seen in real time, and digitally enhanced and archived. The construction of such a system involves the MV photon beam passing through the patient, striking and causing excitation of a metal fluorescent screen producing an image [30]. The image produced is reflected by a 45° mirror toward a video camera system which in turn transmits the image to a screen at the control console. Over time, more sophisticated systems have been developed such as the Varian Medical Systems Portal Vision, which uses detectors based on amorphous silicon providing a larger sensitive area and higher spatial resolution. However, as with film-based portal imaging, soft-tissue visualization is poor, and patient positioning is based on bony landmarks.

CT-on-Rails

The CT-on-rails setup involves a CT scanner placed in the same room as the linear accelerator. The CT system is placed on rails and can be moved to allow CT imaging of patient anatomy in the treatment position, image verification, and treatment delivery without the need to move the patient off the treatment couch.

Two such systems have been described [31]. Siemens Medical Systems has developed the PRIMATOM™ system consisting of a Siemens PRIMUS® linear accelerator and a SOMATOM™ CT scanner with Sliding Gantry™. The CT scanner moves on two rails by a motor-driven carriage. To obtain images, the linear accelerator couch is rotated 180° and then rotated back to the treatment position while the patient remains immobilized. A similar system was also designed combining a General Electric Smart Gantry CT scanner and a Varian 2100EX linear accelerator. The positional accuracy of this system was found to be between 0.18 ± 0.13 mm and 0.39 ± 0.10 mm in various directions [32]. The advantage of the CT-on-rails system is the kilovoltage (kV) image acquisition with good soft-tissue delineation.

In-Room Orthogonal X-Ray Systems

In-room orthogonal systems utilize two floor- or ceiling-mounted x-ray sources with opposing

amorphous silicon flat-panel detectors. After the patient is placed in the treatment position, orthogonal films are obtained and digitally reconstructed for verification of isocenter placement based on bony anatomy.

Two such systems are commonly used clinically. One is the BrainLAB ExacTrac® system. This uses floor-mounted x-ray sources with detectors in the ceiling. Additionally, an infrared camera system is also combined with this to allow optical tracking of the patient's surface anatomy. Ball-shaped infrared reflectors are placed on the patient at the time of simulation such that no two reflectors are in the same CT axial plane and their positions recorded. At the time of treatment, these reflectors are placed in the same position and couch movements performed to match initial setup.

Cone-Beam Computed Tomography (CBCT)

The cone-beam technology is being provided as an option by most linear accelerator manufacturers nowadays and can be either kilovoltage CBCT (Varian Trilogy, Novalis TX, Elekta) or megavoltage CBCT (Siemens).

In the kV-CBCT systems, a kV source of x-rays is mounted on a retractable arm at 90° to the treatment gantry. On another retractable arm, directly opposite the x-ray source, a flat-panel detector is placed. To obtain cone-beam images, the x-ray source is turned on as the gantry rotates 180° or more around the patient in the treatment position. Multiple planar projection images are acquired and 3-dimensional images reconstructed using a filtered back-projection algorithm [33, 34]. Unlike a conventional helical CT scanner where the images are obtained by longitudinal translation of the patient through a narrow x-beam being generated by a rotating x-ray source, CBCT uses a broad beam of x-rays with a 2D detector array to provide a larger field of view. MV CBCTs use the linear accelerator as the source of x-rays. The gantry can rotate 200° in 45 s with one image per degree being captured on the EPID [35]. The 3D images are again reconstructed using the filtered back-projection algorithm.

Both systems are widely used clinically and are associated with certain advantages and disadvantages [36]. The MV CBCT system does not require any physical modification of the linear accelerator. The source of x-rays and detector are already part of the system. It provides superior images with minimal artifacts when metallic prostheses or implants are in the path of the beam such as in prostate cancer patients with hip replacements. Also, doses being delivered to the tissues in the field by the MV beam are modeled and known. The kV-CBCT system, on the other hand, provides better soft-tissue imaging and can be used in the fluoroscopy mode to assess tumor motion. The disadvantage of this system is the additional equipment that needs to be installed on the linear accelerator gantry. This additional equipment requires its own quality assurance checks for accuracy. Jaffray et al. noted that corrections of up to 2 mm were required to compensate for gravity-induced flex in the support arms of the source and detector [34]. This flex, if uncorrected, resulted in loss of detail, misregistration, and streak artifacts (Fig. 40.6).

Helical Megavoltage Computed Tomography (MVCT)

The idea of tomotherapy or "slice therapy" was first proposed by Mackie et al. in 1993 [37]. The concept was further developed for commercial use and is now available as the Hi-Art® treatment system (TomoTherapy Inc., Madison, WI). In this design, the MV linear accelerator is mounted on a CT-like gantry. As with the acquisition of helical CT scan, the patient is translated through the rotating gantry to produce images in the treatment position. These images can be matched and compared with the treatment planning CT. If shifts are required, the couch allows six degrees of freedom of movement to allow matching. After a proper match, the patient is treated on the same couch and gantry without any need for moving the patient. This MV imaging system provides the same imaging advantages as outlined above.

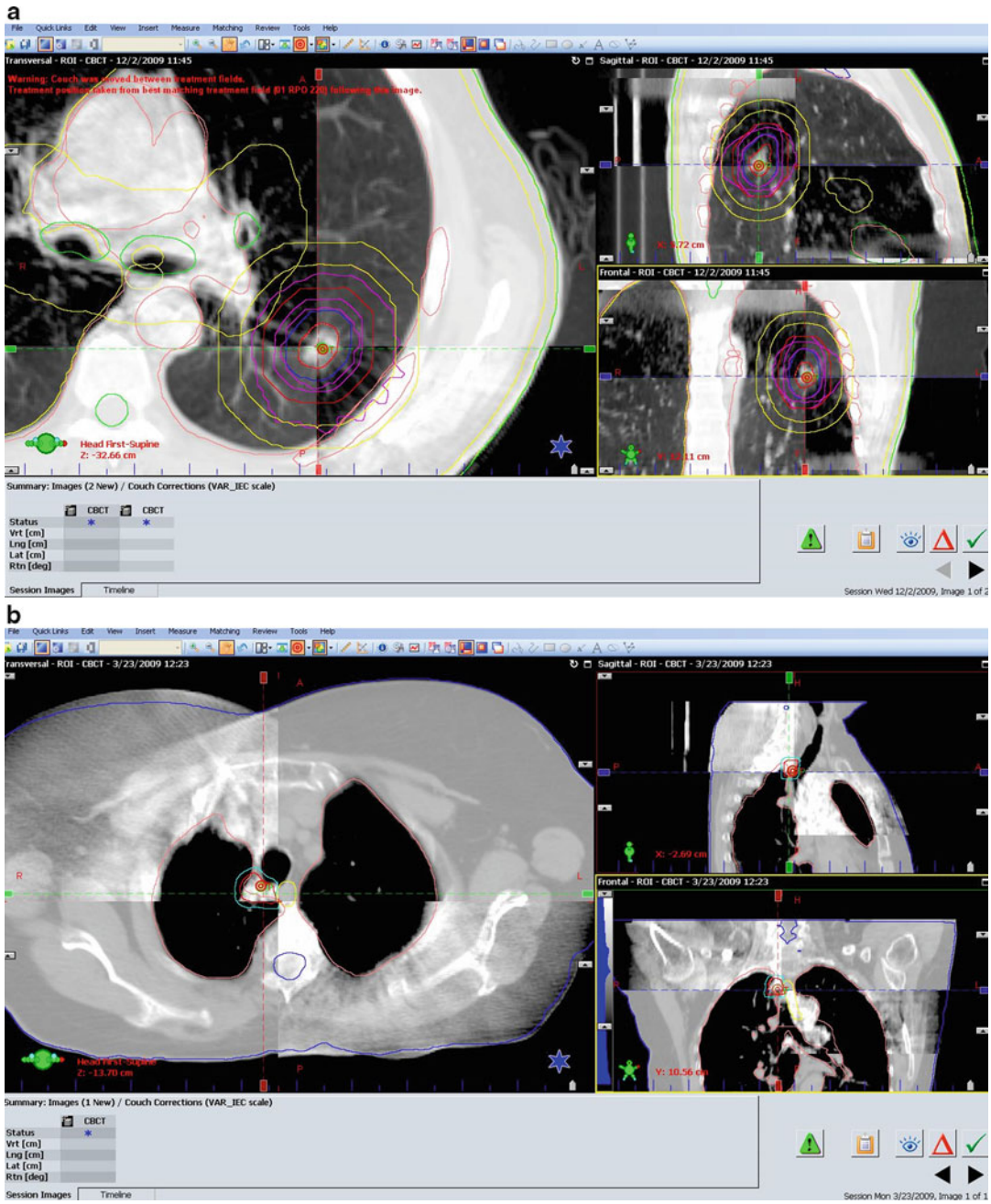

Fig. 40.6 Cone-beam CT (CBCT) acquired prior to each treatment and fused with the simulation CT for verification and adjustment of SBRT setup for (**a**) peripheral and (**b**) central stage I non-small cell lung cancer

A study by Zhou et al. compared shifts in lateral, longitudinal, and vertical directions and rotational variations for lung cancer patients being treated using SBRT [38]. They found no correlation between patient characteristics and setup uncertainties. Studies such as this highlight the difficulties in trying to predict isocenter shifts based on lung function, tumor location, or other patient characteristics and emphasize the need for image guidance.

ExacTrac-6D System

The ExacTrac X-Ray 6D stereotactic IGRT system (BrainLAB AG, Feldkirchen, Germany) uses a combination of optical positioning and kV radiographic imaging to position patients and perform online positioning corrections. The system consists of two main subsystems: (1) an infrared (IR)-based optical positioning system (ExacTrac) for initial patient setup and precise control of couch movement, using a robotic couch, and (2) a radiographic kV x-ray imaging system (X-Ray 6-D) for position verification and readjustment based on the internal anatomy or implanted fiducial markers. In addition, the IR system can be used to monitor a patient's respiration and provide a signal to the linac for tracking and gating of the treatment beam. In conjunction with the x-ray system, image-guided verification of target position relative to the gating window can be performed throughout the duration of the gated delivery. A detailed review of the ExacTrac technology is provided in the article by Jin et al. [39].

The infrared tracking system detects patient position based on external markers for the initial pre-positioning of the patient. The x-ray system is a stereoscopic planar kV x-ray system for detecting target positions based on internal anatomic references. The planning system establishes a locational relation between the infrared localization markers and the planning isocenter. With this information, the initial patient positioning is achieved through an infrared positioning system which consists of a pair of cameras in the treatment room that generate and detect infrared radiation reflected from markers placed on the patient. Data are disseminated to yield real-time positional information. Translation and rotation in all three major axes are displayed in the treatment and control rooms. The treatment couch is driven automatically to position the patient near the isocenter of the linear accelerator based on information derived from the infrared positioning system. The video camera system is linked to the infrared system and provides a qualitative visual check for patient positioning.

The final patient positioning is achieved with radiographic image guidance based on internal bony anatomy or radiopaque markers. The radiographic image-guidance system consists of a pair of amorphous silicon detectors suspended from the ceiling and two floor-mounted kV x-ray sources. X-ray sources project obliquely onto the two flat-panel detectors from lateral to medial, posterior to anterior, and superior to inferior. A pair of radiographs is obtained following infrared positioning to determine the current patient position relative to the planned position. This is achieved with a 2D-3D registration called "6D fusion" by the manufacturer (BrainLAB, AG, Feldkirchen, Germany). An additional analysis tool, Snap Verification (SV, BrainLAB AG, Feldkirchen, Germany), has been implemented to monitor intrafraction motion based on single oblique digital radiographs. This is a monoscopic imaging tool for detecting motion during the treatment (intrafraction motion).

Recently, a new technology, which couples the ExacTrac optical guidance and x-ray-based localization with the onboard imaging system (MV, kV x-rays, and kV-CBCT) on a multiphoton/electron beam linear accelerator, the Novalis Tx™, (Varian Medical Systems, Palo Alto, CA), has been introduced [40]. As with the Novalis system, Novalis Tx™ includes a robotic couch to perform translational and rotational (tilt, roll, and yaw), "6-D", positioning of the patient [41].

Cyberknife

The Accuray CyberKnife® Robotic Radiosurgery (Accuray Inc., Sunnyvale, CA) system [42] consists of a compact x-band linear accelerator mounted on an industrial robotic manipulator arm. The manipulator arm is configured to direct the radiation beams to the region of beam intersection of two orthogonal x-ray imaging systems integrated to provide image guidance for the treatment process. The patient under treatment is positioned on an automated robotic couch such that the lesion to be treated is located within this radiation beam accessible region.

The movements of the robotic manipulator arm and the robotic patient support assembly are under the direct control of a computer system that is in turn controlled by the radiation therapist or medical physicist.

In routine clinical use, the x-ray system is used for patient alignment before the treatment and to compensate for patient motion during treatment. The x-ray image pairs taken during patient setup and treatment are saved in the patients' digital record. The result of the tracking algorithm, that is, the patient shift from the simulation position, is recorded in a log file. For the fiducial tracking, individual fiducial positions and the center of mass of all fiducials are also recorded in a log file. These data can be post-processed later to study, for example, the accuracy of tracking algorithms under development compared to clinically used tracking algorithms. During the treatment, images are taken every *n*-th beam (*n* being a user-selected skip factor) or, for prostate, on a preset time interval.

Currently, four different image registration algorithms are used. The cranial tracking algorithm [43] and spine tracking algorithm [44–46] both use bony anatomy for a 2D-3D registration. The fiducial tracking algorithm [47, 48] uses high-density markers such as gold seeds, steel screws, or titanium clips or screws as surrogate markers for tumor tracking. A soft-tissue tracking algorithm is available for dense tumors with diameter >15 mm in the peripheral areas of the lung. Fiducial tracking is also used for mobile soft-tissue targets or targets in the extremities.

The benefit of the stereoscopic x-ray system with 2D-3D registration is its robustness and speed of image processing [43]. Because it is an established technology, the use of an x-ray-based image-guidance system, calibration, and 2D-3D image registration is familiar to most users. One of the disadvantages is the use of ionizing radiation for imaging, although the dose is very small compared to the treatment dose, and even the dose from scatter and leakage radiation [49]. In soft-tissue fiducial tracking, the quality of the tracking is dependent on the quality of the fiducial placement. The surrogate markers have to be placed inside the target and not migrate between simulation and treatment [50, 51]. Localization algorithms rely on the marker position of the simulation CT [52]. Differential marker motion relative to the tumor can usually not be identified by the tracking algorithm. CyberKnife can also be combined with the Synchrony® Respiratory Tracking System or Xsight® Lung Tracking System to track tumor motion without fiducial implantation.

Camera-Based Systems

External beam planning for radiation therapy with modern imaging and treatment planning allows radiation oncologists to deliver very conformal dose distributions with modern delivery techniques. In many cases, image guidance can enhance the ability to deliver these conformal plans. Optical imaging allows for the continual monitoring of patient surface during the actual treatment and can be used to monitor interfraction motion. Imaging the patient surface is also an elegant method for setting up patients for which the body surface is closely related to tumor location, such as breast cancer patients. The use of optical imaging for the setup of radiation therapy patients is hardly new [53], but this technology has experienced resurgence in interest as treatment delivery techniques and image guidance have become more prevalent. Advantages of the technology include speed and the fact that they operate without ionizing radiation.

Currently, two products are available: AlignRT® (VisionRT, London, UK) and C-Rad Sentinel (C-RAD AB, Uppsala, Sweden), both with the ability to perform rapid surface imaging of patients during a radiotherapy treatment. Using photogrammetry, these devices can generate 3D models of the patient surface. The AlignRT system utilizes two cameras for stereotactic imaging whereas the C-Rad Sentinel system scans using a line scanning mode with a single camera and laser system. These devices must be calibrated so all reading will be relative to the room isocenter. For planning CT-based alignment, they also need a reference RT structure set that includes the reference 3D model of

the patient surface as well as its geometric relationship to the room isocenter. Using rigid body transformations, the systems perform a least square fit to minimize the difference in space between the planned 3D model of the patient relative to isocenter and the observed surface model of the patient.

Without a planning, CT-based reference alignment can be done from an acquired optical 3D reference image of the patient. This is useful when the patient alignment is established with other means, that is, a different patient positioning system, and the surface-matching-based system is used to verify consistent patient position, either between fractions or during the course of a fraction. In the latter mode, AlignRT can also be used without precise isocenter calibration if a single system is being employed and patients will not be transferred from room to room.

These imaging methods allow not only daily image verification for patient setup but also help with adaptive radiation therapy in which a new treatment plan may need to be generated in case the tumor size or shape changes considerably.

Adaptive Radiation Planning for Fractionated Course of Standard External Beam RT

As defined in the original article by Yan et al. [54], adaptive radiation therapy (ART) refers to the process whereby a treatment plan can be modified by a systematic feedback of measurements. Image-guided adaptive radiation therapy (or IGART) involves the use of image-guidance technologies to monitor treatment variations and incorporate them into the planning process to possibly re-optimize the plan during treatment. The goal of IGART is to provide additional sparing of dose to normal tissues, thereby allowing for escalation of dose to the target. In principle, any imaging modality, be it planar imaging or volumetric assessment of the target, can be used to monitor treatment variations to provide feedback in the IGART loop. There have been a number of publications on the use of daily planar images to monitor setup uncertainties and possibly adjust PTV margins based on trends observed during a given number of fractions [55]. The ability to image the tumor volumetrically, using, for instance, CBCT or helical tomotherapy, allows one to monitor the tumor response during the course of radiation. Studies using helical tomotherapy have shown that volumetric assessment of lung tumor regression is possible during the course of treatment [56] and that significant reduction in the dose to healthy lung tissue is achievable if one were to re-optimize the planning margins based on tumor volume regression during the course of treatment [57]. Although the reduction of margins by assessment of volumetric tumor regression during the course of treatment appears plausible, the issue of how to reduce margins in light of tumor microscopic extension remains controversial [57]. Using kV-CBCT for daily image guidance of lung tumors, Bissonnette et al. [58] analyzed random and systematic setup errors and showed that significant reductions in setup margins were possible, thereby facilitating the use of IGART.

Radiobiology Considerations

IGRT provides the ability to deliver high doses of radiation per fraction. The maximum dose per fraction and the total dose delivered are still largely empiric. Data generated for tumor control, normal tissue toxicity, and outcomes have largely been based on daily doses of 1.8–2 Gy per fractions. Most of the mathematical models used to explain dose–response or cell-survival curves, like the single-hit multi-target, multi-hit multi-target, repair-misrepair model, lethal-potentially lethal model, and the linear-quadratic (LQ) model, are based on a multi-fractionated course of treatment. The radiobiology of large doses per fraction is still not well understood.

The most commonly used model is the LQ model. In its simplest form, it was used to derive the conclusion that biologically effective doses of $\geq$100 Gy provided superior outcomes compared to BED $<$100 Gy in SBRT protocols for lung cancer [59, 60]. However, the LQ model does

not take into account the vascular and stromal damage that is believed to be caused by high doses per fraction as used in SBRT and also ignores the impact of radioresistant populations of cells [61]. There is evidence that vascular endothelial cell damage may be triggered at doses greater than 10 Gy given in a single fraction [62, 63].

Others, however, are of the opinion that the LQ model has been validated experimentally and theoretically for doses up to 10 Gy per fraction and it would be reasonable to use this formalism for doses up to 18 Gy per fraction [64]. Due to lack of availability of any other theoretical or mathematical model for high doses per fraction, the LQ model continues to be used for comparison of fractionation schemes. Clinical data are being generated at a rapid pace for SBRT in lung cancers, and the development of such a model may become possible in the near future. There are data for tumor response and local control, and data are also becoming available for early and late normal tissue toxicities. A recent review summarizes the clinical experience and toxicities in lung SBRT including pneumonitis, pulmonary function, esophagitis, rib fractures/chest wall pain, brachial plexopathy, and radiographic changes [65].

Indeed, such a model has been proposed by Park et al. [66]. They combined the LQ and multi-target models in a single "universal survival curve" (USC). The rationale for doing so was the fact that the LQ model for cell survival, which is continuously bending, does a better job of predicting cell survival at low doses and overpredicts the biologically effective dose at high doses per fraction. On the other hand, cell survival at high doses is better modeled by the multi-target equation. The universal cell-survival curve follows the LQ line at low doses and multi-target line at high doses with transition occurring at a dose D_T. Based on reports of 12 NSCLC cell lines from the National Cancer Institute, the authors calculated D_T to be 6.2 Gy. The experimental validity of the universal survival curve was tested in the H460 non-small cell lung cancer cell line by comparing the theoretical fits of the LQ and USC models with clonogenic cell survival. The USC model fit the experimental data better. The concept of single fraction effective dose (SFED) for clinical data in lung SBRT trials was also presented in this article.

Treatment Planning: Motion and Dose Calculation

As discussed in the section on CT simulation, the use of 4D CT techniques for modeling respiratory-induced patient motion is a useful approach for motion compensation in lung cancer treatment planning, in particular for those tumors exhibiting large motion amplitudes, for example, tumors located in the vicinity of the diaphragm [67]. Methods proposed for incorporating motion include convolution approaches, in which either the dose [68] or the fluence [69] is convolved with a Gaussian function to account for random setup errors. Fluence translation has also been proposed to account for respiratory-induced motion of the tumor in primary lung cancer treatment planning [70]. Approaches for incorporating 4D imaging in the treatment planning and delivery process can generally be classified into two schemes: (a) "real-time" adaptive delivery and (b) nonadaptive delivery. In the adaptive delivery method, organ segmentation and planning are performed on all phases of the 4D dataset, the dose from each phase is accumulated onto the reference planning dataset (e.g., the exhale or free-breathing scan) for plan evaluation, and the radiation delivery is performed by synchronizing the breathing phases with the beam poses for the treatment plans at the respective phases [71]. The advantage of this approach is that dose to normal lung tissue is limited. A disadvantage is that phase differences exist between the motion of the tumor and MLC leaf motion, which may result in a lack of synchronization between the target position and the intended MLC-shaped delivery field. In the nonadaptive delivery scheme, the GTVs from each phase of the 4D dataset are composited to form an internal target volume (ITV), which is generally defined on the reference planning dataset for planning purposes [72]. Treatment

delivery is performed based on the reference treatment plan. Although ITV-based delivery may produce somewhat higher doses to normal lung relative to the adaptive delivery approach, it circumvents the problem of phase differences between the delivered radiation fields and target motion. Using ITV-based planning, studies have been performed to assess the optimal number of phases in the 4D dataset required to produce accurate estimates of planning dose indices. Generally, results have shown that even a few datasets (e.g., the composite inhale and exhale datasets) [72] or the time-averaged CT dataset [73] produces treatment plans of equivalent quality with respect to target coverage and normal tissue sparing as plans performed with up to ten datasets between the inhale and exhale phases.

The presence of low-density lung tissue in the vicinity of or surrounding thoracic tumors significantly confounds the radiation dose computation problem in lung cancer treatment planning. Conditions of loss of charged-particle equilibrium are produced when the field size is reduced such that the lateral ranges of the secondary electrons become comparable to (or greater than) the field size [74]; such conditions occur for larger field sizes in lung than in water-equivalent tissues due to the increased electron range in lung. Under such circumstances, the dose to the target is determined primarily by the secondary electron interactions and dose deposition. Because conventional dose algorithms do not account explicitly for transport of secondary electrons, they can be severely limited in accuracy under nonequilibrium conditions. Moreover, in low-density, lung-equivalent tissues, the range of the secondary electrons along (parallel to) the beam axis contributes to the dose "build-down" effect at the edges of the tumor (at the lung tumor interface if the tumor is located proximal to the lung), an effect which increases with beam energy. The article by Reynaert et al. [75] and AAPM Task Group No. 105 [76] provide examples of numerous studies reported on the inaccuracies associated with conventional algorithms for dose calculations in the lung. Therefore, for lung cancer treatment planning, in general, and especially when dealing with smaller tumors, where the field sizes are less than 5×5 cm^2 in lung, more advanced dose algorithms such as convolution/superposition [77] or the Monte Carlo (MC) method AAPM TG-105 [76], the latter of which accounts explicitly for electron transport, are preferred. Das et al. [74] provided the following summary of the role of MC: "It is also expected that the Monte Carlo techniques will increasingly be used in assessing the accuracy, verification, and calculation of dose, and will aid perturbation calculations of detectors used in small and highly conformal radiation beams." It is appealing to consider a properly commissioned MC dose algorithm in the quality assurance (QA) of small-field IMRT treatment plans for lung cancer. Such a QA device is likely to provide more accurate and realistic estimates of the doses delivered to the actual patient targets and normal tissues than current methods for IMRT verification, often involving measurements in a solid-water phantom. In addition, careful measurements under small-field, nonequilibrium conditions are fraught with uncertainties and in practice are difficult to perform to within errors of 2 % [74, 76].

Clinical Outcomes

A review of literature shows that since the late 1990s, stereotactic body radiation therapy (SBRT) has gained increasing acceptance as a treatment option for medically inoperable patients with early-stage lung cancer. This increase has been possible partly because of increasing use of IGRT to guide tumor/target delineation and delivery of radiation. The safety and efficacy of image-guided SBRT for lung cancer is evident when results from various studies are compared (Table 40.1).

Results of RTOG 0236, a phase II trial of SBRT in medically inoperable NSCLC, were recently presented [78]. Patients with T1-3N0M0 tumors were treated to a dose of 60 Gy in 3 fractions (heterogeneity-corrected dose of 54 Gy in 3 fractions). The primary endpoint of this study was local control. With a median follow-up of 25 months, the 2-year

Table 40.1 Selected trials of stereotactic body radiation therapy for early-stage lung cancers

Study	No. of patients	Stage	Dose/no. of fr	Prescription point	Local control/overall survival (yrs)	Toxicity
Uematsu et al. [97]	45	Primary^{+}mets	30–75 Gy/ 5–15	80 % isodose	97 %/NA	NA
Nyman et al. [98]	45	I	45 Gy/3	100 % at PTV periphery	80 %/30 % (5 year)	4, gr I esophagitis; 9, skin reactions; 4, transient chest pain; 4, infections. Late: 2 rib fractures, 3 atelectasis
Nagata et al. [99]	45	I	48 Gy/4	Isocenter	98 %/IA, 83 % (3 year); IB, 72 % (3 year)	No gr 3 or greater toxicities
Onishi et al. [100]	257	I	18–75 Gy/ 1–22	Isocenter	92 % (BED > = 100 Gy); 57 % (BED < 100 Gy)/ 70.8 % (BED > =100 Gy); 30.2 % (BED < 100 Gy) (5 year)	5.4 % pulmonary grade 2 or more
Videtic et al. [101]	26	I	50 Gy/5	PTV	94 %/52 % (3 year)	3.6 % developed acute grade 3 dyspnea
Timmerman et al. [79]	70	I, up to 7 cm	60–66 Gy/ 3	80 % isodose includes > =95 % PTV	95 %/54.7 % (2 year)	20 % gr 3–5 toxicity; central lesions, 46 % versus peripheral, 17 %
Fakiris et al. [102]	70	I, up to 7 cm	60–66 Gy/ 3	80 % isodose	88 %/43 % (3 year)	Grade 3+ toxicity in peripheral 10 % versus central 27 % (p = 0.09)
Baumann et al. [103]	138	I	45 Gy/3; 30 Gy/3	100 % isodose at PTV periphery	88 %/26 % (5 year)	14 % gr 3–4
Lagerwaard et al. [104]	206	I	60 Gy/3; 60 Gy/5; 60 Gy/ 8 (central tumors)	80 % isodose at PTV periphery	97 %/64 % (2 year)	<3 %

PTV planning target volume

local control rate was 93.7 %, and the disease-free and overall survival rates at 2 years were 66.6 % and 72 %, respectively. A follow-up RTOG study is protocol 0618 which is a phase II trial in operable stage I–II NSCLC. Patients will be treated to a dose of 60 Gy in 3 fractions and will be followed for local control, toxicity, and survival. In case enlargement of tumor is noted on CT scans, a PET scan or biopsy will be performed followed by a surgical resection of the tumor if positive.

The Indiana University experience had cautioned against the use of SBRT in central lung lesions [79]. Central lesions are defined as tumors within or touching a volume 2 cm in all directions around the proximal bronchial tree. The RTOG has an ongoing phase I/II dose-escalation trial to address this issue (RTOG 0813). This trial will be escalating doses from 50 to 60 Gy for centrally located lesions in 10 to 12 Gy per fraction. Our institutional experience suggested that delivering 48 Gy in 4 fractions is safe in these lesions [80].

The RTOG has initiated a randomized phase II trial in patients with stage I peripheral NSCLC (RTOG 0915). This trial randomizes between 34 Gy in one fraction and 48 Gy in 4 fractions. Such an approach would never be feasible without image guidance.

Such efforts are also being undertaken internationally. The Japan Clinical Oncology Group has a trial enrolling patients with stage I disease, delivering 48 Gy in 4 fractions (JCOG 0403) [81].

This trial has a planned accrual of 165 patients (65, operable; 100, inoperable). A Dutch study (ROSEL) is randomizing operable stage IA NSCLC patients to surgery versus SBRT with a planned dose of 60 Gy in 3 or 5 fractions [82]. The results of this trial will be interesting and could bring about a paradigm change in the way early-stage lung cancers are managed.

In addition to the pivotal role image guidance plays in SBRT for lung cancers, it can also be used for adaptive radiation therapy (ART). This refers to a closed-loop radiation treatment process in which the treatment plan can be modified using a systematic feedback of measurements [54]. During the 6–7-week course of fractionated RT for lung cancers, the tumor can change its size and shape, atelectasis may resolve, or the mediastinum may shift. A traditional fractionated course of RT uses a plan developed at the start of treatment and implements that to the end of treatment. Sometimes, a re-simulation may be done at the 36–40-Gy point to see if any modifications in the plan are possible or needed. ART uses continuous image guidance to monitor these changes and may help in better defining the RT field. This may allow escalation of dose to the tumor while maintaining or reducing the risk of normal tissue complications.

This approach was tested by Harsolia et al. in a dosimetric study in 8 patients with lung lesions (7 – NSCLC, 1 – metastatic rectal cancer) [83]. A Siemens onboard imaging system was used to obtain cone-beam CT scans, and four treatment plans were generated. The 3D conformal plan served as the baseline against which other 4D plans were compared. The 4D plans included (a) 4D-union plan, a union of GTVs from six phases of the 4D-CBCT with a 5 mm expansion; (b) offline ART, a 4D adaptive plan with a single correction; and (c) online ART, a 4D adaptive plan with daily correction. The standard 3D plan did not provide adequate coverage of the ITV in 25 % cases because of respiratory motion. Image guidance and 4D planning were able to achieve a significant reduction in normal tissue irradiated. Compared to 3D plans, the 4D-union, offline ART, and online ART were able to reduce PTV volume by 15 %, 39 %, and 44 %, respectively. Consequently, there was a reduction in lung V20 and mean lung doses of 21 %, 23 %, 31 %, and 16 %, 26 %, and 31 % for the three 4D methods, respectively.

Another interesting study included 114 NSCLC patients with clinical stages T1N0 to T4N3 treated using 45–87.75 Gy over 5–6 weeks [84]. An average of nine CBCTs were obtained in these patients. Considerable anatomic change was noted in 51 % of patients (40 %, tumor regression; 1 %, tumor progression; 10 %, other changes). Changes were also noted in the degree of atelectasis (decreased in 23 %; increased in 6 %) and pleural effusion. In the 46 patients with tumor regression, the volume decreased on average 37 % during the course of treatment, with 11 patients showing greater than 50 % reduction. Another study in 10 patients who underwent IGRT with weekly CBCTs also found an 11.9 % decrease in dose to 95 % of the PTV and 2.5 % decrease in dose to 95 % of the ITV [85].

The use of image-guided ART need not be limited to the anatomic definition of the target volume. Combination with PET scans may allow better biological targeting. Kong et al. studied FDG uptake 1 week before starting RT, during the course of RT (day 29), and 3 months post-RT [86]. Of the 15 lung cancer patients in the study, 11 achieved partial metabolic response at a dose of 45 Gy, 2 had complete metabolic responses, and 2 were stable. The mean SUV decreased from 5.2 pre-RT to 2.5 during RT and to1.7 three months post-radiation therapy. The location of the low and high FDG-uptake areas is also noted to be relatively stable during the course of RT when PET scans were done in 23 patients with stage I–III NSCLC on days 0, 7, and 14 of RT [87]. This suggests that biological targeting of a FDG-avid area of the tumor might be a possible approach and needs to be systematically studied.

Ongoing Research

The field of IGRT in the treatment of lung cancer remains a “hotbed” of research. Areas of technological development include the following,

among others: improvement of CBCT image quality by, for instance, reducing scatter in kV-CBCT [88]; reduction of dose in CBCT lung imaging using limited projection techniques, such as digital tomosynthesis [89] and associated novel reconstruction techniques [90]; deformable image registration algorithms [91, 92]; and dose reconstruction techniques [93–95] for determining dose accurate in adaptive therapy. With improvements in patient simulation, treatment planning and targeting, and subsequently the ability to reduce treatment margins and spare healthy lung tissue, it is expected that dose escalation to lung tumors will be feasible, thereby leading to improved outcomes for patients with lung cancer [96].

References

1. Parkin DM, Bray F, Ferlay J, et al. Global cancer statistics, 2002. CA Cancer J Clin. 2005;55:74–108.
2. American Cancer Society. Global cancer facts and figures. Atlanta: American Cancer Society; 2007.
3. Jemal A, Siegel R, Ward E, et al. Cancer statistics, 2009. CA Cancer J Clin. 2009;59:225–49.
4. Le Chevalier T, Arriagada R, Quoix E, et al. Radiotherapy alone versus combined chemotherapy and radiotherapy in nonresectable non-small-cell lung cancer: first analysis of a randomized trial in 353 patients. J Natl Cancer Inst. 1991;83:417–23.
5. Bradley J, Graham MV, Winter K, et al. Toxicity and outcome results of RTOG 9311: a phase I-II dose-escalation study using three-dimensional conformal radiotherapy in patients with inoperable non-small-cell lung carcinoma. Int J Radiat Oncol Biol Phys. 2005;61:318–28.
6. Rosenzweig KE, Fox JL, Yorke E, et al. Results of a phase I dose-escalation study using three-dimensional conformal radiotherapy in the treatment of inoperable nonsmall cell lung carcinoma. Cancer. 2005;103:2118–27.
7. Hayman JA, Martel MK, Ten Haken RK, et al. Dose escalation in non-small-cell lung cancer using three-dimensional conformal radiation therapy: update of a phase I trial. J Clin Oncol. 2001;19:127–36.
8. Kong FM, Hayman JA, Griffith KA, et al. Final toxicity results of a radiation-dose escalation study in patients with non-small-cell lung cancer (NSCLC): predictors for radiation pneumonitis and fibrosis. Int J Radiat Oncol Biol Phys. 2006;65:1075–86.
9. Sura S, Gupta V, Yorke E, et al. Intensity-modulated radiation therapy (IMRT) for inoperable non-small cell lung cancer: the Memorial Sloan-Kettering Cancer Center (MSKCC) experience. Radiother Oncol. 2008;87:17–23.
10. Liao ZX, Komaki RR, Thames Jr HD, et al. Influence of technologic advances on outcomes in patients with unresectable, locally advanced non-small-cell lung cancer receiving concomitant chemoradiotherapy. Int J Radiat Oncol Biol Phys. 2009;76(3):775–81.
11. Gould MK, Maclean CC, Kuschner WG, et al. Accuracy of positron emission tomography for diagnosis of pulmonary nodules and mass lesions: a meta-analysis. JAMA. 2001;285:914–24.
12. Toloza EM, Harpole L, Detterbeck F, et al. Invasive staging of non-small cell lung cancer: a review of the current evidence. Chest. 2003;123:157S–66.
13. Gould MK, Kuschner WG, Rydzak CE, et al. Test performance of positron emission tomography and computed tomography for mediastinal staging in patients with non-small-cell lung cancer: a meta-analysis. Ann Intern Med. 2003;139:879–92.
14. Reed CE, Harpole DH, Posther KE, et al. Results of the American College of Surgeons Oncology Group Z0050 trial: the utility of positron emission tomography in staging potentially operable non-small cell lung cancer. J Thorac Cardiovasc Surg. 2003;126:1943–51.
15. Bentel GC, Marks LB, Krishnamurthy R. Impact of cradle immobilization on setup reproducibility during external beam radiation therapy for lung cancer. Int J Radiat Oncol Biol Phys. 1997;38:527–31.
16. Baba F, Shibamoto Y, Tomita N, et al. Stereotactic body radiotherapy for stage I lung cancer and small lung metastasis: evaluation of an immobilization system for suppression of respiratory tumor movement and preliminary results. Radiat Oncol. 2009;4:15.
17. Fox T, Elder E, Crocker I. Image registration and fusion techniques. In: Paulino AC, Teh BS, editors. PET-CT in radiotherapy treatment planning. Philadelphia: Saunders/Elsevier; 2008.
18. Paulino AC, Johnstone PA. FDG-PET in radiotherapy treatment planning: Pandora's box? Int J Radiat Oncol Biol Phys. 2004;59:4–5.
19. Nestle U, Kremp S, Schaefer-Schuler A, et al. Comparison of different methods for delineation of 18F-FDG PET-positive tissue for target volume definition in radiotherapy of patients with non-Small cell lung cancer. J Nucl Med. 2005;46:1342–8.
20. Liu BJ, Dong JC, Xu CQ, et al. Accuracy of 18F-FDG PET/CT for lymph node staging in non-small-cell lung cancers. Chin Med J (Engl). 2009;122:1749–54.
21. Munley MT, Marks LB, Scarfone C, et al. Multimodality nuclear medicine imaging in three-dimensional radiation treatment planning for lung cancer: challenges and prospects. Lung Cancer. 1999;23:105–14.
22. Deniaud-Alexandre E, Touboul E, Lerouge D, et al. Impact of computed tomography and 18F-deoxyglucose coincidence detection emission tomography image fusion for optimization of

conformal radiotherapy in non-small-cell lung cancer. Int J Radiat Oncol Biol Phys. 2005;63:1432–41.
23. Bradley J, Thorstad WL, Mutic S, et al. Impact of FDG-PET on radiation therapy volume delineation in non-small-cell lung cancer. Int J Radiat Oncol Biol Phys. 2004;59:78–86.
24. Bradley JD, Bae K, Choi N, et al. A phase II comparative study of Gross tumor volume definition with or without PET/CT fusion in dosimetric planning for non–small-cell lung cancer (NSCLC): primary analysis of Radiation Therapy Oncology Group (RTOG) 0515. Int J Radiat Oncol Biol Phys. 2009;75:S2.
25. Jin JY, Ajlouni M, Chen Q, et al. A technique of using gated-CT images to determine internal target volume (ITV) for fractionated stereotactic lung radiotherapy. Radiother Oncol. 2006;78:177–84.
26. Underberg RW, Lagerwaard FJ, Cuijpers JP, et al. Four-dimensional CT scans for treatment planning in stereotactic radiotherapy for stage I lung cancer. Int J Radiat Oncol Biol Phys. 2004;60:1283–90.
27. Underberg RW, Lagerwaard FJ, Slotman BJ, et al. Use of maximum intensity projections (MIP) for target volume generation in 4DCT scans for lung cancer. Int J Radiat Oncol Biol Phys. 2005;63:253–60.
28. Droege RT, Bjarngard BE. Influence of metal screens on contrast in megavoltage x-ray imaging. Med Phys. 1979;6:487–93.
29. Droege RT, Bjarngard BE. Metal screen-film detector MTF at megavoltage x-ray energies. Med Phys. 1979;6:515–8.
30. Antonuk LE, El-Mohri Y, Huang W, et al. Initial performance evaluation of an indirect-detection, active matrix flat-panel imager (AMFPI) prototype for megavoltage imaging. Int J Radiat Oncol Biol Phys. 1998;42:437–54.
31. Ma CM, Paskalev K. In-room CT techniques for image-guided radiation therapy. Med Dosim. 2006;31:30–9.
32. Kuriyama K, Onishi H, Sano N, et al. A new irradiation unit constructed of self-moving gantry-CT and linac. Int J Radiat Oncol Biol Phys. 2003;55:428–35.
33. Feldkamp IA, Davis LC, Kress JW. Practical cone-beam algorithm. J Opt Soc Am A. 1984;1:612–9.
34. Jaffray DA, Siewerdsen JH, Wong JW, et al. Flat-panel cone-beam computed tomography for image-guided radiation therapy. Int J Radiat Oncol Biol Phys. 2002;53:1337–49.
35. Morin O, Gillis A, Chen J, et al. Megavoltage cone-beam CT: system description and clinical applications. Med Dosim. 2006;31:51–61.
36. Khan FM. The physics of radiation therapy. 3rd ed. Philadelphia: Lippincott Williams & Wilkins; 2009.
37. Mackie TR, Holmes T, Swerdloff S, et al. Tomotherapy: a new concept for the delivery of dynamic conformal radiotherapy. Med Phys. 1993;20:1709–19.
38. Zhou J, Uhl B, Dewitt K, et al. Image-guided stereotactic body radiotherapy for lung tumors using bodyloc with tomotherapy: clinical implementation and set-up accuracy. Med Dosim. 2010;35(1): 12–8. doi: 10.1016/j.meddos.2008.12.003. Epub 2009 Jan 30.
39. Jin JY, Yin FF, Tenn SE, et al. Use of the BrainLAB ExacTrac X-Ray 6D system in image-guided radiotherapy. Med Dosim. 2008;33:124–34.
40. Chang Z, Wang Z, Wu QJ, et al. Dosimetric characteristics of novalis Tx system with high definition multileaf collimator. Med Phys. 2008;35:4460–3.
41. Walls NM, Nurushev T, Jin JY, et al. Assessment of 2D X-ray and volumetric-based localization imaging for patients treated with SRS and SBRT. Int J Radiat Oncol Biol Phys. 2009;75:S-682.
42. Adler Jr JR, Chang SD, Murphy MJ, et al. The Cyberknife: a frameless robotic system for radiosurgery. Stereotact Funct Neurosurg. 1997;69: 124–8.
43. Fu D, Kuduvalli G. A fast, accurate, and automatic 2D-3D image registration for image-guided cranial radiosurgery. Med Phys. 2008;35:2180–94.
44. Fu D, Kuduvalli G. Enhancing skeletal features in digitally reconstructed radiographs. In: Reinhardt JM, Pluim JP, editors. Medical imaging 2006: image processing. Vol 6144. San Diego: The International Society for Optical Engineering; 2006. p. Abstract 61442 M.
45. Fu D, Kuduvalli G, Maurer CJ, et al. 3D target localization using 2D local displacements of skeletal structures in orthogonal x-ray images for image-guided spinal radiosurgery. Int J CARS. 2006;1:198–200.
46. Ho AK, Fu D, Cotrutz C, et al. A study of the accuracy of cyberknife spinal radiosurgery using skeletal structure tracking. Neurosurgery. 2007;60: ONS147–56. discussion ONS156.
47. Mu Z, Fu D, Kuduvally G. Multiple fiducial identification using the hidden Markov model in image guided radiosurgery. In: Proceedings of the conference on computer vision and pattern recognition workshop: IEEE. New York, June 17–22, 2006; pp. 0-7695-2646-7692/7606.
48. Murphy MJ. Fiducial-based targeting accuracy for external-beam radiotherapy. Med Phys. 2002; 29:334–44.
49. Chuang CF, Larson DA, Zytkovicz A, et al. Peripheral dose measurement for CyberKnife radiosurgery with upgraded linac shielding. Med Phys. 2008;35:1494–6.
50. Kothary N, Heit JJ, Louie JD, et al. Safety and efficacy of percutaneous fiducial marker implantation for image-guided radiation therapy. J Vasc Interv Radiol. 2009;20:235–9.
51. Kothary N, Dieterich S, Louie JD, et al. Percutaneous implantation of fiducial markers for imaging-guided radiation therapy. AJR Am J Roentgenol. 2009;192:1090–6.
52. West JB, Fitzpatrick JM, Toms SA, et al. Fiducial point placement and the accuracy of point-based,

rigid body registration. Neurosurgery. 2001;48: 810–6. discussion 816–817.
53. Mitchell H, Newton I. Medical photogrammetric measurement: overview and prospects. ISPRS J Photogramm. 2002;56:286–94.
54. Yan D, Vicini F, Wong J, et al. Adaptive radiation therapy. Phys Med Biol. 1997;42:123–32.
55. Yan D, Wong J, Vicini F, et al. Adaptive modification of treatment planning to minimize the deleterious effects of treatment setup errors. Int J Radiat Oncol Biol Phys. 1997;38:197–206.
56. Kupelian PA, Ramsey C, Meeks SL, et al. Serial megavoltage CT imaging during external beam radiotherapy for non-small-cell lung cancer: observations on tumor regression during treatment. Int J Radiat Oncol Biol Phys. 2005;63:1024–8.
57. Ramsey CR, Langen KM, Kupelian PA, et al. A technique for adaptive image-guided helical tomotherapy for lung cancer. Int J Radiat Oncol Biol Phys. 2006;64:1237–44.
58. Bissonnette JP, Purdie TG, Higgins JA, et al. Cone-beam computed tomographic image guidance for lung cancer radiation therapy. Int J Radiat Oncol Biol Phys. 2009;73:927–34.
59. Onishi H, Araki T, Shirato H, et al. Stereotactic hypofractionated high-dose irradiation for stage I nonsmall cell lung carcinoma: clinical outcomes in 245 subjects in a Japanese multiinstitutional study. Cancer. 2004;101:1623–31.
60. Guckenberger M, Wulf J, Mueller G, et al. Dose–response relationship for image-guided stereotactic body radiotherapy of pulmonary tumors: relevance of 4D dose calculation. Int J Radiat Oncol Biol Phys. 2009;74:47–54.
61. Kirkpatrick JP, Meyer JJ, Marks LB. The linear-quadratic model is inappropriate to model high dose per fraction effects in radiosurgery. Semin Radiat Oncol. 2008;18:240–3.
62. Fuks Z, Kolesnick R. Engaging the vascular component of the tumor response. Cancer Cell. 2005; 8:89–91.
63. Garcia-Barros M, Paris F, Cordon-Cardo C, et al. Tumor response to radiotherapy regulated by endothelial cell apoptosis. Science. 2003;300:1155–9.
64. Brenner DJ. The linear-quadratic model is an appropriate methodology for determining isoeffective doses at large doses per fraction. Semin Radiat Oncol. 2008;18:234–9.
65. Milano MT, Constine LS, Okunieff P. Normal tissue toxicity after small field hypofractionated stereotactic body radiation. Radiat Oncol. 2008;3:36.
66. Park C, Papiez L, Zhang S, et al. Universal survival curve and single fraction equivalent dose: useful tools in understanding potency of ablative radiotherapy. Int J Radiat Oncol Biol Phys. 2008;70:847–52.
67. Liu HH, Balter P, Tutt T, et al. Assessing respiration-induced tumor motion and internal target volume using four-dimensional computed tomography for radiotherapy of lung cancer. Int J Radiat Oncol Biol Phys. 2007;68:531–40.
68. Leong J. Implementation of random positioning error in computerised radiation treatment planning systems as a result of fractionation. Phys Med Biol. 1987;32:327–34.
69. Beckham WA, Keall PJ, Siebers JV. A fluence-convolution method to calculate radiation therapy dose distributions that incorporate random set-up error. Phys Med Biol. 2002;47:3465–73.
70. Chetty IJ, Rosu M, McShan DL, et al. Accounting for center-of-mass target motion using convolution methods in Monte Carlo-based dose calculations of the lung. Med Phys. 2004;31:925–32.
71. Keall PJ, Joshi S, Vedam SS, et al. Four-dimensional radiotherapy planning for DMLC-based respiratory motion tracking. Med Phys. 2005;32:942–51.
72. Rosu M, Balter JM, Chetty IJ, et al. How extensive of a 4D dataset is needed to estimate cumulative dose distribution plan evaluation metrics in conformal lung therapy? Med Phys. 2007;34:233–45.
73. Wolthaus JW, Schneider C, Sonke JJ, et al. Mid-ventilation CT scan construction from four-dimensional respiration-correlated CT scans for radiotherapy planning of lung cancer patients. Int J Radiat Oncol Biol Phys. 2006;65:1560–71.
74. Das IJ, Ding GX, Ahnesjo A. Small fields: nonequilibrium radiation dosimetry. Med Phys. 2008;35:206–15.
75. Reynaert N, van der Marck SC, Schaart DR, et al. Monte Carlo treatment planning for photon and electron beams. Rad Phys Chem. 2007;76:643–86.
76. Chetty IJ, Curran B, Cygler JE, et al. Report of the AAPM Task Group No. 105: issues associated with clinical implementation of Monte Carlo-based photon and electron external beam treatment planning. Med Phys. 2007;34:4818–53.
77. Mackie TR, Scrimger JW, Battista JJ. A convolution method of calculating dose for 15-MV x rays. Med Phys. 1985;12:188–96.
78. Timmerman RD, Paulus R, Galvin J, et al. Stereotactic body radiation therapy for medically inoperable early-stage lung cancer patients: analysis of RTOG 0236. Int J Radiat Oncol Biol Phys. 2009;75:S3.
79. Timmerman R, McGarry R, Yiannoutsos C, et al. Excessive toxicity when treating central tumors in a phase II study of stereotactic body radiation therapy for medically inoperable early-stage lung cancer. J Clin Oncol. 2006;24:4833–9.
80. Patel AH, Ajlouni M, Jin J, et al. Is stereotactic body radiotherapy (SBRT) safe for central non-small cell lung cancer (NSCLC) lesions? Int J Radiat Oncol Biol Phys. 2008;72:S434–5.
81. Hiraoka M, Ishikura S. A Japan clinical oncology group trial for stereotactic body radiation therapy of non-small cell lung cancer. J Thorac Oncol. 2007;2: S115–7.
82. Hurkmans CW, Cuijpers JP, Lagerwaard FJ, et al. Recommendations for implementing stereotactic

radiotherapy in peripheral stage IA non-small cell lung cancer: report from the quality assurance working party of the randomised phase III ROSEL study. Radiat Oncol. 2009;4:1.
83. Harsolia A, Hugo GD, Kestin LL, et al. Dosimetric advantages of four-dimensional adaptive image-guided radiotherapy for lung tumors using online cone-beam computed tomography. Int J Radiat Oncol Biol Phys. 2008;70:582–9.
84. van Zwienen M, van Beek S, Belderbos J, et al. Anatomical changes during radiotherapy of lung cancer patients. Int J Radiat Oncol Biol Phys. 2008;72:S111.
85. Britton KR, Starkschall G, Liu H, et al. Consequences of anatomic changes and respiratory motion on radiation dose distributions in conformal radiotherapy for locally advanced non-small-cell lung cancer. Int J Radiat Oncol Biol Phys. 2009;73:94–102.
86. Kong FM, Frey KA, Quint LE, et al. A pilot study of [18F]fluorodeoxyglucose positron emission tomography scans during and after radiation-based therapy in patients with non small-cell lung cancer. J Clin Oncol. 2007;25:3116–23.
87. Aerts HJ, Bosmans G, van Baardwijk AA, et al. Stability of 18F-deoxyglucose uptake locations within tumor during radiotherapy for NSCLC: a prospective study. Int J Radiat Oncol Biol Phys. 2008;71:1402–7.
88. Siewerdsen JH, Daly MJ, Bakhtiar B, et al. A simple, direct method for x-ray scatter estimation and correction in digital radiography and cone-beam CT. Med Phy. 2006;33:187–97.
89. Godfrey DJ, Ren L, Yan H, et al. Evaluation of three types of reference image data for external beam radiotherapy target localization using digital tomosynthesis (DTS). Med Phys. 2007;34:3374–84.
90. Ren L, Godfrey DJ, Yan H, et al. Automatic registration between reference and on-board digital tomosynthesis images for positioning verification. Med Phys. 2008;35:664–72.
91. Wijesooriya K, Weiss E, Dill V, et al. Quantifying the accuracy of automated structure segmentation in 4D CT images using a deformable image registration algorithm. Med Phys. 2008;35:1251–60.
92. Zhong H, Kim J, Chetty IJ. Analysis of deformable image registration accuracy using computational modeling. Med Phys. 2009;37:970–9.
93. Heath E, Seuntjens J. A direct voxel tracking method for four-dimensional Monte Carlo dose calculations in deforming anatomy. Med Phys. 2006;33:434–45.
94. Rosu M, Chetty IJ, Balter JM, et al. Dose reconstruction in deforming lung anatomy: dose grid size effects and clinical implications. Med Phys. 2005;32:2487–95.
95. Siebers JV, Zhong H. An energy transfer method for 4D Monte Carlo dose calculation. Med Phys. 2008;35:4096–105.
96. Kong FM, Ten Haken RK, Schipper MJ, et al. High-dose radiation improved local tumor control and overall survival in patients with inoperable/unresectable non-small-cell lung cancer: long-term results of a radiation dose escalation study. Int J Radiat Oncol Biol Phys. 2005;63:324–33.
97. Uematsu M, Shioda A, Tahara K, et al. Focal, high dose, and fractionated modified stereotactic radiation therapy for lung carcinoma patients: a preliminary experience. Cancer. 1998;82:1062–70.
98. Nyman J, Johansson KA, Hulten U. Stereotactic hypofractionated radiotherapy for stage I non-small cell lung cancer–mature results for medically inoperable patients. Lung Cancer. 2006;51:97–103.
99. Nagata Y, Takayama K, Matsuo Y, et al. Clinical outcomes of a phase I/II study of 48 Gy of stereotactic body radiotherapy in 4 fractions for primary lung cancer using a stereotactic body frame. Int J Radiat Oncol Biol Phys. 2005;63:1427–31.
100. Onishi H, Shirato H, Nagata Y, et al. Hypofractionated stereotactic radiotherapy (HypoFXSRT) for stage I non-small cell lung cancer: updated results of 257 patients in a Japanese multi-institutional study. J Thorac Oncol. 2007;2:S94–100.
101. Videtic GM, Stephans K, Reddy C, et al. Intensity-modulated radiotherapy-based stereotactic body radiotherapy for medically inoperable early-stage lung cancer: excellent local control. Int J Radiat Oncol Biol Phys. 2010;77(2):344–9. doi: 10.1016/j.ijrobp.2009.05.004. Epub 2009 Sep 18.
102. Fakiris AJ, McGarry RC, Yiannoutsos CT, et al. Stereotactic body radiation therapy for early-stage non-small-cell lung carcinoma: four-year results of a prospective phase II study. Int J Radiat Oncol Biol Phys. 2009;75:677–82.
103. Baumann P, Nyman J, Lax I, et al. Factors important for efficacy of stereotactic body radiotherapy of medically inoperable stage I lung cancer. A retrospective analysis of patients treated in the Nordic countries. Acta Oncol. 2006;45:787–95.
104. Lagerwaard FJ, Haasbeek CJ, Smit EF, et al. Outcomes of risk-adapted fractionated stereotactic radiotherapy for stage I non-small-cell lung cancer. Int J Radiat Oncol Biol Phys. 2008;70:685–92.

Chemotherapy for the Lungs

41

Corey J. Langer and Jared Weiss

Abstract

The addition of chemotherapy to definitive radiation for both non-small cell lung cancer (NSCLC) and small cell lung cancer (SCLC) improves survival. Although the initial data for superior survival with chemotherapy came from studies using induction chemotherapy before definitive radiation, subsequent studies have shown superior outcomes with concurrent therapy. The combination of cisplatin and etoposide remains the standard of care for patients able to tolerate the regimen. In the context of concurrent definitive chemoradiation with full dose chemotherapy, there is no proven benefit to additional chemotherapy given either before or after chemoradiation. However, consolidation with full dose therapy remains standard following low-dose regimens used for patients unable to tolerate cisplatin and etoposide. Perhaps, the most accepted of these regimens is the locally advanced multimodality protocol (LAMP) regimen of weekly carboplatin and paclitaxel, which in Japan proved equivalent to a cisplatin-containing regimen in combination with radiation. The combination of full dose carboplatin and pemetrexed is also of increasing interest for patients with non-squamous histology. No targeted agent is currently indicated in combination with radiation.

Introduction

The dominant image-guided therapy for lung cancer is radiation. While other locally ablative procedures such as radiofrequency ablation have been explored for small primary lung tumors, combination of these modalities with chemotherapy has not been addressed by any major studies. When given before or after radiation therapy, chemotherapy has the potential to both eliminate distant micrometastatic disease and to cytoreduce the primary site. When given simultaneously

C.J. Langer (✉)
Department of Medicine, Division of Hematology-Oncology, Hospital of the University of Pennsylvania, Philadelphia, PA, USA
e-mail: corey.langer@uphs.upenn.edu

J. Weiss
Department of Medicine, Division of Hematology-Oncology, University of North Carolina at Chapel Hill, Chapel Hill, NC, USA

D.E. Dupuy et al. (eds.), *Image-Guided Cancer Therapy*, DOI 10.1007/978-1-4419-0751-6_43,

Table 41.1 Concurrent therapy versus sequential therapy

Trial	Outcome	N	F/U	Concurrent	sequential	P
Furuse [3]	(+)	320	5 year	16 %	9 %	.04
RTOG 9410 [4]	(+)	597	5 year	16 %	10 %	.038
GLOT [5]	(−)	205	4 year	21 %	14 %	.24
Czech	(+)	207	2 year	42 %	15 %	.021
Aupérin (meta-analysis) [6]	(+)	1,205 from 6 trials	5 year	15.1 %	10.6 %	.004

with radiation, it can also sensitize cancer cells to the damage caused by radiation therapy, thereby improving local control. In stage III non-small cell lung cancer (NSCLC), chemotherapy has been proven to act as an adjunct to the curative potential of radiation therapy. For small cell lung cancer (SCLC), chemotherapy plays the primary curative role, with image-guided radiation providing adjunctive cell kill at the primary site. Our challenge over the next several years is to pair systemic therapy with new technologies, including 3D conformal radiation, proton beam, intensity-modluated radiotherapy (IMRT), and stereotactic radiotherapy (SBRT).

Induction Chemotherapy for Stage III NSCLC

The addition of chemotherapy to radiation for stage III NSCLC was first proven in the context of induction chemotherapy. Cancer and leukemia group B 8433 trial (CALGB 8433) randomized 155 patients with stage III non-small cell lung cancer to receive 6,000 CGy in 30 fractions, starting either day 1 (radiation arm) or day 50, following cisplatin and vindesine induction therapy (induction arm). The addition of induction chemotherapy improved median survival from 9.6 to 13.7 months and 6 years survival from 6 % to 13 % [1]. These results were confirmed by a subsequent intergroup trial which randomized 452 patients to three arms – the same standard radiation regimen; this regimen is preceded by cisplatin and vinblastine induction chemotherapy and hyperfractionated radiation (1.2 Gy twice daily to 69.6 Gy). The addition of cisplatin, but not hyperfractionated radiation, significantly improved survival. Median overall survival was 11.4 months for standard radiation, 13.2 months for induction chemotherapy followed by radiation, and 12 months for hyperfractionated radiation; corresponding 5-year overall survival rates were 5 %, 8 %, and 6 %, respectively [2]. These studies laid the groundwork for combined modality treatment in locally advanced (LA) NSCLC.

Concurrent Chemoradiotherapy for Stage III NSCLC

Although induction chemotherapy remains a viable option in select patients, concurrent administration allows for immediate delivery of optimal therapy for distant control of metastatic disease while also taking maximal advantage of the radiosensitizing properties of chemotherapy for local control. At least three major studies and a meta-analysis have confirmed superior local control and overall survival for concurrent therapy over sequential therapy (Table 41.1).

In addition to demonstrating improved survival, the meta-analysis underscored a theme consistent throughout trials comparing induction chemotherapy to sequential chemoradiotherapy – increased toxicity. In particular, acute esophageal toxicity grades 3–4 increased from 4 % to 18 % ($p < .001$). There was no significant increase in long-term pulmonary toxicity.

High-Dose Versus Low-Dose Chemotherapy

In an effort to mitigate the toxicity of concurrent radiation and to make more patients eligible for this approach, investigators have evaluated a number of low-dose chemotherapy regimens that feature more frequent administration. These regimens have frequently been termed

"radiosensitizing" regimens in contrast to "systemic-dose" regimens, although it is not clear if these lower doses lack systemic activity. Nonetheless, most of these trials incorporated traditional dose chemotherapy either before or following chemoradiation to compensate for the presumed lack of systemic efficacy of low-dose chemotherapy (Table 41.2).

Low-dose chemotherapy has never been directly compared to the same regimen with high-dose chemotherapy in a randomized phase III trial. The WJTOG study and the Dutch study compare high-dose to low-dose regimens, but the specific drugs in each regimen were not the same. Thus, no definitive conclusions about the merits of more frequent, low-dose concurrent chemotherapy compared to less frequent, systemic, high-dose chemotherapy can be made. However, a consistent theme emerges from the bulk of non-randomized data that low-dose chemotherapy represents a reasonable and generally effective treatment option.

Other Regimens

The OLCSG007 study compared the second generation regimen of mitomycin, vindesine, and cisplatin to the third-generation regimen cisplatin plus docetaxel, both concurrent with a modified Furuse regimen [3] of radiation. At initial report [13], the third-generation regimen improved overall survival at 2 years, but on further follow-up, this advantage was lost at 3 years [14]. The authors argued that given the early survival advantage for this regimen as well as numerous changes in care such as improvements in radiation techniques, this "modern" regimen was nonetheless worthy of further study.

A recent trial demonstrated superior survival in the metastatic setting for treatment with the multi-folate-targeted pemetrexed in patients with non-adenocarcinoma histology [15]. These efficacy results combined with pemetrexed's superior tolerability have led to increased interest in pemetrexed-containing chemoradiation regimens. One arm of a randomized phase II study presented at ASCO in 2009 demonstrated a 22-month median overall survival with a good toxicity profile [16] when carboplatin and pemetrexed were administered concomitantly with XRT for two cycles, followed by two additional combination cycles, then four cycles of consolidative pemetrexed. Additional study of pemetrexed-containing regimens is ongoing. In particular, the PROCLAIM trial is comparing the cisplatin-pemetrexed combination to standard etoposide/cisplatin[17]. In the "standard" therapy arm of this trial, patients receive two cycles of cisplatin and etoposide, monthly, concurrent with radiation, followed by the clinician's choice of consolidative therapy for two cycles, with options including additional cisplatin and etoposide, cisplatin and vinorelbine, and carboplatin and paclitaxel. In the experimental arm, patients are treated with three cycles of pemetrexed and cisplatin, given every 3 weeks, followed by four cycles of consolidative pemetrexed. Numerous phase II trials are evaluating modified pemetrexed-containing schedules.

Lack of Proven Benefit to Targeted Agents Concurrent with Radiation

The epidermal growth factor antibody cetuximab improves survival when added to definitive radiation for squamous cell carcinoma of the head and neck [18] and when added to cisplatin plus vinorelbine chemotherapy for metastatic NSCLC [19]. These results led to the hypothesis that cetuximab might also improve outcomes from definitive radiation in NSCLC. This hypothesis has been evaluated in the phase II setting both in conjunction with carboplatin and paclitaxel and with carboplatin and pemetrexed. RTOG 0324 evaluated 87 patients treated with weekly carboplatin (AUC 2), paclitaxel (45 mg/m^2), cetuximab (400 mg/m^2 loading dose followed by 250 mg/m^2), and radiation (63 Gy) over 7 weeks followed by consolidation carboplatin and paclitaxel [20]. The treatment was well tolerated with a median survival time of 22.7 months, leading the authors to conclude it worthy of further study. RTOG 0617 is an ongoing phase III trial with a 2 by 2 design testing whether the addition of cetuximab to

Table 41.2 Low-dose chemotherapy regimens

Trial	Regimen	Month OS	2year OS	5year OS
LAMP [7]	Sequential: Carboplatin (AUC6) + paclitaxel (200mg/m^2) Q3w x 2 then QD TRT to 63Gy	12.5		
	Induction/concurrent: Carboplatin (AUC6) + paclitaxel (200mg/m^2) Q3w x 2 then Carboplatin (AUC2) + paclitaxel (45mg/m^2) weekly + QD TRT to 63Gy	11		
	Concurrent/adjuvant: Carboplatin (AUC2) + paclitaxel (45mg/m^2) weekly + QD TRT to 63Gy then Carboplatin (AUC6) + paclitaxel (200mg/m^2) Q3w x 2	16.1		
CALGB 39801 [8]	Induction/concurrent: Carboplatin (AUC6) + paclitaxel (200mg/m^2) Q3w x 2 then Carboplatin (AUC2) + paclitaxel (50mg/m^2) weekly + QD TRT to 66Gy	14	31 %	
	Concurrent Carboplatin (AUC2) + paclitaxel (50mg/m^2) + QD TRT to 66Gy	12	29 %	
RTOG 9801 [9, 10]	Control: Carboplatin (AUC6) + paclitaxel (225mg/m^2) Q3w x 2 then Carboplatin (AUC2) + paclitaxel (50mg/m^2) weekly + BID TRT to 69.6Gy	17.9	40 %	16 %
	Experimental: Carboplatin (AUC6) + paclitaxel (225mg/m^2) Q3w x 2 then Carboplatin (AUC2) + paclitaxel (50mg/m^2) weekly + BID TRT to 69.6Gy + amifostine 500mg/m^2 4x/week	17.3	38 %	17 %

(*continued*)

Table 41.2 (continued)

Trial	Regimen	Month OS	2year OS	5year OS
WJTOG 0105 [11]	Older generation chemotherapy: Cisplatin 80 mg/m2 d1 + VDS 3mg/m2 d1, 8 + MMC 8mg/m^2 d1 q4w× 2 cycles + QD TRT to 60Gy (2 Gy/fr. split) then Cisplatin 80 mg/m2 d1 + VDS 3mg/m^2 d1, 8 + MMC 8mg/m2 d1 q4w× 2 cycles	20.5		17.5 %
	Weekly with irinotecan: Carboplatin AUC2 + irinotecan 20mg/m^2 d1, 8, 15, 22, 29, 36 with TRT QD to 60 Gy then Carboplatin AUC2 + irinotecan 50mg/m^2 day 1, 8 Q3w x 2	19.8		17.8 %
	Weekly with paclitaxel: Carboplatin AUC2 + paclitaxel 40mg/m^2 both weekly with TRT QD to 60Gy then Carboplatin AUC5 + paclitaxel 200mg/m^2 q3w x 2	22		19.5 %
Dutch study [12]	Radiation alone: QD TRT 3Gy/d X 10 then 3 weeks rest then QD TRT 2.4 Gy/d x 10		13 %	
	Weekly chemotherapy: 3Gy/d X 10 with cisplatin 30mg/m^2 weekly during XRT then 3 weeks rest then 2.4 Gy/d x 10 with cisplatin 30mg/m^2 weekly during XRT		19 %	
	Daily chemotherapy: 3Gy/d X 10 with 6mg/m^2 cisplatin daily during XRT then 3 weeks rest then 2.4 Gy/d x 10 with 6mg/m^2 cisplatin daily during XRT		26 %	

chemoradiation with paclitaxel and carboplatin is superior to chemoradiation alone; in addition, it compares 3D conformal RT to standard delivery of radiation. As of November 2010, this study was more than half accrued. Finally, CALGB 30407 was a randomized phase II study evaluating the combination of XRT, carboplatin, and pemetrexed chemoradiation with or without cetuximab. In this study, all patients received carboplatin (AUC 5), pemetrexed (500 mg/m^2) intravenously every 3 weeks, and radiation (70 Gy) with half randomized to also receive cetuximab [21]. Although cetuximab did not add substantially to toxicity, there was no clear difference in treatment outcomes between the two arms. Follow-up on this study was fairly immature at last report, with median follow-up of only 17 months, leading the authors to conclude that additional time would be needed before concluding definitely that cetuximab did not confer benefit in this setting.

Bevacizumab is a monoclonal antibody that targets the vascular endothelial growth factor receptor and improves survival in the treatment of metastatic NSCLC [22]. However, both in NSCLC and SCLC, its combination with radiation therapy has proven problematic. In one study, the addition of bevacizumab to chemoradiation in SCLC resulted in a heightened incidence of tracheoesophageal fistulae [23]. A phase II SCLC trial treated 39 patients with carboplatin, irinotecan, and bevacizumab concurrent with radiation therapy, followed by maintenance bevacizumab. Three patients developed tracheoesophageal fistula, which is very rare with carboplatin and irinotecan, whether alone or combined with radiation. In the NSCLC trial, five patients were treated with pemetrexed, carboplatin, bevacizumab, and radiation; two patients developed tracheoesophageal fistula. Heretofore, tracheoesophageal fistula was a rare event not associated with these agents, either alone or in combination with radiation. Therefore, while alternative schedules of bevacizumab might be considered in the context of carefully conducted clinical trials, it should not be used concurrently with radiation therapy for lung cancer outside the context of such a trial.

Numerous other targeted agents are being studied in various combinations and schedules together with radiation for lung cancer. At this time, none can be considered validated approaches, and these agents should not be considered outside the context of a carefully conducted clinical trial.

Lack of Benefit to Additional Chemotherapy Before or After Chemoradiotherapy for Stage III NSCLC

Investigators from the CALGB noted that the results of trials demonstrating that induction chemotherapy provided less benefit than concurrent therapy did not rule out a benefit to induction therapy as an addition to concurrent chemoradiotherapy. CALGB 39801 randomized patients to receive either chemoradiation alone (weekly carboplatin and paclitaxel simultaneous with daily radiation to 66 Gy) or identical therapy preceded by two cycles of induction carboplatin (AUC 6) and paclitaxel (200 mg/m^2). There was no difference between the two arms overall [8] or in the subgroups of good or poor prognosis patients [24]. Induction chemotherapy before definitive chemoradiation is now rarely used but may be considered when the patient is considered of borderline functional status for combined modality therapy. In this situation, the treating clinicians use chemotherapy to give the cancer an opportunity to "prove" its chemosensitivity and the patient to "prove" his/her ability to tolerate chemotherapy before employing potentially more toxic multimodality therapy. Patients unable to tolerate chemotherapy alone and patients whose cancers are destined to metastasize despite therapy can thus be spared the greater toxicity of concurrent chemoradiotherapy.

The SWOG 9504 phase II study of cisplatin plus etoposide chemoradiation followed by consolidation docetaxel yielded impressive results, with a median survival time of 26 months and 5-year survival of 29 %. These results appeared superior to the previous SWOG 9019 trial, which administered identical chemoradiotherapy but continued cisplatin plus etoposide consolidation.

In this older trial, median survival was 15 months, and 5-year survival was 17 % [25]. As a result of the favorable comparison, some oncologists concluded, without randomized data, that docetaxel consolidation was superior to cisplatin/etoposide consolidation and thus considered this approach the new standard of care. However, the Hoosier Oncology Group launched the HOG LUN01-24/USO 02–033 trial to test the hypothesis that docetaxel consolidation indeed contributed to therapeutic outcome [26]. All patients received cisplatin (50 mg/m^2 on days 1, 8, 29, and 33) plus etoposide (50 mg/m^2 on days 1–5 and 29–33) chemoradiation to 59.4 Gy and were then randomized to three cycles of docetaxel consolidation (75 mg/m^2 every 3 weeks) or observation. Treatment results were not improved by the addition of docetaxel. Median survival time for the consolidation arm was 21.2 months, with a 3-year survival rate of 27.1 %. Median survival time for the observation arm was similar at 23.2 months ($p = 0.833$), and the 3-year survival rate was 26.1 %. Grade 3–5 toxicities with docetaxel included 11 % infections and 9.6 % pneumonitis. Some have argued that the HOG results demonstrate the folly of comparing phase II trials and the failure of docetaxel consolidation to improve outcomes. A vocal minority have argued that pulmonary reserve in the two groups was not balanced and that this could account for a failure to demonstrate a real improvement – FEV1 of > 2 L was present in 59.5 % of the observation group but only 41.1 % of the docetaxel group ($p = 0.066$). Majority opinion seems to have lined up with the first impression, as the use of docetaxel for consolidation has fallen out of favor [27]. But the concept of testing consolidation after definitive chemoradiation has not been discarded.

Lack of Benefit to Additional Targeted Agents After Chemoradiotherapy for Stage III NSCLC

The tyrosine kinase inhibitors gefitinib [28] and erlotinib [25] have demonstrated single-agent activity in metastatic NSCLC, and gefitinib has demonstrated superiority over chemotherapy for patients with the epidermal growth factor receptor mutation [29]. Further, erlotinib has demonstrated a modest progression-free survival advantage when given as maintenance after 1st-line chemotherapy for metastatic disease [30]. Investigators from SWOG noted a high distant relapse rate after chemoradiotherapy for stage III NSCLC and hypothesized that maintenance gefitinib following cisplatin plus etoposide chemoradiation might improve outcomes. SWOG 0023 treated all patients with the standard regimen of cisplatin (50 mg/m^2 on days 1, 8, 29, and 33) plus etoposide (50 mg/m^2 on days 1–5 and 29–33) concurrent with radiation to 61 Gy. All patients received consolidation docetaxel for three cycles at 70 mg/m^2 and were then randomized to observation or a maximum of 5 years of gefitinib at 250 mg per day. The results were surprising – not only did gefitinib fail to improve survival; it resulted in a significant decrease in survival: the median OS was 35 months in the placebo arm versus 23 months in the gefitinib arm (p. 01) [31].

Chemoradiation for LS-SCLC

Small cell lung cancer is an extremely chemosensitive disease, with high response rates, including durable complete response with chemotherapy alone in patients with limited-stage disease [32]. However, local control can also be a significant issue in SCLC, with local progression in a high proportion of patients treated with chemotherapy alone. One meta-analysis [33] demonstrated a 3-year survival advantage of 5.4 % for the addition of radiation to chemotherapy for LS-NSCLC. Another meta-analysis showed a 25.3 % improvement in intrathoracic tumor control and a 5-year absolute survival advantage of 5.4 % [34]. Further, in a separate meta-analysis, prophylactic cranial irradiation has demonstrated a similar survival advantage [35]. Therefore, radiation has a key role to play in improving treatment outcomes. Nonetheless, because of the proclivity of SCLC for early systemic spread, rapid delivery of

optimal chemotherapy remains paramount in the care of the patients with limited-stage disease.

Recognizing the importance of early chemotherapy, some clinicians initially favored planned sequential therapy. However, evidence from randomized trials and meta-analysis clearly support the delivery of early concurrent chemoradiation. The NCI Canada [36] treated all patients with alternating cycles of cisplatin plus etoposide and cyclophosphamide, doxorubicin, and vincristine chemotherapy for six cycles, followed by prophylactic cranial irradiation. All patients received 40 Gy of thoracic radiation, delivered over 15 fractions in three weeks with randomization to receive this radiation concurrent with the first or final cycle of cisplatin plus etoposide. Both progression-free (15.4 vs. 11.8 months, $p = .036$) and overall survival (21.2 months, 16.0 months, $p = .008$) favored the early radiation group. The JCOG 9304 [37] trial found similar results. All patients were treated with BID XRT to 45 Gy over 3 weeks and were randomized to receive it concurrent with the first cycle or following the fourth cycle of cisplatin and etoposide. Survival strongly trended in favor of the concurrent arm (27.2 vs. 19.7 months, $p = .097$).

The bulk of the data supporting chemoradiation for SCLC were derived from regimens incorporating cisplatin plus etoposide. Further, the pivotal trial demonstrating the merits of accelerated hyperfractionation radiotherapy utilized this regimen [38]. At this time, cisplatin plus etoposide is the standard regimen for patients who are able to tolerate this combination, with substitution of carboplatin for cisplatin acceptable when the patient is not a cisplatin candidate. Attempts to improve outcome by adding other cytotoxics (taxanes [39]) or using vaccine therapy [40] after chemoradiation have not succeeded.

References

1. Dillman RO, et al. Improved survival in stage III non-small-cell lung cancer: seven-year follow-up of cancer and leukemia group B (CALGB) 8433 trial. J Natl Cancer Inst. 1996;88(17):1210–5.
2. Sause W, et al. Final results of phase III trial in regionally advanced unresectable non-small cell lung cancer: Radiation Therapy Oncology Group, Eastern Cooperative Oncology Group, and Southwest Oncology Group. Chest. 2000;117(2):58–64.
3. Furuse K, et al. Phase III study of concurrent versus sequential thoracic radiotherapy in combination with mitomycin, vindesine, and cisplatin in unresectable stage III non-small-cell lung cancer. J Clin Oncol. 1999;17(9):2692–9.
4. Curran W, Paulus R, Langer CJ, Komaki R, Lee JS, Hauser S, Movsas B, Wasserman T, Russell A, Byhardt R, Machtay M, Sause W, Cox JD. Phase III comparison of sequential vs. concurrent chemo-radiation for patients with unresected stage III non-small cell lung cancer (NSCLC): Report of Radiation Therapy Oncology Group (RTOG) 9410. In Press at JNCI, 2010.
5. Fournel P, et al. Randomized phase III trial of sequential chemoradiotherapy compared with concurrent chemoradiotherapy in locally advanced non-small-cell lung cancer: Groupe Lyon-Saint-Etienne d'Oncologie Thoracique-Groupe Francais de Pneumo-Cancerologie NPC 95–01 Study. J Clin Oncol. 2005;23(25):5910–7.
6. Auperin A, et al. Meta-analysis of concomitant versus sequential radiochemotherapy in locally advanced non-small-cell lung cancer. J Clin Oncol. 2010; 28(13):2181–90.
7. Choy H, WJ, CJ, Scott CB, Bonomi P, Travis P, Haluschak J, Belani CP. Preliminary report of locally advanced multimodality protocol (LAMP): ACR 427: a randomized phase II study of three chemo-radiation regimens with paclitaxel, carboplatin, and thoracic radiation (TRT) for patients with locally advanced non small cell lung cancer (LA-NSCLC). Proc Am Soc Clin Oncol. 2002; 21 (abstr 1160).
8. Vokes EE, et al. Induction chemotherapy followed by chemoradiotherapy compared with chemoradiotherapy alone for regionally advanced unresectable stage III Non-small-cell lung cancer: cancer and leukemia group B. J Clin Oncol. 2007;25(13):1698–704.
9. Movsas B, et al. Randomized trial of amifostine in locally advanced non-small-cell lung cancer patients receiving chemotherapy and hyperfractionated radiation: radiation therapy oncology group trial 98–01. J Clin Oncol. 2005;23(10):2145–54.
10. Lawrence YR, Langer C, Werner-Wasik M, Nicolaou N, Komaki R, Machtay M, Wasserman T, Byhardt R, Movsas B. Carboplatin and paclitaxel based chemoradiation in locally advanced non-small cell lung cancer: a long-term follow-up of Radiation Therapy Oncology Group (RTOG) 98–01. 2010: Personal communication from Corey Langer to Jared Weiss, 11/4/2010.
11. Satouchi NY, Chiba Y, Kudoh S, Hida T, Kubo A, Seto T, Nishimura Y, Nakagawa K, Fukuoka M. Randomized, phase III study of mitomycin/vindesine/cisplatin (MVP) versus weekly

irinotecan/carboplatin (IC) or weekly paclitaxel/carboplatin (PC) with concurrent thoracic radiotherapy (TRT) for unresectable stage III non-small cell lung cancer (NSCLC): WJTOG0105. J Clin Oncol 27:15s, 2009 (suppl; abstr 7504).
12. Schaake-Koning C, et al. Effects of concomitant cisplatin and radiotherapy on inoperable non-small-cell lung cancer. N Engl J Med. 1992;326(8):524–30.
13. Kiura NT, Segawa Y, Kamei H, Takemoto M, Tabata M, Ueoka H, Hiraki S, Matsuo K, Tanimoto M. Randomized phase III trial of docetaxel and cisplatin combination chemotherapy versus mitomycin, vindesine, and cisplatin combination chemotherapy with concurrent thoracic radiation therapy for locally advanced non-small-cell lung cancer: OLCSG 0007. J Clin Oncol 26: 2008 (May 20 suppl; abstr 7515).
14. Segawa Y, et al. Phase III trial comparing docetaxel and cisplatin combination chemotherapy with mitomycin, vindesine, and cisplatin combination chemotherapy with concurrent thoracic radiotherapy in locally advanced non-small-cell lung cancer: OLCSG 0007. J Clin Oncol.
15. Scagliotti GV, et al. Phase III study comparing cisplatin plus gemcitabine with cisplatin plus pemetrexed in chemotherapy-naive patients with advanced-stage non-small-cell lung cancer. J Clin Oncol. 2008; 26(21):3543–51.
16. Govindan R, Wang X, Hodgson L, Kratzke R, Vokes EE. Phase II study of pemetrexed, carboplatin, and thoracic radiation with or without cetuximab in patients with locally advanced unresectable non-small cell lung cancer: CALGB 30407. J Clin Oncol 27:15s, 2009 (suppl; abstr 7505).
17. Vokes EE, et al. PROCLAIM: a phase III study of pemetrexed, cisplatin, and radiation therapy followed by consolidation pemetrexed versus etoposide, cisplatin, and radiation therapy followed by consolidation cytotoxic chemotherapy of choice in locally advanced stage III non-small-cell lung cancer of other than predominantly squamous cell histology. Clin Lung Cancer. 2009;10(3):193–8.
18. Bonner JA, et al. Radiotherapy plus cetuximab for locoregionally advanced head and neck cancer: 5-year survival data from a phase 3 randomised trial, and relation between cetuximab-induced rash and survival. Lancet Oncol. 2010;11(1):21–8.
19. Pirker R, et al. Cetuximab plus chemotherapy in patients with advanced non-small-cell lung cancer (FLEX): an open-label randomised phase III trial. Lancet. 2009;373(9674):1525–31.
20. Blumenschein GR, Curran WJ, Robert F, Fossella FV, Werner-Wasik M, Doescher P, Choy H, Komaki R. A phase II study of cetuximab (C225) in combination with chemoradiation (CRT) in patients (PTS) with stage IIIA/B non-small cell lung cancer (NSCLC): A report of the 2 year and median survival (MS) for the RTOG 0324 trial. J Clin Oncol 26: 2008 (May 20 suppl; abstr 7516).
21. Govindan JB, Wang X, Hodgson L, Kratzke R, Vokes EE. Phase II study of pemetrexed, carboplatin, and thoracic radiation with or without cetuximab in patients with locally advanced unresectable non-small cell lung cancer: CALGB 30407. Clin Oncol. 27:15s, 2009 (suppl; abstr 7505).
22. Sandler A, et al. Paclitaxel-carboplatin alone or with bevacizumab for non-small-cell lung cancer. N Engl J Med. 2006;355(24):2542–50.
23. Spigel DR, et al. Tracheoesophageal fistula formation in patients with lung cancer treated with chemoradiation and bevacizumab. J Clin Oncol. 2010;28(1):43–8.
24. Stinchcombe TE, et al. Treatment outcomes of different prognostic groups of patients on cancer and leukemia group B trial 39801: induction chemotherapy followed by chemoradiotherapy compared with chemoradiotherapy alone for unresectable stage III non-small cell lung cancer. J Thorac Oncol. 2009; 4(9):1117–25.
25. Gandara DR, Gaspar LE, Albain KS, Lara PN, Crowley J. Long term survival in stage IIIb non-small cell lung cancer (NSCLC) treated with consolidation docetaxel following concurrent chemoradiotherapy (SWOG S9504). J Clin Oncol, 2005 ASCO Annual Meeting Proceedings. Vol 23, No. 16S, Part I of II (June 1 Supplement), 2005: 7059.
26. Hanna N, et al. Phase III study of cisplatin, etoposide, and concurrent chest radiation with or without consolidation docetaxel in patients with inoperable stage III non-small-cell lung cancer: the Hoosier Oncology Group and U.S. Oncology. J Clin Oncol. 2008;26(35):5755–60.
27. Green MR, et al. Impact of the ASCO 2007 presentation of HOG Lun 01-24/USO-023 on the prescribing plans of American medical oncologists for patients with stage IIIB non-small cell lung cancer. J Thorac Oncol. 2009;4(8):983–7.
28. Kim ES, et al. Gefitinib versus docetaxel in previously treated non-small-cell lung cancer (INTEREST): a randomised phase III trial. Lancet. 2008;372(9652): 1809–18.
29. Mok TS, et al. Gefitinib or carboplatin-paclitaxel in pulmonary adenocarcinoma. N Engl J Med. 2009; 361(10):947–57.
30. Cappuzzo F, et al. Erlotinib as maintenance treatment in advanced non-small-cell lung cancer: a multicentre, randomised, placebo-controlled phase 3 study. Lancet Oncol. 2010;11(6):521–9.
31. Kelly K, et al. Phase III trial of maintenance gefitinib or placebo after concurrent chemoradiotherapy and docetaxel consolidation in inoperable stage III non-small-cell lung cancer: SWOG S0023. J Clin Oncol. 2008;26(15):2450–6.
32. Souhami RL, Law K. Longevity in small cell lung cancer. A report to the Lung Cancer Subcommittee of the United Kingdom Coordinating Committee for Cancer Research. Br J Cancer. 1990;61(4):584–9.

33. Pignon JP, et al. A meta-analysis of thoracic radiotherapy for small-cell lung cancer. N Engl J Med. 1992;327(23):1618–24.
34. Warde P, Payne D. Does thoracic irradiation improve survival and local control in limited-stage small-cell carcinoma of the lung? A meta-analysis. J Clin Oncol. 1992;10(6):890–5.
35. Auperin A, et al. Prophylactic cranial irradiation for patients with small-cell lung cancer in complete remission. Prophylactic Cranial Irradiation Overview Collaborative Group. N Engl J Med. 1999;341(7): 476–84.
36. Murray N, et al. Importance of timing for thoracic irradiation in the combined modality treatment of limited-stage small-cell lung cancer. The National Cancer Institute of Canada Clinical Trials Group. J Clin Oncol. 1993;11(2):336–44.
37. Takada M, et al. Phase III study of concurrent versus sequential thoracic radiotherapy in combination with cisplatin and etoposide for limited-stage small-cell lung cancer: results of the Japan Clinical Oncology Group Study 9104. J Clin Oncol. 2002;20(14): 3054–60.
38. Turrisi 3rd AT, et al. Twice-daily compared with once-daily thoracic radiotherapy in limited small-cell lung cancer treated concurrently with cisplatin and etoposide. N Engl J Med. 1999;340(4):265–71.
39. Ettinger DS, et al. Study of paclitaxel, etoposide, and cisplatin chemotherapy combined with twice-daily thoracic radiotherapy for patients with limited-stage small-cell lung cancer: a Radiation Therapy Oncology Group 9609 phase II study. J Clin Oncol. 2005; 23(22):4991–8.
40. Giaccone G, et al. Phase III study of adjuvant vaccination with Bec2/bacille Calmette-Guerin in responding patients with limited-disease small-cell lung cancer (European Organisation for Research and Treatment of Cancer 08971-08971B; Silva Study). J Clin Oncol. 2005;23(28):6854–64.

Percutaneous Radio Frequency Ablation for Painful Skeletal Metastases

42

Matthew Callstrom

Abstract

Patients with skeletal metastatic disease often have inadequate pain relief and conventional treatments, including external beam radiation therapy and opioid analgesics, often fail to provide pain relief and when relief is obtained, the duration is often short. Side effects of conventional therapies may also markedly decrease their quality of life, and few options are available for pain relief in patients with painful bone metastases who fail standard treatments. Image-guided percutaneous radiofrequency ablation of focal painful metastases has emerged as an effective focal treatment for patients with painful metastatic disease. This treatment offers clinically significant reduction of pain, an improvement in their quality of life and reduction in the use of analgesic medications by these patients.

Introduction

Metastases involving bone are a common problem in cancer patients and are a frequent source of pain and morbidity [1, 2]. In fact, up to 85 % of patients that die from lung, breast, and prostate cancer have bone metastases at the time of death [1]. Patients often suffer reduced performance status and poor quality of life due to complications from skeletal metastases resulting from pain, fractures, and decreased mobility. In addition, these complications can affect a patient's mood, leading to associated depression and anxiety [1]. Although bone metastases usually indicate a poor prognosis, with patients experiencing a median survival of 3 years or less, a significant fraction, 5–40 %, of patients are alive at 5 years dependent on tumor histology and burden [3, 4]. Treatments for patients with bone metastases are primarily palliative and include the following: systemic therapies (chemotherapy, hormonal therapy, radiopharmaceuticals, and bisphosphonates) and analgesics (opioids and nonsteroidal anti-inflammatory drugs) and localized therapies including surgery, radiation, and ablative therapies.

The current standard of care for patients with localized bone pain due to metastatic disease is external beam radiation therapy (RT). A majority of patients experience complete or partial relief

M. Callstrom
Department of Diagnostic Radiology, Mayo Clinic, Rochester, MN, USA
e-mail: Callstrom.matthew@mayo.edu

D.E. Dupuy et al. (eds.), *Image-Guided Cancer Therapy*, DOI 10.1007/978-1-4419-0751-6_44,

of pain following RT: however, it is typically several weeks before relief is achieved, and pain relief response is transient in more than 50 % of the patients that had an initial response to treatment. A prospective trial involving 1,016 patients conducted by the Radiation Therapy Oncology Group (RTOG) found RT resulted in complete relief in 53 % of patients with half of these patients achieving this relief in greater than 4 weeks [5]. Complete or partial relief was observed in a total of 83 % of the patients studied. The median duration of response for those patients that had partial pain relief was 20 weeks and 12 weeks for those that had initial complete relief. In a study comparing single fraction RT using either 8 or 4 Gy in 1,172 patients, the median time to a 2-point reduction in pain (10-point scale) in those that did respond to therapy was 3 weeks; however, approximately 35 % of these patients did not obtain relief until 5–20 weeks posttreatment [6]. Median time to recurrence of the same or higher pain score was dependent on tumor histology with breast cancer patients progressing in 36 weeks, prostate cancer in 20 weeks, lung cancer in 10 weeks, and all other cancers in 8 weeks. Unfortunately, 20–30 % of patients treated with RT do not experience pain relief.

Overall, between 60 % and 70 % of patients will have pain at the same or higher level following RT therapy within a period of 30–40 weeks. While repeat RT may be possible for a small fraction of these patients with recurrent or persistent pain, few other treatment options exist for these patients [7–12]. For most patients, repeat RT for failed treatment or recurrent pain is not offered due to limitations in normal tissue tolerance. Surgery for skeletal metastatic disease is usually employed for those with pathologic fracture or for those at high risk for fracture. In addition, surgery is rarely offered to patients with more than one site of metastatic disease or when patients present with advanced disease and poor functional status. The typical therapy for many patients with focal painful metastatic disease that have failed RT is narcotic analgesics [13]. Many patients balance the analgesia effect of these medications with undesirable common side effects such as sedation, constipation, and nausea.

Several new effective ablation treatment strategies have recently been reported for the treatment of metastatic disease involving bone [14]. These methods are based on using percutaneous image-guided methods to deliver tissue ablative devices into focal metastatic lesions. These include the use of RFA, cryoablation, laser ablation, and microwave ablation. In addition, patients at risk for fracture due to metastases in axially loaded locations (such as vertebral bodies, periacetabular region) may benefit from percutaneous cementoplasty. Of these minimally invasive methods, RFA has been the most studied. This chapter describes the use of RFA for the treatment of patients with painful metastatic skeletal disease.

Patients with limited metastatic disease involving bone that may benefit from image-guided radiofrequency ablation fall into two general categories: (1) patients who have limited painful metastatic disease that have failed conventional therapies or have refused conventional therapy and (2) patients with limited painful metastatic disease at risk for further morbidity with progression of a metastatic lesion that may be at risk for fracture or invasion of adjacent critical structures.

Patient selection and appropriate treatment strategies are important for successful outcomes with the use of RFA for palliation of painful metastases. Expected outcomes using radiofrequency ablation for palliation of painful metastatic disease is based on several recent case reports and series as well as two prospective clinical trials, which are described below.

Patient Selection for Radiofrequency Ablation

Patients appropriate for RFA for painful metastases include those with moderate or severe pain, typically $\geq$4/10 for worst pain in a 24-h period. Treatment of patients with mild pain with RFA is not usually indicated because it is difficult to

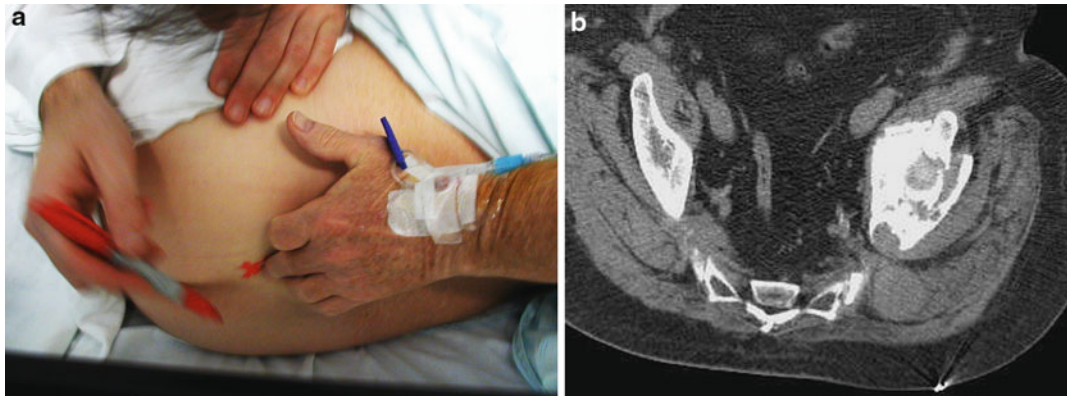

Fig. 42.1 (**a**) Patients are physically examined prior to the thermal ablation procedure for careful identification of the area of focal pain. The area is marked on the skin. (**b**) Following application of a metallic marker, CT imaging is used to correlate imaging findings and patient's identified site of pain. The metallic marker correlates with an osteolytic destructive lesion in the periacetabular region and a soft tissue implant in the gluteal musculature (Reprinted from Callstrom MR, Charboneau JW. Image-guided palliation of painful metastases using percutaneous ablation. Tech Vasc Interv Radiol. 2007;10(2):120–31, with permission from Elsevier)

improve on mild pain and because this type of pain can usually be adequately managed by oral analgesics. It is important that the focal pain is limited to one or two sites and that the site of pain corresponds to a metastasis evident with cross-sectional imaging. A limited physical exam is helpful as part of the process to both localize the patients' focal pain and to correlate with findings on cross-sectional imaging (Fig. 42.1). As seen in Fig. 42.1, careful identification of the site of focal pain found an osteolytic tumor in the periacetabular region as well as a soft tissue tumor in the adjacent musculature. As a result, both sites of disease are treated with RFA, as the pain could be caused by either of the two sites of metastatic disease.

In contrast to identifying a site for treatment with RFA, this examination may lead to a different etiology for focal pain. Figure 42.2 shows a prone CT image of a metastatic osteolytic lesion involving the mid-sacrum. When this patient was examined and a metallic marker placed on the skin overlying the site of greatest pain, CT imaging found the marker overlaid a sacral fracture (Fig. 42.2). Because the patient's pain was well localized to the side

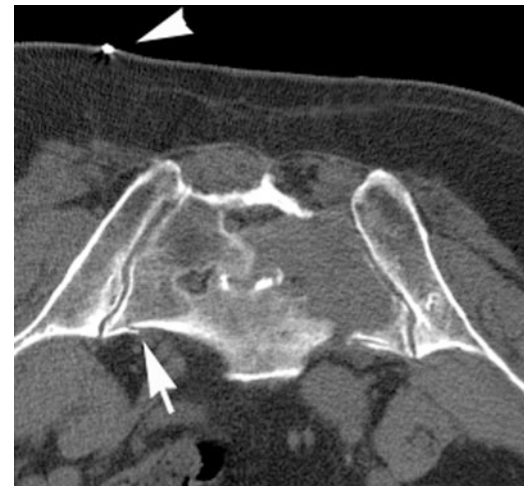

Fig. 42.2 Pain due to sacral fracture rather than osteolytic tumor. Prior to CT examination, the patient was examined, and a metallic marker was placed on the skin overlying the site of focal pain. CT imaging at this level shows an osteolytic destructive lesion involving the right side of the sacrum. The metallic marker (*arrow head*) overlies a sacral fracture (*arrow*). This lesion was not treated because the patient's pain was likely due to the sacral fracture rather than the adjacent osteolytic lesion (Reprinted from Callstrom MR, Charboneau JW, Goetz MP, Rubin, J. Image-Guided Palliation of Painful Skeletal Metastases, in Tumor Ablation, Eds. vanSonnenberg E, McMullen W, Solbiati L Springer, New York, NY, 2005, pgs 377–388, with kind permission of Springer Science+ Business Media)

opposite the metastatic disease, this tumor was not treated. Treatment of this patient's sacral pain may have benefitted from the use of cementoplasty (termed sacroplasty when performed in the sacrum) [15].

Although many patients will have more than one site of metastatic disease, it is common for only a few of the metastases to be symptomatic. However, patients with numerous painful lesions are not treated with these techniques because this type of pain is better treated with a systemic, rather than focal, approach. Finally, treatment of the painful metastatic lesion must be amenable to the use of RF electrodes, typically osteolytic or mixed osteolytic/osteoblastic metastases.

The primary reason for exclusion of patients from treatment is when successful treatment is expected to require treatment of a portion of the lesion located within 1 cm of the spinal cord, major motor nerve, brain, spinal artery of Adamkiewicz, bowel, or bladder. This margin of safety is a general guideline for the deployment of the ablative device adjacent to these critical structures. In practice, the nearest proximity of the ablative device to critical structures is dependent on visibility of the adjacent critical structure, utilization of thermal protection devices or maneuvers, monitoring of temperatures and neural structures, and experience of the interventional oncologist [16, 17].

Radiofrequency Ablation Treatment Analgesia and Sedation

Patients can be treated with RF ablation using either general anesthesia or moderate sedation with or without regional anesthesia. The type of anesthesia employed is often a function of local practice preferences. While moderate conscious sedation may be employed for many patients, the use of a general anesthetic allows complete treatment of the target lesion while providing adequate control of focal pain associated with the RFA treatment. In addition, the use of general anesthesia allows the procedure to be performed without the additional necessity of the performing physician to provide the necessary care management for the patient as is often required with conscious sedation. A general anesthetic is often preferred for treatment of difficult or large lesions because the procedures can be long – lasting greater than an hour depending on the technical difficulty associated with access or the size of the target lesion. Epidural catheters, placed prior to treatment of lesions, may be used to improve patient pain control following the procedure when the lesion is located in the pelvis or lower extremities.

As patients have moderate to severe pain prior to the procedure, it is not unusual for patients to have persistent pain immediately following the ablation treatment and as a result often benefit from either hospital admission or overnight observation. It is also common for some patients to have complete or near-complete relief of focal pain immediately following RFA treatment, and for these patients, observation status or outpatient treatment is possible. For patients with a painful tumor in an extremity or in the pelvis, these patients may benefit from the use of regional anesthesia, including epidural spinal analgesia or focal nerve blocks, for the treatment and for controlling pain in the immediate post ablation period. When an epidural catheter is employed, the duration of use is typically for a 12–24-h period following the ablation treatment. Prior to removal of the catheter, the medication infusion is halted. If the patient's pain has returned to the pretreatment level or improved, the catheter is removed, and the patient is converted to oral opioid analgesics for persistent mild to moderate discomfort or pain.

Radiofrequency Ablation Technique

Dispersive electrodes (grounding pads) are placed on the patient at approximately equidistant sites from the RF source, usually on the patient's thighs. In order to avoid skin burns from the ground pads, placement of skin temperature electrodes (Mallinkrodt Mon-a-therm Model 4070 with 700 series thermistor) can be placed on the corners or leading edges

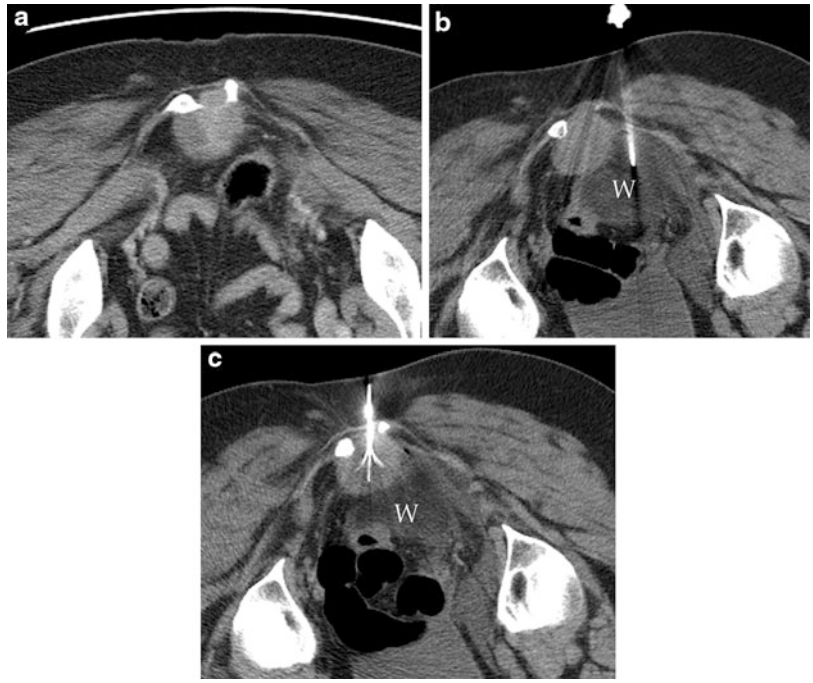

Fig. 42.3 RFA of painful metastatic carcinoid tumor to sacrum. Water displaces bowel and prevents injury. (**a**) Prone CT demonstrates a 4-cm soft tissue mass with associated destruction of the sacrum. A gas-filled loop of rectum is adjacent to the mass. (**b**) CT image shows needle in soft tissues; water (*W*) displaces rectum away from the tumor. (**c**) CT image shows RF electrode within tumor (Reprinted from Callstrom MR, Charboneau JW. Image-guided palliation of painful metastases using percutaneous ablation. Tech Vasc Interv Radiol. 2007;10(2):120–31, with permission of Elsevier)

(nearest the ablation location) of grounding pads. If the skin temperature reaches 38 °C, dry cold packs can be applied over the grounding pads.

Either multi-tined electrodes or cool-tip electrodes can be used, depending on physician preference. The RF electrode tip is directed into the tumor to be treated using image guidance. For deployable multi-tined electrodes, the tines are advanced into the soft tissue portion of the lesion until no further advancement is possible due to placement of the electrode tips against the bone interface with the active portion of the electrode placed in the tumor. The length of exposed electrode controls the diameter of electrode device and approximates the ablation diameter. For RF ablation using a cool-tip device, the electrode is placed into the soft tissue portion of the metastatic lesion against the bone-soft tissue interface.

With both types of electrode systems, electrode tip position is confirmed by CT or ultrasound imaging. For the deployable RF electrode systems, once the target temperature of 100 °C, or roll-off for impedance-controlled systems, is obtained, ablation is typically continued for 5 min with an overall treatment time goal of 5–15 min. Single ablations are usually performed for lesions of $\leq$3 cm in diameter. For larger lesions, the target is systematically treated using multiple 3–5-cm overlapping deployments of the electrode. For these larger lesions (>5 cm in diameter), the entire lesion may not be completely treated; rather, electrode placements are directed to the margin of the lesion involving bone with the goal of treating the majority of the soft tissue/bone interface. For cool-tip RF electrode treatments, either single or cluster electrodes, the treatment is continued with application of energy for approximately 4 min at maximum current [18].

A number of different techniques are utilized to reduce the risk of injury of adjacent normal critical structures. Of these, the use of tissue displacement and thermal monitoring methods is the most commonly employed. For RFA, hydrodisplacement with sterile water, such as D5W, rather than buffered fluids to prevent the theoretical risk of conduction of energy that may be possible with ionic solutions, can be used to displace loops of bowel away from a target lesion (Fig. 42.3) [19]. The use of one or more thermocouples adjacent to a critical structure such as the spinal cord or neural foramen can be used to provide thermal monitoring during an RFA

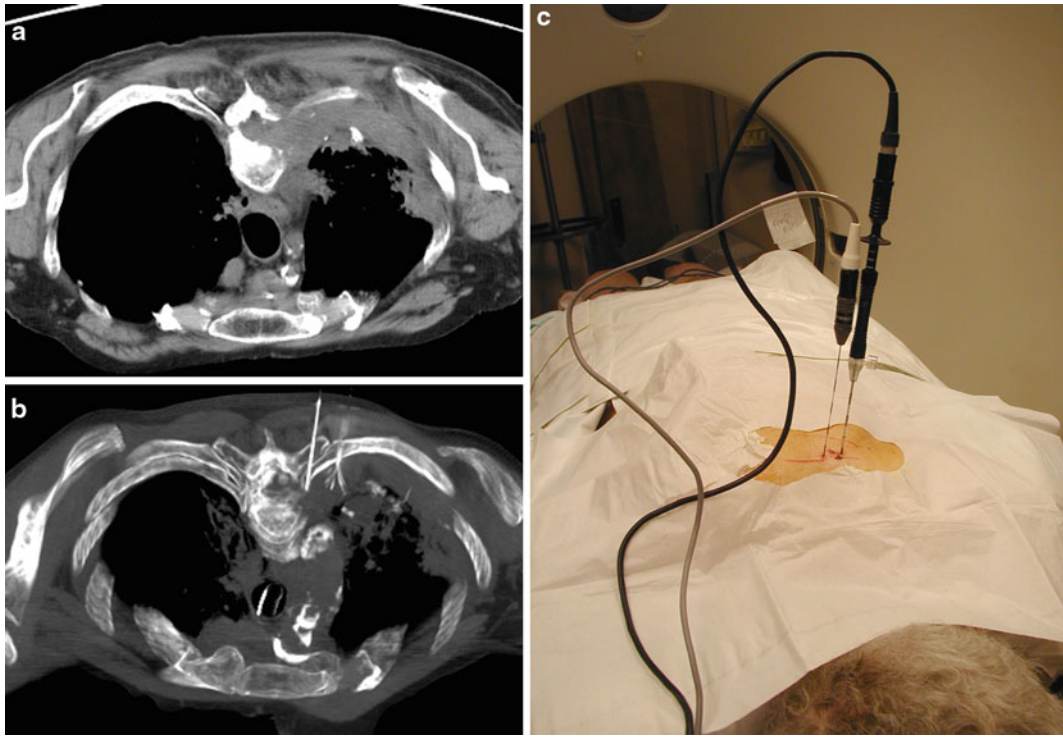

Fig. 42.4 Metastatic colorectal carcinoma to rib, vertebral body, and pleural surface. (**a**) Prone CT demonstrates osteolytic destruction of the lateral portion of the vertebral body with associated soft tissue mass anterior to the rib. (**b**). Prone CT image shows the passive thermocouple probe placed near the vertebral body pedicle with the RF electrode deployed laterally in the metastatic lesion. Ablation was discontinued when the temperature at the passive thermocouple reached 40 °C. (**c**) Photograph of the RF ablation electrode in place with adjacent thermocouple located medially. The patient's pain decreased from 10/10 to 3/10 four weeks following the treatment (Reprinted from Callstrom MR, Charboneau JW, Goetz P, et al. Image-guided ablation of painful metastatic bone tumors: A new and effective approach to a difficult problem. Skeletal Radiol 2006;35:1–15, with kind permission of Springer Science+Business Media)

procedure. Using this approach, RF ablation of painful paraspinal metastatic lesions is possible. Carefully monitoring temperatures allows ablation to be performed when metastatic tumors have destroyed the vertebral body with the resultant loss of the insulative effect of the adjacent bone [20]. This real-time temperature feedback allows ablation of neoplastic tissue as aggressively as possible while avoiding injury to the adjacent neural structures. Figure 42.4 shows a CT image of a large metastatic colorectal carcinoma metastasis involving the chest wall with a thermocouple placed along the lateral aspect of the destroyed pedicle. With the RF electrode deployed in the nearest paraspinal location, the treatment was discontinued when the thermocouple temperature reached 40 °C. This patient reported a reduction in pain from 10/10 prior to the treatment to 3/10 four weeks after the RF ablation procedure.

Treatment of metastatic tumors should include ablation of the bone-tumor interface. This treatment strategy is important as several possible mechanisms responsible for decreased pain involve this interface including (1) destruction of sensory nerve fibers involving the periosteum and bone cortex inhibiting pain transmission, (2) decompression of tumor volume decreasing stimulation of sensory nerve fibers, (3) destruction of tumor cells that produce nerve-stimulating cytokines (tumor necrosis factor-alpha, interleukins, and others) which

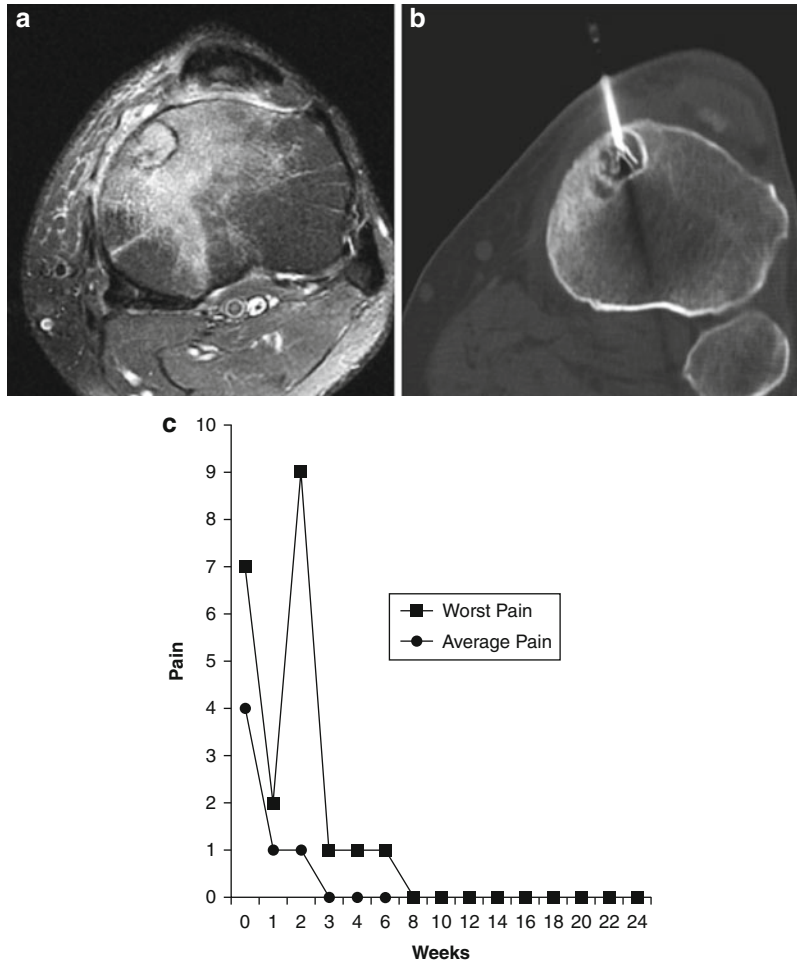

Fig. 42.5 (**a**) Fat-suppressed T2-weighted axial MRI image of the upper tibia and fibula. Metastatic malignant melanoma lesion contained within the tibia (*arrow*) with surrounding bony edema. Metastatic melanoma was also present in the soft tissues overlying the anterior aspect of the tibia (*arrow head*). (**b**) Axial CT image at the corresponding level with an RF electrode (*arrow*) placed within the osteolytic metastatic tumor. (**c**) Patient's worst and average pain scores in a 24-h period before and after treatment with percutaneous RF ablation. Patient's increased worst pain score at the 2-week interview resulted from resumption of strenuous physical activity (racquetball) (Reprinted from Callstrom MR, Charboneau JW. Percutaneous ablation: safe, effective treatment of bone tumors. Oncology (Williston Park). 2005;19(11 Suppl 4):22–6, with permission from UBM Medica)

may sensitize nerve fibers and affect pain transmission, and (4) inhibition of osteoclast activity which may cause pain [21–23]. Figure 42.5 shows the electrode deployed in a small osteolytic focus of metastatic melanoma in the anterior tibia. This treatment illustrates that the RF electrode is advanced into the soft tissue portion of the lesion to be treated and the tips of the tines of the electrode are deployed against the soft tissue/bone interface.

Figure 42.6 shows an example of a large osteolytic destructive lesion involving the most of the sacrum. The patient's oncologic treatment history included resection of the rectum with a diverting colostomy as well as radiation treatment to the pelvis, including the sacrum. The patient had reduced bladder function with difficulty initiating a stream and incomplete emptying of his bladder. With the goal of maintaining the patient's bladder function, we initially treated the

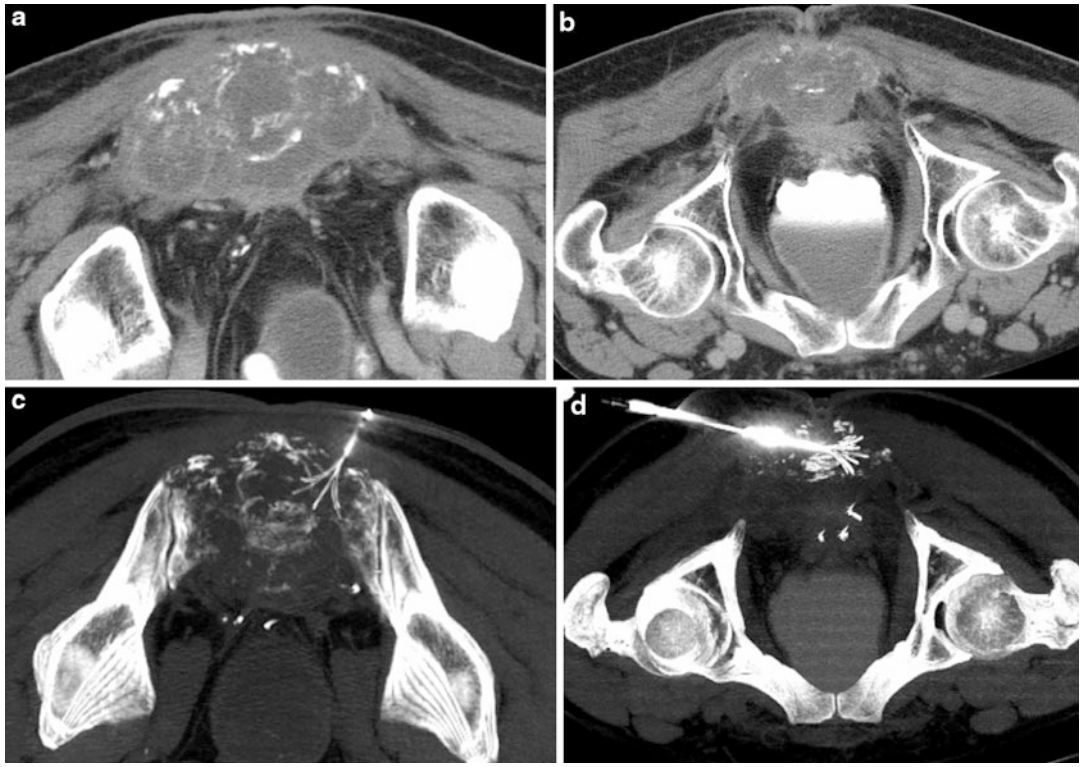

Fig. 42.6 RF ablation of a large sacral metastasis. (**a** and **b**) Prone CT demonstrates near-complete replacement of the sacrum by metastatic rectal carcinoma. (**c** and **d**) RF ablation electrodes were deployed to 5 cm. These were two of seven electrode placements during the first of stage of treatment for the ablation of much of the caudal aspect of the osteolytic lesion. The second-stage treatment of the mid-sacrum was performed 6 weeks later. Patient was unable to sit prior to treatment and had resting pain of 8/10. One day following the ablation, the patient was able to sit. His pain decreased to 3/10 following the first stage and to 0/10 soon after the second stage of treatment (Reprinted from Callstrom MR, Charboneau JW, Goetz P, et al. Image-guided ablation of painful metastatic bone tumors: a new and effective approach to a difficult problem. Skeletal Radiol 2006;35:1–15, with kind permission of Springer Science+Business Media)

caudal aspect of the sacrum with seven separate deployments of the RF electrode avoiding the course of the lumbar plexus and the S1 nerve. Following this treatment, the patient had a marked improvement in pain but with residual 3/10 pain. Because of the patient's desire for greater pain relief, and with the understanding that further RF ablation could lead to complete loss of bladder function, we treated the superior portion of the tumor to the level of the S2 neural foramina in a second stage of treatment. This treatment resulted in complete resolution of his previously reported 8/10 worst pain.

Unfortunately, many patients with rectal carcinoma will have regional metastases involving the presacral region often with direct extension to involve the adjacent sacrum. Figure 42.7 shows a tumor in a patient with previous resection of the rectum measuring approximately 3 cm in diameter located at the level of the lower sacrum/coccyx with 8/10 worst pain. Four weeks following RFA, the patient reported 2/10 worst pain and, at latest follow-up 11 months following treatment, 1/10 pain at the treated site.

Percutaneous Radiofrequency Ablation: Initial Case Reports

Dupuy and colleagues used an animal model to measure the temperature distribution within a vertebral body and the adjacent spinal canal

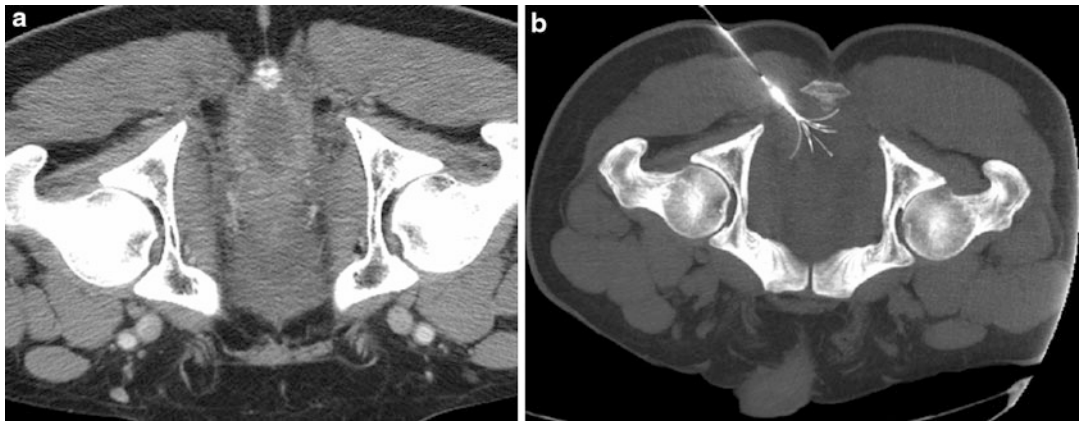

Fig. 42.7 Metastatic presacral rectal carcinoma. (**a**) Prone contrast-enhanced CT demonstrates a peripherally enhancing soft tissue mass anterior to the coccyx. (**b**) Prone CT demonstrates the RF ablation electrode deployed within the mass. Patient's pain decreased from 8/10 to 1/10 four weeks posttreatment. The patient continues to report 0–1/10 pain at this site 24 months posttreatment (Reprinted from Callstrom MR, Charboneau JW, Goetz MP, et al. Image-Guided Ablation of Painful Metastatic Bone Tumors: A New and Effective Approach to a Difficult Problem. Skel Rad. 2006;35:1–15, with kind permission of Springer Science+Business Media)

with the radiofrequency ablation electrode placed within the vertebral body [20]. They reported decreased heat transmission in cancellous bone and an insulative effect of cortical bone. They found that the temperature elevations in the epidural space were not high enough to cause injuries to the adjacent spinal cord or nerve roots. Based on this study, they subsequently treated a woman with a painful osteolytic metastatic hemangiopericytoma lesion in the anterior aspect of a lumbar vertebral body. Using local anesthesia and conscious sedation, a 3-cm exposed tip Radionics radiofrequency electrode (Covidien, Boulder, CO) was placed into the tumor using a far lateral approach after passing through intact cortex with a 14-gauge Ackermann bone biopsy needle (Cook Incorporated, Bloomington, IN). The patient had improved pain control at the latest follow-up evaluation of 13 months.

Gröenemeyer and colleagues used RFA to treat 10 patients with 21 painful spinal metastases using an expandable-type electrode (RITA Medical Systems, Angiodynamics Latham, NY) with a 50-W generator. The patients tolerated the procedure with local anesthesia only. The highest treatment temperature used for the ablations was based on distance of the RF electrode from the spinal cord and patient tolerance for the procedure. Four of the 10 patients were also treated with vertebroplasty receiving 3–5.5 mL of polymethylmethacrylate 3–7 days following the RFA [24]. At last follow-up, 9 of the 10 patients reported reduced pain with an average pain reduction of 74 %.

Percutaneous Radiofrequency Ablation: Clinical Trials

Because of the several reports suggesting the potential benefits of RFA for palliation of pain due to metastatic disease, two separate prospective clinical trials were conducted, one using an multi-tined RF electrode and the second using a cool-tip RF electrode.

An initial feasibility clinical trial was conducted using the multi-tined RF electrode to determine the safety and benefits of RFA in patients with painful metastatic lesions involving bone [25]. This preliminary data showed that this procedure was safe and resulted in significant relief of pain. As a result, the study was expanded to enroll patients from other centers in the United

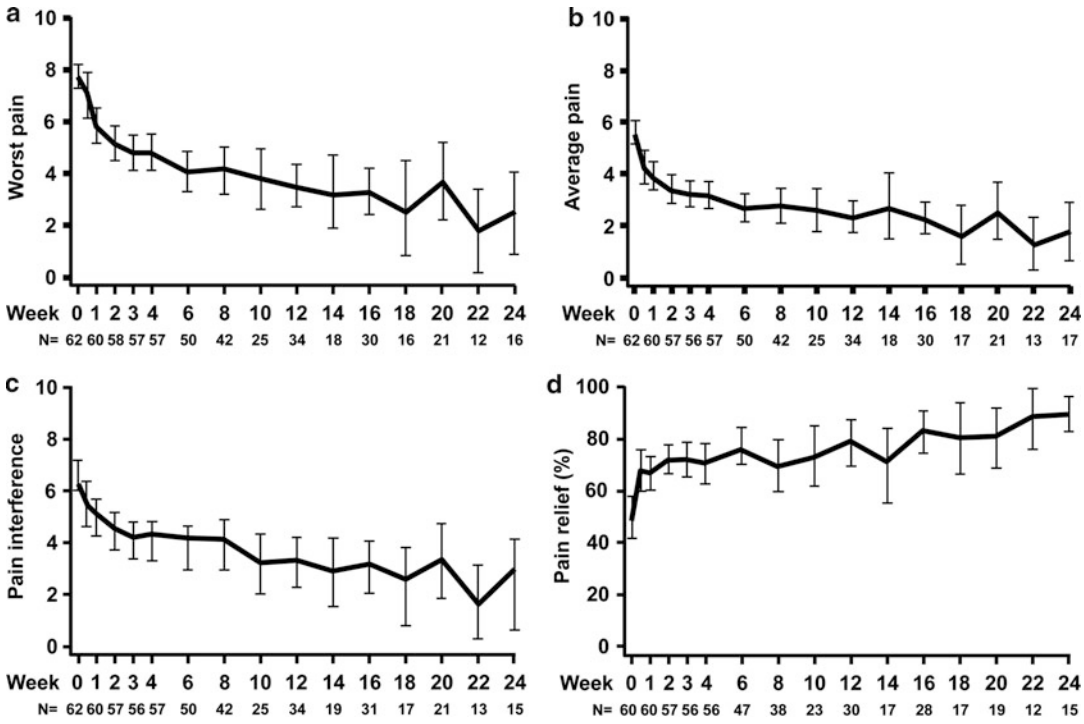

Fig. 42.8 Mean BPI pain scores over time for patients treated with RFA. (**a**) Worst pain, (**b**) average pain, (**c**) interference of pain in daily activities, (**d**) pain relief from RFA and medications. *Error bars* represent the 95 % confidence intervals. N = the number of patients completing BPI at each time point (Reprinted from Callstrom MR, Charboneau JW, Goetz MP, et al. Image-Guided Ablation of Painful Metastatic Bone Tumors: A New and Effective Approach to a Difficult Problem. Skel Rad. 2006;35:1–15, with kind permission of Springer Science+Business Media)

States and Europe [26]. In all, 62 patients at five centers in the United States and Europe with painful metastatic lesions that had failed or refused conventional radiation treatment were treated with RF ablation [27]. For these patients, nearly all patients were treated using general anesthesia [26, 28]. Inclusion criteria included patients that had moderate to severe pain (≥4/10 worst pain over a 24-h period) from ≤2 painful sites of metastasis. The primary measurement tool for response to RF ablation treatment was the Brief Pain Inventory (BPI), a validated numeric scale for the evaluation of pain in cancer patients [29, 30]. This visual analog scale includes several questions related to focal pain. Patients are asked to rate their worst, least, and average pain in the past 24 h, with responses ranging from 0 to 10 (0 = no pain, 10 = pain as bad as you can imagine). Relief of pain secondary to the RFA procedure or to pain medications is scored on a scale of 0 % (no relief) to 100 % (complete relief). In addition to questions related to pain, several questions concerning quality of life are also contained in the inventory. General activity, mood, walking ability, normal work, relations with other people, sleep, and enjoyment of life are scored on a 0–10 scale (0 = no interference, 10 = completely interferes).

Despite patients having failed conventional therapy in the majority, RFA treatment resulted in a clinically significant drop in pain (≥2 point drop in worst pain in a 24-h period) for 59/62 patients (95 %) (Fig. 42.8). Complications were noted in six patients with three patients experiencing exacerbation of preexisting tumor cutaneous fistulae involving the perineum within 1–2 weeks of the procedure due to generation of a large volume of necrotic tissue in the lower pelvis following

RF ablation. The remaining three complications involved one patient who developed transient bowel and bladder incontinence treatment of a previously irradiated leiomyosarcoma metastasis involving the upper sacrum, an acetabular fracture 6 weeks following RFA of a breast cancer metastasis with significant involvement of the periacetabular region, and a second-degree skin burn at the grounding pad site.

In a similar study utilizing the American College of Radiology Imaging Network (ACRIN) involving six centers in the USA, 55 patients with a single painful (>50 on a 1–100-pt scale) osseous metastasis were treated using a single 17-gauge or cluster cool-tip RF electrode [18]. The specific number of patients treated with either general anesthesia or conscious sedation was not reported; however, the majority of these patients were treated using conscious sedation. Conscious sedation, as well as some forms of general anesthesia, allows sensorimotor testing to be performed during the procedure.

Prior to treatment on this trial, patients reported a mean pain score of 54/100 with a range of 51–91/100. The mean treated tumor size was 5.2 cm in diameter ranging in size from 2.0 to 8.0 cm. The most common types of tumors treated included lung, renal, and colon cancer. These tumors were most commonly located in the pelvis, chest wall, spine, or in an extremity. Following treatment with RFA, patients had a statistically significant improvement in pain scores reporting an average decrease in pain at the 1-month and 3-month follow-ups of 27/100 points and 14/100 points, respectively. As noted previously, the RFA treatment can cause a transient increase in pain with 27 % of patients reporting pain greater than the baseline pain score immediately following the procedure.

Many patients had tumors treated that were adjacent to major motor nerves with 27/55 patients with tumors within 3 cm of a major neurovascular bundle. Although sensorimotor testing was available, one patient suffered a motor nerve deficit and three other patients developed neuropathic pain, developing as late as 35 days post-RFA. In total, major complications were found in 3/55 (5.4 %) including one case of foot drop, one patient with increased pain, and one patient with neuropathic pain. Although prior studies found a benefit from both external beam radiation therapy (RT) and RFA, this trial did not find a benefit from prior RT for a reduction in pain intensity [31].

It is difficult to directly compare these two prospective studies using RFA for several reasons. First, the two studies used different visual analog scales for the assessment of pain response. Comparison of the pain response for the two studies at the 3-month time point finds the ACRIN study reported a 14/100 pain score reduction, while the Callstrom et al. study had a corresponding reduction of 28/100. Unfortunately, further comparison beyond the 3-month time point is not possible as durability of pain relief was not assessed beyond this time in the ACRIN study. Continued decreases in pain scores were reported by patients in the Callstrom et al. study with reductions in pain of 53/100 at the 24-week follow-up evaluation.

In addition to using different pain score systems for evaluation of treatment response, the patient demographics and the RFA procedure also differ slightly between these two studies and may explain the relatively decreased pain relief realized in the ACRIN study (Table 42.1). The pain scores prior to treatment with RFA were likely different with mean pain scores of 7.7/10 for the Callstrom et al. study, while the Dupuy et al. study group had a mean pain score of 5.4/10. The majority of patients in the Callstrom et al. trial had received conventional treatments for pain with 74 % receiving RT prior to RFA, while in the ACRIN study, 24 % had received RT prior to treatment. It is possible that the higher percentage of patients that had received RT in the Callstrom et. al. trial may have benefited from the combination treatment, although neither study found that prior treatment with RT had a statistical impact on the pain response. The RF ablation devices used in these trials also differed. The RF electrode utilized as the Callstrom et. al trial was an expandable RF electrode (RITA Medical Systems, Angiodynamics, Latham, NY), while the ACRIN trial used a single or cluster cool-tip electrode (Radionics,

Table 42.1 Characteristics of patients with painful skeletal metastases treated with RFA in multicenter trials

Trial	Callstrom et al. [27]	Dupuy et. al. [18]
Device	Multi-tined	Cool-tip
Number of patients	62	54
Female	22 (35 %)	26 (47 %)
Male	40 (65 %)	29 (53 %)
Age (median, year)	64	62
Age range (year)	28–88	34–85
Tumor type (number)		
Renal CA	14 (23 %)	10 (18 %)
Colorectal CA	12 (19 %)	10 (18 %)
Lung CA	4 (6 %)	17 (31 %)
Breast	4 (6 %)	4 (7 %)
Other	28 (45 %)	14 (25 %)
Tumor size (longest diameter; cm)	6.3	5.2
Tumor size range (cm)	1–18	2–8
Tumor location		
Pelvis	31 (50 %)	22 (40 %)
Rib/chest wall	6 (10 %)	20 (36 %)
Vertebrae	4 (6 %)	8 (15 %)
Other	21 (34 %)	5 (9 %)
Prior radiation to treated site	44 (71 %)	13 (24 %)

Covidien, Boulder, CO). No clear differences are evident with these systems as power output is similar for these systems, and they reach maximal tissue temperatures in approximately the same time frame with similar volumes of tissue ablation. Management of procedurally related pain, which can limit the treatment, also differed in these trials. The Callstrom et al. trial employed general anesthesia, while the ACRIN trial utilized conscious sedation for a majority of cases. It is possible that the total volume of tissue destruction and completeness of treatment could be different between the two studies due to procedural pain limiting the aggressiveness of tumor destruction in the ACRIN trial. Although sensorimotor testing was used in the ACRIN trial, major complications noted in this trial involved damage to major motor nerves or other nerve injury. Unfortunately, this nerve monitoring approach did not completely safeguard against nerve injury. Although it is also possible that the differences in pain response for the patients in these trials could be due to differences in types of tumors treated, the majority of tumor types were the same in both studies, including lung, colon, and renal metastases, and no difference in pain response was observed on the basis of tumor type for either trial.

Despite the differences in treatment approach using RFA, these two multicenter clinical trials demonstrated that RFA is effective at palliation of pain due to skeletal metastatic disease. A couple of important lessons are evident from these trial results. Consideration of treatment of patients with painful metastatic disease using RF ablation should include the following: (1) the ablation margin can only be estimated when using CT monitoring, and patient and tumor selection is based on operator experience; (2) although multiple applicators are now available for RF ablation, this procedure is most commonly performed with multiple, sequential, overlapping ablation sessions in order to better estimate the ablation margin and thereby avoid injury of adjacent normal critical tissues; (3) residual disease is possible at the treatment margins which may not affect pain reduction but may necessitate repeat treatment in patients that may live for an extended period of time with their disease.

Summary

Several case reports and series as well as two completed prospective clinical trials have found highly significant reductions in pain due to focal metastatic disease. These findings are significant, not only because of the magnitude of the benefit, but because the findings were achieved in patients traditionally refractory to most conventional treatments.

These reports and the clinical trials also show that RFA of metastatic lesions involving bone can be performed effectively with either multi-tined or cool-tip electrodes. RFA provides an effective, rapid, and durable method for palliation of localized painful metastases involving bone and provides an alternative for the palliation of painful, bone metastases when standard treatments fail.

References

1. Nielsen OS, Munro AJ, Tannock IF. Bone metastases: pathophysiology and management policy. J Clin Oncol. 1991;9:509–24.
2. Mercadante S. Malignant bone pain: pathophysiology and treatment. Pain. 1997;69(1–2):1–18.
3. Coleman RE. Skeletal complications of malignancy. Cancer. 1997;80(8 Suppl):1588–94.
4. Tubiana-Hulin M. Incidence, prevalence and distribution of bone metastases. Bone. 1991;12(Suppl 1): S9–10.
5. Tong D, Gillick L, Hendrickson FR. The palliation of symptomatic osseous metastases: final results of the study by the radiation therapy oncology group. Cancer. 1982;50(5):893–9.
6. Steenland E, Leer JW, van Houwelingen H, et al. The effect of a single fraction compared to multiple fractions on painful bone metastases: a global analysis of the Dutch Bone Metastasis Study. Radiother Oncol. 1999;52(2):101–9.
7. Massie MJ, Holland JC. The cancer patient with pain: psychiatric complications and their management. J Pain Symptom Manage. 1992;7:99–109.
8. Spiegel D, Sands S, Koopman C. Pain and depression in patients with cancer. Cancer. 1994;74:2570–8.
9. Jeremic B, Shibamoto Y, Acimovic L, et al. A randomized trial of three single-dose radiation therapy regimens in the treatment of metastatic bone pain. Int J Radiat Oncol Biol Phys. 1998;42(1):161–7.
10. Price P, Hoskin PJ, Easton D, Austin D, Palmer SG, Yarnold JR. Prospective randomised trial of single and multifraction radiotherapy schedules in the treatment of painful bony metastases. Radiother Oncol. 1986;6(4):247–55.
11. Cole DJ. A randomized trial of a single treatment versus conventional fractionation in the palliative radiotherapy of painful bone metastases. Clin Oncol (R Coll Radiol). 1989;1:59–62.
12. Gaze MN, Kelly CG, Kerr GR, et al. Pain relief and quality of life following radiotherapy for bone metastases: a randomised trial of two fractionation schedules. Radiother Oncol. 1997;45(2):109–16.
13. Hara S. Opioids for metastatic bone pain. Oncology. 2008;74(Suppl 1):52–4.
14. Callstrom MR, York JD, Gaba RC, et al. Research reporting standards for image-guided ablation of bone and soft tissue tumors. J Vasc Interv Radiol. 2009;20(12):1527–40.
15. Cho CH, Mathis JM, Ortiz O. Sacral fractures and sacroplasty. Neuroimaging Clin N Am. 2010;20(2): 179–86.
16. Sabharwal T, Katsanos K, Buy X, Gangi A. Image-guided ablation therapy of bone tumors. Semin Ultrasound CT MR. 2009;30(2):78–90.
17. Lessard AM, Gilchrist J, Schaefer L, Dupuy DE. Palliation of recurrent Ewing sarcoma of the pelvis with cryoablation and somatosensory-evoked potentials. J Pediatr Hematol Oncol. 2009;31(1):18–21.
18. Dupuy DE, Liu D, Hartfeil D, et al. Percutaneous radiofrequency ablation of painful osseous metastases: a multicenter American College of Radiology Imaging Network trial. Cancer. 2010;116(4):989–97.
19. Farrell MA, Charboneau JW, Callstrom MR, Reading CC, Engen DE, Blute ML. Paranephric water instillation: a technique to prevent bowel injury during percutaneous renal radiofrequency ablation. AJR Am J Roentgenol. 2003;181(5):1315–7.
20. Dupuy DE, Hong R, Oliver B, Goldberg SN. Radiofrequency ablation of spinal tumors: temperature distribution in the spinal canal. AJR. 2000;175:1263–6.
21. Honore P, Luger NM, Sabino MA, et al. Osteoprotegerin blocks bone cancer-induced skeletal destruction, skeletal pain and pain-related neurochemical reorganization of the spinal cord. Nat Med. 2000;6(5):521–8.
22. Mannion RJ, Woolf CJ. Pain mechanisms and management: a central perspective. Clin J Pain. 2000;16: S144–56.
23. Woolf CJ, Allchorne A, Safieh-Garabedian B, Poole S. Cytokines, nerve growth factor and inflammatory hyperalgesia: the contribution of tumour necrosis factor alpha. Br J Pharmacol. 1997;121(3):417–24.
24. Gröenemeyer DHW, Schirp S, Gevargez A. Image-guided radiofrequency ablation of spinal tumors: preliminary experience with an expandable array electrode. Cancer J. 2002;8(1):33–9.
25. Callstrom MR, Charboneau JW, Goetz MP, et al. Painful metastases involving bone: feasibility of percutaneous CT- and US-guided radio-frequency ablation. Radiology. 2002;224(1):87–97.
26. Goetz MP, Callstrom MR, Charboneau JW, et al. Percutaneous image-guided radiofrequency ablation of painful metastases involving bone: a multicenter study. J Clin Oncol. 2004;22(2):300–6.
27. Callstrom MR, Charboneau JW, Goetz MP, et al. Image-guided ablation of painful metastatic bone tumors: a new and effective approach to a difficult problem. Skeletal Radiol. 2006;35:1–15.
28. Callstrom MR, Atwell TD, Charboneau JW, et al. Painful metastases involving bone: percutaneous image-guided cryoablation–prospective trial interim analysis. Radiology. 2006;241(2):572–80.
29. Daut RL, Cleeland CS, Flanery RC. Development of the Wisconsin brief pain questionnaire to assess pain in cancer and other diseases. Pain. 1983;17:197–210.
30. Cleeland CS, Gonin R, Hatfield AK, et al. Pain and its treatment in outpatients with metastatic cancer. N Engl J Med. 1994;330:592–6.
31. Grieco CA, Simon CJ, Mayo-Smith WW, DiPetrillo TA, Ready NE, Dupuy DE. Image-guided percutaneous thermal ablation for the palliative treatment of chest wall masses. Am J Clin Oncol-Canc. 2007;30(4):361–7.

Cryoablation of Bone Tumors

43

Matthew Callstrom

Abstract

Bone and soft tissue metastases can give rise to complications including pain, decreased quality of life, and decreased mobility. The standard palliative treatment for patients with metastatic disease is external beam radiation therapy. When this fails to give pain relief or when relief is transient, analgesics (opioids and nonsteroidal anti-inflammatory drugs) are typically optimized although inadequate pain relief or side effects are often present for these patients. Image-guided percutaneous cryoablation of focal painful metastases has emerged as an effective focal treatment for patients with painful metastatic disease. This treatment offers clinically significant reduction of pain, an improvement in their quality of life, and reduction in the use of analgesic medications by these patients.

Introduction

Skeletal tumors, including primary malignancies and metastases, are a common problem in oncology patients. Up to 85 % of patients with breast, prostate, and lung cancer have bone metastases at the time of death [1]. Complications due to skeletal tumors, including intractable pain, fracture, and decreased mobility, can reduce performance status and quality of life [1, 2]. In addition, these complications can lead to depression and anxiety [1].

External beam radiation therapy (RT) is the current standard of care for patients with localized bone pain due to metastatic disease. Tong and colleagues reported the use of RT resulted in complete relief in 53 % and partial relief in 83 % of the 1,016 patients that were treated as part of a trial conducted by the Radiation Therapy Oncology Group (RTOG) [3]. However, 20–30 % of patients do not experience pain relief, and few options exist for these patients [4–9]. A clinically significant decrease in pain (2/10 reduction in pain) for those that respond to treatment was 3 weeks; however, approximately 35 % of these patients did not obtain relief until 5–20 weeks posttreatment [10]. In addition, pain relief from RT is often transient with 57 % of patients experiencing recurrence of pain at a median of 15 weeks after completion of RT [3]. For many

M. Callstrom
Department of Diagnostic Radiology, Mayo Clinic, Rochester, MN, USA
e-mail: Callstrom.matthew@mayo.edu

D.E. Dupuy et al. (eds.), *Image-Guided Cancer Therapy*, DOI 10.1007/978-1-4419-0751-6_45,

patients with painful metastatic disease that have failed RT, analgesics remain the only treatment option. Unfortunately, in order to obtain sufficient pain control for many of these patients, side effects, such as constipation, nausea, and sedation, can be significant.

As a result of these limitations, investigators have explored several alternative strategies for the treatment of painful metastatic disease, based on using percutaneous image-guided methods to deliver tissue ablative devices into focal metastatic skeletal disease including ethanol [11], laser-induced interstitial thermotherapy (LITT) [12], percutaneous radiofrequency ablation (RFA) [13–15], and most recently, cryoablation [16]. While these treatment methods all involve focal destruction of tissue, they vary in type of energy, image guidance approaches, treatment monitoring, and risk profile. These differences may influence which technique is best suited for a particular patient based on tumor type and tumor location and the goal of pain palliation or when the goal includes achieving complete local control of the tumor when necessary. Of these ablative methods, radiofrequency ablation (RFA) has been the most studied and widely used. RFA was first used to treat benign primary bone lesions, such as osteoid osteomas, as a single modality treatment or as an adjunct to surgical resection [1–4]. As noted in a companion chapter, RFA has emerged as an effective treatment for palliation of painful bone metastases [14, 17, 18].

Of the various percutaneous ablation treatment methods, cryoablation has the longest history of successful treatment of neoplasms in various locations in the body, including prostate, kidney, liver, and lung. Cryoablation has also recently emerged as an exceptional treatment method for treatment of metastatic disease involving bone and soft tissue outside of liver and lung [19–24]. The rationale for using cryoablation for this clinical need is based on the inherent technical advantages with the treatment method to effectively treat often complex metastatic disease while preserving adjacent normal critical tissue. A critical advantage of cryoablation relative to other ablation technologies is that ice generated in the body is well visualized with non-contrast CT imaging. The edge of the ice ball corresponds to 0 °C, and the tissue outside this boundary is not at risk for injury [25]. The CT environment is readily available for intervention in most practices, and wide-bore systems are also becoming more common allowing placement of ablation devices while retaining the ability to image patients without great difficulty. While it is possible to image thermal changes with MRI, the challenges of performing ablation procedures in this environment are considerable and not widely available in many practices. While cryoablation has only recently been applied to the treatment of metastatic disease outside liver and lung, percutaneous cryoablation is a promising technique that offers several advantages over today's conventional palliative treatments and potentially over other ablation technologies.

Percutaneous Cryoablation Technology

Cryoablation was initially limited to intraoperative use because of the large diameter probes necessary with the use of liquid nitrogen for tissue cooling. With the advent of well-insulated probes and the use of Joule-Thompson ports utilizing room-temperature argon gas as a cooling source, percutaneous systems can generate an ice ball, using a single probe, of approximately 3.5 cm diameter. Active thawing is achieved by infusing helium gas into the cryoprobes instead of argon gas. Multiple cryoprobes are used simultaneously to generate large ice balls (>8-cm diameter), to shape the ablation zone through varied geometry of probe placement, and to provide decreased procedure time for treatment of large or complex tumors by avoiding the need to perform time-consuming overlapping ablations needed with other ablation techniques. Importantly, synchronous ablation with several cryoprobes eliminates residual disease at the ablation interfaces that can result from performing overlapping sequential

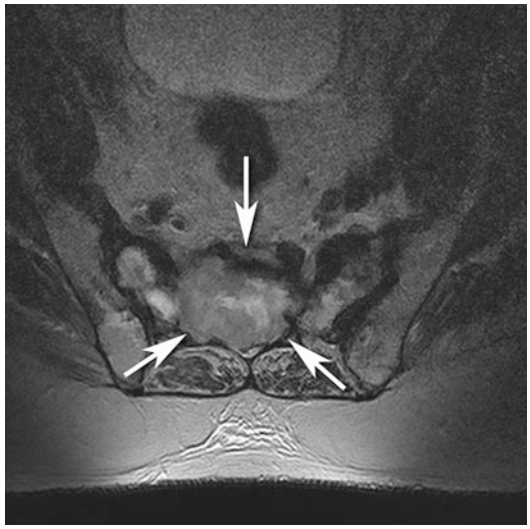

Fig. 43.1 Metastatic medullary thyroid cancer to the central sacrum (*arrows*). Partial or complete treatment of this tumor with cryoablation would likely result in injury of the S1–4 nerve roots

ablations [26]. Cell death from cryoablation occurs within about 3 mm internal to the ice-ball margin [25].

Patient Selection for Cryoablation

The goals of image-guided cryoablation treatment should be clearly defined. If the patient has limited metastatic disease and the treatment goal is local control, the targeted tumor should be aggressively treated while respecting adjacent critical normal structures as these are often limiting boundaries for treatment. For treatment of patients with painful bone lesions, patients should report moderate to severe pain, at least 4 on a 10-point scale for worst pain in a 24-h period. Patients with mild pain may not improve with ablation and typically can be adequately managed with oral analgesics. Patients with one or two painful sites with corresponding abnormalities on cross-sectional imaging can be treated in a single session. Patients with diffuse painful skeletal metastases are better served with systemic therapies rather than a focal approach. Lesions should be osteolytic, mixed osteolytic-osteoblastic, or primarily soft tissue in composition. Osteoblastic lesions can be treated with cryoablation although they are more difficult to access, frequently requiring bone biopsy devices or a bone drill, and are often multifocal when present. Critically, the target lesion must be accessible percutaneously and be sufficiently distant from the spinal cord, major motor nerves, brain, segmental branch artery leading to the spinal artery of Adamkiewicz, bowel, or bladder. For example, a patient with metastatic medullary thyroid cancer with a painful tumor located in the central spinal canal in the sacrum could not be treated without injuring adjacent motor nerves and nerves that innervate the urinary and anal sphincters (S2–4) (Fig. 43.1). An appropriate treatment option for this patient is RT or opioid analgesia. The required margin of safety beyond the targeted tumor depends on the ability to visualize the ablation margin, the use of techniques to displace critical structures, the use of thermal protection and monitoring devices, and the experience of the interventional radiologist.

Cryoablation Treatment Analgesia and Sedation

Patients can be treated with cryoablation using either general anesthesia or moderate sedation without the need for regional anesthesia. The type of anesthesia employed is often a function of local practice preferences. Moderate conscious sedation may be employed for many patients when using cryoablation as the procedure is well tolerated, typically without pain during the freezing or thawing portions of the procedure. However, general anesthesia is often preferred for treatment of large tumors or tumors with difficult access such as tumors necessitating the use of a drill and because the length of the procedures can be long – often 2 h or possibly longer depending on the technical difficulty of the procedure.

Patients that are treated for pain palliation have moderate to severe pain prior to the procedure, and it is not unusual for these patients to have persistent pain immediately following the ablation treatment and as a result often benefit from either hospital admission or overnight

observation. It is also common for some patients to have complete or near-complete relief of focal pain immediately following cryoablation treatment, and for these patients, observation status or outpatient treatment is possible. Most patients that are treated for painful metastatic disease will be discharged from the hospital with the same level of pain or lower on opioid analgesia when necessary. Patients that are treated for other indications, such as local tumor control, most commonly do not have significant pain associated with the procedure, but when it is present, it typically resolves in 6–8 h and is readily controlled with oral analgesics.

Percutaneous Cryoablation Technique

Two cryoablation systems are available for use, the Endocare Cryocare system and the Galil Medical SeedNet system. The Endocare system uses two different sizes of insulated cryoprobes measuring 2.4 mm (13 gauge/7.2 Fr; Perc-24) and 1.7 mm (16 gauge/5.1 Fr; Perc-15 and Perc-17) in diameter. The Galil system employs non-insulated 1.5-mm (17 gauge/4.4 Fr/1.5 mm; IceRod and IceSeed) cryoprobes (similar MR-compatible cryoprobes are available). These systems generate ice balls of various geometries; for example, the Endocare Perc-24 produces an ice ball up to 3.7 cm in diameter and 5.7 cm in length along the probe shaft. For these systems, rapid freezing of tissue with these cryoprobes is based on rapid expansion of argon gas in the distal portion of the sealed probe. This results in rapid cooling reaching −100 °C within a few seconds. Active thawing of the ice ball is achieved by actively instilling helium gas into the cryoprobes instead of argon gas. The Endocare system allows the independent operation of up to eight cryoprobes at a time, while the Galil system allows operation of 5 independent channels for 25 cryoprobes. The diameter of ice ball generated can be controlled by the rate of gas that is delivered to the probe.

Following sterile preparation, one or more cryoprobes are introduced through a skin nick under CT ultrasound or MR guidance. A single freeze-thaw-freeze cycle is performed for each lesion with typical times for these cycles of 10 min, 8 min, and 10 min, respectively. Shorter or longer times are often used for the freezing portions of the cycle depending on the adequacy of coverage of the lesion and the proximity of adjacent critical structures. Most commonly, non-contrast CT imaging is performed approximately every two minutes throughout the freezing portions of the cycle, with body window and level settings (W400, L40), to monitor the growth of the ice ball. For example, a soft tissue and bony metastasis involving the sternum was treated with two cryoprobes placed through the tumor along the superficial surface of the sternum (Fig. 43.2). The evolution of the ice ball showed complete coverage of the tumor as well as the adjacent involved sternum.

In general, more than one cryoprobe is placed into the targeted tumor with probes placed within 1 cm of the tumor margin and at a cryoprobe spacing of 2 cm with the goal of generating sufficiently low temperatures in the ice ball for tissue destruction. For very large lesions (>5 cm in diameter), the entire tumor may not be completely treated when the goal is palliation; rather, ablation treatments are focused on the margin of the lesion involving bone with the goal of treating the soft tissue/bone interface. Ideally, placement of the cryoprobes is based on the geometry of the target tumor so that the shape of the ice matches the shape of the target tumor. The probes are placed along the long axis of the tumor and at an angle to allow slow growth of the ice in the direction of adjacent critical structures. For example, a tumor located in the right paraspinal chest wall involving a rib, transverse process, and adjacent pleura was treated with multiple cryoprobes oriented so that the ice generated would slowly grow toward the central canal (Fig. 43.3). In addition, the probes were placed so that the ice generated would follow the oblong shape of the tumor along the course of the affected rib.

For treatment of skeletal tumors that are treated for palliation of pain, the soft tissue/bone interface is specifically targeted. For example, a metastatic paraganglioma tumor involving the left scapula, resulting in 5/10 worst pain and 2/10

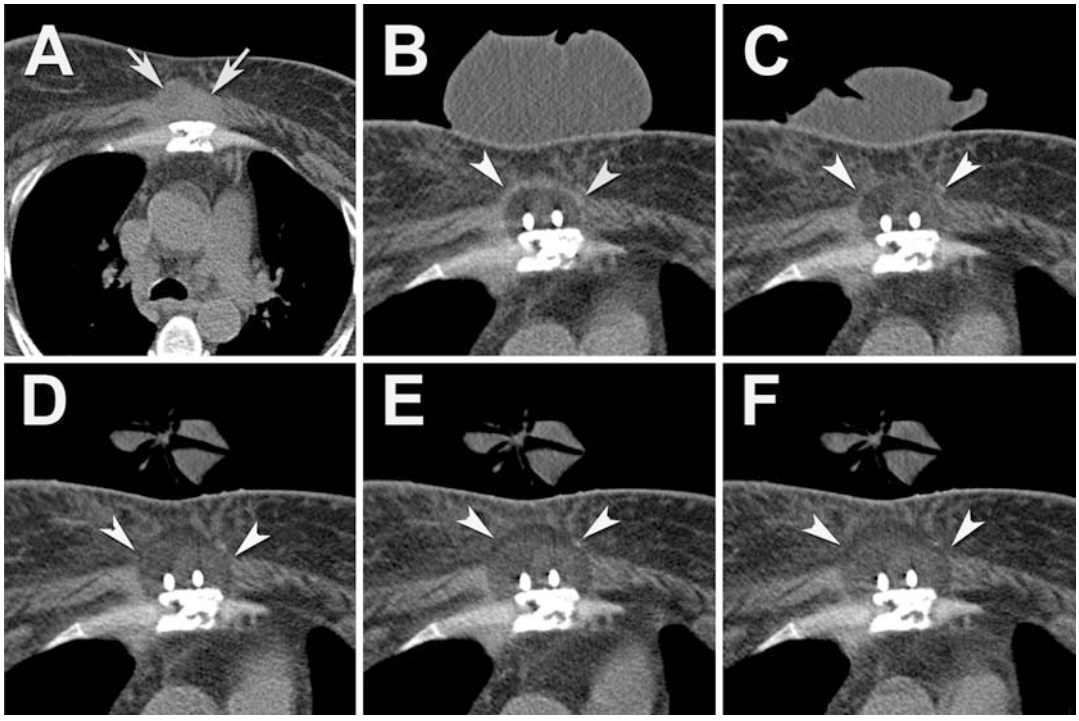

Fig. 43.2 (**a**) Axial non-contrast CT demonstrates breast cancer metastasis to the lower sternum and overlying soft tissues (*arrows*). (**b–f**) Cryoprobes placed along the superficial aspect of the sternum through the soft tissue metastasis following 2, 4, 6, 8, and 10 min of freezing, respectively. Ice (*arrow heads*) encompasses the soft tissue mass and extends into the underlying sternum

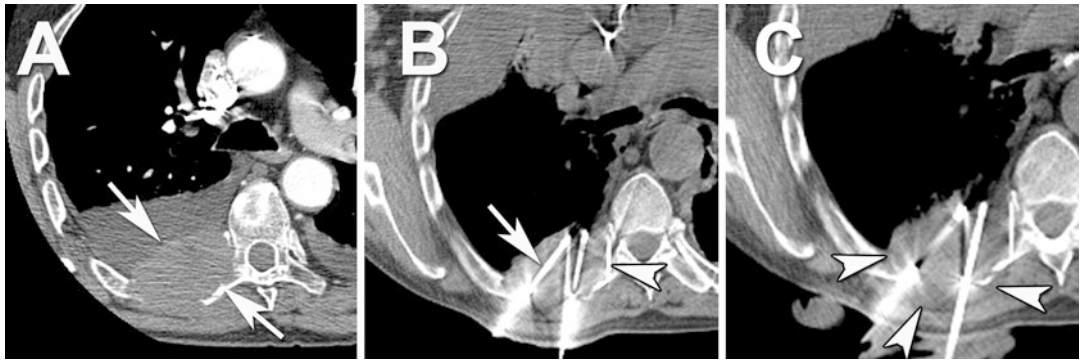

Fig. 43.3 (**a**) Axial contrast-enhanced CT demonstrates a renal cell cancer metastasis involving the transverse process of T7, adjacent right rib, and chest wall (*arrows*), (**b**) two of 4 Perc-24 Endocare cryoprobes (*arrow*) placed in the tumor with a thermistor placed adjacent to the vertebral body pedicle (*arrow head*), and (**c**) ice ball (*arrow heads*) encompassing the tumor with ice extending to the thermistor

average pain in a 24-h period, was treated with cryoablation with complete coverage of the targeted mass (Fig. 43.4). The ice ball that was generated was monitored with CT imaging with careful attention to the adjacent brachial plexus. Follow-up imaging showed no evidence for recurrent tumor, and no pain remained in the treated location throughout the follow-up period.

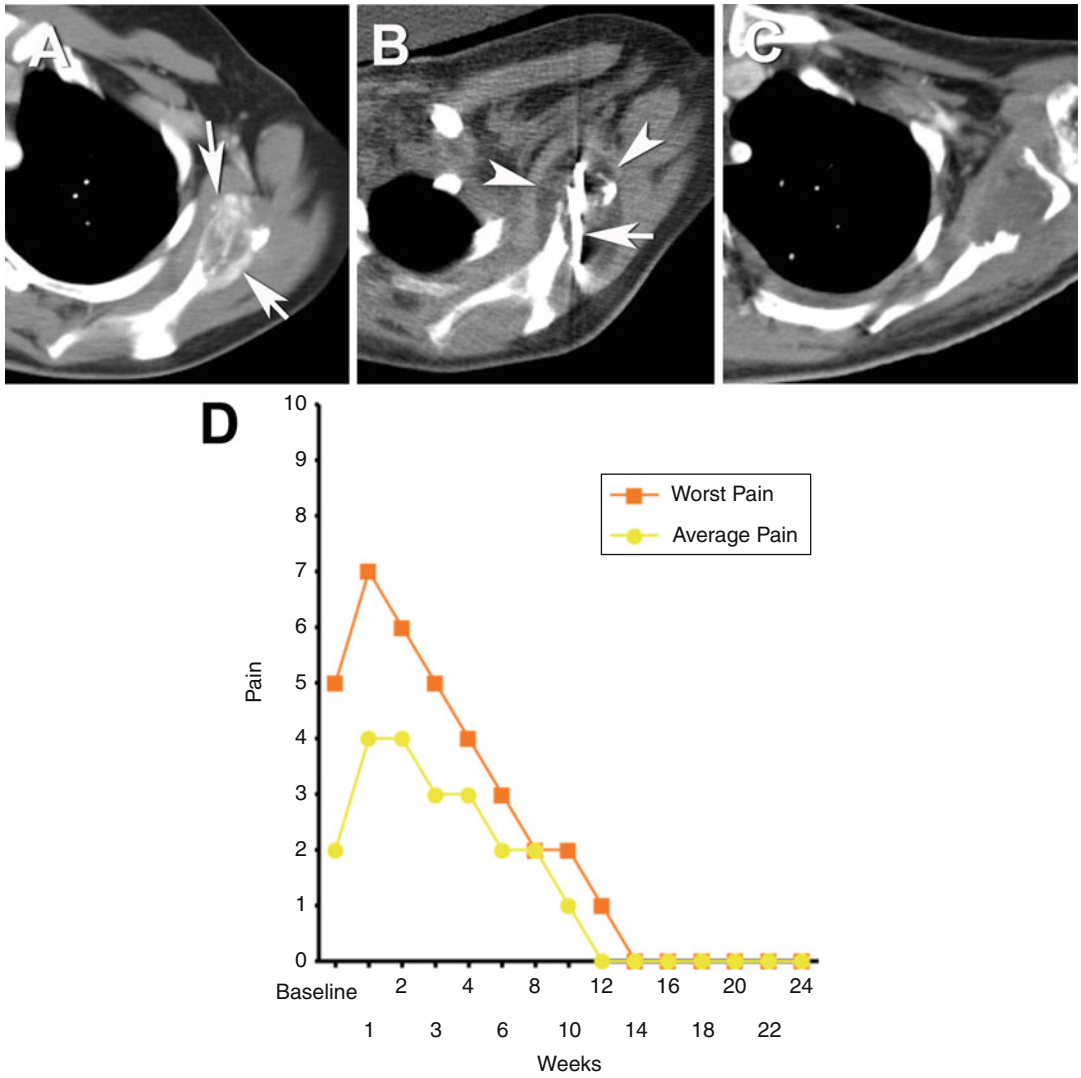

Fig. 43.4 (**a**) Axial contrast-enhanced CT demonstrates a paraganglioma metastasis involving the left scapula (*arrows*), (**b**) two cryoprobes (*arrow*) placed in the tumor and ice ball (*arrow heads*) encompassing the targeted tumor, (**c**) follow-up axial contrast-enhanced CT performed 3 months following ablation showing no residual enhancement in the treated area, and (**d**) graph of worst and average pain in a 24-h period at baseline (prior to treatment) and weeks 1–24 following treatment

Following completion of the second freeze cycle, the cryoprobes are warmed with active heating with helium gas until the temperature is >20 °C. The cryoprobes can be withdrawn at this point although continued warming of the probes over a period of approximately10 min may result in a reduced risk of hematoma formation. Immediate post-procedural pain is typically treated with intravenous fentanyl (Abbott Laboratories, Chicago, IL) and midazolam (Versed; American Pharmaceutical Partners, Los Angeles, CA). For patients with persistent pain, oral analgesics or a patient-controlled analgesia unit can be used and the dose titrated to provide adequate pain relief.

Surgical and Percutaneous Cryoablation Case Series, Reports, and Trials

As image-guided percutaneous cryoablation is finding more common application for treatment of patients with benign and metastatic disease involving bone, it is valuable to consider how this technology has been used in combination with surgical approaches to improve outcomes in patients with skeletal tumors. Surgical experience with cryoablation spans more than 5 decades with the goal of bone conservation treatment of primary and metastatic bone tumors with the goal of local tumor control. The addition of intraoperative cryosurgery, including either liquid nitrogen- or argon gas-based technologies, to surgical curettage results in a reduction of recurrence rates for resection of enchondromas and low-grade chondrosarcomas from 40–100 % to <5 % [27]. In addition to the treatment of benign-aggressive and low-grade malignant lesions, Meller and colleagues reported a surgical conservation strategy for treatment of 79 patients with high-grade and metastatic tumors involving bone with local control achieved in 69/79 (87 %) of patients [28].

Wide resection alone has the potential to achieve local control for the treatment of soft tissue sarcomas; however, adjuvant therapy may be beneficial for improved local control through shrinkage of the tumor, destruction of microsatellites of tumor, and extension of the surgical margin. Although neoadjuvant chemotherapy for treatment of high-grade large extremity soft tissue sarcomas may result in an improved disease-specific survival, use of this therapy remains controversial [29]. Standard adjuvant treatment modalities such as radiation therapy can be beneficial for high-grade tumors but are not as beneficial for low-grade neoplasms [30]. In particular, in the extremities, radiation therapy can cause considerable morbidity including fibrosis, tissue stiffness, delayed wound healing, wound infection, necrosis of underlying bone, peripheral neuropathy, and potentially radiation-induced sarcoma. Ahlmann and colleagues reported the combination treatment of soft tissue sarcomas in 38 patients using cryoablation followed immediately by wide local excision finding a survival advantage for patients that had >95 % tumor destruction vs. those with <95 % tumor destruction following cryoablation [31].

Percutaneous Cryoablation for Treatment of Soft Tissue Masses and Benign Skeletal Tumors

With the success of the intraoperative use of cryoablation for treatment of benign and metastatic skeletal disease, interventional radiologists have explored the use of cryoablation using percutaneous techniques for these same groups of patients. Treatment of locally aggressive tumors has been reported. Kujak and colleagues reported the use of percutaneous cryoablation for treatment of five extra-abdominal desmoids that had failed conventional therapy achieving local control of disease in three patients at latest follow-up [32]. Two patients with large desmoid tumors could not be completely treated due to proximity or encasement of nerves; of these, one patient's tumor was reduced in size, while the second had enlargement following partial treatment. An example among the patients that experienced local control with treatment included a young patient with an extra-abdominal desmoid in the posterior chest wall. This mass had been previously treated with surgical resection and had an area of recurrence along the surgical margin (Fig. 43.5). This was treated with cryoablation with complete resolution of the mass on follow-up imaging.

Image-guided percutaneous cryoablation has been applied to the treatment of benign tumors involving bone. Wu and colleagues reported the use of CT-guided cryoablation for the treatment of osteoid osteoma in the distal femur and patella in six children [33]. Cryoablation, rather than radiofrequency ablation, was utilized in these patients because of reported higher recurrence

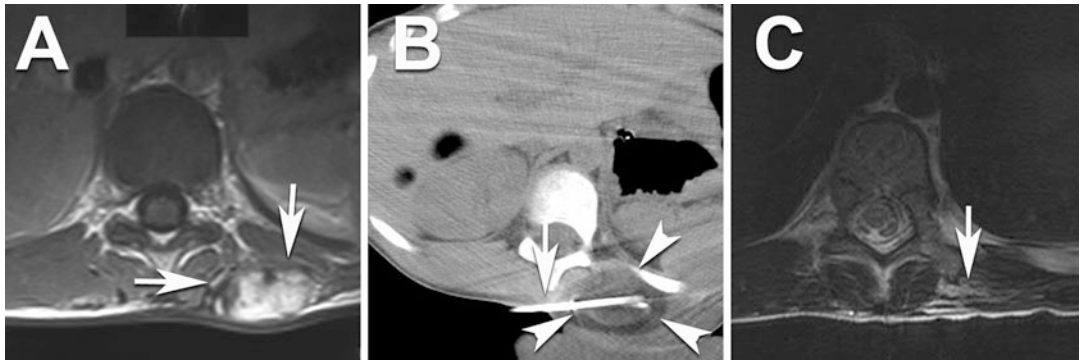

Fig. 43.5 9-year-old female with a posterior chest wall extra-abdominal desmoid tumor previously treated with surgical resection and adjuvant chemotherapy. (**a**) Pretreatment T1-weighted, fat-suppressed gadolinium-enhanced image demonstrates a mass (*arrows*) in the left paraspinal musculature. (**b**) Prone non-contrast CT shows one of the two cryoprobes (*arrow*) with an ice ball (*arrowheads*) that encompasses the mass. A sterile glove filled with warm fluid is placed over the treatment area, and sterile saline has been injected into the subcutaneous fat to displace the overlying dermis, and (**c**) T1-weighted, fat-suppressed gadolinium-enhanced image performed 43 months after cryoablation shows complete resolution of the mass (*arrows*)

rates in this population thought to be due to small body size with associated difficulty with needle placement and fixation. They found clinical success in all treated patients with no complications with latest follow-up at 1 month posttreatment. Liu and colleagues reported the successful use of CT-guided cryoablation for the treatment of two patients with osteoid osteoma in difficult locations, including the inferior femoral neck in a thin patient and first rib. In both cases, the cryoprobe was placed adjacent to the nidus in the soft tissue adjacent to the bone without bone drilling [34]. Ice extended across the lesion evidenced by CT monitoring, and both patients reported complete symptomatic relief.

Percutaneous Cryoablation for Palliation of Skeletal Metastases

Multiple reports have found that percutaneous cryoablation is effective in treating painful primary and secondary bone neoplasms. With excellent visibility of the ice ball with both CT and MR imaging, both imaging technologies have been employed for treatment of painful metastatic disease. The use of MR imaging of cryoablation offers the ability to visualize complex structures, such as important motor nerves, in multiple imaging planes although the environment restricts devices that can be utilized. Sewell and colleagues reported the use of percutaneous cryoablation for palliation of 16 painful tumors in 14 patients using MR guidance and monitoring. They reported a significant reduction in patients' pain in the immediate postoperative period. This pain relief continued over the long term with associated significant improvement in patients' quality of life [35]. Tuncali and colleagues reported the use of MRI-guided and MRI-monitored cryoablation for treatment of patients with refractory or painful metastatic tumors in bone and soft tissue adjacent to critical structures [36]. Pain palliation was at least partially achieved in 17/19 (89 %) of patients with complete pain relief in 6 of the patients and partial relief in ten patients with one patient experiencing initial relief but recurrence of pain. With the visibility of the ice ball with MRI monitoring and with the use of additional measures to reduce the risk of injury including warming urethral catheters, intramedullary rod placement, and skin warming, no immediate complications were noted as a result of immediate thermal injury. One patient suffered a femoral neck fracture 6 weeks after cryoablation of a metastatic renal cell carcinoma in this location that was not treated with an intramedullary rod. Lessard and colleagues reported the use of somatosensory-evoked

potentials to monitor the S1 nerve during ablation of a painful recurrent Ewing sarcoma in the mid and upper right hemisacrum sacrum. This resulted in pain palliation and avoided nerve damage in this distribution; however, the ablation caused incontinence of bowel and bladder, possibly due to ablation injury of the S2–4 nerve roots bilaterally compounded by prior extensive radiation therapy and baseline nerve dysfunction [37].

In most centers, CT suites are more accessible for ablation procedures and have larger bore diameters than those available with current MR systems allowing necessary patient positioning without significant compromise for placement of percutaneous devices. Ullrick and colleagues reported the CT-guided and monitored use of cryoablation for the treatment of three patients with painful metastatic disease involving the pelvis and ribs with palliation in 2/3 patients [38]. Recently published interim results of a single-center prospective clinical trial are also encouraging. Fourteen patients with painful metastatic disease involving bone were treated using percutaneous cryoablation. Patients had one or two painful lesions causing $\geq$4/10 pain in a 24-h period. Using the Cleeland Brief Pain Inventory (BPI) [39, 40], the mean score for worst pain in a 24-h period decreased from 6.7/10–3.8/10 over the course of 4 weeks. All patients who were prescribed narcotics prior to the procedure reported a reduction in these medications (8 out of 8). No serious complications were seen. Pain relief from cryoablation was durable in the patients that were treated. Four of five patients (80 %) reported excellent pain control in the treated area during the 24-week follow-up period. One patient reported transiently increased pain scores at the 24-week follow-up interview but, over the following 6 months, reported worst pain scores of 0–3/10 indicating durable pain control.

Comparison of patient response scores following percutaneous cryoablation to data reported from the treatment of patients with RT is difficult as the methods that have been used in RT trials for measuring patient pain response do not correspond directly with the BPI used in the cryoablation study and the number of patients in this prospective trial is small. However, cryoablation results in significant pain reduction with a 43 % mean reduction in worst pain in 4 weeks, which is considered to be clinically significant [41]. Patients also reported pain relief 4 weeks following cryoablation ranged from 50 % to 100 %, which compares favorably to the reported RT response. It is possible that combination treatment of cryoablation and radiation therapies may be useful for palliation of painful metastatic lesions. However, a randomized prospective trial comparing cryoablation and RT would be necessary to determine the relative response of patients' pain to these treatments, and it is unlikely that this can be accomplished.

Comparison of Cryoablation to RFA

Currently, RFA is the most widely used method of percutaneous focal tumor treatment; however, cryoablation has several inherent advantages over RFA for treatment of painful metastases involving bone. In the event that the target tumor is osteoblastic, the ice ball generated with cryoablation is able to penetrate deeply into bone, whereas RFA poorly penetrates into bone. Therefore, when isolated, a painful osteoblastic metastasis could be treated with cryoablation. For example, a mixed osteoblastic and osteolytic isolated breast metastasis located in the manubrium was treated with multiple overlapping cryoprobes placed through access achieved with a drill using a Steinmann pin. The ice ball encompassed the targeted region and resulted in no tumor evident on follow-up FDG-PET imaging (Fig. 43.6).

There are several technical advantages for the use of cryoablation. First, the ablation margin is poorly visualized during RFA treatment using CT or ultrasound monitoring. However, if MRI monitoring is available, the RFA margin can be visualized although this is impractical in most clinical practices. In contrast, the ice ball generated with cryoablation is readily identified on non-contrast CT as well as MRI. Secondly, an important advantage of cryoablation is the simultaneous independent operation of multiple cryoprobes

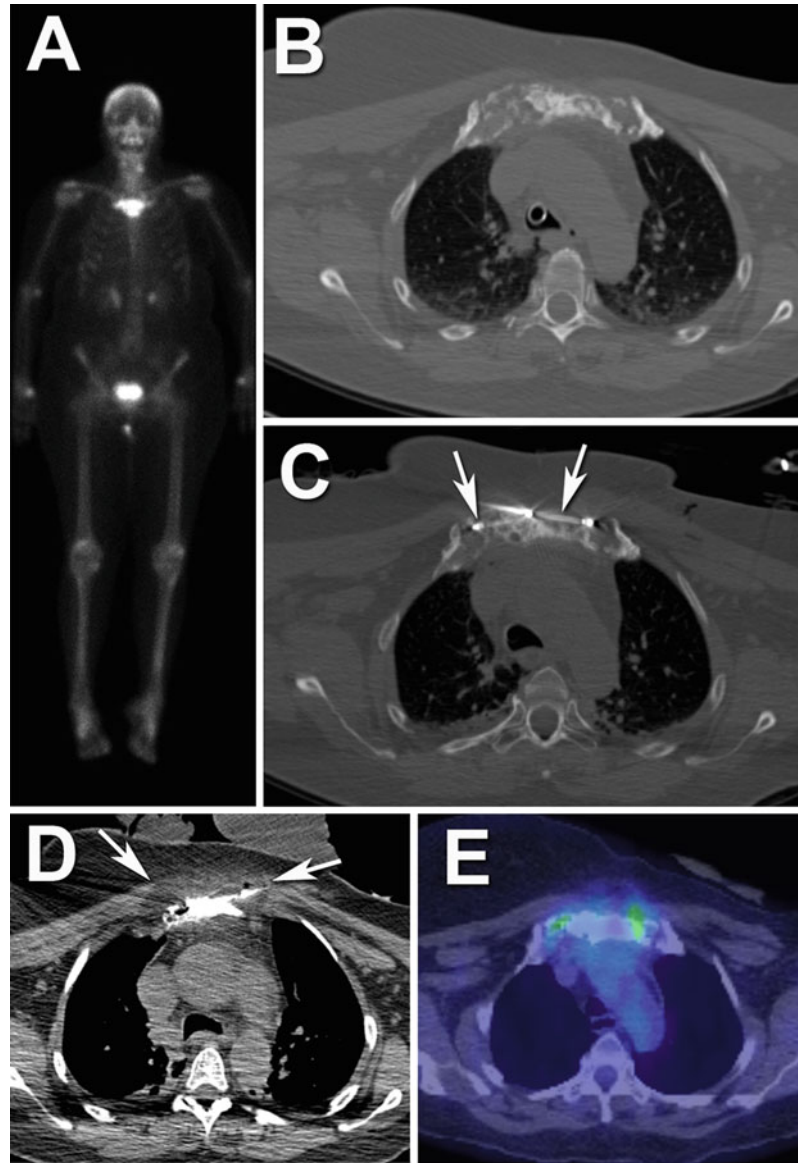

Fig. 43.6 59-year-old female with asymptomatic solitary focus of metastatic breast cancer. (**a**) Anterior 99mTechnitium bone scan demonstrates a solitary focus of uptake in the manubrium and upper sternum. (**b**) Non-contrast CT with bone windows demonstrates a mixed osteolytic and osteoblastic metastasis in the manubrium. (**c**) Two of 4 Perc-24 Endocare cryoprobes (*arrows*) placed into the target area. Access was achieved using a surgical drill with a 2.8-mm Steinmann pin. Subcutaneous tissues were protected by placing the pin through an 8-Fr peel-away sheath. (**d**) Intraprocedural non-contrast CT of the sternum shows an ice ball (*arrows*) encompassing the sternum. (**e**) FDG-PET/CT performed 3 months posttreatment shows no residual uptake in the treated region. Patient developed multifocal FDG-avid skeletal metastases 12 months following the cryoablation treatment

(up to 5 channels with 5 cryoprobes in each channel with the Galil system and 8 cryoprobes with the Endocare system). This allows generation of a large volume of ice (>8 cm diameter) in a shape that matches the geometry of the target tumor with appropriate placement of the cryoprobes. Although 3 RFA electrodes can be operated simultaneously with the use of a switching controller, generation of large ablation zones without visualization is difficult due to increased risk of complications, and instead it is more common to sequentially treat larger tumors with careful attention to the boundaries of each ablation session. Microwave ablation may be a treatment option for larger tumors, but to date there is no published literature comparing this newer technology to RFA or cryoablation. Finally, the cryoablation procedure is less painful for the patient in the immediate posttreatment period. Thacker and colleagues reported a retrospective review of patients that were treated with either cryoablation or RFA for painful

metastatic skeletal disease, finding the opioid analgesia requirements increased following RFA, while they were decreased following cryoablation in the immediate 24-h period following ablation [42].

Summary

Percutaneous cryoablation is an important alternative for treatment of both benign and malignant bone and soft tissue tumors. Cryoablation provides local control of tumors and is effective for palliation of pain due to bony metastatic disease. Significant pain reduction is possible in patients that have failed to achieve benefit from conventional therapies including chemotherapy and external beam radiation. Importantly, the pain reduction that is achieved is durable over many months of observation.

References

1. Nielsen OS, Munro AJ, Tannock IF. Bone metastases: pathophysiology and management policy. J Clin Oncol. 1991;9:509–24.
2. Mercadante S. Malignant bone pain: pathophysiology and treatment. Pain. 1997;69:1–18.
3. Tong D, Gillick L, Hendrickson FR. The palliation of symptomatic osseous metastases: final results of the study by the Radiation Therapy Oncology Group. Cancer. 1982;50(5):893–9.
4. Massie MJ, Holland JC. The cancer patient with pain: psychiatric complications and their management. J Pain Symptom Manage. 1992;7:99–109.
5. Spiegel D, Sands S, Koopman C. Pain and depression in patients with cancer. Cancer. 1994;74:2570–8.
6. Jeremic B, Shibamoto Y, Acimovic L, et al. A randomized trial of three single-dose radiation therapy regimens in the treatment of metastatic bone pain. Int J Radiat Oncol Biol Phys. 1998;42(1):161–7.
7. Price P, Hoskin PJ, Easton D, Austin D, Palmer SG, Yarnold JR. Prospective randomised trial of single and multifraction radiotherapy schedules in the treatment of painful bony metastases. Radiother Oncol. 1986;6:247–55.
8. Cole DJ. A randomized trial of a single treatment versus conventional fractionation in the palliative radiotherapy of painful bone metastases. Clin Oncol (R Coll Radiol). 1989;1:59–62.
9. Gaze MN, Kelly CG, Kerr GR, et al. Pain relief and quality of life following radiotherapy for bone metastases: a randomised trial of two fractionation schedules. Radiother Oncol. 1997;45:109–16.
10. Steenland E, Leer JW, van Houwelingen H, et al. The effect of a single fraction compared to multiple fractions on painful bone metastases: a global analysis of the Dutch Bone Metastasis Study. Radiother Oncol. 1999;52(2):101–9.
11. Gangi A, Kastler B, Klinkert A, Dietemann JL. Injection of alcohol into bone metastases under CT guidance. J Comput Assist Tomogr. 1994;18:932–5.
12. Gröenemeyer DH, Schirp S, Gevargez A. Image-guided percutaneous thermal ablation of bone tumors. Acad Radiol. 2002;9:467–77.
13. Dupuy DE, Safran H, Mayo-Smith WW, Goldberg SN. Radiofrequency ablation of painful osseous metastatic disease. Radiology. 1998;209(P):389.
14. Callstrom MR, Charboneau JW, Goetz MP, et al. Painful metastases involving bone: feasibility of percutaneous CT- and US-guided radio-frequency ablation. Radiology. 2002;224(1):87–97.
15. Goetz MP, Callstrom MR, Charboneau JW, et al. Percutaneous image-guided radiofrequency ablation of painful metastases involving bone: a multicenter study. J Clin Oncol. 2004;22(2):300–6.
16. Beland MD, Dupuy DE, Mayo-Smith WW. Percutaneous cryoablation of symptomatic extraabdominal metastatic disease: preliminary results. AJR Am J Roentgenol. 2005;184(3):926–30.
17. Callstrom MR, Charboneau JW, Goetz MP, et al. Image-guided ablation of painful metastatic bone tumors: a new and effective approach to a difficult problem. Skeletal Radiol. 2006;35(1):1–15.
18. Dupuy DE, Liu D, Hartfeil D, et al. Percutaneous radiofrequency ablation of painful osseous metastases: a multicenter American College of Radiology Imaging Network trial. Cancer. 2010;116(4):989–97.
19. Callstrom MR, Atwell TD, Charboneau JW, et al. Painful metastases involving bone: percutaneous image-guided cryoablation–prospective trial interim analysis. Radiology. 2006;241(2):572–80.
20. Sabharwal T, Katsanos K, Buy X, Gangi A. Image-guided ablation therapy of bone tumors. Semin Ultrasound CT MR. 2009;30(2):78–90.
21. Sabharwal T, Salter R, Adam A, Gangi A. Image-guided therapies in orthopedic oncology. Orthop Clin North Am. 2006;37(1):105-+.
22. Callstrom MR, Kurup AN. Percutaneous ablation for bone and soft tissue metastases–why cryoablation? Skeletal Radiol. 2009;38(9):835–9.
23. Callstrom MR, York JD, Gaba RC, et al. Research reporting standards for image-guided ablation of bone and soft tissue tumors. J Vasc Interv Radiol. 2009;20(12):1527–40.
24. Rybak LD. Fire and ice: thermal ablation of musculoskeletal tumors. Radiol Clin North Am. 2009;47(3):455–69.
25. Chosy SG, Nakada SY, Lee Jr FT, Warner TF. Monitoring renal cryosurgery: predictors of tissue necrosis in swine. J Urol. 1998;159(4):1370–4.

26. Dodd 3rd GD, Frank MS, Aribandi M, Chopra S, Chintapalli KN. Radiofrequency thermal ablation: computer analysis of the size of the thermal injury created by overlapping ablations. AJR Am J Roentgenol. 2001;177(4):777–82.
27. Mohler DG, Chiu R, McCall DA, Avedian RS. Curettage and cryosurgery for low-grade cartilage tumors is associated with low recurrence and high function. Clin Orthop Relat Res. 2010;468(10):2765–73.
28. Meller I, Weinbroum A, Bickels J, et al. Fifteen years of bone tumor cryosurgery: a single-center experience of 440 procedures and long-term follow-up. Eur J Surg Oncol. 2008;34(8):921–7.
29. Grobmyer SR, Maki RG, Demetri GD, et al. Neoadjuvant chemotherapy for primary high-grade extremity soft tissue sarcoma. Ann Oncol. 2004;15(11):1667–72.
30. Bickels J, Meller I, Shmookler BM, Malawer MM. The role and biology of cryosurgery in the treatment of bone tumors. A review. Acta Orthop Scand. 1999;70(3):308–15.
31. Ahlmann ER, Falkinstein Y, Fedenko AN, Menendez LR. Cryoablation and resection influences patient survival for soft tissue sarcomas: impact on survivorship and local recurrence. Clin Orthop Relat Res. 2007;459:174–81.
32. Kujak JL, Liu PT, Johnson GB, Callstrom MR. Early experience with percutaneous cryoablation of extra-abdominal desmoid tumors. Skeletal Radiol. 2010;39(2):175–82.
33. Wu B, Xiao YY, Zhang X, Zhao L, Carrino JA. CT-guided percutaneous cryoablation of osteoid osteoma in children: an initial study. Skeletal Radiol. 2011;40:1303–10.
34. Liu GR, Gao PY, Lin Y, et al. Brain magnetic resonance elastography on healthy volunteers: a safety study. Acta Radiol. 2009;50(4):423–9.
35. Sewell P, Jackson M, Dhillon G. Percutaneous MRI guided cryosurgery of bone tumors. Radiology. 2002;225(P):514.
36. Tuncali K, Morrison PR, Winalski CS, et al. MRI-guided percutaneous cryotherapy for soft-tissue and bone metastases: initial experience. AJR Am J Roentgenol. 2007;189(1):232–9.
37. Lessard AM, Gilchrist J, Schaefer L, Dupuy DE. Palliation of recurrent Ewing sarcoma of the pelvis with cryoablation and somatosensory-evoked potentials. J Pediatr Hematol Oncol. 2009;31(1):18–21.
38. Ullrick SR, Hebert JJ, Davis KW. Cryoablation in the musculoskeletal system. Curr Probl Diagn Radiol. 2008;37(1):39–48.
39. Daut RL, Cleeland CS, Flanery RC. Development of the wisconsin brief pain questionnaire to assess pain in cancer and other diseases. Pain. 1983;17:197–210.
40. Cleeland CS, Gonin R, Hatfield AK, et al. Pain and its treatment in outpatients with metastatic cancer. N Engl J Med. 1994;330:592–6.
41. Farrar JT, Young Jr JP, LaMoreaux L, Werth JL, Poole RM. Clinical importance of changes in chronic pain intensity measured on an 11-point numerical pain rating scale. Pain. 2001;94:149–58.
42. Thacker PG, Callstrom MR, Curry TB, et al. Palliation of painful metastatic disease involving bone with image-guided treatment: comparison of patients immediate response to radiofrequency ablation and cryoablation. AJR Am J Roentgenol. 2011;197(2):510–5.

Bone Therapy

44

Anne Smith Hutchison and Jordan Berlin

Abstract

Both primary and secondary neoplasms of bone can be difficult to treat due to their high likelihood of systemic involvement. Systemic therapy has a role for both local control and for palliation in the presence of more disseminated disease. This chapter will review the current systemic treatments offered to patients with either primary bone malignancies or metastatic bone disease.

Tumors of bone are comprised of the primary bone tumors and, more commonly, osseous metastases from cancers of other primary sites. The primary bone tumors are rare, with an estimated 2,570 new cases and 1,470 deaths due to cancers of the bones and joints in the United States in 2009 [1]. The most common primary bone tumors include osteosarcoma, Ewing sarcoma, and chondrosarcoma. These are more common in children and adolescents, with osteosarcoma and Ewing sarcoma comprising 2.7 % and 1.4 % of all childhood malignancies, respectively [1]. More frequently, tumors involving the bone are metastatic sites from cancers of other primary sites, and they can be primarily osteolytic or osteoblastic, or they can have mixed lesions with both lytic and blastic elements. The most common primary solid tumor malignancies with osseous metastases are cancers of the breast, prostate, kidney, lung, and thyroid; however, almost any cancer type has the potential for spread to the bone. In addition, multiple myeloma, a primary hematologic malignancy of plasma cell origin, causes purely osteolytic lesions of the bone in the majority of affected patients. Metastatic bone lesions are a frequent source of morbidity and mortality in cancer patients, potentially causing pain, fractures, decreased mobility, hypercalcemia, and interference with the activities of daily living, and therapy directed at them is primarily palliative [1].

Chemotherapy for the primary bone tumors is primarily used in the adjuvant or neoadjuvant setting, where combination chemotherapy yields an improved survival compared to surgery alone due to treatment of micrometastatic disease present at the time of diagnosis. Conversely, chemotherapy for metastatic solid tumors is primarily palliative. The individual chemotherapy regimens utilized are specific to the type of cancer being treated.

A.S. Hutchison (✉)
South Carolina Oncology Associates, Columbia, SC, USA
e-mail: ahutchison@sconcology.net

J. Berlin
Department of Medicine, Division of Hematology and Oncology, Vanderbilt University Medical Center, Nashville, TN, USA

D.E. Dupuy et al. (eds.), *Image-Guided Cancer Therapy*, DOI 10.1007/978-1-4419-0751-6_46,

Some of the common regimens will be discussed in further detail below. Specific bone-targeted therapies that are frequently used in osseous metastatic lesions and multiple myeloma include the bisphosphonates, and less commonly, the bone-targeted radioisotopes.

Primary Bone Tumors

Osteosarcoma

Osteosarcomas are rare malignancies of bone, characterized by the development of osteoid or immature bone by the malignant cells [2]. Historically, osteosarcoma has had a high rate of recurrence and death due to metastatic disease despite adequate local resection. With the advent of successful adjuvant chemotherapy regimens in the 1970s, however, the long-term disease-free survival was increased to 48 % at a median follow-up of 7 years compared to less than 20 % in historical comparisons treated with resection alone [3]. Following this, two randomized clinical trials further demonstrated the benefit of adjuvant chemotherapy. These demonstrated an improvement in both disease-free and overall survival with the addition of postoperative combination chemotherapy compared to resection alone in patients with localized high-grade osteosarcoma [4–6]. While these studies employed combination chemotherapy with high-dose methotrexate, doxorubicin, and BCD (bleomycin, cytoxan, dactinomycin), more modern chemotherapy regimens have typically included cisplatin and doxorubicin, with or without high-dose methotrexate [5–9]. With the advent of limb-sparing surgical techniques, the concept of giving preoperative chemotherapy came into favor. A randomized trial showed no difference in event-free survival or incidence of limb salvage when chemotherapy was given preoperatively versus immediate surgery followed by adjuvant chemotherapy [10]. While this study was not powered to determine equivalence between presurgical and postsurgical chemotherapy, it established that neoadjuvant chemotherapy followed by resection can result in a 5-year event-free survival of 61 % which compares favorably to historical outcomes. Furthermore, the use of preoperative chemotherapy has become more frequent in practice as a result of data showing that responsiveness of osteosarcoma to neoadjuvant chemotherapy yields important prognostic information. Numerous studies have demonstrated that the degree of tumor necrosis in the surgical specimen following neoadjuvant chemotherapy is predictive of local recurrence and survival [11–14]. Whether altering the postoperative chemotherapy regimen based on the degree of tumor necrosis confers benefit remains controversial.

Ewing Sarcoma

Ewing sarcoma is a small round blue cell tumor that arises from the bone or rarely the soft tissue. It is part of a spectrum of neoplastic diseases known as the Ewing sarcoma family of tumors (EFT), which also includes the primitive neuroectodermal tumors (PNET) and other rare malignancies. The EFT is characterized by similar pathologic characteristics and chromosomal translocations, most commonly a translocation between chromosomes 11 and 22, and they are believed to share a common cell of origin. In patients treated with local therapy alone, relapse rates are as high as 90 %, and it is therefore presumed that the great majority of patients have micrometastatic disease at the time of diagnosis despite the relatively low rate of overt metastases at diagnosis. Ewing sarcoma and the EFT are therefore treated as a systemic disease with a multimodality approach.

Like osteosarcoma, Ewing sarcoma is most common in children, adolescents, and young adults. There is a lack of available data in adults with Ewing sarcoma, and treatment recommendations are usually extrapolated from data in the pediatric population. Modern adjuvant chemotherapy regimens have largely been shaped by a series of trials by the Intergroup Ewing's Sarcoma Study (IESS). The first of these randomized

patients with localized Ewing sarcoma to radiation therapy to the primary site plus one of the following adjuvant treatment protocols: (1) vincristine, doxorubicin, cyclophosphamide, and dactinomycin (VDCA); (2) vincristine, dactinomycin, and cyclophosphamide (VAC) alone; or (3) VAC with adjuvant bilateral pulmonary irradiation. They found a significant relapse-free and overall survival advantage for the patients that received the doxorubicin-containing regimen [15]. The second intergroup study showed that an increase in the dose intensity of doxorubicin resulted in a further improvement in outcome [16]. In the early 1980s, the use of ifosfamide, with or without etoposide, was shown to have impressive response rates in patients that experienced a relapse after standard therapy for Ewing sarcoma. Based on these results, a study was performed that randomized patients with Ewing sarcoma or PNET to standard therapy with VDCA or to the same four-drug regimen alternating with courses of ifosfamide and etoposide (IE). They found that the non-metastatic patients treated with VDCA alternating with IE had an improved event-free and overall survival compared to patients treated with VDCA alone [17].

Based on the results of the above studies, modern treatment regimens for Ewing sarcoma and PNET include chemotherapy with vincristine, doxorubicin, and cyclophosphamide, with or without dactinomycin (VDCA or VDC), alternating with courses of ifosfamide and etoposide (IE). Surgical resection is generally performed after several courses of preoperative chemotherapy, with the remainder of the course of chemotherapy given postoperatively. In patients in whom a function-preserving surgical resection is not possible, due to the location or extent of the primary tumor, definitive radiation therapy is also an option.

Metastatic Bone Disease

Almost all solid tumor malignancies are capable of osseous metastasis; however, cancers of the breast, prostate, and lung most frequently involve the bone. Curative therapy is very unlikely in advanced disease, and chemotherapy is primarily palliative in these cases, with the goal of prolonging survival or improving quality of life.

Breast Cancer

In metastatic breast cancer, the choice of therapy is determined by the sites of disease involvement and rapidity of progression, as well as tumor specific factors, such as hormone receptor status and the presence of HER2 overexpression. For women with hormone receptor (estrogen and/or progesterone receptor)-positive disease and primarily osseous metastases, endocrine therapy is usually the treatment of choice. The selective estrogen receptor modulators (SERMs), aromatase inhibitors, and antiestrogens have response rates of up to 50–60 % in ER-/PR-positive tumors, and they are generally well-tolerated. The addition of a bisphosphonate is usually warranted for those with osseous metastases.

For patients that have failed endocrine therapy, that have rapidly progressive visceral disease, or that have ER/PR-negative tumors, chemotherapy is the preferred initial therapy. Numerous single agents have activity in breast cancer, the most commonly used being the taxanes, anthracyclines, gemcitabine, vinorelbine, and capecitabine. While combination chemotherapy may have higher response rates, it has not consistently shown a survival benefit when compared to single-agent chemotherapy and the side effect profiles can be significantly worse. Therefore, therapy with serial single agents is generally preferred over combination chemotherapy regimens. One notable exception is the combination of paclitaxel and bevacizumab, which has been shown in a randomized phase III trial to prolong progression-free survival when compared to paclitaxel alone (median, 11.8 vs. 5.9 months, $P < 0.001$). The overall survival rate, however, was similar in both groups [18]. The role of bevacizumab in metastatic breast cancer remains unclear given the increased toxicity and expense of this

combination regimen. Combination chemotherapy may be utilized in patients with symptomatic disease or those entering visceral crisis, where the higher response rate may prove beneficial.

Approximately 20 % of breast cancers overexpress the receptor tyrosine kinase HER2 (also called HER2/neu). Drugs targeting HER2 include trastuzumab, a humanized monoclonal antibody that binds HER2 on the cell surface, and lapatinib, a tyrosine kinase inhibitor that targets both HER2 and the epidermal growth factor receptor (EGFR). These agents have activity in HER2-overexpressing metastatic breast cancers, and they are often given in combination with either chemotherapy or hormonal therapy with minimal increase in toxicity.

Prostate Cancer

Prostate cancer has a propensity to form osseous metastases, and the majority of men with metastatic prostate cancer will have bony involvement at some time during their disease course. Because testosterone promotes the growth of many prostate tumors, initial therapy for metastatic prostate cancer is usually hormonal therapy that negates this androgenic effect. The gold standard of treatment is surgical orchiectomy; however, this is rarely performed in the modern era. Hormonal options include the gonadotropin-releasing hormone (GnRH) agonists and antagonists, which lower serum testosterone levels, and the antiandrogens, which block androgen action. Response rates to initial hormonal therapy are high, with 60–70 % of patients experiencing a decline in PSA values and 30–50 % of patients showing an improvement on serial bone scans or a decrease in the size of measurable tumor masses.

Patients with disease that relapses or progresses during hormonal therapy, and in whom castrate levels of serum testosterone are confirmed, are termed castrate-resistant (or hormone refractory). In many of these patients, further hormonal manipulation can be effective, though responses are usually of short duration. For men on GnRH agonists, a nonsteroidal antiandrogen, such as flutamide or bicalutamide, may be added. Men already taking an antiandrogen in addition to a GnRH agonist at the time of progression may benefit from antiandrogen withdrawal, as these agents have been shown to sometimes promote the growth of prostate cancer in its later stages. Third-line hormonal therapy with agents such as ketoconazole may also be considered.

When hormonal therapy options have been exhausted, or in patients with visceral disease, cytotoxic chemotherapy is generally recommended. Mitoxantrone plus prednisone was shown to provide palliation in symptomatic hormone-resistant prostate cancer; however, overall survival was not prolonged in comparison to prednisone alone [19]. Two subsequent randomized trials showed that docetaxel was superior to mitoxantrone plus prednisone, where docetaxel-containing regimens significantly prolonged the overall survival in men with metastatic castrate-resistant prostate cancer [20–22]. Therefore, docetaxel is the most often utilized chemotherapy regimen after failure of hormonal therapy in men with metastatic prostate cancer, with mitoxantrone reserved for second-line chemotherapy. A recently FDA-approved novel taxane, cabazitaxel, was shown to prolong survival and time to progression after docetaxel therapy failure and may replace mitoxantrone in the second-line setting [23].

Lung Cancer

Chemotherapy is indicated for metastatic small cell lung cancer (SCLC) and non-small-cell lung cancer (NSCLC). Standard therapy for small cell lung cancer is platinum-based chemotherapy, including either cisplatin or carboplatin in combination with etoposide. Small cell lung cancers are highly chemosensitive, with a 50 % response rate among patients with extensive stage disease (and 25 % complete response rate). Despite this high response rate, median survival is less than 1 year for patients with advanced disease.

Chemotherapy for NSCLC has traditionally consisted of a platinum-based combination, and while this is not curative, it may prolong survival and palliate symptoms. Numerous doublet (or

two-agent) chemotherapy options exist; however, none has proven to be superior to the others in a randomized trial comparing 4 platinum-based doublets [24]. More recent studies have suggested that the various histologic types of non-small-cell carcinoma have different chemotherapy responsiveness. For example, a phase III study comparing cisplatin/pemetrexed chemotherapy with cisplatin/gemcitabine found no difference in overall survival between the two regimens. In a prespecified subset analysis, however, patients with adenocarcinoma or large-cell carcinoma histology had a superior overall survival when treated with cisplatin/pemetrexed compared with cisplatin/gemcitabine. Conversely, squamous cell histology was associated with an improved overall survival in the cisplatin-/gemcitabine-treated patients [25]. These data suggest that the tumor histology dictates biologic behavior and response to chemotherapy and that the choice of first-line chemotherapy for metastatic NSCLC should be tailored to the different tumor types. The addition of bevacizumab, a humanized monoclonal antibody that binds and inhibits vascular endothelial growth factor (VEGF), to chemotherapy is also histology dependent. In patients with advanced, nonsquamous NSCLC, the addition of bevacizumab to carboplatin/paclitaxel chemotherapy prolonged survival when compared to carboplatin/paclitaxel alone (12.3 vs. 10.3 months, $P = 0.003$) in a randomized phase III trial. Patients with squamous cell carcinoma were excluded from this study (as were patients with hemoptysis, brain metastases, bleeding disorders, or requiring therapeutic anticoagulation), due to high rates of hemorrhage among patients with predominantly squamous cell carcinomas in the phase II study that preceded this one [26].

Bone-Targeted Therapies

Bisphosphonates

The bisphosphonates are analogues of pyrophosphate that inhibit osteoclastic bone resorption [27], and they are widely used in the treatment of hypercalcemia, in certain bone diseases, and in the treatment and prevention of osteoporosis. While they have numerous potential uses in cancer treatment, they are most commonly used to reduce the risk of skeletal-related events in patients with osteolytic bone lesions of multiple myeloma and with bone metastases from a variety of solid tumors. These skeletal-related events include pathologic fractures, the requirement for surgery or radiation therapy to the bone, and spinal cord compression.

In the mid-1990s, several studies established the efficacy of bisphosphonates in reducing skeletal-related events in patients with multiple myeloma. In 377 patients with stage III multiple myeloma and at least one lytic bone lesion, treatment with nine cycles of pamidronate in addition to antimyeloma chemotherapy significantly reduced the incidence of skeletal-related events (pathologic fracture, irradiation of or surgery on bone, and spinal cord compression) when compared to placebo plus antimyeloma chemotherapy (24 % vs. 41 %, $P < 0.001$). The pamidronate-treated group also experienced a significant decrease in bone pain [28]. A follow-up study after 21 cycles of pamidronate showed a significantly decreased number of skeletal events per year in the pamidronate-treated patients (1.3 vs. 2.2 with placebo, $P = 0.008$) [29]. A subsequent study evaluated the efficacy of zoledronic acid, a more potent bisphosphonate that can be administered more rapidly than pamidronate, in patients with either multiple myeloma or advanced breast cancer and at least one bone lesion. This study randomized 1,648 patients to either pamidronate or zoledronic acid every 3–4 weeks for 24 months. They found that the number of skeletal-related events and the median time to the first skeletal-related event were similar in the treatment groups, and after 25 months of follow-up, there was no increase in nephrotoxicity with the shorter 15-min zoledronic acid infusion [30, 31].

Based on these results, bisphosphonates are recommended for all patients with multiple myeloma and at least one bone lesion for prevention or delay of skeletal-related events and reduction in bone pain. The optimal duration of therapy is

unknown, and there is no definitive data to support the use of one intravenous bisphosphonate over another. It is clear, however, that the oral bisphosphonates currently available in the United States are not beneficial in preventing skeletal-related events in multiple myeloma [32, 33].

Breast cancer is the most common malignancy diagnosed in women, and the second most common cause of cancer death in women. Each year, approximately 40,000 women will die of breast cancer in the United States, and the majority of these have metastatic disease involving the bone [1]. Skeletal complications, including bone pain, pathologic fracture, spinal cord compression, and hypercalcemia, are a frequent source of morbidity in patients with metastatic breast cancer. Bisphosphonates are known to reduce the risk of these complications. The efficacy of intravenous pamidronate was demonstrated in a study that randomized 382 patients with advanced breast cancer receiving chemotherapy and at least one lytic bone lesion to receive pamidronate or placebo. This study demonstrated a significant decrease in the proportion of patients with skeletal complications in the pamidronate-treated arm (43 % vs. 56 % with placebo, $P = 0.008$) and a delay in the time to occurrence of first skeletal event (13.1 vs. 7.0 months, $P = 0.005$) [34]. With 2 years of follow-up, this effect was maintained [35]. A similar study conducted by the same investigators evaluated the effect of pamidronate or placebo in patients with metastatic breast cancer on hormonal therapy and at least one lytic bone lesion. A reduction in the proportion of patients with skeletal complications (56 % vs. 67 %, $P = 0.027$) and a longer time to first skeletal complication (10.4 vs. 6.9 months, $P = 0.049$) was found in the pamidronate-treated patients when compared to placebo [36]. Zoledronic acid has also shown efficacy at reducing the rate of skeletal-related events in patients with bone metastases from breast cancer [37]. There is no definitive data to support the use of one intravenous bisphosphonate over another. As noted previously, a randomized study comparing pamidronate to zoledronic acid in patients with metastatic breast cancer or multiple myeloma and bone lesions showed no difference in outcomes between the two intravenous bisphosphonates, though zoledronic acid is generally considered to be more convenient given its shorter infusion time [30, 31].

The bone is the most common site of metastasis in advanced prostate cancer, occurring in approximately 80 % of patients. Unlike multiple myeloma and breast cancer, in which the majority of bone lesions are osteolytic, bone metastases in prostate cancer are predominantly osteoblastic. Clinical studies have shown, however, that osteolysis also plays a role in the formation and growth of prostate cancer bone metastases, and this provides a rationale for the use of bisphosphonates in patients with metastatic prostate cancer as well [38]. Despite their osteoblastic nature, up to 22 % of men with prostate cancer and bone metastases will have a pathologic fracture [39]. Another factor contributing to bone fractures in men with advanced prostate cancer is osteoporosis secondary to androgen deprivation therapy.

The role of bisphosphonates in advanced prostate cancer has been extensively studied. In a randomized, double-blind, placebo-controlled study of 643 patients with hormone-refractory prostate cancer and bone metastases, there was a significant reduction in skeletal-related events (SREs, including pathologic fractures, spinal cord compression, surgery to bone, radiation therapy to bone, or a change of antineoplastic therapy to treat bone pain). The rate of SREs was decreased from 44 % with placebo to 33 % with zoledronic acid at a dose of 4 mg ($P = 0.021$), and the rate of fracture was decreased from 22 % to 13 % ($P = 0.015$), respectively. They also found a significant delay in time to first SRE in the treatment arm [39]. The role of bisphosphonates in hormone-sensitive prostate cancer remains unclear. While both pamidronate and zoledronic acid have been found to be efficacious in skeletal metastases due to breast cancer and multiple myeloma [30, 31], the less potent pamidronate has shown no benefit in reducing bone pain or skeletal-related events in advanced prostate cancer [40].

Despite the frequency of skeletal metastases in numerous solid tumors, the use of bisphosphonates in cancers other than those of breast and prostate origin has not been extensively studied. One

randomized, double-blind trial evaluated the efficacy of zoledronic acid versus placebo in patients with bone metastases secondary to solid tumors other than breast or prostate cancer. Of 773 patients randomized, approximately 50 % had non-small-cell lung cancer, with the majority of the remaining patients having renal cell carcinoma, small cell lung cancer, or cancer of unknown primary site. Patients with osteolytic and osteoblastic or mixed bone lesions were included, but the relative frequency or osteolytic versus osteoblastic metastases was not reported. They found that zoledronic acid was associated with a decreased rate of skeletal events (38 % vs. 47 % in the placebo group, $P = 0.039$), which were defined as pathologic fracture, spinal cord compression, radiation therapy to bone, surgery to bone, or hypercalcemia in this study. There was also a significant increase in time to first skeletal event with zoledronic acid therapy [41, 42]. Based in large part on this study, the routine use of bisphosphonates on all patients with bone metastases, regardless of the primary tumor site, is generally recommended. The optimal duration of bisphosphonate therapy remains unknown, but a systematic review of the use of bisphosphonates in metastatic cancer recommends continuing bisphosphonates until their use is no longer clinically relevant [43].

Bone-Targeted Radioisotopes

The bone-targeted radioisotopes include strontium 89 (^{89}Sr), samarium 153 (^{153}Sm), and rhenium 188 (^{188}Re), among others. They have been found to have efficacy in the palliation of pain due to multifocal osteoblastic bone metastases. Because they are only active in osteoblastic bone disease, these agents have primarily been studied in men with advanced prostate cancer and women with advanced breast cancer. They can be used, however, in any histologic tumor type with osteoblastic bone metastases.

One of the largest trials of radionuclide therapy randomized 284 men with prostate cancer and painful bone metastases to either radiotherapy or ^{89}Sr. Both treatment arms provided effective pain relief, and this was sustained at 3 months in the majority of patients, with no difference between the treatment arms. Fewer patients reported the development of new painful sites after ^{89}Sr than after radiotherapy ($P < 0.05$), and fewer patients in the ^{89}Sr group required radiation therapy to a new painful site than in the local radiotherapy group ($P < 0.01$) [44]. In a phase III randomized placebo-controlled trial of men with painful bone metastases from metastatic endocrine-resistant prostate cancer, the addition of ^{89}Sr to local field radiotherapy reduced progression of disease, as measured by new sites of pain and the requirement of further radiotherapy, when compared to local field radiotherapy plus placebo. While there was no significant difference in pain relief at the index site, there was a reduction in the need for analgesics in the ^{89}Sr arm [45]. While the previous studies showed no difference in median survival between the treatment arms, a European Organization for Research and Treatment of Cancer (EORTC) study in a similar population of patients showed an improved overall survival with local radiotherapy as compared to ^{89}Sr treatment (11 months vs. 7.2 months, respectively; $P = 0.0457$). There was no difference in subjective response rate [46].

The efficacy of ^{153}Sm in treating painful bone metastases has been demonstrated in two randomized, placebo-controlled phase III trials. The first of these randomized 118 patients with painful bone metastases secondary to a variety of primary malignancies to receive ^{153}Sm at a dose of 0.5 mCi/kg or 1 mCi/kg, or placebo. Patients that received the 1 mCi/kg dose of ^{153}Sm had a significant reduction in pain in each of the first 4 weeks after treatment, when compared to placebo. In the 1 mCi/kg dose group, 72 % of patients experienced pain relief, and this persisted for at least 16 weeks in the majority of patients [47]. The second study randomized 152 patients with painful bone metastases secondary to hormone-refractory prostate cancer to ^{153}Sm at a dose of 1 mCi/kg or a nonradioactive (^{152}Sm) placebo in a 2:1 randomization. There was a significant decrease in pain scores within 1–2 weeks of treatment, and analgesic consumption

was reduced by weeks 3–4, in the ^{153}Sm treatment group compared to placebo [48].

Radionuclide therapy is generally well-tolerated, with hematologic toxicity being the most common adverse event. This is usually mild, with recovery of myelosuppression within 8 weeks after treatment. Because of myelosuppression, the concurrent use of chemotherapy and radioisotopes is generally avoided except in the setting of a clinical trial.

Denosumab

Receptor activator of nuclear factor-kB ligand (RANKL) is expressed by osteoblasts and bone marrow stromal cells. When RANKL binds to its receptor, RANK, on osteoclast precursors, it induces maturation into mature osteoclasts, and these activated osteoclasts then secrete proteases and acid to resorb bone. Denosumab is a fully human monoclonal antibody directed against RANKL. It has proven efficacy in the treatment of postmenopausal osteoporosis and in bone loss associated with androgen deprivation therapy in prostate cancer, and it is under investigation for the treatment of multiple myeloma, metastatic bone disease, and other benign bone diseases. Preliminary studies appear promising, but the results of large phase III studies in multiple myeloma and metastatic solid tumors are pending.

References

1. Cancer Facts & Figures. http://www.cancer.org/docroot/home/index.asp (2009). Accessed 22 Feb 2010.
2. Sissons HA. The WHO, classification of bone tumors. Recent Results Cancer Res. 1976;54:104–8.
3. Rosen G, Marcove RC, Huvos AG, et al. Primary osteogenic sarcoma: eight-year experience with adjuvant chemotherapy. J Cancer Res Clin Oncol. 1983;106(Suppl):55–67.
4. Eilber F, Giuliano A, Eckardt J, Patterson K, Moseley S, Goodnight J. Adjuvant chemotherapy for osteosarcoma: a randomized prospective trial. J Clin Oncol. 1987;5:21–6.
5. Link MP, Goorin AM, Miser AW, et al. The effect of adjuvant chemotherapy on relapse-free survival in patients with osteosarcoma of the extremity. N Engl J Med. 1986;314:1600–6.
6. Link MP, Goorin AM, Horowitz M, et al. Adjuvant chemotherapy of high-grade osteosarcoma of the extremity. Updated results of the multi-institutional osteosarcoma study. Clin Orthop Relat Res. 1991;270:8–14.
7. Bacci G, Ferrari S, Bertoni F, et al. Long-term outcome for patients with nonmetastatic osteosarcoma of the extremity treated at the istituto ortopedico rizzoli according to the istituto ortopedico rizzoli/osteosarcoma-2 protocol: an updated report. J Clin Oncol. 2000;18:4016–27.
8. Bramwell VH, Burgers M, Sneath R, et al. A comparison of two short intensive adjuvant chemotherapy regimens in operable osteosarcoma of limbs in children and young adults: the first study of the European Osteosarcoma Intergroup. J Clin Oncol. 1992;10:1579–91.
9. Souhami RL, Craft AW, Van der Eijken JW, et al. Randomised trial of two regimens of chemotherapy in operable osteosarcoma: a study of the European Osteosarcoma Intergroup. Lancet. 1997;350:911–7.
10. Goorin AM, Schwartzentruber DJ, Devidas M, et al. Presurgical chemotherapy compared with immediate surgery and adjuvant chemotherapy for nonmetastatic osteosarcoma: Pediatric Oncology Group Study POG-8651. J Clin Oncol. 2003;21:1574–80.
11. Picci P, Sangiorgi L, Rougraff BT, Neff JR, Casadei R, Campanacci M. Relationship of chemotherapy-induced necrosis and surgical margins to local recurrence in osteosarcoma. J Clin Oncol. 1994;12:2699–705.
12. Bielack SS, Kempf-Bielack B, Winkler K. Osteosarcoma: relationship of response to preoperative chemotherapy and type of surgery to local recurrence. J Clin Oncol. 1996;14:683–4.
13. Bielack SS, Kempf-Bielack B, Delling G, et al. Prognostic factors in high-grade osteosarcoma of the extremities or trunk: an analysis of 1,702 patients treated on neoadjuvant cooperative osteosarcoma study group protocols. J Clin Oncol. 2002;20:776–90.
14. Petrilli AS, de Camargo B, Filho VO, et al. Results of the Brazilian osteosarcoma treatment group studies III and IV: prognostic factors and impact on survival. J Clin Oncol. 2006;24:1161–8.
15. Nesbit Jr ME, Gehan EA, Burgert Jr EO, et al. Multimodal therapy for the management of primary, nonmetastatic Ewing's sarcoma of bone: a long-term follow-up of the First Intergroup study. J Clin Oncol. 1990;8:1664–74.
16. Burgert Jr EO, Nesbit ME, Garnsey LA, et al. Multimodal therapy for the management of nonpelvic, localized Ewing's sarcoma of bone: intergroup study IESS-II. J Clin Oncol. 1990;8:1514–24.
17. Grier HE, Krailo MD, Tarbell NJ, et al. Addition of ifosfamide and etoposide to standard chemotherapy for Ewing's sarcoma and primitive neuroectodermal tumor of bone. N Engl J Med. 2003;348:694–701.

18. Miller K, Wang M, Gralow J, et al. Paclitaxel plus bevacizumab versus paclitaxel alone for metastatic breast cancer. N Engl J Med. 2007;357:2666–76.
19. Tannock IF, Osoba D, Stockler MR, et al. Chemotherapy with mitoxantrone plus prednisone or prednisone alone for symptomatic hormone-resistant prostate cancer: a Canadian randomized trial with palliative end points. J Clin Oncol. 1996;14:1756–64.
20. Berthold DR, Pond GR, Soban F, de Wit R, Eisenberger M, Tannock IF. Docetaxel plus prednisone or mitoxantrone plus prednisone for advanced prostate cancer: updated survival in the TAX 327 study. J Clin Oncol. 2008;26:242–5.
21. Tannock IF, de Wit R, Berry WR, et al. Docetaxel plus prednisone or mitoxantrone plus prednisone for advanced prostate cancer. N Engl J Med. 2004;351:1502–12.
22. Petrylak DP, Tangen CM, Hussain MH, et al. Docetaxel and estramustine compared with mitoxantrone and prednisone for advanced refractory prostate cancer. N Engl J Med. 2004;351:1513–20.
23. De Bono JS, Oudard S, Ozguroglu M, et al. Cabazitaxel or mitoxantrone with prednisone in patients with metastatic castration-resistant prostate cancer (mCRPC) previously treated with docetaxel: final results of a multinational phase III trial (TROPIC). J Clin Oncol (Meeting Abstracts). 2010;28:4508.
24. Schiller JH, Harrington D, Belani CP, et al. Comparison of four chemotherapy regimens for advanced non-small-cell lung cancer. N Engl J Med. 2002;346:92–8.
25. Scagliotti GV, Parikh P, von Pawel J, et al. Phase III study comparing cisplatin plus gemcitabine with cisplatin plus pemetrexed in chemotherapy-naive patients with advanced-stage non-small-cell lung cancer. J Clin Oncol. 2008;26:3543–51.
26. Sandler A, Gray R, Perry MC, et al. Paclitaxel-carboplatin alone or with bevacizumab for non-small-cell lung cancer. N Engl J Med. 2006;355:2542–50.
27. Rodan GA, Fleisch HA. Bisphosphonates: mechanisms of action. J Clin Invest. 1996;97:2692–6.
28. Berenson JR, Lichtenstein A, Porter L, et al. Efficacy of pamidronate in reducing skeletal events in patients with advanced multiple myeloma. Myeloma Aredia Study Group. N Engl J Med. 1996;334:488–93.
29. Berenson JR, Lichtenstein A, Porter L, et al. Long-term pamidronate treatment of advanced multiple myeloma patients reduces skeletal events. Myeloma Aredia Study Group. J Clin Oncol. 1998;16:593–602.
30. Rosen LS, Gordon D, Kaminski M, et al. Zoledronic acid versus pamidronate in the treatment of skeletal metastases in patients with breast cancer or osteolytic lesions of multiple myeloma: a phase III, double-blind, comparative trial. Cancer J. 2001;7:377–87.
31. Rosen LS, Gordon D, Kaminski M, et al. Long-term efficacy and safety of zoledronic acid compared with pamidronate disodium in the treatment of skeletal complications in patients with advanced multiple myeloma or breast carcinoma: a randomized, double-blind, multicenter, comparative trial. Cancer. 2003;98:1735–44.
32. Brincker H, Westin J, Abildgaard N, et al. Failure of oral pamidronate to reduce skeletal morbidity in multiple myeloma: a double-blind placebo-controlled trial Danish-Swedish co-operative study group. Br J Haematol. 1998;101:280–6.
33. Belch AR, Bergsagel DE, Wilson K, et al. Effect of daily etidronate on the osteolysis of multiple myeloma. J Clin Oncol. 1991;9:1397–402.
34. Hortobagyi GN, Theriault RL, Porter L, et al. Efficacy of pamidronate in reducing skeletal complications in patients with breast cancer and lytic bone metastases. Protocol 19 Aredia Breast Cancer Study Group. N Engl J Med. 1996;335:1785–91.
35. Hortobagyi GN, Theriault RL, Lipton A, et al. Long-term prevention of skeletal complications of metastatic breast cancer with pamidronate. Protocol 19 Aredia Breast Cancer Study Group. J Clin Oncol. 1998;16:2038–44.
36. Theriault RL, Lipton A, Hortobagyi GN, et al. Pamidronate reduces skeletal morbidity in women with advanced breast cancer and lytic bone lesions: a randomized, placebo-controlled trial. Protocol 18 Aredia Breast Cancer Study Group. J Clin Oncol. 1999;17:846–54.
37. Kohno N, Aogi K, Minami H, et al. Zoledronic acid significantly reduces skeletal complications compared with placebo in Japanese women with bone metastases from breast cancer: a randomized, placebo-controlled trial. J Clin Oncol. 2005;23:3314–21.
38. Oades GM, Coxon J, Colston KW. The potential role of bisphosphonates in prostate cancer. Prostate Cancer Prostatic Dis. 2002;5:264–72.
39. Saad F, Gleason DM, Murray R, et al. A randomized, placebo-controlled trial of zoledronic acid in patients with hormone-refractory metastatic prostate carcinoma. J Natl Cancer Inst. 2002;94:1458–68.
40. Small EJ, Smith MR, Seaman JJ, Petrone S, Kowalski MO. Combined analysis of two multicenter, randomized, placebo-controlled studies of pamidronate disodium for the palliation of bone pain in men with metastatic prostate cancer. J Clin Oncol. 2003;21:4277–84.
41. Rosen LS, Gordon D, Tchekmedyian S, et al. Zoledronic acid versus placebo in the treatment of skeletal metastases in patients with lung cancer and other solid tumors: a phase III, double-blind, randomized trial–the Zoledronic Acid Lung Cancer and Other Solid Tumors Study Group. J Clin Oncol. 2003;21:3150–7.
42. Rosen LS, Gordon D, Tchekmedyian NS, et al. Long-term efficacy and safety of zoledronic acid in the treatment of skeletal metastases in patients with nonsmall cell lung carcinoma and other solid tumors: a randomized, phase III, double-blind, placebo-controlled trial. Cancer. 2004;100:2613–21.

43. Ross JR, Saunders Y, Edmonds PM, Patel S, Broadley KE, Johnston SR. Systematic review of role of bisphosphonates on skeletal morbidity in metastatic cancer. BMJ. 2003;327:469.
44. Quilty PM, Kirk D, Bolger JJ, et al. A comparison of the palliative effects of strontium-89 and external beam radiotherapy in metastatic prostate cancer. Radiother Oncol. 1994;31:33–40.
45. Porter AT, McEwan AJ, Powe JE, et al. Results of a randomized phase-III trial to evaluate the efficacy of strontium-89 adjuvant to local field external beam irradiation in the management of endocrine resistant metastatic prostate cancer. Int J Radiat Oncol Biol Phys. 1993;25:805–13.
46. Oosterhof GO, Roberts JT, de Reijke TM, et al. Strontium(89) chloride versus palliative local field radiotherapy in patients with hormonal escaped prostate cancer: a phase III study of the European Organisation for Research and Treatment of Cancer, Genitourinary Group. Eur Urol. 2003;44:519–26.
47. Serafini AN, Houston SJ, Resche I, et al. Palliation of pain associated with metastatic bone cancer using samarium-153 lexidronam: a double-blind placebo-controlled clinical trial. J Clin Oncol. 1998;16:1574–81.
48. Sartor O, Reid RH, Hoskin PJ, et al. Samarium-153-Lexidronam complex for treatment of painful bone metastases in hormone-refractory prostate cancer. Urology. 2004;63:940–5.

High-Intensity Focused Ultrasound Treatment for Bone Metastases

45

Ronit Machtinger, Fiona M. Fennessy, and Mark D. Hurwitz

Abstract

Bone metastases are a frequent complication of cancer which are often associated with severe morbidity, due to pain, pathologic fractures, and spinal cord compression. Current treatment options for bone metastases include external beam radiation, radionuclide therapy, analgesia, surgery, bisphosphonates, and ablation techniques. However, the treatments themselves might be associated with morbidity and side effects, and patients may experience persistent or recurrent pain. Magnetic resonance-guided focused ultrasound surgery (MRgFUS) is a relatively new technique which has been shown to have potential as a noninvasive treatment option for a variety of benign and malignant tumors. Recent clinical trials have shown its benefit in palliative treatment of bone metastasis. This chapter summarizes the data from animal and clinical trials of MRgFUS treatment for bone metastases, with subsequent discussion of future directions for use of MRgFUS for treatment of osseous neoplasm.

Dr. Machtinger is supported by an award from the Focused Ultrasound Surgery Foundation for a part time fellowship in Brigham and Women's Hospital.

R. Machtinger (✉)
Department of Obstetrics and Gynecology, Brigham and Women's Hospital, Boston, MA, USA
e-mail: rmachtinger@sheba.health.gov.il

F.M. Fennessy
Department of Radiation, Brigham and Women's Hospital, Boston, MA, USA
e-mail: ffennessy@partners.org

M.D. Hurwitz
Department of Radiation Oncology, Dana-Farber/Brigham and Women's Cancer Center, Boston, MA, USA
e-mail: mhurwitz@lroc.harvard.edu

Introduction

Metastases are a frequent complication of cancer. Bone is the third most common organ involved by metastatic disease after lung and liver [1]. Breast and prostate cancers metastasize to bone most frequently, with a clinical prevalence of at least 70 % of the patients with metastatic disease. Osseous metastases also occur in 15–30 % of patients with carcinoma of the lung, colon, stomach, bladder, uterus, rectum, thyroid, and kidney [2, 3].

D.E. Dupuy et al. (eds.), *Image-Guided Cancer Therapy*, DOI 10.1007/978-1-4419-0751-6_47,

In patients who die from breast, prostate, and lung cancers, autopsy studies have shown that up to 85–90 % have evidence of bone metastases at the time of death [1, 4–6].

Metastatic bone disease is associated with a variety of skeletal complications, including pathologic fractures, bone pain, impaired mobility, spinal cord compression, and hypercalcaemia [7]. Bone metastases are often associated with severe pain, which can be intractable. Coupled with advances in cancer detection and therapy, the protracted life expectancy of many patients contributes to the high incidence and prevalence of metastatic bone lesions. As more patients are living with bone metastases, improving their quality of life becomes a major challenge. Previous studies showed that approximately half of patients with bone metastases receive only temporary pain relief with treatment [8, 9]. Permanent pain relief is seldom achieved and continues to challenge physicians.

Anatomy and Physiology

The skeletal bones are subdivided to four categories: long bones, short bones, flat bones, and irregular bones. The long bones are composed of a diaphysis, metaphyses, and epiphyses. The diaphysis is composed mainly of thick cortical bone, and the metaphysis and epiphysis are composed of trabecular bone surrounded by a relatively thin layer of cortical bone. The cortical bone has an outer periosteal surface and inner endosteal surface. The periosteum is a connective tissue that surrounds the outer cortical surface and contains nerve fibers, blood vessels, osteoclasts, and osteoblasts. The endosteum contacts the bone marrow and contains blood vessels, osteoclasts, and osteoblasts. The osteoclasts are responsible for bone resorption and the osteoblasts for bone formation. Bones constantly undergo modeling and remodeling throughout life [10].

Bone Metastases and Pain

The process of bone metastases formation is not completely understood involving various elements as metastatic cancer cells, cellular components of the bone marrow microenvironment, and imbalances between bone formation (osteoblasts) and bone resorption (osteoclasts). Bone metastases are classified as osteoblastic when bone formation exceeds bone resorption (i.e., prostate cancer) or osteolytic, when a decrease in bone density occurs via increased bone resorption (i.e., example multiple myeloma) [11–13]. The mechanisms responsible for bone pain are poorly understood. It seems to be a consequence of bone destruction (osteolysis) by the tumor cells but also results from tumor-induced nerve injury [8, 14]. Chemicals derived including cytokines from tumor cells and inflammatory cells appear to be involved simultaneously in driving this frequently difficult-to-control pain state [4]. Experimental animal models showed that bone cancer pain is different from neuropathic or inflammatory pain and causes reorganization and sensitization of the central dorsal horn of the spinal cord [8].

Validated Tools for Assessment of Pain and Quality of Life

Painful bone metastases are a debilitating problem that commonly impacts quality of life for patients with disseminated cancer. Quality of life can be impacted physically, emotionally, socially, and financially. Several pain scores have been used for the assessment of cancer pain, some of which are further detailed in this chapter. Measurements of the quality of life by reliable standard questionnaires might allow comparisons across studies:

1. *Numerical rating scales* (*NRS*): Developed by the World Health Organization (WHO) in 1994 [15], the NRS is an 11-point pain intensity scale (0 = no pain and 10 = worst possible pain) which is widely used for the assessment

Table 45.1 Current treatment options for bone metastases

Treatment	Pros	Cons
External beam radiation therapy (EBRT)	Achieves palliation in more than 60 % of patients with a limited number of well-localized bony metastases	A transient increased risk of pathological fractures.
		Patients who have recurrent pain at a site previously irradiated site may not be eligible for further radiation therapy secondary to normal tissue tolerance
Radionuclide therapy	Ease of administration, 50–70 % of patients experience pain relief	Limited to osteoblastic lesions, hematologic parameters must be in acceptable range
Surgery	Can prevent spinal cord compression and to relieve pressure on the spinal nerves	Invasive, requires anesthesia, postoperative recovery
Bisphosphonates	Also a treatment for associated hypercalcaemia, this therapy has been shown to reduce bone pain and to delay skeletal events	Routine use at earlier points in the disease course not fully established. Side effects include rare but serious events (i.e., jaw osteonecrosis)
Analgesia	Not invasive and does not need hospitalization in most of the cases	Often associated with side effects (lethargy, nausea, constipation)
Ablative techniques (Cryoablation, RFA)	Can be used when conventional therapies are ineffective or cause unacceptable side effects	Invasive, some sites may not be accessible

of cancer pain and has been used to investigate the effectiveness of radiation therapy to relieve pain resulting from bone metastases [16, 17]. The NRS worst pain score is highly correlated with quality of life and with mild, moderate, and severe pain categories [16–18]. A 2-point change on the NRS of pain intensity is accepted as a clinically important change in pain in patients with bone metastases.

2. *Short-form general health questionnaire* (*SF-36*): The SF-36 questionnaire is a short-form health survey with 36 questions. The questions represent domains as physical function, bodily pain, general health, vitality, social function, role emotional, and mental health. This multipurpose questionnaire has been validated in many different languages and countries [19, 20].
3. *Visual analog scores* (*VAS*): The visual analog scales for pain (VAS) are a type of rating scale (0 = death; 100 = perfect or optimal health), in which the patient marks a point on the line that matches the amount of pain he or she feels [21]. Changes in this score are widely used to estimate the efficacy of various treatments/medications for pain palliation.

Current Treatment Options for Bone Metastases

Current treatments for patients with bone tumors are primarily palliative and focus on controlling tumor proliferation, reducing tumor-induced bone loss, and stabilizing painful bones infiltrated with metastases [9]. The available strategies include localized therapies (external beam radiation therapy, surgery) [22], systemic therapies (chemotherapy, hormonal therapy, radionuclide therapy, and bisphosphonates), and analgesics (nonsteroidal anti-inflammatory drugs and opioids). Recently, radiofrequency ablation and cryoablation have been used for treatment of bone metastases [23] (Table 45.1 summarizes the pros and cons for current treatment options).

External Beam Radiation Therapy (EBRT)

EBRT is the standard of care for patients with localized bone pain and results in the palliation of pain in the majority of patients.

More than 60 % of patients with a limited number of well-localized bony metastases can be treated effectively by external beam irradiation [5, 17, 24–30]. A phase III Radiation Therapy Oncology Group study, RTOG 97–14, revealed that approximately one third of patients fail to achieve significant pain relief with radiation for treatment of bone metastases [17]. This randomized study included patients with prostate and breast cancer and investigated whether 8 Gy delivered in a single treatment fraction provides pain and narcotic relief that is equivalent to that of the standard treatment course of 30 Gy delivered in 10 treatment fractions over 2 weeks. Complete and partial response rates were 15 % and 50 %, respectively, in the 8-Gy arm ($n = 455$) compared with 18 % and 48 % in the 30-Gy arm ($n = 443$) ($P = 0.6$). At 3 months, 33 % of all patients no longer required narcotic medications. The incidence of subsequent pathologic fracture was 5 % for the 8-Gy arm and 4 % for the 30-Gy arm. The authors found that both regimens were equivalent in terms of pain and narcotic relief at 3 months post EBRT and were well tolerated with few adverse effects. The 8-Gy arm resulted in less acute toxicity than the 30-Gy arm (10 % vs. 17 %, $p = 0.002$). The retreatment rate was statistically significantly higher in the 8-Gy arm (18 %) than in the 30-Gy arm (9 %) ($P < 0.001$) which may reflect the willingness of physicians to retreat after a single fraction course of treatment.

Radiation therapy can lead to a transient increased risk of pathological fracture due to an induced hyperemic response at the periphery of the tumor. This weakens the adjacent bone and increases the risk of spontaneous fracture, although long-term radiation therapy reduces the risk of fractures. Another limitation is that patients who have recurrent pain at a site previously irradiated may not be eligible for further radiation therapy secondary to normal tissue tolerance.

Radionuclide Therapy

Patients with diffuse osteoblastic metastases may benefit from radionuclide therapy. Radionuclides used for treatment of bone metastases are either direct calcium homologues (i.e., strontium-89) or chelated to an agent such as EDTMP [ethylenediamine tetra(methylene phosphonic acid)] with phosphonic acid groups that target to areas of newly deposited bone (i.e., samarium-153). The radionuclide is administered intravenously in an outpatient setting. Between 50 % and 70 % of patients experience a significant decrease in pain with an average response of 12–16 weeks [31–33]. Typically, patients experience transient mild neutropenia and thrombocytopenia. Repeat dosing of samarium-153, which has a half-life of less than 2 days, has been shown to be feasible and effective [34]. An active area of ongoing clinical research is combination of radionuclide therapy with chemotherapy for not only relief of pain but to also extend patient survival.

Surgery

Surgery is often used in conjunction with, or prior to, other therapy to prevent bone fracture or to reduce pain. Techniques for stabilizing osteolytic lesions include salvage surgery to remove the cancerous area and replace with a prosthesis or surgical insertion of rods and plates. Surgery can prevent spinal cord compression and can relieve pressure on the spinal nerves. More recent advances in spinal surgery for metastatic lesions include minimally invasive procedures such as kyphoplasty where injections of a cement-like material are made directly into the fractured bone, typically the vertebra [14].

Analgesia

The World Health Organization (WHO) proposed three-step analgesic ladder for treatment of pain associated with metastatic cancer [35]. For mild pain, anti-inflammatory adjuvant analgesics (i.e., acetylsalicylate) were proposed

as good initial options. Most patients will benefit from the addition of nonsteroidal anti-inflammatory drugs, but their use might be contraindicated in these patients due to renal impairment or gastrointestinal side effects. Pain that is not relieved by anti-inflammatory drugs might be improved by opioid treatment. Side effects of opioid drugs include cognitive impairment, lethargy, nausea, and constipation. For localized bone pain in the spine that is refractory to systemic palliative therapy, epidural application of analgesics (i.e., local anesthetics, opioids, and others) is an important option to consider. This strategy is especially useful in patients who have slowly progressive tumors and few, but difficult to treat, bone metastases [14].

Bisphosphonates

Morbidity caused by skeletal complications may include not only pain but also hypercalcaemia and pathologic fractures. Some of those adverse effects on bone health result from the cancer treatments themselves. Bisphosphonates are potent inhibitors of bone osteolysis and may inhibit the development of bone metastases and the survival of dormant cells in the marrow microenvironment. They are standard of care for tumor-associated hypercalcaemia and have been shown to reduce bone pain, to improve quality of life, to delay skeletal events, and to reduce lesion number in patients with multiple myeloma and breast cancer [36, 37]. This therapy was recently approved by the FDA for metastatic bone disease [38]. Additionally, bisphosphonates may have direct effects on tumor cells, especially in combination with chemotherapy [39].

Ablation Techniques

Radiofrequency ablation (RFA) and cryoablation are relatively new treatments for metastatic bone pain relief. Both are ablative therapies, but unlike MRI-guided focused ultrasound surgery (MRgFUS), these techniques are invasive in that they require placement of applicators directly in the body. They can be used when conventional therapies are ineffective or cause unacceptable side effects. RFA ablates the interface between the tumor and the pain-sensitive periosteum. A multicenter trial of patients with painful bone metastases, in whom other therapies such as radiotherapy and chemotherapy had failed, found sustained pain relief in 95 % of patients following radiofrequency ablation [40–47].

Cryoablation is another tool for metastatic pain palliation with similar applications to RFA. A recent preliminary report from a prospective clinical trial evaluated bone cryoablation with a standardized pain score (Brief Pain Inventory) [42]. The authors showed an almost 40 % reduction in the mean score of worst pain as well as in the mean pain interfering with daily activities within 4 weeks of treatment.

MRgFUS Technology

MRgFUS is a system that combines a focused ultrasound surgery delivery system and a diagnostic MRI scanner. Focused ultrasound surgery (FUS) is a thermal ablation method that uses sound waves created in tissue as a source of thermal injury. The tissues within the focal point at which the ultrasonic energy is delivered are heated to a critical level (>55 °C) that results in tissue necrosis and apoptosis or cell death. The local tissue structure and content, through which the beam passes, has a considerable effect on the ultimate tissue temperatures achieved, because blood vessels are great conductors of heat and can move heat away from the point of delivery, thereby acting as an inherent cooling system [48]. MR imaging enables treatment monitoring using thermal imaging. The fundamental principle of image-guided therapy is that of maximal therapy to a target tissue, with little or no damage to surrounding tissues [49–51].

MRgFUS has been shown to have potential as a minimally invasive treatment option for a variety of benign and malignant tumors in the human body [52].

Already approved for the treatment of uterine fibroids, MRgFUS is in ongoing clinical trials for

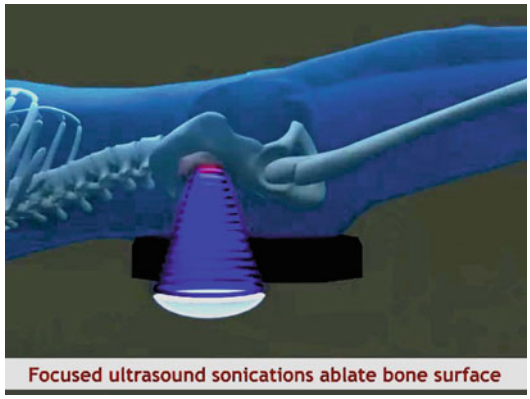

Fig. 45.1 Schematic figure of the MRgFUS bone treatment (courtesy of InSightec, Inc.)

the treatment of breast, liver, prostate, and brain cancer and for the palliation of pain in bone metastasis [53].

The ExAblate system (InSightec, Tirat Carmel Israel) is an MRgFUS device that has been used for the ablation of tissue. This system combines a focused ultrasound surgery delivery system and a conventional diagnostic 1.5 T or 3 T MRI scanner (MRgFUS/MR-guided focused ultrasound surgery). The ExAblate system provides real-time therapy planning algorithm, thermal dosimetry, and closed-loop therapy control. The latter is achieved by utilizing the unique interactive MRI scan control features of the GE SIGNA MRI system (GE Healthcare, Waukesha WI). The ExAblate device is an integrated component of the MRI table. The subject is placed on the MRI table and moved into the MRI scanner (Fig. 45.1).

The treatment process begins with the physician acquiring a set of MR images, identifying target volume(s) of tissue to be treated, and drawing the treatment contours (Fig. 45.2). The therapy planning software computes the type and number of sonications required to treat the defined region while minimizing total treatment time. MR images taken during the sonication provide a diagnostic quality image of the target tissue and a quantitative, real-time temperature map overlay to confirm the therapeutic effect of the treatment. The transducer is then automatically moved to the succeeding treatment point, and the process is repeated until the entire volume has been treated. Typically, 20–50 individual sonications are delivered over approximately 1–2-h period to complete a treatment.

MRgFUS for Bone Metastases

Bone has much higher acoustic absorption of ultrasound energy compared with soft tissue and allows minimal penetration of ultrasound energy. MRgFUS treatment of painful bone metastases utilizes the propensity of bone to absorb this energy to achieve palliation. Specifically, energy absorption is about 50× greater in bone than soft tissues. Animal studies (porcine model) showed that MRgFUS can be used to produce controlled well-localized damage to soft tissue in close proximity to bone, with minimal collateral damage [54]. The exact mechanism of pain relief is thought to be destruction of the periosteal innervation to the affected bone [55, 56], and therefore, selective targeting of periosteum as opposed to more demanding whole lesion ablation can result in significant pain palliation.

MRgFUS Treatment of Metastatic Bone Tumors: Human Clinical Studies

MRgFUS has been shown in phase I/II trials for treatment of bone metastases to have an excellent safety profile and high rates of pain response. An initial feasibility trial to evaluate the safety and initial efficacy of MRgFUS for the palliation of pain caused by bone metastases in patients for whom no other available treatments were effective or feasible included 21 patients at Charite Hospital, Germany, and Sheba Medical Center, Israel [57]. There were a diverse range of primary diagnoses, treatment sites, and mix of osteoblastic and osteolytic lesions. The treatment safety was evaluated by assessing the incidence and severity of device-related complications. Effectiveness of pain palliation was evaluated using the visual analog scale (VAS) pain questionnaires. In this study, there were no device-related deaths, life-threatening injuries, or permanent injuries

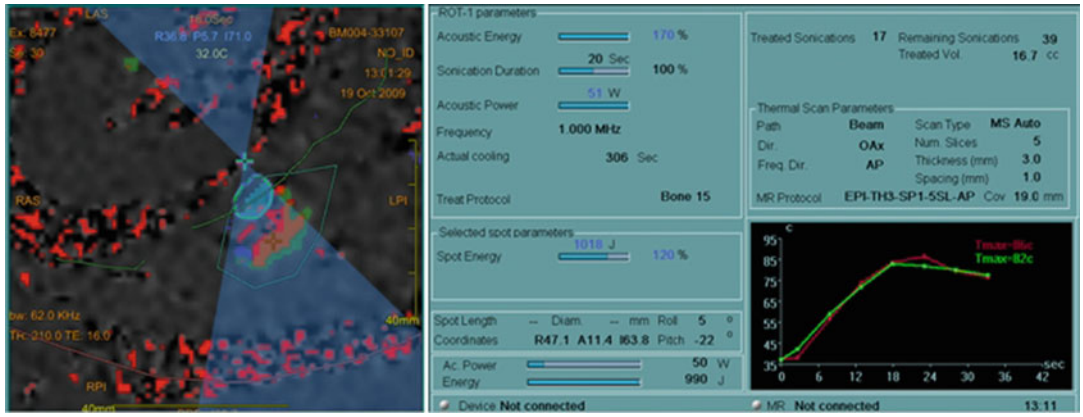

Fig. 45.2 MRI-guided temperature measurements of the treated area (courtesy of InSightec, Inc.)

attributable to the device. Only two adverse events were reported: one event of "moderate" sonication-induced pain resolved when sonication ended, and another event of "mild" urinary tract infection due to catheter insertion which resolved in 3 days without intervention. These events were anticipated side effects that had been identified in the study protocol as possible treatment related complications of ExAblate treatment, based on previous ExAblate MRgFUS treatment experiences. Hence, there was no evidence of new risks or an increase of expected risks in this study. In regard to efficacy, 70 % of patients experienced a significant reduction in pain during the follow-up period with 11/17 evaluable patients having significant improvement at the final 3-month follow-up visit.

A subsequent FDA clinical study was performed to further evaluate the safety and effectiveness of using ExAblate as a treatment for pain palliation in patients with metastatic bone tumors [46]. This study followed the "International Bone Metastases Consensus Working Party" on endpoint measurement for future clinical trials that was established in conjunction with the American Society for Therapeutic Radiology and Oncology, the European Society for Therapeutic Radiology and Oncology, and the Canadian Association of Radiation Oncology. The change in the patient pain relief was assessed using the VAS, whereas patient quality of life was assessed using the SF-36 quality of life questionnaire. These assessments were performed at baseline, on treatment day, and at follow-up time points of 3 days, 2 weeks, and 1 month and 3 months. The safety profile was evaluated using a common description of significant clinical complications for patients treated in this study. Additional data regarding dosage and frequency of analgesic consumption for the management of the metastatic bone tumor-induced pain were also collected. Ten patients were enrolled (Fig. 45.3). One patient's treatment could not be completed due to limited device accessibility, and this patient was excluded from further analysis. Only three adverse events were reported: 2 events of "mild" sonication-induced pain resolved the same day when sonication ended and 1 event of "mild" shivering reaction to conscious sedation medication that lasted a few minutes during the procedure and then resolved. All of these events were anticipated side effects that were already identified in the study protocol as possible treatment-related complications of treatment, based on previous ExAblate treatment experiences. Hence, there was no evidence of new or increased risks during the course of this study. All 9 evaluable patients experienced significant pain relief which persisted through the 3-month follow-up period. In summary, these initial phase I/II trials demonstrated excellent toxicity and rates of pain response. No severe adverse events (SAE) occurred, and 72 % of patients evaluable at 3 months experienced a significant pain response [58].

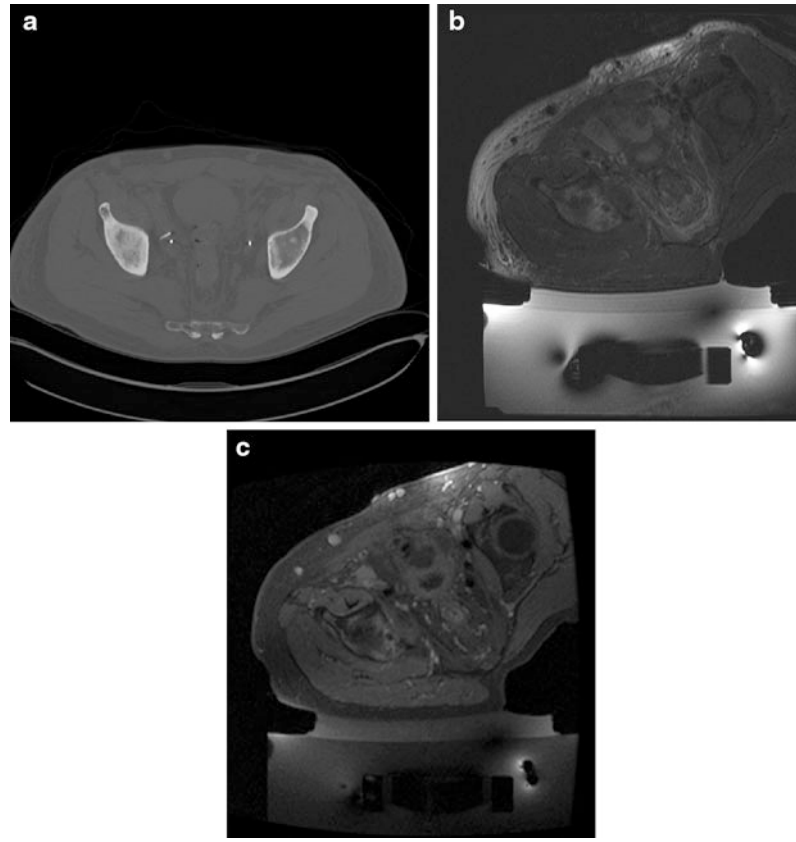

Fig. 45.3 Treatment of a tumor in the right acetabulum, part of the clinical trial at Brigham and Women's Hospital, Boston, MA. (**a**) Screening axial CT demonstrating a sclerotic lesion in the right acetabulum (*black arrow*); (**b**) treatment-planning axial fat-saturated T2-weighted magnetic resonance (MR) image shows the periosteum of the area to be treated (*white arrow*) overlying the ultrasound transducer (*red arrows*); and (**c**) axial T1 MR image post gadopentetate dimeglumine administration after treatment demonstrates no abnormal enhancement within the surrounding soft tissues

At present, over 70 patients have received MRgFUS treatment for bone metastases with the ExAblate system and no SAE have occurred. The phase I/II experience with MRgFUS, typically as second-line therapy, indicates that approximately 77 % of patients experience clinically significant pain relief in this unfavorable scenario with 72 % of patients continuing to experience significant relief at 3 months. This pain relief has been consistently and usually rapidly achieved without the need to ablate the entire lesion in bone but rather by focusing on treating the involved periosteum. The ability to achieve pain relief with selective targeting has the advantage of minimizing risk of complications although when stabilization is an issue, more extensive lesion targeting either alone or in combination with other treatments may need to be considered. Future studies will help to address this issue.

Future Directions

Treatment of bone metastases with high focused ultrasound will likely benefit from improvements in treatment application now in development as well as thoughtful integration of MRgFUS with other treatment modalities. Currently, MRgFUS is delivered with the ultrasound transducer in a fixed position on the treatment table. The lesion to be treated, and therefore the patient, must be positioned to accommodate the location of the transducer. A mobile transducer has been developed which is now being assessed clinically. It is anticipated that the use of this applicator will expand the number of sites in the body that can be treated with MRgFUS. The integration of MRgFUS into multimodality therapy also holds great promise for its expanded use in oncology including treatment of bone metastases.

Significant advances in cancer therapy have often come through multidisciplinary approaches to therapy. While the use of mild temperature hyperthermia in combination with radiation or chemotherapy has been extensively studied, the application of thermal ablative therapies in combination with other common cancer therapies however has not been adequately evaluated in the clinical setting. The rationale for combined RT and thermal therapy is compelling [59, 60]. Radiation and hyperthermia may have complimentary, sensitizing, and synergistic effects. The extension of the compelling biologic rationale for combined hyperthermia and radiation also, as expected, appears to be applicable to combination of thermal ablative therapy with radiation as a hyperthermic rim of heated but not ablated tissue surrounds the high-temperature zone. While preclinical data suggests there is a synergistic effect to the addition of radiation to thermal ablative therapies [61, 62], this treatment approach has not yet been assessed in clinical trials. The combination of MRgFUS and RT may lead to enhanced safety through reduced necessity of ablative therapy delivery at the interface of the tumor and normal tissue interfaces. When used in combination with radiation, MRgFUS may result in more rapid and durable pain relief with enhanced antitumor effects. Future clinical trials will be required to fully assess the potential of MRgFUS as part of combined modality therapy in treatment of pain osseous lesions as well as other oncologic conditions.

References

1. Buckwalter JA, Brandser EA. Metastatic disease of the skeleton. Am Fam Physician. 1997;55(5):1761–8.
2. Roodman GD. Mechanisms of bone metastasis. N Engl J Med. 2004;350(16):1655–64.
3. Coleman RE, Rubens RD. The clinical course of bone metastases from breast cancer. Br J Cancer. 1987;55:61–6.
4. Sabino MA, Mantyh PW. Pathophysiology of bone cancer pain. J Support Oncol. 2005;3(1):15–24.
5. Nielsen OS, Bentzen SM, Sandberg E, Gadeberg CC, Timothy AR. Randomized trial of single dose versus fractionated palliative radiotherapy of bone metastases. Radiother Oncol. 1998;47(3):233–40.
6. Nielsen OS, Munro AJ, Tannock IF. Bone metastases: pathophysiology and management policy. J Clin Oncol. 1991;9(3):509–24.
7. Mundy GR. Metastasis to bone: causes, consequences and therapeutic opportunities. Nat Rev Cancer. 2002;2(8):584–93.
8. Goblirsch MJ, Zwolak PP. Clohisy DR biology of bone cancer pain. Clin Cancer Res. 2006; 12(Suppl 20):6231s–5.
9. Meuser T, Pietruck C, Radbruch L, Stute P, Lehmann KA, Grond S. Symptoms during cancer pain treatment following WHO-guidelines: a longitudinal follow-up study of symptom prevalence, severity and etiology. Pain. 2001;93:247–57.
10. Clarke B. Normal bone anatomy and physiology. Clin J Am Soc Nephrol. 2008;3(Suppl 3):S131–9.
11. Ibrahim T, Flamini E, Mercatali L, Sacanna E, Serra P, Amadori D. Pathogenesis of osteoblastic bone metastases from prostate cancer. Cancer. 2010;116(6): 1406–18.
12. Casimiro S, Guise TA, Chirgwin J. The critical role of the bone microenvironment in cancer metastases. Mol Cell Endocrinol. 2009;310(1–2):71–81.
13. Kakonen SM, Mundy GR. Mechanisms of osteolytic bone metastases in breast carcinoma. Cancer. 2003;97:834–9.
14. von Moos R, Strasser F, Gillessen S, Zaugg K. Metastatic bone pain: treatment options with an emphasis on bisphosphonates. Support Care Cancer. 2008;16(10):1105.
15. Cleeland CS, Ryan KM. Pain assessment: global use of the brief pain inventory. Ann Acad Med Singapore. 1994;23(2):129–38.
16. Chow E, et al. Prospective patient-based assessment of effectiveness of palliative radiotherapy for bone metastases. Radiother Oncol. 2001;61(1):77–82.
17. Hartsell WF, et al. Randomized trial of short- versus long-course radiotherapy for palliation of painful bone metastases. J Natl Cancer Inst. 2005; 97(11):798–804.
18. Serlin RC, et al. When is cancer pain mild, moderate or severe? Grading pain severity by its interference with function. Pain. 1995;61(2):277–84.
19. Ware Jr JE, Sherbourne CD. The MOS 36-item short-form health survey (SF-36). I. Conceptual framework and item selection. Med Care. 1992;30(6):473–83.
20. Veresciagina K, Ambrozaitis KV, Spakauskas B. The measurements of health-related quality-of-life and pain assessment in the preoperative patients with low back pain. Medicina (Kaunas). 2009;45(2):111–22.
21. Torrance GW, Feeny D, Furlong W. Visual analog scales: do they have a role in the measurement of preferences for health states? Med Decis Making. 2001;21(4):329–34.
22. Diederich CJ, Hynynen K. Ultrasound technology for hyperthermia. Ultrasound Med Biol. 1999;25(6): 871–87.

23. Goetz MP, et al. Percutaneous image-guided radiofrequency ablation of painful metastases involving bone: a multicenter study. J Clin Oncol. 2004; 22(2):300–6.
24. Cole DJ. A randomized trial of a single treatment versus conventional fractionation in the palliative radiotherapy of painful bone metastases. Clin Oncol (R Coll Radiol). 1989;1(2):59–62.
25. Gaze MN, et al. Pain relief and quality of life following radiotherapy for bone metastases: a randomised trial of two fractionation schedules. Radiother Oncol. 1997;45(2):109–16.
26. Jeremic B, et al. A randomized trial of three single-dose radiation therapy regimens in the treatment of metastatic bone pain. Int J Radiat Oncol Biol Phys. 1998;42(1):161–7.
27. Konski A, Feigenberg S, Chow E. Palliative radiation therapy. Semin Oncol. 2005;32(2):156–64.
28. Steenland E, et al. The effect of a single fraction compared to multiple fractions on painful bone metastases: a global analysis of the Dutch bone metastasis study. Radiother Oncol. 1999;52(2):101–9.
29. Janjan NA. Radiation for bone metastases: conventional techniques and the role of systemic radiopharmaceuticals. Cancer. 1997;80:1628–45.
30. Kashima M, Yamakado K, Takaki H, Kaminou T, Tanigawa N, Nakatsuka A, Takeda K. Radiofrequency ablation for the treatment of bone metastases from hepatocellular carcinoma. AJR Am J Roentgenol. 2010;194(2):536–41.
31. Lewington VJ, McEwan AJ, Ackery DM, Bayly RJ, Keeling DH, Macleod PM, Porter AT, Zivanovic MA. A prospective, randomised double-blind crossover study to examine the efficacy of strontium-89 in pain palliation in patients with advanced prostate cancer metastatic to bone. Eur J Cancer. 1991;27(8):954–8.
32. Resche I, Chatal JF, Pecking A, Ell P, Duchesne G, Rubens R, Fogelman I, Houston S, Fauser A, Fischer M, Wilkins D. A dose-controlled study of 153Sm-ethylenediaminetetramethylenephosphonate (EDTMP) in the treatment of patients with painful bone metastases. Eur J Cancer. 1997;33:1583–91.
33. Serafini AN, Klein JL, Wolff BG, Baum R, Chetanneau A, Pecking A, Fischman AJ, Hoover Jr HC, Wynant GE, Subramanian R, Goroff DK, Hanna Jr MG. Radioimmunoscintigraphy of recurrent, metastatic, or occult colorectal cancer with technetium 99 m-labeled totally human monoclonal antibody 88BV59: results of pivotal, phase III multicenter studies. J Clin Oncol. 1998;16:1574–81.
34. Sartor O, Reid RH, Hoskin PJ, Quick DP, Ell PJ, Coleman RE, Kotler JA, Freeman LM, Olivier P. Quadramet 424Sm10/11 study group. Samarium-153-Lexidronam complex for treatment of painful bone metastases in hormone-refractory prostate cancer. Urology. 2004;63:940–5.
35. Dalton JA, Youngblood R. Clinical application of the World health organization analgesic ladder. J Intraven Nurs. 2000;23(2):118–24.
36. Yuen KK, Shelley M, Sze WM, Wilt T, Mason MD. Bisphosphonates for advanced prostate cancer. Cochrane Database Syst Rev. 2006;18(4):CD006250.
37. Pavlakis N, Schmidt R, Stockler M. Bisphosphonates for breast cancer. Cochrane Database Syst Rev. Cochrane Database Syst Rev. 2005;20(3):CD003474.
38. Lipton A. Bone continuum of cancer. Am J Clin Oncol. 2010;33(3 Suppl):S1–7.
39. Coleman R, Gnant M. New results from the use of bisphosphonates in cancer patients. Curr Opin Support Palliat Care. 2009;3(3):213–8.
40. Sabharwal T, Katsanos K, Buy X, Gangi A. Image-guided ablation therapy of bone tumors. Semin Ultrasound CT MRI. 2009;30:78–90.
41. Callstrom MR, Atwell TD, Charboneau JW, et al. Painful metastases involving bone: percutaneous image-guided cryoablation-prospective trial interim analysis. Radiology. 2006;241:572–80.
42. Callstrom MR, Charboneau JW, Goetz MP, et al. Image guided ablation of painful metastatic bone tumours: a new and effective approach to a difficult problem. Skeletal Radiol. 2006;35:1–15.
43. Nakatsuka A, Yamakado K, Takaki H, et al. Percutaneous radiofrequency ablation of painful spinal tumors adjacent to the spinal cord with real-time monitoring of spinal canal temperature: a prospective study. Cardiovasc Intervent Radiol. 2009;32:70–5.
44. Nakatsuka A, Yamakado K, Maeda M, et al. Radiofrequency ablation combined with bone cement injection for the treatment of bone malignancies. J Vasc Interv Radiol. 2004;15:707–12.
45. Kodama H, Aikata H, Uka K, et al. Efficacy of percutaneous cementoplasty for bone metastasis from hepatocellular carcinoma. Oncology. 2007;72: 285–92.
46. Kojima H, Tanigawa N, Kariya S, et al. Clinical assessment of percutaneous radiofrequency ablation for painful metastatic bone tumors. Cardiovasc Intervent Radiol. 2006;29:1022–6.
47. Grönemeyer DH, Schirp S, Gevargez A. Image-guided radiofrequency ablation of spinal tumors: preliminary experience with an expandable array electrode. Cancer J. 2002;8:33–9.
48. Fennessy FM, Tempany CM. MRI-guided focused ultrasound surgery of uterine leiomyomas. Acad Radiol. 2005;12(9):1158–66.
49. Jolesz JA. 1996 RSNA Eugene P. Pendergrass New Horizons Lecture: Image-guided procedures and the operating room of the future. Radiology. 1997; 204:601–12.
50. Grimson WE, Kikinis R, Jolesz FA, et al. Image-guided surgery. Sci Am. 1999;280:62–9.
51. Jolesz FA. Interventional and intraoperative MRI: a general overview of the field. J Magn Reson Imaging. 1998;8:3–7.
52. Gianfelice D, Gupta C, Kucharczyk W, Bret P, Havill D, Clemons M. Palliative treatment of painful bone metastases with MR imaging–guided focused ultrasound. Radiology. 2008;249(1):355–63.

53. Jolesz FA. MRI-guided focused ultrasound surgery. Annu Rev Med. 2009;60:417–30.
54. Kopelman D, Inbar Y, Hanannel A, Pfeffer RM, Dogadkin O, Freundlich D, Liberman B, Catane R. Magnetic resonance guided focused ultrasound surgery. Ablation of soft tissue at bone-muscle interface in a porcine model. Eur J Clin Invest. 2008; 38(4):268–75.
55. Ripamonti C, Fulfaro F. Malignant bone pain: pathophysiology and treatment. Curr Rev Pain. 2000;4(3):187–96.
56. Mercadante S. Malignant bone pain: pathophysiology and treatment. Pain. 1997;69(1–2):1–18.
57. Catane R, Beck A, Inbar Y, Rabin T, Shabshin N, Hengst S, Pfeffer RM, Hanannel A, Dogadkin O, Liberman B, Kopelman D. MR-guided focused ultrasound surgery (MRgFUS) for the palliation of pain in patients with bone metastases–preliminary clinical experience. Ann Oncol. 2007;18(1):163–7.
58. Liberman B, Gianfelice D, Inbar Y, Beck A, Rabin T, Shabshin N, Chander G, Hengst S, Pfeffer R, Chechick A, Hanannel A, Dogadkin O, Catane R. Pain palliation in patients with bone metastases using MR-guided focused ultrasound surgery: a multicenter study. Ann Surg Oncol. 2009;16(1):140–6.
59. Dewhirst MW, Vujaskovic Z, Jones E, Thrall D. Re-setting the biologic rationale for thermal therapy. Int J Hyperthermia. 2005;21(8):779–90.
60. Horkan C, Dalal K, Coderre JA, Kiger JL, Dupuy DE, Signoretti S, Halpern EF, Goldberg SN. Reduced tumor growth with combined radiofrequency ablation and radiation therapy in a rat breast tumor model. Radiology. 2005;235(1):81–8.
61. Jernberg A, Edgren MR, Lewensohn R, Wiksell H, Brahme A. Cellular effects of high-intensity focused continuous wave ultrasound alone and in combination with X-rays. Int J Radiat Biol. 2001; 77(1):127–35.
62. Raaphorst GP, Szekely JG. Thermal enhancement of cellular radiation damage: a review of complementary and synergistic effects. Scanning Microsc. 1988; 2(1):513–35.

Image-Guided Radio Frequency Ablation of Renal Cancer

46

Peter Osborn and David J. Breen

Abstract

Incidental small-volume renal tumors are a growing clinical problem, and while partial nephrectomy – open or laparoscopic – remains the standard of care, radiofrequency ablation for sub-4 cm disease has been increasingly confirmed as a viable treatment alternative. This chapter looks at the suitability of renal tumors to percutaneous ablation, radiofrequency ablation equipment, and ablation techniques including imaging, patient sedation, and follow-up regimes. The chapter concludes with a review of the current evidence for RFA and how it compares to surgical treatments of renal cancer.

Trends in Renal Cancer Epidemiology

The incidence of renal cell carcinoma (RCC) has increased in recent years, notably in the USA, from 31,200 in 2000 to 57,760 new cases in 2009 [1, 2]. This has largely been attributed to the incidental detection of small renal cancers by the virtue of increased abdominal imaging [3, 4]. However, even accounting for this increase in imaging-detected tumors, there appears to be an additional background increase in renal cancer incidence [3], which appears to be attributable to increased longevity [4, 5], obesity, and hypertension [6]. The largest rise has been seen in the western hemisphere where the age-standardized incidence rates are currently 11–12 per 100,000 compared with 1–3 per 100,000 in China [5].

Contrary to widespread opinion, not all of the increase in renal mass incidence is due to small clinically irrelevant disease. Indeed, there has been an increase in renal cancer-specific mortality from 4.3 per 100,000 in 1971 to 6.0 per 100,000 in 2008 in males in England and Wales [5]. Despite this, overall renal cancer survival rates have improved from 53.2 % in 1975 to 68.8 % in 2002 [1]. In the background, there is an undoubted stage migration toward smaller, more treatable, sub-4 cm stage T1a disease.

P. Osborn (✉)
Department of Diagnostic Imaging, Queen Alexandra Hospital, Portsmouth, Hampshire, UK
e-mail: peter.osborn@porthosp.nhs.uk

D.J. Breen
Department of Radiology, Southampton University Hospitals, Southampton, UK
e-mail: david.breen@suht.swest.nhs.uk

D.E. Dupuy et al. (eds.), *Image-Guided Cancer Therapy*, DOI 10.1007/978-1-4419-0751-6_48,

Natural History of Renal Cell Carcinoma

Most incidental renal masses detected on imaging for alternative symptomatology are small in size, (<4 cm). Despite optimal imaging it is often not possible to distinguish benign from malignant lesions in this group of lesions. Clinicians must seek to avoid unnecessary, even though minimally invasive, therapies for benign masses.

Frank et al. [7] compared preoperative imaging of solid renal masses with postoperative histology in 2,770 patients. 12.8 % of the 2,935 tumors were benign, largely oncocytomas, and angiomyolipomas. Size has a significant bearing on malignancy risk. In this series, 25 % of sub-3 cm and 46 % of sub-1 cm masses were benign. Ninety percent of masses greater than 4 cm were malignant with 30 % demonstrating high-grade histology (Fuhrman grade 2 and above).

In 1995, Bosniak et al. reviewed historic imaging of 37 patients who had subsequently gone on to have renal lesions removed and reported average growth rate of 3.6 mm/year with a range of 0–11 mm/year [8]. Although the numbers were small, Bosniak noted that those with the most histologically malignant features were toward the upper end of this range of growth rates, whereas those with less malignant features grew more slowly. A meta-analysis by Chawla et al. [9] of 286 lesions demonstrated an average renal mass growth of 2.8 mm/year while the subset histologically proven to be RCC had an average growth rate of 4.0 mm/year. Overall it appears that there is a range of growth patterns with follow-up data suggesting higher histological grades seen in faster growing lesions [9]. Conversely, Kunkle et al. [10] demonstrated 83 % of enhancing renal masses followed up for at least 12 months demonstrating no measurable growth were eventually histologically proven to be RCC.

The meta-analysis by Cary et al. in 2009 with a total of 441 patients [11] found significant rates of malignancy (>60 %) in all renal masses, regardless of size or growth rate. They also reported a 1 % distant metastasis rate during watchful waiting, although these two cases were at 5 and 10 years.

Most authors [12, 13] conclude that renal masses in fit patients should be removed/ablated, while there may be some scope for watchful waiting in less-fit patients where slow-growing renal masses are unlikely to diminish patient longevity (Fig. 46.1).

Should Renal Masses Be Biopsied?

With significant rates of benignity for small renal masses, clinicians should always seek histological verification of the nature of a small renal mass. This can be done either before or, at the very least, immediately prior to the planned ablation. Definitive benign diagnoses of angiomyolipoma or focal infection can be made though there are risks to relying on negative biopsy results. Dechet [14] demonstrated some of the uncertainties of renal biopsy. Intraoperative frozen section results, when compared with extirpative histology, had negative predictive values by two histologists of 69 % and 73 % [14]. Additional more recent renal mass biopsy studies have shown significant improvements in diagnostic accuracy largely due to the advances in immunohistochemistry [15, 16]. Ablation in particular is a non-extirpative technique, and therefore, histological proof of the nature of the treated lesion becomes more critical. For the purposes of treatment planning and follow-up, a histological biopsy should always be sought even though on occasion it will yield a false-negative result (Fig. 46.2).

Device

Radiofrequency ablation causes cell death through heating and tissue coagulation. Radiofrequency ablation utilizes high-frequency alternating current to cause ion agitation of polarized water molecules and subsequent heating through frictional heat loss. There is a concentration of current flux density and thus heating effect around the antenna tip. Most

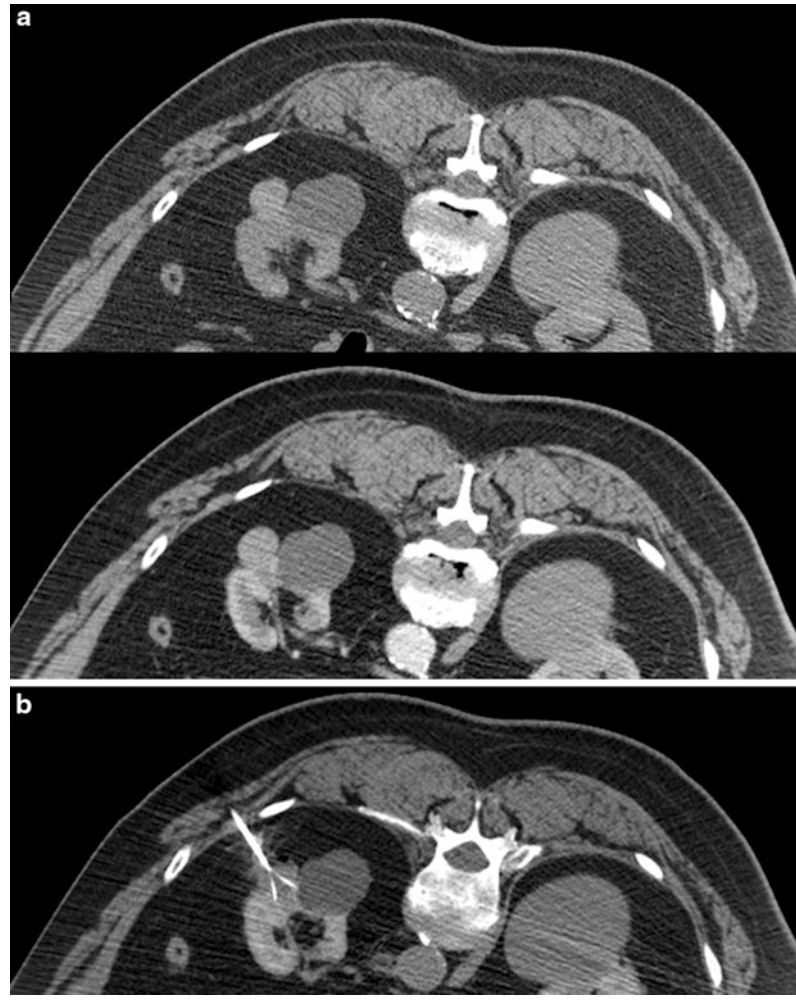

Fig. 46.1 (**a**) A formal diagnostic study is usually performed at the onset of the RFA procedure. This permits accurate probe placement within +/−3 mm. (**b**) Deployed position of tines should be clearly defined by CT

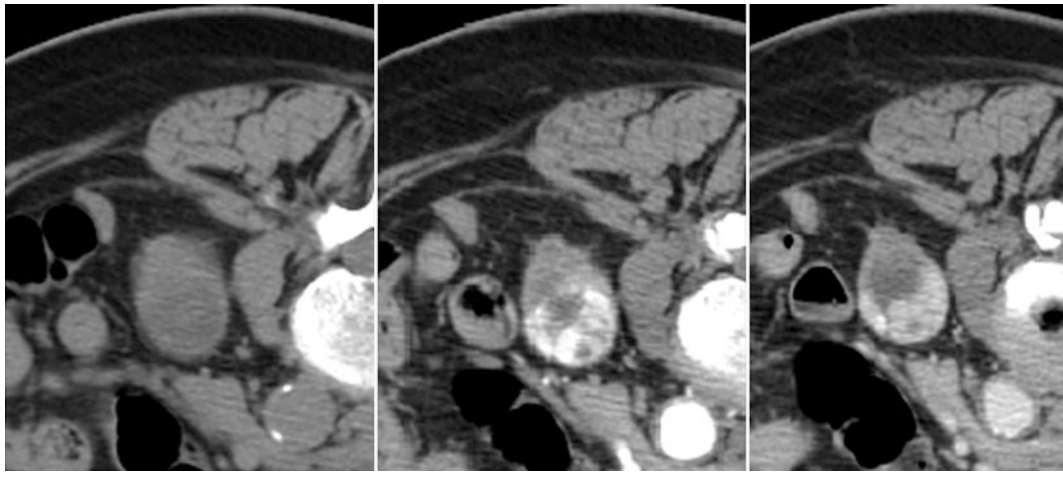

Fig. 46.2 Lower pole renal mass, pre-contrast, 35-s renal phase, and 70-s portal venous phase. Note irregular early enhancement of the mass with cystic or necrotic areas

monopolar systems use a single-exposed probe antenna placed within the target lesion. The electrical circuit is completed by large grounding pads applied to the patient's thighs. When the alternating current is applied, the heating effect is concentrated within 2–3 mm of the probe tip reaching 80–100 °C, whereas the tissue adjacent to the much larger surface area of the grounding pad usually barely records a temperature rise. Although the tissue immediately next to the probe tip is actively heated, the process is otherwise considerably reliant on conductive heating to achieve the overall thermal ablation zone. In order to achieve greater ablation volumes, manufactures have designed clustered or expandable monopolar probes [17]. Hollow probes have also been made which can be coaxially perfused with chilled saline in order to increase the efficiency of heat deposition.

Alternatively the circuit can be completed with multiple bipolar probes instead grounding pads or multiple monopolar probes. This allows one or more probes to be placed (bipolar or multipolar RF ablation) within the target lesion with the current between them resulting in a larger volume of lethal heating [17].

Most authors report using RFA safely in patients with in situ cardiac pacemakers [18, 19], as long as the treatment zone is adequately remote from the pacemaker. A magnet can be placed over the pacemaker to deactivate rhythm sense function. The cardiac devices require formal resetting and checking following the RFA procedure.

Is Renal Cell Cancer Suited to Image-Guided Ablation?

Ignoring the specifics of renal tumors for one moment, we can consider which tumor characteristics imply suitability for image-guided ablation.

Given current RFA device capabilities, an ideal target tumor would be a well-defined, focal tumor of less than 4 cm in size. It should be targetable without critical intervening structures. The tumor should be surrounded by relatively thermally insensitive tissue so as to permit adequate thermal tumor destruction. Lastly, the target lesion itself should be amenable to thermal injury. T1a renal masses [6] fulfill all these physical criteria and are eminently suited to currently available devices and thereby image-guided thermal ablation (Box 46.1).

Box 46.1 Summary

An ideal target tumor would have the following characteristics:

- Well defined, less than 4 cm in size
- Amenable to thermal injury
- Targetable without critical intervening structures
- Surrounded by relatively thermally insensitive tissue

Treatment Trends

The first standardized, low-mortality nephrectomy technique was described by Robson as recently as 1969 [20]. With most other cancers, the intention is to remove the cancer and not the whole organ; however, radical nephrectomy has persisted as an oncologically effective operation due to the availability of a contralateral functioning kidney. Advanced patient age and renal impairment at time of diagnosis have increased the need to preserve functioning renal parenchyma, and thus, the partial nephrectomy was developed. In the1990s, Van Poppel et al. compared open partial renal resection with open radical nephrectomy [21] and confirmed the technical efficacy of partial resection, albeit with an increase in the complication rates. The oncological efficacy of partial nephrectomy was subsequently confirmed by Weight et al. who demonstrated 5-year overall survival rates of 95 % [22].

Laparoscopic partial nephrectomy is a technically demanding procedure occasionally requiring intracorporeal pelvicalyceal suturing. The procedure usually incurs some degree of warm ischemic injury by virtue of the necessity to clamp the renal hilum for the purposes of intraoperative hemostasis [23]. This can be

detrimental to the function of the remaining renal parenchyma and thereby overall renal function if it exceeds 20–30 min [24]. On the other hand, focal renal tumor ablation in patients with single kidneys has been reported to cause no significant functional renal injury [25].

Surgical resection is a well-established treatment which permits histological confirmation of complete tumor removal. Image-guided ablation is inherently an in situ tumor destruction process which relies upon subsequent radiological confirmation of treatment adequacy. Tumor ablation was first reported with an open and then laparoscopic approach using either heat coagulation in the form of radiofrequency ablation or cryotherapy [26]. As ablative probes became smaller, the percutaneous approach became increasingly feasible but highly dependent on accurate image guidance.

There are several advantages to image-guided ablation. Image-guided ablation uses rapid 3-D image reconstruction, usually CT, which can be supplemented with US or MRI, using image fusion technology. This imaging permits precise probe positioning and improves prediction of the ablation zone. From a patient point of view, the percutaneous approach has several advantages. It results in less postoperative pain, can, on occasion, be done with sedation if unable to tolerate a general anesthetic, and is even being performed in many centers as a day-case procedure [18].

In order for image-guided renal tumor ablation to achieve similar outcomes to resectional surgery, it requires precise probe placement or even multiple probe placements with a tolerance of +/−3 mm. This requires the patient to be very still, often for 90–120 min, lying in a prone or prone-oblique position. Although some centers have used RFA under heavy sedation in patients not suitable for general anesthesia, the risks of heavy sedation are often similar. The risks may even be increased as the airway is poorly controlled especially in the prone position with the stomach being compressed. These authors feel strongly that general anesthesia or intravenous (TIVA – total intravenous anesthesia) should be used as it allows complete control, with arrested ventilation permitting a largely stationary target with reproducible organ positioning. As yet, there have been no direct studies comparing general anesthesia to sedation because most centers use either one method or the other. There do not appear to be demonstrable differences in oncological outcome to date [18, 22, 27, 28].

Surgical resection of renal masses yields prognostically important histological information, including the resection margins. RFA cannot provide the physician with that immediate feedback and reassurance. RFA requires serial imaging to assess ablation zone shrinkage, to confirm accepted radiologic surrogates of complete treatment, and to look for tumor recurrence/margin regrowth. This all takes time. For RFA to become successful and widespread, there will have to be sufficient evidence of good long-term oncological outcomes and negligible late local recurrences comparable with the current very low rates of local recurrence after clear margin resectional surgery for small-volume disease.

Image Guidance

While US-guided renal tumor ablation is practiced without significant undertreatment compared to CT guidance [27], the authors feel strongly that US should at least be used in conjunction with CT for confirmation of accurate 3-dimensional probe position. However, in larger patients, US may not be well suited. Furthermore, the echogenic treatment response visualized at US may make it difficult to see the electrode if additional overlapping ablations are to be performed in larger tumors. Also multiprobe placement may be difficult with US as the US transducer may not be able to easily appreciate the position of multiple electrodes. Therefore, deployed electrode positioning is currently best confirmed by orthogonal CT/MRI reformatting. CT also permits careful assessment of tine position in the case of expandable probes. Importantly if all renal tumors are to be targeted, CT most easily allows for careful assessment of adjacent thermally sensitive structures such as colon, adrenal, and the renal hilum. The former can be displaced from the ablation zone by means of hydrodissection (see later).

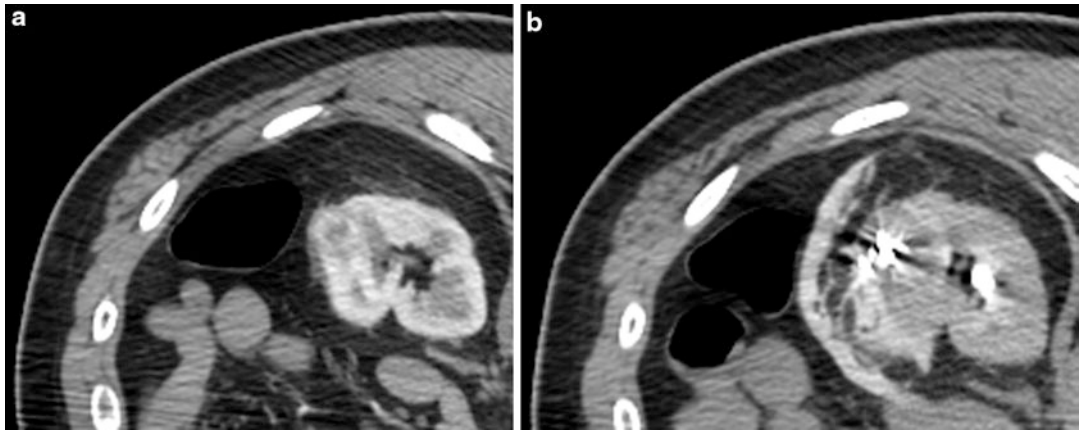

Fig. 46.3 (**a**) Exophytic renal tumor suitable for image-guided ablation but note the close proximity of the adjacent colon. (**b**) Hydrodissection fluid has been injected into the perirenal fat to displace the colon from the ablation zone. The addition of 2 % contrast to the hydrodissection fluid enhances visualization of the dissection process with regard to adjacent bowel, kidney, or even hematoma

Patient Positioning and Technique

To achieve accurate electrode position and therefore good outcomes, it is essential to make the electrode placement as straightforward as possible. Although there are software and technologies in development to dictate electrode position within a volume, most procedures are currently best carried out by a combination of US and CT or CT guidance alone. The patient should be placed in an optimized prone-oblique position, and the spine flexed over pillows (a nephrostomy-style position). This usually ensures that straightforward direct or minimally oblique intercostal puncture can be made to the tumor mass.

Even with the patient and electrodes positioned perfectly, there can be thermally sensitive tissue such as bowel adjacent to the renal mass especially in thinner patients. Laparoscopic ablation allows these tissues to be mechanically moved out of the ablation zone. RFA still requires these tissues to be moved, but this is achieved using fluid or gas (often carbon dioxide) injected into retroperitoneal fat planes to displace adjacent structures. The technique is widely known as "hydrodissection" [29]. The fluid used is typically 5 % dextrose solution, in order to prevent any aberrant electrical conduction. Two to three percent of intravenous iodinated contrast can be added to this fluid to facilitate assessment of the dispersal of the dissection fluid [30]. The ureteropelvic junction (UPJ) is thermally sensitive but cannot be easily displaced using hydrodissection. Tumors close to the collecting system and UPJ are increasingly being treated by RFA and cryoablation. In addition to seeking to displace structures, the ureter and collecting system can, to some extent, be protected if actively cooled. This can be achieved by means of the pressure-bagged circulation of chilled normal saline via a cystoscopically placed retrograde ureteric catheter with "piggy-backed" urethral catheter drainage [31]. There is some anecdotal evidence that this can reduce the risk of thermal injury but the operator should still pay careful attention to the likely ablation zone with particular reference to major vessels and the UPJ [32] (Fig. 46.3).

Renal artery or segmental renal artery embolization prior to RFA may have two potential benefits. Early animal models have shown increased ablation volume in pre-embolized renal tissue [33]. Practice suggests pre-embolization may reduce treatment bleeding and lead to a more effective ablation zone. Larger flowing vessels of greater than 3 mm can cause

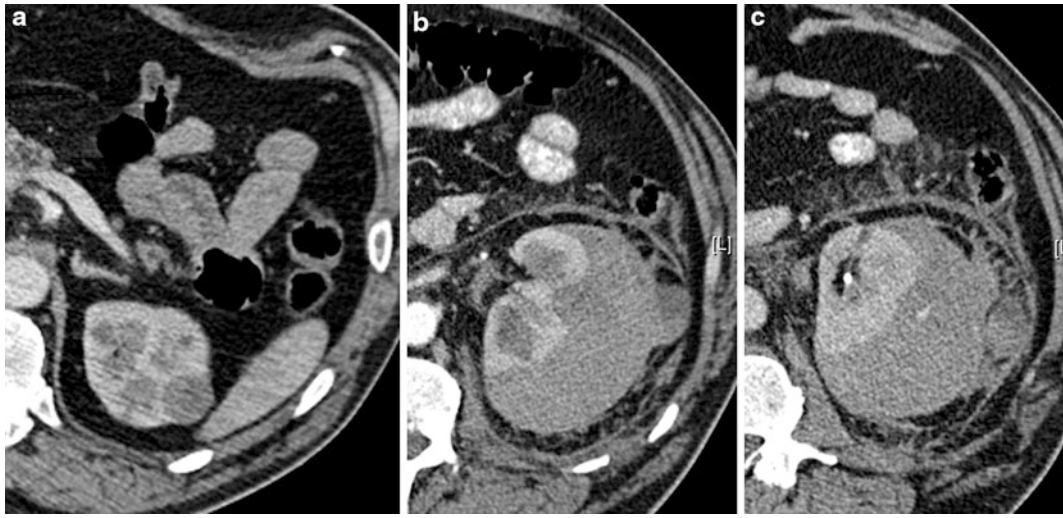

Fig. 46.4 (**a**) Small cortical renal mass; (**b**) post procedure, the patient became hypotensive with severe flank pain. Portal venous phase images show a large post-procedural renal capsular hematoma; (**c**) delayed phase images show a small pool of extravasated contrast. This was treated conservatively, but if it had been more brisk, it could have been embolized/coiled angiographically

a heat-sink effect which segmental pre-embolization may help diminish. However pre-embolization is not used routinely as it comes with its own risks including inadvertent renal and/or vascular injury (Fig. 46.4).

Minimizing Complications

The vascular nature of RCCs means any needling procedure carries a risk of bleeding. Pre-procedural checks should include any patient or family history of bleeding problems and any current medication. The authors' practice is to ensure the platelets are greater than 100 and INR equal to or less than 1.4 [27]. Minimizing the number of passes of the RF probe by using a combination of US and CT for placement, and as discussed earlier, reduces probe placements and the risk of obscuring hematoma. At the end of the procedure, RF-induced tumor coagulation and track ablation are thought to help reduce bleeding risk. Overall significant bleeding is seen in less than 1 % of patients [18] and is usually self-limiting.

Tumors in differing positions within the kidney require different strategies to prevent complication. During treatment of lower pole lesions, care must be taken to prevent injury to the ureteropelvic junction; this can be achieved by careful planning of the ablation zone but also ureteric cooling via ureteric catheters as described earlier. Despite these precautions authors have still reported a ureteral stricture rate of 2 % [18]. One should take similar precautions when dealing with lesions deep within the parenchyma and close to the collecting system to reduce the small risk of pelvicalyceal leak or urinoma, even though this has only been rarely reported. Upper pole lesions may be near the adrenal glands; even with the best ablation zone planning, it is essential to have good communication with the anesthetist who should watch for transient hypertension [34] and be prepared with hypotensive anesthesia. All anterior renal lesions bring the ablation zone near the small or large bowel. The authors currently prescribe an enema pre-procedure to help reduce colon loading and particularly gas. Even after the enema, it is often necessary to carefully consider the ablation zone and perform hydrodissection to displace the bowel in up to 50 % of cases in the authors' experience. Lesions lying anteriorly within the right kidney

need special consideration as the duodenum is often in close proximity. If suitable precautions are taken, the position of the lesion within the kidney does not affect the complication rate [18, 35, 36].

It is vital that the ablation process is performed in a sterile manner as post ablation, the tumor undergoes necrosis and becomes temporarily vulnerable to opportunistic infection, although this complication has been rarely reported without associated gut injury. It is important to ensure the patient is not systemically unwell pre-procedure and in particular does not have active urinary infection. Most authors use prophylactic antibiotics; the authors regime is 24 h of broad-spectrum intravenous antibiotic cover starting at induction (metronidazole 500 mg and cefuroxime 750 mg tds) followed by a 10-day course of oral antibiotics (ciprofloxacin 500 mg bd), although there is little evidence of an absolute requirement for this prophylactic cover.

Immediate Follow-Up

Diligent imaging follow-up of patients post RFA is the only way to ensure complete tumor treatment or to detect incomplete treatment. The first post-ablation imaging assessment is usually carried out at 24 h to 30 days after RFA. Immediate post-ablation CTs are reserved for those with a suspected acute complication and are less accurate in detecting undertreatment as an irregular margin of the ablation zone enhances acutely [37], and the ablation zone becomes better defined over the subsequent 3–14 days. CT densitometry – i.e., assessment of target tumor enhancement – remains central to the determination of treatment success and has been validated by several studies [38]. This is usually performed by careful volumetric CT comparison of unenhanced images with late arterial phase and to a lesser extent nephrographic phase images [39]. Subtotal treatments are usually manifest as marginal crescents or focal areas of persistent enhancement often at the peri-cortical or deep aspects of the tumor. Other CT features help to confirm treatment adequacy [39], a subjacent crescent or wedge of cortical coagulation usually signifies adequate treatment of the cortical margin, and over time a fibrotic halo is often seen (approximately 70 %) in the peri-renal fat and has been confirmed as a feature supporting complete treatment [40, 41] (Fig. 46.5).

In 1.9 % of patients, Lokken [42] described enhancing nodules along the ablation track post RFA which were concerning for track seeding. Some of these lesions were sampled and found to be inflammatory or a small abscess. All lesions subsequently became smaller or resolved completely. Lokken concluded that even though the imaging was initially suspicious for track seeding, the lesions should be biopsied and not diagnosed as tumor seeding which is rare especially with track ablation.

Long-Term Follow-Up Regimes

Radiofrequency-ablated tumors will often appear slightly enlarged at initial post-procedural imaging but do not enhance. The treated tumor slowly diminishes in size and exophytic tumors often "auto-amputate." In the case of RFA, the thermal scar can form a chronic granulomatous nodule and persist for years as a small, stable, and non-enhancing nodule. This is in contradistinction to cryoablation where the nodule appears to involute more quickly and often completely involutes over 2–3 years. In the case of renal failure, MR can be utilized to avoid the risk of contrast-induced nephropathy with attention to the relative risks of nephrogenic systemic fibrosis. Early studies [43] have suggested arterial spin labeling can identify viable tumor as well as contrast-enhanced MRI and may negate the need for IV contrast in future follow-up studies. In severe renal failure, GFR < 25 contrast-enhanced US can be utilized for follow-up. However, US contrast is not approved in the United States (Fig. 46.6).

A multicenter review concluded that follow-up in the first year should consist of imaging at 1, 3, and 12 months with most people also imaging at 6 months [37]. Follow-up regimes are currently

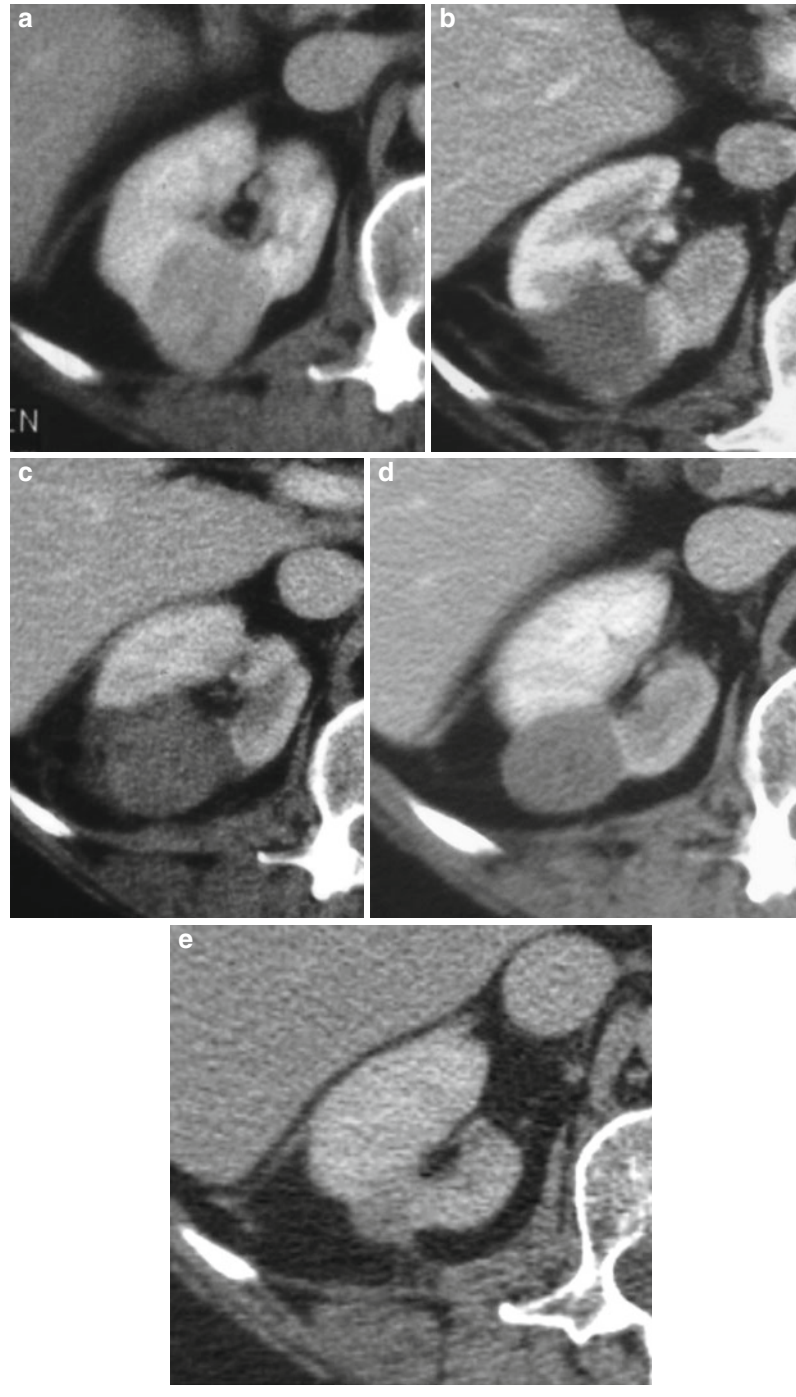

Fig. 46.5 (**a**) Lower pole RCC; (**b**) follow-up imaging after the first ablation, note the crescentic enhancement of local recurrence. (**c**) Immediate post re-ablation confirms subjacent crescent of cortical infarction, treatment margin; (**d**, **e**) longer-term follow-up shows non-enhancing ablation zone reducing in size

intense for the purposes of data collection and validation of RFA outcomes. Some published series have however noted [44] a small (3–4 %) but significant incidence of late local recurrence as late as 2–4 years after treatment. These recurrences are very uncommon and slow growing. As such most centers still perform at least annual imaging out to 5 years.

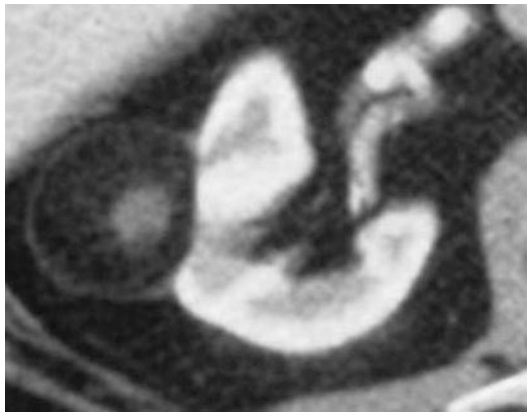

Fig. 46.6 Fibrotic halo with auto-amputated exophytic treated tumor

Radiologic and Oncologic Outcomes for Small Renal Tumors

Radiofrequency ablation (RFA) is a maturing technology, and undoubtedly the clinical effectiveness of these devices, in terms of lethal thermal ablation volumes, has improved significantly over the last 15 years. Similarly, as with any surgical techniques, there is a clearly identifiable learning curve with optimal outcomes dependent upon a standardized technique with appropriate treatment dosimetry and diligent imaging follow-up. Recent natural history papers [45] have also emphasized the relatively indolent growth pattern of many small, incidentally detected renal tumors in older patients, often meaning the growth rate at ~3 mm/year with a low metastatic potential.

It remains the case that some 20–30 % of renal tumors exhibit a significantly faster doubling time and therefore pose a higher risk of progression and metastasis [46]. The decision to treat must, however, be judged against the overall relatively slow growth of these often incidentally detected tumors.

Partial nephrectomy – laparoscopic or open – has been shown to achieve excellent 5- and 10-year cancer-specific survivals [47, 48]. However, given the low metastatic potential of sub-4 cm, T1a tumors, it can be difficult to demonstrate survival differences between treatment modalities. Studies will have to be adequately powered to detect these differences. The reported experience in the literature is confounded by a number of factors:

(a) Often single-center retrospective cases series
(b) Tendency toward biased case selection with percutaneous procedures reserved for patients with significant comorbidities
(c) Some centers comparing mixed modalities of treatment such as laparoscopic cryoablation (CRA) compared with percutaneous radiofrequency ablation (RFA)

For the purposes of this review, we have therefore drawn together larger, more substantial RFA case series and reported longer-term oncologic outcomes.

In 2005, Gervais et al. [28] reported their experience of 100 renal tumors treated by percutaneous, CT-guided RFA in 85 patients. The mean tumor size was 32 mm (90 % biopsy-proven renal cell carcinoma), and they were followed up for a mean of 28 months. Overall 90 % were completely ablated. Multivariate analysis found that small (<3 cm), exophytic tumors were straightforwardly treated but that larger (>3 cm), more deeply set tumors often required additional treatment sessions (Fig. 46.7).

A report by Park et al. [49] in 2006 reported on a mixed series of percutaneous and laparoscopic RFA in 78 patients with 94 tumors, with a mean size of 24 mm. Some 75 % of these tumors were biopsy-proven renal cancer, and the mean follow-up of this cohort was 25 months. The authors reported a cancer-specific survival rate of 98.5 % and an overall survival rate of 92.3 %. They concluded that RFA was comparable with traditional surgical resection for solitary renal masses.

A further large series by Zagoria et al. [18] reported CT-guided renal tumor RFA outcomes in 104 patients with 125 renal tumors. All were biopsy-proven RCC with a mean diameter of 27 mm and a mean follow-up of 13.8 months. Ninety three percent of these tumors were treated in a single session. On subgroup analysis, straightforward, single-session treatment occurred up to a threshold of 37 mm. Increasingly larger tumors resulted in higher level of subtotal treatment, with every 1 cm increase in size-decreasing tumor-free survival by a factor of 2.19.

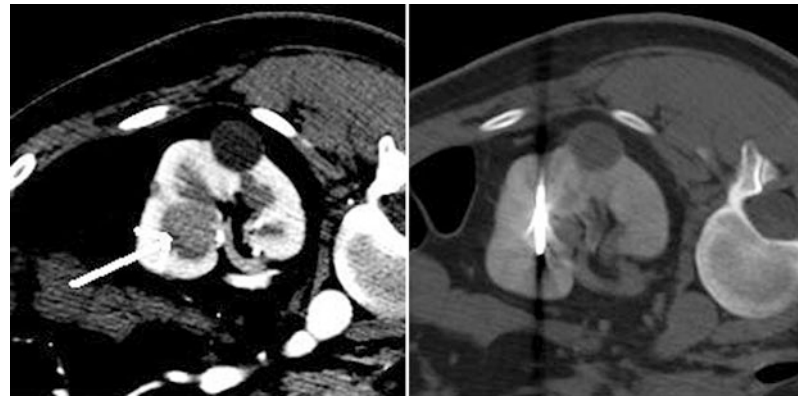

Fig. 46.7 Central renal tumor abutting the collecting system; here pyeloperfusion via a retrograde stent has been used to protect the collecting system/ureter

Breen et al. reported the technical outcomes from the RFA of 105 tumors in 97 patients with a mean tumor size of 32 mm and mean follow-up of 16.7 months [27]. The biopsy outcomes in this cohort were not detailed. They reported an overall technical success rate of 90.5 %, and again logistic regression analysis confirmed 37 mm as an important threshold for single-session treatment success (given technology present during the study period, 1999–2005).

A multicenter, collaborative study by Matin et al. reviewed the experience of seven institutions in terms of residual posttreatment and recurrent disease following percutaneous and laparoscopic radiofrequency and cryoablation of renal tumors [37]. (The cryoablation results are dealt with in a separate chapter). The authors chose to report together residual and recurrent disease rates akin to the practice in the liver of reporting "local tumor progression," making no distinction between primary subtotal treatment and late local recurrence. Of 616 patients treated, 63 patients were found to have residual/recurrent disease of which 8 had undergone cryoablation and 55 RFA. However, these combined cohorts obscured a significant bias with the vast majority of CRA cases performed via a laparoscopic approach and almost certainly the vast majority of those unsuitable for laparoscopic CRA being offered percutaneous RFA. Unfortunately, these selection biases plague the reported renal tumor ablation literature. Most incomplete treatments (70 %) were detected within the first three months – i.e., were likely reportable as primary "subtotal treatments."

Despite reasonable intermediate term results, the long-term oncologic outcome data for renal tumor RFA remains sparse. In 2005, the MGH Boston group reported the 5-year outcome of 16 patients following RFA for biopsy-proven RCC [50]. Five patients had died before completing 4 years of follow-up from unrelated causes. All except one tumor was completely ablated for a cancer-specific survival rate of 93.8 %.

The most substantive long-term data comes from Levinson et al. [44]. Thirty one patients with 34 tumors of between 1 and 4 cm (median 2 cm) were followed up for a mean of 61.6 months. One subtotal treatment was successfully retreated. There were three late local recurrences notably at 7, 13, and 31 months yielding an overall recurrence-free survival of 90.3 %. Of the 18 pathologically confirmed RCCs, the disease-specific, metastasis-free, and recurrence-free survivals were 100 %, 100 %, and 79.9 % at a mean of 57.4 months of follow-up.

Recent studies have continued to show consistent results. Tracy et al. [51] followed 160 patients who had RFA for biopsy-proven RCC for 5 years; their overall 5-year recurrence-free survival was 90 %. Zagoria et al. [36] followed up 41 patients with 48 RCCs; they found no recurrences in those tumors less than 4 cm at time of treatment and an overall 5-year recurrence-free survival of 88 %.

In summary, RFA appears to yield disease-specific survivals comparable with more onerous surgical resection. This is, however, a coarse

measure of outcome in a relatively indolent disease. Larger cohorts with longer follow-up after RFA are required to ensure there is not a small but significant incidence of unacceptable late local recurrence [44] which would question the oncological merit of even this minimally invasive intervention.

References

1. National Cancer Institute. Surveillance, epidemiology and end results. http://seer.cancer.gov. Accessed June 2010.
2. American Cancer Society. Facts and figures downloads. http://www.cancer.org. Accessed June 2010.
3. Chow W, Devesa S, et al. Rising incidence of renal cell cancer in the United States. JAMA. 1999;281:1628–31.
4. Jayson M, Sanders H. Increased incidence of serendipitously discovered renal cell carcinoma. Urology. 1998;51(2):203–5.
5. Quinn M, Babb P, et al. Cancer trends in England and Wales 1950–1999, National statistics. http://www.statistics.gov.uk/downloads/theme_health/cancertrends_5099.pdf. Accessed June 2010. or Vol. SMPS No. 66. 2001: TSO.
6. Adams KF, Leitzmann MF, Albanes D, et al. Body size and renal cell cancer incidence in a large US cohort study. Am J Epidemiol. 2008;168(3):268–77. Epub 9 Jun 2008.
7. Frank I, Blute M, Cheville J, et al. Solid renal tumors: an analysis of pathological features related to tumor size. J Urol. 2003;170(6 Pt 1):2217–20.
8. Bosniak MA, Birnbaum BA, Krinsky GA, Waisman J. Small renal parenchymal neoplasms: further observations on growth. Radiology. 1995;197(3):589–97.
9. Chawla SN, Crispen PL, Hanlon AL, Greenberg RE, Chen DY, Uzzo RG. The natural history of observed enhancing renal masses: meta-analysis and review of the world literature. J Urol. 2006;175(2):425–31.
10. Kunkle DA, Crispen PL, Chen DY, Greenberg RE, Uzzo RG. Enhancing renal masses with zero net growth during active surveillance. J Urol. 2007;177(3):849–53. discussion 853–4.
11. Cary KC, Sundaram CP. Watchful waiting in the treatment of the small renal mass. Indian J Urol. 2009;25(4):489–93.
12. Mattar K, Jewett MA. Watchful waiting for small renal masses. Curr Urol Rep. 2008;9(1):22–5.
13. Mues AC, Landman J. Small renal masses: current concepts regarding the natural history and reflections on the American Urological Association guidelines. Curr Opin Urol. 2010;20(2):105–10.
14. Dechet CB, Sebo T, Farrow G, Blute ML, Engen DE, Zincke H. Prospective analysis of intraoperative frozen needle biopsy of solid renal masses in adults. J Urol. 1999;162(4):1282–4. discussion 1284–5.
15. Beland MD, Mayo-Smith WW, Dupuy DE, Cronan JJ, DeLellis RA. Diagnostic yield of 58 consecutive imaging-guided biopsies of solid renal masses: should we biopsy all that are indeterminate? AJR. 2007;188:792–7.
16. Rybicki FJ, Shu KM, Cibas ES, Fielding JR, vanSonnenberg E, Silverman SG. Percutaneous biopsy of renal masses: sensitivity and negative predictive value stratified by clinical setting and size of masses. AJR Am J Roentgenol. 2003;180(5):1281–7.
17. Goldberg SN, Gazelle GS, Dawson SL, Rittman WJ, Mueller PR, Rosenthal DI. Tissue ablation with radiofrequency using multiprobe arrays. Acad Radiol. 1995;2(8):670–4.
18. Zagoria RJ, Traver MA, Werle DM, Perini M, Hayasaka S, Clark PE. Oncologic efficacy of CT-guided percutaneous radiofrequency ablation of renal cell carcinomas. AJR Am J Roentgenol. 2007;189(2):429–36.
19. Skonieczki BD, Wells C, Wasser EJ, Dupuy DE. Radiofrequency and microwave tumor ablation in patients with implanted cardiac devices: is it safe? Eur J Radiol. 2011;79(3):343–6. Epub ahead of print.
20. Robson CJ, Churchill BM, Anderson W. The results of radical nephrectomy for renal cell carcinoma. J Urol. 1969;101(3):297–301.
21. Van Poppel H, Bamelis B, Oyen R, Baert L. Partial nephrectomy for renal cell carcinoma can achieve long-term tumor control. J Urol. 1998;160(3 Pt 1):674–8.
22. Weight CJ, Lieser G, Larson BT, Gao T, Lane BR, Campbell SC, Gill IS, Novick AC, Fergany AF. Partial nephrectomy is associated with improved overall survival compared to radical nephrectomy in patients with unanticipated benign renal tumours. Eur Urol. 2010;58(2):293–8 [Epub ahead of print].
23. Marszalek M, Meixl H, Polajnar M, Rauchenwald M, Jeschke K, Madersbacher S. Laparoscopic and open partial nephrectomy: a matched-pair comparison of 200 patients. Eur Urol. 2009;55(5):1171–8. Epub 2009 Feb 20.
24. Thompson RH, Lane BR, Lohse CM, Leibovich BC, Fergany A, Frank I, Gill IS, Campbell SC, Blute ML. Comparison of warm ischemia versus no ischemia during partial nephrectomy on a solitary kidney. Eur Urol. 2010;58(3):331–6 [Epub].
25. Krambeck AE, Farrell MA, Callstrom MR, Atwell TD, Charboneau JW, Chow GK, Dimarco DS, Patterson DE. Radiofrequency ablation of renal tumors in the solitary kidney. Can J Urol. 2008;15(4):4163–8. discussion 4168.
26. Zlotta AR, Wildschutz T, Raviv G, Peny MO, van Gansbeke D, Noel JC, Schulman CC. Radiofrequency interstitial tumor ablation (RITA) is a possible new modality for treatment of renal cancer: ex vivo and in vivo experience. J Endourol. 1997;11(4):251–8.

27. Breen D, Rutherford E, Steadman B, et al. Management of renal tumours by image-guided radiofrequency ablation: experience in 105 tumours. CVIR. 2007;30:936–42.
28. Gervais DA, McGovern FJ, Arellano RS, McDougal WS, Mueller PR. Radiofrequency ablation of renal cell carcinoma: part 1, Indications, results, and role in patient management over a 6-year period and ablation of 100 tumors. AJR Am J Roentgenol. 2005;185(1):64–71.
29. Ginat DT, Saad WE. Bowel displacement and protection techniques during percutaneous renal tumor thermal ablation. Tech Vasc Interv Radiol. 2010;13(2): 66–74.
30. DeBenedectis CM, Beland MD, Dupuy DE, et al. Utility of iodinated contrast medium in hydrodissection fluid when performing renal tumor ablation. J Vasc Interv Radiol. 2010;21(5):745–7.
31. Cantwell CP, Wah TM, Gervais DA, Eisner BH, Arellano R, Uppot RN, Samir AE, Irving HC, McGovern F, Mueller PR. Protecting the ureter during radiofrequency ablation of renal cell cancer: a pilot study of retrograde pyeloperfusion with cooled dextrose 5 % in water. J Vasc Interv Radiol. 2008;19:1034–40.
32. Morales JP, Sabharwal T, Georganas M, Dourado R, Cahill D, Adam A. Cold saline irrigation of the renal pelvis during radiofrequency ablation of a central renal neoplasm: a case report. J Med Case Reports. 2008;2:40.
33. Sommer CM, Kortes N, Zelzer S, Arnegger FU, Stampfl U, Bellemann N, Gehrig T, Nickel F, Kenngott HG, Mogler C, Longerich T, Meinzer HP, Richter GM, Kauczor HU, Radeleff BA. Renal artery embolization combined with radiofrequency ablation in a porcine kidney model: effect of small and narrowly calibrated microparticles as embolization material on coagulation diameter, volume, and shape. Cardiovasc Intervent Radiol. 2011;34(1):156–65 [Epub].
34. Mayo-Smith WW, Dupuy DE, Parikh PM, Pezzullo JA, Cronan JJ. Imaging-guided percutaneous radiofrequency ablation of solid renal masses: techniques and outcomes of 38 treatment sessions in 32 consecutive patients. AJR. 2003;180(6):1503–8.
35. Atwell TD, Carter RE, Schmit GD, Carr CM, Boorjian SA, Curry TB, Thompson RH, Kurup AN, Weisbrod AJ, Chow GK, Leibovich BC, Callstrom MR, Patterson DE. Complications following 573 percutaneous renal radiofrequency and cryoablation procedures. J Vasc Interv Radiol. 2012;23(1):48–54.
36. Zagoria RJ, Pettus JA, Rogers M, Werle DM, Childs D, Leyendecker JR. Long-term outcomes after percutaneous radiofrequency ablation for renal cell carcinoma. Urology. 2011;77(6):1393–7.
37. Matin SF, Ahrar K, Cadeddu JA, Gervais DA, McGovern FJ, Zagoria RJ, Uzzo RG, Haaga J, Resnick MI, Kaouk J, Gill IS. Residual and recurrent disease following renal energy ablative therapy: a multi-institutional study. J Urol. 2006;176(5):1973–7.
38. Gervais DA, McGovern FJ, Wood BJ, et al. Radiofrequency ablation of renal cell carcinoma: early clinical experience. Radiology. 2000;217:665–72.
39. Rutherford EE, Cast JE, Breen DJ. Immediate and long-term CT appearances following radiofrequency ablation of renal tumours. Clin Radiol. 2008;63(2): 220–30. Epub 2007 Nov 7.
40. Davenport MS, Caoili EM, Cohan RH, Ellis JH, Higgins EJ, Willatt J, Fox GA. MRI and CT characteristics of successfully ablated renal masses: imaging surveillance after radiofrequency ablation. AJR Am J Roentgenol. 2009;192(6):1571–8.
41. Schirmang TC, Mayo-Smith WW, Dupuy DE, Beland MD, Grand DJ. Kidney neoplasms: renal halo sign after percutaneous radiofrequency ablation – incidence and clinical importance in 101 consecutive patients. Radiology. 2009;253:263–9.
42. Lokken RP, Gervais DA, Arellano RS, Tuncali K, Morrison PR, Tatli S, Mueller PR, Silverman SG. Inflammatory nodules mimic applicator track seeding after percutaneous ablation of renal tumors. AJR Am J Roentgenol. 2007;189:845–8.
43. Boss A, Martirosian P, Schraml C, Clasen S, Fenchel M, Anastasiadis A, Claussen CD, Pereira PL, Schick F. Morphological, contrast-enhanced and spin labeling perfusion imaging for monitoring of relapse after RF ablation of renal cell carcinomas. Eur Radiol. 2006;16(6):1226–36.
44. Levinson AW, Su LM, Agarwal D, Sroka M, Jarrett TW, Kavoussi LR, Solomon SB. Long-term oncological and overall outcomes of percutaneous radio frequency ablation in high risk surgical patients with a solitary small renal mass. J Urol. 2008;180(2): 499–504. discussion 504. Epub 2008 Jun 11.
45. Kunkle DA, Egleston RG. Excise, ablate or observe: the small renal mass dilemma – a meta-analysis and review. J Urol. 2008;179:1227–33.
46. Volpe A, Panzarella T, Rendon RA, Haider MA, Kondylis FI, Jewett MA. The natural history of incidentally detected small renal masses. Cancer. 2004;100:738.
47. Fergany AF, Hafez KS, Novick AC. Long-term results of nephron sparing surgery for localized renal cell carcinoma: 10-year follow up. J Urol. 2000;163(2): 442–5.
48. Aron M, Gill IS. Partial nephrectomy–why, when, how. . .? J Urol. 2008;179(3):811–2. Epub 2008 Jan 25.
49. Park S, Anderson JK, Matsumoto ED, et al. Radiofrequency ablation of renal tumours: intermediate-term results. J Endourol. 2006;20:569–73.
50. McDougal WS, Gervais DA, McGovern FJ, Mueller PR. Long-term follow up of patients with renal cell carcinoma treated with radiofrequency ablation with curative inter. J Urol. 2005;174:61–3.
51. Tracy CR, Raman JD, Donnally C, Trimmer CK, Cadeddu JA. Durable oncologic outcomes after radiofrequency ablation. Experience from treating 243 small renal masses over 7.5 years. Cancer. 2010;116(13):3135–42.

Percutaneous Renal Cryoablation

47

Thomas D. Atwell and Matthew Callstrom

Abstract

Percutaneous cryoablation is an evolving method of definitive renal mass treatment. With growing experience showing durability of treatment, cryoablation is a reasonable treatment option for an expanding patient population. In addition, large tumors may be treated using multiple cryoprobes. Patients may be treated under IV sedation, although general anesthesia may be more appropriate, particularly for larger tumors or technically complicated cases. Follow-up imaging is typically performed several times in the first 12 months following ablation and then every 6–12 months thereafter, depending on the tumor biology and other clinical indications. Outcomes following ablation have shown short- and midterm local control rates of about 95 %. Major complications are rare, occurring in about 5–7 % of patients.

Introduction

Since its original description in 1995 [1], percutaneous cryoablation has slowly evolved into an accepted treatment alternative in the management of renal masses. While early adoption by the surgical community validated the short-term efficacy of renal cryoablation, newer and thinner cryoprobes have allowed cryoablation to be performed percutaneously using image guidance.

T.D. Atwell (✉) • M. Callstrom
Department of Diagnostic Radiology, Mayo Clinic, Rochester, MN, USA
e-mail: atwell.thomas@mayo.edu; Callstrom.matthew@mayo.edu

Technique

Patient Selection

As any new treatment method is introduced, it is compared with a standard treatment until its efficacy is proven. In the case of percutaneous renal ablation, this standard has been surgical extirpation. Without proven durability of cryoablation in the treatment of renal neoplasms, this treatment has typically been reserved for those patients who were unable to undergo surgery. Historically, these patients include those with:

1. Advanced medical comorbidity that would place them at high risk of open surgery. Particularly in elderly patients, surgery carries a relatively high risk of morbidity and

D.E. Dupuy et al. (eds.), *Image-Guided Cancer Therapy*, DOI 10.1007/978-1-4419-0751-6_49,

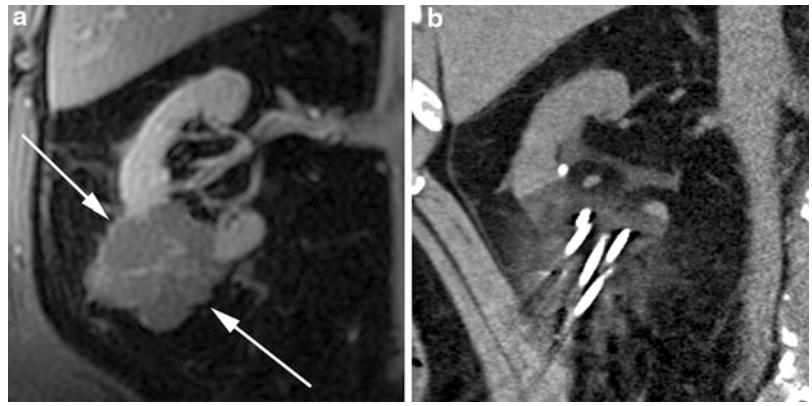

Fig. 47.1 Percutaneous cryoablation of large renal mass. (**a**) Coronal MRI following administration of gadolinium shows 6.0-cm mass in the right kidney (*arrows*), and (**b**) following placement of five cryoprobes, CT shows an ice-ball encompassing the tumor

mortality. One study demonstrated a 32 % complication rate following laparoscopic renal surgery in patients over the age of 80 years, including 8 % mortality [2]. This contrasts with published complication rates of 4–7 % in the percutaneous renal cryoablation experience, which has been biased toward the treatment of older patients [3–6].

2. Hereditary or other metachronous renal cell carcinoma (RCC). Patients with such conditions including von Hippel-Lindau, hereditary papillary renal cell carcinoma, and Birt-Hogg-Dube are at risk for the development of metachronous renal tumors. Initial surgical management of these patients is most appropriate, as it allows optimal debulking of tumor and full pathological evaluation of the tumor(s) for type, stage, and grade. However, repeat partial nephrectomy in these patients can be challenging, with a published major complication rate of 20 % and kidney loss in 6 % [7]. In these patients, ablation is an excellent treatment option with no technical regard to prior surgical intervention.

With increasing acceptance of percutaneous ablation as a viable treatment alternative, these indications are slowly expanding to include the more general patient population. The primary limitations of ablation at this point remain the lack of proven durability beyond 5 years after treatment and the reliance on needle biopsy and its inherent limitations for pathologic tumor evaluation.

Tumor Selection

Several tumor-specific factors need to be considered in assessing feasibility of cryoablation.

Size: In contrast to radiofrequency ablation (RFA), size has not been associated with failure following percutaneous renal cryoablation [8] (Fig. 47.1). Cryoablation allows simultaneous operation of multiple cryoprobes to generate large balls of lethal ice, at least 7 cm in diameter using eight cryoprobes [5]. In fact, too much confidence in cryoablation may lead to undertreatment of small tumors, where phantom studies and clinical experience have suggested that at least two cryoprobes should be used to treat tumors larger than 1 cm [9].

Location: The nonspecific nature of tumor ablation has resulted in some concern of collateral injury in the performance of renal cryoablation. This includes injury to the ureter resulting in stricture [5, 10], injury to the bowel resulting in abscess [6], and freezing of the adrenal gland causing hypertension [11]. Techniques to minimize such injuries include the following:

1. Hydrodisplacement, with injection of fluid to displace adjacent structures [12]
2. Probe retraction to manually pull tumor from adjacent structure [13]
3. Manual displacement of bowel using one's hand [14]

While described for renal RFA [15] and not specifically proven to be effective for cryoablation, a thin (5-French), externalized ureteral

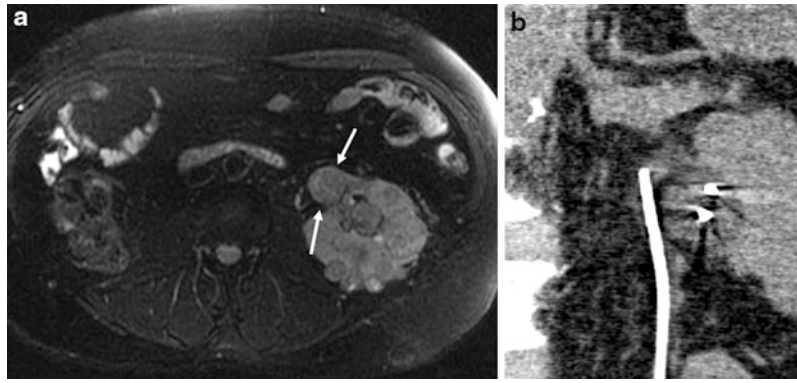

Fig. 47.2 Role of ureteral stent during cryoablation. 65-year-old male with multifocal RCC and prior nephrectomy. (**a**) Axial T2-weighted MRI shows numerous masses in the solitary left kidney, including a 2.8-cm mass medially (*arrows*); (**b**) coronal CT image obtained during cryoablation shows an externalized, irrigated (pyeloperfused) stent within the ureter, allowing the operator to optimally ablate the tumor and minimize urothelial injury. The stent was subsequently internalized and left in place for 6 weeks

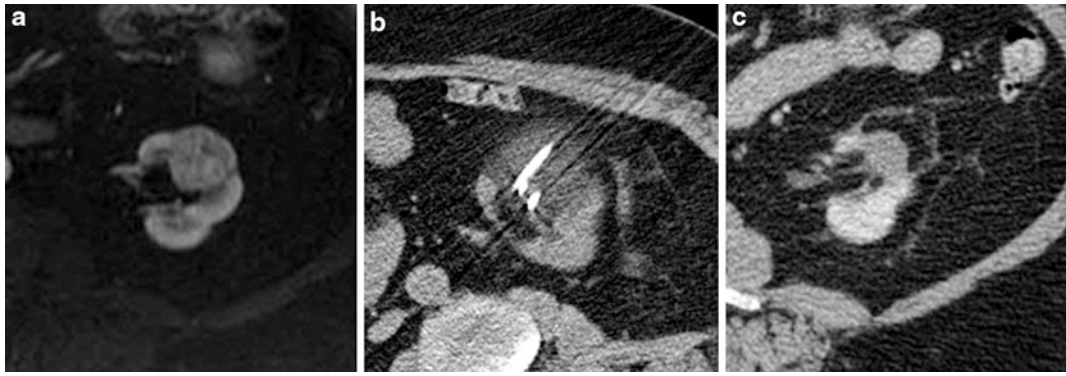

Fig. 47.3 Cryoablation of centrally located mass. (**a**) Contrast-enhanced CT image shows a 4.8-cm tumor in the left kidney with component of tumor extending to renal sinus fat; (**b**) axial CT image obtained at the time of cryoablation shows cryoprobes within the tumor adjacent ice; and (**c**) axial contrast-enhanced CT images obtained 21 months following ablation shows no evidence of recurrent tumor

stent can be placed prior to treatment of tumors located immediately adjacent to the ureter. Not only can this stent be used to irrigate the ureter with warm fluid (and theoretically minimize risk of ureteral injury), but the stent allows precise visualization of the ureter during cryoablation to monitor and limit ice involvement (Fig. 47.2).

Tumors located centrally within the kidney can also be effectively treated with cryoablation (Fig. 47.3). While such tumors have been prone to thermal sink effects with RFA with reduced local control rates [16, 17], accurate monitoring with CT allows confidence in treating tumor margins which extend centrally into the kidney, with success comparable to treatment of intraparenchymal and exophytic tumors [3]. Freezing of the intrarenal collecting system does not appear to result in significant urothelial injury [18]. However, placement of probes centrally into the kidney can result in significant hematuria, with clots resulting in ureteral obstruction.

Biopsy: The role of biopsy in guiding renal mass management is quite controversial. Two studies correlated core needle biopsy of resected renal tumors (i.e., biopsied under direct visualization following extirpation) with subsequent explanted tumor pathology. These studies showed both false negative and nondiagnostic rates

of 20 % [19, 20]. A third, similar study also correlated biopsy of the explanted tumor with ultimate tumor pathology [21]. Despite obtaining five core biopsy samples, the authors were only able to fully characterize tumor pathology in 64 % of cases. Based on these studies, some have been reluctant to use biopsy results to guide tumor management [3–5, 22].

However, it is important to recognize the significant number of benign tumors that exist in patients treated with ablation. It is recognized that 18–25 % of renal masses smaller than 3 cm are benign [23, 24]. It is this same population of tumors that is most frequently treated with ablation. Accordingly, many would argue that treatment in these patients is unnecessary and could be prevented by biopsy prior to ablation [25, 26]. At this time, the role of biopsy in guiding treatment remains based on individual practice patterns.

Pre-ablation Assessment

General considerations immediately prior to treatment include both patient- and tumor-specific characteristics.

Patient: Appropriate coagulation screening labs should be obtained on any patient to be treated with cryoablation. Generally accepted thresholds for treatment include a platelet count of greater than 50,000/L and international normalized ratio (INR) of less than 1.6. Careful attention should be paid to the hemoglobin concentration; some degree of bleeding is common following cryoablation, and if the patient has preexisting anemia, the threshold for pre-procedural blood matching (i.e., type cross) should be lower. Antiplatelet agents such as aspirin and clopidogrel should be held for 7–10 days prior to treatment.

Tumor: Pre-ablative embolization of larger tumors may decrease bleeding during ablation and contribute to local control [27]. Additional adjunctive techniques for the cryoablation should be anticipated, including hydrodisplacement, ureteral stent placement, and need for arterial blood pressure monitoring (particularly for tumors near the adrenal gland). One should recognize potential changes in tumor position relative to other structures when the patient is placed in the decubitus or prone position.

Anesthesia

The level of anesthesia varies among different practices. Compared to RFA, there is less pain associated with cryoablation, requiring diminished levels of analgesia [28]. Accordingly, at some institutions, conscious/moderate sedation has been shown to be sufficient in performing cryoablation [4]. Other ablation centers have elected to perform renal cryoablation under general anesthetic, maximizing patient tolerance of the exam (both psychologically and hemodynamically) and, potentially, optimizing treatment outcome [29].

Probe Placement

The number of cryoprobes placed depends on tumor size and geometry. The operator needs to consider the ice-ball morphology and anticipated lethal isotherms of the given cryoprobe in planning for the ablation. Larger tumors require a greater number of cryoprobes (Fig. 47.4).

Cryoprobes are placed using image guidance. Such imaging includes ultrasound, CT, or MRI, with the latter being reserved for highly specialized practices. Advantages of ultrasound include real-time visualization of probe placement within the tumor and lack of ionizing radiation. CT allows a greater perspective of tumor and probe relationships to other adjacent structures. For many users, placement under CT guidance is much faster and efficient.

Cryoablation

Freezing a tumor twice has been shown to be more effective in achieving tumor death than a single freeze event; in an animal study, a double-freeze cycle produced significantly

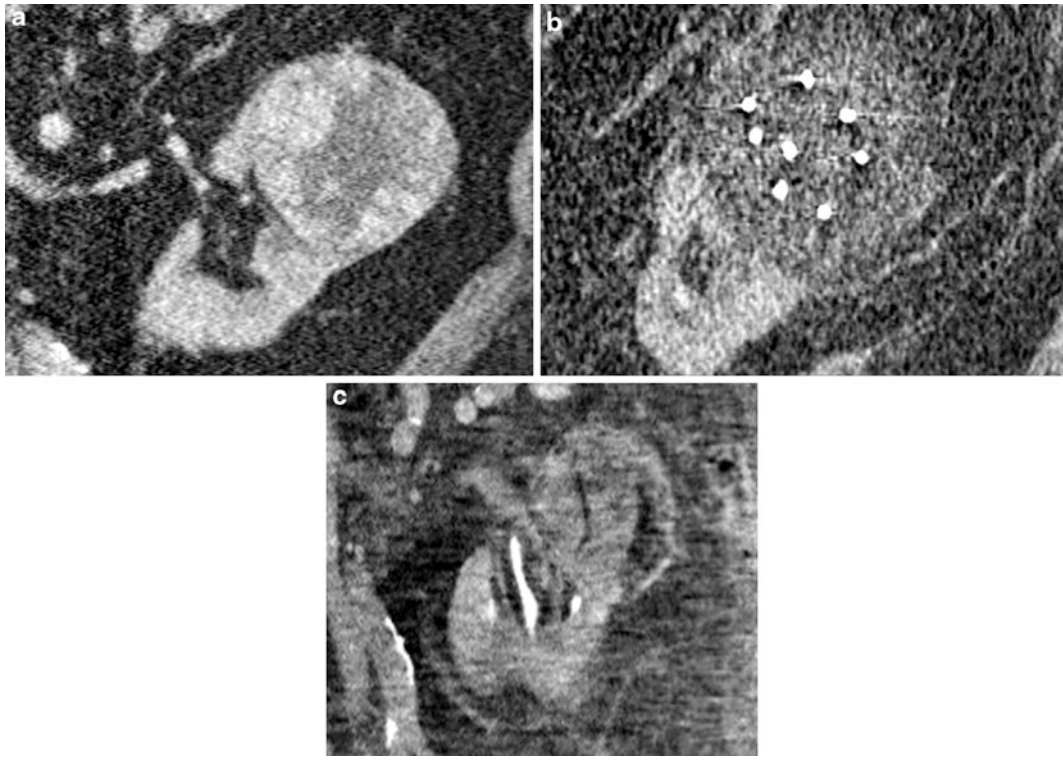

Fig. 47.4 Multiple cryoprobes in the treatment of a large renal mass. (**a**) Coronally reconstructed contrast-enhanced CT image shows a 6.1-cm mass in the upper pole of the left kidney; (**b**) coronally reconstructed image shows eight cryoprobes with the tumor. Note bias of probes toward the renal vasculature side of the tumor, where thermal sink effects are greatest; (**c**) coronally reconstructed CT image with delayed enhancement 14 months following ablation shows involuting ablation defect with no recurrent tumor

larger areas of necrosis [30]. This is likely related to the combination of both slow and fast cooling rates, which have been shown to be critical in the role of cryoinjury [31]. In addition, small vessel thrombosis during the first freeze may reduce thermal sink effects during the second ablation, allowing more ice to form.

Monitoring

Cryoablation is unique to other ablation modalities in the ability to easily monitor the ablation process with standard imaging, including CT, ultrasound, and MRI. Using CT, the leading edge of ice has been shown to represent 0 degrees Celsius (°C) [32]. The leading edge of ice is also clearly visualized with MRI. Both CT and MRI have a notable advantage over ultrasound in the ability to image all margins of the ice ball, whereas ultrasound is only able to demonstrate the leading edge of ice; as such, the role of ultrasound in monitoring cryoablation remains limited.

An important drawback of CT is the radiation associated with monitoring. With aggressive, frequent CT monitoring, radiation doses can quickly escalate. Accordingly, the operator may choose to adjust CT technique to minimize radiation dose yet maintain images of sufficient quality to allow monitoring of ice-ball growth.

Using CT monitoring, the historical goal of renal cryoablation was to extend the ice at least 3 mm beyond the tumor margin. This was based on two studies showing that temperatures below −20 °C are required to achieve complete uniform ablation in renal tissue [33] and that this −20 °C-isotherm occurs 3 mm inside the

outer ice-ball margin in renal parenchyma [34]. More recently, using a −30 °C isotherm for presumed complete necrosis, Littrup et al. showed that lethal ice existed as much as 1 cm within the ice-ball margin [9]. There is likely some variation among the type of cryoprobes used, and one should be aware of specific isotherms for the device that they are using.

Follow-Up Imaging

A CT or MRI is typically obtained within 24 h following cryoablation, ideally performed with intravenous contrast. This allows the following: (1) an assessment of the completeness of ablation, with an ablation defect encompassing the index tumor; (2) an identification of any potential acute complications, such as bleeding; and (3) a baseline for future imaging.

In defining outcomes following ablation, specific terms have been applied [35]. The original Image-Guided Tumor Ablation Working Group defined "technical success" as treatment of the tumor according to protocol and complete coverage of the tumor by the ablation [35, 36]. This contrasts with the group's definition of "technique effectiveness," which is the lack of tumor recurrence (based on imaging) within an undefined period of time. As most recurrences are identified within 3 months, a more recent paper suggested that residual disease be defined as that detected within 3 months and recurrent disease defined as that detected later [37]. Such discrepancies have complicated the reporting of outcomes following ablation, particularly in comparing results with other treatment methods, as treatment success is binary (i.e., was the initial treatment successful?). In comparing surgical outcomes with ablation, a published clinical guideline from the American Urological Association elected to adopt such a binary method for ablation success, recognizing the opportunity for re-treatment [38].

Imaging 3 months following ablation is performed to detect residual tumor and allows potential, timely re-treatment. Subsequent surveillance imaging is typically performed at 6- or 12-month intervals following treatment, largely due to the uncertain durability of ablation treatment. In the surgical patient, follow-up in intermediate- and high-risk patients is typically maintained for 10 years [39]; one would assume that a similar duration would be reasonable after renal ablation until long-term efficacy is proven.

Cell lysis typically results in considerable absorption of the cryoablation defect over time, with the cryoablation defect involuting over the course of a few years (Fig. 47.4). Littrup et al. showed the ablation site to contract to about 50 % of its original size at 6 months and 66 % at $\geq$ 24 months [5]. Calcifications may also develop at the ablation site, possibly due to fat necrosis.

Residual/recurrent tumor manifests as new nodular areas of enhancement, typically at the tumor margin, or as enlargement of the ablation site (Fig. 47.5). Occasionally, intratumoral enhancement may be seen with MRI, which decreases over 6–9 months [40].

Surveillance imaging after ablation may be confounded in the patient with renal insufficiency or allergy which precludes the use of intravenous CT or MRI contrast. In this situation, progressive retraction of the ablation site is a marker for successful treatment; enlargement of the ablation site should indicate recurrent tumor.

Percutaneous Cryoablation Outcomes

Since its initial description in 1995 [1], several retrospective studies have shown favorable short- and midterm outcomes following percutaneous cryoablation (Table 47.1). Generally, local tumor control is achieved in 90–95 % of cases (Fig. 47.6). Recent data shows that tumor size does not appear to be a significant risk factor for tumor recurrence [45].

While the results are encouraging, the limited duration of follow-up is as much proof of feasibility as durability. Fortunately, long-term ($\geq$3 years) local control following laparoscopic cryoablation has been achieved in 88–96 % of tumors [46, 47], thus adding validation to cryoablation as a durable treatment modality. Such long-term results after percutaneous cryoablation have yet to be published.

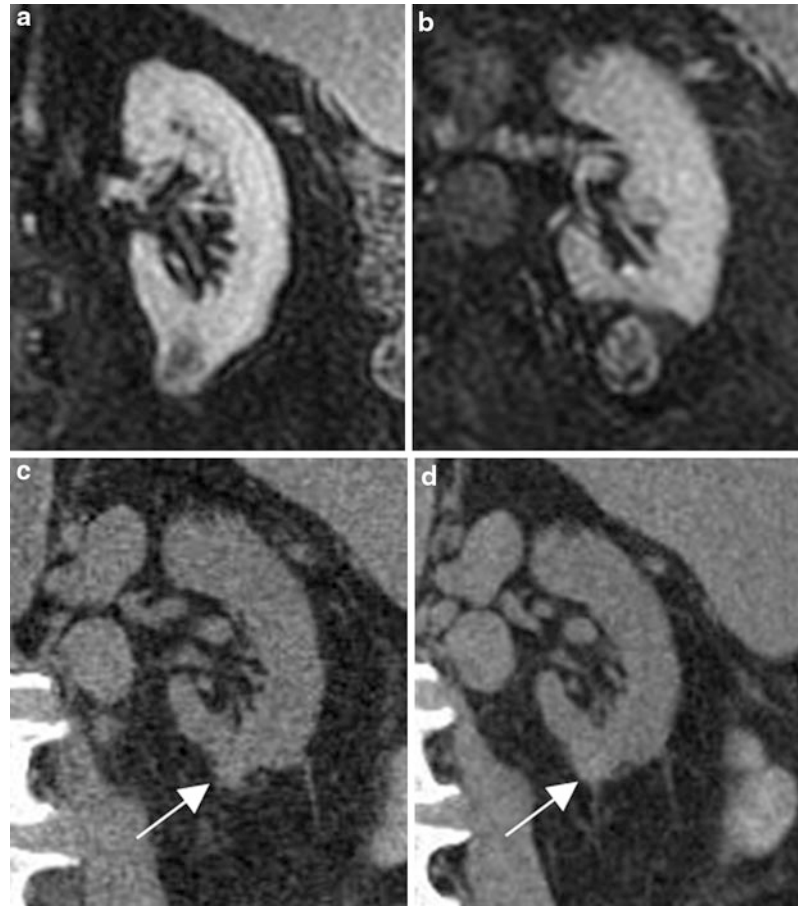

Fig. 47.5 Local progression of RCC following cryoablation. Patient had known leukemia and associated adenopathy. (**a**) Coronal contrast-enhanced MRI shows a 2.1-cm mass in the lower pole of the left kidney; (**b**) coronal contrast-enhanced MRI obtained immediately following ablation using a single cryoprobe shows an ablation defect which encompasses the tumor; (**c**) coronally reconstructed CT image without contrast (due to renal insufficiency) 12 months following ablation shows a contracting ablation defect (*arrow*); and (**d**) coronally reformatted CT image without contrast 14 months following ablation shows enlargement of the ablation defect (*arrow*), consistent with tumor recurrence. Subsequent biopsy confirmed recurrent clear cell RCC

Table 47.1 Percutaneous cryoablation outcomes – select literature

	Year	# Tumors with follow-up	Mean tumor size (cm)	Mean follow-up (mo)	Local control (%)[a]
Shingleton et al. [41]	2001	22	3.2	9	21/22 (95)
Silverman et al. [6]	2005	26	2.6	14	23/26 (88)
Gupta et al. [4]	2006	16	2.4	6	15/16 (94)
Littrup et al. [5]	2007	36	3.3	19	33/36 (92)
Bandi et al. [42]	2007	20	2.2	12	18/20 (90)
Georgiades et al. [43]	2010	81	2.7	17	79/81 (98)
Atwell et al. [44]	2010	93	3.4	26	88/93 (95)

[a]Excluding re-treatments

Complications from Percutaneous Cryoablation

Major complications following percutaneous cryoablation are infrequent, occurring in about 6 % of patients (Table 47.2). Hemorrhage accounts for half of the major published complications, occurring in about 3 % of patients. This may be related to the large size of the cryoprobes, typically measuring 1.5–2.4 mm in outer diameter (17–13 gauge) and the use of multiple probes in tumor treatment. In addition, compromised hemostasis at cold temperatures is a recognized

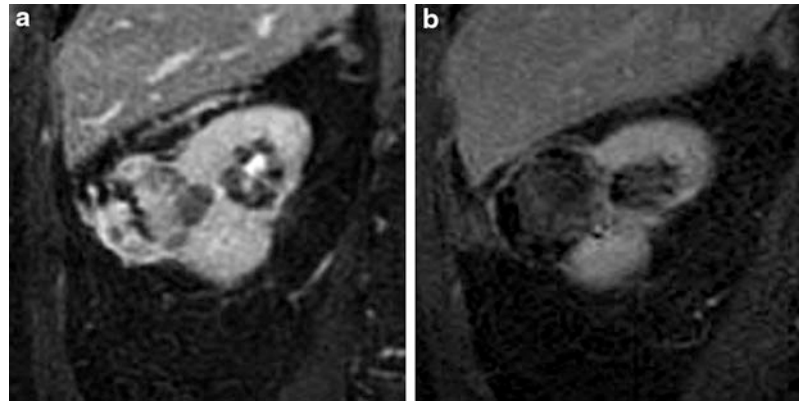

Fig. 47.6 Extended follow-up following cryoablation. (**a**) Coronal MRI following administration of intravenous gadolinium shows a 5.4-cm mass in the right kidney. Biopsy confirmed RCC. (**b**) Enhanced coronal MRI 40 months following ablation shows no recurrent tumor

Table 47.2 Percutaneous cryoablation complications – select literature

	Year	Procedures	Major complication rate (%)[a]
Shingleton et al. [41]	2001	20	1/20 (5)
Silverman et al. [6]	2005	27	2/27 (7)
Gupta et al. [4]	2006	20	1/20 (5)
Littrup et al. [5]	2007	49	3/49 (6)
Bandi et al. [42]	2007	20	0/20 (0)[b]
Atwell et al. [3]	2008	113	7/113 (6)
Georgiades et al. [43]	2010	117	5/117 (4)

[a]≥Grade 3 CTCAE
[b]Neuralgia excluded (insufficient detail to grade using CTCAE)

phenomenon [48] and probably accounts for some level of bleeding tendency during cryoablation. Gross hematuria requiring stent placement can also occur; in select cases, prophylactic ureteral stenting of the solitary kidney prior to cryoablation may be reasonable, particularly for central tumors.

Other complications directly related to ablation may include nerve injury resulting in neuralgia, adjacent organ injury (especially bowel), and infection [6, 43]. Ureteral injury resulting in stricture is exceptionally rare [5, 10].

Cross-References

- Chemotherapy, Targeted Therapies, and Biological Therapies for Renal Cell Carcinoma
- Cryoablation
- Image-Guided Radiation Therapy for Renal Cell Carcinoma
- Image-Guided Radio Frequency Ablation of Renal Cancer
- Surgical Approaches to Treatment of Renal Cell Carcinoma

References

1. Uchida M, et al. Percutaneous cryosurgery for renal tumours. Br J Urol. 1995;75(2):132–6. discussion 136–7.
2. Magrill D, et al. Laparoscopy extirpative renal surgery in the octogenarian population. J Endourol. 2009;23 (9):1499–502.
3. Atwell TD, et al. Percutaneous renal cryoablation: experience treating 115 tumors. J Urol. 2008;179(6): 2136–40. discussion 2140–1.
4. Gupta A, et al. Computerized tomography guided percutaneous renal cryoablation with the patient under conscious sedation: initial clinical experience. J Urol. 2006;175(2):447–52. discussion 452–3.
5. Littrup PJ, et al. CT-guided percutaneous cryotherapy of renal masses. J Vasc Interv Radiol. 2007;18(3):383–92.
6. Silverman SG, et al. Renal tumors: MR imaging-guided percutaneous cryotherapy–initial experience in 23 patients. Radiology. 2005;236(2):716–24.

7. Johnson A, et al. Feasibility and outcomes of repeat partial nephrectomy. J Urol. 2008;180(1):89–93. discussion 93.
8. Atwell TD, et al. Percutaneous cryoablation of large renal masses: technical feasibility and short-term outcome. AJR Am J Roentgenol. 2007;188(5):1195–200.
9. Littrup PJ, et al. Lethal isotherms of cryoablation in a phantom study: effects of heat load, probe size, and number. J Vasc Interv Radiol. 2009;20(10): 1343–51.
10. Bagley DH, et al. Cryosurgery of the ureter in dogs. Invest Urol. 1976;14(3):241–5.
11. Atwell TD, et al. Malignant hypertension during cryoablation of an adrenal gland tumor. J Vasc Interv Radiol. 2006;17(3):573–5.
12. Bodily KD, et al. Hydrodisplacement in the percutaneous cryoablation of 50 renal tumors. AJR Am J Roentgenol. 2010;194(3):779–83.
13. Froemming A, et al. Probe retraction during renal tumor cryoablation: a technique to minimize direct ureteral injury. J Vasc Interv Radiol. 2010;21(1): 148–51.
14. Tuncali K, et al. MRI-guided percutaneous cryoablation of renal tumors: use of external manual displacement of adjacent bowel loops. Eur J Radiol. 2006;59(2):198–202.
15. Wah TM, et al. Radiofrequency ablation of a central renal tumor: protection of the collecting system with a retrograde cold dextrose pyeloperfusion technique. J Vasc Interv Radiol. 2005;16(11): 1551–5.
16. Gervais DA, et al. Radiofrequency ablation of renal cell carcinoma: part 1, Indications, results, and role in patient management over a 6-year period and ablation of 100 tumors. AJR Am J Roentgenol. 2005;185(1):64–71.
17. Varkarakis IM, et al. Percutaneous radio frequency ablation of renal masses: results at a 2-year mean followup. J Urol. 2005;174(2):456–60. discussion 460.
18. Warlick CA, et al. Clinical sequelae of radiographic iceball involvement of collecting system during computed tomography-guided percutaneous renal tumor cryoablation. Urology. 2006;67(5): 918–22.
19. Dechet CB, et al. Prospective analysis of intraoperative frozen needle biopsy of solid renal masses in adults. J Urol. 1999;162(4):1282–4. discussion 1284–5.
20. Dechet CB, et al. Prospective analysis of computerized tomography and needle biopsy with permanent sectioning to determine the nature of solid renal masses in adults. J Urol. 2003;169(1):71–4.
21. Wunderlich H, et al. The accuracy of 250 fine needle biopsies of renal tumors. J Urol. 2005;174(1): 44–6.
22. Heilbrun ME, et al. CT-guided biopsy for the diagnosis of renal tumors before treatment with percutaneous ablation. AJR Am J Roentgenol. 2007;188(6):1500–5.
23. Frank I, et al. Solid renal tumors: an analysis of pathological features related to tumor size. J Urol. 2003;170(6 Pt 1):2217–20.
24. Thompson RH, et al. Tumor size is associated with malignant potential in renal cell carcinoma cases. J Urol. 2009;181(5):2033–6.
25. Silverman SG, et al. Renal masses in the adult patient: the role of percutaneous biopsy. Radiology. 2006;240(1):6–22.
26. Beland MD, et al. Diagnostic yield of 58 consecutive imaging-guided biopsies of solid renal masses: should we biopsy all that are indeterminate? AJR Am J Roentgenol. 2007;188(3):792–7.
27. Woodrum DA, et al. Role of intraarterial embolization before cryoablation of large renal tumors: a pilot study. J Vasc Interv Radiol. 2010;21(6):930–6.
28. Allaf ME, et al. Pain control requirements for percutaneous ablation of renal tumors: cryoablation versus radiofrequency ablation–initial observations. Radiology. 2005;237(1):366–70.
29. Gupta A, et al. General anesthesia and contrast-enhanced computed tomography to optimize renal percutaneous radiofrequency ablation: multi-institutional intermediate-term results. J Endourol. 2009;23(7):1099–105.
30. Woolley ML, et al. Effect of freezing parameters (freeze cycle and thaw process) on tissue destruction following renal cryoablation. J Endourol. 2002; 16(7):519–22.
31. Hoffmann NE, Bischof JC. The cryobiology of cryosurgical injury. Urology. 2002;60(2 Suppl 1): 40–9.
32. Saliken JC, McKinnon JG, Gray R. CT for monitoring cryotherapy. AJR Am J Roentgenol. 1996;166 (4):853–5.
33. Chosy SG, et al. Monitoring renal cryosurgery: predictors of tissue necrosis in swine. J Urol. 1998;159(4):1370–4.
34. Campbell SC, et al. Renal cryosurgery: experimental evaluation of treatment parameters. Urology. 1998;52(1):29–33. discussion 33–4.
35. Goldberg SN, et al. Image-guided tumor ablation: standardization of terminology and reporting criteria. Radiology. 2005;235(3):728–39.
36. Goldberg SN, et al. Image-guided tumor ablation: proposal for standardization of terms and reporting criteria. Radiology. 2003;228(2):335–45.
37. Matin SF, et al. Residual and recurrent disease following renal energy ablative therapy: a multi-institutional study. J Urol. 2006;176(5):1973–7.
38. Campbell SC, et al. Guideline for management of the clinical T1 renal mass. J Urol. 2009; 182(4):1271–9.
39. Chin AI, et al. Surveillance strategies for renal cell carcinoma patients following nephrectomy. Rev Urol. 2006;8(1):1–7.

40. Porter CA, et al. MRI after technically successful renal cryoablation: early contrast enhancement as a common finding. AJR Am J Roentgenol. 2010; 194(3):790–3.
41. Shingleton WB, Sewell Jr PE. Percutaneous renal tumor cryoablation with magnetic resonance imaging guidance. J Urol. 2001;165(3):773–6.
42. Bandi G, et al. Cryoablation of small renal masses: assessment of the outcome at one institution. BJU Int. 2007;100(4):798–801.
43. Rodriguez R, et al. Prospective analysis of the safetyand efficacy of percutaneous cryoablation for pT1NxMx biopsy-proven renal cell carcinoma. Cardiovasc Intervent Radiol. 2011;34(3):573–8.
44. Atwell TD, et al. Percutaneous renal cryoablation: Local control at mean 26 months of followup. J Urol. 2010;184(4):1291–5.
45. Schmit GD, et al. Percutaneous cryoablation of renal masses > or=3 cm: efficacy and safety in treatment of 108 patients. J Endourol. 2010;24(8):1255–62.
46. Davol PE, Fulmer BR, Rukstalis DB. Long-term results of cryoablation for renal cancer and complex renal masses. Urology. 2006;68(1 Suppl):2–6.
47. Gill IS, et al. Renal cryoablation: outcome at 3 years. J Urol. 2005;173(6):1903–7.
48. Sutor AH, Bowie EJ, Owen Jr CA. Effect of temperature on hemostasis: a cold-tolerance test. Blut. 1971;22(1):27–34.

Image-Guided Radiation Therapy for Renal Cell Carcinoma

48

Ying Li, Gregory P. Swanson, and Chul S. Ha

Abstract

The role of radiotherapy in treating renal cell carcinoma (RCC) was thought to be limited for several reasons. RCC was considered to be radioresistant, and clinical data on preoperative or postoperative radiotherapy did not show significant benefits. In recent years, stereotactic body radiation therapy (SBRT) using image guidance has emerged as a favorable radiation technique in treating RCC. This chapter reviews the radiobiology of RCC and clinical experience with hypofractionated radiotherapy and SBRT in palliating metastatic RCC and definitively treating primary RCC.

Introduction

Renal cell carcinoma (RCC) is the third most common genitourinary malignancy (after prostate and bladder cancer), comprising approximately 2–3 % of all malignancies. It is estimated that 64,770 Americans will be diagnosed with renal cancer and 13,570 will die of this disease in the United States in 2012. Approximately 90 % of the renal tumors are RCC, and 85 % of these are clear cell tumors [1]. In the past 65 years, the rate of RCC has increased by 2 % per year. Although the reason for this increase is unknown, it could be in part due to better detection through more frequent use of imaging studies and newer imaging techniques [2], as the majority of all renal cancers are discovered incidentally [3].

Surgical resection remains a mainstay of therapy for localized RCC. Other than total nephrectomy, for small tumors, nephron-sparing surgeries such as partial nephrectomy, radiofrequency ablation, and cryotherapy have become increasingly favorable. Different from these invasive or minimally invasive surgeries, stereotactic body radiotherapy (SBRT) using image guidance shows potential as a noninvasive alternative in patients that are medically inoperable or with poor renal function or single kidney.

The benefit of radiotherapy in treating locally advanced renal cell carcinoma has been debated. Some early studies showed that preoperative

Y. Li (✉)
Department of Radiation Oncology, University of Texas Health Science Center at San Antonio, San Antonio, TX, USA
e-mail: liy8@uthscsa.edu

G.P. Swanson • C.S. Ha
Department of Radiation Oncology, Cancer Therapy and Research Center at the University of Texas Health Science Center, San Antonio, TX, USA
e-mail: swansong@uthscsa.edu; hac@uthscsa.edu

D.E. Dupuy et al. (eds.), *Image-Guided Cancer Therapy*, DOI 10.1007/978-1-4419-0751-6_50,

radiotherapy improves survival [4]. However, other series reported high complication rates, which limited the application of preoperative radiotherapy [5, 6]. There is no benefit of adjuvant treatment to tumor bed after nephrectomy using conventional fractionated radiotherapy [7]. It should be noted that those early studies used conventional radiation techniques with suboptimal sparing of normal tissues.

Radiobiological Consideration in Treating RCC

Although the current dogma is that renal cell cancer is a radioresistant tumor, this impression is not uniform or totally supported by the literature. In an early article on the subject, Waters [8] found hypernephroma (renal cell cancer) to be radiosensitive, and he was an advocate of preoperative radiation to improve operability. He did note that renal cancers show a "considerable variation in the rapidity and degree of response." Subsequent retrospective reviews seemed to support this observation, and in addition, a series of retrospective studies in the 1950s and 1960s strongly suggested a benefit to postoperative radiation. This was considered significant given the likely case selection where only the worst cases were referred for radiation [9]. In spite of these studies that suggested a benefit to pre- and postoperative radiation (i.e., this is a radiosensitive cancer), by the 1970s, the general impression was that carcinoma of the kidney is highly radioresistant. This is probably due to Water's observation that these tumors do not uniformly shrink or can take several months to do so [10]. The observation was also made that the lack of a dramatic response is partially due to having to underdose primary kidney tumors in deference to the radiosensitivity of neighboring structures (i.e., bowel and liver) [11]. Based on the retrospective data, a series of small randomized studies were undertaken to determine the role of preoperative radiation therapy. The radiation doses were modest by today's standards and delivered with nonconformal techniques, often at low energies. Although they were probably not powered to demonstrate this definitively, some seemed to show improved clinical local control (remember that these studies were done in the pre-CT era) and even a decrease in metastasis [12] in the radiation groups. They were uniform in their finding that radiation offered no survival advantage [12, 13]. The use of postoperative radiation was not studied as extensively, but as noted above [9], some early retrospective data appeared promising. Unfortunately, the findings were not uniformly positive [14, 15] although more contemporary data [16, 17] again suggest that there might not only be a local control benefit but a survival benefit. What really curtailed the subsequent evolution of radiation therapy in the neoadjuvant and adjuvant setting was the finding that some patients died of radiation toxicity with the non-sophisticated techniques resulting in overtreating critical organs such as the liver [14, 15].

In the context that renal cell cancer does not seem to respond dramatically and that there does not seem to be a survival advantage to perioperative radiation, in his classic radiation pathology text, Rubin [18] classified renal cell cancer as having a "fairly low" relative radiosensitivity. It is noteworthy that breast cancer, colon cancer, and squamous cell lung cancer were also so classified. This perception was perpetuated by an oft-quoted review of cellular radiosensitivity by Deacon [19] that also placed renal cell cancer in the radioresistant group. This was based on the review of a single study of one cell line. In addition, we are reminded from a previous review [20] that culture conditions are such an artificial environment that it really calls into question the relevance of in vitro data to clinical practice. Subsequently, several studies have shown that some renal cell lines are actually quite sensitive [21–24] to ionizing radiation, while others are not [21]. In addition, in some fascinating studies done on human cancers taken from patients that received preoperative radiation, the radiation stopped the extracted renal cell cancer from growing [25, 26]. In the more recent study [26], malignant renal tumor was taken from 13 patients that had not received preoperative radiation, and when transplanted into mice, in every case the

tumor grew. For the seven patients that had received 25 Gy preoperatively, in only one case was the transplanted tumor able to survive and grow. They then studied three different cell lines, and in two lines, radiation had a dramatic effect on tumor growth, and in the third, there was no change with doses up to 30 Gy. In spite of the differing outcomes in the experimental data, a more recent review of radiosensitivity of different cancers again concluded that renal cell cancer is the most resistant to radiation [27], although they acknowledged that these results are based on a small amount of data that is greatly influenced by the experimental conditions under which the studies are conducted. At the minimum, given the reports discussed above, the conclusion that renal cell cancer is radioresistant may not apply to all renal cell cancers.

Early studies have shown that renal cell carcinoma demonstrates dose response, with higher biologically effective dose (BED) showing higher response rate [28]. Radiobiologically SBRT confers a high BED radiotherapy in delivering a large dose each fraction. SBRT is ideal for treating less radiosensitive tumors, such as RCC. Using a xenograft model involving A498 human RCC cells injected subcutaneously into nude mice, Walsh et al. [29] demonstrated that SBRT treatment (48 Gy in 3 fractions) could result in a sustained decrease in tumor volume and marked cytologic changes when compared to the control group. Using a porcine animal model, Ponsky et al. [30] evaluated the safety and effectiveness of image-guided radiosurgery of renal tissue. It was shown that after 8 weeks, the lesions showed complete fibrosis. The zones of complete fibrosis were characterized by dense, paucicellular connective tissue completely devoid of all normal kidney elements. This technique could ablate a targeted area precisely and completely with relative sparing of the surrounding tissue.

Palliation of Metastatic RCC

Renal cell carcinoma may have prolonged survival despite the presence of metastatic disease. RCC primarily metastasizes to the lung, brain, bone, liver, adrenal gland, opposite kidney, and soft tissue. Having fallen out of favor as an adjunct to the primary treatment of renal cell cancer, radiation has been used primarily for palliation of metastatic disease. The most common sites are in the bone, brain, and soft tissue.

In the treatment of metastatic disease to the bone, the endpoint is usually palliation (i.e., pain relief). In an early retrospective review of Radiation Therapy Oncology Group (RTOG) studies, 32 patients were identified that had renal cell cancer bone metastasis, and at 1 month after radiation, 59 % had at least some relief of pain although complete relief was obtained in only 12 % [31]. These findings were consistent with other histologies. There was no evaluation as to duration of response, so it could be argued that these results were due to the short-term abrogation of local inflammatory responses by the radiation. Other studies done at the same time showed that these responses were indeed durable, indicating at least some destruction of the cancer. In a study by Halperin of patients with renal cell bone metastasis, 78 % of the lesions responded with pain relief, which was durable in most of them. For those with a mass effect, 64 % had a partial or complete response [32]. Not unexpected, there is some variability across studies, for example, Fossa [33] showed an 84 % symptom response and in 50 % masses got smaller or the bone showed signs of healing. Not quite as optimistic was the study by Seitz [34] of patients with not only bone, but other locations of metastasis, with 58 % having improved symptoms and 33 % showing a measurable response, although another 52 % showed disease arrest. This general pattern persists across studies [28, 35–39]. Not easily explained, as they are at variance to the bulk of the literature, are reports that while most patients get relief of symptoms, the duration is actually not durable [40]. There has been some suggestion that more aggressive treatment (i.e., higher total dose or higher doses per fraction) might improve the outcomes [41]. This supports the concept that for radioresistant tumors, it takes a greater dose intensity, especially in the form of higher fractional dose to overcome the inherent cellular resistance [21]. From a radiobiological

standpoint, this would be enough dose to get pass the large "shoulders" of the cell survival curves. In a study of patients with renal cell cancer spinal metastases treated with a single large fraction, 95 % had pain improvement, which was durable in 89 %. Of the measurable tumors, 88 % were thought to be controlled [42]. In a more recent large fraction study (24 Gy in one fraction, 27 Gy in 3 fractions, or 30 Gy in 5 fractions), at 1 year, 82 % of the patients were progression-free in the spine, and 52 % were completely pain-free in that area [43]. In the third study of patients treated with 3 or 4 large fractions, other sites were included (mostly lung), and tumor measurements showed a 52 % partial or complete response, with another 38 % read as stable (for a control rate of 90 %). Interesting was that some tumors took up to 36 months to shrink [44]. Given differences in patient selection and that the large fraction studies were done in an era of better imaging, it is hard to determine if these results are better than those historically, but they certainly appear favorable in both symptom and actual tumor control. The techniques of radiosurgery for bone lesions are explored elsewhere in this book, but it appears that bone metastasis from renal cell cancer responds quite favorably to radiosurgery.

The other common site of metastasis for which patients are referred for palliative radiation is the brain. As with other palliative treatment, the historical measurement of response has been that of a relief of symptoms or maintenance of neurologic function. In an early review of data from the RTOG brain metastasis studies [31], for genitourinary cancers, with the majority being RCC, there was found to be a greater than 80 % improvement of headaches and seizures with 66 % having a complete relief. Motor function improved in 62 %. This was determined to be similar to other histologies with primaries in the lung and breast. In spite of these encouraging results, an oft-sited report by Maor [45] reported only a 30 % clinical response, and in the few patients that had a scan (early in the CT era), 64 % showed progression. A subsequent follow-up study from the same institution utilizing standard palliative doses (30 Gy in 10 fractions) showed that 76 % of the patients died a neurologic (i.e., CNS progressive disease related) death. There was no radiologic evaluation reported [46]. In studies with imaging, the reported response rates (CR/PR) have been 30 % and 32 %, and the control rates (CR/PR and stable) are 52 % and 91 % [47, 48]. Perplexing is a study that reports that although patients uniformly had neurologic improvement, there was no response seen in the 32 patients with follow-up scans [49].

The apparent success of large fraction radiation seen in other metastatic sites has also been explored in the brain. This has been greatly facilitated by sophisticated sterotactic radiotherapy technology. As seen in Table 48.1, numerous studies have evaluated the use of radiosurgery in brain metastasis. The studies have significant variability in patient characteristics with differing combinations of primary radiosurgery, RS with whole brain radiotherapy, RS after surgical failure, RS for radiation failure, and any combination of the above. In spite of those differences, the results are surprisingly consistent with a control rate of better than 80 %. Interesting is the variability of tumor regression with a wide range from 30 % to almost 100 %. Part of this may be related to the length and intensity of follow-up and definition of regression. In general, 30–60 % show at least some shrinkage. While not ideal, the control and response rates with large fraction radiation are favorable and indicate at least some ability to overcome some of the inherent radioresistance attributed to renal cell cancer. This success has led to increased interest in radiosurgery not only for extracranial metastasis but also for primary tumors and local recurrences after surgery.

Treatment of RCC Localized to the Kidney with SBRT

In recent years, SBRT has shown advantages in treating primary and recurrent RCC localized to the kidney, as a noninvasive ablative alternative to surgery in medically inoperable patients or patients with compromised renal function or single remaining kidney.

In treating RCC confined to the kidney, the basic principles of body stereotactic radiation are

Table 48.1 Response of renal cell cancer brain metastasis to radiosurgery

Study	Number of renal cell patients	Number of evaluated lesions	Mean or median follow-up (mo)	"Control" (non-progressed) (%)	Regressed (CR or PR) (%)	1-year control (%)	2-year control (%)
Samlowski [50]	22	42	NR	86	NR	86	74
Mori [51]	35	39	11.0	90	65	100	63
Schoggl [52]	23	NR	NR	96	NR	–	–
Goyal [48]	23	47	6.8	91	32	83	83
Payne [53]	12	23	14.0	100	96	–	–
Brown [54]	16	NR	16.2	85	NR	–	–
Chang [55]	77	NR	8.8	81	NR	64	53
Shiau [56]	10	21	9.3	100	NR	>80	–
Marko [57]	19	NR	NR	95	NR	–	–
Ikushima[58][b]	10	24	5.2	88	NR	90	55
Muacevic [59]	69	NR	NR	96	63	–	–
Sheehan [60]	69	76	NR	96	63	–	–
Shuto [61]	69	132	17.1	83	62	–	–
Wowra [62]	75	350	>6.0	99	NR	–	95[a]
Auchter [63]	12		28.7	100	–	–	–
Hoshi [64]	32	NR	9.5	91	–	–	–
Noel [65]	28	56	14.0	96	35	93	–
Pirzkall [66]	53	NS	4.2	92	–	–	–
Powell [67]	23	NS	4.9			94	87

[a](@1.5 years)
[b]Hypofractionated

germane. Those techniques are discussed in detail in this book, but consist of patient immobilization, target tracking, target delineation, and complex dosimetry. Patients are usually immobilized in a body form, an example of which is a vacuum bag. This can be used in conjunction with a stereotactic body frame. After image acquisition, planning is completed with consideration of the factors of planned dose and fractionation, with strong consideration of dose to normal structures. The latter is a crucial issue as the doses used are ablative to any tissue in the target volume. In addition, in the mid to upper abdomen, other than the kidney itself, consideration has to be given to the dose delivered to the small intestine, the stomach, the liver, the spinal cord, the pancreas, and the large bowel. Dose constraints are placed on partial organ volume based on existing protocol and published literature [68, 69].

An additional consideration is whether the target volume moves during respiration. Several studies have evaluated kidney motion during respiration. With normal respiration, the cranial–caudal movement of the left kidney has been found to be 2–24 mm [70] with a mean of 14 mm [71], 16.9 mm [72], and 9.8 mm [73] and for the right kidney 4–35 mm [70] with a mean of 16 mm [71], 16.1 mm [72], and 9.0 mm [73]. With deep inspiration, it increases dramatically [70, 71], in one study up to 39 mm [71]. With breath-holding techniques, the kidney position is reproducible on the order of 3 mm or less [71], so this technique or some other respiration limiting maneuvers such as abdominal compression is frequently employed to reduce motion. It is critical that either two-dimensional image guidance with fiducial markers or three-dimensional (i.e., CT)-based daily verification is utilized to ensure proper targeting.

Lesions up to 10 cm have been treated [44], but as with SBRT in general, the size that can be treated depends on its location in consideration of the permissible dose to surrounding critical

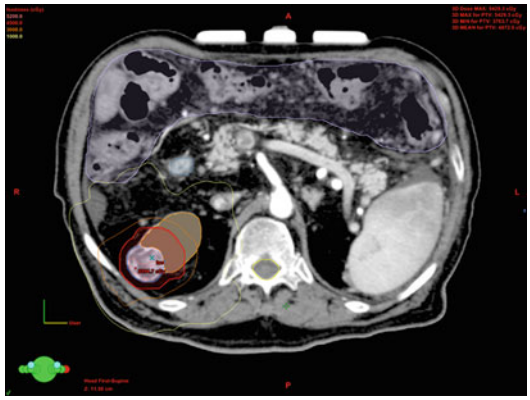

Fig. 48.1 Right kidney renal cell carcinoma treated with SBRT. The patient was immobilized in a BodyFix cast with abdominal compression applied. Prescription was 15 Gy for 3 fractions to a total dose of 45 Gy. Careful attention has to be made to the dose to the surrounding structures

structures. Since renal tumors are usually well defined on imaging, the clinical treatment volume (CTV) is usually the same as the visualized gross treatment volume (GTV). For the final treatment volume (planning treatment volume or PTV), the GTV is usually expanded uniformly (cranial–caudal and transverse) by 1 cm [74]. In deference to the less lateral motion, some utilize a tighter margin of 5–10 mm transversely [44, 75]. There is a wide range of doses utilized, undoubtedly influenced by dose to surrounding structures. These include 8 Gy times 3 fractions [76], 8 Gy times 5 fractions [74], 8 Gy or 10 Gy times 4 fractions [44, 75], 10 Gy times 3 fractions [75], and 15 Gy times 3 fractions [44]. The isodose line to which the dose is prescribed varies from 50 % [44] to 70–90 % [74]. An example of a treatment plan is shown in Fig. 48.1.

Teh et al. used PET–CT in SBRT planning to treat primary RCC [77]. PET–CT is more accurate in differentiating fibrosis/necrosis versus recurrent/residual tumors. PET–CT was performed in the same position as the CT simulation using a special preparation (Lasix and Foley catheter) in order to show any FDG uptake in the kidney mass. Two different fraction sizes were prescribed using simultaneous modulated accelerated radiation therapy (SMART) boost approach, 12 Gy to the PET-avid area and 8 Gy to the larger non-PET-avid area. 4D-CT was performed to assess tumor motion and to define PTV. Fiducial markers (Visicoils) were implanted in the kidney mass for the purpose of image guidance with kV X-ray for each SBRT fraction.

There are limited published data on the efficacy of SBRT for kidney lesions. In some cases, the reports are almost anecdotal. One such example is the report by Teh [76] of patients treated for primary and metastatic renal cell cancer. Only two patients actually received treatment to the renal lesions, and with 24 Gy in 3 fractions and with 9-month median follow-up, there was no change in tumor size, but both patients had palliation of pain. There was reported to be no change in renal function. In a second study evaluating only renal cell cancer in the kidney (both primary and recurrent), with a median follow-up of 26.7 months, utilizing 40 Gy in 5 fractions over 15 days, four of nine patients were still alive. There was no report on local control. A third study [44] included eight patients with inoperable or locally failing tumor in the kidney. Using 8 or 10 Gy for 4 fractions or 1,500 for 2–3 fractions over 1 week, only one patient recurred and median survival had not been reached (>58 months). None of the patients developed uremia. Finally, Svedman et al. [75] evaluated seven patients with new tumors (either metastatic or second primary) in the contralateral kidney. Utilizing 10 Gy times 3 or 4 treatments, six of the seven patients responded with at least radiographically stable tumors. At follow-up, three patients were alive, but four had died of renal cell cancer. Five of the seven had no change in renal function and in the two that did, it was modest (neither required dialysis).

The undeniable success of radiosurgery in treating renal cell brain and bone metastases give strong impetus to explore its use in treating primary or recurrent renal cell cancer in the kidney [31–44, 50–67]. It is the only modality that has the capability of ablating the renal tumor that is noninvasive, so has potentially wide applications. Future directions include optimizing SBRT dose and fraction schemes, comparing SBRT directly with surgery in operable patients, and combining SBRT with novel targeted therapy agents. Only with further research and experience will its utility be fully defined.

References

1. NCCN, Kidney cancer. Version 1. 2013, National Comprehensive Cancer Network clinical practice guidelines in oncology.
2. McLaughlin JK, Lipworth L, Tarone RE. Epidemiologic aspects of renal cell carcinoma. Semin Oncol. 2006;33(5):527–33.
3. Homma Y, et al. Increased incidental detection and reduced mortality in renal cancer–recent retrospective analysis at eight institutions. Int J Urol. 1995; 2(2):77–80.
4. Cox CE, et al. Renal adenocarcinoma: 28-year review, with emphasis on rationale and feasibility of preoperative radiotherapy. J Urol. 1970;104(1):53–61.
5. Kortmann RD, et al. Future strategies in external radiation therapy of renal cell carcinoma. Anticancer Res. 1999;19(2C):1601–3.
6. Cassady JR. Clinical radiation nephropathy. Int J Radiat Oncol Biol Phys. 1995;31(5):1249–56.
7. Kjaer M, Frederiksen PL, Engelholm SA. Postoperative radiotherapy in stage II and III renal adenocarcinoma. A randomized trial by the Copenhagen Renal Cancer Study Group. Int J Radiat Oncol Biol Phys. 1987;13(5):665–72.
8. Waters CA, Frontz WA. Radiation therapy of renal cortical neoplasms. South Med J. 1934;27:290–9.
9. Bloom HJ. Adjuvant therapy for adenocarcinoma of the kidney: present position and prospects. Br J Urol. 1973;45(3):237–57.
10. Caldwell W. Principles of radiation therapy. In: Javadpour N, editor. Principles and management of urologic cancer. 2nd ed. Baltimore: Williams & Wilkins; 1983.
11. Vaeth JM. Proceedings: cancer of the kidney–radiation therapy and its indications in non-Wilms' tumors. Cancer. 1973;32(5):1053–5.
12. van der Werf-Messing B. Proceedings: carcinoma of the kidney. Cancer. 1973;32(5):1056–61.
13. Juusela H, et al. Preoperative irradiation in the treatment of renal adenocarcinoma. Scand J Urol Nephrol. 1977;11(3):277–81.
14. Finney R. The value of radiotherapy in the treatment of hypernephroma–a clinical trial. Br J Urol. 1973;45(3):258–69.
15. Kjaer M, et al. A randomized trial of postoperative radiotherapy versus observation in stage II and III renal adenocarcinoma. A study by the Copenhagen Renal Cancer Study Group. Scand J Urol Nephrol. 1987;21(4):285–9.
16. Stein M, et al. The value of postoperative irradiation in renal cell cancer. Radiother Oncol. 1992;24(1):41–4.
17. Tunio MA, Hashmi A, Rafi M. Need for a new trial to evaluate postoperative radiotherapy in renal cell carcinoma: a meta-analysis of randomized controlled trials. Ann Oncol. 2010;21(9):1839–45.
18. Rubin P. Clinical radiation pathology, vol. II. Philadelphia: WB Saunders & Co; 1968.
19. Deacon J, Peckham MJ, Steel GG. The radioresponsiveness of human tumours and the initial slope of the cell survival curve. Radiother Oncol. 1984;2(4): 317–23.
20. Fertil B, Malaise EP. Inherent cellular radiosensitivity as a basic concept for human tumor radiotherapy. Int J Radiat Oncol Biol Phys. 1981;7(5):621–9.
21. Ning S, et al. Radiobiologic studies of radioimmunotherapy and external beam radiotherapy in vitro and in vivo in human renal cell carcinoma xenografts. Cancer. 1997;80(12 Suppl):2519–28.
22. Chiou RK, et al. Monoclonal antibody-targeted radiotherapy of renal cell carcinoma using a nude mouse model. Cancer. 1988;61(9):1766–75.
23. Weichselbaum RR, Nove J, Little JB. X-ray sensitivity of human tumor cells in vitro. Int J Radiat Oncol Biol Phys. 1980;6(4):437–40.
24. Wei K, Wandl E, Karcher KH. X-ray induced DNA double-strand breakage and rejoining in a radiosensitive human renal carcinoma cell line estimated by CHEF electrophoresis. Strahlenther Onkol. 1993;169(12):740–4.
25. Saksela E, Alfthan O, Malmio K. Effect of preoperative radiotherapy on the growth of human renal carcinoma tissue in vitro. Scand J Urol Nephrol. 1973;7(2):181–3.
26. Otto U, et al. Transplantation of human renal cell carcinoma into NMRI nu/nu mice. III. Effect of irradiation on tumor acceptance and tumor growth. J Urol. 1985;134(1):170–4.
27. Deschavanne PJ, Fertil B. A review of human cell radiosensitivity in vitro. Int J Radiat Oncol Biol Phys. 1996;34(1):251–66.
28. DiBiase SJ, et al. Palliative irradiation for focally symptomatic metastatic renal cell carcinoma: support for dose escalation based on a biological model. J Urol. 1997;158(3 Pt 1):746–9.
29. Walsh L, et al. Efficacy of ablative high-dose-per-fraction radiation for implanted human renal cell cancer in a nude mouse model. Eur Urol. 2006; 50(4):795–800.
30. Ponsky LE, et al. Initial evaluation of Cyberknife technology for extracorporeal renal tissue ablation. Urology. 2003;61(3):498–501.
31. Reddy S, et al. The role of radiation therapy in the palliation of metastatic genitourinary tract carcinomas. A study of the Radiation Therapy Oncology Group. Cancer. 1983;52(1):25–9.
32. Halperin EC, Harisiadis L. The role of radiation therapy in the management of metastatic renal cell carcinoma. Cancer. 1983;51(4):614–7.
33. Fossa SD, Kjolseth I, Lund G. Radiotherapy of metastases from renal cancer. Eur Urol. 1982; 8(6):340–2.
34. Seitz W, Karcher KH, Binder W. Radiotherapy of metastatic renal cell carcinoma. Semin Surg Oncol. 1988;4(2):100–2.
35. Wilson D, et al. The effect of biological effective dose on time to symptom progression in metastatic renal

cell carcinoma. Clin Oncol (R Coll Radiol). 2003;15(7):400–7.
36. Lee J, et al. A phase II trial of palliative radiotherapy for metastatic renal cell carcinoma. Cancer. 2005;104(9):1894–900.
37. Freundt K, et al. Radiotherapy for oligometastatic disease in patients with spinal cord compression (MSCC) from relatively radioresistant tumors. Strahlenther Onkol. 2010;186(4):218–23.
38. Sundaresan N, et al. Surgical treatment of spinal cord compression in kidney cancer. J Clin Oncol. 1986;4(12):1851–6.
39. Rades D, et al. Dose escalation for metastatic spinal cord compression in patients with relatively radioresistant tumors. Int J Radiat Oncol Biol Phys. 2011;80(5):1492–7.
40. Reichel LM, et al. Radiotherapy to bone has utility in multifocal metastatic renal carcinoma. Clin Orthop Relat Res. 2007;459:133–8.
41. Onufrey V, Mohiuddin M. Radiation therapy in the treatment of metastatic renal cell carcinoma. Int J Radiat Oncol Biol Phys. 1985;11(11):2007–9.
42. Gerszten PC, et al. Stereotactic radiosurgery for spinal metastases from renal cell carcinoma. J Neurosurg Spine. 2005;3(4):288–95.
43. Nguyen QN, et al. Management of spinal metastases from renal cell carcinoma using stereotactic body radiotherapy. Int J Radiat Oncol Biol Phys. 2010;76(4):1185–92.
44. Wersall PJ, et al. Extracranial stereotactic radiotherapy for primary and metastatic renal cell carcinoma. Radiother Oncol. 2005;77(1):88–95.
45. Maor MH, Frias AE, Oswald MJ. Palliative radiotherapy for brain metastases in renal carcinoma. Cancer. 1988;62(9):1912–7.
46. Wronski M, et al. External radiation of brain metastases from renal carcinoma: a retrospective study of 119 patients from the M. D. Anderson Cancer Center. Int J Radiat Oncol Biol Phys. 1997;37(4):753–9.
47. Cannady SB, et al. Results of whole brain radiotherapy and recursive partitioning analysis in patients with brain metastases from renal cell carcinoma: a retrospective study. Int J Radiat Oncol Biol Phys. 2004;58(1):253–8.
48. Goyal LK, et al. The role of whole brain radiotherapy and stereotactic radiosurgery on brain metastases from renal cell carcinoma. Int J Radiat Oncol Biol Phys. 2000;47(4):1007–12.
49. Culine S, et al. Prognostic factors for survival in patients with brain metastases from renal cell carcinoma. Cancer. 1998;83(12):2548–53.
50. Samlowski WE, et al. Multidisciplinary treatment of brain metastases derived from clear cell renal cancer incorporating stereotactic radiosurgery. Cancer. 2008;113(9):2539–48.
51. Mori Y, et al. Stereotactic radiosurgery for brain metastasis from renal cell carcinoma. Cancer. 1998;83(2):344–53.
52. Schoggl A, et al. Gamma-knife radiosurgery for brain metastases of renal cell carcinoma: results in 23 patients. Acta Neurochir (Wien). 1998;140(6): 549–55.
53. Payne BR, et al. Gamma surgery for intracranial metastases from renal cell carcinoma. J Neurosurg. 2000;92(5):760–5.
54. Brown PD, et al. Stereotactic radiosurgery for patients with "radioresistant" brain metastases. Neurosurgery. 2002;51(3):656–65. discussion 665–7.
55. Chang EL, et al. Outcome variation among "radioresistant" brain metastases treated with stereotactic radiosurgery. Neurosurgery. 2005;56(5): 936–45. discussion 936–45.
56. Shiau CY, et al. Radiosurgery for brain metastases: relationship of dose and pattern of enhancement to local control. Int J Radiat Oncol Biol Phys. 1997;37(2):375–83.
57. Marko NF, et al. Stereotactic radiosurgery as single-modality treatment of incidentally identified renal cell carcinoma brain metastases. World Neurosurg. 2010;73(3):186–93. discussion e29.
58. Ikushima H, et al. Fractionated stereotactic radiotherapy of brain metastases from renal cell carcinoma. Int J Radiat Oncol Biol Phys. 2000;48(5):1389–93.
59. Muacevic A, Wowra B, Kreth FW. Radiosurgery in renal cell carcinoma. J Neurosurg. 2003; 99(2):441.
60. Sheehan JP, et al. Radiosurgery in patients with renal cell carcinoma metastasis to the rain: long-term outcomes and prognostic factors influencing survival and local tumor control. J Neurosurg. 2003;98(2): 342–9.
61. Shuto T, et al. Gamma knife surgery for metastatic brain tumors from renal cell carcinoma. J Neurosurg. 2006;105(4):555–60.
62. Wowra B, et al. Repeated gamma knife surgery for multiple brain metastases from renal cell carcinoma. J Neurosurg. 2002;97(4):785–93.
63. Auchter RM, et al. A multiinstitutional outcome and prognostic factor analysis of radiosurgery for resectable single brain metastasis. Int J Radiat Oncol Biol Phys. 1996;35(1):27–35.
64. Hoshi S, et al. Gamma-knife radiosurgery for brain metastasis of renal cell carcinoma: results in 42 patients. Int J Urol. 2002;9(11):618–25. discussion 626.
65. Noel G, et al. LINAC radiosurgery for brain metastasis of renal cell carcinoma. Urol Oncol. 2004;22(1): 25–31.
66. Pirzkall A, et al. Radiosurgery alone or in combination with whole-brain radiotherapy for brain metastases. J Clin Oncol. 1998;16(11):3563–9.
67. Powell JW, et al. Gamma Knife surgery in the management of radioresistant brain metastases in high-risk patients with melanoma, renal cell carcinoma, and sarcoma. J Neurosurg. 2008;109(Suppl):122–8.

68. Schefter TE, et al. A phase I trial of stereotactic body radiation therapy (SBRT) for liver metastases. Int J Radiat Oncol Biol Phys. 2005;62(5):1371–8.
69. Kavanagh BD, Timmerman RD. Stereotactic body radiation therapy. Philadelphia: Lippincott Williams & Wilkins; 2005. p. 159.
70. Moerland MA, et al. The influence of respiration induced motion of the kidneys on the accuracy of radiotherapy treatment planning, a magnetic resonance imaging study. Radiother Oncol. 1994;30(2):150–4.
71. Schwartz LH, et al. Kidney mobility during respiration. Radiother Oncol. 1994;32(1):84–6.
72. Bussels B, et al. Respiration-induced movement of the upper abdominal organs: a pitfall for the three-dimensional conformal radiation treatment of pancreatic cancer. Radiother Oncol. 2003;68(1):69–74.
73. van Sornsen de Koste JR, et al. Renal mobility during uncoached quiet respiration: an analysis of 4DCT scans. Int J Radiat Oncol Biol Phys. 2006;64(3):799–803.
74. Beitler JJ, et al. Definitive, high-dose-per-fraction, conformal, stereotactic external radiation for renal cell carcinoma. Am J Clin Oncol. 2004;27(6):646–8.
75. Svedman C, et al. Stereotactic body radiotherapy of primary and metastatic renal lesions for patients with only one functioning kidney. Acta Oncol. 2008;47(8):1578–83.
76. Teh BS, Galli-Guevara M, Doh L, Richardson S, Chiang S, Yeh P, Gonzalez M, Lunn W, Marco R, Jac J, Paulino AC, Lu HH, Butler EB, Amato RJ. The treatment of primary and metastatic renal cell carcinoma (RCC) with image-guided stereotactic body radiation therapy (SBRT). Biomed Imaging Intervent J. 2007;3:e6.
77. Teh BS, Chiang S, Richardson S, Butler EB, Amato R, Paulino AC. Genitourinary cancer. In: Paulino A, Teh BS, editors. PET-CT in radiotherapy treatment planning, Vol. Chapter 11. Philadelphia: Saunders Elsevier; 2008.

Surgical Approaches to Treatment of Renal Cell Carcinoma

49

Jonathan A. Coleman and Paul Russo

Abstract

Radical nephrectomy is historically accepted as standard treatment for localized renal cell carcinoma (RCC). However, the presentation of RCC has changed dramatically over the past 3 decades. Newer alternative interventions aim to reduce the negative impact of open radical nephrectomy, with the natural history of RCC now better understood. This chapter discusses current surgical and management options for localized kidney cancer.

Introduction

Surgical therapies have a central role in the management of kidney cancer, from localized to advanced forms of disease. In 2011, there will be over 58,000 new cases identified in the USA, and approximately 70 % of these patients will have localized tumors at the time of diagnosis [1]. Aside from genetically inherited kidney cancer syndromes, there are no screening recommendations for kidney cancer. It is well recognized that a growing number of cases are identified early, discovered incidentally on imaging studies obtained for unrelated medical conditions. In this setting, surgical management often offers the best curative intervention in achieving durable long-term outcomes with lowest risk for local tumor recurrence and is thus considered the accepted standard of treatment when possible [2]. Approaches to surgical intervention for kidney cancer continue to evolve and, at present, include a variety of modalities, each with unique advantages. This chapter will outline the surgical interventions for small renal masses, the risk factors and complications associated with these approaches, and the basis for recommendations regarding surgical therapy in the management of kidney cancer.

J.A. Coleman (✉)
Department of Surgery, Urology Division, Weill Cornell/Memorial Sloan Kettering Cancer Center, New York, NY, USA
e-mail: colemanj@mskcc.org

P. Russo
Cornell Weill School of Medicine, Memorial Sloan Kettering Cancer Center, New York, NY, USA
e-mail: russop@mskcc.org

Background

Kidney cancer is a disease that affects a growing proportion of individuals in the United States. Since 1971, there has been a fivefold increase in the incidence and twofold increase in the

D.E. Dupuy et al. (eds.), *Image-Guided Cancer Therapy*, DOI 10.1007/978-1-4419-0751-6_51,

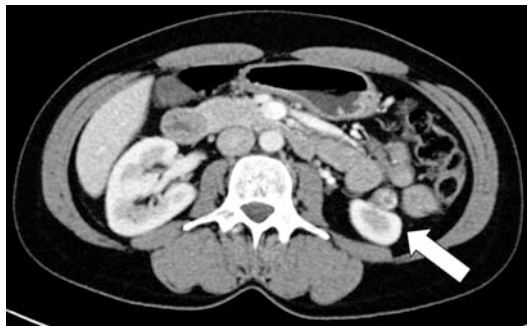

Fig. 49.1 Incidental small renal tumor. CT scan image of a young woman with 1.6 cm anterior lower-pole renal tumor in the left kidney (*arrow*). Note the surrounding loops of small bowel that could be at risk for injury if contemplating percutaneous ablative options

mortality of renal cancer. Risk factors include hypertension, tobacco use, obesity, family history, and race with a noted increase in incidence seen among African Americans. Between 30 % and 40 % of patients with kidney cancer will either present with or later develop metastatic disease. Renal cortical tumors, though often grouped together as a single entity, are several distinct cancer types, defined by their histologic features which reflect variable cytogenetic defects and metastatic potential [3]. Although 55–65 % of resected tumors are conventional clear cell carcinomas, these represent approximately 90 % of metastatic kidney cancers [4]. Over the last decade there has been a proportional increase in the number of incidentally discovered tumors identified during abdominal imaging studies obtained for unrelated indications (Fig. 49.1). In the most recent era, nearly 70 % of cases are identified with tumors <4 cm in diameter, associated with 10-year disease-free survival in over 90 % of these patients following surgical management [5].

Surgical treatment of kidney cancer has evolved as there has been change in the clinical landscape of kidney tumors. Historically, most tumors were discovered when symptomatic. The first evidence of cancer would be the presence of flank mass, hemorrhage, or anorexia. Radical nephrectomy was developed as the standard approach to managing the disease and included resection of the kidney, surrounding fat, and the ipsilateral adrenal gland. In rare cases when smaller tumors were incidentally identified, this approach was still the accepted practice. However, as smaller tumors were increasingly found and concerns grew over iatrogenic renal impairment, the procedure of partial nephrectomy became more commonly used in the elective setting. It has been recognized that nearly 40 % of patients with renal tumors will be discovered to harbor some form of medical renal disease at the time of initial diagnosis, meeting the defined criteria for chronic kidney disease. The indications for partial nephrectomy have thus been expanded and performed in the setting of large invasive tumors, for multiple cancers, and as a cytoreductive procedure in cases of known metastatic disease. Partial nephrectomy, by any approach, is now considered the surgical standard of care for most patients. Reported data show the trend toward partial nephrectomy, now representing over 45 % of cases for tumors <4 cm performed nationally and nearly 70 % of all kidney procedures performed at specialized centers committed to renal tumor surgery.

Oncologic outcomes with nephron-sparing surgery are comparable to radical nephrectomy. Initially, partial nephrectomy procedures were developed for imperative indications as in selected cases of solitary kidney, bilateral or multifocal renal tumors, and renal insufficiency. As data accumulated indicating adequate oncologic control with this approach, partial nephrectomy became increasingly used for elective cases though restricted to tumors less than 4 cm in size. Retrospective studies from large series indicated that PN did not compromise local tumor control or survival when compared to RN for patients with T1a renal tumors (4 cm or less) across all histological subtypes [6–9]. In cases of larger tumors, the approach and indications for partial nephrectomy appeared equally compelling [10], and initial reports from several centers indicated favorable results were achievable in selected cases [11–13]. Combined data from the Mayo Clinic and Memorial Sloan-Kettering Cancer Center evaluated 1,159 patients with renal tumor between 4 and 7 cm (T1b) treated with partial ($N = 286$, 25 %) or radical nephrectomy

($N = 873$, 75 %) and demonstrated no significant difference in survival between these groups [14]. Partial nephrectomy has been performed in selected tumors over 7 cm in size. In one series, partial nephrectomy for these large tumors in 34 patients identified benign tumors in 6 patients (16.2 %) and relatively low-risk tumors (papillary or chromophobe) in 12 patients (35 %). Of patients with malignant tumors, disease-free survival was 71 % at a median follow-up of 17 months [15]. Similar results were found when investigators at the Mayo Clinic reviewed the outcomes of 276 patients with tumors of clinical stage >T2 treated with either partial ($N = 69$, 25 %) or radical nephrectomy ($N = 207$, 75 %) [16]. Though selection factors clearly play a role in these cases, together these data indicate that surgeons are reasonably adept at selecting cases which can be effectively managed by nephron-sparing techniques, for even large tumors, to provide good oncologic control. Although it is not clear what the surgeon selection factors may be, preoperative predictive instruments which take into account features of tumor size, patient age, symptoms, etc., have provided a means for stratifying patients in regard to the optimal approach for surgical intervention with an expectation of reasonable accuracy [4, 17].

Although the associated mortality is high overall, the outcomes for patients with kidney cancer who present with localized tumors are much more favorable. Incidental renal masses have been found to be benign in roughly 20 % of surgical cases. Benign lesions include the histologic subtypes of angiomyolipoma, oncocytoma, metanephric adenoma, or complex cysts. Additionally, 25 % of lesions will represent relatively indolent tumors with limited metastatic potential (papillary and chromophobe carcinoma). Even for patients with T1 conventional clear cell carcinomas, long-term survival exceeding 90 % is anticipated. In the pretreatment setting, consideration for the competing risks of tumor progression, operative risks, and patient comorbidities have combined under the emerging view that preservation of renal function, particularly in elderly and/or comorbidly ill patients, is equally if not more important to the patient's long-term health than resection of a small renal mass. In many cases, the use of surveillance strategies represent the ultimate degree of functional preservation and may be appropriately applied in selected cases with increasing acceptance [6].

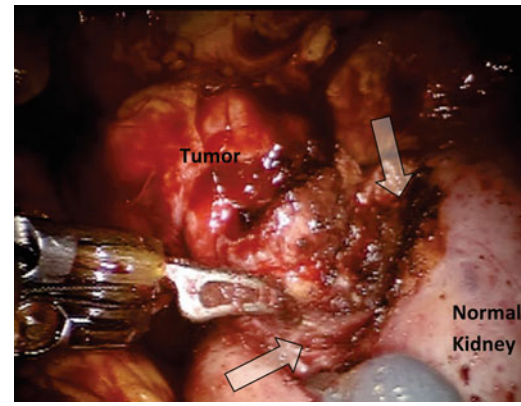

Fig. 49.2 Partial nephrectomy. Surgical resection of lower-pole anterior mass in left kidney of patient from Fig. 49.1. Dissection of the bowel away from the kidney has allowed safe access to the tumor (*upper left*) as it is excised from the normal kidney (*lower right*). The plane of dissection (*arrows*) into the kidney and around the tumor provides a thin rim of normal kidney tissue as a surgical margin to ensure that the entire tumor is removed

The surgical progression toward less invasive techniques was adapted for kidney surgery relatively recently. Introduced in 1991 by Clayman, the initial application of laparoscopic surgery was focused on radical nephrectomy and quickly applied in the field of organ transplantation for donor nephrectomy [18, 19]. The development of these techniques to partial nephrectomy was investigated by McDougal through laboratory research in a porcine model [20], and in 1993 the first successful laparoscopic partial nephrectomy was reported by Winfield [21]. Despite time and experience, laparoscopic partial nephrectomy is still considered an advanced laparoscopic procedure due to the technically demanding components of the operation which requires skills in tumor localization, careful anatomic resection, and suture reconstruction (Fig. 49.2). This approach has been mastered by a number of surgeons at specialized centers though has not been widely adopted. Advances in minimally invasive

instrumentation, including robotic assistance with use of multiple surgical consoles and the introduction of sophisticated training simulators, have been advocated to enhance the utilization of these techniques in the future [22].

Patient Evaluation and Selection

Imaging plays a central role in the evaluation of kidney tumors. Imaging data can provide meaningful data regarding the size, location, depth of invasion, presence of thrombus, lymph node changes, and characterization of tumor features including presence of fat (angiomyolipoma), central scar (oncocytoma), invasive components, calcification, and necrosis. These features have been well studied though difficult to standardize. At Memorial Sloan-Kettering, tumors routinely selected for radical nephrectomy include those large and centrally localized tumors that have effectively replaced the majority of the normal renal parenchyma (Fig. 49.3), often associated with regional adenopathy and renal vein extension [23]. Findings of tumor involvement of major branched renal veins, the main renal vein, or extension into the inferior vena cava can occur in approximately 10 % of patients with renal cell carcinoma. The safety of surgical resection in these cases depends largely on extent of vascular invasion and involvement of adjacent organs which may also be affected (Fig. 49.4). For patients without regional nodal or distant metastatic disease, long-term survival is possible in 50–60 % of patients, whereas the presence of either reduces survival to that of those patients undergoing cytoreductive nephrectomy [24–27]. Radical nephrectomy is commonly performed in this setting on patients with metastatic disease referred for cytoreductive nephrectomy prior to the initiation of systemic therapy [28–30]. This type of multimodality approach for management has been established as the standard of care based on level 1 evidence and extrapolated to the

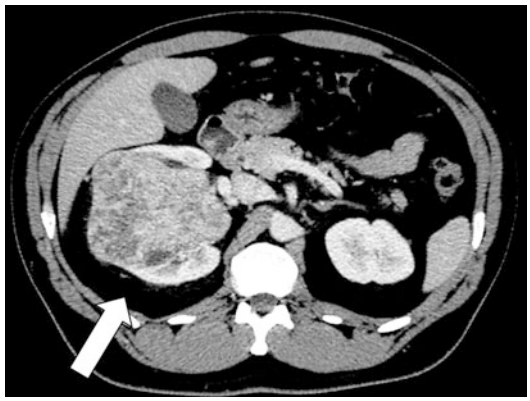

Fig. 49.3 Large kidney tumor. Tumors involving the central renal sinus and vascular hilum of the kidney are less often amenable to partial nephrectomy procedures and more typically managed by radical nephrectomy

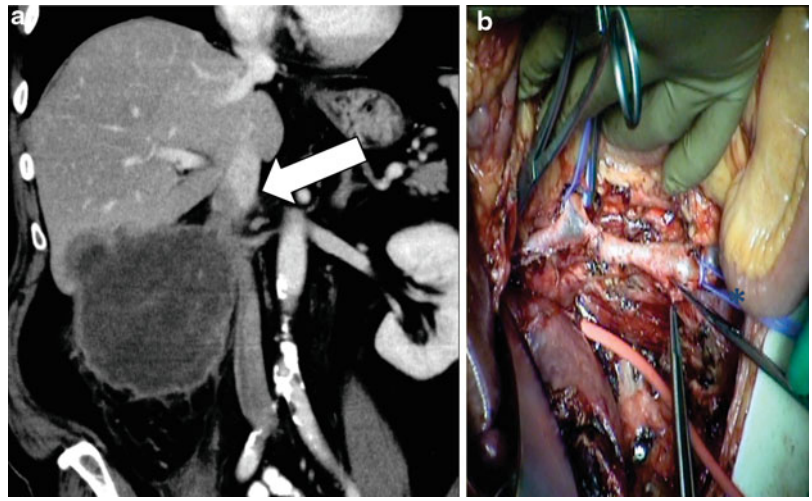

Fig. 49.4 Advanced kidney tumors. CT scan (**a**) of large right-sided renal tumor invading the liver and vena cava with tumor thrombus extending into the vena cava (*arrow*). Surgical resection of the mass was performed (**b**) with reconstruction of the vena cava (*)

present era of targeted molecular therapies [31]. However, in cases demonstrating extensive metastatic disease and a poor Karnofsky Performance Status, surgical intervention may represent excessive risk. In these cases, percutaneous needle biopsy may serve as a diagnostic study to aid in the choice for appropriate systemic therapies.

Preoperative medical evaluation is largely standardized and based on preoperative clinical staging criteria. Routine laboratory evaluation consists of serum chemistries, liver function tests, hemoglobin, platelets, and coagulation profile. Blood type and cross match (or autologous blood donation) may be optional depending on the expected requirements of the operation. Chest X-ray is needed or may be substituted by existing chest CT. Routine brain imaging and bone scans are optional in the setting of existing metastatic disease or site-specific abnormalities evident in the history, physical, or routine preoperative laboratory examination. For patients with significant comorbid conditions, particularly cardiac and pulmonary related, appropriate consultations are obtained with an effort made to optimize patients for operation whenever possible. Patients identified with significant cardiovascular disease may require revascularization prior to considering surgery. Evaluation by anesthesiology before surgical procedures is beneficial in addressing any associated pulmonary concerns or for consideration of epidural perioperative analgesia.

Anatomic Considerations

The location of the kidneys high within the retroperitoneum requires a degree of surgical planning and consideration for some of the anatomic variability which may encountered, often site specific, depending on laterality. The kidneys lie deep to surrounding organ structures including the duodenum, small and large bowel, liver or spleen, and pancreatic tail depending on right or left, respectively. Perinephric fat, which envelopes the kidneys, is contained within a thin membrane of Gerota's fascia. Posteriorly the muscles of the psoas, quadratus lumborum, and diaphragm are in proximity and may require partial resection depending on the localized extent of disease. The surgical approach (e.g., open or minimally invasive, incision location, extent of incision) often depends on factors such as tumor size, extent of local invasion, resection or concern for involvement of adjacent organs, patient's body habitus, and tumor location. In open surgical procedures, different surgical incisions can be used including subcostal, thoracoabdominal, 11th-rib flank, and midline abdominal [23]. When considering large tumors with extensive degree of adjacent organ or vascular involvement, a transabdominal approach is preferred to allow for access to these organs and major vascular structures. Early ligation and division of the renal artery effectively decreases blood flow to the kidney and tumor, decompresses fragile and engorged tumor parasitic vessels, and enhances the mobility of the kidney during its resection, all of which can facilitate the tumor resection and decrease intraoperative bleeding. In selected cases, preoperative renal artery embolization has been utilized to perform this function, potentially limiting some of these factors. Concerns with this approach include the possibility for added morbidity from pain, electrolyte imbalances from tumor lysis syndrome, and the risks of tumor thromboembolism without clear benefits demonstrated from retrospective experience [32].

Much more commonly, however, such requirements are unnecessary, as in the situation of smaller tumors amenable to partial nephrectomy or radical nephrectomy for less advanced cancers. Though transabdominal approaches may also be utilized in such cases, extraperitoneal approaches utilizing a flank incision between the 10th and 11th rib allow direct access to the kidney while avoiding excessive manipulation or exposure of the bowel and other abdominal viscera. Small incisions in this location have been used routinely for these procedures, termed as "miniflank incision" with cited advantages of rapid access to the retroperitoneal space and kidney while avoiding the need for rib resection with a low likelihood (<5 %) of flank incisional bulging which has been noted with other approaches [33].

Although the traditional radical nephrectomy described by Robson included ipsilateral adrenalectomy and regional lymph node dissection, no convincing evidence exists that these component parts offer a therapeutic advantage [34–37]. Contemporary survival data indicates that the involvement of lymph node or the ipsilateral adrenal gland with cancer has a similar negative impact as seen with distant metastatic disease resulting in median survival rates of less than 12 months [38, 39]. Yet these findings provide critical prognostic data regarding the likelihood of disease relapse and help to define a category of patients who could potentially benefit from adjuvant treatment with systemic agents on a clinical trial. Though resection addressing these sites is considered optional, these procedures are commonly performed during surgery for radical or partial nephrectomy. Postoperatively, data regarding pathologic features, combined with clinical variables, can be used to accurately predict risk for disease recurrence and the development of follow-up management strategies [4, 17, 40].

Minimally Invasive Surgery

Similar to the movement toward smaller, miniflank incisions, minimally invasive approaches to kidney surgery have been developed with the intention of offering a less invasive alternative to the classical open nephrectomy with potential for less wound pain and collateral morbidity. Expectations with these techniques have included decreased analgesic requirement, decreased hospitalization, and shorter convalescence. Over time, data regarding survival rates indicated the procedure of laparoscopic nephrectomy was comparable to that achieved with open nephrectomy [41–45]. At the time of this development, radical nephrectomy, either by open or laparoscopic surgery, was still considered the standard for management of most kidney tumors. Retrospective data regarding oncologic outcomes coupled with compelling quality of life data from prospective comparative trials in donor nephrectomy resulted in adoption of these techniques as accepted standards of care [46].

Nephron-sparing surgery proved more difficult to adapt to minimally invasive approaches and is still considered by many as an advanced laparoscopic technique. At centers with expertise in both open and laparoscopic renal surgical techniques, published early experiences indicate dissimilar management of small renal tumors likely based on limitations with laparoscopic approaches and instrumentation. Disparate data regarding the national trends of open partial nephrectomy and laparoscopic radical nephrectomy indicated a fundamental shift in priority away from nephron-sparing procedures toward those that were less invasive but more functionally harmful [47, 48]. In part, these discrepancies were clouded by the preoperative factors of case selection, technical limitations, and patient preference. Indeed, factors such as gender have been identified as an independent risk factor for choice of radical instead of partial nephrectomy in both open and laparoscopic series, though for unclear reasons [49].

More recently, minimally invasive surgical approaches have more rigorously developed techniques to perform partial nephrectomy procedures intended to closely simulate open procedures. These efforts initially appeared isolated to highly selected cases of smaller, exophytic renal tumors though in time progressed to ever more complex and centrally located or cystic renal tumors (Fig. 49.5). The limitations of laparoscopic surgery included the need for complete vascular control and creating the risk of prolonged warm ischemia which is obviated in the open setting by use of externally applied ice slush to achieve renal hypothermia. In several series, efforts have been made to duplicate the renal protective effects of cold ischemia during laparoscopic procedures by use of cold renal arterial and ureteral perfusions as well as externally applied ice slush or surface cooling with cold irrigant. Still, laparoscopic- and robotic-assisted laparoscopic partial nephrectomy remains a challenging procedure which is performed by relatively few surgeons.

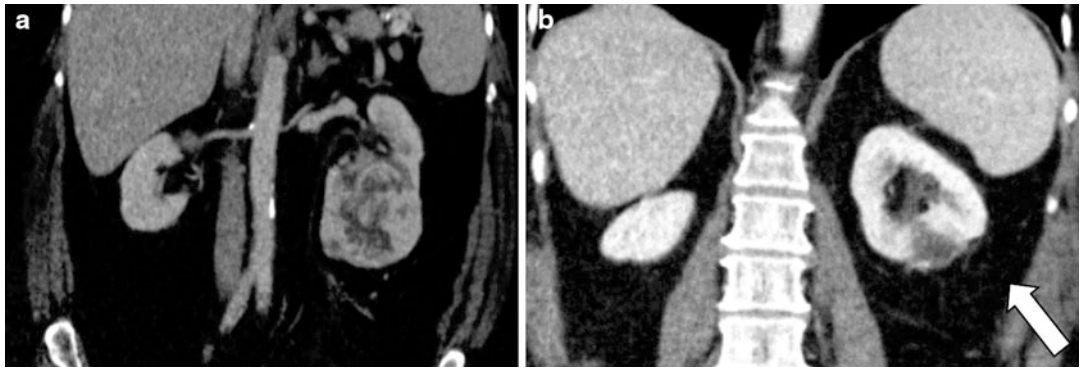

Fig. 49.5 Partial nephrectomy for larger tumors. Selected cases of large renal tumors which about or involve the renal hilum, or collecting system may be candidates for partial nephrectomy. The preoperative CT scan (**a**) in this woman demonstrates a large tumor arising in the lower pole of the left kidney involving the collecting system and adjacent to the ureter. The postoperative scan (**b**) obtained seven weeks after robotic-assisted laparoscopic partial nephrectomy demonstrates normal postoperative radiographic changes and low-density defect from surgically placed absorbable hemostatic agents. These agents (*arrow*) should not be radiographically mistaken for residual tumor

Complications from partial nephrectomy, both open and laparoscopic cases, involve similar events. Much of the published data regarding the adverse event rates from both open and laparoscopic series are retrospectively collected, and few have utilized standardized reporting criteria specific to surgical procedures [50]. Investigators from the Mayo Clinic, Cleveland Clinic, and Johns Hopkins provided pooled data from 1800 partial nephrectomy procedures for T1 tumors, 1,029 open and 771 laparoscopic, from 1998 to 2005 [51]. The groups were dissimilar. Compared to laparoscopic cases, open patients were older, had larger tumors that were more likely centrally located and malignant, and had increased comorbidities, decreased performance status, and decreased baseline renal function. Mean hospital stay favored laparoscopic procedures which stayed on average 2 days less. Patients in the LPN group, however, were more likely to have longer kidney ischemic time, more postoperative complications, and increased number of subsequent procedures to treat complications. Similar results have also been identified in other smaller though comparable series [52]. Studies such as these indicate that minimally invasive partial nephrectomy is a technically challenging operation, even in the hands of experts.

Surgical Complications

Adverse events from surgical interventions are often overlooked or underreported for a variety of reasons, though perhaps foremost due to the fact that all procedures are invasive with the expectation of associated side effects. Until relatively recently, few surgical series have reported adverse events in a standardized and graded manner [53]. In a large series from Memorial Sloan-Kettering Cancer Center, complications of RN ($n = 688$) and PN ($n = 361$) were analyzed using a graded five-tiered scale based on the severity and the intensity of treatment required [50]. For radical nephrectomy there was a 3 % complication rate directly related to the procedure. These events included adjacent organ damage, hemorrhage, and bowel obstruction with a need for surgical re-intervention in 0.6 % of cases. There were three postoperative deaths due to myocardial infarction and pulmonary embolism. For partial nephrectomy, the commonest procedure-related complication was urinary fistula (9 %) with re-interventions (2.5 %) either by percutaneous drainage or endoscopic stent placement in the ureter. Tumor location or indication for the procedure (elective or essential) did

not appear to impact the complication rate in this series. Minimally invasive surgical outcomes from partial nephrectomy at MSKCC were also reported using the same standardized reporting system. Laparoscopically managed patient cohort characteristics (144 cases) were comparable to the open series. Overall complication rates were similar at approximately 20 % in each, yet higher-grade complications were noted among the laparoscopic procedures, notably grade four complications at 2.1 % and 0.2 % for LPN and OPN, respectively. Many of these represented hemorrhagic events [52]. With time and experience, there is evidence that complication rates decrease even with a transition to more challenging cases. At the Cleveland Clinic, minimally invasive surgeons evaluated and compared outcomes in their initial 200 consecutive LPN patients [54] to their later cohort of 200 more recent cases between 2003 and 2005 [55]. Complications were seen in 18.5 % of the more recent cohort, representing a decrease in the overall complications by 44 %, urological complications by 56 %, and hemorrhagic complications by 53 % though cases appeared comparatively more difficult – requiring longer ischemia times [56]. Other studies evaluating learning curve-related features have produced similar results [57]. Risk factors for complications have been evaluated in several series indicating that comorbidity, tumor depth of involvement, and longer ischemia times and imperative indications (solitary kidney) are associated with greater risk of adverse outcome [52, 56]. Notably, age has not proven to pose a risk for adverse outcome, refuting the notion that elderly patients are better managed with radical instead of partial nephrectomy [58].

Kidney Surgery and Renal Function

Kidney surgery, by any approach, is a cause of iatrogenic forms of renal injury and kidney dysfunction. Lately the focus of intense research and debate, the importance of kidney function has been brought to the forefront in developing management strategies for patients with renal tumors. Unlike the population of highly screened, well individuals who volunteer for donor nephrectomy, kidney cancer patients are not screened and are older (mean age 61 years), and many have significant comorbidities affecting baseline kidney function including metabolic syndrome, hypertension, coronary artery disease, obesity, vascular disease, and diabetes. The cumulative effect of aging, particularly beyond 60 years, has a detrimental impact on renal tissue as nephrons atrophy and glomerular filtration rate progressively decreases [59]. A study 110 nephrectomy specimens in which the non-tumor-bearing kidney was examined demonstrated extensive and unsuspected underlying renal disease including vascular sclerosis, glomerular hypertrophy, mesangial expansion, and diffuse glomerulosclerosis [60]. Only 10 % of patients had completely normal renal tissue adjacent to the tumor. Under these conditions, indiscriminant use of radical nephrectomy poses the threat of a profound physiologic impact to the cancer patient.

Evidence of the hyperfiltration injury occurring after radical nephrectomy is well documented. Following kidney surgery procedures for tumors <4 cm, radical nephrectomy patients are more likely than partial nephrectomy patients to have elevated serum creatinine levels to >2.0 ng/mL and proteinuria, even when controlling for associated risk factors including diabetes, smoking history, preoperative serum creatinine, and ASA score [61, 62]. Oncologic outcomes appear equivalent and highly favorable (>90 % survival rates) with either partial or radical nephrectomy in this setting. Current standards for estimating renal function have migrated toward calculated values of glomerular filtration rate utilizing a number of accepted formulas. In a retrospective cohort study of 662 bi-nephric patients with a normal serum creatinine treated by either elective PN or RN for a tumor 4 cm or less in diameter, 171 patients (26 %) had preexisting CKD (GFR < 60) prior to operation, classifying these patients with advanced renal dysfunction. Data was analyzed using two threshold definitions of CKD, a GFR < 60 mL/min/1.73 m^2 or a GFR < 45 mL/min/1.73 m^2. After surgery, the 3-year probability of freedom from

new onset of GFR < 60 was 80 % after PN but only 35 % after RN. Corresponding values for 3-year probability of freedom from a GFR < 45, a more severe level of CKD, were 95 % for PN and 64 % for RN. Multivariable analysis indicated that RN was an independent risk factor for the development of new-onset CKD [63]. Mayo Clinic investigators identified 648 patients from 1989 to 2003 treated with RN or PN for a solitary renal tumor less than or equal to 4 cm with a normal contralateral kidney. In 327 patients younger than 65, it was found that RN was significantly associated with an increased risk of death which persisted after adjusting for year of surgery, diabetes, Charlson-Romano index, and tumor histology [64]. Using the Surveillance, Epidemiology and End Results cancer registry data linked with Medicare claims, MSKCC investigators studied 2,991 patients older than 65 years for resected renal tumors of 4 cm or less from 1995 to 2002. A total of 254 patients (81 %) underwent RN, and 556 patients underwent PN. During a median follow-up of 4 years, 609 patients experienced a cardiovascular event and 892 patients died. After adjusting for preoperative demographic and comorbidity variables, RN was associated with a 1.38 times increased risk of overall mortality and a 1.4 times greater number of cardiovascular events [65].

Similar results were reported in patients undergoing laparoscopic RN and PN [66]. Because of these reports, urologists are now increasingly aware that CKD status can be created or preexisting CKD significantly worsened by the liberal use of RN for the treatment of the small renal mass [67]. Short-term end points, including length of hospital stay, analgesic requirements, and cosmetic elements viewed by many as the reason to elect laparoscopic RN, must now be tempered by concerns that RN causes or worsens preexisting CKD and decreases overall patient survival. The most recent AUA guidelines for the management of the small renal tumor emphasize these points and strongly support the use of PN whenever technically feasible [2].

Despite the above well-described oncological and medical arguments in the contemporary literature supporting PN as an ideal treatment for small renal masses, the urological oncology community continues to use RN as the predominant treatment of the T1a renal mass. A cross-sectional view of clinical practice using the Nationwide Inpatient Sample revealed that only 7.5 % of kidney tumor operations in the United States (1988–2002) were PN [68]. Using the Surveillance, Epidemiology and End Results (SEER) database, investigators from the University of Michigan reported from 2001 that only 20 % of all renal cortical tumors between 2 and 4 cm were treated by PN [69], and using the SEER database linked to Medicare claims, Huang and colleagues from MSKCC reported a utilization rate of only 19 % for T1a tumors (4 cm or less) [65]. Interestingly and for uncertain reasons, women and elderly patients are more likely to be treated with RN [70]. Many urologists believe a "quick" RN in an elderly patient would expose the patient to fewer postoperative complications than would a PN. However, MSKCC investigators evaluated age and type of procedure performed in 1,712 patients with kidney tumors found the interactive term was not significant indicating a lack of statistical evidence that the risk of complications associated with PN increased with advancing age. Furthermore, no evidence was reported linking age to estimated blood loss or operative time. Given the advantages of renal functional preservation, the authors concluded that elderly patients should be perfectly eligible for PN [58].

Although the urology literature has several articles written concerning the use of laparoscopic techniques to resect kidney tumors, the penetrance of laparoscopic RN according to the National Inpatient Sample from 1991 to 2003 was only 4.6 % with a peak incidence of 16 % in 2003. This data indicates that the bulk of "kidney wasting operations" are being done by traditional open surgical approaches [71]. In England, a similar underutilization of PN was reported in 2002 with only 108 (4 %) PN out of 2,671 nephrectomies performed [72]. Investigators at MSKCC tracked nephrectomy use in 1,533 patients between 2000 and 2007 excluding patients with bilateral tumors and tumors in

a solitary kidney and including only patients with an eGFR of greater than 45 mL/min/1.73 m^2. Overall 854 (56 %) patients underwent PN, and 679 (44 %) underwent RN. In the 820 patients with a renal tumor of 4 cm or less, the frequency of PN increased from 69 % in 2000 to 89 % in 2007. In the 365 patients with a renal tumor from 4 to 7 cm, the frequency of PN increased from 20 % in 2000 to 60 % in 2007. Despite a commitment to kidney-sparing operations during this time frame by the MSKCC group, multivariate analysis indicated that PN was a significantly favored approach for males, younger patients, smaller tumors, and open surgeons [49].

Follow-Up After Surgery

No uniform guidelines have been established for the follow-up of patients who have undergone surgical treatment of renal cell carcinoma [73]. Despite emerging evidence that some patients can benefit from aggressive surgical treatment of limited metastatic disease, different practices exist among urologic surgeons regarding the search for and management of recurrent disease. The intensity of follow-up and the tests ordered during follow-up also vary from center to center. In the absence of effective systemic therapy for metastatic disease, overly compulsive follow-up may diagnose asymptomatic metastatic disease earlier but not necessarily provide a therapeutic advantage. Excessive costs and patient anxiety may also occur unnecessarily during this follow-up. In addition, the above-described evidence that radical nephrectomy can have a deleterious impact on renal function requires strict surveillance over renal function as well as surveillance over the contralateral kidney that has a small (<5 %) but real chance of developing an asynchronous renal cortical tumor [74].

Follow-up strategies were proposed from a nephrectomy series by Sandock and colleagues after a detailed analysis of the pattern of metastatic disease progression, sites of metastatic failure, and the efficacy of tests required to diagnose recurrence [75]. These investigators reviewed 137 patients with node-negative, non-metastatic renal cell carcinoma that underwent radical nephrectomy between 1979 and 1993 at the Case Western affiliated hospitals. Recurrence correlated closely with the clinical stage of the tumor at the time of diagnosis. Using the older AJCC classification (T1 < 2.5 cm), no patients with T1 disease relapsed, but 15 % of patients with T2 and 53 % of patients with T3 tumors relapsed. Of the 19 patients in whom pulmonary metastases developed, 14 (74 %) had cough, dyspnea, pleuritic chest pain, or hemoptysis. In all patients with pulmonary metastases, the metastatic disease was diagnosed by a plain chest X-ray. Of the 13 patients in this series that developed intra-abdominal metastatic disease, 12 (92 %) complained of abdominal symptoms or had abnormal liver function studies that lead to the diagnosis. All 10 patients that developed bone metastases complained of new bone pain that directed the diagnosis by plain film and bone scan. Only one patient had an isolated brain metastasis, which was associated with CNS symptoms and was confirmed by brain CT. Two patients developed cutaneous metastases that were detected on physical examination. In this series, 85 % of patients that experienced a recurrence of their disease did so during the first 3 years after nephrectomy with the remaining relapses occurring between 3.4 and 11.4 years.

Levy and colleagues from M.D. Anderson Cancer Center tracked the pattern of recurrence in 286 patients with P1–3N0 or Nx RCC operated upon between 1985 and 1995. Perhaps reflecting the above-described stage migration that has occurred in RCC over the last 10 years, 59/92 (62 %) patients diagnosed with metastatic disease were asymptomatic, including 32 detected by routine chest X-ray and 12 detected by routine blood work. Isolated asymptomatic intra-abdominal metastases were diagnosed by surveillance CT scan in only six patients (9 %) [76]. As in the Sandock study, as the P-stage increased, the likelihood of recurrence increased from 7 % for P1, 27 % for P2, and 39 % for P3 leading the authors to conclude that a stage-specific

surveillance protocol would tailor the follow-up evaluation intensity with the relative risk of recurrence.

At MSKCC, we use postoperative nomograms [4, 17, 40] which incorporate the tumor histological subtype, tumor size, mode of presentation with the P-stage to fashion our follow-ups. Following the postoperative recovery, we generally see P1 (<7 cm) and P2 non-clear cell histology (papillary, chromophobe) patients back every 6 months with renal function studies and yearly with an imaging study of the remaining kidney (CT or US), chest X-ray, and renal function studies for a total of three years and then a yearly visit usually with CT chest/abdomen/pelvis or renal ultrasound and chest X-ray. For tumors >P2 (P3a–c, P4) particularly with conventional clear cell histology, we perform biannual chest X-ray and annual CT scan chest abdomen and pelvis coupled with renal function studies at each visit. Routine brain or bone scans are not performed unless the patient reports symptoms referable to those sites. Renal cell carcinoma is notorious for unusual, late, symptomatic, metastatic recurrences in organs such as the pancreas, thyroid, skin, duodenum, and adrenal glands. These recurrences are often mistaken for new primary tumors, and aggressive surgical resection is undertaken and can be associated with long-term survival depending on the patient age, the number of sites of metastases, and disease-free interval [77, 78]. Whether such metastectomy procedures are truly therapeutic or patient survival is within the confines of the often long and unpredictable natural history of renal cell carcinoma is not known.

Conclusions

An increase in incidental renal tumors due to the prevalent use of imaging studies is largely responsible for the shift in management for renal tumors to smaller lesions, the majority of which are <4 cm in size. The diversity of biologic behavior in these tumors presents a great challenge to the management of these masses, recognizing that radiographic small solid lesions often possess limited malignant potential, yet our ability to definitively determine such potential remains highly limited. Surgical excision remains the most effective form of treatment for renal cancers, and it is now accepted that partial nephrectomy is the appropriate standard of care for small tumors unless there is a contraindication. These procedures may be performed by either open or minimally invasive surgical techniques with equal expectations for oncologic control and comparable functional outcomes. The role of radical nephrectomy is reserved for large tumors, particularly those with central vascular involvement, with the recognition that the adverse impact on renal functional outcomes is more profound. Further research and education is needed in the field to improve on the organ-sparing strategies offered to our patients and the interplay of renal physiology, iatrogenic and biologic forms of renal dysfunction, and cancer biology.

References

1. Jemal A, Siegel R, Xu J, et al. Cancer statistics, 2010. CA Cancer J Clin. 2010;60:277.
2. Campbell SC, Novick AC, Belldegrun A, et al. Guideline for management of the clinical T1 renal mass. J Urol. 2009;182:1271.
3. Linehan WM, Walther MM, Zbar B. The genetic basis of cancer of the kidney. J Urol. 2003;170:2163.
4. Kattan MW, Reuter V, Motzer RJ, et al. A postoperative prognostic nomogram for renal cell carcinoma. J Urol. 2001;166:63.
5. Russo P. Renal cell carcinoma: presentation, staging, and surgical treatment. Semin Oncol. 2000;27:160.
6. Russo P, Huang W. The medical and oncological rationale for partial nephrectomy for the treatment of T1 renal cortical tumors. Urol Clin North Am. 2008;35:635.
7. Uzzo RG, Novick AC. Nephron sparing surgery for renal tumors: indications, techniques and outcomes. J Urol. 2001;166:6.
8. Lee CT, Katz J, Shi W, et al. Surgical management of renal tumors 4 cm or less in a contemporary cohort. J Urol. 2000;163:730.
9. Lesage K, Joniau S, Fransis K, et al. Comparison between open partial and radical nephrectomy for renal tumours: perioperative outcome and health-related quality of life. Eur Urol. 2007;51:614.

10. Russo P, Goetzl M, Simmons R, et al. Partial nephrectomy: the rationale for expanding the indications. Ann Surg Oncol. 2002;9:680.
11. Leibovich BC, Blute ML, Cheville JC, et al. Nephron sparing surgery for appropriately selected renal cell carcinoma between 4 and 7 cm results in outcome similar to radical nephrectomy. J Urol. 2004;171: 1066.
12. Dash A, Vickers AJ, Schachter LR, et al. Comparison of outcomes in elective partial vs radical nephrectomy for clear cell renal cell carcinoma of 4–7 cm. BJU Int. 2006;97:939.
13. Pahernik S, Roos F, Rohrig B, et al. Elective nephron sparing surgery for renal cell carcinoma larger than 4 cm. J Urol. 2008;179:71.
14. Thompson RH, Siddiqui S, Lohse CM, et al. Partial versus radical nephrectomy for 4 to 7 cm renal cortical tumors. J Urol. 2009;182:2601.
15. Karellas ME, O'Brien MF, Jang TL, et al. Partial nephrectomy for selected renal cortical tumours of >/= 7 cm. BJU Int. 2010;106:1484.
16. Breau RH, Crispen PL, Jimenez RE, et al. Outcome of stage T2 or greater renal cell cancer treated with partial nephrectomy. J Urol. 2010;183:903.
17. Lane BR, Kattan MW. Prognostic models and algorithms in renal cell carcinoma. Urol Clin North Am. 2008;35:613.
18. Clayman RV, Kavoussi LR, Soper NJ, et al. Laparoscopic nephrectomy. N Engl J Med. 1991;324:1370.
19. Clayman RV, Kavoussi LR, Soper NJ, et al. Laparoscopic nephrectomy: initial case report. J Urol. 1991;146:278.
20. McDougall EM, Clayman RV, Chandhoke PS, et al. Laparoscopic partial nephrectomy in the pig model. J Urol. 1993;149:1633.
21. Winfield HN, Donovan JF, Godet AS, et al. Laparoscopic partial nephrectomy: initial case report for benign disease. J Endourol. 1993;7:521.
22. Caruso RP, Phillips CK, Kau E, et al. Robot assisted laparoscopic partial nephrectomy: initial experience. J Urol. 2006;176:36.
23. Russo P. Open radical nephrectomy for localized renal cell carcinoma. In: Vogelzang NJ, editor. Comprehensive textbook of genitourinary oncology. 3rd ed. Philadelphia: Lippincott Williams & Wilkins; 2005.
24. Rabbani F, Hakimian P, Reuter VE, et al. Renal vein or inferior vena cava extension in patients with renal cortical tumors: impact of tumor histology. J Urol. 2004;171:1057.
25. Martinez-Salamanca JI, Huang WC, Millan I, et al. Prognostic impact of the 2009 UICC/AJCC TNM staging system for renal cell carcinoma with venous extension. Eur Urol. 2011;59:120.
26. Kaag MG, Toyen C, Russo P, et al. Radical nephrectomy with vena caval thrombectomy: a contemporary experience. BJU Int. 2011;107:1386.
27. Feifer A, Savage C, Rayala H, et al. Prognostic impact of muscular venous branch invasion in localized renal cell carcinoma cases. J Urol. 2011;185:37.
28. Flanigan RC, Salmon SE, Blumenstein BA, et al. Nephrectomy followed by interferon alfa-2b compared with interferon alfa-2b alone for metastatic renal-cell cancer. N Engl J Med. 2001;345:1655.
29. Russo P, O'Brien MF. Surgical intervention in patients with metastatic renal cancer: metastasectomy and cytoreductive nephrectomy. Urol Clin North Am. 2008;35:679.
30. Russo P. Multi-modal treatment for metastatic renal cancer: the role of surgery. World J Urol. 2010;28:295.
31. Motzer RJ, Hutson TE, Tomczak P, et al. Sunitinib versus interferon alfa in metastatic renal-cell carcinoma. N Engl J Med. 2007;356:115.
32. Subramanian VS, Stephenson AJ, Goldfarb DA, et al. Utility of preoperative renal artery embolization for management of renal tumors with inferior vena caval thrombi. Urology. 2009;74:154.
33. Diblasio CJ, Snyder ME, Russo P. Mini-flank supra-11th rib incision for open partial or radical nephrectomy. BJU Int. 2006;97:149.
34. Sagalowsky AI, Kadesky KT, Ewalt DM, et al. Factors influencing adrenal metastasis in renal cell carcinoma. J Urol. 1994;151:1181.
35. Herrlinger A, Schrott KM, Schott G, et al. What are the benefits of extended dissection of the regional renal lymph nodes in the therapy of renal cell carcinoma. J Urol. 1991;146:1224.
36. Ditonno P, Traficante A, Battaglia M, et al. Role of lymphadenectomy in renal cell carcinoma. Prog Clin Biol Res. 1992;378:169.
37. Vasselli JR, Yang JC, Linehan WM, et al. Lack of retroperitoneal lymphadenopathy predicts survival of patients with metastatic renal cell carcinoma. J Urol. 2001;166:68.
38. Blom JH, van Poppel H, Marechal JM, et al. Radical nephrectomy with and without lymph-node dissection: final results of European Organization for Research and Treatment of Cancer (EORTC) randomized phase 3 trial 30881. Eur Urol. 2009;55:28.
39. Whitson JM, Harris CR, Reese AC, et al. Lymphadenectomy improves survival of patients with renal cell carcinoma and nodal metastases. J Urol. 2011;185:1615.
40. Sorbellini M, Kattan MW, Snyder ME, et al. A postoperative prognostic nomogram predicting recurrence for patients with conventional clear cell renal cell carcinoma. J Urol. 2005;173:48.
41. Dunn MD, Portis AJ, Shalhav AL, et al. Laparoscopic versus open radical nephrectomy: a 9-year experience. J Urol. 2000;164:1153.
42. Chan DY, Cadeddu JA, Jarrett TW, et al. Laparoscopic radical nephrectomy: cancer control for renal cell carcinoma. J Urol. 2001;166:2095.
43. Makhoul B, De La Taille A, Vordos D, et al. Laparoscopic radical nephrectomy for T1 renal cancer: the gold standard? A comparison of laparoscopic vs open nephrectomym. BJU Int. 2004;93:67.
44. Matin SF, Gill IS, Worley S, et al. Outcome of laparoscopic radical and open partial nephrectomy for the

sporadic 4 cm or less renal tumor with a normal contralateral kidney. J Urol. 2002;168:1356.
45. Gill IS, Meraney AM, Schweizer DK, et al. Laparoscopic radical nephrectomy in 100 patients: a single center experience from the United States. Cancer. 2001;92:1843.
46. Wolf Jr JS, Merion RM, Leichtman AB, et al. Randomized controlled trial of hand-assisted laparoscopic versus open surgical live donor nephrectomy. Transplantation. 2001;72:284.
47. Scherr DS, Ng C, Munver R, et al. Practice patterns among urologic surgeons treating localized renal cell carcinoma in the laparoscopic age: technology versus oncology. Urology. 2003;62:1007.
48. Russo P. Evolving strategies for renal tumor surgery: whether by open or by laparoscopic approaches, do the right operation! Urol Oncol. 2005;23:456.
49. Thompson RH, Kaag M, Vickers A, et al. Contemporary use of partial nephrectomy at a tertiary care center in the United States. J Urol. 2009;181:993.
50. Stephenson AJ, Hakimi AA, Snyder ME, et al. Complications of radical and partial nephrectomy in a large contemporary cohort. J Urol. 2004;171:130.
51. Gill IS, Kavoussi LR, Lane BR, et al. Comparison of 1,800 laparoscopic and open partial nephrectomies for single renal tumors. J Urol. 2007;178:41.
52. Nogueira L, Katz D, Pinochet R, et al. Critical evaluation of perioperative complications in laparoscopic partial nephrectomy. Urology. 2010;75:288.
53. Shabsigh A, Korets R, Vora KC, et al. Defining early morbidity of radical cystectomy for patients with bladder cancer using a standardized reporting methodology. Eur Urol. 2009;55:164.
54. Ramani AP, Desai MM, Steinberg AP, et al. Complications of laparoscopic partial nephrectomy in 200 cases. J Urol. 2005;173:42.
55. Simmons MN, Gill IS. Decreased complications of contemporary laparoscopic partial nephrectomy: use of a standardized reporting system. J Urol. 2007;177:2067.
56. Turna B, Frota R, Kamoi K, et al. Risk factor analysis of postoperative complications in laparoscopic partial nephrectomy. J Urol. 2008;179:1289.
57. Clark MA, Shikanov S, Raman JD, et al. Chronic kidney disease before and after partial nephrectomy. J Urol. 2011;185:43.
58. Lowrance WT, Yee DS, Savage C, et al. Complications after radical and partial nephrectomy as a function of age. J Urol. 2010;183:1725.
59. Kaplan C, Pasternack B, Shah H, et al. Age-related incidence of sclerotic glomeruli in human kidneys. Am J Pathol. 1975;80:227.
60. Bijol V, Mendez GP, Hurwitz S, et al. Evaluation of the nonneoplastic pathology in tumor nephrectomy specimens: predicting the risk of progressive renal failure. Am J Surg Pathol. 2006;30:575.
61. Lau WK, Blute ML, Weaver AL, et al. Matched comparison of radical nephrectomy vs nephron-sparing surgery in patients with unilateral renal cell carcinoma and a normal contralateral kidney. Mayo Clin Proc. 2000;75:1236.
62. McKiernan J, Simmons R, Katz J, et al. Natural history of chronic renal insufficiency after partial and radical nephrectomy. Urology. 2002;59:816.
63. Huang WC, Levey AS, Serio AM, et al. Chronic kidney disease after nephrectomy in patients with renal cortical tumours: a retrospective cohort study. Lancet Oncol. 2006;7:735.
64. Segev DL, Muzaale AD, Caffo BS, et al. Perioperative mortality and long-term survival following live kidney donation. JAMA. 2010;303:959.
65. Huang WC, Elkin EB, Levey AS, et al. Partial nephrectomy versus radical nephrectomy in patients with small renal tumors–is there a difference in mortality and cardiovascular outcomes? J Urol. 2009;181:55.
66. Foyil KV, Ames CD, Ferguson GG, et al. Long-term changes in creatinine clearance after laparoscopic renal surgery. J Am Coll Surg. 2008;206:511.
67. Lane BR, Poggio ED, Herts BR, et al. Renal function assessment in the era of chronic kidney disease: renewed emphasis on renal function centered patient care. J Urol. 2009;182:435.
68. Hollenbeck BK, Taub DA, Miller DC, et al. National utilization trends of partial nephrectomy for renal cell carcinoma: a case of underutilization? Urology. 2006;67:254.
69. Miller DC, Hollingsworth JM, Hafez KS, et al. Partial nephrectomy for small renal masses: an emerging quality of care concern? J Urol. 2006;175:853.
70. Dulabon LM, Lowrance WT, Russo P, et al. Trends in renal tumor surgery delivery within the United States. Cancer. 2010;116:2316.
71. Miller DC, Taub DA, Dunn RL, et al. Laparoscopy for renal cell carcinoma: diffusion versus regionalization? J Urol. 2006;176:1102.
72. Nuttall M, Cathcart P, van der Meulen J, et al. A description of radical nephrectomy practice and outcomes in England: 1995–2002. BJU Int. 2005;96:58.
73. Montie JE. Follow-up after partial or total nephrectomy for renal cell carcinoma. Urol Clin North Am. 1994;21:589.
74. Patel MI, Simmons R, Kattan MW, et al. Long-term follow-up of bilateral sporadic renal tumors. Urology. 2003;61:921.
75. Sandock DS, Seftel AD, Resnick MI. A new protocol for the follow-up of renal cell carcinoma based on pathological stage. J Urol. 1995;154:28.
76. Levy DA, Slaton JW, Swanson DA, et al. Stage specific guidelines for surveillance after radical nephrectomy for local renal cell carcinoma. J Urol. 1998;159:1163.
77. Kavolius JP, Mastorakos DP, Pavlovich C, et al. Resection of metastatic renal cell carcinoma. J Clin Oncol. 1998;16:2261.
78. Adamy A, Chong KT, Chade D, et al. Clinical characteristics and outcomes of patients with recurrence 5 years after nephrectomy for localized renal cell carcinoma. J Urol. 2011;185:433.

Chemotherapy, Targeted Therapies, and Biological Therapies for Renal Cell Carcinoma

50

Farshid Dayyani and Eric Jonasch

Abstract

The last 5 years have seen a major shift in the treatment of patients with advanced renal cell carcinoma. Since 2005, a total of six new agents were approved for use in advanced RCC, including four antiangiogenic agents and two mammalian targets of rapamycin (mTOR) inhibitors. This chapter reviews currently used agents, describes the integration of surgical management and systemic therapy, and summarizes future directions in the systemic management of patients with advanced RCC.

The last 5 years have seen a major shift in the treatment paradigm for patients with advanced renal cell carcinoma (RCC). In the 1980s and 1990s, metastatic RCC was treated with immunotherapy, and interferon (IFN) and interleukin-2 (IL-2) were the mainstays of therapy. With the cloning of the VHL gene in 1993, and the understanding that VHL mutations result in unbridled angiogenesis, RCC became an obvious place to test a new class of antiangiogenic agents. Since 2005, a total of six additional agents were approved for use in advanced RCC, including four antiangiogenic agents and two mammalian targets of rapamycin (mTOR) inhibitors. This chapter reviews currently used agents, describes the integration of surgical management and systemic therapy, and summarizes future directions in the systemic management of patients with advanced RCC.

F. Dayyani (✉) • E. Jonasch
Division of Hematology-Oncology, The University of Texas MD Anderson Cancer Center, Houston, TX, USA
e-mail: fdayyani@mdanderson.org

Systemic Therapy

Even with the goal of surgical resection of localized disease being "cure," there are still 25–30 % of patients who are diagnosed with primary metastatic disease and up to 30–40 % of patients with a surgical "cure" develop recurrent disease. The long-term survival of patients with metastatic renal cell carcinoma (mRCC) is subject to significant variation and is currently estimated using multiple prognostic factors [1]. Median overall survival rates for MSKCC-based risk categories of favorable, intermediate, and poor are 26, 14.4, and 7.3 months, respectively [1, 2]. Given the large differences in overall survival based on known risk factors, one must always keep in mind the characteristics of the enrolled patient population when evaluating any phase II or III study in mRCC. With better

D.E. Dupuy et al. (eds.), *Image-Guided Cancer Therapy*, DOI 10.1007/978-1-4419-0751-6_52,

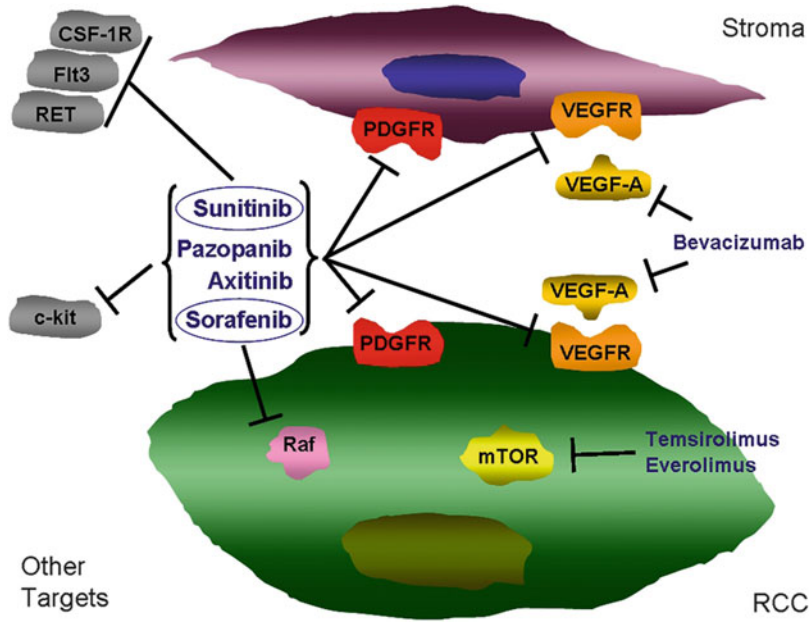

Fig. 50.1 *PDGFR* platelet-derived growth factor receptor, *VEGF(R)* vascular endothelial growth factor (receptor), *mTOR* mammalian target of rapamycin, *CSF-1R* colony-stimulating factor-1 receptor

understanding of the underlying biology, the treatment options have shifted from hormonal therapy, chemotherapy, and immunotherapy to targeted therapy approaches.

Neoadjuvant Therapy

Mature data evaluating targeted agents in the preoperative setting could potentially address two different subsets of patients: (a) patients who present with primary metastatic disease, where response to therapy could guide prognostication with regard to the benefits of cytoreductive nephrectomy and (b) nonmetastatic patients with locally advanced/marginally resectable disease, where an objective response might lead to downstaging of the disease or, at the least, maintain stability of disease, thereby identifying patients who have early presentation of nonresponsive metastases and are likely not appropriate candidates for nephrectomy. To be able to answer these and other questions, the development of clinical trials with appropriately size and power is required. So far, two prospective clinical trials have been published: the first evaluated 50 individuals with metastatic RCC pretreated with bevacizumab therapy for 8 weeks, followed by cytoreductive nephrectomy [3]. The second study assessed pretreatment of patients with advanced RCC with sorafenib for 8 weeks, followed by nephrectomy [4]. In both studies, modest regression of primary tumor lesions was observed, but the degree of shrinkage was not sufficient to substantively change resectability in the majority of cases. Agents capable of substantial downsizing and downstaging will aid in the development of the presurgical paradigm.

Targeted Agents

The identification of the biallelic loss of the VHL gene in a large proportion of patients with RCC and the associated dysregulation of hypoxia-inducible genes including pro-angiogenic growth factors VEGF and PDGF have placed renal cell carcinoma at the forefront of diseases that are particularly suited for antiangiogenic therapy. One must acknowledge that except for monoclonal antibodies, most targeted drugs act on multiple systems within the cell and are multi-targeted (Fig. 50.1) [5, 6], and therefore, the term "targeted agent" might be somewhat misleading.

A number of novel agents have been tested in RCC, and currently, six of these drugs have positively shown an improved PFS or OS in large phase 3 randomized trials, with several more awaiting data maturity. Unfortunately, although higher response rates and better tolerability of these agents have been observed compared to cytokines, durable complete responses are a rarity. Therefore, despite the advances brought by targeted agents, there is still a role for cytokine therapy in select patients. The introduction of a large number of new targeted agents and their next-generation derivatives brings not only more treatment options but also poses new important questions: (a) how to best determine the right sequence of administration of these agents and (b) how and if to combine drugs to develop safe and more effective regimens than single-agent therapy. These questions urge for novel clinical trial designs with multi-institutional and multinational cooperation to obtain the answers that will guide clinical management in the future.

Sunitinib

Sunitinib belongs to the class of small-molecule multi-targeted tyrosine kinase inhibitor (TKI) of VEGFR, PDGFR c-kit, and FLT-3. Its role in cytokine-refractory mRCC was evaluated in two phase II trials. The first trial enrolled 63 patients with mainly clear cell histology and prior nephrectomy. The authors reported a response rate of 40 % and a PFS of 8.1 months, although there were no complete responses [7]. The second trial included only patients with clear cell histology, prior nephrectomy, and progressive disease after cytokine therapy. Among 106 individuals, a 25 % response rate was established after independent review. Sunitinib was approved by the FDA in January 2006 based on these phase II data. The following randomized phase III trial of 750 patients treated with either sunitinib or interferon alpha was completed in July of 2005 [8]. The primary endpoint, PFS, was 11 months in the sunitinib arm versus 5 months in the interferon arm ($p = 0.001$), and overall survival was superior in the sunitinib group, 26.4 versus 21.8 months ($p = 0.049$). While the objective response rate as measured by RECIST criteria was 47 % for sunitinib, there was only a 12 % response rate for INF-α. Grade 3 adverse events in the sunitinib group mainly included hypertension (12 %), fatigue (11 %), diarrhea (9 %), and hand-foot syndrome (9 %). Other studies have reported associated thyroid abnormalities in more than 80 % of patients and warrant serial monitoring [9]. Other studies have identified grade 3 systemic hypertension while on treatment as a potential predictive marker of sunitinib efficacy [10]. Sunitinib is taken orally, and it is dosed within a 6-week cycle: 4 weeks at 50 mg per day, followed by 2 weeks off therapy.

Sorafenib

Another small-molecule TKI is sorafenib, a bis-aryl urea originally developed as a potent inhibitor of both wild-type and mutant (V600E) B-Raf and C-Raf kinase isoforms. Pharmacodynamic studies revealed it was also very active against VEGFR, PDGFR, c-kit, and FLT-3. Sorafenib was tested in 502 patients with mRCC in a phase II randomized discontinuation trial [11]. After receiving 12 weeks of sorafenib, patients who had more than 25 % shrinkage continued the drug, while those with at least 25 % growth of tumor discontinued therapy. All remaining individuals were randomized between continuation of sorafenib and placebo. In this randomized group, sorafenib improved PFS by 18 weeks (24 weeks vs. 6 weeks in the placebo group; $p = 0.0087$).

Sorafenib was FDA approved in December of 2005 for use in advanced renal cell carcinoma based on the phase III TARGET trial (treatment approaches in renal cancer global evaluation trial) [12]. Patients who had metastatic RCC progressive after one prior therapy were randomized between sorafenib and placebo. Median progression-free survival (PFS) was 5.5 months in the sorafenib arm and 2.8 months in the control arm, a 2.7 months difference which was highly statistically significant ($p = 0.000001$). The initial survival analysis showed a difference of 2.6 months in survival (17.8 months in the sorafenib arm vs. 15.2 months in the placebo arm; $p = 0.146$). After censoring

post-crossover data, the differences in survival became significant, 17.8 months versus 14.3 (p =.029) [13]. Sorafenib was also evaluated as first-line therapy against IFN-alpha [14], but no change in PFS could be demonstrated (5.7 months for sorafenib-treated patients and 5.6 months for IFN-treated patients). Crossover was permitted in the upfront IFN arm, and patients who subsequently received sorafenib demonstrated a median PFS of 3.6 months. Since PFS data for sorafenib have not matched those of other antiangiogenic agents, it is not commonly used in the frontline setting.

Pazopanib

Pazopanib is an oral second-generation multi-targeted kinase inhibitor against VEGF-R1,2,3, PDGFR-α, PDGFR-β, and c-kit [15]. It has demonstrated a different tolerability profile compared to other multi-targeted kinase inhibitors based on phase II data, with hypertension in 8 %, grade 4 myelosuppression in 7 %, fatigue in 4 %, and diarrhea in 3 %, with 11 % toxicity-related drug. In 2009, an international phase III trial in treatment-naive ($N = 233$) or prior cytokine-treated ($N = 202$) patients with RCC was reported [16], in which patients were randomized in a 2:1 ratio to receive 800 mg pazopanib orally per day or placebo. The primary endpoint was progression-free survival, and crossover to pazopanib was allowed at the time of progression. There was a highly significant increase in the median PFS by pazopanib (9.2 months in the pazopanib-treated group vs. 4.2 months in the placebo arm, HR = 0.42, 95 % CI 0.34, 0.62, $p < 0.0000001$). In the treatment-naive subset, pazopanib improved the PFS from 2.8 months to 11.1 months, HR = 0.42, 95 % CI 0.27, 0.60, $p < 0.0000001$. Based on these findings, an ongoing trial is comparing upfront pazopanib to sunitinib therapy, with a non-inferiority design.

Axitinib

Axitinib is an oral second-generation multi-targeted kinase inhibitor which blocks VEGF-R1, 2, and 3. In mRCC, a 44.2 % overall response rate (complete + partial by RECIST criteria) was shown in a phase 2 clinical trial with 52 cytokine-refractory patients [17]. Patients were followed up for a median of 20 months, and a median PFS of 15.7 months and median overall survival of 31.1 months were established for this cohort. Serious adverse events (SAEs) led to a dose reduction in 29 % of all study participants. A second phase II study enrolled 62 sorafenib-refractory patients, 72 % of whom had received another prior systemic therapy. The reported overall response rate was 22.6 %, corresponding to a median progression-free and overall survival was 7.4 and 13.6 months, respectively. The most common grade 3 or 4 adverse events were hand-foot syndrome (16.1 %), fatigue (16.1 %), hypertension (16.1 %) diarrhea (14.5 %), dyspnea (14.5 %), and hypotension (6.5 %) [17]. A second-line prospective randomized phase 3 trial of sorafenib versus axitinib was completed in patients with metastatic RCC refractory to a prior first-line therapy. A phase II frontline study was also performed, which randomized patients without hypertension between maintenance of the standard 5 mg PO BID dose of axitinib and dose escalation up to 10 mg PO BID. The hypothesis of the study was that induction of hypertension through dose escalation is a surrogate marker for achieving a biologically relevant dose of drug and will result in improved clinical outcome in patients where the development of hypertension occurs.

Bevacizumab

Bevacizumab is an anti-VEGF human monoclonal antibody with reactivity against all circulating VEGF isoforms, which upon binding are neutralized, thus prohibiting ligand binding to the VEGF receptor and consequently inhibiting signal transduction in the endothelial cell. Bevacizumab was tested in a large phase 3 randomized trial of 649 patients who received either bevacizumab and interferon-α (IFN) or IFN and placebo. Based on a median progression-free survival of 10.4 months versus 5.5 months ($p < 0.0001$) in favor of the bevacizumab combination, this drug was FDA

approved in July 2009 as upfront treatment option for mRCC patients [18]. Similar results were obtained in another randomized phase 3 trial enrolling 723 treatment-naïve patients, who were randomized between bevacizumab and IFN and IFN alone. This study showed a median progression-free survival of 8.5 months versus 5.2 months ($p < 0.001$), again favoring bevacizumab. The combination of bevacizumab and interferon induced a higher degree of overall toxicity, including significantly more grade 3 hypertension (95 % vs. 0 %), anorexia (17 % vs. 8 %), fatigue (35 % vs. 28 %), and proteinuria (13 % vs. 0 %). Despite the PFS advantage, no overall survival difference has been reported in either study for the bevacizumab containing arms [19, 20].

Bevacizumab has been combined with erlotinib (a tyrosine kinase inhibitor to the epidermal growth factor receptor), and the results have been reported [21]. In a phase 2 study with 65 patients, 43 of whom were previously untreated, an 11-month PFS was demonstrated [21]. The benefit of erlotinib was called into question after a 100-patient study randomizing patients between bevacizumab and bevacizumab plus erlotinib [22] showed a PFS for bevacizumab arm of 8.5 months versus 9.9 months for the combination arm ($p = 0.58$), with no survival difference.

Temsirolimus

Temsirolimus, an intravenous drug, is a rapamycin analogue that inhibits mammalian target of rapamycin (mTOR) downstream of AKT. It was evaluated in mRCC in a phase III 3 arm study randomizing patients to (a) 25 mg IV weekly of temsirolimus, (b) IFN 9 MU three times per week, or (c) 15 mg IV weekly temsirolimus plus 6MU three IFN three times per week [23]. There was a significant representation of patients with poor risk features: 80 % of patients had a Karnofsky performance status less than 80; 20 % of patients had non-clear cell histology, and 35 % of patients had not undergone cytoreductive nephrectomy. Survival of patients in the temsirolimus arm was significantly longer than patients who received IFN monotherapy (10.9 months vs. 7.1 months, $p = 0.0069$). No difference in the objective response rates was seen. Median survival of patients receiving temsirolimus and interferon alpha (arm c) was 8.4 months and was not significantly different from the temsirolimus only arm (arm a). The most frequent serious adverse events (SAE) in the temsirolimus only arm were anemia (20 %), asthenia (11 %), and hyperglycemia (11 %). Due to higher proportion of SAEs, in the combination arm (arm c), there were significantly more treatment delays and dose reductions. Based on these data, temsirolimus is currently regarded the drug of choice for upfront single-agent treatment of patients with poor risk mRCC (including non-clear cell histologies).

Everolimus

Everolimus is an orally bioavailable mTOR inhibitor which was FDA approved for second-line treatment of mRCC after anti-VEGF therapy based on a phase III clinical trial of everolimus versus placebo in a 2:1 ratio in patients who progressed after treatment with at least one prior targeted agent [24]. Crossover was permitted in the placebo arm at the time of progression. The treatment with everolimus improved median PFS from 1.9 to 4.9 months, corresponding to a significantly decreased risk of progression (hazard ratio [HR], 0.30; 95 % confidence interval [CI], 0.22–0.40) compared to placebo. No significant differences in overall survival could be shown. Grade 3 or 4 adverse events in the everolimus versus placebo group were stomatitis (3 % vs. 0 %), fatigue (3 % vs. 1 %), and pneumonitis (3 % vs. 0 %). In the community setting, the incidence of significant noninfectious pneumonitis is likely higher than was reported in the phase III study and needs to be monitored carefully.

Sequencing of Therapies

With the emergence of multiple drugs active in RCC within a relatively short-time period, there is unfortunately a paucity of evidence-based

guidelines regarding the sequencing of these systemic agents. Based on a small retrospective chart review, there is a suggestion that salvage cytokine therapy after targeted agents (sunitinib, sorafenib, bevacizumab) is associated with a substantially higher rate of severe cardiac toxicity. Among the patients included in that study, a 40 % rate of severe cardiac toxicities was reported, and only 1 of 23 was able to tolerate a second cycle of IL-2. Complete responses with targeted agents are rare and thus far only described in case reports and small series, and even in those patients, it is not clear how long the response will last. Therefore, most patients are expected to receive different agents during the course of their disease, including chemotherapy. Based on this knowledge, future clinical trial design should (a) accept newer drugs into the sequencing, and (b) include novel multi-institutional and multinational trials, in order to enable progress rather than replication of same data for each new agent. Sequencing may hold promise in extending our responses and adequately treating tumors that become resistant. This can only be accomplished through integration of preclinical data (alternative escape pathways) into large clinical trials.

Chemotherapy

Historically, based on a number of published studies, single-agent chemotherapy has shown minimal or no activity in RCC [25]. In a systematic review of trials with different chemotherapy regimens including 3,635 patient total, the overall response rate was reported as 4 % [26]. A somewhat higher response has been observed more recently with gemcitabine, with response rates as high as 30 % [27–29]. Gemcitabine has also been studied in combination with 5-fluorouracil and its derivative, capecitabine. Forty-one patients with mRCC received gemcitabine with 5-FU, and 17 % of them had an objective response with a median PFS of almost 29 weeks [30]. The addition of capecitabine, the oral prodrug form of 5-FU, to gemcitabine resulted in response rates of 11 % and overall survival of 14 months [31]. The same regimen yielded in a more recent study, a median PFS and overall survival of 4.6 and 17.9 months, respectively [32]. The objective response rate was 8.4 % [95 % CI 3.5–16.6], including six partial responses and one patient had a complete response. In the less frequent subset of collecting duct tumors, the combination of cisplatin with taxanes has shown major responses [33]. A case series from 2004 described the experience with doxorubicin (50 mg/m^2) and gemcitabine (1,500 or 2,000 mg/m^2) every 2–3 weeks with granulocyte colony-stimulating factor support in patients with sarcomatoid renal cell carcinoma and other aggressive renal cell carcinomas, a group of patients with historically very limited treatment options. Nevertheless, overall clinical benefit was seen in 11 patients (two complete responses, five partial responses, three mixed responses, and one stable disease) for a median of 5 months (range, 2–21 + months) [34]. Obviously, prospective studies are required to validate these promising data.

Interleukin-2 Therapy

Starting in the mid-1980s, interleukin-2 (IL-2) was clinically investigated in RCC, with initial studies including high-dose bolus IL-2 and lymphokine-activated killer (LAK) cells, since preceding animal studies had shown a steep dose–response curve for IL-2 and benefit for the addition of LAK cells [35]. But in subsequent trials, the antitumor activity of high-dose bolus IL-2 was basically equivalent to the combination of IL-2 and lymphokine-activated killer cells [36, 37]. More importantly, exposure to high-dose IL-2 led to striking and durable responses, albeit in a small subset of patients [38, 39].

In 1992, the United States Food and Drug Administration approved high-dose bolus IL-2 received for metastatic renal cell carcinoma after reviewing data from 255 patients treated on seven clinical trials at more than 20 institutions. The established regimen was IL-2 (600,000–720,000 IU/kg), administered by 15-min intravenous infusion every 8 h on days 1–5 and

15–19 (maximum, 28 doses), repeated at approximately 3-month intervals in responding patients for up to three cycles. With more mature follow-up (median 8 years), the rate of complete responses improved from 5 % to 7 % and 8 % (20 patients) were classified as having a partial response. The entire cohort had a median overall survival of 16.3 months, but importantly, 10–15 % of patients were estimated to remain alive 5–10 years after treatment with high-dose IL-2. Durable response beyond 2 years and resection of residual disease after initial response to high-dose IL-2 are thought to be indicators for long-term survivors, and some might even consider these patients "cured" [40].

The serious side effects of high-dose IL-2 have led to several trials evaluating alternative routes or lower doses of IL-2 in order to potentially minimize adverse events. As already mentioned, continuous intravenous infusion IL-2 and lymphokine-activated killer cell regimens appeared to produce tumor response rates similar to those seen with single-agent high-dose bolus intravenous IL-2 [40–42]. Interestingly, despite the more convenient mode of administration, continuous-infusion regimens proved to be more toxic than high-dose bolus IL-2 when similar absolute doses were given [42]. In addition, withholding the lymphokine-activated killer cells [43] and/or further dose reductions of IL-2 to facilitate prolonged administration, while producing enhanced immune activation, appeared to decrease antitumor activity [44].

Encouraged by the observed durable responses with high-dose IL-2, there were efforts to increase the proportion of responders by combining IL-2 with agents such as interferon alpha and 5-FU. Studies varied in the route of IL-2 administration: high-dose intravenous bolus injection, continuous intravenous infusion, subcutaneous injection, or in combination with 5-FU [45–48], but despite some promising data published by several groups, the subsequent trials within the Cytokine Working Group were not able to confirm the promise of cytokine combination therapy [49, 50]. None of the combination tests, including IL-2 and interferon alfa administered subcutaneously with or without weekly 5-FU, was able to produce response rates and median survival better than those observed with high-dose IL-2 alone or high-dose IL-2 and interferon; however, the quality and the durability of the responses appeared to be considerably less than those observed with high-dose IL-2 [47].

When compared with either IL-2 or interferon alfa administered alone, intermediate-dose IL-2 administered by continuous intravenous infusion plus subcutaneous interferon alfa had significantly improved response rates and 1 year EFS, as reported in a large-scale, phase III randomized trial [51]. But again, there was no significant difference in overall survival among the three groups. A modified outpatient regimen of this combination was compared by the Cytokine Working Group in a randomized phase III trial with high-dose (HD) IL-2 in 192 patients with mRCC. Similar to the previous trial, there was a response rate benefit in patients receiving the combination (23.2 %, 22 of 95 patients for HD IL-2 vs. 9.9 %, 9 of 91 patients for IL-2/IFN; $P = 0.018$), but although there was a trend for improved median survival (17.5 months vs. 13 months), this difference was not statistically significant ($p = 0.24$). Surprisingly, in subsets of patients with bone or liver metastases ($P = 0.001$) or a primary tumor in place ($P = 0.040$), previously thought to be relatively resistant to immunotherapy, there was a significant improvement in survival with high-dose IL-2.

A three-arm trial conducted by the National Cancer Institute compared in patients with measurable mRCC and a good performance status different doses and schedules of IL-2 [52]. Eligible individuals were randomized to receive either (high-dose [HD]) or 72,000 U/kg (low-dose [LD]), both given by intravenous (IV) bolus every 8 h. After randomly assigning 117 patients, a third arm of low-dose daily subcutaneous IL-2 was added. In 156 patients randomly assigned to HD IV IL-2, and 150 patients to LD IV IL-2, there were no IL-2-related deaths in any arm. HD IV IL-2 produced a higher response rate (21 %) compared to LD IV IL-2 (13 %; $P = 0.048$) but no overall survival difference. The response rate of subcutaneous IL-2 was 10 %. Response durability and survival in completely responding patients was superior with HD IV compared with LD IV therapy ($p = 0.04$).

Immunomodulatory Effects of Novel Agents

The long-lasting remissions seen in a subset of patients treated with HD IL-2 are attributed mainly to immune-activating effects of IL-2. Also, considering that long-term survivors among IL-2-treated patients consist mainly of patients who either had a complete response to therapy or had a good enough partial response to be rendered tumor-free by surgery for oligometastatic disease, one must wonder whether the addition of the novel agents listed above or their sequential use with IL-2 will be able to increase the response rates by modulating the host immune response and thus altering the natural course of the disease. In addition, in the nonmetastatic setting, there is increasing interest in nephron-sparing surgery such as partial nephrectomy. Such procedures are thought to provide comparable oncological control as radical nephrectomies but would be expected to be associated with better preservation of renal function and lower incidence of chronic kidney disease in affected patients. Therefore, it is of great interest to explore whether novel drugs for RCC, alone or in combination, are able to alter the immune milieu of the host such that objective tumor responses are seen and local nephron-sparing procedures are possible without compromising the clinical outcomes.

Several components of the host immune response are affected by anti-VEGF TKIs, and at this point, it is not established if the net effect of TKIs on the immune system activates or suppresses the antitumor immunity of the host. In patients with metastatic RCC, treatment of sunitinib resulted in a significant reduction in the number of circulating myeloid-derived suppressor cells (MDSC), as defined by a CD33+HLA-DR- or CD15+CD14- phenotype [53]. This effect was correlated with increased type 1 T cell activity and at the same time, a decrease in the immunosuppressive Treg population. Similar effects were observed in corresponding in vitro experiments, explaining in part the antitumor effects of sunitinib containing regimens by inhibiting immunosuppressive cells. Additional studies have indicated that granulocyte-macrophage colony-stimulating factor (GM-CSF) is required and may enhance the immunomodulatory effects of sunitinib [54]. The reduction in Treg function in patients with RCC treated with sunitinib has been shown to correlate with an increase in type 1 T cell cytokine response (gamma-interferon [IFN-gamma]) and a reduction in type 2 cytokine (interleukin-4) production [55], providing further rational to a possible combination of sunitinib with IL-2 or alpha-interferon. Another study came to somewhat opposite conclusions, showing that in vitro exposure of sunitinib to peripheral blood mononuclear cells (PBMC) from healthy donors, patients with RCC, and patients with other solid tumors led to cell cycle arrest in T cells and downregulation of activation markers on T cells [56]. Perhaps, these differences are explained by the fact that the latter study did not differentiate between specific T cell subpopulations, and while the former studies included T cells from patients treated in vivo with sunitinib, the latter contained only in vitro experiments, possibly confounding the interpretation of the results because of different drug concentrations. Supporting the importance of drug concentration, differential activity of sunitinib and sorafenib on lymphocyte subsets, specifically the natural killer (NK) cells, was explained in another study by differences of drug levels achieved in patients. Pharmacologic concentrations of sorafenib, but not sunitinib, resulted in inhibition of cytotoxicity and IFN-gamma production in NK cells through inhibition of the PI3 kinase/ERK pathway in NK cells [57]. These findings were confirmed in another study, where sorafenib, at concentrations achieved in patients, caused proliferation arrest of human T cells in vitro, even after drug withdrawal. In contrast to prior reports with sunitinib, sorafenib was also shown to induce apoptosis in T cells at higher concentrations (>10 uM), corresponding with decreased activation marker expression and IL-2 production in these cells [58]. Both sorafenib and the mTOR inhibitor sirolimus were shown in another report to induce T cell apoptosis, and cell death could be prevented by prior administration of IL-2 [59]. This finding is intriguing in the sense that it highlights the importance of considering the

sequence of drug administration when designing trials combining novel targeted agents with cytokine therapies. It is also important to be aware of the potential significance of drug sequence when interpreting the results of ongoing combination trials.

Several of such trials are either currently underway or have already been completed. The Cytokine Working Group (CWG) presented at the ASCO 2007 Annual Meeting an abstract of a trial combining IL-2 with bevacizumab, and in the small cohort of patients reported, this combination appeared to be safe [ASCO 2007: 15524] [60–64]. The combination of sorafenib with IFN-alpha2b was explored in two phase II clinical trials [33, 65, 66]. The objective response rates were 19 % and 33 %, respectively, and the side effects were mostly dominated by known IFN-alpha effects. Randomized trials are needed to establish the superiority of this regimen compared to single agents, but phase III trials of this combination are at the time of writing this chapter (August 2010) not active. IFN-alpha has been shown in two phase III trials to have superior activity when combined with bevacizumab, but although many clinicians suspect that the benefit is mostly derived from the antiangiogenic drug bevacizumab, and formal testing in a randomized setting of bevacizumab versus bevacizumab/IFN-alpha is thus far lacking.

Complicating the matter further, a recent study described the immunological consequences of cryoablation for RCC which might interact with effects of targeted therapies [PMID: 19914660]. In an animal model to deliver in vivo renal cryotherapy, only animals treated with cryoablation showed lymphocytic infiltrate in the tumor with a significant inflammatory response primarily in sublethal tissue injury and perivascular areas. The majority of infiltrating cells were identified as neutrophils, macrophages, and T cells, and using PCR technology, IFN-gamma production was demonstrated in kidneys after cryoablation. Future studies are required to combine novel drugs such as sunitinib with local ablative methods (e.g., cryoablation) to elucidate the immunologic implications of such combinations.

Cytoreductive Nephrectomy

Cytoreductive nephrectomy prior to cytokine therapy was shown to be associated with a significant increase in overall survival in two randomized studies from 2001 [67, 68]. It is important to note that (a) nephrectomy did not alter the response to immunotherapy and (b) the greatest benefit was achieved in patients with a performance score of 0. The case for considering IL-2-based therapy after cytoreductive nephrectomy in metastatic renal cancer is supported by two trials: a Cytokine Working Group study with a 21–24 % response rate in patients who received cytokine therapy following recent nephrectomy [69] and an UCLA-led trial that reported a median survival of 16.7 months and a 19.6 % 5-year survival rate in patients treated with interleukin-2-containing therapy following debulking nephrectomy [70].

Since according to published literature, up to 77 % treated with cytoreductive nephrectomy will never be able to receive cytokine therapy because of complications of treatment or rapid, symptomatic disease progression, it is of great importance to emphasize the careful patient selection if debulking nephrectomy is considered [71–74]. Strict criteria for patient selection for debulking nephrectomy prior to IL-2 treatment have been established by Fallick et al., as displayed in Table 50.1 [75].

Resection of Metastatic Disease

Although the presence of distant metastasis at the time of diagnosis (i.e., synchronous) portends an inferior survival compared to development of metastasis at a later time point after the removal of the primary tumor (i.e., metachronous) [76], it is not unreasonable to consider surgical resection of primary metastatic disease in certain clinical situations. While patients with recurrent disease at a single site might have a 5-year survival probability as high as 50 % [77–79], there are reports in the literature describing durable disease-free survivals even in some patients

Table 50.1 Inclusion criteria for debulking nephrectomy prior to IL-2 treatment

Criteria	Notes
Surgical debulking possible	At least 75 % of the total tumor
No metastases in central nervous system, bone, or liver	
Adequate pulmonary and cardiac function	For age >40 years, normal cardiact stress test
	All patients must have a forced expiratory volume >2 L
Absence of concurrent infection or other co-morbid illness	
ECOG performance status 0 or 1	
Histology predominantly clear cell type	

who underwent resection of solitary or oligometastatic disease, often in the ipsilateral lung or adrenal gland, in conjunction with nephrectomy [80–82]. Nevertheless, when entertaining the idea of metastasectomy, the time to presentation of metastatic disease (after initial nephrectomy) is still a significant prognostic factor.

Cross-References

- Chemotherapy for the Lungs
- Combination Therapies in the Treatment of Primary Liver Cancers
- Combination Therapy for Liver Metastases: Chemotherapy and Radiologic Interventions
- Image-Guided Radiation Therapy for Renal Cell Carcinoma
- Image-Guided Radio Frequency Ablation of Renal Cancer
- Percutaneous Renal Cryoablation
- Surgical Approaches to Treatment of Renal Cell Carcinoma
- Systemic Therapy for Breast Cancer: Success and Challenges

References

1. Motzer RJ, et al. Prognostic factors for survival in previously treated patients with metastatic renal cell carcinoma. J Clin Oncol. 2004;22(3):454–63.
2. Mekhail TM, et al. Validation and extension of the Memorial Sloan-Kettering prognostic factors model for survival in patients with previously untreated metastatic renal cell carcinoma. J Clin Oncol. 2005;23(4):832–41.
3. Jonasch E, et al. Phase II presurgical feasibility study of bevacizumab in untreated patients with metastatic renal cell carcinoma. J Clin Oncol. 2009;27(25):4076–81.
4. Cowey CL, et al. Neoadjuvant clinical trial with sorafenib for patients with stage II or higher renal cell carcinoma. J Clin Oncol. 2010;28(9):1502–7.
5. Rini BI. Metastatic renal cell carcinoma: many treatment options, one patient. J Clin Oncol. 2009; 27(19):3225–34.
6. Rini BI, Campbell SC, Escudier B. Renal cell carcinoma. Lancet. 2009;373(9669):1119–32.
7. Motzer RJ, et al. Phase III randomized trial of sunitinib malate (SU11248) versus interferon-alfa (IFN-α) as first-line systemic therapy for patients with metastatic renal cell carcinoma (mRCC). In: ASCO. 2006.
8. Motzer RJ, et al. Overall survival and updated results for sunitinib compared with interferon alfa in patients with metastatic renal cell carcinoma. J Clin Oncol. 2009;27(22):3584–90.
9. Rini BI, et al. Hypothyroidism in patients with metastatic renal cell carcinoma treated with sunitinib. J Natl Cancer Inst. 2007;99(1):81–3.
10. Rixe O, Billemont B, Izzedine H. Hypertension as a predictive factor of sunitinib activity. Ann Oncol. 2007;18(6):1117.
11. Ratain MJ, et al. Phase II placebo-controlled randomized discontinuation trial of sorafenib in patients with metastatic renal cell carcinoma. J Clin Oncol. 2006; 24(16):2505–12.
12. Escudier B, et al. Sorafenib in advanced clear-cell renal-cell carcinoma. N Engl J Med. 2007;356(2): 125–34.
13. Escudier B, et al. Sorafenib for treatment of renal cell carcinoma: final efficacy and safety results of the phase III treatment approaches in renal cancer global evaluation trial. J Clin Oncol. 2009;27(20):3312–8.
14. Escudier B, et al. Randomized phase II trial of first-line treatment with sorafenib versus interferon Alfa-2a in patients with metastatic renal cell carcinoma. J Clin Oncol. 2009;27(8):1280–9.
15. Sonpavde G, Hutson TE, Sternberg CN. Pazopanib, a potent orally administered small-molecule multitargeted tyrosine kinase inhibitor for renal cell carcinoma. Expert Opin Investig Drugs. 2008; 17(2):253–61.
16. Sternber CN, Lee E, Salman PV, Mardiak J, Davis D. A randomized, double-blind phase III study of

pazopanib in treatment-naive and cytokine-pretreated patients with advanced renal cell carcinoma (RCC). In ASCO 2009. Orlando; 2009.
17. Rixe O, et al. Axitinib treatment in patients with cytokine-refractory metastatic renal-cell cancer: a phase II study. Lancet Oncol. 2007;8(11):975–84.
18. Escudier B, et al. Bevacizumab plus interferon alfa-2a for treatment of metastatic renal cell carcinoma: a randomised, double-blind phase III trial. Lancet. 2007;370(9605):2103–11.
19. Rini B, Rosenberg J, Stadler WM, Vaena DA, Atkins N, Bevacizumab plus interferon-alpha versus interferon-alpha monotherapy in patients with metastatic renal cell carcinoma: results of overall survival for CALGB 90206. In: ASCO 2009. Orlando; 2009.
20. Escudier BJ, Bracarda S, Melichar B, Delva R, Sevin E, Negrier S. Efficacy and safety of first-line bevacizumab (BEV) plus interferon-α2a (IFN) in subgroups of patients (pts) with metastatic renal cell carcinoma (mRCC). In: ASCO 2009. Orlando; 2009.
21. Hainsworth JD, et al. Treatment of metastatic renal cell carcinoma with a combination of bevacizumab and erlotinib. J Clin Oncol. 2005;23(31):7889–96.
22. Bukowski RM, et al. Randomized phase II study of erlotinib combined with bevacizumab compared with bevacizumab alone in metastatic renal cell cancer. J Clin Oncol. 2007;25(29):4536–41.
23. Hudes G, et al. Temsirolimus, interferon alfa, or both for advanced renal-cell carcinoma. N Engl J Med. 2007;356(22):2271–81.
24. Motzer RJ, et al. Efficacy of everolimus in advanced renal cell carcinoma: a double-blind, randomised, placebo-controlled phase III trial. Lancet. 2008; 372(9637):449–56.
25. Harris DT. Hormonal therapy and chemotherapy of renal-cell carcinoma. Semin Oncol. 1983;10(4): 422–30.
26. Yagoda A, Petrylak D, Thompson S. Cytotoxic chemotherapy for advanced renal cell carcinoma. Urol Clin North Am. 1993;20(2):303–21.
27. Casali M, et al. Gemcitabine in pre-treated advanced renal carcinoma: a feasibility study. J Exp Clin Cancer Res. 2001;20(2):195–8.
28. De Mulder PH, et al. Gemcitabine: a phase II study in patients with advanced renal cancer. Cancer Chemother Pharmacol. 1996;37(5):491–5.
29. Mertens WC, et al. Gemcitabine in advanced renal cell carcinoma. A phase II study of the National Cancer Institute of Canada Clinical Trials Group. Ann Oncol. 1993;4(4):331–2.
30. Rini BI, et al. Phase II trial of weekly intravenous gemcitabine with continuous infusion fluorouracil in patients with metastatic renal cell cancer. J Clin Oncol. 2000;18(12):2419–26.
31. Stadler WM, et al. A phase II study of gemcitabine and capecitabine in metastatic renal cancer: a report of Cancer and Leukemia Group B protocol 90008. Cancer. 2006;107(6):1273–9.
32. Tannir NM, et al. A phase II trial of gemcitabine plus capecitabine for metastatic renal cell cancer previously treated with immunotherapy and targeted agents. J Urol. 2008;180(3):867–72. discussion 872.
33. Gollob JA, et al. Long-term remission in a patient with metastatic collecting duct carcinoma treated with taxol/carboplatin and surgery. Urology. 2001;58(6): 1058.
34. Nanus DM, et al. Active chemotherapy for sarcomatoid and rapidly progressing renal cell carcinoma. Cancer. 2004;101(7):1545–51.
35. Mazumder A, Rosenberg SA. Successful immunotherapy of natural killer-resistant established pulmonary melanoma metastases by the intravenous adoptive transfer of syngeneic lymphocytes activated in vitro by interleukin 2. J Exp Med. 1984; 159(2):495–507.
36. Fyfe G, et al. Results of treatment of 255 patients with metastatic renal cell carcinoma who received high-dose recombinant interleukin-2 therapy. J Clin Oncol. 1995;13(3):688–96.
37. Rosenberg SA, et al. Prospective randomized trial of high-dose interleukin-2 alone or in conjunction with lymphokine-activated killer cells for the treatment of patients with advanced cancer. J Natl Cancer Inst. 1993;85(8):622–32.
38. Fisher RI, et al. Metastatic renal cancer treated with interleukin-2 and lymphokine-activated killer cells. A phase II clinical trial. Ann Intern Med. 1988; 108(4):518–23.
39. Rosenberg SA, et al. A progress report on the treatment of 157 patients with advanced cancer using lymphokine-activated killer cells and interleukin-2 or high-dose interleukin-2 alone. N Engl J Med. 1987;316(15):889–97.
40. Fisher RI, et al. High-dose aldesleukin in renal cell carcinoma: long-term survival update. Cancer J Sci Am. 1997;3(Suppl 1):S70–2.
41. Dillman RO, et al. Continuous interleukin-2 and lymphokine-activated killer cells for advanced cancer: a National Biotherapy Study Group trial. J Clin Oncol. 1991;9(7):1233–40.
42. Weiss GR, et al. A randomized phase II trial of continuous infusion interleukin-2 or bolus injection interleukin-2 plus lymphokine-activated killer cells for advanced renal cell carcinoma. J Clin Oncol. 1992;10(2):275–81.
43. Gold PJ, et al. Metastatic renal cell carcinoma: long-term survival after therapy with high-dose continuous-infusion interleukin-2. Cancer J Sci Am. 1997;3(Suppl 1):S85–91.
44. Sosman JA, et al. Repetitive weekly cycles of interleukin-2. II. Clinical and immunologic effects of dose, schedule, and addition of indomethacin. J Natl Cancer Inst. 1988;80(18):1451–61.
45. Atkins MB, et al. Randomized phase II trial of high-dose interleukin-2 either alone or in combination with interferon alfa-2b in advanced renal cell carcinoma. J Clin Oncol. 1993;11(4):661–70.

46. Dutcher JP, et al. Interleukin-2-based therapy for metastatic renal cell cancer: the Cytokine Working Group experience, 1989–1997. Cancer J Sci Am. 1997;3(Suppl 1):S73–8.
47. Dutcher JP, et al. Outpatient subcutaneous interleukin-2 and interferon-alpha for metastatic renal cell cancer: five-year follow-up of the Cytokine Working Group Study. Cancer J Sci Am. 1997;3(3):157–62.
48. Rosenberg SA, et al. Combination therapy with interleukin-2 and alpha-interferon for the treatment of patients with advanced cancer. J Clin Oncol. 1989; 7(12):1863–74.
49. Figlin RA, et al. Concomitant administration of recombinant human interleukin-2 and recombinant interferon alfa-2A: an active outpatient regimen in metastatic renal cell carcinoma. J Clin Oncol. 1992; 10(3):414–21.
50. Atzpodien J, et al. Multiinstitutional home-therapy trial of recombinant human interleukin-2 and interferon alfa-2 in progressive metastatic renal cell carcinoma. J Clin Oncol. 1995;13(2):497–501.
51. Negrier S, et al. Recombinant human interleukin-2, recombinant human interferon alfa-2a, or both in metastatic renal-cell carcinoma. Groupe Francais d'Immunotherapie. N Engl J Med. 1998;338(18): 1272–8.
52. Yang JC, et al. Randomized study of high-dose and low-dose interleukin-2 in patients with metastatic renal cancer. J Clin Oncol. 2003;21(16):3127–32.
53. Ko JS, et al. Sunitinib mediates reversal of myeloid-derived suppressor cell accumulation in renal cell carcinoma patients. Clin Cancer Res. 2009;15(6): 2148–57.
54. Ko JS, et al. Direct and differential suppression of myeloid-derived suppressor cell subsets by sunitinib is compartmentally constrained. Cancer Res. 2010; 70(9):3526–36.
55. Finke JH, et al. Sunitinib reverses type-1 immune suppression and decreases T-regulatory cells in renal cell carcinoma patients. Clin Cancer Res. 2008; 14(20):6674–82.
56. Gu Y, et al. Sunitinib impairs the proliferation and function of human peripheral T cell and prevents T-cell-mediated immune response in mice. Clin Immunol. 2011;135(1):55–62.
57. Krusch M, et al. The kinase inhibitors sunitinib and sorafenib differentially affect NK cell antitumor reactivity in vitro. J Immunol. 2009;183(12):8286–94.
58. Zhao W, et al. Sorafenib inhibits activation of human peripheral blood T cells by targeting LCK phosphorylation. Leukemia. 2008;22(6):1226–33.
59. Molhoek KR, et al. Apoptosis of CD4(+)CD25(high) T cells in response to Sirolimus requires activation of T cell receptor and is modulated by IL-2. Cancer Immunol Immunother. 2009;58(6):867–76.
60. Herman DC, Zhang YM, Miller RM. Rhamnolipid (biosurfactant) effects on cell aggregation and biodegradation of residual hexadecane under saturated flow conditions. Appl Environ Microbiol. 1997;63(9): 3622–7.
61. Huo YY, et al. Marinobacterium nitratireducens sp. nov and Marinobacterium sediminicola sp. nov., isolated from marine sediment. Int J Syst Evol Microbiol. 2009;59:1173–8.
62. Fenwick RB, et al. Resonance assignments for the RLIP76 Ral binding domain in its free form and in complex with the small G protein RalB. Biomol NMR Assign. 2008;2(2):191–4.
63. Koren-Morag N, Goldbourt U, Tanne D. Poor functional status based on the New York Heart Association classification exposes the coronary patient to an elevated risk of ischemic stroke. Am Heart J. 2008;155(3):515–20.
64. Zerza G, Sassara A, Chergui M. Matrix isolation spectroscopy of C-70 – vibrational analysis and assignment of the lowest excited states. Synth Met. 1999;103(1–3):2386–7.
65. Gollob JA, et al. Phase II trial of sorafenib plus interferon alfa-2b as first- or second-line therapy in patients with metastatic renal cell cancer. J Clin Oncol. 2007;25(22):3288–95.
66. Ryan CW, et al. Sorafenib with interferon alfa-2b as first-line treatment of advanced renal carcinoma: a phase II study of the Southwest Oncology Group. J Clin Oncol. 2007;25(22):3296–301.
67. Mickisch GH, et al. Radical nephrectomy plus interferon-alfa-based immunotherapy compared with interferon alfa alone in metastatic renal-cell carcinoma: a randomised trial. Lancet. 2001;358(9286):966–70.
68. Flanigan RC, et al. Nephrectomy followed by interferon alfa-2b compared with interferon alfa-2b alone for metastatic renal-cell cancer. N Engl J Med. 2001;345(23):1655–9.
69. McDermott D, et al. A randomized phase III trial of high-dose interleukin-2 (HD IL2) versus subcutaneous (SC) 112/interferon (IFN) in patients with metastatic renal cell carcinoma (RCC). Proc Am Soc Clin Oncol. 2001;20: abstr 685.
70. Pantuck AJ, Belldegrun AS, Figlin RA. Nephrectomy and interleukin-2 for metastatic renal-cell carcinoma. N Engl J Med. 2001;345(23):1711–2.
71. Bennett RT, et al. Cytoreductive surgery for stage IV renal cell carcinoma. J Urol. 1995;154(1):32–4.
72. Rackley R, et al. The impact of adjuvant nephrectomy on multimodality treatment of metastatic renal cell carcinoma. J Urol. 1994;152(5 Pt 1):1399–403.
73. Taneja SS, et al. Immunotherapy for renal cell carcinoma: the era of interleukin-2-based treatment. Urology. 1995;45(6):911–24.
74. Walther MM, et al. Cytoreductive surgery before high dose interleukin-2 based therapy in patients with metastatic renal cell carcinoma. J Urol. 1997;158(5):1675–8.
75. Fallick ML, et al. Nephrectomy before interleukin-2 therapy for patients with metastatic renal cell carcinoma. J Urol. 1997;158(5):1691–5.

76. Dekernion JB, Ramming KP, Smith RB. The natural history of metastatic renal cell carcinoma: a computer analysis. J Urol. 1978;120(2):148–52.
77. Belldegrun A, et al. Renal cell carcinoma: basic biology and current approaches to therapy. Semin Oncol. 1991;18(5 Suppl 7):96–101.
78. O'Dea MJ, et al. The treatment of renal cell carcinoma with solitary metastasis. J Urol. 1978;120(5):540–2.
79. Tolia BM, Whitmore Jr WF. Solitary metastasis from renal cell carcinoma. J Urol. 1975;114(6):836–8.
80. Kavolius JP, et al. Resection of metastatic renal cell carcinoma. J Clin Oncol. 1998;16(6):2261–6.
81. Dineen MK, et al. Results of surgical treatment of renal cell carcinoma with solitary metastasis. J Urol. 1988;140(2):277–9.
82. Swanson DA. Surgery for metastases of renal cell carcinoma. Scand J Surg. 2004;93(2):150–5.

Focal Therapy of Prostate Cancer by Radiofrequency and Photodynamic Therapy

51

Bob Djavan, Herbert Lepor, Reza Zare, and Seyed Saeid Dianat

Abstract

Prostate cancer is still the most common noncutaneous cancer in male. It is estimated that 217,730 new cases of prostate cancer will be diagnosed, and 32,050 prostate cancer-related deaths will occur in the United States in 2010. Focal therapeutic techniques offer a middle way between the radical surgery and active surveillance in the management of prostate cancer. Two major developments in this field are improvements in tumor localization techniques and new ablative therapies such as high-intensity focused ultrasound (HIFU), cryosurgery, photodynamic therapy, photothermal therapy, and radiofrequency interstitial tumor ablation (RITA) enabling a precise and accurate ablation of tumor foci. RITA therapy is a focal therapeutic modality in which low-level radiofrequency energy is precisely delivered to the target tissue to heat and ablate the malignant tissue. RF energy generates temperatures of around 100 °C and induces irreversible cellular destruction by coagulative necrosis. This chapter reviews the concept of focal therapy for prostate cancer, image-guided biopsy, and the role of imaging before focal therapy and more specifically considers the equipments, procedural technique, and the efficacy of radiofrequency ablation for local prostate cancer. Finally, we briefly reviewed the contribution of photodynamic therapy for the treatment of prostate cancer.

Introduction

Prostate cancer remains the most common noncutaneous cancer in male. Despite of declining incidence of prostate cancer in the developed countries, it is estimated that 217,730 new cases of prostate cancer will be diagnosed and 32,050 prostate cancer-related deaths will occur in the United States in 2010 [1]. More than 80 % of

B. Djavan (✉) • R. Zare • S.S. Dianat
Department of Urology, New York University VA University Hospital, New York, NY, USA
e-mail: bob.djavan@nyumc.org; reza.zare@nyumc.org; saieddianat@gmail.com

H. Lepor
Department of Urology, New York University Langone Medical Center, New York, NY, USA
e-mail: herbert.lepor@nyumc.org

D.E. Dupuy et al. (eds.), *Image-Guided Cancer Therapy*, DOI 10.1007/978-1-4419-0751-6_53,

patients with prostate cancer suffer from a clinically localized tumor, and it is reported that about one-third of this group are likely to be treated with definitive radiation therapy [2]. For patients who do not accept active surveillance, treatment is aimed at local cancer control with minimal treatment-related side effects. However, radical surgery causes several side effects including a 25–50 % chance of impotence, a 1–10 % chance of urinary incontinence, and as high as a 10 % risk of rectal toxicity [3–5].

Advances in image-guided cancer treatment including 3D-conformal planning, inverse planning, and intensity-modulated radiotherapy (IMRT) have revolutionized the techniques of radiation therapy for local control of cancers. The advent of radioactive seed implantation technique has proposed brachytherapy as a therapeutic option for patients with early-stage prostate cancer. However, about 30–50 % of patients with localized prostate cancer who have been treated with radiation therapy experience prostate-specific antigen (PSA) failure within 10 years of treatment [6].

In addition, some patients will have locally recurrent or persistent disease following radiation therapy, and a curative salvage therapy is needed. Curative salvage treatment modalities include salvage prostatectomy, salvage brachytherapy, and salvage cryotherapy. However, these treatments are limited by their complications and side effects. Salvage radical prostatectomy is associated with several major morbidities including rectal injury, bladder neck contracture, reoperation for hemorrhage, ureteral injury, fistulas, deep venous thrombosis, and pulmonary embolism [7, 8].

Salvage cryotherapy has also been applied for eradication of residual prostate cancer and to prevent the need for further intervention. However, this treatment is also limited by low treatment efficacy such as 5-year PSA failure-free rates of 47 % and prostate cancer-specific survival rates of 79 %. Furthermore, some significant treatment-related morbidity has also been reported including urinary incontinence (73 %), obstruction (67 %), and impotence (72 %) [9, 10].

However, there were more favorable outcomes in new reports. Pisters and associates reported the outcome of salvage cryotherapy in 279 patients from several large centers that participated in the COLD (Cryo On-Line Data) registry. They reported higher 5-year PSA failure-free survival rates of 58.9 % and 54.5 % based on two definitions. Post-cryotherapy biopsy showed positive results in 32.6 % of patients. The main advantage over the previous reports was the less complication rates including incontinence (requiring pad use) in 4.4 %, rectal fistula in 1.2 %, and impotence in 69.2 % of patients. Other complications such as urethral sloughing, stricture, and obstruction were not reported. Advances in cryoablation technology have a major impact on the improvement in the outcomes [11]. Salvage brachytherapy is another treatment option with much lower morbidity than the others but is limited by modest efficacy reflected by low rate of 5-year freedom from second PSA relapse of about 34 % [12, 13].

Given the modest treatment efficacy and reported treatment-related morbidities, various research projects and techniques have been implemented for the treatment of patients with recurrent prostate cancer after radiation therapy. Focal therapeutic techniques offer an alternative to radical surgery and active surveillance. Two major developments in this field are improvements in prostate cancer localization techniques using saturation and template biopsy and ablative therapies such as high-intensity focused ultrasound (HIFU), cryosurgery, photodynamic therapy (PDT), photothermal therapy, and radiofrequency interstitial tumor ablation (RITA) enabling a precise and accurate ablation of tumor foci [14]. In this chapter, we will cover the concept of focal therapy in prostate cancer, image-guided biopsy, and the role of imaging before focal therapy and more specifically discuss the equipments, procedural technique, and efficacy of radiofrequency ablation for localized prostate cancer.

Focal Therapy and Pathology of Prostate Cancer

Prostate cancer is usually considered as a multifocal malignant process. However, several studies on radical prostatectomy specimens have revealed that a significant proportion of patients (16–63 %) [15–17] have unilateral disease and 13–26 % of patients have unifocal disease [18–20].

Accordingly, focal therapy could be indicated in approximately one-third of patients. However, a study on 1159 radical prostatectomy specimen showed that unifocal cancers were associated with higher rates of positive surgical margin, Gleason score 8–10 disease, and biochemical recurrence as compared with multifocal disease. However, many of these "unifocal" cancers actually represent collision tumors of a number of smaller tumors [21]. Therefore, they reported worse biochemical recurrence-free survival in unifocal as compared to the multifocal group. Based on the results of this study, an aggressive, disciplined pretreatment evaluation to define the site of the disease, extent, and tumor grade before focal therapy is needed [22].

However, insignificant foci may coexist with significant foci within the same gland in some patients. Index lesion hypothesis has been proposed to define the significance of lesions. Index lesion is defined as the largest tumor focus which drives the natural history and prognosis of tumor [23].

Tumor focus with volume of 0.5 cm^3 (less than a diameter of 9–10 mm) represents a significant disease that can lead to disease progression [24]. In addition, about 90 % of extracapsular extension (ECE) of the disease is originated from index lesion, the lesion occupying 80 % of total tumor volume [25–28].

Local cancer control using focal therapy techniques is achieved by just treating the index lesion. Therefore, significant foci should be identified and localized in each patient, and the lack of metastatic potential in nontreated foci should be ascertained.

Criteria for Candidates of Focal Therapy

There are several recommendations on eligible patients for focal therapy established by different authors in the literature. Group consensus reports from the consensus conference on focal treatment of prostate cancer were published in 2006. They proposed the following criteria for candidates of focal therapy: life expectancy >5 years, stage T1 to T3, PSA <15 ηg/mL, and no M1 disease. They considered lymph node involvement as a relative contraindication. Several parameters such as PSA density, PSA doubling time, Gleason score, and ploidy status were not included in their criteria [29].

International Task Force group suggested more strict criteria for candidates of focal therapy: clinical stage T1–T2a, PSA <10 ηg/mL, PSA density <0.15 ηg/mL, PSA velocity <2 ηg/mL yearly, no Gleason 4 or 5, and no evidence of extraprostatic extension and single lesion [30].

In another study, Sartor et al. [20] stated that modern biopsy strategies, combined with optimal imaging and nomograms to estimate the pathologic stage and risk, all together, provide a basis for the selection of appropriate patient entry into prospective clinical trials of focal therapy. They reported that a single lesion should not exceed the largest dimension of 15 mm in any plane by imaging with capsular contact not to exceed 5 mm on axial images. Furthermore, the regional nodes should not be suspicious for metastatic disease (i.e., they should measure <7 mm in the short axis and have a smooth border, while there should not be an asymmetric cluster of nodes) [20].

There is currently an ongoing focal therapy HIFU trial at the University College London. They include the patients with the following criteria in the focal therapy trial: patients with life expectancy >5 years, PSA ≤15 ηg/mL, multiparametric MRI, and/or template transperineal biopsies performed before treatment all demonstrating stage T1–2 N0 M0 and Gleason score 7 and showing no clinically significant disease elsewhere (either no cancer or

cancer with no Gleason pattern 4 and maximum core length involvement on template biopsies of 3 mm) [14].

Localization

Standard transrectal ultrasound (TRUS) biopsy techniques such as extended biopsy have improved the prostate cancer detection, while not accurate for tumor localization or identification of tumor stage. Enhanced image techniques have been developed to more accurately characterize cancers by biopsy such as color Doppler ultrasonography or magnetic resonance imaging (MRI), transrectal "saturation" biopsies, and transperineal "mapping" biopsies.

Image-Guided Biopsy

Most image-guided biopsy techniques use either ultrasound or MRI platforms. Accuracy of each modality for the diagnosis of prostate cancer has been studied. The use of transperineal mapping biopsy is limited by the intensive requirements such as need for anesthesia (or heavy sedation), with provisions for recovery afterward, time consumption, and high cost of treatment. For initial biopsy, transperineal approach has cancer detection rates similar to those of transrectal biopsies if a comparable number of cores are obtained during each technique [20].

Moran et al. [31] investigated the role of stereotactic transperineal prostate repeated biopsy with three-dimensional mapping for the diagnosis of nonpalpable isoechoic occult prostate malignancy. They identified prostate cancer in 68 (38 %) of patients with previous negative biopsy on repeated biopsy using the transperineal mapping approach. Of these patients, 31 % had Gleason score 7 or greater, and 26 % had an extensive cancer found in at least one-half of the sectors sampled [31].

In another study, the role of systematic transperineal ultrasound-guided template biopsy in the repeated biopsy was evaluated. They similarly found that 37 % of patients had prostate cancer on transperineal biopsy. In addition, about 45 % of patients had Gleason score 7 or greater [32].

Therefore, transperineal template mapping biopsy is a safe method to more accurately diagnose the cancer than the standard transrectal biopsies in patients who are candidates for focal therapy. Mapping biopsies might be a more reliable way to locate the tumor and to reduce the risk of underestimating the stage and grade of prostate cancer. Clinical trials designed to evaluate focal therapy should consider transperineal mapping biopsy for initial assessment and as the primary endpoint of treatment success [20].

Prostate Imaging

Advanced imaging modalities, especially MRI and magnetic resonance spectroscopic imaging (MRSI), could be used to identify patients suitable for focal therapy, plan and implement the treatment, and monitor for the tumor recurrence or progression. Imaging also helps to determine the tumor location, to assess the prostate volume, and to rule out the tumor extension such as extracapsular extension, seminal vesicle invasion, lymph node metastases, and bone metastases [20].

Clinical grading and staging of some tumors may be limited by underestimating the tumor grade as compared with histopathological findings. Therefore, advanced imaging modalities should be used to more accurately assess the tumor stage and exclude patients with intermediate- or high-risk cancer from candidates of focal therapy [20].

In a patient with a PSA level <10 ng/mL, a PSA density <0.15 ng/mL/g, and a Gleason score of 6 (i.e., no grade 4 or 5 cancer) who is candidate for focal therapy, imaging is undertaken. The imaging criteria for identifying unifocal tumor include no more than 1 biopsy-proven lesion, largest tumor dimension of <15 mm in any plane by imaging, capsular contact with the lesion does not exceed 5 mm on axial images, and organ-confined disease, with no evidence of ECE or seminal vesicle invasion.

In addition, the regional lymph nodes should not be suspicious for metastatic disease (i.e., they should measure <7 mm in the short axis and have a smooth border, and there should not be an asymmetric cluster of nodes) [20].

Evaluating Local Tumor Extent and Volume

New imaging modalities are helpful to determine the extent of prostate tumor and to identify organ-confined prostate cancer.

Wang et al. [33] have reported the role of endorectal MRI in 344 consecutive patients with biopsy-proven prostate cancer prior to surgery to predict the extracapsular extension. Clinical variables that were used to predict extracapsular extension were serum PSA level, Gleason score, clinical stage of tumor, greatest percentage of cancer in all core biopsy specimens, percentage of cancer-positive core specimens in all core biopsy specimens, and the presence of perineural invasion. At multivariate analysis, serum PSA level, percentage of cancer in all core biopsy specimens, and endorectal MRI findings ($P = 0.001$, $P = 0.001$, and $P < 0.001$, respectively) were all predictors of ECE. Areas under receiver operating characteristic (ROC) curve for two models for prediction of ECE, with and without endorectal MRI, were 0.838 and 0.772, respectively ($P = 0.022$). They concluded that endorectal MRI findings are significant predictors of ECE before treatment in patients with prostate cancer and add incremental value to clinical variables for prediction [33].

In another study by Wang et al [34] 229 patients who underwent endorectal MRI and 383 who underwent combined endorectal MRI–MRSI before radical prostatectomy were included, and the role of imaging findings on the staging nomogram for prediction of organ-confined prostate cancer (OCPC) was investigated. The likelihood of OCPC was predicted according to the 2001 version of the Partin tables on the basis of the serum PSA level, Gleason grade, and clinical staging [35]. MR findings contributed a significant incremental value to the standard nomogram for predicting organ-confined prostate cancer, increasing the area under the curve (AUC) from 0.80 to 0.88 ($P < 0.01$). Accuracy in the prediction of OCPC with MR was higher when MRSI was used, but the difference was not significant [34].

They have also evaluated the contribution of endorectal MRI for prediction of the likelihood of seminal vesicle invasion (SVI) [36]. MR imaging findings, individual clinical variables (serum PSA level, Gleason grade, clinical stage, greatest percentage of cancer in all biopsy cores, percentage of positive cores in all biopsy cores, and perineural invasion), and the Kattan nomogram were evaluated with respect to SVI prediction. The Kattan staging nomogram is based on presurgical clinical variables (serum PSA level, Gleason grade at biopsy, clinical stage, and systematic needle biopsy cores from the base of the prostate) and is a validated predictive tool that is widely used to help direct adjuvant therapy and to guide postoperative counseling for patients with clinical data suggestive of SVI [37].

They found that endorectal MRI results and all clinical variables except the percentage of positive biopsy cores were significantly associated with SVI at univariate analysis ($P < 0.02$); endorectal MR imaging (0.76) had a larger area under the ROC curve (AUC) than any clinical variable (0.62–0.73). However, at multivariate analysis, endorectal MRI results, Gleason grade, PSA level, and the percentage of cancer in all biopsy cores were significantly associated with SVI ($P \leq 0.02$). The Kattan nomogram plus endorectal MRI (0.87) had a significantly larger ($P < 0.05$) AUC than either endorectal MRI alone (0.76) or the Kattan nomogram alone (0.80). They suggested that endorectal MRI contributes a significant incremental value to the Kattan nomogram for prediction of SVI [36].

In another study [38], the accuracy of combined endorectal and phased-array MRI in detecting pelvic lymph node metastasis (LNM) in patients with prostate cancer has been investigated. MRI was performed at 1.5 T with state-of-the-art imaging systems (Signa Horizon, GE Healthcare) and pelvic phased-array and endorectal coils. Images of the pelvis, extending

from the pubic symphysis to the level of the aortic bifurcation, were obtained. In the evaluation of LNM, MRI had sensitivity and specificity of 27.27 % and 98.46 %, respectively, and positive predictive value and negative predictive value of 50 % and 95.99 %, respectively.

Univariate analysis showed that all variables in Partin nomogram were associated with LNM. In the prediction of LNM, the AUC for MRI was 0.633. In multivariate analysis, MRI ($P = 0.002$), Gleason score ($P = 0.007$), greatest percentage of cancer in all biopsy cores ($P = 0.007$), and PSA ($P = 0.004$) were significant predictors of LNM. They demonstrated that the model constituting all MRI variables (extracapsular extension, seminal vesicle invasion, and LNM) along with the Partin nomogram results had a significantly greater AUC than the univariate model that included only MRI LNM findings [38].

Picture Archiving and Communication System (PACS) technology facilitates the display and distribution of digital images [39]. Using this technology, medical images obtained with various techniques, such as CT, MRI, sonography, and digital projection radiography, are transmitted to various, sometimes remote, locations over networks. This technology enables us to display the images on computer workstations for soft-copy viewing and simultaneous consultations and almost instant reporting from radiologists working in several locations [40].

The PACS workstation (Centricity RA 1000, GE Healthcare) at Memorial Sloan-Kettering Cancer Center has a cross-referencing feature whereby selection of a voxel in any one plane highlights the corresponding voxel in the intersecting planes [41].

Wang and colleagues [41] have assessed whether the use of PACS cross-referencing improves tumor staging of prostate cancer with 3D MRI when pathologic findings are the reference standard. Two radiologists, who were not aware of the clinical data of the patients, retrospectively and independently interpreted MR images without and with cross-referencing to predict the presence of ECE and SVI. Sensitivity and specificity for ECE with MRI alone and with cross-referencing were 43 % and 94 % and 57 % and 100 % for reviewer 1 and 40 % and 93 % and 59 % and 98 % for reviewer 2, respectively. Sensitivity and specificity for SVI with MRI alone and with cross-referencing, respectively, were 23 % and 83 % and 46 % and 93 % for reviewer 1 and 31 % and 91 % and 54 % and 95 % for reviewer 2. They suggested that PACS cross-referencing significantly improves tumor staging of prostate cancer with 3D MRI [41].

With the emergence of some minimally invasive prostate cancer treatment, such as interstitial brachytherapy, intensity-modulated radiotherapy, and cryosurgery, the intraprostatic distribution of tumor is becoming of increasing clinical importance [42]. It has also been reported that anatomic site of positive surgical margin after prostatectomy is important for the risk of tumor recurrence and those with positive margins at the base are more at risk of recurrence than those with positive margins at the apex [43].

The role of MRI for determination of tumor location has been investigated. Wefer et al. [44] compared the accuracy of endorectal MRI and MRSI with that of sextant biopsy for the sextant localization of prostate cancer. They found that MRI and MRSI were more sensitive but less specific than biopsy (67 % and 76 % versus 50 %, and 69 % and 68 % vs. 82 %, respectively). The sensitivity of sextant biopsy was significantly less in the apex than in the mid prostate or prostate base (38 % vs. 52 % and 62 %, respectively). They found that MRI and MRSI had similar efficacy throughout the prostate compared with biopsy but with better sensitivity and specificity in the prostate apex (60 % and 75 %, and 86 % and 68 %, respectively). Using these two imaging, one could determine the intraprostatic location of tumors which helps the physician for decision making on a suitable treatment [44].

Prostate cancer usually occurs in the peripheral zone (PZ); however, it has been shown that the transition zone (TZ) may be involved in up to 25 % of radical prostatectomy specimens [45–47].

Tumors located in the transition zone have different pathological and clinical features from tumors of peripheral zone.

It has been reported that patients with anterior prostate cancer tend to have organ-confined disease, even with higher PSA values [48].

The most striking pathological difference between tumors in both zones is in Gleason grading. Tumors with Gleason score 1 are almost exclusively found in the TZ, and a Gleason 2 pattern is also more frequent in that zone. On the other hand, even small cancers in the PZ are primarily Gleason grade 3 and may contain high-grade (Gleason 4 or 5) tumor [49]. In addition, TZ tumors have a specific feature, as they will attain higher cancer volumes before escaping the prostate. Patients with TZ tumors have a distinctly higher PSA level than those with PZ cancers with comparable pathological stage. However, after radical prostatectomy, if the pathological tumor stages and Gleason scores are comparable, the biochemical recurrence rates of TZ and PZ cancers do not differ [50].

Therefore, the accurate discrimination of TZ tumors with imaging is needed to plan disease-targeting therapies and avoid positive anterior surgical margins at radical prostatectomy [51–53].

Akin and colleagues [54] investigated the accuracy of endorectal MRI in the detection and local staging of TZ prostate cancers, with pathologic analysis as the reference standard, and described the MRI findings of these cancers. Imagings were reported by two reviewers. For identification of patients with TZ cancers, sensitivity and specificity were 75 % and 87 %, respectively, for reader 1 and 80 % and 78 %, respectively, for reader 2, but the interreader agreement was fair. For detection of the location of transition zone cancer, the area under the ROC curve was 0.75 for reader 1 and 0.73 for reader 2, but the interreader agreement was fair. The accuracy of detecting TZ cancer increased significantly when the tumor volume increased. In the detection of extraprostatic extension of TZ cancers, sensitivity and specificity were 56 % and 94 %, respectively, for reader 1 and 28 % and 93 %, respectively, for reader 2. Homogeneous low-T2 signal intensity and lenticular shape were significantly associated with the presence of TZ cancer. This study supports the role of MRI to detect, localize, and stage TZ cancers; however, one should consider that the accuracy of TZ cancer detection at MRI is related to the TZ cancer volume, with higher accuracy for cancers with larger volumes [54].

Coakley et al. [55] have evaluated the accuracy of tumor volume measurement using endorectal MRI or 3D-MRSI. For nodules greater than 0.50 cm^3, tumor volume measurements with MRI, 3D-MRSI, and a combination of both were all positively correlated with histopathological tumor volume (Pearson correlation coefficients of 0.49, 0.59, and 0.55, respectively), but only measurements with 3D-MRSI or a combination of MRI and 3D-MRSI reached the level of statistical significance. The fact that tumor volume measurements for all nodules with the above imaging methods were not correlated with histopathological tumor volume suggests that, although many methods apparently detected small tumor nodules, this may be represented as chance detection [55].

Evaluating Prostate Cancer Aggressiveness

The Gleason scores at biopsy and at postsurgical pathologic evaluation are important factors for prediction of outcome, regardless of therapy undertaken [56, 57].

Biopsy Gleason score is subject to sampling error for the suitable number of biopsy cores. In addition, prostate cancer is usually heterogeneous and multifocal. It has been reported that the biopsy Gleason score is upgraded in as many as 54 % of patients after radical prostatectomy [58].

Thus, a noninvasive technique to predict more accurately the prostate cancer aggressiveness and the pathologic Gleason score is needed to make a better decision in patients with prostate cancer.

MRSI helps to analyze the metabolism of the entire prostate gland. Combination of MR imaging and proton MRSI helps to detect and localize the prostate tumor more sensitively and specifically [59].

Zakian et al. [60] investigated the correlation between MRSI with pathologic analysis of radical prostatectomy samples. They found that overall sensitivity of MRSI was 56 % for tumor detection, increasing from 44 % in lesions with Gleason score of 3 + 3 to 89 % in lesions with Gleason score greater than or equal to 4 + 4. There was a trend toward increasing choline + creatine/citrate with increasing Gleason score in lesions identified correctly with MRSI. Tumor volume assessed with MR spectroscopic imaging increased with increasing Gleason score.

In a study by Shukla et al. [61], the correlation of MRI and MRSI findings with Ki-67, phospho-Akt (pAkt), and androgen receptor (AR) expression in prostatectomy specimen was investigated. In differentiating clinically insignificant from clinically significant prostate cancer, areas under the ROC curves for Ki-67, AR, pAkt, MRI, and combined MRI and MRSI were 0.75, 0.78, 0.80, 0.85, and 0.91, respectively. They reported that the use of pretreatment MRI or combined MRI and MRSI and molecular marker analyses of biopsy samples could facilitate better treatment selection [61].

Wang et al. [62] have investigated the correlation between the signal intensity (SI) of prostate cancer on T2-weighted MRI and the Gleason grade at whole-mount step-section pathological evaluation after radical prostatectomy. They found that higher Gleason grades were associated with lower tumor–muscle SI ratios, while nontumor–muscle SI ratios did not correlate with patients' Gleason grades. They also found that the tumor–muscle SI ratios were lower in transition zone than in peripheral zone tumors ($P < 0.001$). They reported that SI evaluation on T2-weighted MR images may facilitate better and noninvasive assessment of prostate cancer aggressiveness.

Predicting Very-Low-Risk or Indolent Prostate Cancer

Shukla et al. [63] evaluated the role of MRI and MRSI as a model predicting insignificant cancer defined as organ-confined cancer of ≤ 0.5 cm^3 with no poorly differentiated elements. Using the combined model of MRI/MRSI and clinical data, AUC for discriminating insignificant from significant cancer is 0.854. They found that MRI and MRI/MRSI models might be useful in predicting the probability of insignificant cancer. Although they were limited in determining exact tumor volume, combined MRI and MRSI could be used to separate with reasonable accuracy tumors of <0.5 cm^3 from those of >0.5 cm^3 [63].

Follow-Up After Focal Therapy

There are limited data on the role of imaging after focal therapy in prostate cancer. TRUS has not been shown to be an effective and accurate tool to assess the treatment effect, to determine the treated volume, or to detect residual cancer after either cryosurgery or HIFU ablation for prostate cancer [64, 65].

Kalbhen and colleagues investigated the role of posttreatment MRI after cryosurgery. They reported that mean prostate volume decreased by 52 % in patients examined 8 weeks or more after cryosurgery using MRI. Areas of intraprostatic necrosis were detected in about half of the patients. Due to high frequency of loss of zonal differentiation, MRI could not reliably detect residual cancer. Positive and negative predictive values for assessment of recurrent tumor using MRI findings were 44 % and 73 %, respectively [64].

In another study, Parivar et al. [65] have assessed and compared the clinical usefulness of TRUS, MRI, and three-dimensional proton MRSI in detecting local recurrence in patients with detectable serum PSA levels after cryosurgery. In patients with detectable PSA, MRSI identified, location for location, all foci of tumors and benign prostatic tissue that were detected by prostate biopsy. In addition, MRSI could detect more sites of tumoral tissue than did prostate biopsy. In two patients with detectable PSA but negative prostate biopsy, MRSI identified 11 voxels with viable prostatic tissue. In patients with undetectable PSA, both MRSI and prostate biopsy showed necrosis. They reported that ultrasound

and MRI are very poor tools for identifying recurrent cancer and differentiating between viable- and necrotic prostate tissue. Furthermore, the addition of spectroscopy to endorectal MRI increases the sensitivity for detection of local recurrence by providing chemical mapping of the prostate in contiguous voxels [65].

Rouviere and associates evaluated the role of T2-weighted (T2w) and dynamic contrast-enhanced (DCE) MRI in detecting local recurrence after prostate HIFU ablation. Targeted biopsy detected more cancers than routine biopsy. The mean percentages of positive cores per patient and of tumor invasion of the cores were significantly higher for targeted biopsies. The odds ratios of the probability of finding viable cancer and viable prostate tissue (benign or malignant) at targeted versus routine biopsy were, respectively, 3.35 (95 % CI: 3.05–3.64) and 1.38 (95 % CI: 1.13–1.63). They suggested that MRI combining T2-weighted and DCE images is a promising method for guiding post-HIFU biopsy toward areas containing recurrent cancer and viable prostate tissue [66].

Radiofrequency Interstitial Tumor Ablation

Background

Radiofrequency interstitial tumor ablation (RITA) therapy is a focal therapeutic modality in which low-level radiofrequency energy is precisely delivered to the target tissue to heat and ablate the malignant tissue. RF energy generates temperatures of around 100 °C and induces irreversible cellular destruction by coagulative necrosis [67].

RF ablation was initially used to treat liver tumors as early as in 1990 [68].

RITA therapy has been mostly utilized in the treatment of primary and secondary hepatic tumors with excellent results [69].

The efficacy, safety, and feasibility of RITA for the treatment of patients with prostate cancer who are candidates of focal therapy have been initially reported in 1998 [67].

Basic Principles

There are two main objectives for the implementation of focal therapy such as RF thermal tumor ablation. First, focal therapy is aimed at complete eradication of all viable malignant cells within a designated area. There should be an ablative margin to make sure complete eradication of malignant cells. Ablative margin is at least a 1.0 cm for liver tumors, but less may be needed for some tumors such as kidney [70]. Another important objective is the specificity and accuracy of therapy leading to the least damage to the normal tissue.

One of the advantages of RF thermal ablation in comparison with conventional standard surgical resection of tumors is the minimal amount of normal tissue loss during the treatment. This is more sensible in the treatment of primary liver tumors, in which functional hepatic reserve is a primary predictive factor for long-term survival of the patient [71]. This is also important for nephron-sparing treatments in patients with von Hippel–Lindau who are at risk of the development of multiple renal cell carcinomas [72].

Multiple energy sources have been used for focal therapy of various tumors. The energy is delivered through the placement of applicators in the center of a tumor, around which heating occurs. Hyperthermic (>50°C) ablation techniques include those using RF and microwave (electromagnetic), laser (light), and ultrasound energy to generate focal increases in tissue temperature. Cryoablation is another focal therapy for tumor destruction by alternating between sessions of freezing and thawing.

Coagulation Necrosis Induced by RF

Cosman et al. [73] have initially shown that the resistive heating produced by RFA technique leads to heat-based cellular death through the thermal coagulation necrosis.

Cellular homeostatic mechanisms can accommodate slight increases in temperature (to 40 °C). Irreversible cellular damage occurs when cells

are heated to 46 °C for 60 minutes and occurs more rapidly when the temperature rises [74].

Immediate cellular damage occurs with coagulation of proteins located in the cytosol, mitochondrial enzymes, and nucleic acid–histone protein complexes. This type of cellular injury causes cell death after several days of the treatment [75].

Optimal temperatures for thermal ablation range from 50 °C to 100 °C. Extremely high temperatures (>105 °C) result in tissue vaporization which impedes the current flow and restricts total energy deposition [76].

The exact temperature at which cell death occurs is multifactorial and tissue specific. Maximal temperature at the edge of the ablation zone, known as "critical temperature," depends on the duration of heating and the tissue being treated. Critical temperature ranges from 30 °C to 77 °C for normal tissues and from 41 °C to 64 °C for tumor models. In addition, the total amount of heat administered for a given time, known as the thermal dose, varies significantly between different tissues [77].

Equipment

Result of the first study on the feasibility and safety of interstitial radiofrequency ablation for human prostate cancer was published in 1998 [67].

In that study, radiofrequency energy was delivered via a RF generator (RITA Medical Systems Inc, California, USA) with the power of up to 50 W at a frequency of 480 kHz and monopolar or bipolar probes (Fig. 51.1). Controlled parameters on the generator included the power delivered, the impedance, total energy administered, temperature measurements (provided by thermocouples), and timing of the procedure during RF treatment.

The probes were needle electrodes with different configurations either as two-hook or triple-hook electrodes. To deliver the energy to well-defined targeted area, the portions of electrodes are insulated. The primary electrode is a stainless-steel cannula with a 1-cm exposed tip that can be

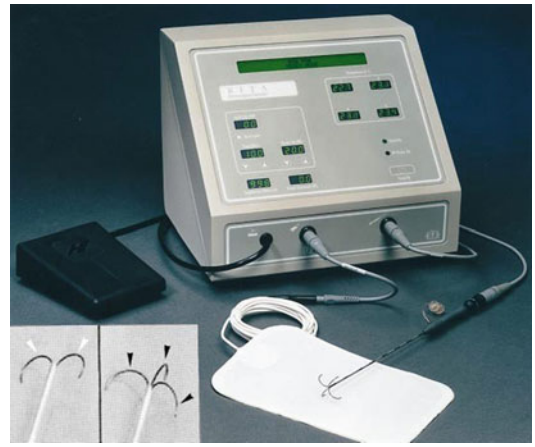

Fig. 51.1 RF generator, foot pedal, neutral electrode, and monopolar needle electrode. Inset: monopolar electrodes and monopolar two-hook electrodes located 180° apart (*white arrow*) or triple hook (*black arrows*). The extendible nickel–titanium hook electrodes (*black arrows*) increase the size of the lesions (Adapted with permission from Zlotta AR, Djavan B, Maton C. Percutaneous transperineal radiofrequency ablation of prostate tumour: Safety, feasibility and pathological effects on human prostate cancer. Br J Urol. 1998 Feb; 81(2): 265–75)

lengthened by retracting the adjustable insulating shield, controlled at the handle of the device. Extendible nickel–titanium hook electrodes are deployed at the distal end of the probe to increase the size of the lesions (Fig. 51.1). Thermocouples have been added to the hooks for continuous interstitial temperature measurement. The handle is marked to show the extent of deployment of the side hooks from the cannula. The diameter of the uncovered needles with triple-hook electrodes is 2 cm. All parameters such as temperature, impedance, time, and power measurements are recorded by a computer connected to the generator.

Using the monopolar electrodes, a neutral electrode is needed to be located on the skin of the patient (lower vertebral column, midline). The energy delivered by this electrode creates a thermal lesion that extends around the active electrode. Using the secondary hooks, the lesion formed is spherical (Fig. 51.2a). When bipolar electrode is applied, two active needles should be placed, with the lesion formed between them and with a variable ovoid or pillow-like shape (Fig. 51.2b).

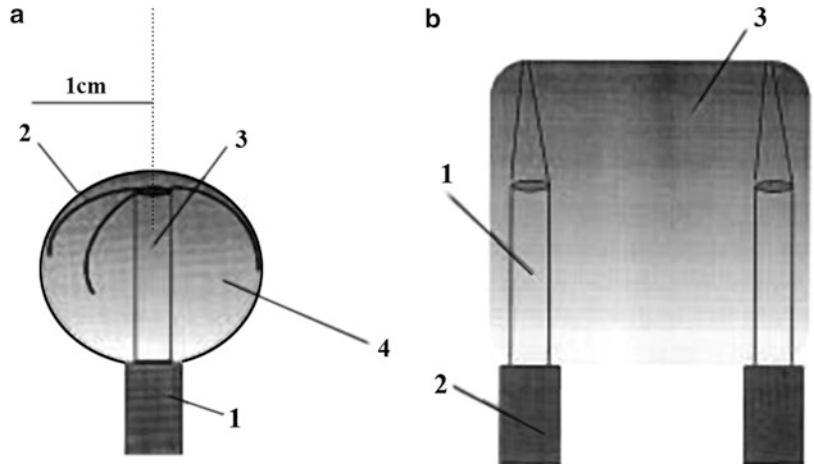

Fig. 51.2 (**a**). The *spherical shape* of lesions produced with triple-hook monopolar needles. Lesions are produced around the two active electrodes. *1*, Shield; *2*, extendible hook; *3*, central probe; and *4*, lesion. (**b**). A bipolar lesion with bipolar energy. The lesions are produced between the active electrodes. *1*, bipolar needle; *2*, shield; and *3*, lesion (Adapted with permission from Zlotta AR, Djavan B, Maton C. Percutaneous transperineal radiofrequency ablation of prostate tumour: Safety, feasibility and pathological effects on human prostate cancer. Br J Urol. 1998 Feb; 81(2): 265–75)

The Bruel & Kjaer (model 1846) ultrasound machine was used to monitor the placement of the electrodes. Prostate volume was estimated using this formula, width × height × length × 0.52. The TRUS machine was equipped with software that shows different longitudinal paths on the screen (on both sagittal and transverse views) corresponding to the various parallel channels of a ring connected to the ultrasound probe (Fig. 51.3).

Procedural Technique

In the study on safety, feasibility, and efficacy of RITA, the procedure was performed under general or spinal anesthesia and the patient positioned in the lithotomy position. For monopolar ablation, the dispersive electrode was placed at the coccyx. Following intravenous administration of antibiotic and urethral catheterization, ultrasonography was performed, and prostate volume was defined, and tumor location was determined. A small perineal incision was made, and under TRUS guidance, the active monopolar needles were introduced transperineally using the ring attached to the transrectal ultrasonic probe. The needles were advanced into one of the lobes and then accurately positioned into the targeted area by visualizing both sagittal and transversal planes. The hooks were then deployed. Placement of needles and their relations in sagittal and transverse planes of ultrasound are showed in Fig. 51.4.

When bipolar electrodes were needed, electrodes were introduced parallel to each other. After proper positioning of electrodes, the power was delivered under the control of parameters. Rectal temperature was monitored using thermosensors attached to the TRUS probe in all patients. Additional thermometry was performed using thermosensors that were introduced into the prostate or adjacent areas during open surgery. One thermocouple was inserted between active bipolar electrodes and one another just outside of the posterior capsule to monitor this potentially endangered area behind the rectum.

For the treatment of entire prostate in the patient not undergoing prostatectomy, three different monopolar electrodes were used. The first electrode was a triple-hook electrode (making a 2-cm diameter spherical lesion) to treat all portions of the prostate (bladder neck, central and transition zones) except for the areas at the

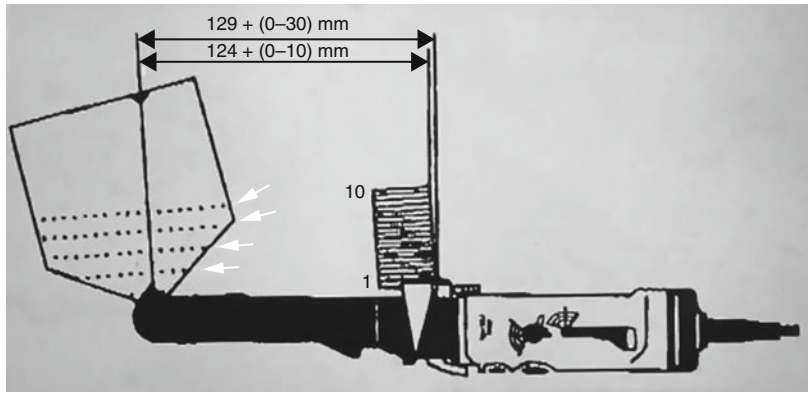

Fig. 51.3 The ring connected to the ultrasound probe; this ring is perforated with longitudinal channels through which the probes are introduced (*white arrows*) (Adapted with permission from Zlotta AR, Djavan B, Maton C. Percutaneous transperineal radiofrequency ablation of prostate tumour: Safety, feasibility and pathological effects on human prostate cancer. Br J Urol. 1998 Feb; 81(2): 265–75)

neurovascular bundles (NVB) and the posterior portion of the prostate on Denonvillier's fascia above the rectum. The second electrode was a two-hook electrode with hooks positioned 180° apart and designed to give a flat, "smile-like" lesion 2 cm across to treat the posterior prostate on the rectum. The third electrode used was a straight needle with a single passive hook and acted simply as temperature monitor.

This needle was used to treat all the areas adjacent to the capsule and neurovascular bundles. An individual independent thermistor was placed perineally through the puncture site along Denonvillier's fascia to the level of the seminal vesicles to monitor the temperature at the prostatorectal interface. Duration of the procedure was about 1.5 h of total operation time.

Finally, cystoscopy was repeated showing no areas of charred or burned urethra. The patient left the operating room and discharged within the same day with the Foley catheter retained [67].

There are several animal studies on the feasibility of some modifications to the technique.

Initially, Leveillee et al. [78] reported the application of liquid conductor for increasing the size of lesions induced by radiofrequency in canine prostate. They reported that rapid increase in electrical impedance secondary to tissue desiccation and charring at the electrode tip in conventional technique makes an impediment to achieve sizable lesions. They created a hollow screw-tip needle electrode that permits fixation to tissue, recording of temperature and impedance, infusion of fluid, and delivery of RF energy. In their experiment, saline infusion into the tissue prevented impedance rise by conducting RF energy away from the metal electrode and permitted induction of large lesions. Large-diameter lesions could be induced by varying the conductivity of the solution either by concentration or temperature. It was suggested that using a liquid conductor in prostate tissue allows a single electrode-placement heating cycle leading to controlled ablation of the prostate with adjustment of duration of RF energy application [78].

Liu and colleagues performed new experiments on the use of contrast-enhanced ultrasound (CEUS) in canine model [79]. In their experiment, Sonazoid® was used as the contrast agent. The contrast agent was continuously infused throughout the procedure with some intravenous bolus injection before ablation, after completing each RF ablation and at the end of the entire ablation procedure. Contrast-enhanced pulse inversion harmonic imaging (PIHI) mode showed normal prostate vasculature as a radial, spoke-like pattern with smaller vessels, resulting in parenchymal enhancement of the entire gland. Real-time monitoring

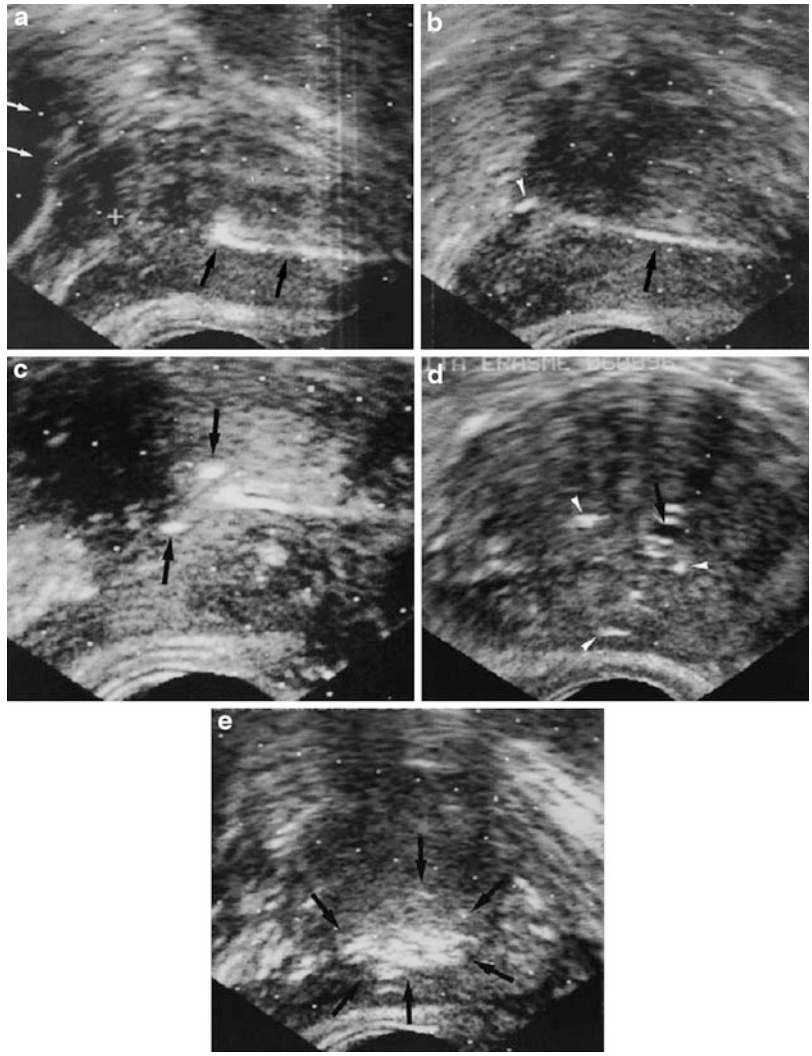

Fig. 51.4 Ultrasonograms of monopolar needle placement before RITA. The guides on the screen (**a**, *white arrows*) facilitate needle placement. Software shows the location on both sagittal and transverse planes of a needle introduced through one of the channels. The needle electrode (*black arrows*) is introduced in the mid prostate (**a**). The active electrode is further deployed in the sagittal plane, close to the base of the prostate (**b**, *white arrow*). Two of the triple hooks (*black arrows*) are clearly visible on the sagittal plane (**c**). The accuracy of needle placement is confirmed on the transverse plane (**d**) and shows the triple hooks deployed (*white arrows*) and the catheter placed in the urethra (*black arrow*). A minimum distance of 5 mm was maintained between the most peripheral hook and the rectum. Ultrasonography during RF ablation is shown in (**e**); note the hyperechoic front that departs from the tip of the active needles, forming a *bullet-shaped* lesion (*arrows*) (Adapted with permission from Zlotta AR, Djavan B, Maton C. Percutaneous transperineal radiofrequency ablation of prostate tumour: Safety, feasibility and pathological effects on human prostate cancer. Br J Urol. 1998 Feb; 81(2): 265–75)

showed peripheral arteries enhancing early in the arterial phase, followed by drainage mainly in the urethral area in the venous phase. Thermal lesions were detected as nonperfused areas during continuous infusion and appeared as well-defined hypoechoic areas relative to surrounding normal prostate parenchyma with bolus injection of contrast agent. Using this technique, the average volume of ablation was 96.3 %. It was identified that contrast-enhanced

PIHI could be used to guide, monitor, and control radiofrequency ablation of the whole gland [79].

In the following study, they evaluated the role of urethral and neurovascular cooling as protective tools to minimize the possibility of injury to the adjacent tissues such as urethra, bladder, and NVB during the whole-gland ablation in the canine model. Damage to the urethra and the NVB was detected in group without any protection. In contrast, urethral cooling significantly reduced urethral damage ($P = 0.002$). However, intra-arterial cooling as a protection for NVB showed a decreased NVB damage which did not reach statistical significance ($P = 0.069$) [80].

Radiofrequency Ablation of Prostate Tumors

In the first study, fourteen patients with biopsy-proven prostate cancer who had been scheduled for radical prostatectomy were included. Prostatectomy was immediately performed after the transperineal RF treatment in eight patients. The other six patients were treated with RF 1 week before radical prostatectomy. In addition, one patient was treated with RF but did not undergo radical prostatectomy and was followed by serial PSA measurement [67].

The last patient was an asymptomatic man with a PSA level of 5.1 ng/mL and no suspicious digital rectal exam findings, but with grade III adenocarcinoma in both lobes of the prostate on biopsy. He successfully underwent androgen blockade, and then RFA was undertaken. RFA was performed with no complication in all patients.

Only bipolar electrodes were used in five patients, while in two patients, both bipolar and monopolar electrodes were applied. In eight patients (including the patient who did not undergo radical prostatectomy), RF energy was delivered with monopolar electrode only.

Examination of specimens obtained immediately after RF treatment showed necrotic hemorrhagic areas in all cases but cavitation with liquefaction and caseated areas just in one specimen.

H&E staining of specimens obtained 7 days after the procedure revealed an intense interstitial edema and fading of the cell borders with cytoplasmic hypereosinophilia. Glands appeared retracted, with their epithelium desquamating in the glandular lumen.

In one specimen recovered 7 days after the RF treatment in which prostate cancer was diagnosed in both lobes on biopsy, in the left lobe, there were no tumor cells in histology, whereas in the right lobe, several tumor cells were still visible. In the other specimens, lesions not targeted to specifically destroy the tumor did not ablate the entire tumor area.

The extent of the lesions induced by bipolar energy was related to the interneedle distance and length of uncovered needle. But, when the low power (3 W) was used, a smaller than expected lesion was induced. They found that the size of the lesion induced by monopolar electrode is poorly correlated with the power of energy delivered.

It has also been shown that RF treatment could be safely delivered via needles placed close to prostate capsule with the lesion not extending into the extraprostatic tissue.

In a patient who underwent radical prostatectomy 7 days after RF treatment, preoperative MRI which was performed at 7 days of RF ablation showed extensive lesions of necrosis corresponding to histological diagnosis. There was also no enhancement using gadolinium contrast.

Finally, it would be suggested that RF can induce reproducible large necrotic lesions in the prostate including the posterior capsule while sparing adjacent organs such as the rectum.

In a study by Patriarca et al. [81], histopathological findings after RITA treatment have been reported. The procedure was performed in ten patients with histologically confirmed prostate cancer. The biopsy Gleason score ranged from 6 (3 + 3) to 7 (4 + 3 or 3 + 4) and 8 (4 + 4). Prostate cancer was clinically organ confined in all patients. Patients underwent radical prostatectomy within 1 to 4 weeks after the RITA treatment. Two ablations were performed per prostate (one for each lobe) in seven cases, a single lobe

was treated in one case, and five ablations were performed in two cases. Urinary retention due to edema induced by the thermal lesions was detected in 60 % of patients between 24 h and 7 days after the treatment.

Formalin-fixed prostatectomy specimens were routinely embedded, and transversal sections 0.5 cm thick were taken macroscopically from all 10 prostates. Then coronal sections were routinely embedded, and histological sections 3 mm thick were stained with hematoxylin and eosin (H&E). Immunohistochemical staining was also performed for bcl-2 antiapoptotic protein.

There were no signs of the RITA treatment or histological evidence of necrosis or inflammation with macroscopic examination in the outer surface of the prostate specimens, while macroscopic examination of the cut surface of the glands revealed the presence of sharply defined, rounded areas of the prostates in one (one case) or both lobes (nine cases).

Treated areas had a gray-white crumbly appearance with a well-defined dark-red peripheral ring. The major diameters of the lesions ranged from 9 to 25 mm.

Histological examination showed a precise compartmentalization of the lesions and massive, homogeneous coagulative necrosis in all cases. "Pink" homogenized coagulative necrosis encompassed the neoplastic tissue, as well as the nonneoplastic epithelial, smooth muscle, and vascular and fibroblastic tissues. Surrounding ring at macroscopic examination showed a well-defined area of hemorrhagic extravasation and capillary ectasia at histological exam. Squamous metaplasia of the ducts was always evident at the periphery of the necrotic area, and scattered foci of squamous metaplasia were detectable in the untreated tissue close to the hemorrhagic ring.

Only two of the 10 cases revealed small foci of non-necrotic neoplastic tissue with a maximal diameter of 3–6 mm and a Gleason score of 6 and 8 and were located in the middle and at the periphery of the necrotic areas. These two cases had a shorter duration of treatment.

bcl-2 immunostaining was negative in the shadows of neoplastic nuclei in coagulative necrotic areas. There was no inflammatory reaction in all but three cases, where confined microfoci of lymphoplasmacellular reaction were seen around the necrotic areas. Giant cell granulomatous reaction was also evident in one case. There were also no correlations between the type of necrosis and the interval between RITA treatment and prostatectomy.

The duration of treatment was in average 10–12 min. Temperatures higher than 100 °C were reached within about 2 min and maintained for 5 min in eight patients, 4 min in one, and 3 min in one to establish how long it took to necrotize all the cells in the treatment area.

During radical prostatectomy procedure, there was no sign of damage to the urethral sphincter, bladder, or rectal wall, and no greater difficulties were encountered in separating cleavage surfaces, apart from the presence of mild reactive fibrosis in the connective tissue of the pelvis and Denonvillier's fascia in a few cases.

Macroscopically, there was an almost perfect consistency between the areas where the hooks were applied and the lesions obtained. The largest diameter of the necrotic volumes ranged from 0.9 to 2.5 cm, whereas the treated areas ranged from 1 to 2.5 cm in diameter.

Finally, they found that RITA treatment induces necrotic lesions of the planned shape and size, with no residual vital tumor in the necrotic areas after RF ablation for more than 5 min. The satisfactory consistency between the expected ablation and the lesions obtained using RF energy delivery might provide the foundations for future research on complete prostate ablation using RITA [81].

Photodynamic Therapy

Background

Photodynamic therapy (PDT) is an ablative therapy using three elements including a photosensitizer agent, light, and oxygen. Photosensitizer agent is usually administered by intravenous infusion and is present in the tissue of interest by perfusion of that organ. Using fiber-optic illumination with certain wavelength for the

specific drug, the photosensitizer agent is activated at the targeted site. Activation of photosensitizing drug might occur either within the tissue or in the vasculature supplying the targeted tissue [82].

Tissue-activated drugs have long drug–light intervals requiring administration of the drug and light at separate treatment sessions. This type of photosensitizing agents remains in the body for a long time and accumulates in the skin, and sunlight exposure should be avoided using covers to prevent sunburn [82].

However, vascular-activated drugs have the advantage of a short drug–light interval, allowing the physician to perform the whole treatment in a single treatment session. Also, these drugs are rapidly removed from the vasculature and do not accumulate within the cutaneous tissue, and no light restrictions might be needed after a few hours [82].

Some of the tissue-activated photosensitizers such as amino levulinic acid (ALA) preferentially accumulate in the proliferating and tumoral cells causing some selectivity for tumor ablation.

Underlying mechanism for tumoral cell destruction is not completely understood. Some mechanisms such as oxygen-dependent cytotoxic effect, vasculotoxic reactions [83], and loss of endothelial integrity leading to vascular thrombosis might be involved [84–86].

Photosensitizers that have been studied include hematoporphyrin derivatives (Photofrin), m-tetrahydroxyphenylchlorin (Foscan), etiopurpurin dichloride (PhotoPoint), lutetium texaphyrin (LuTex), verteporfin (Visudyne), and palladium-bacteriopheophorbide (WST09, also known as Tookad) [87].

Newer vascular-targeting photosensitizers such as verteporfin and Tookad can be used to cause vascular damage and occlusion with better tumor tissue necrosis. Verteporfin is primarily used in preclinical studies [88, 89], while Tookad has been evaluated in preclinical and also early human trials.

This type of focal therapy is usually used for cutaneous lesions but has also been evaluated for breast, central nervous system, head and neck, lung, esophageal, cervical, bladder, and prostate cancers.

As a focal ablative therapy for prostate cancer, PDT can be applied transperineally similar to brachytherapy technique, and the lesions created with PDT can be well followed by perfusion imaging such as gadolinium-enhanced endorectal MRI. However, this treatment is subject to some disadvantages including risk of cutaneous and ocular photosensitivity, localized collateral damage to adjacent organs (including bowel, urethra, bladder, and nerve tissue), and systemic toxicity associated with intravenous administration of photosensitizing drug that may include vasculopathy or involvement of other organs [87].

History and Recent Studies

Windahl and colleagues initially reported the use of PDT for prostate cancer in two patients. Following transurethral resection of the prostate revealing prostate cancer, PDT was applied using transurethral approach and tissue-activated photosensitizing drug. The drug–light interval was 48 or 72 h. One patient died of an undiagnosed lung cancer, but with no evidence of prostate cancer on postmortem histologic study. The other one had a reduction in PSA with no evidence of residual prostate cancer on follow-up biopsy session at 3 months [90].

In a phase I trial study, Nathan et al. [91] evaluated PDT using m-tetrahydroxyphenylchlorin (mTHPC, Foscan®) as a photosensitizer in 14 patients with localized recurrent prostate cancer after radiation therapy. Study was performed at a certain drug dose (0.15 mg/kg), with drug–light interval of 3 to 5 days, and a variety of light doses, using both bare fibers and cylindrical diffusers. PSA decreased in nine patients (to undetectable levels in 2) and five had no evidence of residual tumor on future biopsies. Contrast-enhanced computerized tomography or MRI performed after the treatment showed necrosis involving up to 91 % of the prostate cross section. Complications included stress incontinence (in four patients) and impaired

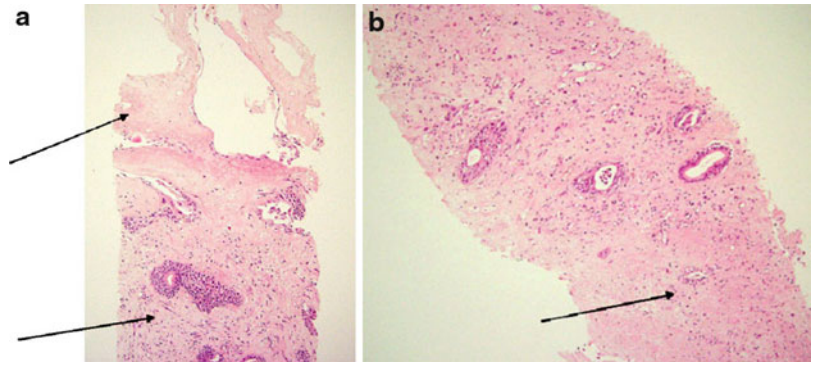

Fig. 51.5 Histological changes following PDT (**a**) biopsy 1 month post-PDT. The *lower arrow* shows unaffected tissue, and the *upper arrow* points to an area of necrosis. Magnification ×10. (**b**): Biopsy 2 months post-PDT. The arrow shows vascular inflammation and fibrosis. Magnification × 10 (Adapted with permission from Moore CM, Nathan TR, Lees WR, Mosse CA, Freeman A, Emberton M, et al. Photodynamic therapy using meso tetra hydroxy phenyl chlorin (mTHPC) in early prostate cancer. Lasers Surg Med. 2006;38: 356–63)

sexual potency (in 4 of the 7 potent men). There were no rectal complications directly related to PDT, but urethrorectal fistula developed after an ill-advised rectal biopsy to assess an abnormal area of rectal mucosa 1 month after therapy in one patient [91].

In another study, they evaluated the efficacy of PDT as the primary treatment of organ-confined prostate cancer (OCPC) in six men who received ten sessions of PDT [92]. Red light (652 nm) was delivered to biopsy-proven cancer areas via fibers inserted through transperineal needles. Results of this phase I study indicated that, after 8 of 10 PDT sessions, the PSA level fell by up to 67 %. Histological examination of treated areas 1 month after PDT showed necrosis and early fibrosis, along with areas of hemorrhage. At 2 months, histological changes indicating healing process following necrosis including established fibrosis and increased vascularity were detected (Fig. 51.5).

Early MRI performed 2–6 days after the procedure showed variable changes in different patients. Diffuse, patchy areas of reduced enhancement were reported in some patients, while in some others, necrosis was more evident in the form of zones of devascularization and marked edema. Subsequent findings at 1 month later indicated healing process, and the major finding at 2–3 months was edema (Fig. 51.6). Treatment complications included irritative voiding symptoms for 2 weeks, temporary recatheterization after two treatments, and one episode of sepsis, despite prophylactic antibiotics [92].

Zaak et al. [93] investigated the use of 5-aminolevulinic acid (5-ALA) for interstitial PDT in five patients. 5-ALA is metabolized to photoactive protoporphyrin IX (PPIX) before being converted to photo inactive hem. Patients received oral 5-ALA of 20 mg/kg, and light of a diode laser (wavelength = 633 nm) was coupled into a fiber with a 1-cm cylindrical diffuser tip and introduced into the tissue transurethrally ($n = 3$) or transperineally ($n = 2$). PSA levels were decreased by 20 % up to 70 % at 6 weeks after the treatment. There was no side effect or complication in their patients [93].

Motexafin lutetium, a vascular-acting photosensitizer for PDT, has been initially used in canine model. The interstitial alone technique resulted in the least amount of toxicity. The prostatic tissue reaction to treatment is characterized by initial inflammation and necrosis, followed by fibrosis and glandular epithelial atrophy [94].

A group of investigators in the University of Pennsylvania have conducted a phase I trial study on PDT using motexafin lutetium with various drug doses, drug–light intervals, and light doses. This study was performed on 17 patients, 8 of

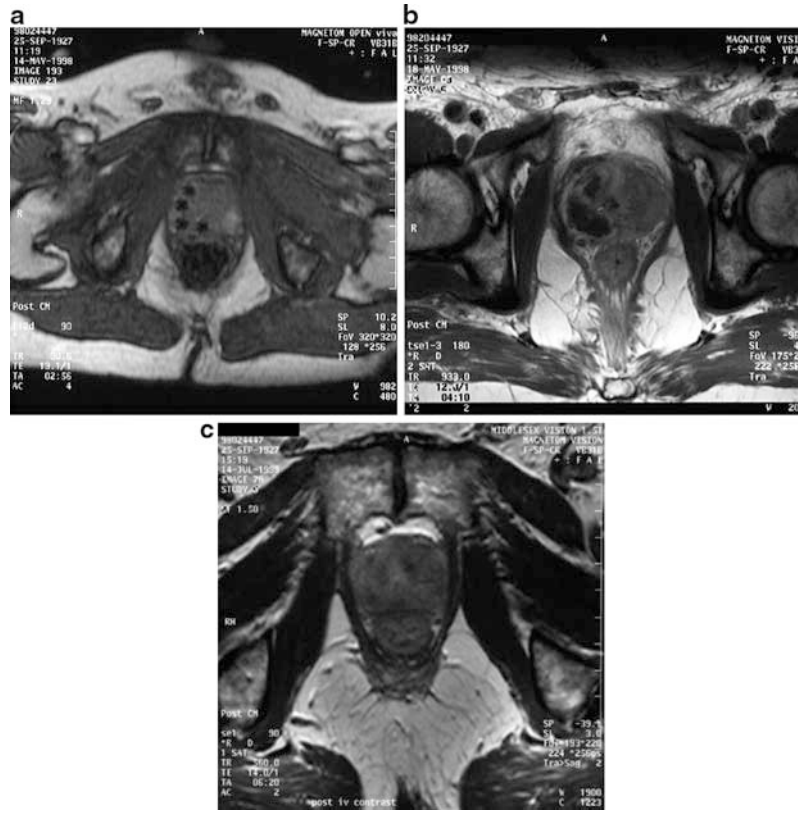

Fig. 51.6 Contrast-enhanced MRI of patient D, first treatment (**a**) four needles in right lobe of the prostate, just prior to light delivery. (**b**): Four days after light delivery, the right lobe shows large areas of loss of enhancement, which indicate early necrosis. (**c**): Two months after treatment, the enhancement pattern is almost entirely returned to that prior to therapy, indicating resolution of necrosis. Histology suggests that healing is by fibrosis (Adapted with permission from Moore CM, Nathan TR, Lees WR, Mosse CA, Freeman A, Emberton M, et al. Photodynamic therapy using meso tetra hydroxy phenyl chlorin (mTHPC) in early prostate cancer. Lasers Surg Med. 2006;38: 356–63)

whom had previously undergone external beam radiotherapy and 9 of whom had undergone brachytherapy. High-dose PDT, defined as using the highest drug dose (2 mg/kg), the highest light dose (150 J/cm^2), and the shortest drug–light interval (3 h), was performed in eight patients. Those patients undergoing high-dose PDT experienced the greatest initial rise in PSA level, followed by a reduction in PSA levels to below baseline values. By contrast, patients who received low-dose PDT (drug dose 0.5 mg/kg, light dose 25 J/cm^2, and drug–light interval 24 h) had a treatment-related rise in PSA level that did not subsequently fall below baseline. Treatment-related adverse effects included grade I urinary toxicity in many patients. Grade II urinary toxicity occurred in one patient (5.88 %) which was believed to be related to catheterization [95–97].

Authors have also extensively studied the heterogeneity of optical properties of the prostate and photosensitizer distribution throughout the prostate, in both canine models and in the group of patients described above [98–101].

Vascular-acting drugs are novel agents used in PDT of prostate cancer. Padoporfin (WST-09, Tookad®) and padeliporfin (WST-11, Stakel®) are palladium-bacteriopheophorbide photosensitizers that were synthesized from the native bacteriochlorophyll, a molecule produced in dark-growing bacteria under aerobic conditions [102–104].

Padoporfin, a lipophilic photosensitizer, needs a carrier (e.g., cremophor) to be given as an intravenous infusion, while padeliporfin is a water-based drug and can be used easily without any additional carrier. Some features have made these two vascular-acting photosensitizers optimal for prostate cancer treatment: water solubility and ease of preparation and administration, selective tissue destruction by being confined to circulation until clearance, rapid clearance from circulation and liver avoiding long sunlight exposure prevention, connective tissue resistance to

photodynamic effects, and deep-tissue penetration allowing large-volume destruction in a short time [82, 84].

Padoporfin is administered by a 20-min intravenous infusion. Delivery of the activating light at 763 nm begins within a few minutes of starting the infusion. Extensive skin testing has shown that no skin phototoxicity occurs 3 h after the treatment, and treatment could be performed in ambulatory care setting [105].

Initial study on the application of Tookad® was performed by Trachtenberg and colleagues. Twenty-four Canadian patients with biopsy-proven recurrent prostate cancer following definitive radiotherapy were enrolled in a phase I/II trial study [106]. Inclusion criteria were life expectancy more than 5 years, no evidence of regional or systemic disease on abdominopelvic CT scan, PSA less than 20 ng/mL, prostate volume less than 50 cm^3, and Gleason score greater than 6. Patients received escalating drug doses of 0.1 to 2 mg/kg at a fixed light dose of 100 J/cm or escalated light doses of 230 and 360 J/cm at the 2 mg/kg dose. Six optical fibers were used including two fibers for light delivery and the four others for light dosimetry. Treatment response was assessed primarily by hypovascular lesion formation on contrast-enhanced magnetic resonance imaging and transrectal ultrasound-guided biopsies targeting areas of lesion formation and secondarily by serum PSA changes [106].

In the lithotomy position and under the general anesthesia, the patients underwent transurethral ultrasound to visualize the prostate. Then, a standard brachytherapy stabilizing frame with the template modified to have 13 gauge holes was used to place transparent, closed-end catheters in the prostate.

One optical fiber was placed transperineally into these catheters in each of the right and left lobes of the prostate. For light dosimetry, four fibers were positioned in urethra, rectum, and hydrodissection space between rectum and prostate. A thermal monitoring probe was also inserted (Fig. 51.7).

The exact delivered light dose was determined using computer planning software program. The threshold light dose (i.e., the minimum light dose required to see an effect on MRI) was found to be 23 J/cm^2 in at least 90 % of the prostate volume. Treatment response was assessed by dynamic gadolinium-enhanced MRI at the end of the first week and 6 months after treatment, prostate biopsy performed at 6 months, and serum PSA measurements at 1, 2, 3, and 6 months. Patients were followed for possible complications affecting potency, continence, voiding symptoms, and rectal symptoms. Neither urinary nor erectile function was compromised in the long term (up to 6 months) following the procedure. All patients had normal urination 1 week after treatment, but 2 of them had urinary catheter for 1 additional week and voided spontaneously afterward. Bowel and erectile function showed no significant change from baseline at 6 months. Transient hypotension occurred early after infusion of the Tookad® solution that responded to fluids and pressors. Decreased urinary function occurred in patients who had an MRI response to treatment ($n = 10$) at 1 month, but returned to baseline status at 6 months [106].

On posttreatment biopsies, regions of avascularity seen on the post-PDT MRI images at 7 days were matched to regions of histopathological fibrosis with no residual viable tumor. In all patients, tissue 3–5 mm outside these avascular zones showed remaining viable tumor and preserved prostatic stroma with no observable photodynamic effect. The lesion diameter ranged between 5 and 10 mm. Even at the highest light dose, no injuries to the rectum or urethra happened. Complete response to treatment occurred in 60 % of the patients who received at least the threshold light dose. Extensive avascular areas at 1-week MRI with no evidence of residual cancer on 6-month biopsy were considered as treatment response [106].

In another phase II trial study, Trachtenberg et al [107] investigated the efficacy of this treatment in 28 patients with recurrent prostate cancer after failed external beam radiotherapy. Whole prostate gland was treated with minimal effects on surrounding organs. An increased light dose improved the tissue response. Avascular lesions detected on contrast-enhanced MRI involved up

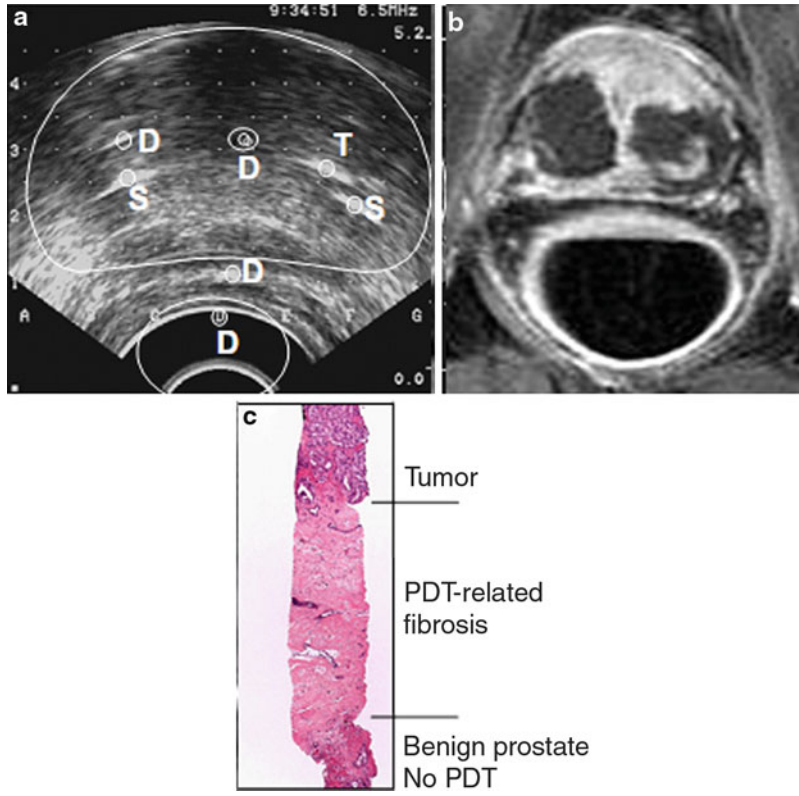

Fig. 51.7 (**a**), Transverse view of prostate under transrectal ultrasound. *White areas* indicate fibers. *Outlines* indicate prostate, urethra, and rectum. *S* Source fibers, *T* Temperature probe, *D* Light dosimetry fibers are positioned in urethra, rectum, and hydrodissection space between rectum and prostate. (**b**), Post-gadolinium-enhanced MRI 7 days after VTP in patient with 2 mg/kg drug dose and 360 J/cm light dose demonstrates necrotic regions. Note large lesions in each lobe. (**c**), Pathological finding in same patient reveals viable tumor adjacent to punched out area of fibrosis attributable to partial VTP effect and preserved prostate stroma containing benign prostate glands. Note entrapped benign atrophic prostate glands in well-defined area of VTP-induced fibrosis. Reduced from × 25 (Adapted from Trachtenberg J, et al. J Urol. 2007; 178: 1974–9, with permission from John Wiley & Sons, Ltd.)

to 80 % of the prostate in some patients. Complete response required at least 23 J/cm^2 of light doses in 90 % of the prostate volume. Thus, they identified the clinical potential of TOOKAD® for PDT to manage recurrence of prostatic cancer following external beam radiotherapy [107].

Despite of developments in PDT for prostate cancer, this technique is subject to several limitations. Whole-gland PDT needs a sufficient dose of drug, light, and oxygen to be delivered to the entire gland. An excess of drug or light might influence the adjacent organs. Also, there is no consensus on the appropriate follow-up protocol for patients undergoing PDT. Major limitations for the use of PDT in focal prostate cancer therapy include accurate identification of cancer within the gland, accurate prediction of the tumor behavior, accurate treatment of the identified target volume, and assessment of the gland after treatment [82].

Conclusion

In conclusion, focal therapy may be considered in approximately one-third of patients with newly diagnosed prostate cancer. There is no clear consensus on the criteria for candidates of focal therapy; however, it could be suggested that a patient with a PSA level <10 ng/mL, a PSA density

<0.15 ng/mL/g, and a Gleason score of 6 (i.e., no grade 4 or 5 cancer) as a candidate for focal therapy undergo imaging before decision making on treatment option. The imaging criteria for identifying unifocal tumor include no more than 1 biopsy-proven lesion, largest tumor dimension of <15 mm in any plane by imaging, capsular contact with the lesion <5 mm on axial images, and organ-confined disease, with no evidence of ECE or seminal vesicle invasion. In addition, the regional lymph nodes should not be suspicious for metastatic disease (i.e., they should measure <7 mm in the short axis and have a smooth border, and there should not be an asymmetric cluster of nodes). Current trend is toward the use of combination of MRI and MRSI to predict the tumor volume, location, extension, invasion, and staging and to plan the suitable treatment alternatives. However, a more extensive study on the efficacy of RITA with long-term follow-up is needed.

PDT has the potential to be used for focal treatment of prostate cancer. Safety, feasibility, and efficacy of vascular-targeted PDT as a focal treatment option have been shown in clinical trials.

Despite of advances in PDT for prostate cancer, this technique is still subject to several limitations. One of the major limitations includes difficulty with accurate identification of tumor location, treatment planning, and lack of real-time feedback of therapeutic effect during the procedure.

References

1. National Cancer Institute, prostate cancer. 2010. http://www.cancer.gov/cancertopics/types/prostate. Accessed 22 July 2010.
2. Jemal A, Murray T, Samuels A, Ghafoor A, Ward E, Thun MJ. Cancer statistics, 2003. CA Cancer J Clin. 2003;53(1):5–26.
3. Hu JC, Gu X, Lipsitz SR, et al. Comparative effectiveness of minimally invasive vs open radical prostatectomy. JAMA. 2009;302(14):1557–64.
4. Cahlon O, Hunt M, Zelefsky MJ. Intensity-modulated radiation therapy: supportive data for prostate cancer. Semin Radiat Oncol. 2008;18(1):48–57.
5. Sharma NL, Shah NC, Neal DE. Robotic-assisted laparoscopic prostatectomy. Br J Cancer. 2009;101(9):1491–6.
6. Shipley WU, Thames HD, Sandler HM, et al. Radiation therapy for clinically localized prostate cancer: a multi-institutional pooled analysis. JAMA. 1999;281(17):1598–604.
7. Rogers E, Ohori M, Kassabian VS, Wheeler TM, Scardino PT. Salvage radical prostatectomy: outcome measured by serum prostate specific antigen levels. J Urol. 1995;153(1):104–10.
8. Pisters LL. Salvage radical prostatectomy: refinement of an effective procedure. Semin Radiat Oncol. 2003;13(2):166–74.
9. Izawa JI, Morganstern N, Chan DM, Levy LB, Scott SM, Pisters LL. Incomplete glandular ablation after salvage cryotherapy for recurrent prostate cancer after radiotherapy. Int J Radiat Oncol Biol Phys. 2003;56(2):468–72.
10. Pisters LL, von Eschenbach AC, Scott SM, et al. The efficacy and complications of salvage cryotherapy of the prostate. J Urol. 1997;157(3):921–5.
11. Pisters LL, Rewcastle JC, Donnelly BJ, Lugnani FM, Katz AE, Jones JS. Salvage prostate cryoablation: initial results from the cryo on-line data registry. J Urol. 2008;180(2):559–63. discussion 563–554.
12. Grado GL, Collins JM, Kriegshauser JS, et al. Salvage brachytherapy for localized prostate cancer after radiotherapy failure. Urology. 1999;53(1):2–10.
13. Beyer DC. Brachytherapy for recurrent prostate cancer after radiation therapy. Semin Radiat Oncol. 2003;13(2):158–65.
14. Lecornet E, Ahmed HU, Moore CM, Emberton M. Conceptual basis for focal therapy in prostate cancer. J Endourol. 2010;24(5):811–8.
15. Mouraviev V, Mayes JM, Madden JF, Sun L, Polascik TJ. Analysis of laterality and percentage of tumor involvement in 1386 prostatectomized specimens for selection of unilateral focal cryotherapy. Technol Cancer Res Treat. 2007;6(2):91–5.
16. Jayram G, Eggener SE. Patient selection for focal therapy of localized prostate cancer. Curr Opin Urol. 2009;19(3):268–73.
17. Mouraviev V, Mayes JM, Sun L, Madden JF, Moul JW, Polascik TJ. Prostate cancer laterality as a rationale of focal ablative therapy for the treatment of clinically localized prostate cancer. Cancer. 2007;110(4):906–10.
18. De Laet K, de la Taille A, Ploussard G, et al. Predicting tumour location in radical prostatectomy specimens: same-patient comparisons of 21-sample versus sextant biopsy. BJU Int. 2009;104(5):616–20.
19. Polascik TJ, Mouraviev V. Focal therapy for prostate cancer is a reasonable treatment option in properly selected patients. Urology. 2009;74(4):726–30.
20. Sartor AO, Hricak H, Wheeler TM, et al. Evaluating localized prostate cancer and identifying candidates for focal therapy. Urology. 2008;72(6 Suppl):S12–24.
21. Hirano D, Werahera PN, Crawford ED, Lucia MS, DeAntoni EP, Miller GJ. Morphological analysis and classification of latent prostate cancer using

a 3-dimensional computer algorithm: analysis of tumor volume, grade, tumor doubling time and life expectancy. J Urol. 1998;159(4):1265–9.
22. Rice KR, Furusato B, Chen Y, McLeod DG, Sesterhenn IA, Brassell SA. Clinicopathological behavior of single focus prostate adenocarcinoma. J Urol. 2009;182(6):2689–94.
23. Ahmed HU. The index lesion and the origin of prostate cancer. N Engl J Med. 2009;361(17):1704–6.
24. Villers A, Lemaitre L, Haffner J, Puech P. Current status of MRI for the diagnosis, staging and prognosis of prostate cancer: implications for focal therapy and active surveillance. Curr Opin Urol. 2009;19(3):274–82.
25. Onik G. Rationale for a "male lumpectomy," a prostate cancer targeted approach using cryoablation: results in 21 patients with at least 2 years of follow-up. Cardiovasc Intervent Radiol. 2008;31(1):98–106.
26. Lindner U, Weersink RA, Haider MA, et al. Image guided photothermal focal therapy for localized prostate cancer: phase I trial. J Urol. 2009;182(4):1371–7.
27. de Senneville BD, Mougenot C, Moonen CT. Real-time adaptive methods for treatment of mobile organs by MRI-controlled high-intensity focused ultrasound. Magn Reson Med. 2007;57(2):319–30.
28. de Senneville BD, Mougenot C, Quesson B, Dragonu I, Grenier N, Moonen CT. MR thermometry for monitoring tumor ablation. Eur Radiol. 2007;17(9):2401–10.
29. Bostwick DG, Waters DJ, Farley ER, et al. Group consensus reports from the Consensus Conference on Focal Treatment of Prostatic Carcinoma, Celebration, Florida, February 24, 2006. Urology. 2007;70(6 Suppl):42–4.
30. Eggener SE, Scardino PT, Carroll PR, et al. Focal therapy for localized prostate cancer: a critical appraisal of rationale and modalities. J Urol. 2007;178(6):2260–7.
31. Moran BJ, Braccioforte MH, Conterato DJ. Re-biopsy of the prostate using a stereotactic transperineal technique. J Urol. 2006;176(4 Pt 1):1376–1381. discussion 1381.
32. Pinkstaff DM, Igel TC, Petrou SP, Broderick GA, Wehle MJ, Young PR. Systematic transperineal ultrasound-guided template biopsy of the prostate: three-year experience. Urology. 2005;65(4):735–9.
33. Wang L, Mullerad M, Chen HN, et al. Prostate cancer: incremental value of endorectal MR imaging findings for prediction of extracapsular extension. Radiology. 2004;232(1):133–9.
34. Wang L, Hricak H, Kattan MW, Chen HN, Scardino PT, Kuroiwa K. Prediction of organ-confined prostate cancer: incremental value of MR imaging and MR spectroscopic imaging to staging nomograms. Radiology. 2006;238(2):597–603.
35. Partin AW, Mangold LA, Lamm DM, Walsh PC, Epstein JI, Pearson JD. Contemporary update of prostate cancer staging nomograms (Partin Tables) for the new millennium. Urology. 2001;58(6):843–8.
36. Wang L, Hricak H, Kattan MW, et al. Prediction of seminal vesicle invasion in prostate cancer: incremental value of adding endorectal MR imaging to the Kattan nomogram. Radiology. 2007;242(1):182–8.
37. Ramsden AR, Chodak G. An analysis of risk factors for biochemical progression in patients with seminal vesicle invasion: validation of Kattan's nomogram in a pathological subgroup. BJU Int. 2004;93(7):961–4.
38. Wang L, Hricak H, Kattan MW, et al. Combined endorectal and phased-array MRI in the prediction of pelvic lymph node metastasis in prostate cancer. AJR Am J Roentgenol. 2006;186(3):743–8.
39. Miyamoto K, Abe S, Kawakami Y. Picture archiving and communication system in Hokkaido University hospital: advantage and disadvantage of HU-PACS chest roentgenogram images in the outpatient clinic. J Digit Imaging. 1991;4(4 Suppl 1):28–31.
40. De Backer AI, Mortele KJ, De Keulenaer BL. Picture archiving and communication system–Part one: filmless radiology and distance radiology. JBR-BTR. 2004;87(5):234–41.
41. Wang L, Zhang J, Schwartz LH, et al. Incremental value of multiplanar cross-referencing for prostate cancer staging with endorectal MRI. AJR Am J Roentgenol. 2007;188(1):99–104.
42. Carroll PR, Presti Jr JC, Small E, Roach 3rd M. Focal therapy for prostate cancer 1996: maximizing outcome. Urology. 1997;49(3A Suppl):84–94.
43. Blute ML, Bostwick DG, Bergstralh EJ, et al. Anatomic site-specific positive margins in organ-confined prostate cancer and its impact on outcome after radical prostatectomy. Urology. 1997;50(5):733–9.
44. Wefer AE, Hricak H, Vigneron DB, et al. Sextant localization of prostate cancer: comparison of sextant biopsy, magnetic resonance imaging and magnetic resonance spectroscopic imaging with step section histology. J Urol. 2000;164(2):400–4.
45. Noguchi M, Stamey TA, Neal JE, Yemoto CE. An analysis of 148 consecutive transition zone cancers: clinical and histological characteristics. J Urol. 2000;163(6):1751–5.
46. Stamey TA, Donaldson AN, Yemoto CE, McNeal JE, Sozen S, Gill H. Histological and clinical findings in 896 consecutive prostates treated only with radical retropubic prostatectomy: epidemiologic significance of annual changes. J Urol. 1998;160(6 Pt 2):2412–7.
47. Reissigl A, Pointner J, Strasser H, Ennemoser O, Klocker H, Bartsch G. Frequency and clinical significance of transition zone cancer in prostate cancer screening. Prostate. 1997;30(2):130–5.
48. Philip J, Manikandan R, Viswanathan P. Prostate cancers in the transition zone: part 2; clinical aspects. BJU Int. 2005;95(6):909.
49. Erbersdobler A, Augustin H, Schlomm T, Henke RP. Prostate cancers in the transition zone: part 1; pathological aspects. BJU Int. 2004;94(9):1221–5.

50. Augustin H, Erbersdobler A, Hammerer PG, Graefen M, Huland H. Prostate cancers in the transition zone: part 2; clinical aspects. BJU Int. 2004;94(9):1226–9.
51. Gelet A, Chapelon JY, Bouvier R, Rouviere O, Lyonnet D, Dubernard JM. Transrectal high intensity focused ultrasound for the treatment of localized prostate cancer: factors influencing the outcome. Eur Urol. 2001;40(2):124–9.
52. Fleshner NE, Fair WR. Indications for transition zone biopsy in the detection of prostatic carcinoma. J Urol. 1997;157(2):556–8.
53. Lui PD, Terris MK, McNeal JE, Stamey TA. Indications for ultrasound guided transition zone biopsies in the detection of prostate cancer. J Urol. 1995;153(3 Pt 2):1000–3.
54. Akin O, Sala E, Moskowitz CS, et al. Transition zone prostate cancers: features, detection, localization, and staging at endorectal MR imaging. Radiology. 2006;239(3):784–92.
55. Coakley FV, Kurhanewicz J, Lu Y, et al. Prostate cancer tumor volume: measurement with endorectal MR and MR spectroscopic imaging. Radiology. 2002;223(1):91–7.
56. Kattan MW, Eastham JA, Stapleton AM, Wheeler TM, Scardino PT. A preoperative nomogram for disease recurrence following radical prostatectomy for prostate cancer. J Natl Cancer Inst. 1998;90(10):766–71.
57. Kattan MW, Wheeler TM, Scardino PT. Postoperative nomogram for disease recurrence after radical prostatectomy for prostate cancer. J Clin Oncol. 1999;17(5):1499–507.
58. Cookson MS, Fleshner NE, Soloway SM, Fair WR. Correlation between Gleason score of needle biopsy and radical prostatectomy specimen: accuracy and clinical implications. J Urol. 1997;157(2):559–62.
59. Scheidler J, Hricak H, Vigneron DB, et al. Prostate cancer: localization with three-dimensional proton MR spectroscopic imaging–clinicopathologic study. Radiology. 1999;213(2):473–80.
60. Zakian KL, Sircar K, Hricak H, et al. Correlation of proton MR spectroscopic imaging with gleason score based on step-section pathologic analysis after radical prostatectomy. Radiology. 2005;234(3):804–14.
61. Shukla-Dave A, Hricak H, Ishill NM, et al. Correlation of MR imaging and MR spectroscopic imaging findings with Ki-67, phospho-Akt, and androgen receptor expression in prostate cancer. Radiology. 2009;250(3):803–12.
62. Wang L, Mazaheri Y, Zhang J, Ishill NM, Kuroiwa K, Hricak H. Assessment of biologic aggressiveness of prostate cancer: correlation of MR signal intensity with Gleason grade after radical prostatectomy. Radiology. 2008;246(1):168–76.
63. Shukla-Dave A, Hricak H, Kattan MW, et al. The utility of magnetic resonance imaging and spectroscopy for predicting insignificant prostate cancer: an initial analysis. BJU Int. 2007;99(4):786–93.
64. Kalbhen CL, Hricak H, Shinohara K, et al. Prostate carcinoma: MR imaging findings after cryosurgery. Radiology. 1996;198(3):807–11.
65. Parivar F, Hricak H, Shinohara K, et al. Detection of locally recurrent prostate cancer after cryosurgery: evaluation by transrectal ultrasound, magnetic resonance imaging, and three-dimensional proton magnetic resonance spectroscopy. Urology. 1996;48(4):594–9.
66. Rouviere O, Girouin N, Glas L, et al. Prostate cancer transrectal HIFU ablation: detection of local recurrences using T2-weighted and dynamic contrast-enhanced MRI. Eur Radiol. 2010;20(1):48–55.
67. Zlotta AR, Djavan B, Matos C, et al. Percutaneous transperineal radiofrequency ablation of prostate tumour: safety, feasibility and pathological effects on human prostate cancer. Br J Urol. 1998;81(2):265–75.
68. McGahan JP, Browning PD, Brock JM, Tesluk H. Hepatic ablation using radiofrequency electrocautery. Invest Radiol. 1990;25(3):267–70.
69. Kudo M. Radiofrequency ablation for hepatocellular carcinoma: updated review in 2010. Oncology. 2010;78(Suppl 1):113–24.
70. Dodd III GD, Soulen MC, Kane RA. Minimally invasive treatment of malignant hepatic tumors: at the threshold of a major breakthrough. Radiographics. 2000;20(1):9–27.
71. Lencioni R, Cioni D, Crocetti L, et al. Early-stage hepatocellular carcinoma in patients with cirrhosis: long-term results of percutaneous image-guided radiofrequency ablation. Radiology. 2005;234(3):961–7.
72. Clark TW, Millward SF, Gervais DA, et al. Reporting standards for percutaneous thermal ablation of renal cell carcinoma. J Vasc Interv Radiol. 2006;17(10):1563–70.
73. Cosman ER, Nashold BS, Ovelman-Levitt J. Theoretical aspects of radiofrequency lesions in the dorsal root entry zone. Neurosurgery. 1984;15(6):945–50.
74. Larson TR, Bostwick DG, Corica A. Temperature-correlated histopathologic changes following microwave thermoablation of obstructive tissue in patients with benign prostatic hyperplasia. Urology. 1996;47(4):463–9.
75. Goldberg SN, Gazelle GS, Compton CC, Mueller PR, Tanabe KK. Treatment of intrahepatic malignancy with radiofrequency ablation: radiologic-pathologic correlation. Cancer. 2000;88(11):2452–63.
76. Goldberg SN, Gazelle GS, Halpern EF, Rittman WJ, Mueller PR, Rosenthal DI. Radiofrequency tissue ablation: importance of local temperature along the electrode tip exposure in determining lesion shape and size. Acad Radiol. 1996;3(3):212–8.

77. Liu Z, Lobo SM, Humphries S, et al. Radiofrequency tumor ablation: insight into improved efficacy using computer modeling. AJR Am J Roentgenol. 2005;184(4):1347–52.
78. Leveillee RJ, Hoey MF, Hulbert JC, Mulier P, Lee D, Jesserun J. Enhanced radiofrequency ablation of canine prostate utilizing a liquid conductor: the virtual electrode. J Endourol. 1996;10(1):5–11.
79. Liu JB, Merton DA, Wansaicheong G, et al. Contrast enhanced ultrasound for radio frequency ablation of canine prostates: initial results. J Urol. 2006;176(4 Pt 1):1654–60.
80. Liu JB, Wansaicheong G, Merton DA, et al. Canine prostate: contrast-enhanced US-guided radiofrequency ablation with urethral and neurovascular cooling–initial experience. Radiology. 2008;247(3):717–25.
81. Patriarca C, Bergamaschi F, Gazzano G, et al. Histopathological findings after radiofrequency (RITA) treatment for prostate cancer. Prostate Cancer Prostatic Dis. 2006;9(3):266–9.
82. Moore CM, Pendse D, Emberton M. Photodynamic therapy for prostate cancer–a review of current status and future promise. Nat Clin Pract Urol. 2009;6(1):18–30.
83. Henderson BW, Dougherty TJ. How does photodynamic therapy work? Photochem Photobiol. 1992;55(1):145–57.
84. Borle F, Radu A, Monnier P, van den Bergh H, Wagnieres G. Evaluation of the photosensitizer Tookad for photodynamic therapy on the Syrian golden hamster cheek pouch model: light dose, drug dose and drug-light interval effects. Photochem Photobiol. 2003;78(4):377–83.
85. Koudinova NV, Pinthus JH, Brandis A, et al. Photodynamic therapy with Pd-Bacteriopheophorbide (TOOKAD): successful in vivo treatment of human prostatic small cell carcinoma xenografts. Int J Cancer. 2003;104(6):782–9.
86. Zilberstein J, Schreiber S, Bloemers MC, et al. Antivascular treatment of solid melanoma tumors with bacteriochlorophyll-serine-based photodynamic therapy. Photochem Photobiol. 2001;73(3):257–66.
87. Eggener SE, Coleman JA. Focal treatment of prostate cancer with vascular-targeted photodynamic therapy. Sci World J. 2008;8:963–73.
88. Zhou X, Chen B, Hoopes PJ, Hasan T, Pogue BW. Tumor vascular area correlates with photosensitizer uptake: analysis of verteporfin microvascular delivery in the Dunning rat prostate tumor. Photochem Photobiol. 2006;82(5):1348–57.
89. Zhou X, Pogue BW, Chen B, et al. Pretreatment photosensitizer dosimetry reduces variation in tumor response. Int J Radiat Oncol Biol Phys. 2006;64(4):1211–20.
90. Windahl T, Andersson SO, Lofgren L. Photodynamic therapy of localised prostatic cancer. Lancet. 1990;336(8723):1139.
91. Nathan TR, Whitelaw DE, Chang SC, et al. Photodynamic therapy for prostate cancer recurrence after radiotherapy: a phase I study. J Urol. 2002;168(4 Pt 1):1427–32.
92. Moore CM, Nathan TR, Lees WR, et al. Photodynamic therapy using meso tetra hydroxy phenyl chlorin (mTHPC) in early prostate cancer. Lasers Surg Med. 2006;38(5):356–63.
93. Zaak D, Sroka R, Höppner M, et al. Photodynamic therapy by means of 5-ALA induced PPIX in human prostate cancer – preliminary results. Med Laser Appl. 2003;18(1):91–5.
94. Hsi RA, Kapatkin A, Strandberg J, et al. Photodynamic therapy in the canine prostate using motexafin lutetium. Clin Cancer Res. 2001;7(3):651–60.
95. Pinthus JH, Bogaards A, Weersink R, Wilson BC, Trachtenberg J. Photodynamic therapy for urological malignancies: past to current approaches. J Urol. 2006;175(4):1201–7.
96. Verigos K, Stripp DC, Mick R, et al. Updated results of a phase I trial of motexafin lutetium-mediated interstitial photodynamic therapy in patients with locally recurrent prostate cancer. J Environ Pathol Toxicol Oncol. 2006;25(1–2):373–87.
97. Patel H, Mick R, Finlay J, et al. Motexafin lutetium-photodynamic therapy of prostate cancer: short- and long-term effects on prostate-specific antigen. Clin Cancer Res. 2008;14(15):4869–76.
98. Zhu TC, Hahn SM, Kapatkin AS, et al. In vivo optical properties of normal canine prostate at 732 nm using motexafin lutetium-mediated photodynamic therapy. Photochem Photobiol. 2003;77(1):81–8.
99. Zhu TC, Finlay JC, Hahn SM. Determination of the distribution of light, optical properties, drug concentration, and tissue oxygenation in-vivo in human prostate during motexafin lutetium-mediated photodynamic therapy. J Photochem Photobiol B. 2005;79(3):231–41.
100. Li J, Zhu TC. Determination of in vivo light fluence distribution in a heterogeneous prostate during photodynamic therapy. Phys Med Biol. 2008;53(8):2103–14.
101. Yu G, Durduran T, Zhou C, et al. Real-time in situ monitoring of human prostate photodynamic therapy with diffuse light. Photochem Photobiol. 2006;82(5):1279–84.
102. Schreiber S, Gross S, Brandis A, et al. Local photodynamic therapy (PDT) of rat C6 glioma xenografts with Pd-bacteriopheophorbide leads to decreased metastases and increase of animal cure compared with surgery. Int J Cancer. 2002;99(2):279–85.
103. Gross S, Gilead A, Scherz A, Neeman M, Salomon Y. Monitoring photodynamic therapy of solid tumors online by BOLD-contrast MRI. Nat Med. 2003;9(10):1327–31.
104. Mazor O, Brandis A, Plaks V, et al. WST11, a novel water-soluble bacteriochlorophyll derivative; cellular uptake, pharmacokinetics, biodistribution and vascular-targeted photodynamic activity using

melanoma tumors as a model. Photochem Photobiol. 2005;81(2):342–51.
105. Weersink RA, Forbes J, Bisland S, et al. Assessment of cutaneous photosensitivity of TOOKAD (WST09) in preclinical animal models and in patients. Photochem Photobiol. 2005;81(1):106–13.
106. Trachtenberg J, Bogaards A, Weersink RA, et al. Vascular targeted photodynamic therapy with palladium-bacteriopheophorbide photosensitizer for recurrent prostate cancer following definitive radiation therapy: assessment of safety and treatment response. J Urol. 2007;178(5):1974–1979. discussion 1979.
107. Trachtenberg J, Weersink RA, Davidson SR, et al. Vascular-targeted photodynamic therapy (padoporfin, WST09) for recurrent prostate cancer after failure of external beam radiotherapy: a study of escalating light doses. BJU Int. 2008;102(5):556–62.

Surgical Approaches to Treatment of Prostate Cancer

52

Simone Thavaseelan and Gyan Pareek

Abstract

Surgical treatment of prostate cancer remains the cornerstone of extirpative therapy for localized disease. Radical prostatectomy affords excellent long-term cancer-specific survival and can be approached by open, perineal, laparosopy, or robotic-assisted laparoscopy. Advances in surgical care have improved the anatomic dissection, reduced the blood loss, and facilitated the preservation of the neurovascular bundles. Significant experience has been gained with robotic prostatectomy which has widely popularized a minimally invasive approach. Cryosurgery continues to evolve as an ablative therapy for prostate cancer although long-term data are limited. This chapter considers the principles of the various surgical approaches to prostate cancer, including open, perineal, laparosopy, robotic assisted, and cryosurgery, as well as their indications, techniques, outcomes, and complications.

General Surgical Considerations

Introduction

Prostate cancer is the most common non-cutaneous malignancy in men and surgical management of prostate cancer is the first-line therapy for patients with localized disease. Radical retropubic prostatectomy (RRP) is the most common operation performed in these patients. The main benefits of an expertly performed radical prostatectomy are complete removal of the prostate for thorough pathologic staging, simplified postoperative monitoring for disease recurrence, low morbidity and mortality, and finally, the potential for curative intent with minimal collateral injury to adjacent structures [1]. Additionally in comparison to other management options such as watchful waiting, radical prostatectomy has been shown to reduce the risk of local progression and distant metastases [2]. Disadvantages of surgery are the short hospitalization, the potential for incomplete removal, and the risks of urinary incontinence and erectile dysfunction (ED). Nevertheless, both urinary continence and erectile function are affected by *all* treatment options, including such treatments as radiation therapy

S. Thavaseelan (✉) • G. Pareek
Department of Surgery, Division of Urology, Warren Alpert Medical School of Brown University, Providence, RI, USA
e-mail: simonethavaseelan@gmail.com; gyan_pareek@brown.edu

D.E. Dupuy et al. (eds.), *Image-Guided Cancer Therapy*, DOI 10.1007/978-1-4419-0751-6_54,

and cryosurgery. Given the overall risk and benefit analysis of surgery, radical prostatectomy is usually reserved for patients with a life expectancy that exceeds 10 years, those who are healthy and reasonable surgical candidates, and those who do not have any evidence of metastatic disease. Various tools in the form of nomograms are frequently used to predict the likelihood of organ-confined disease [3]. Combining PSA, Gleason score, and clinical stage permits risk stratification of disease and helps the clinician counsel patients on appropriate disease management.

Thus, management of prostate cancer is a multidisciplinary effort, involving clinicians across several subspecialties including urology, radiology, medical oncology, and radiation oncology. In order for these clinicians to provide a comprehensive management plan to these patients, knowledge of prostatic anatomy and the surgical approach to the prostate is paramount. Herein, we describe the anatomy of the prostate, with a focus on the surgical approaches. Specifically, techniques, indications, complications, and outcomes for each surgical approach are emphasized for the reader.

Approaches

The surgical approaches to the prostate include open retropubic, perineal, laparoscopic, and robotic-assisted laparoscopy. Open retropubic radical prostatectomy has been the cornerstone of surgical treatment of clinically localized prostate cancer and is the preferred approach by most surgeons due to the familiarity of the anatomy as it has been the technique most commonly taught to residents in training. It offers prompt access for pelvic lymphadenectomy and lower risk of rectal injury. Perineal radical prostatectomy (RPP) is less commonly performed because many urologists are not familiar with this exposure, but despite the higher risk of rectal injury and fecal incontinence, it is associated with less blood loss. Laparoscopic radical prostatectomy (LRP) was originally introduced by French surgeons in 2000 and remains a technically challenging operation with a steep learning curve [4]. Robotic-assisted laparoscopic radical prostatectomy (RALRP) is a more recent advance in the field of minimally invasive prostatectomy that makes use of the da Vinci Surgical System (Intuitive Surgical® Inc., Sunnyvale, CA) to reduce the operative time and learning curve and improve the visualization and technical ease with laparoscopic prostatectomy. This chapter will define the role of each of these techniques with a focus on outcomes and complications.

Regardless of the surgical approach, informed consent includes a discussion regarding the risks of bleeding, infection, urinary incontinence, erectile dysfunction, positive surgical margins, injury to adjacent organs particularly the rectum, anastomotic leak, bladder neck stricture, need for adjuvant therapy, and the risks of anesthesia. Typically, a bowel preparation is administered the night before. The latter is useful in the rare event of a rectal injury and may permit primary closure. Preoperative antibiotic prophylaxis with a second-generation cephalosporin is administered, and antithromboembolic stockings are placed. General anesthesia is induced followed by appropriate patient positioning and the surgical procedure. Standard postoperative course depends on return of bowel function, laboratory stability, and patient teaching to care for the urethral catheter that stents the reconstruction. Pathologic review occurs at the first postoperative visit, and prostate-specific antigen (PSA) is checked starting at 6 weeks following surgery and at regular quarterly, semiannual, and/or annual intervals. Thus, PSA is not only utilized as a screening tool but also as a biochemical marker to monitor for recurrence.

Anatomy and Technique

Radical prostatectomy is typically performed in an extraperitoneal fashion when completed open, while laparoscopic prostatectomy is more commonly performed in an intraperitoneal fashion to increase the working space. Regardless of approach, there are certain principles and actions that are common to the surgical removal of the prostate. These steps include opening of the

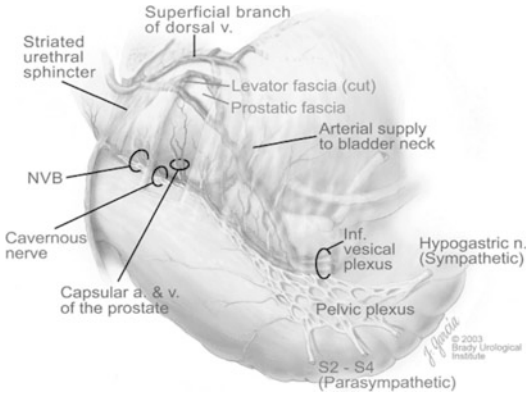

Fig. 52.1 Prostatic anatomy. The superficial branch of the dorsal vein is located on the anterior surface of the prostate. The neurovascular bundle lies on the posterolateral surface of the prostate (Reprinted from Walsh PC, Partin AW. Anatomic Radical Retropubic Prostatectomy. In: Wein AJ, Kavoussi LR, Novick AC, Partin AW, Peters CA, eds. Campbell-Walsh Urology. 9th ed. Philadelphia Pa: Saunders Elsevier; 2007;3:2959, with permission from Elsevier)

endopelvic fascia, incision of the puboprostatic ligaments, and either suture ligation, staple division, or transection of the dorsal venous complex (DVC). The DVC may be a troublesome source of bleeding, especially at the apex of the prostate. Apical dissection of the prostate requires careful manipulation of the urethral stump in order to preserve functional length of the urethra and to ensure a negative surgical margin. This step is essential for continence after the procedure. Dissection of the prostate from its lateral aspects is challenging and involves careful mobilization of the neurovascular bundles, neural structures associated with erectile function. The neurovascular bundles can be approached by either an antegrade or retrograde fashion by incision of the lateral prostatic fascia and careful disengagement from the posterolateral aspect of the prostate while avoiding any thermal injury (Fig. 52.1). Posteriorly, the prostate is dissected off the rectum followed by ligation of the prostate pedicles which receive arterial supply from the inferior vesical arteries. The prostatovesical junction is then transected followed by the reconstruction of the bladder neck. The seminal vesicles and the ampullae of the vasa are removed with the prostate specimen. Extirpation of the prostate is followed by reconstruction of the urinary tract. The goals of the vesicourethral anastomosis are to create a watertight, tension free, vesical to urethral mucosal apposition with absorbable suture. In the open setting, this is usually an interrupted closure with 4–6 sutures, and with laparoscopic and/or robotic assistance, this is usually a running closure [5]. A Jackson-Pratt drain is left to monitor for urinary leak, and a urethral catheter is placed to stent the anastomosis.

Complications

The three goals of radical prostatectomy are oncologic control, preservation of urinary control, and, finally, maintenance of erectile function (Fig. 52.2). Early complications include hemorrhage, rectal injury, ureteral injury, obturator nerve injury, lymphocele formation during and after pelvic lymphadenectomy, urinary leak, urinary tract infection, thromboembolic events, anesthetic complications, urinary incontinence, and erectile dysfunction [6]. Late complications from radical prostatectomy include biochemical recurrence, local or metastatic progression, and anastomotic stricture.

Urinary incontinence occurs on the basis of intrinsic sphincter deficiency likely from a decrease in mean functional urethral length and urethral closure pressure resulting in stress incontinence [7, 8]. Although there is great variation in the definition of incontinence and the method by which it is determined (physician assessment versus patient self report; subjective questionnaires versus objective measures), continence generally improves over the first 12 months after surgery [9]. Modern series report continence rates of 90 % at 12 months follow-up [9]. Postprostatectomy incontinence can be treated by a range of options from noninvasive pelvic floor muscle physiotherapy and urethral bulking agents to male urethral slings or artificial urinary sphincters for severe incontinence.

Potency is often defined as the ability to achieve and maintain an erection sufficient and satisfactory for sexual intercourse. Postoperative

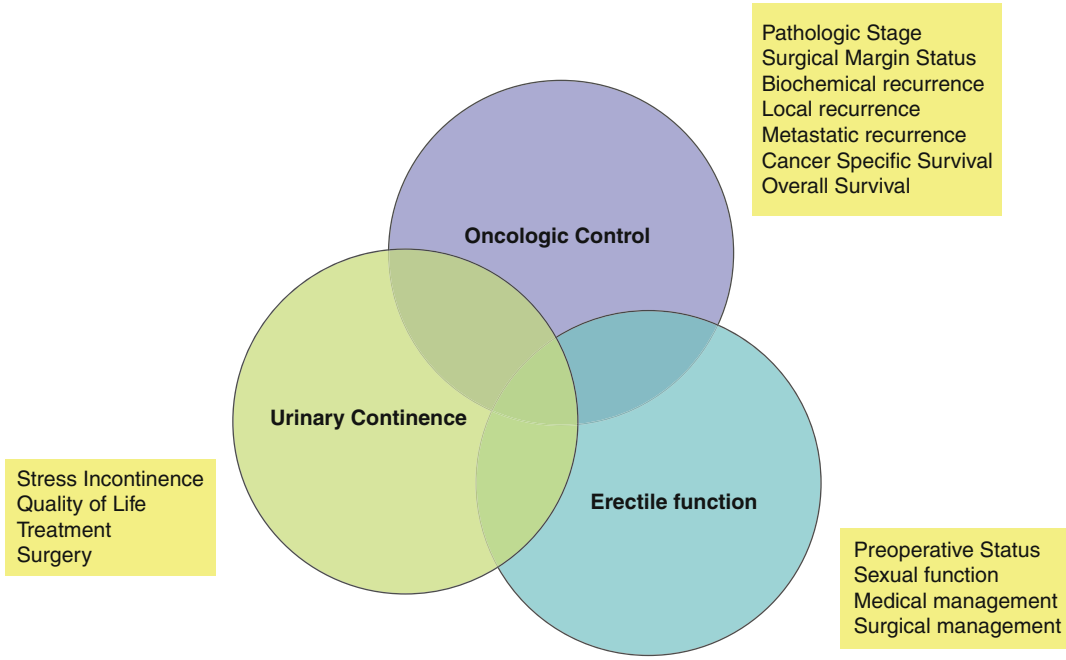

Fig. 52.2 Goals of radical prostatectomy. Oncologic control is the primary objective of radical prostatectomy, and urinary continence and erectile function are secondary and tertiary priorities

erectile function is influenced by preoperative erectile status, age, vascular health, and the extent of nerve sparing that is performed. Potency rates of 75 % are achievable in men with younger age and nerves that are bilaterally spared [10]. Erectile dysfunction can be managed on a continuum of options consisting of phosphodiesterase-5 inhibitors, intraurethral medications, intracavernosal injections, vacuum-assisted erection devices, and penile prostheses.

Outcomes

The principle goal of radical prostatectomy is complete removal of the prostate gland with negative surgical margins. Oncologic control is measured by the following parameters: pathologic stage with negative surgical margins, lack of biochemical recurrence as monitored by PSA, lack of local recurrence or metastases, and cancer-specific and overall survival. Prognostic factors include PSA at diagnosis, Gleason score, and stage. It is challenging to compare outcomes across surgical approaches for radical prostatectomy because there are no randomized studies that compare open to laparoscopic or to robotic-assisted surgery. However, most series have found that minimally invasive prostatectomy is associated with less blood loss [11]. Furthermore, patients are often faced with multiple options for treatment of prostate cancer apart from surgery such as active surveillance, radiation therapy, or cryosurgery, and therefore these patients require comprehensive and individualized counseling.

Open Radical Retropubic Prostatectomy

Anatomy

Open radical retropubic prostatectomy is the "gold standard" and time-tested method of surgical removal of the prostate. Walsh pioneered understanding of prostatic anatomy and modernized the operation. Specifically, Walsh identified the three major branches of the deep dorsal venous complex, the superficial branch and the

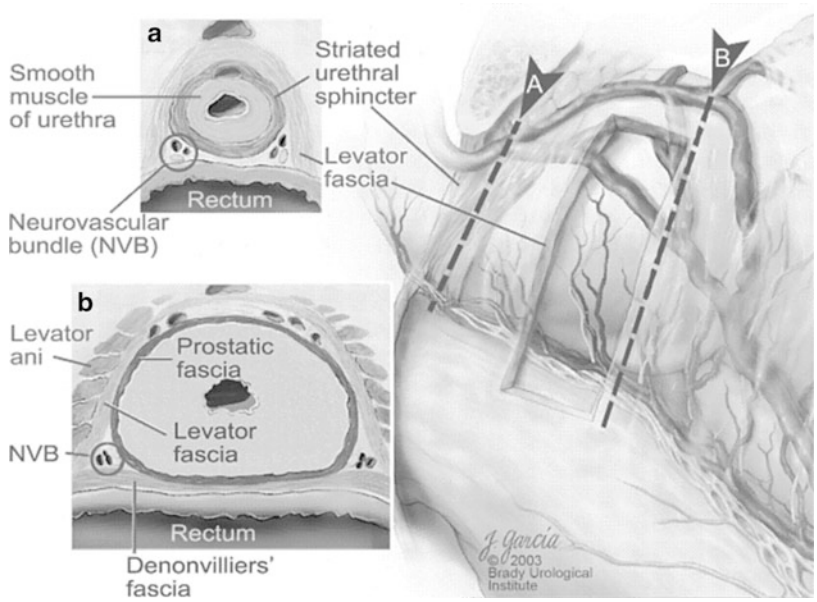

Fig. 52.3 Anatomy of the neurovascular bundle and urethral sphincter. The cross section of the urethra in *A* shows the urethral sphincter is composed of both smooth muscle and striated muscle. The cross section of prostate in *B* shows the relationship between the neurovascular bundle and the investing fasciae of the prostate (Reprinted from Walsh PC, Partin AW. Anatomic Radical Retropubic Prostatectomy. In: Wein AJ, Kavoussi LR, Novick AC, Partin AW, Peters CA, eds. Campbell-Walsh Urology. 9th ed. Philadelphia Pa: Saunders Elsevier; 2007;3:2958, with permission from Elsevier)

right and left venous plexuses, and described its course under Buck's fascia in the penis [12]. These contributions helped urologic surgeons become more comfortable with the deep pelvic anatomy in order to minimize blood loss particularly from the dorsal venous complex. Arterial supply of the prostate originates from the inferior vesical artery. The prostate receives innervation from the pelvic plexus that arise from S2 to S4 and the hypogastric nerve from the thoracolumbar center [13]. The neurovascular bundles lie between the lateral pelvic fascia and the prostatic fascia with variation in volume and distribution [14]. The striated sphincter is composed of slow twitch fibers innervated by the pudendal nerve and provides passive urinary continence (Fig. 52.3).

Technique

A midline extraperitoneal infraumbilical incision is made by splitting the rectus muscle. The space of Retzius is manually mobilized, and the fibroadipose tissue overlying the endopelvic fascia is cleared. The endopelvic fascia is incised lateral to the prostate and medial to the levator ani muscle. After the superficial dorsal vein is cauterized, the puboprostatic ligaments are carefully divided leaving the dorsal venous complex to be controlled. Accessory pudendal arteries are delicately preserved if encountered to prevent arterial insufficiency if possible. Ligation of the dorsal venous complex should be accomplished swiftly and while avoiding the urethra or unintended entry into the prostatic apex. The suture can be placed into the perichondrium of the pubis symphysis to recreate anterior support of the urethra. Apical dissection of the prostate must proceed under vision to prevent a positive margin. The urethra is divided next, and some surgeons will place the anterior 3 anastomotic sutures at this juncture. The neurovascular bundles pierce the urogenital diaphragm at the 5 and 7 o'clock positions below the urethra; therefore, posterior division of the urethra must not cause inadvertent

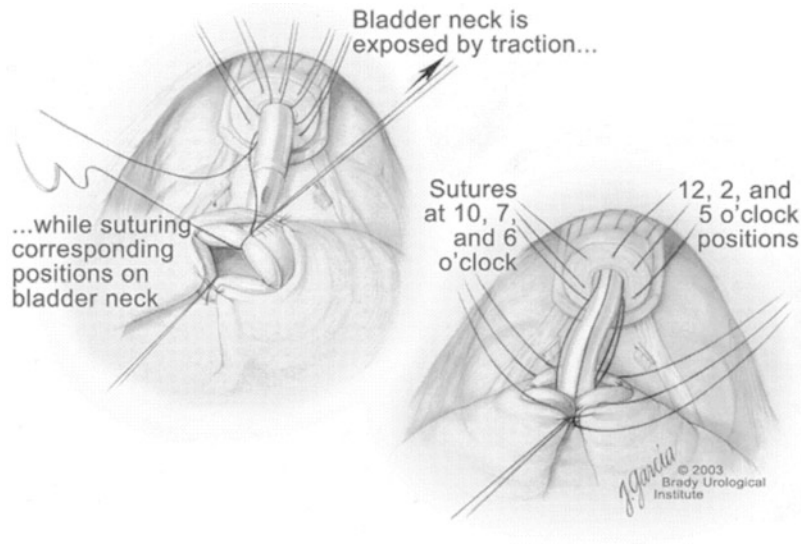

Fig. 52.4 Vesicourethral anastomosis. Circumferential interrupted sutures are placed to approximate the bladder neck and urethra. They are secured sequentially over a urethral catheter (Reprinted from Walsh PC, Partin AW. Anatomic Radical Retropubic Prostatectomy. In: Wein AJ, Kavoussi LR, Novick AC, Partin AW, Peters CA, eds. Campbell-Walsh Urology. 9th ed. Philadelphia Pa: Saunders Elsevier; 2007;3:2972, with permission from Elsevier)

injury to the apical branches. Retrograde release of the neurovascular bundle is achieved by mobilizing them off the prostate between the layers of the levator fascia and the prostatic fascia [15]. Posterior dissection is now performed by entering the plane between the rectum and Denonvilliers' fascia. The vascular supply to the prostate is disconnected with lateral division of the pedicles. The bladder neck is separated at the prostatovesical junction, and dissection of the seminal vesicles and vasa is performed.

If needed, bladder neck reconstruction can recreate a size-appropriate opening to which the urethra will be connected. Care should be taken to avoid injuring the ureteral orifices. Eversion of the bladder neck mucosa will ensure mucosa to mucosa urethrovesical anastomosis. Typically 4–6 interrupted absorbable sutures are placed, and a catheter and drain are positioned (Fig. 52.4).

Complications

Overall mortality for open radical retropubic prostatectomy is extremely low [16]. In modern series of high-volume surgeons, postoperative transfusion rates are approximately 5 % and rectal injury occurs in 1 % [17]. Bladder neck contracture occurs in 0.5–10 % of patients and may arise from inadequate mucosal apposition, urinary extravasation with resultant fibrosis, or distraction from pelvic hematoma [18]. Dilations or incision of scar tissue may alleviate obstruction, but management of recalcitrant contractures can be complex.

Outcomes

Radical prostatectomy remains an important cornerstone of therapy for prostate cancer since radiation does not always eliminate all cancer cells and since hormonal therapy and chemotherapy are not curative. Ten-year prostate-cancer-specific progression-free survival is 85 % for organ-confined disease in a large single-surgeon series of open radical prostatectomy by Catalona in the pre-PSA era [6]. Biochemical recurrence usually precedes clinical metastatic disease by 8 years and prostate-cancer-specific mortality by about 13 years [19].

Salvage Radical Prostatectomy

Although primary radiotherapy for prostate cancer is an excellent treatment option, local recurrence after failure of primary therapy can be treated with salvage radical prostatectomy.

There is controversy surrounding the definition of recurrence after radiation, and many criteria are used (American Society for Therapeutic Radiology and Oncology, Phoenix, PSA bump), but for particular candidates, salvage radical prostatectomy might offer a second chance at definitive local therapy. However, it remains a technically demanding operation best performed in centers of high volume. As for all surgical approaches, patient selection is critical. Patients should have evidence of radiorecurrent prostate cancer that is localized, without evidence of metastatic disease, and life expectancy of at least 10–15 years [15]. It is well known that radiation affects healing and increases the difficulty of the operation though a combination of effects on the tissues from vasculitis, fibrosis, and ischemia [20]. For these reasons, salvage radical prostatectomy is associated with a higher rate of complications [21]. In a review of the literature, Chen et al. reported a rectal injury rate of 6 %, incontinence rate of 50 %, and nearly universal erectile dysfunction and a risk of bladder neck contracture of 30 % [20].

Radical Perineal Prostatectomy

General

Radical perineal prostatectomy (RPP) was first described by Hugh Hampton Young in 1905. Although the prostate is more commonly accessed retropubically from either an extraperitoneal or intraperitoneal fashion, the prostate does lie close to the surface of the perineum, and as such, this approach can provide excellent visualization. Combining the patient's PSA, Gleason score, and clinical stage allows the clinician to predict the likelihood of pathologic stage and lymph node involvement. With this information, the need for pelvic lymphadenectomy can be determined, and for those patients at low risk of lymph node involvement, a perineal approach is reasonable. In comparison to other exposures, the radical perineal prostatectomy offers unhindered visualization of the urethrovesical anastomosis which facilitates reconstruction, good long-term oncologic control, and notably, a shorter hospital stay and convalescence [22].

Patient Selection

As with the other surgical techniques intended to be curative, patient selection for RPP starts with an assessment of the patient's life expectancy that is anticipated to exceed 10 years and in whom there is a high likelihood of organ-confined disease. Laparoscopic pelvic lymphadenectomy can be combined with the procedure if dictated by the patient's preoperative assessment. Given the exaggerated lithotomy position required for this procedure, contraindications include hip and pelvic bone pathology or severe spine disease that will not permit placing the legs in stirrups at a 75° angle. However, there are also unique clinical situations where perineal access is preferred. In the case of renal transplantation to the pelvic fossa, there may be concern to avoid vascular injury. In the case of previously placed preperitoneal mesh during herniorrhaphy, the space of Retzius can be obliterated and prevent a retropubic approach. Relevant to the epidemic of obesity, large BMI may prohibit retropubic access while also precluding a laparoscopic approach since ventilation can be compromised in the morbidly obese by pneumoperitoneum. In these clinical situations, the perineal approach is ideal.

Technique

Bowel preparation is performed the night before, and rectal evacuation is ensured after anesthesia. The patient is placed into exaggerated dorsal lithotomy position. A curved Lowsley tractor is placed transurethrally past the prostate, and the distal wing tips are opened inside the bladder. This allows for palpation of the prostate and retraction of the organ toward the perineum. A curvilinear skin incision is made from one ischial tuberosity to the contralateral one in the fashion of a half moon (Fig. 52.5).

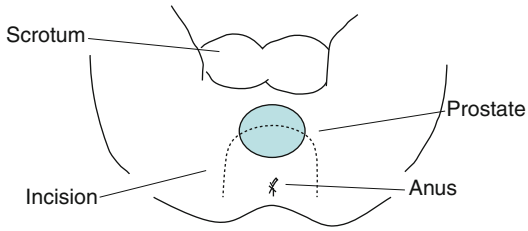

Fig. 52.5 Radical perineal prostatectomy incision. A curvilinear incision is made from one ischial tuberosity to the other to access the prostate for radical perineal prostatectomy. The superficial exposure provides excellent visualization of the vesicourethral anastomosis

The ischiorectal fossae are developed with blunt dissection, and the central tendon is located first and divided by electrocautery. Next, the external anal sphincter is retracted anteriorly and rectourethralis muscle is divided. Care is taken not to injury the rectum as it is tented up by this muscle. Using pressure on the Lowsley tractor, the prostate is delivered into the incision, and blunt dissection with a peanut sponge or manual clearing of the prostate is performed such that the layers of Denonvilliers' fascia can be incised in the midline.

By palpating the Lowsley tractor, the apex of the prostate is identified and the neurovascular bundles are separated away from the urethra which is then cut circumferentially using a scalpel against the metal tractor. The anterior aspect of the prostate is dissected bluntly taking care not to enter or injure the dorsal venous complex. At this point, the posterior, inferior, and anterior prostate has been dissected; the superior aspect or the prostatovesical junction and the lateral pedicles remain. Sharp dissection is preformed preserving the bladder neck which is entered and disengaged completely from the prostate. The vascular pedicles are controlled with sutures or clips. The vasa deferentia and seminal vesicles are grasped, bluntly dissected, and divided.

Vesicourethral anastomosis is now performed to reestablish continuity of the urinary tract by approximating the bladder neck to the membranous urethra. Typically 4–6 interrupted absorbable sutures are placed in circumferential fashion with a urethral catheter positioned to bridge the anastomosis. Hemostasis is confirmed, a Penrose drain is situated, and the central tendon and Colles' fascia are reapproximated. Postoperatively, diet is advanced, rectal stimulation is avoided, the Penrose drain is removed within 24–48 h, and most patients are discharged to home on postoperative day 2 with urethral catheter removal in the office in 10–14 days [23].

Complications

In general, blood loss with RPP is lower than RRP since the dorsal venous complex is outside of the planes of dissection, and therefore troublesome bleeding can be avoided altogether. Transfusions are rare [24]. The rate of rectal injury has been reported to range from 1 % to 10 % [25] and can be repaired primarily if recognized. Urinary continence is an important clinical parameter after prostate surgery, and excellent urinary control is achieved with RPP. Continence rates of 95 % by 10 months are reported [25]. Although erectile function is almost always affected by any treatment for prostate cancer, potency rates range from 35 % to 70 % [26].

Outcomes

Excellent pathological outcomes are possible with RPP. Positive surgical margin rates are 14 % comparing similarly to RRP of 19 % [27]. Summarized in a series of over 1,200 patients undergoing RPP, Paulson showed 5-year biochemical recurrence rate of 8 % in organ-confined disease. Although not a dominant approach, RPP remains a good option for certain patients and permits prostate removal in clinically localized disease with good functional outcomes and minimal morbidity. Furthermore, with an emphasis on comparative cost of treatment for prostate cancer, there may be a resurgence of this surgery as the shorter

hospital stay and no need for costly minimally invasive laparoscopic equipment might contain the overall expense.

Laparoscopic and Robotic-Assisted Laparoscopic Radical Prostatectomy

Introduction

Minimally invasive surgical approaches to radical prostatectomy have had a worldwide explosion because of the recent application of robotic assistance to the technically difficult laparoscopic prostatectomy. Originally described by Schuessler in 1997, laparoscopic prostatectomy was notable for long operative times and a significant learning curve which hampered widespread use [28]. Guillonneau and Vallancien reported their technique in 2000 in which operative times had improved to 4–5 h with a positive margin rate of 15–28 % [4]. However, the da Vinci Surgical System (Intuitive Surgical® Inc., Sunnyvale, CA) has ushered in a new era of minimally invasive prostatectomy by facilitating three-dimensional vision, wristed motion, magnification, and assisting with intracorporeal suturing. Since robotic-assisted laparoscopic radical prostatectomy (RALRP) overcomes many of the limitations of standard laparoscopic prostatectomy such as rigid instrumentation, inadequate depth perception, and higher learning curve, RALRP is now extremely common and is the focus of the rest of this section.

Indications and Patient Selection

The indications for RALRP are the same as open surgery, which are patients with a life expectancy that exceeds 10 years, who are healthy and reasonable surgical candidates, and who have evidence of clinically localized disease. Contraindications are uncorrectable bleeding diatheses and, specific to the laparoscopic approach, include cardiopulmonary disease that prevents adequate ventilation in the face of pneumoperitoneum as well as previous abdominal surgery.

Technique

The da Vinci Surgical System consists of an operator console and a patient side robotic tower that accommodates 3–4 robotic surgical arms (Fig. 52.6). In this master–slave system, the surgeon controls all movements of the robot from a remote position to the patient's bedside [29]. The dual lens camera constructs a three-dimensional visual field for the operating surgeon at the console with 10× magnification (Fig. 52.7). After pneumoperitoneum is established with either a Veress needle or open Hasson technique, the standard template of trocars is placed under direct vision. This typically consists of a camera, 2–3 robot arms, and two assistant ports for suctioning and introduction of sutures or clips. The patient is placed into dorsal lithotomy with steep Trendelenburg to allow for gravity retraction of the bowels and to create space for the robot to be docked at the foot of the table in between the patient's legs. The surgeon manipulates the master controls which effect precise and real-time wristed movements at the terminal ends of the robotic arms [30]. With a posterior approach, the seminal vesicles and vasa are dissected first by incision of the peritoneum overlying the vasa [4]. With anterior retraction of the seminal vesicles and vasa, sharp entry through Denonvilliers' fascia allows for full posterior dissection of the prostate and mobilization of the rectum. The space of Retzius is then developed by releasing the bladder from the anterior abdominal wall with division of the urachus and the medial umbilical ligaments. If an anterior approach is taken, then this latter step is the initial move in the operation, and the seminal vesicles and vasa are dissected after the posterior bladder neck transection. The deep dorsal venous complex is controlled by suture ligation.

Next, the anterior bladder neck is sharply incised until the previously placed urethral catheter is encountered which is used for anterior retraction of the prostate. Care is taken to determine if there is a median prostatic lobe, an area of prostatic hypertrophy which may present a technical challenge during the operation with

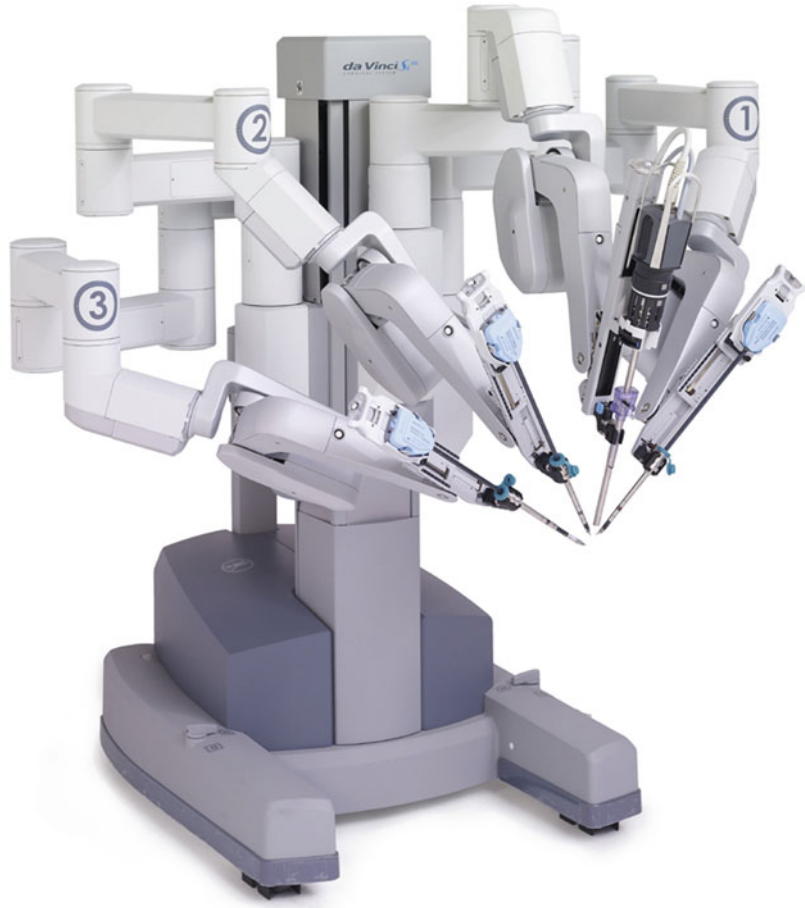

Fig. 52.6 da Vinci Surgical System, Intuitive Surgical®. This patient side tower houses the camera and three additional robotic arms that are controlled by the surgeon seated at the console (© 2010 Intuitive Surgical, Inc.)

the goal of complete removal of these PSA-producing cells. The posterior bladder neck fibers are divided, and with anterior retraction of the seminal vesicles and vasa, the prostatic pedicles are visualized and controlled. In an antegrade fashion, the neurovascular bundles are mobilized off the prostate by incising the lateral prostatic fascia. Once the deep dorsal vein is divided, the prostatic apex is dissected and the urethral is divided. Once the prostate specimen is completely released, it is placed into a laparoscopic entrapment device and later removed via the midline supraumbilical port site.

The critical urinary reconstruction is usually accomplished with a running continuous suture [5]. The robotic assistance greatly facilitates this portion of the procedure and a tension free, watertight vesicourethral anastomosis with mucosal apposition is essential. A urethral catheter and prevesical drain are placed, the robot is undocked, and extraction of the specimen and wound closure are performed. Although transperitoneal RALRP allows for a larger working space, the extraperitoneal method recapitulates the open surgery and confines any urine leak to the space of Retzius. Most studies do not demonstrate any significant differences in the transperitoneal and extraperitoneal techniques [31, 32], and therefore it is mostly surgeon's preference.

Complications

Several institutions have reported their complication rates, although with varying definitions of major and minor complication rates [33, 34].

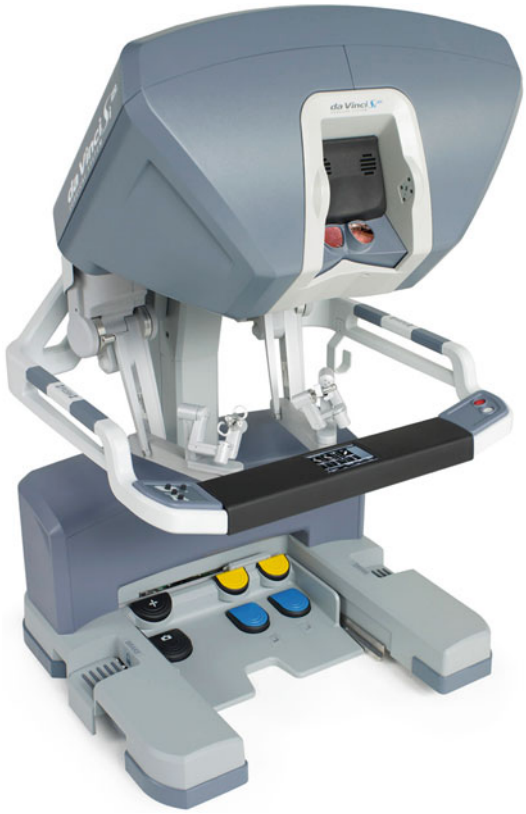

Fig. 52.7 da Vinci Surgical System Console, Intuitive Surgical®. This console allows the surgeon to have a 3-dimensional magnified view of the surgical field and to perform the dissection by controlling the robotic arms with enhanced dexterity, motion scaling and tremor reduction, 7 degrees of freedom, and 90 degrees of articulation (© 2010 Intuitive Surgical, Inc.)

Lasser et al. reported on an independent, blinded, and prospective method of collecting data on 239 consecutive patients who underwent RALRP from initiation of their robotics program. They found a major and minor complication rate of 5 % and 14 %, respectively, using the modified Clavien system to grade complications. Eighty three percent of patients had an uneventful postoperative course in that they were discharged within 2 days and did not have any unscheduled procedures or hospital/emergency room visits. Major complications included percutaneous drainage of pelvic fluid collections, one PE, and one small bowel perforation [35].

Outcome

Positive surgical margin rates are used as a surrogate endpoint for oncologic efficacy since long-term variables such as cancer-specific survival and overall survival have not yet matured for many RALRP series. In a meta-analysis performed by Patel et al., they evaluated 14 articles that contained RALRP case series of at least 250 patients to focus on high-volume centers. They evaluated the following parameters: perioperative outcomes such as operative time, blood loss, and complications; positive surgical margin rates; urinary continence; and potency recovery. RALRP was associated with a mean operative time of 162 min, estimate blood loss of 164 ml, and a complication rate of 10.3 %. The positive surgical margin rate was 9.6 % for pT2 tumors and 37.1 % for pT3 tumors. Urinary continence was defined as either no use of pads or use of one pad only for security and ranged from 82.1 % to 97 % at 12 months follow-up. Finally, RALRP patients who underwent unilateral and bilateral nerve sparing had a potency rate of 59.9 % and 93.5 %, respectively, at 12 months follow-up. This analysis also assessed these parameters in 30 articles for open prostatectomy and concluded that overall when comparing RALRP to open prostatectomy, RALRP is safe, has a similar complication rate, and is associated with decreased blood loss and transfusion, lower mean positive surgical margin rates, and higher continence and potency rates [36]. Nevertheless, randomized comparative trials using standardized outcomes with long-term follow-up of the different surgical approaches to prostatectomy do not exist at this time, and therefore scientifically rigorous comparison is not yet possible [36].

Cryosurgery

Introduction

In 1996, the American Urological Association (AUA) recognized cryosurgery as a therapeutic option for prostate cancer and removed the investigational label for the procedure. In 2007,

the AUA published practice guidelines for the management of clinically localized prostate cancer but concluded that insufficient information is available to include cryosurgery in the data meta-analyses. Therefore, the AUA convened a panel to develop a Best Practice Statement addressing the use of cryosurgery which summarized the published data in concert with expert opinion but without any formal meta-analysis of the literature. There are no published long-term data on the efficacy of cryosurgery on metastasis-free survival, cancer-specific survival, or overall survival as there are with other more established forms of therapy. However, there are several large, single institution experience reports on the efficacy and morbidity of cryosurgery of the prostate, and it remains a valid treatment option for the informed patient. The resurgence of cryosurgery for the treatment of prostate cancer is consistent with the general trend toward more minimally invasive treatment options for prostate cancer.

Evolution

Cryotherapy dates back to the nineteenth century when a mixture of salt and ice was used to reduce the size of breast and cervical tumors, and in this setting, cryotherapy was limited to superficial applications [37]. Cooper and Lee developed the first device for cryosurgery using a liquid nitrogen cryogenic probe [38]. In modern systems, pressurized argon gas is circulated to the tip of the cryogenic probe where it expands. This results in a rapid temperature drop. The expanded argon gases are then circulated back to the cryogenic unit through the large outer lumen of the probe. Thereafter, helium is delivered to the tip of the cryogenic probe where it expands, but in contrast to argon, when helium expands, this causes the temperature to increase resulting in active defrosting. The temperature changes that occur when a particular gas expands are governed by the Joule-Thomson effect and are based on the physical properties of the gases themselves. The main mechanism of cytotoxicity from cryosurgery is the induction of targeted areas of coagulative necrosis. This mechanism is in comparison to radiation which produces mitotic arrest and androgen deprivation which induces apoptosis [39]. With the onset of ice formation, water is extracted from the extracellular solution as pure crystalline ice resulting in an increasingly hyperosmotic solution. This leads to cell shrinkage and damage to the intracellular membrane. Subsequent delayed and indirect destructive effects continue primarily because of vasculature disruption from cell sludging within the vessels leading to coagulation, vascular thrombosis, and cellular hypoxia [40]. With consecutive rapid freeze and slow thaw cycles, temperatures of $-40\ ^{\circ}C$ are achieved to result in lethal cell kill [41]. The double cycle with rapid freezing allows for cells that are initially stressed but not killed to undergo lethal damage in the second cycle, and additionally the rapid freezing rate prevents cellular adaptation to freezing conditions.

Technique

Modern cryosurgery systems employ real-time transrectal ultrasound (TRUS) guidance and a urethral warming catheter to more safely deliver treatment. Real-time imaging demonstrates the freezing process, allows for accurate placement of thermocouple probes as well as the cryoprobes, and maintains constant visualization of the freezing process and the rectum. The urethral warming catheter continuously circulates heated saline to prevent urethral freezing and, therefore, urethral sloughing which can lead to obstruction and stricture. After spinal or general anesthesia is induced, the patient is placed into dorsal lithotomy, and the TRUS probe is maintained in a position within the rectum by a holder secured to the bed. Two-dimensional prostatic anatomy is mapped by ultrasound. Using a brachytherapy-like template drilled with a matrix of holes to accommodate the cryoprobes, each probe is placed percutaneously via the perineum (Fig. 52.8). Multiple probes result in an additive effect of overlapping freezing zones. Thermocouples are placed to monitor tissue temperatures at critical locations such as the

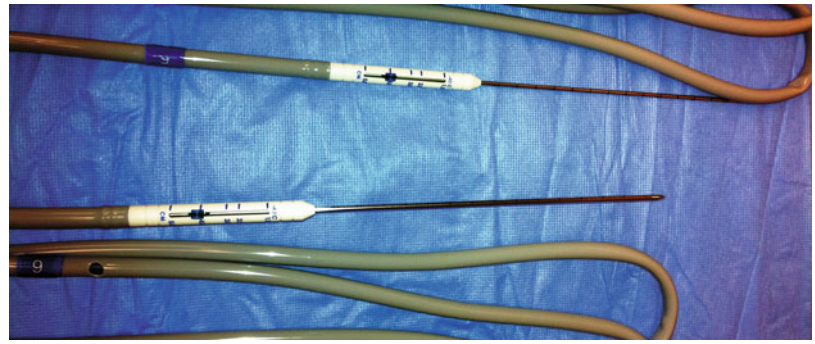

Fig. 52.8 Cryoprobes. Using real-time transrectal ultrasound guidance, these cryoprobes are placed into the prostate via the perineum

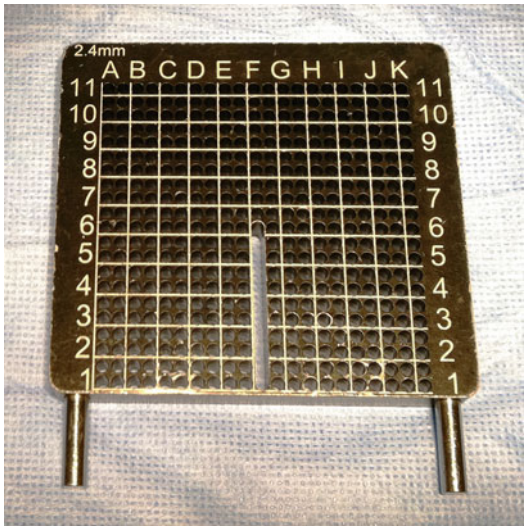

Fig. 52.9 Template used for cryotherapy. Using this grid, precise placement of cryoprobes and thermocouples is achieved with software mapping and ultrasound guidance

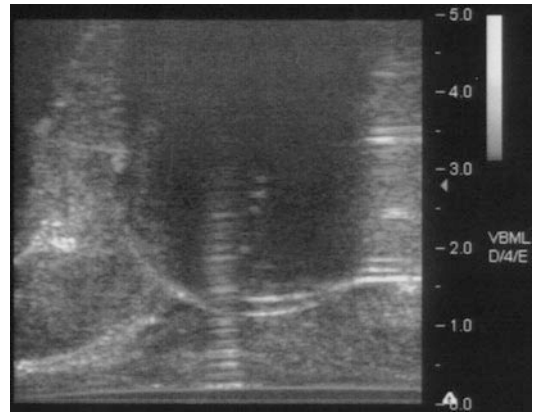

Fig. 52.10 Hypoechoic ice ball formation. During the freezing process, real-time ultrasound monitoring is used to visualize the formation of the hypoechoic ice ball

sphincter, neurovascular bundles, and Denonvilliers' fascia (Fig. 52.9). Double freeze-thaw cycles are performed with real-time monitoring of ice ball formation which is represented as a hypoechoic area on ultrasound (Fig. 52.10). Patients are discharged home the same day with anti-inflammatory medications, alpha blockers, and either a urethral catheter or a temporary suprapubic tube.

Indications and Patient Selection

The consensus opinion of the AUA Best Practice Statement is that cryosurgery is an option for any man with clinically localized or organ-confined disease with a negative metastatic evaluation [42]. Additionally, there are some patients who are not ideal candidates for radical prostatectomy; these include patients with significant rectal pathology, those with extremely large body habitus, or those who have had previous radiation therapy for nonurologic malignancies [42]. Contraindications include advanced local disease, inflammatory bowel disease because of an increased risk of rectourethral fistula, and previous transurethral resection of the prostate. In these patients, the urethral warming catheter will not properly coapt against the resection defect and urethral necrosis is more likely [42]. An additional application of cryosurgery is for those patients who have initially been treated with radiation as primary therapy and are diagnosed with radiorecurrent disease. For this challenging clinical situation, cryosurgery can be

a viable option [43]. Given the increased technical difficulty and rate of complications encountered with salvage prostatectomy, there is great conceptual interested in cryotherapy as a treatment for curative intent in the setting of radiation failure [44]. Patients with biopsy-proven persistent organ-confined prostate cancer, PSA <10 ng/ml, and a negative metastatic evaluation are candidates for salvage cryosurgery [45].

Complications

Immediate complications from cryosurgery for prostate cancer include urinary retention or penile and scrotal swelling. These tend to be self-limiting and are treated with urinary drainage and expectant management, respectively. Delayed complications include rectourethral fistula, urinary incontinence, erectile dysfunction, and urethral sloughing. Most contemporary series report a very low risk of fistula formation, under 1 %, which is similar to the risk of rectal injury with radical prostatectomy [46]. The risk of urinary incontinence from freeze injury to the sphincter ranges in the literature from 1 % to 10 % [47]. With regard to erectile dysfunction, during total gland cryosurgery, the ice ball extends to the prostatic capsule and encompasses the neurovascular bundles. The incidence of ED ranges from 40 % to 80 %, and for this reason, cryotherapy is considered suitable for men with underlying ED at the time of treatment [47].

Outcomes

As with other therapies for prostate cancer, posttreatment PSA is an integral part of follow-up; however, for cryosurgery, there is no universally accepted definition of biochemical failure. Therefore, a variety of endpoints are used such as PSA cutoff values of 1 or 0.5 ng/ml or ASTRO (three consecutive increases in PSA) or Phoenix (PSA nadir + 2 ng/ml) criteria. In many of the earlier published series, follow-up biopsy was performed as part of the treatment protocol. The incidence of negative biopsy after cryotherapy is excellent, ranging from 87 % to 98 % [48]. In one of the larger case series ($n = 590$), Bahn et al. reported on patients with 5.4 years follow-up with a mean age of 70 years and a distribution of low (16 %), intermediate (30 %), and high (54 %) risk disease. Using a definition of PSA recurrence as greater than a cutoff value of 1.0 ng/ml, the 5-year biochemical disease-free survival rates were 87 %, 79 %, and 71 % for low-, intermediate-, and high-risk disease, respectively [48]. Advances in modern cryotherapy for prostate cancer such as real-time imaging, thermocouples for temperature monitoring at critical structures, and the urethral warming catheter have made cryotherapy a viable treatment option for localized prostate cancer. Several large single institution experiences have defined the efficacy and safety of cryosurgery although long-term data on cancer-specific or overall survival are pending. These studies and comparative trials of surgery versus radiation versus cryotherapy will further refine the use of cryotherapy for treatment of prostate cancer.

References

1. Han M, Partin AW, Piantadosi S, et al. Era specific biochemical recurrence-free survival following radical prostatectomy for clinically localized prostate cancer. J Urol. 2001;166:416–9.
2. Bill-Axelson A, Holmber L, Ruutu M, et al. Radical prostatectomy versus watchful waiting in early prostate cancer. N Engl J Med. 2005;342:1977–84.
3. Kattan MW, Eastham JA, Stapleton AM, et al. A preoperative nomogram for disease recurrence following radical prostatectomy for prostate cancer. J Natl Cancer Inst. 1998;90:766–71.
4. Guillonneau B, Vallancien G. Laparoscopic radical prostatectomy. The Montsouris technique. J Urol. 2000;163:418–22.
5. Van Velthoven RF, Ahlering TE, Peltier A, et al. Technique for laparoscopic running urethrovesical anastomosis: the single knot method. Urology. 2003;61:699–702.
6. Catalona WJ, Misop H. Definitive therapy for localized prostate cancer- an overview. In: Wein AJ, Kavoussi LR, Novick AC, Partin AW, Peters CA, editors. Campbell-Walsh urology, vol. 3. 9th ed. Philadelphia: Saunders Elsevier; 2007. p. 2937–8.
7. Ficazzola M, Nitti VW. The etiology of post-radical prostatectomy incontinence and correlation of

symptoms with urodynamic findings. J Urol. 1998;160:1317.
8. O'Donnell PD, Finan BF. Continence following nerve-sparing radical prostatectomy. J Urol. 1989;142:1227.
9. Smither AR, Guralnick ML, Davis NB, See WA. Quantifying the natural history of post-radical prostatectomy incontinence using objective pad test data. BMC Urol. 2007;7:2.
10. Kundu SD, Roehl KA, Eggener SE, Antenor JA, Han M, Catalona WJ. Potency continence and complications in 3,477 consecutive radical retropubic prostatectomies. J Urol. 2004;72(6 Pt 1):2227–31.
11. Parsons JK, Bennett JL. Outcomes of retropubic, laparoscopic, and robotic-assisted prostatectomy. Urology. 2008;72(2):412–6.
12. Reiner WG, Walsh PC. An anatomical approach to the surgical management of the dorsal vein and Santorini's plexus during radical retropubic surgery. J Urol. 1979;121:198–200.
13. Walsh PC. Anatomic radical prostatectomy: evolution of the surgical technique. J Urol. 1998;160:2418–24.
14. Costello AJ, Brooks M, Cole OJ. Anatomical studies of the neurovascular bundle and cavernosal nerves. BJU Int. 2004;94:1071–6.
15. Walsh PC, Partin AW. Anatomic radical retropubic prostatectomy. In: Wein AJ, Kavoussi LR, Novick AC, Partin AW, Peters CA, editors. Campbell-Walsh urology, vol. 3. 9th ed. Philadelphia: Saunders Elsevier; 2007. p. 2977–8.
16. Lepor H, Nieder AM, Ferrandino MN. Intraoperative and postoperative complications of radical retropubic prostatectomy in a consecutive series of 1,000 cases. J Urol. 2001;166(5):1729–33.
17. Lepor H, Kaci L. Contemporary evaluation of operative parameters and complications related to open radical retropubic prostatectomy. Urology. 2003;62:702–6.
18. Huang G, Lepor H. Factors predisposing to the development of anastomotic strictures in a single-surgeon series of radical retropubic prostatectomies. BJU Int. 2006;97(2):255–8.
19. Pound CR, Partin AW, Eisenberger MA, et al. Natural history of progression after PSA elevation following radical prostatectomy. JAMA. 1999;281:1591–7.
20. Chen BT, Wood DP. Salvage prostatectomy in patients who have failed radiation therapy or cryotherapy as primary treatment for prostate cancer. Urology. 2003;62:69–78.
21. Rogers E, Ohori M, Kassabian VS, et al. Salvage radical prostatectomy outcome measured by serum prostate specific antigen levels. J Urol. 1995;153:104–10.
22. Silverstein AD, Weizer AZ, Dowell JM, Auge BK, Paulson DF, Dahm P. Cost comparison of radical retropubic and radical perineal prostatectomy: single institution experience. Urology. 2004;63(4):746–50.
23. Ruiz-Deya G, Davis R, Srivastav S, Wise A, Thomas R. Outpatient radical prostatectomy: impact of standard perineal approach on patient outcome. J Urol. 2001;166(2):581–6.
24. Gillitzer R, Melchior SW, Hampel C, Wiesner C, Fichtner J, Thüroff JW. Specific complications of radical perineal prostatectomy: a single institution study of more than 600 cases. J Urol. 2004;172(1):124–8.
25. Weldon VE, Tavel FR, Neuwirth H. Continence, potency and morbidity after radical perineal prostatectomy. J Urol. 1997;158(4):1470–5.
26. Lerner SE, Fleischmann J, Taub HC, Chamberlin JW, Kahan NZ, Melman A. Combined laparoscopic pelvic lymph node dissection and modified belt radical perineal prostatectomy for localized prostatic adenocarcinoma. Urology. 1994;43(4):493–8.
27. Korman HJ, Leu PB, Goldstein NS. A prospective comparison of anatomic radical perineal and retropubic prostatectomy specimens: are surgical margins equivalent? Prostate Cancer Prostatic Dis. 2000;3(S1):S22.
28. Schuessler WW, Schulam PG, Clayman RV, Kavoussi LR. Laparoscopic radical prostatectomy: initial short-term experience. Urology. 1997;50:854–7.
29. Schneider O, Troccaz J. A six-degree-of-freedom passive arm with dynamic constraints (PADyC) for cardiac surgery application: preliminary experiments. Comput Aided Surg. 2001;6:341–51.
30. Su L, Smith JA. Laparoscopic and robotic assisted laparoscopic radical prostatectomy and pelvic lymphadenectomy. In: Wein AJ, Kavoussi LR, Novick AC, Partin AW, Peters CA, editors. Campbell-Walsh urology, vol. 3. 9th ed. Philadelphia: Saunders Elsevier; 2007. p. 2985.
31. Cathelineau X, Cahill D, Widmer H, et al. Transperitoneal or extraperitoneal approach for laparoscopic radical prostatectomy: a false debate over a real challenge. J Urol. 2004;171(2 pt 1):714–16.
32. Brown JA, Rodin DM, Lee B, Dahl DM. Transperitoneal versus extraperitoneal approach to laparoscopic radical prostatectomy: an assessment of 156 cases. Urology. 2005;65:320–4.
33. Tewari A, Srivasatva A, Menon M, et al. A prospective comparison of radical retropubic and robot-assisted prostatectomy: experience in one institution. BJU Int. 2003;92:205–10.
34. Hu JC, Nelson RA, Wilson TV, et al. Perioperative complications of laparoscopic and robotic assisted laparoscopic radical prostatectomy. J Urol. 2006;175:541–6.
35. Lasser MS, Renzulli J, Pareek G, et al. An unbiased prospective report of perioperative complications of robot-assisted laparoscopic radical prostatectomy. Urology. 2010;75:1083–90.
36. Coelho RF, Rocco B, Patel MB, Orvieto MA, Chauhan S, Ficarra V, Melegari S, Palmer KJ, Patel VR. Retropubic, laparoscopic, and robot-assisted radical prostatectomy: a critical review of outcomes reported by high-volume centers. J Endourol. 2010;Not available-,ahead of print. doi:10.1089/end2010.0295.
37. Arnott J. Practical illustrations of the remedial efficacy of a very low or anesthetic temperature: in cancer. Lancet. 1850;2:257–9.

38. Cooper IS, Lee A. Cryostatic congelation: a system for producing a limited controlled region of cooling or freezing of biologic tissues. J Nerv Ment Dis. 1961;133:259–63.
39. Baust JG, Gage AA, Robilotto AT, Baust MH. The pathophysiology of thermoablation: optimizing cryoablation. Curr Opin Urol. 2009;19:127–32.
40. Hoffmann N, Boschof J. The cryobiology of cryosurgical injury. Urology. 2002;60(2):40–49.
41. Gage AA, Baust JG. Mechanisms of tissue injury in cryosurgery. Cryobiology. 1998;37:171–86.
42. Babaian RJ, Donnelly B, Bahn D, Baust JG, Dinnen M, Ellis D, Katz A, Pisters L, Rukstalis D, Shinohara K, Tharsher JB. Best practice statement on cryosurgery for the treatment of localized prostate cancer. J Urol. 2008;180:1993–2004.
43. Ng CK, Moussa M, Downey DB, Chin JL. Salvage cryoablation of the prostate: follow up and analysis of predictive factors for outcome. J Urol. 2007;178:1253.
44. Miller Jr RJ, Cohen JK, Shuman BA, et al. Percutaneous transperineal cryosurgery of the prostate as salvage therapy for post radiation recurrence of adenocarcinoma. Cancer. 1996;77:1510–4.
45. Pisters LL, Rewcastle JC, Donnelly BJ, Luganni FM, Katz AE, Jones JS. Salvage prostate cryoablation: initial results from the cryo online data registry. J Urol. 2008;180:559–64.
46. Shinohara K, Connolly JA, Presti Jr JC, et al. Cryosurgical treatment of localized prostate cancer (stages T1-T4): preliminary results. J Urol. 1996; 156:115–20.
47. Mouraviev V, Polascik TJ. Update on cryotherapy for prostate cancer in 2006. Curr Opin Urol. 2006; 16:152.
48. Bahn DK, Lee F, Badlament R, Kumar A, Greski J, Chernick M. Targeted cryoablation of the prostate: 7 year outcomes in the primary treatment of prostate cancer. Urology. 2002;60:3.

Image-Guided Radiotherapy and Prostate Cancer

53

Paul S. Rava and Thomas A. DiPetrillo

Abstract

The role of imaging in medicine is in constant flux and utilization now extends well beyond its initial intent as a diagnostic modality. In the field of radiation oncology, imaging has historically been employed to define the treatment field or target at the time of radiation planning. With improvements in imaging and greater accessibility, the incorporation of daily imaging into treatment has improved accuracy and precision of radiation delivery. Early prostate cancer is a very treatable disease, but requires high doses of radiation for optimal local control. Current standard treatment dose is well beyond the tolerance of adjacent normal tissues. Dose escalation for the treatment of prostate cancer is achieved by shrinking field sizes in addition to accurate and precise delivery of radiation. Image-guided radiotherapy (IGRT) involves imaging prior to daily treatment to compensate for organ motion and daily setup errors. The ability to shrink fields and escalate dose has greatly improved outcomes in definitive radiation therapy for early prostate cancer improving local control without increasing treatment-related morbidity.

Introduction

Prostate cancer is an exceptionally manageable disease with treatment decisions respecting the fact that most men have a prolonged life expectancy despite the diagnosis. Effective radiation treatment as a result is a balance between achieving tumoricidal doses while minimizing radiation damage to adjacent normal tissues, thus preserving their biological function. In fact, normal tissue tolerance can be considered the limiting factor in tumor control. This is especially applicable to the definitive treatment of early prostate cancer during which the amount of delivered dose

P.S. Rava (✉)
Department of Radiation Oncology, Tufts Medical Center and Rhode Island Hospital, Boston, MA, USA
e-mail: prava@tuftsmedicalcenter.org

T.A. DiPetrillo
Department of Radiation Oncology, Rhode Island Hospital, Providence, RI, USA
e-mail: tdipetrillo@lifespan.org

D.E. Dupuy et al. (eds.), *Image-Guided Cancer Therapy*, DOI 10.1007/978-1-4419-0751-6_55,

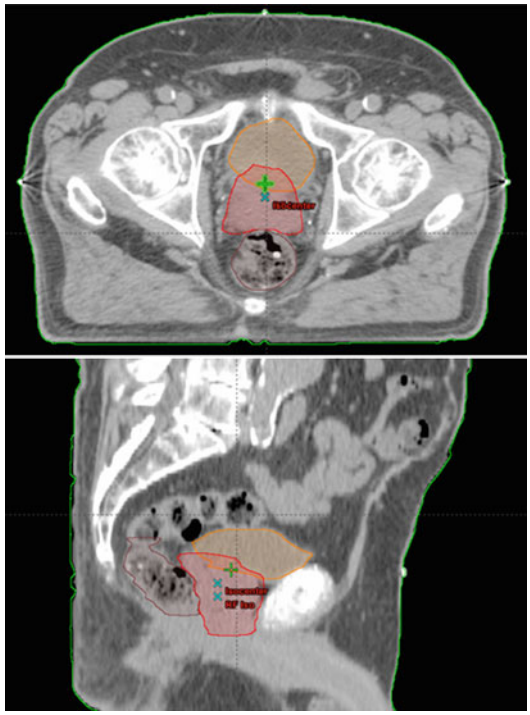

Fig. 53.1 *The anatomical position of the prostate gland and adjacent normal tissues*. The prostate gland and seminal vesicles are outlined in red in both axial and sagittal images. Adjacent organs of interest include the bladder (*orange*) and the rectum (*brown*). The spatial arrangement of these tissues, as well as daily variation in their position, limits the radiation dose that can be delivered using conventional treatment techniques

is restricted by the anatomical relationships between the prostate and adjacent normal structures (Fig. 53.1). Tolerance doses that predict for 5 % complication rate in 5 years for small bowel (50 Gy), bladder (65 Gy), as well as rectum (60 Gy) have been reported and are significantly less than the dose (>76–78 Gy) currently considered necessary for effective local disease control [1–10]. Therefore, to achieve acceptable local control rates, delivered dose must be escalated in excess of tissue tolerance. Dose escalation is feasible if only small volumes of normal tissue exceed predicted tolerance. In addition to advances with radiation delivery, doses of this magnitude can be safely and effectively administered by reducing treatment field size. Small radiation fields require daily monitoring for target motion since the margin for systematic error has been reduced. With the introduction of image-guided radiation therapy (IGRT), precise and accurate treatment of small target volumes can be safely and effectively achieved. IGRT allows for daily identification of the target as well as compensation for motion. Furthermore, it has played an essential role in dose escalation with a significant impact on prostate cancer outcome from the perspective of tumor control as well as treatment toxicity.

Dose Escalation

Historically, prostate cancer was treated with large radiation fields encompassing the entire pelvis, followed by field reductions to boost the prostate itself to higher doses (Fig. 53.2). This approach provided adequate coverage to the clinical target volume and the generous field size compensated for errors in treatment setup as well as target motion. Doses <70 Gy were generally prescribed to the prostate, and local control rates ranged between 60 % and 80 % [11]. In addition to limiting the delivered radiation dose, large field sizes also led to significant toxicity. Early experience suggested that as much as 10 % of patients required hospitalization as a direct consequence of their treatment [12]. Lawton et al. reviewed two early RTOG trials and identified a 3.3 % incidence of grade 3 or greater bowel toxicity with 0.6 % of patients experiencing bowel perforation or stricture [13]. The incidence of grade 3 or greater urinary complications was 7.7 %. Upon further analysis of their data, a total dose >70 Gy was noted to predict for adverse affects. Coincidently, while these and additional studies confirmed the association between dose and toxicity, evidence supporting a direct correlation between radiation dose and tumor control was also accumulating [3–10].

To date, at least five randomized trials evaluating dose escalation using external beam radiation therapy have been reported [3–9]. In an initial study from MD Anderson Cancer Center, 70 Gy versus 78 Gy was evaluated. Freedom from PSA failure was statistically improved for those receiving the higher dose, 70 % versus 64 % [3].

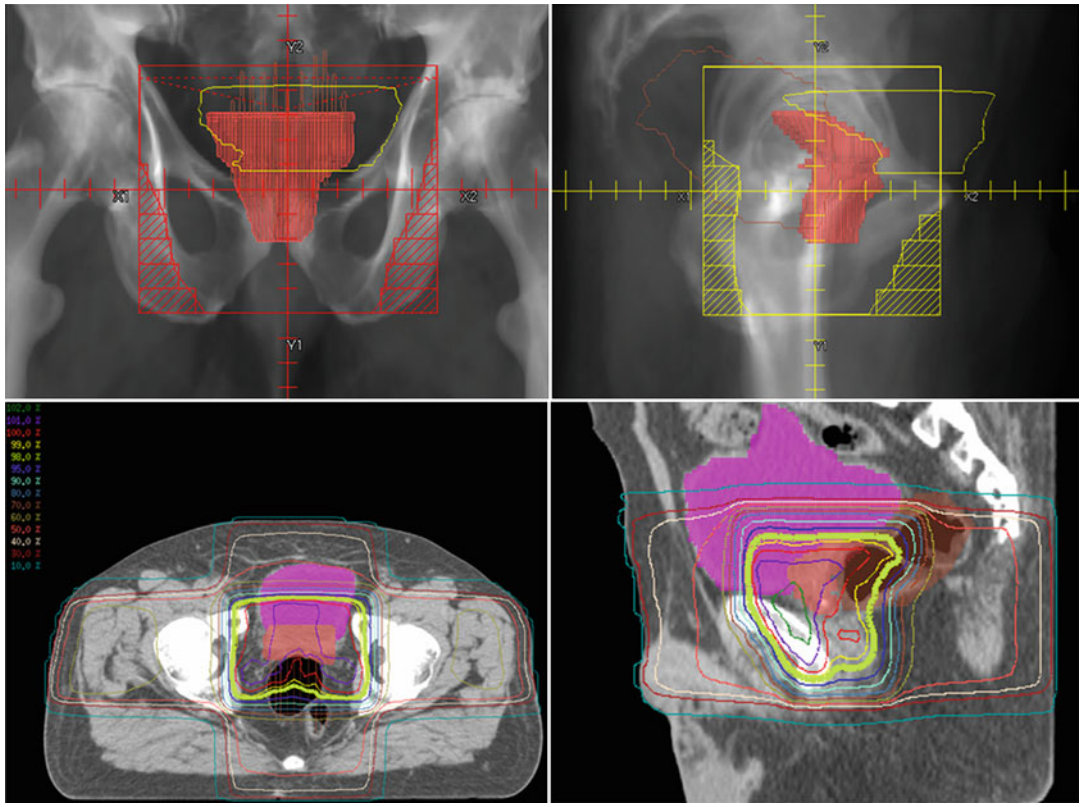

Fig. 53.2 *Conventional radiation fields for treatment of localized prostate cancer*. Prostate cancer was historically treated with AP and lateral fields (4-field technique) (*upper panels*). The prostate target (*red*), rectum (*brown*), and bladder (*yellow*) are shown. Sagittal and axial views (*lower panels*) are also shown with dose distribution. The 99 % isodose line is bolded in *yellow*

At Mass General, conventional treatment of 70.2 Gy was compared with a second arm prescribing an additional 9 Gy for a total dose of 79.2 Gy [4]. Again, an overwhelming benefit in PSA relapse-free survival, 80 % versus 61 %, was noted for the patients receiving higher dose. A recently published meta-analysis evaluated all dose-escalation trials and demonstrated a significant reduction in biochemical failure, 24.8 % versus 34.6 % ($p < 0.0001$) for high-dose radiation treatment [10]. All GI toxicity grade 3 or greater was significantly increased in the high-dose radiation therapy group. However, no difference in GU toxicity was observed. Thus, a clear benefit to dose escalation in reducing biochemical failure rates (a surrogate for local control) exists. With novel radiation delivery systems used in the clinic today, further dose escalation without adding additional toxicity is possible and might further broaden the therapeutic index (Fig. 53.3). However, prescribing even higher doses will require complicated, yet precise treatment, directed to the target with sharp dose gradients. The precision of radiation delivery will likely represent a major limitation to this approach. Thus, one must understand organ motion and compensate for this event to prevent under-dosing the target or unintentionally subjecting critical normal tissues to areas of high dose. Furthermore, precise targeting will become even more crucial as the field of radiation therapy moves toward hypofractionation with larger doses and greater risk/reward compared to conventional treatment.

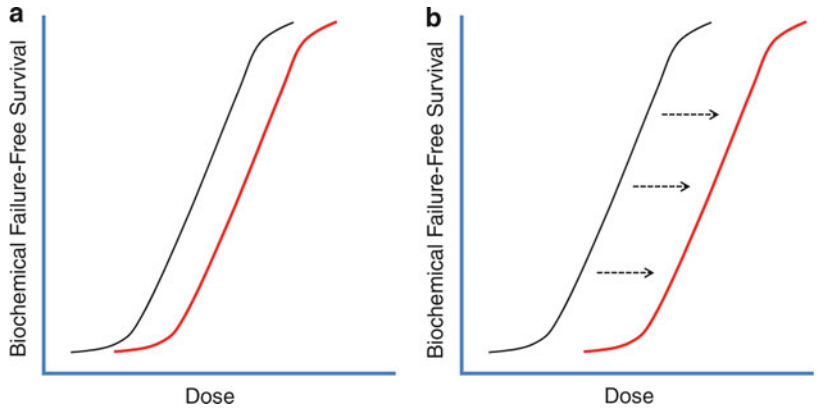

Fig. 53.3 *The effect of modern radiation treatment on the predicted therapeutic index*. Conventional radiation (**a**), with inherently large treatment fields that compensate for organ motion and setup error, results in unacceptable normal tissue toxicity compared to prostate cancer control (biochemical failure-free survival) as the dose is increased. However, improving radiation delivery using small treatment fields and intensity modulation (**b**) results in focused, high-dose radiation, sparing adjacent normal tissue and thus limiting toxicity. Image guidance compensates for the large dose gradients created when radiation is delivered in this fashion, thus eliminating target underdosing or normal tissue overdosing

Target Motion

While the prostate sits in direct contact with the bladder and is located just anterior to the rectum, the complexity of treatment arises from the fact that the pelvic organs are dynamic in nature. Both the bladder and rectum experience changes in volume during a single fraction of radiation as well as throughout the ~9-week course of conventional radiation treatment. Changes in bladder volume have little effect on the prostate's positional status; however, variations in rectal volume result in geometric miss, target underdosing, and poor clinical outcomes [14–16]. A 30 % decrease in biochemical control at 5 years has been observed in patients with distended rectums at the time of CT simulation [15]. A retrospective review of data from the Dutch dose-escalation study showed a 20 % reduction in freedom from PSA failure in their subset of patients with large rectal volumes [16]. A reasonable conclusion to derive from this data is that clinical control is directly related to changes occurring in the local anatomy. An air-filled rectum will shift the prostate anteriorly or tilt the prostate base toward the bladder changing its pitch (Figs. 53.4 and 53.5). Reduced rectal volume during treatment shifts the prostate position more posterior. As a consequence, a portion of the clinical target will be relocated outside the treatment field. In this scenario, the peripheral zone of the prostate (i.e., the region most likely to harbor malignancy) moves toward, or potentially beyond, the field edge, a region with characteristic rapid dose falloff.

In general, two types of positional changes have the greatest effect on the prostate's position within the pelvis. The first, interfractional motion, describes changes that occur between radiation treatments. Intrafractional motion, on the other hand, refers to positional variability during a single treatment. The first impacts prostate cancer treated with conventional radiation delivery, while intrafractional motion likely plays a more significant role when treating prostate cancer with hypofractionationated schedules. In the latter, each treatment interval is increased 3–4 times that of conventional treatment during which time the prostate position can be influenced by the dynamic movements of adjacent pelvic organs. Additionally, using larger dose per fraction and reduced number of fractions requires image guidance as systematic dose errors to target and normal tissues will not be averaged out over >35 treatments. In this setting,

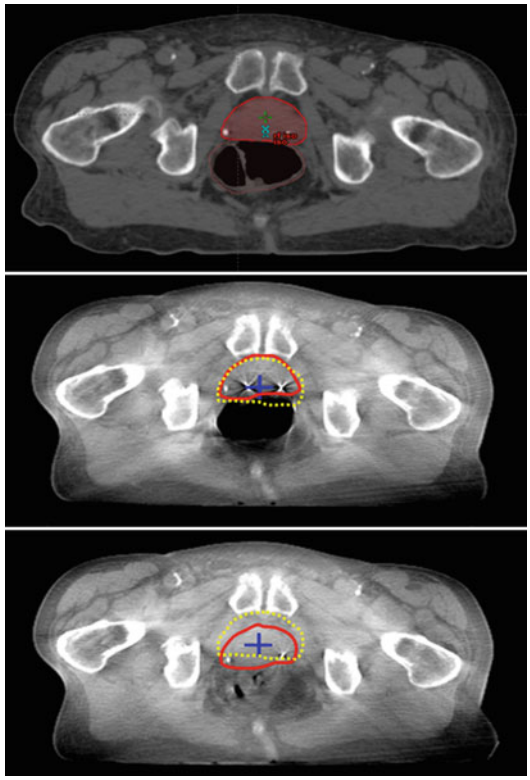

Fig. 53.4 *The variation in rectal volume and its effect on prostate location at the time of a single radiation treatment*. At the time of radiation planning (*top figure*), the rectum is air-filled and the prostate (*red*) is located between the rectum and pubic symphysis. At separate times during the weeks of treatment, the rectal volume has changed shifting the prostate more posteriorly away from the symphysis (*bottom figure*). The prostate position at the time of radiation planning is depicted as a broken *yellow line*. When the rectal volume is significantly reduced compared to the planning CT, the prostate no longer resides within the preplanned target volume. Without appropriate shifting of the target, under-dosing of the posterior portion of the gland would occur as the target volume falls outside of or at the edge of the treatment field

even small motion errors can translate into significant dose excess or under-dosing.

It is accepted that the largest interfractional changes in prostate position occur in the anterior-posterior direction and are the direct consequence of varying rectal volumes [14, 17, 18]. Lateral, as well as superior to inferior, positional changes have also been reported, but only on the order of 1–3 mm [17]. Balter et al. evaluated the position of metallic fiducials placed within the prostate of 10 patients over the course of their treatment [17]. While rotational changes were on average less than 1 mm, translations in the anterior-posterior direction were nearly 5 mm. Maximum differences approached 1 cm. Similarly, the interfraction standard deviation in prostate position assessed by ultrasound was 4.9 mm in the anterior-posterior direction [18]. Studying intrafractional motion requires real-time imaging of the prostate and adjacent tissues over the duration equivalent to a single fraction of radiation. Measuring positional changes using fluoroscopy to define the position of metallic fiducials or ultrasound suggests that most displacements are less than 1–2 mm [19, 20]. Ghilezan et al. quantified prostate motion using cine MRI over the duration of 20–30 min, an interval that is more representative of a single radiation treatment [14]. Intrafraction displacement was dependent on rectal volume and the absolute variations in position were again small, measuring less than 2 mm. More recently, electromagnetic transponders have been used to analyze target motion during prostate treatments [24]. Su et al. reported that the prostate was located within a 5-mm setup margin >91 % of the time [21]. Similarly, Tanyi et al. concluded that prostatic intrafractional motion was on the order of millimeters [22]. Collectively, studies have generally agreed that the prostate position at the time of treatment, compared to its position at the time of CT-simulation, would be within 5 mm 90 % of the time [23]. This is acceptable variation using conventional radiation treatment schedules; however, outcomes with even small changes in position would likely be magnified as total dose continues to be escalated and fractional doses becoming increasingly large.

Imaging Techniques

Large margins are not compatible with escalated doses, especially in the pelvis where sensitive tissues lie in close proximity to the target. Image guidance provides the opportunity to reduce treatment volumes while maintaining appropriate dosimetric coverage to the target.

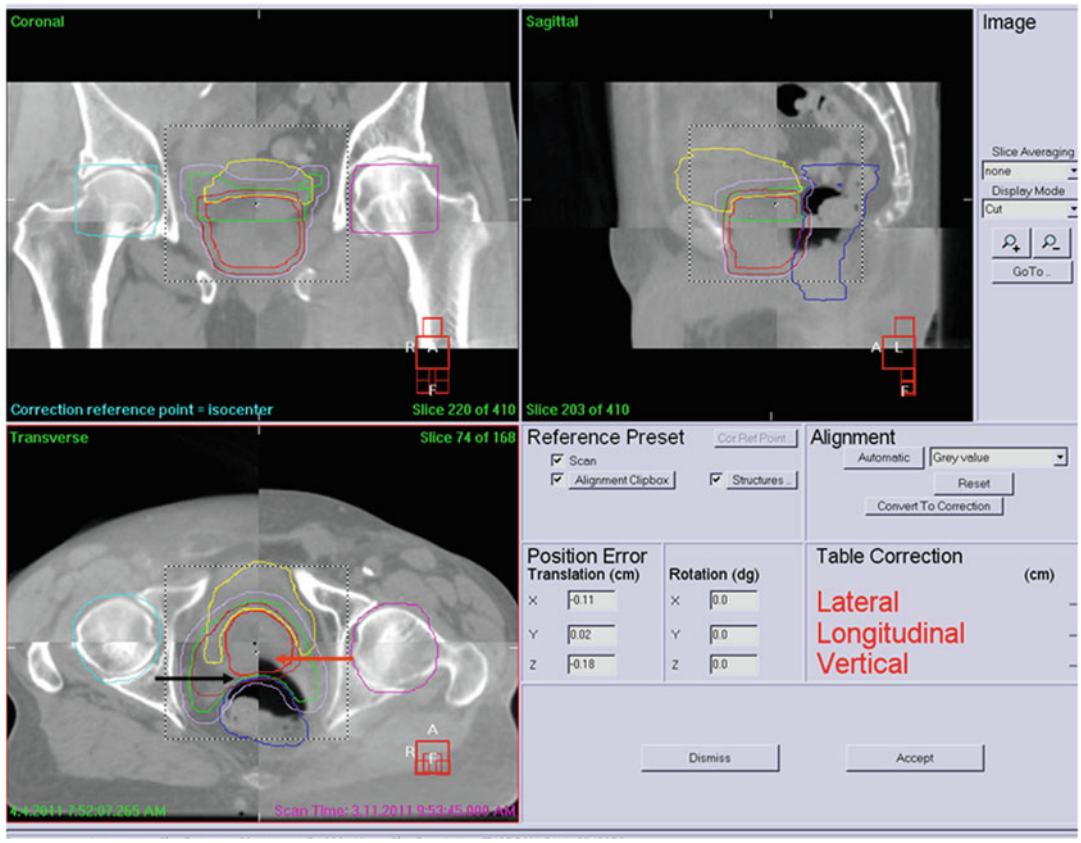

Fig. 53.5 Cone-beam CT scan demonstrating the position of the prostate at the time of first treatment compared to pretreatment simulation with varying rectal volume. The rectum (*blue*), prostate CTV (*red*), and bladder (*yellow*) are depicted in a single axial, sagittal, and coronal view. The anterior wall of the rectum at the time of simulation (*black arrow*) is more posterior compared to its position at the time of treatment (*red arrow*)

CT-based planning provides a static picture of the anatomical relationship between the pelvic bony anatomy, surrounding soft tissues, and radiation target. The intention is to replicate the dosimetry over a 9-week treatment period based upon this initial set of images (Fig. 53.6). Daily setup, with a reproducible target position, is crucial for safe administration of high radiation doses. Laser alignment to skin tattoos does not accurately define the treatment isocenter and can result in discrepancies in the actual prostate location that exceed 10 mm [21]. Even with good immobilization, up to 2-cm margins are proposed to account for daily setup errors [22, 31]. Daily kV imaging with alignment to bony anatomy also does not correlate well with the daily anatomical position of the prostate [25]. Margins in excess of 7 mm have been recommended with this approach [26, 27].

Currently, the most common techniques used for IGRT include kV imaging to identify fiducial markers or CT scanning. Daily ultrasound is also available, but requires additional expertise that restricts its overall utility. Radiofrequency transponders are quite novel, but a benefit beyond current standards requires additional investigation.

Fiducial markers are placed transrectally using ultrasound. Three insertion positions are recommended to triangulate the position of the prostate in its relationship to the bony anatomy (Fig. 53.7). At least one of the markers should be

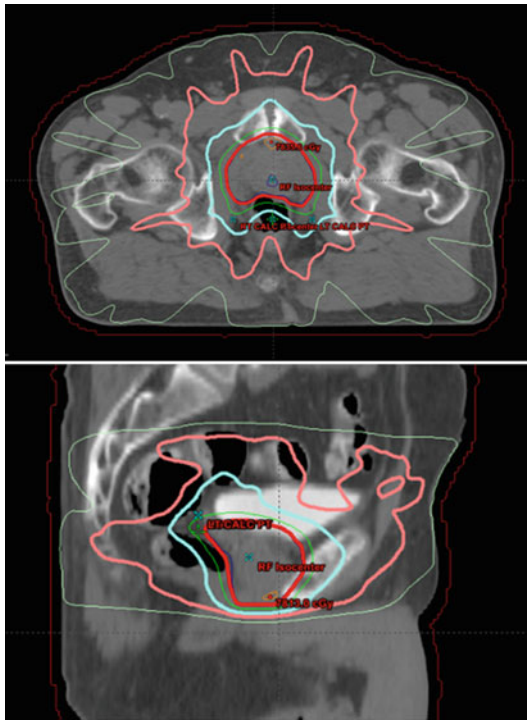

Fig. 53.6 *Dose distribution for localized prostate cancer treated with IMRT*. Typical radiation dose distribution for a 9- and 7-field pelvic IMRT plan for localized prostate cancer. The prescription dose was 75 Gy. The 100 % (*red*), 60 % (*blue*), and 40 % (*pink*) isodose lines are depicted. An acceptable 4.5 % "hot spot" resides in the prostate gland (i.e., target tissue). High radiation dose, beyond bowel and bladder tissue tolerance, can be safely delivered because the radiation is highly focused with steep dose gradients. Daily imaging is required to make certain the target volume does not reside in a dose gradient or known "hot spots" within critical normal tissue

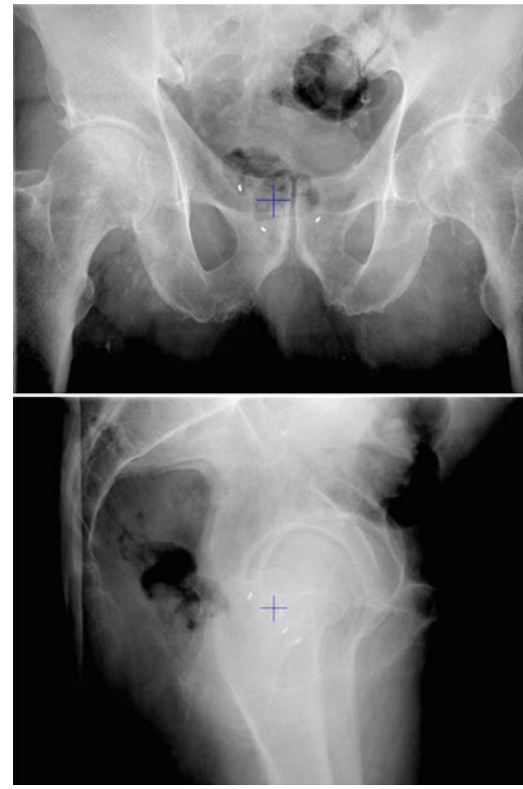

Fig. 53.7 *Daily kV imaging with gold fiducial markers*. Three gold markers were inserted trans-anally under ultrasound guidance. Their position is used to identify the daily location of the prostate on both AP and lateral images. (Note that three markers are located in different planes and a single fiducial is located at the prostatic-rectal interface.) After imaging, the table is shifted to position the prostate within the planning treatment volume

located in the posterior wall of the gland to define the prostatic-rectal interface. This region defines the posterior edge of the target and is important for both tumor control and treatment toxicity [15, 16]. The placement of fiducial markers, either transrectally or transperineally, is associated with limited toxicity. Adverse events include hematuria (15 %), rectal bleeding (4 %), and fever (2 %) [28]. Moman et al. reviewed their experience of 914 patients who received fiducial placement and reported only two grade 3 toxicities (both urosepsis) [29]. In addition to safety and tolerability, another advantage to IGRT with fiducial markers is that minimal imaging expertise is required by the treating therapists to maintain the accuracy and reproducibility of daily treatments. Minor intra- and inter-user variability, both of which have been measured to be less than 1 mm, have been described [30]. This variability is considerably less than for other imaging techniques.

CT on-rails, cone-beam CT, and helical megavoltage CT scanners are in use today. All CT-based techniques provide soft tissue discrimination but still require fiducial alignment for optimal benefits (Fig. 53.8). The prostate can be aligned to soft tissue without the addition of fiducials. This may be necessary for patients on Coumadin or with other contraindications to a minimally invasive procedure. However, even with CT imaging, 5-mm margins are required

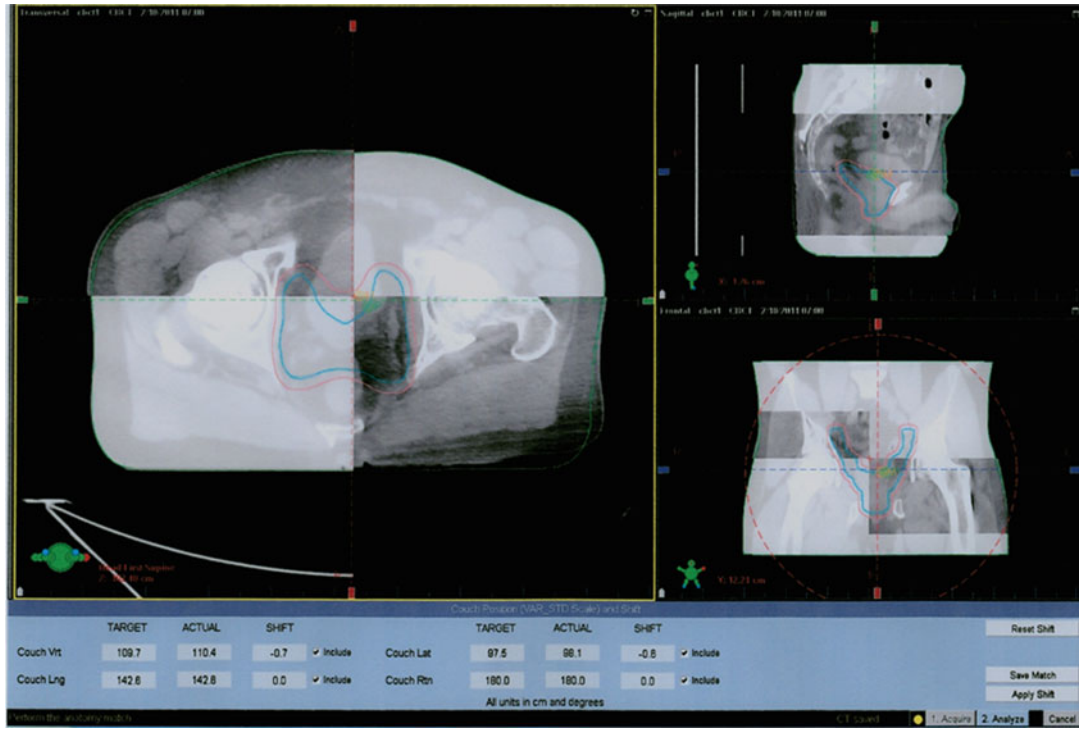

Fig. 53.8 *Cone-beam CT scan*. Prior to treatment, a cone-beam CT is performed. Initially, the bony anatomy is aligned in three planes (axial, sagittal, and coronal). The images then are evaluated to ascertain whether the position of the prostate is similar to the planning CT. If not, the table is shifted to compensate for setup error and organ motion and the patient receives his daily fraction of radiation

when no fiducial marker is used. Yet only 3-mm margins are recommended when using CT imaging in conjunction with fiducial alignment [31–34]. Again, volume of normal tissue receiving dose might become limiting and additional toxicity dulling the therapeutic benefit of dose escalation. An additional benefit to CT scanning is that the interfractional position of bladder, rectum, and small bowel can be evaluated over the course of an entire treatment. Overlays of planned dose and received dose to these structures in association with toxicity data might better define tissue tolerance and assist further dose escalation.

A B-mode acquisition and targeting (BAT) transabdominal system is the most common ultrasound technique available. For radiation treatment, the ultrasound probe is generally docked to the linear accelerator gantry. Sagittal and transverse images of the prostate and seminal vesicles are obtained prior to treatment (Fig. 53.9). Ultrasound images are then overlaid with CT images from patient simulation. The BAT software calculates and displays the recommended couch movements in three orthogonal positions to align the prostate to the planning CT. Although effective, inherent concerns limit the use of ultrasound in radiation clinics. The majority of concern is centered around inter- and intra-user variability. CT target volumes tend to be larger than those defined by ultrasound and can bring individual bias into daily alignment. Displacement of the prostate occurs as a function of transducer pressure on the abdomen [35, 36]. When assessing probe displacement in a stepwise manner, Artignan et al. showed that prostate motion was <5 mm 80–100 % of the time after 1–1.5 cm of displacement [36]. However, 2 cm of displacement resulted in motion of <5 mm only 40 % of the time. In all, 1.2 cm of displacement resulted in

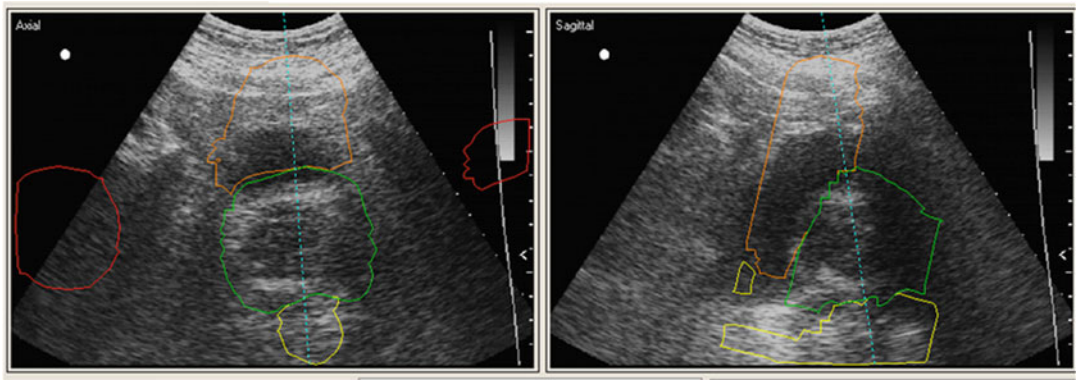

Fig. 53.9 *B-mode acquisition ultrasound* (*BAT*). Axial and sagittal views are shown. The location and position of the target (*red*), bladder (*orange*), and rectum (*yellow*) at the time of planning CT simulation are depicted and overlaid on the ultrasound image. The patient is then shifted to reposition the target within the planning volume. An ultrasound is repeated to demonstrate a correct shift prior to treatment

good-quality imaging and produced 3.1 mm of prostate motion. In addition, ultrasound expertise and patient body habitus may add additional variability beyond that described. In a comparison with implanted fiducials, treatment margins when using ultrasound were determined to range between 0.9 and 1.6 cm for adequate target coverage [37]. Independently, Scarbrough et al. also recommended 9-mm margins when using ultrasound and only 3-mm margins for fiducial markers [38]. Others have also suggested a difference in defining the prostate position between the two modalities, further questioning the ability of ultrasound to correctly define the target [39, 40]. Thus, the additional expertise required by treating therapists, the inherent variability among individual and between users, as well as the accumulating evidence that suggests possible inferiority of ultrasound directed prostate targeting compared to fiducial alignment has restricted its mainstream use.

In addition to deciding on the appropriate modality to provide image guidance, the frequency of patient imaging has also come into question. Unlike diagnostic radiology, imaging prior to treatment does not substantially increase the total radiation dose. Secondly, a majority of patients receiving treatment are older and part of a low-risk group, considering their expected longevity beyond the treatment period, for developing a second radiation-induced cancer. This is in striking contrast to patients treated with radiation therapy for Hodgkin's disease where lifetime risk of secondary radiation-induced cancers is significantly increased and the incidence of breast cancer can approach 30 % [41]. However, in the setting of ALARA, even the appropriate use of imaging for IGRT is under debate. In an effort to evaluate the appropriate frequency of imaging, a cohort of 74 patients who underwent IGRT with metallic fiducials were retrospectively studied [42]. Not surprising, as the frequency of imaging increased, errors exceeding 5 mm decreased from 73 % (no imaging) to 24 % (imaging every other day). More importantly, errors exceeding 1 cm were seen in 20 % of patients receiving no imaging, 12 % of patients receiving weekly imaging, and only 4 % of patients who received imaging every other day. Thus, although daily imaging can be labor and time intensive, in the era of small fields and dose escalation, its potential safety and impact on accuracy is undoubtedly of great benefit. The frequency of cone-beam CT in addition to alignment of fiducial markers using kV imaging still requires further investigation.

Accelerating Delivery of Radiotherapy

Effective image-guided therapy permits both dose escalation and hypofractionation. The first has a proven clinical benefit, while the latter may

improve outcomes but is yet only based on radiobiological models [3–10, 43]. Fractionated radiation (small daily doses) relies on cancer cells being inherently radiation sensitive and the ability of normal tissue to repair sublethal radiation damage. Hypofractionation delivers higher per fractional doses of radiation in fewer treatments. With a hypofractionated schedule, the benefit of sublethal repair is lost and late toxicities can be significant with a negative effect on the therapeutic index. However, there exist scenarios where hypofractionation could result in better tumor control and therefore, widen the therapeutic index, compared to standard fractionation. An example would be for slowly dividing tumor histologies that have an a/b ratio similar to late-responding tissues. This has recently been discussed in the setting of hypofractionated treatment for breast cancer [44].

Hypofractionated radiation therapy for prostate cancer was first described in the United Kingdom during the 1960s [45]. Economic concerns as well as limited resources mandated for shorter treatments. More recently, radiobiological data continues to accumulate that shows prostate cancer cells are slowly proliferating with an a/b ratio estimated to be ~1.85 Gy [46]. This is in comparison to most proliferating tissues whose a/b ratio is considered to be in excess of 10 Gy. The low a/b ratio implies that prostate cancer is highly sensitive to increased dose per fraction and that fractionation might have little benefit to widening the therapeutic index. The feasibility of this approach was described by Madsen et al. who treated 40 patients with a total dose of 33.5 Gy delivered in 5 fractions with only a single grade 3 (GU) toxicity reported [47]. However, biochemical-free survival was slightly lower than expected (~70 %) after a median follow-up of 40 months. Two recent experiences with larger patient numbers have also been published [48, 49]. King et al. reported on 67 patients with localized low-risk prostate cancer treated after implantation of gold fiducials for real-time tracking of prostate motion [48]. An equivalent biological dose at 2 Gy per fraction of 90.6 Gy was prescribed using hypofractionation. With a median follow-up of 2.7 years, two PSA, biopsy-proven failures were documented. There were no grade 4 toxicities and only 3 % of patients experienced late grade III urinary toxicity. Similarly, no grade III rectal toxicity was reported either. This compares well with the late grade III toxicity reported in the MD Anderson Cancer Center dose-escalation study (78 Gy in 2 Gy fractions) in which 3 % of patients reported urinary and 7 % reported rectal grade III late toxicity [3]. Katz et al. published their experience on a much larger patient set treated with image-guided SBRT [49]. Both low- and intermediate-risk patients were treated with either 35 Gy or 36.25 Gy in 5 fractions. 5-month toxicity data revealed that <5 % of patients experienced acute grade II urinary or rectal toxicity independent of the total dose. Furthermore, late toxicity data was also encouraging with only 2–6 % grade II late urinary or rectal toxicity thus far reported and only one patient with grade III toxicity. However, the late toxicity data is still early and additional follow-up is required to fully appreciate the effects of hypofractionation. With high dose per fraction, treatment volumes and high dose gradients become extremely important for administering safe and effective radiation delivery. It is in this scenario where image guidance will have its greatest impact maximizing reward while limiting overall risks.

In all, radiotherapy is a safe, effective approach to managing localized prostate cancer. There exists a balance in long-term cancer control and minimization of treatment-related toxicities. These have been advanced by the technological advances in radiation delivery in addition to careful image guidance. Further advances will reflect a better understanding of disease and normal tissue responses to precisely delivered high-dose radiation.

References

1. Emami B, Lyman J, Brown A, et al. Tolerance of normal tissue to therapeutic irradiation. IJROBP. 1991;21:109–22.
2. Marks LB, Yorke ED, Jackson A, et al. Use of normal tissue complication probability models in the clinic. IJROBP. 2010;76(3):S10–9.

3. Kuban DA, Tucker SL, Dong L, et al. Long-term results of the MD Anderson randomized dose-escalation trial for prostate cancer. IJROBP. 2008;70:67–75.
4. Zeitman AL, DeSilvio ML, Slater JD, et al. Comparison of conventional-dose vs. high-dose conformal radiation therapy in clinically localized adenocarcinoma of the prostate: a randomized control trial. JAMA. 2005;294:1233–40.
5. Sathya JR, Davis IR, Julian JA, et al. Randomized trial comparing iridium implant plus external beam radiation therapy with external beam radiation therapy alone in node-negative locally advanced cancer of the prostate. JCO. 2005;23:1192–200.
6. Peeters ST, Heemsbergen WD, Koper PC, et al. Dose–response in radiotherapy for localized prostate cancer: results of the Dutch multicenter randomized phase III trial comparing 68 Gy of radiotherapy with 78 Gy. JCO. 2006;24:1990–9.
7. Shipley WU, Verhey LJ, Munzenrider JE, et al. Advanced prostate cancer: the results of a randomized comparative trial of high dose irradiation boosting with conformal protons compared with conventional irradiation using photons alone. IJROBP. 1995;32:3–12.
8. Dearnaley DP, Sydes MR, Graham JD, et al. Escalated-dose versus standard-dose conformal radiotherapy in prostate cancer: first results from the MRC RT01 randomized controlled trial. Lancet Oncol. 2007;8:475–87.
9. Beckendorf V, Guerif S, Le Prise E, et al. The GETUG 70 Gy vs. 80 Gy randomized trial for localized prostate cancer: feasibility and acute toxicity. IJROBP. 2004;60:1056–65.
10. Viani GA, Stefano EJ, Afonso SL. Higher-than-conventional radiation doses in localized prostate cancer treatment: a meta-analysis of randomized, controlled trials. IJROBP. 2009;74(5):1405–18.
11. Brabbins D, Kestin L, Yan D, et al. Improvements in clinical outcomes with prostate radiotherapy at a single institute in the PSA era (abstr). Int J Radiat Oncol Biol Phys. 2008;69(suppl):1100–9.
12. Hanks GE, Kramer S, Diamond JJ, et al. Patterns of care outcome survey: national outcome data for six disease sites. Am J Clin Oncol. 1982;5(4):349–53.
13. Lawton CA, Won M, Pilepich MV, et al. Long-term treatment sequelae following external beam irradiation for adenocarcinoma of the prostate: analysis of RTOG studies 7506 and 7706. IJROBP. 1991;21(4):935–9.
14. Ghilezan MJ, Jaffray DA, Siewerdsen JH, et al. Prostate gland motion assessed with cine-magnetic resonance imaging (CINE-MRI). Int J Radiat Oncol Biol Phys. 2005;62(2):406–17.
15. de Crevoisier R, Tucker SL, Dong L, et al. Increased risk of biochemical and local failure in patients with distended rectum on the planning CT for prostate cancer radiotherapy. IJROBP. 2005;62:965–73.
16. Heemsbergen WD, Hoogeman MS, Witte MG, et al. Increased risk of biochemical and clinical failure for prostate patients with a large rectum at radiotherapy planning: results from the Dutch Trial of 68 Gy versus 78 Gy. IJROBP. 2007;67:1418–24.
17. Balter JM, Sandler HM, Lam K, et al. Measurement of prostate movement over the course of routine radiotherapy using implanted markers. IJROBP. 1995; 31(1):113–8.
18. Chandra A, Dong L, Huang E. Experience of ultrasound-based daily prostate localization. Int J Radiat Oncol Biol Phys. 2003;56:73–8.
19. Kitamura K, Shirato H, Seppenwoolde Y, et al. Three-dimensional intrafractional movement of prostate measured during real-time tumor tracking radiotherapy in supine and prone treatment positions. Int J Radiat Oncol Biol Phys. 2002;53:1117–23.
20. Huang E, Dong L, Chandra A, et al. Intrafraction prostate motion during IMRT for prostate cancer. IJROBP. 2002;53(2):261–8.
21. Su Z, Zhang L, Murphy M, et al. Analysis of prostate patient setup and tracking data: potential intervention strategies. IJROBP. 2010;81(3):880–7.
22. Tanyi JA, He T, Summers PA, et al. Assessment of planning target volume margins for intensity-modulated radiotherapy of the prostate gland: role of daily inter- and intrafraction motion. IJROBP. 2010;78(5):1579–85.
23. Kupelian P, Willoughby T, Mahadevan A, et al. Multi-institutional clinical experience with the Calypso System in localization and continuous, real-time monitoring of the prostate gland during external radiotherapy. Int J Radiat Oncol Biol Phys. 2007;67:1088–98.
24. Haisen LS, Chetty IJ, Enke CA, et al. Dosimetric consequences of intrafraction prostate motion. IJROBP. 2008;71(3):801–12.
25. Schallenkamp JM, Herman MG, Kruse JJ, et al. Prostate position relative to pelvic bony anatomy based on intraprostatic gold markers and electronic portal imaging. IJROBP. 2005;63:800–11.
26. Khosa R, Nangia S, Chufal KS, et al. Daily online localization using implanted fiducial markers and its impact on planning target volume for carcinoma prostate. J Cancer Res Ther. 2010;6(2):172–8.
27. Skarsgard D, Cadman P, El-Gayed A, et al. Planning target volume margins for prostate radiotherapy using electronic portal imaging and implanted fiducial markers. Radiat Oncol. 2010;10(5):52.
28. Igdem S, Akpinar H, Alco G, et al. Implantation of fiducial markers for image guidance in prostate radiotherapy: patient-reported toxicity. Br J Radiol. 2009; 82(983):941–5.
29. Moman MR, van der Heide UA, Kotte AN, et al. Long-term experience with transrectal and transperineal implantations of fiducial gold markers in the prostate for position verification in external beam radiotherapy, feasibility, toxicity and quality of life. Radiother Oncol. 2010;96(1):38–42.
30. Ullman KL, Ning H, Susil RC, et al. Intra- and inter-radiation therapist reproducibility of daily isocenter

verification using prostatic fiducial markers. Radiat Oncol. 2006;28(1):2.
31. Langen KM, Zhang Y, Andrews RD, et al. Initial experience with megavoltage (MV) CT guidance for daily prostate alignments. IJROBP. 2005;62:1517–24.
32. Moseley DJ, White EA, Wiltshire KL, et al. Comparison of localization performance with implanted fiducial markers and cone-beam computed tomography for on-line image-guided radiotherapy of the prostate. IJROBP. 2007;67:942–53.
33. Kupelian PA, Langen KM, Willoughby TR, et al. Image-guided radiotherapy for localized prostate cancer: treating a moving target. Semin Radiat Oncol. 2008;18:58–66.
34. Shi W, Li JG, Zlotecki RA, et al. Evaluation of kV cone-beam CT performance for prostate IGRT: a comparison of automatic grey-value alignment to implanted fiducial-marker alignment. Am J Clin Oncol. 2011;34(1):16–21.
35. Serago CF, Chungbin SJ, Buskirk SJ, et al. Initial experience with ultrasound localization for positioning prostate cancer patients for external beam radiotherapy. IJROBP. 2002;53:1130–8.
36. Artignan X, Smitsmans MH, Lebesque JV, et al. Online ultrasound image guidance for radiotherapy of prostate cancer: impact of image acquisition on prostate displacement. IJROBP. 2004;59:595–601.
37. Johnson H, Hilts M, Beckham W, et al. 3D ultrasound for prostate localization in radiation therapy: a comparison with implanted fiducial markers. Med Phys. 2008;35(6):2403–13.
38. Scarbrough TJ, Golden NM, Ting JY, et al. Comparison of ultrasound and implanted seed marker prostate localization methods: implications for image-guided radiotherapy. Int J Radiat Oncol Biol Phys. 2006;65(2):378–87.
39. Serago CF, Buskirk SJ, Igel TC, et al. Comparison of daily megavoltage electronic portal imaging or kilovoltage imaging with marker seeds to ultrasound imaging or skin marks for prostate localization and treatment positioning in patients with prostate cancer. Int J Radiat Oncol Biol Phys. 2006;65(5):1585–92.
40. Fuller CD, Thomas CR, Schwartz S, et al. Method comparison of ultrasound and kilovoltage x-ray fiducial imaging for prostate radiotherapy targeting. Phys Med Biol. 2006;51(19):4981–93.
41. Ng AK, Kenney LB, Gilbert ES, et al. Secondary malignancies across the age spectrum. Semin Radiat Oncol. 2010;20(1):67–78.
42. Kupelian PA, Langen KM, Willoughby TR, et al. Image-guided radiotherapy for localized prostate cancer: treating a moving target. Semin Radiat Oncol. 2008;18(1):58–66.
43. Fowler JF. The radiobiology of prostate cancer including new aspects of fractionated radiotherapy. Acta Oncol. 2005;44(3):265–76.
44. START Trialists' Group, Bentzen SM, Agrawal RK, et al. The UK Standardisation of Breast Radiotherapy (START) Trial A of radiotherapy hypofractionation for treatment of early breast cancer: a randomized trial. Lancet Oncol. 2008;9(4):331–41.
45. Lloyd-Davies RW, Collins CD, Swan AV. Carcinoma of prostate treated by radical external beam radiotherapy using hypofractionation. Twenty-two years' experience (1962–1984). Urology. 1990;36(2):107–11.
46. Dasu A. Is the alpha/beta value for prostate tumours low enough to be safely used in clinical trials. Clin Oncol. 2007;19(5):289–301.
47. Madsen BL, Hsi RA, Pham HT, et al. Stereotactic hypofractionated accurate radiotherapy of the prostate (SHARP), 33.5 Gy in five fractions for localized disease: first clinical trial results. Int J Radiat Oncol Biol Phys. 2007;67(4):1099–105.
48. King CR, Brooks JD, Gill H, et al. Long-term outcomes from a prospective trial of stereotactic body radiotherapy for low-risk prostate cancer. Int J Radiat Oncol Biol Phys. 2012;82(2):877–82.
49. Katz AJ, Santoro M, Ashley R, et al. Stereotactic body radiotherapy for organ-confined prostate cancer. BMC Urol. 2010;10:1.

Embolotherapy in the Management of Gynecologic Neoplasms

54

Robert L. Worthington-Kirsch

Abstract

Endovascular embolization techniques have been used in the treatment of many disorders for over 30 years. In the management of gynecologic neoplasms, embolization is now a standard care option for treatment of symptomatic fibroids. Embolization allows for definitive treatment of fibroid disease in the majority of women, with a lower complication risk and faster recovery than more invasive surgical therapies. Historically embolotherapy has not had a great role to play in the treatment of gynecologic malignancies. New embolic technologies, especially drug-eluting embolics, may hold promise for the future.

Background

Embolotherapy includes both embolization with only an embolic agent ("bland embolization") and embolization using some combination of an embolic agent and a medical agent, typically a chemotherapy drug ("trans-arterial chemoembolization" (TACE)). In general, the object of bland embolization is to obstruct blood flow, often to control or prevent hemorrhage, while the object of TACE is to achieve a cytotoxic effect for the treatment of malignancy.

Interventional radiologists have performed bland embolization using current techniques since the early 1970s, initially for gastrointestinal hemorrhage [1] and trauma [2]. Bland embolization to prevent tumor-associated bleeding was introduced in the late 1970s [3–5]. This technique is now commonly used in benign entities such as angiomyolipoma of the kidney [6] and hepatic hemangioma [7] and other benign tumors. It is also often used as a preoperative therapy to prevent blood loss during resection of both primary renal cell carcinomas [8] and bony metastases from renal cell carcinoma [9], as well as management of active hemorrhage from a wide variety of cancers [5, 10, 11].

TACE was introduced in the early 1980s [12]. While bland embolization has been applied in many different cancers, historically TACE has largely been applied to primary and metastatic lesions of the liver.

In the female reproductive tract, embolotherapy has been used for control of postpartum or postsurgical hemorrhage since the late 1970s [13, 14]. In these situations, embolization has been shown

R.L. Worthington-Kirsch
Vein Clinics of America, Wayne, PA, USA
e-mail: worthingtonkirsch@inbox.com

D.E. Dupuy et al. (eds.), *Image-Guided Cancer Therapy*, DOI 10.1007/978-1-4419-0751-6_56,

to be both safe and effective. Embolotherapy or surgical devascularization of the uterus for these indications does not appear to have an adverse effect on menstrual function or fertility [15, 16]. In these emergent cases, the technique has typically been to perform bland embolization with a resorbable embolic agent – almost always gelatin sponge pledgets and particles. The current primary use of embolotherapy in this anatomic region is fibroid embolization.

Fibroid Embolotherapy

Fibroids are benign tumors of the myometrium (leiomyomas). They are extremely common. By age 35, as many as 70–80 % of African-American women and 40–50 % of Caucasian women will have been diagnosed with fibroids [17, 18]. While fibroids are essentially asymptomatic in at least half of women who have them, they can cause a wide variety of symptoms [19, 20]. These can be grouped into three categories.

The most common fibroid-related symptom is abnormal menstrual bleeding. Fibroids cause both prolongation of menses and increase in menstrual flow. This may or may not be associated with worsened dysmenorrhea. The severity of fibroid-induced menorrhagia varies widely. In some women, the bleeding can be severe enough that they are housebound for part or all of their menses. Fibroid-related menorrhagia can rarely cause life-threatening anemia.

The next most common fibroid-related symptom category is bulk-related. The growing fibroids expand and enlarge the uterus, putting pressure on adjacent organs. In many ways, this is similar to the pressure effects associated with pregnancy. The most common of these is pressure on the urinary bladder, with subsequent urinary frequency, urgency, and nocturia. Less common bulk-related symptoms include episodic bladder outlet obstruction, rectal pressure, sacral or low back pain, dyspareunia, and hydronephrosis.

The last category is the effect of fibroids on fertility [21, 22]. This is still poorly understood. Most women with fibroid disease have fairly normal fertility. Large and/or submucosal fibroids can distort the uterine cavity, leading to repeated pregnancy loss. There do appear to be other untoward effects that fibroids can have on fertility.

Given the success of embolotherapy in controlling post-myomectomy bleeding, in the late 1980s a French gynecologist named Jacques Ravine became interested in the possible utility of preoperative embolization to decrease the risk of operative blood loss during myomectomy. He found that preoperative embolization did indeed decrease perioperative bleeding complications [23]. He also found that the embolization itself could relieve patients' fibroid-related symptoms, allowing them to avoid surgery [24]. Fibroid embolization (also referred to as "uterine artery embolization" (UAE) or "uterine fibroid embolization" (UFE)) was introduced into the USA in 1996 by cooperating teams of a gynecologist and an interventional radiologist in both Los Angeles and Philadelphia [25, 26]. Since that time, there has been rapid spread of the procedure worldwide as well as a plethora of publications related to the procedure.

In all cases, the ideal situation is for the gynecologist and interventional radiologist to cooperate in evaluation and management of women who wish to be evaluated for fibroid embolization [27, 28]. Premenopausal women with symptomatic fibroids are good candidates for UAE if they have no other uterine or adnexal pathology and no contraindications to arteriography [29]. The number, location, and size of fibroids are usually not a relevant consideration [30]. Embolotherapy can also sometimes be offered to postmenopausal women who have persistent bulk-related symptoms [31]. Patients who desire to maintain fertility require even more careful evaluation by all members of the team. The insight of a fertility specialist as well as a general gynecologist may well be important in choosing the best fibroid therapy for these patients [32].

It is crucial to exclude adenomyosis of the uterus, which can have a presentation similar to that of fibroid disease. In adenomyosis, the symptoms of pain (dysmenorrhea, dyspareunia) commonly overshadow the symptoms of excessive bleeding [33]. This is the reverse of the typical

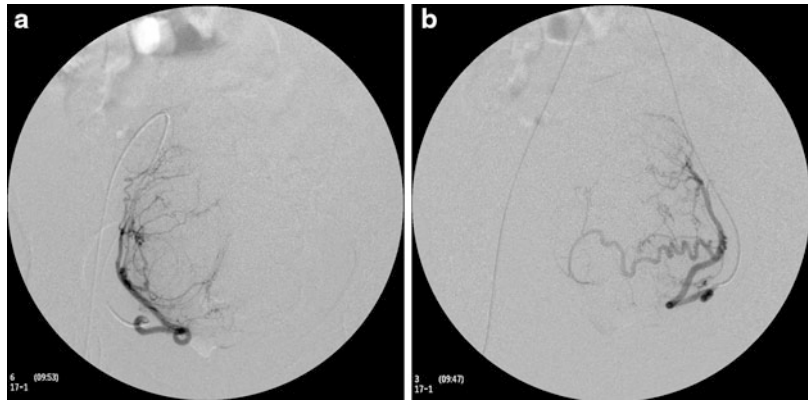

Fig. 54.1 A 42-year-old African-American woman with menorrhagia and pressure symptoms from fibroid disease. Selective injections of the right (**a**) and left (**b**) uterine arteries from embolization procedure. Note the appearance of the vessels stretched around the fibroids. Embolization was performed with 700–900-um calibrated PVA hydrogel microspheres. (Images courtesy of RL Worthington-Kirsch, MD)

presentation of fibroid disease. Ultrasound examination of the uterus is insensitive for distinguishing between the two entities. MRI is the best imaging study for the uterus and reliably distinguishes between adenomyosis and fibroids [34]. There is much less experience with embolotherapy for adenomyosis than for fibroids, and it has been generally disappointing in the medium- to long-term [35, 36]. On the other hand, embolotherapy is the only uterus-sparing treatment available for adenomyosis [37]. The author feels that embolotherapy should not be offered as a treatment for adenomyosis outside of a study protocol except in specific clinical situations [38].

The fibroid embolization procedure is performed [39] under conscious sedation after premedication with antibiotic, anti-inflammatory, and antiemetic medications. The majority of cases are done from a unilateral femoral approach. The uterine arteries are selectively catheterized, either with a 4–5Fr diagnostic catheter or with a microcatheter through a diagnostic catheter (Fig. 54.1). The entire uterine vascular bed is then nonselectively embolized using one of a variety of spherical hydrogel embolic agents. The patient is monitored and pain medications are provided for several hours after the procedure.

In the author's practice, all patients are discharged to home 4–6 h after completion of the procedure. Recovery is rapid, with the majority of patients returning to full activities in 1–3 weeks. Complications such as infection are rare [40]. Follow-up care, including evaluation and initial management of complications, is the responsibility of the interventional radiologist. The cooperating gynecologist also continues to see the patient for all other gynecologic care.

Technical success for fibroid embolization is high. Both uterine arteries are embolized in 98–99 % of patients. Clinical outcomes are also excellent, with approximately 90 % of patients experiencing relief from fibroid-related symptoms [41, 42]. In most patients, embolotherapy provides long-term control of fibroid-related symptoms and is a durable bridge to menopause [43].

One of the concerns raised by both gynecologists and patients when discussing fibroid embolotherapy is the possibility of leiomyosarcoma rather than simple fibroid disease. There is no noninvasive method that will reliably diagnose leiomyosarcoma, and even biopsy is not useful due to sampling error [44]. Fortunately, uterine leiomyosarcoma is several orders of magnitude rarer than fibroid disease [45, 46], and in real practice, both gynecologists and interventional radiologists assume that a patient with the appropriate clinical presentation has benign fibroid disease. Sarcoma is only

suspected when the clinical presentation or response to therapy is atypical. There are a few reports of patients who showed no clinical response to a technically successful UAE and were later found to have sarcoma [47, 48]. It is important that patients be followed carefully after uterine embolotherapy and any unusual or unexpected outcomes be addressed appropriately.

Embolotherapy for Malignant Disease

Intra-arterial chemotherapy without embolization as a potential treatment for gynecologic cancers was first reported in the early 1950s. This was done by the nonselective injection of nitrogen mustard into the aorta in women with cervical carcinoma [49]. Selective intra-arterial chemotherapy was first reported, also without embolization, in 1981 [50].

Embolotherapy for gynecologic malignancy was first reported for the control of hemorrhage in 1989 when Pisco et al. reported embolization of the internal iliac arteries [51]. Over time the technique has become more refined and embolization is usually performed much more selectively than it was in the past [52]. After diagnostic arteriography to define the vascular anatomy and localize the bleeding point, embolization is performed. If no specific bleeding point can be identified, then the area of tumor vascularity can be embolized. However, overembolization can result in further tumor necrosis and sloughing, which can lead to worse bleeding. This usually occurs when too small an embolic agent (e.g., gelatin sponge powder) is used, with subsequent extensive blockade of the microvascular bed.

Agents for such embolization can be divided into three main categories. Permanent particulate embolic agents include metal coils, polyvinyl alcohol (PVA) particles, and calibrated hydrogel microspheres. Metal coils come in a wide variety of sizes and are the most amenable to precise placement. Calibrated hydrogel microspheres are easy to use and appear to perform reliably. Non-hydrogel PVA preparations are historically one of the most commonly used agents but are often more difficult to use than calibrated microspheres with no better performance. Permanent liquid agents include n-butyl cyanoacrylate glues and ethylene vinyl alcohol polymer. These make a cast of the vascular bed. In general they are best used for larger lesions such as arteriovenous malformations. Temporary particulate embolic agents are almost always particles prepared from gelatin sponge sheets. These can be prepared in widely varying sizes depending on the exact needs of the moment. None of these are ideal for all situations, and the operating interventionalist needs to have a variety of devices available.

Embolotherapy is extremely effective in controlling tumor-associated bleeding. Procedure technical success rates are typically over 90 %, bleeding is controlled in almost all patients who have a successful embolization, and the procedure is repeatable if necessary. Embolotherapy should be the procedure of choice for tumor-associated bleeding that does not respond to non-invasive methods such as vaginal packing or surface fulguration [10, 53, 54].

There were studies from Japan published at the end of the 1990s and beginning of 2000s reporting results of TACE for gynecologic cancers [55–57]. These studies showed promising results, suggesting that TACE was superior to traditional IV chemotherapy. It appears that this research has by and large not been pursued further. Shimizu [57] attributes this to a lack of familiarity with intra-arterial chemotherapy and the attraction of newer agents for traditional chemotherapy, particularly taxanes. A recent Cochrane review has indicated that there is probably little or no benefit from neoadjuvant chemotherapy, which would seem to further mitigate against pursuit of TACE in these conditions [58].

In the last few years, we have seen major changes in the technology available for TACE. The most significant of these is the development of drug-eluting embolic particles. These devices make TACE technically easier, since the chemotherapy agent and emboli are delivered together. They also appear to offer tissue pharmacokinetics that are superior to that offered by TACE using a liquid chemotherapy preparation followed by

embolic particles [59, 60]. Drug-eluting particles provide a "depot" effect for drug delivery, with high tissue levels persisting for days rather than just a few hours as happens after older TACE techniques. These advances theoretically make current generation TACE more effective than the previous technology.

Drug-eluting embolic technology is stimulating a tremendous amount of research as a platform for delivery of a variety of agents, most especially chemotherapy. This has created a revolution in treatment of primary and metastatic liver tumors and cancers at other sites, particularly the head and neck. At the same time, we are seeing an explosion in other methods for regional cancer treatment. This includes invasive ablative technologies (e.g., radiofrequency ablation, cryoablation, irreversible electroporation), noninvasive ablative technologies (e.g., CyberKnife™ radiosurgery), and advances in surgical techniques (e.g., da Vinci™ robotic surgery), as well as new chemotherapy agents. Research is also being done into using these techniques in combination, which may well provide synergistic effects on cancer treatment [61–63].

The entire landscape of intra-arterial and other minimally invasive therapies for cancer has changed radically in the last few years. Perhaps it is time to revisit the role of intra-arterial chemotherapy and embolization in gynecologic malignancies.

References

1. Rosch J, Dotter CT, Brown MJ. Selective arterial embolization: a new method for control of acute gastrointestinal bleeding. Radiology. 1972;102:303–6.
2. Margolies MN, Ring EJ, Waltman AC, et al. Arteriography in the management of hemorrhage from pelvic fractures. N Engl J Med. 1972;287:318–21.
3. Chuang VP, Soo CS, Wallace S, et al. Arterial occlusion: management of giant cell tumor and aneurysmal bone cyst. AJR Am J Roentgenol. 1981;136:1127–30.
4. Wallace S, Chuang VP, Swanson D, et al. Embolization of renal cell carcinoma. Radiology. 1981;138:563–70.
5. Lang EK, Deutsch JS, Goodman JR, et al. Transcatheter embolization of hypogastric artery branches in the management of intractable bladder hemorrhage. J Urol. 1979;121:30–6.
6. Soulen MC, Faykus MH, Shlansky-Goldberg RD, et al. Elective embolization for prevention of hemorrhage from renal angiomyolipomas. J Vasc Interv Radiol. 1994;5:587–91.
7. Giavroglou C, Economou H, Ioannidis I. Arterial embolization of giant hepatic hemangiomas. Cardiovasc Intervent Radiol. 2003;26:92–6.
8. Kalman D, Varenhorst E. The role of arterial embolization in renal cell carcinoma. Scand J Urol Nephrol. 1999;33:162–70.
9. Sun S. Bone metastases from renal cell carcinoma: preoperative embolization. In: Golzarian J, Sun S, Sharafuddin MJ, editors. Vascular embolotherapy: a comprehensive approach, vol. 2. Berlin: Springer; 2006. p. 189–99.
10. Yalvac S, Kayikcioglu F, Borna N, et al. Embolization of uterine artery in terminal stage cervical cancers. Cancer Invest. 2002;20:754–8.
11. Morrissey DD, Andersen PE, Nesbit GM, et al. Endovascular management of hemorrhage in patients with head and neck cancer. Arch Otolaryngol Head Neck Surg. 1997;123:15–9.
12. Konno T, Maeda H, Iwai K, et al. Effect of arterial administration of high-molecular-weight anticancer agent SMANCS with lipid lymphangiographic agent on hepatoma. Eur J Cancer Clin Oncol. 1983;19:1053–65.
13. Heaston DK, Mineau DE, Brown BJ, Miller FJ. Transcatheter arterial embolization for the control of persistent massive puerperal hemorrhage after bilateral surgical hypogastric artery ligation. AJR Am J Roentgenol. 1979;133:152–4.
14. Oliver JA, Lance JS. Selective embolization to control massive hemorrhage following pelvic surgery. Am J Obstet Gynecol. 1979;135:431–2.
15. Stancato-Pasik A, Mitty HA, Richard III HM, Eshkkar NS. Obstetric embolotherapy: effect on menses and pregnancy. Radiology. 1996;201:179.
16. Shinagawa S, Nomura Y, Kudoh S. Full-term deliveries after ligation ofbilateral internal iliac arteries and infundibulopelvic ligaments. Acta Gynecol Obstet Scand. 1981;60:439–40.
17. Cramer SF, Patel D. The frequency of uterine leiomyomas. Am J Clin Pathol. 1990;94:435–8.
18. Schwartz SM. Epidemiology of uterine leiomyomata. Clin Obstet Gynecol. 2001;44:316–26.
19. Greenberg MD, Kazamel TIG. Medical and socioeconomic impact of uterine fibroids. Obstet Gynecol Clin North Am. 1995;22:625–36.
20. Stovall DE. Clinical symptomatology of uterine leiomyomas. Clin Obstet Gynecol. 2001;44:364–71.
21. Forman RG, Reidy J, Nott V, Braude P. Fibroids and fertility. Min Invas Ther Allied Technol. 1999;8:415–9.
22. Rice JP, Kay HH, Mahony BS. The clinical significance of uterine leiomyomas in pregnancy. Am J Obstet Gynecol. 1989;8:517–26.
23. Ravina JH, Bouret JM, Fried D, et al. Value of preoperative embolization of uterine fibroma: report of

a multicenter series of 31 cases. Contracept Fertil Sex. 1995;23:45–9.
24. Ravina JH, Herbreteau D, Ciraru-Vigneron N, et al. Arterial embolisation to treat uterine myomata. Lancet. 1995;346:671–2.
25. McLucas B, Goodwin SC. A fibroid treatment with promise – and a catch. OBG Manage. 1996;8:53–7.
26. Worthington-Kirsch RL, Hutchins FL, Popky GL. Uterine artery embolization for the management of leiomyomas: quality of life assessment and clinical response. Radiology. 1998;208:625–9.
27. Zurawin RK, Fischer JH, Amir L. The effect of a gynecologist-interventional radiologist relationship on selection of treatment modality for the patient with uterine myoma. J Min Invas Gynecol. 2010;17: 214–21.
28. Vedantham S, Sterling KM, Goodwin SC, et al. Uterine fibroid embolization: preprocedure assessment. Tech Vasc Interv Radiol. 2002;5:2–16.
29. Andrews RT, Spies JB, Sacks D, et al. Patient care and uterine artery embolization for leiomyomata. J Vasc Interv Radiol. 2004;15:115–20.
30. Firouznia K, Ghanaati H, Sanaati M, Jalali AH, Shakiba M. Uterine artery embolization in 101 cases of uterine fibroids: do size, location, and number of fibroids affect therapeutic success and complications? Cardiovasc Intervent Radiol. 2008;31:521–6.
31. Chrisman HB, Minocha J, Ryu RK, Vogelzang RL, Nikolaidis P, Omary RA. Uterine artery embolization: a treatment option for symptomatic fibroids in postmenopausal women. J Vasc Interv Radiol. 2007;18: 451–4.
32. Usadi R, Marshburn PB. The impact of uterine artery embolization on fertility and pregnancy outcome. Curr Opin Obstet Gynecol. 2007;19:279–83.
33. Azziz R. Adenomyosis: current persectives. Obstet Gynecol Clin North Am. 1989;16:221–35.
34. Dueholm M, Lundorf E, Sorensen JS, Ledertoug S, Olesen F. Reproducibility of evaluation of the uterus by transvaginal sonography, hysterosongraphic examination, hysteroscopy and magnetic resonance imaging. Hum Reprod. 2002;17:195–200.
35. Pelage JP, Jacob D, Fazel A, et al. Midterm results of uterine artery embolization for symptomatic adenomyosis: initial experience. Radiology. 2005;234:948–53.
36. Kim MD, Kim S, Kim NK, et al. Long-term results of uterine artery embolization for symptomatic adenomyosis. AJR Am J Roentgenol. 2007;188:176–81.
37. Goldberg J. Uterine artery embolization for adenomyosis: looking at the glass half full. Radiology. 2005;236:1111–2.
38. Pelage JP, Jacob D, leDref O. Dr Pelage and colleagues respond. Radiology. 2005;236:1111–2.
39. Worthington-Kirsch RL, Andrews RT, Siskin GP, et al. Uterine fibroid embolization: technical aspects. Tech Vasc Interv Radiol. 2002;5:17–34.
40. Worthington-Kirsch RL, Spies JB, Myers ER, et al. The fibroid registry for outcomes data (FIBROID) for uterine embolization: short-term outcomes. Obstet Gynecol. 2005;106:52–9.
41. Spies JB, Myers ER, Worthington-Kirsch R, Mulgund J, Goodwin S, Mauro M. The FIBROID registry: symptoms and quality-of-Life status 1 year after therapy. Obstet Gynecol. 2005;106:1309–18.
42. Goodwin SC, Spies JB, Worthington-Kirsch R, et al. Uterine artery embolization for treatment of leiomyomata: long-term outcomes from the FIBROID registry. Obstet Gynecol. 2008;111:22–33.
43. Spies JB, Bruno J, Czeyda-Pommersheim F, Magee S, Ascher SA, Jha RC. Long-term outcomes of uterine artery embolization of leiomyomata. Obstet Gynecol. 2005;106:933–9.
44. Kempson RL, Bari W. Uterine sarcomas: classification, diagnosis, and prognosis. Hum Pathol. 1970;1: 331–49.
45. Brooks SE, Zhan M, Cote T, Baquet CR. Surveillance, epidemiology, and end results analysis of 2677 cases of uterine sarcoma 1989–1999. Gynecol Oncol. 2004;93:204–8.
46. Leibsohn S, d'Aiblang G, Mishell DR, Schlaerth JB. Leiomyosarcoma in a series of hysterectomies performed for presumed uterine leiomyomas. Am J Obstet Gynecol. 1990;162:968–76.
47. Common AA, Mocarski EJ, Kolin A, Pron G, Soucie J. Therapeutic failure of uterine fibroid embolization caused by underlying leiomyosarcoma. J Vasc Interv Radiol. 2001;12:1449–52.
48. Goldberg J, Burd I, Price FV, Worthington-Kirsch R. Leiomyosarcoma in a premenopausal patient after uterine artery embolization. Am J Obstet Gynecol. 2004;191:1733–5.
49. Cromer JK, Bateman JC, Berry GN, Kennelly JM, Klopp CT, Platt LI. Use of intra-arterial nitrogen mustard therapy in the treatment of cervical and vaginal cancer. Am J Obstet Gynecol. 1952;63:538–48.
50. Carlson JA, Freedman RS, Wallace S, Chuang VP, Wharton JP, Rutledge FN. Intra-arterial cis-platinum in the management of squamous cell carcinoma of the uterine cervix. Gynecol Oncol. 1981;12:92–8.
51. Pisco JM, Martins JM, Correia MG. Internal iliac artery: embolization to control hemorrhage from pelvic neoplasms. Radiology. 1989;172:337–9.
52. Yamashita Y, Harada M, Yamamoto H, et al. Transcatheter arterial embolization of obstetric and gynaecologic bleeding: efficacy and clinical outcome. Br J Radiol. 1994;67:530–4.
53. Vedantham S, Godowin SC, McLucas B, Mohr G. Uterine artery embolization: an underused method of controlling pelvic hemorrhage. Am J Obstet Gynecol. 1997;176:938–48.
54. Hayashi M, Murakami A, Iwasaki N, Yaoi Y. Effectiveness of arterial embolization procedure in uterine cancer patients. J Med. 1999;30:225–34.
55. Adachi S, Yamasaki N, Ogasawara T, Takayasu Y, Takemura T, Koyama K. Combination chemotherapy using intravenous nedaplatin (254-S) and intraarterial cisplatin (CDDP) with transcatheter arterial

embolization (TAE) for a patient with uterine cervical cancer: a case report. Jpn J Clin Oncol. 1997;27: 442–4.
56. Adachi S, Ogasawara T, Tsubamoto H, et al. Intravenous nedaplatin and intraarterial cisplatin with transcatheter arterial embolization for patients with locally advanced uterine cervical cancer. Int J Pharmacol Res. 2001;21:105–10.
57. Shimizu Y. Recent advances in intraarterial chemotherapy in gynecologic malignancy. Gan To Kagaku Ryoho. 2002;29:189–96.
58. Morrison J, Swanton A, Collins S, Kehoe S. Chemotherapy versus surgery for initial treatment in advanced ovarian epithelial cancer. Cochrane Database Syst Rev. 2007;4:Art No. CD005343.
59. Taylor RR, Tang Y, Gonzalez MV, Strafford PW, Lewis AL. Irinotecan drug eluting beads for use in chemoembolization: in vitro and in vivo evaluation of drug release properties. Eur J Pharmacol Sci. 2007;30:7–14.
60. Lewis AL, Taylor RR, Hall B, Gonzalez MV, Willis SL, Stratford PW. Pharmacokinetic and safety study of doxorubicin-eluting beads in a porcine model of hepatic arterial embolization. J Vasc Interv Radiol. 2006;17:1335–43.
61. Cheng BQ, Jia CQ, Liu CT, et al. Chemoembolization combined with radiofrequency ablation for patient with hepatocellular carcinoma larger than 3 cm: a randomized controlled trial. JAMA. 2008;299:1669–77.
62. Yamakado K, Nakatsuka A, Takaki H, et al. Early-stage hepatocellular carcinoma: radiofrequency ablation combined with chemoembolization versus hepatectomy. Radiology. 2008;247:260–6.
63. Xu KC, Niu LZ, Zhou Q, et al. Sequential use of transarterial chemoembolization and percutaneous cryosurgery for hepatocellular carcinoma. World J Gastroenterol. 2009;15:3664–9.

Magnetic Resonance-Guided High-Intensity Focused Ultrasound: Gynecological Applications

55

Nelly Tan and Steven S. Raman

Abstract

High-intensity focused ultrasound (HIFU) is an exciting ablative technology that promises noninvasive direct and indirect treatment of a variety of benign and malignant disorders including solid tumors. Although the HIFU concept has been existent for several decades, its most recent iterations have enabled proof of concept treatment in both benign tumors such as uterine leiomyomas and also malignant tumors in liver, bone, pancreas, and prostate. In this chapter, we focus on HIFU applications for treatment of uterine leiomyomas. We will review clinical manifestations, imaging characteristics, treatment options, and approaches to patients; we will also discuss short- and long-term outcomes of patients with symptomatic leiomyomas treated with HIFU. Finally, we will discuss less common applications of HIFU including cervical ectopy and abdominal wall endometriosis.

High-Intensity Focused Ultrasound (HIFU)

High-intensity focused ultrasound (HIFU) is an exciting ablative technology that promises noninvasive direct and indirect treatment of a variety of benign and malignant disorders including solid tumors [1]. Although the HIFU concept has been existent for several decades, its most recent iterations have enabled proof of concept treatment in both benign tumors such as uterine leiomyomas and also malignant tumors in liver, bone, pancreas, and prostate. In this chapter, we focus on HIFU applications for treatment of uterine leiomyomas. HIFU devices are available from several manufacturers and includes two systems incorporating the therapeutic HIFU transducer with either MR guidance (ExAblate, InSightec, Hiafa, Israel; Sonalleve, Philips, Best, Netherlands) or ultrasound (US) guidance (Seapostar, Chongqing Haifu [HIFU] Technology, Co. Ltd., Chongqing, China) [2] (Fig. 55.1). The InSightec ExAblate 2000 received approval from the United States Food and Drug Administration (FDA) in 2004 for the noninvasive treatment of uterine leiomyomas. It is widely known by its marketing name: MR-guided focused ultrasound surgery (MRgFUS). This technology offers

N. Tan (✉) • S.S. Raman
Department of Radiological Sciences, Ronald Regan UCLA Medical Center, Los Angeles, CA, USA
e-mail: ntan@mednet.ucla.edu; sraman@mednet.ucla.edu

D.E. Dupuy et al. (eds.), *Image-Guided Cancer Therapy*, DOI 10.1007/978-1-4419-0751-6_57,

Fig. 55.1 High-intensity focused ultrasound systems. There are two MRI-guided HIFU systems – InSightec ExAblate 2000 (**a**) and Philips Sonalleve (**b**) – and one ultrasound-guided HIFU system, Chongquin Haifu (**c**) available worldwide (Part A reprinted with permission from InSightec, Haifa, Israel; part B reprinted with permission from Phillips; and part C reprinted with permission from Chongguin Haifu, HIFU Technology Co., Ltd.)

a novel, completely noninvasive option for treatment of common gynecological disorders, including leiomyoma and adenomyosis-related symptoms. A variety of other conditions, such as cervical ectopy and palliative pain therapy, are also being studied. In this chapter, we will review the current state of MRgFUS and its role in the treatment of gynecologic disorders.

Introduction

Uterine leiomyomas (fibroids) are estrogen-driven, benign, well-encapsulated, monoclonal neoplasms originating from uterine smooth muscle. An estimated 20–35 % of all reproductive-age women experience uterine leiomyomas, and some studies report that a cumulative lifetime incidence of leiomyomas occurs in 70 % of US white women and 80 % of African-American women [3]. Risk factors include African or African-American background, family history, early menarche, nulliparity, obesity, hypertension, and polycystic ovary syndrome [4]. Although the majority of women with uterine leiomyomas are asymptomatic, approximately 20–30 % of women have related symptoms [3]. These symptomatic women typically present in their 40s with symptoms lasting into menopause and typically diminishing thereafter.

Uterine fibroid-related symptoms may be divided into those related to mass effect (bulk) or excessive endometrial effect (bleeding). Bulk-related symptoms include pain, pelvic pressure, urinary frequency, dyspareunia, defecatory disorder, and back pain. Bleeding-related symptoms include heavy menstrual bleeding (menorrhagia), irregularity in menstrual cycle (metrorrhagia), or both (menometrorrhagia), and pain with menstruation (dysmenorrhea) [5]. The most common symptoms are menorrhagia with anemia.

Leiomyoma-related symptoms are among the most common of all gynecologic disorders and are thought to be responsible for over 360,000 hysterectomies in the United States annually, with an overall estimated annual cost of care exceeding $2 billion [6, 7].

Imaging Findings

Ultrasound is used primarily to detect uterine fibroids, but MR imaging offers vastly superior soft tissue contrast and the ability to tissue characterize individual leiomyomas. MR imaging also provides multiplanar imaging capability and contrast enhancement help triage patients to one or more therapeutic options including surgical resection, uterine artery embolization, or MRgFUS. Leiomyomas have distinct T1 and T2 tissue MR characteristics and enhancement after intravenous gadolinium contrast. Based on MR imaging and enhancement characteristics, individual leiomyomas can be classified as classical, hypercellular, or degenerating (Fig. 55.2). Classical fibroids appear hypointense on T2-weighted sequences and enhance on gadolinium-enhanced T1-weighted sequences and respond best to MRgFUS. Hypercellular fibroids are hyperintense on T2-weighted sequences, enhance avidly on gadolinium-enhanced T1-weighted sequences, but do not respond as well as classical fibroids to HIFU treatment. Degenerating fibroids have variable T1and T2 signal, do not enhance after gadolinium administration and respond poorly to either HIFU or UFE treatment. Thus, tissue characterizing these different subtypes of fibroids can help determine the best choice of treatment for patients.

Location of Uterine Leiomyomas

Leiomyomas can be described in terms of their location in the uterus. Intramural leiomyomas are the most common and are mostly asymptomatic. Large intramural lesions may cause any combination of bulk and bleeding symptoms. Lesions abutting the outer contour of the uterus are termed subserosal and when large can cause bulk symptoms; conversely lesions abutting or into the endometrial cavity are termed submucosal and even small lesions can cause bleeding symptoms while larger lesions may cause also cause bulk symptoms. Those growing into the endometrial cavity on a fibrovascular stalk are termed intracavitary and result in bleeding symptoms whereas those growing outside the uterus on a fibrovascular stalk are termed pedunculated. The larger ones can cause a mass effect on adjacent organs and structures and cause voiding or defecation symptoms. See Fig. 55.3.

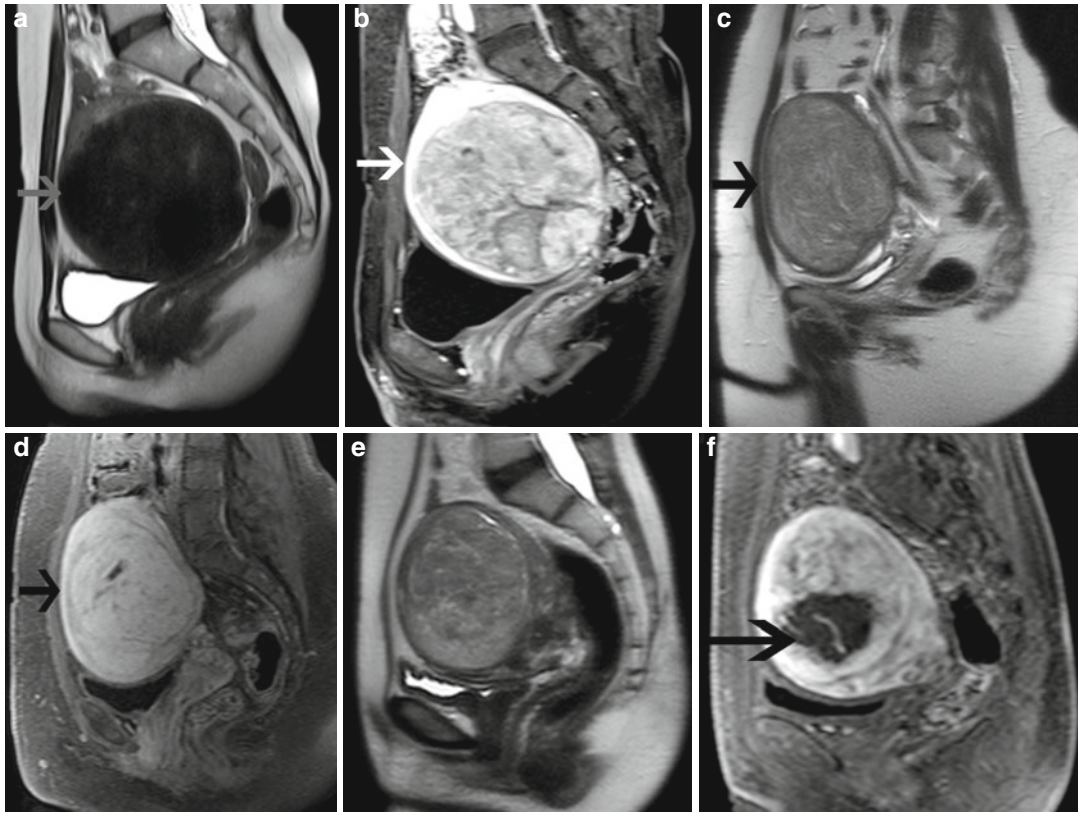

Fig. 55.2 MR imaging and enhancement characteristics of individual leiomyomas can be classified as classical, hypercellular, or degenerating. Classical fibroids appear hypointense on T2-weighted sequences (**a**) and enhance on gadolinium-enhanced T1-weighted sequences (**b**). Hypercellular fibroids are hyperintense on T2-weighted sequences (**c**), enhance avidly on gadolinium-enhanced T1-weighted sequences (**d**). Degenerating fibroids have variable T1and T2 signal (**e**) and do not enhance after gadolinium administration (**f**)

Treatment of Uterine Leiomyoma

Therapy for uterine leiomyoma-related symptoms may be divided into medical, surgical, or alternative/watchful waiting. Medical treatments such as nonsteroidal anti-inflammatory drugs (NSAIDs), contraceptive steroids, and gonadotropin-releasing hormone agonists as well as watchful waiting and alternative therapies such as acupuncture, dietary modification, or herbal therapies may be effective in the short term [8–11]. However, these treatments are considered temporary, and most symptomatic patients progress over time, requiring more durable treatment. A variety of surgical therapies have been the standard the care for treatment of symptomatic uterine leiomyomas. In women who do not desire the option of full future fertility (termed "family complete"), laparoscopic, laparoscopic-assisted robotic, or open hysterectomy is considered the definitive therapy for leiomyoma-related bulk and bleeding symptoms and leiomyoma-related infertility. Although these are extremely common and safe surgical procedures, there is a major complication rate of 8.9 % for abdominal, 14 % for vaginal, and 9 % for laparoscopic hysterectomy. Major complications including postoperative mortality have been reported [12]. Removal of the uterus and surrounding attachments may increase a woman's postmenopausal risk of pelvic floor disorders (pelvic prolapse and laxity) although this is debated [13, 14]. For women who desire the

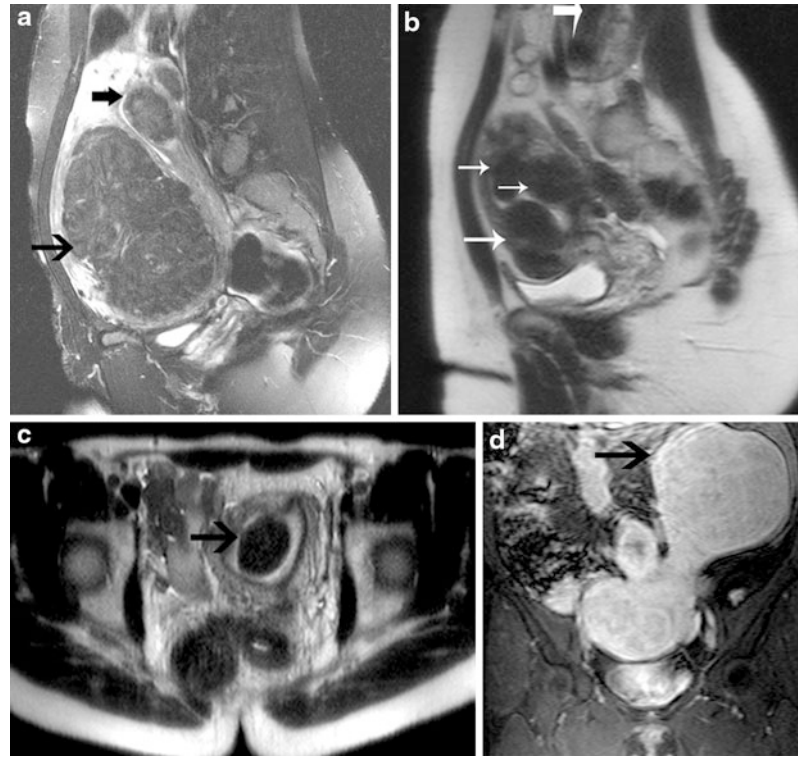

Fig. 55.3 Leiomyomas can be described in terms of their location in the uterus. Intramural leiomyomas are within the myometrium of the uterus (**a**, *thin arrow*); subserosal ones abut the outer contour of the uterus (**a**, *thick arrow*; **b**); intracavitary fibroids project into the endometrial cavity and are on a fibrovascular stalk (**c**); pedunculated leiomyomas project outside the uterus on a fibrovascular stalk (**d**)

option of future fertility or who wish to retain their uterus, surgical resection of individual leiomyomas (myomectomy), either by open or laparoscopic methods, is performed [15, 16]. Although generally safe, complications include possible need for perioperative blood transfusion (20 %), fever (2.9 %), ileus (2.4 %), infection (2 %), wound disruption (1 %), and urinary retention or bladder injury (0.7 %) [17]. After myomectomy, there is a recurrence of up to 51 % over time [18, 19], and 10–25 % of patients will require a major surgery after the first myomectomy [19–22].

Options for Minimally Invasive Treatment of Uterine Leiomyomas

Uterine Artery Embolization

The most widely available nonsurgical procedural treatment option for moderately large symptomatic uterine leiomyomas is uterine artery embolization (UAE or UFE), a technique first developed in the early 1970s for control of postpartum hemorrhage, in 1980s for reducing hemorrhage prior to myomectomy, and finally as therapy for leiomyomas in the early 1990s. Patients who are family complete and have multiple, moderate volume fibroids respond very well to UAE. In this technique, an interventional radiologist introduces a small catheter into the femoral artery after needle puncture and guides it sequentially into the right and left uterine arteries. In each uterine artery, the interventionalist can then select the arteries supplying the individual target fibroids with smaller catheters (microcathers) and then inject one of several types of small embolic particles that lodge into the small arteries of leiomyomas, causing cutoff of blood flow and subsequent infarction [23]. The uterine myometrium is spared due to extensive collateral blood supply. UAE was first introduced into clinical practice in the United States in 1995 and has consistently been shown to be safe and effective for both bulk and

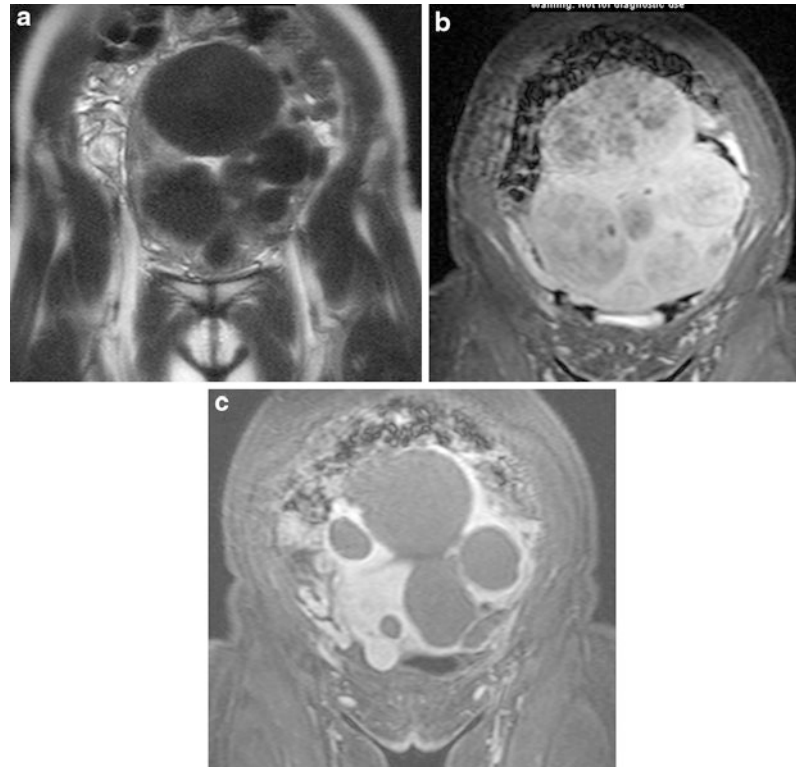

Fig. 55.4 Pre- and post-UAE. Pre-UAE coronal T2-weighted image demonstrates multiple T2 hypointense fibroids (**a**) that are enhancing on gadolinium-enhanced T1-weighted sequence (**b**) which become non-enhancing on post-UAE gadolinium-enhanced T1 images (**c**)

bleeding symptoms with minimal morbidity and patients can avoid general anesthesia [24]. Several large-scale cohort trials as well as randomized trials against myomectomy and hysterectomy have shown that the procedure is safe and effective [25–27] (See Fig. 55.4 for MRI pre- and post-UAE). Major complications are rare and most commonly include post-embolization syndrome associated with high fever, leukocytosis, and general malaise. Other rare major complications include uterine necrosis and infection leading to emergent hysterectomy; ovarian failure; vaginal dryness related to nontarget embolization or over-embolization. In a few case reports, death has also been reported, possibly resulting from acute pulmonary embolism [15, 28]. In addition, patients usually stay in the hospital overnight for observation and pain control, usually with a patient-controlled anesthesia (PCA pump) although they can be managed as outpatients with an aggressive pain control regimen.

MR-Guided Focused Ultrasound Surgery

The InSightec ExAblate 2000 MRgFUS system was approved for clinical treatment of uterine fibroids by the US FDA in 2004 and is the newest and least invasive treatment option of a subset of women with uterine fibroids, particularly for those who wish to retain the option of future fertility [2]. This novel treatment modality incorporates an HIFU transducer unit, which is built into a specially designed table designed to fit into a gantry in the GE 1.5 or 3 T magnet. Two other systems are also available outside the United States for treatment of uterine fibroids that include an MR-guided HIFU system by Philips (Sonalleve, Philips, Best, Netherlands) and an US-guided HIFU system (Seapostar, Chongching HAIFU, Chongching, China).

At this time, direct comparisons between the systems are not possible. MR-guided ablation has several theoretical advantages over

ultrasound-guided thermal ablation: MRI provides much higher, near-real-time, multiplanar-unenhanced soft tissue contrast, and spatial resolution. It also provides near-real-time, MR-based thermal mapping of ablated tissue, and surrounding nontarget soft tissues [29] to monitor target heating. Thus, MRgFUS provides a safe, near-real-time monitored, controlled, and repeatable treatment option that is uniquely noninvasive. With the first-generation technology, minimally mobile lesions like uterine fibroids are an ideal target since motion correction technology is in development and not widely clinically available. To date, over 5,000 women have undergone treatment of one or more uterine fibroids with MRgFUS with minimal complications [30].

Thermal Ablation

Human soft tissue is instantaneously and irreversibly injured through exposure to temperatures exceeding 60 °C due to protein denaturation and coagulative necrosis [31]. Coagulated lesions shrink in size due to water volume loss and also by resorption due to the inflammatory response. The consistency of thermally ablated uterine fibroids also changes from rock-hard to soft and gel-like, which may help explain in part the resolution of symptoms. MRgFUS allows real-time feedback of thermal gradient and, thus, enables a complete ablation of the targeted site that avoids adjacent tissues [31]. MRgFUS allows for the evaluation of thermal sites posttreatment and to assess the need for additional treatment [29, 32].

Ultrasound-Guided HIFU Treatment of Clinical Human Leiomyomas

Use of ultrasound (US)-guided HIFU, available only in Asia and Europe, for treatment of uterine leiomyomas has been shown to be effective. Ren et al. [33] evaluated 119 patients who underwent US-guided HIFU for 187 uterine fibroids. On follow-up images, the treated areas showed no evidence of blood flow, and the average leiomyoma size reduced by 48.7 %. Among the treated patients, 10 % required additional treatment (i.e., surgery) for therapy failure [34]. In regard to clinical outcomes, 85 % of patients reported substantial improvement, and in 59 %, symptoms had completely resolved. The procedures were completed with minimal complications: 6.2 % reported low-grade fever; 3.4 % had nerve injury, characterized by lower extremity pain, which resolved without any intervention, within 2 months of treatment; 3.2 % had skin burns; and 13.1 % had gross hematuria lasting 1–3 days. This study demonstrated that US-guided HIFU is feasible and effective. However, although US-guided HIFU is less expensive and thus theoretically more accessible when compared to MRgFUS, there are substantial disadvantages, including the inability to monitor temperature, distinguishing intervening bowel loops and inferior soft tissue and bone resolution. Nevertheless, ultrasound-guided HIFU is practical and feasible for anterior fibroids. In reported studies, there is no indication of its efficacy for hypercellular fibroids, since these lesions cannot be sonographically characterized.

MR-Guided HIFU Treatment of Clinical Human Leiomyomas

MRI-guided focused ultrasound surgery (MRgFUS) for leiomyomas have been evaluated in multicenter trails and is generally more widely used. We will review the procedure and clinical outcomes in details.

Procedure

Prior to the treatment, patients are informed of risks including bowel, skin or nerve injury, and risk of possible deep venous thrombosis (DVT) from the potential 3-h procedure. The anterior pelvic wall is shaved to the symphysis pubis to minimize the chances of entrapment of air bubbles by hair in the water bath. For the ExAblate system, patients are placed prone on the ExAblate table with the lower abdomen and pelvis lying on a degassed water bath over the transducer. A coupling gel pad is also placed between the

patients' skin and the therapeutic transducer built into the system. A Foley catheter is always placed to either empty or fill the bladder (bladder fill) as necessary to optimally position the uterus. In selected instances, it may be necessary to place a small-gauge rectal tube in the rectum to fill the rectum with sonographic gel, water, or air (rectal fill), and displace the uterus anteriorly and move bowel out of the treatment field. Manual displacement of the bowel via suprapubic massage can also be performed for optimal positioning of the fibroid. A combination of these techniques is necessary for obtaining an optimal treatment window.

An initial pretreatment MR of the pelvis is performed with coronal, sagittal, and axial single-shot or multi-shot T2 sequences using the body coil for reception. This serves as the template scan to plan the procedure and select the individual leiomyomas. The circumference of the target lesions is outlined; the treatment volume is then calculated by system software. Imaging is then performed using the receiver channels built into the ExAblate table to display near-real-time temperature and phase maps. Prior to delivering sonications, the bowel, pubic bone, lumbosacral spine, nerves, and intestine are all demarcated to prevent unintended target sonication.

On the ExAblate 2000 system, transducer power can vary from 0 to 3,000 W/cm^2, with an ultrasound frequency of 1.0–1.3 MHz. Over approximately 20 s energy deposition can vary between 2,000 and 4,000 J into the target site per each sonication. The focal region target site is an ellipsoid with dimensions of 8–40 mm parallel to the sonication beam and 1–10 mm perpendicular to the beam direction at the 17 cm focal distance from therapeutic transducer (up to 13 cm deep to the skin within the patient's pelvis). The newer devices will allow for deeper penetration into the pelvis by physical movement of the transducer. Low-power test sonications are delivered to the target lesions to ensure accurate targeting and to correct for sonication-related distortions in coronal and sagittal planes. Then, high-power treatment sonications lasting from 15 to 20 s are delivered to the selected treatment volume, followed by a cooling duration of 45–90 s to minimize skin burn from excessive energy deposition into skin.

A cluster of up to approximately 120 sonications may be performed in the maximum 3-h period to ablate a given volume. Temperature at the target sonication is noninvasively measured every 3–4 s by phase changes on MR imaging, and an MR thermal map is produced. The therapeutic energy and the sonication time are adjusted based on the feedback from the patient and temperature maps. Post-procedure dynamic contrast-enhanced MRI is performed to assess the non-perfused volume. Patients are monitored for 1–3 h post-procedure to allow for recovery from conscious sedation and are then discharged home. They are free to resume normal activities almost immediately, typically on the following day. A small subset may require a more prolonged recovery. See Fig. 55.5 for MRgFUS treatment planning and representative images captured during a procedure. See Fig. 55.6 for pre- and post-HIFU MRI images.

Patient Selection

Women who want a nonsurgical treatment option for their symptomatic uterine leiomyomas should be evaluated holistically. An essential part of the assessment is to determine if individual symptoms are causally related to uterine fibroids. If related, ideally, all options (medical, interventional radiology, MRgFUS, surgical, and alternative) should be discussed or presented. At our center, most women who desire MRgFUS are evaluated jointly by a radiologist and a gynecologist. Patient selection for MRgFUS is relatively straightforward. Potential patients are excluded if they have contraindications for MR imaging, such as non-MRI compatible implanted metallic devices, uterine pathology other than leiomyoma, active pelvic infection, a pelvic mass outside the uterus, concurrent pregnancy, obesity exceeding table capacity, or the inability to tolerate a prolonged stationary position inside the MRI scanner (restless leg syndrome, etc.). MRgFUS was initially contraindicated for premenopausal women with symptomatic fibroids desiring future fertility by the FDA. However, in 2009, the FDA amended this from

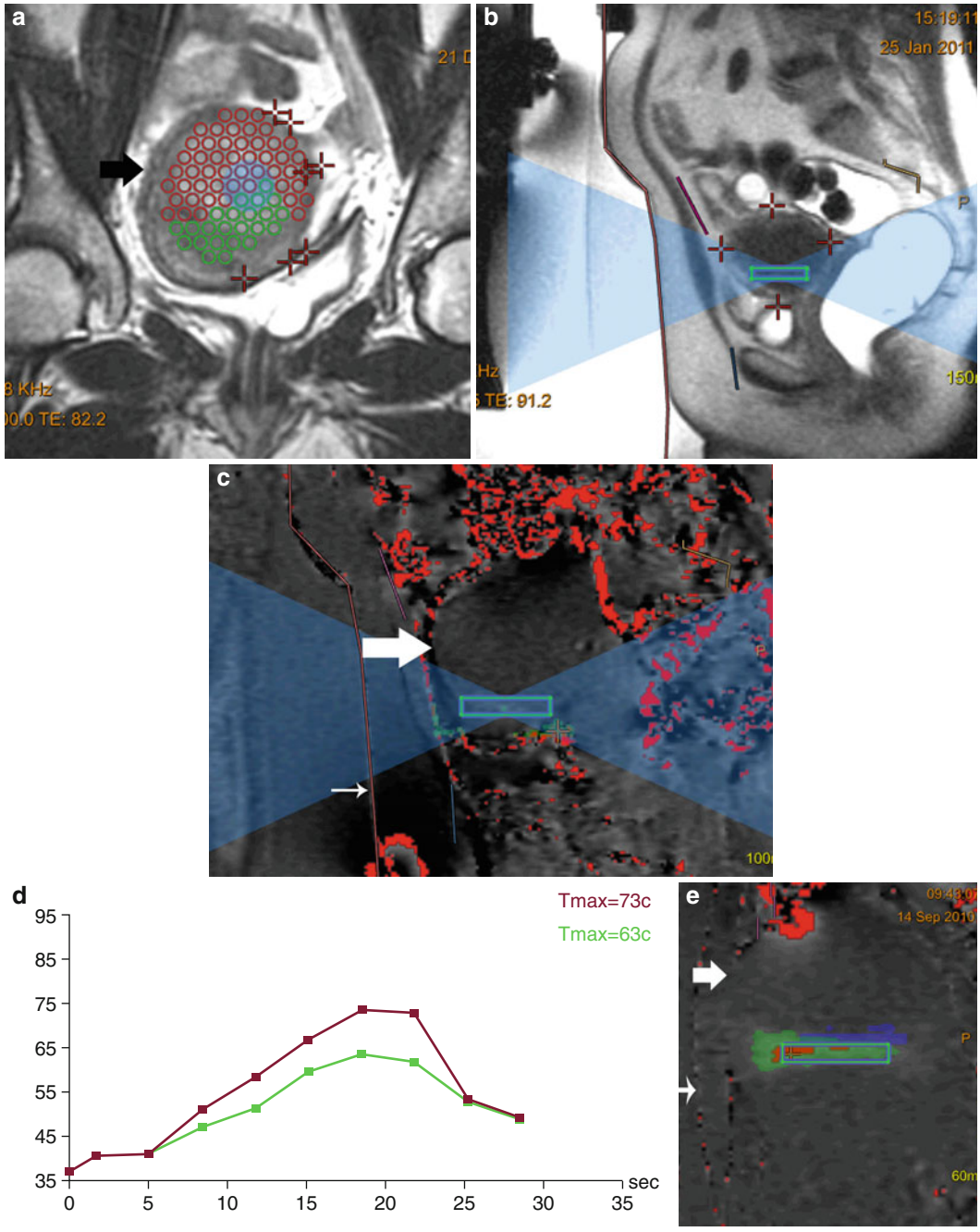

Fig. 55.5 MRgFUS treatment planning and representative images visualized during MRgFUS. (**a**) Sonication targets seen on coronal T2-weighted image; *green circles* indicate safe targets; *red circles* indicate targets which will require angulation of the transducer beam to pass sound waves through a safe, bowel-free window. *Arrrow points* to the fibroid. (**b**) Sagittal T2-weighted image of MRgFUS beam path. (**c**) Real-time sagittal MR phase image during a sonication of a fibroid (*small arrow* points to skin line; *large arrow* points to the outline of the fibroid). (**d**) MRI thermometry map of the treated lesion: *blue box* outlines at the targeted areas and *green* and *red images* portray areas with temperatures greater than 70 °C. (**e**) Temperature graph of treated lesion demonstrate goal temperatures attained during the 20 s sonication session (*small arrow* points to skin line; *thick arrow* points to the fibroid)

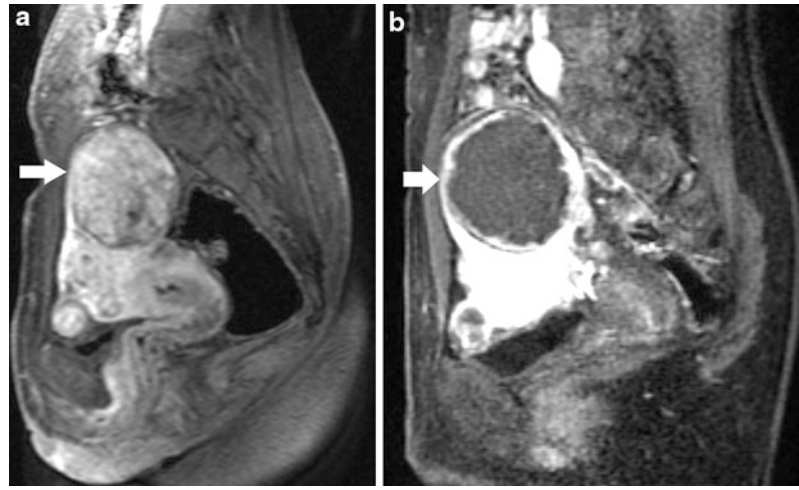

Fig. 55.6 Sagittal gadolinium-enhanced T1-weighted image of a patient pre-MRgFUS (**a**). Post-MRgFUS gadolinium enhancement of the same fibroid demonstrates 80 % non-perfused volume of the ablated fibroid (**b**)

an absolute to a relative contraindication after more studies were published suggesting that women were able to successfully conceive and carry pregnancies to term. Thus, women who desire future fertility may undergo MRgFUS. Relative contraindications include inability to comprehend instructions or communicate sensations during treatment (safe treatment requires that patient communicate sensations such as leg, buttock, skin, or back pain to the operator). Other factors for exclusion are common to any procedure and include severe medical conditions such as unstable cardiac status or cerebrovascular disease, hemolytic anemia, anticoagulation therapy or underlying bleeding disorder [35]. Patients with a non-displaceable bowel that cannot be shifted out of the sonication beam path with provocative measures are also excluded.

Patients with cutaneous scars in the beam path, including those that could not be seen on the MR images, may be excluded since scar tissue may absorb the ultrasound energy and cause cutaneous pain or even a skin burn. However, there have been recent developments, including a scar patch and reflectors applied over the scar to deflect energy absorption into the scar [36, 37].

Patients who have a total classical fibroid volume of more than 500 cc may be pretreated for 3 months with a gonadotropin-releasing hormone (GnRH) agonist (e.g., leuprolide (Lupron®)) which may cause 30–60 % volume reduction of leiomyoma and enable a larger percentage of the overall leiomyoma to be treated by MRgFUS [38].

Currently, at our multidisciplinary UCLA Fibroid Treatment Program, approximately 33 % of the candidates being screened for MRgFUS are not candidates for the procedure due to other pathology or technical factors that would preclude the beam from entering the fibroid (clips/metal in the beam path), history of liposuction, primary adenomyosis, too many fibroids (3 or more $>$ 5 cm) non-enhancing (degenerated) leiomyomas, intracavitary lesions amenable to hysteroscopic resection, pedunculated leiomyomas, T2 hyperintense leiomyomas, and lesions suspicious for cancer (cervical or endometrial carcinoma or sarcoma) [39]. The patients who were not candidates still benefited from the MR screening exam; of the patients with MRI findings, 38 % of patients who had suspicious lesions had pathology proven malignancy [39]. Thus, about 67 % of patients with symptoms and ultrasound findings consistent with fibroids are potential candidates for MRgFUS based on MRI findings. Proper evaluation of images ensures that the procedure could technically be performed to ensure a successful outcome [39].

Certain groups of patients are at risk for failing screening for MRgFUS. A recent study analyzing screen failures prior to MRgFUS for uterine fibroids show that African-American women

were more likely to fail screening because they were found present with a significantly larger number of fibroids when compared to non-African-American women, and they were found to possess significantly more technical problems, which would interfere with safe delivery of treatment [40].

Imaging Characteristics of Fibroids and Predictors of Treatment Success and Failures

If a patient is clinically eligible and interested in MRgFUS, she undergoes a screening MR imaging study in the prone position, which includes multiplanar T2- and T1-weighted sequences and dynamic gradient-echo 2D or 3D T1 sequences after power injection of an extracellular gadolinium chelate (0.1 mmol/kg). A radiologist specializing in abdominal imaging and experienced in MRgFUS analyzes the screening MR images to determine patient suitability for the procedure. Patients are deemed technically suitable for first-generation MRgFUS if their leiomyomas are of appropriate size (<12 cm), number (4–5 < 4 cm or 1 < 12 cm), signal quality (T2 hypointense, enhancing), and depth from skin (<13 cm) [41]. With current technology, larger volumes or numbers of lesions or deep lesions cannot be fully treated in the 3-h treatment window; however, these indications will be expanded as technology improves over currently available equipment.

On pre-procedural MR imaging, leiomyomas should be described in terms of size, location, and T1 and T2 enhancement characteristics. Size and number of leiomyomas directly influence the success of both MRgFUS and UAE; thus, these should be recorded.

Location of lesions within the uterus also independently influences the outcome, although to a lesser extent. Leiomyomas completely within the uterine wall ("intramural") are preferred. Those that protrude from the serosal outer surface of the uterus ("subserosal") may also be acceptable as long as at least 30 % of the circumference of the leiomyoma is within the uterine wall. Conversely, when less than 30 % of the leiomyoma circumference is within the uterine wall, the lesion is considered "pedunculated," and is best treated with surgical resection (myomectomy) due to the theoretical risk of post treatment torsion and detachment into the pelvis. Similarly, leiomyomas completely within the endometrial canal ("intracavitary") are amenable to hysteroscopic resection [42].

In addition to size and location, there are a number of MR signal characteristics empirically observed to be predictive of treatment response with MRgFUS. In general, thermal ablation efficacy from sonication is best for T2 hypointense, enhancing ("classical") leiomyomas. Efficacy is much less for T2 hyperintense, enhancing ("hypercellular") leiomyomas and for non-enhancing (degenerated) or calcified leiomyomas if first-generation ablation equipment is used [43].

Newer generation equipment (e.g., ExAblate 2100, InSightec Ltd,Haifa Israel) will likely enable increased eligibility for a variety of technical innovations including vertical transducer motion positioning the transducer closer to skin and improving focusing while also reducing spot length for more precise sonication. Treatment efficiency should improve due to improved planning algorithm and greater variety of sonication types, likely increasing the rate of tissue ablation. Lastly, this system will improve safety through automatic motion detection, lower energy density on skin, and low-energy density regions [44].

Early Outcomes in MRgFUS

One of the earliest studies was a multicentered study of 109 patients [45]. The actual volume that received a thermal dose was intentionally limited to a small volume of 32–36 cm^3 by MRI. The posttreatment contrast-enhanced images showed that the actual non-perfused volumes were greater than the intended volume 25–29 % of the fibroid volume. Of nine adverse events, the only treatment-related event was transient post-procedure leg pain. At the 6-month follow-up, the mean fibroid volume was reduced by 13.5 %, and the average non-perfused volume at the end of the treatment was approximately 25 %. Even with the small treated volume, on clinical follow-up,

the mean reduction in the Uterine Fibroid Symptoms and Quality of Life (UFS-QOL) Questionnaire symptom severity score was 27.3 points; 79.3 % of patients achieved a greater than 10-point reduction in the UFS-QOL, thereby proving the primary endpoint hypothesis to be correct. Most of the improvement occurred in the first 3 months. A follow-up of this study [46] at the 6-month period reported a significant reduction in all subscales of the UFS-QOL. Of note, 5 % of women had skin burns after MRgFUS, and a single subject had skin ulceration. Skin burns were confined to the areas of the abdominal wall where hair removal was incomplete. The most serious complication after MRgFUS was the development of a transient, sciatic nerve palsy in one woman due to absorption of energy by bone in the far field of the sonication.

Midterm Outcome (After FDA Approval)

After the US FDA approved MRgFUS in April 2004, early restrictions on treatment were relaxed resulting in significant increase in treatment volume and increased treatment time from 120 to 180 min. Sonications which were previously allowed only near the center of leiomyomas were also allowed toward the edge of leiomyomas, both near the endometrium and the serosal surface. In addition, re-treatment was allowed within 14 days [47].

In a study of 160 patients prospectively, comparing outcomes in the restrictive ($n = 96$) and relaxed treatment ($n = 64$) cohorts demonstrated that the NPV increased from 59.4 cm^3 (16.6 % of fibroid volume) to 131.6 cm^3 (25.8 % of fibroid volume), respectively. The UFS-QOL score also showed an increased 10-point decrease in a larger percentage of patients (91 % vs. 72 %) at the 1-year post follow-up. There were no differences in the rates of adverse effects between the two groups. This study demonstrated the correlation between NPV and the change in the UFS-QOL symptom severity score from baseline to 6 months after therapy. In a single center subset of 42 treated patients, excessive bleeding, urinary and bulk symptoms all improved. On average, the number of days of excessive bleeding decreased from 6.1 to 4.9 days. Of 37 patients experiencing pressure symptoms before treatment, 36 (98 %) described either complete or partial symptomatic improvement. Nocturia resolved completely in 68 % of the patients. Funaki et al. [48] corroborated these results in 69 symptomatic patients who reported improvement in urinary frequency and abdominal pressure in the first 3 months, followed by improvement in pain and hemorrhage after 3 months. The majority of the patients had mild to significant improvement after 12 months.

A multicenter clinical trial of 359 demonstrated sustained relief of fibroid-related symptoms after MRgFUS treatment at the 24 months follow-up [49]. They also demonstrated that patients with higher NPV's were significantly less likely to have additional treatments for their fibroids [49].

As discussed previously, hyperintense leiomyomas (high T2 signal) respond relatively poorly to ablation and have a higher re-intervention rate. In one study reporting 24-month follow-up results on 91 patients [50], leiomyomas were classified into three types on the basis of the signal intensity of pretreatment T2-weighted images: type 1, a very low-intensity image comparable to that of skeletal muscle; type 2, an image intensity lower than that of the myometrium and higher than that of the skeletal muscle; and type 3, an image intensity equal to or higher than that of the myometrium [48]. Types 1 and 2 patients had significant fibroid volume reduction at 6 months, with a mean reduction of 40 %; type 3 patients showed a much lower reduction of volume after 12 months. Moreover, patients in types 1 and 2 had ~15-point reduction in their symptom severity score at 3 months, which persisted for 24 months. Type 3 patients, however, had high intervention rates and low response rates. The re-intervention rate for types 1/2 and 3 were 14 % and 21 %, respectively, at 24 months. Thus, they concluded that patients with type 3 lesions have a lower volume reduction and higher re-intervention rate compared to types 1 and 2.

A more recent study [51], using a protocol with greater treatment volumes (50 % of total fibroid volume compared with 33 %) and greater treatment duration (180 min compared with 120 min), reported a mean fibroid shrinkage of 31 %. In addition, a durability of symptom improvement for 1–1.5 years correlated with an NPV between 50 % and 80 %; 2.5–5 years correlated with an NPV exceeding 80 % [52].

In addition to a high non-perfused volume, dynamic contrast-enhanced MRI (DCE-MRI) imaging has also been shown to predict immediate, therapeutic response of MRgFUS for symptomatic fibroids [53]. K^{trans} of baseline DCE-MR, acoustic power, and ultrasound frequency were found to be independent predictors for immediate therapeutic response of volumetric MRgFUS ablation. A high K^{trans} value is deemed to be a significant predictor of poor treatment results. The authors concluded that, in such cases, the choice of higher acoustic power and/or higher ultrasound frequency would enhance the ablation efficacy [54].

In summary, clinical outcomes are improving predictably as treatment volumes have increased due to more relaxed restrictions, longer treatment duration, and technical refinement improving treated volume. Patients who are treated with a higher non-perfused volume ratio have significantly more improvement in symptoms and have a lower re-intervention rate compared with patients treated at a lower volume; the effect is sustained for up to 2 years. Furthermore, imaging characteristics can affect the treatment outcomes: patients with high T2 intensity (hyperintense) leiomyomas are less likely to respond and are more likely to need additional treatment. They require higher energy in each treatment compared to low T2 intensity leiomyomas. Moreover, DCE-MRI may be a helpful imaging adjunct to predict therapeutic response.

Cost-Effectiveness

In comparison to available treatment options, the cost-effectiveness of MRgFUS in the US has been found to be reasonable and comparable to alternative treatments [55]. The quality-adjusted life year (QALY) has been used to measure disease burden, including both the quality and the quantity of life lived. Lifetime total costs (including lost productivity) per patient were lowest for the pharmacotherapy strategy ($9,200). Among procedure-based therapy, hysterectomy has the least upfront cost ($19,800), followed by MRgFUS ($27,300), UAE ($28,900), and myomectomy ($35,100). Treatment with UAE was associated with the most QALYs (17.39), followed by MRgFUS (17.36), myomectomy (17.31), hysterectomy (17.18), and pharmacotherapy (16.70). The results suggested that MRgFUS is in the range of currently accepted criteria for cost-effectiveness, along with hysterectomy and UAE.

A study performed in the National Health Service (NHS) Trusts in England and Wales demonstrated similar results [56]. The total direct medical costs of 1,000 women treated with MRgFUS at age 39 and followed until menopause or age 56 have been estimated at £3,101,644 ($4,817,157), compared with the cost of £3,396,913 ($5,275,740) for 1,000 women treated with currently available procedures. Thus, the incremental cost of an MRgFUS treatment strategy compared with current treatment results in a cost saving of £295,269 ($458,582). Moreover, MRgFUS treatment compared with current practice increased QALYs by 10.658. Both studies suggest that MRgFUS is a cost-effective treatment option for patients.

Need for Additional Treatment

All uterine-preserving strategies have a failure rate requiring potential additional treatment. Stewart et al. reported that leiomyomas with larger treated volumes (as measured by NPV) are less likely to require additional treatment [57]. In one study [58], the rate of additional treatment for the first half of this study was 52 %, but it decreased to 29 % during the second half of the study. Six (35 %) of the 17 women who required additional treatment elected a second course of MRgFUS for either gradually

progressive symptom recurrence or for incomplete symptom relief. Six women had a hysterectomy after MRgFUS treatment. Since the approval of the ExAblate device in 2004 and the increased treated volumes allowed by the FDA (NPV ratios larger than 50 %), the published data suggests that there is a corresponding decreased need for additional treatment as the NPV ratio is increased. Newer series from outside the US that achieve mean NPV ratios of 50 % have demonstrated additional treatment in only 12–17 % of women at ≤12 months [50, 59].

Additionally, having a younger age at treatment and having a single fibroid were associated with the need of additional treatment [60]. Other variables such as weight, smoking status, parity, age at fibroid diagnosis, presenting symptoms, baseline symptom severity score, total fibroid volume, concomitant diagnosis of adenomyosis or endometriosis, prior use of oral contraceptives, or past medical history were not found to be associated with the treatment outcome [60].

Pregnancy Outcomes after MRgFUS

Although pregnancy was initially considered an early absolute contraindication to MRgFUS, the FDA relaxed this requirement and desire for future fertility has now been downgraded to a relative contraindication. Several studies have reported successful pregnancy after leiomyoma treatment with MRgFUS [61–64]. Rabinovici et al. [61] reported a global experience of 54 pregnancies in 51 women, all of which occurred after MRgFUS treatment of symptomatic uterine leiomyomas. The mean time to conception was 8 months after treatment. Live births occurred in 41 % of pregnancies, with a 28 % spontaneous abortion rate, an 11 % rate of elective pregnancy termination, and 20 % ongoing pregnancies beyond 20 gestational weeks. This study demonstrated a high rate of successfully delivered and ongoing pregnancies. In another study, Morita et al. [64] presented a case report of a 29-year-old female with a 6.8 × 8.0 × 7.9 cm uterine fibroid who underwent MRgFUS because concerns were raised about complications which may occur during pregnancy (i.e., spontaneous abortion, preterm labor); the patient was offered myomectomy but refused surgical intervention due to the associated risks involved. The patient successfully became pregnant three menstrual cycles after MRgFUS treatment and had a full-term pregnancy with an uneventful term vaginal delivery of a healthy baby. Another case report [65] described a patient who underwent MRgFUS for leiomyomas, which distorted the uterine cavity. Eighteen months after treatment, the patient uneventfully carried a uterine pregnancy to term with an uncomplicated labor and vaginal delivery. The authors speculate that the pregnancy occurred after a change in the configuration of the endometrial cavity as a result of MRgFUS, and the authors suggest that MRgFUS may have a role in facilitating fertility in patients with fibroids. Despite these anecdotal reports, there is no formal study evaluating the effect of MRgFUS in either facilitating conception or minimizing gestational complications in women with uterine leiomyomas.

Pretreatment with Gonadotropin-Releasing Hormone Agonists

Based on experience from myomectomy where preoperative administration of gonadotropin-releasing hormone agonists (GNRH agonists) is used to temporarily decrease bulk, bleeding-related symptoms, and leiomyoma size. Several groups have extended this application to minimize symptoms and leiomyoma size prior to MRgFUS.

Studies have suggested the use of GnRH agonist prior to MRgFUS for leiomyomas larger than 10 cm can help significantly decrease leiomyoma size, allowing for larger posttreatment NPV's and more effective treatment (Fig. 55.7). In one prospective study [66], women with symptomatic leiomyomas larger than 10 cm in diameter were treated with GnRH agonists – 3.6 mg of subcutaneous goserelin (ZoladexTM, AstraZeneca) – on day 1 or 2 of their menstrual cycle for three

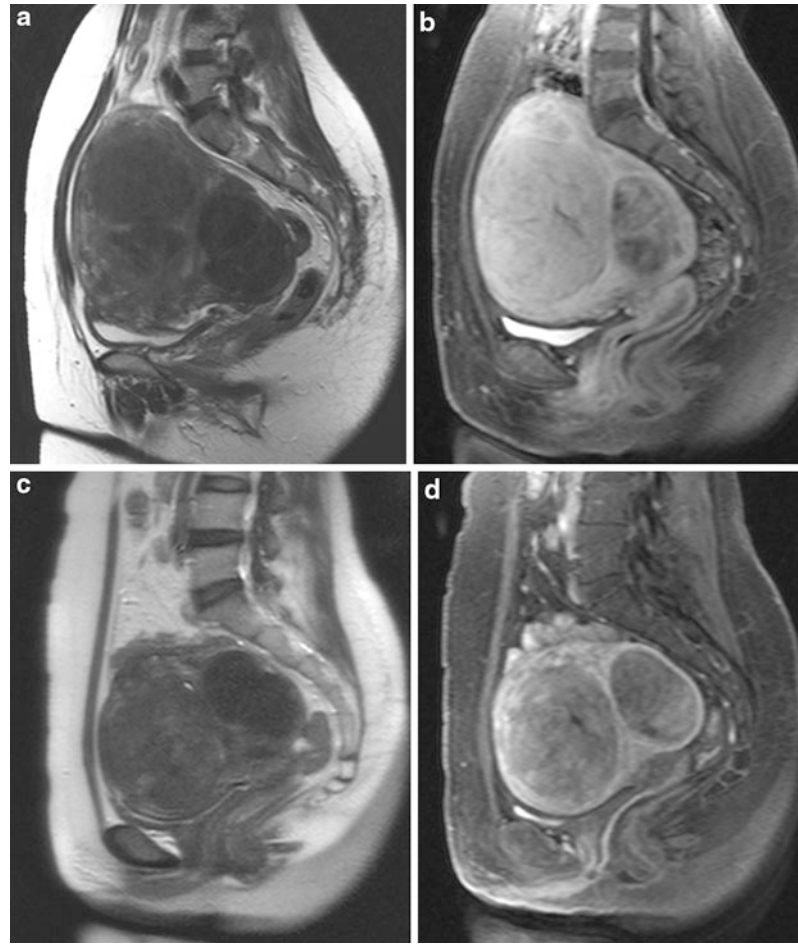

Fig. 55.7 Sagittal T2-weighted image of a patient treated with a T2 hypointense 10-cm leiomyoma (**a**) which enhances on post-gadolinium T1 image (**b**), who underwent 3 months of GnRH agonist treatment and post-therapy had a 50 % reduction in leiomyomas volume (**c**, T2-weighted image, **d**, post-gadolinium T1 image)

consecutive months; MRgFUS was performed 14–21 days after the final injection. The study reported that patients on GnRH-treated patients required half the energy (Joules) for a given NPV, thus confirming that this method was robust in enhancing MRgFUS treatment. In our experience, we have observed significant decrease in enhancement of leiomyomas after GnRH agonist therapy (Fig. 55.8).

Current Practice Patterns

In a survey of 13 providers at the international symposium devoted to clinical MRgFUS in 2008, limitations to patient selection for MRgFUS was assessed on a 10-point Likert scale ranging from 1, which indicated no impediment to therapy, to 10, which represented an absolute contraindication to therapy [67]. Surveys were completed by 13 symposium participants: five gynecologists (39 %) and eight radiologists (61 %). Factors that were not considered impediments (score <3) included concomitant mild adenomyosis, primary complaint being heavy bleeding, bulk pain, pelvic pain; possible impediments (score 3–5) included a desire for future fertility and pedunculated subserosal fibroid; factors that were considered significant impediments (score >5) include abdominal scarring, concomitant severe adenomyosis, gadolinium non-enhancement, high T2 signal intensity, pedunculated submucosal fibroid, size >10 cm, and postmenopausal status.

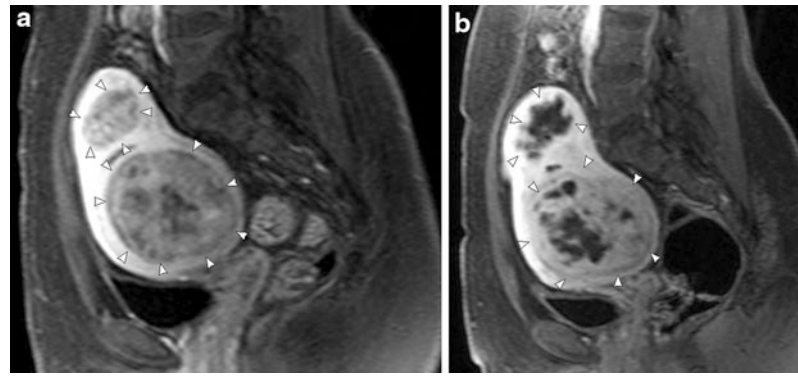

Fig. 55.8 Sagittal gadolinium-enhanced T1-weighted image of a patient with an intramural fibroid (**a**) underwent GnRH agonist therapy and developed spontaneously degenerating areas in her fibroid seen on the post-gadolinium image (**b**)

Other GYN Application of MRgFUS

Use of MRgFUS for Adenomyosis

Adenomyosis is a common and often misdiagnosed gynecologic disorder with symptoms mimicking those of leiomyomas. It is defined by ectopic location of endometrium and fibrous stroma in the myometrium. Symptoms associated with adenomyosis include menometrorrhagia, menstrual cramps, dyspareunia, and dysmenorrhea. Currently, the definitive therapy for uterine adenomyosis is hysterectomy. Medical therapies can provide symptomatic relief, but they are short-lived [68]. There are minor surgical procedures including endomyometrial ablation, laparoscopic myometrial electrocoagulation, and adenomyoma excision, which have been used with varying degrees of success [68]. Although endometrial ablation may be effective in the short term, there is a significant long-term failure rate [68–72]. Hysterectomy is the ultimate solution for women with deep, myometrial involvement or if future fertility is not desired [73, 74]. Uterine artery embolization (UAE) has been applied to treat symptomatic localized adenomyosis [75–77]. Although short-term outcomes are promising, durable, long-term results are significantly less than in women with leiomyomas. Symptoms recur in up to 40–45 % of patients [75, 77, 78].

Although not approved by the US FDA, recently, the use of HIFU for treatment of adenomyosis has shown potential as an effective modality in other countries [79]. There have been multiple case reports of successful MRgFUS treatment of focal adenomyosis with subsequent symptomatic relief [35, 63, 80]. One study reported 20 patients treated with MRgFUS for adenomyosis reported significant symptomatic improvement [81]. Ultrasound-guided HIFU ablation of adenomyosis has also been described. Wang et al [79] reported a phase I clinical trial using ultrasound-guided ablation for 12 patients with adenomyosis. During the 3 months of follow-up, the intensity of pain and dysmenorrhea in all patients was lower than they were before treatment. The results showed that ablation may be safe and effective for treating patients with adenomyosis. Though HIFU has the potential to offer a noninvasive alternative treatment method of adenomyosis, further study is needed to fully evaluate its efficacy.

Treatment of Cervical Ectopy

Cervical ectopy is a normal condition that is due to extension of the columnar epithelium from the endocervix that extends to the ectocervix [82]. For chronic cervicitis that is unresponsive to medical management, surgical options are available to mitigate symptoms and to prevent neoplastic transformation. Cryocautery, electrocoagulation, and laser therapy are popular methods. However, these methods can cause fibrosis of the cervix, secondary cervical stenosis, and subsequent infertility and/or cervical-origin dystocia [83].

High-intensity focused US has been explored as an alternative treatment for cervical ectopy because it has the theoretical advantage of

not disrupting the mucosa and thus, decrease risk of cervical stenosis. A study of 200 patients comparing HIFU versus laser treatments in patients with symptomatic, benign ectopy of the cervix demonstrated no differences in the symptomatic cure rate (97 % vs. 98 %); however, the rate of side effects (vaginal reactive discharge and colporrhagia) was lower in the US group than the laser group (8 % vs. 45 %, respectively) [84], This comparative study demonstrated that US and laser therapies had similar efficacy, but there was less post-procedure bleeding and vaginal discharge in the US group. Ultrasound therapy appears to be a promising new treatment method for symptomatic cervical ectopy, but long-term outcomes are needed.

Abdominal Wall Endometriosis

Abdominal wall endometriosis (AWE) occurs when endometriosis occurs outside the pelvis. Most AWEs are associated with obstetrical or gynecological procedures such as cesarean delivery, hysterotomy, hysterectomy, and amniocentesis [85–87]. Patients who typically have a painful nodule under or close to previous scar have pain that fluctuates with menstruation [88]. Treatment of AWE includes hormonal treatment and surgical resection [89, 90]. HIFU has been evaluated as an alternative, less invasive means of controlling symptoms. In one study, ultrasound-guided HIFU ablation of AWE in 21 patients demonstrated clinical improvement in all patients [91]. The cyclic pain disappeared after a mean follow-up of 18.7 months (range 3–31 months), and the treated nodules gradually reduced in size over time. These results suggested that US-guided HIFU can achieve effective therapeutic benefit for patients and may need to bypass surgical resection.

Summary

Leiomyoma-related bulk and bleeding symptoms are among the most commonly treated gynecological disorders in women. A multidisciplinary approach is necessary to optimize individual treatment. Prior to treatment, MR imaging is essential for triage. MRgFUS provides an attractive noninvasive method to imaging and treatment alternative to currently available therapies for symptomatic classical uterine leiomyomas. However, only a certain percentage of patients with small to moderate volume classical leiomyomas are suitable for therapy with currently available technology. It may be particularly useful for symptomatic women desiring future fertility. Patient and leiomyoma selection is important. Although early reports suggest that reduction in symptom severity is related to robust leiomyoma treatment, randomized trials, and long-term outcomes (> 5 years) have not been reported to date.

References

1. Haar GT, Coussios C. High intensity focused ultrasound: past, present and future. Int J Hyperthermia. 2007;23:85–7.
2. Accessed at http://www.fda.gov/MedicalDevices/ProductsandMedicalProcedures/DeviceApprovalsandClearances/Recently-ApprovedDevices/ucm080704.htm
3. Day Baird D, Dunson DB, Hill MC, Cousins D, Schectman JM. High cumulative incidence of uterine leiomyoma in black and white women: ultrasound evidence. Am J Obstet Gynecol. 2003;188:100–7.
4. Parazzini F, Negri E, La Vecchia C, Chatenoud L, Ricci E, Guarnerio P. Reproductive factors and risk of uterine fibroids. Epidemiology. 1996;7:440–2.
5. Spies JB, Coyne K, Guaou Guaou N, Boyle D, Skyrnarz-Murphy K, Gonzalves SM. The UFS-QOL, a new disease-specific symptom and health-related quality of life questionnaire for leiomyomata. Obstet Gynecol. 2002;99:290–300.
6. Flynn M, Jamison M, Datta S, Myers E. Health care resource use for uterine fibroid tumors in the United States. Am J Obstet Gynecol. 2006;195:955–64.
7. Hartmann KE, Birnbaum H, Ben-Hamadi R, et al. Annual costs associated with diagnosis of uterine leiomyomata. Obstet Gynecol. 2006;108:930–7.
8. Wise LA, Radin RG, Palmer JR, Kumanyika SK, Rosenberg L. A prospective study of dairy intake and risk of uterine leiomyomata. Am J Epidemiol. 2010;171:221–32.
9. Liu JP, Yang H, Xia Y, Cardini F. Herbal preparations for uterine fibroids. Cochrane Database Syst Rev. 2009;2:CD005292. PMID 19370619.

10. Nowak RA. Fibroids: pathophysiology and current medical treatment. Baillieres Best Pract Res Clin Obstet Gynaecol. 1999;13:223–38.
11. Zhang Y, Peng W, Clarke J, Liu Z. Acupuncture for uterine fibroids. Cochrane Database Syst Rev. 2010;1: CD007221. PMID 2009162.
12. McCracken G, Hunter D, Morgan D, Price JH. Comparison of laparoscopic-assisted vaginal hysterectomy, total abdominal hysterectomy and vaginal hysterectomy. Ulster Med J. 2006;75:54–8.
13. Karasick S, Spettell CM. The role of parity and hysterectomy on the development of pelvic floor abnormalities revealed by defecography. AJR Am J Roentgenol. 1997;169:1555–8.
14. Dallenbach P, Kaelin-Gambirasio I, Dubuisson JB, Boulvain M. Risk factors for pelvic organ prolapse repair after hysterectomy. Obstet Gynecol. 2007;110:625–32.
15. Lumsden MA. Embolization versus myomectomy versus hysterectomy: which is best, when? Hum Reprod. 2002;17:253–9.
16. Gupta JK, Sinha AS, Lumsden MA, Hickey M. Uterine artery embolization for symptomatic uterine fibroids. Cochrane Database Syst Rev. 2006;1: CD005073. PMID 16437515.
17. Spilsbury K, Hammond I, Bulsara M, Semmens JB. Morbidity outcomes of 78,577 hysterectomies for benign reasons over 23 years. BJOG. 2008;115:1473–83.
18. Fedele L, Parazzini F, Luchini L, Mezzopane R, Tozzi L, Villa L. Recurrence of fibroids after myomectomy: a transvaginal ultrasonographic study. Hum Reprod. 1995;10:1795–6.
19. Yoo EH, Lee PI, Huh CY, et al. Predictors of leiomyoma recurrence after laparoscopic myomectomy. J Minim Invasive Gynecol. 2007;14:690–7.
20. Malone LJ. Myomectomy: recurrence after removal of solitary and multiple myomas. Obstet Gynecol. 1969;34:200–3.
21. Buttram Jr VC. Uterine leiomyomata–aetiology, symptomatology and management. Prog Clin Biol Res. 1986;225:275–96.
22. Fauconnier A, Chapron C, Babaki-Fard K, Dubuisson JB. Recurrence of leiomyomata after myomectomy. Hum Reprod Update. 2000;6:595–602.
23. Ravina JH, Herbreteau D, Ciraru-Vigneron N, et al. Arterial embolisation to treat uterine myomata. Lancet. 1995;346:671–2.
24. Goodwin SC, Vedantham S, McLucas B, Forno AE, Perrella R. Preliminary experience with uterine artery embolization for uterine fibroids. J Vasc Interv Radiol. 1997;8:517–26.
25. Siskin GP, Shlansky-Goldberg RD, Goodwin SC, et al. A prospective multicenter comparative study between myomectomy and uterine artery embolization with polyvinyl alcohol microspheres: long-term clinical outcomes in patients with symptomatic uterine fibroids. J Vasc Interv Radiol. 2006;17: 1287–95.
26. Volkers NA, Hehenkamp WJ, Birnie E, et al. Uterine artery embolization in the treatment of symptomatic uterine fibroid tumors (EMMY trial): periprocedural results and complications. J Vasc Interv Radiol. 2006;17:471–80.
27. Volkers NA, Hehenkamp WJ, Birnie E, Ankum WM, Reekers JA. Uterine artery embolization versus hysterectomy in the treatment of symptomatic uterine fibroids: 2 years' outcome from the randomized EMMY trial. Am J Obstet Gynecol. 2007;196:519 e1–11.
28. Spies JB, Ascher SA, Roth AR, Kim J, Levy EB, Gomez-Jorge J. Uterine artery embolization for leiomyomata. Obstet Gynecol. 2001;98:29–34.
29. Jolesz FA. MRI-guided focused ultrasound surgery. Annu Rev Med. 2009;60:417–30.
30. http://www.insightec.com/MRgFUSArticles.html
31. Stewart EA, Gedroyc WM, Tempany CM, et al. Focused ultrasound treatment of uterine fibroid tumors: safety and feasibility of a noninvasive thermoablative technique. Am J Obstet Gynecol. 2003;189:48–54.
32. Jolesz FA, Hynynen K, McDannold N, Tempany C. MR imaging-controlled focused ultrasound ablation: a noninvasive image-guided surgery. Magn Reson Imaging Clin N Am. 2005;13:545–60.
33. Ren XL, Zhou XD, Zhang J, et al. Extracorporeal ablation of uterine fibroids with high-intensity focused ultrasound: imaging and histopathologic evaluation. J Ultrasound Med. 2007;26:201–12.
34. Ren XL, Zhou XD, Yan RL, et al. Sonographically guided extracorporeal ablation of uterine fibroids with high-intensity focused ultrasound: midterm results. J Ultrasound Med. 2009;28:100–3.
35. Yoon SW, Lee C, Cha SH, et al. Patient selection guidelines in MR-guided focused ultrasound surgery of uterine fibroids: a pictorial guide to relevant findings in screening pelvic MRI. Eur Radiol. 2008; 18:2997–3006.
36. Yoon S-W. Magnetic resonance-guided focused ultrasound treatment of uterine fibroids in patients with abdominal scars, using an energy-blocking scar patch. In: MR-guided focused ultrasound 2010, Washington, DC;2010. p. 122.
37. Gorny KR, Chen S, Hangiandreou NJ, et al. Initial evaluation of acoustic reflectors for the preservation of sensitive abdominal skin areas during MRgFUS treatment. Phys Med Biol. 2009;54:N125–33.
38. Smart OC, Hindley JT, Regan L, Gedroyc WG. Gonadotrophin-releasing hormone and magnetic-resonance-guided ultrasound surgery for uterine leiomyomata. Obstet Gynecol. 2006;108:49–54.
39. LeBlang SD. Patient selection for MRgFUS in the treatment of uterine fibroids. In: MR-guided focused ultrasound 2010 2nd International Symposium. Washington, DC;2010. p. 116.
40. Machtinger R, Fennessy FM, Stewart EA, Tempany CA. Analyzing screen failures prior to MRgFUS for uterine fibroids: do African American (AA) women

have different characteristics?. In: MR-guided focused ultrasound. Washington, DC; 2010
41. Summary of safety and effectiveness data. http://www.accessdata.fda.gov/cdrh_docs/pdf4/P040003b.pdf (2004). Accessed 3 June 2004.
42. Wamsteker K, Emanuel MH, de Kruif JH. Transcervical hysteroscopic resection of submucous fibroids for abnormal uterine bleeding: results regarding the degree of intramural extension. Obstet Gynecol. 1993;82:736–40.
43. Lenard ZM, McDannold NJ, Fennessy FM, et al. Uterine leiomyomas: MR imaging-guided focused ultrasound surgery–imaging predictors of success. Radiology. 2008;249:187–94.
44. Hananel A. The next generation fo ExAblate. In: Tan N, editor. Los Angeles:2010. http://www.insightec.com/contentManagment/uploadedFiles/fileGallery/brochure_or_brochure.pdf
45. Hindley J, Gedroyc WM, Regan L, et al. MRI guidance of focused ultrasound therapy of uterine fibroids: early results. AJR Am J Roentgenol. 2004;183:1713–9.
46. Stewart EA, Rabinovici J, Tempany CM, et al. Clinical outcomes of focused ultrasound surgery for the treatment of uterine fibroids. Fertil Steril. 2006;85:22–9.
47. Fennessy FM, Tempany CM, McDannold NJ, et al. Uterine leiomyomas: MR imaging-guided focused ultrasound surgery–results of different treatment protocols. Radiology. 2007;243:885–93.
48. Funaki K, Fukunishi H, Funaki T, Sawada K, Kaji Y, Maruo T. Magnetic resonance-guided focused ultrasound surgery for uterine fibroids: relationship between the therapeutic effects and signal intensity of preexisting T2-weighted magnetic resonance images. Am J Obstet Gynecol. 2007;196:184 e1–6.
49. Stewart EA, Gostout B, Rabinovici J, Kim HS, Regan L, Tempany CM. Sustained relief of leiomyoma symptoms by using focused ultrasound surgery. Obstet Gynecol. 2007;110:279–87.
50. Funaki K, Fukunishi H, Sawada K. Clinical outcomes of magnetic resonance-guided focused ultrasound surgery for uterine myomas: 24-month follow-up. Ultrasound Obstet Gynecol. 2009;34:584–9.
51. LeBlang SD, Hoctor K, Steinberg FL. Leiomyoma shrinkage after MRI-guided focused ultrasound treatment: report of 80 patients. AJR Am J Roentgenol. 2010;194:274–80.
52. Kurashvili J, Stepanov A, Batarchina O, et al. MRgFUS treatment for uterine myomas: safety, effectiveness and pathogenesis. In: MR-guided focused ultrasound 2010 2nd International Symposium; 2010 Oct 17; Washington, DC; 2010. p. 117.
53. Kim Y-s, Lim HK, Kim J-H, Rhim H, Keserci B. Dynamic contrast-enhanced magnetic resonance imaging predicts immediate therapeutic response of MR-guided high-intensity focused ultrasound ablation of symptomatic uterine fibroids. In: MR-guided focused ultrasound 2010 2nd International Symposium. Washington, DC; 2010. p. 119.
54. Kim Y-s, Lim HK, Kim J-H, Rhim H, Keserci B. Dynamic contrast-enhanced magnetic resonance imaging predicts immediate therapeutic response of MR-guided high-intensity focused ultrasound ablation of symptomatic uterine fibroids. In: MR-guided focused ultrasound 2010. Washington, DC; 2010. p. 118.
55. O'Sullivan AK, Thompson D, Chu P, Lee DW, Stewart EA, Weinstein MC. Cost-effectiveness of magnetic resonance guided focused ultrasound for the treatment of uterine fibroids. Int J Technol Assess Health Care. 2009;25:14–25.
56. Zowall H, Cairns JA, Brewer C, Lamping DL, Gedroyc WM, Regan L. Cost-effectiveness of magnetic resonance-guided focused ultrasound surgery for treatment of uterine fibroids. BJOG. 2008;115:653–62.
57. Stewart E, editor. Uterine fibroids: the complete guide. 1st ed. Baltimore: Johns Hopkins University Press; 2007.
58. Hesley GK, Felmlee JP, Gebhart JB, et al. Noninvasive treatment of uterine fibroids: early Mayo clinic experience with magnetic resonance imaging-guided focused ultrasound. Mayo Clin Proc. 2006;81:936–42.
59. Rabinovici J, Inbar Y, Revel A, et al. Clinical improvement and shrinkage of uterine fibroids after thermal ablation by magnetic resonance-guided focused ultrasound surgery. Ultrasound Obstet Gynecol. 2007;30:771–7.
60. Bouwsma E, Stewart EA, Gorny K, Hesley G. In: MR-guided focused ultrasound 2010 2nd International Symposium. Washington, DC; 2010. p. 119.
61. Rabinovici J, David M, Fukunishi H, Morita Y, Gostout BS, Stewart EA. Pregnancy outcome after magnetic resonance-guided focused ultrasound surgery (MRgFUS) for conservative treatment of uterine fibroids. Fertil Steril. 2010;93:199–209.
62. Gavrilova-Jordan LP, Rose CH, Traynor KD, Brost BC, Gostout BS. Successful term pregnancy following MR-guided focused ultrasound treatment of uterine leiomyoma. J Perinatol. 2007;27:59–61.
63. Rabinovici J, Inbar Y, Eylon SC, Schiff E, Hananel A, Freundlich D. Pregnancy and live birth after focused ultrasound surgery for symptomatic focal adenomyosis: a case report. Hum Reprod. 2006;21:1255–9.
64. Morita Y, Ito N, Ohashi H. Pregnancy following MR-guided focused ultrasound surgery for a uterine fibroid. Int J Gynaecol Obstet. 2007;99:56–7.
65. Hanstede MM, Tempany CM, Stewart EA. Focused ultrasound surgery of intramural leiomyomas may facilitate fertility: a case report. Fertil Steril. 2007;88:497 e5–7.
66. Smart OC, Hindley JT, Regan L, Gedroyc WM. Magnetic resonance guided focused ultrasound surgery of uterine fibroids–the tissue effects of GnRH agonist pre-treatment. Eur J Radiol. 2006;59:163–7.
67. Taran FA, Hesley GK, Gorny KR, Stewart EA. What factors currently limit magnetic resonance-guided

focused ultrasound of leiomyomas? A survey conducted at the first international symposium devoted to clinical magnetic resonance-guided focused ultrasound. Fertil Steril. 2010;94:331–4.
68. Farquhar C, Brosens I. Medical and surgical management of adenomyosis. Best Pract Res Clin Obstet Gynaecol. 2006;20:603–16.
69. Banu NS, Manyonda IT. Alternative medical and surgical options to hysterectomy. Best Pract Res Clin Obstet Gynaecol. 2005;19:431–49.
70. Rabinovici J, Stewart EA. New interventional techniques for adenomyosis. Best Pract Res Clin Obstet Gynaecol. 2006;20:617–36.
71. Roman JD. Surgical treatment of endometriosis in private practice: cohort study with mean follow-up of 3 years. J Minim Invasive Gynecol. 2010;17:42–6.
72. McCausland V, McCausland A. The response of adenomyosis to endometrial ablation/resection. Hum Reprod Update. 1998;4:350–9.
73. Keckstein J. Hysteroscopy and adenomyosis. Contrib Gynecol Obstet. 2000;20:41–50.
74. Levgur M. Therapeutic options for adenomyosis: a review. Arch Gynecol Obstet. 2007;276:1–15.
75. Kim MD, Kim S, Kim NK, et al. Long-term results of uterine artery embolization for symptomatic adenomyosis. AJR Am J Roentgenol. 2007;188:176–81.
76. Pelage JP, Le Dref O, Jacob D, et al. Uterine artery embolization: anatomical and technical considerations, indications, results, and complications. J Radiol. 2000;81:1863–72.
77. Bratby MJ, Walker WJ. Uterine artery embolisation for symptomatic adenomyosis–mid-term results. Eur J Radiol. 2009;70:128–32.
78. Pelage JP, Jacob D, Fazel A, et al. Midterm results of uterine artery embolization for symptomatic adenomyosis: initial experience. Radiology. 2005;234:948–53.
79. Wang W, Wang Y, Tang J. Safety and efficacy of high intensity focused ultrasound ablation therapy for adenomyosis. Acad Radiol. 2009;16:1416–23.
80. Yoon SW, Kim KA, Cha SH, et al. Successful use of magnetic resonance-guided focused ultrasound surgery to relieve symptoms in a patient with symptomatic focal adenomyosis. Fertil Steril. 2018;2008(90):2018 e13–5.
81. Fukunishi H, Funaki K, Sawada K, Yamaguchi K, Maeda T, Kaji Y. Early results of magnetic resonance-guided focused ultrasound surgery of adenomyosis: analysis of 20 cases. J Minim Invasive Gynecol. 2008;15:571–9.
82. Singer A. The uterine cervix from adolescence to the menopause. Br J Obstet Gynaecol. 1975;82:81–99.
83. Mayeaux Jr EJ, Spigener SD, German JA. Cryotherapy of the uterine cervix. J Fam Pract. 1998;47:99–102.
84. Chen J, Zhou D, Liu Y, et al. A comparison between ultrasound therapy and laser therapy for symptomatic cervical ectopy. Ultrasound Med Biol. 2008;34:1770–4.
85. Patterson GK, Winburn GB. Abdominal wall endometriomas: report of eight cases. Am Surg. 1999;65:36–9.
86. Dwivedi AJ, Agrawal SN, Silva YJ. Abdominal wall endometriomas. Dig Dis Sci. 2002;47:456–61.
87. Hughes ML, Bartholomew D, Paluzzi M. Abdominal wall endometriosis after amniocentesis. A case report. J Reprod Med. 1997;42:597–9.
88. Gunes M, Kayikcioglu F, Ozturkoglu E, Haberal A. Incisional endometriosis after cesarean section, episiotomy and other gynecologic procedures. J Obstet Gynaecol Res. 2005;31:471–5.
89. Blanco RG, Parithivel VS, Shah AK, Gumbs MA, Schein M, Gerst PH. Abdominal wall endometriomas. Am J Surg. 2003;185:596–8.
90. Kocakusak A, Arpinar E, Arikan S, Demirbag N, Tarlaci A, Kabaca C. Abdominal wall endometriosis: a diagnostic dilemma for surgeons. Med Princ Pract. 2005;14:434–7.
91. Wang Y, Wang W, Wang L, Wang J, Tang J. Ultrasound-guided high-intensity focused ultrasound treatment for abdominal wall endometriosis: preliminary results. Eur J Radiol. 2011;79(1):56–9

Image-Guided Radiation Therapy in Gynecology Applications

56

Tony Y. Eng, Daniel Baseman, Dominic Nguyen, and Chul S. Ha

Abstract

The current image-guided radiation therapy (IGRT) incorporates anatomical, functional, or biological information into radiation treatment design, planning, and delivery. The rationale for the use of IGRT in gynecologic malignancies includes three-dimensional assessment of tumor extent and surrounding organs, compensation for organ motion, adaptation to rapid tumor shrinkage, and potential dose escalation. The utilization of advanced imaging has led to improved target delineation and localization, a more realistic assessment of dose to critical structures, and the ability to increase tumor dose in a way not possible before. Currently, CT, MRI, and PET-CT are the most commonly used imaging methods in gynecologic IGRT as they are widely available and reasonably affordable. Many bulky tumors shrink rapidly during radiation therapy with concomitant chemotherapy. Daily IGRT may allow plans to be adapted as tumors shrink with treatments; thus, more normal tissues can be spared. The incorporation of IGRT and intensity-modulated radiation therapy (IMRT) into clinical practice allows a reduction in both systematic and random errors. IGRT/IMRT has gained increasing momentum as a component of treatment planning and delivery for gynecologic malignancies. Guidelines Consensus Working Group and

T.Y. Eng (✉) • D. Baseman • D. Nguyen
Department of Radiation Oncology, Cancer Therapy and Research Center & The University of Texas Health Science Center at San Antonio, San Antonio, TX, USA
e-mail: eng@uthscsa.edu; basemand@uthscsa.edu; eng@uthscsa.edu

C.S. Ha
Department of Radiation Oncology, Cancer Therapy and Research Center at the University of Texas Health Science Center, San Antonio, TX, USA
e-mail: hac@uthscsa.edu

D.E. Dupuy et al. (eds.), *Image-Guided Cancer Therapy*, DOI 10.1007/978-1-4419-0751-6_58,

Radiation Therapy Oncology Group Consensus Conference have proposed guidelines for delineation of various target and nontarget volumes for cervical and endometrial cancer patients. Clinical outcome data are slowly emerging and prospective randomized trials are anticipated.

Introduction

Radiation therapy has always been "image-guided" either clinically (electron beam therapy) or radiographically. Imaging is often near real time with pre-port or post-port planar x-ray films. The recent advances in imaging technology have redefined the concept of image-guided radiation therapy (IGRT) in treatment planning and delivery. However, the current definition of IGRT is not universally standardized and open to various interpretations. Most radiation oncologists view anatomical CT or MR-based treatment planning and delivery as IGRT, whereas others may view any aspect of treatment involving weekly fluoroscopic imaging as IGRT. The Radiation Therapy Oncology Group (RTOG) IGRT Committee [1] defines IGRT as radiation treatment design and delivery using modern imaging methods, such as computed tomography (CT), magnetic resonance imaging (MRI), positron emission tomography (PET), and ultrasound (US), in target and nontarget structures. Examples of IGRT include three-dimensional conformal radiation therapy (3DCRT), intensity-modulated radiation therapy (IMRT), stereotactic radiosurgery, stereotactic body radiation therapy (SBRT), and most brachytherapy procedures utilizing 3D imaging. Modern imaging, like on-board imager (OBI) systems, can be used to adjust for target motion and positional changes and adapt treatment to tumor response (adaptive IGRT). Fast high-quality 3D images of the patient in treatment position can be obtained daily immediately prior to treatment to more accurately guide radiation delivery based on internal anatomy without the need for implanted fiducial markers.

As imaging has steadily improved, current IGRT/IMRT incorporates anatomical, functional, or biological information into radiation treatment design, planning, and delivery. It has been well accepted in head and neck and genitourinary tumors with very encouraging outcome data [2–6]. For gynecologic malignancies, IGRT/IMRT has gained acceptance only in recent years with limited clinical data emerging. It has been used in gynecologic malignancies to augment target delineation and improve treatment delivery. Molecular imaging will likely lead to early cancer detection and diagnosis, improve image-guided cancer therapy, and enable better monitoring response to treatment. Parallel with advance in imaging, combined modality therapy in multidisciplinary setting has lead to improved survival and lower morbidity and mortality. This chapter focuses on the current use of IGRT/IMRT, mostly PET/CT-based, in the treatment of gynecologic malignancies and offers some guidelines for its appropriate utilization, especially in cervical and endometrial cancers, where radiation therapy plays a sentinel role in their management.

Background

The incidence and mortality from invasive cervical cancer have declined substantially in developed countries due in large part to successful cytologic screening programs. Still, cervical cancer remains a major global problem especially in medically underserved regions. In the United States, it is estimated that 12,200 new cases of cervical cancer were diagnosed in 2010, with 4,210 deaths as a result [7]. Worldwide, invasive cervical cancer is the second most common cancer in women behind breast cancer, with an estimated 555,094 cases and 309,808 deaths [8]. Risk factors for the development of cervical cancer are similar to those associated with other sexually transmitted diseases (STD) and include multiple sexual partners, history of other STDs, first coitus at a young age, and high parity.

Endometrial cancer is the most frequently diagnosed gynecologic malignancy in the United

States and Europe, with an estimated 43,470 new cases in the USA in 2010 [7]. Outcomes are very favorable: most patients present with early-stage disease given the propensity for early symptomatic presentation, classically with postmenopausal abnormal uterine bleeding. The majority of endometrial cancers are adenocarcinomas, with endometrioid type the most common by far.

Vulvar carcinoma is a rare disease accounting for 3–4 % of gynecologic malignancies with an estimated 3,900 new cases diagnosed in 2010 resulting in approximately 920 deaths [7]. Immunosuppression, human papillomavirus infection, and advanced age are the strongest risk factors associated with vulvar neoplasms [9]. The most common pathology is squamous cell carcinoma accounting for 90 % of primary disease.

While the estimated incidence of ovarian cancer is 21,880 with 13,850 deaths [7], radiation therapy plays a very limited role in its current management. The incidence of vaginal and other gynecologic malignancies are relatively low. The management of these gynecologic malignancies may be different from each other. When radiation therapy is needed, however, the technical aspect is similar. Therefore, these cancer sites will not be discussed separately.

General Management

Cervical Carcinoma

Patients with cervical cancer are variably managed depending on their stage of presentation. Early-stage small lesions can be managed by surgery alone which can include procedures as conservative as a cone biopsy and as extensive as an extended radical hysterectomy. Larger and more advanced stage lesions are managed nonsurgically, typically with chemotherapy and radiation. One landmark study that helped shape the current paradigm for cervical cancer management was published by Landoni et al. [10] and examined patients with stage Ib and IIa cervical cancer, randomizing them to surgery vs. radical radiotherapy. Surgery was a class III radical abdominal hysterectomy, and radiation included external beam radiation therapy (EBRT) to a median dose of 47 Gy to the pelvis followed by intracavitary brachytherapy bringing total point A dose to a median of 76 Gy. The para-aortic nodes were treated when lymphangiogram demonstrated involvement. Adjuvant radiation therapy was administered for high-risk pathological features including positive nodes, involved parametria, <3-mm safe cervical stroma, or cut-through of disease. They found equivalent rates of disease control in both arms and increased toxicity with combined surgery and radiation. Given that a great proportion of large tumors require adjuvant radiation due to high-risk pathological features, nonoperative management for stage ≥ IB2 (except some small IIA lesions) has become a standard of care.

Several other randomized controlled trials have been conducted to determine the optimal nonsurgical management of patients with cervical cancer. RTOG 7920 examined patients with stage IIB and >4-cm IB/IIA disease and revealed improved 10-year overall survival (55 vs. 44 %) when patients were treated with extended-field radiotherapy (with para-aortic treatment) instead of whole pelvic radiation therapy [11]; there was no effect on locoregional control (65 %) or distant metastasis (25–30 %). It was later revealed that the addition of platinum-based chemotherapy to radiation improved nearly every outcome for patients with at least stage IB2 disease; this was demonstrated in several randomized controlled trials including Gynecologic Oncology Group (GOG) 85/Southwest Oncology Group (SWOG) 8695, RTOG 90–01, GOG 120, and GOG 123 [12–15]. While adjuvant chemotherapy has shown to improve survival and local control (LC) as supported by multiple randomized trials, neoadjuvant chemotherapy has not shown clear benefits in randomized trials. Some non-cisplatinum (CDDP)-based chemotherapy also showed similar benefit, and extended adjuvant chemotherapy may have further benefit [16].

In addition to demonstrating improved survival with the addition of adjuvant chemotherapy to radiation, RTOG 90–01 also called into question the need for para-aortic radiation [13]. In this study, patients with stage IB (≥5 cm) and higher disease were randomized to extended-field radiation therapy (EFRT) or whole pelvic radiation

therapy (WPRT) with CDDP/5-FU. The experimental arm of the study, WPRT with cisplatin-based chemotherapy, has become a de facto standard of care for nonsurgical management of cervical cancer, and the benefit of EFRT with chemotherapy is uncertain. Still, most advocate the use of EFRT if the para-aortic lymph nodes are involved, and some advocate prophylactic para-aortic radiation for high-risk patients given that those patients with stage IIB–IVA disease have rates of para-aortic lymph node involvement ranging from ~15–50 % [17, 18].

Endometrial Carcinoma

Patients with endometrial carcinomas are primarily managed with surgery. The standard surgical procedure is the total abdominal hysterectomy and bilateral salpingo-oophorectomy (TAH-BSO). In addition to removal of the uterus, ovaries, and fallopian tubes, peritoneal fluid is sent for cytology, and lymph node sampling is typically performed at the level of the pelvic, common iliac, and para-aortic nodes. In 2009, results of the Medical Research Council ASTEC (A Study in the Treatment of Endometrial Cancer) trial of systematic pelvic lymphadenectomy were published [19]. In this study, 1,408 women with endometrial carcinoma of all stages were randomized to standard surgery (TAH-BSO, peritoneal washings, palpation of para-aortic nodes) or standard surgery and lymphadenectomy. They found no benefit in terms of overall or recurrence-free survival for pelvic lymphadenectomy and concluded pelvic lymphadenectomy cannot be recommended as routine treatment for patients with endometrial cancer. Still, many advocate the continued use of lymph node sampling and/or dissection at the time of surgery, and the specific operation undertaken will depend on the clinician's preference.

Even after definitive surgery, the risk of both locoregional and distant recurrence has for years prompted the use of adjuvant treatment with radiation therapy, chemotherapy, and hormonal therapy. Three multicenter randomized trials have been published documenting the efficacy of postoperative radiation therapy in terms of improved locoregional control [20–22]. In addition, data from one of the aforementioned studies, GOG 99, was used to help define a high-intermediate-risk group of patients – those who may benefit more from the use of adjuvant radiation therapy [22]. This group consisted of patients with outer third myometrial invasion, lymphovascular invasion, and moderately poorly differentiated tumor, patient's age 50 years or greater with two of the above risk factors, and patient's age 70 years or greater with one of the above risk factors. In this group of patients, radiation therapy decreased the risk of locoregional recurrence from 26 % to 6 % (as opposed to 6–2 % for low-intermediate-risk patients).

Historically, treatment plans in radiation therapy for endometrial cancer (both EBRT and brachytherapy) have been calculated utilizing two-dimensional (2D) x-ray images. In EBRT, fields were drawn on simulator radiographs utilizing bony anatomy as surrogates for the location of target structures, organs at risk (OAR), and lymph nodes. For brachytherapy doses have been prescribed depending on the applicator used. Examples include prescribing to a distance of 0.5 cm from the surface of a vaginal cylinder along the area of interest or prescribing to Point A using tandem and ovoids. Details of these methods are described elsewhere [23].

Vulva Cancer

Historically, radical vulvectomy was performed with excellent LC rates. However, radical surgery was associated with excessive morbidity and unacceptable mortality [24]. Modern therapy has shifted from radical surgery for all patients irrespective of stage of disease toward an individualized approach. For early-stage disease, wide local excision with surgical margins >8 mm in the postoperative fixed specimen is appropriate when the primary lesion measures less than 2 cm in maximum diameter and the depth of invasion is less than 1 mm (International Federation of Gynecologists and Obstetricians Stage 1A disease), as the risk of groin lymph node metastases is extremely small (<1 %) in these

patients [25]. In patients with more extensive local disease, groin lymph node dissection is carried out in conjunction with wide local excision of the vulva. Primary tumors involving the clitoris, labia minora, perineum, or Bartholin's gland, (>Stage 1b) require bilateral groin lymphadenectomy. Radical vulvectomy and bilateral groin lymphadenectomy may be required for locally advanced disease or extensive disease [26]. Neoadjuvant cisplatin-based chemotherapy with or without radiotherapy can be utilized to shrink the tumor sufficiently to render an otherwise inoperable tumor operable or as a second-line therapy [27, 28]. In a phase II GOG trial, 73 patients with stage III/IV vulvar cancer deemed unresectable without an exenterative procedure were given neoadjuvant concurrent chemoradiotherapy. Surgery was later possible in 69 patients [29].

Postoperative radiotherapy has been found to improve survival in patients with vulvar cancer [30]. The patients who have been shown to benefit from adjuvant radiotherapy are those with involved margins, with two or more malignant lymph nodes, or with complete replacement of nodal tissue with malignant cells and/or evidence of extracapsular spread for any single node [31]. Treatment is usually to both the groin and the pelvic nodes. Adjuvant radiotherapy to malignant groin and pelvic nodes is associated with lower recurrence rates and improved 2-year survival rates compared with pelvic lymphadenectomy.

The Rationale for IGRT/IMRT

As the world of diagnostic imaging has evolved, so have radiation treatment techniques which now commonly utilize imaging modalities such as CT, MRI, and PET. The utilization of these techniques has led to improved target delineation and localization, a more realistic assessment of dose to critical structures (and hopefully decreased side effects as a result), and the ability to increase tumor dose in a way not possible before.

Treatment of gynecologic malignancies often involves large pelvic fields to encompass the gross disease and subclinical extension. Generous margins are employed to account for potential setup errors and organ motion on a daily basis while avoiding excessive dose to adjacent normal critical tissues such as bowels, bladder, and femoral heads. Inaccurate setup, organ motion, and tumor regression can lead to potential underdosing the tumor and overdosing the normal tissues. The rationale for the use of IGRT/IMRT in gynecologic malignancies includes three-dimensional (3D) assessment of tumor extent and surrounding organs, compensation for organ motion, adaptation to rapid tumor shrinkage and potential dose escalation. Image-guided therapy, for example, on-board cone-beam CT (CBCT), could assess the patient's treatment delivery in 3D in near real time and improve daily setup [32]. Thus, it reduces volume of small bowel, bladder, and rectum irradiated that can lead to lower toxicities. Since most patients with cervical cancer also receive systemic chemotherapy, with proper treatment planning, IGRT/IMRT can potentially reduce the volume of pelvic bone marrow irradiated. Therefore, lower hematologic sequelae may be expected. Conventionally, to overcome internal organ motion issues, particularly in patients with an intact uterus and large tumor, generous clinical target volume-planning target volume (CTV-PTV) margins are used. IGRT/IMRT can reduce these margins, improving sparing of normal tissues [33]. Many gynecologic tumors, especially bulky tumors, may change in volume and shape during the course of therapy, and treatment plan needs to adapt to these changes to spare more normal tissues. Dynamic adaptive radiation therapy has addressed these changes. In a study of 14 patients undergoing IMRT for cervical cancer, replanning after 30-Gy tumor dose demonstrated 46 % reduction of gross tumor volume (GTV) and improved sparing of the rectum and overall bowel volume [34]. Thus, IGRT/IMRT may eliminate some of the conventional limitations and improve target delineation and dose delivery, allowing safe margin reduction, opening the way for potential dose escalation, or as an alternative boost technique for patients who are not amenable to brachytherapy because of anesthesia risks or other medical comorbidities. Potentially, it can

improve tumor control while reducing normal tissue toxicity, as LC still remains a major clinical problem in patients with locally advanced cervical carcinoma [35].

Imaging

Oncologic imaging plays a crucial role in screening, diagnosis, staging, treatment planning, and posttreatment surveillance. As diagnostic imaging has advanced, so have treatment techniques in gynecologic cancer, which now commonly utilize imaging modalities such as CT, MRI, and PET. The utilization of these techniques has led to improved target delineation and localization, a more realistic assessment of dose to critical structures (and hopefully decreased side effects as a result), and the ability to increase tumor dose in a way not possible before.

Currently, CT and MRI are the most commonly used imaging methods in gynecologic IGRT/IMRT as they are widely available and reasonably affordable. They offer 3D assessment of anatomical, structural, and physical tumor extension. MR-CT registration (fusion) can create color wash overlay of anatomy correlation and help identify tumors and nodes for targeting and normal tissues for sparing during treatment planning (Fig. 56.1). However, the identification criteria of metastatic lymph nodes are based on size, where >1-cm short-axis diameter being the most commonly accepted criterion for pathologic involvement [36]. Normal-sized pathologic and reactive enlarged lymph nodes cannot be reliably identified leading to false negatives and positives, respectively [37]. The combination of PET with CT, which is approved by the Centers for Medicare and Medicaid Services for cervical cancer staging and management as an adjunct to conventional imaging, has further added metabolic information to anatomical images. Malignant tumors and pathologically involved lymph nodes tend to manifest themselves with high ^{18}Fluorodeoxyglucose (FDG) uptake on PET.

Since nodal involvement is a strong predictor for survival, accurate assessment of nodal status is crucial. PET-CT provides higher diagnostic accuracy and is being increasingly preferred over CT scanning alone [38]. Abnormal lymph nodes are also better detected by PET-CT than CT alone (Fig. 56.2). The node-based accuracy of integrated PET-CT is reportedly high (>99 %) for tumor involvement in patients with invasive cervical cancer [39]. The positive predictive value of PET-CT in the pelvis and para-aortic region appears to be 75–94 % [40]. In a retrospective study of 101 patients with cervical cancer who underwent CT and PET, Grigsby and associates found positive pelvic nodes as detected by PET in 67 % of the patients vs. 20 % detected by CT. Abnormal para-aortic nodes were 21 % detected by PET versus 7 % detected by CT. The 2-year disease progression-free survival was 64 % for those with negative CT and PET

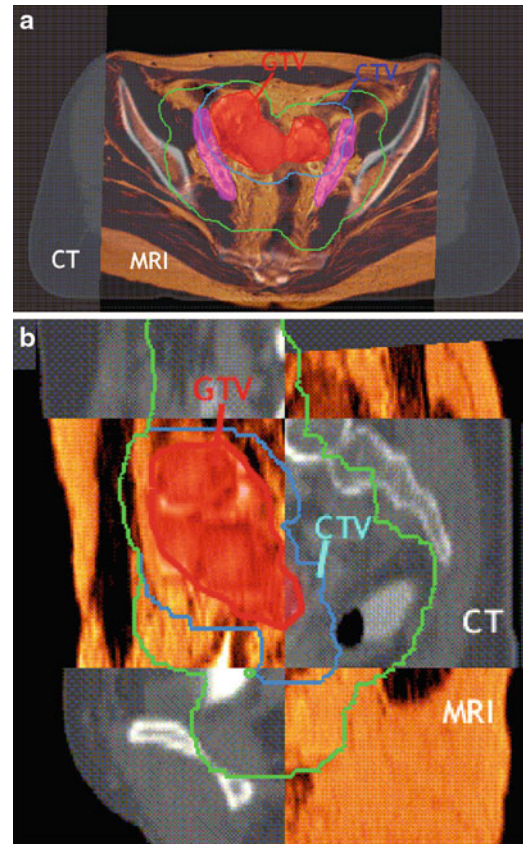

Fig. 56.1 A 27-year-old female with a large squamous cell carcinoma of the cervical stump. MR-CT fusion helps identify and delineate the gross disease. Axial view (**a**) and Sagittal view (**b**)

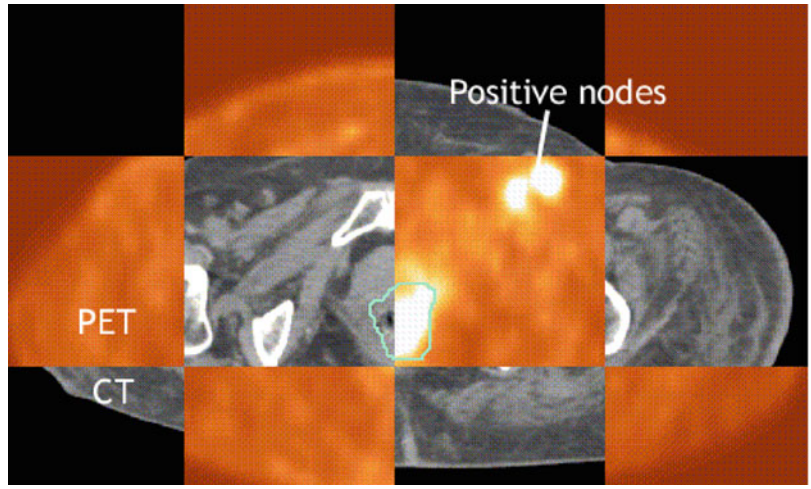

Fig. 56.2 PET-CT detection of nodal metastasis

compared with 18 % for those with positive PET only and 14 % for those with positive CT and PET [41, 42]. Therefore, noninvasive PET-CT imaging can detect pathological nodes accurately and may obviate the need for surgical intervention in patients with advanced cervical cancer.

For endometrial cancer, preoperative imaging of 30 patients with endometrial cancer compared with postoperative pathologic findings showed a higher sensitivity (96.7 %) of FDG-PET for identification of primary endometrial cancer compared to that (83.3 %) of CT or MRI. The sensitivity of FDG-PET for detection of extrauterine lesions was also superior to that of CT or MRI [43]. In a recently reported series of 34 patients, positive and negative predictive values of FDG-PET imaging in the post-therapy surveillance of endometrial carcinomas were 78 % and 90 %, respectively [44]. Thus, FDG-PET was reasonably accurate in detecting early recurrence and evaluating therapeutic response. FDG-PET also appeared to have a possibility to predict the outcome of these patients [45].

The role of PET-CT in evaluating patients with gynecologic cancer recurrence is emerging. Recent reports suggest that PET-CT is a useful tool not only for defining initial tumor extent and regional involvement but for posttreatment detection of distant disease in patients with recurrence [46]. In patients with a suspicion of recurrence of cervical cancer, PET-CT may have a significant impact on treatment planning and predict disease-free survival [47]. Serum tumor markers such as squamous cell carcinoma antigen (SCC-Ag) and CEA have been used in combination with CT and MRI for post-therapy surveillance with promising results [48].

Among the metabolic tracers used in cancer imaging, FDG is the most commonly used radiotracer metabolite in the management of cervical cancer patients. The local tumor extension is more precisely assessed with the metabolic tumor activity. Parametrial and endometrial involvements are more frequently identified beyond anatomical boundary. Regional pelvic nodal involvement and extrapelvic disease may be detected even if the CT and MRI are normal. Such findings will alter the course of patient management. Furthermore, follow-up of persistent or identification of early recurrence can play a crucial role in the patient's prognosis and survival [49]. Figure 56.3 illustrates early asymptomatic local recurrence detected by PET-CT.

Both MR spectroscopy and single-photon emission computed tomography (SPECT) can be used to map bone marrow. They can be a useful tool for identifying "red" marrow. However, they are not widely available or employed. Clinical data are slowly emerging. Although other modalities are less commonly used, they may also help better define normal tissues including MR-PET,

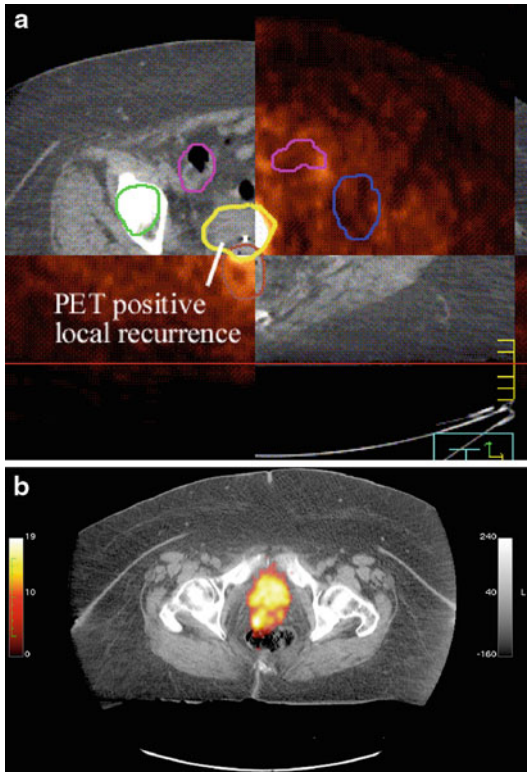

Fig. 56.3 Follow-up PET-CT shows early asymptomatic local recurrence

MR spectroscopy (MRS), Cu-ATSM PET, and nanoparticle MRI which may further improve the definition of tumor and target tissues [50].

External Beam Radiation Therapy

From Conventional 4-Field to IGRT/IMRT

Conventional adjuvant radiation treatments typically use 2D, 4-field plans (anteroposterior, posteroanterior, right lateral, and left lateral) based on visualized bony anatomy. Contrast may be used to define normal tissues such as bowels and bladder. A significant portion of small and large bowel is usually in the treatment fields and consequently acute GI toxicity such as diarrhea and nausea is common. In GOG 99, two women in the treatment arm died from intestinal complications thought to be radiation-related and six women experienced grade 3–4 obstruction (vs. 1 in the observation arm). In addition to toxicity concerns, pelvic lymphangiography shows great variability in lymph node location, and there is also evidence that the use of bony landmarks yields inadequate coverage of lymph nodes in a substantial proportion of patients [51]. In one study of 43 patients with cervical cancer, 95 % had inadequate (<1.5-cm vessel to block edge) nodal coverage, and 56 % had too generous coverage (>2.0 cm) with 2D based fields [52]. Because of this, and the availability of improved imaging and conformal dose delivery platforms, IGRT/IMRT is increasingly used in treatment of endometrial cancer and in pelvic malignancies in general.

The incorporation of IGRT/IMRT into clinical practice in place of classic conventional fields requires increased attention to and accounting for uncertainties in setup and motion of both targets and normal tissues. If not accounted for, tumor and normal tissue movement can significantly detract from the benefits of IMRT and potentially lead to geographic miss and increased toxicity. This highlights the potential benefit of using IGRT, in which imaging (either 2D or 3D) is used to accurately align the patient. In addition to accurately aligning the patient, IGRT can also monitor and account for motion during the course of treatment leading to a reduction in both systematic and random error (on-line correction strategy – described elsewhere in this chapter).

Lim et al. [53] examined the effect of internal anatomic changes during a course of radiotherapy for cervical cancer and explored its effect on dose delivered to tumor and OAR. The 20 women comprising this study underwent CT and MRI scans initially and then weekly MRI scans during the course of radiation therapy; contours were drawn on all obtained scans, and software with deformation capability was used for dose accumulation in the face of motion and disease regression. Three types of plan were computed and compared: conventional, large-margin IMRT (20-mm PTV except inferiorly which was 10 mm), and small-margin IMRT (5-mm PTV). While there was no difference between planned and delivered doses to GTV and primary disease

CTV (pCTV) for the conventional and large-margin IMRT plans, there was a significant reduction found in delivered dose to the GTV and pCTV for the small-margin IMRT plan, and in one patient, the pCTV was underdosed (4,656 cGy instead of planned 5,000 cGy). They concluded that the adequacy of primary tumor coverage using a 5-mm PTV (commonly used in institutions today) is contingent on the use of daily image-guided setup.

In reviewing patients with early-stage endometrial cancer treated with IMRT and those treated with whole pelvic RT followed by vaginal high-dose-rate intracavitary brachytherapy (HDR-ICBT) [54], the maximum rectal doses were lower with IMRT than those with HDR-ICBT (89 % vs. 143 %, $p < 0.05$). Mean rectal doses in IMRT were also lower than in HDR-ICBT (14.8 % vs. 21.4 %, $p < 0.05$). IMRT also resulted in lower maximum bladder doses (66.2 % vs. 74.1 %, $p < 0.05$). Plans provided comparable coverage to the PTV with IMRT plans resulting in less dose heterogeneity. However, clinical outcomes are only slowly emerging.

Nodal Management

The use of IGRT/IMRT requires detailed anatomic information regarding the location of the primary tumor, nearby normal tissues, and at-risk lymph nodes. Some guidelines for delineating lymph node target volumes in pelvic IMRT plans have been published. By using MRI images obtained with ultrasmall particles of iron oxide (USPIO), a contrast agent developed for assessment of lymph nodes, Taylor and associates [55] determined that the pelvic vessels expanded with a 7-mm margin (with small modifications described in the publication) would ensure 99 % anatomical coverage of the pelvic lymph nodes. In addition, the RTOG has published guidelines [56] for contouring in IMRT plans for cancers of various organ systems, including head and neck, gynecologic, male genitourinary, and anorectal. Figure 56.4 shows the RTOG contour atlas used for postoperative endometrial cancer. Table 56.1 shows commonly used dose constraints in IMRT treatment planning; these particular constraints are culled from a recent RTOG trial [56] investigating the addition of chemotherapy to radiation therapy in the adjuvant setting following hysterectomy for high-risk cervical cancer patients.

Results of patients treated with whole pelvic IMRT have been reported with encouraging results. An Austrian study [57] analyzed both cervical cancer patients treated with definitive radiation therapy and endometrial cancer patients treated postoperatively. They compared dose-volume histogram data on conventional 4-field and IMRT plans and also examined anatomical factors that could impact bowel sparing. There was a statistically significant improvement in the irradiated volume of rectal wall and bladder with IMRT over conventional plans; in addition, they found that an intact uterus had a displacing effect on large bowel, and as a result, the postoperative patients (i.e., endometrial cancer) might especially benefit from the use of IMRT in facilitating bowel sparing. Figure 56.5 is a dose-volume histogram comparing a conventional radiation plan using bony landmarks (solid lines) to an IMRT (dotted lines) plan. The prescribed dose was 4,600 cGy in 200-cGy fractions. The IMRT plan yielded improved doses to all delineated critical structures, including the rectum, bladder, sigmoid colon, and small intestine.

IMRT allows delivery of higher than conventional doses in patients with positive para-aortic nodes or positive margins after surgery while sparing normal bowels [58]. In ten patients with advanced cervical cancer undergoing extended-field (pelvic and para-aortic nodes) radiation therapy, IMRT, compared to 2- and 4-field techniques with comparable target coverage, demonstrated significantly lower volume of normal tissues (bowel, bladder, and rectum) receiving prescription dose [59].

IGRT/IMRT Patient Selection

Image-guided treatment planning and delivery has gained rapid acceptance steadily. Although most gynecologic patients can be potentially treated with IGRT/IMRT, patient selection is

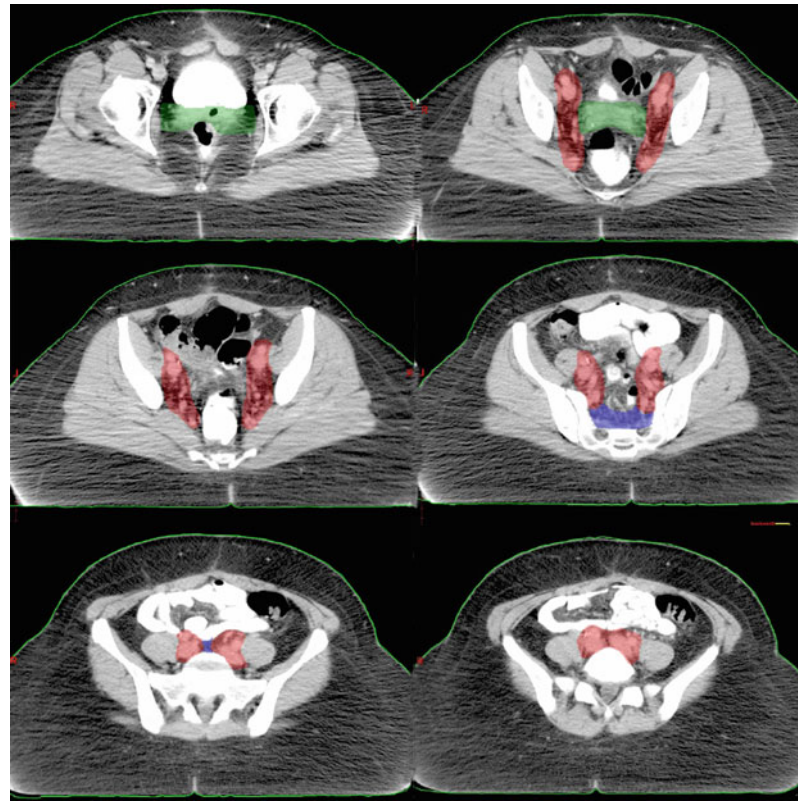

Fig. 56.4 The RTOG contour atlas guide for postoperative endometrial cancer. Color wash volumes represent CTVs. (Reprinted from [66], with permission from Elsevier. Also available at www.rtog.org)

Table 56.1 Treatment planning constraints used in whole pelvic radiotherapy for cervical cancer (RTOG Constraints)

Target or organ at risk	Volume and dose constraints
Planning target volume	97 % of volume covered by prescription dose
	≥0.03 cc cannot receive <93 % or >110 % of prescription dose
Bowel	30 % to receive ≤ 4,000 cGy
Rectum	60 % to receive ≤ 4,000 cGy
Bladder	35 % to receive ≤ 4,500 cGy
Kidneys	2/3 of each to receive ≤ 1,800 cGy
Spinal cord	4,500 cGy any point in volume

(Prescription dose is 4,500–5,040 cGy)

crucial for successful treatment planning and delivery. Patients who are uncooperative for various reasons and who cannot tolerate moderately longer time on the table for simulation and treatment delivery are not good candidates for IGRT/IMRT. Such patients likely miss treatment sessions, have more treatment interruptions, and cause more treatment delays. Very obese patients are generally not the ideal patients for IGRT/IMRT because of potential difficulties with daily setup due to body motion and with imaging to capture the entire external body contour. Moreover, potential dosimetric compromise in obese patients may offset the intended benefits. Patients with advanced or metastatic disease who require just a short course of palliative treatment or those who require urgent therapy because of uncontrolled bleeding are not good candidates for IGRT/IMRT. On the other hand, most patients who were previously irradiated may be better candidates for IGRT/IMRT because more normal tissues can be spared (Fig. 56.6). For those patients who cannot tolerate brachytherapy because of comorbidities or anesthesia risks, using IGRT/IMRT as a last resort to deliver a curative dose of radiation to the target volume may be feasible [60].

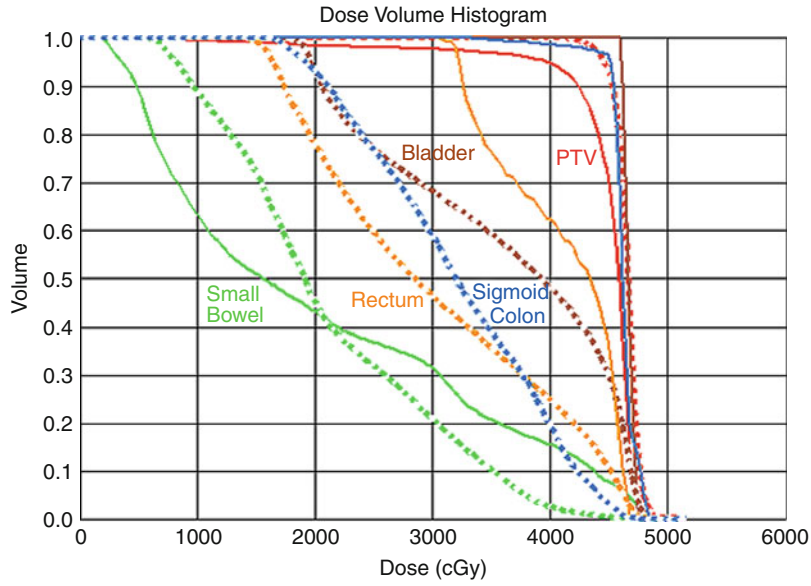

Fig. 56.5 Dose-volume histogram comparing a conventional pelvic radiation plan using bony landmarks (*solid lines*) to an IMRT plan (*dotted lines*). IMRT plan improves coverage of PTV while better sparing of organs at risk

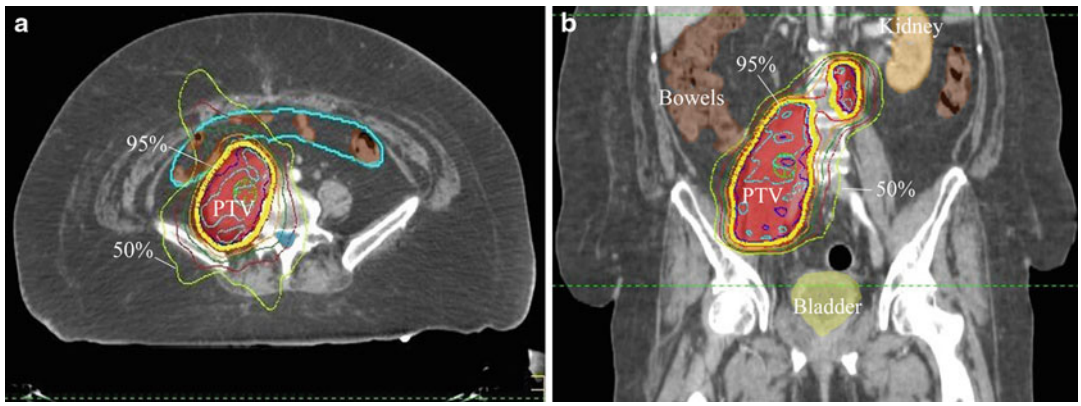

Fig. 56.6 Treatment of recurrent cervical cancer with a pelvic mass. IGRT/IMRT allows sparing of remaining kidney and previously irradiated pelvic tissues, axial (**a**) and coronal (**b**) views

IGRT/IMRT Treatment Simulation

IGRT/IMRT planning begins with a CT or PET-CT simulation. Although some institutions prefer simulating the patient in prone position for potential dosimetric advantages [61], we generally favor the supine treatment position for better patient comfort, stability, and reproducibility, especially if the patient requires inguinal treatment. Proper immobilization of upper and lower body during simulation and treatment delivery is paramount in IGRT. We commonly immobilize patients with customized thermoplastic molds, Alpha Cradles (Smithers Medical Products, Inc., North Canton, OH), VacLoc bags (Med Tec Inc., Orange City, IA), or BodyFix systems (Medical Intelligence, Schwabmuenchen, Germany) to maximize repositioning accuracy and patient stability. These are indexed to the treatment table for reference during simulation and treatment delivery. Figure 56.7 illustrates a simulation setup with BodyFix system.

Planning CT scan is done with contrast to help delineate normal and target tissues. Rectal contrast outlines the rectal and sigmoid colon. IV (intravenous) contrast identifies the pelvic

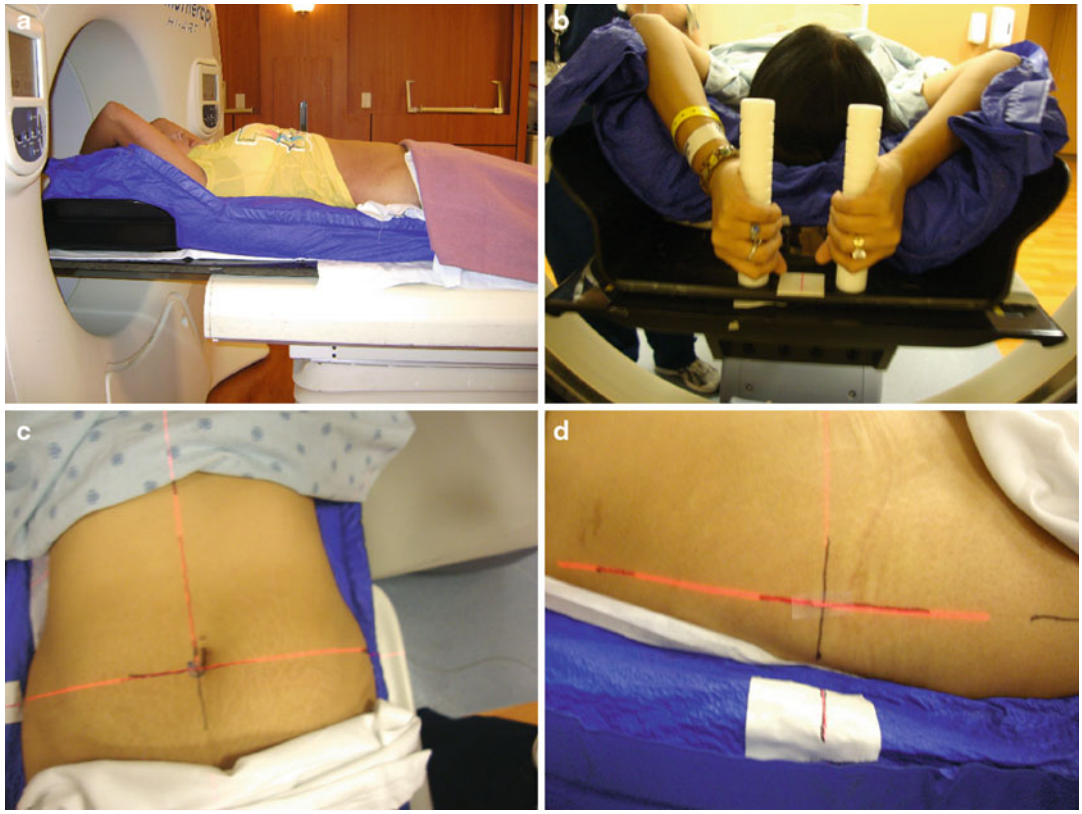

Fig. 56.7 Simulation setup with BodyFix system (**a**–**d**). It provides accurate and reproducible setups daily

vessels and lymphatics. Bladder is visualized by IV contrast with Foley catheter clamped after initial drainage to gravity. With experience, oral contrast, which fills the small bowel, is less needed. A vaginal marker is also placed during simulation to help delineate the lower extent of disease and during treatment delivery unless such maneuver is judged to be clinically traumatic causing bleeding or pain, especially in advanced cases. In those cases, the entire vagina is treated. The extent of scan is determined by disease status. Typically, we scan the abdomen from level L2–L3 vertebral body to 3–4 cm below the ischial tuberosities flashing the vulva. Higher levels, T10–T11, are used for extended field to cover the para-aortics, and a more generous lower border is used as clinically indicated for treating the inguinal nodes or advanced diseases. Slice thickness is commonly set for 3 mm for small field and 5 mm for extended fields.

IGRT/IMRT

Treatment Planning and Delivery

There are various commercially available IGRT/IMRT treatment planning and delivery systems. In our experience, we have not found any particular system standing out from others. We utilize Novalis Tx with ExacTrac and Rapid Arc systems and on-board CBCT/KV (kilovoltage CT) imaging capabilities, or TomoTherapy with MVCT (megavoltage CT) IGRT system. Figure 56.8 illustrates CBCT/KV and TomoTherapy IGRT images. Rapid Arc is a form of volumetric-modulated arc therapy that delivers a precisely sculpted 3D dose distribution with one or multiple rotations of the linear accelerator gantry. It is made possible by a treatment planning algorithm that simultaneously changes

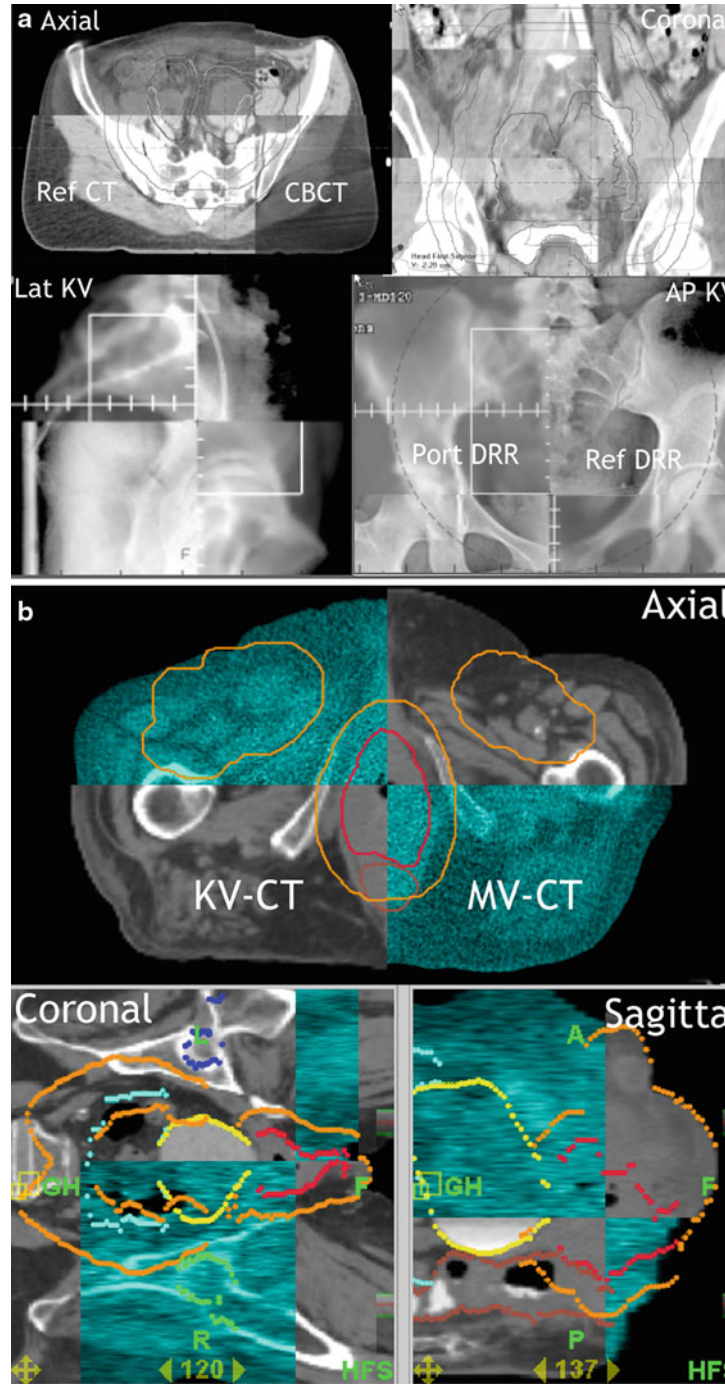

Fig. 56.8 CBCT/KV (**a**) and TomoTherapy (**b**) IGRT images for visual verification of treatment delivery

the rotation speed of the gantry, the shape of the treatment aperture using the movement of multi-leaf collimator, and the delivery dose rate during treatment. It delivers dose to the target volume during the rotation rather than beam by beam (stop and shoot) and substantially reduces treatment time. We normally use 6-MV photon energy since higher energy, like 15–18 MV,

shows no significant dosimetric advantages, having higher exit and integral total body doses. Helical therapy with the TomoTherapy treatment system can accommodate large extended fields. We typically deliver 45–50.4 Gy at 1.8-Gy daily fraction to the CTV in most patients. For those postoperative patients, we deliver 45 Gy plus 10 Gy in two fractions using vaginal brachytherapy. Infrequently, we consider higher fraction doses of more than 2 Gy by "dose painting" using simultaneous integrated boost (SIB) in patients with large tumors, grossly positive nodes, or positive surgical margins.

Defining the Target and Nontarget Volumes

The incorporation of PET-CT Imaging in treatment planning has improved target definition while sparing surrounding normal tissues [62]. While PET-CT can aid with tumor volume delineation, the delineation of target volumes should be done by an experienced physician and assisted by a radiologist when necessary. GTV may be visualized and defined on CT with contrast. Modest margins (1.5–2.0 cm) are generally used around the cervix and fundus. Further modifications of margins based on tumor extent are common and can be made based on PET images. Because of tumor inhomogeneity with nonuniformed FDG uptake, especially large tumors that have moderate necrotic and hypoxic tissues, there is no absolute standardized uptake value (SUV) or threshold SUV to define GTV. The GTV may be systematically defined using a predetermined threshold SUV based on experience. While others have suggested a threshold SUV of >2.5 for contouring GTVs dependent on the mean target SUV, some investigators have used a percentage of >40 % the maximum SUV. When the PET volume does not coincide with the CT volume, both volumes may be contoured as the target if clinically indicated.

In post-hysterectomy setting, without cervical or uterine organ motion, only a clinical target volume (CTV) is delineated. Depending on the pathologic findings, the CTV consists of the contrast-enhanced vessels plus a 0.7-cm margin for noninvolved nodes and up to 1.5 cm for involved nodes by encompassing surrounding fat and connective tissues. Starting at L5, the CTV nodal groups include the common, external, and internal nodal regions, at least the upper half of the vagina (length depending on stage and involvement), parametrial tissues, presacral nodes, and entire uterus if present. The CTV includes approximately 0.5–1.0 cm of bladder and rectum adjacent to GTV. If different doses are planned, CTV can be contoured as separate structures (CTVnodes, CTVtumor bed, or CTV1, CTV2). One should avoid following external iliacs into the groins except when they are at risk or involved. This also applies to patients with endometrial cancer involving the cervix; the presacral nodal coverage can be excluded if there is no tumor extension to the cervix. At the level of the vaginal cuff, more generous margins should be employed.

A PTV may be added to the CTV based on setup uncertainty, internal organ motion, and differential filling status of the bladder and rectum [63]. The amount of expansion of CTV to PTV remains subjective. Expansion of CTV by 0.5–1.5 cm has been used to form PTV. As setup uncertainty varies from institution to institution, independent institutional study of their setup uncertainty is recommended to determine the appropriate PTV expansion. Such expansion is done in 3D, and therefore, the margins are not always equal on each axial slice as portions of the expansion are not necessarily on same axial plane. At the University of Texas Health Science Center in San Antonio (UTHSCSA), we commonly use a 1-cm expansion with customization based on adjacent critical organs. Modifications of GTV/CTV/PTV are also made by replanning when large tumors regress during radiation treatment, so that less normal tissue is treated.

Depending on the clinical circumstances, normal organ delineation includes small bowel, rectum, and bladder. Since there is variable filling of bowel and bladder and the cervix and vagina are mobile, integrated target volume (ITV) may be

used to incorporate internal motion into consideration utilizing 4D-CT data [64]. Other structures that may be informative include the femoral heads, kidneys, spinal cord, and liver if extended fields are used. Organs should be contoured by the outer wall to the extent of the visible anatomy. Although anatomical variability occurs, the rectum extends from anus to the sigmoid flexure, whereas colon above the sigmoid flexure at L4–L5 interspace is included in the small bowel volume. The bowel contour commonly dips posteriorly into the concave CTV to improve dose conformity and reduce small bowel dose [65].

A Guidelines Consensus Working Group and RTOG Consensus Conference have proposed guidelines for delineation of CTV in cervical and uterine cancer patients treated with IMRT used by RTOG trials, including the recently closed RTOG 0418, which is a phase II study of intensity-modulated radiation therapy (IMRT) to the pelvis +/− chemotherapy for postoperative patients with either endometrial or cervical carcinoma [66, 67]. The freely accessible atlas is also available on the RTOG website [56].

Organ Motion-Integrated Target Volume

An ITV takes internal motion into account. Two planning CT scans are done, one with full and the other with empty bladder. The target volume is drawn on both full and empty bladder scans. The target volume should encompass the cuff and parametria on both scans. Scans are then fused together to generate the ITV. ITV may be expanded by 0.5 cm to form PTV [65]. Vaginal cuff motion can be compensated by vaginal immobilization, or on-board CBCT. Reasonably generous CTV expansion of 1–1.5 cm to form PTV around the vaginal cuff should be considered as we have observed variations of tumor motion up to 1.5 cm from bony landmarks in postoperative patients. Individualized smaller margins may be considered if higher than conventional doses are used with IGRT. Nonetheless, tighter volumes could result in less toxicity.

In patients with unfavorable anatomy for brachytherapy, an "applicator-guided" IMRT approach has been utilized [68]. A PET/MRI compatible vaginal cylinder-type applicator is inserted into the cervix and vagina to localize the cervix and to position the bladder and rectum on a daily basis during treatment. It spatially registers the tumor and internal organs for planning and treatment. IMRT can cover the target volume while reducing the dose to the bladder and rectum. Potentially it may provide better target coverage compared to HDR brachytherapy in selected patient.

Bone Marrow

In patients receiving concomitant or sequential systemic chemotherapy, sparing of bone marrow (BM) may be considered and has been advocated by some investigators to incorporate BM volume into the treatment planning process [69, 70]. Within the conventional pelvic field, the bone marrow represents approximately 30–40 % of the total body BM reserve. Increasing the dose conformity with IMRT while sparing the contoured intramedullary canal of the iliac crests and sacrum can potentially reduce the volume of the pelvic bone marrow irradiated. Functional BM imaging may further help identify areas of active BM to be contoured and spared. By reducing the pelvic BM in the target volume, the patients receiving concurrent chemotherapy with pelvic radiation therapy may tolerate the treatment better with less hematologic toxicities. BM-sparing techniques have recently been shown to reduce hematologic toxicity in cervical cancer patients undergoing concurrent IMRT and chemotherapy. In a study of 37 cervical cancer patients treated with pelvic IMRT and CDDP, the major predictors of acute hematologic toxicity included total pelvic BM irradiated and lumbar sacral spine BM volume (V10 and V-20) [71]. There were less acute hematologic toxicities in those who were treated with pelvic IMRT. While we are aware and mindful of the volume of bone marrow within the target volume during

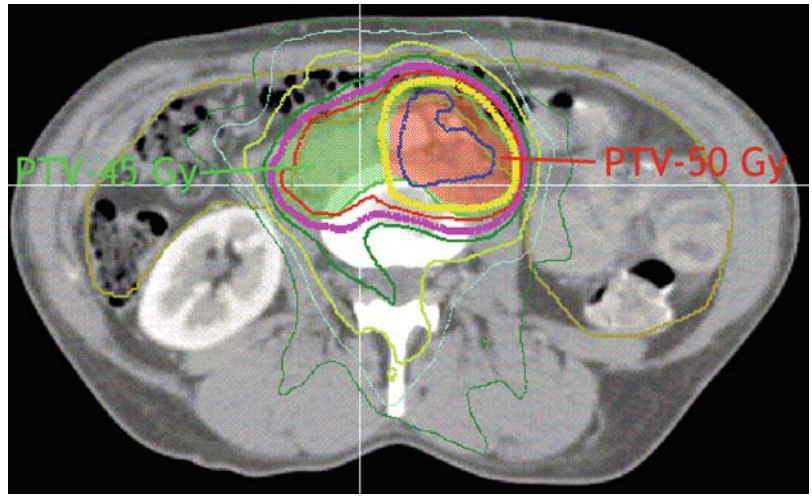

Fig. 56.9 Example of a SIB plan showing two dose levels to different targets while sparing the remaining kidney

treatment planning and evaluation, technically, such BM sparing is challenging because of the proximity of the target volume to the pelvic BM which is exquisitely radiosensitive. BM sparing requires additional time and efforts. The clinical impact of daily IGRT/IMRT on bone marrow sparing in cervical cancer patients is inconclusive [72]. As such, we normally do not delineate bone marrow.

Dose Painting

With appropriate software, one can "dose paint" or "dose sculpt" various organs or tissues at risk so that different doses are simultaneously delivered based on tumor burden. This is referred to as SIB [73]. Such method is commonly employed in the management of patients with head and neck or prostate cancer treated with IMRT [2–6]. SIB approach can potentially improve bowel and bladder sparing while the overall treatment time is shortened to 5 weeks. For CT-PET-negative nodes, 4,500 cGy should be adequate, especially with concurrent chemotherapy. The CT-PET-detected positive nodes can be treated to 50 Gy or higher for larger nodes with SIB, depending on its size and location [58, 74]. One approach is to deliver 45 Gy in 1.8-Gy fractions for 25 daily fractions to the pelvic lymphatics while the positive nodes and gross cervical mass receive up to 70 Gy in 2.8 Gy per daily fraction [75]. Figure 56.9 illustrates a SIB plan with different dose levels to various targets. Radiobiologically, such regimen is equivalent to 45-Gy whole pelvis and 30-Gy HDR-ICBT in five fractions conventionally. Ahmed et al. [74] have demonstrated the dosimetric feasibility of hypofractionated SIB to involved para-aortic nodes in patients with cervical cancers. Although there are no specific guidelines in fraction size and total dose for the SIB technique in patients with cervical cancer, patients with involved nodes can be treated with 45 Gy to the pelvis, while involved nodes receive 56 Gy or higher dose simultaneously [76].

IGRT/IMRT Treatment Plan and Evaluation

As no consensus guidelines exist for the planning and delivery of IGRT/IMRT for gynecologic malignancies, various institutional planning parameters have been used by many investigators [70–76]. The Gynecologic IMRT Working Group was formed to develop standards [66, 67]. Currently, there is no consensus on plan evaluation and acceptability. The beam energy, arrangement, number, and angles are optimized to meet the input parameters. Typically, 6-MV photons and six to nine equally spaced beams at various angles are used [77]. The optimal balance of covering the PTV and sparing the normal tissues is not known and is

subject to individual experience and interpretations. Increasing conformity will lead to decreasing homogeneity. We strive to minimize the volume of normal tissue receiving more than the prescription dose. Frequently, more than one plan per patient are evaluated, slice by slice, for conformality of the target volume and homogeneity of the target dose. The sizes of the hot and cold spots and their locations are reviewed. At UTHSCSA, we assess the dose-volume histograms (DVH) of surrounding normal tissue and PTV/CTV coverage to ensure doses are within organ tolerances and target volume coverage is adequate. The prescribed dose (100 % isodose line) should cover >96–98 % of the PTV, while "hot spots" of >110 % of prescription dose should be <5–10 % of the PTV, preferably located within the GTV and not along the mucosal wall of bladder and rectum. Hot spots of >115 % should be less than 2–3 % of PTV. Cold spots (<95 % of the prescribed dose) should not be located within the GTV or CTV.

Evaluation of normal tissue complications may be estimated based on the normal tissue complication probability (NTCP) curve [78]. To minimize the incidence of acute gastrointestinal toxicity, for example, the small bowel constraint should be less than 200 cc of the small bowel receiving 45 Gy. Some institutions also define bone marrow constraints for patients receiving concomitant chemotherapy. As CT does not define active bone marrow well, SPECT may be used to define active bone marrow, and it can be fused with the planning CT or projected on to the digitally reconstructed radiograph (DRR) so that it can overlay the images [77].

Various organ-dose constraints have been used and consensus has not been established. In general, tighter constraints for maximal conformality and sparing, while they can be met, do not necessarily result in the maximal sparing of the OAR. The benefits of IGRT/IMRT can be compromised in trading off dose homogeneity with more heterogeneity in the target volume. Table 56.2 shows the typical volume parameters used at UTHSCSA.

Table 56.2 Volume parameters used at the University of Texas Health Science Center in San Antonio

Volume	Expansion	Comments
GTV_{cervix}	As drawn	Gross disease on PET-CT, MRI, and clinical disease on exam
CTV_{cervix}	GTV_{cervix} + subclinical disease	Cervix, uterus, upper half vagina, paravaginal and parametrial tissues, and presacral region
GTV_{node}	As drawn	Involved nodes based on PET-CT, MRI
CTV_{node}	GTV_{node} + vessels + 0.7–1.5 cm	Internal, external, and common iliac vessels
		Para-aortics/IVC if high-stage disease
		Larger margin for involved nodes
PTV	CTV + 0.5–1.0 cm	Institution-based setup uncertainty (0.5–1.5 cm)
Bladder	0–0.5 cm	Neutral filling (average volume)
Rectum	0–0.5 cm	Variable due to rectal gas
Colon	0–0.5 cm	Variable due to gas and colonic motility
Small bowel	0–0.5 cm	Variable due to intestinal motility
Kidney	0.5 cm	Most radiosensitive organ
Spinal cord	0.5 cm	Most critical organ

IGRT/IMRT Treatment Delivery and Quality Assurance

On-board electronic portal imaging devices (EPID) are commonly used to monitor patient setup before treatment delivery. This gives a planar projection view of the patient's bony anatomy. Based on bony landmarks, on-line setup corrections can be made [79]. Radiopaque tantalum fiducials can be implanted on cervix and help track cervical movement. However, many such markers tend to be lost before completing the course of radiation treatment [80]. Commercial real-time tumor tracking system (e.g., CyberKnife) with separate diagnostic x-ray imagers can track an implanted tumor marker continuously during treatment. The treatment beam is triggered on only if the tracking marker

is within a set tolerance. Using real-time tumor tracking, the necessary CTV-PTV margin can potentially be reduced to less than 10 mm [81]. OBI system with a mounted kV source can generate high-quality planar images (e.g., Elekta Synergy and Varian OBI) while delivering much less dose than an EPID system. Volumetric-based IGRT uses the treatment MV beam (e.g., TomoTherapy) or KV cone-beam CT (e.g., Novalis CBCT) to generate a 3D view by reconstructing multiple planar images to monitor target coverage both on-line or off-line. Such images are overlaid with the planning CT images for setup adjustment prior to treatment daily (Fig. 56.8).

All major delivery systems have been used successfully, and there is no clear best delivery approach. At UTHSCSA, Varian Novalis and TomoTherapy are the main IGRT/IMRT delivery systems. Depending on the patient's setup and clinical factors, treatment and setup accuracy is verified daily with volumetric imaging (MVCT or KVCT) or with CBCT on the first day followed by KV films on other days. When field sizes exceed MLC travel limits, fields must be split into two or more carriage movements [73, 82]. Independent monitor unit verification calculation (MUVC) is done by comparing the doses calculated by planning system with that by an independent dose calculation software (MU Check or RadCal). The acceptable mean disparity at a point is less than 5 %. In addition to a point dose calculation, a measurement is performed for all IGRT/IMRT patients using a 2D detector, such as film, a diode array, or an ion chamber array (e.g., Matrixx and PTW 729). A gamma analysis (3 % and 3 mm) is performed between the measurement in phantom and the planned dose, which typically results in more than 95 % passing rate for all the pixels analyzed [83, 84].

Tumor Shrinkage (Adaptive IGRT)

Many bulky cervical tumors shrink rapidly during radiation therapy (especially with concomitant chemotherapy). Even tight margins early on can be too generous by the later treatments. Daily IGRT imaging (like CBCT) may allow plans to be adapted as tumors shrink with treatments. Normal tissues, like small bowels, bladder, and rectum are better spared while coverage of the tumor is preserved and organ motion is compensated accordingly. While target shrinkage increases margins and may reduce the chance of a geographic miss, it changes the conformity of the original plan and treating more normal tissue. The rate of shrinkage in cervical cancers is variable. A periodic exam is often necessary to assess tumor response, especially bulky tumors. Proper replanning improves bowel and bladder sparing. It is often seen in women with bulky (>30 cc) tumors. Daily imaging allows us to determine whether replanning is necessary and at what doses. Lee et al. [64] reported a mean of 50 % tumor reduction by physical exam after 30.8 Gy. FDG-PET imaging has been used to assess physiologic volume response during radiotherapy in cervix cancer. In a prospective study of 32 patients with cervical cancer undergoing EBRT to the pelvis and HDR brachytherapy, a 50 % physiologic tumor volume reduction occurs within 20 days of therapy after 24.9 Gy [85]. Likewise, investigators at MD Anderson reported a mean reduction of 64 % using weekly CT measurements. Others have used MRI to monitor tumor regression and noted an average of 46 % GTV reduction, and re-optimizing the treatment plan at 30 Gy improved the sparing of the rectum. The average rectal volume receiving $\geq$95 % of the prescription dose was 75 cc (range, 20–145 cc) with no replanning and was 67 cc (range, 15–106 cc) after replanning ($P = 0.009$) [34, 86, 87]. However, the cost benefits of adaptive IGRT have not been adequately addressed at present time. The potential beneficial differences between the new plan and the old plan could be very small, while the task of target and normal tissue delineation, timing, and replanning is labor intensive and time consuming. More rapid and better quality of OBI is needed. The use of adaptive IGRT, therefore, should be individualized based on the institutional capabilities and resources available.

Definitive Radiation

A small number of patients (3–10 %) diagnosed with endometrial cancer present with severe medical comorbidities for which they are deemed inoperable; this is often due to morbid obesity or cardiovascular disease. For these patients, radiation therapy has been utilized as definitive management with good results, often employing either brachytherapy alone or a combination of EBRT and brachytherapy. Incorporation of multiple imaging modalities is critical; the American Brachytherapy Society recommends determining uterine wall thickness using CT, MRI, or US, with MRI offering information regarding the depth of myometrial or cervical invasion [23]. The target volume would ideally include the entire uterus, cervix, and upper 3–5 cm of the vagina. Dose specification for endometrial brachytherapy varies widely, as do the applicators used, which can include double or triple tandems (with or without ovoids depending on degree of lower uterine segment or cervical involvement) and Simon-Heyman capsules. Clinical outcomes of patients with endometrial cancer treated nonsurgically have generally been good, with rates of disease-free survival up to 85 % [88, 89], though this depends on several prognostic factors including stage, grade, age, and histologic cell type.

A comparison of 2D and 3D treatment planning using Rotte "Y" applicator (double tandem) in the primary management of inoperable endometrial cancer has been reported [90]. In this study, the 2D calculation was performed using a uterine point (2 cm below the center of a line drawn between the tips of the two ends of the Rotte applicator extending laterally from the tandem by half the maximum uterine width), point A, and 0.5-cm depth along the upper 3 cm of the vagina. Doses used were 7 Gy × 5 fractions if using brachytherapy alone or 4 Gy × 5 fractions if following EBRT. They found that doses to critical organs were reduced with 3D optimization with the following percent decreases in dose: 5.6 % for rectum, 20.6 % for bladder, and 26.8 % for sigmoid. In addition, use of 2D prescription points was found to overestimate dose to the target volumes. With additional information such as MRI and US, it may be possible to delineate a GTV in addition to a CTV and thereby increase dose to gross disease while decreasing dose to adjacent critical structures.

Another method for administering high dose to the intact uterus involves the use of Heyman capsules, in which multiple applicators are inserted into a distended uterus in an attempt to provide a uniform dose distribution. Patients have been treated with this technique since the 1930s, when Heyman first introduced the procedure using radium. As with other brachytherapy techniques, the use of 3D imaging has also revolutionized how this treatment is administered, and 3D dosimetric analysis and clinical outcomes have been published using a modified Heyman technique in 16 patients (three of whom received EBRT as well) [91]. On average, 68 % of the CTV (which was by definition the entire uterus and proximal vagina) and 92 % of the GTV (delineated by MRI, US, or hysteroscopy) were encompassed by the 60-Gy reference volume, which was the isoeffective target dose. Out of 13 patients completing treatment with curative intent, 12 had LC at a median follow-up of 47 months, and severe acute and late side effects did not occur.

Indications for the use of EBRT to the pelvis in addition to brachytherapy can include cervical involvement, high-grade disease, deep invasion (e.g., seen by MRI), or even a large uterine volume. As one would expect, the same advantages and techniques for IMRT in treating pelvic lymph nodes mentioned above in the section on adjuvant radiation therapy apply in the definitive setting as well.

In medically or technically inoperable vulvar cancer patients, primary EBRT, followed by interstitial brachytherapy, surface mold or electron boost with or without chemotherapy has been used with acceptable levels of late tissue damage [92]. Complete response rates range from 53 % to 89 % and disease-free survival rates of 47–84 % after a median 37 months' follow-up [93].

Detection and Management of Disease Recurrence

The optimal surveillance program for endometrial cancer following definitive management is unclear. Recurrences occur both locoregionally and at distant sites and are often asymptomatic highlighting the importance of effective surveillance. The National Comprehensive Cancer Network (NCCN) recommends clinical visits and vaginal cytology at varying intervals depending on elapsed time since treatment [94]. Others have proposed that routine vaginal cytology benefits less than 1 % of patients and should therefore be avoided due to cost [95]. The utility of CT in the posttreatment period is similarly unclear. While its usefulness in identifying sites of recurrence in both symptomatic and asymptomatic women has been reported [96], others have described low detection rates in asymptomatic women (~4 %) and no survival advantage in women with subclinical disease recurrence detected by CT scan [97].

More recently, metabolic imaging such as PET and PET-CT has been incorporated into posttreatment surveillance of endometrial cancer with promising results. A Korean study [98] reported on the use of PET and PET-CT in both symptomatic and asymptomatic women following definitive management for endometrial cancer and reported high sensitivity and specificity; in addition, the incorporation of PET data resulted in a change in clinical decisions on treatment in 21.9 % of women. Figure 56.3b shows an example of an asymptomatic rectovaginal recurrence detected by PET-CT in our own patient population. Until there is level 1 evidence describing an advantage to one method of surveillance over another, clinicians must determine which patients they believe to be at highest risk of recurrence and order studies accordingly.

As mentioned above, recurrences of endometrial cancer occur both locally and at distant sites; advances in IGRT have changed the approach to management in both situations, enabling increasing doses of radiation to be administered with greater conformality in an attempt to yield improved outcomes. In early-stage patients treated initially with surgery alone, the majority of recurrences are isolated vaginal recurrences. LC rates for the patients with recurrent disease not previously treated with radiation have been very good, approaching >80 % for those with recurrences confined to the mucosa, though patients with more advanced lesions have fared poorer, likely due to the inability of brachytherapy to uniformly treat larger lesions [99–101].

SBRT involves the use of large doses per fraction (often ablative doses) administered to well-defined targets throughout the body. This technique necessitates the use of 3D imaging, often with CT and MRI, and very reproducible immobilization. Most experience with SBRT has been with tumors in the lung and liver, though it is being increasingly used in other sites as well, including the pancreas, kidney, and spine. A study from Germany [102] examined the use of SBRT for unfavorable local recurrences in 19 patients with cervical and endometrial cancer; in all of these patients, use of vaginal brachytherapy as sole boost modality was precluded by the tumor size. Patients were treated with whole pelvic radiotherapy to 50 Gy which was then followed by SBRT of three 5-Gy fractions prescribed to 65 % isodose line (median dose). Three of the patients also received vaginal brachytherapy. The LC at 3 years was 81 %, though systemic progression was the leading cause of death.

Isolated para-aortic lymph node (PALN) recurrences represent a small subgroup of uterine cervix and corpus recurrences; historically these patients have done very poorly. Grigsby et al. reported [103] on a group of 20 cervical cancer patients with isolated PALN recurrence, all of whom were treated with EBRT. All patients died within 2 years of recurrence, and the median survival for the group was 8.7 months. A more recent report [104] describing the use of chemotherapy and radiation for isolated para-aortic recurrence of cervical cancer is more encouraging, with a 5-year survival of 51.2 % in 14 patients who received salvage concurrent chemoradiation. Image guidance has enabled the escalation of dose to this area and outcomes are promising. A recent study [105] from Korea

reported on 30 patients with either uterine corpus or cervix cancers with isolated PALN recurrences treated with SBRT via CyberKnife. Gold fiducial markers were placed for tumor localization, and the doses used ranged from 33 to 45 Gy administered in three fractions. Four patients also received EBRT, and 25 patients received chemotherapy as a component of their treatment. The 4-year rates of LC and overall survival were 67.4 % and 50.1 %, and $\geq$ grade 3 late complications requiring hospitalization were reported in only only patient (ureteral stricture).

Brachytherapy

IGRT Brachytherapy

More advanced cervical cancers are usually managed nonsurgically, necessitating the escalation of dose beyond what can safely be given using EBRT. Because of the limitation imposed by adjacent critical structures, brachytherapy is used following EBRT in order to escalate dose while sparing the bladder, rectum, and sigmoid colon. This is accomplished with brachytherapy techniques. Brachytherapy, either intracavitary or interstitial, involves very high dose to tumor with very steep dose gradients; thus, it can spare adjacent critical tissue better and minimize complications. It is the most conformal treatment when applied properly and an integral part of radiation therapy for gynecologic malignancies. The complexity and variability of image-guided interstitial brachytherapy that often rely on the operator experience and skills are beyond the scope of this chapter. We will focus on intracavitary brachytherapy that is routinely used in gynecologic malignancies.

The most common method of prescription for intracavitary brachytherapy to this day is the Manchester System, which utilizes orthogonal radiographs and in which dose is prescribed to point A, defined as 2 cm above the distal end of the lowest source of the tandem and 2 cm lateral to the tandem bilaterally. Bladder and rectal points have been previously described by the International Commission of Radiological Units and Measurements (ICRU) [106] and are used to help facilitate the minimization of OAR toxicity; the bladder point is defined as the posterior surface of the Foley balloon on the lateral and center of balloon on AP film, and the rectal point is 5 mm behind posterior vaginal wall between ovoids at the inferior point of the last intrauterine tandem source. Ideally, one attempts to give the full prescription to point A on both sides and limit the bladder and rectal points to less than 70–80 % of the prescribed dose. This technique has been utilized for decades in low-dose-rate (LDR) treatment and more recently in HDR treatment, yielding good LC and acceptable toxicity. Figure 56.10 illustrates orthogonal radiographs used in intracavitary brachytherapy. Intravaginal balloons were used in addition to conventional packing to reduce bladder and rectum doses [107].

As many institutions have switched from LDR to HDR-ICBT, accurate tumor targeting and normal tissue sparing with image guidance are paramount to improve the therapeutic ratio. There is clinical evidence supporting that HDR-ICBT, which commonly utilizes 3D CT-image-guided treatment planning, offers better CTV coverage with lower late radiation side effects and complications than LDR-ICBT that utilizes 2D orthogonal x-ray-image-guided treatment planning [108, 109]. CT or MR imaging can detect unsuspected uterine perforation that can be missed with orthogonal x-rays. Figure 56.11 demonstrates an unsuspected posterior uterine perforation performed by an experienced gynecologic surgeon with over 40 years of practice. Intraoperative ultrasound-based IGRT has been utilized for cervical cancer, especially when technically difficult implants are encountered [110].

As is the case with EBRT, the incorporation of 3D imaging into treatment planning and delivery has the potential to revolutionize brachytherapy, enabling a more accurate assessment of the dose to critical structures and more conformal coverage of targets. This technique is sometimes called image-guided brachytherapy (IGBT) (Fig. 56.12). This can hopefully lead to improved locoregional control and decreased toxicity. Some studies [111] have suggested that point A dose is a poor

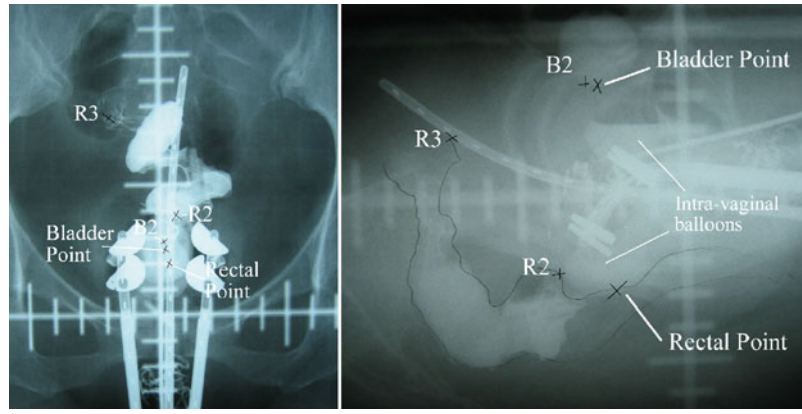

Fig. 56.10 Orthogonal radiographs used in intracavitary brachytherapy. Intravaginal balloons were used in addition to conventional packing to reduce bladder and rectum doses

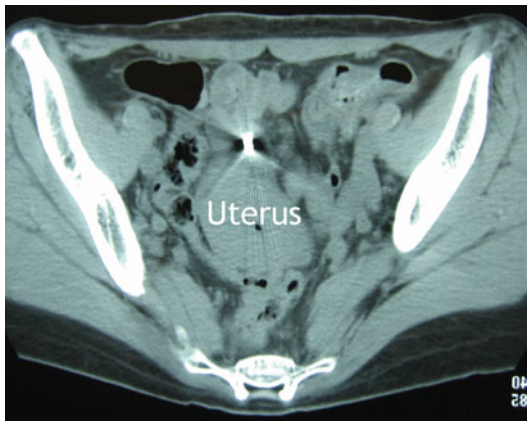

Fig. 56.11 An unsuspected anterior uterine perforation performed by an experienced gynecologic surgeon with over 40 years of experience

surrogate of target dosing. Three-dimensional volumetric dose parameters are slowly emerging but have not been well established and accepted so far. Guidelines and standards for GTV and CTV are yet to be defined [112]. The Groupe European de Curietherapie (GEC) and European Society for Therapeutic Radiology and Oncology (ESTRO) have published joint guidelines [113, 114] for the implementation of 3D volumetric planning using MRI imaging, as has the American Brachytherapy Society (ABS) Image-Guided Working Group [115]. For MRI planning, the ABS recommendations are the same as GEC-ESTRO; CT-based recommendations are also given.

In the 3D approach, contours are drawn on the CT or MRI images and include GTV, CTV, rectum, bladder, and sigmoid colon. When using MRI, the CTV can be further broken down into a high-risk CTV (CTV-HR) corresponding to residual gross disease and an intermediate-risk CTV (CTV-IR) corresponding to areas that initially had gross disease that has since resolved during the course of EBRT (Table 56.3). The volumetric parameter D_{2cc} (as well as D_{1cc}, $D_{0.1cc}$, and D_{5cc}) is a proven predictor for clinical and endoscopic changes and is calculated for the rectum, bladder, and sigmoid. It is defined as the minimum dose to the most exposed 2 cc (or 1 cc, 0.1 cc, 5 cc, etc.) of the OAR. Koom et al. [116] reported that $D_{0.1cc}$, D_{1cc}, D_{2cc}, and D_{5cc} all predicted for radiation-induced telangiectasia evaluated by sigmoidoscopy. In this study, the probability of telangiectasia was increased when the D_{2cc} was >70 Gy. Another study [117] published by Georg et al. confirmed the predictive power of D_{2cc} for endoscopic changes and also examined clinical late effects. They found that all symptomatic patients had evidence of telangiectasia on sigmoidoscopy. In this study, the patients were broken down into two groups: group 1 consisted of asymptomatic patients with no endoscopic changes and group 2 consisted of both symptomatic and asymptomatic patients with endoscopic changes. They found that dose differences between the two groups were significant using $D_{0.1cc}$, D_{1cc}, and D_{2cc}. It is important to account for biological equivalence when reporting a total dose to a target or OAR; this is especially true for HDR brachytherapy which has a greater biological effect for the same dose due to the dose rate effect. This is usually accounted

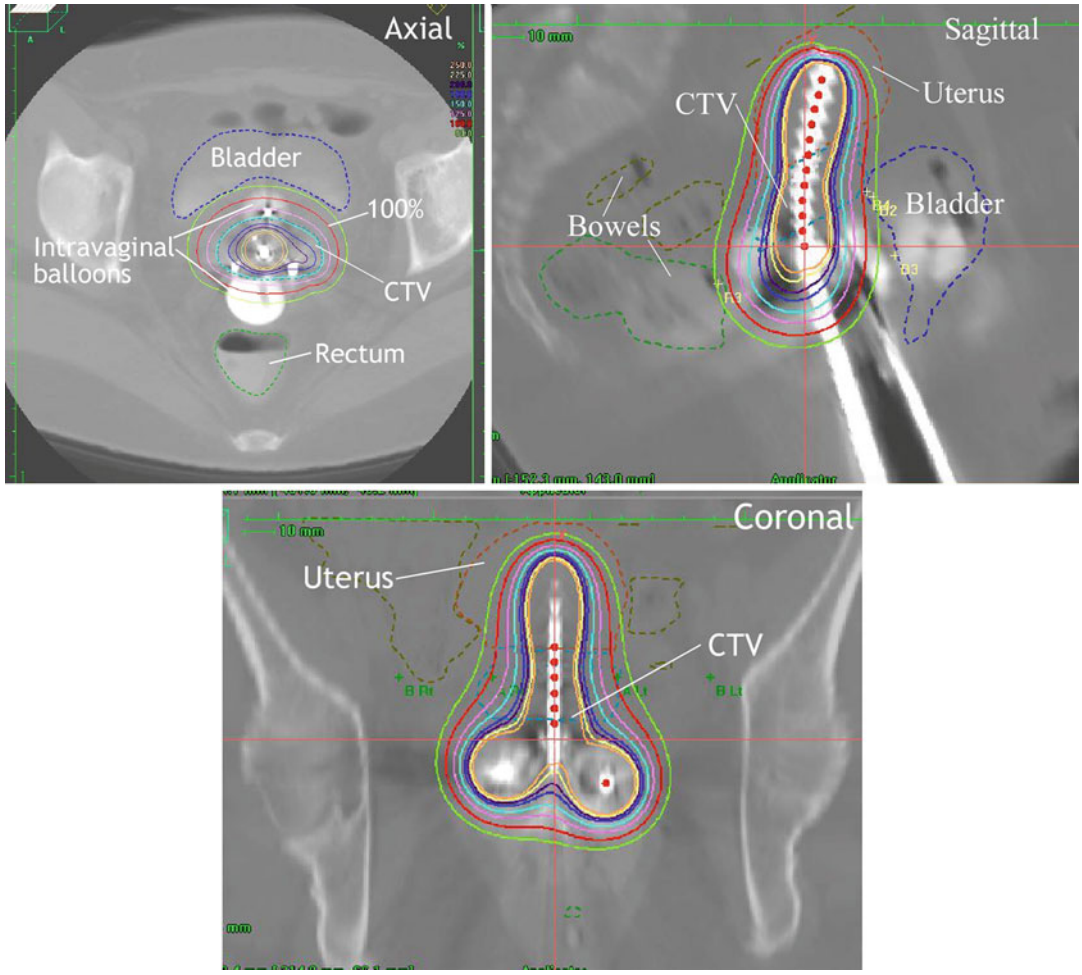

Fig. 56.12 CT-IGBT allows visualization of isodose lines over the target and normal tissues in 3D. The CT window is set to decrease scatter from the T&O apparatus: axial view (**a**), sagittal view (**b**)

for using equivalent dose in 2-Gy fractions (EQD_2) calculated from the linear-quadratic model; this is what should be reported for both the target as well as OARs. The most commonly recommended α/β is 10 for tumors/targets and 3 for OAR. Details for calculating EQD_2 are described in the supplementary data section of the GEC-ESTRO recommendations [114].

Clinical outcomes using MRI-based brachytherapy have been encouraging thus far. Potter et al. reported [118] on 145 patients treated with systematic image-guided MRI brachytherapy during two time periods; for the patients treated most recently (2001–2003), 3-year LC rates were 96 % for tumors 2–5 cm and 82 % for tumors >5 cm. In the same group of patients, the rate of gastrointestinal and urinary late morbidity, LENT SOMA (late effects of normal tissues, subjective, objective, management, analytic) grades 3–4, was 2 %. A recent Danish study [111] compared MRI-based volumetric treatment planning with conventional point A prescription; they found that point A dose is a poor surrogate for CTV coverage and that MRI-based planning improved target coverage as well as OAR dosing. They also found that using point A prescription, small tumors were often overdosed and large tumors underdosed. For example, the mean

Table 56.3 Volumetric definitions and recommended doses

Volume	Definition	Recommended total dose
GTV	Gross tumor volume as defined by imaging (preferably MR) plus clinical exam findings	–
GTV_D	GTV at diagnosis	–
GTV_{B1}	GTV at time of first brachytherapy	4–7 Gy (ICBT)
GTV_{B2}	GTV at time of second brachytherapy	4–7 Gy (ICBT)
CTV	Clinical target volume includes GTV plus areas of various risks of subclinical disease (local recurrence)	–
CTV_{HR}	High-risk CTV includes the GTV_B plus the entire cervix	80–90 Gy[a] (EBRT + ICBT)
CTV_{IR}	Intermediate-risk CTV includes the GTV_D if no gross disease at time brachytherapy or CTV_{HR} plus 0.5–1.5-cm margin	≥60–65 Gy[a] (EBRT + ICBT)
CTV_{LR}	Low-risk CTV includes GTV_D, entire uterus, upper vagina (>2 cm beyond GTV_D), parametrium, pelvic sidewall, and pelvic lymphatics (iliac vessels with 1.5-cm margin)	45–50 Gy (EBRT)

Source: Adapted from Nag et al. [112], with permission from Elsevier
[a]Bioequivalent doses at 2 Gy/d ($\alpha/\beta = 10$)

CTV-HR D_{90} for small tumors was 123 % and was as high as 167 %. On the other hand, for large tumors, the mean CTV-HR D_{90} was 82 % and was as low as 36 %.

Lin et al. reported the use of sequential FDG-PET imaging for brachytherapy treatment planning in 24 patients with carcinoma of the cervix [119]. Sequential FDG-PET imaging can identify patient-specific tumor response and potentially make patient-specific brachytherapy treatment planning possible. At UTHSCSA, we employ CT-image-guided treatment planning using thin-slice axial CT images. Coronal and sagittal images are reconstructed digitally. The OARs (bladder, rectum, small bowel) are identified, delineated, monitored, and spared as well as possible by optimizing the dwell times and positions along the tandem and ovoids. Figure 56.13 illustrates that optimization helps reduce the rectal dose. Although controversies still exist, GTV and CTV are defined individually mostly according to GEC-ESTRO Working Group [112, 113, 115]. Customized geometric optimization in treatment planning is preferred to avoid overdosing adjacent organs [120]. Maximum OAR doses are determined, and DVHs generated are analyzed prior to treatment as D90 and D100 (dose to 90 % and 100 % of volume) for CTV have been shown to correlate with LC [121, 122] and should be ≥100 % and 95 %, respectively, of the prescribed dose. Although we did not find any advantage of using point H as defined by the American Brachytherapy Society (ABS) [123, 124], we follow the guidelines for dosing recommended by the ABS, while dose customization and modification based on surround critical organs are frequently made.

Several national and multinational groups have offered recommendations for the implementation of IGBT using either CT or MRI, including the ABS [115], GEC-ESTRO [113, 114], as well as UK Royal College of Radiologists [125]. The recommended prescription doses, prescription methodologies, and dose limits to OARs are similar between the groups, so only the ABS recommendations will be briefly reviewed here. When using CT imaging, only CTV-HR (CT image-based) is defined. The superior border of the cervix should extend at least 1 cm above the uterine vessels if identified, or the locations of where the uterus begins to enlarge. If these landmarks are difficult to define, a length of 3 cm above the cervix is recommended. When using MRI imaging, both CTV-HR and CTV-IR (described above) are delineated. The total dose prescribed should be >85 Gy (EQD_2). It is worth noting that the UK group [125] recommends a slightly lower dose of 75–80 Gy. The most common HDR prescription regimens are 5.5 Gy × 5, 6 Gy × 5, and 7 Gy × 4. LDR should be given at 40–60 cGy/hr to yield the desired total dose. Point A dose should continue to be reported, but the intended target coverage D90 (dose to 90 % of the target) should be

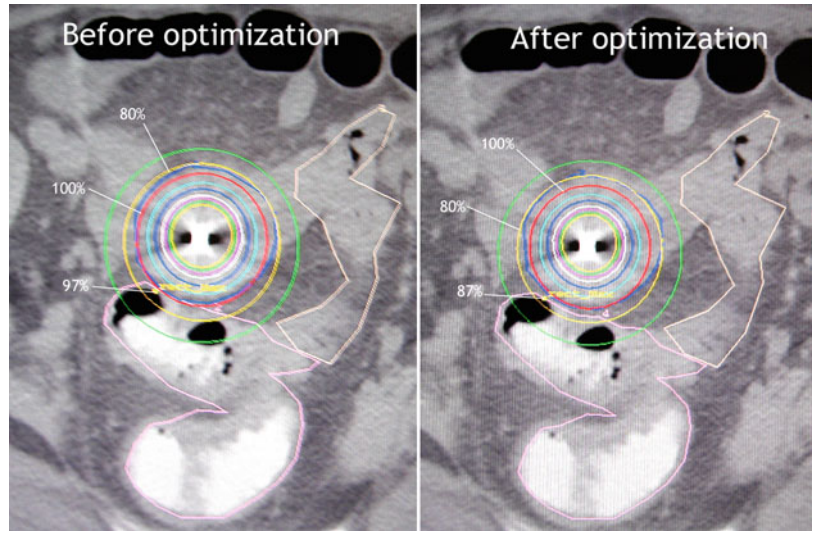

Fig. 56.13 Before and after optimization to reduce the sigmoid dose

100 % of the prescription. The D_{2cc} to the sigmoid and rectum should be <75 Gy, and while dose-limiting toxicity to the bladder has been harder to define, a D_{2cc} of <95 Gy is currently recommended. Similar to the target prescription, ICRU bladder and rectal points should continue to be reported.

As the use of point A dose over the past several decades has produced predicable results in terms of LC, survival, and complications, we must adapt 3D volumetric dose specification cautiously. Treatment plans should be tailored for each patient's anatomy, disease, and response for every brachytherapy procedure.

IGRT Vaginal Cuff Brachytherapy

It should be noted that many in the radiation oncology community are moving away from the use of whole pelvic EBRT. The PORTEC-2 study [126] compared whole pelvic EBRT with vaginal brachytherapy (VBT) in high-intermediate-risk patients, similar to those included in the aforementioned adjuvant RT trials. The doses used were 46 Gy in 23 fractions for EBRT and 30-Gy LDR or 21 Gy in three fractions HDR for VBT administered with a vaginal cylinder. There was no difference in 3-year vaginal relapse (0.9 % with VBT vs. 2.0 % with EBRT, p = 0.97), relapse-free survival (89.5 % vs. 89.1 %, p = 0.38), or overall survival (90.4 % vs. 90.8 %, p = 0.55). There was a difference in 3-year pelvic relapse (3.6 % with VBT vs. 0.7 % with EBRT, p = 0.03) though the absolute difference was small. They concluded that in light of improved patient-reported quality of life after VBT alone, this should be the treatment of choice for high-intermediate-risk patients.

Determining the size of the vaginal cylinder and proper imaging are critical in vaginal cuff brachytherapy. Conventionally, a vaginal cylinder is inserted into the vagina until it meets resistance, and x-ray imaging is obtained to verify its position. However, the vaginal apex is not necessarily against the tip of the cylinder, leading to underdosing of the apex. Therefore, a metallic marker or clip is placed to identify the vaginal apex. Figure 56.14 shows marking of the vaginal apex with a metallic seed and the difference between initial insertion of vaginal cylinder until resistance and reinsertion with a different diameter cylinder. At our institution, we have been using reconstructed CT images in different planes to identify the apex and facilitate treatment planning routinely in brachytherapy with vaginal cylinder treatments (Fig. 56.15). A full CT dataset is taken at the first treatment, and calculations are performed considering doses to the rectal wall, bladder, and small and large

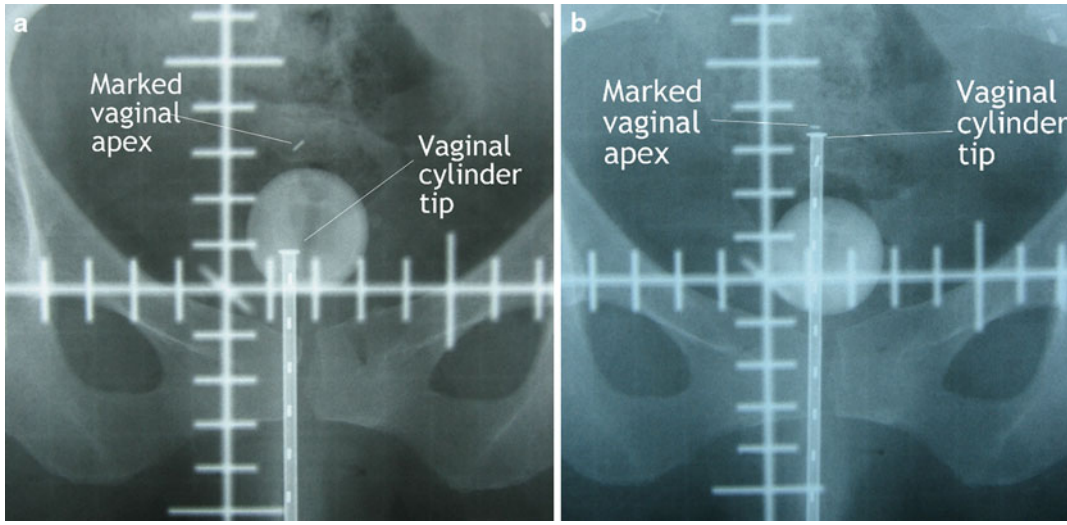

Fig. 56.14 The difference between initial insertion of vaginal cylinder until resistance and reinsertion with a smaller diameter cylinder. If the vaginal apex was not visualized by placing a metallic marker, initial insertion could potentially miss the vaginal apex

bowel (as applicable). At subsequent treatments, 2D scout images are taken to verify positioning of the cylinder, and doses to critical structures should be similar to the initial treatment.

IGRT/IMRT/SBRT Replacing ICBT

IGRT/IMRT has been used to deliver higher than conventional doses while reducing the volume of normal tissues irradiated. Promising clinical results have been published on head and neck and prostate cancers [2–6]. The same paradigm could be applied to cervical cancer [127]. IMRT may provide a potential alternative to ICBT in selected cases [128]. Molla et al. [127] reported 16 patients with either endometrial or cervical cancer undergoing a final SBRT boost instead of ICBT to the areas at higher risk for relapse. The CTV included the vaginal vault, the upper vagina, the parametria, or the uterus (if not operated) plus 6–10-mm expansion to form the PTV. No patient developed severe acute urinary or low-intestinal toxicity. SBRT improved dose homogeneity to the PTV and in reducing the maximum dose to the rectum, when compared to brachytherapy. Aydogan et al. [54] reported a dosimetric comparison of IMRT with HDR-ICBT with vaginal cylinder (7 Gy $\times$ 3 fractions) in ten endometrial cancer patients following surgery. While the bladder maximum and mean doses were comparable, the rectal maximum and mean doses were lower with IMRT. IMRT PTV coverage was also comparable and appeared more homogeneous than HDR-ICBT. Some of the major concerns with IMRT are the higher average integral dose and internal organ motion, as small movements in the target and normal tissues may significantly affect the doses to them. Although IGRT/IMRT appears to be a potential alternative to ICBT, more clinical studies are still needed to define its role in these patients. Currently, IGRT-ICBT with advanced equipment and techniques is the standard of care.

Conclusion and Future Directions

IGRT/IMRT has gained increasing momentum as a component of treatment planning and delivery for gynecologic malignancies. It is a major advancement in the treatment of patients with gynecologic malignancies. Current effort is focusing on developing consensus guidelines and incorporating sophisticated imaging for IGRT approaches. The three main areas of benefit

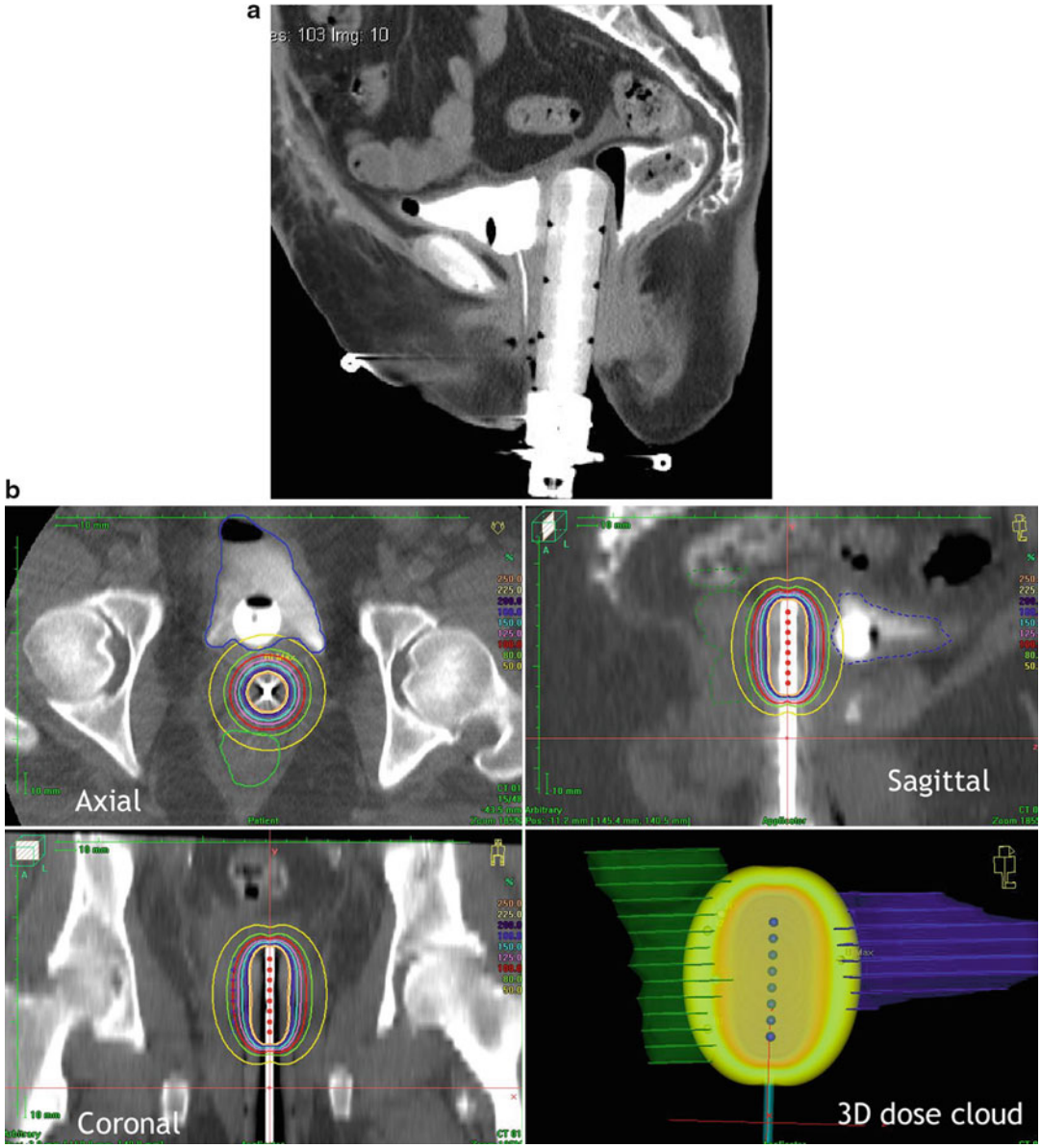

Fig. 56.15 CT-IGBT allows visualization of vaginal apex (**a**) during treatment planning and delivery (**b**)

include reduction of geometric misses, less normal tissue irradiated to high dose, and adaptation to tumor shrinking during the course of treatment. In addition, IGRT/IMRT approaches may potentially replace brachytherapy in selected cases. IGRT/IMRT treatment planning is a multistep process. Careful consideration throughout the entire process is necessary to ensure that an optimal plan is achieved. Decisions made at the time of simulation, target and normal tissue delineation, planning and the delivery/verification process themselves can impact the overall treatment plan.

However, IGRT/IMRT results in higher volumes of normal tissue receiving lower doses. The long-term effects of increased integral total body dose are not known. Target and normal tissue delineation and IGRT/IMRT delivery are

time-consuming and complex processes with only limited existing guidelines. Variations in contouring techniques, planning parameters, and plan optimization methods in addition to available data limited to short follow-up make clinical outcome comparison of tumor control, survival, and treatment sequelae difficult. Nevertheless, clinical data are slowly emerging and prospective randomized trials are anticipated. The future of IGRT/IMRT relies on the incorporation of improved diagnostic quality images, accurate tumor targeting, adaptation to physiologic changes over the course of treatment, lower integral dose to normal tissue, shortened time required for treatment planning and delivery, and cost containment. Improved sparing of normal tissue allows dose escalation, and hence, improved clinical outcomes, particularly in early-stage disease, may be realized in time.

References

1. Michalski J, Purdy JA, Gaspar L, et al. The RTOG research plan 2002–2006, IGRT committee report. Int J Radiat Oncol Biol Phys. 2001;51:60–5.
2. Nath SK, Simpson DR, Rose BS, et al. Recent advances in image-guided radiotherapy for head and neck carcinoma. J Oncol 2009;2009:1–10(752135).
3. Nguyen NP, Ceizyk M, Vos P, et al. Effectiveness of image-guided radiotherapy for laryngeal sparing in head and neck cancer. Oral Oncol. 2010;46(4):283–6.
4. Stephans KL, Xia P, Tendulkar RD, et al. The current status of image-guided external beam radiotherapy for prostate cancer. Curr Opin Urol. 2010;20(3):223–8.
5. Kupelian PA, Langen KM, Willoughby TR, et al. Image-guided radiotherapy for localized prostate cancer: treating a moving target. Semin Radiat Oncol. 2008;18(1):58–66.
6. Valicenti RK, Dicker AP, Jaffray DA, editors. Image-guided radiation therapy of prostate cancer. London: Informa Healthcare; 2008.
7. Jemal A, Siegel R, Xu J, et al. Cancer statistics 2010. CA Cancer J Clin. 2010;60:277–300.
8. Global Cancer Facts & Figures 2007 – www.cancer.org.
9. Anil K, Chaturvedi AK, Madeleine MM, et al. Risk of human papillomavirus-associated cancers among persons with AIDS. J Natl Cancer Inst. 2009;101(16):1120–30.
10. Landoni F, Maneo A, Colombo A, et al. Randomised study of radical surgery versus radiotherapy for stage Ib-IIa cervical cancer. Lancet. 1997;350:535–40.
11. Rotman M, Pajak TF, Choi K. Prophylactic extended field irradiation of para-aortic lymph nodes in stages IIB and bulky IB and IIA cervical carcinomas. Ten-year treatment results of RTOG 79–20. JAMA. 1995;274:387–93.
12. Whitney CW, Sause W, Bundy BN, et al. Randomized comparison of fluorouracil plus cisplatin versus hydroxyurea as an adjunct to radiation therapy in stage IIB-IVA carcinoma of the cervix with negative para-aortic lymph nodes: a Gynecologic Oncology Group and Southwest Oncology Group study. J Clin Oncol. 1999;17(5):1339–48.
13. Morris M, Eifel PJ, Lu J, et al. Pelvic radiation with concurrent chemotherapy compared with pelvic and para-aortic radiation for high risk cervical cancer. N Engl J Med. 1999;340:1137–43.
14. Rose PG, Bundy BN, Watkins EB, et al. Concurrent cisplatin-based radiotherapy and chemotherapy for locally advanced cervical cancer. N Engl J Med. 1999;340(15):1144–53.
15. Keys HM, Bundy BN, Stehman FB. Cisplatin, radiation, and adjuvant hysterectomy compared with radiation and adjuvant hysterectomy for bulky stage IB cervical carcinoma. N Engl J Med. 1999;340(15):1154–61.
16. Tierney JF, Vale C, Symonds P. Concomitant and neoadjuvant chemotherapy for cervical cancer. Clin Oncol (Royal College of Radiologists). 2008;20(6):401–16.
17. Lagasse LD, Creasman WT, Shingleton HM, et al. Results and complications of operative staging in cervical cancer: experience of the Gynecologic Oncology Group. Gynecol Oncol. 1980;9:90–8.
18. Nelson JH, Boyce J, Macasaet M, et al. Incidence, significance, and follow-up of para-aortic lymph node metastases in late invasive carcinoma of the cervix. Am J Obstet Gynecol. 1977;128:336–40.
19. Kitchener H, Swart AM, Qian Q, et al. ASTEC study group: efficacy of systematic pelvic lymphadenectomy in endometrial cancer (MRC ASTEC trial): a randomized study. Lancet. 2009;373(9658):125–36.
20. Aalders JG, Abeler V, Kolstad P, et al. Postoperative external irradiation and prognostic parameters in stage I endometrial carcinoma: clinical and histopathologic study of 540 patients. Obstet Gynecol. 1980;56(4):419–27.
21. Creutzberg CL, van Putten WL, Koper PC, et al. Surgery and postoperative radiotherapy versus surgery alone for patients with stage I endometrial carcinoma: a multicentre randomised trial. PORTEC Study Group. Lancet. 2000;355:1404–11.
22. Keys HM, Roberts JA, Brunetto VL, et al. A phase III trial of surgery with or without adjunctive external pelvic radiation therapy in intermediate risk endometrial adenocarcinoma: a Gynecologic Oncology Group study. Gynecol Oncol. 2004;92:744–51.
23. Nag S, Erickson B, Parikh S, et al. The American Brachytherapy Society recommendations

for high-dose-rate brachytherapy for carcinoma of the endometrium. Int J Radiat Oncol Biol Phys. 2000;48(3):779–90.
24. Magrina JF, Gonzalez-Bosquet J, Weaver AL, et al. Primary squamous cell cancer of the vulva: radical versus modified radical vulvar surgery. Gynecol Oncol. 1998;71(1):116–21.
25. Heaps JM, Fu YS, Montz FJ, et al. Surgical-pathologic variables predictive of local recurrence in squamous cell carcinoma of the vulva. Gynecol Oncol. 1990;38(3):309–14.
26. Hoffman MS, Cavanagh D, Roberts WS, et al. Ultraradical surgery for advanced carcinoma of the vulva: an update. Int J Gynecol Cancer. 1993;3(6): 369–72.
27. Gerszten K, Selvaraj RN, Kelley J, et al. Preoperative chemoradiation for locally advanced carcinoma of the vulva. Gynecol Oncol. 2005;99(3):640–4.
28. Domingues AP, Mota F, Durão M, et al. Neoadjuvant chemotherapy in advanced vulvar cancer. Int J Gynecol Cancer. 2010;20(2):294–8.
29. Moore DH, Thomas GM, Montana GS, et al. Preoperative chemoradiation for advanced vulvar cancer: a phase II study of the Gynecologic Oncology Group. Int J Radiat Oncol Biol Phys. 1998;42(1): 79–85.
30. Faul CM, Mirmow D, Huang Q, et al. Adjuvant radiation for vulvar carcinoma: improved local control. Int J Radiat Oncol Biol Phys. 1997;38(2):381–9.
31. Homesley HD, Bundy BN, Sedlis A, et al. Radiation therapy versus pelvic node resection for carcinoma of the vulva with positive groin nodes. Obstet Gynecol. 1986;68(6):733–40.
32. Nielsen M, Bertelsen A, Westberg J, et al. Cone beam CT evaluation of patient set-up accuracy as a QA tool. Acta Oncol. 2009;48:271–6.
33. Huh SJ, Park W, Han Y. Interfractional variation in position of the uterus during radical radiotherapy for cervical cancer. Radiother Oncol. 2004;71(1):73–9.
34. van de Bunt L, van der Heide UA, Ketelaars M, et al. Conventional, conformal, and intensity-modulated radiation therapy treatment planning of external beam radiotherapy for cervical cancer: the impact of tumor regression. Int J Radiat Oncol Biol Phys. 2006;64(1):189–96.
35. Monk BJ, Tewari KS, Koh WJ. Multimodality therapy for locally advanced cervical carcinoma: state of the art and future directions. J Clin Oncol. 2007;25(20):2952–65.
36. Kim SH, Choi BI, Lee HP, et al. Uterine cervical carcinoma: comparison of CT and MR findings. Radiology. 1990;175:45–51.
37. Williams AD, Cousins C, Soutter WP, et al. Detection of pelvic lymph node metastases in gynecologic malignancy: a comparison of CT, MR imaging, and positron emission tomography. Am J Roentgenol. 2001;177:343–8.
38. Tatsumi M, Cohade C, Bristow RE, et al. Imaging uterine cervical cancer with FDG-PET/CT: direct comparison with PET. Mol Imaging Biol. 2009;11(4):229–35.
39. Sironi S, Buda A, Picchio M, et al. Lymph node metastasis in patients with clinical early-stage cervical cancer: detection with integrated FDG PET/CT. Radiol. 2006;238:272–9.
40. Loft A, Berthelsen AK, Roed H, et al. The diagnostic value of PET/CT scanning in patients with cervical cancer: a prospective study. Gynecol Oncol. 2007;106(1):29–34.
41. Grigsby PW, Siegel BA, Dehdashti F. Lymph node staging by positron emission tomography in patients with carcinoma of the cervix. J Clin Oncol. 2001;19(17):3745–9.
42. Grigsby PW, Singh AK, Siegel BA, et al. Lymph node control in cervical cancer. Int J Radiat Oncol Biol Phys. 2004;59(3):706–12.
43. Suzuki R, Miyagi E, Takahashi N, et al. Validity of positron emission tomography using fluoro-2-deoxyglucose for the preoperative evaluation of endometrial cancer. Int J Gynecol Cancer. 2007;17(4):890–6.
44. Belhocine T, De Barsy C, Hustinx R, et al. Usefulness of (18)F-FDG PET in the post-therapy surveillance of endometrial carcinoma. Eur J Nucl Med Mol Imaging. 2002;29:1132–9.
45. Saga T, Higashi T, Ishimori T, et al. Clinical value of FDG-PET in the follow up of post-operative patients with endometrial cancer. Ann Nucl Med. 2003;17:197–203.
46. Subhas N, Patel PV, Pannu HK, et al. Imaging of pelvic malignancies with in-line FDG PET-CT: case examples and common pitfalls of FDG PET. Radiographics. 2005;25:1031–43.
47. Chung HH, Jo H, Kang WJ, et al. Clinical impact of integrated PET/CT on the management of suspected cervical cancer recurrence. Gynecol Oncol. 2007;104:529–34.
48. Esajas MD, Duk JM, de Bruijn HW, et al. Clinical value of routine serum squamous cell carcinoma antigen in follow-up of patients with early-stage cervical cancer. J Clin Oncol. 2001;19:3960–6.
49. Jover R, Lourido D, Gonzalez C, et al. Role of PET/CT in the evaluation of cervical cancer. Gynecol Oncol. 2008;110(3, Suppl 2):S55–9.
50. Belhocine T. Whole-body 18FDG PET plus pelvic MRI in the pre-treatment assessment of cervical cancers: an alternative to the FIGO clinical staging. Gynecol Surg. 2004;1(2):95–100.
51. Bonin SR, Lanciano RM, Corn BW, et al. Bony landmarks are not an adequate substitute for in defining pelvic lymph node location for the treatment of cervical cancer with radiotherapy. Int J Radiat Oncol Biol Phys. 1996;34(1):167–72.
52. Finlay MH, Ackerman I, Tirona RG, et al. Use of CT simulation for treatment of cervical cancer to assess the adequacy of lymph node coverage of conventional pelvic fields based on bony landmarks. Int J Radiat Oncol Biol Phys. 2006;64:205–9.

53. Lim K, Kelly V, Stewart J. Pelvic radiotherapy for cancer of the cervix: is what you plan actually what you deliver? Int J Radiat Oncol Biol Phys. 2009;74(1):304–12.
54. Aydogan B, Mundt AJ, Smith BD, et al. A dosimetric analysis of intensity- modulated radiation therapy (IMRT) as an alternative to adjuvant high-dose-rate (HDR) brachytherapy in early endometrial cancer patients. Int J Radiat Oncol Biol Phys. 2006;65:266–73.
55. Taylor A, Rockall AG, Reznek RH, et al. Mapping pelvic lymph nodes: guidelines for delineation in intensity-modulated radiotherapy. Int J Radiat Oncol Biol Phys. 2005;63(5):1604–12.
56. Radiation Therapy Oncology Group Contouring Atlases and Protocols. 2012. http://www.rtog.org/pdf_document/GYN-Atlas.pdf.
57. Georg P, Georg D, Hillbrand M, et al. Factors influencing bowel sparing in intensity modulated whole pelvic radiotherapy for gynaecological malignancies. Radiother Oncol. 2006;80:19–26.
58. Mutic S, Malyapa RS, Grigsby PW, et al. PET-guided IMRT for cervical carcinoma with positive para-aortic lymph nodes-a dose-escalation treatment planning study. Int J Radiat Oncol Biol Phys. 2003;55(1):28–35.
59. Portelance L, Chao KS, Grigsby PW, et al. Intensity-modulated radiation therapy (IMRT) reduces small bowel, rectum, and bladder doses in patients with cervical cancer receiving pelvic and para-aortic irradiation. Int J Radiat Oncol Biol Phys. 2001;51(1):261–6.
60. Ahamad A, D'Souza W, Salehpour M, et al. Intensity-modulated radiation therapy (IMRT) for post-hysterectomy pelvic radiation: selection of patients and planning target volume (PTV). Int J Radiat Oncol Biol Phys. 2002;54:42(abs).
61. Adli M, Mayr NA, Kaiser HS, et al. Does prone positioning reduce small bowel dose in pelvic radiation with intensity-modulated radiotherapy for gynecologic cancer? Int J Radiat Oncol Biol Phys. 2003;57(1):230–8.
62. Miller TR, Grigsby PW. Measurement of tumor volume by PET to evaluate prognosis in patients with advanced cervical cancer treated by radiation therapy. Int J Radiat Oncol Biol Phys. 2002;53(2):353–9.
63. Haslam JJ, Lujan AE, Mundt AJ, et al. Setup errors in patients treated with intensity-modulated whole pelvic radiation therapy for gynecological malignancies. Med Dosim. 2005;30(1):36–42.
64. Lee CM, Shrieve DC, Gaffney DK. Rapid involution and mobility of carcinoma of the cervix. Int J Radiat Oncol Biol Phys. 2004;58(2):625.
65. Jhingran A, Salehpour M, Brooks B. Endometrial cancer: case study. In: Mundt AJ, Roeske JC, editors. Intensity modulated radiation therapy: a clinical perspective. 1st ed. Hamilton: BC Decker; 2005. p. 513–7.
66. Small Jr W, Mell LK, Anderson P, et al. Consensus guidelines for delineation of clinical target volume for intensity-modulated pelvic radiotherapy in post-operative treatment of endometrial and cervical cancer. Int J Radiat Oncol Biol Phys. 2008;71(2):428–34.
67. Lim K, Small W Jr, Portelance L, et al. Consensus guidelines for delineation of clinical target volume for intensity-modulated pelvic radiotherapy for the definitive treatment of cervix cancer. Int J Radiat Oncol Biol Phys. 2011;79(2):348–355.
68. Low DA, Grigsby PW, Dempsey JF, et al. Applicator-guided intensity modulated radiation therapy. Int J Radiat Oncol Biol Phys. 2002;52:1400–6.
69. Mell LK, Kochanski JD, Roeske JC, et al. Dosimetric predictors of acute hematologic toxicity in cervical cancer patients treated with concurrent cisplatin and intensity-modulated pelvic radiotherapy. Int J Radiat Oncol Biol Phys. 2006;66(5):1356–65.
70. Lujan AE, Mundt AJ, Yamada SD, et al. Intensity-modulated radiotherapy as a means of reducing dose to bone marrow in gynecologic patients receiving whole pelvic radiotherapy. Int J Radiat Oncol Biol Phys. 2003;57(2):516–21.
71. Mell LK, Tiryaki H, Ahn K, et al. Dosimetric comparison of bone marrow-sparing intensity-modulated radiotherapy versus conventional techniques for treatment of cervical cancer. Int J Radiat Oncol Biol Phys. 2008;71(5):1504–10.
72. Lewis JH, Tyagi N, Yashar CM, et al. Impact of daily image-guided patient setup on bone marrow sparing in cervical cancer patients undergoing IMRT. Int J Radiat Oncol Biol Phys. 2008;72(1,Suppl):S582–3.
73. Vandecasteele K, De Neve W, De Gersem W, et al. Intensity-modulated arc therapy with simultaneous integrated boost in the treatment of primary irresectable cervical cancer. Treatment planning, quality control, and clinical implementation. Strahlenther Onkol. 2009;185(12):799–807.
74. Ahmed RS, Kim RY, Duan J, et al. IMRT dose escalation for positive PA nodes in locally advanced cervical cancer. Int J Radiat Oncol Biol Phys. 2004;60:505–12.
75. Guerrero M, Li XA, Ma L, et al. Simultaneous integrated intensity-modulated radiotherapy boost for locally advanced gynecological cancer: radiobiological and dosimetric considerations. Int J Radiat Oncol Biol Phys. 2005;62:933.
76. Vandecasteele K, De Neve W, De Gersem W, et al. Intensity-modulated arc therapy with simultaneous integrated boost in the treatment of primary irresectable cervical cancer. Treatment planning, quality control, and clinical implementation. Strahlenther Onkol. 2009;185(12):799–807.
77. Roeske JC, Lujan A, Reba RC, et al. Incorporation of SPECT bone marrow imaging into intensity modulated whole-pelvic radiation therapy treatment

planning for gynecologic malignancies. Radiother Oncol. 2005;77(1):11–7.
78. Dale E, Hellebust TP, Skjonsberg A, et al. Modeling normal tissue complication probability from repetitive computed tomography scans during fractionated high-dose-rate brachytherapy and external beam radiotherapy of the uterine cervix. Int J Radiat Oncol Biol Phys. 2000;47(4):963–71.
79. Stroom JC, Olofsen-van Acht MJ, Quint S, et al. On-line set-up corrections during radiotherapy of patients with gynecologic tumors. Int J Radiat Oncol Biol Phys. 2000;46(2):499–506.
80. Kaatee RS, Olofsen MJ, Verstraate MB, et al. Detection of organ movement in cervix cancer patients using a fluoroscopic electronic portal imaging device and radiopaque markers. Int J Radiat Oncol Biol Phys. 2002;54(2):576–83.
81. Yamamoto R, Yonesaka A, Nishioka S, et al. High dose three-dimensional conformal boost (3DCB) using an orthogonal diagnostic X-ray set-up for patients with gynecological malignancy: a new application of real-time tumor-tracking system. Radiother Oncol. 2004;73(2):219–22.
82. Kamath S, Sahni S, Ranka S, et al. Optimal field splitting for large intensity-modulated fields. Med Phys. 2004;31(12):3314–23.
83. Haslam JJ, Bonta DV, Lujan AE, et al. Comparison of dose calculated by an intensity modulated radiotherapy treatment planning system and an independent monitor unit verification program. J Appl Clin Med Phys. 2003;4(3):224–30.
84. Low DA, Dempsey JF. Evaluation of the gamma dose distribution comparison method. Med Phys. 2003;30(9):2455–64.
85. Lin LL, Yang Z, Mutic S, et al. FDG-PET imaging for the assessment of physiologic volume response during radiotherapy in cervix cancer. Int J Radiat Oncol Biol Phys. 2006;65(1):177–81.
86. Beadle BM, Jhingran A, Salehpour M, et al. Cervix regression and motion during the course of external beam chemoradiation for cervical cancer. Int J Radiat Oncol Biol Phys. 2009; 73(1):235–41.
87. Mayr NA, Yuh WT, Taoka T, et al. Serial therapy-induced changes in tumor shape in cervical cancer and their impact on assessing tumor volume and treatment response. Am J Roentgenol. 2006;187:65–72.
88. Nguyen TV, Petereit DG. High-dose-rate brachytherapy for medically inoperable stage I endometrial cancer. Gynecol Oncol. 1998;71(2):196–203.
89. Fishman DA, Roberts KB, Chambers JT, et al. Radiation therapy as exclusive treatment for medically inoperable patients with stage I and II endometrioid carcinoma with endometrium. Gynecol Oncol. 1996;61(2):189–96.
90. Beriwal S, Kim H, Heron D, et al. Comparison of 2D vs. 3D dosimetry for Rotte 'Y' applicator high dose rate brachytherapy for medically inoperable endometrial cancer. Technol Cancer Res Treat. 2006;5(5):521–7.
91. Weitmann HD, Potter R, Waldhausl C, et al. Pilot study in the treatment of endometrial carcinoma with 3D image-based high-dose-rate brachytherapy using modified Heyman packing: clinical experience and dose-volume histogram analysis. Int J Radiat Oncol Biol Phys. 2005;62(2):468–78.
92. KohWJ, Wallace 3rd HJ, Greer BE, et al. Combined radiotherapy and chemotherapy in the management of local-regionally advanced vulvar cancer. Int J Radiat Oncol Biol Phys. 1993;26(5):809–16.
93. Landrum LM, Skaggs V, Gould N, et al. Comparison of outcome measures in patients with advanced squamous cell carcinoma of the vulva treated with surgery or primary chemoradiation. Gynecol Oncol. 2008;108(3):584–90.
94. Teng N, Abu-Rustum NR, Bahador A, et al. Cervical cancer guidelines. Clinical practice guidelines in oncology. J Natl Compr Cancer Netw. 2004;2(6):612–30.
95. Bristow RE, Purinton SC, Santillan A, et al. Cost-effectiveness of routine vaginal cytology for endometrial cancer surveillance. Gynecol Oncol. 2006;103(2):709–13.
96. Suarez LS, Mariani A, Cliby WA, et al. Endometrial cancer recurrence: the role of surveillance regimens. Gynecol Oncol. 2007;107(2):375.
97. Connor JP, Andrews J, Anderson B, et al. Computed tomography in endometrial carcinoma. Obstet Gynecol. 2000;95(5):692–6.
98. Park JY, Kim EN, Kim DY, et al. Clinical impact of positron emission tomography or positron emission tomography/computed tomography in the posttherapy surveillance of endometrial carcinoma: evaluation of 88 patients. Int J Gynecol Cancer. 2008;18(6):1332–8.
99. Pai HH, Souhami L, Clark BG, et al. Isolated vaginal recurrences in endometrial carcinoma: treatment results using high-dose-rate intracavitary brachytherapy and external beam radiotherapy. Gynecol Oncol. 1997;66(2):300–7.
100. Nag S, Yacoub S, Copeland L, et al. Interstitial brachytherapy for salvage treatment of vaginal recurrences in previously unirradiated endometrial cancer patients. Int J Radiat Oncol Biol Phys. 2002;54(4): 1153–9.
101. Hart KB, Han I, Shamsa F, et al. Radiation therapy for endometrial cancer in patients treated for postoperative recurrence. Int J Radiat Oncol Biol Phys. 1998;41(1):7–11.
102. Guckenberger M, Bachmann J, Wulf J, et al. Stereotactic body radiotherapy for local boost irradiation in unfavorable locally recurrent gynaecological cancer. Radiother Oncol. 2010;94:53–9.
103. Grigsby PW, Vest ML, Perez CA. Recurrent carcinoma of the cervix exclusively in the paraaortic nodes following radiation therapy. Int J Radiat Oncol Biol Phys. 1994;28(2):451–5.

104. Chou HH, Wang CC, Lai CH, et al. Isolated paraaortic lymph node recurrence after definitive irradiation for cervical carcinoma. Int J Radiat Oncol Biol Phys. 2001;51(2):442–8.
105. Choi CW, Cho CK, Yoo SY, et al. Image-guided stereotactic body radiation therapy in patients with isolated para-aortic lymph node metastases from uterine cervical and corpus cancer. Int J Radiat Oncol Biol Phys. 2009;74(1):147–53.
106. International Commission of Radiological Units and Measurements. ICRU report 38. Dose and volume specification for intracavitary therapy in gynecology. Bethesda: ICRU; 1985.
107. Eng TY, Fuller CD, Cavanaugh SX, et al. Significant rectal and bladder dose reduction via utilization of Foley balloon catheters in high-dose-rate tandem and ovoid intracavitary brachytherapy of the uterine cervix. Int J Radiat Oncol Biol Phys. 2004;59(1):174–8.
108. Narayan K, van Dyk S, Bernshaw D, et al. Comparative study of LDR (Manchester system) and HDR image-guided conformal brachytherapy of cervical cancer: patterns of failure, late complications, and survival. Int J Radiat Oncol Biol Phys. 2009;74(5):1529–35.
109. Shin KH, Kim TH, Cho JK, et al. CT-guided intracavitary radiotherapy for cervical cancer: comparison of conventional point A plan with clinical target volume-based three-dimensional plan using dose-volume parameters. Int J Radiat Oncol Biol Phys. 2006;64(1):197–204.
110. Davidson MT, Yuen J, D'Souza DP, et al. Optimization of high-dose-rate cervix brachytherapy applicator placement: the benefits of intraoperative ultrasound guidance. Brachytheraphy. 2008;7(3):248–53.
111. Tanderup K, Nielsen S, Nyvang G, et al. From point A to the sculpted pear: MR image guidance significantly improves tumor dose and sparing of organs at risk in brachytherapy of cervical cancer. Radiother Oncol. 2010;94:173–80.
112. Nag S. Controversies and new developments in gynecologic brachytherapy: image-based intracavitary brachytherapy for cervical carcinoma. Semin Radiat Oncol. 2006;16(3):164–7.
113. Haie-Meder C, Potter R, Van Limbergen E, et al. Recommendations from gynaecological GEC-ESTRO working group (I): concepts and terms in 3D image based 3D treatment planning in cervix cancer brachytherapy with emphasis on MRI assessment GTV and CTV. Radiother Oncol. 2005;74:235–45.
114. Potter R, Haie-Meder C, Van Limbergen E, et al. Recommendations from gynaecological GEC-ESTRO working group (II): concepts and terms in 3D image based 3D treatment planning in cervix cancer brachytherapy – 3D dose volume parameters and aspects of 3D image based anatomy, radiation physics, radiobiology. Radiother Oncol. 2006;78:67–77.
115. Nag S, Cardenes H, Chang S, et al. Proposed guidelines for image-based intracavitary brachytherapy for cervical carcinoma: report from Image-Guided Brachytherapy Working Group. Int J Radiat Oncol Biol Phys. 2004;60(4):1160–72.
116. Koom WS, Dohn DF, Kim JY, et al. Computed tomography-based high-dose-rate intracavitary brachytherapy for uterine cervical cancer: preliminary demonstration of correlation between dose-volume parameters and rectal mucosal changes observed by flexible sigmoidoscopy. Int J Radiat Oncol Biol Phys. 2007;68(5):1446–54.
117. Georg P, Kirisits C, Goldner G, et al. Correlation of dose-volume parameters, endoscopic and clinical rectal side effects in cervix cancer patients treated with definitive radiotherapy including MRI-based brachytherapy. Radiother Oncol. 2009;91(2):173–80.
118. Potter R, Dimopoulos J, Georg P, et al. Clinical impact of MRI assisted dose volume adaptation and dose escalation in brachytherapy of locally advanced cervix cancer. Radiother Oncol. 2007;83:148–55.
119. Lin LL, Mutic S, Malyapa RS, Low DA. Sequential FDG-PET brachytherapy treatment planning in carcinoma of the cervix. Int J Radiat Oncol Biol Phys. 2005;63(5):1494–501.
120. Gao M, Sinacore J. Single versus customized treatment planning for image-guided high-dose-rate brachytherapy for cervical cancer: dosimetric comparison and predicting factor for organs at risk overdose with single plan approach. Int J Radiat Oncol Biol Phys. 2009;75(1):309–14.
121. Dimopoulos JC, Potter R, Lang S, et al. Dose-effect relationship for local control of cervical cancer by magnetic resonance image-guided brachytherapy. Radiother Oncol. 2009;93(2):311–5.
122. Wang B, Kwon A, Zhu Y, et al. Image-guided intracavitary high-dose-rate brachytherapy for cervix cancer: a single institutional experience with three-dimensional CT-based planning. Brachyther. 2009;8(2):240–7.
123. Nag S, Erickson B, Thomadsen B, et al. The American Brachytherapy Society recommendations for high-dose-rate brachytherapy for carcinoma of the cervix. Int J Radiat Oncol Biol Phys. 2000;48(1):201–11.
124. Eng TY, Cummins S, Baake D. Point A or point H in prescribing high-dose-rate (HDR) intracavitary brachytherapy for cervical Carcinoma? Int J Radiat Oncol Biol Phys. 2007;69(3S):S396–S397.
125. The Royal College of Radiologists. Implementing image-guided brachytherapy for cervix cancer in the UK. Board of the Faculty of Clinical Oncology. The Royal College of Radiologists. 2009. (https://www.rcr.ac.uk/docs/oncology/pdf/BFCO(09)1_cervix.pdf).

126. Nout RA, Smit VT, Putter H, et al. Vaginal brachytherapy versus pelvic external beam radiotherapy for patients with endometrial cancer of high-intermediate risk (PORTEC-2): an open-label, non-inferiority, randomised trial. Lancet. 2010; 375(9717):781–2.
127. Molla M, Escude L, Nouet P, et al. Fractionated stereotactic radiotherapy boost for gynecologic tumors: an alternative to brachytherapy? Int J Radiat Oncol Biol Phys. 2005;62:118–24.
128. Roeske JC, Lujan AE, Rotmensch J, et al. A feasibility study of IMRT for the treatment of cervical cancer patients unable to receive intracavitary brachytherapy. Eng Med Biol Soc. Proceedings of the 22nd annual international conference of the IEEE, Chicago, IL, 2000;1:463–465.

Ablation of Gynecologic Cancers

57

Fady Khoury-Collado and Yukio Sonoda

Abstract

The use of ablative therapies in gynecologic malignancies can be divided into direct (surgical or intraoperative) and image-guided tumor ablation. In advanced-stage ovarian and endometrial cancers, the primary treatment is surgery, with the goal of removing all visible tumors. In that setting, direct ablative techniques are extremely useful and have become part of the standard modern surgical tools. The most commonly used techniques (argon beam coagulator, ultrasonic surgical aspirator, plasma surgery) along with the evidence supporting their use will be reviewed.

On the other hand, the use of image-guided therapies (radiofrequency ablation, cryotherapy, embolization) in gynecologic cancers is limited and mostly reported in the palliative setting in recurrent disease. Radiofrequency ablation is occasionally used to ablate tumors metastatic to the liver, although there is still no evidence showing a benefit to this practice. Embolization of pelvic vessels is a commonly used modality in the palliative treatment of advanced recurrent pelvic malignancies presenting with genitourinary or gastrointestinal bleeding.

Intraoperative ultrasound has been used to assist in the identification of suspicious lymph nodes, in the assessment of myometrial invasion, and in the diagnoses of adnexal masses. Unfortunately, results have been disappointing for the most part, and the use of intraoperative ultrasound remains investigational.

Introduction

One of the unique characteristics of gynecologic malignancies (ovarian and endometrial cancer in particular) is their susceptibility to the available chemotherapy agents. Thus, despite widespread metastases, surgical cytoreduction (followed by chemotherapy) is the treatment of choice in ovarian and endometrial cancers, and successful

F. Khoury-Collado (✉) • Y. Sonoda
Gynecology Service, Department of Surgery, Memorial Sloan-Kettering Cancer Center, New York, NY, USA
e-mail: fcollado@maimonidesmed.org; sonoday@mskcc.org

D.E. Dupuy et al. (eds.), *Image-Guided Cancer Therapy*, DOI 10.1007/978-1-4419-0751-6_59,

"debulking" surgery is consistently associated with a survival benefit. Direct ablative therapies are commonly used in the surgical cytoreduction of gynecologic malignancies. In the first part of the chapter, we will focus on direct ablative therapies.

The use of image-guided ablative therapies in the primary management of gynecologic malignancies has been limited for several reasons. Gynecologic cancers typically present at an age when most women have completed their childbearing; since gynecologic organs function primarily for reproduction, they are expendable in these women and can be removed with limited long-term side effects. The spread pattern of the more common gynecologic cancers tends to be widespread peritoneal disease, as with ovarian cancer, or via the lymphatic channels, as with endometrial and cervical cancers, and a significant portion of these metastases are not detectable by current imaging modalities. Since image-guided modalities require the tumor to be localized and visible by imaging, primary surgical excision remains the management of choice at this time. Image-guided therapy in gynecologic cancers has therefore been limited to a palliative role in the recurrent setting for the most part. In the second part of this chapter, we will focus on image-guided ablative therapies.

Cytoreduction for Gynecologic Malignancies

Ovarian Cancer

Ovarian cancer is the leading cause of gynecologic cancer deaths annually, mainly due to a lack of effective screening techniques. Patients with newly diagnosed ovarian cancer often present with widespread peritoneal disease. Griffiths was the first to demonstrate the potential benefit of surgical debulking in cases of advanced ovarian cancer. His initial study demonstrated a significant survival benefit for patients in whom residual disease could be minimized to less than 1.5 cm [1]. The traditional management for advanced epithelial ovarian and peritoneal cancers is to perform maximal cytoreductive surgery, with the intent to remove all large-volume disease. This led to the current definition of "optimal" cytoreduction—debulking to no remaining tumor nodule greater than 1 cm in maximal diameter [2].

The current concept of optimal debulking has been challenged recently, and a growing body of literature has shown that complete gross resection is associated with more favorable outcomes [3, 4].

In 2006, Chi et al. reported on 465 patients with bulky International Federation of Gynecology and Obstetrics (FIGO) stage IIIC epithelial ovarian cancer at a single institution [3]. In an attempt to maintain a homogeneous cohort, the authors excluded patients with stage IIIC disease based on nodal metastases alone, and those with fallopian tube, primary peritoneal, and borderline tumors. Multivariate analysis identified the amount of residual disease as a significant prognostic factor. Patients were classified into one of five categories of residual disease: no gross disease, $\leq$0.5 cm, 0.6–1.0 cm, 1–2 cm, and $\geq$2 cm. Statistical comparisons of these five categories revealed significantly different survival between patients with no gross residual disease, residual disease $\leq$1 cm, and residual disease $>$1 cm. With a median survival of 106 months for the patients with no gross residual disease, the authors concluded that complete gross resection should be the goal of surgery. Others have reported a similar correlation of improved survival with complete cytoreduction [2, 5].

Endometrial Cancer

Endometrial cancer is the most common gynecologic malignancy in the United States. The vast majority of these cases present at an early stage, mainly with organ-confined disease. According to the new FIGO staging system, patients with intra-abdominal metastases are designated as stage IVB. In general, the prognosis of the 3–5 % of patients with endometrial carcinoma who have stage IV disease is poor, with an overall 5-year survival rate of 5–20 %. There is no

consensus as to the most effective postoperative treatment for stage IVB disease, and the role of surgery in these patients has not been clearly defined. With the response rates afforded by current chemotherapy regimens, however, some have adapted the principles of cytoreductive surgery to patients who present with intra-abdominal spread.

In 2004, Lambrou and colleagues [6] reported on 85 patients with stage III and IV disease. All patients underwent initial surgical treatment, and 45.25 % received postoperative radiation therapy, and 27.4 % and 21.2 % received chemotherapy and/or hormonal therapy, respectively. In their analysis of stage IIIC (39 patients) and stage IV (19 patients), the median survival was 17.8 months for patients with optimal cytoreduction (maximum tumor nodules of 2 cm or less) compared with 6.7 months for patients with suboptimal cytoreduction ($P = 0.001$).

Looking specifically at stage IV disease, Goff et al. [7] reported a median survival of 18 months in 29 patients who underwent total abdominal hysterectomy/bilateral salpingo-oophorectomy (TAH/BSO), omentectomy, and tumor cytoreduction for stage IV endometrial carcinoma compared with 8 months for 18 patients with stage IV disease who did not undergo tumor cytoreduction. Of the 18 patients who did not undergo cytoreduction, 15 were considered to have disease too extensive to be resected on preoperative evaluation. The remaining three patients were found to have unresectable, diffuse peritoneal carcinomatosis at exploratory laparotomy. No patient who underwent tumor cytoreduction was left with gross bulky disease; residual disease was not quantified. In their multivariate analysis, successful cytoreduction was the only statistically significant prognostic variable.

To further delineate the impact of surgical cytoreduction on survival, Chi and colleagues [8] compared 55 patients divided among three groups who underwent surgery as part of their primary treatment for stage IV disease. Twenty-four patients underwent TAH/BSO, omentectomy, and optimal tumor cytoreduction (diameter of the largest residual tumor nodule $\leq$2 cm). The second group consisted of 21 patients who also underwent TAH/BSO and omentectomy but had suboptimal surgical cytoreduction (residual disease $>$2 cm). The third group consisted of ten patients who underwent laparotomy without cytoreduction because they had unresectable carcinomatosis. The median survival in each group was 31 months, 12 months, and 3 months, respectively. Within the first group of optimally cytoreduced patients, there was no statistically significant difference in survival between those patients found at laparotomy to have metastatic disease $\leq$2 cm compared to those cytoreduced to $\leq$2 cm residual. On multivariate analysis, only the extent of surgical cytoreduction had prognostic significance on survival. The authors concluded that aggressive surgical cytoreduction may improve survival in patients with stage IV endometrial carcinoma.

Bristow and associates [9] also reported on surgical cytoreduction in 65 patients with stage IVB endometrial carcinoma. Defining optimal debulking as disease $\leq$1 cm, they found that patients who underwent optimal cytoreduction had a median survival of 34 months compared with 11 months for those who had suboptimal disease at surgical completion. On multivariate analysis, residual disease and performance status were the only independent predictors of survival. Given the extent and location of metastatic disease, not all patients are surgical candidates. However, it seems clear that patients with advanced endometrial carcinoma who can undergo optimal cytoreduction obtain a survival benefit from aggressive surgical debulking.

Cervical Cancer

Ablative techniques for the management of invasive cervical cancer are not routinely employed. Unlike ovarian and endometrial cancers, chemotherapy for cervical cancer is not very effective. When cervical cancer is found at its earliest stages, it is usually treated with excision, which entails some form of hysterectomy. If cancer has spread outside the cervix, but still remains

localized, radiation with chemotherapy is the treatment of choice. If cervical cancer has spread in the peritoneum, cytoreduction is not performed. Although not the focus of this chapter, ablative techniques (primarily with the CO_2 laser) have been used for premalignant disease of the cervix. Studies have demonstrated efficacy of ablation of the precursor lesions when compared to the excisional procedures; however, cost and lack of a pathologic specimen are reasons why the excision is favored.

Direct Ablative Techniques for Surgical Cytoreduction

As discussed earlier, the goal of surgical cytoreduction is to remove all visible tumors (complete gross resection). Setting the bar at this level requires meticulous technique and the removal of numerous gross tumor implants. In order to accomplish these goals, gynecologic oncologists must employ a variety of surgical techniques, including the direct ablative techniques that will be reviewed.

Argon Beam Coagulator (ABC)

Electrosurgical ablation of tumor implants and diffuse tumor plaques using the ABC has been a useful tool to eradicate disease in areas not amenable to conventional surgical excision or areas that would require extensive resections, in which the morbidity and long-term consequences can be significant (i.e., diffuse small bowel mesenteric implants) [10]. In addition to tumor ablation, the ABC has a hemostatic effect, and its utility has been demonstrated in surgeries associated with extensive blood loss [11, 12].

Brand et al. first described the use of the ABC in ovarian cancer in 1990 [13]; since then, it has been a commonly used surgical instrument in ovarian cancer surgery and appears to significantly increase the feasibility of achieving optimal debulking as well as complete cytoreduction in patients with metastatic ovarian cancer, with no reported increase in perioperative complications [10, 12]. Venous gas embolism leading to cardiac arrest associated with the use of the ABC has been reported but seems to be a rare event [14].

Mechanism of Action

The ABC uses a beam of inert argon to conduct unipolar current in a noncontact, directed fashion. The energy transmitted (40–150 W) is in the same range as standard monopolar electrocautery. A sensor in the handpiece automatically initiates the electrical current only when the tip is within 10 mm of the target tissue. "Arc tunnels" are then generated and interconnect, leading to a reticular network in the treated tissue. The current spreads out on the tissue surface with a more homogeneous distribution of energy than standard electrocautery, because it distributes the energy in a more even pattern and more uniform depth within the tissue. In addition to tissue destruction, bleeding vessels up to 2–3 mm in diameter can be coagulated during this process. Visibility is enhanced because the flow of argon displaces the blood and debris from the immediate operative field [13, 15].

Histopathologic Effect

Pathologic effects have been reported in experimental animal models on a variety of tissue types (small intestine, liver, spleen, and kidney) [16–18]. A consistent finding in these experimental models is that both power setting and interaction time increase amount of tissue damage.

In the small intestinal injury canine model [16], a 40-W application for 1 s resulted in an injury that reached the muscularis propria in 50 % of cases. At 3 s, tissue damage extended into the submucosa in the majority of applications, and full-thickness injury was seen in all cases after 5 s. In the dogs that were not immediately sacrificed, a 3-s application was associated with delayed (5–7 days after the injury) bowel perforation at 50 % of the application sites [16]. Based on these findings, caution should be exercised when using the ABC close to the bowel serosa [16]. While a short accidental burst could probably be tolerated, direct application on the serosa to ablate tumor should be avoided. If applied

inadvertently for a period longer than 1 s, the area of the small bowel injured should be oversewn or resected. As delayed perforation can occur (up to 7 days after surgery), vigilance should be exercised during the postoperative period for early detection of these complications.

In their initial report on the use of the ABC in ovarian cancer surgery, Brand et al. indicated that the depth of tissue damage was fixed at 2–3 mm [13]. A more detailed evaluation of the histopathologic effects of electrosurgical tumor destruction of metastatic ovarian cancer by the ABC was reported by Bristow et al. [15]. Using 1 cm^3 of epithelial ovarian cancer tumor specimens, the total depth of destruction produced by the ABC was composed of three distinct zones of tissue injury, in order of depth: vaporization (immediate tissue/current interface), carbonized eschar, and coagulative necrosis (deepest layer). They found that the depth of destruction increased from 1.7 mm to 5.5 mm as the power setting of the ABC increased (60, 80, and 100 W) and the interaction time between the ABC and the tissue increased (1 s, 3 s, and 5 s). The increase in depth of destruction was primarily due to the increased tissue vaporization zone. Interestingly, at all power settings and interaction intervals, the ratio of coagulative necrosis/carbonized eschar was highly consistent (ranging from 1 to 1.3), indicating that for any given thickness of carbonized eschar (which is usually grossly visible at the time of surgery), an equivalent or greater degree of underlying coagulative necrosis (despite a grossly "normal" appearing tissue) is also present. Knowing the precise depth of tissue destruction has important clinical and surgical implications when eradicating all visible tumors is the goal. This information is crucial in allowing the surgeon to destroy the tissue to a level that will maximize tumor destruction while preserving as much normal tissue as possible. Typically, 60–80-W settings are used for ablation of subcentimeter implants and tumor nodules on the bowel mesentery, while higher power settings (100–110 W) are used for larger tumor plaques and for disease located on the diaphragm, liver, and abdominal peritoneum (Fig. 57.1).

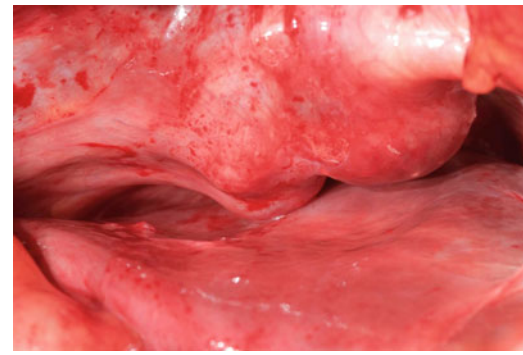

Fig. 57.1 Ovarian cancer diaphragm tumor indenting the liver surface

Cavitron Ultrasonic Surgical Aspirator (CUSA)

The ultrasonic surgical aspirator was first applied in the 1960s for phacoemulsification of cataracts [19] and then in the 1970s for the removal of neurologic tumors [20]. Its surgical advantages, which include reduced blood loss, reduced tissue injury, and improved visibility, have been reported in hepatic, splenic, and renal resections [19, 20]. In the late 1980s, case reports and small series were reported describing its use for female genital tract malignancies. The ultrasonic surgical aspirator is designed to be used in combination with standard operative techniques to aid in the debulking of gynecologic malignancies, mainly ovarian cancer.

Mechanism of Action

The ultrasonic surgical aspirator consists of a handpiece with a high-frequency (23,000 Hz) ultrasonic vibrator, which destroys tissue by cavitation, and an irrigation and aspiration system, which cleans the operative field and cools the tip of the instrument [20]. The instrument disrupts tissue by repetitive striking [21]. The tip is hollow, and broken pieces of tumor are aspirated with saline through the handpiece and into a specimen trap at the bottom of the machine [19]. Cavitation induces selective tissue fragmentation: tissue with high water content (fat, muscle, carcinoma) is destroyed easily, whereas tissue with a high content of collagen and elastic

fibers (blood vessels, nerves, ureters, serosa) is more difficult to damage. The amplitude of vibration controls the excursion of the instrument tip and the depth of tissue disruption. The amplitude setting most commonly used for tumor resection is 0.7–0.8 (210–240 μm) [22]. In contrast to lesions removed with laser or the ABC, the tissue removed can be used to establish a histologic diagnosis [23].

Histopathologic Effect

Thompson et al. compared hematoxylin and eosin-stained histologic sections of tumor removed by CUSA with tumors removed by cold knife. They found that the ultrasound irradiation caused minimal tissue distortion on light microscopy, and the diagnosis was the same for both groups. In addition, tumor cell viability and physiology was not significantly different between the two groups. They used these findings to conclude that the effects of CUSA in vivo on tissues remaining in situ adjacent to the tumor are negligible. This is in agreement with findings in neurologic studies that also showed an absence of neurologic deficit attributable to the use of CUSA for tumor excision [19].

Clinical Application

The CUSA has been used in tumor debulking of gynecologic malignancies, mainly ovarian cancer, in which it seems to be a useful adjunct in achieving complete tumor eradication from the abdomen. Specifically, it is reported to help in the removal of tumor nodules from the diaphragm, liver surface, major vessels, ureters, and bowel and bladder serosa (Fig. 57.2) [10, 20, 21]. It does not seem to be associated with a higher incidence of operative complications. One of the criticisms of the CUSA is that the dissection and removal of tumor can be tedious and time consuming [20]. However, increased operative time may be offset if extensive dissection and reconstruction required by standard techniques can be avoided [22].

The CUSA has also been used in other gynecologic malignancies and premalignant conditions, although the experience has been limited. Deppe et al. reported favorable results when the CUSA is used for palliative control of bleeding in recurrent tumors invading the vagina in patients who had failed standard treatment [24]. Rader et al. reported rapid healing, minimal patient discomfort, and excellent cosmetic results using the CUSA in 27 patients with noninvasive disease of the vulva [25]. Matsuo et al. successfully used the CUSA for the treatment of vaginal intraepithelial neoplasia, with excellent correlation between the histologic diagnosis of the excised specimen and the pretreatment biopsy [26].

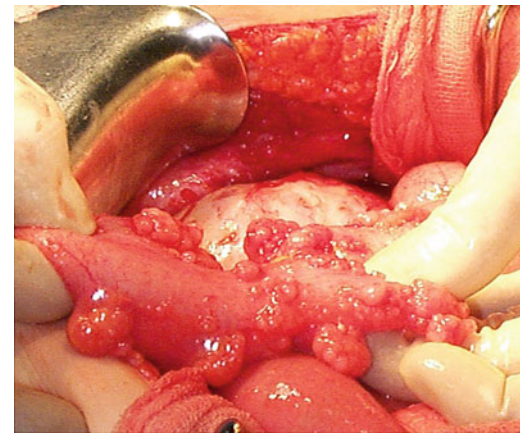

Fig. 57.2 Bowel serosal tumor (Courtesy of Dr. Dennis S. Chi)

Some experts have expressed concern over the CUSA's association with unique complications. Donovan et al. suggested there may be an increased risk of coagulopathy with extended use of the CUSA [27], although this was not seen in others studies [10, 20]. It seems more likely that the extent of surgery required in a significant number of patients with ovarian cancer is probably associated with the development of coagulopathy, rather than the use of the CUSA.

Another concern is whether the "mist" created by the instrument can transport tumor cells and cause local dissemination of the tumor. Ultrasonic cell destruction, combined with continuous irrigation, causes a cloud of fine droplets to form above the surgical field [28]. This mist attaches itself to the surgical mask, and viable cancer cells have been detected in this mist [29]. When using the CUSA for disseminated tumors

(i.e., cytoreduction for advanced ovarian cancer), this may not have meaningful clinical implications. On the other hand, when using the CUSA for removal of other localized tumors, caution should be exercised [28].

Plasma Energy

Pure plasma energy is a new technology that achieves optimal coagulation with minimal tissue damage. This form of coagulation does not require conduction of an electrical current through the patient. Instead, a low-voltage electrical current (30 V) is used only to ionize argon gas to form plasma. Very high temperatures are then created within the plasma, but at a very low mass flow rate. The argon plasma transfers this heat (kinetic) energy to coagulate tissue for rapid and complete hemostasis. The surface temperature of the affected coagulated tissue reaches approximately 100° C; this high temperature causes the liquid component of the tissue to vaporize.

A review of 96 ovarian cancer specimens showed that greater power and tissue interaction resulted in more tumor vaporization, as seen with the ABC; interestingly, the lateral spread remained minimal at all levels [30]. There are no published data on its use in gynecologic malignancies.

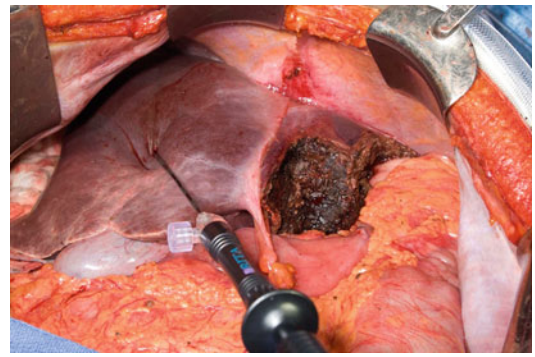

Fig. 57.3 Ovarian cancer liver tumor debulking combining liver resection and intraoperative radiofrequency ablation (Courtesy of Dr. Dennis S. Chi)

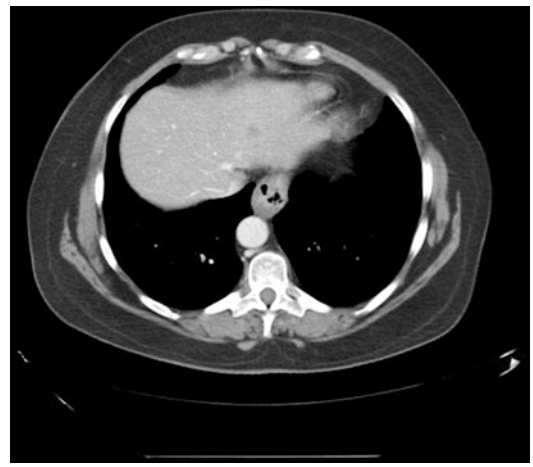

Fig. 57.4 Ovarian cancer intrahepatic tumor treated with intraoperative radiofrequency ablation

Image-Guided Ablation

Radiofrequency Ablation

Radiofrequency ablation (RFA) destroys tumor by generating heat within a lesion, resulting in necrosis of the tumor and surrounding tissue. Since the mid-1990s, RFA has been studied extensively in the treatment of primary and metastatic liver tumors [31]. Its use has since expanded to other solid tumors (kidney, lung) [32]. Its use in the treatment of metastatic gynecologic malignancies has been limited to case reports and small series [31, 33, 34]. The purpose of primary ovarian cancer surgery is to remove all gross disease, and a potential role for RFA would be to allow optimal cytoreduction by ablating intraparenchymal liver metastases that otherwise would not have been removed or would have required major hepatic resections (Figs. 57.3 and 57.4). Another role would be in the recurrent setting, where it could be a useful tool for secondary debulking or for palliation of symptomatic lesions.

Gervais et al. reported on their experience in percutaneous RFA of ovarian cancer hepatic metastases in five women with isolated surface liver disease and one patient with an intraparenchymal lesion [31]. The diameter of the tumors ablated ranged from 1.5 to 5.3 cm. RFA was

performed with CT or sonographic guidance. Overlapping ablations were performed, ranging from one to three ablations per tumor. The entire volume of the tumor, including a small margin of normal liver parenchyma, was covered. A CT scan was performed 1 month after treatment for identification of residual tumor necessitating additional ablation. Technique effectiveness was defined as complete ablation of macroscopic tumor on imaging 3 months after treatment. Absence of enhancement was considered to represent complete necrosis, while residual tumor enhancement within or at the periphery of the target tumor was considered viable tumor. Additional CT scans were performed at 3-month intervals. When CT findings were equivocal, a PET scan was performed. At 3 months, complete necrosis was achieved in 83 % of cases (five patients). After a median follow-up period of 23 months, four of the five patients had no evidence of tumor progression on subsequent imaging, while the fifth patient had an area of increased enhancement at 9 months. This tumor was treated successfully by a second RFA. There were no major complications. Of note, some of the patients treated in this series have received concurrent chemotherapy, and therefore, the exact contribution of each treatment (RFA vs. chemotherapy) on the tumors identified is unknown. These same authors also reported on successful RFA of an isolated retroperitoneal node metastasis in a patient with recurrent ovarian cancer [32].

Mateo et al. reported on the use of RFA combined with hepatectomy in the treatment of three patients with recurrent ovarian cancer in order to achieve optimal tumor cytoreduction [35]. The RFA was performed during laparotomy using intraoperative ultrasound. Jacobs et al. reported on a case of recurrent granulosa cell tumor metastatic to the liver treated successfully with RFA during laparotomy [33]. Bojalian et al. reported on the successful percutaneous RFA treatment of an isolated recurrence to the liver from an epithelial ovarian cancer in an 81-year-old patient after a diagnostic laparoscopy with biopsies and a PET scan failed to identify other sites of disease [34]. Schumacher et al. reported on the successful ablation of an isolated liver metastasis in a patient with ovarian cancer using a hand-assisted laparoscopic approach [36]. Other large series of RFA of liver tumors include few patients with gynecologic cancers, and do not include specific clinical details on the patients treated [37].

Intraoperative use of RFA is probably favored over percutaneous treatment for several reasons. Despite the use of CT, liver surface metastases can be mistaken for parenchymal lesions, while miliary diaphragm disease may not be detected by CT. In addition, intraoperative ultrasound may detect lesions not seen on a preoperative CT scan, and these additional lesions may be amenable to ablation [35]. Finally, CT may not detect disseminated peritoneal disease, whose presence may influence the treatment decision and whether ablating the liver lesions remains a sound option. In this setting, a laparoscopic approach may be particularly attractive as it can allow visualization of the abdominal surfaces, as well as intraoperative ultrasound and RFA of liver lesions if indicated. Percutaneous RFA would then be the preferred option in patients with symptomatic tumors on imaging who are not candidates for surgical exploration.

The role of RFA in gynecologic malignancies, particularly in the management of liver metastases, remains to be defined. The published literature is very limited and pertains mainly to small series and case reports proving technical feasibility. Larger series with oncologic outcome data are needed to better define RFA's role in the treatment of gynecologic malignancies.

Cryotherapy

Recent advances in cryotherapy technology have allowed this therapy to be used for image-guided ablation of several solid tumors, with a large portion of the literature relating to prostate cancer and colorectal cancer liver metastases. Cellular damage is caused by direct injury due to ice crystal formation and microcirculatory failure [38]. The use of cryotherapy in gynecologic malignancies has been limited to the palliative setting, mainly to manage recurrent symptomatic

metastases refractory to conventional therapy where surgical treatment has been considered clinically inappropriate either due to the overall condition of the patient or to an unusual location where surgery would entail significant risk [39].

Solomon et al. reported on their experience in using cryotherapy in 15 patients with recurrent symptomatic gynecologic malignancies for which surgical removal was not deemed appropriate [39]. Twenty-eight ablation procedures were performed for 41 metastatic foci. CT guidance was used for all cases. Ten patients received concurrent chemotherapy. Tumor locations included the lungs, liver, spleen, and perivaginal, intraperitoneal, retroperitoneal, and superficial soft tissues. The average tumor size was 2.57 cm (range, 1.2–4.6 cm). The goal for visible ice was chosen to extend approximately 1 cm beyond the tumor margins. The median percent decrease in tumor dimension was 21.4 % at 1 month, 43.6 % at 3 months, 53.7 % at 6 months, and 58.2 % at 9 months, with some tumors decreasing in size by up to 88 %. Reported complications included a liver capsule hematoma and an enterocutaneous fistula.

Embolization

Embolization of the hypogastric arteries to control bleeding from an advanced cervical cancer was first described in 1976 [40]. Since then, embolization of pelvic vessels (hypogastric arteries or smaller branches) has been used with increased frequency in gynecologic malignancies to control bleeding from advanced or recurrent malignancies when other treatments (radiation, surgery) have failed, carry significant risk, or are technically not feasible (Fig. 57.5).

Advanced gynecologic malignancies in the pelvis can present with either vaginal or rectal bleeding. When the patient presents with vaginal bleeding, the traditional initial steps in management include vaginal packing and radiation [41]. When these fail, embolization of the tumor is a reasonable option. It is particularly indicated when surgery is associated with significant risks and/or may not be able to achieve control of the bleeding (previous radiation, previous surgeries, unresectable tumors in the pelvis eroding into pelvic vessels). In addition, surgical ligation of the internal iliac arteries may not necessarily control the bleeding [42] and may result in the inability to access additional bleeding vessels by percutaneous methods should bleeding recur from collaterals.

The evidence for the efficacy of embolization in controlling pelvic hemorrhage comes from case reports, case series, and small studies [41, 43–46].

Lang et al. reported on 24 patients with pelvic neoplasms who developed uncontrollable bleeding [44]. Among them, 12 patients had cervical cancer. All were treated successfully. Delayed complications included a vesicovaginal and a ureterovaginal fistulas in two patients, respectively (2 months after the embolization). Of note, their tumor was already invading the bladder, and the fistulas were thought to be also related to tumor progression and necrosis rather than exclusively a result of embolization.

Yamashita et al. reported on 17 patients with primary advanced or recurrent cervical cancer who developed massive hemorrhaging and were treated by arterial embolization [47]. The immediate response was 100 %; however, seven patients (40 %) had recurrent bleeding within 2 weeks, of which three required a second embolization. Complications were reported in two patients—transient numbness in the lower extremity in one patient and a buttock ulcer that healed after 2 weeks in the other.

Spinosa et al. reported on the successful treatment of two patients with massive lower gastrointestinal bleeding from advanced cervical carcinoma [43]. In both cases, the bleeding originated from the internal iliac arteries or their branches and was treated with percutaneous embolization. In cases presenting with heavy rectal bleeding, colonoscopy is commonly not able to visualize or treat the source of the bleeding. If an angiogram is performed to identify the source of bleeding, imaging should not be limited to visualization of the branches of the superior and inferior mesenteric arteries (most common sources of lower gastrointestinal bleeding) but should also

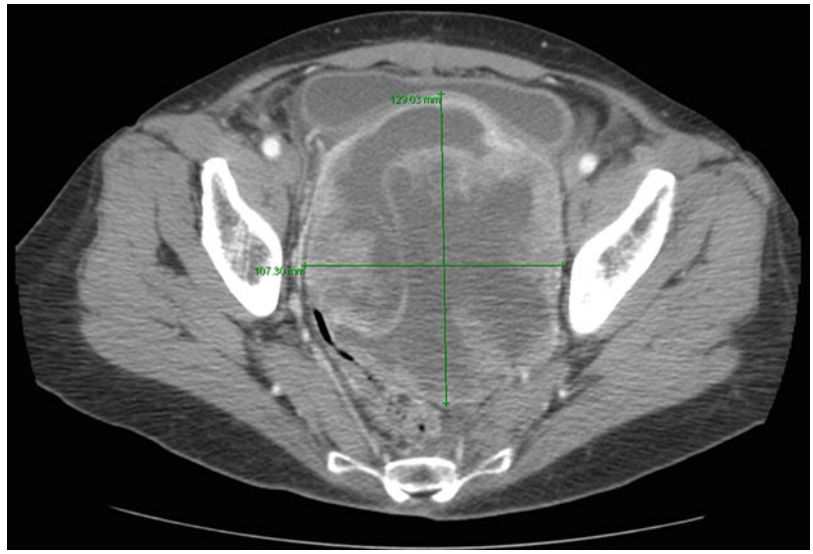

Fig. 57.5 Pelvic tumor embolized prior to surgical removal

include the pelvic vessels, as the bleeding can be from the pelvic tumor eroding into a pelvic vessel and into the bowel wall [43].

Uterine artery embolization has also been successfully used in controlling life-threatening hemorrhaging from gestational trophoblastic disease, allowing uterine and fertility preservation [46].

Intraoperative Ultrasound

Intraoperative ultrasound has not gained widespread use in gynecologic oncology and is not part of the standard tools used in the surgical management of gynecologic malignancies. The current evidence to support its role comes from a few single-institution reports, with no large validated data available [48]. Other reports have shown disappointing results [49].

Assessment of Lymph Nodes

Ryo evaluated the role of intraoperative ultrasonography in detecting enlarged aortic nodes in 163 women with ovarian or uterine corpus malignancies [48]. He defined a node as abnormal when its diameter in the transverse plane was larger than 5 mm. The sensitivity, specificity, and positive and negative predictive values of intraoperative ultrasound in detecting metastatic aortic nodes were 91.4 %, 69.5 %, 45.1 %, and 96.7 %, respectively. In this series, the sensitivity and negative predictive values of intraoperative ultrasonography were higher than either preoperative CT or intraoperative palpation and thus could be used to decrease the number of aortic lymph node dissections; if only sonographically suspicious nodes were removed, the number of lymphadenectomies could have been reduced by 43.6 % while missing aortic node metastasis in 1.8 % of the patients. The duration of the intraoperative ultrasonography was less than 5 min.

Yang et al. compared laparoscopic ultrasound with surgical pathology in the evaluation of pelvic nodes in 31 women with cervical cancer [50]. A lymph node that was rounded (longitudinal-transverse ratio <2) or showed absence of central hilum was defined as positive for metastasis. Size was not a criterion. The duration of the laparoscopic ultrasound examination was completed in approximately 20 min after an initial learning period of 4 months. Laparoscopic sonography was able to detect only 59 % of metastatic lymph nodes. Similarly, Cheung et al. [51] evaluated laparoscopic ultrasound in 90 patients with cervical carcinoma. The sensitivity, specificity, and positive and negative predictive values of laparoscopic ultrasound in detecting pelvic lymph node metastasis were 63.6 %, 95.6 %,

82.4 %, and 89 %, respectively. The reduced sensitivity was mainly attributable to the failure of the ultrasound to detect solitary metastatic foci less than 3 mm in size.

Teefey et al. evaluated intraoperative ultrasound to detect myometrial invasion in 16 patients with endometrial carcinoma and concluded it was inaccurate in predicting the location and depth of myometrial invasion, performing no better than transvaginal ultrasound or gross visual inspection [49].

Yang et al. used intraoperative ultrasound to assess adnexal masses in 58 women. The scanning time was approximately 10–15 min. When compared to transvaginal ultrasonography, laparoscopic sonography showed greater morphologic detail, was able to demonstrate the presence of residual ovarian tissue more frequently, and, most importantly, allowed detection of additional adnexal lesions not evident on preoperative transvaginal sonography [52]. Laparoscopic sonography may therefore play a potential role in the surgical management of early-stage ovarian carcinoma and borderline tumors in women of young age with a strong desire for childbearing, in whom a unilateral salpingo-oophorectomy may be considered. In those cases, an intraoperative ultrasound may allow better evaluation of the contralateral ovary. However, its role in this setting has not been studied yet.

Magnetic Resonance (MR)-Guided High Intensity Focused Ultrasound (HIFU)

MR-HIFU is a treatment technique in which an ultrasound beam is guided to selectively ablate tissues within its focus, in parallel with MR imaging used for anatomic visualization, beam guidance, real-time thermometry, and post-procedure assessment [53]. Its main gynecologic application at this time has been in the noninvasive treatment of benign uterine leiomyomas with apparently high rates of patients' satisfaction (up to 80–90 % patient satisfaction at 12 months) with an almost absent incidence of serious side effects [54]. Although the use MR-HIFU is being investigated in the treatment of a variety of tumors, there is currently no data for its role in the management of gynecologic malignancies.

Conclusion

Direct ablative techniques are commonly used in the management of gynecologic malignancies, particularly in advanced ovarian and endometrial cancers. These techniques have become more important as an increasing body of literature shows that complete gross resection translates into improved outcomes for patients with advanced ovarian and endometrial cancers.

There remains a paucity of data on the use of image-guided therapy for the management of gynecologic malignancies. This primarily has to do with the multifocal spread patterns of these cancers. However, as the field of gynecologic oncology continues to evolve and patient outcomes improve, new situations may arise that warrant the application of more image-guided therapy.

References

1. Griffiths CT. Surgical resection of tumor bulk in the primary treatment of ovarian carcinoma. Natl Cancer Inst Monogr. 1975;42:101–4.
2. Armstrong DK, Bundy B, Wenzel L, Gynecologic Oncology Group, et al. Intraperitoneal cisplatin and paclitaxel in ovarian cancer. N Engl J Med. 2006;354:34–43.
3. Chi DS, Eisenhauer EL, Lang J, et al. What is the optimal goal of primary cytoreductive surgery for bulky stage IIIC epithelial ovarian carcinoma? Gynecol Oncol. 2006;103:559–64.
4. Winter 3rd WE, Maxwell GL, Tian C, et al. Prognostic factors for stage III epithelial ovarian cancer: a Gynecologic Oncology Group Study. J Clin Oncol. 2007;25:3621–7.
5. Eisenkop SM, Friedman RL, Wang HJ. Complete cytoreductive surgery is feasible and maximizes survival in patients with advanced epithelial ovarian cancer: a prospective study. Gynecol Oncol. 1998;69:103–8.
6. Lambrou NC, Gómez-Marín O, Mirhashemi R, et al. Optimal surgical cytoreduction in patients with stage III and stage IV endometrial carcinoma: a study of morbidity and survival. Gynecol Oncol. 2004;93:653–8.

7. Goff BA, Goodman A, Muntz HG, et al. Surgical stage IV endometrial carcinoma: a study of 47 cases. Gynecol Oncol. 1994;52:237–40.
8. Chi DS, Welshinger M, Venkatraman ES, Barakat RR. The role of surgical cytoreduction in stage IV endometrial carcinoma. Gynecol Oncol. 1997;67:56–60.
9. Bristow RE, Zerbe MJ, Rosenshein NB, Grumbine FC, Montz FJ. Stage IVB endometrial carcinoma: the role of cytoreductive surgery and determinants of survival. Gynecol Oncol. 2000;78:85–91.
10. Eisenkop SM, Nalick RH, Wang HJ, Teng NN. Peritoneal implant elimination during cytoreductive surgery for ovarian cancer: impact on survival. Gynecol Oncol. 1993;51:224–9.
11. Rusch VW, Schmidt R, Shoji Y, Fujimura Y. Use of the argon beam electrocoagulator for performing pulmonary wedge resections. Ann Thorac Surg. 1990;49:287–91.
12. Bristow RE, Montz FJ. Complete surgical cytoreduction of advanced ovarian carcinoma using the argon beam coagulator. Gynecol Oncol. 2001; 83:39–48.
13. Brand E, Pearlman N. Electrosurgical debulking of ovarian cancer: a new technique using the argon beam coagulator. Gynecol Oncol. 1990;39:115–8.
14. Kizer N, Zighelboim I, Rader JS. Cardiac arrest during laparotomy with argon beam coagulation of metastatic ovarian cancer. Int J Gynecol Cancer. 2009;19:237–8.
15. Bristow RE, Smith Sehdev AE, Kaufman HS, Montz FJ. Ablation of metastatic ovarian carcinoma with the argon beam coagulator: pathologic analysis of tumor destruction. Gynecol Oncol. 2001;83:49–55.
16. Go PM, Bruhn EW, Garry SL, Hunter JG. Patterns of small intestinal injury with the argon beam coagulator. Surg Gynecol Obstet. 1990;171:341–2.
17. Go PM, Goodman GR, Bruhn EW, Hunter JG. The argon beam coagulator provides rapid hemostasis of experimental hepatic and splenic hemorrhage in anticoagulated dogs. J Trauma. 1991;31:1294–300.
18. Hernandez AD, Smith Jr JA, Jeppson KG, Terreros DA. A controlled study of the argon beam coagulator for partial nephrectomy. J Urol. 1990;143:1062–5.
19. Thompson MA, Adelson MD, Jozefczyk MA, Coble DA, Kaufman LM. Structural and functional integrity of ovarian tumor tissue obtained by ultrasonic aspiration. Cancer. 1991;67:1326–31.
20. van Dam PA, Tjalma W, Weyler J, van Oosterom AT, Buytaert P. Ultraradical debulking of epithelial ovarian cancer with the ultrasonic surgical aspirator: a prospective randomized trial. Am J Obstet Gynecol. 1996;174:943–50.
21. Deppe G, Malviya VK, Malone Jr JM, Christensen CW. Debulking of pelvic and para-aortic lymph node metastases in ovarian cancer with the cavitron ultrasonic surgical aspirator. Obstet Gynecol. 1990;76:1140–2.
22. Rose PG. The cavitational ultrasonic surgical aspirator for cytoreduction in advanced ovarian cancer. Am J Obstet Gynecol. 1992;166:843–6.
23. Deppe G, Malviya VK, Malone Jr JM. Debulking surgery for ovarian cancer with the Cavitron Ultrasonic Surgical Aspirator (CUSA)–a preliminary report. Gynecol Oncol. 1988;31:223–6.
24. Deppe G, Malviya VK, Malone Jr JM. Use of Cavitron Ultrasonic Surgical Aspirator (CUSA) for palliative resection of recurrent gynecologic malignancies involving the vagina. Eur J Gynaecol Oncol. 1989; 10:1–2.
25. Rader JS, Leake JF, Dillon MB, Rosenshein NB. Ultrasonic surgical aspiration in the treatment of vulvar disease. Obstet Gynecol. 1991;77:573–6.
26. Matsuo K, Chi DS, Walker LD, Rosenshein NB, Im DD. Ultrasonic surgical aspiration for vaginal intraepithelial neoplasia. Int J Gynaecol Obstet. 2009;105:71–3.
27. Donovan JT, Veronikis DK, Powell JL, Lundy LE, Préfontaine M. Cytoreductive surgery for ovarian cancer with the Cavitron Ultrasonic Surgical Aspirator and the development of disseminated intravascular coagulation. Obstet Gynecol. 1994;83:1011–4.
28. van Dam PA, Coppens M, van Oosterom AT, Van Marck E, Buytaert P. Is there an increased risk for tumor dissemination using ultrasonic surgical aspiration in patients with vulvar carcinoma? Eur J Obstet Gynecol Reprod Biol. 1994;55:145–7.
29. Nahhas WA. A potential hazard of the use of the surgical ultrasonic aspirator in tumor reductive surgery. Gynecol Oncol. 1991;40:81–3.
30. Sonoda Y, Olvera N, Chi DS, Brown CL, Abu-Rustum NR, Levine DA. Pathologic analysis of ex vivo plasma energy tumor destruction in patients with ovarian or peritoneal cancer. Int J Gynecol Cancer. 2010;20(8):1326–30.
31. Gervais DA, Arellano RS, Mueller PR. Percutaneous radiofrequency ablation of ovarian cancer metastasis to the liver: indications, outcomes, and role in patient management. AJR Am J Roentgenol. 2006; 187:746–50.
32. Gervais DA, Arellano RS, Mueller PR. Percutaneous radiofrequency ablation of nodal metastases. Cardiovasc Intervent Radiol. 2002;25:547–9.
33. Jacobs IA, Chang CK, Salti G. Hepatic radiofrequency ablation of metastatic ovarian granulosa cell tumors. Am Surg. 2003;69:416–8.
34. Bojalian MO, Machado GR, Swensen R, Reeves ME. Radiofrequency ablation of liver metastasis from ovarian adenocarcinoma: case report and literature review. Gynecol Oncol. 2004;93:557–60.
35. Mateo R, Singh G, Jabbour N, Palmer S, Genyk Y, Roman L. Optimal cytoreduction after combined resection and radiofrequency ablation of hepatic metastases from recurrent malignant ovarian tumors. Gynecol Oncol. 2005;97:266–70.
36. Schumacher G, Eisele R, Spinelli A, et al. Indications for hand-assisted laparoscopic radiofrequency ablation for liver tumors. J Laparoendosc Adv Surg Tech A. 2007;17:153–9.

37. Bleicher RJ, Allegra DP, Nora DT, Wood TF, Foshag LJ, Bilchik AJ. Radiofrequency ablation in 447 complex unresectable liver tumors: lessons learned. Ann Surg Oncol. 2003;10:52–8.
38. Baust JG, Gage AA. The molecular basis of cryosurgery. BJU Int. 2005;95:1187–91.
39. Solomon LA, Munkarah AR, Vorugu VR, et al. Image-guided percutaneous cryotherapy for the management of gynecologic cancer metastases. Gynecol Oncol. 2008;111:202–7.
40. Smith DC, Wyatt JF. Embolization of the hypogastric arteries in the control of massive vaginal hemorrhage. Obstet Gynecol. 1977;49:317–22.
41. Lin YC, Kudelka AP, Lawrence D, et al. Transcatheter arterial embolization for the control of life-threatening pelvic hemorrhage in a patient with locally advanced cervix carcinoma. Eur J Gynaecol Oncol. 1996;17:480–3.
42. Burchell RC. Physiology of internal iliac artery ligation. J Obstet Gynaecol Br Commonw. 1968;75:642–51.
43. Spinosa DJ, Angle JF, McGraw JK, Maurer EJ, Hagspiel KD, Matsumoto AH. Transcatheter treatment of life-threatening lower gastrointestinal bleeding due to advanced pelvic malignancy. Cardiovasc Intervent Radiol. 1998;21:503–5.
44. Lang EK. Transcatheter embolization of pelvic vessels for control of intractable hemorrhage. Radiology. 1981;140:331–9.
45. Mihmanli I, Cantasdemir M, Kantarci F, et al. Percutaneous embolization in the management of intractable vaginal bleeding. Arch Gynecol Obstet. 2001;264:211–4.
46. Frati A, Ducarme G, Wernet A, Chuttur A, Vilgrain V, Luton D. Uterine artery embolization as treatment for life-threatening haemorrhage from a cervical choriocarcinoma: a case report. Eur J Obstet Gynecol Reprod Biol. 2008;141:87–8.
47. Yamashita Y, Harada M, Yamamoto H, et al. Transcatheter arterial embolization of obstetric and gynaecological bleeding: efficacy and clinical outcome. Br J Radiol. 1994;67:530–4.
48. Ryo E. Diagnostic value of intraoperative ultrasonography to assess para-aortic lymph nodes in women with ovarian and uterine corpus malignancy. Ultrasound Obstet Gynecol. 2008;32:91–6.
49. Teefey SA, Roarke MC, Brink JA, et al. Bowel wall thickening: differentiation of inflammation from ischemia with color Doppler and duplex US. Radiology. 1996;198:547–51.
50. Yang WT, Cheung TH, Ho SS, Yu MY, Metreweli C. Comparison of laparoscopic sonography with surgical pathology in the evaluation of pelvic lymph nodes in women with cervical cancer. AJR Am J Roentgenol. 1999;172:1521–5.
51. Cheung TH, Lo WK, Yu MY, Yang WT, Ho S. Extended experience in the use of laparoscopic ultrasound to detect pelvic nodal metastasis in patients with cervical carcinoma. Gynecol Oncol. 2004;92:784–8.
52. Yang WT, Yuen PM, Ho SS, Leung TN, Metreweli C. Intraoperative laparoscopic sonography for improved preoperative sonographic pathologic characterization of adnexal masses. J Ultrasound Med. 1998;17:53–61.
53. Cline HE, Hynynen K, Watkins RD, et al. Focused US system for MR imaging-guided tumor ablation. Radiology. 1995;194:731–7.
54. Gorny KR, Woodrum DA, Brown DL, et al. Magnetic resonance-guided focused ultrasound of uterine leiomyomas: review of a 12-month outcome of 130 clinical patients. J Vasc Interv Radiol. 2011;22:857–64.

Breast Ablation for Breast Imagers and Interventional Radiologists

58

Peter J. Littrup

Abstract

The long history of success with less-invasive, breast conservation surgery in combination with radiation therapy and systemic chemo-hormonal therapy serves as an excellent background to address recent rapid advancements in technology for both imaging and ablation. This chapter primarily will address the complexities of breast cancer ablation, although over one million benign resections are still being performed in the USA every year for growing or painful fibroadenomas. The choice of different imaging modalities for baseline workup extends to their role in guidance and follow-up. Ablation technologies also need to be carefully evaluated in relation to their optimum usage with the various imaging choices and guidance. Breast MRI has rapidly become the "gold standard" but has severe incompatibility issues with several ablation technologies and may never be cost-effective enough to address large sectors of the breast cancer population. We attempt to balance these crucial issues at a time when a new paradigm for breast tumor ablation is emerging.

Introduction

The preceding chapters emphasized the changing landscape of breast cancer treatment for both radiation oncologists and breast surgeons. Radiation oncologists view their role in treating breast cancer from a stable perspective, since for the near future, they can continue to follow decades of experience in assisting the outcomes of surgical resection. Meanwhile, breast surgeons are rapidly adopting the concept that palpable surgical guidance has been nearly replaced by the greater accuracy of imaging for diagnosis, as well as planning the extent of their resections. Surgeons see this imaging transition as more of an adjunct to their current procedures of open surgical biopsy and cancer resection as needed. Yet, image guidance has been the primary domain of breast imaging by nearly all diagnostic radiologists, as well as the ablation domain of interventional radiologists.

We are thus at a crossroads in the changing paradigm for breast cancer screening and treatment, both for patients with newly diagnosed as

P.J. Littrup
Imaging Division, Karmanos Cancer Institute, Detroit, MI, USA
e-mail: littrupp@karmanos.org

D.E. Dupuy et al. (eds.), *Image-Guided Cancer Therapy*, DOI 10.1007/978-1-4419-0751-6_60,

well as locally recurrent breast cancer. As breast surgeons become more facile with image-guided techniques, the role of breast imagers and/or interventional radiologists also needs clarification. Namely, there are few breast imagers with tumor ablation experience in other organ sites; similarly, few interventional radiologists are certified breast imagers. Inside radiology practices, a paucity of ablation experience exists for most breast imagers. Rather than focus on the territoriality of subspecialties as they evolve to meet the changing needs and capabilities of radiologists or surgeons, the intent of this chapter is to highlight key *imaging* issues that will facilitate interventional oncology's role for benign and malignant breast tumors. In this manner, modern imaging now impacts the spectrum of breast care, extending from surgical pathology as a "gold standard" for screening outcomes to clinicians and oncologists managing the subsequent outcomes of ablation. Regardless of which subspecialty will have accepted the technical and clinical responsibilities of performing breast tumor ablation, attention to state-of-the-art imaging and technology options will provide the best outcomes for women.

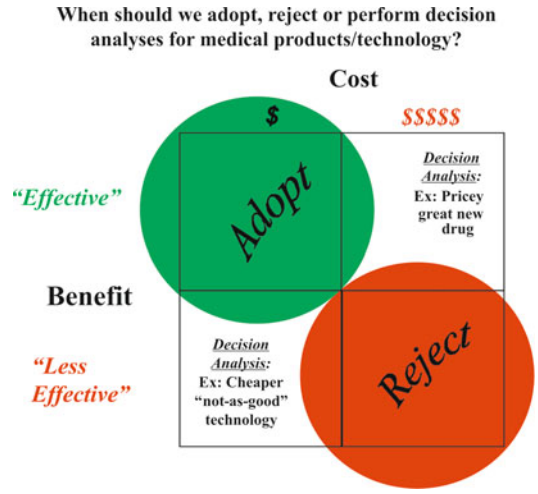

Fig. 58.1 *Need for decision analyses*: Basic 2-by-2 decision analysis box for assessing new medical drugs or technology. A low-cost highly effective product (*green*) should lead to rapid acceptance and implementation. Conversely, a costly but less effective product (*red*) should lead to prompt rejection. Decision analyses are thus required for products which are costly but effective products or inexpensive and less effective. Relative costs are thus balanced against efficacy, frequently referred to as the incremental cost-effectiveness ratio (ICER). Acceptance has been justified as an ICER less than $50,000 per life year saved [13]

Pathology as a Gold Standard

Impact upon Screening and Ablation Concepts

Fortunately or unfortunately, the multifaceted aspects of breast cancer research also contributed to recent controversies in breast cancer screening by mammography, once considered the gold standard for all of breast imaging [1–4]. Saving lives through cost-effective screening is only part of a large, complex puzzle of breast cancer issues. Breast imaging has now extended well beyond mammography, with magnetic resonance imaging (MRI) now considered optimal for screening high-risk women due to its superior diagnostic performance for tumor differentiation and malignant extent [5–7]. Breast MRI may also have 90 % sensitivity for detecting the premalignant or coexisting condition of high-grade ductal carcinoma in situ (DCIS) [8, 9]. Autopsy series suggest that not all DCIS is clinically relevant [9], nor does it always progress in the contralateral breast if undetected or left untreated [10]. MR thus has exceptionally high negative predictive value to exclude the presence of nearly all clinically relevant tumors. However, the superb performance of breast MRI does not validate it as a broad screening tool due to access by all women and costs.

Breast-imaging controversies and/or uncertain treatment efficacy should not prevent us from performing thoughtful benefit-cost analyses, similar to that we initiated for prostate cancer screening when clear mortality benefits could not be defined for prostate specific antigen as a screening test [11, 12]. Such considerations are beyond the scope of this chapter, but Fig. 58.1 helps simplify the need for decision analyses and when to accept or reject any new medical products, drugs, or technology [13]. Much of what will be considered for ablation

imaging involves not only the performance of screening modalities but also the type of tumor that is being diagnosed and the role of imaging in treatment follow-up. Emerging new imaging technologies will be briefly covered in the next chapter after the type of tumor and pathologic extent are considered for current imaging options.

Screening for breast cancer favors the simplistic idea that a "window of curability" exists for nearly all detected tumors, when in fact most consider breast cancer an early systemic disease. The contemporary view of breast cancer is that it is NOT a single disease that remains well localized as a small tumor for an extended period time. The widespread availability of tumor markers has better characterized breast cancer as a heterogeneous disease with many subtypes, commonly distinguished by the presence of estrogen, progesterone, and HER2/neu receptor amplification (ER, PR, and HER2) [14]. Indeed, triple-negative breast cancers have now been better defined at the time of diagnosis as larger, occurring in younger women and having greater risk for local occurrence, yet with lower likelihood of early lymphatic spread [15]. Similarly, breast density not only increases the risk of breast cancer [16] but also may make cancers more likely to be multicentric and mammographically occult, despite being associated with more calcifications and architectural distortion [17]. Cancers in dense breasts also tend to have greater incidence of luminal or lobular cancer subtypes and result in more frequent mastectomy, despite showing no greater propensity for increased size or lymph node involvement. The breast density conundrum again emphasizes the need for breast MRI screening in high-risk women.

Much of the controversy about ablation of newly diagnosed cancers relates to the lack of tissue confirmation afforded by resection. However, rigid adherence to the pathologic specimen may also be outdated, or at least biased, by changing perspectives caused by advances in imaging and biopsy. After tumors are initially detected and undergo lumpectomy, treatment decisions for additional chemo and/or radiation therapy currently depend upon tumor size and biomarker status from the resection specimen. While tumor size may be less accurate by US or MRI, histologic tumor measurements may not be practical or accurate, especially for smaller tumors. Breast specimens also have variability due to both tumor and tissue shrinkage during fixation [18, 19]. Distortion of tumor measurements from the resection specimens is common following large core, vacuum-assisted biopsy especially for small tumors [20]. Tumor measurements from lumpectomy specimens are thus unreliable when little, or even no, residual tumor remains. Techniques need to be defined for measuring a representative tumor length on biopsy core biopsy specimens. Some suggest that US-guided core biopsies are comparable to the surgical specimen for all prognostic markers [21]. Finally, a new era of individual tumor markers is also beginning, such that tumor size criteria may not be as important for chemotherapy decisions, at least for estrogen-receptor-positive, node-negative patients [22–24]. The absolute size of tumor foci within a tumor core relative to the actual specimen also raises the issue of the need for frequent re-resection [25].

How Beneficial Is Resection in Relation to Identifying Positive Surgical Margins?

Currently, if there is a positive surgical margin, residual tumor can be found at the time of re-resection in up to 50 % of specimens [25]. US guidance of lumpectomy localization may decrease the rate of positive surgical margins to ~11 %, down from a high of 50 % for mammographically guided wire localization of breast cancers. Positive surgical margins could be decreased to as low as 5 % if a freeze margin is extended >6 mm beyond the US-visible breast tumor and then resecting the iceball in a procedure known as cryo-assisted lumpectomy [26]. These factors suggest

> Most surgeons would state that performing a lumpectomy is one of the most imprecise procedures they perform: determining an accurate margin even around an easily palpable lesion can

be limited by the composition of the tissue. Frequently in young women the tissue is dense and the tumor can be difficult to differentiate from fibrocystic breast tissue. In older women, or in women with fatty breasts, trying to preserve fatty breast tissue around a tumor that is determined to separate from the tumor can be a source of frustration. [26]

While surgeons and pathologists are still not willing to relinquish any tissue data gained by even inaccurate resections, surgeons already acknowledge that imaging will play a crucial role in improving the outcomes of local treatment. Thereby, we need to consider not only the paradigm of tissue confirmation but also the reliability and accuracy that it currently provides. We can now consider the role of ablation in the changing landscape of imaging, guidance, and treatment follow-up.

Ablation Guidance

US/CT/MRI and Their Impact Upon Ablation Options

Breast ***MRI*** represents the most accurate imaging modality for breast cancer detection and characterization of tumor size and extent, including DCIS [5–8]. Techniques and utility of MR for biopsy and guidance have also been established [27]. MR also remains the only imaging technology that can reliably map hyperthermic changes to validate thorough necrosis (e.g., >60° C), as well as clearly define the 0° C rim of a progressing iceball. Nevertheless, MR compatibility of percutaneous ablation technology has so far been limited to single companies producing *laser* (Visualase, Inc.) (Fig. 58.2) and *cryoablation* (Galil, Inc.) products, but neither have adapted their products to be specifically compatible with current MR breast biopsy fixtures for the treatment of either benign or malignant breast masses. Only *high-intensity focused ultrasound* (*HIFU*) has been clinically used for breast tumors in conjunction with MRI-guided temperature mapping [28–30] (Fig. 58.3). MRI-guided HIFU remains a technically complex procedure with high equipment costs and even more restricted patient access. In addition, MRI-guided HIFU is currently limited to smaller masses (e.g., <2 cm) due to extended treatment times of up to 2 h for tumors up to 2-cm. Broad applicability to the spectrum of breast cancer patients may only be possible with newer treatment regimens that avoid multiple pinpoint ablations (Fig. 58.3). By volumetrically heating an entire target region, decreased total treatment time or much larger volumes appear feasible (Siemens communication).

Equipment compatibility and access to interventional MR units make ***CT and/or US guidance*** the preferred methods for guiding ablation in most organ sites. MRI is currently limited for percutaneous ablation guidance yet well suited as a "roadmap" for US/CT guidance since it accurately defines breast cancer extent and multicentricity. MRI-guided breast procedures need to become more accessible and cost-effective in order to effectively utilize emerging MRI-compatible ablation technologies. Until then, the MR roadmap for procedural guidance by US and/or CT provides an excellent transition.

US alone remains highly operator and equipment dependent. The weaker performance of US alone for screening [31] and evaluation of tumor size and extent [7, 32] thus appears to outweigh its superior cost efficacy compared to breast MRI. Again, this is an example of a low-cost test with worse clinical performance needing to be better evaluated by future decision analyses (Fig. 58.1). In addition, newer ultrasound technology will be described later which may alter these cost analyses by providing better diagnostic and operator-independent performance. Nevertheless, US targeting of breast MRI findings has been described [33, 34], as well as the potential for MR biopsy to leave a range of clips that are US visible [35]. Ultrasound alone probably provides the best real-time procedure guidance but also suffers from distinct artifacts that may limit monitoring of many ablation procedures (Fig. 58.4).

US guidance appears ideal for outpatient-based procedures since the relative low cost of these machines is amenable to office, clinic and/or, breast center settings. However, US guidance of tumor ablation is more complex than

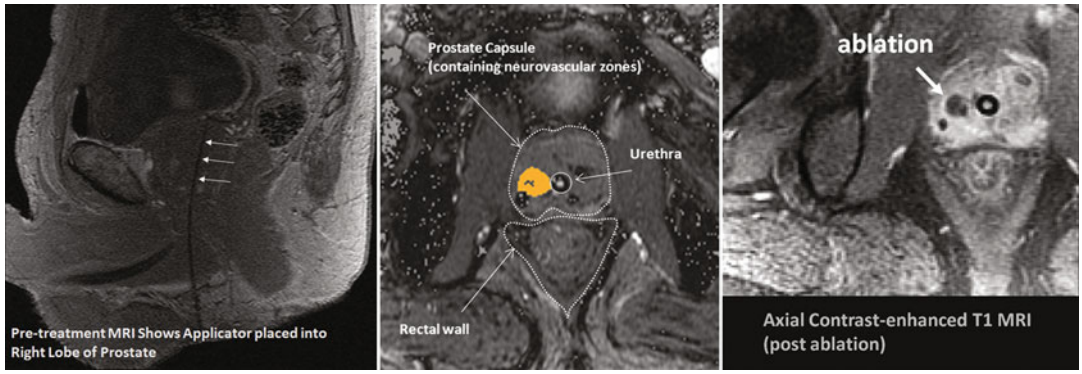

Fig. 58.2 *MR guidance and thermometry for laser ablation*: Sagittal (*far left* and *far right*) and axial (*central*) MR images during prostate ablation show 1.6-mm OD laser probe (Visualase Inc., Houston Texas) in place (*left*). Colorized thermal monitoring during ablation (*middle left*) and resultant axial and sagittal post-ablation lesions (*middle right*) help monitor ablation extent. Currently, this technology is targeted primarily for brain and prostate ablation

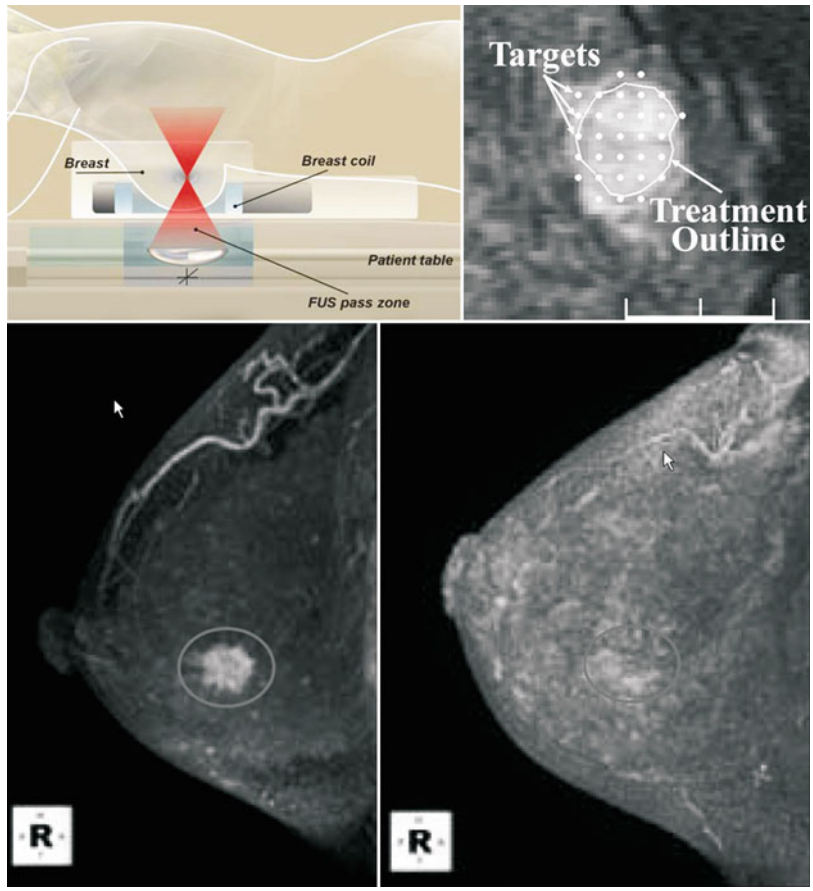

Fig. 58.3 *MR guidance of breast HIFU*: While it is truly noninvasive and provides excellent thermal monitoring, MR-guided HIFU is still limited to smaller masses. Long treatment times may be improved in the future with more efficient volumetric treatment protocols. Top left image graphically demonstrates ablation technique generated from HIFU unit within the MR table/breast coil which targets a tumor within the breast while the woman lies prone (From Schmitz [29]). Top right image shows the multiple target points for each sonication that eventually coalesce to form an ablation zone covering the target tumor(From Hynynen [27]). Bottom row shows sagittal MR images pre- (*left*) and post-ablation (*right*) of a small local breast cancer (From Wu [30])

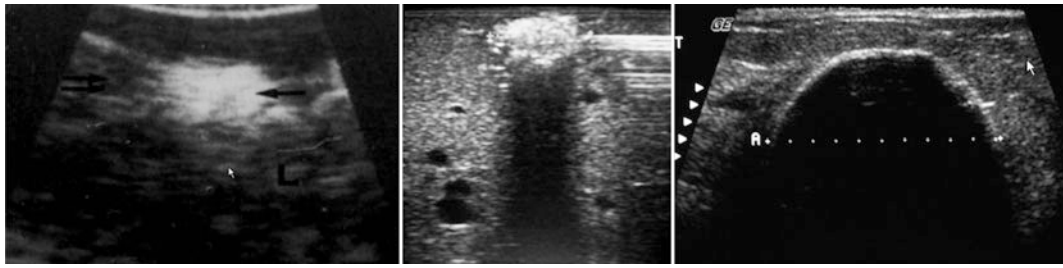

Fig. 58.4 *Imaging difficulties for US guidance during laser, RF, and cryoablation:* Left sagittal US image shows echogenic coagulation zone (*black arrow* on *left image*) during interstitial laser ablation. Middle sagittal US image shows similar echogenic "cloud" causing severe posterior shadowing. Right axial US image during cryoablation causes severe shadowing from the leading ice edge. Upon initiation of all ablations, US guidance may limit evaluation of underlying tumor margins and ablation zone extent

biopsy or drainage procedures, requiring experienced physicians, or healthcare personnel, to also become facile ultrasonographers. Artifacts are inherent to ultrasound evaluation and even help characterize breast masses (e.g., through transmission), but US artifacts rapidly degrade procedure visualization when more than one needle is used or even when minor hemorrhage occurs with multiple punctures. In addition, the tissue effects of ablation modalities also create disruptive shadowing of posterior tumor margins and adjacent structures. Microbubbles produced by heat-based ablations (*RF, laser, microwave, HIFU*) and the leading edge of the ice margin during *cryoablation* are seen in Fig. 58.4. US visualization of all tumor and ablation zone margins can usually only be safely accomplished for superficial lesions. Deep breast lesions, or those near the chest wall, are very difficult to monitor. For percutaneous tumor ablations using a single RF or laser probe, repositioning of the needle to assure full tumor coverage may also cause residual tumor foci between ablation sites [36–39]. For *cryoablation*, multiple cryoprobes not only allow careful planning and placement prior to initiating an ablation but also ensure thorough cytotoxicity (e.g., $<-20^{\circ}$ C) throughout a tumor due to their synergistic effect [40]. We have found that US guidance may also provide an excellent adjunct to CT-guided procedures in order to simplify needle/probe placement, even for deeper procedures near the chest wall.

CT guidance of breast ablation has continued to grow for our cryoablation program. CT guidance is well served for nearly all deep breast ablations or those involving the chest wall. Near real-time CT visualization of needle/probe placement and ablation monitoring can be achieved with judicious use of CT fluoroscopy. While radiation dose exposure is of much less concern for therapeutic procedures, care should be taken to limit fluoroscopy time during needle/probe placements. CT ablation monitoring, especially during cryotherapy, should be limited to standard helical scans encompassing only the ablation zone every few minutes. In general, CT fluoroscopy is of great assistance during the targeting phase and only requires short bursts of CT exposure during monitoring.

The circumferential visualization and monitoring of the ablation zone is perhaps the main benefit of CT. However, this really only applies to *cryoablation* since ice causes a clear density reduction of 20–60 Hounsfield units, depending upon the target tumor and surrounding tissue. Despite ongoing research for subtle density changes during heat-based ablations, no practical regimens are noted for percutaneous *RF, laser*, or *microwave* ablations. Some have noted the slight decrease in density throughout a heat ablation zone at the conclusion of the ablation, likely due to the diffuse microbubble formation, but does not allow for continuous imaging and ablation control. Most practitioners of heat-based ablations in other organ sites try to confirm the final extent of ablation with contrast-enhanced CT but again does not provide for *intra-procedure* control. More detail of CT guidance will be given in the next section, with procedure details for cryoablation.

Which Ablation Modality Is the Current Leader for Breast Tumors?

As physicians, we frequently get caught up in the merits of a specific ablation modality and/or image guidance preference without objectively balancing the multiple combinations or options. This balance is difficult to achieve as new products merge for each ablation modality, continual improvements occur with all imaging equipment, and then the personal experience and/or bias of each physician or hospital setting. The only clear imaging winner between US, CT, and MRI for breast cancer is currently MRI. Table 58.1 attempts to highlight the relative merits of the most common ablation modalities in relation to their ability to be guided and monitored by US, CT, or MRI. Nearly all imaging modalities can provide basic needle placement. CT has no apparent guidance role for current HIFU products. Table 58.1 shows the overall imaging superiority of MRI for breast cancer but also notes its severe incompatibility issues. Perhaps it is even generous to consider that MR-compatible research prototypes have undergone limited testing for RF, microwave, and irreversible electroporation (IRE) probes. Other than HIFU, only laser and cryoablation have great potential for MR compatibility but have not yet defined a viable product for breast cancer. IRE is quite new and may have good application for breast cancer in the future due to its apparent superb healing noted in other body sites but has not been tested in breast cancer to our knowledge [41]. The near-complete resorption of IRE-ablated tumors is likely due to its non-thermal effects that preserve nearly all underlying collagenous architecture. However, many uncertainties exist regarding IRE near the skin and the heart, which need to be much better defined for breast applications, as well as its MR compatibility.

Table 58.1 also elucidates why the 2008 FDA Thermal Ablation Workshop focused a lot of their attention on potential future multicenter trial options for MR-guided HIFU and cryoablation. Overall, cryoablation appears to have the greatest potential for broad application to the US population as an entirely outpatient procedure that can be performed at nearly any imaging site. What is not mentioned in an upcoming review of that meeting is the procedural flexibility of cryotherapy in terms of protection of adjacent structures and most importantly overlying skin. Therefore, the following section will emphasize some of the techniques, observations, and outcomes we have found with our emphasis on breast cryoablation.

Table 58.1 Based solely on ablation zone visualization and guidance options, *cryoablation* has the flexibility for US/CT guidance using an MRI tumor roadmap. *MRI* provides the best overall breast imaging for evaluation of tumor size, extent, and multicentricity but has severe compatibility problems for visualization of nearly all heat-based percutaneous ablation probes, except *laser*. Until MR costs and procedure times are markedly improved, MRI-guided *HIFU* will be limited to small tumors in select patient populations, while MR-guided laser and cryoablation have yet to be commercially implemented for breast cancer

Ablation modalities	Imaging/guidance			
	US	*CT*	*MRI*	Comments
Laser	++	+	+++	US microbubble only; MR compatible
RF	++	+	+	US microbubble only
Microwave	++	+	+	US microbubble only
Electroporation	++	+	+	US hypoechoic changes
HIFU	+	0	+++	Possible by US; MR greatly favored
Cryoablation	+++	+++	+++	Superb visualization of ice margins; MR best contrast – possible isotherms

US-/CT-Guided Breast Cryoablation with Pre- and Post-MR Evaluation

This section will convey the flexibility and future potential of cryoablation, noting its strengths and current procedural weaknesses.

Patient Selection

Cryoablation differs from all the other ablation modalities by its technical potential to sculpt a volume of thoroughly cytotoxic tissue temperatures (e.g., $<-20^{\circ}$ C), thereby easily covering a small mass or a 6-cm tumor region as needed. The following section will describe cryoprobe placement parameters needed to consistently achieve a cytotoxic volume of varying sizes. *Patient selection* has been facilitated by the technical flexibility of cryoablation and allowed us to address a spectrum of breast cancer ablation, from the newly diagnosed small mass to large tumor recurrences [42]. It should be noted that we only began breast cancer ablation after years of treating benign breast fibroadenomas with excellent tissue outcomes [43–45]. We have also gained insight to treatment flexibility from early animal models [46] and over 1000 clinical ablations in multiple organ sites [47–51]. Several additional cryoablation manuscripts are also in preparation, detailing hepatic and pulmonary cryoablation, as well as our recently observed mortality benefits for soft tissue ablation of renal, lung and colon metastases [52–54]. We have been careful to acknowledge the distinct sensitivities surrounding patient selection for breast cancer.

Breast cancer patients considered for *cryotherapy* at our institution [42] are predominantly limited to breast cancer recurrences. For this patient group, there is little controversy due to their lack of treatment options or their refusal to accept the higher morbidities from repeated surgeries. We have also considered an unusual group of patients that absolutely refused surgery and would have otherwise chosen alternative treatments and may not have entered the standard medical system. These patients sign a special informed consent, noting that they have been fully informed of surgical, radiation, and/or chemo-hormonal treatment options and acknowledge the risks of choosing cryoablation as a lumpectomy alternative. These patients must also agree to follow additional post-cryoablation treatment recommendations, as appropriate, for local-regional or systemic control by radiation therapy and/or chemo-hormonal therapy, respectively. We heartily endorse the concept of a larger multicenter trial that uses appropriate cryoablation and imaging guidance parameters as noted below. With careful clinical screening of patients who refuse all surgery, cryoablation may at least offer a thoroughly ablative treatment producing excellent local control, while we continue to gather valuable data until more definitive trials are launched. We have thereby assessed long-term tissue effects of cryoablation for a broad range of breast tumor sizes, locations, and extent throughout the breast. Work is still needed to standardize associated techniques and approaches.

Cryoablation Technique Considerations

It is very encouraging that the American College of Surgeons Oncology Group (ACOSOG) has also acknowledged the broad treatment potential of cryoablation and launched trial Z-1072 for the treatment of early breast cancer [55]. However, basic technology assessments from both cryoablation and imaging perspectives within Z-1072 have not been adequately controlled to avoid prior technical difficulties. Namely, single cryoprobes are still being used at the discretion of the treating surgeon with minimal consideration of appropriate cytotoxic isotherms. In addition, Z-1072 will attempt to assess the negative predictive value of MRI after less than 28 days post-cryoablation in an ablate-and-resect format. Within even 3 months after cryoablation, we have noted continued surrounding inflammatory changes and associated rim enhancement that would be virtually indistinguishable from residual enhancing tumor [42]. Therefore, the likelihood of prospectively identifying residual tumor caused by single-probe undertreatment is exceedingly low and may simply confirm a well-known imaging fact – MRI is not a microscope.

We have previously summarized the well-documented history of cryoablation parameters, specifically required to achieve thorough cytotoxicity for breast cancer [42]. Detailed freeze rate factors were not fully considered in reporting early outcomes of human breast cryoablation [56–58]. Lumpectomy specimens were obtained 5 days after cryoablation from 15 patients with 16 breast cancers, averaging over 2 cm [56, 58].

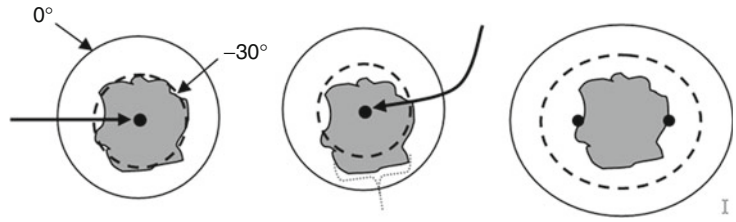

Fig. 58.5 *Basic isotherms for single and double cryoprobes:* Accurate central placement of a single 2.4-mm cryoprobe (*left – arrow*) within a simulated 1.2 cm × 1.2 cm tumor (*dark gray*) may still not produce sufficient lethal ice to cover all tumor margins (*dashed line* ~ <−30° C diam. ~ 1.2cm). Even though visible ice (*solid outer line*) may appear to cover all tumor margins, slight off-center placement (*middle – curved arrow*) leaves grossly untreated tumor (*wide bracket*) beyond the lethal isotherm (*dashed line*). Tumor on right is covered by lethal ice due to synergy produced by two cryoprobes [40]

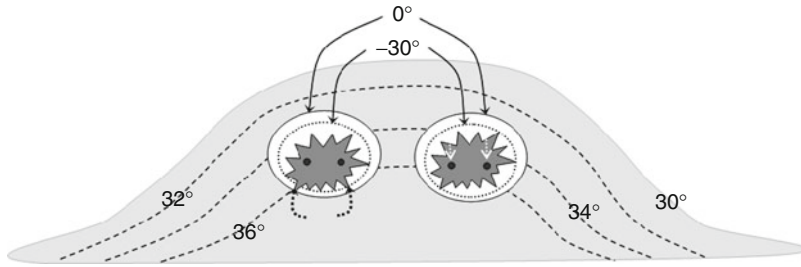

Fig. 58.6 *Avoiding posterior positive margins: heat load effects of the chest wall:* The estimated temperature difference between skin surface (30° C) and chest wall/body (36° C) causes greater heat load along the posterior margin of ice propagation, which narrows the posterior distance between the visible (0° C) and lethal (−30° C) isotherms (*curved solid arrows*). Ablation on left shows central position of cryoprobes and greater anterior extension of visible ice beyond tumor margin (*brackets*); however, incomplete coverage of posterior tumor margins (*curved black dashed arrows*) is noted similar to prior series [53–55]. Ablation on right shows through tumor coverage by lethal ice due to more posterior placement of cryoprobes in tumor (*straight arrows*), thus overcoming heat sink effect along chest wall

They reported only temperatures from *within* a single cryoprobe, thus limiting cooling rate estimates to only a few mm from the cryoprobe (~100 °C/min). Nevertheless, five patients with tumor diameters <16 mm showed complete destruction of the invasive tumor component using only a single probe. Of these, two showed ductal carcinoma in situ (DCIS) in the vicinity of the cryosite. They also concluded that multiple cryoprobes are needed, especially for tumors >16 mm which showed incomplete treatment and residual tumor along the posterior ablation margins.

The concept of *heat sink* has long been known and not only applies to adjacent vasculature but also for breast tumors; the chest wall serves as a relative heat source, particularly when insufficient probe power or numbers are used. Figures 58.5 and 58.6 [40, 42] demonstrate the high risk for residual tumor when a single cryoprobe was used and the need for eccentric posterior placements in most breast masses. Figure 58.7 and Table 58.2 shows the minimum probe configurations for small breast masses favoring a faster freeze with three probes, two of them posterior, over even two well-placed cryoprobes. An ovoid configuration with two cryoprobes thus has a slower, less cytotoxic freeze rate and greater susceptibility to heat sink effects, requiring longer freeze times. Figure 58.7 also suggests that smaller less powerful cryoprobes (e.g., 1.7-mm OD) generally require longer treatment times

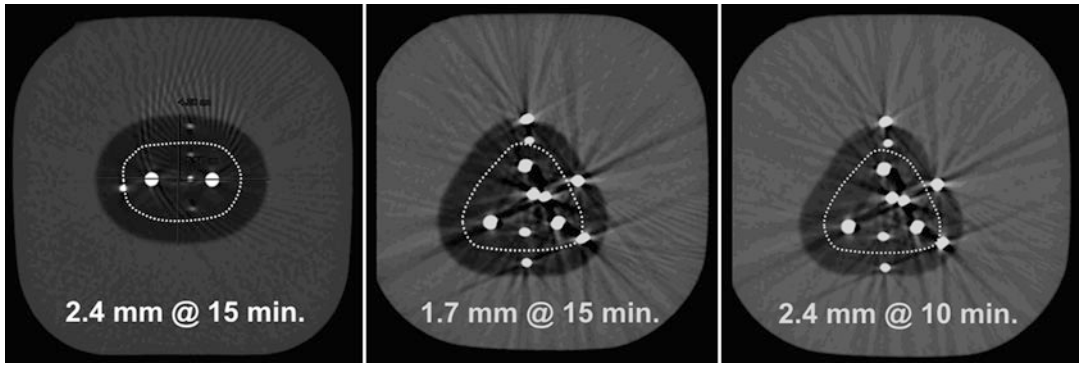

Fig. 58.7 *Cryoablation outcomes according to time, probe size, and number:* Options are shown that could conceivably cover a ~1-cm irregular tumor with a generous 3-cm-diameter lethal ice ablation zone. A double 2.4-mm cryoprobe configuration run to its longest practical extent at ~15 min produces similar overall ice and lethal zone as a triple configuration of 1.7-mm cryoprobes at 15 min or triple 2.4-mm probes run for only 10 min

Table 58.2 Impact upon cross-sectional area and diameter of ice depending upon probe number and sizes

	A Double 2.4 mm @ 15 min	B Triple 1.7 mm @ 15 min	C Triple 2.4 mm @ 10 min
Total ice (cm^2)	17.7	22.6	19.9
Lethal ice (cm^2)	8.1	9.9	9.0
Lethal diameter (cm)	3.3	3.5	3.4

and usually an additional overall cryoprobe than would have been required for larger diameter probes (e.g., four 1.7-mm versus three 2.4-mm OD cryoprobes) [40].

Special techniques for breast cryoablation procedures also emphasize its flexibility. Figures 58.8 and 58.9 provide technical details for a breast cryoablation procedure that coincidentally combines aspects of our two major patient groups. Namely, the patient already had two lumpectomies, definitive radiation and chemo-hormonal therapy, but developed a small recurrent mass, similar to a patient with a small newly diagnosed cancer, and she now refused additional surgical resection. *Patient position* for US- and/or CT-guided cryoablation is supine or at a partial decubitus angle. The CT image in Fig. 58.8 shows how the supine position significantly distorts and flattens the breast, thus requiring careful US scanning to confirm the target mass and adjacent landmarks from the prone MRI scans. For superficial lesions and smaller breasts, distortion is not as significant, but deeper masses in larger breasts may move considerably from its original position on MRI. Color Doppler can be useful in locating more ill-defined tumors, and the tumor vasculature by US also helps confirm the relative enhancement seen on breast MR (Fig. 58.8).

Figure 58.9 demonstrates some important breast cryoablation technique considerations. The approach and puncture site should be chosen to avoid the upper inner quadrants, if at all possible, since even small puncture scars may be "cleavage" visible for several months. A sagittal approach from below readily targeted the tumor in her upper inner periareolar region. Cryoprobes should generally be placed with their tip approximately 5 mm beyond the distal tumor margin, especially since most cryoprobes have a freeze length of 4 cm. Since faster freeze rates produce even greater cell lethality [40, 42], we also favor using three over two probes when possible to achieve overall shorter procedure times (Fig. 58.7). This also allows two probes to be placed along the posterior tumor margin to address the greater heat sink near the chest wall (Fig. 58.6).

Perhaps the most important *safety* aspects of Fig. 58.9 are the skin and chest wall protection

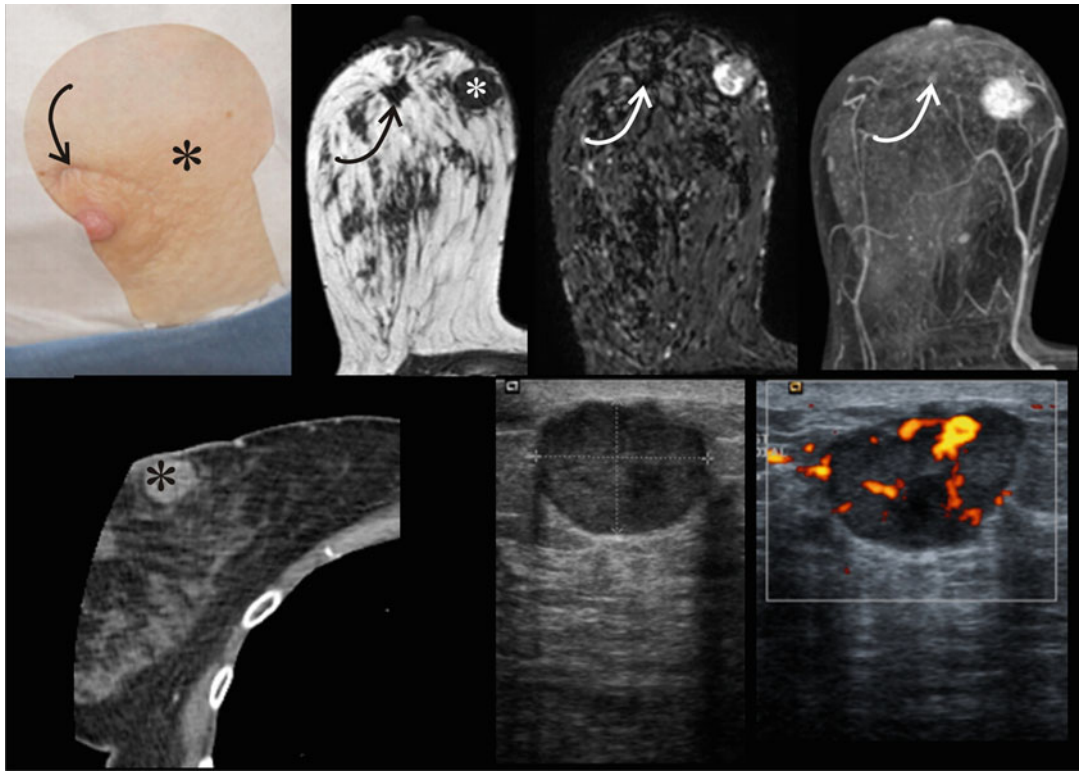

Fig. 58.8 *Cryotherapy for repeat local recurrence guided solely by US – planning:* A 56-year-old woman with her third recurrence of invasive ductal carcinoma in the right breast, following two prior lumpectomies, radiation therapy, and chemo-hormonal therapy. *Top row:* Left clinical image shows periareolar skin retraction from prior lumpectomy site (*curved arrow*) and adjacent underlying tumor (*). Prone axial T1, T2, and MIP 3T-MR images show retraction from the previous surgical scar (curved arrows) and no T2 signal or enhancement. Conversely, the medial tumor (*) shows high T2 signal and distinct enhancement. *Bottom row:* Left axial CT image at the level of the tumor (*) shows significant distortion of the breast in the supine position, encountered during US imaging. Right US images show axial measurements of the 17 mm ×14 mm hypoechoic mass lying only 2–3 mm beneath the skin surface, and the sagittal power Doppler image confirms a 21-mm-long hypervascular tumor. The tumor's longer craniocaudal extent and cosmetic considerations (i.e., avoiding visible cleavage) determined an inferior approach for subsequent cryoablation seen in Fig. 58.9

measures. Since this tumor is so close to the skin surface, aggressive infiltration of the overlying skin needs to be done throughout both freeze cycles. When the iceball approaches the anterior tumor margin, we also place a warmed sterile saline bag (e.g., 250 mL bag in microwave for ~30 s) directly over the tumor. This superficial warmth helps keep the dermis pliable for continued injection to prevent full-thickness freeze into the skin. We have then been able to treat tumors within 1 mm of the skin surface. *A good clinical rule* of thumb to assure that a tumor has not invaded the skin is to assess skin mobility directly over the mass, which should feel similar to your skin moving smoothly over the flexed knuckles on your fingers. Beyond safety, aggressive saline infiltration of thin overlying skin was also important for the clinical cases in Figs. 58.12, 58.13, 58.14, and 58.15 to achieve thorough ablation outcomes.

Long-Term Ablation Follow-up

Role of Imaging

MRI has also been well described as the most accurate imaging tool in following multiple forms of therapy [59–67]. Nevertheless, differing

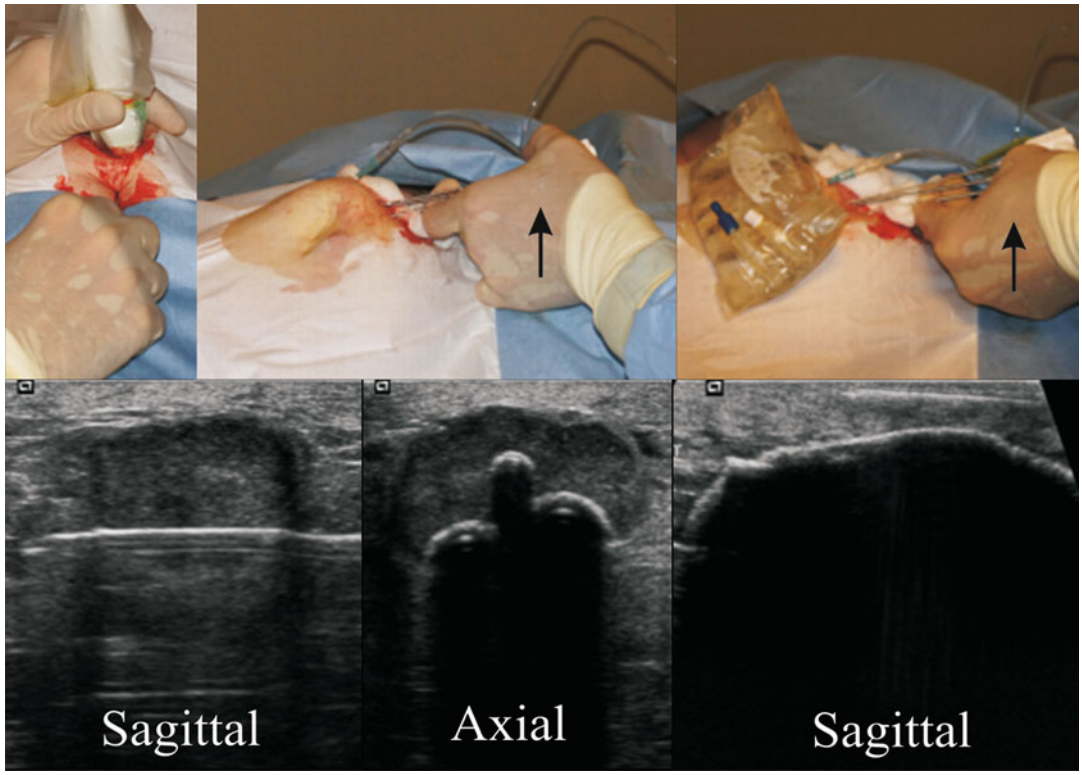

Fig. 58.9 *Cryotherapy for repeat local recurrence guided solely by US – procedure:* Images during cryoablation of the patient seen in Fig. 58.8, showing an inferior approach for three 1.7-mm cryoprobes placed in the optimum configuration (Figs. 58.6 and 58.7) compensate for the greater heat sink along the posterior tumor margin and facilitate easier anterior control for skin protection. *Top row:* Clinical images during phases of ablation demonstrate an inferior percutaneous approach with ultrasound transducer in place (*left*). Middle and right clinical images demonstrate both skin protection by subcutaneous saline injection throughout the case in conjunction with an overlying warm sterile saline bag, and intermittent anterior retraction of all cryoprobes (*arrows*) easily keeping the iceball off the chest wall. *Bottom row:* US images approximate the phases of ablation seen in the top row. Left sagittal US image confirms 5-mm extension of the cryoprobe beyond the superior margin of the tumor. Middle axial US image shows the ideal configuration of three 1.7-mm cryoprobes at the initiation of the first freeze cycle. Right sagittal US image during the maximum freeze shows complete coverage of all apparent tumor margins and a 25-gauge injection needle lying just beneath the skin surface to maintain skin protection throughout the case. The overlying warm saline bag kept the subcutaneous tissues pliable for continuous saline injection

opinions on the utility of breast MRI may arise from the context and clinical scenario for which MRI has been used to evaluate complicated treatment outcomes. There is no question that MRI after *breast-conserving surgery* (BCS) is too expensive, with ipsilateral tumor recurrence rates of only 1.7 % that usually occur 5–10 years after treatment [59, 61]. If standard DCE-MRI is used to assess for residual tumor following *neoadjuvant chemotherapy*, overestimation of pathologic complete response rate (pCR) (i.e., 20 % instead of the actual 9 % pCR) appears related to false negatives due to scattered tumor cells within residual granulomatous or fibromatous changes that occurred within the primary tumor site [60]. Residual tumor foci in a primary tumor site are quite different from assuming residual tumor surrounding an ablation rim, yet the authors made the erroneous assumption that this also applies to RF and HIFU without

associated data. Again, MRI cannot be expected to be a microscope, and current biopsy criteria for MR screening and biopsy are generally limited to a suspiciously enhancing focus over 5 mm.

As MR techniques continue to advance, greater confidence is emerging for evaluating treatment outcomes over time [62–67]. Volume reductions of the ablation zone that we noted for cryoablation of breast and renal tumors [42, 50] have also been validated as treatment response criteria for outcomes of MR-guided laser ablation of liver masses [62]. Newer techniques of MR spectroscopy [63] and diffusion-weighted imaging [64] also hold promise for evaluation of any nodular rim of DCE surrounding a breast ablation site. Continued follow-up of a suspicious focus of enhancement over 6–12 months may also help differentiate areas of chronic inflammatory change from slow-growing residual tumor. Indeed, most chronic inflammation following any breast cancer treatment tends to resolve by 6–12 months, but 37 % of patients following BCS had persistent enhancement surrounding the lumpectomy site beyond 12 months [66]. Finally, neoadjuvant chemo-hormonal therapy may not only affect the primary tumor but has also been noted to reduce overall breast density in the contralateral breast due to systemic effects upon normal breast parenchyma [67].

Long-Term Cryoablation Follow-Up

Figures 58.10, 58.11, 58.12, 58.13, 58.14, and 58.15 present longer-term follow-up of three very different cases, extending from our first patient with newly diagnosed breast cancer (Figs. 58.10 and 58.11) to more extensive cases requiring local control of a residual primary tumor (Figs. 58.12 and 58.13) and a sternal metastasis (Figs. 58.14 and 58.15). The patient in Figs. 58.10 and 58.11 was our first patient to thoroughly refuse surgical resection, yet agreed to receive radiation therapy 3 months post-cryoablation and subsequent tamoxifen. The three months delay until radiation therapy was arbitrarily chosen to allow thorough healing, but the patient noted that resorption of the mass effect appeared to "stall" during radiation therapy. Delayed healing is well known as a consequence of radiation therapy but did not appear to cause any further delay of ablation zone resorption after radiation therapy was concluded. Further work is needed on the ideal timing of radiation therapy, before or after cryoablation, but no apparent problems have been seen for radiation therapy and prostate cancer. Prostate cancer patients have received radiation following limited cases of incomplete cryoablation, as well as salvage cryoablation having been performed after radiation therapy without any specific complications or healing difficulties. Our patient continues to do well now 6 1/2 years after cryoablation with a recent unremarkable PET-CT and breast MRI.

The two cases in Figs. 58.12, 58.13, 58.14, and 58.15 also demonstrate the flexibility of cryoablation as an overall tumor control technique in diverse soft tissue locations. The bulging tumor within the breast of the patient seen in Figs. 58.12 and 58.13 also directly abutted underlying breast implants and caused her increasing pain. The implant was not affected by cryoablation, although we did achieve some saline infiltration between the tumor and the implant. However, it is usually quite difficult to maintain continuous saline flow during deep injections since the infusion needle frequently becomes engulfed in ice. Posterior protection is usually sufficient by anterior retraction of the iceball (Fig. 58.9). Despite an extensive freeze covering over 5 cm of irregular tumor, she did very well and had prompt pain relief. Her tumor underwent marked resorption by 15 months, and she was very pleased. She did require an additional ablation session at 12 months for a new tumor focus beyond the ablation site and an enlarging node in the lower axilla. These sites also responded well with good local control, but she unfortunately succumbed to her diffuse systemic disease 2 years later.

The patient in Figs. 58.14 and 58.15 demonstrates superb local control of an isolated sternal metastasis and exemplifies the excellent

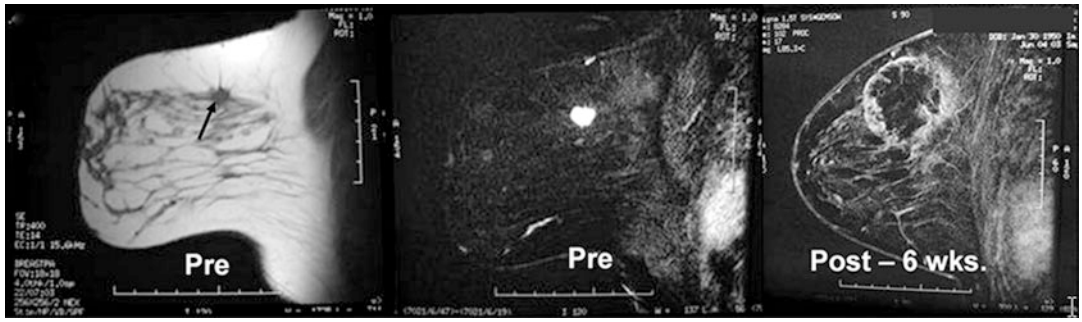

Fig. 58.10 *Pre-cryotherapy MRI – multifocal left upper outer quadrant cancer: Left*: T1-weighed axial image shows the spiculated, 1.6-cm dominant mass in the left outer quadrant (*black arrow*). Another biopsy confirmed cancer in the same quadrant was in different image planes. *Middle*: Fat-subtracted T1-weighted image following gadolinium (T1FS-Gd) showing brisk tumor enhancement. *Right*: T1FS-Gd image showing rim of enhancement corresponding to healing cryotherapy rim which also covered the other cancer. The micro-lumpectomy sampling (i.e., Mammotome removal) of the tumor region prior to initiating the freeze made our first BC procedure more complex. US visualization of the tumor site became distorted by blood during the vacuum-assisted biopsies, which are no longer used. Despite poor visualization of any remaining tumor margin, thorough ablation margins were still achieved by placement of the cryoprobes along the outer margins of these micro-lumpectomy sites. Biopsy of three slightly nodular areas of rim enhancement showed no residual cancer or DCIS

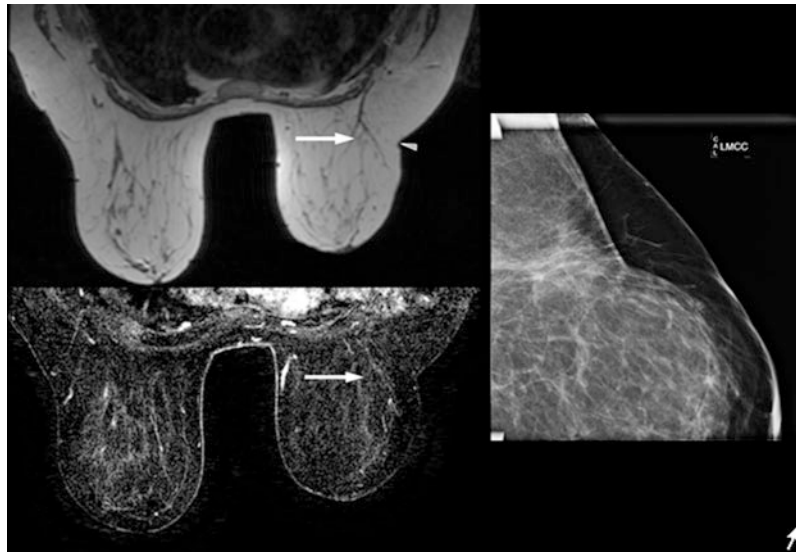

Fig. 58.11 *Five-year follow-up: Top*: T1-weighed axial image shows minimal scarring and/or distortion at cryosite (*arrow*). Slightly smaller left breast was initially present, and lateral scar indentation (arrowhead) is a scar from abscess debridement 1 year prior to this study (i.e., 4 year after cryotherapy), which also confirmed no residual tumor throughout the original cryotherapy site. *Middle*: T1FS-Gd image showing no enhancement of prior ablation and subsequent resection site (arrow). *Bottom*: Compression mammogram of left upper outer quadrant shows no mass effect and minimal scarring, likely related to resection 1 year ago than original cryotherapy 5 year ago

cryoablation outcomes we have noted in other metastatic sites. Namely, we have an upcoming publication of 100 patients treated for non-organ locations which we arbitrarily categorized as retroperitoneal, intraperitoneal, superficial/extremities, and bone locations. Only 17 local recurrences of 195 tumor sites (9 %) were noted, of which ten (59 %) occurred within the

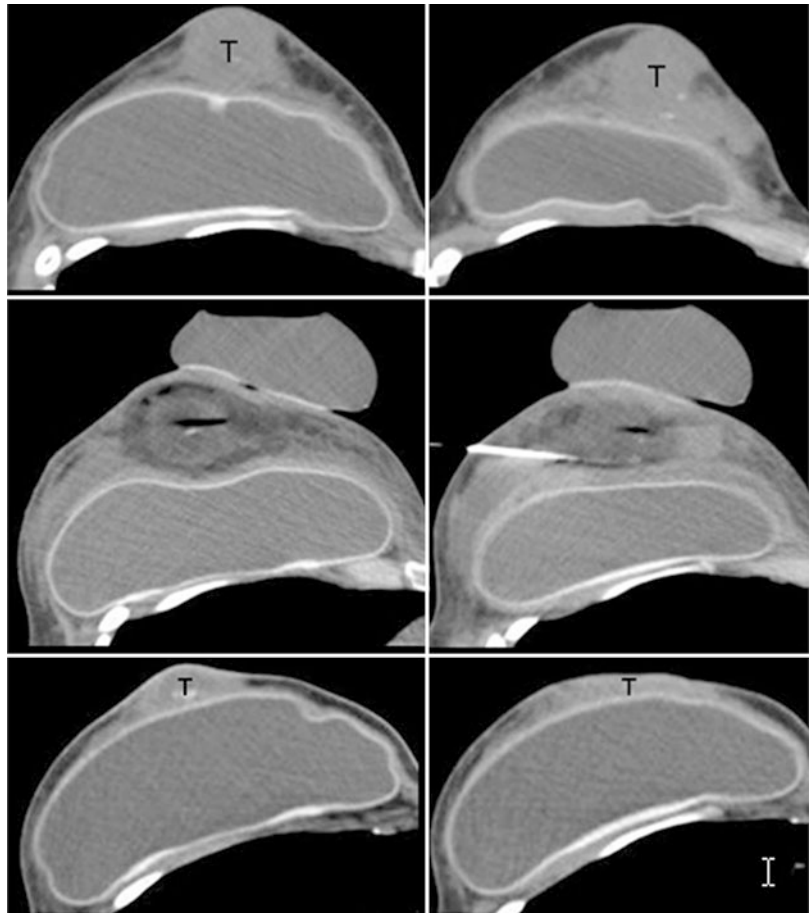

Fig. 58.12 *CT guidance, pre- and post-cryotherapy: Top line:* Non-enhanced CT images at level of the nipple and superior breast, showing extensive tumor involvement (T). The skin (*) and tumor appear inseparable but was NOT fixed on physical exam or involved by US or MR (Fig. 58.6). *Middle line:* CT images at the same levels immediately after cryotherapy and probe removal, leaving air in tracts. The tumors are covered by hypodense ice, except for image on right where the ice had already melted after cryoprobes had been retracted from an earlier medial freeze cycle. Saline injection needle remains between tumor and implant, and skin had also been infiltrated. *Bottom line:* CT images at the same anatomic levels 15 months after cryotherapy showing marked resolution of prior bulky tumors. Random biopsies at 6 weeks post-ablation showed no residual tumor (T) but cancer recurred in two sites beyond the ablation zone at 7 months. Repeat cryotherapy was done for a 6-mm new nodule in the far upper central breast and a 17-mm lower axillary node

ablation zone and seven (41 %) were satellite lesions less than 10 mm beyond. A true procedure failure rate of only 5 % (10/195) was noted with an average time to recurrence of 4.1 months. Our overall mean follow-up is now over 12 months with no apparent late recurrences. Similar to what we see for the patient in Figs. 58.14 and 58.15, the average ablation volume reduction of 94 % was noted at 24 months. This patient has continued to do well and remains disease-free nearly 10 years post-cryoablation of a painful tumor that was also about to break through the 1-mm-thick overlying skin. We purposely froze into the majority of the underlying sternum where her pain appeared to originate. This case shows the great potential for cryoablation control of oligometastatic disease and its potential impact on mortality reduction or at least marked morbidity control.

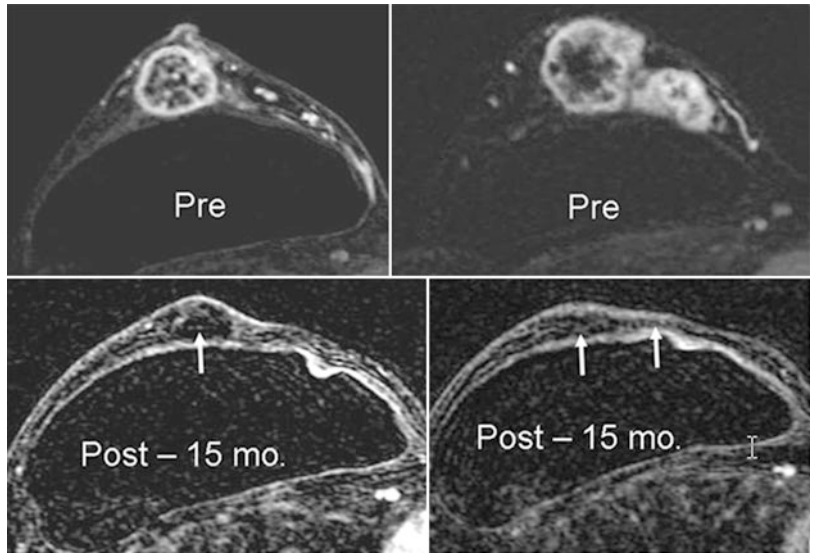

Fig. 58.13 *MR evaluation: pre- and post-cryotherapy: Top line:* Before cryotherapy, T1FS Gd axial MR images show brisk enhancement throughout the tumor nodularity of the retro-areolar (*left*) and superior breast (*right*). Note also the lack of skin enhancement. *Bottom line:* T1FS-Gd MR images at the same levels 15 months after cryotherapy showing marked reduction of prior bulky tumors and no residual enhancement of any margin (*arrows*)

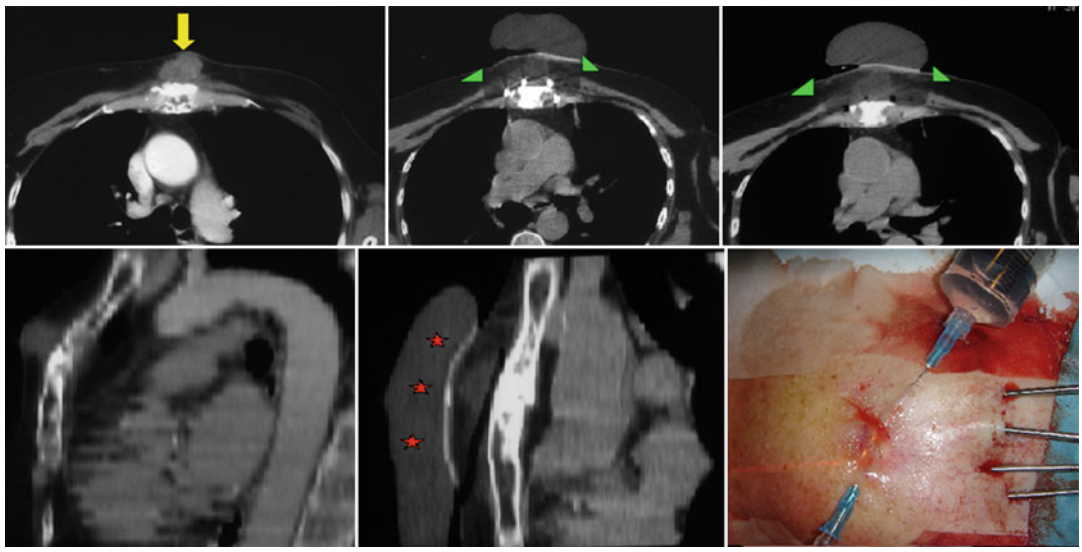

Fig. 58.14 *Chest wall cryotherapy for a bone metastasis about to break through skin:* A 68-year-old woman with continuously growing sternal and soft-tissue tumor but otherwise stable, PET-negative bone metastases from breast cancer. There was only a very thin layer of intact skin overlying the tumor. The top line shows the sagittal reconstruction of the 4.2 × 3.0 × 4.5-cm enhancing mass (*arrow*) tumor (*arrow*), then covered in ice (*arrowhead*) extending to the skin surface. Overlying skin was successfully protected by continuous injection of the dermal layer by saline (*stars*) and warmed saline bags seen on the skin surface

Summary

Ablation of both benign and malignant breast tumors will have a large impact upon current paradigms of breast cancer treatment, mostly due to marked improvements in breast imaging and procedure guidance. Breast MRI has demonstrated the greatest advances in the last 10 years to become the screening modality of choice for high-risk women, as well as the most accurate evaluation of primary tumor and DCIS extent for

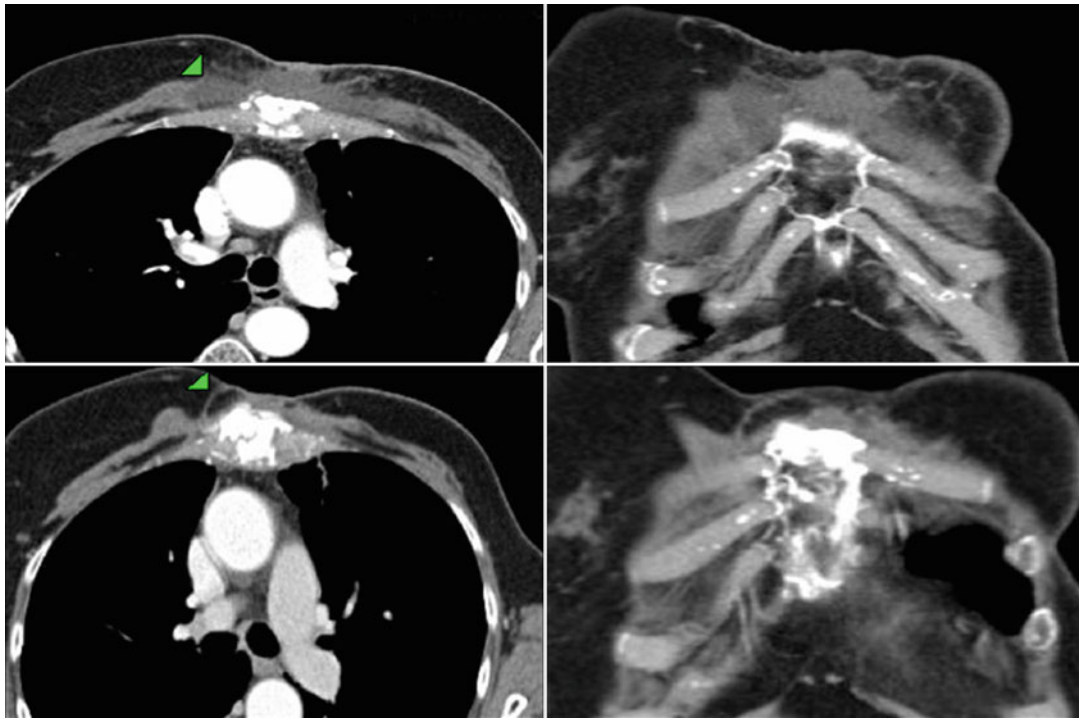

Fig. 58.15 *Chest wall cryotherapy – follow-up:* The hypovascular zone at 1 month post-BC (*top row arrowheads*) corresponding to the approximate visible ice extent 1 cm beyond lateral tumor margins. Enhanced axial and coronal CT images 18 months post-BC (*Bottom line*) show near-complete resorption of tumor mass with good remodeling of adjacent normal tissues. This area also remains negative on PET and bone scan at 36 months with no other distant disease recurrences

staging and therapy planning. Careful pretreatment MR evaluation with subsequent combined US- and CT-guided ablation appears to hold the greatest prospect for addressing the broadest sector of the population. In the near future, MR-guided HIFU may become more cost-effective, while advances in MRI-compatible laser and cryotechnology will also allow more interactive control and guidance. Breast ablation may then be performed in the prone position, similar to current stereotactic and MR-guided biopsies, and facilitates direct comparisons of intraprocedural ablation extent with subsequent follow-up scans. The next chapter will also address the prospect of emerging imaging technologies that may be also more cost-effective than breast MRI to allow even broader, cost-effective patient access to the benefits of breast tumor ablation.

References

1. US Preventive Services Task Force. Screening for breast cancer: US Preventive Services Task Force recommendation statement. Ann Intern Med. 2009;151:716–26.
2. Woolf SH. The 2009 breast cancer screening recommendations of the US Preventive Services Task Force. JAMA. 2010;303:162–3.
3. Petitti DB, Calonge N, LeFevre ML, Melnyk BM, Wilt TJ, Schwartz JS, U.S. Preventive Services Task Force. Breast cancer screening: from science to recommendation. Radiology. 2010;256:8–14.
4. Kopans DB. The 2009 US Preventive Services Task Force (USPSTF) guidelines are not supported by science: the scientific support for mammography screening. Radiol Clin North Am. 2010;48:843–57.
5. Lehman CD, Isaacs C, Schnall MD, Pisano ED, Ascher SM, Weatherall PT, et al. Cancer yield of mammography, MR, and US in high-risk women: prospective multi-institution breast cancer screening study. Radiology. 2007;244:381–8.

6. Saslow D, Boetes C, Burke W, Harms S, Leach MO, Lehman CD, American Cancer Society Breast Cancer Advisory Group, et al. American Cancer Society guidelines for breast screening with MRI as an adjunct to mammography. CA Cancer J Clin. 2007;57:75–89.
7. Uematsu T, Yuen S, Kasami M, Uchida Y. Comparison of magnetic resonance imaging, multidetector row computed tomography, ultrasonography, and mammography for tumor extension of breast cancer. Breast Cancer Res Treat. 2008;112:461–74.
8. Neubauer H, Li M, Kuehne-Heid R, Schneider A, Kaiser WA. High grade and non-high grade ductal carcinoma in situ on dynamic MR mammography: characteristic findings for signal increase and morphological pattern of enhancement. Br J Radiol. 2003;76:3–12.
9. Nielsen M, Thomsen JL, Primdahl S, et al. Breast cancer and atypia among young and middle-aged women: a study of 110 medicolegal autopsies. Br J Cancer. 1987;56:814–9.
10. Schnitt SJ, Silen W, Sadowsky NL, et al. Ductal carcinoma in situ (intraductal carcinoma) of the breast-current concepts. N Engl J Med. 1988;318:898–903.
11. Littrup PJ, Goodman AC, Mettlin CJ. The benefit and cost of prostate cancer early detection. The Investigators of the American Cancer Society-National Prostate Cancer Detection Project. CA Cancer J Clin. 1993;43:134–49.
12. Littrup PJ, Goodman AC, Mettlin CJ, Murphy GP. Cost analyses of prostate cancer screening: frameworks for discussion. Investigators of the American Cancer Society-National Prostate Cancer Detection Project. J Urol. 1994;152(5 Pt 2):1873–7.
13. Pauker SG, Kassirer JP. Decision analysis. N Engl J Med. 1987;316:250–8.
14. Sotiriou C, Pusztai L. Gene-expression signatures in breast cancer. N Engl J Med. 2009;360:790–800.
15. Billar JA, Dueck AC, Stucky CC, Gray RJ, Wasif N, Northfelt DW, McCullough AE, Pockaj BA. Triple-negative breast cancers: unique clinical presentations and outcomes. Ann Surg Oncol. 2010;17 Suppl 3:384–90. Epub 2010 Sep 19.
16. Boyd NF, Martin LJ, Bronskill M, Yaffe MJ, Duric N, Minkin S. Breast tissue composition and susceptibility to breast cancer. J Natl Cancer Inst. 2010;102: 1224–37. Epub 2010 Jul 8.
17. Arora N, King TA, Jacks LM, Stempel MM, Patil S, Morris E, Morrow M. Impact of breast density on the presenting features of malignancy. Ann Surg Oncol. 2010;17 Suppl 3:211–8. Epub 2010 Sep 19.
18. Yeap BH, Muniandy S, Lee SK, Sabaratnam S, Singh M. Specimen shrinkage and its influence on margin assessment in breast cancer. Asian J Surg. 2007;30:183–7.
19. Pritt B, Tessitore J, Weaver D, Blaszyk H. The effect of tissue fixation and processing on breast cancer size. Hum Pathol. 2005;36:756–60.
20. Yang JH, Lee WS, Kim SW, Woo SU, Kim JH, Nam SJ. Effect of core-needle biopsy vs. fine-needle aspiration on pathologic measurement of tumor size in breast cancer. Arch Surg. 2005;140:125–8.
21. Ozdemir A, Voyvoda NK, Gultekin S, Tuncbilek I, Dursun A, Yamac D. Can core biopsy be used instead of surgical biopsy in the diagnosis and prognostic factor analysis of breast carcinoma? Clin Breast Cancer. 2007;7:791–5.
22. Flanagan MB, Dabbs DJ, Brufsky AM, Beriwal S, Bhargava R. Histopathologic variables predict Oncotype DXtrade mark Recurrence Score. Mod Pathol. 2008 Mar 21. Epub ahead of print
23. Habel LA, Shak S, Jacobs MK, et al. A population-based study of tumor gene expression and risk of breast cancer death among lymph node-negative patients. Breast Cancer Res. 2006;8:R25. Epub 2006 May 31.
24. Conlin AK, Seidman AD. Use of the Oncotype DX 21-gene assay to guide adjuvant decision making in early-stage breast cancer. Mol Diagn Ther. 2007;11: 355–60.
25. Miller AR, Brandao G, Prihoda TJ, et al. Positive margins following surgical resection of breast carcinoma: analysis of pathologic correlates. J Surg Oncol. 2004;86:134–40.
26. Tafra L, Smith SJ, Woodward JE, Fernandez KL, Sawyer KT, Grenko RT. Pilot trial of cryoprobe-assisted breast-conserving surgery for small ultrasound-visible cancers. Ann Surg Oncol. 2003; 10:1018–24.
27. Heywang-Köbrunner SH, Sinnatamby R, Lebeau A, Lebrecht A, Britton PD, Schreer I; Consensus Group. Interdisciplinary consensus on the uses and technique of MR-guided vacuum-assisted breast biopsy (VAB): results of a European consensus meeting. Eur J Radiol. 2008 Aug 22. Epub ahead of print.
28. Hynynen K, Pomeroy O, Smith DN, Huber PE, McDannold NJ, Kettenbach J, Baum J, Singer S, Jolesz FA. MR imaging-guided focused ultrasound surgery of fibroadenomas in the breast: a feasibility study. Radiology. 2001;219:176–85.
29. Schmitz AC, Gianfelice D, Daniel BL, Mali WP, van den Bosch MA. Image-guided focused ultrasound ablation of breast cancer: current status, challenges, and future directions. Eur Radiol. 2008;18:1431–41.
30. Wu F, Wang ZB, Cao YD, Zhu XQ, Zhu H, Chen WZ, Zou JZ. "Wide local ablation" of localized breast cancer using high intensity focused ultrasound. J Surg Oncol. 2007;96:130–6.
31. Berg WA, Blume JD, Cormack JB, Mendelson EB, Lehrer D, Böhm-Vélez M, ACRIN 6666 Investigators, et al. Combined screening with ultrasound and mammography vs mammography alone in women at elevated risk of breast cancer. JAMA. 2008;299: 2151–63.
32. Berg WA, Gutierrez L, NessAiver MS, Carter WB, Bhargavan M, Lewis RS, Ioffe OB. Diagnostic accuracy of mammography, clinical examination, US, and MR imaging in preoperative assessment of breast cancer. Radiology. 2004;233:830–49.

33. Hollingsworth AB, Stough RG, O'Dell CA, Brekke CE. Breast magnetic resonance imaging for preoperative locoregional staging. Am J Surg. 2008;196:389–97.
34. Wiratkapun C, Duke D, Nordmann AS, Lertsithichai P, Narra V, Barton PT, Hildebolt CF, Bae KT. Indeterminate or suspicious breast lesions detected initially with MR imaging: value of MRI-directed breast ultrasound. Acad Radiol. 2008;15:618–25.
35. Genson CC, Blane CE, Helvie MA, Waits SA, Chenevert TL. Effects on breast MRI of artifacts caused by metallic tissue marker clips. AJR Am J Roentgenol. 2007;188:372–6.
36. Fornage BD, Sneige N, Ross MI, Mirza AN, Kuerer HM, Edeiken BS, Ames FC, Newman LA, Babiera GV, Singletary SE. Small (< or = 2-cm) breast cancer treated with US-guided radiofrequency ablation: feasibility study. Radiology. 2004;231:215–24.
37. Noguchi M, Earashi M, Fujii H, Yokoyama K, Harada K, Tsuneyama K. Radiofrequency ablation of small breast cancer followed by surgical resection. J Surg Oncol. 2006;93:120–8.
38. Dowlatshahi K, Fan M, Gould VE, Bloom KJ, Ali A. Stereotactically guided laser therapy of occult breast tumors: work-in-progress report. Arch Surg. 2000; 135:1345–52.
39. van Esser S, Stapper G, van Diest PJ, van den Bosch MA, Klaessens JH, Mali WP, Borel Rinkes IH, van Hillegersberg R. Ultrasound-guided laser-induced thermal therapy for small palpable invasive breast carcinomas: a feasibility study. Ann Surg Oncol. 2009;16:2259–63.
40. Littrup PJ, Jallad B, Vorugu V, et al. Lethal isotherms of cryoablation in a phantom study: effects of heat load, probe size, and number. J Vasc Interv Radiol. 2009;20:1343–51.
41. Rubinsky B. Irreversible electroporation in medicine. Technol Cancer Res Treat. 2007;6:255–60.
42. Littrup PJ, Jallad B, Chandiwala-Mody P, D'Agostini M, Adam BA, Bouwman D. Cryotherapy for breast cancer: a feasibility study without excision. J Vasc Interv Radiol. 2009;20:1329–41.
43. Kaufman CS, Bachman B, Littrup PJ, White M, Carolin KA, Freeman-Gibb L, Francescatti D, Stocks LH, Smith JS, Henry CA, Bailey L, Harness JK, Simmons R. Office-based ultrasound-guided cryoablation of breast fibroadenomas. Am J Surg. 2002;184:394–400.
44. Kaufman CS, Littrup PJ, Freeman-Gibb LA, et al. Office-based cryoablation of breast fibroadenomas with long-term follow-up. Breast J. 2005;11:344–50.
45. Littrup PJ, Freeman-Gibb L, Andea A, White M, Amerikia KC, Bouwman D, Harb T, Sakr W. Cryotherapy for breast fibroadenomas. Radiology. 2005; 234:63–72.
46. Littrup PJ, Mody A, Sparschu R, Prchevski P, Montie J, Zingas AP, Grignon D. Prostatic cryotherapy: ultrasonographic and pathologic correlation in the canine model. Urology. 1994;44:175–83. discussion 183–174.
47. Kam AW, Littrup PJ, Walther MM, Hvizda J, Wood BJ. Thermal protection during percutaneous thermal ablation of renal cell carcinoma. J Vasc Interv Radiol. 2004;15:753–8.
48. Wang H, Littrup PJ, Duan Y, Zhang Y, Feng H, Nie Z. Thoracic masses treated with percutaneous cryotherapy: initial experience with more than 200 procedures. Radiology. 2005;235:289–98.
49. Ahmed A, Littrup P. Percutaneous cryotherapy of the thorax: safety considerations for complex cases. AJR Am J Roentgenol. 2006;186:1703–6.
50. Littrup P, Ahmed A, Aoun H, Noujaim DL, Harb T, Nakat S, Abdallah K, Adam BA, Venkatramanamoorthy R, Sakr W, Pontes JE, Heilbrun LK. CT-guided percutaneous cryotherapy of renal masses. J Vasc Interv Radiol. 2007;18:383–92.
51. Solomon LA, Munkarah AR, Vorugu VR, Deppe G, Adam B, Malone Jr JM, Littrup PJ. Image-guided percutaneous cryotherapy for the management of gynecologic cancer metastases. Gynecol Oncol. 2008;111:202–7.
52. Bang HJ, Littrup PJ, Currier BP, Aoun HD, Heilbrun LK, Vaishampayan U, Adam B, Goodman AC. Percutaneous cryoablation of metastatic lesions from non-small-cell lung carcinoma: Initial survival, local control, and cost observations. Journal of Vascular and Interventional Radiology. 2012;23:761–9.
53. Bang HJ, Littrup PJ, Currier BP, Goodrich DJ, Aoun HD, Klein LC, Kuo JC, Heilbrun LK, Gadgeel S, Goodman AC. Percutaneous cryoablation of metastatic renal cell carcinoma for local tumor control: Feasibility, outcomes, and estimated cost effectiveness for palliation. Journal of Vascular and Interventional Radiology. 2012;23:770–7.
54. Bang HJ, Littrup PJ, Currier BP, Goodrich DJ, Choi M, Heilbrun LK, and Goodman AC. Percutaneous cryoablation of metastatic lesions from colorectal cancer: Efficacy and feasibility with survival and cost-effectiveness observations. ISRN Minimally Invasive Surgery. 2012;2012:1–10.
55. http://clinicaltrials.gov/ct2/show/NCT00723294
56. Pfleiderer SO, Freesmeyer MG, Marx C, Kuhne-Heid R, Schneider A, Kaiser WA. Cryotherapy of breast cancer under ultrasound guidance: initial results and limitations. Eur Radiol. 2002;12:3009–14.
57. Roubidoux MA, Sabel MS, Bailey JE, Kleer CG, Klein KA, Helvie MA. Small (< 2.0-cm) breast cancers: mammographic and US findings at US-guided cryoablation–initial experience. Radiology. 2004;233:857–67.
58. Pfleiderer SO, Marx C, Camara O, Gajda M, Kaiser WA. Ultrasound-guided, percutaneous cryotherapy of small (< or = 15 mm) breast cancers. Invest Radiol. 2005;40:472–7.
59. Khatcheressian JL, Wolff AC, Smith TJ, Grunfeld E, Muss HB, Vogel VG, Halberg F, Somerfield MR, Davidson NE, American Society of Clinical Oncology. American Society of Clinical Oncology 2006 update of the breast cancer follow-up and management guidelines in the adjuvant setting. J Clin Oncol. 2006;24:5091–7.

60. Nakamura S, Ishiyama M, Tsunoda-Shimizu H. Magnetic resonance mammography has limited ability to estimate pathological complete remission after primary chemotherapy or radiofrequency ablation therapy. Breast Cancer. 2007;14:123–30.
61. Gorechlad JW, McCabe EB, Higgins JH, Likosky DS, Lewis PJ, Rosenkranz KM, Barth Jr RJ. Screening for recurrences in patients treated with breast-conserving surgery: is there a role for MRI? Ann Surg Oncol. 2008;15:1703–9.
62. Vogl TJ, Naguib NN, Eichler K, Lehnert T, Ackermann H, Mack MG. Volumetric evaluation of liver metastases after thermal ablation: long-term results following MR-guided laser-induced thermotherapy. Radiology. 2008;249:865–71.
63. Baek HM, Chen JH, Nie K, Yu HJ, Bahri S, Mehta RS, Nalcioglu O, Su MY. Predicting pathologic response to neoadjuvant chemotherapy in breast cancer by using MR imaging and quantitative 1H MR spectroscopy. Radiology. 2009;251:653–62.
64. Sharma U, Danishad KK, Seenu V, Jagannathan NR. Longitudinal study of the assessment by MRI and diffusion-weighted imaging of tumor response in patients with locally advanced breast cancer undergoing neoadjuvant chemotherapy. NMR Biomed. 2009;22:104–13.
65. Kim SH, Jung SE, Kim HL, Hahn ST, Park GS, Park WC. The potential role of dynamic MRI in assessing the effectiveness of high-intensity focused ultrasound ablation of breast cancer. Int J Hyperthermia. 2010;26:594–603.
66. Li J, Dershaw DD, Lee CF, Joo S, Morris EA. Breast MRI after conservation therapy: usual findings in routine follow-up examinations. AJR Am J Roentgenol. 2010;195:799–807.
67. Chen JH, Nie K, Bahri S, Hsu CC, Hsu FT, Shih HN, Lin M, Nalcioglu O, Su MY. Decrease in breast density in the contralateral normal breast of patients receiving neoadjuvant chemotherapy: MR imaging evaluation. Radiology. 2010;255:44–52.

The Role of Image-Guided Surgery in Breast Cancer

59

Kambiz Dowlatshahi, Rosalinda Alvarado, and Katherine Kopckash

Abstract

The surgical management of breast cancer has changed drastically over the past three decades. These improvements have been possible due to advances in imaging and ablative therapies. This chapter gives a brief overview of the historical management of breast cancer and describes the modern imaging techniques of the breast and axilla, including digital mammography, ultrasound, magnetic resonance imaging (MRI), and positron emission mammography (PEM). We discuss the devices currently used for breast biopsy and the techniques employed for minimally invasive surgery. Finally, the chapter provides a summary of the available ablative therapies, which include cryoablation, laser therapy, radiofrequency ablation, microwave thermotherapy, and high-intensity focused ultrasound.

Historical Background

The surgical management of breast cancer has significantly changed since Halsted introduced radical mastectomy in 1894. Before that, wide excision was practiced resulting in very high local recurrence and poor survival [1]. Radical mastectomy (en bloc removal of the breast, skin, pectoralis major, pectoralis minor, and axillary contents) improved disease control but left the patient mutilated. The underlying premise was that breast cancer was an orderly disease that progresses in a contiguous manner from the primary site by direct extension to the lymphatic nodes and then to the distant sites. This concept was followed even to an even greater degree by extending the surgical removal of the internal mammary lymph nodes in the form of extended radical mastectomy as practiced by Urban [2]. Radical mastectomy, however, was the standard of care for many years until the emergence of the modified radical mastectomy (MRM), spearheaded by Patey and Crile, sparing resection of the muscles [3, 4]. A number of prospective randomized trials were able to show equivalent survival between MRM and radical

An erratum to this chapter can be found at http://dx.doi.org/10.1007/978-1-4419-0751-6_66

K. Dowlatshahi (✉) • R. Alvarado
Department of General Surgery, Rush University Medical Center, Chicago, IL, USA
e-mail: kdowlat@gmail.com; rosalinda_alvarado@rush.edu

K. Kopckash
Department of Surgery, Rush University Medical Center, Chicago, IL, USA
e-mail: katherine_kopkash@rush.edu

D.E. Dupuy et al. (eds.), *Image-Guided Cancer Therapy*, DOI 10.1007/978-1-4419-0751-6_61,

mastectomy [5–8]. While MRM became more favorable as compared to radical mastectomy, it was still not ideal as it involved the loss of the breast.

In the early 1960s, Dr. Bernard Fisher, a distinguished oncologic investigator, announced that breast cancer is a systemic disease involving a complex spectrum of host tumor interactions and that variations in local /regional treatment are unlikely to affect survival substantially [9]. Drs. Fisher in Pittsburgh and Veronesi in Milan are accredited in popularizing breast conservation therapy (BCT), consisting of lumpectomy with axillary lymph node dissection/ sampling followed by radiation [10, 11]. Several prospective, randomized clinical trials comparing BCT to mastectomy [12–14] have shown equivalent survival, making it a viable option in carefully selected women.

Modern Trends

Image-guided treatment of breast cancer has its roots in screening mammography which was first introduced into the United States by Shapiro et al. in the 1960s [15] and in Sweden by Laslo Tabar in the 1970s [16]. The reports from both of these studies revealed a 25–32 % reduction in mortality among women with breast cancer. The report from a larger multicenter trial, Breast Cancer Detection and Demonstration Project, by Baker in 1981 [17] strongly supported the concept that early detection of cancer leads to better outcome. Unfortunately, the positive predictive value of screening mammography for breast cancer was approximately 20 %. In practical terms, this meant that 80 % of women with abnormal mammogram had unnecessary surgery. To overcome this problem, a group of investigators at Karolinska Institutet in Stockholm developed the stereotactic needle biopsy, an image-guided technique for tissue sampling with a fine needle to rule out malignancy [18–20] (Figs. 59.1 and 59.2). The device consisted of a table with an opening for the breast on which the patient would lie and the suspended breast be immobilized for radiographic examination at fixed angles to determine the exact location of the lesion (Fig. 59.3). Under local anesthesia, cytology samples would be taken for diagnosis.

In 1985, the technology was introduced into the United States, installed at the University of Chicago, and its accuracy was validated against open biopsy [21, 22]. Due to a nationwide shortage of experienced cytopathologists in this country, cytology was replaced with needle core biopsy [23, 24]. Early in its development, surgeons rejected the concept of "needle instead of knife," and the radiologists took over and popularized this technology. The shift to larger samples through bigger vacuum-assisted needles came partly on behest of pathologists who recommended more tissue for definitive diagnosis and partly due to medicolegal climate in the United States. Currently, needle core biopsy has become accepted by the majority of physicians and the public to be as good as open biopsy for diagnosis of breast lesions [25].

Breast Imaging Technologies

Although film mammography is the mainstay of breast imaging, other modalities for diagnosis and treatment purposes have been introduced into the field; a brief account of these options are given below.

Digital Mammography

Introduction of digital mammography to replace film screen mammography in the early 1990s was a major progress in breast imaging. Digital mammography has a greater contrast resolution [26] at lower average dose [27] in dense breasts of younger women at risk for breast cancer. Additionally, images can be post-processed, displayed on multiple viewing stations, and transmitted to remote locations for interpretation and consultation.

Mammography reports are also standardized with the use of the Breast Imaging Reporting and Data System (BI-RADS) [28]. The system simplifies the interpretation of images and communication among physicians of different specialties

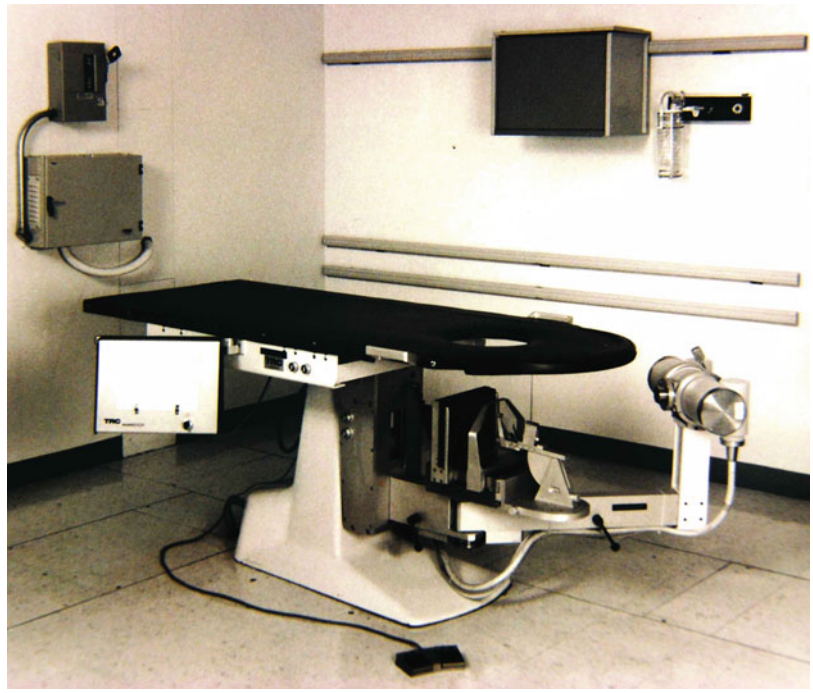

Fig. 59.1 Stereotactic table developed at Karolinska Institutet Stockholm, Sweden

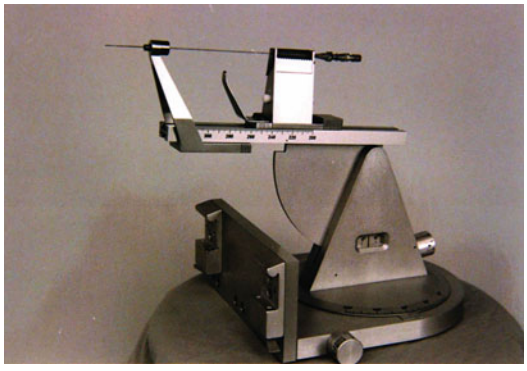

Fig. 59.2 Stereotactic module with a mounted biopsy needle – manually operated

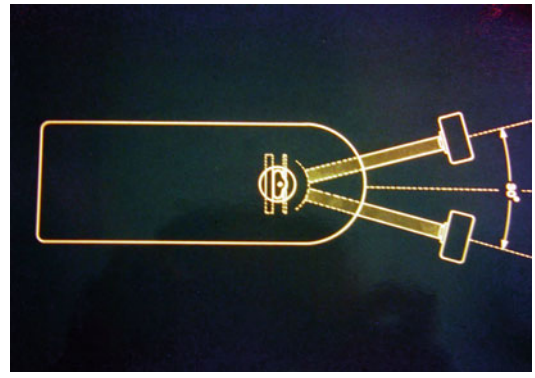

Fig. 59.3 Diagrammatic representation of the stereotactic principle of imaging breast lesion

caring for the patient. By assigning numbers on a scale of I–V, the interpreter predicts the likelihood of malignancy in the case under consideration [29].

Ultrasound

Breast ultrasound is an important imaging adjunct which has been increasingly deployed since its development in the 1990s [30, 31]. It was initially used to differentiate between solid and cystic lesions in the breast but is now often used as a complementary imaging device with mammography and guides the practitioner in interventional procedures. When compared with other breast imaging modalities, ultrasound has excellent image contrast and spatial resolution. The benefits of ultrasound include its relatively

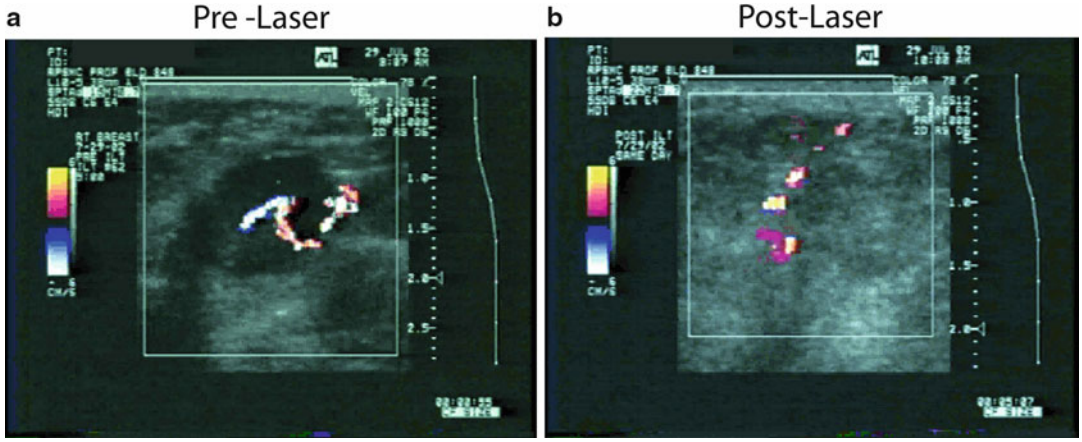

Fig. 59.4 Interstitial laser therapy (ILT) causes thrombosis of breast cancer blood vessel: (**a**) pre- and (**b**) post-ILT

low cost, its availability, and its portability in the clinic and operating room. The penetration of denser breast tissue of younger women and the absence of patient exposure to radiation are the features which have made the breast US a stethoscope-like tool for the physician. The primary disadvantage of ultrasound is that it is highly operator dependent. A 7-MHz linear array transducer is the minimum frequency that can be used for breast examination. However, 10–13 MHz transducers offer more near-field quality imaging.

Ultrasound characteristics which are considered when determining the malignant potential of breast lesions include margins, echogenicity, compressibility, and lateral/anterior–posterior dimension ratio. Malignant lesions often have irregular and indistinct margins and a heterogeneous interior, which results in an irregular posterior shadowing pattern. Such lesions are usually minimally compressible and have a vertical growth appearance, i.e., "taller than wider" [30].

CDUS (Color Doppler Ultrasound)

CDUS provides information regarding vasculature and blood flow of breast tissue. In general, vessels supplying tumors are numerous and tortuous with high velocity and low resistance flow. CDUS has been used in demonstrating the extent of zone of necrosis in interstitial laser therapy of breast cancer [31] (Fig. 59.4). It has also been shown to demonstrate local recurrence of laser-treated breast cancer by the appearance of neo-vasculature before the development of the tumor mass (K. Dowlatshahi, personal observation, 2008) (Fig. 59.5).

Role of Ultrasound in Surgical Practice

The availability of ultrasound in the office and clinic makes it the instrument of choice for a surgeon to differentiate cyst from solid, benign from malignant and to guide a needle for biopsy under local anesthesia. Its intraoperative application to better visualize the tumor and its extensions into the surrounding tissue is exploited to minimize the margin positivity and the need for second operation [32, 33]. Ultrasound also provides in real time the changes in the thermally treated breast fibroadenoma either by freezing or by heat [34–36] (Figs. 59.6 and 59.7).

MRI (Magnetic Resonance Imaging)

Breast MRI is increasingly used for screening as well as diagnosis of breast cancer (Fig. 59.8).

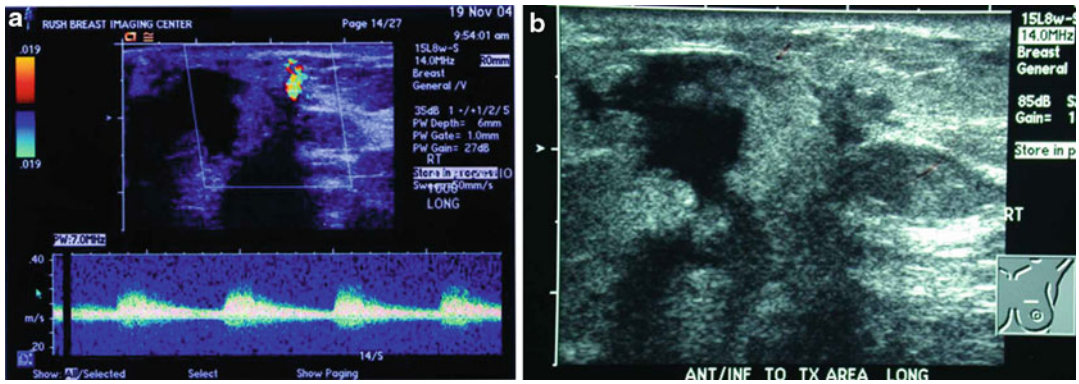

Fig. 59.5 Color Doppler appearance of neo-vascular: (**a**) *left image*, generated six months before detection of local recurrence shown on (**b**) *right image*

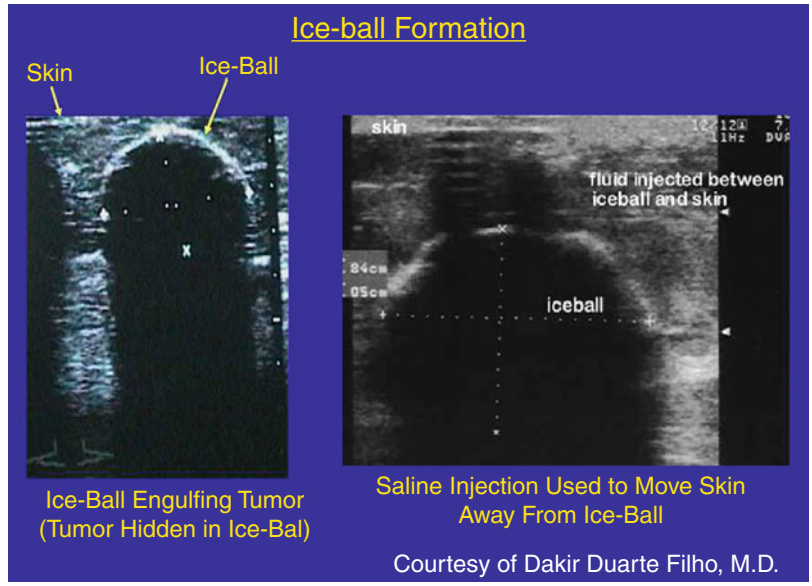

Fig. 59.6 Ice ball formation induced around a fibroadenoma by a cryoprobe

MRI is advantageous in that there is no ionizing radiation to the patient and the breast density is not a limiting factor. It is also used to rule out multicentricity and suspicion of recurrence in a patient previously treated for breast cancer [37]. Known disadvantages include cost, limited availability, and low specificity. Breast MRI is best performed on a machine with a high-field strength magnet (>1.5 T) and a dedicated breast coil. Contrast enhancement with gadolinium is used to identify cancers and distinguish them from benign lesions. Cancers have a rapid wash-in of contrast and either a rapid washout or leveling off of contrast, while benign lesions have a slow progressive wash-in. Lesion morphology is characterized using high-resolution imaging [38, 39]. Spiculated margins and irregular rim enhancement indicate malignant lesions, while smooth borders with uniform enhancement are more suggestive of benign lesions [40].

MRI is particularly helpful in surgical decision making by more accurately determining the size of the tumor and ruling out multicentricity.

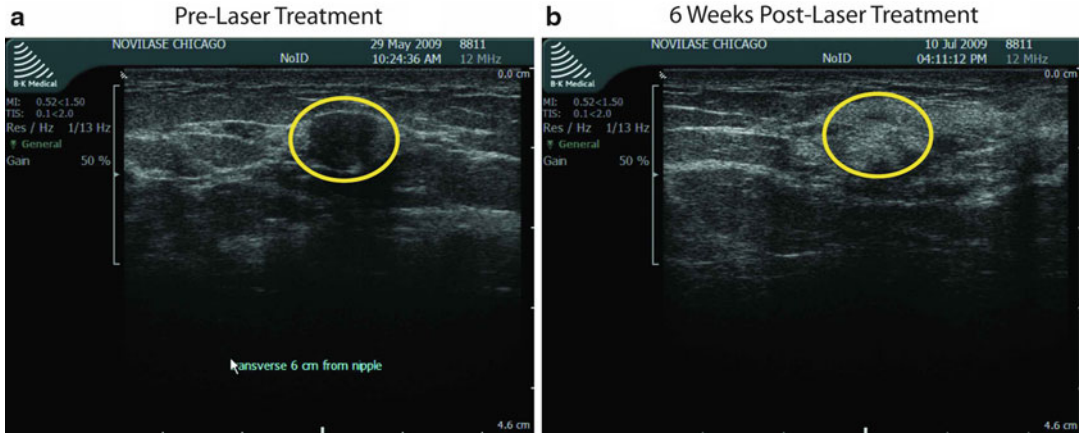

Fig. 59.7 Breast fibroadenoma treated with ILT: (**a**) pre- and (**b**) posttreatment

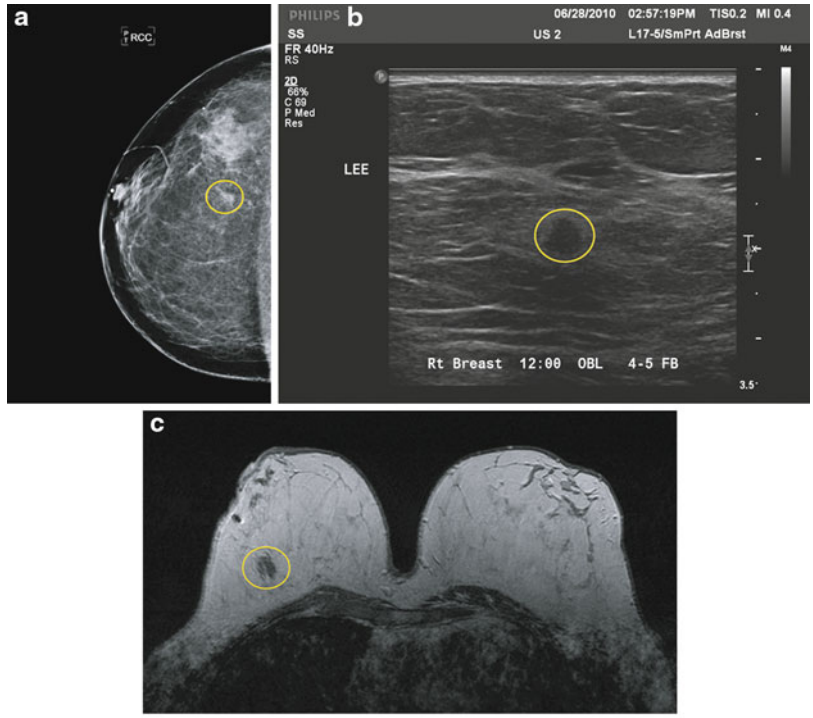

Fig. 59.8 Breast cancer imaged by (**a**) mammogram, (**b**) ultrasound, and (**c**) MRI

MRI can also aid in distinguishing scar tissue from recurrent cancer and to assess the effects of chemotherapy. It has been investigated in regard to screening of high-risk patients, including women with genetic mutations. The American Cancer Society recommends MRI screening in combination with mammography for women with a greater than 20 % lifetime risk for breast cancer. Included in this group are women with a strong family history of breast or ovarian cancer and women with history of radiation to the chest wall [41].

MRI Intervention

Breast abnormalities discovered by MRI are often difficult to localize with ultrasound or

mammography. MRI is deployed to wire localize for surgical intervention with excellent results. Patient positioning and access to the lesion can be challenging using MRI, and accurate radiological–pathological correlation is always of the utmost importance. The marked advantage of MRI may lie in its guidance of ablative therapies as it is an imaging technique that is able to sense changes in tissue temperature. Thus, the treatment region may be monitored closely with adjustments made to therapy as needed. Research in this area is ongoing, and early results are promising [42].

PEM (Positron Emission Mammography)

Like MRI, PEM is a functional test. The patient is given an intravenous infusion of FDG (fluorodeoxyglucose), a glucose analog, which accumulates in glucose-avid cells. FDG will accumulate in both inflammatory and cancerous states as they have higher metabolic rate than normal cells. PEM can be useful in women with newly diagnosed breast cancer who are thought to be candidates for breast conservation therapy, where conventional imaging and clinical breast examination often do not describe the full extent of cancer. In preliminary studies [43], PEM appears to be as sensitive as and probably more specific than MRI. It can be used to aid in diagnosis and staging. In recent studies, PEM has been shown to detect in situ cancers better than any other modality. This is very significant, given that quite frequently when lumpectomy margins are positive, it is secondary to ductal carcinoma in situ (DCIS) rather than invasive tumor. Therefore, PEM may be very valuable in decreasing the rate of re-excision [44].

In patients with locally advanced disease, PEM can help determine the extent of disease and spread to the lymph nodes [45]. The overall specificity for PEM is about 86 % with a specificity of 91 % and an overall diagnostic accuracy of 89 % [46]. PEM has thus far proven to be a useful adjunct to breast cancer diagnosis and more importantly surgical planning. Current and future studies are looking at the use of PEM as an in vitro assay of breast cancer tumor biology and tumor responsiveness to treatment.

Minimally Invasive Techniques in Surgical Treatment of Breast Cancer

Mammography and other breast imaging technologies have fundamentally changed our approach to the diagnosis and treatment of breast disease. We are witnessing a major paradigm shift from tactile to visual in the management of patients with breast cancer. With the advent of widespread annual screening mammography, an increasing number of detected breast cancers are non-palpable or smaller than 1 cm. The diagnosis of such lesions (microcalcifications, masses, or architectural distortions) is made by image-guided needle biopsy in the physician's office or in an outpatient setting. In the past decade, several minimally invasive treatments have emerged and are under consideration for wider clinical application. Broadly, they can be divided into two categories:

- *Excisional*: The tumor is removed through a 1–2-cm skin incision either in small segments, e.g., vacuum-assisted Mammotome, or in one piece using a special probe (Intact and Site-Select). In either case, the procedure is guided by US or stereotactic images.
- *In situ ablation* by freezing (cryotherapy) or by heating (laser, radiofrequency, microwave, and high-intensity focused ultrasound), whereby the tumor is destroyed within the breast and left on-site to be removed by the immune system.

The main difference between the two approaches is that in the first, the pathologist is provided with tissue to report on margin status – important information needed prior to adjuvant radiation therapy. In cases of in situ ablation, reliance is placed on imaging to inform the operator of total destruction of the cancer

resulting in "clear margins." A recent US Food and Drug Administration (FDA) workshop addressed the role of thermal ablation and the reliability of the current imaging technologies to evaluate selected tumors before and after treatment. The FDA is also considering creation of a registry to track the results. The imaging technologies under consideration include digital mammography, high-resolution gray scale and color Doppler ultrasound, and MRI. Newer technologies, such as tomosynthesis, breast-specific gamma imaging (BSGI), and PEM, are also expected to play significant roles in the future management of breast cancer – especially in dense breasts of younger patients. A brief account of these therapies is presented.

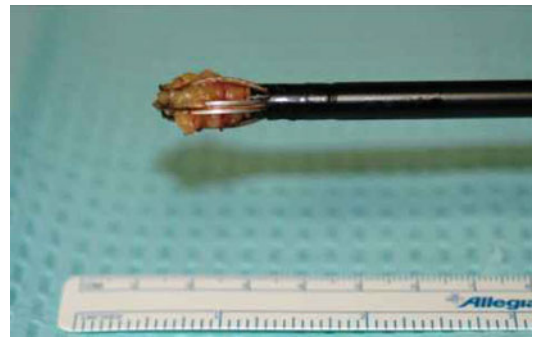

Fig. 59.9 Radiofrequency probe with its basket containing the breast lesion electrically excised and removed

Image-Guided Excision Devices

Several technologies at different phases of development are available for removal of the breast lesions. They are the following:

1. *Mammotome*: This is a vacuum-assisted biopsy device (VABD), originally introduced as a diagnostic tool. However, improvement in technology (by production of larger caliber tools) has now extended its use to therapeutic procedures. VABD has been used in treatment of benign breast disease such as fibroadenoma [47]. These investigators have shown that fibroadenomas can be safely removed under local anesthesia with ultrasound guidance using eight-gauged VABD probes [48]. A recent long-term report on ultrasound-guided vacuum-assisted removal of benign palpable breast masses showed 61 % success rate with no residual tumor [49].
2. *Site-Select*: A second manually operated device is Site-Select, which is used in conjunction with a stereotactic table [50]. With the patient lying on the table in a prone position and under local anesthesia, a 10–15-mm skin incision is made, and an appropriately sized cylinder is driven into the breast to engulf the targeted lesion. Stereotactic images confirm correct capture of the lesion before it is electrically severed at its distal and proximal borders, including a cuff of normal tissue. The specimen is then removed for histological examination, and the incision is closed with sutures or surgical tapes.
3. *Intact*: This device utilizes radiofrequency energy to cut and separate the breast tumor and a margin of normal tissue around it. The procedure is performed on a stereotactic table or guided by ultrasound under local anesthesia. The resected tissue is removed in one piece from the breast either in a bag or by the device itself through an 8–12-mm skin incision for the pathologist's assessment of the margin status (Fig. 59.9). At present, these devices can remove only sub-centimeter tumors with enough surrounding tissue to obtain a clear margin [51].

In Situ Thermal Ablation

Currently, five technologies are available for ablation of tumors within the breast and without their removal:

1. *Cryoablation*: This is tumor destruction by freezing. With ultrasound guidance and under local anesthesia, the cryoprobe, a special size 16-G needle, is inserted into the center of the tumor. Its tip is then cooled

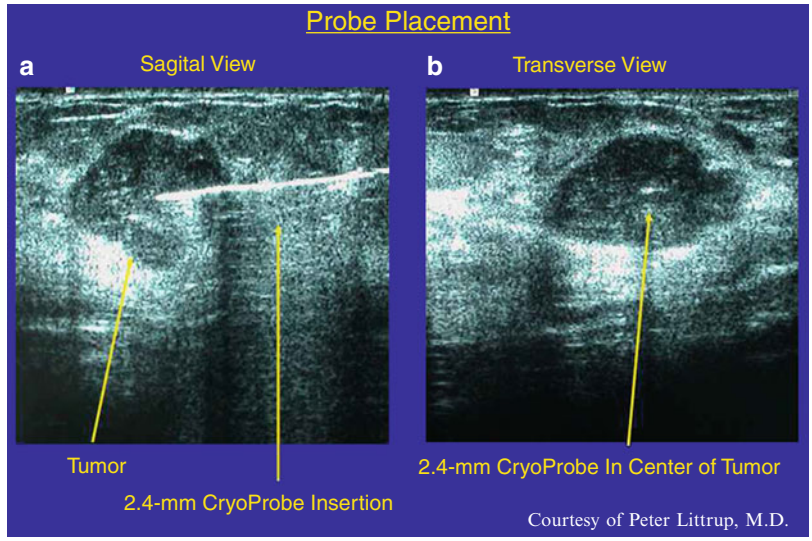

Fig. 59.10 Ultrasound-guided placement of a cryoprobe in a breast fibroadenoma, (**a**) sagittal and (**b**) coronal views

with a circulating liquid, resulting in an ice ball that encompasses the tumor and a rim of normal tissue around it (Fig. 59.10). At least two cycles of freezing and thawing may be necessary to complete the ablation [52, 53]. In addition to ablating small invasive breast cancers, cryoablation has also been shown to initiate an inflammatory response which is believed to induce an antitumor immune response. Studies by Sabel et al. using a murine model have shown that cryoablation leads to induction of a tumor-specific T cell response and increased NK cell activity [54].

2. *Laser Ablation*: Interstitial laser therapy has been reported by several investigators from the UK and USA. [55–59]. Computerized tomography, stereotactic technique, and more recently ultrasound have been deployed for treatment monitoring. The patient lies on a stereotactic table with the indexed breast being immobilized. Under local anesthesia, the laser probe (14-G needle) is inserted into the center of the tumor, and a thermal probe is inserted parallel with the laser probe and 1 cm away from it so that its tip comes to lie 1 cm beyond the laser probe. (Figs. 59.11 and 59.12) The breast tissue around the tumor is anesthetized with 20–25 cc of ½ % Marcaine.

Fig. 59.11 Operational position for a patient lying on a stereotactic table showing the laser and thermal probes inserted into the breast under local anesthesia

Low-power (5 w) laser energy is given until the peripheral temperatures reach 60 °C (Fig. 59.13). A necrotic sphere of 2.0–2.5 cm in diameter is created (Fig. 59.14) which engulfs the 1.0–1.5-cm tumor (Fig. 59.15). The completeness of the process is demonstrated by MRI. This technique is currently approved for the treatment of benign breast tumors such as fibroadenomas. A multicenter clinical trial for treatment of breast cancers is planned.

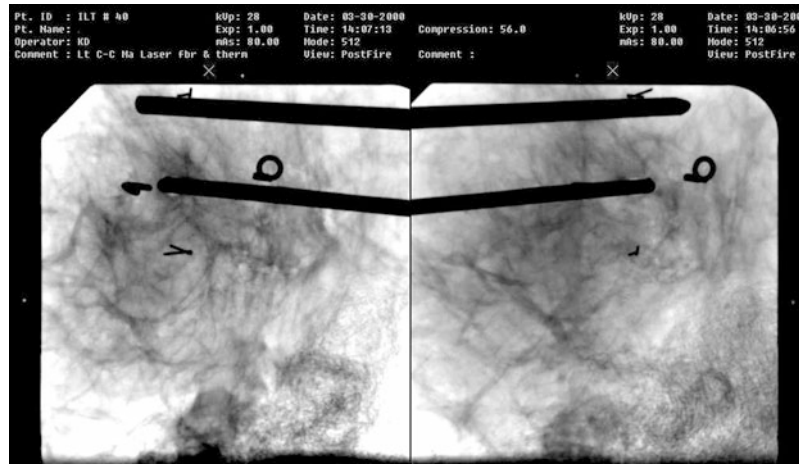

Fig. 59.12 Stereotactic images of the laser and thermal probes inserted into the breast

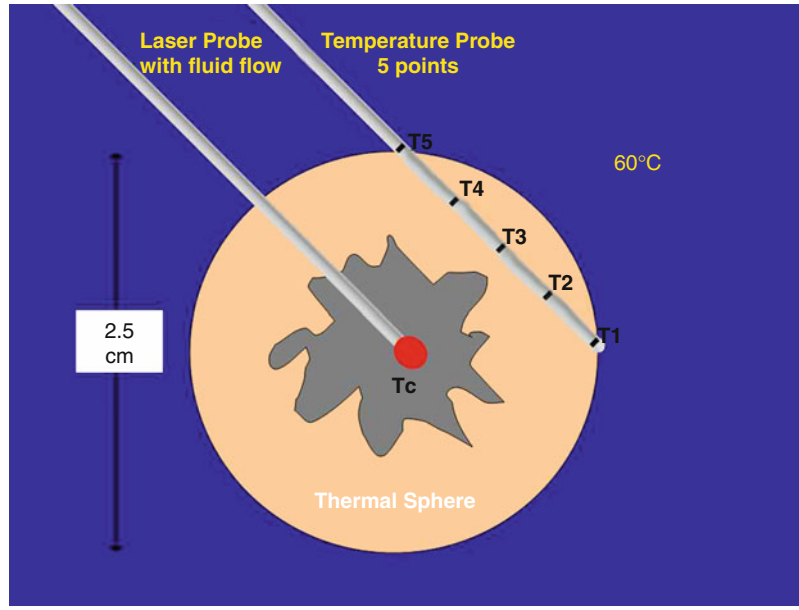

Fig. 59.13 Diagrammatic representation of the laser and thermal probes placed in the breast tumor

3. *Radiofrequency Ablation*: Another potential ablative technology is radiofrequency ablation (RFA) with image guidance, utilizing the radiofrequency energy to create molecular movement and frictional heating within the tumor [60]. The generated heat destroys the cancer cells. This technology is extensively employed for treatment of intrahepatic tumors up to 3 cm in size. Therefore, it can be considered as an option for treatment of inoperable tumors in neoadjuvant setting [61]. With regard to breast cancer, RFA is used to ablate residual malignant cells post-lumpectomy [62, 63]. Klimberg et al. have shown that this technique reduces re-excision rate by 86 %, thus addressing the problem of positive margins [63].
4. *Microwave Thermotherapy*: Focused microwave phased array thermotherapy for ablation

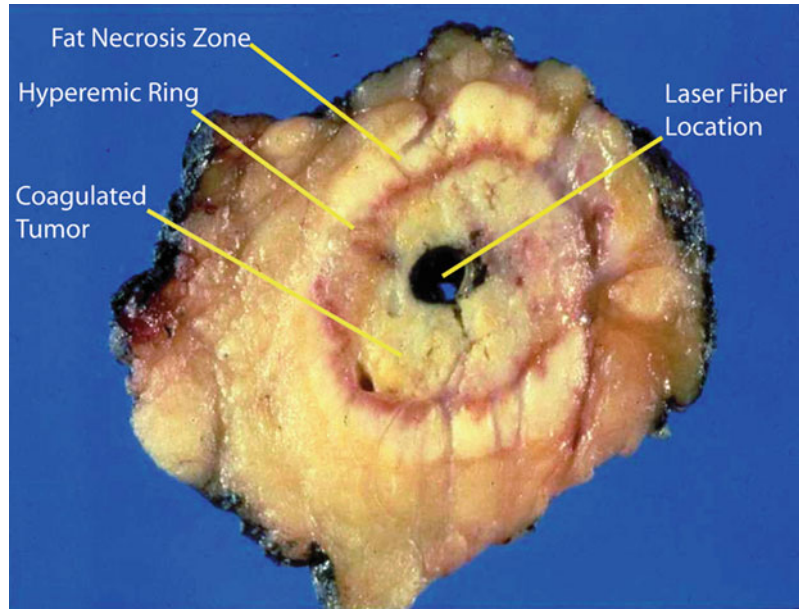

Fig. 59.14 A cross section representative of a laser-treated breast cancer showing necrotic tumor marked by a hyperemic ring and a zone of outer fat necrosis

of small breast cancers was tested and reported in a multicenter, non-randomized group of 25 patients. Microwaves were guided by an antenna–temperature sensor placed percutaneously into the tumor. Pathological necrosis was achieved in 68 % of patients. The degree of the tumor necrosis was noted to be a function of the thermal dose. With sufficient skin cooling, minimal morbidity was noted [64].

5. *High-Intensity Focused Ultrasound*: High-intensity focused ultrasound (HIFU) uses an external ultrasonic energy source to induce 3D conformal ablation of the tumor through intact skin. It is guided to the breast lesion with MRI, which also measures and displays the temperature of the tumor in real time. The largest experience in this field has been reported from China [65]. This technology is truly noninvasive as no skin incision is made to insert a device. High-intensity focused ultrasound achieves a positive response in breast cancer patients resulting in regression of tumors postoperatively. Biopsies of the treated area show coagulation necrosis and replacement by fibroblastic tissue. Ninety-five percent 5-year disease-free survival and 89 % recurrence-free survival have been reported [66].

Summary

In today's practice, detection and diagnosis of breast cancer at sub-centimeter size has become a common experience. Emergence of sophisticated imaging technologies have replaced "knife with needle" with equal accuracy and to the satisfaction of the patient [67]. The treatment has lagged behind diagnosis. Lumpectomy is a misnoma because there is no palpable lump in the breast. More importantly, the management of such tumors can be done with image-guided thermal energies as briefly outlined in this chapter. The paradigm shift from tactile to visual is critical and is not without its inherent difficulties. Nevertheless, it behooves us as breast oncologists to take up the challenge of mastering the new approach in treatment of patients with breast cancer and to move on to the next phase of treating the disease at subcellular level.

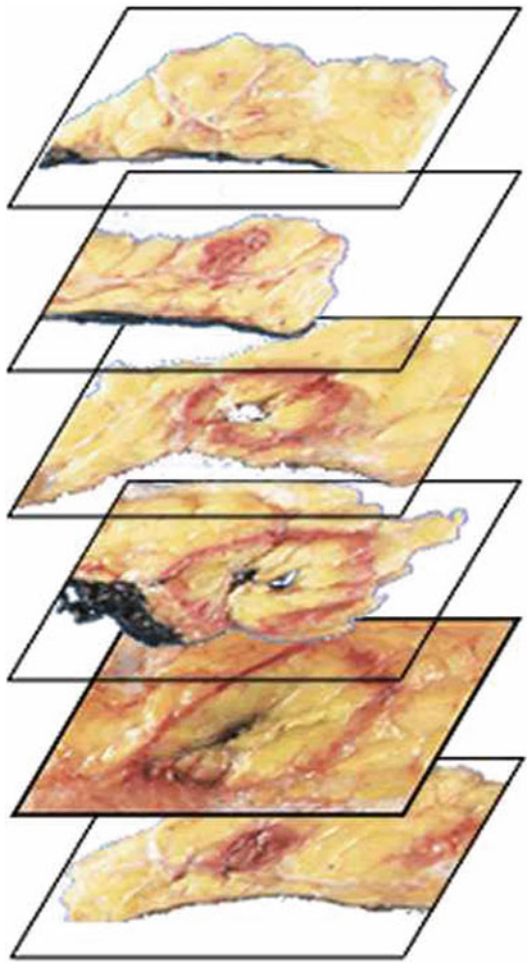

Fig. 59.15 Serial sections of a laser-treated breast cancer depicting the extent of necrosis three dimensionally

References

1. Halsted W. The results of radical operations for the cure of carcinoma of the breast. Ann Surg. 1907;46:1.
2. Urban JA. Current cancer concepts. What is the rationale for an extended radical procedure in early cases? JAMA. 1967;199(10):742–3.
3. Patey DH, Dyson WH. The prognosis of carcinoma of the breast in relation to the type of operation performed. Br J Cancer. 1948;2(1):7–13.
4. Crile Jr G. Results of simple mastectomy without irradiation in the treatment of operative stage I cancer of the breast. Ann Surg. 1968;168(3):330–6.
5. Turner L, Swindell R, Bell WG, et al. Radical versus modified radical mastectomy for breast cancer. Ann R Coll Surg Engl. 1981;63:239.
6. Maddox WA, Carpenter JT, Laws HL, et al. A randomized prospective trial of radical (Halsted) mastectomy versus modified radical mastectomy in 311 breast cancer patients. Ann Surg. 1983; 198:207.
7. Fisher B, Redmond C, Fisher E, et al. Ten year result of a randomized clinical trial comparing radical mastectomy and total mastectomy with or without irradiation. N Engl J Med. 1985;312:674.
8. Fisher B, Jeong JH, Anderson S, et al. Twenty-five-year follow-up of a randomized trial comparing radical mastectomy, total mastectomy, and total mastectomy followed by irradiation. N Engl J Med. 2002;347:567.
9. Fisher B. Laboratory and clinical research in breast cancer–a personal adventure: the David A Karnofsky memorial lecture. Cancer Res. 1980;40(11):3863–74.
10. Fisher B, Anderson S, Bryant J, et al. Twenty-year follow-up of a randomized trial comparing total mastectomy, lumpectomy, and lumpectomy plus irradiation for the treatment of invasive breast cancer. N Engl J Med. 2002;347:1233.
11. Veronesi U, Cascinelli N, Mariani L, et al. Twenty-year follow-up of a randomized study comparing breast-conserving surgery with radical mastectomy for early breast cancer. N Engl J Med. 2002;347:1227.
12. van Dongen JA, Voogd AC, Fentiman IS, et al. Long-term results of a randomized trial comparing breast-conserving therapy with mastectomy: European Organization for Research and Treatment of Cancer 10801 Trial. J Natl Cancer Inst. 2000;92:1143.
13. Jacobson JA, Danforth DN, Cowan KH, et al. Ten-year results of a comparison of conservation with mastectomy in the treatment of stage I and II breast cancer. N Engl J Med. 1995;332:907.
14. Poggi MM, Danforth DN, Sciuto LC, et al. Eighteen-year results in the treatment of early breast carcinoma with mastectomy versus breast conservation therapy: the National Cancer Institute Randomized Trial. Cancer. 2003;98:697.
15. Shapiro S, Strax P, Venet L. Periodic breast cancer screening. The first two years of screening. Arch Environ Health. 1967;15:547–53.
16. Tabar L, Fagerberg CJ, Gad A, et al. Reduction in mortality from breast cancer after mass screening with mammography. Randomised trial from the Breast Cancer Screening Working Group of the Swedish National Board of Health and Welfare. Lancet. 1985;1:829–32.
17. Baker LH. Breast Cancer Detection Demonstration Project: five-year summary report. CA Cancer J Clin. 1982;32:194–225.
18. Bolmgren J, Jacobson B, Nordenstrom B. Stereotaxic instrument for needle biopsy of the mamma. AJR Am J Roentgenol. 1977;129:121–5.
19. Svane G, Silfversward C. Stereotaxic needle biopsy of non-palpable breast lesions. Cytologic and histopathologic findings. Acta Radiol Diagn (Stockh). 1983;24:283–8.

20. Azavedo E, Svane G, Auer G. Stereotactic fine-needle biopsy in 2594 mammographically detected non-palpable lesions. Lancet. 1989;1(8646):1033–6.
21. Gent HJ, Sprenger E, Dowlatshahi K. Stereotaxic needle localization and cytological diagnosis of occult breast lesions. Ann Surg. 1986;204(5):580–4.
22. Dowlatshahi K, Yaremko ML, Kluskens LF, Jokich PM. Nonpalpable breast lesions: findings of stereotaxic needle-core biopsy and fine-needle aspiration cytology. Radiology. 1991;181:745–50.
23. Parker SH, Lovin JD, Jobe WE, Burke BJ, Hopper KD, Yakes WF. Nonpalpable breast lesions: stereotactic automated large-core biopsies. Radiology. 1991;180:403–7.
24. Doyle AJ, Murray KA, Nelson EW, Bragg DG. Selective use of image-guided large-core needle biopsy of the breast: accuracy and cost-effectiveness. AJR Am J Roentgenol. 1995;165(2):281–4.
25. Jackman RJ, Nowels KW, Shepard MJ, Finkelstein SI, Marzoni Jr FA. Stereotaxic large-core needle biopsy of 450 nonpalpable breast lesions with surgical correlation in lesions with cancer or atypical hyperplasia. Radiology. 1994;193(1):91–5.
26. Kettritz U, Rotter K, Schreer I, Murauer M, Schulz-Wendtland R, Peter D, et al. Stereotactic vacuum-assisted breast biopsy in 2874 patients: a multicenter study. Cancer. 2004;100(2):245–51.
27. Pisano ED, Yaffe MJ. Digital mammography. Radiology. 2005;234:353–62.
28. Skaane P, Skjennald A. Screen-film mammography versus full-field digital mammography with soft-copy reading: randomized trial in a population-based screening program–the Oslo II Study. Radiology. 2004;232(1):197–204.
29. Bassett L, Winchester DP, Caplan RB, Dershaw DD, Dowlatshahi K, Evans 3rd WP, et al. Stereotactic core-needle biopsy of the breast: a report of the Joint Task Force of the American College of Radiology, American College of Surgeons, and College of American Pathologists CA. Cancer J Clin. 1997;47(3):171–90.
30. Kerlikowske K, Grady D, Barclay J, et al. Variability and accuracy in mammographic interpretation using the American College of Radiology Breast Imaging Reporting and Data System. J Natl Cancer Inst. 1998;90:1801–9.
31. Staren ED, Fine R. Breast ultrasound for surgeons. Am Surg. 1996;62:108–12.
32. Jackson VP, Reynolds HE, Hawes DR. Sonography of the breast Semin. Ultrasound CT MR. 1996;17(5):460–75.
33. Kopans DB, Feig SA, Sickles EA. Malignant breast masses detected only by ultrasound: a retrospective review. Cancer. 1996;77(1):208–9.
34. Dowlatshahi K, Dieschbourg J. Shift in the surgical treatment of non-palpable breast cancer: tactile to visual. Breast Cancer Online. 2005;9:1–10.
35. Smith LF, Rubio IT, Henry-Tillman R, Korourian S, Klimberg VS. Intraoperative ultrasound-guided breast biopsy. Am J Surg. 2000;180(6):419–23.
36. Kaufman CS, Jacobson L, Bachman B, Kaufman L. Intraoperative ultrasound facilitates surgery for early breast cancer. Ann Surg Oncol. 2002;9(10):988–93.
37. Kaufman CS, Bachman B, Littrup PJ, White M, Carolin KA, Freman-Gibb L, Francescatti D, Stocks LH, Smith S, Henry CA, Bailey L, Harness JK, Simmons R. Office-based ultrasound-guided cryoablation of breast fibroadenomas. Am J Surg. 2002;184:394–400.
38. Sabel MS, Kaufman CS, Whitworth P, et al. Cryoablation of early-stage breast cancer: work-in-progress report of a multi-institutional trial. Ann Surg Oncol. 2004;11:542–9.
39. Littrup PJ, Jallad B, Chandiwala-Mody P, D'Agostini M, Adam BA, Bouwman D. Cryotherapy for breast cancer: a feasibility study without excision. J Vasc Interv Radiol. 2009;20(10):1329–41.
40. Nunes LW, Schnall MD, Orel SG, et al. Breast MR imaging: interpretation model. Radiology. 1997;202:833–41.
41. Morris EA, Liberman L, Ballon DJ, et al. MRI of occult breast carcinoma in a high-risk population. AJR Am J Roentgenol. 2003;181:619–26.
42. Eby PR, Lehman CD. Magnetic resonance imaging–guided breast interventions. Top Magn Reson Imaging. 2008;19(3):151–62.
43. Leach MO. Breast cancer screening in women at high risk using MRI. NMR Biomed. 2009;22:17–27.
44. Pickles MD, Lowry M, Manton DJ, Gibbs P, Turnbull LW. Role of dynamic contrast enhanced MRI in monitoring early response of locally advanced breast cancer to neoadjuvant chemotherapy. Breast Cancer Res Treat. 2005;91(1):1–10.
45. Breast Cancer: Early Detection, Diagnosis, and Staging. Available at: http://www.cancer.org/Cancer/BreastCancer/DetailedGuide/breast-cancer-detection (2010). Accessed 27 Sep 2010.
46. Kriege M, Brekelmans CT, Boetes C, Besnard PE, Zonderland HM, Obdeijn IM, et al. Efficacy of MRI and mammography for breast-cancer screening in women with a familial or genetic predisposition. N Engl J Med. 2004;351(5):427–37.
47. Berg WA, Weinberg IN, Narayanan D, Lobrano ME, Ross E, Amodei L, et al. High-resolution fluorodeoxyglucose positron emission tomography with compression ("positron emission mammography") is highly accurate in depicting primary breast cancer. Breast J. 2006;12(4):309–23.
48. Tafra L. Positron Emission Tomography (PET) and Mammography (PEM) for breast cancer: importance to surgeons. Ann Surg Oncol. 2007;14:3–13.
49. Fine RE, Staren ED. Percutaneous radiofrequency-assisted excision of fibroadenomas. Am J Surg. 2006;192:545–7.
50. Fine RE, Whitworth PW, Kim JA, Harness JK, Boyd BA, Burak Jr WE. Low-risk palpable breast masses removed using a vacuum-assisted hand-held device. Am J Surg. 2003;186:362–7.

51. Kim MJ, Park BW, Kim SI, Youk JH, Kwak JY, Moon HJ, et al. Long-term follow-up results for ultrasound-guided vacuum-assisted removal of benign palpable breast mass. Am J Surg. 2010;199(1):1–7.
52. Corn CC. Review of 125 SiteSelect stereotactic large-core breast biopsy procedures. Breast J. 2003;9:147–52.
53. Sie A, Bryan DC, Gaines V, et al. Multicenter evaluation of the breast lesion excision system, a percutaneous, vacuum-assisted, intact-specimen breast biopsy device. Cancer. 2006;107:945–9.
54. Sabel MS, Nehs MA, Su G, Lowler K, Ferrara JLM, Chang AE. Immunologic response to cryoablation of breast cancer. Breast Cancer Res Treat. 2005;90(1):97–104.
55. Dowlatshahi K, Dieschbourg JJ, Bloom KJ. Laser therapy of breast cancer with 3-year follow-up. Breast J. 2004;10:240–3.
56. Dowlatshahi K, Fan M, Gould VE, Bloom KJ, Ali A. Stereotactically guided laser therapy of occult breast tumors: work-in-progress report. Arch Surg. 2000; 135:1345–52.
57. Dowlatshahi K, Francescatti DS, Bloom KJ. Laser therapy for small breast cancers. Am J Surg. 2002;184:359–63.
58. Goldstein NS. Laser therapy for small breast cancers. Am J Surg. 2004;187:149–50.
59. Mumtaz H, Hall-Craggs MA, Wotherspoon A, et al. Laser therapy for breast cancer: MR imaging and histopathologic correlation. Radiology. 1996;200:651–8.
60. Izzo F, Thomas R, Delrio P, et al. Radiofrequency ablation in patients with primary breast carcinoma: a pilot study in 26 patients. Cancer. 2001; 92:2036–44.
61. Singletary SE. Applications of radiofrequency ablation in the treatment of breast cancer. Breast Cancer Online. 2005;8(9):1–4.
62. Burak Jr WE, Agnese DM, Povoski SP, et al. Radiofrequency ablation of invasive breast carcinoma followed by delayed surgical excision. Cancer. 2003;98:1369–76.
63. Klimberg VS, Kepple J, Shafirstein G, Adkins L, Henry-Tilman R, Youssef E, Brito J, Talley L, Korourian S. eRFA: excision followed by RFA-a new technique to improve local control in breast cancer. Ann Surg Oncol. 2006;13(11):1422–33.
64. Vargas HI, Dooley WC, Gardner RA, Gonzalez KD, Venegas R, Heywang-Kobrunner SH, Fenn AJ. Focused microwave phased array thermotherapy for ablation of early-stage breast cancer: results of thermal dose escalation. Ann Surg Oncol. 2004;11: 139–46.
65. Wu F, Wang ZB, Cao YD, et al. Heat fixation of cancer cells ablated with high-intensity-focused ultrasound in patients with breast cancer. Am J Surg. 2006;192:179–84.
66. Wu F, Wang ZB, Zhu H, Chen WZ, Zou JZ, Bai J, Li KQ, Jin CB, Xie FL, Su HB. Extracorporeal high intensity focused ultrasound treatment for patients with breast cancer. Breast Cancer Res Treat. 2005;92(1):51–60.
67. Dowlatshahi K, Snider H, Lerner AG. Who should perform image-guided breast biopsy and treatment? Am J Surg. 2007;194(3):275–7.

Radiation Oncology in Breast Cancer

60

Chirag Shah, Samuel McGrath, and Frank Vicini

Abstract

With the advent of breast-conserving therapy (BCT), radiation therapy is utilized in noninvasive and early-stage breast cancer as well as locally advanced and metastatic breast cancer. With ductal carcinoma in situ (DCIS) and early-stage breast cancer, radiation therapy is delivered following surgery, utilizing whole breast irradiation. Boost treatments have been shown to improve local control, especially in younger patients. There have been no subsets of patients with DCIS or early-stage breast cancer that have been identified in which radiation therapy may be omitted in spite of improved surgical and hormonal treatments. Postmastectomy radiation therapy (PMRT) has been found to provide a benefit in overall survival and locoregional control in patients with locally advanced breast cancer. Current recommendations for PMRT include patients with four or more lymph nodes involved with tumors greater than 5 cm and 1–3 lymph nodes involved being controversial at this time.

Radiation therapy techniques have evolved in order to increase compliance including new techniques in hypofractionation and accelerated partial breast irradiation, which shorten the overall length of adjuvant treatment. These new techniques have demonstrated promising initial results with long-term follow-up limited at this time. New techniques in radiation therapy planning including intensity-modulated radiation therapy (IMRT) are being developed in order to help reduce the acute and long-term morbidity associated with radiation therapy. Toxicity following radiation therapy is primarily dermatological, and the frequency of good/excellent cosmesis has improved with the use of modern surgical and radiotherapy techniques.

C. Shah (✉) • S. McGrath • F. Vicini
Department of Radiation Oncology, William Beaumont Hospital, Royal Oak, MI, USA
e-mail: chirag.shah@beaumont.edu; smcgrath@beaumont.edu; fvicini@beaumont.edu

D.E. Dupuy et al. (eds.), *Image-Guided Cancer Therapy*, DOI 10.1007/978-1-4419-0751-6_62,

Introduction

The management of breast cancer has evolved over the past several decades from primarily surgical management to one requiring a multidisciplinary approach. This change in paradigm requires a team of specialists from surgery, medical oncology, and radiation oncology to come together to help formulate an individualized treatment plan for each patient. Further, with the advent of breast-conserving therapy (BCT), radiation therapy is utilized in noninvasive and early-stage breast cancer as well as locally advanced and metastatic breast cancer.

The purpose of this chapter is to discuss how radiation therapy is integrated into interventional oncology of the breast and its role in the multidisciplinary approach to breast cancer.

DCIS

DCIS presents primarily as a mammographic abnormality with approximately 75 % of cases being associated with microcalcifications on mammography. The disease represents approximately one-third of all new breast cancers [1–3]. DCIS was a rare diagnosis prior to the advent of population wide mammographic screening in the 1980s representing approximately 5 % of breast malignancies at that time [4]. Currently, more than 50,000 cases of DCIS are diagnosed yearly, representing nearly 85 % of noninvasive breast malignancies [5, 6]. DCIS is treated similarly to early-stage breast cancer (from a local standpoint) with treatment options including mastectomy, BCT, and excision alone. The rate of ipsilateral breast tumor recurrence (IBTR) is commonly cited at 2–4 % per year with excision alone and 0.5–1 % per year with the addition of adjuvant radiation therapy. Most recurrences develop at or near the index lesion with half of recurrences being invasive and the other half noninvasive (regardless whether post-excision radiation is used) [7]. Currently, the National Comprehensive Cancer Network (NCCN) lists mastectomy and lumpectomy with adjuvant radiation therapy as Category 1 recommendations, while lumpectomy alone is a Category 2B recommendation for the management of in situ disease [8]. BCT is considered the standard of care in the management of DCIS due to the psychological benefits of preserving the breast and the acceptable rates of local control achieved. Mastectomy is often reserved for cases with multicentric or diffuse disease, patients who cannot receive radiation therapy, and cases where breast conservation would lead to an unacceptable cosmetic outcome.

Breast-Conserving Therapy

There are no prospective randomized trials comparing mastectomy to BCT in patients presenting with pure DCIS. However, retrospective data have demonstrated excellent outcomes with BCT. A large series of cases from multiple institutions by Solin, with a median follow-up of 8.5 years, found the 15-year overall survival to be 89 % and the cause-specific survival 98 % in 1,003 patients with DCIS treated with BCT [9].

In four randomized trials, breast-conserving surgery alone was compared with surgery with adjuvant radiation therapy; these trials are listed in Table 60.1 [10–13]. The conclusions from these four studies confirm that adjuvant radiation therapy following breast-conserving surgery reduces the risk of local recurrence by approximately 60 %. No overall survival benefit has been found in these four trials individually or as a pooled analysis; however, the National Surgical Adjuvant Breast and Bowel Project (NSABP), European Organisation for Research and Treatment of Cancer (EORTC), and Swedish trials reported benefits in disease-free or event-free survival.

NSABP-B17 was a prospective trial randomizing 818 patients with DCIS following lumpectomy to radiation therapy or observation. Radiation therapy was delivered to the whole breast to a dose of 50 Gy without the use of a tumor bed boost. At 12 years, the rate of local recurrence was 31 % in the observation alone arm compared with 15 % in the radiation therapy arm, with similar rates of invasive and noninvasive

recurrences. Predictors of ipsilateral recurrence included uncertain or positive margins and moderate to marked comedonecrosis [10]. The EORTC 10853 trial consisted of 1,010 women with DCIS measuring less than 5 cm and negative margins following lumpectomy. Patients were randomized to 50 Gy of adjuvant whole breast radiation therapy without a boost or observation. Ten-year results demonstrated a decrease in local recurrence from 26 % to 15 %. Risk factors for local recurrence included grade 2 or 3 histology, excision alone, closer margins, and age less than 40 [11]. The United Kingdom Coordinating Committee on Cancer Research (UKCCR) conducted a 2 × 2 factorial trial with 1,701 DCIS patients. Patients were randomized to observation, Tamoxifen, radiation therapy, or radiation and Tamoxifen. Radiation therapy was 50 Gy and Tamoxifen was prescribed for 5 years at a dosage of 20 mg per day. With a mean follow-up of 4 years, ipsilateral breast events were 22 %, 18 %, 8 %, and 6 % in the four arms, respectively, with radiation therapy reducing the risk of both invasive and noninvasive ipsilateral breast events [12]. A meta-analysis of these four trials performed by Viani demonstrated that the addition of radiation therapy following surgery reduced local recurrences by approximately 60 % [14].

Omission of Radiation Therapy

Previous studies evaluating the role of adjuvant radiation therapy in DCIS were conducted when lesions presented primarily as a palpable finding. However, the majority of women with DCIS now present with incidental, non-palpable lesions detected solely on mammographic examination. This has led many to question the role of adjuvant radiation therapy with modern surgical techniques. However, despite improved radiographic and surgical techniques, local recurrence with surgery alone in mammographically detected DCIS approaches 20 % [15].

A prospective trial from the Massachusetts General Hospital (MGH) examined withholding adjuvant radiation therapy after excision in grade I/II DCIS with tumors less than 2.5 cm and margins greater than 1 cm. No hormonal treatment was administered. At 5 years, the risk of local recurrence was found to be 12 % [16]. A prospective nonrandomized trial performed by Eastern Cooperative Oncology Group (ECOG) consisted of 670 patients with grade I/II DCIS less than 2.5 cm or grade III DCIS less than 1 cm and margins greater than 3 mm treated with lumpectomy alone. All patients received Tamoxifen. At 5 years, the risk of local recurrence was 6.1 % in the grade I/II group and 15.3 % in the grade III group [17].

A retrospective series by Silverstein et al. followed 706 patients with DCIS with 426 managed with excision alone and 280 with adjuvant radiation therapy. No statistically significant difference in local recurrence was noted between the groups. Independent predictors of local recurrence were found to be age, grade, size of tumor, and surgical margin status. Based on theses parameters, the Van Nuys Prognostic Index (VNPI) was created (Table 60.2). The authors suggested that those cases with intermediate and high VNPI scores benefited from adjuvant radiation therapy, while those with low scores may forgo adjuvant treatment (Table 60.3) [18]. While several other institutions have attempted

Table 60.1 Rates of local recurrence in DCIS: observation versus adjuvant radiation

Study	Observation (%)	Radiation (%)
NSABP-B17	31	15
EORTC 10853	26	15
UKCCR	22	8
SweDCIS	22	10

NSABP National Surgical Adjuvant Breast and Bowel Project, *EORTC* European Organisation for Research and Treatment of Cancer, *UKCCR* United Kingdom Coordinating Committee on Cancer Research

Table 60.2 Van Nuys Prognostic Index

	1 point	2 points	3 points
Age (years)	>60	40–60	<40
Grade	I/II without necrosis	I/II with necrosis	III
Margin (mm)	> = 10	1–9	<1
Size (cm)	< = 1.5	1.5–4.0	>4.0

Table 60.3 Risk of local recurrence by treatment and VNPI score

Score	No radiation (%)	Radiation (%)
4–6	3	3
7–9	36	21
10–12	88	41

VNPI Van Nuys Prognostic Index

to validate the VNPI, this prognostic score has not been found to consistently predict the risk of local recurrence [19, 20].

Radiation therapy oncology group (RTOG) 9,804 randomized patients with low-risk DCIS who underwent excision with adequate margins (3 mm) to observation alone or followed by whole breast irradiation. The trial was set to accrue 1,800 patients but closed due to poor enrollment. Final results are pending at this time.

Boost

There are limited data examining the role of a boost in patients with DCIS treated with BCT. A retrospective analysis of the NSABP B-24 phase III trial was performed to assess the role of a lumpectomy cavity boost in DCIS. 44 % of patients received a boost dose of 1–20 Gy. Boost was used more frequently in patients with positive surgical margins (46 % vs. 37 %), but the rate of IBTR was no different regardless of margin status [21]. However, a boost is often employed based on data from invasive breast cancers showing a local recurrence benefit with the addition of boost treatment to whole breast radiation therapy [22, 23].

Accelerated Partial Breast Irradiation in DCIS

Currently, the use of accelerated partial breast irradiation (APBI) to treat patients with DCIS remains investigational. However, multiple series have evaluated the use of APBI in DCIS utilizing the MammoSite (Hologic Inc., Bedford, Massachusetts) applicator. Analysis of the American Society of Breast Surgeons trials and a prospective manufacturer sponsored trial has found that the rate of local recurrence was approximately 2.5 % at 4 years [24–26].

Early-Stage Breast Cancer

The paradigm in the management of early-stage breast cancer has changed over the past 30 years. With follow-up greater than 20 years in multiple prospective trials, it has become clear that there is no difference in overall survival (OS) or disease-free survival (DFS) between mastectomy and breast-conserving surgery followed by adjuvant radiation in properly selected patients. Further, breast conservation yields good-to-excellent cosmetic results when modern techniques are utilized. Newer techniques including APBI and intensity-modulated radiation therapy (IMRT) are currently being investigated. BCT can be offered to the majority of women with early-stage breast cancer. Absolute contraindications to breast conservation include persistently positive margins following lumpectomy, multicentric disease, diffuse malignant appearing calcifications, prior radiation therapy to the breast or chest wall, and pregnancy [8]. Relative contraindications include active connective tissue disease, tumors greater than 5 cm, and focally positive margins [8].

Mastectomy Versus Breast-Conserving Therapy

Multiple prospective randomized clinical trials have been performed comparing mastectomy with breast-conserving surgery and adjuvant radiation therapy in early-stage invasive breast cancer. Table 60.4 lists the results of the major trials comparing mastectomy with BCT [27–32].

EORTC 10801 was a landmark trial in which 868 patients with invasive tumors less than or equal to 5 cm were randomized to modified radical mastectomy or lumpectomy with axillary lymph node dissection followed by adjuvant radiation therapy. Radiation was delivered to a dose of 50 Gy in 25 fractions with a 25 Gy boost administered via an Ir-192 interstitial implant. At 10 years, there was no difference in OS

Table 60.4 Rates of local recurrence following BCT compared with mastectomy

	n	F/U (years)	Local recurrence	
			Mastectomy	Lumpectomy
NSABP B-06	1,851	20	10	14
EORTC 10801	868	10	12	20
NCI	237	18	0	22
Milan	701	20	2	9
Institut Gustave-Roussy	179	15	14	9
Dutch	793	20	6.5	4.6

NSABP National Surgical Adjuvant Breast and Bowel Project, *EORTC* European Organisation for Research and Treatment of Cancer, *NCI* National Cancer Institute

(66 % vs. 65 %); however, there were significantly more local recurrences in the lumpectomy arm (12 % vs. 20 %) [27]. Of note, 48 % of patients in the lumpectomy arm had positive margins. These results were confirmed by the NSABP B-06 trial, which randomized 1,851 patients with stage I–II invasive breast cancer less than 4 cm size to total mastectomy, lumpectomy, or lumpectomy and adjuvant radiation therapy. Radiation therapy was delivered to a total dose of 50 Gy without a boost. At 20 years, no difference in OS was seen between the arms. The rate of IBTR was significantly increased in the lumpectomy arm without radiation when compared to the arm receiving radiation (39 % vs. 14 %). No difference in locoregional recurrence (LRR) was seen between the mastectomy and lumpectomy with radiation therapy arms [30]. The Milan I trial randomized 701 patients with tumors less than or equal to 2 cm to radical mastectomy or quadrantectomy with adjuvant radiation. Radiation therapy was delivered as 50 Gy of whole breast irradiation followed by a 10 Gy boost. At 20 years, there was no difference in OS (48 %), although there was a significant difference in IBTR favoring the mastectomy arm (2 % vs. 9 %) [31].

When looking at these studies, note should be made that three of these trials found an increase in local recurrence with lumpectomy and radiation therapy when compared to mastectomy. However, in the EORTC and National Cancer Institute (NCI) trials, positive margins were included in the lumpectomy arm and the Milan trial randomized patients to a radical mastectomy (RM) rather than a modified radical mastectomy (MRM), which was used in the other studies. Data from Maddox et al. demonstrated a trend for increased local recurrence with MRM compared to RM [33]. Furthermore, the NSABP B-06, Institut Gustave-Roussy, and the Dutch trials failed to demonstrate a difference in local recurrence between mastectomy and BCT. With modern surgical and radiotherapy techniques, the rate of local recurrence is thought to be approximately 0.5 % per year, in line with previous mastectomy series [34, 35].

Concern has been raised over the rates of increased IBTR in younger patients. In a pooled analysis of the EORTC 10801 and Danish Breast Cancer Cooperative Group (DBCCTG) 82TM trials, Voogd et al. found that the hazard for local recurrence following BCT was 9.24 in patients 35 years old or younger when compared to patients older than 60 years of age. Ten-year rates of local recurrence in the cohort less than 35 years old were 35 % with BCT when compared to 7 % in the mastectomy arm [36].

Analysis of a prospectively accrued database in British Columbia looked at approximately 2,500 patients between 20 and 49 years of age treated for breast cancer. As previously reported, younger patients were found to have worse clinical outcomes as compared to older patients. When the cohort of younger patients was analyzed, there was no difference in local recurrence free survival (RFS), locoregional RFS, or distant RFS based on surgical procedure received. There was a trend for improved breast cancer specific survival in the BCT arm [37]. A retrospective review performed at MD Anderson Cancer Center (MDACC) looked at 650 patients 35 years or younger treated with BCT,

mastectomy, or mastectomy with adjuvant radiation therapy. At 10 years, the rate of LRR was decreased in the mastectomy with adjuvant radiation arm when compared to mastectomy alone. The benefit was only seen in stage II patients [38].

Boost

The concept of a tumor bed boost refers to the delivery of an additional dose of radiation therapy to the area surrounding the lumpectomy cavity following whole breast radiation. The rationale for utilizing a boost is that since the majority of local recurrences develop in close vicinity to the index lesion, the additional dose to the tumor bed will improve local control.

Many of the prospective trials comparing BCT with mastectomy incorporated the use of a boost in the adjuvant radiation therapy, including the Milan, EORTC, DBCCG, NCI, and Gustave-Roussy trials. EORTC 22881 accrued 5,318 patients with stage I/II breast cancer who underwent lumpectomy followed by whole breast irradiation. Patients were then randomized to receive a 16 Gy boost to the tumor bed or no further radiation. At 10 years, there was a significant decrease in local recurrences (6 % vs. 10 %) when utilizing the boost. No difference was noted in OS. In the subset of patients less than 40 years old, the benefit of boost on local recurrence was magnified (13 % vs. 24 %) [22]. Multivariate analysis of the EORTC trial found that age less than 50 years old and high-grade histology were associated with an increased risk of local recurrence and that boost treatments halved the risk of local recurrence in these patients [39]. The findings of the EORTC trial were confirmed by a French trial randomizing 1,024 patients with tumors 3 cm or less. Patients were randomized to receive a 10 Gy boost or observation. At 5 years, there was a significant decrease in local recurrence (3.6 % vs. 4.5 %) [23].

A current trial accruing in the Netherlands is randomizing patients to receive a 16 Gy boost following 50 Gy of whole breast irradiation or observation. Younger patients are to be randomized to receive a 26 Gy boost or observation.

Alternative Radiation Schedules: Hypofractionation

One of the concerns with the use of breast conservation therapy is the protracted 6–7 week course of adjuvant radiation therapy. The lack of compliance by patients in receiving their radiation treatments has been documented, with up to 20 % of patients not receiving radiation therapy [40, 41]. Multiple techniques and dose strategies have been studied to shorten the course of radiation therapy while delivering biologically equivalent doses, including hypofractionation and accelerated partial breast irradiation (APBI). Hypofractionation refers to delivering larger than normal daily fraction sizes in order to deliver the treatment in a shorter interval of time.

Two trials were performed in the United Kingdom looking at the feasibility of hypofractionation. Standardisation of Breast Radiotherapy (START) A randomized 2,236 patients to the traditional whole breast irradiation (50 Gy/25 fractions) or 1 of 2 hypofractionated arms. The hypofractionated arms were 39 or 41.6 Gy delivered in 13 fractions over 5 weeks. Boost was at the discretion of the treating physician. At 5 years, no difference in local control was seen (3.6 % vs. 3.5 % vs. 5.2 %) [42]. START B randomized patients to whole breast irradiation (50 Gy/25 fractions) over 5 weeks or 40 Gy delivered in 15 fractions over 3 weeks, an accelerated hypofractionated arm. 2,215 patients were enrolled, and at 5 years, no difference in local recurrence was seen (3.3 % vs. 2.2 %). Adverse effects were reduced in the hypofractionated arm [43]. In a prospective trial performed by the Ontario Clinical Oncology Group, 1,200 patients with T1-2, node-negative, invasive breast cancer were randomized to whole breast irradiation (50 Gy/25 fractions) or 42.5 Gy in 16 fractions delivered over 3 weeks. At 10 years, no difference was noted in IBTR. However, an increase in local recurrence was noted with high-grade tumors in the hypofractionated arm [44].

Limitations of these studies are that boost was not used consistently, the role of chemotherapy with these regimens has not been addressed, and patients with larger breasts were usually

excluded. Currently, the Medical Research Council (MRC) is conducting a trial randomizing patients to adjuvant whole breast irradiation, 30 Gy in 5 fractions, or 28.5 Gy in 5 fractions delivered over 5 weeks.

Alternative Radiation Schedules: Accelerated Partial Breast Irradiation

APBI is an alternative to hypofractionation that allows for the delivery of adjuvant radiation therapy in a shortened interval of time. The rationale for whole breast radiation is the assumption that clinically undetectable microscopic disease may be present in areas distant from the lumpectomy site. However, pathologic data has suggested that the majority of residual tumor following surgery is within 1–2 cm of the lumpectomy cavity [45]. Further, because the majority of IBTR are in close proximity to the primary lesion, the rationale behind APBI is that targeting solely the lumpectomy cavity would provide adequate local control. Treatment times may be reduced from 6 weeks to 5 days or less. Several techniques have been utilized to deliver APBI. Initially, treatment was performed with low dose rate interstitial catheters and transitioned to high dose rate catheters. These implants have been replaced with balloon brachytherapy, simplifying treatment delivery. A noninvasive form of APBI has been developed utilizing a linear accelerator and a 3-D conformal technique.

Currently, the NSABP B-39/RTOG 0413 trial is accruing patients with stage I-II invasive ductal carcinoma (IDC) or DCIS. Patients are randomized to adjuvant whole breast irradiation or APBI delivered via interstitial, 3-D conformal, or intracavitary techniques. The Ontario Randomized Trial of Accelerated Partial Breast Irradiation (RAPID) trial is currently accruing and seeks to compare hypofractionation (42.5 Gy/6 fractions) with APBI delivered with a 3-D CRT technique delivering 38.5 Gy in 10 fractions on a twice daily basis. Eligible patients include those older than 40 years of age with DCIS or invasive cancer that are lymph node negative and have adequate surgical resection margins.

Multicatheter interstitial brachytherapy was the original technique devised to deliver APBI and therefore has the longest follow-up of any of the APBI techniques. A retrospective series from William Beaumont Hospital reported the outcomes of 199 patients with stage I/II breast cancer treated with interstitial brachytherapy (LDR/HDR). The 5-year rate of IBTR was 1.2 %, and excluding elsewhere breast failures, the rate of IBTR was 0.5 %. Cause-specific survival at 5 years was 99 % with 92 % good/excellent cosmesis [46]. Matched-pair analysis of this cohort with 199 women treated with whole breast irradiation revealed no differences in outcomes [47]. A Hungarian prospective trial testing the non-inferiority of APBI randomized 258 patients with T1, grade 1–2, non-lobular breast cancer to whole breast irradiation (50 Gy/25 fractions) or APBI (36.4 Gy/7 fractions BID) delivered with multicatheter HDR treatments or limited electron fields. At 5 years, no difference was seen in local recurrence (3.4 % vs. 4.7 %). Excellent/good cosmesis was significantly improved in the APBI arm [48]. These trials prompted RTOG 9517, a phase II trial in which 99 patients with invasive non-lobular breast cancers less than 3 cm were given adjuvant radiation therapy via LDR (45 Gy) or HDR (34 Gy/10 fractions BID) following lumpectomy. The 5-year rates of in-breast, regional, and contralateral failures were 6 %, 0 %, and 6 %, respectively [49].

Over the past decade, interstitial brachytherapy has been replaced by the use of balloon brachytherapy as a way to reduce the technical complexity and breast trauma seen with the multicatheter interstitial techniques. The initial MammoSite device was a balloon catheter with a single lumen allowing for HDR brachytherapy. Dose distributions were found to be similar to those achieved by the multicatheter interstitial techniques. Limitations of this technique include minimum skin and chest wall separations, nonconforming balloons to the lumpectomy cavity, and less flexibility in creating conformal dose distributions. An initial FDA trial conducted with 43 patients found a 5-year IBTR of 0 % and improved cosmesis with skin distances greater than 7 mm [50]. A registry trial performed by

Table 60.5 Criteria for off-protocol use of APBI per ASTRO consensus panel guidelines

	Consensus panel category		
Criteria	Suitable	Cautionary	Unsuitable
Age	≥60 years old	50–59 years old	<50 years old
Size	≤2 cm	2.1–3.0 cm	>3 cm
Margins	Negative	Close (<2 mm)	Positive
BRCA	Negative	–	Positive
LVSI	Negative	Limited/focal	Extensive
Histology	No pure DCIS	Pure DCIS ≤ 3 cm	Pure DCIS ≥ 3 cm
	No ILC	ILC ≤ 3 cm	ILC ≥ 3 cm
EIC	Absent	≤3 cm	>3 cm

APBI Accelerated Partial Breast Irradiation, *ASTRO* American Society for Therapeutic Radiology and Oncology, *LVSI* Lymphovascular Space Invasion, *EIC* Extensive Intraductal Component

the American Society of Breast Surgeons accrued 1,440 patients with a median follow-up 2.5 years. Local recurrences were seen in 1.6 % of patients with 93 % of patients reporting excellent/good cosmesis [51]. This was confirmed in a multi-institutional trial in which 483 patients underwent MammoSite placement, receiving 34 Gy in 10 fractions BID. 2-year outcomes demonstrated a 1 % IBTR with two-third of these recurrences occurring away from the lumpectomy site [52]. With the success of the MammoSite applicator, multiple other devices are currently being developed.

An alternative to balloon or catheter based APBI is 3-D CRT that allows for the delivery of localized treatment with minimal breast trauma and without HDR equipment. This technique utilizes a traditional linear accelerator to deliver a dose to the lumpectomy cavity; however, margins are larger than with brachytherapy in order to compensate for setting up uncertainties and breathing motion, which can increase normal tissue dose. A benefit to utilizing 3-D CRT is the increased homogeneity, reducing hot spots and potentially improving cosmesis. Treatment is administered twice a day in 1 week delivering a total dose of 38.5 Gy. Chen et al. presented a 4-year data with this technique and found an IBTR of 1.1 % with 97 % OS and 99 % cause-specific survival (CSS) [53]. Furthermore, RTOG 0319 accrued 52 patients with stage I/II breast cancer with tumors 3.0 cm or less to receive 3D-CRT APBI. APBI was delivered as 38.5 Gy/10 fractions BID. 4-year IBTR was 6 % (67 % in field) with 84 % DFS, and 96 % OS [54].

At this time, ASTRO has released guidelines regarding suitable, cautionary, and unsuitable patients for APBI [55]. Table 60.5 lists the criteria set forth in these guidelines. At this time, the NCCN recommends that APBI be performed only as part of a clinical trial [8].

Omission of Radiation Therapy

Due to the duration of administering adjuvant radiation therapy, the question arises as to whether there is a subset of patients who would be adequately treated with lumpectomy alone. A meta-analysis performed by the Early Breast Cancer Trialists' Collaborative Group (EBCTG) demonstrated that local recurrences were decreased by approximately 20 % with the addition of radiation therapy. This improvement in local control translated into a 5 % overall survival benefit at 15 years [56]. Despite multiple trials and subset analyses, no study has definitively identified a subset of patients that may be treated with excision alone.

Table 60.6 lists prospective trials that examined the omission of adjuvant radiation therapy [30, 57–60]. While Tamoxifen has been shown to decrease the IBTR rate, the question arises as to whether it obviates the need for adjuvant radiation therapy. NSABP B-21 randomized 1,000 women with invasive breast cancers less than

Table 60.6 Rate of local recurrence with and without the omission of radiation therapy following breast-conserving surgery

	N	Randomization	Patient and tumor characteristics	Local recurrence	
				RT (%)	No RT (%)
CALGB 9343	636	Tamoxifen ± RT	>70 years old	1	4
Canadian	769	Tamoxifen ± RT	>50 years old	0.6	7.7
NSABP B-06	1,851	Lumpectomy ± RT		14	39
Milan III	580	Quadrantectomy ± RT	T ≤ 2.5 cm	5.8	23.5
NSABP B-21	1,009	Lumpectomy + Tamoxifen ± RT	T < 1 cm	3	16

CALGB Cancer and Leukemia Group B, *NSABP* National Surgical Adjuvant Breast and Bowel Project

1 cm in diameter to adjuvant Tamoxifen, radiation therapy, or Tamoxifen and radiation therapy. With 8 years of follow-up, the rate of local recurrence was 16 %, 9 %, and 3 % in the Tamoxifen, radiation, and Tamoxifen + radiation arms, respectively [60].

Postmastectomy Radiation

With the treatment of early-stage breast cancer, patients who opt for mastectomy generally do not require postmastectomy radiation (PMRT) unless close or positive margins are present. However, with locally advanced breast cancers, multiple studies have established risk factors for LRR and have recommended PMRT in multiple settings. A pooled analysis of NSABP trials looked at LRR following mastectomy and chemotherapy without PMRT. Rates of LRR based on tumor size were 14.9 % T < 2 cm, 21.3 % T 2–5 cm, and 24.6 % T > 5 cm. Analysis by LN status found the risk of LRR to be 13 % with 1–3 LNs positive, 24.4 % with 4–9 LNs positive, and 31.9 % with > 10 LNs positive. Of note, 85 % of LRR were on the chest wall [61]. An analysis performed by the ECOG found tumors greater than 5 cm and/or ≥ 4 lymph nodes positive to be significant predictors of LRR [62]. Currently, the ASTRO consensus statement recommends PMRT in patients with four or more positive lymph nodes [63]. NCCN guidelines recommend PMRT with four or more lymph nodes involved (Category 1) and to consider PMRT with 1–3 lymph nodes involved or tumors greater than 5 cm [8].

Multiple large prospective trials have examined the role of PMRT following surgery and chemotherapy. The Danish 82b trial enrolled 1,700 premenopausal women with one or more of the following: positive axillary lymph nodes, tumor greater than 5 cm, and/or invasion into the skin or pectoralis fascia. Patients were randomized to PMRT + CMF chemotherapy, CMF alone, or CMF + Tamoxifen. The third arm was closed early due to increased mortality. Radiation therapy was delivered to the chest wall as well as the supraclavicular, infraclavicular, and internal mammary lymph nodes to a total dose of 50 Gy. At 10 years, the addition of PMRT improved OS (54 % vs. 45 %), DFS (48 % vs. 34 %), and LRR (9 % vs. 32 %) [64]. A prospective trial randomized 318 premenopausal patients with lymph node-positive disease to radiation therapy with CMF chemotherapy or chemotherapy alone for nine cycles. Radiation therapy was given to the chest wall, supraclavicular and axillary regions along with bilateral internal mammary chains. The radiation dose was 37.5 Gy in 16 fractions delivered between the fourth and fifth cycle of chemotherapy. With 20 years of follow-up, PMRT improved breast cancer specific survival (BCSS) (53 % vs. 38 %), OS (47 % vs. 37 %), and locoregional control (LRC) (90 % vs. 74 %) [65]. Postmenopausal patients were evaluated in the Danish 82c trial which randomized 1,460 patients with the same criteria as the 82b trial to PMRT + Tamoxifen or Tamoxifen alone. At 10 years, the OS (45 % vs. 36 %), DFS (36 % vs. 24 %), and LRR (8 % vs. 35 %) were significantly improved with PMRT [66]. A meta-analysis of 18 trials performed by Whelan which included 6,400

patients found that the addition of PMRT reduced the rate of local recurrence, any recurrence, and mortality [67].

Currently, controversy remains as to the benefit of PMRT in patients with T3N0 tumors or 1–3 lymph nodes involved. A multi-institutional review of 70 patients with tumors greater than 5 cm and no lymph node involvement found that the locoregional failure (LRF) was 8 % without PMRT. However, lymphovascular space invasion (LVSI) was found to be a predictor of LRF in this subset of patients with LRF rates of 20 % compared with 4 % without LVSI [68]. Further, analysis by the EBCTG group found that while the rate of LR was decreased with PMRT (6 % vs. 2 %), no difference in 15-year survival was noted [56]. Analysis of the Danish 82b/c trials looked at the rates of LRR in patients with 1–3 lymph nodes involved and found that PMRT significantly decreased the rates of LRR while improving overall survival [69]. A retrospective review from British Columbia found that the rates of LRR were increased with the omission of PMRT in patients with 1–3 lymph nodes involved and one or more of the following: <45 years old, ER negative tumors, medially located primary lesion, or >25 % of lymph nodes sampled positive [70].

Radiation Therapy Planning

Over the past two decades, treatment planning for breast cancer radiation therapy has changed drastically. Older techniques utilized two-dimensional planning. Modern radiotherapy has forgone the use of conventional simulators for virtual simulation and CT-based planning. At the time of simulation, the patient is placed on the CT table and immobilization devices are fabricated. The boundaries of the breast or chest wall are marked (wired), as is the scar. Traditional borders for the breast include the head of the clavicle superiorly, 2 cm below the inframammary fold inferiorly, mid-sternum medially, and the midaxillary line laterally. A detailed analysis of these anatomic borders was recently published by the RTOG [71]. Following this, the patient undergoes a CT scan.

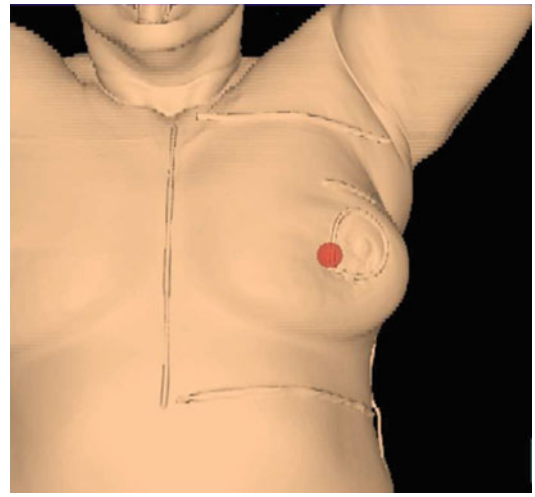

Fig. 60.1 Three-dimensional reconstruction of a patient following virtual simulation

After the simulation is complete, the images from the CT scan are transferred to a treatment planning computer allowing for the creation of a three-dimensional model of the patient as displayed in Fig. 60.1. In early-stage breast cancer patients, the lumpectomy cavity is defined by contouring the seroma cavity (with or without the assistance of surgically placed clips) as demonstrated in Fig. 60.2.

Radiation therapy is often delivered using opposed tangential beams. The posterior borders of the tangential fields are set to align to minimize divergence into the lungs. Beam modifiers such as wedges are often utilized to improve the homogeneity of the dose distribution due to the fact that the breast is not uniformly thick. An example of tangential fields with wedge placements with dose distributions is displayed in Fig. 60.3. An example of an en face treatment plan used to treat the chest wall following mastectomy is displayed in Fig. 60.4. In more advanced cases, lymph node regions, including levels I–III of the axilla and the supraclavicular fossa, can be contoured and treated as displayed in Fig. 60.5. Use of 3-D conformal radiation therapy (CRT) has allowed for more homogeneous treatment of the target while minimizing dose to the ipsilateral lung and heart.

Newer techniques in radiation therapy planning include both "field in field" techniques and

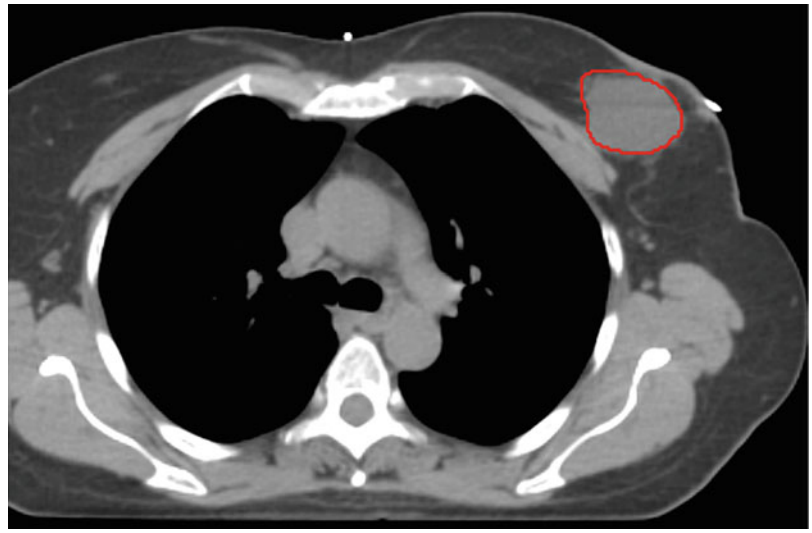

Fig. 60.2 CT visualization of the seroma cavity

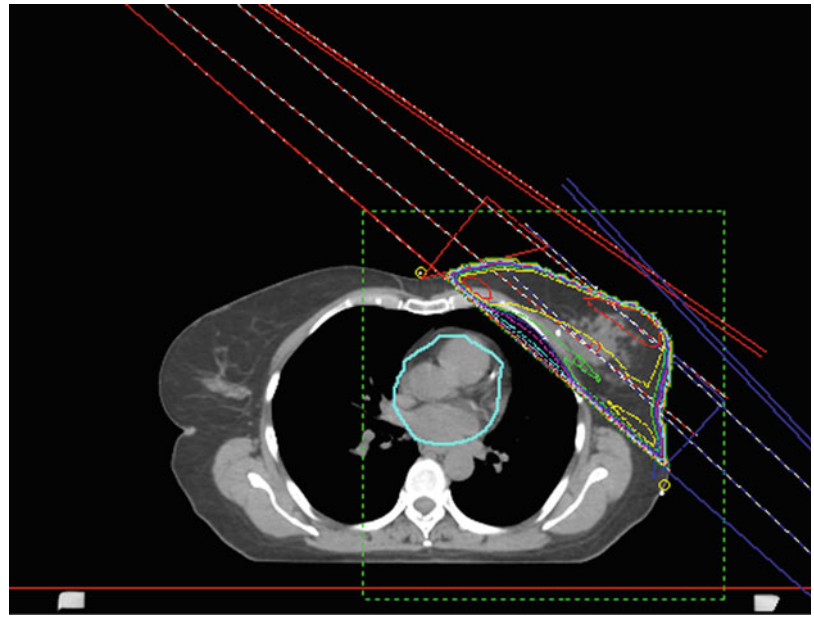

Fig. 60.3 Tangential beam plan with 15° wedges

conventional intensity-modulated radiation therapy (IMRT). The goals of these techniques are to reduce inhomogeneity within the breast and reduce the hot spots that plagued conventional treatments. One of the first reports of IMRT was from William Beaumont Hospital where 281 patients with early-stage breast cancer were treated with IMRT. Toxicity was minimal and 99 % of patients rated their cosmesis as good/excellent at 1 year [72, 73]. A randomized trial of 300 patients with early-stage breast cancer compared 2-D planned treatments with IMRT and found that IMRT decreased the risk of moist desquamation [74]. Further, series from individual institutions have found that IMRT reduced the rate of breast changes, palpable induration, and the whole body exposure when compared to traditional treatments [75, 76]. An example IMRT dosimetry is illustrated in Fig. 60.6.

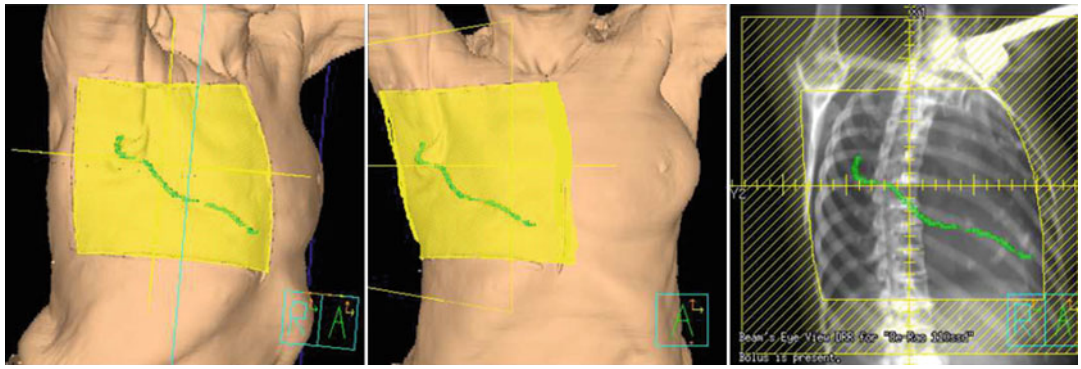

Fig. 60.4 Monoisocentric treatment for locally advanced breast cancer

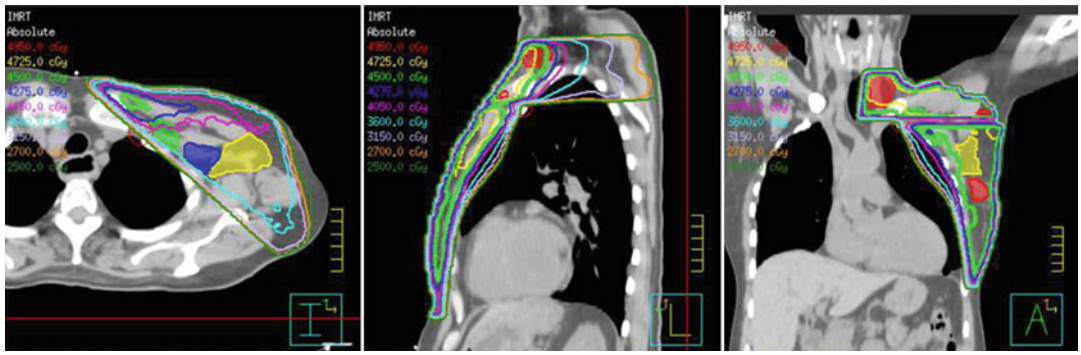

Fig. 60.5 Treatment plan to the chest wall and level I–III lymph nodes

In cases of left-sided breast cancer, concern arises over dose to the heart and the potential late cardiac toxicity. Techniques such as assisted breathing control (ABC) have been devised as illustrated in Fig. 60.7. With ABC, radiation therapy delivery is coordinated with inspiration, increasing the distance between the heart and chest wall and therefore minimizing potential cardiac toxicity. Data from William Beaumont Hospital have shown that the use of ABC decreased volumetric doses to the heart as well as the normal tissue complication probability (NTCP) [77].

Radiation Therapy Toxicity

Side effects from breast irradiation can include acute, subacute, and chronic side effects. Acute and subacute side effects of radiation therapy can include fatigue, erythema, hyperpigmentation, dry desquamation, moist desquamation, chest wall myositis, and radiation pneumonitis. Acute radiotherapy toxicity has been classified by the RTOG scoring system which is displayed in Table 60.7 [78]. Using these criteria, a series by Back et al. found that 5 % of cases had a peak RTOG score of 3 and 1 % of cases had a peak RTOG score of 4 using conventional radiotherapy techniques and doses. 31.4 % of patients in this study were found to have any desquamation [79]. Chronic side effects of radiation therapy may include hyper- or hypopigmentation of the skin, induration or fibrosis, telangiectasias, cardiac toxicity, persistent breast discomfort, and second malignancies. Acute toxicity with APBI is often less than whole breast irradiation but can also include radiation dermatitis and infection. The risk of infection has been documented as being less than 5 %

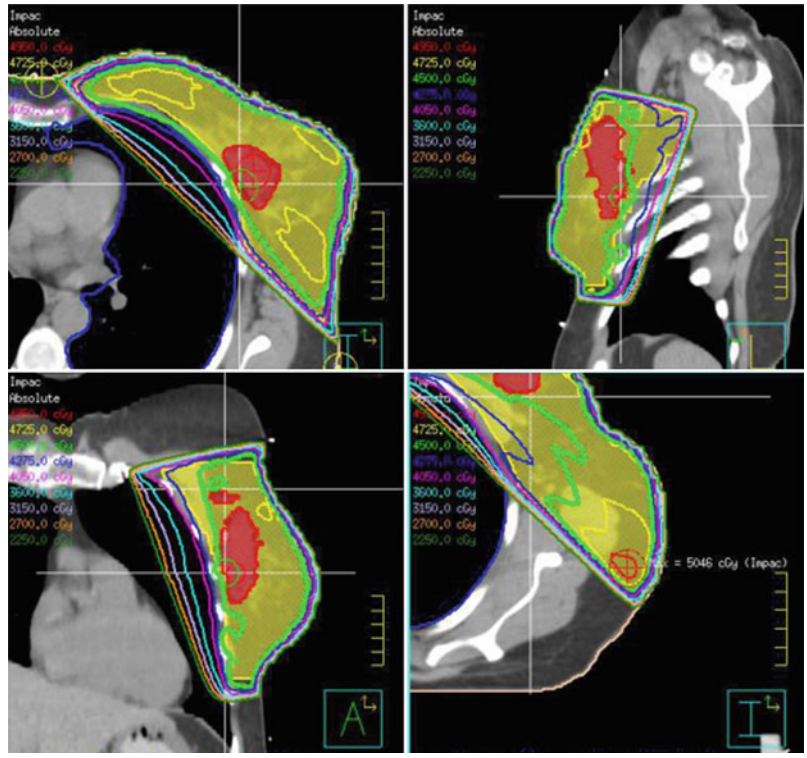

Fig. 60.6 IMRT plan for early-stage breast cancer

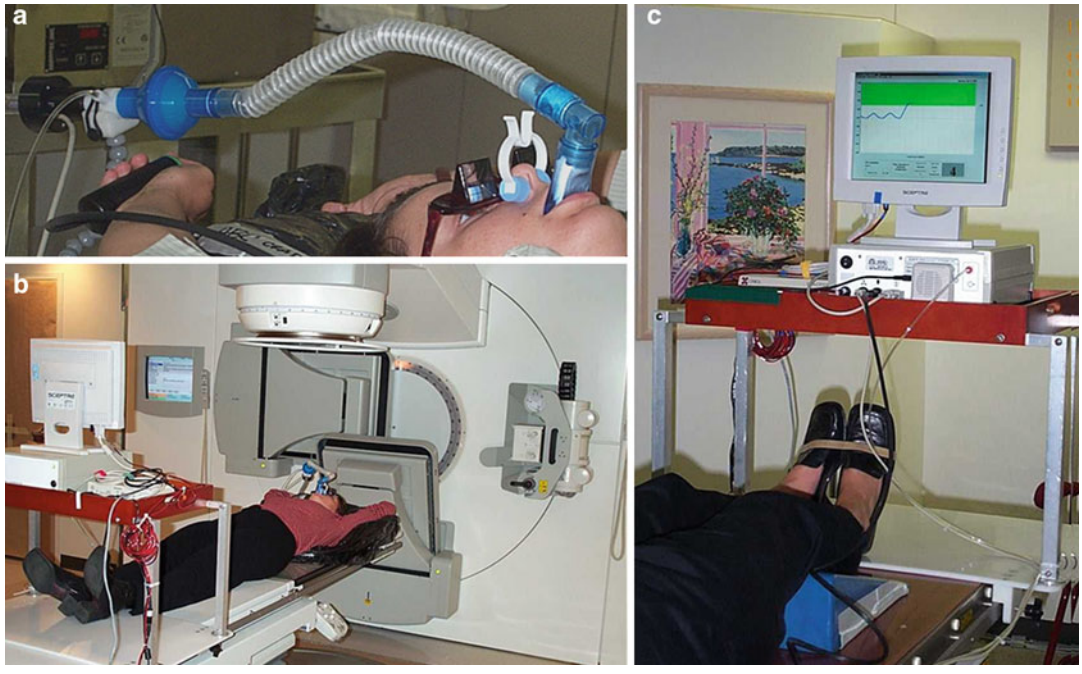

Fig. 60.7 Active breathing control mouthpiece assembly (**a**). Patient setup on linear accelerator (**b**). Breath control readout for patient (**c**)

Table 60.7 RTOG acute cutaneous toxicity scoring

Grade	
0	No change
1	Faint or dull erythema, dry desquamation, or epilation
2	Moderate edema, non-confluent moist desquamation, bright or tender erythema
3	Confluent moist desquamation(other than folds)
4	Ulceration, necrosis, hemorrhage

RTOG Radiation Therapy Oncology Group

with utilization of closed techniques [52]. Late effects of APBI are similar to whole breast irradiation and include hyperpigmentation, fibrosis, and telangiectasias [80].

Studies regarding chronic toxicities following breast radiotherapy are often limited by objective endpoints and quality follow-up. A review of 727 patients with early-stage breast cancer treated with whole breast radiation therapy via tangential fields found the rates of lymphedema to be 4 % at 10 years. Rates were increased with axillary treatment to 9 % [81]. A University of Pennsylvania review of 62 patients with left-sided breast cancer who underwent radiation therapy found that there was an increase in cardiac test abnormalities in symptomatic patients [82]. In an analysis of patients undergoing BCT compared with a cohort of mastectomy patients who did not receive PMRT, the rates of secondary malignancies were not found to be different. Further, no difference in second breast primaries was noted [83]. However, a series assessing patients under 40 years old found the rates of contralateral breast cancer to be 2.5 times greater when doses in excess of 1.0 Gy were delivered to the contralateral breast [84].

Ablative Techniques and Radiation Therapy

Currently, ablative techniques are being investigated in patients who are nonsurgical candidates or wish to forgo surgery. Ablation can be performed using radiofrequency ablation, laser, or cryotherapy. Advantages to ablative techniques include no scars, general anesthesia, or tissue loss. Drawbacks include the lack of pathological specimen which precludes analysis of grade, receptor status, margins, and genetic markers. At this time, the feasibility of ablative techniques has been demonstrated in studies where ablative procedures were performed followed by excision. Complete ablation rates range from 70 % to 100 %, and though limited by small numbers, toxicity was minimal in the majority of cases [85–89].

The question arises as to the role of radiation therapy in the adjuvant setting following ablative procedures. Limited data are available regarding the role of radiation therapy following ablative procedures; however, due to the risk of residual microscopic foci, radiation therapy could be offered. With regard to technique and doses, limited data are available and would be expected to be extrapolated from traditional breast treatments.

References

1. Cady B, Stone MD, Schuler JG, et al. The new era in breast cancer: invasion, size and nodal involvement dramatically decreasing as a result of mammographic screening. Arch Surg. 1996;31:301–8.
2. Tabar L, Fagerberg CJ, Gad A, et al. Reduction in mortality from breast cancer after mass screening with mammography. Randomised trial from the Breast Cancer Screening Working Group of the Swedish National Board of Health and Welfare. Lancet. 1985;1:829–32.
3. Tabar L, Gad A, Parson WC, et al. Mammographic appearances of in situ carcinomas. In: Silverstein MJ, editor. Ductal Carcinoma in situ of the breast. 2nd ed. Philadelphia: Lippincott Williams & Wilkins; 2002. p. 87–104.
4. Wilson RE, Donegan WL, Mettlin C, et al. The 1982 national survey of carcinoma of the breast in the United States by the American College of Surgeons. Surg Gynecol Obstet. 1984;159:309–18.
5. Burstein HJ, Polyak K, Wong JS, et al. Ductal carcinoma in situ of the breast. N Engl J Med. 2004;350:1430–41.
6. Ernster VL, Barclay J, Kerlikowske K, et al. Incidence of and treatment for ductal carcinoma in situ of the breast. JAMA. 1996;275:913–18.
7. Fisher ER, Sass R, Fisher B, et al. Pathologic findings from the National Surgical Adjuvant Breast Project (protocol 6). II. Relation of local breast recurrence to multicentricity. Cancer. 1986;57:1717–24.

8. NCCN Clinical Practice Guidelines in Oncology: Breast Cancer. http://www.nccn.org/professionals/physician_gls/f_guidelines.asp. Accessed 14 Apr 2010.
9. Solin LJ, Fourquet A, Vicini FA, et al. Long-term outcome after breast-conservation treatment with radiation for mammographically detected ductal carcinoma in situ of the breast. Cancer. 2005;103:1137–46.
10. Fisher B, Land S, Mamounas E, et al. Prevention of invasive breast cancer in women with ductal carcinoma in situ: an update of the National Surgical Adjuvant Breast and Bowel Project experience. Semin Oncol. 2001;28:400–18.
11. Bijker N, Meijnen P, Peterse JL, et al. Breast-conserving treatment with or without radiotherapy in ductal carcinoma-in-situ: ten-year results of European Organisation for Research and Treatment of Cancer randomized phase III trial 10853–a study by the EORTC Breast Cancer Cooperative Group and EORTC Radiotherapy Group. J Clin Oncol. 2006;24:3381–7.
12. Houghton J, George WD, Cuzick J, et al. Radiotherapy and tamoxifen in women with completely excised ductal carcinoma in situ of the breast in the UK, Australia, and New Zealand: randomised controlled trial. Lancet. 2003;362:95–102.
13. Holmberg L, Garmo H, Granstrand B, et al. Absolute risk reductions for local recurrence after postoperative radiotherapy after sector resection for ductal carcinoma in situ of the breast. J Clin Oncol. 2008;26:1247–52.
14. Viani GA, Stefano EJ, Afonso SL, et al. Breast-conserving surgery with or without radiotherapy in women with ductal carcinoma in situ: a meta-analysis of randomized trials. Radiat Oncol. 2007;2:28.
15. Schwartz GF, Finkel GC, Garcia JC, et al. Subclinical ductal carcinoma in situ of the breast. Treatment by local excision and surveillance alone. Cancer. 1992;70:2468–74.
16. Wong JS, Kaelin CM, Troyan SL, et al. Prospective study of wide excision alone for ductal carcinoma in situ of the breast. J Clin Oncol. 2006;24:1031–6.
17. Hughes LL, Wang M, Page DL, et al. Local excision alone without irradiation for ductal carcinoma in situ of the breast: a trial of the Eastern Cooperative Oncology Group. J Clin Oncol. 2009;27:5319–24.
18. Silverstein MJ. An argument against routine use of radiotherapy for ductal carcinoma in situ. Oncology. 2003;17:1511–33.
19. Di Saverio S, Catena F, Santini D, et al. 259 Patients with DCIS of the breast applying USC/Van Nuys prognostic index: a retrospective review with long term follow up. Breast Cancer Res Treat. 2008;109:405–16.
20. Boland GP, Chan KC, Knox WF, et al. Value of the Van Nuys Prognostic Index in prediction of recurrence of ductal carcinoma in situ after breast-conserving surgery. Br J Surg. 2003;90:426–32.
21. Julian TB, Land SR, Wang Y, et al. Is boost therapy necessary in the treatment of DCIS? ASCO Breast Symposium Abstract; 2007.
22. Bartelink H, Horiot JC, Poortmans PM, et al. Impact of a higher radiation dose on local control and survival in breast-conserving therapy of early breast cancer: 10-year results of the randomized boost versus no boost EORTC 22881–10882 trial. J Clin Oncol. 2007;25:3259–65.
23. Romestaing P, Lehingue Y, Carrie C, et al. Role of a 10-Gy boost in the conservative treatment of early breast cancer: results of a randomized clinical trial in Lyon, France. J Clin Oncol. 1997;15:963–8.
24. Jeruss JS, Vicini FA, Beitsch PD, et al. Initial outcomes for patients treated on the American Society of Breast Surgeons MammoSite clinical trial for ductal carcinoma-in-situ of the breast. Ann Surg Oncol. 2006;13:967–76.
25. Benitez PR, Streeter O, Vicini F, et al. Preliminary results and evaluation of MammoSite balloon brachytherapy for partial breast irradiation for pure ductal carcinoma in situ: a phase II clinical study. Am J Surg. 2006;192:427–33.
26. Keisch M, Vicini F, Beitsch P, et al. American Society of Breast Surgeons MammoSite Radiation Therapy System Registry Trial: ductal carcinoma-in-situ subset analysis–4-year data in 194 treated lesions. Am J Surg. 2009;198:505–7.
27. van Dongen JA, Voogd AC, Fentiman IS, et al. Long-term results of a randomized trial comparing breast-conserving therapy with mastectomy: European Organization for Research and Treatment of Cancer 10801 trial. J Natl Cancer Inst. 2000;92:1143–50.
28. Poggi MM, Danforth DN, Sciuto LC, et al. Eighteen-year results in the treatment of early breast carcinoma with mastectomy versus breast conservation therapy: the National Cancer Institute Randomized Trial. Cancer. 2003;98:697–702.
29. Blichert-Toft M, Nielsen M, Düring M, et al. Long-term results of breast conserving surgery vs. mastectomy for early stage invasive breast cancer: 20-year follow-up of the Danish randomized DBCG-82TM protocol. Acta Oncol. 2008;47:672–81.
30. Fisher B, Anderson S, Bryant J, et al. Twenty-year follow-up of a randomized trial comparing total mastectomy, lumpectomy, and lumpectomy plus irradiation for the treatment of invasive breast cancer. N Engl J Med. 2002;347:1233–41.
31. Veronesi U, Cascinelli N, Mariani L, et al. Twenty-year follow-up of a randomized study comparing breast-conserving surgery with radical mastectomy for early breast cancer. N Engl J Med. 2002;347:1227–32.
32. Arriagada R, Lê MG, Rochard F, et al. Conservative treatment versus mastectomy in early breast cancer: patterns of failure with 15 years of follow-up data. Institut Gustave-Roussy Breast Cancer Group. J Clin Oncol. 1996;14:1558–64.

33. Maddox WA, Carpenter Jr JT, Laws HL, et al. A randomized prospective trial of radical (Halsted) mastectomy versus modified radical mastectomy in 311 breast cancer patients. Ann Surg. 1983;198:207–12.
34. Cabioglu N, Hunt KK, Buchholz TA, et al. Improving local control with breast-conserving therapy: a 27-year single-institution experience. Cancer. 2005;104: 20–9.
35. Fisher B, Jeong JH, Dignam J, et al. Findings from recent National Surgical Adjuvant Breast and Bowel Project adjuvant studies in stage I breast cancer. J Natl Cancer Inst Monogr. 2001;30:62–6.
36. Voogd AC, Nielsen M, Peterse JL, et al. Differences in risk factors for local and distant recurrence after breast-conserving therapy or mastectomy for stage I and II breast cancer: pooled results of two large European randomized trials. J Clin Oncol. 2001;19: 1688–97.
37. Coulombe G, Tyldesley S, Speers C, et al. Is mastectomy superior to breast-conserving treatment for young women? Int J Radiat Oncol Biol Phys. 2007;67:1282–90.
38. Beadle BM, Woodward WA, Tucker SL, et al. Ten-year recurrence rates in young women with breast cancer by locoregional treatment approach. Int J Radiat Oncol Biol Phys. 2009;73:734–44.
39. Jones HA, Antonini N, Hart AA, et al. Impact of pathological characteristics on local relapse after breast-conserving therapy: a subgroup analysis of the EORTC boost versus no boost trial. J Clin Oncol. 2009;27:4939–47.
40. Lazovich D, Solomon CC, Thomas DB, et al. Breast conservation therapy in the United States following the 1990 National Institutes of Health Consensus Development Conference on the treatment of patients with early stage invasive breast carcinoma. Cancer. 1999;86:628–37.
41. Morrow M, White J, Moughan J, et al. Factors predicting the use of breast-conserving therapy in stage I and II breast carcinoma. J Clin Oncol. 2001;19:2254–62.
42. START Trialists' Group, Bentzen SM, Agrawal RK, et al. The UK Standardisation of Breast Radiotherapy (START) Trial A of radiotherapy hypofractionation for treatment of early breast cancer: a randomised trial. Lancet Oncol. 2008;9:331–41.
43. START Trialists' Group, Bentzen SM, Agrawal RK, et al. The UK Standardisation of Breast Radiotherapy (START) Trial B of radiotherapy hypofractionation for treatment of early breast cancer: a randomised trial. Lancet. 2008;371:1098–107.
44. Whelan TJ, Pignol JP, Levine MN, et al. Long-term results of hypofractionated radiation therapy for breast cancer. N Engl J Med. 2010;36:513–20.
45. Haffty BG, Carter D, Flynn SD, et al. Local recurrence versus new primary: clinical analysis of 82 breast relapses and potential applications for genetic fingerprinting. Int J Radiat Oncol Biol Phys. 1993;27: 575–83.
46. Benitez PR, Chen PY, Vicini FA, et al. Partial breast irradiation in breast conserving therapy by way of intersitial brachytherapy. Am J Surg. 2004;188: 355–64.
47. Antonucci JV, Wallace M, Goldstein NS, et al. Differences in patterns of failure in patients treated with accelerated partial breast irradiation versus whole-breast irradiation: a matched-pair analysis with 10-year follow-up. Int J Radiat Oncol Biol Phys. 2009;74:447–52.
48. Polgár C, Fodor J, Major T, et al. Breast-conserving treatment with partial or whole breast irradiation for low-risk invasive breast carcinoma–5-year results of a randomized trial. Int J Radiat Oncol Biol Phys. 2007;69:694–792.
49. Arthur DW, Winter K, Kuske RR, et al. A Phase II trial of brachytherapy alone after lumpectomy for select breast cancer: tumor control and survival outcomes of RTOG 95–17. Int J Radiat Oncol Biol Phys. 2008;72:467–73.
50. Benitez PR, Keisch ME, Vicini F, et al. Five-year results: the initial clinical trial of MammoSite balloon brachytherapy for partial breast irradiation in early-stage breast cancer. Am J Surg. 2007;19:456–62.
51. Vicini F, Beitsch PD, Quiet CA, et al. Three-year analysis of treatment efficacy, cosmesis, and toxicity by the American Society of Breast Surgeons MammoSite Breast brachytherapy registry Trial in patients treated with accelerated partial breast irradiation. Cancer. 2008;112:758–66.
52. Cuttino LW, Keisch M, Jenrette JM, et al. Multi-institutional experience using the MammoSite radiation therapy system in the treatment of early-stage breast cancer: 2-year results. Int J Radiat Oncol Biol Phys. 2008;71:107–14.
53. Chen PY, Wallace M, Mitchell C, et al. Four-year efficacy, cosmesis, and toxicity using three-dimensional conformal external beam radiation therapy to deliver accelerated partial breast irradiation. Int J Radiat Oncol Biol Phys. 2010;76:991–7.
54. Vicini F, Winter K, Wong J, et al. Initial efficacy results of RTOG 0319: three-dimensional conformal radiation therapy (3D-CRT) confined to the region of the lumpectomy cavity for stage I/II breast carcinoma. Int J Radiat Oncol Biol Phys. 2010;77(4):1120–7.
55. Smith BD, Arthur DW, Buchholz TA, et al. Accelerated partial breast irradiation consensus statement from the American Society for Radiation Oncology (ASTRO). Int J Radiat Oncol Biol Phys. 2009;15: 987–1001.
56. Clarke M, Collins R, Darby S, et al. Effects of radiotherapy and of differences in the extent of surgery for early breast cancer on local recurrence and 15-year survival: an overview of the randomised trials. Lancet. 2005;366:2087–106.
57. Hughes KS, Schnaper LA, Berry D, et al. Lumpectomy plus tamoxifen with or without irradiation in women 70 years of age or older with early breast cancer. N Engl J Med. 2004;351:971–7.

58. Fyles AW, McCready DR, Manchul LA, et al. Tamoxifen with or without breast irradiation in women 50 years of age or older with early breast cancer. N Engl J Med. 2004;351:963–70.
59. Veronesi U, Marubini E, Mariani L, et al. Radiotherapy after breast-conserving surgery in small breast carcinoma: long-term results of a randomized trial. Ann Oncol. 2001;12:997–1003.
60. Fisher B, Bryant J, Dignam JJ, et al. Tamoxifen, radiation therapy, or both for prevention of ipsilateral breast tumor recurrence after lumpectomy in women with invasive breast cancers of one centimeter or less. J Clin Oncol. 2001;20:4141–9.
61. Taghian A, Jeong JH, Mamounas E, et al. Patterns of locoregional failure in patients with operable breast cancer treated by mastectomy and adjuvant chemotherapy with or without tamoxifen and without radiotherapy: results from five National Surgical Adjuvant Breast and Bowel Project randomized clinical trials. J Clin Oncol. 2004;22:4247–54.
62. Fowble B, Gray R, Gilchrist K, et al. Identification of a subgroup of patients with breast cancer and histologically positive axillary nodes receiving adjuvant chemotherapy who may benefit from postoperative radiotherapy. J Clin Oncol. 1988;6:1107–17.
63. Harris JR, Halpin-Murphy P, McNeese M, et al. Consensus Statement on postmastectomy radiation therapy. Int J Radiat Oncol Biol Phys. 1999;44:989–90.
64. Overgaard M, Hansen PS, Overgaard J, et al. Postoperative radiotherapy in high-risk premenopausal women with breast cancer who receive adjuvant chemotherapy. Danish Breast Cancer Cooperative Group 82b Trial. N Engl J Med. 1997;337:949–55.
65. Ragaz J, Olivotto IA, Spinelli JJ, et al. Locoregional radiation therapy in patients with high-risk breast cancer receiving adjuvant chemotherapy: 20-year results of the British Columbia randomized trial. J Natl Cancer Inst. 2005;97:116–26.
66. Overgaard M, Jensen MB, Overgaard J, et al. Postoperative radiotherapy in high-risk postmenopausal breast-cancer patients given adjuvant tamoxifen: Danish Breast Cancer Cooperative Group DBCG 82c randomised trial. Lancet. 1999;353:1641–8.
67. Whelan TJ, Julian J, Wright J, et al. Does locoregional radiation therapy improve survival in breast cancer? A meta-analysis. J Clin Oncol. 2000;18:1220–9.
68. Floyd SR, Buchholz TA, Haffty BG, et al. Low local recurrence rate without postmastectomy radiation in node-negative breast cancer patients with tumors 5 cm and larger. Int J Radiat Oncol Biol Phys. 2006;66:358–64.
69. Overgaard M, Nielsen HM, Overgaard J. Is the benefit of postmastectomy irradiation limited to patients with four or more positive nodes, as recommended in international consensus reports? A subgroup analysis of the DBCG 82 b&c randomized trials. Radiother Oncol. 2007;82:247–53.
70. Truong PT, Olivotto IA, Kader HA, et al. Selecting breast cancer patients with T1-T2 tumors and one to three positive axillary nodes at high postmastectomy locoregional recurrence risk for adjuvant radiotherapy. Int J Radiat Oncol Biol Phys. 2005;61:1337–47.
71. RTOG- Breast Cancer Atlas. http://www.rtog.org/pdf_file2.html?pdf_document=BreastCancerAtlas.pdf. Accessed 26 Apr 2010.
72. Kestin LL, Sharpe MB, Frazier RC, et al. Intensity modulation to improve dose uniformity with tangential breast radiotherapy: initial clinical experience. Int J Radiat Oncol Biol Phys. 2000;48:1559–68.
73. Vicini FA, Sharpe M, Kestin L, et al. Optimizing breast cancer treatment efficacy with intensity-modulated radiotherapy. Int J Radiat Oncol Biol Phys. 2002;54:1336–44.
74. Pignol JP, Olivotto I, Rakovitch E, et al. A multicenter randomized trial of breast intensity-modulated radiation therapy to reduce acute radiation dermatitis. J Clin Oncol. 2008;26:2085–92.
75. Evans PM, Donovan EM, Partridge M, et al. The delivery of intensity modulated radiotherapy to the breast using multiple static fields. Radiother Oncol. 2000;57:79–89.
76. Woo TC, Pignol JP, Rakovitch E, et al. Body radiation exposure in breast cancer radiotherapy: impact of breast IMRT and virtual wedge compensation techniques. Int J Radiat Oncol Biol Phys. 2006;65:52–8.
77. Remouchamps VM, Letts N, Vicini FA, et al. Initial clinical experience with moderate deep-inspiration breath hold using an active breathing control device in the treatment of patients with left-sided breast cancer using external beam radiation therapy. Int J Radiat Oncol Biol Phys. 2003;56:704–15.
78. Cox JD, Stetz J, Pajak TF, et al. Toxicity criteria of the Radiation Therapy Oncology Group (RTOG) and the European Organization for Research and Treatment of Cancer (EORTC). Int J Radiat Oncol Biol Phys. 1995;31:1341–6.
79. Back M, Guerrieri M, Wratten C, et al. Impact of radiation therapy on acute toxicity in breast conservation therapy for early breast cancer. Clin Oncol. 2004;16:12–6.
80. Chao KK, Vicini FA, Wallace M, et al. Analysis of treatment efficacy, cosmesis, and toxicity using the MammoSite breast brachytherapy catheter to deliver accelerated partial-breast irradiation: the William Beaumont Hospital experience. Int J Radiat Oncol Biol Phys. 2007;69:32–40.
81. Coen JJ, Taghian AG, Kachnic LA, et al. Risk of lymphedema after regional nodal irradiation with breast conservation therapy. Int J Radiat Oncol Biol Phys. 2003;55:1209–15.
82. Correa CR, Das IJ, Litt HI, et al. Association between tangential beam treatment parameters and cardiac abnormalities after definitive radiation treatment for left-sided breast cancer. Int J Radiat Oncol Biol Phys. 2008;72:508–16.
83. Obedian E, Fischer DB, Haffty BG, et al. Second malignancies after treatment of early-stage breast

cancer: lumpectomy and radiation therapy versus mastectomy. J Clin Oncol. 2000;18:2406–12.
84. Stovall M, Smith SA, Langholz BM, et al. Dose to the contralateral breast from radiotherapy and risk of second primary breast cancer in the WECARE study. Int J Radiat Oncol Biol Phys. 2008;72:1021–30.
85. Jeffrey SS, Birdwell RL, Ikeda DM, et al. Radiofrequency ablation of breast cancer: first report of an emerging technology. Arch Surg. 1999;134:1064–8.
86. Burak Jr WE, Agnese DM, Povoski SP, et al. Radiofrequency ablation of invasive breast carcinoma followed by delayed surgical excision. Cancer. 2003;98:1369–76.
87. Earashi M, Noguchi M, Motoyoshi A, et al. Radiofrequency ablation therapy for small breast cancer followed by immediate surgical resection or delayed mammotome excision. Breast Cancer. 2007;14:39–47.
88. Dowlatshahi K, Fan M, Gould VE, et al. Stereotactically guided laser therapy of occult breast tumors: work-in-progress report. Arch Surg. 2000;135:1345–52.
89. Littrup PJ, Jallad B, Chandiwala-Mody P, et al. Cryotherapy for breast cancer: a feasibility study without excision. J Vasc Interv Radiol. 2009;20:1329–41.

Systemic Therapy for Breast Cancer: Success and Challenges

61

Zeina Nahleh

Abstract

We have come a long way in the management of breast cancer over the last few decades as evidenced by decreasing breast cancer mortality since the 1990s. The improved understanding of breast cancer as a heterogenous disease led to the development of newer systemic chemotherapies, hormonal therapies, and targeted (biologic therapies). The classification of breast cancer has been refined into distinct molecular subtypes. However, important questions remain regarding how to further tailor therapy based on better predictive and prognostic markers. In this chapter, we review the progress achieved in the systemic treatment of breast cancer and highlight some of the remaining challenges in this field.

Introduction

Over the last few decades, enormous progress has been achieved in the understanding and treatment of breast cancer. Breast cancer has evolved from a disease of whispers to one that receives increased public awareness and powerful advocacy. The contribution of federal and private financial support to breast cancer research has also been palpable and added to the advances in this disease. Only one in four women with breast cancer were alive after 10 years in the 1950s, whereas three in four women remain alive now [1]. Mortality from breast cancer has declined by more than 25 % over the past 20 years [2, 3].

The past two decades have seen the most rapid pace of progress characterized by a greater understanding of the molecular biology of breast cancer, rational drug design, development of agents with specific cellular targets and pathways, development of better prognostic and predictive multigene assays, and marked improvements in supportive care. Three main factors brought us closer to using the term "cure" for many breast cancers. One is early detection through mammography [4–6]; another is a better understanding of breast cancer as both a local and a systemic disease leading to the demonstration that breast-conserving surgery (lumpectomy) followed by radiation therapy is unequivocally comparable to mastectomy [7–9] and the implementation of early systemic therapy [10]; and third is the understanding that breast cancer is

Z. Nahleh
Department of Internal Medicine, Division of Hematology-Oncology, TTUHSC-Paul L. Foster School of Medicine, El Paso, TX, USA
e-mail: zeina.nahleh@ttuhsc.edu

D.E. Dupuy et al. (eds.), *Image-Guided Cancer Therapy*, DOI 10.1007/978-1-4419-0751-6_63,

a heterogenous disease which led to the development of newer systemic chemotherapies, hormonal therapies, and targeted (biologic therapies) [11]. In this chapter, we focus on the current progress in the systemic treatment of breast cancer and highlight some of the remaining challenges in this field. We emphasize the treatment in early and locally advanced breast cancer as it presents a nice multidisciplinary model compared to the treatment of more advanced stages of breast cancer with distant metastatic disease.

Principles of Systemic Therapy

The improvement in breast cancer mortality over the past two decades has been a direct result of both improvements in early detection through screening and advances in adjuvant treatment [12]. Depending on the model of risk reduction, adjuvant therapy has been estimated to be responsible for 35–75 % of that reduction [13]. Adjuvant treatment of breast cancer is the term given to systemic therapies (chemotherapy, endocrine/hormonal therapy, or targeted biologic therapy) designed to treat micrometastatic disease or breast cancer cells that have escaped the breast and regional lymph nodes but have not yet established an identifiable metastasis. Treatment is aimed at reducing the risk of future recurrence, thereby reducing breast cancer-related morbidity and mortality [14].

Historically, the main methods of cancer management were based on radiation treatment and surgery. It was first in the middle of the twentieth century that chemotherapy has joined the team and was represented by a single toxic medication, nitrogen mustard [15]. In recent years, we have seen an explosion of new endocrine and chemotherapeutic advances against breast cancer. Drugs were developed based on the fundamental investigations of the normal and cancer cells, their pathophysiological peculiarities, and the intracellular pathway signals [16]. Combination chemotherapy regimens became standardly recommended in the adjuvant setting [17]. The decision to give chemotherapy is typically based on the cancer's stage; lymph nodes status; hormone receptors, estrogen receptor (ER) and progesterone receptor (PR); human epidermal growth factor 2 (HER2) status; and more recently on multigene assays. More aggressive treatment is usually recommended for premenopausal women with invasive breast cancer.

We have now been using adjuvant systemic therapy in early breast cancer for decades, but the main challenge still remains to figure out how to use each optimally and in what particular patient. Advances in genomic profiling, mostly based upon gene expression microarrays, have permitted simultaneous examinations of thousands of genes and pathways in a specific tumor and the description of comprehensive portraits of malignant cells [11]. At least four discrete breast tumor subtypes with distinct clinical behavior have been identified: luminal A (ER+ and/or PR+/HER2−), the most common subtype and typically associated with increasing age, lower histologic grade, good prognosis, and hormone responsiveness; luminal B (ER+ and/or PR− or +/HER2 − or +), similar to luminal A but more frequently ER+/PR− and with worse outcome than luminal A; HER2+ (ER−/PR−), less common, generally aggressive subtype with high-grade histology, and more common at younger age; and basal-like (ER−/PR−/HER2−), also known collectively as triple negative, aggressive subtype with high-grade histology and high mitotic rate, and common at younger age and in premenopausal African American women [18, 19].

In view of this refined classification of breast cancer, we now need to address these important questions:

- What patient subsets really need both chemotherapy and endocrine therapy?
- Are there some women who should not take endocrine therapy?
- What specific type of chemotherapy each woman would respond to?
- What is the differential response and toxicity to chemotherapy based on each woman's unique pharmacogenomic makeup?
- Are there some women who could receive just endocrine therapy or targeted therapy despite advanced stage on presentation?

- Can we identify patients who are not going to respond to hormonal therapy and steer them toward more appropriate therapies?

Evolution of Adjuvant Chemotherapy

The first chemotherapy combination regimen used on a large scale for breast cancer was the CMF (cyclophosphamide, methotrexate, and 5-fluorouracil) regimen [20]. Six cycles of CMF were the gold standard of adjuvant chemotherapy in breast cancer for decades, and it significantly improved early and long-term results and conferred better rates of relapse-free survival and overall survival compared with no chemotherapy [21]. Multiple subsequent regimens were developed and contributed to improved outcome in breast cancer (Table 61.1).

Table 61.1 Evolution of chemotherapy in breast cancer

Class	Drug	Years
Chemotherapy	Monotherapy alkylating agents, nitrogen mustard	1950s–1960s
	Polychemotherapy Cooper schedule, alkylating	1960s
	Adjuvant chemotherapy CMF	1970s
	Anthracyclines, combination chemotherapy	1980s
	Adjuvant and neoadjuvant anthracyclines, taxanes	1990s
Targeted (biologic therapy)	Adjuvant chemotherapy combination with anti-HER2 trastuzumab	2000s

Anthracyclines

Anthracycline-containing adjuvant chemotherapy regimens were introduced for the treatment of early-stage breast cancer in the early 1980s. Compared with standard CMF, anthracycline-containing regimens reduced both the annual risk of recurrence and the annual risk of death by more than 10 %, equating to about 5 % absolute reduction in recurrence and a 3 % absolute reduction in mortality at 5 years [22–24]. This small but real difference established anthracyclines (epirubicin, doxorubicin) as the most active drugs for breast cancer. Multiple schedules, dose densities, and intensities have been tested; common regimens in use contain three or more agents including cyclophosphamide(C), fluorouracil (F), epirubicin (E) or doxorubicin (A) (e.g., CEF and CAF, FAC, FEC), or 2-drug regimens (e.g., AC or EC) which appears to be equivalent to six cycles of CMF. Anthracyclines remain the most commonly used drugs for breast cancer but not without concerns regarding anthracycline-associated cardiotoxicity or leukemogenic potential.

In the 2000 Early Breast Cancer Trialists' Collaborative Group (EBCTCG) meta-analysis overview [23], anthracycline-based regimens were associated with an annual risk of cardiac mortality of 0.08 % per year as compared with 0.06 % per year in patients treated with nonanthracycline-based regimens. This is the largest of any meta-analyses of individual patients in cancer care that included data from 145,000 women with breast cancer at an early stage, randomized in 194 trials of adjuvant systemic therapy (chemotherapy and/or hormonal therapy). However, the question of long-term cardiac safety remains, particularly for older women with early-stage breast cancer.

Multiple subsequent trials conducted by the Cancer and Leukemia Group B (CALGB) over the last few decades using anthracycline regimens confirmed the advantages of this chemotherapy in terms of improving disease-free and overall survival particularly in patients with estrogen receptor-negative disease, without significant nonhematologic toxicity [25–28]. Additionally, a recent meta-analysis of eight trials comprised of 6,564 women with early-stage breast cancer to anthracycline- versus nonanthracycline-based regimens suggested a benefit with anthracycline administration only in patients with HER2+ disease [29]. The role of predictive markers of response to anthracyclines remains an area of active research. Biologically, anthracyclines inhibit topoisomerase IIa, whose gene (TOP2A) lies adjacent to the HER2 gene on chromosome 17 and is coamplified in

approximately 35 % of HER2-overexpressing breast cancers [30, 31]. The role of ER, HER2, as well as other biomarkers like TOP2A as predictive markers of response to anthracyclines needs further validation. Until then, many experts believe that patients should not be deprived of anthracycline-based adjuvant chemotherapy if their risk assessment so determines it [32].

Taxanes

Among the novel chemotherapeutic drugs introduced in the 1990s, the taxanes have emerged as among the most active and commonly used chemotherapeutic agents for the treatment of early-stage breast cancer. The CALGB 9344 was one of the largest trials evaluating taxanes in the adjuvant setting for early-stage breast cancer and included more than 3,000 women with node-positive breast cancer [28]. This study demonstrated a 5-year survival benefit of 80 % versus 77 % for the sequential use of paclitaxel following AC (doxorubicin, cyclophosphamide) chemotherapy, compared to AC alone. This important trial led to the incorporation and recommendation of paclitaxel following AC administration for adjuvant polychemotherapy in women with lymph node-positive disease.

The main unanswered question remains:

- What patient subsets will benefit most from taxane chemotherapy?

In a recent retrospective analysis of CALGB 9344 testing for HER2 status using 1,322 original participant tumor blocks [33], HER2 positivity irrespective of estrogen receptor status predicted a significant benefit from paclitaxel in terms of reduced disease recurrence (HR 0.59, $p = 0.01$). Patients with estrogen receptor-positive, HER2-negative, node-positive breast cancer did not seem to benefit from the addition of a taxane [33]. However, the Breast Cancer International Research Group (BCIRG) 001 docetaxel trial, in which significant improvement was documented in disease-free survival with 6 × TAC (docetaxel, doxorubicin, cyclophosphamide) compared with 6 × FAC (82 % vs. 74 %), showed significant benefit of taxane-anthracycline regimen over the anthracycline-nontaxane regimen in both ER-positive and ER-negative tumors [34]. A recent Cochrane meta-analysis including 12 studies and more than 21,000 patients evaluated the role of taxanes in the adjuvant treatment of operable breast cancer (stage I–III) [35]. The results showed a statistically significant overall survival (HR 0.81, $p < 0.00001$) and disease-free survival (HR 0.81, $p < 0.00001$) for the taxane-containing regimens compared with the nontaxane regimens [35]. This review did not identify a subgroup of patients where taxane-containing treatment may have been more or less effective [35]. The totality of evidence, therefore, supports the use of taxane-containing adjuvant chemotherapy regimens with improvement of overall survival and disease-free survival for women with operable early breast cancer. To date, there is not enough evidence to support withdrawing taxane therapy in any subgroup of breast cancer patients.

Although the precise role of adjuvant taxane therapy remains controversial, the optimal scheduling of taxane administration has been determined. The Eastern Cooperative Oncology Group (ECOG) 1199 randomized 4,950 women with lymph node-positive or high-risk lymph node-negative early-stage breast cancer to four cycles of AC followed by four different taxane regimens: (1) paclitaxel at 175 mg/m^2 q3wk, (2) paclitaxel at 80 mg/m^2 weekly, (3) docetaxel at 100 mg/m^2 q3wk, and (4) docetaxel 35 mg/m^2 weekly. After a 64-month median follow-up, paclitaxel weekly and docetaxel every 3 weeks were superior to the other two regimens in terms of disease-free survival [36].

In an effort to identify nonanthracyclines and therefore potentially less cardiotoxic regimens for the treatment of early-stage breast cancer, the US Oncology 9735 trial randomized 1,016 women with operable breast cancer (stages I–III) to four cycles of TC (docetaxel plus cyclophosphamide) versus four cycles of standard-dose AC [37]. After a median of 7-year follow-up, both disease-free survival and overall survival were superior in the TC arm with less cardiotoxicity. This trial introduced TC as a viable option for treating women with early-stage breast cancer, especially those at high risk of cardiotoxicity or requiring only 12 weeks of therapy.

Table 61.2 Evolution of therapeutic hormonal therapy methods in breast cancer

Class	Drug/method	Toxicities	Years
Hormonal therapy	Testosterone, progesterone, estrogen, prednisolone, aminogluthemide, adnexectomy, ovarian irradiation	Hirsutism, acne	1950–1970s
	Tamoxifen	Hot flashes, mood changes, thromboembolic events, cancer of uterus	1980s
	Aromatase inhibitors	Arthralgias, decreased bone density, hot flashes	1990s

In summary, it appears that an anthracycline followed by or concurrent with a taxane is the most optimal adjuvant therapy for breast cancer patients, especially those with estrogen receptor-negative tumors with no medical contraindications, using either weekly paclitaxel or every-3-week docetaxel-dosing schedules. However, it remains unclear what the optimal combination chemotherapy regimen is for each subset of breast cancer, especially for ER+, HER2− tumors. Currently, CMF, TC, or an anthracycline-based regimen may all be additional reasonable options.

Adjuvant Therapy for HER2+ Breast Cancer

Clinicians have long recognized that breast cancer is a heterogenous disease. One of the most important success stories in breast cancer over the past two decades was the identification of HER2 as a driver of prognosis by Slamon and his colleagues, reported in the 1988 seminal *Science* paper [38]. Overexpression of HER2 occurs in approximately 20 % of breast cancers and correlates with a more aggressive phenotype and worse prognosis overall. However, the development of HER2-targeted therapies with the advent of trastuzumab, a monoclonal antibody (mAb) targeting the extracellular domain of the receptor, has changed the treatment paradigm and history for HER2-positive breast cancer. Trastuzumab was approved by the US Food and Drug Administration (FDA) in combination with chemotherapy for the treatment of HER2+ disease in the adjuvant setting in 2005. To date, results are available from five studies [39–42] (BCIRG006 [42], HERA [40], FinHer [41], N9831 [39], and NSABP B31 [39]) that randomized 11,650 women with early-stage HER2+ breast cancer to trastuzumab versus non-trastuzumab-based adjuvant chemotherapy. All five trials have demonstrated that the inclusion of trastuzumab produces roughly a 50 % improvement in disease-free survival and 35 % improvement in overall survival regardless of the chemotherapy regimen or sequence of trastuzumab delivery. Ongoing trials are currently testing whether the combination of two anti-HER2-targeted therapies with chemotherapy will prove beneficial in early-stage disease in the phase III ALTTO (Adjuvant Lapatinib and/or Trastuzumab Treatment Optimization) trial [43].

Adjuvant Hormonal Therapy

In 1896, Dr. George Beatson removed the ovaries from a 33-year-old woman with locally advanced breast cancer and noted visible tumor regression [44]. He was intrigued by the physiology when studying lactation in sheep in West Scotland and observing farmers using oophorectomy to maintain lactation in cows and ensure milk supply. By the first half of the twentieth century, endocrine (also known as hormonal) therapy which involves reducing the amount of estrogen in the body or blocking the effect of estrogen became recognized as a viable treatment for breast cancer (Table 61.2). This was based on strong evidence that estrogen plays a role in the development and progression of breast cancer [45, 46]. This process depends on the presence of the hormone

receptors: ER and/or PR [46, 47]. About 70–80 % of breast cancers are ER+. Almost 65 % of ER+ breast cancers are also PR+. Nearly 10 % cases are ER+ and PR−. From this point, all breast tumors can be generally divided into hormone-receptor-positive (HR+) and hormone-receptor-negative (HR−) cases and hormonal receptor; specifically ER can be considered the first target of biological therapy in breast cancer. Hormonal therapy is now considered the main systemic treatment for HR+ breast cancers and is not effective against HR− breast cancer [48].

There are currently four main different modalities of hormonal therapies [14]: (1) ovarian suppression or ablation using irreversible oophorectomy, irradiation, or more commonly the utilization of luteinizing hormone-releasing hormone (LHRH) analogs, which effects a temporary loss of ovarian function; (2) selective estrogen receptor modulators (SERM) (e.g., tamoxifen, toremifene); (3) aromatase inhibitors (anastrozole, examestane, letrozole); and (4) estrogen receptors downregulators (fulvestrant). The first three modalities are used for the treatment of early stages of breast cancer while all four modalities can be used for the treatment for advanced metastatic breast cancer.

Tamoxifen is the oldest and most-prescribed SERM, which binds to, and inhibits estrogen receptor signaling in the breast [49]. As a receptor antagonist, it is effective in both premenopausal and postmenopausal women. It has ER-stimulating effects in other tissues, including bone (resulting in preservation of bone density) and endometrium (leading to a two- to fourfold increased risk of endometrial cancer) [22, 23]. Tamoxifen has been approved for breast cancer treatment since the early 1980s. It has been shown in multiple studies to decrease breast cancer-associated mortality and recurrence in the adjuvant treatment of breast cancer. Five years of tamoxifen therapy has been the standard resulting in about 50 % reduction in recurrence and 25 % reduction in mortality [22, 23]. Common side effects associated with tamoxifen use include hot flashes (up to 80 %), vaginal bleeding (2–25 %) or discharge (10–55 %), urinary frequency or urgency (10 %), and mood changes (15–20 %) or depression (2–12 %).

For premenopausal women diagnosed with HR+ breast cancer, tamoxifen remains the hormonal therapy treatment standard [17]. Ongoing studies are testing whether ovarian suppression, using (LHRH) analogs, e.g., goserelin and leuprolide (temporary) or by surgically removing the ovaries (permanent suppression), is also necessary in premenopausal women diagnosed with HR + breast cancer where estrogens are mostly produced in the ovaries [48]. An area of controversy exists regarding how to determine who benefits the most from tamoxifen?

Tamoxifen is a prodrug that is metabolized primarily by the cytochrome P450 (CYP2D6) system to its active metabolite, endoxifen [50]. More than 80 different alleles of the CYP2D6 gene have been identified with varying activity levels. Consequently, patients can be categorized by their level of CYP2D6 activity into high/extensive or low/poor metabolizers. Around 10 % of the populations are poor metabolizers of tamoxifen. Poor metabolizers have been shown in several retrospective studies to have lower disease-free survival and higher recurrence rates compared to extensive metabolizers. Poor metabolizers also seem to tolerate tamoxifen better as they have less severe hot flashes and endocrine-related toxicities. Several laboratories now offer CYP2D6 testing for patients treated with tamoxifen, but recommendation for this testing is still controversial, especially in women who have no alternative treatment options. However, considerable attention has been paid to the use of concomitant medications especially potent inhibitors of CYP2D6 activity such as the selective serotonin-reuptake inhibitors (SSRIs) fluoxetine and paroxetine. These drugs can decrease conversion of tamoxifen to endoxifen, but their association with increased cancer recurrence has been controversial [51, 52]. The concomitant use of potent CYP2D6 inhibitors like SSRIs should be avoided if possible in patients on tamoxifen.

For postmenopausal women, a number of studies have compared ***aromatase inhibitors*** (AIs) with tamoxifen [48, 53]. Aromatase is the

enzyme (found in body fat, adrenal glands, and breast tissue as well as tumor cells) responsible for converting other steroid hormones into estrogen [54]. Aromatase is the sole source of estrogen in postmenopausal women. Having no effect on ovarian estrogen production, AIs are therefore only effective in postmenopausal women. Based on the overall evidence, it appears that AIs are slightly superior in decreasing breast cancer recurrence (by around 4 %) in postmenopausal women with early-stage HR + breast cancer and may carry fewer serious side effects but no improvement in overall survival compared to tamoxifen [53]. Common side effects of AIs include hot flashes (10–35 %), arthralgia/arthritis (20 %), headache (10–15 %), vaginal dryness (2 %), and mood changes (20 %) [55, 56]. Aromatase inhibitors are approved for the adjuvant treatment of postmenopausal women with HR+ breast cancer [48]. Other acceptable options include switching to an aromatase inhibitor after taking tamoxifen for 2 or 3 years (for a total of 5 years of hormonal therapy) as it has been shown to offer more benefits than 5 years of tamoxifen [57, 58]. The Breast International Group (BIG) completed a randomized, double-blind phase three trial (BIG 1–98) to evaluate the optimal treatment strategy with an aromatase inhibitor, letrozole, in postmenopausal women with endocrine-responsive breast cancer [56]. Patients ($n = 6{,}182$) were randomly assigned to receive 5 years of tamoxifen, 5 years of letrozole, letrozole for 2 years followed by tamoxifen for 3 years, or tamoxifen for 2 years followed by letrozole for 3 years. The primary endpoint, disease-free survival, was not significantly better among either sequential treatment group compared with letrozole monotherapy, but all were better than tamoxifen alone. In addition, overall survival was not statistically different among the groups.

To date, the optimal duration and sequence for the use of aromatase inhibitors have not been clearly defined, but their benefits in terms of breast cancer recurrence and survival clearly support their use in all postmenopausal women [48]. The Canadian lead MA.17 trial randomized patients to an additional 5 years of AI therapy with letrozole after completion of 5 years of tamoxifen therapy [59]. The additional 5 years of AI therapy resulted in improved disease-free survival in all patients randomized and improved overall survival in the higher risk lymph node-positive subset of patients. This study was the first to suggest that prolonged hormonal therapy may be more effective than 5 years of therapy. Ongoing trials are now comparing 5 versus 10 years of AI therapy including a continuation of the MA.17 trial, which will include patients receiving hormonal therapies for up to 15 years, and studying whether the sequence of hormonal agent (i.e., tamoxifen followed by AI vs. AI followed by tamoxifen) affects the efficacy.

In summary, in HR-positive early-stage breast cancer, hormonal therapy plays a major role in the adjuvant treatment, either alone or in combination with chemotherapy. Hormonal treatments function to decrease estrogen's ability to stimulate existing micro-metastases or dormant cancer cells. Adjuvant hormonal therapy can reduce the relative risk of distant, ipsilateral, and contralateral breast cancer recurrence by up to 50 % in tumors with high ER expression. Hormonal therapy is used typically after other breast cancer local and systemic treatments are completed. FDA-approved endocrine therapies for adjuvant treatment of breast cancer include tamoxifen (all women) and the aromatase inhibitors (only in postmenopausal women) (anastrozole, letrozole, exemestane) given upfront or sequentially after 2–3 years of tamoxifen [48]. To date, there are no robust clinically available tools that can be used to reliably identify patients that are likely to be selectively responsive to an aromatase inhibitor compared to tamoxifen. The decision to use an aromatase inhibitor upfront is primarily guided by consideration of recurrence risk and contraindication to tamoxifen.

Neoadjuvant Therapy

Neoadjuvant, also known as preoperative therapy, is used mainly in two distinct groups of breast cancer patients: (1) women who have large but technically operable primary tumors

when the goal of neoadjuvant therapy is to shrink the tumor and increase the chances for breast-conserving surgery (BCS), i.e., stages T3N0M0 (IIB) and T3N1M0 (IIIA), and (2) women who have disease that meets the original criteria of locally advanced breast cancer (LABC) or inflammatory breast cancer (IBC), for whom the administration of systemic treatment is essential to make definitive local treatment possible with the intent of cure, mainly stages IIIB, IIIC, or IBC. As expected, patients with stages IIB and IIIA breast cancer have improved disease-free and overall survival compared to those with LABC and also a higher likelihood of achieving a pathologic complete response (pCR) following neoadjuvant treatment, a well-recognized surrogate for long-term outcome [60–62].

Locally Advanced Breast Cancer (LABC)

Epidemiologically, locally advanced breast cancer is associated with lower socioeconomic class and with African American ethnicity in the United States [63]. It encompasses both relatively indolent neglected tumors and those that have grown rapidly due to their inherent biology. It is as heterogeneous as invasive breast cancer in general, and in most series, locally advanced breast cancer has a better long-term outcome than inflammatory breast cancer. Inflammatory breast cancer is a clinical diagnosis that implies presentation with the cardinal signs of inflammation (calor, rubor, and tumor) involving the breast and represents around 1–2 % of all breast cancers in western countries [64]. Pathologically, it is associated with the classic finding of involvement of subdermal lymphatics, although this finding is not in itself necessary for the diagnosis of inflammatory breast cancer, and it may occur with locally advanced breast cancer as a secondary phenomenon [65]. Inflammatory breast cancer tends to occur at a younger age than locally advanced breast cancer. It is more likely to stain negatively by IHC for ER and PR, somewhat more likely to be positive for HER2/neu overexpression, and both angiogenesis and lymphangiogenesis appear to be increased [65].

Neoadjuvant Chemotherapy

Most programs of neoadjuvant therapy used in the United States have been anthracycline-taxane based, following proven therapies in the adjuvant setting. The landmark NSABP-B18 trial was the first to prove that preoperative chemotherapy was equivalent to postoperative standard chemotherapy, in operable breast cancer. This trial also found that pathologic complete response (pCR) in the primary tumor predicts excellent overall survival and is now considered an excellent surrogate for long-term disease-free survival and overall survival [60]. In the subsequent NSABP B-27 trial, three arms compared four cycles of standard-dose AC to four cycles of standard-dose AC followed by docetaxel, with a third arm sandwiching primary surgery between the neoadjuvant four cycles of AC and the adjuvant four cycles of docetaxel [66]. This trial found that the addition of four cycles of taxanes to standard AC increased pathologic complete response from 14 % to 26 %, and that sandwiching surgery in between the chemotherapy regimens was less effective than administering all chemotherapy upfront. About 15 % of initially node-positive patients who achieve pCR in the breast have residual disease in the axilla. Patients who have no residual disease in both the primary (pCR) and lymph nodes (N0) have the best overall prognosis with a markedly prolonged disease-free survival.

For patients with HER2/neu overexpression, the value of adding trastuzumab in the adjuvant setting led to its incorporation into neoadjuvant therapies for patients with the HER2+ phenotype. This resulted in higher rates of pCR for operable patients, as high as 65 % as initially reported by the MD Anderson group, when trastuzumab was given concurrent with an epirubicin-containing regimen [67]. Though not yet tested on a large scale, it appears likely the addition of agents with antiangiogenesis activity may also be of value as targeted therapy especially in IBC, given its profile of excessive blood vessel formation. The Southwest Oncology Group (SWOG) is currently conducting a randomized phase II trial (S0800) to address this question in patients with locally advanced and inflammatory breast cancer [68].

Local-Regional Therapy

Patients with operable breast cancer who achieve good tumor reduction with neoadjuvant systemic treatment are good candidates for subsequent breast-conserving surgery. Breast-conserving surgery is certainly feasible among some with locally advanced breast cancer, but it is not yet clear whether the rates of locoregional recurrence are unacceptable. Patients with inflammatory breast cancer are best served by having mastectomy as their standard definitive surgery [65]. Immediate reconstruction is not recommended for locally advanced (stage IIB or stage III) and inflammatory breast cancer patients because it may compromise their oncologic care by interfering with the administration of chemotherapy or radiation therapy. Radiation therapy is recommended following surgery for all patients who do not have a medical contraindication.

The preoperative versus postoperative evaluation of lymph nodes remain an area of controversy. Patients with locally advanced breast cancer or inflammatory breast cancer with clinically positive nodes should undergo a core biopsy prior to initiating chemotherapy. Those with clinically negative nodes may undergo sentinel node biopsy before they start treatment, or sentinel node determination may be delayed until after treatment is completed. The proponents of upfront sentinel node sampling argue that chemotherapy might eradicate preexistent disease in the sentinel node and result in a false positive and/or altered lymphatic drainage in large tumors, which might affect the accuracy of the procedure. However, data from the NSABP B-27 neoadjuvant trial suggest that the false-negative rate for sentinel node biopsies performed after neoadjuvant chemotherapy is about 11 %, comparable to the false-negative rate for patients undergoing initial resection [66].

In summary, neoadjuvant chemotherapy is used successfully to downsize tumors and improve the chances of BCS in operable tumors as well as cure in LABC and IBC. The recurrent question of how to better tailor therapy is extremely relevant to neoadjuvant treatment. It appears that the best candidates for neoadjuvant chemotherapy are patients with ER- or HER2+-expressing tumors where pCR rates are generally above 20 % [60, 62, 66]. Patients with ER+, HER2− locally advanced breast cancer are unlikely to achieve a pCR from presently available chemotherapy [66]. Neoadjuvant hormonal therapies appear to be effective in shrinking tumor size to enable breast-conserving surgery, but pCR is rare [69]. Further studies should address how to optimize neoadjuvant therapy in this group. Also to date, there is a lack of evidence-based guidance of what additional treatment to administer after surgery when the surgical result is suboptimal.

Other areas of future research should include how to optimize the role of imaging to evaluate the response assessment during neoadjuvant therapy. Currently, most tumors show a good clinical response (>50 %) but with discordant pathological response [60]. Currently, ultrasound is among the most commonly used test to evaluate the status of measurable tumors. The mass often appears larger on physical examination than it does on ultrasound, which can more effectively discriminate hypoechoic masses from surrounding stroma and/or hematoma. In inflammatory breast cancer, MRI may be an important adjunct to response assessment. The role of PET in the routine assessment of response remains to be determined. No present imaging technique appears to be highly accurate for the prediction of pathologic complete response. Thus, the purpose of regular size assessment is to exclude continuation of therapy in a patient with a growing tumor (seen in <5 % with the initial treatment) and to suggest when maximal response of grossly evident disease has been achieved, as this may be the optimal time to proceed to resection. Alternatively, future research efforts should focus on determining who is most likely to achieve complete pathological response based on clinical and molecular techniques as well as optimal imaging and consequently, who may not require prolonged courses of neoadjuvant therapy nor perhaps extensive surgical resection. This is the biggest challenge of the next decade.

Future Directions

We have certainly come a long way in the past few years, witnessed by the steady decrease in breast cancer mortality that began in the 1990s and has continued since. The improved understanding that breast cancer is a systemic heterogenous disease with identifiable subsets led to significant improvement in scientific research and its clinical application. The ability to selectively target a driving molecule of importance is best illustrated by the isolated inhibition of ER and HER2 which led to improving the cure rate in the adjuvant setting and providing long-term disease control in the metastatic setting. Today, we are working to further refine treatment recommendations and tailor therapy.

Identifying women who benefit most from hormonal and chemotherapy through evaluation of molecular and genomic features of the tumor is now becoming possible. A practical example is the 21 gene recurrence (Oncotype DX; Genomic Health Inc, Redwood city, CA), currently available in clinical practice but limited to the use for ER+ tumors [70]. The Oncotype DX allows for the prediction of benefit of the addition of chemotherapy to hormonal therapy compared with hormonal therapy alone. The routine clinical use of Oncotype DX, which classifies patients with node-negative, HR+ tumors in terms of low-, intermediate-, and high-risk categories for the future development of distant metastatic disease, has lead to a reduction in the use of chemotherapy, without apparent worsening of clinical outcomes. However, prediction of tumor sensitivity to the different types of systemic therapies has not reached a high level of confidence, and further efforts are urgently needed. Currently, high-throughput genomic techniques are promising but not widely available, so clinical decisions continue to be actually based on immunohistochemistry, fluorescence in situ hybridization (FISH), and other, broadly available assays. But continued progress in molecular diagnostics and therapeutics is evolving quickly and is likely to result in additional improvements in targeted therapies and outcome.

It is important to note that the next generation of targeted therapies in oncology are likely to be very expensive, however, and not without toxicity. Therefore, predictive tests geared toward trimming unnecessary treatments and tailoring therapy will be even more crucial. Understanding further the biology of breast cancer will require that we move to a more sophisticated era of incorporated tissue-based and functional imaging studies into clinical trials, in addition to far more routine and far more routine acquisition of target tissue for diagnostic and therapeutic discovery. The theme of the last two decades will continue to dominate. We will continue to move away from maximal-tolerated treatment and one-size-fits-all approach to minimum effective treatment, less invasive procedures, and more tailored therapy. A refined newer classification of breast cancer based on molecular features may allow a better prediction of prognosis and response to several types of treatment and would allow a more optimal design of clinical trials. Neoadjuvant therapeutic approaches are ideal venues for research aimed at a better understanding of breast cancer biology and improving individualized therapy. Neoadjuvant therapy offers the unique potential to study predictor of treatment responses in a relatively short duration with a fewer number of patients compared to adjuvant trials. Ongoing and future trials should further refine optimal locoregional management. Finally, breast cancer will continue to offer a great multidisciplinary model for clinical and research progress in oncology.

References

1. Buzdar A. Improving survival of patients with breast cancer over the past 6 decades: the University of Texas M. D. Anderson Cancer Center experience – ASCO 2010 Breast Cancer Symposium; 2010 Oct: Washington, D.C, Abstract 172.
2. Jemal A, Ward E, Thun ML. Declining death rates reflect progress against cancer. PLoS One. 2010;5(3): e9584. Published online 2010 March 9.
3. Peto R, Boreham J, Clarke M, et al. UK and USA breast cancer deaths down 25 % in year 2000 at ages 20–69 years. Lancet. 2000;355:1822.
4. Tabar L, Fagerberg G, Gad A, et al. Reduction in mortality from breast cancer after mass screening

with mammography: randomized trial from the Breast Cancer Screening Working Group of the Swedish National Board of Health and Welfare. Lancet. 1985;1:829–32.
5. Kerlikowske K, Grady D, Rubin S, et al. Efficacy of screening mammography: a meta-analysis. JAMA. 1995;273:149–54.
6. Hellquist BN, Duffy SW, Abdsaleh S et al. Effectiveness of population-based service screening with mammography for women ages 40 to 49 years: evaluation of the Swedish Mammography Screening in Young Women (SCRY) cohort. Cancer. 2011;117:714–22.
7. Fisher B, Redmond C, Fisher ER, et al. Ten-year results of a randomized clinical trial comparing radical mastectomy and total mastectomy with or without radiation. N Engl J Med. 1985;312(11): 674–81.
8. Fisher B, Bauer M, Margolese R, et al. Five-year results of a randomized clinical trial comparing total mastectomy and segmental mastectomy with or without radiation in the treatment of breast cancer. N Engl J Med. 1985;312(11):665–73.
9. Fisher B, Anderson S, Bryant J, et al. Twenty-year follow-up of a randomized trial comparing total mastectomy, lumpectomy, and lumpectomy plus irradiation for the treatment of invasive breast cancer. N Engl J Med. 2002;347(16):1233–41.
10. Early Breast Cancer Trialists' Collaborative Group (EBCTCG). Effects of chemotherapy and hormonal therapy for early breast cancer on recurrence and 15-year survival: an overview of the randomised trials. Lancet. 2005;365(9472):1687–717.
11. Carey L. Through a glass darkly: advances in understanding breast cancer biology, 2000–2010. Clin Breast Cancer. 2010;10(3):188–95.
12. Berry DA, Cronin KA, Plevritis SK, et al. Effect of screening and adjuvant therapy on mortality from breast cancer. N Engl J Med. 2005;353:1784–92.
13. Bilynskyj BT. The breast cancer treatment as a marker of progress in oncology. Exp Oncol. 2010;32(3):190–4.
14. Winer E, Morrow M, Osborne K, et al. Cancer of the breast. In: Devita VT, Hellman S, Rosenberg SA, editors. Principles and practice of oncology. 6th ed. Philadelphia: J.B. Lippincott Co; 2001. p. 1651–717.
15. Shingleton WW. Chemotherapy of breast cancer. N C Med J. 1962;23:465–8.
16. Bedard PL, Cardoso F. Recent advances in adjuvant systemic therapy for early-stage breast cancer. Ann Oncol. 2008;19:122–7.
17. National Institute of health Consensus Statement. Adjuvant therapy for breast cancer. J Natl Cancer Inst. 2001;93:979–89.
18. Perou CM, Sorlies T, Eisen MB, et al. Molecular portraits of human breast tumors. Nature. 2000;406:747–52.
19. Sorlie T. Molecular portraits of breast cancer: tumor subtypes as distinct disease entities. Eur J Cancer. 2004;40(18):2667–75.
20. Bonadonna G, Brusamolino E, Valagussa P, et al. Combination chemotherapy as an adjuvant treatment in operable breast cancer. N Engl J Med. 1976;294(8):405–10.
21. Bonadonna G, Rossi A, Valagussa P. Adjuvant CF chemotherapy in operable breast cancer: ten years later. Lancet. 1985;325:976–7.
22. Early Breast Cancer Trialists' Collaborative Group. Effects of adjuvant tamoxifen and of cytotoxic therapy on mortality in early breast cancer: an overview of 61 randomised trials among 28 896 women. N Engl J Med. 1988;319:1681–92.
23. Early Breast Cancer Trialists' Collaborative Group. Effects of chemotherapy and hormonal therapy for early breast cancer on recurrence and 15-year survival: an overview of the randomised trials. Lancet. 2005;365(9472):1687–717.
24. Coombes RC, Bliss JM, Wils J, et al. Adjuvant cyclophosphamide, methotrexate, and fluorouracil versus fluorouracil, epirubicin, and cyclophosphamide chemotherapy in premenopausal women with axillary node-positive operable breast cancer: results of a randomized trial. The International Collaborative cancer Group. J Clin Oncol. 1996;14:35–45.
25. Wood WC, Budman DR, Korzun AH, et al. Dose and dose intensity of adjuvant chemotherapy for stage II, node-positive breast carcinoma. N Engl J Med. 1994;330:1253–9.
26. Budman DR, Berry DA, Cirrincione CT, et al. Dose and dose intensity as determinants of outcome in the adjuvant treatment of breast cancer. J Natl Cancer Inst. 1998;90:1205–11.
27. Citron ML, Berry DA, Cirrincione C, et al. Randomized trial of dose-dense versus conventionally scheduled and sequential versus concurrent combination chemotherapy as postoperative adjuvant treatment of node-positive primary breast cancer: first report of Intergroup trial C9741/Cancer and Leukemia Group B trial 9741. J Clin Oncol. 2003;21:1431–9.
28. Henderson IC, Berry DA, Demetri GD, et al. Improved outcomes from adding sequential paclitaxel but not from escalating doxorubicin dose in an adjuvant chemotherapy regimen for patients with node-positive primary breast cancer. J Clin Oncol. 2003;21:976–83.
29. Gennari A, Sormani MP, Pronzato P, et al. HER2 status and efficacy of adjuvant anthracyclines in early breast cancer: a pooled analysis of randomized trials. J Natl Cancer Inst. 2008;100(1):14–20.
30. Slamon DJ, Mackey J, Robert N et al. Role of anthracycline-based therapy in the adjuvant treatment of breast cancer: efficacy analyses determined by molecular subtypes of the disease. San Antonio Breast Cancer Symposium 2007, Symposium; 2007: Abstract 13.
31. Konecny GE, Pauletti G, Untch M, et al. Association between HER2, TOP2A, and response to anthracycline-based preoperative chemotherapy in high-risk primary breast cancer. Breast Cancer Res Treat. 2010;120(2):481–9.

32. Gianni L, Norton L, Wolmark N, et al. Role of anthracyclines in the treatment of early breast cancer. J Clin Oncol. 2009;27(28):4798–808.
33. Hayes DF, Thor AD, Dressler LG, et al. HER2 and response to paclitaxel in node-positive breast cancer. Cancer and Leukemia Group B (CALGB) Investigators. N Engl J Med. 2007;357(15):1496–506.
34. Martin M, Pienkowski T, Mackey J, et al. Adjuvant docetaxel for node-positive breast cancer. N Engl J Med. 2005;352:2302–13.
35. Ferguson T, Wilcken N, Vagg R, et al. Taxanes for adjuvant treatment of early breast cancer. Cochrane Database Syst Rev. 2007:Issue 4. Art. No.: CD004421. doi: 10.1002/14651858.CD004421.
36. Sparano J, Wang M, Martino S. Weekly paclitaxel in the adjuvant treatment of breast cancer. N Engl J Med. 2008;358:1663–71.
37. Jones SE, Savin MA, Holmes FA, et al. Phase III trial comparing doxorubicin plus cyclophosphamide with docetaxel plus cyclophosphamide as adjuvant therapy for operable breast cancer. J Clin Oncol. 2006;24:5381–7.
38. Slamon DJ, Clark GM. Amplification of c-erbB-2 and aggressive human breast tumors? Science. 1988;240: 1795–8.
39. Romond EH, Perez EA, Bryant J, et al. Trastuzumab plus adjuvant chemotherapy for operable HER2-positive breast cancer. N Engl J Med. 2005;353: 1673–84.
40. Piccart-Gebhart M, Procter M, Leyland-Jones B, et al. Trastuzumab after adjuvant chemotherapy in HER2-positive breast cancer. N Engl J Med. 2005;353: 1659–72.
41. Joensuu H, Kellokumpu-Lehtinen P, Bono P. Adjuvant docetaxel or vinorelbine with or without trastuzumab for breast cancer. N Engl J Med. 2006;354:809–20.
42. Slamon D, Eiermann W, Robert N, et al. Phase III randomized trial comparing doxorubicin and cyclophosphamide followed by docetaxel (AC→T) with doxorubicin and cyclophosphamide followed by docetaxel and trastuzumab (AC→TH) with docetaxel, carboplatin and trastuzumab (TCH) in Her2neu Positive Early Breast Cancer Patients: BCIRG 006 Study. Presented at the 32nd Annual San Antonio Breast Cancer Symposium; 2009 Dec: Abstract 62.
43. ALTTO (Adjuvant Lapatinib And/Or Trastuzumab Treatment Optimisation) Study; BIG 2-06/N063D. http://www.cancer.gov/#StudyIdInfo_CDR0000558836.
44. Beatson GT. On the treatment of inoperable carcinoma of the mamma. Sugestions for new method of treatment. Lancet. 1896;II:104–7.
45. Block GE, Jensen EV, Polley TZ. The prediction of hormonal dependency of mammary cancer. Ann Surg. 1975;182(3):342–52.
46. McGuire WL. Hormone receptors: their role in predicting prognosis and response to endocrine therapy. Semin Oncol. 1978;5:428–33.
47. Gustafsson JA. Therapeutic potential of selective estrogen receptor modulators. Curr Opin Chem Biol. 1998;2:508–11.
48. Burstein HJ, Prestrud AA, Seidenfeld J, et al. American society of clinical oncology clinical practice guideline: update on adjuvant endocrine therapy for women with hormone receptor-positive breast cancer. J Clin Oncol. 2010;28(23):3784–96.
49. Heel RC, Brogden RN, Speight TM, et al. Tamoxifen: a review of its pharmacological properties and therapeutic use in the treatment of breast cancer. Drugs. 1978;16(1):1–24. Review.
50. Higgins MJ, Stearns V. CYP2D6 polymorphisms and tamoxifen metabolism: clinical relevance. Curr Oncol Rep. 2010;12(1):7–15.
51. Dezentjé VO, van Blijderveen NJ, Gelderblom H, et al. Effect of concomitant CYP2D6 inhibitor use and tamoxifen adherence on breast cancer recurrence in early-stage breast cancer. J Clin Oncol. 2010; 28(14):2423–9.
52. Aubert RE, Stanek EJ, Yao J, et al. Risk of breast cancer recurrence in women initiatingtamoxifen with CYP2D6 inhibitors. J Clin Oncol. 2009;27:18s.
53. Dowsett M, Cuzick J, Ingle JN, et al. Meta-analysis of breast cancer outcomes in adjuvant trials of aromatase inhibitors versus tamoxifen. J Clin Oncol. 2010;28:509–18.
54. Johnston SRD. Dowsett M Aromatase inhibitors for breast cancer: lessons from the laboratory. Nat Rev Cancer. 2003;3:821–31.
55. Arimidex, Tamoxifen, Alone or in Combination (ATAC) Trialists' Group, Forbes JF, Cuzick J, et al. Effect of anastrozole and tamoxifen as adjuvant treatment for early-stage breast cancer: 100-month analysis of the ATAC trial. Lancet Oncol. 2008;9:45–53.
56. Breast International Group (BIG) 1–98 Collaborative Group, Thürlimann B, Keshaviah A, et al. A comparison of letrozole and tamoxifen in postmenopausal women with early breast cancer. N Engl J Med. 2005;353:2747–57.
57. Kaufmann M, Jonat W, Hilfrich J, et al. Improved overall survival in postmenopausal women with early breast cancer after anastrozole initiated after treatment with tamoxifen compared with continued tamoxifen: the ARNO 95 Study. J Clin Oncol. 2007;25(19):2664–9.
58. Coombes RC, Kilburn LS, Snowdon CF, et al. Survival and safety of exemestane versus tamoxifen after 2–3 years' tamoxifen treatment (Intergroup Exemestane Study): a randomised controlled trial. Lancet. 2007;369:559–70.
59. Mann BS, Johnson JR, Kelly R, et al. Letrozole in the extended adjuvant treatment of postmenopausal women with history of early-stage breast cancer who have completed 5 years of adjuvant tamoxifen. Clin Cancer Res. 2005;11(16):5671–7.
60. Fisher B, Bryant J, Wolmark N, et al. Effect of preoperative chemotherapy on the outcome of women with

operable breast cancer. J Clin Oncol. 1998;16: 2672–85.
61. Kuerer HM, Newman LA, Smith TL, et al. Clinical course of breast cancer patients with complete pathologic primary tumor and axillary lymph node response to doxorubicin-based neoadjuvant chemotherapy. J Clin Oncol. 1999;17:460–9.
62. Guarneri V, Broglio K, Kau SW, et al. Prognostic value of pathologic complete response after primary chemotherapy in relation to hormone receptor status and other factors. J Clin Oncol. 2006;24:1037–44.
63. Newman LA, Mason J, Cote D, et al. African-American ethnicity, socioeconomic status, and breast cancer survival: a meta-analysis of 14 studies involving over 10,000 African-American and 40,000 White American patients with carcinoma of the breast. Cancer. 2002;94:2844–54.
64. Levine PH, Steinhorn SC, Ries LG, et al. Inflammatory breast cancer: the experience of the surveillance, epidemiology, and end results (SEER) program. J Natl Cancer Inst. 1985;74:291–2.
65. Dawood S, Merajver SD, Viens P. International expert panel on inflammatory breast cancer: consensus statement for standardized diagnosis and treatment. Ann Oncol. 2011;22(3):515–523.
66. Bear HD, Anderson S, Brown A, et al. The effect on tumor response of adding sequential preoperative docetaxel to preoperative doxorubicin and cyclophosphamide: preliminary results from National Surgical Adjuvant Breast and Bowel Project Protocol B-27. J Clin Oncol. 2003;21(22):4165–74.
67. Buzdar AU, Ibrahim NK, Francis D, et al. Significantly higher pathologic complete remission rate after neoadjuvant therapy with trastuzumab, paclitaxel, and epirubicin chemotherapy: results of a randomized trial in human epidermal growth factor receptor 2-positive operable breast cancer. J Clin Oncol. 2005;23(16):3676–85.
68. http://www.cancer.gov/clinicaltrials/SWOG-S0800
69. Dienstmann R, Bines J. Evidence-based neoadjuvant endocrine therapy for breast cancer. Clin Breast Cancer. 2006;7(4):315–20.
70. Paik S, Tang G, Shak S, et al. Gene expression and benefit of chemotherapy in women with node-negative, estrogen receptor-positive breast cancer. J Clin Oncol. 2006;24(23):3726–34.

Percutaneous Image-Guided Treatment of Pediatric Malignancy

62

William E. Shiels, II and Mark J. Hogan

Abstract

Interventional radiologists continue to expand the diagnostic and therapeutic options available for pediatric oncology patients. Percutaneous radiofrequency ablation (RFA) and transarterial chemoembolization (TACE) are performed safely in children, providing new adjuncts in the armamentarium of therapies for childhood cancer. Percutaneous image-guided radiofrequency ablation (RFA) provides a viable and effective therapeutic option in the treatment of benign and malignant solid tumors in a variety of locations to include the skeleton, liver, spleen, kidney, adrenal gland, lung, and pancreas. Primary and metastatic malignancies as large as 8 cm in children are now effectively treated with RFA. The most common indications for RFA in children include hepatoblastoma, hepatocellular carcinoma (HCC), metastatic osteosarcoma, and Wilms tumor. TACE is an additional therapy, safely performed in children, providing effective therapy options for children with multifocal hepatoblastoma, paraganglioma, neuroblastoma, HCC, osteogenic sarcoma, and Wilms tumor. When TACE and surgery are combined, blood loss and operative time are reduced, while providing more efficacious therapy when combined to surgery alone. In conclusion, RFA and TACE provide children with safe and effective options for treatment of pediatric malignancy.

Interventional radiologists continue to expand the diagnostic and therapeutic options available for pediatric oncology patients. Pediatric oncologists and surgeons increasingly rely on partnership with pediatric interventional radiology for precise and effective percutaneous biopsy, tumor ablation, drainage, and vascular access procedures. With specific reference to image-guided therapy procedures and protocols, discussions of percutaneous radiofrequency ablation and transarterial chemoembolization in children will be the focus of this chapter.

W.E. Shiels, II (✉) • M.J. Hogan
Department of Radiology, School of Medicine,
The University of Toledo Medical Center, Columbus, OH, USA
e-mail: shiels.2@osu.edu; hogan.90@osu.edu

D.E. Dupuy et al. (eds.), *Image-Guided Cancer Therapy*, DOI 10.1007/978-1-4419-0751-6_64,

Radiofrequency Tumor Ablation

Percutaneous image-guided radiofrequency ablation (RFA) provides a viable and effective therapeutic option in the treatment of benign and malignant solid tumors in a variety of locations to include the skeleton, liver, spleen, kidney, adrenal gland, lung, and pancreas [1–31]. In these applications, the basic concepts of radiofrequency tumor ablation are similar: delivery of localized and contained heat induces focal coagulative necrosis and cell death. Cytotoxicity is best induced when regional temperatures are maintained between 50 °C and 100 °C. In the recent decade, the majority of RFA experience documented in pediatric and adult medical literature focuses on primary applications of RFA in the treatment of hepatocellular carcinoma (HCC) and osteoid osteoma [1–6]. Percutaneous RFA has expanding indications in the treatment of pediatric malignancy, most evolving in the treatment of multifocal, recurrent, or metastatic malignancies of bone, liver, kidney, and face with successful treatment of children as young as 1 year old [8–12]. This section will review details of pediatric unique care issues in percutaneous RFA with respect to general patient care and organ-specific RFA applications in the treatment of pediatric malignancy.

General Procedural Issues

Although adult percutaneous RFA in organs such as the liver, lung, and kidney may be successfully performed in adults with conscious sedation, children do not tolerate similar pain experiences, and thus, general anesthesia is required for RFA procedures in children. In the authors' clinical experience, pain, even with general anesthesia, can be significant enough to cause elevations in blood pressure and heart rate when the RFA heat contacts sensitive structures such as the pleura during lung RF ablation.

The use of prophylactic antibiotics is variable among authors and in specific tissue applications, especially when treating focal hepatic and renal malignancies [2, 5, 6, 8]. In the authors' pediatric experience, a single dose of preprocedural antibiotics is administered when treating focal liver, bone, and lung lesions, and to date, none of our cases have been complicated by abscess formation or sepsis.

The potential for skin burns exists with RFA due to heat distribution at the skin site of grounding pads used with monopolar RFA systems or if coaxial needles are not fully withdrawn adjacent to the insulated portion of the RFA needle. Thermal burns are best avoided with the use of large surface area foil-grounding pads, placed with the longest surface edge facing the RFA electrode, at a distance of 25–50 cm from the electrode [22]. In larger children, the thigh is often recommended as a good location for placement of up to four large (100 cm^2 each) foil pads. In young children, the thighs may be too small for placement of large foil pads. As an alternative large surface area structure, the buttocks serve well as a site for the foil pads when RFA is performed in the upper body.

Young children present with smaller body surface areas than their adult counterparts. Algorithms have been published that predict the range of core temperature elevation with RFA [13]. Given the relatively greater ratio of tumor volume to body surface area, the potential exists of greater total body-heating effect when large surface areas are treated with RF in children [8, 13]. In the authors' experience, total body temperature elevation has not been encountered in the treatment of focal liver tumors. On the other hand, body core temperature elevation as high as 40°C has been documented when treating large metastatic lung lesions, responding well to the use of a hypothermic blanket. When treating large volume tumors (5–8 cm diameter), patients are placed on a hypothermic blanket prior to beginning the RFA procedure. The use of a hypothermic blanket as cool as 20°C maintains body temperature at or below 38°C during prolonged RFA treatment of large volume malignancy in the chest [8, 13].

Pain control is critical in children, requiring a plan for each specific organ system and lesion being treated with RFA. In bone, liver, and lung, pain from RFA usually requires the

administration of intravenous narcotic analgesics for effective pain management. Pain following RFA is reported to be greatest 12–24 h following treatment, usually subsiding after a few days and is well managed with narcotic analgesia [8].

Hepatic Tumor Ablation

Hepatoblastoma and hepatocellular carcinoma are the most common hepatic malignancies in children [14–16]. In adults, the primary focus of hepatic tumor RFA is in treatment of hepatocellular carcinoma (HCC) or metastatic disease from organs such as the colon, pancreas, lung, and breast [1, 2, 5, 6]. Radiofrequency ablation treatment of hepatic malignancy (hepatoblastoma, HCC, metastatic leiomysarcoma) in children has been sporadically reported [8–10]. Hepatoblastoma patients that present the greatest clinical challenge are those with Beckwith-Wiedemann, with multiple hepatoblastomas developing over time. These patients are ideal candidates for RFA, given the risks of repeated surgeries for resection (Fig. 62.1). A percutaneous approach is used in the majority of reported pediatric hepatic tumor RF ablations. Overlapping RFA burns is performed in larger tumors, each site reaching a target temperature of at least 60°C over 12 min.

In the treatment of focal liver tumors, the authors would apply guidelines similar to adult literature, such that we expect complete tumor RFA in 90 % of patients with tumors smaller than 2.5 cm. Tumors 2.5–3.5 cm can be ablated in 70–90 % of cases; ablation of tumors 3.5–5.0 cm will be effectively ablated in 50–70 % of cases [2, 5, 25]. In large tumors (greater than 3.5 cm), and with conditions such as Beckwith-Wiedemann with recurrent hepatoblastoma, palliative RF ablation is a reasonable goal, if treatment can prolong life expectancy with limited systemic symptoms and few minor complications. Radiofrequency ablation, in combination with chemoembolization, is effective in the treatment of adult patients with HCC larger than 3.5 cm [27] and should be considered in similar situations in the pediatric patient.

Lung and Renal Malignancy Ablation

Radiofrequency ablation is an effective percutaneous option for treatment of solid lung malignancies in adults and children. The most common indication for lung RFA in children is metastasis such as osteogenic sarcoma primarily for patients who are not operative candidates [2, 8, 9, 28–30]. Both ultrasound and CT guidance for lung RF ablation cases have been utilized for metastatic lesions as large as 8 cm (Fig. 62.2), with CT most useful when lung precludes an effective sonographic window. In large bilateral lung tumor ablations, core body temperature elevations are maintained at 38–39°C with the use of a hypothermic blanket system (Medi-Therm II; Gaymar, Orchard Park, NY), with blanket cooling temperatures as low as 20°C [8]. Although initial experience shows that RFA ablation in the pediatric lung is well tolerated, the potential for fatal complications is reported in adult lung RFA treatment [28, 29].

The limited reported experience with percutaneous RFA of Wilms tumor and renal cell carcinoma developing in children with von Hippel-Lindau disease is promising [8, 19–21]. In these situations, percutaneous RFA is well tolerated, providing an effective nephron-sparing alternative to surgery especially for recurrent and multifocal Wilms tumor and Wilms tumor in patients with solitary kidney. Recent literature has shown that RF ablation of renal lesions during renal artery balloon occlusion results in larger effective zones of ablation, with a higher rate of infarction of normal renal tissue peripheral to the treated focus [31].

RFA Conclusion

Radiofrequency tumor ablation in children is rapidly evolving and is proving to offer effective therapeutic options in a variety of pediatric disorders. Radiofrequency ablation is well tolerated in children with few complications. As the pediatric experience grows, new opportunities for interdisciplinary treatment regimens that include

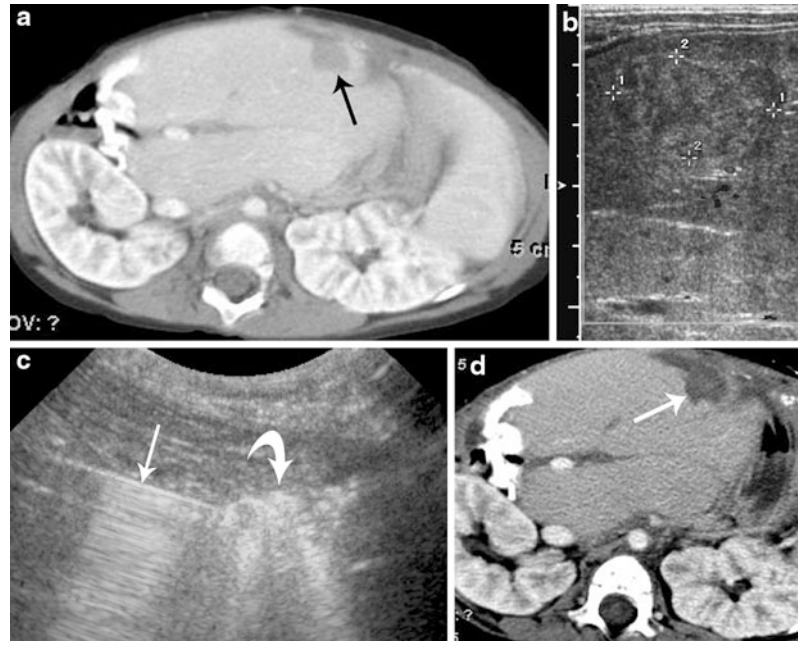

Fig. 62.1 Two-year-old male with Beckwith-Wiedemann syndrome and focal HB, treated with RFA. (**a**) Pretreatment CT (*arrow* indicates the focal HB). (**b**) Ultrasound with cursors *1* and *2* delineating the focal HB. (**c**) Sonogram during RF ablation with watercooled electrode (*straight arrow*)-inducing echogenic RF coagulation necrosis (*curved arrow*) in the tumor. (**d**) CT image at 1 month follow-up demonstrating complete ablation (*arrow*) of the focal HB

RF ablation will develop, defining clear roles for this versatile minimally invasive therapy.

Chemoembolization in Children

Chemoembolization is uncommonly performed in children. Reports are confined to case reports and case studies, with no randomized controlled studies available [32]. Pediatric chemoembolization has been performed for primary and metastatic hepatic malignancies (Fig. 62.3), osteogenic sarcoma, and Wilms tumor [33–44].

The basic principles of transarterial chemoembolization (TACE) are the same in both children and adults. Direct injection of the chemotherapeutic agent into the tumor allows for a greater concentration of the drug into the tumor with fewer systemic toxicities, while the embolization provides a longer dwell time and produces ischemia.

Pediatric Liver TACE

Indications for hepatic TACE in children include primary liver malignancies (predominately hepatoblastoma (HB) and hepatocellular carcinoma (HCC)) and metastatic disease such as sarcomas or neuroblastoma [33–44]. Hepatoblastoma accounts for 1 % of all pediatric malignancies [38]. While overall survival from HB is 63 %, a 90 % cure rate is possible if the tumor is resectable and the patient has no metastatic disease at diagnosis [36]. Complete surgical resection is the key [33]. Unfortunately, the tumor is initially unresectable in approximately 50 % [40, 42]. Systemic chemotherapy may shrink the tumor and allow later resection in up to 70 % of those patients [35, 36]. Unresectable patients receiving orthotopic liver transplantation (OLT) have a survival of 20–40 % and a recurrence rate of 50 % [35]. Otherwise, the outcome is dismal in tumors that remain unresectable. Due to toxicities of systemic chemotherapy, several investigators have attempted TACE to provide a greater tumor response while avoiding these complications [32, 33, 35–42]. The indications for TACE are not well established. TACE has been advocated for treating unresectable patients after failed systemic chemotherapy, for replacing primary systemic chemotherapy, as a bridge to OLT, and for palliative care [32, 35–40]. Initial attempts at TACE with HB were in patients with unresectable tumors despite systemic

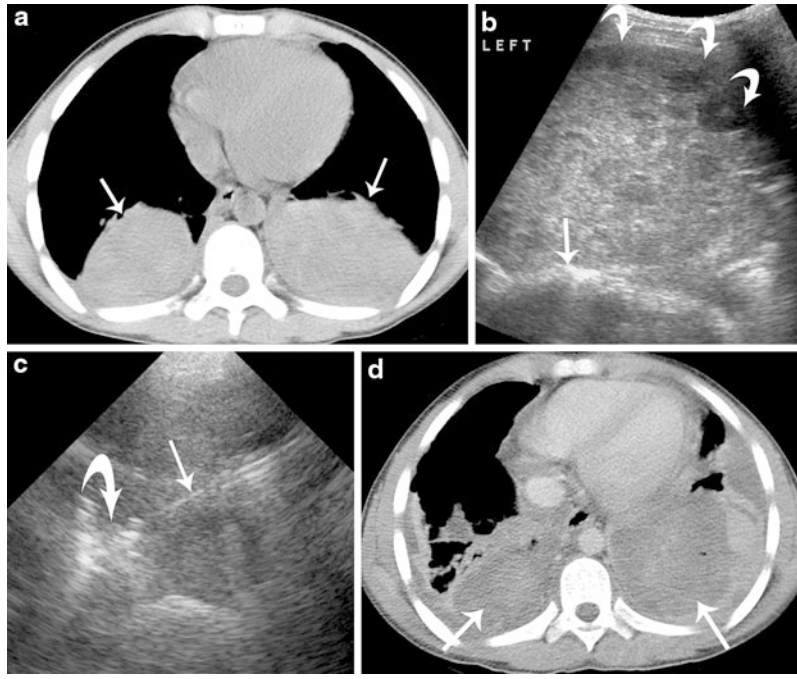

Fig. 62.2 Twelve-year-old male undergoing palliative RFAfor bilateral pulmonary metastatic ostoesarcoma. (**a**) CT image of the chest demonstrating bilateral pulmonary metastatic lesions (*arrows*), measuring 5 cm (*right*) and 8 cm (*left*). (**b**) Sonogram of the osteosarcoma (*curved arrows*) adjacent to normal lung (*straight arrow*) prior to RFA. (**c**) Sonogram during US-guided RF ablation (*straight arrow*-RF electrode) of the left metastatic lesion, demonstrating early coagulation necrosis echogenicity (*curved arrow*) during RFA. (**d**) CT image during second palliative RFA session demonstrating significant bilateral necrosis following the first RFA (*arrows*)

chemotherapy. Subsequently, TACE has been studied as the primary treatment for liver-only disease.

Arcement et al. reported on seven patients with unresectable HB treated by TACE [36]. These patients received cisplatin (90–150 mg/m^2) and/or adriamycin (30 mg/m^2) with gelatin sponge embolization in five of these patients. Lipiodol was not included in the TACE. One of these patients had significant reduction in the tumor size, but none became resectable. Three patients survived to the point of receiving OLT, with two still alive at the conclusion of the study. An additional patient was alive and awaiting OLT at 18 months. They concluded that TACE could be used as a bridge to OLT in unresectable patients who do not respond to systemic chemotherapy.

Malogolowkin et al. treated six children with HB, all of which remained unresectable after systemic chemotherapy [35]. Their protocol consisted of cisplatin (100 mg) and doxorubicin (30 mg), with one patient also receiving mitomycin (30 mg). This was mixed with bovine collagen (Angiostat, Regional Therapeutics, Inc, Pacific Palisades, CA) as an embolic agent and nonionic contrast to a volume of 8.75 ml. They did not use lipiodol and limited treatment to no more than 70 % of total liver volume and a maximum injected volume of 8.75 ml. All six children had a partial response (>50 % reduction in tumor volume). Three patients became resectable by imaging criteria, although two of these had residual microscopic disease. The patient with complete resection died of a recurrence in the residual liver. Both of the patients with microscopic residual disease survived, one after additional systemic chemotherapy and one after OLT.

Czanderna et al. reported on four patients with unresectable HB treated with TACE [39].

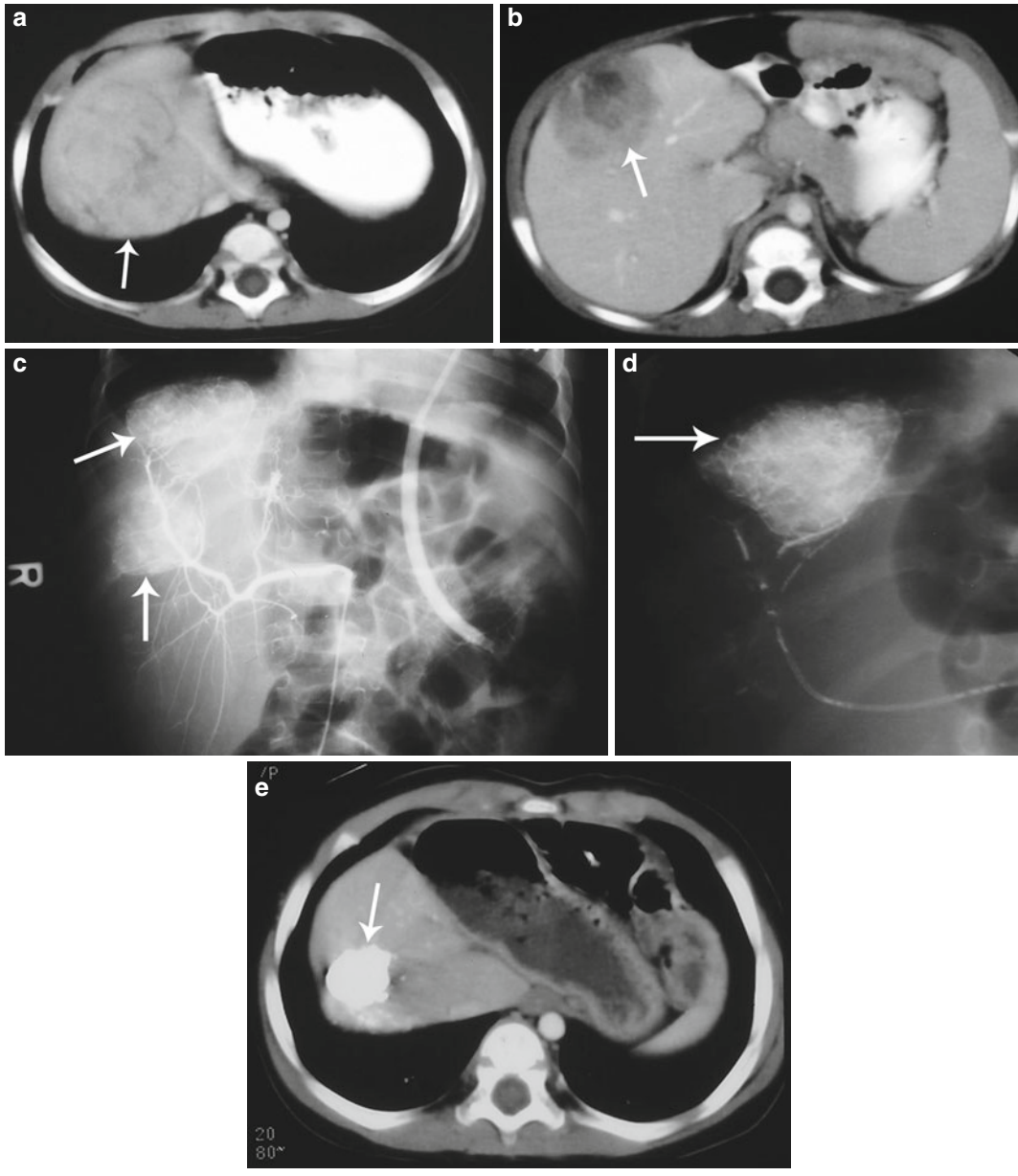

Fig. 62.3 Nine-month-old male with residual hepatoblastoma following partial hepatectomy, effectively treated with TACE (with no recurrence). (**a**) and (**b**) CT images demonstrating the two residual foci of HB (*arrows*). (**c**) Arteriogram with *arrows* indicating two foci of HB with well-defined arterial supply. (**d**) Microcatheter access with lipiodol contrast defining one of two foci treated with TACE (*arrow*). (**e**) Posttreatment CT demonstrating dense contrast in shrunken and necrotic focus (*arrow*) of previously treated HB

All patients had received systemic chemotherapy, using cisplatin (60 mg/m^2), doxorubicin (30 mg/m^2), and mitomycin (20 mg/m^2) mixed with 10 ml or less of lipiodol, and embolized with gelatin sponge. Patients received 1–3 courses of treatment. Three of the patients had a reduction in volume of between 25 % and 33 % and a decrease AFP 83–99 %. One patient died of systemic myelotoxicity before response could be assessed. One patient received OLT, and two were

resected. One patient died after resection, presumably as a cardiac complication from prior systemic chemotherapy.

Xuewu and colleagues reported on eight patients with unresectable HB [38]. They performed 1–3 TACE procedures on each patient with adriamycin (20 mg/m^2), vincristine (1.5 mg/m^2), and cisplatin (40 mg/m^2) mixed with 5–10 ml of lipiodol. They performed coil embolization afterward. Six of the eight (75 %) became resectable after the first TACE procedure, and the two others became resectable after further TACE procedures. One patient died of pneumonia. Six had surgery, and one patient refused surgery but elected to have TACE 3 times and no longer has detectable disease. All were disease-free 15–49 months after TACE.

Li et al. reported on 16 patients with unresectable HB treated with TACE [37]. Their protocol included cisplatin (40–50 mg/m^2), adriamycin (20–30 mg/m^2), and lipiodol. After infusing the chemotherapy, embolization was performed with gelatin sponge particles. Total treatment was limited to <70 % of the liver volume and no more than 10 ml of solution. Patients received 1–3 treatments. The tumors demonstrated a 19–82 % reduction in size (mean = 59.2 %), with reduction in the alpha fetoprotein (AFP) of 29–99 % (mean = 60 %). The tumor became completely resectable in 13/16 patients, with the additional 3/16 patients having a partial resection 4 weeks after the last TACE. Survival at 1, 2, and 5 years was 87.5 %, 68.7 %, and 50 %, respectively, with all receiving systemic chemotherapy after surgery. No patients had chemotoxicity from the TACE. The authors thought TACE may be a first-line treatment in patients without metastatic disease.

Ohtsuka and colleagues were the first to report on using TACE as the primary treatment for HB without metastatic disease [40]. They did not limit TACE to unresectable patients, with seven children in their study. Four patients were without metastatic disease and did not receive systemic chemotherapy. The three children with metastases received systemic chemotherapy prior to TACE. TACE used pirarubicin (30 mg/m^2) mixed with lipiodol (1 ml/maximum tumor diameter with 15 ml being the maximum volume given) and gelatin sponge embolization. Tumor volume reduced by 12–57 %. Complications included transient liver insufficiency in one patient who recovered in 6 days and pulmonary artery embolization of lipiodol in one patient who recovered in 2 weeks (lipiodol volume of 0.8 ml/maximum tumor diameter). They stated they believe the optimum lipiodol volume is 0.6 ml/maximum tumor diameter. All patients without metastatic disease at diagnosis had subsequent resection and were disease-free at the time of the report. The patients with metastatic disease all died, two of their metastatic disease and one from a secondary malignancy.

A similar study by Oue and colleagues had eight patients with HB [42]. Six patients had primary TACE and two had prior systemic chemotherapy before TACE. Only one patient had metastatic disease at diagnosis. This patient received systemic chemotherapy. The additional patient with systemic chemotherapy received it at an outside hospital prior to referral for TACE. TACE consisted of adriamycin (20–30 mg/m^2) and cisplatin (4–60 mg/m^2) mixed with lipiodol followed by gelatin sponge embolization. Tumor shrinkage varied from 0.9 % to 45 % with a mean of 25.8 %; after resection, pathology showed 71.1 % necrosis. All patients received systemic chemotherapy after surgery. Of the eight patients, six were disease-free and alive at the time of the report, although three received bone marrow transplantation due to elevated AFP levels. Two patients died of metastatic disease.

A case report by Xianliang et al. demonstrated a patient with an unresectable tumor treated solely by TACE and systemic chemotherapy [41]. The original tumor occupied 90 % of the total liver volume. TACE consisted of doxorubicin (20 mg/m^2), vincristine (1.5 mg/m^2), and cisplatin (40 mg/m^2) in 10 ml of lipiodol followed by coil embolization. Tumor volume reduction was 75 % after the first TACE, and after three TACE sessions, no discernable residual tumor was present. He then had six courses of systemic chemotherapy (vincristine and cisplatin) followed by an additional TACE. His disease-free survival was 33 months at the time of the study.

These reports and an additional case report demonstrate that TACE has utility in treating patients with HB [33]. Response rates seem to be better when lipiodol is used in the TACE procedure. The role of TACE as a primary treatment option after failed systemic chemotherapy, bridge to OLT, or for palliation cannot be known due to the lack of randomized control trials.

While HB is the most reported liver tumor in pediatric TACE, other tumors have been treated with this technique. Hepatocellular carcinoma (HCC), sarcomas, neuroblastoma, and a paraganglioma have been treated as well with TACE [34–36, 39, 43, 44]. In one study, three patients with HCC and two patients with undifferentiated sarcoma were treated with TACE [35]. All HCC patients had a partial response. Two became resectable with one survivor. The other resectable patient had microscopic residual, received two additional course of TACE, and died of liver failure. There was no response in the sarcoma patients, both of which died. Arcement in the same study as above had seven patients with HCC [36]. Four received intra-arterial chemotherapy. All of these patients died, two after OLT. Three patients had gelatin sponge embolization after intra-arterial chemotherapy. One patient had OLT and was alive at 14 months. A single patient with HCC was treated by TACE in another study; this patient died from pulmonary embolization of lipiodol [39]. There is a case report on TACE for neuroblastoma; this patient had Stage 4S and was treated with TACE due to the large mass effect from the tumor causing pulmonary and hepatic compromise [43]. This patient received 10 mg of cisplatin and 7 mg of doxorubicin with polyvinyl alcohol particle embolization. The tumor reduced in volume by 50 % and improved symptoms. Another case report showed TACE for metastatic paraganglioma [34]. This patient had anemia unresponsive to erythropoietin and iron supplementation from a paraneoplastic syndrome and would not receive blood products due to religious beliefs. He had intra-arterial infusion of 5-fluorouracil and then two rounds of TACE with doxorubicin and cisplatin mixed with lipiodol. Gelatin sponge embolization was then performed. His hemoglobin increased from 5.6 mg/dL to 17 mg/dL. He died of a postsurgical complication after resection of his primary chest mass.

TACE for Osteogenic Sarcoma

Osteogenic sarcoma is the most common primary bone malignancy in children. Limb salvage surgery is the preferred treatment, supplemented with chemotherapy. Intra-arterial administration of the chemotherapy directed into bone tumors has been described [45]. In addition, case series have been published describing TACE in patients with osteogenic sarcoma [46, 47]. In one series, pirarubicin (30–50 mg) and cisplatin (40–80 mg) were infused into the arteries supplying the primary tumor followed by gelatin sponge embolization [46]. Limb salvage surgery was then performed within a week. In this series of 47 patients, the authors found that there was significantly less blood loss, the operating time was less, and the resection was easier as the tumors had developed a pseudocapsule of fibrous edematous tissue in 43/47 patients. Mean tumor necrosis was 82.9 %. Follow-up was short, and it is unknown what will be the effect on local recurrence. The only complication was skin blistering in three patients.

Another study of 32 patients received an infusion of methotrexate (1–2 gm), pharmorubicin (30–50 mg), and cisplatin (60–100 mg) [47]. The embolic agents included adriblastine gelatin microspheres, anhydrous alcohol with lipiodol, common bletilla tuber with lipiodol, and gelatin sponge. Necrosis occurred in 85.5 % of patients with extent being 81.6–87.9 %, although gelatin sponge results were significantly lower than the others. All patients also received systemic chemotherapy and had limb salvage surgery. The surgery was aided by the stable to decreased tumor size and less blood loss. Survival at 1, 2, and 5 years was 95.5 %, 72 %, and 42 %, respectively. Local recurrence occurred in three between 3 and 6 months after the procedure.

TACE for Wilms Tumor

Two reports are published on TACE for Wilms tumor, although both are on the same patient population [48, 49]. They treated 24 patients with TACE and compared them to a control group of 20. Their protocol was doxorubicin (20 mg/m^2), cisplatin (50 mg/m^2) mixed with lipiodol (0.5 ml/kg), and saline (5–15 ml) with gelatin sponge embolization. Mean tumor size reduction was 48.2 %. At 2-year follow-up, their conclusion was that TACE and surgery was superior to surgery alone. Survival at 2 years was 83.3 % in the TACE group and 10 % in the surgical group. At 1 year, 16.6 % of the TACE group was alive and disease-free as compared to the control group with only 40 %. Pathological specimens showed tumor cell necrosis, degeneration, and apoptosis; increased interstitial fibrous tissue hyperplasia; and lymphocyte infiltration [49].

References

1. Goldberg SN, Dupuy DE. Image-guided radiofrequency tumor ablation: challenges and opportunities-part I. J Vasc Interv Radiol. 2001;12:1021–32.
2. Dupuy DE, Goldberg SN. Image-guided radiofrequency tumor ablation: challenges and opportunities-part II. J Vasc Interv Radiol. 2001;12:1135–48.
3. Rosenthal DI, Hornicek FJ, Wolfe MW, Jennings LC, Gephart MC, Mankin HJ. Changes in the management of osteoid osteoma. J Bone Joint Surg. 1998;80:815–21.
4. Woertler K, Vestring T, Boettner F, Winkelmann W, Heindel W, Lindner N. Osteoid osteoma: CT-guided percutaneous radiofrequency ablation and follow-up in 47 patients. J Vasc Interv Radiol. 2001;12:717–22.
5. Ahmed M, Goldberg SN. Thermal ablation therapy for hepatocellular carcinoma. J Vasc Interv Radiol. 2002;13:S231–43.
6. Livraghi T, Solbiati L, Meloni MF, Gazelle GS, Halpern EF, Goldberg SN. Treatment of focal liver tumors with percutaneous radiofrequency ablation: complications encountered in a multicenter study. Radiology. 2003;226:441–51.
7. Rocourt DV, Shiels WE, Hammond S, Besner GE. Contemporary management of benign hepatic adenoma using percutaneous radiofrequency ablation. J Pediatr Surg. 2006;41(6):1149–52.
8. Shiels WE, Brown SD. Radiofrequency tumor ablation in children. In: van Sonnenberg E, McMullen W, Solbiati L, editors. Tumor ablation: principles and practice. New York: Springer; 2005. p. 488–95.
9. Hoffer FA. Pediatric applications of radiofrequency ablation. Semin Interv Radiol. 2003;20(4):323–31.
10. Jingjing Y, Qiang S, Minju L, Tian-an J. Percutaneous radiofrequency ablation for treatment of hepatoblastoma recurrence. Pediatr Radiol. 2008;38(9):1021–3.
11. Nashida Y. Radiofrequency ablation used for the treatment of frequently recurrent rhabdomyosarcoma in the masticator space in a 10-year-old girl. J Pediatr Hematol/Oncol. 2007;29:640–2.
12. Brown SD, van Sonnenberg E, Morrison PR, Diller L, Shamberger R. CT-guided radiofrequency ablation of pediatric Wilms tumor in a solitary kidney. Pediatr Radiol. 2005;35(9):923–8.
13. Sawada M, Watanabe S, Tsuda H, Kano T. An increase in body temperature during radiofrequency ablation of liver tumors. Anesth Analg. 2002;94(6):1416–20.
14. Katzenstein HM, Krailo MD, Malogolowkin MH, et al. Hepatocellular carcinoma in children and adolescents: results from the pediatric oncology group and the children's cancer group intergroup study. J Clin Oncol. 2002;20:2789–97.
15. Bellani FF, Massimino M. Liver tumors in childhood: epidemiology and clinics. J Surg Oncol. 1993;53:119–21.
16. Exelby PR, Filler RM, Grosfeld JL. Liver tumors in children in the particular reference to hepatoblastoma and hepatocellular carcinoma. American Academy of Pediatrics Surgical Section Survey 1974. J Pediatr Surg. 1975;10:329–37.
17. Iannitti DA, Dupuy DE, Mayo-Smith WW, Murphy B. Hepatic radiofrequency ablation. Arch Surg. 2002;137:422–6. discussion 427.
18. Gervais DA, McGovern FJ, Arellano RS, McDougal WS, Mueller PR. Renal cell carcinoma: clinical experience and technical success with radiofrequency ablation of 42 tumors. Radiology. 2003;226:417–24.
19. Gervais DA, McGovern FJ, Wood BJ, et al. Radiofrequency ablation of renal cell carcinoma: early clinical experience. Radiology. 2000;217:665–72.
20. Roy-Choudhury SH, Cast JE, Cooksey G, Puri S, Breen DJ. Early experience with radiofrequency ablation of small solid renal masses. AJR Am J Roentgenol. 2003;180:1055–61.
21. Goldberg SN, Solbiati L, Halpern EF, Gazelle GS. Variables affecting proper system grounding for radiofrequency ablation in an animal model. J Vasc Interv Radiol. 2000;11:1069–75.
22. Ramnath RR, Rosenthal DI, Cates J, Gebhardt M, Quinn RH. Intracortical chondroma simulating osteoid osteoma treated by radiofrequency. Skeletal Radiol. 2002;31(10):597–602.
23. Chopra S, Dodd GD, Chanin MP, Chintapalli KN. Radiofrequency ablation of hepatic tumors adjacent to the gallbladder; feasibility and safety. AJR Am J Roentgenol. 2003;180:697–701.

24. Livraghi T, Lazzaroni S, Meloni F. Radiofrequency thermal ablation of hepatocellular carcinoma. Eur J Ultrasound. 2001;13:159–66.
25. Ahmed M, Lobo SM, Weinstein J, Kruskai JB, Gazelle GS, Halpern EF, Afzal SK, Lenkinski RE, Goldberg SN. Improved coagulation with saline solution pretreatment during radiofrequency tumor ablation in a canine model. J Vasc Interv Radiol. 2002;13: 717–24.
26. Bloomston M, Binitie O, Fraiji E, et al. Transcatheter arterial chemoembolization with or without radiofrequency ablation in the management of patients with advanced hepatic malignancy. Am Surg. 2002;68:827–31.
27. Shankar S, van Sonnenberg E, Silverman SG, Tuncali KT, Morrison PR. Combined radiofrequency and direct alcohol infusion for percutaneous tumor ablation. Presented at the 88th Scientific Assembly and Annual meeting, RSNA. Chicago; 2002 Dec.
28. Dupuy DE, Zagoria RJ, Akerley W, Mayo-Smith WM, Kavanagh PV, Safran H. Percutaneous radiofrequency ablation of malignancies in the lung. AJR Am J Roentgenol. 2000;174:57–9.
29. Simon CJ, Dupuy DE, DiPetrillo TA, et al. Pulmonary radiofrequency ablation: long-term safety and efficacy in 153 patients. Radiology. 2007;243:268–75.
30. Nakamura T, Matsumine A, Yamakado K, et al. Lung radiofrequency ablation in patients with pulmonary metastases from musculoskeletal sarcomas. Cancer. 2009;115(16):3774–81.
31. Kariya Z, Yamakado K, Nakatuka A, Onaoda M, Kobayasi S, Takeda K. Radiofrequency ablation with and without balloon occlusion of the renal artery: an experimental study in porcine kidneys. J Vasc Interv Radiol. 2003;14:241–5.
32. Guvnén P. Liver embolizations in oncology; a review. Part I. Arterial (chemo) embolizations. Med Oncol. 2008;25(1):1–11.
33. Tashjian DB, Moriarty KP, Courtney RA, Bean MS, Steele DA. Preoperative chemoembolization for unresectable hepatoblastoma. Pediatr Surg Int. 2002;18(2–3):187–9.
34. Mutabagani KH, Klopfenstein KJ, Hogan MJ, Caniano DA. Metastatic paraganglioma and paraneoplastic-induced anemia in an adolescent: treatment with hepatic arterial chemoembolization. J Pediatr Hematol Oncol. 1999;21(6):544–7.
35. Malogolowkin MH, Stanley P, Steele DA, Ortega JA. Feasibility and toxicity of chemoembolization for children with liver tumors. J Clin Oncol. 2000;18(6):1279–84.
36. Arcement CM, Towbin RB, Meza MP, Gerber DA, Kaye RD, Mazariegos GV, Carr BI, Reyes J. Intrahepatic chemoembolization in unresectable pediatric liver malignancies. Pediatr Radiol. 2000;30(11):779–85.
37. Li JP, Chu JP, Yang JY, Chen W, Wang Y, Huang YH. Preoperative transcatheter selective arterial chemoembolization in treatment of unresectable hepatoblastoma in infants and children. Cardiovasc Intervent Radiol. 2008;31(6):1117–23.
38. Xuewu J, Jianhong L, Xianliang H, Zhongxian C. Combined treatment of hepatoblastoma with transcatheter arterial chemoembolization and surgery. Pediatr Hematol Oncol. 2006;23(1):1–9.
39. Czauderna P, Zbrzezniak G, Narozanski W, Korzon M, Wyszomirska M, Stoba C. Preliminary experience with arterial chemoembolization for hepatoblastoma and hepatocellular carcinoma in children. Pediatr Blood Cancer. 2006;46(7):825–8.
40. Ohtsuka Y, Matsunaga T, Yoshida H, Kouchi K, Okada T, Ohnuma N. Optimal strategy of preoperative transcatheter arterial chemoembolization for hepatoblastoma. Surg Today. 2004;34(2):127–33.
41. Xianliang H, Jianhong L, Xuewu J, Zhongxian C. Cure of hepatoblastoma with transcatheter arterial chemoembolization. J Pediatr Hematol Oncol. 2004;26(1):60–3.
42. Oue T, Fukuzawa M, Kusafuka T, Kohmoto Y, Okada A, Imura K. Transcatheter arterial chemoembolization in the treatment of hepatoblastoma. J Pediatr Surg. 1998;33(12):1771–5.
43. Weintraub M, Bloom AI, Gross E, Revel-Vilk S, Shahroor S, Koplewitz BZ, Freeman AI. Successful treatment of progressive state 4s hepatic neuroblastoma in a neonate with intra-arterial chemoembolization. Pediatr Blood Cancer. 2004;43(2):148–51.
44. Uemura S, Todani T, Watanabe Y, Toki A, Sato Y, Morotomi Y, Ohkawa M, Kojima K, Seo H. Successful left hepatectomy for hepatocellular carcinoma in a child after transcatheter arterial chemoembolization; report of a survival. Eur J Pediatr Surg. 1993;3(1): 54–6.
45. Wang MQ, Dake MD, Wang ZP, et al. Isolated lower extremity chemotherapeutic infusion for treatment of osteogenic sarcoma; experimental study and preliminary clinical report. J Vasc Interv Radiol. 2001;12: 731–7.
46. Zhang HJ, Yang JJ, Lu JP, Lai CJ, Sheng J, Li YX, Hao Q, Zhang SM, Gupta S. Use of intra-arterial chemotherapy and embolization before limb salvage surgery for osteosarcoma of the lower extremity. Cardiovasc Intervent Radiol. 2009;32(4):672–8.
47. Chu JP, Chen W, Li JP, Zhuang WQ, Huang YH, Huang ZM, Yang JY. Clinicopathologic features and results of transcatheter arterial chemoembolization for osteosarcoma. Cardiovasc Intervent Radiol. 2007;30(2):201–6.
48. Liu WG, Gu WZ, Zhou YB, Tang HF, Li MJ, Ma WX. The prognostic relevance of preoperative transcatheter arterial chemoembolizaton (TACE) and PCNA/VEGF expression in patients with Wilms' tumour. Eur J Clin Invest. 2008;38(12):931–8.
49. Li JP, Chu JP, Oh P, Li Z, Chen W, Huang YH, Yang JY. Characterizing clinicopathological findings of transarterial chemoembolization for Wilms tumor. J Urol. 2010;183(3):1138–44.

Perspectives in Image-Guided Cancer Therapy: Comments from Patients and Families

63

Damian E. Dupuy and Derek Tessier

Abstract

Medicine remains an art that not only treats the patient, but also treats their family as well. The following excerpts are but one of many chapters in the lives of patients, families, friends undergoing cancer treatment. Lives and relationships began well before there was cancer and will forever be changed by cancer.

Case # 1 RV

My diagnosis of kidney cancer started in the most peculiar of ways. I was originally diagnosed with stage IV renal cancer in October of 2000. I had a slowly enlarging bump on my forehead. I was surprised that the doctor wanted to even biopsy it. I was quite a bit more surprised at the results of the biopsy. Much to my dismay, the biopsy showed that I had metastatic kidney cancer. I thought, "seriously, kidney cancer on my forehead!" After the initial shock and an even shorter period of time, I had thrown at me tests I never thought I would ever need. The truly bad news came in the form of a 6-cm tumor in my left kidney.

D.E. Dupuy
Department of Diagnostic Imaging, Rhode Island Hospital, Providence, RI, USA

D. Tessier
Department of Radiology, Rhode Island Hospital, Providence, RI, USA
e-mail: dtessier@lifespan.org

My doctors were also concerned about an area in my liver. This is not how my life plan was supposed to unfold. I went on to undergo surgery to remove the tumor in my left kidney. The only treatment the doctors would consider for me was to remove the entire kidney or what is referred to as a radical left nephrectomy. So, in December of 2000, I went to get my kidney, but, more importantly, my tumor removed. An intraoperative ultrasound of my liver at the time of my kidney surgery was negative for tumor. Luckily or unluckily, depending on how you view it, during my cancer staging, I was also found to have a multinodular goiter in my thyroid. I ultimately had the left side of my thyroid gland removed. Much to my chagrin, this too proved to be a cancer, completely separate from my kidney. While we are on the subject, the other side of my thyroid gland eventually became abnormal and was removed in 2001. This too was positive for cancer.

After surgery for my kidney cancer, I felt I needed some time to absorb all this. I did have an opportunity to participate in a clinical trial, but I chose not to do so at the time. Many follow up

D.E. Dupuy et al. (eds.), *Image-Guided Cancer Therapy*, DOI 10.1007/978-1-4419-0751-6_65,

CAT scans and time went on and I thought I was in the clear. Then, 2005 came along, and with it, a presumed small metastases appeared in my lungs. Apparently I was more concerned about this than the doctors were. The doctors reassured me that this type of cancer is very slow growing. This was palatable considering all the CAT scans I had done had shown such a slow progression.

Over the next several years, I was closely observed. One tumor, two tumors, and eventually a few tumors arose in my lungs. I was reassured that these were not considered large or serious enough for systemic or surgical treatment. Then, in January of 2009, I learned about a new 3-cm tumor in my remaining kidney. The situation went from bad to worse. In addition to the kidney tumor, I now also had three new metastases in my pancreas. Naturally, not only was I concerned, surprised, and very worried about issues such as kidney failure, dialysis, or breathing, now the thought of death loomed in my mind.

When I started losing hope, my oncologist, Dr. Constantinou, described a potential treatment process to me, radiofrequency ablation. It seemed like science fiction. They were going to heat up and cook my tumor? She referred me to Dr. Mayo-Smith in the image-guided tumor ablation department at Rhode Island Hospital. I was seen very promptly. I was met with friendly, helpful, and knowledgeable staff. In my case, Dr. William Mayo-Smith and Derek Tessier his nurse practitioner explained to me a procedure that could not only salvage my kidney but also save me from going on dialysis. I have to say that I met with an incredibly professional staff that explained every minute detail in a way that I fully understood. No one spoke above or beyond me. Now, I had to make the decision to move forward as this was the way I felt I needed to go.

Other possible treatments including systemic treatment like Sutent versus a local treatment for my kidney like ablation were discussed in depth with numerous doctors including Dr. Constantinou and Dr. Mayo-Smith. I also received second opinions on this matter from a local Providence urologist as well as a second urologist/oncologist at the Bertucci Clinic for Genitourinary Cancers at Massachusetts General Hospital.

After carefully considering my treatment options, I would ultimately end up choosing ablation because it seemed to me to be the most effective and least toxic way of dealing with the most threatening tumor, the one in my kidney. After all, I did not and do not like the prospect of going on any type of dialysis. Since my prior nephrectomy, my kidney function has gotten slightly worse, and the thought of dialysis has been a constant on my mind.

Prior to ablation, the recommendation was to have a biopsy, which, not surprisingly, came back positive for another renal cell cancer. I carefully weighed all my options again and proceeded with radiofrequency ablation. Very matter of fact, I responded very well to both the biopsy and ablation treatment. Healing and pain management were handled very well, and after 2 weeks and another CAT scan, I found out that the ablation had successfully ridded my body of the tumor. All sorts of thoughts and scenarios go through your mind when you hear the word "cancer." After receiving the unwelcomed information that I had a tumor in my only remaining kidney and the prospect of my whole life changing and being dictated and dominated by dialysis treatments, the possibility of ablation was and will always remain a gift. It was a huge relief to know that such an option was available to me.

I feel that I was thoroughly and accurately prepared for the possible risks, benefits, and outcomes of the ablation. Although my choices were limited, remaining off dialysis and continuing to work full time are things that are very important to both me and my wife. The ablation itself was practically painless. I feel like I remember much of the procedure, or at least think I do. The medications make for quite a surreal experience. You get pictures or thoughts in your head of what is happening. They're actually cooking a cancerous tumor in my kidney.

To my delight, the ablation and its recovery was less painful than I had prepared for. It was amazing that I was literally back on my feet only a few hours later. Ultimately, I was off my pain medications within 24 h and returned to work within 4 days of the procedure. It was quite

interesting to learn that my results are quite typical. After all this bad luck, my procedure like many before and many after went on without a single glitch. If I'd been able to have coffee during the ablation and the subsequent couple of hours in the recovery area, I'd say the experience would have been perfect.

I am not completely out of the woods, but I do feel very lucky and very good. It has been 1 year since the procedure, and subsequent CAT scans have shown the tumor in my kidney to be dead and only minimal growth of the remaining tumors in my lungs and pancreas. I have a continued sense of gladness despite all that has happened. It is even more interesting to hear people say how "lucky" I am. I wouldn't necessarily call myself being lucky as calling myself being blessed.

Please see the attached copy of a letter that my wife later wrote to the chairman of the radiology department concerning how we *both* felt not only about the ablation process but also about the people and the quality of care I received during the treatment.

I'm writing this letter a couple of months later than I would have liked, but life has been hectic.

On behalf of my husband RV and myself, I simply wish to make you aware of the exceptional level of care RV received throughout this winter and spring from the entire staff at the Department of Interventional Radiology. Most notably, Dr. Mayo-Smith and Clinical Manager Derek Tessier have earned our deepest respect, confidence and gratitude. My husband's medical situation is fraught with renal complications that make treatment, in particular, radiologic diagnostics and treatment, knotty at best. During RV's treatment, Dr. Mayo-Smith and his colleagues showed a degree of attention to detail, inventive problem-solving and most important: coordination of care, that we never expected – despite Dr. Mayo-Smith's acknowledged and sterling reputation. RV and I have spent nearly a decade dealing with his renal (and other) cancer and the attendant medical fallout thereof. During this time we have received nearly all of his care at Rhode Island Hospital, and we've met some exceptional doctors. Invariably, it's been difficult to express our thanks to these MDs in person: they tend to become self-effacing and evasive, or suddenly they have someplace else they needed to be ten minutes ago – zoom! (We have always found this hugely comical, given the apocryphal and ubiquitous stories one hears concerning doctors and their insatiable egos). Hence, RV and I are hopeful that in writing you, we are expressing our thanks in a way that is both meaningful and bearable (heavy sarcasm on the 'bearable') to you, Dr. Mayo-Smith, Derek Tessier, Amy Doorley, the receptionists, the ablation secretary and the recovery room nurses – the list goes on and on.

Thank you for taking the time to read this letter. Thank you even more for the standard of care which your department provides.

Very Truly Yours,
KT

Case # 2 BL

I never thought it would take cancer to bring me from Denmark to the United States. For quite some time, I was experiencing pain in my back, which did not dissipate in spite of massage, exercise, and pain killers. I saw my general practitioner several times before they finally diagnosed [cancer].

At first I did simply not believe it. Then I got sort of a shock, and the first thing I did was immediately stop smoking and have not done since. Together with my husband, we decided to fight as much as possible against the disease. Unfortunately, I was diagnosed at a stage 4 non-small cell lung cancer (NSCLC). In addition to a tumor in my right lung, I also had metastasis to vertebral bodies and several lymph nodes in my mediastinum.

A radiologist friend in Spain told me about radiofrequency ablation (RFA). I did as much research on this topic as possible and came across Dr. Damian Dupuy at Rhode Island Hospital. My radiologist friend encouraged me to contact Rhode Island Hospital in Providence. I did not even know it was possible to do such a procedure in the lung, since it seemed to be such a delicate intervention in moving tissue. He said that Professor Dupuy was among the best in the world at performing RFA.

We still had to get by the first round of treatment before we were even considered for RFA. This would mean many months of treatment before Dr. Dupuy would consider treating me. As it was already, the doctors did not want to perform an operation or remove the tumor in the lung, since I already had metastases. They offered chemotherapy, a combination of carboplatin and vinorelbine, as well as radiation to the metastasis in the spine.

For many reasons, the most of which is the socialized aspect of European medicine, I had traveled Spain to get test done after my chemotherapy, more specifically a PET/CT. This scan showed that the lung tumor was still "hot" in spite of its decreased size. There was a reduction of the lung tumor by 30 % and a significant response in the lymph nodes. Being in Europe, we felt our options were quite limited, and the oncologists were debating to put me on more chemotherapy. We did not feel that this would be aggressive enough.

We decided then and there that although I did get some response for the chemotherapy, we still needed to pursue any reasonable treatment that may offer me a better prognosis, even if it meant leaving home to get it. Since RFA not only seemed like a promising opportunity, it was one the few remaining options we had left to choose from. When we made this decision, we wanted to receive the best care possible. So, we sent my latest scans across the Atlantic Ocean to Dr. Dupuy for review. Once we heard the wonderful news that he felt I would be a suitable patient, we headed over to Providence, Rhode Island. While in Providence, we also met with the medical oncologist to get their opinion on treatment regimens. We met with Professor Dupuy the day before the ablation. By our previous correspondence and after meeting with the doctor, we were well prepared for what was going to occur. We all felt that a biopsy of the right lung tumor was a good idea prior to the ablation to check for genetic mutations.

The actual ablation itself was without any special physical problems. We returned home a short 3 days later. The weeks that followed did come with some cough and residues from the tumor coming up from the lung. I also experienced a small inflammation in the lung, and as a precaution, I was admitted to the hospital and treated with antibiotics. The biopsy showed that I may be sensitive to Tarceva, so I was eventually placed on this medication. Thus far, I have had a moderately positive response.

I am very happy I got the ablation. To be diagnosed and to learn that your cancer is too far advanced to be considered for surgery is a lonely and helpless place. It seemed like all I was getting was bad news. I was told that an operation could not be done. To know that the tumors growing inside me were more aggressive and ever, can make one panic and sink into a depression. Luckily, chemotherapy and radiation allowed me to advance to the next step of therapy, ablation.

Ablation for me was a good thing. I am extremely grateful to Professor Dupuy and his entire staff – they are all so kind and highly professional. The RFA was, in my opinion, the only opportunity for me a year ago, and it was simply fantastic it could be done in such a place as Rhode Island Hospital in Providence. Despite my trip being a medical one, the experience I had was no less than rewarding. I felt encouraged by the doctors and well taken care of by the staff. I am still sending my follow-up scans from Denmark and Spain to get Professor Dupuy's opinion on my progress.

On the flip side of the physical aspect of cancer, there is the emotional side. This was and is a whole separate arena. On one hand, it was a considerable relief to get the tumor inside you treated. The "devil" inside, inside my lung, is now dead. But, in your mind and in my case, literally in my bones, he still lurks.

For quite a while since my ablation, I was having a normal life without much interruption. I was still playing golf from time to time. I have recently needed to be restarted on chemotherapy. I feel that I have realistic expectations and continually hope that the worst is over. I continue also to be grateful for each passing day and to all those around me.

Case # 3 GC

I was first diagnosed with a "spot" on my kidney. As if it was not already bad enough that I was being worked up for serious back pain that eventually required corrective surgery. As I was being worked up for herniated disk, the orthopedic surgeon mentioned that the MRI taken for my back and spine revealed a spot on my left kidney. I was in disbelief and skeptical. I knew I would have to have this checked out sooner than later by a specialist whoever that may eventually be. It was psychologically difficult having to wait to get an answer about what was happening in my kidney.

Following my return to health from the disk surgery, my primary care physician referred me to a kidney specialist. It seemed at times that my life was moving in slow motion as I was waiting to be seen by the urologist. This tumor in my kidney certainly prompted me to look into resources such as the Internet to help me satisfy my own inquisitiveness. I found Internet and the resources out there were really overwhelming.

I was finally referred to a urologist, Dr. Joseph Renzulli, who would operate on my kidney if that was to be the final recommendation. I voiced my concerns to Dr. Renzulli about having yet another surgery following my two recent disk surgeries. Follow-up corrective surgery to my original disk surgery, a second surgery, was necessary because of a postoperative infection. He sent me to the team led by Dr. Damian Dupuy at Rhode Island Hospital to meet and discuss my situation. I was informed that my case was not exactly unique. I was told that a majority of kidney cancers were found incidentally while having imaging studies for an unrelated medical issues. In my case, they discovered my cancer while I was having imaging for my disk herniation. I was also informed that up to 25 % of tumors my size could be benign. Dr. Dupuy recommended a biopsy procedure to determine the etiology of this tumor. At that same meeting, I was also made aware of the ablation process as a method of treating tumors if they came back as cancer.

Many doctors may say and agree that it is not necessarily an emergency when they find a tumor in the kidney, but when that tumor is in your own kidney, it can be quite nerve racking. The biopsy was promptly performed by Dr. Dupuy. I went into the biopsy optimistic, but being a realist, I knew the odds were against me. I was reassured that a vast majority of these kidney tumors are also very slow growing and that I could have had this tumor for years. This was scary but reassuring.

Following receipt of the biopsy results which were positive for cancer, Dr. Renzulli met with me, and we discussed the options to have the tumor removed. They were partial nephrectomy, total nephrectomy, or tumor ablation, as well as the probability of total correction of this problem by any of these methods. Based on my feelings about going through another major surgery and the size and location of the tumor, Dr. Renzulli then sent me back to see Dr. Dupuy to further discuss ablation to treat my kidney tumor. I needed some time to think about my options. I met with my closest family members, my wife, and children. Discussions with others, whose opinions I trust, confirmed my feelings that I wanted to go through with the less invasive tumor ablation process. Dr. Dupuy described the tumor ablation procedure and prepared me for what he proposed. He discussed radiofrequency ablation and cryoablation as my options. He selected the latter with an explanation of this would be safer for me given the tumor's location in the kidney.

The procedure seemed to be incredibly noninvasive. I was really surprised that several long needles were being placed directly into the tumor. My only major reaction to the procedure was one of mild discomfort and some physical pressure, but, to my surprise if not delight, no real pain physically or psychologically.

I was mobile on my feet and home later that day. At this age, I am not certain that I believe in miracles, but I do consider myself incredibly fortunate to have been introduced to this procedure and the professionals performing it.

My experience was totally positive. Obviously, I did not want to be diagnosed with a cancer, but from the time that I first met

with Dr. Renzulli, and through my total experience with Dr. Dupuy and the entire staff at Rhode Island Hospital, I feel that I have been treated by consummate, caring professionals.

I have lived my adult life in excellent health and prior to this experience had never had any major health issues, other than a knee that was surgically repaired years ago following my years of running. I am quite sure my days of running are long gone, but there are still many roads for me to walk down. I feel as though a great weight has been lifted off my shoulders. Hopefully all the fuss with cancer is now behind me, and I can move ahead with my life. I feel in very good health now and expect to be back in perfect health in the near future.

Case # 4 FF

I had lived what I considered to be a relatively healthy life. That was about to change very quickly and without much warning. I was soon to find out about my lung cancer in the fall of 2006 as a result of a routine checkup and chest x-ray. This led to a bevy of other tests that I wish I had never heard of. Because of the abnormal chest x-ray, I went on to have a CT scan then a PET scan, all of which indicated the presence of sugar-avid lesion in the right upper lobe [lung] as well as several lesions elsewhere in the lung which were not, however, avid. Concomitantly, there appeared two lymph nodes in my right neck. The nodes in my neck were biopsied and there proved the presence of thyroid cancer. The doctors also wanted to biopsy the area in my lung, but this proved more difficult than anticipated. In a strange twist, I was eventually found to have a primary lung cancer as well as a metastasis of my thyroid cancer in my lung.

I couldn't believe all this was happening. Obviously, I reacted with shock and in many ways disbelief. How I wished I hadn't smoked for 36 years. How I wished I had quit sooner, better yet never smoked at all. But, I was also spurred to action trying to learn as much as possible about my treatment options. I discussed my case with a number of great doctors at Johns Hopkins and other institutions. I am always seeking to gather more than one opinion and do what makes the most sense to me and, of course, the represented consensus of the treating doctors. I really felt as if I became a member of the treating crew. These diagnoses fueled me into actively pursuing a vested interest in not only my health but my mortality. I almost felt as if I was a third party doing research on this strange case of two primary cancers in the same organ.

After the thyroid biopsy, I underwent thyroid surgery and shortly thereafter had radioactive iodine treatments. Without much time for recovery, I went on to have surgery on my right upper lobe lung tumor. As you know, this proved to be a second primary lung cancer. Unfortunately, there were some tumor cells around the resected cancer, and it was recommended that I go on to have additional treatments with chemotherapy. After all this, there was still another tumor in the lower part of my right lung that didn't respond to either treatment that we were all keeping a close eye on.

This began my road to ablation, which was arduous and actually quite round about. Luckily, I had the resources to do my own form of clinical research for my condition. I was fastidious about researching my condition, my treatment options, and those providers with the most experience performing these particular diagnostic tests and treatments. I went from John Hopkins' oncologist favoring a second traditional thoracotomy where they surgically remove the part or lobe of the lung. After having all too recently gone through this incredibly invasive surgery, I had another doctor speak to me about performing a biopsy at MD Anderson. I opted for the less invasive biopsy at MD Anderson.

After the biopsy, we learned that the lesion in my lung was indeed metastatic thyroid cancer rather than another primary lung carcinoma or worse yet metastatic lung cancer. I went back to Hopkins for more consultation and finally decided that I did not and could not withstand another surgery.

Learning of your diagnosis is a double-edged scenario. On one hand, you are relieved of sorts that now we have an answer. On the other hand, you ask now what do we do with this

information? It is important to note from all the information that I gathered from my many e-mails, conversations, and consultations with a whole slew of excellent doctors, that I became totally convinced that I could not suffer through another surgery. Thus, ablation looked to be the solution for my current problem and without hesitation went for ablation.

I knew what I had to do, what I had been doing, I educated myself about alternatives to thoracotomy, and once I decided on ablation, the obvious choice, which as an alternative to surgery, was eventually recommended by both MD Anderson and Hopkins knowledgeable people. The next step was figuring out who I would entrust to undertake this procedure. For me, the answer was to go and see Dr. Damian Dupuy. The rest of the story just falls into place. My ablation experience was pretty flawless. I had sent my medical information up to Providence for Dr. Dupuy's review. I spoke to his nurse practitioner and afterward traveled up to Providence to meet up with Dr. Dupuy and his team. I had a consultation of the first day, my lung ablation on the second, and after a quick stop at his office on the third day, I was headed to the airport to fly home.

This seemed almost surreal as I was conjuring thoughts of my previous surgical treatments and the whirlwind of events occurring during my recoveries. I was a bit surprised that my ablation experience was not that unique. How the team at Rhode Island Hospital described the course of my treatment and how this course played actually out was not only typical, according to them, but expected.

My physical response was no less than stellar. I guess I was also very lucky that no complications arose. In turn, my emotional response was equally positive because the physical response was positive. I felt very confident in Dr. Dupuy. He and his team really accorded me a VIP treatment topped with a final cappuccino and pastry after the treatment.

As aforementioned, my experiences with surgery were very negative. I had experienced unexpected and unforeseen complications associated with my hospital stays (including a falling in the hospital, retinal detachment in the middle of chemotherapy, and innumerable other disasters). Considering my past, I was frankly expecting a lot worse out of the ablation. After my ablation, I was very pleasantly surprised that I could walk out of the hospital the same day I was admitted and fly back home the next.

In my condition, I feel remarkably well. Not a single doctor nor myself expected my surviving to this day. Thus, all things considered, each day, each activity, and each interaction I consider to be a gift.

Case # 5 CS

This case is being written on behalf of my mother CS. Although CS was and remains a relatively independent woman, I have been intimately caring for her medical needs for many years. Her and my story all begin in 2004 when she had complained of shortness of breath. She had two appointments with her primary physician about 6 months apart. When symptoms did not seem to improve, her doctor ordered a chest x-ray. The first x-ray did not show much of anything. Her cough persisted and fortunately or unfortunately the second x-ray did show a "spot." With a smoking history spanning about 60 years, we were prepared for the worst. At 83 years of age, my mother was scheduled to have a biopsy. The biopsy confirmed our and the doctor's suspicion. CS, me, and her whole family would now be contending with cancer. We learned shortly after the first CAT scan that we were not only dealing with a single area in the lung, there was a second spot in the back of her lung.

We thought about what we needed to do. The major obstacle was that we really did not know where or who to turn to get this knowledge. In many if not all ways, we really felt like we were at the mercy of the doctors. Luckily, all the doctors with whom we would eventually meet with, seemed to not only be great at what they do, but also work with my mom as person, not just another patient. Better yet, we really sensed a comprehensiveness the doctors had with each other.

The thoracic surgeon was the first to evaluate my mother. He felt that her age, lung function, and the presence of two tumors rendered her to be not best served by surgery. We were then referred to the radiation oncologist, Dr. DiPetrillo, who despite probably being able to treat my mother felt that a team approach to address both tumors would require us to see another doctor for consideration of a more lung sparing treatment. This treatment, we would learn, was radiofrequency ablation.

We were anxious to get the lung tumors treated and saw each passing day as a delay. Why we're seeing so many doctors? Our situation was put into perspective. There were just so many necessary steps to ensure that all of our bases were covered. We were soon more thankful and glad to have doctors making not only standard treatments available to us, but also made treatments that they felt were more appropriate for my mother's own particular health needs. At this point, we were introduced to Dr. Dupuy.

Dr. Dupuy and Dr. DiPetrillo coordinated a treatment plan that allowed CS to get both of her lung tumors treated while causing as little damage to her more normal surrounding lung tissue. After learning the disheartening news that surgery was too risky, we were relieved that CS was not out of options. Luckily, now, there was a treatment. There was hope.

CS eventually had a total of four ablations. The first ablation was the easiest for her. She really does not recall a single uncomfortable response. The second ablation was followed by a planned additional radiation treatment. This also went exceedingly well. Unfortunately, the tumors reared their ugly heads again! We were really hopeful that we were out of the woods. The third ablation was not as easy as the first two. She experienced a collapsed lung and had to be admitted to the hospital. After a few days, she felt fine and returned to her everyday routines. The fourth ablation, mind you 4 years later, did take a toll on CS.

The procedure itself went very well, and CS was discharged home under my care. Later that evening, she started to experience chills, nausea, and flu-like symptoms. Dr. Dupuy told us that a small percentage of patients do experience flu-like symptoms. She was hospitalized for a couple of days and was released from the hospital with oxygen. Even though this was not completely unexpected and unanticipated, we were anticipating the fourth ablation to go as smoothly as the first couple. That being said, CS was off her oxygen in a matter of weeks and back to her old self and playing bridge with friends.

My mother is in her late 80s and has experienced a total of four ablations. All in all, I am convinced that all of these treatments have allowed CS to live longer. Of course, the last ablation was a bit trickier than the previous ones for both her and me. Being her closest daughter, working full time, and dealing with a family of my own, it was slightly difficult helping care for an otherwise healthy independent woman. Seeing the situation from another perspective, it actually allowed me to spend more time with her.

Currently, CS is still living independently. She has seen many years of holiday gatherings, graduations, weddings, the births of great grandchildren, and a lifetime worth of memories. Recently, my mother's cancer has yet again returned. As a family, we determined it was best not to have any further treatments or ablations after two new tumors were detected in 2010. Luckily, even with the new tumors, CS does not have any ill feelings other than an occasional flare up of her emphysema. She is, and I know I am, forever grateful for the caring doctors and staff and for the additional time – measured in years – we are still enjoying together.

Derek, my mother asked me to add that she feels that she received great treatment from Dr. Dupuy and you and that you are both truly and genuinely concerned and considerate. That includes Robin [your ablation secretary] as well. I second that emotion!

Case # 6 AK

My name is Ray, and I am writing this on behalf of my recently deceased wife, AK. Our journey began many years ago when we first met in college, but our story began in December of 2003 when a routine chest x-ray showed a shadow on

my wife's lung. So began many chapters in our life that lasted 6 years and sadly came to an end this past fall.

We were first seen by the lung doctor and in turn referred to a thoracic surgeon. AK went on to have a mediastinoscopy prior to her proposed surgery to remove the tumor. Within days of meeting the surgeon and without much warning, we were told that the tumor cells from the lung were now in the lymph nodes and surgery was not an option. We were soon off to the medical and radiation oncologist for chemotherapy and eventual radiation.

We were handed a second heavy blow that her cancer was not only inoperable it was also incurable. Believe me, rather upsetting news to the two of us. But, if you knew my wife and you were in the room the very same minute this information was told to us, you would have thought we each received different news. She reacted with such great poise. She was a fighter and vowed to fight to the very end. She kept her promise.

She did not begin chemotherapy right away, as the doctors were concerned that there may not be a place in her treatment for this. Bam! More bad news. We went on to see the radiation oncologist, Dr. DiPetrillo. They "restaged" her cancer, and the new recommendations were radiation treatments along with chemotherapy.

We were incredibly relieved to know something could now be done. We were so discouraged initially to learn that AK had cancer and there wasn't much we or anyone could do much about. We were even more encouraged after her course of treatment. Her cancer had responded. This was obviously what we hoped and prayed for, but we also had been schooled on cancer and the statistics, and the literature was filled with grim facts, black and white facts. We had realistic expectations. But within a year, we had already gone from no treatment options to a CAT scan 12 months later showing that the doctors could not see any cancer at all.

Unfortunately, the excitement of this news was relatively short lived. In September of 2005, we were hit with more disturbing news. The cancer was back. Each time we received bad news, we would always try to see the positive side. In AK's mind, the fact remained that despite this setback, there was still other treatment available; there was still hope. Most of our hope came in the form of family and prayer. We had chosen to limit the knowledge of AK's cancer to very few family members and even fewer friends. So, we depended on the support from not only a relatively small group of friends but from her doctors.

Our prayers did not go unanswered, and our next wave of hope came in the form of Dr. Damian Dupuy. When that new spot in the right lung was detected after a PET scan in September 2005, Dr. Dipetrillo referred us over to see if AK was a good candidate for a new procedure, one we had never heard of which literally involved cooking the tumor.

We met with Dr. Dupuy and were explained the procedure known as radiofrequency ablation. We were amazed about his technology. Our hope hit a small bump in the road when we were disheartened to learn that our insurance company would not pay for the procedure. That would be the end of our story had we listened to our insurance company. But, you don't know my wife like I do. With many phone calls and borderline "threats," we inevitably got approval for the ablation procedure from our insurance company. We never even rescheduled the procedure. AK confidently disagreed and fought with our insurance and would not let them determine her treatment, determine her fate, or determine if she lived or died.

With butterflies in our stomachs, we arrived to the hospital for AK's ablation only to receive rather good news, no, great news. No treatment was necessary. The CAT scan that Dr. Dupuy performed before the anticipated ablation had shown that the "tumor" had shrunk and was possibly just inflammation. Scheduling the procedure and the insurance issue provoked a lot of emotions. We wished in some ways that would be the last we needed to see of Dr. Dupuy.

Another whole year went by before we eventually received more bad news. A PET scan from September 2006 showed the area in the right lung had grown again. We weren't sure if this is how tumors behaved. Do they come and go? This time it was the real deal. A biopsy showed the cancer

was back, and we were back at Dr. Dupuy's discussing the biopsy results and scheduling her lung ablation shortly thereafter.

The ablation went well. We won't kid you though, it hurt like hell. They told us that the tumor was right up against the lining of the lung and to expect pain. Admittedly, AK was not one for pills and did not take her pain medications as prescribed and paid for it with a trip to the emergency room. We were wondering if we had made the right decision. The short answer came with some IV pain medications and her follow-up CAT scan images which had shown that the ablation had killed the tumor. The pain improved and the positive results of the follow-up CAT scan certainly relieved much if not all of the anxiety we were having.

Fast forward almost a year and as an aside, during routine follow-up for her lung tumor, we were back in Dr. Dupuy's office discussing an incidental tumor found in her left kidney. As luck would have it, this area was completely unrelated to her lung cancer, and the kidney tumor was zapped with yet another ablation procedure without much fanfare. I was relieved that this was not only covered by my insurance without so much as a peep but, practically, pain-free. We were all so relieved that she did so well with the procedure.

So many things were happening in our lives. Why couldn't cancer give us a break? There were engagements, marriages, birthdays, holidays, bills, and work. But, AK always found time to put her cancer on the shelf sometimes for minutes, sometimes for hours, or even days at a time. She learned more than I'll ever know how to appreciate the events in each and every day as a seemingly small milestone.

AK was already a statistic anomaly. She kept motoring. However, by March of 2008, we received more bad news. You well know the cancer was back in her lung. Still though, she always looked at the silver lining. She looked at the fact that while some people were at the end of their rope with emotions or worse yet treatment options, there was still a treatment for her. There was still hope to rid herself of this. There was still one more ablation.

She did very well with her last ablation treatment, and we wish we could say that the cancer was kept away. The most we can say is that it was kept at bay. Like clockwork, her cancer eventually returned. Then again, we know it never really left her physically; it just left for brief periods of time. When June came around, she was not feeling well. The spiral began, and AK's health began to unravel. You can guess how this story, how this life, and how my partnership with this beautiful woman of 41 years ends. I do not need to recount the days.

We will always remember our doctors and the time, care, and compassion they had shown to the both of us. We will remember extra time spent explaining what was going on and what we could do. They eased my and AK's suffering both physically and emotionally. I won't necessarily miss our visits to the hospital. However, I will miss the people who cared for my wife, and I will always really miss my wonderful lady.

Erratum to: The Role of Image-Guided Surgery in Breast Cancer

Kambiz Dowlatshahi, Rosalinda Alvarado, and Katherine Kopkash

Owing to an unfortunate oversight the family name of the third author, Katherine Kopkash, was misspelled in this chapter.

The online version of the original chapter can be found at http://dx.doi.org/10.1007/978-1-4419-0751-6_61

D.E. Dupuy et al. (eds.), *Image-Guided Cancer Therapy*, DOI 10.1007/978-1-4419-0751-6_66,

Index

D.E. Dupuy et al. (eds.), *Image-Guided Cancer Therapy*, DOI 10.1007/978-1-4419-0751-6,